

J. SEBAG
EDITOR

Vitreous

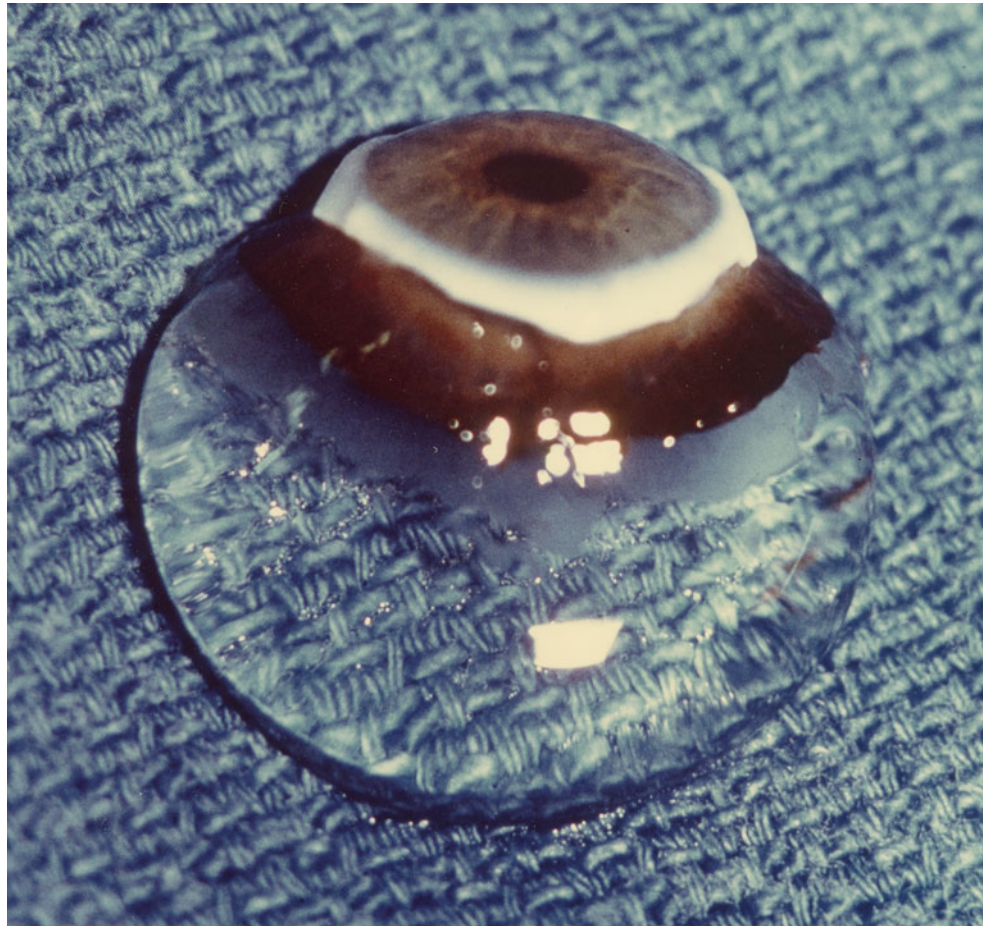
in Health and Disease

Vitreous

J. Sebag
Editor

Vitreous

in Health and Disease



Editor-in-Chief

J. Sebag, MD, FACS, FRCOphth, FARVO
VMR Institute for Vitreous Macula Retina
Huntington Beach
California
USA

Videos to this book can be accessed at
<http://www.springerimages.com/videos/978-1-4939-1085-4>

ISBN 978-1-4939-1085-4 ISBN 978-1-4939-1086-1 (eBook)
DOI 10.1007/978-1-4939-1086-1
Springer New York Heidelberg Dordrecht London

Library of Congress Control Number: 2014951881

© Springer Science+Business Media New York 2014

This work is subject to copyright. All rights are reserved by the Publisher, whether the whole or part of the material is concerned, specifically the rights of translation, reprinting, reuse of illustrations, recitation, broadcasting, reproduction on microfilms or in any other physical way, and transmission or information storage and retrieval, electronic adaptation, computer software, or by similar or dissimilar methodology now known or hereafter developed. Exempted from this legal reservation are brief excerpts in connection with reviews or scholarly analysis or material supplied specifically for the purpose of being entered and executed on a computer system, for exclusive use by the purchaser of the work. Duplication of this publication or parts thereof is permitted only under the provisions of the Copyright Law of the Publisher's location, in its current version, and permission for use must always be obtained from Springer. Permissions for use may be obtained through RightsLink at the Copyright Clearance Center. Violations are liable to prosecution under the respective Copyright Law.

The use of general descriptive names, registered names, trademarks, service marks, etc. in this publication does not imply, even in the absence of a specific statement, that such names are exempt from the relevant protective laws and regulations and therefore free for general use.

While the advice and information in this book are believed to be true and accurate at the date of publication, neither the authors nor the editors nor the publisher can accept any legal responsibility for any errors or omissions that may be made. The publisher makes no warranty, express or implied, with respect to the material contained herein.

Printed on acid-free paper

Springer is part of Springer Science+Business Media (www.springer.com)

Foreword

Notwithstanding its position at the center of the eye, vitreous has historically been mostly ignored by the world. Although vitreous integrity is required for a clear optical pathway and intraocular pressure maintenance, these are passive qualities, and this, the largest structure of the eye, was never regarded as possessing critical active functions. The ever-expanding body of basic and clinical science knowledge, however, has led to a growing appreciation of the importance of vitreous in health as well as disease. Additionally, a recent surge of novel therapeutics for vitreoretinal disorders prompts a thorough reexamination of the vitreous body. Given that there is even promise of newer, more effective, and less invasive avenues of therapy (both curative and preventive), it is imperative that we understand vitreous, beginning with the recognition of its status as an organ and not just a space.

Vitreous is more than a vestigial space filler within the eye. Charles Luc Schepens, 1989

In 1930, Sir Stewart Duke-Elder authored a monograph published in the British Journal of Ophthalmology entitled *The Nature of the Vitreous Body*. It was 72 pages long and contained very little clinical information. A monograph written by Sebag in 1989 entitled *The Vitreous – Structure, Function, and Pathobiology* was 173 pages long and provided considerable insights into the relevance of basic science information on vitreous to our understanding of vitreoretinal disease. By 2002, a single-author treatise on vitreous was no longer possible, as evidenced by the Rapport de la Société Française d’Ophtalmologie entitled *Pathologie du Vitré*, edited by Gerard Brasseur. Six section editors and 31 authors produced a comprehensive treatise that was 493 pages in length. In 2014, we find ourselves the beneficiaries of a sufficient extension in our understanding of vitreous that it has taken five section editors and 90 authors to produce a tome of nearly 1,000 pages, inspired, compiled, and edited by Jerry Sebag. This present volume appears on the 25th anniversary of the editor’s first book on vitreous. That landmark achievement by a single author has been widely regarded as the definitive text for more than two decades but can now be supplanted. Fortunately, Dr. Sebag himself has undertaken the Herculean task of assembling the current knowledge of the vitreous body by internationally respected experts and integrating the chapters with extensive cross-referencing, thereby greatly enriching the tome.

In this book, vitreous comes into its own in terms of its importance in the eye and, therefore, its contribution to the most amazing sense—vision. Vitreous has long been respected, and even feared, when disrupted by trauma or with surgical invasion (a surgeon’s “bête noire” as termed by Machemer) but has not been the subject of as much investigation as the retina or cornea. Indeed, vitreous has been considered simply an optical pathway by optical specialists, a space filler that maintains pressure to keep the eye inflated by glaucoma specialists, an environment for inflammation/infection by cataract surgeons, and a possible impediment before the retina by retinal surgeons. To mitigate these shortfalls, this book discusses in depth the role of vitreous in ocular physiology (*health*) and pathology (*disease*).

Of note, this book is written for both clinicians and scientists—to update the former on where we are and the latter on where we need to go. Thus, there are many fundamental perspectives presented herein, as evidenced by dedicating four sections to basic sciences: Biochemistry (section editor Paul Bishop of Manchester, England); Anatomy, Development, and Aging; Pathology and Pathobiology; as well as Physiology and Pharmacotherapy (section editor Einar Stefánsson of Reykjavik, Iceland). However, throughout the book, this material is presented with a view to clinical relevance. Further, in contrast to the first installment in 1989, this book has assembled considerable information on therapy as performed today by surgery (section editors Susanne Binder of Vienna, Austria, and Larry Chong of Los Angeles, California) and as will be performed tomorrow by pharmacologic vitreolysis and gene therapy.

One of the basic premises of this book is that while it is important to review and examine what is known, it is just as important to consider what is not known and frame questions for future exploration in our never-ending quest to preserve and restore vision. Before you can seek the answers, you must understand and appreciate the questions. This book strives to do much of the former and even more of the latter.

Learn from yesterday, live for today, hope for tomorrow.

The important thing is not to stop questioning. Albert Einstein, 1916

New York, New York

D. Jackson Coleman, MD, FACS, FARVO

New York, New York

Harvey A. Lincoff, MD

Preface

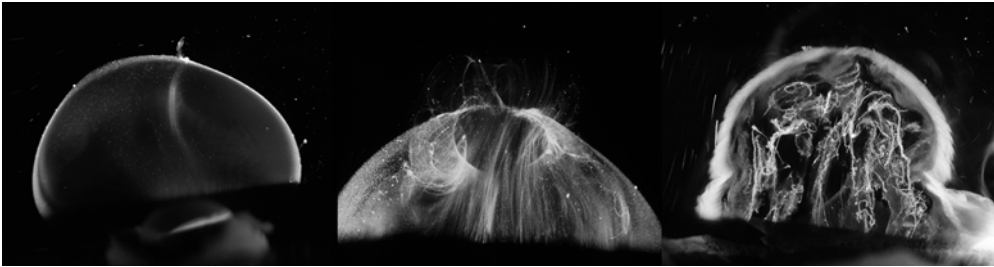
This project began a few years ago at the suggestion of many colleagues who proposed that it was time for a new book on vitreous. In 2014, we celebrate the 25th anniversary of the first vitreous book published by Springer (as well as Springer's 50th anniversary of publishing in America), and this new book reflects how much more has been learned about vitreous since 1989. As was true of the first book, however, this work still aims to bridge the gap between basic and clinical sciences, providing clinicians with a better understanding of the scientific basis of health and disease and scientists with an appreciation of where their expertise is needed to solve clinical problems. Though I initially conceived of this project as a monograph like the first book, it rapidly became apparent that at this time in our advancement, the topic of vitreous is too vast and complex to be adequately addressed by a single author. Thus, a multi-author platform was chosen to garner a richness of experience and diversity of opinion. The authors come from various backgrounds with different skills and styles. Yet, they have allowed their immense and varied experiences to be blended into a compendium of today's knowledge that will hopefully serve readers for years to come. The team that was assembled consists of individuals from around the world who were familiar with each other and, in many cases, were already close friends. We labored long and hard, with the process bringing us all even closer. Indeed, this book has formed a connection that will link us forever. For that, I thank each and every author, for I will cherish this bond for the rest of my life.

There are many others to thank for their notable and important contributions.

My Jewish heritage instilled in me the spirit of the quest for knowledge and learning. With their support, encouragement, and love, my parents showed me how this quest could be pleasurable and personally rewarding. They further made it possible for me to pursue studies at the finest institutions, surrounded by brilliant and stimulating people. In 1978, I met Endre Balazs, who introduced me to vitreous from the critical perspective of basic science and encouraged me to seek a better understanding of its composition, organization, and role in health and disease. Charles Schepens supported the continued development of this research at the Eye Research Institute of Retina Foundation in Boston where he taught me the relevance of a scientific basis to our understanding of disease. Always eager to help patients, Dr. Schepens emphasized the essential role science plays in the development of better ways to manage their illnesses. One day, however, the teaching stopped. Yet, learning is lifelong. In 1986, my venerable professors at Columbia and Harvard were replaced by a new group of teachers—my patients. To them I am indebted for allowing me the privilege of participating in their experiences and learning from the momentous events in their lives that we shared. They, as is life, were the best teachers of all.

Of special note is the important role played by Alfredo Sadun, my longtime friend and colleague. We met more than three decades ago at Harvard, where he allowed me the use of his camera to photograph human vitreous structure. Many of those images appear in this book. As the consummate renaissance man of science and philosophy, Alfredo has continued to support my quest and graciously has not only facilitated my work but also amplified my scientific research and development as a collaborator and valuable colleague.

Of course, the most critical role of all was played by my closest friend and mate for life, my wonderful wife Jacqui. Resilient, patient, tender, loving, and filled with a very deep understanding of life and me, my Mukai has been extraordinary. It is, indeed, her time that went into the writing of this book.

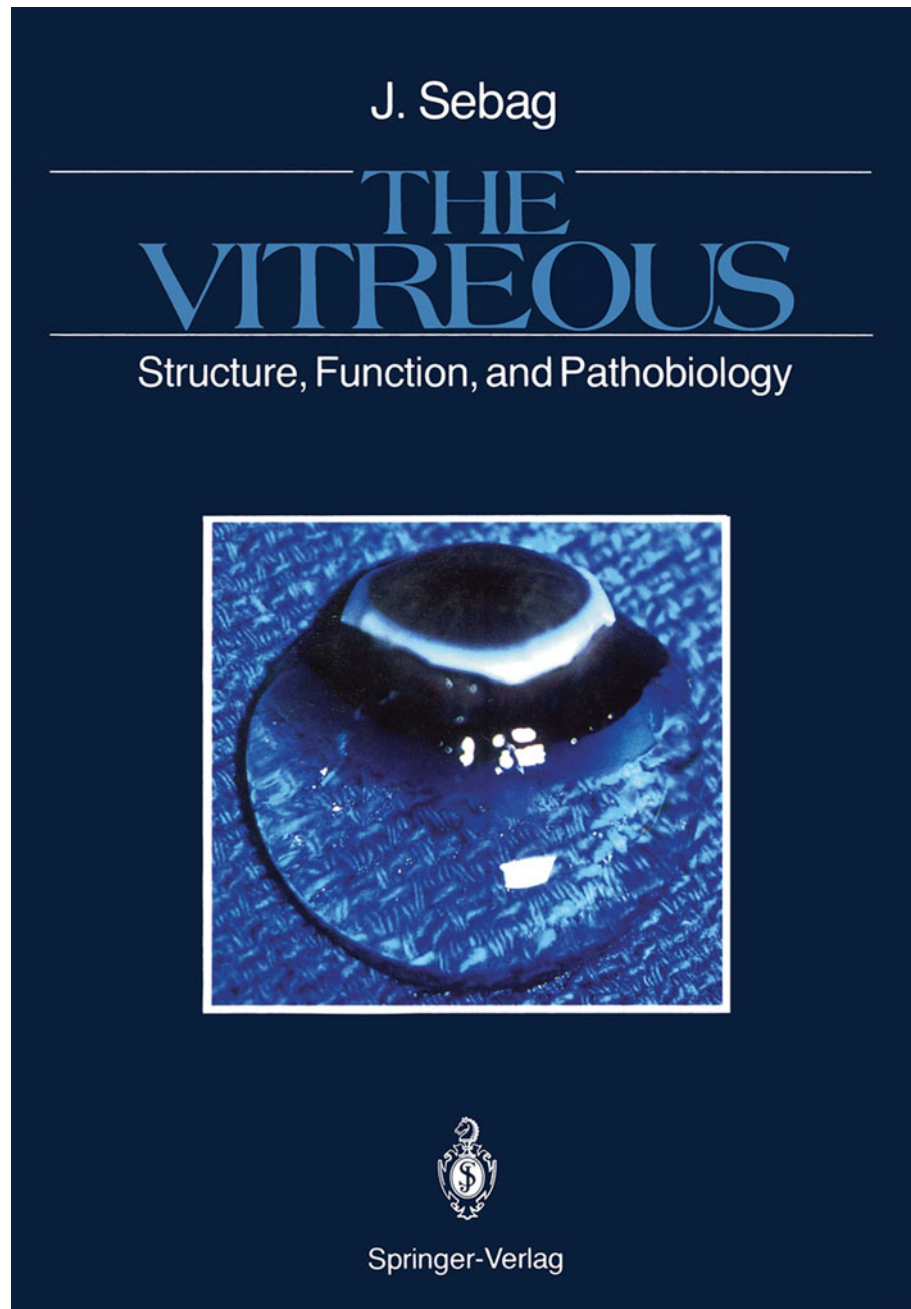


Look at vitreous, not just through it

CALIFORNIA, USA

J. Sebag, 2014

Commemoration



2014

25th Anniversary Springer Publication of Vitreous

50th Anniversary Springer Publishing in New York

Contents

Part I	Biochemistry	
	Paul N. Bishop	
I.A.	Vitreous Proteins	3
	Paul N. Bishop	
I.B.	Hyaluronan and Other Carbohydrates in the Vitreous	13
	Janet L. Denlinger and Endre A. Balazs	
I.C.	Hereditary Vitreo-Retinopathies	21
	Martin P. Snead and Allan J. Richards	
I.D.	Vitreous Cytokines and Regression of the Fetal Hyaloid Vasculature	41
	Kenneth M.P. Yee, Edward P. Feener, Benbo Gao, Lloyd Paul Aiello, Michele C. Madigan, Jan Provis, Fred N. Ross-Cisneros, Alfredo A. Sadun, and J. Sebag	
I.E.	Diabetic Vitreopathy	57
	Jesse Gale, Lloyd Paul Aiello, and J. Sebag	
I.F.	Vitreous Biochemistry and Artificial Vitreous	81
	Sven Crafoord, Fredrik Ghosh, and J. Sebag	
Part II	Anatomy, Development and Aging	
	J. Sebag	
II.A.	Development and Developmental Disorders of Vitreous	95
	Zabrina S. Kingston, Jan M. Provis, and Michele C. Madigan	
II.B.	Myopic Vitreopathy	113
	Jesse Gale and Yasushi Ikuno	
II.C.	Vitreous Aging and Posterior Vitreous Detachment	131
	Kevin Tozer, Mark W. Johnson, and J. Sebag	
II.D.	Hyalocytes: Essential Vitreous Cells in Vitreoretinal Health and Disease	151
	Takeshi Kita, Taiji Sakamoto, and Tatsuro Ishibashi	
II.E.	Vitreoretinal Interface and Inner Limiting Membrane	165
	Willi Halfter, J. Sebag, and Emmett T. Cunningham Jr.	
II.F.	To See the Invisible: The Quest of Imaging Vitreous	193
	J. Sebag, Ronald H. Silverman, and D. Jackson Coleman	

Part III Pathology/Pathobiology

J. Sebag

III.A.	Congenital Vascular Vitreoretinopathies	223
	Ronald Paul Hobbs and Mary Elizabeth Hartnett	
III.B.	Anomalous Posterior Vitreous Detachment and Vitreoschisis	241
	J. Sebag, Moritz Niemeyer, and Michael J. Koss	
III.C.	Pathology of Vitreomaculopathies	265
	Arnd Gandorfer, Ricarda G. Schumann, Christos Haritoglou, and Anselm Kampik	
III.D.	Vitreo-Macular Adhesion/Traction and Macular Holes: Pseudo, Lamellar, and Full-Thickness	287
	Miriam Englander, Jay S. Duker, and Peter K. Kaiser	
III.E.	Vitreo-Papillary Adhesion and Traction	299
	Michelle Y. Wang, Alfredo A. Sadun, and J. Sebag	
III.F.	Vitreous in the Pathobiology of Macular Pucker	311
	Kevin Tozer and J. Sebag	
III.G.	Vitreous in Age-Related Macular Degeneration	329
	Ilse Krebs, Carl Glittenberg, and Susanne Binder	
III.H.	Peripheral Vitreo–Retinal Pathologies	347
	J. Sebag, Stephan Dunker, and W. Richard Green	
III.I.	Role of Vitreous in the Pathogenesis of Retinal Detachment	375
	Wallace S. Foulds	
III.J.	Cell Proliferation at the Vitreoretinal Interface in Proliferative Vitreoretinopathy and Related Disorders	395
	Sonia Mehta, Rui Zhang, and Hans E. Grossniklaus	
III.K.	Vitreous in Retinovascular Diseases and Diabetic Macular Edema	407
	Gabriele E. Lang	
III.L.	Proliferative Diabetic Vitreoretinopathy	421
	Peter Kroll, Eduardo B. Rodrigues, and Carsten H. Meyer	

Part IV Physiology and Pharmacotherapy

Einar Stefánsson

IV.A.	Vitreous Physiology	437
	Einar Stefánsson	
IV.B.	Oxygen in Vitreoretinal Physiology and Pathology	459
	Nancy M. Holekamp, David C. Beebe, and Ying-Bo Shui	
IV.C.	Vitreous and Iris Neovascularization	477
	David McLeod	
IV.D.	Physiology of Accommodation and Role of the Vitreous Body	495
	D. Jackson Coleman, Ronald H. Silverman, and Harriet Lloyd	

IV.E.	Principles and Practice of Intravitreal Application of Drugs	509
	Phoebe Lin, Shivali Menda, and Eugene de Juan Jr.	
IV.F.	Pharmacotherapy of Proliferative Vitreoretinopathy	523
	Philip J. Banerjee, David G. Charteris, and David Wong	
IV.G.	Physiology of Vitreous Substitutes	537
	Ian Y. Wong, Ning Cheung, and David Wong	
Part V.A.	Posterior Vitreo-Retinal Surgery	
	Susanne Binder	
V.A.1.	Age-Related Macular Degeneration Surgery	553
	Susanne Binder and Lawrence P. Chong	
V.A.2.	Vitreomaculopathy Surgery	571
	Marta S. Figueroa and Inés Contreras	
V.A.3.	Chromodissection in Vitreoretinal Surgery	601
	Christos Haritoglou, Arnd Gandorfer, and Anselm Kampik	
V.A.4.	Macular Hole and Macular Pucker Surgery with Special Emphasis on Reoperations	613
	Billy X. Pan, Kenneth M.P. Yee, Fred N. Ross-Cisneros, Alfredo A. Sadun, and J. Sebag	
V.A.5.	Surgery of Diabetic Vitreo-Retinopathy and Diabetic Macular Edema	629
	Simon Brunner and Susanne Binder	
V.A.6.	Vitreous Surgery of Arterial and Venous Retinovascular Diseases	647
	Jose Garcia-Arumi, Susanne Binder, Mahmoud Leila, and Miguel Angel Zapata Victori	
Part V.B.	Peripheral Vitreo-Retinal Surgery	
	Lawrence P. Chong	
V.B.1.	The History of Vitrectomy Instrumentation: A Personal Account of a Transoceanic Australian-USA Collaboration	665
	Jean-Marie Parel	
V.B.2.	Modern Vitrectomy Cutters: An Improved Understanding of Vitreous Cutting	693
	Lawrence P. Chong	
V.B.3.	The Future of Vitrectomy	699
	Jean-Pierre Hubschman, Sanket U. Shah, and Vinod B. Voleti	
V.B.4.	Prophylaxis and Cure of Rhegmatogenous Retinal Detachment	713
	C. Pat Wilkinson	
V.B.5.	Management of Proliferative Vitreoretinopathy	731
	Ankur N. Mehta and Gary W. Abrams	

V.B.6.	Retinectomy for Recalcitrant Retinal Detachments	749
	Lawrence P. Chong	
V.B.7.	Pneumatic Retinopexy	757
	Kenneth M.P. Yee and J. Sebag	
V.B.8.	Vitreous Floaters and Vision: Current Concepts and Management Paradigms	771
	Laura C. Huang, Kenneth M.P. Yee, Christianne A. Wa, Justin N. Nguyen, Alfredo A. Sadun, and J. Sebag	
V.B.9.	Rare Indications for Vitrectomy: Tumor Excision, Optic Nerve Pits, and Malignant Glaucoma	789
	Lawrence P. Chong	
Part VI	Pharmacologic Vitreolysis	
	J. Sebag	
VI.A.	Pharmacologic Vitreolysis	799
	J. Sebag	
VI.B.	The History of Pharmacologic Vitreolysis	817
	Wallace S. Foulds	
VI.C.	Pharmacologic Vitreolysis with Tissue Plasminogen Activator	825
	Peter Kroll and Lutz Hesse	
VI.D.1.	Pharmacologic Vitreolysis with Plasmin: Basic Science Experiments	831
	Thierry C. Verstraeten	
VI.D.2.	Pharmacologic Vitreolysis with Plasmin: Clinical Studies	837
	Hiroko Terasaki and Tetsu Asami	
VI.E.1.	Pharmacologic Vitreolysis with Ocriplasmin: Basic Science Studies	845
	Marc D. de Smet and Bart Jonckx	
VI.E.2.	Pharmacologic Vitreolysis with Ocriplasmin: Clinical Studies	853
	Peter Stalmans	
VI.F.	Hyaluronidase as a Vitreous Liquefactant	863
	Marc D. de Smet and Lisa Grillone	
VI.G.	Pharmacologic Vitreolysis with Purified Dispase (Vitreolysin™)	869
	Tongalp H. Tezel, Lucian V. Del Priore, and Henry J. Kaplan	
VI.H.	Chondroitinase as a Vitreous Interfactant: Vitreous Disinsertion in the Human	881
	Stephen R. Russell and Gregory S. Hageman Chondroitinase Study Group (Addendum 1)	
Erratum		E1
Index		895

Contributors

Gary W. Abrams, MD, FARVO Department of Ophthalmology,
Kresge Eye Institute, Wayne State University School of Medicine, Detroit, MI, USA

Lloyd Paul Aiello, MD, PhD, FARVO Beetham Eye Institute, Joslin Diabetes Center,
Boston, MA, USA
Department of Ophthalmology, Harvard Medical School, Boston, MA, USA

Tetsu Asami, MD, PhD Department of Ophthalmology, Nagoya University School
of Medicine, Nagoya, Japan

Endre A. Balazs, MD Matrix Biology Institute, Edgewater, NJ, USA

Philip J. Banerjee, MD Vitreo-Retinal Department, Moorfields Eye Hospital,
London, England, UK

David C. Beebe, PhD, FARVO Department of Ophthalmology and Visual Sciences,
Washington University, St. Louis, MO, USA

Susanne Binder, MD Department of Ophthalmology, and Ludwig Boltzmann Institute for
Retinology and Biomicroscopic Laser Surgery, Rudolf Foundation Clinic, Vienna, Austria

Paul N. Bishop, MD, PhD Centre for Hearing and Vision Research, Institute of Human
Development/University of Manchester, Manchester Academic Health Science Centre,
Manchester, England, UK
Manchester Royal Eye Hospital, Central Manchester University Hospitals
NHS Foundation Trust, Manchester, England, UK

Simon Brunner, MD Department of Ophthalmology, Rudolph Foundation Hospital,
Vienna, Austria
The Ludwig Boltzmann Institute for Retinology and Biomicroscopic Laser Surgery,
Vienna, Austria

David G. Charteris, MD Vitreo-Retinal Department, Moorfields Eye Hospital,
London, England, UK

Ning Cheung, MD Department of Ophthalmology, University of Hong Kong,
Hong Kong, China
Singapore Eye Research Institute, Singapore National Eye Centre, Singapore

Lawrence P. Chong, MD Doheny Retina Institute, Los Angeles, CA, USA
VMR Institute for Vitreous Macula Retina, Huntington Beach, CA, USA

D. Jackson Coleman, MD, FACS, FARVO Department of Ophthalmology,
College of Physicians and Surgeons, Columbia University Medical Center,
Edward S. Harkness Eye Institute, New York, NY, USA

Inés Contreras, MD, PhD Department of Ophthalmology,
Hospital Universitario Ramón y Cajal, Instituto Ramón y Cajal de Investigaciones
Sanitarias (IRYCIS), Madrid, Spain
Clínica Rementería, Madrid, Spain

Sven Crafoord, MD, PhD Department of Ophthalmology, Örebro University Hospital,
Örebro, Sweden
School of Health and Medical Sciences, Örebro University, Örebro, Sweden

Emmet T. Cunningham Jr., MD, PhD, MPH The Uveitis Service,
West Coast Retina Medical Group, Department of Ophthalmology,
California Pacific Medical Center, Stanford University School of Medicine,
San Francisco, CA, USA

Eugene de Juan Jr., MD ForSight Labs, Menlo Park, CA, USA

Marc D. de Smet, MDCM, PhD, FRCSC, FRCOphth, FMH Department of Retina
and Inflammation, MIOS sa, Lausanne, Switzerland

Lucian V. Del Priore, MD, PhD, FARVO Department of Ophthalmology and Visual
Sciences, Medical University of South Carolina, Charleston, SC, USA

Janet L. Denlinger, PhD Matrix Biology Institute, Edgewater, NJ, USA

Jay S. Duker, MD Department of Ophthalmology, New England Eye Center,
Tufts Medical Center, Tufts University School of Medicine, Boston, MA, USA

Stephan Dunker, MD VMR Institute for Vitreous Macula Retina, Huntington Beach, CA, USA

Miriam Englander, MD Cole Eye Institute of the Cleveland Clinic, Cleveland, OH, USA

Edward P. Feener, PhD Department of Medicine, Harvard Medical School,
Boston, MA, USA

Beetham Eye Institute, Joslin Diabetes Center, Boston, MA, USA

Marta S. Figueroa, MD, PhD Department of Ophthalmology, Hospital Universitario Ramón
y Cajal, Instituto Ramón y Cajal de Investigaciones Sanitarias (IRYCIS), Madrid, Spain
Vissum Madrid, Madrid, Spain

Wallace S. Foulds, MD, DSc, FRCS, FRCOphth Singapore Eye Research Institute,
Singapore National Eye Centre, Singapore, Singapore
Retina Research, Glasgow University (Emeritus), Glasgow, Scotland

Jesse Gale, MB, ChB, MD Doheny Eye Institute, Los Angeles, CA, USA
VMR Institute for Vitreous Macula Retina, Huntington Beach, CA, USA
Addenbrooke's Hospital, Cambridge University Hospitals, Cambridge, England, UK

Arnd Gandorfer, MD Department of Ophthalmology,
MVZ Memmingen and Ludwig Maximilian University, Munich, Germany
Department of Ophthalmology, University Eye Hospital, Ludwig Maximilians University,
Munich, Germany

Benbo Gao, PhD Beetham Eye Institute, Joslin Diabetes Center, Boston, MA, USA

Jose Garcia-Arumi, MD, PhD Department of Ophthalmology, Hospital Vall d'Hebron,
Barcelona, Spain

Fredrik Ghosh, MD, PhD Dept. of Ophthalmology, Skåne University Hospital, Lund, Sweden
Lund University, Lund, Sweden

Carl Glittenberg, MD Department of Ophthalmology and Ludwig Boltzmann Institute for Retinology and Biomicroscopic Laser Surgery, Rudolf Foundation Clinic, Vienna, Austria

W. Richard Green, MD (posthumously) Wilmer Eye Institute, Johns Hopkins University, Baltimore, MD, USA

Lisa Grillone, PhD PharmaQuest Associates LLC, San Diego, CA, USA

Hans E. Grossniklaus, MD, MBA Department of Ophthalmology, Emory Eye Center, Emory University School of Medicine, Atlanta, GA, USA

Gregory S. Hageman, PhD, FARVO Department of Ophthalmology and Moran Eye Institute, University of Utah Health Care, Salt Lake City, UT, USA

Laboratory of Ocular Cell Biology, Salt Lake City, UT, USA

Willi Halfter, PhD Department of Neurobiology, University of Pittsburgh, Pittsburgh, PA, USA

Christos Haritoglou, MD Department of Ophthalmology, Duke Carl Theodor Eye Clinic, Ludwig Maximilian University, Munich, Germany

Department of Ophthalmology, University Eye Hospital, Ludwig Maximilians University, Munich, Germany

Mary Elizabeth Hartnett, MD Vitreoretinal Service and Surgery, Retinal Angiogenesis Laboratory, University of Utah, John A. Moran Eye Center, Salt Lake City, UT, USA

Lutz Hesse, MD Augenklinik der SLK-Kliniken, Heilbronn, Germany

Ronald Paul Hobbs, MD Vitreoretinal Fellow, University of Utah, John A Moran Eye Center, Salt Lake City, UT, USA

Nancy M. Holekamp, MD Department of Ophthalmology and Visual Sciences, Washington University, St. Louis, MO, USA

Laura C. Huang, BA VMR Institute for Vitreous Macula Retina, Huntington Beach, CA, USA

University of Miami Miller School of Medicine, Miami, FL, USA

Doheny Eye Institute, Los Angeles, CA, USA

Jean-Pierre Hubschman, MD Jules Stein Eye Institute at UCLA, University of California Los Angeles, Los Angeles, CA, USA

Yasushi Ikuno, MD Department of Ophthalmology, Osaka University Graduate School of Medical, Suita, Japan

Tatsuro Ishibashi, MD, PhD Department of Ophthalmology, Graduate School of Medical Sciences, Kyushu University, Higashi-Ku, Fukuoka, Japan

Mark W. Johnson, MD, FARVO Department of Ophthalmology and Visual Sciences, Kellogg Eye Center, University of Michigan, Ann Arbor, MI, USA

Bart Jonckx, PhD Thrombogenics nv, Leuven, Belgium

Peter K. Kaiser, MD Cole Eye Institute, The Cleveland Clinic, Cleveland, OH, USA

Anselm Kampik, MD, FARVO Department of Ophthalmology, Ludwig Maximilian University, Munich, Germany

Department of Ophthalmology, University Eye Hospital, Ludwig Maximilians University, Munich, Germany

Henry J. Kaplan, MD, FARVO Department of Ophthalmology and Visual Sciences, University of Louisville, School of Medicine, University of Louisville School of Medicine, Kentucky Lions Eye Center, Louisville, KY, USA

Z.S. Kingston, MBBS ANU Medical School, John Curtin School of Medical Research, The Australian National University, Canberra, ACT, Australia

T. Kita, MD, PhD Department of Ophthalmology, Graduate School of Medical Sciences, Kyushu University, Higashi-Ku, Fukuoka, Japan

Michael J. Koss, MD Doheny Eye Institute, Los Angeles, CA, USA
Department of Ophthalmology, Rupprecht Karls University, Heidelberg, Germany

Ilse Krebs, MD Department of Ophthalmology and Ludwig Boltzmann Institute for Retinology and Biomicroscopic Laser Surgery, Rudolf Foundation Clinic, Vienna, Austria

Peter Kroll, MD Department of Ophthalmology, Philipps-University, Marburg, Germany

Gabriele E. Lang, MD Department of Ophthalmology, University Eye Hospital Ulm, Ulm, Germany

Mahmoud Leila, MD Department of Ophthalmology, Hospital Vall d'Hebron, Barcelona, Spain

Phoebe Lin, MD, PhD Division of Retina and Vitreous Diseases/Surgery, Ocular Inflammation, Casey Eye Institute, Oregon Health and Science University, Portland, OR, USA

Harriett Lloyd, MS Department of Ophthalmology, College of Physicians and Surgeons, Columbia University Medical Center, New York, NY, USA

Michele C. Madigan, PhD School of Optometry and Vision Science, University of New South Wales, Sydney, NSW, Australia
Save Sight Institute, The University of Sydney, Sydney, NSW, Australia

David McLeod, MD Manchester Royal Eye Hospital, University of Manchester, Manchester, England, UK

Ankur N. Mehta, MD Department of Ophthalmology, Kresge Eye Institute, Wayne State University School of Medicine, Detroit, MI, USA

Sonia Mehta, MD Department of Ophthalmology, Emory Eye Center, Emory University School of Medicine, Atlanta, GA, USA

Shivali Menda, MD Department of Ophthalmology, UCSF School of Medicine, San Francisco, CA, USA

Carsten H. Meyer, MD, FEBO, FMH Department of Ophthalmology, Pallas Clinic, Aarau, Switzerland

Justin N. Nguyen, BA VMR Institute for Vitreous Macula Retina, Huntington Beach, CA, USA

Moritz Niemeyer, MD Doheny Eye Institute, Los Angeles, CA, USA
VMR Institute for Vitreous Macula Retina, Huntington Beach, CA, USA

Billy X. Pan, MD Doheny Eye Institute, Los Angeles, CA, USA
VMR Institute for Vitreous Macula Retina, Huntington Beach, CA, USA

Jean-Marie Parel, Ing ETS-G, PhD, FARVO Ophthalmic Biophysics Center, Bascom Palmer Eye Institute, University of Miami Miller School of Medicine, Miami, FL, USA

Jan M. Provis, PhD, FARVO ANU Medical School, John Curtin School of Medical Research, The Australian National University, Canberra, ACT, Australia

Allan J. Richards, MD, PhD Cambridge University NHS Foundation Trust, Addenbrooke's Hospital, Cambridge, England, UK
Department of Pathology, University of Cambridge, Cambridge, UK

Eduardo B. Rodrigues, MD Department of Ophthalmology, Philipps-University, Marburg, Germany

Department of Ophthalmology, Federal University of São Paulo, São Paulo, Brazil

Fred N. Ross-Cisneros, BS Doheny Eye Institute/UCLA, Los Angeles, CA, USA

Stephen R. Russell, MD Department of Ophthalmology and Visual Sciences, The University of Iowa Carver College of Medicine, Iowa City, IA, USA
Carver Center for Macular Degeneration, Institute of Visual Research, Carver College of Medicine, University of Iowa, Iowa City, IA, USA

Alfredo A. Sadun, MD, PhD, FARVO Doheny Eye Institute/UCLA, Los Angeles, CA, USA

Taiji Sakamoto, MD, PhD, FARVO Department of Ophthalmology, Kagoshima University Graduate School of Medical and Dental Sciences, Kagoshima, Japan

Ricarda G. Schumann, MD Department of Ophthalmology, Ludwig Maximilians University, Munich, Germany
Department of Ophthalmology, University Eye Hospital, Ludwig Maximilians University, Munich, Germany

J. Sebag, MD, FACS, FRCOphth, FARVO VMR Institute for Vitreous Macula Retina, Huntington Beach, CA, USA

Sanket U. Shah, MD Retina Division, Department of Ophthalmology, Jules Stein Eye Institute, UCLA, Los Angeles, CA, USA

Ying-Bo Shui, MD, PhD Department of Ophthalmology and Visual Sciences, Washington University, St. Louis, MO, USA

Ronald H. Silverman, PhD Department of Ophthalmology, College of Physicians and Surgeons, Columbia University Medical Center, New York, NY, USA

Biomedical Engineering Laboratory, Frederic L. Lizzi Center for Biomedical Engineering, Riverside Research, New York, NY, USA

Martin P. Snead, MA, MD, DO, FRCS, FRCOphth Addenbrooke's Eye Hospital, University of Cambridge, Cambridge, England, UK
Vitreoretinal Service, Cambridge University NHS Foundation Trust, Addenbrooke's Hospital, Cambridge, England, UK

Peter Stalmans, MD, PhD Department of Ophthalmology, Universitaire Ziekenhuizen Leuven, Leuven, Belgium

Einar Stefánsson, MD, PhD, FARVO Department of Ophthalmology, National University Hospital, University of Iceland, Reykjavik, Iceland

Hiroko Terasaki, MD, PhD Department of Ophthalmology, Nagoya University School of Medicine, Nagoya, Japan

Tongalp H. Tezel, MD College of Physicians and Surgeons, Columbia University,
New York, NY, USA

Edward S. Harkness Eye Institute, Columbia University Medical Center, New York,
NY, USA

Kevin Tozer, MD Doheny Eye Institute, Los Angeles, CA, USA
VMR Institute for Vitreous Macula Retina, Huntington Beach, CA, USA
Department of Ophthalmology and Visual Sciences, Kellogg Eye Center,
University of Michigan, Ann Arbor, MI, USA

Thierry C. Verstraeten, MD Department of Ophthalmology, Allegheny General Hospital,
Drexel University College of Medicine, Pittsburgh, PA, USA

Miguel Angel Zapata Victori, MD Department of Ophthalmology, Hospital Vall d'Hebron,
Barcelona, Spain

Vinod B. Voleti, MD New Jersey Retina, Vauxhall, NJ, USA

Christianne A. Wa, BA Doheny Eye Institute, Los Angeles, CA, USA
VMR Institute for Vitreous Macula Retina, Huntington Beach, CA, USA

Michelle Y. Wang, MD Doheny Eye Institute, Los Angeles, CA, USA
VMR Institute for Vitreous Macula Retina, Huntington Beach, CA, USA

C. Pat Wilkinson, MD Department of Ophthalmology, Greater Baltimore Medical Center,
Baltimore, MD, USA

David Wong, MD Vitreo-Retinal Department, The Royal Liverpool University Hospital,
Liverpool, England, UK
Department of Ophthalmology, LKS Faculty of Medicine, University of Hong Kong,
Hong Kong, China

Ian Y. Wong, MD Department of Ophthalmology, University of Hong Kong,
Hong Kong, China

Kenneth M.P. Yee, BS VMR Institute for Vitreous Macula Retina, Huntington Beach,
CA, USA
Doheny Eye Institute, Los Angeles, CA, USA

Rui Zhang, MD Department of Ophthalmology, Case Western Reserve University,
Cleveland, OH, USA

Is Your Vitreous Really Necessary?

Wallace S. Foulds

I. Introduction

Some 25 years ago, I published a paper entitled rather flippantly *Is Your Vitreous Really Necessary?* [1], in which I attempted to identify features of the vitreous body that might have an important role in the eye. I came to the conclusion that although the rather complex structure of the vitreous body had a number of identifiable and important roles, vitreous was present mainly as an insurance, not really being needed except in exceptional circumstances. On reflection, this was too simplistic a conclusion. On the other hand, one might be excused for thinking that the vitreous serves no useful purpose, for its removal by vitrectomy is now commonplace and the eye seems to get along well without it. Indeed, following vitrectomy, the vitreous chamber is filled with an aqueous fluid, albeit with a proportion of hyaluronan previously believed to be secreted by the hyalocytes in the peripheral cortical vitreous [2], although the ciliary body may well be the source. Indeed, one might ask why the vitreous chamber should not be filled with aqueous fluid in the first place rather than with vitreous with its well-known intricately organized structure of highly polymerized hyaluronan-stabilizing fine collagen fibrils [3, 4]. Even animals with a largely liquid vitreous such as the owl monkey have a layer of vitreous gel in the peripheral vitreous cavity that is in contact with the retina, indicative of a need for at least some vitreous gel rather than aqueous fluid filling the posterior eye.

An obvious mechanical role for the vitreous, which in spite of its high content of water has a prominent gel-like nature, is the prevention of the complete collapse of the globe following a penetrating injury, something that would certainly result if the vitreous chamber were filled with aqueous. Indeed, the injection of a viscoelastic gel into the vitreous chamber has been used in the surgical management of severe penetrating eye injuries [5]. However, in general, the vitreous can be regarded as not only maintaining the homeostasis within the posterior segment of the eye and providing support to the structures with which it is in contact but playing a role in the molecular exchanges with these structures that may be necessary for their metabolism and their integrity. This homeostasis can be regarded in two categories: mechanical and molecular.

W.S. Foulds, MD, DSc, FRCS, FRCOphth
Singapore Eye Research Institute, Singapore National Eye Centre, 11 Third Hospital Avenue, Singapore 168751, Singapore

Retina Research, Glasgow University (Emeritus),
Kinnoull Place, 68 Dowanside Road,
Glasgow G129DL, Scotland
e-mail: wallace.stewart.foulds@seri.com.sg

II. Mechanical Homeostasis

Vitreous is not only a gel but is viscoelastic, a characteristic recognized by Sir Stewart Duke-Elder as long ago as 1929 [6–8] and investigated by him using an intravitreal nickel particle subjected to electromagnetic pulses. While the gel-like characteristics of the vitreous are largely the result of its constituent hyaluronan [9], its elastic characteristics result from the combined contributions of vitreous collagen and hyaluronan [10, 11]. As is well known, the vitreous body contains a network of long fine collagen fibers running from the vitreous base anteriorly to the cortical vitreous posteriorly, where they fuse with the inner limiting membrane of the retina [3, 4]. These anteroposterior fibers are accompanied by other fibers running nasotemporally, crisscrossing with the former fibers with which they form attachments to establish a network. Within the spaces between these collagen fibers are highly hydrated polymerized molecules of hyaluronan. These hyaluronan molecules attract water and swell to establish a Donnan equilibrium [10]. The swelling hyaluronan forces the collagen fibers apart, preventing their adherence to each other that otherwise would degrade the optical clarity of the vitreous body. It is suggested that the swollen hyaluronan molecules also stretch the load-bearing collagen fibers longitudinally and thus contribute to the elastic properties of the vitreous body [10].

If the vitreous body is removed from the eye, there is a rapid initial loss of its volume, with water (and contained solutes) and hyaluronan being ejected from the isolated vitreous as a result of the contraction of the stretched collagen fibers that have been relieved of their normal constraints. The previously stretched and taught fibers become relaxed and tortuous as the effect of the hydrated hyaluronan is lost. This is followed by a slower loss of vitreous volume in which gravity and diffusion are involved [10]. Liquefaction of the aging vitreous [12–14] is also accompanied by a loss of hyaluronan and a relaxation of collagen fibrils that not only become tortuous but tend to adhere together, so reducing the clarity of the vitreous [13] [see chapter II.C. Vitreous aging and posterior vitreous detachment].

The viscoelastic properties of the vitreous body allow it to absorb energy rapidly and release it slowly, the former associated with vitreous collagen and the latter with interacting hyaluronan and collagen [11]. This characteristic not only protects the retina in head injuries but also prevents sudden changes in vitreous volume that might result from pressure on the globe during eye closure or from tension in the extraocular muscles during eye movements that otherwise would have obvious adverse effects on the optics of the eye. The evaluation of these and other attributes has long been rendered difficult by the fact that *in vivo* investigation of an optically clear vitreous is difficult [15], although many ingenious techniques have been successfully developed [15–20] [see chapter II.F. Imaging vitreous].

III. Molecular Homeostasis

The stabilized hydrated molecules of hyaluronan within the vitreous collagen network slow or prevent the movement of molecules or cells within the vitreous body and control the entry into the vitreous of molecules from surrounding tissues and the clearance of molecules from the vitreous body into surrounding tissues [see chapter IV.A. Vitreous physiology]. These effects lead to molecular homeostasis within vitreous that can be beneficial, usefully prolonging the therapeutic effects of intravitreally injected therapeutic agents [see chapter IV.E. Principles and practice of intravitreal application of drugs], but equally disadvantageous when, for example, there is a breakdown in the blood-ocular barrier and release into the vitreous body of molecules not usually present such as inflammatory cytokines or angiogenic factors, the persistence of which may be detrimental. The diffusion of water molecules within and from the vitreous body plays an important role in retinal attachment and detachment [see chapter III.I. Role of vitreous in the pathogenesis of retinal detachment].

A. Oxygen Physiology

Oxygen levels within the normal vitreous body are low [21], probably related to the high levels of ascorbic acid within vitreous [22]. It has been shown that normal vitreous absorbs and metabolizes oxygen to keep oxygen levels low (around 1 %) [23]. Following vitrectomy, ascorbate levels within the vitreous chamber fall, and oxygen levels increase. The resulting exposure of surrounding structures (retina and lens) to molecular oxygen may result in oxidative damage. Thus, it has been suggested that the high prevalence of nuclear cataract following vitrectomy among those of 50+ years of age (95 % within 2 years) may be the effect of oxidative damage to the lens coupled with an age-related predilection [24] [see chapter IV.B. Oxygen in vitreo-retinal physiology and pathology].

Even more surprising is the suggestion that increased oxygen levels after vitrectomy may cause late-onset open-angle glaucoma [25]. In one study, 67.6 % of those developing postvitrectomy late-onset open-angle glaucoma only did so in the vitrectomized eye [26]. Following vitrectomy, oxygen levels increase not only within the vitreous chamber but also in the posterior chamber in front of the lens and behind the iris [23], perhaps accounting for this phenomenon, for the posterior chamber is in molecular continuity with the anterior chamber and the trabecular tissues in the anterior chamber angle. There are, however, other studies that dispute a relationship between vitrectomy and the subsequent development of glaucoma [see chapter IV.A. Vitreous physiology].

B. Angiogenic and Pro-Inflammatory Factors

Vitreous itself may be antiangiogenic (and antineoplastic), possibly related to its thrombospondin content, a property that may be reduced in conditions such as diabetes [27]. In all conditions of retinal hypoxia including diabetes, there is a breakdown in the inner blood-retinal barrier [28] that allows the diffusion of angiogenic and pro-inflammatory molecules into the vitreous body. It has been shown, for example, that vascular endothelial growth factor (VEGF) is present in the vitreous body at increased levels in diabetic eyes [29] and in eyes with retinal vein occlusion [30]. The gel structure of vitreous promotes the persistence of angiogenic factors such as VEGF and aids its eventual dispersion throughout the vitreous body. Thus, angiogenic factors originating in the hypoxic peripheral retina may cause neovascularization in the posterior retina or optic nerve head from the presence within the contiguous vitreous of retained angiogenic factors. Similarly, angiogenic factors that arise from the posterior retina can induce iris neovascularization, especially in ischemic retinal vein occlusions. Vitrectomy in these circumstances may be beneficial in reducing the amount of VEGF in the vitreous chamber not only as a result of its initial removal but also subsequently by its increased clearance from the now liquefied vitreous, although increased clearance to the anterior chamber following vitrectomy may increase the risk of anterior segment neovascularization. An additional advantage of vitrectomy in conditions of retinal hypoxia would be the increased oxygen levels that follow vitrectomy with a consequent increase in the availability of oxygen to the hypoxic retina that, however, would have to be balanced against the risks of oxidative damage [see chapter IV.A. Vitreous physiology].

IV. Intravitreal Pharmacotherapy

The injection of therapeutic agents into the vitreous body has become common practice, especially in the treatment of wet age-related macular degeneration (AMD). Persistence of the injected drug is obviously desirable to avoid the need for frequent intravitreal injections. The gel structure of vitreous with its resistance to molecular diffusion does help to prolong the availability of intravitreal drugs, but their persistence is greatly affected by molecular size. The half-life in

vitreous of bevacizumab (unified atomic mass 148kD) (~8.5 days) is significantly longer than that of ranibizumab (unified atomic mass 48kD) (~4.5 days). However, the relatively short half-life in vitreous of intravitreal drugs has prompted the development of slow-release agents to prolong their persistence in the vitreous [see chapter IV.E. Principles and practice of intravitreal application of drugs].

Although VEGF is an important angiogenic molecule involved in AMD and diabetic retinopathy, many other molecules are involved in what is a very complex process [31]. These include transcriptional factors such as hypoxia-inducible factor-1 (HIF-1 α) and a number of nitric oxide synthases such as iNOS (inducible), nNOS (neuronal), and eNOS (endothelial) nitric oxide synthases [32]. Increased retinal glutamate activates microglia with release of inflammatory cytokines and the production of reactive oxygen species [33]. All of these molecules will penetrate the vitreous body via a defective inner blood-retinal barrier so that the vitreous body will contain a mélange of angiogenic and inflammatory molecules rather than one solitary factor such as VEGF with obvious implications for therapy.

V. Ocular and Refractive Development

Although vitreous undoubtedly plays an active role in ocular and refractive development, the details of how this is achieved are sparse. It has been suggested that factors promoting ocular growth and refractive development may be elaborated in peripherally situated retinal amacrine cells [34]. Experimentally induced myopia (e.g., by form deprivation) is accompanied by a reduction in dopamine levels and an increase in vasoactive intestinal peptide (VIP) [34] in the vitreous. As ocular growth involves scleral growth that is excessive in eyes developing myopia, one must ask how factors of amacrine origin might reach the sclera. An obvious route is via the vitreous chamber and subsequent diffusion across the retina to the retinal pigment epithelium (RPE) and stimulation of scleral fibroblast proliferation directly or indirectly by growth factors secondarily generated in the RPE [35]. Undoubtedly, vitreous is further involved in the development of the eye and its refractive state, but at present, understanding of the factors involved is limited.

The vitreous body can also provide a physical restraint to ocular enlargement since destruction of cortical vitreous or the inner limiting membrane, for example, promotes eye enlargement [36]. An interesting molecule shown to be present in high concentration in the vitreous chamber of the developing eye is the amino acid taurine that has antioxidative and neuroprotective properties vasculature for the normal development of many tissues including the retina [37].

Within the fetal vitreous, the nonvascularized retina is oxygenated from the hyaloid vascular system that remains functional until shortly before birth, by which time vascularization of the retina renders the hyaloid system unnecessary [see chapter I.D. Vitreous cytokines and regression of the fetal hyaloid vasculature]. Persistence of the hyaloid in the vitreous body is common in the eyes of premature babies [see chapter III.A. Congenital vascular vitreo-retinopathies].

VI. Vitreous Evolution

Fossils of soft-bodied animals and their organs such as the eye are rarely found. Much can be deduced, however, from the study of currently extant animal forms both invertebrate and vertebrate that can provide insight into the likely features of the evolving forebearers of higher vertebrates including humans. Evolutionary developments that fail to have survival benefit will, however, have died out and will not be represented among currently extant species. Much is known about the evolution of the eye but much less about the vitreous during evolution. Only a simplified account of the evolution of the eye would therefore be appropriate.

Although Charles Darwin (1809–1882) is rightly credited with the identification of the mechanisms by which evolution can alter species and create new life-forms by natural selection, the idea of evolution has a long history extending back in time to the ancient Greeks some

2,500 years ago [38]. Emedocles of Agrigentum (495–435BC) suggested that animals were derived from plants, and according to Aristotle (384–322 BC), Emedocles also suggested that the fittest forms of life could have arisen by chance rather than by body design [38]. Aristotle considered evolution to be a gradual chain of events leading from simple sea creatures to fish and then land animals in a progression in which nature aimed at perfection.

A very long time would be required for chance variation to allow the survival of those animal forms best suited to a changing environment that is the basis for Darwinian evolution, and it was Avicenna (980–1037) who noted the presence of fossils of sea creatures and of land animals high in the mountains and was the first to suggest that the formation and erosion of mountains would take an extremely long time [38]. Currently, the age of the Earth is believed to be 4.54 ± 0.05 billion years [39].

In Victorian times, it was generally accepted that developing fetuses passed through the evolutionary stages that preceded the extant form and that in humans, congenital abnormalities could be related to particular stages of evolutionary development, it being held that a developmental abnormality in a higher animal was equivalent to normal development in a lower animal [40]. The simplest form of life, i.e., an anaerobic cell capable of growth and replication, is thought to have developed some 3.6 billion years ago (BYA) [41]. Organisms capable of photosynthesis (blue-green algae, cyanophytes) are thought to have developed some 2.3 BYA and continued to exist for at least 1.7 billion years [41]. The forerunners of protozoa developed around 1.2 BYA, and by 570 million years ago (MYA), organs including light-sensitive organs had developed. Flagellate protozoa are thought to have been light sensitive, possibly as a result of symbiosis with ingested cyanophytes [42]. It has been suggested that genes from ingested cyanophytes may have been the precursors of those for visual pigments in currently extant eyes [42].

Although it has been suggested that eyes have been repeatedly developed and subsequently lost at different times during evolution [43], more recent genetic studies indicate that the eyes of all extant species evolved from one type of primitive light-sensitive cell in company with a pigment-bearing cell [44, 45]. Light-sensitive cells are found in or beneath the skin of many primitive life-forms (e.g., hagfish [46]) but lack focus and provide only low-definition sensitivity to light rather than vision. Such cells can be considered as having a nonvisual function being responsible for the control of the circadian rhythm. In conjunction with this, in marine organisms, light-sensitive cells can act as depth gauges based on the decreasing intensity of light with increasing depth of water [47]. This had the evolutionary advantage of ensuring that night-feeding or day-feeding organisms were at an appropriate depth to locate their specific food [47].

The phylogenetic development of eyes started with the aggregation of light-sensitive cells to form a light-sensitive patch or eye spot [48]. Such aggregated cells in early marine animals had no focus, would be bathed in seawater, and had no equivalent to a vitreous or any real resemblance to an eye. A further development was the so-called cup eye (ocellus), where a group of light-sensitive cells lined a cup-like depression in the skin or other surface membrane in conjunction with pigment cells that could control the intensity of ambient light (and especially potentially damaging UV light). Simple cup eyes provided some directional information but did not provide true vision and lacked any of the features of a formed eye including the vitreous body. Starfish have such cup eyes at the tip of each of their arms. In starfish, the light-sensitive cells have nervous connections to a primitive nervous system that allows a rapid response to a change in light intensity such as a shadow [48]. Improved directional light sensitivity would result from a deepening of cup eyes with some survival benefit. As a result, a progressive deepening of cup eyes during evolution led to the development of eyes with a more spherical shape and a decreasing size of anterior opening until in some species (e.g., Nautilus), only a very small anterior opening remained. This opening functioned like a pinhole camera with the advantage of a formed (but low-intensity) image.

An expanding spherical shape of the primitive eye was accompanied by an increase in photoreceptor numbers, thereby increasing light sensitivity [46]. The interior of the almost closed spherical cup eye, however, continued to be filled with seawater rather than vitreous.

The next step in evolution was the development of a lens, the most primitive lens being modified vitreous as seen in pelagic carnivorous polychaete worms that have large spherical eyes with, in their simplest form, a covering of epidermis over a shallow anterior chamber and a spherical “vitreous” filling the eye (so-called ventral lens) in contact with a primitive retina capable of image formation [48]. More advanced polychaete worms have a crystalline lens just under the covering epidermis. This lens, derived from surface ectoderm, is cellular, spherical in shape, and surrounded by a dense anterior (“distal”) vitreous separated from a less dense posterior (“proximal”) vitreous that is in contact with a well-developed retina. The nature of this vitreous is not clear, but it is to be noted that as a general rule, connective tissues have a network of insoluble fibers interspersed with proteoglycans and glycosaminoglycans, and it has been suggested that radiation played an important role in the evolution of such structural characteristics [49]. The eye would be a prime candidate for radiation to have played a role in the evolution of transparent ocular media including the cornea, lens, and vitreous. Eventually, an eye with the characteristics of the human eye became widespread among vertebrates including humans and a not dissimilar complex eye developed among cephalopods (squid, cuttlefish, and octopus) that, however, had the retinal nerve fiber layer beneath rather than in front of the photoreceptors [48].

According to Schwab [50], the first mention of a vitreous body was in comb jellies (ctenophores) and jellyfish (cnidarians) during the Ediacaran Period (650–543 MYA). These eyes were simple cup eyes (ocelli) overlain by condensed tissue that formed a primitive cuticular lens and the forerunner of vitreous. He concluded that such organisms demonstrated both positive and negative phototaxis. In jellyfish, the ocelli have a direct neural connection to muscles responsible for locomotion and have been regarded as having a role in the maintenance of jellyfish posture in conjunction with a statocyst (a primitive vestibular system) that also has a direct neural connection to locomotor muscles [48]. The development of a closed eye with a need for nutrition of intraocular structures and disposal of the waste products of intraocular cellular metabolism demanded the continuous ingress and egress of an aqueous fluid and the formation of a vitreous body with its known multifactorial properties. As evolving eyes became more complex, an increasing complexity in the structure and function of vitreous would have been required.

Although in general the posterior segments of all vertebrate eyes are filled with vitreous, there is considerable variation in the composition of the vitreous body among species. As early as 1834 [40], it was noted that *the vitreous humor in lower “vertebrated” animals has the consistence and chemical properties of cerebral fluid*. In fish, the posterior and peripheral vitreous is in a gel state, while the central and anterior vitreous is liquid, extending around the lens into the anterior chamber that has no aqueous. The polysaccharides in fish vitreous (tuna) have been shown to contain ichthyosan in addition to hyaluronan [51], the latter showing varying degrees of polymerization [52] and thus varying degrees of viscosity in differing locations within the vitreous body. The fish lens is spherical, and accommodation is achieved by movements of the lens along its anteroposterior axis [see chapter IV.D. Physiology of accommodation and role of vitreous]. The fluid vitreous around the lens allows unhindered movement of the lens during accommodation that would be hindered by a formed viscoelastic vitreous. The owl monkey also has a fluid vitreous but retains a narrow layer of viscoelastic vitreous in contact with the retina. The vitreous body in cattle, dogs, and rabbits is much denser than in humans, while in the dog, the anterior vitreous is firmly adherent to the posterior lens capsule.

It is usually held that the development of vertebrate eyes during early gestation is a response to the outgrowth of the optic vesicles from the developing forebrain. It has been suggested, however, that the brain’s evolutionary development was a response to the progressive development of sensory organs, with each evolutionary advance in such organs permitting new sensory tasks with survival benefit [47]. The increasing acquisition of external information from sensory organs including the developing eye is thought to have necessitated a centralized processing ability in the developing nervous system. The complexity of information provided by complex sensory organs such as the eye, therefore, necessitated the development of an increasingly complex brain [47].

VII. Summary

In summary, one might consider vitreous as being “conditionally essential.” In differing situations, vitrectomy may be beneficial or disadvantageous. Undoubtedly, a risk/benefit assessment should be made before removing the vitreous body with its complex and at present incompletely understood involvement in the health of the eye. From an evolutionary standpoint, early primitive eyes in marine creatures did not provide vision, were bathed in seawater, and did not require a vitreous body. Only with the development of a closed spherical complex eye was there the need for the mechanical and molecular homeostasis that is provided by the vitreous body, with the characteristics seen in vertebrate eyes.

Abbreviations

AMD	Age-related macular degeneration
BYA	Billion years ago
eNOS	Endothelial nitric oxide synthase
HIF-1 α	Hypoxia-inducible factor 1 α
iNOS	Inducible nitric oxide synthase
kD	Kilodalton
MYA	Million years ago
NOS	Nitric oxide synthase
nNOS	Neuronal nitric oxide synthase
RPE	Retinal pigment epithelium
UV	Ultraviolet (light)
VEGF	Vascular endothelial growth factor receptor
VIP	Vasoactive intestinal peptide

References

1. Foulds WS. Is your vitreous really necessary? The role of the vitreous in the eye with particular reference to retinal attachment, detachment and the mode of action of vitreous substitutes. *Eye*. 1987;1:641–64.
2. Balazs EA. Molecular morphology of the vitreous body. In: Smelser GK, editor. *Structure of the eye*. New York: Academic Press Inc; 1961. p. 293–310.
3. Sebag J. *The vitreous – structure, function and pathobiology*. New York: Springer; 1989.
4. Bishop PN. Structural macromolecules and supramolecular organisation of the vitreous gel. *Prog Retin Eye Res*. 2000;19:323–44.
5. Yucel A, Suner K, Sanli O, et al. Viscoelastic protection of the retina after severe penetrating eye injury with vitreous loss. *Invest Ophthalmol Vis Sci*. 2003;44:E-Abstract 1837.
6. Duke-Elder WS. The physico-chemical properties of the vitreous body. *J Physiol*. 1929;68:855–65.
7. Robertson EB, Duke-Elder WS. The elasticity of the vitreous body. *Proc Roy Soc Lond*. 1933;112: 215–24.
8. Duke-Elder WS, Robertson EB. The viscous-elastic properties of the vitreous body and its reaction to external forces. *Brit J Ophthalmol*. 1934;18:433–42.
9. Lee B, Litt M, Buchsbaum G. Rheology of the vitreous body. 1. Visco-elasticity of human vitreous. *Biorheology*. 1992;29:521–33.
10. Nickerson CS. In: *The vitreous humor: mechanics and structure*. Chapter 3. 2006. http://thesis.library.caltech.edu/974/3/CSN_CH3.pdf.
11. Sharif-Kashani P, Hubschman J-P, Sassoon D, Kavehpour HP. Rheology of the vitreous gel: effects of macromolecule organization on the viscoelastic properties. *J Biomech*. 2011;44:419–23.
12. Le Goff MM, Bishop PN. Adult vitreous structure and postnatal changes. *Eye*. 2008;22:1214–22.
13. Sebag J. Age-related changes in human vitreous structure. *Graefes Arch Clin Exp Ophthalmol*. 1987;225:89–93.
14. Merala I, Bilgilia Y. Diffusion changes in the vitreous humor of the eye during aging. *AJNR Am J Neuroradiol*. 2011;32:1563–6.
15. Sebag J. Seeing the invisible: the challenge of imaging vitreous. *J Biomed Opt*. 2004;9:38–46.
16. Piccirelli M, Bergamin O, Landau K, et al. Vitreal viscoelasticity revealed by motion-encoded MRI. www.mr.ethz.ch/abstracts/files/ismrm09_00710.pdf.

17. Zimmerman RL. In vivo measurements of the viscoelasticity of the human vitreous humor. *Biophys J*. 1980;29:539–44.
18. Rossi T, Querzoli G, Pasqualitto G, et al. Ultrasound imaging velocimetry of the human vitreous. *Exp Eye Res*. 2012;99:98–104.
19. Pokki J, Ergeneman O, Bergeles C, et al. Localized viscoelasticity measurements with untethered intravitreal microrobots. *Conf Proc IEEE Eng Med Biol Soc*. 2012;2012:2813–16.
20. Dholakia K, Watts F, Tan LE, et al. The viscoelastic properties of the vitreous humor measured using an optically trapped local probe. In: *Optical Trapping and Optical Micromanipulation VIII*, 2011, San Diego.
21. Sakaue H, Negi A, Hondo Y. Comparative study of vitreous oxygen tension in human and rabbit eyes. *Invest Ophthalmol Vis Sci*. 1989;30:1933–37.
22. Shui Y-B, Holekamp NM, Kramer BC, et al. The gel state of the vitreous and ascorbate-dependent oxygen consumption: relationship to the etiology of nuclear cataracts. *Arch Ophthalmol*. 2009;127:475–82.
23. Doran M. (Interviewing Holekamp NM, Seigfried CJ, Trese MT). A new view of the vitreous in health and disease. *Am J Ophthalmol*. 2005;139:302–10.
24. Holekamp NM, Shui Y-B, Beebe DC, Doran M. Vitrectomy surgery increases oxygen exposure to the lens: a possible mechanism for nuclear cataract formation. *Am J Ophthalmol*. 2005;139:302–10.
25. Siegfried CJ, Shui Y-B, Holekamp NM, et al. Oxygen distribution in the human eye: relevance to the etiology of open-angle glaucoma after vitrectomy. *Invest Ophthalmol Vis Sci*. 2010;51:5731–38.
26. Chang S. LXII Edward Jackson lecture: open angle glaucoma after vitrectomy. *Am J Ophthalmol*. 2006;141:1033–43.
27. Sheibani N, Sorenson CM, Cornelius LA, Frazier WA. Thrombospondin-1, a natural inhibitor of angiogenesis is present in vitreous and aqueous humor and is modulated by hyperglycemia. *Biochem Biophys Res Commun*. 2000;267:257–61.
28. Kaur C, Foulds WS, Ling EA. Blood-retinal barrier in hypoxic-ischemic conditions: basic concepts, clinical features and management. *Prog Retin Eye Res*. 2008;27:622–647.
29. Malik RA, Li C, Aziz W, et al. Elevated plasma CD105 and vitreous VEGF levels in diabetic retinopathy. *J Cell Mol Med*. 2005;9:692–97.
30. Pe'er J, Folberg R, Itin A, et al. Vascular endothelial growth factor upregulation in human central retinal vein occlusion. *Ophthalmology*. 1998;105:412–26.
31. Matsumoto Y, Takahashi M, Ogata M. Relationship between Glycoxidation and cytokines in the vitreous of eyes with diabetic retinopathy. *Jpn J Ophthalmol*. 2002;46:406–12.
32. Kaur C, Sivakumar V, Foulds WS. Early response of neurons and glial cells to hypoxia in the retina. *Invest Ophthalmol Vis Sci*. 2006;47:1126–41.
33. Sivakumar V, Foulds WS, Luu CD, Ling EA, Kaur C. Hypoxia induced retinal cell damage through activation of AMPA receptors and the neuroprotective effects of DNQX. *Exp Eye Res*. 2013;109:1–15.
34. Stone RA, Lin T, Iuvone PM, Laties AM. Postnatal control of ocular growth: dopaminergic mechanisms. In: *CIBA Foundation Symposium*. Chichester: Wiley; 1990. p. 45–57.
35. Wallman J. Retinal influences on sclera underlie visual deprivation myopia. In: *Myopia and the control of eye growth*. CIBA Foundation Symposium. Chichester: Wiley; 1990. p. 126–33.
36. Halfter W, Winzen U, Bishop PN, Eller A. Regulation of eye size by the retinal basement membrane and vitreous body. *Invest Ophthalmol Vis Sci*. 2006;47:3586–94.
37. Ripps H, Shen W. Review: taurine, a “very essential” amino acid. *Mol Vis*. 2012;18:2673–86.
38. White M, Gribbin J. Evolution before Darwin. In: *Darwin: a life in science*, chapter 2. London: Simon & Schuster; 1995. p. 27–48.
39. http://en.wikipedia.org/wiki/Age_of_the_Earth.
40. von Seiler M. Observations on the original malformation and total want of eyes. *Medico-Chirurgical Review*. 1834;20:370–80.
41. Dando M, Burchett M. The origin of life in the sea. In: Waller G, editor. *Sealife*. Sussex: Smithsonian; 1996. p. 32–34.
42. Gehring WJ. New perspectives on eye development and the evolution of eyes and photoreceptors. *J Heredity*. 2005;96:171–84.
43. Salvini-Plawen I, Mayr E. In: Hecht MK, Steere WC, Wallace B, editors. *Evolutionary biology*. New York: Plenum Press; 1961. p. 207–63.
44. Gehring WJ, Ikeo K. Pax 6: mastering eye morphogenesis and eye evolution. *Trends Genet*. 1999;15:371–77.
45. Arendt D. Evolution of eyes and photoreceptor cell types. *Int J Dev Biol*. 2003;47:563–571.
46. Lamb TD, Pugh Jr EN, Collin SP. The origin of the vertebrate eye. *Evo Edu Outreach*. 2008;1:415–26.
47. Nilsson D-E. The evolution of eyes and visually guided behaviour. *Phil Trans R Soc B*. 2009;364:2833–47.
48. Dando M. Marine invertebrates. In: Waller G, editor. *Sealife*. Sussex: Smithsonian; 1996. p. 113–190.
49. Scott JE. Physiological function and chemical composition of pericellular proteoglycan (an evolutionary view). *Trans R Soc B*. 1975;271:235–42.
50. Schwab IR. *Evolution's witness – how eyes evolved*. New York: Oxford University Press; 2012.
51. Armand G, Balazs EA, Meyer K, Reyes M. Isolation and characterization of ichthyosan from tuna vitreous. *Connect Tissue Res*. 1983;11:21–33.
52. Amagai I, Tashiro Y, Ogawa H. Improvement of the extraction procedure for hyaluronan from fish eyeball and the molecular characterization. *Fisheries Science*. 2009;75:805–10.

Part I

Biochemistry

Paul N. Bishop

Paul N. Bishop

Outline

- I. **Introduction**
- II. **Extracellular Matrix Proteins of the Vitreous**
 - A. Vitreous Collagens
 - 1. Collagen Structure
 - a. Type II Collagen
 - b. Type V/XI Collagen
 - c. Type IX Collagen
 - d. Type VI Collagen
 - 2. Heterotypic Collagen Fibrils of Vitreous
 - 3. Synthesis and Turnover of Vitreous Collagen
 - 4. Spacing Between Vitreous Collagen Fibrils and Aging Changes
 - B. Non-collagenous Extracellular Matrix Components of Vitreous
 - 1. Fibrillins
 - 2. Fibulins
 - 3. Versican and Link Proteins
 - 4. Agrin and Type XVIII Collagen
- III. **Vitreous Macromolecules That Regulate Angiogenesis**
 - A. Opticin
 - B. Pigment Epithelium-Derived Factor
 - C. Leucine-Rich Alpha-2 Glycoprotein (LRG1)
 - D. Thrombospondins

References

P.N. Bishop, MD, PhD
Centre for Hearing and Vision Research, Institute of Human
Development, University of Manchester, Manchester Academic
Health Science Centre, Oxford Road, Manchester M13 9PL, UK

Manchester Royal Eye Hospital,
Central Manchester University Hospitals NHS Foundation Trust,
Oxford Road, Manchester M13 9WH, UK
e-mail: paul.bishop@manchester.ac.uk

Keywords

Vitreous • Extracellular matrix • Angiogenesis •
Protein • Glycoprotein • Proteoglycan • Collagen

Key Concepts

1. The gel state of the vitreous body is maintained by a network of fine heterotypic (mixed composition) collagen fibrils that are composed of collagens II, V/XI and IX.
2. The adult vitreous collagens are mainly synthesized during embryonic and early postnatal life.
3. Vitreous is normally anti-angiogenic as it contains proteins/glycoproteins that inhibit angiogenesis including opticin, PEDF and thrombospondins.

I. Introduction

The overall protein concentration in human vitreous is between 0.5 and 1 mg/ml. Proteomic analyses have identified a large number of proteins in vitreous. For example, a 2013 study by Aretz et al. [1] identified over a 1,000 proteins in vitrectomy samples from three human subjects, and 261 of these proteins were consistently identified in all three samples. The embryonic human vitreous proteome has also been studied with the aim of identifying changes (up as well as down regulation) that could be related to the regression the hyaloid vasculature during the second trimester. This study identified 896 unique proteins, with significant changes during the second trimester, both up- and downregulation. [see chapter I.D. Vitreous cytokines and regression of the fetal hyaloid vasculature].

A high proportion of the protein content of vitreous is derived from the plasma, so albumin and immunoglobulins represent over 80 % of the protein in human vitreous [2].

These plasma proteins are probably derived from fenestrated capillaries in the ciliary body stroma, although there may be low-level leakage across the blood-retinal barrier, which when compromised becomes markedly increased. Many intracellular proteins have been identified either because of the presence of a small number of resident cells (i.e. hyalocytes) and/or they are released from degraded cells in the vitreous or surrounding ocular tissues and then sequestered in the vitreous.

This chapter will focus on two groups of proteins. Firstly, an overview of the extracellular matrix proteins of vitreous will be provided. These are structural molecules that are known to or may contribute to the physical properties of vitreous, such as collagens. Many of these proteins are modified with carbohydrates and they will be referred to as glycoproteins if they have short oligosaccharide side chains and proteoglycans if they have one or more glycosaminoglycan chain attached. The second group that will be reviewed are endogenous proteins/glycoproteins that may have a role in regulating pathological angiogenesis in vitreous. Growth factors/cytokines that regulate angiogenesis will be discussed elsewhere in this book [see chapter IV.C. Vitreous and iris neovascularization].

II. Extracellular Matrix Proteins of the Vitreous

A. Vitreous Collagens

The overall concentration of collagen in vitreous is low and in the human vitreous is approximately 300 µg/ml [3], i.e. only 0.5 % of the total protein content. Nonetheless, it is the dilute network of collagen fibrils that imparts gel-like properties to the vitreous. So, if the collagen fibrils are removed, vitreous is converted into a viscous liquid. Furthermore, in various vitreous pathologies it is this network of collagen fibrils that transmits tractional forces. The collagen is not uniformly distributed in vitreous, the highest concentration being present at the vitreous base, reflecting the main site of synthesis. The collagen concentration decreases towards the central and posterior parts of vitreous, but then increases in the posterior vitreous cortex adjacent to the retina. In the adult eye virtually all of this collagen is cross-linked into fibrils. The collagen fibrils of vitreous contain a co-assembly of collagen types II, V/XI and IX, i.e. they are heterotypic fibrils. Mutations in collagen types II and V/XI cause Stickler syndrome [see chapter I.C. Hereditary vitreo-retinopathies].

1. Collagen Structure

The collagens are a group of extracellular matrix proteins that constitute about 30 % of the body's total protein. More than 28 different types of collagen molecule have been

identified. Each collagen molecule is composed of three polypeptide chains, called α -chains. Some collagen molecules contain three identical α -chains, but others contain mixtures of α -chains that are derived from different collagen genes. The individual collagen molecules typically assemble into elongated fibrils or sheet-like structures which possess high tensile strength.

The three collagen α -chains wind around each other as the collagen molecule is assembled in the cellular endoplasmic reticulum. They assemble in this way because the α -chains have a characteristic amino acid sequence with glycine (the smallest amino acid) at every third amino acid, whilst the other two amino acids in the repeating triplets starting with glycine are often proline or hydroxyproline. Hydroxyproline is unique to collagens, so measurement of the amount of hydroxyproline in a tissue is a way of determining its collagen concentration. This repetitive amino acid sequence allows the three α -chains to assemble into a collagenous triple-helix which has a stiff, rod-like structure. Collagen molecules are not entirely composed of triple-helical regions; some have short non-triple-helical domains at the end of the molecules called telopeptides, whereas others, such as type IX collagen, have non-collagenous regions interspersed between the collagenous regions.

The individual triple-helical collagen molecules are secreted and then assemble outside cells to form fibrous assemblies. For example, the major collagens of vitreous assemble into very long, thin fibrils, whereas the type IV collagen of basement membranes, such as the inner limiting membrane (ILM), forms sheet-like structures. Some collagen molecules, such as the fibril-forming collagens of vitreous, are initially synthesized as longer procollagens. Once secreted from the cells, proteolytic removal of the ends of the procollagen molecules by specific enzymes results in the production of "mature" collagen molecules, and this facilitates their assembly into fibrils. The collagen molecules within fibrils are highly organised, so in fibrils they are in staggered arrays.

Collagen molecules undergo various post-translational modifications prior to secretion by the cells that synthesize them. Short carbohydrate chains are added to hydroxylysine residues, composed of just galactose or glucosyl1 α 1,2galactose. Non-collagenous regions within collagen molecules may have N- or O-linked oligosaccharides attached. Some collagens, such as type IX collagen, have a glycosaminoglycan chain added to a non-collagenous region, so they are proteoglycans.

As they assemble into fibrils, collagen molecules rapidly become cross-linked together, thereby adding tensile strength and mechanical stability to the fibrils. Cross-links form between lysyl and hydroxylysyl residues. Cross-link formation is catalysed by the copper-dependent enzyme lysyl oxidase resulting in the formation of lysine/hydroxylysine

Table I.A-1 Summary of α -chain composition of the collagen molecules that assemble into heterotypic fibrils in vitreous and cartilage

Collagen type	Genes encoding α -chains	Vitreous collagen α -chains	Cartilage collagen α -chains
II	COL2A1	$\alpha 1(\text{II})_3^a$	$\alpha 1(\text{II})_3$
V/XI	COL11A1	$\alpha 1(\text{XI})_2$	$\alpha 1(\text{XI})$
	COL11A2		$\alpha 2(\text{XI})$
	COL11A3		$\alpha 3(\text{XI})$
	COL5A2	$\alpha 2(\text{V})$	
IX	COL9A1	$\alpha 1(\text{IX})^b$	$\alpha 1(\text{IX})$
	COL9A2	$\alpha 2(\text{IX})$	$\alpha 2(\text{IX})$
	COL9A3	$\alpha 3(\text{IX})$	$\alpha 3(\text{IX})$

^aAlternative mRNA splicing results in long and short forms of type II procollagen in vitreous

^bAlternative mRNA splicing results in a shortened $\alpha 1(\text{IX})$ chain in vitreous

aldehydes. These then spontaneously undergo a series of chemical reactions to form di- or tri-functional intra- and intermolecular cross-links.

a. Type II Collagen

Type II collagen is the predominant collagen in vitreous, accounting for approximately 75 % of the total collagen [4]. It is a member of the fibril-forming group of collagens along with collagen types I, III, V, XI, V/XI, XXIV and XXVII. The type II collagen molecule is composed of three identical α -chains [$\alpha 1(\text{II})_3$] (Table I.A-1). When type II collagen molecules are secreted, they are procollagens, which have terminal extensions called the amino-propeptide and the carboxy-propeptide, alternatively referred to as the N- and C-propeptides (Figure I.A-1). Once in the extracellular environment, these extensions are removed or “processed” by specific enzymes leaving short non-collagenous telopeptides at each end of the main triple-helical region. Processing reduces the solubility of the type II collagen molecules and allows them to participate in fibril formation.

The N-propeptide of type II procollagen contains a region that undergoes alternative splicing at the mRNA level where exon 2 is present (IIA procollagen) or absent (IIB procollagen). The IIA procollagen contains an additional 69 amino acid cysteine-rich domain in the N-propeptide. In mature cartilage type IIB procollagen is expressed, but in prechondrogenic tissue and a number of other embryonic tissues, the IIA form is expressed [5]. In foetal and adult bovine vitreous, both forms are present, but the IIA form predominates [6]. The N-propeptides of type IIA procollagen once cleaved can remain non-covalently bound to the surface of adult bovine vitreous collagen fibrils [7]. One consequence of this alternative splicing is that there is an ocular-only form of Stickler syndrome in which there are mutations in this alternatively spliced exon 2 [8] [see chapter I.C. Hereditary vitreoretinopathies]. As cartilage only has the IIB form, it is not affected by this condition, but as the type II procollagen of vitreous is predominantly in the IIA form, there is a vitreous phenotype in this condition.

b. Type V/XI Collagen

Type V and type XI collagens were initially identified as distinct collagen types with type V collagen being found in skin and other tissues with various chain compositions (e.g. [$\alpha 1(\text{V})_2\alpha 2(\text{V})$], [$\alpha 1(\text{V})_3$], [$\alpha 1(\text{V})\alpha 2(\text{V})\alpha 3(\text{V})$]) and type XI collagen [$\alpha 1(\text{XI})\alpha 2(\text{XI})\alpha 3(\text{XI})$] in cartilage. However, it later became apparent that hybrid molecules exist in various tissues including vitreous, which contain chains from both collagen types, so the term type V/XI collagen has been adopted. Type V/XI collagen represents approximately 10 % of the collagen in vitreous [4]. In bovine vitreous, this collagen was shown to contain $\alpha 1(\text{XI})$ and $\alpha 2(\text{V})$ chains [9]. The stoichiometry of the chains in the molecules is uncertain, but is most probably [$\alpha 1(\text{XI})_2\alpha 2(\text{V})$], that is to say that each molecule contains two $\alpha 1(\text{XI})$ chains and one $\alpha 2(\text{V})$ chain (Table I.A-1).

Type V/XI collagen is secreted from cells as a procollagen with N- and C-propeptides (Figure I.A-1). However, whilst the C-propeptide is removed by processing, the N-propeptide is only partially processed and a large globular region is retained on the type V/XI collagen molecule [10]. The type V/XI collagen assembles into heterotypic (mixed composition) fibrils in the vitreous along with type II and type IX collagen. Studies of other tissues demonstrate that type V/XI collagen has roles in nucleating collagen fibril formation and regulating collagen fibril diameter [10].

c. Type IX Collagen

Type IX collagen is not a fibril-forming collagen although it is found in the surface of collagen fibrils. Instead it belongs to the FACIT (fibril-associated collagens with interrupted triple helices) group of collagens which also includes collagens XII, XIV, XVI and XIX. Type IX collagen is composed of three different α -chains, i.e. $\alpha 1(\text{IX})$, $\alpha 2(\text{IX})$ and $\alpha 3(\text{IX})$ (Table I.A-1). It has a rather more complex structure than that of the fibril-forming collagens described above as it possesses three collagenous regions (COL1, COL2 and COL3) interspersed between four non-collagenous regions (NC1, NC2, NC3 and NC4) (Figures I.A-1 and I.A-2). Type IX collagen is secreted as a mature collagen so it does not undergo processing

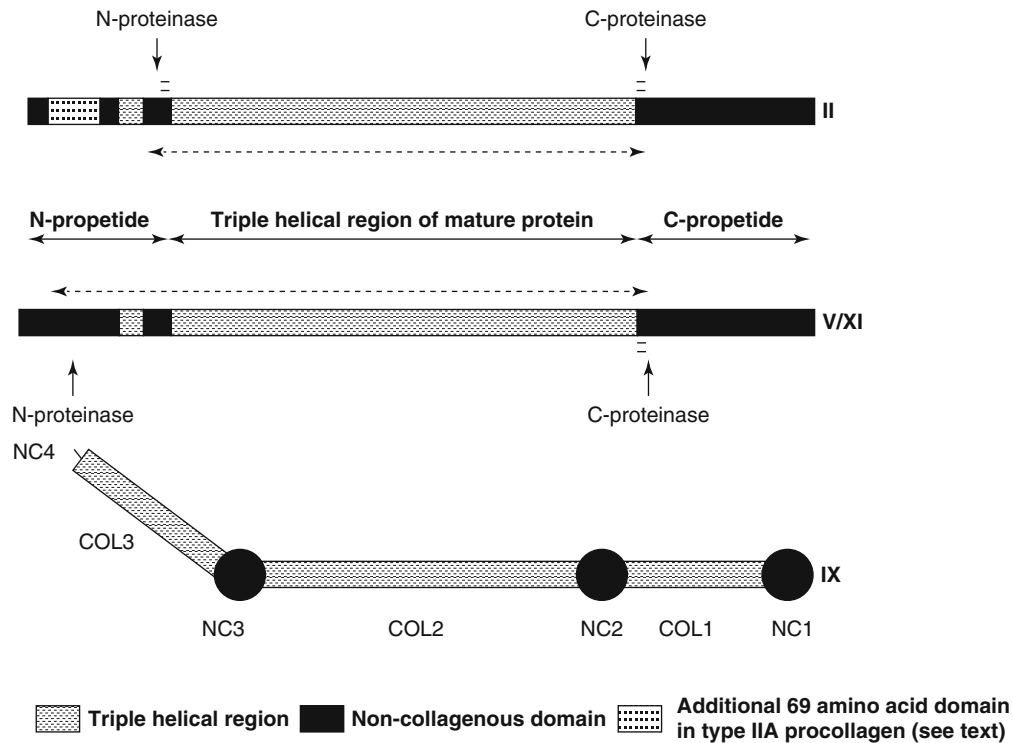


Figure I.A-1 Diagrammatic representation of the three collagens that co-assemble to form vitreous collagen fibrils, i.e. collagen types II, V/XI and IX. In the case of collagen types II and V/XI, these are synthesized as procollagens that then undergo processing (cleavage with *N*- and *C*-proteinases) prior to incorporation into fibrils. The *dotted line* represents the mature collagen molecule that remains after processing. The mature type II collagen has short telopeptides remaining after processing

represented by the *double line* (=); this is also the case for the C-terminus of the type V/XI collagen, but a large part of the N-propeptide is retained. The N-propeptide of type II procollagen has a 69 amino acid sequence that results from alternative splicing of mRNA, so long and short forms exist. The IX collagen has a complex structure with three collagenous (*COL*) domains and four non-collagenous (*NC*) domains. Type IX collagen does not undergo processing (Reproduced from Bishop [42])

prior to incorporation onto the surface of heterotypic collagen fibrils. Type IX collagen in vitreous is a proteoglycan with a 15–60 kDa chondroitin sulphate glycosaminoglycan chain attached to the $\alpha 2(\text{IX})$ chain of the NC3 domain [4].

d. Type VI Collagen

Type VI collagen forms distinct beaded microfibrils and small amounts of these microfibrils have been identified in vitreous isolates (Figure I.A-3) [11]. Subsequent studies indicate that the type VI collagen is present specifically in the ILM, vitreous cortex or both [12]. Given the location of the type VI collagen microfibrils and that they are known to bind collagen types II and IV, it is conceivable that they contribute to vitreoretinal adhesion.

2. Heterotypic Collagen Fibrils of Vitreous

The heterotypic collagen fibrils of vitreous are composed of collagen types II, V/XI and IX. The fibrils are very long, unbranched and thin; they have a uniform diameter of between 10 and 20 nm depending upon species [13] (Figure I.A-4). Cartilage has collagen fibrils with a very

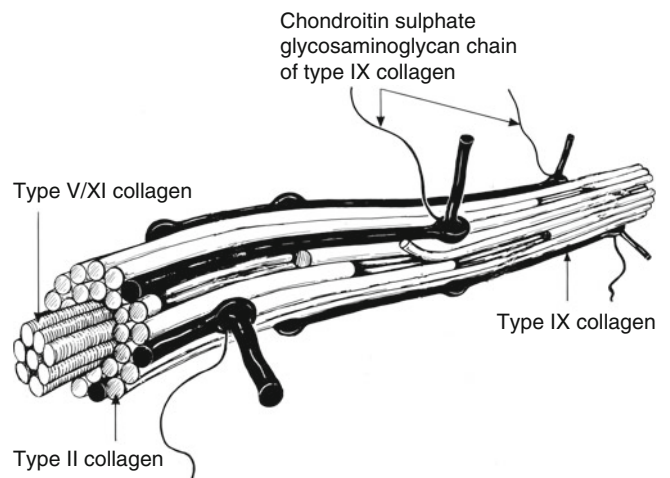


Figure I.A-2 Schematic diagram showing how molecules of collagen types II, V/XI and IX may co-assemble into heterotypic collagen fibrils. The triple-helical region of type V/XI is probably largely buried in the fibril but its retained N-propeptide extends to the surface. Type II collagen is the predominant collagen type in the fibrils and is arranged in staggered arrays. Type IX collagen is on the surface of the fibrils and has a chondroitin sulphate chain attached to its NC3 domain (Reproduced from Bishop [43])

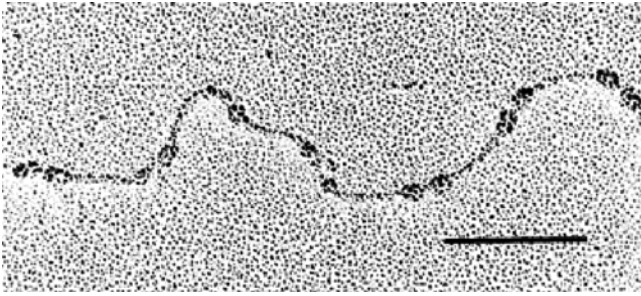


Figure I.A-3 Rotary shadowing electron microscopy of a type VI collagen microfibril isolated from vitreous. These have a characteristic double-beaded appearance (bar 100 nm)

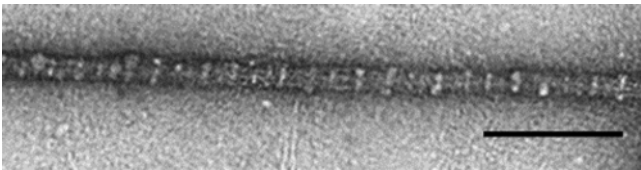


Figure I.A-4 Electron micrograph showing a section of a negatively stained bovine vitreous collagen fibril. The diameter of the fibril is approximately 15 nm and the banding pattern has a 64 nm periodicity due to the ordered, staggered arrays of collagen molecules (bar 100 nm)

similar composition, containing collagen types II, IX and XI (i.e. a form of type V/XI). Cartilage contains a mixture of thick and thin collagen fibrils, and the thin cartilage fibrils structurally resemble those found in vitreous.

The core of vitreous collagen fibrils is a copolymer of collagen II and collagen V/XI. In other tissues there is evidence that forms of collagen V/XI are deposited initially as rudimentary fibrils and they provide a nucleation site for the subsequent deposition of other fibrillar collagens, which in the case of vitreous would be type II collagen. The collagen molecules within the fibrils are assembled in a highly ordered manner, resulting in the fibrils having a repetitive banding pattern when examined under electron microscopy using particular staining techniques. In the case of the vitreous fibrils, because they are very thin, the banding pattern is difficult to visualise clearly; however, it is detectible with careful examination and this has allowed a detailed analysis of the organisation of the collagen molecules within the fibrils to be performed [14]. Collagen types II and V/XI are aligned in staggered arrays and are cross-linked together to form the long thin fibrils. Studies in other tissues suggest that the triple-helical portions of collagen V/XI are not exposed on the fibril surfaces and are buried within the fibrils, possibly because the V/XI collagen forms a nucleation site for the subsequent deposition of type II collagen (Figure I.A-2). However, the V/XI collagen has a retained N-propeptide that is located on fibrillar surfaces (its globular structure preventing it from being buried within the fibrils), and there is evidence that the N-propeptide is important in controlling fibril diameter.

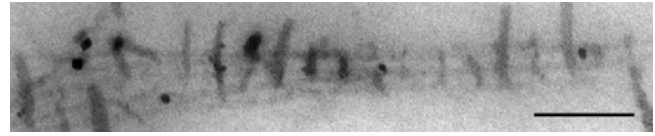


Figure I.A-5 Electron micrograph showing vitreous collagen fibrils stained with uranyl acetate and Alcian blue using the critical electrolyte concentration method. The faint horizontal strands are vitreous collagen fibrils and the more intensely stained components projecting away from the collagen fibrils are the chondroitin sulphate chains of type IX collagen. The chondroitin sulphate chains appear to both space apart and interlink the collagen fibrils as they run in small bundles (bar 200 nm)

Type IX collagen is regularly distributed along, and cross-linked to, the fibril surfaces. COL1 and COL2 are thought to be aligned antiparallel to the surface of the collagen fibril and COL2 provides sites for cross-linking to type II collagen molecules [15]. The NC3 region acts as a hinge allowing COL3 to extend in a strut-like manner away from the surface of the fibril with the NC4 domain attached to the end of this strut. In cartilage, a globular NC4 domain can be seen at the end of this strut by rotary shadowing electron microscopy, but in vitreous the NC4 domain is not visible [16, 17]. The large globular NC4 domain of cartilage type IX collagen is almost entirely composed of an extended $\alpha 1(\text{IX})$ chain, but in vitreous the $\alpha 1(\text{IX})$ chain is shorter as a result of the use of alternative splicing and transcription start sites. As type IX collagen in vitreous is a chondroitin sulphate proteoglycan, chondroitin sulphate chains are regularly distributed along the surface of the fibrils (Figure I.A-5), and as discussed below these are thought to be important in spacing the collagen fibrils apart.

3. Synthesis and Turnover of Vitreous Collagen

The synthesis of secondary (adult-type) vitreous begins at the end of the 6th week of human embryonic life [see chapter II.A. Development and Developmental Disorders of Vitreous]. Vitreous collagens are mainly derived from the ciliary body region, but there is also evidence for synthesis of vitreous collagen by the developing retina. A possible explanation for the distribution and orientation of the vitreous collagen fibrils in the developed eye is that the cortical vitreous collagen is derived mainly from retina, whereas the basal and central vitreous collagen is secreted by the ciliary body into the vitreous body. The optimal way to determine where vitreous collagen is synthesized is to use in situ hybridisation to detect the collagen mRNA in histological sections. This has not been done in embryonic human eyes, so we have to draw conclusions from research on animal eyes. Studies on embryonic chick eyes demonstrated type II collagen expression throughout the inner layer of the optic cup in early embryonic development

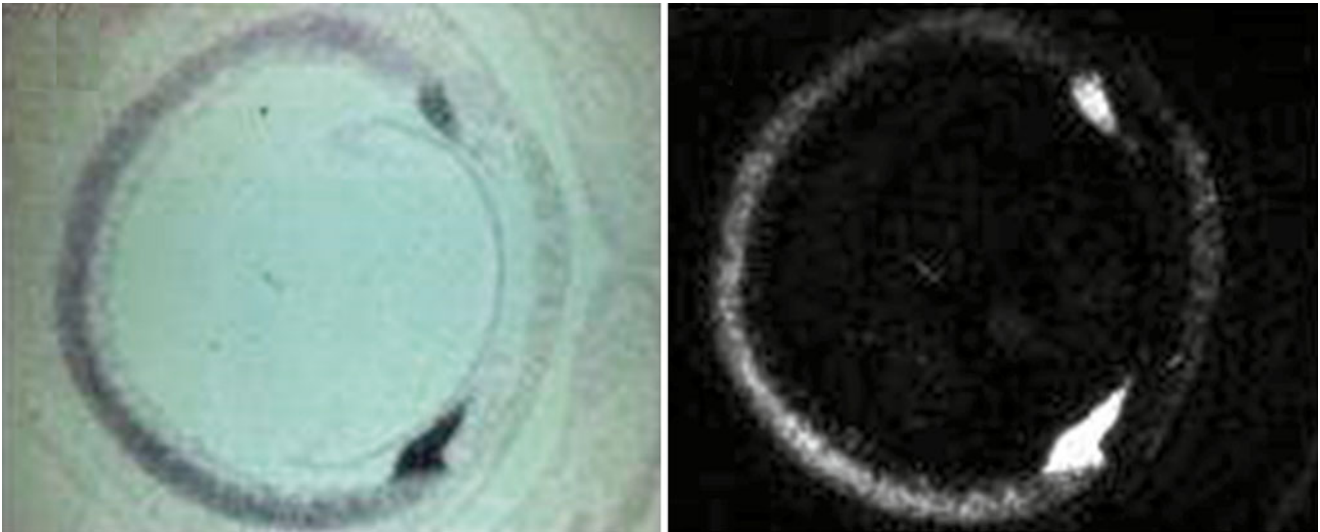


Figure I.A-6 *In situ* hybridization showing the expression of the COL9A1 gene (encoding the $\alpha 1(\text{IX})$ chain of type IX collagen) in the embryonic day 17.5 mouse eye. *Left*, bright field image; *right* dark field

image showing COL9A1 expression. There is a strong signal in the ciliary body and a weak signal in the retina and cornea (Reproduced from Takanosu et al. [44])

(embryonic days 3.5–5); then by embryonic day 7 type II collagen expression was localised to the presumptive ciliary body [18]. By embryonic days 13–15 the ciliary body has formed and type II and type IX collagen mRNA expression was then just localised to the ciliary body. Another study of the developing chick eye confirmed that type IX collagen expression at embryonic day 10 was confined to the developing ciliary body [19]. We observed a similar pattern in the embryonic mouse eye (embryonic day 17.5) and the adult mouse eye, with type IX collagen chains mainly being expressed by the ciliary body, although some weak expression was observed in the retina and lens (Figure I.A-6) [20]. However, type II collagen is widely expressed in the developing and adult mouse eye.

The soluble collagens in vitreous were analysed by Western blotting in embryonic and postnatal human eyes [19]. A rapid postnatal decline in the amount of soluble collagen in vitreous was observed with very little being detected by 6 months of age, and the soluble collagen was undetectable in the adult eye. Collagen was still present in the postnatal and adult vitreous, but it was virtually all cross-linked into fibrils and therefore not soluble and detectable by Western blotting. However, evidence has been found by other groups for some synthesis of vitreous collagen in adult human eyes including the detection of small amounts of soluble type II procollagen, immature collagen cross-links in the fibrils and type II collagen mRNA in retinectomy samples [21]. In addition, there is morphological evidence for the synthesis of vitreous collagen by the peripheral retina [22, 23]. The overall concentration of collagen in human vitreous remains fairly constant throughout life at approximately 300 $\mu\text{g}/\text{ml}$ [11], and the vitreous gel does not reform to any

significant degree after vitrectomy. Therefore, this new synthesis of collagen in the adult eye is likely to be at a low level unless there is also significant degradation of collagen so that these constant levels are maintained. Ponsioen et al. [21] suggest that there is a considerable degradation of collagen and active turnover of collagen in the adult vitreous through the actions of trypsin and metalloproteinases [24]. This is possible, but the complete destruction of the heavily cross-linked collagen fibrils by these enzymes is difficult to achieve. Another possibility is that these enzymes act on the surface of collagen fibrils leading to some surface remodelling without complete destruction of the fibrils. In this context we have observed an age-dependent loss of type IX collagen from the fibril surfaces leading to surface exposure of type II collagen [25].

4. Spacing Between Vitreous Collagen Fibrils and Ageing Changes

As discussed above, vitreous collagen fibrils run in small bundles through the vitreous body and within these bundles the collagen fibrils are spaced apart by the chondroitin sulphate chains of type IX collagen. The bundles of collagen fibrils are then interlinked by collagen fibrils running from one bundle to another thereby forming an extended network that maintains the gel state of vitreous [26]. Hyaluronan forms a network by entanglement and is expansile due to the ability of hyaluronan to attract water and counter ions, thereby pushing the bundles of collagen fibrils apart and inflating the collagen network.

During ageing the collagen within and between the bundles aggregates together due to a loss of the type IX collagen, and hence chondroitin sulphate chains, from the

surface of the fibrils [25]. The aggregation of the collagen fibrils results in areas within the vitreous body becoming devoid of collagen fibrils, and this then leads to vitreous liquefaction.

B. Non-collagenous Extracellular Matrix Components of Vitreous

1. Fibrillins

Vitreous contains fibrillin-1 and fibrillin-2. Fibrillins assemble into distinct microfibrils, i.e. fibrillin-containing microfibrils [15]. These are much less abundant than the heterotypic collagen fibrils in vitreous. Whilst it is unknown as to whether these microfibrils make a significant contribution to the structure of vitreous, bundles of fibrillin-containing microfibrils, containing fibrillin-1 and fibrillin-2, are the main components of the ocular zonules [27]. In many tissues fibrillin-containing microfibrils are associated with elastin, but this does not appear to be the case in vitreous or in ocular zonules. Fibrillin-containing microfibrils are 10–12 nm in diameter and have a characteristic beaded appearance by rotary shadowing electron microscopy (Figure I.A-7).

Mutations in the gene encoding fibrillin-1 cause Marfan syndrome. This syndrome is characterised by ocular, cardiovascular and skeletal malformations. The ocular phenotype includes ectopia lentis, myopia and a propensity towards developing rhegmatogenous retinal detachments. The increased risk of retinal detachment could be due to structural abnormalities of the vitreous gel as a result of abnormal fibrillin-containing microfibrils within vitreous, or it could be secondary to lens instability and myopia. Defects in the fibrillin-2 gene cause contractural arachnodactyly; an ocular phenotype is uncommon in this condition, but there is a possible association with ectopia lentis [see chapter I.C. Hereditary Vitreo-Retinopathies].

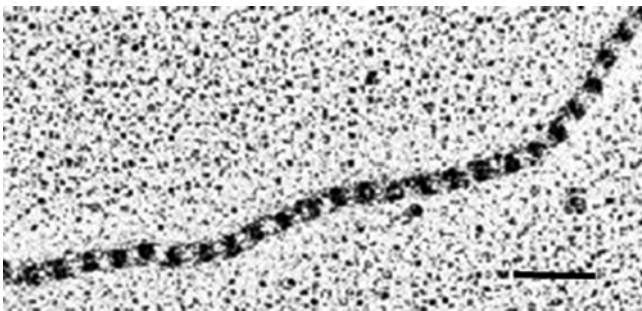


Figure I.A-7 Rotary shadowing electron microscopy of a fibrillin-containing microfibril isolated from vitreous. These fibrils have a characteristic beaded structure (bar 50 nm)

2. Fibulins

Fibulins are a family of extracellular matrix glycoproteins that are defined by the presence of tandem epidermal growth factor-like repeats and a unique C-terminal fibulin-type module [28]. There are seven members of this family of extracellular matrix molecules and of these fibulin-1 and fibulin-3 (also called EFEMP1) have been identified in vitreous [1]. These molecules are thought to have bridging roles in extracellular matrix assemblies. For example, fibulin-1 is known to interact with versican and fibronectin, both of which are known to be present in vitreous. However, it is not known whether fibulins 1 and 3 contribute significantly to the structural stability of the vitreous gel.

3. Versican and Link Proteins

Our group first identified the large chondroitin sulphate proteoglycan versican in vitreous [29]. It consists of an N-terminal hyaluronan binding domain, a central chondroitin sulphate substituted domain and a C-terminal globular domain. There are four isoforms of versican of different sizes and with different numbers of chondroitin sulphate attachment sites. The N-terminal domain binds to hyaluronan and this binding is stabilised by link proteins. We identified link proteins in vitreous in a 1:1 molar ratio with versican suggesting that the versican in vitreous is bound to hyaluronan and this binding is stabilised by the link proteins [29]. Wagner syndrome/erosive vitreoretinopathy is a hereditary condition with vitreous abnormalities that is caused by splice site mutations in the versican gene which are likely to result in an imbalance in the amounts of the four isoforms [see chapter I.C. Hereditary vitreo-retinopathies].

4. Agrin and Type XVIII Collagen

These are both heparan sulphate proteoglycans that are present in basement membranes including the ILM. In addition they have been identified in the vitreous, but it is unclear whether they play a role in maintaining the structural stability of the vitreous gel or whether their presence in vitreous represents a by-product of ILM synthesis or degradation.

III. Vitreous Macromolecules That Regulate Angiogenesis

A. Opticin

Analysis of molecules associated with vitreous collagen fibrils by SDS-PAGE revealed a major band that migrated at approximately 45 kDa (Figure I.A-8). This gel band was subjected to proteomic analysis and found to be a novel glycoprotein that was subsequently cloned and sequenced and called opticin [30]. Opticin is a member of a family of extracellular matrix molecules called the small leucine-rich repeat

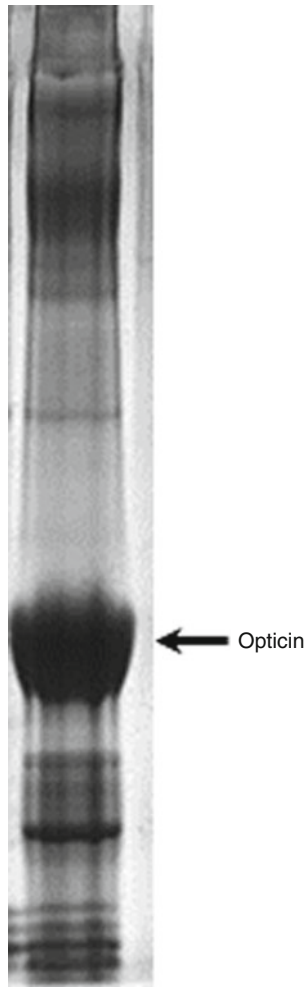


Figure I.A-8 Coomassie Blue stained SDS-PAGE gel of a 4 M guanidine hydrochloride extract from vitreous collagen fibrils. This technique identified proteins and glycoproteins that are strongly bound to the surface of the collagen fibrils. The major band, which runs at approximately 45 kDa, is monomeric opticin

proteoglycan (SLRP) family and is the only member of this family of molecules that has been identified conclusively in vitreous. Opticin is a homodimeric glycoprotein of approximately 90 kDa that dimerises through its leucine-rich repeat domains [31]. Each monomer in the homodimer consists of a region containing seven leucine-rich repeats that are flanked by cysteine clusters and an N-terminal region that contains a domain that is heavily substituted with sialylated O-linked oligosaccharides. Opticin is expressed by the non-pigmented ciliary epithelium, and unlike other extracellular matrix molecules of vitreous, high level expression is maintained throughout life [20]. Immunohistochemistry demonstrates that opticin is present throughout the vitreous body and there is strong labelling of the ILM, but only relatively small amounts cross the ILM into the retina (Figure I.A-9) [32] [see chapter II.E. Vitreo-retinal interface & inner limiting membrane].

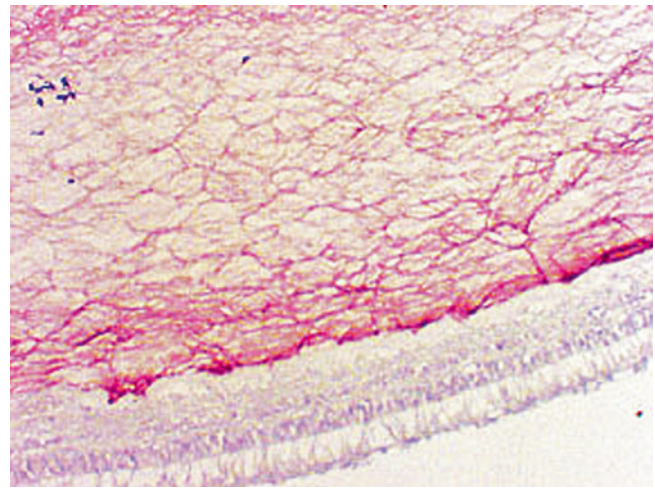


Figure I.A-9 Immunolocalization of opticin in the adult human eye. The bright magenta stain demonstrates the Immunolocalization of opticin in the eye. The opticin coats the collagen fibrils and there is strong labelling near the vitreoretinal interface. However, very little opticin crosses into the neurosensory retina, which is counterstained with hematoxylin (blue)

Experiments were undertaken to determine whether opticin influenced pathological angiogenesis in vitreous, i.e. preretinal neovascularization. The well-established murine oxygen-induced retinopathy model was used, and it was shown that there is increased preretinal neovascularization in opticin knockout mice compared to wild-type mice [33]. A second set of experiments demonstrated that the injection of recombinant opticin into the wild-type mouse vitreous inhibited preretinal neovascularization in this model. From these experiments it was concluded that opticin is anti-angiogenic and that it inhibits preretinal neovascularization in a dose-dependent manner. Other anti-angiogenic molecules have been described in vitreous, but opticin is the only one in which the genetic knockout of the molecule leads to increased neovascularization in the oxygen-induced retinopathy model. This suggests that whilst several molecules are likely to contribute to the anti-angiogenic properties of vitreous, opticin may be the most important.

In a series of experiments the mechanism underpinning the anti-angiogenic actions of opticin was elucidated [34]. Vitreous collagen fibrils are required for preretinal neovascularization to occur. The collagen fibrils provide mechanical support for the growth of new blood vessels. In addition, signals that are critical for angiogenesis to occur are transmitted from the collagen via the collagen binding integrins (including $\alpha 1\beta$ and $\alpha 2\beta 1$ integrins) into the endothelial cells. Opticin coats the collagen fibrils, weakens integrin-mediated endothelial cell adhesion to the collagen and inhibits the outside-to-inside integrin-mediated signalling that is required for angiogenesis.

B. Pigment Epithelium-Derived Factor

Pigment epithelium-derived factor (PEDF) is a 50 kDa secreted protein. It has multiple biological activities and is neuroprotective and neurotrophic; it can regulate cell survival, differentiation and migration and has anti-angiogenic properties [35]. It has several ligands and cell surface receptors. Its N-terminal domain was identified as being anti-angiogenic. Whilst the overall levels of PEDF are not altered in diabetic vitreous, there is a shift to a higher molecular weight isoform and it was suggested that this may contribute to a pro-angiogenic shift [36]. However, whilst PEDF knockout mice have an enhanced rate of retinal vascular expansion during development and show heightened retinal obliteration in the oxygen-induced retinopathy model, they do not show increased preretinal neovascularization [37]. Vitreous PEDF levels underwent three-fold upregulation during the second trimester of human embryogenesis, consistent with its role as an inhibitor of angiogenesis [see chapter I.D. Vitreous cytokines and regression of the fetal hyaloid vasculature].

C. Leucine-Rich Alpha-2 Glycoprotein (LRG1)

LRG1 is a secreted 35 kDa leucine-rich repeat containing glycoprotein that is present in vitreous [1]. It has been shown to be pro-angiogenic by causing a switch in transforming growth factor beta signalling in endothelial cells via binding to endoglin and promoting signalling via the smad1/5/8 pathway [38]. When the LFG1 knockout mice were analysed using the oxygen-induced retinopathy model, there was significantly less neovascularization as compared to controls. Therefore, endogenous LRG1 stimulates angiogenesis in vitreous, at least in this mouse model.

D. Thombospondins

Thombospondin-1 is a large (360 k kDa) homotrimeric glycoprotein that has anti-angiogenic properties. It inhibits the proliferation and migration of endothelial cells through its interaction with receptors including CD36, CD47 and integrins. Thombospondin-1 is present in vitreous and levels have been found to be decreased in diabetic vitreous, which could predispose to proliferative diabetic retinopathy [36]. Thombospondin-1 knockout mice were less sensitive to retinal vaso-obliteration in the oxygen-induced retinopathy model, but there was a similar level of neovascularization comparing knockout mice with controls [39].

Thombospondin-2 has a similar structure to thombospondin-1 and is anti-angiogenic, acting through similar mechanisms [40]. It was found to be in higher concentration

in diabetic vitreous than controls and at higher levels in active vascularised preretinal membranes compared to quiescent membranes [41]. It was suggested that upregulation of thrombospondin-2 is a protective mechanism in proliferative diabetic retinopathy.

Abbreviations

C-	Carboxy-
FACIT	Fibril-associated collagens with interrupted triple helices
kDa	Kilodaltons
LRG1	Leucine-rich alpha-2 glycoprotein
mRNA	Messenger ribonucleic acid
N-	Amino-
NC	Non-collagenous
PEDF	Pigment epithelium-derived factor
SDS-PAGE	Sodium dodecyl sulphate-polyacrylamide gel electrophoresis
SLRP	Small leucine-rich repeat proteoglycan

References

1. Aretz S, Krohne TU, Kammerer K, Warnken U, Hotz-Wagenblatt A, Bergmann M, Stanzel BV, Kempf T, Holz FG, Schnölzer M, Kopitz J. In-depth mass spectrometric mapping of the human vitreous proteome. *Proc Natl Acad Sci U S A*. 2013;11:22.
2. Angi M, Kalirai H, Coupland SE, Damato BE, Semeraro F, Romano MR. Proteomic analyses of the vitreous humour. *Mediators Inflamm*. 2012;2012:148039.
3. Balazs EA. Physiology of the vitreous body. In: Schepens CL, editor. Importance of the vitreous body in retinal surgery with special emphasis on re-operation. St. Louis: C.V. Mosby Co; 1960. p. 29–57.
4. Bishop PN, Crossman MV, McLeod D, Ayad S. Extraction and characterization of the tissue forms of collagen types II and IX from bovine vitreous. *Biochem J*. 1994;299:497–505.
5. Oganessian A, Zhu Y, Sandell LJ. Type IIA procollagen amino propeptide is localized in human embryonic tissues. *J Histochem Cytochem*. 1997;45:1469–80.
6. Bishop PN, Reardon AJ, McLeod D, Ayad S. Identification of alternatively spliced variants of type II procollagen in vitreous. *Biochem Biophys Res Commun*. 1994;203:289–95.
7. Reardon A, Sandell L, Jones CJ, McLeod D, Bishop PN. Localization of pN-type IIA procollagen on adult bovine vitreous collagen fibrils. *Matrix Biol*. 2000;19:169–73.
8. McAlinden A, Majava M, Bishop PN, Perveen R, Black GC, Pierpont ME, Ala-Kokko L, Männikkö M. Missense and nonsense mutations in the alternatively-spliced exon 2 of COL2A1 cause the ocular variant of Stickler syndrome. *Hum Mutat*. 2008;29:83–90.
9. Mayne R, Brewton RG, Mayne PM, Baker JR. Isolation and characterization of the chains of type V/type XI collagen present in bovine vitreous. *J Biol Chem*. 1993;268:9381–6.
10. Smith SM, Birk DE. Focus on molecules: collagens V and XI. *Exp Eye Res*. 2012;98:105–6.
11. Bishop P, Ayad S, Reardon A, McLeod D, Sheehan J, Kieley C. Type VI collagen is present in human and bovine vitreous. *Graefes Arch Clin Exp Ophthalmol*. 1996;234:710–3.

12. Ponsioen TL, van Luyn MJ, van der Worp RJ, van Meurs JC, Hooymans JM, Los LI. Collagen distribution in the human vitreoretinal interface. *Invest Ophthalmol Vis Sci.* 2008;49:4089–95.
13. Balazs EA, Denlinger JL. Ageing changes in the vitreous. In: Dismukes K, Sekular R, editors. *Ageing and human visual function.* New York: Alan R Liss, Inc; 1982. p. 45–57.
14. Bos KJ, Holmes DF, Kadler KE, McLeod D, Morris NP, Bishop PN. Axial structure of the heterotypic collagen fibrils of vitreous humour and cartilage. *J Mol Biol.* 2001;306:1011–22.
15. Wu JJ, Woods PE, Eyre DR. Identification of cross-linking sites in bovine cartilage type IX collagen reveals an antiparallel type II-type IX molecular relationship and type IX to type IX bonding. *J Biol Chem.* 1992;267:23007–14.
16. Vaughan L, Mendler M, Huber S, Bruckner P, Winterhalter KH, Irwin MI, Mayne R. D-periodic distribution of collagen type IX along cartilage fibrils. *J Cell Biol.* 1988;106:991–7.
17. Ren ZX, Brewton RG, Mayne R. An analysis by rotary shadowing of the structure of the mammalian vitreous humor and zonular apparatus. *J Struct Biol.* 1991;106:57–63.
18. Linsenmayer TF, Gibney E, Gordon MK, Marchant JK, Hayashi M, Fitch JM. Extracellular matrices of the developing chick retina and cornea. Localization of mRNAs for collagen types II and IX by in situ hybridization. *Invest Ophthalmol Vis Sci.* 1990;31:1271–6.
19. Halfter W, Dong S, Schurer B, Ring C, Cole GJ, Eller A. Embryonic synthesis of the inner limiting membrane and vitreous body. *Invest Ophthalmol Vis Sci.* 2005;46:2202–9.
20. Bishop PN, Takanosu M, Le Goff M, Mayne R. The role of the posterior ciliary body in the biosynthesis of vitreous humour. *Eye.* 2002;16:454–60.
21. Ponsioen TL, Hooymans JM, Los LI. Remodelling of the human vitreous and vitreoretinal interface—a dynamic process. *Prog Retin Eye Res.* 2010;29:580–95.
22. Wang J, McLeod D, Henson DB, Bishop PN. Age-dependent changes in the basal retinovitreal adhesion. *Invest Ophthalmol Vis Sci.* 2003;44:793–800.
23. Ponsioen TL, van der Worp RJ, van Luyn MJ, Hooymans JM, Los LI. Packages of vitreous collagen (type II) in the human retina: an indication of postnatal collagen turnover? *Exp Eye Res.* 2005;80:643–50.
24. van Deemter M, Kuijter R, Harm Pas H, Jacoba van der Worp R, Hooymans JM, Los LI. Trypsin-mediated enzymatic degradation of type II collagen in the human vitreous. *Mol Vis.* 2013;19:1591–9.
25. Bishop PN, Holmes DF, Kadler KE, McLeod D, Bos KJ. Age-related changes on the surface of vitreous collagen fibrils. *Invest Ophthalmol Vis Sci.* 2004;45:1041–6.
26. Bos KJ, Holmes DF, Meadows RS, Kadler KE, McLeod D, Bishop PN. Collagen fibril organisation in mammalian vitreous by freeze etch/rotary shadowing electron microscopy. *Micron.* 2001;32:301–6.
27. Yamanouchi K, Tsuruga E, Oka K, Sawa Y, Ishikawa H. Fibrillin-1 and fibrillin-2 are essential for formation of thick oxytalan fibers in human nonpigmented ciliary epithelial cells in vitro. *Connect Tissue Res.* 2012;53:14–20.
28. de Vega S, Iwamoto T, Yamada Y. Fibulins: multiple roles in matrix structures and tissue functions. *Cell Mol Life Sci.* 2009;66:1890–902.
29. Reardon A, Heinegård D, McLeod D, Sheehan JK, Bishop PN. The large chondroitin sulphate proteoglycan versican in mammalian vitreous. *Matrix Biol.* 1998;17:325–33.
30. Reardon AJ, Le Goff M, Briggs MD, McLeod D, Sheehan JK, Thornton DJ, Bishop PN. Identification in vitreous and molecular cloning of opticin, a novel member of the family of leucine-rich repeat proteins of the extracellular matrix. *J Biol Chem.* 2000;275:2123–9.
31. Le Goff MM, Hindson VJ, Jowitt TA, Scott PG, Bishop PN. Characterization of opticin and evidence of stable dimerization in solution. *J Biol Chem.* 2003;278:45280–7.
32. Ramesh S, Bonshek RE, Bishop PN. Immunolocalisation of opticin in the human eye. *Br J Ophthalmol.* 2004;88:697–702.
33. Le Goff MM, Lu H, Ugarte M, Henry S, Takanosu M, Mayne R, Bishop PN. The vitreous glycoprotein opticin inhibits preretinal neovascularization. *Invest Ophthalmol Vis Sci.* 2012;53:228–34.
34. Le Goff MM, Sutton MJ, Slevin M, Latif A, Humphries MJ, Bishop PN. Opticin exerts its anti-angiogenic activity by regulating extracellular matrix adhesiveness. *J Biol Chem.* 2012;287:28027–36.
35. Crawford SE, Fitchev P, Veliceasa D, Volpert OV. The many facets of PEDF in drug discovery and disease: a diamond in the rough or split personality disorder? *Expert Opin Drug Discov.* 2013;8:769–92.
36. Wang S, Gottlieb JL, Sorenson CM, Sheibani N. Modulation of thrombospondin 1 and pigment epithelium-derived factor levels in vitreous fluid of patients with diabetes. *Arch Ophthalmol.* 2009;127:507–13.
37. Huang Q, Wang S, Sorenson CM, Sheibani N. PEDF-deficient mice exhibit an enhanced rate of retinal vascular expansion and are more sensitive to hyperoxia-mediated vessel obliteration. *Exp Eye Res.* 2008;87:226–41.
38. Wang X, Abraham S, McKenzie JA, Jeffs N, Swire M, Tripathi VB, Luhmann UF, Lange CA, Zhai Z, Arthur HM, Bainbridge JW, Moss SE, Greenwood J. LRG1 promotes angiogenesis by modulating endothelial TGF- β signalling. *Nature.* 2013;499:306–11.
39. Wang S, Wu Z, Sorenson CM, Lawler J, Sheibani N. Thrombospondin-1-deficient mice exhibit increased vascular density during retinal vascular development and are less sensitive to hyperoxia-mediated vessel obliteration. *Dev Dyn.* 2003;228:630–42.
40. Lawler PR, Lawler J. Molecular basis for the regulation of angiogenesis by thrombospondin-1 and -2. *Cold Spring Harb Perspect Med.* 2012;2:a006627.
41. Abu El-Asrar AM, Nawaz MI, Ola MS, De Hertogh G, Opendakker G, Geboes K. Expression of thrombospondin-2 as a marker in proliferative diabetic retinopathy. *Acta Ophthalmol.* 2013;91:e169–77.
42. Bishop PN. Structural macromolecules and supramolecular organisation of the vitreous gel. *Prog Retin Eye Res.* 2000;19:434–344.
43. Bishop PN. The biochemical structure of mammalian vitreous. *Eye.* 1996;10:664–70.
44. Takanosu M, Boyd TC, Le Goff M, Henry SP, Zhang Y, Bishop PN, Mayne R. Structure, chromosomal location, and tissue-specific expression of the mouse opticin gene. *Invest Ophthalmol Vis Sci.* 2001;42:2202–10.

Janet L. Denlinger and Endre A. Balazs

Outline

- I. Introduction
- II. Vitreous Structure
- III. Hyaluronan
- IV. Proteoglycans of the Vitreous
- V. Aging of the Vitreous
- VI. Miscellaneous Considerations
 - A. Species Variations
 - B. Hyaluronidase and the Vitreous
 - C. Hyaluronan and its Derivatives as Viscoelastics in Medicine

References

Keywords

Vitreous • Gel vitreous • Liquid vitreous • Hyaluronan • Proteoglycan

Key Concepts

1. Adult vitreous may consist totally of gel (cattle, rabbit) or may be a combination of gel and liquid (humans, monkeys). The gel is composed of a network of a very thin, fibrous collagen network, and the liquid is viscoelastic hyaluronan.
2. Vitreous viscoelasticity is produced by a combination of the concentration and the molecular size of the hyaluronan molecules.
3. After birth no new collagen fibrils, but only hyaluronan (liquid vitreous), is produced to keep pace with and fill the globe as it develops. With aging, gel vitreous liquefies in nearly all animals and in humans.

As elected by the authors of this chapter, *vitreus* will be used as a noun, designating the connective tissue surrounded by the lens, ciliary body, and retina. Thus, vitreus will replace vitreous humor, vitreous body, and vitreous (if used as a noun). The two rheological states of the vitreous will be designated as *gel vitreus* and *liquid vitreus*. *Vitreous* will be used, as an adjective, in the following manner: vitreous anomalies, vitreous strands, vitreous implants, etc. [1].

J.L. Denlinger, PhD (✉) • E.A. Balazs, MD
Matrix Biology Institute, 720 River Road, Suite 205,
Edgewater, NJ 07020, USA
e-mail: jdenlinger@matrixbio.org; eabalazs@matrixbio.org

I. Introduction

Why vitreous? Why any connective tissue? In the eye, vitreous is responsible for the stability and general good health of the adjacent structures retina, lens, ciliary body, and zonules. Unlike other connective tissues, vitreous fulfills its function of transparency with solidity in order to serve as a stabilizer and shock absorber for movement or mechanical impact that could harm these delicate tissues. In addition, its high permeability permits free diffusion of most molecules reaching its border [see chapter IV.A. Vitreous physiology]. The authors have spent several decades studying vitreous, despite the fact that many years ago someone once noted that there is nothing more to know about the vitreous; everything is known. This chapter explains how the

hyaluronan (formerly hyaluronic acid, hyaluronate) content and function in human vitreous contribute to development and aging in this most interesting tissue. Most of the work on this subject has been done before the mid-1980s and was reviewed and summarized by us [1] and updated in 1992 and 1998 by Sebag [2, 3] and in 1994 by Balazs [4]. In the last three decades, there has been additional work on human and animal vitreous, noting the similarities and differences between them. Unfortunately, since 1998 until today fewer than ten nonclinical papers were published with the words “hyaluronan” and “vitreous” in the title. In this paper we will review only a select group of those papers that represent important research findings on this subject.

As early as 1852, the German pathologist Rudolf Virchow observed that there were two parts to vitreous: a viscous liquid that could pass through a filter and a white, fibrous residue that was retained on the filter [5]. It was not, however, until the work of Meyer and Palmer [6] in 1934 that this substance was isolated, characterized, and given the name hyaluronic acid (from *hyaloid* (glassy, vitreous)) and *uronic acid* (for a review on the history of vitreous research from 1852, see [7]). In 1986, the name *hyaluronan* was adopted to replace the inaccurate name *hyaluronic acid* [8].

II. Vitreous Structure

The adult human vitreous has three distinct parts: liquid vitreous, gel vitreous, and posterior vitreous cortex, 100–300 μm thick, which contains in its posterior and lateral portions the only cells in the vitreous (hyalocytes) and is attached to the basal lamina of the retina and ciliary body [9, 10]. Its anterior portion, known as the *annular gap* [11], represents a “diffusion barrier” for liquid vitreous so that it cannot directly flow, but can only diffuse, out of the vitreous space into the anterior chamber. This anterior portion of the cortical gel vitreous does not contain cells. In a few primates such as the owl monkey (*Aotus trivirgatus*) and bush baby (*Galago galago*) in whom the entire vitreous space is filled with viscous liquid vitreous, the cortical gel still exists as a thin shell completely surrounding the liquid [12].

The human gel is made of collagen fibers, and in between the fibers is a large amount of hyaluronan. The gel vitreous fills the vitreous space in embryos and for a short period postnatally. After birth liquid vitreous is produced to keep pace with and fill the eyeball as it develops [13]. From development until adulthood, the vitreous doubles in volume. The concentration of hyaluronan in the normal human eye during this same period more than doubles increasing from approximately 0.07–1.8 mg/mL. The number of

collagen fibrils responsible for the gel state of the vitreous (10–20 μm in size), forming a completely non-cross-linked, random network, remains constant. These fibers are very similar to type II collagen and crisscross the vitreous space, from basal lamina to basal lamina without detectable ends [2, 14]. Collagen fibers that are part of the gel vitreous are formed during prenatal development, and their number remains constant thereafter. There is no evidence that this collagen fibrillar network metabolizes in the normal adult vitreous. Following vitrectomy, the gel-forming collagen fibrils do not regenerate, provided that surgical trauma that could lead to wound-related connective tissue formation is minimal. The formation of liquid vitreous during normal growth and development of the eye is a result of the fact that the number of collagen fibrils does not increase, and hyaluronan (liquid vitreous) fills the space between the fibrils. The molecular size of hyaluronan is the same in young and old eyes, as well as in the liquid and gel vitreous [13, 15].

Also of note are differences in the topographical distribution of the insoluble (fibrillar) and soluble macromolecules in the human vitreous. The collagen fibrillar network is densest in the cortical vitreous gel next to the ciliary epithelium and near the ora serrata of the retina. In other areas of the cortical gel, it is less dense. Liquid vitreous, whether visualized during development or aging, is always located in the center and anterior part of the vitreous where the collagen fibrillar network is the least dense. Collapse of the sparse collagen network in this area (syneresis) can result in pools of liquid vitreous.

III. Hyaluronan

Hyaluronan is a unique, pure polysaccharide in the human and animal body – present in all intercellular matrices (also intercellular spaces) of the body. It is a polydisperse molecular system above the molecular size of 30,000; therefore, the molecular weight must always be expressed as an “average.” Consequently the term “Dalton” cannot be used for characterizing hyaluronan because it is not monodisperse. The average molecular weight of hyaluronan varies in the human and animal body according to the intercellular space of the tissue where it is present. In vitreous the average molecular weight is very high; consequently the solution of the molecules represents a viscoelastic fluid system. The viscoelasticity of the hyaluronan solution depends not only on the average molecular weight but also on the concentration of the molecules. Hyaluronan is also unevenly distributed, being the highest in the posterior cortical gel in which the hyalocytes are

embedded. A concentration gradient toward the retrolental space exists and is maintained by a continuous production of hyaluronan by the hyalocytes. It must be pointed out, however, that the evidence for hyalocyte synthesis of hyaluronan is circumstantial and not direct.

The filtering effect of the basal laminae prevents the hyaluronan from diffusing into the intercellular spaces of the adjacent structures. Hyaluronan can slowly diffuse (it does not “flow”) through the anterior cortical gel of vitreus into the posterior chamber [11]. From the posterior chamber, it is washed by the aqueous to the anterior chamber and leaves the eye through the trabecular meshwork to Schlemm’s canal. The turnover time (half-life) of hyaluronan in the eyes of two monkey species was found to be several months, indicating a very slow diffusion (not flow) of these molecules out of the eye [1, 16]. This type of organization is typical of connective tissue matrices that separate tissues and protect them against friction and vibration caused by natural dislocation and stress (eye movements, heart beats, rubbing the eye). Examples of such matrices, in addition to vitreus, are synovial tissue and fasciae. These matrices are also more viscoelastic, as they protect against weak mechanical stress of higher frequency. Borzacchiello et al. [17] studied the rheological properties of vitreus in pigs, sheep, and rabbits in the frequency range of 0.05–10 Hz. The dynamic elastic modulus (G') was always higher than the viscous modulus (G'') within this frequency range. It was possible to reproduce the rheological behavior of the animal vitreus qualitatively by increasing the molecular weight or the concentration of pure hyaluronan. This demonstrated that the molecular network of high average molecular weight hyaluronan can “mimic” the rheological properties of vitreus. Soluble protein concentration follows approximately the same distribution pattern as for hyaluronan, being highest in the posterior cortical gel vitreus and lowest in the central and anterior part [9, 18].

The hyaluronan molecule in vitreus has approximately the same average molecular weight in humans and animals, except in the case of hyaluronan in vitreus of macaques (ages 6–21 years), which was found to be significantly lower than that found in adult human liquid vitreus (2.9×10^6 versus 4.6×10^6) [19]. The hyaluronan molecular network consists of a spheroidal system with a molecular weight range of two to ten million and a diameter about ten times larger (200–300 nm) than that of the individual collagen fibrils. The domain of the hyaluronan molecular network consists of polysaccharide chains of 1–2 nm long random coils in which the space between the coils is filled with water. This special structure, with random distribution of thin molecular

networks with relatively low concentration, is responsible for vitreus transparency. Reports of hyaluronan with lower-than-normal molecular size are thought to be due to artifacts resulting from damage to the molecule during the purification process or, as is the case in bovine vitreus, exposure to atmospheric oxygen during dissection. This rapid oxygen-sensitive degradation system does not manifest itself in vitreus of other species [10, 20].

There are considerable variations in the concentration of hyaluronan among species, with the highest concentrations found in the vitreus of the owl monkey, cattle, human, and rhesus monkey and the lowest in guinea pig, rabbit, cat, dog, and chicken [1]. In searching for an appropriate animal model for human vitreus, the rhesus monkey (*Macaca mulatta*) eye was found to have the most similarities to the human eye with regard to physical state, collagen, hyaluronan content, and aging [19]. The hyaluronan concentration is about ten times higher in the vitreus than in the aqueous in both macaque and human eyes. In both species, the hyaluronan concentration is similar and changes with age in the same manner [19, 21].

There are only a few connective tissue compartments that contain mainly one major structural polysaccharide – hyaluronan – and these are the vitreus, the umbilical cord, the rooster comb, and the synovial tissue around the joint space. In all of these tissues, one of the functions of hyaluronan is to stabilize a collagen fibrillar network. This interaction between the collagen fibrils and hyaluronan molecules is predominantly frictional, meaning that these two elements of the vitreus can be separated by mechanical forces such as filtration and centrifugation without denaturing or destroying them. Either of these two mechanical processes, however, will destroy the gel itself, as the collagen fibrils accumulate at the bottom of the centrifuge tube or on the filter. In animals that have a predominantly gel vitreus (rabbit, dog, cat, rodent, chicken), the concentration of hyaluronan is low and the collagen fibril concentration is higher than in species which have more hyaluronan in their vitreus. Thus, one can surmise that the role of hyaluronan as a stabilizer of collagen fibrils becomes more and more important as the human eye grows during development and the distance between the collagen fibrils increases.

Hyaluronan plays an important role in the physical properties of the vitreus. It was suggested by several authors that this provides an important “linkage” between the collagen-gel network of the vitreus and hyaluronan. One must realize that an interaction between the collagen network and the hyaluronan filling the space in between does not create a permanent contact (covalent binding) between the collagen and hyaluronan [22].

IV. Proteoglycans of the Vitreus

While the major molecular components of the human (as well as most animals) vitreus are the collagen and hyaluronan, there are also proteoglycans present in smaller quantities. The name proteoglycan indicates that the molecules are made up of a molecular complex of proteins and carbohydrates of various types. These are present in the liquid vitreus, but are not attached to the collagen fibers or to hyaluronan. One such proteoglycan is called *versican* [23–25]. This large molecule has a mass of 37 kDa (kDa) and contains a large amount of sulfated disaccharides. The presence of versican-like proteoglycans in different species represents a common structural component of the mammalian vitreus. A second important proteoglycan is *type IX collagen*. Like versican, it also contains both uronic acid and chondroitin sulfate [23, 26, 27].

The most important question from the point of view of stability of the vitreus is whether or not these proteoglycan interact with collagen fibers or with hyaluronan [28]. If an interaction exists, then the hyaluronan could not be removed from the gel part of the vitreus by washing with water. The proteoglycans could also be removed from the gel. In general, recent opinion is that if a direct interaction between hyaluronan and collagen fibers exists at all, it is very weak. Recent (1990–2008) studies were carried out using animal vitreus (cattle, pig, rabbit, sheep, and goat). The first biochemical evidence that hyaluronan-binding macromolecules are present in the vitreous was published in 1998 [24]. Noulas et al. [22] published investigations on pig vitreus gel. The aim was to study the “macromolecular composition of the vitreus,” with particular interest in hyaluronan-binding proteoglycans. Their study confirmed the presence of hyaluronan and that the pig vitreus contained lower levels than human vitreus. This was the first time the existence of a population of hyaluronan-binding proteoglycans in the pig vitreus gel was shown. These molecules show structural and immunological characteristics similar to versican. Their findings are in agreement with the data obtained in human vitreus, as well as from bovine vitreus gel [24]. The molar ratio of versican and link proteins is approximately 1:1, suggesting that they form aggregates with hyaluronan in cattle vitreus. The functional significance of versican and link proteins remains uncertain.

V. Aging of the Vitreus

The human vitreus continues to develop after birth, nearly doubling its volume (Figure I.B-1). This volume increase occurs in parallel with the production of hyaluronan that fills

the enlarging vitreous body and provide support and stabilization for the collagen fibrillar network (Figure I.B-2). This stabilizing effect is especially important because the production of collagen fibers does not continue after birth and the space between the fibrils increases as the gel becomes less and less dense.

No liquid vitreus is found in human eyes below the age of 4 years [13]. As the eye develops, up to the age of 20 years, the liquid volume slowly increases and fills about 20 % of the total vitreous volume. This may increase in some cases to 50 % in old adult eyes. In animals that have a predominantly gel vitreus (cattle, dogs, sheep, cats, horses, rabbits, and most monkeys), liquid vitreus does not form [30], but in humans and rhesus monkeys, aging results in important and parallel changes in the vitreus. From the age of 45–50 years in humans, the volume of the liquid vitreus increases as the volume of the gel vitreus steadily decreases (Figure I.B-1).

From early adulthood to old age, the hyaluronan concentration in the vitreus does not change in either the gel or liquid vitreus (Figure I.B-2 [31–35]). After 70 years, an increase in hyaluronan concentration was found in most individuals studied, with a greater increase in the liquid than the gel vitreus with no change in molecular size of the hyaluronan [1, 13, 30]. Eisner [36] has described this process as beginning with the occurrence of narrow channels and then pockets and pools of liquid vitreus that begin to coalesce after 40–45 years of age, resulting in a central liquid pocket that in later years occupies slightly more than half the volume of the vitreus. A parallel result is the increase in collagen concentration in the gel vitreus during the aging process due to the collapse or contraction of the collagen fibrillar network during the formation of these channels and pools of liquid vitreus (see [1] for review).

Another aging change that occurs in the vitreus and has only been documented in the human eye is called posterior vitreous detachment [37, 38] [see chapter II.C. Vitreous Aging and PVD]. Since this change occurs in a large number of the aging population and usually does not lead to any serious pathological change or impairment of vision, it is assumed to be part of the normal aging process. The fundamental structural changes that influence the vitreus during aging are a thickening of the basal lamina of the retina accompanied by an increase in the volume of the liquid vitreus with simultaneous collapse of the gel and aggregation/coalescence of the collagen fibrils. The rhesus monkey (*Macaca mulatta*) vitreus is the only one described thus far that shows developmental and aging changes similar to those that occur in humans. Posterior vitreous detachment, however, was not observed in rhesus monkeys as old as 21 years to 30 years. Posterior vitreous detachment can also

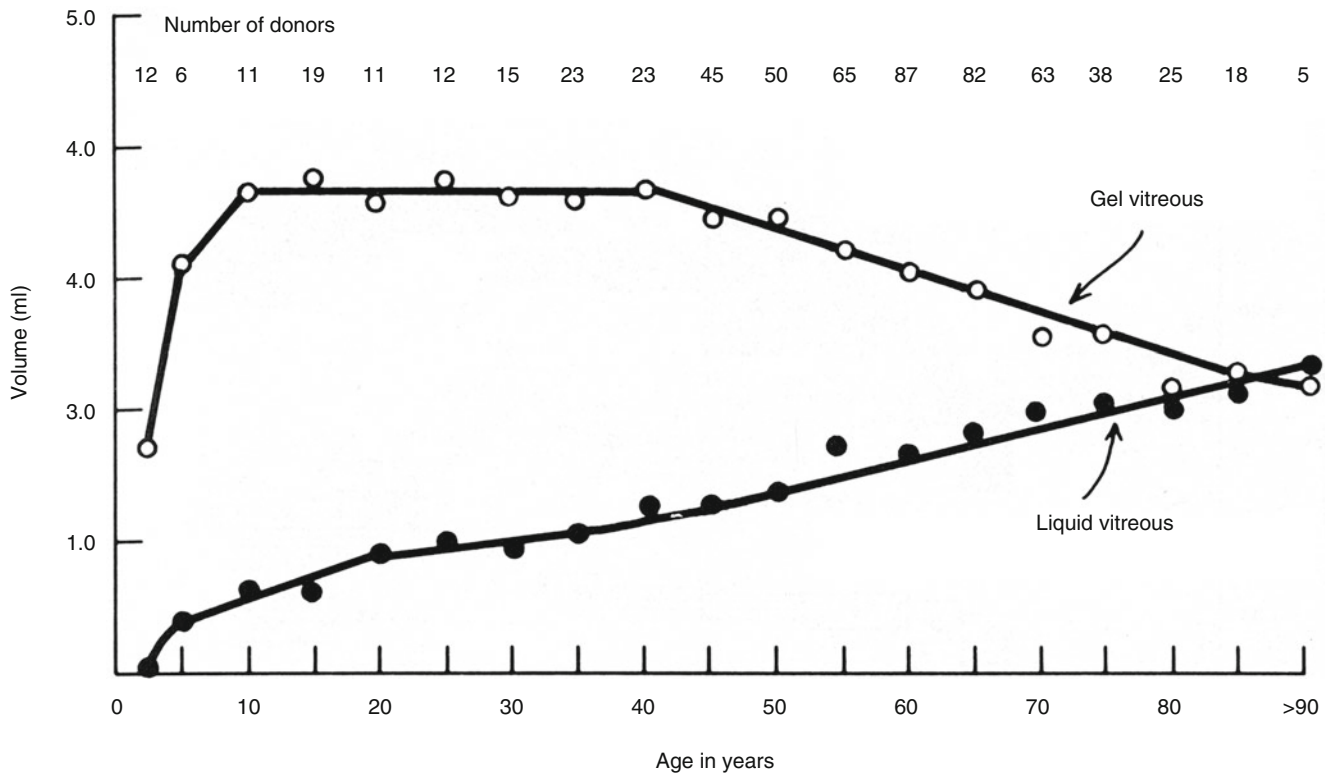


Figure I.B-1 Rheology of human vitreous [29]. Fresh unfixed human eyes were studied postmortem and the volumes of gel vitreous (open circles) as well as liquid vitreous (closed circles) were measured. The y-axis displays the volume in ml and the x-axis the age groups of the donors. Each point represents the mean value

obtained from various numbers of donor eyes (shown at top of graph). It can be appreciated that after growth of the eye ceases (age 10–20), the gel volume is stable until age 40 when it begins to steadily decline throughout the remainder of life. The volume of liquid vitreous increases throughout life

occur at any age as a result of chronic intraocular inflammation, severe trauma to the eye, and in aphakic or highly myopic young individuals [19]. Molecular weight determinations of hyaluronan from human diabetic and nondiabetic vitreous showed no significant difference [39], although there are known changes in vitreous collagen [see chapter I.E. Diabetic vitreopathy]. Itakura et al. [40], using eyes from patients with diabetic retinopathy or macular holes, found that there was a significant decrease in the “level” (concentration) of hyaluronan in the vitreous with aging under these pathological conditions. In our opinion their reported data does not prove their assumption.

The age-related partial liquefaction of human vitreous was studied by electron microscopy, and a breakdown of collagen fibers into smaller fragments was found [41]. The mechanism of the process – especially from the point of view of its cellular or extracellular origin – could not be determined. However, they “tentatively concluded that an extracellular process is involved.” However, in biomicroscopic studies of macaque eyes, it was found that the coalescence of

the liquid pockets results from dislocation and collapse of the tractus vitrealis rather than a breakdown of the collagen into smaller fragments [19].

VI. Miscellaneous Considerations

A. Species Variations

In fish eyes, Balazs, for the first time in 1956 [42], found that gel vitreous is attached to the entire retina and that in front of it is a viscoelastic liquid vitreous that completely surrounds the rigid, spherical lens. Balazs gave the name ichthyosan A to this very viscoelastic liquid that surrounds the lens and ichthyosan V to the gel in front of the retina. These two molecular complexes are non-covalent aggregates composed of hyaluronan, a sulfate-free chondroitin proteoglycan, and a keratin-like molecule [43, 44]. Ichthyosan V is in between the collagen fibrils in the vitreous and stabilizes the structure of the vitreous gel. The anterior chamber is

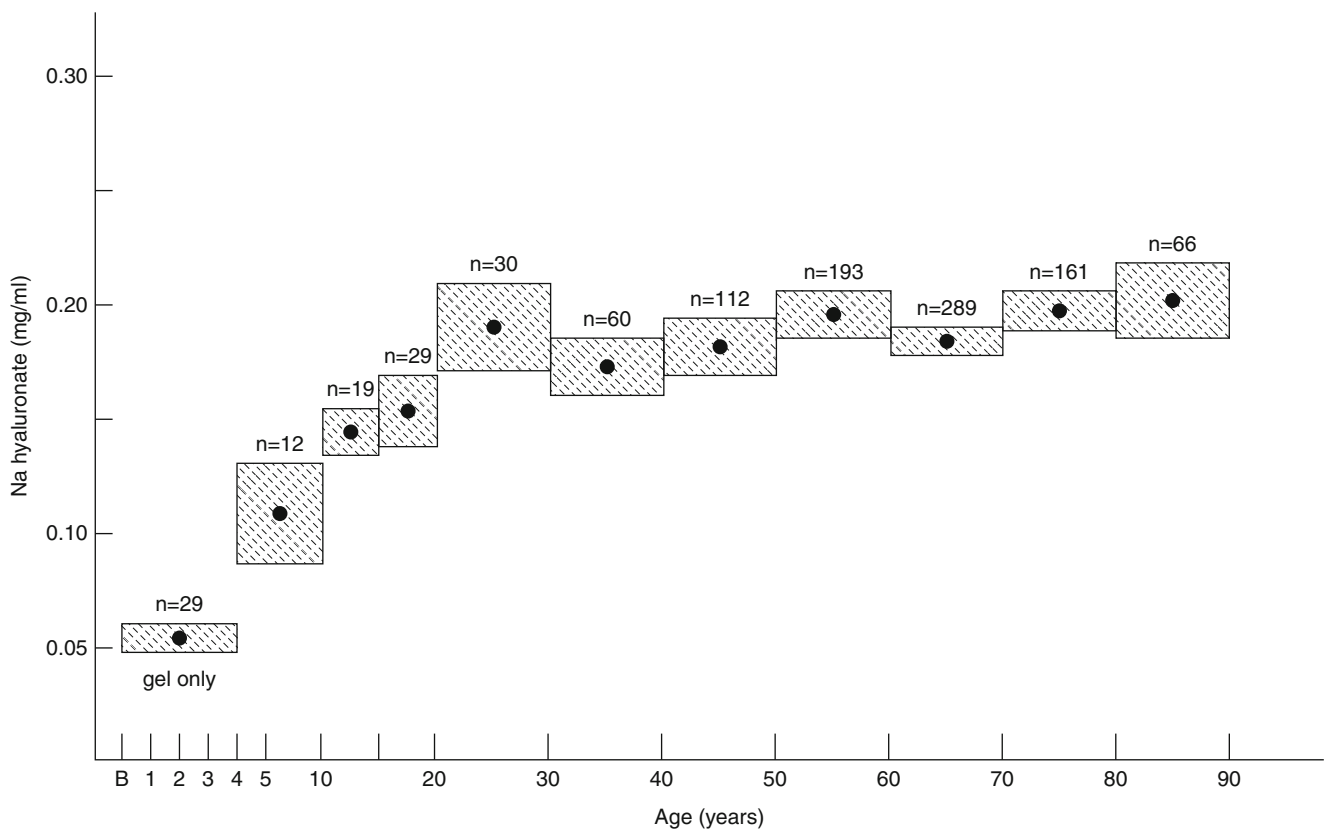


Figure I.B-2 Concentration of hyaluronan in human gel vitreous during life [30]. The sides of the boxes indicate the standard error of the means; the horizontal shows the age range of individuals included in the

group. The number of samples in each group is indicated by “n”. There is a steady increase in hyaluronan concentration until a plateau is reached at about age 25

filled with the same liquid as the vitreous. Because the lens cannot be deformed in fish eyes, it accommodates (focuses) by moving the lens back, forward, and sideways in this very elastoviscous liquid. The average molecular weight of ichthyosan varies from 5.2 to 13.0 million in various species of fish [43, 44].

B. Hyaluronidase and the Vitreous

Hyaluronidase has been found in the human and animal vitreous, but at physiological pH in the range of 6.5–8.0, it has no activity [45]. Consequently, hyaluronan is not affected by degrading enzymes in the vitreous in vivo [31–35]. Highly purified ovine hyaluronidase (Vitrane® [46]) has been prepared for the treatment of vitreous hemorrhage in human eyes. No serious safety issues were reported after a single intravitreal injection of this enzyme. Iritis, manifesting as an acute, self-limited inflammation, was the most common adverse event [47, 48]. This agent failed FDA testing and is thus not indicated for intraocular use.

C. Hyaluronan and its Derivatives as Viscoelastics in Medicine

After more than 15 years of research and development to produce hyaluronan that could be used therapeutically in humans and animals, Balazs [49] published the first comprehensive report on this subject. Two conclusions could be drawn from this work: first hyaluronan could be purified in such a way that the fraction of the molecule that was responsible for the production of acute inflammation in animals and humans was removed and second the medical utility of hyaluronan is based on its mechanical properties of viscosity and elasticity, and thus its ability to be a physical barrier, rather than having a chemical effect. The first such non-inflammatory fraction of sodium hyaluronate (known by the acronym NIF-NaHA) was tested during the late 1960s for two medical applications: use in humans and animals (mainly horses) to treat traumatic and idiopathic osteoarthritis and for ophthalmic surgery in the anterior chamber and in the vitreous [49–52].

The concept of using hyaluronan for viscosurgery [53–55] in the eye was based on its rheological properties. Solutions

of hyaluronan and its derivatives have a very high viscosity at low shear (e.g., during the insertion of a plastic lens) where they can be used to make and maintain space, and they exhibit low viscosity and high elasticity at high shear, making it possible to deliver the solutions through narrow channels such as a small gauge needle with ease. In such cases the elastoviscous solution serves as a shock-absorbing body and serves to protect delicate tissues and cell layers, such as the corneal endothelium, the iris, and the retina [56]. In 1982, the first clinical symposium was organized [57] to review the clinical benefits of viscosurgery with Healon®, the name given by Balazs to the first viscosurgical tool made available for ophthalmic viscosurgery.

Abbreviations

FDA	Food and Drug Administration
kDa	Kilodaltons
mg	Milligrams
NIF-NaHA	Noninflammatory fraction of sodium hyaluronate
mL	Milliliters
nm	Nanometers
PVD	Posterior vitreous detachment
µm	microns

References

- Balazs EA, Denlinger JL. The vitreus. In: Davson H, editor. Vegetative physiology and biochemistry, vol. IA. New York: Academic; 1984. p. 533–89.
- Sebag J. The vitreous. In: Hart Jr WJ, editor. Adler's physiology of the eye. St. Louis: Mosby; 1992. p. 268–92.
- Sebag J. Macromolecular structure of the corpus vitreus. Prog Polym Sci. 1998;23:415–46.
- Balazs EA. Functional anatomy of the vitreous. In: Tasman W, editor. Duane's foundations of clinical ophthalmology. Philadelphia: J.B. Lippincott Co; 1994. p. 1–17.
- Virchow R. Notiz über den glaskörper (notes on the vitreous body). Archiv Pathol Anat Physiol. 1852;4:468.
- Meyer K, Palmer J. The polysaccharide of the vitreous humor. J Biol Chem. 1934;107:629–34.
- Balazs EA, Hargittai I, Hargittai M. The early history of hyaluronan research. In: Balazs EA, editor. History of hyaluronan science-hyaluronan: from basic science to clinical applications. Edgewater: PubMatrix; 2011. p. 1–70.
- Balazs EA, Laurent TC, Jeanloz RW. Nomenclature of hyaluronic acid. Biochem J. 1986;235:903.
- Balazs EA. Physiology of the vitreous body. In: Schepens CL, editor. Importance of the vitreous body in retina surgery with special emphasis on reoperations. The Second Conference of the Retinal Foundation. Ipswich, May 30–31, 1958; 1960. p. 29–48.
- Balazs EA. Molecular morphology of the vitreous body. In: Smelser GK, editor. The structure of the eye. New York: Academic; 1961. p. 293–310.
- Denlinger JL, Balazs EA. The fate of exogenous viscoelastic hyaluronan solutions in the primate eye. In: Rosen ES, editor. Viscoelastic materials: basic science and clinical applications. Manchester/Oxford: Pergamon Press; 1989. p. 185–99.
- Österlin SE, Balazs EA. Macromolecular composition and fine structure of the vitreous in the owl monkey. Exp Eye Res. 1968;7:534–45.
- Balazs EA, Flood MT. Age related changes in the physical and chemical structure of human vitreous. Osaka: Third International Congress of Eye Research; 1978.
- Balazs EA. The vitreous. In: Zinn K, editor. Ocular fine structure for the clinician. Boston: Little, Brown and Company; 1973. p. 169–87.
- O'Malley P. The pattern of vitreous synthesis. A study of 800 autopsy eyes. In: Irvine AR, O'Malley CO, editors. Advances in vitreous surgery. Springfield: Charles Thomas; 1976. p. 17–33.
- Denlinger JL. Metabolism of sodium hyaluronate in articular and ocular tissues [dissertation]. Lille: Université des Sciences et Techniques de Lille; 1982.
- Borzacchiello A, Netti P, Ambrosio L, Nicolais L. Hyaluronic acid derivatives mimic the rheological properties of vitreous body. In: Abatangelo G, Weigel P, editors. New frontiers in medical sciences: redefining hyaluronan. Amsterdam: Elsevier; 2000. p. 195–202.
- Balazs EA. Structure of the vitreous gel. Acta XVII Cong Ophth. 1954;11:1019–24.
- Denlinger JL, Eisner G, Balazs EA. Age-related changes in the vitreous and lens of rhesus monkeys (*Macaca mulatta*). Exp Eye Res. 1980;31(1):67–79.
- Sundblad L, Balazs EA. Chemical and physical changes of glycosaminoglycans and glycoproteins caused by oxidation-reduction systems and radiation. In: Balazs EA, Jeanloz RW, editors. The amino sugars: the chemistry and biology of compounds containing amino sugars, Metabolism and interactions, vol. IIB. New York: Academic; 1966. p. 229–50.
- Flood MT, Balazs EA. Hyaluronic acid content in the developing and aging human liquid and gel vitreous. ARVO Ann Meeting Assoc Res Vis Ophthal; 1977.
- Noulas AV, Theocharis AD, Feretis E, Papageorgakopoulou N, Karamanos NK, Theocharis DA. Pig vitreous gel: macromolecular composition with particular reference to hyaluronan-binding proteoglycans. Biochimie. 2002;84:295–302.
- Brewton RG, Wright DW, Mayne R. Structural and functional comparison of Type IX collagen-proteoglycan from chicken cartilage and vitreous humor. J Biol Chem. 1991;266(8):4752–7.
- Reardon A, Heinegård D, McLeod D, Sheehan JK, Bishop PN. The large chondroitin sulphate proteoglycan versican in mammalian vitreous. Matrix Biol. 1998;17(5):325–33.
- Theocharis AD, Papageorgakopoulou N, Feretis E, Theocharis DA. Occurrence and structural characterization of versican-like proteoglycan in human vitreous. Biochimie. 2002;84(12):1235–41.
- Mayne R, Brewton RG, Mayne PM, Baker JR. Isolation and characterization of the chains of type-V, type-XI collagen present in bovine vitreous. J Biol Chem. 1993;268(13):9381–6.
- Zhidkova NI, Justice SK, Mayne R. Alternative messenger-RNA processing occurs in the variable region of the pro-alpha-1 (Xi) and pro-alpha-2 (Xi) collagen chains. J Biol Chem. 1995;279:9486–93.
- Theocharis DA, Skandalis SS, Noulas AV, Papageorgakopoulou N, Theocharis AD, Karamanos NK. Hyaluronan and chondroitin sulfate proteoglycans in the supramolecular organization of the mammalian vitreous body. Conn Tiss Res. 2008;49(3–4):124–8.
- Balazs EA. Functional anatomy of the vitreus. In: Jacobiec F, editor. Ocular anatomy, embryology and teratology. New York: Harper and Row; 1982. p. 425–40.
- Balazs EA, Denlinger JL. Aging changes in the vitreus. In: Sekuler R, Kline D, Desmukes K, editors. Aging and human visual function. New York: Alan R. Liss, Inc.; 1982. p. 45–57.

31. Breen M, Bizzell JW, Weinstein MG. A galactosamine-containing proteoglycan in human vitreous. *Exp Eye Res.* 1977;24:409–12.
32. Allen W, Otterbein SC, Wardi AH. Isolation and characterization of the sulfated glycosaminoglycans of the vitreous body. *Biochem Biophys Acta.* 1977;498:167–75.
33. Kamei A, Totani A. Isolation and characterization of minor glycosaminoglycans in the rabbit vitreous body. *Biochem Biophys Res Comm.* 1982;109(3):881–7.
34. Hultsch E, Freeman MI, Balazs EA. Transport and regeneration of hyaluronic acid in extracellular ocular compartments. *Sarasota: Annual Meeting of the Association for Research in Vision and Ophthalmology (ARVO); 1974.* p. 97.
35. Sweeney DB, Balazs EA. Fate of collagen and hyaluronic acid gels in solutions injected into the vitreous of the owl monkey. *Invest Ophth.* 1964;3:473.
36. Eisner G. Zur Anatomie des glaskörpers. *Albrecht v Graefes Arch Klin Exp Ophthal.* 1975;193:33–56.
37. Pischel DK, Kronfeld PC. The scleral resection operation for retinal detachment. *Am J Ophth.* 1953;36(5):629–40.
38. Goldman VH. Senescenz des Glaskörpers. *Ophthalmology.* 1962;143:253–79.
39. Laurent U, Tornquist P, Granath K, Liljaenglind K, Ytterberg D. Molecular weight and concentration of hyaluronan in vitreous humor from diabetic patients. *Acta Ophthal.* 1990;68:109–12.
40. Itakura H, Kishi S, Kotajima N, Murakami M. Decreased vitreal hyaluronan levels with aging. *Ophthalmology.* 2009;223(1):32–5.
41. Los LI, van der Worp RJ, van Luyn MJA, Hooymans JMM. Age-related liquefaction of the human vitreous body: LM and TEM evaluation of the role of proteoglycans and collagen. *Invest Ophth Vis Sci.* 2003;44(7):2828–33.
42. Balazs EA. Chemical composition of aqueous humor and vitreous body of different animal species. *Am J Ophthal.* 1956;42:137.
43. Armand G, Balazs EA. Ichthyosan in fish eye. *Struct Chem.* 2009;20:337–40.
44. Armand G, Balazs EA, Meyer K, Reyes M. Isolation and characterization of ichthyosan from tuna vitreous. *Conn Tiss Res.* 1983; 11(1):21–33.
45. Schwartz DM, Shuster S, Jumper MD, Chang A, Stern R. Human vitreous hyaluronidase: isolation and characterization. *Curr Eye Res.* 1996;15(12):1156–62.
46. Bhavsar AR, Grillone LR, McNamara TR, Gow JA, Hochberg AM, Pearson RK, et al. Predicting response of vitreous hemorrhage after intravitreal injection of highly purified ovine hyaluronidase (Vitrace) in patients with diabetes. *Invest Ophthal Vis Sci.* 2008; 49(10):4219–25.
47. Kuppermann BD, Thomas EL, de Smet MD, Grillone LR. Pooled efficacy results from two multinational randomized controlled clinical trials of a single intravitreal injection of highly purified ovine hyaluronidase (Vitrace®) for the management of vitreous hemorrhage. *Am J Ophthal.* 2005;140(4):573–84.
48. Kuppermann BD, Thomas EL, de Smet MD, Grillone LR. Safety results of two Phase III trials of an intravitreal injection of highly purified ovine hyaluronidase (Vitrace®) for the management of vitreous hemorrhage. *Am J Ophthal.* 2005;140(4): 585–97.
49. Balazs EA, Freeman MI, Klöti R, Meyer-Schwickerath G, Regnault F, Sweeney DB. Hyaluronic acid and the replacement of vitreous and aqueous humor. In: Streiff EB, editor. *Modern problems in ophthalmology (secondary detachment of the retina, Lausanne, 1970).* Basel: S. Karger; 1972. p. 3–21.
50. Balazs EA, Sweeney DB. The use of hyaluronic acid and collagen preparations in eye surgery. In: Schepens CL, Regan CDJ, editors. *Controversial aspects of the management of retinal detachment.* Boston: Little, Brown and Company; 1965. p. 200–2.
51. Balazs EA, Sweeney DB. The replacement of the vitreous body in the monkey by reconstituted vitreous and by hyaluronic acid. In: Streiff EB, editor. *Modern problems in ophthalmology (surgery of retinal vascular diseases).* Basel: S. Karger; 1966. p. 230–2.
52. Balazs EA, Sweeney DB. The injection of hyaluronic acid and reconstituted vitreous into the vitreous cavity. In: McPherson A, editor. *New and controversial aspects of retinal detachment.* New York: Hoeber Medical Division, Harper & Row; 1968. p. 371–6.
53. Balazs EA, Miller D, Stegmann R. Viscosurgery and the use of Na-hyaluronate in intraocular lens implantation. *Cannes: International Congress and First Film Festival on Intraocular Implantation; 1979.* p. 1–6.
54. Pape LG, Balazs EA. The use of sodium hyaluronate (Healon®) in human anterior segment surgery. *Ophthalmology.* 1980;87(7): 699–705.
55. Miller D, Stegmann R. Use of Na-hyaluronate in anterior segment eye surgery. *Am Intraoc Implant Soc J.* 1980;6(1):13–5.
56. Denlinger JL. Hyaluronan and its derivatives as viscoelastics in medicine. In: Laurent TC, editor. *The chemistry, biology and medical applications of hyaluronan and its derivatives.* London: Portland Press Ltd.; 1998. p. 235–42.
57. Balazs EA. Pharmakologische eigenschaften von natriumhyaluronat im auge. In: *Viskochirurgie des auges (Beiträge des ersten nationalen Healon®/Symposiums, Oct. 15–16, 1982).* Stuttgart: Ferdinand Enke Verlag; 1984. p. 1–13.

Martin P. Snead and Allan J. Richards

Outline

I. Introduction

A. Vitreous Embryology

II. Classification of Inherited Vitreo-Retinopathies

A. Diagnosis and Clinical Features

1. Vitreo-retinopathies with Skeletal Abnormalities

a. Stickler Syndrome

- i. Epidemiology
- ii. Diagnosis and Differential Diagnosis
- iii. Clinical Features
 1. Ophthalmologic Features
 2. Orofacial Features
 3. Hearing Loss
 4. Musculoskeletal Features
- iv. Molecular Genetic Analysis of Stickler Syndrome
 - a. Type 1 Stickler Syndrome
 - b. Type 2 Stickler Syndrome
 - c. Type 3, “Non-ocular” Stickler Syndrome
 - d. Types 4, 5, and 6 Stickler Syndrome
 - e. “Ocular-Only” Stickler Syndrome
 - f. Stickler Syndrome with Profound Deafness
 - g. Unresolved

b. COL2A1-Related Disorders

- i. Kniest Dysplasia
 - ii. Spondyloepiphyseal Dysplasia Congenita (SEDC)
 - iii. Vitreoretinopathy with Phalangeal Epiphyseal Dysplasia (V-PED)
 - iv. Marshall Syndrome
 - v. Knobloch Syndrome
 - vi. Marfan Syndrome
- ##### 2. Vitreoretinopathies with Progressive Retinal Dysfunction
- a. Wagner Vitreoretinopathy/Erosive Vitreoretinopathy
 - b. Goldmann-Favre Syndrome/Enhanced S-Cone Dystrophy
- ##### 3. Vitreoretinopathies with Abnormal Retinal Vasculature
- a. Familial Exudative Vitreoretinopathy
 - b. Autosomal Dominant Vitreoretinopathy (ADVIRC)
- ##### 4. Vitreoretinopathy Associated with Corneal Changes
- ##### 5. Vitreoretinopathies Associated with Dominant and/or Bilateral Rhegmatogenous Retinal Detachment (DRRD/BRDD)

III. Screening and Ancillary Investigations

IV. From Laboratory To Bedside: Current Research on Mechanisms for Variability in Clinical Phenotype

- #### A. Phenotypic Differences Due to Splicing Variations
1. Phenotypic Differences Due to Missense Mutations
 2. Phenotypic Differences Due to Mosaicism
- #### B. Future Developments

V. Prophylaxis

VI. Summary

References

Electronic supplementary material Supplementary material is available in the online version of this chapter at [10.1007/978-1-4939-1086-1_3](https://doi.org/10.1007/978-1-4939-1086-1_3). Videos can also be accessed at <http://www.springerimages.com/videos/978-1-4939-1085-4>.

M.P. Snead, MA, MD, DO, FRCS, FRCOphth (✉)
Vitreoretinal Service, Cambridge University NHS Foundation Trust, Addenbrooke’s Hospital,
Hill Road, Cambridge CB2 0QQ, England, UK
e-mail: mps34@cam.ac.uk

A.J. Richards, PhD
Department of Pathology, University of Cambridge,
Tennis Court Rd, Cambridge CB2 1QP, UK
Cambridge University NHS Foundation Trust,
Addenbrooke’s Hospital, Cambridge, England, UK
e-mail: ar204@cam.ac.uk

Keywords

Vitreous • Congenital vitreoretinopathy • Collagen • Retinal detachment • Stickler syndrome • Wagner syndrome • Genetics

Key Concepts

1. The ophthalmologist has a key role to identify the emerging array of ocular-only vitreo-retinopathies at risk of retinal detachment but which would be overlooked or excluded using historic criteria constrained by the requirement for systemic involvement. Genetic analysis for inherited (non-syndromic) rhegmatogenous retinal detachment is now a realistic possibility.
2. Functional studies are likely to become increasingly relevant as diagnostic molecular genetic analysis moves away from exon sequencing to whole-gene analysis by next-generation sequencing.
3. Molecular genetic diagnosis and subtyping now provide a much more precise stratification of risk for retinal detachment so that effective prophylaxis can, for the first time, be deployed in high-risk subgroups.

I. Introduction

Inherited vitreoretinopathies mostly result from genetic abnormalities of types II, IX, or V/XI collagen [see chapter I.A. Vitreous proteins] and proteoglycans, [see chapter I.F. Vitreous biochemistry and artificial vitreous] expressed principally and collectively in the eye but also in articular and hyaline cartilage. The phenotypes can be variable but affected patients classically exhibit high degrees of congenital myopia and visual loss from retinal detachment with varying degrees of associated hearing loss, arthropathy, and orofacial abnormalities.

The Stickler syndromes form by far the largest subgroup and are the most common cause of inherited retinal detachment. Originally considered a single-gene disorder, at least 8 subgroups of Stickler syndrome have now been characterized and recent laboratory research has shed much new light on the basis for the clinical and phenotypic variability between patients that now extends to encompass familial retinal detachment in the general population. This chapter provides a clinical overview of these important disorders of vitreous embryogenesis together with a review of the recent advances in their molecular genetic analysis, including minigene splicing reporter analysis. Such functional studies are likely to become increasingly relevant as diagnostic molecular genetic analysis moves away from exon sequencing to whole-gene analysis by next-generation sequencing. The emergence and availability of rapid, accurate molecular genetic diagnosis and subtyping provide much more precise stratification of risk, and as a result protocols for effective prophylaxis against retinal detachment can, for the first time, be deployed in high-risk subgroups.

A. Vitreous Embryology

For a detailed description of vitreous embryogenesis, see chapter II.A. Development and developmental disorders of vitreous. The largest of ocular components, vitreous's major structural components are collagen types II, IX, and V/XI [47] together with hyaluronan as the quantitatively major glycosaminoglycan associated with the binding molecules versican and proteoglycan link protein in lower concentrations [9, 14, 15, 27, 43, 55]. The collagen fibrils are co-expressed with a number of other proteins including opticin, vitrin, fibulin-1, and nidogen-1 [13, 32, 63].

Due to the early embryogenesis of vitreous and negligible postnatal turnover, mutations in the genes encoding this unique extracellular matrix result in an array of anatomical and architectural variations in vitreous development evident on slit-lamp biomicroscopy and fundus examination. Expression of some of these genes in other connective tissues frequently, but not invariably, results in associated extraocular systemic manifestations, and recent laboratory research has shed significant new light on the role of tissue-specific or idiosyncratic alternative splicing as the underlying basis for some of the phenotypic variation seen within and between individual families and siblings.

II. Classification of Inherited Vitreo-Retinopathies

Inherited vitreoretinopathies may be classified according to either their genetic basis or phenotype. For the vitreoretinal surgeon faced with making a differential diagnosis upon which to direct any subsequent ancillary investigations, the phenotypic approach provides a useful starting point and a modified classification from Meredith and Snead [50] on which to base such a clinical approach is given below:

1. *Vitreo-retinopathies with skeletal abnormalities*
2. *Vitreo-retinopathies with progressive retinal dysfunction*
3. *Vitreo-retinopathies with abnormal retinal vasculature*
4. *Vitreo-retinopathies with corneal changes*
5. *Vitreo-retinopathies with dominant and/or bilateral rhegmatogenous retinal detachment (DRRD/BRRD) ocular-only phenotypes*

A. Diagnosis and Clinical Features

1. Vitreo-Retinopathies with Skeletal Abnormalities

The vitreoretinopathies associated with skeletal abnormalities contribute the bulk of inherited vitreoretinopathies, comprising at least a dozen recognized subgroups, which are summarized in Table I.C-1.

Table I.C-1 Vitreoretinopathies associated with skeletal abnormalities

Syndrome		Gene	Distinguishing features	MIM no.
Stickler syndrome				
	<i>Type 1</i>	COL2A1	Membranous congenital vitreous anomaly, congenital megalophthalmos, deafness, arthropathy, cleft palate	108300
	<i>Ocular only</i>	COL2A1	Membranous congenital vitreous anomaly (usually), congenital megalophthalmos. No systemic features	609508
	<i>Type 2</i>	COL11A1	Beaded congenital vitreous anomaly, congenital megalophthalmos, deafness, arthropathy, cleft palate	604841
	<i>Type 2 recessive</i>	COL11A1	Autosomal recessive, beaded congenital vitreous anomaly, congenital megalophthalmos, cleft palate, profound severe congenital deafness	<i>TBC</i>
	<i>Type 3</i>	COL11A2	Normal vitreous and ocular phenotype, deafness, arthropathy, cleft palate	184840
	<i>Type 4</i>	COL9A1	Recessive inheritance, sensorineural deafness, myopia, vitreoretinopathy, epiphyseal dysplasia	614134
	<i>Type 5</i>	COL9A2	Recessive inheritance, sensorineural deafness, myopia, vitreoretinopathy, epiphyseal dysplasia	614284
	<i>Type 6</i>	COL9A3	Recessive inheritance, sensorineural deafness, myopia, vitreoretinopathy, epiphyseal dysplasia	<i>TBC</i>
	<i>Other</i>	Unknown	Hypoplastic vitreous, deafness, arthropathy, cleft palate	<i>Not assigned</i>
Kneist dysplasia		COL2A1	Severe arthropathy, short stature, phalangeal dysplasia	156550
Spondyloepiphyseal dysplasia congenital (SEDC)		COL2A1	Severe short stature, rhizomelic limb shortening, barrel chest	183900
V-PED		COL2A1	Vitreoretinopathy associated with severe phalangeal dysplasia	Not assigned
Marshall syndrome		COL11A1	Sparse hair, reduced sweating, congenital/ juvenile cataract	154780
Knobloch syndrome		COL18A1	Occipital encephalocoele, renal abnormalities, abnormal palmar creases	267750
Marfan syndrome		FBN1	Cornea plana, ectopia lentis, arachnodactyly, aortic root dilatation	154700

a. Stickler Syndrome

The Stickler syndromes are a range of inherited disorders of type II, IX, and V/XI collagen associated with congenital megalophthalmos, retinal detachment and giant retinal tear, deafness, cleft palate, Pierre-Robin sequence, joint hypermobility, and premature arthritis. Initially considered a single-gene disorder, possibly allelic with Wagner vitreoretinopathy (see below), at least nine clinical subgroups have been characterized.

i. Epidemiology

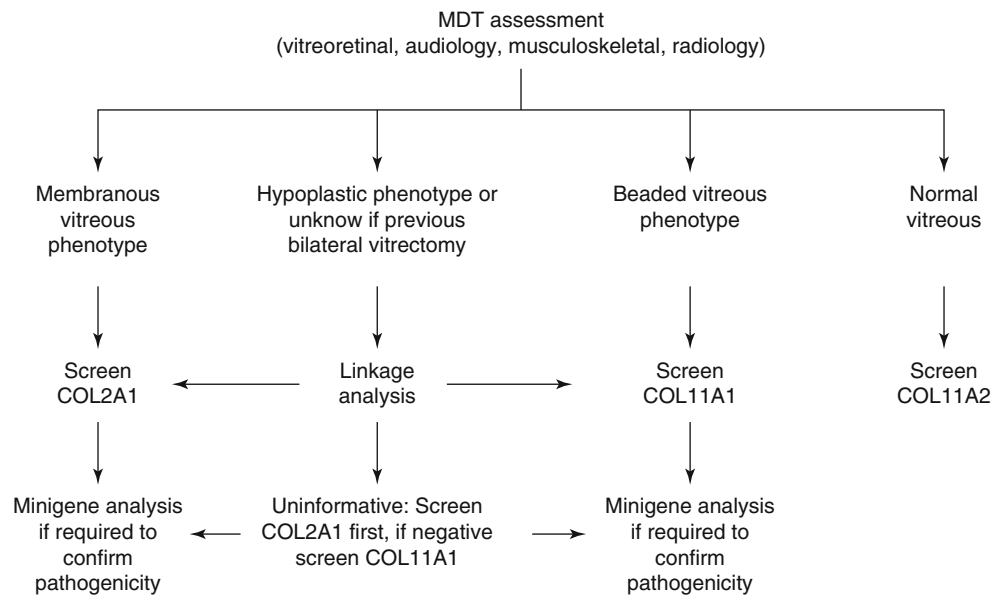
No reliable studies to determine the prevalence of Stickler syndrome have been undertaken. It has been reported previously to be approximately one case in 10,000 newborns [18], but given the past difficulties with diagnosis prior to reliable molecular genetic analysis and the varied and subtle clinical presentation, this figure is likely to be a considerable underestimate. Prevalence estimates by the UK Genetic

Testing Network and those based on extrapolation of data regarding the incidence of Pierre Robin sequence (PRS) in newborns suggest a higher figure at between 1:7,500 and 1:9,000 [60].

ii. Diagnosis and Differential Diagnosis

The classical clinical features of Stickler syndrome are a variable combination of congenital high myopia, retinal detachment, deafness, joint hypermobility, premature arthropathy, and cleft palate. There is much inter- and intra-familial variability and patients may present with a combination of any or all of the classical clinical features or remain undiagnosed until retinal detachment in adulthood. Such clinical variability means that patients may present to an array of different clinical subspecialties, and such subtle clinical phenotypic variations can make the diagnosis difficult. It is not uncommon for patients within or between

Figure I.C-1 Clinical algorithm for gene selection and mutation analysis in Stickler syndrome based on vitreous phenotype (Reproduced with permission from Snead et al. [85])



families to receive different clinical diagnoses. In the majority of cases the diagnosis can now be confirmed relatively easily and quickly using a combination of clinical assessment and molecular genetic analysis according to the algorithm depicted in (Figure I.C-1) [70, 73].

iii. Clinical Features

1. Ophthalmologic Features

Of all the various clinical features, statistical analysis by Hoornaert et al. [37] concluded that an eye examination was the key and most important evaluation for patients. The pathognomonic hallmark of Stickler syndrome is a congenital arrest in vitreous embryological development, manifest postnatally as an abnormal vitreous architecture visible on slit-lamp biomicroscopy. This feature is present at birth and in the absence of surgical intervention remains evident throughout life. The four common vitreous phenotypes are depicted in Figure I.C-2. Vitreous examination is especially important for the clinical diagnosis of the ocular-only subgroups (see Table I.C-1 and below) which without systemic involvement are likely to pass undiagnosed until sudden visual loss from retinal detachment occurs [85].

The majority of patients are significantly myopic, but unlike the more common developmental myopia in the population at large (which develops typically during school age), the refractive error in Stickler syndrome is characteristically congenital, of high degree, and largely nonprogressive. Interestingly, unlike developmental myopia, the optic disc in Stickler syndrome is frequently normal and does not show the peripapillary changes usually associated with the developmentally progressive myopia in the general population. There is often an associated significant astigmatic error, but it is important to be aware that in some series up to a quarter

of patients exhibit only a mild or moderate level of myopia [57]. Radial, perivasculature lattice retinopathy is a frequent finding in older patients but this is a later-onset feature, and the fundus appearance in children may be unremarkable despite the fact that the risk of retinal detachment and blindness is high in both the major subgroups of Stickler syndrome [7, 57, 59]. The high risk of giant retinal tear and detachment (Video I.C-1), particularly in children, has formed one of the principal drives to provide quick and reliable molecular genetic analysis so that patients can be identified and, where appropriate, offered prophylactic treatment (see below).

2. Orofacial Features

Apart from the congenital megalophthalmos, patients with Stickler syndrome may also exhibit certain other characteristic facial features that include retrognathia, midfacial flattening, and a shortened nose with anteverted nares and associated long philtrum. These features are often most striking in childhood and become progressively less obvious with age [84]. The similarity between some of these facial features and those of an allied disorder Marshall syndrome (Table I.C-1) has led to some controversy in the literature as to whether these two disorders are one and the same or distinct separate clinical entities (see below). What is clear from the published literature to date is that mutations in the gene for the $\alpha 1$ chain of type XI collagen (COL11A1) can result in both the Stickler and Marshall phenotypes and that genetically confirmed type 1 Stickler syndrome can exhibit the same facial features. For these reasons, analysis of facial phenotype alone should not be considered reliable for differential diagnosis nor to reliably differentiate between the subgroups of Stickler syndrome.

Patients with systemic involvement may also exhibit clefting abnormalities of the hard or soft palate. This may be

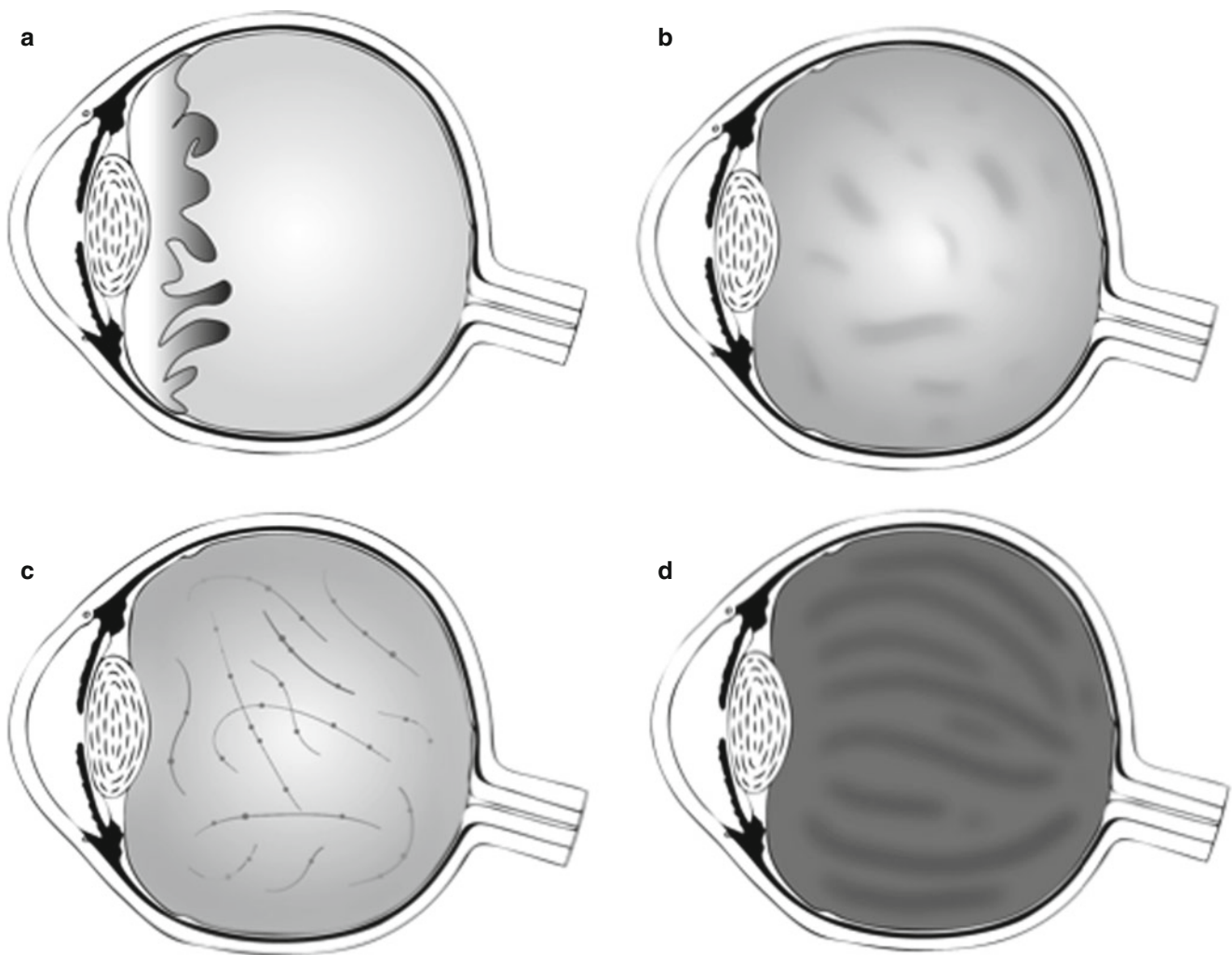


Figure I.C-2 Schematic illustration of the 4 most common vitreous phenotypes found in Stickler syndrome. (**a: top left**): Membranous type 1 vitreous anomaly (premature termination or frame-shift mutations COL2A1). (**b: top right**): Hypoplastic vitreous phenotype (usually

splice site mutations COL2A1). (**c: bottom left**): Type 2 beaded vitreous anomaly (COL11A1 mutations). (**d: bottom right**): Healthy compact gel architecture. Unaffected or non-ocular Stickler syndrome (COL11A2 mutations)

asymptomatic and unrecognized by the patient and is distinct from other causes of midline clefting associated with cleft lip, the latter feature being only rarely associated with Stickler syndrome. In patients without an obvious history of palate repair, direct examination and palpation will help identify those with subclinical clefts – a helpful diagnostic sign for the clinician but easily overlooked.

3. Hearing Loss

In common with all midline clefting disorders, impairment of eustachian tube function may lead to a secondary conductive hearing loss and serous otitis media is a common association, often compounded by associated tympanic membrane or middle ear ossicle abnormalities. Furthermore, the associated collagen abnormalities in the cochlea can cause a combined sensorineural hearing defect that is typically high tone and may be mild or asymptomatic. An audiogram is a simple and useful first-line investigation to identify and differentiate conductive from sensorineural

components. In addition to the raised hearing thresholds, abnormal tympanic membrane mobility (measured using tympanometry) has been observed in individuals identified with Stickler syndrome, although interestingly this is not always linked to a conductive hearing loss [1, 85, 90].

4. Musculoskeletal Features

Many younger patients with Stickler syndrome have joint hypermobility and the diagnosis should certainly be considered in hypermobile patients who are myopic with hearing loss or midline clefting. Joint mobility can be assessed objectively using the Beighton scoring system to allow comparison with an age, sex, and race matched population. With increasing age the hypermobility reduces or is lost completely and a degenerative arthropathy of variable severity typically affecting the knees, hips, and spine is common by the third or fourth decade (Figure I.C-3) [21, 61, 78]. Radiological features can include enlargement of the epiphyses, overtubulation of long bones, rhizomelic limb shortening,



Figure I.C-3 Joint hypermobility and dysplasia in adolescence typically gives way to premature arthritis later in life. Arthropathy and hip dysplasia in a 60 year old lady with type 1 Stickler syndrome

flattening and irregularity of the femoral epiphyses, and flaring of the metaphyses. Spinal changes are characterized by irregularity, platyspondyly, and anterior wedging of the vertebral bodies, but in a significant proportion of patients with genetically confirmed Stickler syndrome, the radiology is unremarkable and cannot therefore be relied upon in isolation for exclusion of the diagnosis. This is especially true for the ocular-only subgroups (see below), where the diagnosis will be dismissed using algorithms overly reliant on radiological criteria. Stickler patients are occasionally given an erroneous diagnosis of Perthes disease as the appearances in some patients are similar radiologically. Osgood-Schlatter's disease is also a common association [3], but since this is a clinical rather than a radiological diagnosis and is common in adolescence generally, the true nature of this association is uncertain [85].

iv. Molecular Genetic Analysis of Stickler Syndrome

Stickler syndrome may be caused by mutations in the genes for type II, type IX, and type V/XI collagen, and 9 distinct subgroups are currently recognized and classified on the basis of genetic analysis.

a. Type 1 Stickler Syndrome

The majority of patients (75–80 %) will have type 1 Stickler syndrome resulting from mutations in the gene for type II collagen (COL2A1) usually via haploinsufficiency either from point mutations resulting in a direct premature termination codon or a deletion/insertion frameshift resulting in premature termination further downstream. These premature termination codons are recognized by the cell as abnormal

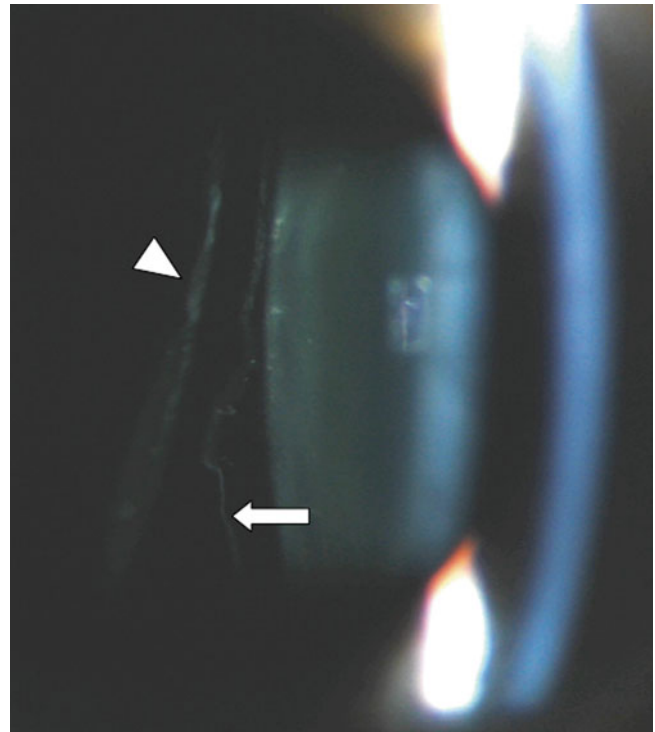


Figure I.C-4 Posterior vitreous detachment in type 1 Stickler syndrome. Posterior vitreous cortex (PVC) (*arrow head*) visible as second membrane behind type 1 congenital membranous vitreous anomaly (*arrow*). In type 2 Stickler syndrome, the ophthalmologist should be wary of mistakenly confusing the PVC with the type 1 anomaly – examination of fellow eye may help (Reproduced with permission from Snead et al. [85])

and the mutant mRNA is targeted for degradation via the nonsense-mediated decay pathway [67]. Although there are a small number of recurrent mutations, most families have unique mutations private to themselves. In addition to premature termination codons, there are many splice site mutations and it has been presumed that these result in the use of cryptic splice sites (see below) that cause shifts in the reading frame and haploinsufficiency, although this has only been demonstrated in a few cases [37, 70, 101].

b. Type 2 Stickler Syndrome

Patients with type 2 Stickler syndrome exhibit a different vitreous phenotype [59, 64, 66, 83, 84] (Table I.C-1, Figure I.C-2c) and result from dominant-negative mutations in the gene encoding the $\alpha 1$ chain of type XI collagen (COL11A1). As yet there are no clear genotype/phenotype correlations within this subgroup. Although there are some reports of the type 1 vitreous phenotype being associated with mutations in COL11A1 [45, 48], the weight of accumulated published data strongly suggests that these are more likely to be due to posterior vitreous detachment leading to an erroneous identification of the detached posterior vitreous cortex as the type 1 vitreous anomaly [70, 85]. The difference between the two membranes is illustrated in (Figure I.C-4).

c. Type 3, “Non-ocular” Stickler Syndrome

The gene encoding the $\alpha 2$ chain of type XI collagen (COL11A2) is not expressed in the eye and is replaced by an additional $\alpha 1$ (XI) chain or the $\alpha 2$ chain of type V collagen (COL5A2 gene) thereby forming a type V/XI collagen [47]. So patients with mutations affecting COL11A2 present with arthropathy and deafness, but without ophthalmic involvement [82]. Both dominant and recessive mutations in the same gene have also been found in patients with otospondyloomegaepiphyseal dysplasia.

d. Types 4, 5, and 6 Stickler Syndrome

Rarely, an autosomal recessive form of Stickler syndrome due to biallelic null mutations in the genes encoding either the $\alpha 1$, $\alpha 2$, or $\alpha 3$ chains of type IX collagen is reported [10, 25, 96]. These genes are more commonly associated with multiple epiphyseal dysplasia (MED2 and MED3; MIM 600204, 600696).

e. “Ocular-Only” Stickler Syndrome

As part of natural, tissue-dependent mRNA splicing variation, exon 2 of the gene for type II collagen (COL2A1) is not expressed in mature cartilage but is expressed in the eye. Mutations falling by chance within this exon will be naturally removed from the mature type II collagen transcript in cartilage tissue, and such patients therefore typically present to the clinician with minimal (if any) of the skeletal abnormalities more usually associated with the disorder. Since exon 2 of COL2A1 is normally expressed in the eye, however, patients harboring such specific mutations have an identical vitreoretinal and ocular phenotype to type 1 Stickler syndrome and a similarly high risk of retinal detachment [57, 65].

f. Stickler Syndrome with Profound Deafness

Reviews of published information on hearing loss in Stickler syndrome suggest that although hearing loss is common, it is usually mild to moderate in nature [1, 85]. Combinations of null alleles and missense mutations or biallelic null alleles in COL11A1 have been shown to result in the severe recessive disorder fibrochondrogenesis which is usually lethal. Carriers show only mild clinical features such as myopia or hearing loss and are not considered to have Stickler syndrome [2, 93].

COL11A1, COL11A2, and COL2A1 are all subject to alternative splicing [79, 102] where inclusion or exclusion of exons encoding the N-propeptide region of the molecules results in isoforms that can vary in their interaction with other components of the extracellular matrix [98] and growth factors such as TGF β 1 and BMP-2. A novel form of Stickler syndrome associated with severe, profound deafness has been identified in which mutations affecting the alternatively

spliced exon 9 (also referred to as exon 8 or V2) of COL11A1 and modified by the natural alternative splicing result in a recessive variant of the disorder with total deafness and severe myopia but mild arthropathy [75].

The expression of the alternatively spliced exon 9 of COL11A1 is similar to that of exon 2 of COL2A1 (see above and [51]). Both are present in immature chondrocytes but disappear as these cartilage precursors differentiate and mature. This explains why the resulting phenotype in these individuals manifests as a vitreoretinopathy rather than (severe) fibrochondrogenesis. Just as mutations in exon 2 of COL2A1 result in a nonsystemic form of Stickler syndrome (see above), so the natural alternative splicing of COL11A1 exon 9 modifies and reduces the severity of abnormal skeletal development. Exon 9 of the COL11A1 gene is however expressed in Meckel’s cartilage [22] – the origin of the malleus and incus of the inner ear, and anterior ligament of the malleus tympanic plate [20] accounting for the profound deafness associated with this recessive form of Stickler syndrome [75].

g. Unresolved

There are several reports of pedigrees with the full Stickler syndrome phenotype including vitreous abnormality, in which linkage to all the known loci has been excluded indicating that there is further genetic heterogeneity still to be resolved [46, 99].

b. COL2A1-Related Disorders

i. Kniest Dysplasia

Kniest dysplasia is an autosomal dominant disorder that shares many similarities with Stickler syndrome and the same genetic locus. Mutations are found in the same gene as for type 1 Stickler syndrome (COL2A1, Table I.C-1) but result in dominant-negative effects rather than haploinsufficiency resulting in a more severe arthropathy (Figure I.C-5) and short stature combined with variable degrees of cleft palate, Pierre Robin sequence, and deafness. Clinical features present at birth include shortened trunk and limbs, congenital megalophthalmos, and a flattened nasal bridge. The joints are often large at birth and with pronounced phalangeal epiphyseal dysplasia. Both conductive and sensorineural hearing loss may be present as with Stickler syndrome and all the type II collagenopathies [86].

ii. Spondyloepiphyseal Dysplasia Congenita (SEDC)

SEDC presents at birth with shortening of the trunk and to a lesser extent the extremities (rhizomelic limb shortening) with or without midline cleft and Pierre Robin sequence (Figure I.C-6). It is inherited as an autosomal dominant disorder and characteristically results from dominant-negative mutations in the gene for type II collagen (COL2A1). In common with other type II collagenopathies, they exhibit

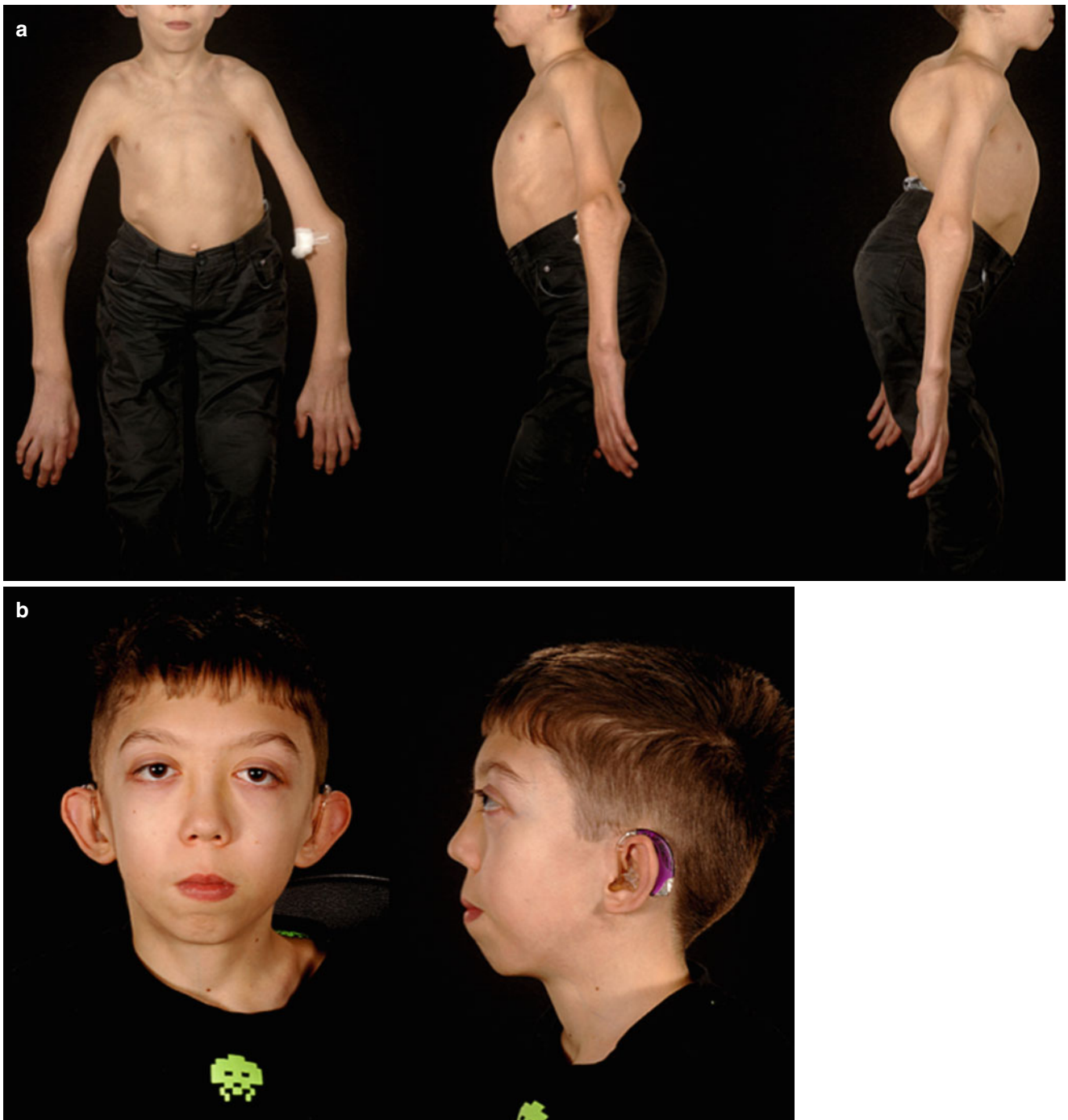


Figure I.C-5 (a, b) Kniest dysplasia. Note megalophthalmos and severe arthropathy particularly spine, knees, elbows, and phalangeal dysplasia

congenital abnormalities of vitreous development, hearing loss (both conductive and sensorineural). Patients classically develop a barrel-shaped chest associated with an exaggerated lumbar lordosis, which may compromise respiratory function. Odontoid hypoplasia may be present, predisposing to cervicomedullary instability. In parallel with the other type II/XI collagenopathies, patients with SEDC are at significant risk of giant retinal tear (GRT) and rhegmatogenous retinal detachment.

iii. Vitreoretinopathy with Phalangeal Epiphyseal Dysplasia (V-PED)

Richards et al. [68] described a novel form of dominantly inherited rhegmatogenous retinal detachment in which affected individuals also displayed an unusual but characteristic and severe phalangeal epiphyseal dysplasia resulting in brachydactyly. Analysis identified a novel mutation in the C-propeptide region of COL2A1 in a region that is highly conserved in all fibrillar collagen molecules. The phenotype



Figure I.C-6 Spondyloepiphyseal dysplasia congenita. Note short stature, barrel chest and rhizomelic (proximal) limb shortening. Patients typically exhibit the membranous congenital vitreous anomaly and congenital megalophthalmos

appears to represent a distinct separate entity from other the type II collagenopathies (SEDC, Kniest, Strudwick, and Stickler) (Figure I.C-7).

iv. Marshall Syndrome

There is some uncertainty as to whether or not the type 2 Stickler and Marshall syndromes are clinically separate entities. Many features are shared such as midfacial hypoplasia, spondyloepiphyseal abnormalities, cleft palate, and sensorineural hearing loss, but patients with Marshall syndrome were originally reported to also have ectodermal dysplasia with hypertrichosis and hypohydrosis, calvarial thickening, and ocular hypertelorism. Some authors link certain mutations

in COL11A1 with the Marshall facial phenotype, others taking an opposing view [8, 31, 81]. Regardless of nomenclature, what is clear from the published literature to date is that not all mutations in COL11A1 result in the Marshall phenotype [8, 45, 59] and also that genetically confirmed COL2A1 Stickler syndrome can exhibit the same facial features. The term Marshall-Stickler syndrome has been used but is potentially even more confusing and is best avoided until the original entity reported by Marshall is better characterized on clinical and molecular genetic grounds.

Recessive mutations have been described in both Marshall syndrome and a more severe and usually lethal disorder fibrochondrogenesis [2, 93]. These include substitutions of a

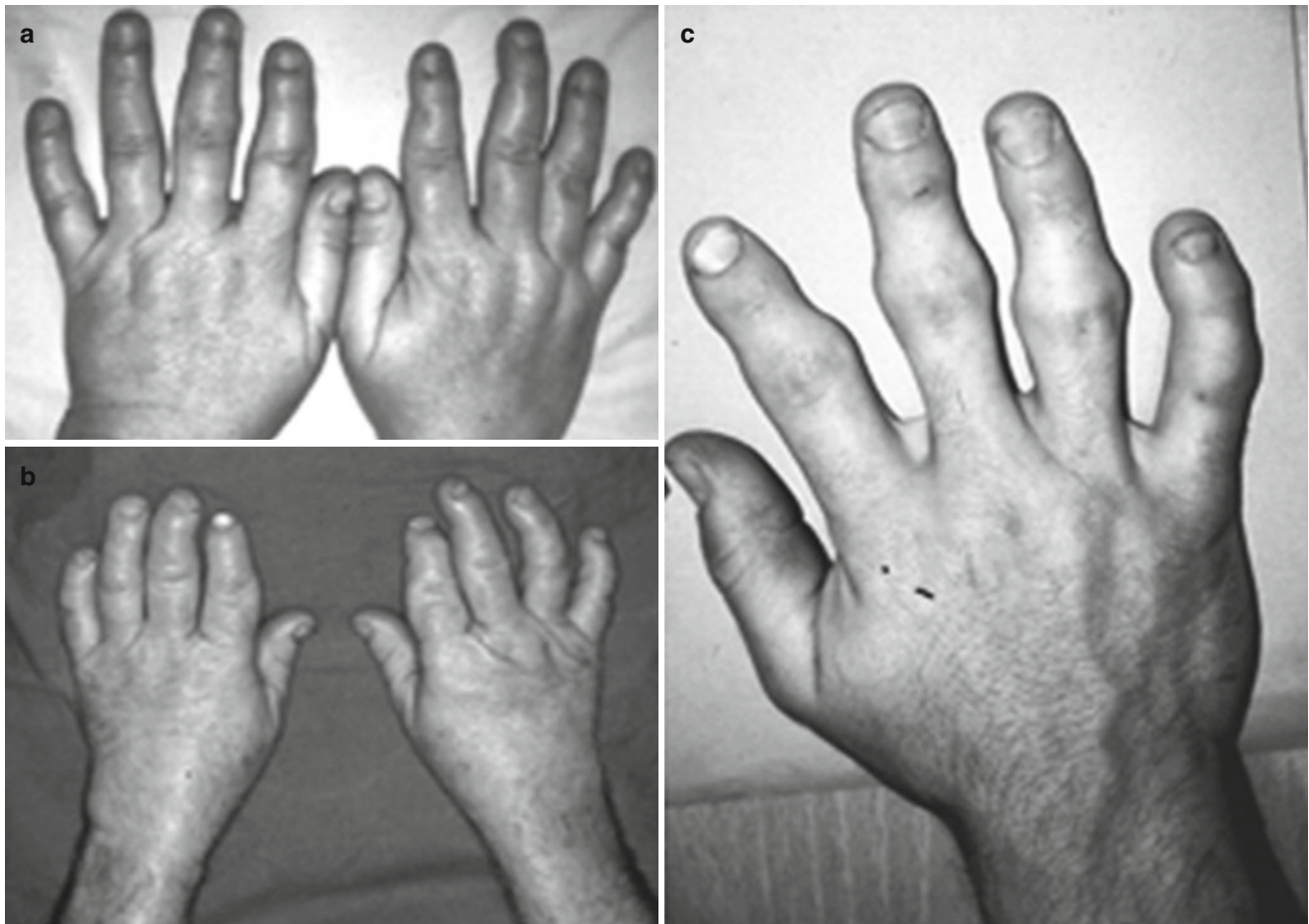


Figure I.C-7 Brachydactyly in vitreoretinopathy with phalangeal epiphyseal dysplasia (V-PED) (Reproduced with permission from Richards et al. [68])

glycine residue within the $\alpha 1(XI)$ collagen triple helical domain. This type of mutation usually has a dominant-negative effect but these recessive mutations highlight the need for caution in assuming the mode of inheritance. Clinical and molecular analysis of both parents is recommended when assessing apparently sporadic cases of Stickler/Marshall syndrome (see below).

v. Knobloch Syndrome

Knobloch syndrome is an autosomal recessive vitreoretinopathy which features high myopia, nystagmus, featureless iris, cataract, ectopia lentis, retinal detachment, and severe RPE atrophy resulting in prominent choroidal vasculature (Figure I.C-8). Systemic associations are congenital occipital encephalocele, unusual palmar creases, nail hypoplasia, and dental caries. In instances where the occipital encephalocele is subclinical, CT or MRI imaging may be required to support the clinical diagnosis. Molecular genetic analysis most commonly implicates homozygous splice site changes in the gene encoding the $\alpha 1$ chain of type XVIII collagen (COL18A1), although compound heterozygotes have also

been identified. The gene is expressed in two distinct isoforms, the longer isoform in retina (with a putative role in retinal structure) as well as in the closure of the neural tube, and associations with spina bifida have been reported. Mice that are COL18a1 knockouts show abnormalities in the uveal tract.

vi. Marfan Syndrome

Marfan syndrome is an autosomal dominant vitreoretinopathy associated with an abnormal vitreous architecture, myopic astigmatism, cornea plana, ectopia lentis, and characteristic skeletal and cardiovascular features. Although there is a significant association with myopia, this is characteristically developmental in contrast to the congenital nonprogressive myopia found in type 1 Stickler syndrome (see above). Increased height with disproportionately long limbs and digits; scoliosis; lumbar lordosis; joint laxity; a crowded, high-arched (but not cleft) palate; and anterior chest deformities characterize the classical phenotype. Mitral valve prolapse, mitral regurgitation, dilatation of the aortic root, aortic regurgitation, aneurysm

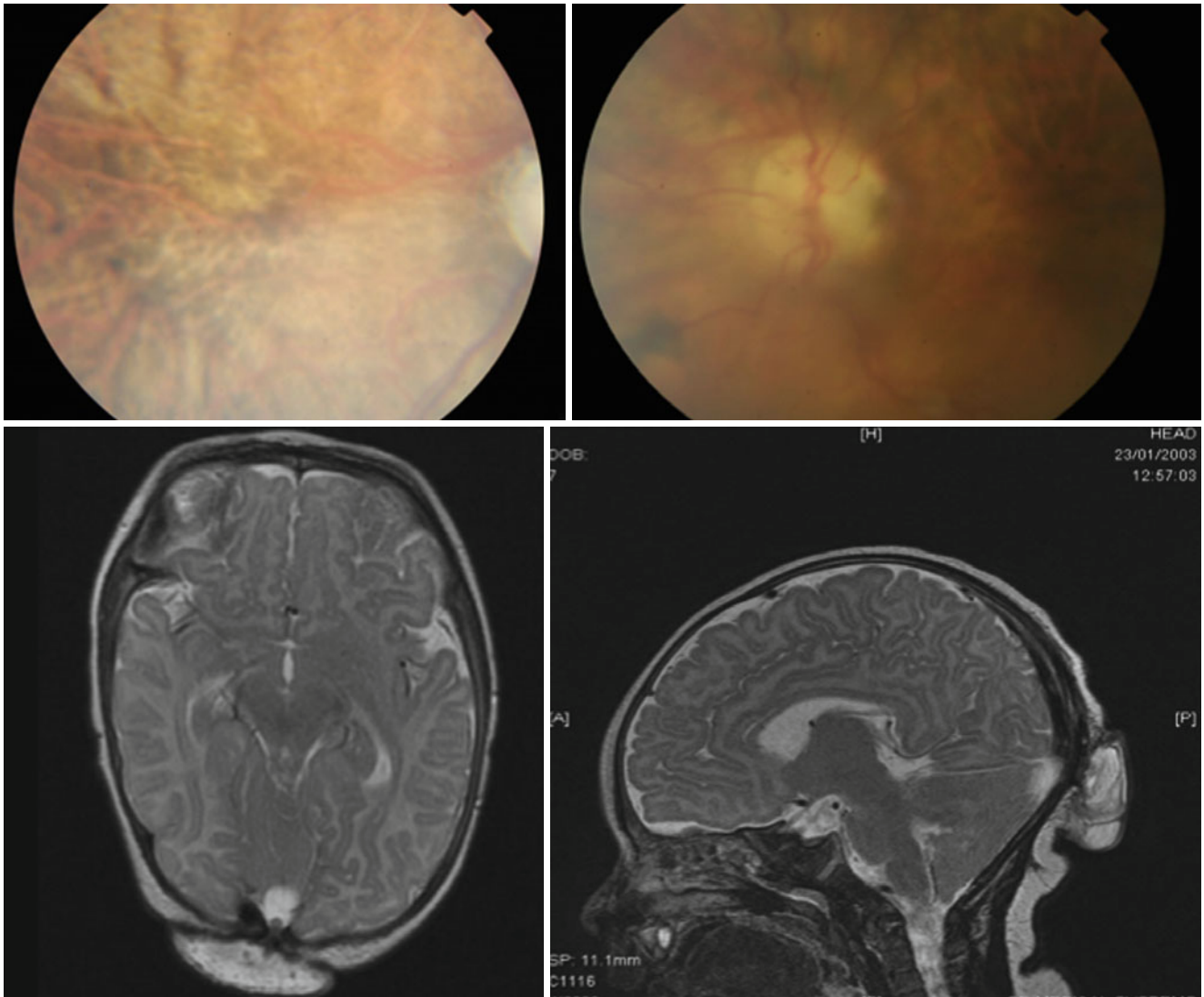


Figure I.C-8 Knobloch syndrome. a type XVIII collagenopathy associated with vitreoretinopathy and retinal detachment. Left inferior macula off retinal detachment associated with high myopia and occipital encephalocele (Reproduced with permission from Snead et al. [85])

of the aorta, and aortic dissection are the major life-threatening cardiovascular complications. Other atypical findings include striae distensae, pulmonary blebs (predisposing to spontaneous pneumothorax), and spinal arachnoid cysts or diverticula. All “true” cases of Marfan syndrome appear to be due to heterozygous mutations in the fibrillin-1 gene (FBN1) on chromosome 15q21.1 that encodes fibrillin – a high-molecular-weight extracellular glycoprotein. Mutations in the fibrillin gene cause both Marfan syndrome and dominant ectopia lentis. Loeys-Dietz syndrome (LDS), an autosomal dominant disorder characterized by the triad of arterial tortuosity and aneurysms, hypertelorism, and bifid uvula or cleft palate, forms part of the clinical differential diagnosis but without associated vitreous abnormality.

2. Vitreoretinopathies with Progressive Retinal Dysfunction

a. Wagner Vitreoretinopathy/Erosive Vitreoretinopathy

Wagner syndrome is a rare autosomal dominant vitreoretinopathy associated with myopia, glaucoma, chronic uveitis, liquid vitreous, premature cataract, night blindness, and retinal detachment. Clear lenses in childhood typically develop anterior and posterior cortical opacities in puberty with rapid progression during the third or fourth decades. The anterior lens capsule is unusually tough and highly elastic making the capsulorrhexis challenging and secondary capsular opacity and phimosis common.

The cardinal vitreous features are the absence of the normal vitreous architecture and a very pronounced thickening

and incomplete separation of the posterior vitreous cortex [16, 49] that tends to occur in a circumferential band. Ectopia of the macula with an associated “W-shaped” nasal displacement of retinal vessels is associated with pseudoexotropia [49, 52]. Many patients show elevated rod and cone thresholds on dark adaptation, and the majority will have subnormal b-wave amplitudes on ERG. Visual field analysis may demonstrate ring scotomas with eventual loss of central visual acuity. Even in the absence of retinal detachment, the progressive nature of the chorioretinal pathology results in progressive nyctalopia and visual field loss, the clinical phenotype at the end-stage being referred to as erosive vitreoretinopathy – the two disorders being allelic.

A heterozygous mutation in the gene encoding versican (CSPG2) was first identified in Wagner syndrome by Miyamoto et al. [52]. Versican is a chondroitin sulfate proteoglycan expressed in many tissues including the vitreous gel, where it represents 2.5 % of the total protein content [62]. The amino-terminal of versican binds to hyaluronan, resulting in the formation of very large complexes. Natural alternative splicing results in 4 isoforms, and mutations identified in Wagner vitreoretinopathy usually result in a significant imbalance and increase of the V2 and V3 isoforms as a result of exon 8 skipping which is required for the V0 and V1 transcripts [16, 40, 49, 53, 77].

b. Goldmann-Favre Syndrome/ Enhanced S-Cone Dystrophy

Goldmann-Favre syndrome is a recessive vitreoretinopathy characterized by night blindness, liquefaction and fibrillar changes of the vitreous, equatorial chorioretinal atrophy and pigment clumping, peripheral and macular schisis, and diffuse vascular leakage on fluorescein angiography. This syndrome is now known to be caused by mutations in the same gene that causes enhanced S-cone syndrome (ESCS the NR2E3 gene). The ERG findings show severely reduced rod-isolated responses and reduced combined rod-cone responses.

3. Vitreoretinopathies with Abnormal Retinal Vasculature

During embryogenesis vitreous undergoes a remarkable transformation from a vascularized structure during the first trimester to an avascular and largely acellular clear structure at birth [see chapter I.D. Vitreous cytokines and regression of the hyaloid vasculature]. There are a variety of abnormalities that can occur during this process resulting in different phenotypic expressions [see chapter III.A. Congenital vascular vitreoretinopathies]. As the following describes, these phenotypes are beginning to be reclassified in terms of genotype.

a. Familial Exudative Vitreoretinopathy

Familial exudative vitreoretinopathy (FEVR) is an inherited vitreoretinopathy characterized by premature arrest of retinal

angiogenesis and vascular differentiation resulting in incomplete vascularization of the peripheral retina. The clinical phenotype shows wide inter- and intrafamilial variation ranging from bilateral total retinal detachment and blindness in infancy to a subclinical, asymptomatic vascular change only identifiable on fundus fluorescein angiography. Other features include retinal vascular exudates, peripheral snowflake vitreous changes, and tractional or combined tractional and rhegmatogenous retinal detachment. The frequent occurrence of an associated premacular membrane can cause severe retinal distortion and macular ectopia.

The condition is genetically heterogenous. Familial exudative vitreoretinopathy-1 (EVR1) is caused by heterozygous mutations in the frizzled-4 gene (FZD4) on chromosome 11q14, and an X-linked form of familial exudative vitreoretinopathy (EVR2) is caused by mutations in the NDP gene. EVR3 maps to chromosome 11p13-p12, EVR4 can be caused by heterozygous or homozygous mutations in the LRP5 gene on 11q13.4, and EVR5 is caused by heterozygous mutations in the TSPAN12 gene on 7q31.

b. Autosomal Dominant Vitreoretinochoroidopathy (ADVIRC)

Autosomal Dominant Vitreoretinochoroidopathy (ADVIRC) is an inherited vitreoretinopathy characterized by peripheral pigmentary changes at the equatorial region with a pathognomonic discrete posterior boundary [39]. There is marked intrafamilial variability but the characteristic band of retinal hyperpigmentation is a constant feature irrespective of age. Other associated developmental ocular abnormalities include microcornea, presenile cataracts, angle closure glaucoma, iris dysgenesis (absence of crypts and abnormal pupillary ruff), retinal detachment, and optic nerve dysplasia [97]. BEST1 is proposed to have a role in normal ocular development. Ex vivo studies reveal that all BEST1 mutations known to cause ADVIRC result in aberrant mRNA splicing [17].

4. Vitreoretinopathy Associated with Corneal Changes

Snowflake vitreoretinal degeneration (SVD) [24, 35] is characterized by the association of corneal endothelial guttata, premature cataract, atypical “fibrillar” vitreous gel architecture, retinal detachment, and peripheral retinal abnormalities including minute crystalline “snowflake-like” deposits. Minor vascular abnormalities of small retinal vessels have also been noted. Visual acuity is generally normal and retinal function tests show minimal or no abnormality. The disorder appears to result in a superficial retinal degeneration in contrast to the rather deeper retinal and choroidal disturbances characteristic of Wagner vitreoretinopathy

Molecular genetic analysis has identified a heterozygous missense mutation in the potassium channel gene KCNJ13 in Hirose’s original pedigree [34], although analysis in other SVD families indicates that there is still further clinical and

genetic heterogeneity to be resolved [19, 30, 41, 58, 76]. Interestingly, homozygous mutations in *KCNJ13* have been identified in patients with Leber congenital amaurosis in whom heterozygous carriers have a normal fundal appearance [80].

5. Vireoretinopathies Associated with Dominant and/or Bilateral Rhegmatogenous Retinal Detachment (DRRD/BRRD)

Mutations affecting the genes encoding all three of the principle fibrillar collagens found in human vitreous (II, IX and V/XI) are known to cause Stickler syndrome (see above), the majority being due to defects in the major structural constituent, type II collagen. In addition to the natural, tissue-dependent splicing variations of the gene for type II collagen resulting in “ocular-only” Stickler syndrome, investigations using Stickler syndrome as a model of high-risk retinal detachment have unveiled the wider involvement of these loci in other more common forms of retinal detachment, particularly dominant rhegmatogenous retinal detachment (DRRD) and bilateral rhegmatogenous retinal detachment (BRRD). Alternatively spliced exons, splice site mutations resulting in alternatively spliced transcripts and differential effects of various amino acid substitutions have all been shown to result in either DRRD or BRRD but without the systemic features associated with generalized Stickler syndrome [66, 67, 69, 85]. Research into the extent of the involvement of these loci in the wider issue of retinal detachment in the general population continues.

III. Screening and Ancillary Investigations

Pedigree drawing and a thorough family history are helpful in assessing inheritance pattern, and assessment of affected family members or siblings can prove invaluable information in instances where it is difficult to assess vitreous phenotype in a young infant or where gel examination is not possible because of previous vitrectomy surgery. The fundus assessment and screening algorithm of vitreous phenotypes depicted in Figure I.C-2 will form an essential cornerstone evaluation for patients, the majority of whom are likely to present with one or other variant of the Stickler syndromes. Ancillary ophthalmic investigations may include keratometry (cornea plana in Marfan syndrome), lens changes (ectopia in Marfan or Knobloch syndrome, quadrant lamellar opacities and zonule defects in Stickler syndrome), orthoptic assessment, visual fields, electrodiagnostic evaluation, as well as OCT, and fundus fluorescein angiography. Audiology and tympanometry can provide invaluable information with regard to identification of hearing loss that is frequently subclinical and

asymptomatic as well as differentiating between conductive and sensorineural elements. Associated connective tissue abnormalities of tympanic membrane mobility can be identified on tympanometry.

The association between midline palate abnormalities and retinal detachment was recognized even before the original report of hereditary arthro-ophthalmopathy by Stickler and colleagues in 1965. Stickler syndrome, Kniest dysplasia, Knobloch syndrome, SEDC, Marshall syndrome, and Marfan syndrome may all exhibit variable abnormalities in palate development from full-blown cleft to an asymptomatic submucous cleft or bifid uvula. Even in the absence of a history of cleft repair, examination of the palate can be a helpful and should be included as part of the clinical assessment.

Systemic assessment should pay particular attention to arthropathy affecting the limbs and joints. Hypermobility in adolescence is common but typically superseded by restricted movements and a degenerative arthropathy in the third and fourth decades. Joint hypermobility can be assessed using the Beighton scoring system, allowing comparison with age and sex matched controls. Radiological investigations are important to identify associated features of skeletal dysplasia (enlarged epiphyses, flattened and irregular femoral epiphyses, flared metaphyses, platyspondyly, anterior wedging of vertebral bodies) as well as subclinical encephalocele, or occult spina bifida in Knobloch syndrome.

The criteria for diagnosis of mitral valve prolapse have been modified over the years and are a recognized finding in the population at large but a formal cardiology assessment including echo studies will be needed in cases of suspected Marfan syndrome.

IV. From Laboratory To Bedside: Current Research on Mechanisms for Variability in Clinical Phenotype

Vitreoretinopathies associated with skeletal abnormalities form by far the largest subgroup of inherited vitreoretinopathies, and of these the Stickler syndromes in their various forms are the most likely to be encountered in clinical practice. Originally considered a single-gene disorder, recent research has identified at least five different molecular mechanisms for the clinical and phenotypic variability between patients and families and now extends to encompass familial retinal detachment in the general population. This latter group is perhaps the most important but most difficult to identify since lacking any systemic involvement to suggest the diagnosis; they are frequently undiagnosed until sudden loss of vision from retinal detachment presents.

For the most common variant of Stickler syndrome (type 1 – see above), the finding that most unique private mutations

result in a common theme of haploinsufficiency of type II collagen raises the conundrum as to why the phenotype is so variable both between and within these families. One emerging explanation for this lies in the differential effects that such mutations can have on pre-mRNA processing.

A. Phenotypic Differences Due to Splicing Variations

Correct pre-mRNA processing requires the accurate recognition of donor, branch, and acceptor splice sites by the spliceosome – the macromolecular assembly that removes intronic sequences from messenger RNA. Many genes exhibit tissue-specific or temporal variations in this process and are alternatively spliced, that is to say certain exons are either included or excluded during production of the mature mRNA transcript. By this mechanism, similar but subtly different protein isoforms can be synthesized from the same gene by different tissues and the diversity of proteins encoded by the genome is greatly enhanced according to the varying needs of individual tissue expression. In humans, approximately 95 % of genes are alternatively spliced [56] in a tissue-dependent manner and both COL2A1 and COL11A1 are no exception [79, 102].

Because of the nature of collagen molecules and the exon structure of the genes, which almost always contain complete codons, mutations that result in exon skipping have a dominant-negative effect. That is to say, the mutant protein co-assembles with the normal protein synthesized from the wild-type allele and disrupts its normal function [11]. Complete exon skipping in COL2A1 therefore usually results in severe chondrodysplasias [87]. However, many COL2A1 “Stickler” mutations disrupt splice sites, and because most COL2A1 exons contain complete codons, it is presumed that rather than causing exon skipping, these mutations result in the use of alternative cryptic splice sites, leading to shifts in the reading frame and ultimately nonsense-mediated decay. However, this has only been demonstrated in a few cases [37, 70, 101].

Nonsense-associated exon skipping is a mechanism whereby some premature termination codons actually cause exon skipping by disrupting exon definition and has been well documented [23, 42]. It is not known if this contributes to phenotypic variability in Stickler syndrome, but if even a small proportion of exon-skipped transcripts result from nonsense mutations in COL2A1, this would be enough to influence the resulting phenotype, by switching mRNAs away from the nonsense-mediated decay pathway towards a product that would exert a dominant-negative effect [72]. Ocular and cartilage tissue are not readily available for direct examination and so to investigate this problem, research using an elegant minigene model to study mutations is often

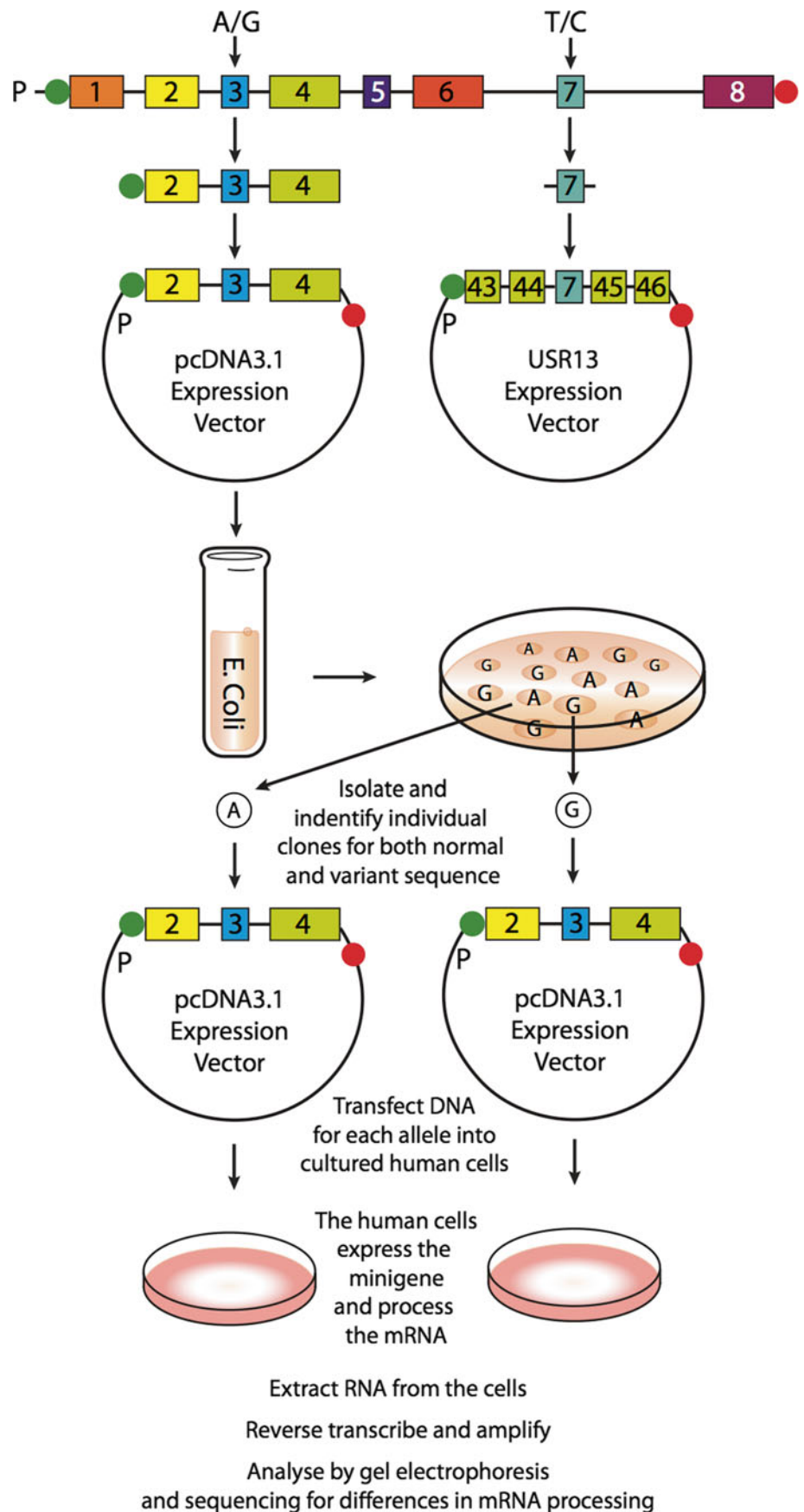
utilized [28]. As the name suggests only part of a gene is examined. The DNA variant under test is amplified either within neighboring exons and cloned into a vector that can express the minigene in cultured human cells. Alternatively if the gene structure does not allow this, then a test exon can be amplified and inserted into a cassette of unrelated exons (Figure I.C-9). This technique has been used to elucidate the effect of a number of mutations that alter pre-mRNA processing in COL2A1 associated vitreoretinopathies [71, 74]. Recently it has been demonstrated that apparently straightforward single-point mutations can produce a variety of transcripts. Some mutations result in nonsense-mediated decay leading to haploinsufficiency but also produce a proportion of exon-skipped transcripts that exert a dominant-negative effect. Other mutations have been shown to produce a mixture of normal and missplicing. The resulting phenotype from these mutations will potentially vary from tissue to tissue and person to person depending upon the ratio of the normal/haploinsufficient/dominant-negative transcripts produced [72].

1. Phenotypic Differences Due to Missense Mutations

Other variations in phenotype can be caused by alterations in the amino-acid sequence. Fibrillar collagens are characterized by a highly conserved repeating Gly-Xaa-Yaa amino acid sequence, whereby glycine, the smallest amino acid, occupies every third position. This repeating motif is believed to be essential for correct trimerization of the polypeptide chains during assembly of the triple helical domain and construction of the mature collagen molecule. Substitution of any of the glycine residues is generally considered to be pathogenic, but in type II collagen, these can result in phenotypes ranging from the lethal achondrogenesis type II to dominantly inherited retinal detachment, depending upon the effect that the missense change has upon the structure and function of the collagen molecule. Studies of similar mutations in type I collagen have shown factors that influence phenotype to include the nature of the substituting amino acid, disruption to cell-matrix interaction, and intracellular quality control mechanisms [11, 12, 44]. The substitution of a cysteine amino acid into the collagen helix is also pathogenic. Although these are usually milder phenotypically than the glycine substitutions, phenotypes can range from Czech dysplasia through Stickler syndrome to dominantly inherited osteoarthritis [36, 66, 100].

In comparison with type 1 Stickler syndrome, far fewer mutations have been characterized for type 2 Stickler syndrome (COL11A1). The majority have altered donor and acceptor splice sites and where analyzed have resulted in exon skipping, leaving the message in-frame thereby exerting a dominant-negative effect. Only a few substitutions of

Figure I.C-9 Minigenes as splicing reporters. Exons/introns with variants under examination can be amplified either within a product that includes neighboring exons (i.e., within the natural genetic environment) or as a single exon including some surrounding intronic sequence. Multi-exon products are cloned into the expression vector pcDNA3.1, and single exons are cloned into the splicing reporter USR13 which already contains COL2A1 exon 43–46 and includes a cloning site in intron 44 for insertion of the single exon under test. Recombinant molecules are inserted into *E. coli*, and clones for each allele are identified by PCR and sequencing. DNA prepared from each of the normal and variant constructs is transfected separately into cultured human cells. These cells express the minigene and process the mRNA transcribed from it. Differences between the normal and variant alleles can then be examined by RT-PCR and sequencing. *P* promoter, *green circle* start signal, *red circle* stop signal



glycine have been reported [8, 64, 73]. The recent identification of COL11A1 as the gene locus for the recessive disorder fibrochondrogenesis [93] demonstrated that the carrier parents with a nonsense mutation had a relatively normal phenotype with myopia or mild hearing loss as the only clinical signs. A similar finding was reported for the carrier parents with a glycine substitution, and so in parallel with type II collagen, it seems likely there will be a range of phenotypes resulting from glycine substitutions in $\alpha 1(\text{XI})$ collagen (COL11A1), some of which may result in few, if any, clinical symptoms. A recent report of recessive “Marshall syndrome” due to homozygous glycine substitutions in $\alpha 1(\text{XI})$ collagen supports this hypothesis [38].

2. Phenotypic Differences Due to Mosaicism

In addition to alternative splicing of exons, alternatively spliced transcripts, and missense mutations, phenotypic variation has also been reported as a result of somatic mosaicism [4, 54, 88]. Although rare, such cases emphasize the importance of detailed clinical and molecular genetic analysis even in clinically normal parents of affected individuals.

B. Future Developments

As new DNA sequencing technologies are introduced into hospital diagnostic services, it will become possible to analyze complete genes, rather than current techniques that examine merely the exons and their short surrounding sequences. At present whole genome sequencing and exome sequencing (sequencing of the coding regions of the genome) are more suited to research projects than routine diagnostic analysis. It is this approach that can be utilized to identify as yet unknown loci for uncharacterized inherited vitreoretinopathies. For some genetic eye disorders (not discussed under this section) with many possible pathogenic loci (such as retinitis pigmentosa), it is also possible to use a strategy that screens a panel of exonic regions of all candidate genes. This approach is suitable for routine diagnostic testing but may not result in 100 % coverage of all exons.

Advances in sequencing technology also means it is now possible to economically sequence a complete gene (i.e., all of the introns and exons of COL2A1) in diagnostic laboratories. Although an attractive and exciting prospect, the benefits of such comprehensive DNA analysis will be mitigated by many more sequence variants being identified of uncertain influence or pathogenicity. For example, using current techniques for type 1 Stickler syndrome, approximately 5 % of cases have no detectable mutation within the regions currently analyzed. Recent research [74] suggests that many of these 5 % will harbor deep intronic mutations and more are

likely to be detected when complete gene analysis replaces exon only sequencing. Although identification of these rarer mutations is technically possible, confirming their pathogenicity will remain problematic and a combination of approaches will be necessary which might include absence or very low frequency of such a change in the DNA sequence variation databases, co-segregation of the variant with disease, in silico prediction software, and functional studies (Figure I.C-9). The minigene analysis approach developed for Stickler syndrome is a model for the latter category and has also been used to study mutations in many other genetic disorders such as breast cancer, muscular dystrophy, and cystic fibrosis [29, 33, 94]. As an alternative to minigene analysis, when cells from a patient are available, it is also possible to culture these cells so that nonsense-mediated decay can be inhibited. This enables cDNA from the mutant allele to be synthesized and sequenced following RT-PCR [37, 67, 70, 101]. The algorithm depicted in Figure I.C-1 illustrates an assessment and diagnostic pathway for Stickler syndrome.

V. Prophylaxis

Successful primary repair of retinal detachment [see chapter V.B.4. Prophylaxis and cure of retinal detachment] is now possible with a single operation in over 90 % of cases [5, 6, 91, 92, 95,], but even with successful surgery, macular and binocular function may still be compromised, especially in pediatric vitreoretinopathy patients who often present late or who are diagnosed only on second eye involvement [see chapter III.A. Congenital vascular vitreo-retinopathies]. In contrast to many other retinal blinding disorders, blindness through retinal detachment in such cases is potentially avoidable if a rationale for the prediction and prevention of retinal tears could be developed. This has, until recently, been frustrated by a lack of availability of the genetic analysis defining subgroups at highest risk. This void is rapidly being filled, and surveys of unselected cohorts of patients with a clinical diagnosis of Stickler syndrome in both the UK and US report that over 50 % of patients had already suffered a retinal detachment [7, 57, 89].

Patients with type 1 Stickler syndrome are the subgroup at highest risk of developing retinal detachment, typically as a result of a giant retinal tear (GRT), that is to say a circumferential break at the pars plana junction caused by a separation of the vitreous and posterior vitreous cortex much more anteriorly than would normally be the case. Prophylactic retinopathy designed and specifically positioned to prevent GRT progression appears to substantially reduce the risk of retinal detachment and blindness from this type of break in type 1 Stickler syndrome. Detachment due to retinal breaks at other more posterior locations can occur but are impossible to

predict in terms of position, making effective prophylaxis in a 100 % of cases impractical. In one large cohort of over 200 patients with genetically confirmed type 1 Stickler syndrome, 73 % of 111 patients who had not had prophylactic retinopathy (preventative retinal adhesion treatment) had suffered retinal detachment and 48 % of these had both eyes affected. Of the cohort of patients who had had preventative treatment, only 8 % had suffered retinal detachment and there were no cases of bilateral detachment [7].

A more recent study of the long-term efficacy of a standardized prophylaxis protocol (the Cambridge Prophylactic Cryotherapy Protocol) in a cohort analysis of 487 type 1 Stickler syndrome patients confirmed that untreated patients ($n=194$) had a greater than seven-fold increased risk of detachment compared to the prophylaxis group ($n=229$) (hazard ratio [HR], 7.40; 95 % confidence interval [CI], 4.5–12.1; $p<0.001$) [26]. The risk in type 2 Stickler syndrome appears to be slightly less but remains to be quantified; surveys suggest that between 40 and 50 % of patients had suffered retinal detachment ([59] and unpublished data in preparation). In the non-ocular subgroup (type 3), the risk appears to be no greater than the population at large.

VI. Summary

Inherited vitreoretinopathies for the most part result from genetic abnormalities of type II, IX, or V/XI collagen and proteoglycans expressed in the vitreous [see chapters I.A. Vitreous proteins; I.F. Vitreous biochemistry & artificial vitreous]. The Stickler syndromes form by far the largest subgroup and are the most common cause of inherited retinal detachment. Originally considered a single-gene disorder, at least 9 subgroups of Stickler syndrome have now been characterized and recent laboratory research has shed much new light on the basis for the clinical and phenotypic variability within and between inherited vitreoretinopathies that now extends to encompass familial retinal detachment in the general population. This chapter provides an update and clinical overview of these important disorders of vitreous embryogenesis together with the recent advances in their molecular genetic analysis, including minigene splicing reporter analysis. Such functional studies are likely to become increasingly relevant as diagnostic molecular genetic analysis moves away from exon sequencing to whole-gene analysis by next-generation sequencing.

The emergence and availability of rapid, accurate molecular genetic diagnosis and subtyping provides much more precise stratification of risk, and as a result protocols for effective prophylaxis against retinal detachment can, for the first time, be deployed in high-risk subgroups.

Abbreviations

ADVIRC	Autosomal dominant Vitreoretinopathies
BMP2	Bone morphogenetic protein 2
BRRD	Bilateral rhegmatogenous retinal detachment
cDNA	Complementary deoxyribonucleic acid
CI	Confidence interval
CT	computerized tomography
DNA	Deoxyribonucleic acid
DRRD	Dominant rhegmatogenous retinal detachment
ERG	Electroretinogram
FEVR	Familial exudative vitreoretinopathy
GRT	Giant retinal tear
HR	Hazard ratio
LDS	Loeys-Dietz syndrome
MED	Multiple epiphyseal dysplasia
MRI	Magnetic resonance imaging
mRNA	Messenger ribonucleic acid
OCT	Optical coherence tomography
PRS	Pierre Robin sequence
RNA	ribonucleic acid
RPE	Retinal pigment epithelium
RT-PCR	Reverse transcription polymerase chain reaction
SEDC	Spondyloepiphyseal dysplasia congenita
SVD	Snowflake vitreoretinal degeneration
TGF β	Transforming growth factor β
V-PED	Vitreoretinopathy with phalangeal epiphyseal dysplasia

References

1. Acke FR, Dhooge IJ, Malfait F, De Leenheer EM. Hearing impairment in Stickler syndrome: a systematic review. *Orphanet J Rare Dis.* 2012;7:84.
2. Akawi NA, Al-Gazali L, Ali BR. Clinical and molecular analysis of UAE fibrochondrogenesis patients expands the phenotype and reveals two COL11A1 homozygous null mutations. *Clin Genet.* 2012;82:147–56.
3. Al Kaissi A, Klaushofer K, Grill F. Osteochondritis dissecans and Osgood Schlatter disease in a family with Stickler syndrome. *Pediatr Rheumatol Online J.* 2009;7:4.
4. Ala-Kokko L, Shanske AL. Mosaicism in Marshall syndrome. *Am J Med Genet A.* 2009;149A:1327–30.
5. Alexander P, Ang A, Poulson A, Snead MP. Prevention and control of proliferative vitreo-retinopathy: primary retinal detachment surgery using silicone oil as a planned 2-stage procedure in high risk cases. *Eye.* 2008;22:815–8.
6. Alexander P, Ang A, Poulson A, Snead MP. Scleral buckling combined with vitrectomy for the management of rhegmatogenous retinal detachment associated with inferior retinal breaks. *Eye.* 2008;22:200–3.

7. Ang A, Poulson AV, Goodburn SF, Richards AJ, Scott JD, Snead MP. Retinal detachment and prophylaxis in type 1 Stickler syndrome. *Ophthalmology*. 2008;115:164–8.
8. Annunen S, Korkko J, Czarny M, et al. Splicing mutations of 54-bp exons in the COL11A1 gene cause Marshall syndrome, but other mutations cause overlapping Marshall/Stickler phenotypes. *Am J Hum Genet*. 1999;65:974–83.
9. Azuma N, Tajima S, Konomi H, Hida T, Akiya S, Uemura Y. Glycosaminoglycan and collagen distribution in the developing human vitreous. *Graefes Arch Clin Exp Ophthalmol*. 1998;236:679–87.
10. Baker S, Booth C, Fillman C, Shapiro M, Blair MP, Hyland JC, et al. A loss of function mutation in the COL9A2 gene cause autosomal recessive Stickler syndrome. *Am J Med Genet A*. 2011;155:1668–72.
11. Bateman JF, Boot-Handford RP, Lamande SR. Genetic diseases of connective tissues: cellular and extracellular effects of ECM mutations. *Nat Rev Genet*. 2009;10:173–83.
12. Beck K, Chan VC, Shenoy N, Kirkpatrick A, Ramshaw JA, Brodsky B. Destabilization of osteogenesis imperfecta collagen-like model peptides correlates with the identity of the residue replacing glycine. *Proc Natl Acad Sci U S A*. 2000;97:4273–8.
13. Bishop PN, Takanosu M, Le Goff M, Mayne R. The role of the posterior ciliary body in the biosynthesis of vitreous humour. *Eye*. 2002;16:454–60.
14. Bremer FM. Histochemical study on glycosaminoglycans in the developing mouse vitreous. *Histochemistry*. 1987;87:579–83.
15. Bremer FM, Rasquin F. Histochemical localisation of hyaluronic acid in vitreous during embryonic development. *Invest Ophthalmol Vis Sci*. 1998;39:2466–9.
16. Brézin AP, Nedelec B, Barjol A, Rothschild PR, Delpech M, Valleix S. A new VCAN/versican splice acceptor site mutation in a French Wagner family associated with vascular and inflammatory ocular features. *Mol Vis*. 2011;17:1669–78.
17. Burgess R, MacLaren RE, Davidson AE, Urquhart JE, Holder GE, Robson AG, Moore AT, Keefe RO, Black GC, Manson FD. ADVIRC is caused by distinct mutations in BEST1 that alter pre-mRNA splicing. *J Med Genet*. 2009;46:620–5.
18. Carroll C, Papaioannou D, Rees A, Kaltenthaler E. The clinical effectiveness and safety of prophylactic retinal interventions to reduce the risk of retinal detachment and subsequent vision loss in adults and children with Stickler syndrome: a systematic review. *Health Technol Assess*. 2011;15:1–62.
19. Chen CJ, Everett TK, Marascalco D. Snowflake degeneration: an independent entity or a variant of retinitis pigmentosa? *South Med J*. 1986;79:1216–23.
20. Chung KS, Park HH, Ting K, Takita H, Apte SS, Kuboki Y, Nishimura I. Modulated expression of type X collagen in Meckel's cartilage with different developmental fates. *Dev Biol*. 1995;170:387–96.
21. Couchouron T, Masson C. Early-onset progressive osteoarthritis with hereditary progressive ophthalmopathy or Stickler syndrome. *Joint Bone Spine*. 2011;78:45–9.
22. Davies GB, Oxford JT, Hausafus LC, Smoody BF, Morris NP. Temporal and spatial expression of alternative splice-forms of the alpha1(XI) collagen gene in fetal rat cartilage. *Dev Dyn*. 1998;213:12–26.
23. Dietz HC, Valle D, Francomano CA, Kendzior Jr RJ, Pyeritz RE, Cutting GR. The skipping of constitutive exons in vivo induced by nonsense mutations. *Science*. 1993;259:680–3.
24. Edwards AO. Clinical features of the congenital vitreo-retinopathies. *Eye*. 2008;22:1233–42.
25. Faletra F, D'Adamo AP, Bruno I, Athanasakis E, Biskup S, Esposito L, et al. Autosomal recessive Stickler syndrome due to a loss of function mutation in the COL9A3 gene. *Am J Med Genet A*. 2013; Part A, 9999:1–6.
26. Fincham, GS, Pasea L, Carroll, C, McNinch AM, Poulson AV, Richards AJ, Scott JD, Snead MP. Prevention of retinal detachment in Stickler syndrome: the Cambridge Prophylactic Cryotherapy protocol. *Ophthalmology*. 2014, pii: S0161-6420(14)00186–9. doi:10.1016/j.ophtha.2014.02.022.
27. Fitch JM, Mentzer A, Mayne R, Linsenmayer TF. Acquisition of type IX collagen by the developing avian primary corneal stroma and vitreous. *Dev Biol*. 1988;128:396–405.
28. Gaillardat P, Killian A, Martins A, Tournier I, Frébourg T, Tosi M. Use of splicing reporter minigene assay to evaluate the effect on splicing of unclassified genetic variants. *Methods Mol Biol*. 2010;653:249–57.
29. Gaillardat P, Krieger S, Théry JC, Killian A, Rousselin A, Berthet P, Frébourg T, Hardouin A, Martins A, Tosi M. The BRCA1 c.5434C->G (p.Pro1812Ala) variant induces a deleterious exon 23 skipping by affecting exonic splicing regulatory elements. *J Med Genet*. 2010;47:398–403.
30. Gheiler M, Pollack A, Uchenik D, Godel V, Oliver M. Hereditary snowflake vitreoretinal degeneration. *Birth Defects Orig Artic Ser*. 1982;18:577–80.
31. Griffith AJ, Sprunger LK, Sirko-Osadsa DA, Tiller GE, Meisler MH, Warman ML. Marshall syndrome associated with a splicing defect at the COL11A1 locus. *Am J Hum Genet*. 1998;4:816–23.
32. Halfter W, Dong S, Dong A, Eller AW, Nischt R. Origin and turnover of ECM proteins from the inner limiting membrane and vitreous body. *Eye*. 2008;22:1207–13.
33. Hefferon TW, Groman JD, Yurk CE, Cutting GR. A variable dinucleotide repeat in the CFTR gene contributes to phenotype diversity by forming RNA secondary structures that alter splicing. *Proc Natl Acad Sci U S A*. 2004;101:3504–9.
34. Hejtmanec JF, Jiao X, Li A, Sergeev YV, Ding X, Sharma AK, Chan CC, Medina I, Edwards AO. Mutations in KCNJ13 cause autosomal-dominant snowflake vitreoretinal degeneration. *Am J Hum Genet*. 2008;82:174–80.
35. Hirose T, Lee KY, Schepens CL. Snowflake degeneration in hereditary vitreoretinal degeneration. *Am J Ophthalmol*. 1974;77:143–53.
36. Hoornaert KP, Marik I, Kozłowski K, Cole T, Le Merrer M, Leroy JG, Coucke PJ, Sillence D, Mortier GR. Czech dysplasia metatarsal type: another type II collagen disorder. *Eur J Hum Genet*. 2007;15:1269–75.
37. Hoornaert KP, Vereecke I, Dewinter C, et al. Stickler syndrome caused by COL2A1 mutations: genotype-phenotype correlation in a series of 100 patients. *Eur J Hum Genet*. 2010;18:872–80.
38. Khalifa O, Imtiaz F, Allam R, et al. A recessive form of Marshall syndrome is caused by a mutation in the COL11A1 gene. *J Med Genet*. 2012;49:246–8.
39. Kaufman SJ, Goldberg MF, Orth DH, Fishman GA, Tessler H, Mizuno K. Autosomal dominant vitreoretinopathy. *Arch Ophthalmol*. 1982;100:72–8.
40. Kloeckener-Gruissem B, Neidhardt J, Magyar I, Plauchu H, Zech JC, Morlé L, Palmer-Smith SM, Macdonald MJ, Nas V, Fry AE, Berger W. Novel VCAN mutations and evidence for unbalanced alternative splicing in the pathogenesis of Wagner syndrome. *Eur J Hum Genet*. 2013;21:352–6.
41. Lang GE, Laudi B, Pfeiffer RA. Autosomal dominant vitreoretinal dystrophy with skeletal dysplasia in one generation. *Klin Monatsbl Augenheilkd*. 1991;198:207–14.
42. Liu HX, Cartegni L, Zhang MQ, Krainer AR. A mechanism for exon skipping caused by nonsense or missense mutations in BRCA1 and other genes. *Nat Genet*. 2001;27:55–8.
43. Linsenmayer TF, Gibney E, Gordon EG, Marchant JK, Hayashi M, Fitch JM. Extracellular matrices of the developing chick retina and cornea. *Invest Ophthalmol Vis Sci*. 1990;31:1271–6.
44. Marini JC, Forlino A, Cabral WA, et al. Consortium for osteogenesis imperfecta mutations in the helical domain of type I collagen:

- regions rich in lethal mutations align with collagen binding sites for integrins and proteoglycans. *Hum Mutat.* 2007;28:209–21.
45. Marjava M, Hoornaert KP, Bartholdi D, et al. A report on 10 new patients with heterozygous mutations in the COL11A1 gene and a review of genotype-phenotype correlations in type XI collagenopathies. *Am J Med Genet.* 2007;143A:258–64.
 46. Martin S, Richards AJ, Yates JR, Scott JD, Pope M, Snead MP. Stickler syndrome: further mutations in COL11A1 and evidence for additional locus heterogeneity. *Eur J Hum Genet.* 1999;7:807–14.
 47. Mayne R, Brewton RG, Mayne PM, Baker JR. Isolation and characterization of the chains of type V/type XI collagen present in bovine vitreous. *J Biol Chem.* 1993;268:9381–6.
 48. McLeod D, Black GC, Bishop PN. Vitreous phenotype: genotype correlation in Stickler syndrome. *Graefes Arch Clin Exp Ophthalmol.* 2002;240:63–5.
 49. Meredith SP, Richards AJ, Flanagan DW, Scott JD, Poulson AV, Snead MP. Clinical characterisation and molecular analysis of Wagner syndrome. *Br J Ophthalmol.* 2007;91:655–9.
 50. Meredith S, Snead MP. Inherited Vitreo-retinopathies. In: Besharse JC, Bok DP, editors. *The retina and its disorders.* San Diego: Elsevier/Academic Press; 2011. p. 252–62.
 51. Morris NP, Oxford JT, Davies GB, Smoody BF, Keene DR. Developmentally regulated alternative splicing of the $\alpha 1$ (XI) collagen chain: spatial and temporal segregation of isoforms in the cartilage of fetal rat long bones. *J Histochem Cytochem.* 2000;48:725–41.
 52. Miyamoto T, Inoue H, Sakamoto Y, Kudo E, Naito T, Mikawa T, Mikawa Y, Isashiki Y, Osabe D, Shinohara S, Shiota H, Itakura M. Identification of a novel splice site mutation of the CSPG2 gene in a Japanese family with Wagner syndrome. *Invest Ophthalmol Vis Sci.* 2005;46:2726–35.
 53. Mukhopadhyay A, Nikopoulos K, Maugeri A, de Brouwer AP, van Nouhuys CE, Boon CJ, Perveen R, Zegers HA, Wittebol-Post D, van den Biesen PR, van der Velde-Visser SD, Brunner HG, Black GC, Hoyng CB, Cremers FP. Erosive vitreo-retinopathy and Wagner disease are caused by intronic mutations in CSPG2/Versican that result in an imbalance of splice variants. *Invest Ophthalmol Vis Sci.* 2006;47:3565–72.
 54. Nagendran S, Richards AJ, McNinch A, Sandford RN, Snead MP. Somatic mosaicism and the phenotypic expression of COL2A1 mutations. *Am J Med Genet A.* 2012;158A(5):1204–7.
 55. Newsome DA, Linsenmayer TF, Trelstad RL. Vitreous body collagen. Evidence for a dual origin from the neural retina and hyalocytes. *J Cell Biol.* 1976;71:59–67.
 56. Pan Q, Shai O, Lee LJ, Frey BJ, Blencowe BJ. Deep surveying of alternative splicing complexity in the human transcriptome by high-throughput sequencing. *Nat Genet.* 2008;40:358–63.
 57. Parma ES, Körkkö J, Hagler WS, Ala-Kokko L. Radial perivascular retinal degeneration: a key to the clinical diagnosis of an ocular variant of Stickler syndrome with minimal or no systemic manifestations. *Am J Ophthalmol.* 2002;134:728–34.
 58. Pollack A, Uchenik D, Chemke J, Oliver M. Prophylactic laser photocoagulation in hereditary snowflake vitreoretinal degeneration. A family report. *Arch Ophthalmol.* 1983;101:1536–9.
 59. Poulson AV, Hooymans JM, Richards AJ, Bearcroft P, Murthy R, Baguley DM, Scott JD, Snead MP. Clinical features of type 2 Stickler syndrome. *J Med Genet.* 2004;41:e107.
 60. Printzlau A, Andersen M. Pierre Robin sequence in Denmark: a retrospective population-based epidemiological study. *Cleft Palate Craniofac J.* 2004;41:47–52.
 61. Rai A, Wordworth P, Coppock JS, Zaphiropoulos GC, Struthers GR. Hereditary arthro-ophthalmopathy (Stickler syndrome): a diagnosis to consider in familial premature osteoarthritis. *Br J Rheumatol.* 1994;33:1175–80.
 62. Reardon A, Heinegård D, McLeod D, Sheehan JK, Bishop PN. The large chondroitin sulphate proteoglycan versican in mammalian vitreous. *Matrix Biol.* 1998;17:325–33.
 63. Reardon AJ, Le Goff M, Briggs MD, McLeod D, Sheehan JK, Thornton DJ, Bishop PN. Identification in vitreous and molecular cloning of opticin, a novel member of the family of leucine-rich repeat proteins of the extracellular matrix. *J Biol Chem.* 2000;275:2123–9.
 64. Richards AJ, Yates JR, Williams R, Payne SJ, Pope FM, Scott JD, et al. A family with Stickler syndrome type 2 has a mutation in the COL11A1 gene resulting in the substitution of glycine 97 by valine in alpha 1 (XI) collagen. *Hum Mol Genet.* 1996;5:1339–43.
 65. Richards AJ, Martin S, Yates JRW, Baguley DM, Pope FM, Scott JD, et al. COL2A1 exon 2 mutations: relevance to the Stickler and Wagner syndromes. *Br J Ophthalmol.* 2000;84:364–71.
 66. Richards AJ, Baguley DM, Yates JR, Lane C, Nicol M, Harper PS, Scott JD, Snead MP. Variation in the vitreous phenotype of Stickler syndrome can be caused by different amino acid substitutions in the X position of the type II collagen Gly-X-Y triple helix. *Am J Hum Genet.* 2000;67:1083–94.
 67. Richards AJ, Scott JD, Snead MP. Molecular genetics of rhegmatogenous retinal detachment. *Eye.* 2002;16:388–92.
 68. Richards AJ, Morgan J, Bearcroft PW, Pickering E, Owen MJ, Holmans P, Williams N, Tysoe C, Pope FM, Snead MP, Hughes H. Vitreo-retinopathy with phalangeal epiphyseal dysplasia, a type II collagenopathy resulting from a novel mutation in the C-propeptide region of the molecule. *J Med Genet.* 2002;39:661–5.
 69. Richards AJ, Meredith S, Poulson A, Bearcroft P, Crossland G, Baguley DM, Scott JD, Snead MP. A novel mutation of COL2A1 resulting in dominantly inherited rhegmatogenous retinal detachment. *Invest Ophthalmol Vis Sci.* 2005;46:663–8.
 70. Richards AJ, Laidlaw M, Whittaker J, Treacy R, Rai H, Bearcroft P, et al. High efficiency of mutation detection in type 1 stickler syndrome using a two stage approach: vitreoretinal assessment coupled with exon sequencing for screening COL2A1. *Hum Mutat.* 2006;27:696–704.
 71. Richards AJ, Laidlaw M, Meredith SP, Shankar P, Poulson AV, Scott JD, Snead MP. Missense and silent mutations in COL2A1 result in Stickler syndrome but via different molecular mechanisms. *Hum Mutat.* 2007;28:639.
 72. Richards AJ, Snead MP. The influence of pre-mRNA splicing on phenotypic modification in Stickler's syndrome and other type II collagenopathies. *Eye.* 2008;22:1243–50.
 73. Richards AJ, McNinch A, Martin H, Oakhill K, Rai H, Waller S, et al. Stickler syndrome and the vitreous phenotype: mutations in COL2A1 and COL11A1. *Hum Mutat.* 2010;31:E1461–71.
 74. Richards AJ, McNinch A, Whittaker J, Treacy B, Oakhill K, Poulson A, Snead MP. Splicing analysis of unclassified variants in COL2A1 and COL11A1 identifies deep intronic pathogenic mutations. *Eur J Hum Genet.* 2012;20:552–8.
 75. Richards AJ, Fincham GS, McNinch AM, Hill D, Poulson AV, Castle B, et al. Alternative splicing modifies the effect of mutations in COL11A1 and results in recessive type 2 Stickler syndrome with profound hearing loss. *J Med Genet.* 2013;50(11):765–71.
 76. Robertson DM, Link TP, Rostvold JA. Snowflake degeneration of the retina. *Ophthalmology.* 1982;89:1513–7.
 77. Ronan SM, Tran-Viet KN, Burner EL, Metlapally R, Toth CA, Young TL. Mutational hot spot potential of a novel base pair mutation of the CSPG2 gene in a family with Wagner syndrome. *Arch Ophthalmol.* 2009;127:1511–9.
 78. Rose PS, Ahn NU, Levy HP, Ahn UM, Davis J, Liberfarb RM, et al. Thoracolumbar spinal abnormalities in Stickler syndrome. *Spine.* 2001;26:403–9.
 79. Ryan MC, Sandell LJ. Differential expression of a cysteine-rich domain in the amino-terminal propeptide of type II (cartilage)

- procollagen by alternative splicing of mRNA. *J Biol Chem.* 1990;265:10334–9.
80. Sergouniotis PI, Davidson AE, Mackay DS, Li Z, Yang X, Plagnol V, Moore AT, Webster AR. Recessive mutations in *KCNJ13*, encoding an inwardly rectifying potassium channel subunit, cause Leber congenital amaurosis. *Am J Hum Genet.* 2011;89:183–90.
 81. Shanske A, Bogdanow A, Shprintzen RJ, Marion RW. Marshall syndrome and a defect at the *COL11A1* locus. *Am J Hum Genet.* 1998;63:1558–61.
 82. Sirko-Osadsa DA, Murray MA, Scott JA, Lavery MA, Warman ML, Robin NH. Stickler syndrome without eye involvement is caused by mutations in *COL11A2*, the gene encoding the alpha 2(XI) chain of type XI collagen. *J Pediatr.* 1998;132:368–71.
 83. Snead MP, Yates JRW, Williams R, Payne SJ, Pope FM, Scott JD. Stickler syndrome Type 2 and linkage to the *COL11A1* gene. *Ann N Y Acad Sci.* 1996;785:331–2.
 84. Snead MP, Yates JR. Clinical and molecular genetics of Stickler syndrome. *J Med Genet.* 1999;36:353–9.
 85. Snead MP, McNinch AM, Poulson AV, Bearcroft P, Silverman B, Gomersall P, Parfect V, Richards AJ. Stickler syndrome, ocular only variants and a key diagnostic role for the ophthalmologist. *Eye.* 2011;25:1389–400.
 86. Snead MP. Retinal detachment in childhood. In: Hoyt CS, Taylor D, editors. *Pediatric ophthalmology and strabismus.* 4th ed. Edinburgh: Saunders/Elsevier; 2013. p. 530–42.
 87. Spranger J, Winterpacht A, Zabel B. The type II collagenopathies: a spectrum of chondrodysplasias. *Eur J Pediatr.* 1994;153:56–65.
 88. Spranger J, Menger H, Mundlos S, Winterpacht A, Zabel B. Kniest dysplasia is caused by dominant collagen II (*COL2A1*) mutations: parental somatic mosaicism manifesting as Stickler phenotype and mild spondyloepiphyseal dysplasia. *Pediatr Radiol.* 1994;24:431–5.
 89. Stickler GB, Hughes W, Houchin P. Clinical features of hereditary progressive arthro-ophthalmopathy (Stickler syndrome): a survey. *Genet Med.* 2001;3:192–6.
 90. Szymko-Bennett YM, Mastroianni MA, Shotland LI, Davis J, Ondrey FG, Balog JZ, et al. Auditory dysfunction in stickler syndrome. *Arch Otolaryngol Head Neck Surg.* 2001;127:1061–8.
 91. Thompson JA, Snead MP, Billington BM, Barrie T, Thompson JR, Sparrow JM. National audit of the outcome of primary surgery for rhegmatogenous retinal detachment. I Samples and methods. *Eye.* 2002;16:766–70.
 92. Thompson JA, Snead MP, Billington BM, Barrie T, Thompson JR, Sparrow JM. National audit of the outcome of primary surgery for rhegmatogenous retinal detachment. II. Clinical outcomes. *Eye.* 2002;16:771–7.
 93. Tompson SW, Bacino CA, Safina NP, Bober MB, Proud VK, Funari T, Wangler MF, Nevarez L, Ala-Kokko L, Wilcox WR, et al. Fibrochondrogenesis results from mutations in the *COL11A1* type XI collagen gene. *Am J Hum Genet.* 2010;87:708–12.
 94. Tran VK, Takeshima Y, Zhang Z, Yagi M, Nishiyama A, Habara Y, Matsuo M. Splicing analysis disclosed a determinant single nucleotide for exon skipping caused by a novel intraexonic four-nucleotide deletion in the dystrophin gene. *J Med Genet.* 2006;43:924–30.
 95. Ung T, Comer MB, Ang AJS, Sheard R, Lee C, Poulson AV, Newman DK, Scott JD, Richards AJ, Snead MP. Clinical features and surgical management of retinal detachment secondary to round retinal holes. *Eye.* 2005;19:665–9.
 96. Van Camp G, Snoeckx RL, Hilgert N, van den Ende J, Fukuoka H, Wagatsuma M, et al. A new autosomal recessive form of Stickler syndrome is caused by a mutation in the *COL9A1* gene. *Am J Hum Genet.* 2006;79:449–57.
 97. Vincent A, McAlister C, Vandenhoven C, Héon E. BEST1-related autosomal dominant vitreoretinopathopathy: a degenerative disease with a range of developmental ocular anomalies. *Eye.* 2011;25:113–8.
 98. Warner LR, Brown RJ, Yingst SM, Oxford JT. Isoform-specific heparan sulfate binding within the amino-terminal noncollagenous domain of collagen $\alpha 1(XI)$. *J Biol Chem.* 2006;281:39507–16.
 99. Wilkin DJ, Mortier GR, Johnson CL, Jones MC, de Paepe A, Shohat M, et al. Correlation of linkage data with phenotype in eight families with Stickler syndrome. *Am J Med Genet.* 1998;80:121–7.
 100. Williams CJ, Considine EL, Knowlton RG, Reginato A, Neumann G, Harrison D, Buxton P, Jimenez S, Prockop DJ. Spondyloepiphyseal dysplasia and precocious osteoarthritis in a family with an Arg75->Cys mutation in the procollagen type II gene (*COL2A1*). *Hum Genet.* 1993;92:499–505.
 101. Yaguchi H, Ikeda T, Osada H, Yoshitake Y, Sasaki H, Yonekura H. Identification of the *COL2A1* mutation in patients with type I Stickler syndrome using RNA from freshly isolated peripheral white blood cells. *Genet Test Mol Biomarkers.* 2011;15:231–7.
 102. Zhidkova NI, Justice SK, Mayne R. Alternative mRNA processing occurs in the variable region of the pro- $\alpha 1(XI)$ and pro- $\alpha 2(XI)$ collagen chains. *J Biol Chem.* 1995;270:9486–93.

Vitreous Cytokines and Regression of the Fetal Hyaloid Vasculature

I.D.

Kenneth M.P. Yee, Edward P. Feener, Benbo Gao,
Lloyd Paul Aiello, Michele C. Madigan, Jan Provis,
Fred N. Ross-Cisneros, Alfredo A. Sadun, and J. Sebag

Outline

- I. Introduction
- II. Structure of the Hyaloid Vasculature
- III. Timeline of Fetal Hyaloid Vasculature Regression
 - A. Lower Mammals
 - B. Humans
- IV. Vitreous Cytokine Expression
 - A. Comparative Analysis to a Murine Model of Vitreous Embryogenesis
- V. Mechanisms of Fetal Vessel Regression
 - A. Apoptosis
 - B. Macrophagy
 - 1. Macrophage Adhesion to Hyaloid Vessels
 - 2. Macrophage-Induced Apoptosis
 - C. Antiangiogenesis
 - 1. Angiogenesis Promoters
 - 2. Angiogenesis Inhibitors
 - D. Autophagy
 - E. External Stimuli

VI. Miscellaneous Proteins

VII. Genetic Influences

Conclusions

References

Keywords

Vitreous • Embryogenesis • Hyaloid artery • Vasa hyaloidea propria • Tunica vasculosa lentis • Pupillary membrane • Vascular regression • Cytokines • Ingenuity Pathways Bioinformatic Analysis • Immunohistochemistry

Key Concepts

1. Regression of the fetal hyaloid vasculature is a vital process required for vision that can impact the proper development of vitreous, retina, and other ocular structures.
2. Although the timing of hyaloid vasculature regression is well defined, little is known about the molecular mechanisms involved. Recent proteomic studies in mice identified 770 proteins, while studies of human embryonic vitreous identified 896 unique proteins. Changes in the human fetal proteome during the second trimester and differences in comparison to young adult human vitreous are being studied to identify molecules and pathways that may be involved in the regression of the hyaloid vasculature.
3. Many complex mechanisms must occur sequentially and concurrently for proper and complete hyaloid vasculature regression. Apoptosis, increased expression of antiangiogenic factors, reduced expression of endothelial survival factors, macrophagy, and perhaps external stimuli are all involved in regression of the hyaloid vasculature.

K.M.P. Yee, BS • J. Sebag, MD, FACS, FRCOphth, FARVO (✉)
VMR Institute for Vitreous Macula Retina, 7677 Center Avenue,
suite 400, Huntington Beach, CA 92647, USA

Doheny Eye Institute, Los Angeles, CA USA
e-mail: jsebag@VMRinstitute.com

E.P. Feener, PhD • B. Gao, PhD
Department of Medicine, Harvard Medical School, Boston, MA, USA

Beetham Eye Institute, Joslin Diabetes Center, Boston, MA, USA

L.P. Aiello, MD, PhD, FARVO
Beetham Eye Institute, Joslin Diabetes Center, Boston, MA, USA

Department of Ophthalmology, Harvard Medical School,
Boston, MA, USA

M.C. Madigan, PhD, OD
School of Optometry and Vision Science, University of New South
Wales, Sydney, NSW, Australia

Save Sight Institute, Sydney University, Sydney, NSW, Australia

J. Provis, PhD, FARVO
ANU Medical School, Australian National University, Canberra,
Australia

A.A. Sadun, MD, PhD, FARVO • F.N. Ross-Cisneros
Doheny Eye Institute/UCLA, Los Angeles, CA, USA

I. Introduction

The fetal hyaloid vasculature plays a critical role in many aspects of proper ocular development. The hyaloid artery (HA) is a large vessel that extends from the optic disc through the vitreous body where it branches and extends to the posterior surface of the lens to anastomose with the tunica vasculosa lentis (TVL) which supplies nutrients to the developing lens in the fetus (Figure I.D-1). In humans, the entire embryonic vascular system regresses by birth, which is necessary for media clarity and normal vision. Regression of the hyaloid vasculature is a very complex process likely requiring the participation of many events. The mechanisms of hyaloid vessel regression are not known, but insight could be obtained by understanding how this fetal vasculature forms. One study of human embryonic vitreous revealed the presence of blood islands composed of aggregates of primitive erythroblasts and hemangioblasts, as early as the seventh week of gestation (WG) [1]. These cell aggregates express hematopoietic stem cell markers, and the ligands for these markers are expressed in high concentrations in the lens and retina, probably functioning to guide the cells into the vitreous body assembling the fetal vitreous vasculature by hemo-vasculogenesis [2].

A better understanding of the mechanisms of fetal hyaloid vasculature formation and regression would help in understanding conditions that impair vision due to hyaloid vessel persistence in youth, since it is necessary that fetal vitreous vessels regress to establish a clear medium through which light can traverse to reach the retina. The mechanisms of this process may also provide insight into how nature induces blood vessel regression. Unraveling these secrets could enable new avenues of research to develop ever more-effective therapies for pathological neovascularization in diseases such as exudative age-related macular degeneration, ischemic proliferative (diabetic and other) retinopathies, and metastatic carcinomas.

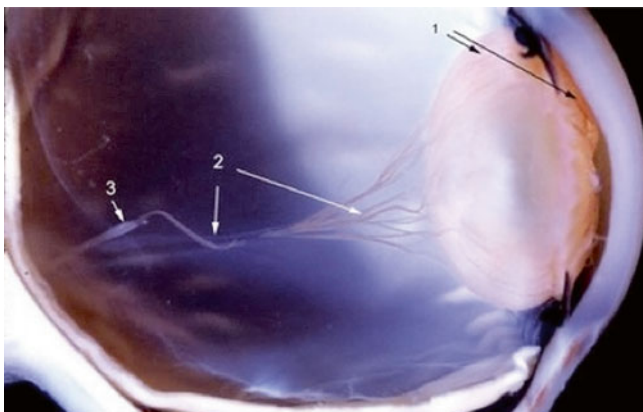


Figure I.D-1 The tunica vasculosa lentis (TVL) surrounds and feeds the developing lens (1). The vasa hyaloidea propria (2) arises from the hyaloid artery (3) and forms anastomoses with the TVL

II. Structure of the Hyaloid Vasculature

The anatomy of the hyaloid vasculature was first described by Ida Mann in 1928 [2]. During this time, studying the hyaloid vasculature was difficult because fixation methods would destroy hyaloid structures and because freshly excised eyes were difficult to dissect while preserving fetal vitreous structures. Slit-lamp biomicroscopy made it possible to observe Cloquet's canal, a clear central space through the central vitreous that was once occupied by the hyaloid artery *in utero*. More thorough examination of the hyaloid vasculature has been made possible by advances of *in vivo* and fixed tissue imaging.

The hyaloid vasculature is first seen in humans at approximately the fourth week of fetal development [see chapter II.A. Development and developmental disorders of vitreous]. It is comprised of the main trunk of the *hyaloid artery* (HA) which divides into the *vasa hyaloidea propria* (VHP), a vascular network which divides further to form a dense capillary network called the *tunica vasculosa lentis* (TVL) that approaches and attaches to the posterior lens [2]. The *pupillary membrane* (PM) is an extension of the TVL that covers the anterior lens (Figure I.D-1). The well-developed primate hyaloid artery has the ultrastructural characteristics of an arteriole with a non-fenestrated intima, a multilayered smooth muscular media, a connective tissue adventitia, and a perivascular sheath. The branching networks of the HA which include the VHP, the TVL, and the pupillary membrane appear to be type A-1 alpha capillaries with non-fenestrated endothelium, incomplete pericyte layer, and a basement membrane surrounding each layer [3].

The hyaloid vasculature contains junctional complexes including zonulae and macula adherens and possible zonulae occludens between adjacent endothelial cells [4]. The hyaloid artery and its branch systems do not exhibit leakage of fluorescein dye, consistent with the presence of endothelial tight junctions [3]. A heterogeneous population of leukocyte-derived hyalocytes associated with the human hyaloid vasculature has also been demonstrated [4]. The hyaloid vasculature is further characterized by the absence of veins. All vessels of the hyaloid system are arteries, and venous drainage is accomplished through the choroidal vessels [5].

III. Timeline of Fetal Hyaloid Vasculature Regression

A. Lower Mammals

The pattern of normal hyaloid vasculature development is basically the same in mice as in rats and rabbits. In contrast to humans, the hyaloid system in these species regresses after birth. In mice the hyaloid vascular system forms at

embryonic day (ED) 10.5 and is fully developed by ED 13.5. Apoptosis of the endothelial cells that constitute the TVL occurs as early as ED 17.5, but the TVL persists until post-gestational day (PGD) 16 and undergoes gradual regression from PGD 14–30 [6, 7]. The VHP and PM disappear between PGD 12 and 16 in rodents and between PGD 10 and 12 in rabbits [8]. During vascular regression in rats, apoptosis occurs in pericytes as well as in endothelial cells. Capillary apoptosis occurs mostly from day 10 to 20 after birth [9]. The earliest detectable regression-related changes are apparent around day 3 and initially involve the capillaries surrounding the posterior lens, then proceed posteriorly [10].

B. Humans

At about the 48 mm stage of embryologic development (ninth week of gestation, WG), the fetal intraocular blood system has reached maximal development, and thereafter every subsequent stage reveals signs of vessel regression [2, 4]. Regression of the hyaloid vasculature begins at 12–13 WG, and complete involution is achieved by 35–36 WG [1, 6, 11, 12]. Variability in the timeline of regression may exist, as another human study showed that regression is not evident until 18 WG and is complete by 29 WG [13]. *In vivo* ultrasonography has suggested that the hyaloid vessels are detectable at 20 WG and that regression begins in the early third trimester. By 30 WG, the hyaloid artery is normally not detectable [14]. What is likely, however, is that all cytokine stimuli for hyaloid vessel regression predate the aforementioned cellular events.

After the 65 mm stage, atrophy of the fetal vascular system becomes apparent beginning with the elongation and thinning of the vessels of the VHP then the TVL, followed by the PM. Complete involution of the VHP, TVL, and PM occurs by about 8.5 months. During the eighth month of gestation, the main trunk of the hyaloid artery gradually atrophies and eventually disappears. Cellular debris and macrophages fill the lumen forming a plug that occludes blood flow and promotes necrosis and phagocytosis of the vessel [15]. Remnants of the atrophied vessels can sometimes form corkscrew configurations after they lose connection with the main trunk due to the elastic properties of endothelial cells and/or their basal laminae [2].

Before birth and up to the fourth week after birth, the vessel walls appear atrophic as well as acellular and the lumen is occluded by a thrombus [3]. Although the timeline for hyaloid development and regression is well defined, the exact molecular mechanisms are not well understood, especially in humans. Insight into this aspect of hyaloid regression may be gained by study of cytokine expression and the key signals and mechanisms underlying the fetal vessel regression.

IV. Vitreous Cytokine Expression

Recent proteomic studies of embryonic human vitreous, aged 14 to 20 WG (during the early period of hyaloid regression), identified the presence of 896 unique protein peptides [16]. Studies are ongoing to ascertain how the human fetal vitreous proteome compares to the young adult and to determine whether any changes in the levels of protein expression can be identified that may have relevance to the phenomenon of fetal hyaloid vasculature regression.

Bioinformatic evaluation of some of this data with Ingenuity Pathway Analysis (IPA) determined that there was generalized decrease in protein synthesis pathways [16], consistent with a decrease in cell metabolism during apoptosis and cell death as the vessels regress. Figure I.D-2a demonstrates that many of the detected proteins with a significant decrease in expression in vitreous during the period of regressing hyaloid vessels are involved with protein synthesis pathways and most of these are known to be cytoplasmic.

Since the cellular *primary* vitreous is replaced by an acellular collagenous *secondary* vitreous, an increase in proteins involved in connective tissue pathways is to be expected. Figure I.D-2b demonstrates that many of the proteins with significantly increased expression during the period of hyaloid vascular regression are involved in collagen synthesis and connective tissue formation [16]. The connective tissue pathway proteins that increased in expression were mostly extracellular.

During this period, there was also a marked decrease in the free radical scavenging pathway [16]. Reactive oxygen species (ROS) have been shown to induce apoptosis in many tissue types. Free radicals can start chain reactions of oxidation, which cause cell damage or death. Antioxidant binding of free radical intermediates halts these processes. Thus, a reduction in free radical scavenging during hyaloid regression would promote the induction of apoptosis via ROS during this period. Consistent with this, IPA bioinformatic analysis revealed that many of the proteins with decreased expression during hyaloid regression are involved in free radical scavenging.

Proteins involved in small molecule biochemistry were also markedly decreased in vitreous from 14 to 20 WG [16]. Small molecules (<900 Da) typically regulate biological processes and can rapidly diffuse across membranes, a characteristic necessary for bioavailability, allowing these regulatory molecules to reach and interact with intracellular action sites [19, 20]. As the cellular primary vitreous is replaced by an acellular secondary vitreous during development, the biological requirement for small molecule-dependent regulation of cellular processes likely diminishes, consistent with the observed decreased expression.

According to the Science Signaling Journal (<http://stke.sciencemag.org/about/help/cm.dtl>), canonical pathways are “idealized or generalized pathways that represent common

properties of a particular (specific to tissues, cell lines, etc.) signaling module or pathway.” In human embryonic vitreous, the two most relevant canonical pathways determined by IPA bioinformatic analysis were EIF2 signaling and protein ubiquitination [16]. Molecules involved in these canonical pathways decreased in detection from 14 to 20 WG. EIF2 activity regulates mRNA translation and regulates protein synthesis in response to various stimuli. Decreased EIF2 activity concurrent with hyaloid vasculature regression may be explained by a reduced need for cellular protein synthesis as a mostly acellular vitreous is formed. The protein ubiquitination pathway plays a major role in the degradation of short-lived regulatory proteins involved in many cellular processes including apoptosis, cell proliferation, and transcription regulation [21]. Decreased detection of molecules involved in protein ubiquitination pathways may be due to reduced need for signals involved in endothelial cell proliferation, pro-apoptotic factors, or complex proteins in general, as the acellular secondary vitreous is formed.

A. Comparative Analysis to a Murine Model of Vitreous Embryogenesis

A previous histologic and proteomic study was performed on vitreous of developing postnatal mice [22]. In this model, the hyaloid network is still prominent at post-gestation day 1 (PGD 1) but is mostly regressed and nonfunctional by PGD 16. Two-dimensional electrophoresis was utilized to investigate the protein profile of the mouse vitreous spanning the period of hyaloid regression (PGD 1–16) and found 770 protein spots [21]. Both the number of detected protein spots and the volume of the spots decreased from PGD 1–16. These findings are similar to the human embryonic vitreous study where three times as many proteins decreased as increased during hyaloid vessel regression [16]. In the mouse vitreous, the number of proteins that had an increased spot volume compared to PGD 1 decreased at PGD 16. The active protein expression and existence in the earlier post-gestation days may indicate that these particular proteins are involved in the actual process of vessel degradation. This study also found that proteins with decreased spot volume relative to PGD 1 increased in number at PGD 16 [21].

A decrease in the number of different proteins and the levels of protein expression during hyaloid vessel regression is consistent with the replacement of a highly vascularized primary vitreous with a largely acellular secondary vitreous during this period. Although the overall changes in protein profiles are similar in human and mice, there were no proteins identified that changed expression significantly in both humans and mice, perhaps limiting the applicability of animal studies to humans. In mice, proteins that were found to be upregulated in PGD 1 were involved in energy metabo-

lism as well as cell proliferation and development. Proteins upregulated in PGD 16 were cancer- and apoptosis-related or inflammatory proteins.

V. Mechanisms of Fetal Vessel Regression

Many processes have been implicated in normal hyaloid vascular regression. Vitreous itself has been shown to be an inhibitor of angiogenesis and inhibits tumor-induced neovascularization in the rabbit cornea by as much as 37 % [23]. Apoptosis, autophagy, macrophagy, antiangiogenesis, reduced expression of survival factors, and some external environmental factors have all been associated with the regression of the hyaloid vasculature. All these biological processes are likely initiated and promoted by cytokines under the influence of protein synthesis regulation, both up and down, as defined above.

A. Apoptosis

Apoptosis has been definitively proven to contribute to the regression of the fetal intraocular vasculature system. *Pro-apoptotic proteins*, *Bax* and *Bak*, of the B-cell lymphoma 2 (*bcl-2*) family may serve overlapping functions in the promotion of hyaloid vessel regression. Complete involution of the hyaloid vessels was not observed in the eyes of *bax(-/-) bak(-/-)* mice, indicating that only deficiencies in both proteins would lead to pathological persistence of the hyaloid vasculature [24]. In the aforementioned study of human embryonic vitreous, isoform alpha of Bax protein decreased during the period of maximal hyaloid regression [16]. As hyaloid regression progresses, there are fewer endothelial cells remaining to undergo apoptosis, and this may explain the decreased detection of pro-apoptotic Bax at the end phase of hyaloid regression [21]. The presence of either of these pro-apoptotic *bcl-2* apoptosis promoters is sufficient for complete hyaloid regression [23].

Bim is another member of the *bcl-2* family that may influence apoptosis of the hyaloid vessels. In mice that do not express *Bim*, there is significant attenuation of hyaloid vessel regression [25]. Interestingly, hyaloid vessel regression is not affected in the absence of *bcl-2* in mice [26].

Vitreous hyalocytes are the only cell type in the eye that express all four forms of *transforming growth factor-β* (TGF-β) [27]. Hyalocyte production of TGF-β may contribute to the apoptotic process of hyaloid regression [see chapter II.D. Hyalocytes]. TGF-β can induce apoptosis through the SMAD or DAXX pathways and can inhibit vascular endothelial cell proliferation, although TGF-β has also been shown to be pro-angiogenic [28]. TGF-β is also required for *Arf* promoter activation that is induced before hyaloid vessel regression [29]. *Arf* regulates vascular regression in a tumor protein 53

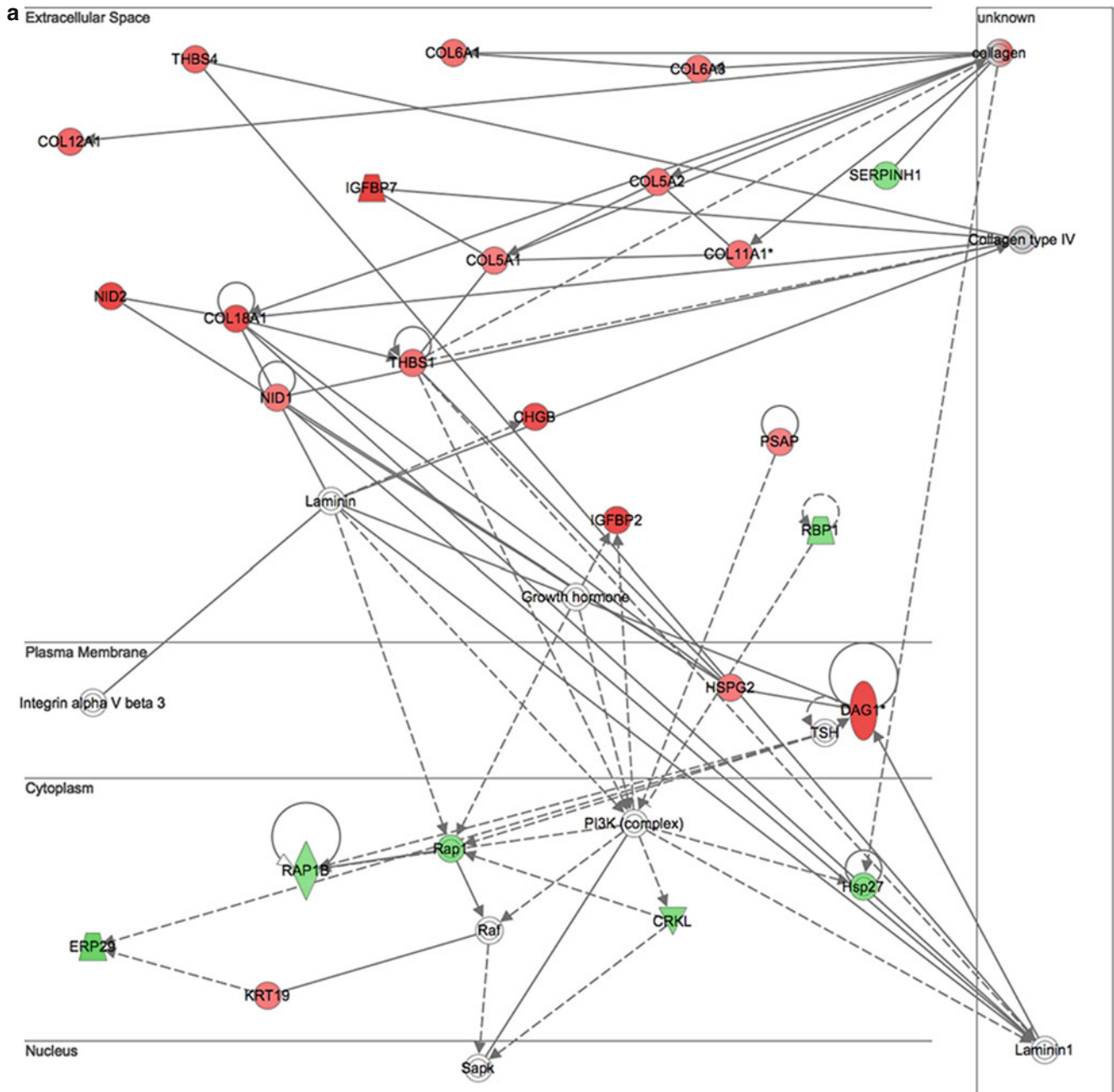


Figure I.D-2 (a) The connective tissue pathway was upregulated consistent with the formation of a collagenous secondary vitreous (Bonferroni adjusted P -value < 0.00005). The overwhelming majority

of this activity occurs in the extracellular compartment [red=upregulated]. Of note is the localization in the extracellular space

(p53) independent manner [30]. *Activin receptor-like kinase-1* (ALK-1), a type 1 receptor for TGF- β , may also play a role in the regression of the hyaloid vasculature as ALK-1 overexpression has been shown to inhibit basic fibroblast growth factor-induced corneal neovascularization [31]. TGF- β 2 has been detected in human vitreous during early development, and its localization has been associated with the development and regression of the hyaloid vascular network [32]. In mice with *p53* deficiency, there is persistence

of parts of the hyaloid vasculature, and these parts eventually develop into fibrovascular plaques that are analogous to persistent hyperplastic primary vitreous. This indicates a role for p53-dependent apoptosis in hyaloid vascular regression [33].

Prolactin (PRL) is proteolytically processed to 16 K-PRL fragments with potent pro-apoptotic and antiangiogenic properties. Apoptosis of the hyaloid vessels in neonatal rats is inhibited by intravitreal injections of neutralizing anti-PRL antibodies, suggesting a role for PRL in hyaloid regression [34].

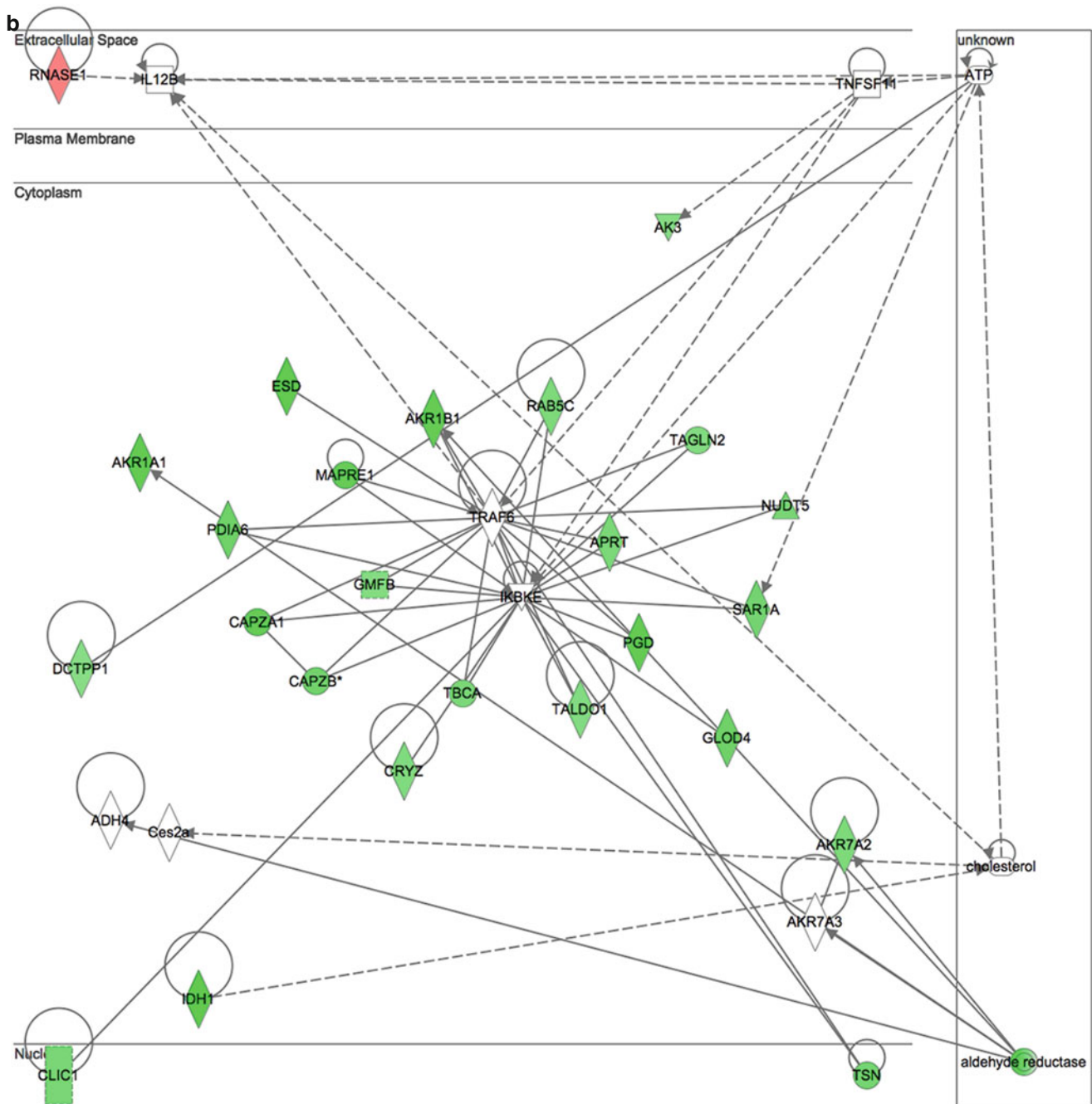


Figure I.D-2b (continued) **(b)** The small molecule biochemistry pathway showed reduced activity during the same period, suggesting a role for reactive oxygen species-driven apoptosis and a reduction in

cellular processes as the acellular secondary vitreous is formed and the hyaloid vasculature regresses (Bonferroni adjusted P -value < 0.00005) [green = downregulated]. Of note is the localization in the cytoplasm

Bovine endothelial cells have decreased viability when cultured in the presence of vitreous, and ascorbic acid from the vitreous has been identified as an apoptosis-inducing factor [35]. Concentrations of ascorbic acid similar to vitreous levels can reduce endothelial cell viability and may function as an inhibitor of neovascularization, which can be completely inhibited by antioxidants [36].

B. Macrophagy

Macrophages induce ocular tissue remodeling and hyaloid vessel regression by phagocytosis of dead cells and by inducing vascular endothelial cell apoptosis [35]. Disruption of mature macrophages in mice leads to persistence of the hyaloid vasculature with the PM retained for up to 14 days

after normal regression [37]. This suggests that macrophages are actively involved in targeted cell death of the hyaloid vessels. Human vitreous and hyalocyte-conditioned culture medium were shown to inhibit human vascular endothelial cell growth *in vitro* [38, 39] in a dose- and time-dependent manner [40]. Macrophages and hyalocytes (macrophage-like cells) have been found adjacent to hyaloid vessels by electron microscopy and immunostaining and are believed to be essential for regression of the hyaloid vascular system [8, 36, 41]. Morphological and immunophenotypic characteristics of the macrophages surrounding the PM are similar to hyalocytes in adult rat vitreous [42]. Macrophage-vascular endothelial cell interactions allow for cooperation between the Wnt and angiopoietin (Ang) pathways, although it remains unclear how macrophages are activated or the exact mechanism of their interaction with vascular endothelial cells.

1. Macrophage Adhesion to Hyaloid Vessels

Ninjurin 1 (nerve injury-induced protein; *Ninj1*) has been shown to be temporarily upregulated in macrophages, which enhances cell-cell and cell-matrix adhesion of macrophages and stimulates the expression of Wnt7b in macrophages. *Ninj1* overexpressing macrophages decrease Ang1 and increase Ang2 in pericytes, triggering apoptosis of hyaloid vascular endothelial cells [35]. Macrophages may express *Ninj1* to increase apoptotic signals through cell-cell adhesion.

Periostin (POSTN) also supports cell adhesion and migration. Periostin is secreted by intraocular macrophages and seems to enhance regression of the hyaloid system by intensifying the adhesion of macrophages to hyaloid vessels [43]. Periostin was detected in human embryonic vitreous with no appreciable change in the level of expression over the 2nd trimester [16].

Overexpression of *Aquaporin 4* (AQP4) in the astrocytes of rats delays hyaloid regression [44]. In persistent fetal vasculature conditions, astrocytes abnormally migrate into the vitreous, ensheath the hyaloid vessels and impede the normal macrophage-endothelial cell adhesion and the process of macrophage-dependent hyaloid regression [44].

2. Macrophage-Induced Apoptosis

Impeding macrophage-vascular endothelial cell adhesion delays hyaloid vasculature regression by preventing phagocytosis. Another role of macrophages is the direct induction of programmed cell death in capillary regression. Elimination of macrophages results in persistence of the normally transient endothelial cells; these cells lack apoptotic morphology, express intracellular esterases, and continue to synthesize DNA [45]. Macrophages elicit targeted cell death by inducing apoptosis of PM endothelial cells. During

regression of the PM, cells have characteristics of apoptosis, specifically apoptotic bodies with condensed chromatin and nucleosomal fragmented DNA. Apoptosis can occur in single cells of healthy vessels or along the entire length of a capillary segment [41]. In mice, lack of *norrin*, a secreted regulatory protein normally required for ocular angiogenesis in mice impairs macrophage-induced apoptosis of hyaloid endothelial cells delaying vessel regression [46, 47]. Apoptosis and macrophage-dependent apoptosis are key to hyaloid regression although a two-step process has been proposed in previous studies. Regression of the mouse PM begins with macrophage-initiated apoptosis followed by the synchronous death of endothelial cells as a consequence of the cessation of blood flow and/or the loss of survival factors such as VEGF [48].

C. Antiangiogenesis

Many mechanisms of vascular inhibition and antiangiogenesis play significant roles in hyaloid regression. Hyaloid regression can be influenced by the downregulation and neutralization of angiogenic promoters, and/or upregulation and enhancement of angiogenic inhibitors.

1. Angiogenesis Promoters

Regression of the hyaloid vessels may be initiated by the reduction of endogenous survival factors below a critical threshold [2]. Platelet-derived growth factor (PDGF) plays a significant role in angiogenesis [49], and overexpression of PDGF-B under control of the *nestin enhancer* causes delayed regression of the hyaloid vasculature in mice [50].

Vascular endothelial growth factors (VEGFs) are another large family of signaling proteins involved in vasculogenesis (formation of new blood vessels where none exist) and angiogenesis (formation of new blood vessels from existing ones). VEGF-A is necessary for the formation of the normal hyaloid vascular system. Absence of VEGF-A in the mouse lens prevents the formation of the capillary vessels of the pupillary membrane, but does not alter the nearby hyaloid vessels at the surface of the retina [51]. Neutralization of VEGF-A causes a significant reduction in the hyaloid and retinal vasculature [52]. During the regression phase of the hyaloid vascular system, VEGF expression increases in the lens and also persists in adults. VEGF-A secreted by the lens may promote the formation of fetal vasculature, but reduction of VEGF-A does not likely cause regression of these vessels [53].

Angiopoietin-2 (Ang2) is a growth factor that is critical in physiological and pathologic angiogenesis, and physiological but not oxygen-induced vascular regression. Ang2-deficient mice show a lack of regression of the hyaloid vasculature [54].

Fibroblast growth factor (FGF) proteins are potent mitogens for endothelial cells and induce the assembly of these cells into vascular-like structures. FGF inhibition in transgenic mice causes failed regression of the hyaloid vessels and eventual massive intravitreal neovascularization [55].

2. Angiogenesis Inhibitors

Vitreous has been shown to be an effective inhibitor of neovascularization and many molecules have been identified [56]. Luty et al. showed that the anti-neovascular activity of vitreous is dose dependent and effective upon capillary endothelial cells and aortic endothelium. They also found that common glycosaminoglycans such as keratan sulfate, chondroitin sulfate-C, and hyaluronan, all found in vitreous, apparently did not inhibit angiogenesis [57]. On the other hand, a partially purified protein of MW = 6.2 K was found to inhibit vascular endothelial cell proliferation *in vitro* [58]. In another study, a 5.7 K glycoprotein has been derived from bovine vitreous, which inhibits angiogenesis possibly by disrupting collagenase activity [59].

Thrombospondins (TSP or THBS) are potent angiogenic inhibitors that directly affect endothelial cell migration, proliferation, survival, and apoptosis and antagonize VEGF activity [60]. In mice lacking thrombospondin 1 (TSP-1^{-/-}), there is a delay in the regression of hyaloid vessels. In the aforementioned proteomic studies of embryonic human vitreous during hyaloid regression, precursors of thrombospondins 1 and 4 were found to have increased expression, respectively. Increased expression of the VEGF antagonizing thrombospondins is consistent with a regressing vascular system [16].

Collagen type XVIII, alpha 1 (Col18A), is one of the multiplex in extracellular matrix proteins [61]. Proteolytic cleavage of Col18A produces endostatin, an endogenous angiogenesis inhibitor found in mice and humans [62, 63]. *Endostatin* affects many pathways that involve cell mobility or viability, thus suppressing angiogenesis. Endostatin can repress cell cycle control and anti-apoptotic mechanisms in proliferating endothelial cells and also potently inhibits endothelial cell migration [64]. Endostatin inhibits endothelial cell migration by altering FGF signal transduction disrupting cell-to-cell adhesion, cell-to-matrix adhesion, and reorganization [65]. Col18A knockout mice show delayed regression of the hyaloid vascular system, most likely due to the absence of endostatin [66]. The aforementioned proteomic study of embryonic human vitreous discovered that Col18A has increased expression during the period of hyaloid vessel regression, consistent with its potent antiangiogenic properties and a putative role in regression of the hyaloid vasculature [16].

Pigment epithelium-derived factor (PEDF), also known as serpin F1 (SERPINF1), is a multifunctional secretory

protein that has antiangiogenic functions [67–69]. PEDF has been shown to affect malignant peripheral nerve sheath tumors, prevents progression of liver metastasis in a mouse model of uveal melanoma, and has been used for therapy in multiple cancer types [70–72]. In the eye, PEDF suppresses retinal neovascularization and endothelial cell proliferation [73, 74]. In mice, PEDF knockout has a minimal effect on the regression of hyaloid vasculature; [75] however, in the aforementioned proteomic studies of embryonic human vitreous, there was an increase in expression of PEDF [16]. The lack of congruity with the mouse models casts further doubt upon the value of these models for studying human hyaloid vessel regression (see above).

It is also possible that the responsiveness to endogenous factors that induce regression can be modified, thus effecting vessel growth or regression. Such a mechanism is present in the vitreous of patients with proliferative diabetic retinopathy (PDR) where lysophosphatidic acid (LPA) has been recently shown to promote regression of blood vessels. However, PDR-vitreous mediates an insensitivity to LPA, which can be overcome pharmacologically. Thus, a decline in the responsiveness to regression factors such as LPA, which are naturally present in the vitreous, may contribute to the pathophysiology of PDR [76]. Whether this concept applies to regression of the hyaloid vasculature is presently unknown.

D. Autophagy

Autophagy is morphologically unique from apoptosis because cell death occurs in the absence of chromatin condensation with concurrent cytoplasmic vacuolization [77]. Also, phagocytes are not associated with cells that die with autophagic morphology [78, 79]. In a murine model, Kim et al. found LC3 and cleaved caspase-3 expression on regressing hyaloid vessels; these are considered respective markers of autophagy and apoptosis. Transmission EM also demonstrated cytoplasmic segregation into autophagosomes, characteristic of autophagy. Autophagic LC3-positive cells progressively decreased in a time-dependent manner. A hypoxia model revealed that LC3-II increased in a treatment time-dependent manner and that autophagy can be induced by a lack of oxygen. Activation of the autophagy pathway by >100 ng/ml of rapamycin decreased the viability of vascular endothelial cells and enhanced hyaloid regression [79]. 3-methyladenine, an autophagy blocker, however, did not completely inhibit hyaloid regression, but significantly attenuated it. Kim et al. demonstrated, for the first time, that hyaloid regression is induced by apoptosis as well as autophagy and that autophagy activation could further enhance regression of hyaloid vessels [80].

E. External Stimuli

It has been proposed that regression of the hyaloid vasculature and the PM occurs in a two-step process beginning with macrophage-dependent apoptosis, followed by the synchronous death of endothelial cells as a direct result of the cessation of blood flow and/or reduced survival factors [8, 36, 81]. Hyaloid vessel regression coincides with a progressive decrease in blood flow and velocity that is thought to be a major trigger in the regression of hyaloid vessels [82]. Arterial vasoconstriction precedes regression of the hyaloid vasculature, which has been reported to be dependent on proximal arterial vasoconstriction [83].

A scanning electron microscopy study showed that exposure to various concentrated gas mixtures of carbon dioxide, oxygen, and nitrogen created marked differences in hyaloid regression of mice when compared to control mice in air; neovascularization was not evident in these mice [84].

Ocular blood vessel development also critically depends on a light-response pathway in mice, where dark-reared mice have been observed to display persistent hyaloid structures as much as eight days postpartum. By post-gestational day (PD) 15 the persistent vessels had regressed, indicating that dark rearing results in a delayed regression. Also quantification of apoptosis at PD5 showed a reduced level, similar to that previously characterized in conditions with persistent hyaloid vasculature [85]. Melanopsin has been implicated as a candidate to mediate light-dependent vascular development because it is expressed early in both humans and mice and is known to be functional from as early as PD10 in mice and because it is expressed in retinal cells adjacent to both the retinal and hyaloid vasculatures [86]. Mice mutated in the *Opn4* melanopsin-encoding gene (*Opn4*^{-/-}) showed

normal hyaloid vessels at PD1 but persistence at PD8 and eventual complete regression by PD15, indicating that the hyaloid persistence was not long term. Dark-reared mice and *Opn4*^{-/-} mutants had VEGFA levels that were seven-fold higher than in controls, which may explain the delay in hyaloid regression. Also, dark rearing from late gestation or in the presence of an *Opn4* mutation produced the same disruption of vascular development, indicating involvement of a melanopsin-dependent light-response pathway [85]. Surprisingly, it was determined that the critical light-response period that stimulates hyaloid regression occurs *in utero* and not at birth.

VI. Miscellaneous Proteins

Dystroglycan is a lamin receptor dystrophin-associated glycoprotein which consists of two subunits, α and β . It has an important role in the formation of glio-vascular connections, cerebral vascularization, and formation of the blood-brain barrier, and thus is involved in many basic processes such as basement membrane assembly, cell survival, and cell migration [87–89]. Dystroglycan also functions as a transmembrane scaffold protein involved in adhesion and adhesion-mediated signaling. Dystroglycan can be a signal transducer from the outside of a cell to the inside or serve as a physical connection between the extracellular matrix and cytoskeleton [90].

Immunostaining (Figure I.D-3) confirmed the presence of dystroglycan on cell membranes and cell junctions of the endothelial cells in the hyaloid vessels of a 14 WG eye, consistent with dystroglycan being a transmembrane protein [16]. The role of dystroglycan in hyaloid vessel regression remains unknown, although loss of dystroglycan was shown

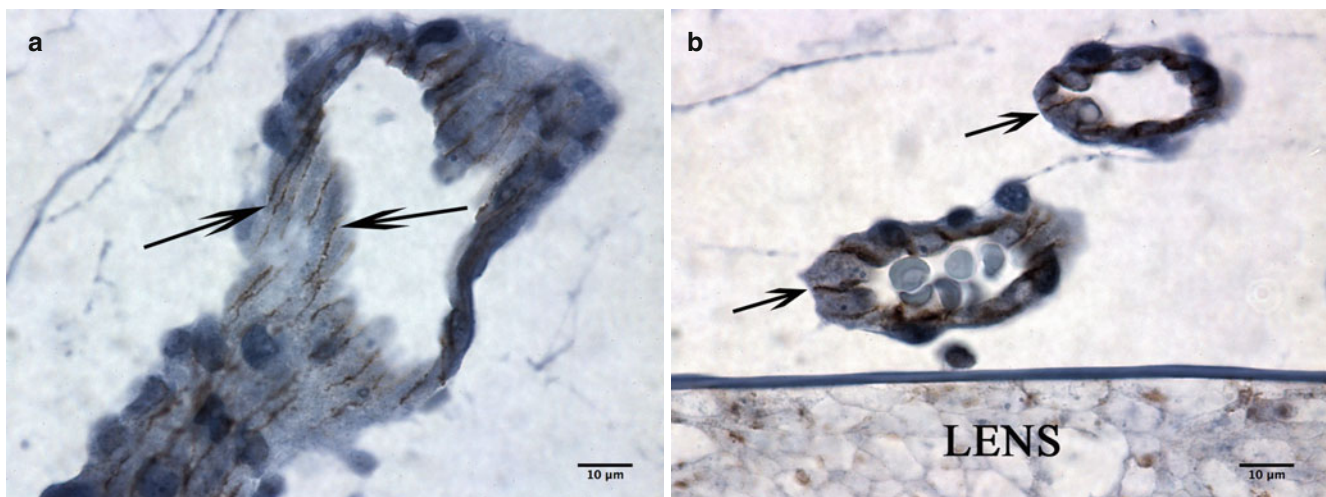


Figure I.D-3 Immunostaining for dystroglycan showed the protein localized to the cell membranes of endothelial cells at the cell junctions of hyaloid vascular endothelium (arrows). In the vitreous of a 14 WG

human, dystroglycan is seen at cell junctions of the endothelium in the (a) hyaloid trunk and the (b) tunica vasculosa lentis

to increase tumor formation in prostate cancer [91, 92], and thus further study in the eye is warranted.

Profilin-1, a cytoskeletal and cytoplasmic protein, was confirmed by immunostaining to localize to hyalocytes of the vitreous and the endothelial cells of the hyaloid artery (Figure I.D-4a) and tunica vasculosa lentis (Figure I.D-4b). However, there was no appreciable difference in immunostaining intensity throughout the 2nd trimester of development [16]. Profilin-1 has been shown to inhibit endothelial cell migration and proliferation [93]. Interruption of endothelial cell migration and proliferation is necessary for hyaloid vessel regression.

Clusterin (Apolipoprotein J) is a secreted chaperone protein involved in cell death, tumor growth, and neurodegenerative disorders such as Alzheimer's. Clusterin inhibits the movement of (pro-apoptotic) Bax into the mitochondria and thus can prevent the induction of apoptosis [94]. It has also been suggested that Clusterin may be involved in atherosclerosis although its role is controversial. Some studies suggest an anti-inflammatory effect, while others indicate Clusterin can either inhibit or induce vascular smooth muscle cell hyperplasia, as well as protect endothelial cells [95].

Immunohistochemistry in human fetal eyes found positive staining for clusterin in the hyaloid vasculature. Although the study was constrained by a limited number of eyes, the results suggested that at 14 WG (Figure I.D-5a), clusterin was not detected on the structures of the hyaloid vasculature, but at 18 WG (Figure I.D-5b), clusterin expression was observed on hyaloid vessels [16].

Neural cadherin (N-Cadherin, Cadherin-2), part of the cadherin superfamily, is a calcium-dependent cell-to-cell adhesion glycoprotein. N-cadherin is critical for cancer metastasis because it disrupts endothelial cell-cell junctions speeding up

the process of transendothelial migration [96]. Disruption of endothelial cell junctions may also be important in the process of regression of the hyaloid vasculature. By immunostaining, N-cadherin was not found in endothelial cells of the hyaloid vasculature in a 14 WG human (Figure I.D-6a), but was observed in the endothelium of 18 WG eyes (Figure I.D-6b) [16]. Given the limited number of specimens studied, this finding needs corroboration by future research.

Platelet endothelial cell adhesion molecule 1 (PECAM-1), also known as cluster of differentiation 31 (CD31), is involved in leukocyte migration, angiogenesis, and integrin activation [97]. In a mouse model of retinal neovascularization during oxygen-induced ischemic retinopathy (OIR), PECAM-1 deficiency (PECAM-1^{-/-}) was shown to decrease retinal vasculature and increase apoptosis of retinal vessels. PECAM-1^{-/-} does not appear to affect the development or regression of the nearby hyaloid vasculature [98].

Opticin is an extracellular matrix glycoprotein that is present throughout the vitreous body and is associated with vitreous collagen fibrils [99, 100]. Opticin is an antiangiogenic protein that regulates extracellular matrix adhesion characteristics by competitively inhibiting endothelial cell interactions with collagen preventing the strong adhesion that is necessary for pro-angiogenic signaling [101]. Opticin production is reduced by hypoxic conditions and by secreted VEGF in human retinal pigment epithelium (RPE) cells [102]. Although opticin is antiangiogenic and inhibits pre-retinal neovascularization, it does not appear to influence hyaloid vascular regression or retinal vasculature development [102, 103]. This is consistent with the finding that although Opticin precursors and fragments were detected in embryonic human vitreous, there was no significant increase or decrease in their levels during the 2nd trimester [16].

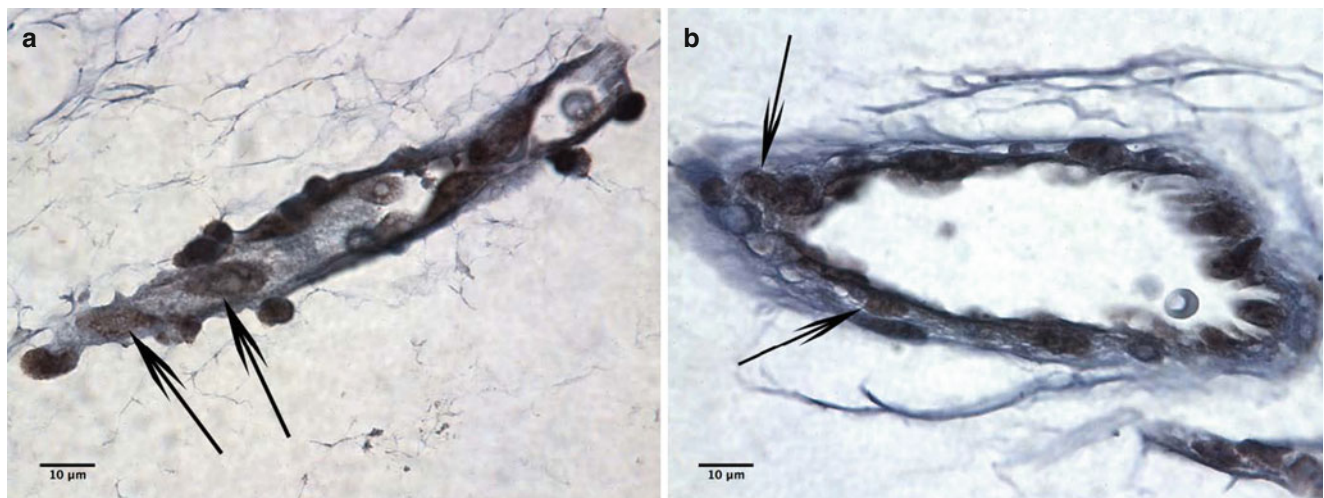


Figure I.D-4 Profilin-1. Profilin-1 was found in endothelial cells (arrows) of the hyaloid artery (a) and of the vasa hyaloidea propria (b) in the vitreous of a 14 WG human

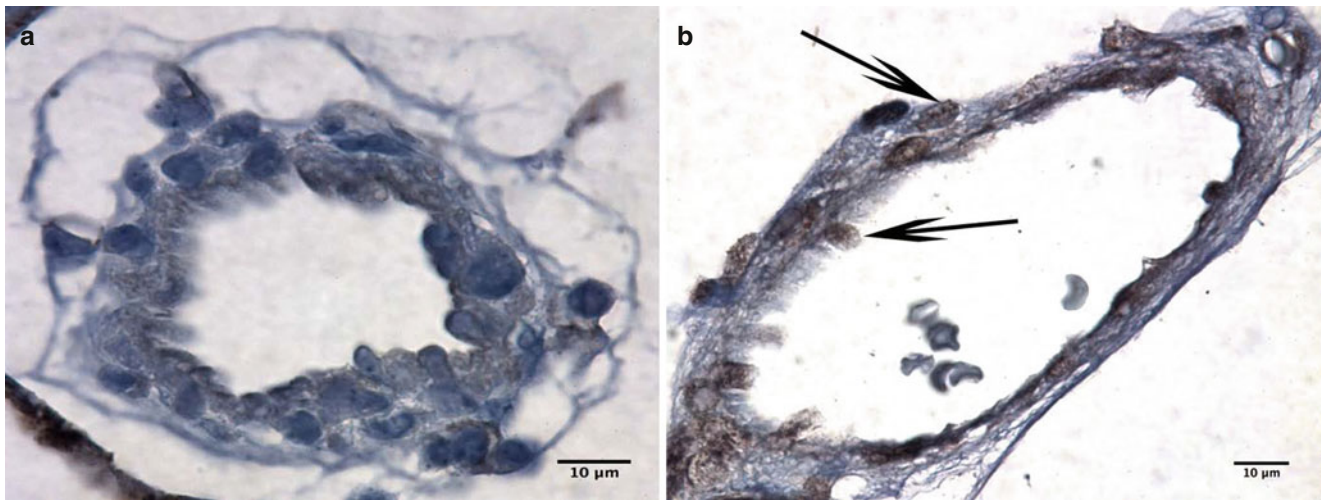


Figure I.D-5 Clusterin. Clusterin was not detected in the hyaloid vessels of 14 WG human vitreous (a). In 18 WG eyes, clusterin was found in the endothelial cells (arrows) of the tunica vasculosa lentis (b)

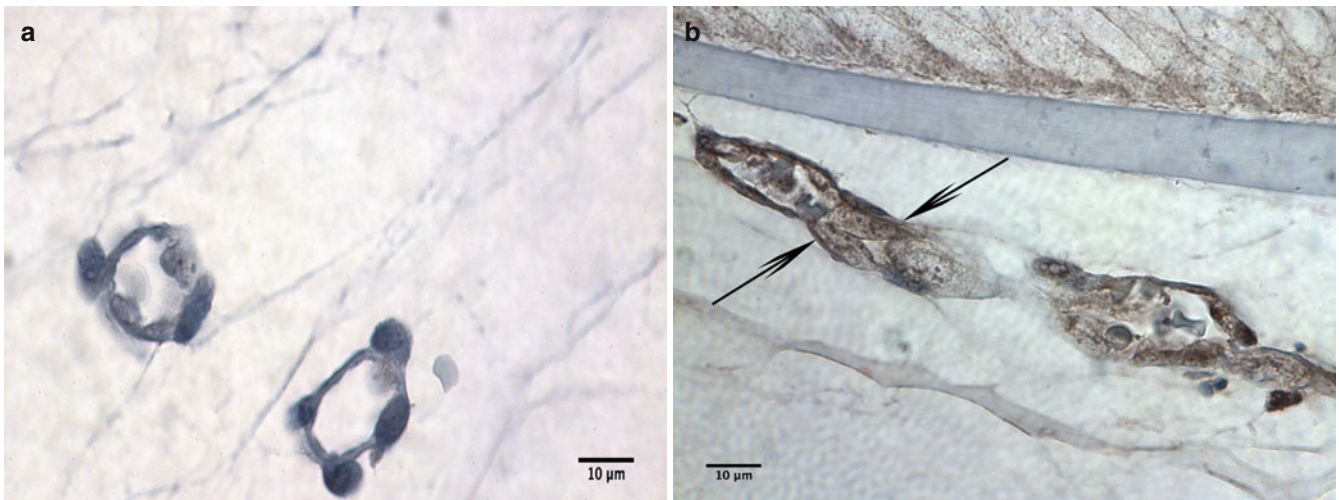


Figure I.D-6 N-Cadherin. In 14 GW eyes (a), N-Cadherin was not detected in endothelial cells of the hyaloid vessels. (b) However, in 18 WG eyes, N-Cadherin was found in the cytoplasm of endothelial cells that make up the endothelium of the TVL (arrows)

VII. Genetic Influences

While many proteins have been shown to have an influence on the regression of the fetal hyaloid vasculature, less is known about the upstream, genetic influences on normal or pathological vitreous development. Several studies have identified specific genes that can influence hyaloid vessel regression.

Endothelial cell-specific gene ablation of either the *transcription factor serum response factor (SRF)* or its cofactors *myocardin-related transcription factors A and B* (but not SRF cofactors Eph-like kinase 1 and 4) impairs protrusion of endothelial tip cell filopodia, resulting in the persistence of hyaloid vessels in mice [104].

A spontaneous mouse mutation named *fierce (frc)* involves a deletion for the nuclear receptor Nr2e1 gene (also known as Tix, mouse homologue of *Drosophila tailless*) that is important for normal development. The impaired regression of the hyaloid system has been observed in *frc* mouse on three defined genetic backgrounds (C57BL/6 J, 129P3/JEmS, and B6129F1) [105]. In these mice, both large and small vessels were observed in the vitreous body, close to the optic nerve and the peripheral retina, suggesting the hyaloid vessels had failed to undergo apoptosis and regress [104]. The murine INK4a locus encodes *tumor suppressor proteins p16 (INK4a)* and *p19 (ARF)*. INK4a^{-/-} mice showed defects in the regression of the hyaloid vasculature [106].

Mice that are mutated in the atypical *opsin melanopsin* gene (*Opn4*) or are dark reared were recently reported to have persistent hyaloid vessels at 8 days postpartum and an overgrown retinal vasculature that may be explained by the fact that a light-response pathway is critical to ocular blood vessel patterning [85]. This study found that the melanopsin light-response pathway normally suppresses the number of retinal neurons, limiting hypoxia and, as a consequence, local expression of VEGF-A by retinal neurons [84].

Conclusions

Regression of the human fetal hyaloid vasculature is critical for development of vitreous, retina, and surrounding ocular structures. Although the timing of hyaloid vessel regression is established, especially in lower mammals, little is known about the exact processes and molecular mechanisms involved in the human. Recent proteomic studies of embryonic mouse and human vitreous have suggested various protein and pathways that may be involved in the regression of the hyaloid vasculature. These proteomic studies suggest that complex and highly orchestrated mechanisms are required for proper and complete hyaloid vasculature regression. Apoptosis, increased expression of antiangiogenic factors, reduced expression of endothelial survival factors, macrophagy, and perhaps external stimuli are all implicated in the regression of hyaloid vasculature. Understanding these processes will further our knowledge about pathological neovascularization in the eye and perhaps other parts of the body and might guide our approaches to new therapies.

Abbreviations

Alk-1	Activin receptor-like kinase
Ang	Angiopoietin
AQP	Aquaporin
CD	Cluster of differentiation
CO ₂	Carbon dioxide
Col18	Collagen type XVIII
ED	Embryonic day
EM	Electron microscopy
FGF	Fibroblast growth factor
HA	Hyaloid artery
IPA	Ingenuity Pathway Analysis
LPA	Lysophosphatidic acid
MPNST	Malignant peripheral nerve sheath
N ₂	Nitrogen
Ninj1	Nerve injury-induced protein
O ₂	Oxygen
OIR	Oxygen-induced ischemic retinopathy
PDGF	Platelet-derived growth factor
PDR	Proliferative diabetic retinopathy

PECAM	Platelet endothelial cell adhesion molecule
PEDF	Pigment epithelium derived factor
PGD	Post gestational day
PM	Pupillary membrane
POSTN	Periostin
PRL	Prolactin
ROS	Reactive oxygen species
RPE	Retinal pigment epithelium
SEM	Scanning electron microscopy
TEM	Transmission electron microscopy
TGFβ	Transforming growth factor-β
TSP, THBS	Thrombospondin
TVL	Tunica vasculosa lentis
VEGF	Vascular endothelial growth factor
VHP	Vasa hyaloidea propria
WG	Weeks of gestation

References

- McLeod DS, Hasegawa T, Baba T, Grebe R, Galtierd'Auriac I, Merges C, Edwards M, Luty GA. From blood islands to blood vessels: morphologic observations and expression of key molecules during hyaloid vascular system development. *Invest Ophthalmol Vis Sci.* 2012;53(13):7912–27.
- Mann IC. The relations of the hyaloid canal in the foetus and in the adult. *J Anat.* 1928;62(3):290–6.
- Hamming NA, Apple DJ, Gieser DK, Vygantas CM. Ultrastructure of the hyaloid vasculature in primates. *Invest Ophthalmol Vis Sci.* 1977;16(5):408–15.
- Zhu M, Provis JM, Penfold PL. The human hyaloid system: cellular phenotypes and inter-relationships. *Exp Eye Res.* 1999;68(5):553–63.
- Saint-Geniez M, D'Amore PA. Development and pathology of the hyaloid, choroidal and retinal vasculature. *Int J Dev Biol.* 2004;48(8–9):1045–58.
- Mitchell CA, Risau W, Drexler HC. Regression of vessels in the tunica vasculosa lentis is initiated by coordinated endothelial apoptosis: a role for vascular endothelial growth factor as a survival factor for endothelium. *Dev Dyn.* 1998;213(3):322–33.
- Barishak YR. Embryology of the eye and its adnexae. *Dev Ophthalmol.* 1992;24:1–142.
- Ito M, Yoshioka M. Regression of the hyaloid vessels and pupillary membrane of the mouse. *Anat Embryol (Berl).* 1999;200(4):403–11.
- Taniguchi H, Kitaoka T, Gong H, Amemiya T. Apoptosis of the hyaloid artery in the rat eye. *Ann Anat.* 1999;181(6):555–60.
- el-Hifnawi E, el-Hifnawi A, Frankenberg C, Keeler C. Ultrastructure and regression of the tunica vasculosa lentis in newborn Wistar rats. *Ann Anat.* 1994;176(2):143–9.
- Zhu M, Madigan MC, van Driel D, Maslim J, Billson FA, Provis JM, et al. The human hyaloid system: cell death and vascular regression. *Exp Eye Res.* 2000;70(6):767–76.
- Ko MK, Chi JG, Chang BL. Hyaloid vascular pattern in the human fetus. *J Pediatr Ophthalmol Strabismus.* 1985;22(5):188–93.
- Achiron R, Kreiser D, Achiron A. Axial growth of the fetal eye and evaluation of the hyaloid artery: in utero ultrasonographic study. *Prenat Diagn.* 2000;20(11):894–9.

14. Birnholz JC, Farrell EE. Fetal hyaloid artery: timing of regression with US. *Radiology*. 1988;166(3):781–3.
15. Jack RL. Regression of the hyaloid vascular system. An ultrastructural analysis. *Am J Ophthalmol*. 1972;74(2):261–72.
16. Sebag J, Yee KMP, Madigan MC, Aiello LP, Sadun AA. Bioinformatic analysis of embryonic human vitreomics. *Invest Ophthalmol Vis Sci (ARVO Abstract 4928)*. 2012.
17. Armstrong RA. When to use the Bonferroni correction. *Ophthalmic Physiol Opt*. 2014. Epub ahead of print.
18. Aickin M, Gensler H. Adjusting for multiple testing when reporting research results: the Bonferroni vs. Holm methods. *Am J Public Health*. 1996;86(5):726–8.
19. Dougherty TJ, Pucci MJ. Antibiotic discovery and development. New York: Springer; 2011.
20. Veber DF, Johnson SR, Cheng HY, Smith BR, Ward KW, Kopple KD. Molecular properties that influence the oral bioavailability of drug candidates. *J Med Chem*. 2002;45(12):2615–23.
21. Komander D. The emerging complexity of protein ubiquitination. *Biochem Soc Trans*. 2009;37(Pt 5):937–53.
22. Albè E, Chang JH, Azar NF, Ivanov AR, Azar DT. Proteomic analysis of the hyaloid vascular system regression during ocular development. *J Proteome Res*. 2008;7(11):4904–13.
23. Preis I, Langer R, Brem H, Folkman J. Inhibition of neovascularization by an extract derived from vitreous. *Am J Ophthalmol*. 1977;84(3):323–8.
24. Hahn P, Lindsten T, Tolentino M, Thompson CB, Bennett J, Dunaief JL. Persistent fetal ocular vasculature in mice deficient in bax and bak. *Arch Ophthalmol*. 2005;123(6):797–802.
25. Wang S, Park S, Fei P, Sorenson CM. Bim is responsible for the inherent sensitivity of the developing retinal vasculature to hyperoxia. *Dev Biol*. 2011;349(2):296–309.
26. Wang S, Sorenson CM, Sheibani N. Attenuation of retinal vascular development and neovascularization during oxygen-induced ischemic retinopathy in Bcl-2^{-/-} mice. *Dev Biol*. 2005;279(1):205–19.
27. Luttly GA, Merges C, Threlkeld AB, Crone S, McLeod DS. Heterogeneity in localization of isoforms of TGF-beta in human retina, vitreous, and choroid. *Invest Ophthalmol Vis Sci*. 1993;34(3):477–87.
28. Elliott RL, Blobe GC. Role of transforming growth factor beta in human cancer. *J Clin Oncol*. 2005;23(9):2078–93.
29. Zheng Y, Devitt C, Liu J, Iqbal N, Skapek SX. Arf induction by Tgfβ is influenced by Sp1 and C/ebpβ in opposing directions. *PLoS One*. 2013;8(8):e70371.
30. McKeller RN, Fowler JL, Cunningham JJ, Warner N, Smeyne RJ, Zindy F, Skapek SX. The Arf tumor suppressor gene promotes hyaloid vascular regression during mouse eye development. *Proc Natl Acad Sci USA*. 2002;99(6):3848–53.
31. Albe E, Escalona E, Rajagopal R, Javier JA, Chang JH, Azar DT. Proteomic identification of activin receptor-like kinase-I as a differentially expressed protein during hyaloid vascular system regression. *FEBS Lett*. 2005;579(25):5481–6.
32. Sukhikh GT, Panova IG, Smirnova YA, Milyushina LA, Firsova NV, Markitantova YV, et al. Expression of transforming growth factor-β2 in vitreous body and adjacent tissues during prenatal development of human eye. *Bull Exp Biol Med*. 2010;150(1):117–21.
33. Reichel MB, Ali RR, D'Esposito F, Clarke AR, Luthert PJ, Bhattacharya SS, et al. High frequency of persistent hyperplastic primary vitreous and cataracts in p53-deficient mice. *Cell Death Differ*. 1998;5(2):156–62.
34. Dueñas Z, Rivera JC, Quiróz-Mercado H, Aranda J, Macotela Y, Montes de Oca P. Prolactin in eyes of patients with retinopathy of prematurity: implications for vascular regression. *Invest Ophthalmol Vis Sci*. 2004;45(7):2049–55.
35. Hanashima C, Namiki H. Reduced viability of vascular endothelial cells by high concentration of ascorbic acid in vitreous humor. *Cell Biol Int*. 1999;23(4):287–98.
36. Lee HJ, Ahn BJ, Shin MW, Jeong JW, Kim JH, Kim KW. Ninjurin1 mediates macrophage-induced programmed cell death during early ocular development. *Cell Death Differ*. 2009;16(10):1395–407.
37. Lang RA, Bishop JM. Macrophages are required for cell death and tissue remodeling in the developing mouse eye. *Cell*. 1993;74(3):453–62.
38. Jacobson B, Basu PK, Hassany SM. Vascular endothelial cell growth inhibitor of normal and pathologic vitreous. *Arch Ophthalmol*. 1984;102:1543–5.
39. Jacobson B, Dorfman T, Basu PK, et al. Inhibition of vascular endothelial cell growth and trypsin activity by vitreous. *Exp Eye Res*. 1985;41:581–95.
40. Zhu M, Penfold PL, Madigan MC, Billson FA. Effect of human vitreous and hyalocyte-derived factors on vascular endothelial cell growth. *Aust N Z J Ophthalmol*. 1997;25 Suppl 1:S57–60.
41. Lang R, Lustig M, Francois F, Sellinger M, Plesken H. Apoptosis during macrophage-dependent ocular tissue remodeling. *Development*. 1994;120:3395–403.
42. McMenamin PG, Djano J, Wealthall R, Griffin BJ. Characterization of the macrophages associated with the tunica vasculosa lentis of the rat eye. *Invest Ophthalmol Vis Sci*. 2002;43(7):2076–82.
43. Arima M, Yoshida S, Nakama T, Ishikawa K, Nakao S, Yoshimura T, et al. Involvement of periostin in regression of hyaloid vascular system during ocular development. *Invest Ophthalmol Vis Sci*. 2012;53(10):6495–503.
44. Zhang C, Asnaghi L, Gongora C, Patek B, Hose S, Ma B, et al. A developmental defect in astrocytes inhibits programmed regression of the hyaloid vasculature in the mammalian eye. *Eur J Cell Biol*. 2011;90(5):440–8.
45. Diez-Roux G, Lang RA. Macrophages induce apoptosis in normal cells in vivo. *Development*. 1997;124(18):3633–8.
46. Luhmann UF, Lin J, Acar N, Lammel S, Feil S, Grimm C, et al. Role of the Norrie disease pseudoglioma gene in sprouting angiogenesis during development of the retinal vasculature. *Invest Ophthalmol Vis Sci*. 2005;46(9):3372–82.
47. Ohlmann AV, Adamek E, Ohlmann A, Lütjen-Drecoll E. Norrie gene product is necessary for regression of hyaloid vessels. *Invest Ophthalmol Vis Sci*. 2004;45(7):2384–90.
48. Meeson AP, Argilla M, Ko K, Witte L, Lang RA. VEGF deprivation-induced apoptosis is a component of programmed capillary regression. *Development*. 1999;126(7):1407–15.
49. Schultz GS, Grant MB. Neovascular growth factors. *Eye (Lond)*. 1991;5(2):170–80.
50. Edqvist PH, Niklasson M, Vidal-Sanz M, Hallböök F, Forsberg-Nilsson K. Platelet-derived growth factor over-expression in retinal progenitors results in abnormal retinal vessel formation. *PLoS One*. 2012;7(8):e42488.
51. Garcia CM, Shui YB, Kamath M, DeVillar J, Johnson RS, Gerber HP, et al. The function of VEGF-A in lens development: formation of the hyaloid capillary network and protection against transient nuclear cataracts. *Exp Eye Res*. 2009;88(2):270–6.
52. Feeney SA, Simpson DA, Gardiner TA, Boyle C, Jamison P, Stitt AW. Role of vascular endothelial growth factor and placental growth factors during retinal vascular development and hyaloid regression. *Invest Ophthalmol Vis Sci*. 2003;44(2):839–47.
53. Shui YB, Wang X, Hu JS, Wang SP, Garcia CM, Potts JD. Vascular endothelial growth factor expression and signaling in the lens. *Invest Ophthalmol Vis Sci*. 2003;44(9):3911–9.
54. Hackett SF, Wiegand S, Yancopoulos G, Campochiaro PA. Angiopoietin-2 plays an important role in retinal angiogenesis. *J Cell Physiol*. 2002;192(2):182–7.
55. Rousseau B, Larrieu-Lahargue F, Bikfalvi A, Javerzat S. Involvement of fibroblast growth factors in choroidal angiogenesis and retinal vascularization. *Exp Eye Res*. 2003;77(2):147–56.

56. Felton SM, Brown GC, Felberg NT, Federman JL. Vitreous inhibition of tumor neovascularization. *Arch Ophthalmol*. 1979;97(9):1710–3.
57. Luty GA, Thompson DC, Gallup JY. Vitreous – an inhibitor of retinal extract-induced neovascularization. *Invest Ophthalmol Vis Sci*. 1983;24:52–6.
58. Raymond L, Jacobson B. Isolation and identification of stimulatory and inhibiting growth factors in bovine vitreous. *Exp Eye Res*. 1982;34:267–86.
59. Taylor CM, Weiss JB. Partial purification of a 5.7K glycoprotein from bovine vitreous which inhibits both angiogenesis and collagenase activity. *Biochem Biophys Res Commun*. 1985;133(3):911–6.
60. Lawler PR, Lawler J. Molecular basis for the regulation of angiogenesis by thrombospondin-1 and -2. *Cold Spring Harb Perspect Med*. 2012;2(5):a006627.
61. Felbor U, Dreier L, Bryant RA, Ploegh HL, Olsen BR, Mothes W. Secreted cathepsin L generates endostatin from collagen XVIII. *EMBO J*. 2000;19(6):1187–94.
62. O'Reilly MS, Boehm T, Shing Y, Fukai N, Vasios G, Lane WS, Flynn E, Birkhead JR, Olsen BR, Folkman J. Endostatin: an endogenous inhibitor of angiogenesis and tumor growth. *Cell*. 1997;88(2):277–85.
63. Ständker L, Schrader M, Kanse SM, Jürgens M, Forssmann WG, Preissner KT. Isolation and characterization of the circulating form of human endostatin. *FEBS Lett*. 1997;420(2–3):129–33.
64. Shichiri M, Hirata Y. Antiangiogenesis signals by endostatin. *FASEB J*. 2001;15(6):1044–53.
65. Dixelius J, Larsson H, Sasaki T, Holmqvist K, Lu L, Engström A. Endostatin-induced tyrosine kinase signaling through the Shb adaptor protein regulates endothelial cell apoptosis. *Blood*. 2000;95(11):3403–11.
66. Hurskainen M, Eklund L, Hägg PO, Fruttiger M, Sormunen R, Ilves M, et al. Abnormal maturation of the retinal vasculature in type XVIII collagen/endostatin deficient mice and changes in retinal glial cells due to lack of collagen types XV and XVIII. *FASEB J*. 2005;19(11):1564–6.
67. Tombran-Tink J, Aparicio S, Xu X, Tink AR, Lara N, Sawant S, et al. PEDF and the serpins: phylogeny, sequence conservation, and functional domains. *J Struct Biol*. 2005;151(2):130–50.
68. Sawant S, Aparicio S, Tink AR, Lara N, Barnstable CJ, Tombran-Tink J. Regulation of factors controlling angiogenesis in liver development: a role for PEDF in the formation and maintenance of normal vasculature. *Biochem Biophys Res Commun*. 2004;325(2):408–13.
69. Rychli K, Huber K, Wojta J. Pigment epithelium-derived factor (PEDF) as a therapeutic target in cardiovascular disease. *Expert Opin Ther Targets*. 2009;13(11):1295–302.
70. Sundararajan V, Bohensky MA, Moore G, Brand CA, Lethborg C, Gold M, Murphy MA, Collins A, Philip J. Mapping the patterns of care, the receipt of palliative care and the site of death for patients with malignant glioma. *J Neurooncol*. 2014;116:119–26.
71. Shoji S, Nakano M, Tomonaga T, Kim H, Hanai K, Usui Y, et al. Value of metastin receptor immunohistochemistry in predicting metastasis after radical nephrectomy for pT1 clear cell renal cell carcinoma. *Clin Exp Metastasis*. 2013;30(5):607–14.
72. Zheng D, Chen H, Davids J, Bryant M, Lucas A. Serpins for diagnosis and therapy in cancer. *Cardiovasc Hematol Disord Drug Targets*. 2013;13(2):123–32.
73. Mori K, Duh E, Gehlbach P, Ando A, Takahashi K, Pearlman J, et al. Pigment epithelium-derived factor inhibits retinal and choroidal neovascularization. *J Cell Physiol*. 2001;188(2):253–63.
74. Duh EJ, Yang HS, Suzuma I, Miyagi M, Youngman E, Mori K, et al. Pigment epithelium-derived factor suppresses ischemia-induced retinal neovascularization and VEGF-induced migration and growth. *Invest Ophthalmol Vis Sci*. 2002;43(3):821–9.
75. Huang Q, Wang S, Sorenson CM, Sheibani N. PEDF-deficient mice exhibit an enhanced rate of retinal vascular expansion and are more sensitive to hyperoxia-mediated vessel obliteration. *Exp Eye Res*. 2008;87(3):226–41.
76. Aranda J, Motiejunaite R, Silva P, Aiello LP, Kazlauskas A. Regression activity that is naturally present in vitreous becomes ineffective as patients develop proliferative diabetic retinopathy. *Diabetologia*. 2013;56(6):1444–53.
77. Kroemer G, Galluzzi L, Vandenabeele P, Abrams J, Alnemri ES, Baehrecke EH, et al. Classification of cell death: recommendations of the Nomenclature Committee on Cell Death 2009. *Cell Death Differ*. 2009;16(1):3–11.
78. Baehrecke EH. Autophagy: dual roles in life and death? *Nat Rev Mol Cell Biol*. 2005;6:505–10.
79. Clarke PG. Developmental cell death: morphological diversity and multiple mechanisms. *Anat Embryol (Berl)*. 1990;181:195–213.
80. Kim JH, Kim JH, Yu YS, Mun JY, Kim KW. Autophagy-induced regression of hyaloid vessels in early ocular development. *Autophagy*. 2010;6(7):922–8.
81. Meeson A, Palmer M, Calfon M, Lang R. A relationship between apoptosis and flow during programmed capillary regression is revealed by vital analysis. *Development*. 1996;122(12):3929–38.
82. Brown AS, Leamen L, Cucevic V, Foster FS. Quantitation of hemodynamic function during developmental vascular regression in the mouse eye. *Invest Ophthalmol Vis Sci*. 2005;46(7):2231–7.
83. Browning J, Reichelt ME, Gole GA, Massa H. Proximal arterial vasoconstriction precedes regression of the hyaloid vasculature. *Curr Eye Res*. 2001;22(6):405–11.
84. Bischoff PM, Wajer SD, Flower RW. Scanning electron microscopic studies of the hyaloid vascular system in newborn mice exposed to O₂ and CO₂. *Graefes Arch Clin Exp Ophthalmol*. 1983;220(6):257–63.
85. Rao S, Chun C, Fan J, Kofron JM, Yang MB, Hegde RS, et al. A direct and melanopsin-dependent fetal light response regulates mouse eye development. *Nature*. 2013;494(7436):243–6.
86. Tarttelin EE, Bellingham J, Bibb LC, Foster RG, Hankins MW, Gregory-Evans K, Gregory-Evans CY, Wells DJ, Lucas RJ. Expression of Opsin genes early in ocular development of humans and mice. *Exp Eye Res*. 2003;76(3):393–6.
87. Kálmán M, Mahalek J, Adorján A, Adorján I, Pócsai K, Bagyura Z, Sadeghian S. Alterations of the perivascular dystrophin-dystroglycan complex following brain lesions. An immunohistochemical study in rats. *Histol Histopathol*. 2011;26:1435–52.
88. Sotgia F, Lee H, Bedford MT, Petrucci T, Sudol M, Lisanti MP. Tyrosine phosphorylation of beta-dystroglycan at its WW domain binding motif, PPxY, recruits SH2 domain containing proteins. *Biochemistry*. 2001;40(48):14585–92.
89. Rambukkana A, Yamada H, Zanazzi G, Mathus T, Salzer JL, Yurchenco PD, Campbell KP, Fischetti VA. Role of alpha-dystroglycan as a Schwann cell receptor for Mycobacterium leprae. *Science*. 1998;282(5396):2076–9.
90. Moore CJ, Winder SJ. Dystroglycan versatility in cell adhesion: a tale of multiple motifs. *Cell Commun Signal*. 2010;8:3.
91. Mitchell A, Mathew G, Jiang T, Hamdy FC, Cross SS, Eaton C. Dystroglycan function is a novel determinant of tumor growth and behavior in prostate cancer. *Prostate*. 2013;73(4):398–408.
92. Sgambato A, De Paola B, Migaldi M, Di Salvatore M, Rettino A, Rossi G, Faraglia B, Boninsegna A, Maiorana A, Cittadini A. Dystroglycan expression is reduced during prostate tumorigenesis and is regulated by androgens in prostate cancer cells. *J Cell Physiol*. 2007;213(2):528–39.
93. Ding Z, Joy M, Bhargava R, Gunsaulus M, Lakshman N, Miron-Mendoza M, Petrol M, Condeelis J, Wells A, Roy P. Profilin-1 downregulation has contrasting effects on early vs late steps of

- breast cancer metastasis. *Oncogene*. 2013. doi:10.1038/onc.2013.166 [Epub ahead of print].
94. Er E, Oliver L, Cartron PF, Juin P, Manon S, Vallette FM. Review: Mitochondria as the target of the pro-apoptotic protein Bax. *Biochim Biophys Acta*. 2006;1757:1301–11.
95. Kim HJ, Yoo EK, Kim JY, Choi YK, Lee HJ, Kim JK, et al. Protective role of clusterin/apolipoprotein J against neointimal hyperplasia via antiproliferative effect on vascular smooth muscle cells and cytoprotective effect on endothelial cells. *Arterioscler Thromb Vasc Biol*. 2009;29(10):1558–64.
96. Qi J, Chen N, Wang J, Siu CH. Transendothelial migration of melanoma cells involves N-Cadherin-mediated adhesion and activation of the β -Catenin signaling pathway. *Mol Biol Cell*. 2005;16(9):4386–97.
97. “Gene ID: PECAM1 platelet/endothelial cell adhesion molecule 1,” last modified 25 Feb 2014, <http://www.ncbi.nlm.nih.gov/gene/18613>.
98. Dimaio TA, Wang S, Huang Q, Scheef EA, Sorenson CM, Sheibani N. Attenuation of retinal vascular development and neovascularization in PECAM-1-deficient mice. *Dev Biol*. 2008;315(1):72–88.
99. Ramesh S, Bonshek RE, Bishop PN. Immunolocalisation of opticin in the human eye. *Br J Ophthalmol*. 2004;88(5):697–702.
100. Le Goff MM, Bishop PN. Focus on molecules: opticin. *Exp Eye Res*. 2007;85(3):303–4.
101. Le Goff MM, Sutton MJ, Slevin M, Latif A, Humphries MJ, Bishop PN. Opticin exerts its anti-angiogenic activity by regulating extracellular matrix adhesiveness. *J Biol Chem*. 2012;287(33):28027–36.
102. Ma J, Zhu TP, Moe MC, Ye P, Yao K. Opticin production is reduced by hypoxia and VEGF in human retinal pigment epithelium via MMP-2 activation. *Cytokine*. 2012;59(1):100–7.
103. Le Goff MM, Lu H, Ugarte M, Henry S, Takanosu M, Mayne R, et al. The vitreous glycoprotein opticin inhibits preretinal neovascularization. *Invest Ophthalmol Vis Sci*. 2012;53(1):228–34.
104. Weint C, Riehle H, Park D, Stritt C, Beck S, Huber G, et al. Endothelial SRF/MRTF ablation causes vascular disease phenotypes in murine retinae. *J Clin Invest*. 2013;123(5):2193–206.
105. Young KA, Berry ML, Mahaffey CL, Saionz JR, Hawes NL, Chang B, et al. Fierce: a new mouse deletion of Nr2e1; violent behaviour and ocular abnormalities are background-dependent. *Behav Brain Res*. 2002;132(2):145–58.
106. Cheong C, Sung YH, Lee J, Choi YS, Song J, Kee C, Lee HW. Role of INK4a locus in normal eye development and cataract genesis. *Mech Ageing Dev*. 2006;127(7):633–8.

Jesse Gale, Lloyd Paul Aiello, and J. Sebag

Outline

- I. **Introduction**
- II. **Biochemistry of Diabetes**
 - A. Advanced Glycation End Products
 - B. Protein Kinase C
 - C. Aldose Reductase
 - D. Hexosamine
 - E. Oxidative Stress
- III. **Diabetic Retinopathy**
 - A. Epidemiology
 - B. Pathophysiology of Diabetic Retinopathy
 - 1. Diabetic Retinopathy and the Neurosensory Retina
 - 2. Diabetic Retinal Vasculopathy
- IV. **Diabetic Vitreopathy**
 - A. Molecular Alterations
 - 1. Collagen
 - 2. Hyaluronan
 - 3. Extracellular Matrix Constituents
 - B. Structural Alterations
 - 1. Vitreoretinal Interface
 - 2. Vitreous Body
- V. **Physiological Considerations in Diabetic Vitreopathy**
 - A. Oxygen Physiology
 - B. Paracrine Depot
- VI. **Treatment Considerations in Diabetic Vitreopathy**
 - A. Pharmacotherapy
 - 1. Aminoguanidine
 - 2. Alagebrium
 - 3. Vitamin B Derivatives
 - B. Surgery
 - C. Pharmacologic Vitreolysis
- VII. **Asteroid Hyalosis (AH)**
- VIII. **Summary**

References

Keywords

Vitreous • Collagen • Diabetes • Advanced glycation end products • Inflammation • Diabetic Vitreopathy • Diabetic Retinopathy • Asteroid hyalosis

Key Concepts

1. Hyperglycemia causes intracellular production of superoxide, which initiates a complex network of metabolic derangements, transcription factors, and extracellular signaling pathways. An important outcome is the oxidation of sugars and formation of advanced glycation end products, which have widespread pathologic effects both as ligands of their receptor(s) and as abnormally cross-linked proteins in extracellular matrices throughout the body, including vitreous.
2. Not unlike aging, diabetic vitreous undergoes metabolic derangements leading to cross-linking of collagen and depolymerization of hyaluronan, resulting in premature liquefaction. In diabetes, the cortical vitreous is a toxic reservoir of pathological signals and a barrier to retinal oxygenation that is tethered by neovascular tufts with increased vitreoretinal adhesion leading to vitreoretinal traction, vitreochisis, and complex preretinal membranes.

J. Gale, MB, ChB, MD
VMR Institute for Vitreous Macula Retina,
7677 Center Avenue, Suite 400,
Huntington Beach, CA 92647, USA

Addenbrooke's Hospital, Cambridge University
Hospitals NHS Foundation Trust, Cambridge, UK
e-mail: jesse.gale@gmail.com

L.P. Aiello, MD, PhD, FARVO
The Beetham Eye Institute, Joslin Diabetes Center
Harvard Medical School, Boston, MA, USA

J. Sebag, MD, FACS, FRCOphth, FARVO (✉)
VMR Institute for Vitreous Macula Retina,
7677 Center Avenue, Suite 400,
Huntington Beach, CA 92647, USA
e-mail: jsebag@VMRinstitute.com

- Emerging treatments to reduce the effects of protein glycation and other metabolic derangements, as well as alternative approaches to eliminate vitreoretinal attachment via pharmacologic vitreolysis, will likely have expanding roles in the future management of diabetic eye disease.

I. Introduction

Diabetes mellitus, hereafter called diabetes, is a systemic disorder of insulin signaling, resulting in hyperglycemia. Hypertension and dyslipidemia are frequent associations. The pathological results of diabetes are microvascular complications, notably retinopathy, nephropathy, and peripheral neuropathy, and accelerated atherosclerosis, resulting in major cardiovascular complications. Overnutrition is causing an international diabetes epidemic of extraordinary proportions [1]. The purpose of this discussion is to summarize the disordered metabolic pathways in diabetes with

an emphasis on ocular manifestations, placing particular emphasis on how these biochemical changes alter vitreous structure and function, contributing to retinopathy and vision loss.

II. Biochemistry of Diabetes

At a molecular and cellular level, the myriad downstream consequences of diabetes all appear to have some association with an increase in superoxide production [2, 3]. Intracellular hyperglycemia causes an oversupply of metabolites from glycolysis into the tricarboxylic acid cycle (TCA cycle, also known as Krebs cycle or citric acid cycle). This causes oversupply of electrons to the electron transport chain of mitochondria. Beyond a certain level, this causes a dramatic and specific increase in superoxide production from mitochondria [2]. This acts as a step function or switch, activating the multiple downstream pathological pathways of diabetes [4].

The following delineates the major biochemical pathways that are important in diabetes, which are summarized in Figure I.E-1.

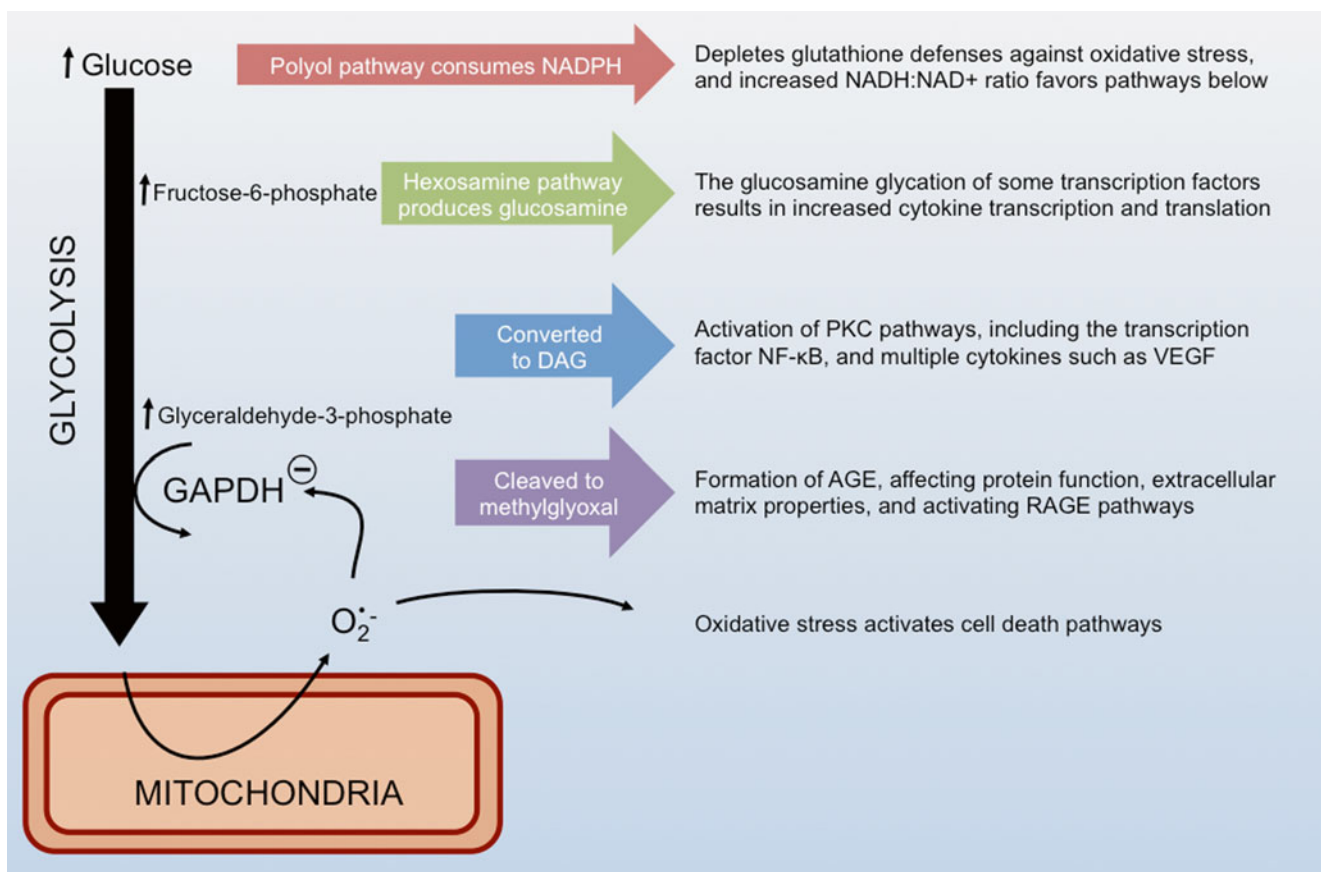


Figure I.E-1 Summary of pathological pathways in diabetes. The pathological effects of intracellular hyperglycemia are mediated by the increased production of superoxide in the electron transport chain. Superoxide causes inhibition of GAPDH, which results in accumulation of metabolites and diversion into polyol and hexosamine pathways and creation of DAG and methylglyoxal. Data summarized from Refs.

[2–4]. [AGE advanced glycation end products, DAG diacyl glycerol, GAPDH glyceraldehyde phosphate dehydrogenase, NADPH reduced nicotinamide adenine dinucleotide phosphate, NADH reduced nicotinamide adenine dinucleotide, NF-κB nuclear factor – kappa B, PKC protein kinase C, RAGE receptor for AGE, VEGF vascular endothelial growth factor]

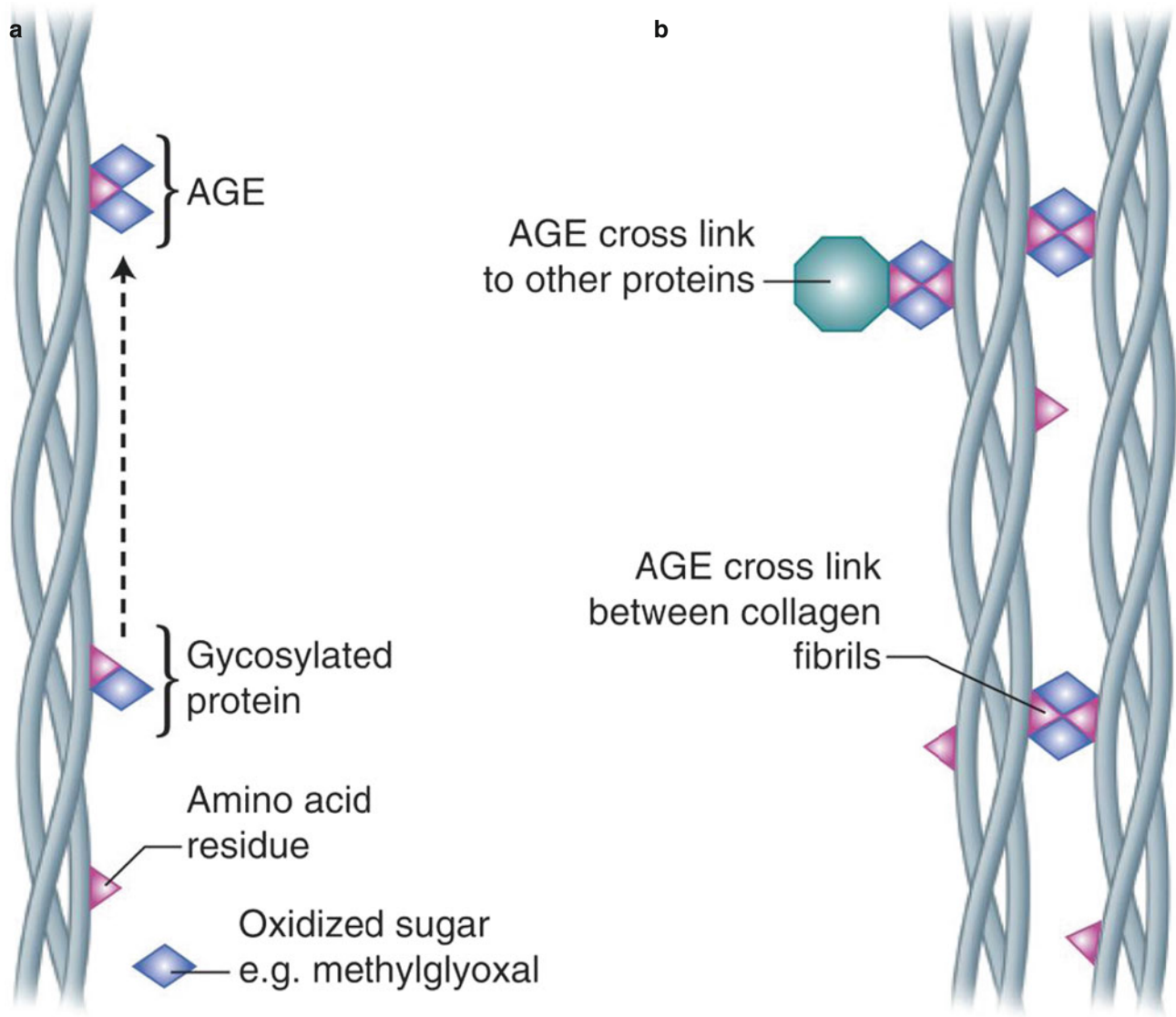


Figure I.E-2 Diagram of advanced glycation end products (AGE) formation on collagen fibril (a), showing cross-linking between collagen fibrils and to other proteins (b)

A. Advanced Glycation End Products

The Maillard reaction occurs normally with aging, but is accelerated in diabetes [5]. Oxidized sugar molecules, notably methylglyoxal, attach to proteins by formation of a Schiff base and then slowly rearrange to a more stable Amadori adduct [6]. Glycosylated proteins can rearrange and dehydrate further to produce brown and fluorescent pigments, which also act as cross-links between proteins [5]. In structural proteins such as collagen, this can reduce protein solubility and affect mechanical properties (Figure I.E-2). These oxidized, dehydrated, cross-linked protein compounds are irreversibly altered and are collectively termed advanced glycation end products (AGE) [6]. Although AGE formation is “normal,” it is greatly accelerated in diabetes beyond the first order kinetics expected from hyperglycemia alone [6]. Superoxide inhibits glyceraldehyde-3-phosphate dehydrogenase (GAPDH),

resulting in increased levels of glyceraldehyde-3-phosphate, which fragments into methylglyoxal [3, 4].

The glycosylated precursors of AGE have pathological effects by altering protein structure and function within cells, as well as altering extracellular matrix (ECM) components and ECM interactions with cell receptors such as integrins [3]. Systemically, AGE precursors target the receptor of AGE (RAGE) on endothelial cells, mesangial cells, glia, and macrophages, resulting in production of reactive oxygen species and phosphorylation of numerous kinases, activating the pleiotropic transcription factor NF- κ B [7, 8]. This factor NF- κ B links AGE to several inflammation-related cellular pathways such as apoptosis, motility, and cytokine expression [6, 9]. The more complex interlinked AGE can also make long-term alterations to the function of long-lived structural proteins in the ECM, in particular collagen, resulting in a chronic functional change and creating a depot

of pathological signaling at RAGE [6]. Collagen cross-linking also increases vascular stiffness and provides a molecular link between diabetes and hypertension [10, 11].

B. Protein Kinase C

The inhibition of GAPDH by intracellular hyperglycemia and superoxide production also increases production of the metabolite diacyl glycerol (DAG), which is the specific physiologic activator of the protein kinase C (PKC) family of enzymes [3, 12]. Activation of RAGE and increased activity of the aldose reductase pathway may also activate PKC by increasing reactive oxygen species and inhibiting GAPDH. When activated, PKC forms a key messenger in the pathological processes of diabetes with downstream effects that include reduced nitric oxide production and increased endothelin-1 activity, both contributing to a reduction in microvascular blood flow [3]. Activated PKC also activates NF- κ B and affects the expression of vascular endothelial growth factor (VEGF), transforming growth factor beta (TGF- β), and plasminogen activator inhibitor-1. Each of these factors has direct relevance to the pathological processes in diabetic retinopathy, such as vascular permeability, angiogenesis, capillary occlusion, vascular occlusion, and proinflammatory gene expression. Hyperglycemia also activates PKC- δ which contributes to cell death of retinal vascular pericytes specifically [13].

Orally administered, isoform-selective inhibition of PKC- β has been shown to have a beneficial effect in animal models of diabetic retinopathy [14–17] and has also been shown to ameliorate diabetes-induced retinal hemodynamic abnormalities in patients with diabetes [18]. Two 3-year, randomized, double-masked, placebo-controlled phase 3 trials (PKC-DRS and PKC-DRS2) [19, 20] demonstrated an approximately 50 % reduction in the occurrence of vision loss in patients treated with the isoform-selective PKC β inhibitor ruboxistaurin (RBX). Although one study attained statistical significance, the other (PKC-DRS) was not adequately powered to do so [19]. Two subsequent randomized clinical trials using RBX showed slowing in the development of diabetic macular edema (DME) and its attendant visual loss in patients, consistent with that observed in the previous trials, although these also failed to meet their primary outcome measure [21]. The relative risk of sustained moderate vision loss from DME was reduced by 40–50 % with RBX. Vision benefit exceeded the benefit on morphologic severity, suggesting a potential neuroprotective effect of PKC- β inhibition. Given the only modest clinical benefit and lack of statistical significance in several clinical trials, RBX is not currently being pursued for the treatment of diabetic retinopathy or macular edema.

C. Aldose Reductase

Aldose reductase is the first enzyme of the polyol pathway, catalyzing the reduction of glucose to sorbitol with the oxidation of NADPH to NADP⁺. With a low affinity for glucose, aldose reductase only converts significant amounts of glucose into sorbitol in a diabetic hyperglycemic setting. Increased flux in the polyol pathway depletes the cell of NADPH, which limits the replenishment of glutathione, and thus depletes the cell defenses against reactive oxygen species (ROS). Also, corresponding increases in cytosolic NADH:NAD⁺ ratio can result in downstream increases of AGE precursor methylglyoxal and DAG which activates PKC [3].

Although multicenter clinical studies to date have not detected a structural or functional benefit for nephropathy from blockade of this pathway, beneficial effects of the angiotensin-converting enzyme inhibitor enalapril and the aldose reductase blocker losartan have been noted in terms of reducing the risk of progression of nonproliferative diabetic retinopathy [22, 23].

D. Hexosamine

Intracellular hyperglycemia also causes increased flux through alternative glucose metabolic pathways including the hexosamine pathway, where fructose-6-phosphate is converted into glucosamine-6-phosphate. Inhibition of GAPDH by superoxide also underlies this pathway activation in diabetes [3]. Enzymatic glycation of certain transcription factors with glucosamine alters the expression of relevant pathological cytokines such as TGF- β 1 [3]. Thus, the increased hexosamine flux contributes to changes in gene expression and release of signaling molecules that contribute to the pathogenic milieu of diabetes.

E. Oxidative Stress

Finally, superoxide itself contributes to the pathological effects of hyperglycemia. Superoxide causes oxidative stress, which directly damages cells and leads to degenerative pathways such as apoptosis. Oxidative stress also arises from RAGE activation and from the aldose reductase pathway as described above. Oxidative stress is also a potent inducer of RAGE expression, forming a positive feedback cycle [8]. An important regulator of oxidative stress is the transcription factor nuclear factor erythroid-2-related factor 2 (also known as NFE2L2 or NRF2). This molecule also has anti-inflammatory activities. Studies suggest that NRF2 is an important protective factor regulating the progression of diabetic retinopathy [24, 25].

III. Diabetic Retinopathy

A. Epidemiology

Diabetic retinopathy (DR) is the leading cause of visual loss in adults of working age [26, 27]. Population-based studies found DR is common among diabetic individuals (prevalence 20–40 %), and vision-threatening features occur in 5–10 %, but these estimates vary as diabetes becomes more prevalent and treatments improve. The Wisconsin Epidemiologic Study of Diabetic Retinopathy provided some of the most complete longitudinal data on the incidence of DR [28]. Over 25 years, nearly all patients (97 %) with diabetes develop some DR at a rate of around 15 % per year for type 1 and 8 % per year for type 2 diabetes and continue to progress at similar probabilities each year [28]. The risk of developing DR increases with duration of diabetes and with poor control of hyperglycemia [27]. The other modifiable risk factors for DR include hypertension, dyslipidemia, inflammation, and obesity. Non-modifiable risks include puberty, pregnancy, and ethnicity [27]. Long-term follow-up of patients with DR demonstrate high mortality (and a specific mortality risk associated with macular edema), demonstrating that DR is an important marker of widespread pathologic changes [29–31].

Two landmark clinical trials established that improved glycemic control ($HbA_{1C} < 7\%$) reduced the risk of development and progression of DR [32, 33]. Other trials have failed to show a benefit of improved glycemic control for patients with existing DR, which might indicate that hyperglycemia has a gradual incremental and cumulative effect on DR [27]. More important and interestingly, the two large randomized trials of glycemic control showed that rates of DR progression were slowed in the original treatment group even many years after the glycemic control between treated and non-treated groups had merged once the trials had concluded [33, 34]. This long-term benefit from earlier treatment was termed “metabolic memory.” The mechanisms for metabolic memory are not fully known, but vitreous may be highly relevant in the storage of this long-term signal.

B. Pathophysiology of Diabetic Retinopathy

Initial observations established the understanding of DR as a prototypical microangiopathy, where capillary changes underlie the entire spectrum of disease. However, in view of the systemic processes described above and with current methods to investigate ocular biochemistry and neuronal function, a modern understanding of DR recognizes that the visible vascular changes are the result of a

long process of biochemical derangement [35]. In particular, the cellular and biochemical processes described above cause stress and dysfunction in retinal neurons, glia, and vascular cells, resulting in capillary loss and subsequently hypoxia, which causes production of vascular endothelial growth factor (VEGF). There are, however, other sources of VEGF in the diabetic eye, including a chronic inflammatory response and upregulated renin-angiotensin hormones acting on ocular angiotensin II receptors [36]. In addition, VEGF-independent pathways may contribute to retinopathy and angiogenesis, such as erythropoietin signaling within the eye [37] and release of extracellular carbonic anhydrase-I that stimulates the kallikrein pathway [38].

1. Diabetic Retinopathy and the Neurosensory Retina

It has been recognized for 50 years that in addition to causing retinal vascular changes, diabetes disrupts the neurosensory retina [39, 40], and recent techniques to measure these changes have further improved our understanding of diabetic retinal neuropathy [35, 41]. Measures of outer retinal function such as dark adaptation are reduced in diabetic patients [35, 42]. These outer retinal functions should not be affected by inner retinal vasculopathy as they are supplied by the choroid. It is possible that a diabetic choroidal vasculopathy influences outer retinal function. Subtle tests of inner retinal function with frequency doubling technology visual field testing, and sensitive structural measures such as OCT, reveal inner neurosensory changes before retinal vascular changes of DR are seen [43–45]. Multifocal electroretinography (mfERG) was found to correlate closely with vascular DR [46], but more interestingly, abnormalities of mfERG were shown to precede and predict vascular abnormalities with sensitivity and specificity [47, 48].

Together these studies demonstrate not only that the neural retina may be affected by diabetes before vascular changes appear but also that these correlations of neural and vascular dysfunction are precise [43]. The interaction can be conceptualized as a neurovascular unit with a pathological feed-forward cycle (Figure I.E-3) [1, 35]. That is, neural degeneration from diabetes results in release of vascular permeability factors (notably VEGF), to the detriment of cells forming the blood-retina barrier, while damage to retinal capillary endothelium and pericytes leads to loss of the supply of nutrients and breakdown in the integrity of the important blood-retina barrier, leading to the accumulation of macrophages, release of harmful cytokines, and further damage to retinal neurons. This is an amplifying cycle driven by hyperglycemic stress. This model also has implications for vitreous, which is a major paracrine depot for signals such as cytokines (see below).

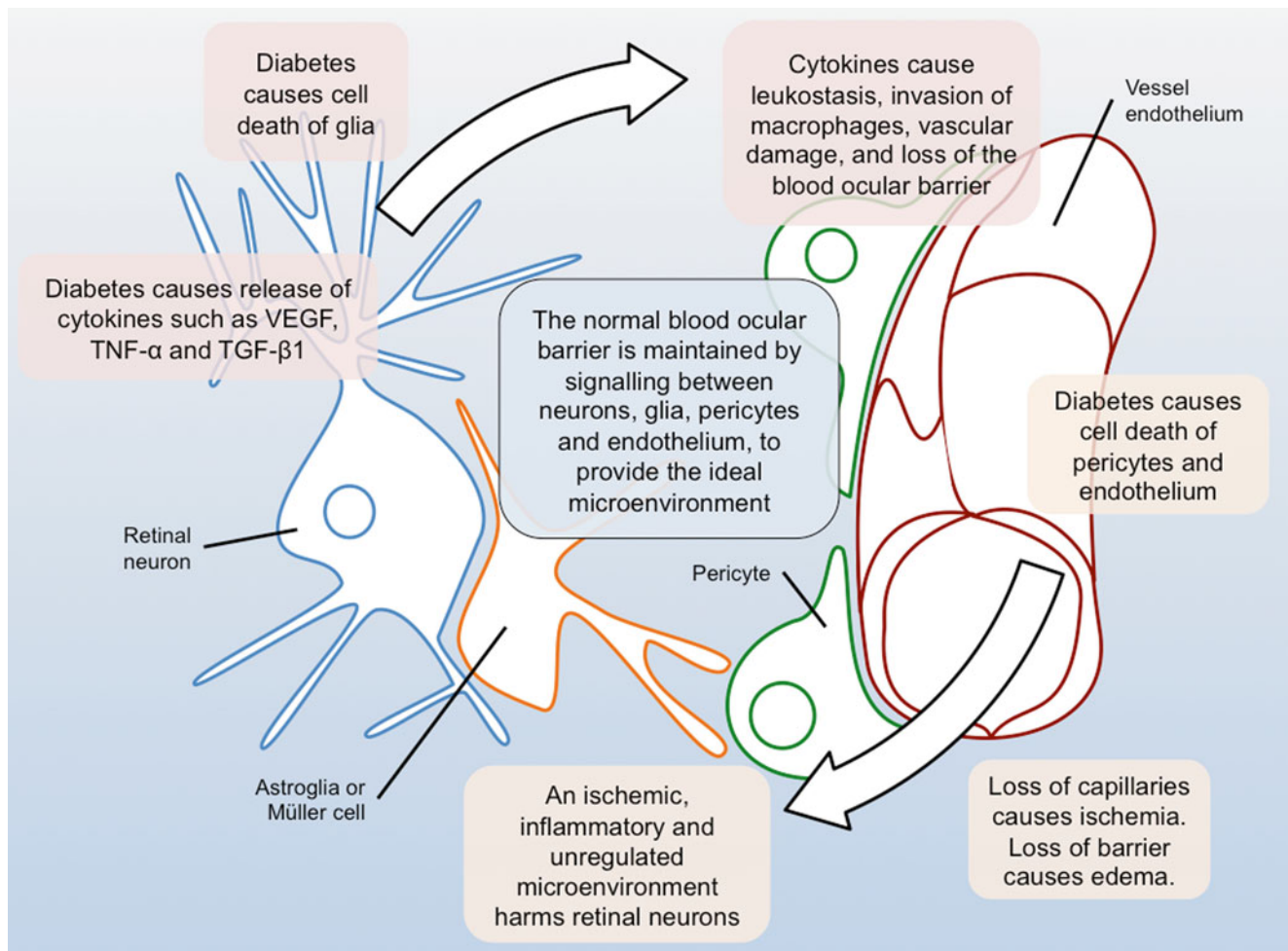


Figure I.E-3 Positive feedback cycle between vascular and neuronal elements in diabetic retinopathy. Diabetes damages both to the vascular and neural cells of the retina and damage to either the vessels or the

neurons results in secondary damage to the other. [*TNF- α* tumor necrosis factor alpha, *TGF- β 1* transforming growth factor beta, *VEGF* vascular endothelial growth factor]

2. Diabetic Retinal Vasculopathy

To date, the medical profession historically awaits the appearance of retinal vascular changes before establishing the diagnosis of diabetic retinopathy (DR). It is clear from the foregoing that derangements in physiology predate the visible histopathology. Thus, the established classification of DR is based on the visible vascular changes on funduscopy. Venous dilatation, perhaps the earliest fundoscopic change, is a physiologic adaptation to the altered physiologic milieu, especially hypoxia. Apoptosis of capillary pericytes results in retinal microaneurysms, another early change, and then as capillaries are lost and ischemia develops, hemorrhages and cotton wool spots are seen. Vascular dysfunction, increased permeability, and loss of the blood-retina barrier result in retinal edema and the deposition of hard exudates. At advanced stages, severe ischemia results in high levels of VEGF and abnormal new vessel proliferation. When these blood vessels grow into the vitreous, they can bleed easily and may also contract against the vitreous scaffold and create areas of tractional retinal detachment. Together these findings represent the classical concepts of DR (Figure I.E-4).

It is important, however, to appreciate the limitations of these concepts and develop new methods [see chapter II.F. Imaging vitreous] to assess ocular biochemistry and physiology, so as to diagnose diabetic eye disease in the stage of physiopathology and not await the more advanced stages of clinically evident histopathology that frame our current concepts of this disease. The earlier diagnosis afforded by this approach will enable intervention at an earlier stage in the natural history of disease when abnormalities are more likely to be reversible, and disease progression can more effectively be mitigated.

Inflammation is now recognized as an important component of DR [9]. As discussed, pathological cytokines such as TGF- β 1, tumor necrosis factor alpha (TNF α), and interleukin 1-beta (IL-1 β) are produced and released by cells experiencing the oxidative stress of hyperglycemia. Also AGE formation in the extracellular space directly activates inflammatory pathways and pleiotropic transcription factors such as NF- κ B [6]. These extracellular signals affect retinal capillaries, increasing vascular permeability, but also affect circulating leukocytes [49]. It was found that the early

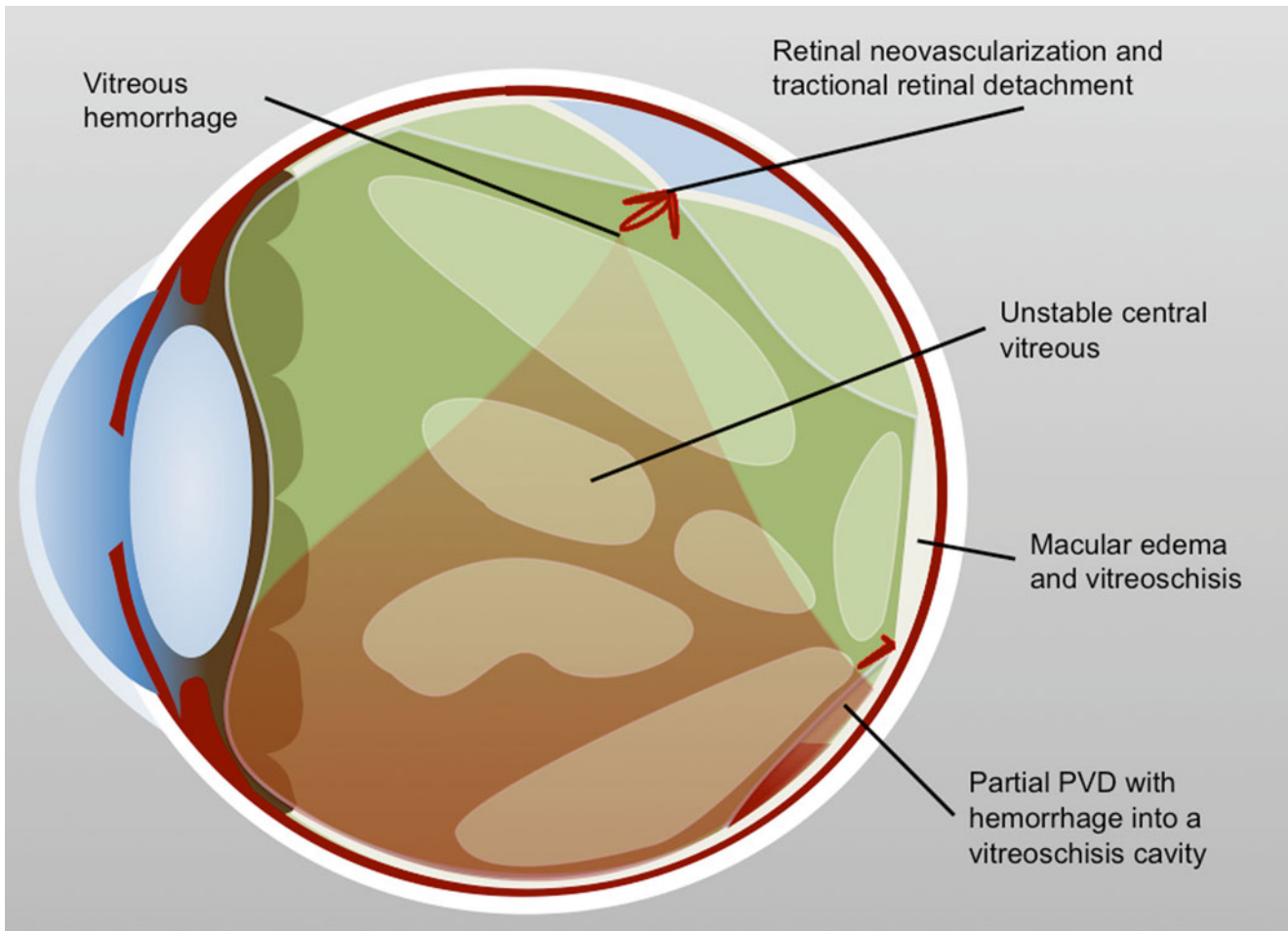


Figure I.E-4 The vitreoretinal complications of proliferative diabetic retinopathy. Elements of diabetic vitreopathy contribute to the structural complications of advanced proliferative diabetic retinopathy [PVD posterior vitreous detachment]

inflammatory event of leukostasis is an important component in DR [49], and this may contribute to capillary closure and loss [9].

IV. Diabetic Vitreopathy

Vitreous plays a central role in much of the visual loss associated with diabetic retinopathy (DR). Firstly, vitreous is an obvious factor in complications of proliferative diabetic retinopathy (PDR) such as vitreous hemorrhage and tractional retinal detachment (Figure I.E-4). Secondly, vitreous has a clear role in the development of macular edema, the leading cause of vision loss in diabetic patients, through both biochemical and mechanical pathways [see chapter III.K. Vitreous in retino-vascular diseases and diabetic macular edema]. Thirdly, vitreous may act as a biochemical depot or reservoir to mitigate or worsen the biochemical derangements of diabetes. Fourthly, vitreous affects the physiology of oxygen in the eye [see chapters IV.A. Vitreous physiology; IV.B. Oxygen in vitreo-retinal physiology and pathology]. Many of these effects are due to specific and intrinsic

changes in vitreous that occur in response to diabetes. This phenotype has been termed diabetic vitreopathy [50].

A. Molecular Alterations

In general, vitreous levels of small molecules such as glucose reflect the circulation of aqueous, and these levels may change in response to serum levels or tonicity [51, 52]. Glucose is usually lower in the vitreous than the serum, but has been found to be higher in people with diabetes [51]. Early experiments in diabetic rabbits detected changes in vitreous such as increased viscosity and reduced vitreous volume, but methodologic limitations limit interpretation of these data [53]. Modern proteomic techniques can quantify the proteins in human vitreous with or without diabetes [54]. Many hundreds of vitreous proteins have been identified with these techniques, including many of the signaling pathways implicated in DR [55]. It is difficult to interpret these studies directly for a number of reasons. Firstly, there is a wide variety of methods and each study reports different results that cannot be compared. Secondly, quantification of signaling proteins, such as VEGF, for example, does not necessarily

relate to potency of signaling and low concentrations of cytokines may not be detected. Thirdly, an increase of some proteins in the vitreous of diabetic patients does not imply their relevance to diabetic pathology, for example, the protein may be increased due to vascular permeability. Fourthly, the key structural proteins such as collagen are not often identified with these methods. Fifthly, many of the samples are collected during vitrectomy for vitreous hemorrhage and the effect of this pathology on the results is not known [54–56].

1. Collagen

Monnier and colleagues established a correlation between advanced glycation of collagen (measured as fluorescence in a skin biopsy) and severity of diabetic retinopathy [10]. Lundquist and Österlin showed vitreous glucose levels can be increased in excess of 11 mmol/L in diabetes, and then Sebag and colleagues showed that as a result, nonenzymatic glycation of human vitreous collagen was indeed increased [51, 57]. Additional enzymatic cross-linking of collagen, such as the dihydroxylysinoxidation, was also found by Sebag and colleagues to be elevated in diabetic vitreous [45], as was previously detected in other diabetic connective tissues such as skin [57, 58]. The diabetic cross-linking of human vitreous collagen was further characterized by Sebag and coinvestigators using Fourier transform Raman spectroscopy [59, 60].

Collagen cross-linking by AGE is believed to underlie the observed structural alterations in human diabetic vitreous [61–63]. Indeed, the term diabetic vitreopathy was initially coined to describe this premature aging of vitreous structure in response to glycation and cross-linking [50]. Interestingly, the accumulation of AGE in skin collagen, which correlated with vascular stiffness and joint stiffness, was also found to correlate with DR [10]. These biochemical abnormalities induce premature liquefaction and earlier posterior vitreous detachment (PVD) [64]. In particular, a partial PVD is much more common than complete PVD in diabetes [64–66], causing vitreo-macular traction or vitreoschisis forming a preretinal membrane, hallmarks of anomalous PVD [67].

2. Hyaluronan

The second major macromolecule of vitreous is hyaluronan (HA) [see chapter I.F. Vitreous biochemistry and artificial vitreous]. It is hypothesized that glycation of the protein core of HA contributes to depolymerization, dissociating HA from collagen and contributing to liquefaction in aging and diabetes. This hypothesis has yet to be tested in experimental models and humans. However, in the process of vitreous liquefaction, HA is hypothesized to be depolymerized and also dissociated from proteins such as collagen fibers. This might also occur with some cytokines, such as longer isoforms of

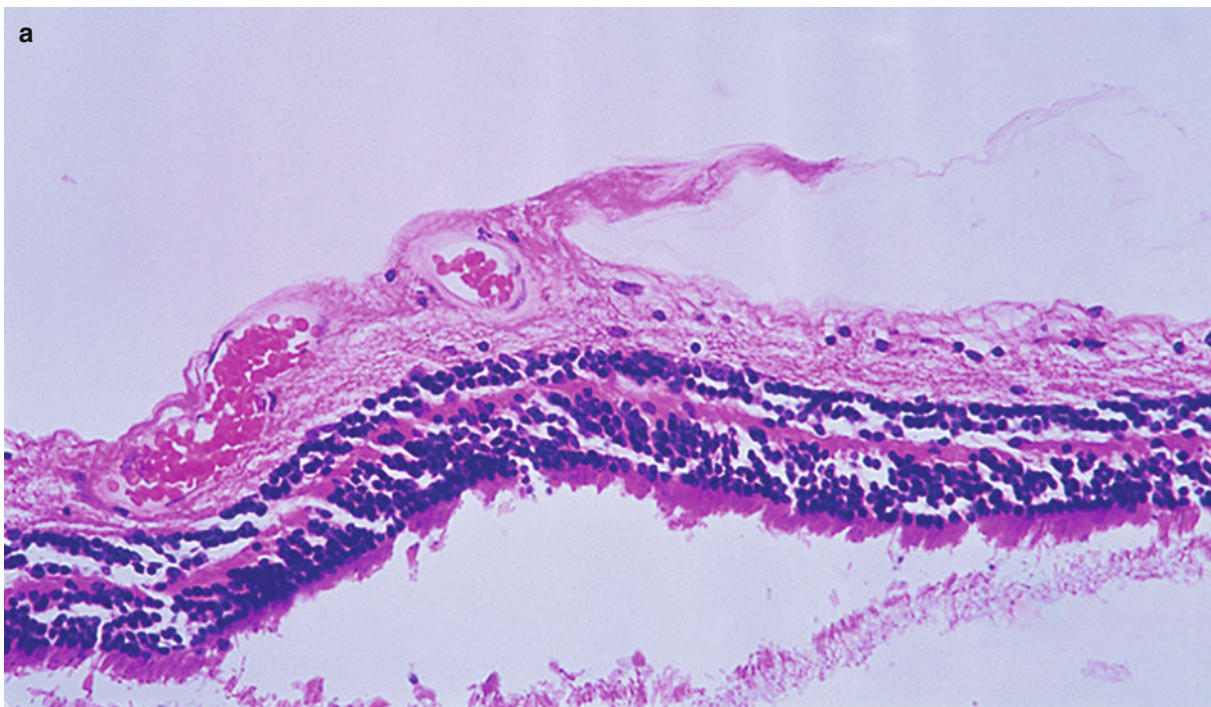


Figure I.E-5 Neovascularization at the human vitreoretinal interface in proliferative diabetic retinopathy. Proliferation of new blood vessels from the human retina (*below* in each image) into the posterior vitreous cortex (*above* in each image) demonstrates the insertion of vitreous fibers onto the neovascular complexes. This pathologic structural arrangement transmits traction from the collapsing vitreous body that

has undergone pathologic effects of diabetic vitreopathy. The traction stimulates further proliferation and can rupture the new vessels causing vitreous hemorrhage. Severe traction can also induce traction retinal detachment. (**a** is stained with hematoxylin and eosin; **b** is From Faulborn and Bowald [77] with permission)

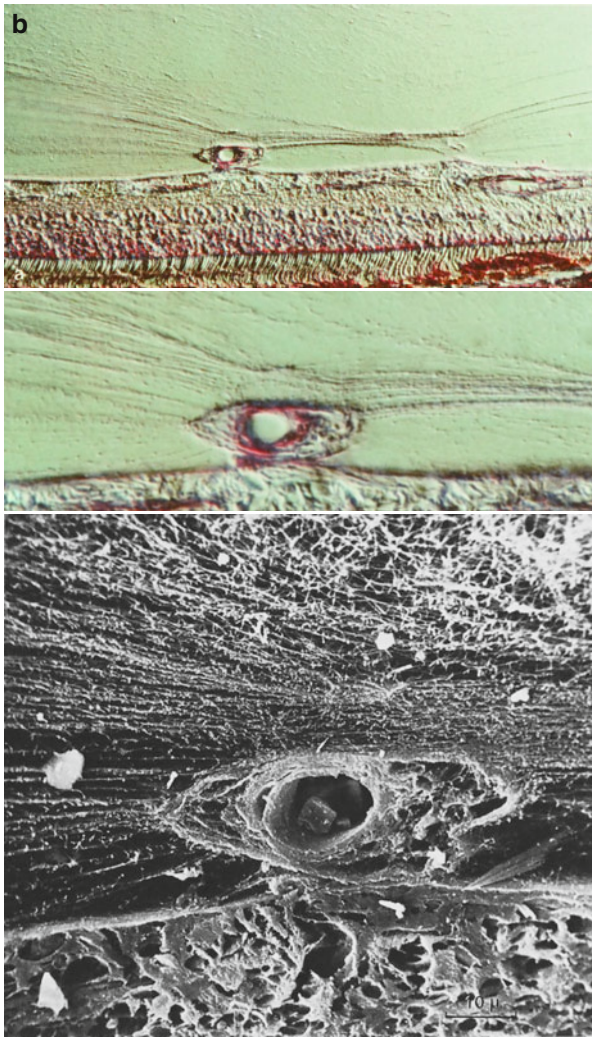


Figure I.E-5 (continued)

VEGF, which may be inactive when tightly bound to normal HA, but with depolymerization of HA, there may be dissociation and activation of this and other cytokines potentiating the cytokine effect. In this way the premature liquefaction of diabetic vitreous may also directly stimulate the pathological pathways of DR.

It has been identified that AGE in diabetic vitreous may accelerate the depolymerization of HA. Initial studies showed that UV light causes oxidative damage and light-induced depolymerization of HA when in the presence of a photosensitizer (riboflavin) [68, 69]. Collagen in the same samples accumulated and precipitated, presumably due to cross-linking [68]. In experimental diabetes or incubation with sugars, AGE formation in ocular proteins occurs within hours and results in light-induced oxidative stress [70, 71]. These AGEs were specifically shown to induce light-associated depolymerization of HA in vitreous through oxidative stress, leading to vitreous liquefaction and reduced viscosity [72, 73]. This is a second mechanism by which dia-

betic vitreopathy can be seen to resemble premature aging through AGE formation and oxidative stress.

3. Extracellular Matrix Constituents

In addition to the two major molecular components of vitreous described above, there are many lesser (in quantity, albeit probably not in importance) constituents that are molecules typically found in extracellular matrices throughout the body. These too are likely to be affected by the biochemical abnormalities of diabetes. Of greatest significance in this regard is that these extracellular matrix molecules are concentrated at the vitreoretinal interface and thus are likely to play an important role in the pathophysiology of both proliferative diabetic retinopathy and diabetic macular edema.

B. Structural Alterations

1. Vitreoretinal Interface

The vitreoretinal interface is a site of complex dysfunction in the diabetic eye and is the site where diabetic vitreopathy has most clinical relevance. There is an unusual and strong interface between vitreous and retinal vessels (Figure I.E-5a) [see chapter II.E. Vitreo-retinal interface and inner limiting membrane]. Thus, early observers noted that contraction of the posterior vitreous was associated with the important tractional and hemorrhagic complications of proliferative DR (PDR) [74]. Liquefaction of the central vitreous was found to be accelerated by diabetes and accompanied by early posterior vitreous detachment (PVD), although this is often incomplete and/or anomalous due to a high incidence of vitreoschisis, especially in proliferative retinopathy [64, 65, 75]. The presence of a partial PVD also portends a poorer prognosis [75, 76]. In pathological studies of PDR, it was noted that retinal neovascularization tended to occur at sites of vitreoretinal adhesion, where new vessels would breach the inner limiting membrane (ILM) and entangle in the posterior vitreous cortex [77] (Figure I.E-5b). Complete PVD was found to be uncommon among those diabetic patients with PDR or macular edema [78, 79], and conversely vitrectomy prevented recurrence of retinal neovascularization [80]. In areas of PVD new vessel outgrowths were “abortive” or limited in that they did not fan out to insert into the posterior vitreous cortex [81]. Together these observations forged the concept that DR is worse in regions with firm vitreoretinal adhesion and that these points of adhesion contribute to complications, while PVD was protective against florid neovascularization and aggressive PDR.

In eyes from patients with diabetes, scanning electron micrographs of the retinal surface after PVD showed that the normally smooth ILM was textured and cellular, with remnants of cortical vitreous collagen commonly remaining on the ILM [82, 83], although similar findings can occur in nondiabetic

eyes [70]. When these remnants are in the form of sheets, which is quite often, this splitting of the cortical vitreous is known as vitreoschisis [84] [see chapter III.B. Anomalous posterior vitreous detachment and vitreoschisis]. By OCT, vitreoschisis was found in half of patients with macular holes and macular pucker and is likely to be prevalent in diabetes as well [85, 86]. Indeed, ultrasonography in cases of diabetic vitreous hemorrhage revealed a previously unrecognized high prevalence of vitreoschisis in PDR [87]. In 270 non-vitreotomized eyes of diabetic patients with vitreous hemorrhage, 45 had clear evidence of vitreoschisis on ultrasonography, usually in the premacular region. The posterior wall of the schisis cavity created by the split in the posterior vitreous cortex is able to exert significant traction [87], especially at the points where the inner and outer walls meet to reunite into full-thickness posterior vitreous cortex (Figure I.E-6). A pathological study of diabetic preretinal membranes removed during vitrectomy suggested that many of the multilayered membranes were the result of vitreoschisis of the posterior vitreous cortex, as a collagen II layer was identified under all membranes [88]. The Munich group found that membranes, most often the result of vitreoschisis, were also excessively cellular in diabetic patients [89]. While the premacular lacuna (Bursa Premacularis of Worst) has also been identified in nondiabetic vitreous [90], it appeared that in diabetes the thin outer wall was more likely to remain adherent to the retina after collapse of the central vitreous and apparent PVD [91], owing perhaps to the effects of diabetes upon extracellular matrix components at the vitreoretinal interface.

Diabetes causes changes in the posterior vitreous cortex and inner limiting membrane (ILM) that increase vitreoretinal adhesion and contribute to the tendency for vitreoschisis. The accelerated cross-linking due to nonenzymatic glycation and the formation of AGEs may occur between proteins of the cortical vitreous (primarily type II collagen) and the ILM (primarily type IV collagen). Both AGE and RAGE are found in the ILM, resulting in long-lasting pathological signaling of and by Müller cells [92]. The AGEs within the ILM can also disrupt other normal interactions between Müller cells and the extracellular matrix such as integrin signaling [6]. There are also changes in Müller cell physiology due to DR that may specifically increase vitreoretinal adhesion. An important inflammatory cytokine that is upregulated in DR and is important for diabetic retinal vasculopathy (see above) is the intercellular adhesion molecule (ICAM-1) [9, 49]. The expression of ICAM-1 is upregulated in Müller cells following activation of RAGE [6, 93], and soluble cell adhesion molecules are also excessively present in diabetic vitreous [94]. These ICAM-1 and vascular cell adhesion molecule (VCAM-1) are also important cell migration agents and may recruit retinal glia and inflammatory cells onto the retinal surface and into the cortical vitreous in diabetes. The preretinal membranes common in both inflammatory conditions and in DR express high levels of ICAM-1 and VCAM-1 [93].

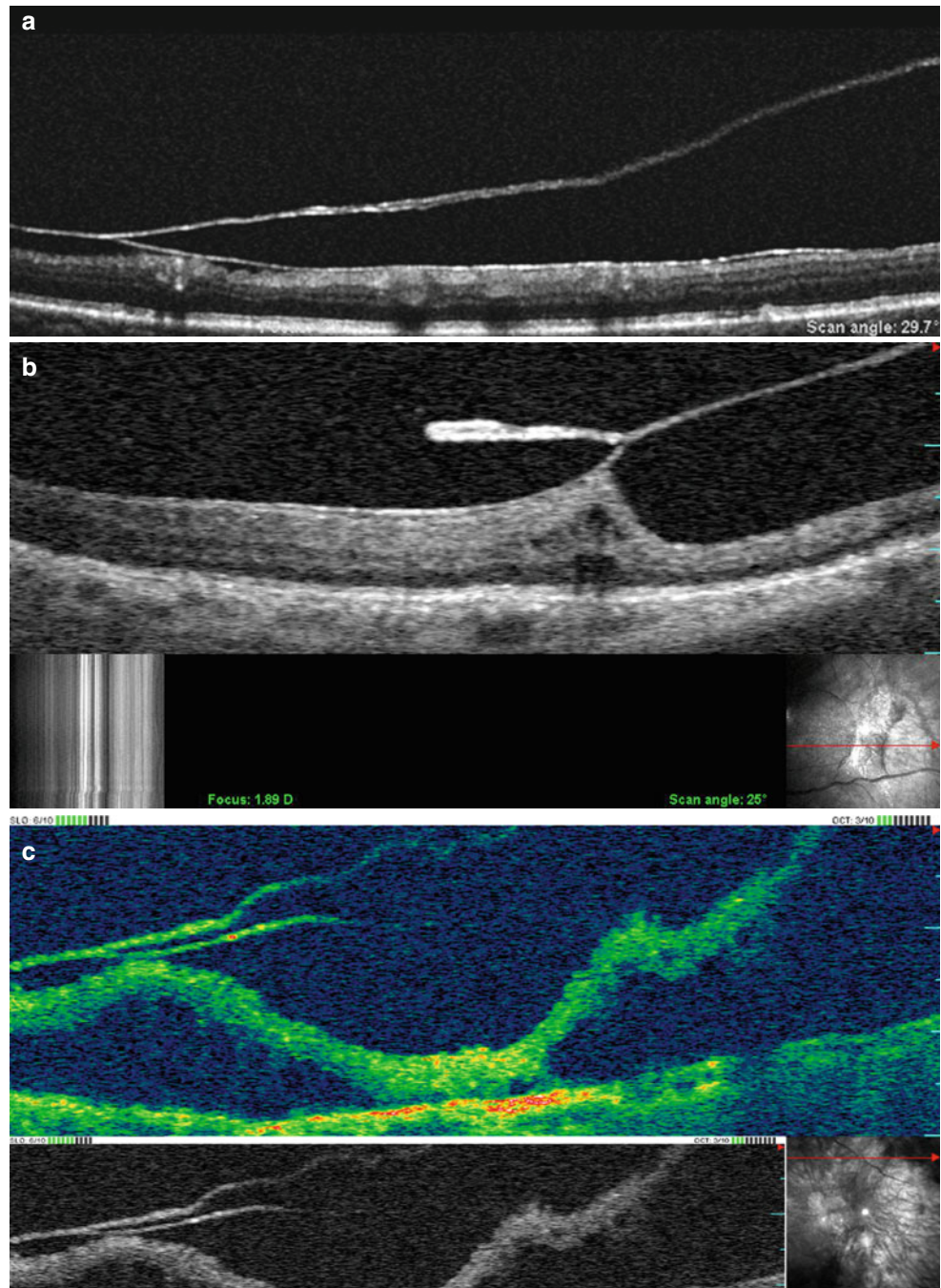
On histological examination, ILM thickness was increased to around twice normal in eyes with diabetic maculopathy, with invasion of macrophages [95]. It is hypothesized that this thickened and cellular ILM is less conductive, preventing egress of fluid from the edematous diabetic macula. Since the ILM is essentially the basement membrane of neuroectodermal Müller cells, it has some homology to the mesangium of the kidney and to the endothelial basement membrane of retinal capillaries that are also damaged and thickened by diabetes (see above). Molecules such as interleukin-6 and VEGF are known to be important in the pathology of both nephropathy and the preretinal membranes of DR [93, 96, 97]. Therefore, the cause of vitreoschisis in diabetic vitreopathy represents converging factors: liquefied collapsing unstable central vitreous; regions of increased cortical vitreous adhesion from a thickened, cross-linked, and cellular ILM with increased cell adhesion from Müller cells; and in advanced cases points of firm adhesion at foci of neovascularization.

These changes at the vitreoretinal interface in diabetes result in a proliferating cellular vitreous, forming pathological preretinal membranes. The cells of these membranes are themselves a source of further cytokines [96]. Furthermore, these invading blood or glial cells change into fibroblasts or myofibroblasts, forming contractile sheets between retinal anchor points. This cellular contraction of the vitreous results in tangential traction that contributes to macular edema, vitreous hemorrhage, and even traction retinal detachment (Figures I.E-4 and I.E-6c). When these planes of traction are created, normal forces such as eye movements or changes in vitreous tonicity can have severe consequences. A majority of diabetic vitreous hemorrhages were found to occur between midnight and 6:00 am suggesting changes in systemic glucose or tonicity may have significant mechanical effects in the eye [98]. An alternative hypothesis for this observation is that sleep apnea, a common comorbidity in diabetic patients, causes nocturnal vitreous hemorrhage by creating peaks of systemic hypertension. In a chronic context, however, macular edema, particularly the honeycomb pattern, is strongly associated with the elements of diabetic vitreopathy such as traction, cytokine production, and a thickened (glycated) impermeable ILM [99, 100].

2. Vitreous Body

As mentioned, diabetes alters the structure of the vitreous body, primarily by glycation (and thus cross-linking) collagen, dissociating hyaluronan, and accelerating liquefaction. In normal youthful vitreous, hyaluronan interacts with collagen fibrils to organize a bimolecular three-dimensional network that stabilizes vitreous and maintains transparency by separating collagen fibrils and thus minimize light scattering and maximize photon transmission to the retina (Figure I.E-7a). With changes in both collagen and hyaluronan due to diabetes, there is disruption of the collagen-

Figure I.E-6 (a) Vitreoschisis in nonproliferative diabetic retinopathy. Combined OCT/SLO imaging of a split in the posterior vitreous cortex demonstrates the lambda sign at the point of reunification of the inner and outer walls of the vitreoschisis cavity into full-thickness posterior vitreous cortex. This patient had nonproliferative diabetic retinopathy. (b) Vitreoschisis in proliferative diabetic retinopathy. Significant axial traction at the reunification point exerts considerable traction on the retina with elevation of the retina. (c) Vitreoschisis in proliferative diabetic retinopathy with traction retinal detachment. The classic lambda sign of vitreoschisis is seen on the left where the inner and outer walls of the vitreoschisis cavity rejoin to form full-thickness posterior vitreous cortex. Retinal traction is typically significant at this site of reunification and in this case has produced traction retinal detachment. The grayscale image at the bottom is included for slightly better resolution of this OCT whose image quality is compromised by slight vitreous hemorrhage and lens opacification



hyaluronan association, resulting in cross-linking of collagen fibrils and displacement of hyaluronan that draws water and forms liquid vitreous. The formation of macroscopic fibers can be seen with dark-field slit microscopy [49] (Figure I.E-8). The collagenous nature of these structures has been confirmed by electron microscopy (Figure I.E-9). Dynamic light scattering is able to detect these changes *in vitro* [101] and may provide a clinical method for detection and quantification *in vivo* [60], while Raman spectroscopy could offer further molecular characterization [59].

The clinical effects of these diabetes-induced changes with the vitreous body are liquefaction with destabilization of the gel and antero-inferior collapse of the vitreous body. Given the aforementioned abnormalities at the diabetic vitreoretinal interface, this destabilization will place traction at the vitreoretinal interface with a variety of possible consequences that are not mutually exclusive:

- If there is sufficient weakening of vitreoretinal adhesion, an innocuous PVD will occur and the long-term prognosis will be significantly ameliorated.

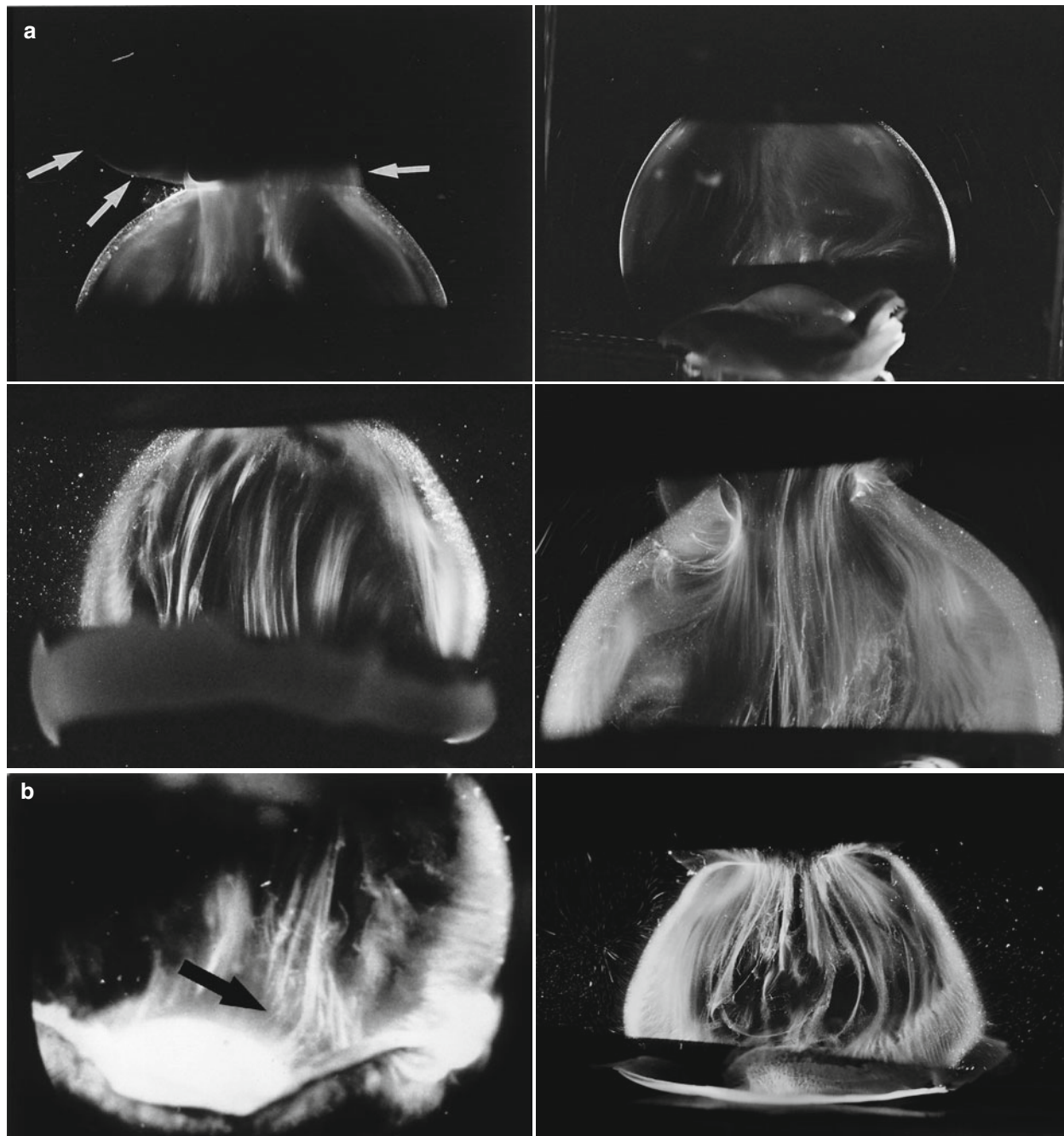


Figure I.E-7 Vitreous structure in non-diabetic eyes. All images are photographs of fresh, unfixed human eyes with the sclera, choroid, and retina dissected off the vitreous cortex. Each specimen was suspended in an isotonic solution and illuminated from the side with a slit lamp beam, creating a horizontal optical section. The anterior segment is below and the posterior pole is above in all images. **(a)** Dark-field microscopy of human vitreous structure in children (*top panel*) and adults (*middle panel*). There is considerable light scattering from the peripheral and posterior vitreous cortex, owing to the dense matrix of collagen fibrils. Within the central vitreous, however, there is little light scattering in children due to a homogenous distribution of collagen fibrils separated by hyaluronan molecules. This is apparent not only in the specimen from a 4-year-old child (*upper right*) but also in the specimen from an 11-year-old child (*upper left*) where vitreous is seen

extruding out through a dehiscence in the premacular region (*white arrows*) where the posterior vitreous cortex is thinner than elsewhere. In spite of this significant traction, there are no macroscopic fibrous structures in the vitreous body. In the adult eyes (*middle left*, 56 years old; *middle right*, 59 years old), however, there are visible fibers with an antero-posterior orientation. These fibers are continuous from the posterior pole to anterior periphery where they insert into the vitreous base surrounding the lens. **(b)** Vitreous fibers course anteriorly to insert into the vitreous base (*black arrow*). The *left* image demonstrates fiber insertion both anterior and posterior to the ora serrata. The *right* image shows the continuity of fibers from the posterior pole to the anterior periphery where they insert into the vitreous base. [see chapter III.H. Peripheral vitreo-retinal pathology]

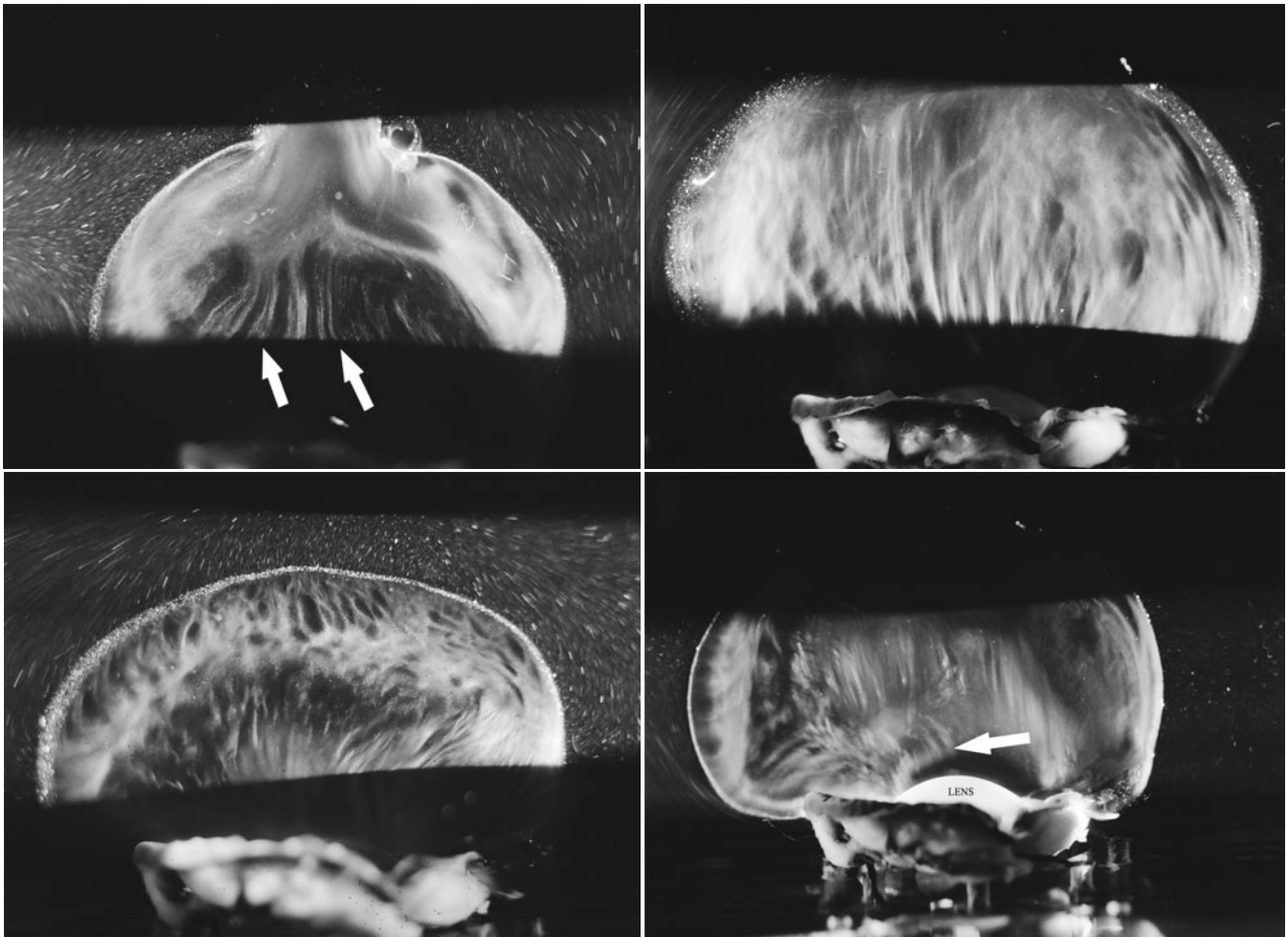


Figure I.E-8 Structural effects of diabetic vitreopathy. Dark-field microscopy of vitreous structure in the two eyes of a 9-year-old girl with a 5-year history of type I diabetes and no evidence of diabetic retinopathy. There are macroscopic fibers (*white arrows*) with an antero-

posterior orientation coursing from the posterior vitreous to insert into the vitreous base around the lens (*lower right image*). This structure is far more similar to middle-aged adults (*bottom panel figure I.E-7b*) than age-matched controls without diabetes (*top panel figure I.E-7a*)

- If there is persistent adhesion at the vitreoretinal interface, there can be traction upon abnormal new vessels with rupture and vitreous hemorrhage.
- If there is persistent adhesion over a broad area at the vitreoretinal interface, there can be traction upon the retina with “table-top” tractional retinal detachment.
- If there is traction upon the macula, diabetic macular edema can be exacerbated.
- If there is insufficient weakening of vitreoretinal adhesion there can be vitreoschisis, providing a scaffold for cellular preretinal membranes and further traction.

V. Physiological Considerations in Diabetic Vitreopathy

A. Oxygen Physiology

As described by Holekamp and Beebe [see chapter IV.B. Oxygen in vitreo-retinal physiology and pathology], vitreous

plays an important role in oxygen physiology of the eye, and these effects have heightened relevance in diabetes where widespread retinal ischemia and altered vitreous structure are concurrent. It is known that oxygen gradients exist within the eye [102, 103]. Oxygen in the clear optical tissues of the anterior chamber, lens, and vitreous arises from retinal and iris vessels and from diffusion across the cornea, with oxygen concentration lowest around the ciliary body and surrounding the lens [102]. These gradients suggest oxygen consumption by vitreous and the crystalline lens, supported by the observation that cataract surgery and vitrectomy cause persistently elevated oxygen tension postoperatively [103]. However, there is debate about whether oxygen diffusion rates are altered by vitrectomy [104–106]. Movement of small molecules may be affected by convection currents or affected by their association with larger molecules [105]. Ascorbate is thought to be responsible for the chemical consumption of oxygen in the vitreous, and it is proposed that an association between ascorbate and the gel macromolecules of vitreous results in the higher ascorbate levels and

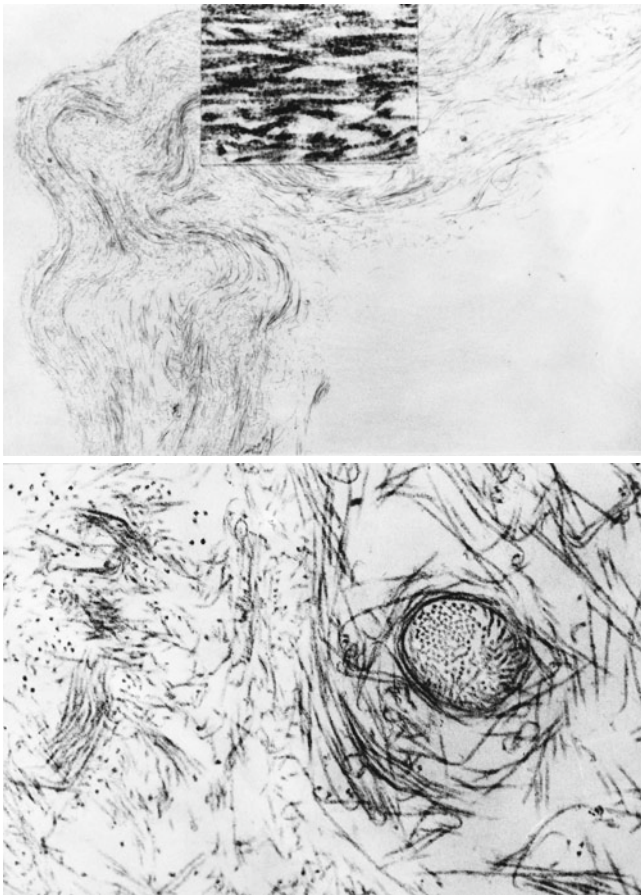


Figure I.E-9 Ultrastructure of human vitreous fibers. Transmission electron microscopy of human vitreous in middle age demonstrates bundles of collagen fibrils shown longitudinally (*top image*) and in cross section (*bottom image*). The inset in the upper image is a high magnification view of the bundle of fibrils demonstrating their collagenous nature. The biochemical changes of diabetic vitreopathy, in particular the nonenzymatic glycation that results in advanced glycation end products within the vitreous collagen fibrils and promotes cross-linking of collagen fibrils (Figure I.E-2), cause these fibers to form much earlier in life than in nondiabetic individuals

faster oxygen consumption in gel vitreous than liquid vitreous [102]. Therefore, an intact vitreous gel consumes oxygen from the retinal surface, providing a barrier to oxygen flow from vascularized retina to ischemic areas while also protecting the lens and trabecular meshwork from oxidative stress [107]. This model has obvious relevance to diabetes, where an ischemic retina meets an abnormal vitreoretinal interface and increased liquefaction of the vitreous body with a prominent fibrous structure. It is not known whether oxygen circulates differently in diabetic eyes, but this would seem likely. Different factors may affect whether the adherent cortical vitreous or the increased liquefaction of central vitreous has a dominant effect on oxygen circulation, and further investigation is warranted.

B. Paracrine Depot

As described above, intracellular hyperglycemia results in release of numerous locally acting factors (paracrine signals), particularly cytokines, into the retinal interstitium, the vitreous body, and at the vitreoretinal interface. The micro-environment surrounding retinal neurons is normally closely controlled by glia (particularly Müller cells) and yet in diabetic retinopathy, Müller cells are affected early. Thus, extracellular cytokines accumulate in diabetic retina [8, 9] because the scavenging and regulating functions of retinal glia are impaired. The relative circulation of these cytokines into and out of lacunae within vitreous is unknown, but a stagnant pocket of liquid within a vitreoschisis cavity could concentrate cytokines and produce a depot effect. Furthermore, certain cytokines can bind vitreous components tightly and be essentially prevented from acting locally by this sequestration. The longer isoforms of VEGF are classic examples with regard to heparin binding. However, with either cleavage of the cytokine or the scaffold, the cytokines may be released in active form [108]. Vitreous can thus form an overwhelming “reservoir” of pathological paracrine signals, such as AGE, VEGF, and others [93], especially in the presence of a premacular vitreoschisis cavity which may increase the duration and potency of the cytokines released by the cells within diabetic retina that produce these factors [109, 110]. Proteomic analysis of vitreous in diabetes confirms the presence of many locally acting signals that are known to be involved in DR [54, 111] whose duration of action may be further prolonged because turnover and remodeling of vitreous is slow in adulthood [112].

As mentioned above, it was long ago observed that retinal neovascularization grows into the cortical vitreous, growing away from the retinal surface and entangling with the cortical vitreous fibers (Figure I.E-5), but in areas of vitreous detachment, the new vessels breach the internal limiting membrane (ILM) and grow along the retinal surface or form abortive clumps [77, 81]. This phenomenon could represent simply a mechanical scaffolding effect, or it could indicate that vitreous itself was attracting the neovascularization, or both. Faulborn and Bowald even proposed the term diabetic vitreopathy in passing, to describe a vitreous that had become trophic and recruited its own blood supply [77]. It is likely that vitreous detachment or vitrectomy allows clearance of angiogenic factors away from the retinal surface [107] or oxygenation from the ciliary body [see chapter IV.B. Oxygen in vitreo-retinal physiology and pathology]

The various aspects of diabetic vitreopathy and its role in diabetic retinopathy are summarized schematically in Figure I.E-10.

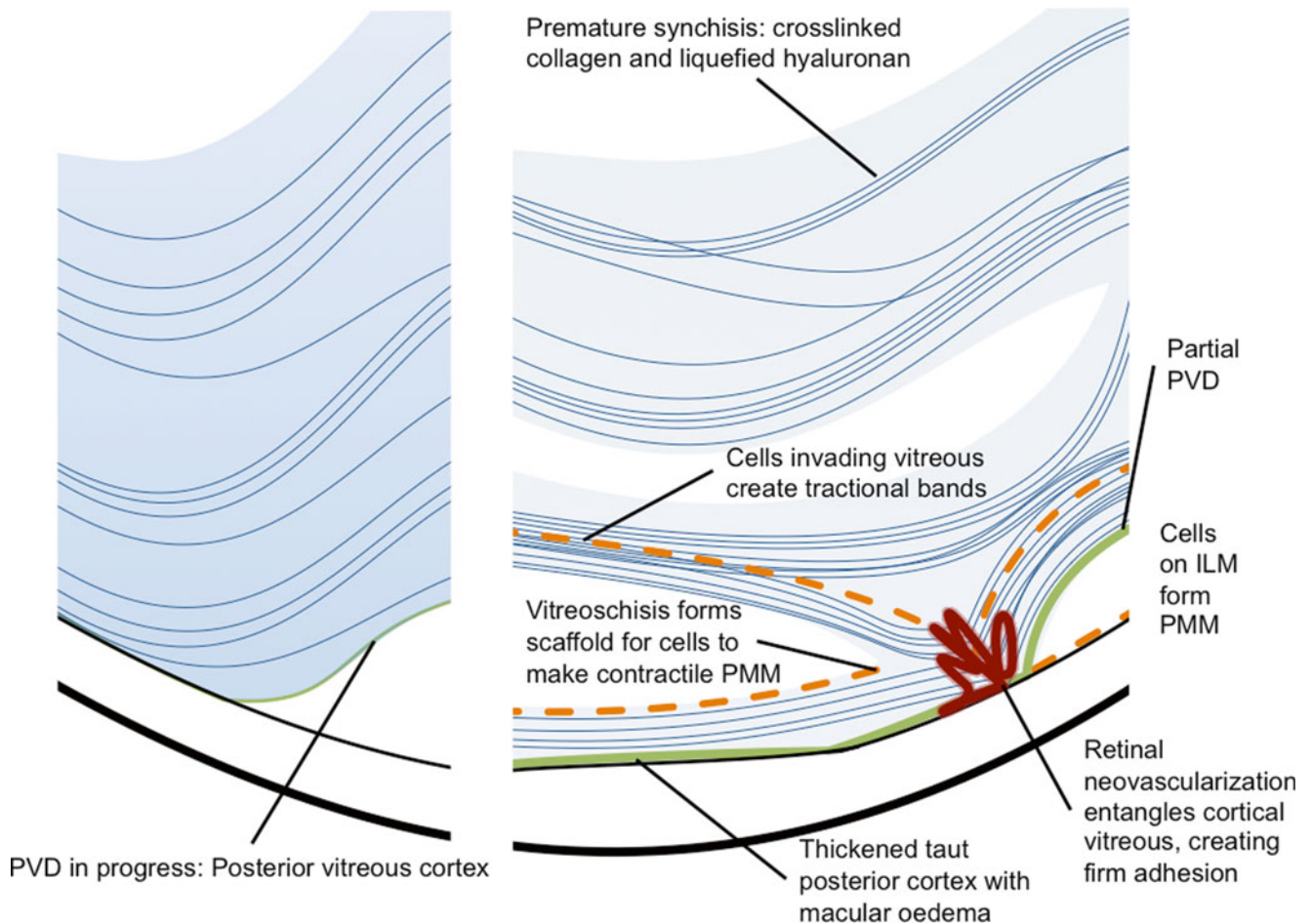


Figure I.E-10 Summary of the major elements of diabetic vitreopathy. Normal vitreous undergoing a PVD is shown on the left and diabetic vitreopathy on the right. Cells in the vitreous are illustrated as orange

dashed lines; the posterior vitreous cortex is illustrated as a *green line* [ILM inner limiting membrane, PMM premacular membrane, PVD posterior vitreous detachment]

VI. Treatment Considerations in Diabetic Vitreopathy

The treatment of diabetic vitreopathy can be preventative or therapeutic. Induction of PVD, either surgically or pharmacologically, would prevent the structural and some physiologic effects of diabetic vitreopathy described above. However, preventing diabetic vitreopathy at a molecular level would obviate the need for PVD either with surgery or pharmacologic vitreolysis and may mitigate many of the aforementioned biochemical derangements.

A. Pharmacotherapy

Pharmacologic options for preventing and managing diabetic retinopathy are expanding, but currently there are no agents in development specifically for managing diabetic

vitreopathy [26, 113]. The importance of nonenzymatic glycation and AGE in diabetic vitreopathy and diabetic retinopathy raises the possibility that prevention of vitreous AGE formation could reduce complications [8]. Extracellular AGE has also been implicated as a source of “metabolic memory,” conveying a long-term risk of complications after a period of hyperglycemia [33, 34], and in this regard blockade of the RAGE pathway may be a suitable approach [8].

1. Aminoguanidine

Aminoguanidine showed early promise as an AGE inhibitor. *In vitro* studies of bovine vitreous showed that the glycation and cross-linking of vitreous collagen can be inhibited by aminoguanidine [62]. Further, experimental studies in rats and dogs have shown that aminoguanidine can prevent DR [114–116]. In dogs this effect was not specifically related to AGE formation, and it was subsequently found that aminoguanidine is also an inhibitor of nitric oxide synthase

[6, 115]. A randomized human trial of aminoguanidine for diabetic nephropathy was neither designed nor powered to examine effects in the eye, but the risk of significant DR progression appeared to fall from 16 % with placebo to 10 % with aminoguanidine ($p=0.030$) [117]. However, a trial in older diabetic subjects appeared to show unfavorable early results and was terminated without publication. Lingering safety concerns related to nitric oxidase inhibition and the creation of oxidative stress are likely to prevent further use of aminoguanidine in humans [113].

2. Alagebrium

A specific breaker of AGE cross-links, alagebrium, was discovered in 1996 and led to several promising experimental studies [118]. In contrast to aminoguanidine, this agent is not designed to prevent AGE formation, but to reverse these cross-links, a remarkable and potentially exciting pharmacotherapy, not only for diabetes but aging as well. Alagebrium reversed myocardial and vascular stiffness in nonhuman primates [119, 120]. Although four human trials were completed for hypertension and heart failure, several other trials were never completed, and the role of this molecule in DR has never been assessed [113]. The concept of breaking cross-links has intuitive appeal in diabetic vitreopathy, to reverse rather than prevent complications of diabetes. It could be that the ability to release AGE cross-links can reduce an adherent vitreoretinal interface or mitigate the tendency for vitreoschisis, promoting a more complete PVD pharmacologically (see below) or facilitating vitrectomy with surgical induction of PVD in advanced DR. Thus, experimental investigation is warranted.

3. Vitamin B Derivatives

The B vitamins *pyridoxamine* and a synthetic derivative of thiamine *benfotiamine* have both shown promise in preventing complications of diabetes through AGE inhibition. Both agents had promising results in preventing diabetic retinopathy in experimental diabetes in rats [121, 122]. Human trials for these agents have had inconsistent and unimpressive results in reducing circulating AGE levels [113] and neither agent has been studied in humans in relation to the effects on the eye, in particular diabetic vitreopathy.

B. Surgery

In advanced diabetic retinopathy, vitrectomy has traditionally been reserved for structural indications: clearing vitreous hemorrhage or relieving traction retinal detachment. Results in these cases have been mixed, because these eyes have already sustained a great deal of damage from DR before surgery [123]. The major randomized trials of vitrectomy for complications of DR showed that benefits of vitrectomy were modest and that patients with type one diabetes with vitreous hemorrhage benefited most [124, 125]. That

said, it is important to point out that vitrectomy technology has improved greatly over four decades [see chapter V.B.1. History of vitrectomy instrumentation] and now minimally invasive, small gauge, sutureless surgery is common [see chapter V.B.2. Modern vitrectomy cutters] with even greater advances to come [see chapter V.B.3. The future of vitrectomy] to further lessen the inflammation associated with surgery. Given the importance of inflammation in DR and complications of vitrectomy, this is an important advance. It may be that surgery has increasing roles in the future management of DR as results and technology improve [123]. At some point it may prove to be salubrious and indeed reasonable to remove vitreous so as to eliminate the paracrine depot (see above) and facilitate the departure of injurious cytokines while simultaneously increasing oxygenation from the ciliary body to the ischemic inner retina of diabetic eyes.

There is specific interest in the role of vitrectomy for diabetic macular edema (DME). Ever since vitreous was recognized to be of relevance to macular edema over two decades ago [78, 126], vitrectomy has been increasingly performed in eyes with thickened and taut posterior vitreous cortex inducing obvious macular traction, and results were good [127–129]. Subsequently, vitrectomy surgery was offered to patients with an attached posterior vitreous cortex without traction [99, 130, 131], and initial results were promising. Controlled prospective trials, however, had more mixed outcomes [132–134]. Some groups reported better results for vitrectomy with peeling of the ILM whether or not traction was present [135, 136]. The intention of ILM peel is to completely remove any residual vitreous cortex relieving any residual traction, to remove a scaffold for future proliferation, and potentially to alter Müller cell physiology [91, 137]. Compared to laser or observation, vitrectomy and ILM peel appeared superior [138–140]. However, when patients undergoing bilateral vitrectomy for DME were randomized to have ILM peel only in one eye, no significant anatomic or visual benefit was seen [91]. Further, a substantial review of over 30 reports could not identify any advantage to ILM peeling in clinical trials [141]. Longer-term studies of vitrectomy for DME had more equivocal success rates, with or without ILM peeling [142–144].

To address many of these uncertainties, a large prospective trial was conducted by the DR-CR.net consortium, which found a macular edema but not acuity improvement with vitrectomy [145]. Factors associated with improving vision were poor baseline acuity and preretinal membrane peel, while factors associated with anatomic improvement in DME included preoperative poor vision and thick retina, ILM peel, and tractional vitreoretinal abnormalities. However, even in patients with a tractional component to their DME, the results remained less impressive than the earlier uncontrolled and retrospective reports [146].

One explanation for these disparate findings could be that there has been no uniform approach to preoperative assessment and the methods undertaken at surgery where not

only can approaches differ but even the choice of instruments can vary widely. For example, the lack of appreciation of the role of vitreoschisis in diabetic vitreopathy could influence the extent of preoperative diagnostic evaluation, and the plan for surgery might thus be insufficient in some cases. Certainly, not controlling for this in different clinical trials would influence the results. Because vitreoschisis is common, it is the experience of many vitreoretinal surgeons that diabetic vitrectomies can be extremely challenging, requiring removal of many layers and membranes before traction to the retina and neovascular tufts can be fully relieved. In addition, pathologic preretinal membranes can be extensive with numerous points of fibrovascular attachment between vitreous and retina. These aspects are summarized in Figure I.E-10 and demonstrate that in general the findings during diabetic vitrectomy demonstrate our conceptual understanding of diabetic vitreopathy and retinopathy [107].

C. Pharmacologic Vitreolysis

Pharmacologic vitreolysis represents a radically different approach than inhibitors of diabetic vitreopathy. This approach aims to separate vitreous from retina in the same innocuous way as naturally occurs in the vast majority of people, thereby eliminating much of the clinical significance of diabetic vitreopathy. To date, pharmacologic vitreolysis has primarily been employed to treat nondiabetic anomalous PVD inducing vitreo-macular traction with or without macular hole [147], to create a safe and complete PVD [see chapter VI.A. Pharmacologic vitreolysis]. There is nonetheless immediate application of this concept to diabetic vitreopathy. Although premature aging of vitreous may lead to early PVD in diabetes [64], too often the cortical vitreous remains attached and plays a role in the development of diabetic retinopathy and complications as described above. Induction of a complete PVD early in the natural history would be a potentially powerful preventive treatment in all patients with early changes of DR. There may also be a role for pharmacologic vitreolysis of more advanced DR in the period immediately before vitrectomy [148]. The case of diabetic macular edema (DME) may be particularly relevant in this context. Indeed, a study of patients with refractory DME reported induction of PVD in all 16 eyes that were injected with plasmin and moderate improvements in vision and DME that were not observed in the fellow controlled eyes [149]. This same group recently reported a larger cohort (63 eyes) where PVD was induced in 38 % after the first injection and 51 % after a second injection 1 month later [150]. Visual acuity and DME improved in 89 %, including patients without a complete PVD [150]. These interesting findings await corroboration before wider implementation. It seems clear, however, that pharmacologic vitreolysis will have an expanding role in diabetic vitreopathy if the principles are borne out by clinical evidence [151].

A word of caution would seem appropriate with respect to the development of all forms of pharmacotherapy for diabetic vitreopathy and retinopathy. The foregoing clearly and comprehensively makes the case for there being significant differences between diabetic and non-diabetic vitreous. Thus, preclinical testing of clinical therapies for both diabetic vitreopathy and diabetic retinopathy (which might employ intravitreal injections) must be performed in diabetic animal models in order to maximize the chances that subsequent clinical testing will be successful. Consider, for example, that hyaluronidase failed clinical FDA trials, in part because preclinical testing was not performed in diabetic animal models [see chapter VI.A. Pharmacologic vitreolysis]. This principle is important not only for pharmacologic vitreolysis of diabetic eye diseases, where the target is the vitreous body and the vitreoretinal interface [see chapter VI.A. Pharmacologic vitreolysis], but also for pharmacotherapy of diabetic retinopathy where vitreous is the pathway to treating the retina [see chapter IV.E. Principles and practice of intravitreal application of drugs]. Clearly, the effects of diabetic vitreopathy will influence the pharmacodynamics and pharmacokinetics of any drug placed into this milieu.

VII. Asteroid Hyalosis (AH)

First described by Benson in 1894, AH fills the vitreous body with yellow-white round structures (Figure I.E-11), yet it usually has little impact on vision and thus does not often require vitrectomy. In the Beaver Dam Study ($n=4,952$), AH was present in 0.2 % of subjects 43–54 years of age and 2.9 % aged 75–86 years. AH was primarily unilateral and more prevalent in men. The Australian Blue Mountains Eye Study ($n=3,654$) found that AH prevalence increased from 0 % in those 49–55 years old, to 2.1 % in ages 75–97 years,

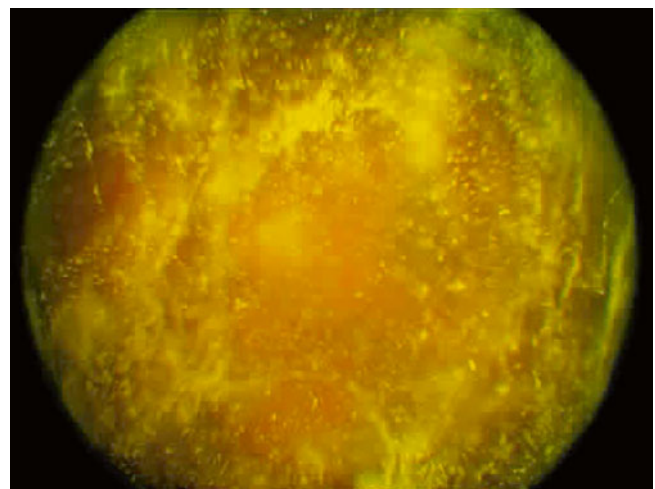


Figure I.E-11 Color fundus photograph of Asteroid Hyalosis. A clear view of the fundus is made very difficult, yet the patient's vision is not disturbed

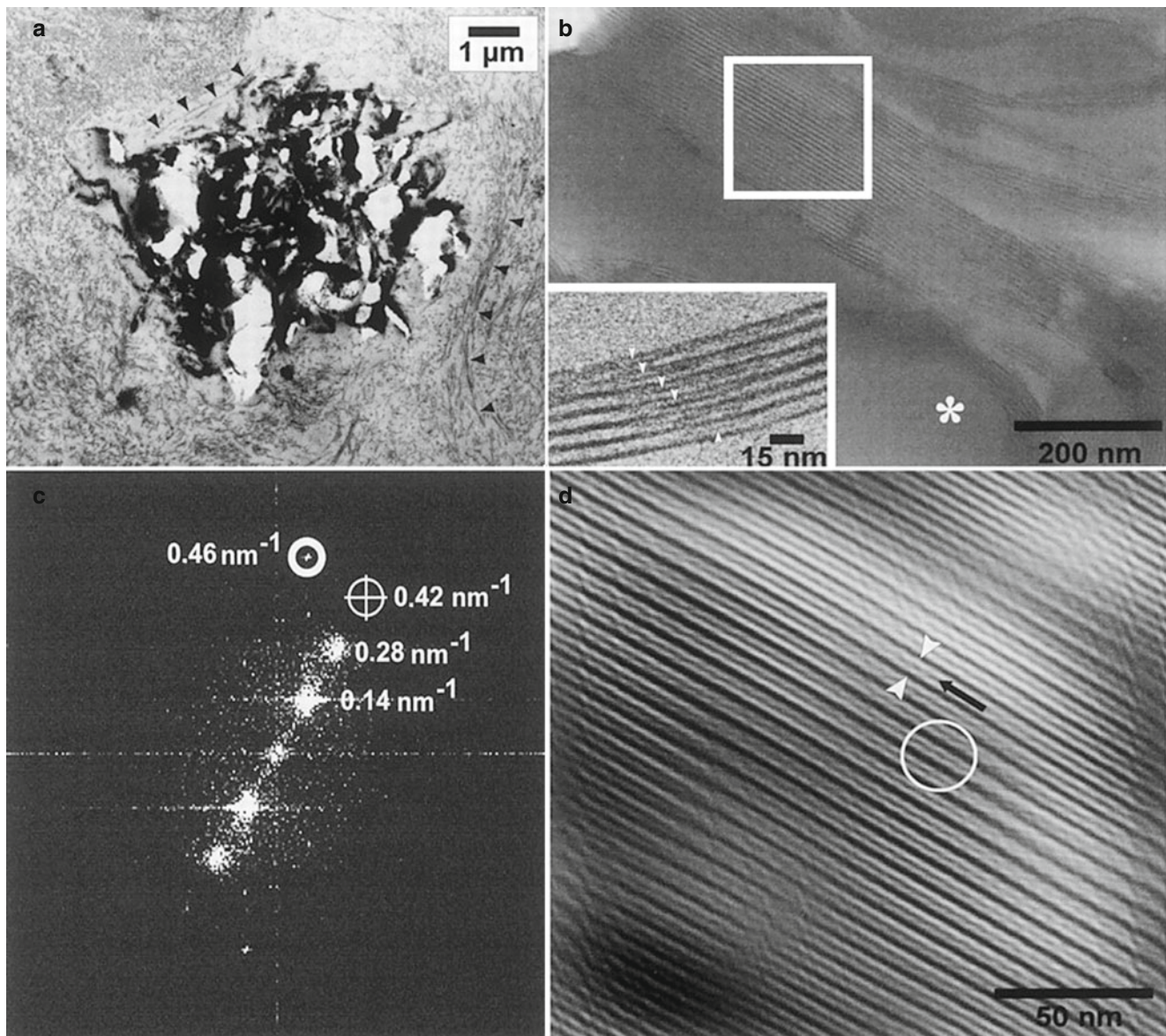


Figure I.E-12 Ultrastructure of Asteroid Hyalosis. (a) Asteroid body (AB) comprised of opaque ribbons embedded in an amorphous matrix. The AB is surrounded by fibrillar collagen-like structures (*arrowheads*). (b) Detailed survey of multi-lamellar stacks oriented parallel (*squared box*) or oblique (*asterisk*) to the incident electron beam. *Inset*: lamellar stack with a bipartite organization, indicated by the weak inter-layer lines (*arrowheads*). (c) Fourier transform of the 256×256 square

boxed area from (b), which shows an ultimate resolution of 0.46 nm^{-1} (*circle*). *Crossed circled spot*: a third-order diffraction spot. (d) Inverted Fourier transform, filtered of noise, showing the thickness of the lamellar unit (*opposing arrowheads*), separated by a dense interlayer (*arrow*), indicating a sandwich organization. A granular, particulate ultrastructure is obvious (*circle*) (With permission from Jorg and Heinrich. *IOVS* 2001;42(5):902–7)

again more prevalent in men. A prevalence of 1.96 % was found in the UCLA eye autopsy database of 10,801 eyes. Although numerous studies have claimed an association between AH and diabetes, this was not found in 547 cases reported in 11 studies. No relation to diabetes is further supported by AH unilaterality.

Asteroid bodies (ABs) readily stain for the presence of lipids (Sudan black B and oil red O) and calcium (von Kossa), but do not dissolve in common fat solvents. Rodman et al. confirmed Vorhoeff's 1920 finding that calcium is bound to

the main acidic lipid components of ABs. Two types were observed: I. ABs suspended in and surrounded by vitreous fibrils; II. ABs composed of a large inner zone filled with birefringent particles, and a thin cortical rim composed of condensed non-birefringent particles. This suggested potential differences in pathogenesis. EM found that ABs contain intertwined ribbons of multi-laminar membranes with a 10–60 Å periodicity characteristic of phospholipids, along with calcium and phosphate. Based on finding a lamellar arrangement with a periodicity of 4.6 nm (Figure I.E-12),

typical of the crystalline phase of lipids in water, Miller et al. suggested that ABs are not true crystals but rather liquid crystals of phospholipids. Using element mapping with electron spectroscopy, Winkler and Lunsdorff demonstrated that the electron energy loss spectra of calcium, phosphorus, and oxygen in ABs are similar to those in hydroxyapatite.

VII. Summary

To summarize, diabetes has its major systemic effects through hyperglycemia, which among its many actions triggers a sharp increase in superoxide production from mitochondria. Superoxide inhibits GAPDH, causing accumulation of glycolysis metabolites that are diverted into alternative pathways with pathologic results. One central consequence is glycation of proteins (AGE), with myriad downstream effects including extracellular matrix alteration, inflammation, vascular occlusion, cytokine production, and cell death. These pathways are summarized in Figure I.E-1.

Diabetic vitreopathy represents a combination of pathological changes. Glycation of collagen and depolymerization of HA destabilize the vitreous body, while cellular pathways (particularly of Muller cells) and retinal neovascularization create local areas of increased vitreoretinal adhesion. Together these create vitreoretinal traction, and further cellular invasion creates slowly contractile preretinal membranes that underlie the cicatricial stages of advanced complications in PDR. The firmly attached vitreous also represents a paracrine depot for pathological signals and a barrier to oxygen circulation, which contribute to diabetic retinopathy. These concepts are summarized in Figure I.E-10.

The importance of diabetic vitreopathy in the pathophysiology of some important forms of diabetic retinopathy prompts therapeutic considerations. Agents to prevent or reverse the molecular changes warrant further exploration, and there are immediate prospects for pharmacologic vitreolysis in diabetes. In spite of impressive advances in surgical instrumentation and strategies, successful implementation of this approach may one day obviate the need for vitreous surgery.

Acknowledgements The authors are indebted to Matin Khoshnevis of the University of California, Irvine for preparing the section on Asteroid Hyalosis, and Christianne Wa of the Doheny Eye Institute for her assistance with literature research for this chapter.

Abbreviations

AGE	Advanced glycation end products
AH	Asteroid hyalosis
DAG	Diacyl glycerol
DME	Diabetic macular edema
DR	Diabetic retinopathy
DRCR.net	Diabetic retinopathy clinical research network
ECM	Extracellular matrix
GAPDH	Glyceraldehyde-3-phosphate dehydrogenase
HA	Hyaluronan
ICAM-1	Intercellular adhesion molecule 1
IL-1 β	Interleukin 1-beta
ILM	Internal limiting membrane
mfERG	Multifocal electroretinography
NAD ⁺	Nicotinamide adenine dinucleotide (oxidized form)
NADH	Nicotinamide adenine dinucleotide (reduced form)
NADP ⁺	Nicotinamide adenine dinucleotide phosphate (oxidized form)
NADPH	Nicotinamide adenine dinucleotide phosphate (reduced form)
NFE2L2	Erythroid-2-related factor 2
NF- κ B	Nuclear factor kappa-B
NRF2	Erythroid-2-related factor 2
OCT	Optical coherence tomography
PDR	Proliferative diabetic retinopathy
PKC	Protein kinase C
PKC-DRS	Protein kinase C diabetic retinopathy study
PKC-DRS2	Protein kinase C diabetic retinopathy study 2
PKC- β	Protein kinase C beta
PKC- δ	Protein kinase C delta
PVD	Posterior vitreous detachment
RAGE	Receptor for advanced glycation end products
RBX	Ruboxistaurin
ROS	Reactive oxygen species
TCA	Tricarboxylic acid
TGF- β	Transforming growth factor beta
TNF- α	Tumor necrosis factor alpha
UV	Ultraviolet
VCAM-1	Vascular cell adhesion molecule 1
VEGF	Vascular endothelial growth factor

References

- Antonetti DA, Klein R, Gardner TW. Diabetic retinopathy. *N Engl J Med*. 2012;366:1227–39.
- Nishikawa T, Edelstein D, Du XL, Yamagishi S, Matsumura T, Kaneda Y, et al. Normalizing mitochondrial superoxide production blocks three pathways of hyperglycaemic damage. *Nature*. 2000;404:787–90.
- Brownlee M. Biochemistry and molecular cell biology of diabetic complications. *Nature*. 2001;414:813–20.
- Du XL, Edelstein D, Rossetti L, Fantus IG, Goldberg H, Ziyadeh F, et al. Hyperglycemia-induced mitochondrial superoxide overproduction activates the hexosamine pathway and induces plasminogen activator inhibitor-1 expression by increasing Sp1 glycosylation. *Proc Natl Acad Sci U S A*. 2000;97:12222–6.
- Monnier VM, Kohn RR, Cerami A. Accelerated age-related browning of human collagen in diabetes mellitus. *Proc Natl Acad Sci U S A*. 1984;81:583–7.
- Stitt AW. AGEs and diabetic retinopathy. *Invest Ophthalmol Vis Sci*. 2010;51:4867–74.
- Goh SY, Cooper ME. Clinical review: the role of advanced glycation end products in progression and complications of diabetes. *J Clin Endocrinol Metab*. 2008;93:1143–52.
- Zong H, Ward M, Stitt AW. AGEs, RAGE, and diabetic retinopathy. *Curr Diab Rep*. 2011;11:244–52.
- Tang J, Kern TS. Inflammation in diabetic retinopathy. *Prog Retin Eye Res*. 2011;30:343–58.
- Monnier VM, Vishwanath V, Frank KE, Elmets CA, Dauchot P, Kohn RR. Relation between complications of type I diabetes mellitus and collagen-linked fluorescence. *N Engl J Med*. 1986;314:403–8.
- Charonis AS, Tsilibary EC. Structural and functional changes of laminin and type IV collagen after nonenzymatic glycation. *Diabetes*. 1992;41 Suppl 2:49–51.
- Koya D, King GL. Protein kinase C activation and the development of diabetic complications. *Diabetes*. 1998;47:859–66.
- Geraldes P, Hiraoka-Yamamoto J, Matsumoto M, Clermont A, Leitges M, Marette A, et al. Activation of PKC-delta and SHP-1 by hyperglycemia causes vascular cell apoptosis and diabetic retinopathy. *Nat Med*. 2009;15:1298–306.
- Aiello LP, Bursell SE, Clermont A, Duh E, Ishii H, Takagi C, et al. Vascular endothelial growth factor-induced retinal permeability is mediated by protein kinase C in vivo and suppressed by an orally effective beta-isoform-selective inhibitor. *Diabetes*. 1997;46:1473–80.
- Danis RP, Bingaman DP, Jirousek M, Yang Y. Inhibition of intracellular neovascularization caused by retinal ischemia in pigs by PKCbeta inhibition with LY333531. *Invest Ophthalmol Vis Sci*. 1998;39:171–9.
- Nonaka A, Kiryu J, Tsujikawa A, Yamashiro K, Miyamoto K, Nishiwaki H, et al. PKC-beta inhibitor (LY333531) attenuates leukocyte entrapment in retinal microcirculation of diabetic rats. *Invest Ophthalmol Vis Sci*. 2000;41:2702–6.
- Yokota T, Ma RC, Park JY, Isshiki K, Sotiropoulos KB, Rauniyar RK, et al. Role of protein kinase C on the expression of platelet-derived growth factor and endothelin-1 in the retina of diabetic rats and cultured retinal capillary pericytes. *Diabetes*. 2003;52:838–45.
- Aiello LP, Clermont A, Arora V, Davis MD, Sheetz MJ, Bursell SE. Inhibition of PKC beta by oral administration of ruboxistaurin is well tolerated and ameliorates diabetes-induced retinal hemodynamic abnormalities in patients. *Invest Ophthalmol Vis Sci*. 2006;47:86–92.
- Group P-DS. The effect of ruboxistaurin on visual loss in patients with moderately severe to very severe nonproliferative diabetic retinopathy: initial results of the Protein Kinase C beta Inhibitor Diabetic Retinopathy Study (PKC-DRS) multicenter randomized clinical trial. *Diabetes*. 2005;54:2188–97.
- Group P-D, Aiello LP, Davis MD, Girach A, Kles KA, Milton RC, et al. Effect of ruboxistaurin on visual loss in patients with diabetic retinopathy. *Ophthalmology*. 2006;113:2221–30.
- Sheetz MJ, Aiello LP, Davis MD, Danis R, Bek T, Cunha-Vaz J, et al. The effect of the oral PKC beta inhibitor ruboxistaurin on vision loss in two phase 3 studies. *Invest Ophthalmol Vis Sci*. 2013;54:1750–7.
- Perkins BA, Aiello LP, Krolewski AS. Diabetes complications and the renin-angiotensin system. *N Engl J Med*. 2009;361:83–5.
- Mauer M, Zinman B, Gardiner R, Suissa S, Sinaiko A, Strand T, et al. Renal and retinal effects of enalapril and losartan in type 1 diabetes. *N Engl J Med*. 2009;361:40–51.
- Xu Z, Wei Y, Gong J, Cho H, Park JK, Sung ER, et al. NRF2 plays a protective role in diabetic retinopathy in mice. *Diabetologia*. 2014;57:204–13.
- Wei Y, Gong J, Yoshida T, Eberhart CG, Xu Z, Kombairaju P, et al. Nrf2 has a protective role against neuronal and capillary degeneration in retinal ischemia-reperfusion injury. *Free Radic Biol Med*. 2011;51:216–24.
- Cheung N, Mitchell P, Wong TY. Diabetic retinopathy. *Lancet*. 2010;376:124–36.
- Ding J, Wong TY. Current epidemiology of diabetic retinopathy and diabetic macular edema. *Curr Diab Rep*. 2012;12:346–54.
- Klein R, Knudtson MD, Lee KE, Gangnon R, Klein BE. The Wisconsin Epidemiologic Study of Diabetic Retinopathy: XXII the twenty-five-year progression of retinopathy in persons with type 1 diabetes. *Ophthalmology*. 2008;115:1859–68.
- Wei M, Gaskill SP, Haffner SM, Stern MP. Effects of diabetes and level of glycemia on all-cause and cardiovascular mortality. The San Antonio Heart Study. *Diabetes Care*. 1998;21:1167–72.
- Chew EY, Ferris FL, Csaky KG, Murphy RP, Agrón E, Thompson DJS, et al. The long-term effects of laser photocoagulation treatment in patients with diabetic retinopathy. *Ophthalmology*. 2003;110:1683–9.
- Hirai FE, Knudtson MD, Klein BE, Klein R. Clinically significant macular edema and survival in type 1 and type 2 diabetes. *Am J Ophthalmol*. 2008;145:700–6.
- The effect of intensive treatment of diabetes on the development and progression of long-term complications in insulin-dependent diabetes mellitus. The Diabetes Control and Complications Trial Research Group. *N Engl J Med*. 1993;329:977–86.
- Holman RR, Paul SK, Bethel MA, Matthews DR, Neil HA. 10-year follow-up of intensive glucose control in type 2 diabetes. *N Engl J Med*. 2008;359:1577–89.
- White NH, Sun W, Cleary PA, Danis RP, Davis MD, Hainsworth DP, et al. Prolonged effect of intensive therapy on the risk of retinopathy complications in patients with type 1 diabetes mellitus: 10 years after the Diabetes Control and Complications Trial. *Arch Ophthalmol*. 2008;126:1707–15.
- Gardner TW, Abcouwer SF, Barber AJ, Jackson GR. An integrated approach to diabetic retinopathy research. *Arch Ophthalmol*. 2011;129:230–5.
- Giese MJ, Speth RC. The ocular renin-angiotensin system: a therapeutic target for the treatment of ocular disease. *Pharmacol Ther*. 2014;142(1):11–32.
- Watanabe D, Suzuma K, Matsui S, Kurimoto M, Kiryu J, Kita M, et al. Erythropoietin as a retinal angiogenic factor in proliferative diabetic retinopathy. *N Engl J Med*. 2005;353:782–92.
- Gao BB, Clermont A, Rook S, Fonda SJ, Srinivasan VJ, Wojtkowski M, et al. Extracellular carbonic anhydrase mediates hemorrhagic retinal and cerebral vascular permeability through prekallikrein activation. *Nat Med*. 2007;13:181–8.
- Bloodworth Jr JM. Diabetic retinopathy. *Diabetes*. 1962;11:1–22.
- Wolter JR. Diabetic retinopathy. *Am J Ophthalmol*. 1961;51:1123–41.
- Antonetti DA, Barber AJ, Bronson SK, Freeman WM, Gardner TW, Jefferson LS, et al. Diabetic retinopathy: seeing beyond glucose-induced microvascular disease. *Diabetes*. 2006;55:2401–11.

42. Greenstein VC, Holopigian K, Hood DC, Seiple W, Carr RE. The nature and extent of retinal dysfunction associated with diabetic macular edema. *Invest Ophthalmol Vis Sci.* 2000;41:3643–54.
43. Ghirlanda G, Di Leo MA, Caputo S, Cercone S, Greco AV. From functional to microvascular abnormalities in early diabetic retinopathy. *Diabetes Metab Rev.* 1997;13:15–35.
44. van Dijk HW, Kok PH, Garvin M, Sonka M, Devries JH, Michels RP, et al. Selective loss of inner retinal layer thickness in type 1 diabetic patients with minimal diabetic retinopathy. *Invest Ophthalmol Vis Sci.* 2009;50:3404–9.
45. van Dijk HW, Verbraak FD, Kok PH, Garvin MK, Sonka M, Lee K, et al. Decreased retinal ganglion cell layer thickness in patients with type 1 diabetes. *Invest Ophthalmol Vis Sci.* 2010;51:3660–5.
46. Fortune B, Schneck ME, Adams AJ. Multifocal electroretinogram delays reveal local retinal dysfunction in early diabetic retinopathy. *Invest Ophthalmol Vis Sci.* 1999;40:2638–51.
47. Harrison WW, Bearse Jr MA, Ng JS, Jewell NP, Barez S, Burger D, et al. Multifocal electroretinograms predict onset of diabetic retinopathy in adult patients with diabetes. *Invest Ophthalmol Vis Sci.* 2011;52:772–7.
48. Fletcher EL, Phipps JA, Ward MM, Puthussery T, Wilkinson-Berka JL. Neuronal and glial cell abnormality as predictors of progression of diabetic retinopathy. *Curr Pharm Des.* 2007;13:2699–712.
49. Jousseaume AM, Poulaki V, Le ML, Koizumi K, Esser C, Janicki H, et al. A central role for inflammation in the pathogenesis of diabetic retinopathy. *FASEB J.* 2004;18:1450–2.
50. Sebag J. Diabetic vitreopathy. *Ophthalmology.* 1996;103:205–6.
51. Lundquist O, Osterlin S. Glucose concentration in the vitreous of nondiabetic and diabetic human eyes. *Graefes Arch Clin Exp Ophthalmol.* 1994;232:71–4.
52. Xiong H, Cheng HM. Aqueous/vitreous tonicity in “sugar” cataracts. *Ophthalmic Res.* 1989;21:292–6.
53. Christiansson J. Changes in mucopolysaccharides during alloxan diabetes in the rabbit. I. Comparative studies on serum and the hyaluronic acid of the vitreous body. *Acta Ophthalmol (Copenh).* 1958;36:141–62.
54. Walia S, Clermont AC, Gao BB, Aiello LP, Feener EP. Vitreous proteomics and diabetic retinopathy. *Semin Ophthalmol.* 2010;25:289–94.
55. Kim T, Kim SJ, Kim K, Kang UB, Lee C, Park KS, et al. Profiling of vitreous proteomes from proliferative diabetic retinopathy and nondiabetic patients. *Proteomics.* 2007;7:4203–15.
56. Gao BB, Chen X, Timothy N, Aiello LP, Feener EP. Characterization of the vitreous proteome in diabetes without diabetic retinopathy and diabetes with proliferative diabetic retinopathy. *J Proteome Res.* 2008;7:2516–25.
57. Sebag J, Buckingham B, Charles MA, Reiser K. Biochemical abnormalities in vitreous of humans with proliferative diabetic retinopathy. *Arch Ophthalmol.* 1992;110:1472–6.
58. Buckingham B, Reiser KM. Relationship between the content of lysyl oxidase-dependent cross-links in skin collagen, nonenzymatic glycosylation, and long-term complications in type I diabetes mellitus. *J Clin Invest.* 1990;86:1046–54.
59. Sebag J, Nie S, Reiser K, Charles MA, Yu NT. Raman spectroscopy of human vitreous in proliferative diabetic retinopathy. *Invest Ophthalmol Vis Sci.* 1994;35:2976–80.
60. Fankhauser 2nd F. Analysis of diabetic vitreopathy with dynamic light scattering spectroscopy—problems and solutions related to photon correlation. *Acta Ophthalmol.* 2012;90:e173–8.
61. Sebag J. Abnormalities of human vitreous structure in diabetes. *Graefes Arch Clin Exp Ophthalmol.* 1993;231:257–60.
62. Stitt AW, Moore JE, Sharkey JA, Murphy G, Simpson DA, Bucala R, et al. Advanced glycation end products in vitreous: structural and functional implications for diabetic vitreopathy. *Invest Ophthalmol Vis Sci.* 1998;39:2517–23.
63. Avery NC, Bailey AJ. The effects of the Maillard reaction on the physical properties and cell interactions of collagen. *Pathol Biol.* 2006;54:387–95.
64. Foos RY, Kreiger AE, Forsythe AB, Zakka KA. Posterior vitreous detachment in diabetic subjects. *Ophthalmology.* 1980;87:122–8.
65. Tagawa H, McMeel JW, Furukawa H, Quiroz H, Murakami K, Takahashi M, et al. Role of the vitreous in diabetic retinopathy. I. Vitreous changes in diabetic retinopathy and in physiologic aging. *Ophthalmology.* 1986;93:596–601.
66. Faulborn J, Dunker S, Bowald S. Diabetic vitreopathy – findings using the celloidin embedding technique. *Ophthalmologica.* 1998;212:369–76.
67. Sebag J. Anomalous posterior vitreous detachment: a unifying concept in vitreo-retinal disease. *Graefes Arch Clin Exp Ophthalmol.* 2004;242:690–8.
68. Akiba J, Ueno N, Chakrabarti B. Mechanisms of photo-induced vitreous liquefaction. *Curr Eye Res.* 1994;13:505–12.
69. Ueno N, Sebag J, Hirokawa H, Chakrabarti B. Effects of visible-light irradiation on vitreous structure in the presence of a photosensitizer. *Exp Eye Res.* 1987;44:863–70.
70. Obayashi H, Nakano K, Shigeta H, Yamaguchi M, Yoshimori K, Fukui M, et al. Formation of crossline as a fluorescent advanced glycation end product in vitro and in vivo. *Biochem Biophys Res Commun.* 1996;226:37–41.
71. Ortwerth BJ, Prabhakaram M, Nagaraj RH, Linetsky M. The relative UV sensitizer activity of purified advanced glycation endproducts. *Photochem Photobiol.* 1997;65:666–72.
72. Deguine V, Menasche M, Ferrari P, Fraisse L, Pouliquen Y, Robert L. Free radical depolymerization of hyaluronan by Maillard reaction products: role in liquefaction of aging vitreous. *Int J Biol Macromol.* 1998;22:17–22.
73. Katsumura C, Sugiyama T, Nakamura K, Obayashi H, Hasegawa G, Oku H, et al. Effects of advanced glycation end products on hyaluronan photolysis: a new mechanism of diabetic vitreopathy. *Ophthalmic Res.* 2004;36:327–31.
74. Davis MD. Vitreous contraction in proliferative diabetic retinopathy. *Arch Ophthalmol.* 1965;74:741–51.
75. Takahashi M, Trempe CL, Maguire K, McMeel JW. Vitreoretinal relationship in diabetic retinopathy. A biomicroscopic evaluation. *Arch Ophthalmol.* 1981;99:241–5.
76. Jalkh A, Takahashi M, Topilow HW, Trempe CL, McMeel JW. Prognostic value of vitreous findings in diabetic retinopathy. *Arch Ophthalmol.* 1982;100:432–4.
77. Faulborn J, Bowald S. Microproliferations in proliferative diabetic retinopathy and their relationship to the vitreous: corresponding light and electron microscopic studies. *Graefes Arch Clin Exp Ophthalmol.* 1985;23:130–8.
78. Nasrallah FP, Jalkh AE, Van Coppenolle F, Kado M, Trempe CL, McMeel JW, et al. The role of the vitreous in diabetic macular edema. *Ophthalmology.* 1988;95:1335–9.
79. Akiba J, Arzabe CW, Trempe CL. Posterior vitreous detachment and neovascularization in diabetic retinopathy. *Ophthalmology.* 1990;97:889–91.
80. Blankenship GW, Machermer R. Long-term diabetic vitrectomy results. Report of 10 year follow-up. *Ophthalmology.* 1985;92:503–6.
81. Wong HC, Sehmi KS, McLeod D. Abortive neovascular outgrowths discovered during vitrectomy for diabetic vitreous haemorrhage. *Graefes Arch Clin Exp Ophthalmol.* 1989;27:237–40.
82. Kishi S, Numaga T, Yamazaki S. Structure of the inner retinal surface in simple diabetic retinopathy. *Jpn J Ophthalmol.* 1982;26:141–9.
83. Kishi S, Demaria C, Shimizu K. Vitreous cortex remnants at the fovea after spontaneous vitreous detachment. *Int Ophthalmol.* 1986;9:253–60.
84. Sebag J. Vitreoschisis. *Graefes Arch Clin Exp Ophthalmol.* 2008;246:329–32.

85. Sebag J, Gupta P, Rosen RR, Garcia P, Sadun AA. Macular holes and macular pucker: the role of vitreoschisis as imaged by optical coherence tomography/scanning laser ophthalmoscopy. *Trans Am Ophthalmol Soc.* 2007;105:121–9; discussion 9–31.
86. Gupta P, Yee KM, Garcia P, Rosen RB, Parikh J, Hageman GS, et al. Vitreoschisis in macular diseases. *Br J Ophthalmol.* 2011;95:376–80.
87. Chu TG, Lopez PF, Cano MR, Freeman WR, Lean JS, Liggett PE, et al. Posterior vitreoschisis. *Ophthalmology.* 1996;103:315–22.
88. Schwartz SD, Alexander R, Hiscott P, Gregor ZJ. Recognition of vitreoschisis in proliferative diabetic retinopathy. *Ophthalmology.* 1996;103:323–8.
89. Gandorfer A, Rohleder M, Grossefinger S, Haritoglou C, Ulbig M, Kampik A. Epiretinal pathology of diffuse diabetic macular edema associated with vitreomacular traction. *Am J Ophthalmol.* 2005;139:638–52.
90. Kishi S, Shimizu K. Posterior precortical vitreous pocket. *Arch Ophthalmol.* 1990;108:979–82.
91. Bahadir M, Ertan A, Mertoglu O. Visual acuity comparison of vitrectomy with and without internal limiting membrane removal in the treatment of diabetic macular edema. *Int Ophthalmol.* 2005;26:3–8.
92. Barile GR, Pachydaki SI, Tari SR, Lee SE, Donmoyer CM, Ma W, et al. The RAGE axis in early diabetic retinopathy. *Invest Ophthalmol Vis Sci.* 2005;46:2916–24.
93. Pachydaki SI, Tari SR, Lee SE, Ma W, Tseng JJ, Sosunov AA, et al. Upregulation of RAGE and its ligands in proliferative retinal disease. *Exp Eye Res.* 2006;82:807–15.
94. Barile GR, Chang SS, Park LS, Reppucci VS, Schiff WM, Schmidt AM. Soluble cellular adhesion molecules in proliferative vitreoretinopathy and proliferative diabetic retinopathy. *Curr Eye Res.* 1999;19:219–27.
95. Matsunaga N, Ozeki H, Hirabayashi Y, Shimada S, Ogura Y. Histopathologic evaluation of the internal limiting membrane surgically excised from eyes with diabetic maculopathy. *Retina.* 2005;25:311–6.
96. Yamamoto T, Akabane N, Takeuchi S. Vitrectomy for diabetic macular edema: the role of posterior vitreous detachment and epimacular membrane. *Am J Ophthalmol.* 2001;132:369–77.
97. Sun YM, Su Y, Li J, Wang LF. Recent advances in understanding the biochemical and molecular mechanism of diabetic nephropathy. *Biochem Biophys Res Commun.* 2013;433:359–61.
98. Tasman W. Diabetic vitreous hemorrhage and its relationship to hypoglycemia. *Mod Probl Ophthalmol.* 1979;20:413–4.
99. Ikeda T, Sato K, Katano T, Hayashi Y. Vitrectomy for cystoid macular oedema with attached posterior hyaloid membrane in patients with diabetes. *Br J Ophthalmol.* 1999;83:12–4.
100. Ikeda T, Sato K, Katano T, Hayashi Y. Attached posterior hyaloid membrane and the pathogenesis of honeycombed cystoid macular edema in patients with diabetes. *Am J Ophthalmol.* 1999;127:478–9.
101. Sebag J, Ansari RR, Dunker S, Suh KI. Dynamic light scattering of diabetic vitreopathy. *Diabetes Technol Ther.* 1999;1:169–76.
102. Shui YB, Fu JJ, Garcia C, Dattilo LK, Rajagopal R, McMillan S, et al. Oxygen distribution in the rabbit eye and oxygen consumption by the lens. *Invest Ophthalmol Vis Sci.* 2006;47:1571–80.
103. Siegfried CJ, Shui YB, Holekamp NM, Bai F, Beebe DC. Oxygen distribution in the human eye: relevance to the etiology of open-angle glaucoma after vitrectomy. *Invest Ophthalmol Vis Sci.* 2010;51:5731–8.
104. Stefansson E, Loftsson T. The Stokes-Einstein equation and the physiological effects of vitreous surgery. *Acta Ophthalmol Scand.* 2006;84:718–9.
105. Barton KA, Shui YB, Petrash JM, Beebe DC. Comment on: the Stokes-Einstein equation and the physiological effects of vitreous surgery. *Acta Ophthalmol Scand.* 2007;85:339–40.
106. Gisladottir S, Loftsson T, Stefansson E. Diffusion characteristics of vitreous humour and saline solution follow the Stokes Einstein equation. *Graefes Arch Clin Exp Ophthalmol.* 2009;247:1677–84.
107. Stefansson E. Physiology of vitreous surgery. *Graefes Arch Clin Exp Ophthalmol.* 2009;247:147–63.
108. Yamazaki Y, Morita T. Molecular and functional diversity of vascular endothelial growth factors. *Mol Divers.* 2006;10:515–27.
109. Aiello LP, Avery RL, Arrigg PG, Keyt BA, Jampel HD, Shah ST, et al. Vascular endothelial growth factor in ocular fluid of patients with diabetic retinopathy and other retinal disorders. *N Engl J Med.* 1994;331:1480–7.
110. Funatsu H, Yamashita H, Noma H, Mimura T, Yamashita T, Hori S. Increased levels of vascular endothelial growth factor and interleukin-6 in the aqueous humor of diabetics with macular edema. *Am J Ophthalmol.* 2002;133:70–7.
111. Abu El-Asrar AM, Nawaz MI, Kangave D, Siddiquei MM, Ola MS, Opdenakker G. Angiogenesis regulatory factors in the vitreous from patients with proliferative diabetic retinopathy. *Acta Diabetol.* 2013;50:545–51.
112. Ponsioen TL, Hooymans JM, Los LI. Remodelling of the human vitreous and vitreoretinal interface – a dynamic process. *Prog Retin Eye Res.* 2010;29:580–95.
113. Engelen L, Stehouwer CD, Schalkwijk CG. Current therapeutic interventions in the glycation pathway: evidence from clinical studies. *Diabetes Obes Metab.* 2013;15:677–89.
114. Gardiner TA, Anderson HR, Stitt AW. Inhibition of advanced glycation end-products protects against retinal capillary basement membrane expansion during long-term diabetes. *J Pathol.* 2003;201:328–33.
115. Kern TS, Engerman RL. Pharmacological inhibition of diabetic retinopathy: aminoguanidine and aspirin. *Diabetes.* 2001;50:1636–42.
116. Hammes HP, Martin S, Federlin K, Geisen K, Brownlee M. Aminoguanidine treatment inhibits the development of experimental diabetic retinopathy. *Proc Natl Acad Sci U S A.* 1991;88:11555–8.
117. Bolton WK, Cattran DC, Williams ME, Adler SG, Appel GB, Cartwright K, et al. Randomized trial of an inhibitor of formation of advanced glycation end products in diabetic nephropathy. *Am J Nephrol.* 2004;24:32–40.
118. Vasani S, Zhang X, Zhang X, Kapurniotu A, Bernhagen J, Teichberg S, et al. An agent cleaving glucose-derived protein crosslinks in vitro and in vivo. *Nature.* 1996;382:275–8.
119. Asif M, Egan J, Vasani S, Jyothirmayi GN, Masurekar MR, Lopez S, et al. An advanced glycation endproduct cross-link breaker can reverse age-related increases in myocardial stiffness. *Proc Natl Acad Sci U S A.* 2000;97:2809–13.
120. Vaitkevicius PV, Lane M, Spurgeon H, Ingram DK, Roth GS, Egan JJ, et al. A cross-link breaker has sustained effects on arterial and ventricular properties in older rhesus monkeys. *Proc Natl Acad Sci U S A.* 2001;98:1171–5.
121. Hammes HP, Du X, Edelstein D, Taguchi T, Matsumura T, Ju Q, et al. Benfotiamine blocks three major pathways of hyperglycemic damage and prevents experimental diabetic retinopathy. *Nat Med.* 2003;9:294–9.
122. Stitt A, Gardiner TA, Alderson NL, Canning P, Frizzell N, Duffy N, et al. The AGE inhibitor pyridoxamine inhibits development of retinopathy in experimental diabetes. *Diabetes.* 2002;51:2826–32.
123. Mohamed Q, Gillies MC, Wong TY. Management of diabetic retinopathy: a systematic review. *JAMA.* 2007;298:902–16.
124. Early vitrectomy for severe vitreous hemorrhage in diabetic retinopathy. Two-year results of a randomized trial. *Diabetic Retinopathy Vitrectomy Study report 2. The Diabetic Retinopathy*

- Vitrectomy Study Research Group. *Arch Ophthalmol*. 1985;103:1644–52.
125. Early vitrectomy for severe proliferative diabetic retinopathy in eyes with useful vision. Results of a randomized trial—Diabetic Retinopathy Vitrectomy Study Report 3. The Diabetic Retinopathy Vitrectomy Study Research Group. *Ophthalmology*. 1988;95:1307–20.
 126. Hikichi T, Fujio N, Akiba J, Azuma Y, Takahashi M, Yoshida A. Association between the short-term natural history of diabetic macular edema and the vitreomacular relationship in type II diabetes mellitus. *Ophthalmology*. 1997;104:473–8.
 127. Lewis H, Abrams GW, Blumenkranz MS, Campo RV. Vitrectomy for diabetic macular traction and edema associated with posterior hyaloidal traction. *Ophthalmology*. 1992;99:753–9.
 128. Harbour JW, Smiddy WE, Flynn Jr HW, Rubsamen PE. Vitrectomy for diabetic macular edema associated with a thickened and taut posterior hyaloid membrane. *Am J Ophthalmol*. 1996;121:405–13.
 129. Pendergast SD, Hassan TS, Williams GA, Cox MS, Margherio RR, Ferrone PJ, et al. Vitrectomy for diffuse diabetic macular edema associated with a taut premacular posterior hyaloid. *Am J Ophthalmol*. 2000;130:178–86.
 130. Tachi N, Ogino N. Vitrectomy for diffuse macular edema in cases of diabetic retinopathy. *Am J Ophthalmol*. 1996;122:258–60.
 131. La Heij EC, Hendrikse F, Kessels AG, Derhaag PJ. Vitrectomy results in diabetic macular oedema without evident vitreomacular traction. *Graefes Arch Clin Exp Ophthalmol*. 2001;239:264–70.
 132. Otani T, Kishi S. A controlled study of vitrectomy for diabetic macular edema. *Am J Ophthalmol*. 2002;134:214–9.
 133. Thomas D, Bunce C, Moorman C, Laidlaw DA. A randomised controlled feasibility trial of vitrectomy versus laser for diabetic macular oedema. *Br J Ophthalmol*. 2005;89:81–6.
 134. Kralinger MT, Pedri M, Kralinger F, Troger J, Kieselbach GF. Long-term outcome after vitrectomy for diabetic macular edema. *Ophthalmologica*. 2006;220:147–52.
 135. Gandorfer A, Messmer EM, Ulbig MW, Kampik A. Resolution of diabetic macular edema after surgical removal of the posterior hyaloid and the inner limiting membrane. *Retina*. 2000;20:126–33.
 136. Dillinger P, Mester U. Vitrectomy with removal of the internal limiting membrane in chronic diabetic macular oedema. *Graefes Arch Clin Exp Ophthalmol*. 2004;42:630–7.
 137. Sonoda KH, Sakamoto T, Enaida H, Miyazaki M, Noda Y, Nakamura T, et al. Residual vitreous cortex after surgical posterior vitreous separation visualized by intravitreal triamcinolone acetate. *Ophthalmology*. 2004;111:226–30.
 138. Yanyali A, Horozoglu F, Celik E, Ercalik Y, Nohutcu AF. Pars plana vitrectomy and removal of the internal limiting membrane in diabetic macular edema unresponsive to grid laser photocoagulation. *Eur J Ophthalmol*. 2006;16:573–81.
 139. Yanyali A, Nohutcu AF, Horozoglu F, Celik E. Modified grid laser photocoagulation versus pars plana vitrectomy with internal limiting membrane removal in diabetic macular edema. *Am J Ophthalmol*. 2005;139:795–801.
 140. Stolba U, Binder S, Gruber D, Krebs I, Aggermann T, Neumaier B. Vitrectomy for persistent diffuse diabetic macular edema. *Am J Ophthalmol*. 2005;140:295–301.
 141. Hartley KL, Smiddy WE, Flynn Jr HW, Murray TG. Pars plana vitrectomy with internal limiting membrane peeling for diabetic macular edema. *Retina*. 2008;28:410–9.
 142. Figueroa MS, Contreras I, Noval S. Surgical and anatomical outcomes of pars plana vitrectomy for diffuse nontractional diabetic macular edema. *Retina*. 2008;28:420–6.
 143. Yanyali A, Horozoglu F, Celik E, Nohutcu AF. Long-term outcomes of pars plana vitrectomy with internal limiting membrane removal in diabetic macular edema. *Retina*. 2007;27:557–66.
 144. Kumagai K, Furukawa M, Ogino N, Larson E, Iwaki M, Tachi N. Long-term follow-up of vitrectomy for diffuse nontractional diabetic macular edema. *Retina*. 2009;29:464–72.
 145. Flaxel CJ, Edwards AR, Aiello LP, Arrigg PG, Beck RW, Bressler NM, et al. Factors associated with visual acuity outcomes after vitrectomy for diabetic macular edema: diabetic retinopathy clinical research network. *Retina*. 2010;30:1488–95.
 146. Diabetic Retinopathy Clinical Research Network Writing C, Haller JA, Qin H, Apte RS, Beck RR, Bressler NM, et al. Vitrectomy outcomes in eyes with diabetic macular edema and vitreomacular traction. *Ophthalmology*. 2010;117:1087–93.e3.
 147. Stalmans P, Benz MS, Gandorfer A, Kampik A, Girach A, Pakola S, et al. Enzymatic vitreolysis with ocriplasmin for vitreomacular traction and macular holes. *N Engl J Med*. 2012;367:606–15.
 148. Benz MS, Packo KH, Gonzalez V, Pakola S, Bezner D, Haller JA, et al. A placebo-controlled trial of microplasmin intravitreal injection to facilitate posterior vitreous detachment before vitrectomy. *Ophthalmology*. 2010;117:791–7.
 149. Diaz-Llopis M, Udaondo P, Arevalo F, Salom D, Garcia-Delpech S, Quijada A, et al. Intravitreal plasmin without associated vitrectomy as a treatment for refractory diabetic macular edema. *J Ocul Pharmacol Ther*. 2009;25:379–84.
 150. Diaz-Llopis M, Udaondo P, Millan JM, Arevalo JF. Enzymatic vitrectomy for diabetic retinopathy and diabetic macular edema. *World J Diabetes*. 2013;4:319–23.
 151. de Smet MD, Castilla M. Ocriplasmin for diabetic retinopathy. *Expert Opin Biol Ther*. 2013;13:1741–7.

Sven Crafoord, Fredrik Ghosh, and J. Sebag

Outline

- I. **Introduction**
 - A. Rationale: Why an Artificial Vitreous?
 - B. Vitreous Biochemistry
 1. Glycosaminoglycans (GAGs)
 - a. Hyaluronan
 - b. Chondroitin Sulfate (CS)
 - c. Heparan Sulfate (HS)
 2. Proteins
 3. HA-Collagen Interaction
 4. Miscellaneous Components
 - a. Metabolites and Enzymes
 - b. Ascorbic Acid
 - c. Amino and Fatty Acids
 - d. Prostaglandins
- II. **Roles of an Artificial Vitreous**
- III. **Properties of an Artificial Vitreous**
 - A. Anatomic Considerations: Do We Need a Posterior Vitreous Cortex?
- IV. **Vitreous Substitutes in Vitreoretinal Surgery**
 - A. Natural and Semisynthetic Polymers and Hyaluronic Hydrogels
 - B. Synthetic Hydrogels and “Smart Hydrogels”
- V. **Developing an Artificial Vitreous**
 - A. Experimental Models for Testing Artificial Vitreous *In Vivo*
 1. Polyalkylimide
 2. Polyethylene Glycol
 - B. Experimental Model for Testing Artificial Vitreous *In Vitro*

References

S. Crafoord, MD, PhD (✉)
Department of Ophthalmology, Örebro
University Hospital, Örebro SE-701 85, Sweden

School of Health and Medical Sciences,
Örebro University, Örebro, Sweden
e-mail: sven.crafoord@gmail.com

F. Ghosh, MD, PhD
Department of Ophthalmology, Skåne
University Hospital, Lund, Sweden
Lund University, Lund, Sweden

Keywords

Vitreous • Biochemistry • Collagen • Hyaluronan • Artificial vitreous • Hydrogels • Polyalkylimide • Polyethylene glycol • Cross-linked hyaluronic acid hydrogels

Key Concepts

1. Vitreous is not an inert substance but has a complex biochemistry and plays an important role in ocular physiology.
2. To date, vitreous substitutes have only been developed for short-term use during or, typically, after vitreoretinal surgery, without consideration for the optical and physiologic properties necessary for long-term homeostasis. Cross-linked hyaluronic acid hydrogels possess many of the needed physiologic properties without the untoward effects of polyalkylimide and polyethylene glycol.
3. Future development of artificial vitreous gels must confirm biocompatibility as tested with electrophysiology, morphology, and histology both *in vitro* and *in vivo*. Future objectives will be to determine whether a synthetic posterior vitreous cortex is needed and whether “smart hydrogels” and hydrogels containing hyaluronic acid and cross-linked, enzyme-stable gels will be the best future options for an artificial vitreous.

J. Sebag, MD, FACS, FRCOphth, FARVO
VMR Institute for Vitreous Macula Retina
Huntington Beach, CA, USA

Doheny Eye Institute, Los Angeles, CA, USA
e-mail: jsebag@VMRinstitute.com

I. Introduction

A. Rationale: Why an Artificial Vitreous?

Aging of vitreous involves a degenerative process where glycosaminoglycans (GAGs) dissociate from collagen and the gel disintegrates into fluid adjacent to which collagen fibrils adhere to each other and cross-link [1–4]. In most eyes this process is accompanied by dehiscence at the vitreoretinal interface progressing to posterior vitreous detachment and nothing more happens [see chapter II.C. Vitreous aging and posterior vitreous detachment]. In several pathologic conditions, vitreous is hazy due to hemorrhage and/or cell proliferation forming membranes that contract, leading to traction retinal detachment [see chapters III.J. Cell proliferation at the vitreo-retinal interface in proliferative vitreoretinopathy and related disorders; III.L. Proliferative diabetic vitreo-retinopathy]. Vitreoretinal surgery for these conditions includes complete removal of the vitreous gel (Figure I.F-1), removal of pre- and subretinal membranes, and injection of a tamponade such as silicone oil or expanding gases. All the presently used intravitreal tamponade substances carry different side effects making them unsuitable for permanent or long-standing use. Many authors [5–9] have suggested an ideal single artificial vitreous gel covering all needs, but no gel has yet been found to fit these demands [10].

This chapter reviews the biochemical composition and organization of vitreous, the currently used vitreous substitutes, and the rationale as well as approaches to developing an artificial vitreous.

B. Vitreous Biochemistry

More than 95 % of the vitreous gel weight is water. About 15–20 % of this water is bound to glycosaminoglycans (GAGS) and proteins. The vitreous body of all species is composed of essentially the same extracellular matrix elements organized to fill the center of the eye with a clear viscous substance surrounded by a dense cortex that is attached to the basal laminae of surrounding cells. There are, however, species variations in the relative concentrations of the major structural components [2, 11] of vitreous, i.e., hyaluronan (HA) and collagen. These differences account for variations in the rheologic (gel-liquid) state of the vitreous body in different species. It should be emphasized that in more advanced species there are also age-related differences. Consequently, the selection of an appropriate animal with which to model human diseases for scientific investigation must take into consideration these species variations and age-related differences. HA is present in the vitreous body of all species studied except for fishes.

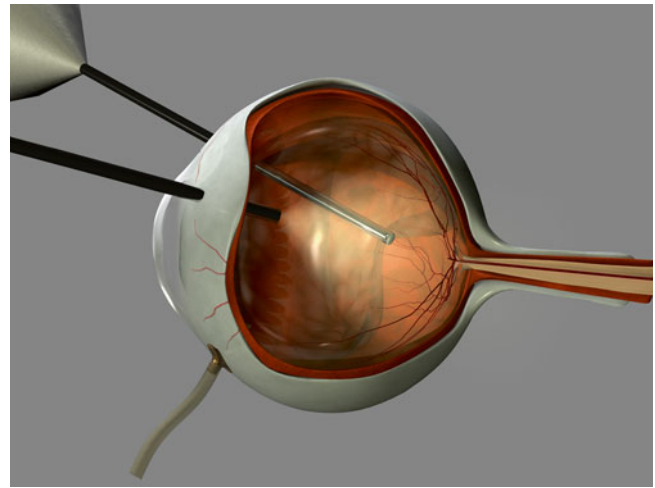


Figure I.F-1 Pars plana vitrectomy with removal of the vitreous gel (Copyright Fredrik Ghosh)

1. Glycosaminoglycans (GAGs)

GAGs are polysaccharides composed of repeating disaccharide units, each consisting of hexosamine (usually *N*-acetyl glucosamine or *N*-acetyl galactosamine) glycosidically linked to either uronic (glucuronic or iduronic) acid or galactose. The nature of the predominant repeating unit is characteristic for each GAG and the relative amount, molecular size, and type of GAG are said to be tissue specific [12]. A sulfated group is attached to oxygen or nitrogen in all GAGs except HA. GAGs do not normally occur *in vivo* as free polymers but are covalently linked to a protein core, the ensemble called a proteoglycan. There are three types of GAGs present in the vitreous body: hyaluronan (HA), chondroitin sulfate (CS) and heparan sulfate (HS).

a. Hyaluronan

Hyaluronan (HA; previously called hyaluronic acid) is the major GAG present in the human vitreous. Meyer and Palmer 1934 [13] first isolated this macromolecule from bovine vitreous. HA's name is derived from the fact that it was first discovered in the clear, colorless vitreous ("hyalos," means glass in Greek) and that it contains uronic acid. Balazs et al. [14, 15] documented the presence of sulfated galactosamine-containing GAGS in bovine vitreous (less than 5 % heparin sulfate). Meyer [16] and Balazs [17] first identified HA as a long, unbranched polymer of repeating disaccharide (glucuronic acid beta 1–3 *N*-acetylglucosamine) linked by beta 1-4 bonds. HA first appears after birth and is believed to be synthesized primarily by hyalocytes. Although the synthesis of HA plateaus in the adult, there does not appear to be any extracellular degradation [18–21], so HA levels remain constant because there is escape of HA molecules from vitreous via the anterior segment of the eye [22] and there is reuptake by hyalocytes. Laurent and Fraser [23] showed

that the escape of HA from the vitreous to the anterior segment is strongly molecular weight dependent, indicating a diffusion-controlled process. In contrast, disappearance of HA from the anterior chamber is independent of molecular weight, suggesting that this is controlled by bulk flow. Later studies noted a marked linear decrease of HA levels with age in human vitreous [24]. Laurent and Granath [25] used gel chromatography and found the average molecular weight of rabbit vitreous to be $2\text{--}3 \times 10^6$ and of bovine vitreous to be $0.5\text{--}0.8 \times 10^6$. These studies found age-related differences in the bovine vitreous since the HA molecular weight dropped from 3×10^6 in the newborn calf to 0.5×10^6 in old cattle.

The volume of the unhydrated HA molecule is about $0.66 \text{ cm}^3/\text{g}$, whereas the hydrated specific volume is $2\text{--}3,000 \text{ cm}^3/\text{g}$ [15]. Thus, the degree of hydration (and any pathologic condition that alters hydration) can have a significant influence on the size and configuration of the molecular network in vitreous. Because the solution domains are so large, the long unbranched HA chains form widely open coils, which at concentrations greater than $1 \text{ mg}/\text{cm}^3$, become highly entangled [26]. Due to its entanglement and immobilization in tissue, HA acts much like an ion-exchange resin in that an electrostatic interaction can occur between the small charges of mobile ions in the tissue and the electrostatic envelope of the stationary polyelectrolyte. This electrostatic interaction forms the basis for various properties of HA including its influence upon osmotic pressure, ion transport and distribution, and electric potentials within vitreous [27]. A compressed HA chain has extensive “interdigitations” since it interacts with nearest antiparallel as well as parallel neighbors (totalling 8 molecules), whereas extended forms only interact with 3 antiparallel neighbors [28].

b. Chondroitin Sulfate (CS)

CS is a major component in the extracellular matrix throughout the body, likewise in vitreous. In Wagner’s vitreoretinal degeneration a mutation in the gene for versican (one of the CS) was found to be the cause [29, 30]. This and other hereditary vitreo-retinopathies are discussed extensively in chapter I.C. Hereditary vitreo-retinopathies.

c. Heparan Sulfate (HS)

HS is a renewable proteoglycan present in vitreous in small amounts and presumed to maintain adequate distance between the collagen fibrils [31].

2. Proteins

The total protein content in vitreous is rather small in percentage, variable, and complex in nature. Among the soluble proteins, albumin and iron-binding proteins play the major role. Transferrin and other iron-binding proteins may have a protective capability by reducing iron toxicity in vitreous hemorrhage [32]. Collagens are the most frequent insoluble

proteins and it has been shown that the Muller cells can synthesize vitreous collagens *in vitro* [33]. Vitreous proteins are extensively discussed in chapter I.A. Vitreous proteins. An important consideration is the interaction of collagen and HA.

3. HA-Collagen Interaction

Vitreous is composed of interpenetrating networks of HA molecules and collagen fibrils. The collagen fibrils provide a solid structure to the vitreous that is “inflated” by the hydrophilic HA. Comper and Laurent [27] found that if collagen is removed, the remaining HA forms a viscous solution; if HA is removed, the gel shrinks. There exists interaction between HA and collagen, and the structure and function of these macromolecules is influenced by this interaction [34]. In all extracellular matrices collagen–proteoglycan interaction determines the morphology of the matrix. The nature of this interaction is a function of collagen type and proteoglycan concentration. Type I collagen is associated with small amounts of proteoglycan and has a weak interaction with this proteoglycan, thus appearing as compact fibrils. The appearance is different in extracellular matrices with predominantly type II collagen, which is rich in proteoglycans and has strong collagen–proteoglycan interaction. Thus, in such extracellular matrices, the type II collagen fibrils are widely separated and the spaces between are filled with proteoglycan.

Physiologic observations also suggest the existence of an important interaction between HA and collagen. Jackson [35] was the first to propose that proteoglycans had a “stabilizing effect” upon collagen. Gelman and Blackwell and Gelman et al. [36, 37] have shown that several glycosaminoglycans, including HA, stabilized the helical structure of collagen so that the melting temperature of collagen was increased from 38 to $46 \text{ }^\circ\text{C}$. Measurements of the dynamic viscoelasticity of bovine vitreous showed that the shapes of the master relaxation curves of vitreous are quite similar to those of lightly cross-linked polymer systems [38]. Notably, the behavior of these relaxation curves is different from that of solutions of HA and collagen. This suggests that the physicochemical properties of vitreous *in vivo* are not simply the result of a combination of these two molecular elements but that HA and collagen form a “lightly” cross-linked polymer system. Furthermore, these investigations suggest that the molecular weight at the cross-linking points is about 10^6 . This corresponds closely to the molecular weight of HA and according to these investigators suggests that this molecule might serve as the cross-linking element in this polymer system.

HA-collagen interaction in the vitreous may be mediated by a third molecule. Swann et al. [39] have demonstrated large amount of noncollagenous protein associated with collagen in the insoluble residue fraction of vitreous. There are filaments connecting the collagen fibrils and these amorphous masses. These filaments may represent “link”

structures of either a glycoprotein or proteoglycans nature. HA is known to interact with link proteins [40] as well as an HA-binding glycoprotein, hyaluronectin [41]. Thus, HA could bind to vitreous collagen fibrils via such linkage molecules, most probably in a repeating, ordered manner. This type of arrangement would not be consistent with the concept of random distribution of HA molecules spreading apart the collagen fibrils. Rather, binding to collagen fibrils of the protein core of a proteoglycan such as chondroitin sulfate would “organize” the network in a manner to keep the vitreous collagen fibrils at a critical distance apart [41] to minimize light scattering. Many investigators believe that HA-collagen interaction occurs on a physicochemical rather than chemical level. It may well be that there are several types of collagen-HA interactions that are at play in different circumstances. Further investigation must be undertaken to identify the nature of HA-collagen interaction(s) in vitreous. This question is important not only with respect to the normal physiology of vitreous and its structure but also to understand the aging phenomena of vitreous liquefaction and posterior vitreous detachment, as well as to aid in the development of an artificial vitreous.

4. Miscellaneous Components

a. Metabolites and Enzymes

Glucose and lactic acid are found in vitreous mostly due to cellular metabolism in adjacent tissues. Glucose is supposed to support the enzymatic activity in vitreous in connection with HA turnover [42]. In diabetes, there are elevated levels of glucose in vitreous [43] leading to the formation of advanced glycation at end products in the gel [44] and presumably at the vitreoretinal interface as well.

Renin–angiotensin-converting enzyme has been isolated from the vitreous [45]. Vitreous lactate seems to be a major metabolite in the human vitreous [46].

b. Ascorbic Acid

Ascorbic acid is found in higher levels in the vitreous body compared to plasma.

It is postulated that ascorbic acid is associated with liquefaction during aging and after cataract extraction [47], but it could also be an inhibitor for neovascularization [48] and increase proliferation of hyalocytes [49]. Recent studies also implicate that ascorbic acid may play an important role as antioxidant and thereby decreasing the amount of free oxygen near the lens and thus preventing cataract formation [50] [see chapter IV.B. Oxygen in vitreo-retinal physiology and pathology.]

c. Amino and Fatty Acids

Some amino acids have been detected in vitreous at the same concentration as in plasma. Unsaturated fatty acids (50 % of all fatty acids in vitreous) have been found to have a constant level throughout age [51].

d. Prostaglandins

Prostaglandins have been measured in concentration of about 100 pg/ml in the human vitreous [52].

II. Roles of an Artificial Vitreous

With an ever-increasing appreciation of the role of vitreous in ocular health [see chapters IV.A. Vitreous in ocular physiology; IV.B. Oxygen in vitreo-retinal physiology and pathology; IV.D. Physiology of accommodation and role of vitreous], there is growing interest in the development of an artificial vitreous. The diversity of demands on artificial vitreous candidates is notable (Figure I.F-2):

1. Volume filler: In hypotonous and phthisical eyes where aqueous production is diminished or absent, there is a need for a *volume filler* to hold the form of the eye globe.
2. Tamponade: In severe forms of retinal detachment, it is mandatory to seal the breaks by gel adhesion or “glueing” with a *tamponade*.
3. Drug vehicle: In diseases such as age-related macular degeneration (AMD), a suitable *vehicle for drugs* such as synthetic gels capable of slow release of pharmacologic substances is desired [53–55].
4. Free radical scavenger: After vitrectomy, the oxygen balance is changed and the pO_2 near the lens increases causing cataract progression. With a suitable gel, cataract formation might be prevented [56–58].
5. Refract incident light: Refractive error such as high myopia can be difficult to adjust with optical aid. A vitreous gel with *refractive properties* may be useful (compare to silicone oil).

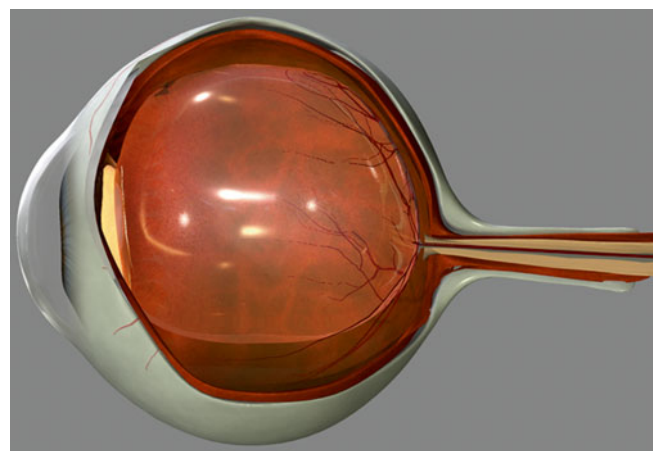


Figure I.F-2 There is a diversity of demands on artificial vitreous candidates such as: (a) volume filler, (b) tamponade, (c) drug vehicle, (d) free radical scavenger, (e) refract incident light, (f) hemostasis, (g) maintain optical clarity (Copyright Fredrik Ghosh)

6. Hemostasis: In diabetic and other vascular retinal diseases, patients may suffer recurrent intravitreal hemorrhage. A suitable synthetic vitreous tamponade (similar to silicone oil or a gel containing anti-VEGF) might *stop further bleeding*.
7. Maintain optical clarity: Cell migration and proliferation must be inhibited and protein exudation must be mitigated to maintain a clear medium through which photons can pass unhindered to undergo photoreception and begin vision.

III. Properties of an Artificial Vitreous

An artificial vitreous gel should possess certain physical properties such as being injectable through a small cannula without disintegration (shearing). To avoid thermal damage, the gelation process should not produce high temperature once inside the eye. The gel must be inert, have the ability to allow transfer of metabolites, be nonabsorbable or slow disintegrating, and carry high clarity and transparency. It seems that for different indications and purposes we might not be able to identify one single gel. Instead a variety of different gels with various properties (such as long or short lasting, drug delivery, glue, volume, or tamponade) for specified indications may be interesting.

A. Anatomic Considerations: Do We Need a Posterior Vitreous Cortex?

During removal of the natural vitreous in patients, we consider it necessary to induce a posterior vitreous detachment sometimes in combination with peeling of the inner limiting membrane (ILM). This is to ensure that all vitreous remnants are removed together with fibrous membranes and other traction components. We leave the retina without cover and the protection of ILM or the posterior vitreous cortex. If we inject an artificial gel into the vitreous cavity in such an eye, it will come in close contact with the neural retina and have a higher potential of toxic influences on the retinal cells. Histological findings [59] suggested a direct toxic effect at sites where a polyacrylamide hydrogel came in direct contact with the neural retina. In sections where a PVD was not complete and the natural posterior vitreous cortex persisted, the neural retina appeared normal on histology. Could it be that constructing a thin, semipermeable membrane around the artificial vitreous gel is a solution to prevent destruction of the neural retina seen in experimental studies? Gao et al. [60] tested a capsular silicone elastomer 0.01 mm thick which inside the eye on rabbits was filled with physiological balanced salt solution and included a tube–valve system for pressure regulation. During the 8 weeks the experiment

lasted, there were no negative effects or malfunction detected by ERG or histology.

IV. Vitreous Substitutes in Vitreoretinal Surgery

Besides the currently used clinical vitreous substitutes (silicone oil, expanding gases, perfluorocarbon liquids, semi-fluorinated alkanes, and mixtures such as heavy silicone oil; see chapter IV.G. Physiology of vitreous substitutes), many different gels with various chemical and physical properties have been tested *in vitro* and *in vivo* in animal and humans experiments.

A. Natural and Semisynthetic Polymers and Hyaluronic Hydrogels

Cross-linked hyaluronic acid is in most perspectives identical to one component of the natural vitreous gel and has been found to be nontoxic to the retina [61–63]. The compound is used clinically for viscodissection of intraocular tissue or to maintain a filtering bleb in glaucoma surgery and has also been tested as temporary or partial retinal tamponade. This compound has a high degradation tendency and lasts for a short period of time, inducing elevated intraocular pressure while disintegrating [64–69]. By employing different cross-linking methods and techniques, the rapid disintegration and small molecule formation may be halted and tolerance enhanced [70] (Figure I.F-3).

Gels containing gelatin and collagen have been tested as vitreous substitutes but after a short duration, there was rapid disintegration. Polysaccharides, e.g., dextran, sodium alginate, and chondroitin sulfate did not elicit inflammation, but vitreous haze and high dissolving tendency were reported [71]. A natural crustacean product, chitosan, was tested with promising results regarding biocompatibility and gel stability [72].

B. Synthetic Hydrogels and “Smart Hydrogels”

Hydrogels are synthetic three-dimensional polymers that swell in aqueous solution and do not display any dissolution, resorption, or disintegration inside the eye. They are becoming popular due to their physical and chemical properties meaning that they stay stable, show biocompatibility, keep transparent, are highly hydrophilic, and do not shear when injected through small gauge cannulas [59, 73–76]. However, polyacrylamide and similar hydrogels are highly neurotoxic when in monomer form and only biocompatible

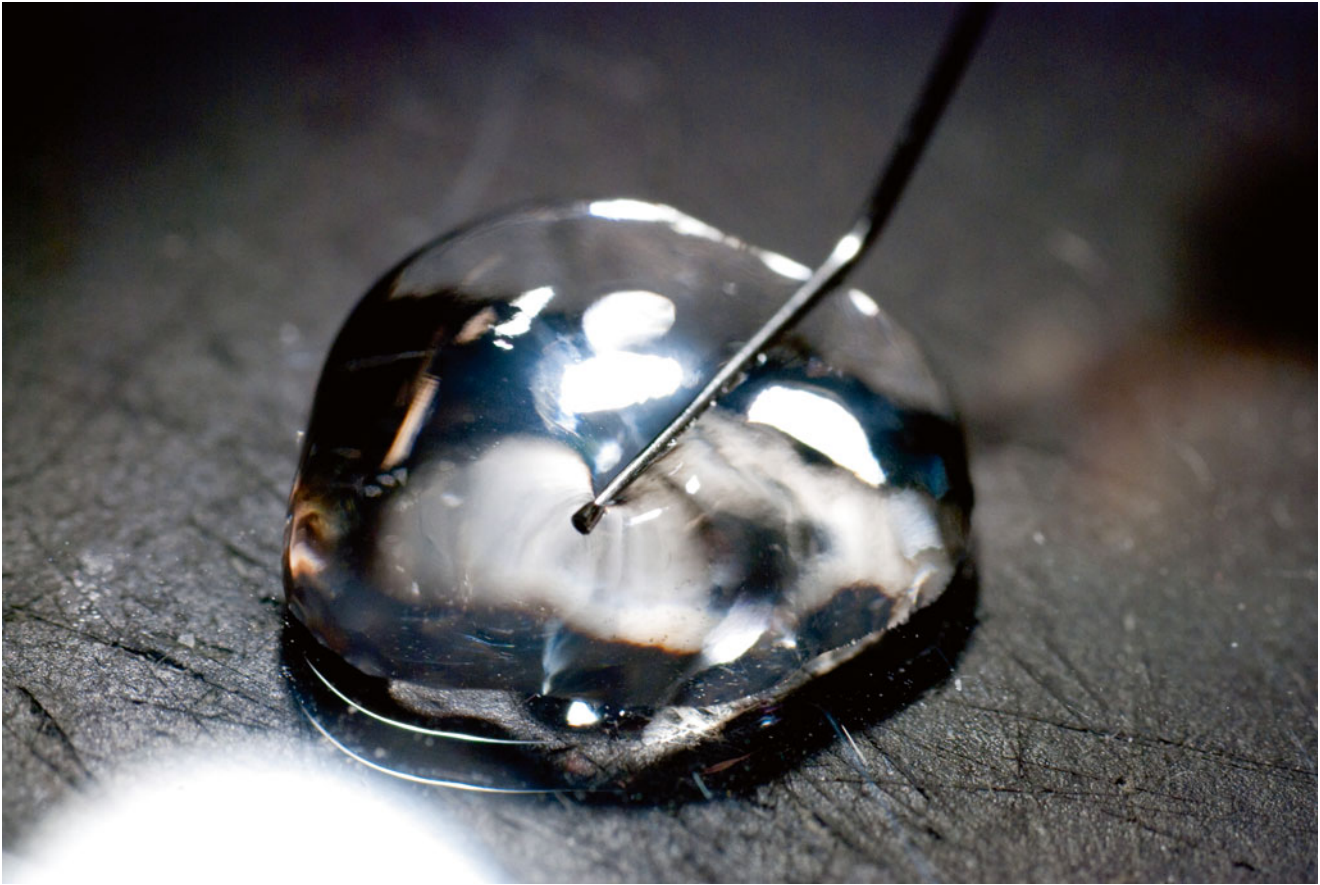


Figure I.F-3 By employing different cross-linking methods and techniques, a more stable hydrogel was achieved such as sodium hyaluronic acid hydrogel (Healaflo[®])

after complete polymerization. To minimize toxicity and increase injectability, many investigators have used different methods such as cross-linking or chemical modifications making the (*smart-*) gel liquid during injection but spontaneously gelating inside the eye. This can occur due to a temperature-sensitive gel [77–80], or a gel responsive to the oxygen rich environment inside the eye [81]. Tai [82] has reported a polyethylene glycol gel, which is thermoresponsive and, after gelation, forms a covalently cross-linked hydrogel.

V. Developing an Artificial Vitreous

A. Experimental Models for Testing Artificial Vitreous *In Vivo*

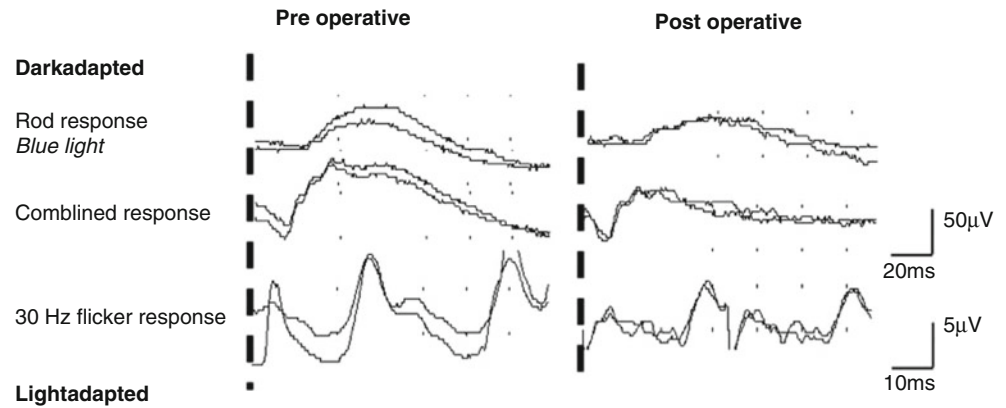
Several animal models have been used to explore physical and biochemical properties of novel vitreous substitute candidates. The rabbit eye is one of the most commonly used

since it is well suited for the vitrectomy procedure and is well characterized regarding retinal structure and function. We recently developed an *in vivo* rabbit model using vitrectomy and subsequent infusion of the candidate compound followed by morphological and electrophysiological retinal evaluation [72, 83].

1. Polyalkylimide

Polyalkylimide is a gel polymer comprised exclusively of networks of alkylimide groups (approximately 4 %) and non-pyrogenic water (approximately 96 %). Alkylimide belongs to the family of acryl derivatives, and its polymeric structure does not contain free monomers. The gel is commercially available and is used clinically in plastic surgery as nondegradable filler in esthetic lipoatrophic conditions and after post-traumatic or therapeutic atrophy of subcutaneous tissue [75, 84, 85]. When placed in the subcutaneous space, the gel forms a thin collagen capsule, and it is extractable even after several years without signs of degrading. This gel has been found to be nontoxic when

Figure I.F-4 Full-field ERG demonstrating reduction of a- and b-wave amplitudes in all stimulation protocols, indicating diminished cone and rod function 28 days after injection of Bio-Alcamid®



applied on the human skin or on cultured fibroblast but did induce swelling and hyperemia after subcutaneous injection in the rat [86].

In a first experiment, we performed a regular 20G vitrectomy including posterior vitreous detachment, central vitrectomy, and infusion of approximately 1.0 ml of polyalkylimide (Bio-Alcamide®) hydrogel [59]. Hydrogel-filled eyes were compared with eyes filled with balanced salt solution. We found that the viscoelastic polyalkylimide hydrogel could be injected with ease into the vitreous cavity. The gel remained clear with retained viscosity for at least 28 days. In contrast to previous reports in reconstructive surgery, a surrounding capsule was not found, but the gel displayed uninterrupted apposition with the retinal surface. Pathological reactions were present early in the postoperative period in the form of neuroretinal swelling and posterior capsule opacification. In addition, ERG recordings showed a radical decrease in rod- and cone-derived b-wave amplitudes performed [87, 88] (Figure I.F-4). In histological sections, degenerative retinal changes were seen almost exclusively in central parts of the retina and not in the periphery, where the natural vitreous remained, suggesting that direct gel-to-retina contact was responsible for the adverse morphological effects on the retina (Figure I.F-5). In this setting, the rabbit retina may be especially vulnerable to biochemical changes due to its merangiotic (partly vascularized) nature, i.e., lack of retinal circulation, making it dependent on support from the vitreous and choroid [89] (Figure I.F-6). The conclusion of this experiment was that the intravitreal polyalkylimide gel displays excellent physical requirements of an ideal vitreous tamponade but that it induces severe retinal pathological reactions which limits its use as a potential artificial vitreous (Figure I.F-7). The reasons for the adverse intraocular reactions are not

readily known, but recent evidence points to an inflammation-inducing capacity when used subcutaneously [90], so perhaps also in the eye.

2. Polyethylene Glycol

For the next experiment [91] we used polyethylene glycol (PEG) [92], a synthetic water-soluble polymer approved by the FDA for use in a wide range of biomedical applications, including injectable hydrogels [93]. PEG has also been tested in formulations for intravitreal drug delivery, repair of scleral incisions, and sealing retinal detachments [54, 94, 95]. We used the same surgical protocol as in the polyalkylimide experiment but instead injected viscoelastic PEG sols of high molecular weight (>200 kDa) in phosphate-buffered saline (PBS). Molecular weights and concentration of PEG were chosen to approximate the mechanical properties of the natural vitreous. Sols of 5 wt.% PEG with a molecular weight of 400 kDa in PBS were shown to have mechanical and optical properties similar to the natural vitreous and were well tolerated by the retina, with minimal histological or electrophysiological changes, with the exception GFAP upregulation over a period of 41 days. However, the sols were not retained in vitreous throughout the postoperative period and were found to be completely dissolved. These results indicate that PEG displays excellent biocompatibility within the eye, but to extend its use to clinical application, further modification of the gel is needed.

B. Experimental Model for Testing Artificial Vitreous *In Vitro*

To provide an alternative to relatively costly and cumbersome *in vivo* testing, we developed a new model for primary *in vitro* assessment of novel artificial vitreous

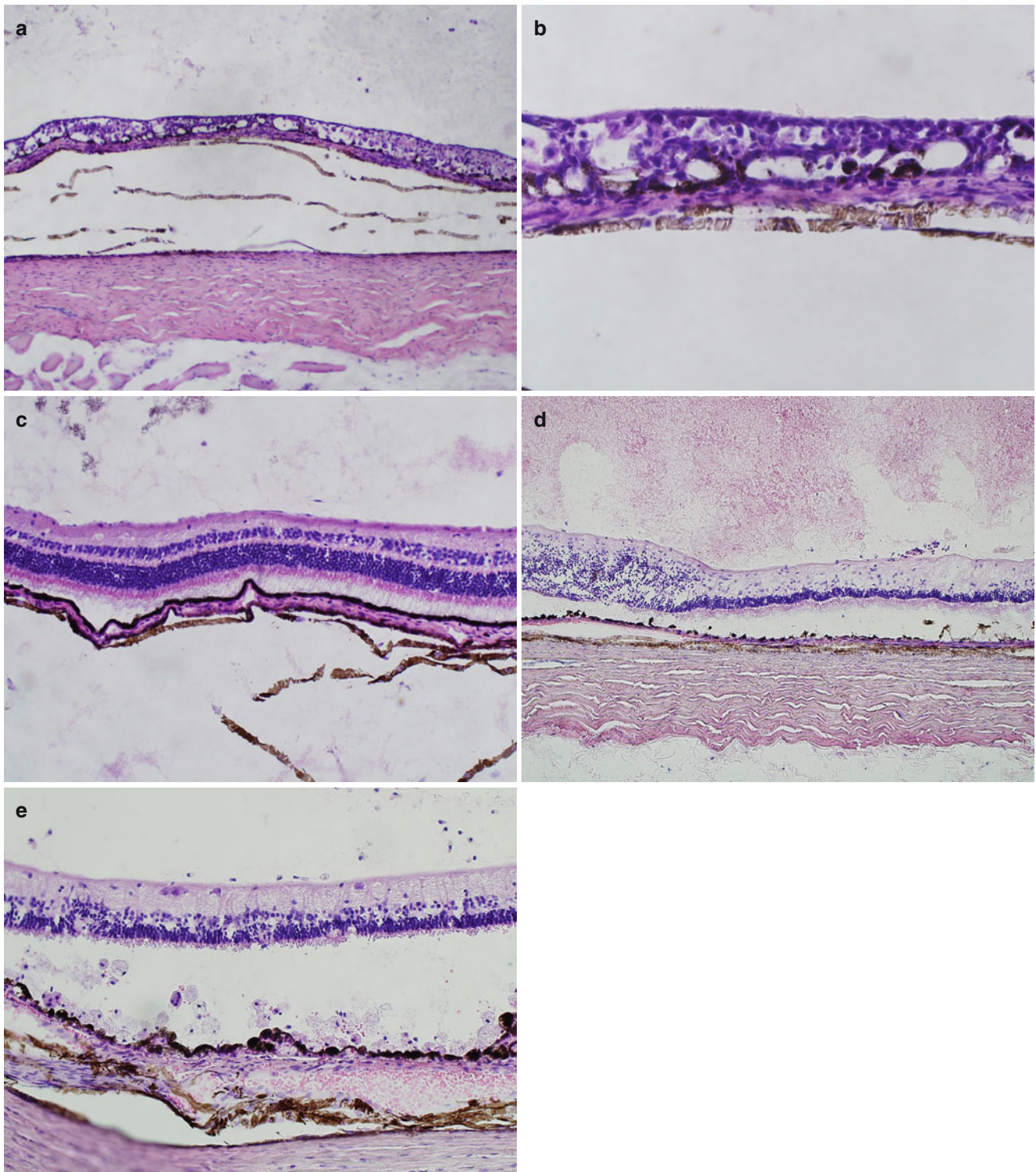


Figure I.F-5 Histology of experimental rabbit operations with polyalkylimide. (a–c) Hematoxylin and eosin staining, cryosections. There is choroidal edema and total neuroretinal destruction centrally (a, b) 6 days postoperatively. The peripheral neuroretina appears normal (c). (d) In another rabbit the border between severe neuroretinal degenera-

tion and less affected tissue is seen. (e) In yet a third rabbit, invasion of inflammatory cells can be seen in the subretinal space. The RPE is disrupted, and degeneration of photoreceptors as well as inner retinal cells is evident

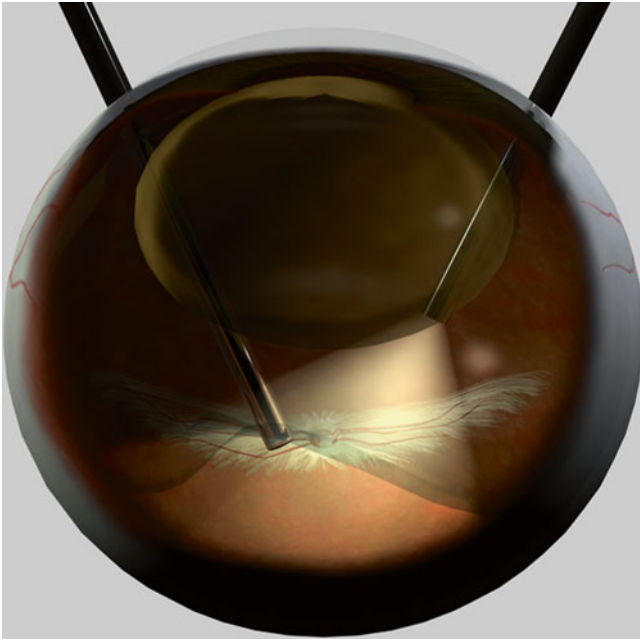


Figure I.F-6 The rabbit retina may be especially vulnerable to biochemical changes due to its merangiotic (partly vascularized) nature, i.e., lack of retinal circulation, making it dependent on support from the vitreous and choroid (Copyright Fredrik Ghosh)

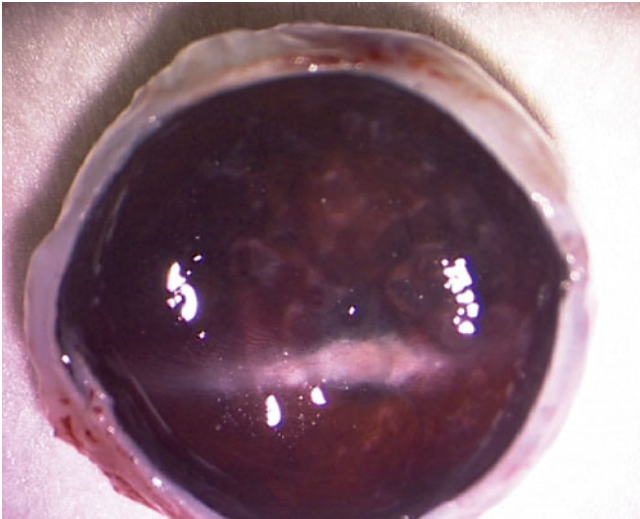


Figure I.F-7 Dissection of rabbit eye displays clear Bio-Alcamid gel with no apparent fragmentation 28 days postoperatively. The gel is well-apposed to the retinal surface

candidates [96]. For this experiment, the biological impact of three artificial vitreous candidates was explored in a retinal explant culture model: polyalkylimide (Bio-Alcamid®), a two-component hydrogel of 20 wt.% poly-(ethylene

glycol) in phosphate-buffered saline (PEG), and a cross-linked sodium hyaluronic acid hydrogel (Healaflo®) (Figure I.F-3). The gels were applied to explanted adult rat retinas and then kept in culture for 5 days after which morphological evaluation using immunohistochemistry, TUNEL, and hematoxylin–eosin staining were performed. Explants kept under standard conditions as well as PEG-exposed explants displayed disruption of retinal layers with moderate pyknosis of first-, second-, and third-order neurons. They also showed moderate fragmentation of DNA (TUNEL). Polyalkylimide-exposed explants displayed severe thinning and disruption of retinal layers with massive cell death. In contrast, cross-linked sodium hyaluronic acid hydrogel-treated explants showed normal retinal lamination with significantly better preservation of retinal neurons compared with control specimens and almost no DNA fragmentation. We conclude that the explant culture system under standard conditions imposes reactions within the retina that can be used when evaluating artificial vitreous candidates. In our particular experiment, polyalkylimide adversely affected the *in vitro* retina, consistent with the results of prior *in vivo* trials. PEG gel imposed reactions similar to the control retinas, whereas Healaflo® showed protection from culture-induced trauma, indicating a favorable biocompatibility. The *in vitro* retinal explant model provides a method of biocompatibility testing prior to more costly and cumbersome *in vivo* experiments.

Abbreviations

AMD	Age-related macular degeneration
CS	Chondroitin sulfate
DNA	Deoxyribonucleic acid
ERG	Electroretinography
G	Gauge
GAG	Glycosaminoglycans
GFAP	Glial fibrillar acid protein
HA	Hyaluronan
HS	Heparan sulfate
ILM	Inner limiting membrane
kDa	Kilodalton
PBS	Phosphate-buffered saline
PEG	Polyethylene glycol
pg.ml	Picograms/milliliter
pO ₂	Partial pressure of oxygen
TUNEL	Terminal deoxynucleotidyl transferase dUTP nick end labeling
VEGF	Vascular endothelial growth factor

References

- Sebag J. Age-related changes in human vitreous structure. *Graefes Arch Clin Exp Ophthalmol*. 1987;225(2):89–93.
- Sebag J. The vitreous: structure, function, and pathobiology. New York: Springer; 1989.
- Chuo JY, Lee TY, Hollands H, Morris AH, Reyes RC, Rossiter JD, et al. Risk factors for posterior vitreous detachment: a case-control study. *Am J Ophthalmol*. 2006;142(6):931–7.
- Los LI, van der Worp RJ, van Luyn MJ, Hooymans JM. Age-related liquefaction of the human vitreous body: LM and TEM evaluation of the role of proteoglycans and collagen. *Invest Ophthalmol Vis Sci*. 2003;44(7):2828–33.
- Kleinberg TT, Tzekov RT, Stein L, Ravi N, Kaushal S. Vitreous substitutes: a comprehensive review. *Surv Ophthalmol*. 2011;56(4):300–23.
- Pruett RC, Calabria GA, Schepens CL. Collagen vitreous substitute. I. Experimental study. *Arch Ophthalmol*. 1972;88(5):540–3.
- Pruett RC, Schepens CL, Freeman HM. Collagen vitreous substitute. II. Preliminary clinical trials. *Arch Ophthalmol*. 1974;91(1):29–32.
- Pruett RC, Schepens CL, Swann DA. Hyaluronic acid vitreous substitute. A six-year clinical evaluation. *Arch Ophthalmol*. 1979;97(12):2325–30.
- Maruoka S, Matsuura T, Kawasaki K, Okamoto M, Yoshiaki H, Kodama M, et al. Biocompatibility of polyvinylalcohol gel as a vitreous substitute. *Curr Eye Res*. 2006;31(7–8):599–606.
- Baino F. Towards an ideal biomaterial for vitreous replacement: historical overview and future trends. *Acta Biomater*. 2011;7(3):921–35.
- Jacobson B. Degradation of glycosaminoglycans by extracts of calf vitreous hyalocytes. *Exp Eye Res*. 1984;39(3):373–85.
- Toledo OM, Dietrich CP. Tissue specific distribution of sulfated mucopolysaccharides in mammals. *Biochim Biophys Acta*. 1977;498(1):114–22.
- Meyer K, Palmer JW. The polysaccharide of vitreous humour. *J Biol Chem*. 1934;107:629–34.
- Balazs EA, Sundblad L, Toth LXJ. In vitro formation of hyaluronic acid by cells in the vitreous body and by comb tissue. *Abstr Fed Proc*. 1958;17:184.
- Balazs EA, Denlinger JL. The vitreous. In: Davson H, editor. *The eye*, vol. 1A. London: Academic; 1984. p. 533–89.
- Meyer K. Chemical structure of hyaluronic acid. *Fed Proc*. 1958;17(4):1075–7.
- Balazs EA. Molecular morphology of the vitreous body. In: Smelser GK, editor. *Structure of the eye*. New York: Academic; 1961. p. 293–310.
- Breen M, Bizzell JW, Weinstein HG. A galactosamine containing proteoglycan in human vitreous. *Exp Eye Res*. 1977;24(4):409–12.
- Allen WS, Otterbein EC, Wardi AH. Isolation and characterization of the sulfated glycosaminoglycans of the vitreous body. *Biochim Biophys Acta*. 1977;498(1):167–75.
- Kamei A, Totani A. Isolation and characterization of minor glycosaminoglycans in the rabbit vitreous body. *Biochem Biophys Res Commun*. 1982;109(3):881–7.
- Hultsch E, Freeman MI, Balazs EA. Transport and regeneration of hyaluronic acid in extracellular ocular compartments. Annual meeting of the Association for Research in Vision and Ophthalmology (ARVO). *Invest Ophthalmol*. 1974;11:97.
- Borzacchiello A, Netti PA, Ambrosio L, Nicolais L. Hyaluronic acid derivatives mimic the rheological properties of vitreous body. In: Abatangelo G, Weigel PH, editors. *New frontiers in medical sciences: redefining hyaluronan: proceedings of the symposium held in Padua, Italy, 17–19 June 1999*. Amsterdam: Elsevier; 2000. p. 195–202.
- Laurent UB, Fraser JR. Turnover of hyaluronate in the aqueous humour and vitreous body of the rabbit. *Exp Eye Res*. 1983;36(4):493–503.
- Itakura H, Kishi S, Kotajima N, Murakami M. Decreased vitreal hyaluronan levels with aging. *Ophthalmologica*. 2009;223(1):32–5.
- Laurent UB, Granath KA. The molecular weight of hyaluronate in the aqueous humour and vitreous body of rabbit and cattle eyes. *Exp Eye Res*. 1983;36(4):481–92.
- Noulas AV, Theocharis AD, Feretis E, Papageorgakopoulou N, Karamanos NK, Theocharis DA. Pig vitreous gel: macromolecular composition with particular reference to hyaluronan-binding proteoglycans. *Biochimie*. 2002;84(4):295–302.
- Comper WD, Laurent TC. Physiological function of connective tissue polysaccharides. *Physiol Rev*. 1978;58(1):255–315.
- Chakrabarti B, Park JW. Glycosaminoglycans: structure and interaction. *CRC Crit Rev Biochem*. 1980;8:255–313.
- Reardon A, Heinegard D, McLeod D, Sheehan JK, Bishop PN. The large chondroitin sulphate proteoglycan versican in mammalian vitreous. *Matrix Biol*. 1998;17(5):325–33.
- Kloetkener-Gruissem B, Bartholdi D, Abdou MT, Zimmermann DR, Berger W. Identification of the genetic defect in the original Wagner syndrome family. *Mol Vis*. 2006;12:350–5.
- Goes RM, Nader HB, Porcionatto MA, Haddad A, Laicine EM. Chondroitin sulfate proteoglycans are structural renewable constituents of the rabbit vitreous body. *Curr Eye Res*. 2005;30(5):405–13.
- Wong RW, Richa DC, Hahn P, Green WR, Dunaief JL. Iron toxicity as a potential factor in AMD. *Retina*. 2007;27(8):997–1003.
- Ponsioen TL, van Luyn MJ, van der Worp RJ, Pas HH, Hooymans JM, Los LI. Human retinal Muller cells synthesize collagens of the vitreous and vitreoretinal interface in vitro. *Mol Vis*. 2008;14:652–60.
- Junqueira LC, Montes GS. Biology of collagen-proteoglycan interaction. *Arch Histol Jpn*. 1983;46(5):589–629.
- Jackson DS. Chondroitin sulphuric acid as a factor in the stability of tendon. *Biochem J*. 1953;54(4):638–41.
- Gelman RA, Blackwell J. Collagen-mucopolysaccharide interactions at acid pH. *Biochim Biophys Acta*. 1974;342(2):254–61.
- Gelman RA, Blackwell J, Kefalides NA, Tomichek E. Thermal stability of basement membrane collagen. *Biochim Biophys Acta*. 1976;427(2):492–6.
- Tokita M, Fujiya Y, Hikichi K. Dynamic viscoelasticity of bovine vitreous body. *Biorheology*. 1984;21(6):751–6.
- Swann DA, Constable IJ, Caulfield JB. Vitreous structure. IV. Chemical composition of the insoluble residual protein fraction from the rabbit vitreous. *Invest Ophthalmol*. 1975;14(8):613–6.
- Scott JE. Supramolecular organization of extracellular matrix glycosaminoglycans, in vitro and in the tissues. *FASEB J*. 1992;6(9):2639–45.
- Scott JE. The chemical morphology of the vitreous. *Eye (Lond)*. 1992;6(Pt 6):553–5.
- Rhodes RH, Mandelbaum SH, Minckler DS, Cleary PE. Tritiated fucose incorporation in the vitreous body, lens and zonules of the pigmented rabbit. *Exp Eye Res*. 1982;34(6):921–31.
- Lundquist O, Osterlin S. Glucose concentration in the vitreous of nondiabetic and diabetic human eyes. *Graefes Arch Clin Exp Ophthalmol*. 1994;232(2):71–4.
- Sebag J, Buckingham B, Charles MA, Reiser K. Biochemical abnormalities in vitreous of humans with proliferative diabetic retinopathy. *Arch Ophthalmol*. 1992;110(10):1472–6.
- Sramek SJ, Wallow IH, Tewksbury DA, Brandt CR, Poulsen GL. An ocular renin-angiotensin system. Immunohistochemistry of angiotensinogen. *Invest Ophthalmol Vis Sci*. 1992;33(5):1627–32.

46. Berkowitz BA, Bansal N, Wilson CA. Non-invasive measurement of steady-state vitreous lactate concentration. *NMR Biomed*. 1994;7(6):263–8.
47. Worst JGF, Los LI. Functional anatomy of the vitreous. In: Worst JGF, Los LI, editors. *Cisternal anatomy of the vitreous*. Amsterdam: Kugler Publications; 1995. p. 33–50.
48. Hanashima C, Namiki H. Reduced viability of vascular endothelial cells by high concentration of ascorbic acid in vitreous humor. *Cell Biol Int*. 1999;23(4):287–98.
49. Sommer F, Brandl F, Weiser B, Tesmar J, Blunk T, Gopferich A. FACS as useful tool to study distinct hyalocyte populations. *Exp Eye Res*. 2009;88(5):995–9.
50. Shui YB, Fu JJ, Garcia C, Dattilo LK, Rajagopal R, McMillan S, et al. Oxygen distribution in the rabbit eye and oxygen consumption by the lens. *Invest Ophthalmol Vis Sci*. 2006;47(4):1571–80.
51. Reddy TS, Birkle DL, Packer AJ, Dobard P, Bazan NG. Fatty acid composition and arachidonic acid metabolism in vitreous lipids from canine and human eyes. *Curr Eye Res*. 1986;5(6):441–7.
52. Thomas MA, O'Grady GE, Swartz SL. Prostaglandin levels in human vitreous. *Br J Ophthalmol*. 1985;69(4):275–9.
53. Park D, Shah V, Rauck BM, Friberg TR, Wang Y. An anti-angiogenic reverse thermal gel as a drug-delivery system for age-related wet macular degeneration. *Macromol Biosci*. 2013;13(4):464–9.
54. Duvvuri S, Janoria KG, Pal D, Mitra AK. Controlled delivery of ganciclovir to the retina with drug-loaded Poly(D, L-lactide-co-glycolide) (PLGA) microspheres dispersed in PLGA-PEG-PLGA Gel: a novel intravitreal delivery system for the treatment of cytomegalovirus retinitis. *J Ocul Pharmacol Ther*. 2007;23(3):264–74.
55. Pritchard CD, O'Shea TM, Siegwart DJ, Calo E, Anderson DG, Reynolds FM, et al. An injectable thiol-acrylate poly(ethylene glycol) hydrogel for sustained release of methylprednisolone sodium succinate. *Biomaterials*. 2011;32(2):587–97.
56. Shui YB, Holekamp NM, Kramer BC, Crowley JR, Wilkins MA, Chu F, et al. The gel state of the vitreous and ascorbate-dependent oxygen consumption: relationship to the etiology of nuclear cataracts. *Arch Ophthalmol*. 2009;127(4):475–82.
57. Holekamp NM, Shui YB, Beebe DC. Vitrectomy surgery increases oxygen exposure to the lens: a possible mechanism for nuclear cataract formation. *Am J Ophthalmol*. 2005;139(2):302–10.
58. Stefansson E. Physiology of vitreous surgery. *Graefes Arch Clin Exp Ophthalmol*. 2009;247(2):147–63.
59. Crafoord S, Andreasson S, Ghosh F. Experimental vitreous tamponade using polyalkylimide hydrogel. *Graefes Arch Clin Exp Ophthalmol*. 2011;249(8):1167–74.
60. Gao Q, Mou S, Ge J, To CH, Hui Y, Liu A, et al. A new strategy to replace the natural vitreous by a novel capsular artificial vitreous body with pressure-control valve. *Eye (Lond)*. 2008;22(3):461–8.
61. Hruby K. Hyaluronic acid as vitreous body substitute in retinal detachment. *Klin Monbl Augenheilkd Augenarztl Fortbild*. 1961;138:484–96.
62. Balazs EA, Sweeney DB. The replacement of the vitreous body in the monkey by reconstituted vitreous and by hyaluronic acid. *Bibl Ophthalmol*. 1966;70:230–2.
63. Nakagawa M, Tanaka M, Miyata T. Evaluation of collagen gel and hyaluronic acid as vitreous substitutes. *Ophthalmic Res*. 1997;29(6):409–20.
64. Hong Y, Chirila TV, Vijayasekaran S, Shen W, Lou X, Dalton PD. Biodegradation in vitro and retention in the rabbit eye of cross-linked poly(1-vinyl-2-pyrrolidinone) hydrogel as a vitreous substitute. *J Biomed Mater Res*. 1998;39(4):650–9.
65. Hong Y, Chirila TV, Cuypers MJ, Constable II. Polymers of 1-vinyl-2-pyrrolidinone as potential vitreous substitutes: physical selection. *J Biomater Appl*. 1996;11(2):135–81.
66. Suri S, Banerjee R. In vitro evaluation of in situ gels as short term vitreous substitutes. *J Biomed Mater Res A*. 2006;79(3):650–64.
67. Denlinger JL, Balazs EA. Replacement of the liquid vitreous with sodium hyaluronate in monkeys. I. Short-term evaluation. *Exp Eye Res*. 1980;31(1):81–99.
68. Denlinger JL, El-Mofty AA, Balazs EA. Replacement of the liquid vitreous with sodium hyaluronate in monkeys. II. Long-term evaluation. *Exp Eye Res*. 1980;31(1):101–17.
69. Koster R, Stilma JS. Comparison of vitreous replacement with Healon and with HPMC in rabbits' eyes. *Doc Ophthalmol*. 1986;61(3–4):247–53.
70. Schramm C, Spitzer MS, Henke-Fahle S, Steinmetz G, Januschowski K, Heiduschka P, et al. The cross-linked biopolymer hyaluronic acid as an artificial vitreous substitute. *Invest Ophthalmol Vis Sci*. 2012;53(2):613–21.
71. Gombos GM, Berman ER. Chemical and clinical observations on the fate of various vitreous substitutes. *Acta Ophthalmol (Copenh)*. 1967;45(6):794–806.
72. Yang H, Wang R, Gu Q, Zhang X. Feasibility study of chitosan as intravitreal tamponade material. *Graefes Arch Clin Exp Ophthalmol*. 2008;246(8):1097–105.
73. Swindle KE, Ravi N. Recent advances in polymeric vitreous substitutes. *Expert Rev Ophthalmol*. 2007;2(2):255–65.
74. Soman N, Banerjee R. Artificial vitreous replacements. *Biomed Mater Eng*. 2003;13(1):59–74.
75. Clauue BL, Rabineau P. The polyalkylimide gel: experience with Bio-Alcamid. *Semin Cutan Med Surg*. 2004;23(4):236–40.
76. Baino F. The use of polymers in the treatment of retinal detachment: current trends and future perspectives. *Polymers*. 2010;2(3):286–322.
77. Katagiri Y, Iwasaki T, Ishikawa T, Yamakawa N, Suzuki H, Usui M. Application of thermo-setting gel as artificial vitreous. *Jpn J Ophthalmol*. 2005;49(6):491–6.
78. Cohn D, Sosnik A, Garty S. Smart hydrogels for in situ generated implants. *Biomacromolecules*. 2005;6(3):1168–75.
79. Dong Y, Saeed AO, Hassan W, Keigher C, Zheng Y, Tai H, et al. "One-step" preparation of thiol-ene clickable PEG-based thermoresponsive hyperbranched copolymer for in situ crosslinking hybrid hydrogel. *Macromol Rapid Commun*. 2012;33(2):101–71.
80. Dong Y, Hassan W, Zheng Y, Saeed AO, Cao H, Tai H, et al. Thermoresponsive hyperbranched copolymer with multi acrylate functionality for in situ cross-linkable hyaluronic acid composite semi-IPN hydrogel. *J Mater Sci Mater Med*. 2012;23(1):25–35.
81. Swindle-Reilly KE, Shah M, Hamilton PD, Eskin TA, Kaushal S, Ravi N. Rabbit study of an in situ forming hydrogel vitreous substitute. *Invest Ophthalmol Vis Sci*. 2009;50(10):4840–6.
82. Tai H, Howard D, Takae S, Wang W, Vermonden T, Hennink WE, et al. Photo-cross-linked hydrogels from thermoresponsive PEGMEMA-PPGMA-EGDMA copolymers containing multiple methacrylate groups: mechanical property, swelling, protein release, and cytotoxicity. *Biomacromolecules*. 2009;10(10):2895–903.
83. Imai K, Loewenstein A, de Juan Jr E. Translocation of the retina for management of subfoveal choroidal neovascularization I: experimental studies in the rabbit eye. *Am J Ophthalmol*. 1998;125(5):627–34.
84. Protopapa C, Sito G, Caporale D, Cammarota N. Bio-Alcamid in drug-induced lipodystrophy. *J Cosmet Laser Ther*. 2003;5(3–4):226–30.
85. Lahiri A, Waters R. Experience with Bio-Alcamid, a new soft tissue endoprosthesis. *J Plast Reconstr Aesthet Surg*. 2007;60(6):663–7.
86. Ramires PA, Miccoli MA, Panzarini E, Dini L, Protopapa C. In vitro and in vivo biocompatibility evaluation of a polyalkylimide hydrogel for soft tissue augmentation. *J Biomed Mater Res B Appl Biomater*. 2005;72(2):230–8.
87. Wallenten KG, Andreasson S, Ghosh F. Retinal function after vitrectomy. *Retina*. 2008;28(4):558–63.

88. Gjorloff K, Andreasson S, Ehinger B. Standardized full-field electroretinography in rabbits. *Doc Ophthalmol*. 2004;109(2):163–8.
89. De Schaepdrijver L, Simoons P, Lauwers H, De Geest JP. Retinal vascular patterns in domestic animals. *Res Vet Sci*. 1989;47(1):34–42.
90. Nelson L, Stewart KJ. Early and late complications of polyalkylimide gel (Bio-Alcamid)(R). *J Plast Reconstr Aesthet Surg*. 2011;64(3):401–4.
91. Pritchard CD, Crafoord S, Andreasson S, Arner KM, O'Shea TM, Langer R, et al. Evaluation of viscoelastic poly(ethylene glycol) sols as vitreous substitutes in an experimental vitrectomy model in rabbits. *Acta Biomater*. 2011;7(3):936–43.
92. Brandl F, Henke M, Rothschenk S, Gschwind R, Breunig M, Blunk T, et al. Poly(ethylene glycol) based hydrogels for intraocular applications. *Adv Eng Mater*. 2007;9(12):1141–9.
93. Sawhney AS, Pathak CP, Hubbell JA. Bioerodible hydrogels based on photopolymerized poly(ethylene glycol)-co-poly(.alpha.-hydroxy acid) diacrylate macromers. *Macromolecules*. 1993;26(4):581–7.
94. Wathier M, Johnson MS, Carnahan MA, Baer C, McCuen BW, Kim T, et al. In situ polymerized hydrogels for repairing scleral incisions used in pars plana vitrectomy procedures. *ChemMedChem*. 2006;1(8):821–5.
95. Ufret R, Yu S-Y, Christoforidis J, D'Amico DJ. Evaluation of a polyethylene glycol (PEG)-derived glue as a potential bioadhesive for vitreoretinal applications. *Invest Ophthalmol Vis Sci*. 2004;45(5):E-Abstract 2054.
96. Barth H, Crafoord SW, Vinchon C, O'Shea TM, Pritchard CD, Ghosh FK. A new model for in vitro testing of vitreous substitute candidates. ARVO meeting, May 6–10, 2012, Ft Lauderdale, USA.

Part II

Anatomy, Development and Aging

J. Sebag

Zabrina S. Kingston, Jan M. Provis,
and Michele C. Madigan

Outline

- I. **Introduction**
- II. **Overview of Eye Development**
 - A. Embryonic Origins
 - B. The Optic Vesicle, Cup, and Fissure
- III. **Embryology of the Vitreous Body**
 - A. Primary Vitreous
 - B. Secondary Vitreous
- IV. **Structural and Molecular Factors in Vitreous Development**
 - A. Structure of the Hyaloid Vascular System
 - B. Molecular Factors in Formation and Regression of the Hyaloid Vasculature
 - C. Cells in the Developing Vitreous
 - D. Molecular Changes During Vitreous Development
- V. **Disorders of the Developing Vitreous**
 - A. Pathologies of the Primary Vitreous
 - 1. Persistent Primary Vitreous
 - 2. Persistent Hyperplastic Primary Vitreous Persistent Fetal Vasculature
 - B. Pathologies of the Secondary Vitreous
 - 1. Syndromic disorders
 - C. Hyaloid Vascular System
 - 1. Persistent Hyaloid Artery
 - 2. Mittendorf's Dot
 - 3. Bergmeister's Papilla
 - 4. Persistent Pupillary Membranes
 - 5. Vitreous Cyst

Conclusion

References

Z.S. Kingston, MBBS • J.M. Provis, PhD, FARVO
ANU Medical School, John Curtin School of Medical Research,
The Australian National University, Canberra, ACT, Australia
e-mail: zabrina.kingston@gmail.com; jan.provis@anu.edu.au

M.C. Madigan, PhD (✉)
School of Optometry and Vision Science,
University of New South Wales, Sydney, NSW, Australia

Save Sight Institute, The University of Sydney,
Sydney, NSW, Australia
e-mail: m.madigan@unsw.edu.au

Keywords

Vitreous • Embryology • Primary vitreous • Secondary vitreous • Hyaloid vessels • Hyalocytes • Vascular regression • Vitreous congenital disorders

Key Concepts

1. Primary vitreous is the collective cellular vitreous that is an extension of the hyaloid vasculature adventitia during the first trimester, which later regresses during the second trimester as the secondary vitreous is formed.
2. Secondary vitreous is the acellular material comprised mainly of type II collagen, proteoglycans, and other macromolecules that fill the space between the retina and the lens.
3. Understanding the molecular processes involved in vitreous development and hyaloid regression may provide insights for the treatment and future management of various ocular diseases.

I. Introduction

Vitreous is a highly hydrated, avascular extracellular matrix located between the lens and retina that serves a variety of structural and physiological functions [1, 2]. Formation of the vitreous is a complex process that has been studied for over a century and still is not clearly understood. Two overlapping developmental phases have been described, the primary and secondary vitreous then followed by formation of the lens zonules previously referred to as tertiary vitreous [3], all closely tied to development of the retina, lens, and retinal vasculature. For this reason, errors in ocular development are often associated with severe congenital disorders

that are reflected in the vitreous. In this chapter we provide a brief overview of the embryology of the eye and explore in detail vitreous development and its anomalies.

II. Overview of Eye Development

A. Embryonic Origins

By the third week of development, the embryonic plate comprises the three primary germ layers – the ectoderm, mesoderm, and endoderm [3]. Towards the end of

gastrulation, the ectoderm anterior to the primitive streak differentiates into the columnar neural ectoderm, which forms of the neural plate, then neural groove, and, subsequently, the neural tube. By 20 days of gestation (DG), the first morphological sign of the developing eye, the optic sulcus, is evident in the anterior-most portion of the neural tube. The optic sulci become internalized when the neural tube closes at ~4 weeks of gestation (WG) and the embryo is entirely covered by surface ectoderm. Optic vesicles form when the optic primordia enlarge and evaginate outwards to make contact with the surface ectoderm (*se*) (Figure II.A-1a) [4–6]. As development progresses, the surface and neural ectoderm

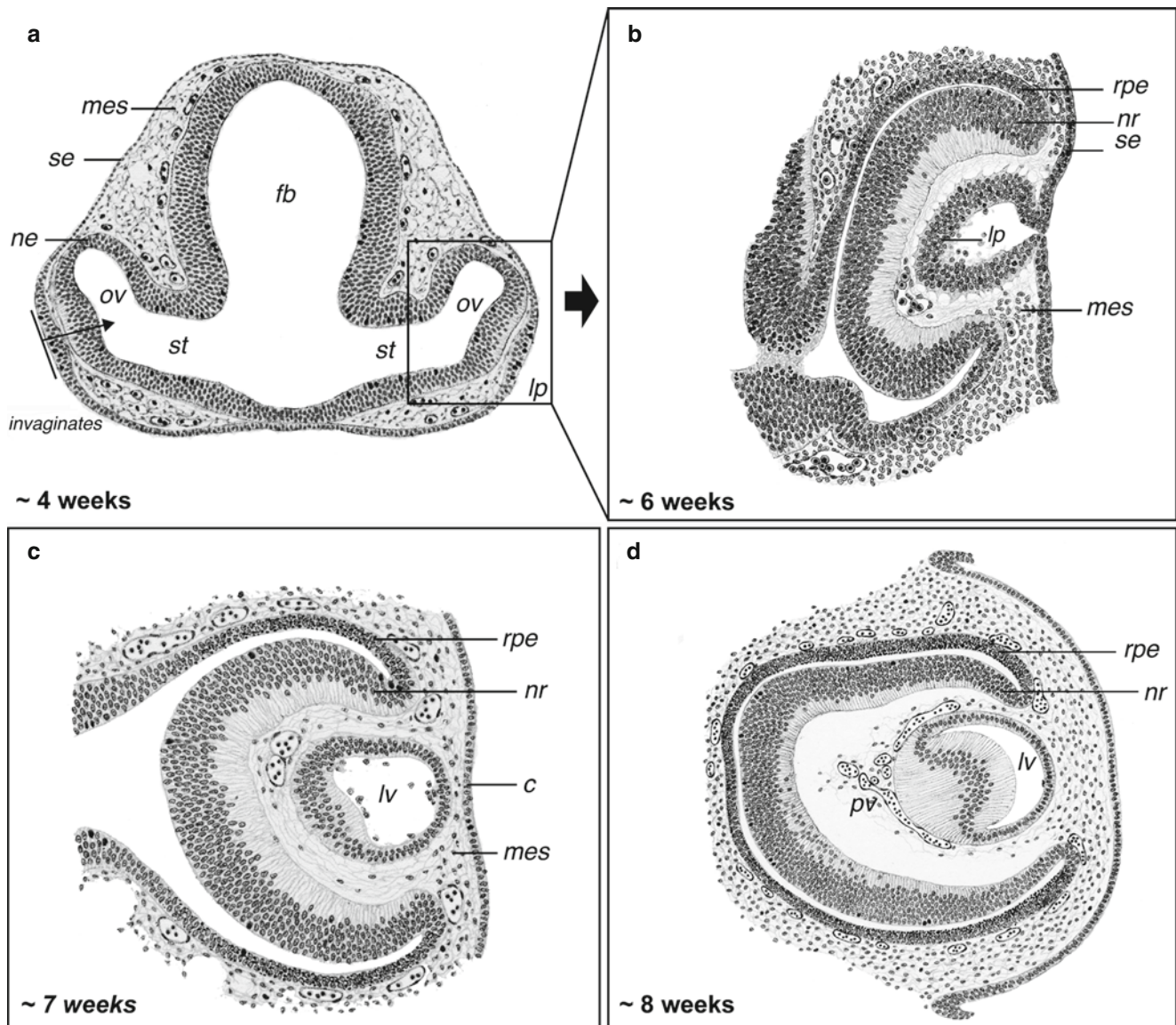


Figure II.A-1 Overview of ocular development. (a–d) Drawings of sections through the developing eye of human embryos ranging from approximately 4–8 weeks of gestation (WG). (a) At around 4 WG the germ layers involved in ocular development are evident, including neural ectoderm (*ne*), surface ectoderm (*se*), and mesoderm (*mes*). The early development of the forebrain (*fb*) is connected to evaginated optic vesicle (*ov*) by the optic stalk (*st*). (b) The lens placode (*lp*) pinches off from the surface ectoderm and invaginates to form the lens vesicle (*lv*). Invagination of the neural retina (*nr*) results in a double-layer optic cup

comprising neural retina (*nr*) and retinal pigmented epithelium (*rpe*). (c) By around 7 WG the lens vesicle (*lv*) has separated from the surface ectoderm that will subsequently become the cornea (*c*). (d) By around 8 WG the primary vitreous (*pv*) is clearly discernable, between the lens vesicle and neural retina. Abbreviations: *c* cornea, *fb* forebrain, *lv* lens vesicle, *mes* mesenchyme, *ne* neuroepithelium, *nr* neural retina, *ov* optic vesicle, *pl* lens placode, *pv* primary vitreous, *rpe* retinal pigmented epithelium, *se* surface ectoderm, *st* optic stalk [132]

Table II.A-1 Embryonic derivation of ocular tissues

Embryonic origin	Ocular structure	
Surface ectoderm	Lens	
	Corneal epithelium	
	Conjunctival epithelium	
	Epithelium of eyelids and cilia	
	Lacrimal apparatus	
	Meibomian glands and glands of Zeis and Moll	
Neural ectoderm	Neural retina	
	Retina pigment epithelium	
	Epithelium of ciliary body	
	Epithelium of iris	
	Iris sphincter and dilator muscles	
	Optic nerve fibers	
Neural crest	Corneal stroma and endothelium	
	Stroma of iris and ciliary body	
	Perivascular connective tissue and smooth muscle cells	
	Sclera (except caudal region)	
	Trabecular meshwork cells	
	Ciliary muscles	
	Vitreous	
	Orbital cartilage and bone	
	Mesoderm	Extraocular muscles
		Endothelium of blood vessels
Caudal region of sclera		

(*ne*), neural crest, and mesoderm (*mes*) will each contribute to the formation of ocular structures, as summarized in Table II.A-1 [4, 7].

B. The Optic Vesicle, Cup, and Fissure

The optic vesicles remain connected to the lumen of the primitive forebrain by the optic stalk (*os*), which at first comprises a layer of neuroepithelium surrounding a narrowing lumen (Figure II.A-1a) [8]. Neural crest cells located between the vesicles and the surface ectoderm are modified as these layers come into closer proximity and subsequently will form the bulk of the connective tissues of the eye [4, 9]. Contact between the neural and surface ectoderm, at around 27 DG, triggers a cascade of induction signals that result in formation of the lens placode (*lp*), the precursor to the lens [10–12]. A double-layered optic cup is formed as the lens placode and neuroectoderm together invaginate (Figure II.A-1a), partially obliterating the cavity of the optic vesicle (*ov*). This results in the first appearance of a structure recognizable as a mammalian eye (Figure II.A-1b) [13]. At around 33 DG the lens vesicle (*lv*) detaches from the surface ectoderm (Figure II.A-1c) under the influence of AP-2 transcription factors [14], and the separated surface ectoderm along with

resident neural crest cells begin to form the cornea [15, 16]. Differentiation of the optic cup into the neurosensory retina (*nr*) (inner layer) and retinal pigmented epithelium (*rpe*) (outer layer) starts at around 47 DG (Figure II.A-1c, d). Both the ciliary body and iris are later derived from cells located at the junction of the neurosensory and RPE layers of the optic cup [17].

III. Embryology of the Vitreous Body

A. Primary Vitreous

Invagination of the optic cup occurs in an eccentric manner such that initially the cup is open inferiorly, at the optic fissure (*of*) (Figure II.A-2a) [8]. From around 4 WG mesodermal cells surrounding the optic fissure and cup differentiate into the hyaloid artery, marking the beginning of differentiation of the vascularized primary vitreous (Figure II.A-1d). The hyaloid vessels traverse the optic stalk then directly cross the optic cup to reach the lens vesicle, providing a transient blood supply to the developing anterior eye [3, 4].

As the neural ectoderm of the optic vesicle separates from the surface ectoderm (3–4 WG), a fibrillar meshwork of periodic acid-Schiff (PAS)-positive and Alcian-blue-positive material bridges the space [3, 4, 18]. This is the primordial vitreous – a collection of ectodermal and mesodermal-derived cells. The ectodermal fibrillar components are produced by the inner layer of the future neurosensory retina, as well as by cells on the posterior surface of the lens vesicle. The mesodermal cells enter the emerging eye cup inferiorly during invagination of the optic vesicle, via the patent optic fissure (4–5 WG), and are the anlage of the hyaloid vascular system (*hvs*), comprising the vasa hyaloidea propria (*vhp*), posterior tunica lentis (*tl*), pupillary membrane (*pm*), and the hyaloid artery (Figure II.A-3) [3, 4]. They are surrounded by fibroblasts which, from the outset, synthesize a collagen that is similar to that found in the adult vitreous [19]. This collective cellular vitreous is considered the “primary vitreous” and conceptually can be thought of as an extension the adventitia of the hyaloid vasculature (Figure II.A-2a, orange shading) [18].

In addition to entering the eye posteriorly along with the hyaloid vessels, mesodermal cells also enter the eye cup anteriorly, through the space between the anterior rim of the optic cup and the lens vesicle [13, 20, 21]. These cells include the monocyte-lineage hyalocytes [19]. Recent studies suggest that some mesodermal cells entering the optic cup at this stage are hemangioblasts, which later differentiate into hyalocytes [22, 23]. By 6 WG the hyaline lens capsule has formed a barrier between the lens proper and the matrix of the optic cup, marking the end of lens ectodermal contributions to the vitreous [21].

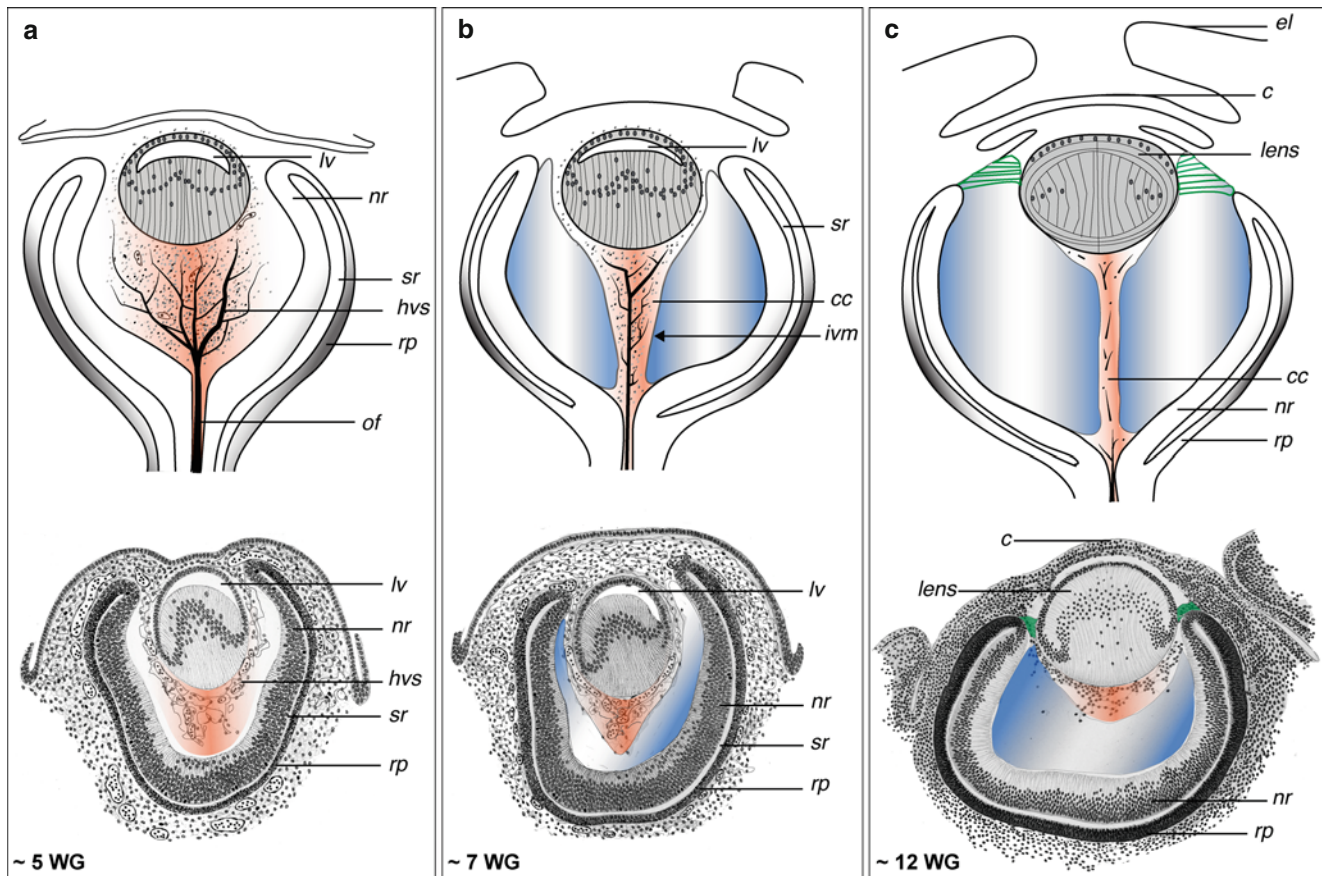


Figure II.A-2 Three stages in development of the vitreous. (a) The primary vitreous (red) may be considered to be an extension of the adventitia of the hyaloid vascular system (*hvs*) and comprises ectodermal and mesodermal cells that have invaded the developing eyecup. (b) By around 7 weeks of gestation (WG), the secondary vitreous (blue) has increased in volume and is separated from primary vitreous by the intravitreal

membrane (*ivm*). (c) By around 12 WG vitreous continued deposition of secondary vitreous and *hvs* regression within Cloquet's canal (*cc*), concurrent development indicated by formation of the zonule fibers (green). Abbreviations: *c* cornea, *el* eyelids, *lv* lens vesicle, *nr* neural retina, *of* optic fissure, *rpe* retinal pigmented epithelium, *sr* subretinal space, WG weeks of gestation [25, 132]

Following closure of the optic fissure, the hyaloid artery rapidly extends anteriorly, ramifying within the primary vitreous to create the anastomotic *vhp*, which in turn anastomoses with the posterior portion of the *tv* surrounding the posterior lens capsule (Figure II.A-4c) and the *pm* adherent to the anterior surface of the lens capsule and iris diaphragm (Figure II.A-3). By approximately 10 WG the *hvs* has reached its zenith, nourishing the growing lens and adjacent mesoderm (Figure II.A-4b). Thereafter, the hyaloid vasculature slowly regresses, in concert with the very early phases of retinal vessel development [24]. The early stages of regression of the hyaloid system are seen around 11–12 WG in the peripheral *vhp*, closely followed by the *tv*. This regression is characterized by gradual shrinkage of vessel walls and reduction in lumen diameters, leaving behind thread-like acellular strands of tissue [24, 25]. The initiating and regulatory factors are not clearly understood. However, apoptosis is a significant feature in the early stages, and migration of hyalocytes into the adventitia of the hyaloid vessels is also part of the regression process and

may involve cytolysis [24]. At 13–15 WG, there is clear morphological evidence of vessel regression, including thinning and narrowing of the *vhp* vessels, thinning and stretching of the interconnecting vessels of the *tv*, and decreased tortuosity and loss of anastomoses in the pupillary membrane (Figure II.A-4a, d) [24]. End-stage changes in endothelial cells, pericytes, and macrophages progress, with complete regression of the hyaloid system and atrophy of the primary vitreous not complete until 35–36 WG (Figure II.A-4e, f) [21].

B. Secondary Vitreous

The secondary vitreous is derived entirely from neural crest cells and forms between 6 and 13 WG [25]. This acellular material fills the space between the retina and posterior *vhp* as the eye enlarges (Figure II.A-2b, blue shading) [3, 21, 26, 27]. By 9 WG it has increased significantly in volume, forcing the fully developed vascularized primary vitreous

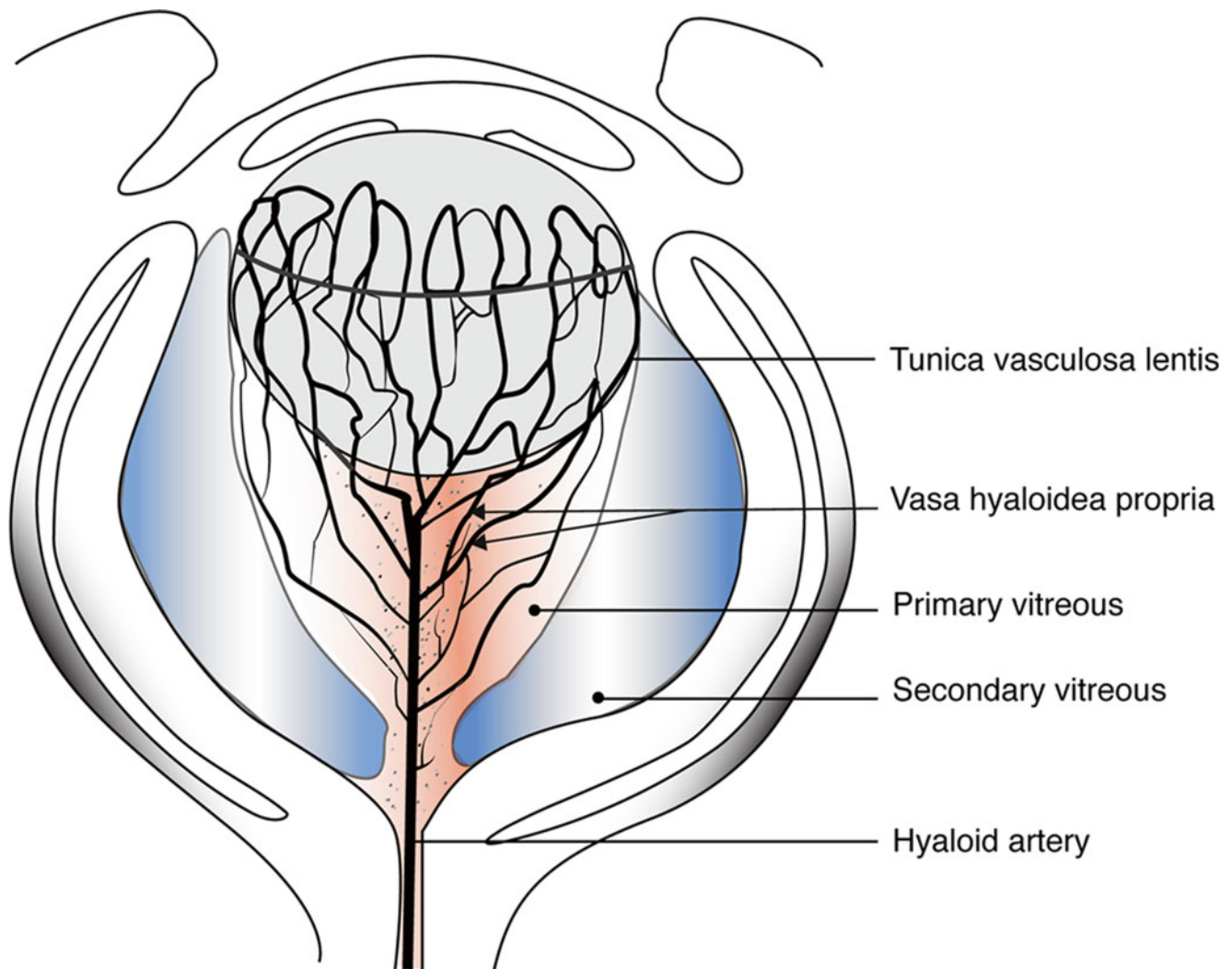


Figure II.A-3 Hyaloid vascular system. Following closure of the optic fissure, the hyaloid artery rapidly extends anteriorly, ramifying within the primary vitreous (*orange shading*) to create the anastomotic vasa hyaloidea propria, which in turn anastomoses with the posterior portion

of the tunica vasculosa lentis surrounding the posterior lens capsule and the pupillary membrane adherent to the anterior surface of the lens capsule and iris diaphragm. Collectively the hyaloid vascular system has reached its zenith by 10 WG [25]

into a central position [3, 21, 25, 27, 28], and by 12 WG, a layer of condensed funnel-like fibers known as the “intra-vitreous membrane” (*ivm*) is apparent along the junction between the primary and secondary vitreous. The classical view is that this membrane forms the walls of Cloquet’s canal (*cc*), a tubular structure running through the vitreous from the optic disc to the posterior lens capsule and which contains remnants of the hyaloid artery and primary vitreous (Figure II.A-2b, c). Recent morphological evidence suggests, however, that retracting hyaloid vessels act as a scaffold along which fibers of the secondary vitreous organize themselves [29–31]. Such a process – formation of the secondary vitreous by a method of continuous and gradual remodeling of the primary vitreous – has also been proposed by Jokl (1927) and Pau (1957) [31, 32]. In this latter view, the terms “primary” and “secondary” vitreous refer to the

temporal transformation of vitreous materials, rather than to a process of replacement.

Secondary vitreous is essentially an extracellular matrix comprising a compact meshwork of type II collagen, proteoglycans, and other macromolecules [33–35]. Prenatally, hyaluronan content of the vitreous is quite low, but increases after birth [36]. The collagen fibers of the secondary vitreous are thought to be synthesized by, and continuous with, the footplates of retinal Müller cells, which are the radial glia of the mature retina and the end-stage cell type that differentiates from the retinal progenitor cells [21, 37, 38]. Around 10 WG, Müller cell processes vitreoretinal border at the posterior pole start to form lateral junctions with each other, comprising the inner limiting membrane (*ilm*) of the retina [21, 38, 39] [see chapter II.E. Vitreoretinal interface and inner limiting membrane].

Posteriorly, collagen fibrils of the vitreous cortex lie almost parallel to the *ilm*. In contrast, anteriorly the secondary vitreous fibers become thickened, forming the margins of the bundle of Druault or “*faisceau isthmique*” that extends from the anterior rim of the optic cup to the equator

of the lens. A portion of the bundle of Druault will later define the anterior extent of the vitreous base. Neural crest-derived mesenchymal cells that accompany the hyaloid vessels may also contribute to the formation of the mature vitreous [21].

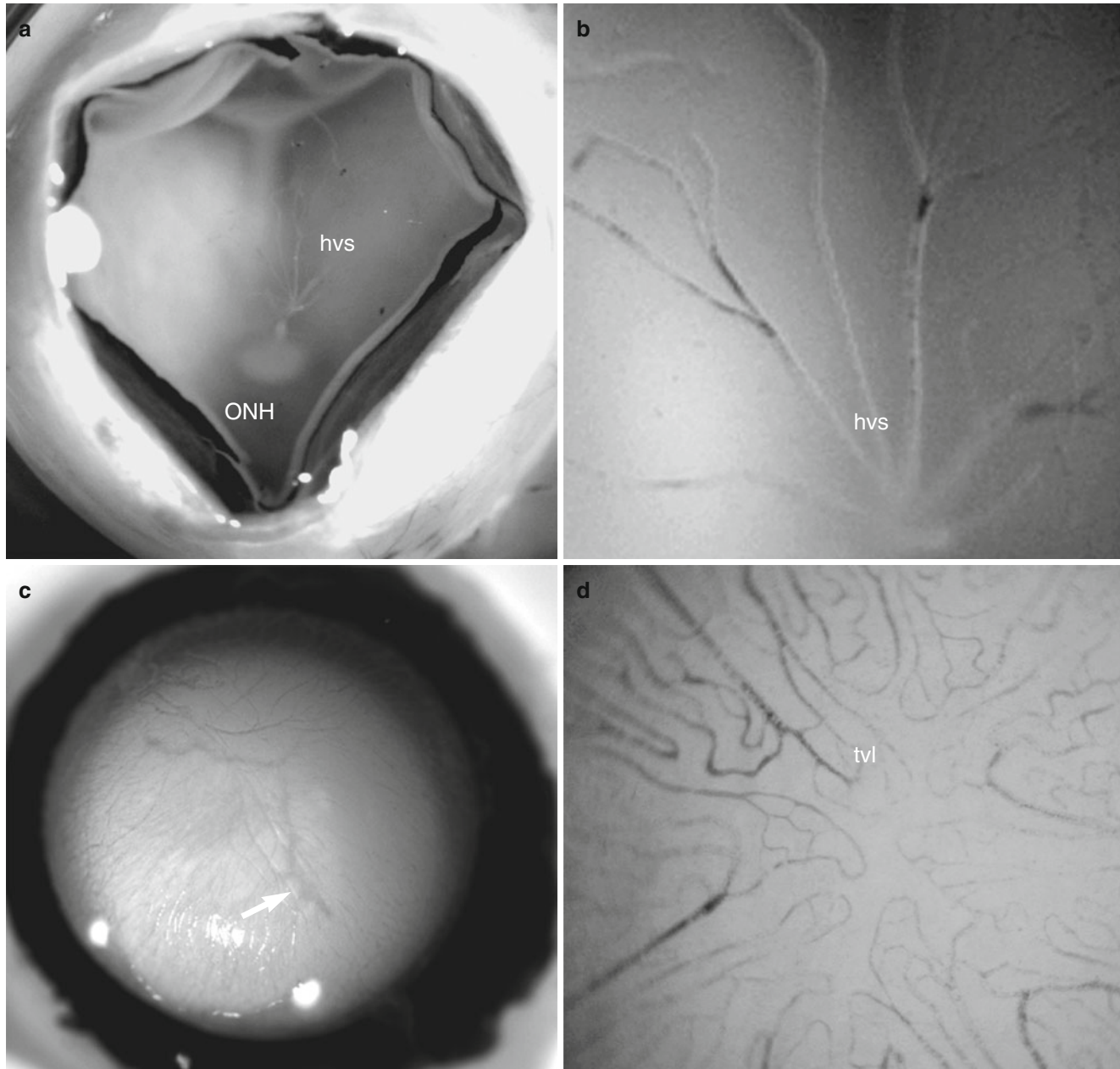


Figure II.A-4 Hyaloid vascular system, tunica vasculosa lentis, and hyalocytes. **(a)** A 17 weeks of gestation (WG) human fetal eyecup with the anterior segment, including the lens, removed. The hyaloid vascular system (*hvs*) is seen extending into the vitreous from the optic nerve head (*ONH*). **(b)** A high-power image of the hyaloid vascular system (*hvs*) showing branches from the hyaloid artery. Some vessel segments are filled with red blood cells (*arrow heads*). **(c)** Anterior segment of a ~17 WG human fetal eye showing the posterior lens surface with vessels of the *tunica vasculosa lentis* (*tv*). Out-of-focus lens sutures (*small*

arrow) can also be seen. **(d)** A high-power image showing the network of vessels on the posterior lens surface (*tv*). **(e, f)** Electron micrographs from a ~18 to 20 WG human fetal eye, showing the typical morphological features of different types of hyalocytes. **(e)** A hyalocyte (*H*) with a bilobed nucleus, fimbriated cytoplasmic processes, and electron-dense cytoplasmic granules is shown (*arrow*) (Bar=2 μ m). **(f)** This hyalocyte (*H*) features a single-lobed nucleus, smooth cell surface, and electron-dense granules (*arrow*) (Bar=2 μ m)

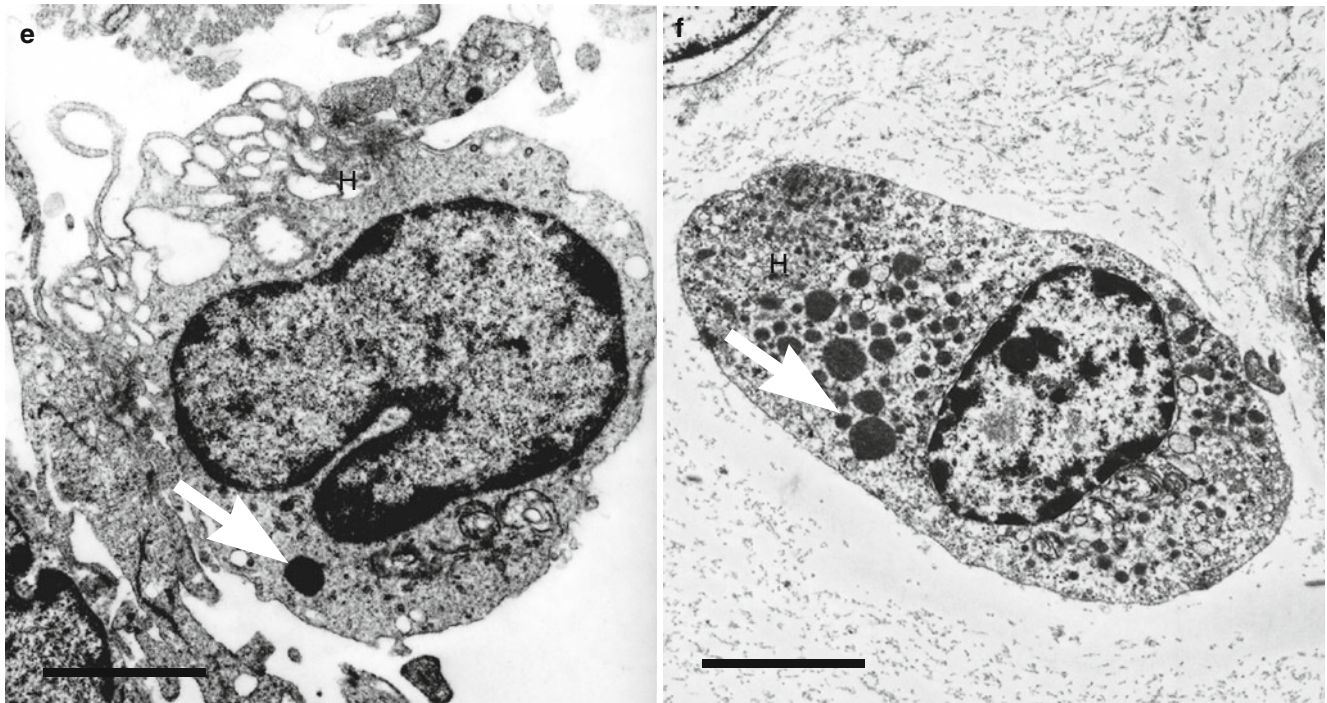


Figure II.A-4 (continued)

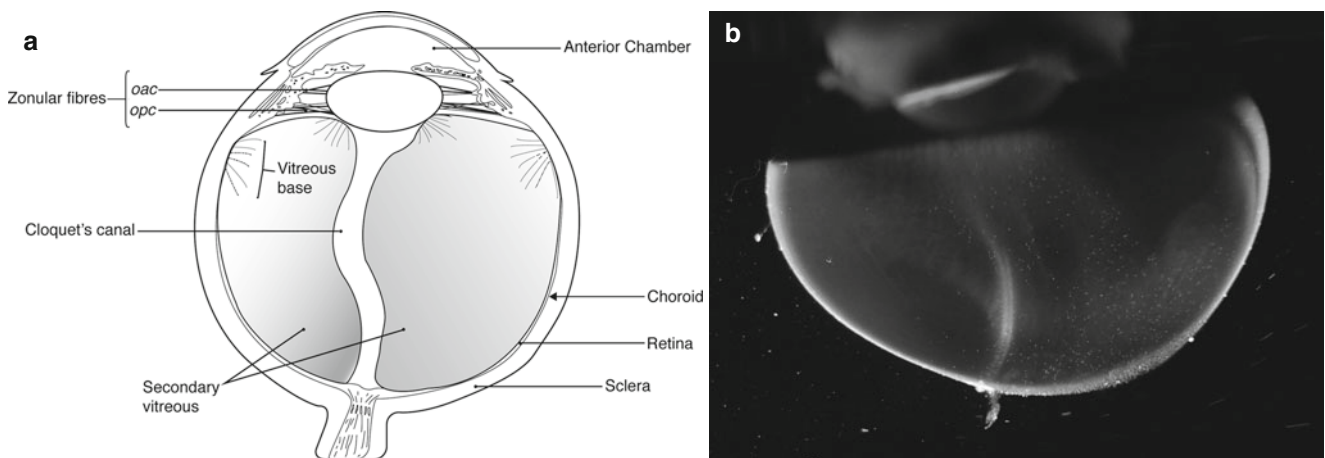


Figure II.A-5 Developed vitreous. (a) Formation of the vitreous is marked by the final stages of secondary vitreous development and the regression of the primary vitreous and hyaloid vasculature. This occurs concurrently with the growth of the lens zonular system, which extends from the *pars plana* of the ciliary body and to the equator of the lens. The zonular fibers form two distinct bundles, the orbiculo-anterocapsular and orbiculo-posterocapsular fibers [25]. (b) Appearance of the formed vitreous body in a 33 weeks of gestation (WG) human post-mortem. The eye underwent dissection of the sclera, choroid, and retina

exposing the vitreous body, which was left attached to the anterior segment. A slit lamp beam illuminated a horizontal section that was photographed from above at a 90° illumination-observation angle maximizing the Tyndall effect. The anterior segment is above and the posterior pole is below. The posterior aspect of the lens can be seen above. There is considerable light scattering from the peripheral vitreous cortex due to the dense collagen matrix at this location. Cloquet's canal is seen in the central and posterior vitreous oriented towards the prepapillary region (Courtesy of J. Sebag, MD)

Around 12–16 WG the zonular system is produced, and approximately two-thirds of the optic cup is filled with secondary vitreous and the primary vitreous is located centrally and axially (between the optic rim and lens) (Figure II.A-2c) [3]. The rim of the optic cup has grown forwards to form the ciliary body, with the secondary vitreous occupying the area

between the ciliary region and the lens [19]. During the final period of antenatal vitreous development (~7 month), the blood flow in the hyaloid artery ceases, followed by regression of hvs and the primary vitreous [20, 28, 40]. The vitreous finally acquires characteristics of fully developed vitreous (Figure II.A-5).

IV. Structural and Molecular Factors in Vitreous Development

A. Structure of the Hyaloid Vascular System

The hyaloid artery (Figure II.A-4b) fine structure is typical of an arteriole [41]. The *tunica intima* consists of flattened endothelial cells connected by tight junctions [24] with an underlying basement membrane. The *tunica media* includes concentric layers of smooth muscle with basement membranes around each contractile fiber [41], surrounded by an *adventitia* of fibroblasts and collagen [42]. Ultrastructural studies show that vessels of the *pm*, *tv*, and *vhp* are similar in structure. These are small capillaries of the “A-1-alpha” structure [43] with a continuous, single layer of non-fenestrated endothelial cells, joined by intervening tight junctional complexes containing zonulae adherens, *macula adherens*, and possible *zonulae occludens* [24, 44]. They have a continuous basement membrane and an incomplete layer of pericytes [24]. Studies in zebra fish suggest that the *FoxC1* gene regulates integrity of this basement membrane and influences the morphology of the *hvs* [45].

B. Molecular Factors in Formation and Regression of the Hyaloid Vasculature

The genes and signaling pathways involved in the formation and regression of the hyaloid vasculature remain poorly defined. Much of the experimental work in this area is derived from rodent and zebra fish models, which provide a good basis for understanding eye development. Many studies have demonstrated the involvement of vascular endothelial growth factor (VEGF-A) as a key regulator of physiological angiogenesis in the eye, particularly in the retina. Changes in VEGF-A mRNA expression in the lens, in the proximity of the developing TVL and PM, suggest that VEGF-A may be one of the factors that trigger the growth of these two vascular networks [46–49]. Indeed, overexpression of VEGF-A in the lens of transgenic mice leads to vascular endothelial cell hyperplasia adjacent to the lens [50–52], and VEGF-A deletion from the developing lens results in failure of the hyaloid vessels to form adjacent to the lens capsule, although the capillary network in proximity of the retina is not affected [46]. A recent study of dark-reared mice demonstrated an association between increased levels of retinal VEGF-A, hyaloid persistence, and deregulated retinal angiogenesis during development [53]. This is consistent with retinal VEGF-A being critical for development of the hyaloid vasculature.

Several hypotheses have been proposed to explain regression of the hyaloid vessels. While the trigger for regression is not well understood, the most widely accepted hypothesis is that hyaloid vessel involution is macrophage dependent.

Several studies in humans and other mammals now show that the ocular macrophages, or hyalocytes (Figure II.A-4e, f), are directly involved in apoptosis of the vascular endothelial cells in the pupillary membrane and the hyaloid vascular system [24, 54–57]. Recent studies in mice demonstrated that a particular class of macrophage (LYVE-1⁺) is attached to the hyaloid vessels during regression [58] and secrete the protein, periostin, which enhances HVS regression by mediating and strengthening the adhesion of macrophages to the hyaloid vessels [59].

In the early stages of hyaloid regression, apoptosis is prevalent and knockout of proapoptotic genes attenuates hyaloid vascular regression [60, 61]. Some features of necrosis are also detected and cytolitic processes appear to be in effect in the later stages of regression [24, 62]. Other studies have shown that a decrease in capillary blood flow is correlated with an increase in programmed cell death in vascular endothelial cells, suggesting that a hemodynamic disadvantage may be a triggering factor [63, 64].

Throughout development both pro- and antiangiogenic proteins are detected in the vitreous with the balance moving towards an antiangiogenic environment in the later stages of development [65–67] [see chapter I.D. Vitreous proteomics and regression of the fetal hyaloid vasculature]. Antiangiogenic molecules including transforming growth factor- β (TGF- β) [68–72], pigment epithelium-derived factor (PEDF) [73–77], endostatin [78–80], thrombospondin-1 (TSP-1) [81–83], and opticin [84, 85] have been identified in the vitreous in rodents and humans, suggesting that these proteins play a role in hyaloid regression and inhibit angiogenesis in the normal adult vitreous. The canonical Wnt signaling pathway is also emerging as having a critical role in hyaloid regression. Optimal Wnt signaling requires the transmembrane Frizzled family receptors and the coreceptors Lrp5 and Lrp6. Studies in mice have shown that the production of Wnt7b by macrophages in the vitreous is a mediating factor [86]. Wnt7b is promoted by angiopoietin-2 (Ang-2), which may induce regression by inhibiting cell-survival signals [87]. In mice, both Wnt7b and Ang-2 are regulated by the production of Ninjurin-1 by resident vitreous macrophages [88]. Furthermore, mutation in the Wnt pathway coreceptor Lrp5 is linked with the syndrome *osteoporosis pseudoglioma*, which features persistence of the hyaloid vessel [89]. Phenotypes of the Fzd4 and Norrie disease protein (Ndp) mutant mice also include a persistent hyaloid, further implicating the canonical Wnt signaling pathway in hyaloid regression [90].

C. Cells in the Developing Vitreous

Vitreous normally contains relatively few cells of which hyalocytes represent approximately 90 % and fibroblasts the remainder [91]. In the postnatal eye, hyalocytes reside

in the peripheral or cortical region of the vitreous body abutting the inner surface of the retina (preretinal) [18, 92]. They are concentrated anteriorly in the vitreous base, surface of the ciliary processes, and posteriorly in the vicinity of the optic papilla, at an average distance of 50 μm from the inner retinal surface [19, 20, 93]. Hyalocytes vary in morphology depending on the stage of development and most likely are comprised of heterogeneous, distinct subpopulations of cells (Figure II.A-4e, f) [94]. Hyalocytes are more numerous in fetal than in adult vitreous, and while their function in the adult eye is unclear, they play a major role in regression of the hyaloid vasculature during fetal life. They are evident in the vitreous at an early embryonic stage, and several studies suggest that they secrete vitreous collagen and hyaluronan (HA) [95–97]. It has been suggested that hyalocytes are remnants of the primary vitreous [18], and studies in animals and humans indicate that hyalocytes may originate from mesenchymal cells in the optic cup, the embryonic fissure, or migrate from the hyaloid vessel wall [18, 98–100]. In the postnatal human eye, hyalocytes derive from blood monocytes and are replenished on the order of every several months [see chapter II.D. Hyalocytes: essential vitreous cells in vitreo-retinal health and disease].

Human hyalocytes express macrophage-like characteristics and leukocyte-associated antigens, CD45 and CD11a and CD64 (Fc receptor I), although, they do not express CD68 (a marker for a major subpopulation of macrophages) [101]. They do not express glial fibrillary acidic protein (GFAP), cellular retinaldehyde-binding protein, or cytokeratin, indicating that they are not of glial or RPE cell lineages [101–106]. Hyalocytes migrate into the vitreous cavity under physiological conditions, most likely from the bone marrow, and begin to accumulate in the cortical vitreous by the fifth month of gestation [107, 108].

While the exact role of hyalocytes is unclear, they are involved in modulation of intraocular immune responses, regression of the hyaloid vascular system, and the synthesis of extracellular matrix. The eye is an immune-privileged site, and hyalocytes have been shown to provide phagocytic defense against invading organisms with surface receptors for IgG and complement components [102, 109]. At the same time, however, hyalocytes are actively involved in the inhibition of immune reactions [110, 111] and enzymatic removal of fibrin and related products [103] to maintain vitreous transparency.

D. Molecular Changes During Vitreous Development

The vitreous body is subject to an ongoing process of matrix remodeling, starting in embryonic stages and continuing after birth. In very early development the majority of vitreous

collagen is type III; however, at 8 WG this is replaced by type II collagen, which comprises approximately 75 % of the total vitreous [112]. The vitreous extracellular matrix is synthesized by numerous cells including retinal cells (most likely Müller cells), cells of the hyaloid vascular system, early lens cells, and presumably cells of the ciliary body [2, 35, 112–114]. In human eyes, there appears to be a high rate of collagen type II production during embryogenesis, which decreases within 2 years after birth [113, 114]. Some evidence suggests that a low level of postnatal synthesis of collagen occurs in cells in the peripheral human retina until adulthood [115]. Hyaluronan is the major GAG in all stages of vitreous development and throughout adulthood [112, 116]. Hyalocytes, Müller cells, and possibly cells associated with the hyaloid vessels secrete hyaluronic acid [95, 116]. Researchers recently hypothesized that collagens and GAGs are synthesized by the mesenchymal cells during the primary vitreous stage, by the retina during the secondary vitreous stage and by hyaloid vessels throughout both these stages [91]. Interestingly, analyses of primary and secondary vitreous failed to show differences in the types and distribution of GAGs and collagens; rather, they are distinguished by the presence of the hyaloid vascular system per se [112].

V. Disorders of the Developing Vitreous

A. Pathologies of the Primary Vitreous

1. Persistent Primary Vitreous

Regression of the primary vitreous occurs during normal eye development; however, its remnants including the anterior, posterior, or the entire hyaloid artery may persist in the adult eye. Anterior hyaloid artery remnants may be seen in the vitreous as small posterior lens opacities (Mittendorf’s dot). Posterior remnants of the hyaloid artery may remain at the optic disc, extending into Cloquet’s canal, associated with glial tissue known as Bergmeister’s papilla (see descriptions below).

2. Persistent Hyperplastic Primary Vitreous Persistent Fetal Vasculature

Persistent hyperplastic primary vitreous (PHPV) is a rare congenital condition that results from a failure of the primary vitreous and the hyaloid vasculature to regress normally (Figure II.A-6). This is associated with hyperplasia of the primary vitreous, *tvI*, and hyaloid system. PHPV can occur in isolation or associated with other congenital disorders or syndromes, such as anterior segment dysgenesis disorders (including Axenfeld-Rieger syndrome), Aicardi syndrome, neurofibromatosis, and morning glory syndrome (reviewed Shastry, 2009) [117]. The term “persistent fetal vasculature (PFV)” was introduced in 1997 by Goldberg

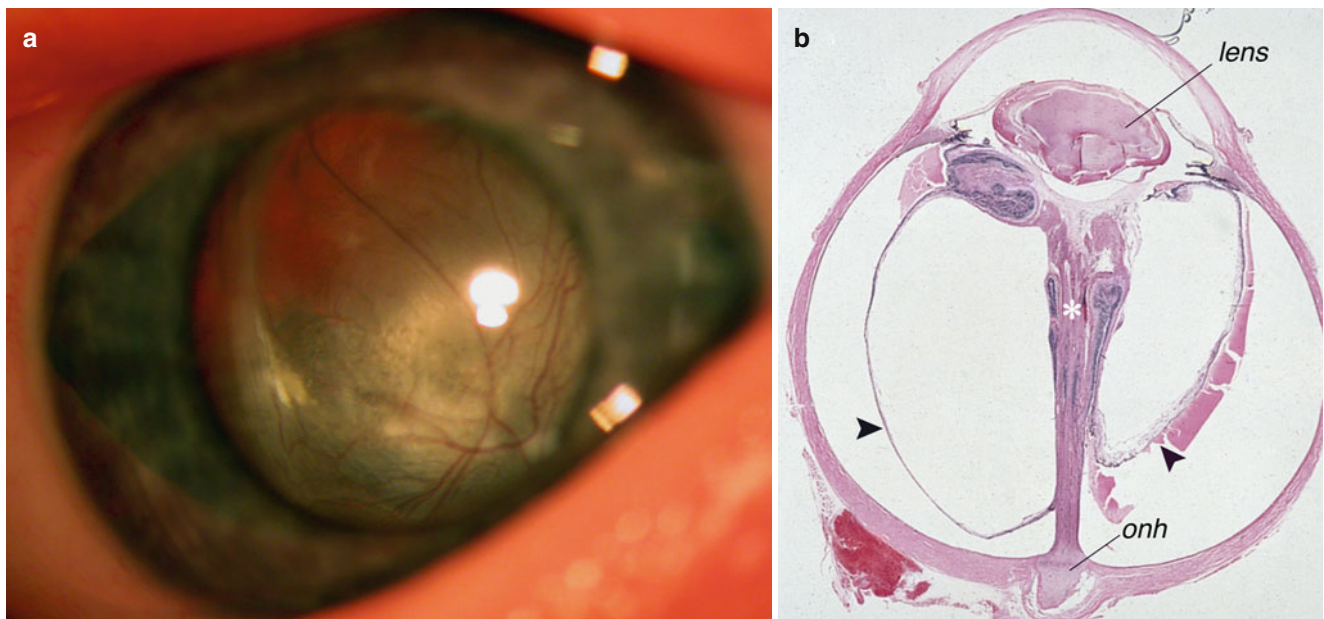


Figure II.A-6 Persistent hyperplastic primary vitreous. **(a)** A photograph of the right eye of a patient showing a persistent hyperplastic primary vitreous (Courtesy of John Grigg, MD, Save Sight Institute, Sydney Medical School). **(b)** Section of an eye with persistent hyperplastic primary vitreous showing a curved fold of detached dysplastic

retina (*arrowheads*) that encircles the persistent hyaloid artery and primary vitreous (*asterisk*). The primary vitreous extends from the optic nerve head (*onh*) to the posterior lens, forming a fibrovascular mass (hematoxylin and eosin) (http://commons.wikimedia.org/wiki/Category:The_Armed_Forces_Institute_of_Pathology_Public_Domain_Images)

to provide an inclusive name for the various forms of congenital persistent anterior and posterior intraocular vasculature and associated clinical features, encompassing PHPV, intravitreal vascular remnants such as Mittendorf dot, persistent hyaloid artery and Bergmeister's papilla, persistent pupillary membrane, congenital retinal folds or dysplasia, or optic nerve dysplasia [118]. The clinical implications of these disorders for vision are significant. PHPV may be considered to refer more specifically to vitreous and hyaloid system-related hyperplasia; however, it continues to be used within contemporary literature, often interchangeably with PFV, to describe the various presentations of a complex and heterogeneous group of disorders. These varied presentations are usually classified as “anterior,” “posterior,” or “combined.” Anterior PHPV is more common and presents as a posterior lens fibrovascular (retrolental) opacity, elongated ciliary processes, or cataract. Congenital fibrovascular pupillary membranes, extending from the posterior iris surface across the anterior lens surface, have also been reported as a variant of PHPV/PFV [119]. Posterior PHPV typically shows one or more features including elevated vitreous membranes or a stalk extending from the optic nerve (a remnant of Cloquet's canal), retinal folds or hypoplasia, retinal detachment, or optic nerve hypoplasia. Combined, they encompass features of both anterior and posterior PHPV. The molecular mechanisms

involved in the pathogenesis of PHPV are not fully understood, although mutations in several candidate genes have been reported including *FZD4* and *NDP* [120, 121].

B. Pathologies of the Secondary Vitreous

1. Syndromic disorders

Several syndromic human disorders that feature congenital high myopia result from mutations in genes that encode ECM proteins that are prominent in the vitreous, ILM, the vitreoretinal border, and the sclera. In Stickler (and Wagner) syndromes, for example, the vitreous is more liquid than gel like, related to dominant mutations of collagen II and V/XI [122]. In particular, mutations in type II collagen gene *COL2A1*, *COL2A*, and the type XI collagen gene *COL11A1* have been shown to result in the membranous phenotype of Stickler syndrome [123, 124] [see chapter I.C. Hereditary vitreo-retinopathies]. Stickler syndrome is an autosomal dominant inherited congenital disorder that affects type II and XI fibrillar collagens in cartilage and vitreous. Sporadic cases and ocular-only variants are also reported. Numerous mutations in *COL2A1*, *COL2A*, and *COL11A1* genes have been characterized associated with Stickler syndrome [123, 124], and the systemic phenotype is widely variable. At least

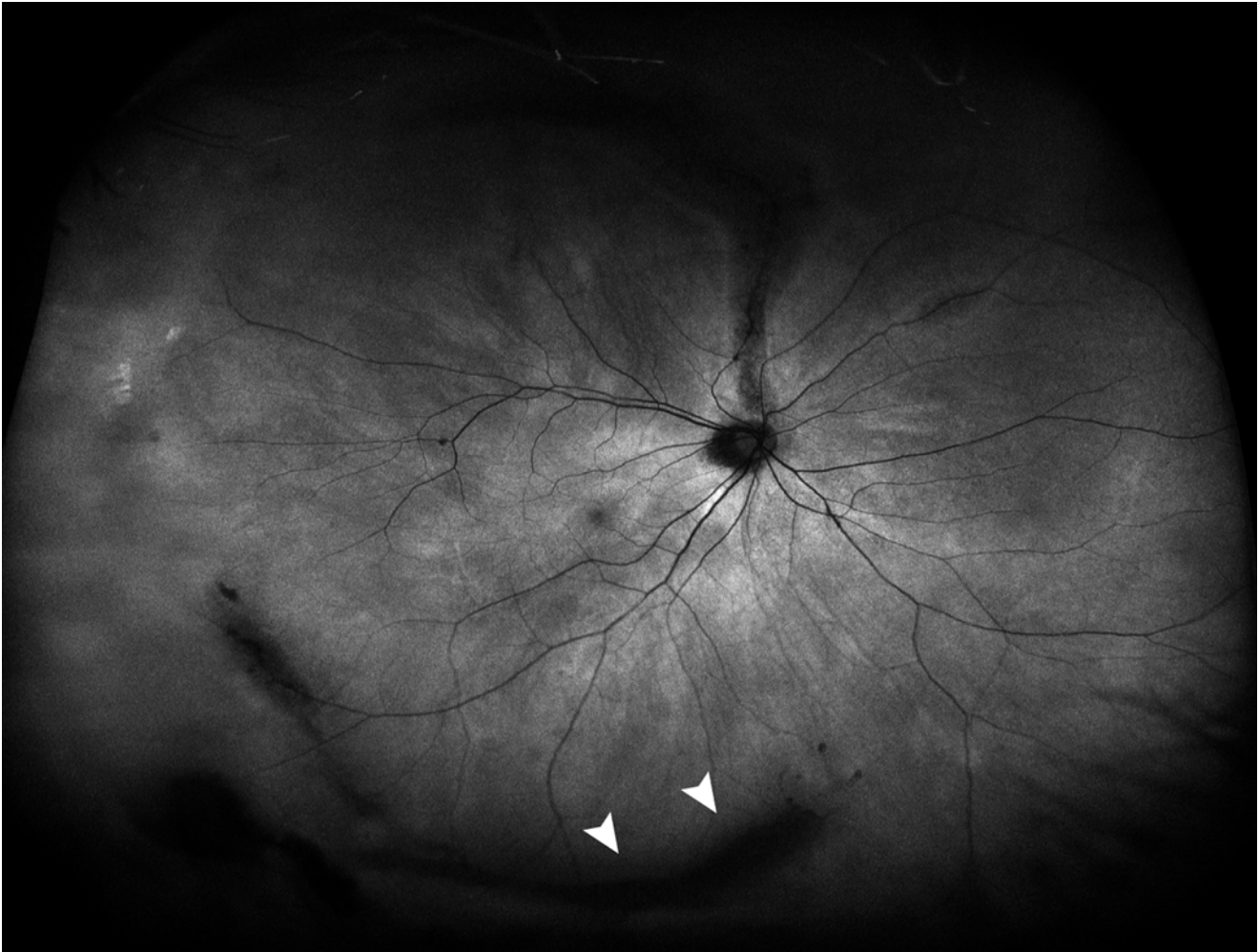


Figure II.A-7 Vitreous veils. A wide-field fundus image showing a vitreous veil (*arrowheads*) in a patient with Stickler syndrome (Courtesy of John Grigg, MD, Save Sight Institute, Sydney Medical School)

five subgroups or types of Stickler syndrome are currently recognized [125]. Vitreous phenotypes are considered a pathognomonic feature, particularly for type I (membranous vitreous) and type II (beaded vitreous). These phenotypes in particular are characterized by an optically empty posterior chamber with the exception of retrolenticular hypoplastic vitreous also known as “vitreous veils” (Figure II.A-7) or comprises sparse irregular, collagen lamellae associated with mutations in both *COL2A1* and *COL11A1* [122].

C. Hyaloid Vascular System

1. Persistent Hyaloid Artery

A persistent hyaloid artery presents as a single vessel that may (fully or in parts) extend from the optic nerve head, through Cloquet’s canal, and to the point of attachment

(Mittendorf’s dot) at the posterior lens capsule. Persistent hyaloid artery, resulting from a failure of vessel regression during development, contrasts with the complex variants that comprise PHPV (Figure II.A-6).

2. Mittendorf’s Dot

Mittendorf’s dot is an embryologic remnant of the anterior attachment of the hyaloid artery to the posterior lens capsule, where the hyaloid artery joins the *tunica vasculosa lentis*. The dot or opacity is typically at an inferonasal location on the posterior pole of the lens. A stalk of hyaloid artery or fibrovascular tissue may sometimes be seen attached at Mittendorf’s dot, floating freely in the anterior vitreous.

3. Bergmeister’s Papilla

Remnants of the cone of posterior glial tissue, that envelops the central hyaloid artery – Bergmeister’s papilla (BP) – can extend from the optic nerve head disc and may persist in the

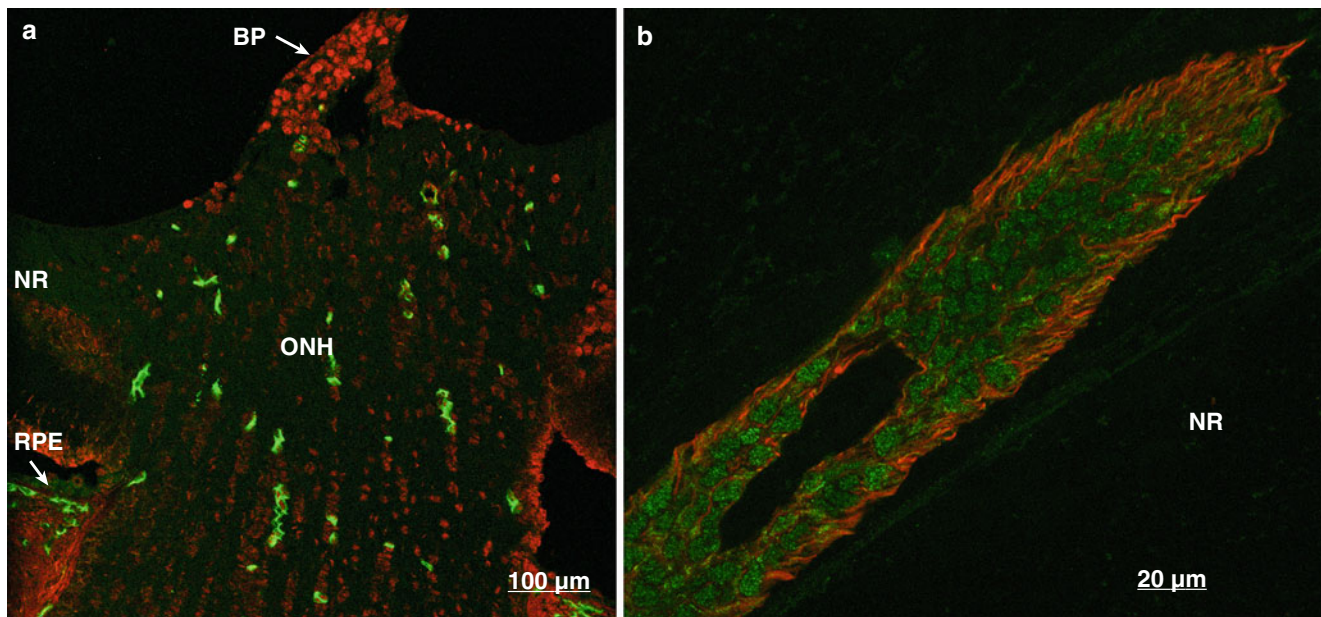


Figure II.A-8 Immunohistochemistry of a Bergmeister's Papilla. Confocal microscopy images of a developing macaque monkey eye at 55 days of gestation, equivalent to approximately 12 WG in the human. (a) Optic nerve head, showing endothelial cells (green) labeled with antibody to CD34 antigen among cells within the optic nerve. The base of Bergmeister's papilla (BP) extends vitread from the optic nerve head at

this stage and includes cells immunoreactive for ephrinA1 (red). No endothelial cells are present in the retina (NR). (b) Section through Bergmeister's papilla of a 55-day-gestation macaque monkey. EphrinA1-positive cells of the papilla (green) are ensheathed with GFAP-immunoreactive astrocyte processes (red). Abbreviations: BP Bergmeister's papilla, ONH optic nerve head, NR neural retina, RPE retinal pigmented epithelium

vitreous of adult human eyes. BP and the glial sheath, but not the hyaloid artery, expressed intense GFAP immunoreactivity in fetal human eyes, indicating ensheathment by astrocytes derived from the optic nerve (Figure II.A-8) [106]. A recent study in mice has suggested that ensheathment of the hyaloid artery by abnormal astrocytes may limit normal macrophage-pericyte contact and interfere in the macrophage-mediated hyaloid vessel regression that normally occurs during development [126].

4. Persistent Pupillary Membranes

During embryogenesis, the anterior *tunica vasculosa lentis* forms the iris vasculature and pupillary membrane. Normally, involution of the pupillary membrane and vessels occurs during the third trimester (7–9 months of gestation) and is complete by 34 WG, forming the pupillary aperture. Failure to completely regress can produce persistent pupillary membranes (PPM) that can occur either sporadically or associated with other ocular or syndromic conditions. These membranes are attached at the iris collarette on one side and may extend across the anterior lens surface as free-floating pigmented strands or with focal

attachments to the lens anterior capsule or to the iris on the opposite side; these often persist into adulthood (Figure II.A-9). Histopathology of surgically removed PPM showed evidence of thickened iris fibrocellular stroma and pigmented cells [127].

5. Vitreous Cyst

Primary (congenital) free-floating vitreous cysts are translucent, semitransparent, or pigmented spherical or oval forms that may also be multilobed and can vary in size from 0.15 to 12 mm diameter [128]. These rare benign cysts are thought to be the remnants of the primary hyaloid or Bergmeister's papilla (translucent cysts) or associated with iris, ciliary body, or retinal pigment epithelium. Cysts from Bergmeister's papilla are observed to be small, round, and located in posterior vitreous [129]. Several case reports showed connection of cysts and hyaloid remnants and cysts frequently located within Cloquet's canal, consistent with a primary hyaloid origin [130, 131]. One group has proposed that cysts with immature melanosomes (not seen in adults) provide evidence of congenital vitreous cysts being primary hyaloid choriostomas [129].

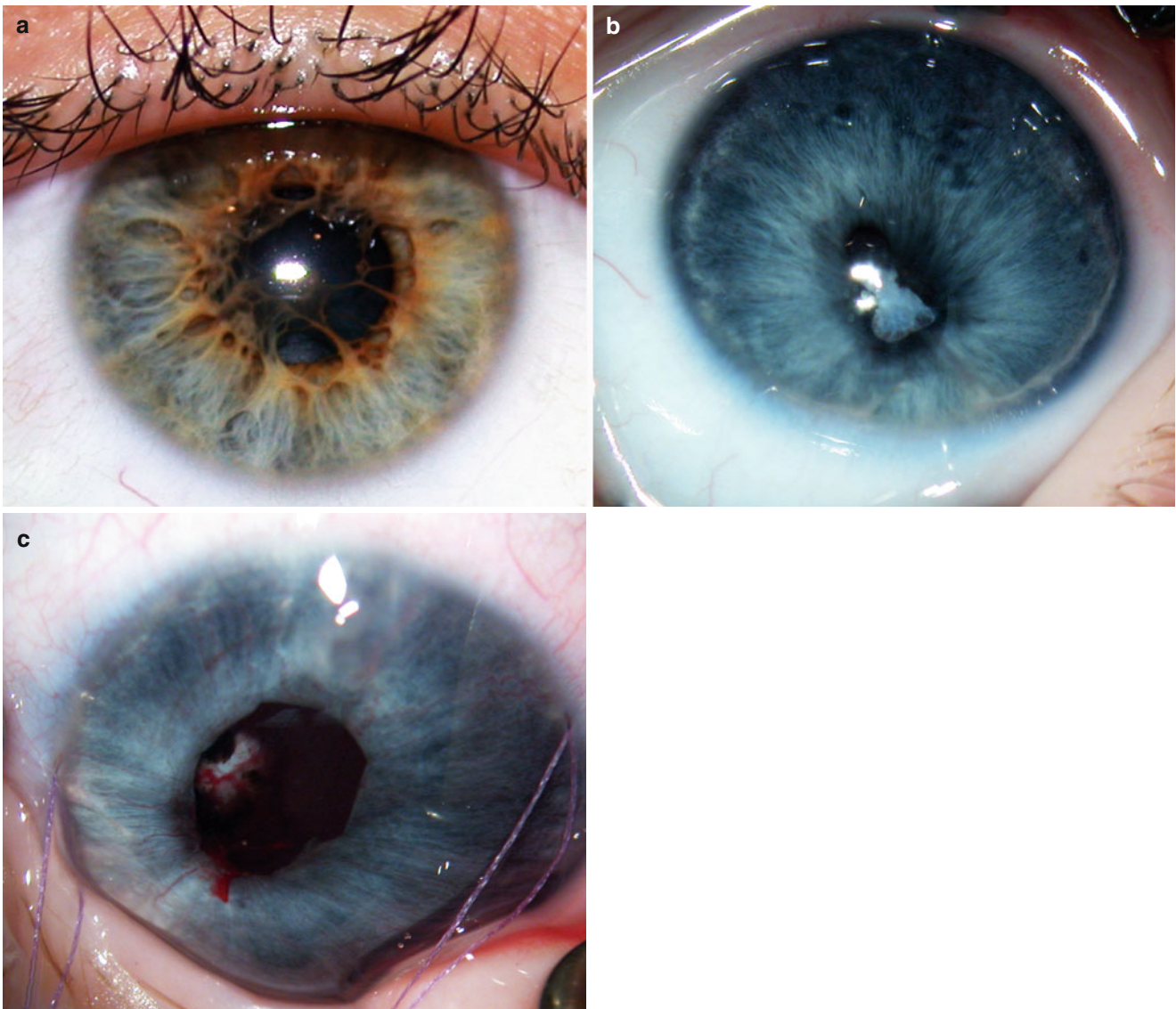


Figure II.A-9 Persistent pupillary membranes. (a) Anterior eye photograph of a patient with a persistent pupillary membrane (*ppm*), seen as fine iris strands bridging the pupil to form intricate webs with attachments to the lens. (b) A patient with a severe form of *ppm*. (c) This

image shows the postoperative appearance following surgical management of the severe form of *ppm* (Courtesy of John Grigg MD, Save Sight Institute, Sydney Medical School)

Abbreviations

Ang-2	Angiopoietin-2
AP-2	Activating protein 2
<i>cc</i>	Cloquet's canal
COL	Collagen
DG	Days of gestation
ECM	Extracellular matrix
FoxC1	Forkhead box C1
Fzd	Frizzled protein
GAG	Glycosaminoglycan
GFAP	Glial fibrillary acidic protein

HA	Hyaluronan
<i>hvs</i>	Hyaloid vascular system
<i>ilm</i>	Inner limiting membrane
<i>Ivm</i>	Intravitreal membrane
<i>lp</i>	Lens placode
<i>lv</i>	Lens vesicle
LYVE-1	Lymphatic vessel endothelial receptor 1
<i>mes</i>	Mesoderm
Ndp	Norrie disease protein
<i>ne</i>	Neural ectoderm
<i>nr</i>	Neurosensory retina

<i>of</i>	Optic fissure
<i>os</i>	Optic stalk
PAS	Periodic acid-Schiff
PEDF	Pigment epithelium-derived factor
PFV	Persistent fetal vasculature
PHPV	Persistent hyperplastic primary vitreous
<i>pm</i>	Pupillary membrane
PPM	Persistent pupillary membranes
<i>rpe</i>	Retinal pigmented epithelium
<i>se</i>	Surface ectoderm
TGF- β	Transforming growth factor- β
TSP-1	Thrombospondin-1
<i>tvf</i>	Posterior tunica lentis
VEGF-A	Vascular endothelial growth factor
<i>vhp</i>	Vasa hyaloidea propria
WG	Weeks of gestation

Conclusion

Vitreous serves a variety of structural and physiological functions during development and throughout life. This is reflected in the transition from the primary fetal vascularized vitreous that supports the development of surrounding intraocular structures to the mature highly hydrated, optically clear, avascular extracellular matrix gel seen in adult eyes. Understanding the molecular processes involved in vitreous development and hyaloid regression may provide insights for the treatment and future management of various ocular diseases.

References

- Balazs EA. The biological function of the vitreous body. *Bibl Ophthalmol.* 1969;79:1–4.
- Bishop PN. Structural macromolecules and supramolecular organization of the vitreous gel. *Prog Retin Eye Res.* 2000;19(3):323–44.
- Duke-Elder D, Cook C. System of ophthalmology, vol. III, part I. In: Cook C, editor. *Embryology.* London: Henry Kimpton; 1963.
- Mann I. *The development of the human eye.* 3rd ed. New York: Grune & Stratton; 1964.
- Tripathi BJ, Tripathi RC. Neural crest origin of human trabecular meshwork and its implications for the pathogenesis of glaucoma. *Am J Ophthalmol.* 1989;107(6):583–90.
- Schook P. A review of data on cell actions and cell interaction during the morphogenesis of the embryonic eye. *Acta Morphol Neerl Scand.* 1978;16(4):267–86.
- Tripathi BJ, Tripathi RC, Livingston AM, Borisuth NS. The role of growth factors in the embryogenesis and differentiation of the eye. *Am J Anat.* 1991;192(4):442–71.
- Ozanic V, Jakobiec F. Prenatal development of the eye and its adnexa. In: *Ocular anatomy, embryology and teratology.* Philadelphia: Harper and Row; 1982. p. 11–96.
- Johnston MC, Noden DM, Hazelton RD, Coulombre JL, Coulombre AJ. Origins of avian ocular and periocular tissues. *Exp Eye Res.* 1979;29(1):27–43.
- Lewis W. Experimental studies on the development of the eye in amphibia. I On the origins of the lens. *Am J Anat.* 1904;3: 505–36.
- McAvoy JW, Chamberlain CG, de Iongh RU, Hales AM, Lovicu FJ. Lens development. *Eye (Lond).* 1999;13(Pt 3b):425–37.
- Spemann H. Über organisatoren in der tierischen entwicklung. *Naturwissenschaften.* 1924;48:1092–4.
- O’Rahilly R. The prenatal development of the human eye. *Exp Eye Res.* 1975;21(2):93–112.
- West-Mays JA, Zhang J, Nottoli T, Hagopian-Donaldson S, Libby D, Strissel KJ, et al. AP-2alpha transcription factor is required for early morphogenesis of the lens vesicle. *Dev Biol.* 1999; 206(1):46–62.
- Hay E. Development of the vertebrate cornea. *Int Rev Cytol.* 1986;63:263–322.
- Nishina S, Kohsaka S, Yamaguchi Y, Handa H, Kawakami A, Fujisawa H, et al. PAX6 expression in the developing human eye. *Br J Ophthalmol.* 1999;83(6):723–7.
- Beebe DC. Development of the ciliary body: a brief review. *Trans Ophthalmol Soc U K.* 1986;105(Pt 2):123–30.
- Balazs EA, Toth LZ, Ozanics V. Cytological studies on the developing vitreous as related to the hyaloid vessel system. *Albrecht Von Graefes Arch Klin Exp Ophthalmol.* 1980;213(2):71–85.
- Balazs EA. Fine structure of the developing vitreous. *Int Ophthalmol Clin.* 1975;15(1):53–63.
- Sebag J, Balazs EA. Morphology and ultrastructure of human vitreous fibers. *Invest Ophthalmol Vis Sci.* 1989;30(8):1867–71.
- Mann IC. The vitreous and suspensory ligaments of the lens. In: *The development of the human eye.* London: Cambridge University Press; 1928. p. 151–89.
- Lutty GA. Anti-Angiogenic Properties of vitreous. In: Dartt D, Dana R, D’Amore P, Niederkorn J, editors. *Immunology, inflammation and diseases of the eye.* Academic Press, Oxford: Elsevier; 2010. p. 112–9.
- Lutty GA, Hasegawa T, Baba T, Grebe R, Bhutto I, McLeod DS. Development of the human choriocapillaris. *Eye (Lond).* 2010;24(3):408–15.
- Zhu M, Madigan MC, van Driel D, Maslim J, Billson FA, Provis JM, et al. The human hyaloid system: cell death and vascular regression. *Exp Eye Res.* 2000;70(6):767–76.
- Sang DN. Embryology of the vitreous. Congenital and developmental abnormalities. *Bull Soc Belge Ophthalmol.* 1987;223 Pt 1:11–35.
- Hogan MJ. The vitreous, its structure, and relation to the ciliary body and retina. Proctor Award Lecture. *Invest Ophthalmol.* 1963;2:418–45.
- Sebag J. Structure, function, and age-related changes of the human vitreous. *Bull Soc Belge Ophthalmol.* 1987;223(Pt 1):37–57.
- Barishak YR. Embryology of the eye and its adnexa. *Dev Ophthalmol.* 1992;24:1–142.
- Los LI. The rabbit as an animal model for post-natal vitreous matrix differentiation and degeneration. *Eye (Lond).* 2008;22(10): 1223–32.
- Los LI, van Luyn MJ, Egli PS, Dijk F, Nieuwenhuis P. Vascular remnants in the rabbit vitreous body. II. Enzyme digestion and immunohistochemical studies. *Exp Eye Res.* 2000;71(2): 153–65.
- Pau H. Development of the structures of vitreous body and of the zonula. *Ophthalmologica.* 1957;134(5):320–31.
- Jokl A. Vergleichende Untersuchungen über den Bau und die Entwicklung des Glaskörper und seiner Inhaltsgebilde bei Wirbeltieren und beim Menschen. Uppsala: Almqvist & Wiksells; 1927. p.183–90.

33. Linsenmayer TF, Gibney E, Little CD. Type II collagen in the early embryonic chick cornea and vitreous: immunoradiochemical evidence. *Exp Eye Res.* 1982;34(3):371–9.
34. Sebag J, Balazs EA. Human vitreous fibres and vitreoretinal disease. *Trans Ophthalmol Soc U K.* 1985;104(Pt 2):123–8.
35. Smith Jr GN, Linsenmayer TF, Newsome DA. Synthesis of type II collagen in vitro by embryonic chick neural retina tissue. *Proc Natl Acad Sci U S A.* 1976;73(12):4420–3.
36. Bremer FM, Rasquin F. Histochemical localization of hyaluronic acid in vitreous during embryonic development. *Invest Ophthalmol Vis Sci.* 1998;39(12):2466–9.
37. Foos RY. Vitreoretinal juncture; topographical variations. *Invest Ophthalmol.* 1972;11(10):801–8.
38. Walcott JC, Provis JM. Muller cells express the neuronal progenitor cell marker nestin in both differentiated and undifferentiated human foetal retina. *Clin Experiment Ophthalmol.* 2003;31(3):246–9.
39. Diaz CM, Macnab LT, Williams SM, Sullivan RK, Pow DV. EAAT1 and D-serine expression are early features of human retinal development. *Exp Eye Res.* 2007;84(5):876–85.
40. Jack RL. Regression of the hyaloid vascular system. An ultrastructural analysis. *Am J Ophthalmol.* 1972;74(2):261–72.
41. Rhodin JA. The ultrastructure of mammalian arterioles and precapillary sphincters. *J Ultrastruct Res.* 1967;18(1):181–223.
42. Hamming NA, Apple DJ, Gieser DK, Vygantas CM. Ultrastructure of the hyaloid vasculature in primates. *Invest Ophthalmol Vis Sci.* 1977;16(5):408–15.
43. Jack RL. Ultrastructure of the hyaloid vascular system. *Arch Ophthalmol.* 1972;87(5):555–67.
44. Gergely K, Gerinec A. A consonant construction of the hyaloid and retinal vascular systems by the angiogenic process. *Bratisl Lek Listy.* 2011;112(3):143–51.
45. Skarie JM, Link BA. FoxC1 is essential for vascular basement membrane integrity and hyaloid vessel morphogenesis. *Invest Ophthalmol Vis Sci.* 2009;50(11):5026–34.
46. Garcia CM, Shui YB, Kamath M, DeVillar J, Johnson RS, Gerber HP, et al. The function of VEGF-A in lens development: formation of the hyaloid capillary network and protection against transient nuclear cataracts. *Exp Eye Res.* 2009;88(2):270–6.
47. Gogat K, Le Gat L, Van Den Berghe L, Marchant D, Kobetz A, Gadin S, et al. VEGF and KDR gene expression during human embryonic and fetal eye development. *Invest Ophthalmol Vis Sci.* 2004;45(1):7–14.
48. Mitchell CA, Risau W, Drexler HC. Regression of vessels in the tunica vasculosa lentis is initiated by coordinated endothelial apoptosis: a role for vascular endothelial growth factor as a survival factor for endothelium. *Dev Dyn.* 1998;213(3):322–33.
49. Shui YB, Wang X, Hu JS, Wang SP, Garcia CM, Potts JD, et al. Vascular endothelial growth factor expression and signaling in the lens. *Invest Ophthalmol Vis Sci.* 2003;44(9):3911–9.
50. Ash JD, Overbeek PA. Lens-specific VEGF-A expression induces angioblast migration and proliferation and stimulates angiogenic remodeling. *Dev Biol.* 2000;223(2):383–98.
51. Mitchell CA, Rutland CS, Walker M, Nasir M, Foss AJ, Stewart C, et al. Unique vascular phenotypes following over-expression of individual VEGFA isoforms from the developing lens. *Angiogenesis.* 2006;9(4):209–24.
52. Rutland CS, Mitchell CA, Nasir M, Konerding MA, Drexler HC. Microphthalmia, persistent hyperplastic hyaloid vasculature and lens anomalies following overexpression of VEGF-A188 from the alphaA-crystallin promoter. *Mol Vis.* 2007;13:47–56.
53. Rao S, Chun C, Fan J, Kofron JM, Yang MB, Hegde RS, et al. A direct and melanopsin-dependent fetal light response regulates mouse eye development. *Nature.* 2013;494(7436):243–6.
54. Albe E, Chang JH, Azar NF, Ivanov AR, Azar DT. Proteomic analysis of the hyaloid vascular system regression during ocular development. *J Proteome Res.* 2008;7(11):4904–13.
55. Diez-Roux G, Lang RA. Macrophages induce apoptosis in normal cells in vivo. *Development.* 1997;124(18):3633–8.
56. Lang R, Lustig M, Francois F, Sellinger M, Plesken H. Apoptosis during macrophage-dependent ocular tissue remodelling. *Development.* 1994;120(12):3395–403.
57. Lang RA, Bishop JM. Macrophages are required for cell death and tissue remodeling in the developing mouse eye. *Cell.* 1993;74(3):453–62.
58. Zhang H, Tse J, Hu X, Witte M, Bernas M, Kang J, et al. Novel discovery of LYVE-1 expression in the hyaloid vascular system. *Invest Ophthalmol Vis Sci.* 2010;51(12):6157–61.
59. Arima M, Yoshida S, Nakama T, Ishikawa K, Nakao S, Yoshimura T, et al. Involvement of periostin in regression of hyaloidvascular system during ocular development. *Invest Ophthalmol Vis Sci.* 2012;53(10):6495–503.
60. Wang S, Park S, Fei P, Sorenson CM. Bim is responsible for the inherent sensitivity of the developing retinal vasculature to hyperoxia. *Dev Biol.* 2011;349(2):296–309.
61. Wang S, Sorenson CM, Sheibani N. Attenuation of retinal vascular development and neovascularization during oxygen-induced ischemic retinopathy in Bcl-2–/– mice. *Dev Biol.* 2005;279(1):205–19.
62. Kim JH, Yu YS, Mun JY, Kim KW. Autophagy-induced regression of hyaloid vessels in early ocular development. *Autophagy.* 2010;6(7):922–8.
63. Kaiser D, Freyberg MA, Friedl P. Lack of hemodynamic forces triggers apoptosis in vascular endothelial cells. *Biochem Biophys Res Commun.* 1997;231(3):586–90.
64. Meeson A, Palmer M, Calfon M, Lang R. A relationship between apoptosis and flow during programmed capillary regression is revealed by vital analysis. *Development.* 1996;122(12):3929–38.
65. Felton SM, Brown GC, Felberg NT, Federman JL. Vitreous inhibition of tumor neovascularization. *Arch Ophthalmol.* 1979;97(9):1710–3.
66. Luttly GA, Thompson DC, Gallup JY, Mello RJ, Patz A, Fenselau A. Vitreous: an inhibitor of retinal extract-induced neovascularization. *Invest Ophthalmol Vis Sci.* 1983;24(1):52–6.
67. Preis I, Langer R, Brem H, Folkman J. Inhibition of neovascularization by an extract derived from vitreous. *Am J Ophthalmol.* 1977;84(3):323–8.
68. Luttly GA, Merges C, Threlkeld AB, Crone S, McLeod DS. Heterogeneity in localization of isoforms of TGF-beta in human retina, vitreous, and choroid. *Invest Ophthalmol Vis Sci.* 1993;34(3):477–87.
69. Blobel GC, Schiemann WP, Lodish HF. Role of transforming growth factor beta in human disease. *N Engl J Med.* 2000;342(18):1350–8.
70. Bottinger EP, Letterio JJ, Roberts AB. Biology of TGF-beta in knockout and transgenic mouse models. *Kidney Int.* 1997;51(5):1355–60.
71. Saika S, Liu CY, Azhar M, Sanford LP, Doetschman T, Gendron RL, et al. TGFbeta2 in corneal morphogenesis during mouse embryonic development. *Dev Biol.* 2001;240(2):419–32.
72. Sommer F, Pollinger K, Brandl F, Weiser B, Tessmar J, Blunk T, et al. Hyalocyte proliferation and ECM accumulation modulated by bFGF and TGF-beta1. *Graefes Arch Clin Exp Ophthalmol.* 2008;246(9):1275–84.
73. Becerra SP. Focus on molecules: pigment epithelium-derived factor (PEDF). *Exp Eye Res.* 2006;82(5):739–40.
74. Matsuoka M, Ogata N, Minamino K, Matsumura M. Expression of pigment epithelium-derived factor and vascular endothelial growth factor in fibrovascular membranes from patients with proliferative diabetic retinopathy. *Jpn J Ophthalmol.* 2006;50(2):116–20.
75. Ogata N, Nishikawa M, Nishimura T, Mitsuma Y, Matsumura M. Unbalanced vitreous levels of pigment epithelium-derived factor

- and vascular endothelial growth factor in diabetic retinopathy. *Am J Ophthalmol*. 2002;134(3):348–53.
76. Ogata N, Tombran-Tink J, Jo N, Mrazek D, Matsumura M. Upregulation of pigment epithelium-derived factor after laser photocoagulation. *Am J Ophthalmol*. 2001;132(3):427–9.
 77. Stitt AW, Graham D, Gardiner TA. Ocular wounding prevents pre-retinal neovascularization and upregulates PEDF expression in the inner retina. *Mol Vis*. 2004;10:432–8.
 78. Fukai N, Eklund L, Marneros AG, Oh SP, Keene DR, Tamarkin L, et al. Lack of collagen XVIII/endostatin results in eye abnormalities. *EMBO J*. 2002;21(7):1535–44.
 79. Hurskainen M, Eklund L, Hagg PO, Fruttiger M, Sormunen R, Ilves M, et al. Abnormal maturation of the retinal vasculature in type XVIII collagen/endostatin deficient mice and changes in retinal glial cells due to lack of collagen types XV and XVIII. *FASEB J*. 2005;19(11):1564–6.
 80. Marneros AG, Olsen BR. Physiological role of collagen XVIII and endostatin. *FASEB J*. 2005;19(7):716–28.
 81. Brown AS, Leamen L, Cucevic V, Foster FS. Quantitation of hemodynamic function during developmental vascular regression in the mouse eye. *Invest Ophthalmol Vis Sci*. 2005;46(7):2231–7.
 82. Sheibani N, Sorenson CM, Cornelius LA, Frazier WA. Thrombospondin-1, a natural inhibitor of angiogenesis, is present in vitreous and aqueous humor and is modulated by hyperglycemia. *Biochem Biophys Res Commun*. 2000;267(1):257–61.
 83. Wang S, Wu Z, Sorenson CM, Lawler J, Sheibani N. Thrombospondin-1-deficient mice exhibit increased vascular density during retinal vascular development and are less sensitive to hyperoxia-mediated vessel obliteration. *Dev Dyn*. 2003;228(4):630–42.
 84. Le Goff MM, Lu H, Ugarte M, Henry S, Takanosu M, Mayne R, et al. The vitreous glycoprotein opticin inhibits preretinal neovascularization. *Invest Ophthalmol Vis Sci*. 2012;53(1):228–34.
 85. Ramesh S, Bonshek RE, Bishop PN. Immunolocalisation of opticin in the human eye. *Br J Ophthalmol*. 2004;88(5):697–702.
 86. Lobov IB, Rao S, Carroll TJ, Vallance JE, Ito M, Ondr JK, et al. WNT7b mediates macrophage-induced programmed cell death in patterning of the vasculature. *Nature*. 2005;437(7057):417–21.
 87. Rao S, Lobov IB, Vallance JE, Tsujikawa K, Shiojima I, Akunuru S, et al. Obligatory participation of macrophages in an angiopoietin 2-mediated cell death switch. *Development*. 2007;134(24):4449–58.
 88. Lee HJ, Ahn BJ, Shin MW, Jeong JW, Kim JH, Kim KW. Ninjurin1 mediates macrophage-induced programmed cell death during early ocular development. *Cell Death Differ*. 2009;16(10):1395–407.
 89. Luhmann UF, Lin J, Acar N, Lammel S, Feil S, Grimm C, et al. Role of the Norrie disease pseudoglioma gene in sprouting angiogenesis during development of the retinal vasculature. *Invest Ophthalmol Vis Sci*. 2005;46(9):3372–82.
 90. Ohlmann AV, Adamek E, Ohlmann A, Lutjen-Drecoll E. Norrie gene product is necessary for regression of hyaloid vessels. *Invest Ophthalmol Vis Sci*. 2004;45(7):2384–90.
 91. Ponsioen TL, Hooymans JM, Los LI. Remodelling of the human vitreous and vitreoretinal interface – a dynamic process. *Prog Retin Eye Res*. 2010;29(6):580–95.
 92. Hamburg A. Some investigations on the cells of the vitreous body. *Ophthalmologica*. 1959;138:81–107.
 93. Vagaja NN, Chinnery HR, Binz N, Kezic JM, Rakoczy EP, McMenamin PG. Changes in murine hyalocytes are valuable early indicators of ocular disease. *Invest Ophthalmol Vis Sci*. 2012;53(3):1445–51.
 94. Sommer F, Brandl F, Weiser B, Tesmar J, Blunk T, Gopferich A. FACS as useful tool to study distinct hyalocyte populations. *Exp Eye Res*. 2009;88(5):995–9.
 95. Osterlin SE, Jacobson B. The synthesis of hyaluronic acid in vitreous. I. Soluble and particulate transferases in hyalocytes. *Exp Eye Res*. 1968;7(4):497–510.
 96. Newsome DA, Linsenmayer TF, Trelstad RL. Vitreous body collagen. Evidence for a dual origin from the neural retina and hyalocytes. *J Cell Biol*. 1976;71(1):59–67.
 97. Rittig M, Flugel C, Prehm P, Lutjen-Drecoll E. Hyaluronan synthase immunoreactivity in the anterior segment of the primate eye. *Graefes Arch Clin Exp Ophthalmol*. 1993;231(6):313–7.
 98. Ogawa K. Scanning electron microscopic study of hyalocytes in the guinea pig eye. *Arch Histol Cytol*. 2002;65(3):263–8.
 99. Saga T, Tagawa Y, Takeuchi T, Nerome K, Matsuda H. Electron microscopic study of cells in vitreous of guinea pig. *Jpn J Ophthalmol*. 1984;28(3):239–47.
 100. Salu P, Claeskens W, De Wilde A, Hijmans W, Wisse E. Light and electron microscopic studies of the rat hyalocyte after perfusion fixation. *Ophthalmic Res*. 1985;17(3):125–30.
 101. Lazarus HS, Hageman GS. In situ characterization of the human hyalocyte. *Arch Ophthalmol*. 1994;112(10):1356–62.
 102. Grabner G, Boltz G, Forster O. Macrophage-like properties of human hyalocytes. *Invest Ophthalmol Vis Sci*. 1980;19(4):333–40.
 103. Noda Y, Hata Y, Hisatomi T, Nakamura Y, Hirayama K, Miura M, et al. Functional properties of hyalocytes under PDGF-rich conditions. *Invest Ophthalmol Vis Sci*. 2004;45(7):2107–14.
 104. Jacobson B. Degradation of glycosaminoglycans by extracts of calf vitreous hyalocytes. *Exp Eye Res*. 1984;39(3):373–85.
 105. Schonfeld CL. Hyalocytes inhibit retinal pigment epithelium cell proliferation in vitro. *Ger J Ophthalmol*. 1996;5(4):224–8.
 106. Zhu M, Provis JM, Penfold PL. The human hyaloid system: cellular phenotypes and inter-relationships. *Exp Eye Res*. 1999;68(5):553–63.
 107. Qiao H, Hisatomi T, Sonoda KH, Kura S, Sassa Y, Kinoshita S, et al. The characterisation of hyalocytes: the origin, phenotype, and turnover. *Br J Ophthalmol*. 2005;89(4):513–7.
 108. Sakamoto T. Cell biology of hyalocytes. *Nihon Ganka Gakkai Zasshi*. 2003;107(12):866–82; discussion 83.
 109. Stein-Streilein J. Immune regulation and the eye. *Trends Immunol*. 2008;29(11):548–54.
 110. Jiang LQ, Streilein JW. Immune privilege extended to allogeneic tumor cells in the vitreous cavity. *Invest Ophthalmol Vis Sci*. 1991;32(1):224–8.
 111. Sonoda KH, Sakamoto T, Qiao H, Hisatomi T, Oshima T, Tsutsumi-Miyahara C, et al. The analysis of systemic tolerance elicited by antigen inoculation into the vitreous cavity: vitreous cavity-associated immune deviation. *Immunology*. 2005;116(3):390–9.
 112. Azuma N, Tajima S, Konomi H, Hida T, Akiya S, Uemura Y. Glycosaminoglycan and collagen distribution in the developing human vitreous. *Graefes Arch Clin Exp Ophthalmol*. 1998;236(9):679–87.
 113. Halfter W, Dong S, Dong A, Eller AW, Nischt R. Origin and turnover of ECM proteins from the inner limiting membrane and vitreous body. *Eye (Lond)*. 2008;22(10):1207–13.
 114. Halfter W, Dong S, Schurer B, Ring C, Cole GJ, Eller A. Embryonic synthesis of the inner limiting membrane and vitreous body. *Invest Ophthalmol Vis Sci*. 2005;46(6):2202–9.
 115. Wang J, McLeod D, Henson DB, Bishop PN. Age-dependent changes in the basal retinovitreal adhesion. *Invest Ophthalmol Vis Sci*. 2003;44(5):1793–800.
 116. Azuma N, Hida T, Akiya S, Uemura Y, Kohsaka S, Tsukada Y. Histochemical studies on hyaluronic acid in the developing human retina. *Graefes Arch Clin Exp Ophthalmol*. 1990;228(2):158–60.
 117. Shastry BS. Persistent hyperplastic primary vitreous: congenital malformation of the eye. *Clin Experiment Ophthalmol*. 2009;37(9):884–90.

118. Goldberg MF. Persistent fetal vasculature (PFV): an integrated interpretation of signs and symptoms associated with persistent hyperplastic primary vitreous (PHPV). LIV Edward Jackson Memorial Lecture. *Am J Ophthalmol.* 1997;124(5):587–626.
119. Lambert SR, Buckley EG, Lenhart PD, Zhang Q, Grossniklaus HE. Congenital fibrovascular pupillary membranes: clinical and histopathologic findings. *Ophthalmology.* 2012;119(3):634–41.
120. Pelcastre EL, Villanueva-Mendoza C, Zenteno JC. Novel and recurrent NDP gene mutations in familial cases of Norrie disease and X-linked exudative vitreoretinopathy. *Clin Experiment Ophthalmol.* 2010;38(4):367–74.
121. Robitaille JM, Wallace K, Zheng B, Beis MJ, Samuels M, Hoskin-Mott A, et al. Phenotypic overlap of familial exudative vitreoretinopathy (FEVR) with persistent fetal vasculature (PFV) caused by FZD4 mutations in two distinct pedigrees. *Ophthalmic Genet.* 2009;30(1):23–30.
122. Snead MP, Yates JR. Clinical and molecular genetics of Stickler syndrome. *J Med Genet.* 1999;36(5):353–9.
123. Donoso LA, Edwards AO, Frost AT, Ritter 3rd R, Ahmad N, Vrabec T, et al. Clinical variability of Stickler syndrome: role of exon 2 of the collagen COL2A1 gene. *Surv Ophthalmol.* 2003;48(2):191–203.
124. Richards AJ, Baguley DM, Yates JR, Lane C, Nicol M, Harper PS, et al. Variation in the vitreous phenotype of Stickler syndrome can be caused by different amino acid substitutions in the X position of the type II collagen Gly-X-Y triple helix. *Am J Hum Genet.* 2000;67(5):1083–94.
125. Snead MP, McNinch AM, Poulson AV, Bearcroft P, Silverman B, Gomersall P, et al. Stickler syndrome, ocular-only variants and a key diagnostic role for the ophthalmologist. *Eye (Lond).* 2011;25:1389–400.
126. Zhang C, Asnaghi L, Gongora C, Patek B, Hose S, Ma B, et al. A developmental defect in astrocytes inhibits programmed regression of the hyaloid vasculature in the mammalian eye. *Eur J Cell Biol.* 2011;90(5):440–8.
127. Ramappa M, Murthy SI, Chaurasia S, Singhla R, Rathi VM, Vemuganti GK, et al. Lens-preserving excision of congenital hyperplastic pupillary membranes with clinicopathological correlation. *J AAPOS.* 2012;16(2):201–3.
128. Cruciani F, Santino G, Salandri AG. Monolateral idiopathic cyst of the vitreous. *Acta Ophthalmol Scand.* 1999;77(5):601–3.
129. Nork TM, Millecchia LL. Treatment and histopathology of a congenital vitreous cyst. *Ophthalmology.* 1998;105(5):825–30.
130. Francois J. Pre-papillary cyst developed from remnants of the hyaloid artery. *Br J Ophthalmol.* 1950;34(6):365–8.
131. Lisch W, Rochels R. Pathogenesis of congenital vitreous cysts. *Klin Monbl Augenheilkd.* 1989;195(6):375–8.
132. Bach L and Seefelder R. *Atlas zur Entwicklungsgeschichte des menschlichen Auges.* Leipzig, Berlin W. Engelmann 1911.

Jesse Gale and Yasushi Ikuno

Outline

- I. **Introduction**
 - A. Definition of Myopia
 - B. Emmetropization and Axial Length
- II. **Myopia**
 - A. Epidemiology
 - B. Etiology
 - 1. Genetic Factors
 - 2. Environmental Factors
 - 3. Vitreous Factors
 - C. Ocular Features of Myopia
 - 1. Scleral changes and Axial length
 - 2. Myopic Vitreopathy
 - 3. Retina and Choroid
 - D. The Pathologies of Myopic Vitreopathy
 - 1. Retinal Detachment
 - a. Retinal Detachment After Anterior Segment Surgery
 - 2. Myopic Maculopathy
 - a. Myopic Macular Degeneration
 - i. Choroidal Neovascularization
 - b. Myopic Foveoschisis
 - c. Premacular Membranes
 - d. Macular Hole
 - i. Macular Hole with Retinal Detachment
 - e. Paravascular Retinal Microholes
 - 3. Cataract

References

Electronic supplementary material Supplementary material is available in the online version of this chapter at [10.1007/978-1-4939-1086-1_8](https://doi.org/10.1007/978-1-4939-1086-1_8). Videos can also be accessed at <http://www.springerimages.com/videos/978-1-4939-1085-4>.

J. Gale, MB, ChB, MD (✉)
VMR Institute for Vitreous Macula Retina,
7677 Center Ave, Suite 400, Huntington Beach, CA 92647, USA

Doheny Eye Institute, Los Angeles, CA USA

Addenbrooke's Hospital, Cambridge University
Hospitals NHS Foundation Trust,
Cambridge, CB2 0QQ, England, UK
e-mail: jesse.gale@gmail.com

Keywords

Myopia • Vitreous • Myopic vitreopathy • Posterior vitreous detachment • Anomalous PVD • Retinal detachment • Macular hole • Choroidal neovascularization • Vitreoretinal interface • Myopic foveoschisis

Key Concepts

1. Myopia is increasing rapidly in recent decades, associated with increasing education and urbanization of many populations. Elements of the modern environment such as prolonged reading and time spent indoors are disturbing the normal homeostasis of eye growth known as emmetropization.
2. Mutations of extracellular matrix proteins can result in both myopia and myopic vitreopathy, supporting the concept that vitreous is part of the myopic phenotype. Myopia is associated with increased liquefaction of vitreous, which resembles premature synchysis. This happens in younger myopes when vitreoretinal adhesion remains strong, thus creating anomalous posterior vitreous detachments with a full range of vitreoretinal complications.
3. All degrees of myopia have associated risks of blinding complications, including retinal detachment, maculopathy of various types, cataract, and glaucoma. Maculopathy and retinal detachment have direct connection to myopic vitreopathy. Prophylaxis for myopia and the various complications of myopic vitreopathy requires continued research.

Y. Ikuno, MD
Department of Ophthalmology, Osaka University Graduate
School of Medicine, 2-2 Yamadaoka, Suite 5650871, Japan
e-mail: ikuno@ophthal.med.osaka-u.ac.jp

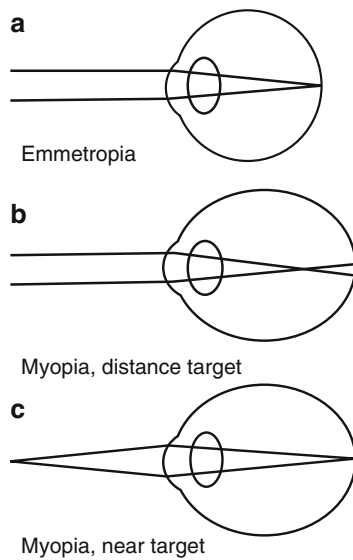


Figure II.B-1 (a) Schematic representation of emmetropia. Parallel light from the distance is brought to focus onto the fovea. (b) Schematic representation of myopia. Parallel light from the distance is brought to focus anterior to the retina in this elongated globe. This creates a blur circle on the retina. (c) Schematic representation of myopia. Divergent light from a near target is brought to focus on the fovea

I. Introduction

Myopia is gaining public health importance because it is a major cause of correctable blindness and visual impairment globally [1]. In some populations the complications of myopia are now the major cause of uncorrectable blindness [2, 3]. Historically, the mild phenotype of low myopia has been separated from the potentially blinding associations of pathological myopia with an arbitrary refractive error of -6.0D [4]. However it is becoming clear that there is no threshold effect and that common myopia of all levels contributes to risks of uncorrectable visual loss such as cataract, glaucoma, retinal detachment, and maculopathy [5, 6].

A. Definition of Myopia

Myopia, defined by refractive error, is the product of multiple optical variables in the eye. Parallel light from infinity is brought to focus anterior to the retina, and divergent light from near targets may focus at the retina, hence “nearsightedness” (Figure II.B-1). The anatomic substrate of this abnormality can be summarized as either an excessively powerful converging optical apparatus of the cornea and lens or an excessively long distance to the retina (axial length). There are many ways to classify or define myopia. At a population level, the main causes of myopia can be grouped

Table II.B-1 Simple classification of myopia

1. <i>Syndromic myopia</i> with systemic associations; for example: <i>Stickler syndrome type 1</i> with clefting, arthropathy, vitreoretinal abnormalities, hearing loss, collagen 2A1 mutation <i>Marfan syndrome</i> with long limbs, ectopia lentis, cardiac abnormalities, fibrillin mutation
2. <i>Nonsyndromic autosomal dominant myopia</i> Isolated ocular hereditary myopia E.g., early-onset high myopia with dominant inheritance and associated loci on genome-wide analysis
3. <i>Nonsyndromic myopia acquired in childhood</i> Common myopia, school myopia

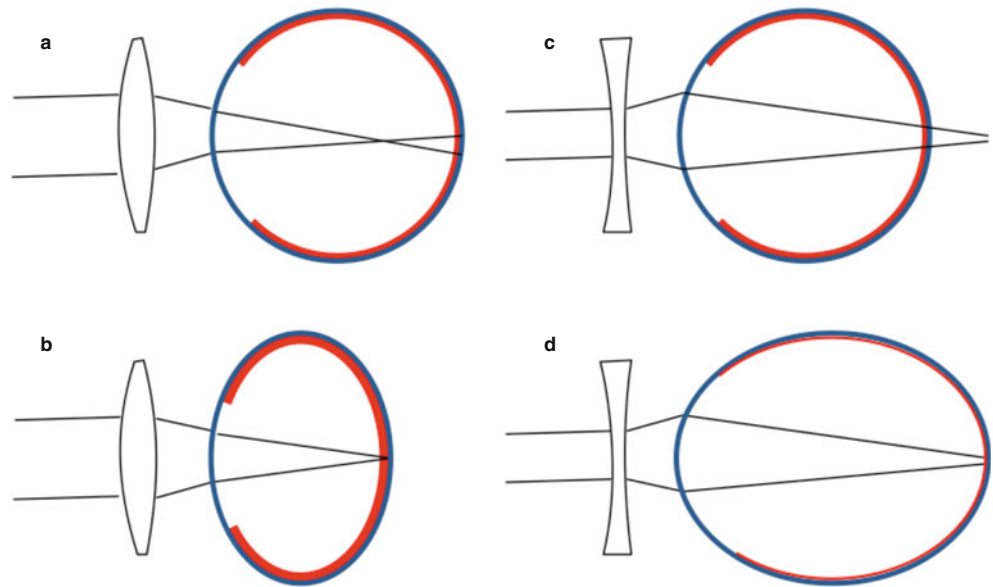
as: (1) myopia with systemic associations or syndromes, (2) isolated ocular hereditary myopia, or (3) acquired myopia without associations (Table II.B-1). The first two groups have a clear genetic component. The first group demonstrates connections between the genetic causes of myopia, vitreous, and extracellular matrix in general. It is the third group, however, often known as school myopia or common myopia, which has more environmental causes and is becoming a major cause of correctable and uncorrectable vision loss worldwide.

B. Emmetropization and Axial Length

The process by which the normal eye maintains emmetropia during growth and development is termed emmetropization. Myopia represents a failure of this process. Thus, common myopia may best be characterized as dysregulated eye growth [7]. A rich and expanding scientific literature has illuminated numerous elements of this emmetropization process, particularly through animal studies [8]. A positive lens over a developing chick eye will induce myopic defocus and corresponding shortening of the eye through reduced scleral growth and thickening of the choroid, while hyperopic focus or form deprivation will accelerate scleral growth and thin the choroid (Figure II.B-2). These changes are direction-specific, reversible, and can occur locally within the eye [8, 9]. There are important parallels between these animal findings and humans, as discussed below.

An implication of this understanding is that the failure of emmetropization that results in common myopia does so through an increased axial length. This can be observed in children developing myopia, with an increasing vitreous chamber [10]. Thus, axial length can be considered an important endophenotype of myopia, with greater sensitivity and specificity for the deranged emmetropization process than refractive error in general [11]. That is, the specific anatomic changes of myopia are most apparent in the measurement of the vitreous chamber. Whether cause or effect,

Figure II.B-2 Emmetropization in developing animals. (a) A positive lens will induce myopic defocus. (b) Axial growth will slow and the choroid will thicken, to bring the image into focus. (c) A negative lens will induce hyperopic defocus. (d) Axial growth accelerates and the choroid thins, to bring the image into focus



the associated changes within the vitreous constitute myopic vitreopathy. This chapter will discuss the various etiologic (both genetic and environmental) aspects of myopia, the effects on the vitreous that result in myopic vitreopathy, how this causes anomalous PVD, and its various clinical consequences.

II. Myopia

A. Epidemiology

Refractive error is the leading cause of correctable visual impairment worldwide and therefore a major international public health issue [1, 12]. Myopia is common, and prevalence varies between populations [13]. The complications of myopia are the major causes of uncorrectable blindness at a population level in European and Asian populations [2, 3].

Many large cross-sectional studies have found the prevalence of myopia $> -0.5D$ in adults, to range from 15 % in older Australians [14] to 49 % in 44-year-old Britons [15]. In the United States, the overall prevalence has been measured around 25–35 % in adults [16–19] with lower prevalence in Black and Latino people [17, 18, 20, 21]. Asian populations, particularly those of Chinese ethnicity, appear to be mildly more susceptible to myopia [13, 22, 23].

In cross-sectional studies of adults, the prevalence of myopia is found to decline with age, which is due to two factors: the gradual hypermetropization during adulthood [24–26] and an increasing prevalence of myopia in recent generations [27, 28]. Initially noted in Inuit populations in the 1960s [29, 30] and then strikingly documented in Taiwan

and Singapore [27, 31], the increasing prevalence of myopia in recent birth cohorts is now clear [28, 32–34]. In Taiwan, for example, the prevalence of myopia in 7-year-old children has increased from 6 % in 1983 to 21 % in 2000, and in those aged 16–18 years, the prevalence of myopia has increased from 74 to 84 % with doubled prevalence of high myopia $> -6.0D$ from 11 % in 1983 to 21 % in 2000. Thus, myopia is beginning earlier and also increasing in severity, especially in young urban educated Asian people. This increase has occurred within three generations, highlighting aspects of the modern environment that are associated with this epidemic of myopia [34, 35].

B. Etiology

It is likely that myopia, like cardiovascular disease, for example, represents a complex interaction of genetic and environmental factors. The increasing prevalence of myopia associated with ethnicity, urbanization, and education highlights the multifactorial etiology, rather than simply nature versus nurture [36].

1. Genetic Factors

Human myopia is etiologically heterogeneous at a genetic level, with more than 300 associations identified. As briefly summarized in Table II.B-1, several syndromes of ocular and systemic abnormality can include high myopia, such as Marfan, Weill-Marchesani (both fibrillin mutations), Stickler types 1 and 2 (collagen II and XI mutations), Ehlers-Danlos (type 4, collagen III mutation), Knobloch (collagen XVIII mutation), and congenital stationary night blindness syndromes [37]. These syndromes often include abnormalities

of the vitreous and relate to mutations of the extracellular matrix [see chapter I.C. Hereditary vitreo-retinopathies].

There are also isolated ocular forms of familial high myopia, which is often early-onset and severe [37]. In general, high myopia may have a stronger genetic component [38]. These familial forms of myopia (e.g., associated with chromosomes 18p or 12q) do not seem to relate to the common school myopia, which has a greater environmental component [39, 40].

The heritability of myopia appears to diminish between generations. Children of myopic parents have a higher prevalence of myopia, but in China this relationship has changed dramatically in two generations [35]. For the parents' generation, being born to myopic parents resulted in an odds ratio (OR) of 6.71 for developing myopia, but for their children's generation, myopic parents only conveyed an OR of 1.85 [35]. This indicates the genetic risk has been diluted by the environmental risks. In general, the heritability estimates that are derived from correlations of refractive error are greater from sibling to sibling correlations than parent-child correlations (particularly in times of intergenerational change), indicating shared environments are a large part of these correlations [37, 38].

Eye size is heritable, but this does not seem relevant to myopia. Children of myopic parents were found to have larger eyes before they developed myopia and after controlling for near work and education [41]. However, eye size and axial length are poor predictors of myopia because the process of emmetropization adjusts ocular growth to match focal length [42]. There is scant evidence to suggest that larger eyes are more vulnerable to derangement of emmetropization [37, 40]. The implication of this is that the larger eyes in children of myopes may simply reflect shared environmental factors or irrelevant covariates such as height, rather than a genetic determinant of myopia. On the other hand, some carefully controlled observational studies find parental myopia far more strongly associated with myopia than environmental factors in multivariate models that adjust for both [40].

Twin studies are a powerful method for testing heritability, and several early results showed extremely high estimates of heritability (summarized and tabulated in Guggenheim et al. [38]). The assumptions concerning twins sharing environments have been challenged, and these studies will consistently overestimate heritability at a population level [37].

Genome-wide association studies provide a powerful method to establish genetic causes of the disease and understand pathophysiology. Hammond et al. [43] performed a linkage analysis in 280 dizygotic twins (with any type of myopia), revealing the 11p13 locus overlying PAX6 as a possible association, as well as other loci of interest at 3q26, 8p23, and 4q12. Genetic investigation of dizygotic twins shares the power of twin studies by controlling environments

to a large degree. Stambolian et al. [44] were the first to perform genome-wide analysis exclusively for the common school myopia, with methods designed to increase the likelihood of linkage, and identified one locus at 22q12 for further study. In recent years, a rapidly growing number of genome-wide association studies have established a growing number of loci of interest, though differences in populations and differences in the types of myopia that are included can make interpretation difficult. Now, very large consortia have examined the entire genome of many thousands of participants for associations with myopia [45–49]. Fan et al. [45] identified a locus of interest in 1q41 among three large Singapore genome-wide studies. Verhoeven et al. [46] validated an association of myopia with 15q14 (GDJ2) among many cohorts across Europe and Asia and also commented on a gene for Connexin36 and actin proteins that could have relevance to retinal signaling or scleral remodeling. Cheng et al. [49] limited their analysis to loci associated with axial length, as this is a suitable endophenotype for myopia, and tested over 12,000 Europeans and 8,000 Asians, then validated the findings in another independent group of over 23,000. They found nine loci common to both European and Asian cohorts to be associated with myopia, including 1q41 (ZC3H11B) and 15q14 (GJD2), as well as laminin alpha-2 subunit (LAMA2) on chromosome 6. Two other loci were associated with Wnt signaling pathways. Verhoeven et al. [47] performed a similar large consortium-derived genome-wide analysis of refractive error in many thousands of participants in multiple continents. They identified 24 loci, including GDJ2 and LAMA2 again but also candidate genes with functions in neurotransmission (GRIA4), ion transport (KCNQ5), retinoic acid metabolism (RDH5), and eye development (SIX6 and PRSS56). Kiefer et al. [48] found 22 loci associated with myopia in another large genome-wide study of Europeans, including LAMA2 and candidate genes involved in photopigment regeneration and retinal development and signaling. These powerful studies and enticing findings require considerable follow-up investigation to understand the relevant genetic and molecular pathways in common myopia.

The genetic associations of myopia can be summarized by stating that mutations of extracellular matrix proteins commonly result in both myopia and vitreopathy, supporting the concept that vitreopathy is part of the myopic phenotype. Common myopia represents failure of the emmetropization process, and the genetic associations include signaling pathways and the LAMA2 subunit of laminin, an important extracellular protein in the vitreoretinal interface.

2. Environmental Factors

Animal studies, particularly with chicks, rodents, and nonhuman primates, have clearly shown that the homeostasis of ocular growth is guided by vision [5, 8]. Form deprivation

results in myopia in monkeys [50] and children [51] as well as other animals. In chicks as in other animals, a positive lens providing myopic defocus results in thickening of the choroid and slowing of scleral growth, while hyperopic defocus from a negative lens results in ocular elongation and choroidal thinning [52] (Figure II.B-2). These responses are partially preserved with optic nerve transection and can be generated locally in only half of one eye using partial lenses [9, 53–55], indicating that an important signal for eye growth is generated locally in the retina. Thus it appears that the developing retina can detect blur but can also detect the sign of the defocus, in order to slow or accelerate growth in the correct direction, which may be mediated by combining cues from chromatic and non-chromatic aberrations and from accommodation [8, 56]. These findings implicate a signaling pathway from the retina, through the choroid to the sclera. Although the pathways involved have not been clearly demonstrated, retinoic acid production in the choroid is likely to be involved because it is upregulated by myopic defocus and inhibits scleral proteoglycan synthesis and downregulated in hyperopic defocus when the sclera elongates and causes increased scleral proteoglycan synthesis [57]. The effector mechanism of emmetropization involves changes in fluid lacunae in the choroid [58] and changes in the scleral growth, with scleral thinning, remodeling, and increased viscoelasticity (“creep”). The abnormalities of myopic sclera are described below. Together these findings elucidate mechanisms by which environmental factors can affect the normal process of emmetropization.

Education and urbanization are the two environmental factors that are closely associated with myopia at a population level. Common myopia correlates strongly with education across all major population groups of the world [37]. This association exists with the duration of education, intensity of study and final academic achievement, and professional training in law, medicine, or engineering. The progression of myopia may even occur in parallel with the school terms in some populations [59]. Similarly, in regions with very similar genetic background, people in urban centers have consistently higher prevalence of myopia than in rural areas, even after adjusting for education, affluence, and activities [37].

Near work is the environmental factor that is used to explain these associations mechanistically at an individual level. The mechanism here is not excessive accommodative effort, but accommodative lag or deficiency. Accommodation is driven by a blur-feedback loop, so there is a tendency to accommodate only to the point of acceptable blur, resulting in mild hyperopic defocus for near targets (accommodative lag). Myopes have more accommodative lag than emmetropes, but it is unclear whether this accommodative lag precedes myopia development and whether this lag is a specific defect in pre-myopes [60–63]. Thus, the association between near

work and myopia is sometimes weak and difficult to quantify. Other factors such as the relative potency of different types of defocus for eye growth, peripheral refraction patterns, and the variations in defocus due to physical environments are all explanations for why these associations can be hard to measure [5].

A more recently revealed association between time spent outdoors and a reduced risk of myopia may also explain much of the associations of myopia with urbanization, population, and education [64–66]. This was hypothesized to be related to UV light stimulation of dopamine release from amacrine cells, a pathway that is shown to reduce eye growth and myopia in animal studies [33, 64].

In summary, the normal processes of emmetropization may be deranged or confused by aspects of the environment to create myopia. The retina has the central role in detecting not only the blur but also the direction of defocus and changing ocular growth to compensate. Near work could result in persistent low-grade hyperopic defocus to drive excessive ocular growth, although multiple optical considerations can make this association tenuous at a population level. Certainly, education and urbanization are strongly associated with myopia, and both near work and time spent outdoors might partially explain these associations. Clinical trials of outdoor education and optical interventions continue [33, 67].

3. Vitreous Factors

Curtin [68] and Seltner [69] proposed a role for the vitreous in the development of myopia, suggesting excessive vitreous formation was a cause for ocular enlargement. As mentioned, hereditary abnormalities of collagen can result in syndromic vitreopathy and myopia, linking the two with common causation [70]. In line with this concept, Wilkinson [71] correlated intraocular pressure with ocular growth in experimental chick models, and Quinn [72] showed a slightly increased IOP among myopic children. On the other hand, the rate of passive scleral creep in experimental situations is two orders of magnitude greater than the maximal rate of ocular elongation [73], and scleral remodeling appears to be an active cellular process rather than a passive stretching process [8]. Also in opposition to this theory of “overinflation,” tree shrews showed scleral contraction in response to experimentally increased IOP [74]. It is hard to propose a complete model by which vitreous expansion could lead to axial growth, when the formation of the vitreous in the mature eye is not well understood.

C. Ocular Features of Myopia

1. Scleral Changes and Axial Length

The characteristic changes of myopia are seen in the size and shape of the globe. Axial length accounts for more than 40 %

of refractive error and is considered an important endophenotype of myopia [10, 49, 75, 76]. Axial length also correlates more closely with complications of myopia than does refractive state [77].

Myopic sclera is thin and distensible, particularly in the posterior globe, with good agreement between mammalian models and the limited human data reported [7, 78–81]. At a histological level, myopic sclera has thin collagen fibrils distributed uniformly through the scleral wall in a lamellar pattern, compared to normal sclera with thicker fibrils in the outer layers and greater interweaving [80, 82, 83]. In experimental myopia induced with hyperopic defocus or deprivation, the posterior scleral collagen fibers are lost first, and overall scleral dry weight decreases, implicating a remodeling process rather than stretching and redistribution of fibers [83, 84]. The viscoelastic stretching known as scleral creep is increased, particularly in the posterior sclera [73, 85, 86]. The posterior sclera matures later than the anterior sclera, and these changes of experimental myopia have been described as delayed maturation of the posterior sclera [8]. Corresponding to this, the sensitive period through which deprivation can induce myopia corresponds to the maturation of the sclera [87].

At a biochemical level, several changes can be detected in the elongating myopic sclera. Collagen content and collagen synthesis in the sclera are reduced in experimental myopia, and prevention of collagen cross-linking also worsened deprivation-induced myopia but did not affect the open contralateral eyes [88]. Specifically, collagen I synthesis is reduced, with increased proportions of collagen III and collagen V, which may explain the reduced collagen fibril diameters [89]. In mammalian models of deprivation myopia, in contrast to avian models, which have different scleral structure, glycosaminoglycans (GAG) synthesis is reduced [88, 90]. Scleral metalloproteinases are upregulated in experimental myopia, further reducing collagen content [91, 92], and there is differential expression of regulating proteins (TIMPs) which can further activate metalloproteinases [88, 93]. At a cellular level too, differentiation of dormant scleral fibroblasts into contractile myofibroblasts appears to have an important role in scleral biomechanics, but the exact relevance to myopic sclera has not been established [7].

In summary, signals from the retina lead to elongation of the globe and scleral thinning through changes in the sclera which include reduced collagen production, increased viscoelasticity, remodeling and thinning, and potentially changes in cellular activity.

2. Myopic Vitreopathy

The vitreous is particularly liquefied in myopic eyes [94, 95]. Nonspecific vitreous degeneration is observed in myo-

pic eyes, but histology cannot differentiate specific myopic changes from age-related synchysis [96]. This myopic liquefaction could be because the vitreous chamber is of increased volume and production of gel components does not keep pace with the expanding chamber. In measuring the molecular components of myopic vitreous with early techniques, Berman and Michaelson [97] found reduced protein concentration, collagen content, and estimated hyaluronate concentrations in myopic vitreous compared to controls. Total protein of the vitreous was not directly measured.

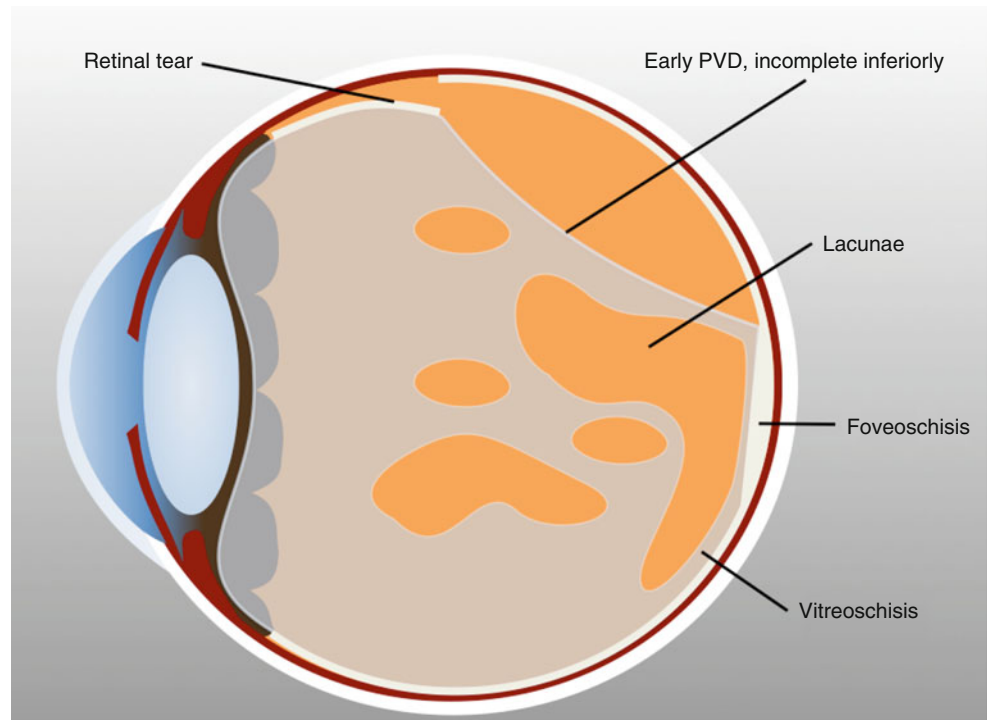
In experimental deprivation myopia in chicks, it is relevant to understand the normal development: vitreous protein concentration declines during embryonic development, as a blood ocular barrier and vitreous macromolecules form, both of which exclude plasma proteins. By hatching, there is a formed gel vitreous anterior to a 20–30 % chamber of liquid vitreous posteriorly, which is surrounded by a thin cortical layer [98, 99]. This liquid component increases to 60 % volume by adulthood. When a diffuser is used to create deprivation myopia in one eye in the first days after hatching, the vitreous chamber expands and total volume increases, with the increase entirely due to liquid vitreous [69, 100]. The gel vitreous did not change in size or protein composition, but the myopic liquid vitreous had mildly reduced protein concentration (although not significantly) [100]. This implies that in aging of the chicken vitreous, or in experimental deprivation myopia, the liquid vitreous gains in size and reduces in protein concentration.

Together these findings imply that the production of vitreous gel occurs in the vascular and cellular embryonic vitreous and that myopic ocular growth during postnatal development is not matched by production of additional vitreous gel. Thus, the elongation of the globe is accompanied by increased liquid, low-protein vitreous.

As a result, myopic vitreous has a phenotype resembling premature synchysis, and posterior vitreous detachment (PVD) occurs earlier in highly myopic eyes [101, 102]. Akiba [101] found PVD occurred around 10 years earlier in myopia > -6.0D (compared to emmetropes). Indeed, 23 % of these myopes had PVD between age 30 and 40 years, with 100 % over 70 years, compared to no PVD among emmetropes under 40 years, with PVD in 74 % of those 70–80 years old. Morita [102] found PVD to occur closer to 20 years earlier in those with axial length >26.0 mm (myopia > -8.25D), compared to age-matched controls who were low myopes, emmetropes, or hypermetropes.

Premature vitreous liquefaction occurring in younger people who have strong vitreoretinal adhesion [103] creates the conditions for an anomalous PVD and pathological vitreoretinal interactions [104]. Stirpe and Heimann [105]

Figure II.B-3 Features of myopic vitreopathy. Increased liquefaction and early synchysis result in lacunae, vitreous collapse, and premature posterior vitreous detachment (PVD) when vitreoretinal adhesion persists. This may lead to an anomalous PVD, with risk of retinal tears or maculopathy such as foveoschisis



found that among 496 highly myopic eyes undergoing retinal detachment surgery, there were 17.5 % with prominent posterior vitreous lacunae overlying posterior staphyloma with a thin but strongly adherent vitreous cortex, and among these posterior retinal breaks such as macular holes were common. Forty-six of the 496 eyes had incomplete PVD inferiorly, with partial PVD and retinal breaks in the superior globe, and a tendency for delayed postoperative retinal tears inferiorly. Similarly, Sakaguchi and colleagues [106] found vitreoschisis, preretinal proliferation, and a firmly adherent ILM during vitrectomy in a 73-year-old highly myopic woman with macular hole, requiring three layers of membrane peeling [see chapter III.B. Anomalous PVD and vitreoschisis]. Thus, PVD and peripheral retinal breaks have an ominous prognosis in myopia, due to persistence of the normal vitreoretinal adhesion of youth. These changes are summarized in Figure II.B-3.

3. Retina and Choroid

Changes in the myopic retina have long been observed by clinicians. In humans and experimental models, the choroid is thinner, and may sometimes lack the choriocapillaris, with overlying retinal thinning that is presumed to be secondary [33, 80]. The clinical relevance of these changes in the retinal periphery has been hard to define precisely [107]. The vision-threatening manifestations of this chorioretinal thinning at the macula are discussed below.

a. Retinal Lattice

Retinal lattice (also called “lattice degeneration”) is associated with myopia, particularly over $-6.0D$, and is of interest in this review of myopic vitreopathy because abnormal vitreoretinal adhesions are a key part of this pathology. As summarized by Saw [108], the evidence for an association between myopia and lattice is not strong because there are few prospective studies. In the United States, Karlin and Curtin [109] examined over 1,400 asymptomatic myopic eyes, and Pierro [110] examined 513 asymptomatic myopic patients and found an association between retinal lattice and axial length. On the other hand, Yura [111] examined 542 high myopes in Japan and did not find an association with axial length, while Celorio [112] even found the prevalence of lattice to be decreased in extreme myopia. In preoperative evaluations of 165 eyes in patients with pathological myopia ($>-8.0D$ or 26.0 mm axial length) undergoing clear lens extraction, retinal lattice was detected in 10 % of patients [113]. Histological evaluation of 308 eyes with pathological myopia revealed peripheral retinal degeneration in 31 %, cobblestone degeneration in 14 %, and retinal lattice in 5 % [114]. A variant of retinal lattice was present in an additional 11 %. A total of around 16 % was in agreement with another study of 436 eyes with myopia of $>-6.0D$, among patients with retinal detachments [115]. It is tempting to speculate that retinal lattice, as a feature most prominent in those with moderate and high myopia, represents a feature of common myopia (rather than the more severe isolated

heritable myopia). Another intriguing connection is with Stickler syndrome [see chapter I.C. Hereditary vitreo-retinopathies], where a mutation of collagen II results in vitreopathy, myopia, and widespread lattice. Because collagen II is predominant in the vitreous, this could suggest that lattice is a manifestation of a myopic vitreopathy. Prospective observation of lattice in child populations at high risk of myopia (e.g., urban Taiwan, Singapore) could establish the temporal connection between these peripheral retinal changes and the development of axial elongation.

D. The Pathologies of Myopic Vitreopathy

1. Retinal Detachment

As discussed above, myopia results in premature vitreous sychysis combined with vitreoschisis and firm vitreoretinal adhesion, creating the conditions for anomalous PVD and retinal tears with persistent vitreous traction. Retinal tears are common in myopia. Hyams and Neumann [116] found peripheral retinal breaks in 10.5 % of low myopes and 13 % of high myopes from a total of 332 asymptomatic myopes in the clinic. Consequently, there is a clear association between rhegmatogenous retinal detachment (RRD) and myopia. Two case–control studies found elevated odds ratio for myopia among those with RRD compared to controls [115, 117], and this was confirmed in a large multicenter case–control study [118]. Excluding pathological myopia, there was an odds ratio of 7.8 for myopia overall, increasing from 4.4 for myopia between $-1.0D$ and $-3.0D$ to almost ten-fold increased risk for those over $-3.0D$ [118].

Prophylaxis for retinal detachment in myopia remains controversial [119]. While laser retinopexy is recommended for retinal tears under traction before cataract surgery, prospective evidence should be collected, and trials of pharmacologic vitreolysis or primary vitrectomy could be considered.

a. Retinal Detachment After Anterior Segment Surgery

Retinal detachment is an uncommon complication after cataract surgery, with incidence rates between 0.3 and 1.2 % in the general cataract population [120–124]. This incidence of RRD after cataract surgery presumably relates to surgical forces on the anterior vitreous cortex and postoperative inflammation, resulting in anomalous PVD and vitreoretinal traction [125]. The rate of RRD after cataract surgery in myopes is of particular interest to ophthalmologists, particularly as clear lens extraction gains popularity for refractive correction. Initial studies from the 1980s using predominantly extracapsular cataract extraction (ECCE) showed pseudophakic RRD incidence of 1.6 % in myopes $> -6.0D$ (or 4.1 % in those with axial length >26.5 mm) [77]. With retrospective comparison Badr [126] found that intraocular lenses resulted in fewer RD among myopes, compared with

aphakia. A population-based case–control study [127] comparing 291 cases of RD after cataract surgery to 870 matched uncomplicated cataract operations found that the odds ratio of RD increased by 0.92 for each diopter of myopia and by 1.21 for each millimeter of axial elongation, potentially supporting the concept that axial length predicts RRD risk better than refraction [77].

However, as phacoemulsification technology improves, cataract surgery appears to be getting safer for myopes. In a large retrospective cohort of 2,356 eyes (1,519 patients) all with >27.0 mm axial length, the incidence of pseudophakic RRD after phacoemulsification was 1.5–2.2 % (the minimum value excluding RRD that could be attributed to other causes) [128]. Across a range of similar retrospective cohorts, the incidence of RRD among high myopes after phacoemulsification ranges from 0 to 8.1 % depending on the age, indication, and severity of myopia [129–134].

Clear lens extraction for myopia may have an even greater risk of RRD, simply because it is offered to younger patients with stronger vitreoretinal adhesion. In young patients receiving clear lens extraction for high myopia, some of the greatest rates of pseudophakic RD have been reported, for example, 8.1 % [129], 7.3 % with ECCE [113], and 8.0 % with very high myopia $>-15.0D$. However, some argue that these rates are not greatly higher than the incidence of spontaneous RRD among cohorts of similar severe myopia [128].

Refractive corneal surgery such as laser-assisted in-situ keratomileusis (LASIK) induces PVD in some high myopes due to physical forces from the suction ring [135]. However, LASIK appears to have a lower incidence of RRD than lens extraction, estimated 0.19 % at 10 years postoperatively among 11,594 myopes $<-10.0D$ [136]. Other posterior segment complications of LASIK for myopia also appear to be rare [137].

2. Myopic Maculopathy

Myopic maculopathy encompasses a range of vision-threatening pathologies [4, 138], many of which bear direct connection to myopic vitreopathy. The regular presence of vitreoschisis, large lacunae, and anomalous PVD results in specific myopic maculopathies such as foveoschisis and macular hole with extensive retinal detachment. There are also some indications that CNV can relate to the vitreoretinal interface [see chapter III.G. Vitreous in age-related macular degeneration], although this has not been shown in myopia [139]. Anomalous PVD with vitreomacular traction can be different in myopia than emmetropia (Video II.B-1). Pharmacologic vitreolysis [see chapter VI.A. Pharmacologic vitreolysis] and dye-assisted chromodissection [see chapter V.A.3. Chromodissection in vitreoretinal surgery] to remove vitreoschisis layers during surgery will likely assist greatly in management [140].

a. Myopic Macular Degeneration

There are two types of atrophic degenerations in high myopia: patchy atrophy is seen as a whitish lesion and well demarcated

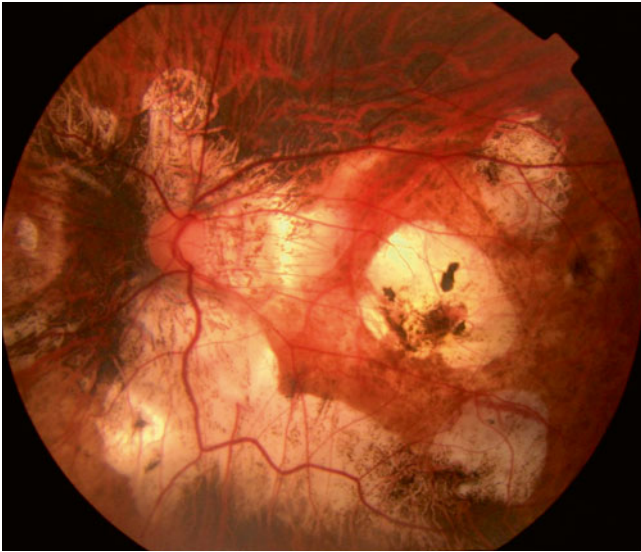


Figure II.B-4 Patchy chorioretinal atrophy. Several whitish lesions with well-identifiable margins are typically seen at the posterior pole

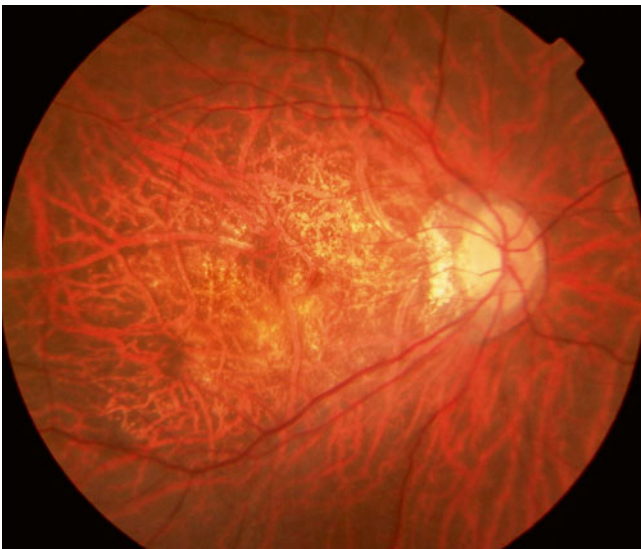


Figure II.B-5 Diffuse atrophy. The area inside the posterior staphyloma is yellowish-white, and the margin is ill-defined

(Figure II.B-4), and diffuse atrophy is yellowish-white and harder to demarcate or identify (Figure II.B-5). Lacquer cracks are whitish linear or crisscrossing lesions that sometimes are accompanied by a myopic subretinal hemorrhage. These atrophic changes appear to relate to loss of underlying choriocapillaris and splits in Bruch's membrane (lacquer cracks). The presence of lacquer cracks implies that stretching and redistribution of the scleral collagen and the underlying mechanical stretching and thinning of the choroid are part of the pathological process in myopic development. No treatment currently exists for these changes, and there are no prospective data to quantify the risk of vision loss, which can be severe.

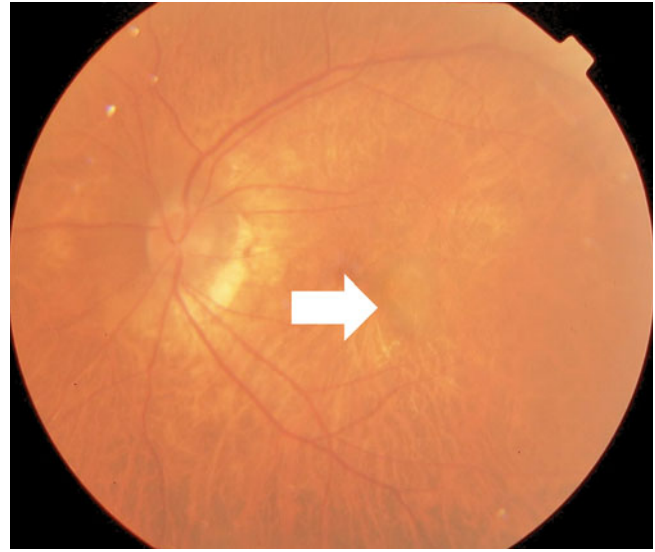


Figure II.B-6 Representative case of choroidal neovascularization (CNV) from pathological myopia. A small, grayish round lesion can be seen (*arrow*)

i. Choroidal Neovascularization

Choroidal neovascularization (CNV) is the main complication of degenerative myopic maculopathy and lacquer cracks [138]. Myopia is the second leading cause of CNV after age-related macular degeneration and the most common predisposing factor in younger patients [4]. The CNV in myopia is also referred to as a Forster-Fuchs' spot and commonly presents as a mound-shaped, grayish, small, and round lesion (Figure II.B-6). The incidence is unknown; however, Curtin and Karlin [141] reported it in 5.2 % of postmortem eyes with axial lengths exceeding 26.5 mm. Unfortunately, prospective clinical data are lacking [108]. The etiology is not fully understood, but lacquer crack formation and consequent upregulation of vascular endothelial growth factor (VEGF) may play critical roles. As in the case in AMD [see chapter III.G. Vitreous in age-related macular degeneration], the vitreous may play a role in the pathophysiology of myopic CNV, but this has yet to be investigated. While a range of treatments have been successfully offered for myopic CNV, anti-VEGF therapy currently appears to have the best risk-benefit profile with excellent visual outcomes [138].

b. Myopic Foveoschisis

Prior to the widespread use of optical coherence tomography (OCT), myopic foveoschisis was potentially mislabeled as a retinal detachment of the macula overlying a posterior staphyloma, without a macular hole [142, 143]. The term foveoschisis includes a variety of pathologies: a foveal cyst in 47 %, a lamellar hole in 29 %, and a foveal detachment in 29 % [144]. The inner retina is often split from the outer retina by traction that includes residual adherent vitreous cortex, with or without vitreoschisis [see chapter III.B.

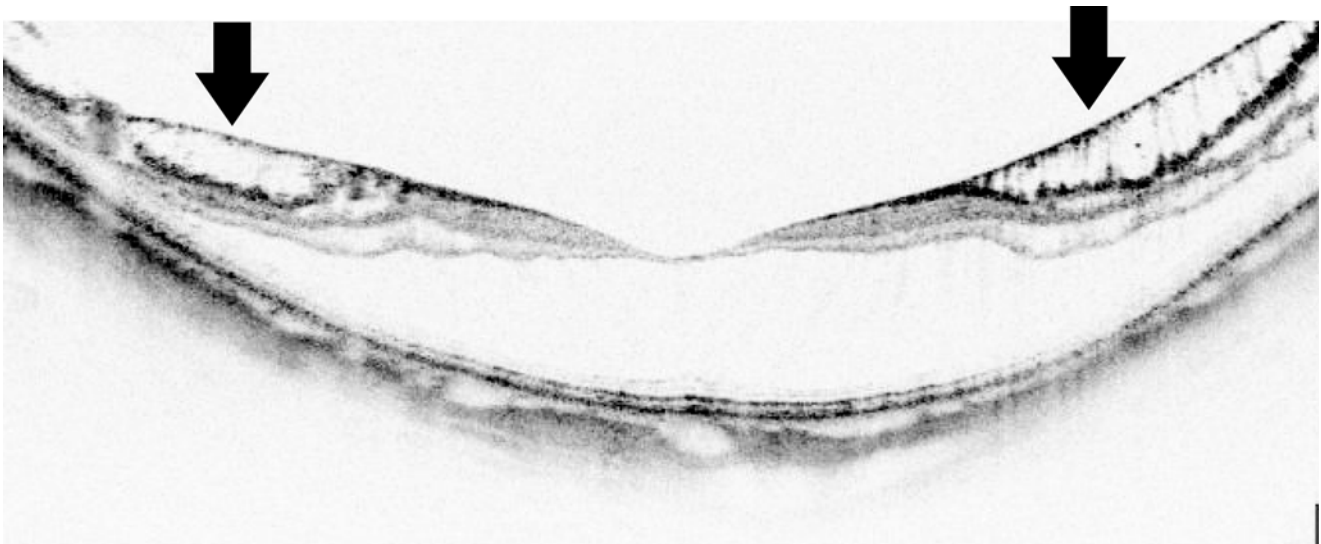


Figure II.B-7 Optical coherence tomography (OCT) appearance of an inner limiting membrane (ILM) detachment in myopic foveoschisis (*arrows*). A thin sheet is separated from the other retinal layers. Columns bridge the split between the layers



Figure II.B-8 Typical optical coherence tomography (OCT) image of retinal microfolds from retinal vascular traction (*arrows*). A tentlike lesion can be seen with retinal arterioles on the top

Anomalous PVD and vitreoschisis], and a rigid inner limiting membrane (ILM). The foveoschisis sometimes leads to macular hole formation and consequent retinal detachment [145]. The so-called ILM detachment is observed and is an indicator of the tractional force upon the ILM (Figure II.B-7) [146]. A tentlike peak of the inner retina is seen on OCT images coincident with retinal vessels and the so-called retinal microfolds (Figure II.B-8) [147]. The inner segment/outer segment (IS/OS) junction of the photoreceptors sometimes disappears in the area of the retinal detachment [148]; however, the IS/OS line is typically well preserved in the area of the retinoschisis, suggesting that the photoreceptor

function is not affected in this subtype. Retinoschisis has two stages before macular hole formation [149]. The first is the retinoschisis type, in which only retinoschisis and not a retinal detachment is present (Figure II.B-9). A retinal detachment later begins from the fovea. The next stage is the foveal detachment type (Figure II.B-10). After a while, the inner retina above the detachment is stretched and torn (Figure II.B-11). This is the appearance of a macular hole as a result of retinoschisis with a retinal detachment. The OCT images from these myopic eyes led to the hypothesis that the inner retina is less flexible than the outer retina because the vitreous cortex adheres to the retina [149]. The pattern

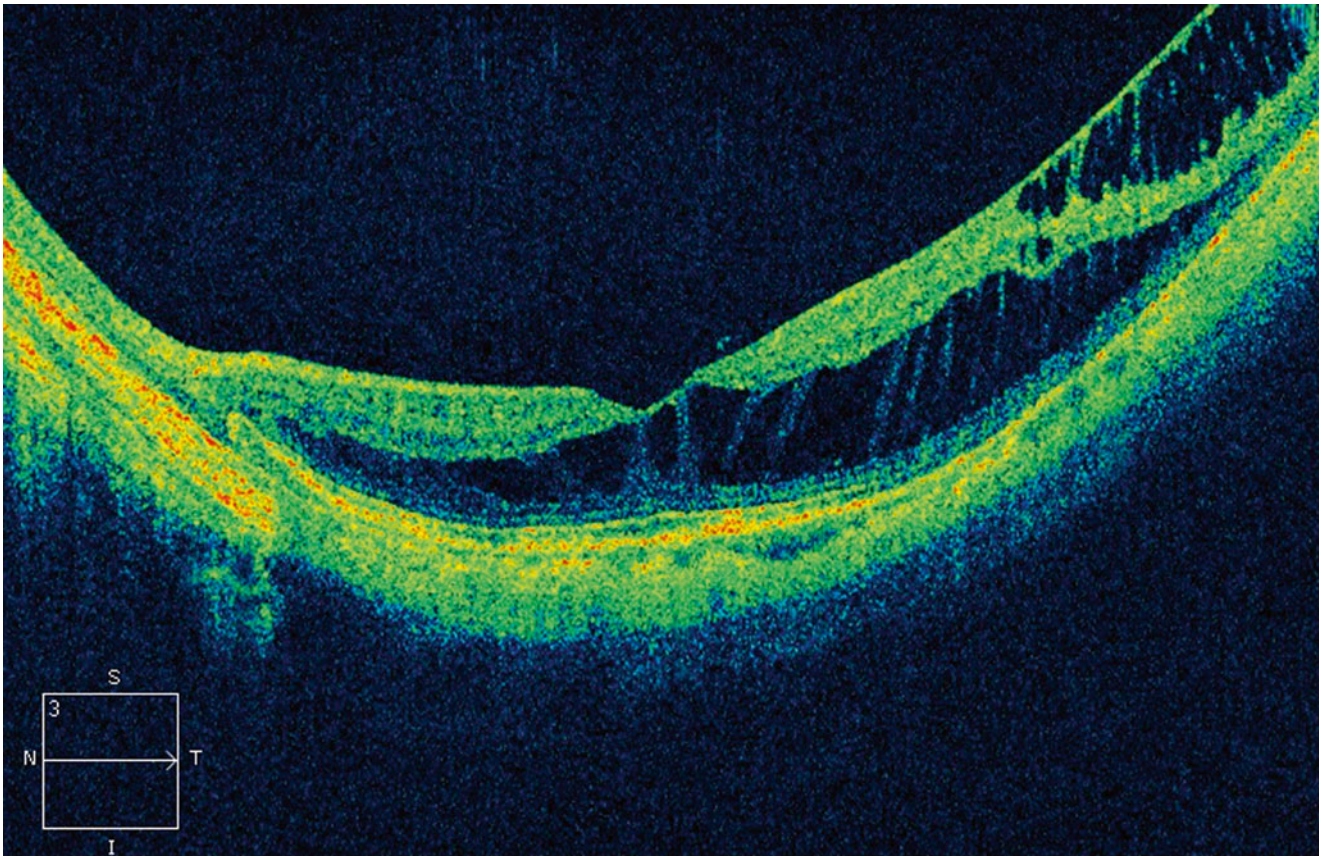


Figure II.B-9 Optical coherence tomography (OCT) image of retinoschisis type of myopic foveoschisis. The inner and outer retina is split and connected by columns. The photoreceptors are still attached to the retinal pigment epithelium (RPE)

of ILM detachments illustrates the underlying traction from the ILM, which is anchored at blood vessels on the retinal surface (Figure II.B-7) [146, 147]. An OCT study of over 200 highly myopic eyes reported ILM detachments in 6 %, retinoschisis in 13.5 %, and retinal vascular microfolds in 20 % [150].

c. Premacular Membranes

Premacular membrane (PMM) formation and retinal thickening are common in highly myopic eyes. The membrane is often difficult to find without OCT. A PMM sometimes causes retinoschisis with retinal wrinkling or macular lamellar holes (i.e., distorted foveal contour without full thickness macular hole) [144]. Histological membrane specimens from macular holes and myopic foveoschisis revealed a thin collagenous vitreoschisis and a fibroblast PMM in many myopic eyes [106, 151].

d. Macular Hole

Macular holes may develop more frequently in highly myopic eyes, and while vitrectomy appears to be successful, it

can be difficult to judge closure clinically on an atrophic myopic macula [152]. OCT has indicated that the presence of schisis in the retina surrounding the macular hole is of poor prognosis [153].

i. Macular Hole with Retinal Detachment

Retinal detachments from the macular hole are a typical finding in high myopia and uncommon in other settings besides trauma (see Figure II.B-12). Residual adherent vitreous cortex (vitreoschisis) on the retinal surface around the hole causes tangential traction that generates an anterior vector in a deep staphyloma [154]. Releasing the retinal traction is critical to anatomic success, and vitrectomy with vitreous cortex and membrane removal is the most common treatment.

e. Paravascular Retinal Microholes

A paravascular microhole and consequent retinal detachment are specific to high myopia. They are typically small, round, or oval, and sometimes there are multiple retinal

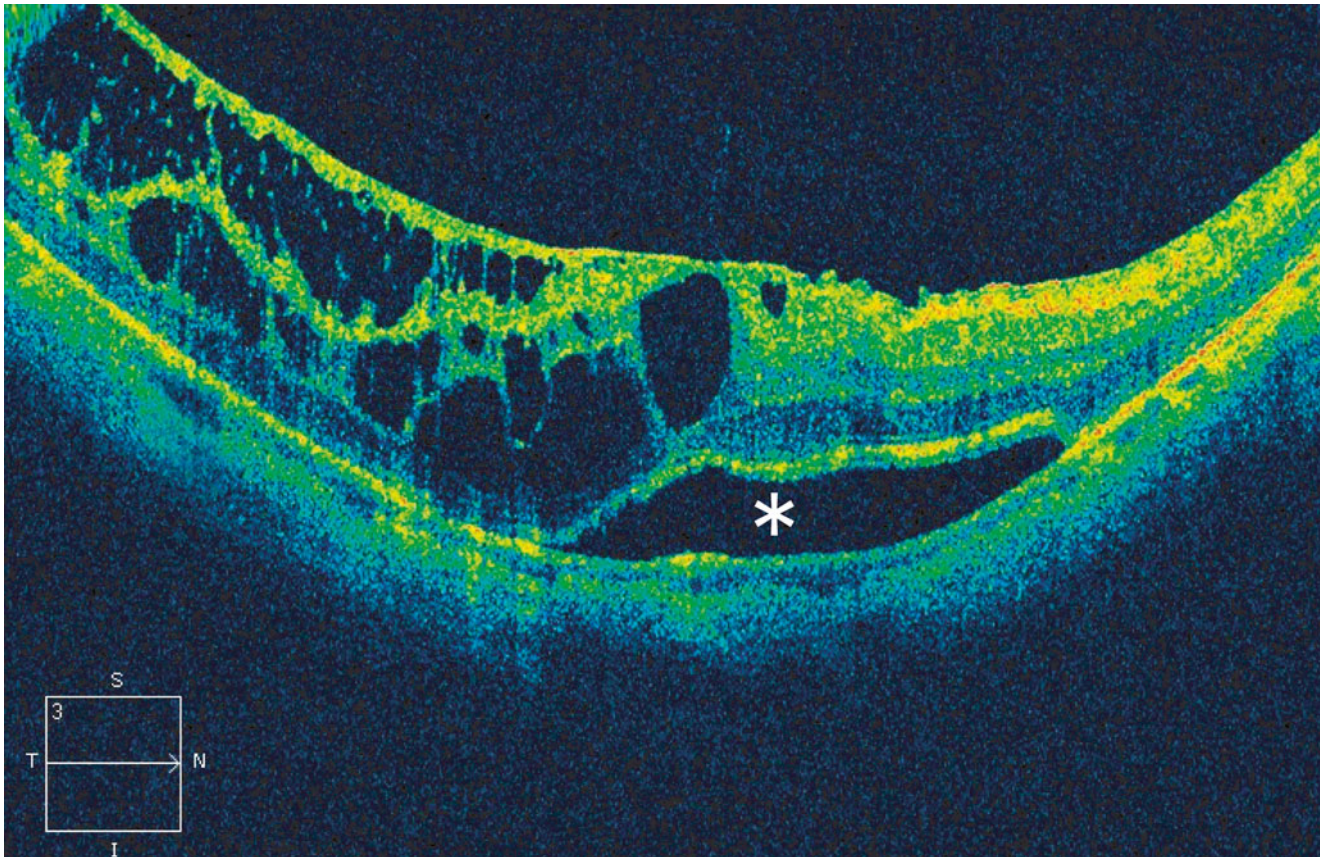


Figure II.B-10 Typical appearance of the foveal detachment type of myopic foveoschisis. The photoreceptors detach from the retinal pigment epithelium (RPE) (*asterisk*)

holes adjacent to posterior major vessels [155]. An OCT study of highly myopic eyes reported that the incidence rates of retinal cysts and paravascular holes were 50 % and 27 %, respectively. The vitreoretinal adhesion is normally strong at the paravascular site, and traction from the vitreous is believed to be the main cause [156]. Paravascular microholes often co-localize with vascular microfolds and retinoschisis, indicating a common pathology.

3. Cataract

The effect of myopia on cataract is relevant to this discussion of vitreopathy because some cataracts may be accelerated by vitreous liquefaction and because the increased risks of cataract are not confined to pathological or high myopia.

Some of the major population-based cross-sectional and cohort studies of eye disease have addressed the connection between myopia and cataract [6]. Early case-control studies showed no meaningful association [157]. In the Blue Mountains Eye Study of Australia, a cross-sectional study of 3,654 people found that increasing severity of early-onset myopia was associated with increasing odds ratio of poste-

rior subcapsular (PSC) cataracts [158]. This same study found an increased risk of incident cataract over 5 years, particularly PSC, associated with myopia [159]. Another Australian cross-sectional study found increased risk of both nuclear and PSC cataracts among myopes [160]. In the prospective Barbados Eye Study, myopia was associated with an odds ratio of 2.8 for developing a nuclear opacity over 4 years [161] but not PSC or cortical cataract [162]. In the United States, the Beaver Dam Eye Study reported that myopia was associated with prevalent nuclear cataract, but not the 5-year incidence of cataract [163], although the incidence of cataract surgery was higher in myopes [164] by an OR of 1.89.

To summarize, cataracts and myopia may be associated because nuclear sclerosis causes myopia; however, the prospective cohort studies also indicate that cataract development is accelerated in those with longstanding myopia. It is possible that an increasingly liquefied vitreous in myopic vitreopathy is a mechanism by which retinal oxygenation can affect the lens more in myopia, accelerating cataract development [see chapter IV.B. Oxygen in vitreoretinal physiology and pathology].

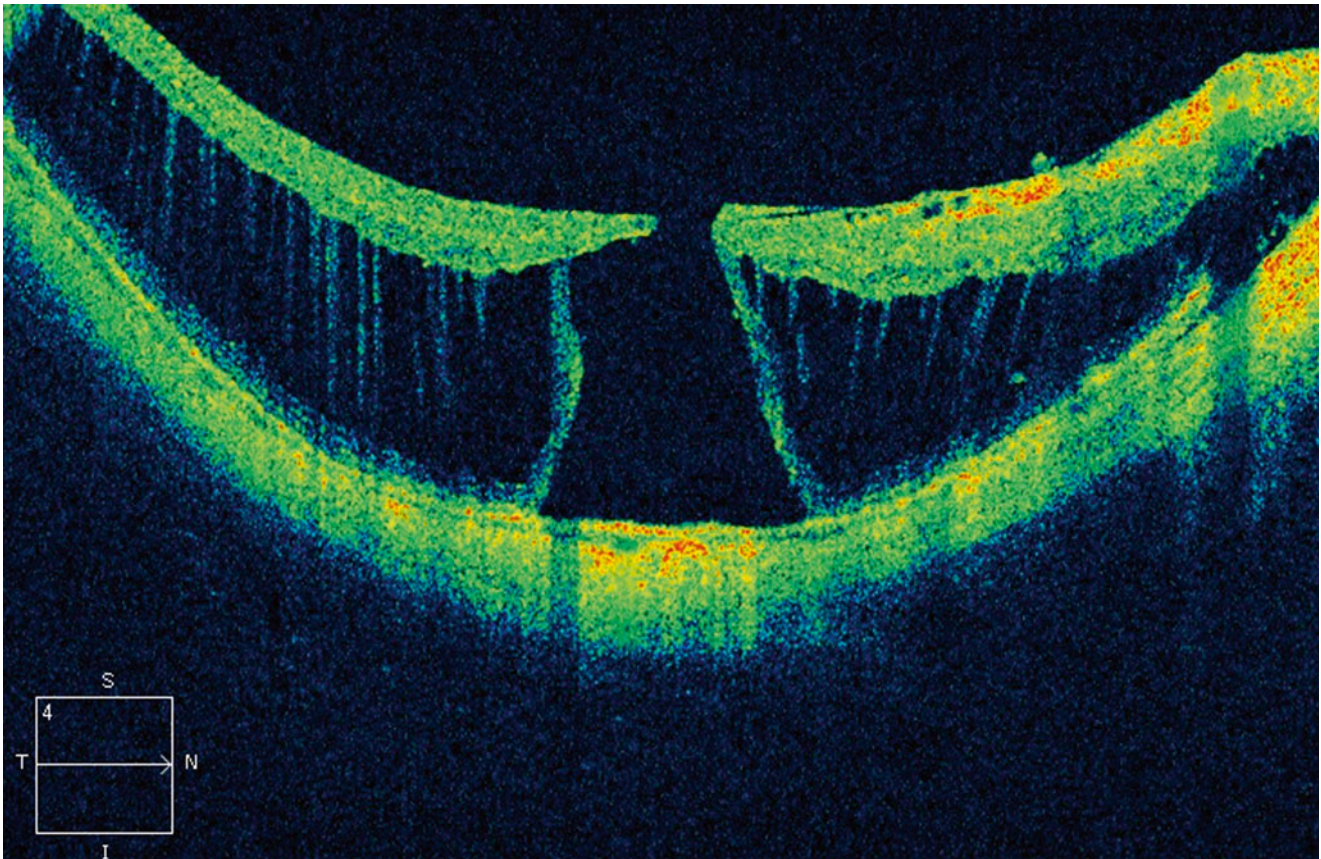


Figure II.B-11 A macular hole surrounded by retinoschisis. This type often occurs after myopic foveoschisis and with underlying traction. This type is at high risk for retinal detachment

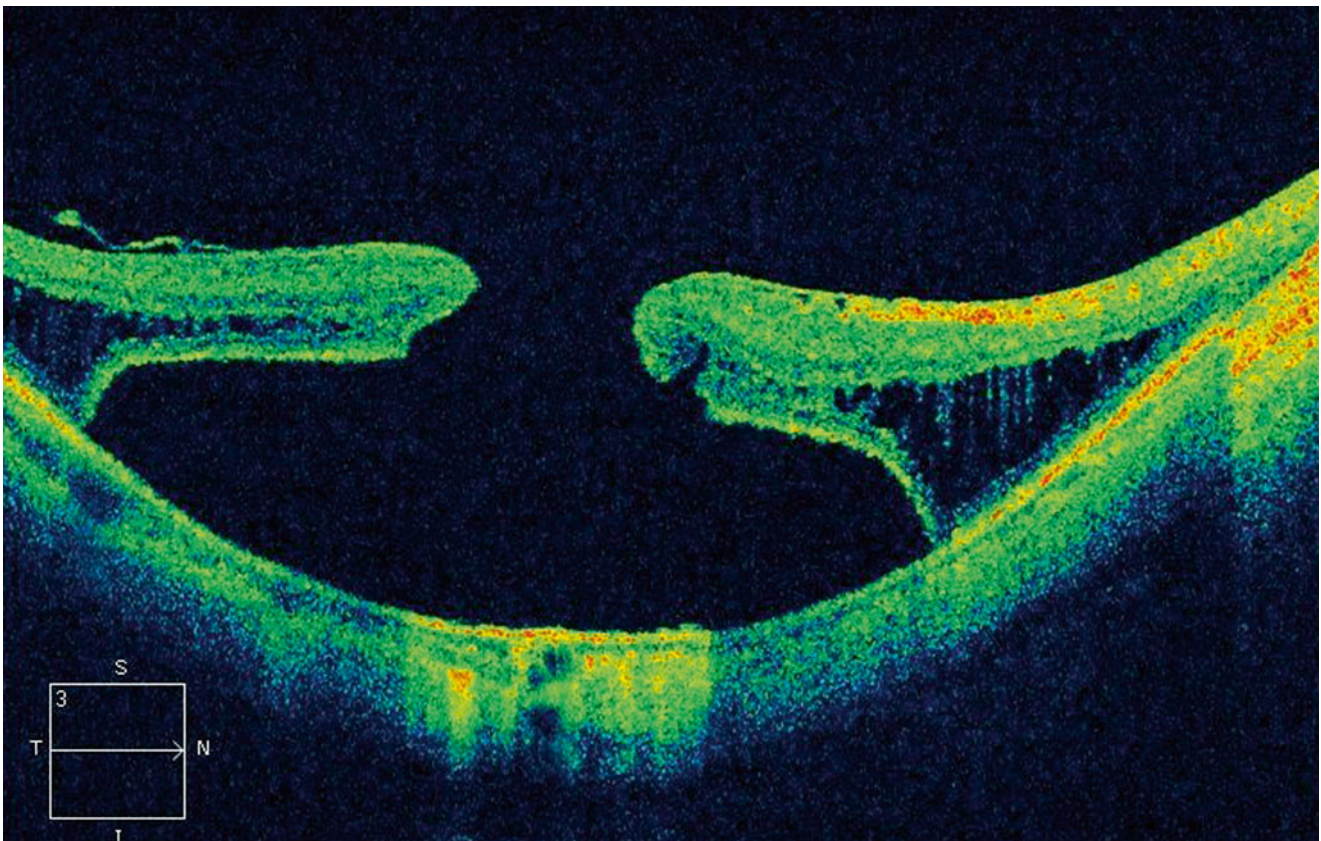


Figure II.B-12 Optical coherence tomograph (OCT) of a myopic staphyloma with full thickness macular hole and central retinal detachment

Abbreviations

CNV	Choroidal neovascularization
ECCE	Extracapsular cataract extraction
GAG	Glycosaminoglycans
ILM	Inner limiting membrane
IOP	Intraocular pressure
IS/OS	Inner segment/outer segment (junction of photoreceptors)
LAMA2	Laminin alpha-2 subunit gene
LASIK	Laser-assisted in-situ keratomileusis
OCT	Optical coherence tomography
OR	Odds ratio
PMM	Premacular (formerly “epiretinal”) membrane
PSC	Posterior subcapsular cataract
PVD	Posterior vitreous detachment
RD	Retinal detachment
RRD	Rhegmatogenous retinal detachment
TIMPs	Tissue inhibitors of metalloproteases
UV	Ultraviolet
VEGF	Vascular endothelial growth

References

- Resnikoff S. Global magnitude of visual impairment caused by uncorrected refractive errors in 2004. *Bull World Health Organ.* 2008;86:63–70.
- Klaver CC, Wolfs RC, Vingerling JR, Hofman A, de Jong PT. Age-specific prevalence and causes of blindness and visual impairment in an older population: the Rotterdam Study. *Arch Ophthalmol.* 1998;116:653–8.
- Iwase A, Araie M, Tomidokoro A, Yamamoto T, Shimizu H, Kitazawa Y, et al. Prevalence and causes of low vision and blindness in a Japanese adult population: the Tajimi Study. *Ophthalmology.* 2006;113:1354–62.
- Ohno-Matsui K, Ikuno Y, Yasuda M, Murata T, Sakamoto T, Ishibashi T. Myopic macular degeneration. In: Ryan SJ, Schachar AP, Sadda SVR, editors. *Retina*. 5th ed. London: Elsevier; 2013. p. 1256–66.
- Flitcroft DI. The complex interactions of retinal, optical and environmental factors in myopia aetiology. *Prog Retin Eye Res.* 2012; 31:622–60.
- Saw SM, Gazzard G, Shih-Yen EC, Chua WH. Myopia and associated pathological complications. *Ophthalmic Physiol Opt.* 2005; 25:381–91.
- McBrien NA, Jobling AI, Gentle A. Biomechanics of the sclera in myopia: extracellular and cellular factors. *Optom Vis Sci.* 2009; 86:E23–30.
- Wallman J, Winawer J. Homeostasis of eye growth and the question of myopia. *Neuron.* 2004;43:447–68.
- Diether S, Schaeffel F. Local changes in eye growth induced by imposed local refractive error despite active accommodation. *Vision Res.* 1997;37:659–68.
- Ip JM, Huynh SC, Kifley A, Rose KA, Morgan IG, Varma R, et al. Variation of the contribution from axial length and other oculometric parameters to refraction by age and ethnicity. *Invest Ophthalmol Vis Sci.* 2007;48:4846–53.
- Meng W, Butterworth J, Malecaze F, Calvas P. Axial length: an underestimated endophenotype of myopia. *Med Hypotheses.* 2010;74:252–3.
- Fricke TR, Holden BA, Wilson DA, Schlenker G, Naidoo KS, Resnikoff S, et al. Global cost of correcting vision impairment from uncorrected refractive error. *Bull World Health Organ.* 2012; 90:728–38.
- Pan CW, Ramamurthy D, Saw SM. Worldwide prevalence and risk factors for myopia. *Ophthalmic Physiol Opt.* 2012;32:3–16.
- Attebo K, Ivers RQ, Mitchell P. Refractive errors in an older population: the Blue Mountains Eye Study. *Ophthalmology.* 1999;106: 1066–72.
- Rahi JS, Cumberland PM, Peckham CS. Myopia over the life-course: prevalence and early life influences in the 1958 British birth cohort. *Ophthalmology.* 2011;118:797–804.
- Sperduto RD, Seigel D, Roberts J, Rowland M. Prevalence of myopia in the United States. *Arch Ophthalmol.* 1983;101:405–7.
- Framingham Offspring Eye Study G. Familial aggregation and prevalence of myopia in the Framingham Offspring Eye Study. *Arch Ophthalmol.* 1996;114:326–32.
- Katz J, Tielsch JM, Sommer A. Prevalence and risk factors for refractive errors in an adult inner city population. *Invest Ophthalmol Vis Sci.* 1997;38:334–40.
- Wang Q, Klein BE, Klein R, Moss SE. Refractive status in the Beaver Dam Eye Study. *Invest Ophthalmol Vis Sci.* 1994;35:4344–7.
- Wu SY, Nemesure B, Leske MC. Refractive errors in a black adult population: the Barbados Eye Study. *Invest Ophthalmol Vis Sci.* 1999;40:2179–84.
- Tarczy-Hornoch K, Ying-Lai M, Varma R, Los Angeles Latino Eye Study G. Myopic refractive error in adult Latinos: the Los Angeles Latino Eye Study. *Invest Ophthalmol Vis Sci.* 2006;47:1845–52.
- Sawada A, Tomidokoro A, Araie M, Iwase A, Yamamoto T, Tajimi Study G. Refractive errors in an elderly Japanese population: the Tajimi study. *Ophthalmology.* 2008;115:363–70.e3.
- Xu L, Li J, Cui T, Hu A, Fan G, Zhang R, et al. Refractive error in urban and rural adult Chinese in Beijing. *Ophthalmology.* 2005;112:1676–83.
- Lee KE, Klein BE, Klein R. Changes in refractive error over a 5-year interval in the Beaver Dam Eye Study. *Invest Ophthalmol Vis Sci.* 1999;40:1645–9.
- Mutti DO, Zadnik K. Age-related decreases in the prevalence of myopia: longitudinal change or cohort effect? *Invest Ophthalmol Vis Sci.* 2000;41:2103–7.
- Rose K, Smith W, Morgan I, Mitchell P. The increasing prevalence of myopia: implications for Australia. *Clin Experiment Ophthalmol.* 2001;29:116–20.
- Lin LL, Shih YF, Hsiao CK, Chen CJ. Prevalence of myopia in Taiwanese schoolchildren: 1983 to 2000. *Ann Acad Med Singapore.* 2004;33:27–33.
- Vitale S, Sperduto RD, Ferris 3rd FL. Increased prevalence of myopia in the United States between 1971–1972 and 1999–2004. *Arch Ophthalmol.* 2009;127:1632–9.
- Morgan RW, Speakman JS, Grimshaw SE. Inuit myopia: an environmentally induced “epidemic”? *Can Med Assoc J.* 1975;112:575–7.
- van Rens GH, Arkeell SM. Refractive errors and axial length among Alaskan Eskimos. *Acta Ophthalmol (Copenh).* 1991;69:27–32.
- Tay MT, Au Eong KG, Ng CY, Lim MK. Myopia and educational attainment in 421,116 young Singaporean males. *Ann Acad Med Singapore.* 1992;21:785–91.
- Bar Dayan Y, Levin A, Morad Y, Grotto I, Ben-David R, Goldberg A, et al. The changing prevalence of myopia in young adults: a 13-year series of population-based prevalence surveys. *Invest Ophthalmol Vis Sci.* 2005;46:2760–5.
- Morgan IG, Ohno-Matsui K, Saw S-M. Myopia. *Lancet.* 2012;379:1739–48.

34. Matsumura H, Hirai H. Prevalence of myopia and refractive changes in students from 3 to 17 years of age. *Surv Ophthalmol*. 1999;44 Suppl 1:S109–15.
35. Wu MM, Edwards MH. The effect of having myopic parents: an analysis of myopia in three generations. *Optom Vis Sci*. 1999;76:387–92.
36. Mutti DO, Zadnik K, Adams AJ. Myopia. The nature versus nurture debate goes on. *Invest Ophthalmol Vis Sci*. 1996;37:952–7.
37. Morgan I, Rose K. How genetic is school myopia? *Prog Retin Eye Res*. 2005;24:1–38.
38. Guggenheim JA, Kirov G, Hodson SA. The heritability of high myopia: a reanalysis of Goldschmidt's data. *J Med Genet*. 2000;37:227–31.
39. Ibay G, Doan B, Reider L, Dana D, Schlifka M, Hu H, et al. Candidate high myopia loci on chromosomes 18p and 12q do not play a major role in susceptibility to common myopia. *BMC Med Genet*. 2004;5:20.
40. Mutti DO, Mitchell GL, Moeschberger ML, Jones LA, Zadnik K. Parental myopia, near work, school achievement, and children's refractive error. *Invest Ophthalmol Vis Sci*. 2002;43:3633–40.
41. Zadnik K, Satariano WA, Mutti DO, Sholtz RI, Adams AJ. The effect of parental history of myopia on children's eye size. *JAMA*. 1994;271:1323–7.
42. Ojaimi E, Morgan IG, Robaei D, Rose KA, Smith W, Rochtchina E, et al. Effect of stature and other anthropometric parameters on eye size and refraction in a population-based study of Australian children. *Invest Ophthalmol Vis Sci*. 2005;46:4424–9.
43. Hammond CJ, Andrew T, Mak YT, Spector TD. A susceptibility locus for myopia in the normal population is linked to the PAX6 gene region on chromosome 11: a genomewide scan of dizygotic twins. *Am J Hum Genet*. 2004;75:294–304.
44. Stambolian D, Ibay G, Reider L, Dana D, Moy C, Schlifka M, et al. Genomewide linkage scan for myopia susceptibility loci among Ashkenazi Jewish families shows evidence of linkage on chromosome 22q12. *Am J Hum Genet*. 2004;75:448–59.
45. Fan Q, Barathi VA, Cheng CY, Zhou X, Meguro A, Nakata I, et al. Genetic variants on chromosome 1q41 influence ocular axial length and high myopia. *PLoS Genet*. 2012;8:e1002753.
46. Verhoeven VJ, Hysi PG, Saw SM, Vitart V, Mirshahi A, Guggenheim JA, et al. Large scale international replication and meta-analysis study confirms association of the 15q14 locus with myopia. The CREAM consortium. *Hum Genet*. 2012;131:1467–80.
47. Verhoeven VJM, Hysi PG, Wojciechowski R, Fan Q, Guggenheim JA, Höhn R, et al. Genome-wide meta-analyses of multiethnicity cohorts identify multiple new susceptibility loci for refractive error and myopia. *Nat Genet*. 2013;45:314–8.
48. Kiefer AK, Tung JY, Do CB, Hinds DA, Mountain JL, Francke U, et al. Genome-wide analysis points to roles for extracellular matrix remodeling, the visual cycle, and neuronal development in myopia. *PLoS Genet*. 2013;9:e1003299.
49. Cheng CY, Schache M, Ikram MK, Young TL, Guggenheim JA, Vitart V, et al. Nine loci for ocular axial length identified through genome-wide association studies, including shared loci with refractive error. *Am J Hum Genet*. 2013;93:264–77.
50. Wiesel TN, Raviola E. Myopia and eye enlargement after neonatal lid fusion in monkeys. *Nature*. 1977;266:66–8.
51. Hoyt CS, Stone RD, Fromer C, Billson FA. Monocular axial myopia associated with neonatal eyelid closure in human infants. *Am J Ophthalmol*. 1981;91:197–200.
52. Wildsoet C, Wallman J. Choroidal and scleral mechanisms of compensation for spectacle lenses in chicks. *Vision Res*. 1995;35:1175–94.
53. Smith 3rd EL, Hung LF, Huang J, Blasdel TL, Humbird TL, Bockhorst KH. Effects of optical defocus on refractive development in monkeys: evidence for local, regionally selective mechanisms. *Invest Ophthalmol Vis Sci*. 2010;51:3864–73.
54. Troilo D, Gottlieb MD, Wallman J. Visual deprivation causes myopia in chicks with optic nerve section. *Curr Eye Res*. 1987;6:993–9.
55. Smith 3rd EL, Huang J, Hung LF, Blasdel TL, Humbird TL, Bockhorst KH. Hemiretinal form deprivation: evidence for local control of eye growth and refractive development in infant monkeys. *Invest Ophthalmol Vis Sci*. 2009;50:5057–69.
56. Ashby R, McCarthy CS, Maleszka R, Megaw P, Morgan IG. A muscarinic cholinergic antagonist and a dopamine agonist rapidly increase ZENK mRNA expression in the form-deprived chicken retina. *Exp Eye Res*. 2007;85:15–22.
57. Mertz JR, Wallman J. Choroidal retinoic acid synthesis: a possible mediator between refractive error and compensatory eye growth. *Exp Eye Res*. 2000;70:519–27.
58. Junghans BM, Crewther SG, Liang H, Crewther DP. A role for choroidal lymphatics during recovery from form deprivation myopia? *Optom Vis Sci*. 1999;76:796–803.
59. Tan NW, Saw SM, Lam DS, Cheng HM, Rajan U, Chew SJ. Temporal variations in myopia progression in Singaporean children within an academic year. *Optom Vis Sci*. 2000;77:465–72.
60. Gwiazda J, Thorn F, Bauer J, Held R. Myopic children show insufficient accommodative response to blur. *Invest Ophthalmol Vis Sci*. 1993;34:690–4.
61. Gwiazda JE. Accommodation and related risk factors associated with myopia progression and their interaction with treatment in COMET children. *Invest Ophthalmol Vis Sci*. 2004;45:2143–51.
62. Mutti DO, Mitchell GL, Hayes JR, Jones LA, Moeschberger ML, Cotter SA, et al. Accommodative lag before and after the onset of myopia. *Invest Ophthalmol Vis Sci*. 2006;47:837–46.
63. Seidel D, Gray LS, Heron G. The effect of monocular and binocular viewing on the accommodation response to real targets in emmetropia and myopia. *Optom Vis Sci*. 2005;82:279–85.
64. Rose KA, Morgan IG, Ip J, Kifley A, Huynh S, Smith W, et al. Outdoor activity reduces the prevalence of myopia in children. *Ophthalmology*. 2008;115:1279–85.
65. Rose KA, Morgan IG, Smith W, Burlutsky G, Mitchell P, Saw SM. Myopia, lifestyle, and schooling in students of Chinese ethnicity in Singapore and Sydney. *Arch Ophthalmol*. 2008;126:527–30.
66. Jones LA, Sinnott LT, Mutti DO, Mitchell GL, Moeschberger ML, Zadnik K. Parental history of myopia, sports and outdoor activities, and future myopia. *Invest Ophthalmol Vis Sci*. 2007;48:3524–32.
67. Wu PC, Tsai CL, Wu HL, Yang YH, Kuo HK. Outdoor activity during class recess reduces myopia onset and progression in school children. *Ophthalmology*. 2013;120:1080–5.
68. Curtin BJ. The myopias—basic science and clinical management. Philadelphia: Harper & Row; 1985.
69. Seltner RL, Sivak JG. A role for the vitreous humor in experimentally-induced myopia. *Am J Optom Physiol Opt*. 1987;64:953–7.
70. Snead MP. Hereditary vitreopathy. *Eye (Lond)*. 1996;10(Pt 6):653–63.
71. Wilkinson JL, Hodos W. Intraocular pressure and eye enlargement in chicks. *Curr Eye Res*. 1991;10:163–8.
72. Quinn GE, Berlin JA, Young TL, Ziylan S, Stone RA. Association of intraocular pressure and myopia in children. *Ophthalmology*. 1995;102:180–5.
73. Phillips JR, Khalaj M, McBrien NA. Induced myopia associated with increased scleral creep in chick and tree shrew eyes. *Invest Ophthalmol Vis Sci*. 2000;41:2028–34.
74. Phillips JR. Pressure-induced changes in axial eye length of chick and tree shrew: significance of myofibroblasts in the sclera. *Invest Ophthalmol Vis Sci*. 2004;45:758–63.
75. Pan CW, Wong TY, Chang L, Lin XY, Lavanya R, Zheng YF, et al. Ocular biometry in an urban Indian population: the Singapore

- Indian Eye Study (SINDI). *Invest Ophthalmol Vis Sci.* 2011;52:6636–42.
76. Shufelt C, Fraser-Bell S, Ying-Lai M, Torres M, Varma R, Los Angeles Latino Eye Study G. Refractive error, ocular biometry, and lens opalescence in an adult population: the Los Angeles Latino Eye Study. *Invest Ophthalmol Vis Sci.* 2005;46:4450–60.
 77. Percival SP. Redefinition of high myopia: the relationship of axial length measurement to myopic pathology and its relevance to cataract surgery. *Dev Ophthalmol.* 1987;14:42–6.
 78. Curtin BJ, Teng CC. Scleral changes in pathological myopia. *Trans Am Acad Ophthalmol Otolaryngol.* 1958;62:777–88; discussion 88–90.
 79. Curtin BJ. The posterior staphyloma of pathologic myopia. *Trans Am Ophthalmol Soc.* 1977;75:67–86.
 80. Curtin BJ, Iwamoto T, Renaldo DP. Normal and staphylomatous sclera of high myopia. An electron microscopic study. *Arch Ophthalmol.* 1979;97:912–5.
 81. Avetisov ES, Savitskaya NF, Vinetskaya MI, Iomdina EN. A study of biochemical and biomechanical qualities of normal and myopic eye sclera in humans of different age groups. *Metab Pediatr Syst Ophthalmol.* 1983;7:183–8.
 82. Funata M, Tokoro T. Scleral change in experimentally myopic monkeys. *Graefes Arch Clin Exp Ophthalmol.* 1990;228:174–9.
 83. McBrien NA, Cornell LM, Gentle A. Structural and ultrastructural changes to the sclera in a mammalian model of high myopia. *Invest Ophthalmol Vis Sci.* 2001;42:2179–87.
 84. McBrien NA, Lawlor P, Gentle A. Scleral remodeling during the development of and recovery from axial myopia in the tree shrew. *Invest Ophthalmol Vis Sci.* 2000;41:3713–9.
 85. Phillips JR, McBrien NA. Form deprivation myopia: elastic properties of sclera. *Ophthalmic Physiol Opt.* 1995;15:357–62.
 86. Siegwart Jr JT, Norton TT. Regulation of the mechanical properties of tree shrew sclera by the visual environment. *Vision Res.* 1999;39:387–407.
 87. Siegwart Jr JT, Norton TT. The susceptible period for deprivation-induced myopia in tree shrew. *Vision Res.* 1998;38:3505–15.
 88. McBrien N. Role of the sclera in the development and pathological complications of myopia. *Prog Retin Eye Res.* 2003;22:307–38.
 89. Gentle A, Liu Y, Martin JE, Conti GL, McBrien NA. Collagen gene expression and the altered accumulation of scleral collagen during the development of high myopia. *J Biol Chem.* 2003;278:16587–94.
 90. Norton TT, Rada JA. Reduced extracellular matrix in mammalian sclera with induced myopia. *Vision Res.* 1995;35:1271–81.
 91. Rada JA, Brenza HL. Increased latent gelatinase activity in the sclera of visually deprived chicks. *Invest Ophthalmol Vis Sci.* 1995;36:1555–65.
 92. Guggenheim JA, McBrien NA. Form-deprivation myopia induces activation of scleral matrix metalloproteinase-2 in tree shrew. *Invest Ophthalmol Vis Sci.* 1996;37:1380–95.
 93. Siegwart Jr JT, Norton TT. Steady state mRNA levels in tree shrew sclera with form-deprivation myopia and during recovery. *Invest Ophthalmol Vis Sci.* 2001;42:1153–9.
 94. Nguyen N, Sebag J. Myopic vitreopathy: significance in anomalous PVD and vitreoretinal disorders. In: Midena E, editor. *Myopia and related diseases.* New York: Ophthalmic Communications Society; 2005. p. 137–45.
 95. Sebag J, Yee KMP. Vitreous: from biochemistry to clinical relevance. In: Tasman W, Jaeger EA, editors. *Duane's foundations of clinical ophthalmology, vol. 1.* Philadelphia: Lippincott Williams & Wilkins; 2007.
 96. Van Alphen GWHM. Emmetropization in the primate eye. In: Boch G, Widdows K, editors. *Myopia and the control of eye growth.* New York: Wiley; 1990. p. 115.
 97. Berman ER, Michaelson IC. The chemical composition of the human vitreous body as related to age and myopia. *Exp Eye Res.* 1964;3:9–15.
 98. Balazs EA, Toth LZ, Jutheden GM, Collins BA. Cytological and biochemical studies on the developing chicken vitreous. *Exp Eye Res.* 1965;4:237–48.
 99. Beebe DC, Latker CH, Jebens HA, Johnson MC, Feagans DE, Feinberg RN. Transport and steady-state concentration of plasma proteins in the vitreous humor of the chicken embryo: implications for the mechanism of eye growth during early development. *Dev Biol.* 1986;114:361–8.
 100. Pickett-Seltner RL, Doughty MJ, Pasternak JJ, Sivak JG. Proteins of the vitreous humor during experimentally induced myopia. *Invest Ophthalmol Vis Sci.* 1992;33:3424–9.
 101. Akiba J. Prevalence of posterior vitreous detachment in high myopia. *Ophthalmology.* 1993;100:1384–8.
 102. Morita H, Funata M, Tokoro T. A clinical study of the development of posterior vitreous detachment in high myopia. *Retina.* 1995;15:117–24.
 103. Sebag J. Age-related differences in the human vitreoretinal interface. *Arch Ophthalmol.* 1991;109:966–71.
 104. Sebag J. Anomalous posterior vitreous detachment: a unifying concept in vitreo-retinal disease. *Graefes Arch Clin Exp Ophthalmol.* 2004;42:690–8.
 105. Stirpe M, Heimann K. Vitreous changes and retinal detachment in highly myopic eyes. *Eur J Ophthalmol.* 1996;6:50–8.
 106. Sakaguchi H, Ikuno Y, Choi JS, Ohji M, Tano T. Multiple components of epiretinal tissues detected by triamcinolone and indocyanine green in macular hole and retinal detachment as a result of high myopia. *Am J Ophthalmol.* 2004;138:1079–81.
 107. Burton TC. The influence of refractive error and lattice degeneration on the incidence of retinal detachment. *Trans Am Ophthalmol Soc.* 1989;87:143–55; discussion 55–7.
 108. Saw SM, Chua WH, Gazzard G, Koh D, Tan DT, Stone RA. Eye growth changes in myopic children in Singapore. *Br J Ophthalmol.* 2005;89:1489–94.
 109. Karlin DB, Curtin BJ. Peripheral chorioretinal lesions and axial length of the myopic eye. *Am J Ophthalmol.* 1976;81:625–35.
 110. Pierro L, Camesasca FI, Mischi M, Brancato R. Peripheral retinal changes and axial myopia. *Retina.* 1992;12:12–7.
 111. Yura T. The relationship between the types of axial elongation and the prevalence of lattice degeneration of the retina. *Acta Ophthalmol Scand.* 1998;76:90–5.
 112. Celorio JM, Pruett RC. Prevalence of lattice degeneration and its relation to axial length in severe myopia. *Am J Ophthalmol.* 1991;111:20–3.
 113. Barraquer C, Cavelier C, Mejia LF. Incidence of retinal detachment following clear-lens extraction in myopic patients. Retrospective analysis. *Arch Ophthalmol.* 1994;112:336–9.
 114. Grossniklaus HE, Green WR. Pathologic findings in pathologic myopia. *Retina.* 1992;12:127–33.
 115. Ogawa A, Tanaka M. The relationship between refractive errors and retinal detachment—analysis of 1,166 retinal detachment cases. *Jpn J Ophthalmol.* 1988;32:310–5.
 116. Hyams SW, Neumann E. Peripheral retina in myopia. With particular reference to retinal breaks. *Br J Ophthalmol.* 1969;53:300–6.
 117. Austin KL, Palmer JR, Seddon JM, Glynn RJ, Rosenberg L, Gragoudas ES, et al. Case-control study of idiopathic retinal detachment. *Int J Epidemiol.* 1990;19:1045–50.
 118. Risk factors for idiopathic rhegmatogenous retinal detachment. The Eye Disease Case-control Study Group. *Am J Epidemiol.* 1993;137:749–57.
 119. Mehdizadeh M, Nowroozadeh MH. Effect of preoperative laser therapy of retinal degeneration on retinal detachment after phacemulsification. *J Cataract Refract Surg.* 2009;35:960–1; author reply 1–2.
 120. Sheu SJ, Ger LP, Chen JF. Axial myopia is an extremely significant risk factor for young-aged pseudophakic retinal detachment in Taiwan. *Retina.* 2006;26:322–7.

121. Russell M, Gaskin B, Russell D, Polkinghorne PJ. Pseudophakic retinal detachment after phacoemulsification cataract surgery: ten-year retrospective review. *J Cataract Refract Surg.* 2006;32:442–5.
122. Boberg-Ans G, Henning V, Villumsen J, la Cour M. Longterm incidence of rhegmatogenous retinal detachment and survival in a defined population undergoing standardized phacoemulsification surgery. *Acta Ophthalmol Scand.* 2006;84:613–8.
123. Bhagwandien AC, Cheng YY, Wolfs RC, van Meurs JC, Luyten GP. Relationship between retinal detachment and biometry in 4262 cataractous eyes. *Ophthalmology.* 2006;113:643–9.
124. Norregaard JC, Thoning H, Andersen TF, Bernth-Petersen P, Javitt JC, Anderson GF. Risk of retinal detachment following cataract extraction: results from the International Cataract Surgery Outcomes Study. *Br J Ophthalmol.* 1996;80:689–93.
125. Ripandelli G, Coppe AM, Parisi V, Olzi D, Scassa C, Chiaravalloti A, et al. Posterior vitreous detachment and retinal detachment after cataract surgery. *Ophthalmology.* 2007;114:692–7.
126. Badr IA, Hussain HM, Jabak M, Wagoner MD. Extracapsular cataract extraction with or without posterior chamber intraocular lenses in eyes with cataract and high myopia. *Ophthalmology.* 1995;102:1139–43.
127. Tielsch JM, Legro MW, Cassard SD, Schein OD, Javitt JC, Singer AE, et al. Risk factors for retinal detachment after cataract surgery. A population-based case-control study. *Ophthalmology.* 1996;103:1537–45.
128. Neuhann IM, Neuhann TF, Heimann H, Schmickler S, Gerl RH, Foerster MH. Retinal detachment after phacoemulsification in high myopia: analysis of 2356 cases. *J Cataract Refract Surg.* 2008;34:1644–57.
129. Colin J, Robinet A, Cochener B. Retinal detachment after clear lens extraction for high myopia: seven-year follow-up. *Ophthalmology.* 1999;106:2281–4; discussion 5.
130. Fernandez-Vega L, Alfonso JF, Villacampa T. Clear lens extraction for the correction of high myopia. *Ophthalmology.* 2003;110:2349–54.
131. Horgan N, Condon PI, Beatty S. Refractive lens exchange in high myopia: long term follow up. *Br J Ophthalmol.* 2005;89:670–2.
132. Alio JL, Ruiz-Moreno JM, Shabayek MH, Lugo FL, Abd El Rahman AM. The risk of retinal detachment in high myopia after small incision coaxial phacoemulsification. *Am J Ophthalmol.* 2007;144:93–8.
133. Ripandelli G, Scassa C, Parisi V, Gazzaniga D, D'Amico DJ, Stirpe M. Cataract surgery as a risk factor for retinal detachment in very highly myopic eyes. *Ophthalmology.* 2003;110:2355–61.
134. Ravalico G, Michieli C, Vattovani O, Tognetto D. Retinal detachment after cataract extraction and refractive lens exchange in highly myopic patients. *J Cataract Refract Surg.* 2003;29:39–44.
135. Luna JD, Artal MN, Reviglio VE, Pelizzari M, Diaz H, Juarez CP. Vitreoretinal alterations following laser in situ keratomileusis: clinical and experimental studies. *Graefes Arch Clin Exp Ophthalmol.* 2001;239:416–23.
136. Arevalo JF, Lasave AF, Torres F, Suarez E. Rhegmatogenous retinal detachment after LASIK for myopia of up to –10 diopters: 10 years of follow-up. *Graefes Arch Clin Exp Ophthalmol.* 2012;250:963–70.
137. Arevalo JF. Posterior segment complications after laser-assisted in situ keratomileusis. *Curr Opin Ophthalmol.* 2008;19:177–84.
138. Silva R. Myopic maculopathy: a review. *Ophthalmologica.* 2012;228:197–213.
139. Robison CD, Krebs I, Binder S, Barbazetto IA, Kotsolis AI, Yannuzzi LA, et al. Vitreomacular adhesion in active and end-stage age-related macular degeneration. *Am J Ophthalmol.* 2009;148:79–82.e2.
140. Bababegy SR, Sebag J. Chromodissection of the vitreo-retinal interface. *Retin Physician.* 2009;6:16–21.
141. Curtin BJ, Karlin DB. Axial length measurements and fundus changes of the myopic eye. *Am J Ophthalmol.* 1971;71:42–53.
142. Phillips CI. Retinal detachment at the posterior pole. *Br J Ophthalmol.* 1958;42:749–53.
143. Takano M, Kishi S. Foveal retinoschisis and retinal detachment in severely myopic eyes with posterior staphyloma. *Am J Ophthalmol.* 1999;128:472–6.
144. Benhamou N, Massin P, Haouchine B, Erginay A, Gaudric A. Macular retinoschisis in highly myopic eyes. *Am J Ophthalmol.* 2002;133:794–800.
145. Ikuno Y. Pathogenesis and treatment of myopic foveoschisis. *Nippon Ganka Gakkai Zasshi.* 2006;110:855–63.
146. Sayanagi K, Ikuno Y, Tano Y. Tractional internal limiting membrane detachment in highly myopic eyes. *Am J Ophthalmol.* 2006;142:850–2.
147. Ikuno Y, Gomi F, Tano Y. Potent retinal arteriolar traction as a possible cause of myopic foveoschisis. *Am J Ophthalmol.* 2005;139:462–7.
148. Sayanagi K, Ikuno Y, Soga K, Tano Y. Photoreceptor inner and outer segment defects in myopic foveoschisis. *Am J Ophthalmol.* 2008;145:902–8.
149. Ikuno Y, Sayanagi K, Soga K, Oshima Y, Ohji M, Tano Y. Foveal anatomical status and surgical results in vitrectomy for myopic foveoschisis. *Jpn J Ophthalmol.* 2008;52:269–76.
150. Forte R, Cennamo G, Pascotto F, de Crecchio G. En face optical coherence tomography of the posterior pole in high myopia. *Am J Ophthalmol.* 2008;145:281–8.
151. Bando H, Ikuno Y, Choi JS, Tano Y, Yamanaka I, Ishibashi T. Ultrastructure of internal limiting membrane in myopic foveoschisis. *Am J Ophthalmol.* 2005;139:197–9.
152. Garcia-Arumi J, Martinez V, Puig J, Corcostegui B. The role of vitreoretinal surgery in the management of myopic macular hole without retinal detachment. *Retina.* 2001;21:332–8.
153. Jo Y, Ikuno Y, Nishida K. Retinoschisis: a predictive factor in vitrectomy for macular holes without retinal detachment in highly myopic eyes. *Br J Ophthalmol.* 2012;96:197–200.
154. Stirpe M, Michels RG. Retinal detachment in highly myopic eyes due to macular holes and epiretinal traction. *Retina.* 1990;10:113–4.
155. Shimada N, Ohno-Matsui K, Nishimuta A, Moriyama M, Yoshida T, Tokoro T, et al. Detection of paravascular lamellar holes and other paravascular abnormalities by optical coherence tomography in eyes with high myopia. *Ophthalmology.* 2008;115:708–17.
156. Spencer LM, Foos RY. Paravascular vitreoretinal attachments. Role in retinal tears. *Arch Ophthalmol.* 1970;84:557–64.
157. Brown NA, Hill AR. Cataract: the relation between myopia and cataract morphology. *Br J Ophthalmol.* 1987;71:405–14.
158. Lim R, Mitchell P, Cumming RG. Refractive associations with cataract: the Blue Mountains Eye Study. *Invest Ophthalmol Vis Sci.* 1999;40:3021–6.
159. Younan C, Mitchell P, Cumming RG, Rochtchina E, Wang JJ. Myopia and incident cataract and cataract surgery: the blue mountains eye study. *Invest Ophthalmol Vis Sci.* 2002;43:3625–32.
160. McCarty CA, Mukesh BN, Fu CL, Taylor HR. The epidemiology of cataract in Australia. *Am J Ophthalmol.* 1999;128:446–65.
161. Leske MC, Wu SY, Nemesure B, Hennis A, Barbados Eye Studies G. Risk factors for incident nuclear opacities. *Ophthalmology.* 2002;109:1303–8.
162. Hennis A, Wu SY, Nemesure B, Leske MC, Barbados Eye Studies G. Risk factors for incident cortical and posterior subcapsular lens opacities in the Barbados Eye Studies. *Arch Ophthalmol.* 2004;122:525–30.
163. Wong TY, Klein BE, Klein R, Tomany SC, Lee KE. Refractive errors and incident cataracts: the Beaver Dam Eye Study. *Invest Ophthalmol Vis Sci.* 2001;42:1449–54.
164. Klein BE, Klein R, Moss SE. Incident cataract surgery: the Beaver Dam eye study. *Ophthalmology.* 1997;104:573–80.

Vitreous Aging and Posterior Vitreous Detachment

I.I.C.

Kevin Tozer, Mark W. Johnson, and J. Sebag

Outline

- I. **Introduction**
- II. **Molecular Composition of Vitreous**
 - A. Collagens
 - B. Non-collagenous Components
- III. **Vitreous Structure**
 - A. Vitreous Body
 - B. Posterior Vitreous Cortex
 - C. Vitreous Base
 - D. Vitreoretinal Interface
- IV. **Aging Changes in the Vitreous Body**
 - A. Liquefaction
 - B. Structural Changes
 - 1. Fibrous Aggregation
 - 2. Vitreous Base Migration
 - 3. Vitreoretinal Interface Weakening
- V. **Posterior Vitreous Detachment**
 - A. Epidemiology
 - B. Pathophysiology
 - C. Clinical Presentation
 - 1. Time Course
 - D. Anomalous PVD

References

Keywords

Posterior vitreous detachment • Vitreoretinal interface • Liquefaction • Synchysis • Syneresis • Vitreous aging • Hyaluronan • Collagen • Myopia

Key Concepts

1. Posterior vitreous detachment is not an acute process, but is instead a series of aging changes in the vitreous body that take place over many years.
2. Changes to both hyaluronan and type IX collagen have been implicated as the cause of vitreous liquefaction. The mechanisms underlying dehiscence at the vitreoretinal interface are less well understood.
3. Pathology from posterior vitreous detachment results from liquefaction without concurrent vitreoretinal interface dehiscence, known as *anomalous posterior vitreous detachment*.

Electronic supplementary material Supplementary material is available in the online version of this chapter at [10.1007/978-1-4939-1086-1_9](https://doi.org/10.1007/978-1-4939-1086-1_9). Videos can also be accessed at <http://www.springerimages.com/videos/978-1-4939-1085-4>.

K. Tozer, MD
Doheny Eye Institute, Los Angeles, CA, USA

VMR Institute for Vitreous Macula Retina, 7677 Center Avenue, Suite 400, Huntington Beach, CA 92647, USA

Department of Ophthalmology and Visual Sciences, Kellogg Eye Center, University of Michigan, 1000 Wall Street, Ann Arbor, MI 48105, USA
e-mail: ktozer@med.umich.edu

M.W. Johnson, MD
Department of Ophthalmology and Visual Sciences, Kellogg Eye Center, University of Michigan, 1000 Wall Street, Ann Arbor, MI 48105, USA
e-mail: markwj@med.umich.edu

J. Sebag, MD, FACS, FRCOphth, FARVO (✉)
Doheny Eye Institute, Los Angeles, CA, USA

VMR Institute for Vitreous Macula Retina, 7677 Center Avenue, Suite 400, Huntington Beach, CA 92647, USA
e-mail: jsebag@VMRinstitute.com

I. Introduction

Vitreous undergoes dramatic changes with age, the most notable called “synchysis senilis,” which refers to the liquefaction of the gel with age. An understanding of synchysis from molecular to macroscopic levels is crucial because it is directly responsible for many important pathologic conditions that form a large and diverse group of ocular diseases. Remarkably, these changes start in the first few years of life and thus, untoward consequences are not confined to the elderly, but have the potential to afflict anyone. The most important event that is directly related to vitreous aging is posterior vitreous detachment (PVD). This seminal event is the ultimate outcome of a series of vitreous changes that occur throughout life in two locations: in the gel vitreous body and at the vitreoretinal interface. Although remarkably common and usually harmless, PVD is the single most important factor underlying pathology that results from the aging process in the vitreous body [see chapter III.B. Anomalous posterior vitreous detachment and vitreoschisis].

II. Molecular Composition of Vitreous

Understanding the process of aging in the vitreous requires knowledge of the molecular components that are ultimately responsible for the changes on a macroscopic level. A more detailed review of all aspects of vitreous biochemistry is available elsewhere in this book [see chapters I.A. Vitreous proteins; I.F. Vitreous biochemistry and artificial vitreous].

A. Collagens

Type II collagen comprises 60–70 % of all vitreous collagen [1]. Alternative splicing within the second exon creates two different forms, IIA and IIB [2]. Mutations in exon 2, such as in Stickler syndrome, result in significant ocular pathology that includes very liquefied vitreous [3] and a substantially higher risk of retinal detachment arising from large posterior retinal breaks [see chapter I.C. Hereditary vitreoretinopathies]. Type IX collagen comprises 20–25 % of vitreous collagen [1, 4]. Unlike type II, it is a heterotrimer and cannot form fibrils, but it does interact with the fibrils of other collagens. Alterations in the quantity and location of type IX collagen have been proposed as a reason for some of the most important age-related vitreous changes [5, 6]. Type V/XI collagen makes up about 10–15 % of all vitreous collagen [2]. Type II and the hybrid type V/XI collagen combine to form a heterotypic fibril. Type IX collagen attaches to the COL2 domain of type II collagen and helps keep the fibrils spaced from one another [2].

Current evidence suggests that during life vitreous collagens change dramatically in structure, with both aggregation and enzymatic cleavage, but there is also evidence of colla-

gen turnover. Advanced glycation end products (AGEs), specifically pentosidine, have been documented, suggesting vitreous turnover [7]. Based on rate of accumulation of pentosidine in nondiabetic individuals, the average half-life of vitreous collagen is likely around 15 years, similar to that of skin [7]. In diabetes, there are significant increases in vitreous AGEs [8, 9] [see chapter I.E. Diabetic vitreopathy].

B. Non-collagenous Components

Hyaluronan (HA) is a highly hydrophilic glycosaminoglycans (GAG) [see chapter I.F. Vitreous biochemistry and artificial vitreous] that keeps vitreous collagen sufficiently spaced to minimize light scattering [10]. Loss of this HA-collagen association has been implicated as an important part of vitreous aging [11]. Other important non-collagenous molecules include chondroitin sulfate (CS) and heparin sulfate, as well as opticin, a structural protein. CS and HS both attach to protein cores to form proteoglycans [2]. CS interacts with type IX collagen and may be important in fibril aggregation with aging [5, 6], while HS is also found at the vitreoretinal interface [2]. Opticin, which is not a GAG, is found at the vitreoretinal interface as well as on the surface of heterotypic collagen fibrils [12, 13]. Its role may be important in vitreoretinal adhesion and in preventing neovascularization [see chapter IV.C. Vitreous and iris neovascularization].

III. Vitreous Structure

A. Vitreous Body

Comprised mostly of water, the vitreous body is important in maintaining both optical clarity and structural integrity of the eye. For transparency, collagen fibrils are spread apart in youth by association with HA molecules. The collagen fibers attain their highest concentration at the vitreous base and lowest concentration in the central vitreous body. At the vitreous base the fibers course perpendicular to the eye wall which results in strong mechanical vitreoretinal adhesion in the periphery [14, 15].

B. Posterior Vitreous Cortex

The posterior vitreous cortex is the outer shell of the vitreous that extends from the vitreous base posteriorly to adhere to the entire posterior retina. Similarly, there is an anterior vitreous cortex that courses anteriorly from the vitreous base and adheres to the posterior lens surface. The posterior vitreous cortex varies in thickness between 100 and 110 μm [16] and is actually absent over the optic disc (i.e., the prepapillary

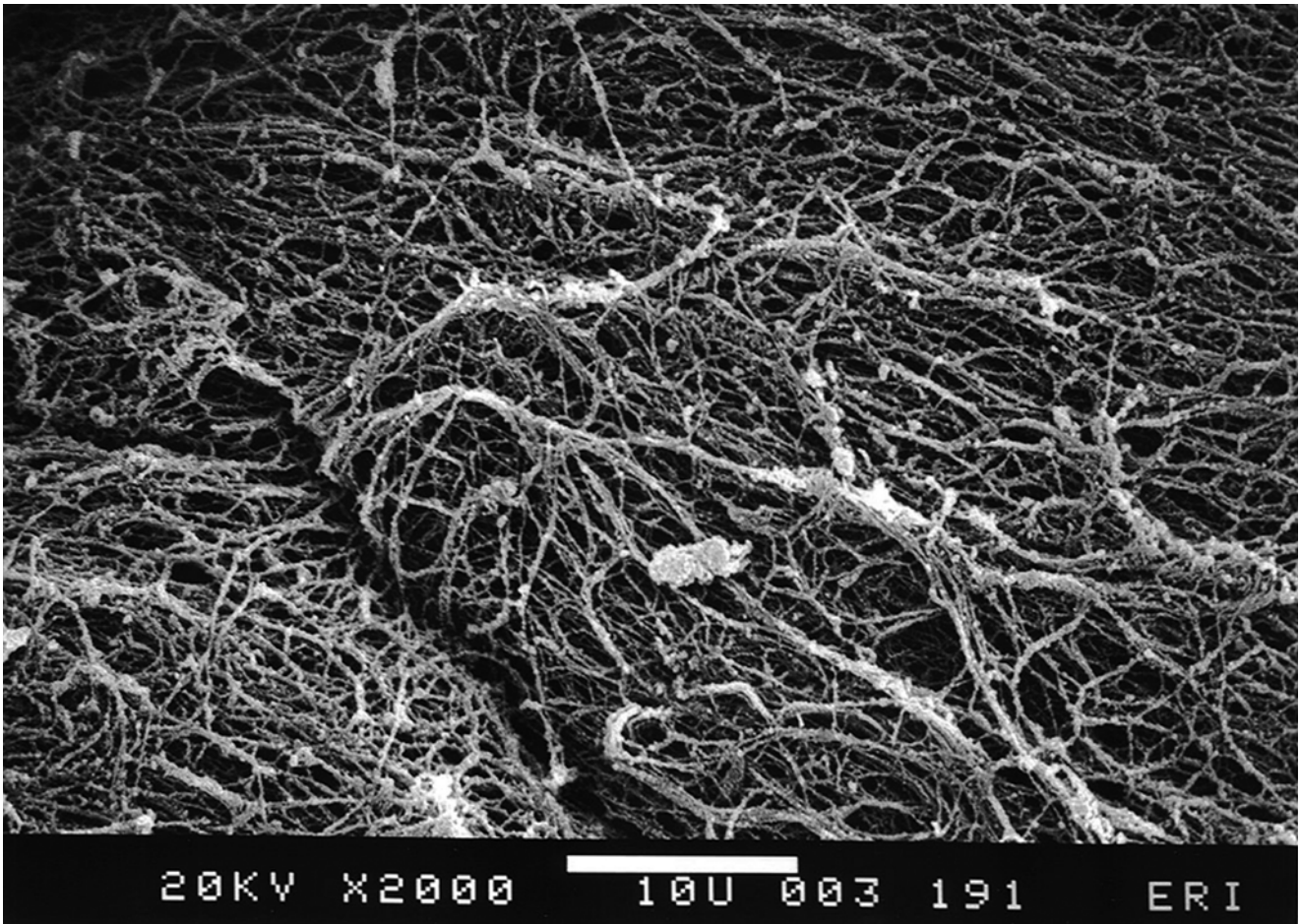


Figure II.C-1 Scanning electron micrograph demonstrating the dense matrix of collagen fibrils in the human posterior vitreous cortex

hole) [15, 17]. The cortex is thinnest in the fovea and increases in thickness as it extends outward [18] [see chapter III.E. Vitreo-papillary adhesion and traction]. Unlike at the vitreous base, the collagen fibrils in the posterior vitreous cortex run parallel to the plane of the retina (Figure II.C-1). This orientation does not allow any direct insertion into the retina and accounts for the weaker adhesion along this zone [15, 19].

An important structural feature of the posterior vitreous cortex is its lamellar organization. Much like an onion, the posterior vitreous cortex is comprised of layers that are potential cleavage planes through which the structure can split, a phenomenon known as “vitreschisis” which can occur endogenously or during membrane peel surgery [see chapter III.B. Anomalous posterior vitreous detachment and vitreschisis]. Indeed, Gupta et al. [20] showed that vitreschisis is present in a much higher percentage of patients with macular hole and macular pucker than normal controls [see chapters III.F. Vitreous in the pathobiology of macular pucker; III.C. Pathology of vitreomaculopathies]. Another unique feature of the posterior vitreous cortex is that hyalocytes are embedded within it. These cells, which are located approximately 20–50 μm from the retina, form a monolayer in the posterior vitreous cortex [10]. Their main function is to serve as important immunomodulating cells

and help maintain vitreous clarity through their phagocytic activity. Pathologically, they are likely to be important in early stages of a number of disease entities involving preretinal membranes, like macular pucker, and serve as the main contractile elements by differentiating into myofibroblasts [see chapters II.D. Hyalocytes: essential vitreous cells in vitreoretinal health and disease; III.F. Vitreous in the pathobiology of macular pucker].

C. Vitreous Base

The vitreous base “anchors” the vitreous body and is the point of insertion for vitreous collagen fibrils. Its anterior border is approximately 2 mm anterior to the ora serrata, and the posterior border, which extends posteriorly over time, is between 1 and 3 mm posterior to the ora serrata [21, 22]. Additionally, the vitreous base is not a flat structure but actually extends into the anterior vitreous body as well. As mentioned above, the vitreous base is the location of highest collagen concentration and the only zone where collagen fibers course perpendicular to the retina. These fibers insert anterior and posterior to the ora serrata (Figure II.C-2) forming a dense doughnut-like structure that straddles the ora

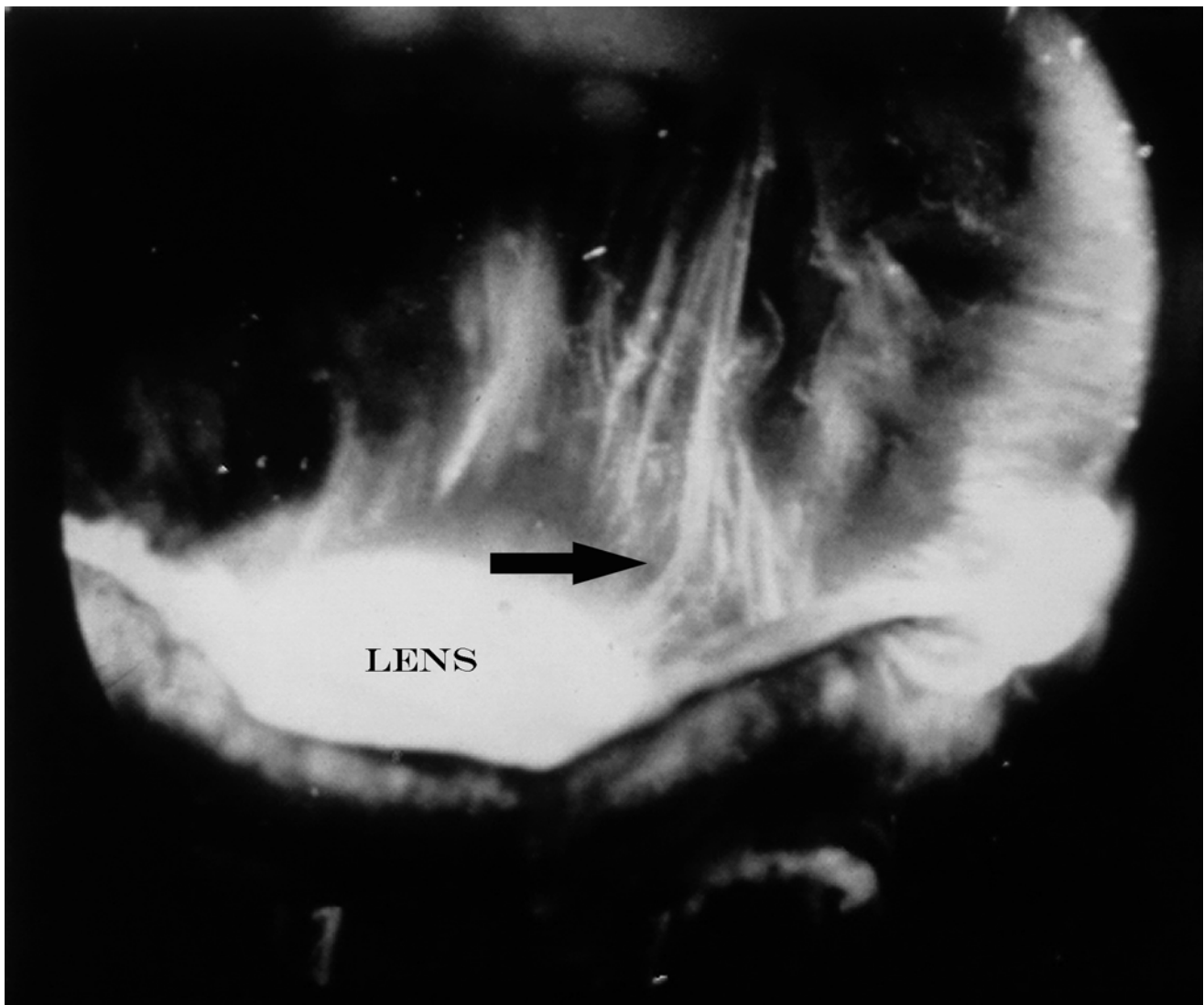


Figure II.C-2 Dark-field slit micrograph demonstrating the collagen fibrils of the vitreous base inserting anterior and posterior to the ora serrata (arrow). The posterior aspect of the lens is seen [24]

serrata. While biochemical interactions may underlie vitreoretinal adhesion elsewhere in the fundus, mechanical insertion is a unique property of the vitreous base where vitreous collagen fibrils directly interdigitate with the nonpigmented epithelium of the ciliary body and the neuroglia of the peripheral retina. This strong mechanical adhesion is likely responsible for persistent attachment along the vitreous base [15] despite PVD elsewhere and explains the propensity for retinal tears to occur at the posterior border of the vitreous base [see chapter III.H. Peripheral vitreo-retinal pathologies].

D. Vitreoretinal Interface

Possibly the most complex region of the vitreous is the narrow zone of adhesion between the vitreous and the retina, known as the vitreoretinal interface. The vitreoretinal interface is made of three distinct components: the posterior vitreous cortex (see above), the inner limiting membrane of the retina [see chapter II.E. Vitreoretinal interface and inner limiting membrane], and the extracellular matrix between the two. The inner limiting membrane (ILM) is the basal lamina of the retina and serves as the basement membrane for the Müller cells. Over the optic disc, the ILM actually ceases and transitions to the inner limiting membrane of Elschnig and the membrane of Khunt [10, 15, 23] [see chapter III.E. Vitreo-papillary adhesion and traction]. These topographical variations are important because numerous studies have demonstrated an inverse relationship between strength of vitreoretinal adhesion and ILM thickness [15, 24]. Studies [25] demonstrated that there were persistent remnants of vitreous cortex in the fovea after spontaneous posterior vitreous detachment with diameters of approximately 500 and 1,500 μm , both areas with thin ILM.

The other important component of the vitreoretinal interface is the extracellular matrix (ECM), also called the

The other important component of the vitreoretinal interface is the extracellular matrix (ECM), also called the

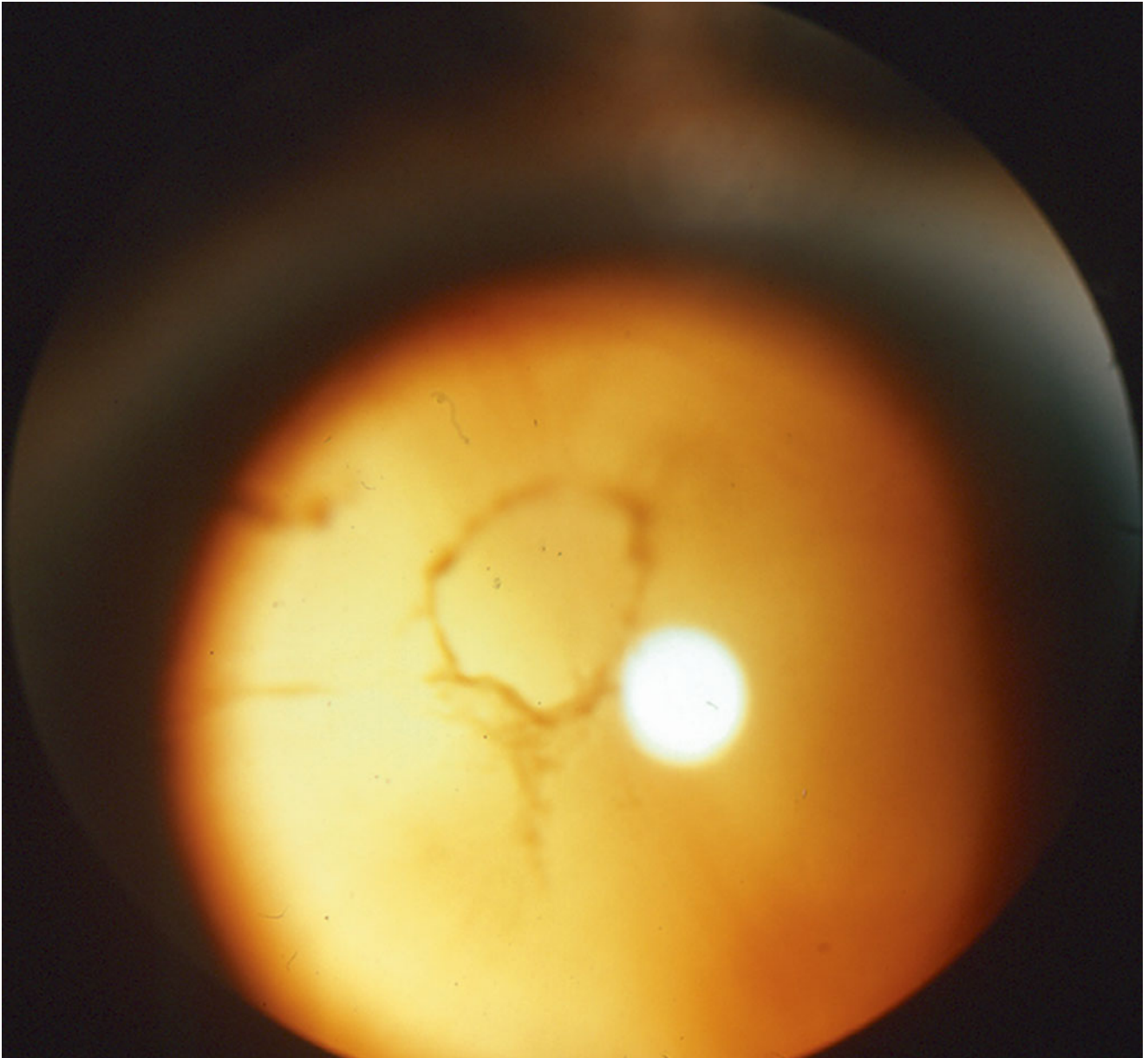


Figure II.C-3 Slit-lamp photo of a Weiss ring in the posterior vitreous cortex following PVD

vitreoretinal border region of Heegaard. The ECM functions as the biochemical glue that keeps the two structures adherent in the absence of mechanical adhesions. The molecular components of the ECM are numerous but are known to include fibronectin, laminin, opticin, and chondroitin sulfate proteoglycans. Russell [12] proposed a model by which the ECM maintains integrity of the vitreoretinal interface. In his theory a 240-kDa protein core is bound to the type IV collagen of the ILM. Attached to the protein core are a series of chondroitin sulfate glycosaminoglycans (GAG) that are present on the vitreal side of the ILM. The GAGs bind to a fibrillar protein, most likely opticin, which then interacts with type II collagen of the cortical vitreous. Through this chain of interaction, ILM to core protein to GAG to opticin to cortical vitreous, a relatively strong bio-

chemical adhesion is formed [12]. This type of biochemical adhesion appears to present throughout the retina, not just along the posterior pole. Evidence for this fact comes from studies examining the effect of ABC chondroitinase on the vitreoretinal interface. Chondroitinase causes an enzymatic destruction of the chondroitin sulfate adhesion process, and exposure to it caused complete dissociation of the vitreous from the retina, even along the vitreous base [26, 27] [see chapter VI.H. Chondroitinase as a vitreous interfactant: vitreous disinsertion in the human].

Another important consideration in the topographical variations of the vitreoretinal adhesion is the optic disc. Over the optic disc head, there is no posterior vitreous cortex and no inner limiting membrane, only the very thin membranes of Elschnig and Khunt [28]. Along the borders of the optic

disc, however, there are strong vitreoretinal adhesions. The nature of these adhesions likely falls somewhere between the biochemical adhesions of the remaining posterior pole and mechanical insertions of the vitreous base. What is known is that this peripapillary adhesion is often the last area of the retina, other than the vitreous base, to separate during a posterior vitreous detachment. Additionally, this separation is often associated with a rim of neuroglial tissue coming off the retina along with the vitreous, a finding clinically identified as a Weiss ring [29] (Figure II.C-3).

That PVD can tear away peripapillary tissue suggests a strong adhesion between the fibers of the vitreous cortex and glial tissue of the optic nerve head. In fact, cortical vitreous fibers have been shown to mechanically intertwine with the basal lamina and astroglial epipapillary membranes present in that area [30]. Whether this adhesion is purely mechanical or a mixture of mechanical and biochemical remains to be determined. Interestingly, in diabetic patients the peripapillary vitreous often remain persistently attached. The mechanism for this is likely related to the presence of neovascular membranes that preferentially proliferate through the prepapillary hole in the vitreous cortex [31]. These membranes function as additional anchors strengthening peripapillary vitreoretinal adhesion [see chapter III.E. Vitreo-papillary adhesion and traction].

IV. Aging Changes in the Vitreous Body

Vitreous aging is characterized by two separate processes that occur in parallel: gel liquefaction and vitreoretinal interface weakening. Each contributes to the principal aging event of the adult vitreous, posterior vitreous detachment.

A. Liquefaction

The first appearance of liquid vitreous is actually in childhood [32, 33]. Age-related liquefaction is called “synchysis senilis”; however, liquid vitreous has been documented at all ages (Figure II.C-4). In many young individuals a major cause of vitreous liquefaction is myopia which is known to lead to PVD at an earlier age than in emmetropia. Yonemoto [34] found that 0.91 years could be subtracted from the average age of PVD development (61 years) for each diopter of myopic refractive error. This is presumably at least in part related to precocious vitreous liquefaction. The pathway through which myopia affects PVD may be a decrease in HA concentration [35]. Others have suggested that in myopic eyes there may actually be an increase in synthesis of liquid vitreous more so than an increase in liquefaction of existing gel vitreous [36, 37]

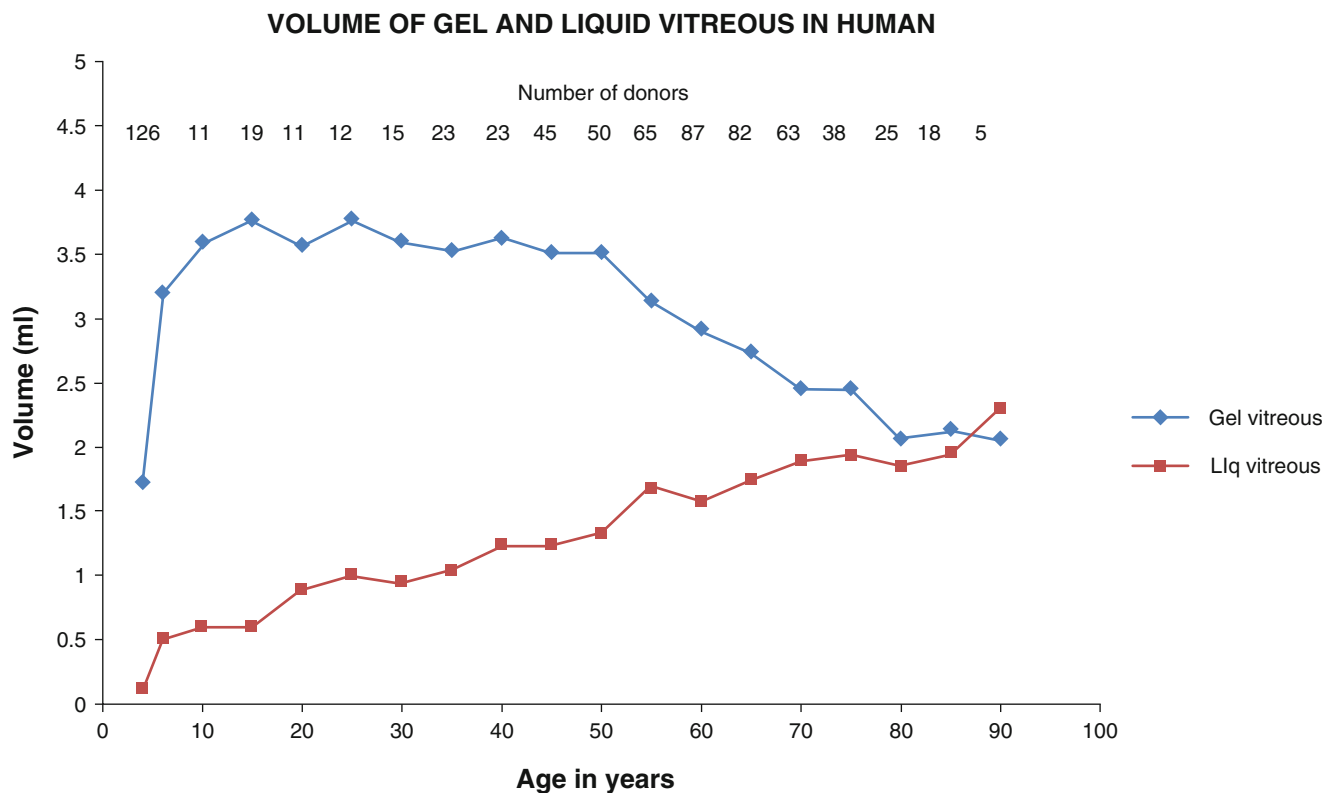


Figure II.C-4 Graph depicting the volume of gel and liquid vitreous throughout life. Note that liquid vitreous begins appearing, albeit in small quantities, during the first 5 years of life. Each data point represents the average derived from the number of eyes listed across the top of the graph

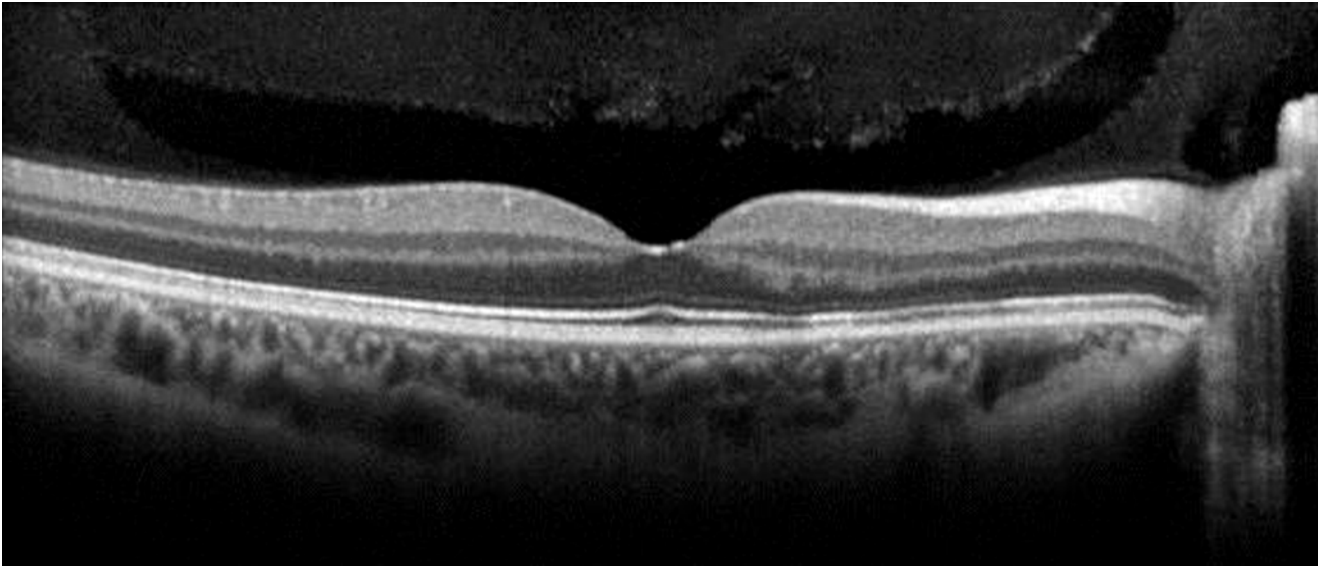


Figure II.C-5 Optical coherence tomography image demonstrating a premacular lacuna in the posterior vitreous of a 22-year-old female

[see chapter II.B. Myopic vitreopathy]. In addition, there are number of conditions that may cause increased liquefaction at an earlier age, most related to inborn errors of collagen metabolism. Collagen disorders such as Marfan, Ehlers-Danlos, Stickler [38], and Knobloch syndromes [39] all have substantial ocular manifestations usually associated with advanced vitreous liquefaction [see chapter I.C. Hereditary vitreoretinopathies].

With advancing vitreous liquefaction, pockets of liquid vitreous called lacunae form within the gel. As originally described by Worst [40], the first lacunae form in the premacular vitreous (Figure II.C-5). The reason for this specific location is unclear, but several theories exist. One is that the macula is the site that the majority of the light, and therefore light radiation, is focused. Visible light radiation exposure is thought to produce free radicals [41] that predispose the premacular vitreous to breakdown at a younger age than other parts of the vitreous body [42, 43]. A second theory is similarly reliant on free-radical damage but posits that the free radicals are a byproduct of being located near the highly metabolically active macula [44]. It is also plausible that like Cloquet's canal, this bursa is an embryologic vascular remnant.

By the teenage years, 20 % of the total vitreous has undergone synchysis [32], and by 70 years of age, this increases to 50 % [45]. Importantly, it is usually around the age of 40 that enough vitreous has liquefied to produce findings evident on clinical slit-lamp biomicroscopy as gray linear structures and pockets of liquid vitreous devoid of any light scattering. Dark-field slit microscopy has documented the presence of fibers in the adult human vitreous and characterized their distribution (Figure II.C-6a). Transmission electron microscopy has determined that

these visible fibers are aggregated vitreous collagen fibrils organized into bundles [46] (Figure II.C-6b). Indeed, all theories of vitreous liquefaction maintain a central role for collagen. Although there is evidence of vitreous collagen turnover throughout life (see section I above), turnover alone would not account for the dramatic structural changes that vitreous undergoes. Three theories to be discussed include changes in the hyaluronan-collagen association, loss of type IX collagen from the surface of heterotypic collagen fibrils, and enzymatic collagen destruction.

One of the leading theories explaining vitreous liquefaction explores the role of hyaluronan (HA). As described above HA is a hydrophilic glycosaminoglycans that is important in short- and long-range spacing of collagen fibrils [see chapter I.F. Vitreous biochemistry and artificial vitreous]. While the collagen provides the matrix, HA draws the water that effectively provides the matrix structure by hydrating it [47, 48]. In theory, if the nature of the HA-collagen interaction were to change, either through loss of HA or another mechanism, the collagen matrix would collapse and the liquid inside would form pockets. Following HA dissociation from collagen, the collagen fibrils cross-link with one another and undergo lateral fusion into larger aggregates. Increasing the collagen content in the residual gel vitreous while simultaneously decreasing it elsewhere leads to liquid lacunae (Figure II.C-6c). This theory is supported by the finding that eyes with posterior vitreous detachment had a lower concentration of HA than eyes with an intact vitreous [11]. Circumstantial evidence derives from the observation that as HA concentration decreases the volume of the vitreous gel decreases as well [6]. There may also be HA structural changes that alter its interaction with collagen. Free-radical

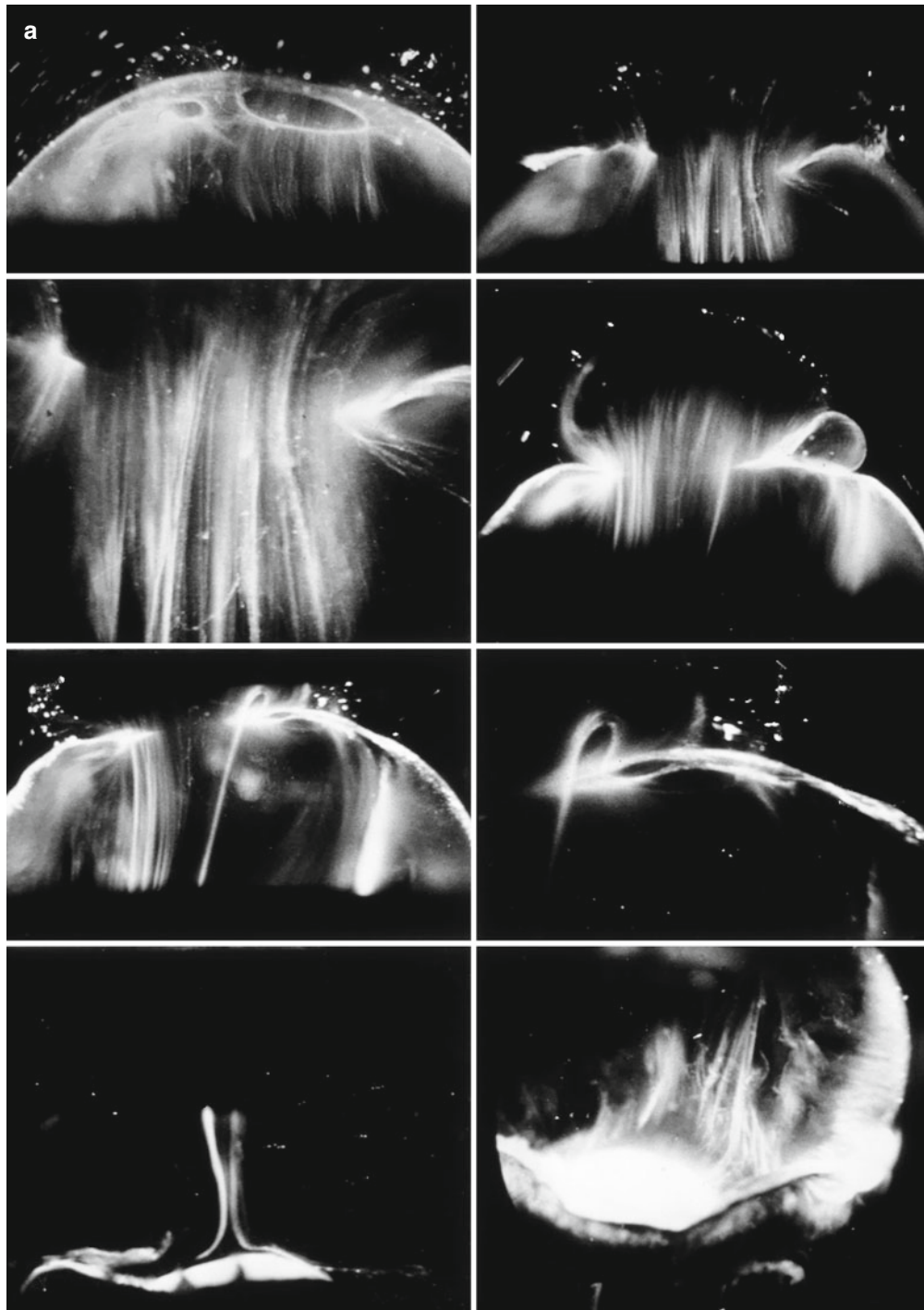


Figure II.C-6 (a) Dark-field slit microscopy of human vitreous structure. The sclera, choroid, and retina were dissected off the vitreous body which is left attached to the anterior segment. Illumination is provided by a slit-lamp beam shining in from the side, creating a horizontal optical section through the eye. All photographs are oriented with the anterior segment below and the posterior pole above. *Top left:* Posterior vitreous in the left eye of a 52-year-old man. The vitreous body is enclosed by the vitreous cortex. There is a hole in the prepapillary (small, to the left) vitreous cortex. Vitreous fibers are oriented toward the premacular region. *Top right:* Posterior vitreous in a 57-year-old man. A large bundle of prominent fibers is seen coursing anteroposteriorly and entering the retrocortical space by way of the prepapillary hole (to the right) and premacular (large extrusion to

the left) vitreous cortex. Fibers course anteroposteriorly out into the retrocortical space. *Row 3 left:* Horizontal optical section of the same specimen as row 2 right at a different level. A large fiber courses posteriorly from the central vitreous and inserts into the premacular vitreous cortex. *Row 3 right:* Same view as row 3 left at higher magnification. The large fiber has a curvilinear appearance because of traction by the vitreous extruding into the retrocortical space. However, because of its attachment to the posterior vitreous cortex, the fiber arcs back to its point of insertion. *Bottom left:* Anterior and central vitreous in a 33-year-old woman. The canal of Cloquet is seen forming the retrolental space of Berger. *Bottom right:* Anterior and peripheral vitreous in a 57-year-old man. The specimen is tilted forward to enable visualization of the posterior aspect of the lens and the peripheral anterior vitreous. To the right of the lens, there are fibers coursing anteroposteriorly that insert into the vitreous base. These fibers splay out to insert anterior and posterior to the ora serrata (From Sebag [24])

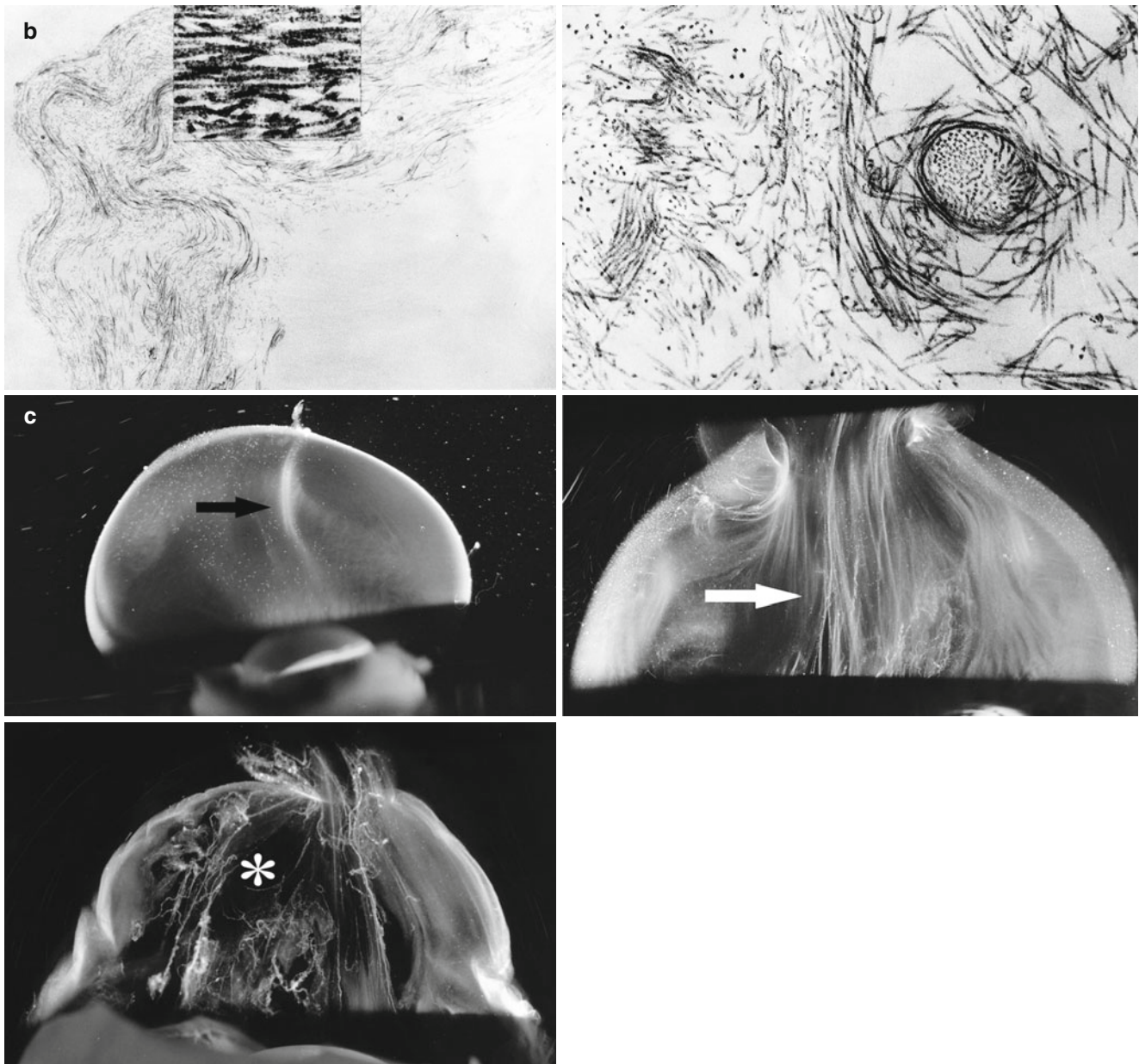


Figure II.C-6 (continued) (b) Transmission electron microscopy of human vitreous detected bundles of collagen fibrils shown longitudinally to the left and in cross section to the right. The inset in the left image is a high magnification of the bundle of fibrils demonstrating their collagenous nature [46]. (c) Left image (*middle*) shows the homogenous gel vitreous of a 33-week gestational age human. The

only light-scattering structure is the remnant of the hyaloid artery (*black arrow*). *Right image* demonstrates the formation of central vitreous fibers (*white arrow*) in a 59-year-old subject. *Bottom left image* shows the extensive degeneration of the gel structure in an 88-year-old human with dense fibrous aggregation and adjacent gel liquefaction, sometimes forming lacunae (*asterisk*)

damage has been shown to change the average molecular weight of HA [49]. Additionally, the chromatographic elution profile and optical properties of HA have been shown to be different in gel versus liquefied vitreous [50], suggesting that changes in structural properties play an important role in vitreous liquefaction. Additionally, it provides a plausible explanation for the development of more extensive vitreous liquefaction earlier in life in diabetic patients compared to nondiabetics. Since diabetes increases glucose concentration

in the vitreous [51], collagen is more likely to develop non-enzymatic glycation [8, 52] and with free-radical damage to HA [49] lead to earlier vitreous liquefaction [see chapter I.E. Diabetic vitreopathy].

One problem with the HA theory, however, is that experimental studies showed that even with almost complete removal of HA, vitreous did not liquefy. Although the volume of the gel did decrease, there was not extensive gel liquefaction even after over 90 % of the HA had been

depolymerized using *Streptomyces* HA lyse [6]. Thus, another mechanism that has been proposed for the liquefaction of vitreous over time is the loss of type IX collagen from the surface of the heterotypic collagen fibrils [5, 53]. As described above, type IX collagen binds to the type II collagen in the heterotypic collagen fibrils. This is important in maintaining spacing between collagen fibrils because unbound type II collagen has a natural propensity to aggregate with other type II collagen molecules. Studies [53] have shown that type IX collagen has shorter half-life (approximately 11 years), as compared to other forms of collagen. Additionally, loss of type IX collagen has been shown to cause type II collagen aggregation. This has been proven by enzymatically cleaving the CS chains of type IX collagen using ABC lyase and observing subsequent type collagen bundling [53].

While most of the prevailing theories on vitreous liquefaction involve collagen aggregation, a third theory actually proposes that collagen breakdown is the primary cause. Los and colleagues [54] demonstrated an increase in collagen fragments associated with aging. Further studies on the topic suggested that enzymatic breakdown, possibly from matrix metalloproteinases or other enzymes, is responsible specifically for collagen type II destruction over time.

B. Structural Changes

1. Fibrous Aggregation

As vitreous liquefies, collagen aggregates into bundles (Figure II.C-6b) that become visible with biomicroscopy [32, 46] (Figure II.C-6a, c). Liquefaction and concomitant dehiscence at the vitreoretinal interface results in entry of liquid vitreous between the inner limiting membrane of the retina and posterior vitreous cortex. This volume displacement from within the vitreous body to the space forming between vitreous and retina results in collapse (“syneresis”) of the vitreous body, an important event in vitreous aging. Aside from being a crucial step in the process of posterior vitreous detachment, to be discussed below, the rheological changes caused by liquefaction play an important role in ocular physiology [see chapter IV.A. Vitreous physiology] and many disease entities, ranging from nuclear sclerotic cataract formation to primary open-angle glaucoma and proliferative diabetic retinopathy. The critical pathway by which liquefied vitreous affects these disease states is oxygen diffusion [see chapter IV.B. Oxygen in vitreoretinal physiology and pathology]. Oxygen is known to move from retinal arterioles into [55] the vitreous via diffusion. However, oxygen in gel vitreous can only reach other parts of the vitreous via further diffusion, a relatively slow process. Once the

vitreous has liquefied, however, fluid currents generated by eye movements quickly disperse the oxygen throughout the entire vitreous, greatly altering the geographical oxygen concentration gradients in the vitreous [56]. Additionally, as vitreous liquefies it consumes less oxygen than it does in its gel state [57]. This results in a higher oxygen concentration in the vitreous cavity. It is this alteration in oxygen distribution and consumption that has been proposed as the cause of pathological changes in the eye associated with vitreous liquefaction [55, 57].

2. Vitreous Base Migration

Like the vitreous body and vitreoretinal interface, the vitreous base undergoes changes over time. The most significant change is that the posterior border of the vitreous base migrates posteriorly. At birth the posterior border of the vitreous base is usually at or minimally past the posterior edge of the ora serrata. As the vitreous ages, however, this border migrates farther posteriorly into the peripheral retina itself [21]. This process is possibly due to synthesis of new collagen in the anterior retina that migrates through the ILM and intertwines with existing vitreous collagen [22]. Interestingly, this process appears to happen to a greater extent on the temporal side as compared to the nasal side. This fact may explain the phenomenon that retinal tears occur with greater frequency temporally rather than nasally.

3. Vitreoretinal Interface Weakening

Gel liquefaction with vitreous body collapse can only result in an innocuous posterior vitreous detachment (PVD) if there is concurrent weakening of the vitreoretinal interface. Foos demonstrated that despite a substantial part of the vitreous being liquefied earlier, posterior vitreous detachment rarely occurred before the age of 60, a fact that has been attributed to persistent vitreoretinal adhesion [45]. While the vitreoretinal interface does weaken, and often dehisce, one area that does not separate is the vitreous base, where strong mechanical adhesions prevent vitreoretinal separation, even in the setting of complete PVD. Other sites of firm adhesion are at the optic disk, macula, and along retinal blood vessels but it is important to appreciate that rather than just focal adherence at these locations, vitreous adheres to the entire posterior pole in a fascial manner (Figure II.C-7a). At times, the circular edge of the central zone of the premacular vitreous cortex is the site of membrane formation in proliferative diabetic retinopathy or the site of vitreo-macular traction (larger circle to the right in Figure II.C-7b and Video II.C-1).

There are many theories about the mechanisms underlying vitreoretinal interface weakening. One theory states that Müller cells play an important role. Müller cells are known

to synthesize some of the extracellular matrix components of the vitreoretinal interface. Kloti and colleagues demonstrated that Müller cell infarction led to dissolution of the attachment between the ILM and the PVC and hypothesized that this was underlying mechanism behind age-related vitreoretinal interface changes [59]. Along a similar line of reasoning, other studies have hypothesized that it is thickening of the ILM over time [60] that mechanically prevents Müller cells from getting ECM proteins into the vitreoretinal interface [58]. Progressive ILM thickening over time is a well-documented phenomenon and thus provides at least a temporal association with vitreoretinal interface weakening [see chapter II.E. Vitreoretinal interface and inner limiting membrane].

Another popular theory centers on the collagen content, specifically type XVIII, in the ECM [61, 62]. As mentioned above, vitreoretinal adhesion involves the interaction of GAGs, collagen, and opticin. Type XVIII collagen has been proposed as one of the crucial collagens in that chain of interactions because it forms a heparin sulfate proteoglycan which binds to opticin [2, 13]. In fact, knock-out mice deficient in type XVIII collagen have increased vitreoretinal disinsertion. Opticin knock-out mice, however, do not appear to have increased rate of dehiscence [62].

V. Posterior Vitreous Detachment

Posterior vitreous detachment (PVD) is the final step in the long process of vitreous aging. It is defined as a complete separation of the vitreous from the retina in all areas posterior to the vitreous base (Figure II.C-8). It occurs without untoward sequelae if both liquefaction and vitreoretinal dehiscence have occurred in a sufficient amount and is instigated by static and dynamic forces associated with eye movement. Although PVD is a natural part of aging and usually does not result in any problems, PVD can be the inciting event for numerous vitreoretinal pathologies. Studies suggest up to 24 % of symptomatic PVDs result in retinal complications [34, 63, 64] [see chapter III.B. Anomalous posterior vitreous detachment and vitreoschisis]. Thus, understanding the process of PVD is helpful in defining the pathophysiology behind many important clinical conditions.

A. Epidemiology

PVD is one of the most common events that occur in vitreous. Autopsy studies [45] show that by the seventh decade of life, PVD is present in 51 % of all eyes and by the eighth decade the prevalence increases to 63 %. Similarly, clinical

studies have shown a prevalence of 65 % after the age of 65 [65]. Overall, the average age of onset is approximately 61 years [34]. Comparing prevalence to degree of liquefaction shows a significant increase in PVD when over 60 % of the vitreous has liquefied as compared to only 50 % liquefaction [45]. Several other factors can influence the onset of PVD. One interesting factor is female gender. The average age of onset for females has been shown to be statistically significantly earlier than males [34, 45, 66]. The mechanism for the age disparity has been attributed to postmenopausal loss of estrogen [63]. The decrease in estrogen may cause a decrease in hyaluronan synthesis leading to increased liquefaction as described above [11, 45]. This theory is supported by animal evidence showing a decrease in hyaluronan with decreased exposure to sex hormones [67]. Another proposed pathway is that the antioxidant and insulin-dependent glucose regulation roles of estrogen are affected by menopause. Van Deemter et al. showed that females accumulate advanced glycation end products (AGEs) at a faster rate than men, particularly after menopause [7].

Another risk factor for earlier PVD is myopia [63]. Yonemoto et al. [34] found that 0.91 years could be subtracted from the average age of PVD (61 years) for each diopter of myopic refractive error. That study included eyes that had undergone either complete posterior vitreous detachment or partial PVD with residual retinal adhesions. The pathway through which myopia affects PVD is likely related to a decrease in hyaluronan concentration [35]. Others have suggested that in myopic eyes there may actually be an increase in synthesis of liquid vitreous more so than an increase in liquefaction of existing gel vitreous [36, 37].

Additionally, many disorders of collagen metabolism affect PVD incidence. As mentioned above, increased vitreous liquefaction is seen in Marfan, Stickler, Ehlers-Danlos, and other collagen disorders [see chapter I.C. Hereditary vitreoretinopathies]. An important distinction for this group of disorders is that the liquefaction occurs at a rate far out of proportion to vitreoretinal dehiscence. Due to that fact, patients with these collagen disorders often have persistent vitreoretinal adhesion even after near complete vitreous liquefaction and thus may not undergo an innocuous PVD. Other factors that have been shown to increase vitreous liquefaction and PVD are trauma, aphakia, inflammation, retinal vascular diseases, and vitreous hemorrhage [68].

B. Pathophysiology

The most important processes in the pathophysiology of PVD are gel liquefaction and vitreoretinal dehiscence. While

these are necessary, they may not be sufficient since there are other events that contribute to complete PVD. One important event is that liquid vitreous must enter the retrocortical/preretinal space, essentially the vitreoretinal border region of Heegaard [23]. The path through which the gel obtains access to this area is unclear. One widely accepted route is through the prepapillary hole in the posterior vitreous cortex. The presence of this hole is documented on numerous histologic studies and provides a logical explanation for liquid vitreous entry into the retrocortical/preretinal space [24, 45, 69]. However, as pointed out by Johnson [29], vitreopapillary adhesion is usually the last to release during

PVD. Thus, another possible route is through the premacular vitreous cortex. While a “hole” can sometimes be seen in the premacular vitreous cortex after vitreo-macular separation (Figure II.C-7b), it was long ago pointed out by Sebag and recently confirmed by OCT imaging [29, 70, 71] that such a hole usually does not exist *in vivo*. In some cases of PVD, there can be a prolapse of vitreous through this region, as first proposed by Jaffe in 1968 [72] and as identified by Kishi who found an oval-shaped defect in the premacular cortex through which vitreous herniated in 10/36 cases at autopsy [33]. Indeed, Gärtner likened this to herniation of the intervertebral disk and questioned whether the two events were

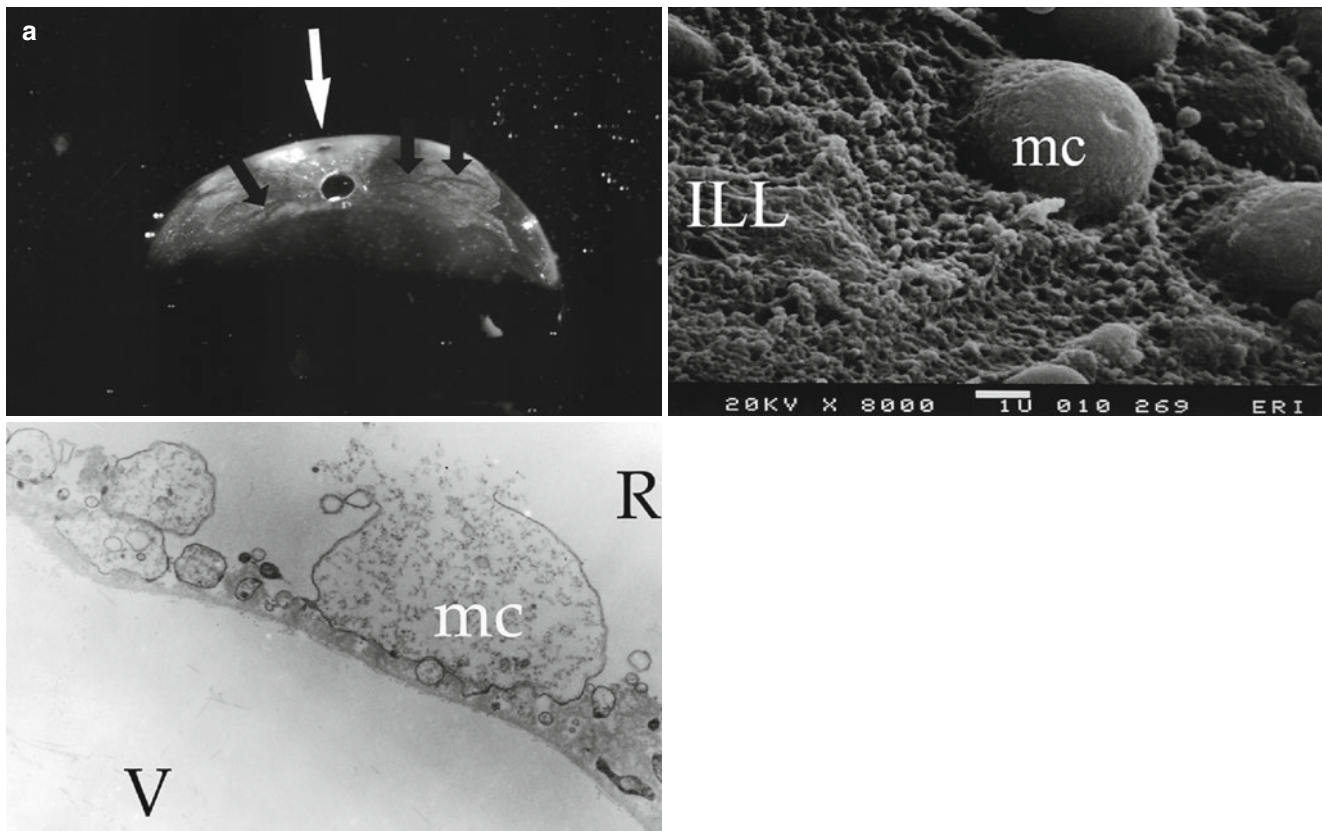


Figure II.C-7 Age-related differences at the vitreoretinal interface. There is firm adhesion of vitreous to the vitreous base, optic disc, macula, and along retinal blood vessels. In addition, there is strong adhesion throughout the posterior pole in a fascial (rather than focal) distribution. This is demonstrated by the different appearance of the posterior pole following peeling of the retina off the posterior vitreous in young subjects (a) as compared to middle-aged subjects (b). (a) Imaging of the posterior vitreous cortex in youth. After peeling the retina off the posterior vitreous, there is a different appearance from that obtained in all middle-aged subjects (see Figure II.C-7b). By dark-field slit microscopy, there appears to be an additional layer of tissue adherent to the posterior vitreous (top left image, this page). Within this tissue is a hole corresponding to the prepapillary posterior vitreous with linear branching structures that have a pattern identical to retinal blood vessels (black arrows). The white arrow indicates the site correspond-

ing to the fovea. This tissue was processed for scanning electron microscopy (upper right image) which revealed the presence of mound-like structures (mc) adherent to the inner limiting membrane (ILL). Transmission electron microscopy (lower left image) identified these mounds as the inner segment footplates of Müller cells (mc) adherent to the ILM [R retina, V vitreous]. Thus, in youth the adhesion of vitreous to retina was stronger than the Müller cells themselves. This occurred only in subjects younger than 20 years of age and only in the posterior pole (From Sebag [58]). (b, see next page) Dark-field slit microscopy imaging of the posterior vitreous cortex in middle age. Demonstrated are the peripapillary hole (smaller “hole” to the left; black arrows) with extruding vitreous (white arrows) and the premacular hole (larger “hole” to the right) with extruding vitreous fibers. Hyalocytes appear as bright punctate structures embedded within the peripheral and posterior vitreous cortex

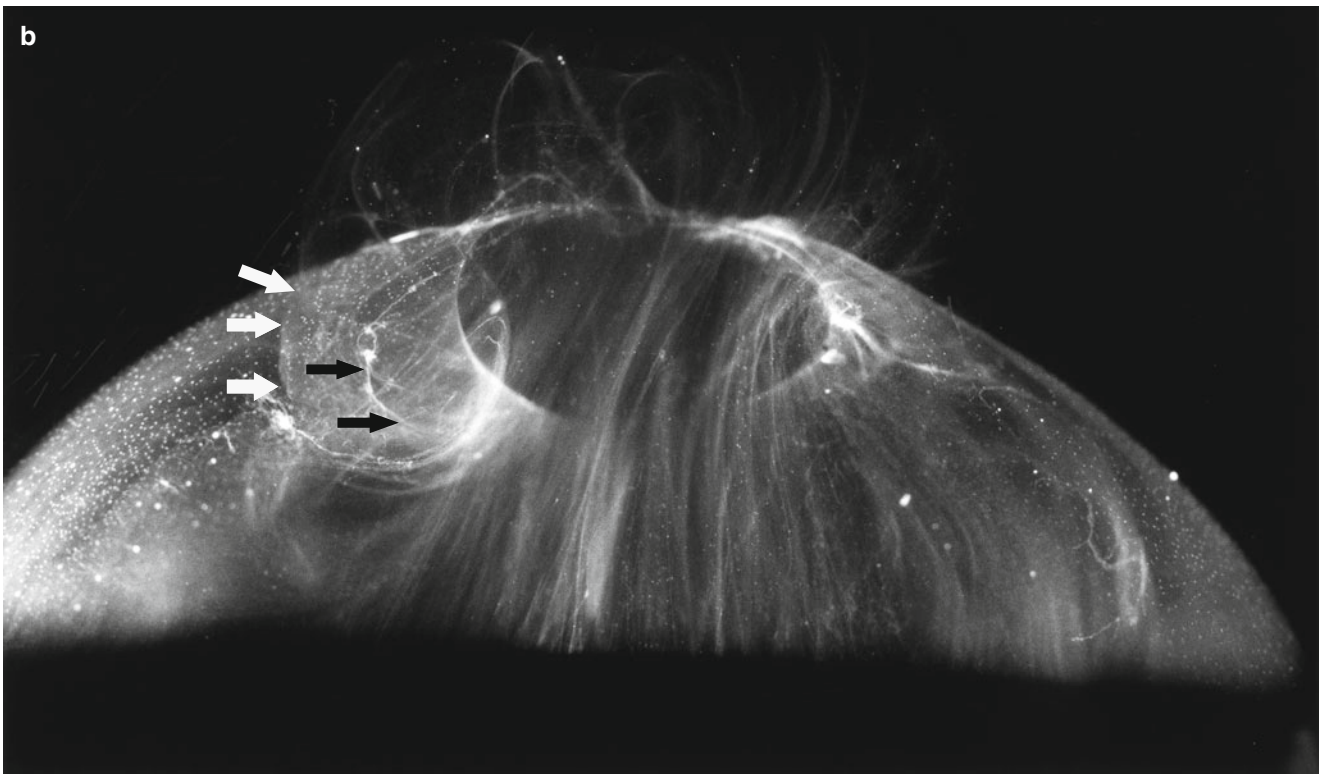


Figure II.C-7 (continued)

not somehow related [73]. Given the biochemical similarities between vitreous and joints [see chapter I.F. Vitreous biochemistry and artificial vitreous], this is plausible. Even if a true hole is not present, the premacular vitreous cortex likely does play a role in liquid vitreous dissection of a plane between the posterior vitreous cortex and the ILM since as the vitreous liquefies this region of the cortex becomes thin and thus more prone to microscopic defects [68, 74].

Once liquid vitreous enters the retrocortical/preretinal space, it begins to hydrodissect a plane separating vitreous from retina. Extensive mathematical modeling has been done to explore the role of saccadic eye movements on vitreous movement. Most early models failed to account for the unique geometry of the eye. For instance, early work by Lindner [75] and later Rosengren [76] utilized a cylindrical chamber to model the complex fluid dynamics of the eye. A more recent model presented by David et al. [77] assumed a spherical shape for the vitreous body. That model, while more accurate, failed to account for lens-induced flattening of the anterior vitreous. Even so, it presented an interesting representation and directly related shear stress on the retina induced by vitreous movement to axial length of the eye. Finally, the most recent model, as described by Abouali, accounted for lens geometry while

also comparing the effect of changing viscosity in the aging vitreous. This model suggested that as vitreous liquefies the intensity of secondary flow increases by as much as 500 % as compared to a complete gel state. This suggests that the movement of vitreous, particularly near its boundaries, increases dramatically as the vitreous liquefies [78]. Other work that used a similar anatomically correct model for the eye showed that this effect is not so much influenced by the amplitude of saccadic eye movements as it is frequency of movement [79]. This suggests that is the frequent smaller movements that play the largest role in moving the liquefied vitreous.

The process of hydrodissection often follows a well-defined sequence that is influenced by previously described areas of increased vitreoretinal adhesion. This sequence has been described by Johnson [68, 80] as a 5-stage process (Stages 0–4; Figure II.C-9). Stage 0 is complete attachment throughout the fundus. Stage 1 involves detachment of the perifoveal posterior vitreous cortex, probably because this is the area where the liquefied gel first gains access to the retrocortical/preretinal space. Although there is perifoveal vitreous detachment, there is persistent vitreo-foveal adhesion at this early stage. As described above, studies have documented a 500- μm diameter area of strong vitreoretinal

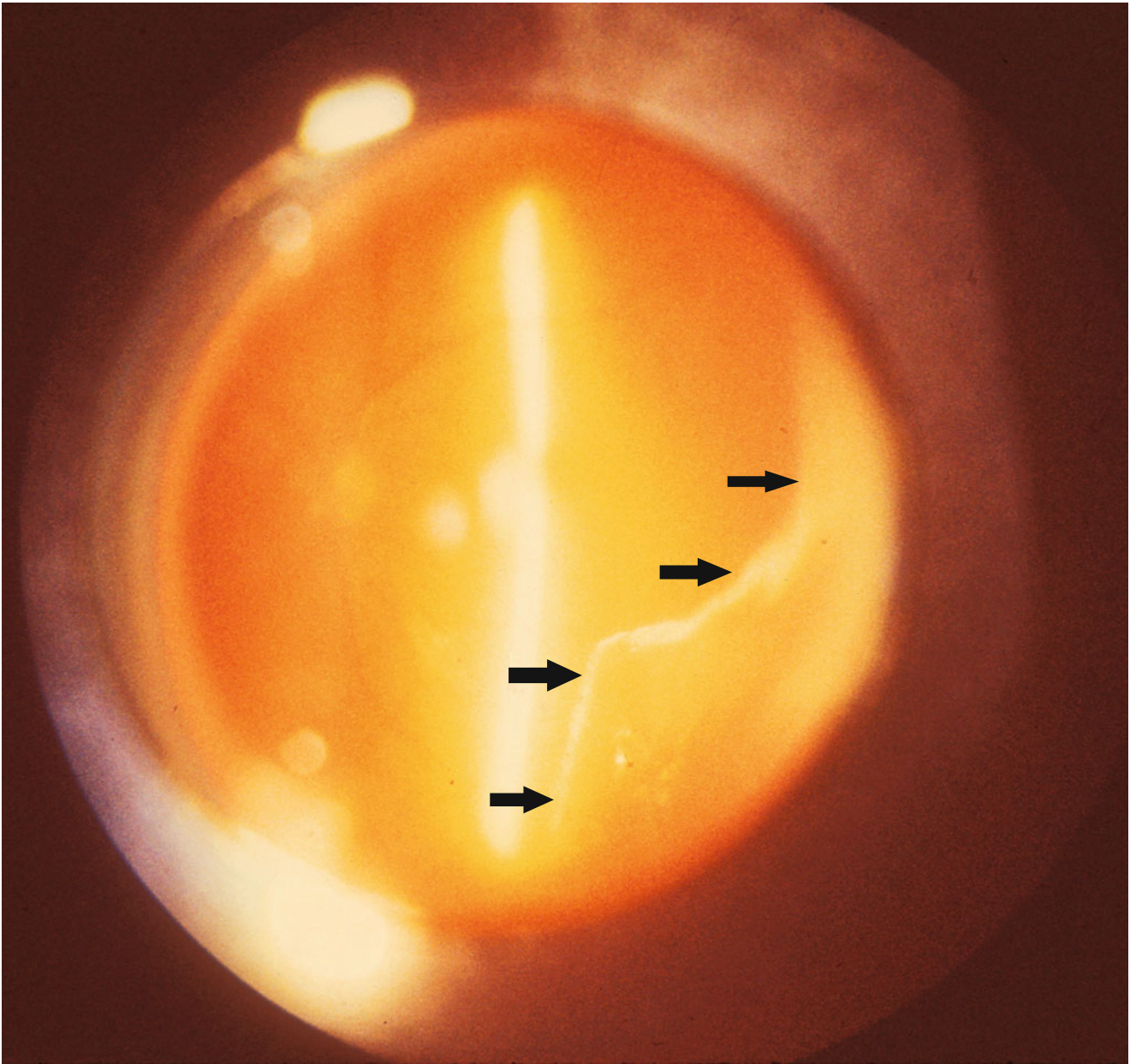


Figure II.C-8 Preset lens biomicroscopy of posterior vitreous detachment *in vivo*. The posterior vitreous cortex (*black arrows*) is detached away from the disc (to the left), macula, and retinal vessels (seen emanating from the optic disk). Commonly seen on clinical ultrasonography,

the typical sigmoid configuration of the detached posterior vitreous is due to the effects of gravity upon the superior vitreous which descends inferiorly after detaching from the retina (Courtesy of Clement Trempe, MD)

adhesion in the foveola [25]. This strongly adherent foveolar zone does not detach until stage 2, at which point there is complete macular separation. In stage 3, there is a near-total PVD involving the entire retina except for the vitreo-papillary zone. Apart from the vitreous base, the immediate peripapillary zone is the area of strongest vitreoretinal adhesion and thus is the last site of vitreoretinal separation in the posterior fundus. In stage 4, there is release of the

vitreo-papillary adhesion and total PVD. It is this last stage that is most often the clinically recognized event [29, 68].

C. Clinical Presentation

When describing the clinical presentation of PVD, it is important to make a distinction about where in the process of

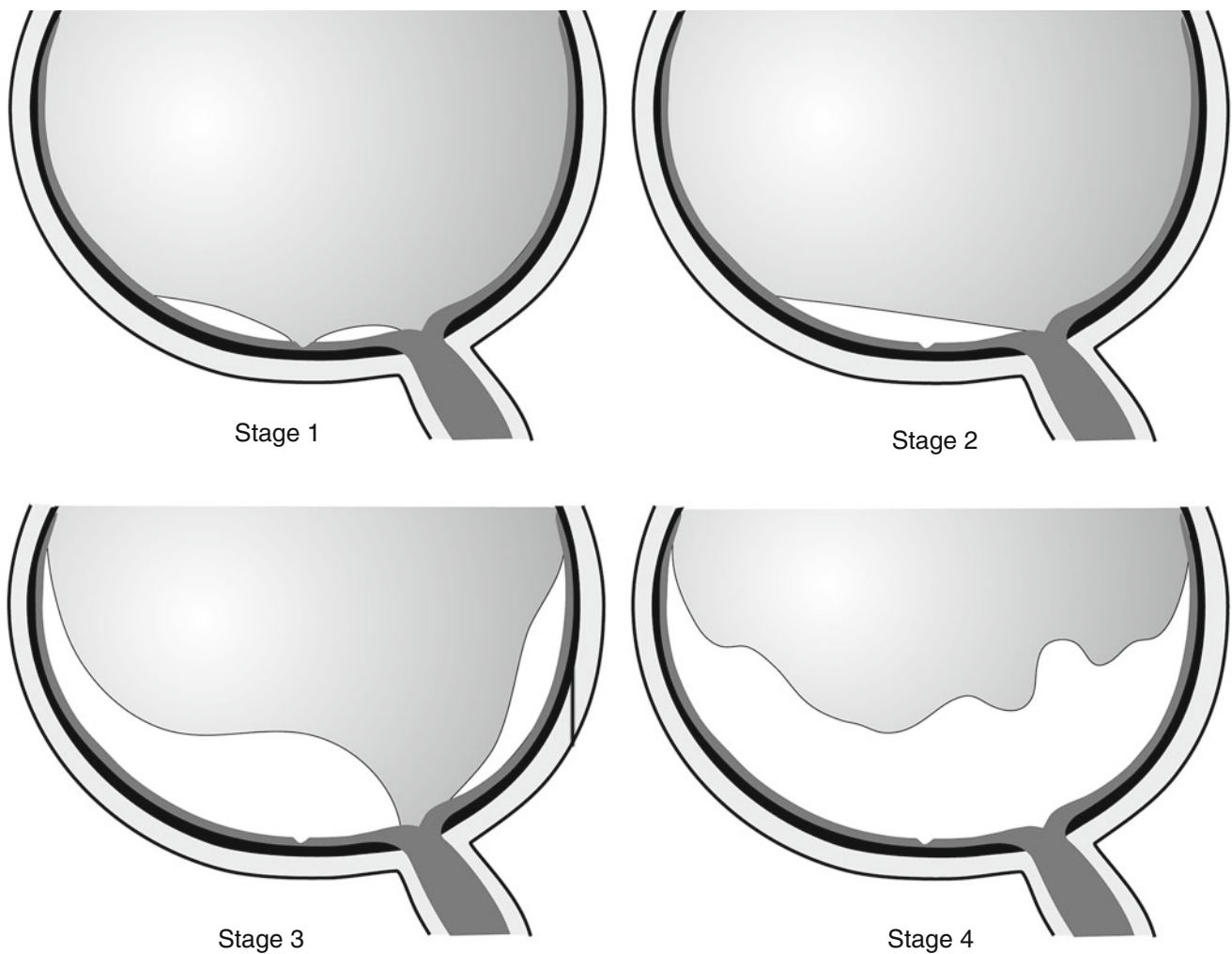


Figure II.C-9 Schematic representation of the last 4 stages (stage 0 not shown) of posterior vitreous detachment (d'après Johnson [68])

PVD symptoms occur. Barring a complication in an early stage (as described below), PVD is usually asymptomatic until the final stage of vitreo-papillary dehiscence. Even then, many PVDs occur with no symptoms at all. The symptoms described in this section are only those caused by a complete PVD and not those caused by all previous stages, which will be discussed later.

The most common symptom resulting from PVD is *floaters* [see chapter V.B.8. Vitreous floaters and vision: current concepts and management paradigms]. Floaters can result from shadows cast by Weiss ring, intravitreal blood, or condensed vitreous fibers. Their movement during saccadic eye movements is characterized by over-damping which creates a noticeable visual phenomenon in many patients. Recent studies suggest that these symptoms have a significantly negative impact on patients' quality of life [81, 82]. Since the floaters have a different acoustic reflectivity than normal

gel vitreous, they can be visualized on B-scan ultrasound and are represented by increased speckling of the image. B-scan image speckle density has been shown to increase with age. Additionally, by quantifying the motion of the speckles on ultrasound, the movement and viscosity of the vitreous can be measured *in vivo* [83] [see chapter II.F. Imaging vitreous].

Another common clinical symptom in PVD is photopsia or Moore's light flashes. Symptomatic flashes occur in between 27 and 42 % of PVD cases [72]. These are thought to result from either traction [84] or impact [85] exerted by the vitreous onto the retina and may signify a higher risk of retinal tears [72]. It is especially useful to query patients whether photopsia can be triggered by head movement or ocular saccades. If this is the case and the photopsia are described as a c-shaped arc of light that flashes off to the side, then it is likely they are experiencing vitreous traction

upon the peripheral retina with an increased risk of retinal tears. Interestingly, mathematical models of vitreous motion have shown that eyes with longer axial length experience larger shear forces exerted onto the retina by the movement of vitreous during saccadic eye movements. This is another possible explanation for the increased incidence of retinal tears and detachments in myopic individuals [77]. Similar traction upon retinal or optic disk blood vessels [72, 86] can induce hemorrhage, noted in 21 % of eyes with symptomatic PVD [66].

1. Time Course

PVD has long been perceived as a relatively acute process that occurs following a long process of gel liquefaction and weakening of the vitreoretinal adhesion. However, this is only true of the final stage of PVD, i.e., vitreo-papillary separation. With only perpendicular B-scan ultrasonography [70, 87], true high-resolution documentation of early PVD was difficult [88, 89]. With the advent of optical coherence tomography (OCT) (Figure II.C-10), however, early PVD can now be reliably identified [89]. Consequently, PVD is now perceived as a slow process occurring over the course of many years. In healthy, asymptomatic adults over the age 30, over 62 % of people have been found to have between a stage 1 and stage 3 PVD [90], suggesting a very high prevalence of early PVD. In eyes with various vitreoretinal pathologies the prevalence may be as high as 90 % [29]. Also, longitudinal studies have documented a very slow progression of PVD. Over the course of 30 months, 10 % of eyes with stage 1 or 2 PVD progressed to complete PVD [29]. Even progression from stage 1 to stage 2 PVD occurred in only 29 % of patients observed over 24 months [91]. While the process maybe slow, it is largely bilateral and occurs at approximately the same rate in each eye. After development of acute PVD in one eye, PVD will occur in 47 % of fellow eyes within 18 months and 90 % of fellow eyes within 36 months [92].

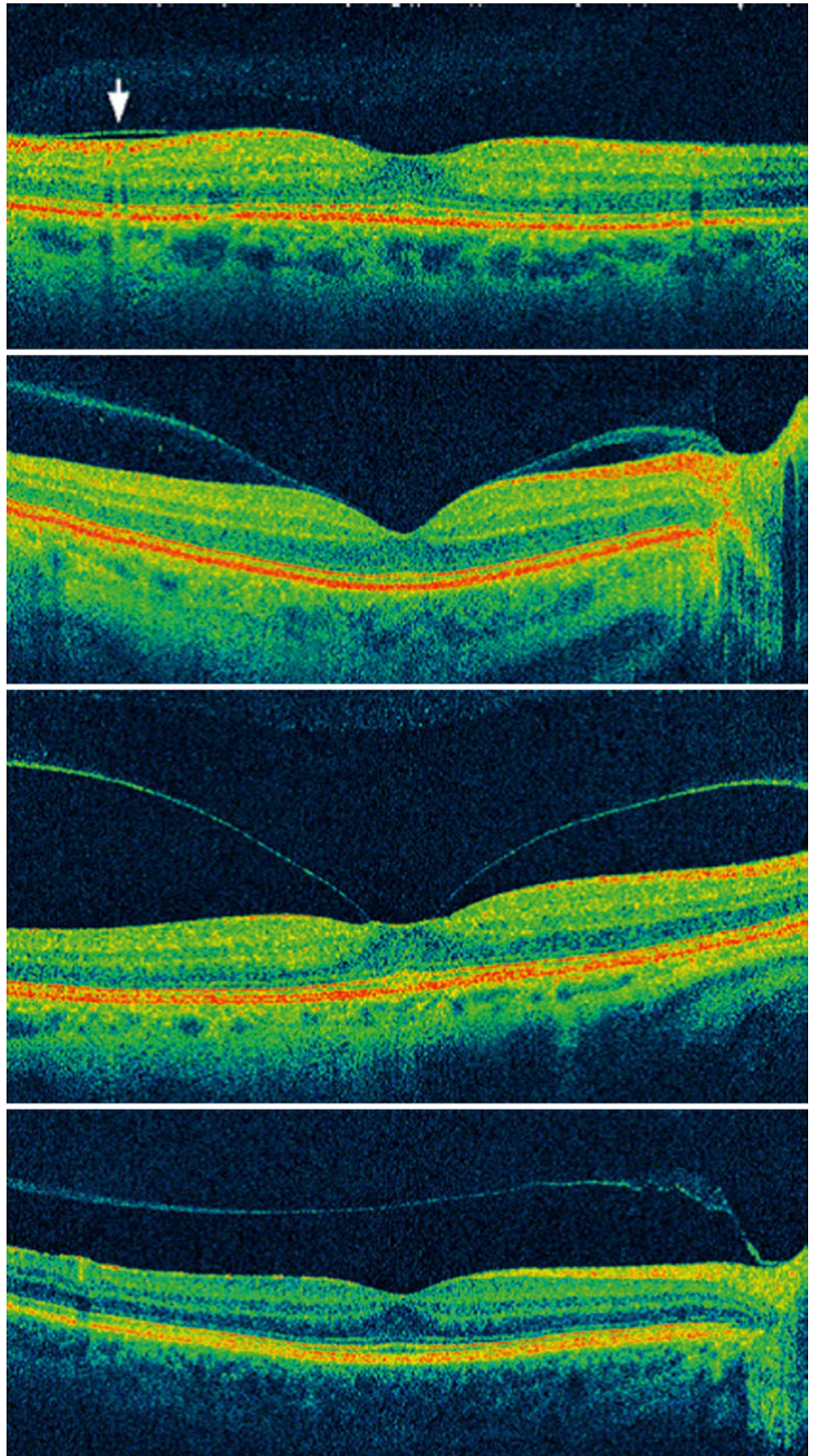
D. Anomalous PVD

Although early PVD often goes undetected, the clinical implications of these early stages have recently been defined. Several authors have described events that may occur prior to a complete PVD that can result in substantial vitreoretinal pathology. One such description by Sebag [10, 93] utilizes the concept of “anomalous PVD” (APVD) [see chapter III.B. Anomalous posterior vitreous detachment and vitreoschisis]. Sebag’s APVD theory states that pathology arises from a disconnection between liquefaction and gel dehiscence. This can be the result of any number of underlying conditions, such as inborn errors of type II collagen metabolism, myopia, or diabetes, or may occur in the

absence of underlying systemic conditions. Therefore, in this model, the term “anomalous” does not necessarily imply the presence of an underlying condition affecting vitreous liquefaction, such as Marfan or high myopia, but simply means that a disconnection between liquefaction and interface dehiscence exists. Within the APVD theory framework, the exact pathological manifestation of APVD is determined by a few factors. First, the location of persistent gel adhesion is important. For example, persistent adhesion at the macula results in vitreo-macular traction syndrome, while persistent adhesion at the disk or over blood vessels may cause vitreo-papillary traction or retinal hemorrhage, respectively. The second important consideration is the structural integrity of the vitreous cortex. Known to have lamellar structure, the posterior vitreous cortex can split (*vitreoschisis*) during early PVD resulting in the more posterior layers remaining adherent to the retinal surface [see chapter III.B. Anomalous posterior vitreous detachment and vitreoschisis].

Johnson [29, 68, 80] has further advanced our understanding of early PVD by grouping the manifestations of early PVD according to the anatomical site of persistent adhesion. Utilizing the 500- and 1,500- μm regions of increased vitreo-macular adhesion described by Kishi [25], Johnson gathered seemingly disparate conditions into two categories based on the size of the adhesion. With smaller adhesion sizes (500 μm or less), the tractional force is very localized, resulting in high stress over a small area of the central macula. This may cause full-thickness macular hole, pseudo-operculum, lamellar macular hole, or vitreo-foveal traction syndrome. Macular microhole and most cases of foveal red spot syndrome are likely due to the smallest zones of adhesion (50–150 μm), which result in even higher force per unit area traction stress. Conversely, larger adhesion zones (typically 1,500 μm or greater) disperse the traction force over a larger area. This lower traction stress is unlikely to result in macular hole states but can cause vitreo-macular traction syndrome or traction diabetic macular edema and can exacerbate myopic traction maculopathy [94] and possibly neovascular age-related macular degeneration [95]. Premacular membranes, which most likely develop from vitreoschitic remnants on the retinal surface, can begin to form as soon as there are areas of vitreoretinal separation and may therefore be seen in eyes with or without residual vitreo-macular adhesions [68]. Johnson’s model also discusses the nature of the traction forces being applied to the persistent vitreoretinal adhesion. He describes both static and dynamic forces as being important contributors. Static traction results from the inherent trampoline-like elasticity of the detaching posterior vitreous cortex and possibly from gravitational forces acting on the partially separated vitreous body. Dynamic traction forces are generated by

Figure II.C-10 Optical coherence tomography (OCT) images of the early stages of posterior vitreous detachment. Many of the early stages were undetectable prior to the advent of OCT imaging [see chapter II.F. To see the invisible - the quest of imaging vitreous]. The top panel demonstrates the appearance of the posterior vitreous cortex (*arrow*) slightly elevated off the inner limiting membrane (*ILM*) of the retina. The third panel down demonstrates anomalous PVD with vitreo-macular traction, defined by the 2013 IVTS classification system as persistent vitreo-macular adhesion with structural alteration of the retina, in this case slight elevation of the fovea. The bottom panel demonstrates PVD with persistent attachment to the optic disc [68]



ocular saccades. It is likely the dynamic forces that are responsible for the greater part of the tractional stress placed on the retina [29, 68, 80].

The two models share many similarities. Both models contrast physiologic, uncomplicated PVDs with PVDs that are complicated by vitreoretinal pathology. Both Sebag and Johnson ascribe vitreoretinal pathology to age-related vitreous degeneration and detachment in the presence of persistent focal vitreoretinal adhesions. Both recognize that the macular and peripapillary areas are the most common sites of adhesion and that slight variations in the size and strength of the adhesion can determine the resulting retinal pathology. Johnson's model emphasizes the evolution and complications of the early stages of PVD, and Sebag emphasizes the role of vitreoschisis, particularly with respect to the pathogenesis of macular pucker [see chapter III.F. Vitreous in the pathobiology of macular pucker] and macular hole [see chapter III.B. Anomalous posterior vitreous detachment and vitreoschisis]. Both models suggest that most late complications of PVD (e.g., retinal tear, retinal detachment, vitreous hemorrhage) occur only after vitreo-papillary separation, which allows for large saccadic movements of the vitreous body and increased dynamic traction forces [68]. Other late complications of PVD, like cataract formation, are likely due to changes in oxygen tension in the vitreous cavity [57]. In summary, both descriptions serve to underscore the pathogenic role of early PVD stages in the development of many serious vitreoretinal pathologies.

Abbreviations

AGEs	Advanced glycation end products
APVD	Anomalous posterior vitreous detachment
CS	Chondroitin sulfate
ECM	Extracellular matrix
GAG	Glycosaminoglycans
HA	Hyaluronan
HS	Heparan sulfate
ILM	Inner limiting membrane
PVC	Posterior vitreous cortex
PVD	Posterior vitreous detachment

References

- Bishop P, Crossman M, McLeod D, Ayad S. Extraction and characterization of the tissue forms of collagen types II and IX from bovine vitreous. *Biochem J*. 1994;299(Pt 2):497.
- Le Goff M, Bishop P. Adult vitreous structure and postnatal changes. *Eye*. 2008;22(10):1214–22.
- Richards AJ, Martin S, Yates JRW, Scott JD, Baguley DM, Pope FM, et al. COL2A1 exon 2 mutations: relevance to the Stickler and Wagner syndromes. *Br J Ophthalmol*. 2000;84(4):364–71.
- Bishop P, McLeod D, Ayad S. Extraction and characterisation of the intact form of bovine vitreous type IX collagen. *Biochem Biophys Res Commun*. 1992;185(1):392–7.
- Bos K, Holmes D, Meadows R, Kadler K, McLeod D, Bishop P. Collagen fibril organisation in mammalian vitreous by freeze etch/rotary shadowing electron microscopy. *Micron*. 2001;32(3):301–6.
- Bishop PN, McLeod D, Reardon A. Effects of hyaluronan lyase, hyaluronidase, and chondroitin ABC lyase on mammalian vitreous gel. *Invest Ophthalmol Vis Sci*. 1999;40(10):2173–8.
- Van Deemter M, Ponsioen T, Bank R, Snabel J, Van der Worp R, Hooymans J, et al. Pentosidine accumulates in the aging vitreous body: a gender effect. *Exp Eye Res*. 2009;88(6):1043–50.
- Sebag J, Buckingham B, Charles MA, Reiser K. Biochemical abnormalities in vitreous of humans with proliferative diabetic retinopathy. *Arch Ophthalmol*. 1992;110(10):1472.
- Sebag J, Nie S, Reiser K, Charles MA, Yu NT. Raman spectroscopy of human vitreous in proliferative diabetic retinopathy. *Invest Ophthalmol Vis Sci*. 1994;35(7):2976–80.
- Sebag J. Vitreous – from biochemistry to clinical relevance. In: Tasman W, Jaeger E, editors. *Duane's foundations of clinical ophthalmology*. Philadelphia: Lippincott Williams & Wilkins; 1998. p. 1–34.
- Larsson L, Österlin S. Posterior vitreous detachment. *Graefes Arch Clin Exp Ophthalmol*. 1985;223(2):92–5.
- Russell SR. What we know (and do not know) about vitreoretinal adhesion. *Retina*. 2012;32:S181–6.
- Hindson VJ, Gallagher JT, Halfter W, Bishop PN. Opticin binds to heparan and chondroitin sulfate proteoglycans. *Invest Ophthalmol Vis Sci*. 2005;46(12):4417–23.
- Bishop PN. Structural macromolecules and supramolecular organisation of the vitreous gel. *Prog Retin Eye Res*. 2000;19(3):323–44.
- Foos RY. Vitreoretinal juncture; topographical variations. *Invest Ophthalmol Vis Sci*. 1972;11(10):801–8.
- Balazs E. Molecular morphology of the vitreous body. The structure of the eye. New York: Academic Press; 1961. p. 295.
- Theopold H, Faulborn J. Scanning electron microscopy of the vitreous body. *Graefes Arch Clin Exp Ophthalmol*. 1979;211(3):259–64.
- Sebag J. Anatomy and pathology of the vitreo-retinal interface. *Eye*. 1992;6(6):541–52.
- Balazs EA. Fine structure of the developing vitreous. *Int Ophthalmol Clin*. 1975;15(1):53.
- Gupta P, Yee KMP, Garcia P, Rosen RB, Parikh J, Hageman GS, et al. Vitreoschisis in macular diseases. *Br J Ophthalmol*. 2011;95(3):376–80.
- Teng C, Chi H. Vitreous changes and the mechanism of retinal detachment. *Am J Ophthalmol*. 1957;44(3):335.
- Wang J, McLeod D, Henson DB, Bishop PN. Age-dependent changes in the basal retinovitreal adhesion. *Invest Ophthalmol Vis Sci*. 2003;44(5):1793–800.
- Heegaard S. Morphology of the vitreoretinal border region. *Acta Ophthalmol Scand Suppl*. 1997;222:1.
- Sebag J. The vitreous: structure, function, and pathobiology. New York: Springer; 1989.
- Kishi S, Demaria C, Shimizu K. Vitreous cortex remnants at the fovea after spontaneous vitreous detachment. *Int Ophthalmol*. 1986;9(4):253–60.
- Hageman GS, Johnson LV. Biochemical characterization of the major peanut agglutinin binding glycoproteins in vertebrate retinae. *J Comp Neurol*. 1986;249(4):499–510.
- Hageman G, Russell S. Chondroitinase-mediated disinsertion of the primate vitreous body. *Invest Ophthalmol Vis Sci*. 1994;35(4):1260.

28. Heegaard S, Jensen O, Prause J. Structure of the vitread face of the monkey optic disc (Macacca mulatta). *Graefes Arch Clin Exp Ophthalmol*. 1988;226(4):377–83.
29. Johnson MW. Perifoveal vitreous detachment and its macular complications. *Trans Am Ophthalmol Soc*. 2005;103:537.
30. Foos RY, Roth A. Surface structure of the optic nerve head. 2. Vitreopapillary attachments and posterior vitreous detachment. *Am J Ophthalmol*. 1973;76(5):662.
31. Kroll P, Wiegand W, Schmidt J. Vitreopapillary traction in proliferative diabetic vitreoretinopathy. *Br J Ophthalmol*. 1999;83(3):261–4.
32. Balazs EA, Denlinger J. Aging changes in the vitreous. Aging and human visual function. New York: Alan R Liss; 1982. p. 45–7.
33. Kishi S, Shimizu K. Posterior precortical vitreous pocket. *Arch Ophthalmol*. 1990;108(7):979–82.
34. Yonemoto J, Ideta H, Sasaki K, Tanaka S, Hirose A, Oka C. The age of onset of posterior vitreous detachment. *Graefes Arch Clin Exp Ophthalmol*. 1994;32(2):67–70.
35. Berman E, Michaelson I. The chemical composition of the human vitreous body as related to age and myopia. *Exp Eye Res*. 1964;3(1):9–15.
36. Balazs EA, Toth LZ, Jutheden GM, Collins B-A. Cytological and biochemical studies on the developing chicken vitreous. *Exp Eye Res*. 1965;4(3):237–IN26.
37. Pickett-Seltner R, Doughty M, Pasternak J, Sivak J. Proteins of the vitreous humor during experimentally induced myopia. *Invest Ophthalmol Vis Sci*. 1992;33(12):3424–9.
38. Maumenee IH. Vitreoretinal degeneration as a sign of generalized connective tissue diseases. *Am J Ophthalmol*. 1979;88(3 Pt 1):432.
39. Knobloch WH. Inherited hyaloideoretinopathy and skeletal dysplasia. *Trans Am Ophthalmol Soc*. 1975;73:417.
40. Worst J. Cisternal systems of the fully developed vitreous body in the young adult. *Trans Ophthalmol Soc U K*. 1977;97(4):550.
41. Ueno N, Sebag J, Hirokawa H, Chakrabarti B. Effects of visible-light irradiation on vitreous structure in the presence of a photosensitizer. *Exp Eye Res*. 1987;44(6):863–70.
42. Akiba J, Ueno N, Chakrabarti B. Mechanisms of photo-induced vitreous liquefaction. *Curr Eye Res*. 1994;13(7):505–12.
43. Kakehashi A, Ueno N, Chakrabarti B. Molecular mechanisms of photochemically induced posterior vitreous detachment. *Ophthalmic Res*. 1994;26(1):51–9.
44. Sebag J. Ageing of the vitreous. *Eye*. 1987;1(2):254–62.
45. Foos R, Wheeler N. Vitreoretinal juncture. Synchysis senilis and posterior vitreous detachment. *Ophthalmology*. 1982;89(12):1502–12.
46. Sebag J, Balazs E. Morphology and ultrastructure of human vitreous fibers. *Invest Ophthalmol Vis Sci*. 1989;30(8):1867–71.
47. Comper W, Laurent TC. Physiological functions of connective tissue polysaccharides. *Physiol Rev*. 1978;58:255.
48. Scott JE. The chemical morphology of the vitreous. *Eye*. 1992;6(6):553–5.
49. Deguine V, Menasche M, Ferrari P, Fraisse L, Pouliquen Y, Robert L. Free radical depolymerization of hyaluronan by Maillard reaction products: role in liquefaction of aging vitreous. *Int J Biol Macromol*. 1998;22(1):17–22.
50. Armand G, Chakrabarti B. Conformational differences between hyaluronates of gel and liquid human vitreous: fractionation and circular dichroism studies. *Curr Eye Res*. 1987;6(3):445–50.
51. Lundquist O, Österlin S. Glucose concentration in the vitreous of nondiabetic and diabetic human eyes. *Graefes Arch Clin Exp Ophthalmol*. 1994;32(2):71–4.
52. Stitt AW, Moore JE, Sharkey JA, Murphy G, Simpson D, Bucala R, et al. Advanced glycation end products in vitreous: structural and functional implications for diabetic vitreopathy. *Invest Ophthalmol Vis Sci*. 1998;39(13):2517–23.
53. Bishop PN, Holmes DF, Kadler KE, McLeod D, Bos KJ. Age-related changes on the surface of vitreous collagen fibrils. *Invest Ophthalmol Vis Sci*. 2004;45(4):1041–6.
54. Los LI, van der Worp RJ, van Luyn MJA, Hooymans JMM. Age-related liquefaction of the human vitreous body: LM and TEM evaluation of the role of proteoglycans and collagen. *Invest Ophthalmol Vis Sci*. 2003;44(7):2828–33.
55. Beebe DC, Holekamp NM, Siegfried C, Shui Y-B. Vitreoretinal influences on lens function and cataract. *Philos Trans Roy Soc B: Biol Sci*. 2011;366(1568):1293–300.
56. Stocchino A, Repetto R, Siggers JH. Mixing processes in the vitreous chamber induced by eye rotations. *Phys Med Biol*. 2010;55(2):453.
57. Holekamp NM. The vitreous gel: more than meets the eye. *Am J Ophthalmol*. 2010;149(1):32–6.e1.
58. Sebag J. Age-related differences in the human vitreoretinal interface. *Arch Ophthalmol*. 1991;109:966–71.
59. Klöti R. Experimental occlusion of retinal and ciliary vessels in owl monkeys: I. Technique and clinical observations of selective embolism of the central retinal artery system. *Exp Eye Res*. 1967;6(4):393–IN28.
60. Kohno T, Sorgente N, Ishibashi T, Goodnight R, Ryan SJ. Immunofluorescent studies of fibronectin and laminin in the human eye. *Invest Ophthalmol Vis Sci*. 1987;28(3):506–14.
61. Ponsioen TL, Hooymans JMM, Los LI. Remodelling of the human vitreous and vitreoretinal interface – a dynamic process. *Prog Retin Eye Res*. 2010;29(6):580–95.
62. Fukai N, Eklund L, Marneros AG, Oh SP, Keene DR, Tamarkin L, et al. Lack of collagen XVIII/endostatin results in eye abnormalities. *EMBO J*. 2002;21(7):1535–44.
63. Chuo JY, Lee TY, Hollands H, Morris AH, Reyes RC, Rossiter JD, et al. Risk factors for posterior vitreous detachment: a case-control study. *Am J Ophthalmol*. 2006;142(6):931–7.e1.
64. Hikichi T, Trempe CL. Relationship between floaters, light flashes, or both, and complications of posterior vitreous detachment. *Am J Ophthalmol*. 1994;117(5):593.
65. Favre M, Goldmann H. Zur Genese der hinteren Glaskörperabhebung. *Ophthalmologica*. 1956;132(2):87–97.
66. Novak M, Welch R. Complications of acute symptomatic posterior vitreous detachment. *Am J Ophthalmol*. 1984;97(3):308–14.
67. Larsen G. The hyaluronic acid in the rabbit vitreous body: variations following hormonal treatment. *Arch Ophthalmol*. 1958;60(5):815.
68. Johnson MW. Posterior vitreous detachment: evolution and complications of its early stages. *Am J Ophthalmol*. 2010;149(3):371–82.
69. Sebag J. Age-related changes in human vitreous structure. *Graefes Arch Clin Exp Ophthalmol*. 1987;225(2):89–93.
70. Johnson MW, Van Newkirk MR, Meyer KA. Perifoveal vitreous detachment is the primary pathogenic event in idiopathic macular hole formation. *Arch Ophthalmol*. 2001;119(2):215.
71. Tanner V, Chauhan D, Jackson T, Williamson T. Optical coherence tomography of the vitreoretinal interface in macular hole formation. *Br J Ophthalmol*. 2001;85(9):1092–7.
72. Jaffe NS. Complications of acute posterior vitreous detachment. *Arch Ophthalmol*. 1968;79(5):568–71.
73. Gärtner J. Photoelastic and ultrasonic studies on the structure and senile changes of the intervertebral disc and of the vitreous body. *Bibl Ophthalmol*. 1969;79:136.
74. Kishi S, Hagimura N, Shimizu K. The role of the premacular liquefied pocket and premacular vitreous cortex in idiopathic macular hole development. *Am J Ophthalmol*. 1996;122(5):622–8.
75. Lindner K. Über die Herstellung von Modellen zu Modellversuchen der Netzhautabhebung. *Klin Monatsbl Augenheilkd*. 1933;90:289–300.

76. Rosengren B, Österlin S. Hydrodynamic events in the vitreous space accompanying eye movements. *Ophthalmologica*. 1976;173(6):513–24.
77. David T, Smye S, Dabbs T, James T. A model for the fluid motion of vitreous humour of the human eye during saccadic movement. *Phys Med Biol*. 1998;43(6):1385.
78. Abouali O, Modareszadeh A, Ghaffariyeh A, Tu J. Numerical simulation of the fluid dynamics in vitreous cavity due to saccadic eye movement. *Med Eng Phys*. 2012;34(6):681–92.
79. Repetto R, Stocchino A, Cafferata C. Experimental investigation of vitreous humour motion within a human eye model. *Phys Med Biol*. 2005;50(19):4729.
80. Johnson MW. Posterior vitreous detachment: evolution and role in macular disease. *Retina*. 2012;32:S174–8.
81. Wagle AM, Lim W-Y, Yap T-P, Neelam K, Au Eong K-G. Utility values associated with vitreous floaters. *Am J Ophthalmol*. 2011;152(1):60–5.e1.
82. Sebag J. Floaters and the quality of life. *Am J Ophthalmol*. 2011;152(1):3–4.e1.
83. Walton KA, Meyer CH, Harkrider CJ, Cox TA, Toth CA. Age-related changes in vitreous mobility as measured by video B scan ultrasound. *Exp Eye Res*. 2002;74(2):173–80.
84. Wise G. Relationship of idiopathic preretinal macular fibrosis to posterior vitreous detachment. *Am J Ophthalmol*. 1975;79(3):358–62.
85. Verhoeff F. Are Moore's lightning streaks of serious portent? *Am J Ophthalmol*. 1956;41(5):837.
86. Lindner B. Acute posterior vitreous detachment and its retinal complications. *Acta Ophthalmol*. 1966;87:1–108.
87. Van Newkirk M, Gass J, Callanan D, Byrne S, Hughes JR. Follow-up and ultrasonographic examination of patients with macular pseudo-epithelium. *Am J Ophthalmol*. 1994;117(1):13–8.
88. Sebag J. Imaging vitreous. *Eye*. 2002;16(4):429–39.
89. Mirza RG, Johnson MW, Jampol LM. Optical coherence tomography use in evaluation of the vitreoretinal interface: a review. *Surv Ophthalmol*. 2007;52(4):397–421.
90. Uchino E, Uemura A, Ohba N. Initial stages of posterior vitreous detachment in healthy eyes of older persons evaluated by optical coherence tomography. *Arch Ophthalmol*. 2001;119(10):1475.
91. Niwa H, Terasaki H, Ito Y, Miyake Y. Macular hole development in fellow eyes of patients with unilateral macular hole. *Am J Ophthalmol*. 2005;140(3):370–5.
92. Hikichi T. Time course of posterior vitreous detachment in the second eye. *Curr Opin Ophthalmol*. 2007;18(3):224–7.
93. Sebag J. Anomalous posterior vitreous detachment: a unifying concept in vitreo-retinal disease. *Graefes Arch Clin Exp Ophthalmol*. 2004;42(8):690–8.
94. VanderBeek BL, Johnson MW. The diversity of traction mechanisms in myopic traction maculopathy. *Am J Ophthalmol*. 2012;153(1):93–102.
95. Krebs I, Brannath W, Glittenberg C, Zeiler F, Sebag J, Binder S. Posterior vitreomacular adhesion: a potential risk factor for exudative age-related macular degeneration? *Am J Ophthalmol*. 2007;144(5):741–6.e1.

Takeshi Kita, Taiji Sakamoto, and Tatsuro Ishibashi

Outline

- I. **Introduction**
- II. **Characteristics of Hyalocytes**
 - A. Existence and Distribution of Hyalocytes
 - 1. Morphological Characteristics of Hyalocytes
 - a. Cell Surface Antigenic Characteristics
 - 2. Origin of Hyalocytes
- III. **Physiological Functional Properties of Hyalocytes**
 - A. Role of Hyalocytes During Development
 - B. Phagocytic and Fibrinolytic Activity of Hyalocytes
 - C. Modulator of Intraocular Immune System: Vitreous Cavity-Associated Immune Deviation
- IV. **Functional Properties of Hyalocytes in Vitreoretinal Interface Pathology**
 - A. Proliferative Vitreoretinal Diseases
 - 1. Formation of Proliferative Membranes
 - 2. Cicatricial Contraction of Proliferative Membranes
 - 3. Macular Pucker
 - 4. Macular Holes
- V. **Treatment**
 - A. Surgical Approach
 - B. Pharmacotherapy
- VI. **Summary**

References

T. Kita, MD, PhD • T. Ishibashi, MD, PhD
Department of Ophthalmology,
Graduate School of Medical Sciences, Kyushu University,
3-1-1 Maidashi, Higashi-Ku, Fukuoka 812-8582, Japan
e-mail: kita@eye.med.kyushu-u.ac.jp;
ishi@eye.med.kyushu-u.ac.jp

T. Sakamoto, MD, PhD (✉)
Department of Ophthalmology,
Kagoshima University Graduate School
of Medical and Dental Sciences,
8-35-1 Sakuragaoka, Kagoshima 890-8520, Japan
e-mail: tsakamot@m3.kufm.kagoshima-u.ac.jp

Keywords

Vitreous • Hyalocytes • α -smooth muscle actin (α -SMA) • Cicatricial contraction • Macrophage • Myofibroblast • Rho kinase • Transforming growth factor- β (TGF- β) • Vitreous cavity-associated immune deviation (VCAID) • Vitrectomy

Key Concepts

1. Hyalocytes are the cells located in the posterior vitreous cortex abutting the inner surface of the retina that play a significant role in the maintenance of vitreous transparency under physiological conditions.
2. Hyalocytes might be involved in the progression of various vitreoretinal interface diseases, such as proliferative diabetic retinopathy, proliferative vitreoretinopathy, macular pucker, and macular hole, under pathological conditions.
3. Hyalocytes could be a novel therapeutic target for surgical and pharmacological approaches to better manage vitreoretinal interface diseases.

I. Introduction

Vitreoretinal interface diseases are common causes of vision loss or metamorphopsia in spite of recent advances in clinical ophthalmology including vitreoretinal surgery, pharmacological therapy such as anti-VEGF agents, and gene-mediated therapy. The vitreous body is often used as a therapeutic depot or platform for these therapies; therefore, more detailed knowledge about the environment of the vitreous is required.

Under physiological condition, only small number of cells currently called “hyalocytes” are present in vitreous, located mainly in the posterior vitreous cortex abutting the inner surface of the retina. According to previous publications [1–3], hyalocytes were regarded as resting cells, and hyalocytes have been studied less extensively compared to other intraocular cells, such as retinal pigment epithelium (RPE), glial cells, and retinal vascular endothelial cells. However, hyalocytes have recently been shown to actively play a significant role in maintaining the vitreous body as a transparent and avascular system [4–7]. In addition, hyalocytes have also been found to play pivotal roles under pathological conditions which involve proliferative vitreoretinal diseases such as proliferative diabetic retinopathy (PDR) and proliferative vitreoretinopathy (PVR), macular pucker, and others [5, 7–9]. This chapter reviews the characteristics of hyalocytes and their functional properties in physiological and pathological conditions to improve our understanding of vitreoretinal pathophysiology and to promote/facilitate the development of novel therapeutic strategies.

II. Characteristics of Hyalocytes

A. Existence and Distribution of Hyalocytes

The vitreous body occupies the greatest volume of the eye. Vitreous is a clear, jellylike substance composed mainly of water and delicate collagenous network associated with hyaluronan. The vitreous not only offers support to the structures within the eye but helps maintain the transparency of the media. The embryonic vitreous contains relatively numerous cells, the number of which gradually decreases, and only a small number of the cells are in the vitreous of the adult eyes under physiological condition. In 1840, Hannover first described cells in the vitreous body of the eye [10]. The term “hyalocytes” was introduced by Balazs [11] in order to define a homogeneous population of cells in the cortical layer of the vitreous body of various animal species. Hyalocytes are located in the cortical region of the vitreous body, at an average distance of 50 μm from the inner surface of the retina, and a certain number of hyalocytes subsist entangled with collagen fibrils in the vitreous cortex

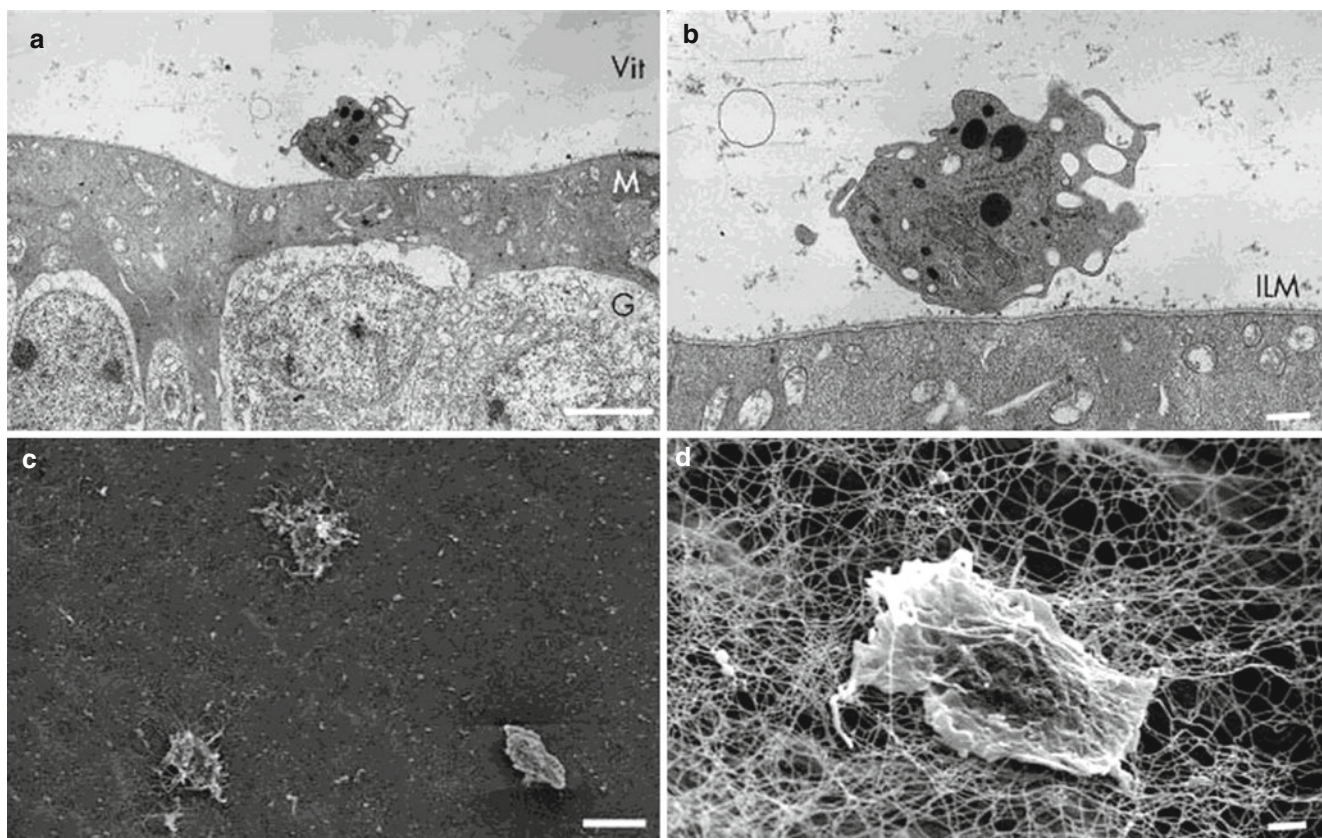


Figure II.D-1 The morphological characteristics and the distribution of hyalocytes in the vitreoretinal interface. (a) Transmission electron micrograph shows a hyalocyte situated in the posterior vitreous cortex close to the retina. (b) Higher magnification shows that hyalocytes are completely free from but close to the inner limiting membrane (ILM) of the retina. The hyalocyte possesses lysosome-like granules, mitochondria, and micropinocytotic vesicles, presenting the characteristics of cells of macrophage lineage. (c) Scanning electron micrograph shows

free hyalocytes in the vitreous cortex that are very close to the retina, which lies in the background of the image. (d) A higher magnification view showing that the cell is entangled in a collagen fibril network in the vitreous cortex and a few protuberances are observed at the cell surface (Original magnification a, 62,600 \times , bar 5 μm ; b, 66,000 \times , bar 1 μm ; c, 61,100 \times , bar 10 μm ; d, 64,300 \times , bar=1 μm) (Ref. [12]). *Vit* vitreous, *M* Mueller cell endplate, *G* ganglion cell)

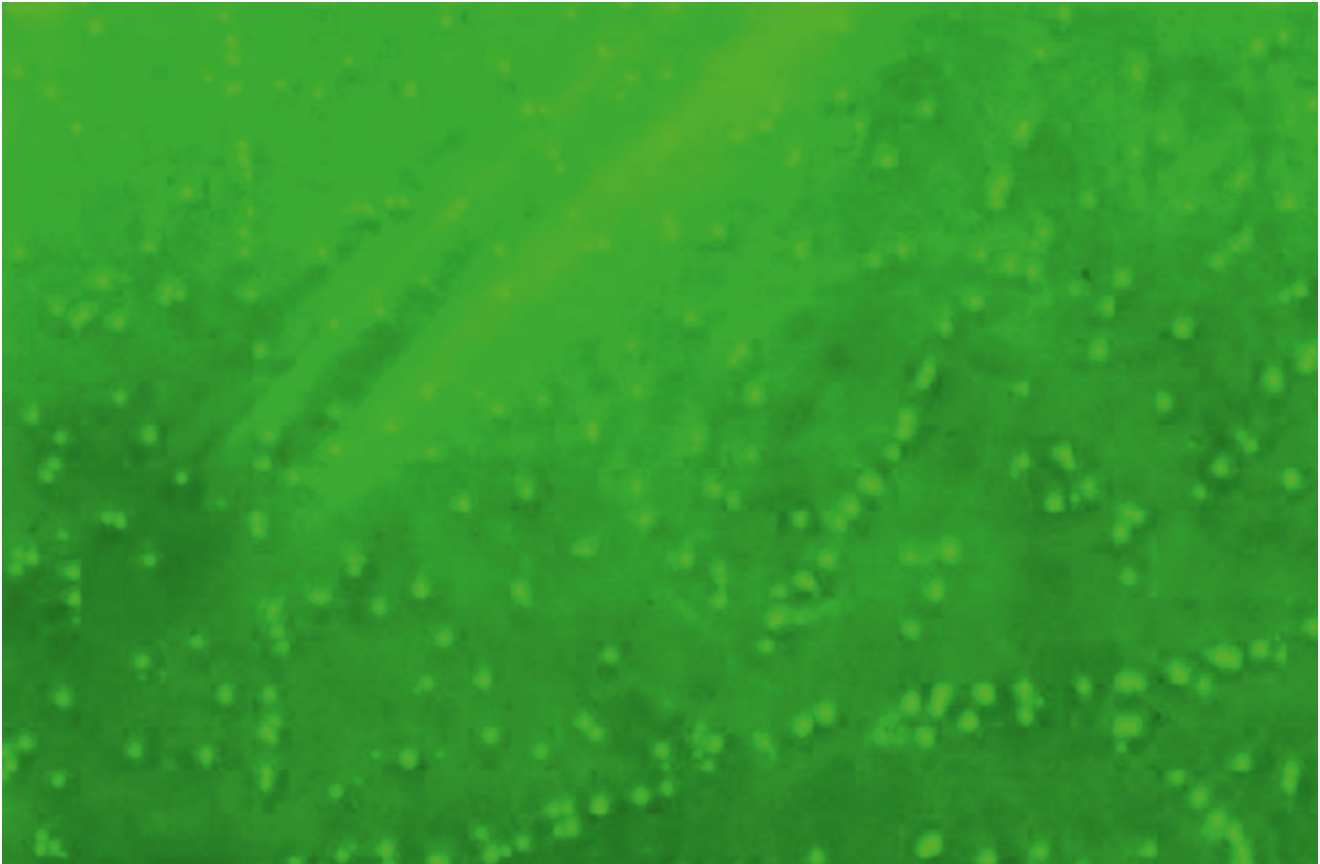


Figure II.D-2 Hyalocytes in the extracted vitreous. The hyalocytes were present mainly on the vitreous gel surface and arranged in branching patterns that are thought to follow the patterns of blood vessels in the retina (Ref. [6])

(Figure II.D-1a–d) [12]. The average number of hyalocytes in human cortical and basal vitreous is about 150 per mm^2 and in pig or bovine eyes is reported to be around 100 per mm^2 . It has been noted that the hyalocytes are arranged in treelike branching patterns, possibly following the course of the retinal vessels [6] (Figure II.D-2).

1. Morphological Characteristics of Hyalocytes

Morphological studies using both light and electron microscopy demonstrate that the shape of hyalocytes varies from oval to spindle or stellate shape and that hyalocytes possess lysosomes, mitochondria, ribosomes, and micropinocytotic vesicles with numerous microvilli on their surface [2], indicating that hyalocytes are morphologically very similar to so-called macrophages. Therefore, hyalocytes are considered to belong to monocyte/macrophage lineage (Figure II.D-1b), although Hogan et al. [13] reported that hyalocytes differ from macrophages because of a paucity of lysosomes. Immunocytochemical analyses found that hyalocytes possess antigenic determinants that react with antibodies directed against CD45 (leukocyte common antigen), CD64 (Fc receptor I), CD11a (leukocyte-function antigen-1), histocompatibility complex (MHC) class II antigens, and S100 protein [14]. The presence of CD45, which is selectively expressed by all hematopoietic cells, excluding mature

erythroid cells, and CD11a, which is present on virtually all leukocytes, strongly suggests that hyalocytes are derived from a leukocytic cell lineage. In addition, Fc receptor I is the particular IgG receptor which is expressed constitutively only by monocytes and tissue macrophages. The expression of MHC class II antigens and S100 protein, although not unique to the monocyte/macrophage lineage, is consistent with this cellular origin.

a. Cell Surface Antigenic Characteristics

Although hyalocytes do not react with CD11b, CD11c, or CD14, these antigenic determinants are variably expressed by tissue macrophages. They differ from other cells of the mononuclear phagocytic system in that they lack immunocytochemically detectable CD68 antigen, an epitope that is highly expressed by peripheral blood monocytes and macrophages of virtually all tissues [14]. Furthermore, antigens that are typically associated with epithelial cells (cytokeratin and epithelial membrane antigen), fibroblasts (prolyl 4-hydroxylase and vimentin), endothelial cells (CD31 and von Willebrand factor), neuroglial cells (glial fibrillary acidic protein: GFAP), neuronal cells (neuron-specific enolase) and RPE cells, and Muller cells (cellular retinaldehyde binding protein) do not react with hyalocytes. In addition, other immunophenotypic analysis demonstrated that most (80 %) of

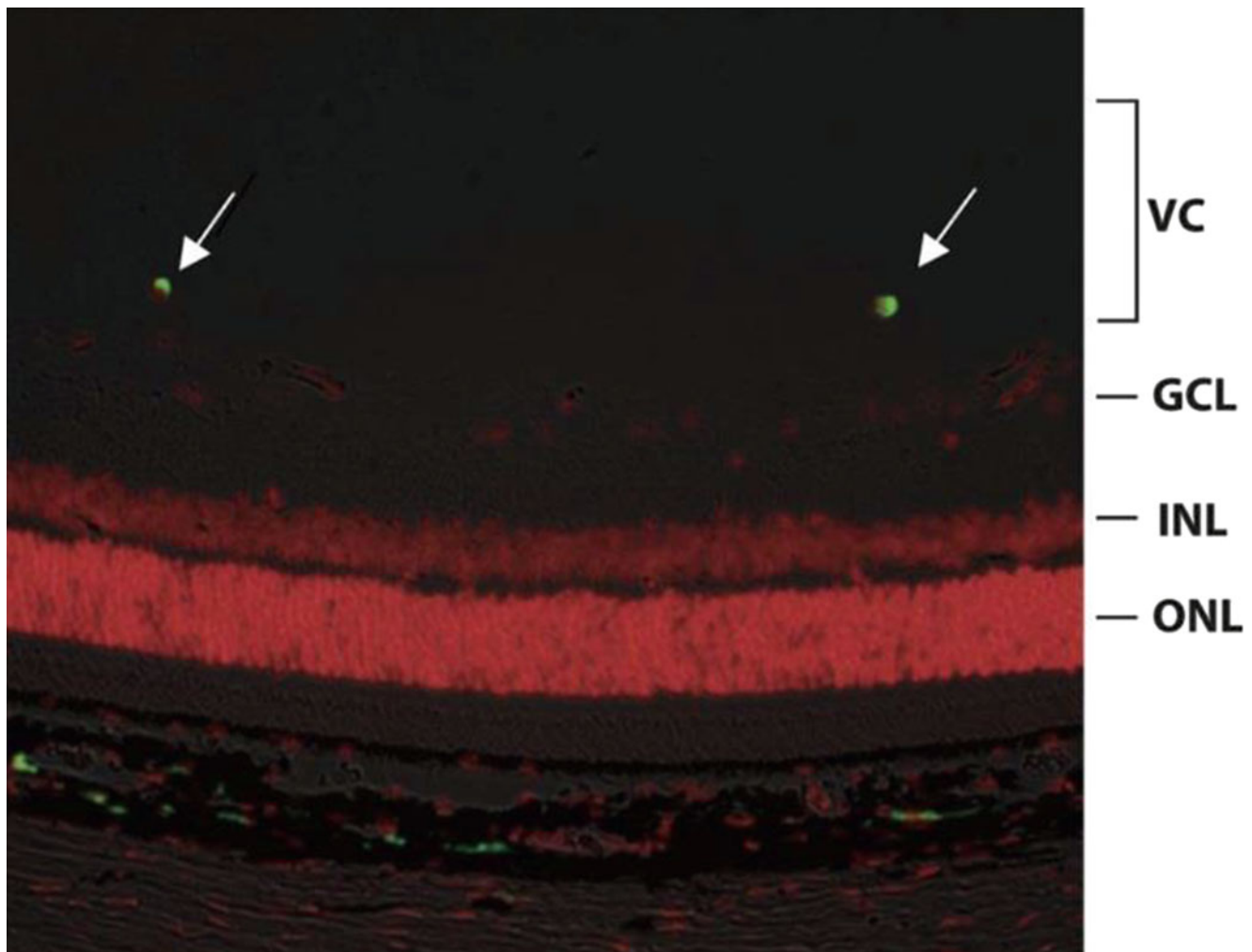


Figure II.D-3 Fluorescent microscopic photograph of GFP chimeric mouse. The hyalocytes (*arrows*) are GFP positive, indicating their bone marrow origin. *VC* vitreous cortex, *GCL* ganglion cell layer, *INL* inner

nuclear layer, *ONL* outer nuclear layer, *GFP* green fluorescent protein (Original magnification = 340x) (Ref. [15])

of the hyalocytes are positive against ED2 antibody, which recognizes membrane and cytoplasmic antigens of tissue macrophages, and a few (15 %) hyalocytes were positive against ED1 antibody, which recognizes an antigen in monocytes and in most macrophages, free and fixed. Only 5 % of hyalocytes showed both ED1 and ED2 positive staining. Antibodies directed against ED1, bearing the characteristic phenotype of monocyte derived macrophages, only label a small proportion of hyalocytes. Antibodies directed against ED2 typically associated with hyalocytes, illustrating that vitreous hyalocytes have the characteristic phenotype of tissue macrophages [15].

2. Origin of Hyalocytes

Numerous theories regarding the origin of the vitreous hyalocytes, including derivation from neuroglia of the retina, mesenchymal cells of the retinal vasculature, or cells of the hyaloid system, have been proposed. However, evidence to

date suggests that hyalocytes belong to the monocyte/macrophage lineage; thus, the recent popular concept about their origin has proposed that hyalocytes originate from the blood monocytes. To confirm this origin of hyalocytes, we created chimeric mice by transplanting the bone marrow cells from enhanced green fluorescent protein (GFP) mice to them [5, 12]. In these chimeric mice, hyalocytes were GFP negative immediately after transplantation of bone marrow cells. However, more than 60 % of total vitreous hyalocytes were replaced with GFP-positive cells within 4 months and approximately 90 % within 7 months under physiological condition [15] (Figure II.D-3). The levels of residual macrophages might not have been maintained by their proliferation but by being produced in bone marrow under a physiological condition with a turnover time of several months [12]. However, van Meurs et al. [16] showed that the half-life of vitreous macrophage was 4.8 days by allowing vitreous macrophages to phagocytose $^{141}\text{Cerium}$ (γ -emitter)-labeled

microspheres. It is difficult to conclude that the same type of vitreous cells was studied in these reports; however, there might be several different cell lineages within the so-called hyalocytes.

Conversely, Gloor [17] described that hyalocytes would be in an independent tissue layer, in which the cells are replaced by reproduction because the hyalocytes showed increased mitotic activity after photocoagulation. Haddad and Andre observed that ^3H -thymidine was detected in the hyalocytes of the cortical vitreous after ^3H -thymidine injection and concluded that hyalocytes renew themselves inside the eye [18]. It is not clear whether hyalocytes are composed of cells of different origins or those of the same origin at different developmental stages. Although more detailed studies are necessary to answer these questions, however, it is safe to say that most hyalocytes originate from bone marrow, at least under physiological conditions.

III. Physiological Functional Properties of Hyalocytes

A. Role of Hyalocytes During Development

An interesting example of tissue regression occurs during development of the mouse eye, where arcades of the hyaloid capillary network (called the vasa hyaloidea propria) disappear from the vitreous between 5 and 7 days after birth and other branches (called the tunica vasculosa lentis) between 7 and 21 days after birth [see chapter I.D. Proteomics of fetal hyaloid vasculature regression]. Histological studies have shown that the embryonic vitreous contains relatively numerous hyalocytes and the hyalocytes are closely associated with the hyaloid vasculature prior to and during the phase of remodeling. The two transient ocular structures, the hyaloid vasculature and the pupillary membrane, which normally regress according to a defined developmental timetable, are found to persist in the macrophage ablation transgenic mice [19]. Hyalocytes are associated with the loss of capillary integrity, leakage of erythrocytes into the vitreous compartment, and phagocytosis of the apoptotic endothelium. It has also been reported that hyalocytes are directly responsible for the endothelial cell death in the system [20]. Furthermore, it has been reported that hyalocytes secrete some antiangiogenic factors. Those experiments provided direct evidence for the active involvement of macrophages in developmentally programmed tissue remodeling and identify the hyaloid vessels and the pupillary membrane in the eye as targets of macrophage-mediated remodeling, suggesting that hyalocytes actively elicit targeted cell death during development of the mouse eye.

Hyalocytes are also considered to have a function in the formation of the vitreous' ground substance. Hyalocytes are purported to be involved in the synthesis of collagen and hyaluronic acid during later stage of development [21, 22], whereas the neural retina is the chief source of the protein during early vitreous development, a period of rapid increase in size of the vitreous body. Recently, it has been further confirmed that the production of hyaluronan is modulated by cytokines, such as transforming growth factor- β (TGF- β) or platelet-derived growth factor-BB (PDGF-BB) using cultured hyalocytes [23].

B. Phagocytic and Fibrinolytic Activity of Hyalocytes

Hyalocytes are thought to function as resident macrophages of the vitreous cavity under physiological condition. Phagocytic activity of hyalocytes with surface receptors for IgG and complement components has been confirmed experimentally by the injection of foreign substances into the vitreous and in experiments with cultured hyalocytes [24]. Thus, hyalocytes are thought to be active in maintaining vitreous as an avascular and transparent tissue.

Hyalocytes also show fibrinolytic activity. PDGF (platelet-derived growth factor) enhances the expression of urokinase-type plasminogen activator (uPA) by hyalocytes and stimulates (uPA)-plasmin activity. This activity was demonstrated *in vitro* where plated fibrin was shown to be lysed using fibrin zymographic analysis [6]. The humoral element circulates poorly in the vitreous because of the gelatinous structure of the vitreous. Therefore, a vitreous hemorrhage tends to remain in the cavity for a long time. It is thus reasonable to suggest that hyalocytes digest the fibrinous material in the vitreous cavity, indicating that one of the physiological properties of these cells is the maintenance of vitreous transparency.

C. Modulator of Intraocular Immune System: Vitreous Cavity-Associated Immune Deviation

The eye is an immune-privileged site that is styled to keep the visual pathway clear while at the same time to provide defenses against invading organisms [25]. Above all, the anterior chamber-associated immune deviation (ACAID) is a unique system to keep the eye immune privileged. ACAID can be induced by antigen injection for peripheral tolerance to that antigen [26]. It has been demonstrated that ACAID is induced by bone marrow-derived antigen-presenting cells (APCs), which are positive for F4/80, a marker of a wide range of mature tissue macrophages, localized in the iris and ciliary body in the eye and carrying an antigen-specific signal to the spleen [25, 27]. We investigated the mechanisms

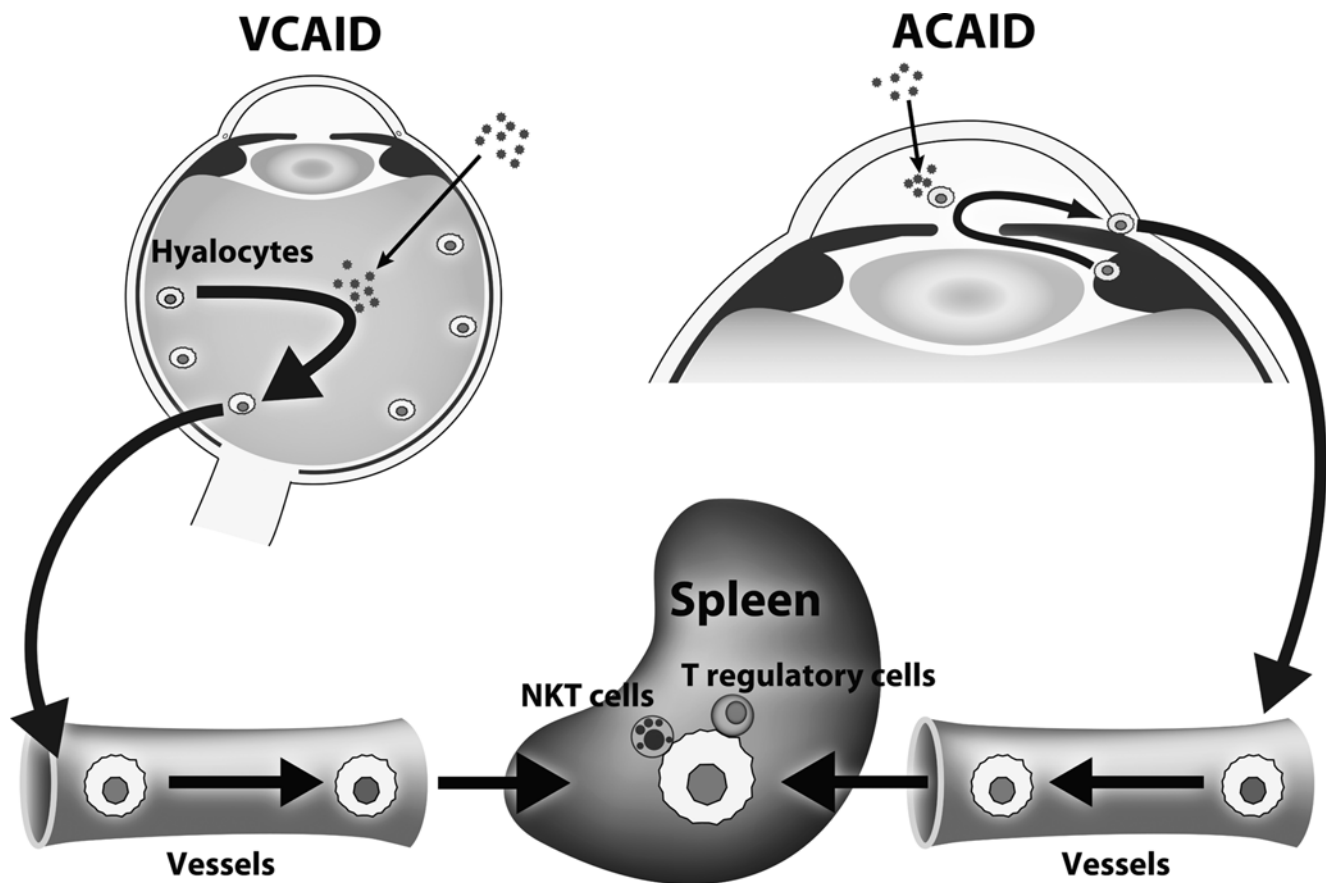


Figure II.D-4 Schema of vitreous cavity-associated immune deviation (VCAID) and anterior chamber-associated immune deviation (ACAID). Antigens inoculated into the vitreous cavity are captured by resident macrophage hyalocytes and carried via the bloodstream to the spleen.

Both VCAID and ACAID require eye-derived antigen-presenting cells and CD1d-restricted natural killer T cells to induce antigen-specific regulatory T cells (Ref. [15])

by which ocular inflammation associated with the vitreous cavity is reduced by injecting either ovalbumin or allogeneic splenocytes into the vitreous cavities of mice and assessed the effects of this on delayed-type hypersensitivity response. After antigen inoculation into the vitreous cavity, antigen-specific delayed-type hypersensitivity responses were significantly impaired, and we named this phenomenon the vitreous cavity-associated immune deviation (VCAID) [28]. VCAID could also be induced by inoculating antigen-pulsed macrophages into vitreous. However, VCAID did not develop either in mice with inflamed eyes, whether as a result of experimental autoimmune uveitis, or coadministration of interleukin-6 (IL-6) in the vitreous cavity, or in knockout mice deficient in natural killer T cells [28]. In this system, we found that hyalocytes are the only cells present in the vitreous. Interestingly, hyalocytes express F4/80, suggesting that hyalocytes are candidate APCs responsible for mediating VCAID [15, 28] (Figure II.D-4). These findings suggest that hyalocytes

could play a pivotal role in inhibiting intraocular inflammation in non-inflamed eyes, which could also serve to maintain vitreous transparency.

IV. Functional Properties of Hyalocytes in Vitreoretinal Interface Pathology

A. Proliferative Vitreoretinal Diseases

Proliferative vitreoretinal diseases such as proliferative diabetic retinopathy (PDR) and proliferative vitreoretinopathy (PVR) still remain common causes of severe vision loss in spite of the dramatic advances in vitreoretinal surgery. PDR and PVR cause traction retinal detachment due to the formation of contractile preretinal fibrous membranes as a result of excessive wound healing under pathological conditions. Previous studies revealed that various types of ocular cells, such as RPE, which contribute especially to the pathogenesis

of PVR, glial cells, vascular endothelial cells, myofibroblast-like cells of unknown origin, and hyalocytes, organize to form the proliferative membranes. Specifically, in human diabetic eyes the hyalocytes have a different shape compared with those in normal eyes, and their numbers appear to be increased. Hyalocytes may participate in the initiation and progression of PDR and PVR through the formation of proliferative membranes and subsequent cicatricial contraction.

1. Formation of Proliferative Membranes

The formation of proliferative membranes is characterized by the proliferation and migration of cells and the excessive synthesis and deposition of extracellular matrix (ECM) proteins. This tissue repair process is regulated by a number of polypeptide including cytokines and growth factors. Growth factors such as PDGF, HGF (hepatocyte growth factor), and MCP-1 (monocyte chemoattractant protein-1) regulate the proliferation and migration of the cells. PDGF stimulates the proliferation of hyalocytes through p44/p42 MAPK, PI3 kinase, and p38 MAPK and promotes migration of hyalocytes through PI3 kinase and p38 MAPK, but not p44/p42 MAPK [29]. In addition, TGF- β , which is overexpressed in the vitreous and proliferative membranes in those diseases, is involved in the production of extracellular matrix proteins such as collagen and fibronectin by various types of cells. Also in hyalocytes, TGF- β promotes the expression of fibronectin, which is one of the major extracellular matrix proteins observed in the preretinal proliferative membranes [30]. Furthermore, TGF- β stimulates the expression of its downstream mediator, CTGF (connective tissue growth factor), by hyalocytes via activation of Smad signaling, which is mediated through Rho kinase (ROCK) pathway and at least partially through p38 MAPK [31]. Various types of vitreoretinal cells other than hyalocytes, such as RPE, Muller cells, and retinal capillary endothelial cells, can also be the sources of CTGF, and CTGF stimulates cell growth and ECM synthesis by hyalocytes and RPE cells [30, 31]. It was also shown that cultured porcine hyalocytes produce glycosaminoglycans and ECM, which is modulated by basic fibroblast growth factor (b-FGF) and TGF- β 1 [32]. Those reports indicate that hyalocytes might modulate the formation of proliferative fibrous membranes together with other neighboring cells, in both an autocrine and paracrine manner. In addition, cytokines such as CTGF, hypoxia-inducible factor-1 (HIF-1), and tumor necrosis factor- α (TNF- α) [30, 33] stimulate the expression of VEGF (vascular endothelial growth factor), a major angiogenic factor, by hyalocytes, which suggests that hyalocytes might have a proangiogenic effect on retinal endothelial cells in a paracrine manner, leading to retinal neovascularization.

2. Cicatricial Contraction of Proliferative Membranes

Cicatricial contraction of preretinal proliferative membranes causes traction retinal detachment, which leads to photoreceptor apoptosis and ultimately to permanent vision loss. Hyalocytes are incorporated into the proliferative membranes and exhibit contractile properties in response to various contractile promoting factors, the expression of which is enhanced in PDR or PVR vitreous or in proliferative membranes. Recent investigations have revealed some of the responsible growth factors and their cellular mechanisms in hyalocytes.

Human vitreous samples collected from PDR or PVR patients significantly enhanced the contraction of hyalocyte-containing collagen gels, an established *in vitro* cicatricial contraction model, compared with vitreous from patients with nonproliferative diseases such as macular hole and rhegmatogenous retinal detachment. In addition, PDR/PVR-induced collagen gel contraction is dramatically but incompletely suppressed by TGF- β blockade. Furthermore, contraction of hyalocyte-containing collagen gels strongly correlates with the concentration of activated TGF- β 2 in the vitreous [34] (Figure II.D-5).

In addition, PDR/PVR vitreous enhances α -smooth muscle actin (α -SMA) expression and phosphorylation of myosin light chain (MLC) in hyalocytes and RPEs, both of which were dramatically suppressed by TGF- β blockade [34]. Overexpression of α -SMA indicates transdifferentiation of hyalocytes and RPEs into myofibroblasts, and phosphorylation of MLC is associated with actin-myosin interaction to form stress fibers and contractile rings, facilitating cell contraction and motility. Therefore, PDR/PVR vitreous may exert their contractile properties by furthering myofibroblastic transdifferentiation and MLC phosphorylation in target cells such as hyalocytes. Furthermore the results single out TGF- β as one of the main factors responsible for the procontractile properties of PDR/PVR vitreous. Certainly, recombinant TGF- β 2, the predominant isoform of three TGF- β isoforms (TGF- β 1, 2, and 3) in the posterior segment of the eye, remarkably stimulates the contraction of hyalocyte-embedded collagen gels and enhances α -SMA expression and MLC phosphorylation by hyalocytes. However, as TGF- β blockade does not abolish the procontractile property of PDR/PVR vitreous, other factors such as PDGF, IGF-1 (insulin-like growth factor-1), and endothelins may also significantly contribute to the cicatricial contraction of the proliferative membrane, albeit to a lesser extent than TGF- β [34].

These data suggest that hyalocytes play a crucial role in the formation and contraction of proliferative membrane in response to growth factors overexpressed in eyes

with proliferative vitreoretinal diseases such as PDR and PVR, even though RPEs play a central role specifically in PVR which is a complication of rhegmatogenous retinal detachment.

3. Macular Pucker

Macular pucker [see chapters III.F. Vitreous in the pathobiology of macular pucker; III.C. Pathology of vitreo-maculopathies] results from fibrous premacular membranes containing various cells that are located on the inner retinal surface and contract to cause mild to moderate visual disturbance or metamorphopsia. The literature often refers to these as “epiretinal membranes (ERM)”; however, this term is inaccurate. The term “epi” refers to a location next to or

beside a structure, in this case the retina. Thus, the term “epiretinal” could refer to a subretinal as well as preretinal membrane. Since the membrane in question is almost always in front of the retina, the prefix “pre-” is more accurate and will be used instead of “epi.” Furthermore, since all of the conditions of clinical relevance are maculopathies, not retinopathies, the term “premacular membrane (PMM)” is the more precise terminology and will be employed herein to refer to what has previously been described as “ERM.”

Machemer in 1978 first showed that these membranes could be removed using vitrectomy techniques. Since then, there have been several ultrastructural and histopathologic studies of specimens removed during vitreous surgery. Those studies demonstrated that several types of cells were observed

Figure II.D-5 Role of TGF- β in vitreous-induced collagen gel contraction. **(a)** Hyalocyte-containing collagen gels were exposed to control (DMEM), recombinant TGF- β 2 (0.3 nM), or patient vitreous, with anti-TGF- β mAb (10 ng/ml) or control IgG (10 ng/ml) ($n=6$ in each group). Rows representative wells per condition, 3 days after stimulation, are shown. **(b)** The diameters of the gels treated with vitreous (Lane 5 from left in **(a)**) and vitreous with anti-TGF- β mAb (Lane 6 in **(a)**) were measured and expressed as a percentage of the diameter of control (Lane 1 in **(a)**). * $P=0.01$ vs. MH and $P=0.007$ vs. RRD, ** $P=0.007$ vs. MH and $P=0.004$ vs. RRD, respectively, and *** $P<0.0001$ vs. each disease without anti-TGF- β mAb. **(c, d)** The correlation of the diameters of the gels with concentration of total TGF- β 2 in the vitreous ($n=24$, $r=0.39$, $P=0.06$) **(c)** and with activated TGF- β 2 ($n=24$, $r=0.82$, $P<0.0001$) **(d)**. MH macular hole, RRD rhegmatogenous retinal detachment, PDR proliferative diabetic retinopathy, PVR proliferative vitreoretinopathy (Ref. [34])

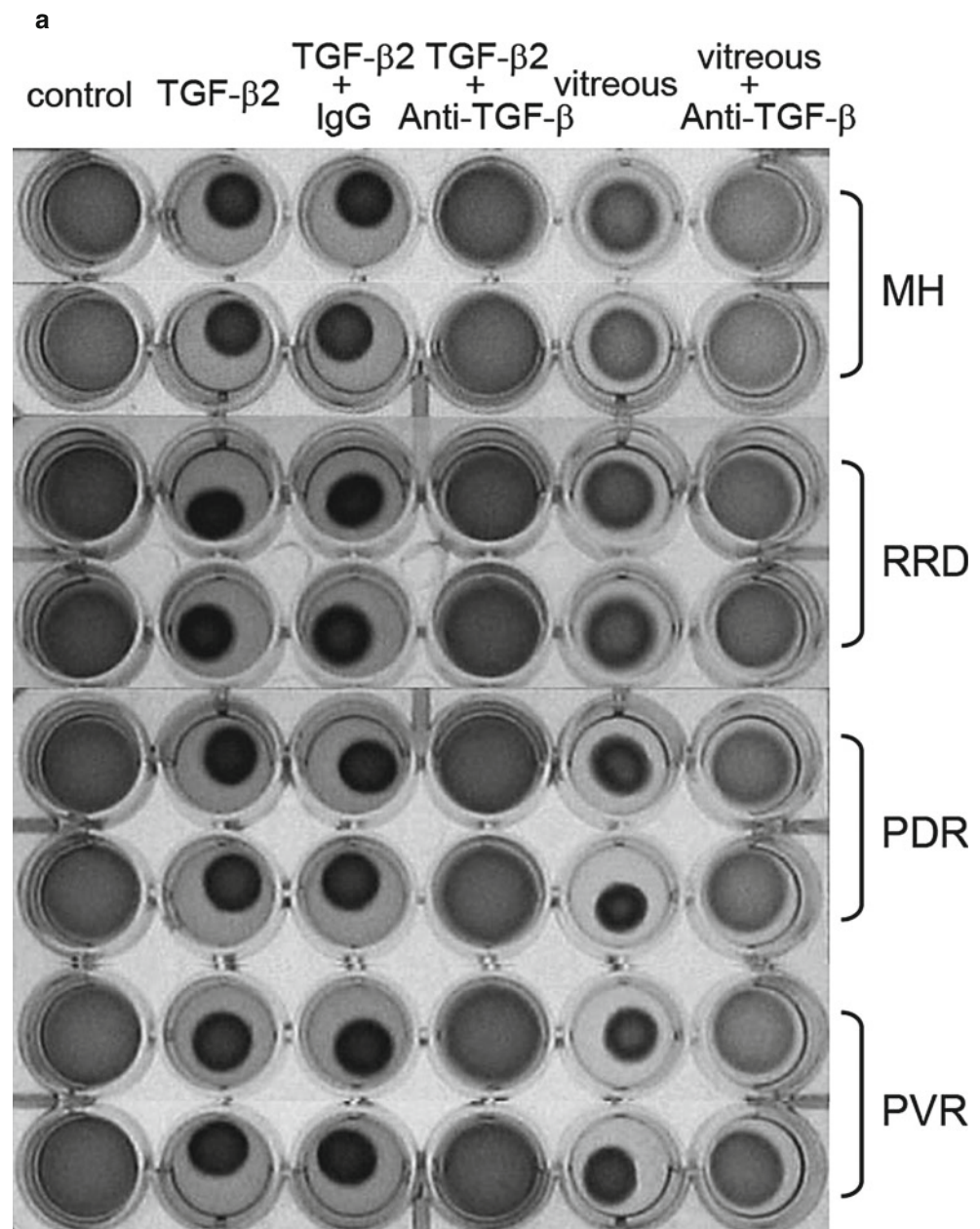
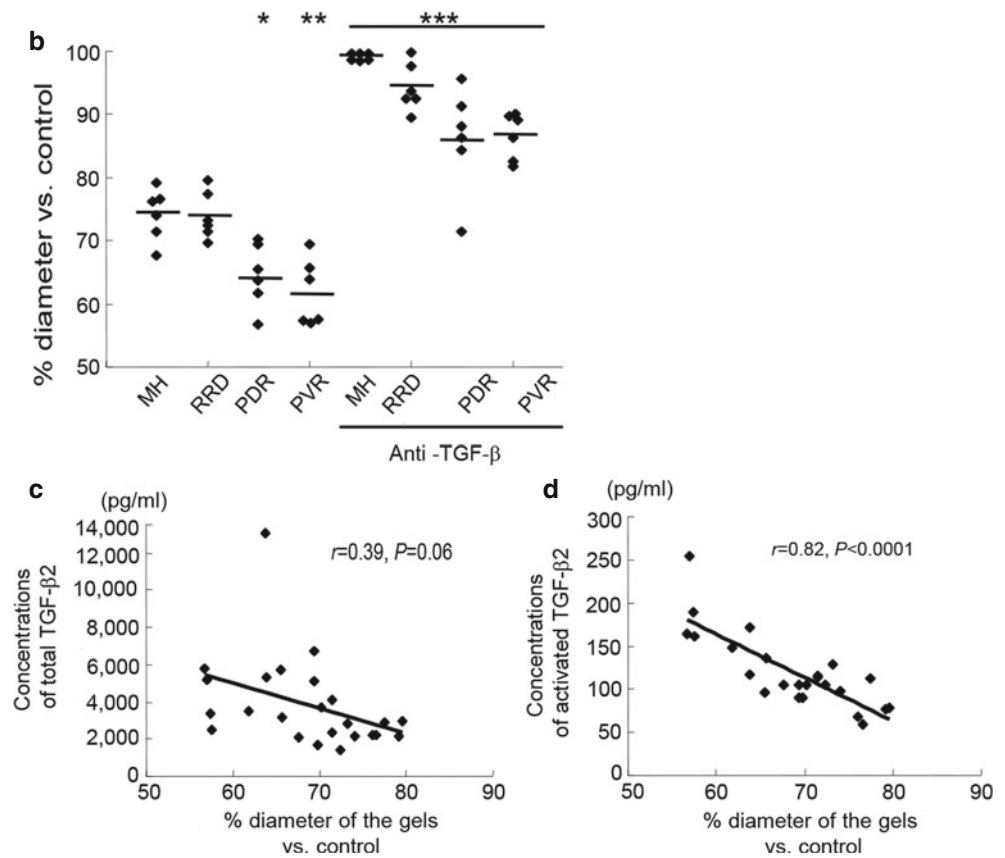


Figure II.D-5 (continued)



and macrophage-like cells were found frequently [4, 7, 35–40]. [see chapters III.J. Cell proliferation at the vitreoretinal interface in PVR and related disorders; III.C. Pathology of vitreo-maculopathies] It is likely that some of these cells are hyalocytes [5] (Figure II.D-6).

Regarding the pathogenesis of macular pucker formation, older theories hypothesized that posterior vitreous detachment (PVD) could result in dehiscences in the inner limiting membrane and subsequent glial cell migration, and process extension onto the retinal surface then causes PMM formation. However, this hypothesis has never been confirmed histologically. It has, on the other hand, been shown that anomalous PVD may leave a portion of posterior vitreous cortex attached to the macula [41, 42] [see chapter III.B. Anomalous PVD and vitreoschisis], and even in the absence of PVD, a premacular liquefied pocket is often present in adult eyes as a result of age-related vitreous liquefaction, and the vitreous cortex then forms the posterior wall of the premacular liquefied pocket [43]. This premacular vitreous cortex may play a key role in the development of macular pucker membranes. In addition, it has been suggested that anomalous PVD results in vitreoschisis, which may contribute to the formation of macular pucker membranes [44, 45].

A recent immunohistochemical study has demonstrated that macular pucker membranes contain both GFAP immunopositive cells and α -SMA immunopositive cells. α -SMA

immunopositive cells were located mainly at the contracted foci of these membranes. On the other hand, GFAP immunopositive cells were present at the periphery of PMMs. In addition, no double positive cells were observed [46]. In line with previous report, the cells were myofibroblast-like cells which are thought to be the main contributor to the membrane contraction similar to PDR and PVR.

In vitro studies showed that the diameter of hyalocyte-containing collagen gels decreased and α -SMA was overexpressed in the presence of TGF- β 2 or vitreous from patients with macular pucker, which was almost completely abolished by anti-TGF- β 2 antibody. In contrast, cultured human astrocytes had no apparent contractile properties of collagen gels in the presence of TGF- β 2, and TGF- β 2 had little effect on human astrocytes and did not cause myofibroblastic transdifferentiation [46]. TGF- β 2 is constitutively expressed to some level and is expressed in macular pucker specimens, so hyalocytes may be the primary component of the contracted membrane foci since they abound in the posterior vitreous cortex and they undergo myofibroblastic transdifferentiation and have contractile properties in the presence of TGF- β . Therefore, the premacular vitreous cortex containing hyalocytes might cause the membrane formation, consistent with the theory of anomalous PVD with vitreoschisis. Once the premacular membrane contracts, it may cause dehiscence in the inner limiting membrane with subsequent glial cell

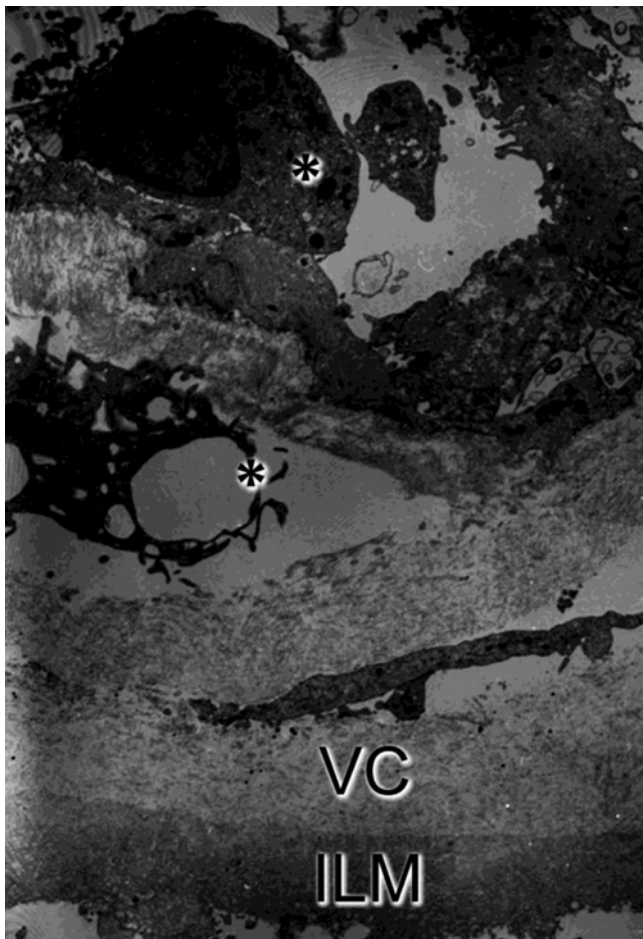


Figure II.D-6 Transmission electron microscopic photograph of surgically removed inner limiting membrane (*ILM*) from the eye of ERM. Macrophage-like cells (*) are present on the vitreal cortex (*VC*) and *ILM*. They are presumably hyalocytes (Reproduced with permission from Ref. [5] (Original magnification = 31,800x))

processes extension or migration onto the retinal surface. That could provide an explanation as to why glial cells are observed only at the periphery of macular pucker membranes.

4. Macular Holes

Several histological studies examining postmortem cases of macular hole have noted a high incidence of premacular membranes, which contain macrophages, fibrocyte-like cells, glial cells, and myofibroblast-like cells, indicating that the histological appearance is very similar to that of macula [47]. These thin, delicate, hypocellular preretinal membranes were mostly associated with lamellar and full-thickness macular holes and do not likely contain hyalocytes near the macular hole, although they may be present in the peripheral parts of the membrane, as observed in macular pucker. Indeed, coronal plane (*en face*) OCT imaging has shown eccentric macular pucker in 40 % of cases of macular holes [48]. Thus, premacular membranes are also considered likely to play an important role in the pathogenesis of macular hole forma-

tion, especially in the presence of persistent vitreo-papillary adhesion [49]. Furthermore, myofibroblastic differentiation has been observed in premacular membranes associated with idiopathic macular holes suggesting that contraction of these cells is at least partly responsible for formation and/or enlargement of macular holes. The similarities between premacular membranes associated with macular holes and macular pucker membranes indicate a common pathogenesis of these two entities. In addition, because these membranes result from cellular proliferation, migration, and myofibroblastic transdifferentiation resulting in membrane contraction, they share many features in common with PDR and PVR, so these diseases might be interpreted as “quiet PVR.”

One of the recent hypotheses underlying these diseases is the unifying concept of anomalous PVD [41]. Collapse of the liquefied vitreous body without sufficient dehiscence at the vitreoretinal interface can induce vitreoschisis, a split within the posterior vitreous cortex, leaving the outermost layer of the posterior vitreous cortex attached to the macula. If anomalous PVD is an important event in macular hole formation and PMMs, there must be some other factors to account for the dissimilar clinical and topographic features of the two conditions. PMM tissues are reported to be hypercellular, whereas the tissue surrounding macular holes is hypocellular in composition [48]. Sebag has hypothesized that the difference could be due to the level at which vitreoschisis splitting occurs during anomalous PVD [41]. If vitreoschisis occurs anterior to the hyalocytes, then the residual membrane is hypercellular, but if it is posterior to the hyalocytes, the membranes are hypocellular, and this results in macular hole formation.

V. Treatment

A. Surgical Approach

To treat the pathological conditions caused by the formation of preretinal proliferative membrane observed in PDR, PVR, macular pucker, and macular hole as described above, removing the membrane and posterior vitreous cortex is the preferred and logical approach at present because these membranes contain a number of cells including hyalocytes. The maneuver itself is not necessarily easy, and recurrence is not rare. Adjunctive use of triamcinolone acetonide during vitrectomy surgery is beneficial to remove these membranes securely and effectively [50, 51]. Although this procedure is not always necessary in most of the cases, it might be beneficial for selected cases to reduce the incidence of postoperative preretinal fibrotic complications [51]. Complete removal of preretinal membranes together with inner limiting membrane (*ILM*) peeling resulted in a lower recurrence rate than incomplete removal, probably because the residual

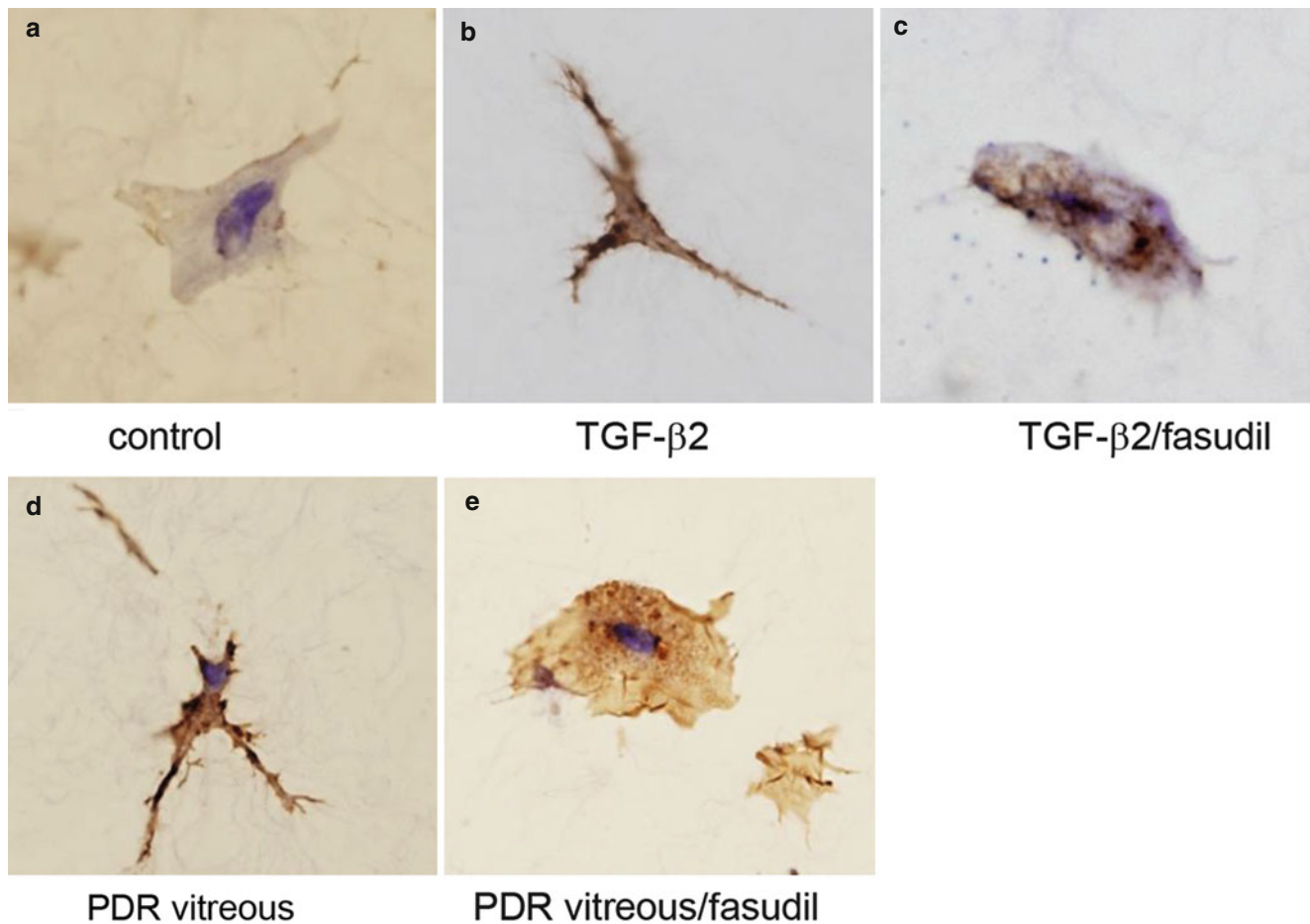


Figure II.D-7 Immunocytochemical analysis of α -SMA (brown) in hyalocytes embedded in collagen gels. Representative micrographs, showing hyalocyte-containing collagen gels that were treated with (a) control (DMEM), (b) recombinant TGF- β 2, (c) recombinant TGF- β 2

with fasudil (20 μ M), (d) PDR vitreous, and (e) PDR vitreous with fasudil (20 μ M). TGF- β 2 and PDR vitreous treatment increases α -SMA expression. Fasudil disrupted α -SMA organization without affecting its expression (Ref. [34])

posterior vitreous cortex or membrane becomes a scaffold of cell proliferation and ECM production by these cells [52]. If the residual posterior vitreous cortex or ILM was left alone without any cells, recurrence, namely, reproduction of ECM by cellular elements after surgery, would not occur.

B. Pharmacotherapy

Recent investigations have also suggested hopeful pharmacological strategies for the management of these pathologies. Rho kinase (ROCK), a target protein of Rho, regulates MLC phosphorylation both directly and via inactivation of the MLC phosphatase. In an *in vitro* study, fasudil, a potent and selective ROCK inhibitor, abolished the PDR-/PVR-induced hyalocyte-containing collagen gel contraction as well as contraction induced by recombinant TGF- β 2. Fasudil almost completely suppressed MLC phosphorylation by hyalocytes, which is a common downstream mediator of various contractile growth factors including TGF- β , PDGF,

IGF-1, and endothelins. In addition, while PDR-/PVR-induced α -SMA expression by hyalocytes was unaffected by fasudil, α -SMA organization, which modulates the contractile property of myofibroblastic cells, was effectively disrupted [34] (Figure II.D-7). This suggests that fasudil might diminish the contractile property of proliferative membranes, which are supposed to be at least partly composed of trans-differentiated hyalocytes, by abolishing MLC phosphorylation and affecting α -SMA organization. Therefore, ROCK inhibition might become a novel therapeutic strategy in the management of these diseased states.

Dexamethasone has been demonstrated to decrease proliferation of hyalocytes induced by TNF- α [53] and also decreased hypoxic- and TNF- α -dependent induction of VEGF expression in hyalocytes [33].

However, in contrast, dexamethasone further increased TNF- α -induced collagen gel contraction embedded by hyalocytes. This suggests that steroid treatment appears to inhibit the activation of hyalocytes in the early stages of these diseases, but might have adverse effects in the late

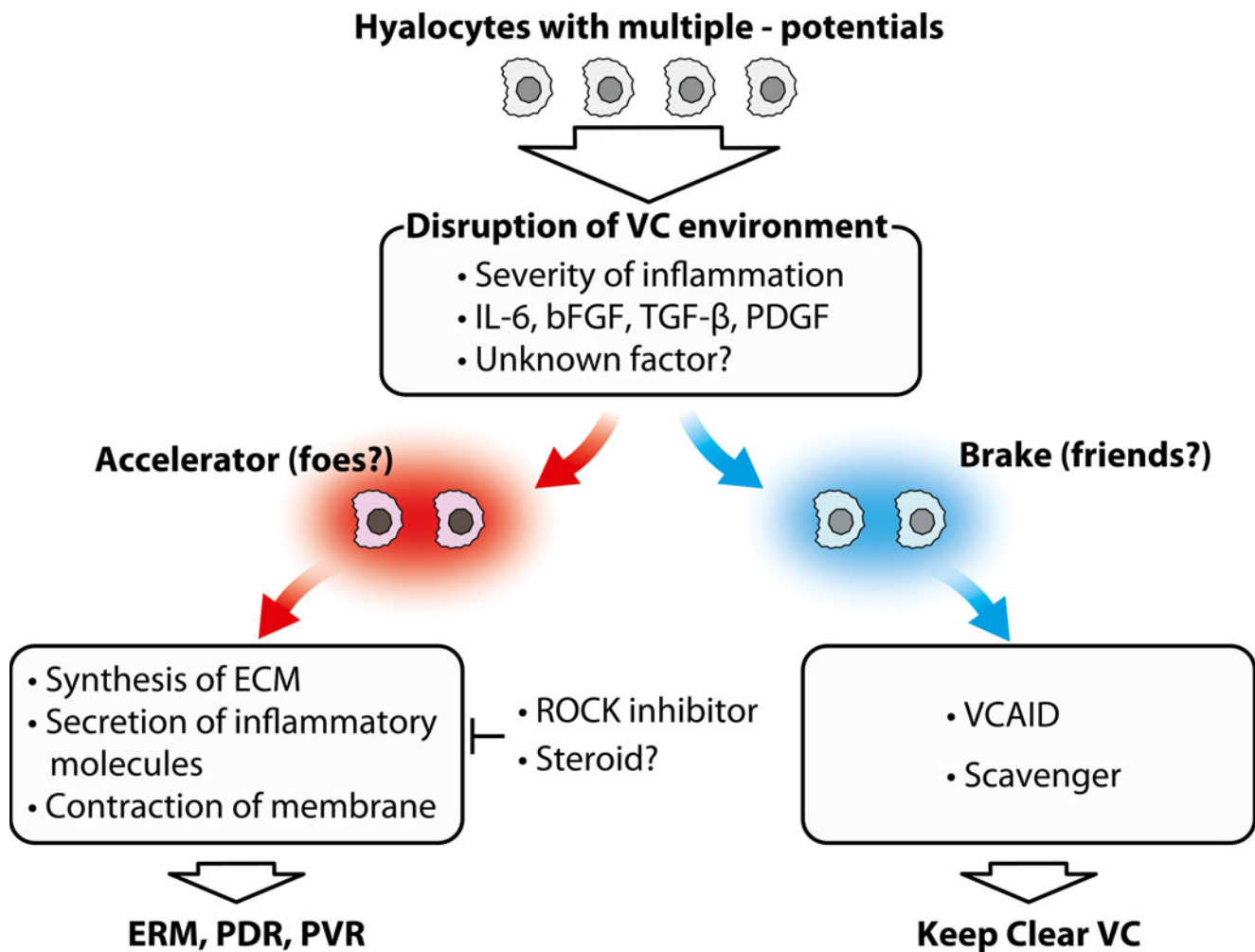


Figure II.D-8 Schema of possible roles of hyalocytes in ocular pathology. Hyalocytes are resident cells in vitreous chamber (VC) with multiple potentials. In the disruption of the VC environment, hyalocytes may act as an accelerator or a brake to destroy the clear vitreous depen-

dent on unknown mechanisms. *IL-6* interleukin-6, *bFGF* basic fibroblast growth factor, *PDGF* platelet-derived growth factor, *PDR* proliferative diabetic retinopathy, *PVR* proliferative vitreoretinopathy (Ref. [15])

stage through membrane contraction, although it might be beneficial for the angiogenesis observed in PDR.

VI. Summary

While there is no strict definition of “hyalocytes,” cells located in the peripheral shell of vitreous are called hyalocytes. The accumulating evidence indicates that hyalocytes can act as “friends” to keep the vitreous cavity transparent by their phagocytic or fibrinolytic activity and their inhibi-

tion of immune reaction through VCAID under physiological conditions. At the same time, hyalocytes can act as “foes” by producing cytokines and ECM followed by cicatricial contraction of the membrane under pathological conditions. Unfortunately, at present, it is difficult to tell what makes hyalocytes “friends” or “foes” [15] (Figure II.D-8). Further studies to answer this question might provide a key to a better understanding of microenvironment of the vitreous and lead to better management of intraocular diseases by surgical and/or pharmacological treatment.

Abbreviations

α -SMA	α -smooth muscle actin
ACAID	Anterior chamber-associated immune deviation
APCs	Antigen-presenting cells
b-FGF	Basic fibroblast growth factor
CTGF	Connective tissue growth factor
ECM	Extracellular matrix
ERM	Epiretinal (actually premacular) membrane
GFAP	Glial fibrillary acidic protein
GFP	Green fluorescent protein
HGF	Hepatocyte growth factor
HIF-1	Hypoxia-inducible factor-1
IGF-1	Insulin-like growth factor-1
ILM	Inner limiting membrane
MCP-1	Monocyte chemoattractant protein-1
MLC	Myosin light chain
PDGF	Platelet-derived growth factor
PDR	Proliferative diabetic retinopathy
PMM	Premacular membrane
PVD	Posterior vitreous detachment
PVR	Proliferative vitreoretinopathy
ROCK	Rho kinase
RPE	Retinal pigment epithelium
TGF- β	Transforming growth factor- β
TNF- α	Tumor necrosis factor- α
uPA	Urokinase-type plasminogen activator
VCAID	Vitreous cavity-associated immune deviation
VEGF	Vascular endothelial growth factor

References

- Gloor BP. Development of the vitreous body and zonula. *Graefes Arch Clin Exp Ophthalmol.* 1973;187:21–44.
- Salu P, et al. Light and electron microscopic studies of the rat hyalocyte after perfusion fixation. *Ophthalmic Res.* 1985;17:125–30.
- Uehara M, et al. Morphological studies of the hyalocytes in the chicken eye: scanning electron microscopy and inflammatory response after the intravitreal injection of carbon particles. *J Anat.* 1996;188:661–9.
- Zhu M, et al. The human hyaloid system: cellular phenotypes and inter-relationships. *Exp Eye Res.* 1999;68:553–63.
- Sakamoto T. Cell biology of hyalocytes. *Nippon Ganka Gakkai Zasshi.* 2003;107:866–82.
- Noda Y, et al. Functional properties of hyalocytes under PDGF-rich conditions. *Invest Ophthalmol Vis Sci.* 2004;45:2107–14.
- Matsumoto H, et al. Triamcinolone acetate-assisted pars plana vitrectomy improves residual posterior vitreous hyaloid removal: ultrastructural analysis of the inner limiting membrane. *Retina.* 2007;27:174–9.
- Ueno A, et al. Long-term clinical outcomes and therapeutic benefits of triamcinolone-assisted pars plana vitrectomy for proliferative vitreoretinopathy: a case study. *Eur J Ophthalmol.* 2007;17:392–8.
- Gandorfer A, et al. Pathology of the macular hole rim in flat-mounted internal limiting membrane specimens. *Retina.* 2009;29:1097–105.
- Hannover A. Muller's Arch. 1840, cited in: Hamburg A: Some investigations on the cells on the vitreous body. *Ophthalmologica.* 1959;138:81–107.
- Balazs EA. Molecular morphology of the vitreous body. In: Smelser GK, editor. *Structure of the eye.* New York: Academic; 1961. p. 293–310.
- Qiao H, et al. The characterization of hyalocytes: the origin, phenotype, and turnover. *Br J Ophthalmol.* 2005;89:513–7.
- Hogan MJ, et al. *Histology of the human eye.* Philadelphia: WB Saunders; 1971.
- Lazarus HS, Hageman GS. In situ characterization of the human hyalocyte. *Arch Ophthalmol.* 1994;112:1356–62.
- Sakamoto T, Ishibashi T. Hyalocytes: essential cells of the vitreous cavity in vitreoretinal pathophysiology? *Retina.* 2011;31:222–8.
- van Meurs JC, et al. Clearance rate of macrophages from the vitreous in rabbits. *Curr Eye Res.* 1990;9:683–6.
- Gloor BP. Mitotic activity in the cortical vitreous cells (hyalocytes) after photocoagulation. *Invest Ophthalmol.* 1969;8:633–46.
- Haddad A, Andre JC. Hyalocyte-like cells are more numerous in the posterior chamber than they are in the vitreous of the rabbit eye. *Exp Eye Res.* 1998;66:709–18.
- Lang RA, Bishop JM. Macrophages are required for cell death and tissue remodelling in the developing mouse eye. *Cell.* 1993;74:453–62.
- Zhu M, et al. The human hyaloid system: cell death and vascular regression. *Exp Eye Res.* 2000;70:767–76.
- Osterlin SE, Jacobson B. The synthesis of hyaluronic acid in vitreous. I. Soluble and particulate transferases in hyalocytes. *Exp Eye Res.* 1968;7:497–510.
- Rittig M, et al. Hyaluronan synthase immunoreactivity in the anterior segment of the primate eye. *Graefes Arch Clin Exp Ophthalmol.* 1993;231:313–7.
- Nishitsuka K, et al. Hyaluronan production regulation from porcine hyalocyte cell line by cytokines. *Exp Eye Res.* 2007;85:539–45.
- Grabner G, et al. Macrophage-like properties of human hyalocytes. *Invest Ophthalmol Vis Sci.* 1980;19:333–40.
- Stein-Streilein J. Immune regulation and the eye. *Trends Immunol.* 2008;29:548–54.
- Streilein JW. Ocular immune privilege: therapeutic opportunities from an experiment of nature. *Nat Rev Immunol.* 2003;3:878–89.
- Streilein JW, et al. Blood-borne signals that induce anterior chamber-associated immune deviation after intracameral injection of antigen. *Invest Ophthalmol Vis Sci.* 1997;38:2245–54.
- Sonoda KH, et al. The analysis of systemic tolerance elicited by antigen inoculation into the vitreous cavity: vitreous cavity-associated immune deviation. *Immunology.* 2005;116:390–9.
- Hirayama K, et al. The involvement of the rho-kinase pathway and its regulation in cytokine-induced collagen gel contraction by hyalocytes. *Invest Ophthalmol Vis Sci.* 2004;45:3896–903.
- Kita T, et al. Functional characteristics of connective tissue growth factor on vitreoretinal cells. *Diabetes.* 2007;56:1421–8.
- Kita T, et al. Transforming growth factor- β 2 and connective tissue growth factor in proliferative vitreoretinal diseases: possible involvement of hyalocytes and therapeutic potential of Rho kinase inhibitor. *Diabetes.* 2007;56:231–8.

32. Sommer F, et al. Hyalocyte proliferation and ECM accumulation modulated by bFGF and TGF-beta1. *Graefes Arch Clin Exp Ophthalmol*. 2008;246:1275–84.
33. Hata Y, et al. Vascular endothelial growth factor expression by hyalocytes and its regulation by glucocorticoid. *Br J Ophthalmol*. 2008;92:1540–4.
34. Kita T, et al. Role of TGF- β in proliferative vitreoretinal diseases and ROCK as a therapeutic target. *Proc Natl Acad Sci U S A*. 2008;105:17504–9.
35. Wiedemann P, Kohlmann H. Perioperative analysis of vitreous cell components by immunoprecipitation cytology. *Graefes Arch Clin Exp Ophthalmol*. 1996;123:463–6.
36. Gandorfer A, et al. Epiretinal pathology of diffuse diabetic macular edema associated with vitreomacular traction. *Am J Ophthalmol*. 2005;139:638–52.
37. Kampik A, et al. Epiretinal and vitreous membranes: comparative study of 56 cases. *Arch Ophthalmol*. 1981;99:1445–54.
38. Faulborn J, et al. Diabetic vitreopathy: findings using the celloidin embedding technique. *Ophthalmologica*. 1998;212:369–76.
39. Kishi S, et al. Structure of the inner retinal surface in simple diabetic retinopathy. *Jpn J Ophthalmol*. 1982;26:141–9.
40. Hisatomi T, et al. A new method for comprehensive bird's-eye analysis of the surgically excised internal limiting membrane. *Am J Ophthalmol*. 2005;139:1121–2.
41. Sebag J. Anomalous posterior vitreous detachment: a unifying concept in vitreo-retinal disease. *Graefes Arch Clin Exp Ophthalmol*. 2004;242:690–8.
42. Sebag J. Vitreous anatomy, aging, and anomalous posterior vitreous detachment. In: Dartt DA, Besharse JC, Dana R, editors. *Encyclopedia of the eye*, vol. 4. Oxford: Elsevier; 2010. p. 307–15.
43. Kishi S, Shimizu K. Oval defect in detached posterior hyaloid membrane in idiopathic preretinal macular fibrosis. *Am J Ophthalmol*. 1994;118:451–6.
44. Sebag J. Vitreoschisis. *Graefes Arch Clin Exp Ophthalmol*. 2008;246:329–32.
45. Gupta P, et al. Vitreoschisis in macular diseases. *Br J Ophthalmol*. 2011;95:376–80.
46. Kohno RI, et al. Possible contribution of hyalocytes to idiopathic epiretinal membrane formation and its contraction. *Br J Ophthalmol*. 2009;93:1020–6.
47. Messmer EM, et al. Ultrastructure of epiretinal membranes associated with macular holes. *Graefes Arch Clin Exp Ophthalmol*. 1998;236:248–54.
48. Sebag J, et al. Macular holes and macular pucker: the role of vitreoschisis as imaged by optical coherence tomography/scanning laser ophthalmoscopy. *Trans Am Ophthalmol Soc*. 2007;105:121–9.
49. Wang MY, Nguyen D, Hindoyan N, Sadun AA, Sebag J. Vitreopapillary adhesion in macular hole and macular pucker. *Retina*. 2009;29:644–50.
50. Enaida H, et al. Possible benefits of triamcinolone-assisted pars plana vitrectomy for retinal diseases. *Retina*. 2003;23:764–70.
51. Sakamoto T, Ishibashi T. Visualizing vitreous in vitrectomy by triamcinolone. *Graefes Arch Clin Exp Ophthalmol*. 2009;247:1153–63.
52. Shimada H, et al. Double staining with brilliant blue G and double peeling for epiretinal membranes. *Ophthalmology*. 2009;116:1370–6.
53. Hata Y, et al. Role of tumour necrosis factor- α (TNF α) in the functional properties of hyalocytes. *Br J Ophthalmol*. 2011;95:261–5.

Willi Halfter, J. Sebag, and Emmett T. Cunningham Jr.

Outline

- I. **Introduction**
- II. **Inner Limiting Membrane**
 - A. Anatomy
 - 1. Structure
 - 2. Topographic Variations
 - B. Biochemical Composition of the ILM
 - C. Biosynthesis and Assembly of the ILM
 - D. Role of the ILM in Ocular Development
 - E. Aging of the ILM
 - F. Role of the ILM in Disease
 - 1. ILM and Diabetes
 - 2. Proliferative Diseases and the ILM
 - 3. Tractional Disorders and the ILM
 - a. Biophysical Properties of the ILM
 - 4. Uveitis
- III. **Posterior Vitreous Cortex**
 - A. Structure
 - B. Cells of the Posterior Vitreous Cortex
 - 1. Hyalocytes
 - 2. Fibroblasts
- IV. **Vitreovascular Interface**
- V. **Unresolved Questions**
 - A. Diffusion Through the ILM
 - 1. Trans-ILM Diffusion from Vitreous to Retina and Choroid
 - 2. Trans-ILM Diffusion from Chorioretinal Compartment to Vitreous
 - B. Viral Penetration Through the ILM into the Retina
 - C. Trans-ILM Cell Migration
 - D. Vitreous-ILM Adhesion

References

Keywords

Vitreous • Vitreoretinal interface • Inner limiting membrane • Extracellular matrix • Biochemistry Ultrastructure • Development • Aging • Disease

Key Concepts

1. The vitreoretinal interface has three components: the inner limiting membrane, the posterior vitreous cortex, and an intervening extracellular matrix responsible for vitreoretinal adhesion.
2. Aging and disease alter the vitreoretinal interface and play an important role in tractional as well as proliferative disorders at the vitreoretinal interface.
3. The vitreoretinal interface influences oxygenation, nutrition, drug delivery, and viral penetration as vectors for future retinal therapeutics.

W. Halfter, PhD
Department of Neurobiology, University of Pittsburgh,
200 Lothrop Street STE W1415, Pittsburgh, PA 15261, USA
e-mail: whalfter@pitt.edu

J. Sebag, MD, FACS, FRCOphth, FARVO (✉)
VMR Institute for Vitreous Macula Retina,
7677 Center avenue, Huntington Beach, CA 92647, USA

Doheny Eye Institute, Los Angeles, CA, USA
e-mail: jsebag@VMRinstitute.com

E.T. Cunningham Jr., MD, PhD, MPH
The Uveitis Service, West Coast Retina Medical Group,
Department of Ophthalmology, California Pacific Medical Center,
Stanford University School of Medicine,
2340 Clay Street, Fifth Floor, San Francisco, CA 94115, USA
e-mail: emmett_cunningham@yahoo.com

I. Introduction

The vitreoretinal interface is the site of many pathogenic events associated with sequences that lead to vision loss. The interface consists of a complex formed by the inner limiting



Figure II.E-1 Human vitreoretinal interface. At the *top* of the figure, vitreous collagen fibrils are densely packed within a layer known as the posterior vitreous cortex (*PVC*), which overlies the ILM of the retina.

Between these two structures is an intervening extracellular matrix (*ECM*), called by Heergaard the “vitreoretinal border region”

lamina of the retina, commonly called the inner limiting membrane (ILM), the posterior vitreous cortex, and an intervening extracellular matrix that is thought to be responsible for vitreoretinal adhesion (Figure II.E-1). Changes in each of these three components occur with aging and in certain diseases, such as myopia and diabetes. These aging and disease-related changes contribute a variety of vitreoretinal disorders. There are special interfaces between vitreous and the optic disc (see chapter III.E. Vitreo-papillary adhesion/traction) and retinal blood vessels, with the latter contributing to various retinovascular disorders (see chapters III.A. Congenital vascular vitreo-retinopathies; III.K. Vitreous in retino-vascular diseases and diabetic macular edema; V.A.6. Vitreous surgery of arterial and venous retino-vascular diseases)

II. Inner Limiting Membrane

For years there was disagreement regarding the existence of an inner limiting membrane (ILM) of the retina. Some believed that the limiting membrane of the vitreous (*membrana hyaloidea*) served as the inner limiting membrane of the retina. Others believed that there was an ILM but that no limiting membrane existed around the vitreous. In 1912, Salzmann proposed a middle ground by stating that *In any case, one must say that this membrane has just as much relation to the vitreous as it has to the retina, and that it looks like the inner glass membrane of the retina in one preparation and like the outer border membrane of the vitreous in another* [1]. In point of fact, both concepts were right. There are

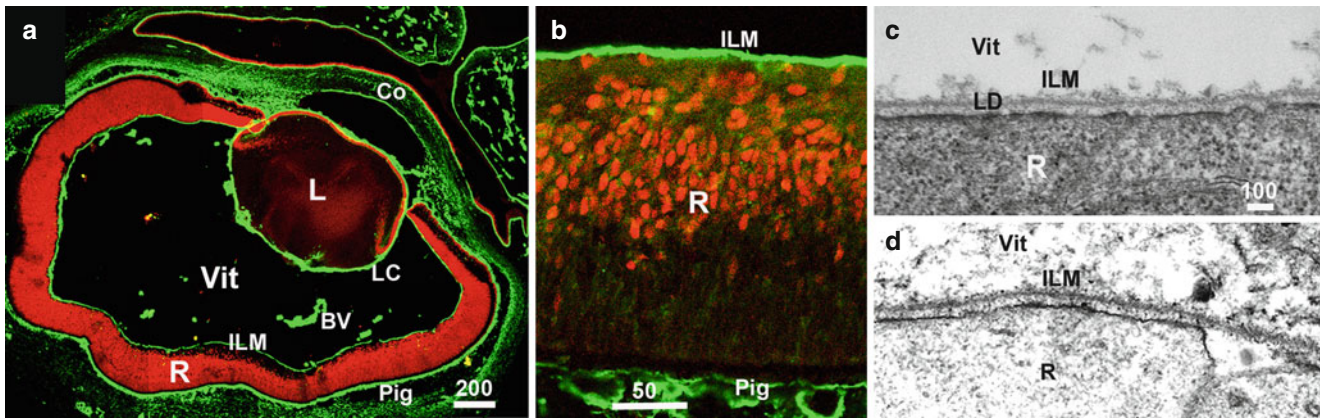


Figure II.E-2 Location and ultrastructure of the fetal human ILM. Fluorescence micrograph showing a cross section of a 10-week-old fetal human eye. (a) This section was stained for collagen IV (green) and shows the location of the ILM, the vascular BMs of the hyaloid blood vessels (BV), the corneal BMs (Co), the BMs of the pigment epithelium (Pig) in Bruch's membrane, and the lens capsule (LC). The section had been counterstained with an antibody to Pax6, a nuclear transcription factor that is present in all ocular cells (red). (b) A high power view of the fetal human retina stained for agrin, a BM proteoglycan (green) shows the ILM and the BM of the pigment

epithelium (Pig). Counterstaining with Islet 1 shows the location of the differentiated ganglion cells at the vitread side of the retina. (c) A TEM micrograph of the vitread surface of the fetal human retina shows that the ILM appears as a thin sheet of ECM at the vitreoretinal border region with a distinctive lamina densa (LD). The ultrastructure of the fetal ILM resembles the classic textbook morphology of a typical BM. (d) The neonatal mouse ILM is shown for comparison. The mouse ILM is morphologically very similar to the fetal human ILM (compare c, d). BM basement membrane, ILM inner limiting membrane, R retina, L lens (Bars: a: 200 μm; b: 50 μm; c, d: 100 nm)

distinct “limiting membranes” demarcating the boundary of both the retina and adjacent vitreous, although neither is a membrane in the classic histological sense of a cell membrane and they are often therefore called “laminae.”

The “limiting membrane” of the retina is formed by the contiguous basement membranes of Müller cells. The “limiting membrane” of the vitreous, in contrast, is formed by the posterior vitreous cortex, a structure composed of densely packed vitreous collagen fibrils [1]. Between the two is an interdigitating extracellular matrix that contains elements of each, described by Heegaard as the “vitreoretinal border region” [2].

A. Anatomy

1. Structure

Despite the fact that the ILM is not a true membrane in the lipid-rich, cell membrane sense, Salzmann [1] preferred the term “membrana limitans interna,” primarily because the ILM is a basement membrane (BM) functionally analogous with the BM covering the inner surface of the ciliary epithelium. Embryologically, the ILM shares ontogeny with the pial BM which envelops the entire central nervous system. In the eye, the ILM is one of six BMs that includes (1) the lens capsule, which is the thickest BM of the body; (2) the hyaloid vascular BMs of the vitreous and the retina; (3) the two corneal BMs; (4) the ILM; (5) the BM of the pigment epithelium; and (6) the BM sub-layer of Bruch's membrane (Figure II.E-2).

The ILM, like all other BMs, is transparent, very thin, and difficult to localize by conventional histology. The ILM can, however, be readily detected by either immunocytochemistry using antibodies specific to BM proteins (Figure II.E-2a, b) or transmission electron microscopy (TEM; Figures II.E-1 and II.E-2c, d). High-resolution TEM of fetal human eyes shows the ILM to be an extracellular matrix sheet with a thickness of less than 100 nm. The fetal human ILM can be subdivided into an outer lamina lucida layer that faces the ECM of the vitreoretinal border region, a central electron-dense lamina densa, and a second inner lamina lucida that faces the end feet of the retinal Müller glial cells [2].

The thickness and morphology of the fetal human ILM resembles the ultrastructure of the classical textbook BMs. Heegaard described that the human ILM increases markedly in thickness during the first months/years of life in the equatorial and macular regions. The thickness is stable from the second decade and remains unchanged throughout subsequent decades. In all human adult eyes that were studied, the ILM was the thickest in the macular region [2].

This information may not be accurate, however, as TEM, which is traditionally used to determine the thickness of BMs and the ILM, may be fraught with artifacts. Since TEM requires chemical fixation and dehydration of tissues, this may result in distortion and artifacts. Recently, Atomic force microscopy (AFM) has been introduced to examine the morphology and biomechanical properties of isolated and flat-mounted BMs [3, 4], including measurements of ILM thickness. AFM uses a fine tip on the flexible cantilever that

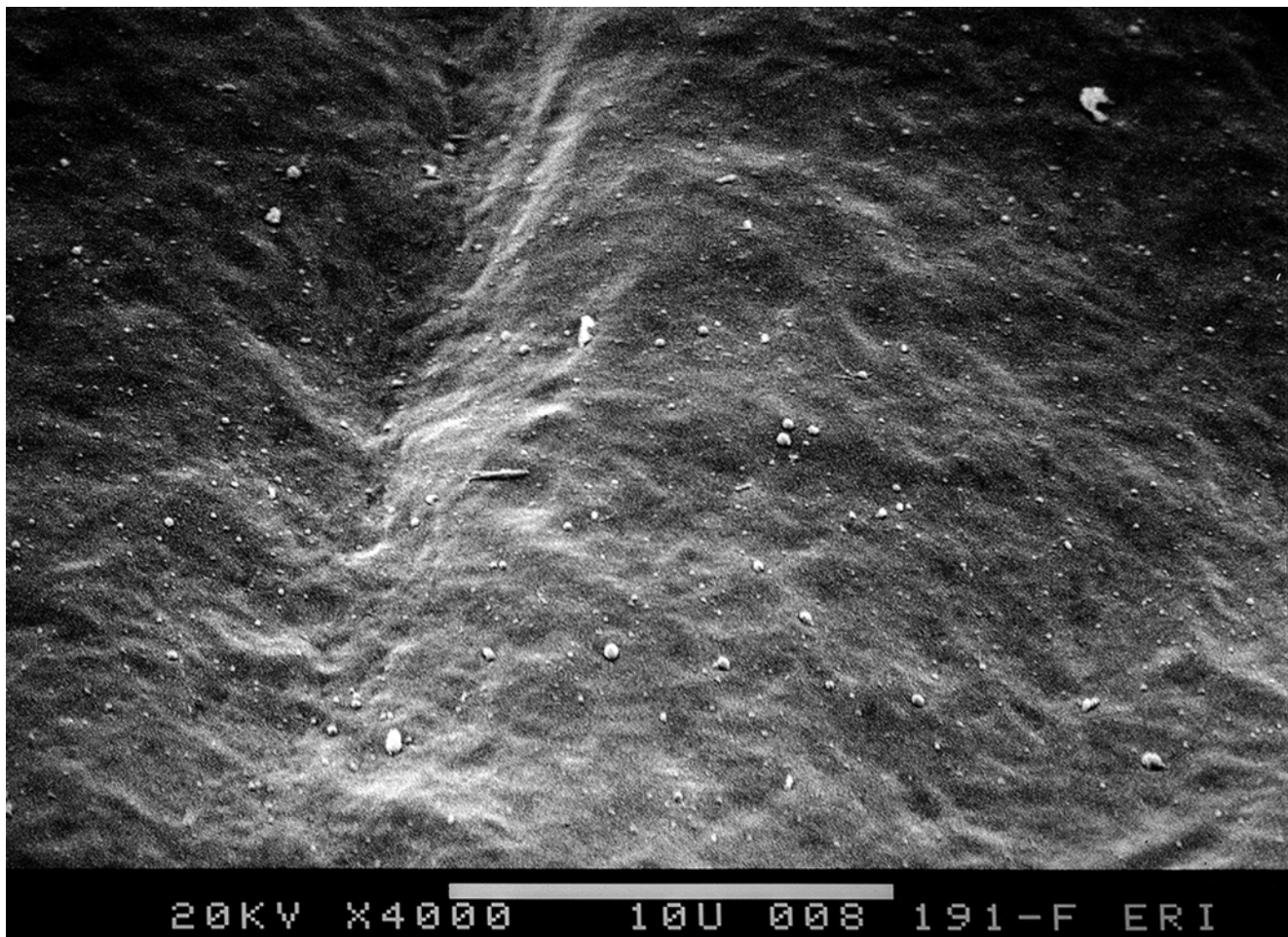


Figure II.E-3 Scanning electron microscopy of the anterior aspect of human ILM, after peeling the retina off the vitreous postmortem in a human adult. The anterior (vitread) surface of the ILM is smooth: (magnification bar = 10 microns)

scans over the surface of the samples. The degree of cantilever deflection, as recorded by a laser beam, can be used to (a) image the sample at atomic resolution, (b) measure its thickness, and (c) assess its stiffness [5–9]. Since AFM can also scan the samples when they are submerged in PBS, AFM can be used to examine unfixed and fully hydrated BMs.

AFM examination revealed that the thickness of the embryonic chick and adult human ILMs is, under native conditions, between two to four times greater than previously measured by TEM [3, 4]. The fact that AFM-based thickness measurements of dehydrated ILMs are very similar to the thickness data obtained by TEM shows that sample preparation, most importantly, its dehydration, results in a dramatic 50 % shrinkage [3]. An independent study measuring lens capsule thickness by confocal microscopy, also under native conditions, showed that hydrated lens capsules are at least twice thicker than previously determined by TEM [10]. Thus, sample preparation for TEM introduces massive shrinkage and possibly a distortion of BM morphology.

The massive shrinkage of the ILM after dehydration is due to the loss of water that is tightly bound by the glycosaminoglycans of proteoglycans that are abundantly present

in BMs. Proteoglycans are highly glycosylated proteins with glycosaminoglycan side chains that carry a large net negative charge. The high density of negative charge of proteoglycans is responsible for substantial water retention in cartilage [11] and vitreous [12] and indicates a similar function of proteoglycans in the ILM. Experimental confirmation for this concept comes from the ILM thickness and stiffness data after enzymatic removal of the GAG side chains that results in 50 % shrinkage and a doubling of the ILM stiffness [4, 13]. Based on the AFM data, we can infer that about 50 % of the ILM mass is water, tightly bound by proteoglycans, and that water is the most abundant component of the ILM. Further, the hydration status determines the stiffness of the ILM.

2. Topographic Variations

In the entire fundus, the anterior aspect of the ILM has a smooth appearance (Figure II.E-3). However, the posterior aspect of the ILM varies in structure by location: in the periphery (Figure II.E-4b), the posterior aspect of the ILM is smooth and resembles the anterior aspect. However, in the posterior pole (Figure II.E-4a), the posterior aspect of

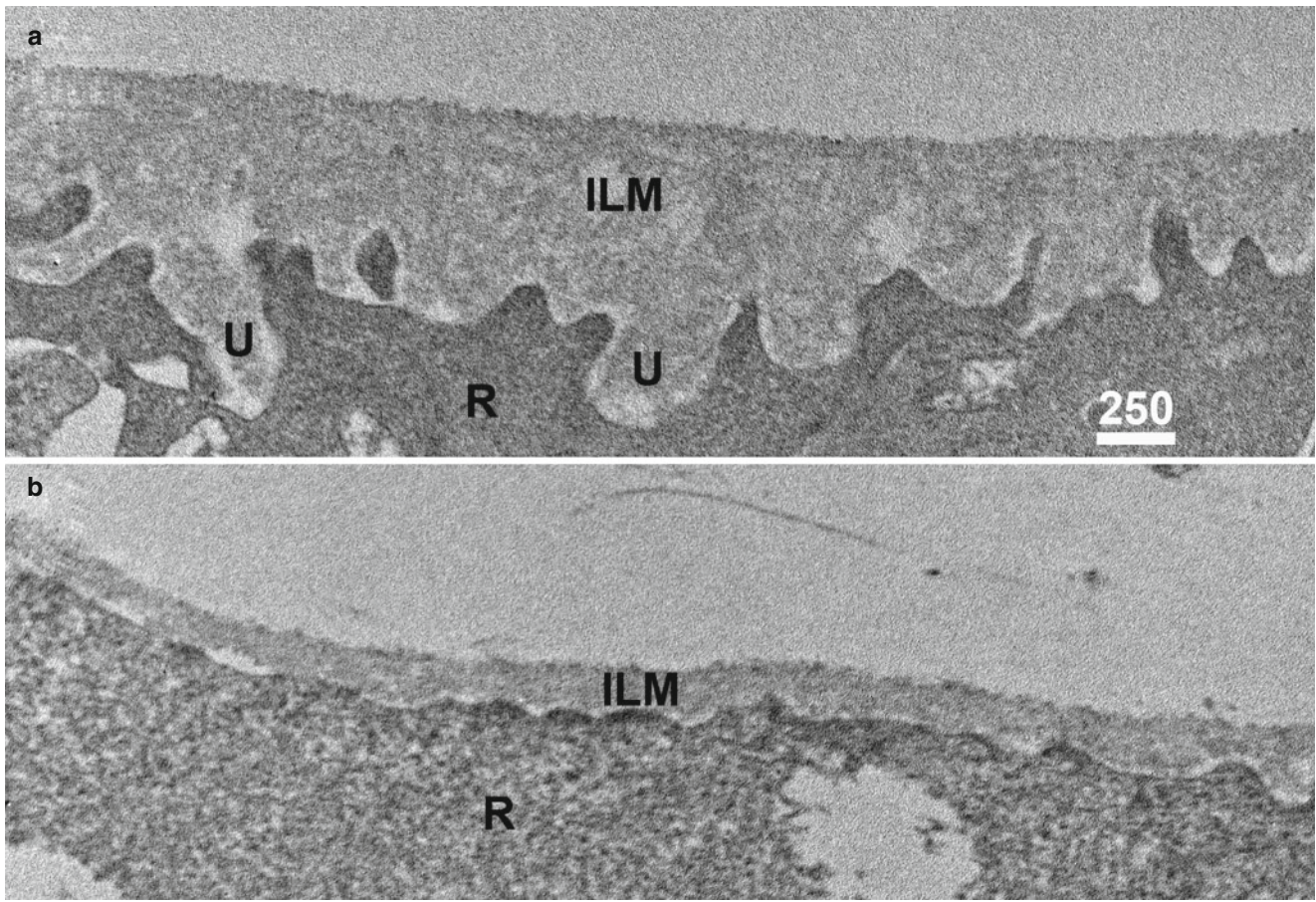


Figure II.E-4 Topographic variation in the human ILM. (a) Transmission electron microscopy of the inner limiting membrane (ILM) in the posterior pole of a 27-year-old human demonstrating “undulations” (U) in the posterior aspect of the ILM that fills the crevices between the underlying

retinal (R) cells (Bar=250 nm). (b) Transmission electron microscopy of the ILM in the peripheral fundus of the same eye as in (a) demonstrates that the posterior aspect of the ILM resembles the anterior aspect of the ILM with a continuous surface and minimal undulations (Bar=250 nm)

the ILM “undulates” in an irregular configuration filling the crevices between underlying retinal glia and nerve fibers.

At the rim of the optic disc (see chapter III.E. Vitreopapillary adhesion and traction), the retinal ILM ceases, although the basement membrane continues as the “inner limiting membrane of Elschnig” [14]. This membrane is 50 nm thick and is believed to be formed by the basal lamina of the astroglia in the optic nerve head. At the central-most portion of the optic disc, the membrane thins to 20 nm, follows the irregularities of the underlying cells of the optic nerve head, and is composed only of glycosaminoglycans and no collagen [14]. This structure is known as the “central meniscus of Kuhnt.” Balazs [12] has stated that the Müller cell basal lamina prevents the passage of cells as well as any molecules larger than 15–20 nm and proposed that the complex of the posterior vitreous cortex and ILM could act as a “molecular sieve.” Consequently, the thinness and chemical composition of the central meniscus of Kuhnt and the membrane of Elschnig may account for, among other phenomena, the frequency with which abnormal cell proliferation arises from or near the optic nerve head in proliferative diabetic retinopathy and premacular membrane formation.

The ILM at the fovea is unique, as it is very thin. The foveal ILM is detectable in ILM whole mounts after immunostaining for collagen IV or laminin as a distinct circular area. AFM measurements showed that the foveal ILM has a thickness of approximately 100 nm, whereas the parafoveal ILM has a thickness of up to 3 μm (Figure II.E-5) [15]. The *in vitro* data are consistent with earlier TEM reports [16] (Figure II.E-5b–e), showing a very thin ILM at the fovea and a much thicker ILM at parafoveal regions. The very thin ILM at the fovea and near large blood vessels in the nerve fiber layer [17] suggests that both areas are possible exit points for retinal cells to migrate and then proliferate and form premacular membranes as well as possible entry sites of macromolecules and viruses from the vitreous into the retina.

B. Biochemical Composition of the ILM

The ILM is a basement membrane (BM). BMs are extracellular matrix (ECM) sheets that underlie all epithelia in the body and outline muscle fibers and the vascular endothelium. As such,

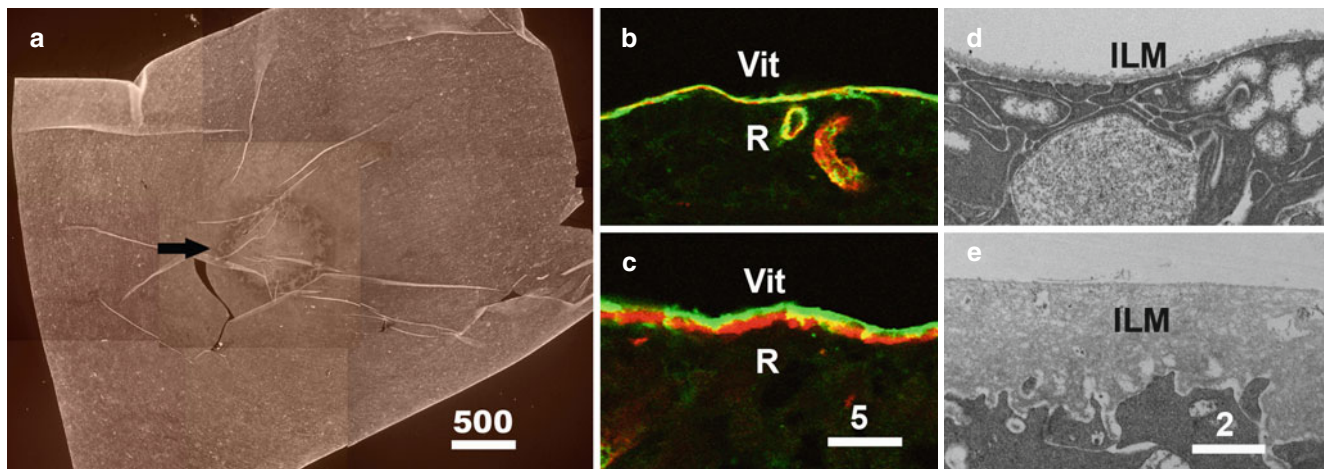


Figure II.E-5 The ILM of the fovea. (a) ILM whole mount from the foveal area of a retina, stained for collagen IV. The fovea is detectable (arrow) as a distinct circular area in the center of the ILM preparation. (b) Fluorescence micrograph showing cross section of the human retina at the foveal center and at the parafoveal area of the same retina. (c) The sections were stained for laminin (red) and collagen IV 7S $\alpha 3$ (green). The foveal

ILM is very thin, and the laminin and collagen IV layers seem to blend and overlap. In contrast, the parafoveal ILM (c) is thick and the laminin and collagen IV layers are clearly distinguishable. (d) TEM micrograph of the human retina in the center of the fovea and at a parafoveal area. (e) The foveal ILM is approximately 100 nm thin, whereas the parafoveal ILM has a thickness of over 2,000 nm (Bars: a: 500 μm ; b, c: 5 μm ; d, e: 2 μm)

the ILM has similar molecular constituents as other BMs. The identification of BM proteins has been complicated by the fact that BMs are not easily isolated in large quantities. Further, the fact that their protein components are highly insoluble in physiological salt concentrations precludes conventional biochemistry and thus is not a useful approach for BM protein analysis.

It was the discovery of two murine yolk sac tumors that synthesize large quantities of a BM like ECM [18–20] that led to the identification of the dominant BM proteins, including laminin-111 [21, 22], nidogen-/entactin-1 [23, 24], perlecan [25], and collagen IV $\alpha 1/\alpha 2$ [26]. In contrast to *in vivo*-derived BMs, the mouse tumor matrix can be solubilized, its components isolated, and its peptide sequenced by conventional biochemistry [27]. More BM proteins were later discovered by means of monoclonal antibodies and by using homology cDNA cloning [28, 29]. Data showed that all of the previously discovered major BM proteins are members of larger protein families. These include the heterotrimeric laminins with five different α -chains, three β -chains, and three γ -chains that form over ten trimeric members [30, 31]. The heterotrimeric collagen IV family members are composed of six genetically different α -chains that assemble into three stable collagen IV trimers [32]. Additional BM components are nidogen-/entactin-1 and nidogen-/entactin-2 [33], and perlecan, agrin, and collagen XVIII are the three dominant BM-associated proteoglycans [34]. All BM proteins are high-molecular-weight proteins of at least 150 kD. The laminin trimers have a molecular weight of 1,000 kD, the collagen IVs over 600 kD, and the proteoglycans between 300 and 600 kD.

Traditionally, protein analysis of BMs *in situ* was done by immunostaining using antibodies to candidate proteins that are

usually present in BMs [35, 36]. More recently, proteomic analysis has been employed for definitive and more comprehensive identification of all BM proteins [13, 37]. Proteomic data from embryonic chick and human ILM, lens capsule, and Descemet's membrane showed that all of these BMs consist of approximately 20 proteins with multiple laminins, multiple collagen type IVs, nidogen-/entactin-1 and nidogen-/entactin-2, and agrin, perlecan, and collagen XVIII. The predominant protein in human ILM is a collagen-type IV, with a chain composition of $\alpha 3/\alpha 4/\alpha 5$. It is of note that the human lens capsule and BMs of the retina vessels have little collagen IV $\alpha 3/\alpha 4/\alpha 5$ but an abundant amount of collagen IV $\alpha 1/\alpha 1/\alpha 2$ [37]. The dominant laminin family member is laminin 521, and the most prominent proteoglycans in the ILM is perlecan, followed by agrin and collagen XVIII [37]. The proteoglycans are responsible for the high water content in the ILM and vitreous [12, 38].

C. Biosynthesis and Assembly of the ILM

All BM proteins are multi-domain molecules that polymerize (laminins, collagen type IVs), cross-link (collagen type IVs), or bind to each other (laminin, agrin, nidogen/entactin, perlecan, collagen type IV). The evidence of polymerization, the mutual binding, and high resolution TEM imaging of individual BM proteins led to a model of BM structure that postulated a two-dimensional network of collagen type IV that combines with a layer of side-to-side polymerized laminin. Nidogen-1 has binding sites for laminin and collagen type IV and was proposed to connect the two polymers [39–43]. Recent data are not entirely consistent with this model,

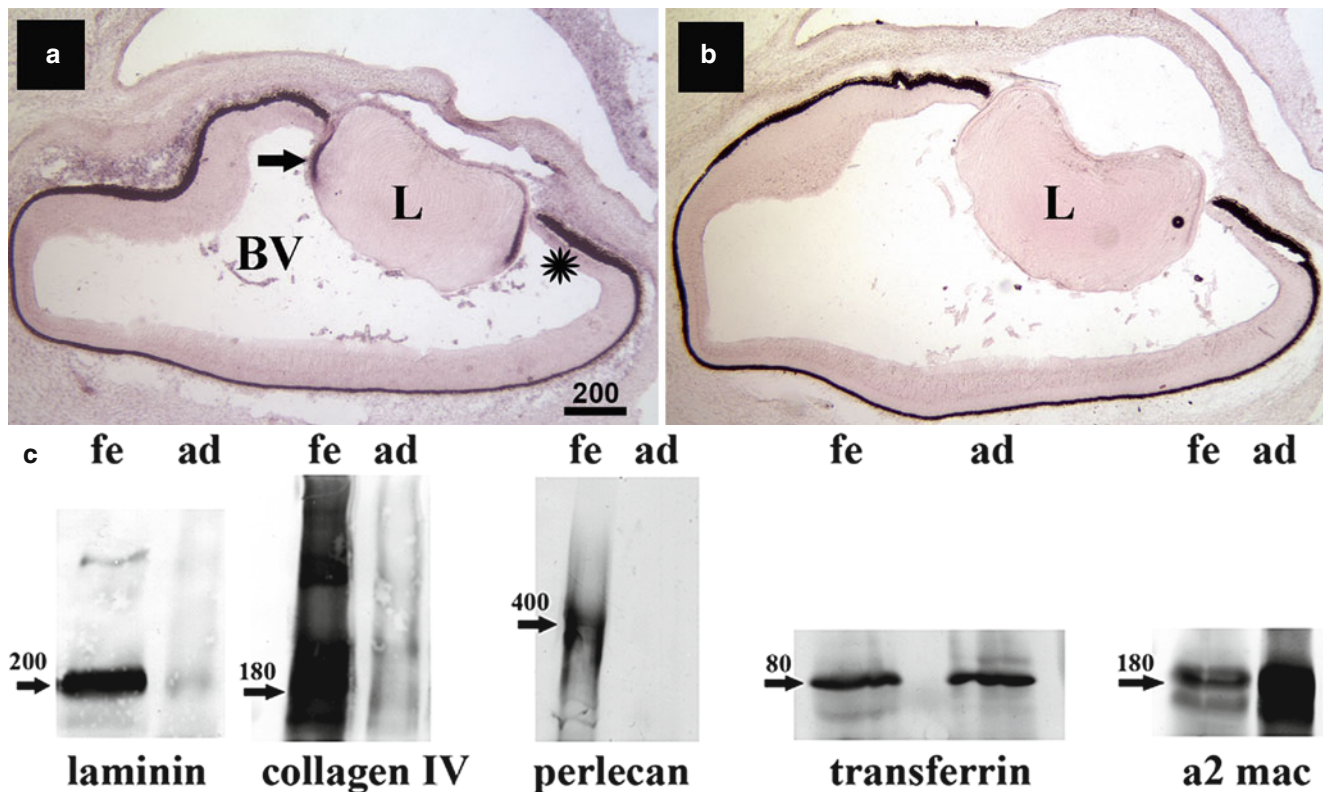


Figure II.E-6 Origin and biosynthesis of the human ILM. *In situ* hybridization. (a) Section of a 10-week-old fetal human eye hybridized *in situ* with antisense RNA for the detection of nidogen-1 mRNA. The nidogen-1/entactin-1 protein is a major component in the human ILM. The labeled cells expressing nidogen/entactin mRNA are located in the lens epithelium (arrow), the ciliary body (star), and the endothelium of the hyaloid vasculature (BV). The absence of any detectable label in the retina indicates that the synthesis of this ILM protein occurs in extraretinal tissues, such as the lens, ciliary body, and intravitreal vasculature. (b) Control section of the same fetal eye labeled with nidogen-1

sense RNA. The *in situ* data suggest that ILM proteins should be detectable in the fetal vitreous. (c) Western blots of fetal (*fe*) and adult (*ad*) vitreous showed that BM proteins are indeed abundant in fetal stages of human eye development and very low in the adult. The blots also showed that transferrin, a non-ILM protein, is not downregulated in the adult eye and that $\alpha 2$ macroglobulin, a typical serum protein, is even more abundant in the adult than in the fetal human vitreous. The data combined indicate that BM protein synthesis occurs in nonretinal tissues of the eye. It is high in fetal stages and selectively downregulated to very low levels in the adult human eye (Bar: a, b: 200 μ m). *L* lens

particularly the finding that BMs assemble properly in the absence of nidogen-1 [44, 45].

Because of the propensity for proteins to polymerize, it was previously thought that BMs spontaneously assemble when BM proteins are present at sufficiently high concentrations [46]. It later became clear that cell receptors are also required for BM assembly. Cell receptors for BM assembly are members of the integrin family and dystroglycan. The best evidence for a central role of cellular receptors in BM assembly comes from targeted mutations of dystroglycan and integrins in mice that lead to defects in BM assembly, which are very similar to BM disruption caused by mutations of essential BM proteins [47, 48].

The presence of the ILM adjacent to the end feet of the Müller glial cells suggested that the retina, specifically Müller cells, is the major source of ILM proteins. However, with the exception of the mRNA for agrin, ILM protein mRNAs were not detected in the neural retina [49–52]. Since the ILM is composed of secretory proteins, however, the

origin of ILM proteins could theoretically be any cell layer lining the interior of the eye. Indeed, *in situ* hybridization of embryonic mouse and human eyes revealed that almost all ILM proteins are synthesized by the lens epithelium, the future ciliary epithelium, and the endothelial cells of the hyaloid vasculature (Figure II.E-6) [49, 50, 53, 54].

The *in situ* hybridization data suggested the hypothesis that ILM proteins are secreted by the lens and ciliary body into the vitreous and that they diffuse to the retinal surface where they assemble into the ILM. The hypothesis further proposes that the role of the retina is to provide the cell surface receptors of the neuroepithelial cells for ILM assembly. In support of this hypothesis, studies have shown that large quantities of laminin, collagen IV, nidogen, perlecan, and agrin are present in the embryonic chick and fetal and neonatal human vitreous. The highest concentrations of ILM proteins in the vitreous coincide with the timing of most active ILM assembly during rapid eye growth [53, 54]. The analysis of the vitreous also showed that the concentrations of ILM proteins decline to very

low levels in the adult human vitreous, and an extended study in chick showed a precipitous decrease of the ILM protein synthesis at late fetal/neonatal stages [53, 55]. The current data suggest that the ILM is primarily assembled during embryonic, fetal, and neonatal stages of development and that this activity is greatly reduced in the adult life. However, given the continuous increase in human ILM thickness during aging, it is probable that there is continued low level of the ILM protein synthesis throughout life.

It is currently not known if the ILM regenerates. The fact that the expression of human vitreous proteins undergoes similar age-related downregulation as ILM proteins and that the vitreous gel does not regenerate after vitrectomy suggests that a complete ILM regeneration does not occur. Consistent with this proposition is experimental data in rabbits showing that a damaged ILM does not regenerate [56]. On the other hand, it has recently been shown that *in vitro* Müller cells can synthesize ILM collagens [57]. Furthermore, studies in monkey found that ILM peeling is followed by resynthesis of the ILM over the course of several months [58].

D. Role of the ILM in Ocular Development

It is of great interest to note that during ocular embryogenesis the ILM can be readily identified during invagination of the optic vesicle (Figure II.E-7). Just prior to completion of invagination, it can be clearly appreciated that there is continuity of the ILM and Bruch's membrane. This suggests that although these two BM interfaces are considered separate and distinct entities, their origin is likely coded by the same genes and their composition is likely identical, at least at the origin of life. Thus, phenomena such as aging, glycosylation, cell adhesion, cell migration, and cell proliferation at these two sites share a common pathway, at least as it concerns the underlying BM substrate upon which these processes occur [59, 60].

The ILM is essential in early ocular and retinal development. Evidence comes from the retinal phenotype of a series of targeted deletions of BM proteins, their processing enzymes, and their receptors in mice and a number of spontaneous mutations in humans. Targeted mutations of the genes encoding laminin chains [61–63] or the binding site of laminin γ -1 for nidogen/entactin-1 [53], collagen IV [64], and enzymes responsible for the glycosylation of dystroglycan, such as LARGE, fukutin, fukutin-related protein, POMT1 and POMT2, and POMGnT1 [65–67], cause major breaks in the ILM and result in retinal ectopia. In eyes with these mutations, retinal cells migrate through breaks in the ILM into the vitreous (Figure II.E-8a–d). Further, approximately 50 % of the retinal ganglion cells undergo apoptosis, resulting in major optic nerve hypoplasia [53]. The underlying cause for this retinal dysplasia is that the mutations cause a weakening of the biomechanical strength of the ILM, leading

to breaks in the ILM due to the rapid expansion of the retina during development. The breaks in the ILM are accompanied by the retraction of the neuroepithelial cells, most likely the cause of ganglion cell death and optic nerve hypoplasia [53]. AFM measurement showed that the stiffness of the ILM in these mutations is lowered by at least 50 %, explaining the numerous stretch-related breaks in the ILM (Figure II.E-8e, f). Similar retinal phenotypes are also recorded for spontaneous mutations of Walker-Warburg syndrome, muscle-eye-brain diseases, and Fukujama muscular dystrophy in humans [68–71].

In addition to massive eye phenotypes, the mutations also affect brain development and, in many cases, result in muscular dystrophy and rupture of ocular and cerebral blood vessels [65, 72–74]. The retinal, cortical, vascular, and muscular phenotypes provide strong evidence that the mechanical strength of BMs is essential in the development of the retina, cerebral cortex, blood vessels, and muscles.

The ILM can be peeled off in the adult human eye and represents a medical intervention for macular hole closure and the cure of other vitreomaculopathies. Peeling the ILM assures removal of an abnormal posterior vitreous cortex and other pathologic membranes. This is only innocuous when partial thickness of the ILM is removed. Further, the ILM is probably regenerated, at least in part, by Müller cells during the months following surgery.

E. Aging of the ILM

Like many connective tissues of the human body, the ILM changes its molecular composition and structure with age. Biochemically, age-related variations were observed in the relative concentration of laminin, which is higher during early stages of ILM assembly than later, and the relative concentration of collagen IV that increases with age [13, 37]. This may underlie the most obvious age-related change of the human ILM, that being an age-dependent increase in thickness with progressing age. During fetal stages, the ILM has a thickness of less than 100 nm and the classical trilaminar BM structure of BMs (Figure II.E-2c). This changes with aging, as the ILM becomes thicker and loses its trilaminar structure to become amorphous (Figure II.E-9). Further, the retinal side of the ILM develops indentation that become more dramatic with progressing age. A systematic analysis of ILMs from over 20 patients (Figure II.E-9f) shows the progressive increase in the ILM thickness with advancing age [4]. The continued age-related increase in the ILM thickness indicates that ILM protein synthesis occurs in the adult human eye over the entire life span but at a very reduced level. The absolute number of years of age counts to a major degree, since increases in the ILM thickness have only been recorded for the long-lived humans and primates and not in any of the short-lived animal species [75].

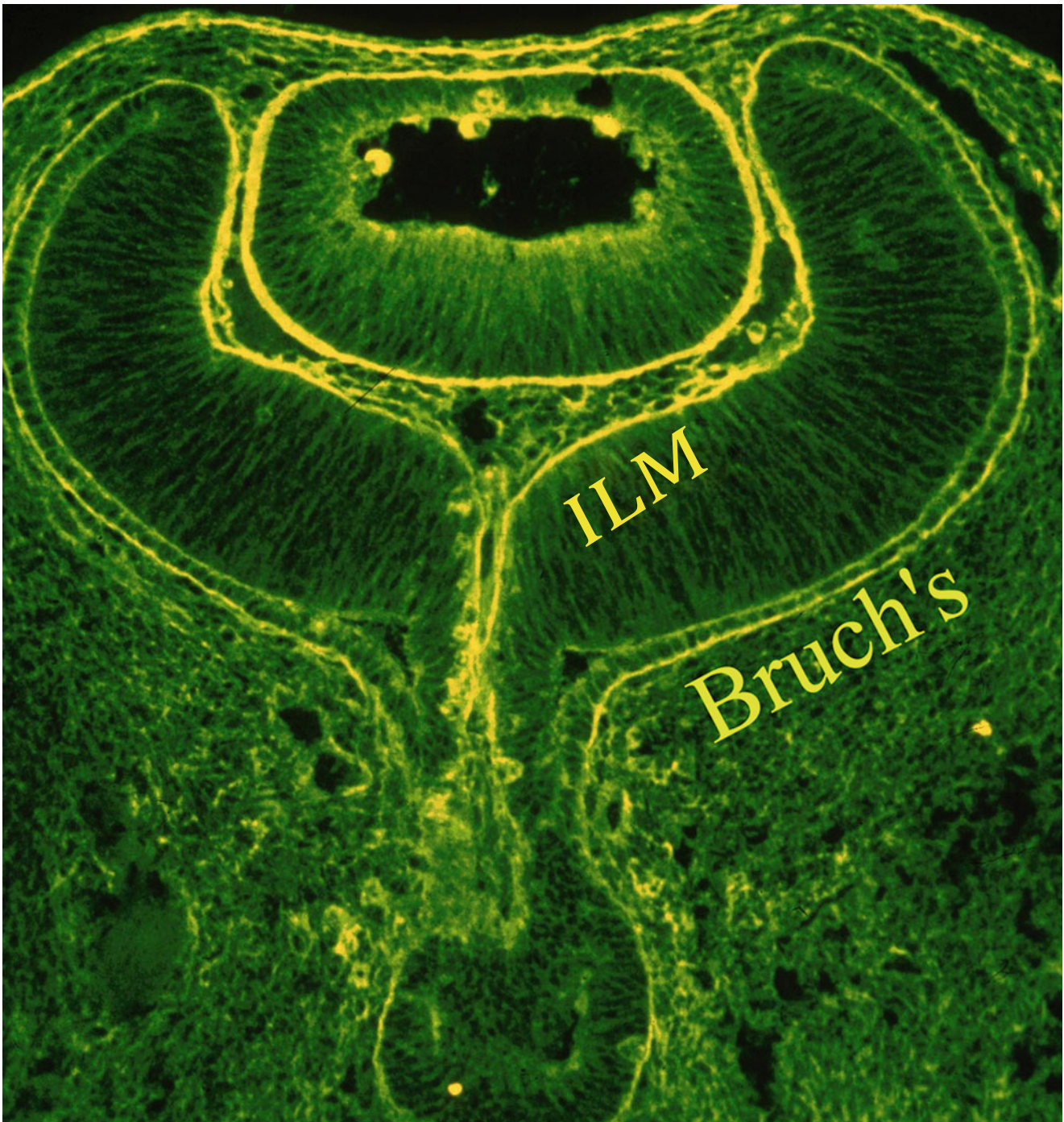


Figure II.E-7 Immunohistochemistry of the human embryonic eye following invagination of the eye cup at about 8 weeks gestation. The section is stained with immunofluorescent antibodies to *Agaricus bisporus* (ABA) that intensely stain basement membranes. The *yellow line* labeled “Bruch’s” is the chorioretinal interface destined to become Bruch’s membrane, while the *yellow line*

labeled “ILM” (*inner limiting membrane*) is the vitreoretinal interface destined to become the ILM. Note that the two structures are continuous and represent the same identical membrane folded over inside the eye. Thus, pathologic events such as cell migration and proliferation at these two interfaces are occurring upon the same identical substrate (Courtesy of Dr. Greg Hageman)

In addition to an increase in thickness, the ILM also becomes stiffer with advancing age [4]. It is conceivable that the progressive change in the protein composition to more collagen IV and less laminin is responsible for this age-related increase in the ILM stiffness.

F. Role of the ILM in Disease

1. ILM and Diabetes

Diabetes alters tissues throughout the body via nonenzymatic glycosylation of proteins. This has been demonstrated

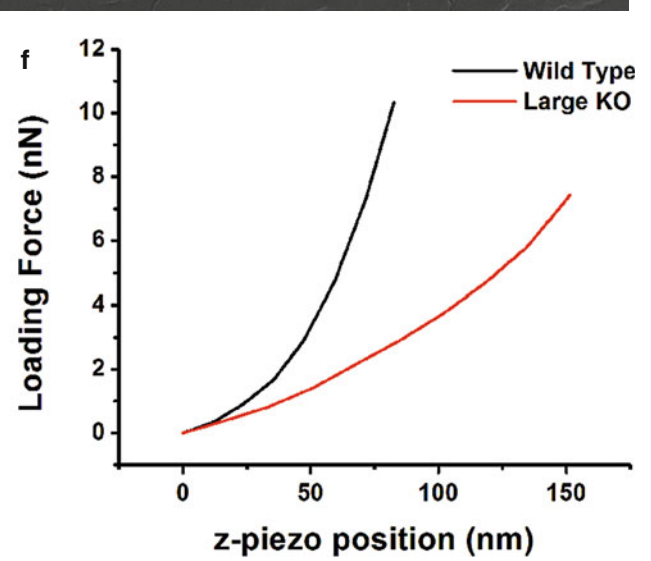
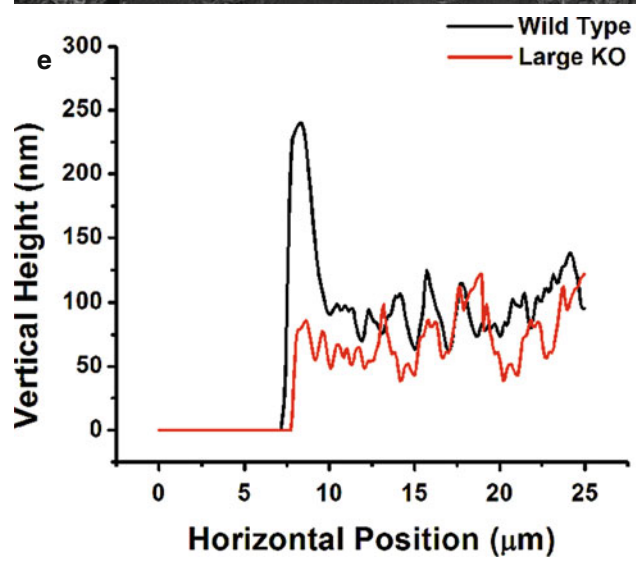
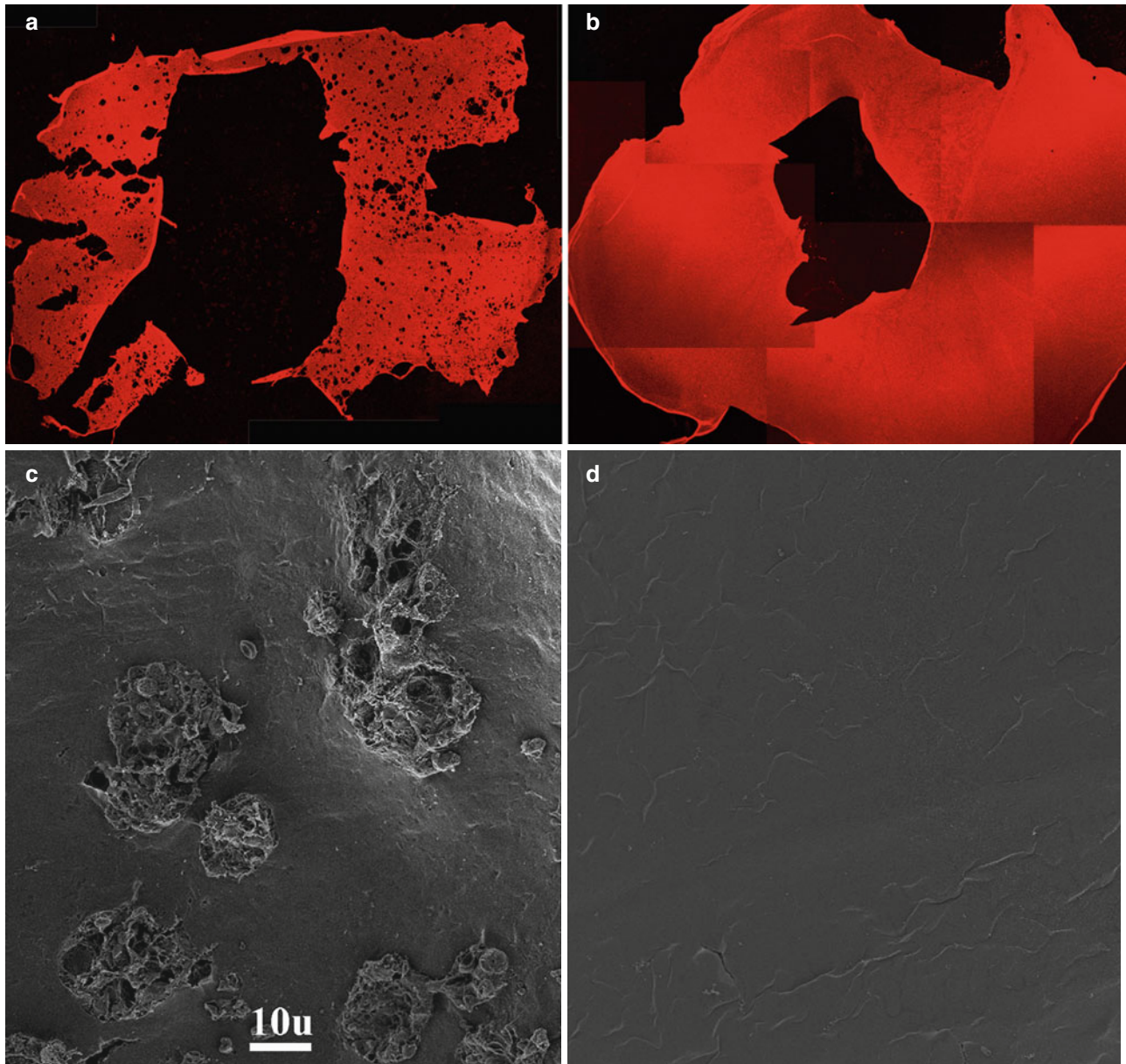


Figure II.E-8 Biomechanical properties of the ILM and retinal development. Mice with a targeted mutation of LARGE or POMGnT1 have fragile BMs. Both mutations affect enzymes that are essential for the glycosylation of dystroglycan, one of the receptors for laminin that is essential for BM assembly. (a) An ILM flat mount from a neonatal mouse with a homozygous mutation for either of the two enzymes shows numerous holes as the ILM is fragile and ruptures during eye growth. (b) An intact control ILM from a heterozygous mouse.

(c) SEM images of the vitread surface of retinas from a mutant animal show the multiple ruptures in the ILM that lead to the migration of retinal cells into the vitreous. (d) The continuous and smooth surface of the ILM from control retina. (e) AFM height measurements showed that the ILM from the mutant mouse is slightly thinner. (f) Stiffness measurements showed a dramatically weaker ILM from the mutant mouse as compared to the control mouse ILM (Bar: c, d: 10 μm)

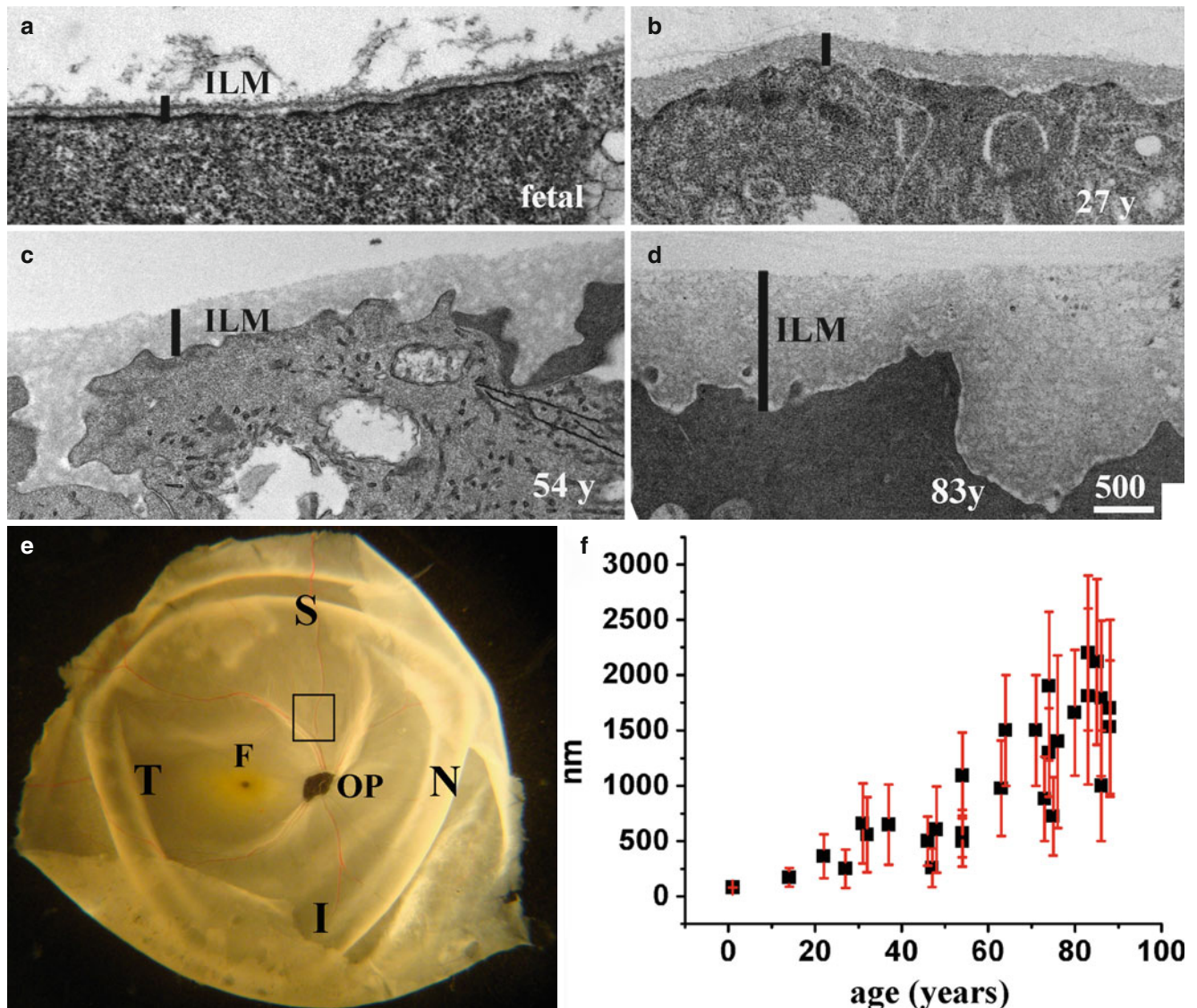


Figure II.E-9 Age-dependent increase in ILM thickness. TEM micrographs show the vitread surface of the retina from a 16-week fetal human eye (a) and from 27, 54 and 83-year-old adult human eyes (b–d). The ILM from the fetal eye (a) has the typical morphology of a BM – it is 70 nm thick with a typical lamina densa and three-layered ultrastructure. Between 22 and 83 years of age (b–d), the ILM dramatically increases in thickness, becomes highly irregular at its retinal surface, and no longer

contains a distinct lamina densa. The black bars in (a) to (d) indicate the thickness of the ILM. Panel (e) shows an adult human retina with the location in the superior posterior pole of the right eye (boxed) where the retina was sampled. The graph in panel (f) shows the age-dependent increase in ILM thickness. Each of the data points represents averages from measurements of one pair of eyes of a single patient. F fovea, OP optic papilla, S superior, I inferior, T temporal, N nasal (Bar: a–d: 500 nm)

to alter vitreous molecules [76, 77] and structure [78], and the term “diabetic vitreopathy” has been proposed to refer to these effects [79] (see chapter I.E. Diabetic vitreopathy). Insofar as the ILM is similarly proteinaceous, advanced glycosylation end products could accumulate in this tissue and alter its physiology.

It is well established that BMs increase in thickness during long-term diabetes. This applies also to the ILM [80–82]. The increase in the ILM thickness occurs in patients suffering from type 1 and type 2 diabetes (Figure II.E-10). However, the increase in thickness is only detectable after several years of the diabetes condition and is not detectable in diabetic mice [83]. What is presently still unknown is the nature of the proteins that are responsible for diabetes-related BM thickening. It is possible that the normal BM proteins are excessively synthesized and incorporated into the ILM at an accelerated rate or that new, diabetes-specific proteins are expressed and incorporated leading to an altered, diabetes-specific protein composition of the ILM. There are some findings that support the latter: fibronectin, normally not present in the human ILM, is detected in ILMs from diabetic eyes [35, 82]. However, several studies have also shown that collagen IV is excessively synthesized in long-term diabetes, which would indicate that normal ILM proteins are expressed at a higher than normal rate [84]. It is of note that only negligible differences in protein compositions of the ILM were detected in diabetic mice showing that mouse models are inadequate to study the diabetic-related pathological changes that are detectable in long-term diabetic human patients [83].

2. Proliferative Diseases and the ILM

Cell proliferation at the vitreoretinal interface plays an important role in proliferative diabetic retinopathy, proliferative vitreoretinopathy (see chapter III.J. Cell proliferation at vitreo-retinal interface in PVR and related disorders), and macular pucker formation (see chapter III.F. Vitreous in the pathobiology of macular pucker). The interaction of the involved cell, which differs in each condition, with the underlying substrate can influence the course of the disease. This is critical to our understanding of disease pathogenesis with respect to cell adhesion, cell migration, and cell proliferation.

Under normal conditions the vitread surface of the human retina is cell-free (Figure II.E-11a, b). However, there are various age- and disease-related conditions where membranes form on the retinal surface. Foos [16, 17] termed these epiretinal membranes, although this is a misnomer since the term “epiretinal” is not adequately specific. Subretinal membranes are also “epiretinal.” The membranes in question here are all actually “premacular” (Figure II.E-11c–e). Foos further described that these membranes arise via cell migration from the retina through the ILM. While this is probably true in proliferative diabetic retinopathy, where there is migration and proliferation of vascular endothelial cells arising from the retina, and proliferative vitreoretinopathy, where retinal

pigment epithelial cells play an important role (although they don’t traverse the ILM but rather enter vitreous via breaks in the retina) [17].

This is not true for macular pucker, the most common case of premacular membrane formation that disturbs vision. Premacular membranes that cause macular pucker most often result from anomalous posterior vitreous detachment [85, 86] with vitreoschisis [87–90] (see chapter III.B. Anomalous PVD and vitreoschisis). The hyalocytes that are embedded in the outer posterior vitreous cortex are left attached to the retina and elicit monocyte migration from retinal vessels as well as glial cell migration from the retina to form the premacular membranes that contract and induce macular pucker. The contractile forces that induce this pucker likely originate from hyalocytes (see chapter II.D. Hyalocytes).

The ILM plays an important role in proliferative disorders at the vitreoretinal interface in several ways. The formation of cellular membranes on the retinal surface requires the migration of cells, their adhesion to a substrate, and then proliferation. Vascular endothelial cell migration through the ILM is important in proliferative diabetic retinopathy as well as trans-ILM migration of glial cells from the retina. Monocytes from the circulation are important in macular pucker. It is not clear whether or not there is alteration of the normal ILM that allows cells to migrate from the retinal vessels, although the foregoing section on diabetes and the ILM would suggest that the ILM in diabetic patients is not normal. In the case of macular pucker, there is no evidence that the ILM is abnormal.

Cell adhesion to normal or pathologic surfaces is mediated by laminin [91]. In the eye, laminin has been shown to play a critical role in retinal vascular development [92], and it would seem a reasonable extrapolation to implicate similar roles in pathologic neovascularization. Thus, the attributes of the ILM and its impact on cell adhesion are important considerations. Studies [93] have shown that the human ILM has side-specific properties that are detectable by side-specific labeling of a flat-mounted ILM preparation using antibodies to laminin or collagen IV. Laminin is most abundant on the retinal side of the ILM, whereas an antibody to the 7S domain of collagen IV $\alpha 3$ labels the vitread side (Figure II.E-12a–c). When dissociated MDCK, corneal, or retinal cells were plated on flat-mounted and folded ILMs, the cells adhered preferentially to the retinal side of the ILM (Figure II.E-12d). This finding suggests that there is a change in proliferative pathologies that facilitates cell adhesion to the vitread side of the ILM. Alternatively, the presence of remnant posterior vitreous cortex on the ILM as a result of anomalous PVD with vitreoschisis could provide the substrate needed for cell adhesion and subsequent proliferation. Contractile effects upon the retina would then arise from this layer of remnant posterior vitreous cortex that has become hypercellular and is still attached to the ILM via the intervening ECM, called the vitreoretinal border region by Heergaard (see above).

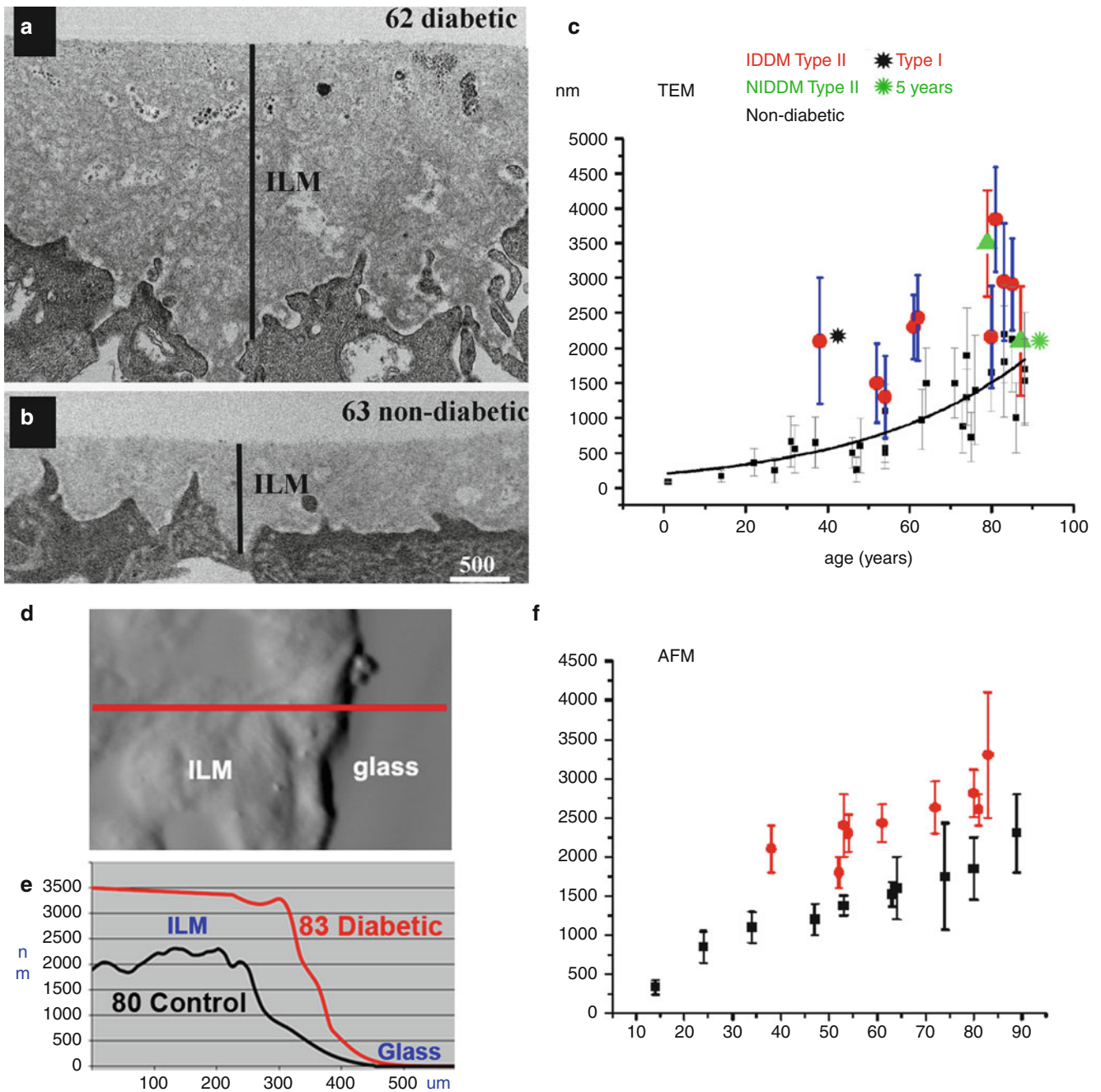


Figure II.E-10 Diabetes-related increase in ILM thickness. **(a)** TEM micrograph of ILM from a 62-year-old diabetic patient. **(b)** TEM micrograph of ILM from a 63-year-old nondiabetic patient. **(c)** Graph showing that the thickness of ILMs increases with age, but the thickness of ILMs from diabetic patients is approximately double the thickness of ILMs from age-matched nondiabetic subjects. **(d)** A similar difference in the thickness of diabetic and nondiabetic ILMs was detected by probing the ILM samples with atomic force microscopy (AFM). An AFM image of the edge of an ILM from a diabetic patient is shown. The ILM had been flat mounted on a glass slide, and the glass surface served as a reference for the height measurements. The red line indicates the trace of the AFM probe used to determine the thickness of the sample.

(e) Representative height traces of a diabetic and a nondiabetic ILM quantitatively demonstrate the increased thickness of the ILM in diabetic patients. **(f)** AFM thickness measurements of nondiabetic and diabetic ILMs show that diabetic ILMs (red) are on average twice as thick as ILMs from similarly aged nondiabetic subjects (Bar: **a**, **b**: 500 nm). Notes: The patient's medical history, time of harvesting of eyes after death, and the time of tissue delivery to the laboratory are available for every ILM sample analyzed in this graph. Except for the sample marked by a star, all samples came from patients with type II diabetes. The duration of diabetes was at least 10 years, except for the ILM marked by a green star (5 years). *IDDM* insulin-dependent diabetic, *NIDDM* non-insulin-dependent diabetic

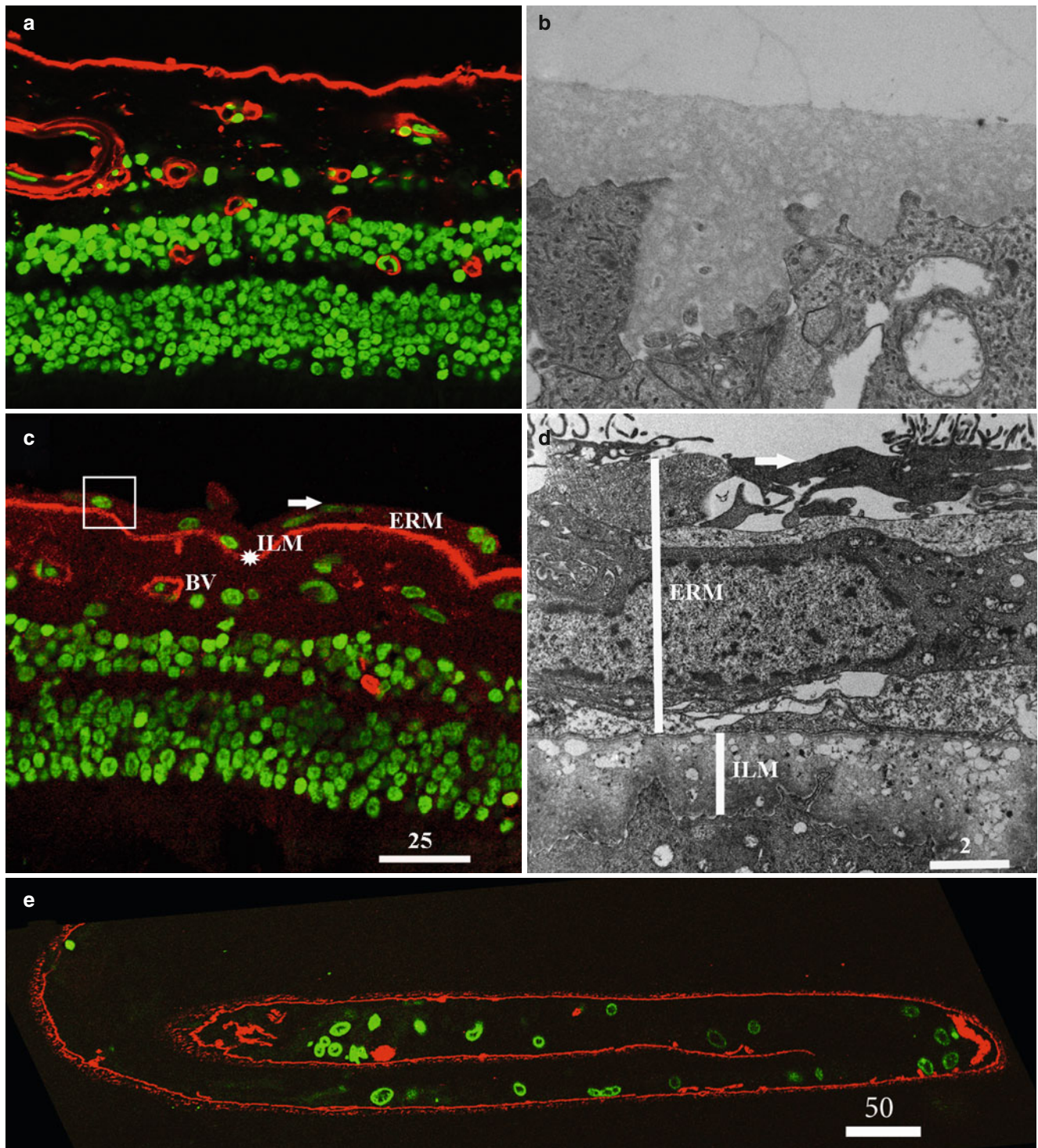


Figure II.E-11 Premacular (“epiretinal”) membranes. The vitread surface of the ILM from a normal human retina is cell-free as shown by immunostaining for collagen IV (**a**; *red*) or by TEM (**b**). (**c**) A premacular cell layer is detectable in a cross section by staining the specimen for

collagen IV (*red*) and cell nuclei (*green*) or by TEM (**d**). (**e**) A surgical specimen following ILM peeling shows the excised ILM with attached cells stained for collagen IV (*red*) and cell nuclei (*green*) (Bars: **a**, **c**: 25 μm ; **b**, **d**: 2 μm ; **e**: 50 μm)

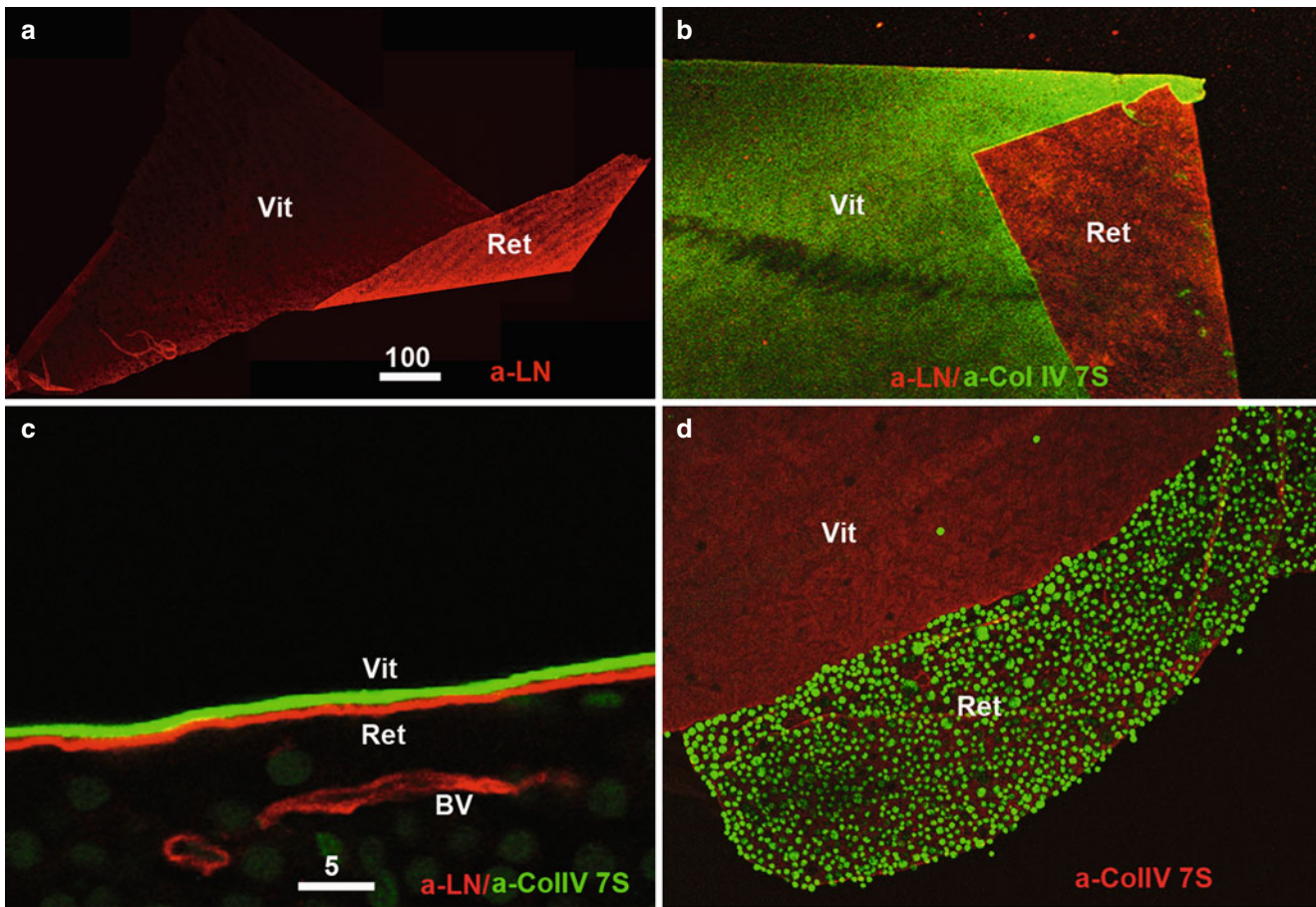


Figure II.E-12 Cell adhesion on the ILM. The human ILM has side-specific properties that are detectable by the side-specific labeling of a flat-mounted ILM using antibodies to laminin (**a**, **b**) or collagen IV (**b**, **c**). Laminin is most abundant on the retinal side of the ILM (**a**, **b**), whereas an antibody to the 7S domain of collagen IV $\alpha 3$ labels the vitread side (**b**, **c**, *green*). The abundance of both proteins on either

the retinal or vitread side is best appreciated by double labeling (**b**, **c**). When dissociated MDCK, corneal, or retinal cells were plated on flat-mounted and folded ILMs, the cells adhere preferentially to the retinal side of the ILM (**d**). The vitread side of this preparation was labeled with an antibody to the 7S domain of collagen IV $\alpha 3$ (*red*). The adherent cells were labeled *green*.

3. Tractional Disorders and the ILM

The ILM is the site of pathologic traction at the vitreoretinal interface. Traditionally, this has been conceived as axial in direction, resulting in anteroposterior traction upon the retina. Gass [94] first proposed that tangential traction at the vitreoretinal interface can also disturb the macula and reduce vision via distortions (macular pucker), blurring (macular edema), and/or scotomata (macular hole). It is not clear whether these tangential forces are exerted uniquely by the posterior vitreous cortex or whether the ILM plays a role as well. Thus, the biophysical properties of the ILM are important to study so as to elucidate this potential role.

a. Biophysical Properties of the ILM

Biophysical properties, such as elasticity and stiffness, are important determinants of the ILM role in disease. For elasticity studies and stiffness measurements, the ILM has to be isolated as a clean preparation, which is done by dissolving

the retinal tissue in detergent [4, 93, 95–97]. These ILM sheets are transparent and invisible under bright-field illumination but detectable under dark-field illumination (Figure II.E-13a, lower left-hand corner inset). Isolated ILMs have the ultrastructure of ILMs in situ, with a smooth vitread surface and an indented and irregular retinal surface (Figures II.E-13a, b). Interestingly, the ILM sheets scroll, with the retinal side consistently facing outward and the vitread surface inward (Figure II.E-13a). This scrolling phenomenon with the epithelial side on the outside of the scroll and the connective tissue side on the inside of the scroll is also observed for the lens capsule and Descemet's membrane of the cornea, thus suggesting an inherent property of BMs [97]. AFM showed that the retinal side of the ILM is at least twice as stiff as the vitread side [15, 93].

It is important to appreciate that during any vitreous surgery that includes ILM peeling, this scrolling effect is only observed when full-thickness ILM is surgically removed

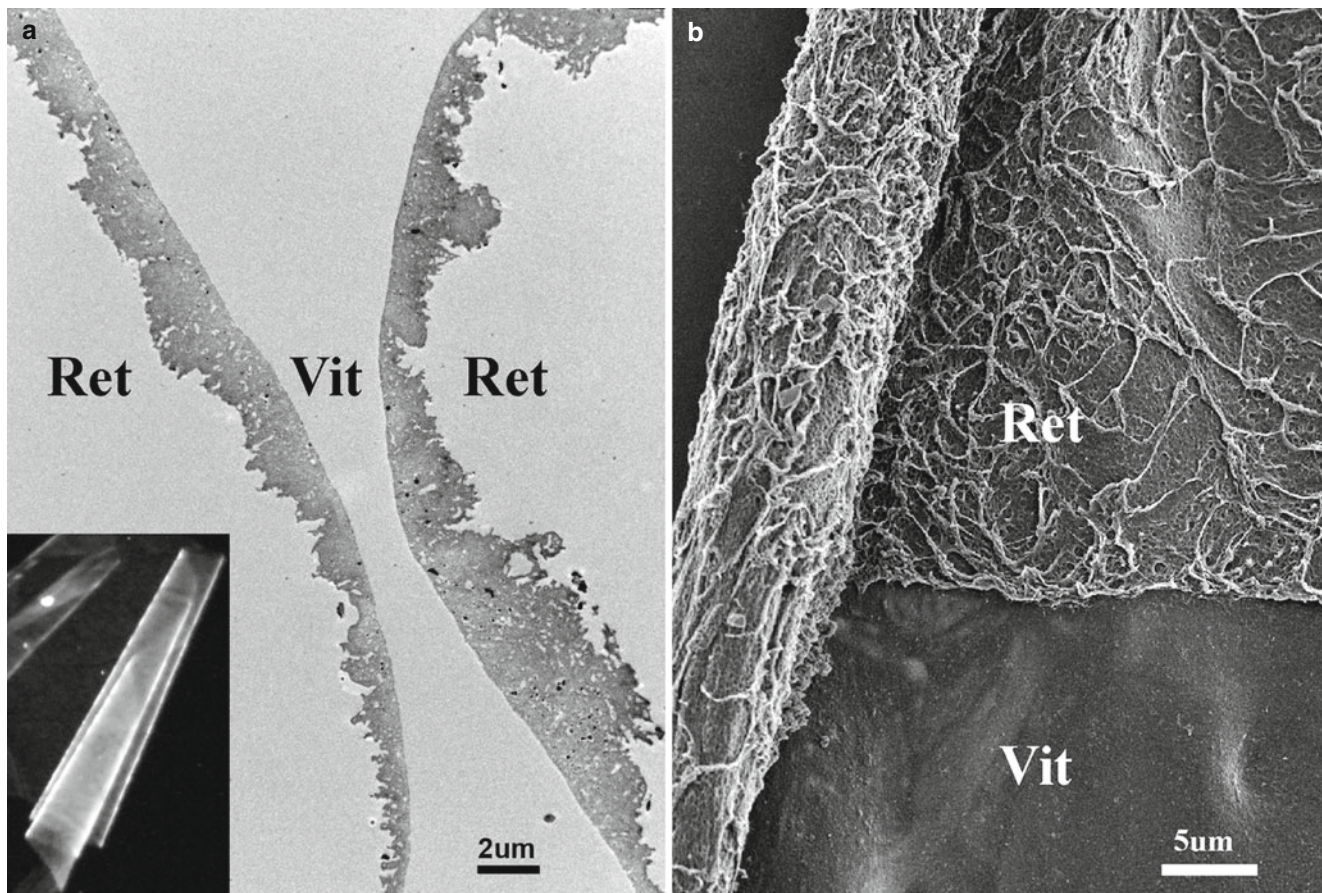


Figure II.E-13 Isolated human ILM. ILMs can be isolated from human retina by dissolving the retinal cells in detergent. The detergent-insoluble BMs are collected under a dissecting microscope using dark-filed illumination (**a**, *insert*). The isolated ILMs scroll up with the retinal surface facing outward and the vitread surface facing inward. TEM

(**a**) and SEM (**b**) micrographs of isolated ILMs show that the retinal surface (*Ret*) is highly irregular, whereas the vitread surface (*Vit*) is even and smooth. The images also show that the ILM preparations are clean and not contaminated with cellular debris or non-BM ECM (Bar: **a**: 2 μm ; **b**: 5 μm)

from the retina. This is fortunately not common, since the overwhelming majority of the time the peeled tissue is partial (not full) thickness ILM, which does not scroll. Thus, splitting of the ILM occurs (perhaps between the lamina lucida interna and the lamina densa) and only the inner (anterior) portion of the ILM is being peeled. This explains why ILM peeling is associated with better surgical outcomes and good vision. Full-thickness ILM peeling will likely not have good postoperative vision due to damage to the underlying retinal nerve fiber layer as well as Müller cells. Thus, surgeons witnessing scrolling of the tissue being peeled off the retina may be well advised to establish a different surgical plane.

The availability of isolated and clean ILM allowed collecting data on its biomechanical properties. By using the force-indentation mode of the AFM, the stiffness of isolated and flat-mounted mouse, chick, and human ILMs were recorded in the high kPa to low MPa range [3, 4]. This corresponds to the stiffness of hyaline cartilage [9] and characterizes the ILM and all other BMs as tough connective tissue

structures. It is of note that the stiffness of cell layers is in the low kPa range [98], and thus BM, including the ILM, is several hundred-times more stable than cell layers and explains why cell layers fail when their BMs or BM assembly receptors are defective [67].

4. Uveitis

Abnormalities of the vitreoretinal interface are common in patients with uveitis and include posterior vitreous detachment, preretinal membrane formation, retinal neovascularization, and vitreomacular traction with or without cystoid macular edema [99, 100]. Partial and full-thickness macular holes, although uncommon in patients with uveitis, have also been described and are typically attributed to accelerated anteroposterior or tangential traction forces [101]. More than half of the nearly 60 uveitic macular holes that have been described in the literature have occurred in patients with Behcet's syndrome – although it remains unclear whether the development of macular holes in patients with uveitis in the setting of Behcet's represents a relative predisposition for

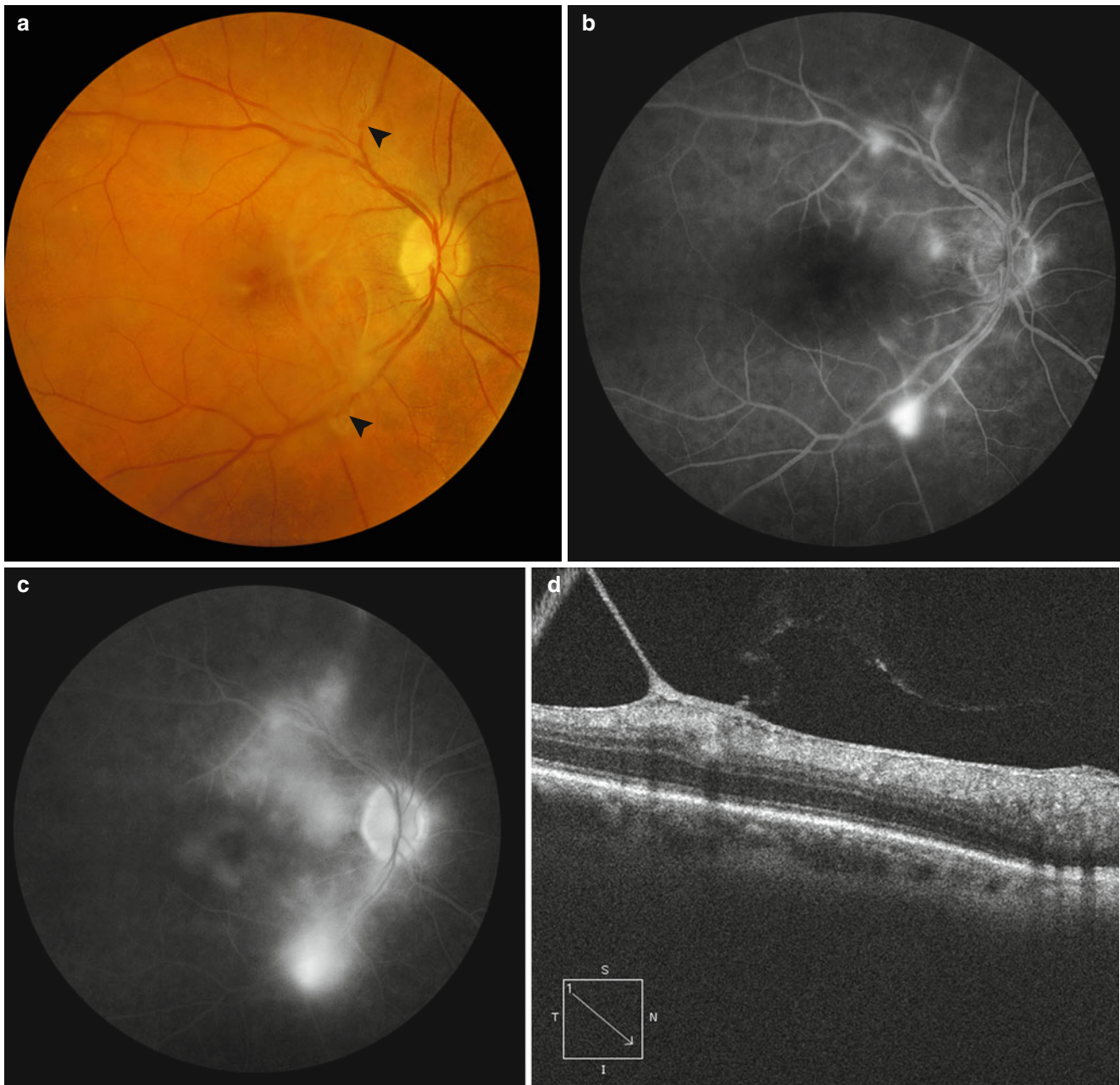


Figure II.E-14 Color fundus photograph (a), early (b), and late (c) fluorescein angiography photographs, and spectral domain ocular coherence tomography (SD-OCT, d) of a 63-year-old woman with extensive vitreoretinal traction throughout the posterior pole producing both retinal neovascularization (*arrowheads*) and diffuse retinal

vascular leakage mimicking vasculitis. The SD-OCT image was taken along the superior temporal arcade vessels. No vitreous cells were present and a workup for causes of uveitis or vasculitis was unrevealing. The patient had no history of radiation or evidence of diabetes mellitus. Similar findings were present in the fellow eye

macular hole formation [102], related perhaps to intrinsic ILM abnormalities. Sullu and associates recently described a case of widespread vitreoretinal traction involving the macula, optic disc, and major retinal vessels that produced diffuse leakage on fluorescein angiography mimicking uveitic retinal vasculitis [103] (Figure II.E-14). This may relate to the special structural interface between the posterior vitreous cortex and the ILM over retinal blood vessels (see below).

III. Posterior Vitreous Cortex

A. Structure

The posterior vitreous cortex is 100–110 μm thick [104, 105] and consists of densely packed collagen fibrils [104–106] (Figure II.E-15). The term “posterior hyaloid” is often used to refer to this structure, but “hyaloid” is best reserved for the

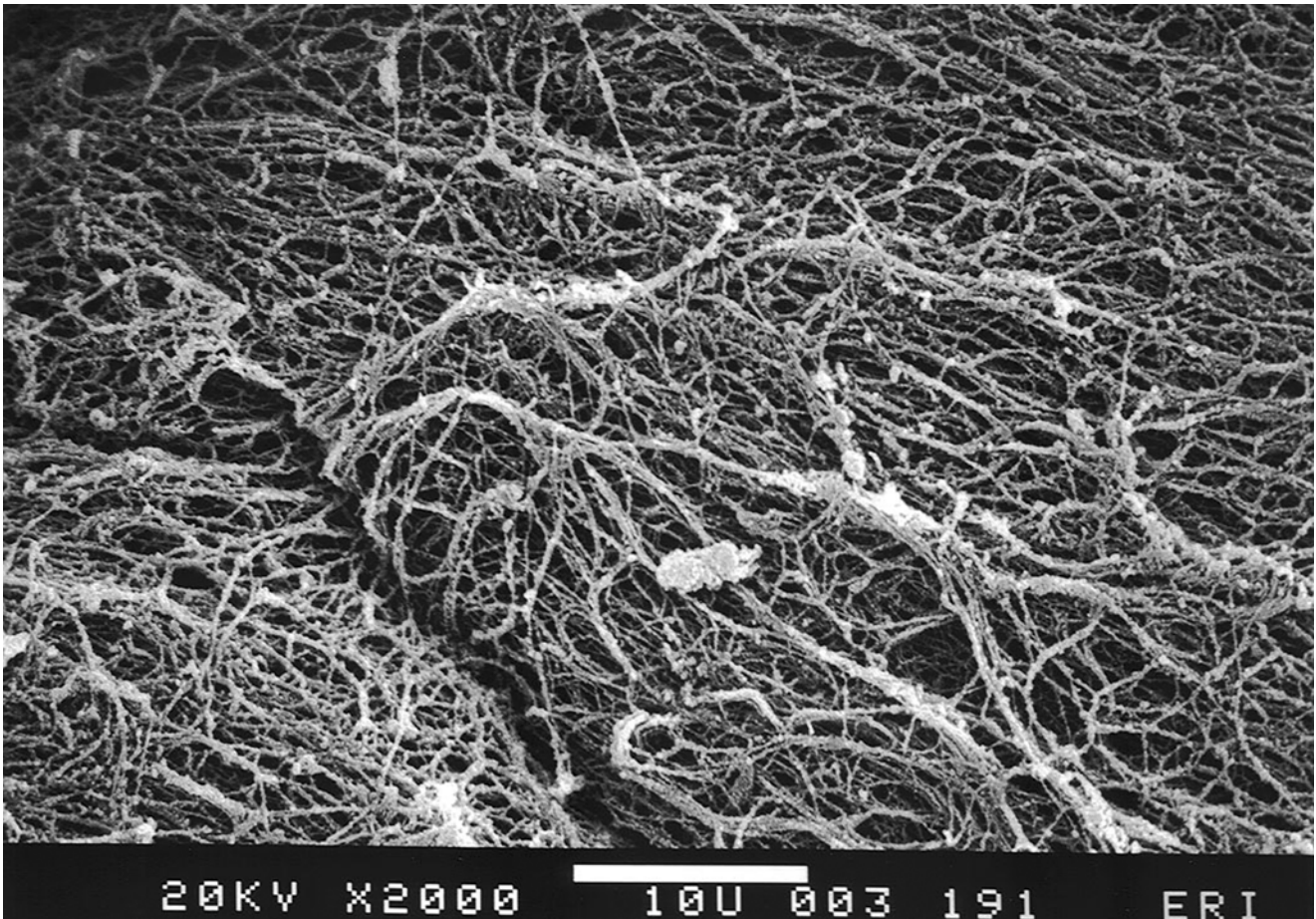


Figure II.E-15 Scanning electron microscopy of the posterior aspect of the human posterior vitreous cortex. Scanning electron microscopy demonstrates the dense packing of collagen fibrils in the vitreous

cortex. To some extent this arrangement is exaggerated by the dehydration that occurs during specimen preparation for scanning electron microscopy (Bar= 10 μ m) [107]

hyaloid artery present during embryogenesis and “face” is to be reserved for the front of the vitreous, not the back, since the face is on the front of the head not the back. Thus, there is an anterior hyaloid face, but not a posterior hyaloid face.

A lamellar organization of these collagen fibrils results in the appearance of sheets on immunohistochemistry (Figure II.E-16). These potential cleavage planes are important not only as sites of tissue separation during posterior vitreous detachment (see chapter III.B. Anomalous PVD and vitreoschisis), but also as potential cleavage planes during membrane peel surgery. Because of vitreoschisis many experienced surgeons have peeled what was thought to represent full-thickness posterior vitreous cortex membranes, only to find additional membranes still attached to the macula.

There is no posterior vitreous cortex over the optic disc, and the cortex is thin over the macula due to rarefaction of the collagen fibrils, allowing vitreous to extrude and give the appearance of two holes. The premacular hole in the posterior vitreous is sometimes referred to as the premacular bursa. The prepapillary hole in the vitreous cortex can sometimes be visualized clinically when the posterior

vitreous is detached from the retina. If the peripapillary glial tissue is torn away during PVD and remains attached to the vitreous cortex about the prepapillary hole, it is referred to as Vogt’s or Weiss’ ring. Vitreous can extrude through the prepapillary hole in the vitreous cortex (Figure II.E-17) but does so to a much lesser extent than through the premacular vitreous cortex.

B. Cells of the Posterior Vitreous Cortex

1. Hyalocytes

Reeser and Aaberg [109] considered the vitreous cortex to be the “metabolic center” of vitreous because of the presence of hyalocytes. These cells were first described in 1845 by Hannover. Schwalbe [110] placed these cells into the group of “Wanderzellen” (wandering cells, *i.e.*, leukocytes or macrophages) on the basis of their morphology, distribution, and behavior. He later named them “subhyaloidale Zellen” [111]. Balazs [112] modified this term and named the cells “hyalocytes.” The origin of hyalocytes is unknown, although

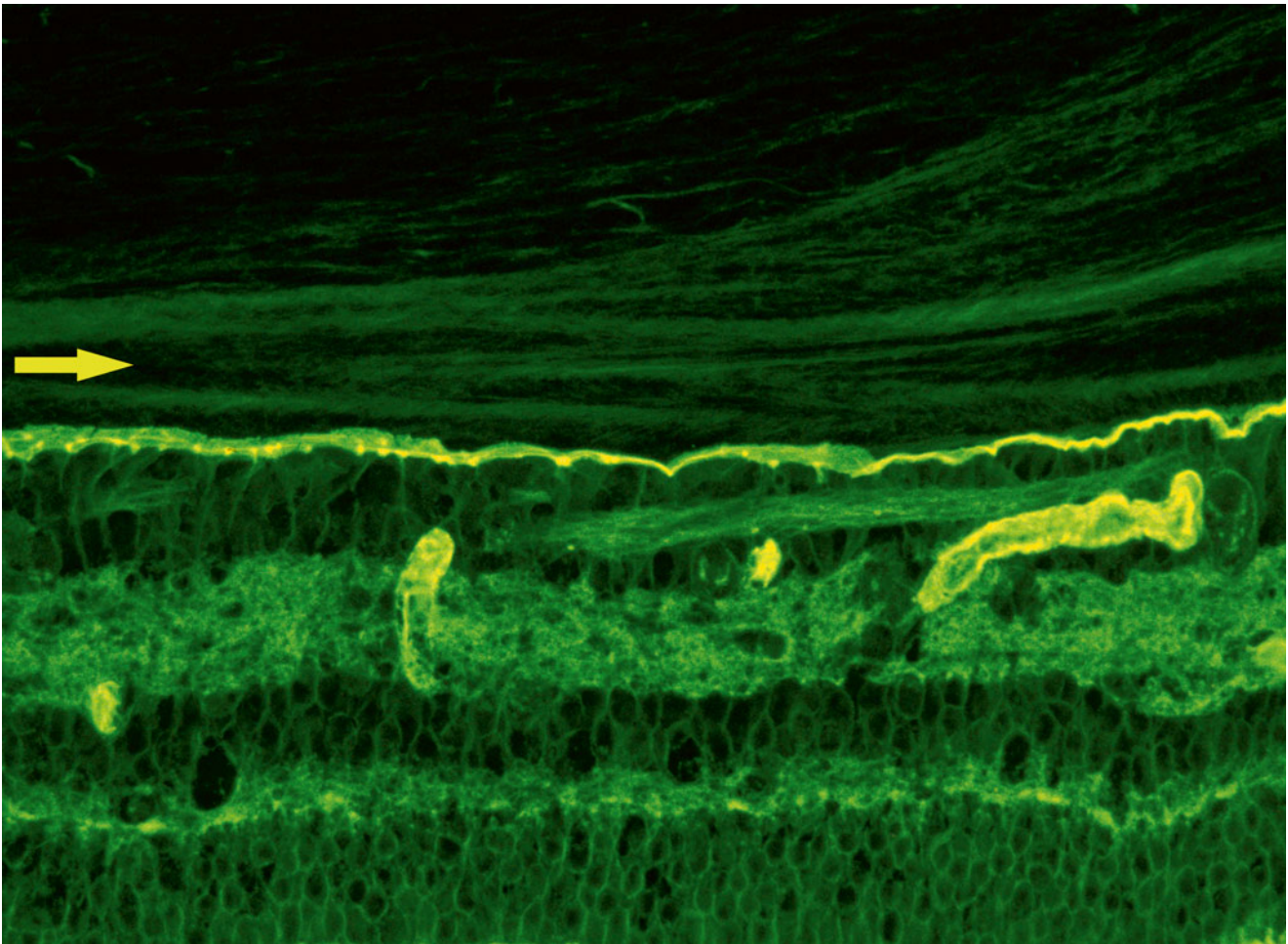


Figure II.E-16 Lamellar organization of the posterior vitreous cortex in the monkey. Immunohistochemistry with anti-ABA lectin antibodies of the monkey vitreoretinal interface demonstrates lamellae in the posterior vitreous cortex (*arrow*) just above the ILM of the retina

(intensely staining *yellow line*). These lamellae represent potential cleavage planes during anomalous PVD with vitreoschisis (Courtesy of Greg Hageman, PhD; Reprinted with Permission [90])

Balazs considered them to be remnants of the adventitia of the hyaloid blood vessels that fill the vitreous body early during embryogenesis. Recent studies identified that rodent hyalocytes contain macrophage cell surface markers, that these cells are derived from bone marrow, and that they are replaced every 7 months (see chapter II.D. Hyalocytes).

Hyalocytes are embedded in the posterior vitreous cortex (Figures II.E-18 and II.E-19), widely spread apart in a single layer situated 20–50 μm from the inner limiting lamina of the retina posteriorly and the basal lamina of the ciliary body epithelium at the pars plana and vitreous base.

Quantitative studies of cell density in the bovine [113] and rabbit [114] vitreous found the highest density of hyalocytes in the region of the vitreous base, followed next by the posterior pole, with the lowest density at the equator. As shown in Figure II.E-19, hyalocytes are oval or spindle shaped, are 10–15 μm in diameter, and contain a lobulated nucleus, a well-developed Golgi complex, smooth and rough endoplasmic reticula, and many large periodic acid-Schiff-positive lysosomal granules and phagosomes [104, 115]. Hogan and

colleagues [116] described that the posterior hyalocytes are flattened and spindle shaped, whereas anterior hyalocytes are larger, rounder, and at times star shaped. Saga and associates [117] have described that different ultrastructural features can be present in different individual cells of the hyalocyte population in an eye. Whether this relates to different origins for the different cells or different states of cell metabolism or activity is not clear.

Balazs [118, 119] pointed out that hyalocytes are located in the region of highest HA concentration and suggested that these cells are responsible for vitreous HA synthesis. In support of this hypothesis is the finding that the enzymes needed for HA synthesis are present within hyalocytes [120]. Osterlin [121] demonstrated that labeled intermediates destined to become incorporated into HA are taken up and internalized by hyalocytes. Several *in vivo* [122, 123] and *in vitro* [123, 124] studies have shown that hyalocytes synthesize large amounts of HA. Bleckmann [125] found that in contrast to *in vivo* metabolism, HA synthesis by hyalocytes grown *in vitro* is reduced in favor of sulfated polysaccharide

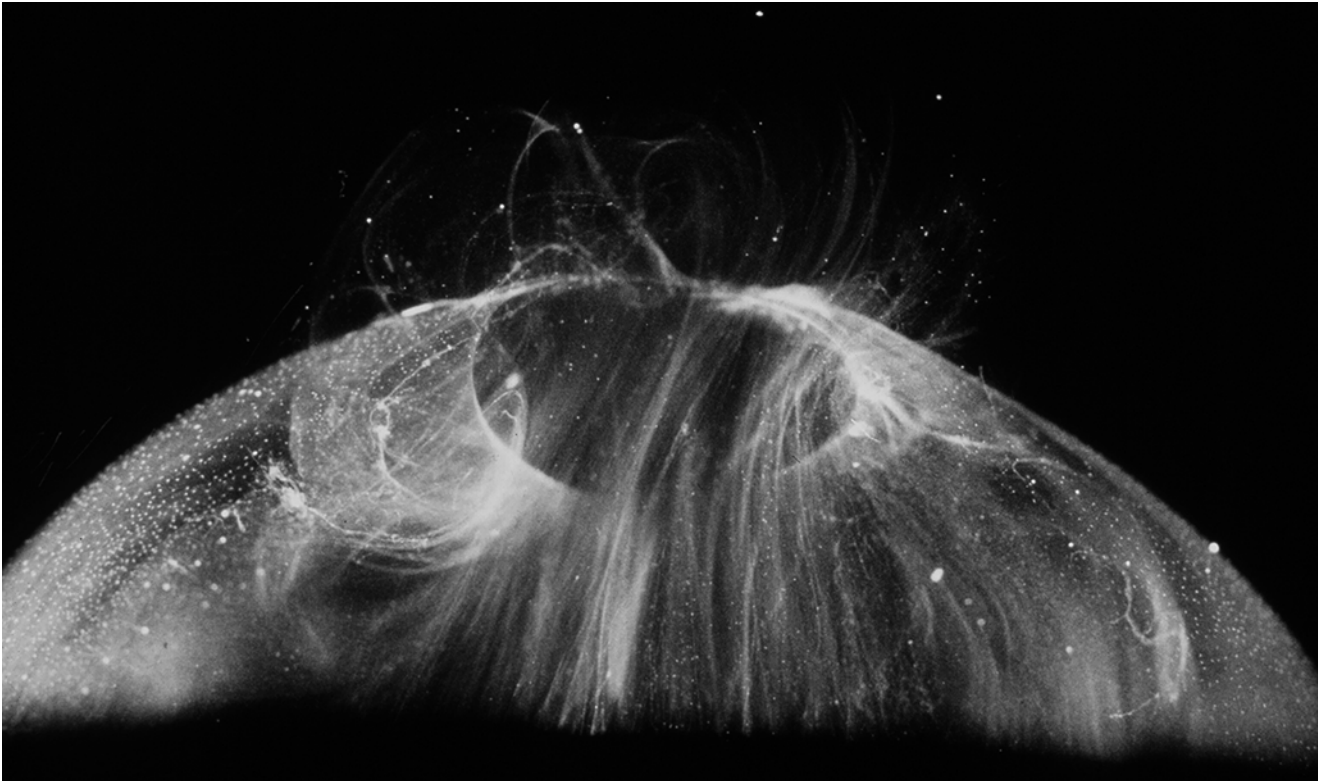


Figure II.E-17 Human posterior vitreous cortex. Posterior vitreous in the left eye of a 59-year-old man. The vitreous cortex envelops the vitreous body and contains multiple, small points that scatter light intensely, which are mononuclear cells known as hyalocytes. There is a

“hole” in the prepapillary posterior vitreous cortex through which vitreous extrudes into the retro-cortical space. Larger amounts of vitreous extrude through the premacular vitreous cortex and fibers course from the central vitreous into the retro-cortical space [108]

synthesis. He suggested that when these cultured cells are reimplanted into vitreous, there must be a retransformation of hyalocyte glycosaminoglycans synthesis to the normal state since vitreous clarity is maintained in these experimental conditions [126]. Swann, however, claimed that there is no evidence that hyalocytes are responsible for the synthesis of vitreous HA. There is no evidence to suggest that hyalocytes maintain ongoing synthesis and metabolism of glycoproteins within the vitreous. Thereafter, Rhodes and coworkers [127] used autoradiography to demonstrate the active incorporation of fucose into rabbit vitreous glycoproteins. In another study [128], sialyl and galactosyl transferase activity was demonstrated in calf vitreous hyalocytes, suggesting that these cells are responsible for vitreous glycoprotein synthesis. An alternate hypothesis, however, states that vitreous glycoproteins originate as secretory products of the inner layer of the ciliary epithelium [129, 130] (see chapter I.F. Vitreous biochemistry and artificial vitreous).

Hyalocyte capacity to synthesize collagen was first demonstrated by Newsome and colleagues [131]. Studies by Ayad and Weiss [132] showed the presence of CPS-1 and CPS-2 collagens adjacent to hyalocytes. These investigators concluded that in similar fashion to chondrocyte metabolism, hyalocytes synthesize these collagens. Hoffman and

coworkers [133] also proposed that the distribution of high-molecular-weight substances in vitreous, including enzymes, suggests synthesis by hyalocytes.

The phagocytic capacity of hyalocytes has been described *in vivo* [134] and demonstrated *in vitro* [113, 126]. This activity is consistent with the presence of pinocytic vesicles and phagosomes [114, 135] and the presence of surface receptors that bind IgG and complement [136]. Interestingly, HA may have a regulatory effect on hyalocyte phagocytic activity [137, 138]. Balazs [12] has proposed that in their resting state, hyalocytes synthesize matrix glycosaminoglycans and glycoproteins and that the cells internalize and reuse these macromolecules by way of pinocytosis. In such a state, hyalocytes may prevent cell migration and proliferation, as has been shown for RPE cells and vascular endothelial cells. However, in response to inducing stimuli and inflammation, hyalocytes may become phagocytic as well as stimulatory for monocyte recruitment from the circulation, beginning the cascade of events associated with inflammation and wound repair. This type of transformation may underlie the observations of Saga and associates [117], who identified different appearances in the various cells of a hyalocyte population in a given eye. It is also important to consider that hyalocytes as well as resident fibroblasts are the

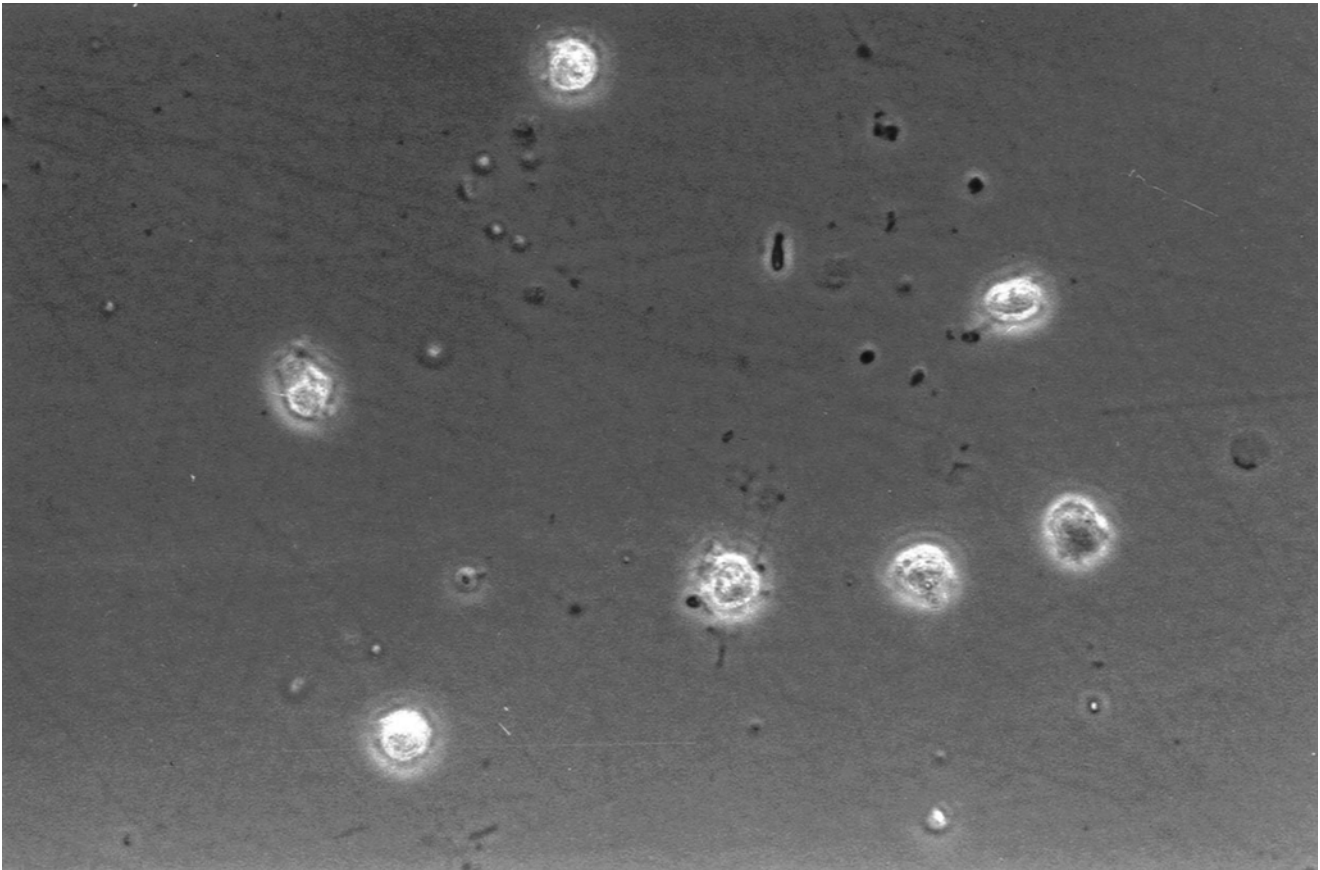


Figure II.E-18 Human hyalocytes *in situ*. Phase contrast microscopy of *in situ* preparation of hyalocytes in the vitreous cortex from the eye of an 11-year-old girl obtained at autopsy. No stains or dyes were used

in this preparation. Pseudopodia are visible in some cells (Original magnification=290x. Specimen courtesy of the New England Eye Bank)

first cells to be exposed to any migratory or mitogenic stimuli. Thus, the response of these cells must be considered in defining the pathophysiology of all proliferative disorders at the vitreoretinal interface, especially PVR and premacular (“epiretinal”) membrane formation.

2. Fibroblasts

There is a second population of cells in the vitreous cortex that in some cases may be mistaken for hyalocytes. Several investigations [113, 139, 140] have determined that fibroblasts are present in the vitreous cortex. These cells constitute less than 10 % of the total vitreous cell population and are localized within the vitreous base, adjacent to the ciliary processes and the optic disc. It may be that these cells are involved in vitreous collagen synthesis, especially in pathologic situations. The argument for a role in normal vitreous collagen synthesis is mostly by analogy to studies of fibrillogenesis in tendon where investigators [141] have found that secreted collagen molecules are assembled into fibrils within invaginations of secreting fibroblasts. The locations of fibroblasts in the anterior peripheral vitreous (vitreous base and near the ciliary processes) and posterior vitreous

may explain how vitreous fibers become continuous structures spanning the distance between these locations. Balazs and coworkers [113] found that near the pars plana ciliaris, vitreous fibroblasts decrease in number with age. Gartner [139] has suggested that changes in these cells are responsible for aging changes in the collagen network of the vitreous base.

IV. Vitreovascular Interface

While the precise nature of the vitreoretinal interactions in and around retinal blood vessels remains incompletely understood, specialized vitreovascular structures and interrelationships do exist [142]. Kuwabara and Cogan [143] described “spiderlike bodies” in the peripheral retina that coiled about blood vessels and connected with the ILM. Pedler [144] found that the ILM was thin over blood vessels and hypothesized that this was due to the absence of Müller cell inner processes (Figure II.E-20). Wolter [145] noted the existence of pores in the ILM along blood vessels and found vitreous strands inserted where the pores were

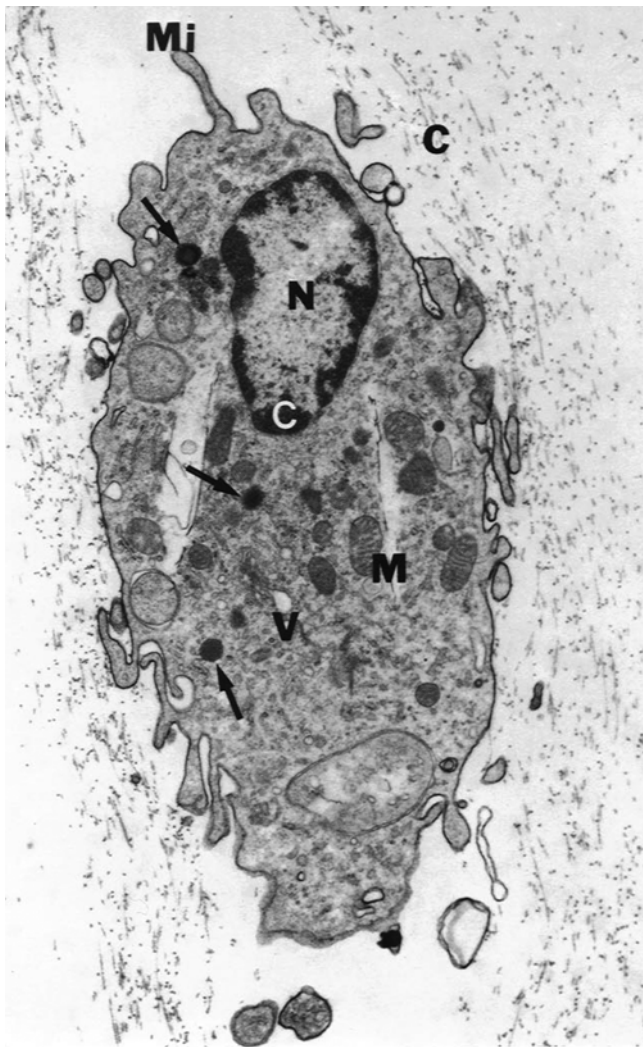


Figure II.E-19 Ultrastructure of human hyalocyte. A mononuclear cell is seen embedded within the dense collagen fibril (black C) network of the vitreous cortex. There is a lobulated nucleus (N) with dense marginal chromatin (white C). In the cytoplasm there are mitochondria (M), dense granules (arrows), vacuoles (V), and microvilli (Mi) ($\times 1,670$) (Courtesy of JL Craft and DM Albert, Harvard Medical School, Boston) (From Sebag [107])

located. Mutlu and Leopold [146] described these strands as extending through the ILM to branch and surround vessels in what they termed “vitreo-retinal-vascular bands.” Such structures might explain the strong adhesion between vitreous and retinal blood vessels, as well as the tendency for vitreous traction to be associated with retinal vascular leakage, retinal neovascularization, and hemorrhage.

Foos [147] proposed a sequence of events in the development of traction associated with retinal blood vessels beginning initially with thinning of the ILM, then subsurface retinal degeneration, and eventually transmigration of macrophages. Small defects in the ILM, when complicated by vitreous incarceration or by simple epiretinal membrane formation can provoke more complex proliferative lesions of the vitreo-vascular interface. Cystic degeneration occurring along the retinal vessels is present in the nerve fiber layer, is seen before the vitreous is detached at that area, and is referred to as paravascular rarefaction [147–150] (see chapter III.H. Peripheral vitreo-retinal pathology). In a study of eyes of 126 consecutive autopsy cases of subjects 21 years or older at death, Spencer and Foos [148] observed retinal paravascular rarefaction in 30%. The process was bilateral in 83% of affected cases and was present in 25% of the 252 eyes in the study. These paravascular cysts are believed to be a common precursor to both paravascular lamellar retinal tears, also called retinal pits, and many full-thickness retinal tears [148, 149]. This correlation between irregular vitreo-vascular adherence, paravascular cyst formation, and the development of localized retinal tears has been identified most convincingly in highly myopic eyes [151, 152].

Polk et al. [153] described the clinicopathologic features of a new sheen retinal dystrophy-familial inner limiting membrane dystrophy. Cystic spaces were present under the ILM and in the inner nuclear layer. Numerous areas of separation of the ILM from the retina were present. A filamentous material was present in some of these areas. Endothelial cell swelling and partial degeneration, pericyte degeneration,

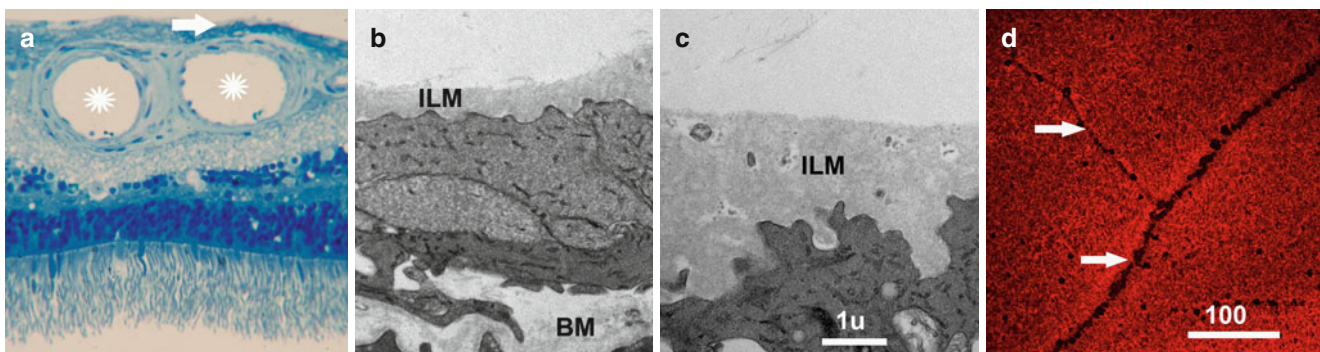


Figure II.E-20 Vitreo-retinal-vascular interface in the human retina. (a) Cross section of an 80-year-old human retina with two large vessels (white stars) near the ILM. TEM shows that the ILM adjacent to those vessels is thinner (b) as compared to the ILM further away from the vessels. BM basement membrane of a retinal vessel close to the

ILM (c). Further, ILM whole mounts stained for laminin show less staining at sites where blood vessels had been in the retina and outline the course of the vessels, confirming that the ILM is thinner when retinal vessels are close to the vitread surface of the retina (d) Bars: b, c: 1um; d: 100 um

and basement membrane thickening of retinal capillaries suggested that this condition is primarily a retinal vascular problem with chronic edema, swelling, and degeneration of Müller cells and separation of the ILM.

The risk of hemorrhage is particularly high when abnormal neovascular vessel complexes grow into the posterior vitreous cortex, as shown by Falbourn and Bowald [154]. However, even in the absence of neovascularization, vitreous traction upon retinal vessels can induce vitreous hemorrhage. This can occur in innocuous posterior vitreous detachment (PVD) or in anomalous PVD. Indeed, studies have shown that in nondiabetic patients with fundus-obscuring hemorrhage, there is a 67 % incidence of retinal tears, 39 % with retinal detachment [155]. Traction-mediated avulsion of retinal veins and/or arteries is believed to be an important contributor to the occurrence of vitreous hemorrhage in the absence of new blood vessel formation [see chapter III.H. Peripheral vitreo-retinal pathology].

Irregularities or defects in vitreovascular adherence are common and appear to correspond to areas of cystic degeneration in the nerve fiber layer, also referred to as paravascular rarefaction [147–149]. These paravascular cysts are believed to be a common precursor to both paravascular lamellar retinal tears, also called retinal pits, and many full-thickness retinal tears [147–149]. This correlation between irregular vitreovascular adherence, paravascular cyst formation, and the development of localized retinal tears has been identified most convincingly in highly myopic eyes [151, 152].

V. Unresolved Questions

While the foregoing presents a comprehensive body of information regarding the vitreoretinal interface and particularly the ILM, there are many important questions that remain unresolved.

A. Diffusion Through the ILM

1. Trans-ILM Diffusion from Vitreous to Retina and Choroid

It is currently not known what size particles and proteins can penetrate the ILM. The successful use of avastin, a humanized monoclonal antibody, to treat VEGF-induced subretinal neovascularization in age-related macular degeneration (AMD) shows that antibodies with a molecular weight of 150 kD can penetrate the ILM. Similar experiments in chick embryos also showed that other antibodies could diffuse through the ILM in matter of hours [156]. The upper molecular weight size and the diffusion kinetics, however, are unknown. While peptides and proteins <150 kD can diffuse through BMs, it is unknown whether lipids, lipophilic compounds, and lipoproteins can penetrate the ILM. Another

question in this regard relates to the observation that eyes of diabetic patients with vitreoretinal adhesion have a greater risk of having proliferative diabetic retinopathy. One hypothesis is that the vitreoretinal interface in these cases interferes with oxygenation of the inner retina, but there are no studies of trans-ILM oxygen transport/diffusion in diabetics vs. nondiabetics.

2. Trans-ILM Diffusion from Chorioretinal Compartment to Vitreous

Studies have shown that in AMD eyes with vitreomacular adhesion have a higher incidence of choroidal neovascularization than eyes with PVD [157, 158]. One of the hypotheses to explain this observation is that the vitreoretinal interface in these eyes represents a barrier to the egress of proangiogenic cytokines from the chorioretinal compartment. There are no studies that address this possibility.

B. Viral Penetration Through the ILM into the Retina

A convenient way to induce a medically relevant transduction of retinal cells would be an intravitreal injection of virus particles that carry a cDNA to transfect the retinal cells. Preliminary data plating adenoviruses on top of ILM whole mounts showed that these viruses were unable to infiltrate the ILM (Halfter, unpublished). Potential entry sites for viruses are the foveal area, where the ILM is very thin and potentially damaged, and sites with large blood vessels in the nerve fiber layer, where the ILM is also very thin and fragile [153] or segments of the ILM that are damaged. Furthermore, it might be desirable to temporarily alter the integrity of the ILM so as to facilitate viral penetration for therapeutic transfection of the retina.

C. Trans-ILM Cell Migration

The mechanism(s) by which circulating monocytes and retinal glial cells migrate through the ILM to form contractile premacular membranes and cause macular pucker are unknown. Similarly, it is not known how vascular endothelial cells migrate through the ILM to form new blood vessels in ischemic retinopathies such as proliferative diabetic retinopathy.

D. Vitreous-ILM Adhesion

TEM imaging of the vitreoretinal interface showed a connectivity of vitreous ECM proteins and the ILM (Figure II.E-1). The adhesion of both ECM structures is strong in youth. In human eyes from patients before the age

of 30, the vitreous and the ILM are almost inseparable and make vitrectomy problematic. Further, high myopia lead to PVD at a relative early age and may cause retinal detachment. This happens at a high frequency in Knobloch syndrome patients, where high myopia lead to a precocious and consequently anomalous PVD followed by giant retinal detachments.

Russell [159] proposes a model by which the ECM maintains integrity of the vitreoretinal interface. In his theory, a 240 kDa protein core is bound to the type IV collagen of the ILM. Attached to the protein core are series of chondroitin sulfate glycosaminoglycans (GAG) that are present on the vitread side of the ILM. The GAGs bind to a fibrillar protein, most likely opticin, which then interacts with type II collagen of the cortical vitreous. Through this chain of interaction, ILM to core protein to GAG to opticin to cortical vitreous, a relatively strong biochemical adhesion is formed. The adhesion of vitreous and ILM becomes progressively weaker with advancing age, and at the age of 60 and older, the vitreous separates by itself from the ILM during posterior vitreous detachment (PVD). What is currently unknown is what molecular partners in ILM and vitreous connect both structures. Since this connectivity is most likely the cause for retinal tears and other pathologies during anomalous PVD, it would be important to have a better understanding of the molecular partners that provide the junction between the vitreous and the ILM.

Abbreviations

AFM	Atomic force microscopy
AMD	Age-related macular degeneration
BM	Basement membrane
GAG	Glycosaminoglycans
IgG	Immunoglobulin G
ILM	Inner limiting membrane
kD	Kilodalton
PBS	Phosphate-buffered saline
PVD	Posterior vitreous detachment
PVR	Proliferative vitreoretinopathy
TEM	Transmission electron microscopy
VEGF	Vascular endothelial growth factor

References

- Salzmann as cited by Hogan MJ, Alvarado JA, Weddel JE. *Histology of the human eye: an atlas and textbook*. Philadelphia: WB Saunders; 1971. 488 p.
- Heegaard S. Morphology of the vitreoretinal border region. *Acta Ophthalmol Scand Suppl*. 1997;222:1–31.
- Candiello J, Balasubramani M, Schreiber EM, Cole GJ, Mayer U, Halfter W, et al. Biomechanical properties of native basement membranes. *FEBS J*. 2007;274:2897–908. PMID: 17488283.
- Candiello J, Cole GJ, Halfter W. Age-dependent changes in the structure, composition and biophysical properties of a human basement membrane. *Matrix Biol*. 2010;29:402–10. PMID: 20362054.
- Binning G, Quate CF, Gerber C. Atomic force microscope. *Phys Rev Lett*. 1986;56:930–3. PMID: 10033323.
- Laney DE, Garcia RA, Parsons SM, Hansma HG. Changes in the elastic properties of cholinergic synaptic vesicles as measured by atomic force microscopy. *Biophys J*. 1997;72:806–13. PMID: 9017205.
- A-Hassan E, Heinz WF, Antonik MD, D'Costa NP, Nageswaran S, Schoenenberger CA, et al. Relative microelastic mapping of living cells by atomic force microscopy. *Biophys J*. 1998;74:1564–78. PMID: 9512052.
- Quist AP, Rhee SK, Lin H, Lal R. Physiological role of gap-junctional hemichannels. Extracellular calcium-dependent isotonic volume regulation. *J Cell Biol*. 2000;148:1063–74. PMID: 10704454.
- Loparic M, Wirz D, Daniels AU, Raiteri R, Vanlandingham MR, Guex G, et al. Micro- and nanomechanical analysis of articular cartilage by indentation-type atomic force microscopy: validation with a gel-microfiber composite. *Biophys J*. 2010;98:2731–40. PMID: 20513418.
- Danysh BP, Czymbek KJ, Olurin PT, Sivak JG, Duncan MK. Contributions of mouse genetic background and age o anterior lens capsule thickness. *Anat Rec*. 2008;291:1619–27. PMID: PMC2699617.
- Kiani C, Chen L, Wu YJ, Yee AJ, Yang BB. Structure and function of aggrecan. *Cell Res*. 2002;12:19–32.
- Balazs EA. Functional anatomy of the vitreous. In: Duane TD, Jaeger EA, editors. *Biomedical foundations of ophthalmology*. Philadelphia: JB Lippincott; 1984.
- Balasubramani M, Schreiber EM, Candiello J, Balasubramani GK, Kurtz J, Halfter W. Molecular interactions in the retinal basement membrane system: a proteomic approach. *Matrix Biol*. 2010;29:471–83. PMID: 20403434.
- Heergaard S, Jensen OA, Prause JU. Structure of the vitread face of the monkey optic disc (*Macaca mulatta*): SEM on frozen resin-cracked optic nerve heads supplemented by TEM and immunohistochemistry. *Graefes Arch Clin Exp Ophthalmol*. 1988;226:377.
- Henrich PB, Monnier CA, Halfter W, Haritoglou C, Strauss RW, Lim RY, et al. Nanoscale topographic and biomechanical studies of the human internal limiting membrane. *Invest Ophthalmol Vis Sci*. 2012;53:2561–70. PMID: 22410559.
- Foos RY. Posterior vitreous detachment. *Trans Am Acad Ophthalmol Otolaryngol*. 1972;76:480.
- Foos RY. Vitreoretinal juncture over retinal vessels. *Albrecht Von Graefes Arch Klin Exp Ophthalmol*. 1977;204:223–34. PMID: 304681.
- Chung AE, Freeman IL, Braginski JE. A novel extracellular membrane elaborated by a mouse embryonal carcinoma-derived cell line. *Biochem Biophys Res Commun*. 1977;79:859–68. PMID: 597311.
- Chung AE. Embryonal carcinoma and the basement membrane glycoproteins laminin and entactin. *Int J Dev Biol*. 1993;37:141–50. PMID: 8507559.
- Kleinman HK, Martin GR. Matrigel: basement membrane matrix with biological activity. *Semin Cancer Biol*. 2005;15:378–86. PMID: 15975825.
- Chung AE, Jaffe R, Freeman IL, Vergnes JP, Braginski JE, Carlin B. Properties of a basement membrane-related glycoprotein synthesized in culture by a mouse embryonal carcinoma-derived cell line. *Cell*. 1979;16:277–87. PMID: 88263.
- Timpl R, Rohde H, Robey PG, Rennard SI, Foidart JM, Martin GR. Laminin – a glycoprotein from basement membranes. *J Biol Chem*. 1979;254:9933–7. PMID: 114518.
- Carlin B, Jaffe R, Bender B, Chung AE. Entactin, a novel basal lamina-associated sulfate glycoprotein. *J Biol Chem*. 1981;256:5209–14. PMID: 6262321.

24. Timpl R, Dziadek M, Fujiwara S, Nowack H, Wick G. Nidogen: a new self-aggregating basement membrane protein. *Eur J Biochem.* 1983;137:455–65. PMID: 6420150.
25. Hassell JR, Robey PG, Barrach HJ, Wilczek J, Rennard SI, Martin GR. Isolation of a heparan sulfate-containing proteoglycan from basement membrane. *Proc Natl Acad Sci.* 1980;77:4494–8.
26. Kleinman HK, McGarvey ML, Liotta LA, Robey PG, Tryggvason K, Martin GR. Isolation and characterization of type IV procollagen, laminin, and heparan sulfate proteoglycan from the EHS sarcoma. *Biochemistry.* 1982;21:6188–93.
27. Paulsson M, Aumailley M, Deutzmann R, Timpl R, Beck K, Engel J. Laminin-nidogen complex. Extraction with chelating agents and structural characterization. *Eur J Biochem.* 1987;166:11–9. PMID: 3109910.
28. Timpl R, Brown JC. Supramolecular assembly of basement membranes. *Bioassays.* 1996;18:123–32. PMID: 8851045.
29. Erickson AC, Couchman JR. Still more complexity in mammalian basement membranes. *J Histochem Cytochem.* 2000;48:1291–306. PMID: 10990484.
30. Miner JH, Yurchenco PD. Laminin functions in tissue morphogenesis. *Annu Rev Cell Dev Biol.* 2004;20:255–84. PMID: 15473841.
31. Hohenester E, Yurchenco PD. Laminins in basement membrane assembly. *Cell Adh Migr.* 2013;7:56–63. PMID: 23076216.
32. Khoshnoodi J, Pedchenko V, Hudson BG. Mammalian collagen IV. *Microsc Res Tech.* 2008;71:357–70.
33. Ho MS, Böse K, Mokkalapati S, Nischt R, Smyth N. Nidogens-extracellular matrix linker molecules. *Microsc Res Tech.* 2008;71:387–95. PMID: 18219668.
34. Iozzo RV. Basement membrane proteoglycans: from cellar to ceiling. *Ant Rev Mol Cell Biol.* 2005;6:646–56. PMID: 16064139.
35. Ljubimov AV, Burgeson RE, Butkowski RJ, Couchman JR, Zardi L, Ninomiya Y, et al. Basement membrane abnormalities in human eyes with diabetic retinopathy. *J Histochem Cytochem.* 1996;44:1469–79. PMID: 8985139.
36. Libby RT, Champliand M-F, Claudepierre T, Xu Y, Gibbons EP, Koch M, et al. Laminin expression in adult and developing retinae: evidence of two novel CNS laminins. *J Neurosci.* 2000;20:6517–28. PMID: 10964957.
37. Uechi G, Sun Z, Schreiber E, Halfter W, Balasubramani M. A proteomic view of basement membranes from human retinal blood vessels, inner limiting membranes and lens capsules. *J Proteomic Res.* [in press]
38. Balazs EA. The vitreous. *Int Ophthalmol Clin.* 1973;15:53–63.
39. Timpl R, Wiedemann H, van Delden V, Furthmayr H, Kuehn K. A network model for the organization of type IV collagen molecules in basement membranes. *Eur J Biochem.* 1981;120:203–11. PMID: 6274634.
40. Schittny JC, Timpl R, Engel J. High resolution immunoelectron microscopic localization of functional domains of laminin, nidogen, and heparan sulfate proteoglycan in epithelial basement membrane of mouse cornea reveals different topological orientations. *J Cell Biol.* 1988;107:1599–610. PMID: 2459133.
41. Yurchenco PD, Ruben GC. Basement membrane structure in situ: evidence for lateral associations in the type IV collagen network. *J Cell Biol.* 1987;105:2559–68. PMID: 3693393.
42. Fox JW, Mayer U, Nischt R, Aumailley M, Reinhardt D, Wiedemann H, et al. Recombinant nidogen consists of three globular domains and mediates binding of laminin to collagen type IV. *EMBO J.* 1991;10:3137–46. PMID: 1717261.
43. Yurchenco PD, Patton BL. Developmental and pathogenic mechanisms of basement membrane assembly. *Curr Pharm Des.* 2009;15:1277–94.
44. Murshed M, Smyth N, Miosge N, Karolat J, Krieg T, Paulsson M, et al. The absence of nidogen 1 does not affect murine basement membrane formation. *Mol Cell Biol.* 2000;20:7007–12. PMID: 10958695.
45. Bader BL, Smyth N, Nedbal S, Miosge N, Baranowsky A, Mokkalapati S, et al. Compound genetic ablation of nidogen 1 and 2 causes basement membrane defects and perinatal lethality in mice. *Mol Cell Biol.* 2005;25:6846–56.
46. Grant DS, Leblond CP, Kleinman HK, Inoue S, Hassell JR. The incubation of laminin, collagen IV, and heparan sulfate proteoglycan at 35 degrees C yields basement membrane-like structures. *J Cell Biol.* 1989;108:1567–74.
47. Stephens LE, Sutherland AE, Klimanskaya IV, Andrieux A, Meneses J, Pedersen RA, et al. Deletion of beta 1 integrins in mice results in inner cell mass failure and peri-implantation lethality. *Genes Dev.* 1995;9:1883–95. PMID: 7544312.
48. Henry MD, Campbell KP. A role for dystroglycan in basement membrane assembly. *Cell.* 1998;95:859–70. PMID: 9865703.
49. Dong LJ, Chung AE. The expression of genes for entactin, laminin A, laminin B1 and laminin B2 in murine lens morphogenesis and eye development. *Differentiation.* 1991;48:157–72. PMID: 1725162.
50. Halfter W, Dong S, Schurer B, Osanger A, Schneider W, Ruegg M, et al. Composition, synthesis, and assembly of the embryonic chick retinal basal lamina. *Dev Biol.* 2000;220:111–28. PMID: 10753504.
51. Dong L, Chen Y, Lewis M, Hsieh JC, Reing J, Chaillet JR, Howell CY, Melhem M, Inoue S, Kuszak JR, DeGeest K, Chung AE. Neurological defects and selective disruption of basement membranes in mice lacking entactin-1/nidogen-1. *Lab Invest.* 2002;82:1617–30. PMID: 12480912.
52. Halfter W, Willem M, Mayer U. Basement membrane-dependent survival of retinal ganglion cells. *Invest Ophthalmol Vis Sci.* 2005;46:1000–9.
53. Halfter W, Dong S, Schurer B, Ring C, Cole GJ, Eller A. Embryonic synthesis of the inner limiting membrane and vitreous body. *Invest Ophthalmol Vis Sci.* 2005;46:2202–9. PMID: 15914642.
54. Sarthy V, Collagen IV. mRNA expression during development of the mouse retina: an in situ hybridization study. *Invest Ophthalmol Vis Sci.* 1993;34:145–52. PMID: 7678834.
55. Halfter W, Dong S, Dong A, Eller AW, Nischt R. Origin and turnover of ECM proteins from the inner limiting membrane and vitreous body. *Eye (Lond).* 2008;22:1207–13. PMID: 18344966.
56. Foos RY, Gloor BP. Vitreoretinal juncture; healing of experimental wounds. *Albrecht Von Graefes Arch Klin Exp Ophthalmol.* 1975;196:213–20.
57. Ponsioen TL, van Luyn MJA, van der Worp RJ, Pas HH, Hooymans JMM, Los LI. Human retinal Müller cells synthesize collagens of the vitreous and vitreo-retinal interface *in vitro*. *Mol Vis.* 2008;14:652–60.
58. Nakamura T, Murata T, Hisatomi T, Enaida H, Sassa Y, Ueno A, et al. Ultrastructure of the vitreoretinal interface following the removal of the internal limiting membrane using indocyanine green. *Curr Eye Res.* 2003;27(6):395–9.
59. Sebag J, Hageman GS. Interfaces. *Eur J Ophthalmol.* 2000;10:1–3.
60. Sebag J, Hageman GS. Interfaces. *Fondazione GB Bietti Per lo Studio e la Ricerca in Oftalmologia.* Roma: Farina Publishers; 2000.
61. Lee J, Gross JM. Laminin beta1 and gamma1 containing laminins are essential for basement membrane integrity in the zebrafish eye. *Invest Ophthalmol Vis Sci.* 2007;48:2483–90.
62. Edwards MM, Mammadova-Bach E, Alpy F, Klein A, Hicks WL, Roux M, et al. Mutations in Lama1 disrupt retinal vascular development and inner limiting membrane formation. *J Biol Chem.* 2010;285(10):7697–711.
63. Pinzón-Duarte G, Daly G, Li YN, Koch M, Brunken WJ. Defective formation of the inner limiting membrane in laminin beta2- and gamma3-null mice produces retinal dysplasia. *Invest Ophthalmol Vis Sci.* 2010;51:1773–82. PMID: 19907020.
64. Labelle-Dumais C, Dilworth DJ, Harrington EP, de Leau M, Lyons D, Kabaeva Z, et al. COL4A1 mutations cause ocular dysgenesis, neural localization defects, myopathy in mice and Walker-Warburg syndrome in humans. *PLoS Genet.* 2011;7:e1002062. PMID: 21625620.

65. Takeda S, Kondo M, Sasaki J, Kurahashi H, Kano H, Arai K, et al. Fukutin is required for maintenance of muscle integrity, cortical histogenesis and normal eye development. *Hum Mol Genet.* 2003;12:1449–59. PMID: 12783852.
66. Lee Y, Kameya S, Cox GA, Hsu J, Hicks W, Maddatu TP, Smith RS, Naggert JK, Peachey NS, Nishina PM. Ocular abnormalities in Large (myd) and Large (vls) mice, spontaneous models for muscle, eye, and brain diseases. *Mol Cell Neurosci.* 2005;30:160–72.
67. Hu H, Candiello J, Zhang P, Ball SL, Cameron DA, Halfter W. Retinal ectopias and mechanically weakened basement membrane in a mouse model of muscle-eye-brain (MEB) disease congenital muscular dystrophy. *Mol Vis.* 2010;16:1415–28. PMID: 20680099.
68. Silan F, Yoshioka M, Kobayashi K, Simsek E, Tunc M, Alper M, et al. A new mutation of the fukutin gene in a non-Japanese patient. *Ann Neurol.* 2003;53:392–6.
69. Beltra'n-Valero de Bernabe D, van Bokhoven H, van Beusekom E, Van den Akker W, Kant S, Dobyns B, et al. A homozygous nonsense mutation of the Fukutin gene causes a Walker-Warburg Syndrome phenotype. *J Med Genet.* 2003;40:845–8.
70. Taniguchi K, Kobayashi K, Saito K, Yamanouchi H, Ohnuma A, Hayashi YK, et al. Distribution and broader clinical spectrum of muscle-eye-brain disease. *Hum Mol Genet.* 2003;12:527–34.
71. Clement E, Mercuri E, Godfrey C, Smith J, Robb S, Kinali M, Straub V, Bushby K, Manzur A, Talim B, Cowan F, Quinlivan R, Klein A, Longman C, McWilliam R, Topaloglu H, Mein R, Abbs S, North K, Barkovic J, Rutherford M, Muntoni F. Brain involvement in muscular dystrophies with defective dystroglycan glycosylation. *Ann Neurol.* 2008;64:573–82.
72. Halfter W, Dong S, Yip YP, Willem M, Mayer U. A critical function of the pial basement membrane in cortical histogenesis. *J Neurosci.* 2002;22:6029–40.
73. Gould DB, Phalan FC, Breedveld GJ, van Mil SE, Smith RS, Schimenti JC, et al. Mutations in Col4A1 cause perinatal cerebral hemorrhage and porencephaly. *Science.* 2005;308:1167–71.
74. Muntoni F, Torelli S, Brockington M. Muscular dystrophies due to glycosylation defects. *Neurotherapeutics.* 2008;5:627–32.
75. Matsumoto B, Blanks JC, Ryan SJ. Topographic variations in the rabbit and primate internal limiting membrane. *Invest Ophthalmol Vis Sci.* 1984;1:71–82.
76. Sebag J, Buckingham B, Charles MA, Reiser K. Biochemical abnormalities in vitreous of humans with proliferative diabetic retinopathy. *Arch Ophthalmol.* 1992;110:1472–9.
77. Sebag J, Nie S, Reiser KA, Charles MA, Yu NT. Raman spectroscopy of human vitreous in proliferative diabetic retinopathy. *Invest Ophthalmol Vis Sci.* 1994;35:2976–80.
78. Sebag J. Abnormalities of human vitreous structure in diabetes. *Graefes Arch Clin Exp Ophthalmol.* 1993;231:257–60.
79. Sebag J. Diabetic vitreopathy. *Ophthalmology.* 1996;103:205–6.
80. Matsunaga N, Ozeki H, Hirabayashi Y, Shimada S, Ogura Y. Histopathological evaluation of the inner limiting membrane surgically excised from eyes with diabetic maculopathy. *Retina.* 2005;25:311–6. PMID: 15805908.
81. Tamura K, Yokoyama T, Ebihara N, Murakami A. Histopathologic analysis of the internal limiting membrane surgically peeled from eyes with diffuse diabetic macular edema. *Jpn J Ophthalmol.* 2012;56:280–7. PMID: 22438196.
82. To M, Goz M, Camenzind L, Oertle P, Candiello J, Sullivan M, Henrich PB, Loparic M, Safi F, Eller A, Halfter W. Diabetes-induced morphological, biomechanical and compositional changes of ocular basement membranes. *Exp Eye Res.* 2013;116:298–307.
83. Abari E, Kociok N, Hartman U, Semkova I, Paulsson M, Lo A, et al. Alterations in basement membrane immunoreactivity of the diabetic retina in three diabetic mouse models. *Graefes Arch Clin Exp Ophthalmol.* 2013;251:763–75.
84. Roy S, Maiello M, Lorenzi M. Increased expression of basement membrane collagen in human diabetic retinopathy. *J Clin Invest.* 1994;93:38–442.
85. Sebag J. Anomalous PVD, – a unifying concept in vitreo-retinal diseases. *Graefes Arch Clin Exp Ophthalmol.* 2004;242:690–8.
86. Sebag J. Vitreous anatomy, aging, and anomalous posterior vitreous detachment. In: Dartt DA, Besharse JC, Dana R, editors. *Encyclopedia of the eye*, vol. 4. Oxford: Elsevier; 2010. p. 307–15.
87. Sebag J, Gupta P, Rosen R, Garcia P, Sadun AA. Macular holes and macular pucker: the role of vitreoschisis as imaged by optical coherence tomography/scanning laser ophthalmoscopy. *Trans Am Ophthalmol Soc.* 2007;105:121–31.
88. Sebag J. Vitreoschisis. *Graefes Arch Clin Exp Ophthalmol.* 2008;246:329–32.
89. Sebag J. Vitreoschisis in diabetic macular edema. *Invest Ophthalmol Vis Sci.* 2011;52(11):8455–6.
90. Gupta P, Yee KMP, Garcia P, Rosen RB, Parikh J, Hageman GS, et al. Vitreoschisis in macular diseases. *Br J Ophthalmol.* 2011;95(3):376–80.
91. Yurchenco PD. Basement membranes: cell scaffoldings and signaling platforms. *Cold Spring Harb Perspect Biol.* 2011;3.
92. Edwards MM, Lefebvre O. Laminins and retinal vascular development. *Cell Adh Migr.* 2013;7(1):82–9.
93. Loparic M, Henrich PB. The bi-functional organization of human basement membranes. *PLoS One.* 2013;8:e67660. PMID: 23844050.
94. Gass JDM. Vitreous maculopathies. In: *Stereoscopic atlas of macular diseases*. St Louis: Mosby; 1987. p. 676–713.
95. Meezan E, Hjelle JT, Brendel K, Carlson EC. A simple, versatile, nondisruptive method for the isolation of morphologically and chemically pure basement membranes from several tissues. *Life Sci.* 1975;17:1721–32. PMID: 1207385.
96. Duhamel RC, Meezan E, Brendel K. Selective solubilization of two populations of polypeptides from bovine retinal basement membranes. *Exp Eye Res.* 1983;36:257–67. PMID: 6297940.
97. Halfter W, Candiello J, Hu H, Zhang P, Schreiber E, Balasubramani M. Protein composition and biomechanical properties of in vivo-derived basement membranes. *Cell Adh Migr.* 2013;7:64–71. PMID: 23154404.
98. Janney PA, McCulloch CA. Cell mechanics: integrating cell responses to mechanical stimuli. *Annu Rev Biomed Eng.* 2007;9:1–34. PMID: 17461730.
99. Ossewaarde-van Norel A, Rothova A. Imaging methods for inflammatory macular edema. *Int Ophthalmol.* 2012;52(4):55–66.
100. Onal S, Tugal-Tutkun I, Neri P, Herbort CP. Optical coherence tomography imaging in uveitis. *Int Ophthalmol.* 2013;34(2):401–35.
101. Nussenblatt RB. Macular alterations secondary to intraocular inflammatory disease. *Ophthalmology.* 1986;93:984–8.
102. Bonnin N, Cornut PL, Chaise F, Labeille E, Manificat HJ, Feldman A, et al. Spontaneous closure of macular holes secondary to posterior uveitis: case series and a literature review. *J Ophthalmic Inflamm Infect.* 2013;3(1):34–40.
103. Sullu Y, Sariaydin G, Kuruoglu S, Bened U. Widespread vitreo-retinal traction simulating retinal vasculitis in a patient with uveitis. *Retin Cases Brief Rep.* 2012;6:379–82.
104. Streeten BA. Disorders of the vitreous. In: Garner A, Klintworth GK, editors. *Pathobiology of ocular disease – a dynamic approach*, part B, chap 49. New York: Marcel Dekker; 1982. p. 1381–419.
105. Balazs EA. Molecular morphology of the vitreous body. In: Smelser GK, editor. *The structure of the eye*. New York: Academic; 1961. p. 293–310.
106. Theopold H, Faulborn J. Scanning electron microscopic aspects of the vitreous body. *Mod Probl Ophthalmol.* 1979;20:92.
107. Sebag J. *The vitreous—structure, function and pathobiology*. New York: Springer; 1989.
108. Sebag J, Balazs EA. Human vitreous fibres and vitreoretinal disease. *Trans Ophthalmol Soc U K.* 1985;104:123.
109. Reeser FH, Aaberg T. Vitreous humor. In: Records PE, editor. *Physiology of the human eye and visual system*. Hagerstown: Harper & Row; 1979. p. 1–31.

110. Schwalbe G. In: Engelmann W, editor. Von Graefe–Saemisch's Handbuch der Gesamten Augenheilkunde, vol 1. Leipzig; 1874. P. 457.
111. Schwalbe G. Lehrbuch der Anatomie des Auges. Erlangen: E Besold; 1887. p. 288.
112. Balazs EA. In: Acta XVIII. Concilium ophthalmologicum, vol 2. Brussels: 1958. p. 1296.
113. Balazs EA, Toth LZ, Eckl EA, Mitchell AP. Studies on the structure of the vitreous body: XII. Cytological and histochemical studies on the cortical tissue layer. *Exp Eye Res.* 1964;3:57.
114. Gloor BP. Cellular proliferation on the vitreous surface after photocoagulation. *Graefes Arch Clin Exp Ophthalmol.* 1969;178:99.
115. Bloom GD, Balazs EA. An electron microscope study of hyalocytes. *Exp Eye Res.* 1965;4:249.
116. Hogan MJ, Alvarado JA, Weddel JE. Histology of the human eye: an atlas and textbook. Philadelphia: WB Saunders; 1971. p. 607.
117. Saga T, Tagawa Y, Takeuchi T, et al. Electron microscopic study of cells in vitreous of guinea pig. *Jpn J Ophthalmol.* 1984;28:239.
118. Balazs EA. Structure of vitreous gel. In: Acta XVII concilium ophthalmologicum, vol. 11. 1954. p. 1019.
119. Balazs EA. Studies on structure of vitreous body: absorption of ultraviolet light. *Am J Ophthalmol.* 1954;38:21.
120. Jacobson B, Osterlin S, Balazs EA. A soluble hyaluronic acid synthesizing system from calf vitreous. *Proc Fed Am Soc Exp Biol.* 1966;25:588.
121. Osterlin SE. The synthesis of hyaluronic acid in the vitreous. III. *In vivo* metabolism in the owl monkey. *Exp Eye Res.* 1968;7:524.
122. Osterlin SE. The synthesis of hyaluronic acid in the vitreous: IV. Regeneration in the owl monkey. *Exp Eye Res.* 1969;8:27.
123. Berman ER, Gambos GM. Studies on the incorporation of U-14 C-glucose into vitreous polymers *in vitro* and *in vivo*. *Invest Ophthalmol.* 1969;18:521.
124. Balazs EA, Sundblad L, Toth LZJ. *In vitro* formation of hyaluronic acid by cells in the vitreous body and by lamb tissue. *Abstr Fed Proc.* 1958;17:184.
125. Bleckmann H. Glycosaminoglycan metabolism of cultured fibroblasts from bovine vitreous. *Graefes Arch Clin Exp Ophthalmol.* 1984;22:90.
126. François J, Victoria-Troncoso V, Maudgal PC. Immunology of the vitreous body. *Mod Probl Ophthalmol.* 1976;16:196.
127. Rhodes RH, Mandelbaum SH, Minckler DS, Cleary PE. Tritiated fucose incorporation in the vitreous body, lens and zonules of the pigmented rabbit. *Exp Eye Res.* 1982;34:921.
128. Jacobson B. Degradation of glycosaminoglycans by extracts of calf vitreous hyalocytes. *Exp Eye Res.* 1984;39:373.
129. Haddad A, Almeida JC, Laicine EM, et al. The origin of the intrinsic glycoproteins of the rabbit vitreous body: an immunohistochemical and autoradiographic study. *Exp Eye Res.* 1990;50:555.
130. Haddad A, Laicine EM. Studies on the origin of the glycoproteins of the rabbit vitreous body using a protein synthesis inhibitor and radioactive fucose and amino acids. *Germ J Ophthalmol.* 1993;2:127.
131. Newsome DA, Linsemayer TF, Trelstad RJ. Vitreous body collagen: evidence for a dual origin from the neural retina and hyalocytes. *J Cell Biol.* 1976;71:59.
132. Ayad S, Weiss JB. A new look at vitreous humour collagen. *Biochem J.* 1984;218:835.
133. Hoffmann K, Baurwieg H, Riese K. Über Gehalt und Verteilung niederund hoch molekularer Substanzen in Glaskörper: II. Hoch molekulare Substanzen (LDH, MDH, GOT). *Graefes Arch Clin Exp Ophthalmol.* 1974;191:231.
134. Teng CC. An electron microscopic study of cells in the vitreous of the rabbit eye: I. The macrophage. *Eye Ear Nose Throat Month.* 1969;48:91.
135. Freeman MI, Jacobson B, Toth LZ, Balazs EA. Lysosomal enzymes associated with hyalocyte granules: I. Intercellular distribution patterns of enzymes. *Exp Eye Res.* 1968;7:113.
136. Grabner G, Baltz G, Forster O. Macrophage-like properties of human hyalocytes. *Invest Ophthalmol Vis Sci.* 1980;19:333.
137. Forrester JV, Balazs EA. Inhibition of phagocytosis by high molecular weight hyaluronate. *Immunology.* 1980;40:435.
138. Sebag J, Balazs EA, Eakins KE, Kulkarni P. The effect of Na-hyaluronate on prostaglandin synthesis and phagocytosis by mononuclear phagocytes. *Invest Ophthalmol Vis Sci.* 1981;20:33.
139. Gartner J. Electron microscopic study on the fibrillar network and fibrocyte-collagen interactions in the vitreous cortex at the ora serrata of human eyes with special regard to the role of disintegrating cells. *Exp Eye Res.* 1986;42:21.
140. Fine BS, Tousimis AJ. The structure of the vitreous body and the suspensory ligaments of the lens. *Arch Ophthalmol.* 1961;65:95,119.
141. Birck DE, Zychard EI. Collagen fibrillogenesis *in situ*: fibril segments are intermediates in matrix assembly. *Proc Natl Acad Sci U S A.* 1989;86:4549.
142. Gloor BP, Daicker BC. Pathology of the vitreo-retinal border structures. *Trans Ophthalmol Soc U K.* 1975;95:387.
143. Kuwabara T, Cogan DG. Studies of retinal vascular patterns: I. Normal architecture. *Arch Ophthalmol.* 1960;64:904.
144. Pedler C. The inner limiting membrane of the retina. *Br J Ophthalmol.* 1961;45:423.
145. Wolter JR. Pores in the internal limiting membrane of the human retina. *Acta Ophthalmol.* 1964;42:971.
146. Mutlu F, Leopold IH. Structure of the human retinal vascular system. *Arch Ophthalmol.* 1964;71:93.
147. Foos RY. Vitreo-retinal juncture over retinal vessels. *Graefes Arch Clin Exp Ophthalmol.* 1977;204:223–34.
148. Spencer LM, Foos RY. Paravascular vitreoretinal attachments: role in retinal tears. *Arch Ophthalmol.* 1970;84:557–64.
149. Sebag J, Green WR. Vitreous and vitreo-retinal interface. In: Ryan SJ, editor. *Retina.* Philadelphia: Elsevier; 2012.
150. Sebag J. Vitreoretinal interface and the role of vitreous in macular disease. In: Brancato R, Coscasa G, Lumbrosos B, editors. *Proceedings of the retina workshop.* Amsterdam: Kugler & Ghedini; 1987. p. 3–6.
151. Hayashi W, Shimada N, Hayashi K, Moriyama M, Yoshida T, Tokoro T, et al. Retinal vessels and high myopia. *Ophthalmology.* 2011;118(4):791.
152. Komeima K, Kikuchi M, Ito Y, Terasaki H, Miyake Y. Paravascular inner retinal cleavage in a highly myopic eye. *Arch Ophthalmol.* 2005;123(10):1449–50.
153. Polk TD, Gass DM, Green WR, et al. Familial internal limiting membrane dystrophy: a new sheen retinal dystrophy. *Arch Ophthalmol.* 1997;115:878–85.
154. Faulborn J, Bowald S. Microproliferations in proliferative diabetic retinopathy and their relationship to the vitreous: corresponding light and electron microscopic studies. *Graefes Arch Clin Exp Ophthalmol.* 1985;223(3):130–8.
155. Sarrafzadeh R, Hassan TS, Ruby AJ, Williams GA, Garretson BR, Capone Jr A, Trese MT, Margherio RR. Incidence of retinal detachment and visual outcome in eyes presenting with posterior vitreous separation and dense fundus-obscuring vitreous hemorrhage. *Ophthalmology.* 2001;108(12):2273–8.
156. Halfter W, Winzen U, Bishop PN, Eller A. Regulation of eye size by retinal basement membrane and vitreous body. *Invest Ophthalmol Vis Sci.* 2006;47:3586–94. PMID: 16877433.
157. Krebs I, Brannath W, Glittenberg K, Zeiler F, Sebag J, Binder S. Posterior vitreo-macular adhesion: a potential risk factor for exudative age-related macular degeneration. *Am J Ophthalmol.* 2007;144:741–6.
158. Robison C, Krebs I, Binder S, Barbazetto IA, Kostolis AI, Yannuzzi LA, et al. Vitreo-macular adhesion in active and end-stage age-related macular degeneration. *Am J Ophthalmol.* 2009;148:79–82.
159. Russell SR. What we know (and do not know) about vitreoretinal adhesion. *Retina.* 2012;32:S181–6.

To See the Invisible: The Quest of Imaging Vitreous

I.I.F.

J. Sebag, Ronald H. Silverman, and D. Jackson Coleman

Outline

- I. Introduction
- II. In Vitro Imaging
- III. In Vivo Imaging
 - A. Physical Examination
 - 1. Direct Ophthalmoscopy
 - 2. Indirect Ophthalmoscopy
 - 3. Slit-Lamp Biomicroscopy
 - a. Preset Lens Biomicroscopy
 - b. Contact Lens Biomicroscopy
 - B. Clinical Imaging Technologies
 - 1. Optical Imaging
 - a. Scanning Laser Ophthalmoscopy
 - b. Optical Coherence Tomography
 - 2. Acoustic Imaging: Ultrasonography
 - 3. Magnetic Resonance Imaging Spectroscopy
- IV. Future Imaging Technologies
 - A. Raman Spectroscopy
 - B. Dynamic Light Scattering

References

“Vision is the art of seeing what is invisible to others.”
Jonathan Swift (1667–1745)

J. Sebag, MD, FACS, FRCOphth, FARVO (✉)
VMR Institute for Vitreous Macula Retina,
7677 Center Avenue, Huntington Beach, CA 92647, USA

Doheny Eye Institute, Los Angeles, CA, USA
e-mail: jsebag@VMRinstitute.com

R.H. Silverman, PhD
Department of Ophthalmology, College of Physicians
and Surgeons, Columbia University Medical Center,
635 West 165th Street, #42, New York, NY 10032, USA
e-mail: rs3072@cumc.columbia.edu

D.J. Coleman, MD, FACS, FARVO
College of Physicians and Surgeons, Columbia
University Medical Center, Edward S. Harkness Eye Institute,
635 West 165th Street, New York, NY 10032, USA
e-mail: djceye@gmail.com

Keywords

Vitreous • Imaging • Dark-field slit microscopy • Physical examination • Ultrasonography • Optical coherence tomography • Magnetic resonance imaging • Dynamic light scattering • Raman spectroscopy

Key Concepts

1. Vitreous is invisible *by design*, making imaging a great challenge, both *in vitro* and *in vivo*. The importance of vitreous imaging, however, is underscored not only by the need to understand the role vitreous plays in various ocular disorders but also because vitreous is an extended extracellular matrix that is relatively accessible by light and sound, making it possible to assess extracellular matrix biology in vitreous as an index for the entire body.
2. Dark-field slit microscopy has been used to characterize vitreous anatomy *in vitro* without dehydration or tissue fixatives, but has limitations *in vivo*. Slit-lamp biomicroscopy; direct, indirect, and scanning laser ophthalmoscopies; ultrasonography; and optical coherence tomography are useful in clinical practice, but have limitations imposed by resolution constraints. The combined use of more than one technique could provide better imaging for investigational and clinical purposes.
3. Magnetic resonance imaging, Raman spectroscopy, and dynamic light scattering are promising future technologies for noninvasive evaluation of vitreous macromolecules and their organization. This and other nanotechnologies will provide opportunities to rewrite the textbooks of ophthalmology in terms of physiopathology rather than the current concepts of ocular disease that are dependent upon histopathologic changes to establish a diagnosis.

I. Introduction

Imaging vitreous is an attempt to view what is *by design* invisible (Figure II.F-1). The inability to adequately image vitreous hinders a more complete understanding of its normal structure and function, its role in ocular health, and how things change in aging and disease. As described by Duke-Elder [1], the theories of vitreous anatomy that were prevalent during the mid-eighteenth century proposed that the vitreous is composed of “loose and delicate filaments sur-

rounded by fluid,” a description that is remarkably close to present-day concepts. During the eighteenth and nineteenth centuries, there were no less than four very different theories of vitreous structure: in 1741 Demours proposed the alveolar theory; in 1780 Zinn offered the concentric, lamellar configuration theory; in 1845 Hannover suggested the radial sector theory; and in 1848 Sir William Bowman proposed the fibrillar theory, later championed by Retzius and Szent-Gyorgi. Unfortunately, as pointed out by Redslob [2], the techniques employed in all these studies were flawed by artifacts that

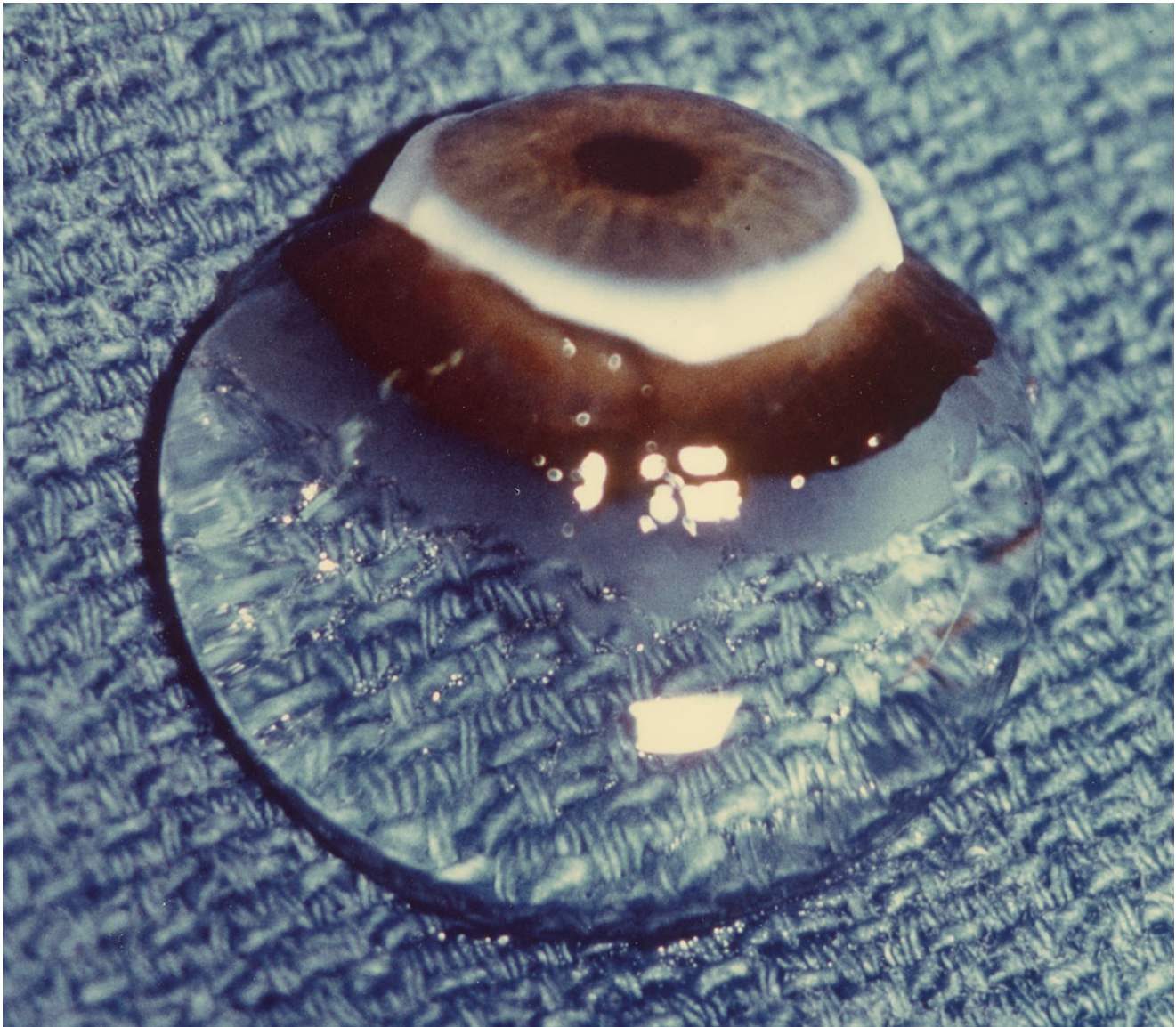


Figure II.F-1 The *invisible* human vitreous postmortem. Intact whole vitreous body from a 9-month-old child with the sclera, choroid, and retina dissected off the vitreous body which remains attached to the anterior segment. A band of gray tissue can be seen posterior to the ora serrata. This is neural retina that was firmly adherent to the vitreous

base and could not be dissected. The vitreous body is solid and although situated on a surgical towel exposed to room air maintains its shape; because of the young age of the donor, the vitreous is almost entirely gel (Specimen courtesy of the New England Eye Bank, Boston, Mass)

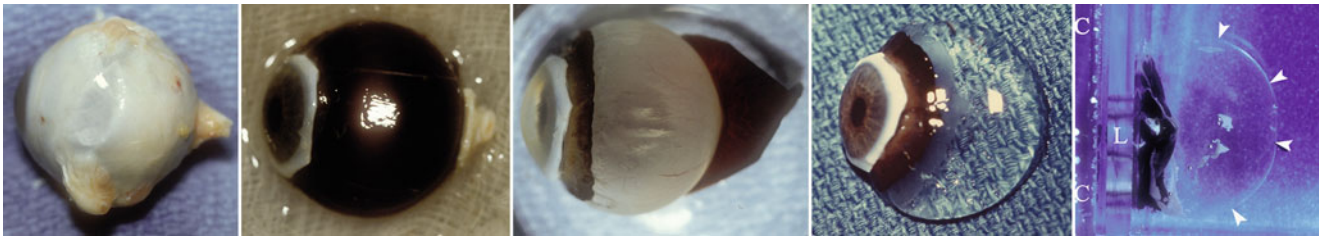


Figure II.F-2 Human vitreous dissection for dark field slit microscopy *in vitro*. Fresh unfixed human eyes were obtained courtesy of the Eye Bank For Sight Restoration in New York City (1978–79) and The New England Eye Bank in Boston (1980–1986). The sclera was dissected from the limbus posteriorly, leaving a region around the optic nerve intact. The choroid was peeled off the retina exposing the posterior surface of the retina. This is the opposite view obtained by ophthalmoscopy and other forms of imaging, although the retinal blood vessels and the

xanthochromic pigment of the fovea can still be identified and used as landmarks for orientation. The retina is then peeled off the vitreous body with the specimen maintained in an isotonic saline solution. Placing sutures through the limbus enables mounting of the specimen onto an L-shaped lucite frame (L) which is then placed in a vertically rectangular lucite chamber (C) filled with isotonic saline to maintain buoyancy of the dissected vitreous body still attached to the anterior segment (image to the far right). *Arrowheads* indicate the posterior vitreous cortex

biased the results of the investigations, since they employed acidic tissue fixatives that precipitated what we recognize today as the glycosaminoglycans, hyaluronan. Thus, the development of slit-lamp biomicroscopy by Gullstrand in 1911¹ held great promise, as it was anticipated that this technique would enable imaging of vitreous structure without the introduction of fixation artifacts. Yet, as described by Redslob [2], a varied set of descriptions resulted over the years, ranging from a fibrous structure to sheets, “chain-linked fences,” and various other interpretations. This problem has even persisted in more recent investigations. Eisner [3] described “membranelles”; Worst [4] “cisterns”; Sebag and Balazs [5] “fibers”; and Kishi and Shimizu [6] “pockets” in the vitreous body [7].

Previously considered a vestigial organ, vitreous is now regarded as an important ocular structure, at least with respect to several important pathological conditions of the posterior segment, but also in terms of ocular physiology, especially regarding the crystalline lens. Vitreous is in essence an extended extracellular matrix, composed largely of water, with a very small amount of structural macromolecules [8, 9]. Nevertheless, in the normal state it is a solid and clear gel, especially in youth (Figure II.F-1). Because of the predominance of water within vitreous, effective imaging of this structure *in vitro* is best performed by methods that overcome the *intended* transparency of this tissue yet avoid dehydration. Imaging the vitreous *in vivo* is even more challenging. The following reviews some of the most important methods available and currently in development for imaging vitreous *in vitro* and *in vivo*.

¹Allvar Gullstrand won the 1911 Nobel Prize for Physiology or Medicine, the only Nobel Prize ever awarded for work in Ophthalmology. [as cited by Ehinger, Grzybowski A. Allvar Gullstrand (1862-1930) - the gentleman with the lamp. *Acta Ophthalmol.* 2011;89(8):701–8].

II. In Vitro Imaging

Dark-field slit microscopy of a whole human vitreous body in the fresh, unfixed state (Figure II.F-2) was extensively employed by Sebag and Balazs to characterize the fibrous structure of vitreous [10] (Figure II.F-3), age-related changes within the central vitreous body [11] (Figure II.F-4) and at the vitreoretinal interface, [12] and the effects of diabetes on the human vitreous structure [13, 14]. This imaging method has successfully demonstrated the anatomy of the posterior vitreous cortex (Figure II.F-5) and the fibers in the anterior peripheral vitreous (Figure II.F-6) that transmit traction to the peripheral retina in rhegmatogenous retinal detachment [see chapters III.I. Role of vitreous in the pathogenesis of retinal detachment and V.B.4. Prophylaxis and cure of rhegmatogenous retinal detachment]. Fibers in this region also play a role in the formation of the so-called “anterior loop” configuration of anterior proliferative vitreoretinopathy [see chapter V.B.6 Retinectomy in Recalcitrant Retinal Detachments].

Pathological fibers, [14] believed to be the consequence of nonenzymatic glycation of vitreous collagen fibrils, [15] were also visualized in cases of diabetic vitreopathy (Figure II.F-7) [see chapter I.E. Diabetic vitreopathy].

The reason that these normal and pathological structures are visible with dark-field slit microscopy is that this technique achieves a 90° illumination/observation angle that maximizes the Tyndall effect. Eisner employed slit microscopy to characterize his system of membranelles [3] (Figure II.F-8).

An important method for *in vitro* imaging was developed by Jan Worst wherein he injected India ink to characterize the cisternal anatomy of vitreous (Figure II.F-9). His findings have particular relevance in this era of frequent intravitreal

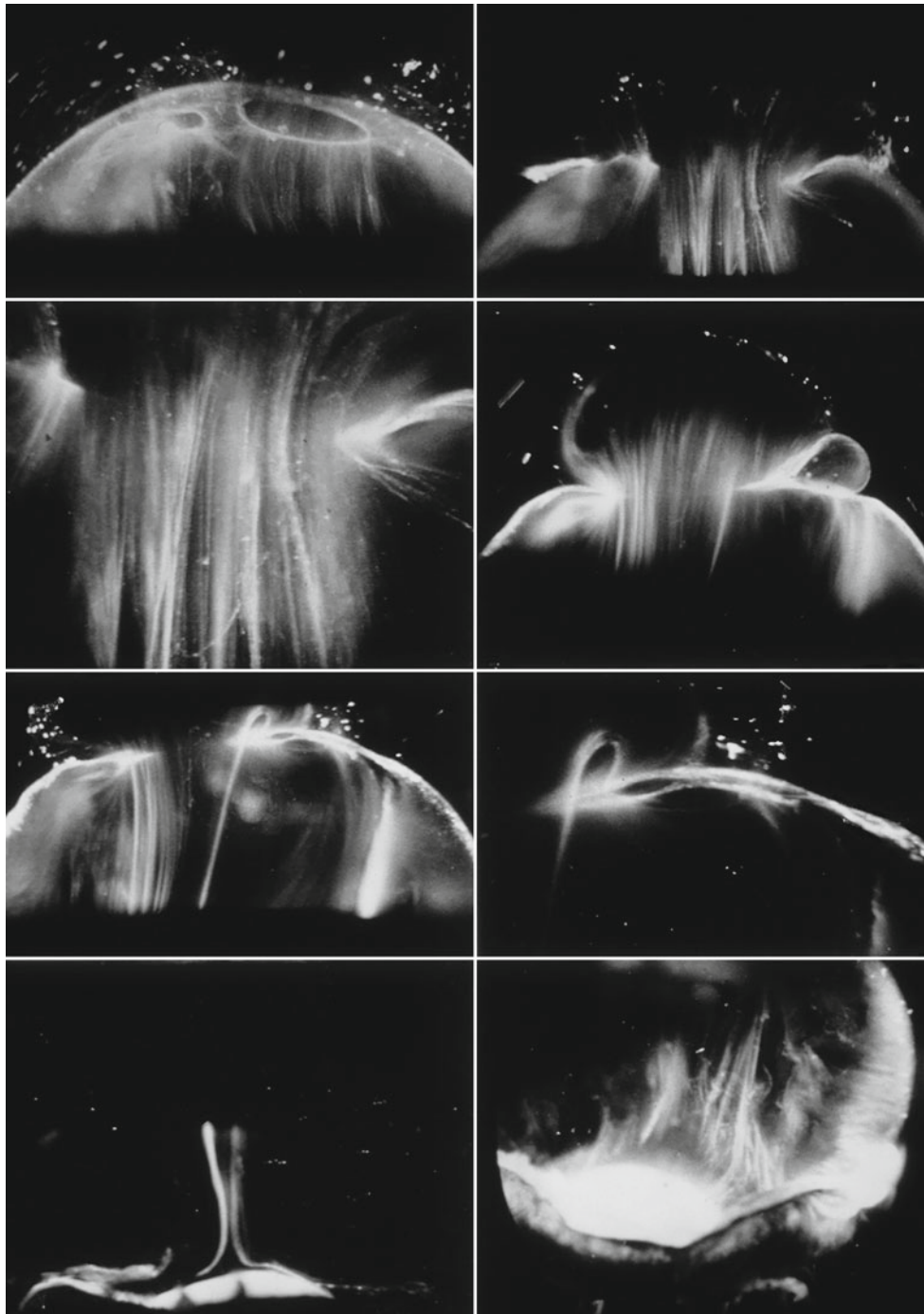


Figure II.F-3 Adult Human Vitreous Structure Visualized by Dark-Field Slit Microscopy. Specimens were prepared as described in **Figure II.F-2**. A slit lamp was used to shine a horizontally oriented beam through the vitreous body, creating a horizontal optical section. When viewed from above, the illuminated plane has a 90° illumination/observation angle that maximizes the Tyndall effect, especially when viewed in a completely dark room. All photographs shown are oriented with the anterior segment below and the posterior pole above. *Top left:* Posterior vitreous in the left eye of a 52-year-old man. The vitreous body is enclosed by the vitreous cortex. There is a hole in the prepapillary (small, to the left) vitreous cortex. Vitreous fibers are oriented towards the premacular region. *Top right:* Posterior vitreous in a 57-year-old man. A large bundle of prominent fibers is seen coursing anteroposteriorly and entering the retrocortical space by way of the premacular vitreous cortex. *Row 2, left:* Same photograph as upper right, at higher magnification. *Row 2, right:* Posterior vitreous in the right eye of a 53-year-old woman. There is posterior extrusion of vitreous out the prepapillary hole (to the right) and premacular (large extrusion to the left)

vitreous cortex. Fibers course anteroposteriorly out into the retrocortical space. *Row 3, left:* Horizontal optical section of the same specimen as row 2 right, at a different level. A large fiber courses posteriorly from the central vitreous and inserts into the premacular vitreous cortex. *Row 3, right:* Same view as row 3 left, at higher magnification. The large fiber has a curvilinear appearance because of traction by the vitreous extruding into the retrocortical space (see row 2 right). However, because of its attachment to the posterior vitreous cortex, the fiber arcs back to its point of insertion. *Bottom left:* Anterior and central vitreous in a 33-year-old woman. The canal of Cloquet is seen forming the retrolental space of Berger. *Bottom right:* Anterior and peripheral vitreous in a 57-year-old man. The specimen is tilted forward to enable visualization of the posterior aspect of the lens and the peripheral anterior vitreous. To the right of the lens, there are fibers coursing anteroposteriorly that insert into the vitreous base. These fibers splay out to insert anterior and posterior to the ora serrata (Reproduced with permission from Sebag and Balazs [94]; Sebag and Balazs [5]; Sebag [9]) (Specimens were courtesy of the New York Bank for Sight and Restoration, New York, NY)

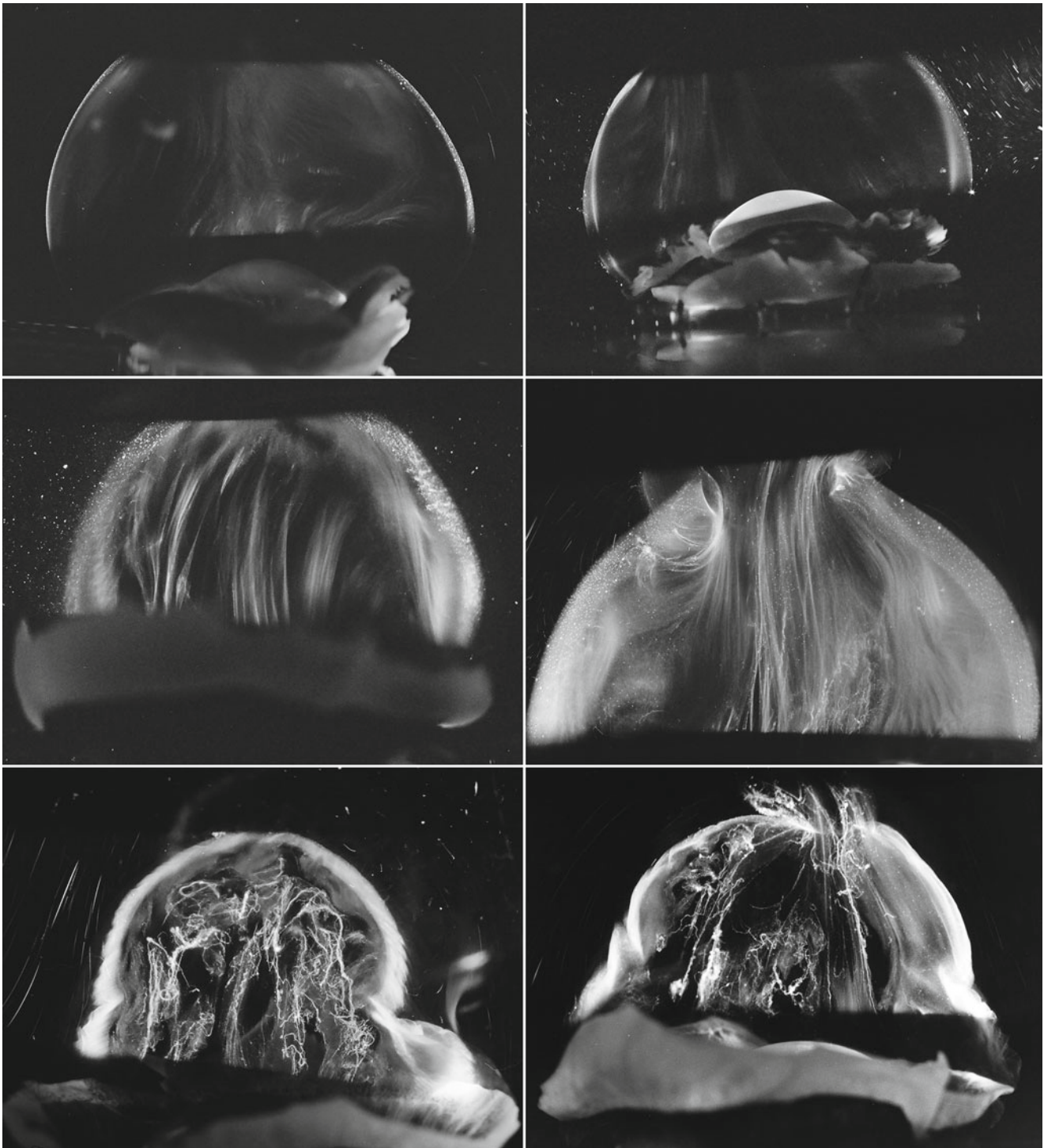


Figure II.F-4 Age-Related Differences in Human Vitreous Structure. Dark-field slit microscopy of fresh unfixed whole human vitreous with the sclera, choroid, and retina dissected off the vitreous body, which remains attached to the anterior segment. The anterior segment is below and the posterior pole is above in all images. *Top row:* The vitreous bodies of an 11-year-old girl (*left*) and a 14-year-old body (*right*) demonstrate a homogeneous structure with no significant light scattering within the vitreous body, only at the periphery where the vitreous cortex is comprised of a dense matrix of collagen fibrils. The posterior aspect of the

lens is visible at the bottom of each image. *Middle row:* Vitreous structure in a 56-year-old (*left*) and a 59-year-old (*right*) subject features macroscopic fibers in the central vitreous body with an anteroposterior orientation. These form when hyaluronan molecules no longer separate collagen fibrils, allowing cross-linking and aggregation of collagen fibrils into visible fibers. *Bottom row:* In old age the fibers of the central vitreous become significantly thickened and tortuous, as demonstrated in the two eyes of an 88-year-old woman. Adjacent to these large fibers are areas of liquid vitreous, at times forming pockets, called lacunae



Figure II.F-5 Dark-field slit microscopy imaging of posterior and central vitreous in a 59-year-old man postmortem. The premacular hole is at the top center. Fibers course anteroposteriorly in the center of the vitreous and exit the vitreous body posteriorly to enter the retrocortical (preretinal) space via the premacular region of the vitreous cortex. The

prepapillary “hole” in the posterior vitreous cortex is to the left. Within the posterior vitreous cortex are many small “dots” that scatter light intensely. The larger, irregular dots are debris. The small punctate dots are hyalocytes (Sebag [9])

injections where there is little attention paid to exactly where within the vitreous body drugs are being injected. For example, it is very plausible that an injection into Cloquet’s canal will have very different drug distribution than an injection into the bursa premacularis of Worst. [see chapter IV.E. Principles and practice of intravitreal application of drugs].

III. In Vivo Imaging

One of the major challenges to imaging vitreous *in vivo* is the limitation imposed by the size of the pupil and the anatomy of the anterior segment, which work against achieving a wide illumination/observation angle with a slit-lamp beam.

A. Physical Examination

Examination of vitreous essentially consists of visualizing a structure intended to be virtually invisible [16]. The clarity of

vitreous and its position within the inner recesses of the eye make clinical examination difficult. Optical transparency necessitates maximizing the Tyndall effect for visualization. Although this can be achieved *in vitro* (see above), there are limitations in the illumination/observation angle that can be achieved *in vivo*. This is even more troublesome in the presence of meiosis, corneal and lenticular opacities, and poor patient compliance. Essential to the success of achieving an adequate Tyndall effect are maximizing pupil dilation in the patient, because the Tyndall effect increases with an increasingly subtended angle between the axis of illumination and the line of observation (up to a maximum of 90°) and dark adaptation in the examiner [17]. Some observers [18] propose that green light further enhances the Tyndall effect. In a fundus camera this can be achieved with red-free illumination.

1. Direct Ophthalmoscopy

With direct ophthalmoscopy, light rays emanating from a point in the patient’s fundus emerge as a parallel beam that is focused on the observer’s retina, and an image is formed. However, incident light reaches only that part of the fundus onto which the image of the light source falls, and only light

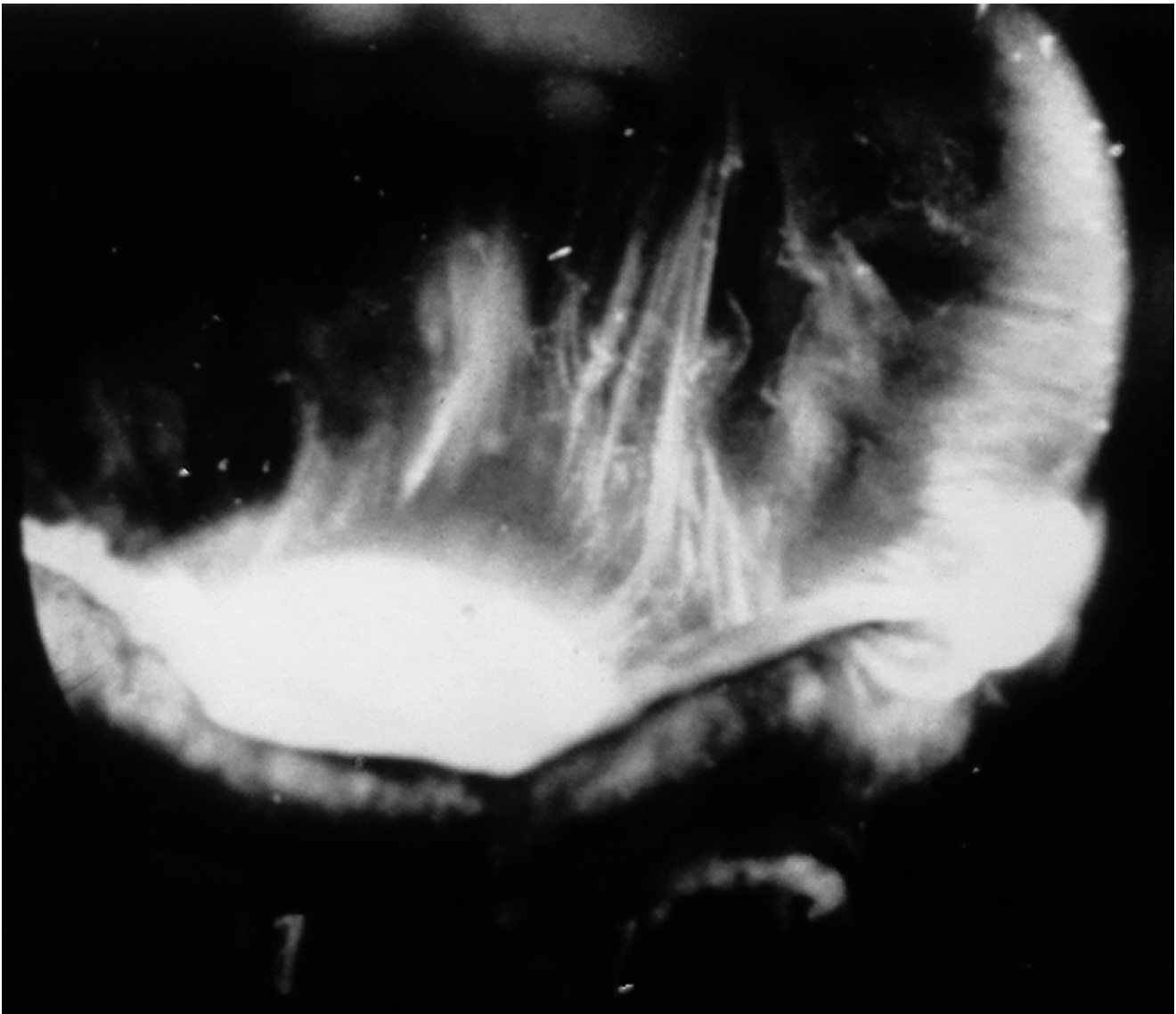


Figure II.F-6 Post-mortem dark-field slit microscopy imaging of vitreous base morphology. Central and peripheral vitreous structure in a 57-year-old male. The posterior aspect of the lens is seen below. Fibers

course anteroposteriorly in the central vitreous and insert at the vitreous base. Vitreous fibers insert into the vitreous base by splaying out to insert anterior and posterior to the ora serrata (Sebag [9])

from the fundus area onto which the observer's pupil is imaged reaches that pupil. Thus, the fundus can be seen only where the observed and the illuminated areas overlap and where the light source and the observer's pupil are aligned optically. This restricts the extent of the examined area, and also because of a limited depth of field, this method is rarely used to assess vitreous structure.

2. Indirect Ophthalmoscopy

Indirect ophthalmoscopy extends the field of view by using an intermediate lens to gather rays of light from a wider area of the fundus. Although binocularity provides stereopsis, the image size is considerably smaller than with direct

ophthalmoscopy and only significant alterations in vitreous structure, such as the hole in the prepapillary posterior vitreous cortex, vitreous hemorrhage, or asteroid hyalosis, are reliably diagnosed by indirect ophthalmoscopy. There is also difficulty in examining the peripheral vitreous resulting from a loss of stereopsis since examining the periphery renders the circular pupil an elliptic aperture, making it difficult to obtain an adequate view with both of the observer's eyes. This is more of a problem in the horizontal meridians than in the vertical, because the examiner's two eyes are positioned horizontally. Scleral indentation during indirect ophthalmoscopy decreases this limitation, but more so for peripheral fundus examination than for the vitreous.

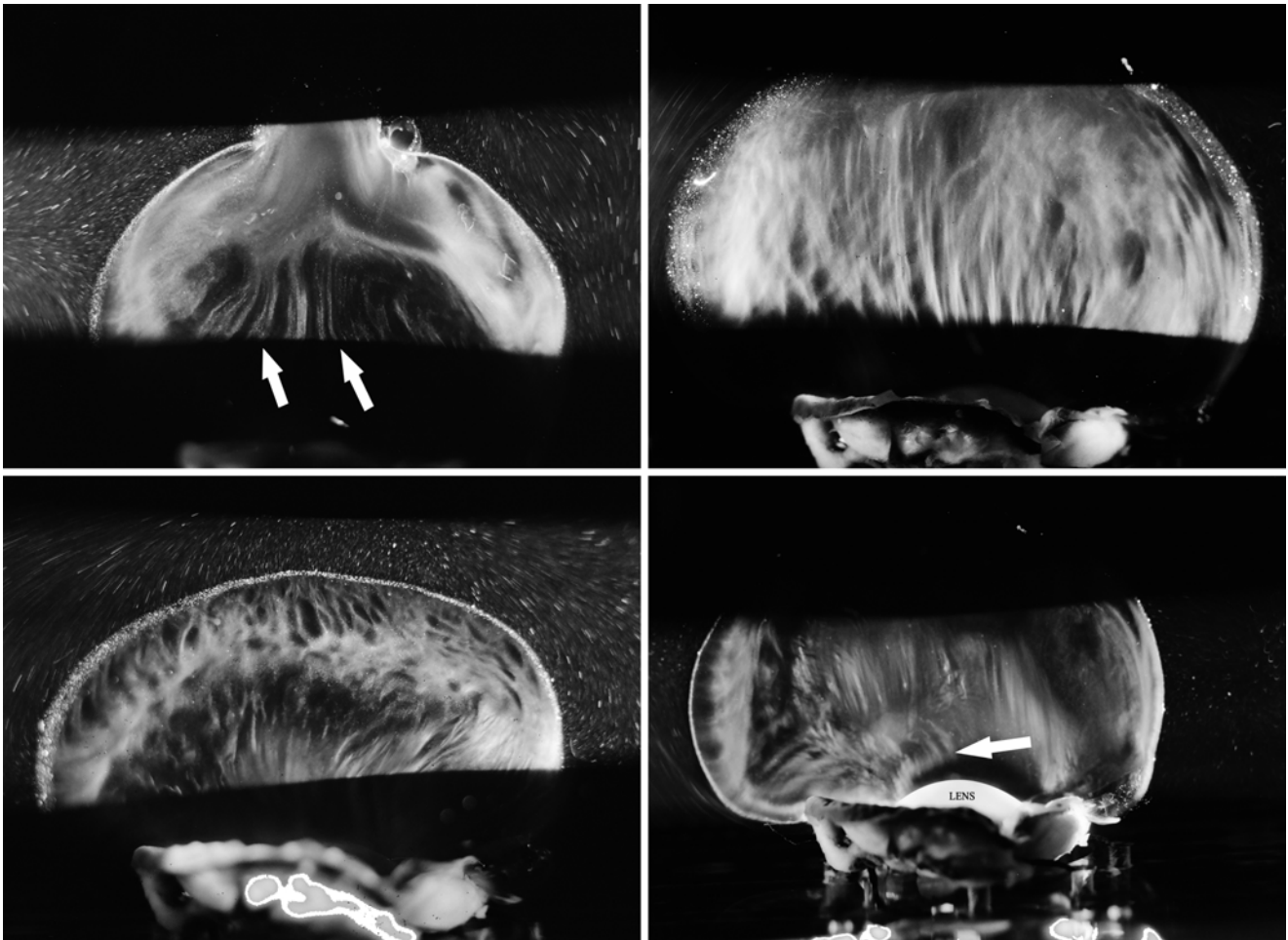


Figure II.F-7 Post-mortem dark-field slit microscopy imaging of diabetic vitreopathy *in vitro*. *Upper left*: The right eye of a 9-year-old girl with a 5 year history of type I diabetes and no evidence of diabetic retinopathy shows extrusion of the central vitreous through the posterior vitreous cortex into the retrocortical (preretinal) space. The subcortical vitreous appears very dense and scatters light intensely. Centrally, there are fibers (*arrows*) with an anteroposterior orientation and adjacent

areas of liquefaction. *Upper right*: Central vitreous in the left eye of the same subject shows prominent fibers that resemble those seen in non-diabetic adults. *Lower left*: Peripheral vitreous of the left eye in the same subject shows fibers inserting into the vitreous cortex with adjacent collections of liquid vitreous. *Lower right*: Anterior vitreous of the right eye in the same subject shows fiber insertion into the vitreous base about the lens (*arrow*) (Reprinted with permission from Sebag [89])

3. Slit-Lamp Biomicroscopy

The anterior vitreous is easily examined at the slit lamp without preset or contact lenses. In the absence of a crystalline or artificial intraocular lens, vitreous prolapse into the anterior chamber could be important in vitreo-corneal touch and the risks of corneal endothelial cell dysfunction [19]. Vitreous adhesions to a cataract wound or to the iris may be important in the pathogenesis of postoperative cystoid macular edema [20]. Particulate opacities in the anterior vitreous can be seen at the slit lamp and can give important clues as to the possible presence of posterior pathology, such as retinitis pigmentosa [21]. Cells can be the augury of retinal infection, inflammation, tears, and/or detachments. Lacqua and Machemer [22] described that an increase in the number and size of pigmented cells in the vitreous of patients with retinal detachment (pre- or

postoperatively) heralds the development of proliferative vitreoretinopathy. Bleeding can be associated with red blood cells in the anterior vitreous. Various neoplastic diseases, for example, endophytic retinoblastoma, choroidal melanoma, and reticulum cell sarcoma, can result in anterior vitreous cells. Anterior vitreous structures such as the Mittendorf dot, a remnant of fetal hyaloid vessel regression, can be seen at the slit lamp and should alert the examiner to the possibility of other developmental disorders, such as persistent hyperplastic primary vitreous in the fellow eye [23] [see chapter III.A. Congenital vascular vitreo-retinopathies].

Effectively using slit-lamp biomicroscopy to overcome vitreous transparency necessitates maximizing the Tyndall effect. Although this can be achieved *in vitro*, as described previously (and for the anterior vitreous), there are limitations to the illu-

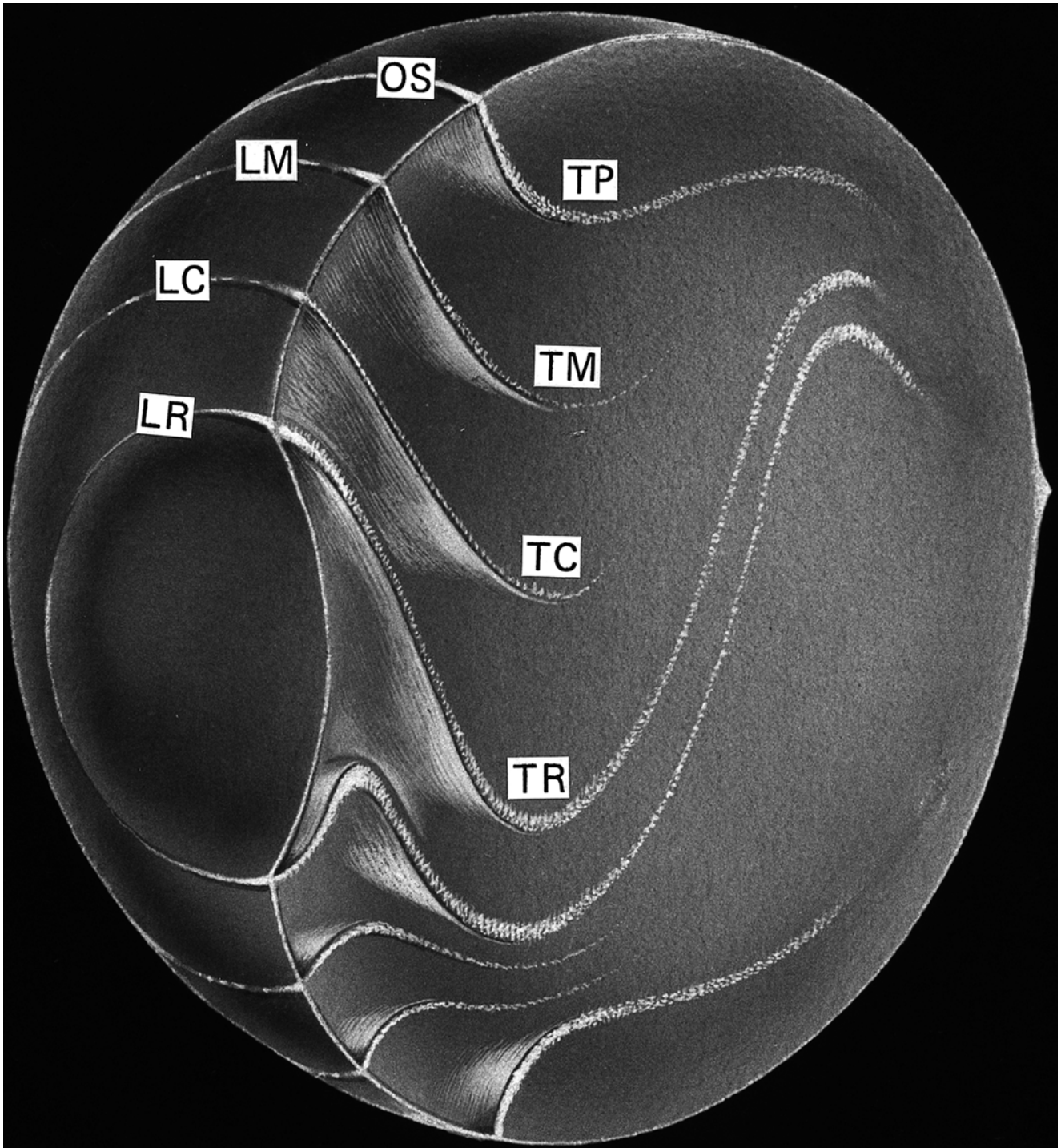


Figure II.F-8 Vitreous structure (d'après Eisner). Schematic diagram of the system of membranelles described by Georg Eisner. These course posteriorly from linear anterior insertion sites, called ligamenta (*LR*,

LC, *LM*) or the ora serrata (*OS*). Each membranelle is called a tractus (*TR* retrolental tract, *TC* coronary tract, *TM* median tract, *TP* preretinal tract) (Eisner [95])

mination/observation angle that can be achieved clinically in the mid-vitreous and posterior vitreous. This is even more troublesome in the presence of meiosis, corneal and/or lenticular opacities, and limited patient cooperation. Pupil dilation

in the patient should be maximized to achieve an adequate Tyndall effect, because the Tyndall effect increases with an increasingly subtended angle between the plane of illumination and the line of observation (up to a maximum of 90°) and

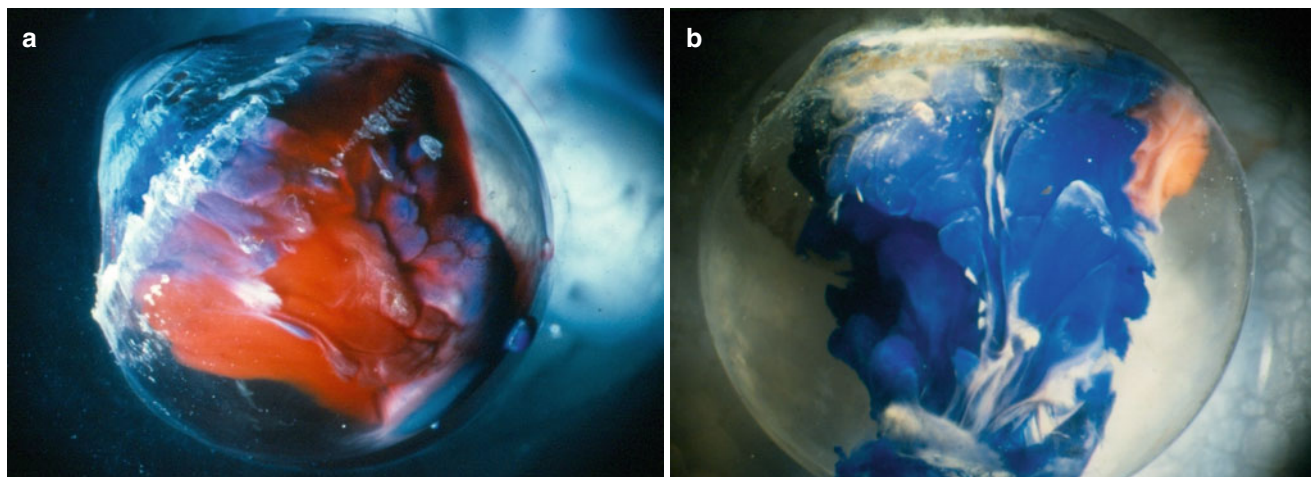


Figure II.F-9 Post-mortem vitreous structure (d'après Worst). Injection of India ink identifies separate cisternal systems. (a) Premacular Bursa of Worst (red). (b) Cloquet's (prepapillary) cisternal system (blue) (Courtesy of Professor Jan Worst)

dark adaptation in the examiner. Some observers purport that green light enhances the Tyndall effect, although this has never been explained or tested scientifically.

a. Preset Lens Biomicroscopy

This method attempts to increase the available illumination/observation angle, offers dynamic inspection of vitreous *in vivo*, and provides the capability of recording the findings in real time [24]. Initially introduced on a wide scale for use with a Hruby lens and currently practiced by using a handheld 90.00 diopter [25] lens at the slit lamp, this technique can be performed either with a plano concave lens (e.g., -55.00 to -58.60 D Hruby lenses) or various convex lenses (e.g., $+32.00$, $+58.60$, $+60.00$, or $+90.00$ D). Plano concave lenses produce a highly magnified, narrow-field, erect image and enable visualization of the posterior pole, although it is difficult to achieve an adequate illumination/observation angle to examine the posterior vitreous. Peripheral examination can only be performed by varying the position of the fixation point of the eye (s) which introduces optical distortions that reduce image quality. El-Bayadi [26] first proposed the use of a $+55.00$ D preset lens and advised maintaining at least a 10° illumination/observation angle. The resultant image is inverted and can be photographed. The advantage offered by this form of posterior vitreous biomicroscopy is that the avoidance of a contact lens facilitates the “ascension/descension” examination technique [27], whereby eye movements are used to displace the vitreous. This can be helpful in visualizing structures such as an operculum or Vogt (or Weiss) ring, which may have descended inferiorly in the presence of a PVD with vitreous syneresis [28]. It is principally this feature that makes the approach superior to contact lens systems for examination of the posterior vitreous [29]. A $+90.00$ D double aspheric

lens can similarly be used in a preset manner, also with photographic capabilities [30]. To examine the peripheral vitreous, Schepens [27] suggests reducing the illumination/observation angle, rotating the slit beam to the axis of the meridian being observed, and reducing the interpupillary distance of the slit-lamp eyepieces as ways of minimizing the loss of stereopsis.

b. Contact Lens Biomicroscopy

Peripheral vitreous examination has been traditionally performed with the various mirrors of the Goldmann lens. Both Schepens [27] and Jaffe [31] give excellent detailed accounts of the procedure to be followed for peripheral vitreous examination. Each describes the use of the oscillation technique of rocking the slit-lamp joystick to alternate between direct and retro-illumination for visualization of particulate or cellular opacities in the posterior vitreous. Schepens [27] further describes the use of a tilted slit-lamp column to enhance visualization of the peripheral vitreous. Eisner [3] has devised a cone-shaped apparatus that fits onto a three-mirror Goldmann lens and enables peripheral scleral indentation during slit-lamp biomicroscopy with a contact lens. Binocular indirect ophthalmoscopy with scleral indentation can also permit such examination. The recent development of inverted image contact lenses with various-size fields has greatly enhanced stereoscopic examination of the vitreous and fundus, and they are now routinely used for laser photocoagulation therapy of the fundus. The Mainster retina laser lens [32] is a $+61.00$ D convex aspheric contact lens that produces a real inverted image of about 45° of the posterior fundus with excellent stereopsis. The panfunduscope lens is a $+85.00$ D convex spheric lens that provides less magnification and image clarity but offers a wider-angle view. It is useful for peripheral examination to 60° or 70° with a 15° tilt.

B. Clinical Imaging Technologies

1. Optical Imaging

a. Scanning Laser Ophthalmoscopy

The scanning laser ophthalmoscope (SLO) that was first developed at the Schepens Eye Research Institute in Boston is now on display at the Smithsonian Institute in Washington, D.C. This instrument features tremendous depth of field and offers real-time recording of findings. Monochromatic green, as well as other wavelengths of light are available for illumination [33]. To date, however, the SLO has really only improved the ability to image vitreous in the prepapillary posterior vitreous, such as viewing the Weiss ring. Unfortunately, despite the dramatic depth of field possible with this technique, SLO does not adequately image the vitreous body and an attached posterior vitreous cortex, probably because of limitations in resolution. Thus, PVD, by far the most common diagnosis to be entertained when imaging vitreous clinically, is not reliably determined by SLO. Indeed, there is an increasing awareness among vitreous surgeons that the reliability of the clinical diagnosis of total PVD by any existing technique is woefully inadequate. This awareness arises because vitreous surgery following clinical evaluation often reveals findings that are contradictory to preoperative assessments. It is hoped that the combination of SLO imaging with optical coherence tomography [34–36] will enable better visualization of vitreous and the vitreoretinal interface.

b. Optical Coherence Tomography

OCT of the retina was introduced in the seminal paper by Huang, Fujimoto, and their coworkers in a paper published in *Science* in 1991 in which they demonstrated high-resolution images of the *ex vivo* retina [37]. *In vivo* OCT images of the human retina were reported shortly thereafter in independent papers by Fercher [38] and Swanson [39] and their respective coworkers. By 1996, the first commercial ophthalmic OCT system was introduced by Carl Zeiss Meditec.

OCT signals are generated by reflection and scattering of light by refractive index inhomogeneities present in tissue. In Huang's implementation of this technique, a Michelson interferometer is used to measure the range and backscatter amplitude along numerous lines-of-sight to form a cross-sectional image. In the interferometer, the tissue is illuminated by infrared low-coherence light (830 nm wavelength) from a superluminescent diode. The emitted light is divided by a beam splitter in two paths or arms, one of which (the reference arm) goes towards a mirror and the other (the sample arm) towards the tissue (in this case, the eye). Reflected light from the sample is combined with the reflection from the reference arm mirror. Interference fringes are produced and recorded on the detector as the reference arm is scanned in the range axis and

path length difference is less than the coherence length. Coherence is a measure of the ability of a light source to produce high contrast interference fringes when interfered with itself. Coherence length is inversely related to the bandwidth of the light source, i.e., the range of wavelengths present in the emitted light. A monochromatic light source will have a long coherence length and hence provide poor resolution. Conversely, a broadband source (emitting over a range of wavelengths) will have a short coherence length and provide good resolution. Lateral resolution is determined by the focusing optics in the sample arm, which are similar to confocal microscopy, such that light scattered from outside the focal spot is suppressed [40]. To obtain a two-dimensional image, the light beam must be scanned laterally across the retina, typically by an electromechanically actuated mirror. Following the ultrasound nomenclature, a one-dimensional representation of amplitude along one line-of-sight is called an "A-scan," while a two-dimensional cross-sectional image formed from a series of lines-of-sight is called a "B-scan."

Once developed, OCT technology was quickly used for many clinical applications in ophthalmology, including retinal imaging [41], glaucoma imaging [42], and imaging of the anterior segment [43]. While the first generation of OCTs was based on the above "time-domain" technology and provided a significant advantage over other imaging technologies in cross-sectional depiction of the retina, there was relatively low imaging speed and consequent motion artifacts and relatively poor sensitivity and resolution by today's standards. A major advance in addressing these shortcomings was the development of spectral- or Fourier-domain OCT. In time-domain systems, imaging speed is low due to the requirement for mechanical scanning of the mirror in the reference arm. In spectral-domain OCT (SD-OCT), first proposed by Fercher in 1995 [44], the interference pattern between a reference mirror and the sample is broken into a spectrum by an optical grating and the spectrum recorded. Fourier transformation of the spectrum into the time domain allows an A-scan to be acquired without depth scanning. Acquisition speed is only limited by data-processing speed of the line scan CCD camera used to record the spectrum of the backscattered light. This technique was first applied clinically for retinal imaging in 2002 [45]. An example of an SD-OCT demonstrating PVD is presented in Figure II.F-10.

Another form of spectral-domain OCT uses a wavelength swept light source rather than an optical grating. Swept-source OCT (SS-OCT) was described by Chinn, Swanson, and Fujimoto in 1997 [46]. It offers several advantages over grating-based SD-OCT, including better sensitivity with imaging depth, longer imaging range, and higher detection efficiencies (because there are no spectrometer grating losses [47]). The first swept-source OCT of the human retina *in vivo* was presented in 2006 by Lim et al. using an 800 nm band source [48]. Srinivasan et al. demonstrated high speed

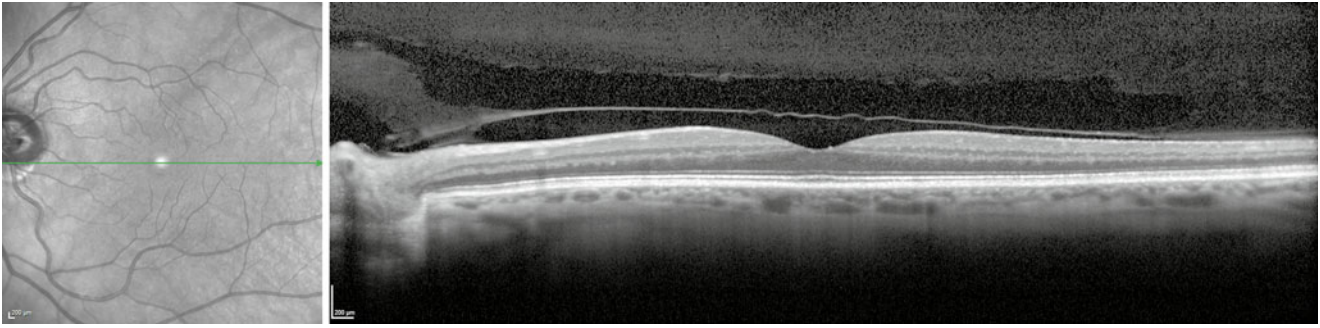


Figure II.F-10 SD-OCT Imaging of posterior vitreous detachment *in vivo*. SD-OCT of left eye of asymptomatic 64-year-old male subject demonstrating PVD extending from the edge of the optic nerve head and fully detached at the fovea. The image was produced with the

Heidelberg Spectralis 820 nm system (Heidelberg Engineering, Heidelberg, Germany). Images were post-processed to enhance low-level backscatter from formed vitreous

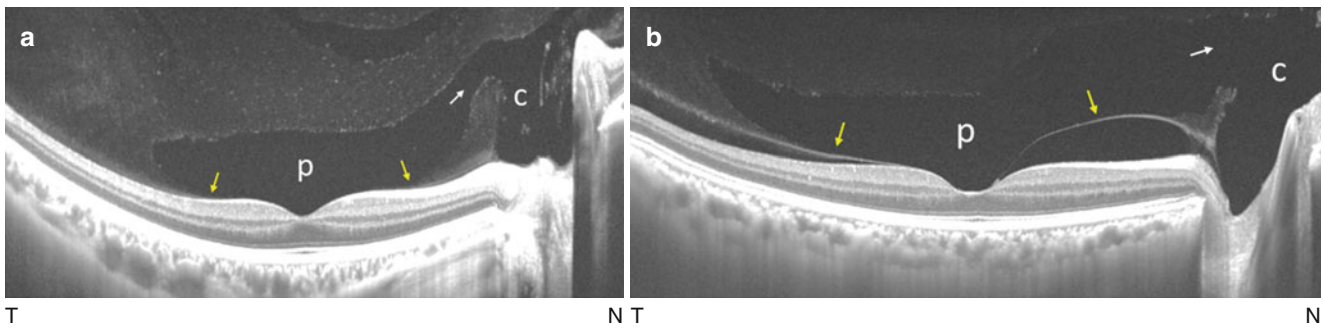


Figure II.F-11 SS-OCT Imaging of posterior precortical vitreous pocket (PPVP, labeled p) *in vivo*. Swept-source optical coherence tomography (SS-OCT) of vitreous structure in young vs. older subjects. (a) Left eye of 22-year-old female (horizontal scan). The anterior border of the PPVP is vitreous gel and the posterior wall is comprised of a thin layer of the vitreous cortex attached to the retina [52]. SS-OCT revealed the existence of a connecting channel between a boat-shaped

PPVP and Cloquet's canal (c) [50]. (b) Left eye of 64-year-old female (horizontal scan). The posterior wall of the PPVP initially detaches at the paramacular area and extends to the perifoveal area, which results in a perifoveal PVD. p PPVP, c Cloquet's canal, T temporal, N nasal, white arrow connecting channel between a PPVP and Cloquet's canal, yellow arrow posterior wall of PPVP (Images courtesy of Hirokazu Itakura, MD, Gunma University, Japan)

(249,000 lines/s) swept-source imaging of the retina and optic nerve head in the 1,060 nm band in 2008 [49]. The high sensitivity of SS-OCT provides excellent depiction of vitreous and the vitreoretinal interface. Itakura et al. have utilized SS-OCT to examine the structure of the vitreous in the region of the macula [50]. Figure II.F-11 shows SS-OCT depiction of a precortical posterior vitreous pocket, a liquefied lacuna anterior to the macula that is physiologically present in the vitreous of adults [51, 52].

Modern SD-OCTs acquire about 50,000 vectors per second, with research units, especially SS-OCTs, achieving an order of magnitude higher speed. The chief disadvantage of OCT stems from its limited capacity to image through light scattering or absorbing structures such as the iris and sclera. Thus, for retinal or vitreous imaging, OCT must be introduced through the pupil and will potentially be degraded by pathologic optical opacities such as corneal scars, cataract, or hemorrhage along the optical path. For anterior segment imaging, OCT can produce excellent depictions of the cornea; anterior chamber, including the

angle; and the anterior lens surface within the pupil, but the ciliary body is generally poorly visualized as is the lens periphery and zonules. A second disadvantage of OCT, at least until recently, was limited depth of field, with images depicting only 2–3 mm axially. This limits its value to assessment of the vitreoretinal interface rather than the full extent of the vitreous. To mitigate this limitation, SS-OCT systems operating in the 1 μ m band have been able to achieve greater depth of field [47]. Figure II.F-12 demonstrates an extended depth SS-OCT image of the anterior segment including the cornea and posterior lens capsule. Grulkowski et al. recently reported a prototype 1,065 nm SS-OCT capable of capturing the full axial length of the eye [53].

One interesting apparatus combines optical coherence tomography (OCT) with scanning laser ophthalmoscopy (SLO) and is able to perform OCT imaging in the coronal plane simultaneously to SLO imaging with exact point-to-point registration (Figure II.F-13) enabling the superimposition of the OCT image onto the SLO image (Figure II.F-14). The results

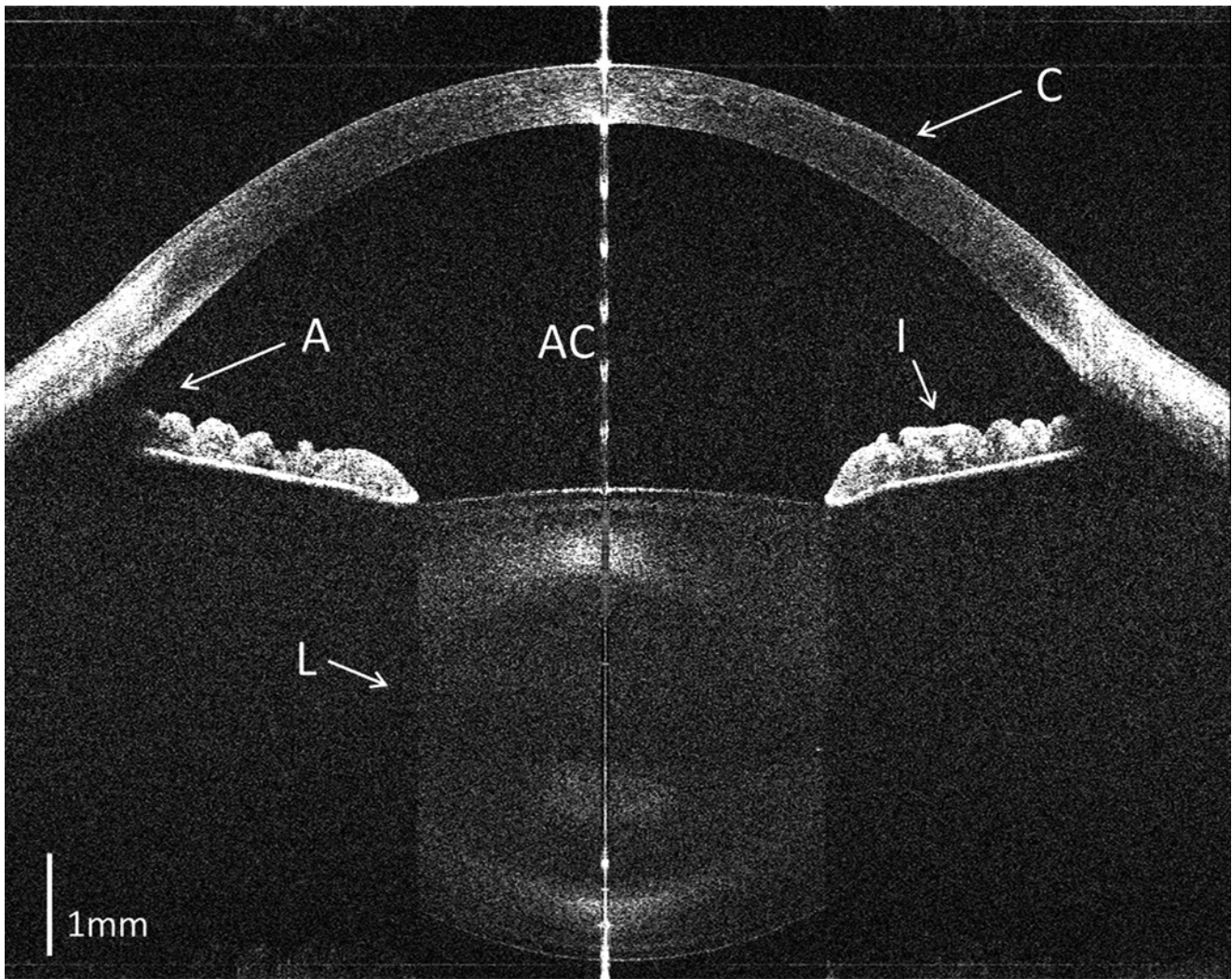


Figure II.F-12 SD-OCT imaging of the anterior segment *in vivo*. Cross-sectional image of the anterior segment of a 35-year-old human eye in the relaxed state acquired with extended depth SD-OCT at 840 nm. The axial resolution of the system is 8 μm in air. The main ocular structures are indicated: cornea (C), anterior chamber (AC), crystalline lens (L), iris (I), and angle (A). The image consists of 1,000

A-lines of 2,556 (axial) pixels each. The size of the frame in the axial direction is 9.5 mm when the mean group refractive index of the anterior segment is taken to be 1.37 at 840 nm. The lateral scanning length was set to 16 mm (Image courtesy of Marco Ruggeri, Bascom Palmer Eye Institute, University of Miami, Miami, FL)

showed that in one study, 40 % of eyes with macular hole also had eccentric macular pucker [35]. In comparison to the eyes that had macular pucker without macular holes, these membranes were three-fold larger ($P=0.006$). In eyes with macular holes and eccentric macular pucker, the center of retinal contraction was twice as far from the fovea as in eyes with only macular pucker ($P=0.0001$). In another study [54] using combined OCT/SLO and coronal plane imaging, macular pucker was found to feature more than one center of retinal contraction (Figure II.F-14) in half of the cases. The number of centers was positively correlated with the presence or absence of retinal cystoid spaces ($P<0.05$) and the degree of retinal thickening ($P<0.05$) [see chapter III.F. Vitreous in the pathobiology of macular pucker].

Visualization of the vitreo-macular interface is sufficiently enhanced with OCT/SLO imaging that the role of vitreoretinal adhesion in macular diseases is being defined as it relates to exudative age-related macular degeneration (AMD) [55, 56] and new preventative strategies are being forged. As previously described [57], vitreoschisis (Figure II.F-15) appears to be an important factor in the pathogenesis of macular holes and macular pucker [35].

Furthermore, recent studies [34, 58] have determined that visualizing the vitreo-papillary interface (Figure II.F-16) may be important in understanding the pathophysiology of various vitreo-maculopathies. In 117 subjects, SD-OCT/SLO detected vitreo-papillary adhesion (VPA) in 15 of 17 (88.2 %) eyes with full-thickness macular holes, 11 of 28

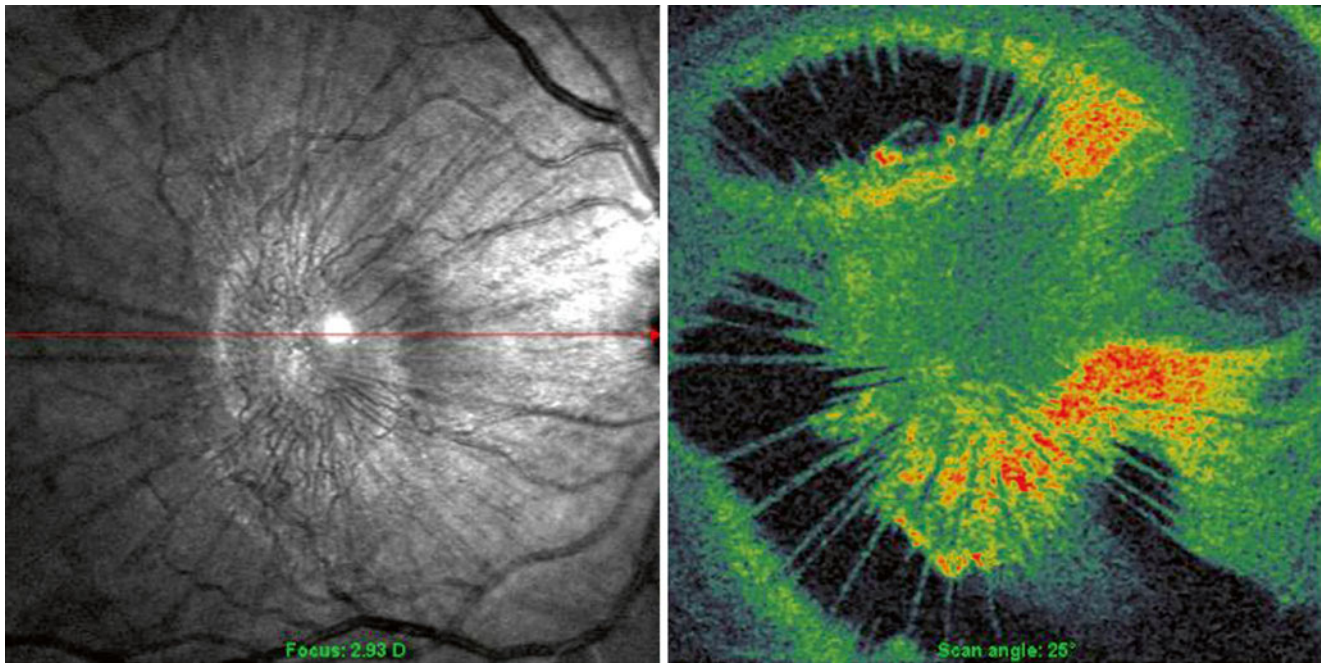


Figure II.F-13 Combined OCT/SLO coronal plane imaging of macular Pucker *in vivo*. Coronal plane optical coherence tomography (OCT) imaging (color to right) and scanning laser ophthalmoscope (SLO) imaging (grayscale to left). There is point-to-point registration of these

two images, enabling an accurate superimposition with exact localization of posterior vitreous pathology (see Figure II.F-14) (Courtesy of VMR Institute©)

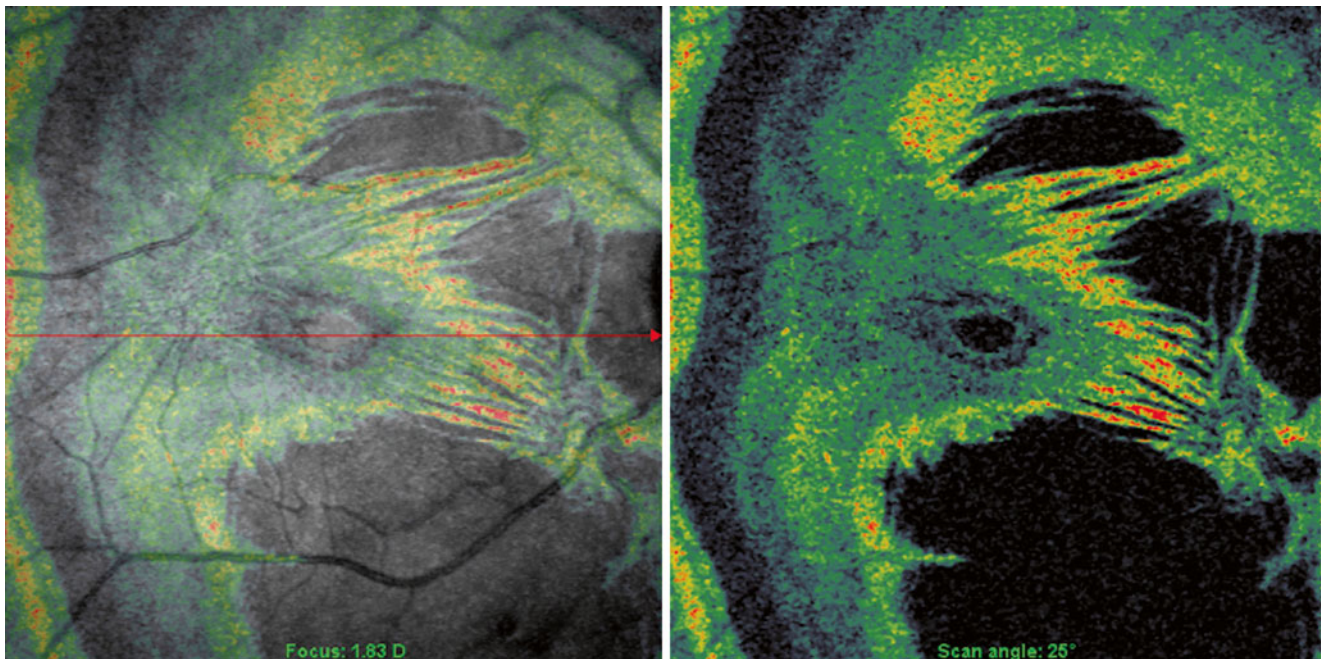


Figure II.F-14 Combined OCT/SLO coronal plane imaging of multifocal retinal contraction in macular pucker *in vivo* by superimposition of images. Coronal plane imaging demonstrates a case of macular pucker in the right eye with three separate centers of retinal contraction

and retinal striae extending between each of the three centers of contraction. The image on the left is a composite overlay of the coronal plane OCT image (color) superimposed upon the SLO image (grayscale) with point-to-point registration (Courtesy of VMR Institute©)

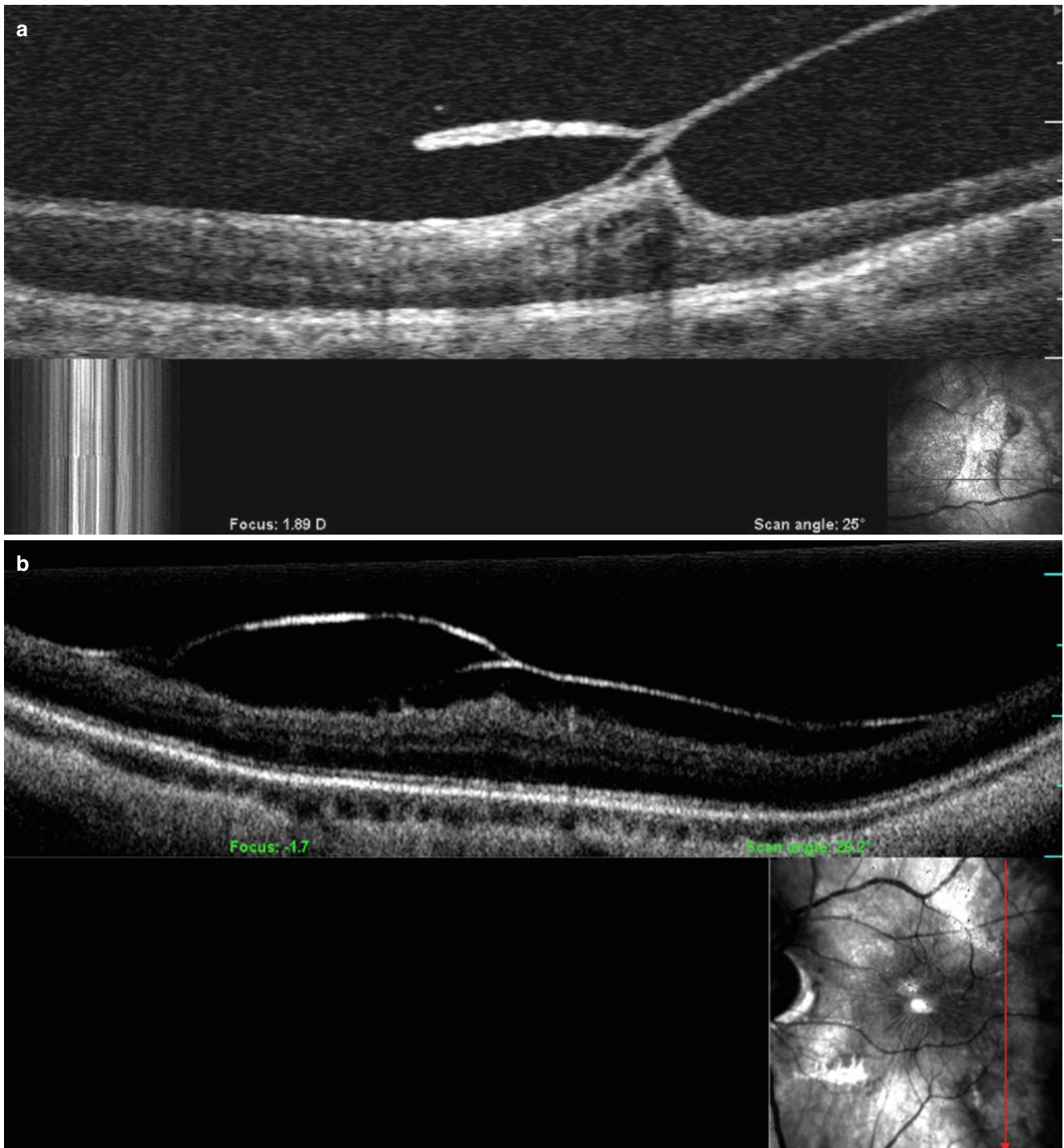


Figure II.F-15 Combined OCT/SLO imaging of posterior vitreoschisis *in vivo*. (a) OCT/SLO longitudinal imaging demonstrates a split in the posterior vitreous cortex, with the inner (anterior) layer rejoining the outer (posterior) layer forming the “lambda sign” where full-thickness posterior vitreous cortex exerts traction lifting the inner

retina (Courtesy of VMRI Institute©). (b) OCT/SLO imaging of vitreoschisis in macular pucker demonstrates the “lambda” sign, created by the rejoining of the two walls or layers of the split into full-thickness posterior vitreous cortex (Reproduced with permission from Sebag et al. [35])

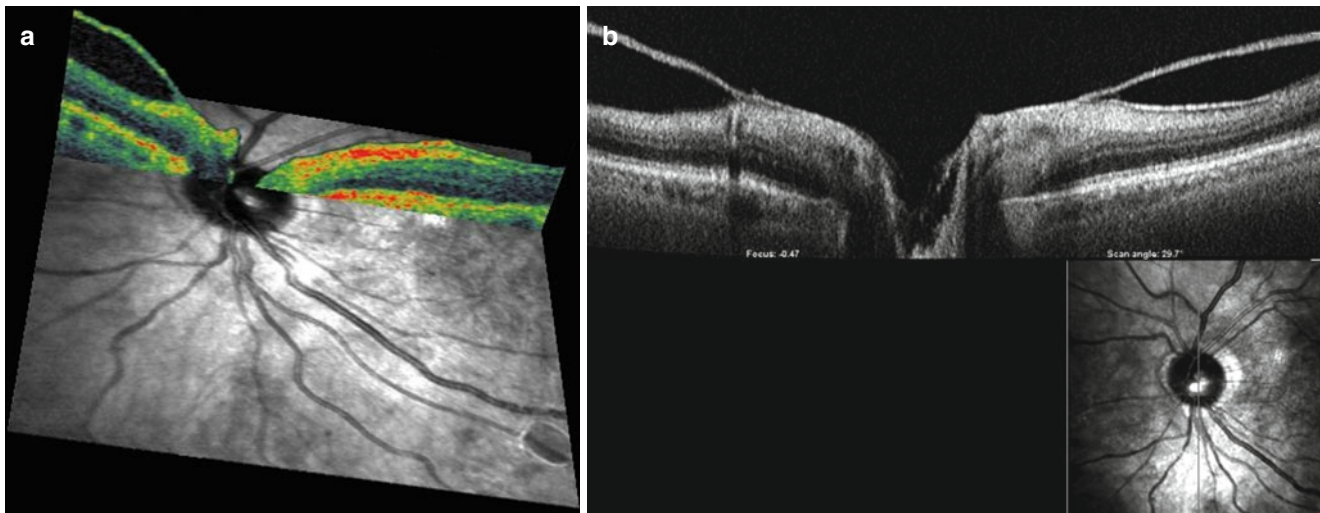


Figure II.F-16 Combined OCT/SLO imaging of vitreo-papillary adhesion *in vivo*. (a) ‘Intersecting planes’ display of longitudinal OCT (color) imaging and SLO (grayscale) imaging showing attachment of the posterior vitreous cortex to the edge of the optic disc following anomalous PVD (Courtesy of VMR Institute©). (b) Longitudinal OCT

imaging of vitreo-papillary adhesion showing vitreous attachment on both sides of the optic disc. Note that the posterior vitreous cortex on the right side of the optic disc in this image is split, constituting vitreoschisis (Courtesy of VMR Institute©)

(39.3 %) age-matched controls ($P=0.002$), 4 of 11 (36.4 %) eyes with lamellar holes ($P=0.01$), 4 of 15 (26.7 %) with dry AMD ($P=0.0008$), and 5 of 28 (17.9 %) eyes with macular pucker ($P=0.000005$). Intraretinal cysts were present in 15 of 15 (100 %) macular hole eyes with VPA. In macular pucker eyes, 4 of 5 (80 %) with VPA had intraretinal cysts, but only 1 of 23 (4.3 %) macular pucker eyes without VPA had intraretinal cysts ($P=0.001$) [see chapter III.E. Vitreo-papillary adhesion and traction].

2. Acoustic Imaging: Ultrasonography

When examination of vitreous is made difficult by opacification of the cornea, lens, or vitreous, there can, nevertheless, be worthwhile information garnered from careful study. As pointed out by Charles [59] much can be learned from studying the geometric configuration of an opaque or semiopaque vitreous. When opacification is advanced, however, ultrasonography can be helpful in defining the nature of the opacification, the three-dimensional configuration of the opaque vitreous, and the presence or absence of structural pathology behind the vitreous body. Of note, however, is that even in the absence of media opacification that precludes light-based imaging, ultrasound can provide useful information about the molecular structure of vitreous and its relation to adjacent structures. Diagnostic ultrasound (US) imaging of the eye has a longer history than either MRI or OCT, with the first A-mode studies performed by Mundt and Hughes in the 1950s [60] and B-mode by Baum shortly thereafter [61]. Coleman and Carlin developed the first A-mode system for axial length determination [62]. Coleman, Konig, and Katz developed the first commercially available combined A- and

B-mode system in 1969 [63]. A handheld contact B-mode instrument was developed by Bronson and Turner in the early 1970s [64]. Conventional US probes operating at a frequency of 10–12 MHz allow visualization of the globe and orbit. High-resolution US, often referred to as ultrasound biomicroscopy (UBM), was developed in the early 1990s primarily as an outgrowth of the work of Pavlin, Sherar, and Foster [65]. UBM systems operate at 35–50 MHz, but acoustic attenuation (which increases exponentially with frequency) limits such systems to visualization of the anterior segment.

The physical basis of ultrasound is the reflection or scattering of high-frequency sound waves by acoustic impedance inhomogeneities or interfaces. Acoustic impedance is the product of speed of sound and density. This is similar to OCT, where refractive index variation causes light to scatter or reflect, and US and OCT images thus bear a qualitative similarity to each other. US wavelengths (150 μm at 10 MHz, 30 μm at 50 MHz), however, are much longer than optical wavelengths (which are on the order of a micron), and hence, resolution is substantially lower. The chief advantage of US over OCT is its penetration. US can readily visualize the lens and vitreous in its entirety, despite the presence of the intervening iris and sclera. In terms of temporal resolution, typical ophthalmic US instruments produce about ten images per second, significantly slower than OCT, but much faster than MRI. Ultrasound’s disadvantage compared to OCT is requiring some form of acoustic coupling, such as a water bath in an immersion exam or gel in a contact exam. Unlike OCT, the US exam is performed without a camera view of

the area being scanned, making registration more difficult. Nevertheless, the ability of US to image optically occult structures in real time gives it an irreplaceable role in ophthalmic imaging.

On US, the posterior vitreous cortex is not detectable when attached to the retinal surface, but presents a sharp, smooth interface when detached sufficiently from the retinal surface to be resolved. Because this interface is often smooth, it presents a specular surface and normal incidence between the US beam and the surface optimizes reflectivity. Figure II.F-17 is an example of the typical appearance of

the detached vitreous. A more shallow detachment, previously shown by SD-OCT in Figure II.F-10, is shown by US in Figure II.F-18. In this case, the detachment is barely resolvable from the retina, as the separation is less than 200 μm at most. US, however, allows the vitreous as a whole to be imaged, and in this patient, intracortical strands suggestive of vitreoretinal tension are seen inferiorly near the equator.

US, like OCT, also has a finite depth of field. A typical 10 MHz transducer would have a depth of field of about 10 mm, which makes simultaneous assessment of the anterior

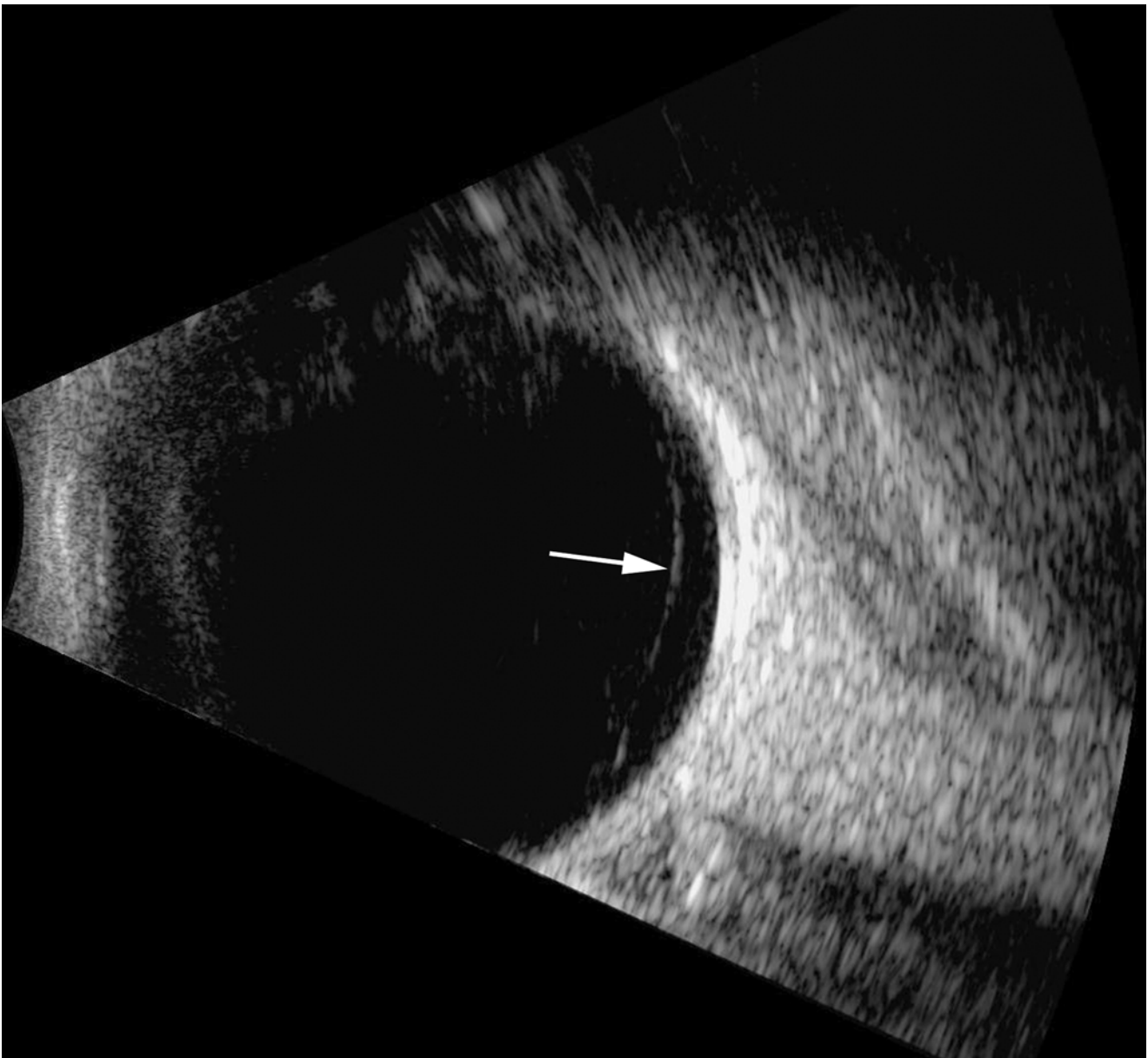
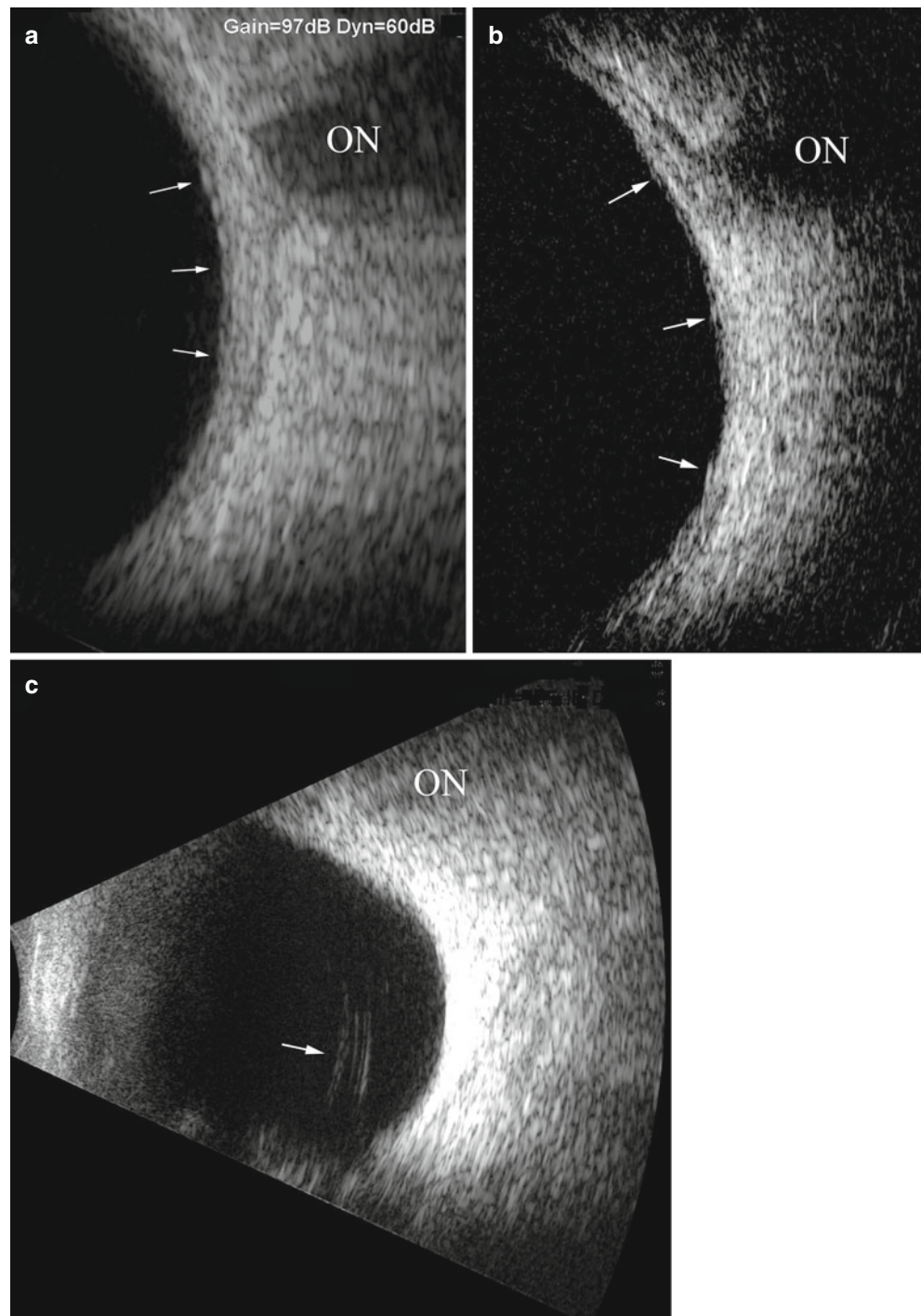


Figure II.F-17 10 MHz ultrasound B-scan of vitreous demonstrating posterior vitreous detachment in the right eye of a 60-year-old female. The arrow indicates the detached posterior vitreous cortex.

Figure II.F-18 Ultrasound imaging of the same eye imaged by SD-OCT in Figure II.F-10. (a) 10 MHz image in horizontal plane across optic nerve and region of the macula demonstrates irregular vitreoretinal interface, although the separation from retinal surface (estimated to be $<200\ \mu\text{m}$ from OCT) is not resolved. (b) 20 MHz image in same plane as image A more clearly depicts vitreous detachment from retinal surface. (c) High-gain 10 MHz B-mode image of same eye in vertical plane depicting the inferior aspect of the eye. Note striations within the vitreous cortex, suggestive of peripheral vitreoretinal tension



segment and retina problematic. UBM systems typically have a depth of field of about 1 mm. As with OCT technology, methods have been developed to extend depth of field for ophthalmic US. Ketterling et al. developed annular array probes consisting of concentric piezoelectric elements that can individually emit and receive ultrasound [66]. Twenty megahertz and forty megahertz probes of this design have been utilized for imaging the globe and the anterior segment, respectively, as

reported by Silverman et al [67, 68]. By post-processing echo signals received at each element, synthetic focusing [69] allows a six-fold improvement in depth of field, enabling imaging of the entire globe, for instance, at 20 MHz, and the anterior segment from cornea to lens posterior at 40 MHz. Examples of 20 and 40 MHz annular array synthetically focused images are provided in Figures II.F-19 and II.F-20. An additional enhancement of this technology is pulse

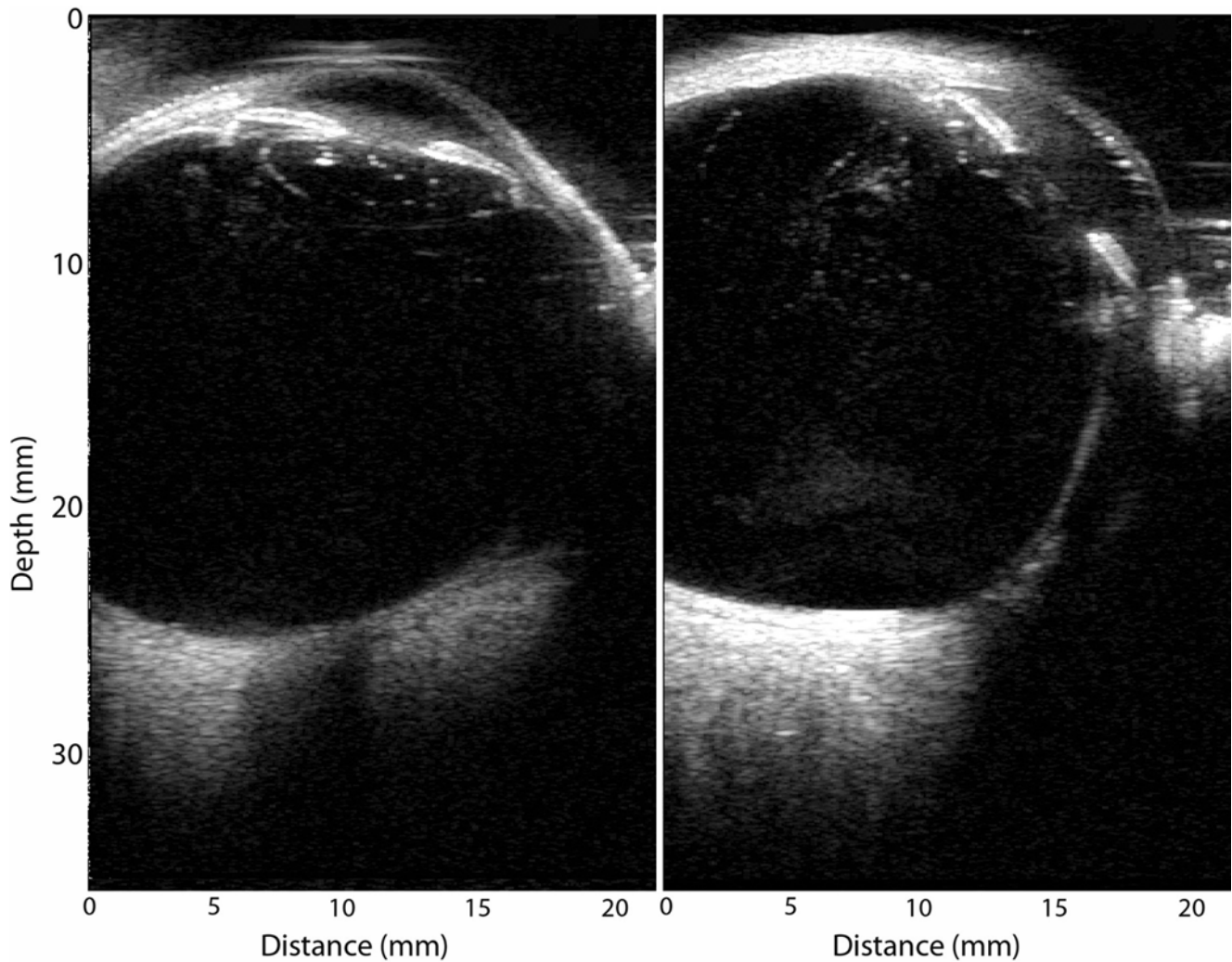


Figure II.F-19 20 MHz annular array images of the left eye in a 65-year-old male obtained in an immersion exam. *The left image* demonstrates the full contour of a cataractous lens, which was evident clinically. The image on the right, avoiding the attenuating and refracting

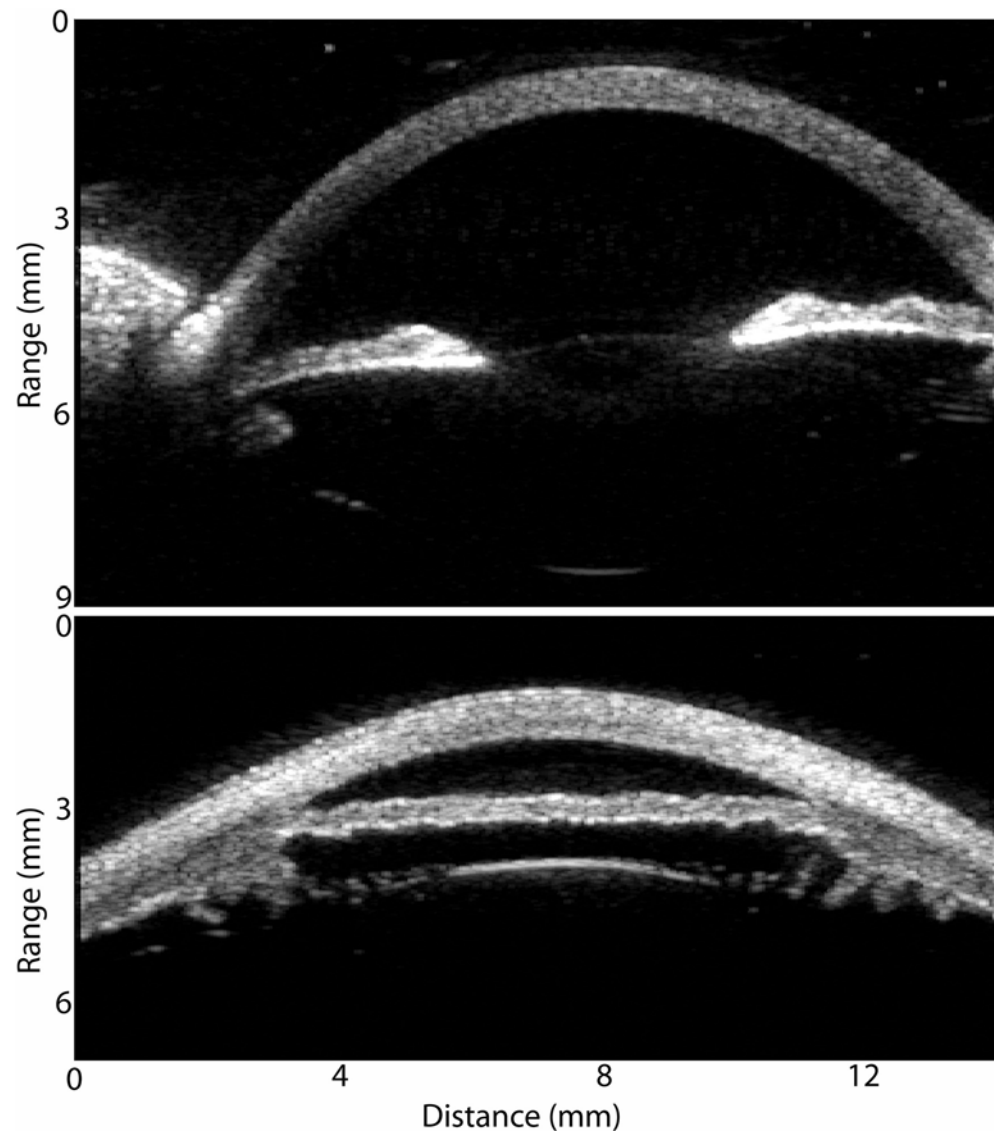
lens, demonstrates inhomogeneities in the anterior vitreous that were mobile on kinetic exam. Note excellent depth of field, with all structures from cornea to optic nerve well resolved

encoding by “chirp” excitation of the transducer [70], which can provide a major improvement in sensitivity. A chirp is a frequency-swept waveform ranging over the useful bandwidth of the transducer. Because of the relatively long duration of the chirp compared to conventional impulse excitation, greater sensitivity is achieved, with high resolution recovered by post-processing of echo data using a compression filter in the Fourier domain. Silverman et al. [71] have described application of a pulse-encoded 20 MHz annular array for imaging the vitreous. An example of pulse-encoded annular array imaging is provided in Figure II.F-21.

The clinical utility of ultrasonography results from strong echoes produced at acoustic interfaces found at the junctions of media with different densities and sound velocities, and the greater the difference in density between the two media that create the acoustic interface, the more prominent the

echo. Thus, age-related or pathologic phase alterations within the vitreous body are detectable by ultrasonography. Oksala [72], among the first to use B-scan ultrasonography to image vitreous in the late 1950s and early 1960s, summarized his findings of aging changes in 1978. In that report of 444 “normal” subjects, Oksala defined the presence of acoustic interfaces within the vitreous body as evidence of vitreous aging and determined that the incidence of such interfaces was 5 % between the ages of 21 and 40 years and was 80 % in individuals older than 60 years of age. In clinical practice, however, only profound entities such as asteroid hyalosis, vitreous hemorrhage, and intravitreal foreign bodies (if sufficiently large) are imaged by ultrasonography. At the vitreoretinal interface, the presence of a PVD is often suspected on the basis of B-scan ultrasonography but vitreous cortex structure cannot be defined, because the level of resolution is not

Figure II.F-20 40 MHz annular array images of a normal anterior segment in the right eye of a 40-year-old woman. The *top image* through the pupil plane demonstrates high resolution from the cornea to the posterior lens capsule as a result of synthetic focusing. Note eyelid to left of image, which produces some shadowing of the ciliary body. The *lower image*, acquired horizontally inferior to the pupil, provides excellent depiction of the ciliary body and processes



sufficient to reliably image the posterior vitreous cortex, which is only a little more than 100 μm thick at its thickest portion. However, recent studies have successfully used this technique to determine the presence of a split in the posterior vitreous cortex, called vitreoschisis, in patients with proliferative diabetic vitreoretinopathy [73]. The success achieved in using ultrasound to identify this important pathologic entity is probably because in advanced cases this tissue is significantly thickened by nonenzymatic glycation of vitreous collagen and other proteins [74] in the posterior vitreous cortex. Future studies should determine if vitreoschisis can be identified by ultrasound in other conditions, especially premacular membranes with pucker and macular holes. However, it may turn out that the thickness of these tissue planes is below the level of resolution presently available

with ultrasonography. When the posterior vitreous cortex is sufficiently displaced anteriorly the diagnosis of complete PVD can be reliably established by ultrasonography.

The solid and fluid components of vitreous undergo complex motions in response to saccades. US imaging allows real-time visualization of such motions, including regions where vitreo-macular traction are present. Rossi et al. recently developed a quantitative approach to characterization of such motions [75]. During a saccade, the vitreous lags a fraction of second behind the sclera and keeps moving after the sclera stops, pulling on the retina. Energy transmission from the eyewall to the vitreous follows two basic mechanisms: where the vitreous is separated, viscosity determines a shear flow parallel to the retina. When incomplete PVD exists, the partially attached mass of gel retains kinetic

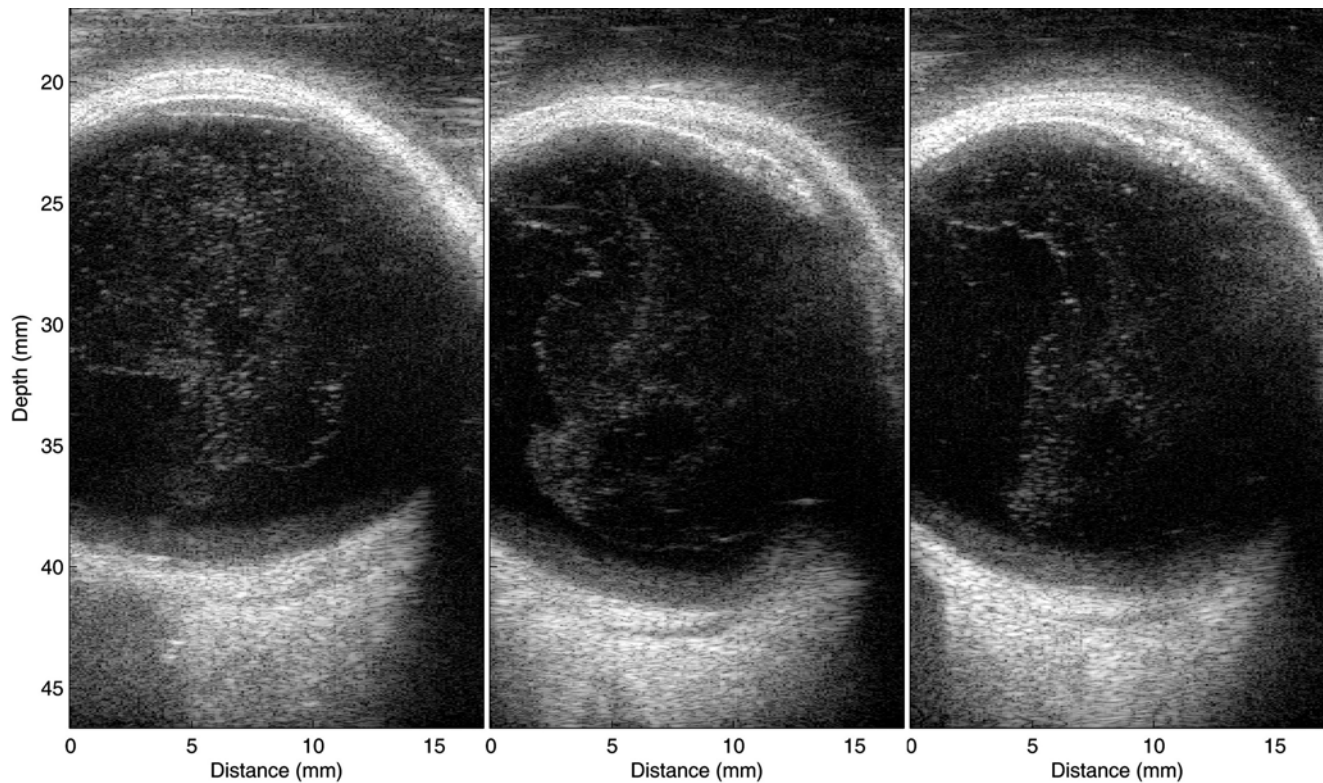


Figure II.F-21 Ultrasound images of the eye of a 59-year-old man 3 months after incomplete posterior vitreous detachment. The images were acquired in a supine immersion exam using a prototype 20 MHz annular array transducer with chirp pulse encoding. Synthetic focusing

provides an extended depth-of-field, while chirp excitation provides increased sensitivity, allowing visualization of faintly reflective vitreous inhomogeneities that were not detectable with conventional 10 MHz probes

energy for a longer time, exerting traction at points of residual retinal adhesion [75]. Figure II.F-22 demonstrates computer analysis of saccade-induced vitreous motion.

Recent studies have employed US to quantify vitreous echodensities in order to improve diagnostics and clinical decision-making. One application for quantitative ultrasound (QUS) is the evaluation of vitreous echodensity in patients complaining of floaters [see chapter V.B.8. Floaters and vision – current concepts and management paradigms]. Studies [76] have determined that floaters impact vision by lowering contrast sensitivity by 67 % in comparison to age-matched controls. In another study [77], patients suffering from floaters sufficiently severe to warrant vitrectomy surgery had 43 % lower contrast sensitivity than a control group of subjects with floaters who were not sufficiently bothered to need vitrectomy. In these subjects, the backscatter envelope in B-mode ultrasound data was quantified within different regions of the vitreous compartment. Echo amplitude, energy, and clustering were determined and correlated with contrast sensitivity. QUS parameters were found to be strongly correlated with contrast sensitivity, with backscatter

energy having a correlation coefficient of from 0.64 to 0.78 ($P < 0.0001$) for different parameters, suggesting that this approach provides a useful index of the structural abnormalities that underlie the functional deficits induced by floaters.

3. Magnetic Resonance Imaging Spectroscopy

MRI is based on interaction of hydrogen nuclei (protons) with a magnetic field and radio waves to produce radiologic images. To acquire an MRI image, the body is placed in a static magnetic field. A second transient field produced by a transmitter coil placed in proximity to the region under study flips the spin of protons into alignment. After this field is discontinued, nuclei return to spin equilibrium with the static field, inducing nuclear magnetic resonance signals in the receiver coil from which the MRI image is constructed. The amplitude of the MRI image relates to the spatial concentration and the relaxation time of specific nuclei. In the case of the eye, both the aqueous and vitreous have high water content and so will produce high contrast in relation to solid components such as the sclera in proton density or

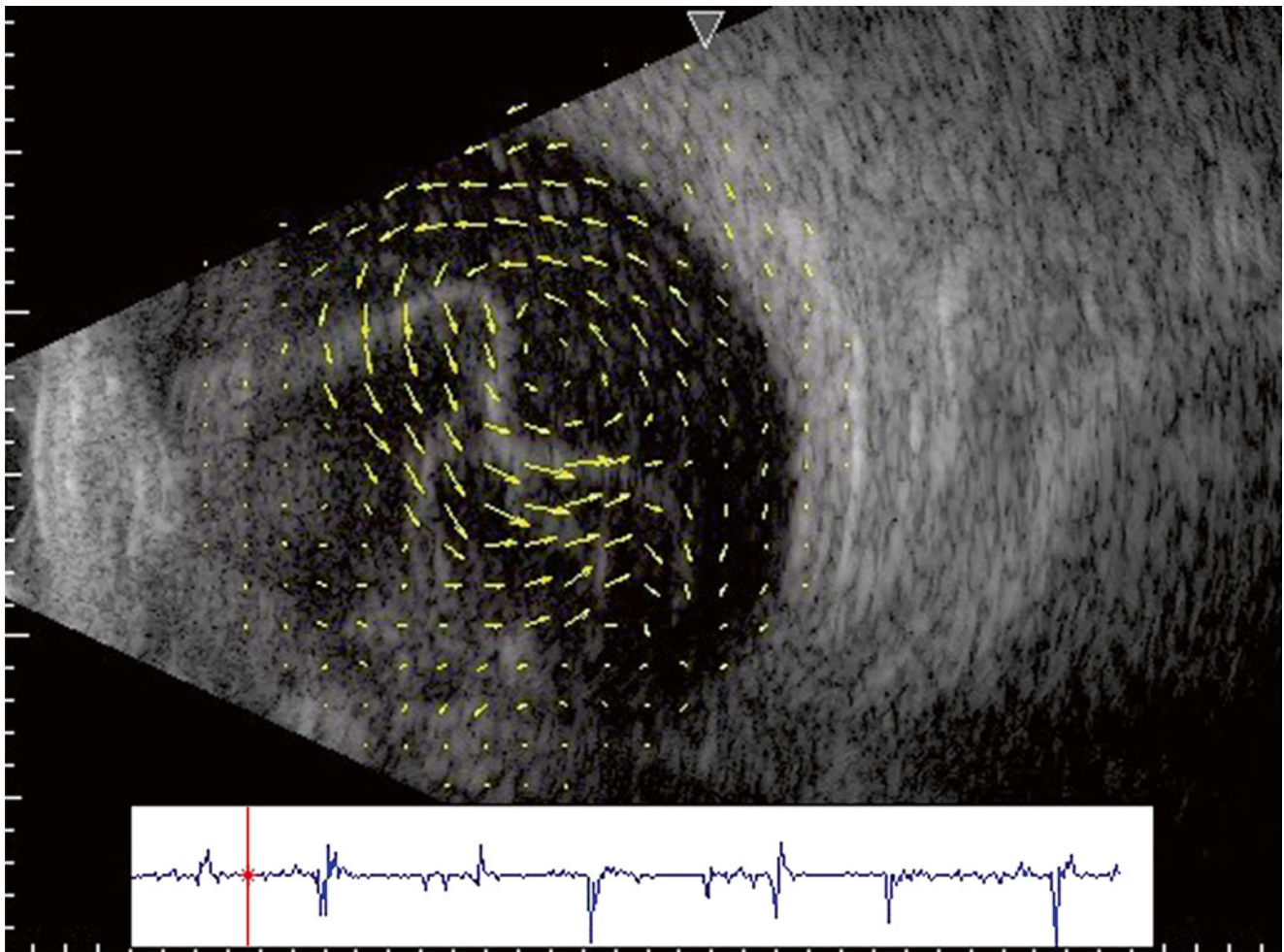


Figure II.F-22 Particle velocity image of a 64-year-old male suffering from vitreous hemorrhage with incomplete posterior vitreous detachment. The image is a single 20 MHz ultrasound frame from a real-time (20 frames/s) sequence obtained while the supine patient looked from side to side. The *yellow arrows* are velocity vectors whose length is proportional to linear velocity. The plot at the *bottom* represents overall kinetic energy over time course of the imaging sequence, with positive and negative values representing energy of saccadic movement to the

right and left, respectively. The *red line* indicates the temporal position of the displayed frame. Note the presence of a vortex of liquefied vitreous as the posterior vitreous cortex undergoes rapid motion in response to the saccade. It is also noteworthy that velocity inside the vitreous is higher than scleral velocity, signifying an amplification of energy due to the elastic properties of vitreous and to the tight vitreoretinal adherence at the vitreous base (Image courtesy of Giorgio Querzoli PhD and Tommaso Rossi MD)

relaxation-time-weighted images. Despite relatively lower resolution, MRI is advantageous compared to US and OCT because it is unaffected by absorption, scattering, refraction, or reflection of light or ultrasound by ocular tissue structures such as the cornea, sclera, iris, and lens [78].

When placed in a magnetic field, magnetic nuclei such as water protons tend to orient their magnetic vectors along the direction of the field. The time constant for this orientation, known as the longitudinal relaxation time T_1 , reflects the thermal interactions of protons with their molecular environment. Magnetic vectors that have previously been induced to be in phase with each other undergo a dephasing relaxation process that is measured by the transverse relaxation time T_2 . It is the transverse relaxation time T_2 that reflects inhomogeneities within the population of protons. Protons oriented by a magnetic field absorb radio waves of the appropriate frequency to induce transactions between their two orientations.

This absorption is the basis of the NMR signal used to index relaxation times. Relaxation times in biologic tissues vary with the concentration and mobility of water within the tissue. Because the latter is influenced by the interaction of water molecules with macromolecules in the tissue, this noninvasive measure can assess the gel-to-liquid transformation that occurs in vitreous during aging [79] and in disease states, such as diabetic vitreopathy [80]. These considerations led Aguayo et al. [81] to use NMR in studying the effects of pharmacologic vitreolysis [82] of bovine and human vitreous specimens and intact bovine eyes *in vitro*. Collagenase induced measurable vitreous liquefaction, more so than hyaluronidase. Thus, this noninvasive method could be used to evaluate age- and disease-induced synchysis (liquefaction) of the vitreous body, although it is not clear that this technique would adequately evaluate the vitreoretinal interface. There have, curiously, been few recent studies that

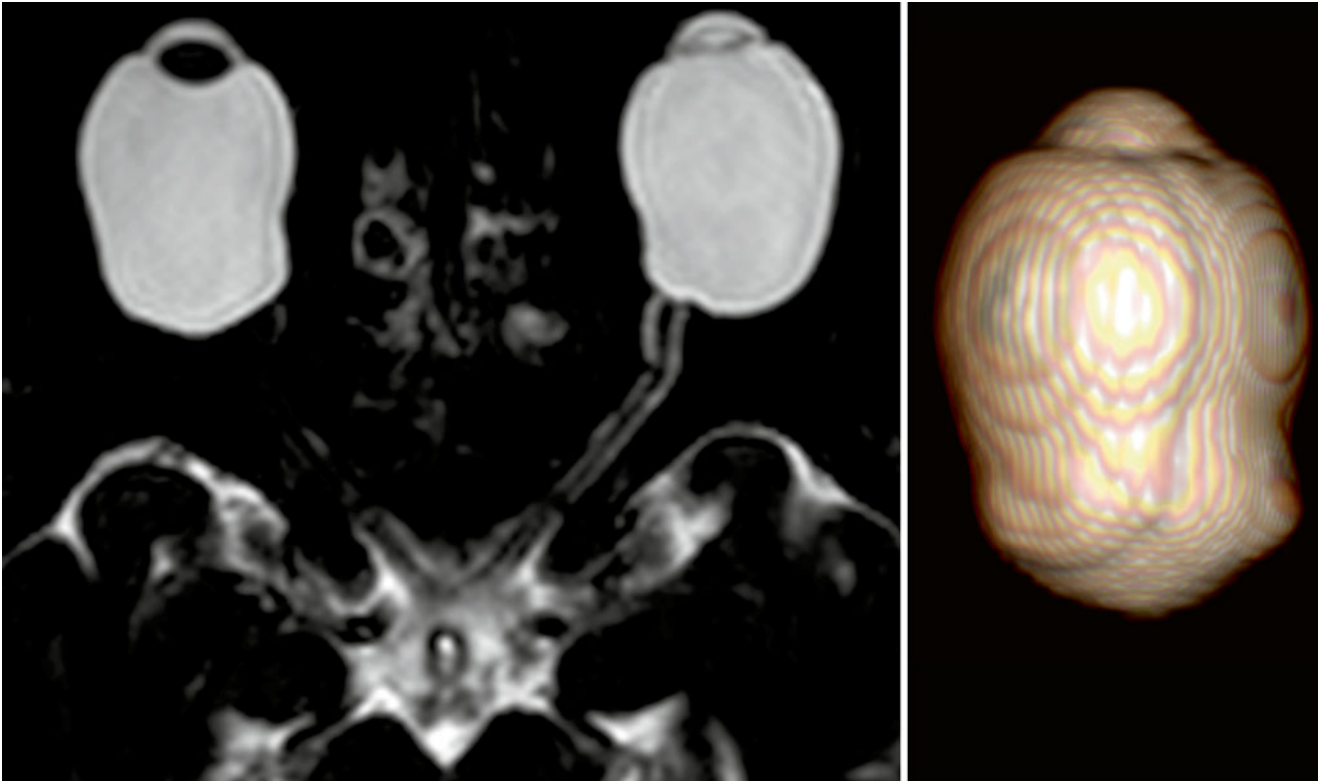


Figure II.F-23 Magnetic resonance imaging of human vitreous *in vivo*. Imaging staphyloma in highly myopic eyes can be problematic due to their aspherical and oftentimes asymmetric nature. MRI can take advantage of the hyperintense characteristic of the vitreous on T_2 -weighted imaging to create a 3D representation of the vitreous. We scanned a 59-year-old woman with -31 diopter spherical equivalent of myopia (axial length 37.0 mm right

eye, OD and 35.5 mm left eye, OS) with posterior polar staphyloma and widespread atrophy in both eyes. *Left*: Transverse scan using standard T_2 -weighted MRI scanning parameters demonstrating a hyperintense vitreous with relatively little intensity of the surrounding tissue. *Right*: Volumetric mold of the vitreous body created from the same MRI scan (Images courtesy of Quan V. Hoang, MD, PhD, Columbia University)

have used NMR spectroscopy in research or clinical applications on vitreous.

MRI can take advantage of the hyperintense characteristic of the vitreous on T_2 -weighted imaging to create a 3D model of the vitreous. In high myopia, such a model can depict the conformation of the pathologic sclera and staphyloma, as illustrated in Figure II.F-23. Because T_1 relaxation time decreases with increasing levels of paramagnetic O_2 , oxygen saturation can be determined from MRI images of the eye, as demonstrated by Berkowitz et al., who used T_1 -weighted MRI images to image and measure preretinal oxygen tension changes in response to breathing of room air versus pure oxygen [83]. Simpson et al. recently utilized this method to demonstrate changes in the distribution of oxygen saturation in the vitreous compartment following pars plana vitrectomy [84].

IV. Future Imaging Technologies

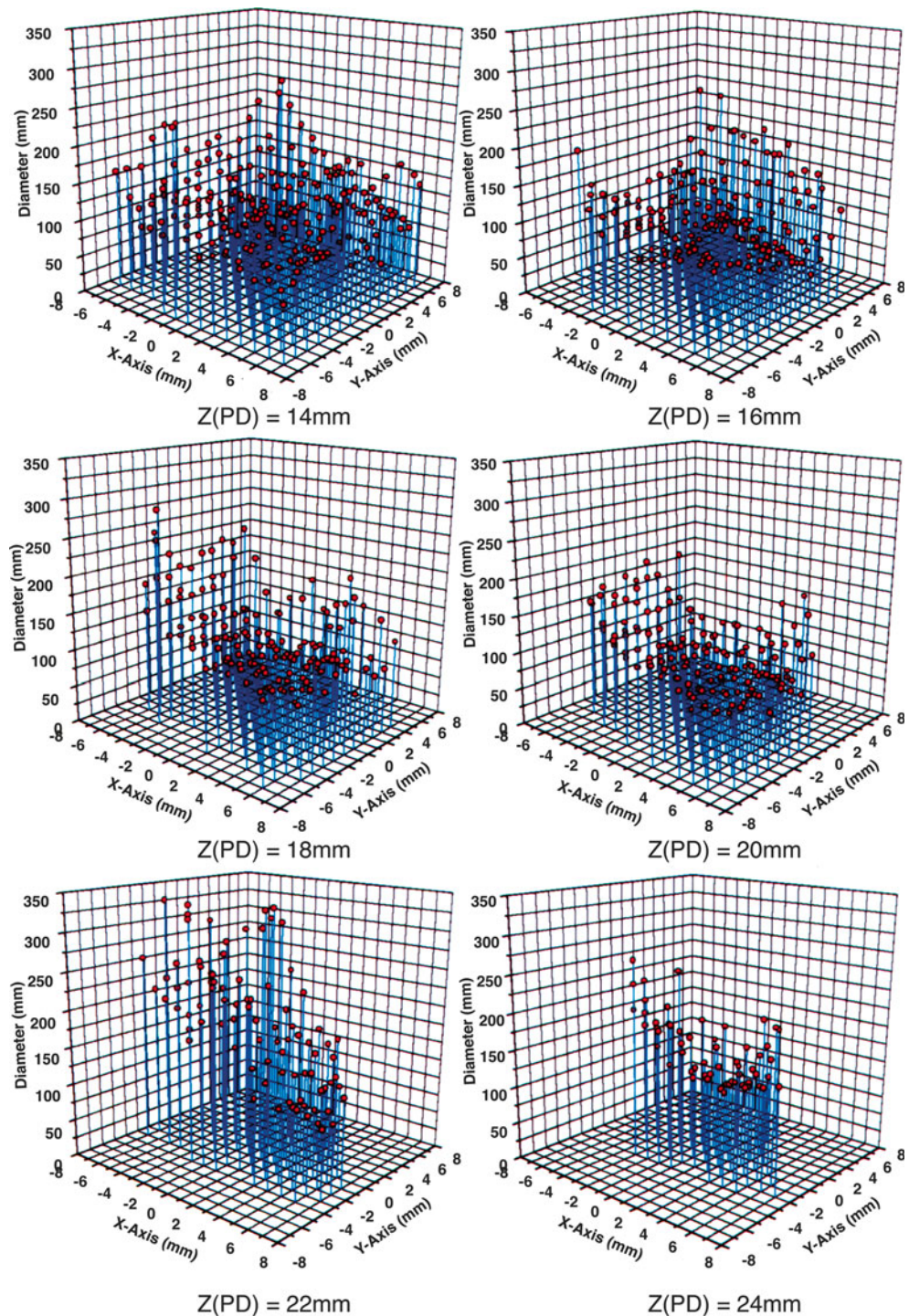
A. Raman Spectroscopy

This form of spectroscopy was first described in 1928 by C.V. Raman in India. Raman spectroscopy is an inelastic light-scattering technique wherein molecules in the study

specimen, in the vibrational mode, absorb energy from incident photons, causing a downward frequency shift, which is called the Raman shift. Because the signal is relatively weak, current techniques use laser-induced stimulation with gradual increases in the wavelength of the stimulating laser to detect the points at which the Raman signal becomes apparent as peaks superimposed on the broad background fluorescence. The wavelengths at which these peaks are elicited are characteristic of the chemical bonds, such as aliphatic C-H ($2,939\text{ cm}^{-1}$), water O-H ($3,350\text{ cm}^{-1}$), and C-C and C-H stretching vibrations in π -conjugated and aromatic molecules ($1,604$ and $3,057\text{ cm}^{-1}$). To date, most applications of this technique in the eye have been for analysis of lens structure and pathology. The use of near-infrared (IR) excitation wavelengths is particularly effective in the lens, because these wavelengths have better penetration through cataractous lenses.

Studies [85] of samples of excised human vitreous obtained during surgery used near-IR excitation at $1,064\text{ nm}$ provided by a diode-pumped neodymium:yttrium-aluminum-garnet (Nd:YAG) CW laser with a diameter of 0.1 mm and a power setting of 300 mW . Backscattering geometry with an optical lens collected scattered light that was passed through a Rayleigh light rejection filter into a spectrophotometer.

Figure II.F-24 Dynamic light-scattering analysis of vitreous structure *in vitro*. 3D plots of average particle size measurement obtained from bovine vitreous *in vitro* at various depths along the optical axis measured from the front surface of the lens. The plots from left to right *top row* to *bottom row* were obtained at depths of 14, 16, 18, 20, 22, and 24 mm, respectively (Courtesy of Jim King and Dr. Rafat Ansari, NASA Glenn Research Center, Cleveland, Ohio; Reprinted with permission from: Ansari et al. [86])



The results showed that this technique was able to detect peaks at 1,604 and 3,057 cm^{-1} in vitreous of diabetic patients that were not present in controls. Further research and development is needed to reliably interpret such results and refine the methodology for noninvasive use *in situ*. Although this has already been achieved in the lens, it is not clear that this will be possible for vitreous applications.

B. Dynamic Light Scattering

Dynamic light scattering (DLS) is an established laboratory technique to measure average size (or size distribution) of microscopic particles as small as 3 nm in diameter that are suspended in a fluid medium in which they undergo random Brownian motion. Light scattered by a laser beam passing

through such a dispersion will have intensity fluctuations in proportion to the Brownian motion of the particles. Because the size of the particles influences their Brownian motion, analysis of the scattered light intensity yields a distribution of the size (s) of the suspended particles. Visible light from a laser diode (power $50 \mu\text{W}$) is focused into a small scattering volume inside the specimen (excised lens or vitreous, autopsy or living eye). The detected signal is processed via a digital correlator to yield a time autocorrelation function (TCF). For dilute dispersions of spherical particles, the slope of the TCF provides a quick and accurate determination of the particle's translational diffusion coefficient, which can be related to its size via a Stokes-Einstein equation, provided that the viscosity of the suspending fluid, its temperature, and its refractive index are known. For the lens and vitreous, a viscosity of $\eta=0.8904$ centipoise, a refractive index of $n=1.333$, and a temperature of 25°C for *in vitro* studies and 37°C for *in vivo* studies were used to determine macromolecule sizes.

Studies [86–89] in the lens and vitreous have used DLS instrumentation that was developed by Dr. Rafat Ansari at the National Aeronautics and Space Administration (NASA) to conduct fluid physics experiments onboard the space shuttle and space station orbiters. The input beam from a semiconductor laser (670 nm wavelength) at $50 \mu\text{W}$ power was projected into the specimens, and the scattered signal was collected by the DLS probe for a duration of 10 s. The signal was then detected by an avalanche photodiode detector system. A TCF was constructed using a digital correlator card. The slope of the TCF provided a measure of particle sizes in the selected measurement sites (volume = $50 \mu\text{m}^3$). Studies [87] in the lens found that DLS was significantly more sensitive than the Scheimpflug photography in detecting early changes in the lens. When the DLS probe was used to obtain measurements from the entire vitreous body, scanning was performed in conjunction with a micropositioning assembly, which controlled detector position in the X, Y, and Z planes. This enabled semiautomated measurements from a sufficient number of sites within the bovine vitreous body to create a three-dimensional map of the distribution of the average particle sizes of vitreous macromolecules (Figure II.F-23). Furthermore, in studies [88] of autopsy human eyes, DLS was able to detect the structural changes [89] resulting from diabetic vitreopathy [90].

Recent studies have used DLS to evaluate the biophysical properties of vitreous in various circumstances. Following pharmacologic vitreolysis [82] with ocriplasmin, DLS was able to demonstrate a significant increase in the diffusion coefficient of porcine vitreous *in vitro* [91]. The use of DLS to study vitreous biophysical properties is increasing [92, 93], and the future will likely see this instrument in routine clinical use for the evaluation of the “invisible” vitreous (Figure II.F-24).

Abbreviations

A	Angle
AC	Anterior chamber
AMD	Age-related macular degeneration
C	Carbon
$^\circ\text{C}$	Degrees centigrade
CCD	Charge-coupled device
cm	Centimeter
CW	Continuous wave
D	Diopter
DLS	Dynamic light scattering
H	Hydrogen
I	Iris
IR	Infrared
L	Lens
MHz	MegaHertz
MRI	Magnetic resonance imaging
N	Nasal
Nd:YAG	Neodymium:yttrium-aluminum-garnet
nm	Nanometer
NMR	Nuclear magnetic resonance
O	Oxygen
OCT	Optical coherence tomography
PPVP	Posterior precortical vitreous pocket
PVD	Posterior vitreous detachment
QUS	Quantitative ultrasound
SD	Spectral domain
SLO	Scanning laser ophthalmoscope (y)
SS	Swept source
T	Temporal
TCF	Time correlation function
UBM	Ultrasound biomicroscopy
μm	Microns
μW	Microwatt
US	Ultrasound ultrasonography
VPA	Vitreo-papillary adhesion
3D	Three dimensional

References

1. Duke-Elder W. The nature of the vitreous body. *Br J Ophthalmol.* 1930;14:6.
2. Redslob E. *Le corps vitre.* Paris: Masson; 1932.
3. Eisner G. *Biomicroscopy of the peripheral fundus.* New York: Springer; 1973.
4. Worst J. Cisternal systems of the fully developed vitreous body in the young adult. *Trans Ophthalmol Soc U K.* 1977;97:550–4.
5. Sebag J, Balazs E. Morphology and ultrastructure of human vitreous fibers. *Invest Ophthalmol Vis Sci.* 1989;30:1867–71.
6. Kishi S, Shimizu K. Posterior precortical vitreous pocket. *Arch Ophthalmol.* 1990;108:979–82.
7. Sebag J. Letter to the editor. *Arch Ophthalmol.* 1991;190:1059.

8. Foulds W. Is your vitreous really necessary? The role of the vitreous in the eye with particular reference to retinal attachment, detachment and the mode of action of vitreous substitutes. *Eye*. 1987;1:641–64.
9. Sebag J. *The Vitreous: Structure, Function and Pathobiology*. New York: Springer; 1989.
10. Ayad S, Weiss J. A new look at vitreous humour collagen. *Biochem J*. 1984;218:835–40.
11. Rest MV. Type IX collagen. *Structure and Function of Collagen Types*. New York: Academic; 1987. p. 195–221.
12. Schmut O, Mallinger R, Paschke E. Studies on a distinct fraction of bovine vitreous body collagen. *Graefes Arch Clin Exp Ophthalmol*. 1984;221:286–9.
13. Eyre D, Apon S, Wu J, et al. Collagen type IX: Evidence for covalent linkages to type II collagen in cartilage. *Fed Eur Biochem Soc*. 1987;220:337–41.
14. Wright D, Mayne R. Vitreous humor of chicken contains two fibrillar systems: An analysis of their structure. *J Ultrastr Mol Struct Res*. 1988;100:224–34.
15. Stitt AW, Moore JE, Sharkey JA, et al. Advanced glycation end products in vitreous: Structural and functional implications for diabetic vitreopathy. *Invest Ophthalmol Vis Sci*. 1998;39(13):2517–23.
16. Sebag J. Classifying posterior vitreous detachment: A new way to look at the invisible. *Br J Ophthalmol*. 1997;81:521.
17. Packer A, Newsome D. Practical guidelines for posterior segment biomicroscopy. In: *Retinal Dystrophies and Degenerations*. New York: Raven; 1988. p. 1–4.
18. Jalkh A, Trempe C. Clinical methods of vitreous examination. In: *The Vitreous and Vitreoretinal Interface*. New York: Springer; 1987. p. 73–83.
19. Boruchoff S. Corneo-vitreous contact. *Trans Ophthalmol Soc U K*. 1975;95:417–21.
20. Jaffe N. *The Vitreous in Clinical Ophthalmology*. St Louis: Mosby; 1968.
21. Pruett R. Retinitis pigmentosa: Clinical observations and correlations. *Trans Am Ophthalmol Soc*. 1983;81:693–735.
22. Lacqua H, Machemer R. Clinical-pathologic correlation in massive preretinal proliferation. *Am J Ophthalmol*. 1975;80:913–29.
23. Awan K, Thurmayan M. Changes in the contralateral eye in uncomplicated persistent hyperplastic primary vitreous. *Am J Ophthalmol*. 1985;99:122–4.
24. Schepens C, Trempe C, Takahashi M. *Atlas of Vitreous Biomicroscopy*. Boston: Butterworth-Heinemann; 1999.
25. Newsome D, Linsemayer T, Trelstad R. Vitreous body collagen – evidence for a dual origin from the neural retina and hyalocytes. *J Cell Biol*. 1976;71:59–67.
26. El-Bayadi G. A new method of slit-lamp micro-ophthalmoscopy. *Br J Ophthalmol*. 1953;37:625–8.
27. Schepens C. *Methods of Examination in Retinal Detachment and Allied Diseases*. Philadelphia: WB Saunders; 1983.
28. Sebag J. *Vitreous pathobiology*. Clinical Ophthalmology. Philadelphia: JB Lippincott Co; 1992.
29. Buzney S, Welter J, Furukawa H, et al. Examination of the vitreous. A comparison of biomicroscopy using the Goldmann and El-Bayadi-Kajiura lenses. *Ophthalmology*. 1985;92(12):1745–8.
30. Kakehashi A, Akiba J, Trempe C. Vitreous photography with a +90 diopter double aspheric preset lens vs the El Bayadi-Kajiura preset lens. *Arch Ophthalmol*. 1991;109:962–5.
31. Jaffe N. Methods of examination of the vitreous and fundus. In: *The Vitreous in Clinical Ophthalmology*. St Louis: Mosby; 1968. p. 75–82.
32. Mainster M, Grossman J, Erickson P, et al. Retinal laser lenses: Magnification, spot size, and field of view. *Br J Ophthalmol*. 1990;74:177–9.
33. Mainster M, Timberlake G, Webb R, Hughes G. *Scanning laser ophthalmology. Clinical applications*. *Ophthalmology*. 1982;89:852–7.
34. Sebag J. Vitreous: The resplendent enigma. *Br J Ophthalmol*. 2009;93(8):989–91.
35. Sebag J, Gupta P, Rosen R, et al. Macular holes and macular pucker: The role of vitreoschisis as imaged by optical coherence tomography/scanning laser ophthalmology. *Trans Am Ophthalmol Soc*. 2007;105:121–31.
36. Sebag J, Wang M, Nguyen D, Sadun A. Vitreopapillary adhesion in macular diseases. *Trans Am Ophthalmol Soc*. 2009;107:35–44.
37. Huang D, Swanson E, Lin C, et al. Optical coherence tomography. *Science*. 1991;254(5035):1178–81.
38. Fercher AF, Hitzenberger CK, Drexler W, et al. In vivo optical coherence tomography. *Am J Ophthalmol*. 1993;116:113–4.
39. Swanson EA, Izatt JA, Hee MR, et al. In vivo retinal imaging by optical coherence tomography. *Opt Lett*. 1993;18:1864–6.
40. Izatt JA, Hee MR, Owen GM, Swanson EA, Fujimoto JG. Optical coherence microscopy in scattering media. *Opt Lett*. 1994;19:590–2.
41. Hee MR, Izatt JA, Swanson EA, et al. Optical coherence tomography of the human retina. *Arch Ophthalmol*. 1995;113:325–32.
42. Schuman JS, Hee MR, Puliafito CA, et al. Quantification of nerve fiber layer thickness in normal and glaucomatous eyes using optical coherence tomography. *Arch Ophthalmol*. 1995;113:586–96.
43. Izatt JA, Hee MR, Swanson EA, et al. Micrometer-scale resolution imaging of the anterior eye in vivo with optical coherence tomography. *Arch Ophthalmol*. 1994;11:1584–9.
44. Fercher AF, Hitzenberger CK, Kamp G, El-Zaiat SY. Measurement of intraocular distances by backscattering spectral interferometry. *Optics Commun*. 1995;117:43–8.
45. Wojtkowski M, Leitgeb R, Kowalczyk A, Bajraszewski T, Fercher AF. In vivo human retinal imaging by Fourier domain optical coherence tomography. *J Biomed Opt*. 2002;7(3):457–63.
46. Chinn SR, Swanson EA, Fujimoto JG. Optical coherence tomography using a frequency-tunable optical source. *Opt Lett*. 1997;22(5):340–2.
47. Potsaid B, Baumann B, Huang D, et al. Ultrahigh speed 1050 nm swept source/Fourier domain OCT retinal and anterior segment imaging at 100,000 to 400,000 axial scans per second. *Opt Expr*. 2010;8(19):20029–48.
48. Lim H, Mujat M, Kerbage C, et al. High speed imaging of human retina *in vivo* with swept-source optical coherence tomography. *Opt Expr*. 2006;14(26):12902–8.
49. Srinivasan VJ, Adler DC, Chen Y, et al. Ultrahigh-speed optical coherence tomography for three-dimensional and en face imaging of the retina and optic nerve head. *Invest Ophthalmol Vis Sci*. 2008;49(11):5103–10.
50. Itakura H, Kishi S, Li D, Akiyama H. Observation of posterior precortical vitreous pocket using swept source optical coherence tomography. *Invest Ophthalmol Vis Sci*. 2013;54:3102–7.
51. Kishi S, Shimizu K. Posterior precortical vitreous pocket. *Arch Ophthalmol*. 1990;108(7):979–82.
52. Itakura H, Kishi S. Aging changes of vitreomacular interface. *Retina*. 2011;31:1400–4.
53. Grulkowski I, Liu JJ, Zhang JY. Reproducibility of a long-range swept-source optical coherence tomography ocular biometry system and comparison with clinical biometers. *Ophthalmology*. 2013;120:2184–90.
54. Gupta P, Sadun A, Sebag J. Multifocal retinal contraction in macular pucker analyzed by combined optical coherence tomography/scanning laser ophthalmoscopy. *Retina*. 2008;28:447–52.
55. Krebs I, Brannath W, Glittenberg C, et al. Posterior vitreomacular adhesion: A potential risk factor for exudative age-related macular degeneration? *Am J Ophthalmol*. 2007;144:741–6.

56. Robison C, Krebs I, Binder S, et al. Vitreo-macular adhesion in active and end-stage age-related macular degeneration. *Am J Ophthalmol*. 2009;148:79–82.
57. Sebag J. Vitreoschisis. *Graefes Arch Clin Exp Ophthalmol*. 2008;246:329–32.
58. Wang M, Nguyen D, Hindoyan N, et al. Vitreo-papillary adhesion in macular hole and macular pucker. *Retina*. 2009;29:644–50.
59. Charles S. *Vitreous Microsurgery*. Baltimore: Williams & Wilkins; 1981.
60. Mundt G, Hughes W. Ultrasonics in ocular diagnostics. *Am J Ophthalmol*. 1956;41:488–98.
61. Baum G, Greenwood I. The application of ultrasonic locating techniques to ophthalmology, Part I: Reflective properties. *Am J Ophthalmol*. 1958;46:319–29.
62. Coleman D, Carlin B. A new system for visual axis measurements in the human eye using ultrasound. *Arch Ophthalmol*. 1967;77:124–7.
63. Coleman D, Konig W, Katz L. A hand-operated ultrasound scan system for ophthalmic evaluation. *Am J Ophthalmol*. 1969;68:256–63.
64. Bronson NR, Turner FT. A simple B-scan ultrasonoscope. *Arch Ophthalmol*. 1973;90:237–8.
65. Pavlin C, Sherar M, Foster F. Subsurface ultrasound microscopic imaging of the intact eye. *Ophthalmology*. 1990;97:244–50.
66. Ketterling J, Lizzi F, Aristizabal O, Turnbull D. Design and fabrication of a 40-MHz annular array transducer. *IEEE Trans Ultrason Ferroelectr Freq Control*. 2005;52(4):672–81.
67. Silverman R, Ketterling J, Coleman D. High-frequency ultrasonic imaging of the anterior segment using an annular array transducer. *Ophthalmology*. 2007;114(4):816–22.
68. Silverman R, Ketterling J, Mamou J, Coleman D. Improved high-resolution ultrasonic imaging of the eye. *Arch Ophthalmol*. 2008;126(1):94–7.
69. Ketterling J, Filoux E. Synthetic-focusing strategies for real-time annular-array imaging. *IEEE Trans Ultrason Ferroelectr Freq Control*. 2012;59(8):1830–9.
70. Mamou J, Ketterling J, Silverman R. Chirp-coded excitation with a high-frequency ultrasound annular array. *IEEE Trans Ultrason Ferroelectr Freq Control*. 2008;55(2):508–13.
71. Silverman R, Ketterling J, Mamou J, Lloyd H, Filoux E, Coleman D. Pulse-encoded ultrasound imaging of the vitreous with an annular array. *Ophthalmic Surg Lasers Imag*. 2012;43(1):82–6.
72. Oksala A. Ultrasonic findings in the vitreous body at various ages. *Graefes Arch Clin Exp Ophthalmol*. 1978;207:275–80.
73. Chu T, Lopez P, Cano M, et al. Posterior vitreoschisis. An echographic finding in proliferative diabetic retinopathy. *Ophthalmology*. 1996;103:315–22.
74. Sebag J, Buckingham B, Charles M, Reiser K. Biochemical abnormalities in vitreous of humans with proliferative diabetic retinopathy. *Arch Ophthalmol*. 1992;110:1472–6.
75. Rossi T, Querzoli G, Pasqualitto G, et al. Ultrasound imaging velocimetry of the human vitreous. *Exp Eye Res*. 2012;99:98–104.
76. Sebag J, Yee K, Huang L, Wa C, Sadun A. Vitrectomy for floaters – prospective efficacy analyses and retrospective safety profile. *Retina*. 2014;34(6):1062–8.
77. Mamou J, Yee KMP, Wa CA. Quantitative ultrasonography of vitreous correlates with contrast sensitivity in patients with floaters. *Invest Ophthalmol Vis Sci*. Submitted for publication.
78. Fanea L, Fanan A. Review: Magnetic resonance imaging techniques in ophthalmology. *Molec Vis*. 2012;18:2538–60.
79. Sebag J. Age-related changes in human vitreous structure. *Graefes Arch Clin Exp Ophthalmol*. 1987;225:89–93.
80. Sebag J. Ageing of the vitreous. *Eye*. 1987;1:254–62.
81. Aguayo J, Glaser B, Mildyan A, et al. Study of vitreous liquefaction by NMR spectroscopy and imaging. *Invest Ophthalmol Vis Sci*. 1985;26:692–7.
82. Sebag J. Pharmacologic vitreolysis. *Retina*. 1998;18:1–3.
83. Berkowitz BA, McDonald C, Ito Y, et al. Measuring the human retinal oxygenation response to a hyperoxic challenge using MRI: eliminating blinking artifacts and demonstrating proof of concept. *Magn Reson Med*. 2001;46:412–6.
84. Simpson AR, Dowell NG, Jackson TL, Tofts PS, Hughes EH. Measuring the effect of pars plana vitrectomy on vitreous oxygenation using magnetic resonance imaging. *Invest Ophthalmol Vis Sci*. 2013;54(3):2028–34.
85. Sebag J, Nie S, Reiser K, et al. Raman spectroscopy of human vitreous in proliferative diabetic retinopathy. *Invest Ophthalmol Vis Sci*. 1994;35:2976–80.
86. Ansari R, Dunker S, Suh K, et al. Quantitative molecular characterization of bovine vitreous and lens with non-invasive dynamic light scattering. *Exp Eye Res*. 2001;73:859–66.
87. Datiles MB 3rd, Ansari RR, Suh KI, Vitale S, Reed GF, Zigler JS Jr, Ferris FL 3rd. Clinical detection of precataractous lens protein changes using dynamic light scattering. *Arch Ophthalmol*. 2008;126(12):1687–93.
88. Sebag J, Ansari R, Dunker S, Suh K. Dynamic light scattering of diabetic vitreopathy. *Diabetes Technol Ther*. 1999;1:169–76.
89. Sebag J. Abnormalities of human vitreous structure in diabetes. *Graefes Arch Clin Exp Ophthalmol*. 1993;231:257–60.
90. Sebag J. Diabetic vitreopathy. *Ophthalmology*. 1996;103:205–6.
91. Sebag J, Ansari R, Suh K. Pharmacologic vitreolysis with microplasmin increases vitreous diffusion coefficients. *Graefes Arch Clin Exp Ophthalmol*. 2007;245:576–80.
92. Matsuura T, Hara Y, Taketani F, et al. Volume phase transition of bovine vitreous body in vitro and determination of its dynamics. *Biomacromolecules*. 2004;5:1296–302.
93. Annaka M, Okamoto M, Matsuura T, et al. Dynamic light scattering study of salt effect on phase behavior of pig vitreous body and its microscopic implication. *J Phys Chem B*. 2007;111:8411–8.
94. Sebag J, Balazs EA. Pathogenesis of cystoid macular edema: Anatomic consideration of vitreoretinal adhesions. *Surv Ophthalmol*. 1984;28(Suppl):493.
95. Eisner G. Zur anatomie des glaskorpers. *Alb v Graefes Arch Klin Exp Ophthalmol*. 1975;93:33–56.

Part III

Pathology/Pathobiology

J. Sebag

Ronald Paul Hobbs and Mary Elizabeth Hartnett

Outline

- I. **Introduction**
- II. **Retinopathy of Prematurity**
 - A. Classification
 - B. Pathophysiology
 - 1. Mechanism of Retinal Detachment
 - C. Risk Factors
 - D. Prevention
 - 1. Screening
 - E. Treatment
 - 1. Cryotherapy
 - 2. Laser Photocoagulation
 - 3. Pharmacotherapy
 - a. Bevacizumab
 - b. Pharmacologic Vitreolysis
 - 4. Treatment of Retinal Detachment
- III. **Persistent Fetal Vasculature**
 - A. Anterior Persistent Fetal Vasculature
 - 1. Persistent Pupillary Membrane
 - 2. Iridohyaloid Blood Vessels
 - 3. Mittendorf's Dot
 - 4. Muscae Volitantes
 - 5. Retrolental Membrane
 - B. Posterior Persistent Fetal Vasculature
 - 1. Bergmeister's Papilla
 - 2. Persistent Hyaloid Artery
 - 3. Congenital Nonattachment of the Retina and Retinal Detachment
 - 4. Globe Malformations
 - 5. Macular Abnormalities
 - 6. Optic Nerve Head Abnormalities
 - C. Genetics
 - D. Treatment of Persistent Fetal Vasculature

IV. Familial Exudative Vitreoretinopathy

- A. Clinical Presentation
- B. Clinical Classification
- C. Genetics
 - 1. Ancillary Testing
 - 2. Systemic Associations
- D. Treatment
 - 1. FEVR Treatment Outcomes

References

Keywords

Retinopathy of prematurity (ROP) • Neovascularization • Angiogenesis • Vasculogenesis • Bevacizumab • Pharmacologic vitreolysis • Persistent fetal vasculature (PFV) • Hyaloid vessels • Familial exudative vitreoretinopathy (FEVR) • Retinal detachment

Key Concepts

1. Retinopathy of prematurity (ROP) continues to cause serious problems in developed countries and has seen a recent dramatic increase in developing countries. Our improved understanding of its pathogenesis has led to a useful classification system of ROP and reasonably effective therapies being utilized today with potential new therapies on the horizon.
2. Persistent fetal vasculature results from failure(s) of regression of the fetal vitreous circulations including the vasa hyaloidea propria. Resulting pathologies have variable clinical presentations, genetic associations, and treatment options.
3. Familial exudative vitreoretinopathy was first described in 1969 and since been identified to have tremendous variability in the clinical presentation, course, and even inheritance patterns. When severe, FEVR can be a lifelong retinal vascular disease with variable periods of quiescence.

R.P. Hobbs, MD
Vitreoretinal Fellow, University of Utah, John A Moran Eye Center, 65 Mario Capecchi Drive, Salt Lake City, UT 84132, USA
e-mail: ronald.hobbs@hsc.utah.edu

M.E. Hartnett, MD (✉)
Director of Pediatric Retina, Vitreoretinal Service and Surgery, Retinal Angiogenesis Laboratory, University of Utah, John A. Moran Eye Center, 65 Mario Capecchi Drive, Salt Lake City, UT 84132, USA
e-mail: me.hartnett@hsc.utah.edu

I. Introduction

Congenital vitreoretinopathies manifest in the pediatric or adult population in a variety of ways and cause varying levels of vision loss. These conditions can also be influenced by environmental factors, as in retinopathy of prematurity (ROP), or be associated with inheritance involving autosomal dominant, autosomal recessive, or X-linked patterns or be sporadic, as with familial exudative vitreoretinopathy (FEVR). As more is learned regarding gene associations, it is anticipated that complex genetic interactions may also play a role in the pathophysiology. Given the rarity of the diseases and their variable manifestations, along with the difficulty of obtaining longitudinal clinical information in the pediatric population, correct diagnosis and treatment can be quite challenging.

The goal of this chapter is to describe the presentations and classifications of ROP, persistent fetal vasculature (PFV), and FEVR that will be helpful to the caregiver to identify these diseases. In order to accomplish this goal, ancillary tests that are helpful in distinguishing different vitreoretinopathies will also be reviewed. In addition, up-to-date treatment options will be discussed. A history of past treatment options and studies that have led to current treatment recommendations for ROP will be included. Whereas fewer analogous studies exist for PFV and FEVR, the current literature and treatment recommendations will also be reviewed. Finally, the expanding knowledge of the genetic components of these diseases will be reviewed as well as systemic associations.

II. Retinopathy of Prematurity

Retinopathy of prematurity (ROP) was first described by Terry in 1942 as the most advanced stage, stage 5 ROP, then described as retrolental fibroplasia. ROP involves aberrant developmental angiogenesis in preterm infants associated with first a delay in physiologic retinal vascular development and later vasoproliferation into the vitreous, which can lead to complete retinal detachment and blindness. In the United States alone, it is estimated that 14,000–16,000 infants are affected by some degree of ROP annually with 1,100–1,500 requiring treatment and 400–600 becoming legally blind [1].

Studies by Patz [2] in 1952 and Kinsey [3] in 1956 demonstrated a link between high oxygen concentrations at birth and the development of ROP. A 40 % limit of oxygen delivered was recommended and was associated with decreased blindness from ROP. However, the reduction in oxygen delivered to the preterm infant was associated with increased mortality and a greater prevalence of cerebral palsy among survivors [4]. Today it is understood that low birth weight and young gestational age are highly associated with increased risk of developing ROP [5]. However, ROP remains the second most common cause of childhood blindness in the United States and other developed countries, next to cortical

blindness [6]. More recent data from middle-income and low-income countries have shown an explosive increase in severe ROP worldwide. Indeed, it is thought that two-thirds of the 50,000 children who are blind from ROP worldwide live in Latin America [5]. This is largely believed to be due to increased survival in premature babies; however, oxygen regulation, screening programs, prenatal care, and therapies may be limited due to reduced financial and personnel resources. This section will review current classifications of ROP, our changing understanding of its pathogenesis, and current and potential therapies utilized in its treatment.

A. Classification

The International Classification of Retinopathy of Prematurity (ICROP) provides standards for documenting the extent and severity of ROP. Four parameters are used: zone, stage, extent of stage, and presence or absence of plus disease. Since physiologic retinal vascular development proceeds peripherally to the ora serrata from the optic nerve, the optic nerve is considered the center of the diagram that divides the retina into zones. The zone is indicated as the highest zone into which vascularization in any clock hour occurs.

- *Zone I* corresponds to a circle, the center of which is the optic disk, with a radius of twice the distance from the optic disk to the center of the fovea.
- *Zone II* forms a circle peripheral to zone I with a radius from the optic nerve to the nasal ora serrata.
- *Zone III* is made up of the remaining temporal crescent of retina outside zones I and II.

The vascular stages of ROP (stages 1–3) are defined according to the appearance of the junction between vascularized and avascular retina. Staging is based on the most severe stage present in any location within the eye.

- *Stage 1* is characterized by a flat white line that separates vascularized from avascular retina.
- *Stage 2* is a ridge with volume in the region between the vascularized and avascular retina. Small tufts of new vessels may be seen in the vascularized retina posterior to the ridge (Figure III.A-1).
- *Stage 3* is characterized by neovascularization growing along the ridge and into the vitreous and may cause vitreous hemorrhage (Figure III.A-2).
- In *stage 4*, with advancing fibrovascular proliferation, traction is exerted on the retina, and progressive stage 4 ROP develops with a partial retinal detachment as a result. Stage 4 ROP is divided into stages 4A and 4B. In 4A, the detachment does not involve the macula, whereas in 4B, it does (Figure III.A-3).
- *Stage 5* denotes a total retinal detachment, sometimes with a peripheral attached trough anteriorly. These are almost always funnel shaped and further classified as “open” or “closed” anteriorly or posteriorly depending on the shape of the funnel.

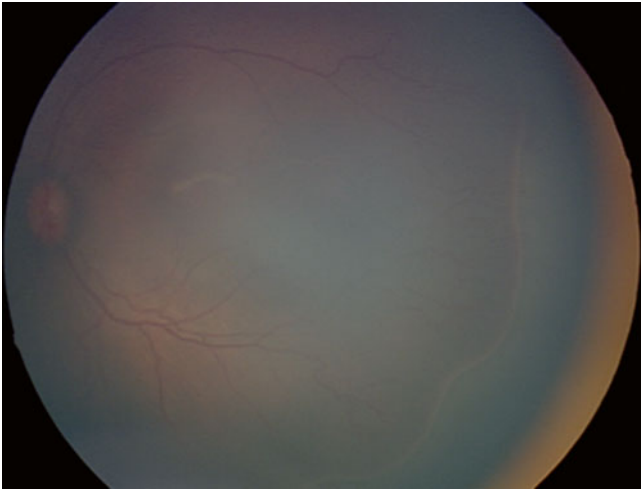


Figure III.A-1 Left eye of premature infant demonstrating Stage 2 ROP (RetCam image, Clarity)

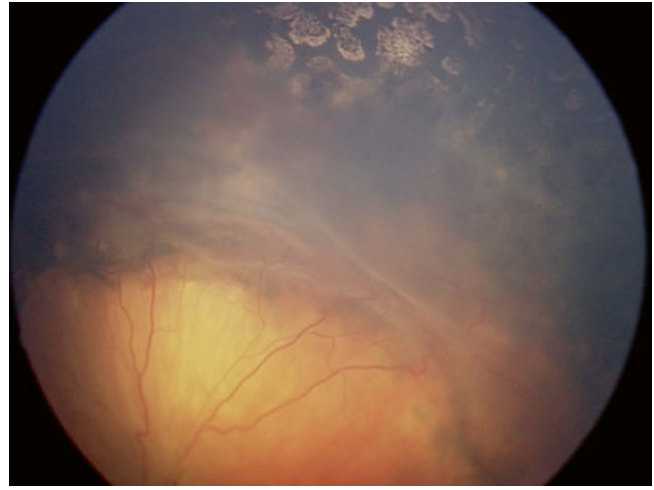


Figure III.A-3 Left eye of premature infant with stage 4A ROP demonstrating peripheral retinal detachment not involving the macula. Note the previous laser therapy to the surrounding avascular retina (RetCam image, Clarity)

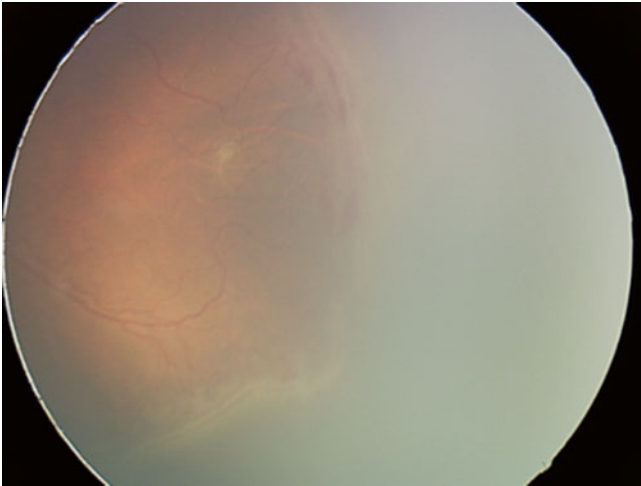


Figure III.A-2 Left eye of a premature infant with stage 3 ROP with small hemorrhages and prominent neovascular vessels along the ridge (RetCam image, Clarity)

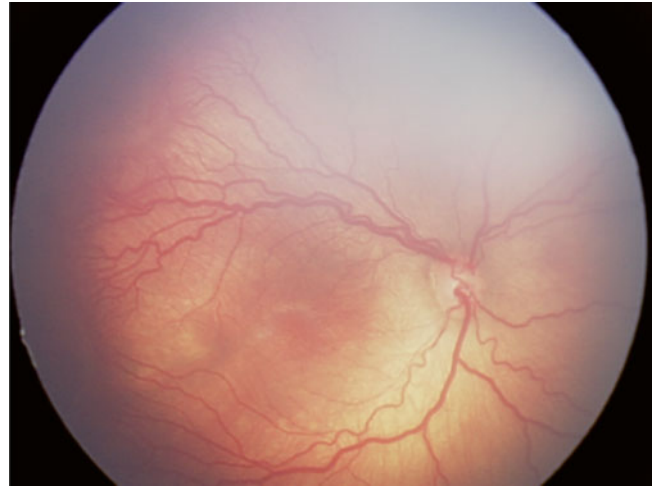


Figure III.A-4 Infant with ROP demonstrating plus disease (RetCam image, Clarity)

Plus disease refers to dilation and tortuosity of the retinal arterioles and veins and is defined by a standard photograph published in the CRYO-ROP study [6] (Figure III.A-4). Recently, “pre-plus disease” and “aggressive posterior ROP” (APROP) were added as categories. Pre-plus disease is defined as abnormal dilation and tortuosity of the posterior pole arterioles and veins that are insufficient for the diagnosis of plus disease. APROP is a severe plus disease in posterior zone II or zone I, which behaves in an aggressive manner with rapid progression often not adhering to the progression of stage of severity and with a higher likelihood of complete retinal detachment.

“*Threshold ROP*” was defined in the Cryotherapy for Retinopathy of Prematurity (CRYO-ROP) study as 5

contiguous clock hours or 8 total clock hours of stage 3 ROP and plus disease in zone I or zone II. A “prethreshold ROP” classification defined eyes at risk of developing threshold ROP and was further subdivided into high-risk (type 1) and low-risk (type 2) prethreshold disease in the Early Treatment for Retinopathy of Prematurity (ETROP) study. High-risk (type I) eyes were estimated to have a $\geq 15\%$ chance of an unfavorable outcome, whereas low-risk (type II) eyes had $< 15\%$ chance.

Type 1 ROP – (high-risk) prethreshold ROP – was defined as:

- Zone I, any stage with plus disease
- Zone I, stage 3 with or without plus disease
- Zone II, stage 2 or 3 with plus disease

Type 2 ROP – (low-risk) prethreshold ROP – was defined as:

- Zone I, stage 1 or 2 without plus disease
- Zone II, stage 3 without plus disease

Results from the ETROP study recommended peripheral laser ablation to the entire avascular retina for type 1 ROP and weekly or twice weekly observation of type 2 ROP. Early treatment of infants resulted in fewer unfavorable structural outcomes and significantly reduced unfavorable visual acuity at 6 years' follow-up compared with conventional treatment [7, 8].

B. Pathophysiology

In utero, retinal development takes place in a relatively hypoxic environment with an arterial oxygen level (PaO₂) of approximately 30 mmHg and a saturation level of approximately 70 % [9]. This physiologic hypoxia is believed to induce growth factors that promote blood vessel development [10]. The hyaloid artery is the first vessel within the eye, appearing at approximately 6 weeks' gestation. The retina begins undergoing vascularization at approximately 16 weeks' gestation with vessels extending from the posterior pole toward the ora serrata and completes its extent by 40 weeks or term birth [11]. Initially, the retinal vascularization is believed to occur by vasculogenesis from endothelial precursor cells or angioblasts that arise from the deeper layers of the retina [12]. Angioblasts cover the posterior pole of the retina through at least 22 weeks' gestation. Following that, less is known about what happens in humans and, therefore, studies are based on other species. Retinal vascularization is believed to progress by angiogenesis, i.e., proliferation of endothelial cells from existing blood vessels that then migrate toward a gradient of vascular endothelial growth factor (VEGF) [13]. Other cells and growth factors, such as insulin-like growth factor-1 (IGF-1) and erythropoietin, can interact with VEGF and play a role [13–15].

From human observation and animal studies, ROP has been characterized as having two phases. In the first phase, a delay in physiologic retinal vascular development occurs. Premature infants have retinas that are not yet fully vascularized, and, therefore, there are areas of peripheral avascular retina when a preterm infant is born. The premature infant experiences fluctuations in blood oxygen levels that likely alter the oxygen status of the retinal tissue and the concentration of hypoxia-inducible factor-regulated growth factors, including vascular endothelial growth factor (VEGF). In addition, other angiostatic factors, such as pigment epithelium-derived factor, are upregulated during hyperoxia and downregulated during hypoxia. Oxygen fluctuations increase the expression of VEGF and also trigger signaling pathways related to reactive oxygen species

from oxidative signaling that slows vascular development [16–18]. As the infant matures, supplementation of oxygen is reduced and the hyaloid vasculature regresses, contributing to hypoxia in the avascular retina. VEGF signaling through VEGF receptor 2 (KDR or Flk-1) increases and affects downstream pathways to delay physiologic retinal vascular development [19] and cause disordered growth of vessels into the vitreous rather than into the retina during the second phase of ROP at around 32–37 weeks' gestation. The abnormal vessels and later fibrovascular scarring can place traction on the retina and thus cause subsequent retinal detachment.

1. Mechanism of Retinal Detachment

Retinal detachments associated with ROP are divided into stages 4A, 4B, and 5. Others use the terms “predominantly effusive” or “predominantly tractional” to further classify these detachments [20]. The retina in a *predominantly effusive* detachment is convex toward the lens with fluid extending posterior to the ridge and toward the macula. This detachment is believed to result as vascular structures leak fluid into the subretinal space. It is seen less frequently after laser treatment than following cryotherapy. In a *predominantly tractional* detachment, peaked retinal folds pull the retina toward the center of the eye. Often, a central stalk and spokes of traction extend posteriorly when associated with regression of posterior hyaloid vessels and extend anteriorly when predominantly associated with delayed regression of the tunica vasculosa lentis. Both components can be seen (Figure III.A-5). Additionally, excessive growth factors in the eyes with ROP are associated with upregulation of hyaluronan and disproportionately liquefied vitreous that then provides reduced internal tamponade allowing the retina to be pushed (*effusive*) or pulled (*tractional*) away from the underlying choroid. A retrospective analysis by Hartnett et al. [21] reported that ridge elevation, recurrent or persistent plus disease, or vitreous haze and the appearance of vitreous organization in front of the lens in eyes treated for threshold ROP predicted progressive stage 4 ROP. In addition, Coats reported that vitreous organization and vitreous hemorrhage were associated with progressive stage 4 ROP [22].

Vitreous liquefaction is often unidentified [23] in stages 1 and 2 ROP and likely occurs as a result of both reactive oxygen species [24] and inadequate synthesis by the underlying peripheral retina where immature Müller cells do not support typical gel vitreous synthesis and may account for the vitreous trough apparent during surgery for stage 4 ROP. The disrupted molecular composition may limit the inherent vitreous ability to inhibit cell invasion [25–27], thereby permitting neovascularization in stage 3 ROP to grow [28, 29] between posterior gel and peripheral liquid vitreous anteriorly [29] (Figure III.A-6). Instability at the interface between gel and

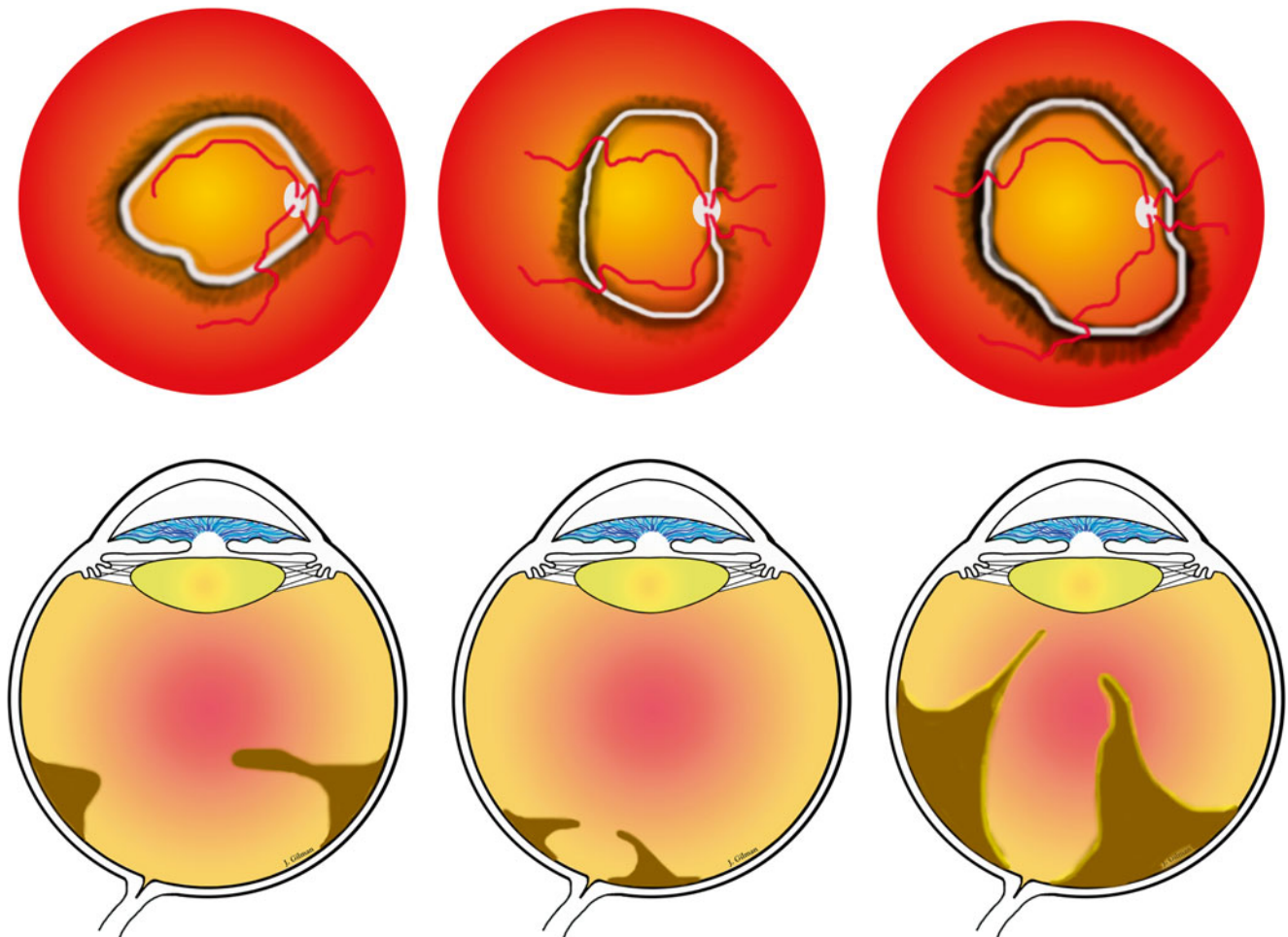


Figure III.A-5 Artist's rendition of a traction retinal detachment due to retinopathy of prematurity. *Left:* Asymmetrical traction associated with posterior elements of hyaloid vasculature. *Center:* Symmetrical traction

of the posterior hyaloid vasculature. *Right:* Traction secondary to anterior hyaloid, i.e., tunica vasculosa lentis. *Top row* corresponds with view through indirect ophthalmoscopy (adapted from [20])

liquid vitreous causes localized collapse of the peripheral vitreous at the ridge exerting traction on the underlying ridge, contributing to tractional retinal detachment.

C. Risk Factors

Prior to the ability to regulate oxygen to preterm infants, high oxygen at birth was recognized as a cause of ROP [2]. Now, other oxygen conditions including fluctuations in oxygenation [30], hypoxia, hyperoxia (see below), and other stresses have been associated with ROP. The most important risk factors for developing ROP are young gestational age and low birth weight. However, more than 50 separate risk factors have been identified. Multivariate analyses demonstrate that low birth weight, young gestational age, poor postnatal weight gain, low IGF-1 levels, hyperglycemia, artificial ventilation more than 7 days, need for blood transfusions, surfactant therapy, and systemic infections are all independently associated with higher rates of ROP [31].

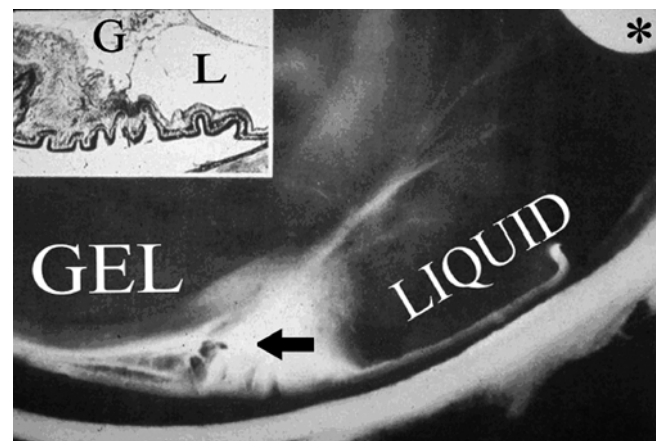


Figure III.A-6 Photomicrograph of the peripheral fundus in retinopathy of prematurity. The lens (*) is in the upper right-hand corner. Below, a fibrovascular membrane is present at the interface between the posterior gel vitreous and the peripheral liquid vitreous. Ridge elevation is seen (arrow). The inset (upper left) shows the histopathology that clearly distinguishes between gel (G) and liquid (L) vitreous (Courtesy of Maurice Landers, MD; reprinted with permission from: Sebag and Nguyen [132])

D. Prevention

Many interventions have been studied in an effort to limit the development or progression of ROP. Identifying strategies to prolong gestation through good prenatal care [32], reduced teenage pregnancies [33], and avoidance of illegal drugs [34] may reduce the morbidity experienced in association with premature birth.

In the 1990s interest in treating the hypoxic stimulus for neovascularization developed, and the Supplemental Therapeutic Oxygen for Prethreshold ROP (STOP-ROP), a multicenter trial to study the efficacy of supplemental oxygen in reducing the progression of ROP to threshold, was undertaken [35]. Six hundred and forty-nine patients with prethreshold ROP were randomly assigned to maintain oxygen saturation at 96–99 % (supplemented group) vs. 89–94 % (conventional group). Progression to threshold was not statistically significant between the two groups (41 vs. 48 %), but adverse pulmonary effects occurred more frequently in the oxygen-supplemented group. On the other hand, several studies in recent years have shown a benefit to carefully regulating oxygen saturation levels. One such study by Chow et al. [36] utilized strict oxygen management with saturation limits of 85–93 % SaO_2 for infants younger than 32 weeks' gestation. They demonstrated a reduction in incidence of stages 3 and 4 ROP from 12.5–2.5 % and decreased need for laser treatment from 4.5–0 %. In 2006, VanderVeen et al. [37] reported a dramatic reduction in the incidence of prethreshold disease in at least one eye of infants weighing less than 1,250 g from 17.5 to 5.6 % after lowering oxygen alarm levels from 87 to 97 % to 85–93 %. Britt and Sandoval [38] also instituted a policy to maintain oxygen saturation at 85–93 % for infants younger than 30 weeks' gestation and found that the incidence of stage 3 or more advanced ROP decreased from 49 to 15 % and the need for laser decreased from 38 to 15 %.

Recent clinical trials [39], the Surfactant Positive Airway Pressure Pulse Oximetry Randomized Trial (SUPPORT), in the US, Benefits of Oxygen Saturation Targeting Study II (BOOST II) in Australia, UK, and New Zealand and the Canadian Oxygen Trial (COT) in Canada, US, Argentina, Finland, Germany and Israel tested the role of oxygen saturation targets (85–89 % SaO_2) compared to infants with high oxygen saturation targets (91–95 % SaO_2) and the association with ROP. In SUPPORT and BOOST II, there was increased death in the infants with low oxygen saturation targets (85–89 % SaO_2) compared to infants with high oxygen saturation targets (91–95 % SaO_2), but in survivors, ROP was reduced in infants with low oxygen saturation targets. In the COT, neither ROP nor survival was affected.

Currently, the recommendation for oxygen level is still unclear. Generally, low-birth-weight infants are maintained at oxygen saturation levels in the high 80s or low 90s with ventilators set to avoid frequent changes in oxygen in

response to variation in saturation levels [39]. Research is needed to determine the best appropriate oxygen levels to reduce the risk of severe ROP and optimize development of other organs. In addition, studies in relevant animal models can provide knowledge of signaling pathways that have been altered by stresses associated with prematurity and lead to targeted treatment to reduce specifically the risk of ROP.

Antioxidant therapies such as vitamin E and D-penicillamine have been studied; however, results are controversial to this point [40–45]. Early promising results have been demonstrated in murine models involving triamcinolone [46] and 17- α -estradiol [47], a 5- α -reductase inhibitor. However, further studies are required.

1. Screening

Successful preventative treatment of ROP is predicated on timely screening. Evaluation consists of pupil dilation and a comprehensive fundus examination with scleral depression. Monitoring the infant throughout the exam is essential as both manipulation of the eye and the use of dilating drops can produce apnea or bradycardia. The American Academy of Pediatrics (AAP) and the American Academy of Ophthalmology (AAO) have joint recommendations for ROP screening [48]. They recommend screening for all infants with a birth weight $\leq 1,500$ g or a gestational age (GA) of ≤ 30 weeks and infants with a birth weight between 1,500 g and 2,000 g or a GA of more than 30 weeks whose clinical course places them at increased risk for ROP. Since it is estimated that less than 10 % of infants screened will require treatment [49], models using various combinations of GA, birth weight, postnatal weight gain, and serum IGF-1 levels to predict ROP risk have been developed [50–55]. Validation studies show that these models have potential but further validation is needed prior to changes in screening recommendations.

The first examination should be performed prior to hospital discharge at 4–6 weeks after birth or 31 weeks' postmenstrual age (PMA), whichever is later. Routine screening before 30 weeks' PMA is difficult as the cornea is hazy [56]. The AAP/AAO recommend follow-up examinations at intervals of 1–3 weeks depending on the severity of disease evident. Exams are continued until criteria for discontinuation are reached.

E. Treatment

The current recommendation is treatment be initiated for ROP for those with type I ROP [48]. This recommendation is based on the ETROP study [57], which reported that unfavorable visual outcomes can be reduced from 19.5 to 14.5 % and unfavorable structural outcomes from 15.6 to 9.1 % at 9 months' corrected age with early treatment. However, infants in the early treatment group experienced more apnea and bradycardia and required re-intubation more frequently. At 6 years of age, early treated eyes continued to have fewer

unfavorable structural outcomes (8.9 % vs. 15.2 %) and relatively preserved peripheral vision [58]. At 6 years, visual acuity outcomes were no longer statistically superior in the early treatment group (24.6 % vs. 29.0 % unfavorable); however, subgroup analysis showed improved visual acuity for “higher-risk” zone I prethreshold eyes in the early treatment group. Additionally, a large retrospective review performed by Alme et al. [59] in 2008 found a decrease in the incidence of retinal detachment from 10.3 to 1.9 % with the change in guidelines. This occurred even though this later study group had lower birth weights and younger gestational ages, on average.

Current treatment options which are discussed in detail below consist of ablation of avascular retina by laser photocoagulation, cryotherapy, or potentially the use of intravitreal anti-vascular endothelial growth factor (VEGF) for some zone I eyes. In general, laser therapy remains the treatment of choice by ophthalmologists throughout the world.

1. Cryotherapy

Cryotherapy was the primary treatment of ROP for many years but has now been largely replaced by laser photocoagulation [60]. The benefit of cryotherapy was demonstrated in the large multicenter trial CRYO-ROP. In this study, 291 infants with birth weights of less than 1,251 g who developed threshold ROP were randomized to observation or treated with cryotherapy within 72 h of diagnosis. Cryotherapy was found to significantly decrease unfavorable outcomes (31 % in treated vs. 51 % in observed), defined as posterior retinal detachment, posterior retinal fold, or retrolental tissue that obscured visualization of the posterior pole at 3 months. At the 15-year follow-up, 254 survivors of the original study [61] continued to have benefit with significantly fewer eyes in the treated group having poor ocular structure, new retinal folds, retinal detachments, and obstruction of the view of the posterior pole (30 % treated vs. 52 % observed). Treated eyes also demonstrated a lower incidence of poor visual acuity, defined as 20/200 or worse (45 % treated vs. 64 % observed). Cryotherapy is not as common now that laser delivery with the indirect ophthalmoscope is possible.

2. Laser Photocoagulation

In the past 20 years, laser photocoagulation using the diode or green laser on an indirect ophthalmoscope has almost completely replaced cryotherapy in the treatment for ROP. Generally, laser is better tolerated than cryotherapy with less conjunctival chemosis, inflammation, pain, or apnea and bradycardia. Laser is applied to peripheral avascular retina with gray to gray-white burns spaced one-half width apart, completely filling the avascular retina from the ora serrata, up to 360° [62]. Care should be taken to avoid “skip areas.” Structural and visual outcomes suggest that laser photocoagulation is superior to cryotherapy. Paysse et al. [63] retrospectively compared 70 infants receiving laser treatment with 63 infants treated with cryotherapy at a single institution and

found that 88 % of the laser-treated group vs. 56 % of the cryotherapy-treated group had resolution of ROP. There was not a statistically significant difference in cycloplegic refraction at 1 year. Visual acuity was better in the laser-treated group vs. the cryotherapy-treated group (20/49 vs. 20/103). A 10-year follow-up study of 44 eyes from 25 patients by Ng and associates [64, 65] demonstrated that when compared to cryotherapy, laser resulted in a better mean best-corrected visual acuity (20/66 vs. 20/182), and these eyes were seven times less likely to develop retinal dragging and developed less myopia (−4.48 vs. −7.65 diopters). These findings have been verified by other studies including a Cochrane systematic review [66].

3. Pharmacotherapy

a. Bevacizumab

Recent studies have tested bevacizumab, an anti-VEGF monoclonal antibody utilized in the treatment of many neovascular eye conditions. Potential advantages to its use in ROP include the ease of administration, rapidity of response, and ability to use this treatment when corneal, lens, or vitreous opacities preclude treatment with laser. Concerns exist because dose and safety studies have not yet been performed and intravitreally administered bevacizumab can enter the systemic circulation and has also been shown to suppress systemic VEGF levels for more than 2 weeks after a single intravitreal injection [67]. The potential effects on the development of the kidneys, lungs, and brain remain unknown, but it is possible that anti-VEGF may further compromise organs that have reduced function because of the premature state.

A multicenter randomized trial by Mintz-Hittner and associates [68] compared bevacizumab (0.625 mg in .025 mL of solution) to conventional laser therapy in 150 infants with stage 3+ ROP in zone I or posterior zone II. In this study, bevacizumab was associated with decreased rates of recurrence (4 % vs. 22 %) and fewer structural abnormalities (macular dragging and retinal detachment) at 1 year. Specifically, among infants with zone I disease (with the highest rate of treatment failure after conventional laser therapy), the recurrence rate was 6 % in the intravitreal bevacizumab subgroup vs. 42 % in the laser-treated group. The differences in outcomes were not significant in infants with posterior zone II disease. No systemic or local toxic effects were observed; however, the study was too small to adequately assess ocular and systemic safety, and the follow-up period was only 54 weeks. A recent single institution study by Hu and associates [69] demonstrated a later recurrence of severe ROP on average than that seen with laser therapy, and in one case recurrence occurred over 1 year later. The authors of this study concluded that although intravitreal bevacizumab treatment is effective in inducing regression of ROP, the effect may be transient. In addition, the use of anti-VEGF in an experimental model led to reduced body weight gain and recurrent intravitreal neovascularization and activation of angiogenic pathways that not only included VEGF but

also erythropoietin, which is independent of VEGF signaling, suggesting that treatment for recurrent neovascularization with anti-VEGF may not be effective [70].

The AAP/AAO guidelines [48] currently state that consideration may be given to treatment of infants with zone I, stage 3+ ROP with an intravitreal injection of bevacizumab—however, only after a thorough discussion for informed consent, since there remain unanswered questions involving dosage, timing, safety, visual outcomes, and other long-term effects. Bevacizumab is not FDA approved for the treatment of ROP. The guidelines also advise weekly monitoring of infants after injection until retinal vascularization is completed. The antibody fragment ranibizumab has a shorter serum half-life in monkeys [71] (3.5 days vs. 12.3 days for bevacizumab [72]) and may be an alternative for use in preterm infants, since bevacizumab reduced VEGF levels in preterm infants for at least 2 weeks following a single intravitreal dose [73]. A study in adults showed that ranibizumab did not reduce serum VEGF levels, whereas intravitreal bevacizumab lowered serum levels [74]. However, in preterm infants who have smaller blood volumes, a case report found that VEGF levels were significantly reduced following intravitreal ranibizumab; [75] thus, more study is needed.

b. Pharmacologic Vitreolysis

Pharmacologic vitreolysis [76, 77] is a new therapeutic paradigm to alter the vitreous on a macromolecular level to induce gel liquefaction and vitreoretinal dehiscence to detach vitreous from the retina [see chapter VI.A. pharmacologic vitreolysis]. Some have suggested using forms of plasmin (e.g., ocriplasmin) to cleave fibronectin and reduce intravitreal neovascularization in stage 3 ROP or vasoproliferation in stage 4 ROP. However, using forms of plasmin in stage 3 may not safely reduce intravitreal neovascularization without affecting physiologic retinal vascular development, because fibronectin and other components of the extracellular matrix that are cleaved by plasmin, such as laminin, are important in normal retinal vascular development [78]. Inhibition of plasmin activity reduces intravitreal neovascularization without adversely affecting physiologic retinal vascular development in the oxygen-induced retinopathy model in rats [79]. Therefore, using plasmin to cleave the vitreoretinal interface may be counterproductive in reducing intravitreal neovascularization and may adversely affect retinal vascular development. Using ocriplasmin in infant vitrectomy for stage 4 or 5 ROP may hold promise by facilitating retinal reattachment in the eyes that develop retinal breaks and recurrent retinal detachments after ROP surgery [80]. Ocriplasmin is therefore being considered in pediatric retinal conditions that are associated with retinal detachments [81] [see chapters VI.E.1. Pharmacologic vitreolysis with ocriplasmin: basic science studies and VI.E.2. Pharmacologic vitreolysis with plasmin: clinical studies.].

4. Treatment of Retinal Detachment

Laser treatment of avascular retina is effective in reducing vascular activity and subsequent retinal detachment in a majority of cases; however, one large study reported retinal detachment in 14 % of the eyes 6–12 weeks after laser treatment [82]. When ROP progresses to partial or total retinal detachment, surgical intervention is undertaken to promote retinal reattachment in the posterior pole, minimize distortion, and preserve vision.

Scleral buckling (SB) and vitrectomy have been used with some success to manage retinal detachments with ROP. One study utilizing these methods demonstrated light perception or better vision in 72 % of eyes with a visual acuity of 20/300 or better in 15 % [83]. Poor outcomes for all surgical interventions are predicted by the presence of plus disease, vitreous haze, and continued neovascularization; [84] therefore, treatment to reduce vascular activity is recommended before proceeding with vitreous surgery. Scleral buckling involves the placement of a silicone band around the eye, sometimes with drainage of subretinal fluid. High degrees of myopia, anisometropia, and amblyopia are associated with scleral buckles [85]. Scleral buckles are the initial treatment for rhegmatogenous detachments and can be used in cases with limited tractional components located near or anterior to the equator. Placement of a scleral buckle almost always necessitates a second procedure 6–9 months later to remove the band and allow the eye to grow.

Vitrectomy with or without a scleral buckle is considered especially for posterior disease and many forms of tractional detachments. A lens-sparing vitrectomy (LSV) allows for the removal of the vitreous and any tractional membranes present, thus enabling the retina to be reattached to the wall of the eye. It also allows better visual development by retaining the lens (Figure III.A-7). A direct comparison of stage 4 detachments repaired by vitrectomy vs. scleral buckle demonstrated a 73 % reattachment rate for eyes treated with a primary LSV vs. 31 % in eyes with a primary scleral buckle [86]. Complications associated with LSV include retinal tears, cataracts, and glaucoma. The incidence of cataract following an LSV varies between 5 and 15 % [87, 88].

III. Persistent Fetal Vasculature

The hyaloid vasculature consists of the vasa hyaloidea propria, tunica vasculosa lentis, and pupillary membrane. Hyaloid vessel development and regression are complex [see chapter II.A. Development and developmental disorders of vitreous failure can result in several ocular pathologies, which are part of a spectrum known as persistent fetal vasculature (PFV). The vasa hyaloidea propria is made up of the hyaloid artery that enters the eye through the optic stalk and its anterior branches that extend through the vitreous toward the lens. The tunica vasculosa lentis is a capillary network

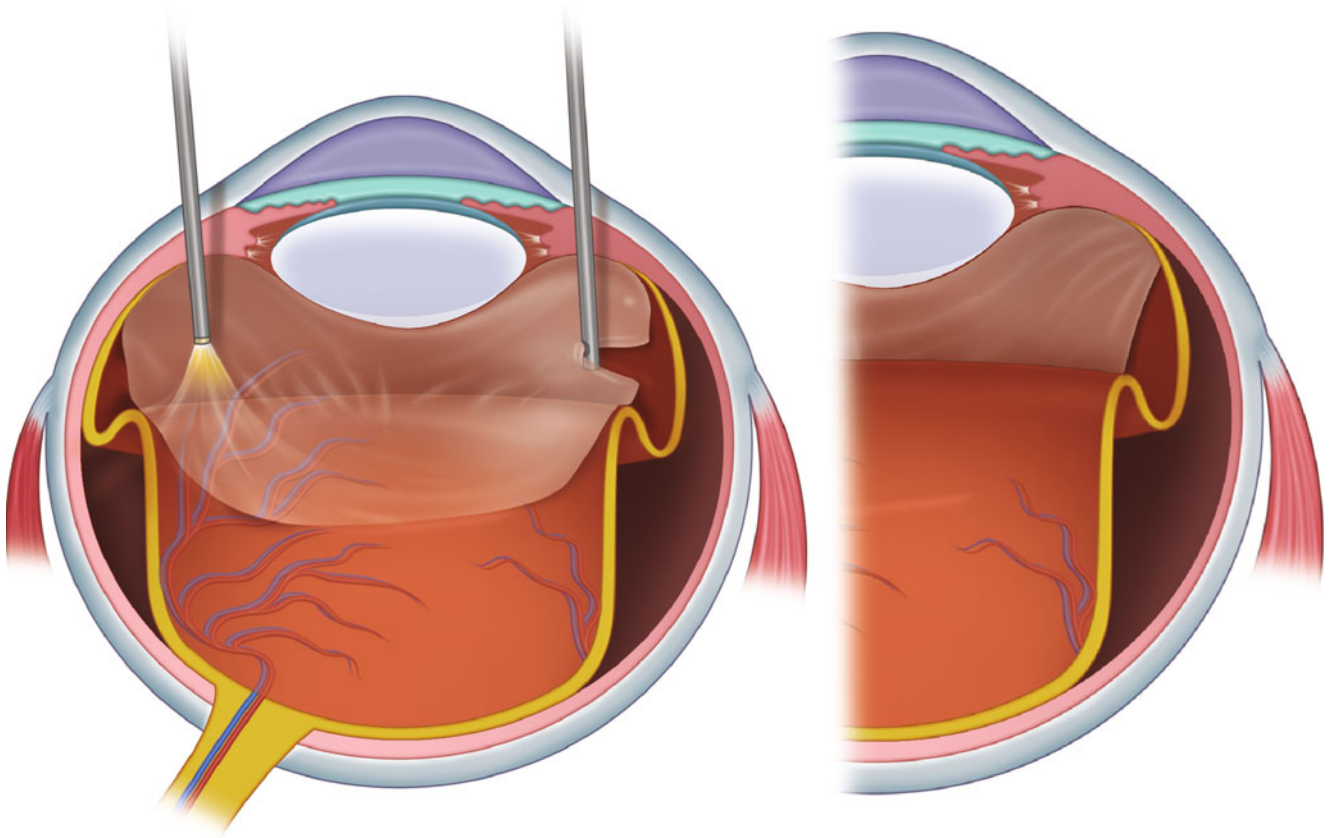


Figure III.A-7 Left rendering demonstrates location of ports in lens-sparing vitrectomy. Right rendering more clearly shows traction component to retinal detachment. Removing this traction is key to successfully reattaching the retina

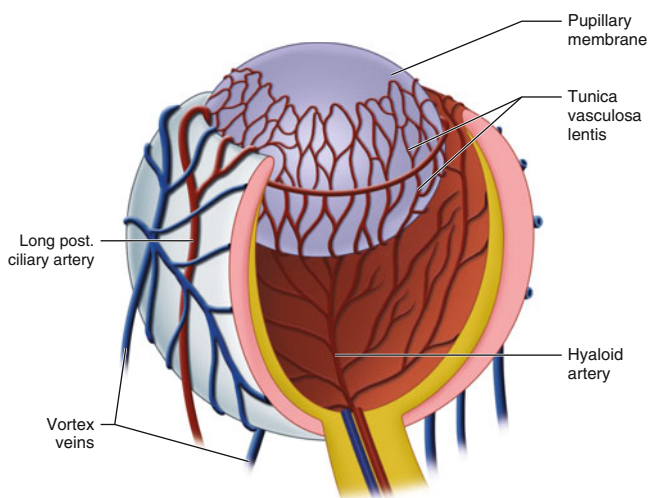


Figure III.A-8 Extensive anastomoses of fetal vasculature (Redrawn based on Goldberg MF. Persistent fetal vasculature [PFV]: an integrated interpretation of signs and symptoms associated with persistent primary vitreous [PHPV]. LIV Edward Jackson Memorial Lecture [107])

that encompasses the posterior developing lens and connects to the lens equator with the pupillary membrane, which covers the anterior lens capsule (Figure III.A-8). The hyaloid artery first appears in humans during the fourth week of

gestation and peaks in prominence during approximately the ninth week of gestation [89]. In early stages of development, the retina and optic nerve lack blood vessel support and are oxygenated by the choroidal and hyaloidal vessels [90–92].

As the eye enlarges and retinal angiogenesis ensues, hyaloid vasculature regression occurs [93, 94]. The first elements to undergo regression are the vasa hyaloidea propria, followed by the tunica vasculosa lentis and pupillary membrane, and lastly the main hyaloid artery trunk. Cessation of blood flow in the hyaloid artery is seen at roughly 7 months and culminates with the involution of the entire hyaloid vessel complex by approximately 36 weeks' gestation [89, 95]. As the vascular structures regress, the primary vitreous retracts, and collagen fibers with a ground substance of collagen, fibronectin, laminin, and other extracellular matrix components (but not hyaluronan) are produced to form the secondary vitreous [see chapter II.A. Vitreous embryology]. By the sixth month of gestation, the posterior segment is largely composed of the secondary vitreous, and the primary vitreous is reduced to a small central portion of the posterior segment that extends from the optic disk to the posterior lens surface and is referred to as Cloquet's canal (Figure III.A-9).

PFV is the term used to describe the array of pathology that results from failed involution of the primary vitreous and

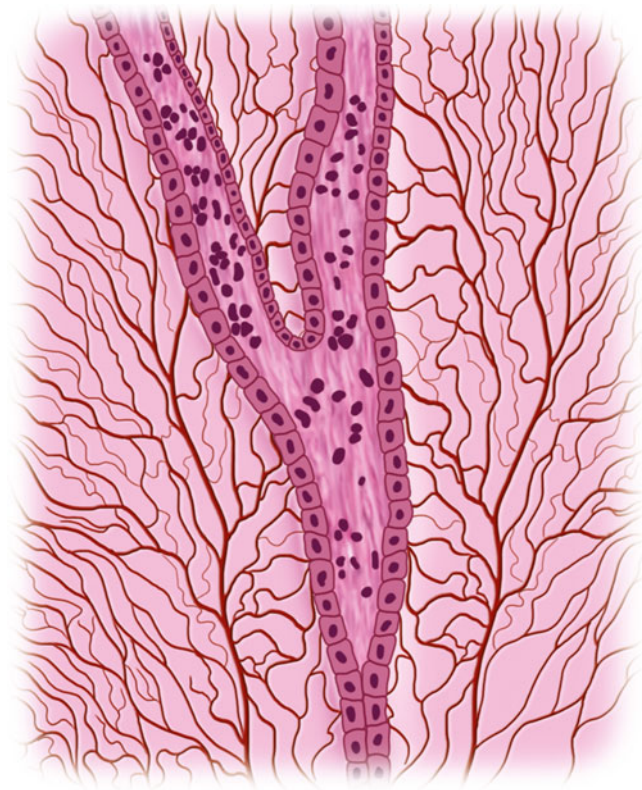


Figure III.A-9 Artist's rendering of longitudinal section of Cloquet's canal and the contained hyaloid artery. The condensation between primary and secondary vitreous is seen forming the wall of Cloquet's canal. (adapted from Ida Mann [89], p. 174 – Figure 147)

regression of the fetal hyaloid vasculature [see chapters I.D. Proteomics of fetal hyaloid vasculature regression and II.A. Vitreous embryology] involving the anterior or posterior compartments of the eye. Mild changes from PFV commonly affect the eye; however, functional complications are rare. Prior studies have estimated that 3 % of full-term infants display some degree of PFV [96] and more than 90 % of those born earlier than 36 weeks of gestation demonstrate incomplete regression of the embryonic hyaloid vessel system [97]. A recent review of individuals at one US institution for the visually impaired found that 4.8 % of blind patients had PFV [98]. Individual components of the fetal vasculature often persist in combination with others; however, any anatomically identifiable vascular remnant may present individually as well. When present in full-term infants, persistent fetal intraocular vessels frequently are compatible with normal ocular and visual functions. However, more severe manifestations of PFV can cause secondary abnormalities resulting in defective physiology and decreased visual acuity. Ancillary tests consisting of ultrasonography, fluorescein angiography (FA), OCT, computed tomography (CT), magnetic resonance imaging (MRI), electroretinography (ERG), and visual evoked potential (VEP) can all be helpful in evaluating PFV.

PFV can be classified as anterior or posterior depending on the intraocular structures involved. The most common complications are seen anteriorly and are frequently associated with abnormal regression of the tunica vasculosa lentis. Common manifestations include cataract formation with associated lens swelling and risk of induced angle closure glaucoma. Frequently, engorgement of iris vessels, pain, and microphthalmia are also present. Posterior PFV, most commonly associated with abnormal regression of the vasa hyaloidea propria, is much less common. It presents with a tractional retinal detachment and adherent preretinal membranes emanating from a persistent stalk, which places traction on the retina. Accompanying retinal dysplasia and optic nerve abnormalities can be seen. As with anterior PFV, microphthalmia and leukokoria may be present.

A. Anterior Persistent Fetal Vasculature

1. Persistent Pupillary Membrane

Noted in approximately 95 % of healthy newborns, a persistent pupillary membrane consists of fine vessels along the pupillary margin. They are non-pathologic and almost always disappear shortly after birth [99]. When associated with cataract or retrolental membranes, they should clue the diagnostician to the possibility of other manifestations of PFV.

2. Iridohyaloid Blood Vessels

Iridohyaloid blood vessels connect the posterior tunica vasculosa lentis to the pupillary membrane vessels. Normal regression of these vessels is required for the development of the zonule at the equator of the lens [100]. The presence of iridohyaloid vessels often manifests as a subtle pupillary sphincter notch [101] or a prominent superficial iris vessel. A severe manifestation would be ectopia lentis et pupillae [102].

3. Mittendorf's Dot

Mittendorf's dot is a remnant of the primary vitreous that corresponds to the location of previous junction of the hyaloid artery to the tunica vasculosa lentis and is almost always on the inferior and nasal posterior lens capsule. It is usually asymptomatic and can be seen in 0.7–2 % of the population [103] (Figure III.A-10).

4. Muscae Volitantes

Latin for “flying flies,” muscae volitantes are vitreous remnants of the regressed vasa hyaloidea propria [see chapter I.D. Proteomics of fetal hyaloid vasculature regression]. They are usually found floating in the anterior vitreous. Sometimes, small corkscrew remnants are seen attached to the posterior capsule. Associated visual symptoms are rare, but floaters would be the only clinical manifestations [see chapter V.B.8.



Figure III.A-10 Mittendorf's dot – Mittendorf's dot located on posterior lens capsule at the site of the former anastomosis of the tunica vasculosa lentis to the hyaloid vasculature. It is almost always located inferonasally without associated visual dysfunction (Courtesy of Dr Parag Shah)

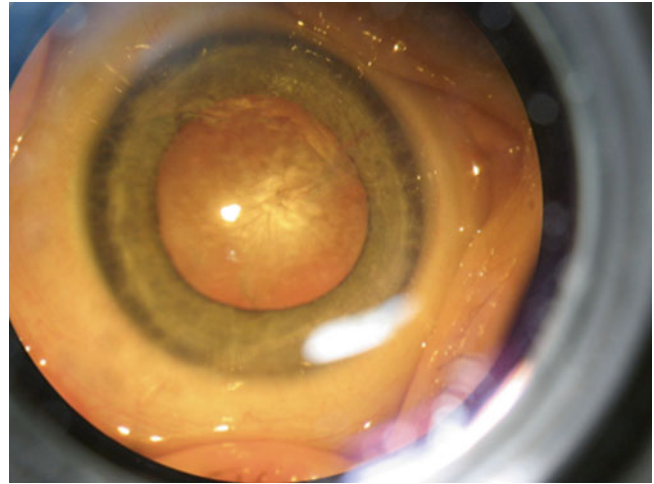


Figure III.A-11 Prominent retrolental membrane obscuring the entire visualized posterior lens capsule with associated iridohyaloid vessel (Courtesy of Dr David Dries, Moran Eye Center)

Floater and vision – current concepts and management paradigms].

5. Retrolental Membrane

Associated with persistence of the posterior tunica vasculosa lentis, these membranes are variable in presentation, ranging from 1.0 mm to more extensive, covering the entire posterior surface of the lens [104]. They result from fibrovascular tissue that attaches to the ciliary processes and draws them to the center of the pupil. They are most commonly seen with corresponding radially oriented blood vessels that are seen clearly on fluorescein angiography and distinguish PFV from Coats disease, retinoblastoma, or stage 5 ROP. Frequently, abnormalities in lens development are also present (Figure III.A-11).

B. Posterior Persistent Fetal Vasculature

1. Bergmeister's Papilla

First described by Austrian Ophthalmologist O. Bergmeister, Bergmeister's papilla arises from the center of the optic disk and consists of a small tuft of fibrous tissue that at one time ensheathed the hyaloid artery.

2. Persistent Hyaloid Artery

Most commonly seen as a flaccid vascular remnant attached to the posterior pole of the lens, this occurs when the hyaloid artery fails to involute completely. Normally, the hyaloid artery cleaves near its center, with both ends retracting and regressing completely [105] [see chapter II.A. Development and Developmental Disorders of Vitreous]. Very rarely, the entire hyaloid artery may persist from the optic nerve head and extend to the posterior lens capsule or into the anterior vitreous with

branches of the vasa hyaloidea propria present. Rarely, a persistent hyaloid artery is associated with vitreous hemorrhage.

3. Congenital Nonattachment of the Retina and Retinal Detachment

Retinal detachments have been noted in 56 % of patients with PFV [106]. Two different mechanisms are believed to contribute to retinal detachment. In the first, adhesion of the primary vitreous and its blood vessels from one portion of the optic cup prevents the secondary vitreous from forming between the primary vitreous and the retina [107]. This causes traction and detachment of the retina as the eye enlarges. Later, a continuous stalk of hyaloidal tissue can be seen to extend from the optic disk to the posterior lens or ciliary body. Contraction of the stalk or growth of the eye results in tractional retinal detachment. In these cases the retina may be adherent to the ciliary body, dragged centrally, or drawn anteriorly and elevated around the optic nerve.

4. Globe Malformations

Microphthalmos and microcornea are two common malformations associated with PFV. However, variations in the size and shape of the globe, cornea, or lens can be seen. In the presence of leukokoria, corresponding microphthalmos or microcornea can be helpful in diagnosing PFV.

5. Macular Abnormalities

Often subtle macular changes can be associated with posterior PFV. Most commonly the result of traction, there is failure of the foveal pit to develop and irregularities in retinal layers can occur. Often these changes are noted on optical coherence tomography (OCT).

6. Optic Nerve Head Abnormalities

Optic nerve head hypoplasia and dysplasia are believed to result from abnormal traction associated with PFV.

C. Genetics

Most cases of PFV are sporadic, but autosomal recessive and autosomal dominant patterns of familial transmission have been documented. Defects in the *NDP* and *FZD4* genes have been identified in cases of unilateral and bilateral PFV. These genes are also associated with familial exudative vitreoretinopathy (see below) and Norrie disease. These genes are associated with the Wnt signaling pathway, and experimental evidence exists to support Wnt signaling in the development of PFV [108]. In addition, mice with defects in genes, *Atoh7* and *Lama1*, responsible for the genesis of retinal ganglion cells, have a high incidence of phenotypes similar to PFV [109, 110]. Also, transgenic mice lacking tumor suppressor genes *arf* [111], *p53* [112], and *frizzled-5* [113] or overexpressing *vegfa188* [114] have also been shown to develop a PFV phenotype similar to human PFV. Finally, PFV has also been reported in association with trisomies 13, 15, and 18. If bilateral disease is suspected, Norrie disease and trisomy 13 should be ruled out. In general, infants presenting with unilateral PFV and no other developmental anomalies are not subjected to testing for other conditions unless other symptoms are present.

D. Treatment of Persistent Fetal Vasculature

Surgical intervention to clear media opacities, to relieve tractional forces, or simply to preserve the globe from the natural course of PFV can be helpful. In eyes with visual potential, visual rehabilitation is important, and the need for careful follow-up must be conveyed to parents. Studies have demonstrated that the eyes with anterior disease have a greater chance of achieving form vision than eyes with posterior malformations. Posterior PFV, microphthalmia, glaucoma, and amblyopia are known to limit visual acuity outcomes even after aggressive intervention. In our experience, tractional effects on the lens or retina due to a stalk can often be relieved with surgical division of the stalk. This can release traction and allow subsequent flattening of the retina, which is particularly important as the eye lengthens during development. In cases of cataract, a limbal-based surgical approach is preferred to removal of the lens during vitrectomy, because the pars plicata/pars plana area can be abnormal, and there is risk of creating a tear in the peripheral retina when the media are too cloudy for direct visualization. Also, the peripheral

retina can be drawn anteriorly into the retrolental membrane. In cases with clear lenses, a pars plana/pars plicata approach can be performed with careful examination of the ora serrata to avoid injury to the retina. Relieving the traction on the stalk is usually sufficient, and complete amputation of the stalk is neither necessary to allow the retina to reattach nor safe, since the peripapillary retina can also be drawn into the stalk and tissue. Complete removal of the stalk may then lead to retinal injury and inoperable retinal detachment. These cases are complicated and often require expertise and training in the procedure.

IV. Familial Exudative Vitreoretinopathy

Familial exudative vitreoretinopathy (FEVR) is a vitreoretinal dystrophy that was first described in 1969 by Criswick and Schepens [115] when they noted retinal changes similar to retinopathy of prematurity (ROP) in children and adolescents who had no risk factors for ROP. They described bilateral involvement, although often asymmetric, of peripheral neovascularization with thick fibrovascular membranes causing traction on the retina and distorting the macula and optic disk. Some eyes were noted to develop peripheral subretinal exudates with associated exudative and traction retinal detachments. Since that time, many studies have identified tremendous variability in the presentation, course, and even inheritance pattern of FEVR. When severe, FEVR can be a lifelong retinal vascular disease with variable periods of quiescence.

A. Clinical Presentation

Due to its rarity and many variable manifestations, the diagnosis of FEVR can be challenging and is likely underdiagnosed. FEVR has been described in all ethnic groups. In a recent review by Ranchodetal [116], only 41/145 or 28 % of patients referred to their practice with FEVR had been correctly diagnosed prior to referral. Many were misdiagnosed as having unspecified retinal detachment, persistent fetal vasculature syndrome (PFV), ROP, retinal folds, or Coats disease. Of note, the average age at presentation for patients in this study was 6 years. Young patients with FEVR can also be referred with a diagnosis of leukokoria, poor vision, retrolental plaque, strabismus associated with a positive angle Kappa, cataract, or even premacular membrane with pucker. Other diseases not already mentioned that should be considered in the differential diagnosis of FEVR include the Norrie disease, retinoblastoma, incontinentia pigmenti, sickle cell disease, and toxocariasis.

FEVR can present with various combinations of macular dragging, radial retinal folds, retinal neovascularization, pre-

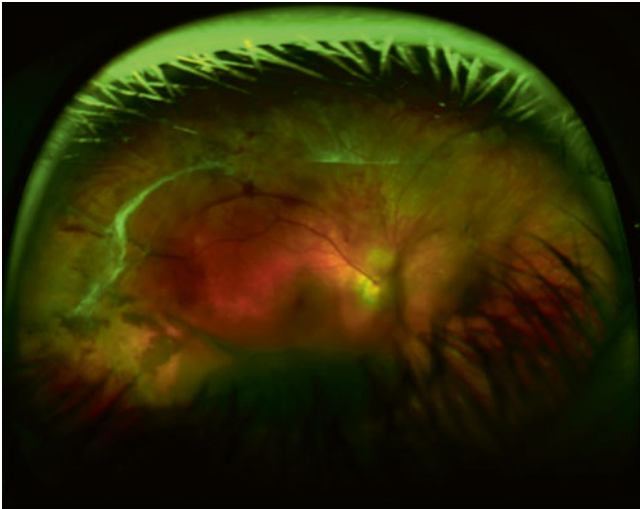


Figure III.A-12 A 10-year-old female presented with vitreous hemorrhage. Following clearing of the hemorrhage, fibrovascular changes were noted with traction on the retina and preretinal hemorrhages (Optos)

retinal vitreous organization, vitreous hemorrhage, tractional retinal detachment, and subretinal exudation [117] (Figure III.A-12). The most prominent feature is the abrupt cessation of peripheral retinal vessels, commonly at the temporal equator; however, they can extend 360° [118]. These vessels take on a scalloped pattern that is often referred to as a “brush border” when seen on fluorescein angiography and frequently demonstrate vascular buds at the junction of avascular and vascularized retina. Subretinal exudates are often present and can be massive resembling the Coats disease. Partial or total retinal detachment due to exudative and fibrovascular proliferative tractional forces can be seen. Miyakubo et al. [119] and van Nouhuys [120] noted that approximately 20 % of patients with FEVR developed retinal detachments and almost all within the first decade of life. Benson [117] noted that children presenting in the first 3 years of life had a worse prognosis than those presenting later in life. In his review of FEVR, Trese [121] also noted a poor prognosis in infants presenting in the first year of life. The presence of bilateral findings can also be helpful in the diagnosis of FEVR. Pendergast [122] reported that 85 % of eyes had bilateral involvement in FEVR and only 15 % had unilateral involvement.

B. Clinical Classification

Different systems have been used to classify FEVR. The most recently recommended system parallels the International Classification of Retinopathy of Prematurity (ICROP) guidelines with five stages ranging from avascular retina to total retinal detachment [121]. They are defined as:

- Stage 1: Avascular periphery
- Stage 2: Retinal neovascularization
 - 2A Without exudates
 - 2B With exudates
- Stage 3: Extramacular retinal detachment
 - 3A Without exudates
 - 3B With exudates
- Stage 4: Macula-involving retinal detachment, subtotal
 - 4A Without exudates
 - 4B With exudates
- Stage 5: Total retinal detachment

C. Genetics

The most common mode of inheritance of FEVR is autosomal dominant (AD); however, many individuals with autosomal dominant FEVR are asymptomatic due to reduced penetrance. In addition, there are known lines of X-linked and autosomal recessive inheritance, as well. In the review by Ranchod et al. [116], 18 % of patients had a diagnosed family history of FEVR upon referral and 37 % had histories consistent with FEVR but had not been diagnosed. Mutations in one of three genes are known to be responsible for the autosomal dominant FEVR. *FZD4* encoding the protein frizzled-4, *LRP5* encoding low-density lipoprotein receptor-related protein 5, and *TSPAN12* encoding tetraspanin-12 are responsible for fewer than 50 % of autosomal dominant FEVR cases. Another locus, *EVR3*, has been mapped, but the gene is unknown at this time. Molecular genetic testing for mutations in *FZD4*, *LRP5*, and *TSPAN12* is available at this writing. However, more than 50 % of the time, a known genetic mutation will not be detected in patients presenting with clinical features of FEVR. *NDP* encoding the Norrie disease protein is associated with X-linked inheritance, and *LRP5* is also associated with autosomal recessive inheritance [123]. Genetic counseling can be very helpful as offspring of a patient with autosomal dominant FEVR will have a 50 % risk of inheriting the mutation, and prenatal testing is currently available. Molecular genetic testing should begin with the sequence analysis of *FZD4*; if the pathologic mutation is not identified, then sequence analysis of *LRP5* and then *TSPAN12* should be performed in that order. All genes associated with AD FEVR have not been identified, so failure to identify a mutation in the above genes does not rule out the diagnosis.

1. Ancillary Testing

The diagnosis of FEVR is based on typical clinical findings in the absence of prematurity or other risks of ROP. A positive family history is helpful. In suspicious cases of asymptomatic stage 1 or 2 FEVR, examination of parents, siblings, and children can help in the diagnosis. Shukla et al. [124] noted in a review that 41 % of patients with FEVR were in

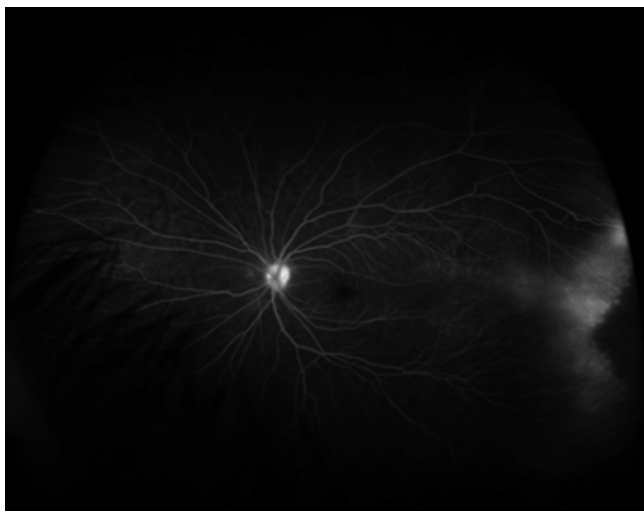


Figure III.A-13 Left eye of patient in Figure III.A-12. Note the leakage of capillaries at the junction of vascular and avascular retina (Optos)

the mild end of the spectrum with normal vision and only a sector of peripheral retinal avascularity noted. Wide-angle fluorescein angiography is helpful to identify avascular retina and vascular abnormalities that may be otherwise missed. Depending on patient cooperation, this can be performed in clinic or while under anesthesia for an examination. Contrasts between peripheral avascular and vascularized retinas are clearly highlighted with fluorescein angiography, and characteristic straightening of peripheral vessels in a “brush border” pattern can be identified. Fluorescein angiography is very useful to detect the vascular/avascular junction and identify leakage of capillaries (Figure III.A-13). ERG changes other than possible mild reductions in b-wave amplitude are not seen with FEVR.

2. Systemic Associations

Individuals with AD FEVR and mutations in *LRP5* have been noted to have reduced bone mass [125]. This does not appear with other forms of FEVR. Reduced bone mass is often only evident upon examination with dual x-ray absorptiometry and leaves affected patients predisposed to fractures.

D. Treatment

As noted with many vitreoretinopathies, early intervention often results in better vision for patients. Screening with wide angle fluorescein angiography of family members of patients with known disease is important as is the need to emphasize that the course of FEVR can wax and wane, and lifelong follow-up is pivotal. Currently, we recommend treating the peripheral avascular retina of stage 2 or greater FEVR with near-confluent laser to the avascular retina, regardless

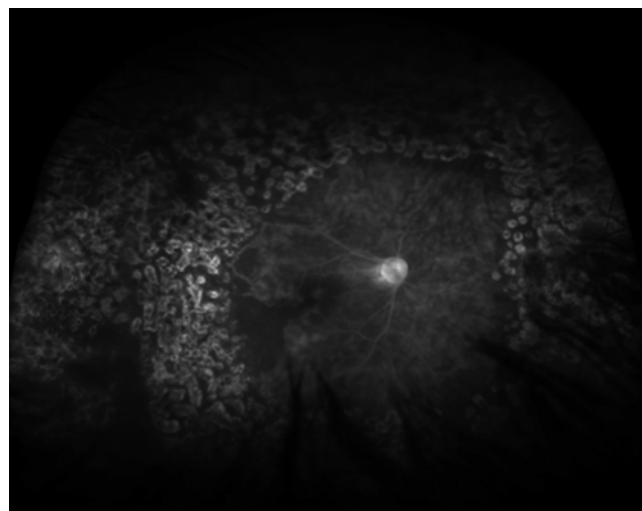


Figure III.A-14 Fluorescein angiogram of same eye as Figure III.A-12 after vitrectomy and extensive laser applied over multiple sessions to treat recurring vitreous hemorrhages (RetCam Image, Clarity). Persistent avascular retina extends to fovea

of whether exudates are present (Figure III.A-14). In addition, FEVR may progress with new capillary involvement resulting in avascular retina later in life. Therefore, until more is known about this condition, patients should be examined regularly throughout their lives.

Vitreous plays a major role in the pathogenesis of FEVR and, specifically, often leads to formation of retinal folds or traction retinal detachment through firm attachment of the posterior vitreous cortex to the retina. With this in mind, vitrectomy might be useful in the eyes with severe FEVR [118, 122, 126, 127]. Ikeda et al. [126] noted in their case series that peripheral vitreoretinal adhesions overlying avascular retina caused iatrogenic breaks during surgery in 22 of 28 eyes. In all their cases, bimanual technique with vitreous scissors and forceps was required to dissect the posterior vitreous cortex from the retinal surface. Vitrectomy was then combined with a lensectomy and scleral buckle placement to help relieve residual vitreoretinal traction. Utilizing these techniques, they successfully reattached the retina in 86 % of cases and improved visual acuity in 71 %. Others report success using similar bimanual techniques for vitrectomy, but reserving the scleral buckle for eyes with a rhegmatogenous component to their retinal detachment [122, 128]. However, vitreous is very adherent to the retina in youth, and care must be exercised to avoid creating retinal breaks.

Recent reports advocate using autologous plasmin to assist with pharmacologic vitreolysis [129, 130] [see chapters VI.D.1. Pharmacologic vitreolysis with plasmin: basic science studies and VI.D.2. Pharmacologic vitreolysis with plasmin: clinical studies. Pharmacologic vitreolysis with plasmin]. Wu et al. [130] noted that a combination of reduced suction and a high cutting rate made it possible to remove sheets of vitreous off the retina but that a clean retinal surface was almost impossible to



Figure III.A-15 Demonstration of new-onset iris neovascularization which occurred ~6 weeks following intravitreal anti-VEGF injection in a child with FEVR who had previously been treated with lens-sparing vitrectomy and extensive ablation of peripheral avascular retina

achieve by mechanical dissection only. They propose that plasmin can remove vitreous from the retinal surface and silicone oil can then be used to stabilize the eye by providing long-term tamponade and reducing the stimulus for vascular leakage. As described above, promising results have been seen recently in the treatment of some forms of ROP with injection of forms of anti-vascular endothelial growth factor (anti-VEGF) agents to reduce abnormal neovascularization. Anti-VEGF agents have been reported for a patient with vitreous hemorrhage and neovascularization attributed to FEVR [131]. However, in our experience, new-onset iris neovascularization can occur in eyes treated with intravitreal anti-VEGF (personal observation, MEH 01/13) (Figure III.A-15). Therefore, much further study is needed before recommending anti-VEGF at this point.

1. FEVR Treatment Outcomes

It can be difficult to accurately quantify successful surgical outcomes in FEVR due to its progressive nature and associated periods of waxing and waning. Success rates of retinal reattachment range from 96 to 63 % [118, 122, 126–128]. Some authors feel that silicone oil decreases the frequency of recurrence and may be considered in eyes that have previously undergone vitrectomy and still show signs of activity [121].

Abbreviations

AAO	American Academy of Ophthalmology
AAP	American Academy of Pediatrics
AD	Autosomal dominant
APROP	Aggressive posterior retinopathy of prematurity
CRYO-ROP	Cryotherapy for Retinopathy of Prematurity

CT	Computed tomography
ERG	Electroretinography
ETROP	Early Treatment for Retinopathy of Prematurity
FA	Fluorescein angiography
FEVR	Familial exudative vitreoretinopathy
GA	Gestational age
ICROP	International classification for retinopathy of prematurity
IGF-1	Insulin-like growth factor-1
LSV	Lens-sparing vitrectomy
MRI	Magnetic resonance imaging
OCT	Optical coherence tomography
PFV	Persistent fetal vasculature
PMA	Postmenstrual age
ROP	Retinopathy of prematurity
SB	Scleral buckling
STOP-ROP	Supplemental therapeutic oxygen for prethreshold retinopathy of prematurity
VEGF	Vascular endothelial growth factor
VEP	Visual evoked potential

References

1. NEI press release. <http://www.nei.nih.gov/health/rop/rop.asp>. October 2009.
2. Patz A, Hoek LE, DeLaCruz E. Studies on the effect of high oxygen administration in retrolental fibroplasias. I. Nursery observations. *Am J Ophthalmol.* 1952;35:1248–53.
3. Kinsey VE. Cooperative study of retrolental fibroplasia and the use of oxygen. *Arch Ophthalmol.* 1956;56:481–543.
4. Crosse VM, Evans PJ. Prevention of retrolental fibroplasias. *AMA Arch Ophthalmol.* 1952;48(1):83–7.
5. Gilbert C, Fielder A, Gordillo L, Quinn G, Semiglia R, Visintin P, et al. Characteristics of infants with severe retinopathy of prematurity in countries with low, moderate, and high levels of development: implication for screening programs. *Pediatrics.* 2005;115:e510–25.
6. Schaffer DB, Palmer EA, Plotsky DF, Metz HS, Flynn JT, Tung B, et al. Prognostic factors in the natural course of retinopathy of prematurity. The Cryotherapy for Retinopathy of Prematurity Cooperative Group. *Ophthalmology.* 1993;100:230–7.
7. Early Treatment for Retinopathy of Prematurity Cooperative Group, Good WV, Hardy RJ, et al. Final visual acuity results in the early treatment for retinopathy of prematurity study. *Arch Ophthalmol.* 2010;128:663–71.
8. Early Treatment for Retinopathy of Prematurity Cooperative Group, Dobson V, Quinn GE, et al. Grating visual acuity results in the early treatment for retinopathy of prematurity study. *Arch Ophthalmol.* 2011;129:840–6.
9. Chen J, Smith LE. Retinopathy of prematurity. *Angiogenesis.* 2007;10(2):133–40.
10. Chan-Ling T, Gock B, Stone J. Supplemental oxygen therapy: basis for noninvasive treatment of retinopathy of prematurity. *Invest Ophthalmol Vis Sci.* 1995;36:1215–30.
11. Ashton N. Retinal angiogenesis in the human embryo. *Br Med Bull.* 1970;26:103–6.

12. Hasegawa T, McLeod DS, Prow T, Merges C, Grebe R, Luttj GA. Vascular precursors in developing human retina. *Invest Ophthalmol Vis Sci.* 2008;49:2178–92.
13. Chan-Ling T, Gock B, Stone J. The effect of oxygen on vasoformative cell division: evidence that ‘physiological hypoxia’ is the stimulus for normal retinal vasculogenesis. *Invest Ophthalmol Vis Sci.* 1995;36:1201–14.
14. Hellstrom A, Carlsson B, Niklassen A, et al. IGF-1 is critical for normal vascularization of the human retina. *J Clin Endocrinol Metab.* 2002;87:3413–6.
15. Smith LE. IGF-1 and retinopathy of prematurity in the preterm infant. *Biol Neonate.* 2005;88:237–44.
16. Hartmann JS, Thompson H, Wang H, Kanekar S, Huang W, Budd SJ, Hartnett ME. Expression of vascular endothelial growth factor and pigment epithelial-derived factor in a rat model of retinopathy of prematurity. *Mol Vis.* 2011;17:1577–87.
17. Hartnett ME. Studies on the pathogenesis of avascular retina and neovascularization into the vitreous in peripheral severe retinopathy of prematurity (an american ophthalmological society thesis). *Trans Am Ophthalmol Soc.* 2010;108:96–119.
18. Hartnett ME, Penn JS. Mechanisms and management of retinopathy of prematurity. *N Engl J Med.* 2012;367(26):2515–26.
19. Wang H, Byfield G, Jiang Y, Smith GW, McCloskey M, Hartnett ME. VEGF-mediated STAT3 activation inhibits retinal vascularization by down-regulating local erythropoietin expression. *Am J Pathol.* 2012;180(3):1243–53.
20. Evolution of Stage 4 Retinopathy of Prematurity Capone A and Trese MT in Pediatric Retina, volume 2 Lippincott Wolters Kluwer. Chapter 44, 2013;568–573.
21. Hartnett ME, McColm JR. Retinal features predictive of progression to stage 4 ROP. *Retina.* 2004;24:237–41.
22. Coats DK. Retinopathy of prematurity: involution, factors predisposing to retinal detachment, and expected utility of preemptive surgical reoperation. *Trans Am Ophthalmol Soc.* 2005;103:281–312.
23. Sebag J. Imaging vitreous. *Eye.* 2002;16(4):429–39.
24. Ueno N, Sebag J, Hirokawa H, Chakrabarti B. Effects of visible-light irradiation on vitreous structure in the presence of a photosensitizer. *Exp Eye Res.* 1987;44(6):863–70.
25. Raymond L, Jacobson B. Isolation and identification of stimulatory and inhibitory cell growth factors in bovine vitreous. *Exp Eye Res.* 1982;34(2):267.
26. Luttj GA, Mello RJ, Chandler C, Fait C, Bennett A, Patz A. Regulation of cell growth by vitreous humour. *J Cell Sci.* 1985;76(1):53–65.
27. Jacobson B, Dorfman T, Basu P, Hasany S. Inhibition of vascular endothelial cell growth and trypsin activity by vitreous. *Exp Eye Res.* 1985;41(5):581–95.
28. Machemer R. Description and pathogenesis of late stages of retinopathy of prematurity. *Ophthalmology.* 1985;92(8):1000.
29. Foos R. Chronic retinopathy of prematurity. *Ophthalmology.* 1985;92(4):563–74.
30. Cunningham S, Fleck BW, Elton RA, et al. Transcutaneous oxygen levels in retinopathy of prematurity. *Lancet.* 1995;346:1464–5.
31. Seiberth V, Linderkamp O. Risk factors in retinopathy of prematurity. A multivariate statistical analysis. *Ophthalmologica.* 2000;214:131–5.
32. Vintzileos AM, Ananth CV, Smulian JC, et al. The impact of prenatal care in the United States on preterm births in the presence and absence of antenatal high-risk conditions. *Am J Obstet Gynecol.* 2002;187:1254–7.
33. Akinbami LJ, Schoendorf KC, Kiely JL. Risk of preterm birth in multiparous teenagers. *Arch Pediatr Adolesc Med.* 2000;154:1101–7.
34. Datta-Bhutada S, Johnson HL, Rosen TS. Intrauterine cocaine and crack exposure: neonatal outcome. *J Perinatol.* 1998;18:183–8.
35. The STOP-ROP Multicenter Study Group. Supplemental therapeutic oxygen for prethreshold retinopathy of prematurity (STOP-ROP), a randomized, controlled trial. I: Primary outcomes. *Pediatrics.* 2000;105:295–310.
36. Chow LC, Wright KW, CSMC Oxygen Administration Study Group. Can changes in clinical practice decrease the incidence of severe retinopathy of prematurity in very low birth weight infants? *Pediatrics.* 2003;111(2):339–45.
37. VanderVeen DK, Mansfield TA, Eichenwald EC. Lower oxygen saturation alarm limits decrease the severity of retinopathy of prematurity. *J AAPOS.* 2006;10(5):445–8.
38. Britt MT, Sandoval M, Siegel LM. Decreased incidence of laser surgery for severe retinopathy of prematurity with supplemental oxygen protocol. *J AAPOS.* 2005;9(1):89.
39. Lane RH, Hartnett ME. Effects of oxygen on the development and severity of retinopathy of prematurity. *J AAPOS.* 2013;17(3):229–34.
40. Raju TNK, Langenberg P, Bhutani V, et al. Vitamin E prophylaxis to reduce retinopathy of prematurity: a reappraisal of published trials. *J Pediatr.* 1997;131:844–50.
41. Johnson L, Bowen Jr FW, Abbasi S, et al. Relationship of prolonged pharmacologic serum levels of Vitamin E to incidence of sepsis and incidence of necrotizing enterocolitis in infants with birth weight 1500 grams or less. *Pediatrics.* 1985;75:619–38.
42. Phelps DL, Lakatos L, Watts JL. D-Penicillamine for preventing retinopathy of prematurity in preterm infants. *Cochrane Database Syst Rev.* 2001;(1):CD001073.
43. Christensen RD, Alder SC, Richard SC, et al. D-Penicillamine administration and the incidence of retinopathy of prematurity. *J Perinatol.* 2007;27(2):103–11.
44. Tandon M, Dutta S, Dogra MR, Gupta A. Oral D-Penicillamine for the prevention of retinopathy of prematurity in very low birth weight infants: a randomized, placebo controlled trial. *Acta Paediatr.* 2010;99(9):1324–8.
45. Siatkowski RM, Yanovitch TL, Ash JD, Moreau A. The effects of D-penicillamine on a murine model of oxygen-induced retinopathy. *J AAPOS.* 2001;15(4):370–3.
46. May CA. The influence of triamcinolone on endostatin-like proteins in oxygen-induced retinopathy of prematurity. *Exp Eye Res.* 2012;100:86–7.
47. Zhang HB, Sun NX, Liang HC, et al. 17-Alpha-estradiol ameliorating oxygen induced retinopathy in a murine model. *Jpn J Ophthalmol.* 2012;56(4):407–15.
48. American Academy of Pediatrics Section on Ophthalmology, American Academy of Ophthalmology, American Association for Pediatric Ophthalmology and Strabismus, American Association of Certified Orthoptists. Screening examination of premature infants for retinopathy of prematurity. *Pediatrics.* 2013;131:189–95.
49. Early Treatment For Retinopathy Of Prematurity Cooperative Group. Revised indications for the treatment of retinopathy of prematurity: results for the early treatment of retinopathy of prematurity randomized trial. *Arch Ophthalmol.* 2003;121:1684–94.
50. Lofqvist C, Hansen-Pupp I, Anderssen E, et al. Validation of a new retinopathy of prematurity screening method monitoring longitudinal postnatal weight and insulin-like growth factor I. *Arch Ophthalmol.* 2009;127:622–7.
51. Hellstrom A, Hard AL, Engstrom E, et al. Early weight gain predicts retinopathy in preterm infants: new, simple, efficient approach to screening. *Pediatrics.* 2009;123:e638–45.
52. Wu C, Lofqvist C, Smith LE, et al. Importance of early postnatal weight gain for normal retinal angiogenesis in very preterm infants: a multicenter study analyzing weight velocity deviations

- for the prediction of retinopathy of prematurity. *Arch Ophthalmol.* 2012;130:992–9.
53. Wu C, Vanderveen DK, Hellstrom A, et al. Longitudinal postnatal weight gain measurements for the prediction of retinopathy of prematurity. *Arch Ophthalmol.* 2010;128:443–7.
 54. Binenbaum G, Ying GS, Quinn GE, et al. The CHOP postnatal weight gain, birth weight, and gestational age retinopathy of prematurity risk model. *Arch Ophthalmol.* 2012;130:1560–5.
 55. Binenbaum G, Ying GS, Quinn GE, et al. A clinical prediction model to stratify retinopathy of prematurity using postnatal weight gain. *Pediatrics.* 2011;127:e607–14.
 56. O’Keefe M, Kirwan C. Screening for retinopathy of prematurity. *Early Hum Dev.* 2008;84:89–94.
 57. Good WV, Hardy RJ, Dobson V, et al. Early Treatment for Retinopathy of Prematurity Cooperative Group. Final visual acuity results in the early treatment for retinopathy of prematurity study. *Arch Ophthalmol.* 2010;128(6):663–71.
 58. Quinn GE, Dobson V, Hardy R, et al. Visual field extent at 6 years of age in children who had high-risk prethreshold retinopathy of prematurity. *Arch Ophthalmol.* 2011;129:127–32.
 59. Alme AM, Mulhern ML, Hejkal TW, et al. Outcome of retinopathy of prematurity patients following adoption of revised indications for treatment. *BMC Ophthalmol.* 2008;8(1):23.
 60. Simpson JL, Melia M, Yang MB, et al. Current role of cryotherapy in retinopathy of prematurity: a report by the American Academy of Ophthalmology. *Ophthalmology.* 2012;119:873–7.
 61. Palmer EA, Hardy RJ, Dobson V, et al. 15 year outcomes following threshold retinopathy of prematurity: final results from the multicenter trial of cryotherapy for retinopathy of prematurity. *Arch Ophthalmol.* 2005;123:311–8.
 62. Banach MJ, Ferrone PJ, Trese MT. A comparison of dense versus less dense diode laser photocoagulation patterns for threshold retinopathy of prematurity. *Ophthalmology.* 2000;107:324–8.
 63. Paysse EA, Lindsey JL, Coats DK, et al. Therapeutic outcomes of cryotherapy versus transpupillary diode laser photocoagulation for threshold retinopathy of prematurity. *J AAPOS.* 1999;3(4):234–40.
 64. Ng EY, Connolly BP, McNamara JA, et al. A comparison of laser photocoagulation with cryotherapy for threshold retinopathy of prematurity at 10 years: part 1. Visual function and structural outcome. *Ophthalmology.* 2002;109(5):928–34.
 65. Connolly BP, Ng EY, McNamara JA, et al. A comparison of laser photocoagulation with cryotherapy for threshold retinopathy of prematurity at 10 years: part 2. Refractive outcome. *Ophthalmology.* 2002;109(5):936–41.
 66. Andersen CC, Phelps DL. Peripheral retinal ablation for threshold retinopathy of prematurity in preterm infants. *Cochrane Database Syst Rev.* 2000;(2): CD001693.
 67. Matsuyama K, Ogata N, Matsuoka M, Wada M, Takahashi K, Nishimura T. Plasma levels of vascular endothelial growth factor and pigment epithelium-derived factor before and after intravitreal injection of bevacizumab. *Br J Ophthalmol.* 2010;94:1215–8.
 68. Mintz-Hittner HA, Kennedy KA, Chuang AZ, BEAT-ROP Cooperative Group. Efficacy of intravitreal bevacizumab for stage 3+ retinopathy of prematurity. *N Engl J Med.* 2011;364:603–15.
 69. Hu J, Blair MP, Shapiro MJ, et al. Reactivation of retinopathy of prematurity after bevacizumab injection. *Arch Ophthalmol.* 2012;130:1000–6.
 70. McCloskey M, Wang H, Jiang Y, Smith GW, Strange J, Hartnett ME. Anti-VEGF antibody leads to later atypical intravitreal neovascularization and activation of angiogenic pathways in a rat model of retinopathy of prematurity. *Invest Ophthalmol Vis Sci.* 2013;54(3):2020–6.
 71. Gaudreault J, Fei D, Rusit J, Suboc P, Shiu V. Preclinical pharmacokinetics of ranibizumab (rhuFabV2) after a single intravitreal administration. *Invest Ophthalmol Vis Sci.* 2005;46:726–33.
 72. Miyake T, Sawada O, Kakinoki M, Sawada T, Kawamura H, Ogasawara K, et al. Pharmacokinetics of bevacizumab and its effect on vascular endothelial growth factor after intravitreal injection of bevacizumab in macaque eyes. *Invest Ophthalmol Vis Sci.* 2010;51:1606–8.
 73. Sato T, Wada K, Arahori H, et al. Serum concentrations of bevacizumab (avastin) and vascular endothelial growth factor in infants with retinopathy of prematurity. *Am J Ophthalmol.* 2012;153(2):327–33.
 74. Zehetner C, Kirchmair R, Huber S, et al. Plasma levels of vascular endothelial growth factor before and after intravitreal injection of bevacizumab, ranibizumab and pegaptanib in patients with age-related macular degeneration, and in patients with diabetic macular oedema. *Br J Ophthalmol.* 2013;97(4):454–9.
 75. Hoerster R, Muether P, Dahlke C, et al. Serum concentrations of vascular endothelial growth factor in an infant treated with ranibizumab for retinopathy of prematurity. *Acta Ophthalmol.* 2013;91(1):e74–5.
 76. Sebag J. Pharmacologic vitreolysis. *Retina.* 1998;18(1):1–3.
 77. Sebag J. Pharmacologic vitreolysis – premise and promise of the first decade. *Retina.* 2009;29(7):871–4.
 78. Stenzel D, Lundkvist A, Sauvaget D, et al. Integrin-dependent and -independent functions of astrocytic fibronectin in retinal angiogenesis. *Development.* 2011;138:4451–63.
 79. Pepper MS. Role of the matrix metalloproteinase and plasminogen activator-plasmin systems in angiogenesis. *Arterioscler Thromb Vasc Biol.* 2001;21:1104–17.
 80. Wu W-C, Drenser KA, Lai M, Capone A, Trese MT. Plasmin enzyme-assisted vitrectomy for primary and reoperated eyes with stage 5 retinopathy of prematurity. *Retina.* 2008;28:S75–80. doi:10.1097/IAE.0b013e318158ea0e.
 81. Wong SCC, Jr A. Microplasmin (ocriplasmin) in pediatric vitreoretinal surgery: update and review. *Retina.* 2013;33:339–48.
 82. Coats DK, Miller AM, Hussein MA, et al. Involution of retinopathy of prematurity after laser treatment: factors associated with development of retinal detachment. *Am J Ophthalmol.* 2005;140:214–22.
 83. Trese MT, Droste PJ. Long-term postoperative results of a consecutive series of stages 4 and 5 retinopathy of prematurity. *Ophthalmology.* 1998;105:992–7.
 84. Hartnett ME. Features associated with surgical outcome in patients with stages 4 and 5 retinopathy of prematurity. *Retina.* 2003;23(3):322–9.
 85. Clark D, Mandal K. Treatment of retinopathy of prematurity. *Early Hum Dev.* 2008;84:95–9.
 86. Hartnett ME, Magaluri S, Thompson HW, McCollm JR. Comparison of retinal outcomes after scleral buckle or lens-sparing vitrectomy for stage 4 retinopathy of prematurity. *Retina.* 2004;24:753–7.
 87. Ferrone PJ, Harrison C, Trese MT. Lens clarity after lens-sparing vitrectomy in a pediatric population. *Ophthalmology.* 1997;104:273–8.
 88. Lakhanpal RR, Davis GH, Sun RL, et al. Lens clarity after three port lens-sparing vitrectomy in stage 4A and 4B retinal detachments secondary to retinopathy of prematurity. *Arch Ophthalmol.* 2006;124(1):20–3.
 89. Mann I. The development of the human eye. New York: Grune & Stratton Inc.; 1950.
 90. Hamming NA, et al. Ultrastructure of the hyaloid vasculature in primates. *Invest Ophthalmol Vis Sci.* 1977;16:408–15.
 91. Gergely K, Gerinec A. A consonant construction of the hyaloids and retinal vascular systems by the angiogenic process. *Bratisk Lek Listy.* 2011;112(3):143–51.
 92. Alvarez Y, et al. Genetic determinants of hyaloid and retinal vasculature in zebrafish. *BMC Dev Biol.* 2007;7:114.

93. Jack RL. Regression of the hyaloid artery system: an ultrastructural analysis. *Am J Ophthalmol*. 1972;74:261–72.
94. Latker CH, Kuwabara T. Regression of the tunica vasculosalensis in the postnatal rat. *Invest Ophthalmol Vis Sci*. 1981;21:689–99.
95. Duke-Elder S. System of ophthalmology. Vol. 3. Normal and abnormal development. Part 1: embryology. St. Louis: The C.V. Mosby Company, 1964. In: Hamming NA, Apple DJ, Gieser DK, Vygantas CM. Ultrastructure of the hyaloid vasculature in primates. *Invest Ophthalmol Vis Sci*. 1977;16:408–15.
96. Delaney WV. Prepapillary hemorrhage and persistent hyaloid artery. *Am J Ophthalmol*. 1980;90:419–21.
97. Renz B, Vygantas C. Hyaloid vascular remnants in human neonates. *Ann Ophthalmol*. 1977;9:179–84.
98. Mets MB. Childhood blindness and visual loss: an assessment at two institutions including a “new” cause. *Trans Am Ophthalmol Soc*. 1999;97:653–96.
99. Gans B. The pupillary membrane in premature infants. *Arch Dis Child*. 1959;34:292–7.
100. Hollenberg MJ, Dickson DH. Scanning electron microscopy of the tunica vasculosa lentis of the rat. *Can J Ophthalmol*. 1971;6:301–10.
101. Meisels H, Goldberg MF. Vascular anastomoses between the iris and persistent hyperplastic primary vitreous. *Am J Ophthalmol*. 1979;88:179–85.
102. Goldberg MF. Clinical manifestations of ectopia lentis et pupillae in 16 patients. *Ophthalmology*. 1988;95:1080–7.
103. Gifford SR, Latta JS. Pseudoglioma and remains of the tunica vasculosalensis. *Am J Ophthalmol*. 1923;6:565–71.
104. Sellheyer K, Spitznas M. Ultrastructure of the human posterior tunica vasculosalensis during early gestation. *Graefes Arch Clin Exp Ophthalmol*. 1987;225:377–83.
105. Hittner HM, Hirsch NJ, Rudolph HJ. Assessment of gestational age by examination of the anterior vascular capsule of the lens. *J Pediatr*. 1977;91:455–8.
106. Pollard ZF. Persistent hyperplastic primary vitreous, diagnosis, treatment, and results. *Am Ophthalmol Soc*. 1997;95:487–549.
107. Goldberg MF. Persistent fetal vasculature (PFV): an integrated interpretation of signs and symptoms associated with persistent hyperplastic primary vitreous (PHPV) LIV Edward Jackson Memorial Lecture. *Am J Ophthalmol*. 1997;124:587–626.
108. Xu O, Wang YS, Dabdoub A, et al. Vascular development in the retina and inner ear: control by norrin and frizzled 4, a high affinity ligand receptor pair. *Cell*. 2004;116:883–95.
109. Prasov L, et al. ATOH7 mutations cause autosomal recessive persistent hyperplasia of the primary vitreous. *Hum Mol Genet*. 2012;21(16):3681–94.
110. Edward MM, Mcleone DS, Grebe R, Heng C, Lefebvre O, Luty GA. Lama1 mutations lead to vitreoretinal blood vessel formation, persistence of fetal vasculature, and epiretinal membrane formation in mice. *BMC Dev Biol*. 2011;11:60.
111. Martin AC, Thornton JD, Liu J, et al. Pathogenesis of persistent hyperplastic primary vitreous in mice lacking the arf tumor suppressor gene. *Invest Ophthalmol Vis Sci*. 2004;45:3387–96.
112. Reichel MB, Ali RR, D’Esposito F, et al. High frequency of persistent hyperplastic primary vitreous and cataracts in p-53 deficient mice. *Cell Death Differ*. 1998;5:156–62.
113. Zhang J, Fuhrmann S, Vetter ML. A nonautonomous role for retinal frizzled-5 in regulating hyaloids vitreous vasculature development. *Invest Ophthalmol Vis Sci*. 2008;49:5561–7.
114. Rutland CS, Mitchell CA, Nasir M, Konerding MA, Drexler HC. Microphthalmia, persistent hyperplastic hyaloid vasculature and lens anomalies following overexpression of VEGF-A188 from the alpha A-crystallin promoter. *Mol Vis*. 2007;13:47–56.
115. Criswick VG, Schepens CL. Familial exudative vitreoretinopathy. *Am J Ophthalmol*. 1969;68:578–94.
116. Ranchod TM, Ho LY, Dresner KA, Capone Jr A, Trese MT. Clinical presentation of familial exudative vitreoretinopathy. *Ophthalmology*. 2011;118:2070–5.
117. Benson WE. Familial exudative vitreoretinopathy. *Trans Am Ophthalmol Soc*. 1995;93:473–521.
118. Tasman W, Augsburger JJ, Shields JA, et al. Familial exudative vitreoretinopathy. *Trans Am Ophthalmol Soc*. 1981;79:211–26.
119. Miyakubo H, Inohara N, Hashimoto K. Retinal involvement in familial exudative vitreoretinopathy. *Ophthalmologica*. 1982;185:125–35.
120. Van Nouhuys CE. Dominant exudative vitreoretinopathy and other vascular developmental disorders of the peripheral retina [thesis]. *Doc Ophthalmol*. 1982;54:1–415.
121. Trese MT, Capone Jr A. Familial exudative vitreoretinopathy. In: *Pediatric retina*. Philadelphia: Lippincott Williams & Wilkins; 2005. p. 425–8.
122. Pendergast SD, Trese MT. Familial exudative vitreoretinopathy: results of surgical management. *Ophthalmology*. 1998;105:1015–23.
123. Toomes C, Downey L. Familial exudative vitreoretinopathy: autosomal dominant. *GeneReviews*. Available at www.genetests.org. Accessed Mar 2013.
124. Shukla D, Singh J, Sudheer G, et al. Familial exudative vitreoretinopathy (FEVR). Clinical profile and management. *Indian J Ophthalmol*. 2003;51:323–8.
125. Toomes C, Bottomley HM, Jackson RM, et al. Mutations in LRP5 or FZD4 underlie the common familial exudative vitreoretinopathy locus on chromosome 11q. *Am J Hum Genet*. 2004;74:721–30.
126. Ikeda T, Tano Y, Tsujikawa K, et al. Vitrectomy for rhegmatogenous or tractional retinal detachment with familial exudative vitreoretinopathy. *Ophthalmology*. 1999;106:1081–5.
127. Glazer LC, Maguir A, Blumenkranz MS, et al. Improved surgical treatment of familial exudative vitreoretinopathy in children. *Am J Ophthalmol*. 1995;120:471–9.
128. Chen SN, Hwang JF, Lin CJ. Clinical characteristics and surgical management of familial exudative vitreoretinopathy-associated rhegmatogenous retinal detachment. *Retina*. 2012;32(2):220–5.
129. Williams JG, Trese MT, Williams GA, et al. Autologous plasmin enzyme in the surgical management of diabetic retinopathy. *Ophthalmology*. 2001;108:1902–5.
130. Wu WC, Dresner KA, Trese MT, et al. Pediatric traumatic macular hole: results of autologous plasmin enzyme-assisted vitrectomy. *Am J Ophthalmol*. 2007;144(5):668–72.
131. Tagami M, Kusuhara S, Honda S, et al. Rapid regression of retinal hemorrhage and neovascularization in a case of familial exudative vitreoretinopathy treated with intravitreal bevacizumab. *Graefes Arch Clin Exp Ophthalmol*. 2008;246(12):1787–9.
132. Sebag J, Nguyen N. Vitreous embryology and vitreo-retinal developmental disorders. In: Hartnett ME et al., editors. *Pediatric retina*. Philadelphia: Lippincott; 2005. p. 13–28.

J. Sebag, Moritz Niemeyer, and Michael J. Koss

Outline

- I. **Introduction**
- II. **Vitreous Biochemistry**
- III. **Aging**
 - A. Vitreous Body Aging
 1. Pathogenesis of Liquefaction
 2. Structural Changes
 - B. Aging of the Vitreoretinal Interface
- IV. **Posterior Vitreous Detachment**
 - A. Diagnosis of PVD
 1. Ultrasound
 2. Optical Coherence Tomography (OCT)
 - a. Vitreoretinal Interface by OCT
 - b. Vitreous Body Imaging by OCT
 - B. Conditions Predisposing to PVD
 1. Cataract Surgery
 2. Myopia
 3. Trauma
 - a. Blunt Trauma
 - b. Penetrating Trauma
- V. **Anomalous Posterior Vitreous Detachment (APVD)**
 - A. Etiology of Anomalous PVD
 - B. Retinal Effects of Anomalous PVD

1. Peripheral Retinal Effects of APVD
2. Macular Effects of Anomalous PVD
 - a. Full-Thickness Vitreomacular Traction
 - i. Vitreomacular Traction (VMT)
 - ii. Age-Related Macular Degeneration
 - iii. Cystoid Macular Edema (CME) and Macular Cysts
 - iv. Diabetic Macular Edema
 - b. Partial-Thickness Vitreomacular Traction (Vitreoschisis)
 - i. Anterior vs. Posterior Split
 - ii. Macular Pucker
 - iii. Macular Hole

References

Keywords

Vitreous • Vitreoretinal interface • Hyalocytes • Aging • Liquefaction • Vitreoretinal dehiscence • Posterior vitreous detachment (PVD) • Anomalous PVD • Vitreomacular traction • Vitreo-papillary adhesion • Vitreoschisis • Macular hole • Macular pucker

Key Concepts

1. Vitreous gel liquefaction without vitreoretinal dehiscence leads to anomalous PVD with untoward effects on both the vitreous and retina.
2. Peripheral vitreoretinal separation with persistent full-thickness attachment of the vitreous to the posterior pole places traction upon the macula causing various maculopathies. Moreover, vitreomacular adhesion is highly associated with exudative AMD and diabetic macular edema, while vitreo-papillary adhesion contributes to macular cysts and holes.
3. Vitreoschisis occurs when anomalous PVD splits the posterior vitreous cortex, resulting in macular pucker via centripetal (inward, toward the fovea) tangential contraction or macular hole via outward centrifugal tangential contraction.

Electronic supplementary material Supplementary material is available in the online version of this chapter at [10.1007/978-1-4939-1086-1_14](https://doi.org/10.1007/978-1-4939-1086-1_14). Videos can also be accessed at <http://www.springerimages.com/videos/978-1-4939-1085-4>.

J. Sebag, MD, FACS, FRCOphth, FARVO (✉)
M. Niemeyer, MD
VMR Institute for Vitreous Macula Retina,
7677 Center Avenue, suite 400,
Huntington Beach, CA 92647, USA

Doheny Eye Institute, Los Angeles, CA, USA
e-mail: jsebag@VMRinstitute.com; moritz.niemeyer@googlemail.com

M.J. Koss, MD, FEBO
Department of Ophthalmology, Rupprecht Karls University,
Heidelberg, Germany

Doheny Eye Institute, Los Angeles, CA, USA
e-mail: michael.koss@me.com

I. Introduction

Alterations in the molecular composition, organization, and structure of the human vitreous body are an inevitable consequence of aging. Complete and innocuous posterior vitreous detachment (PVD) is the most common ultimate consequence of vitreous aging [see chapter II.C. Vitreous aging and PVD], but this can often be disturbed by anomalies in this complex process. Insufficient dehiscence at the vitreoretinal interface, excessive gel liquefaction, or both can result in an anomalous PVD (APVD), sometimes associated with vitreoschisis (VS), which is a lamellar split in the posterior vitreous cortex. APVD and VS are associated with various clinical pathologies. A detailed analysis of vitreous pathophysiology that leads to APVD and VS will enable a better understanding of vitreoretinal disease pathogenesis, improve diagnostic acumen, and provide new directions for therapeutic approaches that will ultimately lead to effective preventative strategies.

II. Vitreous Biochemistry

Vitreous has a high content of water, but its consistency is mainly determined by the structural macromolecules collagen [see chapter I.A. Vitreous proteins] and hyaluronan [see chapter I.F. Vitreous biochemistry and artificial vitreous]. Extracellular matrix components and miscellaneous compounds further contribute to vitreous morphology especially at the vitreoretinal interface [see chapter II.E. Vitreoretinal interface and ILM].

Collagen is the major structural protein, and type II collagen comprises the largest part of the total collagen content in the human vitreous [1]. Type II collagen combines with types IX, and V/XI collagen to form fibrils. It is believed that collagen fibrils are spaced apart by hyaluronan via interaction with the chondroitin sulfate chains of type IX collagen [2]. Other proteoglycans and likely other components (like opticin) further stabilize this macromolecular network that constitutes gel vitreous. With aging, chondroitin sulfate, opticin, and/or other components are lost or altered promoting aggregation of vitreous collagen fibrils into visible fibers, both *in vivo* at the slit lamp and *in vitro* by dark-field slit microscopy. These extend from the vitreous base to the posterior vitreous cortex in an anteroposterior direction, somewhat concentric with the globe peripherally (Figure III.B-1).

The areas adjacent to these large fibers have a low density of collagen fibrils and higher concentration of hyaluronan (HA) molecules with water [3], resulting in less light scattering. This process advances with aging, and hyaluronan–collagen molecules further dissociate resulting in profound liquefaction and ultimate collapse of the vitreous body [3]. This is driven by liquid vitreous, which dissects a plane between the posterior vitreous cortex and the inner limiting membrane of the retina. If there are no abnormal adhesions at this interface, an innocuous PVD is the result [see chapter II.C. Vitreous aging and posterior vitreous detachment]. Liquefaction without dehiscence at the vitreoretinal interface causes anomalous PVD. This chapter will describe the current understanding of anomalous PVD as a unifying concept in vitreoretinal diseases.

reous cortex and the inner limiting membrane of the retina. If there are no abnormal adhesions at this interface, an innocuous PVD is the result [see chapter II.C. Vitreous aging and posterior vitreous detachment]. Liquefaction without dehiscence at the vitreoretinal interface causes anomalous PVD. This chapter will describe the current understanding of anomalous PVD as a unifying concept in vitreoretinal diseases.

III. Aging

Throughout life, changes in the composition and organization of the molecular components of vitreous play an important role in alterations of vitreous structure and very likely physiologic functions. This primarily consists of changes within the vitreous body, where the gel transforms to liquid, and at the vitreoretinal interface. The biochemical manifestations of aging are described in chapters I.A. Vitreous proteins; I.F. Vitreous biochemistry and artificial vitreous; II.C. Vitreous aging and posterior vitreous detachment.

A. Vitreous Body Aging

After the age of 40 there is a significant decrease in the gel volume and concurrent increase in the volume of liquid vitreous, primarily centrally [1, 2] (Figure III.B-2).

Within the vitreous body these changes ultimately form pockets of liquid vitreous, called “lacunae.” While it was previously held that a posterior lacuna is solely a manifestation of age-related liquefaction, recent studies [4, 5] have identified a premacular area of low collagen density (mostly HA and water, hence minimal light scattering) that probably corresponds to Worst’s premacular bursa [6] and may be important in various physiologic and pathologic processes (Figure III.B-3).

1. Pathogenesis of Liquefaction

The gel state of the vitreous primarily results from the interaction of vitreous collagen fibrils and HA. Changes can occur in HA–collagen interaction, either as a result of changes in collagen structure, the conformation of HA and/or other components such as the minor glycosaminoglycans and chondroitin sulfate profile of the vitreous [7] or reactive oxygen species generated by metabolism and/or photons. These promote dissociation of collagen and HA [8–11] with subsequent cross-linking and aggregation of vitreous collagen fibrils into bundles that are visible at the slit lamp and by dark-field slit microscopy (Figure III.B-4a). Ultrastructural studies have confirmed the collagenous nature of these fibrous structures (Figure III.B-4b). Concurrently, HA, which is very hydrophilic, pools and draws water forming liquid vitreous [12, 13] visible as dark spaces or lacunae by dark-field slit microscopy.

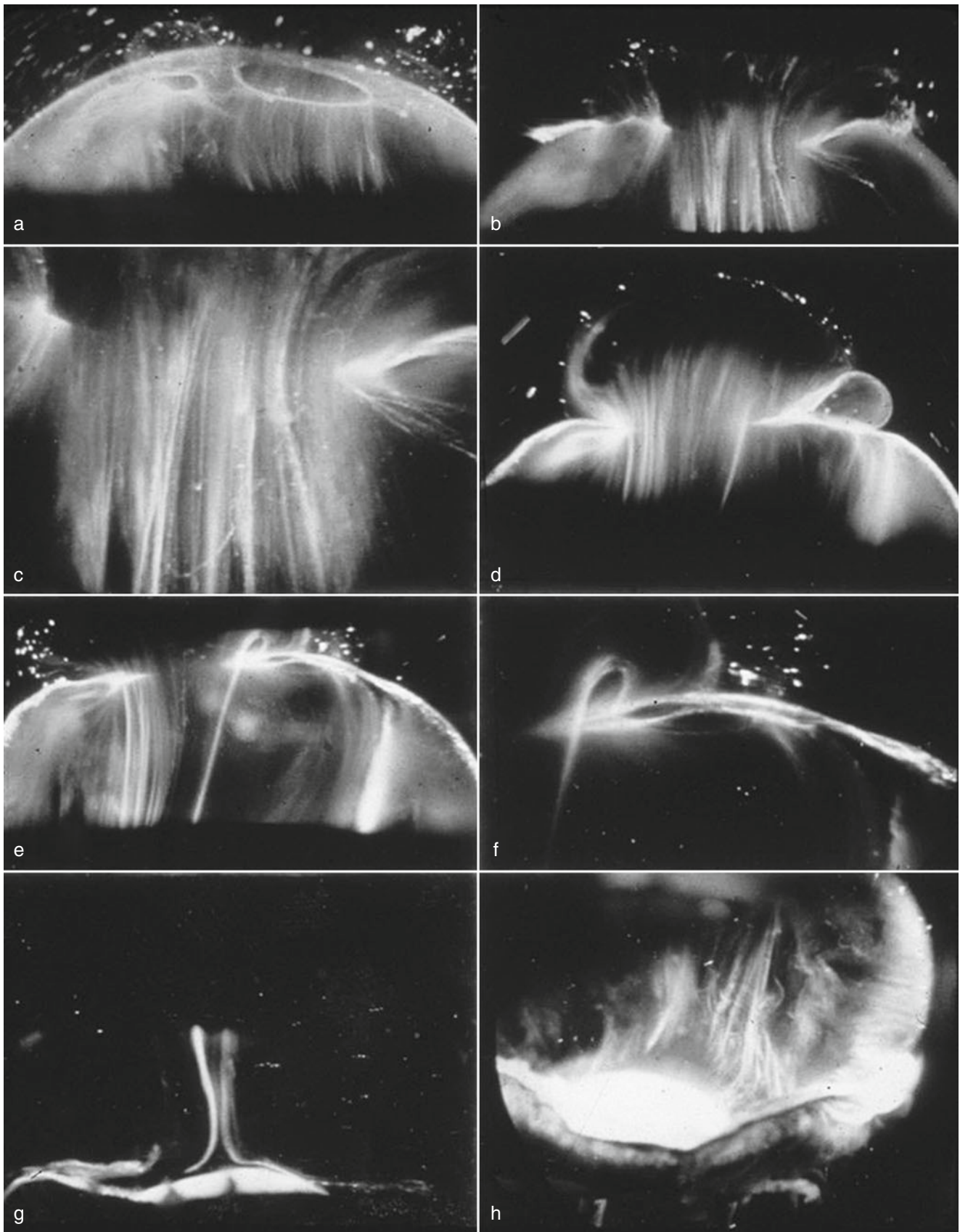


Figure III.B-1 Vitreous structure. Dark-field slit microscopy of the human vitreous demonstrates that the posterior vitreous in middle age features a hole in the pre-papillary posterior vitreous cortex (small circle to left in (a)) and the dehiscence in the premacular posterior vitreous cortex (b) through which fibers extrude into the retro-cortical (preretinal)

area (c, d). Vitreous structure in adults is characterized by macroscopic fibers with an anteroposterior orientation (c, e), inserting into the posterior vitreous cortex (e, f) and the vitreous base (h). Cloquet's canal is shown in (g) imaged in a 32 year old woman (note lens at bottom) (Reprinted with permission from Sebag [25])

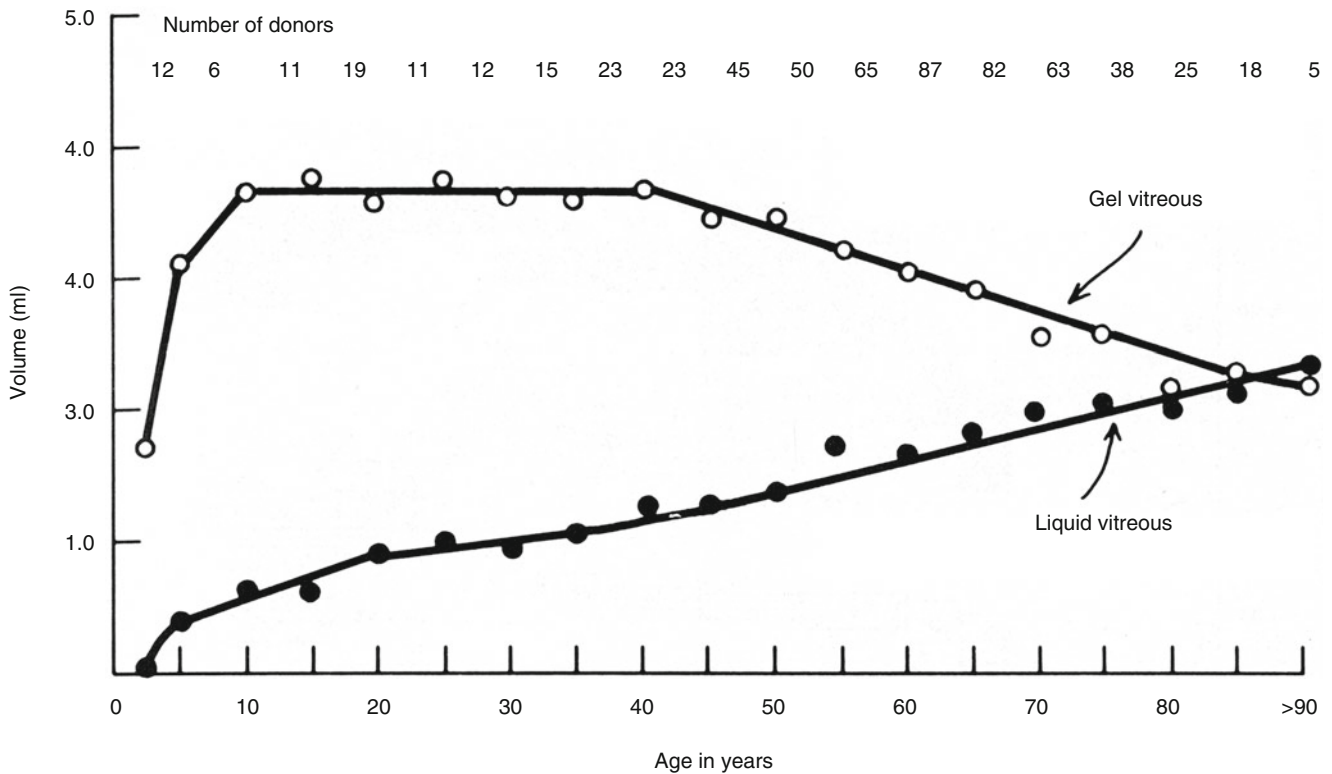


Figure III.B-2 Age-related rheologic changes in human vitreous. The volume of gel vitreous increases during growth and development, remains constant during young adulthood, then decreases significantly during old age. The volume of liquid vitreous appears to increase steadily throughout life (Reprinted with permission from Balazs and Denlinger [27])

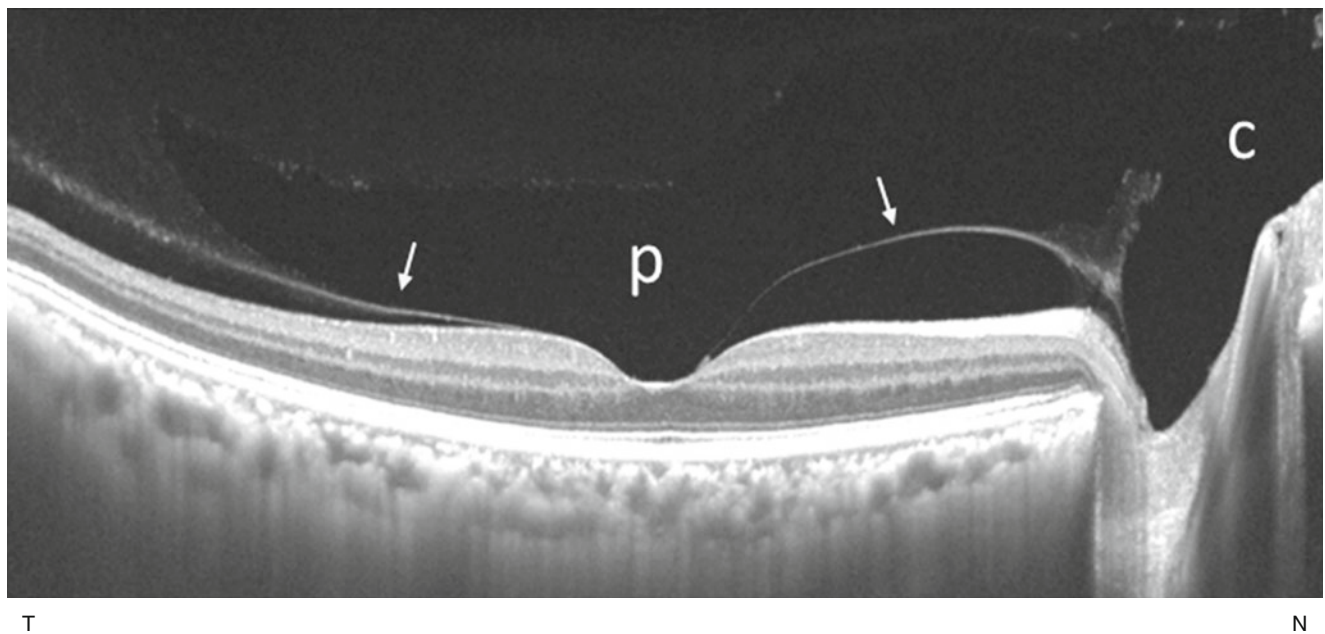


Figure III.B-3 SS-OCT imaging of perifoveal PVD with persistent central adhesion. p precortical pocket, C Cloquet's canal, N nasal, T temporal; arrows indicate the posterior vitreous cortex (Courtesy of Hiroataka Itakura, MD, via Ron Silverman, PhD)

2. Structural Changes

Liquefaction and vitreous collapse (syneresis) are the predominant morphologic changes of aging vitreous. On the one hand there is a progressive increase in liquefied spaces

and on the other an increase in optically dense areas. This results in a transition from a clear gel in youth to a fibrous structure in adults (Figure III.B-4). In old age advanced liquefaction with thickening and tortuosity of vitreous

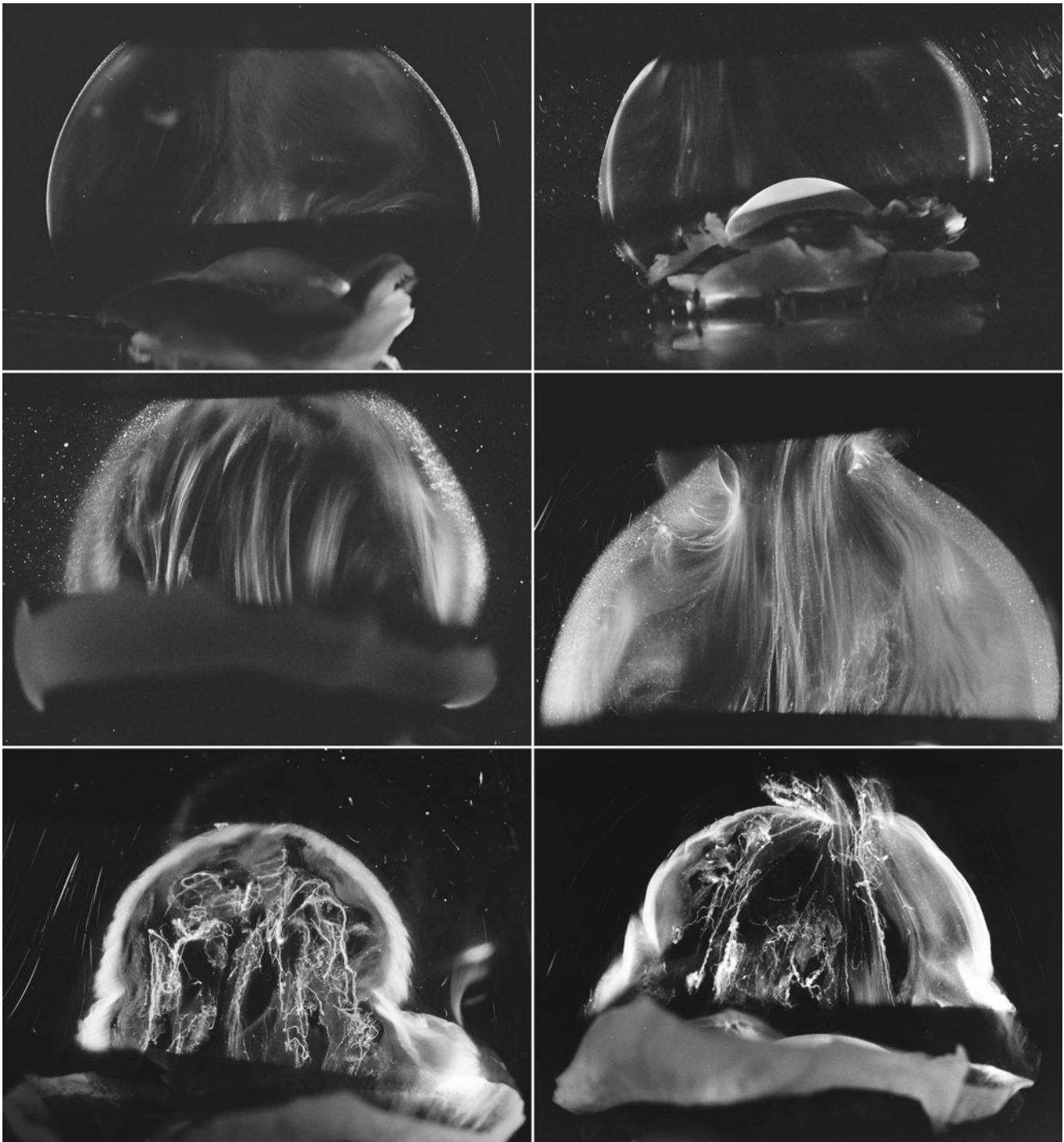


Figure III.B-4a Aging changes in human vitreous structure. (a) Dark-field slit microscopy of fresh unfixed whole human vitreous body with the sclera, choroid, and retina dissected off the vitreous body, which remains attached to the anterior segment. A slit lamp beam illuminates from the side, creating a horizontal optical section with an illumination-observation angle of 90° , maximizing the Tyndall effect. The anterior segment is below and the posterior pole is above in all specimens. *Top row*: the vitreous bodies of an 11-year-old girl (*left*) and a 14-year-old boy (*right*) demonstrate a homogeneous structure with no significant light scattering within the vitreous body, only at the periphery where the vitreous cortex is comprised of a dense matrix of collagen fibrils. The

posterior aspect of the lens is visible at the *bottom* of each image. *Middle row*: vitreous structure in a 56-year-old (*left*) and a 59-year-old (*right*) subject features macroscopic fibers in the central vitreous body with an anteroposterior orientation. These form when hyaluronan molecules no longer separate collagen fibrils, allowing cross-linking and aggregation of collagen fibrils into visible fibers. *Bottom row*: in old age the fibers of the central vitreous become significantly thickened and tortuous, as demonstrated in the two eyes of an 88-year-old woman. Adjacent to these large fibers are areas of liquid vitreous, at times forming pockets, called lacunae

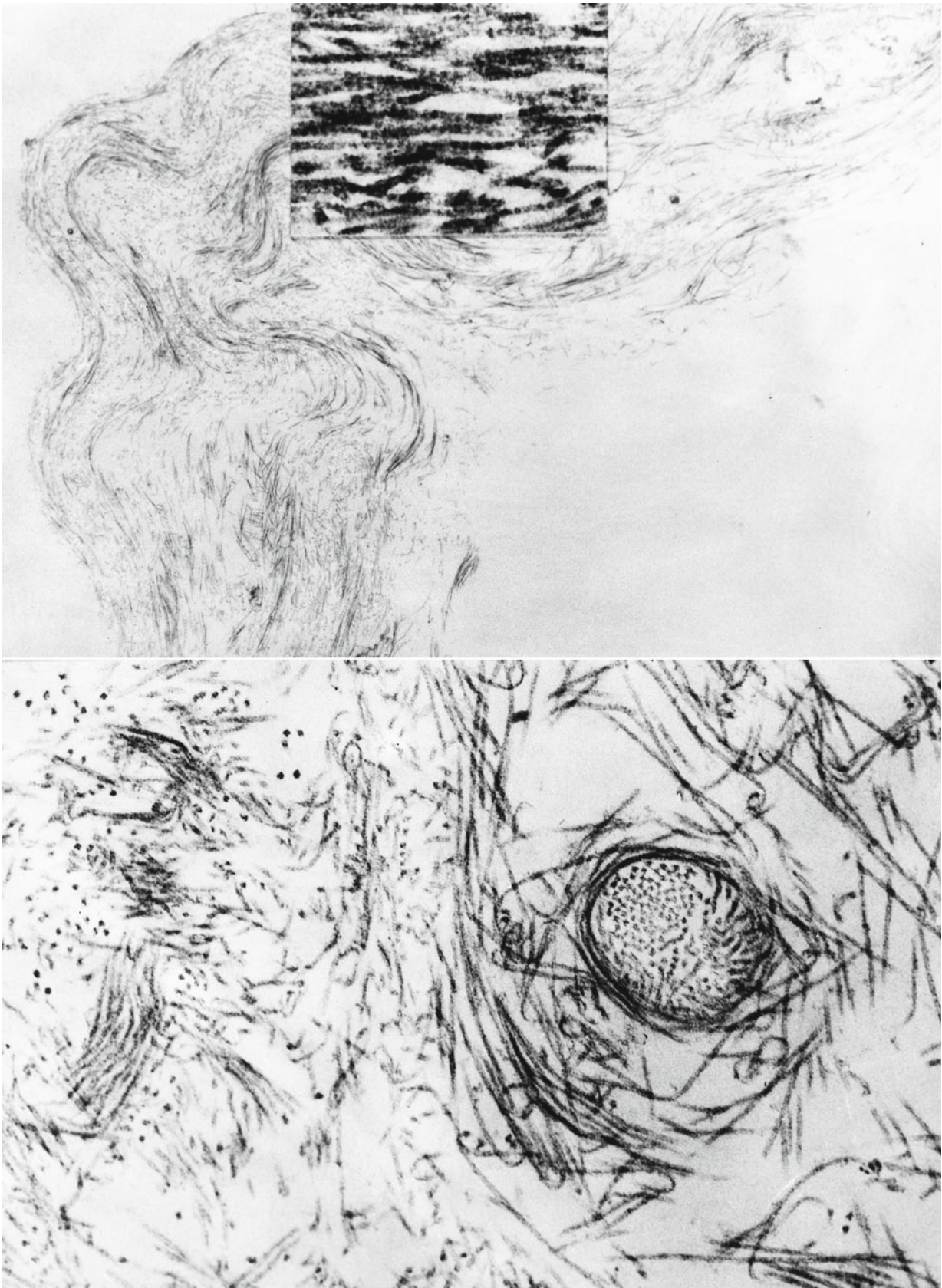


Figure III.B-4b Ultrastructure of human vitreous fibers. Transmission electron microscopy of human vitreous detected bundles of collagen fibrils shown longitudinally in the *upper image* and in cross section in

the *lower image*. The inset in the *upper image* is a high-magnification view of the bundle of fibrils demonstrating their collagenous nature (From Sebag and Balazs [126])

fibers goes along with syneresis. Postmortem studies found syneresis in 70 % of subjects in the eighth decade [14, 15]. Syneresis occurs earlier and is more extensive in myopic eyes and is accelerated with inflammation, trauma, and arthro-ophthalmopathies [14–16] [see chapter I.C. Hereditary vitreo-retinopathies].

B. Aging of the Vitreoretinal Interface

The collagen fibrils of the posterior vitreous cortex are organized in sheets or lamellae (Figure III.B-5). During youth, there is strong adhesion between the posterior vitreous cortex and the inner limiting membrane (ILM) of the retina, primarily at

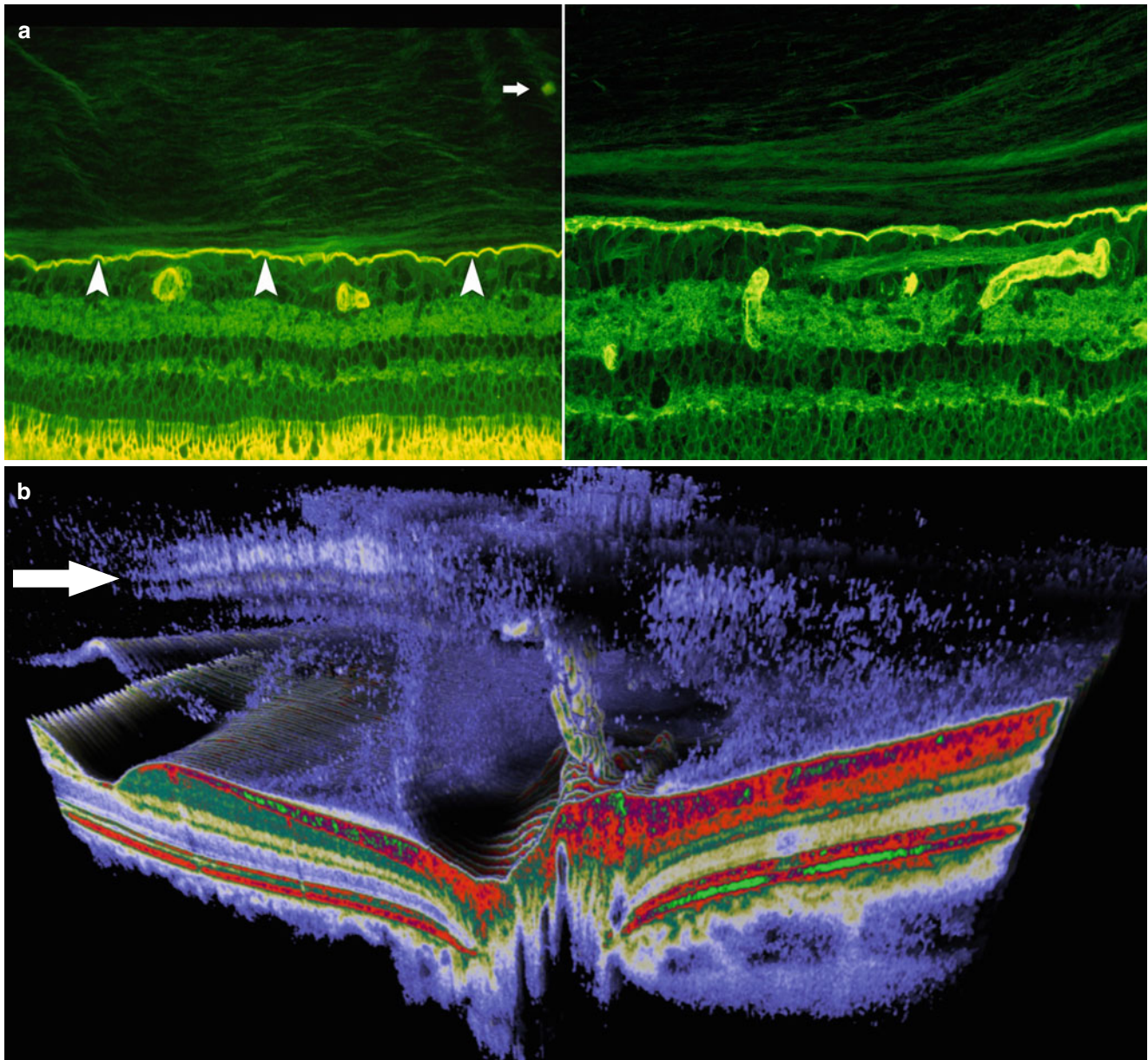


Figure III.B-5 (a) The lamellar structure of the mammalian posterior vitreous cortex is demonstrated in an adult monkey eye stained with fluorescein-conjugated ABA lectin stain. The vitreoretinal interface is shown with the vitreous above and the retina below. The ILM (*arrowheads*) is the intensely bright horizontal line across the image. Above the ILM is the posterior vitreous cortex whose lamellar structure is clearly evident at higher magnification (image to the *right*). These potential cleavage planes can separate during anomalous PVD or during vitrectomy surgery with membrane peeling, in each instance leaving a layer of vitreous attached to the macula. The *arrow* is pointed to a

hyalocyte embedded in the posterior vitreous cortex (Courtesy of Greg Hageman, PhD; original magnification=400×). (b) 3D OCT imaging of the vitreoretinal interface in a normal adult demonstrates a multilamellar structure. In this image at least three layers of the posterior vitreous cortex can be discerned (*large white arrow*). During anomalous PVD there can be splitting between these lamellae leaving the outermost layer attached to the retina. This can also occur during surgery, accounting for some cases of failed surgery (Courtesy of Carl Glittenberg, MD, and Professor Susanne Binder of Vienna, Austria)

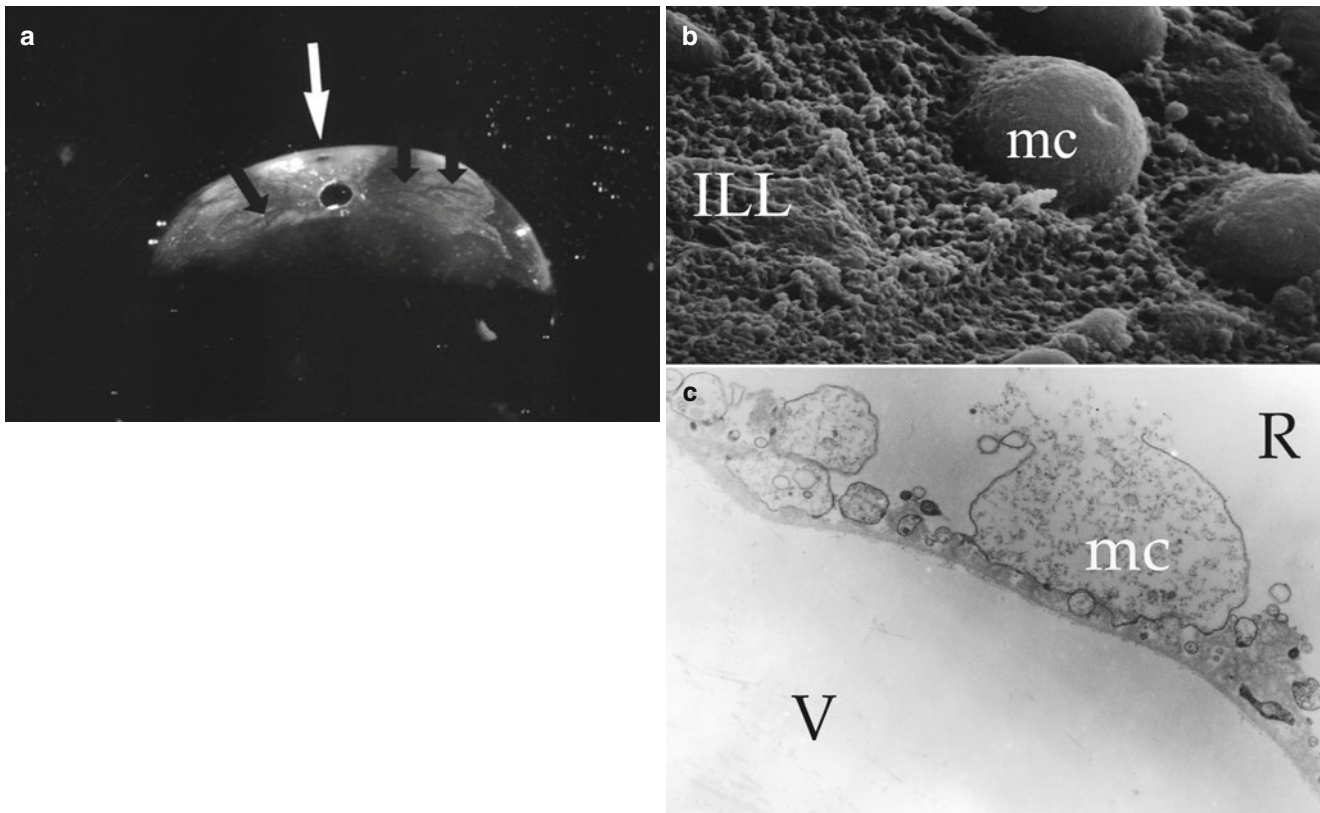


Figure III.B-6 Human vitreoretinal interface in youth. (a) Dark-field slit microscopy of posterior vitreous in a 14-year-old boy after dissection of the sclera, choroid, and retina. A cap of tissue adheres to the vitreous with a hole corresponding to the optic disc, linear structures resembling retinal vessel patterns (*black arrows*), and the fovea (*white arrow*). (b) Scanning electron microscopy of tissue shown in (a). Mueller cell (*MC*) end plates inserted onto the inner limiting membrane

(labeled here as *ILL*) of the retina. (c) Transmission electron microscopy identifies the tissue as the inner limiting membrane the retina (*R*) attached to the posterior vitreous cortex (*V*), with the broken inner segments of Mueller cells adherent to the posterior aspect of the inner limiting membrane (Courtesy of the Eye Research Institute of Retina Foundation, Boston MASS; reprinted with permission from Sebag [17])

the vitreous base and at the posterior pole [17–19]. However, rather than focal adhesions at the disc, fovea, and along retinal blood vessels, vitreoretinal adhesion at the posterior pole appears to be more fascial (Figure III.B-6). In a study of 59 dissected human eyes, age-related differences in vitreoretinal adhesions were investigated using dark-field slit and electron microscopies. In 40 % of young eyes the ILM remained adherent to the vitreous cortex in an area that involved the macula, temporal arcades, and the peripapillary posterior pole [17]. Teng and Chi found that the width (in the radial dimension) of the vitreous base posterior to the ora serrata increases with age to over 3.0 mm [20]. Similarly Wang et al. reported a clear widening of the posterior vitreous base with increasing age. In addition they described the slowly evolving vitreoretinal adhesions as a result of retinal synthesis of collagen fibrils, which penetrate the ILM and become incorporated into the basal vitreous cortex [20, 21]. Whether the posterior migration of the vitreous base with age is greater nasally than temporally is being discussed [22, 23]. Gartner additionally found “lateral aggregation” of the collagen fibrils in the vitreous base of older individuals [24].

IV. Posterior Vitreous Detachment

Complete PVD is a separation between the posterior vitreous cortex and the ILM of the retina, usually occurring without clinically relevant pathologies. It can be localized, partial, or total (throughout the entire posterior pole up to the posterior border of the vitreous base) [3, 17, 25, 26]. For PVD to occur without complications, two different processes are initiated simultaneously and develop to a similar extent: weakening of vitreoretinal adhesion and vitreous liquefaction. Regarding the former, there must be sufficient weakening of vitreoretinal adherence, so when the critical amount of liquefaction has formed, the collapsing vitreous separates away from the retina, and a PVD occurs without untoward consequences [25, 27–29]. Regarding the latter, there are many theories as to the cause of gel liquefaction [30]. Whether due to age-related changes in collagen structure, HA conformation and/or concentration, light-induced or metabolically derived free radicals, hormonal effects, or combinations of all these factors [25, 31], there is a disruption of the normal

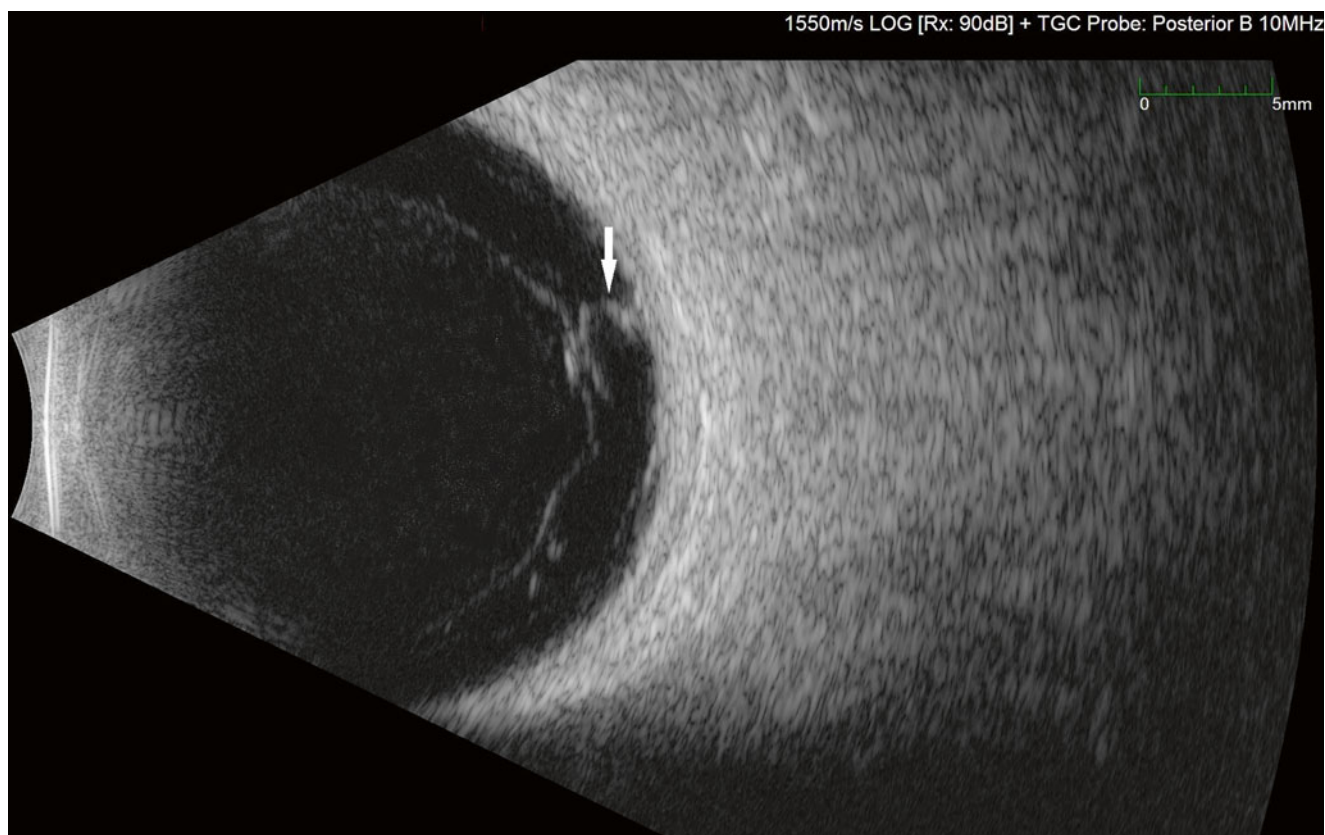


Figure III.B-7 Ultrasound B-scan image of anomalous posterior vitreous detachment with axial vitreomacular traction (*white arrow*)

HA–collagen association transforming the gel vitreous to liquid. Dissolution of the ILM to vitreous cortex adhesion at the posterior pole allows this liquid vitreous to dissect a retro-cortical plane, resulting in the collapse of the vitreous body [25, 32, 33].

A. Diagnosis of PVD

1. Ultrasound

B-scan ultrasonography is an established method to detect and characterize PVD. This application is still superior to biomicroscopy and OCT, especially in the presence of opacities, such as cataract, hyphema, hypopyon, and vitreous hemorrhage [34–36] [see chapter II.F. Imaging vitreous]. Typically, the posterior vitreous cortex can be easily imaged by ultrasound when separated from the retina (Figure III.B-7), but rarely when it is attached. Oksala used clinical ultrasound to detect echoes from gel–liquid interfaces in 444 human eyes [37]. He confirmed that the vitreous body is homogeneous in young eyes with increasing incidence of inhomogeneity in age. Ultrasound is also very helpful to visualize lacunae as a sign of age-related vitreous liquefaction [38]. Liquefaction and the resulting PVD influence

intraocular biomechanics and therefore change the tractional forces exerted by the posterior vitreous cortex on the retina. Walton et al. quantified those effects with kinetic B-scan ultrasound using a grading system based upon the movement of the speckle density (hyperreflective areas in the vitreous) relative to the angle of the eye [39]. Zimmerman evaluated the rheologic state of the vitreous using ultrasound and concluded that the gravitational effect dominates the elastic torque following head movement [40].

Besides conventional B-scan, high-frequency ultrasound complements *in vivo* imaging of the eye. It has higher resolution with the limitation of reduced depth of field due to short wavelength. The latest development represents the pulse-encoded ultrasound [41]. Silverman et al. demonstrated an improved characterization of vitreous mobility with multielement probes and synthetic focusing device (pulse-encoded US). With higher sensitivity and resolution, it may provide a better visualization of the formed and fluid components of the vitreous [36, 42].

2. Optical Coherence Tomography (OCT)

OCT imaging provides extremely good retinal details, less detail at the vitreoretinal interface, and the least detail within the vitreous body itself.

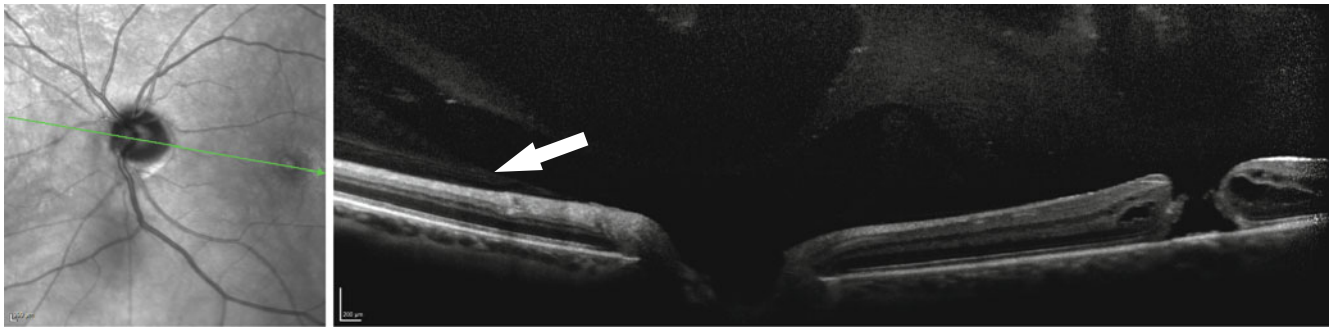


Figure III.B-8 SS-OCT imaging of the posterior pole in an eye with a full-thickness macular hole. This modality enables simultaneous imaging of the anterior optic nerve and macula. Posterior vitreous structure

is seen quite well, including the lamellar configuration of the posterior vitreous cortex (*white arrow*) (Courtesy of Dr. Michael Engelbert, New York, NY)

a. Vitreoretinal Interface by OCT

Conventional time domain OCT is able to detect vitreomacular adhesions, but with relatively low resolution [43–46]. Combined OCT-SLO (scanning laser ophthalmoscopy) imaging, multi-depth scanning with spectral domain-OCT (SD-OCT), or the use of broadband light sources provide a more detailed delineation of the posterior vitreous cortex and the inner limiting membrane (ILM) [47, 48]. On OCT the vitreoretinal interface appears as a hyperreflective line separating the neurosensory retina from the vitreous. A useful feature in both time domain and SD-OCT is *en face* imaging that enables topographic visualization of the retinal surface. Instead of providing single images from longitudinal scans, three-dimensional reconstructions and visualization of the retinal surface following the concavity of the posterior pole of the eye allow topographic characterization of alterations in vitreoretinal relationship [49]. In macular pucker, for example, this type of imaging identified multiple foci of retinal contraction that correlated with disease severity [47]. Furthermore, the topographic and structural features of this and other forms of imaging have contributed considerably to a better understanding of the pathogenesis of macular holes (MH) and macular pucker (MP) by detecting and characterizing anomalous PVD [see chapter III.F. Vitreous in the pathobiology of macular pucker]. Using combined OCT-SLO, Sebag et al. found vitreoschisis in half of their investigated population with MP and MH, which is likely to be related to the underlying multilamellar structure of the posterior vitreous cortex [50].

b. Vitreous Body Imaging by OCT

Within the vitreous body, Itakura et al. were able to detect and describe a large lacuna, called the posterior vitreous pocket (PVP), in the precortical posterior vitreous on SD-OCT [4]. They classified PVD stages on the basis of the posterior wall of the lacuna. The lacuna initially encompasses the

paramacular area and extends to the perifoveal area, inducing a perifoveal PVD. Once the vitreous detaches from the optic disc, a complete PVD can be seen [51, 52]. Mojana et al. used SD-OCT combined with scanning laser ophthalmoscopy (SLO) in patients with PVD symptoms [53]. They identified a strong correlation for a complete PVD between clinical examination and OCT, but a partial PVD was detected more frequently by OCT. Furthermore they could demonstrate high agreement between ultrasound and OCT in a small subset.

Swept source-OCT (SS-OCT) represents the latest development in vitreous imaging. Since it has long coherence length and adjustable frequency sweep range, it enables integration of multiple ophthalmic applications (such as Doppler OCT angiography) in a single instrument. Besides wide field retinal and vitreoretinal interface delineation, it gives a comprehensive volumetric data of the entire eye and vitreous body. Furthermore it improves image quality in combined anterior and posterior segment OCT, which usually needs different wavelengths (1,310 and 840 nm). Using a light source of 1,060 nm, it reduces vitreous absorption [54, 55]. SS-OCT seems to be a promising instrument in describing the state of PVD based on its high resolution and capability to provide a detailed view on the vitreoretinal interface [4] (Figures III.B-3 and III.B-8).

B. Conditions Predisposing to PVD

1. Cataract Surgery

With removal of the lens comes loss of one of the three anchors of the vitreous body, the vitreous base and optic disc being the other two. As a result, all regions of vitreoretinal adherence, both physiologic and pathologic, experience a greater amount of torsional force for any given movement. The loss of the ring of vitreous attachment at Egger's line

adds to the increased workload for the remaining vitreoretinal attachments [56, 57]. Lens extraction has also been shown to result in a reduction in vitreous hyaluronan concentration [58], attributed to facilitated diffusion into the anterior chamber due to disruption of the anterior vitreous face and the absence of the lens and posterior capsule [58, 59]. With the loss of hyaluronan comes decreased stability of the vitreous on a molecular level, resulting in decreased viscosity [60] and shock-absorbing ability; loss of vitreous “lag and slack,” with exaggeration of vitreous currents; and a resultant increase in forces transmitted to remaining vitreoretinal attachments during saccades. An intact posterior lens capsule is thought to prevent this loss of hyaluronan by posing a barrier to diffusion into the anterior chamber [58]. This is supported by owl monkey studies that demonstrated dramatic differences in vitreous hyaluronan concentration following intracapsular and extracapsular cataract extraction, with a rapid 90 % reduction in hyaluronan concentration after ICCE and almost no change in hyaluronan concentration after ECCE and an intact posterior capsule [58]. Osterlin further analyzed the vitreous from human aphakic eyes and found a 63 % reduction of hyaluronan concentration after intracapsular surgery, but only a 16 % reduction after extracapsular surgery with an intact posterior capsule [61]. Clinically, the removal of the crystalline lens results in a higher incidence of complete PVD [62, 63]. The role of an intact posterior capsule was determined in 201 consecutive aphakic and pseudophakic eyes studied postmortem [64]. PVD was present in 84 % of eyes following ICCE and 76 % of eyes following ECCE and surgical capsular discission, but only 40 % of eyes following ECCE with an intact posterior capsule. Clinical studies have claimed that the frequency of PVD in aphakic eyes is 66–100 % [65, 66]; however post-mortem studies have shown that while the incidence of PVD is clearly increased in aphakic eyes, PVD is overdiagnosed clinically, in part, because of erroneous diagnosis in eyes with large central lacunae [67].

2. Myopia

PVD occurs more often in individuals with axial myopia [68–70] [see chapter II.B. Myopic vitreopathy]. In 2004, Hayreh and Jonas confirmed in a hospital-based study of 2,962 eyes that there was a high frequency of complete PVD correlating with myopia and concluded that over a lifetime the onset of complete PVD occurs earlier with increasing myopic refractive error [71]. The study was performed without OCT, and therefore not all complete PVDs may have been detected, and a stage-dependent PVD classification was thus also not possible. Although the Beijing Eye Study consists of a different design (population-based) and demographic (Chinese vs Whites), their findings in 3,468 eyes that were examined for PVD in a stage-dependent manner by OCT seemed to confirm Hayreh’s findings [72]. Interestingly, they concluded

that the prevalence of an incomplete PVD is correlated with hyperopia but that the different OCT-defined stages of incomplete PVD are then associated with myopia [72, 73].

3. Trauma

a. Blunt Trauma

Blunt trauma may be transmitted to the retina in a “coup/contrecoup” fashion, resulting in concussive forces and commotio retinae during the “coup” phase and a variety of rhegmatogenous sequelae [74] during the “contrecoup” phase. Dialysis at the anterior border of the vitreous base typically occurs inferonasally. Less common are avulsion of the vitreous base and retinal dialysis at the posterior border of the vitreous base. Circular macular folds with a sub-ILM schisis cavity containing serosanguinous material [75] and vitreous detachment with ILM throughout the fundus, especially at the vitreous base, and peripapillary hemorrhage are typical of shaken baby syndrome.

b. Penetrating Trauma

Wound healing at the perforation site allows fibrocellular proliferation into the eye, inducing traction retinal detachment. Histopathologic studies revealed cyclitic and periretinal membranes [76]. Intraocular proliferation starts 2–4 days after injury [77], PVD develops at 1–2 weeks [78], and traction retinal detachment occurs at 7–11 weeks. Proliferation can be prevented by vitrectomy [79], less hazardous after 2 weeks because of the development of PVD [80, 81] and more effective if complete [82]. Yet, Miller et al. [83] found that the vitreous plays a role in normal healing of retinal wounds.

V. Anomalous Posterior Vitreous Detachment (APVD)

Anomalous PVD (APVD) occurs when gel liquefaction exceeds the degree of weakening of vitreoretinal adherence and traction is exerted at this interface. There are various possible consequences of APVD, depending upon where the gel is most liquefied and where the posterior vitreous cortex is most firmly adherent to the retina (Figure III.B-9).

A. Etiology of Anomalous PVD

The aforementioned aging changes are the most common cause of gel liquefaction, followed by myopia, diabetes, and several less common conditions. If the degree of vitreoretinal dehiscence is sufficient to allow syneresis (collapse), the vitreous body pulls away from the retina without untoward sequelae. When there is insufficient vitreoretinal dehiscence, the destabilized, liquefied vitreous cannot pull away

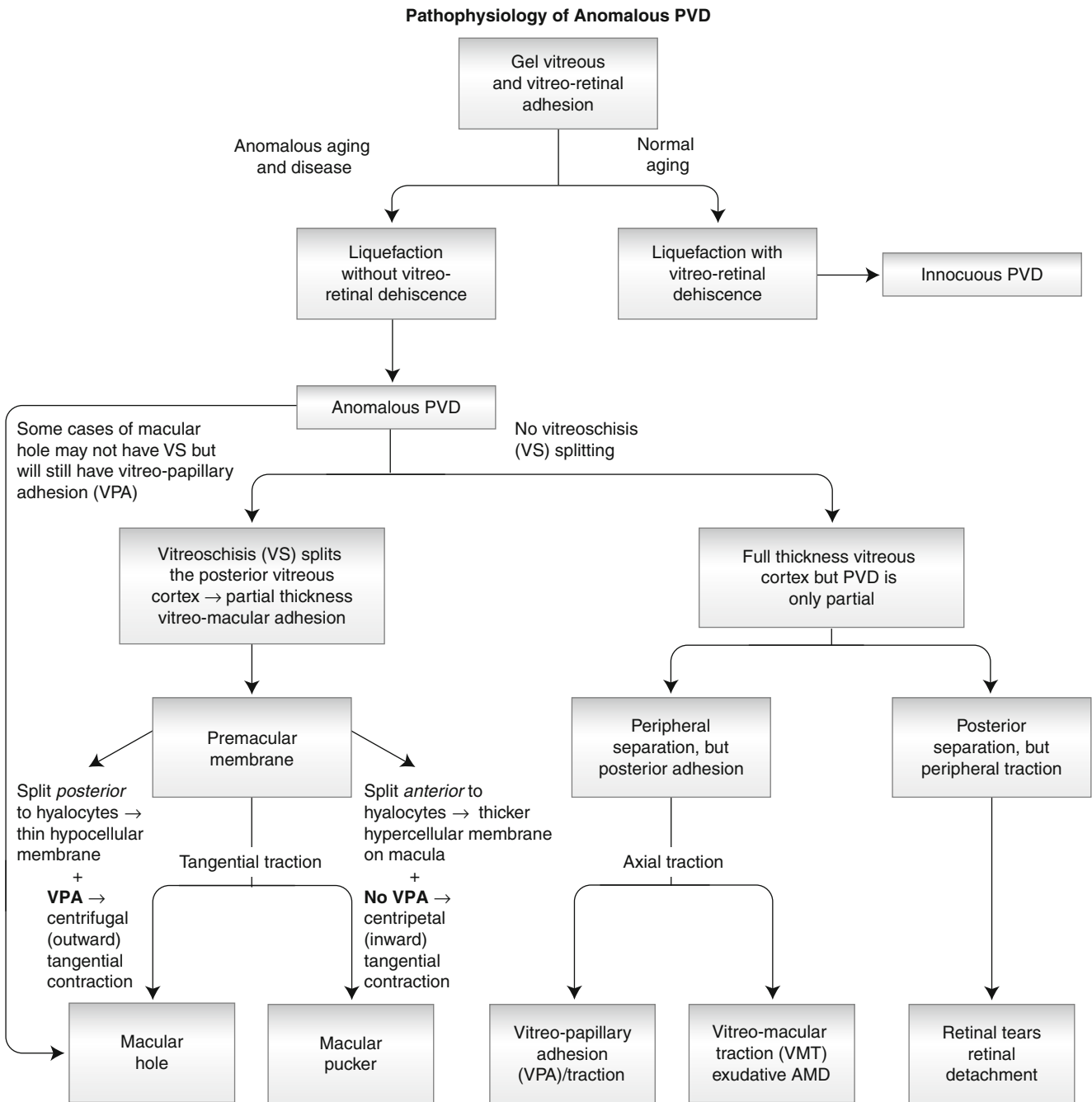


Figure III.B-9 Schematic diagram of anomalous PVD. This unifying concept explains the pathogenesis of several vitreoretinal diseases that were previously considered very disparate but are actually all manifestations of the same underlying pathophysiology – anomalous PVD. Note that vitreo-papillary adhesion and traction can cause primary optic neuropathy but also play a role in facilitating/promoting cell migration and proliferation during pathologic neovascularization of the disc.

Additionally, vitreo-papillary adhesion seems to alter the vector of tangential forces exerted by a membrane (in some cases full-thickness posterior vitreous cortex and in some cases the outer layer of the posterior vitreous cortex left attached to the macula after vitreoschisis). While not all cases of macular holes have vitreoschisis, they feature vitreomacular adhesion and traction almost always with vitreo-papillary adhesion (VPA)

cleanly, resulting in APVD. This process can happen as full-thickness APVD, meaning the entire posterior vitreous cortex stays attached to an area of the retina, or partial-thickness, which means that there is a split in the posterior vitreous cortex, called vitreoschisis (VS). APVD with VS leaves the

outer layer of the posterior vitreous cortex attached to the retina.

There are various causes for this imbalance between the degree of gel liquefaction and weakening of vitreoretinal adhesion. Inborn errors of collagen metabolism, such as

those present in Marfan, Ehlers-Danlos, and Stickler syndromes [84] result in extreme gel liquefaction at an early age with persistent vitreoretinal adherence [see chapter I.C. Hereditary vitreo-retinopathies]. Systemic conditions such as diabetes induce biochemical [85] and structural [86] alterations in the vitreous. The result is diabetic vitreopathy [87], an important contributor to the pathobiology of proliferative diabetic vitreo-retinopathy and diabetic macular edema [see chapter I.E. Diabetic vitreopathy]. Changes associated with myopia can similarly be considered as myopic vitreopathy, where there is excess vitreous liquefaction for the degree of vitreoretinal adhesion, resulting in anomalous PVD and undue traction at the vitreoretinal interface [see chapter II.B. Myopic vitreopathy].

B. Retinal Effects of Anomalous PVD

As a result of abnormal traction at the vitreoretinal interface, there can be deleterious effects upon the retina as well as the vitreous. Depending on where persistent vitreoretinal adhesions are located, various pathologies can develop in a variety of locations in the fundus [26, 88].

1. Peripheral Retinal Effects of APVD

Autopsy studies found that PVD is associated with retinal breaks in 14.3 % of all cases. A degree of vitreous hemorrhage occurs in 13–19 % of cases with PVD, and, when patients suffer a severe vitreous hemorrhage that obscures the view of the fundus on ophthalmoscopy, there is a high incidence of retinal tears (67 %) and retinal detachments (39 %) [85]. Retinal holes unrelated to PVD were observed in 326 (13.9 %) of 2,334 autopsy cases by Foos et al. [89]. Retinal tears can also result from vitreous fluid movement [90]. When the vitreous remains attached to the posterior margin of a retinal flap, this may be avulsed leaving a round or oval hole. The flap of retina remains attached to the posterior surface of the detached vitreous, forming an operculum. Large detached flaps may form a cystic structure [see chapter III.H. Peripheral vitreo-retinal pathology].

The clinical incidence of retinal tears [91] varies from 7.2 % [92] to 5.8 % [93] with a high of 13.75 % [94] and a low of 0.59 % [19]. Postmortem incidences were 3.9 % [20], 8.6 % [95], 4.7 % [96], 8.8 % [97], 3.7 % [89], and 7.3 % [89]. Although the role of retinal tears in causing RD is undisputed, management is controversial [see chapter V.B.4. Prophylaxis and cure of retinal detachment]. Byer [98] concluded that prophylactic treatment is not justified for asymptomatic retinal breaks in phakic eyes. However, in a natural history study of 166 eyes with retinal breaks, Rutnin [94] observed that 31 (18 %) progressed to RD. Neumann and Hyams [99] reported that 2 % of 153 eyes with retinal breaks developed RD. The incidence of

retinal tears is much greater than RD, which varies between nine (0.009 %) [100] and 24.4 (0.02 %) per 100,000 per year [101]. Benson [102] promoted patient education, while Combs and Welch [103] concluded that prophylactic treatment of acute horseshoe tears with vitreous traction significantly reduces the incidence of retinal detachment [see chapter V.B.4. Prophylaxis and Cure of Rhegmatogenous Retinal Detachment]. A particularly high-risk group are patients with vitreous hemorrhage that obscures fundus visualization (see above). Ultrasound may be an effective means of identifying retinal tears in such eyes [104], but misdiagnosis at presentation bodes poorly, since there is 67 % incidence of retinal tears [105].

2. Macular Effects of Anomalous PVD

a. Full-Thickness Vitreomacular Traction

i. Vitreomacular Traction (VMT)

VMT is defined as vitreomacular adhesion with structural alteration of the underlying neural retina [106]. There is often perifoveal vitreous cortex detachment from the retinal surface with persistent adhesion of the vitreous cortex within a 3-mm radius of the fovea. VMT can be classified by the size of the vitreous attachment (focal, if less than 1,500 μm , or broad, if greater than 1,500 μm), associated with intraretinal structural changes, and/or elevation of the fovea above the RPE, but no full-thickness interruption of all retinal layers [106, 107]. Recently, an international panel of experts (International Vitreomacular Traction Study Group, IVTS) convened to develop a new classification system of vitreomacular traction based upon anatomic criteria alone, primarily the findings on OCT evaluation. To determine the presence of VMT requires that the following anatomic criteria be in evidence on at least one B-mode OCT scan: (1) evidence of perifoveal vitreous cortex detachment from retinal surface, (2) macular attachment of the vitreous cortex within a 3-mm radius of the fovea, and (3) association of attachment with distortion of the foveal surface, intraretinal structural changes, elevation of the fovea above the RPE, or a combination thereof [106] [see chapter III.D. Vitreomacular traction and holes (pseudo, lamellar and full-thickness macular holes)].

ii. Age-Related Macular Degeneration

Full-thickness vitreomacular adhesion/traction may also be important in patients with age-related macular degeneration (AMD). Recent studies have identified that true PVD is protective against wet AMD, while anomalous PVD with persistent vitreomacular adhesion may promote choroidal neovascularization. Krebs et al. investigated the state of the posterior vitreous using ultrasound and OCT in exudative AMD with nonexudative and controls. Eyes with exudative AMD had significantly lower rates of detached vitreous compared to the nonexudative eyes and controls

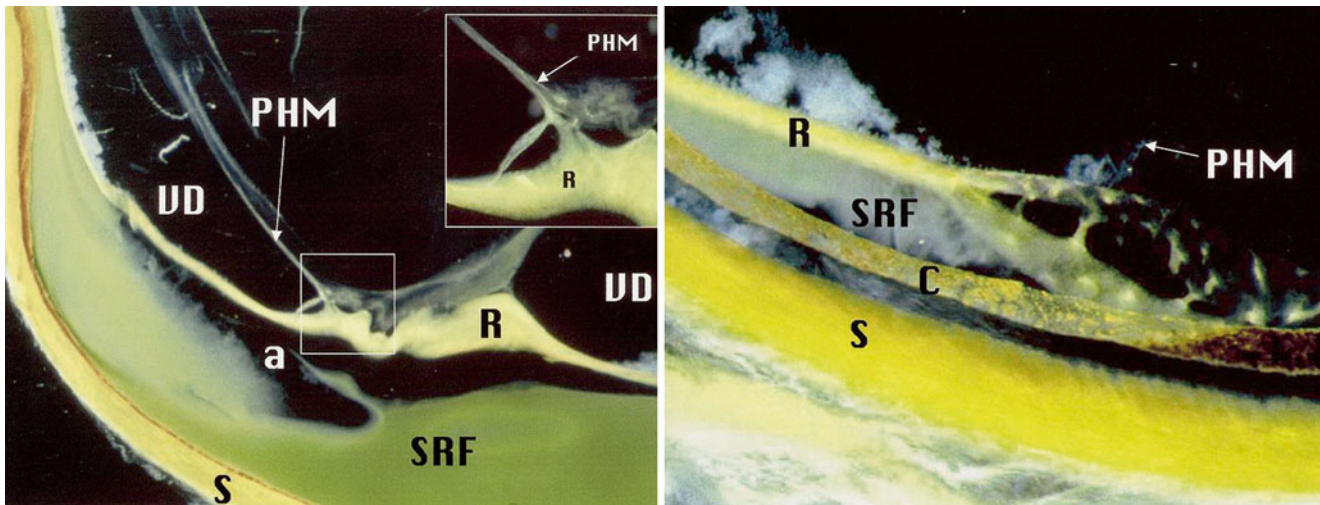


Figure III.B-10 Gross pathology of shrunken vitreous body (syneresis), which is detached in most areas. Anomalous PVD with persistent adherence of the posterior vitreous cortex (PHM) to the retina results in two phenomena of vitreoretinal traction in the same location – a tractional retinal detachment with subretinal fluid (SRF) and a tractional retinoschisis (see image to right). Material is found beneath the detached

retina as well as in the split retina. Higher magnification (right image) of the transition from the attached retina to the elevated retina also shows some small areas of tractional retinoschisis (VD vitreous detachment, R retina, C choroid, S sclera) (Reprinted with permission from Faulborn and Ardjomand [127])

[108]. OCT found significantly higher rates of vitreomacular adhesion in wet AMD. These findings are supported by Robison et al. [109], who reported similar findings in a study that also ruled out genetic and environmental factors. Anomalous PVD was determined to be a risk factor for the development of exudative AMD, and several hypothetical mechanisms were proposed [see chapter III.G. Vitreous in AMD] [110, 111].

iii. Cystoid Macular Edema (CME) and Macular Cysts

CME can be associated with VMT and can occur in cases of unifocal vitreo-foveal traction arising from partial PVD [112]. Broad areas of attachment with traction can cause generalized thickening of the macula, vascular leakage on fluorescein angiography, macular schisis, and CME. Macular cysts that result from chronic edema need to be distinguished from the cystoid spaces created by vitreous traction in macular holes (lamellar and full-thickness) and macular pucker with vitreopapillary adhesion [113] [see chapter III.E. Vitreo-papillary adhesion/traction]. The presence of macular traction cysts is usually associated with decreased vision (acuity and distortion), but generally resolves quickly after the release of traction with little remaining visual deficit [114].

iv. Diabetic Macular Edema

Systemic conditions such as diabetes induce biochemical [85] and structural [86] alterations in the vitreous. The result is diabetic vitreopathy [87] [see chapter I.E. Diabetic vitreopathy], an important contributor to the pathobiology of proliferative diabetic vitreo-retinopathy. Histopathologic

findings showed that retinal traction by “shrinking” of the vitreous body may result in a combination of retinoschisis and retinal detachment (Figure III.B-10). Ultrasound [115] and histopathology [116] studies have shown that patients with proliferative diabetic retinopathy have clear evidence of vitreoschisis. OCT studies have found vitreoschisis in diabetic macular edema [117], which is the most common cause of vision loss in diabetic patients.

b. Partial-Thickness Vitreomacular Traction (Vitreoschisis)

Posterior vitreous detachment (PVD) is associated with vitreous cortex remnants at the fovea in 44 % of human eyes studied at autopsy with scanning electron microscopy [33]. When these remnants are a layer or sheet of posterior vitreous cortex, the term *vitreoschisis* is employed. The proliferation of hyalocytes and migration of glial cells result in a cellular membrane that is often referred to as an “epiretinal” or “ERM.” This term is inappropriate, however, because “epi” refers to a location next to or beside the retina; thus, the term “epiretinal” could refer to a subretinal as well as preretinal location. Following vitreoschisis the membrane location is in front of the retina, thus the prefix “pre” is more accurate than “epi.” Furthermore, vitreoschisis with membrane formation is most often clinically relevant in the macula; thus, the term “premacular membrane,” or “PMM,” is the more precise term than “epiretinal membrane,” or “ERM.” The term “macular pucker” should be used to refer to one (but not the only) clinical consequence of an abnormal premacular membrane, i.e., the distortion or puckering of the macula. Furthermore, the term “idiopathic ERM” is no longer



Figure III.B-11 Ultrasonography of vitreoschisis. B-scan ultrasound of vitreoschisis in a human demonstrates the inner (*I*) and outer (*P*) walls of a split posterior vitreous cortex. The *arrow* indicates the schisis

cavity created by the split (Courtesy of Ron Green, MD; Reprinted with permission from Sebag [25])

appropriate, since we now know that this condition is not idiopathic and that vitreous is the cause.

On clinical examination, the inner wall of the vitreoschisis cavity may be clinically confused with a PVD when the posterior layer of the split vitreous cortex remains attached to the ILM of the retina. Ultrasonography can, at times, detect the split layers in vitreoschisis depending upon the thickness of the layers (Figure III.B-11). Vitreoschisis has been detected by ultrasound in 20 % of eyes with proliferative diabetic retinopathy [115], and optical coherence tomography detected vitreoschisis in about one-half of patients with macular pucker and macular holes [118], but is also present in other vitreomaculopathies (Figure III.B-12).

i. Anterior vs. Posterior Split

The partial-thickness aspect of vitreoschisis can have varying effects on the vitreoretinal interface, depending

upon the level of the split (Figure III.B-13) and whether or not there is persistent vitreo-papillary adhesion [see chapter III.E. Vitreo-papillary adhesion/traction]. Concerning the former, the split can occur at various levels within the vitreous cortex since this tissue is composed of multiple layers or lamellae. Recall that the posterior vitreous cortex contains mononuclear phagocytes called hyalocytes embedded in a monolayer approximately 50–75 μm anterior to the inner limiting membrane of the retina [see chapter II.D. Hyalocytes]. If the vitreoschisis split occurs anterior to the level of the hyalocytes, vitreoschisis leaves a relatively thick, cellular membrane attached to the macula. Inward (centripetal to the fovea) contraction of this membrane induces macular pucker. A vitreoschisis split posterior to the hyalocytes leaves a relatively thin and hypocellular premacular membrane. Outward (centrifugal from the fovea) tangential traction can induce a macular

hole, especially in the presence of vitreo-papillary adhesion, found in 88.2 % of cases [119].

ii. Macular Pucker

Following APVD with vitreoschisis, premacular membranes can contract and cause significant visual impairment and metamorphopsia, sometimes necessitating surgical intervention (Figure III.B-14). Studies of excised tissue

have demonstrated the presence of astrocytes and retinal pigment epithelium (RPE) cells, but there can likely be other cells that can have similar appearances – such as hyalocytes [see chapter II.D. Hyalocytes]. Zhao et al. examined surgically gained histologic ILM specimens from 79 eyes with macular pucker or vitreomacular traction syndrome and found that hyalocytes constitute one of the major cell types of premacular cell proliferation [120]. It has been hypoth-

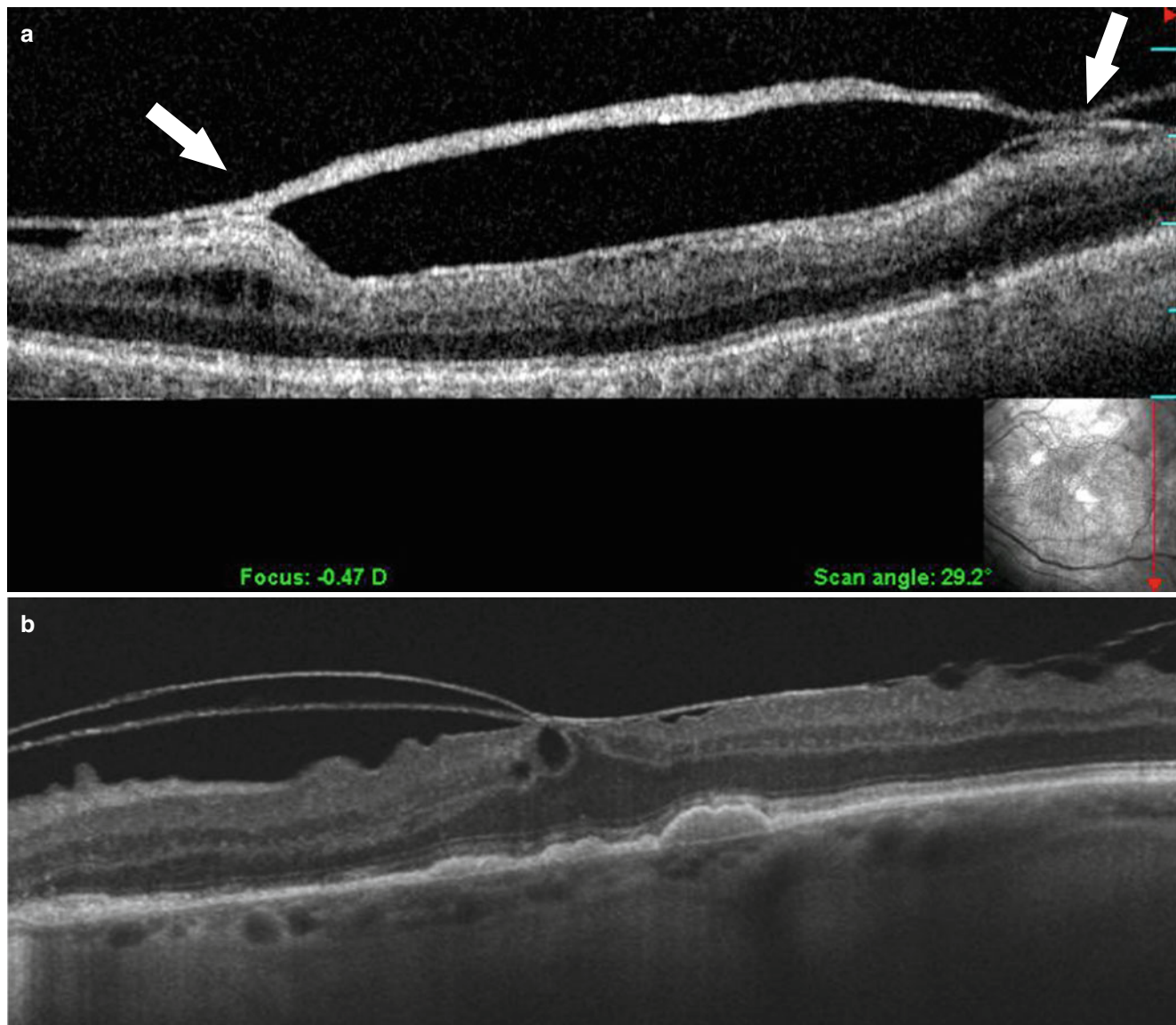


Figure III.B-12 Vitreoschisis. (a) Spectral domain-optical coherence tomography combined with scanning laser ophthalmoscopy demonstrates the split in the posterior vitreous cortex, known as vitreoschisis. The inner and outer walls of the vitreoschisis cavity rejoin to form full-thickness posterior vitreous cortex in two locations (*arrows*). Considerable traction is exerted upon the retina in these two locations, enough to lift the retina on one side (to the *left*) to create tractional retinoschisis. (b) OCT imaging of vitreoschisis demonstrating that the tractional force generated at the point of rejoining by the inner and outer

walls of the vitreoschisis into full-thickness posterior vitreous cortex is sufficiently strong to induce an underlying foveal cyst. Note, this patient also has age-related macular degeneration (Courtesy of Jay S. Duker, MD). (c) Spectral domain-optical coherence tomography combined with scanning laser ophthalmoscopy demonstrates that there can be multiple levels of vitreoschisis due to the fact that there are multiple lamellae comprising the posterior vitreous cortex. Significant traction is placed upon the retina at the point of reunification by two of the three vitreoschisis layers seen in this case

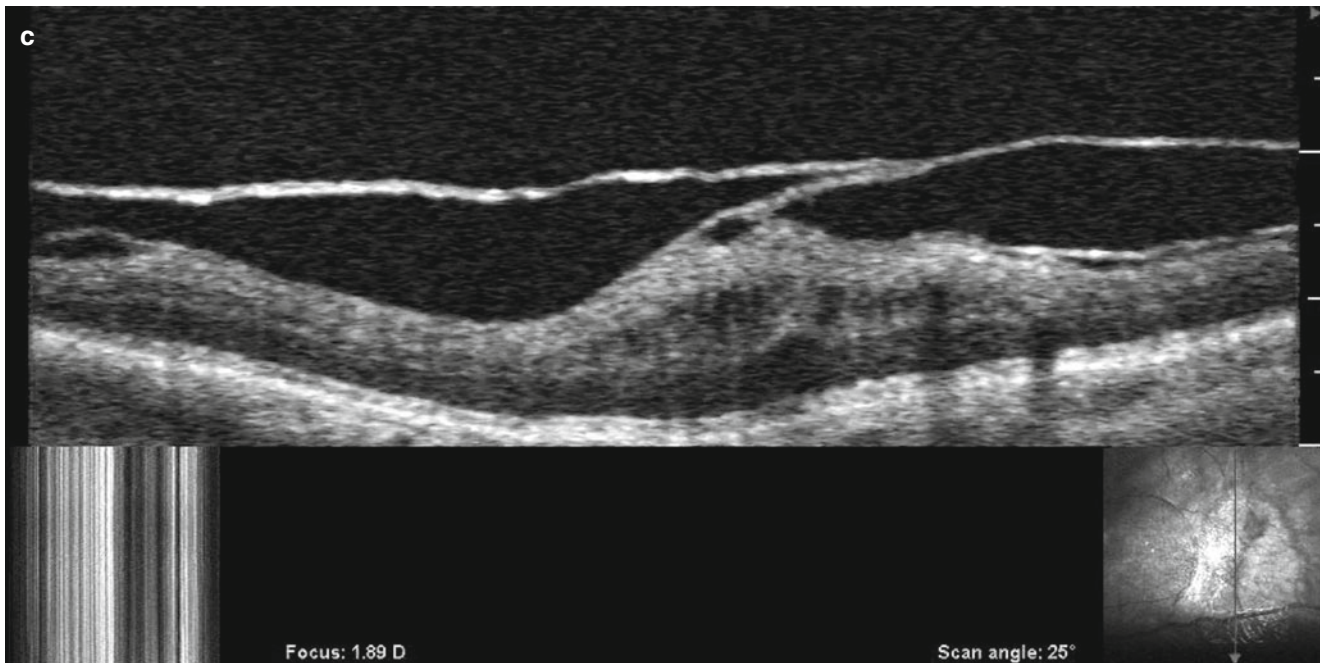


Figure III.B-12 (continued)

esized that macular pucker results when vitreoschisis splits the vitreous cortex anterior to hyalocytes leaving a thick and cellular membrane attached to the macula. Furthermore, recent studies [47] have identified that nearly one-half of all eyes with macular pucker have more than one site of retinal contraction. There is a higher incidence of intraretinal cysts and significantly more macular thickening with increasing foci of retinal contraction [47].

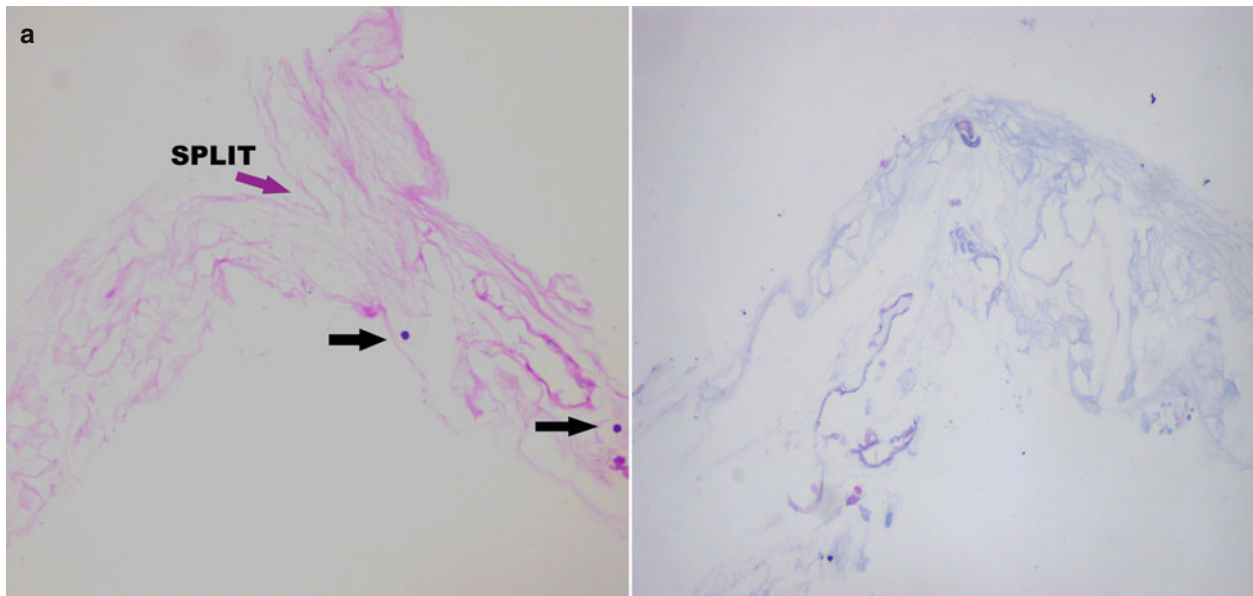
iii. Macular Hole

Full-thickness macular hole (FTMH) is defined as a foveal lesion with interruption of all retinal layers from the internal limiting membrane (ILM) to the retinal pigment epithelium and is usually detected by OCT. There have been various theories of FTMH pathogenesis, such as primary (vitreous traction) or secondary causes (trauma, foveal degeneration, high myopia, exudative AMD, and involutional thinning with PVD). Recently, the International Vitreomacular Traction Study Group differentiated FTMHs based on size (small $\leq 250 \mu\text{m}$; medium ≥ 250 to $\leq 400 \mu\text{m}$; large $\geq 400 \mu\text{m}$), status of the vitreous (with or without vitreomacular traction), and associated conditions (primary or secondary) [106]. This classification is important, as the hole size and presence or absence of vitreomacular traction are predictive of anatomic and functional success after pharmacologic or surgical treatment [107].

It is clear from recent surgical experience [121] that APVD is the cause of FTMH. Johnson and Gass [122] formulated the tangential traction theory by suggesting that

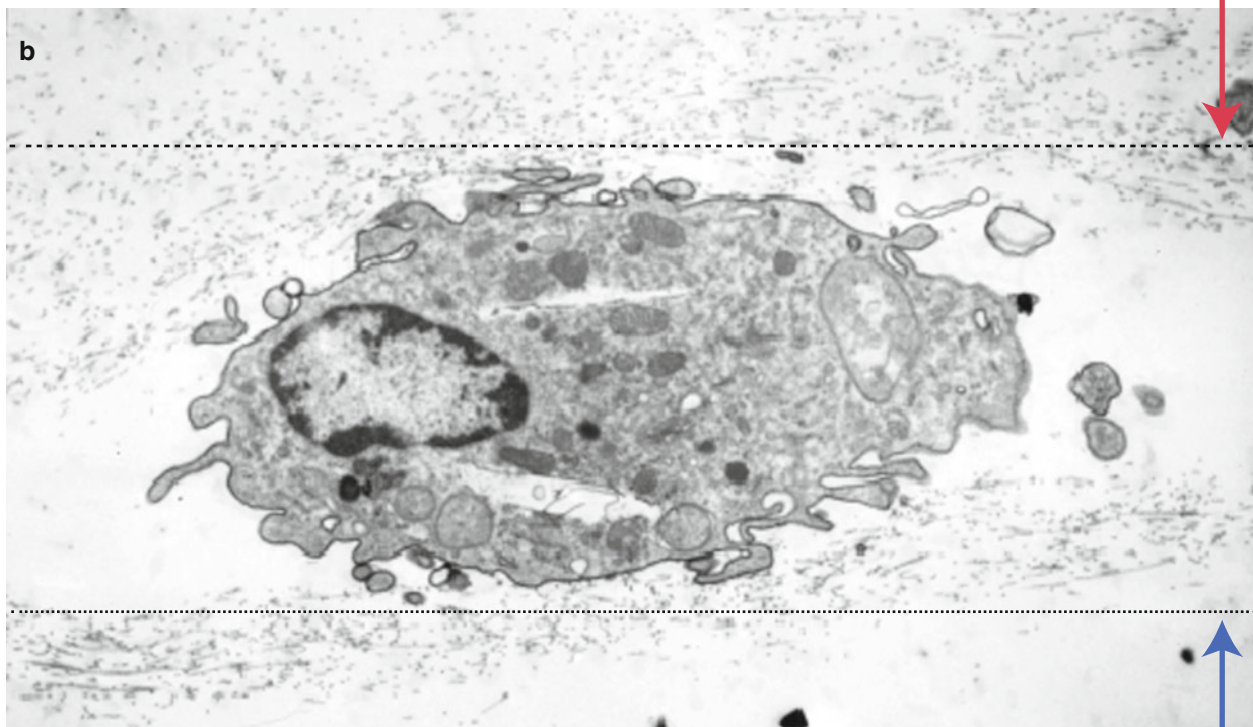
shrinkage of the perifoveal vitreous induces FTMH formation in four stages. While the Gass classification has been used in the past, OCT-based data have added much to our understanding of the pathogenesis and the progression of FTMH in the last two decades. Thus the IVTS classification system, which is OCT-based, should now be the standard system routinely employed [see chapter III.D. Vitreomacular traction and holes (pseudo, lamellar and FTMH)]. There are three possible mechanisms of tangential vitreous traction: fluid vitreous movements and countercurrents, cellular remodeling of cortical vitreous, and contraction of a cellular membrane on the tapered cortical vitreous after vitreoschisis [26, 123, 124]. OCT-SLO imaging found vitreoschisis in half of eyes with MH [50]. In the remaining half of the cases, it is plausible that there is full-thickness separation of the vitreous from the retina peripherally with persistent adhesion of full-thickness vitreous cortex posteriorly exerting traction on the macula. In an ultrastructural study of premacular tissue removed during vitrectomy for impending macular holes, Smiddy et al. [125] observed cortical vitreous in all eyes.

Vitreopapillary adhesion (VPA; see chapter III.E. Vitreopapillary adhesion/traction) may play an important role, as this is present in 88.2 % of MH eyes (Figure III.B-15). VPA is also prevalent in eyes with intraretinal cystoid spaces in both lamellar macular holes and macular pucker [119]. These cystoid spaces are not the result of exudation, but the consequence of tangential traction; thus they are “cystoid spaces” and not “cysts.” VPA influences the vector of tangential



Macular pucker - vitreoschisis splits anterior to hyalocytes

They remain attached to ILM and recruit cells from retina and blood hypercellular membranes, highly contractile



Macular hole vitreoschisis splits posterior to hyalocytes

Hypocellular membranes that are thinner than macular pucker membranes

Figure III.B-13 Vitreoschisis. (a) Histopathology of vitreoschisis. Histopathology of surgical specimen from a patient with vitreoschisis and macular pucker. Image to the upper left is stained with periodic acid Schiff to demonstrate the split (purple arrow) in the premacular membrane removed at surgery. Embedded in this tissue are two hyalocytes (black arrows), consistent with the concept that this tissue is the posterior vitreous cortex (Courtesy of N Rao, MD; magnification=225 \times). Image to the upper right is the tissue from the same subject showing positive staining with alcian blue, confirming its identity as the posterior vitreous cortex (Courtesy of N Rao, MD; magnification=300 \times) (From Gupta et al. [118]).

(b) Ultrastructure of vitreoschisis. Transmission electron micrograph demonstrates a human hyalocyte embedded in the dense collagen matrix of the posterior vitreous cortex (original magnification, $\times 11,670$). The anterior aspect of the posterior vitreous cortex is above, and the posterior aspect is below. Depending upon the level of the vitreoschisis split, a hypercellular and thick membrane can be left on the macula following anomalous PVD, if the split occurs anterior to the hyalocytes (large dashed line below the red arrow). If the split occurs posterior to the level of the monolayer of hyalocytes (dotted dashed line above the blue arrow), then a thin and hypocellular membrane is left attached to the macula (Modified from Sebag [25])

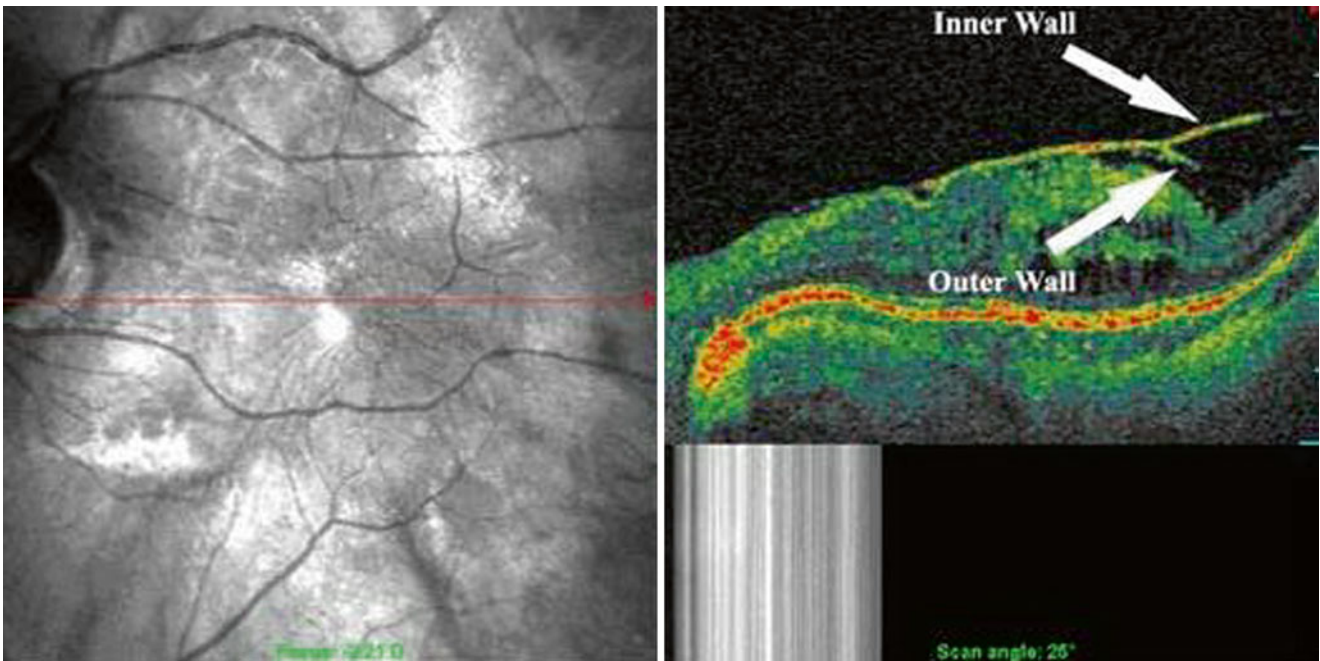


Figure III.B-14 SLO (left) and OCT images of the vitreoretinal interface illustrate the two walls of vitreoschisis in macular pucker (inner wall is anterior, toward the *top* of the photo; outer wall is posterior, toward the *bottom*) (From Gupta et al. [118])



Figure III.B-15 OCT-SLO imaging of foveal region illustrating full-thickness macular hole with tangential vitreous traction. The persistent adhesion of full-thickness vitreous cortex posteriorly exerts traction on the macula. Vitreoschisis is evident on the right side of the image

forces on the macula and induces outward (*centrifugal*) traction opening a central dehiscence. In macular pucker, there is usually no VPA, and the vector of tangential traction is inward (*centripetal*), causing a macular pucker. As indicated

in Figure III.B-9, there may be cases of FTMH that do not involve vitreoschisis. It is nonetheless likely that these cases have vitreo-papillary adhesion influencing the vector of forces at play during and following anomalous PVD.

Abbreviations

AMD	Age-related macular degeneration
APVD	Anomalous posterior vitreous detachment
CME	Cystoid macular edema
DME	Diabetic macular edema
PDR	Proliferative diabetic retinopathy
ECCE	Extracapsular cataract extraction
FTMH	Full-thickness macular hole
HA	Hyaluronan
ICCE	Intracapsular cataract extraction
ILM	Inner limiting membrane
MH	Macular hole
MP	Macular pucker
OCT	Optical coherence tomography
PVD	Posterior vitreous detachment
PVP	Posterior vitreous pocket
SD-OCT	Spectral domain-optical coherence tomography
OCT-SLO	Combined optical coherence tomography-scanning laser ophthalmoscopy
SS-OCT	Swept source-optical coherence tomography
VMTS	Vitreomacular traction syndrome
VPA	Vitreo-papillary adhesion

References

- Schmut O, Mallinger R, Paschke E. Studies on a distinct fraction of bovine vitreous body collagen. *Graefes Arch Clin Exp Ophthalmol*. 1984;221(6):286–9.
- Scott JE, Chen Y, Brass A. Secondary and tertiary structures involving chondroitin and chondroitin sulphates in solution, investigated by rotary shadowing/electron microscopy and computer simulation. *Eur J Biochem*. 1992;209(2):675–80.
- Sebag J. Vitreous anatomy, aging, and anomalous posterior vitreous detachment. In: Dartt DA, editor. *Encyclopedia of the eye*. Oxford: Academic Press; 2010. p. 307–15.
- Itakura H, Kishi S, Li D, Akiyama H. Observation of posterior precortical vitreous pocket using swept-source optical coherence tomography. *Invest Ophthalmol Vis Sci*. 2013;54(5):3102–7.
- Shimada H, Hirose T, Yamamoto A, Nakashizuka H, Hattori T, Yuzawa M. Depiction of the vitreous pocket by optical coherence tomography. *Int Ophthalmol*. 2011;31(1):51–3.
- Takehashi A, Kado M, Akiba J, Hirokawa H. Biomicroscopic findings of premacular posterior vitreous. *Nihon Ganka Gakkai Zasshi*. 1995;99(3):323–8.
- Kamei A, Totani A. Isolation and characterization of minor glycosaminoglycans in the rabbit vitreous body. *Biochem Biophys Res Commun*. 1982;109(3):881–7.
- Akiba J, Ueno N, Chakrabarti B. Age-related changes in the molecular properties of vitreous collagen. *Curr Eye Res*. 1993;12(10):951–4.
- Brown D, Hamdi H, Bahri S, Kenney MC. Characterization of an endogenous metalloproteinase in human vitreous. *Curr Eye Res*. 1994;13(9):639–47.
- Brown DJ, Bishop P, Hamdi H, Kenney MC. Cleavage of structural components of mammalian vitreous by endogenous matrix metalloproteinase-2. *Curr Eye Res*. 1996;15(4):439–45.
- Los LI, van der Worp RJ, van Luyn MJ, Hooymans JM. Age-related liquefaction of the human vitreous body: LM and TEM evaluation of the role of proteoglycans and collagen. *Invest Ophthalmol Vis Sci*. 2003;44(7):2828–33.
- Aguayo J, Glaser B, Mildvan A, Cheng HM, Gonzalez RG, Brady T. Study of vitreous liquefaction by NMR spectroscopy and imaging. *Invest Ophthalmol Vis Sci*. 1985;26(5):692–7.
- Snowden JM. The stabilization of in vivo assembled collagen fibrils by proteoglycans/glycosaminoglycans. *Biochim Biophys Acta*. 1982;703(1):21–5.
- Takahashi M, Jalkh A, Hoskins J, Trempe CL, Schepens CL. Biomicroscopic evaluation and photography of liquefied vitreous in some vitreoretinal disorders. *Arch Ophthalmol*. 1981;99(9):1555–9.
- Goldmann H. Senile changes of the lens and the vitreous. The Arthur J. Bedell lecture. *Am J Ophthalmol*. 1964;57:1–13.
- Sebag J. Age-related changes in human vitreous structure. *Graefes Arch Clin Exp Ophthalmol*. 1987;25(2):89–93.
- Sebag J. Age-related differences in the human vitreoretinal interface. *Arch Ophthalmol*. 1991;109(7):966–71.
- Sebag J. Anatomy and pathology of the vitreo-retinal interface. *Eye (Lond)*. 1992;6(Pt 6):541–52.
- Smith RE, Ganley JP. Ophthalmic survey of a community. I. Abnormalities of the ocular fundus. *Am J Ophthalmol*. 1972;74(6):1126–30.
- Teng CC, Katzin HM. An anatomic study of the periphery of the retina. I. Nonpigmented epithelial cell proliferation and hole formation. *Am J Ophthalmol*. 1951;34(9):1237–48.
- Wang J, McLeod D, Henson DB, Bishop PN. Age-dependent changes in the basal retinovitreal adhesion. *Invest Ophthalmol Vis Sci*. 2003;44(5):1793–800.
- Sebag J. Vitreous base. The vitreous: structure, function, and pathobiology. New York: Springer; 1989. p. 39–40.
- Sebag J, Hageman GS. Interfaces. *Eur J Ophthalmol*. 2000;10(1):1–3.
- Gartner J. Electron microscopic observations on the cilio-zonular border area of the human eye with particular reference to the aging changes. *Z Anat Entwicklungsgesch*. 1970;131(3):263–73.
- Sebag J. The vitreous – structure, function, and pathobiology. New York: Springer; 1989.
- Sebag J. Anomalous posterior vitreous detachment: a unifying concept in vitreo-retinal disease. *Graefes Arch Clin Exp Ophthalmol*. 2004;42(8):690–8.
- Balazs EA, Denlinger JL. Aging changes in the vitreous. In: Sekuler R, Kline D, Dismukes K, editors. *Aging and human visual function*. New York: Liss; 1982. p. 45–57.
- Eisner G. Posterior vitreous detachment. *Klin Monbl Augenheilkd*. 1989;194(5):389–92.
- Foos RY, Wheeler NC. Vitreoretinal juncture. Synchysis senilis and posterior vitreous detachment. *Ophthalmology*. 1982;89(12):1502–12.
- Kishi S, Hagimura N, Shimizu K. The role of the premacular liquefied pocket and premacular vitreous cortex in idiopathic macular hole development. *Am J Ophthalmol*. 1996;122(5):622–8.
- Larsson L, Osterlin S. Posterior vitreous detachment. A combined clinical and physicochemical study. *Graefes Arch Clin Exp Ophthalmol*. 1985;23(2):92–5.
- Johnson MW. Posterior vitreous detachment: evolution and complications of its early stages. *Am J Ophthalmol*. 2010;149(3):371–82 e1.
- Kishi S, Demaria C, Shimizu K. Vitreous cortex remnants at the fovea after spontaneous vitreous detachment. *Int Ophthalmol*. 1986;9(4):253–60.

34. Arzabe CW, Akiba J, Jalkh AE, Quiroz MA, Trempe CL, McMeel JW, et al. Comparative study of vitreoretinal relationships using biomicroscopy and ultrasound. *Graefes Arch Clin Exp Ophthalmol*. 1991;229(1):66–8.
35. Kicova N, Bertelmann T, Irle S, Sekundo W, Mennel S. Evaluation of a posterior vitreous detachment: a comparison of biomicroscopy, B-scan ultrasonography and optical coherence tomography to surgical findings with chromodissection. *Acta Ophthalmol*. 2012;90(4):e264–8.
36. Mamou J, Aristizabal O, Silverman RH, Ketterling JA, Turnbull DH. High-frequency chirp ultrasound imaging with an annular array for ophthalmologic and small-animal imaging. *Ultrasound Med Biol*. 2009;35(7):1198–208.
37. Oksala A. Ultrasonic findings in the vitreous body at various ages. *Albrecht Von Graefes Arch Klin Exp Ophthalmol*. 1978;207(4):275–80.
38. Spaide RF. Measurement of the posterior precortical vitreous pocket in fellow eyes with posterior vitreous detachment and macular holes. *Retina*. 2003;23(4):481–5.
39. Walton KA, Meyer CH, Harkrider CJ, Cox TA, Toth CA. Age-related changes in vitreous mobility as measured by video B scan ultrasound. *Exp Eye Res*. 2002;74(2):173–80.
40. Zimmerman RL. In vivo measurements of the viscoelasticity of the human vitreous humor. *Biophys J*. 1980;29(3):539–44.
41. Silverman RH, Ketterling JA, Mamou J, Coleman DJ. Improved high-resolution ultrasonic imaging of the eye. *Arch Ophthalmol*. 2008;126(1):94–7.
42. Silverman RH, Ketterling JA, Mamou J, Lloyd HO, Filoux E, Coleman DJ. Pulse-encoded ultrasound imaging of the vitreous with an annular array. *Ophthalmic Surg Lasers Imaging*. 2012;43(1):82–6.
43. Barak Y, Ihnen MA, Schaal S. Spectral domain optical coherence tomography in the diagnosis and management of vitreoretinal interface pathologies. *J Ophthalmol*. 2012;2012:876472.
44. Folgar FA, Toth CA, DeCroos FC, Girach A, Pakola S, Jaffe GJ. Assessment of retinal morphology with spectral and time domain OCT in the phase III trials of enzymatic vitreolysis. *Invest Ophthalmol Vis Sci*. 2012;53(11):7395–401.
45. Gallemore RP, Jumper JM, McCuen 2nd BW, Jaffe GJ, Postel EA, Toth CA. Diagnosis of vitreoretinal adhesions in macular disease with optical coherence tomography. *Retina*. 2000;20(2):115–20.
46. Hillenkamp J, Kraus J, Framme C, Jackson TL, Roider J, Gabel VP, et al. Retreatment of full-thickness macular hole: predictive value of optical coherence tomography. *Br J Ophthalmol*. 2007;91(11):1445–9.
47. Gupta P, Sadun AA, Sebag J. Multifocal retinal contraction in macular pucker analyzed by combined optical coherence tomography/scanning laser ophthalmoscopy. *Retina*. 2008;28(3):447–52.
48. Koizumi H, Spaide RF, Fisher YL, Freund KB, Klanck Jr JM, Yannuzzi LA. Three-dimensional evaluation of vitreomacular traction and epiretinal membrane using spectral-domain optical coherence tomography. *Am J Ophthalmol*. 2008;145(3):509–17.
49. Le Rouic JF, Rispoli M. Vitreomacular interface alteration: a new semiology with en face optical coherence tomography. In: Lumbroso B, Huang D, Romano A, Rispoli M, Coscas G, editors. *Clinical enface OCT atlas*. New York: Jaypee Brothers; 2013. p. 355–65.
50. Sebag J, Gupta P, Rosen RR, Garcia P, Sadun AA. Macular holes and macular pucker: the role of vitreoschisis as imaged by optical coherence tomography/scanning laser ophthalmoscopy. *Trans Am Ophthalmol Soc*. 2007;105:121–9. discussion 9–31.
51. Itakura H, Kishi S. Aging changes of vitreomacular interface. *Retina*. 2011;31(7):1400–4.
52. Itakura H, Kishi S. Evolution of vitreomacular detachment in healthy subjects. *JAMA Ophthalmol*. 2013;131:1348–52.
53. Mojana F, Kozak I, Oster SF, Cheng L, Bartsch DU, Brar M, et al. Observations by spectral-domain optical coherence tomography combined with simultaneous scanning laser ophthalmoscopy: imaging of the vitreous. *Am J Ophthalmol*. 2010;149(4):641–50.
54. Grulkowski I, Liu JJ, Potsaid B, Jayaraman V, Lu CD, Jiang J, et al. Retinal, anterior segment and full eye imaging using ultra-high speed swept source OCT with vertical-cavity surface emitting lasers. *Biomed Opt Express*. 2012;3(11):2733–51.
55. Liu JJ, Grulkowski I, Kraus MF, Potsaid B, Lu CD, Baumann B, et al. In vivo imaging of the rodent eye with swept source/Fourier domain OCT. *Biomed Opt Express*. 2013;4(2):351–63.
56. Hilding AC. Normal vitreous, its attachments and dynamics during ocular movement. *AMA Arch Ophthalmol*. 1954;52(4):497–514.
57. Hilding AC. Alterations in the form, movement, and structure of the vitreous body in aphakic eyes. *AMA Arch Ophthalmol*. 1954;52(5):699–709.
58. Osterlin S. Macromolecular composition of the vitreous in the aphakic owl monkey eye. *Exp Eye Res*. 1978;26(1):77–84.
59. Osterlin S. Changes in the molecular morphology of the vitreous after intraocular surgery. *Acta Ophthalmol*. 1970;48(4):829.
60. Kawano SI, Honda Y, Negi A. Effects of biological stimuli on the viscosity of the vitreous. *Acta Ophthalmol*. 1982;60(6):977–91.
61. Osterlin S. Changes in the vitreous with age. *Trans Ophthalmol Soc U K*. 1975;95(3):372–7.
62. Gregor Z, Ryan SJ. Combined posterior contusion and penetrating injury in the pig eye. II. Histological features. *Br J Ophthalmol*. 1982;66(12):799–804.
63. Heller MD, Straatsma BR, Foos RY. Detachment of the posterior vitreous in phakic and aphakic eyes. *Mod Probl Ophthalmol*. 1972;10:23–36.
64. McDonnell PJ, Patel A, Green WR. Comparison of intracapsular and extracapsular cataract surgery. Histopathologic study of eyes obtained postmortem. *Ophthalmology*. 1985;92(9):1208–25.
65. Hauer Y, Barkay S. Vitreous detachment in aphakic eyes. *Br J Ophthalmol*. 1964;48:341–3.
66. Jaffe NS, Light DS. Vitreous changes produced by cataract surgery. A study of 1,058 aphakic eyes. *Arch Ophthalmol*. 1966;76(4):541–53.
67. Foos RY. Posterior vitreous detachment. *Trans Am Acad Ophthalmol Otolaryngol*. 1972;76(2):480–97.
68. Akiba J. Prevalence of posterior vitreous detachment in high myopia. *Ophthalmology*. 1993;100(9):1384–8.
69. Weber-Krause B, Eckardt C. Incidence of posterior vitreous detachment in the elderly. *Ophthalmologie*. 1997;94(9):619–23.
70. Kobayashi H, Ogino N. Incidence of posterior detachment in healthy eyes with age, sex and refraction as variables. *Rinsho Ganka*. 1985;39:514–5.
71. Hayreh SS, Jonas JB. Posterior vitreous detachment: clinical correlations. *Ophthalmologica*. 2004;218(5):333–43.
72. Shao L, Xu L, You QS, Wang YX, Chen CX, Yang H, et al. Prevalence and associations of incomplete posterior vitreous detachment in adult Chinese: the Beijing Eye study. *PLoS One*. 2013;8(3):e58498.
73. You QS, Peng XY, Xu L, Chen CX, Wang YX, Jonas JB. Myopic maculopathy imaged by optical coherence tomography: the Beijing Eye study. *Ophthalmology*. 2013;16.
74. Cox MS, Schepens CL, Freeman HM. Retinal detachment due to ocular contusion. *Arch Ophthalmol*. 1966;76(5):678–85.
75. Massicotte SJ, Folberg R, Torczynski E, Gilliland MG, Luckenbach MW. Vitreoretinal traction and perimacular retinal folds in the eyes of deliberately traumatized children. *Ophthalmology*. 1991;98(7):1124–7.
76. Winthrop SR, Cleary PE, Minckler DS, Ryan SJ. Penetrating eye injuries: a histopathological review. *Br J Ophthalmol*. 1980;64(11):809–17.
77. Faulborn J, Topping TM. Proliferations in the vitreous cavity after perforating injuries. A histopathological study. *Albrecht Von Graefes Arch Klin Exp Ophthalmol*. 1978;205(3):157–66.

78. Cleary PE, Ryan SJ. Histology of wound, vitreous, and retina in experimental posterior penetrating eye injury in the rhesus monkey. *Am J Ophthalmol.* 1979;88(2):221–31.
79. Abrams GW, Topping TM, Machemer R. Vitrectomy for injury: the effect on intraocular proliferation following perforation of the posterior segment of the rabbit eye. *Arch Ophthalmol.* 1979; 97(4):743–8.
80. Cleary PE, Ryan SJ. Vitrectomy in penetrating eye injury. Results of a controlled trial of vitrectomy in an experimental posterior penetrating eye injury in the rhesus monkey. *Arch Ophthalmol.* 1981;99(2):287–92.
81. Spalding SC, Sternberg Jr P. Controversies in the management of posterior segment ocular trauma. *Retina.* 1990;10 Suppl 1:S76–82.
82. Gregor Z, Ryan SJ. Complete and core vitrectomies in the treatment of experimental posterior penetrating eye injury in the rhesus monkey. II. Histologic features. *Arch Ophthalmol.* 1983;101(3):446–50.
83. Miller B, Miller H, Patterson R, Ryan SJ. Effect of the vitreous on retinal wound-healing. *Graefes Arch Clin Exp Ophthalmol.* 1986;224(6):576–9.
84. Snead MP, Yates JR. Clinical and molecular genetics of Stickler syndrome. *J Med Genet.* 1999;36(5):353–9.
85. Sebag J, Buckingham B, Charles MA, Reiser K. Biochemical abnormalities in vitreous of humans with proliferative diabetic retinopathy. *Arch Ophthalmol.* 1992;110(10):1472–6.
86. Sebag J. Abnormalities of human vitreous structure in diabetes. *Graefes Arch Clin Exp Ophthalmol.* 1993;231(5):257–60.
87. Sebag J. Diabetic vitreopathy. *Ophthalmology.* 1996;103(2):205–6.
88. Streeten BA. Disorders of the vitreous. In: Garner A, Klintworth GK, editors. *Pathobiology of the ocular disease – a dynamic approach.* New York/Basel: Marcel Dekker; 1982. p. 1381–419.
89. Foos RY. Tears of the peripheral retina; pathogenesis, incidence and classification in autopsy eyes. *Mod Probl Ophthalmol.* 1975;15:68–81.
90. Machemer R. The importance of fluid absorption, traction, intraocular currents, and chorioretinal scars in the therapy of rhegmatogenous retinal detachments. XLI Edward Jackson memorial lecture. *Am J Ophthalmol.* 1984;98(6):681–93.
91. Sigelman J. Vitreous base classification of retinal tears: clinical application. *Surv Ophthalmol.* 1980;25(2):59–70.
92. Halpern JJ. Routine screening of the retinal periphery. *Am J Ophthalmol.* 1966;62(1):99–102.
93. Byer NE. Clinical study of retinal breaks. *Trans Am Acad Ophthalmol Otolaryngol.* 1967;71(3):461–73.
94. Rutnin U, Schepens CL. Fundus appearance in normal eyes. II. The standard peripheral fundus and developmental variations. *Am J Ophthalmol.* 1967;64(5):840–52.
95. Boniuk M, Butler FC. An autopsy study of lattice degeneration, retinal breaks, and retinal pits. In: McPherson A, editor. *New and controversial aspects of retinal detachment.* New York: Hoeber; 1968.
96. Spencer LM, Foos RY. Paravascular vitreoretinal attachments. Role in retinal tears. *Arch Ophthalmol.* 1970;84(5):557–64.
97. Barishak YR, Stein R. Retinal breaks without retinal detachment in autopsy eyes. *Acta Ophthalmol.* 1972;50(2):147–59.
98. Byer NE. The natural history of asymptomatic retinal breaks. *Ophthalmology.* 1982;89(9):1033–9.
99. Neumann E, Hyams S. Conservative management of retinal breaks. A follow-up study of subsequent retinal detachment. *Br J Ophthalmol.* 1972;56(6):482–6.
100. Haimann MH, Burton TC, Brown CK. Epidemiology of retinal detachment. *Arch Ophthalmol.* 1982;100(2):289–92.
101. Bohringer HR. Statistics on the frequency and risks on retinal detachment. *Ophthalmologica.* 1956;131(4–5):331–4.
102. Kramer SG, Benson WE. Prophylactic therapy of retinal breaks. *Surv Ophthalmol.* 1977;22(1):41–7.
103. Combs JL, Welch RB. Retinal breaks without detachment: natural history, management and long term follow-up. *Trans Am Ophthalmol Soc.* 1982;80:64–97.
104. DiBernardo C, Blodi B, Byrne SF. Echographic evaluation of retinal tears in patients with spontaneous vitreous hemorrhage. *Arch Ophthalmol.* 1992;110(4):511–4.
105. Sarrafzadeh R, Hassan TS, Ruby AJ, Williams GA, Garretson BR, Capone Jr A, et al. Incidence of retinal detachment and visual outcome in eyes presenting with posterior vitreous separation and dense fundus-obscuring vitreous hemorrhage. *Ophthalmology.* 2001;108(12):2273–8.
106. Duker JS, Kaiser PK, Binder S, de Smet MD, Gaudric A, Reichel E, Sadda SR, Sebag J, Spaide RF, Stalmans P. The International Vitreomacular Traction Study Group classification of vitreomacular adhesion, traction, and macular hole. *Ophthalmology.* 2013;17.
107. Stalmans P, Duker JS, Kaiser PK, Heier JS, Dugel PU, Gandorfer A, Sebag J, Haller JA. OCT-based interpretation of the vitreomacular interface and indications for pharmacologic vitreolysis. *Retina.* 2013;33(10):2003–11.
108. Krebs I, Brannath W, Glittenberg C, Zeiler F, Sebag J, Binder S. Posterior vitreomacular adhesion: a potential risk factor for exudative age-related macular degeneration? *Am J Ophthalmol.* 2007;144(5):741–6.
109. Robison CD, Krebs I, Binder S, Barbazetto IA, Kotsolis AI, Yannuzzi LA, Sadun AA, Sebag J. Vitreomacular adhesion in active and end-stage age-related macular degeneration. *Am J Ophthalmol.* 2009;148(1):79–82 e2.
110. Mayr-Sponer U, Waldstein SM, Kundi M, Ritter M, Golbaz I, Heiling U, et al. Influence of the vitreomacular interface on outcomes of Ranibizumab therapy in neovascular age-related macular degeneration. *Ophthalmology.* 2013;120(12):2620–9.
111. Uney GO, Unlu N, Acar MA, Hazirolan D, Altiparmak UE, Yalniz-Akkaya Z, et al. Role of posterior vitreous detachment on outcome of anti-vascular endothelial growth factor treatment in age-related macular degeneration. *Retina.* 2014;34:32–7.
112. Bottos J, Elizalde J, Arevalo JF, Rodrigues EB, Maia M. Vitreomacular traction syndrome. *J Ophthalmic Vis Res.* 2012;7(2):148–61.
113. Wang MY, Nguyen D, Hindoyan N, Sadun AA, Sebag J. Vitreopapillary adhesion in macular hole and macular pucker. *Retina.* 2009;29(5):644–50.
114. Haouchine B, Massin P, Gaudric A. Foveal pseudocyst as the first step in macular hole formation: a prospective study by optical coherence tomography. *Ophthalmology.* 2001;108(1): 15–22.
115. Chu TG, Lopez PF, Cano MR, Freeman WR, Lean JS, Liggett PE, et al. Posterior vitreoschisis. An echographic finding in proliferative diabetic retinopathy. *Ophthalmology.* 1996;103(2):315–22.
116. Schwatz SD, Alexander R, Hiscott P, Gregor ZJ. Recognition of vitreoschisis in proliferative diabetic retinopathy. A useful landmark in vitrectomy for diabetic traction retinal detachment. *Ophthalmology.* 1996;103(2):323–8.
117. Sebag J. Vitreoschisis in diabetic macular edema. *Invest Ophthalmol Vis Sci.* 2011;52(11):8455–6. author reply 6–7.
118. Gupta P, Yee KM, Garcia P, Rosen RB, Parikh J, Hageman GS, Sadun AA, Sebag J. Vitreoschisis in macular diseases. *Br J Ophthalmol.* 2011;95(3):376–80.
119. Sebag J, Wang MY, Nguyen D, Sadun AA. Vitreopapillary adhesion in macular diseases. *Trans Am Ophthalmol Soc.* 2009; 107:35–44.
120. Zhao F, Gandorfer A, Haritoglou C, Scheler R, Schaumberger MM, Kampik A, et al. Epiretinal cell proliferation in macular pucker and vitreomacular traction syndrome: analysis of flat-mounted internal limiting membrane specimens. *Retina.* 2013; 33(1):77–88.

121. Haritoglou C, Reiniger IW, Schaumberger M, Gass CA, Priglinger SG, Kampik A. Five-year follow-up of macular hole surgery with peeling of the internal limiting membrane: update of a prospective study. *Retina*. 2006;26(6):618–22.
122. Johnson RN, Gass JD. Idiopathic macular holes. Observations, stages of formation, and implications for surgical intervention. *Ophthalmology*. 1988;95(7):917–24.
123. Gartner J. Electron-microscopic study on the fibrillar network and fibrocyte–collagen interactions in the vitreous cortex at the ora serrata of human eyes with special regard to the role of disintegrating cells. *Exp Eye Res*. 1986;42(1):21–33.
124. Sebag J. Vitreous: the resplendent enigma. *Br J Ophthalmol*. 2009;93(8):989–91.
125. Smiddy WE, Green WR, Michels RG, de la Cruz Z. Ultrastructural studies of vitreomacular traction syndrome. *Am J Ophthalmol*. 1989;107(2):177–85.
126. Sebag J, Balazs EA. Morphology and ultrastructure of human vitreous fibers. *Invest Ophthalmol Vis Sci*. 1989;30:1867–71.
127. Faulborn J, Ardjomand N. Tractional retinoschisis in proliferative diabetic retinopathy: a histopathologic study. *Graefes Arch Clin Exp Ophthalmol*. 2000;238:40–4.

Arnd Gandorfer, Ricarda G. Schumann,
Christos Haritoglou, and Anselm Kampik

Outline

- I. Introduction
- II. Vitreomacular Traction Syndrome
- III. Macular Pucker
 - A. Cell Types
 - B. Cell Locations
 - C. Cell Origins
- IV. Macular Hole
 - A. Immunocytochemistry

References

Keywords

Vitreous • Posterior vitreous cortex • Inner limiting membrane • Anomalous posterior vitreous detachment
Vitreoschisis • Vitreomaculopathies • Histopathology
Immunocytochemistry • Hyalocytes • Myofibroblasts
Alpha-SMA-mediated contraction

Key Concepts

1. Anomalous PVD with vitreoschisis plays a major role in allowing cells to grow on the ILM and a layer of vitreous cortex collagen left behind as a result of vitreoschisis. These cells undergo myofibroblastic transdifferentiation leading to contractile cellular membranes.
2. While glial cells can cross the ILM and form cell proliferations on the vitreal side of the ILM, these do not cause retinal distortion and thus are not likely prominent players in pathogenesis. In contrast, hyalocytes embedded in the vitreous cortex and left behind after anomalous PVD are the major cellular part of premacular membranes causing visual disturbances.
3. Vitreomacular traction is generated by alpha-SMA-mediated contraction following transdifferentiation of glial cells and in particular by hyalocytes.

A. Gandorfer, MD (✉)
Department of Ophthalmology,
MVZ Memmingen and Ludwig Maximilian University,
Munich, Germany

Department of Ophthalmology,
University Eye Hospital, Ludwig-Maximilians-University,
Mathildenstr 8, Munich 80336, Germany
e-mail: arnd.gandorfer@me.com

R.G. Schumann, MD • A. Kampik, MD
Department of Ophthalmology, Ludwig-Maximilians-University,
Munich, Germany

Department of Ophthalmology,
University Eye Hospital, Ludwig-Maximilians-University,
Mathildenstr 8, Munich 80336, Germany
e-mail: ricarda.schumann@med.uni-muenchen.de;
anselm.kampik@med.uni-muenchen.de

C. Haritoglou, MD
Department of Ophthalmology, Duke Carl Theodor Eye Clinic,
Ludwig Maximilian University, Munich, Germany

Department of Ophthalmology, University Eye Hospital,
Ludwig-Maximilians-University, Mathildenstr 8,
80336 Munich, Germany
e-mail: christos.haritoglou@med.uni-muenchen.de

I. Introduction

The hallmark of vitreomaculopathies is traction exerted onto the macula. This traction is generated by tension forces between the vitreous, in particular the posterior vitreous cortex, and the inner limiting membrane (ILM) of the retina. In theory, traction arising from vitreomacular adhesions can either be tangential to the retinal surface or perpendicular (axial). In reality, both pathologies are frequently found in combination, forming characteristic pathologic features of clinical diseases such as macular pucker, macular hole, and vitreomacular traction syndrome.

Attachments of vitreous to the macula are a rare finding in pathology specimens. As mostly causing no symptoms, no therapy is performed and no surgical specimen is available. In enucleated eyes, pathology is often changed markedly, including the vitreoretinal interface, and the observer's attention is drawn to other pathologies, such as a tumor or changes

following phthisis bulbi. This does, however, not mean that vitreomacular adhesions are rare. Modern imaging techniques such as optical coherence tomography (OCT) frequently demonstrate these vitreomacular adhesions which cannot be detected by biomicroscopy alone. In contrast, remnants of the vitreous cortex can frequently be found in pathology specimens. Given their transparency and thinness, they are often not visible in light microscopy. However, they can be seen by scanning electron microscopy (Figure III.C-1).

The literature contains frequent reference to epiretinal membranes (ERM). This term is inaccurate for two reasons: The term "epi-" refers to a location next to or beside a structure, in this case the retina. Thus, the term "epiretinal" could refer to a subretinal and preretinal location. In all of the situations discussed herein, the membrane location is in front of the retina; thus, the prefix "pre-" is more accurate and will be used instead of "epi-." Furthermore, all of the conditions discussed herein are maculopathies, not retinopathies. Thus,

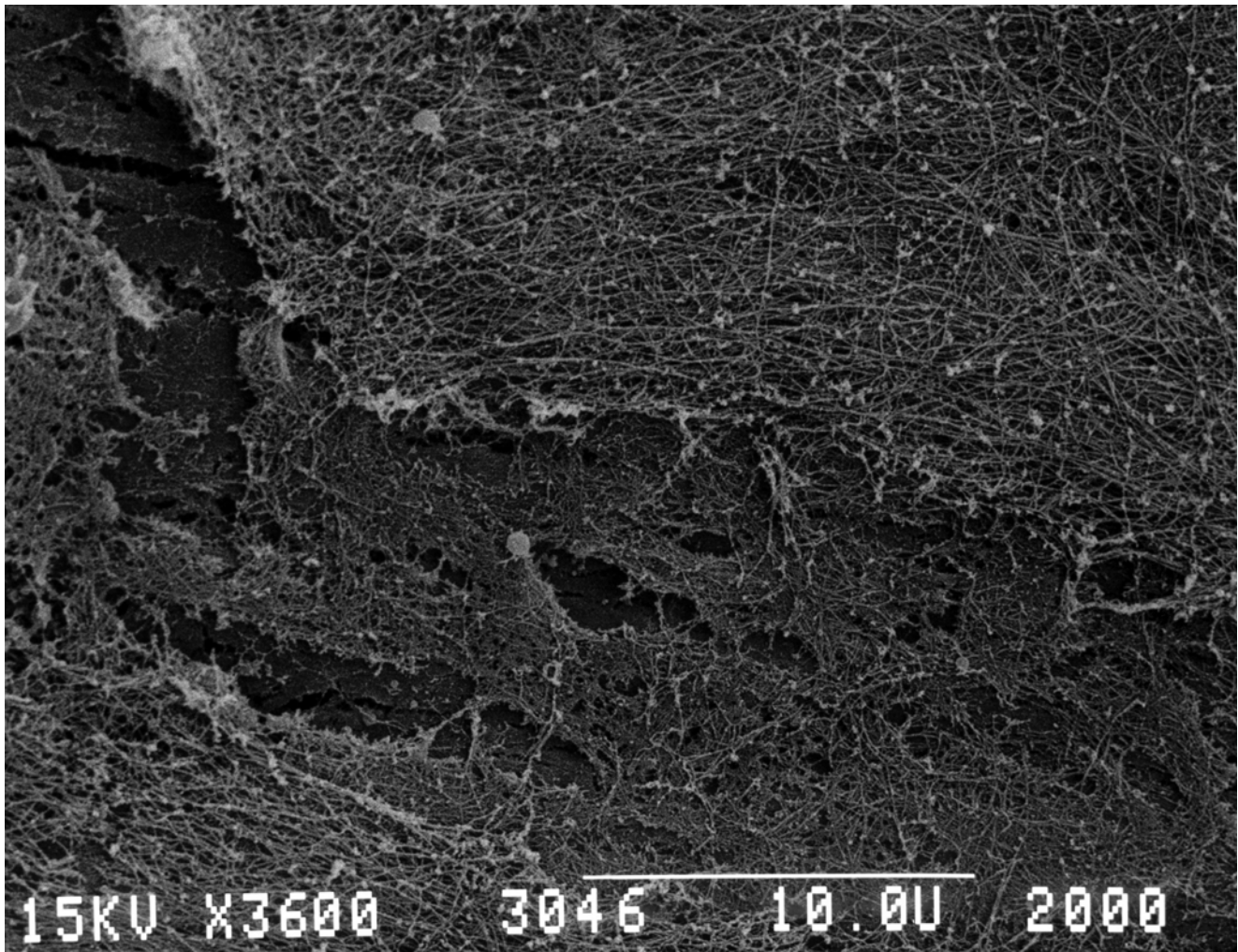


Figure III.C-1 Remnants of the vitreous cortex on the ILM. Scanning electron microscopy showing a dense network of collagen fibrils. Magnification 3,600× (With permission from Gandorfer et al. [1])

the term “premacular membrane (PMM)” is the more precise terminology and will be employed herein to refer to what has previously been described as “ERM.” The term “macular pucker” will be used to refer to one clinical consequence of an abnormal premacular membrane. Furthermore, the term “idiopathic” ERM is no longer an appropriate term to refer to macular pucker, since we now know that vitreous is the cause of this condition, as discussed below [see chapter III.F. Vitreous in the pathobiology of macular pucker].

II. Vitreomacular Traction Syndrome

If vitreomacular adhesions exert traction onto the macula over a prolonged period of time, macular function can be disturbed and the patient becomes symptomatic. The pathology of vitreomacular traction syndrome had been researched by several investigators, who described the histopathology and ultrastructure of surgical specimens. It is important to differentiate between specimens of premacular membranes removed by localized peeling and those of en bloc peelings. In the first case, when the premacular membrane is removed, a conclusion regarding the relationship between the vitreous cortex, premacular cells, and ILM of the retina is limited to areas where the ILM had been removed unintentionally. In the case of en bloc peeling, the specimen can be investigated by serial sectioning and reliably reflects the interaction between the vitreous, premacular cells, and ILM. En bloc specimens demonstrate attachments of the vitreous cortex to the ILM in eyes with vitreomacular traction syndrome. Ultrastructural analysis reveals native vitreous collagen with a characteristic fibril diameter of 8–15 nm and a regular arrangement of fibrils. In our experience, these vitreomacular adhesions are a consequence of incomplete posterior vitreous separation, described by Sebag as *anomalous posterior vitreous detachment* [2], often combined with splitting of the vitreous cortex, so-called vitreoschisis as previously described clinically [3] and histopathologically [4] [see chapter III.B. Anomalous PVD and vitreoschisis].

Cell proliferation is a common finding in vitreomacular traction syndrome, forming premacular membranes which are not always seen by biomicroscopy (Figure III.C-2). The cellular membranes typically grow along the vitreomacular attachment from the retinal surface onto the posterior surface of the detached part of the vitreous cortex. If a layer of native vitreous collagen is sandwiched between the premacular membrane and the ILM, the cells grow along the inner surface of the vitreoschisis cavity. In both situations, the cellular membranes create a firm attachment between the vitreous and the retina and cement the vitreomacular adhesion by cellular proliferation.

In 2002, we published a consecutive series of surgical specimens from patients with vitreomacular traction

syndrome who had been peeled en bloc [5]. Due to this technique, this was the first study demonstrating the in situ arrangement of cellular proliferation, the vitreous cortex, and the ILM in a systematic manner (Figure III.C-3). Half of the eyes showed mostly single cells or a cellular monolayer covering the vitreal side of the ILM, resulting neither in a biomicroscopically detectable premacular proliferation nor in wrinkling of the vitreomacular interface. The other half of the eyes revealed premacular fibrocellular tissue which was separated from the ILM by a layer of native vitreous collagen (Figure III.C-4), resembling the clinical features of macular pucker from premacular membranes in the eyes with complete posterior vitreous detachment.

III. Macular Pucker

Premacular membranes from the eyes with macular pucker were the first surgical specimens investigated following the advent of vitrectomy [7]. The eyes undergoing surgery showed advanced pathology in terms of marked premacular cellular proliferation with macular distortion and vision loss. These studies aimed at describing the cells contributing to preretinal proliferation [8, 9]. In brief, the following cells varied in quantity depending on the underlying disease, but in terms of quality, premacular membranes from the eyes with macular pucker showed uniform ultrastructural features. Five morphologically distinguishable cell types were observed in 56 premacular and vitreous membranes obtained surgically from the eyes with various ocular diseases: (1) retinal pigment epithelial (RPE) cells, evident only in association with retinal detachment; (2) macrophages; (3) fibrocytes; (4) fibrous astrocytes, which were characteristic of all disease groups; and (5) myofibroblast-like cells that had mostly the characteristics of fibrocytes and, occasionally, of RPE cells or fibrous astrocytes. The combination of cell types varied in different types of premacular membranes, but the formation of collagen and the development of cells with myofibroblast-like properties were common features and seemed to be within the capacity of several cell types. These two common features seem to be the basis for the contractile properties of premacular and vitreous membranes [8, 9]. Since then, cells in premacular membranes have been classified according to their ultrastructural features.

A. Cell Types

1. *Fibrous astrocytes* are characterized by masses of intracytoplasmic intermediate-type 10 nm filaments, junctional complexes of the adherence type, and polarization with basement membrane production.

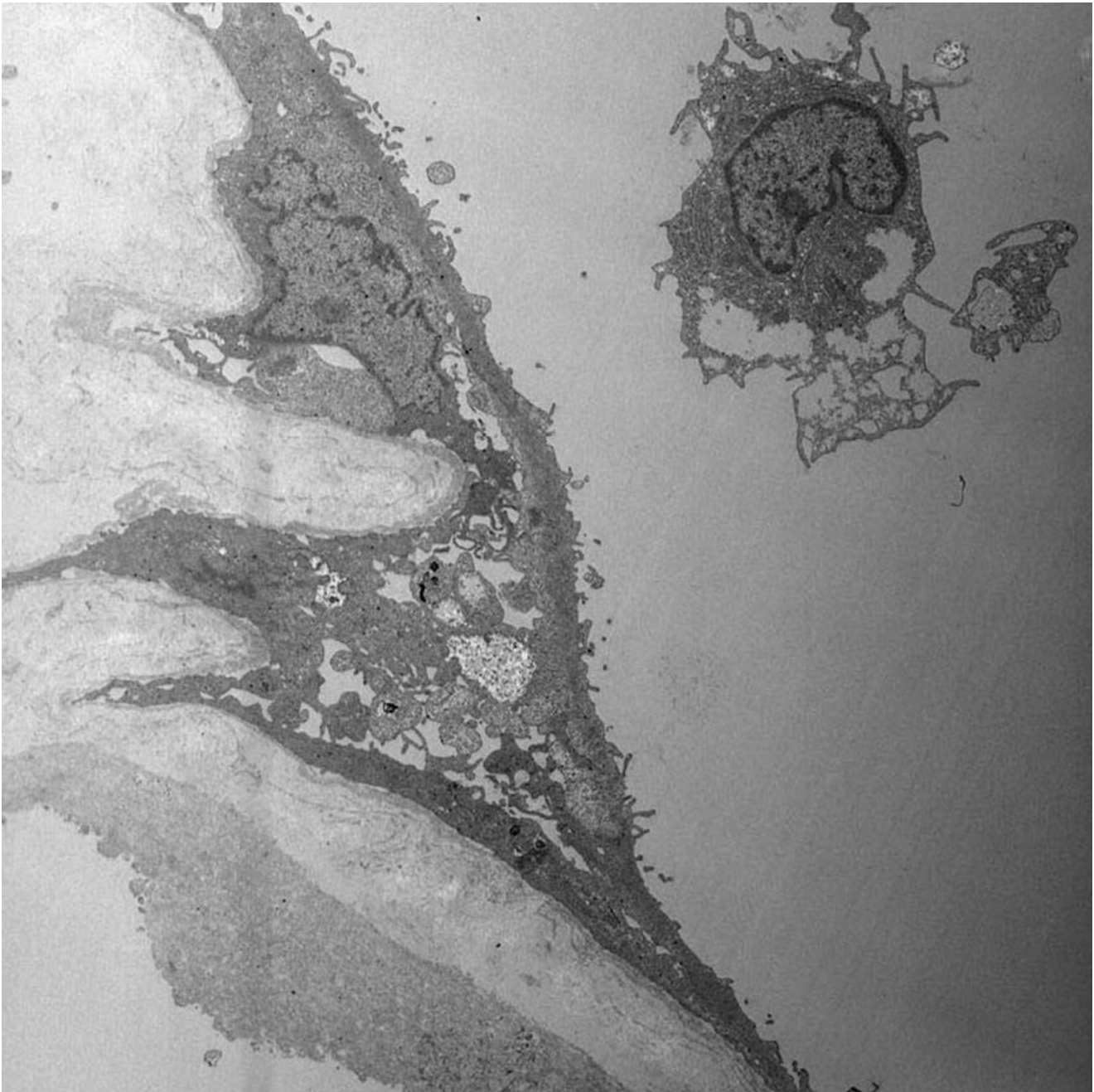


Figure III.C-2 Vitreomacular traction syndrome. A cellular multilayer is situated on vitreous cortex covering the ILM, growing along the vitreous strand. Magnification 1,800 \times (With permission from Gandorfer et al. [5])

2. *Myofibroblasts* are characterized by rough endoplasmic reticulum, a fusiform nucleus and cell body, the absence of intracytoplasmic intermediate-type 10 nm filaments or basement membrane, but aggregates of 5–7 nm subplasmalemmal cytoplasmic filaments with fusiform densities.
3. *Fibrocytes* are characterized by abundant rough endoplasmic reticulum and a prominent Golgi complex, fusiform shape of the cell body and nucleus, and absence of intracytoplasmic filaments or basement membrane.
4. *Hyalocytes* are described as resembling macrophages that usually possess a lobulated nucleus, a well-developed Golgi complex, a rough and smooth endoplasmic reticulum, and many large lysosomal granules and phagosomes. They are embedded in the vitreous cortex situated 20–50 μm from the ILM at the posterior retina, belong to the macrophage/monocyte system, and are bone marrow derived [10].

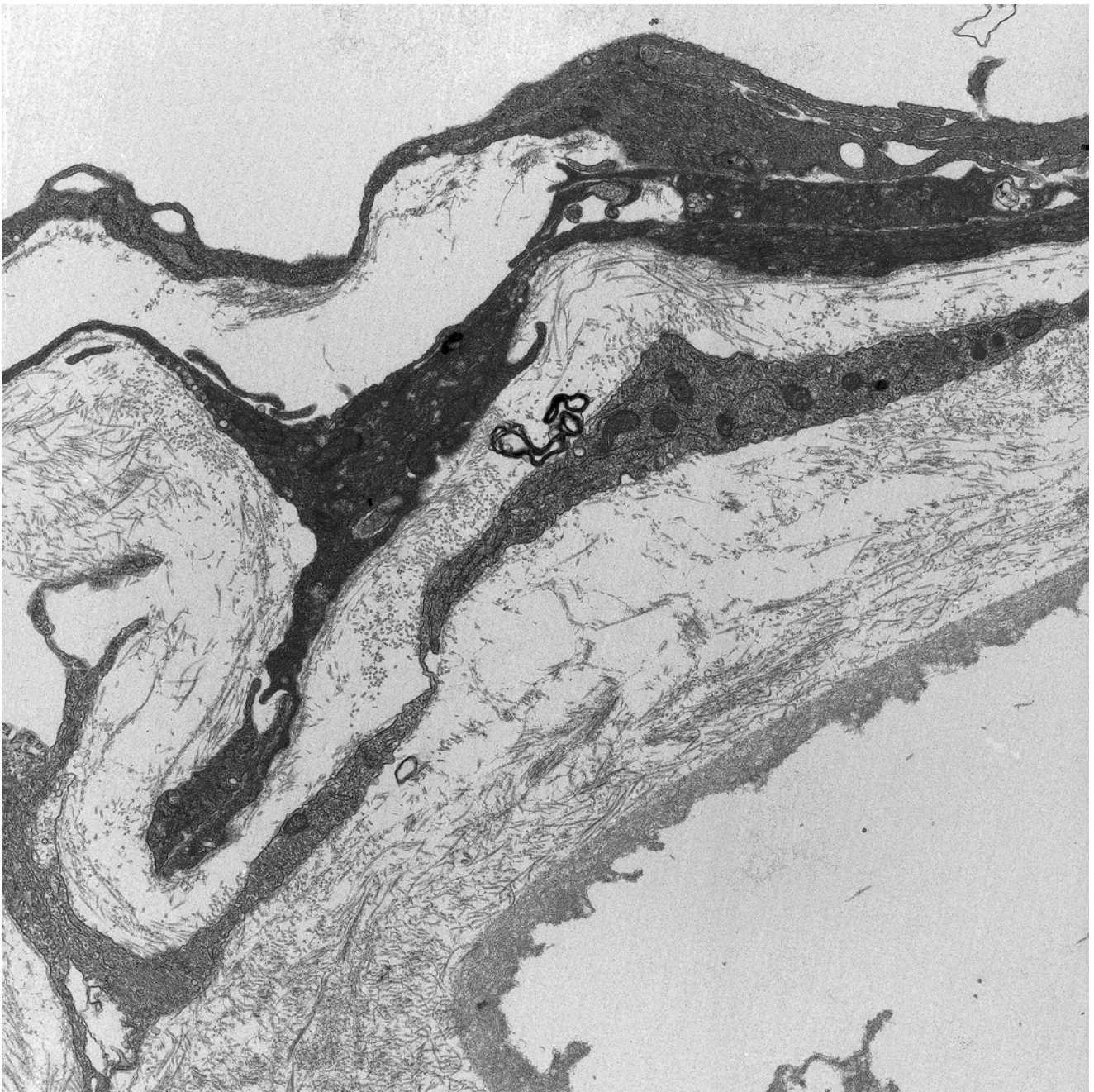


Figure III.C-3 Premacular membrane on a layer of native vitreous collagen. Magnification 4,800 \times (With permission from Gandorfer et al. [6])

B. Cell Locations

In the early studies, cell proliferation was marked due to advanced disease chronicity, and the ILM was removed unintentionally in more than half of the cases, not because of aggressive peeling, but caused by the infoldings of the ILM in advanced premacular proliferation. However, these specimens gave insight into the arrangement of cells in relation to the ILM of the retina. In most instances, a layer of vitreous collagen was sandwiched between the cells and

the ILM. This was confirmed by subsequent studies, when the premacular membrane was intentionally peeled en bloc together with the ILM [11]. As mentioned, the relationship between the vitreous and premacular membranes was not primarily addressed in early studies, as modern imaging techniques did not exist and vitreous removal preceded premacular membrane removal. In addition, no dye was available to stain the different structures of the vitreomacular interface. Dye-assisted macular surgery, called chromodissection [12] [see chapter V.A.3. Chromodissection

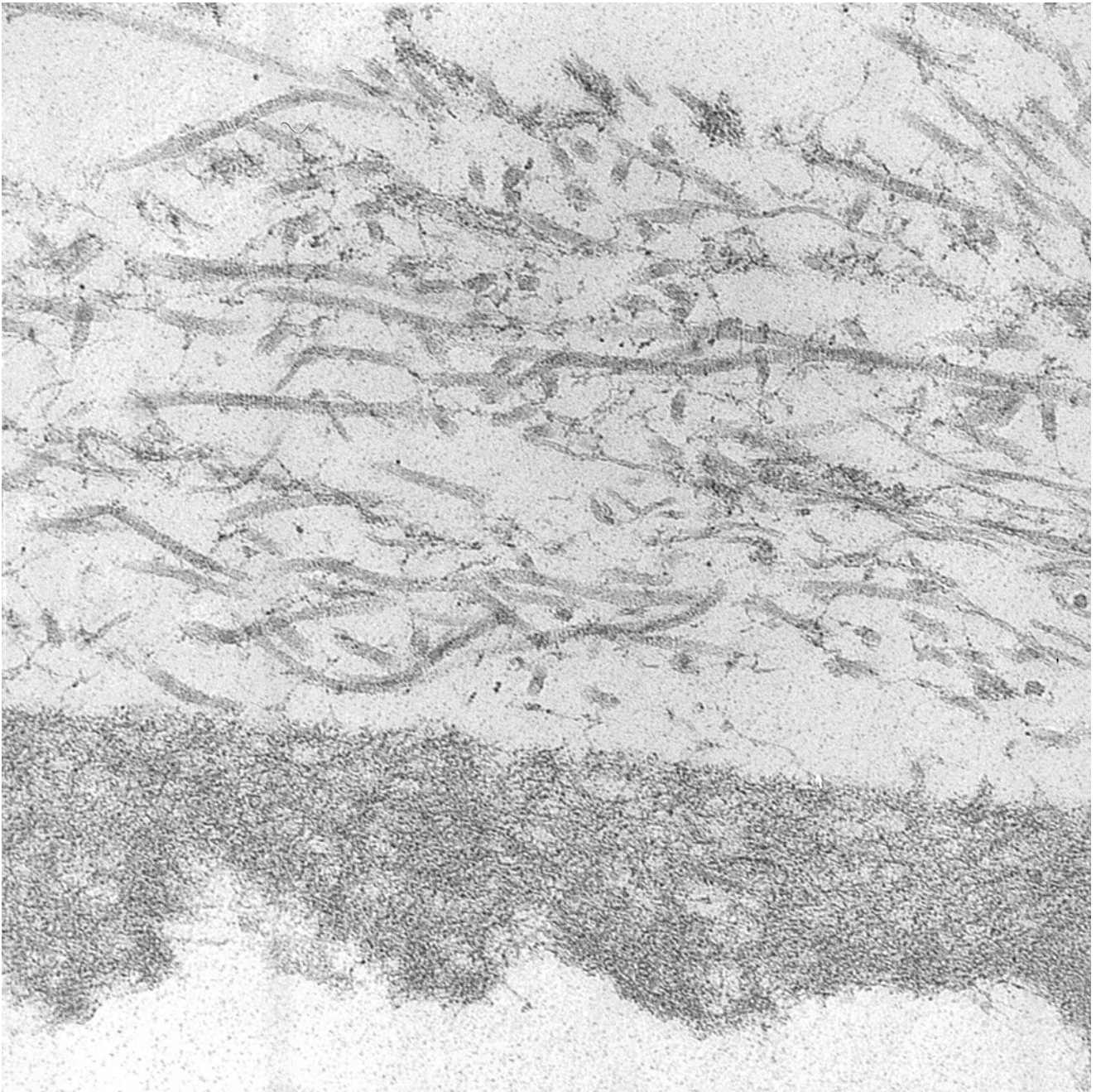


Figure III.C-4 Native vitreous collagen on the ILM. Higher magnification from Figure III.C-3. Regular arrangement of collagen fibrils typical for native vitreous cortex collagen. Magnification 40,000 \times (With permission from Gandorfer et al. [6])

in vitreo-retinal surgery], enables us to investigate premacular tissue with the understanding that “what we see we will get,” i.e., what we’ve stained and removed during surgery, such as vitreous cortex, premacular proliferation, and ILM, we will find again in ultrastructural evaluations [13, 14]. This offers a clear distinction which tissue had been removed and makes a separate investigation of premacular membranes and the ILM possible. Together with interference and phase-contrast microscopy of flat-embedded

surgical specimens, a conclusion regarding the quantity of cells removed or left behind at the ILM can now be drawn.

In 2012, we published a paper on sequential peeling of premacular membranes and the pathology features seen in the removed specimens [15] (Figure III.C-5). In roughly one third of the cases, the premacular membrane and the ILM were removed together. In these specimens, cellular proliferation was seen directly growing on the ILM. In two thirds of the eyes, however, the ILM was still present at the macula

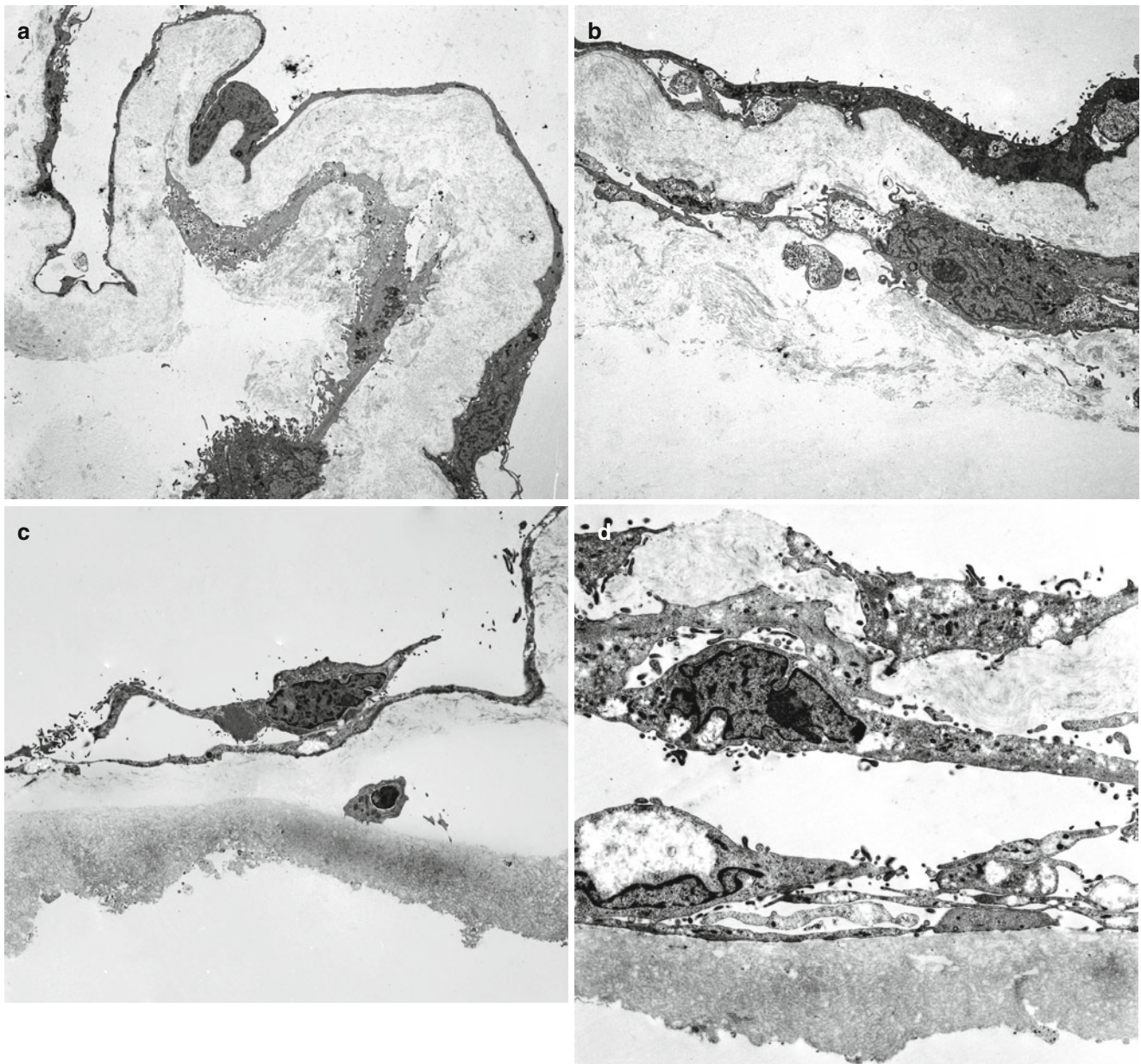


Figure III.C-5 Transmission electron microscopy of ERM and ILM specimens. (a, b) are from the sequential peeling group. (a) Premacular membrane specimen shown in Figure III.C-6. A continuous cellular proliferation is present on a collagenous layer. (b) Higher magnification reveals a multilayered membrane composed of cells and collagen. Note that no ILM is present. (c, d) belong to the complete peeling group.

(c) The ILM was removed together with a thin collagenous layer and cellular proliferation on top of it. A single cell is present close to the ILM. (d) A multilayered cellular membrane in direct contact with the ILM. Note that there is no collagen between the cells and the ILM. Magnification: (a) 31,000 \times ; (b) 31,600 \times ; (c) 31,800 \times ; (d) 33,000 \times (With permission from Gandorfer et al. [15])

after membrane removal and contained an average of 20 % of the total cell count which would have been left behind if the ILM had not been peeled in addition. In the majority of the eyes, premacular membrane removal resulted in splitting of the vitreous cortex with subsequent creation of vitreoschisis, leaving cells and collagen attached to the macula. The cells left behind were mainly glial cells and hyalocytes. The findings of these studies are interesting in two respects. (1) Premacular membranes grow either on a layer of vitreous

collagen following anomalous posterior vitreous detachment with vitreoschisis or directly on the ILM if PVD was complete. (2) The origin of cells and subsequently the composition of premacular membranes as well as their impact on macular function seem to differ between the two types and reflect the distinction Foss and others have made previously, when speaking of “simple” premacular membranes without visual disturbances compared with those impairing visual function [16] (Figure III.C-6).

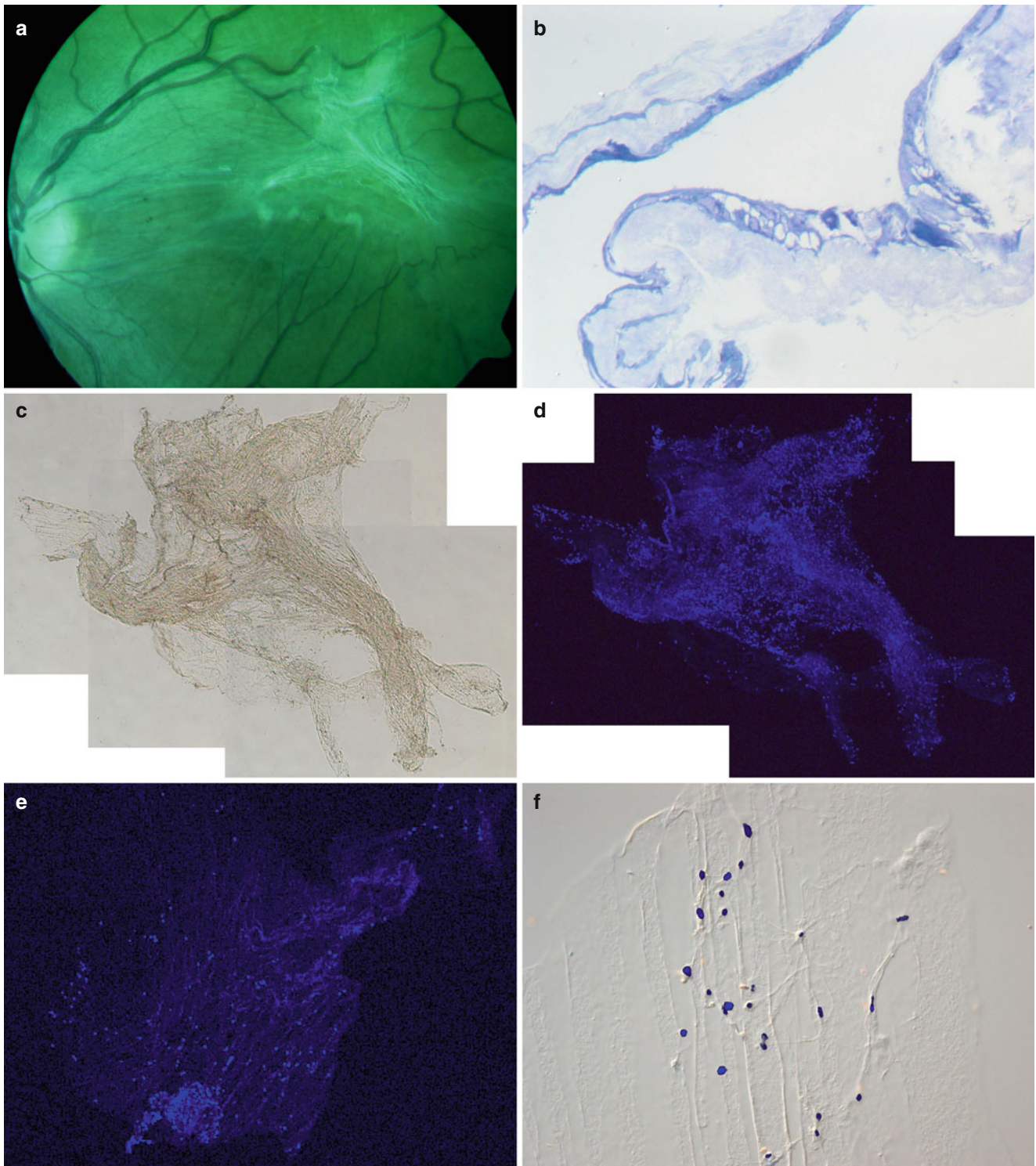


Figure III.C-6 Sequential premacular membrane peeling. (a) Fundus photograph of a 48-year-old patient with PMM formation. (b) Premacular membrane removal resulted in dissection of the premacular cellular membrane on a thick layer of collagen. (c) Flat-mount preparation of the membrane shows the premacular membrane as it was in situ. (d) 4',6-Diamidino-2-phenylindole staining reveals 6,000 cells corresponding to a cell density of 1,040 cells per mm². (e) The ILM was

peeled consecutively. Flat-mount preparation shows 500 cells that were left behind at the vitreomacular interface after premacular membrane removal (8 % of total cell count). (f) Interference microscopy reveals cellular protrusions and interconnections, forming cell clusters. Magnification: (b) 3,400x; (c-e) 350x; (f) 3,200x (With permission from Gandorfer et al. [15])

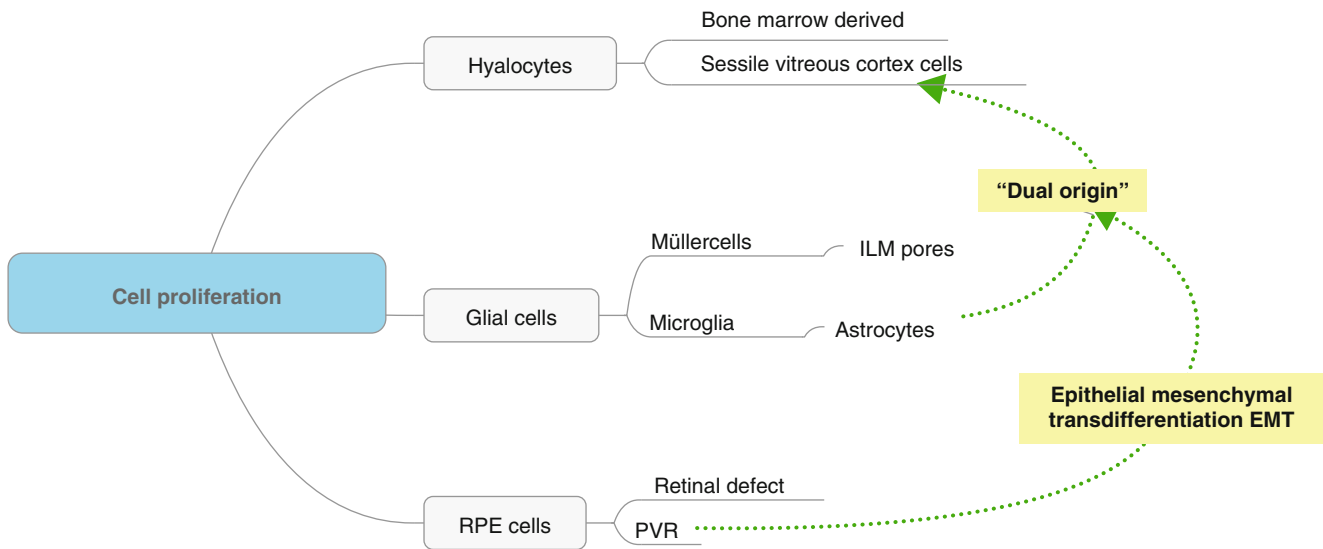


Figure III.C-7 Overview of cells contributing to premacular cell proliferation and their origin

C. Cell Origins

The origin of the cells causing premacular proliferation is still a matter of debate. It is only clear in the case of retinal pigment epithelial cells, but they only play a role in retinal detachment and proliferative vitreoretinopathy (PVR) or in traction maculopathies combined with retinal tears [see chapter III.J. Cell proliferation at VRI in PVR and related disorders]. The majority of cases undergoing macular surgery, however, don't show RPE cells in surgical specimens.

Hyalocytes are bone marrow-derived sessile vitreous cortex cells. It is not entirely understood whether they reach the vitreous body via the vascular system or via the ciliary body [see chapter II.D. Hyalocytes] (Figure III.C-7).

Fibrous astrocytes are derived from retinal glia. They represent the source of “simple” premacular membranes without causing retinal distortion [17]. Proliferating glial cells have also been found on the retinal side of the ILM removed from a patient with cellophane maculopathy [18]. It has been previously proposed that fibrous astrocytes enter the vitreous body via pores in the ILM. Although this can certainly happen, the question arises how much they contribute to premacular membranes causing visual disturbances [17]. This skepticism is supported by a recent study when we looked at ILM pores in the macular hole eyes in a systematic manner (Figure III.C-8). In that study we investigated 112 ILM specimens from the macular hole eyes undergoing surgery and performed serial sectioning to detect pores in the ILM [19]. Only three pores were found. Although undoubtedly glial cells can cross the ILM, there is no evidence to assume that they account for the majority of cells in premacular

membranes causing visual disturbances. Hyalocytes are a much more reasonable source of premacular proliferation, as will be shown by immunohistochemical findings in the following.

IV. Macular Hole

Since the advent of ILM peeling in the 1990s, we have routinely removed the ILM in macular hole eyes and processed the specimens for ultrastructural analysis [20]. Early studies aimed at demonstrating the feasibility of surgical ILM removal, up to the year 2000 without chromodissection, afterwards with the use of indocyanine green (ICG) and later with the application of trypan blue or brilliant blue G. These studies showed that it was the ILM that had been removed and, moreover, that premacular cell proliferation was frequently present in macular hole eyes [21, 22]. The majority of specimens demonstrated mono- or multilayers of fibrous astrocytes with single macrophage- or fibrocyte-like cells. The vitreous and newly formed collagen occupied the space between the ILM and the cells [21]. Obviously, the similar ultrastructure of premacular membranes associated with macular holes and “simple epiretinal membranes” as described by Foos shared a common pathogenesis.

In a larger series of one hundred consecutive eyes with en bloc removal of the ILM and premacular tissue performed by one surgeon, 218 specimens were processed for light and transmission electron microscopy, coming from 80 eyes with stage III macular holes and 20 eyes with stage IV macular holes [23]. Given that many of the specimens had been

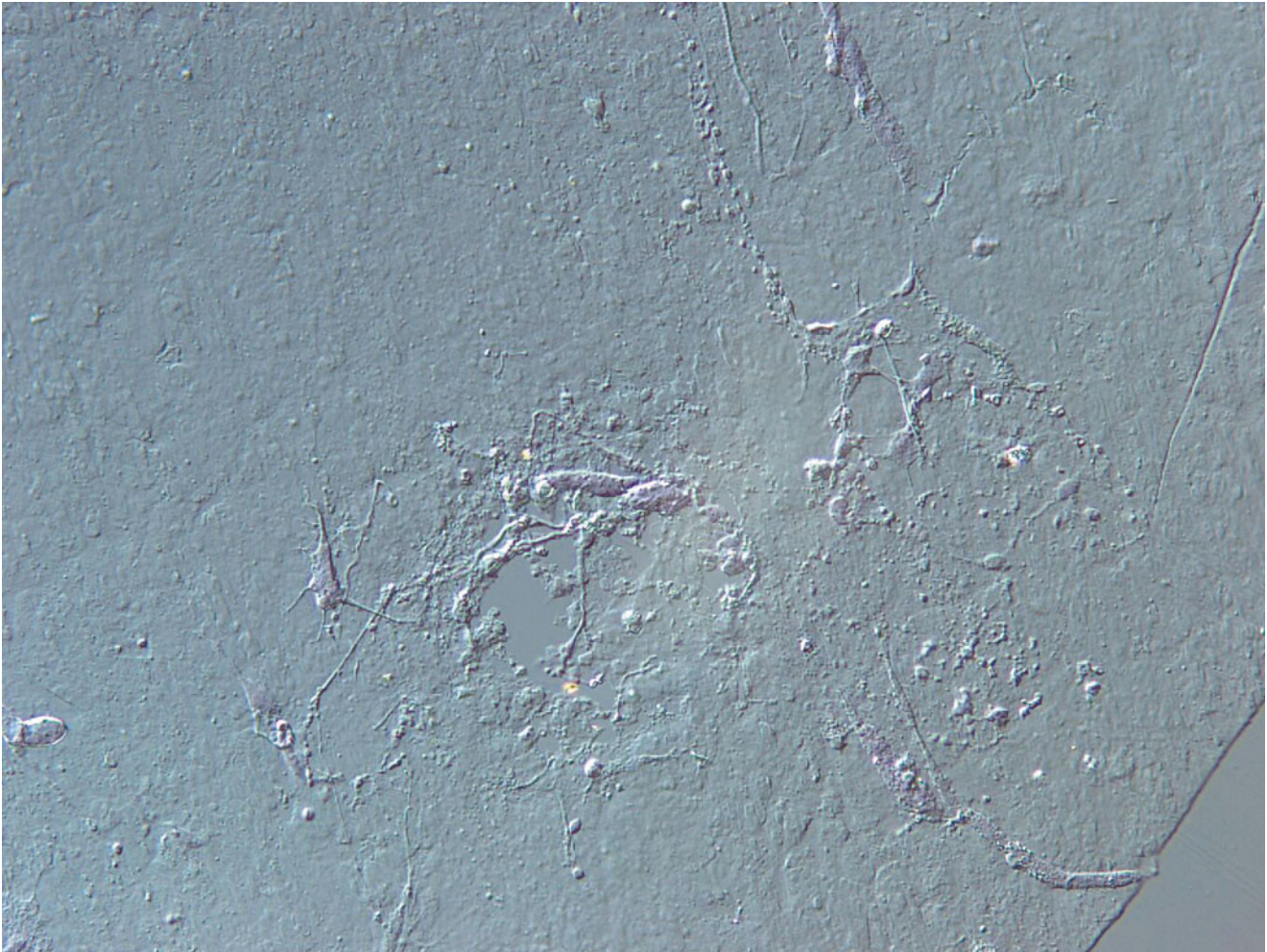


Figure III.C-8 ILM pore. Flat-mount preparation showing the ILM pore surrounded by single cells. Magnification 200× (With permission from Gandorfer et al. [19])

removed before the availability of OCT, the classification whether stage III or stage IV was solely based on intraoperative findings, i.e., total PVD in stage IV macular holes. Fibrocellular proliferation at the vitreal side of the ILM was found in 57 cases. Native vitreous collagen (NVC) was attached to the ILM in 36 eyes. The presence of NVC was considerably more frequent in the eyes with stage IV (70 %) than in the eyes with stage III macular holes (26 %). Mono- and multilayered cellular membranes were seen more frequently in stage IV macular holes. It is of note that NVC, if present, was always associated with fibrocellular proliferation. In 39 eyes with stage III and in four eyes with stage IV macular holes, the ILM was devoid of any cells and collagen. We concluded that fibrocellular proliferation was a secondary event instead of a primary feature in macular hole development. Two issues are obvious from this study: (1) The severity of fibrocellular proliferation is associated with the

presence of native vitreous collagen, emphasizing the importance of vitreoschisis in promoting cell proliferation. (2) Incomplete vitreoretinal separation contributes to the development of premacular membranes in eyes with idiopathic macular holes.

In 2008, we introduced a new method to investigate the vitreoretinal interface of surgical ILM specimens [24]. In contrast to conventional cross section techniques, such as light or transmission electron microscopy, flat-mount preparation was established and combined with interference and phase-contrast microscopy and with in situ immunocytochemistry. Compared with conventional microscopy, phase-contrast and interference microscopy of flat-mounted ILM specimens gives new insights into the distribution of cellular proliferations at the vitreomacular interface and allows for determination of the cell density at the ILM. Given that the entire ILM peeled is seen en face, these techniques offer

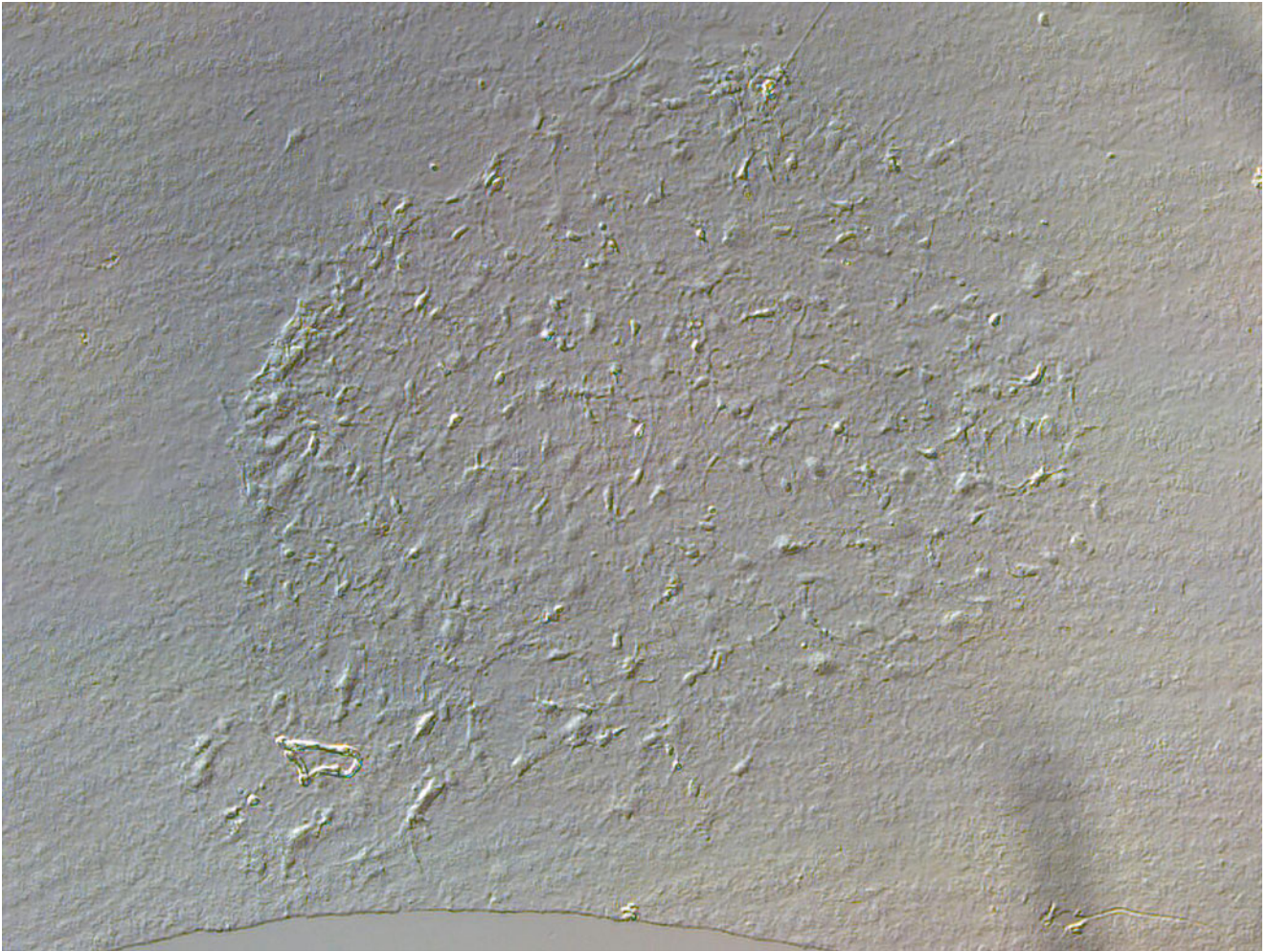


Figure III.C-9 Nidus of cell proliferation. Flat-mount preparation and interference microscopy show a cluster of cells on the ILM. Magnification 100×

a more reliable method to investigate the vitreoretinal interface in terms of cellular distribution. Moreover, it allows for in situ immunocytochemistry and characterization of cellular antigens with precise determination of cell localization. With these techniques, we were able to demonstrate the cell distribution on the ILM in macular hole eyes and investigated the macular hole rim both en face and cross-sectioned in ultrastructural and immunohistological terms [25]. Premacular cell proliferation was found in all ILM specimens, irrespective of the stage of the macular hole. Cell density showed a broad range. There were single cells, cell clusters, and continuous cellular proliferations. The cell clusters seemed to form the nidus for continuous cell membranes (Figure III.C-9). Even if a continuous cellular proliferation covered the ILM, the macular hole rim was spared, and the cells did not reach the edge of the macular hole (Figure III.C-10).

In immunocytochemistry, collagen type II was present surrounding the macular hole rim. This was confirmed by transmission electron microscopy, where the vitreous cortex collagen was a continuous layer covering the foveal ILM and spreading beyond the edge of the foveal dehiscence, thus representing the vitreomacular attachment, which is now frequently seen in OCT, and indicating an abnormal vitreofoveal adhesion in macular hole eyes leading to foveal dehiscence and macular hole development (Figure III.C-11). Again it was obvious that anomalous PVD was responsible for disease development and its sequelae. Vitreomacular adhesion caused a dehiscence in the fovea and the presence of a layer of vitreous cortex collagen on the ILM promoted cellular proliferation, growing along the vitreous adhesion and cementing the adherence of the vitreous to the retina.

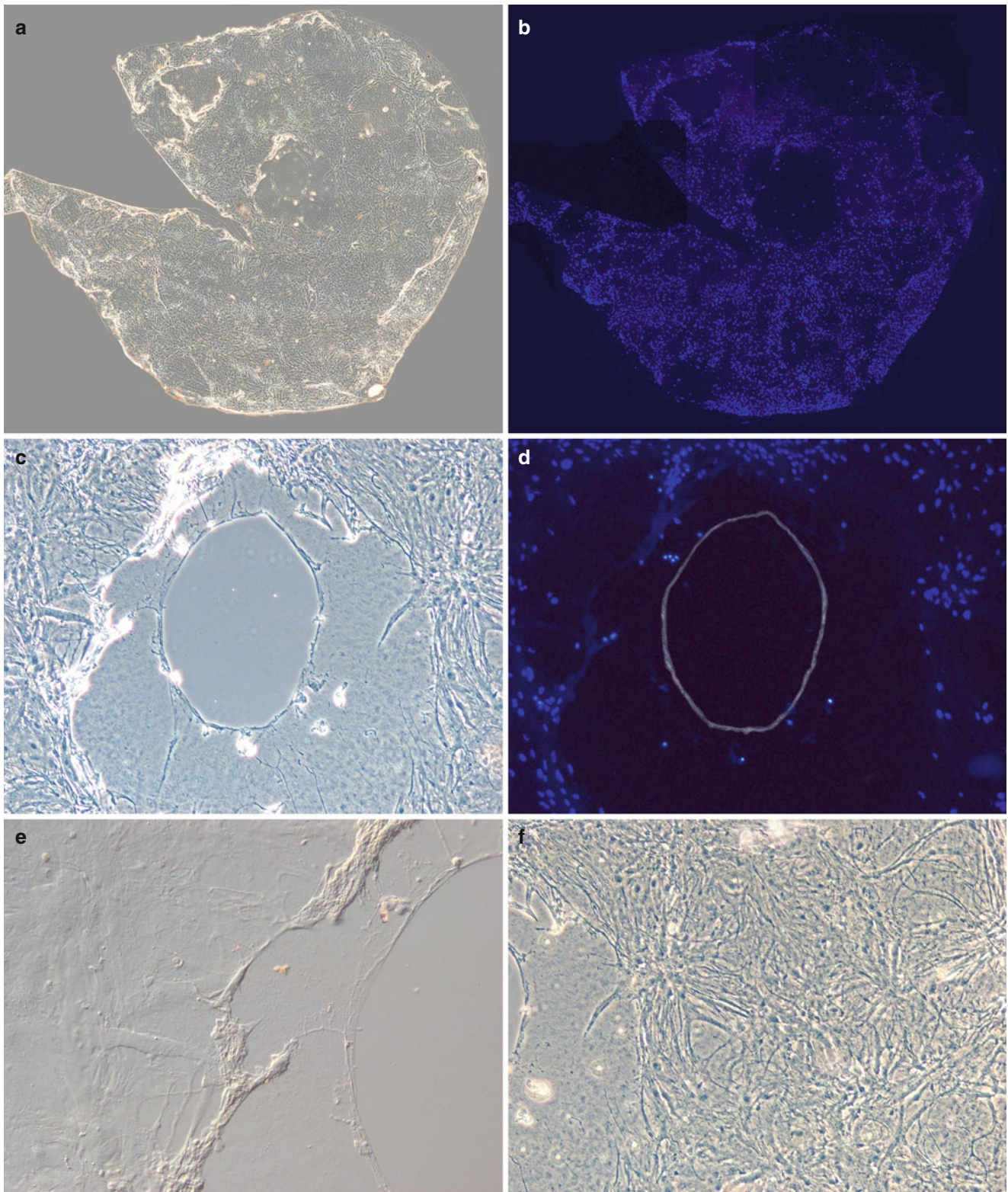


Figure III.C-10 Macular hole rim flat mount. **(a)** Flat-mount preparation of the ILM from a 69-year-old woman with a stage IV macular hole. The area of the ILM peeled is 16.62 mm². **(b)** DAPI staining of cell nuclei shows 6,729 cells attached to the ILM. **(c)** Phase-contrast microscopy of the macular hole rim. The macular hole aperture measures 380 μ m. **(d)** DAPI staining of cell nuclei surrounding the macular hole rim. The edge of the macular hole is indicated by the *gray line*. There are only a few cells ($n=13$) in close

proximity to the macular hole rim. **(e)** Interference microscopy of the area surrounding the macular hole rim. The rim of the macular hole shows a flat ILM with single cells only. Proliferation is located distant from the macular hole rim. The distance between the edge of the macular hole and proliferation is between 80 and 370 μ m. **(f)** From thereon, phase-contrast microscopy shows a continuous network of cells. Magnification: **(a, b)** 10 \times ; **(c, d, and f)** 200 \times ; **(e)** 400 \times (With permission from Gandorfer et al. [25])

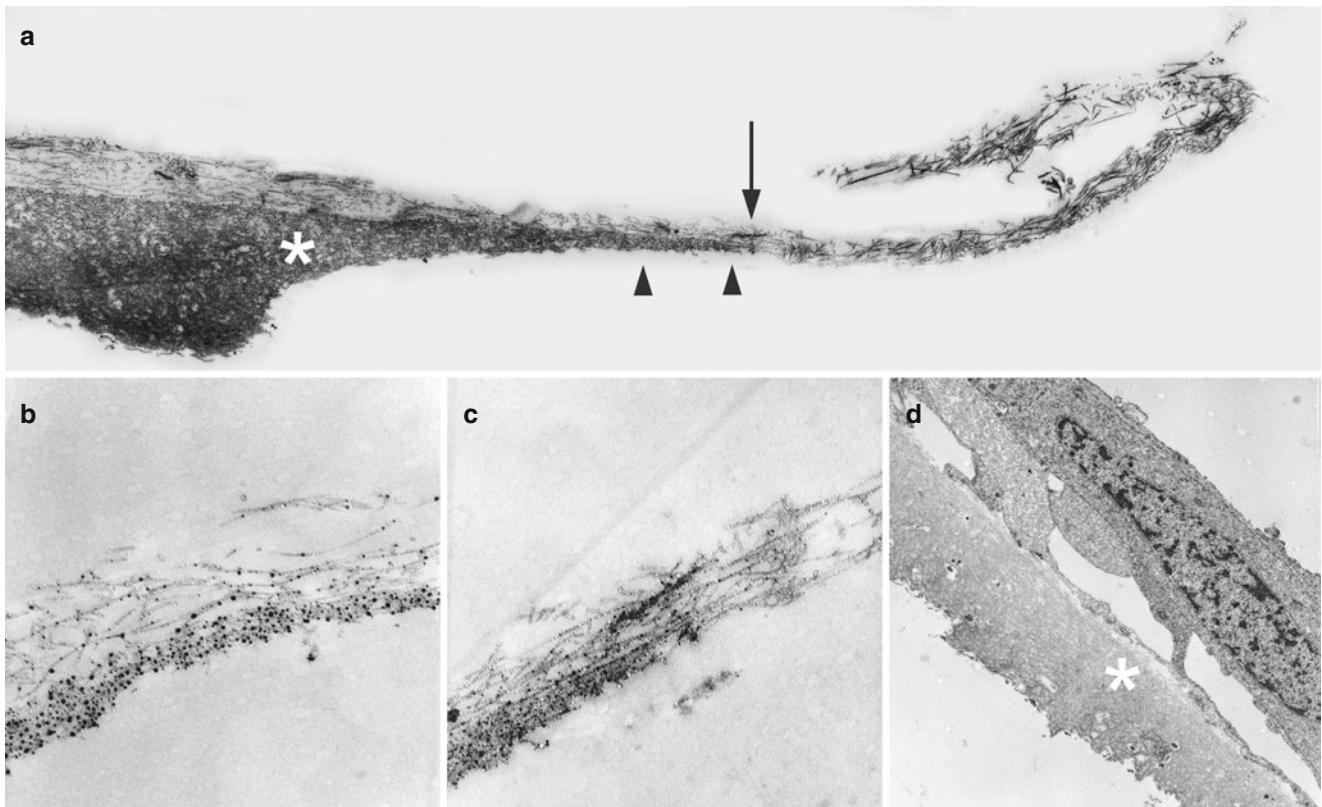


Figure III.C-11 Transmission electron microscopy of the macular hole rim. (a) The macular ILM (*asterisk*) attenuates toward the fovea. The foveolar ILM is only several nanometers thick (*arrowheads*). Collagen fibrils are covering the retinal side of the specimen and extend beyond the ILM (*arrow*). (b) Collagen fibrils are 16 nm in diameter and are regularly arranged, indicating native vitreous collagen. (c) At the end of

the foveal ILM representing the macular hole edge, native vitreous collagen fibrils are directly inserting into the collagen network of the ILM. (d) A multilayered premacular membrane is present distant from the macular hole edge. *Asterisk* marks the ILM. Magnification: (a, d) 4,800 \times ; (b, c) 28,000 \times (With permission from Gandorfer et al. [25])

A. Immunocytochemistry

In the past, glial fibrillar acidic protein (GFAP) was believed to be unique to glia. Therefore, immunolabeling against this intermediate filament protein appeared to be specific for detecting glial cells in premacular membranes. However, retinal Müller cells are known to upregulate (GFAP) in response to retinal injury and cell activation, although they do not label with anti-GFAP under normal conditions except at their end feet [17, 26]. Regarding premacular cells being immunoreactive for GFAP but not for hyalocyte cell markers, it is conceivable that these cells constitute activated and migrated retinal glial cells [17]. It was assumed that all glia-derived cells in premacular tissue would be GFAP positive and that GFAP-negative cells would not be of glial origin. However, more recent studies demonstrated positive GFAP staining in cell populations other than glia, in particular in hyalocytes [27, 28].

Hyalocytes were shown to be immunoreactive for CD45 and CD64, to belong to the monocyte/macrophage lineage,

and to derive from bone marrow. By immunocytochemistry of flat-mounted ILM specimens, we found a proportion of premacular cells showing simultaneous expression of GFAP and hyalocyte cell markers, such as CD45 and CD64 [19, 29] (Figure III.C-12).

Concerning the co-localization of GFAP and hyalocyte cell markers, it remains questionable whether these cells, presumably hyalocytes, are immunoreactive due to an endogenous expression of GFAP or due to phagocytosis of GFAP-positive debris or apoptotic cells. If GFAP labeling in hyalocytes results from endogenous expression, one might hypothesize that these cells have some progenitor potential. If GFAP labeling results from phagocytic activity, these cells may have engulfed Müller cell end feet, activated Müller cells, apoptotic microglia, or astrocytes.

Transdifferentiation of cells with changes in phenotype and antigen expression further complicates the determination of cell type and cell origin (Figure III.C-13). Myofibroblast-like transdifferentiation with positive

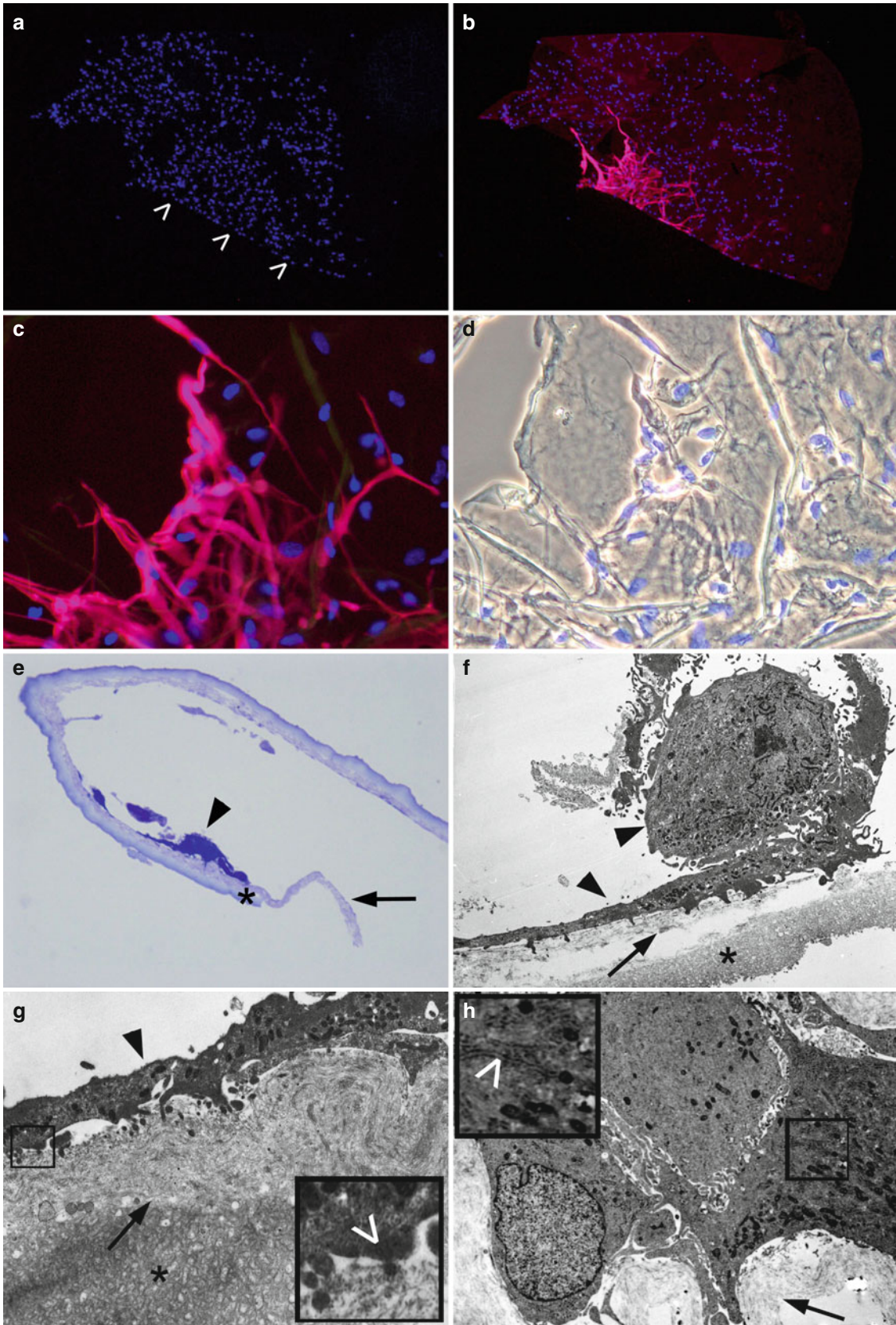


Figure III.C-12 Macular hole immunocytochemistry. Correlation of flat-mount preparation with serial sectioning preparation procedures. Specimen of the ILM removed from a patient with stage III macular hole. (a–d) One half of the specimen was processed for phase-contrast microscopy, interference microscopy, and immunocytochemistry. (e–h) The other half was embedded for conventional light microscopy and transmission microscopy. (a) Cell nuclei staining by DAPI showed large cell count and homogeneously distributed cells at the ILM. *Arrowheads*: cutting line. (b) Only a small cell cluster was positively marked by immunocytochemical staining. (c) A cell cluster labeled with anti-GFAP and anti-CD45 in co-localization, but negative for anti-CK8. All other cells outside of the cluster were not labeled at all by this antibody combination. (d) Phase-contrast microscopy combined with DAPI presents same detail as image (c). (e) Light micrograph

of the ILM prepared by serial sectioning shows the ILM (*asterisk*) with epiretinal cell proliferation (*arrowhead*) and interposition of collagen strand (*arrow*). (f) Transmission electron micrograph demonstrates the vitreal side of the ILM (*asterisk*) with native vitreous collagen (*arrow*) and premacular cell proliferation (*arrowheads*). (g) Epiretinal cell multilayer predominantly composed of myofibroblasts (*arrowhead*) characterized by aggregates of subplasmalemmal cytoplasmic filaments (*white arrowhead*, higher magnification *inset*). (h) Multilayered cell proliferation situated on a collagen strand (*arrow*) composed of fibroblast-like cells with abundant rough endoplasmic reticulum and mitochondria and absence of intracytoplasmic filaments. *Arrowhead*, higher magnification *inset*: rough endoplasmic reticulum. Original magnification: (a, b) 50×; (c, d) 400×; (e) 1,000×; (f) 1,800×; (g, h) 4,800× (With permission from Schumann et al. [29])

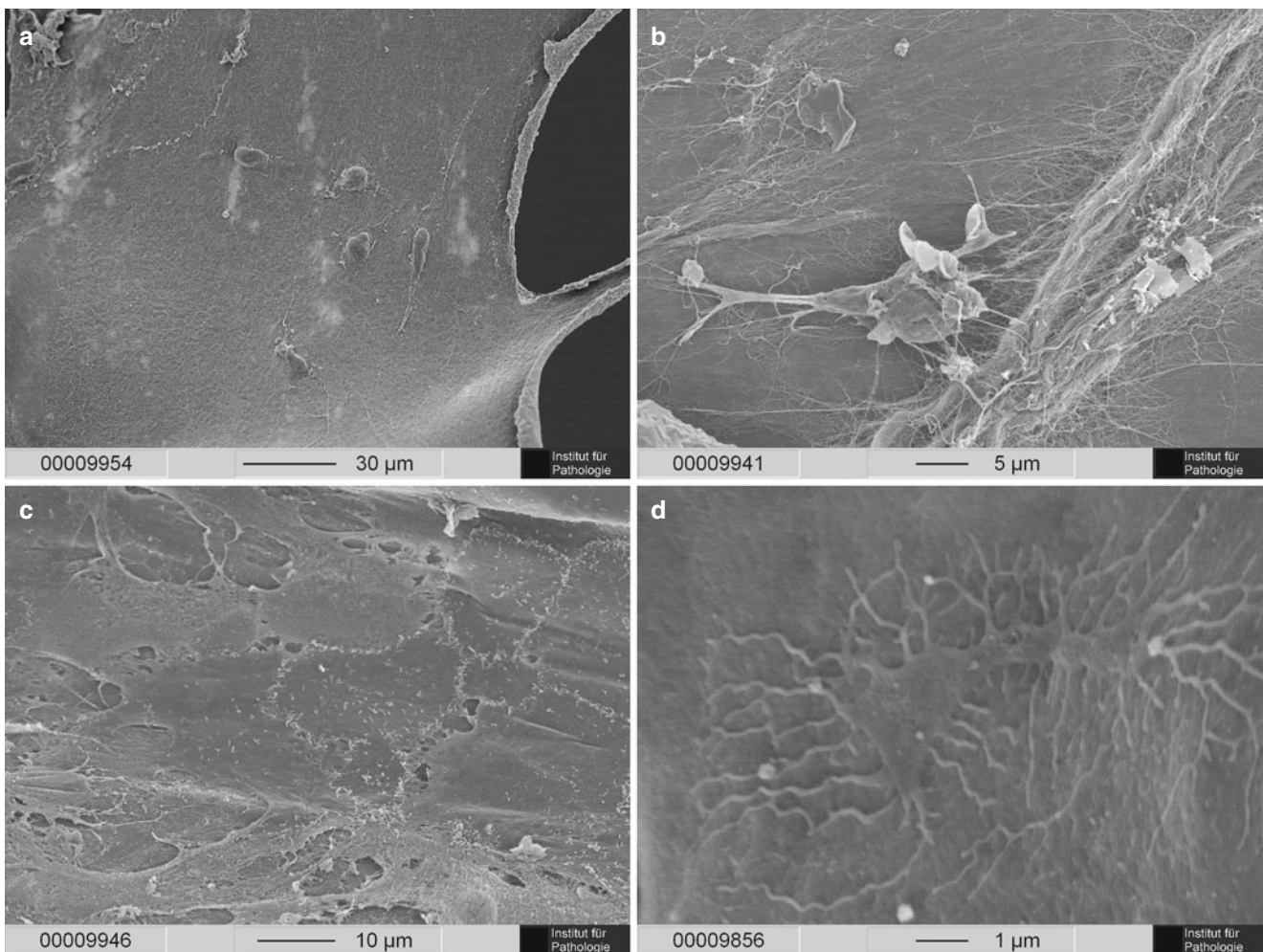


Figure III.C-13 Ultrastructural observations of diverse cell morphology by SEM. (a) Single, round cells with sparse cytoplasm separately distributed on the vitreal side of the ILM. (b) Premacular single cell with irregular short processes near strand-like cell processes embedded in vitreous cortex collagen fibrils. (c) Premacular multilayer of flat,

polygonal cells with broad interdigitating processes and some small microvilli. (d) A single, stretched cell of irregular shape and numerous elongations on the vitreal side of the ILM. Original magnification: (a) 600×; (b) 2,000×; (c) 1,500×; (d) 10,000× (With permission from Schumann et al. [29])



Figure III.C-14 Interference microscopy of polygonal cells with interdigitating processes forming cell clusters on the ILM. Magnification 200× (With permission from Gandorfer et al. [15])

alpha-SMA expression was shown for both hyalocytes and glial cells [29]. Ultrastructural examinations revealed confluent multilayers of glial cells by scanning electron microscopy and myofibroblast-like appearance of premacular cells by transmission electron microscopy.

Moreover, we frequently found alpha-SMA-positive cells in direct proximity, but rarely in co-localization, with GFAP and with hyalocyte cell markers, such as CD45 and CD64. This is consistent with other studies reporting a loss of GFAP with concurrent gains of alpha-SMA immunoreactivity. Since we found alpha-SMA immunoreactivity in all macular hole stages, transdifferentiation appears to take place early in disease development. Based on our findings of glial cells and

hyalocytes as predominating cell types in macular holes, we presume that both glial and hyalocyte cell populations are possible candidates for myofibroblast-like transdifferentiation (Figure III.C-14).

In a recent study of premacular membranes, we found co-localization of anti-alpha-SMA with the hyalocyte marker anti-CD163 [30]. Co-localization of anti-CD163/alpha-SMA further indicates that hyalocytes can transdifferentiate into myofibroblast-like cells (Figure III.C-15). In essence, myofibroblast-like transdifferentiation with positive alpha-SMA expression has been shown for both glial cells and hyalocytes, both in the eyes with premacular membranes and in the eyes with macular holes.

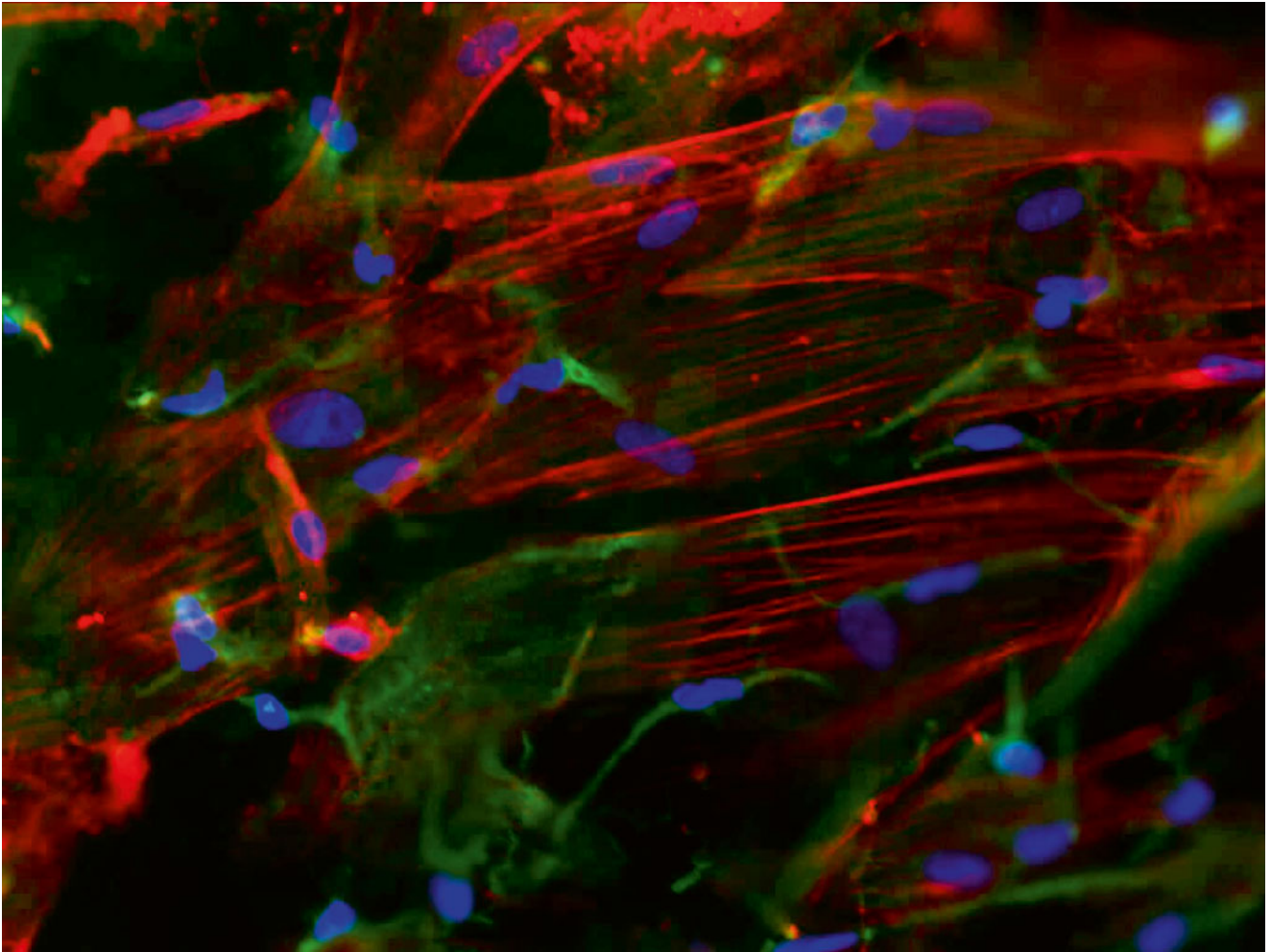


Figure III.C-15 Alpha-SMA-positive cells (*red*) are of similar shape and morphology as cells shown in Figures III.C-14 and III.C-13c. They have undergone myofibroblastic transdifferentiation and are able to exert traction forces. Magnification 400 \times

Myofibroblast-like cells, being immunoreactive for alpha-SMA, represent the contractile elements of premacular tissue as a consequence of cell transdifferentiation. In a recent study on premacular membranes with various forms of PVD, including anomalous PVD and vitreomacular traction syndrome (VMTS), alpha-SMA-positive cells were more frequently found in specimens from VMTS and macular pucker with anomalous PVD than in those from macular pucker with complete PVD [30]. This emphasizes the role of anomalous PVD in the development of vitreomacular traction and shows that the completeness of vitreomacular separation modulates the cellular composition of premacular membranes and their ability to exert traction by expression of contractile filaments (Figures III.C-16 and III.C-17).

CD68 was demonstrated in VMTS and macular pucker with incomplete PVD. CD68 was not found in specimens from premacular membranes with complete PVD [30]. There is no cell-specific marker to differentiate between vitreous-derived macrophages and retinal microglia. There is, however, an obvious difference between the eyes with complete PVD and those with incomplete PVD in immunocytochemical terms, indicating that anomalous PVD supports hyalocyte proliferation and transdifferentiation into alpha-SMA-positive myofibroblast-like cells exerting traction at the vitreomacular interface (Figure III.C-18). Figure III.C-19 summarizes these observations and interpretations.

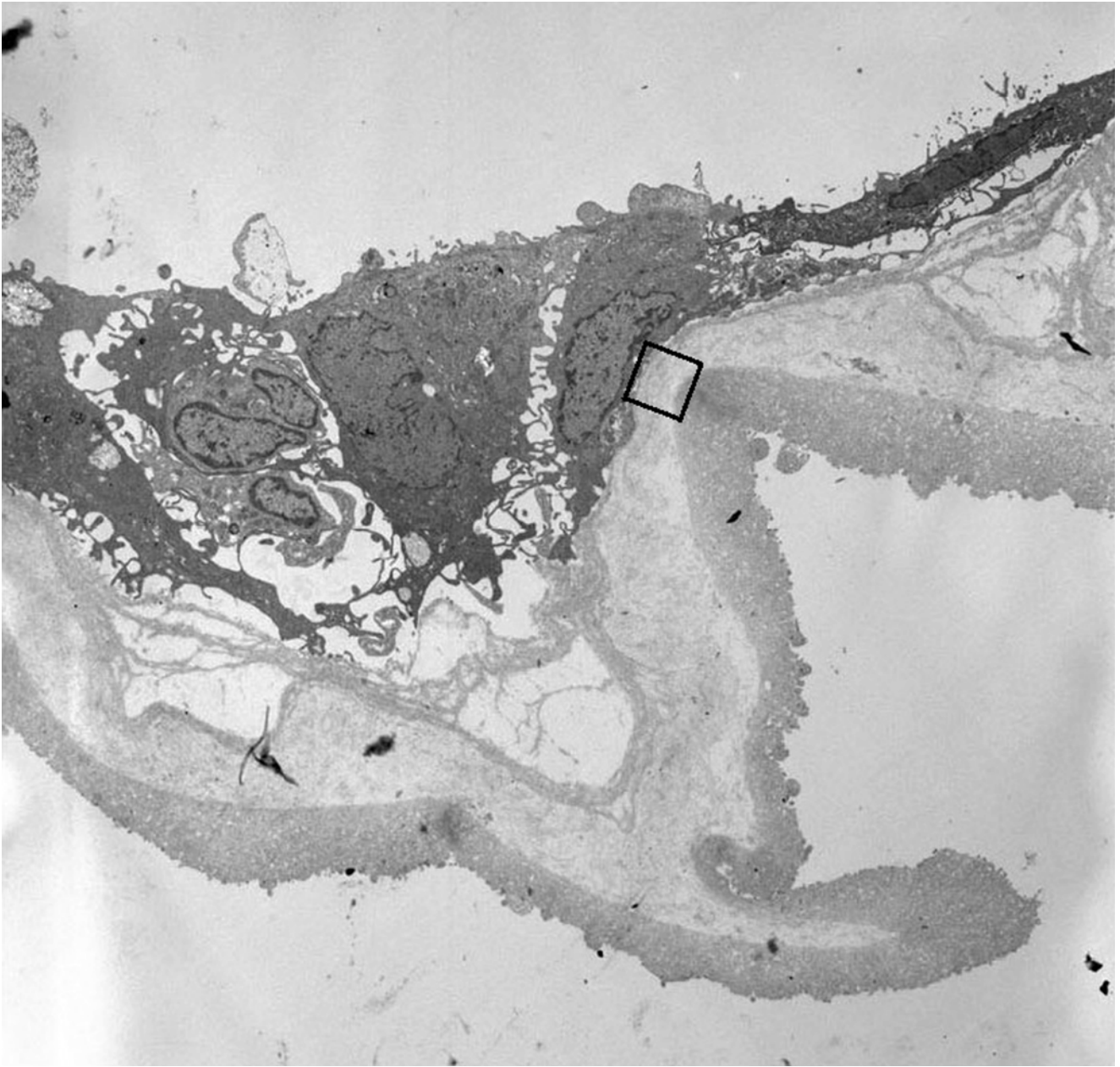


Figure III.C-16 *Vitreoschisis* enables the ILM to form infoldings and outfoldings of the vitreoretinal interface caused by contraction of premacular membranes. Magnification 1,800 \times (With permission from Gandorfer et al. [5])

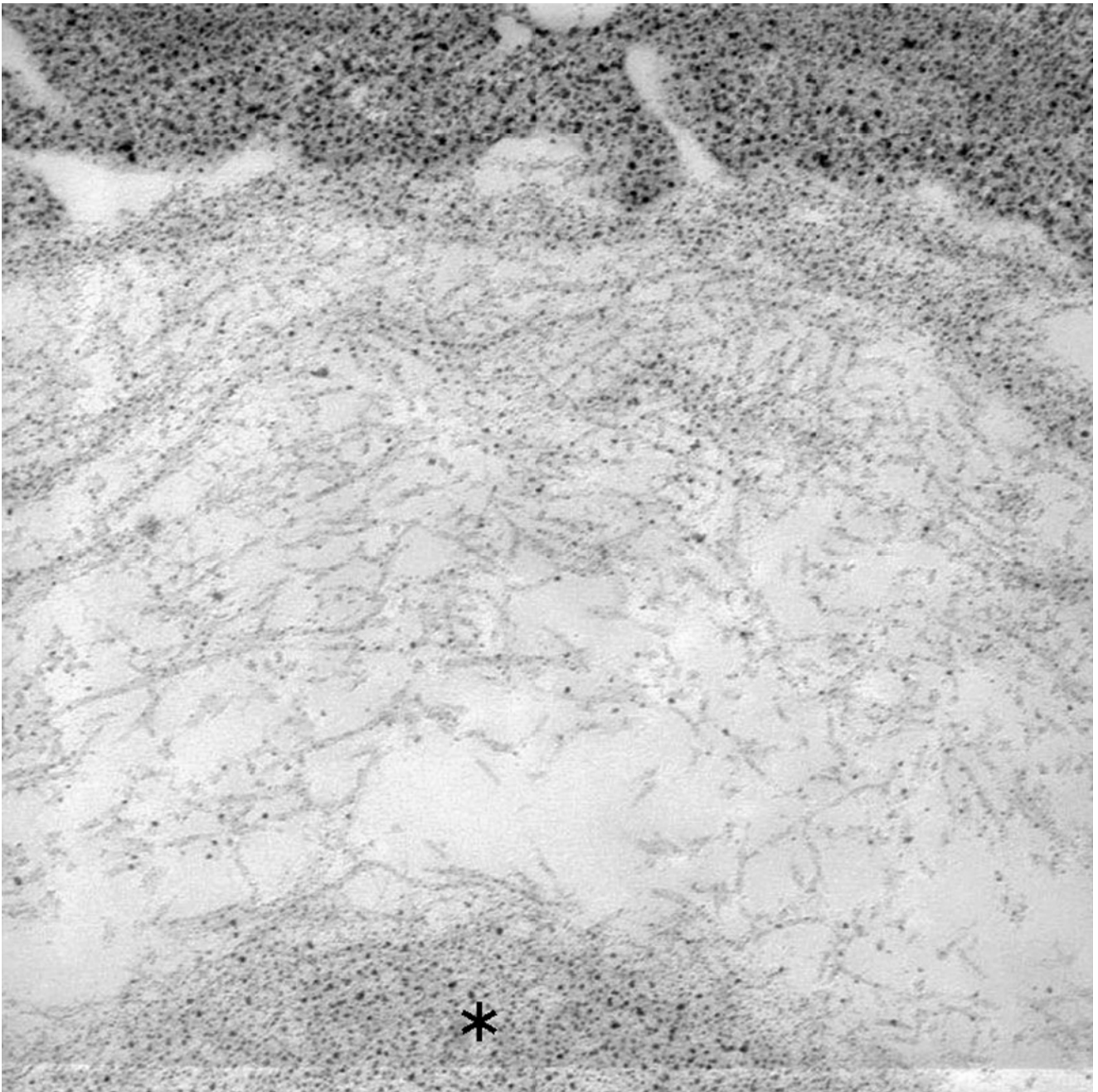


Figure III.C-17 The native vitreous collagen forms the basis of vitreoschisis after splitting of the vitreous cortex. Inset box in Figure III.C-16. Magnification 28,000 \times . *Asterisk* marks the ILM (With permission from Gandorfer et al. [5])

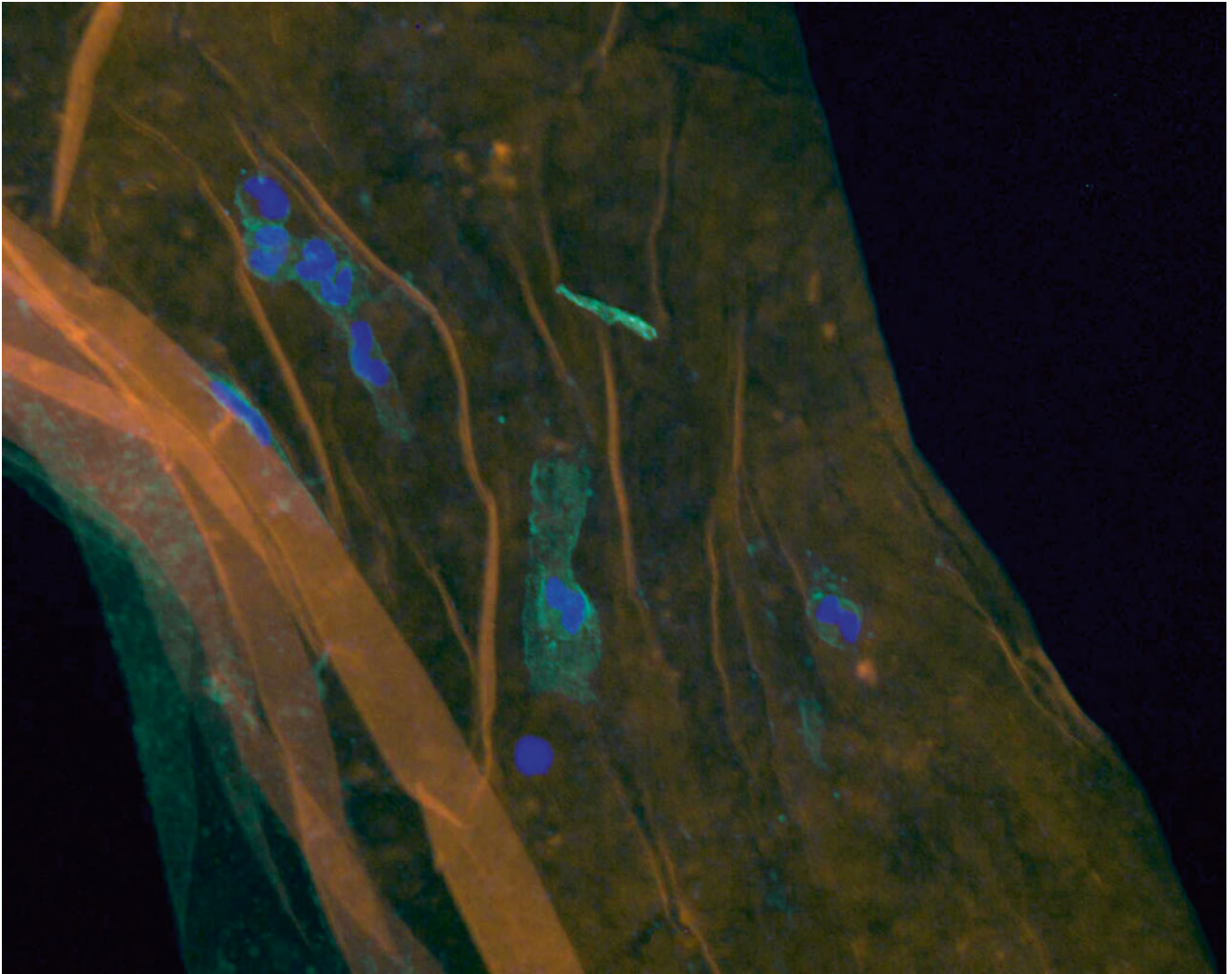


Figure III.C-18 Vitreoschisis immunocytochemistry. Flat-mount preparation shows the ILM stained with anti-collagen type IV (*green*) and a continuous layer of vitreous collagen type II (*orange*) on top of it.

Some cells are embedded in the vitreous cortex. Their nuclei are stained *blue* by DAPI. Magnification 400×

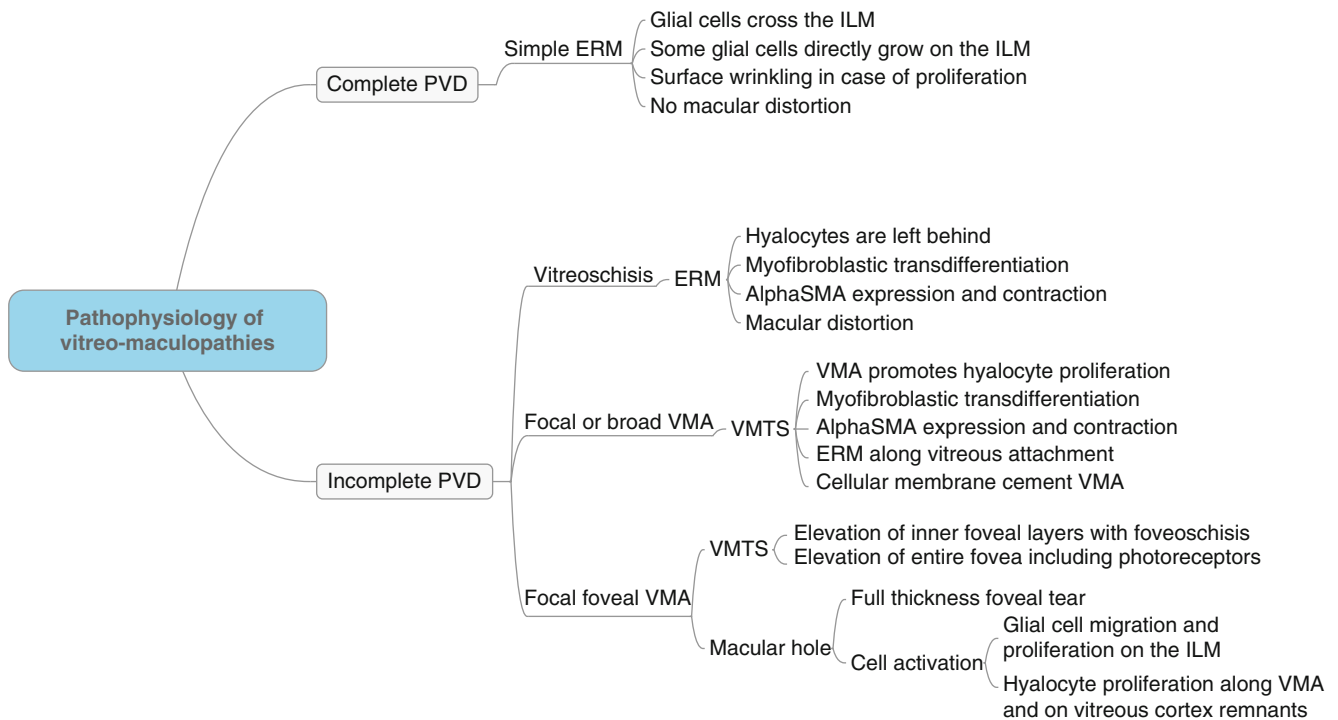


Figure III.C-19 Summary of premacular cell proliferation in vitreomaculopathies

Summary

1. Premacular cell proliferation is a unifying pathologic feature in vitreomaculopathies.
2. Anomalous PVD plays a major role in promoting cell proliferation and myofibroblastic transdifferentiation, leading to contractile cellular membranes.
3. In case of vitreoschisis, the cells grow on a layer of vitreous cortex collagen left behind at the ILM after incomplete PVD.
4. If focal or broad vitreomacular adhesions persist, cells grow along the adhesion from the retinal surface onto the vitreous strand, thereby cementing the vitreomacular attachment.
5. Persistent vitreomacular attachments promote transdifferentiation of cells to myofibroblasts with expression of alpha-SMA, indicating their contractile potential.
6. Both glial cells and hyalocytes are capable of myofibroblastic transdifferentiation.
7. Cell proliferation is a continuous process of cell migration and proliferation, from single cells to cell clusters which can then become confluent and form continuous cellular membranes.
8. Glial cells can cross the ILM and form cell proliferations on the vitreal side of the ILM without causing retinal distortion and thus are not likely prominent players in pathogenesis.
9. Hyalocytes embedded in the vitreous cortex and left behind after incomplete PVD have the potential to represent the major cellular part of premacular membranes causing visual disturbances.
10. Traction is generated by alpha-SMA-mediated contraction following transdifferentiation of glial cells and in particular by hyalocytes.

Abbreviations	
Alpha-SMA	Alpha-smooth muscle actin (a contractile intracellular protein)
GFAP	Glial fibrillary acid protein
ILM	Inner limiting membrane
nm	Nanometer
PVD	Posterior vitreous detachment
RPE	Retinal pigment epithelium
VMTS	Vitreomacular traction syndrome

References

1. Gandorfer A, Ulbig M, Kampik A. Plasmin-assisted vitrectomy eliminates cortical vitreous remnants. *Eye (Lond)*. 2002;16(1):95–7.
2. Sebag J. Anomalous posterior vitreous detachment: a unifying concept in vitreo-retinal disease. *Graefes Arch Clin Exp Ophthalmol*. 2004;242(8):690–8.

3. Sebag J, Gupta P, Rosen R, Garcia P, Sadun AA. Macular holes and macular pucker: the role of vitreoschisis as imaged by optical coherence tomography/scanning laser ophthalmoscopy. *Trans Am Ophthalmol Soc.* 2007;105:121–9; discussion 129–31.
4. Gupta P, et al. Vitreoschisis in macular diseases. *Br J Ophthalmol.* 2011;95(3):376–80.
5. Gandorfer A, Rohleder M, Kampik A. Epiretinal pathology of vitreomacular traction syndrome. *Br J Ophthalmol.* 2002;86(8):902–9.
6. Gandorfer A, et al. Epiretinal pathology of diffuse diabetic macular edema associated with vitreomacular traction. *Am J Ophthalmol.* 2005;139(4):638–52.
7. Rentsch FJ. The ultrastructure of preretinal macular fibrosis. *Graefes Arch Clin Exp Ophthalmol.* 1977;203(3–4):321–37.
8. Kampik A, et al. Ultrastructural features of progressive idiopathic epiretinal membrane removed by vitreous surgery. *Am J Ophthalmol.* 1980;90(6):797–809.
9. Kampik A, et al. Epiretinal and vitreous membranes. Comparative study of 56 cases. *Arch Ophthalmol.* 1981;99(8):1445–54.
10. Sebag J. *The vitreous – structure, function, pathobiology.* New York: Springer; 1989.
11. Gandorfer A. *Ultrastruktur und Chirurgie traktiver Makulopathien.* München: Habilitationsschrift; 2002.
12. Haritoglou C, Sebag J. Indications and considerations for chromodissection. *Retinal Physician.* 2014;11(5):34–39.
13. Schumann RG, et al. Sequential epiretinal membrane removal with internal limiting membrane peeling in brilliant blue G-assisted macular surgery. *Br J Ophthalmol.* 2010;94:1369–72.
14. Haritoglou C, et al. Heavy brilliant blue G for internal limiting membrane staining. *Retina.* 2011;31(2):405–7.
15. Gandorfer A, et al. Residual cellular proliferation on the internal limiting membrane in macular pucker surgery. *Retina.* 2012;32(3):477–85.
16. Foos RY. Vitreoretinal juncture—simple epiretinal membranes. *Albrecht Von Graefes Arch Klin Exp Ophthalmol.* 1974;189(4):231–50.
17. Hiscott PS, et al. Retinal and epiretinal glia—an immunohistochemical study. *Br J Ophthalmol.* 1984;68(10):698–707.
18. Haritoglou C, et al. Glial cell proliferation under the internal limiting membrane in a patient with cellophane maculopathy. *Arch Ophthalmol.* 2007;125(9):1301–2.
19. Gandorfer A, et al. Pores of the inner limiting membrane in flat-mounted surgical specimens. *Retina.* 2011;31(5):977–81.
20. Eckardt C, et al. Removal of the internal limiting membrane in macular holes. Clinical and morphological findings. *Ophthalmologie.* 1997;94(8):545–51.
21. Messmer EM, Heidenkummer HP, Kampik A. Ultrastructure of epiretinal membranes associated with macular holes. *Graefes Arch Clin Exp Ophthalmol.* 1998;236(4):248–54.
22. Haritoglou C, et al. Evaluation of the internal limiting membrane after conventional peeling during macular hole surgery. *Retina.* 2006;26(1):21–4.
23. Schumann RG, et al. Ultrastructure of the vitreomacular interface in full-thickness idiopathic macular holes: a consecutive analysis of 100 cases. *Am J Ophthalmol.* 2006;141(6):1112–9.
24. Gandorfer A, et al. Interference microscopy delineates cellular proliferations on flat mounted internal limiting membrane specimens. *Br J Ophthalmol.* 2009;93(1):120–2.
25. Gandorfer A, et al. Pathology of the macular hole rim in flat-mounted internal limiting membrane specimens. *Retina.* 2009;29(8):1097–105.
26. Gandorfer A, et al. Staining and peeling of the internal limiting membrane in the cat eye. *Curr Eye Res.* 2005;30(11):977–87.
27. Nishitsuka K, et al. Hyaluronan production regulation from porcine hyalocyte cell line by cytokines. *Exp Eye Res.* 2007;85(4):539–45.
28. Kohno RI, et al. Possible contribution of hyalocytes to idiopathic epiretinal membrane formation and its contraction. *Br J Ophthalmol.* 2009;93(8):1020–6.
29. Schumann RG, et al. Immunocytochemical and ultrastructural evidence of glial cells and hyalocytes in internal limiting membrane specimens of idiopathic macular holes. *Invest Ophthalmol Vis Sci.* 2011;52(11):7822–34.
30. Zhao F, et al. Epiretinal cell proliferation in macular pucker and vitreomacular traction syndrome: analysis of flat-mounted internal limiting membrane specimens. *Retina.* 2013;33(1):77–88.

Vitreo-Macular Adhesion/Traction and Macular Holes: Pseudo, Lamellar, and Full-Thickness

III.D.

Miriam Englander, Jay S. Duker, and Peter K. Kaiser

Outline

- I. **Pathophysiology and Classification of Vitreo-Macular Adhesion (VMA) and Vitreo-Macular Traction (VMT)**
 - A. Pathophysiology of Posterior Vitreous Detachment (PVD) and Effects on the Vitreo-Macular Interface (VMI)
 - B. Definition and Classification of VMA
 - C. Definition and Classification of VMT
- II. **Pathophysiology and Classification of Macular Holes**
 - A. Pseudohole
 - B. Lamellar Hole
 - C. Full-Thickness Macular Hole (FTMH)

Conclusion

References

Keywords

Vitreous • Macula • Anomalous posterior vitreous detachment • Vitreoschisis • Vitreo-macular adhesion • Vitreo-macular traction • Pseudoholes • Lamellar holes • Full-thickness macular holes • IVTS classification • Pharmacologic vitreolysis

Key Concepts

1. Anomalous posterior vitreous detachment causes a variety of vitreo-maculopathies with significant impacts on central vision.
2. The various pathologic manifestations of vitreo-macular traction can be classified solely on the basis of anatomical changes (not clinical symptoms or findings) as imaged by optical coherence tomography.
3. The International Vitreomacular Traction Study (IVTS) classification provides a useful method to characterize vitreo-maculopathies for proper case selection to undergo surgery or pharmacologic vitreolysis.

M. Englander, MD • P.K. Kaiser, MD (✉)
Vitreo-Retinal Division, Department of Ophthalmology,
Cole Eye Institute, Cleveland Clinic Foundation,
9500 Euclid Avenue, Desk i3, Cleveland, OH 44195, USA
e-mail: englander.miri@gmail.com; pkkaiser@gmail.com

J.S. Duker, MD
Department of Ophthalmology, New England Eye Center,
Tufts Medical Center, Tufts University School of Medicine,
Washington Street, # 450, Boston, MA 02111, USA
e-mail: jduker@tuftsmedicalcenter.org

Financial Disclosures Consultant: Alcon (PKK, JSD), Novartis (PKK), Genentech (PKK), Ophthotech (PKK, JSD), Allegro (PKK) Thrombogenics (PKK, JSD), Research Grant: Carl Zeiss (JSD), Optovue Inc. (JD); Research to Prevent Blindness (PKK)

I. Pathophysiology and Classification of Vitreo-Macular Adhesion (VMA) and Vitreo-Macular Traction (VMT)

A. Pathophysiology of Posterior Vitreous Detachment (PVD) and Effects on the Vitreo-Macular Interface (VMI)

Vitreous consists of approximately 98 % water and 2 % structural macromolecules [1, 2]. It is attached to all contiguous structures of the inner eye, including the inner limiting membrane (ILM) of the retina. The ILM is primarily composed of type IV collagen. The interface between the ILM and posterior vitreous cortex contains a macromolecular attachment complex, which is composed of fibronectin, laminin, and other extracellular components such as glycoproteins and several collagen types [3–5]. This complex, along with the chondroitin sulfate present throughout the vitreo-retinal interface, plays a major role in vitreo-retinal adhesion [see chapter II.E. Vitreo-retinal interface and ILM]. Chondroitin sulfate may also play a role in mediating hyaluronan-collagen interaction in the gel vitreous [6, 7].

Posterior vitreous detachment (PVD) is an age-related, synchronized process of liquefaction of the gel and progressive posterior vitreous cortex separation from the retina, which ultimately leads to complete vitreous separation without pathology. This may or may not be symptomatic for the patient. The process of vitreo-retinal separation is initiated concurrently at the perifoveal macula and at multiple sites throughout the peripheral fundus [8–11]. The final separation of the vitreous from the macula and optic nerve may take up to several years. Using optical coherence tomography (OCT), a staging system for PVD has been proposed with four distinct stages:

- Stage 0=absence of PVD
- Stage 1=focal perifoveal PVD with persistent attachment to the fovea, optic nerve head, and mid-peripheral retina
- Stage 2=perifoveal PVD across all quadrants, with persistent attachment to the fovea, optic nerve head, and mid-peripheral retina
- Stage 3=detachment of the posterior vitreous cortex from the fovea, with persistent attachment to the optic disc
- Stage 4=complete PVD, with biomicroscopically identified detachment of the posterior vitreous cortex with Weiss ring [10] [see chapter II.C. Vitreous aging and PVD]

Abnormalities in this process can result in an anomalous PVD with the potential of consequent vitreo-macular interface (VMI) pathology. Several anomalous macular conditions, such as premacular membrane with macular pucker, lamellar hole, and full-thickness macular hole, can result from this anomalous adhesion of the posterior vitreous cortex to the ILM. Other contributing factors, including high myopia, blunt trauma, inflammation, and previous intraocular

surgery, may play a role in the pathological progression of anomalous PVD at the VMI.

Over the past two decades, OCT technology has allowed ophthalmologists to visualize and understand VMI pathologies and monitor the progression of the ensuing disorders. Combining these imaging capabilities with advances in surgical and medical management of the VMI pathologies has allowed us to better define and classify these disorders.

B. Definition and Classification of VMA

At birth, most eyes have complete vitreo-macular attachment throughout the fundus. This is represented by stage 0 in the above classification system. Vitreo-macular adhesion (VMA) is a term that represents a specific stage of vitreo-retinal separation in which partial detachment of the vitreous in the perifoveal area has occurred, without retinal abnormalities. This stage is the equivalent of a stage 1 PVD in the PVD classification schemes [8–11] and is an asymptomatic part of the normal process of separation. On OCT, VMA is characterized by an elevation of the cortical vitreous above the retinal surface, with the vitreous remaining attached within a 3-mm radius of the fovea (defined arbitrarily). The angle between the posterior vitreous cortex and the inner retinal surface is acute. Importantly, the retina displays no change in contour or morphology on OCT.

An OCT-based classification scheme has allowed us to categorize VMA according to size of adhesion into either: (1) focal ($\leq 1,500 \mu\text{m}$) or (2) broad ($> 1,500 \mu\text{m}$) (Figure III.D-1) widths. This measurement is taken to encompass the width of the adhesion roughly parallel to the retinal pigment epithelium (RPE) in a single B-scan image on OCT. The 1,500- μm cutoff used in this classification scheme was chosen because it is a known area of increased vitreous adhesion to the central macula. In addition, this size has been routinely used to distinguish focal from broad VMA in the vitreo-retinal literature and at most OCT reading centers [12, 13]. It is unclear if this distinction between focal and broad adhesion has any clinical or prognostic significance. When VMA is the only abnormality seen, it is considered “isolated VMA,” whereas if there are other associated abnormalities such as age-related macular degeneration (AMD), retinal vein occlusion (RVO), or diabetic macular edema (DME) are present, it should be termed “concurrent VMA.”

Patients with VMA report no visual symptoms. Although it is generally considered to be part of the natural course of PVD, a recent observational cohort study showed that VMA released spontaneously in only 30 % of patients, while 53 % remained stable and 16 % progressed from VMA to develop vitreo-macular traction (VMT) or full-thickness macular hole (FTMH) [14].

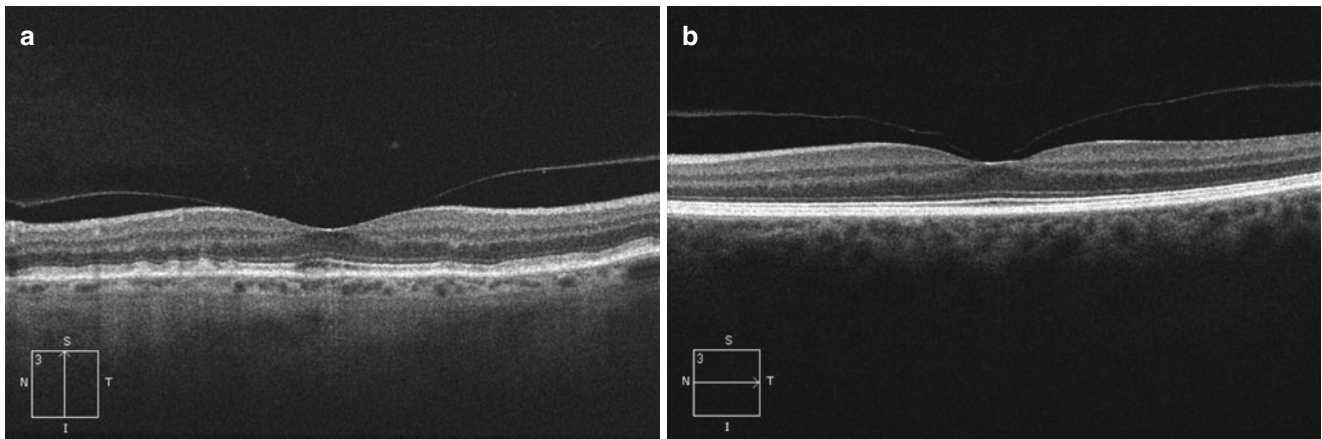


Figure III.D-1 (a) OCT of broad vitreo-macular adhesion (VMA) (>1,500 μm). (b) OCT of focal vitreo-macular adhesion (VMA) (<1,500 μm)

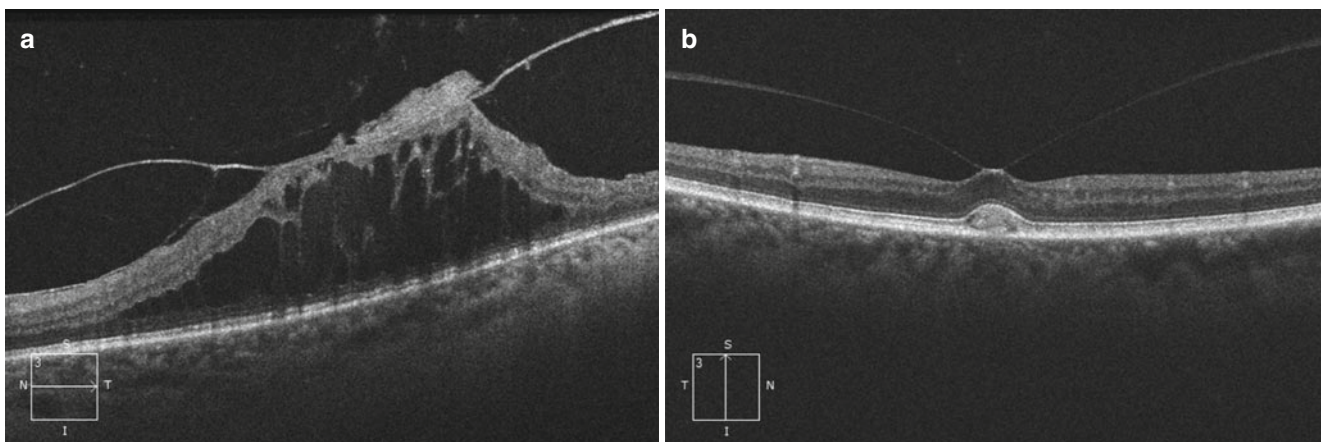


Figure III.D-2 (a) OCT of broad vitreo-macular traction (VMT) (>1,500 μm). (b) OCT of focal vitreo-macular traction (VMT) (<1,500 μm)

C. Definition and Classification of VMT

Vitreo-macular traction (VMT) occurs when the progression of a PVD causes enough traction on the macula to result in anatomical changes. Unlike VMA, VMT is often symptomatic. The focal area of traction can lead to various pathologic changes including distortion the foveal surface, elevation of the foveal floor, and pseudocysts within the central macula. These structural changes lead to diminished visual acuity and visual distortion. Diagnosis of VMT can easily be made with OCT. It may also be identified using fluorescein angiography, ultrasonography, as well as intraoperatively. It is important to recognize VMT and distinguish it from other pathologies in order to provide the patient with appropriate management.

On OCT, VMT is characterized by perifoveal vitreous cortex detachment from the retinal surface with macular attachment of the vitreous cortex within a 3-mm radius of the fovea with associated distortion of the foveal surface, intraretinal structural changes, and/or elevation of the fovea above the RPE, but no full-thickness interruption of all retinal layers.

Vitreo-retinal adhesion in VMA is identical to VMT, but is distinguished by the absence of retinal changes. VMT is VMA plus changes of the retina identified on OCT. In more advanced cases of VMT, persistent vitreous attachment may appear abnormally thickened or even multi-laminate, suggestive of vitreoschisis [15].

Similar to VMA, VMT is subclassified as either focal ($\leq 1,500 \mu\text{m}$) or broad ($> 1,500 \mu\text{m}$) and isolated or concurrent (Figure III.D-2). Unlike VMA, the differentiation is clinically significant. Broad areas of attachment with traction can cause generalized thickening of the macula, vascular leakage on fluorescein angiography, macular schisis, and cystoid macular edema (CME). Focal areas of vitreous attachment with traction can cause distortion of the foveal surface, elevation the foveal floor, and/or formation pseudocysts within the central macula. Occasionally, spontaneous PVD occurs with VMT release, regression of symptoms, and return of the normal foveal contours [16].

In some instances, even with the progression of a PVD, the vitreous may remain adherent to the retina, resulting

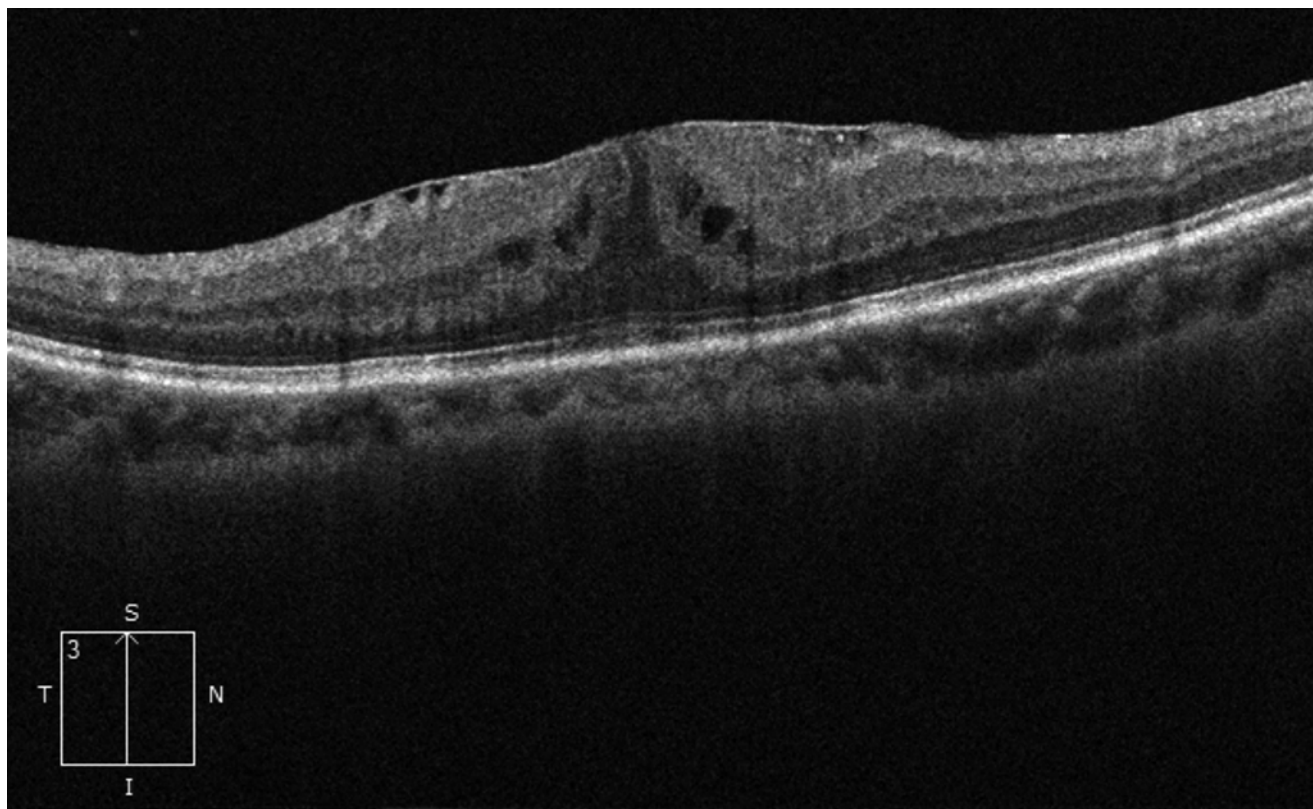


Figure III.D-3 OCT of premacular membrane (PMM; previously called ERM)

in vitreoschisis [15]. The cells embedded within residual vitreous, primarily hyalocytes, can proliferate and result in the formation of a premacular membrane. Hyalocytes also stimulate the migration and proliferation of circulating monocytes and retinal glial cells, as well as occasional RPE cells [see chapters II.D. Hyalocytes; III.F. Vitreous in the pathobiology of macular pucker]. These cells attach to a scaffold of posterior vitreous cortex remnants on the inner retinal surface. Contraction and thickening of the premacular membrane can cause macular abnormalities that may be difficult to distinguish on OCT from an attached posterior vitreous cortex. The diagnosis of vitreoschisis can occasionally be made with B-scan ultrasonography, but has been more reliably identified with OCT, which found vitreoschisis in 53 % of full-thickness macular holes and 43 % of macular pucker cases [17, 18].

II. Pathophysiology and Classification of Macular Holes

A. Pseudohole

A macular pseudohole is difficult to distinguish from a true full-thickness hole on clinical examination alone, hence the term pseudohole. On clinical exam, it appears

as a discrete, reddish, round, or oval lesion in the fovea that is typically 200–400 μm in diameter and similar in clinical appearance to a small- or medium-sized full-thickness hole. The appearance of a pseudohole involves anatomical changes of the vitreo-macular interface (VMI), namely, the formation of premacular membrane (Figure III.D-3). The presence of a defect in the prefoveal portion of a premacular membrane may simulate the appearance of a full-thickness macular hole. This appearance is due to a defect in the premacular tissue itself, as well as of the anterior and central displacement of the perifoveolar retina during contraction of the premacular membrane. Unlike eyes that have true macular holes, those with pseudoholes are usually minimally symptomatic and have normal or near-normal visual acuities.

OCT can readily distinguish between full-thickness macular holes and pseudoholes. Characteristically, there is no loss of foveal tissue, and the central foveal thickness is usually normal or slightly thin. The main features of a pseudohole on OCT include invaginated or heaped foveal edges, concomitant premacular membrane with central opening, steep macular contour to the central fovea with near-normal central foveal thickness, and most importantly, no loss of retinal tissue (Figure III.D-4).

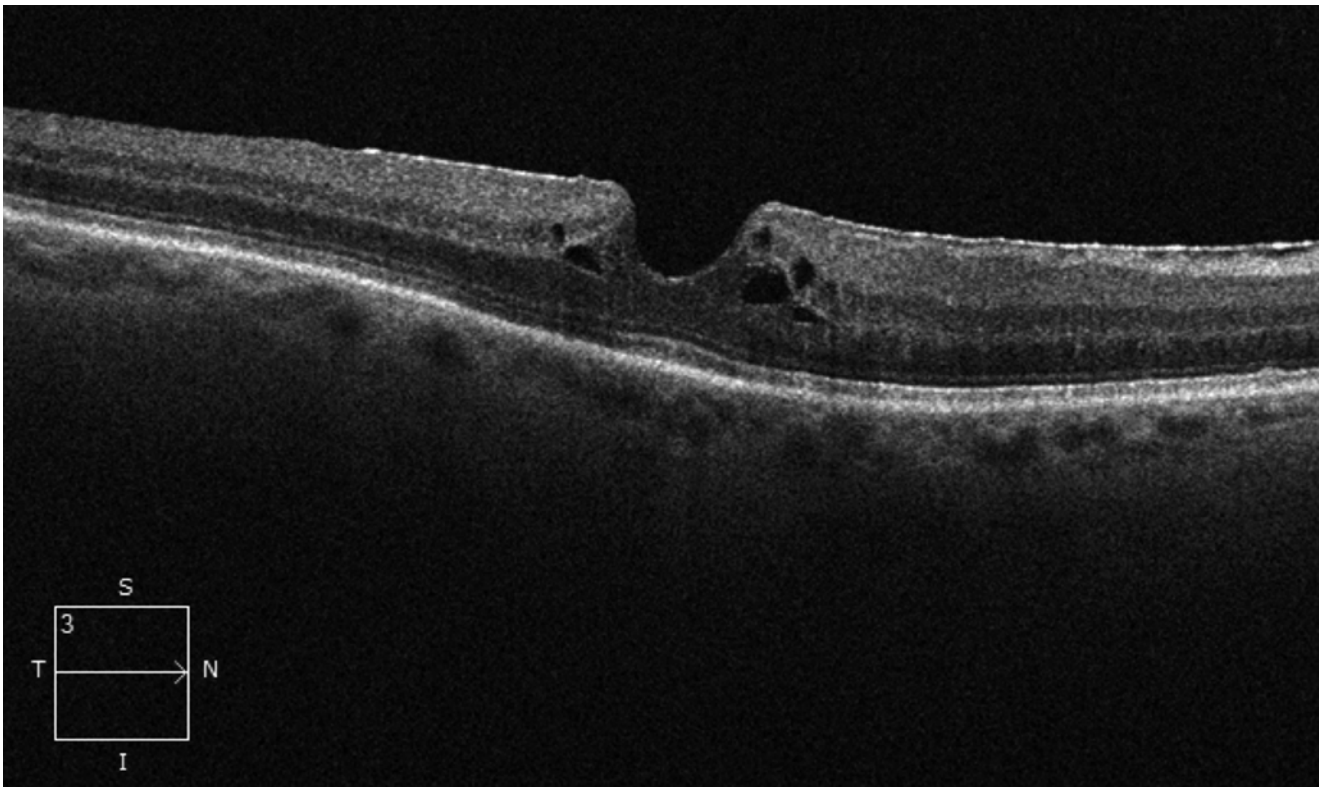


Figure III.D-4 OCT of pseudohole

B. Lamellar Hole

Lamellar macular hole was originally described by Gass as a macular lesion resulting from cystoid macular edema [19]. Prior to OCT, the term lamellar hole was used to describe an abortive process in full-thickness macular hole development where the patient had relatively preserved visual acuity (20/40 or better) and the clinical exam consisted of a stable, round, and well-circumscribed reddish lesion, but no full-thickness hole [9, 15, 19–24]. With the advent of OCT, distinguishing a lamellar hole from similar, but distinct, macular conditions became easy. This distinction is important since the various conditions have different treatment implications.

On OCT, a lamellar macular hole has the following features (Figure III.D-5):

- Irregular foveal contour; a defect in the inner fovea (may or may not have actual loss of retinal tissue)
- Intraretinal splitting (schisis) that typically occurs between the outer plexiform (OPL) and outer nuclear layers (ONL)
- Maintenance of an intact photoreceptor layer

The presence of an intact photoreceptor layer separates this condition from full-thickness macular hole. The separation of the inner from the outer retinal layers occurs typically either between the high-backscattering OPL and the low-backscattering ONL or only within the OPL. Often spanning

this separation are strands of retinal tissue, which may signify Müller cell processes and/or photoreceptor axons (Henle fibers). Müller cell strands spanning the separation between the inner and outer retina may help to prevent dehiscence of the outer retinal layers [25].

There may be several etiologies for the formation of a lamellar hole. Premacular membrane is a common finding on OCT of eyes with lamellar holes. Contraction of the premacular membrane is postulated to contribute to the formation of lamellar holes. In a study by Haouchine et al. [21], pseudopericula, suggestive of an aborted macular hole, were observed on OCT in 24 % of patients. The presence of vitreo-papillary adhesion (VPA), where the vitreous remains attached to the optic disc and peripapillary retina with peripheral detachment is observed in approximately 50 % of patients, suggesting that outward (centrifugal from the fovea) tangential traction by the posterior vitreous cortex plays a role as well [26, 27].

C. Full-Thickness Macular Hole (FTMH)

Full-thickness macular hole (FTMH) is an anatomic defect in the fovea, characterized by interruption of all neural retinal layers extending from the ILM to the RPE. Although the pathogenesis remains incompletely understood, there may be

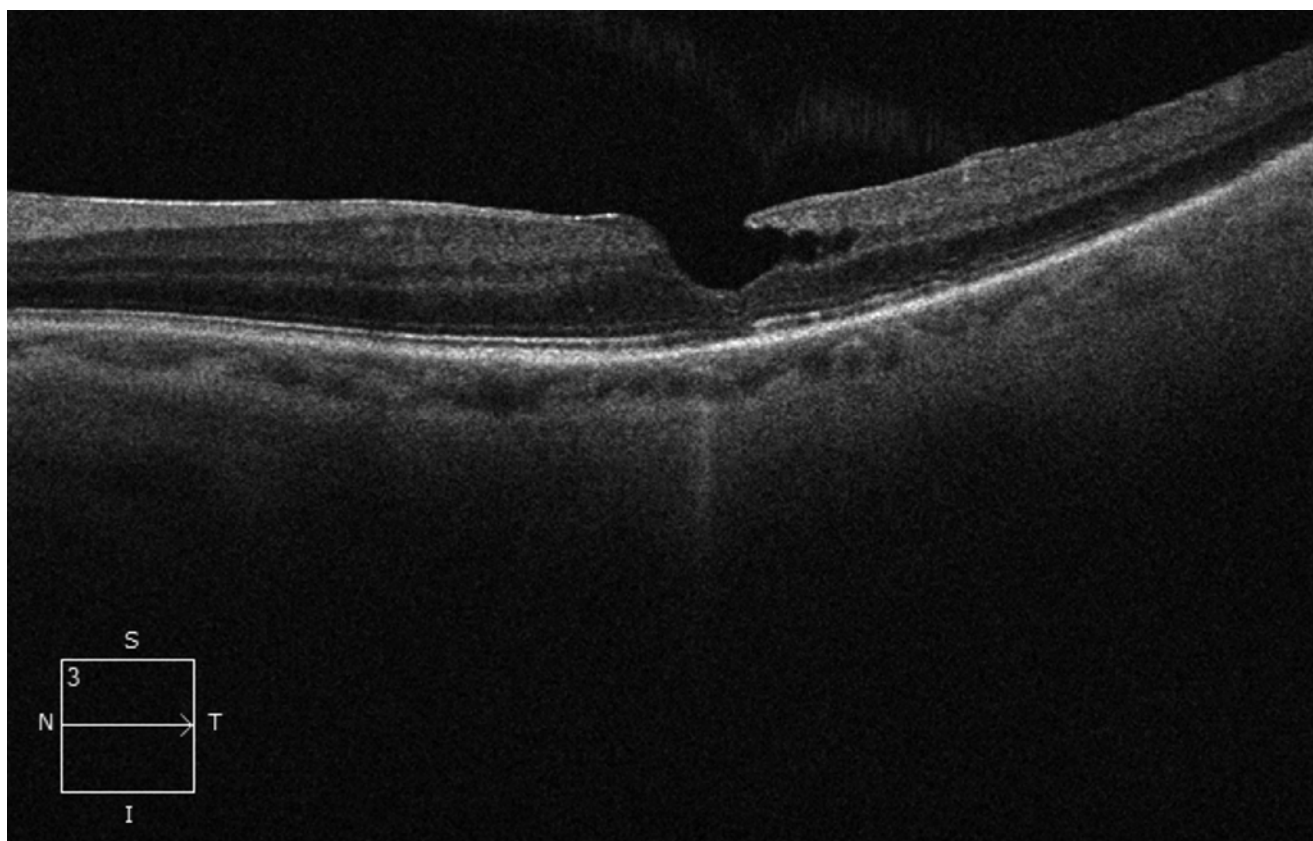


Figure III.D-5 OCT of lamellar hole

several mechanical possibilities, including the formation of tractional foveal cystoid space, breakdown and elevation of central photoreceptors, and traction on the inner retina. The edge may also be thicker than neighboring retinal tissue due to accumulation of intraretinal fluid (the result of tangential traction, not an exudative process) and may appear slightly elevated from the RPE plane. The vitreous may or may not be seen as attached to the edge of the macular hole, but it is very likely that this is present case in all cases.

While the majority of the holes are primary, several pathologic processes, such as blunt trauma, cystoid macular edema, premacular membrane, vitreo-macular traction, rhegmatogenous retinal detachment, inadvertent exposure to laser energy, Best's disease, high myopia with posterior staphyloma, lightning strike injury, hypertensive retinopathy, and proliferative diabetic retinopathy, can induce a FTMH [28–31]. These cases should be considered secondary.

Gass proposed a classification system based on biomicroscopic observations. It was based on clinically observed appearances of macular holes and their precursor lesions [22, 23, 32]. In a stage 1 macular hole, no true neural retinal defect is present, the photoreceptor layer is intact, and no vitreo-foveal separation has occurred. Stage 1 holes are further divided into stage 1a and stage 1b, based on the clinical appearance. In a stage 1a macular hole, a small central yellow spot is seen on ophthalmoscopy. The fovea may be thickened

along with a loss of the normal foveal contour. In a stage 1b macular hole, a yellow ring is visible in the foveal area. With continued shrinkage of the perifoveal vitreous cortex, a stage 1 hole advances to a stage 2 hole. Stage 2 holes have a small (100–200 μm), full-thickness neural retinal defect, either centrally or eccentrically. During this stage, a pseudopericulus, which represents condensed vitreous, may overlie the hole. As the vitreo-foveal traction on a stage 2 hole continues to a stage 3, the hole is developed and consisting of around 350–600- μm full-thickness neural retinal defect with smooth edges and a small, surrounding, doughnut-shaped rim of subretinal fluid. Yellow deposits can be seen in the base of the defect, and perifoveal cystic retinal changes are present. In this stage, vitreo-foveal separation still has not occurred. A stage 4 macular hole has all the features of a stage 3 hole, but with complete posterior separation of the vitreous from the fovea.

While the Gass classification is still widely used, OCT-based anatomic images have added much to our understanding of the pathogenesis and progression of macular holes. Moreover, using an OCT-based system, FTMH can be anatomically defined, quantitatively, and reproducibly. It can also help predict the success of treatment with either medications or surgery [33–37]. OCT classification system of FTMH is based on hole size, the presence or absence of VMT, and the cause.

OCT-based anatomic classification systems have categorized full-thickness macular holes by aperture size into

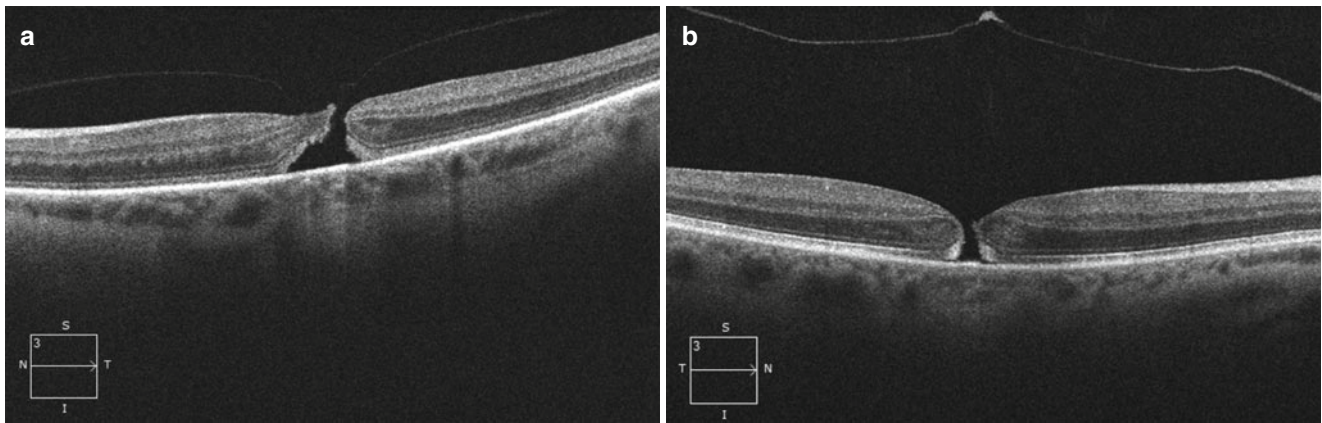


Figure III.D-6 (a) OCT of small full-thickness macular hole (FTMH) (<250 μm) with traction on edge of hole. (b) OCT of small full-thickness macular hole (FTMH) (<250 μm) without traction

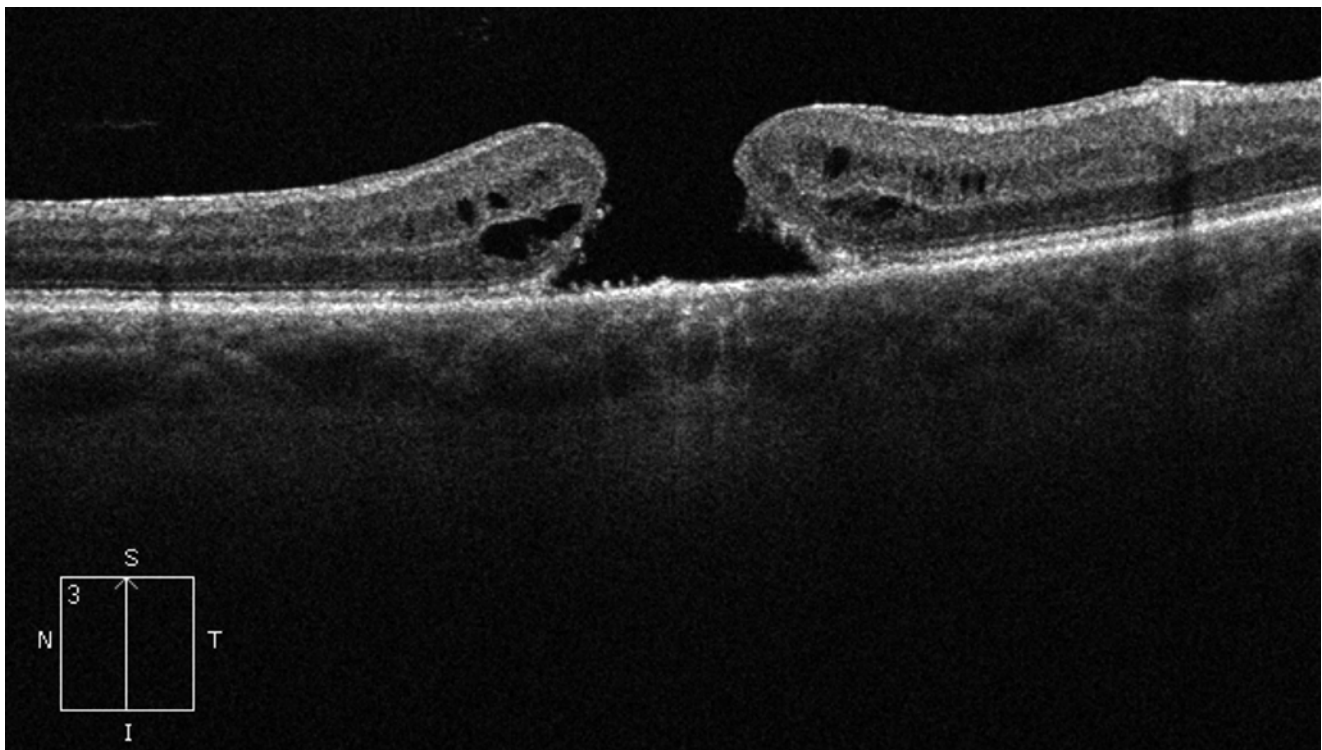


Figure III.D-7 OCT of large full-thickness macular hole (FTMH) (>400 μm)

small, medium, or large FTMH. The aperture size is defined as the minimum hole width measured as a line drawn roughly parallel to the RPE at the narrowest hole point in the mid-retina. A small hole is defined as an aperture size less than 250 μm (Figure III.D-6). This cutoff was chosen due to the fact that although these holes rarely close spontaneously, they have very high success rate with surgical and pharmacological treatments [34, 35]. A medium hole is defined as aperture size ranging from 250 to 400 μm . These holes have slightly lower success rate with vitrectomy and pharmacologic vitreolysis [33, 34, 36, 37]. A large hole is defined as an aperture size greater than 400 μm (Figure III.D-7).

Vitrectomy alone for these holes has a lower success rate, but the rate increases to 90–95 % if ILM peeling is included [38]. Anatomical success is exceedingly low pharmacologically in these large holes [35].

In the OCT-based anatomic system, FTMHs are secondarily categorized according to the absence or presence of vitreous traction. The reason for this is that only macular holes with concurrent VMT should be considered for pharmacologic vitreolysis (Figure III.D-8). Finally, FTMH can be further classified as primary or secondary. Primary holes, also referred to as idiopathic holes, are due to VMT from an anomalous PVD. A secondary FTMH is caused by

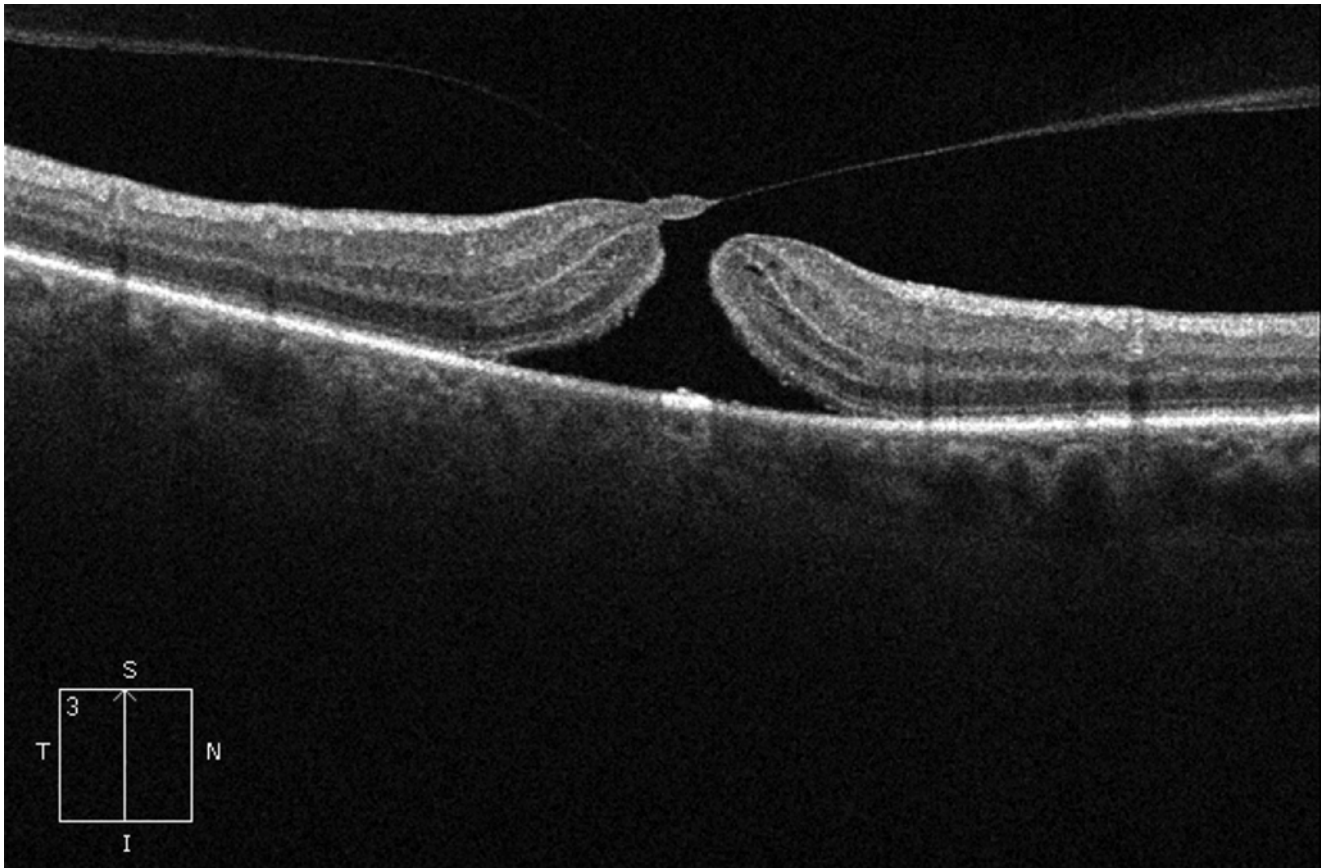


Figure III.D-8 OCT of small full-thickness macular hole (FTMH) with traction

a different mechanism and by definition does not exhibit VMT. Secondary causes of FTMH include blunt trauma, cystoid macular edema, rhegmatogenous retinal detachment, inadvertent exposure to laser energy, Best's disease, high myopia with posterior staphyloma, lightning strike injury, hypertensive retinopathy, proliferative diabetic retinopathy, macular schisis, macular telangiectasia type 2, macroaneurysm, and surgical trauma [39–46]. In addition, FTMH can occur concomitantly with macular edema that is associated with a variety of retinal diseases, including DME, AMD, retinal vascular occlusions, and uveitis [47–49]. Some of these cases should be classified as primary macular holes if VMT is shown to play a role.

Conclusion

Abnormalities in the process of vitreous detachment can result in an anomalous PVD with subsequent vitreo-macular interface (VMI) pathology leading to pathologic macular conditions such as VMT, macular pucker, lamellar hole, and FTMH. VMA, VMT, and FTMH can now be defined by anatomic criteria that are present on OCT and classified by size of attachment or lesion and the presence of concomitant retinal or vitreo-retinal conditions (Table III.D-1). It is solely anatomically based, regardless of symptoms or visual acuity. This new classification system [50] allows for standardization of the diagnosis and management of pathologies of the VMI.

Table III.D-1 The IVTS classification of vitreo-maculopathies

VMA	<p><i>Definition</i></p> <p>Evidence of perifoveal vitreous cortex detachment from the retinal surface</p> <p>Macular attachment of the vitreous cortex within a 3-mm radius of the fovea</p> <p>No detectable change in foveal contour or underlying retinal tissues</p> <p><i>Classification</i></p> <p>By size of attachment area</p> <p>Focal ($\leq 1,500$ mm)</p> <p>Broad ($> 1,500$ mm, parallel to RPE and may include areas of dehiscence)</p> <p>By presence of concurrent retinal conditions</p> <p>Isolated</p> <p>Concurrent</p>
VMT	<p><i>Definition</i></p> <p>Evidence of perifoveal vitreous cortex detachment from the retinal surface</p> <p>Macular attachment of the vitreous cortex within a 3-mm radius of the fovea</p> <p>Association of attachment with distortion of the foveal surface, intraretinal structural changes, and/or elevation of the fovea above the RPE, but no full-thickness interruption of all retinal layers</p> <p><i>Classification</i></p> <p>By size of attachment area</p> <p>Focal (1,500 mm)</p> <p>Broad (> 1500 mm, parallel to RPE and may include areas of dehiscence)</p> <p>By presence of concurrent retinal conditions</p> <p>Isolated</p> <p>Concurrent</p>
LMH	<p><i>Definition</i></p> <p>Irregular foveal contour</p> <p>Defect in the inner fovea (may not have actual loss of tissue)</p> <p>Intraretinal splitting (schisis) between the outer plexiform and outer nuclear layers</p> <p>Maintenance of an intact photoreceptor layer</p>
Macular pseudohole	<p><i>Definition</i></p> <p>Invaginated or heaped foveal edges</p> <p>Concomitant premacular or epiretinal membrane with central opening</p> <p>Steep macular contour to the central fovea with near-normal central foveal thickness</p> <p>No loss of retinal tissue</p>
FTMH	<p><i>Definition</i></p> <p>Full-thickness foveal interruption of all macular layers from the ILM to the RPE</p> <p><i>Classification</i></p> <p>By size (horizontal measure of width across hole at narrowest point, not ILM)</p> <p>Small (250 mm)</p> <p>Medium (> 250 and ≤ 400 mm)</p> <p>Large (> 400 mm)</p> <p>By presence or absence of VMT</p> <p>By cause</p> <p>Primary (initiated by VMT)</p> <p>Secondary (directly due to associated disease or trauma known to cause macular hole in the absence of prior VMT)</p>

Adapted/Modified from: Duker et al. [50]

Abbreviations: *FTMH* full-thickness macular hole, *ILM* internal limiting membrane, *IVTS* International Vitreo-macular Traction Study, *LMH* lamellar macular hole, *RPE* retinal pigment epithelium, *VMA* vitreo-macular adhesion, *VMT* vitreo-macular traction

Abbreviations

AMD	Age-related macular degeneration
CME	Cystoid macular edema
DME	Diabetic macular edema
FTMH	Full-thickness macular hole
ILM	Inner limiting membrane
IVTS	International Vitreo-macular Traction Study
MH	Macular hole
MP	Macular pucker
OCT	Optical coherence tomography
ONL	Outer nuclear layer
OPL	Outer plexiform layer
PMM	Premacular membrane
PVD	Posterior vitreous detachment
RPE	Retinal pigment epithelium
RVO	Retinal vein occlusion
VMA	Vitreo-macular adhesion
VMI	Vitreo-macular interface
VMT	Vitreo-macular traction
VPA	Vitreo-papillary adhesion

References

- Bishop PN. Structural macromolecules and supramolecular organization of the vitreous gel. *Prog Retin Eye Res.* 2000;19(3):323–44.
- Sebag J. Macromolecular structure of the corpus vitreous. *Prog Polym Sci.* 1998;23(3):415–46.
- Bhutto IA, Kim SY, McLeod DS, Merges C, Fukai N, Olsen BR, et al. Localization of collagen XVIII and the endostatin portion of collagen XVIII in aged human control eyes and eyes with age-related macular degeneration. *Invest Ophthalmol Vis Sci.* 2004;45(5):1544–52.
- Sebag J. Age-related changes in human vitreous structure. *Graefes Arch Clin Exp Ophthalmol.* 1987;225(2):89–93.
- Russell SR, Shepherd JD, Hageman GS. Distribution of glycoconjugates in the human retinal internal limiting membrane. *Invest Ophthalmol Vis Sci.* 1991;32(7):1986–95.
- Reardon A, Heinegård D, McLeod D, Sheehan JK, Bishop PN. The large chondroitin sulphate proteoglycan versican in mammalian vitreous. *Matrix Biol.* 1998;17(5):325–33.
- Theocharis DA, Skandalis SS, Noulas AV, Papageorgakopoulou N, Theocharis AD, Karamanos NK. Hyaluronan and chondroitin sulfate proteoglycans in the supramolecular organization of the mammalian vitreous body. *Connect Tissue Res.* 2008;49(3):124–8.
- Johnson MW. Perifoveal vitreous detachment and its macular complications. *Trans Am Ophthalmol Soc.* 2005;103:537–67.
- Gaudric A, Haouchine B, Massin P, Paques M, Blain P, Erginay A. Macular hole formation: new data provided by optical coherence tomography. *Arch Ophthalmol.* 1999;117(6):744–51.
- Uchino E, Uemura A, Ohba N. Initial stages of posterior vitreous detachment in healthy eyes of older persons evaluated by optical coherence tomography. *Arch Ophthalmol.* 2001;119(10):1475–9.
- Johnson MW. Posterior vitreous detachment: evolution and complications of its early stages. *Am J Ophthalmol.* 2010;149(3):371–82.
- DeCroos FC, Toth CA, Folgar FA, Pakola S, Stinnett SS, Heydary CS, et al. Characterization of vitreoretinal interface disorders using OCT in the interventional phase 3 trials of ocriplasmin. *Invest Ophthalmol Vis Sci.* 2012;53(10):6504–11.
- Koizumi H, Spaide RF, Fisher YL, Freund KB, Klancnik Jr JM, Yannuzzi LA. Three-dimensional evaluation of vitreomacular traction and epiretinal membrane using spectral-domain optical coherence tomography. *Am J Ophthalmol.* 2008;145(3):509–17.
- John VJ, Flynn Jr HW, Smiddy WE, Carver A, Leonard R, Tabandeh H, Boyer DS. Clinical course of vitreomacular adhesion managed by initial observation. *Retina.* 2014;34(3):442–6.
- Sebag J. Vitreoschisis. *Graefes Arch Clin Exp Ophthalmol.* 2008;246(3):329–32.
- Haouchine B, Massin P, Gaudric A. Foveal pseudocyst as the first step in macular hole formation: a prospective study by optical coherence tomography. *Ophthalmology.* 2001;108(1):15–22.
- Sebag J, Gupta P, Rosen R, Garcia P, Sadun AA. Macular holes and macular pucker: the role of vitreoschisis as imaged by optical coherence tomography/scanning laser ophthalmoscopy. *Trans Am Ophthalmol Soc.* 2007;105:121–31.
- Gupta P, Yee KMP, Garcia P, Rosen RB, Parikh J, Hageman GS, Sadun AA, Sebag J. Vitreoschisis in macular diseases. *Br J Ophthalmol.* 2011;95(3):376–80.
- Gass JD. Lamellar macular hole: a complication of cystoid macular edema after cataract extraction: a clinicopathologic case report. *Trans Am Ophthalmol Soc.* 1975;73:230–50.
- Tanner V, Chauhan DS, Jackson TL, Williamson TH. Optical coherence tomography of the vitreoretinal interface in macular hole formation. *Br J Ophthalmol.* 2001;85:1092–7.
- Haouchine B, Massin P, Tadayoni R, et al. Diagnosis of macular pseudoholes and lamellar macular holes by optical coherence tomography. *Am J Ophthalmol.* 2004;138:732–9.
- Gass JD. Idiopathic senile macular hole. Its early stages and pathogenesis. *Arch Ophthalmol.* 1988;106:629–39.
- Gass JD. Reappraisal of biomicroscopic classification of stages of development of a macular hole. *Am J Ophthalmol.* 1995;119:752–9.
- Smiddy WE, Gass JD. Masquerades of macular holes. *Ophthalmic Surg.* 1995;26:16–24.
- Gass JD. Stereoscopic atlas of macular diseases: diagnosis and treatment. 4. 1. St. Louis: Mosby; 1997. p. 1–18.
- Wang MY, Nguyen D, Hindoyan N, Sadun AA, Sebag J. Vitreopapillary adhesion in macular hole and macular pucker. *Retina.* 2009;29:644–50.
- Sebag J, Wang MY, Nguyen D, Sadun AA. Vitreopapillary adhesion in macular diseases. *Trans Am Ophthalmol Soc.* 2009;107:35–44.
- Aaberg TM. Macular holes: a review. *Surv Ophthalmol.* 1970;15:139–62.
- Brown GC. Macular hole following rhegmatogenous retinal detachment repair. *Arch Ophthalmol.* 1988;106:765–6.
- Cohen SM, Gass JDM. Macular hole following severe hypertensive retinopathy. *Arch Ophthalmol.* 1994;112:878–9.
- Flynn HW. Macular hole surgery in patients with proliferative diabetic retinopathy. *Arch Ophthalmol.* 1994;112:877–8.
- Johnson RN, Gass JDM. Idiopathic macular holes: observations, stages of formation, and implications for surgical intervention. *Ophthalmology.* 1988;95:917–24.
- Ip MS, Baker BJ, Duker JS, Reichel E, Bauman CR, Gangnon R, et al. Anatomical outcomes of surgery for idiopathic macular hole as determined by optical coherence tomography. *Arch Ophthalmol.* 2002;120(1):29–35.
- Pieramici DJ, Boyer DS. The phase III MIVI-TRUST clinical trial data: subgroup responder analysis of a single intravitreal injection of ocriplasmin in patients with full thickness macular hole. Presented at: 2012 annual meeting of the association for research in vision and ophthalmology. Fort Lauderdale; 6–9 May 2012.
- Stalmans P, Benz MS, Gandorfer A, Kampik A, Girach A, Pakola S, et al. Enzymatic vitreolysis with ocriplasmin for vitreomacular traction and macular holes. *N Engl J Med.* 2012;367(7):606–15.

36. Trese MT, Williams GA, Hartzler MK. A new approach to stage 3 macular holes. *Ophthalmology*. 2000;107(8):1607–11.
37. Ullrich S, Haritoglou C, Gass C, Schaumberger M, Ulbig MW, Kampik A. Macular hole size as a prognostic factor in macular hole surgery. *Br J Ophthalmol*. 2002;86(4):390–3.
38. Chang S. Controversies regarding internal limiting membrane peeling in idiopathic epiretinal membrane and macular hole. *Retina*. 2012;32 Suppl 2:S200–3; discussion S203–4.
39. Shukla D, Naresh KB, Rajendran A, Kim R. Macular hole secondary to X-linked retinoschisis. *Eye (Lond)*. 2006;20(12):1459–61.
40. Shukla D. Evolution and management of macular hole secondary to type 2 idiopathic macular telangiectasia. *Eye (Lond)*. 2011;25(4):532–3.
41. Chaudhry NA, Tabandeh H, Flynn HWJ, Konjara V, Liggett PE. Spontaneous development and closure of full thickness macular hole during intravitreal anti-VEGF therapy for neovascular age-related macular degeneration. Presented at: 2012 annual meeting of the association for research in vision and ophthalmology. Fort Lauderdale; 6–9 May 2012.
42. Sagara N, Kawaji T, Koshiyama Y, Inomata Y, Fukushima M, Tanihara H. Macular hole formation after macular haemorrhage associated with rupture of retinal arterial macroaneurysm. *Br J Ophthalmol*. 2009;93(10):1337–40.
43. Sato R, Yasukawa T, Hirano Y, Ogura Y. Early-onset macular holes following ruptured retinal arterial macroaneurysms. *Graefes Arch Clin Exp Ophthalmol*. 2008;246(12):1779–82.
44. Tashimo A, Mitamura Y, Ohtsuka K, Okushiba U, Imaizumi H, Takeda M. Macular hole formation following ruptured retinal arterial macroaneurysm. *Am J Ophthalmol*. 2003;135(4):487–92.
45. Fabian ID, Moisseiev E, Moisseiev J, Moroz I, Barak A, Alhalel A. Macular hole after vitrectomy for primary rhegmatogenous retinal detachment. *Retina*. 2012;32(3):511–9.
46. Garcia-Arumi J, Boixadera A, Martinez-Castillo V, Zapata MA, Fonollosa A, Corcostegui B. Macular holes after rhegmatogenous retinal detachment repair: surgical management and functional outcome. *Retina*. 2011;31(9):1777–82.
47. Sivaprasad S, Ikeji F, Xing W, Lightman S. Tomographic assessment of therapeutic response to uveitic macular oedema. *Clin Experiment Ophthalmol*. 2007;35(8):719–23.
48. Taylor SR, Lightman SL, Sugar EA, Jaffe GJ, Freeman WR, Altaweel MM, et al. The impact of macular edema on visual function in intermediate, posterior, and panuveitis. *Ocul Immunol Inflamm*. 2012;20(3):171–81.
49. Tsukada K, Tsujikawa A, Murakami T, Ogino K, Yoshimura N. Lamellar macular hole formation in chronic cystoid macular edema associated with retinal vein occlusion. *Jpn J Ophthalmol*. 2011;55(5):506–13.
50. Duker JS, Kaiser PK, Binder S, de Smet MD, Gaudric A, Reichel E, Sadda SR, Sebag J, Spaide RF, Stalmans P. The International Vitreomacular Traction Study Group classification of vitreomacular adhesion, traction, and macular hole. *Ophthalmology*. 2013;120(12):2611–9.

Vitreo-Papillary Adhesion and Traction

III.E.

Michelle Y. Wang, Alfredo A. Sadun, and J. Sebag

Outline

- I. Introduction
- II. Anatomy
 - A. Vitreo-Retinal Interface
 - B. Vitreo-Papillary Interface
- III. Pathology
 - A. Vitreo-Papillary Adhesion and Traction
 - B. Retinal Disorders
 - 1. Macular Diseases
 - 2. Intraretinal Cysts
 - 3. Vascular Disorders
 - a. Peripapillary, Subretinal, and Intrapapillary Hemorrhage
 - b. Diabetic Vitreo-Retinopathy
 - c. Central Retinal Vein Occlusion
 - C. Optic Neuropathies
 - 1. Non-arteritic Anterior Ischemic Optic Neuropathy
 - 2. Gaze-Evoked Amaurosis
 - 3. Optic Nerve Pit

Conclusion

References

Keywords

Vitreous • Vitreo-papillary interface • Vitreo-papillary adhesion • Vitreo-papillary traction • Gaze-evoked amaurosis • Intraretinal cysts • Macular hole • Macular pucker • Non-arteritic anterior ischemic optic neuropathy • Optic nerve pit

Key Concepts

1. The vitreo-papillary interface is different from the vitreo-retinal interface, as there is no inner limiting membrane and no posterior vitreous cortex, but there is firm adhesion of the peripapillary cortex to the rim of the optic disc.
2. Vitreo-papillary adhesion may contribute to a wide spectrum of maculopathies by altering the vector of tangential forces at the vitreo-macular interface, inducing intraretinal cystoid spaces as well as lamellar and even full-thickness macular holes.
3. Anomalous posterior vitreous detachment with vitreo-papillary traction may disturb the cellular architecture of the optic disc inducing or contributing to optic neuropathies via the membrane of Elschnig and/or pathologic attachments.

M.Y. Wang, MD • J. Sebag, MD, FACS, FRCOphth, FARVO (✉)
VMR Institute for Vitreous Macula Retina,
7677 Center Avenue, suite 400, Huntington Beach,
CA 92647, USA

Doheny Eye Institute, Los Angeles, CA USA
e-mail: michellewusc@gmail.com; jsebag@VMRinstitute.com

A.A. Sadun, MD, PhD, FARVO
Doheny Eye Institute/UCLA, Los Angeles, CA USA
e-mail: alfredo.sadun@gmail.com

I. Introduction

Vitreo-papillary adhesion (VPA) is characterized by persistent adhesion of the posterior vitreous cortex to the optic disc as a direct consequence of anomalous posterior vitreous detachment (PVD) [see chapter III.B. Anomalous PVD and Vitreoschisis]. The significance of this pathology has gained

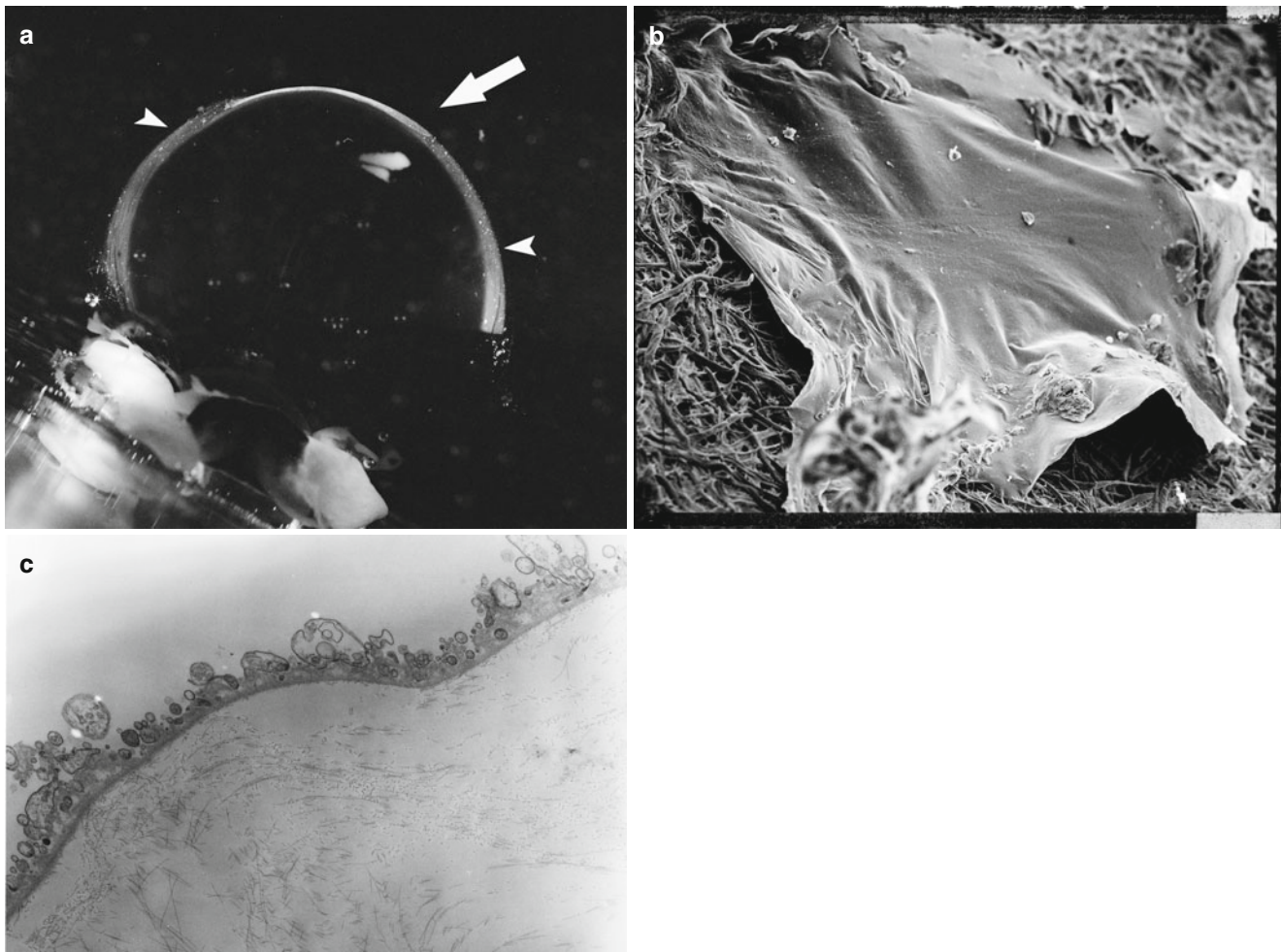


Figure III.E-1 Human vitreo-retinal interface. Vitreous adherence to the retina is mediated by an extracellular matrix “glue” that results in strong fascial adhesion throughout the posterior pole as well as strong focal adhesion at the optic disc. Early studies [80] investigated vitreo-retinal interface anatomy by peeling the retina off the vitreous body. In all adults, the separation between vitreous and retina occurred between the inner limiting membrane of the retina and the posterior vitreous cortex of the vitreous body. In 40 % of individuals younger than 20 years of age, there was a different cleavage plane due to strong vitreo-retinal adherence. (a) Postmortem dark-field slit microscopy of the vitreous

body in a 4-year-old subject reveals the typical appearance of the posterior vitreous cortex with embedded hyalocytes in the mid-peripheral fundus (*arrowheads*). However, in the posterior pole, there appeared to be an additional cap of tissue (*arrow*). (b) Scanning electron microscopy identified a layer of tissue attached to the posterior vitreous. (c) Transmission electron microscopy identified this tissue as the inner limiting membrane of the retina with the inner segments of Müller cells still attached to the posterior aspect of the ILM (*top* of image c), which was firmly adherent to the posterior vitreous cortex (*below*). Note the dense matrix of collagen fibrils in the posterior vitreous cortex

increasing attention in the medical literature as traction at the adhesion site can lead to various pathologies depending on the directions of the force vector. As a result, VPA has been implicated in a wide range of retinal disorders such as macular holes and macular puckers, intraretinal cysts, and vascular disorders including peripapillary/subretinal/intrapapillary hemorrhages, proliferative diabetic vitreo-retinopathy, and central retinal vein occlusion. Due to direct traction on the optic disc, it may also play a role in a number of optic neuropathies such as non-arteritic anterior ischemic optic neuropathy, gaze-evoked amaurosis, and optic nerve pit. Optical coherence tomography (OCT) provides direct visualization of the vitreo-papillary interface, allowing us to better understand the underlying pathophysiology of vitreo-papillary adhesion and traction.

II. Anatomy

A. Vitreo-Retinal Interface

The vitreo-retinal interface consists of the posterior vitreous cortex, the inner limiting membrane (ILM) of the retina, and an extracellular matrix of fibronectin, laminin, and other components. It was once thought that the vitreous cortex was directly affixed to the retina. However, more recent studies support existence of an extracellular matrix between the vitreous and retina, causing fascial adhesion rather than focal attachments [1–3] [see chapter II.E. Vitreo-retinal interface and ILM]. In youth, this fascial adherence of vitreous to the retina and optic disc is strong, indeed stronger than the Müller cells themselves (Figure III.E-1).

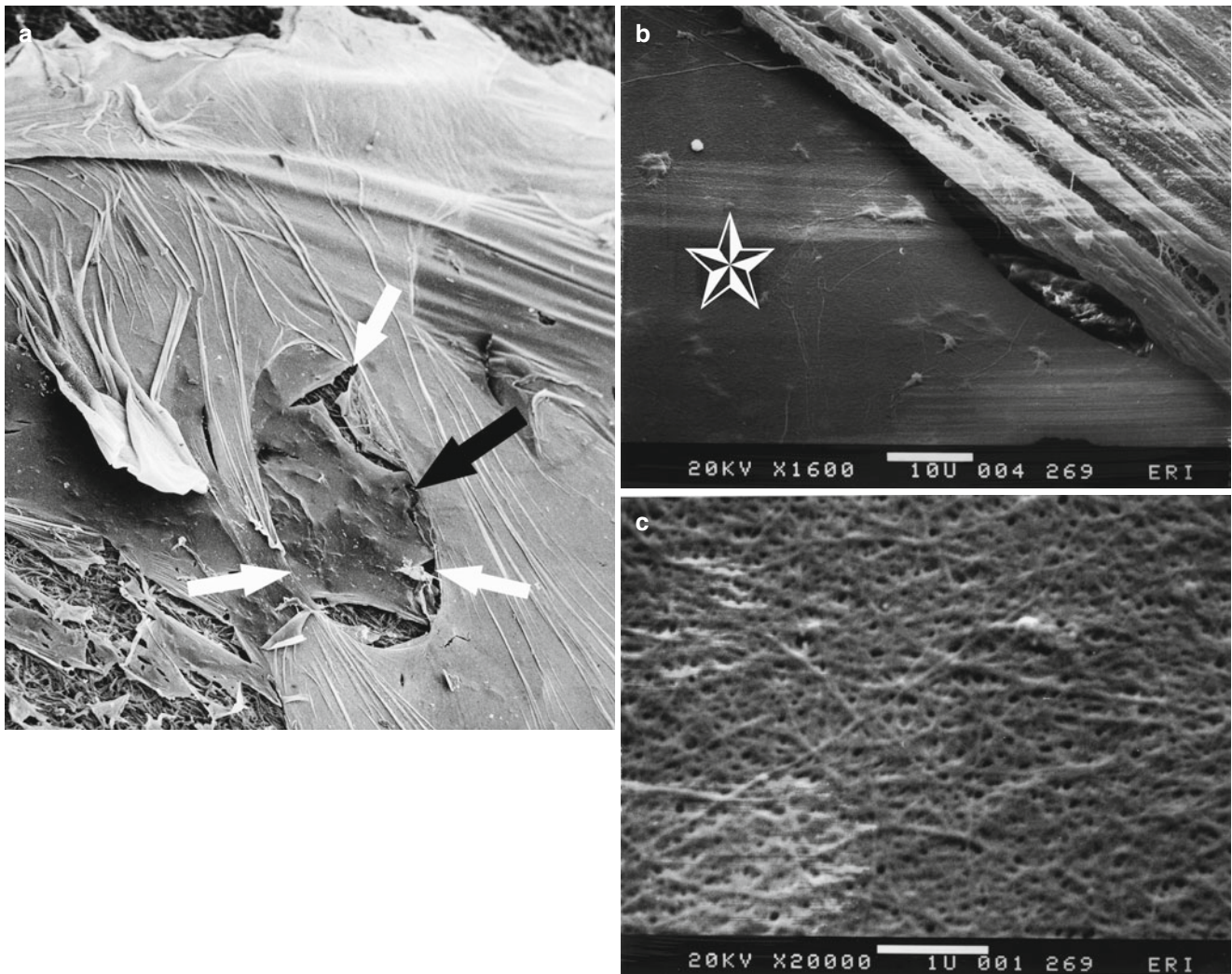


Figure III.E-2 Human vitreo-papillary interface. (a) Scanning electron micrograph of human inner limiting membrane with an oval-shaped structure corresponding to the vitreo-papillary interface (*white arrows*). It can be seen that this area is not a hole devoid of tissue, but has a thin membrane known as the membrane of Elschnig (see c). This specimen was prepared by peeling the retina and optic disc off the posterior vitreous and then mounting and processing for scanning electron microscopy of the peripapillary retina/disc complex. The large *black arrow* indicates the region that was

examined at higher magnification in b. (b) The vitreo-retinal interface at the edge of the optic disc has a thick fibrous structure that is sometimes torn away during posterior vitreous detachment making the Weiss ring discernible. The *star* indicates the region that was examined by higher power in c. (c) Scanning electron microscopy at high magnification demonstrates that the center of the vitreo-papillary interface has thin tissue known as the membrane of Elschnig and central meniscus of Kuhnt

Posterior vitreous detachment (PVD) results from weakening of the vitreous cortex and ILM adhesion in conjunction with liquefaction of the vitreous body, allowing the posterior vitreous cortex to detach from the inner limiting membrane [see chapter II.C. Vitreous aging and PVD]. However, when the extent of vitreous gel liquefaction exceeds the degree of vitreo-retinal dehiscence, anomalous PVD occurs. This imbalance leads to an abnormal traction at the vitreo-retinal interface and is associated with a wide spectrum of disorders depending on the site of the strongest adhesion [4, 5] [see chapter III.B. Anomalous PVD and vitreoschisis].

B. Vitreo-Papillary Interface

The ILM of the retina is not present over the optic disc but is delineated at the rim of the disc; however, the basement membrane continues as the membrane of Elschnig [6] (Figure III.E-2). This membrane is believed to derive from the basal lamina of the astroglia in the optic nerve head, measuring 50 nm in thickness. The center of the membrane, known as the central meniscus of Kuhnt, is only 20 nm in thickness and consists of glycosaminoglycans without collagen. The ILM of the retina functions to prevent passage of cells [7]. Hence, the lack of ILM and thin composition of the central meniscus of Kuhnt may explain the frequent cellular proliferation at or near the optic disc.

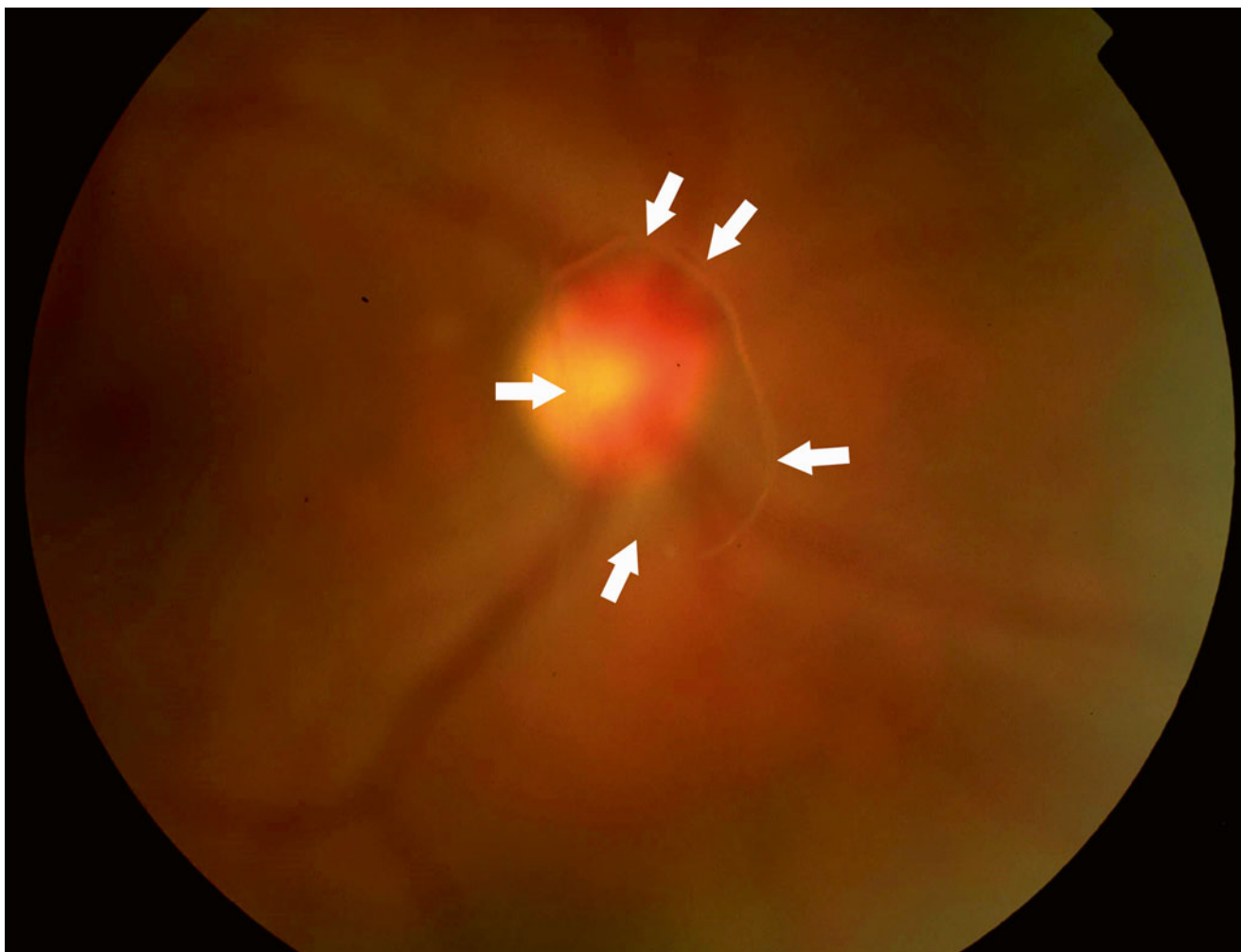


Figure III.E-3 Weiss ring. Fundus photograph of Weiss ring (*arrows*), visible following PVD that tore away peripapillary fibrous tissue demonstrated in Figure III.E-2b

III. Pathology

A. Vitreo-Papillary Adhesion and Traction

Vitreous attachment to the optic disc may be fortified by epipapillary membranes [8], which form due to the relative lack of inhibition against cell migration and proliferation mentioned above, and this attachment may persist after PVD elsewhere [9]. If following PVD, peripapillary tissue tears away from the retina/disc junction and remains attached around the prepapillary hole in the posterior vitreous cortex anterior to the optic disc, a Vogt or Weiss ring can be visualized by ophthalmoscopy (Figure III.E-3). Vitreo-papillary adhesion itself cannot usually be visualized in this manner, but requires imaging, such as with ultrasound or optical coherence tomography (OCT) (Figure III.E-4a). Due to a lack of methods to measure tractional forces inside the eye, traction can in truth only be surmised based upon the appearance on imaging. (Figure III.E-4b).

Vitreo-macular traction syndrome has been well documented in the literature; however, very few studies have investigated vitreo-papillary traction. In 1954, Schepens described the histopathology of “pseudopapilledema” with incomplete PVD from the optic disc and vitreo-papillary traction [10]. This condition is characterized by a contracted fibrocellular posterior vitreous membrane (at its origin the posterior vitreous cortex) causing tractional force at the optic disc. PVD with persistent adhesion to the optic disc, called vitreo-papillary adhesion (VPA), constitutes a manifestation of anomalous PVD, which may contribute to a wide spectrum of diseases such as macular holes [11], maculopathies with intraretinal cystoid spaces [12], hemorrhage [13], exacerbation of neovascularization in proliferative diabetic vitreo-retinopathy [14], non-arteritic anterior optic neuropathy [15], and gaze-evoked visual disturbances [16]. Vitreo-papillary traction appears to play a role in papillopathies, retinopathies, and some vitreo-maculopathies. In children and young adults, vitreous adhesion

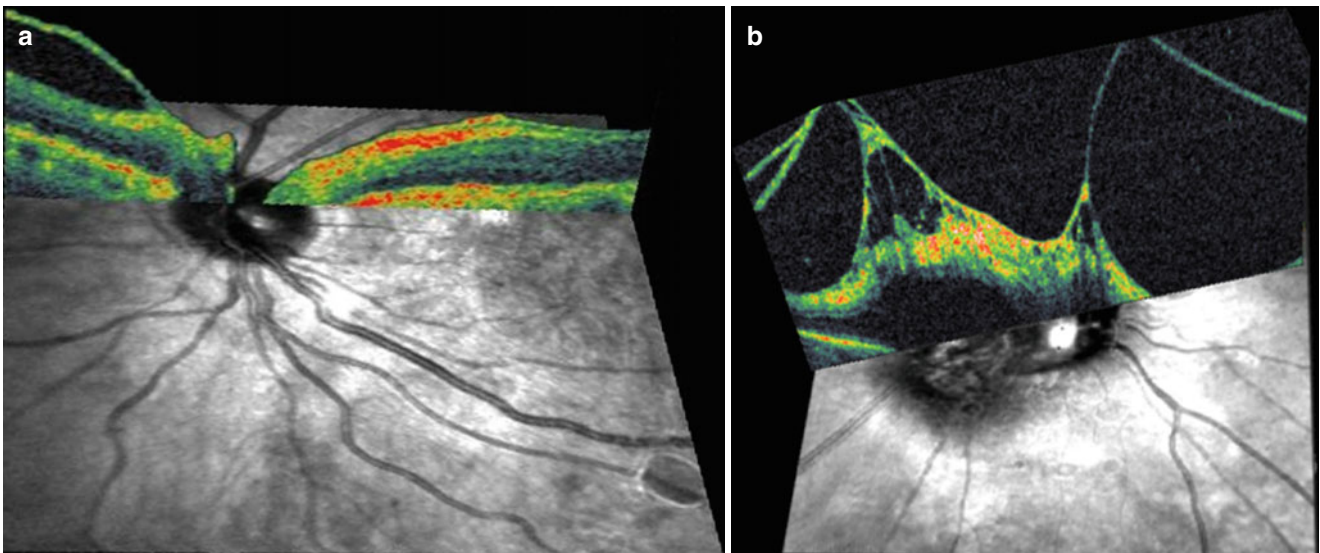


Figure III.E-4 Vitreo-papillary adhesion (VPA). (a) A composite (intersecting planes) longitudinal OCT image (color) with scanning laser ophthalmoscopy imaging of the optic disc (grayscale) demonstrating persistent VPA following anomalous posterior vitreous detachment. (b) Composite (intersecting planes) longitudinal OCT imaging (color) with

scanning laser ophthalmoscopy imaging of the optic disc (grayscale) demonstrating severe vitreo-papillary traction elevating the optic disc anteriorly in a 58-year-old woman with concurrent vitreo-macular traction, both due to anomalous PVD. Note vitreoschisis on the left-hand side of the image

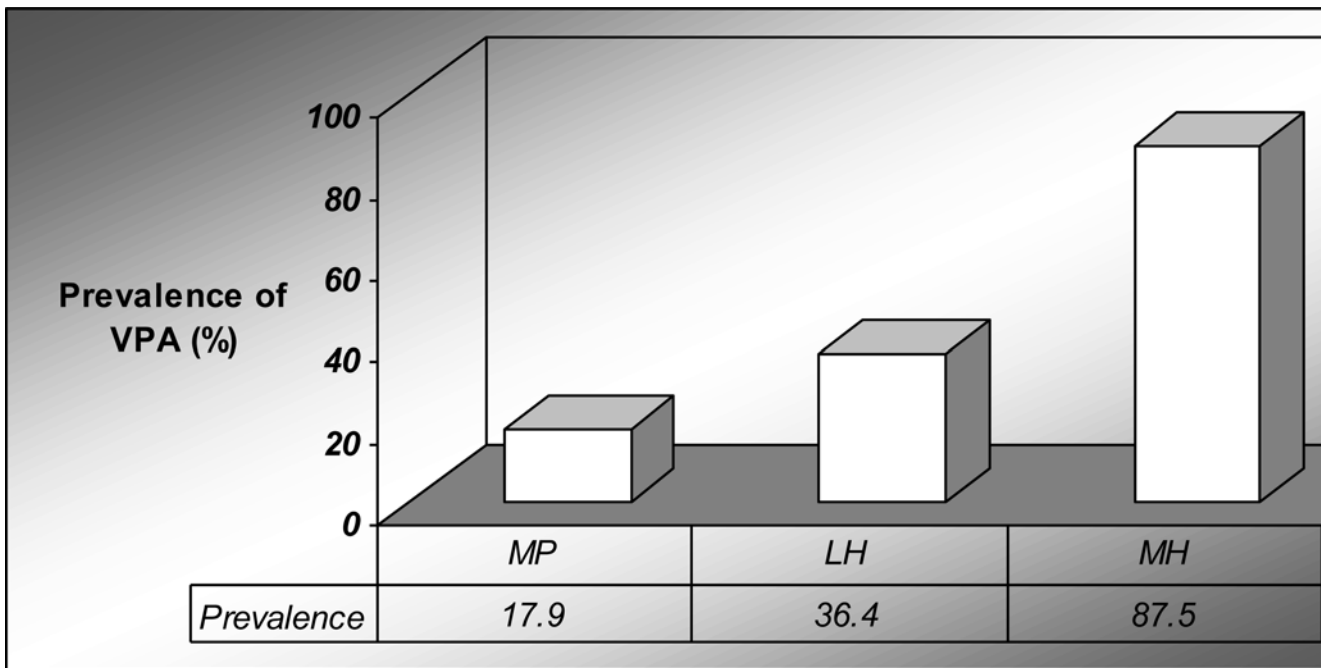


Figure III.E-5 The prevalence of vitreo-papillary adhesion (VPA) is greater in eyes with full-thickness macular holes (MH: 87.5 %) than lamellar macular holes (LH: 36.4 %) and least in eyes with macular pucker (MP: 17.9 %) (Reprinted with permission from Wang et al. [11])

at the posterior pole is strong and distributed in a diffuse, sheetlike configuration encompassing the macula and peripapillary region [17] (Figure III.E-1). This strong interface includes VPA, predisposing individuals to pathologic vitreo-papillary traction (Figure III.E-4b). Similar to the vitreo-retinal interface, however, VPA weakens with aging.

B. Retinal Disorders

1. Macular Diseases

VPA has been shown to be far more prevalent in full-thickness macular holes (MH) than lamellar holes (LH) and macular pickers (MP) [11, 12] (Figure III.E-5). The reason

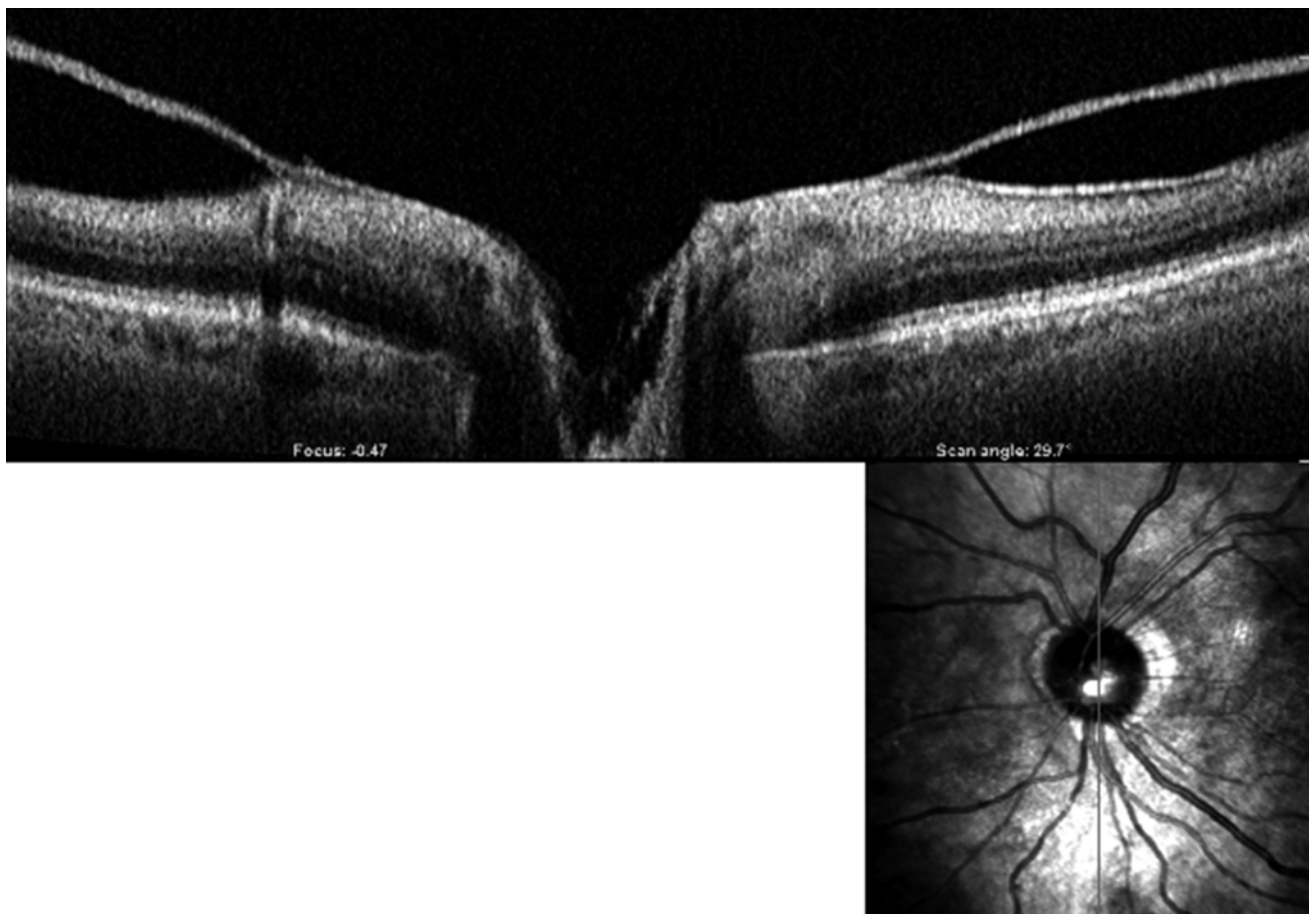


Figure III.E-6 Vitreo-papillary adhesion and vitreoschisis. Combined OCT-SLO demonstrates vitreo-papillary adhesion on both sides of the optic disc. On the *right side*, there is evidence of vitreoschisis

may relate to the effects of persistent VPA on the remaining tissue attached to the macula. Anomalous PVD may be the first event in the pathophysiology of both MH and MP [18–20]. If anomalous PVD induces vitreoschisis, the outer layer of the split posterior vitreous cortex remains attached to the macula. In the absence of VPA, inward (centripetal towards the fovea) tangential traction by this outer layer of the split posterior vitreous cortex throws the underlying retina into folds, resulting in MP. However, if vitreous is still attached to the optic disc, the vectors of force are different, resulting in outward (centrifugal) tangential traction that induces central retinal dehiscence and MH formation. Figure III.E-6 demonstrates a case where vitreoschisis occurred adjacent to the vitreo-papillary interface.

Papillo-foveal traction has previously been implicated in the pathogenesis of MH [21]. Hence, while anomalous PVD may be the precipitating event, the presence or absence of VPA may influence the subsequent course and vectors of traction. In the absence of VPA, a MP is more likely to be present. In the presence of VPA, a MH is more likely to occur, with LH possibly representing an intermediate stage. Previous

studies [19] have suggested that LHs represent an “abortive” process of MH formation [22] and that foveal pseudocysts with partial PVD become LHs if the base is preserved and full-thickness MHs if the outer retinal layer is disrupted [23]. However, many patients live for many years with lamellar holes that do not progress to full-thickness macular holes.

Three years after Wang et al. initially described the role of VPA in MH, LH, and macular pucker, Romano et al. evaluated the role of VPA in LH and pseudohole and found that VPA is more prevalent in LH (37 %) compared to pseudohole (27 %) and that the presence of VPA is associated with worse visual function and impaired integrity of both outer limiting membrane and inner segment and outer segment junction [24]. The authors speculated that in the presence of vitreoschisis, adhesion of vitreous to the optic disc influences tangential traction at the macula with subsequent damage to the outer retinal layers, leading to progression of pseudoholes and LH to the outer retinal layers, similar to the mechanism previously described for MH and MP. Furthermore, in the presence of VPA, surgical removal of preretinal and prepapillary tissue leads to better visual outcomes.

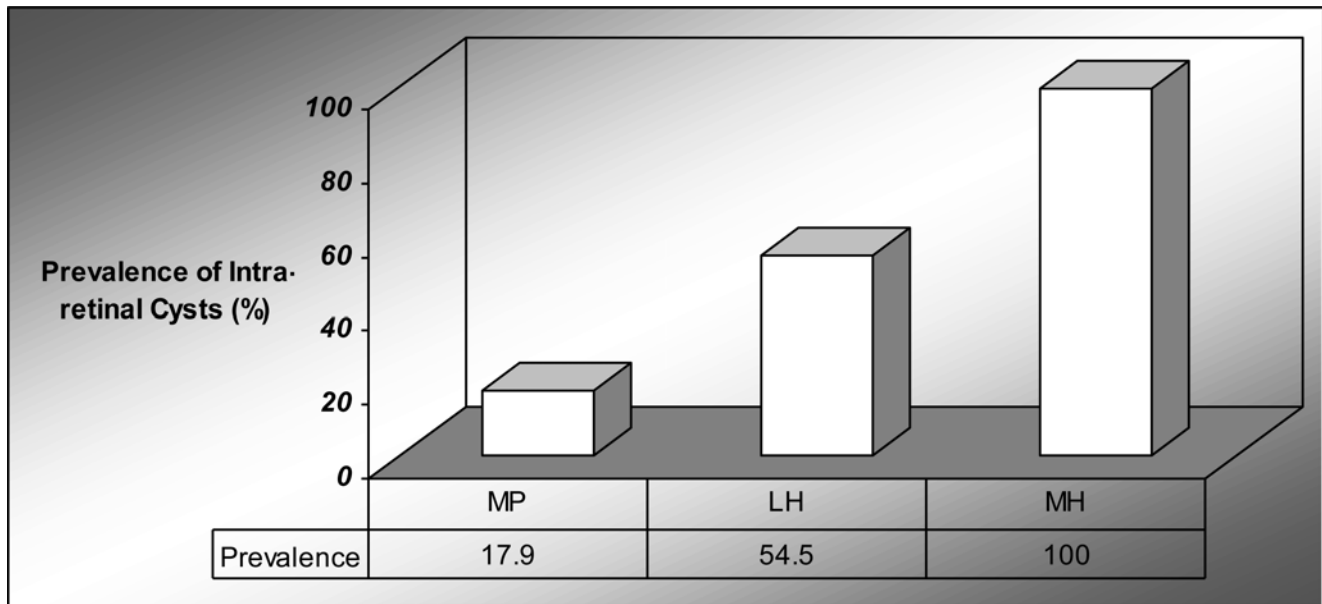


Figure III.E-7 The prevalence of intraretinal cystoid spaces is greater in full-thickness macular holes (MH: 100 %) than lamellar holes (LH: 54.5 %) and macular pucker (MP: 17.9 %) (Reprinted with permission from Wang et al. [11])

2. Intraretinal Cysts

Foveal cysts are believed to be the precursors of either full-thickness MHs or LHs [19, 23, 25]. MH with VPA has been shown to be strongly associated with perifoveal intraretinal cysts, more so than LHs [11], followed by MP (Figure III.E-7). MH and LH may have more cysts compared with MP because the inner layers of the retina are severely disrupted. There was nonetheless a significantly higher prevalence of cysts in MP when VPA was present compared with when there was no VPA in MP (80 % vs. 4.3 %). These cystoid spaces are probably different from intraretinal cyst formation in exudative maculopathies (wet AMD, diabetic macular edema, etc.) where the spaces are caused by fluid, although in MP with cysts both mechanisms may contribute to cyst formation. Of course, in macular disorders with VPA, these cysts are not empty but contain fluid, yet this fluid accumulation is secondary to the pathologic tangential traction, as opposed to exudative maculopathies where it is the primary cause.

When both the specific vitreo-maculopathy and the presence or absence of intraretinal cystoid spaces are considered together, VPA is more common in MH (87.5 %), than MP with cysts (80 %), LH with cysts, (50 %) LH without cysts (20 %), and MP without cysts (4.3 %) (Figure III.E-8).

3. Vascular Disorders

a. Peripapillary, Subretinal, and Intrapapillary Hemorrhage

Peripapillary hemorrhages have been reported in patients with optic disc drusen [26–29], optic disc edema [30–32], peripapillary subretinal neovascular membranes [33, 34], and bleeding diatheses [35]. Cibis et al. first suggested a

casual relationship between PVD and retinal hemorrhages in healthy patients with moderately severe myopia based on biomicroscopic examination [13]. This was supported by another study that showed that intrapapillary hemorrhage with adjacent peripapillary subretinal hemorrhage is more common in young myopic eyes with incomplete PVD [36]. The hemorrhage usually resolves spontaneously without sequelae. Katz and Hoyt postulated that mildly dysplastic discs as seen in young myopic eyes may have unusual vitreous attachments which predispose them to premature vitreous separation except for the tenacious attachment at the optic disc [36]. Vitreo-papillary traction may traumatize disc vessels, causing hemorrhage at or near the optic disc. The shearing force may tear superficial vessels on the optic disc, causing intrapapillary hemorrhage, while transmission of the force through the retina may cause peripapillary subretinal hemorrhage.

VPA has also been hypothesized to be the inciting factor for hemorrhages due to the anatomically vulnerable prelaminar blood vessels of an elevated nasal edge of tilted optic discs in myopic eyes [37]. The cause may be multifactorial as small crowded discs are more vulnerable to vascular events and the vessels from the peripapillary choriocapillaris, choroidal branches supplying the prelaminar nerve head and branches of the posterior ciliary artery that traverse the border tissue of Elschnig in the nasal disc may all be prone to stretching, kinking, or compression in crowded-tilted optic discs [38]. An interplay of tractional forces of vitreous acting on a crowded-tilted optic disc, external forces generated by eye movements, and thinning of the sclera may all contribute to hemorrhage from the area around

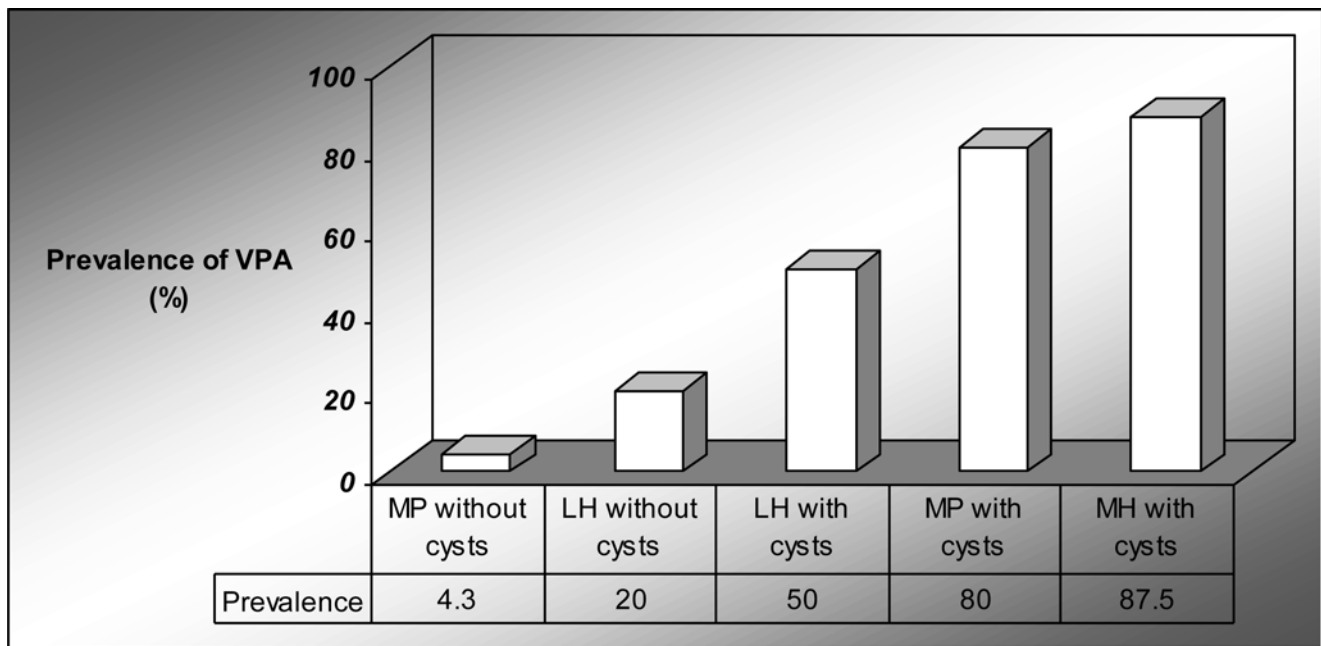


Figure III.E-8 The prevalence of vitreo-papillary adhesion (VPA) is greater in eyes with full-thickness macular holes (MH: 87.5 %) than macular pucker with cysts (MP: 80 %), lamellar macular holes

with cysts (LH: 50 %), and LH without cysts (20 %) and least in eyes with MP and no cysts (4.3 %) (Reprinted with permission from Wang et al. [11])

morphologically predisposed optic discs. The presence of myopia, nasal location of the hemorrhage, crowded and tilted disc, incomplete PVD, and preservation of visual acuity characterize this benign condition.

b. Diabetic Vitreo-Retinopathy

Diabetes is known to have biochemical and structural effects that contribute to liquefaction and destabilization of vitreous that can cause diabetic vitreopathy [39] [see chapter I.E. Diabetic vitreopathy]. This process might promote the migration and proliferation of the cells that form neovascular complexes arising from the optic disc [40]. By liquefying vitreous without weakening adhesion at the vitreo-papillary interface, diabetic vitreopathy can induce pathologic traction at the optic disc. VPA has been investigated in eyes with and without diabetic retinopathy and may be part of the natural course of diabetic retinopathy [36, 41–44]. Some have suggested that VPA may damage the anterior optic nerve by decreasing axoplasmic flow (neurogenic theory) and/or mechanical reduction of perfusion in the posterior ciliary arteries (vasogenic theory), leading to reversible changes as demonstrated by improvement in visual acuity, visual-evoked potential (VEP) latency, and amplitude following surgical removal of VPA [14]. However, irreversible optic nerve atrophy can result in the long run. In proliferative diabetic vitreo-retinopathy, VPA was mostly commonly found localized to the nasal side of the optic disc. Tractional forces on the optic disc may elongate the nerve fibers, distort the normal anatomy, and interrupt the axoplasmic transmission,

resulting in impairments of visual acuity and VEP. The abnormal contour of nerve fibers may reduce the diameter of the blood vessels, causing ischemia of the optic nerve head. Early vitrectomy may be helpful in eyes with VPA that is due to proliferative diabetic vitreo-retinopathy.

Diffuse macular edema, unresponsive to laser treatment, can be seen in some eyes with proliferative or nonproliferative diabetic retinopathy associated with VPA [45]. Two patterns of diffuse macular edema were described: one with maximum VPA thickness adjacent to the elevated optic nerve head and the other at the fovea. Contraction of the posterior vitreous cortex was thought to cause elevation and traction of the optic disc. This elevation may result in stretching and kinking of ganglion cell axons and negatively affects the prelaminar blood flow, leading to peripapillary detachment or diffuse disc edema. It was thought that posterior detachment of the vitreous begins in the macula superiorly and continues nasally towards the optic disc [46]. OCT demonstrated that age-related PVD occurs initially as a focal detachment in one quadrant of perifoveal region with persistent attachment to the fovea and optic nerve head [47]. The detachment process occurred slowly for years with the vitreo-papillary adhesion being the last thing to separate. Vitrectomy was found beneficial in some of the eyes with diabetic macular edema and without macular traction [48], suggesting that there might be other factors such as VPA playing a role in the underlying pathophysiology. Vitrectomy at the optic disc should be performed meticulously to avoid inadvertent damage to the axons that would cause permanent loss of visual acuity or visual field loss [49].

c. Central Retinal Vein Occlusion

VPA has been reported in patients with ischemic central retinal vein occlusion (CRVO), resulting in secondary serous retinal detachment involving the macula [50]. The thickened peripapillary tissue may be due to the growth of peripapillary fibrous tissue following the hemorrhagic CRVO. Lysis of vitreo-papillary and epipapillary adhesions by subretinal administration of tissue plasminogen activator, vitrectomy, and peripheral photocoagulation improved vision in a case with CRVO [43]. Release of VPA may be beneficial in some resilient cases of chronic CRVO. Vitrectomy with radial optic neurotomy has also been developed as a treatment for CRVO [see chapter V.A.6. Surgery of arterial and venous retino-vascular diseases].

C. Optic Neuropathies

1. Non-arteritic Anterior Ischemic Optic Neuropathy

Non-arteritic anterior ischemic optic neuropathy (NAION) is characterized by acute loss of vision with an associated afferent pupillary defect, an altitudinal field defect, and an optic disc edema [51–53]. The “disc at risk” is typically characterized by a small cup-to-disc ratio [54–56]. Cardiovascular diseases that might reduce perfusion pressure or increase resistance to flow within the optic nerve head, such as hypertension and diabetes, are the major risk factors. Acute systemic hypotension, obstructive sleep apnea, migraine, optic disc drusen, vasculitis, idiopathic vaso-occlusive disease, hyperopia, smoking, erectile dysfunction drugs, and hyperlipidemia have been proposed as potential risk factors [57–63]. After the initial episode, about a third of cases demonstrate modest spontaneous improvement of visual acuity (three or more Snellen lines) [52]. By 6 weeks, the optic disc starts to become atrophic.

VPA has been described in a case of NAION that included the usual manifestation of afferent pupillary defect, optic disc elevation with blurring of the disc margin, and inferior altitudinal defect [64]. VPA was confirmed on three-dimensional spectral domain OCT. It was hypothesized that the eyes with small crowded discs may be more vulnerable to the distorting force of vitreous traction. The disc elevation may be asymptomatic initially and resolve if the posterior vitreous detaches from the optic nerve head. However, if VPA persists, the microvascular circulation and/or axoplasmic flow may result in dysfunction and swelling of the optic nerve, leading to the clinical picture of NAION. This was initially proposed by Hoyt as an important cause of NAION [36]. Modarres et al. performed vitrectomy on 16 patients with vitreo-papillary traction and NAION, and this resulted in ≥ 3 lines of improvement in visual acuity for 56 % as compared to 39.5 % in the nontreatment group in the Ischemic

Optic Neuropathy Decompression Trial [15], confirming that VPA may have a causative role in some cases of NAION and its removal may be beneficial in such cases.

2. Gaze-Evoked Amaurosis

Gaze-evoked amaurosis (GEA) is a rare condition described as transient obscuration of vision occurring during and precipitated by eccentric positions of gazes [65–69]. GEA most often is a result of intraconal pathology such as optic nerve sheath meningiomas and cavernous hemangiomas, but it can also be caused by extraorbital processes that exert pressure on the orbit and optic nerve. The common etiology appears to be compromise of the retinal or optic nerve circulation by disruption of the central retinal artery or optic nerve microvasculature [70]. Although historically GEA was associated with an orbital mass, it has infrequently been associated with non-orbital mass such as idiopathic intracranial hypertension (IIH) [71, 72]. Eccentric eye movements may cause pressures to increase within an already tensely dilated optic nerve sheath in IIH, precipitating amaurosis. GEA has also been associated with incomplete PVD and vitreo-papillary traction [16]. Katz et al. reported four patients with gaze-evoked GEA who had disc edema associated with VPA. The authors speculated that the initiating vitreous separation is incomplete with persistent juxtapapillary adherence, which tugs at the optic disc and elevates the optic nerve head. This may represent one phase of a slowly evolving vitreous separation with some temporary VPA and traction to the peripapillary retina, disc, and nerve fibers. The transient visual phosphenes noted by patients and precipitated by eye movements may be caused by traction transmitted from the vitreous to the superficial nerve fibers of the optic disc. Furthermore, the inertial drag induced by the posterior vitreous may cause physical deformation of the nerve fibers and interfere with the transmission of axonal discharge either in an anterograde or retrograde direction. This may serve as a mechanically induced transient blockade of sensory neuroretinal signal and induce transient GEA [73]. All patients who present with GEA should be carefully evaluated for underlying orbital processes. Although VPA is a rare cause, patients with otherwise unexplained GEA should also undergo evaluation of the vitreo-retinal interface.

VPA can cause optic nerve head elevation, which can lead to obscuration of the optic disc margins, peripapillary hemorrhage, and disc leakage on fluorescein angiography, simulating optic disc edema or papilledema [74], which may confound the diagnosis. In such cases, OCT can help make the correct diagnosis and avoid unnecessary expensive and more invasive procedures such as contrast neuroimaging and lumbar puncture [75, 76].

Meyer et al. described a case of chronic visual impairment induced by VPA [77]. The authors reported immediate

functional improvement after surgical release and speculated that physical deformation, via stretching and thinning of the retinal nerve fiber layer, reduced the axoplasmic flow. They felt that this produced a sensory blockade as evidenced by visual-evoked potentials. Mechanical restrictions of the central retinal blood vessels may have also decreased the prelaminar blood flow. This and similar reports suggest that vitrectomy may be a reasonable treatment strategy in some cases with VPA.

3. Optic Nerve Pit

An optic nerve pit is a rare condition typically presents unilaterally in the inferotemporal segment of the optic disc, frequently associated with serous detachment of the macula or cystoid retinal edema. Many have considered optic nerve pits as a variant of optic disc coloboma secondary to incomplete closure of the optic fissure during development. However, the pathophysiology of optic nerve pits remains controversial due to the unilateral and sporadic nature as well as lack of systemic association. Lincoff et al. documented the natural progression of optic nerve pits based on stereoscopic transparency studies of 15 eyes with optic pits in 1988 [78]. Initially, fluid from the pit leads to elevation of the nerve fiber layer, resulting in schisis-like separation of the internal layers of the retina. Beneath the inner layer, an outer macular hole develops, which eventually leads to an outer layer detachment around the macular hole due to movement of the fluid. Later, the outer layer detachment increases, resembling serous detachment. Optic nerve pits are usually asymptomatic unless the macula is involved.

There is no standardized single treatment for optic nerve pits. More recently, the release of vitreous traction has become an important factor in the management of those patients [see chapter V.B.9. Rare indications for vitrectomy: tumor excision, optic nerve pits, malignant glaucoma]. Hirakata et al. studied the outcome of pars plana vitrectomy without gas tamponade or laser photocoagulation in eight patients with unilateral macular detachment associated with optic disc pit [79]. Complete retinal reattachment was achieved in seven of eight eyes without recurrence. Postoperative OCT demonstrated a reduction in the retinal elevation adjacent to the optic disc and a decrease in the inner retinoschisis-like separation, followed by slow but complete resolution of macular detachment. Hence, VPA-induced traction alone appears to be an important factor in the pathogenesis of optic disc pit maculopathy. The OCT analyses suggest that VPA may create a passage for fluid to enter the retina through the pit, resulting in schisis-like separation seen in optic disc pit maculopathy. Vitrectomy alone, by removing the traction around the entrance cavity, can be an effective treatment for optic disc pit maculopathy.

Conclusion

The vitreo-retinal interface and its role in retinal diseases have recently gained considerable attention. However, VPA and its role in a wide spectrum of diseases are still insufficiently recognized. It is important for clinicians to understand that the vitreo-papillary interface consists of many intricate cellular relations and that anomalous PVD with persistent VPA may induce distortion of cellular architecture. Stretching and thinning of the retinal nerve fiber layer, reductions in axonal transmission, and impairment of the peripapillary microvascular supply may all contribute to visual loss. OCT is an important tool to visualize the vitreo-papillary interface and detect VPA, allowing us to detect previously unrecognizable diseases in a noninvasive manner. Visualization of the vitreo-papillary interface helps elucidate the pathogenesis of various diseases characterized by VPA and allows for a more cogent approach to treatment.

Abbreviations

CRVO	Central Retinal Vein Occlusion
GEA	Gaze-Evoked Amaurosis
IIH	Idiopathic Intracranial Hypertension
ILM	Inner Limiting Membrane
LH	Lamellar Hole
MH	Macular Hole
MP	Macular Pucker
NAION	Non-Arteritic Anterior Ischemic Optic Neuropathy
OCT	Optical Coherence Tomography
PVD	Posterior Vitreous Detachment
VEP	Visual Evoked Potential
VPA	Vitreo-Papillary Adhesion

References

1. Russell SR, Shepherd JD, Hageman GS, et al. Distribution of glycoconjugates in the human internal limiting membrane. *Invest Ophthalmol Vis Sci.* 1991;32:1986.
2. Nishitsuka K, Kashiwagi Y, Tojo N, et al. Hyaluronan production regulation from porcine hyalocyte cell line by cytokines. *Exp Eye Res.* 2007;85:539–45.
3. Kita T, Hata Y, Kano K, et al. Transforming growth factor-beta2 and connective tissue growth factor in proliferative vitreoretinal diseases: possible involvement of hyalocytes and therapeutic potential of Rho kinase inhibitor. *Diabetes.* 2007;56:231–8.
4. Sebag J. Anomalous posterior vitreous detachment: a unifying concept in vitreo-retinal disease. *Graefes Arch Clin Exp Ophthalmol.* 2004;42:690–8.

5. Sebag J. Classifying posterior vitreous detachment: a new way to look at the invisible. *Br J Ophthalmol*. 1997;81:521.
6. Heergaard S, Jensen OA, Prause JU, et al. Structure of the vitreal face of the monkey optic disc (*Macaca mulatta*): SEM on frozen resin-cracked optic nerve heads supplemented by TEM and immunohistochemistry. *Graefes Arch Clin Exp Ophthalmol*. 1988;226:377.
7. Grabner G, Baltz G, Forster O, et al. Macrophage-like properties of human hyalocytes. *Invest Ophthalmol Vis Sci*. 1980;19:333.
8. Roth AM, Foos RY. Surface structure of the optic nerve head. I. Epipapillary membranes. *Am J Ophthalmol*. 1972;74:977–85.
9. Foos RY, Roth AM. Surface structure of the optic nerve head. II. Vitreopapillary attachments and posterior vitreous detachment. *Am J Ophthalmol*. 1973;76:662–71.
10. Schepens CL. Clinical aspects of pathologic changes in the vitreous body. *Am J Ophthalmol*. 1954;38:8–21.
11. Wang MY, Nguyen D, Hindoyan N, et al. Vitreo-papillary adhesion in macular hole and macular pucker. *Retina*. 2009;29:644–50.
12. Sebag J, Wang M, Nguyen D, et al. Vitreopapillary adhesion in macular diseases. *Trans Am Ophthalmol Soc*. 2009;107:35–44.
13. Cibis GW, Watzke RC, Chua J, et al. Retinal hemorrhages in posterior vitreous detachment. *Am J Ophthalmol*. 1975;80:1043–6.
14. Kroll P, Wiegand W, Schmidt J, et al. Vitreopapillary traction in proliferative diabetic vitreoretinopathy. *Br J Ophthalmol*. 1999;83:261–4.
15. Modarres M, Sanjari MS, Falavarjani KG. Vitrectomy and release of presumed epipapillary vitreous traction for treatment of nonarteritic anterior ischemic optic neuropathy associated with partial posterior vitreous detachment. *Ophthalmology*. 2007;114:340–4.
16. Katz B, Hoyt C. Gaze-evoked amaurosis from vitreopapillary traction. *Am J Ophthalmol*. 2005;139:631–7.
17. Sebag J. Anatomy and pathology of the vitreo-retinal interface. *Eye (Lond)*. 1992;6:541–52.
18. Sebag J, Gupta P, Rosen R, Garcia P, Sadun AA. Macular holes and macular pucker: the role of vitreoschisis as imaged by optical coherence tomography/scanning laser ophthalmoscopy. *Trans Am Ophthalmol Soc*. 2007;105:121–31.
19. Gaudric A, Haouchine B, Massin P, Paques M, Blain P, Erginay A. Macular hole formation: new data provided by optical coherence tomography. *Arch Ophthalmol*. 1999;117:744–51.
20. Tanner V, Chauhan DS, Jackson TL, Williamson TH. Optical coherence tomography of the vitreoretinal interface in macular hole formation. *Br J Ophthalmol*. 2001;85:1092–7.
21. Chauhan DS, Antcliff RJ, Rai PA, Williamson TH, Marshall J. Papillofoveal traction in macular hole formation: the role of optical coherence tomography. *Arch Ophthalmol*. 2000;118:32–8.
22. Haouchine B, Massin P, Tadayoni R, Erginay A, Gaudric A. Diagnosis of macular pseudoholes and lamellar macular holes by optical coherence tomography. *Am J Ophthalmol*. 2004;138:732–9.
23. Haouchine B, Massin P, Gaudric A. Foveal pseudocyst as the first step in macular hole formation: a prospective study by optical coherence tomography. *Ophthalmology*. 2001;108:15–22.
24. Romano MR, Vallejo-Garcia JL, Camesasca FI, Vinciguerra P, Costagliola C. Vitreopapillary adhesion as a prognostic factor in pseudo- and lamellar macular holes. *Eye (Lond)*. 2012;26:810–5.
25. Jaffe GJ, Caprioli J. Optical coherence tomography to detect and manage retinal disease and glaucoma. *Am J Ophthalmol*. 2004;137:156–69.
26. Harris MJ, Fine SL, Owens SL. Hemorrhagic complications of optic nerve drusen. *Am J Ophthalmol*. 1981;92:70–6.
27. Hitchings RA, Corbett JJ, Winkleman J, et al. Hemorrhages with optic nerve drusen: a differentiation from early papilledema. *Arch Neurol*. 1976;33:675–7.
28. Sanders TE, Gay AJ, Newman M. Hemorrhagic complications of drusen of the optic disk. *Am J Ophthalmol*. 1971;71:204–17.
29. Sanders TE, Gay AJ, Newman M. Drusen of the optic disk hemorrhagic complications. *Trans Am Ophthalmol Soc*. 1970;68:186–218.
30. Orcutt JC, Page NG, Sanders MD. Factors affecting visual loss in benign intracranial hypertension. *Ophthalmology*. 1984;91:1303–12.
31. Castellarin AA, Sugino IK, Nasir M, et al. Clinicopathological correlation of an excised choroidal neovascular membrane in pseudotumour cerebri. *Br J Ophthalmol*. 1997;81:994–1000.
32. Suzuki N, Takeda M, Takeda M, et al. Preretinal and retinal hemorrhage due to chronic subdural hematoma. *Ann Ophthalmol*. 1985;17:494–7.
33. Browning DJ, Fraser CM. Ocular conditions associated with peripapillary subretinal neovascularization, their relative frequencies, and associated outcomes. *Ophthalmology*. 2005;112:1054–61.
34. Meredith TA, Aaberg TM. Hemorrhagic peripapillary lesions in presumed ocular histoplasmosis. *Am J Ophthalmol*. 1977;84:160–8.
35. Shiono T, Abe S, Watabe T, et al. Vitreous, retinal and subretinal hemorrhages associated with von Willebrand's syndrome. *Graefes Arch Clin Exp Ophthalmol*. 1992;30:496–7.
36. Katz B, Hoyt WF. Intrapapillary and peripapillary hemorrhage in young patients with incomplete posterior vitreous detachment: signs of vitreopapillary traction. *Ophthalmology*. 1995;102:349–54.
37. Kokame GT, Yamamoto I, Kishi S, et al. Intrapapillary hemorrhage with adjacent peripapillary subretinal hemorrhage. *Ophthalmology*. 2004;111:926–30.
38. Sibony P, Fourman S, Honkanen R, El Baba F. Asymptomatic peripapillary subretinal hemorrhage: a study of 10 cases. *J Neuroophthalmol*. 2008;28:114–9.
39. Sebag J, Buckingham B, Charles MA, Reiser K. Biochemical abnormalities in vitreous of humans with proliferative diabetic retinopathy. *Arch Ophthalmol*. 1992;110:1472–9.
40. Sebag J. Diabetic vitreopathy [editorial]. *Ophthalmology*. 1996;103:205–6.
41. de Bustros S, Thompson JT, Michels RG, Rice TA. Vitrectomy for progressive proliferative diabetic retinopathy. *Arch Ophthalmol*. 1987;105:196–9.
42. Kroll P, Wiegand W, Schmidt J. Traction vitreoretinal opticopathy in proliferative diabetic vitreoretinopathy. *Ophthalmologie*. 1995;92:687–91.
43. Lam HD, Blumenkranz MS. Treatment of central retinal vein occlusion by vitrectomy with lysis of vitreopapillary and epipapillary adhesions, subretinal peripapillary tissue plasminogen activator injection and photocoagulation. *Am J Ophthalmol*. 2002;134:609–11.
44. Wisotsky BJ, Magat-Gordon CB, Puklin JE. Vitreopapillary traction as a cause of elevated optic nerve head. *Am J Ophthalmol*. 1998;126:137–8.
45. Karatas M, Ramirez JA, Ophir A. Diabetic vitreopapillary traction and macular oedema. *Eye (Lond)*. 2005;19:676–82.
46. Foos RY. Posterior vitreous detachment. *Trans Am Acad Ophthalmol Otolaryngol*. 1972;76:480–97.
47. Uchino E, Uemura A, Ohba N. Initial stages of posterior vitreous detachment in healthy eyes of older persons evaluated by optical coherence tomography. *Arch Ophthalmol*. 2001;119:1475–9.
48. La Heij EC, Hendrikse F, Kessels AG, Derhaag PJ. Vitrectomy results in diabetic macular edema without evident vitreomacular traction. *Graefes Arch Clin Exp Ophthalmol*. 2001;239:264–70.
49. Pendergast SD, Martin DF, Proia AD, Jaffe GJ, McCuen II BW. Removal of optic disc stalks during diabetic vitrectomy. *Retina*. 1995;15:25–8.
50. Rumelt S, Karatas M, Pikkel J, Majlin M, Ophir A. Optic disc traction syndrome associated with central retinal vein occlusion. *Arch Ophthalmol*. 2003;121:1093–7.

51. Hayreh SS, Zimmerman MB. Nonarteritic anterior ischemic optic neuropathy: natural history of visual outcome. *Ophthalmology*. 2008;115:298–305.e2.
52. Hayreh SS. Ischemic optic neuropathy. *Prog Retin Eye Res*. 2009;28:34–62.
53. Hayreh SS. Anterior ischemic optic neuropathy. VIII. Clinical features and pathogenesis of post-hemorrhagic amaurosis. *Ophthalmology*. 1987;94:1488–502.
54. Arnold AC. Pathogenesis of nonarteritic anterior ischemic optic neuropathy. *J Neuroophthalmol*. 2003;23:157–63.
55. Hayreh SS. Risk factors in AION. *Ophthalmology*. 2001;108:1717–8.
56. Burde RM. Optic disk risk factors for nonarteritic anterior ischemic optic neuropathy. *Am J Ophthalmol*. 1993;116:759–64.
57. Hayreh SS, Zimmerman MB, Podhajsky P, Alward WL. Nonarteritic anterior ischemic optic neuropathy: role of nocturnal arterial hypotension. *Arch Ophthalmol*. 1997;115:942–5.
58. Hayreh SS. Erectile dysfunction drugs and non-arteritic anterior ischemic optic neuropathy: is there a cause and effect relationship? *J Neuroophthalmol*. 2005;25:295–8.
59. Hayreh SS, Jonas JB, Zimmerman MB. Nonarteritic anterior ischemic optic neuropathy and tobacco smoking. *Ophthalmology*. 2007;114:804–9.
60. Hayreh SS, Joos KM, Podhajsky PA, Long CR. Systemic diseases associated with nonarteritic anterior ischemic optic neuropathy. *Am J Ophthalmol*. 1994;118:766–80.
61. Hayreh SS. Postcataract extraction ischemic optic neuropathy. *Arch Ophthalmol*. 1982;100:1853–4.
62. Bilgin G, Koban Y, Arnold AC. Nonarteritic anterior ischemic optic neuropathy and obstructive sleep apnea. *J Neuroophthalmol*. 2013;33:232–4.
63. Fraunfelder FW, Pomeranz HD, Egan RA. Nonarteritic anterior ischemic optic neuropathy and sildenafil. *Arch Ophthalmol*. 2006;124:733–4.
64. Nomura Y, Tamaki Y, Yanagi Y. Vitreopapillary traction diagnosed by spectral domain optical coherence tomography. *Ophthalmic Surg Lasers Imaging*. 2010;41(Suppl):S74–6.
65. Otto C, Coppit G, Mazzoli R, et al. Gaze-evoked amaurosis : a report of five cases. *Ophthalmology*. 2003;110:322–6.
66. Hampton G, Krohel G. Gaze-evoked blindness. *Ann Ophthalmol*. 1983;15:74–6.
67. Brown G, Shields J. Amaurosis fugax secondary to presumed cavernous hemangioma of the orbit. *Ann Ophthalmol*. 1981;13:1205–9.
68. Orcutt J, Tucker W, Mills R, Smith C. Gaze-evoked amaurosis. *Ophthalmology*. 1987;94:213–8.
69. Knapp ME, Flaharty P, Sergott R, Savino P, Mazzoli R, Flanagan J. Gaze-induced amaurosis from central retinal artery compression. *Ophthalmology*. 1992;99:238–40.
70. Manor RS, Yassur Y, Hoyt WF. Reading-evoked visual dimming. *Am J Ophthalmol*. 1996;121:212–4.
71. O'Duffy D, James B, Elston J. Idiopathic intracranial hypertension presenting with gaze-evoked amaurosis. *Acta Ophthalmol Scand*. 1998;76:119–20.
72. Pascual J, Combarros O, Berciano J. Gaze-evoked amaurosis in pseudotumor cerebri. *Neurology*. 1988;38:1654–5.
73. Nebel B. The phosphenes of quick eye motion. *Arch Ophthalmol*. 1957;58:235.
74. Houle E, Miller NR. Bilateral vitreopapillary traction demonstrated by optical coherence tomography mistaken for papilledema. *Case Rep Ophthalmol Med*. 2012;2012:682659.
75. Cabrera S, Katz A, Margalit E. Vitreopapillary traction: cost-effective diagnosis by optical coherence tomography. *Can J Ophthalmol*. 2006;41:763–5.
76. Hedges 3rd TR, Flattem NL, Bagga A. Vitreopapillary traction confirmed by optical coherence tomography. *Arch Ophthalmol*. 2006;124:279–81.
77. Meyer CH, Schmidt JC, Mennel S, Kroll P. Functional and anatomical results of vitreopapillary traction after vitrectomy. *Acta Ophthalmol Scand*. 2007;85:221–2.
78. Lincoff H, Lopez R, Kreissig I, Yannuzzi L, Cox M, Burton T. Retinoschisis associated with optic nerve pits. *Arch Ophthalmol*. 1988;106:61–7.
79. Hirakata A, Inoue M, Hiraoka T, McCuen 2nd BW. Vitrectomy without laser treatment or gas tamponade for macular detachment associated with an optic disc pit. *Ophthalmology*. 2012;119:810–8.
80. Sebag J. Age-related differences in the human vitreo-retinal interface. *Arch Ophthalmol*. 1991;109:966–71.

Kevin Tozer and J. Sebag

Outline

- I. **Introduction**
- II. **Epidemiology**
- III. **Anatomy**
 - A. Vitreoretinal Interface
- IV. **Pathology**
 - A. Structure and Composition of Macular Pucker Membranes
- V. **Pathophysiology**
 - A. Pathophysiology of Visual Disturbance in Macular Pucker
- VI. **Clinical Presentation**
 - A. Distinguishing Macular Pucker from Vitreo-Macular Traction Syndrome
 - B. Measuring the Impact of Macular Pucker on Vision

Conclusion

References

Electronic supplementary material Supplementary material is available in the online version of this chapter at [10.1007/978-1-4939-1086-1_18](https://doi.org/10.1007/978-1-4939-1086-1_18). Videos can also be accessed at <http://www.springerimages.com/videos/978-1-4939-1085-4>.

K. Tozer, MD
VMR Institute for Vitreous Macula Retina,
7677 Center Avenue, suite 400, Huntington Beach,
CA 92647, USA

Doheny Eye Institute, Los Angeles, CA USA

Department of Ophthalmology and Visual Sciences,
Kellogg Eye Center, University of Michigan,
1000 Wall Street, Ann Arbor, MI 48105, USA
e-mail: ktozer@med.umich.edu

J. Sebag, MD, FACS, FRCOphth, FARVO (✉)
VMR Institute for Vitreous Macula Retina,
7677 Center Avenue, suite 400, Huntington Beach,
CA 92647, USA

Doheny Eye Institute, Los Angeles, CA USA
e-mail: jsebag@VMRinstitute.com

Keywords

Vitreous • Anomalous posterior vitreous detachment • Vitreoschisis • Premacular membrane • Hyalocytes • Macular pucker • Vitreo-macular traction • Vitreo-foveal traction syndrome • IS/OS junction • Distortions • Inner limiting membrane (ILM)

Key Concepts

1. Macular pucker pathogenesis begins with anomalous posterior vitreous detachment and vitreoschisis, leaving the outer layer of the posterior vitreous cortex attached to the macula, forming a relatively thick premacular membrane.
2. The vitreoschisis split occurs anterior to the level of hyalocytes, leaving these cells attached to the retina while the rest of the vitreous cortex detaches away from the macula and optic disc. Hyalocytes elicit cell migration from the circulation and retina to form hypercellular membranes with contractile properties in a tangential plane.
3. Visual disturbance in macular pucker is due to disruption in multiple layers of the retina. Quantifying distortions will provide a useful means for clinical assessment of disease severity and an outcome measure for therapeutic intervention.

I. Introduction

First described in 1865 by Iwanoff [1], macular pucker has been extensively studied and researched under a variety of names, including *cellophane maculopathy*, *epiretinal membrane*, *preretinal fibrosis*, *epiretinal fibrosis*, and *surface wrinkling retinopathy* [2, 3]. Macular pucker can be defined

as a premacular, avascular, fibrocellular membrane with folds and striae in the underlying inner retina and disturbed cytoarchitecture in the outer retina [4, 5]. The term “epiretinal membrane (ERM)” is most often employed, although it is not as accurate as the term “premacular membrane (PMM).” One reason why PMM is more accurate is that the membrane is always anterior to the retina, while the term “epiretinal” means adjacent to the retina and can refer to subretinal membranes. Further, the membrane is only clinically relevant when attached to the macula. Thus, the preferred terminologies are “premacular membrane (PMM)” to refer to the pathologic membrane itself and “macular pucker (MP)” to refer to the effects of this membrane on the macula. This chapter will review the prevailing theories of pathophysiology and the mechanism(s) of visual impairment caused by macular pucker.

II. Epidemiology

Macular pucker is quite common. With approximately 30 million people affected in the US alone, it ranks as one of the most common vitreoretinal disorders. In the general adult population, the overall prevalence of macular pucker is between 6 and 11.8 % [6–8]. Over the age of 70, the prevalence has been reported as high as 15.1 % [8]. In a population of healthy adults over age of 50, the 5-year incidence of developing macular pucker may be as high as 5.3 % [3].

Risk factors for the development of macular pucker include both modifiable and non-modifiable characteristics. The greatest risk factor is advanced age, with most cases of MP diagnosed after the age of 50 [9, 10]. However, macular pucker has also been described in people under 30 [11, 12]. Other documented risk factors include high cholesterol, diabetes (even without retinopathy), smoking, and recent eye surgery, especially scleral buckling [2, 6, 13]. There does not appear to be a gender preference in adults [6, 8], but among pediatric cases, boys are preferentially affected [13]. Regarding ethnicity, Asians (specifically Chinese) may have a higher prevalence than do Caucasians, African Americans, or Hispanics [2].

III. Anatomy

As is the case throughout the body, macular pucker’s appearances are the consequence of the underlying anatomy, in this case involving both vitreous and the macula. Figure III.F-1 presents a schematic of vitreous anatomy, but a more thorough discussion of vitreoretinal interface anatomy can be found elsewhere in this book [see chapter II.F. Vitreo-retinal interface and ILM].

A. Vitreoretinal Interface

To fully understand macular pucker pathobiology requires an appreciation of vitreoretinal interface anatomy, which consists of three parts: the inner limiting membrane (ILM), posterior vitreous cortex (PVC), and the intervening extracellular matrix (ECM). [see chapter II.E. Vitreo-retinal interface and inner limiting membrane].

The ILM is the innermost layer of the retina. Its embryologic origin is the neural ectoderm that enters the eye during the invagination of the optic vesicle. In effect, it is the basal lamina for the interface between the retina and the vitreous [14]. Structurally, it is composed mainly of type IV collagen and associated glycoproteins. It has a lamina rara that is immediately adjacent to the Müller cells of the retina and is between 0.03 and 0.06 μm thick, which is consistent throughout the fundus. Anterior to the lamina rara is the lamina densa, which borders the posterior vitreous cortex. It can be as thick as 3.2 μm in some areas, but is thinnest (only 0.01–0.02 μm) around the fovea. Knowing the relative thickness of the ILM is important, because numerous studies have demonstrated that the vitreous is more adherent to the retina in areas where the ILM is thinnest, i.e., in the perifoveal region [15, 16]. In the posterior pole the posterior aspect of the ILM is irregular with interdigitating glial cells, while the anterior surface is smooth [17] (Figure III.F-2). The ILM ceases at the edge of the optic disc where the basal lamina of the optic nerve astroglia form the inner limiting membrane of Elschnig [18] [see chapter III.E. Vitreo-papillary adhesion/traction].

The posterior vitreous cortex (PVC) extends posteriorly from the posterior border of the vitreous base and is composed mostly of vitreous collagen fibrils and hyaluronan. The thickness of the PVC is fairly constant between 100 and 110 μm except in the macula where it thins considerably. Embedded within the PVC are numerous hyalocytes approximately 20–50 μm from the ILM (Figure III.F-3). Hyalocytes are oval-shaped mononuclear phagocytes that are members of the reticuloendothelial system [19]. One of their main functions in vitreous is to help maintain transparency via their phagocytic and anti-migratory/proliferative activity. Equally important is their role as sentinel cells. Residing at the vitreo-retinal interface, these cells are the first to be exposed to any noxious stimuli and respond by eliciting monocyte migration from the circulation into the region. This accounts for the hypercellularity of a variety of disorders at the vitreoretinal interface. Additionally, hyalocytes likely play a key role in the development and contraction of premacular membranes inducing pucker [20–22] [see chapter II.D. Hyalocytes].

Between the ILL and PVC is the extracellular matrix (ECM), which serves as the “glue” that anchors vitreous to the ILL and in turn to the retina. Components of this ECM include fibronectin, laminin, chondroitin sulfate, heparin sulfate, and opticin among others [22, 23]. Further characterizing

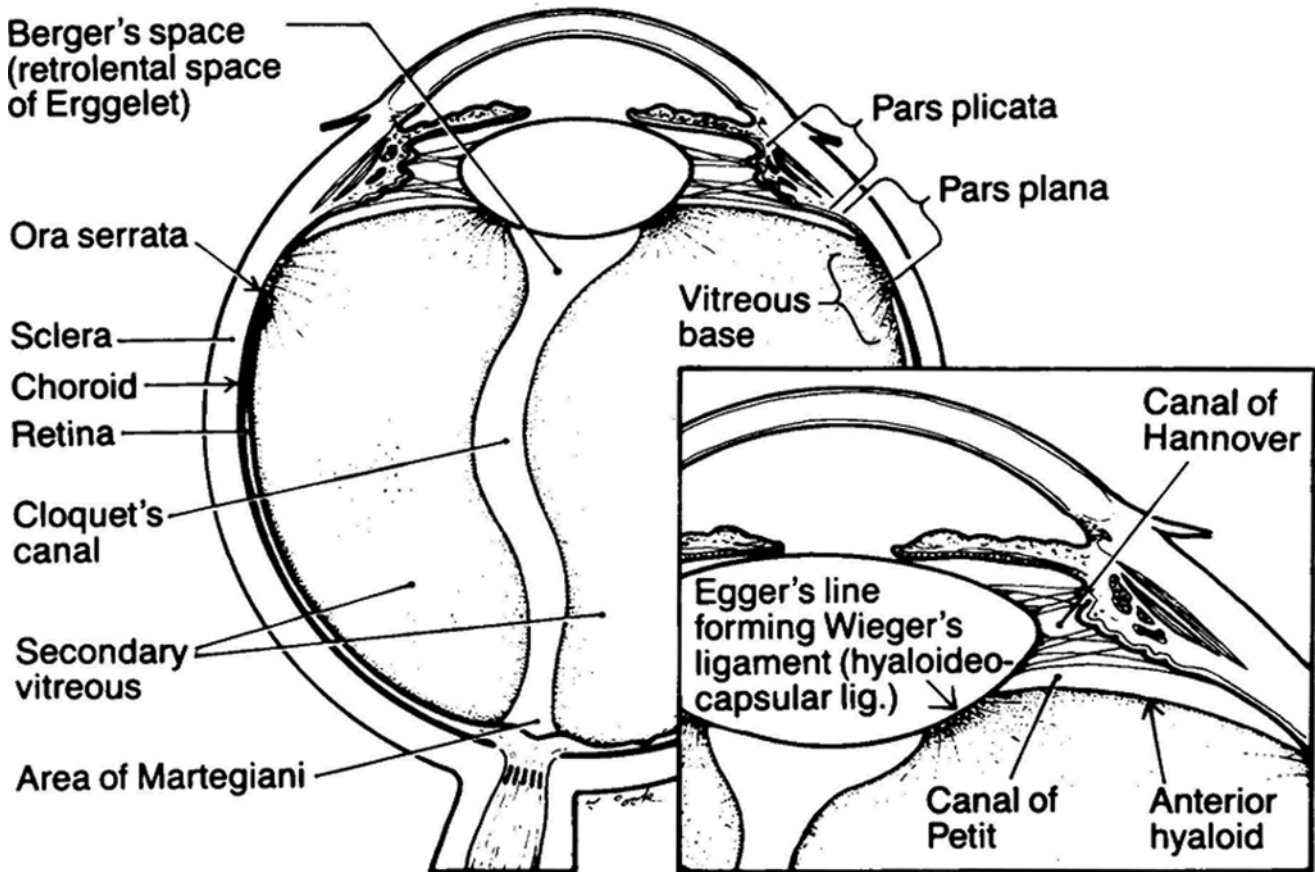


Figure III.F-1 Schematic diagram of vitreous anatomy [40]

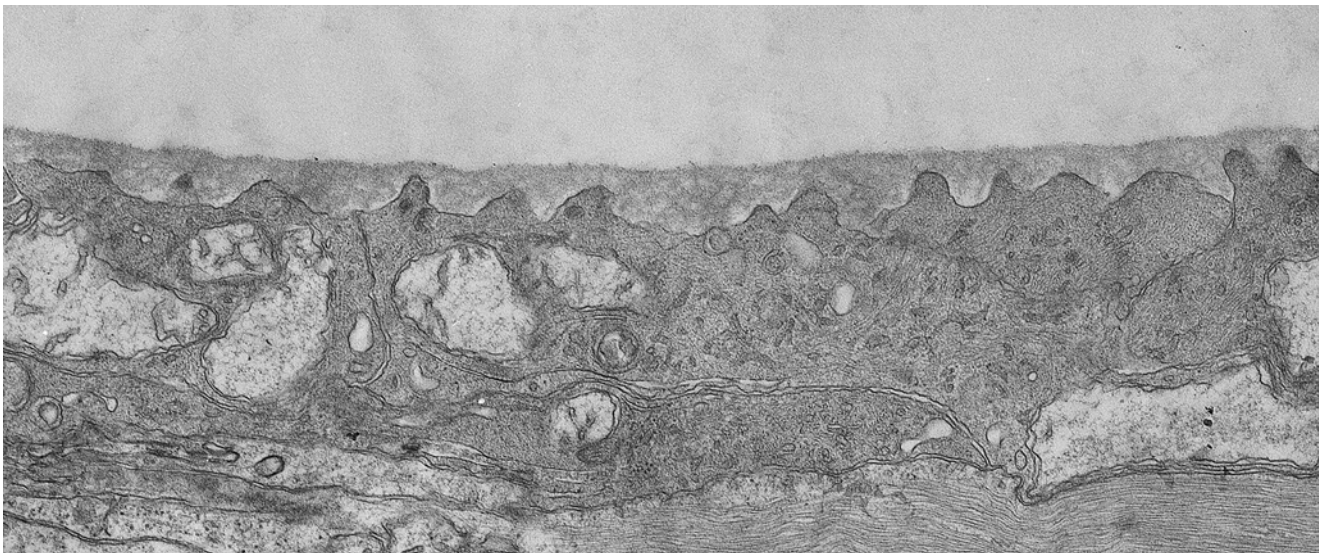


Figure III.F-2 Transmission electron micrograph demonstrating the smooth anterior surface and the irregular, undulating posterior surface of the human inner limiting membrane (ILM). This configuration is only seen in the posterior pole. At the equator, both anterior and posterior aspects of the ILM are smooth, without undulations

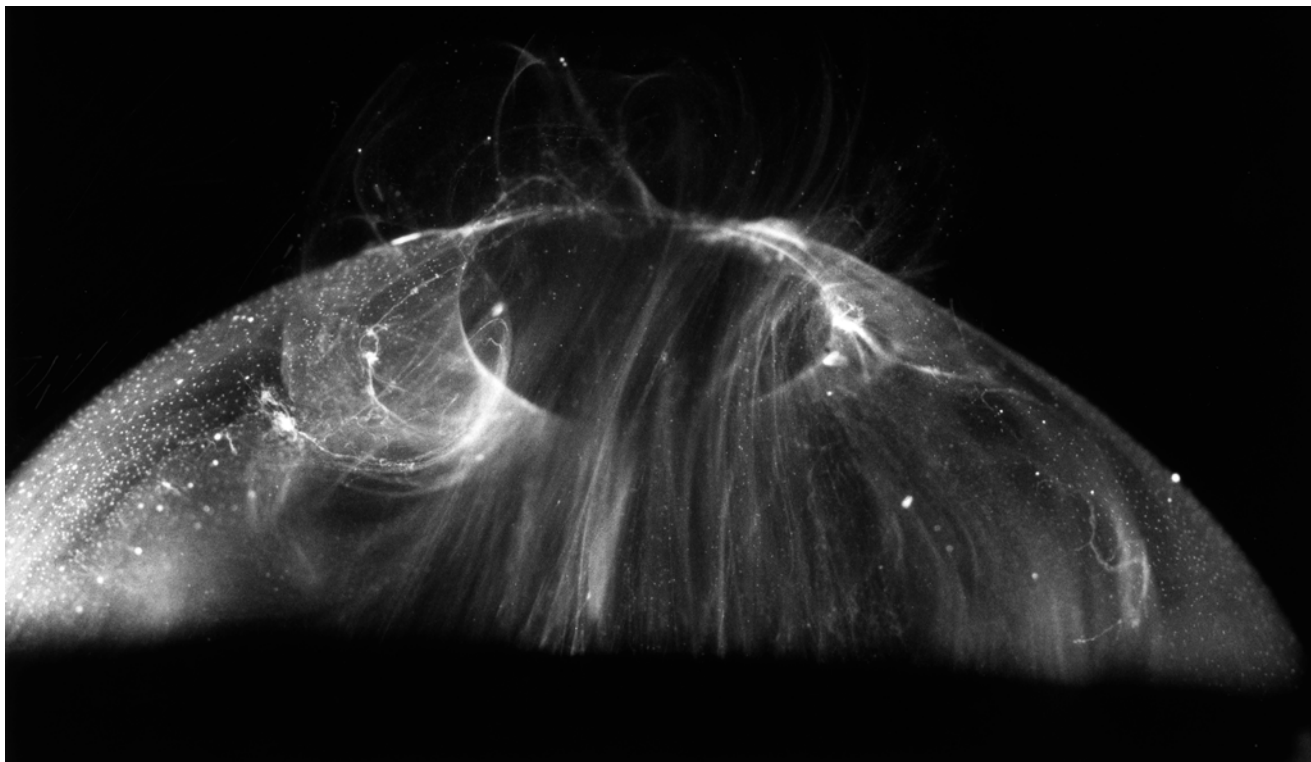


Figure III.F-3 Human hyalocytes *in situ* visualized with postmortem dark-field slit microscopy of the whole vitreous body from a 59-year-old male. Hyalocytes appear as small white dots in the posterior vitreous cortex. Large dots are debris

these extracellular components is crucial because they serve as therapeutic targets for a new treatment modality known as pharmacologic vitreolysis [24–30] that is intended to liquefy the gel vitreous and weaken vitreoretinal adhesion [see chapter VI.A. Pharmacologic vitreolysis].

IV. Pathology

Given the aforementioned prevalence of macular pucker and the frequent and growing incidence of surgical correction, there has been ample opportunity to study the histopathology of macular pucker in both human autopsy specimens and tissue removed at surgery.

A. Structure and Composition of Macular Pucker Membranes

The original studies on ultrastructure of simple premacular membranes responsible for macular pucker were performed by Foos [4, 31] in the early 1970s. His microscopic examinations concluded that the membranes are made exclusively of astroglial cells and their long flat processes. Each individual glial cell could cover a distance of up to 300 μm along the surface of the retina. Additionally the glial cells could be stacked verti-

cally several cells thick or are thin as only two cells in some places. According to his studies, the vitreous fibers only rarely intermingled with the glial cell process. Instead, the vitreous was simply adjacent to, but not mixed in with, the premacular membrane [31]. This is in contrast to epipapillary membranes where the vitreous was found to interdigitate more frequently [32], perhaps related to the strong adhesion between vitreous and the optic disc and immediate peripapillary retina. Foos concluded that the cells were derived from accessory glia in the retina that had migrated through microbreaks in the retina, although such breaks were only rarely found in the samples studied [4, 31]. Further studies by this group went on to describe the nature of more complex premacular membranes. The term “complex” was used to describe membranes associated with the production of a novel basement membrane and underlying retinal wrinkling [33]. Snead and colleagues [34] have coined the term “laminocytes” to describe the main cellular components of premacular membranes. Immunohistochemistry was positive for glial fibrillary acidic protein (GFAP) confirming their glial origin (Figure III.F-4). Laminocytes also stained positively for cytokeratin marker AE1/AE3 which can indicate epithelial cell origin, but is also broadly reactive and very non-specific. Indeed, histologically, laminocytes are the same cells described by Foos as astroglial cells [35] and thus the term “*laminocytes*” has not found widespread acceptance and use [36] and will not be employed herein.

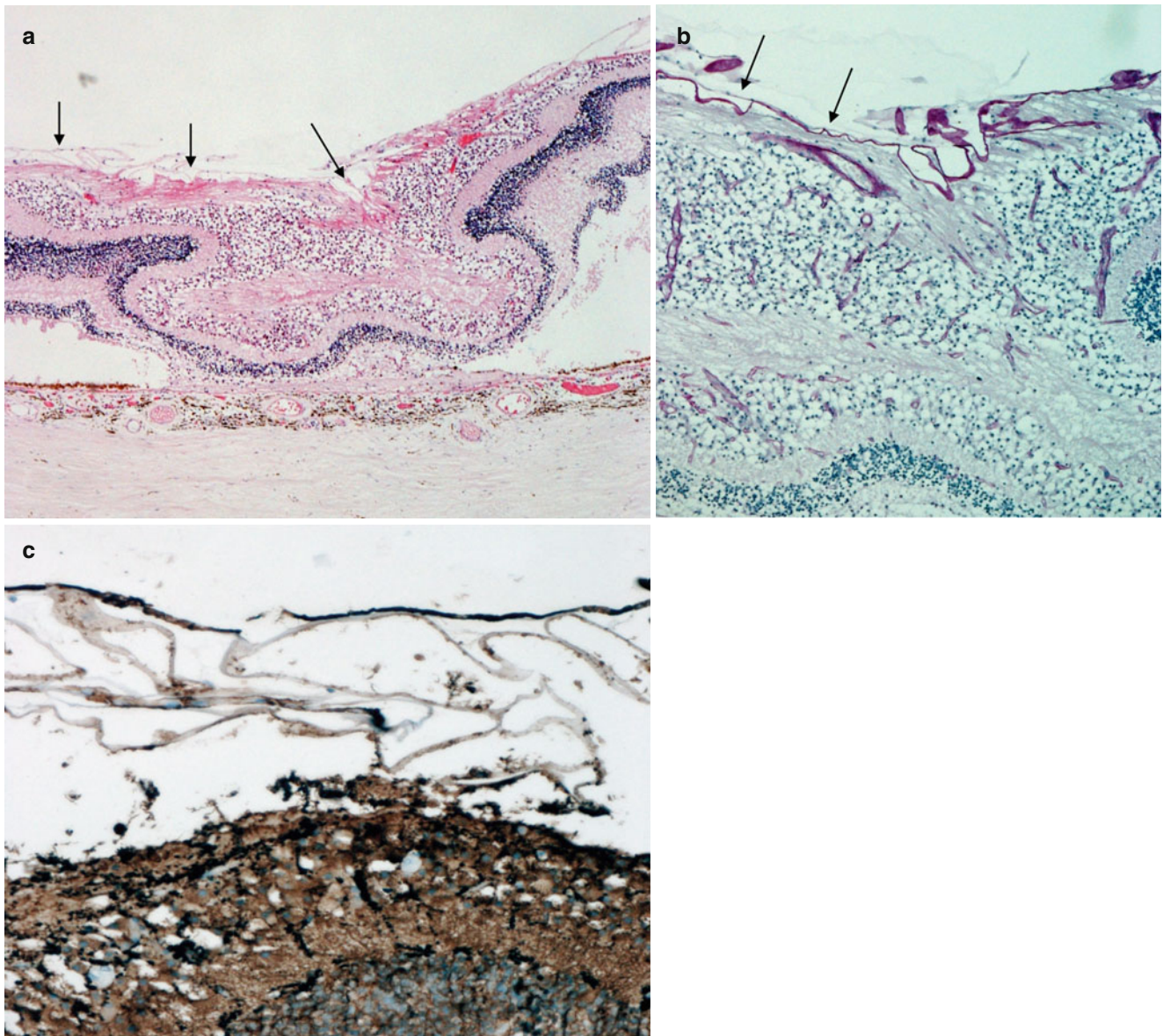


Figure III.F-4 Postmortem specimens from a case of macular pucker. Hematoxylin and eosin stain (a) and DPAS stain (b) of retina showing hyperconvolution of the ILM (arrows). GFAP positivity is demon-

strated as well (c), confirming the glial cell origin of these cells. Original magnification (a) 100 \times ; (b) 200 \times ; (c) 400 \times [34]

While these early studies did not implicate a role for vitreous, other studies showed a higher degree of vitreous involvement with the premacular membranes [37]. Indeed, the immunofluorescence studies of Snead et al. showed positive staining for type II collagen inside the cells [34, 35]. Similar results were seen on studies examining premacular membranes from macular holes [38]. The most recent studies of premacular membranes have identified other important cells. Hyalocytes, known to reside in the posterior vitreous cortex [39, 40], have been implicated as important in the early stages of macular pucker [41–44]. These cells have many of the known synthetic functions that are consistent with theorized function of cells in simple premacular (epiretinal) membranes

[21, 45]. Additionally, studies have shown that hyalocytes have the potential to transdifferentiate into myofibroblasts under the right conditions, thus explaining the contractile nature of premacular membranes [41]. Also, as a member of the reticular endothelial system, hyalocytes may recruit monocytes from the circulation and glial cells from the retina into the premacular membrane.

Finally, Hiscott and colleagues characterized structural changes in premacular membranes over time. In their study, membranes from surgical specimens were divided into two categories, those that were removed in less than 4 months from time of diagnosis and those older than 4 months. The younger membranes had more cellular components but less

collagen. Older membranes had increased production of collagen and progressive cell death. The authors related these findings as being similar to that of a healing scar from a skin wound [5].

V. Pathophysiology

The pathophysiologic mechanism(s) of macular pucker is a topic of much debate. Proposed theories have ranged from trauma [46] to ocular angiospasm [47]. Earlier theories focused on the retina and largely ignored the important role of vitreous. The two modern theories, retinal breaks with glial cell migration and anomalous posterior vitreous detachment, both underscore and integrate the importance of vitreous into their explanations of premacular membrane formation in macular pucker. Common to both theories is the critical role of posterior vitreous detachment [PVD] [see chapter II.C. Vitreous Aging and PVD].

PVD can be defined as vitreous separation away from the retina with the plane of dissection at the level of the ECM between the posterior vitreous cortex and the ILM. PVD can be complete or partial and innocuous or anomalous, as described in chapter III.C. Even in complete and innocuous PVD, vitreous remains attached in the peripheral fundus due to particularly strong adhesion at the vitreous base. The first evidence that PVD is important in macular pucker comes from the fact that it is documented in 80–95 % of all macular pucker cases [9, 16, 48–51]. This is significantly higher than the 53 % prevalence of PVD in the general population over age 50 or even the 63 % by age 70 [52, 53].

Posterior vitreous detachment is the result of a process of age-related changes in the vitreous resulting in gel liquefaction and weakening of vitreo-retinal adhesion. In youth, the vitreous is a gel-like structure that is 98 % water with the rest composed largely of collagen and hyaluronan. Collagen fibrils are stabilized in a lattice-like pattern by the hydrophilic hyaluronan [19, 54]. Liquefaction begins as early as 4 years of age [55], but by the 8th decade of life may account for over 50 % of the total vitreous volume [52]. Congenital defects in type II collagen metabolism, such as Marfan's, Ehlers-Danlos, or Stickler's syndromes, can lead to early vitreous gel liquefaction [see chapter I.C. Hereditary vitreo-retinopathies]. With advanced age, pockets of liquid vitreous, or "lacunae," form. The second critical component in the development of PVD is weakening of vitreoretinal adhesion. Because the exact source of adhesion is not known, it is difficult to say what causes weakened adhesion. Progressive weakening at the vitreoretinal interface allows for extravasation of liquefied vitreous into the retrocortical (preretinal) space. This often begins via the prepapillary hole or through the perifoveal vitreous cortex. The perifoveal vitreous cortex is a likely site because vitreous is thinnest and the adhesions are inherently

weakest there (while remaining strongest directly over the fovea as mentioned above) [19, 55–58]. The liquefied vitreous then dissects through the remaining vitreoretinal interface to progress from a partial PVD to complete PVD.

The first popular theory on the pathogenesis of retinal contraction centers in macular pucker rests on the idea that microbreaks in the retina result from PVD (or trauma) and create pores through which glial cells of the inner retina migrate. Once these glial cells gain access to the preretinal space, they migrate and proliferate along the retinal surface. This theory is supported by the fact that the cells in membranes strongly resemble glial cells in both structure [31] and immunofluorescence staining pattern [34]. The evidence against this theory is that retinal breaks are not usually documented on histological examination.

The second theory on the origin of the premacular membranes in macular pucker more directly implicates vitreous. Originally proposed by Jaffe and Tanenbaum [59–62] in the 1960s and later refined by Sebag [43, 54], this theory involves the concept of anomalous PVD (APVD), which is defined as vitreous liquefaction without sufficient concurrent vitreoretinal interface dehiscence to allow vitreous separation from the retina. When this occurs, segments of the vitreous remain adherent to the retina despite other portions of the vitreous pulling away. According to this theory, variations in the exact location and nature of the anomalous PVD help explain the pathogenesis of not only macular pucker but also macular hole, vitreo-macular traction syndrome, and numerous other vitreo-retinal diseases [63] [see chapter III.B. Anomalous PVD and Vitreoschisis].

One manifestation of anomalous PVD is vitreoschisis. First proposed by Balazs [64] and later Schepens et al. [65], vitreoschisis refers to splitting of the posterior vitreous cortex into layers. It is well documented that the posterior vitreous cortex has a lamellar structure (Figure III.F-5). Each layer of the cortex runs tangential to the retina with the outermost layer connected to the ILM in a fascial manner via the extracellular matrix. Surgical and *in vivo* imaging studies have demonstrated that the vitreous can split along any of these layers leaving behind a portion of vitreous during APVD [42, 66]. In fact, OCT documentation of vitreoschisis has been seen in 53 % of macular hole and 42 % macular pucker eyes [67]. Additionally, 80 % of macular pucker eyes have evidence of vitreoschisis during surgery [66]. The APVD theory states that vitreoschisis during APVD leaves the outermost layer of the posterior vitreous cortex attached to the macula and that this is the seminal event of premacular membrane formation in macular pucker.

The idea that portions of the posterior vitreous cortex are a structural component of premacular membranes in macular pucker has support in histological studies. Messmer and Heilskov documented native vitreous collagen between the premacular and the retina [38, 68]. Also, Kishi showed in multiple studies that the vitreous is heavily interspersed into

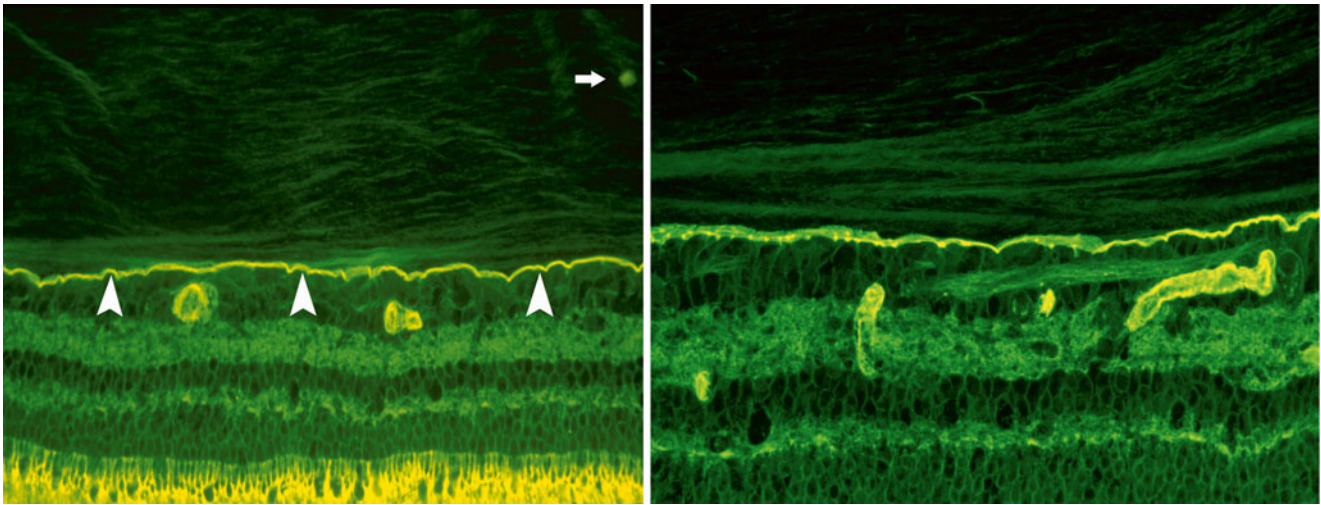


Figure III.F-5 The lamellar structure of the mammalian posterior vitreous cortex is demonstrated in an adult monkey eye stained with fluorescein-conjugated ABA lectin stain. The vitreoretinal interface is shown with vitreous above and retina below. The ILM (*arrowheads*) is the intensely bright horizontal line across the image. Above the ILM is the posterior vitreous cortex whose lamellar structure is clearly

evident at higher magnification (image to the *right*). These potential cleavage planes can separate during anomalous PVD or during vitrectomy surgery with membrane peeling, in each instance leaving a layer of vitreous attached to the macula. The *arrow* is pointed to a hyalocyte embedded in the posterior vitreous cortex (Courtesy of Greg Hageman, PhD; original magnification = 400 \times)

the premacular membrane [49, 69]. The APVD theory further states that the hyalocytes embedded in the posterior vitreous cortex are responsible for the hypercellularity of the premacular membrane. As described above, hyalocytes are cells present in the posterior vitreous cortex that have both phagocytic functions and transdifferentiation potential. Hyalocytes are known to not only secrete collagen, which is found in the premacular membranes, but can also transdifferentiate into myofibroblasts [44, 70]. A study by Kohno and colleagues [41] demonstrated this unique potential by exposing cultured hyalocytes to transforming growth factor beta-2 (TGF- β 2). In the presence of TGF- β 2 the hyalocytes contracted and became positive for alpha smooth muscle actin (α SMA) and negative for GFAP on immunofluorescence indicating a conversion into a myofibroblast. Other cultured astrocytes did not exhibit such ability. Additionally, immunofluorescence of surgically removed premacular membranes showed GFAP-stained cells in non-contracted areas and α SMA-positive cells in areas of contraction. They hypothesized that TGF- β 2 is secreted by the vitreous and induces hyalocytes to transdifferentiate into myofibroblasts [41] (Figure III.F-6).

Kita et al. [71] have offered a potential explanation for how hyalocytes-turned-myofibroblasts go on to induce membrane contraction. The TGF- β 2 critical in the transdifferentiation process also appears to induce hyalocytes to secrete connective tissue growth factor (CTGF). CTGF is well known to cause fibrosis and collagen contraction in other fibrotic disorders, such as liver cirrhosis and scleroderma. CTGF has been shown to exist in the vitreous in higher concentrations when there are proliferative vitreoretinal disorders

present [71]. Others have implicated platelet-derived growth factor (PDGF) working with TGF- β 2 to phosphorylate myosin light chain via rho kinase pathway. Myosin light chains are important in contraction of both muscle fibers and non-muscle cells [72]. Interestingly, by focusing on the role of hyalocytes, some researchers have started developing unique pharmacologic treatments for macular pucker. For instance, blockage of the rho and rho kinase (ROCK) pathways may impact myosin light chain contraction. Therefore a targeted ROCK inhibitor could alter and possibly prevent hyalocyte-mediated membrane contraction [44].

The APVD theory proposed by Sebag has one other important tenet. It states that the exact layer vitreous through which the vitreoschisis occurs ultimately dictates the final pathology [42]. As mentioned above (“vitreoretinal interface anatomy”), hyalocytes are embedded in the posterior vitreous cortex 20–50 μ m anterior to the ILM. If vitreoschisis splits the posterior vitreous cortex anterior to the hyalocytes, they remain adherent to the macula in the premacular membrane and begin the process of macular pucker. Once this has happened, hyalocytes recruit monocytes from the circulation and possibly glial cells from the retina. These cells cause membrane contraction via the mechanisms described above and create an inward or centripetal tangential force on the retina. It is this action that causes an irregular retinal contour typical of macular pucker.

While the APVD/vitreoschisis theory is well developed and has numerous studies documenting many of its components, it is not universally accepted. One issue is that the theory proposes the membranes of macular hole and macular pucker are initially structurally different owing to the different

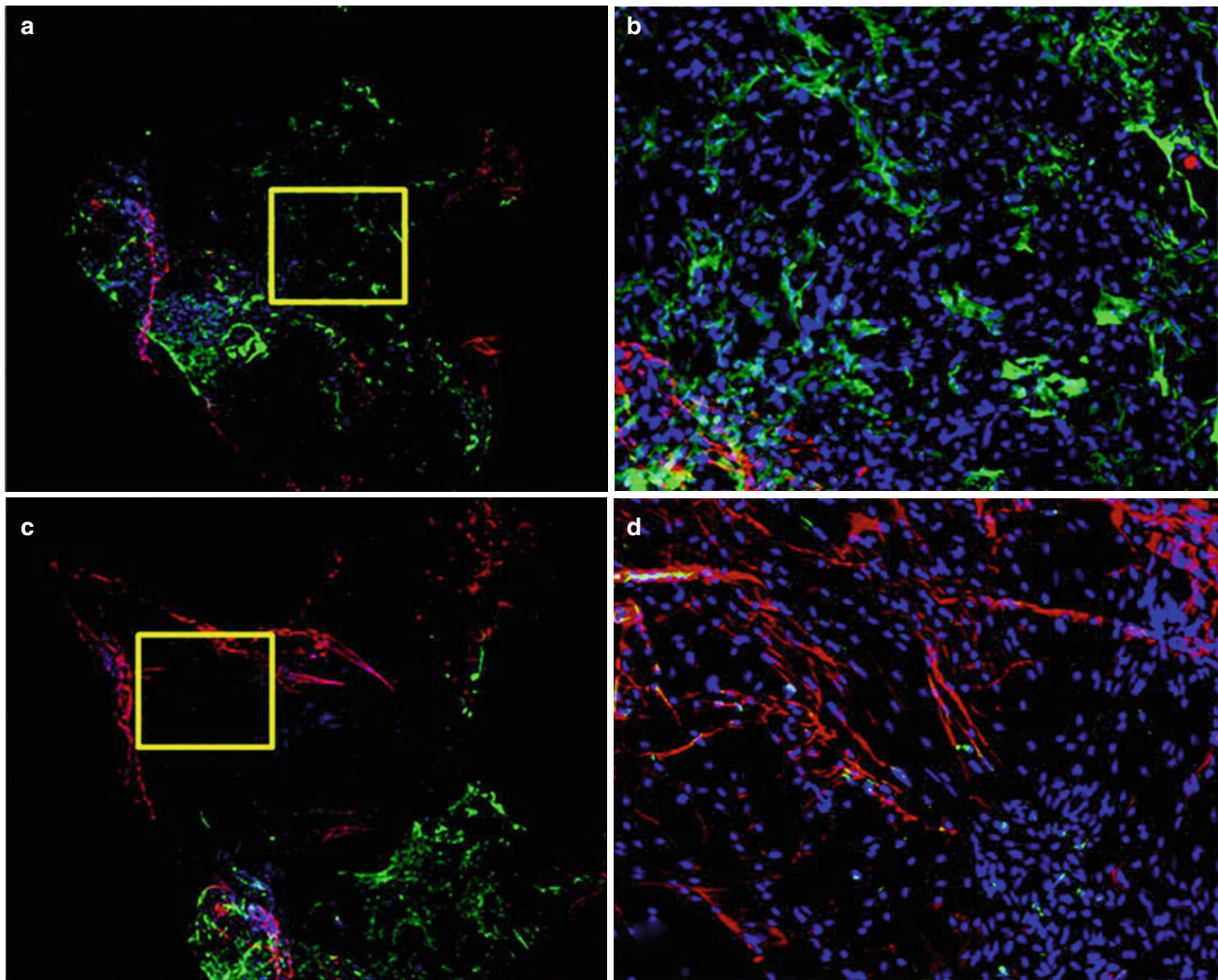


Figure III.F-6 (a, c) Whole mount of premacular membrane from a case of macular pucker demonstrating both glial fibrillar acidic protein (GFAP) in red and alpha-smooth muscle actin (α SMA) in green. The yellow boxes indicate the areas shown to the right in higher magnifica-

tion (b) Higher magnification of thick α SMA cells with large amounts of cytoplasm compared to (d) the elongated GFAP+ cells. No double-stained cells were documented on any section [41]

location of the split during vitreoschisis. However, studies have shown that late in the natural history of disease, the membranes of macular hole and macular pucker are quite similar on an ultrastructural level [38]. Another issue is that studies have failed to correlate the location of retained cortical vitreous after PVD to the location of premacular membrane formation. Chen and colleagues showed in all seven of the patients in their study who developed premacular membranes after PVD, none of them had retained cortical vitreous in the area of membrane formation [73]. Whether it is glial cell migration through retinal breaks or hyalocyte-mediated membrane contraction, both theories underscore the important role the vitreous plays in the pathogenesis of macular pucker. Clearly, posterior vitreous detachment, anomalous or not, is a critical event in initiating this vitreoretinal disorder and disturbing vision.

A. Pathophysiology of Visual Disturbance in Macular Pucker

While *on the surface* macular pucker appears to be a disorder solely of the inner retina where distortions induce metamorphopsia and blurred vision, the true mechanism of visual disturbance is likely more complicated. Clearly, contraction of the premacular membrane with subsequent wrinkling of the inner retina is a necessary event for visual impairment. Even very early researchers recognized that a simple membrane which exerted no force onto the retina rarely caused symptoms. The more difficult question, however, is how does such wrinkling actually affect vision.

One of the earliest and most prevalent theories on the underlying cause of vision changes is retinal edema. It is

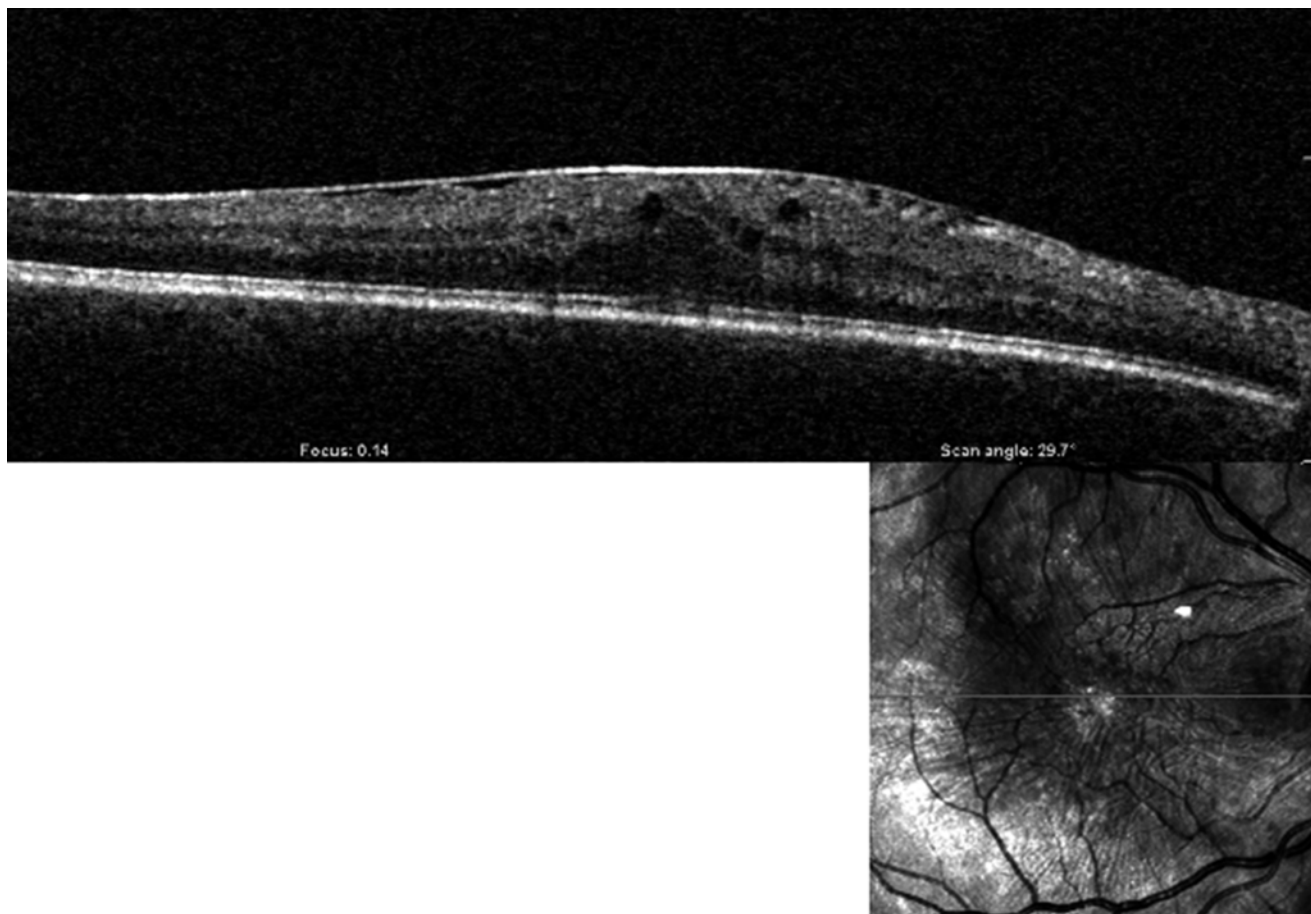


Figure III.F-7 Spectral domain OCT imaging combined with scanning laser ophthalmoscopy of an eye with macular pucker demonstrating marked retinal thickening and multiple intraretinal cystoid spaces,

well documented that premacular membranes frequently cause an increase in central retinal thickness and even intraretinal cysts [74, 75] (Figure III.F-7). With the advent of OCT in the 1990s, researchers were able to accurately quantify this change. Early studies did show correlation between central retinal thickness and visual acuity [74]. More recent studies, however, have shown that retinal thickening alone, while often correlated with visual acuity, is unlikely to explain the entire process [76, 77].

Another popular theory on the pathophysiology of the visual changes is that the photoreceptor inner segment/outer segment (IS/OS) junction is affected. The IS/OS junction is a hyper-reflective line just anterior to the retinal pigment epithelium, which is identifiable on OCT. Disturbances of this line on OCT correspond to anatomical changes in the photoreceptors (Figure III.F-8). The theory that alterations in IS/OS junction integrity affect visual function originates from a study by Niwa that showed a predominance of a-wave alteration on electroretinogram in patients with epiretinal membranes. Since the a-wave represents the activity of the photoreceptors and off-bipolar cells, dysfunction in the inner

probably the result of tangential traction, but at times also due to exudation from distorted retinal blood vessels

retina was hypothesized [77]. Later studies, using OCT, confirmed that IS/OS junction disruptions strongly correlated with either visual acuity or metamorphopsia scores. Oster and colleagues showed that the IS/OS junction was a statistically significant predictor of poor visual acuity. In their study patients with IS/OS junction disruptions were almost seven times more likely to have a visual acuity of 20/50 or worse than those without disruptions [78]. Similar results were seen by other studies [76].

IS/OS junction further appears to predict surgical outcomes. One study of 120 patients with idiopathic epiretinal membranes showed that patients who had IS/OS junction disruptions preoperatively had statistically significantly less visual recovery postoperatively than those with intact junctions at baseline. Additionally, this study showed that eye with preoperative disruptions rarely had intact junctions postoperatively. This suggests that IS/OS junction disruptions are not only important in the pathophysiology of visual disturbance but are also largely irreversible if not treated promptly [79].

Other studies have looked at additional OCT parameters to gauge clinical severity in macular pucker. Movement of

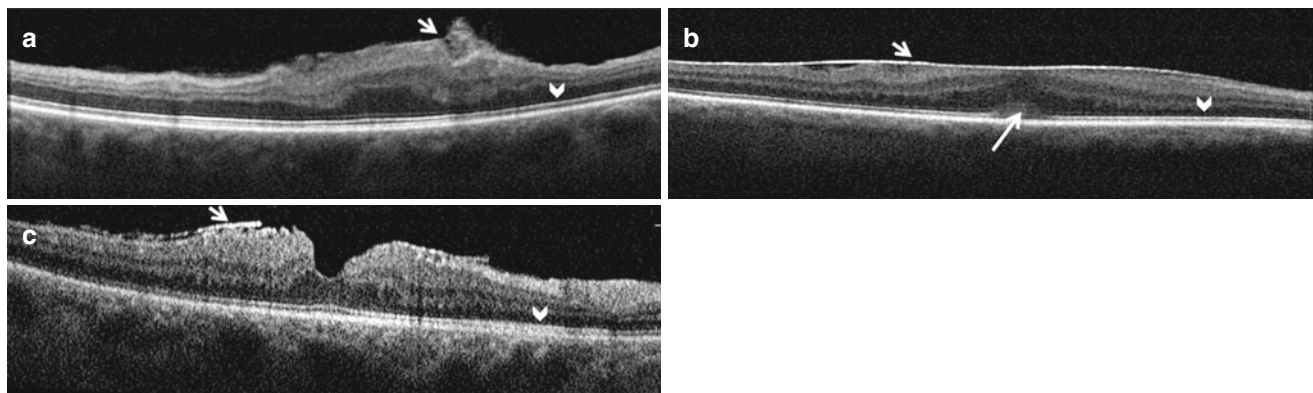


Figure III.F-8 Optical coherence tomography imaging of macular pucker. (a) demonstrates premacular membrane (*short arrow*) and completely intact inner segment/outer segment (IS/OS) junction (*arrowhead*) throughout the macula. (b) demonstrates distinct disruption of

the IS/OS junction (*long arrow*) in the macula. (c) Another example of a premacular membrane (*short arrow*) and completely intact inner segment/outer segment (IS/OS) junction (*arrowhead*) throughout the macula

retinal vessels has been suggested as a possible marker of disease severity. One study showed that over time, eyes with worsening visual acuity had more tangential movement of the retinal vessels underlying the premacular membranes [80]. Similarly, retinal contraction in general may correlate with the degree of metamorphopsia [81]. Other factors that have been shown to affect visual acuity or severity of metamorphopsia include inner nuclear layer thickness and overall thickening of the outer retina [76, 82].

Although the premacular membrane, which is the primary cause of macular pucker, is conceived of only having clinically relevant effects at the surface of the macula, its effects are felt throughout the entire thickness of the macula. Indeed, macular pucker is a prime example of how vitreoretinal interface pathologies are dynamic diseases that can affect multiple layers of the retina [see chapter II.C. Vitreous aging and PVD].

VI. Clinical Presentation

Macular pucker has a broad clinical spectrum ranging from completely asymptomatic to legal blindness. The earliest form of macular pucker, sometimes referred to as cellophane maculopathy, is often asymptomatic [2, 3, 7, 83]. Initially the membrane is thin, transparent, and minimally contracted. In this early stage superficial vessels in the retina cast a shadow on the membrane to create an area of irregular reflection on exam that has been described as a “cellophane macular reflex” [7, 51]. Later in the clinical course, when the membrane thickens and contracts, symptoms frequently develop. This more advanced form of premacular membrane formation has been referred to as preretinal macular fibrosis [7, 10, 51], often featuring retinal striae (Figure III.F-9). The most common complaints are metamorphopsia and decreased visual acuity, although micropsia and monocular diplopia have also been documented [84]. At presentation, however,

fewer than 15 % of cases will have visual acuity less than 20/70 [85]. Although many cases at presentation are unilateral, within 5 years 13.5 % of patients will develop bilateral symptoms [3]. Overall, the prevalence of bilateral involvement is between 19.5 % [3] and 31 % [7] of cases.

Grading systems exist for staging macular pucker, the most widely used being the Gass criteria. Grade 0 is a simple translucent membrane without any retinal folds. In Grade 1 the membrane causes irregular folds in the inner retinal layer. The most severe stage, Grade 2, has an opaque membrane with vascular and/or retinal distortions in all layers of the retina [83]. In general, the central macular thickness is increased and visual acuity decreases with the higher Gass classification [86]. While these criteria are of limited use in the clinical care setting, they have gained some acceptance for staging purposes in clinical research studies [87, 88]. Other staging protocols have been proposed that utilize more advanced imaging criteria, but none have gained widespread acceptance as of yet [89].

Another important clinical consideration is whether or not the membrane is primary (previously called “idiopathic”) or secondary to another cause. The term “idiopathic” is probably no longer appropriate insofar as it is now known that these cases result from anomalous posterior vitreous detachment (PVD) with vitreoschisis, and thus “primary” is a better term. Primary premacular membranes tend to occur in older individuals who have reasonable visual acuity [86]. They can also be associated with other vitreo-retinopathies, in particular, macular holes. Approximately 40 % of macular holes will have associated eccentric macular pucker that does not directly impact upon foveal vision. In these cases the area of retinal contraction is generally smaller than with primary macular pucker and no macular hole [42]. It is important to appreciate that in these cases both the macular hole and the macular pucker result from anomalous PVD.

Within the secondary membrane category, the predominant causes are diabetes, vein occlusion, retinal detachment,

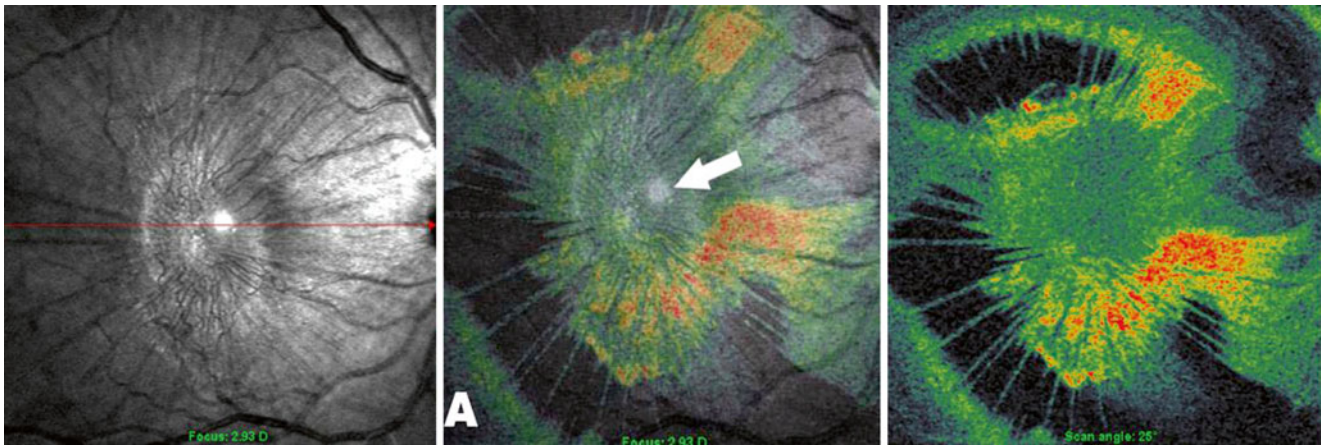


Figure III.F-9 Topographical features of macular pucker by coronal plane imaging. Grayscale scanning laser ophthalmoscopy (SLO) image (left image) displays the right eye of a patient with unifocal macular pucker and prominent retinal striae emanating from the fovea. On the right is the coronal plane OCT image of this retinal contraction center

with emanating retinal striae. In the center is an overlay (A) consisting of the coronal plane OCT image (color) superimposed upon the grayscale SLO image with point-to-point registration. The arrow identifies the center of the retinal contraction in this unifocal case of macular pucker. [courtesy VMR Institute]

postoperative (particularly cataract extraction, scleral buckle, incomplete vitrectomy), post-laser, and sickle cell disease [3, 86, 90–93]. In a pediatric population trauma is the leading cause of secondary macular pucker [13]. In general, macular pucker due to secondary membranes have a greater central macular thickness than idiopathic membranes and worse visual acuity. Additionally only about 6 % of primary membranes have associated cystoid macular edema, while this is present in 42 % of secondary membranes [86]. Also, secondary premacular membranes are more likely to have areas of focal adhesion, while primary membranes tend to have global and more fascial adherence pattern [94]. This finding is consistent with the concept that the cause of primary macular pucker is the outer layer of the posterior vitreous cortex that remains attached to the macula following anomalous PVD with vitreoschisis.

Large prospective population-based studies have detected a variable rate of progression in macular pucker. The Blue Mountain Eye Study followed a cohort of 3,654 people over 5 years. In that group, of the 7 % with macular pucker (either cellophane maculopathy or preretinal macular fibrosis) at baseline, 28.6 % progressed in terms of the area of macular involvement, while 38.8 % remained stable and 25.7 % actually improved. However, of the cases that began with the more severe preretinal fibrosis, only 16.1 % progressed. In terms of visual acuity, no change was seen in eyes that began with preretinal fibrosis, but the study was not adequately powered to detect such a change [3]. Other studies have documented that 13–29 % of cases have deterioration of vision over 2–4 year follow-up period [50, 85]. Overall, less than 5 % of cases will progress to a visual acuity of 20/200 or worse [51]. A separate study looking at a population of patients younger than 20 years old showed that of those with

baseline visual acuity better than 20/50, only 30 % progressed over a mean of 3.7-year follow-up [13]. In rare cases, however, macular pucker has been known to progress rapidly. These are often associated with retinal tears and have membranes with a higher propensity to contract [95].

While clinical exam findings, such as an increased vitreo-macular interface (cellophane) reflex described above, are important for diagnosis, optical coherence tomography (OCT) is useful to fully characterize vitreo-macular morphology [96]. Aside from visualization of the premacular membrane itself, especially regarding vitreoschisis, the classic OCT finding is retinal thickening which can range from minimal to extreme [86, 97]. Another key finding is multifocality of retinal contraction sites or centers, a feature found in nearly half of all cases (Figure III.F-10). Intraretinal cysts, which occur in about 36 % percent of all cases, are seen in over 66 % of cases that have three or more contraction centers. Additionally, there was a statistically significant relationship between increased number of contraction centers and a thicker central retinal thickness. Identifying cases with multifocal retinal contraction is therefore important, because it may be an indicator of more severe retinal damage [48]. Other studies [75, 98] have shown an increased prevalence of cysts in cases of macular pucker that have vitreo-papillary adhesion, suggesting that the direction and force of traction exerted by the contracting membrane are critical in cyst development. Vitreoschisis, or splitting of the vitreous, is identifiable via OCT in over 50 % of macular pucker cases [42, 67]. Vitreoschisis can frequently be visualized as a “lambda” sign where the two membranous layers of the split vitreous join in the shape of a Y (Figure III.F-11). A final OCT finding to consider is inner segment/outer segment (IS/OS) junction disruption. Alterations to the hyper-reflective line representing this

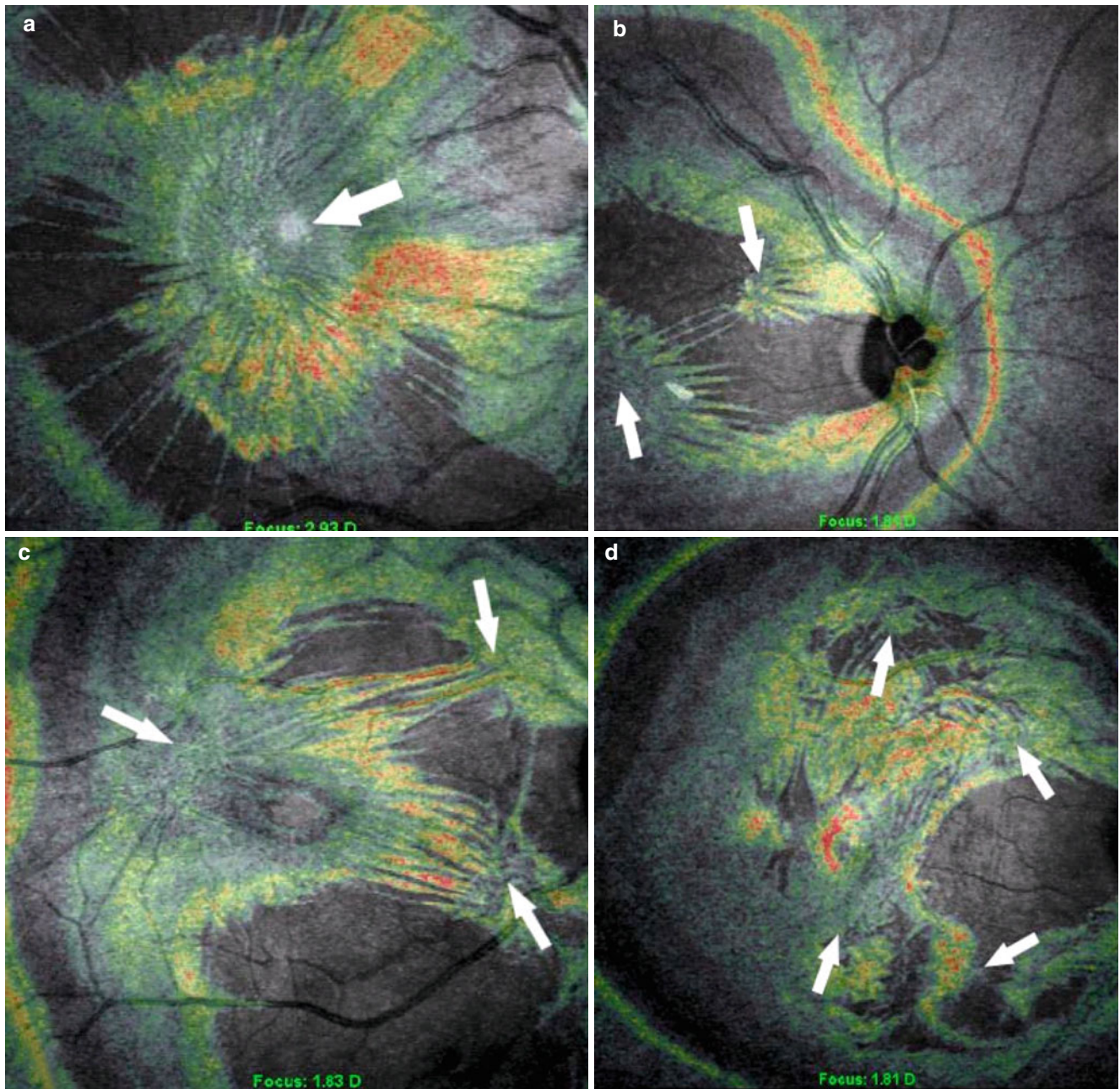


Figure III.F-10 Coronal plane (*en face*) imaging of macular pucker with combined OCT-SLO. Multi-focal retinal contraction is identifiable with this form of imaging, especially given the ability to superimpose the OCT images (*color*) onto the SLO images (*grayscale*) with point-to-point registration. (a) A single center of retinal contraction is present in the central macula (*arrow*). This is the predominant form, found in 54.5 % of cases studied [48]. (b) Two distinct centers of retinal contraction are visible (*arrows*) with radiating retinal striae. This form was found in 25 % of cases [48]. (c) Three retinal contraction centers are

identified (*arrows*) with prominent interconnecting retinal striae. This manifestation of macular pucker was found in 11.4 % of cases [48]. (d) Four centers of retinal contraction (*arrows*) were the most rare manifestation, found in only 9.1 % of cases [48]. There was a statistically significant correlation between the presence of 3 or 4 retinal contraction centers as well as the degree of macular thickening and the presence of intraretinal cystoid space. This suggests that multiple centers of retinal contraction induce more severe effects upon the macula than just one or two foci of retinal contraction [48]

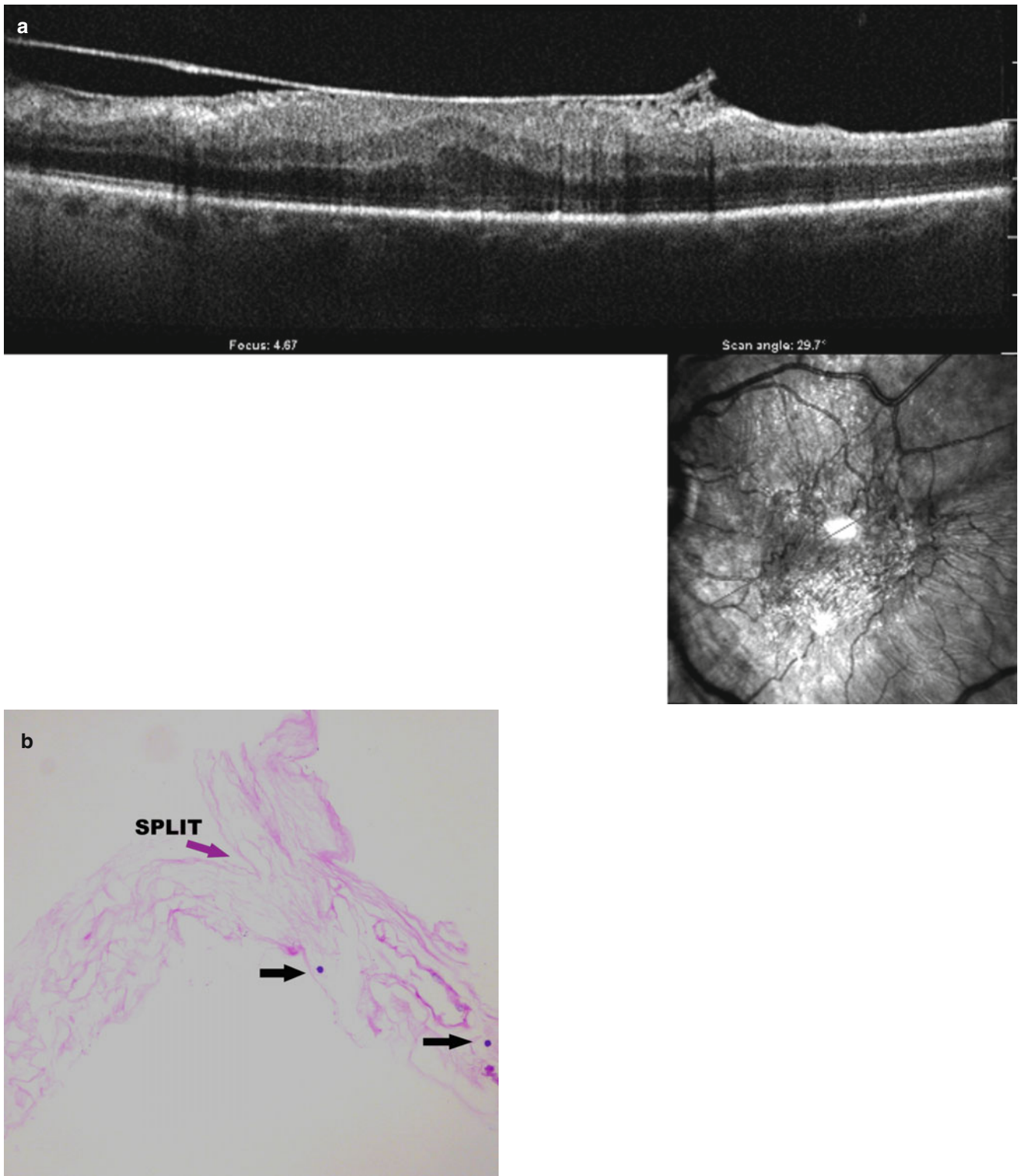


Figure III.F-11 (a) Spectral domain OCT/SLO imaging of macular pucker demonstrating splitting of the posterior vitreous cortex, i.e., vitreoschisis. (b) The case shown in (a) underwent vitrectomy surgery with membrane peeling, and the specimen was stained with periodic acid-Schiff. The area designated as “split” is the site where the posterior

vitreous cortex splits into the inner (anterior) and outer (posterior) walls of the vitreoschisis cavity shown in (a). The *arrows* indicate hyalocytes embedded in the posterior vitreous cortex (Courtesy of Narsing Rao, MD; magnification = 225×; reprinted with permission from [67])

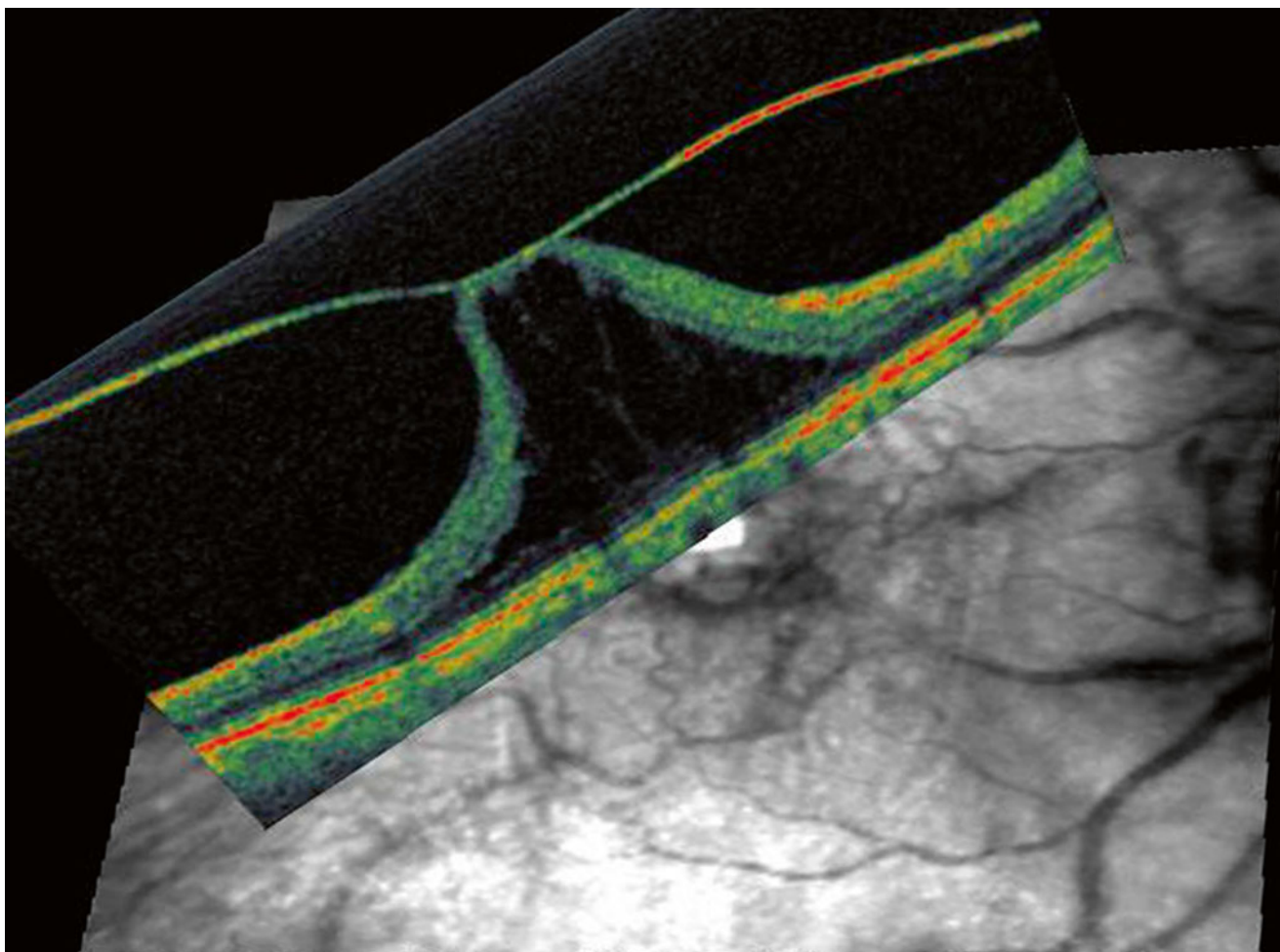


Figure III.F-12 OCT superimposed on a scanning laser ophthalmoscopy image (SLO) demonstrating the axially directed force applied in vitreo-macular traction syndrome (VMTS) and the lack of vitreoschi-

sis, which is characteristic of this syndrome since there is full-thickness posterior vitreous cortex exerting traction upon the macula

photoreceptor layer are frequently seen in macular pucker [30, 76, 78, 97] and have clinical significance.

A. Distinguishing Macular Pucker from Vitreo-Macular Traction Syndrome

Recent studies [see chapter VI.E.2. Pharmacologic Vitreolysis with Ocriplasmin: Clinical Studies] have demonstrated that the presence of a premacular (“epiretinal”) membrane is a poor prognostic sign for a good response to pharmacologic vitreolysis with ocriplasmin, which is indicated for symptomatic vitreo-macular adhesion, or vitreo-macular traction, either in the form of the vitreo-macular traction syndrome (VMTS) or the vitreo-foveal traction syndrome. In the latter case the attachment area is often too small to cause significant elevation of the macula, but does cause a central cyst in the fovea [43]. Thus, distinguishing between macular pucker and VMTS is important.

First described by Reese in 1966 [99], VMTS is similar to macular pucker in that it features a premacular membrane that is vitreous in origin. With VMTS the membrane applies force on the macula in an axial manner (i.e. anteroposteriorly) instead of tangentially, as in macular pucker (Figure III.F-12). This occurs due to an important difference in the nature of the posterior vitreous detachment in this disease. With macular pucker there are not only persistent adhesions of the posterior vitreous cortex to the ILM but also a component of vitreoschisis. Because of vitreoschisis, only partial thickness posterior vitreous cortex remains attached to macula in macular pucker while the rest of the vitreous body pulls away. Due to the aforementioned cell migration and proliferation in macular pucker, the vector of the contractile forces that these cells generate is tangential with the plane of the retina, as first proposed by Gass. In contrast, VMTS results from persistent *full-thickness* vitreous cortex attached to the macula with no vitreoschisis. The tractional forces on the retina in this case are axial, not tangential. While cells can indeed migrate and proliferate in

VMTS membranes, they are not likely to be the main source of the axial traction that is the hallmark of VMTS (Figure III.F-12; Video III.B-1). What such cells might induce, however, is increased vitreo-retinal adhesion. The perifoveal area is known to be the zone of strongest adhesion between the PVC and ILM. In VMTS this already robust connection appears to be further strengthened by fibrocellular proliferation from the retinal surface to the detached portion of the PVC. This increases the strength of perifoveal adhesions and makes spontaneous separation even less likely [100]. The origin of the membrane is unclear, but ultrastructural analysis suggests in some cases it closely resembles the membrane seen in macular pucker, although the membrane in VMTS appears to have a higher concentration of myofibroblasts [101] and fewer retinal pigment epithelial cells as compared to macular pucker [99].

B. Measuring the Impact of Macular Pucker on Vision

Historically, the sole quantitative measure of how macular pucker impacts vision has been Snellen visual acuity. However, this is often an inadequate reflection of patients' complaints of distortions. Further, clinicians are often troubled by decision-making in a patient with relatively good visual acuity who has a prominent premacular membrane inducing significant macular pucker. Thus, additional ways to measure vision in this setting would be helpful.

Studies have shown that distortions can be quantified using 3-dimensional threshold Amsler grid (3D-TAG) testing [102, 103]. This testing paradigm was successful in characterizing differences in patients with macular edema caused by exudative age-related macular degeneration (AMD) as compared to diabetic macular edema [104]. Further, patients with dry AMD could be distinguished from those with wet AMD using 3D-TAG testing [105]. In macular pucker, 3D-TAG has been used to quantify distortions and improvement following vitrectomy with membrane peel [106]. In this study, contrast sensitivity, which has been shown to be a useful measure of the impact of floaters on vision [107] [see chapter V.B.8. Floaters and Vision], was also reduced preoperatively and significantly improved following surgery.

Conclusion

Macular pucker is both common and complex. As the underlying pathobiology is strongly related to changes in the vitreous body, macular pucker underscores the intimate relationship between vitreous and the retina. While much has already been discovered about the origins and nature of the premacular membranes in macular pucker,

future research may help further clarify some of the remaining questions. Hopefully, as our knowledge advances so will our ability to treat and perhaps even prevent this common vitreo-retinal pathology.

Abbreviations

3D-TAG	Three-dimensional threshold Amsler grid
α SMA	Alpha smooth muscle actin
APVD:	Anomalous posterior vitreous detachment
CTGF	Connective tissue growth factor
ECM	Extracellular matrix
GFAP	Glial fibrillary acid protein
ILM	Inner limiting membrane
IS/OS	Inner segment/outer segment
OCT	Optical coherence tomography
PDGF	Platelet-derived growth factor
PMM	Premacular membrane
PVC	Posterior vitreous cortex
PVD	Posterior vitreous detachment
ROCK	Rho and rho kinase
TGF- β 2	Transforming growth factor beta-2
VMTS	Vitreo-macular traction syndrome

References

- Iwanoff A. Beiträge zur normalen und pathologischen Anatomie des Auges. Graefes Arch Clin Exp Ophthalmol. 1865;11(1): 135–70.
- Ng CH, Cheung N, Wang JJ, Islam AFM, Kawasaki R, Meuer SM, et al. Prevalence and risk factors for epiretinal membranes in a multi-ethnic United States population. Ophthalmology. 2011;118(4):694–9.
- Fraser-Bell S, Guzowski M, Rochtchina E, Wang JJ, Mitchell P. Five-year cumulative incidence and progression of epiretinal membranes: the Blue Mountains Eye Study. Ophthalmology. 2003;110(1):34.
- Foos R. Vitreoretinal juncture; epiretinal membranes and vitreous. Invest Ophthalmol Vis Sci. 1977;16(5):416–22.
- Hiscott P, Grierson I, McLeod D. Natural history of fibrocellular epiretinal membranes: a quantitative, autoradiographic, and immunohistochemical study. Br J Ophthalmol. 1985;69(11):810–23.
- Klein R, Klein B, Wang Q, Moss SE. The epidemiology of epiretinal membranes. Trans Am Ophthalmol Soc. 1994;92:403.
- Mitchell P, Smith W, Chey T, Wang JJ, Chang A. Prevalence and associations of epiretinal membranes. The Blue Mountains Eye Study, Australia. Ophthalmology. 1997;104(6):1033.
- McCarty DJ, Mukesh BN, Chikani V, Wang JJ, Mitchell P, Taylor HR, et al. Prevalence and associations of epiretinal membranes in the visual impairment project. Am J Ophthalmol. 2005; 140(2):288–94.
- Appiah A, Hirose T, Kado M. A review of 324 cases of idiopathic premacular gliosis. Am J Ophthalmol. 1988;106(5):533.
- Fraser-Bell S, Ying-Lai M, Klein R, Varma R. Prevalence and associations of epiretinal membranes in latinos: the Los Angeles Latino Eye Study. Invest Ophthalmol Vis Sci. 2004;45(6):1732–6.
- Banach MJ, Hassan TS, Cox MS, Margherio RR, Williams GA, Garretson BR, et al. Clinical course and surgical treatment of

- macular epiretinal membranes in young subjects. *Ophthalmology*. 2001;108(1):23–6.
12. Meyer CH, Rodrigues EB, Mennel S, Schmidt JC, Kroll P. Spontaneous separation of epiretinal membrane in young subjects: personal observations and review of the literature. *Graefes Arch Clin Exp Ophthalmol*. 2004;242(12):977–85.
 13. Khaja HA, McCannel CA, Diehl NN, Mohney BG. Incidence and clinical characteristics of epiretinal membranes in children. *Arch Ophthalmol*. 2008;126(5):632.
 14. Sebag J, Hageman G. Interfaces. *Eur J Ophthalmol*. 2000;10(1):1.
 15. Foos RY. Vitreoretinal junction; topographical variations. *Invest Ophthalmol Vis Sci*. 1972;11(10):801–8.
 16. Johnson MW. Posterior vitreous detachment: evolution and complications of its early stages. *Am J Ophthalmol*. 2010;149(3):371–82.
 17. Sebag J. Anatomy and pathology of the vitreo-retinal interface. *Eye (Lond)*. 1992;6(6):541–52.
 18. Heegaard S, Jensen O, Prause J. Structure of the vitread face of the monkey optic disc (*Macaca mulatta*). *Graefes Arch Clin Exp Ophthalmol*. 1988;226(4):377–83.
 19. Sebag J. Vitreous- from biochemistry to clinical relevance. In: Tasman W, Jaeger E, editors. *Duane's foundations of clinical ophthalmology*. Philadelphia: Lippincott Williams & Wilkins; 1998. p. 1–34.
 20. Kita T, Hata Y, Arita R, Kawahara S, Miura M, Nakao S, et al. Role of TGF-beta in proliferative vitreoretinal diseases and ROCK as a therapeutic target. *Proc Natl Acad Sci USA*. 2008;105(45):17504–9.
 21. Zhao F, Gandorfer A, Haritoglou C, Scheler R, Schaumberger MM, Kampik A, Schumann RG. Epiretinal cell proliferation in macular pucker and vitreomacular traction syndrome: analysis of flat-mounted internal limiting membrane specimens. *Retina*. 2013;33(1):77–88.
 22. Wang MY, Sebag J. Combined SD-OCT/SLO imaging of vitreous and the vitreo-retinal interface. In: *Essentials of Ophthalmology: Medical Retina - Focus on Retinal Imaging* (Holz, Spaide, eds). Springer-Verlag, 2010.
 23. Ramesh S, Bonshek R, Bishop P. Immunolocalisation of opticin in the human eye. *Br J Ophthalmol*. 2004;88(5):697–702.
 24. Sebag J. Pharmacologic vitreolysis. *Retina*. 1998;18(9502274):1–3.
 25. Sebag J, Ansari RR, Suh KI. Pharmacologic vitreolysis with microplasmin increases vitreous diffusion coefficients. *Graefes Arch Clin Exp Ophthalmol*. 2007;245(4):576–80.
 26. Sebag J. Pharmacologic vitreolysis-premise and promise of the first decade. *Retina*. 2009;29(7):871.
 27. Takano A, Hirata A, Ogasawara K, Sagara N, Inomata Y, Kawaji T, et al. Posterior vitreous detachment induced by nattoxinase (subtilisin NAT): a novel enzyme for pharmacologic vitreolysis. *Invest Ophthalmol Vis Sci*. 2006;47(5):2075–9.
 28. Wang ZL, Zhang X, Xu X, Sun XD, Wang F. PVD following plasmin but not hyaluronidase: implications for combination pharmacologic vitreolysis therapy. *Retina*. 2005;25(1):38.
 29. Wang F, Wang Z, Sun X, Wang F, Xu X, Zhang X. Safety and efficacy of dispase and plasmin in pharmacologic vitreolysis. *Invest Ophthalmol Vis Sci*. 2004;45(9):3286–90.
 30. Sakuma T, Tanaka M, Mizota A, Inoue J, Pakola S. Safety of in vivo pharmacologic vitreolysis with recombinant microplasmin in rabbit eyes. *Invest Ophthalmol Vis Sci*. 2005;46(9):3295–9.
 31. Foos RY. Vitreoretinal junction—simple epiretinal membranes. *Graefes Arch Clin Exp Ophthalmol*. 1974;189(4):231–50.
 32. Foos RY, Roth A. Surface structure of the optic nerve head. 2. Vitreopapillary attachments and posterior vitreous detachment. *Am J Ophthalmol*. 1973;76(5):662.
 33. Roth A, Foos R. Surface wrinkling retinopathy in eyes enucleated at autopsy. *Trans Am Acad Ophthalmol Otolaryngol*. 1971;75(5):1047.
 34. Snead D, James S, Snead M. Pathological changes in the vitreo-retinal junction 1: epiretinal membrane formation. *Eye (Lond)*. 2008;22(10):1310–7.
 35. Snead D, Cullen N, James S, Poulson A, Morris A, Lukaris A, et al. Hyperconvolution of the inner limiting membrane in vitreo-maculopathies. *Graefes Arch Clin Exp Ophthalmol*. 2004;242(10):853–62.
 36. Sebag J, Sadun AA. Reflections (Guest Editorial). *Graefes Arch Clin Exp Ophthalmol*. 2004;242:811–3.
 37. Bellhorn M, Friedman A, Wise G, Henkind P. Ultrastructure and clinicopathologic correlation of idiopathic preretinal macular fibrosis. *Am J Ophthalmol*. 1975;79(3):366.
 38. Messmer EM, Heidenkummer HP, Kampik A. Ultrastructure of epiretinal membranes associated with macular holes. *Graefes Arch Clin Exp Ophthalmol*. 1998;236(4):248–54.
 39. Hamburg A. Some investigations on the cells of the vitreous body. *Ophthalmologica*. 1959;138(2):81–107.
 40. Sebag J. *The vitreous: structure, function, and pathobiology*. New York: Springer; 1989.
 41. Kohno R, Hata Y, Kawahara S, Kita T, Arita R, Mochizuki Y, et al. Possible contribution of hyalocytes to idiopathic epiretinal membrane formation and its contraction. *Br J Ophthalmol*. 2009;93(8):1020–6.
 42. Sebag J, Gupta P, Rosen RR, Garcia P, Sadun AA. Macular holes and macular pucker: the role of vitreoschisis as imaged by optical coherence tomography/scanning laser ophthalmoscopy. *Trans Am Ophthalmol Soc*. 2007;105:121.
 43. Sebag J. Vitreoschisis. *Graefes Arch Clin Exp Ophthalmol*. 2008;246(3):329–32.
 44. Sakamoto T, Ishibashi T. Hyalocytes: essential cells of the vitreous cavity in vitreoretinal pathophysiology? *Retina*. 2011;31(2):222.
 45. Jacobson B. Identification of sialyl and galactosyl transferase activities in calf vitreous hyalocytes. *Curr Eye Res*. 1984;3(8):1033–41.
 46. Noyes HD. Detachment of retina with laceration at macula. *Trans Am Ophthalmol Soc*. 1871;1(8):128.
 47. Gifford SR. An evaluation of ocular angiospasm. *Trans Am Ophthalmol Soc*. 1943;48:19.
 48. Gupta P, Sadun AA, Sebag J. Multifocal retinal contraction in macular pucker analyzed by combined optical coherence tomography/scanning laser ophthalmoscopy. *Retina*. 2008;28(3):447–52.
 49. Kishi S, Shimizu K. Oval defect in detached posterior hyaloid membrane in idiopathic preretinal macular fibrosis. *Am J Ophthalmol*. 1994;118(4):451.
 50. Sidd R, Fine S, Owens S, Patz A. Idiopathic preretinal gliosis. *Am J Ophthalmol*. 1982;94(1):44.
 51. Wise G. Clinical features of idiopathic preretinal macular fibrosis. Schoenberg Lecture. *Am J Ophthalmol*. 1975;79(3):349.
 52. Foos R, Wheeler N. Vitreoretinal junction. Synchysis senilis and posterior vitreous detachment. *Ophthalmology*. 1982;89(12):1502–12.
 53. Lindner B. Acute posterior vitreous detachment and its retinal complications. *Acta Ophthalmol*. 1966;87:1–108.
 54. Sebag J. Anomalous posterior vitreous detachment: a unifying concept in vitreo-retinal disease. *Graefes Arch Clin Exp Ophthalmol*. 2004;242(8):690–8.
 55. Balazs EA, Denlinger J. Aging changes in the vitreous. In: *Aging and human visual function*. Vol 2: *Modern Aging Research*. New York: Alan R Liss; 1982. p. 45–57.
 56. Sebag J. Ageing of the vitreous. *Eye (Lond)*. 1987;1(2):254–62.
 57. Sebag J. Age-related changes in human vitreous structure. *Graefes Arch Clin Exp Ophthalmol*. 1987;225(2):89–93.
 58. Johnson MW. Perifoveal vitreous detachment and its macular complications. *Trans Am Ophthalmol Soc*. 2005;103:537.
 59. Jaffe NS. Complications of acute posterior vitreous detachment. *Arch Ophthalmol*. 1968;79(5):568–71.
 60. Jaffe N. Macular retinopathy after separation of vitreo-retinal adherence. *Arch Ophthalmol*. 1967;78:585.
 61. Jaffe N. Vitreous traction at the posterior pole of the fundus clue to alterations in the vitreous posterior. *Trans Am Acad Ophthalmol Otolaryngol*. 1967;71.

62. Tanenbaum HL, Schepens CL, Elzeneiny I, Freeman HM. Macular pucker following retinal detachment surgery. *Arch Ophthalmol*. 1970;83(3):286.
63. Sebag J. Vitreous anatomy, aging, and anomalous posterior vitreous detachment. In: Dartt D, Besharse J, Dana R, editors. *Encyclopedia of the eye*. Oxford: Elsevier; 2010. p. 307–15.
64. Balazs EA. The vitreous. *Int Ophthalmol Clin*. 1973;13(3):169.
65. Kakehashi A, Schepens CL, de Sousa-Neto A, Jalkh AE, Trempe CL. Biomicroscopic findings of posterior vitreoschisis. *Ophthalmic Surg*. 1993;24(12):846.
66. Yamashita T, Uemura A, Sakamoto T. Intraoperative characteristics of the posterior vitreous cortex in patients with epiretinal membrane. *Graefes Arch Clin Exp Ophthalmol*. 2008;246(3):333–7.
67. Gupta P, Yee KMP, Garcia P, Rosen RB, Parikh J, Hageman GS, Sadun AA, Sebag J. Vitreoschisis in macular diseases. *Br J Ophthalmol*. 2011;95(3):376–80.
68. Heilskov TW, Massicotte SJ, Folk JC. Epiretinal macular membranes in eyes with attached posterior cortical vitreous. *Retina*. 1996;16(4):279.
69. Kishi S, Demaria C, Shimizu K. Vitreous cortex remnants at the fovea after spontaneous vitreous detachment. *Int Ophthalmol*. 1986;9(4):253–60.
70. Zhao F, Gandorfer A, Haritoglou C, Scheler R, Schaumberger MM, Kampik A, et al. Epiretinal cell proliferation in macular pucker and vitreomacular traction syndrome: analysis of flat-mounted internal limiting membrane specimens. *Retina*. 2013;33(1):77–88.
71. Kita T, Hata Y, Kano K, Miura M, Nakao S, Noda Y, et al. Transforming growth factor- β 2 and connective tissue growth factor in proliferative vitreoretinal diseases possible involvement of hyalocytes and therapeutic potential of Rho kinase inhibitor. *Diabetes*. 2007;56(1):231–8.
72. Hirayama K, Hata Y, Noda Y, Miura M, Yamanaka I, Shimokawa H, et al. The involvement of the rho-kinase pathway and its regulation in cytokine-induced collagen gel contraction by hyalocytes. *Invest Ophthalmol Vis Sci*. 2004;45(11):3896–903.
73. Chen T, Yang C, Liu K. Intravitreal triamcinolone staining observation of residual undetached cortical vitreous after posterior vitreous detachment. *Eye (Lond)*. 2005;20(4):423–7.
74. Wilkins JR, Puliafito CA, Hee MR, Duker JS, Reichel E, Coker JG, et al. Characterization of epiretinal membranes using optical coherence tomography. *Ophthalmology*. 1996;103(12):2142.
75. Sebag J, Wang MY, Nguyen D, Sadun AA. Vitreopapillary adhesion in macular diseases. *Trans Am Ophthalmol Soc*. 2009;107:35.
76. Okamoto F, Sugiura Y, Okamoto Y, Hiraoka T, Oshika T. Associations between metamorphopsia and foveal microstructure in patients with epiretinal membrane. *Invest Ophthalmol Vis Sci*. 2012;53(11):6770–5.
77. Niwa T, Terasaki H, Kondo M, Piao C-H, Suzuki T, Miyake Y. Function and morphology of macula before and after removal of idiopathic epiretinal membrane. *Invest Ophthalmol Vis Sci*. 2003;44(4):1652–6.
78. Oster SF, Mojana F, Brar M, Yuson R, Cheng L, Freeman WR. Disruption of the photoreceptor inner segment/outer segment layer on spectral domain-optical coherence tomography is a predictor of poor visual acuity in patients with epiretinal membranes. *Retina*. 2010;30(5):713.
79. Suh MH, Seo JM, Park KH, Yu HG. Associations between macular findings by optical coherence tomography and visual outcomes after epiretinal membrane removal. *Am J Ophthalmol*. 2009;147(3):473.
80. Kofod M, la Cour M. Quantification of retinal tangential movement in epiretinal membranes. *Ophthalmology*. 2012;119(9):1886–91.
81. Arimura E, Matsumoto C, Okuyama S, Takada S, Hashimoto S, Shimomura Y. Retinal contraction and metamorphopsia scores in eyes with idiopathic epiretinal membrane. *Invest Ophthalmol Vis Sci*. 2005;46(8):2961–6.
82. Watanabe A, Arimoto S, Nishi O. Correlation between metamorphopsia and epiretinal membrane optical coherence tomography findings. *Ophthalmology*. 2009;116(9):1788–93.
83. Gass JDM. *Stereoscopic atlas of macular diseases: diagnosis and treatment*. St. Louis: Mosby; 1987.
84. Johnson TM, Johnson MW. Epiretinal membrane. In: Yanoff M, Duker JS, editors. *Ophthalmology*. St. Louis: Mosby; 2004. p. 686–7.
85. Wiznia R. Natural history of idiopathic preretinal macular fibrosis. *Ann Ophthalmol*. 1982;14(9):876.
86. Yazici AT, Alagöz N, Çelik HU, Bozkurt E, Alagöz C, Çakir M, et al. Idiopathic and secondary epiretinal membranes: do they differ in terms of morphology? An optical coherence tomography-based study. *Retina*. 2011;31(4):779.
87. Donati G, Kapetanios AD, Pourmaras CJ. Complications of surgery for epiretinal membranes. *Graefes Arch Clin Exp Ophthalmol*. 1998;236(10):739–46.
88. Kinoshita T, Imaizumi H, Okushiba U, Miyamoto H, Ogino T, Mitamura Y. Time course of changes in metamorphopsia, visual acuity, and OCT parameters after successful epiretinal membrane surgery. *Invest Ophthalmol Vis Sci*. 2012;53(7):3592–7.
89. Vingolo EM, Esposito M, Librando A, Huang YH, Salvatore S. New retinal imaging for the visualization and analysis of vitreoretinal interface (VRI) by short-wavelength scanning laser ophthalmoscope (swSLO). *Clin Ophthalmol*. 2011;5:1007.
90. Appiah A, Hirose T. Secondary causes of premacular fibrosis. *Ophthalmology*. 1989;96(3):389.
91. Uemura A, Ideta H, Nagasaki H, Morita H, Ito K. Macular pucker after retinal detachment surgery. *Ophthalmic Surg*. 1992;23(2):116.
92. Benichou C, Flament J. Epiretinal membrane and photocoagulation with argon laser. Discussion of 3 cases. *Bull Soc Ophthalmol Fr*. 1989;89(4):613.
93. Carney MD, Jampol LM. Epiretinal membranes in sickle cell retinopathy. *Arch Ophthalmol*. 1987;105(2):214.
94. Mori K, Gehlbach PL, Sano A, Deguchi T, Yoneya S. Comparison of epiretinal membranes of differing pathogenesis using optical coherence tomography. *Retina*. 2004;24(1):57–62.
95. Sheard RM, Sethi C, Gregor Z. Acute macular pucker. *Ophthalmology*. 2003;110(6):1178–84.
96. Do DV, Cho M, Nguyen QD, Shah SM, Handa JT, Campochiaro PA, et al. Impact of optical coherence tomography on surgical decision making for epiretinal membranes and vitreomacular traction. *Retina*. 2007;27(5):552–6.
97. Michalewski J, Michalewska Z, Cisiecki S, Nawrocki J. Morphologically functional correlations of macular pathology connected with epiretinal membrane formation in spectral optical coherence tomography (SOCT). *Graefes Arch Clin Exp Ophthalmol*. 2007;245(11):1623–31.
98. Wang MY, Nguyen D, Hindoyan N, SADUN AA, Sebag J. Vitreopapillary adhesion in macular hole and macular pucker. *Retina*. 2009;29(5):644–50.
99. Reese A, Jones I, Cooper W. Macular changes secondary to vitreous traction. *Trans Am Ophthalmol Soc*. 1966;64:123.
100. Chang LK, Fine HF, Spaide RF, Koizumi H, Grossniklaus HE. Ultrastructural correlation of spectral-domain optical coherence tomographic findings in vitreomacular traction syndrome. *Am J Ophthalmol*. 2008;146(1):121–7.
101. Gandorfer A, Rohleder M, Kampik A. Epiretinal pathology of vitreomacular traction syndrome. *Br J Ophthalmol*. 2002;86(8):902–9.
102. Wall M, May D. Threshold Amsler grid testing in maculopathies. *Ophthalmology*. 1987;94(9):1126–33.
103. Nazemi PP, Fink W, Lim JI, Sadun AA. Scotomas of age-related macular degeneration detected and characterized by means of a novel three-dimensional computer-automated visual field test. *Retina*. 2005;25(4):446–53.
104. Jivrajka RV, Kim JK, Fink W, et al. Quantitative analysis of central visual field defects in macular edema using three-dimensional

- computer-automated threshold Amsler grid testing. *Graefes Arch Clin Exp Ophthalmol.* 2009;247:165–70.
105. Robison CD, Jivrajka RV, Bababegy SR, Fink W, Sadun AA, Sebag J. Distinguishing wet from dry age-related macular degeneration using three-dimensional computer-automated threshold Amsler grid testing. *Br J Ophthalmol.* 2011;95(10):1419–23.
106. Nguyen J, Yee K, Wa C, Sadun AA, Sebag J. Macular Pucker lowers contrast sensitivity which improves after surgery. *IOVS (ARVO).* 2014.
107. Sebag J, Yee KMP, Huang L, Wa C, Sadun AA. Vitrectomy for floaters – prospective efficacy analyses and retrospective safety profile. *Retina.* 2014;34(6):1062–8. PMID: 24296397.

Ilse Krebs, Carl Glittenberg, and Susanne Binder

Outline

- I. **History**
- II. **Epidemiology of Vitreo-Macular Adhesion in AMD**
 - A. Posterior Vitreous Detachment (PVD) in AMD Study
 - B. Vitreous in Unilateral Exudative AMD Study
- III. **Morphology of Vitreo-Macular Adhesion in AMD**
 - A. Imaging
 1. Three-Dimensional OCT
 - B. Vitreo-Macular Adhesion
 1. Adhesion Versus Traction
 - C. Vitreopapillary Adhesion/Traction
 1. Vitreoschisis
- IV. **Role of Vitreous in Conversion from Dry to Exudative AMD**
- V. **Impact of Vitreous on Treatment of Exudative AMD**
 - A. Spontaneous PVD
 - B. Nonresponders
 - C. Polypoidal Choroidal Vasculopathy and Retinal Angiomatous Proliferation
 - D. Vitrectomy
 - E. Pharmacologic Vitreolysis
- VI. **The Putative Role of Vitreous in the Pathogenesis of AMD**
 - A. Traction
 - B. Low-Grade Inflammation
 - C. Barrier Function
 1. Hypoxia
 2. Macular Cytokine Load

References

Electronic supplementary material Supplementary material is available in the online version of this chapter at [10.1007/978-1-4939-1086-1_19](https://doi.org/10.1007/978-1-4939-1086-1_19). Videos can also be accessed at <http://www.springerimages.com/videos/978-1-4939-1085-4>.

I. Krebs, MD • C. Glittenberg, MD • S. Binder, MD (✉)
Department of Ophthalmology, Ludwig Boltzmann Institute for Retinology and Biomicroscopic Laser Surgery, Rudolf Foundation Clinic, Juchgasse 25, Vienna 1030, Austria
e-mail: Ilse.Krebs@wienkav.at; Carl.Glittenberg@wienkav.at; susanne.binder@wienkav.at

Keywords

Vitreous • Anomalous posterior vitreous detachment
Vitreoschisis • Exudative age-related macular degeneration
Choroidal neovascularization • Vitreo-macular adhesion
Vitreopapillary adhesion • Traction • Vascular endothelial growth factor • Optical coherence tomography • Ultrasound

Key Concepts

1. Anomalous posterior vitreous detachment (assessed by ultrasound) and adhesion of the posterior vitreous (visualized by optical coherence tomography) are significantly correlated to exudative AMD with 100 % co-localization of vitreo-macular adhesion and choroidal neovascularization, often located extrafoveally. Vitreo-papillary adhesion and vitreoschisis are additional morphological changes providing further evidence of an association if not a role for anomalous posterior vitreous detachment in exudative AMD.
2. Vitreo-macular adhesion/traction might promote the development of choroidal neovascularization by low-grade inflammation. Furthermore, the attached posterior vitreous might prevent normal diffusion of oxygen (causing hypoxia) or clearing of vascular endothelial growth factor and other proangiogenic cytokines.
3. Whereas the morphological findings in neovascular AMD are uncontested, the interpretation of these changes regarding their impact on the course of the disease and the role in the etiology of exudative AMD are controversial. The favorable effect of vitrectomy and spontaneous posterior vitreous detachment on the activity of neovascular lesions and the significant correlation of vitreo-macular adherence and the response to pharmacotherapy indicate there is not only a pathogenic role for vitreous but also an influence of vitreo-macular adhesion/traction on the effect of modern anti-VEGF therapy.

I. History

Due to the increasing importance of age-related macular degeneration (AMD) in the modern western world an enormous number of scientific papers have been published concerning the epidemiology, pathogenesis, morphology, and therapy of this disease. All these articles mainly concentrated on changes of the posterior part of the retina, as AMD is a disease of the chorioretinal interface, specifically the retinal pigment epithelium - Bruch's membrane - choriocapillaris complex. In the past, only a few studies examined the relationship of the posterior vitreous cortex to the retina and changes at the vitreo-macular interface in eyes suffering from AMD. Weber-Krause et al. conducted a study based on B-scan ultrasound and reported a higher incidence of incomplete posterior vitreous detachment (PVD) in eyes with AMD compared to age-matched controls [1]. Similarly, Ondes et al. found that complete PVD was more frequent in eyes without AMD compared to eyes with AMD [2]. Neither study specifically evaluated the vitreo-macular relationship in AMD, although it was implicit that anomalous PVD may play a role, as it does in other conditions [see chapter III.B. Anomalous PVD and vitreoschisis].

Interest was drawn to the vitreo-macular interface in AMD by Professor Susanne Binder [3] who performed pars plana vitrectomy, subretinal membrane removal, and transplantation of a suspension of retinal pigment epithelial cells in cases of neovascular AMD. She reported very strong adhesions of the posterior vitreous in the macular region with an incidence of attached posterior vitreous of 83 % in 66 eyes of patients with a mean age of 77.8 years; in contrast to publications concerning age-related changes of the vitreous report an increasing incidence of PVD with age, reaching 63 % in the eighth decade of healthy or not selected cases [4]. The development of optical coherence tomography (OCT) enabled us to get a more detailed insight on the changes of the vitreo-macular interface in AMD. In exudative AMD, eyes treated with photodynamic therapy had central vitreo-macular adhesions surrounded by shallow detachment of the posterior vitreous. The interest aroused by these observations led to clinical studies, whose basis and findings will be presented in detail in this chapter [5].

II. Epidemiology of Vitreo-Macular Adhesion in AMD

A. Posterior Vitreous Detachment (PVD) in AMD Study

Although OCT provides more detailed information concerning localized adhesions of the posterior vitreous, ultrasound is still needed to diagnose PVD. With OCT, only 1 mm

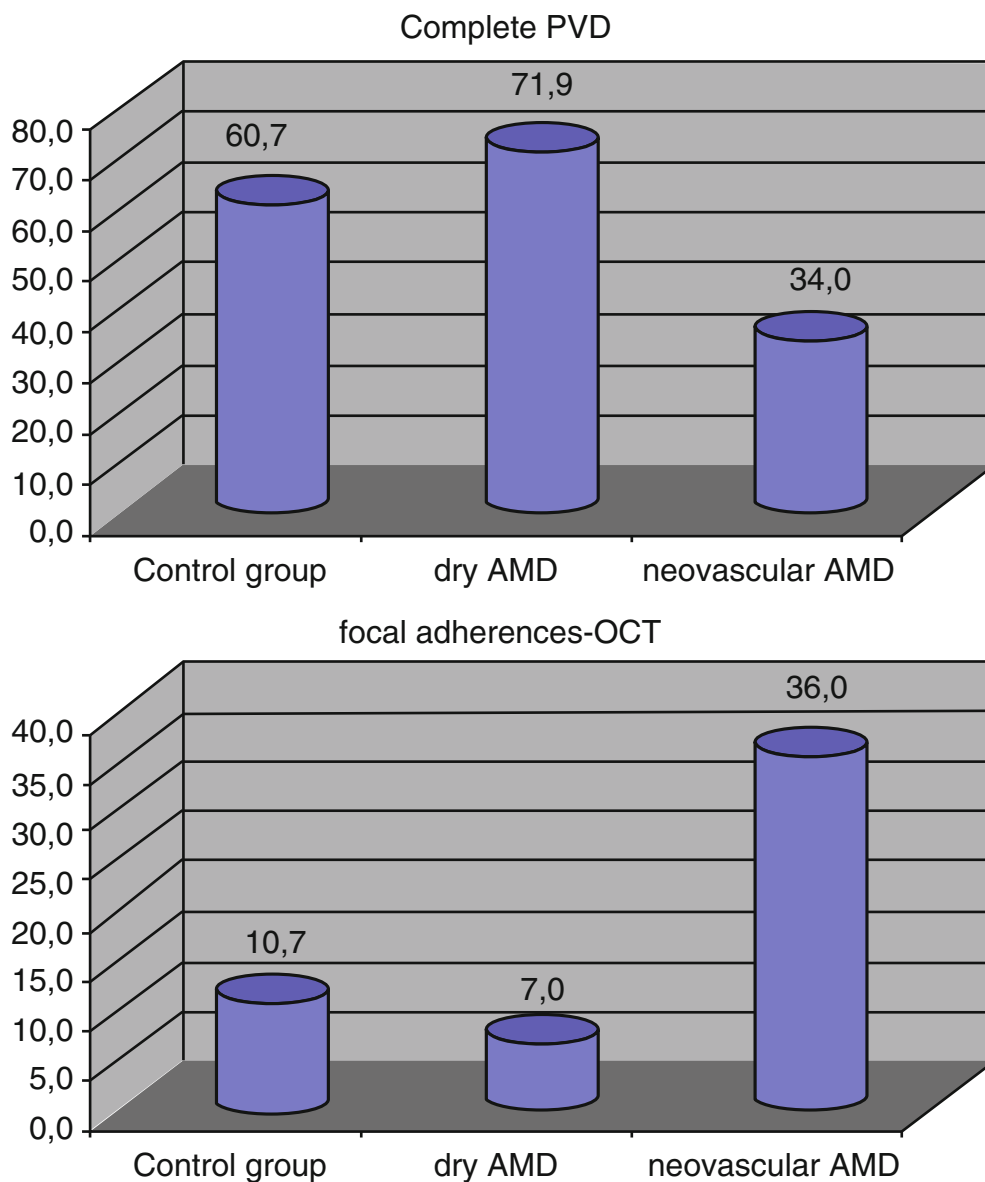
anterior to the retina can be examined; a total vitreous detachment and localized detachments in the periphery can only be detected by ultrasound. Furthermore, the posterior vitreous cortex and the inner limiting membrane cannot be differentiated by OCT; therefore, a total attached vitreous cannot be diagnosed by OCT. Thus, the comparative study of PVD in AMD [5] employed both ultrasound and OCT, to examine the incidence of posterior vitreous detachment and central adhesions (Figure III.G-1).

A consecutive series of eyes at our institution with exudative AMD (50 eyes), nonexudative AMD (57 eyes), and age-matched controls (56 eyes) was assembled. Of the 50 eyes with exudative AMD 34 % had a complete PVD, as compared to 71.9 % with nonexudative AMD ($p=0.00002$) and 60.7 % control eyes ($p=0.014$). In contrast, partial PVD was significantly more frequent in eyes with exudative AMD (30 %) than in eyes with nonexudative AMD (12.3 %, $p=0.02$) and control eyes (5.4 %, $p=0.003$). These results indicate a high percentage of anomalous PVD in eyes with exudative AMD. Another sign of anomalous PVD in exudative AMD were central adhesions surrounded by shallow detachments visualized by OCT. These adhesions were significantly more frequent in exudative AMD (36 %) than in nonexudative AMD (7 %) or controls (11 %), $p<0.0001$ and 0.002, respectively (Figure III.G-1 presents plots of US and OCT results). Therefore, anomalous PVD seemed to play an important role in the etiology of exudative AMD. However, a number of confounding factors might influence the development of exudative AMD, among others genetic and environmental factors. To properly evaluate the importance of anomalous PVD in exudative AMD, such factors should be excluded. This could be achieved by examining patients with exudative AMD only in one eye and nonexudative or no AMD in the fellow eye. In the PVD in AMD study, both eyes of a patient were included, 40 % of the patients with neovascular AMD had this diagnosis only in one eye, 28 % had non-neovascular AMD, and 12 % no AMD in the fellow eye. 22.2 % of the patients showed different behavior of the posterior vitreous cortex in each eye, and half of these patients had different diagnosis in each eye: neovascular AMD in one eye, which means that 36 % of the patients with neovascular AMD presented with different status of the posterior vitreous and different diagnosis concerning both eyes.

B. Vitreous in Unilateral Exudative AMD Study

To address the issue of confounding genetic and environmental factors, a collaborative multicenter study was conducted with the Department of Ophthalmology of the Rudolf Foundation Hospital, with Jerry Sebag, Founding

Figure III.G-1 The plots in the upper part show the incidence of complete PVD (significantly higher in dry AMD and controls than in neovascular AMD, and in the lower part the plots show that the incidence of localized adherences of the posterior vitreous is significantly higher in neovascular AMD than in the other groups

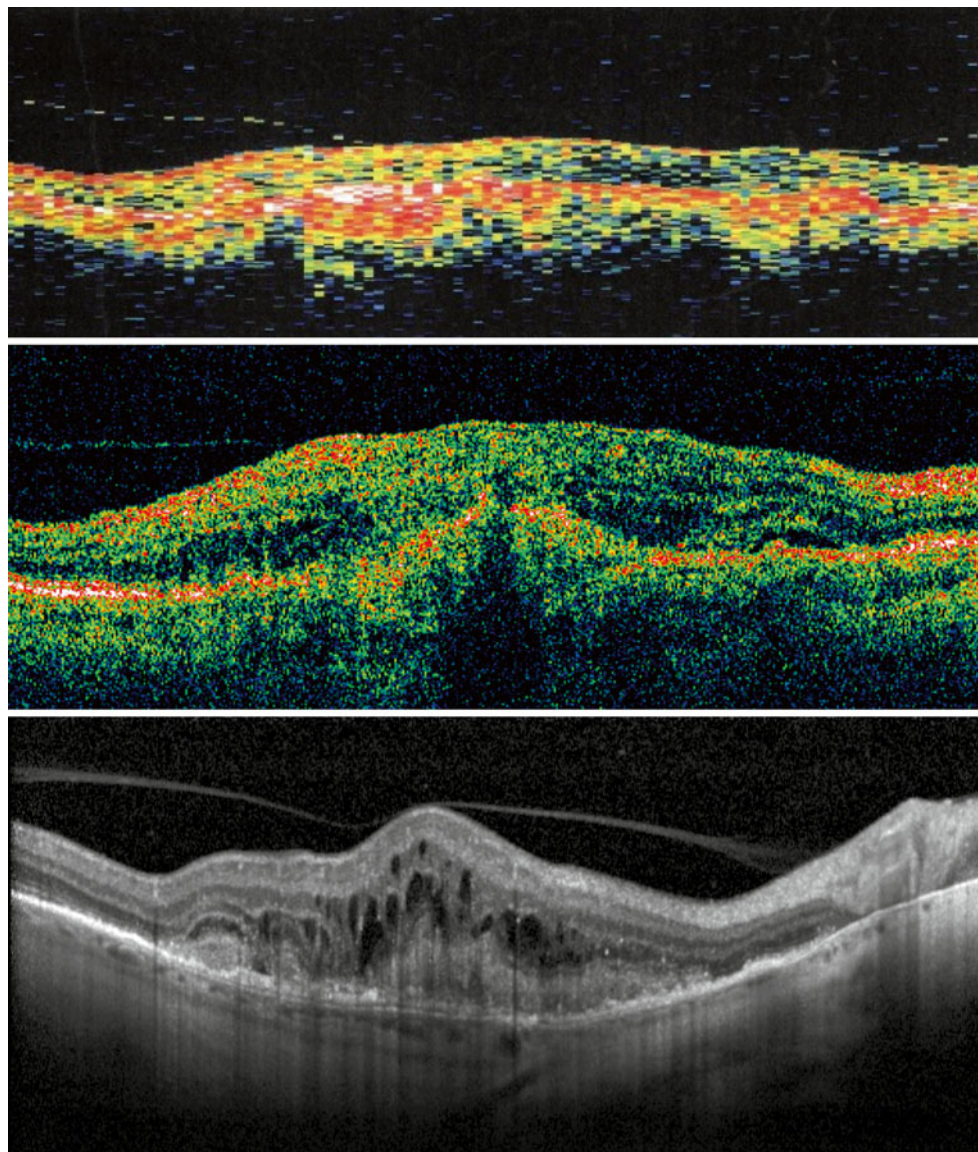


Director of the VMR Institute in Huntington Beach and Lawrence Yanuzzi's group in New York [6]. This study included 39 patients with exudative AMD in one eye and nonexudative AMD in the fellow eye. Eyes with active exudative AMD confirmed the results of the PVD in AMD study, as they had significantly less frequent PVD ($p=0.002$) and more frequent vitreo-macular adhesion ($p=0.008$). When including only eyes with end-stage exudative AMD, PVD was more frequent in exudative AMD, but failed to be significant. To exclude another possible factor, which might have influenced the incidence of PVD, the status of the lens was evaluated. However, the number of pseudophakic eyes was not significantly different between the groups.

A Korean group headed by Sung Jun Lee retrospectively analyzed the records of 251 patients with unilateral

exudative AMD [7]. This study was based on Stratus OCT, and therefore only the status of the vitreo-macular interface was evaluated. Vitreo-macular adhesions were found in 22.3 % of the patients: 18.7 % in eyes with exudative AMD, only 2.4 % in fellow eyes, and 1.2 % in both eyes. In comparison to the data of the PVD in AMD study, vitreo-macular adhesions were found less frequently in the Korean study. However, they were present almost exclusively in eyes with neovascular AMD (83 %). Including a larger number of patients, classification of the lesions was possible: classic lesions in 38 % and occult lesions in 62 % of the vitreo-macular adhesion group, and in 38.3 and 61.7 %, respectively, in the eyes without vitreo-macular adhesions. Furthermore, the localization of the choroidal neovascularization did not reveal any influence on the presence of vitreo-macular adhesions.

Figure III.G-2 Comparison of different generations of OCT. *First line:* OCT of the first generation; *Second line:* time domain OCT (Stratus OCT); *Third line:* spectral domain OCT (Spectralis OCT)



III. Morphology of Vitreo-Macular Adhesion in AMD

A. Imaging

As previously mentioned, ultrasound is indispensable in diagnosing PVD. Resolution of structure at the vitreo-macular interface, however, is not very good. Our understanding of the morphology of the vitreo-macular interface in AMD has benefited greatly from OCT imaging. Spectral domain imaging technology has several advantages compared to time domain OCT. In addition to enhancing resolution, the increased scan velocity considerably improved the evaluation of AMD cases. In Stratus OCT, only 6 (most frequently radial) lines were possible, and in SD OCT, the posterior pole is scanned by a raster of parallel lines. Different machines are on the market, all of them offering higher resolution and increased scan density. We have our own experiences with two of these machines,

the Cirrus OCT (Carl Zeiss Meditec, Dublin, California) and the Spectralis OCT (Heidelberg Engineering, Heidelberg, Germany), both offering special advantages. The Cirrus OCT provides 128 raster scans of very good quality within seconds. The built-in software offers among other tools retinal thickness maps, tissue layer images of the inner limiting membrane, and the retinal pigment epithelium. Furthermore, slabs of different height can be determined. The most prominent advantage of the Spectralis OCT is the eye tracker. A second light source provides that the images are recorded on the correct place and on identical locations in repeated examinations. The course of changes over time of retinal pathologies (such as vitreo-macular adhesions) can therefore be visualized more accurately. Averaging of up to 100 identical scans provides extremely high-quality single scans almost without any disturbing noise. The single scans can be recorded with a length of 8 mm, giving the possibility to record the fovea and the rim of the optic disc in one scan. Figure III.G-2

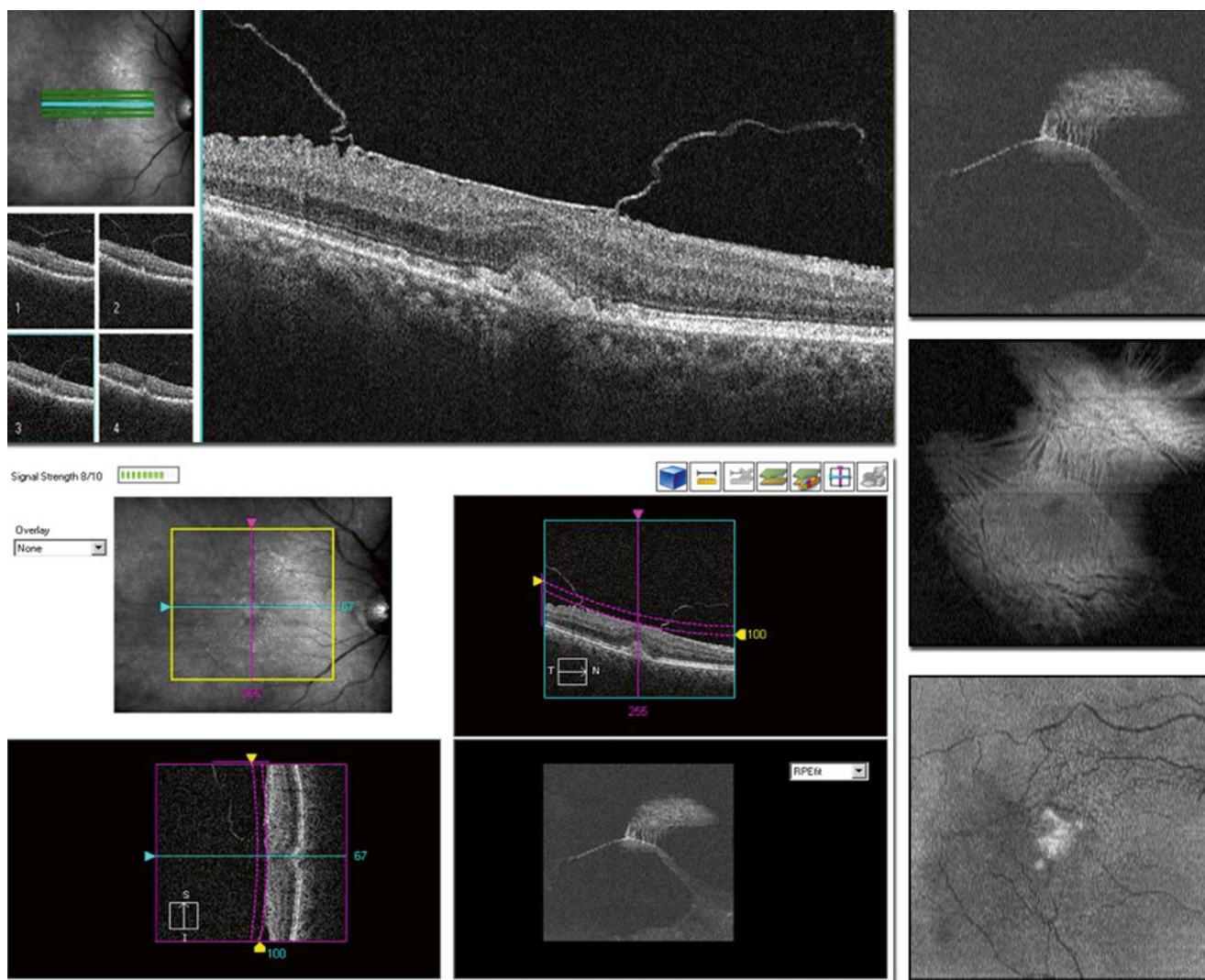


Figure III.G-3 Instrument OCT review. Review of OCT data directly on the instrument (Carl Zeiss Meditec® HD-OCT™). *Top left:* B-mode scan review. *Bottom and right:* Virtual C-mode scan review using an RPE-fit

slab set at 10 μ which is slowly moved from *top to bottom* showing the three-dimensional structure of the lesion as well as the correlation between vitreo-retinal traction and the choroidal neovascularization

presents images of a neovascular AMD case recorded with 3 generations of OCT (see below and chapter III.E. Vitreo-papillary Adhesion and Traction).

1. Three-Dimensional OCT

When ascertaining the relationship between choroidal neovascularization and vitreo-retinal adhesion/traction, it is important to understand the three-dimensional structures of the traction as they relate to the location of the neovascularization. It is also necessary to be able to visualize subtle structures of the vitreo-retinal interface. This can be done in several ways. First of all, it is possible to manually scrub through the B-mode scans of a data set in order to find anatomical relationships (Figure III.G-3, Videos III.G-1 and III.G-2). This is time consuming and difficult. Secondly, it is possible to create virtual C-mode scans. On the Cirrus HD™ OCT, this is achieved by creating an RPE-fit slab of approximately 100 micron thickness and slowly scrubbing through the virtual C-mode scans in

the Z-axis (Figure III.G-3, Videos III.G-1 and III.G-2). This can be very helpful, but is also time consuming and difficult. With both these methods, it is difficult to mentally visualize the three-dimensional correlations between the different areas of the lesions. The third method would be to use three-dimensional visualization. This method is hardly used either clinically or for research purposes because the three-dimensional rendering systems available on commercial OCT equipment do not visualize the data in a useful way as they lack ray-traced shading. This leads to very washed-out, indistinct structures, especially when looking at subtle and small structures of the vitreo-retinal interface. Additionally, structures above the interface inside the vitreous itself tend to be lost due to bad signal-to-noise ratio as the conventional noise reduction algorithms such as tracked averaging are prohibitively time consuming when dealing with large data sets. In order to have a viable method of analyzing these structures, new three-dimensional visualization systems needed to be developed.

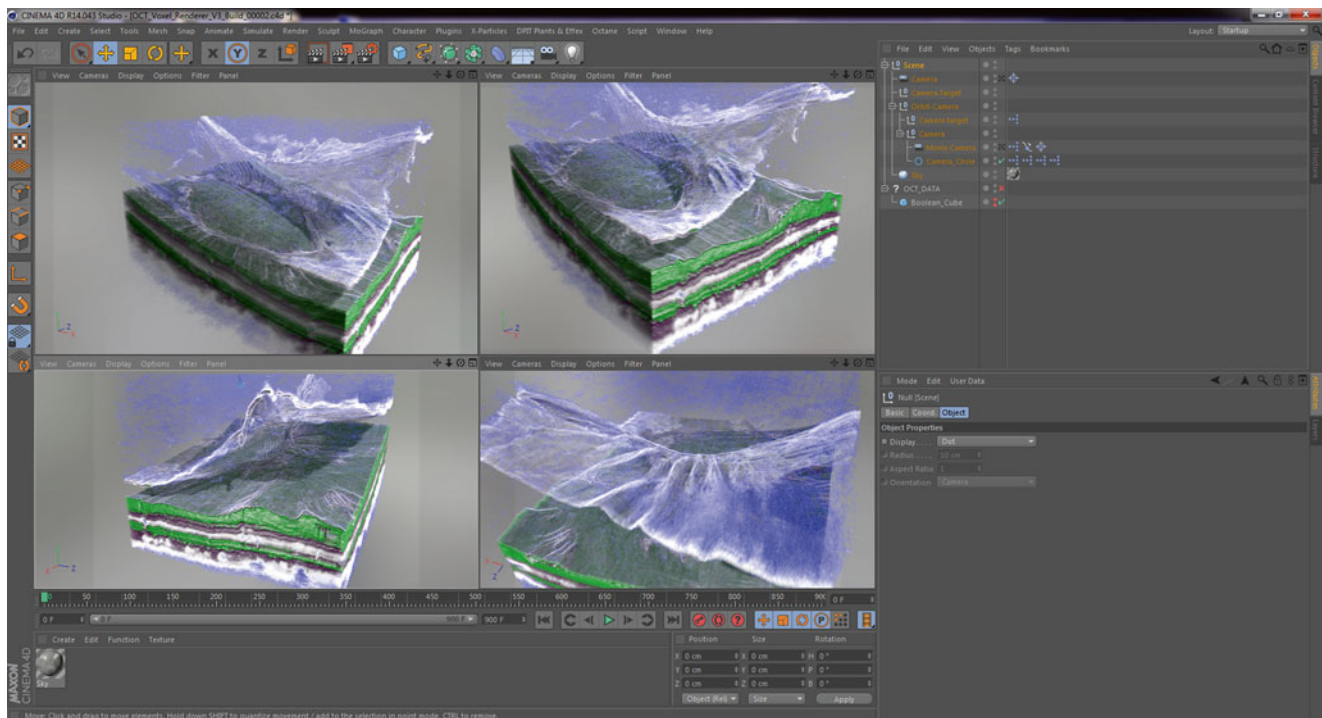


Figure III.G-4 3D voxel-based OCT rendering. Voxel-based 3D visualization of OCT data using a custom-built plug-in for Maxon® Cinema 4D™. This real-time *screenshot* of the interface shows how the

visualization utilizes ray-traced shading to achieve an increased contrast which in turn results in an increased visibility of the vitreous traction forces

With the goal of enhancing the clarity of subtle structures of the vitreo-retinal interface, two different 3D visualization systems were designed, each having different strengths and weaknesses. Both of them employ ray-traced shading which enhances small structures by throwing a shadow from the light source or light sources onto the data behind or below the illuminated structure, making the structure stand out from its surroundings and thereby increasing the contrast of the visualization. The first system (Figure III.G-4, Videos III.G-3 and III.G-4) is voxel based and has the advantage of being usable on almost any computer graphics card (including conventional laptop graphics cards). It also has relatively low preprocessing time and can if necessary use unprocessed raw data directly from the Cirrus OCT™. Additionally, the look-up table range and values can be interactively adjusted during visualization in order to adjust the coloring to specific data sets. The disadvantage is that the visualization becomes diffuse at extreme zoom levels. The second system (Figure III.G-5, Videos III.G-5, III.G-6, and III.G-7) is based on triangle-mesh representation of the data. This requires full nonplanar segmentation of the data, and a large amount of preprocessing is therefore necessary. A second drawback with this method is that it can only be rendered on CUDA (*Compute Unified Device Architecture*)-based graphics cards. This limits the usability of the system to computers running Nvidia™ graphics processor units (GPU). Although

the examples shown in this chapter are created from Cirrus HD™ data sets, any OCT data that has a dense enough scan pattern of approximately 50 micron or less between each B-mode scan, can be used for this type of visualization system.

In order to achieve the first, voxel-based, visualization system (Figure III.G-4), the raw OCT data sets (512×128 macular cube or 200×200 macular cubes) are exported to ImageJ™ in which they are converted into a file format readable by imaging and rendering programs. As the raw data sets we were using did not contain Z-alignment, this had to be added in postprocessing. The data was imported into Adobe After Effects™ where Z-alignment and noise reduction were performed (Figure III.G-6). The noise reduction was based on a temporal filter, which samples empty noise over several frames and removes an averaged noise from the entire set. This increases the signal-to-noise ratio in the vitreous significantly without affecting the detail of actual structure, as this is not averaged (Figure III.G-6). This noise-corrected data is imported into Cinema 4D™ and rendered using a custom-made plug-in which renders the data as voxels with ray-traced shading and a single customizable light source direction.

The second, triangle-mesh-based visualization system (Figure III.G-5) gathers and preprocesses the data similarly to the first method, but before the data is exported to Cinema

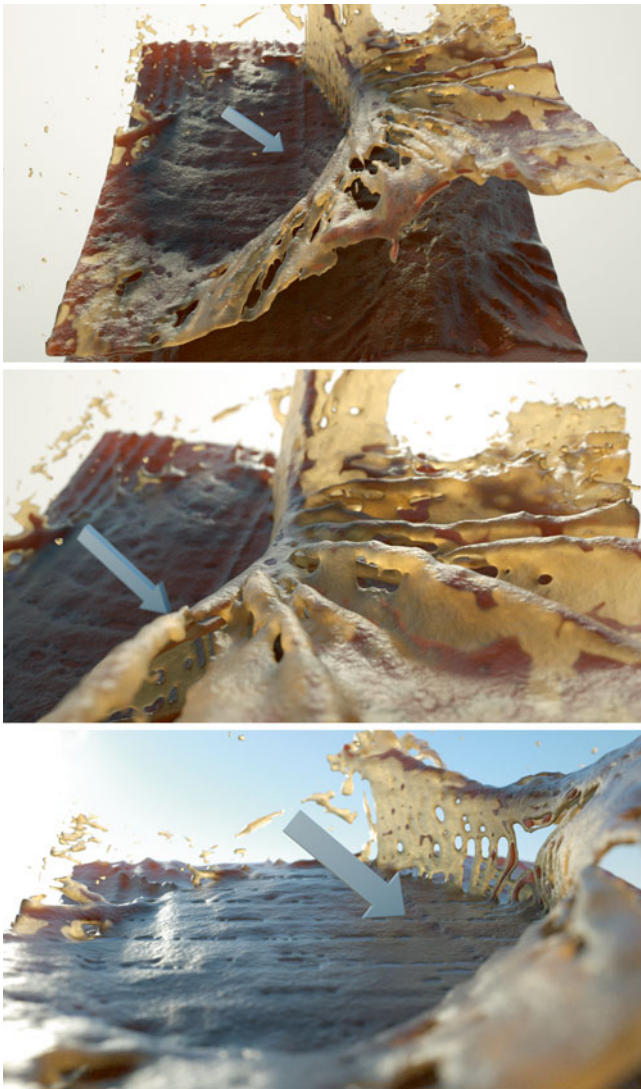


Figure III.G-5 3D mesh-based OCT rendering. Graphics processor (CUDA) based real-time visualization of triangle-meshed OCT data from within Maxon® Cinema 4d™ using the Ottoy® Octane Render™. Clearly visible are the traction force lines which orient to a point on the adhesion (*arrow*) under which the choroidal neovascularization is located

4D™, it is converted into intensity range threshold-based particle clouds in Realflow™ (Figure III.G-6). These particle clouds are used to create triangle meshes of the retinal structures corresponding to the intensity ranges. These meshes are exported to Cinema 4D™ and rendered using a CUDA GPU. The benefit in rendering over the CUDA GPU instead of the central processing unit (CPU) on the computer's motherboard is the possibility of accessing its massive parallel computing capabilities. This means that instead of the 8 computing cores that a traditional computer chip accesses, GPU-based computing can access 1024 CUDA cores simultaneously on a single graphics chip. If two graphics chips are

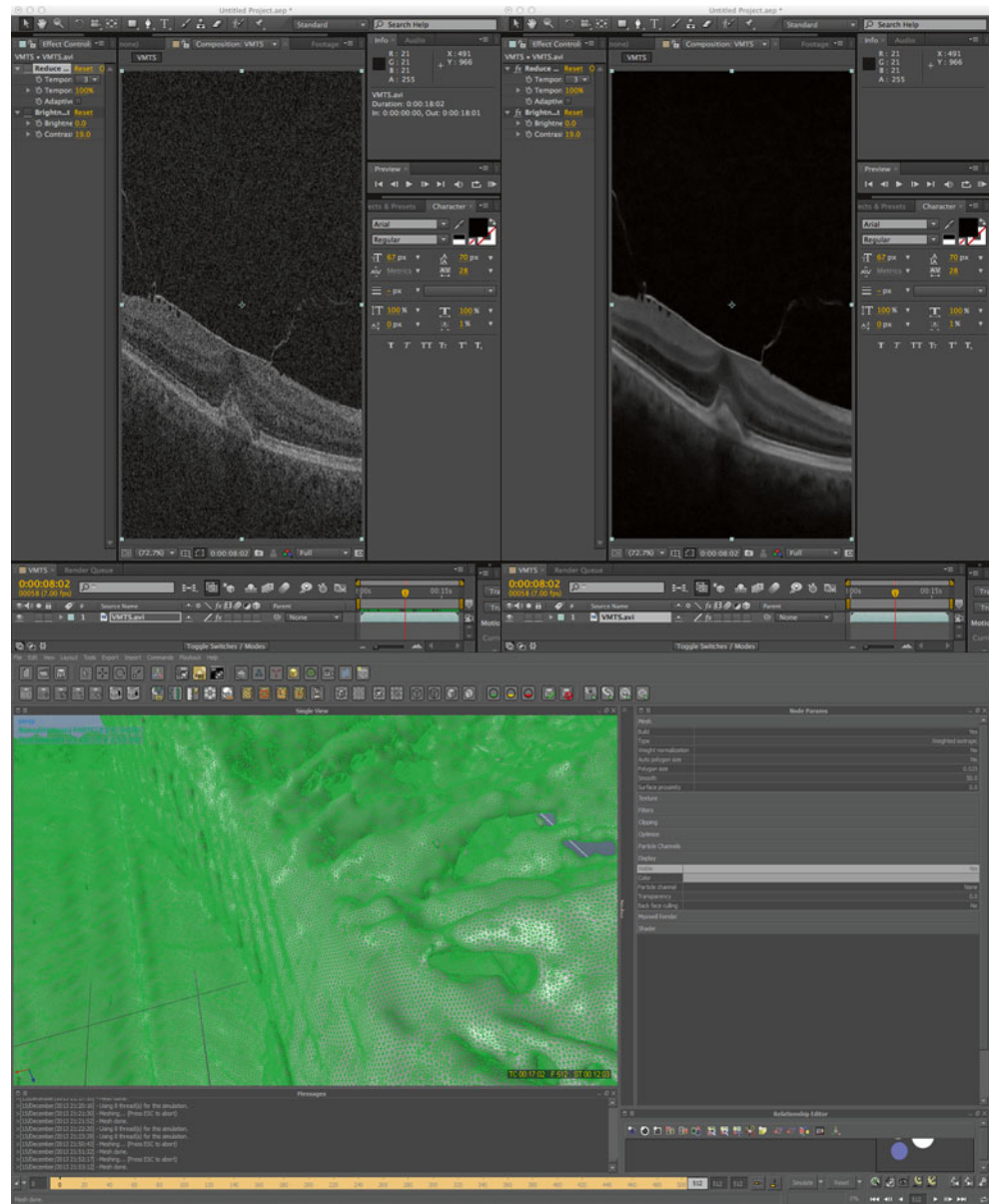
used in parallel, the number of cores accessed increases to 2048. This leads to an exponential increase in the computing speed. This rendering speed increase makes photorealistic rendering in real-time possible. It is even possible to render using multiple freely configurable light sources as well as HDRI (high dynamic range image)-based lighting and automatic depth of field (DOF). The photorealistic rendering and full control of lighting and shading in real time make it possible to visualize very small and subtle structures at the vitreo-retinal interface.

These two methods are very helpful in a research situation, but at this time are too cumbersome to be used effectively in a clinical setting. The transfer of data between the different postprocessing programs needs to be automated. The Z-alignment, noise reduction and the point cloud segmentation need to be moved away from CPU computing towards GPU computing in order to increase processing speed. As computing technology improves this type of data visualization will become an important aid in understanding the three-dimensional relationships between vitreous and age-related macular degeneration. Videos showing the different visualization methods as well as several clinical examples are accessible in the online section of this book.

B. Vitreo-Macular Adhesion

Focal adhesences of the posterior vitreous to the anterior retina surrounded by a shallow vitreous detachment were identified even by time domain OCT. More posterior in the same scans were morphological changes due to neovascular AMD, like fusiform thickening of the retinal pigment epithelium/choriocapillaris band, detachment of the retinal pigment epithelium, and intra- or subretinal fluid. Therefore, correlations between the localization of adhesences and the neovascular complex were determined. Simultaneously recorded video images in Cirrus OCT (in Stratus OCT, the video images were taken at the end of the examination) or even more accurate in Spectralis OCT (due to the eye tracker) allowed for exact localization of the changes on the retinal surface and at the retinal pigment epithelium within the posterior pole. However, the correlation between the localization of adhesences and neovascular complex in 100 % was confirmed with the help of SD-OCT presented in Figure III.G-7 [8]. Of the CNV lesions with vitreo-macular adhesences, adhesions were located in the fovea in 43.3 % and juxtafoveally in 56.7 %. The high incidence of juxtafoveal adhesions may be related to the high percentage of lesions with retinal angiomatous proliferation (88 % of the juxtafoveal lesions). This type of neovascular lesion begins characteristically juxta- or extrafoveally. Whether it does so by proliferation of retinal capillaries or by choroidal vessel

Figure III.G-6 Preprocessing for 3D visualization. *Top:* Adobe® After Effects™ Z-alignment and temporal noise reduction. *Bottom:* Nextlimit® Realflow™ particle cloud formation and triangle meshing



penetration through Bruch's membrane and retinal pigment epithelium is still under discussion [9–11]. The juxtafoveal position of vitreo-macular adhesion in RAP lesions further confirms the correlation between the origin of the neovascularization and the adhesion of the posterior vitreous cortex. In early lesions, this correlation can be demonstrated very well, especially in the 3D animations (Videos III.G-1, III.G-3, III.G-4, III.G-5, and III.G-6). Visualization of the retina in slabs of 100 μm height shows very well the area of adhesion and corresponding neovascularization in the deeper layers. In more advanced lesions, the size of the adhesion is usually smaller than the size of the entire lesion, and the distance of the center of the adhesion and of the neovascular lesion correlates very well as was reported by Mojana et al. [12]. The course of a vitreomacular adhesion over time is presented in Figure III.G-8.

1. Adhesion Versus Traction

Initial studies (PVD in AMD study (see above) and others) were conducted using time domain (Stratus) OCT evaluations that were able to identify vitreo-macular adhesion. However, differentiating between adhesion and traction was not possible without doubt, although traction was suspected in a high percentage of the cases. Sharp angulation of the posterior vitreous cortex present at the site of adhesion or a localized deformation of the retinal profile indicating traction could be detected definitively only with the help of spectral domain imaging. The incidence of vitreo-macular traction was 73.3 % in eyes with neovascular AMD presenting with vitreo-macular adhesion [8]. With the help of 3D animated images, traction lines could be visualized as directed towards the neovascularization. In early lesions with small neovascular membranes, it was even more obvious that

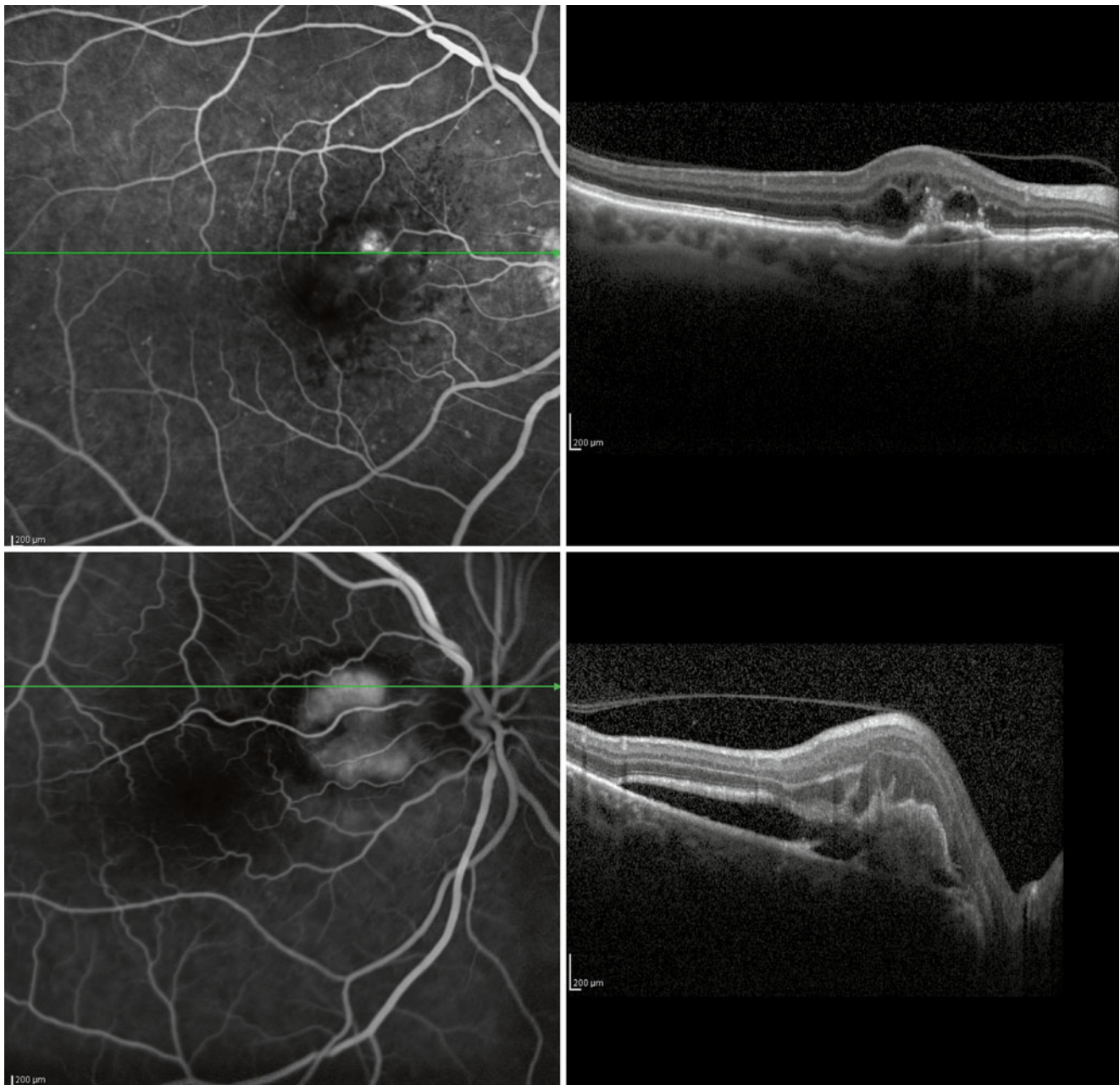


Figure III.G-7 The localization of the vitreo-macular adhesion corresponds to the localization of the choroidal neovascularization even in cases with juxta- or extrafoveal location. In the *upper panel*, a lesion

with retinal angiomatous proliferation localized in the supero-nasal fovea is presented, and in the *lower panel*, a juxtapapillary lesion is shown

the traction forces were directed to the origin of the neovascular membrane. These results of our own studies and examinations were confirmed also by Mojana et al., who found an incidence of traction in 60 % of the cases with vitreo-macular adherences [12].

C. Vitreopapillary Adhesion/Traction

Vitreopapillary adhesion (VPA) has been shown to be present in 87.5 % of full-thickness macular holes and 80 % of

macular pucker cases with intraretinal cysts [13, 14]. Based on these studies, it was proposed that VPA alters the vector of vitreo-macular traction forces inducing macular holes and tractional cystoid spaces [see chapter III.E. Vitreopapillary adhesion and traction]. This might also be a factor in the pathogenesis of exudative AMD. Indeed, in AMD studies, the use of Spectralis OCT has enabled observation of the foveal region and the rim of the optic disk in one single 8 mm scan of high quality in clinical practice. In a retrospective study of exudative AMD, vitreo-papillary adhesion was identified in 83 % of the cases with

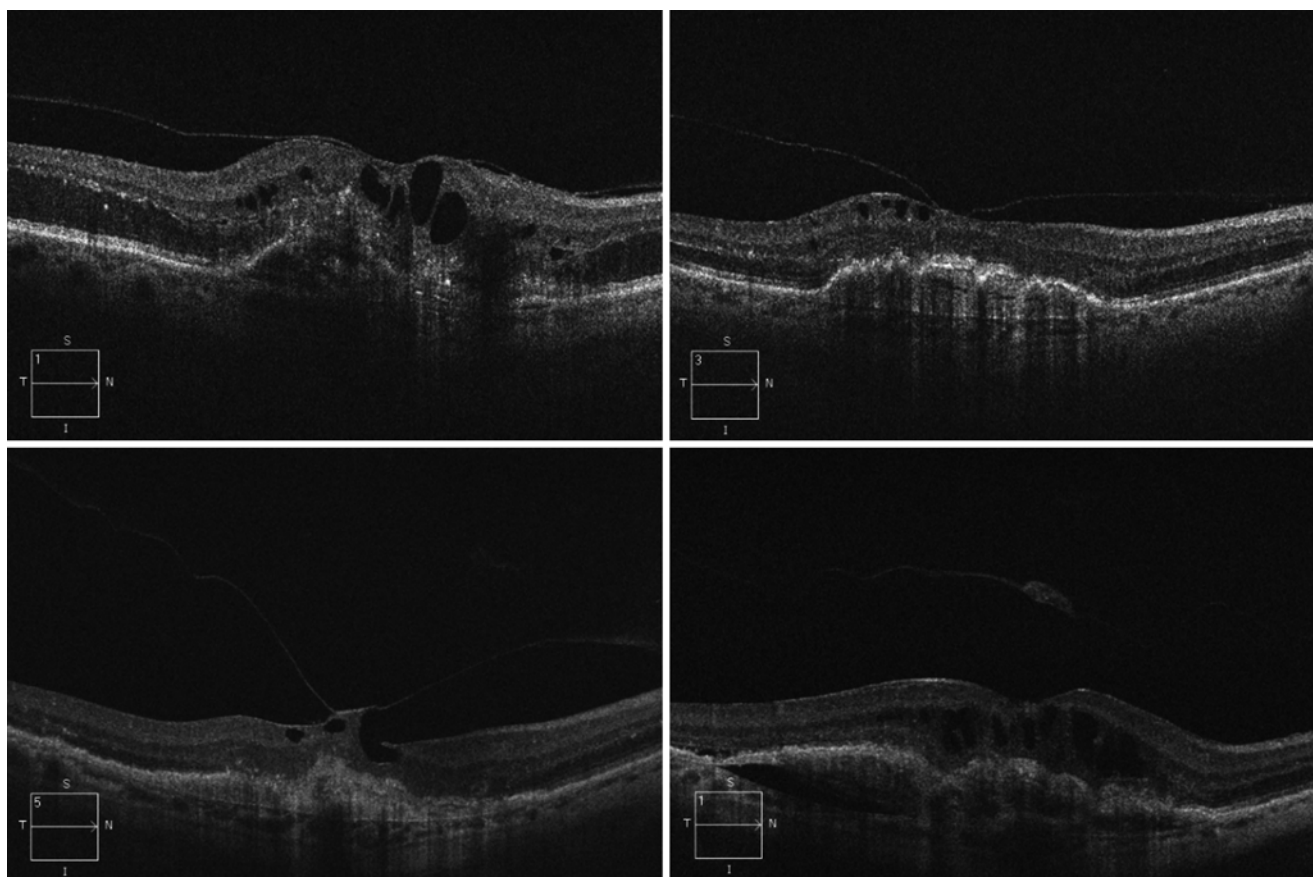


Figure III.G-8 The course of a very tight adherence is presented. At baseline (*upper left*), the vitreo-macular adhesion is broad; at month 6 (*upper right*), it is more localized; after 2 years, traction is obvious with

incipient macular hole; and 6 months later, the pseudo-opsoculum and the detached posterior vitreous cortex are seen

vitreo-macular adhesion [8]. In the remaining 17 %, the scans failed to show the optic disk in spite of the length of the scan. However, vitreo-papillary adhesions were also detected in the PVD in AMD study with Stratus OCT in nearly 60 % of the eyes with vitreo-macular adhesion, because radial lines through the optic disk were part of the study protocol (unpublished data). Obviously, the focal adhesions in AMD cases are in the areas where vitreous is naturally more firmly attached, such as the optic disk and fovea. Vitreo-papillary traction is known to be present also in other diagnoses like proliferative diabetic vitreo-retinopathy and macular hole [13, 14]. In diabetic cases, it has been demonstrated that vitreo-papillary traction can cause possibly reversible damage to the anterior optic nerve combined with a decrease of distance acuity [see chapter III.L. Proliferative diabetic vitreo-retinopathy]. Whether vitreo-papillary adhesion might contribute to a worse outcome of cases of AMD with vitreo-macular adhesion/traction has to be further explored.

1. Vitreoschisis

Anomalous PVD in exudative AMD may not only manifest as vitreo-macular and vitreo-papillary adhesions but also as

vitreoschisis, a split of the posterior vitreous cortex [15, 16]. While the incidence of vitreoschisis in AMD is not as high as vitreo-macular adhesion/traction, only 8 % in exudative AMD [8], there was more frequent vitreoschisis in cases of combined vitreo-papillary and vitreo-macular adhesion where a second layer was noted only adherent at the optic disk. Figure III.G-9 demonstrates splitting of the posterior vitreous. Like vitreo-papillary traction, vitreoschisis is apparent also in other cases associated with anomalous PVD like macular hole, macular pucker, or proliferative diabetic vitreo-retinopathy [see chapter III.B. Anomalous PVD and vitreoschisis].

IV. Role of Vitreous in Conversion from Dry to Exudative AMD

The AREDS study defined the risk of dry AMD cases converting to either geographic atrophy or choroidal neovascularization based on the number and size of drusen and the presence of pigment changes. In the PVD in AMD study (see above), the dry AMD cases were classified according to the AREDS classification [17, 18]. We found

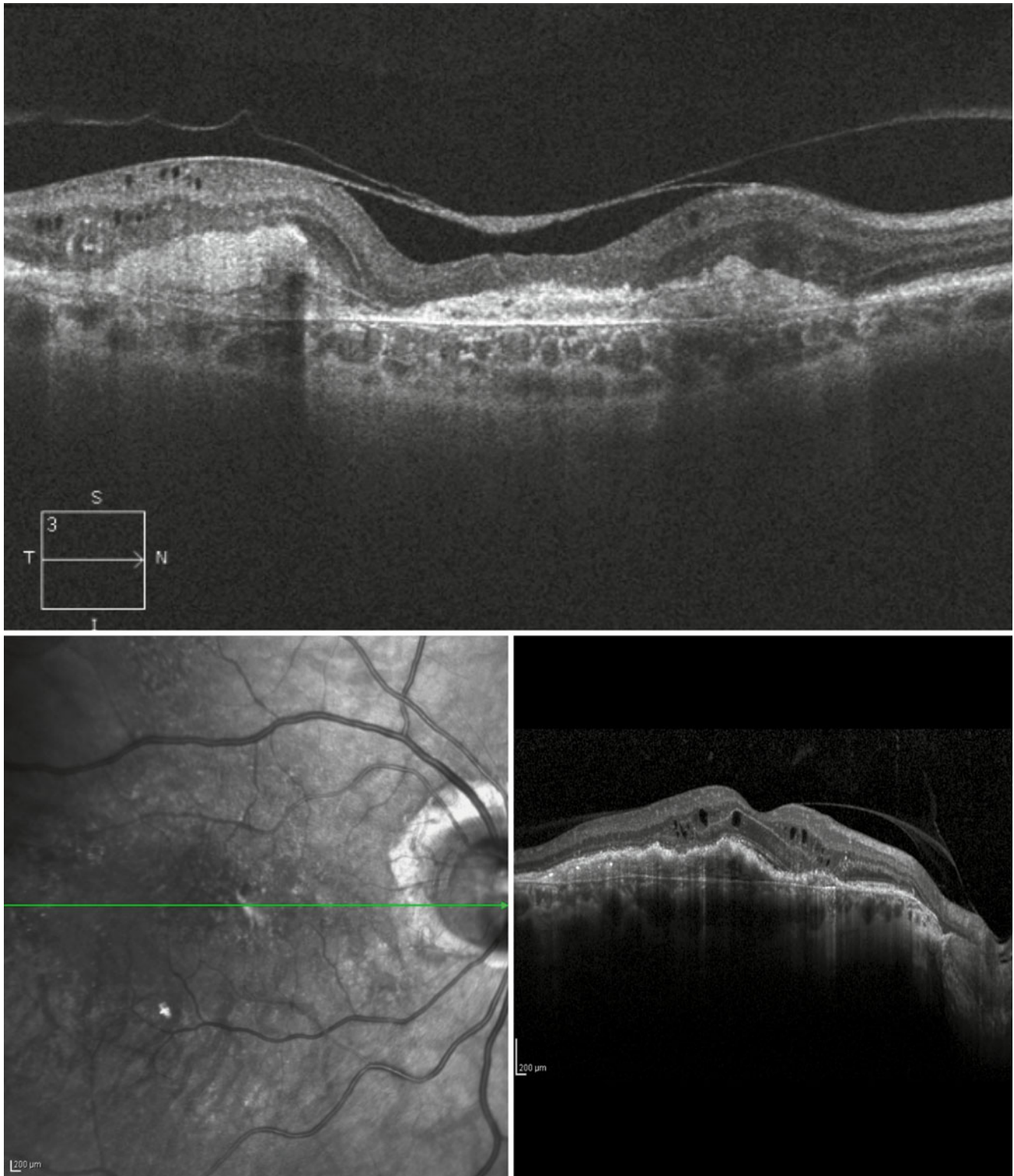


Figure III.G-9 In AMD cases, the posterior vitreous cortex is frequently not a single membrane, but vitreoschisis occurs frequently (in the *upper image* in the foveal region, in the *lower image* peripapillary)

a significant correlation between the AREDS risk to develop CNV in dry AMD and an attached posterior vitreous (odds ratio=0.065, 95 %-CI for odds ratio=[0.012, 0.362], p -value=0.00178). Six of 57 eyes (10.5 %) with

dry AMD developed exudative AMD (3 eyes AREDS III, 1 eye AREDS II, 2 eyes AREDS I), and after 2 years, in five of these six eyes, the vitreous was attached (extension of the PVD in AMD study) [5]. Central adhesion sur-

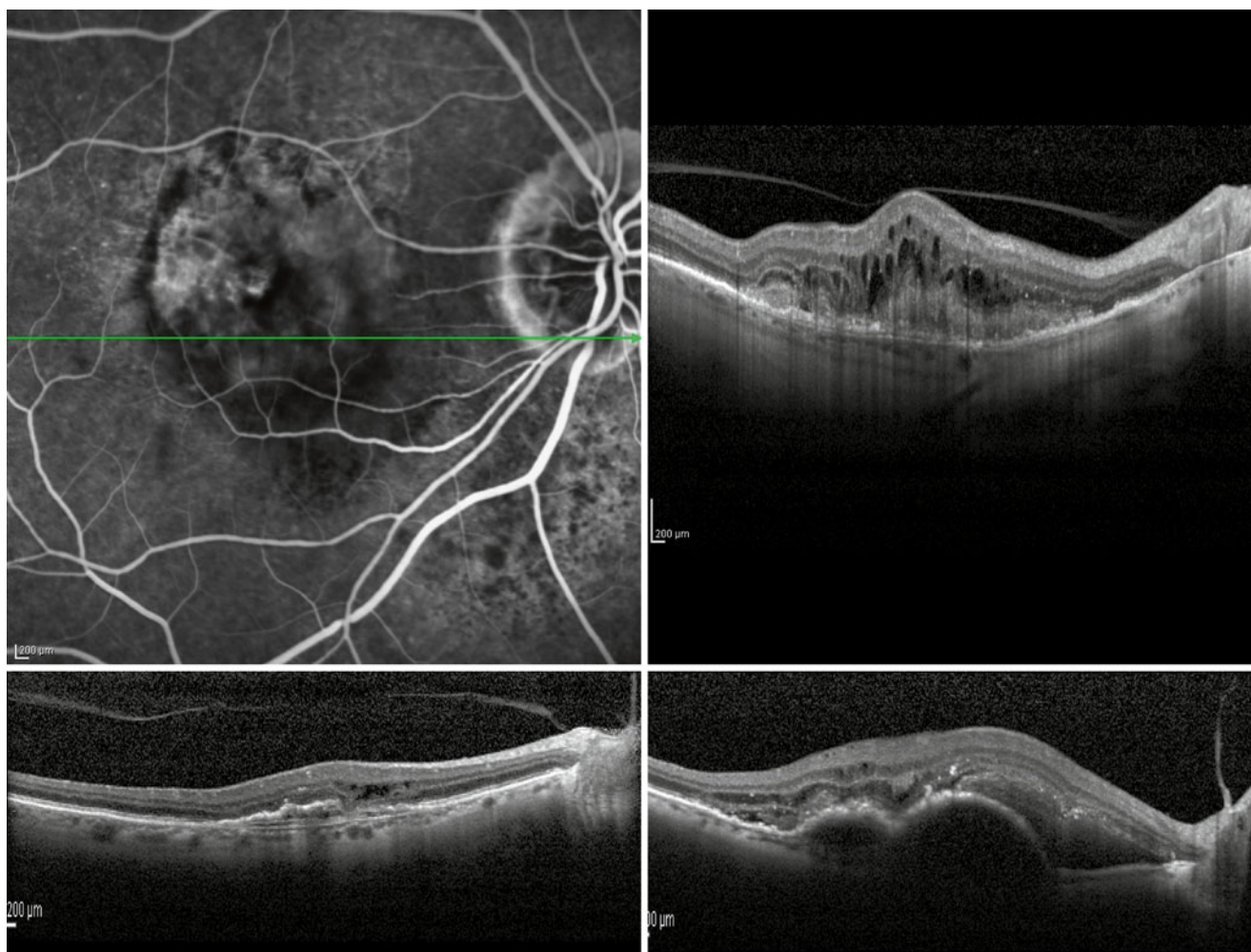


Figure III.G-10 Different stages of vitreo-macular and vitreo-papillary adhesions are presented. In the *upper image*, foveal and papillary adhesions are shown, and in the *lower images*, only vitreo-papillary adhesions are visible in the foveal region since the vitreous is already detached

rounded by elevation of the posterior vitreous cortex on OCT was more frequent in high-risk nonexudative AMD though not significant (p -value=0.670).

In a prospective study conducted at the Medical University of Vienna, the risk to develop exudative AMD in high-risk dry AMD cases was examined. This study was based on SD OCT findings only and did not find a significant influence of vitreo-macular adhesions to develop choroidal neovascularization within a 4-year observation period [19]. However, ultrasound examinations were not performed, and to evaluate the influence of vitreo-macular adhesions, the number of participants was not high enough. We therefore initiated a prospective study to evaluate the risk of developing neovascular AMD in dry AMD cases and calculated that a study population of 320 is mandatory. At present, the results of this study are not yet available.

V. Impact of Vitreous on Treatment of Exudative AMD

A. Spontaneous PVD

In our studies of vitreo-macular adhesion/traction (see above), the status of the posterior vitreous remained unchanged in the majority of eyes (76.7 %) up to 1 year later, in spite of anti-VEGF treatment [8]. In 10 %, a PVD occurred with release of vitreo-macular adhesion. Figure III.G-11 shows the impact of posterior vitreous on the course of the disease in three examples. This was associated with an increase in visual acuity and regression of the neovascular lesion. In contrast, an incidence of nearly 25 % of PVD was found within three months of intravitreal injections for various other conditions (including AMD). The impact on the activity of the disease and the visual acuity are not available [20].

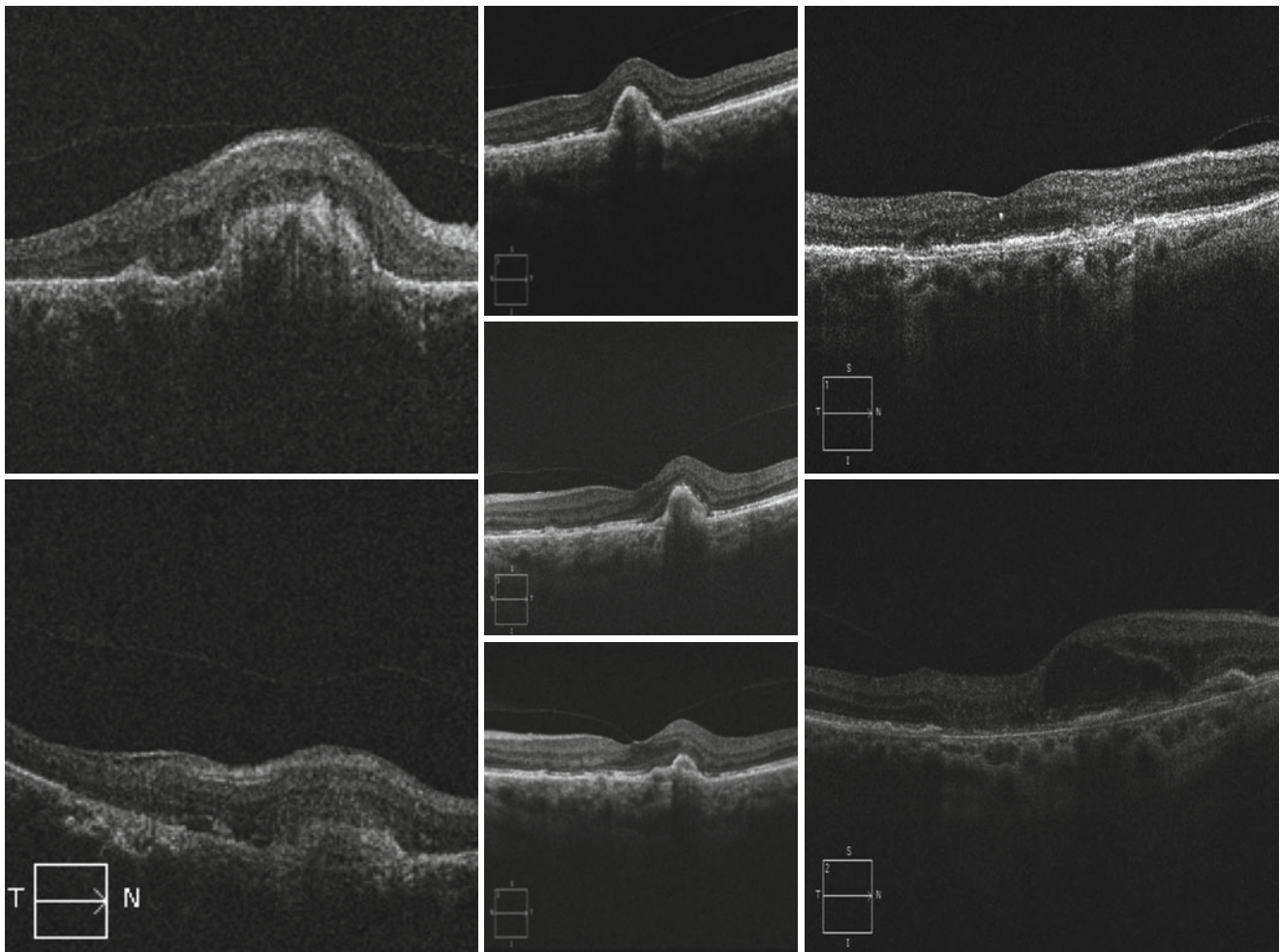


Figure III.G-11 The course of vitreo-retinal adhesions in relation to anti-VEGF treatment is shown. At the *left side*, spontaneous vitreous detachment occurred, and distance visual acuity improved by two lines.

In the *middle*, the adhesions remained unchanged, and distance visual acuity improved by one line. At the *right*, vitreo-macular traction increased, and distance visual acuity decreased by four lines

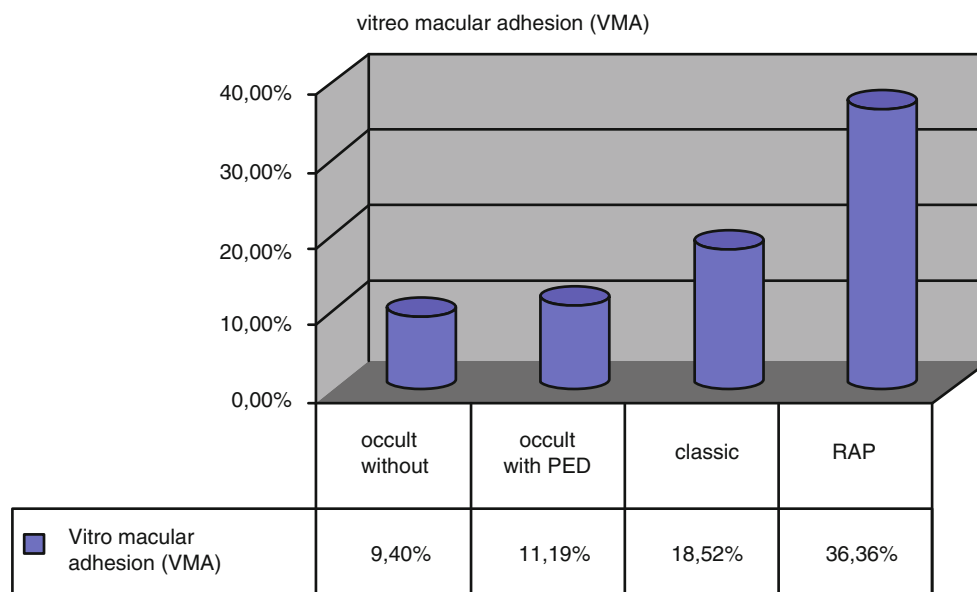
B. Nonresponders

Modern therapy of neovascular AMD consists of intravitreal injection of inhibitors of vascular endothelial growth factor (VEGF). Pegaptanib (Macugen) and ranibizumab (Lucentis) are approved for the therapy of exudative AMD. A third substance bevacizumab (Avastin) is frequently used off-label for treatment in the eye. The effect of Avastin has been shown in comparative studies to be non-inferior to Lucentis [21–23]. Macugen, the first substance approved, provided less favorable results. Whereas the effect of these substances was the subject of many publications, there is little information concerning nonresponders in the literature.

In a retrospective evaluation of 287 patients who completed a 12-month examination, we evaluated distance acuity, retinal thickness measured with OCT, and lesion size at baseline, months 3 and 12. Usually there is a steep increase of distance acuity and decrease of retinal thickness in the first 3

months of therapy, and thereafter the success is maintained. Therefore, we evaluated the cases at month 3 and declared patients exhibiting a loss of ≥ 3 lines distance acuity and/or an increase of retinal thickness and/or lesion size as nonresponders. Vitreo-macular adhesion was present in 12.94 % of responders and 29.17 % of nonresponders. Besides distance acuity at baseline, vitreo-macular adhesion was the only factor significantly associated with nonresponders. Demographic data, the presence of blood, fibrosis, and the type lesion did not reveal a significant influence. Delayed response occurred overall in only 10 %. One of these cases was an eye with vitreo-macular adherence, which exhibited a spontaneous PVD [24]. Another study compared the outcome of anti-VEGF therapy of eyes with and without vitreo-macular adhesions and found a significantly better outcome of lesions without adhesions [25]. A possible bias by including lesions of different composition could not be excluded in this study, because lesion type and composition were not evaluated.

Figure III.G-12 The incidence of vitreo-macular adhesion was higher in classic lesions and especially in lesions with retinal angiomatous proliferation



There are different hypotheses, why lesions with vitreo-macular adhesion might have a worse response to therapy. Mechanical traction during eye movements may potentiate low-grade inflammation [26, 27]. Another possible explanation is the persistence of retinal edema due to traction on the retina. Since retinal edema promotes hypoxia and hypoxia causes VEGF production, it might explain the nonresponse in these cases. It is also plausible that vitreo-macular adhesion/traction prevents flattening of the retinal pigment epithelium (RPE) in cases of RPE detachment or cause tears of the RPE, a feared complication of RPE detachment. Similar processes might be responsible for recurrences in eyes treated by photodynamic therapy exhibiting vitreo-macular adhesion/traction.

C. Polypoidal Choroidal Vasculopathy and Retinal Angiomatous Proliferation

Until recently, the only available therapies of exudative AMD were argon laser photocoagulation and photodynamic therapy. The success of these therapies was related much to the lesion type and composition. In modern anti-VEGF therapy, the lesion type does not play as important a role. However, in clinical practice, some lesion types, like polypoidal choroidal vasculopathy (PCV) and retinal angiomatous proliferation (RAP), are thought to have a worse outcome than other lesions [28, 29]. Concerning PCV, a higher incidence of PVD was found than in typical exudative AMD, and vitreo-macular adhesions tended to be more frequent in eyes without PCV. Therefore, worse outcome in eyes with PCV seems to be not associated with changes at the vitreo-macular interface

[30]. In the nonresponder study, the incidence distribution of vitreo-macular adhesion was quite different between different lesion types. Occult lesions without and with detachment of the RPE had a low incidence of vitreo-macular adhesion (9.4 and 11.2 %, respectively). Vitreo-macular adhesion was more frequent in classic lesions (18.5 %) and most frequent in RAP lesions (36.4 %), results presented in Figure III.G-12. The incidence of nonresponders was higher in the RAP group, but did not reach statistical significance in contrast to the incidence of vitreo-macular adhesion. The association of RAP lesions and vitreo-macular adhesion was also seen in another of our studies where 50 % of the lesions with vitreo-macular adhesion were RAP lesions [8].

D. Vitrectomy

Further evidence of the important role of an adherent posterior vitreous in exudative AMD is provided by the influence of vitrectomy. There are two studies reporting a higher incidence of AMD (geographic atrophy and choroidal neovascularization) in non-vitrectomized eyes compared to the fellow eyes which underwent pars plana vitrectomy for different reasons other than AMD [31, 32]. The first experiences of the effect of vitrectomy on an already established neovascular AMD originate from as early as 2000 [33]. Regression of choroidal neovascularization was achieved in 6 of 12 cases with attached posterior vitreous and an active neovascular lesion. In a series of 54 eyes with vitreous hemorrhage and exudative AMD, regression of choroidal neovascularization was observed in 74 % following pars plana vitrectomy [34]. Furthermore, in eyes with unsuccessfully treated exudative AMD (PDT

or anti-VEGF) and vitreo-macular traction, vitrectomy and release of traction were accompanied by regression of the neovascular membrane, albeit in some cases only transient [12, 35, 36]. The favorable effect of pars plana vitrectomy is not only based on the mechanical removal of vitreo-macular adhesion/traction but also an increase of oxygenation after vitrectomy, verified in eyes with retinal vein occlusion and diabetic retinopathy [37, 38]. The better diffusion and availability of oxygen after vitrectomy have also been demonstrated in animals and also in humans [39] [see chapter IV.B. Oxygen in vitreo-retinal physiology and pathology].

E. Pharmacologic Vitreolysis

Pharmacologic vitreolysis is a term used for the intravitreal application of pharmacologic agents to induce posterior vitreous detachment (vitreoretinal separation and vitreous liquefaction) [40, 41; see chapter VI.A. Pharmacologic vitreolysis]. Concerning age-related macular degeneration, results after pharmacologic vitreolysis are rare so far. In 4 of 4 eyes with vitreo-macular adhesion that were nonresponsive to anti-VEGF treatment, a PVD was achieved by intravitreal injection of 0.3 mL of 100 % perfluoropropane [42]. In nearly 70 % of 27 eyes, a PVD occurred after intravitreally applied tissue plasminogen activator, significantly more frequent than after intravitreal bevacizumab injection [43]. There are a series of studies ongoing using ocriplasmin in various diagnoses [44]. Combined therapy of intravitreally applied ocriplasmin and anti-VEGF might be favorable especially in nonresponders with an attached posterior vitreous cortex.

VI. The Putative Role of Vitreous in the Pathogenesis of AMD

Considering the importance of AMD, especially exudative AMD, there are understandably many studies that have been performed to identify the pathogenesis of this disease. Currently, a multifactorial etiology is suspected. A series of contributing factors have been identified, such as genetic, aging, and environmental factors [45]. Morphological changes at the vitreo-macular interface of exudative AMD, summarized as anomalous PVD, have been proven in a series of studies, but are still only associations. While the aforementioned findings regarding the impact of vitreous on AMD, especially therapy, are highly suggestive, these are not studies that prove causation. Possibly, anomalous PVD and neovascular AMD are caused by a third, up to now unknown, factor. It is also plausible that the developing

neovascularization promotes vitreo-macular adhesion, possibly by localized inflammation or by exudation containing fibrin from new vessels [46]. Certainly, this might strengthen localized adherences between the posterior vitreous and the anterior retina. However, this theory cannot explain why normal age-related PVD did not occur before choroidal neovascularization developed. Furthermore, the size of the adherences is much smaller than the area occupied by the retinal or subretinal fluid exudation [12]. In our opinion, it is more plausible that an anomalous PVD influences the development and/or progression of exudative AMD, perhaps by traction, hypoxia, and/or low-grade inflammation.

A. Traction

Traction has been detected in more than 73 % of exudative AMD eyes with vitreo-macular adhesion [8]. 3D animation visualized the direction of the traction forces from the vitreous towards the retina more specifically towards the choroidal neovascular complex. In these cases, the traction forces are directed from anterior to posterior. But also in eyes with completely attached posterior vitreous, traction forces might be present between areas of loose or tighter adherences [26, 27]. During eye movements, tangential traction forces may act, further exaggerated by vitreo-papillary adhesion, as seen in other vitreo-maculopathies. This thesis is supported by cases presenting first with flat adherences and a more tangential vector of traction. In the course of the disease, the elevation of the posterior vitreous increases, and traction in an anterior posterior direction becomes more prominent [8].

Different pathogenic consequences of traction in the development of neovascular AMD can be imagined. When the anterior part of the retina is pulled apart, the hydrostatic pressure in the posterior retina decreases, and fluid and blood cells might enter the area of lower pressure leading to focal edema [26, 27, 47]. The same mechanism might also be responsible for the decreased responsiveness of neovascular lesions to treatment. Furthermore, the traction forces might cause chronic low-grade inflammation, further contributing to the neovascular stimulus. Lastly, the distortion of structures in the outer retina could prevent the normal supply of nutrients and oxygen (see below).

B. Low-Grade Inflammation

The traction forces might cause chronic low-grade inflammation. Even, when the traction is not yet visible by currently available imaging technologies, the steady stimulus caused by localized tighter vitreo-macular adhesion could be responsible for low-grade inflammation. The importance of inflammation in the development of neovascular AMD

was supported by histopathological examinations of excised neovascular membranes containing inflammatory cells [27]. The findings of examinations of the composition of drusen suggested that activation of the complement system and resultant release of inflammatory mediators play an important role in the etiology of exudative AMD. This was further supported by genetic studies especially of polymorphisms of the complement regulating factor H. The good response of neovascular lesions to anti-inflammatory therapy is additional evidence of the importance of inflammation [48].

C. Barrier Function

1. Hypoxia

Hypoxia is one of the most prominent drivers of angiogenesis and therefore promoters of exudative AMD. The outer two-thirds of the retina are supplied by oxygen and nutrients by the choroidal vasculature, the inner third by the retinal vessels. Oxygen diffuses through the structures of the outer retina and is consumed by the photoreceptors. The partial pressure of O_2 (PO_2) decreases almost linearly with distance from the choriocapillaris to the inner portion of the photoreceptors, where it reaches values of 0 [47]. Thickening of Bruch's membrane, large drusen, and detachment of the retinal pigment epithelium might all increase the distance between choriocapillaris and the photoreceptors and cause hypoxia at the level of the photoreceptors. Vitreous traction might cause localized ischemia and prevent support of the photoreceptors with oxygen. Furthermore, the attached posterior vitreous might prevent oxygen diffusion to the metabolically active cells. Due to the viscous nature of vitreous gel, diffusion of oxygen and other molecules is much slower than in saline solution. In cases of abnormal tissue at the vitreo-macular interface, inadequate diffusion of oxygen might occur comparable to inadequate diffusion through the thickened Bruch's membrane causing hypoxia.

Further support to the theory that the attached vitreous plays an important role concerning the diffusion of oxygen to the retina was provided by studies measuring the PO_2 before and after vitrectomy. They found an increased PO_2 after vitrectomy compared to values before vitrectomy pre-retinal and in the mid-vitreous cavity [35, 36]. Similar examinations were performed before and after pharmacologic vitreolysis with ocriplasmin in rats and guinea pigs [49]. After PVD, there were increased values of PO_2 compared to controls with attached vitreous as well as a faster increase of PO_2 after exposure of 100 % oxygen by face mask. Obviously, oxygen is distributed faster when vitreous is detached. Interestingly, the increase of PO_2 failed to appear when only

liquefaction (by injection of hyaluronidase) of the vitreous occurred without syneresis and PVD.

2. Macular Cytokine Load

Vascular endothelial growth factor (VEGF) is an important angiogenic growth factor also causing hyperpermeability. It has been detected in excised neovascular membranes, and its importance in causing neovascularization in and beneath the macula and other locations in the eye and the whole body in vivo and in vitro has been proven [50, 51]. The production of VEGF and other growth factors is regulated by oxygen. Hypoxia increases the upregulation of VEGF, which causes neovascularization and retinal edema. Retinal edema increases the distance between choriocapillaris and photoreceptors and therefore also increases hypoxia, resulting in a vicious circle [47]. Posterior vitreous attachment can increase local levels of VEGF and cytokines by preventing egress anteriorly. Due to the large size of the VEGF molecule, diffusion might be considerably slowed by the high density of collagen in the posterior vitreous cortex. Vitreous detachment and also vitrectomy can facilitate a higher clearance rate of these substances from the macula [39]. Besides these physiological considerations, VEGF might also be bound by age-altered vitreous collagen fibrils in the posterior vitreous cortex.

Abbreviations

3D	Three-Dimensional
AMD	Age-Related Macular Degeneration
AREDS	Age-Related Eye Disease Study
CNV	Choroidal Neovascularization
CPU	Central Processing Unit
CUDA	Compute Unified Device Architecture
DOF	Depth of Field
GPU	Graphics Processor Units
HDRI	High Dynamic Range Image
mm	Millimeter
OCT	Optical Coherence Tomography
PCV	Polypoidal Choroidal Vasculopathy
PDT	Photodynamic Therapy
PO ₂	Partial Pressure of Oxygen
PVD	Posterior Vitreous Detachment
PVR	Proliferative Vitreo-Retinopathy
RAP	Retinal Angiomatous Proliferation
RPE	Retinal Pigment Epithelium
SD	Spectral Domain
US	Ultrasonography
VEGF	Vascular Endothelial Growth Factor
VPA	Vitreo-Papillary Adhesion
μm	Micron

References

- Weber-Krause B, Eckardt C. Incidence of posterior vitreous detachment in the elderly. *Ophthalmologie*. 1997;94:619–23. German.
- Ondes F, Yilmaz G, Acar MA, Unlu N, Kocaoglan H, Arsan AK. Role of the vitreous in age-related macular degeneration. *Jpn J Ophthalmol*. 2000;44(1):91–3.
- Binder S, Krebs I, Hilgers RD, et al. Outcome of transplantation of autologous retinal pigment epithelium in age-related macular degeneration: a prospective trial. *Invest Ophthalmol Vis Sci*. 2004;45:4151–60.
- Foos RY. Posterior vitreous detachment. *Trans Am Acad Ophthalmol Otolaryngol*. 1972;76:480–97.
- Krebs I, Brannath W, Glittenberg C, Zeiler F, Sebag J, Binder S. Posterior vitreomacular adhesion: a potential risk factor for exudative age-related macular degeneration? *Am J Ophthalmol*. 2007;144(5):741–6. Epub 2007 Sep 20.
- Robison CD, Krebs I, Binder S, Barbazetto IA, Kotsolis AI, Yannuzzi LA, Sadun AA, Sebag J. Vitreomacular adhesion in active and end-stage age-related macular degeneration. *Am J Ophthalmol*. 2009;148:79–82.
- Lee SJ, Lee CS, Koh HJ. Posterior vitreomacular adhesion and risk of exudative age-related macular degeneration: paired eye study. *Am J Ophthalmol*. 2009;147:621–6.
- Krebs I, Glittenberg C, Zeiler F, Binder S. Spectral domain optical coherence tomography for higher precision in the evaluation of vitreoretinal adhesions in exudative age-related macular degeneration. *Br J Ophthalmol*. 2011;95(10):1415–8.
- Yannuzzi LA, Negro S, Iida T, et al. Retinal angiomatous proliferation in age-related macular degeneration. *Retina*. 2001;21:416–34.
- Slakter JS, Yannuzzi LA, Schneider U, et al. Retinal choroidal anastomoses and occult choroidal neovascularization in age-related macular degeneration. *Ophthalmology*. 2000;107:742–53.
- Freund KB, Ho IV, Barbazetto IA, Koizumi H, Laud K, Ferrara D, Matsumoto Y, Sorenson JA, Yannuzzi L. Type 3 neovascularization: the expanded spectrum of retinal angiomatous proliferation. *Retina*. 2008;28:201–11.
- Mojana F, Cheng L, Bartsch DU, Silva GA, Kozak I, Nigam N, Freeman WR. The role of abnormal vitreomacular adhesion in age-related macular degeneration: spectral optical coherence tomography and surgical results. *Am J Ophthalmol*. 2008;146:218–27.
- Wang MY, Nguyen D, Hindoyan N, Sadun AA, Sebag J. Vitreopapillary adhesion in macular hole and macular pucker. *Retina*. 2009;29:644–50.
- Sebag J, Wang MY, Nguyen D, Sadun AA. Vitreopapillary adhesion in macular diseases. *Trans Am Ophthalmol Soc*. 2009;107:35–44.
- Gupta P, Yee KM, Garcia P, Rosen RB, Parikh J, Hageman GS, Sadun AA, Sebag J. Vitreoschisis in macular diseases. *Br J Ophthalmol*. 2011;95(3):376–80. doi:10.1136/bjo.2009.175109. Epub 2010 Jun 28.
- Sebag J. Vitreoschisis. *Graefes Arch Clin Exp Ophthalmol*. 2008;246(3):329–32. doi:10.1007/s00417-007-0743-x. Epub 2008 Jan 29.
- Davis MD, Gangnon RE, Lee LY, Hubbard LD, Klein BE, Klein R, Ferris FL, Bressler SB, Milton RC, Age-Related Eye Disease Study Group. The Age-Related Eye Disease Study severity scale for age-related macular degeneration: AREDS Report No. 17. *Arch Ophthalmol*. 2005;123:1484–98.
- Ferris FL, Davis MD, Clemons TE, Lee LY, Chew EY, Lindblad AS, Milton RC, Bressler SB, Klein R, Age-Related Eye Disease Study (AREDS) Research Group. A simplified severity scale for age-related macular degeneration: AREDS Report No. 18. *Arch Ophthalmol*. 2005;123:1570–4.
- Waldstein SM, Sponer U, Simader C, Sacu S, Schmidt-Erfurth U. Influence of vitreomacular adhesion on the development of exudative age-related macular degeneration: 4-year results of a longitudinal study. *Retina*. 2012;32(3):424–33.
- Geck U, Pustolla N, Baraki H, Atili A, Feltgen N, Hoerauf H. Posterior vitreous detachment following intravitreal drug injection. *Graefes Arch Clin Exp Ophthalmol*. 2013;251(7):1691–5.
- CATT Research Group, Martin DF, Maguire MG, Ying GS, Grunwald JE, Fine SL, Jaffe GJ. Ranibizumab and bevacizumab for neovascular age-related macular degeneration. *N Engl J Med*. 2011;364(20):1897–908. Epub 2011 Apr 28.
- IVAN Study Investigators, Chakravarthy U, Harding SP, Rogers CA, Downes SM, Lotery AJ, Wordsworth S, Reeves BC. Ranibizumab versus bevacizumab to treat neovascular age-related macular degeneration: one-year findings from the IVAN randomized trial. *Ophthalmology*. 2012;119(7):1399–411. Epub 2012 May 11.
- Krebs I, Schmetterer L, Boltz A, Told R, Vécsei-Marlovits V, Egger S, Schönherr U, Haas A, Ansari-Shahrezaei S, Binder S; for the MANTA Research Group. A randomised double-masked trial comparing the visual outcome after treatment with ranibizumab or bevacizumab in patients with neovascular age-related macular degeneration. *Br J Ophthalmol*. 2013. 97(3):266–71.
- Krebs I, Glittenberg C, Ansari-Shahrezaei S, Hagen S, Steiner I, Binder S. Non-responders to treatment with antagonists of vascular endothelial growth factor in age-related macular degeneration. *Br J Ophthalmol*. 2013;97(11):1443–6. doi:10.1136/bjophthalmol-2013-303513. Epub 2013 Aug 21.
- Lee SJ, Koh HJ. Effects of vitreomacular adhesion on anti-vascular endothelial growth factor treatment for exudative age-related macular degeneration. *Ophthalmology*. 2011;118(1):101–10.
- Schulze S, Hoerle S, Mennel S, Kroll P. Vitreomacular traction and exudative age-related macular degeneration. *Acta Ophthalmol*. 2008;86(5):470–81. doi:10.1111/j.1755-3768.2008.01210.x. Epub 2008 Jun 28. Review.
- Simpson AR, Petrarca R, Jackson TL. Vitreomacular adhesion and neovascular age-related macular degeneration. *Surv Ophthalmol*. 2012;57(6):498–509. doi:10.1016/j.survophthal.2012.01.011.
- Cho M, Barbazetto IA, Freund KB. Refractory neovascular age-related macular degeneration secondary to polypoidal choroidal vasculopathy. *Am J Ophthalmol*. 2009;148(1):70–8.
- Rouvas AA, Chatziralli IP, Theodossiadis PG, Moschos MM, Kotsolis AI, Ladas ID. Long-term results of intravitreal ranibizumab, intravitreal ranibizumab with photodynamic therapy, and intravitreal triamcinolone with photodynamic therapy for the treatment of retinal angiomatous proliferation. *Retina*. 2012;32(6):1181–9. doi:10.1097/IAE.0b013e318235d8ce.
- Nomura Y, Ueta T, Iriyama A, Inoue Y, Obata R, Tamaki Y, Yamaguchi T, Yanagi Y. Vitreomacular interface in typical exudative age-related macular degeneration and polypoidal choroidal vasculopathy. *Ophthalmology*. 2011;118(5):853–9. doi:10.1016/j.ophtha.2010.09.001. Epub 2010 Nov 20.
- Roller AB, Mahajan VB, Boldt HC, Abramoff MD, Russell SR, Folk JC. Effects of vitrectomy on age-related macular degeneration. *Ophthalmology*. 2010;117(7):1381–6. doi:10.1016/j.ophtha.2009.11.007. Epub 2010 Feb 21.
- Schulze S, Neugebauer A, Kroll P. Appearance of age-related macular degeneration in vitrectomized and nonvitrectomized eyes: an intraindividual case study. *Acta Ophthalmol*. 2012;90(3):244–7. doi:10.1111/j.1755-3768.2010.01929.x. Epub 2010 May 14.
- Ikeda T, Sawa H, Koizumi K, Yasuhara T, Yamasaki T. Pars plana vitrectomy for regression of choroidal neovascularization with age-related macular degeneration. *Acta Ophthalmol Scand*. 2000;78(4):460–4.
- Sakamoto T, Sheu SJ, Arimura N, Sameshima S, Shimura M, Uemura A, Kawano H, Wu TT, Kubota T, Sohma R, Noda Y. Vitrectomy for exudative age-related macular degeneration with vitreous hemorrhage. *Retina*. 2010;30(6):856–64. doi:10.1097/IAE.0b013e3181c969cb.
- Shah SU, Haller JA. Vitreomacular traction in a case of exudative age-related macular degeneration resistant to anti-VEGF

- therapy. *Acta Ophthalmol.* 2012;90(7):e569–70. doi:[10.1111/j.1755-3768.2011.02372.x](https://doi.org/10.1111/j.1755-3768.2011.02372.x). Epub 2012 Mar 16.
36. Schmidt JC, Mennel S, Hörle S, Meyer CH. High incidence of vitreomacular traction in recurrent choroidal neovascularisation after repeated photodynamic therapy. *Br J Ophthalmol.* 2006;90(11):1361–2. Epub 2006 Jul 19.
 37. Williamson TH, Grewal J, Gupta B, Mokete B, Lim M, Fry CH. Measurement of PO₂ during vitrectomy for central retinal vein occlusion, a pilot study. *Graefes Arch Clin Exp Ophthalmol.* 2009;247(8):1019–23. doi:[10.1007/s00417-009-1072-z](https://doi.org/10.1007/s00417-009-1072-z). Epub 2009 Apr 4.
 38. Maeda N, Tano Y. Intraocular oxygen tension in eyes with proliferative diabetic retinopathy with and without vitreous. *Graefes Arch Clin Exp Ophthalmol.* 1996;234 Suppl 1:S66–9.
 39. Stefánsson E. Physiology of vitreous surgery. *Graefes Arch Clin Exp Ophthalmol.* 2009;247(2):147–63. doi:[10.1007/s00417-008-0980-7](https://doi.org/10.1007/s00417-008-0980-7). Epub 2008 Nov 26. Review.
 40. Sebag J. Pharmacologic vitreolysis (Guest Editorial). *Retina* 1998;18:1–3.
 41. Sebag J. Pharmacologic vitreolysis - premise and promise of the first decade. *Retina.* 2009;29(7):871–4. doi:[10.1097/IAE.0b013e3181ac7b3c](https://doi.org/10.1097/IAE.0b013e3181ac7b3c).
 42. Kim YM, Lee SJ, Koh HJ. Gas-assisted release of vitreomacular adhesion in wet age-related macular degeneration. *Retina.* 2011;31(10):2123–4.
 43. Abrishami M, Moosavi MN, Shoeibi N, Hosseinpour SS. Intravitreal tissue plasminogen activator to treat refractory diabetic macular edema by induction of posterior vitreous detachment. *Retina.* 2011;31(10):2065–70.
 44. Kuppermann BD. Ocriplasmin for pharmacologic vitreolysis. *Retina.* 2012;32 Suppl 2:S225–8; discussion S228–31.
 45. Spaide RF, Armstrong D, Browne R. Continuing medical education review: choroidal neovascularization in age-related macular degeneration—what is the cause? *Retina.* 2003;23:595–614.
 46. Grossniklaus HE, Miskala PH, Green WR, Bressler SB, Hawkins BS, Toth C, Wilson DJ, Bressler NM. Histopathologic and ultrastructural features of surgically excised subfoveal choroidal neovascular lesions: submacular surgery trials report no. 7. *Arch Ophthalmol.* 2005;123(7):914–21.
 47. Stefánsson E, Geirsdóttir A, Sigurdsson H. Metabolic physiology in age related macular degeneration. *Prog Retin Eye Res.* 2011;30(1):72–80. doi:[10.1016/j.preteyeres.2010.09.003](https://doi.org/10.1016/j.preteyeres.2010.09.003). Epub 2010 Oct 15.
 48. Donoso LA, Kim D, Frost A, Callahan A, Hageman G. The role of inflammation in the pathogenesis of age-related macular degeneration. *Surv Ophthalmol.* 2006;51(2):137–52. Review.
 49. Quiram PA, Leverenz VR, Baker RM, Dang L, Giblin FJ, Trese MT. Microplasmin-induced posterior vitreous detachment affects vitreous oxygen levels. *Retina.* 2007;27(8):1090–6.
 50. Kvant A, Algvare PV, Berglin L, Seregard S. Subfoveal fibrovascular membranes in age-related macular degeneration express vascular endothelial growth factor. *Invest Ophthalmol Vis Sci.* 1996;37(9):1929–34.
 51. Adamis AP, Shima DT. The role of vascular endothelial growth factor in ocular health and disease. *Retina.* 2005;25(2):111–8. Review.

J. Sebag, Stephan Dunker, and W. Richard Green

Outline

I. Structure

A. Peripheral Vitreo–Retinal Attachments

1. Vitreous Base
2. Ora Bays
3. Meridional Folds
4. Meridional Complexes
5. Peripheral Retinal Excavations
6. Retinal Tufts
 - a. Non-Cystic Retinal Tufts
 - b. Cystic Retinal Tufts
 - c. Zonular Traction Tufts
7. Spiculated and Nodular Pigment Epithelial Hyperplasia
8. Retinal Lattice
9. White-With-Pressure, White-Without-Pressure
10. Verruca

II. Mechanics of Peripheral Vitreo–Retinal Traction

III. Alterations of Peripheral Vitreo–Retinal Structure

- A. Post-Traumatic Retinal Healing
- B. Aging Changes at the Peripheral Vitreo–Retinal Interface
- C. Retinal Breaks Unrelated to PVD

IV. Effects of Anomalous PVD

- A. Vitreous Traction on Peripheral Retina
 1. Retinal Tags
 2. Retinal Folds
 3. Cystic Degeneration and Peripheral Retinoschisis
 4. Retinal Pits (Lamellar Retinal Tears)
 5. Retinal Tears

V. Vasculopathies of the Peripheral Fundus

- A. Tractional Avulsion of Retinal Vessels
- B. Sickle-Cell Vasculopathies
- C. Coats' Disease

VI. Pars Planitis

- A. Epidemiology and Clinical Presentation
- B. Sequelae
- C. Therapy

References

Keywords

Vitreous • Retina • Anomalous PVD • Peripheral fundus lesions • Retinal lattice • Retinal tears • Retinal detachments • Peripheral vascular disorders • Pars planitis

Key Concepts

1. Vitreous is involved in peripheral fundus diseases; however, its role is unclear due to the lack of adequate imaging of the peripheral vitreous and vitreoretinal interface, limiting our ability to develop pathogenic concepts. Future imaging modalities should address this deficiency to improve diagnosis and management.
2. Anatomic as well as epidemiologic studies help us to understand normal and pathological entities of the vitreoretinal periphery. A review of the knowledge about known structures in health and disease reveals a complex interaction of acellular vitreous, embryonic remnants, connective tissue, and neuronal cells with retinal circulation manifesting in a variety of (sometimes rare) diseases.
3. There are well-defined peripheral lesions that are visible by indirect ophthalmoscopy with scleral depression whose relationship to sight-threatening disease has been well characterized, enabling proper selection of those lesions in need of treatment and those that can be safely observed without treatment.

J. Sebag, MD, FACS, FRCOphth, FARVO (✉)
VMR Institute for Vitreous Macula Retina,
7677 Center Avenue, Huntington Beach, CA 92647, USA

Doheny Eye Institute, Los Angeles, CA, USA
e-mail: jsebag@VMRinstitute.com

S. Dunker, MD
Troisdorf-Sieglar, Germany
e-mail: info@augenarzt-troisdorf.de

W.R. Green, MD (posthumously)
Wilmer Eye Institute, Johns Hopkins University, Baltimore, MD, USA

I. Structure

Vitreous occupies about four-fifths of the volume of the eye and weighs approximately 4 g. The vitreous body is somewhat spherical with slight flattening meridionally and has a cup-shaped depression anteriorly, known as the patellar fossa. The vitreous body is attached to all contiguous structures, but the firmness of the attachment varies with topography and age [1–3]. It is most firmly attached at the vitreous base, a 3-dimensional doughnutlike structure that is 3–6 mm wide and straddles the ora serrata. The vitreous base includes the posterior 2 mm of the pars plana and from 1 to 4 mm of the anterior retina posterior to the ora serrata. The posterior border of the vitreous base is located farther posteriorly in older individuals [4] and is more anterior nasally than temporally [5], which may underlie the greater frequency of retinal tears

temporally than elsewhere in the peripheral retina [4]. The density of vitreous collagen is greatest within the vitreous base, and the collagen fibers are oriented perpendicular to the retinal plane, whereas elsewhere the orientation is tangential to this plane. The vitreous base contains remnants of the fetal hyaloid vasculature, and it has been suggested that fetal antigens in this region of the vitreous [6] or degenerative products of the vitreous [7] may be immunogenic and play a role in ocular inflammatory diseases, such as pars planitis.

Sebag and Balazs [8–11] performed dark-field slit microscopy of normal human eyes from donors aged 33 weeks of gestation to 88 years and described that with aging there appeared fibers coursing in an anteroposterior direction in the central and posterior vitreous which inserted into the vitreous base anterior as well as posterior to the ora serrata (Figure III.H-1). Here Gartner [12] found “lateral aggregation”

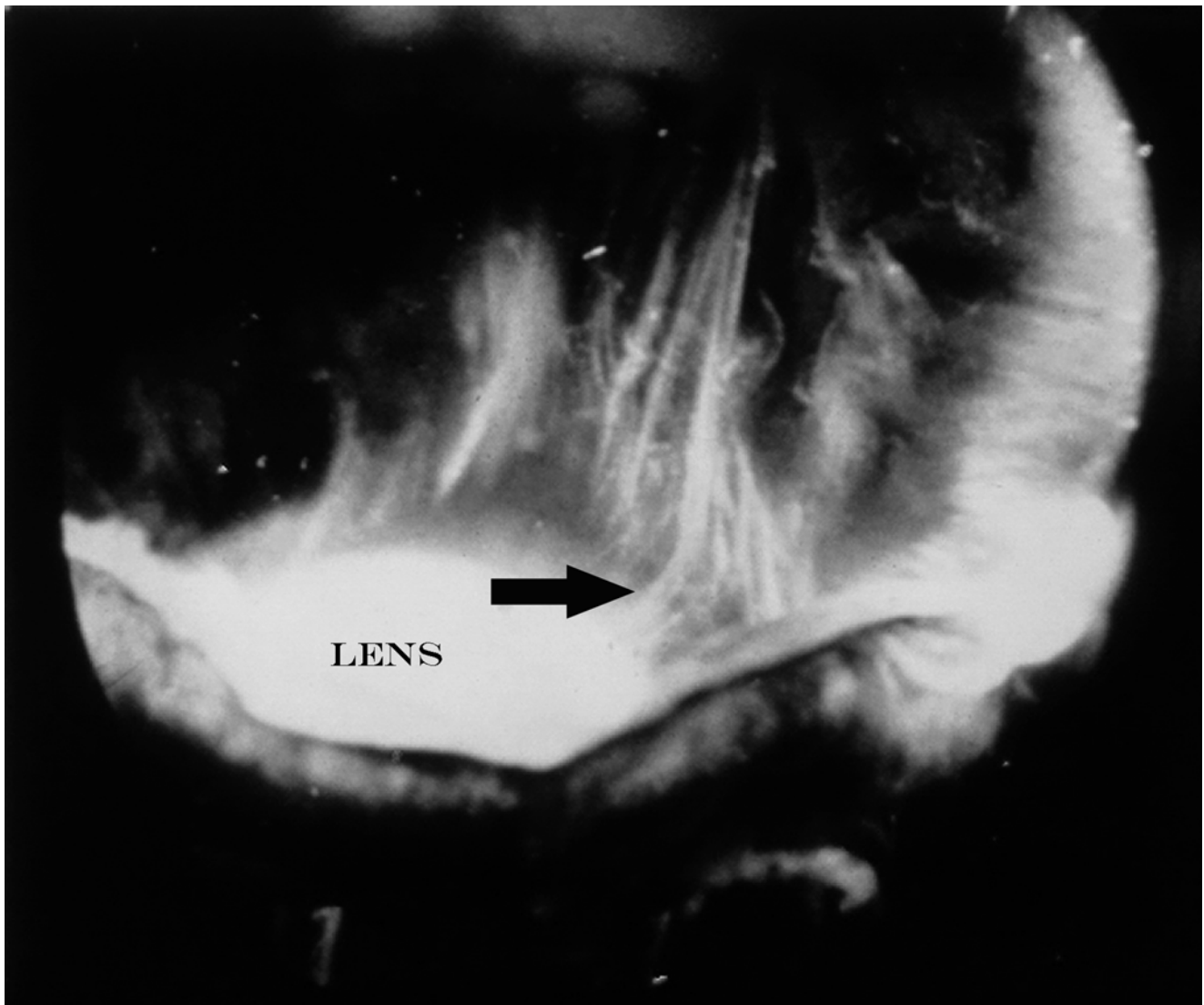


Figure III.H-1 Vitreous base morphology. In this eye of a 58-year-old woman, postmortem studies showed vitreous fibers that are continuous in their course from the posterior vitreous (at the top of the photo) to the

vitreous base, where they “splay out” to insert anterior and posterior to the ora serrata (arrow) (From Sebag and Balazs [181])

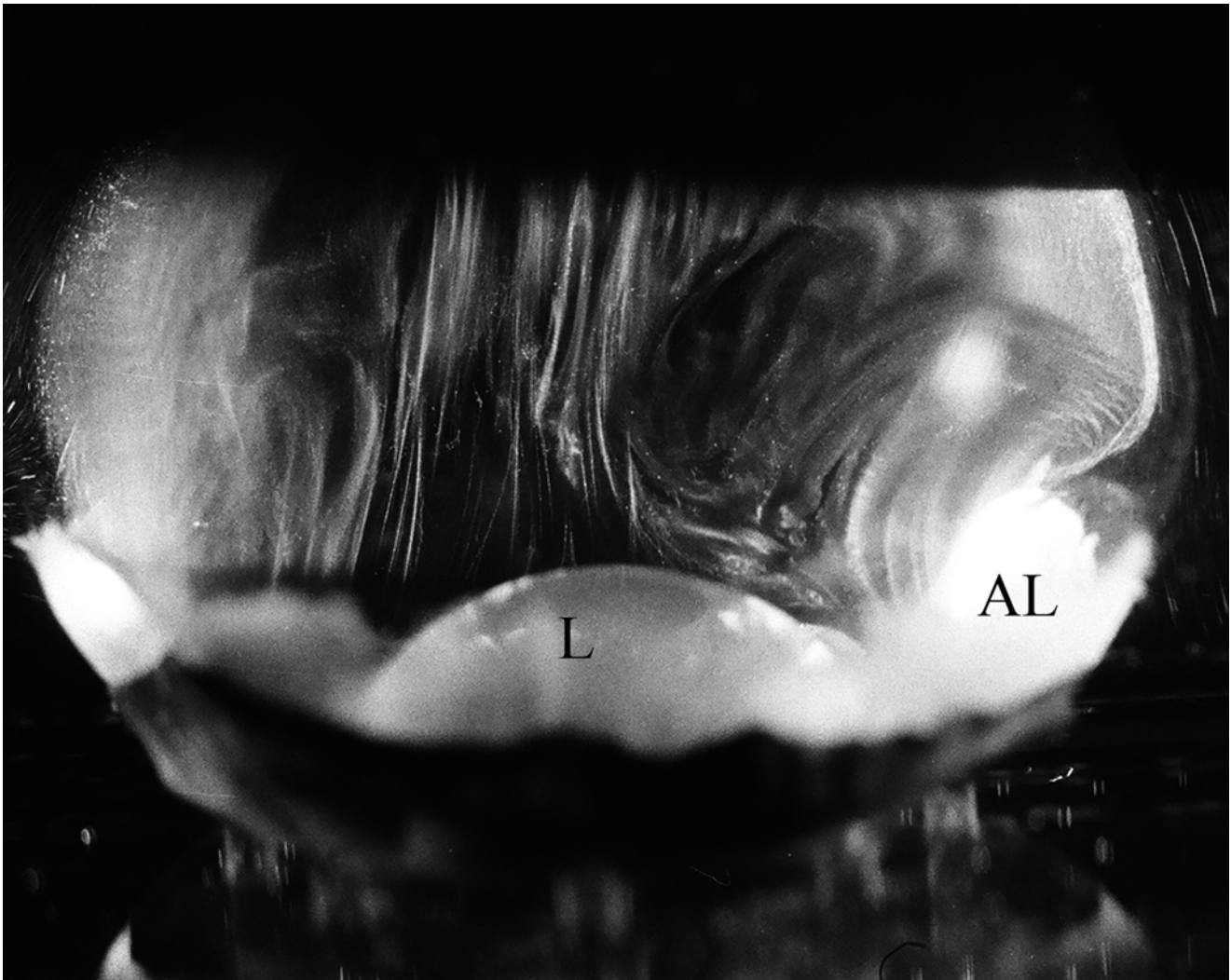


Figure III.H-2 “Anterior loop” of the vitreous base. Central, anterior, and peripheral vitreous structure in a 76-year-old man. The posterior aspect of the lens (*L*) is seen below. Fibers course anteroposteriorly in

the central vitreous and insert into the vitreous base. The “anterior loop” configuration of those fibers inserting into the vitreous base anterior to the ora serrata is seen on the right side of the specimen (*AL*)

of the collagen fibrils in older individuals, similar to aging changes within the central vitreous. Vitreous base collagen fibers inserting anterior to the ora serrata constitute the so-called anterior loop (Figure III.H-2) that plays a role in the formation of anterior proliferative vitreoretinopathy (PVR) membranes [9] and is important in transmitting traction from PVR membranes to both the peripheral retina and ciliary body [13]. Condensed bundles of the fibers inserted into the vitreous cortex in the mid-peripheral and equatorial regions (Figure III.H-3). The areas between the bundles appear as spaces that are devoid of structure, but they do contain liquid vitreous, which is primarily hyaluronan and water.

A. Peripheral Vitreo–Retinal Attachments

In the periphery, vitreous is more firmly adherent in all individuals at the vitreous base, along major retinal vessels, in

areas of retinal lattice, and at retinal tufts. Acquired areas of firm vitreoretinal attachments include postinflammatory lesions, areas of degenerative remodeling [14], and some vitreous base lesions.

1. Vitreous Base

This 3- to 6-mm band is the area of most firm normal attachment of the vitreous gel to contiguous structures (Figures III.H-1 and III.H-2). Vitreous base collagen fibrils lie roughly at right angles to the inner surface of the ciliary epithelium and peripheral retina. The fibrils attach to the basement membrane of the nonpigmented epithelium of the posterior aspect of the pars plana and inner limiting membrane (ILM) of the peripheral retina [15], probably via an intervening extracellular matrix. Within the vitreous base, there are several anatomic variations (minor dysembryogeneses) where vitreous attachments may vary in intensity [16–18]. Some of these are important because of the tendency for associated retinal trophic holes and traction tears [19–21].

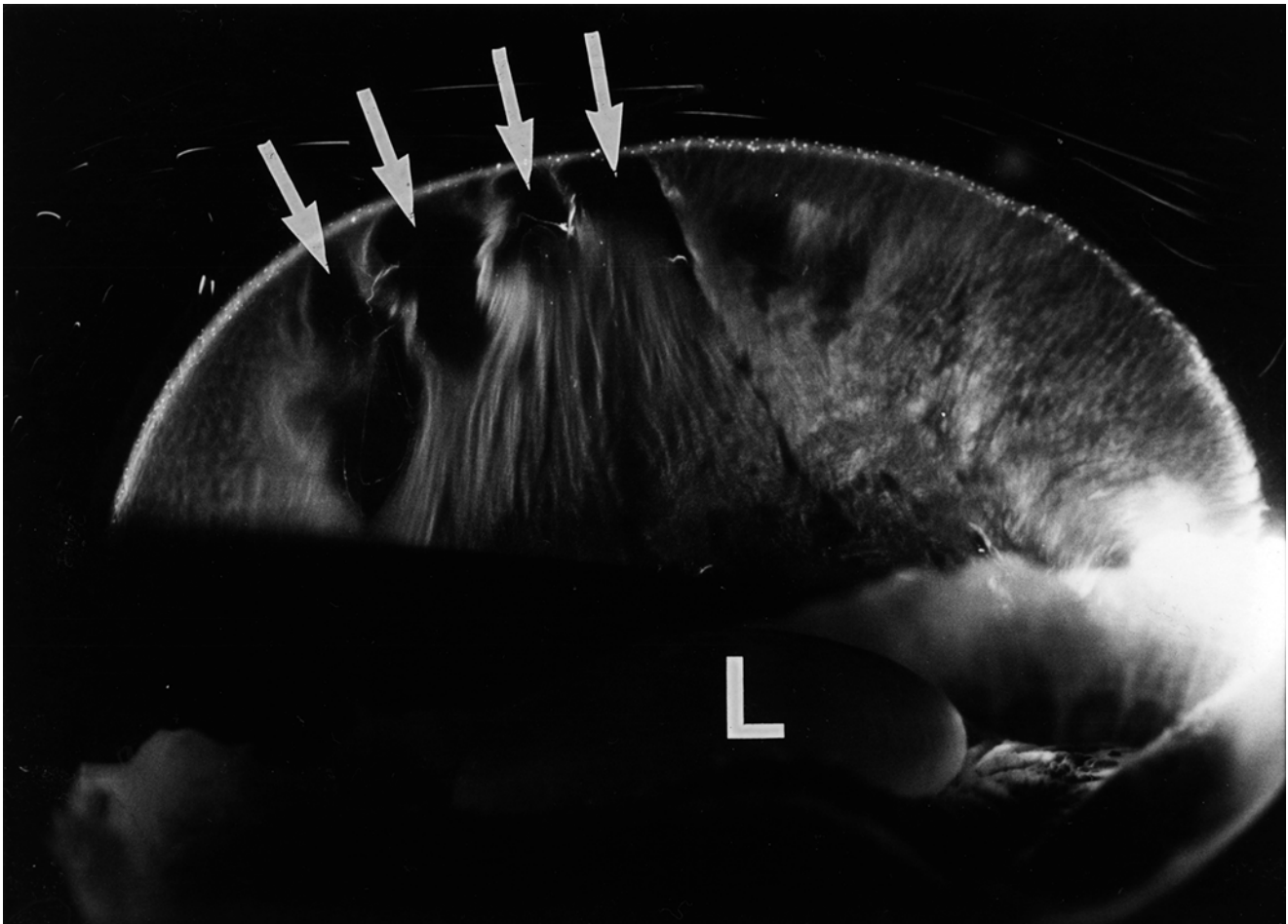


Figure III.H-3 Fibers condense into bundles and insert into the vitreous cortex at the equator. Between these insertions are spaces seemingly devoid of structure (*arrows*) (From Sebag and Balazs [8])

2. Ora Bays

An enclosed ora bay is a posterior indentation in the retina that is separated from the pars plana by retinal tissue [19] (Figure III.H-4). A partially enclosed ora bay is a posterior indentation in the retina that extends more than 0.5 mm posterior to the adjacent retina on both sides and has a width anteriorly that is less than half its maximum width posteriorly [18]. In 1,000 consecutive autopsy eyes, Spencer et al. [22] observed 40 (4.0 %) enclosed ora bays and 6 (0.6 %) partially enclosed ora bays. Retinal tears may occur posteriorly to and meridionally aligned with both types of ora bays. Posteriorly and meridionally aligned retinal tears at the posterior border of the vitreous base were observed in 16.7 % of either type of ora bay, associated with posterior vitreous detachment in all cases. Retinal tears associated with enclosed or partially enclosed ora bays were present in 5 (0.5 %) of the 1,000 eyes.

3. Meridional Folds

Meridional folds are radially oriented, linear elevations of the peripheral retina that are aligned with a dentate process, an ora bay, or a meridional complex (Figure III.H-4). These



Figure III.H-4 Meridional folds, one in line with a meridional complex (*arrowhead*) and the other (*arrow*) in line with a meridional complex and enclosed ora bay (EP 37408) (From Green [182])

folks are most commonly located nasally at or above the horizontal meridian and measure 0.6–6.0 mm long and 0.1–0.6 mm high [18]. Meridional folds were observed in 52



Figure III.H-5 Peripheral retinal excavation (*arrowhead*) in line with a meridional complex and enclosed ora bay (EP 39305) (From Green [182])

(26 %) of 200 autopsy cases, were bilateral in 55 % of affected cases, and were observed in 80 (20 %) of the 400 eyes examined. Of the 80 affected eyes, 73 % had one meridional fold, and the remainder had two to seven folds. A peripheral retinal excavation was present posterior to the meridional fold in 10 (13 %) of the 80 meridional folds. Histologic features of meridional folds include thickened retina with variable cystic degeneration, occasional hyperplasia of the RPE with migration into the retina, occasional foci of ciliary epithelium and glial cells within and along the inner surface of the retina, rare zonular attachments, and rare possible foci of vitreous traction. No retinal breaks were seen associated with the meridional folds in the study of Spencer et al. [18], but these have been observed by others [23].

4. Meridional Complexes

A meridional complex has a configuration in which a dentate process, usually with a meridional fold, is aligned in the same meridian as a ciliary process (Figure III.H-4) and often has a peripheral retinal excavation posteriorly (Figure III.H-5) [18]. This lesion was observed in 31 (16 %) of 200 autopsy cases, was bilateral in 58 % of affected cases, and was present in 49 (12 %) of the 400 eyes examined. Of the affected eyes, 55 % had a single meridional complex, and the remainder had two to five complexes. A peripheral retinal excavation was present posterior to the lesion in 10 (20 %) of the 49 complexes. No retinal breaks were associated with this lesion. An enclosed ora bay was occasionally associated with a meridional complex. Histologic features include the presence of disorganized retina extending over the pars plana. Otherwise, the features of the dentate process are similar to those seen in meridional folds.

5. Peripheral Retinal Excavations

These meridionally oriented, oval-shaped retinal depressions are located between 1.0 and 7.2 mm posterior to the ora

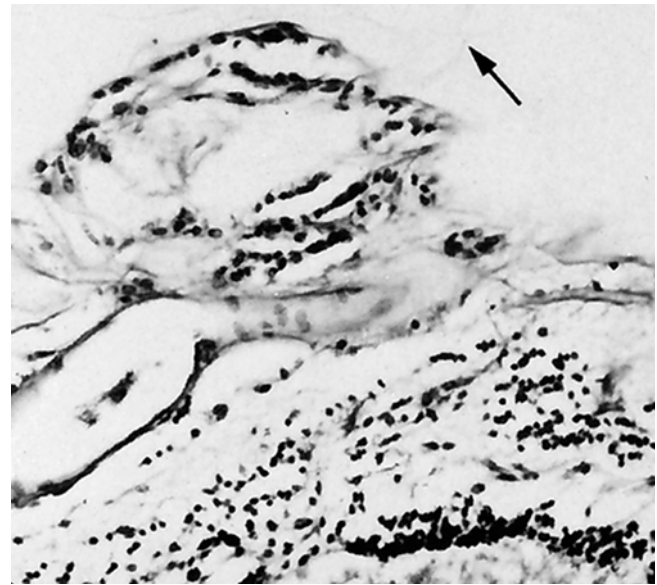


Figure III.H-6 Non-cystic retinal tuft. Microscopic appearance of peripheral retina demonstrates that glial cells and some have strands of vitreous (*arrow*) attached (From Green [183])

serrata. In younger individuals, the margins are elevated and rounded, but in older individuals the lesion has a cystic appearance. A small retinal tuft is on a rare occasion present in the center of the lesion. This lesion was observed in 20 (10 %) of 200 autopsy cases, was bilateral in 43 % of affected cases, and was present in 32 (8 %) of 400 eyes examined [18]. Peripheral retinal excavations are meridionally aligned posterior to meridional folds or complexes (Figure III.H-5) in 60 % of the lesions and are unassociated with any lesion in 40 %. Spencer et al. [18] observed no retinal breaks associated with this lesion. Histologic findings include a circumscribed area of loss or absence of the inner retinal layers. The outer layers of the retina and RPE are usually normal, although minor RPE changes may occasionally be observed. It is reasonable to consider that peripheral retinal excavations (vitreous base excavations) are probably a variant of retinal lattice [24].

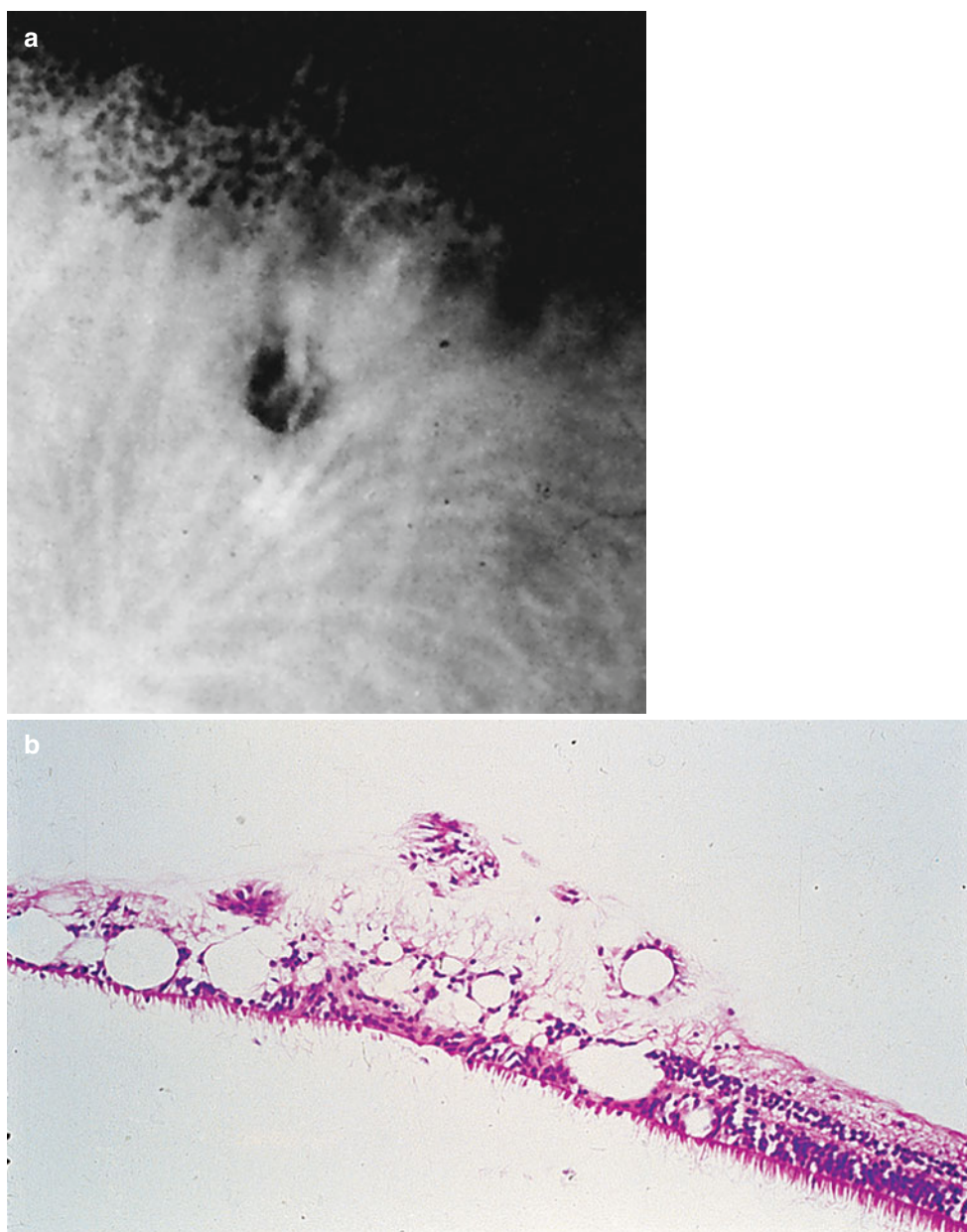
6. Retinal Tufts

Internal projections of the peripheral retina that are located within the vitreous base are called retinal tufts and have been classified as cystic, non-cystic, and zonular tufts [16].

a. Non-Cystic Retinal Tufts

Noncystic retinal tufts are thin, short internal projections of fibroglial tissue that are continuous with vitreous (Figure III.H-6). The base of the tuft is narrow and less than 0.1 mm, and there is no associated cystic degeneration of the retina. Non-cystic tufts often occur in clusters. In a study of 169 autopsy cases [16, 21], non-cystic retinal tufts were observed in 122 (72 %) of cases. The lesions were bilateral in 50 % of affected cases and were observed in 139 (59 %) of

Figure III.H-7 (a) Gross appearance of a cystic retinal tuft. (b) Microscopic appearance demonstrates retinal thickening caused by cystic changes and glial cell proliferation (hemotoxylin & eosin stain; original magnification = 220x) (From Green [182, 183])



the 312 eyes examined. The tufts occurred singly in 36 % of cases, and two to eleven tufts were observed in the remaining cases. The lesions were located in the lower quadrants in 63 % of cases and the nasal quadrants in 79 % of cases. No retinal breaks or retinal detachments were associated with non-cystic retinal tufts [16, 21, 25].

b. Cystic Retinal Tufts

Cystic retinal tufts were defined by Foos and Allen [16] as localized retinal tufts that are cystic; have a base of attachment that is greater than 0.1 mm in diameter; have scant pigmentation; often have condensed strands of vitreous attached to the apex; are often located in the same meridian as a dentate process, meridional fold, or other lesions; and are most often

located within the vitreous base (Figure III.H-7). It is likely that this lesion has been described by others as granular patches [26], globular masses [27], granular tissue [28], and rosettes [29]. In a study of 169 autopsy cases, cystic retinal tufts were observed in 100 (59 %) of cases, were bilateral in 39 % of affected cases, and were found in 139 (44.6 %) of 312 eyes examined [16, 21]. The lesions were observed in all quadrants, but 78 % of lesions were located in the nasal half of the eye [16]. Cystic retinal tufts are probably congenital, for the lesions are found in newborns and are equally represented in all age groups [30]. Some cystic tufts are only slightly elevated and have cystic changes only in the adjacent retina.

Microscopic studies disclose haphazardly arranged cysts in the inner and, sometimes, middle retinal layers



Figure III.H-8 Zonular traction tuft. Microscopically this lesion consists of an area of retinal thickening caused by cystic changes and glial cell proliferation. Vitreous fibers insert into this structure, accounting

for the traction that tears the retina during PVD (Reproduced with permission from Dunker et al. [59])

(see Figure III.H-7). There is loss of the photoreceptor cell layer and alterations in the RPE of lesions in older persons. The lamellar architecture is lost and replaced by cysts and fibroglial tissue. A layer of glial cells with dense cytoplasm is almost always present on the inner surface of the tuft. In rare instances, epithelial cells are present along the inner surface. By electron microscopy, the tuft has deep crypts that are extensively penetrated by vitreous, and the cysts are lined by glial cell processes. Although no traction features were observed in a study of 169 autopsy cases [16], avulsion of the tuft by vitreous traction with or without posterior vitreous detachment has been observed [30]. In a clinical study of 200 consecutive retinal detachment cases, Byer [19] attributed the detachment to retinal holes induced by PVD at points of cystic retinal tufts in 13 (6.5 %) of the cases.

c. Zonular Traction Tufts

Zonular traction tufts consist of a thin strand of tissue that extends to an acute angle from the peripheral retina anteriorly to be continuous with a thickened zonule at the apex [16, 20] (Figure III.H-8). The base of the tuft is located immediately posterior to the ora serrata within the vitreous base. Rarely, the base of the tuft may be located at the posterior border of

the vitreous base, in which case it is longer and thicker and is associated with some pigmentation and cystic degeneration of contiguous retina. Similar, if not the same, structures were described as zonular insertion into crypts of the peripheral retina by Inomata [31] and as “bridging tooth” by Rutnin and Schepens [28]. Microscopically, zonular traction tufts consist of fibroglial tissue that is continuous with a zonular fiber [20]. Rarely, the tufts are composed of embryonal-like epithelium and pigmented epithelium [32]. The retina at the base of the tuft is variably thickened, and the lamellar architecture is replaced by cystic degeneration and fibroglial tissue. The retina may be thin, with lamellar and full-thickness holes with rounded margins. The subjacent RPE may be hypertrophic with some pigment dispersion in larger lesions and those with retinal holes.

Foos [20] observed zonular traction tufts in 112 (15 %) of 750 autopsy cases. The lesions were bilateral in 17 (15 %) cases involved and were present in 135 (9 %) of 1,500 eyes examined. Of the 135 involved eyes, 86 (64 %) had one lesion, 45 (33 %) had two or three, and four (3 %) had four or more. Of the 135 zonular traction tufts, 109 (81 %) were located in the nasal quadrants and 78 (58 %) in the inferior quadrants. Eight (6 %) were longer than 1.0 mm, and 22

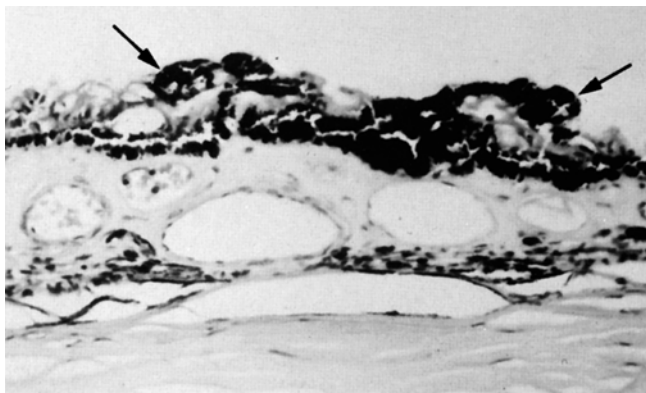


Figure III.H-9 Nodular hyperplasia of pigment epithelium in the pars plana. Hyperplastic pigment epithelium (*arrows*) is present at the inner surface of the pars plana (hematoxylin–eosin stain; $\times 250$) (EP 30655) (From Green [183])

(16 %) were based farther than 0.5 mm behind the ora serrata. Foos [20] classified associated changes into trophic and tractional. Trophic changes included partial holes in 14 (10 %) and full-thickness holes in five (4 %) of the 135 tufts. Traction changes included rupture of the tuft in seven (5 %) and full-thickness tears in three (2.2 %) of the 135 tufts. Two of the ruptured tufts were associated with partial-thickness retinal breaks. Small, lamellar, and full-thickness retinal holes occurring in the vitreous base area and associated with zonular tractional tufts generally do not predispose to retinal detachment. More posteriorly located tufts, however, may be important in the increased incidence of retinal detachment after cataract surgery, with small retinal tears in the nasal periphery [33].

7. Spiculated and Nodular Pigment Epithelial Hyperplasia

Hyperplasia of the pigment epithelium often occurs within the vitreous base, at the ora serrata, and, to a lesser degree, in the posterior aspect of the pars plana in adults. At the ora serrata, the hyperplastic epithelium often has a spiculate appearance as it extends into the vitreous base and along the surface of the peripheral retina and posterior aspect of the pars plana for a short distance. Focal, tiny nodules of hyperplastic pigment epithelium may extend to the inner surface of the posterior portion of the pars plana (Figure III.H-9). These proliferative changes have been interpreted as results of chronic vitreous traction [32].

8. Retinal Lattice

Historical and various other aspects of this condition have been extensively considered in several previous reports [34–37]. Widely referred to as *lattice degeneration*, this readily visible fundus lesion features firm attachment of the vitreous to the retina at the margin of retinal lattice and thus predisposes to retinal tears and detachment. The association of retinal lattice and high myopia is particularly important in



Figure III.H-10 Radial perivascular lattice with sclerotic vessel and hyperplastic retinal pigment epithelium, with migration into the retina in a paravascular location

the pathogenesis of retinal detachment [38]. There is little doubt that some form of inherited pattern exists with regular or irregular autosomal dominant and autosomal recessive patterns, but with the phenomenon of pseudodominant transmission as well [34]. This and the fact that the condition is present in many young individuals prompt the consideration that the name of this condition be changed from lattice degeneration to retinal lattice dystrophy, since the former suggests a primarily age-related pathophysiology, whereas the latter more accurately reflects the genetic basis of this condition with variable expression later in life, during early adulthood and not in old age. In this text, the term “retinal lattice” will be employed.

Retinal lattice lesions vary considerably in their appearance, being of variable size and configuration. Lesions may be round, oval (Figure III.H-10), or linear. The lesions are located anterior to the equator and parallel to the ora serrata. Occasional lesions are located posterior to the equator in a radial paravascular pattern [39] (Figure III.H-10). Most lesions have retinal thinning, and many are readily apparent on ophthalmoscopy because of associated pigmentary changes (Figure III.H-10), the presence of retinal holes, and a *lattice wicker* of sclerotic vessels, although the white lines (lattice wicker), for which the condition was named [39, 40], are not always present [41]. Byer [34] clinically observed white lines in only 3.3 % of patients in the 10- to 19-year age group, but the prevalence increased to 42.9 % after the age of 50.

In a study of 800 consecutive autopsy cases, Straatsma et al. [37] observed that retinal lattice was present in 86 (10.7 %) of cases, was bilateral in 41 (48.1 %) of affected cases, and was present in 126 (7.9 %) of the 1,600 eyes examined. Foos [42] observed retinal lattice in 65 (20.2 %) of 322 autopsy cases of black subjects and in 335 (16.6 %) of 2012 white autopsy subjects. In a clinical study of 1,300 normal patients, Byer [43] found retinal lattice in 92 (7.1 %) of

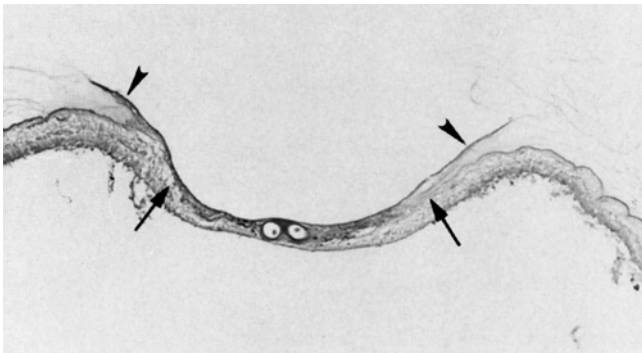


Figure III.H-11 Retinal lattice. Microscopic features of retinal lattice include a pocket of fluid vitreous, discontinuity of the inner limiting membrane (*between arrows*), condensation and adherence of vitreous at the margin (*arrowheads*), and sclerotic retinal vessels centrally (Alcian blue stain; $\times 55$) (EP 43287) (From Green [183])

patients, and this incidence was present in the second decade. Byer [43] further noted that the white lines were present in only 9 % of the lesions and suggested that the white lines and round retinal holes seem to be more frequent in older persons. In an extensive clinical study, Byer [34] observed retinal lattice in 137 (8 %) of 1,700 patients. The lesions were bilateral in 58 (42.3 %) of the affected cases, and 195 (5.7 %) of the 3,400 eyes had 393 lesions. Of the 393 lesions, 64 (16.3 %) had round holes, and 47 (11.9 %) had white lines.

The histopathologic features (Figure III.H-11) of retinal lattice include the following [32, 37]:

- Discontinuity of the ILM
- A pocket of overlying fluid vitreous [17]
- Condensation and adherence of vitreous at the margin of the lesions, which may be fortified by hyperplasia of glial cells and RPE [17, 44]
- Degeneration of the inner retinal layers, which may lead to central atrophic hole formation
- Thickening of the walls and reduced cellularity of larger retinal vessels [25]
- Acellularity of the capillary bed [25] (Figure III.H-12)
- Hypertrophy and hyperplasia of the RPE with migration into the retina, often in a perivascular distribution
- A tractional retinal tear with superimposed posterior vitreous detachment inducing traction

Atrophic holes were observed clinically in 18.2 % of retinal lattice lesions by Rutnin and Schepens [23] and, in 29.2 % of patients, 23.6 % of eyes, and 16.3 % of retinal lattice lesions in the clinical study of 1,700 patients by Byer [34]. In an autopsy study of 800 cases, Straatsma et al. [37] observed atrophic holes in 24.9 % of 125 eyes and 18.2 % of 286 lesions, and traction tears in 3 (2.4 %) of eyes with retinal lattice. In a study of 4,812 autopsy eyes, Foos [45] found 89 (1.9 %) eyes with retinal tears. Fifteen (17 %) of those 89 eyes with tears also had retinal lattice. Of the 29 retinal tears observed in those 15 eyes, only six (20.6 %) directly involved a retinal lattice lesion.

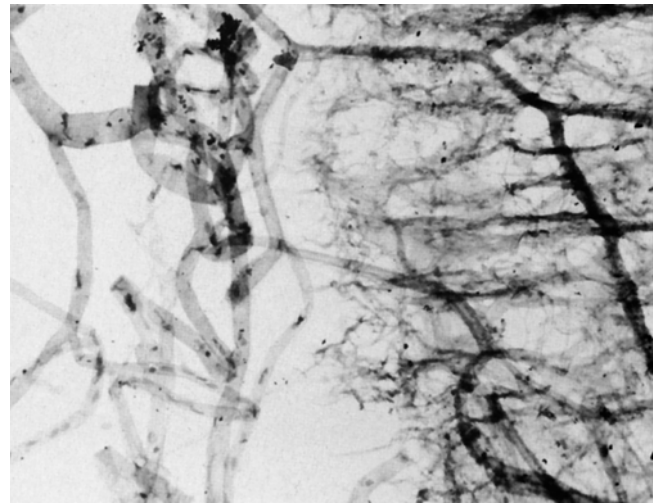


Figure III.H-12 Trypsin-digestion preparation of the retina discloses relatively acellular capillaries in area of retinal lattice (*right*) (hematoxylin–eosin and periodic acid–Schiff stains; $\times 185$). (EP 43287)

Tillery and Lucier [46] reported that during a 3-year period at one institution, 2.8 % of all retinal detachments were caused by round atrophic holes in retinal lattice. Further, Morse and Scheie [47] reported that 31 (13.9 %) of 223 eyes with primary, nontraumatic, rhegmatogenous retinal detachments were caused by atrophic holes occurring within areas of retinal lattice. However, Byer [34, 48] pointed out that given the large population of individuals with retinal lattice, the risk of developing retinal detachment from trophic holes and traction tears is estimated at 0.3–0.5 %. In a prospective study, Byer [34] found tears in only three (1 %) of 289 eyes of patients with retinal lattice followed for 3–10 years. Nonetheless, many opt for prophylaxis in higher-risk cases, especially given the benign nature of the treatment.

There is higher risk for retinal tears to occur at sites of retinal lattice when the retinal lattice is located juxta- or extrabasally [30, 45]. Lattice lesions that occur within the vitreous base (intra-basal) are less likely to be involved with PVD and retinal breaks. It is known (see above), however, that the vitreous base migrates posteriorly with age and, as Byer [34] points out, the posterior border of the vitreous base cannot always be identified. According to Green, the best cases for prophylactic therapy are symptomatic tears, a history of retinal detachment in the fellow eye, the presence of myopia and pseudophakia, or planned cataract surgery [34, 49].

9. White-With-Pressure, White-Without-Pressure

The nature and significance of these findings on indirect ophthalmoscopy remain controversial. These terms refer to geographic areas of whiteness of the mid-peripheral, equatorial, and peripheral fundus. When the white appearance is observed by indirect ophthalmoscopy without scleral depression, it is termed white-without-pressure [50]. When

a white reflex is observed with scleral depression, it is called white-with-pressure. The findings were first described in 1952 by Schepens [40] and were considered to predispose to retinal tears [51]. Freeman [52] noted an increased risk for giant retinal tears in fellow eyes with white-without-pressure at the vitreous base. Others [53], however, attach no diagnostic or prognostic significance to these reflexes. Eisner [54] reported that all lesions internal to the pigment epithelium have a whitish appearance when viewed with scleral depression. This was interpreted as resulting from variations in the angle between the light beam of the indirect ophthalmoscope and the structure being visualized. Another possible explanation is that either phenomenon is a light reflex that occurs when the incident light is tangential to more dense bundles of vitreous collagen. Greater density of collagen is present at the vitreous base and in bundles that insert into the vitreous cortex at the equator and mid-periphery. If the incident light is tangential to such aggregates of collagen, one sees white; if the incident light is mostly parallel with the collagen fibers, no white reflex is seen. Thus, when rolling the eyewall with scleral depression, one may alternately visualize white and no white with pressure. White, with and without pressure, would therefore indicate a zone of greater concentration of collagen fibers in the cortical vitreous, but it does not necessarily imply the presence of a firmer attachment of the vitreous to the retina. This theory may be inconsistent with the observation of migratory white-without-pressure [55]. The cause of migratory white-without-pressure is unknown, but Nagpal et al. [55] suggested that it may be related to separation and recreation of vitreoretinal adhesions.

In a clinicopathologic study, Watzke [56] clinically observed an area of white-with-pressure to correspond to an equatorial area where vitreous remained attached to the retina. This area of white-with-pressure delineated the anterior extent of posterior detachment of the vitreous. Dobbie [50] observed no abnormalities by light and electron microscopy in the study of an eye with white-without-pressure that extended into the posterior pole. Daicker [57] suggested that collagenic formations in the peripheral retina may account for white-with-pressure. Gartner [58] also suggested that irregularities of the inner limiting membrane and condensations of vitreous fibrils near the retinal surface may contribute to white-without-pressure. Other than the incidental association of white-with-pressure and white-without-pressure with posterior vitreous detachment and traction, the significance of these unusual light reflexes is unknown.

10. Verruca

The verruca (Figure III.H-13) has a structure similar to that of a tree [59]. Its “roots” are embedded in the inner layers of the retina. Cellular elements resembling cells of the inner plexiform layer can be seen near the retinal surface. The “trunk” of this structure extends from the retina to the middle

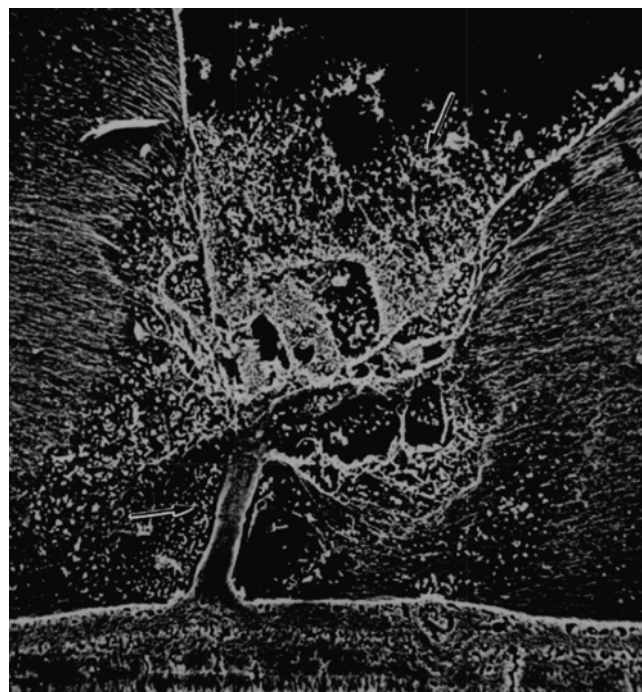


Figure III.H-13 Verruca. On scanning electron microscopy, this structure is seen to arise from the disrupted inner limiting membrane of the retina (*lower arrow*) and insert into disrupted areas of the vitreous cortex (*upper arrow*) (Reproduced with permission from Dunker et al. [59])

parts of the vitreous cortex. The “branches” of the verruca are intertwined with vitreous collagen fibers. Local condensation of collagen fibers exists as well as local collagen destruction and interruption of the inner limiting membrane of the retina. This structure is likely a remnant of the fetal hyaloid vasculature (see tubular structure in Figure III.H-13) and may have immunogenic properties contributing to pars planitis.

II. Mechanics of Peripheral Vitreo–Retinal Traction

During ocular saccades, the rotational force of the eyewall is transmitted to the vitreous body by way of the attachments described above [60–62]. In addition, the lens, with its posterior convexity, bulges into the vitreous and exerts a “grip” or mechanical hold on the vitreous body, above and beyond the vitreolenticular attachment at Egger’s line, imparting rotational forces completely independent of these attachments. On initiation of a saccade, the eyewall accelerates rapidly. This is followed by a latent period before the outer vitreous begins to move. Once the outer vitreous begins to move, angular acceleration is transmitted to successively more internal layers of vitreous until the center is reached. At the conclusion of a saccade, angular deceleration begins in the outer vitreous and is transmitted internally in the same fashion. This internal post-saccadic vitreous movement is dampened by the bulging convexity of the lens, reducing the torsional forces acting on the various vitreous attachments during deceleration. During both

the acceleration and deceleration phases of saccades, the movement of vitreous always lags behind that of the outer eyewall, resulting in markedly reduced velocity and acceleration of the vitreous body relative to the sclera and retina. This inherent property of vitreous, called “slack and lag,” is a function of its unique molecular structure and viscosity and provides another basic mechanism by which the amount of force present at any given internal vitreous attachment is dampened and reduced [61, 62]. The locations of points of greatest strain on the eyewall during saccades are a function of ocular anatomy. The optic disc occupies an eccentric position in the posterior pole, located nasally and slightly inferior. There is thus more vitreous mass temporally and superiorly between the vitreous base and the disc margin than exists nasally and inferiorly. Also, given the shorter distance between the disc margin and ora nasally and inferiorly, the relief of torsional strain on equatorial and anterior vitreoretinal attachments by the anchor of vitreous attachment at the disc margin would theoretically be greater nasally and inferiorly, providing more relative stability in these zones. Accordingly, it has been postulated that the greatest torsional strain on anterior and equatorial vitreous attachments should occur during lateral saccades, with the point of maximum strain located somewhere in the superotemporal quadrant [61, 62]. This is consistent with the observation that peripheral retinal tears occur most frequently superotemporally, followed by inferotemporally, then nasally [see chapters III.I. Role of vitreous in the pathogenesis of retinal detachment; V.B.4. Prophylaxis and cure of retinal detachment].

III. Alterations of Peripheral Vitreo–Retinal Structure

A. Post-Traumatic Retinal Healing

Constable et al. [63] noted that after chorioretinal biopsy in dogs (obtained without vitreous loss) retinal glial cells and fibroblasts filled in the defect and the glial cells produced a new basement membrane that was complete on both the internal and external aspects of the defect. These findings could be interpreted as demonstrating regeneration of the inner limiting membrane (ILM). However, only minimal evidence of regeneration of the ILM was observed in an eye obtained postmortem in which previous stripping of a secondary premacular membrane with ILM had been performed [64]. Foos and Gloor [65] observed two processes of healing after mechanically induced wounds in nonvascularized rabbit retinas. One was “accessory gliosis,” in which accessory glia and their progeny migrated to the wound and differentiated into fibrous astrocytes. The second was “plexiform gliosis,” composed of Müller cell “side branches” proliferation.

Miller et al. [66] studied healing of linear retinal wounds formed internally by a 21-gauge needle in rabbits. Findings included macrophages at the wound surface at 1 week, glial cell processes extension through the defect into the ILL at 2

weeks, subsidence of macrophage response at 6 weeks, and formation of a scar of densely packed glial cells at 10 weeks. No regeneration of ILM was observed over the internal surface of the scar, but it was observed on the undersurface of that portion of the scar that extended over the adjacent intact retina. Retinal pigment epithelium (RPE) did not contribute to healing of the wounds. After vitrectomy, however, the scars were irregular and hypertrophic, leading the authors [67] to suggest that vitreous plays a role in normal healing of retinal wounds.

B. Aging Changes at the Peripheral Vitreo–Retinal Interface

Age-related thickening of the basal laminae that surround the vitreous is believed to be due to synthesis by subjacent retinal Müller cells 2 [see chapter II.E. Vitreo-retinal interface and ILM]. Such thickening of the ILM may ultimately contribute to weakened vitreoretinal adherence, a necessary, but not sufficient, element in the pathogenesis of PVD [see chapter II.C. Vitreous aging and PVD].

C. Retinal Breaks Unrelated to PVD

Retinal holes were observed in 10 (5.9 %) of 169 [68], in 111 (3.9 %) of 2,800 [16], and in 326 (13.9 %) of 2,334 [42] autopsy cases. The range in prevalence of retinal breaks (relationship to PVD unknown) in eyes obtained postmortem was: Teng and Katzin [26] (1951): 4 (3.9 %) of 101 cases
Adamis [69] (1956): 3 (27 %) of 11 eyes
Okun [27] (1961): 12 (4.8 %) of 250 cases, 7.0 % older than 40 years of age
Boniuk and Butler [70] (1968): 13 (8.6 %) of 150 cases
Spencer and Foos [71] (1970): 12 (4.7 %) of 252 eyes
Barishak and Stein [72] (1972): 11 (8.8 %) of 125 cases
Foos [45] (1974): 80 (3.3 %) of 2,406 cases
Foos [73] (1975): 88 (3.7 %) of 2,406 cases
Foos et al. [42] (1983): 172 (7.3 %) of 2,334 cases

IV. Effects of Anomalous PVD

Posterior vitreous detachment (PVD) is defined as complete separation of the posterior vitreous cortex from the ILM of the retina without damage to either. Anomalous PVD results from liquefaction of the gel vitreous without concurrent dehiscence at the vitreoretinal interface [see chapter III.B. Anomalous PVD and vitreoschisis]. The onset of vitreous floaters or a change in the pattern of floaters may be an important clinical sign of PVD, which at times can be anomalous with effects on both vitreous and retina. In vitreous, a study [74] of 589 patients with floaters determined that diffuse dots, many vitreous cells, and vitreous blood were high-risk factors for the development of a retinal tear. Boldrey [74] observed

that 93 of 176 (52.8 %) of eyes with one or more of these risk factors had retinal tears. Spontaneous vitreous hemorrhage may be the result of posterior vitreous detachment and retinal tears [75–77]. Standardized echography may be an effective means of identifying retinal tears in eyes with spontaneous vitreous hemorrhage [78].

Of 100 patients with symptoms of light flashes, floaters, or both, seen by one general ophthalmologist, 10 (10 %) were found to have retinal tears caused by vitreous traction [79]. Murakami et al. [80] used the El Bayadi–Kajiura aspherical lens to examine 148 eyes of patients with sudden onset of floaters. The floaters were attributed to acute PVD in 123 (83 %) of the eyes, and most of those were caused by detached peripapillary glial tissue and minimal hemorrhage. The 25 eyes (17 %) without PVD had central vitreous degeneration with fiber-like opacities. In the patients older than 50 years of age, 95 % had acute PVD. Floaters are now safely cured with minimally invasive vitrectomy [see chapter V.B.8. Floaters and vision – current concepts and management paradigms].

Novak and Welch [81] reported the results of examination within 3 months of the onset of floaters due to acute PVD in 172 eyes of 155 patients (average age = 60 years, range 22–82 years), followed over a 10-year period. Of the 172 eyes, 118 (69 %) had no vitreous or retinal complications. Fourteen (8 %) of 172 eyes had partial (2 cases)- or full-thickness (12 cases) retinal tears, and 36 cases (21 %) had retinal or vitreous hemorrhage (or both). Avulsion of a retinal vessel and congenital retinal tag was observed in two eyes each, and one eye had cystoid macular edema. Of the 155 patients, acute symptomatic PVD subsequently developed in the fellow eye in 17 (11 %) – within 2 years in 15 of the 17 patients. The second eye behaved in a similar fashion to the first eye in regard to complications of PVD.

A. Vitreous Traction on Peripheral Retina

PVD places traction on the peripheral retina at any site where detached vitreous reaches a point of firm adhesion to the retina. Firm vitreoretinal adhesion is known to occur at the peripapillary retina, at the macula, along major retinal vessels, at the vitreous base, and at sites of retinal lattice, enclosed ora bays, retinal tufts, and at points of degenerative remodeling. Traction at such locations may induce retinal tags, retinal folds, cystic degeneration, retinoschisis, traction retinal detachment, retinal pits (lamellar retinal tears), avulsion of retinal vessels, and retinal tears.

1. Retinal Tags

At an early stage of vitreous traction on the retina, a tiny inner portion of the retina may be tented up, producing a retinal tag (Figure III.H-14). There may be a tear in the ILM of the associated retina. Multiple tags are usually aligned circumferentially along a portion of the posterior border of the detached vitreous at the vitreous base. Foss

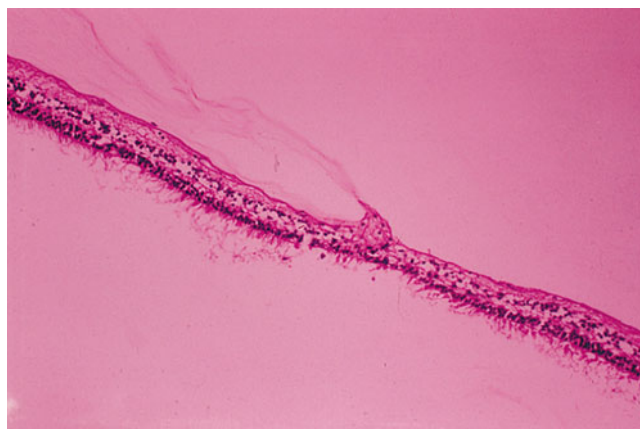


Figure III.H-14 Retinal tag. Posterior vitreous detachment with traction on the retina (hematoxylin–eosin stain; $\times 300$)

and Allen [16] observed retinal tags in 20 (11.8 %) of 169 autopsy cases and in 21 (6.7 %) of 312 eyes examined. Eight eyes had a single retinal tag, and three eyes had 5 to 20 tags.

2. Retinal Folds

Retinal folds related to vitreous traction are uncommon and occur when the vitreous is incarcerated in a corneal wound and has detached posteriorly to a circumferential area of firmer adherence to the retina. With subsequent fibrous tissue proliferation into the incarcerated vitreous and contraction, traction is transmitted posteriorly producing a fold of the retina. An unusual retinal fold associated with a condensed vitreous membrane in an eye with a retinal tear and fibrocellular proliferation was described by Wolter [82].

3. Cystic Degeneration and Peripheral Retinoschisis

Traction retinoschisis (Figure III.H-15) and traction retinal detachment may be produced by vitreous traction at any point of persistent attachment. Firmer vitreoretinal attachment apparently occurs along the major retinal vessels as either a cause or an effect of the frequent tractional changes, including cystic degeneration, retinal pits (lamellar retinal tears), full-thickness retinal tears, and avulsion of retinal vessels [all described below]. The precise nature of the vitreoretinal attachments in paravascular areas is not known [see chapter II.E. Vitreo-retinal interface and ILM]. As noted earlier, there may be defects in the ILM over major blood vessels. Foss [83] proposed a sequence of events in the development of traction associated with retinal blood vessels that begins with developmental thinning of the ILM, subsurface retinal degeneration, and transmigration of macrophages through small defects in the ILM. When complicated by vitreous incarceration, simple preretinal membrane formation leads to firm adhesion.

Cystic degeneration occurring along the retinal vessels is present in the nerve fiber layer, is seen before the vitreous is detached at that area, and is referred to as paravascular rarefaction [71]. In a study of eyes of 126 consecutive autopsy

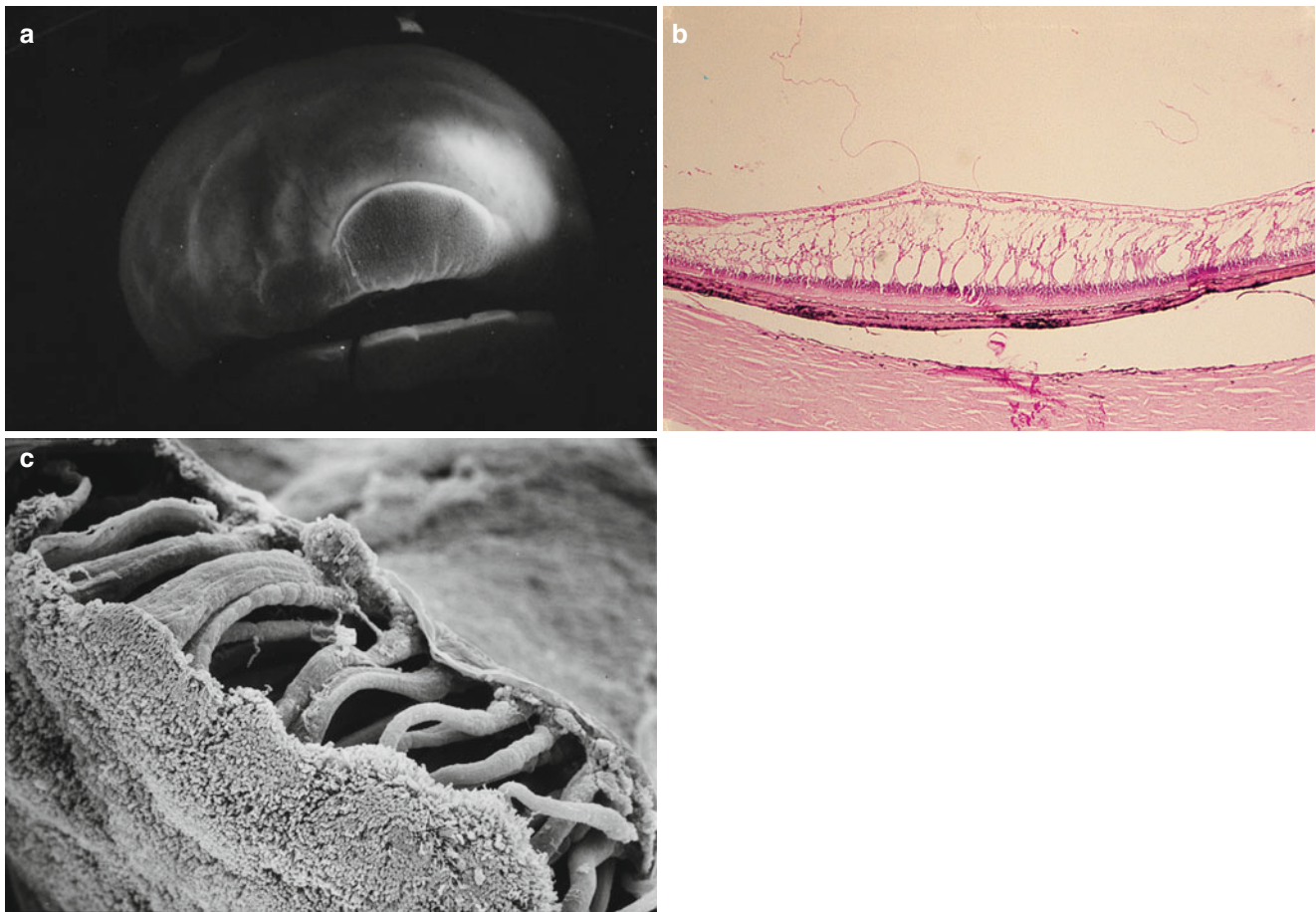


Figure III.H-15 Peripheral retinoschisis. (a) Gross appearance of peripheral retinoschisis in a human eye after peeling the sclera and choroid off the retina then transilluminating the specimen [Specimen courtesy of the New England Eye Bank]. (b) Cystic degeneration

associated with vitreous traction (hematoxylin–eosin stain; $\times 75$) (From Green [183]). (c) Scanning electron microscopy of the same specimen as in (a) demonstrating the columnar structures that are characteristic of peripheral retinoschisis

cases of subjects 21 years or older at death, Spencer and Foos [71] observed retinal paravascular rarefaction in 30 %. The process was bilateral in 83 % of affected cases and was present in 25 % of the 252 eyes in the study.

4. Retinal Pits (Lamellar Retinal Tears)

In a paravascular distribution. The lesions consist of discrete areas where the inner retinal layers are avulsed (Figure III.H-16) as a result of PVD and traction. Meyer and Kurz [84] noted the association with a sclerotic artery in two cases studied. Spencer and Foos [71] observed paravascular lamellar retinal tears (retinal pits) in 17 % of 126 consecutive autopsy cases. The lesions were bilateral in 27 % of affected cases and were present in 11 % of the 252 eyes examined. In the same study of 252 autopsy eyes, Spencer and Foos observed PVD in 96 eyes (38 %); of those, 28 (29 %) had retinal pits, and 12 (13 %) had one or more full-thickness holes. Partial- or full-thickness tears were therefore observed in 44 (46 %) of the 96 eyes with PVD. Spencer and Foos [71] noted the retinal pits were associated with both retinal arteries and veins and that the significance of vascular sclerosis was difficult to assess.

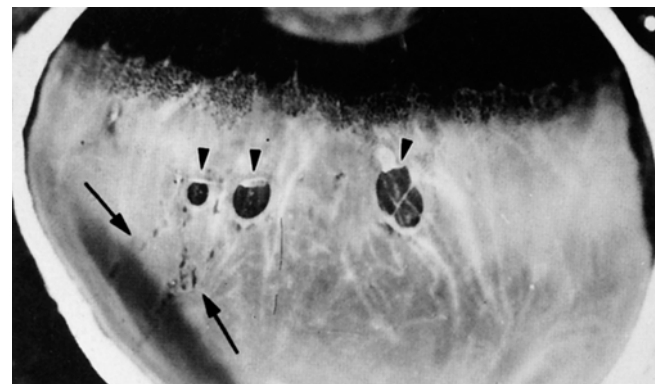


Figure III.H-16 Retinal pits and tears. Gross appearance of eye with posterior vitreous detachment, a string of retinal pits along vessels (arrows), and three horseshoe-shaped retinal tears (arrowheads) (From Green [183])

5. Retinal Tears

Retinal tears occur when the vitreous detaches posteriorly and reaches a point of firmer attachment of the vitreous to the retina [85, 86]. Traction is also induced by fluid movements against the remaining formed vitreous and may lead to a retinal break [87] (Figure III.H-17). Such a break typically

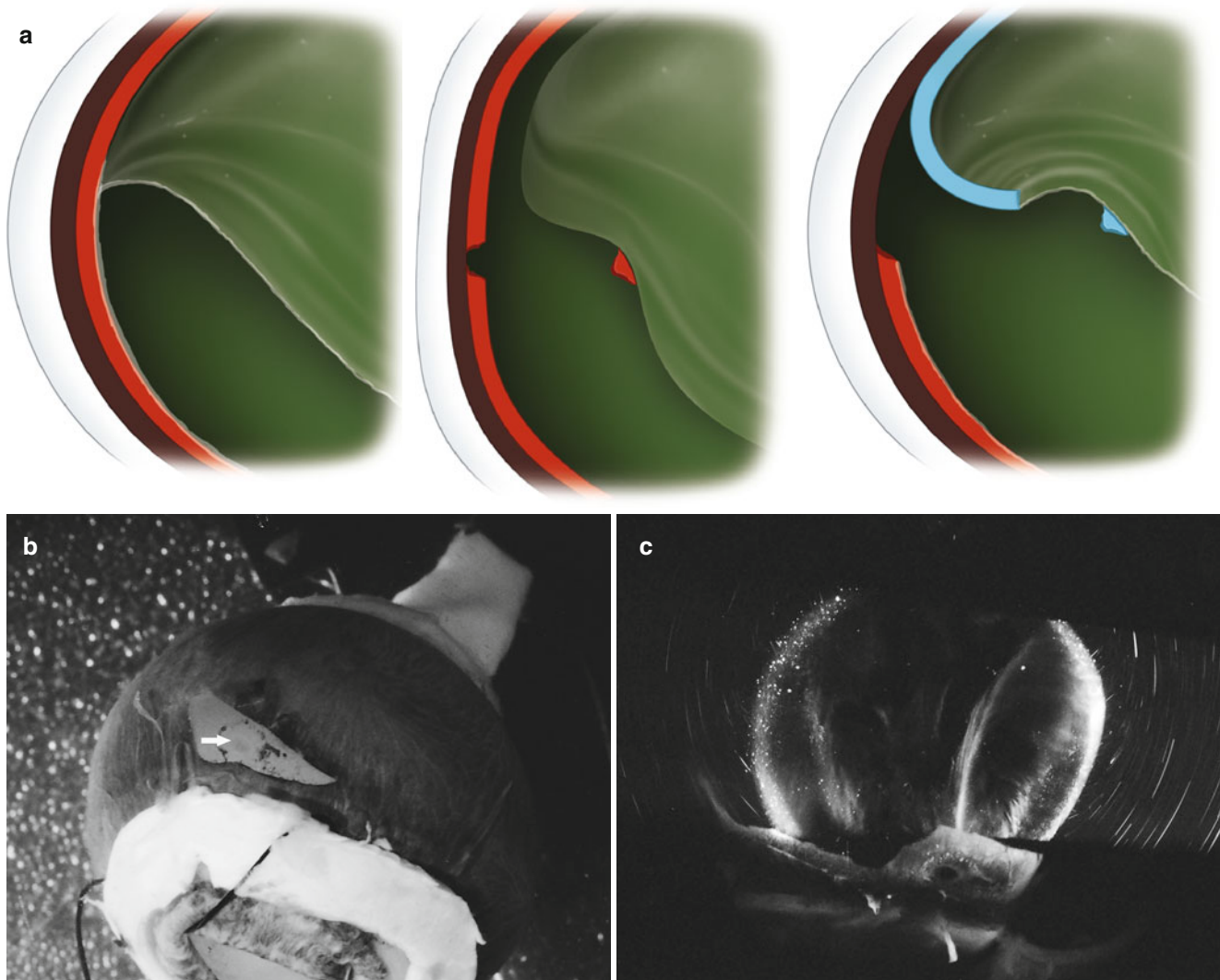


Figure III.H-17 Peripheral retinal holes. (a) Mechanism of retinal hole formation with PVD. Retinal traction occurs at a point of firm vitreo-retinal adhesion causing a tenting up of retina (*left image*). With further traction a break occurs, but without adjacent vitreo-retinal traction, there is no retinal detachment (RD) (*center image*). With persistent traction, an operculum may be detached leaving a round or oval hole, but no RD (*center image*). Traction induces an RD (*right image*) (Modified from Okun [184]). (b) Gross appearance of a peripheral retinal hole after dissecting off the entire

sclera except around the optic disc and at the limbus. The choroid was dissected in a limited triangular-shaped region of the peripheral fundus. There is a retinal hole surrounded by a ring of pigment clumping (*arrow*). (c) Dark-field slit microscopy of the same specimen as in (b) after dissecting the retina up to the edge of the ring of pigment clumping surrounding the retinal hole. A prominent intravitreal fiber can be seen coursing towards the retinal hole. Traction by this fiber likely caused an operculum to break away from the peripheral retina [Courtesy VMR Institute]

has a horseshoe shape, with the open end pointed anteriorly. Vitreous remains attached to the posterior margin of the retinal flap. With further traction, the flap of retinal tissue (operculum) may be avulsed, leaving a round or oval hole. The detached flap of retina remains attached to the posterior surface of the detached vitreous, and large detached flaps may form a cystic structure (Figure III.H-18). Tears may, however, occur at any point and have a variety of configurations. For example, Benson and Tasman [88] observed slit-like paravascular retinal tears caused by vitreous traction in three eyes with posterior retinal detachment that resembled central serous retinopathy.

The reported clinical incidence of retinal tears in patients with acute symptomatic PVD varies from 8 to 15 % and as high as 46 % [88]. It is not always clear that the authors [89] have distinguished between retinal tears caused by vitreous traction and retinal holes not necessarily related to PVD and vitreous traction [90]. The specific clinical series reporting the incidence of retinal tears are:

Halpern [91] (1966): 18 of 250 patients (7.2 %)

Byer [92] (1967): 98 of 1,700 patients (5.8 %)

Rutnin and Schepens [93] (1967): 13.75 % of 102 normal patients (7.8 % of eyes)

Smith and Ganley [94] (1972): 5 of 842 patients (0.59 %)

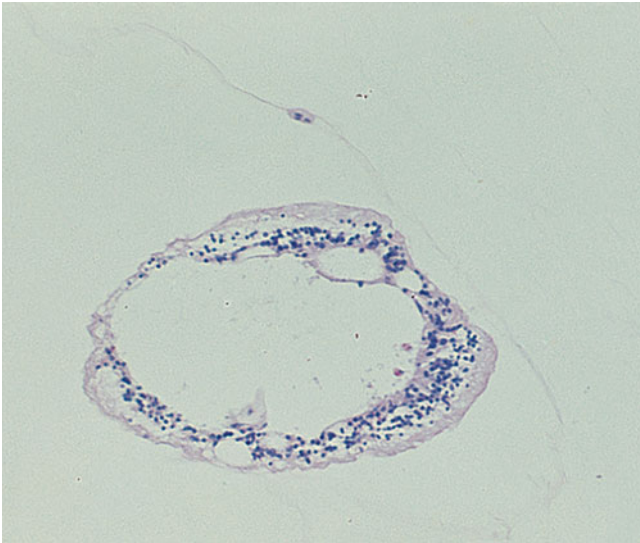


Figure III.H-18 Coiled-up fragment of detached operculum attached to the posterior surface of detached vitreous (periodic acid–Schiff stain; $\times 210$) (EP 34238) (From Green [185])

It seems likely that 15 of the 18 retinal breaks observed in 16 eyes of 14 out of 102 patients in the Rutnin and Schepens [93] study were retinal holes unrelated to PVD.

Although the role of retinal tears in the pathogenesis of retinal detachment is indisputable, the significance of finding a retinal tear in a patient is not entirely clear, but some information is available. Colyear and Pischel [95] reported that five (20 %) of 26 patients with retinal tears developed retinal detachment. Byer [92] observed 98 (5.8 %) asymptomatic retinal breaks in 1,700 presumably normal patients and concluded that prophylactic treatment of retinal breaks is justified only in symptomatic retinal breaks of phakic patients [96, 97]. In a natural history study of 166 eyes with retinal breaks without detachment, Davis [49] observed that 31 (18 %) progressed to retinal detachment. Risk factors for progression included a symptomatic PVD, horseshoe-shaped tear, breaks with subclinical retinal detachment, and aphakia. It is clear that the incidence of retinal tears is much greater than that of retinal detachment; with an incidence of retinal detachment between nine (0.009 %) per 100,000 per year [98–101] and 24.4 (0.02 %) per 100,000 [102], Byer [92] noted the prevalence retinal breaks and retinal detachment in a ratio of 83–1.

Benson [103] reviewed the pros and cons of prophylactic therapy of retinal breaks and pointed out that education of patients with high risk of retinal detachment is probably of equal value to cryotherapy [47] and photocoagulation in preserving visual acuity. Combs and Welch [104] reviewed the literature regarding prophylactic treatment of retinal tears and reported the clinical features and follow-up data from 277 eyes of 248 patients with retinal tears. Based on data from 193 eyes of 171 patients that received prophylac-

tic treatment and 84 eyes of 77 patients that received no treatment, Combs and Welch [104] concluded that the prophylactic treatment of acute horseshoe-shaped tears with continuing vitreous traction significantly reduces the incidence of subsequent retinal detachment. The results and complications of prophylactic treatment of retinal tears have been reported by Robertson and Norton [105] and Smiddy et al. [106] [see chapter V.B.4. Prophylaxis and cure of retinal detachment].

V. Vasculopathies of the Peripheral Fundus

The peripheral fundus is not visible with direct ophthalmoscopy. Introduced by Schepens in the 1950s, indirect ophthalmoscopy revolutionized fundus examination, especially with indentation of the sclera, as it allows the examiner to adequately view the peripheral fundus. Higher magnification examination of the peripheral fundus and pathologic structures can be achieved by using a three-mirror Goldmann contact lens. In case of media opacities (e.g., vitreous hemorrhage), ultrasound can be used to identify retinal detachment or vitreous membranes inducing traction. Photographic documentation of the peripheral fundus requires special wide-field lenses, which in some systems enable peripheral fluorescein angiography as well.

A. Tractional Avulsion of Retinal Vessels

Vitreous traction with avulsion of retinal vessels has been recognized as an important cause of vitreous hemorrhage [107, 108]. Robertson et al. [109] presented 15 patients with vitreous hemorrhage in association with a round retinal break and an avulsed, intact retinal vessel attached to an overlying operculum. They considered these features to be a specific clinical entity having a predictable course of events that includes intermittent vitreous hemorrhage as long as the vessel remains attached to vitreous. In a follow-up study, Robertson and Norton [105] noted the occurrence of vitreous hemorrhage after treatment in 11 patients, five with an avulsed vessel associated with a detached operculum. In a study of 17 cases, Theodossiadis et al. [110] noted that recurrent bleeding was related to the mobility and size of the vessel overlying the break. De Bustros and Welch [111] treated 17 of 19 eyes with avulsed retinal vessels (80 % veins) by a variety of treatment methods. Visual results were good in all but one eye, which developed a massive vitreous hemorrhage and subsequent phthisis bulbi.

Lincoff et al. [112] treated nine avulsed retinal vessels by laser occlusion of the vessel and temporary balloon buckle. The avulsed vessel was an artery in three instances and a vein

in six. The avulsed vessel was associated with a retinal break in six patients, of which five also had a retinal detachment. Five of the nine vessels were occluded with one laser treatment, one required two treatments, two required three treatments, and one required four treatments. No recurrent hemorrhage occurred in follow-up periods of 6–42 months. Theodossiadis and Koutsandrea [113] conducted a prospective study of 87 cases with avulsed retinal vessels associated with retinal tears and rhegmatogenous retinal detachment. They described six patterns of avulsed vessels: avulsion in contact with aperture, arched avulsion at the level of the operculum, arched avulsion higher than the operculum, avulsion with an irregular shape, irregular break with corresponding irregularity of the avulsion, and double avulsion of the same vessel. They further indicated that therapy is directed to seal the tear and occlude or immobilize the vessel. To these ends, they employed a fixed episcleral silastic sponge, applied cryotherapy around the retinal break, released subretinal fluid, applied argon laser coagulation at a later stage (if necessary) to occlude the avulsed vessel, and applied endodiathermy with partial vitrectomy (if necessary). Recurrent vitreous hemorrhage occurred after therapy in six of the 87 cases. Anatomic restoration was achieved in 84 of the 87 cases, and three required a second intervention.

Avulsion of retinal vessels may occur without associated full-thickness retinal tears [114–117]. Hersh et al. [115] conducted a clinicopathologic study of “venous traction loops” in an eye with background diabetic retinopathy. Light microscopy and scanning and transmission electron microscopy disclosed the loops to consist of telangiectatic retinal veins that had passed through a discontinuity in the ILL. The vitreous was detached posteriorly, except at the venous loops and at a few other points at which there was tenting of the ILL.

Chatzoulis et al. [114] reported six patients with recurrent vitreous hemorrhage caused by retinal vessel rupture or injury caused by vitreous traction. In most cases, the avulsed vessel was a small vein in the superior temporal quadrant. Vine [117] observed avulsed retinal veins in eyes of eight patients with a variety of concurrent conditions: resolved Eales’ disease after laser therapy, one; cicatricial retinopathy of prematurity, one; background diabetic retinopathy, two; resolved proliferative diabetic retinopathy after laser therapy, two; elevated preretinal gliosis adherent to contracting vitreous, one; and pars planitis, one. Firm attachments of the vitreous in the vicinity of retinal vessels are an important precursor to traction and avulsion of a retinal vessel. Avulsion of retinal vessels is an important cause of vitreous hemorrhage.

B. Sickle-Cell Vasculopathies

Sickle-cell disease is an inherited hematologic disorder that has no established cure. The molecular lesion of the sickle hemoglobin is a point mutation (GAG→GTG) in exon 1 of the β -globin gene [118]. This single-point mutation renders the

sickle gene with multiple phenotypic expressions associated with complex genetic interactions and modifiers that are not well understood [119, 120]. Vascular occlusions occur from sickling of the erythrocytes, increased viscosity, and venous stasis, especially in the setting of hypoxia, acidosis, and inflammation [121]. The sickle syndromes have the highest incidence in black Africans and African-Americans but are also found in people from Mediterranean countries as well as Saudi Arabia and India [122]. About 8 % of black Americans are heterozygous for hemoglobin S. Approximately 0.15 % of black children in the United States have homozygous hemoglobin S. The prevalence among adults is much lower because patients with sickle-cell anemia have a decreased life expectancy.

In the retina, common findings include salmon-patch hemorrhages, iridescent spots and black sunbursts. *Salmon-patch hemorrhage* is a well-defined area of hemorrhage located within the superficial retina, between the sensory retina and its internal limiting membrane. It usually occurs in the mid-peripheral retina adjacent to an intermediate-sized arteriole [123]. Although the hemorrhage is initially bright red, it turns salmon colored over time because of progressive hemolysis. Resorption may result in a retinoschisis cavity. If the retinoschisis cavity contains refractile, copper-colored granules, it is called an *iridescent spot*. Histologically, these deposits contain hemosiderin-laden macrophages [123, 124]. Intraretinal hemorrhages may track into the subretinal space, dissecting between the neurosensory retina and the retinal pigment epithelium. Retinal pigment epithelium migration into the site may occur with forming of the stellate and spiculate hyperpigmented lesions known as a *black sunburst*. The black sunburst lesion appears as a flat, black patch about 0.5–2 mm in size. Glistening refractile granules, similar to those in iridescent spots, may be present [123]. A large amount of intraretinal and subretinal hemorrhage may rarely alter the extracellular matrix or fibrous component of Bruch’s membrane, allowing development of spontaneous choroidal neovascularization growing within the black sunburst lesion [125] (Figure III.H-19).

Nonproliferative sickle retinopathy with arteriolar occlusions and arteriovenous anastomoses can progress to proliferative sickle retinopathy. In more advanced retinopathy, occlusions can occur in any vessel within the peripheral retinal vasculature and can result in new vascular formations characteristic of sickle-cell disease, such as sea-fan neovascularization (Figure III.H-20) and hairpin loops [126] vitreous hemorrhage, and retinal detachment [127]. Profound visual loss resulting from vitreous hemorrhage and traction retinal detachment have been reported to be as high as 10–20 % in symptomatic patients in a referral setting [128] but rarely found in an observational cohort study [129].

The macular findings in patients with sickle-cell disease include abnormal perfusion and an enlarged foveal avascular zone due to vaso-occlusive episodes. Premacular membranes, schisis, holes, and neovascularization may also occur [130–132]. Spectral domain optical coherence

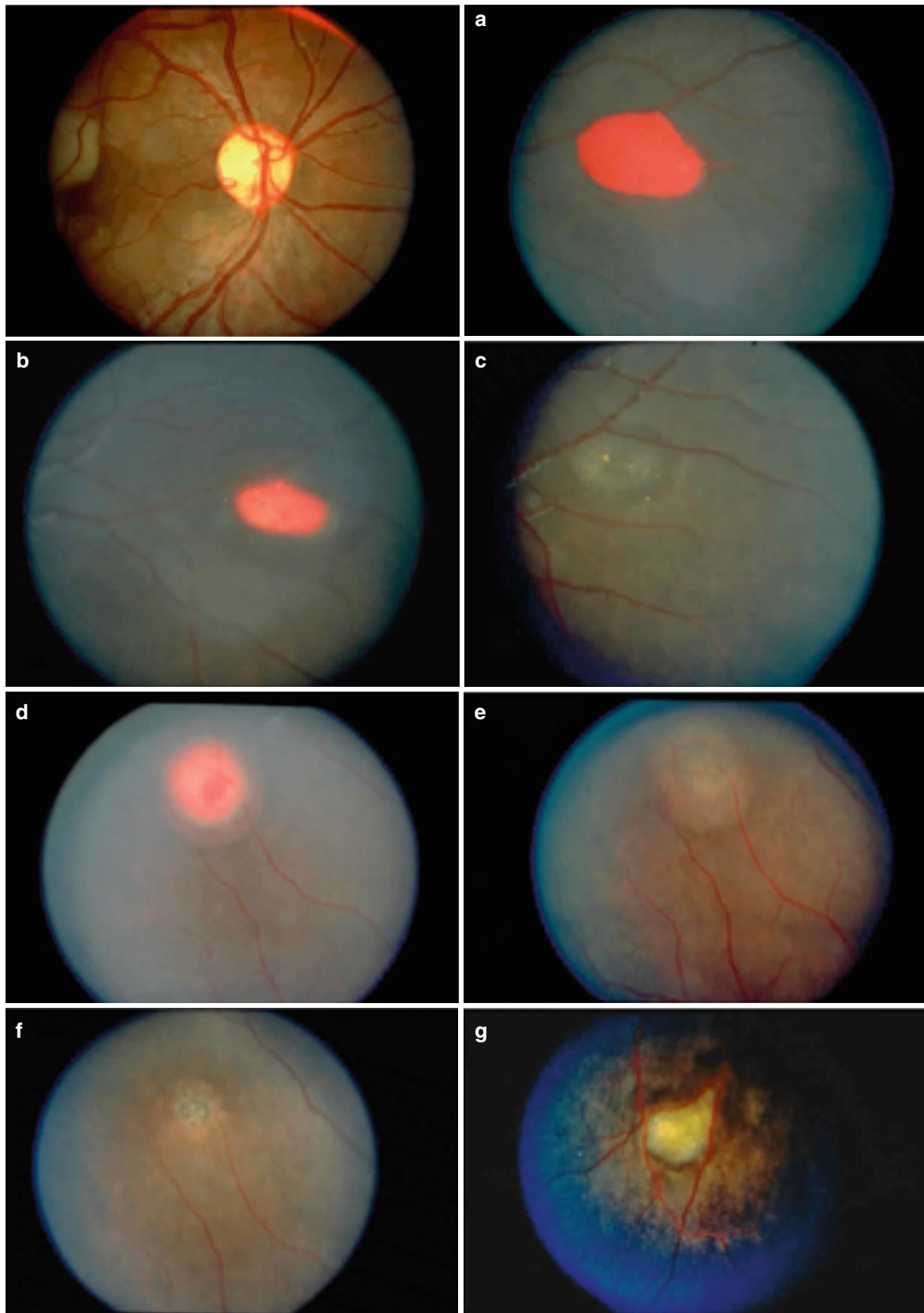


Figure III.H-19 (a) Salmon-patch hemorrhage with preretinal blood obscuring the retinal vasculature. (b) Two weeks later, the hemorrhage shown in (a) has a central grayish-white color as it begins to resolve. (c) Two years later, the hemorrhage shown in (a) and (b) has resolved, and an iridescent spot remains. (d) Salmon-patch hemorrhage with pre-, intra-, and subretinal blood. (e) Two months later, the

hemorrhage shown in (d) has resolved, and a lightly pigmented area surrounded by a depigmented halo is seen. (f) Four years later, a well-pigmented black sunburst adjacent to the arteriole remains from the salmon-patch hemorrhage shown in (e). (g) Iridescent spot with refractile copper-colored granules (With permission from: Gagliano and Goldberg [124])

tomography of the central retina as well as microperimetry are sensitive instruments for the detection of early macular changes due to sickle-cell-associated maculopathy. These anatomical changes might be detected even before they cause symptoms, as such in a preclinical state [133, 134]. In combination with wide-field photographic imaging of the peripheral retina, patients at risk for developing sight-threatening retinopathy can be detected and treated in an early stage. Fluorescein angiography is of great importance in showing the extent of non-perfusion or proliferative retinal disease in this condition as well as in others, such as retinal vein occlusions.

Given the high rate of spontaneous regression and the lack of progression of sea fans in some eyes, indications for treatment of retinal neovascularization vary among different authors. Therapeutic intervention is usually undertaken in cases of bilateral proliferative disease, spontaneous hemorrhage, large elevated sea fans, or rapid growth of the neovascular tissue or in cases in which the fellow eye has already been lost due to proliferative sickle-cell retinopathy [135]. If peripheral neovascularization exceeds 60° of the circumference, therapy is usually implemented. Therapeutic options include feeder vessel photocoagulation and scatter laser coagulation in non-perfused areas. For proliferative disease, cryotherapy, pars planar vitrectomy, and scleral buckling are sometimes indicated. The possible role of anti-VEGF agents is not yet clear.

C. Coats' Disease

Retinal abnormalities characterized by vessel dilatation of small- to medium-sized vessels, with irregular calibers and associated exudative retinal detachment in young male patients were first described by Coats and Leber in the early twentieth century [136, 137]. Reese in 1955 showed the similarities between the two entities known up to that time as "Coats' disease" and "Leber's military aneurysms" [138]. Some authors see these diseases as two stages of the same disease, while others consider them as two different diseases [139, 140]. At the present time, the term Coats' disease refers to the more peripheral retinal lesions, whereas Leber's military aneurysm is seen as a variant of Coats' disease and similar to type 1 idiopathic juxtafoveolar telangiectasia [141].

Coats' disease is a sporadic disease with no association to other diseases and not genetically determined. Coats' disease is typically identified at a median age of 5 years [142] with an estimated incidence of 0.09 per 100,000 in the general population [143]. The disease occurs almost always unilaterally with 75–85 % of the patients being male [142, 143]. The mean age of diagnosis is markedly different with differing modes of presentation. Cases

presenting with leukocoria or strabismus present earlier, while subjective visual loss presents later. A large proportion of eyes (44 %) are blind at diagnosis. The great majority of eyes (71 %) have 6 or fewer clock hours of retinal exudation. More severe forms/stages of Coats' disease are more common in the younger patients [144]. The course of the disease is marked by recurrences. The prognosis is best for the diagnosis in early stages of the disease in older patients (in contrast to late stages in younger patients).

The clinical classification of Coats' disease according to Shields [143] is:

Stage 1 is characterized by telangiectasia only.

Stage 2 demonstrates telangiectasias and exudation (2a) and is further subcategorized depending on involvement of the fovea (2b) (Figures III.H-21 and III.H-22).

Stage 3 demonstrates subtotal retinal detachment (3a), also subcategorized based on foveal involvement (3b).

Stage 4 exhibits total retinal detachment (RD) with glaucoma.

Stage 5 is end-stage disease with a blind, painless or painful eye and total RD, often with cataract and eventual phthisis bulbi.

The hallmark lesion of this disease is idiopathic retinal telangiectasia, which manifest as "lightbulb appearance" on fluorescein angiography. Other features of this disease include irregular retinal vessel dilatations, retinal vessel tortuosity, areas of capillary non-perfusion, intra- and/or subretinal exudation, and retinal detachment. Macular exudation may be caused by macular telangiectasia, peripheral retinal telangiectasia, or both [144]. Coats' disease must be differentiated from several other clinical entities that simulate its fundus picture, especially in children such as retinoblastoma, toxocariasis, persistent fetal vasculature syndrome, retinitis pigmentosa with Coats'-like reaction, and diseases with vascular changes at the vitreo-retinal interface (retinopathy of prematurity, familial exudative vitreo-retinopathy, incontinentia pigmenti). The most important differential diagnosis is retinoblastoma, which justifies the routine use of ultrasound and MRI in the primary diagnosis of the disease [145].

Histopathological examinations of eyes with Coats' disease show thickening of the sensory retina by homogeneous acellular material, typical of lipoproteinaceous exudation. Lipid- and hemosiderin-laden macrophages and cholesterol clefts are present in both the sensory retina and subretinal fluid. Lipid deposition induces foreign-body granulomatous inflammation [143, 146]. In a case study using SD-OCT imaging of the retina in an eye with exudative Coats' disease, intraretinal exudates were identified mainly in the outer plexiform layer of the retina [146]. Treatment options are shown in Table III.H-1 and results are shown in (Figure III.H-23). Enucleation of painful end-stage eyes is necessary in 16 % of cases.

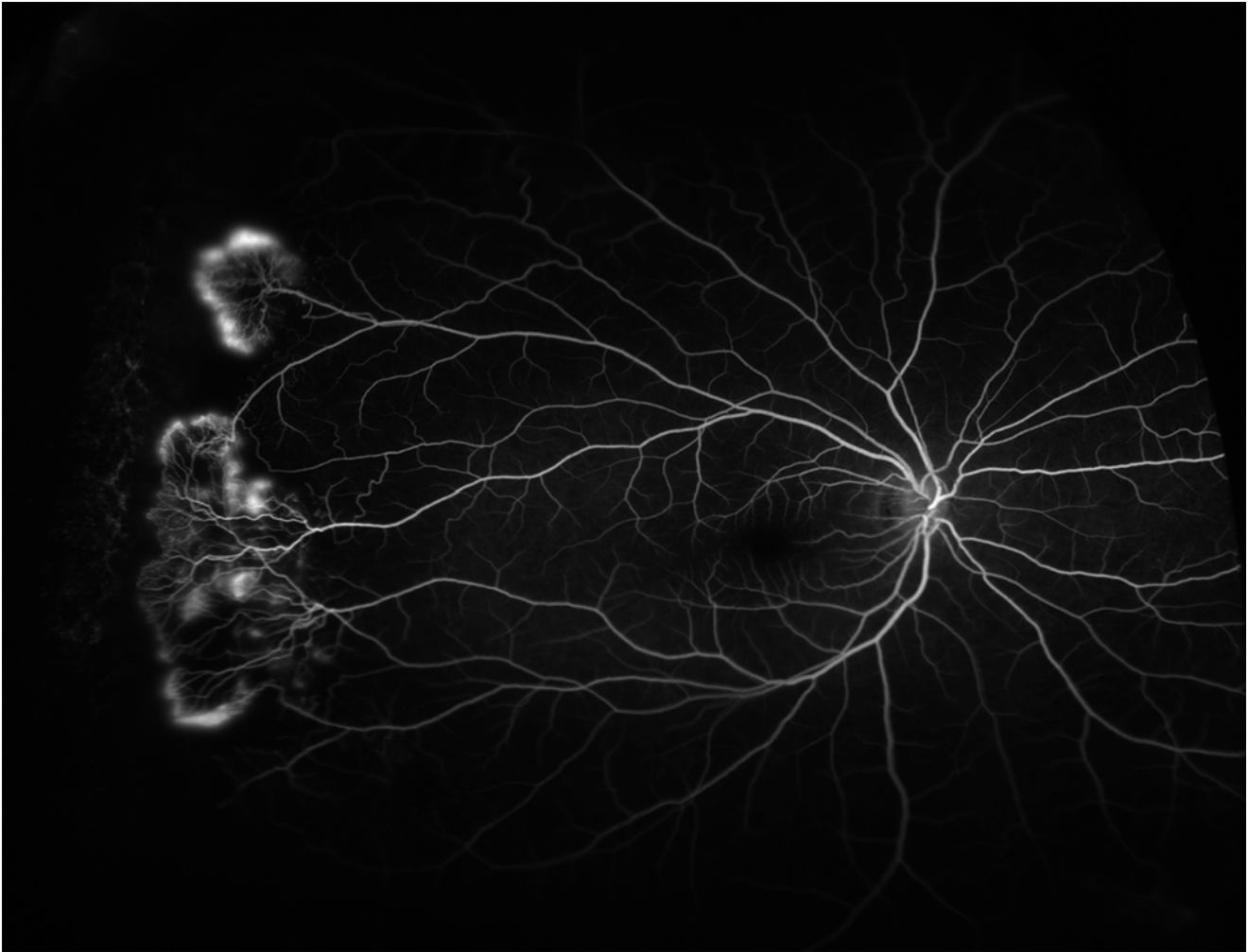


Figure III.H-20 Sickle-cell retinopathy: Fluorescein angiogram in the arteriovenous phase shows peripheral non-perfusion and sea-fan neovascularization at the border of vascularized and nonvascularized retina (Optomap image courtesy of Optos, Inc.)

VI. Pars Planitis

Pars planitis refers to inflammation of the ciliary body, vitreous base, and peripheral retina [153]. Originally, this clinical entity was also known as peripheral uveitis or chronic cyclitis [154–156]. However, the Standardization of Uveitis Nomenclature (SUN) for reporting clinical data established the unique name pars planitis in 2005 [157]. According to the SUN terminology, the term pars planitis should be used only for the subset of intermediate uveitis where there is idiopathic snowball formation (see below) in the absence of systemic disease, such as autoimmune disease, or infection. Nevertheless, the differential diagnosis has to involve a work-up for treatable systemic diseases: sarcoidosis, syphilis, multiple sclerosis with vascular sheathing, toxoplasmosis, and toxocariasis. If biomarkers are found indicating that one of the treatable diseases is present, it has to be treated. In this case, the diagnosis of pars planitis has to be considered a

subset of intermediate uveitis. Further refinements in the standardization of uveitis nomenclature are forthcoming [158]. Herein, the term pars planitis will be used to refer to the anatomical region of the pars plana that is mostly affected, although it could be argued that the term peripheral anterior vitritis might be more appropriate in some cases, given that vitreous may be the stimulus for inflammation and not the pars plana, per se.

Histological studies of the peripheral retina and ciliary body demonstrate condensed vitreous, fibroblasts, spindle cells, blood vessels, and lymphocytes, often with prominent lymphocyte cuffing of retinal veins [159]. Pars plana exudates appear to consist of loose fibrovascular layer containing scattered mononuclear inflammatory cells and a few fibrocyte-like cells adjacent to the hyperplastic nonpigmented epithelium of the pars plana. This fibroglial tissue consists of vitreous collagen, Müller cells, and probably fibrous astrocytes [160]. Pars planitis is associated with an increased frequency of effector memory CD 57+ T cells. CD 57

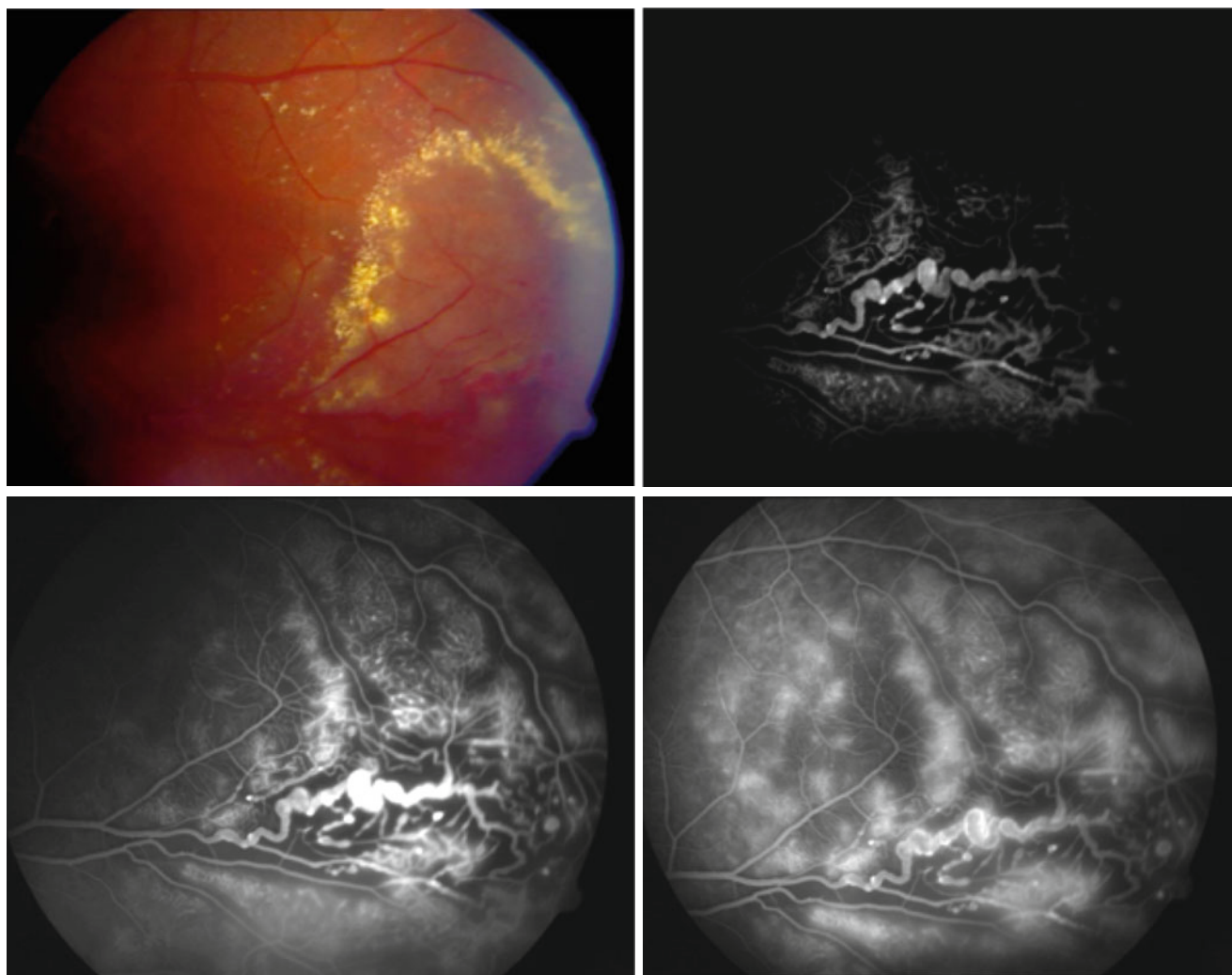


Figure III.H-21 Coats' disease: A 7-year-old boy at primary diagnosis of Coats' disease. Stage 2a according to Shields. Teleangiectasia is well documented in fluorescein angiography (lightbulb appearance). In the

late phase of fluorescein angiography, capillary non-perfusion and leakage of the retinal vessels are present (Courtesy of Prof. Holz and Dr. Herwig of the University Eye Clinic in Bonn, Germany)

expression correlates with late immune responses and some pathologic conditions resulting from persistent stimulation of the immune system [161]. It might be that remnants of the regressed fetal hyaloid vasculature are the antigens that elicit the immune response [7] [see chapters I.D. Proteomics of fetal hyaloid vasculature regression; II.A. Development and Developmental Disorders of Vitreous]. The intact anatomic correlates of these remnants are vitreous tubuli or verrucae (see above), although basement membrane fragments and other remnants of the fetal hyaloid vasculature may remain embedded in the vitreous base.

A. Epidemiology and Clinical Presentation

The incidence of pars planitis in the Rochester Epidemiology Project is 2,077 per 100,000 [162]. The median age of the

patients at onset of the disease is in the early 20 s [163, 164]. More male patients are affected than females, especially in childhood [165, 166]. In fact, intermediate uveitis (pars planitis is synonymous with intermediate uveitis in many studies) accounts for 20–30 % of all uveitis seen in children [167, 168]. Patients usually present with blurred vision followed by red eye and ocular deviation (in children), but symptoms are usually minimal. In severe cases, vision loss might be present due to vitreous opacification or macular edema [167, 169, 170]. The anterior chamber may have signs of inflammation in the form of keratic precipitates or flare and cells, which are usually minimal. Basically vitritis is the characteristic feature of patients, often seen at the slit lamp.

On examination of the posterior pole and the retina, vitreous snowballs typically are yellow–white inflammatory aggregates that are found in the mid-vitreous and inferior periphery. Snow-banks are exudates on the pars plana, when present are usually found inferiorly, but may also

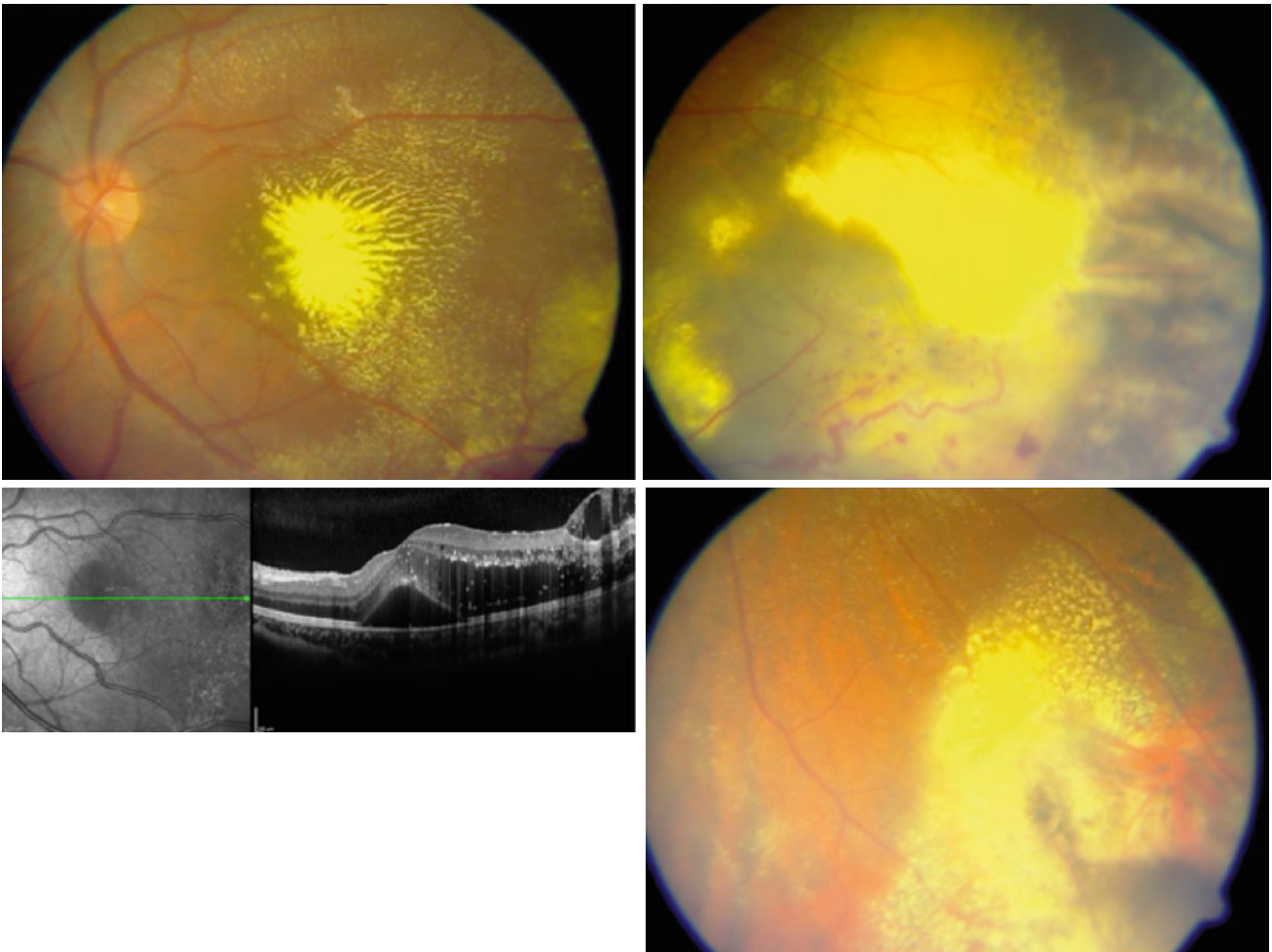


Figure III.H-22 Coats' disease: A 9-year-old boy with stage 2b disease (same as in Figures III.H-21 2 years later). Macular edema is now present: the OCT scan reveals thickening of the outer plexiform layer with

deposits. The decision to treat was taken. Peripheral cryotherapy and intravitreal injection of bevacizumab were done (Courtesy of Prof. Holz and Dr. Herwig of the University Eye Clinic in Bonn, Germany)

extend 360° of the retinal periphery. Snow-banking is usually associated with the more severe form of the disease and warrants aggressive therapy. Retinal changes in pars planitis include tortuosity in arterioles and venules, sheathing of peripheral veins, neovascularization, and retinal detachments [171–173] (Figure III.H-24).

B. Sequelae

Pars planitis is most often a benign form of uveitis. Complications are due to its chronicity, and if left untreated can lead to blindness. The incidence of *glaucoma* in acute uveitis is 7.6 %, and in patients with chronic uveitis, the incidence of glaucoma at 1 and 5 years is 6.5 and 11.1 %, respectively. Active inflammation, steroid usage, increasing age, and number of years since diagnosis are significantly correlated with elevated intraocular pressure [174]. *Cataracts* occur in 15–50 % of eyes. Typically they are

located in the posterior and/or anterior subcapsular, region, or posterior cortex of the lens. Posterior polar cataracts have been reported as well. The incidence of cataracts increases with the duration and severity of the disease. If treated earlier with immunosuppression rather than corticosteroids, cataract formation is less severe [173, 175]. *Macular edema* and maculopathy are the most common causes of visual loss. Incidence varies from 12 to 51 %. Like cataract, their incidence increases with the duration and severity of the disease [173, 175]. Premacular membranes with macular pucker occur in 34.6–36 % eyes, unrelated to duration of disease or chronic cystoid macular edema [161, 176] Retinal vasculitis in the form of *periphlebitis* may also occur and induce neovascularization and cyclitic membrane formation [175]. *Exudative retinal detachments* develop secondary to inflammation, while vitreous traction arising from long-standing vitreous inflammation can cause subsequent peripheral retinal hole formation [177] Peripheral *neovascularization* with and

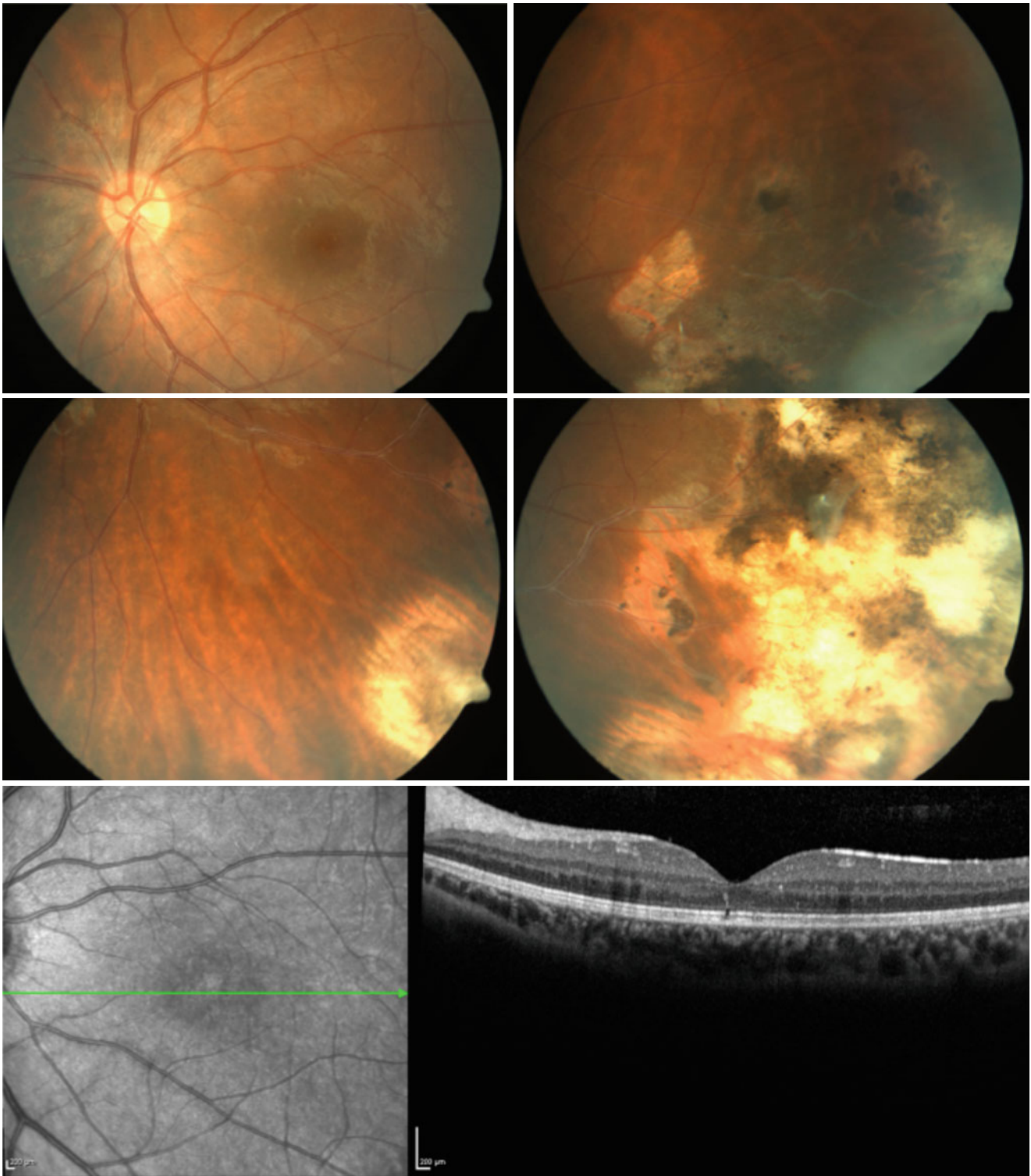


Figure III.H-23 Coats' disease: 3 years after treatment with peripheral cryoapplication and intravitreal bevacizumab: the fovea shows no further edema or deposits. In the periphery, there is scarring of the retina

and some ghost vessels (Courtesy of Prof. Holz and Dr. Herwig University Eye Clinic Bonn, Germany)

Table III.H-1 Treatment options of Coats’ disease according to the classification of Shields [143]

Laser photocoagulation	Cryotherapy	Vitreo-retinal surgery	Intravitreal triamcinolone	Intravitreal anti-VEGF
Stages 1–3a*	Stages 1–3b*	Late stage of the disease	Described in case studies	Described in case studies
Milder forms [143, 147]	Exudative forms [143, 148]	Especially in total retinal detachment [149]	Beneficial as an adjuvant therapy [150]	See triamcinolone [151]
Do not combine with cryotherapy	Used in 42 % of treated eyes		Especially in macular edema	
2 quadrants at a time	Similar to laser		May be used in combination with anti-VEGF	
With 1 month between treatments	Similar to laser			May lead to traction retinal detachment [152]

* According to the classification of Shields [145]

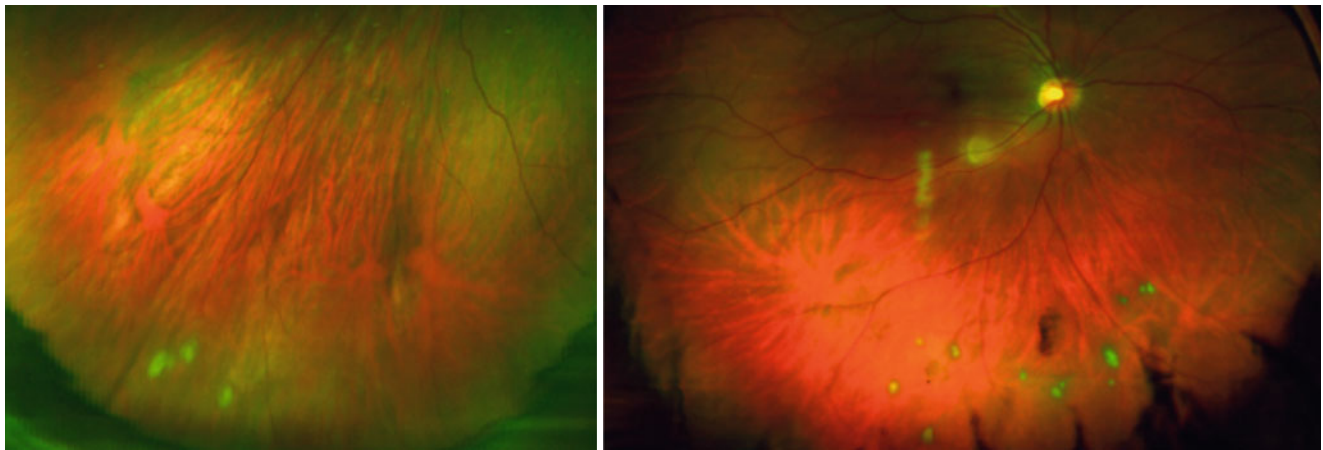


Figure III.H-24 Pars planitis: Snowballs in the inferior vitreous. Snowballs appear as whitish lesions. In these pictures, the camera increases the contrast of these lesions by using the color *green*. P200C image (Optomap image courtesy of Optos, Inc.)

Table III.H-2 Stepwise treatment of pars planitis as recommended by Foster [18, 179] [3]

1st step	2nd step	3rd step	4th step
Kenalog injections (40 mg) peribulbar	Additional nonsteroidal systemic drug (e.g., Naprosyn, 500 mg PO BID)	Pars plana cryopexy	Systemic immunosuppressive chemotherapy (low-dose cyclosporin or low-dose methotrexate)
For 12 weeks	If still active	If still active	If still active or recurrent
Every other week			Alternative: pars plana vitrectomy

without *vitreous hemorrhage* was seen in 6.5 % of cases by Malinowski et al. [176] Optic nerve involvement in the form of *optic disc edema* is seen in 3–38.6 % of eyes with intermediate uveitis [173, 178]. *Optic neuritis* with or without multiple sclerosis was seen in 7.4 % of eyes with pars planitis [173, 176, 178].

C. Therapy

Stepwise treatment of pars planitis is recommended by Foster [179, 180], as shown in Table III.H-2.

Abbreviations

CT	Computerized Tomography
ILM	Inner Limiting Membrane
PO	BID: Orally, Twice a Day
PVD	Posterior Vitreous Detachment
RD	Retinal Detachment
RPE	Retinal Pigment Epithelium
SD-OCT	Spectral Domain Optical Coherence Tomography
VEGF	Vascular Endothelial Growth Factor

References

1. Fine BS, Tousimis AJ. The structure of the vitreous body and the suspensory ligaments of the lens. *Arch Ophthalmol*. 1961;65:95–110.
2. Hogan MJ, Alvarado JA, Weddell JE. *Histology of the human eye: an atlas and textbook*. Philadelphia: WB Saunders; 1971.
3. Sebag J. Age-related differences in the human vitreo-retinal interface. *Arch Ophthalmol*. 1991;109:966–71.
4. Teng CC, Chi HH. Vitreous changes and the mechanism of retinal detachment. *Am J Ophthalmol*. 1957;44:335–56.
5. Schepens CL. Personal communication. 1986.
6. Hultsch E. Vitreous structure and ocular inflammation. In: Silverstein AM, O'Connor GR, editors. *Immunology and immunopathology of the eye*. New York: Masson; 1979.
7. Gartner J. The fine structure of the vitreous base of the human eye and pathogenesis of pars planitis. *Am J Ophthalmol*. 1971;71:1317–27.
8. Sebag J, Balazs EA. Human vitreous fibres and vitreoretinal disease. *Trans Ophthalmol Soc U K*. 1984;104:123–8.
9. Sebag J. *The vitreous: structure, function, and pathobiology*. New York: Springer; 1989.
10. Sebag J. Age-related changes in human vitreous structure. *Graefes Arch Clin Exp Ophthalmol*. 1987;225:89–93.
11. Sebag J, Balazs EA. Morphology and ultrastructure of human vitreous fibers. *Invest Ophthalmol Vis Sci*. 1989;30:1867–71.
12. Gartner J. Electron-microscopic study on the fibrillar network and fibrocyte-collagen interactions in the vitreous cortex at the ora serrata of human eyes with special regard to the role of disintegrating cells. *Exp Eye Res*. 1986;42:21–3.
13. Sebag J. Surgical anatomy of vitreous and the vitreo-retinal interface. In: Tasman W, Jaeger EA, editors. *Duane's clinical ophthalmology*, vol. 6. Philadelphia: JB Lippincott; 1992.
14. Foos RY. Vitreoretinal juncture: topographical variations. *Invest Ophthalmol*. 1972;11:801–8.
15. Hogan MJ. The vitreous, its structure and relation to the ciliary body and retina. *Invest Ophthalmol*. 1963;2:418–45.
16. Foos RY, Allen RA. Retinal tears and lesser lesions of the peripheral retina. *Am J Ophthalmol*. 1967;64:643–55.
17. Foos RY, Simons KB. Vitreous in lattice degeneration of retina. *Ophthalmology*. 1984;91:452–7.
18. Spencer LM, Foos RY, Straatsma BR. Meridional complexes and associated abnormalities of the peripheral retina. *Am J Ophthalmol*. 1970;70:697–713.
19. Byer NE. Cystic retinal tufts and their relationship to retinal detachment. *Arch Ophthalmol*. 1981;99:1788–90.
20. Foos RY. Zonular traction tufts of the peripheral retina in cadaver eyes. *Arch Ophthalmol*. 1969;82:620–32.
21. Spencer LM, Straatsma BR, Foos RY. Tractional degenerations of the peripheral retina. . 1969.
22. Spencer LM, Foos RY, Straatsma BR. Enclosed bays of the ora serrata: relationship to retinal tears. *Arch Ophthalmol*. 1970;83:421–5.
23. Rutnin U, Schepens CL. Fundus appearance in normal eyes. II. The standard peripheral fundus and developmental variations. *Am J Ophthalmol*. 1967;64:840–52.
24. Foos RY, Spencer LM, Straatsma BR. Trophic degenerations of the peripheral retina. In: *Transactions of the New Orleans Academy of Ophthalmology: symposium on retina and retinal surgery*. St Louis: Mosby; 1969.
25. Streeten BW, Bert M. The retinal surface in lattice degeneration of the retina. *Am J Ophthalmol*. 1972;74:1201–9.
26. Teng CC, Katzin KM. An anatomic study of the periphery of the retina. I. Nonpigmented epithelial cell proliferation and hole formation. *Am J Ophthalmol*. 1951;34:1237–48.
27. Okun E. Gross and microscopic pathology in autopsy eyes. III. Retinal breaks without detachment. *Am J Ophthalmol*. 1961;51:369–91.
28. Rutnin U, Schepens CL. Fundus appearance in normal eyes. III. Peripheral degenerations. *Am J Ophthalmol*. 1967;64:1040–62.
29. Cibis PA. *Vitreoretinal pathology and surgery in retinal detachment*. Mosby: St Louis; 1965.
30. Foos RY. Vitreous base, retinal tufts, and retinal tears: pathogenic relationships. In: Pruet RC, Regan CD, editors. *Retina congress*. New York: Appleton-Century-Crofts; 1974.
31. Inomata H. Electron microscopic observations of cystoid degeneration in the peripheral retina. *Jpn J Ophthalmol*. 1966;10:26–40.
32. Green WR. *Retina*. In: Spencer WH, editor. *Ophthalmic pathology: an atlas and text*. 4th ed. Philadelphia: WB Saunders; 1996.
33. Bradford JD, Wilkinson CP, Fransen SR. Pseudophakic retinal detachment: the relationships between retinal tears and the time following cataract surgery at which they occur. *Retina*. 1989;9:181–6.
34. Byer NE. Lattice degeneration of the retina. *Surv Ophthalmol*. 1979;23:213–47.
35. Straatsma BR, Allen RA. Lattice degeneration of the retina. *Trans Am Acad Ophthalmol Otolaryngol*. 1962;66:600–13.
36. Straatsma BR, Foos RY, Feman SS. Degenerative diseases of the peripheral retina. In: Duane TD, editor. *Clinical ophthalmology*, vol. 3. Philadelphia: Harper & Row; 1986.
37. Straatsma BR, Zeegen PD, Foos RY, et al. Lattice degeneration of the retina. *Trans Am Acad Ophthalmol Otolaryngol*. 1974;78:87–113.
38. Burton TC. The influence of refractive error and lattice degeneration on the incidence of retinal detachment. *Trans Am Ophthalmol Soc*. 1990;87:143–57.
39. Parelhoff ES, Wood WJ, Green WR, et al. Radial perivascular lattice degeneration of the retina. *Ann Ophthalmol*. 1980;12:25–32.
40. Schepens CL. Diagnostic and prognostic factors as found in preoperative examination. *Trans Am Acad Ophthalmol Otolaryngol*. 1952;56:398–418.
41. Schepens CL. Subclinical retinal detachments. *Arch Ophthalmol*. 1952;47:593–606.
42. Foos RY, Simons KB, Wheeler NC. Comparison of lesions predisposing to rhegmatogenous retinal detachment by race and subjects. *Am J Ophthalmol*. 1983;96:644–9.
43. Byer NE. Clinical study of lattice degeneration of the retina. *Trans Am Acad Ophthalmol Otolaryngol*. 1965;69:1064–77.
44. Robinson MR, Streeten BW. The surface morphology of retinal breaks and lattice retinal degeneration: a scanning electron microscopic study. *Ophthalmology*. 1986;93:237–46.
45. Foos RY. Posterior peripheral retinal tears. *Ann Ophthalmol*. 1974;6:679–87.
46. Tillery WV, Lucier AC. Round atrophic holes in lattice degeneration: an important cause of phakic retinal detachment. *Trans Am Acad Ophthalmol Otolaryngol*. 1976;81:509–18.
47. Morse PH, Scheie HG. Prophylactic cryoretinopexy of retinal breaks. *Arch Ophthalmol*. 1974;92:204–7.
48. Byer NE. Changes in prognosis of lattice degeneration of the retina. *Trans Am Acad Ophthalmol Otolaryngol*. 1974;78:114–24.
49. Davis MD. Natural history of retinal breaks without detachment. *Arch Ophthalmol*. 1974;92:183–94.
50. Dobbie G. Discussion. New research on the aetiology and surgery of retinal detachment. *Mod Probl Ophthalmol*. 1975;15:113.
51. Tolentino FI, Schepens CL, Freeman HM. *Vitreoretinal disorders: diagnosis and management*. Philadelphia: WB Saunders; 1976. p. 107.
52. Freeman HM. Fellow eyes of giant retinal breaks. *Trans Am Ophthalmol Soc*. 1978;76:343–82.
53. Byer NE. *The peripheral retina in profile: a stereoscopic atlas*. Torrence: Criterion Press; 1982.
54. Eisner G. White with pressure. In: Eisner G, editor. *Biomicroscopy of the peripheral fundus: an atlas and textbook*. New York: Springer; 1973.
55. Nagpal KC, Huamonte F, Constantaras A, et al. Migratory white-without-pressure retinal lesions. *Arch Ophthalmol*. 1976;94:576–9.

56. Watzke RC. The ophthalmoscopic sign, "white with pressure": a clinicopathologic correlation. *Arch Ophthalmol*. 1961;66:812-23.
57. Daicker B. Sind die Symptome "weiss mit druck" und weiss ohne druck durch die periphere netzshantklerose bedingt? *Mod Probl Ophthalmol*. 1975;15:82-90.
58. Gartner J. Discussion. New research on the aetiology and surgery of retinal detachment. *Mod Probl Ophthalmol*. 1975;15:112.
59. Dunker S, Glinz J, Faulborn J. Morphologic studies of the peripheral vitreoretinal interface in humans reveal structures implicated in the pathogenesis of retinal tears. *Retina*. 1997;17:124-30.
60. Balazs EA. Physiology of the vitreous body. In: Schepens CL, editor. *Proceedings of the Second Conference of the Retina Foundation*. St Louis: Mosby; 1960.
61. Hilding AC. Normal vitreous, its attachments and dynamics during ocular movement. *Arch Ophthalmol*. 1954;52:497-514.
62. Hilding AC. Alterations in the form, movement, and structure of the vitreous body in aphakic eyes. *Arch Ophthalmol*. 1954;52:699-709.
63. Constable IJ, Horne R, Slatter DH, et al. Regeneration of retinal limiting membranes after chorioretinal biopsy in dogs. *Invest Ophthalmol Vis Sci*. 1981;20:246-51.
64. Mittleman D, Green WR, Michels RG, et al. Clinicopathologic correlation of an eye after surgical removal of an epiretinal membrane. *Retina*. 1989;9:143-7.
65. Foos RY, Gloor BP. Vitreoretinal junction: healing of experimental wounds. *Graefes Arch Clin Exp Ophthalmol*. 1975;196:213-30.
66. Miller JW, Adamis AP, Shima DT, et al. Vascular endothelial growth factor/vascular permeability factor is temporally and spatially corrected with ocular angiogenesis in a primate model. *Am J Pathol*. 1994;145:574-84.
67. Miller B, Miller H, Patterson R, et al. Effect of the vitreous on retinal wound-healing. *Graefes Arch Clin Exp Ophthalmol*. 1986;224:576-9.
68. Foos RY. Retinal holes. *Am J Ophthalmol*. 1978;86:354-8.
69. Adamis AP, Shima DT, Tolentino MJ, et al. Inhibition of VEGF prevents retinal ischemia associated iris neovascularization in a nonhuman primate. *Arch Ophthalmol*. 1996;114:66-71.
70. Boniuk M, Butler FC. An autopsy study of lattice degeneration, retinal breaks, and retinal pits. In: McPherson A, editor. *New and controversial aspects of retinal detachment*. New York: Hoeber; 1968.
71. Spencer LM, Foos RY. Paravascular vitreoretinal attachments: role in retinal tears. *Arch Ophthalmol*. 1970;84:557-64.
72. Barishak YR, Stein R. Retinal breaks without retinal detachment in autopsy eyes. *Acta Ophthalmol*. 1972;50:147-59.
73. Foos RY. Tears of the peripheral retina: pathogenesis, incidence, and classification in autopsy eyes. *Mod Probl Ophthalmol*. 1975;15:68-81.
74. Boldrey EE. Risk of retinal tears in patients with vitreous floaters. *Am J Ophthalmol*. 1983;96:783-7.
75. Butner RW, McPherson AR. Spontaneous vitreous hemorrhage. *Ann Ophthalmol*. 1982;14:268-70.
76. Morse PH, Aminlari A, Scheie HG. Spontaneous vitreous hemorrhage. *Arch Ophthalmol*. 1974;92:297-8.
77. Winslow RL, Taylor BC. Spontaneous vitreous hemorrhage: etiology and management. *South Med J*. 1980;73:1450-2.
78. DiBernardo C, Blodi B, Byrne SF. Echographic evaluation of retinal tears in patients with spontaneous vitreous hemorrhage. *Arch Ophthalmol*. 1992;110:511-4.
79. Tabotabo MM, Karp LA, Benson WE. Posterior vitreous detachment. *Ann Ophthalmol*. 1980;12:59-61.
80. Murakami K, Jalkh AE, Avila MP, et al. Vitreous floaters. *Ophthalmology*. 1983;90:1271-6.
81. Novak MA, Welch RB. Complications of acute symptomatic posterior vitreous detachment. *Am J Ophthalmol*. 1984;97:308-14.
82. Wolter JR. Circular fixed fold of the retina. *Am J Ophthalmol*. 1965;60:805-11.
83. Foos RY. Vitreoretinal juncture over retinal vessels. *Graefes Arch Clin Exp Ophthalmol*. 1977;204:223-34.
84. Meyer E, Kurz GH. Retinal pits: a study of pathologic findings in two cases. *Arch Ophthalmol*. 1963;70:640-6.
85. Szirmai JA, Balazs EA. Studies on the structure of the vitreous body. III. Cells in the cortical layer. *Arch Ophthalmol*. 1958;59:34-48.
86. Friedman Z, Neumann E, Hyams S. Vitreous and peripheral retina in aphakia: a study of 200 nonmyopic aphakic eyes. *Br J Ophthalmol*. 1973;57:52-7.
87. Machermer R. The importance of fluid absorption, traction, intraocular currents, and chorioretinal scars in the therapy of rhegmatogenous retinal detachments. *Am J Ophthalmol*. 1984;98:681-93.
88. Benson WE, Tasman W. Rhegmatogenous retinal detachments caused by paravascular vitreoretinal traction. *Arch Ophthalmol*. 1984;102:669-70.
89. Tasman WS. Posterior vitreous detachment and peripheral retinal breaks. *Trans Am Acad Ophthalmol Otolaryngol*. 1968;72:217-24.
90. Sigelman J. Vitreous base classification of retinal tears: clinical application. *Surv Ophthalmol*. 1980;25:59-74.
91. Halpern JJ. Routine screening of the retinal periphery. *Am J Ophthalmol*. 1966;62:99-102.
92. Byer NE. Clinical study of retinal breaks. *Trans Am Acad Ophthalmol Otolaryngol*. 1967;71:461-73.
93. Rutnin U, Schepens CL. Fundus appearance in normal eyes. IV. Retinal breaks and other findings. *Am J Ophthalmol*. 1967;64:1063-78.
94. Smith RE, Ganley JP. Ophthalmic survey of a community. I. Abnormalities of the ocular fundus. *Am J Ophthalmol*. 1972;74:1126-30.
95. Colyear BH, Pischel DK. Clinical tears in the retina without detachment. *Am J Ophthalmol*. 1956;41:773-92.
96. Byer NE. Prognosis of asymptomatic retinal breaks. *Arch Ophthalmol*. 1974;92:208-10.
97. Byer NE. The natural history of asymptomatic retinal breaks. *Ophthalmology*. 1982;89:1033-9.
98. Haimann MH, Burton TC, Brown CK. Epidemiology of retinal detachment. *Arch Ophthalmol*. 1982;100:289-92.
99. Michaelson IC, Stein R, Barkai S. A study in the prevention of retinal detachment. *Ann Ophthalmol*. 1969;1:49-55.
100. Michels RG. Vitreous surgery for macular pucker. *Am J Ophthalmol*. 1981;92:628-39.
101. Neumann E, Hyams S, Brakai S. Natural history of retinal holes with specific reference to the development of retinal detachment and time factor involved. In: Michaelson IC, Berman ER, editors. *Causes and prevention of blindness*. New York: Academic Press; 1972.
102. Bohringer HR. Statistisches zu Häufigkeit und Risiko der Netzhautablosung. *Ophthalmologica*. 1956;131:331-4.
103. Benson WE. Prophylactic therapy of retinal breaks. *Surv Ophthalmol*. 1977;22:41-7.
104. Combs JL, Welch RB. Retinal breaks without detachment: natural history, management, and long-term follow-up. *Trans Am Ophthalmol Soc*. 1982;80:64-97.
105. Robertson DM, Norton EWD. Long-term follow-up of treated retinal breaks. *Am J Ophthalmol*. 1973;75:395-404.
106. Smiddy WE, Flynn HW, Nicholson DH, et al. Results and complications in treated retinal breaks. *Am J Ophthalmol*. 1991;112:623-31.
107. Brockhurst RJ, Schepens CL. Vitreous hemorrhages: surgical treatment. *Arch Ophthalmol*. 1961;66:327-35.
108. Clark G. The use of the photocoagulator in conditions associated with retinal detachment. *Trans Am Acad Ophthalmol Otolaryngol*. 1962;66:59-66.

109. Robertson DM, Curtin VT, Norton EWD. Avulsed retinal vessels with retinal breaks: a cause of recurrent vitreous hemorrhage. *Arch Ophthalmol*. 1971;85:669–72.
110. Theodosiadis GP, Velissatopoulos P, Magouritsas N, et al. Behandlung und Nachuntersuchung von Netzhautrissen ohne Netz-hautablosung mit den Riss uberlagerndem abgehobenem Netzhautgefass. *Klin Monatsbl Augenheilkd*. 1977;170:411–5.
111. de Bustros S, Welch RB. The avulsed retinal vessel syndrome and its variants. *Ophthalmology*. 1984;91:86–8.
112. Lincoff H, Kreissig I, Richard G. Treating avulsed vessels with a temporary balloon buckle. *Am J Ophthalmol*. 1986;101:90–4.
113. Theodosiadis GP, Koutsandrea CN. Types of avulsed retinal vessels associated with rhegmatogenous retinal detachment: treatment and results. *Graefes Arch Clin Exp Ophthalmol*. 1987;225:185–8.
114. Chatzoulis D, Theodosiadis GP, Apostolopoulos M, et al. Rezidivierende Glaskorperblutungen infolge cines in die Glaskorperhohle hereingezogenen Netzhautgefalles. *Klin Monatsbl Augenheilkd*. 1983;183:256–8.
115. Hersh PS, Green WR, Thomas JV. Tractional venous loops in diabetic retinopathy. *Am J Ophthalmol*. 1981;92:661–71.
116. Theodosiadis GP, Koutsandrea CN. Avulsed retinal vessels with and without retinal breaks: treatment and extended follow-up. *Trans Ophthalmol Soc U K*. 1985;104:887–9.
117. Vine AK. Avulsed retinal veins without retinal breaks. *Am J Ophthalmol*. 1984;98:723–7.
118. Steinberg MH. Sickle cell anemia, the first molecular disease: overview of molecular etiology, pathophysiology, and therapeutic approaches. *Scientific World Journal*. 2008;8:1295–324.
119. Steinberg MH. Genetic etiologies for phenotypic diversity in sickle cell anemia. *Scientific World Journal*. 2009;9:46–67.
120. Ballas SK, Lief S, Benjamin LJ, et al. Definitions of the phenotypic manifestations of sickle cell disease. *Am J Hematol*. 2010;85(1):6–13.
121. Emerson GG, Harlan JB, Fekrat S, et al. Hemoglobinopathies. In: Ryan SJ, editor. *Retina*. 4th ed. Philadelphia: Elsevier; 2006. p. 1429–45.
122. Clarkson JG. The ocular manifestations of sickle-cell disease: a prevalence and natural history study. *Trans Am Ophthalmol Soc*. 1992;90:481–504.
123. Emerson GG, Luty GA. Effects of sickle cell disease on the eye: clinical features and treatment. *Hematol Oncol Clin North Am*. 2005;19(5):957–73.
124. Gagliano DA, Goldberg MF. The evolution of salmon-patch hemorrhages in sickle cell retinopathy. *Arch Ophthalmol*. 1989;107(12):1814–5.
125. Liang JC, Jampol LM. Spontaneous peripheral chorioretinal neovascularisation in association with sickle cell anaemia. *Br J Ophthalmol*. 1983;67(2):107–10.
126. McLeod DS, Goldberg MF, Luty GA. Dual-perspective analysis of vascular formations in sickle cell retinopathy. *Arch Ophthalmol*. 1993;111(9):1234–45.
127. Goldberg MF. Classification and pathogenesis of proliferative sickle retinopathy. *Am J Ophthalmol*. 1971;71(3):649–65.
128. Moriarty BJ, Acheson RW, Condon PI, Serjeant GR. Patterns of visual loss in untreated sickle cell retinopathy. *Eye*. 1988;2(Pt 3):330–5.
129. Downes SM, Hambleton IR, Chuang EL, et al. Incidence and natural history of proliferative sickle cell retinopathy: observations from a cohort study. *Ophthalmology*. 2005;112(11):1869–75.
130. Murthy RK, Grover S, Chalam KV. Temporal macular thinning on spectral-domain optical coherence tomography in proliferative sickle cell retinopathy. *Arch Ophthalmol*. 2011;129(2):247–9.
131. Raichand M, Dizon RV, Nagpal KC. Macular holes associated with proliferative sickle cell retinopathy. *Arch Ophthalmol*. 1978;96(9):1592–6.
132. Schubert HD. Schisis in sickle cell retinopathy. *Arch Ophthalmol*. 2005;123(11):1607–9.
133. Hoang QV, Chau FY, Shahidi M, Lim JI. Central macular splaying and outer retinal thinning in asymptomatic sickle cell patients by spectral-domain optical coherence tomography. *Am J Ophthalmol*. 2011;151:990–4.
134. Chow CC, Genead MA, Anastasakis A, Chau FY, Fishman GA, Lim JI. Structural and functional correlation in sickle cell retinopathy using spectral domain optical coherence tomography and scanning laser ophthalmoscope microperimetry. *Am J Ophthalmol*. 2011;152:704–11.
135. Emerson GE, Harlan JB, Fekrat S, Luty GA, Goldberg MF. Hemoglobinopathies. *Retina*. 2006;2:1429–45.
136. Coats G. Forms of retinal disease with massive exudation. *R Lond Ophthalmol Hosp Rep*. 1908;17:440–525.
137. Leber T. Über eine durch Vorkommen multipler Miliaraneurysmen charakterisierte Form von Retinaldegeneration. *Albrecht von Graefes Archiv für Ophthalmologie*. 1912;81:1–14.
138. Reese AB. Telangiectasias of the retina and Coats' disease. *Am J Ophthalmol*. 1956;42:1–8.
139. Wessing A, Spitznas M. Morbus Coats und die Leber'sche Miliaraneurysmenretinitis. *Ber dtsh ophthal Ges*. 1977;74:199.
140. Hiller H. Morbus Coats – Miliaraneurysmenretinitis Leber. *Klin Mbl Augenheilk*. 1971;158:225.
141. Gass JD, Blodi BA. Idiopathic juxtafoveal retinal telangiectasis. Update of classification and follow-up study. *Ophthalmology*. 1993;100:1536–46.
142. Shields JA, Shields CL, Honavar SG, Demirci H. Clinical variations and complications of Coats disease in 150 cases: the 2000 Sanford Gifford Memorial Lecture. *Am J Ophthalmol*. 2001;131:561–71.
143. Shields JA, Shields CL, Honavar SG, Demirci H, Cater J. Classification and management of Coats disease: the 2000 Procter Lecture. *Am J Ophthalmol*. 2001;131:572–83.
144. Tarkkanen A, Laatikainen L. Coat's disease: clinical, angiographic, histopathological findings and clinical management. *Br J Ophthalmol*. 1983;76:766–76.
145. de Graaf P, Göricke S, Rodjan F, Galluzi P, Maeder P, Castelijns JA, Brisse HJ, European Retinoblastoma Imaging Collaboration (ERIC). Guidelines for imaging retinoblastoma: imaging principle and MRI standardization. *Pediatr Radiol*. 2012;42:2–14.
146. Kessner R, Barak A, Neudorfer M. Intraretinal exudates in Coats disease as demonstrated by spectral-domain OCT. *Case Rep Ophthalmol*. 2012;3:11–5.
147. Mulvihill A, Morris B. A population-based study of Coats disease in the United Kingdom. II. Investigation, treatment, and outcomes. *Eye*. 2010;24:1802–7.
148. Bergstrom CS, Hubbard 3rd GB. Combination intravitreal triamcinolone injection and cryotherapy for exudative retinal detachments in severe Coats disease. *Retina*. 2008;28:33–7.
149. Kranias G, Krebs TP. Advanced Coats' disease successfully managed with vitreo-retinal surgery. *Eye*. 2002;16:500–1.
150. Böhm MR, Uhlig CE. Use of intravitreal tramcinolone and bevacizumab in Coats' disease with central macular edema. *Graefes Arch Clin Exp Ophthalmol*. 2011;249:1099–101.
151. Entezari M, Ramezani A, Safavizadeh L, Bassirnia N. Resolution of macular edema in Coats' disease with intravitreal bevacizumab. *Indian J Ophthalmol*. 2010;58:80–2.
152. Ramasubramanian A, Shields CL. Bevacizumab for Coats' disease with exudative retinal detachment and risk of vitreoretinal traction. *Br J Ophthalmol*. 2012;96:356–9.
153. Schepens CL. Examination of the Ora serrata region: its clinical significance. *ACTA 16 Concilium Ophthalmologicum Britannia*. London Br Med Assoc. 1950;2:1384–93.
154. Brockhurst RJ, Schepens CL, Okamura ID, Uveitis II. Peripheral uveitis: clinical description and differential diagnoses. *Am J Ophthalmol*. 1960;49:1257–66.
155. Kimura SJ, Hogan MJ. Chronic cyclitis. *Trans Am Ophthalmol Soc*. 1963;61:397–413.

156. Welch RB, Maumenee AE, Wahleu HE. Peripheral posterior segment inflammation, vitreous opacities, and edema of the posterior pole. Pars planitis. *Arch Ophthalmol*. 1960;64:540–9.
157. Jabs DA, Nussenblatt RB, Rosenbaum JT, Standardization of Uveitis Nomenclature (SUN) Working Group. Standardization of uveitis nomenclature for reporting clinical data. Results of the First International Workshop. *Am J Ophthalmol*. 2005;140:509–16.
158. Trusko B, et al. The standardization of Uveitis nomenclature (SUN) project. Development of a clinical base utilizing informatics tools and techniques. *Methods Inf Med*. 2013;51:259–65.
159. Boyd SR, Young S, Lightman S. Immunopathology of noninfectious posterior and intermediate uveitis. *Surv Ophthalmol*. 2001;46:209–33.
160. Pederson JE, Kenyon KR, Green WR, Maumenee AE. Pathology of pars planitis. *Am J Ophthalmol*. 1978;86:762–74.
161. Pedroza-Seres M, Linares M, Jimenez-Martinez MC. Pars planitis is associated with an increased frequency of effector-memory CD57+T cell. *Br J Ophthalmol*. 2007;91:1393–8.
162. Donaldson MJ, Pulido JS, Herman DC, et al. Pars planitis: a 20-year study of incidence, clinical features, and outcomes. *Am J Ophthalmol*. 2007;144:812–7.
163. Petro JF, Dios E, Gutierrez JM, et al. Pars planitis: epidemiology, treatment, and association with multiple sclerosis. *Ocul Immunol Inflamm*. 2001;9:93–102.
164. Althaus C, Sundmacher R. Intermediate uveitis: epidemiology, age and sex distribution. *Dev Ophthalmol*. 1992;23:9–14.
165. Romero R, Peralta J, Sendagorta E, Abeleiras J. Pars planitis in children: epidemiologic, clinical, and therapeutic characteristics. *J Pediatr Ophthalmol Strabismus*. 2007;44:288–93.
166. Nikkah H, Ramezani A, Ahmadi H, et al. Childhood pars planitis; clinical features and outcome. *J Ophthalmol Vis Res*. 2011;6:249–54.
167. Smith JA, Mackensen F, et al. Epidemiology and course of disease in childhood uveitis. *Ophthalmology*. 2009;118:1544–51.
168. Kump L, Cervantes-Castaneda R, Androudi S, Foster CS. Analysis of pediatric uveitis cases at a tertiary referral center. *Ophthalmology*. 2005;112:1287–92.
169. Homayoon N, Alireza R, et al. Childhood pars planitis; clinical features and outcome. *J Ophthalmic Vis Res*. 2011;6:249–54.
170. Babu BM, Rathinam SR. Intermediate uveitis. *Indian J Ophthalmol*. 2010;58:21–7.
171. Nussenblatt RB, Palestine AG. Uveitis: fundamentals and clinical practice. In: Intermediate uveitis. Chicago: Yearbook Medical; 1989. p. 279–88.
172. Felder KS, Brockhurst RJ. Neovascular fundus abnormalities and peripheral uveitis. *Arch Ophthalmol*. 1982;100:750–4.
173. Pruett RC, Brockhurst J, Letts NF. Fluorescein angiography of peripheral uveitis. *Am J Ophthalmol*. 1974;77:448–53.
174. Herbert HM, Viswanathan A, Jackson H, Lightman SL. Risk factors for elevated intraocular pressure in uveitis. *J Glaucoma*. 2004;13:96–9.
175. Vitale AT, Zierhut M, Foster CS. Intermediate uveitis. In: Foster CS, Vitale AT, editors. *Diagnosis and treatment of uveitis*. Philadelphia: W.B. Saunders and Company; 2002. p. 844–57.
176. Malinowski SM, Pulido JS, Folk JC. Long term visual outcome and complication a associated with pars planitis. *Ophthalmology*. 1993;100:818–24.
177. Smith RE, Godfrey WA, Kimura SJ. Complications of chronic cyclitis. *Am J Ophthalmol*. 1976;82:277–82.
178. Prieto JF, Dios E, Gutierrez JM, Mayo A, Calonge M, Herreras JM. Pars planitis: epidemiology, treatment, and association with multiple sclerosis. *Ocul Immunol Inflamm*. 2001;9:93–102.
179. Foster CS: Treatment algorithm for pars planitis. www.uveitis.org/docs/dm/algorithmPars-Planitis.pdf. 2012.
180. Karim R, Sykakis E, Lightman S, et al. Interventions for the treatment of uveitic macular edema: a systemic review and meta-analysis. *Clin Ophthalmol*. 2013;7:1109–44.
181. Sebag J, Balazs EA. Pathogenesis of cystoid macular edema: an anatomic consideration of vitreoretinal adhesions. *Surv Ophthalmol*. 1984;28(Suppl):493–8.
182. Green WR. Pathology of the retina. In: Frayer WC, editor. *Lancaster course in ophthalmic histopathology, unit 9*. Philadelphia: FA Davis; 1981.
183. Green WR. Retina. In: Spencer WH, editor. *Ophthalmic pathology: an atlas and textbook, vol. 2*. Philadelphia: WB Saunders; 1985.
184. Okun E. Mechanism of retinal tear formation with posterior vitreous detachment. *JAMA*. 1960;174:2218–20.
185. Green WR. Pathology of the vitreous. In: Frayer WC, editor. *Lancaster course in ophthalmic histopathology, unit 8*. Philadelphia: FA Davis; 1981.

Role of Vitreous in the Pathogenesis of Retinal Detachment



Wallace S. Foulds

Outline

- I. **Introduction**
- II. **Maintenance of Retinal Apposition**
 - A. Structural Factors
 - B. Molecular Movement Within and from Vitreous
 - 1. Hydrostatic Pressure
 - 2. Colloid Osmotic Pressure
 - 3. Diffusion
 - C. Measurement of Retinal Adhesion
 - D. Retinal Adhesion *In Vivo* and Post-Enucleation
 - E. Effect of pH
 - F. Role of the RPE
 - G. Inhibition of RPE Metabolism
 - H. Surface Energy and Electrostatic Forces
 - I. Flow Conductivity and Retinal Adhesion
- III. **Exudative Retinal Detachment**
- IV. **Rhegmatogenous Retinal Detachment**
 - A. Vitreous Degeneration
 - B. Vitreous Traction
 - 1. Macular Holes
 - 2. Retinal Breaks
 - C. Synchrony, Syneresis, and Vitreous Currents
- V. **Developmental Abnormalities**
- VI. **Effects of Retinal Detachment on Vitreous and Other Ocular Tissues**

References

Keywords

Vitreous • Retinal detachment • Hydrostatic pressure • Osmotic pressure • Retinal pigment epithelium • Flow conductivity • Synchrony • Syneresis • Anomalous PVD • Exudative retinal detachment • Rhegmatogenous retinal detachment

Key Concepts

1. The roles of the vitreous in the pathogenesis of retinal detachment are various and numerous. Factors involved in the maintenance of retinal apposition with the RPE are becoming better understood but are far from a complete understanding and must be appreciated in order to define the mechanisms underlying retinal detachment, including the role of vitreous.
2. The factors that mediate retinal attachment are structural adhesion between retina and RPE (including surface energy and electrostatic forces), hydrostatic and colloid osmotic pressures, and importantly, active fluid transfer by the RPE.
3. Exudative retinal detachment results from blood-retinal barrier breakdown, while rhegmatogenous retinal detachment results from anomalous PVD with retinal breaks and abnormal liquid vitreous currents that lift the retina off the RPE.

W.S. Foulds, MD, PhD
Singapore Eye Research Institute, Singapore National Eye Centre,
11 Third Hospital Avenue, Singapore 168751, Singapore

Retina Research, Glasgow University (Emeritus),
Kinnoull Place, 68 Dowanside Road,
Glasgow G129DL, Scotland
e-mail: wallace.stewart.foulds@seri.com.sg

I. Introduction

Normal vitreous plays important roles in the maintenance of retinal apposition to the retinal pigment epithelium (RPE) and in the prevention of retinal detachment. Conversely an abnormal vitreous can contribute significantly to the development and evolution of retinal detachment. In this context, retinal detachment can be considered a failure of one or more of the factors that maintain retinal-RPE apposition. The forces that maintain retinal apposition are strong and are both active and passive (i.e., structural). Of these, active forces appear to play a major role. An understanding of these factors is of importance in the management of retinal detachment.

Many of the factors contributing to detachment of the retina are age related, and it must be appreciated that as the prevention of aging has long been an unrequited desire of mankind, the prevention of age-related changes in the vitreous is an equally unlikely development in the foreseeable future. Removal of the vitreous and its replacement with an alternative with all the diverse characteristics of normal vitreous may be a more realizable aim but still difficult of attainment [see chapter I.F. Vitreous biochemistry and artificial vitreous]. Early attempts to use highly polymerized hyaluronic acid (using the nomenclature of the time) in the treatment of retinal detachment in which the author was involved were altogether too simplistic, although in one case in the 1950s, total replacement of the vitreous with hyaluronic acid in an only eye with a total retinal detachment following failed surgery had the remarkable effect of preserving vision for the rest of the patient's life.

II. Maintenance of Retinal Apposition

A. Structural Factors

As regards structural factors, the integrity of the retina is obviously important, for retinal breaks are major contributors to the development of retinal detachment although, on their own, retinal breaks do not necessarily result in detachment of the retina. Other structural factors include the fact that the photoreceptor outer segments (OS) are embedded among the apical villi of the RPE and to a degree are adherent there. In experimental retinal detachment, separation of the retina from the RPE may fracture the OS from their inner segments and leave the OS embedded in the RPE [1] (Figure III.I-1a, b) indicating a degree of structural attachment between the photoreceptor OS and the apical RPE. It has been reported that retinal cones are surrounded by an adherent matrix that extends from the external limiting membrane of the retina to the apical cell membranes of the RPE and that specialized RPE apical villi are incorporated within this matrix [2]. The cone matrix sheath is insoluble and acts as bridge between cone

photoreceptors and the apical RPE so contributing to adhesion between them. The interphotoreceptor matrix (IPM) around rods and cones may insulate photoreceptors from each other and the retina from the RPE (Figure III.I-2a, b), but additionally the IPM contributes to adhesion between the outer retina and the apical RPE [3–6]. After retinal adhesion has been weakened by treating the IPM with a variety of enzymes, recovery of adhesion accompanies the reestablishment of IPM glycoconjugates [7]. In the primate eye, it has been reported that galactose is an important constituent of the IPM glycoproteins that are involved in the structural adherence between the retinal photoreceptor OS and the apical villi of the RPE [8]. It has previously been shown that galactose is specifically taken up by retinal cones [9] and that the glycosaminoglycans of the IPM are involved in the phagocytosis of photoreceptor outer segment discs by the RPE [10]. Drug-induced alteration of the morphology of the apical RPE causes a rapid but only temporary reduction in retinal adhesion attributed to actin microfilament dysfunction [11]. In mice [12] it has been shown that a specific integrin with receptors at the RPE-retinal interface plays an important role in retinal attachment but with a marked diurnal variation, retinal attachment being strongest 3.5 h after the onset of light at which time photoreceptor disc phagocytosis is complete. *In vitro* experiments in rabbits have shown that retinal adhesion is greater in the dark than in the light. [13] In rabbits, retinal adhesion is 20 % stronger in light-adapted eyes than in dark-adapted eyes [14].

Although passive structural factors contribute to retinal attachment, active forces including metabolic activity in the RPE may be more important.

B. Molecular Movement Within and from Vitreous

In considering the role of the vitreous in the attachment of the retina to its bed, one must consider the gel nature of the vitreous and the effect that this has on water movement within and from the vitreous cavity and also the fact that the cortical vitreous in contact with the retina contains a higher concentration of collagen and hyaluronan than the mid-vitreous where the concentrations of each are lower [15] (Figure III.I-3). Stabilized hyaluronan (but not hyaluronan in solution) has been shown to have a significant inhibitory effect on diffusion including the diffusion of small molecules such as water [16].

In experiments carried out by the author many years ago [17], it was shown that, in the rabbit, there was a constant movement of water from the vitreous, across the retina, RPE, and Bruch's membrane to the choroid. Using tritiated water ($^3\text{H}_2\text{O}$) injected into the mid-vitreous as a tracer and sampling vortex venous blood at frequent intervals over an

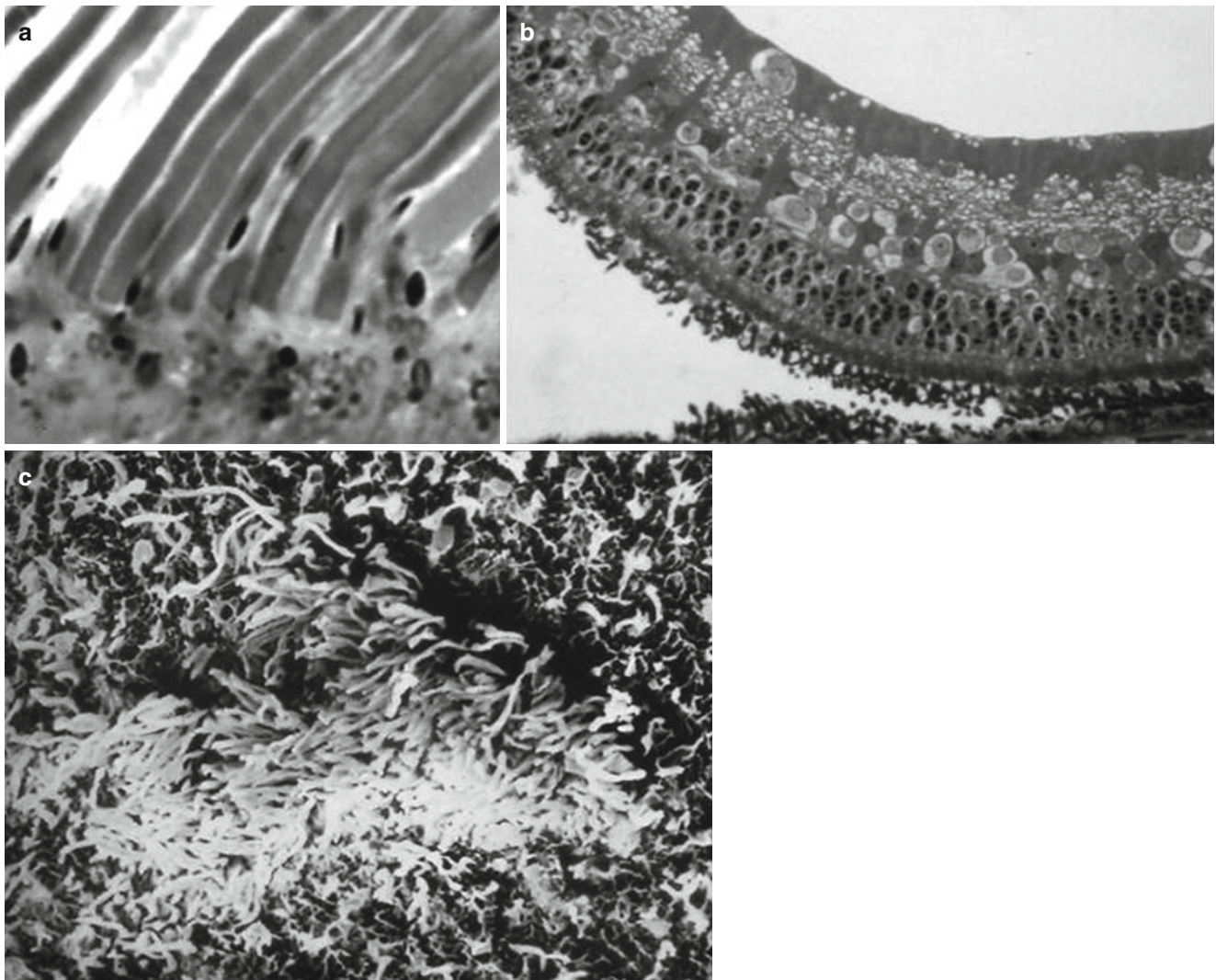


Figure III.I-1 The structural adhesion between photoreceptor outer segments (OS) and the apical RPE cell membrane relates (a) to interdigitation of the RPE apical villi with the OS. (b) In an experimental

retinal detachment in the rabbit, photoreceptor inner segments remain attached to the detaching retina, while (c) OS separated from their inner segments remain embedded among the apical villi of the RPE

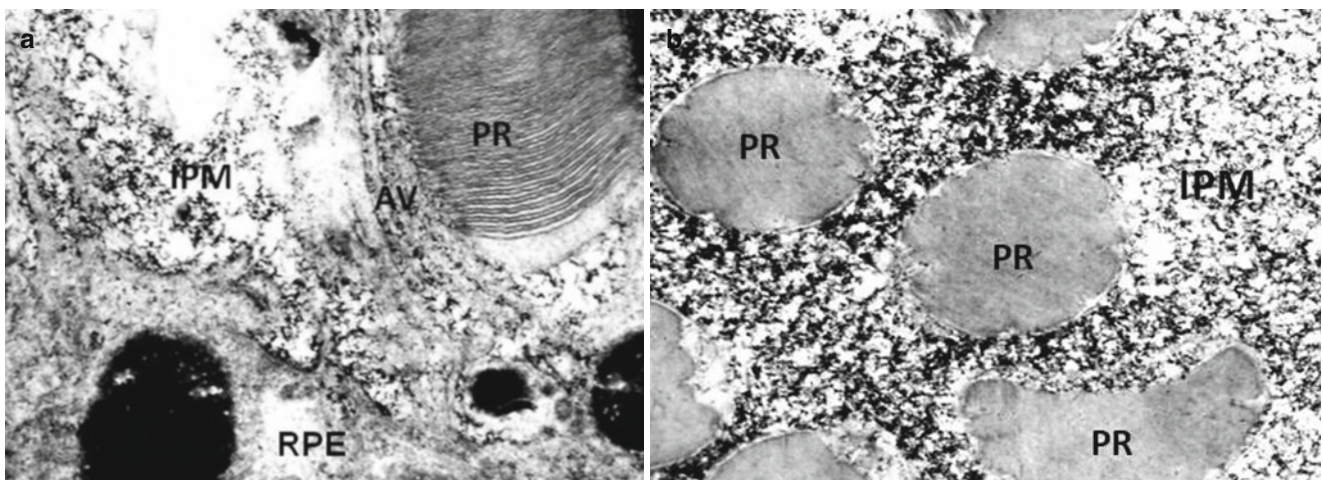


Figure III.I-2 The interphotoreceptor matrix (IPM) stained for glycosaminoglycans is in close apposition (a) to the apical membrane of the RPE and its apical villi (AV) and (b) to the photoreceptor OS (PR)

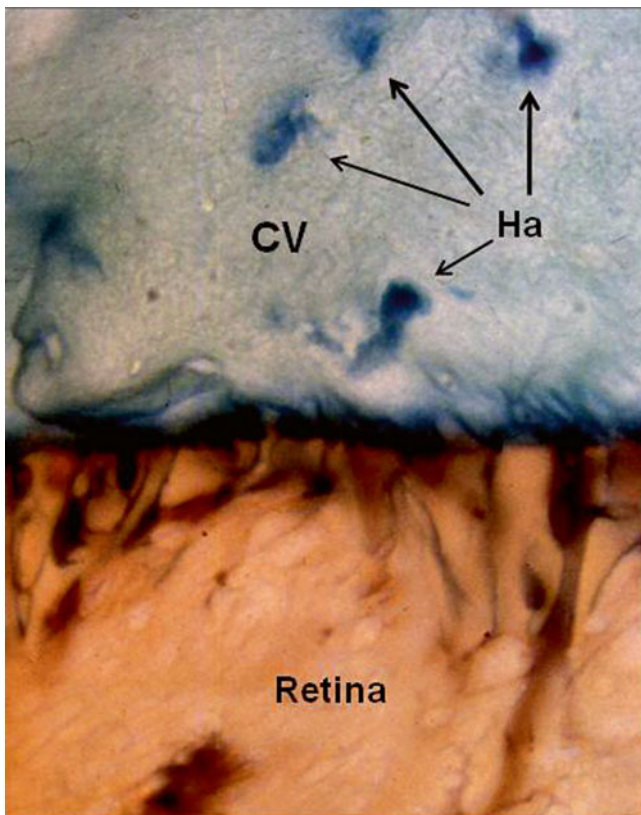


Figure III.I-3 The cortical vitreous (CV) with its contained hyalocytes (Ha), stained (blue) to show its high content of hyaluronan, is in close apposition to the inner limiting membrane of the retina

extended period of time (1–2 h, and exceptionally 5 h), it was found that the mean transit time for a water molecule to pass from the central vitreous to the vortex veins was 32 ± 2 min, with half of the injected tracer leaving the vitreous in 36 min (Figure III.I-4a). Surprisingly, some 94 % of injected tracer could be recovered from the vortex veins, some 2 % from the surface of the sclera, and up to 4 % from the anterior chamber. Depolymerization of vitreous hyaluronan by intravitreal injection of hyaluronidase speeded the mean transit time of tracer from the vitreous to the vortex veins [18] to 19.9 ± 6.1 min compared to a control value of 32 ± 2 min. (Figure III.I-4b), thus confirming the effect that hyaluronan (stabilized by a collagen framework) has on water movement in the vitreous and its transfer to the choroid. Not surprisingly silicone oil in the vitreous prevented water molecules from reaching the area of retina overlying the oil and greatly extended the mean transit time for a water molecule to reach the vortex veins to more than 300 min [19] (Figure III.I-4c).

In considering water movement from the vitreous to the choroid across the many intervening structures (cortical vitreous, retina, IPM, RPE, Bruch's membrane, and choroidal extravascular tissue spaces), an explanation for

the driving forces involved has to be found. Factors that must be considered include physical determinants of fluid movement such as hydrostatic pressure differences, colloid osmotic pressure, diffusion, and active transfer by intervening tissues.

1. Hydrostatic Pressure

Undoubtedly there is a hydrostatic pressure difference between the intraocular pressure in the vitreous cavity and the near-atmospheric pressure in the orbit that may explain the finding in experiments on rabbit eyes that a small amount of intravitreal tracer such as water ($^3\text{H}_2\text{O}^{19}$) or xenon (^{133}Xe [20]) could be recovered from the scleral surface. A hydrostatic pressure difference between the pre-choroidal tissues and the orbit across a relatively permeable sclera [21] probably prevents choroidal detachment in the presence of a normal intraocular pressure [22]. Early attempts to measure pressures within the vitreous and in the subretinal space, however, failed to find any measurable difference in pressure between these two locations [23].

2. Colloid Osmotic Pressure

Vitreous has a low content of soluble protein as has the retina [22, 24], while there is a high concentration of soluble proteins within the blood vessels of the choroid. The retina poses a resistance to molecular passage through it and more so for larger protein molecules than smaller molecules such as water [25]. It has been shown in humans that the outward movement of small molecules such as fluorescein from the vitreous across the retina is some 30 times greater than their inward movement [26]. The RPE with its apical tight junctions between neighboring cells (Figure III.I-5) serves as a semipermeable membrane, the tight junctions preventing the intercellular passage of large molecules in either direction but possibly being permeable to smaller molecules such as water [27]. The difference in protein concentration between the vitreous and choroidal blood, in the presence of intervening semipermeable membranes is capable of generating an oncotic gradient in favor of the movement of small molecules such as water from the vitreous to the choroid.

In support of colloid osmotic pressure as a factor involved in retinal adherence is the finding that the clearance of autologous serum [28] or isotonic sucrose [29, 30] from the subretinal space is much slower than that of saline and that the injection of hyperosmotic solutions into the vitreous can induce retinal detachment [31, 32]. The intravenous administration of hyperosmotic mannitol increased retinal adhesion to 153 % of control values in primates and to 145 % in rabbits [33]. In experiments using the injection of radioactive tracers into the mid-vitreous [17], the intravenous injection of low-molecular-weight dextran, which increased blood volume and reduced the concentration of circulating plasma

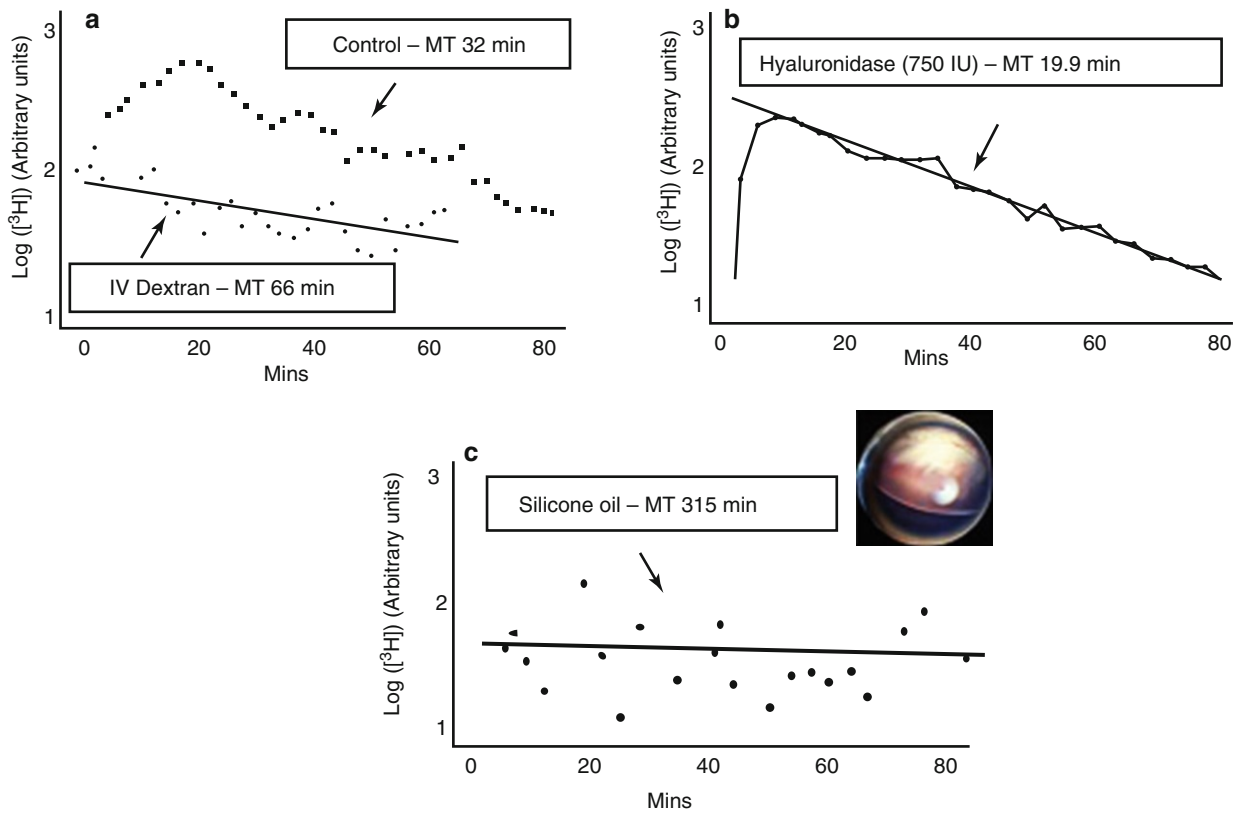


Figure III.I-4 The rate per unit time (mean transit time MT) that an intravitreal tracer ($^3\text{H}_2\text{O}$) could be recovered from rabbit vortex veins is demonstrated (a) in a control animal and following the intravenous injection of a low-molecular-weight dextran that reduced the concentration of circulating plasma proteins and slowed the clearance of tracer from the vitreous in line with a reduction in colloid osmotic pressure between the vitreous and the choroid. Depolymerization of vitreous

hyaluronan by an intravitreal injection of hyaluronidase (b) significantly increased the rate of clearance of tracer from the vitreous to the vortex vein. (c) The presence of a subtotal quantity of silicone oil in the vitreous reduced the area of retina available for the trans-retinal passage of water from the vitreous and greatly slowed the clearance of the tracer from the vitreous

proteins, had an inhibitory effect on water movement from vitreous to choroid [19], prolonging the mean transit time for water molecules to reach the vortex veins to 66 min.

Choroidal capillaries are fenestrated (Figure III.I-6) and allow smaller protein molecules such as albumin to egress into the neighboring extravascular tissue spaces. Retinol, which is required for visual pigment assembly in the photoreceptors, circulates in the blood bound to an albumin retinol-binding protein [34]. Without fenestrations it would not be possible for this molecule to escape from the choroidal circulation on its way to the outer retina.

It is clear from fluorescein angiography that albumin-bound fluorescein leaks from choroidal capillaries into the surrounding choroid. The concentration of plasma proteins in the extravascular choroidal tissues is said to be 60–70 % of that in the plasma [22] although other studies have found large variations between differing methodologies and species [35]. The combination of a significant concentration of protein molecules in the extravascular choroid compared with a low concentration in the vitreous coupled with the reduced

permeability of the retina and RPE is sufficient to generate a colloid osmotic pressure gradient between the vitreous and the extravascular choroid and act as a force for the movement of small molecules between these locations.

3. Diffusion

In spite of the evidence that colloid osmotic pressure is involved in water movement from the vitreous, there remains the problem of explaining how colloid osmotic pressure alone might be sufficient to move water from the extravascular tissues around the choriocapillaris into the lumens of these capillaries, considering the relatively high concentration of protein in the extravascular tissues. Extravascular proteins will attract water across the retina into the choroidal extravascular tissues by colloid osmotic pressure, but the reduced oncotic pressure difference between the extravascular and intravascular choroid will adversely affect the oncotic transfer of water into the choriocapillaris. Mathematical modeling of fluid movement in the posterior eye [36] has shown that this is diffusion limited, and it may well be that

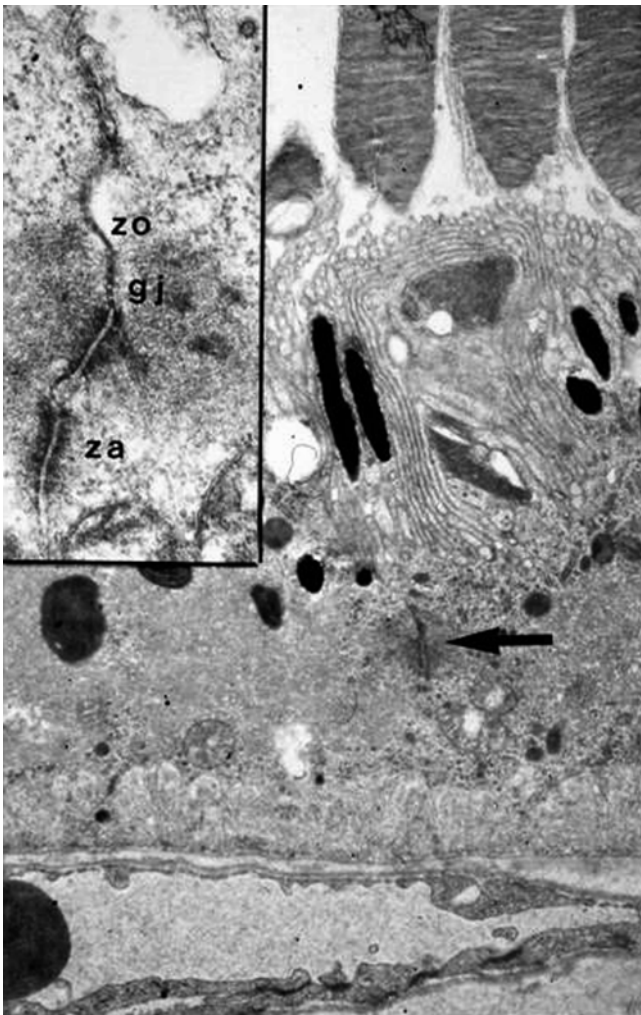


Figure III.I-5 Electron microscopy of the RPE shows details of the intercellular junctions between neighboring RPE cells (*insert*). Types of junction are labeled as follows: tight junction *zo* (*zonula occludens*), gap junction (*gj*), and adherent junction *za* (*zonula adherens*). The apically situated *zo* is impermeable to large (e.g., protein) molecules but may be permeable to small molecules such as water

diffusion is the final force contributing to the transfer of water from the extravascular tissues into the choroidal capillaries. To achieve this, there would have to be a lower concentration of water in the luminal blood as compared with the extravascular tissues. This could be achieved by a high rate of blood flow, so that water reaching the lumen of capillaries was rapidly cleared from there.

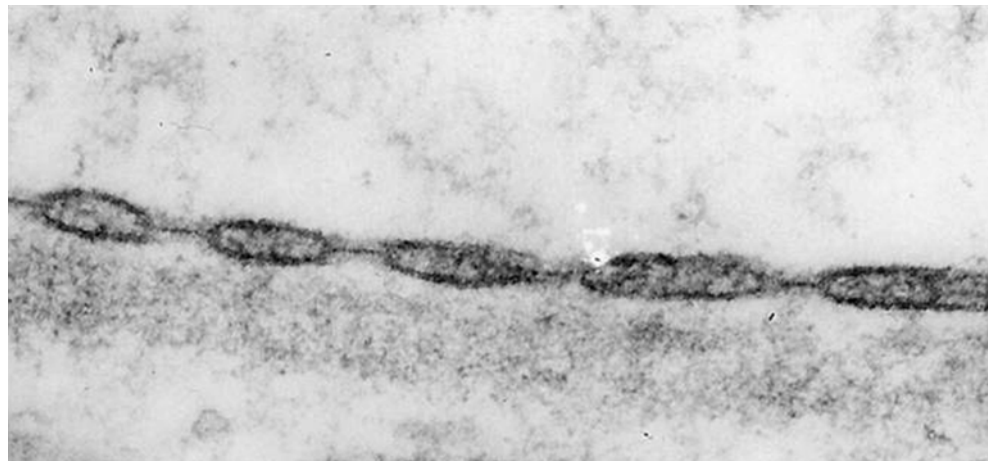
Unlike retinal venules that have a low level of oxygenation, vortex vein blood leaving the eye is known to be highly oxygenated, a fact recently confirmed in the human eye by spectrophotometric oximetry [37], indicating that blood flow in the choroid is in excess of that required for oxygen supply to the outer retina. It has been shown in monkeys that the choroid has the highest rate of blood flow per unit time of any other tissue [38]. A need to transfer water into the choroidal circulation by diffusion would offer an explanation for the high rate of blood flow in the choroid.

Where there is a breakdown in the integrity of the inner blood-retinal barrier as a result of, e.g., hypoxia [39], extravasation of proteins into retinal tissues will attract water into the retina, and the retention of protein molecules within the retina as a result of the barriers to diffusion of large molecules posed by the plexiform layers of the retina [40] and the external limiting membrane [41] will result in retinal edema, compounded by the inability of the RPE to remove water from the retina in this situation [41].

C. Measurement of Retinal Adhesion

A method to study the rate of absorption of tracers injected into the subretinal space was first published in Japanese in 1976 [42], and a further development to measure the actual pressure in the localized retinal detachment created by injection of saline into the subretinal space used a micropipette inserted into the injected saline to measure the pressure in

Figure III.I-6 High-power view of the inner (sub-RPE) wall of a choroidal capillary to show the fenestrations that allow the passage of proteins such as albumin into the extravascular tissue spaces of the choroid with a reduction in the oncotic pressure between the extravascular and intravascular choroid



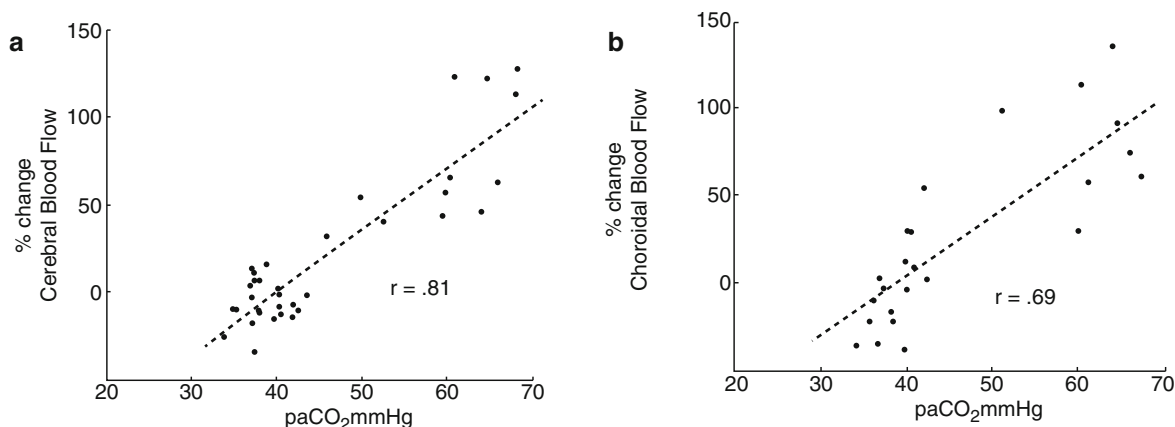


Figure III.I-7 Effects in the nonhuman primate of increasing pCO₂ levels on (a) cerebral and (b) choroidal blood flow. In both locations, increasing pCO₂ results in an increase in blood flow. Systemic acetazolamide has a similar effect

this location [43]. It was found that this pressure was five times greater than had previously been reported [43]. Other techniques used to measure retinal adhesion to the RPE have included the peeling force required to separate the retina from the RPE in isolated strips of eye cups from enucleated eyes [14] and estimation of the amount of pigment left adhering to the retina after its separation from the RPE in the enucleated eye [44].

D. Retinal Adhesion *In Vivo* and Post-Enucleation

Although it is difficult to separate the retina from the RPE in the living eye, after enucleation of the eye and before any detectable changes are observed, the retina separates easily from the RPE [45] indicating that following enucleation there is a loss of those factors present *in vivo*. The loss of adhesion between retina and RPE following enucleation, is extremely rapid in the rabbit (2–3 min) and much slower in monkey eyes [46] and human eyes (40 min) [45]. In both rabbit and primate eyes, retinal attachment to the RPE is oxygen dependent [47, 48], benefits from low temperatures [44, 49], and is reduced by a low pH [45, 49] and by a reduction of calcium [50, 51] or magnesium [51]. Retinal adhesion is also affected by the presence of metabolically active substances introduced into the subretinal space [52]. Ischemia for five minutes or longer causes a complete loss of retinal adhesion in the rabbit eye but after 10 min of ischemia, adhesion can be restored to 80 % of its normal value by restoration of the circulation 5 min before enucleation [49], indicating that choroidal blood flow plays a major role in retinal adhesion in the rabbit eye (that lacks a separate retinal blood circulation). Enucleation of the eye means a cessation of blood flow in the choroid that as already indicated is necessary for the

outward movement of water from the vitreous and from the subretinal space, and this would appear to be one of the many factors responsible for the loss of retinal adhesion following enucleation.

Following enucleation and retinal separation from the RPE, cone and rod sheaths are extended [45] indicating a persistence of structural adherence between photoreceptors and the RPE in the enucleated eye. Thus, the loss of retinal adhesion that follows enucleation is multifactorial, and it appears that the factors maintaining retinal adhesion are qualitatively if not quantitatively similar in rabbit and primate eyes including human eyes [45]. Retinal adhesion in the primate eye, however, is more resistant to adhesive failure than in the rabbit eye [48]. It has been shown that the loss of retinal adhesion after enucleation is reversible, and while a low pH and low calcium/magnesium have additive effects in weakening retinal adhesion, a low temperature can reverse this and restore adhesion [49].

E. Effect of pH

Although it has been shown in the enucleated eye that a low pH decreases retinal adhesion, in the living eye, systemic acetazolamide that lowers pH has been shown to increase retinal adhesion by 133 % in rabbits and by 144 % in primates compared with controls [33]. The differing effects of a reduced pH in enucleated eyes and in the living eye may be explained by the presence or absence of the choroidal circulation for acidosis induced by breathing carbon dioxide causes a significant increase in choroidal and cerebral blood flow in primates [53] (Figure III.I-7a, b) and increased choroidal blood flow in rabbits [54]. Thus, although in enucleated eyes, where there is no choroidal blood flow, retinal adhesion may be reduced in conditions of low pH; in the

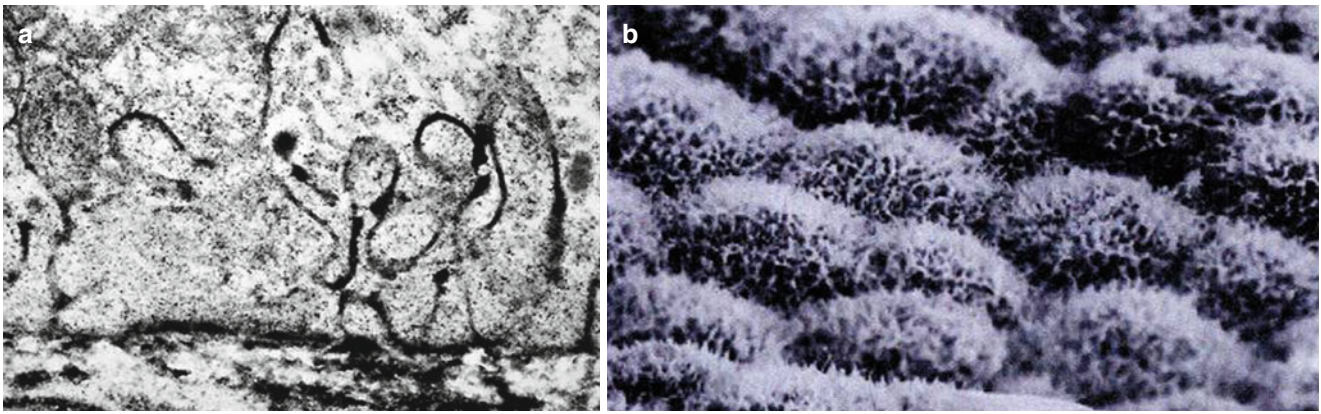


Figure III.I-8 The area for transmembrane transfer of ions is greatly increased by (a) the convolutions of the RPE basal membrane (shown by Indian ink injection) and (b) by the high density of villi on the apical RPE membranes

living eye with an active choroidal blood flow, a low pH is likely to increase retinal adhesion by increasing choroidal blood flow and an increased outward movement of water into the choroidal circulation. Increased choroidal blood flow has been suggested as an explanation (among many others) for the increased retinal adhesion and increased rate of absorption of subretinal fluid demonstrated in rabbits treated with systemic acetazolamide [55]. Additionally, a study of the rate of clearance to the bloodstream of intravitreally injected fluorescein in human volunteers showed an increased rate of clearance when subjects were treated with acetazolamide as compared to placebo [56]. This was attributed to an increased permeability of the outer blood-retinal barrier, but no consideration was given to the possible effect of acetazolamide on choroidal blood flow.

F. Role of the RPE

Among remaining factors to be considered is the active transfer of water molecules across the RPE. RPE cells are metabolically active, related to the multiplicity of their many functions including the inward supply of metabolites to the retina, the phagocytosis of effete photoreceptor OS discs and the disposal of the products of their degradation, the recycling of visual pigment between RPE and retinal photoreceptors, and the transfer via transporting proteins of retinol from the choroidal blood circulation to its destination in the photoreceptor OS [57–60]. The RPE has the difficult task of transferring molecules required by the retina (e.g., oxygen, retinol, and glucose) from the choroidal blood circulation to the outer retina and at the same time transferring water and the waste products of retinal metabolism and photoreceptor outer segment phagocytosis in the opposite direction. There are thus several mechanisms involved in the transfer of ions and molecules across RPE cell membranes in either direction with a preference for the inward transfer of retinal metabo-

lites and the outward transfer of those ions involved in transcellular water movement [60].

The ability of the RPE to transport water is very powerful, and the RPE can pump fluid against a substantial gradient of hydrostatic or osmotic pressure [60]. There are homeostatic mechanisms for maintaining the hydration of the subretinal space to maintain an appropriate relationship between the photoreceptor OS and the apical RPE and other mechanisms removing water from the subretinal space to prevent an undue separation of the OS from the RPE [58, 61]. The basement membranes of RPE cells are highly convoluted (Figure III.I-8a), and this as well as the presence of villi on the apical surface of the RPE (Figure III.I-8b, c) increases the surface areas of the basal and apical cell membranes, with obvious benefit to the inward transfer of oxygen and metabolites from the choroid to the retina and the outward movement of water and waste products of RPE metabolism. Ionic movement across the apical cell membranes of the RPE is thought to be important in the maintenance of ionic homeostasis in the subretinal space. Alterations in the ion content (mainly K^+) of this space accompany light and dark adaptation [61] and may be responsible for the differences found in the measured adherence of the retina in light- and dark-adapted eyes [14]. In the dark-adapted eye, oxygen consumption by the photoreceptors is increased with an increased production of CO_2 and water that are removed by the RPE so maintaining a normal pH in the subretinal space and preventing the accumulation of water that would alter the separation of the photoreceptor OS from the apical RPE [61].

Ion movement across the apical RPE cell membrane involves both ingress and egress of potassium (K^+), secretion of sodium (Na^+) into the subretinal space, and absorption of Cl^- from the subretinal space and its subsequent transfer across the baso-lateral RPE cell membranes towards Bruch's membrane and the choroid. These ionic movements are of importance in the outward transfer of water via the RPE from

the vitreous to the choroid and are thought to involve at least three mechanisms in the apical membrane (a $\text{Na}^+\text{-K}^+$ pump, a $\text{Na}^+\text{-K}^+\text{-Cl}^-$ co-transporter and barium-sensitive K^+ channels that actively recycle K^+ back to the subretinal space) [59]. The chloride pathway across the RPE appears to involve different mechanisms in the apical and baso-lateral membranes, and HCO_3^- transporters appear to play an important role in fluid movement across the RPE. Inhibition of ionic transfer mechanisms can have a significant effect on water movement across the RPE [60] and thus on the maintenance of retinal apposition with the RPE. Indirect evidence that active work by the RPE is involved in the outward movement of water from the subretinal space is the oxygen dependence of such movement [47], the effect that the introduction of metabolically active substances into the subretinal space has on the absorption of saline from the subretinal space [52], and the fact that a low temperature can maintain retinal adhesion in enucleated eyes [44]. It is further claimed that active work by the RPE is a greater contributor to the movement of water from the subretinal space than that effected by oncotic pressure and that active ionic transport across the RPE is responsible for 70 % of trans-RPE fluid movement with oncotic pressure responsible for 30 % [62]. In the subsequent transfer of water to the choroid, however, colloid osmotic pressure may be a more important driving force.

G. Inhibition of RPE Metabolism

Acute toxicity of the RPE with sodium iodate has been shown not only to reduce retinal adhesion to the RPE but also to weaken adhesion of the RPE to Bruch's membrane [63]. Surprisingly, in rabbits, poisoning of the RPE with sodium iodate in a dose sufficient to inhibit RPE metabolism increased the rate at which water was transferred from the vitreous to the choroid (a mean rate of 24 ± 4 min as compared with a control value of 36 ± 4 min) [19]. It has also been reported that sodium iodate speeds up the resorption of subretinal saline but not of serum [64]. It appears that sodium iodate while inhibiting active transport by the RPE also reduces its barrier function, allowing the colloid pressure difference between vitreous and choroid to increase the outward flow of water from the vitreous to the choroid.

H. Surface Energy and Electrostatic Forces

Other forces involved in the maintenance of retinal apposition with its bed that have received less attention but could be significant are surface tension (or more correctly surface energy when considering moist membranes in contact [65]) and electrostatic forces that can determine the macromolecular

structure of tissues such as the vitreous [66]. A difference between a negatively charged vitreous and a positive charge in the apical RPE could contribute to the adhesive force between these tissues. The magnitude of the ocular standing potential that is largely generated across the RPE is an indication of the electrostatic force that could contribute to retinal adhesion. In addition, there is no doubt that electrostatic forces can affect intracellular function and alter ocular cell configuration and cell motility [67]. Lastly, although surface energy between membranes can generate significant adhesive forces [65], once again evidence that this mechanism plays a role in retinal adhesion is lacking.

I. Flow Conductivity and Retinal Adhesion

Irrespective of the mechanism(s) responsible for water movement from the vitreous, there is no doubt that a continuous and significant movement of water from the vitreous to the choroid exists, and one must ask how this might contribute to the attachment of the retina to its bed. The answer undoubtedly lies in the reduced flow conductivity of the retina and of the cortical vitreous. In the case of the retina, this has been measured [68] and although the retina is relatively permeable to water, both the retina and the cortical vitreous offer a significant resistance to the passage of water. With an outward movement of water through the cortical vitreous and retinal tissues and a resistance to its passage through each, water movement will keep the cortical vitreous in contact with the retina (Figure III.I-9a) and maintain contact between the retina and the RPE (Figure III.I-9b). The former will aid the tamponade of retinal holes by cortical vitreous, and the latter will be a major contributor to retinal adhesion and a significant protection against detachment of the retina [68].

III. Exudative Retinal Detachment

As a colloid osmotic pressure difference between the vitreous and the choroid across the intervening tissues is an important factor maintaining retinal apposition, it is no surprise that a breakdown in the posterior blood-retinal barrier can result in an exudative (serous) retinal detachment with a characteristically protein-rich subretinal fluid [69]. Increased permeability of choroidal vessels and damage to the outer blood-retinal barrier can occur in severe inflammation [70], choroidal malignancy, or the rarer uveal effusion syndrome [71]. The volume of an exudative detachment is likely to be maintained by recruitment of water from the vitreous as a result of the colloid osmotic pressure difference between the vitreous and the protein-rich subretinal fluid. Although a breakdown in the posterior blood-retinal barrier

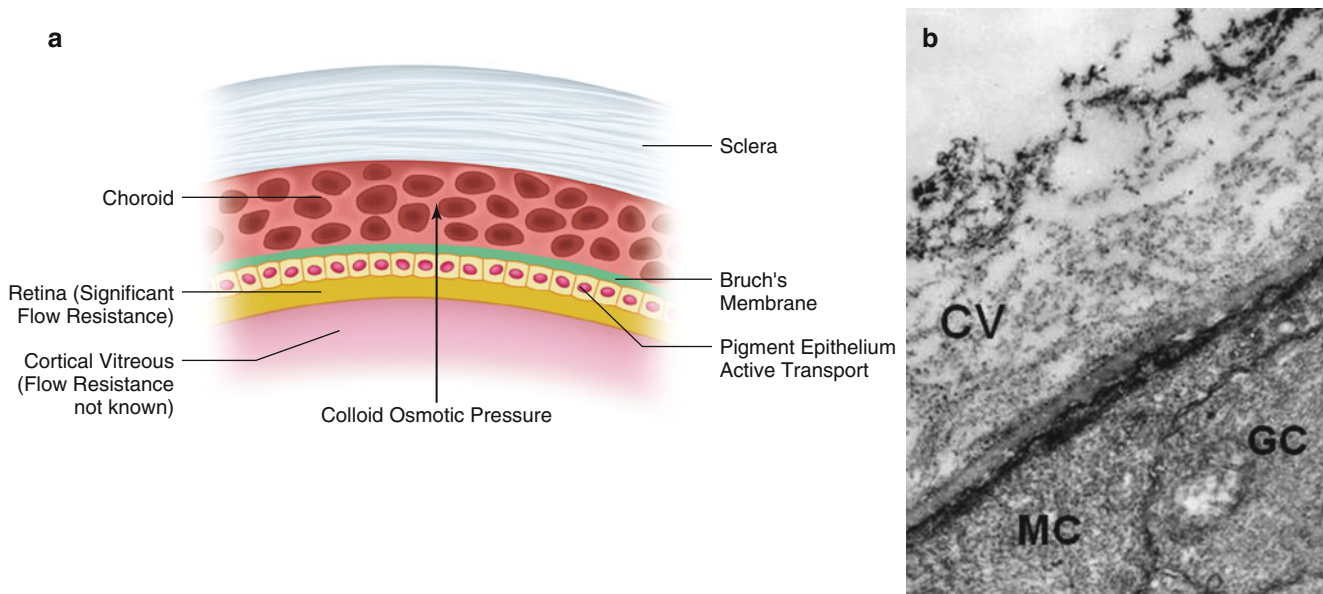


Figure III.I-9 (a) The reduced permeability of the cortical vitreous, retina, and RPE to the outward flow of small molecules such as water ensures that the cortical vitreous remains in close contact with the inner limiting membrane of the retina and that the retina remains in

contact with the RPE and the RPE in contact with Bruch's membrane and choroid. (b) Electron microscopy to demonstrate the close apposition of the cortical vitreous (CV) to the inner limiting membrane (MC Müller cell, GC ganglion cell)

is more usually the cause of an exudative retinal detachment, it has been suggested that some exudative retinal detachments may be the result of a metabolic breakdown in the transport systems of the RPE [72].

In long-standing rhegmatogenous retinal detachments, the subretinal fluid that initially has characteristics akin to aqueous with a low-protein content and a high concentration of ascorbic acid [73–75] gradually becomes more like blood plasma with an increasing content of protein and a decreasing content of ascorbic acid. With subretinal fluid resembling plasma, any colloid osmotic pressure acting across the retina will attract water from the vitreous into the subretinal fluid, while the lack of an osmotic gradient between the subretinal space and the choroid due to the similar concentration of protein in the two locations will act to maintain the retinal detachment.

Following the surgical excision of choroidal melanomas with an accompanying exudative retinal detachment, the retina usually flattens rapidly even in the absence of the RPE and choroid [76]. In these circumstances, a hydrostatic pressure difference between the vitreous and the orbit may account for the flattening of the detached retina as a result of a hydrostatically increased trans-scleral flow of water, the sclera in this type of surgery being reduced to half-thickness.

IV. Rhegmatogenous Retinal Detachment

Having considered the role of the vitreous in maintaining apposition of the retina to the RPE and its possible protective role in the prevention of retinal detachment,

consideration must be given to the role of the vitreous in the onset and evolution of retinal detachments. In simple nontraumatic rhegmatogenous retinal detachment, this is largely a consequence of age-related or myopia-related degenerative changes in the vitreous [see chapters II.B. Myopic vitreopathy and II.C. Vitreous aging and PVD]. Additionally, vitreous involvement in complicated retinal detachments is characterized by fibrous tissue formation such as occurs in proliferative vitreoretinopathy (PVR), proliferative diabetic retinopathy (PDR), and advanced retinopathy of prematurity (ROP) and less commonly inherited genetic disorders affecting the vitreous [see chapter I.C. Hereditary vitreo-retinopathies].

A. Vitreous Degeneration

In vitreous there are at least two mechanisms that may be involved in the etiology and progression of rhegmatogenous retinal detachment. These are liquefaction of the vitreous body and vitreous traction. Age-related changes in vitreous include a loss or reorganization of hyaluronan resulting in collagen fibrils within vitreous adhering to each other and a loss of vitreous volume [77, 78] (Figure III.I-10). Commonly, liquefaction-induced destabilization of the vitreous body results in a posterior vitreous detachment (PVD) where the vitreous severs its posterior connection with the inner limiting membrane of the retina and collapses towards the center of the eye to leave a fluid-filled space between the detached posterior vitreous cortex and the retina

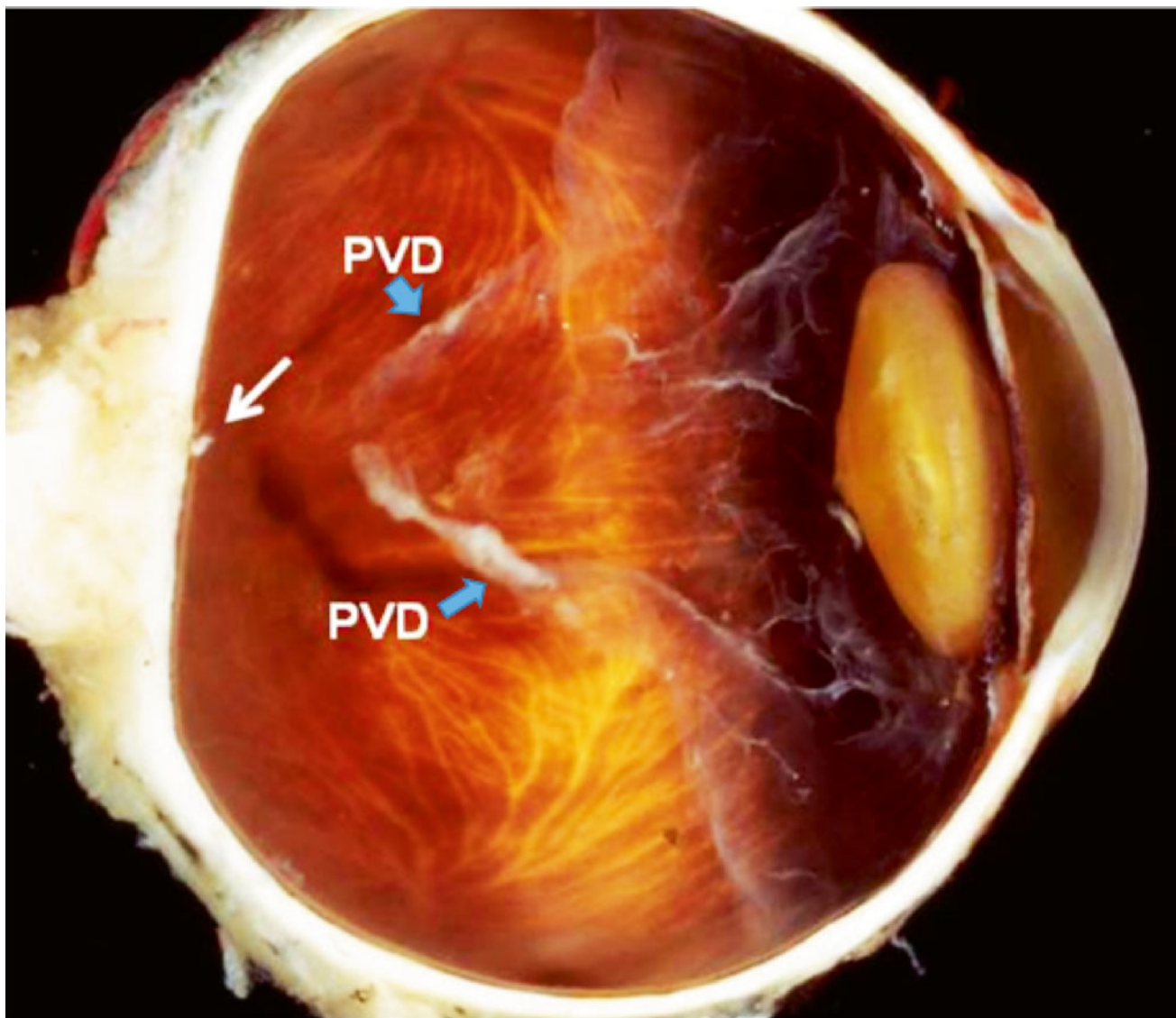


Figure III.I-10 Vitreous syneresis in an elderly human eye. The collagen fibrils that are normally invisible have coalesced together to form large visible vitreous opacities. There is a large posterior vitreous

detachment (*PVD blue arrows*) but an adhesion between the detached vitreous and the optic nerve head persists (*white arrow*)

(Figure III.I-11). The prevalence of PVD increases with increasing age being unusual before the age of 30 years and universal in those aged 70 years or more [79, 80]. Apart from aging, myopia is a risk factor for PVD, the prevalence of PVD increasing in line with the severity of the refractive error [79]. PVD develops earlier (estimated as 10 years earlier) in myopic eyes as compared with emmetropic or hyperopic eyes [79, 80].

B. Vitreous Traction

Collapse of the posterior vitreous can cause traction on the retina [see chapter III.B. Anomalous PVD and

vitreoschisis]. As the posterior attachments of the vitreous are strongest in the vicinity of the optic nerve head (Figure III.I-10) and the macula (Figure III.I-11a, b), a collapsing vitreous exerts most traction at these two locations and is responsible for the occurrence of the vitreo-macular traction syndrome in the case of the former [81–83] and pseudo-papilledema in the latter case [84]. Vitreo-macular traction in turn is an important etiological factor in the development of macular holes [85, 86]. Vitreous traction on the macula is also a common cause of increased vascular permeability at the site of the traction and the development of cystoid macular edema or localized retinal elevation [87–89] (Figure III.I-12). Occasionally, spontaneous separation of the vitreous from

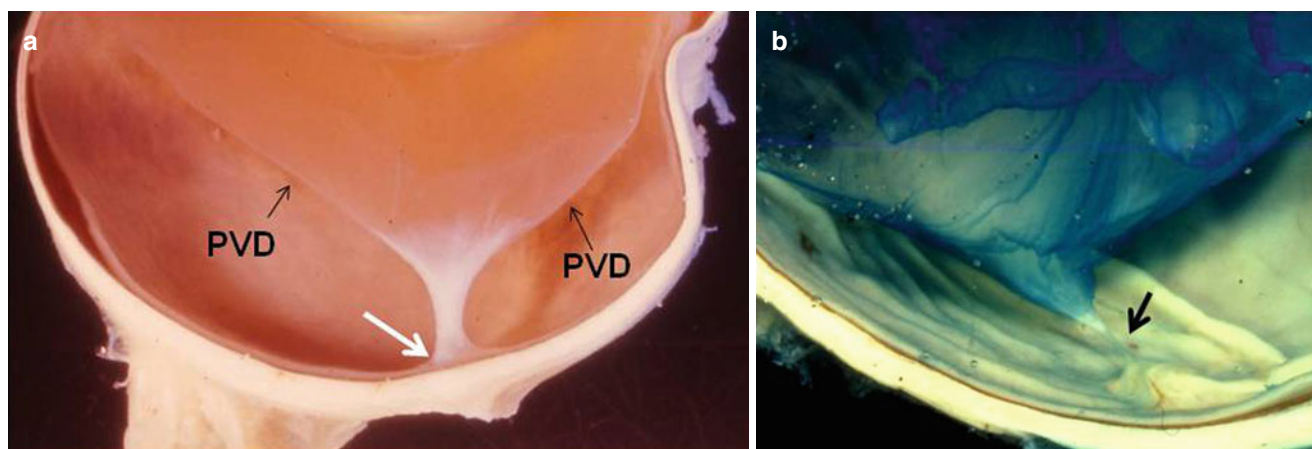


Figure III.I-11 (a) In a human eye with a PVD (*black arrows*), there is a gross attachment between the posterior vitreous cortex and the macula (*white arrow*). (b) In another human eye with a PVD, the hyaluro-

nan in the detached vitreous is stained blue. There is a fine vitreous attachment to the fovea (*arrow*). Symptomatic vitreoretinal traction was likely in each case

its retinal attachment may lead to spontaneous relief of vitreo-macular traction [90, 91].

In the management of retinal detachment, volume-reducing operations (encrochage or plombage) or alternatively vitrectomy may each in their own way reduce vitreoretinal traction with benefit to the outcome of surgery. Volume-reducing surgery may additionally redistribute a detached vitreous body within the vitreous cavity to bring it into contact with an increased area of retina [19] and allow tamponade of any previously detected or undetected peripheral retinal holes with benefit to the cure of the detachment or prevention of its recurrence. An additional benefit from volume-reducing surgery is a reduction in vitreous fluid currents (see below), thus mitigating the risk of continuing accumulation of subretinal fluid.

1. Macular Holes

Because of the optical clarity of vitreous and the absence of visible abnormality in the vicinity of macular holes, the cause of macular holes was for a long time a mystery. The advent of OCT, and particularly OCT capable of providing high-definition images, has revolutionized the understanding of the factors leading to macular hole formation and has established the critical role of vitreous in their development [92–94]. Anteroposterior vitreous traction was thought to be the major etiological factor in macular hole formation until Gass [95] not only developed a classification for macular holes based on their progressive worsening but introduced the concept of tangential traction and the role of contracting adherent cortical vitreous and premacular membrane formation in the development of macular holes. The use of more recently developed high-definition OCT has reestablished anteroposterior vitreous traction as a factor in the etiology of macular holes. Relief of anteroposterior vitreous traction by vitrectomy or the use of newer pharmacologic vitreolytic agents [96] has revolutionized the management of macular

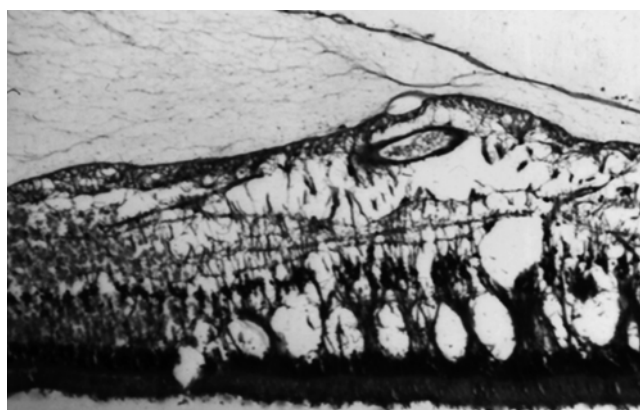


Figure III.I-12 Gross cystoid edema resulting from vitreoretinal traction

holes [see chapters VI.A. Pharmacologic vitreolysis and VI.E. Pharmacologic vitreolysis with ocriplasmin] as has ILM peeling in the relief of tangential traction.

2. Retinal Breaks

Retinal breaks without retinal detachment are commonly seen in postmortem human eyes [97, 98]. Active forces maintaining retinal apposition may explain the absence of retinal detachment in these eyes, but as most of these retinal holes are situated in the retinal periphery, where they are in contact with formed vitreous, tamponade by formed vitreous may be an additional factor preventing retinal detachment [19, 99]. Where there is a PVD, the collapsing vitreous usually retains its contact with the equatorial and pre-equatorial retina. Traction at the interface between attached anterior vitreous and detaching posterior vitreous commonly results in retinal breaks in this location [78]. Retinal breaks without evidence of active vitreous traction, including round holes with an avulsed operculum, seldom cause retinal detachment [100], while continuing traction is a risk factor for detachment [100].

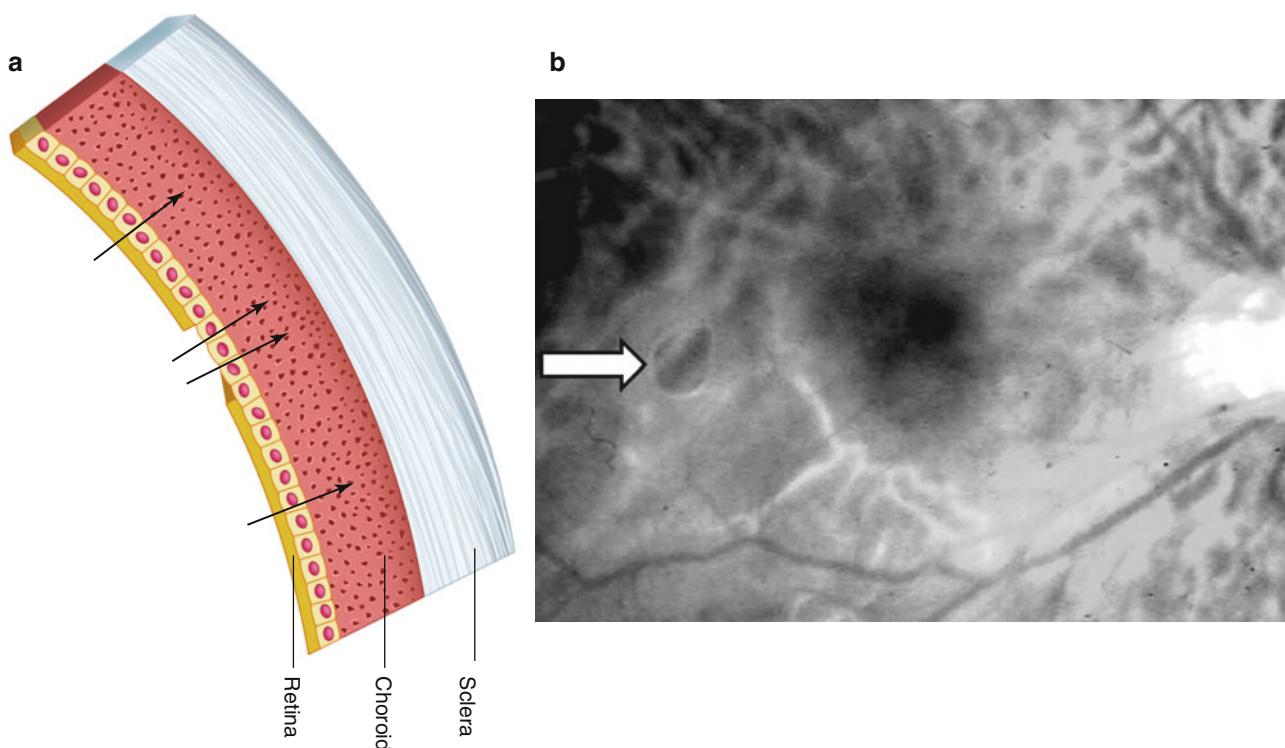


Figure III.I-13 (a) A diagram illustrates that in the absence of vitreoretinal traction, an open hole in a flat retina is unlikely to cause retinal detachment. Water movement through the retina around the hole (*black arrows*) maintains retinal adhesion to the RPE. Increased water move-

ment through the hole itself does not affect this. (b) A flat retina in a lightly pigmented eye with a very visible choroid remains attached in spite of the presence of an open retinal hole (*white arrow*)

A location where vitreoretinal attachment is strong is in the vicinity of major retinal blood vessels, and traction in these locations may result in retinal tears of varying configurations. Retinal tears resulting from vitreous traction are often accompanied by a degree of retinal and vitreous hemorrhage. Occasionally traction on a retinal vessel may result in its avulsion and a major vitreous hemorrhage [101]. Very occasionally an avulsed vessel may remain intact even when crossing a retinal tear resulting from vitreous traction.

In proliferative retinopathies, traction on the retina may be so severe as to cause widespread or total retinal detachment without the presence of a retinal break, a situation that can be challenging to manage. Secondary retinal breaks are common in such eyes and add to the difficulties in management.

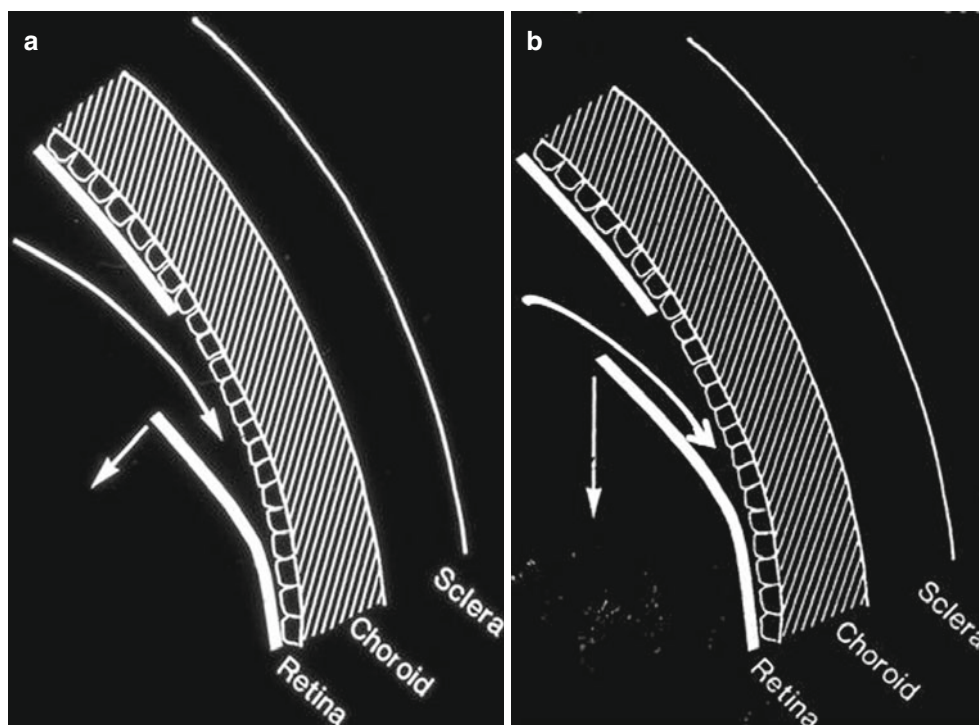
C. Synchysis, Syneresis, and Vitreous Currents

Degenerative changes in aging vitreous include liquefaction of the vitreous gel [77, 78], known as “synchysis” (scattering) or “syneresis” (collapse of a gel that is partially or totally fluid). Liquefaction may be localized forming lacunae or more generalized. As vitreous liquefaction is important in the etiology of retinal detachment, it is worth paying attention to its effects. The viscoelasticity of normal vitreous

absorbs energy and protects the retina from external injury [102]. Viscoelasticity also prevents short-term alterations in vitreous volume [19]. In addition to the loss of these protective effects, liquefaction of the vitreous allows rapid movement of fluid within the vitreous cavity during rotatory eye movements or vigorous movements of the head [103].

The importance of fluid currents within the vitreous cavity in the etiology of retinal detachment was recognized as early as 1933 by Lindner who devised a simple experiment to test this hypothesis [104]. He coated the inner surface of a flask with a continuous film of colloidin and then filled it with fluid. He found that no matter how vigorously he rotated the flask, the colloidin film remained attached to the wall of the flask. Making a small hole in the film especially if its edge was raised completely changed the situation so that any rotation of the flask resulting in rotational currents allowed fluid to enter the hole and rapidly strip the colloidin film from its attachment to the wall of the flask. The importance of vitreous currents in the etiology of rhegmatogenous retinal detachment is now well recognized [19, 105]. Where there is a hole in the retina but no detachment, adhesive forces including the outward movement of water through the retina surrounding the retinal hole will maintain the adhesion of the retina to the RPE even if there is an increased movement of water through the retinal hole itself. In the absence of vitreous traction, a retinal detachment is unlikely to develop [19] (Figure III.I-13a, b.)

Figure III.I-14 (a) In the presence of vitreous traction (*small arrow*), the elevated edge of a retinal tear allows vitreous currents (*long arrow*) to strip the retina from its bed leading to retinal detachment. (b) In the upper retina, gravity (*small arrow*) may be sufficient to elevate the edge of a retinal break and in the presence of vitreous currents (*long curved arrow*) may cause a retinal detachment



Where the edge of a retinal break is elevated by vitreous traction as occurs in operculated holes or where there is a contracting preretinal membrane, a combination of vitreous currents and elevation of the edge of the retinal break makes the onset of a retinal detachment almost inevitable (Figure III.I-14a). In the case of superiorly located retinal breaks even in the absence of vitreous traction, gravity may be sufficient to raise the edge of the retinal break and allow vitreous currents to detach the retina (Figure III.I-14b).

V. Developmental Abnormalities

Although developmental abnormalities of the vitreous including genetically determined conditions are rare, they can have a devastating effect on vision and may greatly increase the risk of retinal detachment and render its management difficult. It is well recognized that the fetal hyaloid vascular system undergoes regression shortly before birth [see chapters I.D. Vitreous proteomics and regression of the fetal hyaloid vasculature and II.A. Development and developmental disorders of vitreous]. A persistent hyaloid system is common within vitreous of premature babies, and remnants of the system such as Bergmeister's papilla with glial elements extending into Cloquet's canal occasionally persist in otherwise normal eyes. A failure of regression of the hyaloid system may be accompanied by cellular proliferation as occurs in persistent hyperplastic primary vitreous [see chapter III.A. Congenital vascular vitreo-retinopathies]. In this condition, there is a mass of proliferating mesenchymal vascular tissue behind the lens that additionally is frequently cataractous. The condition is usually unilateral although when part of a systemic abnormality such

as in trisomy 13, it may be bilateral [106]. Affected eyes are usually microphthalmic. Traction from contracting fibrous tissue may result in total and inoperable retinal detachment.

A large number of hereditary vitreoretinopathies have been described [see chapter I.C. Hereditary vitreoretinopathies]. Most are dominantly inherited genetic abnormalities often affecting the peripheral retina and with variable effects upon the vitreous that may be significantly abnormal from the outset or become abnormal with the late development of secondary vitreous degeneration. Some inherited vitreoretinopathies carry a high risk of retinal detachment from a combination of weakness of the peripheral retina, vitreous traction on the retina, and vitreous degeneration and are sometimes associated with high myopia. Inherited vitreoretinopathies carrying a high risk of retinal detachment include the *Stickler syndrome*, a dominantly inherited connective tissue disorder affecting hyaluronan and type II collagen [107, 108]. The ocular manifestations include vitreous syneresis (optically empty vitreous), vitreous membranes, high myopia, vitreous traction, retinal breaks including giant retinal tears, and a high incidence of retinal detachment in which vitreous abnormalities play a major role. Systemic manifestations of defective collagen synthesis also occur [108].

Wagner's disease and erosive vitreoretinopathy [109] are dominantly inherited, and the affected gene is the same for each [110]. Ocular manifestations are similar to those of Stickler syndrome (but lack systemic abnormalities) and include vitreous syneresis, vitreous bands, and tangential vitreoretinal traction resulting in retinal breaks (including giant retinal tears) and a high incidence of rhegmatogenous retinal detachment.

In *familial exudative vitreoretinopathy (FEVR)* [111, 112], there is a failure of vascularization of the peripheral retina

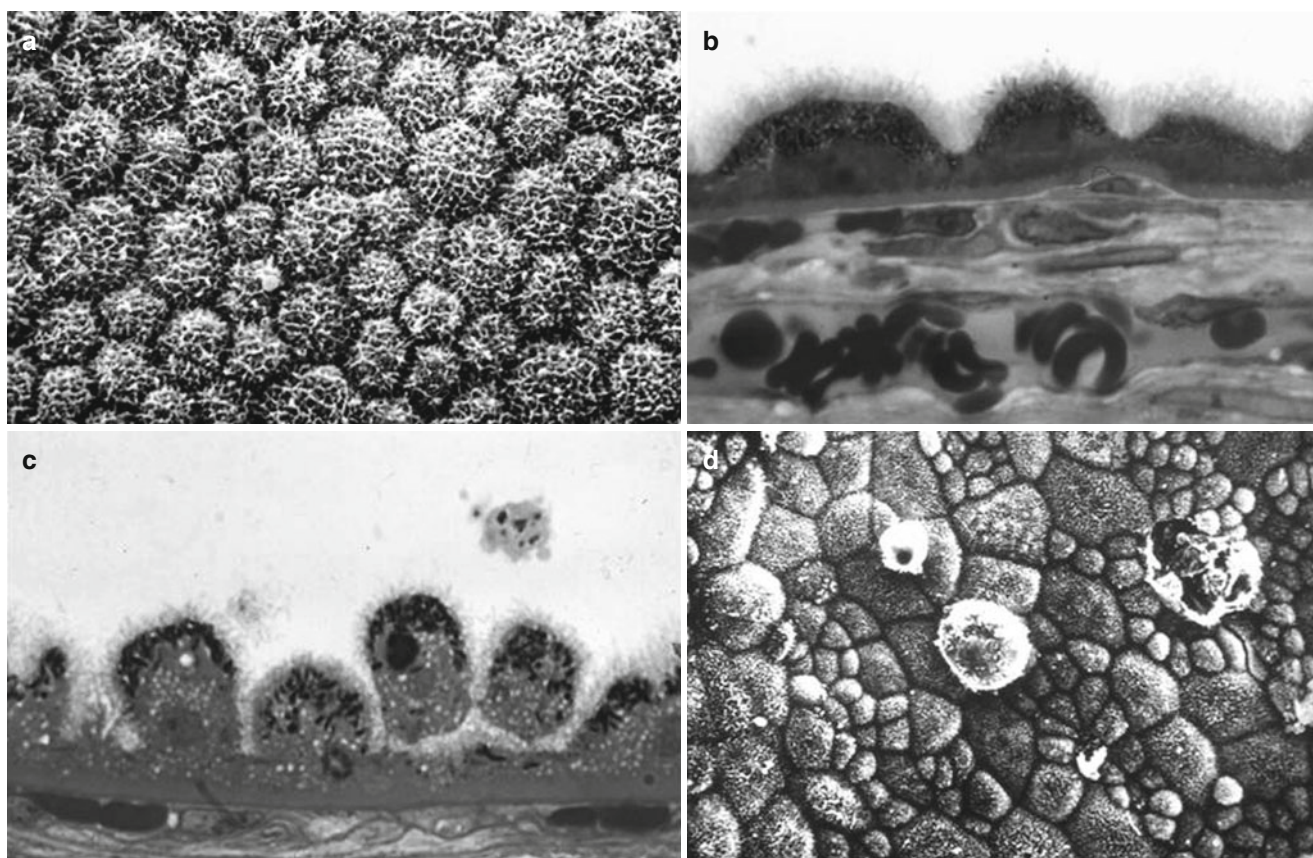


Figure III.I-15 (a) In a recent experimental retinal detachment (4 h) in a rabbit, the RPE retains a normal appearance with equally sized hexagonal cells and retention of apical villi. (b) In cross section, RPE cells are swollen but apical villi are retained. (c) In an experimental retinal detachment of longer duration (4 weeks), RPE cells have rounded up

and are becoming mobile and separated from Bruch's membrane. These are the cells that can give rise to proliferative vitreoretinopathy (PVR). (d) In an eye with a retinal detachment of 4 weeks duration, the RPE shows gross cellular pleomorphism

and an abnormally strong adhesion between the vitreous and the abnormal retina. Vitreoretinal traction accounts for a significant incidence of juvenile retinal detachment although in many cases, the condition may be nonprogressive.

In *lattice degeneration* (more appropriately called *retinal lattice* since this is more likely a dystrophy than a degeneration), which carries an increased risk of retinal detachment, there is an abnormal localized liquefaction of the vitreous over the site of the lesion and adherent vitreous at its edges [113]. Investigations, however, have failed to find associations between the vitreous abnormalities in this condition and the development of retinal detachment [114]. A recent Cochrane review also failed to find any evidence that currently used prophylactic interventions are beneficial [115].

VI. Effects of Retinal Detachment on Vitreous and Other Ocular Tissues

Having considered vitreoretinal interactions that contribute to the pathogenesis of retinal detachment, it may be appropriate to consider what effects retinal detachment may have on the vitreous. The pathological changes that occur following

detachment of the retina include progressive degenerative changes in the retina itself and significant abnormality in the RPE. In long-standing retinal detachments, there is a gradual loss of neural elements affecting the outer retina initially and all retinal layers eventually [116]. Concerning the RPE, shortly after the creation of an experimental retinal detachment, the appearance of the RPE is normal with intact apical villi and retention of a largely hexagonal arrangement of RPE cells (Figure III.I-15a). Very soon, however, RPE cells become swollen (Figure III.I-15b), lose contact with their neighboring cells, and become mobile (Figure III.I-15c), some showing proliferation and others the condensation of nuclear chromatin that denotes apoptosis [117]. Following experimental retinal detachment, the RPE shows loss of apical villi and increasing polymorphism [118] (Figure III.I-15d). In rabbits experimental retinal detachment is followed by acute changes in the morphology of the apical RPE [119]. In long-standing retinal detachment in humans (Figure III.I-16a) and in rabbits (Figure III.I-16b), gross abnormality is seen in the RPE, probably contributing to the poor prognosis for surgery in such cases. Accompanying this is a progressive reduction in the amplitude of the electroretinogram and of the electrooculogram until each is extinguished [120, 121].

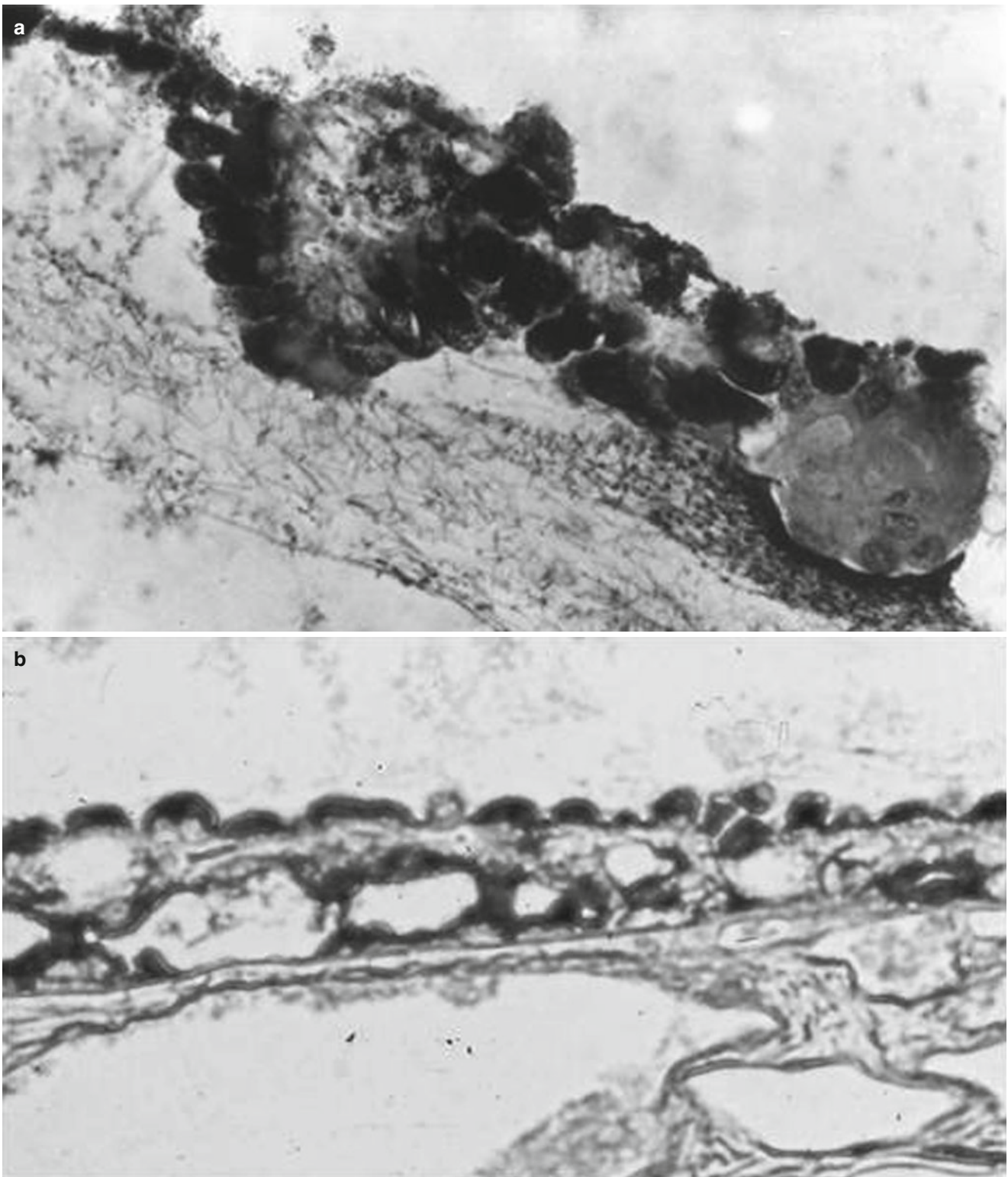


Figure III.I-16 In a human eye (a) and a rabbit eye (b) each with a long-standing retinal detachment (1 year +), the RPE has lost its normal morphology and in the case of (b) has no recordable ERG or electro-oculogram (EOG) and a very reduced response of the EOG to stimula-

tion with sodium azide. The probability is that the role of the RPE in helping to maintain retinal attachment has been irretrievably lost greatly worsening the prognosis for surgical reattachment

In eyes with retinal detachment, the subretinal fluid contains cells of varying origin including glial cells of astrocytic origin and Müller cells [122], but most frequently modified RPE cells [123] that can undergo morphogenesis into macrophages or fibroblasts [see chapter III.J. Cell proliferation at the vitreo-retinal interface in PVR and related disorders]. These cells may not only lay down a subretinal fibrocytic membrane [124] but can induce fibrosis within the retina or invade the vitreous cavity via retinal breaks or by invasion through the retina itself [74]. Within the vitreous cavity, they may create preretinal membranes or proliferate along the surfaces of a detached vitreous to create proliferative vitreoretinopathy (PVR). Contraction of fibrous tissue beneath, within, or on the surface of the retina and within the vitreous cavity can lead to end-stage usually untreatable retinal detachment with its characteristic funnel-shaped configuration.

Abbreviations

$^3\text{H}_2\text{O}$	Tritiated water
Cl^-	Chloride ion
CO_2	Carbon dioxide
FEVR	Familial exudative vitreo-retinopathy
HCO_3^-	Hydrogen carbonate
H_2O	Water
ILM	Inner limiting membrane
IPM	Interphotoreceptor matrix
K^+	Potassium ion
Min	Minute
Na^+	Sodium ion
OS	Outer segments (photoreceptor)
PDR	Proliferative diabetic retinopathy
pH	Power of hydrogen
PVD	Posterior vitreous detachment
PVR	Proliferative vitreo-retinopathy
ROP	Retinopathy of prematurity
RPE	Retinal pigment epithelium
Xe	Xenon

References

- Foulds WS. Factors influencing visual recovery in retinal detachment surgery. *Trans Ophthalmol Soc U K.* 1980;100:72–7.
- Hollyfield JG, Varner HH, Rayborn ME, Osterfeld AM. Retinal attachment to the pigment epithelium. Linkage through an extracellular sheath surrounding cone photoreceptors. *Retina.* 1989;9:59–68.
- Hageman GS, Marmor MF, Yao XY, Johnson LV. The interphotoreceptor matrix mediates primate retinal adhesion. *Arch Ophthalmol.* 1995;113:655–60.
- Sameshima M, Uehara F, Ohba N. Specialization of the interphotoreceptor matrices around cone and rod photoreceptor cells in the monkey retina, as revealed by lectin cytochemistry. *Exp Eye Res.* 1987;45:845–63.
- Fariss RN, Anderson DH, Fisher SK. Comparison of photoreceptor specific matrix domains in the cat and monkey retinas. *Exp Eye Res.* 1990;51:473–85.
- Tien ME, Raybim ME, Holliefield JG. Characterization of the interphotoreceptor matrix surrounding rod photoreceptors in the human retina. *Exp Eye Res.* 1992;55:287–305.
- Yao XY, Hageman GS, Marmor ME. Retinal adhesiveness is weakened by enzymatic modification of interphotoreceptor matrix in vivo. *Invest Ophthalmol Vis Sci.* 1990;31:2051–8.
- Koide H, Suganuma T, Murata F, Ohba N. Ultrastructural localization of lectin receptors in the monkey retinal photoreceptors and pigment epithelium: application of lectin-gold complexes on thin sections. *Exp Eye Res.* 1986;43:343–54.
- Keegan WA, McKechnie NM, Converse CA, Foulds WS. D-(H)-Galactose incorporation in the bovine retina: specific uptake and transport of the radiolabel in cones. *Exp Eye Res.* 1985;40:619–28.
- Gregory CY, Converse CA, Foulds WS. Effect of glycoconjugates on rod outer segment phagocytosis by retinal pigment epithelial explants in vitro assessed by a specific double radioimmunoassay procedure. *Curr Eye Res.* 1990;9:65.
- Chiang RK, Yao XY, Takeuchi A, et al. Cytochalasin D reversibly weakens retinal adhesiveness. *Curr Eye Res.* 1995;14:1109–13.
- Nandrot EF, Emeline F, Anand M, Sircar M, Finnemann SC. Novel role for $\alpha\text{v}\beta 5$ -integrin in retinal adhesion and its diurnal peak. *Am J Physiol Cell Physiol.* 2006;290:C1256–62.
- Marmor MF, Maacka T. Local environmental factors and retinal adhesion in the rabbit. *Exp Eye Res.* 1982;34:727–33.
- Owczarek FR, Marak GE, Pilkerton AR. Retinal adhesion in light- and dark-adapted rabbits. *Invest Ophthalmol.* 1975;14:353–5.
- Balazs EA. Molecular morphology of the vitreous body. In: Smelser GK, editor. *Structure of the eye.* New York: Academic Press Inc; 1961. p. 293–310.
- Ogsten AG, Sherman TF. Effects of hyaluronic acid upon diffusion of solutes and flow of solutes. *J Physiol.* 1961;156:67–74.
- Moseley H, Foulds WS, Allan D, Kyle PM. Routes of clearance of radioactive water from the rabbit vitreous. *Br J Ophthalmol.* 1984;68:145–51.
- Foulds WS, Allan D, Moseley H, Kyle PM. Effect of intravitreal hyaluronidase on the clearance of tritiated water from the vitreous to choroid. *Br J Ophthalmol.* 1985;69:529–32.
- Foulds WS. Is your vitreous really necessary? The role of the vitreous in the eye with particular reference to retinal attachment Detachment and the mode of action of vitreous substitutes. *Eye.* 1987;1:641–64.
- Moseley H, Foulds WS. The movement of Xenon-133 from the vitreous to the choroid. *Exp Eye Res.* 1982;34:169–79.
- Foulds WS. Clinical significance of transscleral fluid transfer. *Trans Ophthalm Soc U K.* 1976;96:290–308.
- Bill A. Some aspects of tissue fluid dynamics in the eye. In: Cant JS, editor. *Vision and circulation.* London: Henry Kimpton; 1976. p. 333–8.
- Maurice DM, Salmon J, Zauberman H. Subretinal pressure and retinal adhesion. *Exp Eye Res.* 1971;12:212–7.
- Bill A. A method to determine osmotically effective albumin and gammaglobulin concentrations in tissue fluids, its application to the uvea and a note on the effects of capillary “leaks” on tissue fluid dynamics. *Acta Physiol Scand.* 1968;73:511–22.
- Marmor MF. Barriers to fluorescein and protein movement. *Jpn J Ophthalmol.* 1985;20:131–8.
- Blair NP, Zeimer RC, Rusin MM, Cuhna-Vaz JC. Outward transport of fluorescein from the vitreous in normal human subjects. *Acta Ophthalmol.* 1983;101:1117–21.
- Mizuno K. Histochemical tracing of fluorescein in retina. *Eye Ear Nose Throat Mon.* 1973;52:15–8.

28. Marmor MF, Negi A, Maurice DM. Kinetics of macromolecules injected into the subretinal space. *Exp Eye Res.* 1985;40:687–96.
29. Negi A, Marmor MF. Mechanisms of subretinal fluid resorption in the cat eye. *Invest Ophthalmol Vis Sci.* 1986;27:1560–3.
30. Negi A, Marmor MF. Effects of subretinal and systemic osmolarity on the rate of subretinal fluid absorption. *Invest Ophthalmol Vis Sci.* 1984;25:616–20.
31. Marmor MF. Retinal detachment from hyperosmotic intravitreal injection. *Invest Ophthalmol Vis Sci.* 1979;18:1237–44.
32. Marmor MF, Martin LJ, Tharpe S. Osmotically induced retinal detachment in the rabbit and primate. Electron microscopy of the pigment epithelium. *Invest Ophthalmol Vis Sci.* 1980;19:1016–29.
33. Kita M, Marmor MF. Retinal adhesive force in living rabbit, cat, and monkey eyes. Normative data and enhancement by mannitol and acetazolamide. *Invest Ophthalmol Vis Sci.* 1992;33:1879–82.
34. Peterson PA. Demonstration in serum of two physiological forms of the human retinol binding protein. *Eur J Clin Invest.* 1971;1:437–44.
35. Toris CB, Pederson JE, Tsuboi Gregerson DS. Extravascular albumin concentration of the uvea. *Invest Ophthalmol Vis Sci.* 1990;31:43–53.
36. Moseley H. Mathematical model of diffusion in the vitreous humour of the eye. *Clin Phys Physiol Meas.* 1981;2:175–82.
37. Kristjansdottir JV, Hardarson SH, Harvey AR, Olafsdottir OB, et al. Choroidal oximetry with a spectrophotometric Oximeter. *Invest Ophthalmol Vis Sci.* 2013;54:3234–9.
38. Cioffi GA, Granstam E, Alm A. Ocular circulation. In: *Adlers physiology of the eye.* 10th ed. St Louis: Mosby; 2003. p. 747–84.
39. Kaur C, Foulds WS, Ling EA. Blood-retinal barrier in hypoxic-ischemic conditions: basic concepts, clinical features and management. *Prog Retin Eye Res.* 2008;27:622–47.
40. Jackson TL, Antcliffe RJ, Hillenkamp J, Marshall J. Human retinal molecular weight exclusion limit and estimate of species variation. *Invest Ophthalmol Vis Sci.* 2003;44:2141–6.
41. Marmor MF. Mechanisms of fluid accumulation in retinal edema. *Doc Ophthalmol.* 1999;97:239–49.
42. Asayama K. In vivo study on the absorption of subretinal fluid.2. Studies of tracers (1125 human serum albumin, lanthanum nitrate) injected between the sensory retina and the pigment epithelium layer. *Nihon Ganka Gakkai Zasshi.* 1976;80:598–607.
43. Kita M, Negi A, Kawano S, Honda Y, Maegawa S. Measurement of retinal adhesive force in the in vivo rabbit eye. *Invest Ophthalmol Vis Sci.* 1990;31:624–8.
44. Endo EG, Yao X-Y, Marmor MF. Pigment adherence as a measure of retinal adhesion: dependence on temperature. *Invest Ophthalmol Vis Sci.* 1988;29:1390–6.
45. Marmor MF, Yao XY, Hageman GS. Retinal adhesiveness in surgically enucleated human eyes. *Retina.* 1994;14:181–6.
46. Yao XY, Hageman GS, Marmor NF. Retinal adhesiveness in the monkey. *Invest Ophthalmol Vis Sci.* 1994;35:744–8.
47. Kim RY, Yao X-Y, Marmor MF. Oxygen dependency of retinal adhesion. *Invest Ophthalmol Vis Sci.* 1993;34:2074–8.
48. Marmor MF, Yao XY. The metabolic dependency of retinal adhesion in rabbit and primate. *Arch Ophthalmol.* 1995;113:232–8.
49. Yao XY, Endo EG, Marmor MF. Reversibility of retinal adhesion in the rabbit. *Invest Ophthalmol Vis Sci.* 1989;30:220–4.
50. Kita M, Negi A, Marmor MF. Lowering the calcium concentration in the subretinal space in vivo loosens retinal adhesion. *Invest Ophthalmol Vis Sci.* 1992;33:23–9.
51. Fang XY, Hayashi A, Cekic O, et al. Effect of Ca(2+)-free and Mg(2+)-free BSS Plus solution on the retinal pigment epithelium and retina in rabbits. *Am J Ophthalmol.* 2001;131:481–8.
52. Kita M, Marmor MF. Effects on retinal adhesive force in vivo of metabolically active agents in the subretinal space. *Invest Ophthalmol Vis Sci.* 1992;33:1883–7.
53. Wilson TM, Strang R, MacKenzie ET. The response of the choroidal and cerebral circulations to changing arterial PCO₂ and acetazolamide in the baboon. *Invest Ophthalmol Vis Sci.* 1977;16:576–80.
54. Strang R, Wilson TM, Johnson NF. The effect of alterations in arterial carbon dioxide tensions on choroidal blood flow in rabbits. *Exp Eye Res.* 1974;18:153–6.
55. Marmor M, Maack T. Enhancement of retinal adhesion and subretinal fluid resorption by acetazolamide. *Invest Ophthalmol Vis Sci.* 1982;23:121–4.
56. Moldow B, Sander B, Larsen M, Lund-Andersen H. Effects of acetazolamide on passive and active transport of fluorescein across the normal BRB. *Invest Ophthalmol Vis Sci.* 1999;40:1770–5.
57. Sparrow JR, Hicks D, Hamel CP. The retinal pigment epithelium in health and disease. *Curr Mol Med.* 2010;10:802–23.
58. Strauss O. The retinal pigment epithelium. In: Kolb H, Nelson R, Fernandez E, Jones B, editors. *The organization of the retina and visual system.* Univ Utah, Webvision, WordPress 2011.
59. Miller SS, Edelman J. Active transport pathways in the bovine retinal pigment epithelium. *J Physiol.* 1990;424:283–300.
60. Marmor MF. Retinal pigment epithelium. In: *Ophthalmology, chapter 100.* Free Medical Textbook, medtextfree. WordPress, 2010.
61. Li J-d, Gallemore RP, Dmitriev A, Steinberg RH. Light-dependent hydration of the space surrounding photoreceptors in chick retina. *Invest Ophthalmol Vis Sci.* 1994;35:2700–11.
62. Negi A, Marmor MF. Quantitative estimation of metabolic transport of subretinal fluid. *Invest Ophthalmol Vis Sci.* 1986;27:1546–68.
63. Yoon YH, Marmor MF. Retinal- pigment epithelium adhesion to Bruch's membrane is weakened by hemicholinium-3 and sodium iodate. *Ophthalmic Res.* 1993;25:386–92.
64. Negi A, Marmor MF. The resorption of subretinal fluid after diffuse damage to the retinal pigment epithelium. *Invest Ophthalmol Vis Sci.* 1983;24:1475–9.
65. Gurkov TD, Kralchevsky PA. Surface tension and surface energy of curved interfaces and membranes. *Colloids Surf.* 1990;41:45–68.
66. Scott JE. Supramolecular organization of extracellular matrix glycosaminoglycans, in vitro and in the tissues. *FASEB J.* 1992;6:2639–45.
67. Zhao M, Chwlmers L, Vieira AC, et al. Electrical signaling in control of ocular cell behaviors. *Prog Retin Eye Res.* 2012;31:65–88.
68. Fatt I, Shantinath K. Flow conductivity of retina and its role in retinal adhesion. *Exp Eye Res.* 1971;12:219–26.
69. Takeuchi A, Kricorian G, Wolfensberger TJ, Marmor MF. The source of fluid and protein in serous retinal detachments. *Curr Eye Res.* 1996;15:764–7.
70. Forrester JV, Liversidge J, Dua HS, et al. Comparison of clinical and experimental uveitis. *Curr Eye Res.* 1990;9:75–8470.
71. Elagouz M, Stanescu-Segall D, Jackson TL. Uveal effusion syndrome. *Surv Ophthalmol.* 2010;55:134–45.
72. Marmor MF. New hypotheses on the pathogenesis and treatment of serous retinal detachment. *Graefes Arch Clin Exp Ophthalmol.* 1988;226:548–52, *Ophthalmol* 2010;55:134–45.
73. Heath H, Beck T, Foulds WS. Chemical composition of subretinal fluid. *Br J Ophthalmol.* 1962;45:385–96.
74. Foulds WS. Pathogenesis of retinal detachment. Thesis for the degree of MD, University of Glasgow. 1964.
75. Chignell AH, Carruthers M, Rahi AHS. Clinical, biochemical and immunoelectrophoretic study of subretinal fluid. *Br J Ophthalmol.* 1975;55:525–32.
76. Foulds WS. Do we need a retinal pigment epithelium (or choroid) for the maintenance of retinal apposition? *Br J Ophthalmol.* 1985;69:237–9.
77. Sebag J. Age-related changes in human vitreous structure. *Graefes Arch Clin Exp Ophthalmol.* 1987;225:89–93.
78. Le Goff MM, Bishop PN. Adult vitreous structure and postnatal changes. *Eye.* 2008;22:1214–22.

79. Akiba J. Prevalence of posterior vitreous detachment in high myopia. *Ophthalmology*. 1883;100:1384–8.
80. Yonemoto J, Ideta H, Sasaki K, et al. The age of onset of posterior vitreous detachment. *Graefes Arch Clin Exp Ophthalmol*. 1884;232:67–70.
81. Reese AB, Jones IR, Cooper WC. Macular changes secondary to vitreous traction. *Am J Ophthalmol*. 1967;51:544–9.
82. Reese AB, Jones IR, Cooper WC. Vitreomacular traction syndrome confirmed histologically. *Am J Ophthalmol*. 1970;69:975–7.
83. Shechtman DL, Dunbar MT. The expanding spectrum of vitreomacular traction. *Optometry*. 2009;80:681–7.
84. Wisotsky BJ, Magat-Gordon CB, Puklin HE. Vitreopapillary traction as a cause of elevated optic nerve head. *Am J Ophthalmol*. 1998;126:137–8.
85. Smiddy WE, Flynn Jr BW. Pathogenesis of macular holes and therapeutic implications. *Am J Ophthalmol*. 2004;137:525–37.
86. Bainbridge J, Herbert E, Gregor Z. Macular holes : vitreoretinal relationships and surgical approaches. *Eye*. 2008;22:1301–9.
87. Sebag J, Balazs EAC. Pathogenesis of cystoid macular edema: an anatomic consideration of vitreoretinal adhesions. *Surv Ophthalmol*. 1984;28:495–8.
88. Gass JDM. Vitreous traction maculopathy in stereoscopic atlas of macular diseases. St Louis: Mosby; 1987. p. 678–83.
89. Johnson MW. Tractional cystoid macular edema: a subtle variant of the vitreomacular traction syndrome. *Am J Ophthalmol*. 2005;140:184–92.
90. Levy J, Klemperer I, Belfair N, et al. Rapid spontaneous resolution of vitreomacular traction syndrome documented by optical coherence tomography. *Int Ophthalmol*. 2004;25:247–51.
91. Rodriguez A, Infante R, Rodriguez FJ, Valencia M. Spontaneous separation in idiopathic vitreomacular traction syndrome associated with contralateral full-thickness macular hole. *Eur J Ophthalmol*. 2006;16:733–40.
92. Gallemore RP, Jumper JM, McCuen 2nd BW, et al. Diagnosis of vitreoretinal adhesions in macular disease with optical coherence tomography. *Retina*. 2000;20:115–20.
93. Koizumi N, Apaide RF, Fisher YL, et al. Three-dimensional evaluation of vitreomacular traction and epiretinal membrane using spectral domain optical coherence tomography. *Am J Ophthalmol*. 2008;145:509–17.
94. Bottos JM, Ezialde J, Rodrigues EB, Maia M. Current concepts in vitreomacular traction syndrome. *Curr Opin Ophthalmol*. 2012;23:195–201.
95. Gass JDM. Idiopathic senile macular hole: its early stages and pathogenesis. *Arch Ophthalmol*. 1988;106:629–39.
96. Stalmans P, Benz MS, Gandorfer A, et al. Enzymatic Vitreolysis with Ocriplasmin for Vitreomacular Traction and Macular Holes. *N Engl J Med*. 2012;367:606–15.
97. Adams ST. Retinal breaks in eye bank eyes. *Arch Ophthalmol*. 1956;55:254–60.
98. Barshak YR, Stein R. Retinal breaks without retinal detachment in autopsy eyes. *Acta Ophthalmol*. 1972;50:147–59.
99. Foulds WS. The vitreous in retinal detachment. *Trans Ophthalmol Soc U K*. 1975;95:412–6.
100. Combs JL, Welch RB. Retinal breaks without detachment: natural history, management and long term follow up. *Trans Am Ophthalmol Soc*. 1982;80:64–97.
101. Vote B, Polkinghorne P. Avulsed retinal vessel with operculated retinal break. *Arch Ophthalmol*. 2002;120:1594–5.
102. Sharif-Kashani P, Hubschman J-P, Sassoon D, Kavehpour HP. Rheology of the vitreous gel: Effects of macromolecule organization on the viscoelastic properties. *J Biomech*. 2011;44:419–23.
103. David T, Smye S, Dabbs T, James T. A model for the fluid motion of vitreous humour of the human eye during saccadic movement. *Phys Med Biol*. 1998;43:1385–99.
104. Lindner K. Uber die Herstellung von mpdellen zu Modellversuchen der netzhaut abhebung. *Mlb Augenheilk*. 1933;90:289–300.
105. Machemer R. The importance of fluid absorption, traction, intraocular currents, and chorioretinal scars in the therapy of rhegmatogenous retinal detachments. *Am J Ophthalmol*. 1984;98:681–93.
106. Kaste SC, Jenkins JJ, Meyer D, Fontanesi J. Persistent hyperplastic primary vitreous of the eye: Imaging findings with pathologic correlation. *AJR Am J Roentgenol*. 1994;162:437–40.
107. Francomano CA, Liberfarb RM, Hirose T, et al. The Stickler syndrome: evidence for close linkage to the structural gene for type II collagen. *Genomics*. 1987;1:293–6.
108. Weingeist TA, Hermsen V, Hanson JVV, et al. Ocular and systemic manifestations of Stickler's syndrome. In: Cotlier E, Maumenee IH, Berman ER, editors. *Genetic eye diseases: retinitis pigmentosa and other inherited eye disorders; proceedings of the International Symposium on Genetics*. New York: Alan R Liss; 1982. p. 539–60.
109. Brown DM, Kimura AK, Weingeist TM, Stone EM. Erosive vitreoretinopathy - a new clinical entity. *Ophthalmology*. 1994;101:694–704.
110. Brown DM, Graemiger RA, Hergersberg M, et al. Genetic linkage of Wagner disease and erosive vitreoretinopathy to chromosome 5q13-14. *Arch Ophthalmol*. 1995;113:671–5.
111. Criswick VB, Schepens CH. Familial exudative vitreoretinopathy. *Am J Ophthalmol*. 1969;68:578–94.
112. Gow J, Oliver GL. Familial exudative vitreoretinopathy. An expanded view. *Arch Ophthalmol*. 1971;86:150–5.
113. Straatsma BR, Zeegan PD, Foos RY, et al. Lattice degeneration of the retina. XXX Edward Jackson Memorial Lecture. *Am J Ophthalmol*. 1974;77:619–49.
114. Foos RY, Simons KB. Vitreous in lattice degeneration of retina. *Ophthalmology*. 1984;91:452–7.
115. Wilkinson CP. Interventions for asymptomatic retinal breaks and lattice degeneration for preventing retinal detachment. *Cochrane Database Syst Rev*. 2012;3, CD003170.
116. Foulds WS. Histology and electrophysiology of induced retinal detachment in rabbits. *Mod Probl Ophthalmol*. 1965;5:249–51.
117. Johnson NF, Foulds WS. Observations on the retinal pigment epithelium and retinal macrophages in experimental detachment. *Br J Ophthalmol*. 1977;61:564–72.
118. Foulds WS. Blood ocular barriers. In: Ryan SJ, Dawson AK, Little HL, editors. *Retinal diseases*. Orlando Fla: Grune and Stratton Inc; 1985. p. 49–52.
119. Immel J, Negi A, Marmor MF. Acute changes in RPE apical morphology after retinal detachment in rabbit. *Invest Ophthalmol*. 1986;27:1770–6.
120. Foulds WS, Ikeda H. Changes in the electrical activity and structure of the retina of rabbit after separation of the pars optica retinae from the pigment epithelium. *J Physiol*. 1964;172:35–7.
121. Foulds WS, Ikeda H. The effects of detachment of the retina on the induced and resting ocular potentials in the rabbit. *Invest Ophthalmol Vis Sci*. 1966;5:93–108.
122. Charteris DG. Proliferative vitreoretinopathy: pathobiology, surgical management, and adjunctive management. *Br J Ophthalmol*. 1995;79:953–60.
123. Machemer R, Laqua H. Pigment epithelial proliferation in retinal detachment (massive periretinal proliferation). *Am J Ophthalmol*. 1975;80:1–23.
124. Hiscott P, Grierson I. Subretinal membranes of proliferative vitreoretinopathy. *Br J Ophthalmol*. 1881;75:53.

Cell Proliferation at the Vitreoretinal Interface in Proliferative Vitreoretinopathy and Related Disorders



Sonia Mehta, Rui Zhang, and Hans E. Grossniklaus

Outline

- I. Introduction
- II. Clinical Features of PVR
 - A. Risk Factors of PVR
 - B. Clinical Signs and Staging of PVR
 - C. Histopathology of PVR
 - D. Pathophysiology of PVR
 1. Cell Types in PVR
 - a. Retinal Pigment Epithelial (RPE) Cells
 - b. Macrophages/Hyalocytes
 - c. Glial Cells
 - d. Myofibroblasts
 - e. Immune Cells
 2. Cytokines of PVR
 - a. Tumor Necrosis Factor- α (TNF- α)
 - b. Transforming Growth Factor- β (TFG- β)
 - c. Platelet-Derived Growth Factor Receptor- α (PDGFR- α)
 - d. Miscellaneous Cytokines
- III. Treatment of PVR
 - A. Surgery of PVR
 - B. Pharmacotherapy of PVR

References

S. Mehta, MD (✉)
Vitreoretinal Diseases and Surgery,
Wills Eye Hospital/Mid-Atlantic Retina,
840 Walnut Street, Suite 1020, Philadelphia, PA 19107, USA
e-mail: soniamehtamd@gmail.com

R. Zhang, MD
Department of Ophthalmology, Case Western Reserve University,
2085 Adelbert Road, Cleveland, OH 44106, USA
e-mail: rxz49@case.edu

H.E. Grossniklaus, MD, MBA (✉)
Department of Ophthalmology, Emory Eye Center,
Emory University School of Medicine,
1365 Clifton Road, Atlanta, GA 30322, USA
e-mail: ophtheg@emory.edu

Keywords

Vitreous • Rhegmatogenous retinal detachment • Proliferative vitreoretinopathy • Preretinal PVR membranes • Subretinal fibrosis • Traction retinal detachment • Histopathology • Pathophysiology • Wound repair • Cytokines

Key Concepts

1. Proliferative vitreoretinopathy is the undesired formation of fibrous contractile membranes at the vitreoretinal interface and on both surfaces of the retina that results from the proliferation of retinal pigment epithelial cells, hyalocytes, and glial cells in the vitreous and on the retinal surface following rhegmatogenous retinal detachment.
2. At the time of retinal break formation, retinal pigment epithelial cells are released and migrate into the vitreous and onto the retinal surface along with fibroblasts, glial cells, and macrophage hyalocytes. Transforming growth factor- β released by retinal pigment epithelial cells stimulates production of collagen and fibronectin which in turn stimulates additional cell migration and proliferation, thus continuing the vicious cycle.
3. Under the influence of cytokines, these cells form contractile membranes leading to recurrent retinal detachment. Much research is being conducted on the specific cytokines and cells involved in this complex pathophysiological process, and it is hoped that additional therapeutic and preventative options will be available in the future.

I. Introduction

Proliferative vitreoretinopathy (PVR) refers to the proliferation of retinal pigment epithelial cells, hyalocytes, and glial cells at the vitreous and on the retinal surface in rhegmatogenous retinal detachment (RRD). Seen in 5–10 % of all cases of RRD [1] and found in 75 % of all recurrent retinal detachment cases [2], PVR is the most common reason for failure of retinal reattachment surgery. PVR results from the dispersion, migration, and proliferation of cells into the vitreous as well as the outer and inner surface of the retina. The cell types involved in the process of PVR formation include retinal pigment epithelial (RPE) cells, fibroblasts, macrophages, hyalocytes, and glial cells [3]. Cytokines such as fibronectin and platelet-derived growth factor (PDGF) have also been implicated in the process of PVR formation [4]. These cells and cytokines lead to membrane formation and contraction of the vitreous and retina resulting in recurrent retinal detachment [4].

II. Clinical Features of PVR

A. Risk Factors of PVR

Multiple factors have been identified that increase the risk of developing PVR. Increased risk has been observed in patients

with large retinal tears, multiple retinal tears, longer duration of retinal detachment, and high levels of vitreous protein such as occurs in vitreous hemorrhage and intraocular inflammation [5]. Presence of preoperative PVR, aphakia, and ocular trauma have also been associated with increased risk of PVR [5].

A model known as the PVR score has been used by many to determine the risk of developing PVR, where $\text{PVR score} = 2.88 \times (\text{grade C PVR}) + 1.85 \times (\text{grade B PVR}) + 2.92 \times (\text{aphakia}) + 1.77 \times (\text{anterior uveitis}) + 1.23 \times (\text{quadrants of detachment}) + 0.83 \times (\text{vitreous hemorrhage}) + 23 \times (\text{previous cryotherapy})$ [6] with one added to the total score if retinal fibrosis is present. A patient is considered high risk if the score is greater than 6.33 [7].

B. Clinical Signs and Staging of PVR

The earliest signs of PVR are the presence of flare, haze, and pigment within the vitreous. As PVR evolves, wrinkling of the inner retinal surface can be seen with vessel tortuosity and rolled edges of retinal breaks. Later states include fixed retinal folds (Figure III.J-1), macular pucker (Figure III.J-2), star folds of the retina (Figure III.J-3), and subretinal fibrotic bands (Figure III.J-4). As the membranes contract, localized detachments can also be seen (Figure III.J-5), which typically



Figure III.J-1 This 53-year-old man with high myopia and a history of rhegmatogenous retinal detachment repaired with scleral buckle and vitrectomy presented 3 months following surgery with fixed retinal folds



Figure III.J-2 A preretinal membrane due to proliferative vitreoretinopathy causing macular pucker

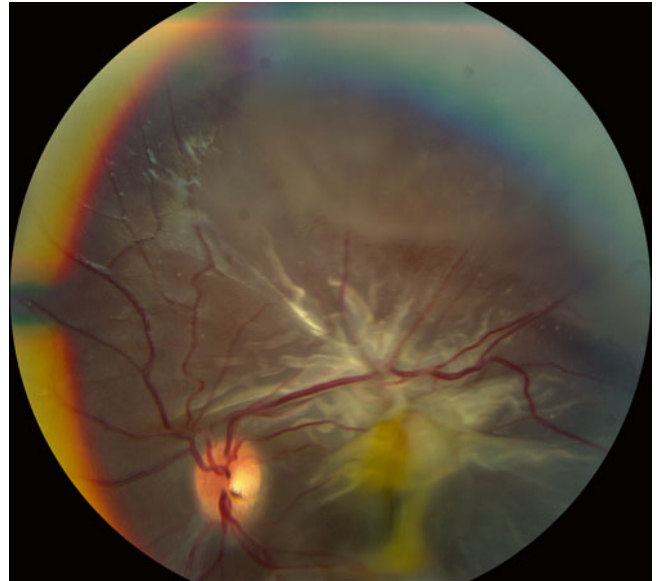


Figure III.J-3 This 6-year-old boy presented with a left exotropia for several months duration and was found to have a rhegmatogenous retinal detachment with proliferative vitreoretinopathy manifesting as star folds of the retina and a macular pucker

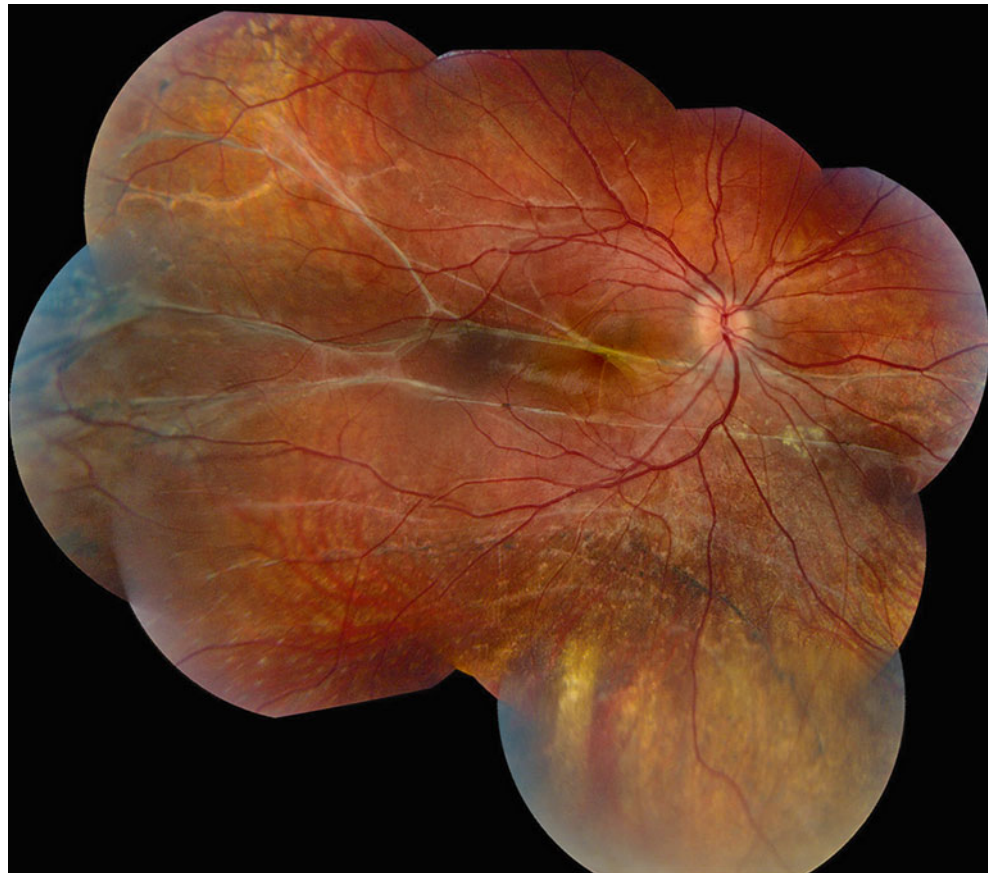


Figure III.J-4 An 11-year-old boy failed a school vision screening and was found to have a rhegmatogenous retinal detachment with proliferative vitreoretinopathy. Fundus examination showed an inferior rhegmatogenous retinal detachment and diffuse subretinal fibrotic bands

Figure III.J-5 This 26-year-old man with a history of a rhegmatogenous retinal detachment and proliferative vitreoretinopathy treated with scleral buckle, vitrectomy, lensectomy, and silicone oil presented 4 months following surgery with inferior proliferative vitreoretinopathy and recurrent inferior retinal detachment under silicone oil

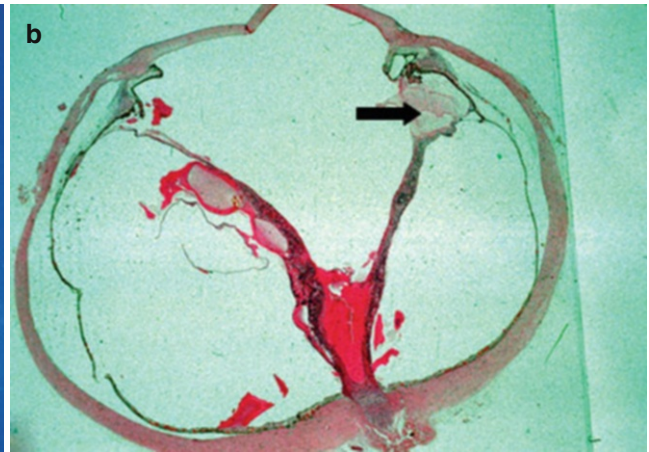
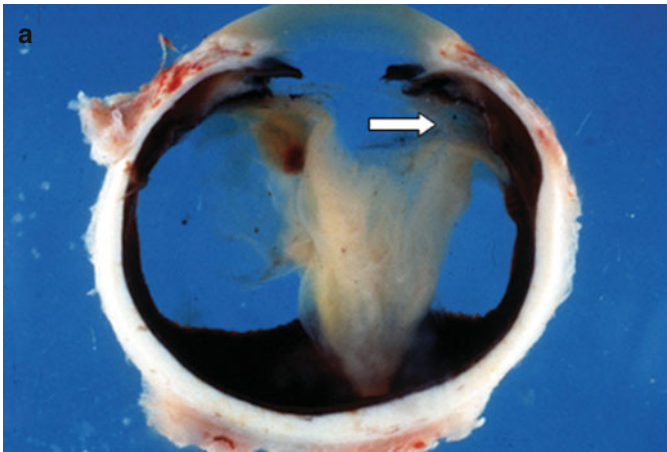
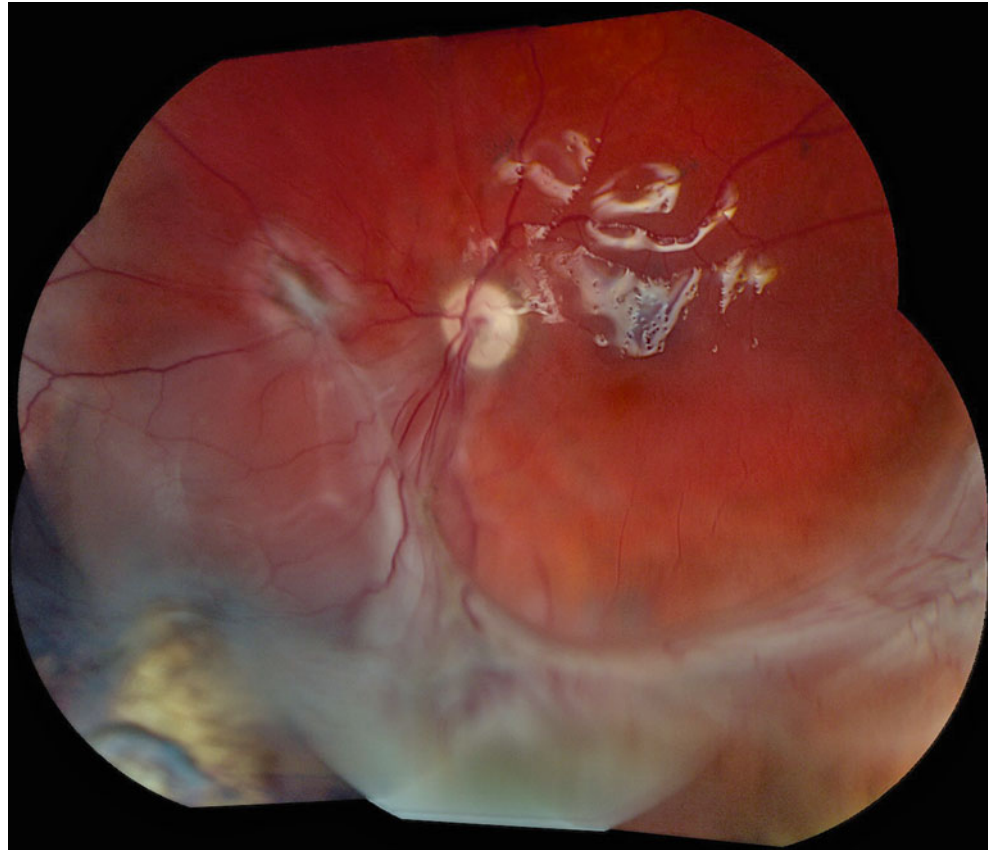


Figure III.J-6 Anterior PVR occurs in the collapsed vitreous base, demonstrated by *arrows* in gross (a) and microscopic (b) sections. Traction from the vitreous base may lead to incorporation and later pro-

liferation of elements from the peripheral retina and ciliary body, thus eventually resulting in hypotony and phthisis (b. H&E, 2 \times)

take on a concave shape versus the convex shape of a rhegmatogenous retinal detachment. Other associated but non-specific signs include flare in the anterior chamber, neovascularization of the iris from ischemia, and hypotony resulting from total retinal detachment (Figures III.J-6 and III.J-7 top) [3], as well as traction by the anterior loop of the

vitreous case upon the ciliary body [see chapter III.H. Peripheral vitreo-retinal pathology].

Two main classification systems have been utilized in the staging of PVR. The first, more widely used classification system, was initially proposed by the Retina Society in 1983 and is organized based on severity and location of ocular findings

(Table III.J-1) [8]. Grade A is presence of haze and pigmented cells within the vitreous. Grade B is wrinkling seen at the edge of the retinal tear or at the inner retinal surface, and grade C is the presence of fixed retinal folds. Three subtypes of grade C PVR exist depending on the location of the PVR: posterior, anterior, or both. The second classification system was proposed by the Silicone Study Group, which categorizes based on type of contraction and location (Table III.J-2) [6].

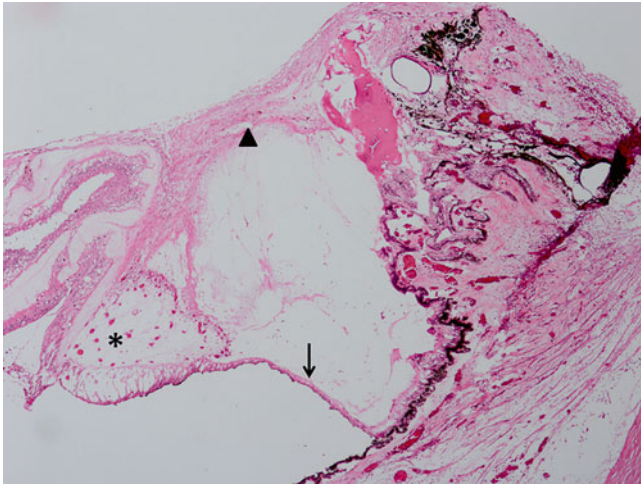


Figure III.J-7 Anterior proliferative vitreoretinopathy consists of ciliary nonpigmented epithelium (*arrow*), gliotic fibrocellular tissue (*arrowhead*), and fibrovascular tissue (*) incorporated into the vitreous base (H&E, 63×)

Table III.J-1 The Retina Society classification of PVR

Grade	Clinical findings
A	Vitreous haze Cells within vitreous Pigment deposition on retina inferiorly
B	Wrinkling seen in retina Vessel tortuosity Irregular edge seen at tear
C	Presence of retinal folds
Ca	Folds within anterior vitreous
Cp	Folds within posterior vitreous

Table III.J-2 Classification of proliferative vitreoretinopathy used in the Silicone Oil Study

Type	Type of contraction	Location	Clinical findings
1	Focal	Posterior	Star fold seen in retina
2	Diffuse	Posterior	Confluent irregular retinal folds present in posterior retina
3	Subretinal	Posterior	“Clothesline” elevation of retina; “napkin ring” around the disc
4	Circumferential	Anterior	Irregular retinal folds present in the anterior retina; peripheral retina within the vitreous base drawn centrally
5	Perpendicular	Anterior	Circumferential retinal fold seen at insertion of posterior vitreous cortex
6	Anterior	Anterior	Circumferential retinal fold at insertion of posterior vitreous cortex drawn forward; ciliary processes stretched with possible hypotony; iris retracted

C. Histopathology of PVR

D. Schwartz et al. studied transmission electron microscopy characteristics of PVR membranes removed from 20 human eyes and noted membranes were composed of RPE cells, fibrous astrocytes, fibrocytes, macrophages (some probably hyalocytes), and cells with myoblastic differentiation [9]. In addition, extracellular matrix consisting of collagen and fibrin was also found in the PVR membranes. We have found a similar composition of PVR membranes at our institution (Figure III.J-8).

D. Pathophysiology of PVR

An understanding of the pathogenesis of PVR is critical in the prevention and treatment of this disease. The development and progression of PVR is a complex interaction between the different cells, inflammatory cytokines, and growth factors leading to fibrous membrane formation [10]. The cycle begins with the dispersion of retinal pigment epithelial cells at the time of retinal break formation [11]. Scleral depression and cryotherapy can cause further release of RPE cells into the vitreous cavity [12]. In addition, RPE cells can migrate through the retinal break into the vitreous and onto the retinal surface, along with other cell types such as fibroblasts, glial cells, and macrophages [13]. The presence of cytokines such as fibronectin and platelet-derived growth factor can stimulate further cell migration and proliferation [14]. Cytokines may be present from vitreous hemorrhage, intraocular inflammation, or breakdown of the blood-retinal barrier as occurs following cryotherapy [12]. RPE cells can release transforming growth factor- β which can stimulate production of collagen and fibronectin which in turn stimulates additional cell migration and proliferation thus continuing this vicious cycle [15]. Hyalocytes are mononuclear phagocytes (macrophages) that reside in the posterior vitreous cortex [see chapter II.D. Hyalocytes] that would be exposed to all these cytokine stimuli. Under the influence of the cytokine stimuli, all these cells migrate, proliferate, and, because they form membranes at the vitreoretinal interface,

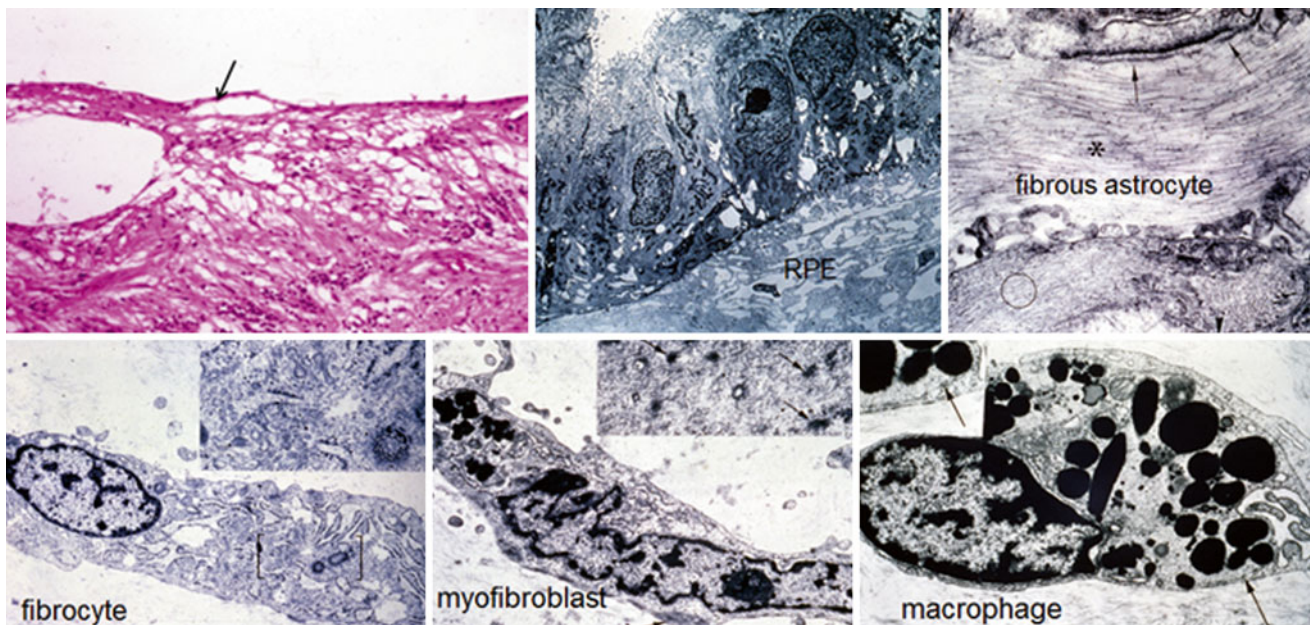


Figure III.J-8 Proliferative vitreoretinopathy (PVR) is composed of fibrocellular tissue (arrow, top left) on the inner surface of the retina. There may be up to five cell types in the tissue as shown, including RPE, fibrous astrocytes containing intermediate filaments (*) and patches of basement membrane (arrows, top right), fibrocytes including rough

endoplasmic reticulum and centrioles (between brackets in the lower left hand image), myofibroblasts containing intracytoplasmic fusiform densities (arrows), and macrophages with intracytoplasmic inclusions of varying electron density (arrows, lower right) (top left, H&E 63 \times ; other images uranyl acetate lead citrate 2,000 \times with insets 25,000 \times)

can contract and pull on the dense collagen matrix of the posterior vitreous cortex [see chapter II.E. Vitreo-retinal interface and ILM]. Eventually, this results in contraction of the PVR membranes in the posterior vitreous that mediates traction upon the retina leading to recurrent retinal detachment.

1. Cell Types in PVR

The main cell types involved in PVR formation are RPE cells, macrophages (including hyalocytes), fibroblasts, and glial cells [13], all noted to migrate into the vitreous and along the vitreoretinal interface following breakdown of the blood-retinal barrier (Figure III.J-9). Their response, typically seen in wound healing, leads to matrix and membrane formation, which leads to increasing traction on the retina and detachment.

a. Retinal Pigment Epithelial (RPE) Cells

RPE cells are postmitotic cells and serve the role of supporting photoreceptor cells. Following a retinal break, RPE cells migrate into the vitreous and form undifferentiated cells within the extracellular matrix (ECM) at the vitreoretinal interface. The RPE neural retinal adhesions and ECM adhesions are lost in the transformation process, and the RPE cells can undergo epithelial-mesenchymal transition and migrate into the vitreous, and also undergo metaplastic transformation [16]. This change of the RPE cells is influ-

enced by the change in environment and the rich abundance of growth factors and cytokines within the vitreous, such as PDGF, FGF, and IGF-1 produced by other cells such as Muller cells, macrophages, and fibroblasts which enter the vitreous via the retina break [17]. The transformed RPE cells lay down fibrotic membranes that form a thick contractile membrane, which leads to contraction and traction of the retina and to a recurrent retinal detachment (Figure III.J-10) [18]. Membrane peeling is usually needed in order to relieve traction and successfully reattach the retina [see chapter V.B.5. Surgical management of retinal detachment with PVR]. Furthermore, the loss of RPE cells also causes loss of support for the photoreceptors, leading to photoreceptor destruction [19].

b. Macrophages/Hyalocytes

Macrophages, including hyalocytes, have also been found to play a key role in the development of PVR (Figure III.J-11) [20]. Studies in rabbits have found that the injection of macrophages into the eyes of rabbits led to an inflammatory response similar to that seen in PVR and also the formation of fibrous membranes [20]. Macrophages are thought to play a multifactorial role, both through the secretion of cytokines and differentiation into fibroblast-like cells [20, 21]. Hyalocytes elicit monocyte migration from the circulation, which is augmented by the breakdown in the blood-ocular barrier that is well documented in PVR, further increasing

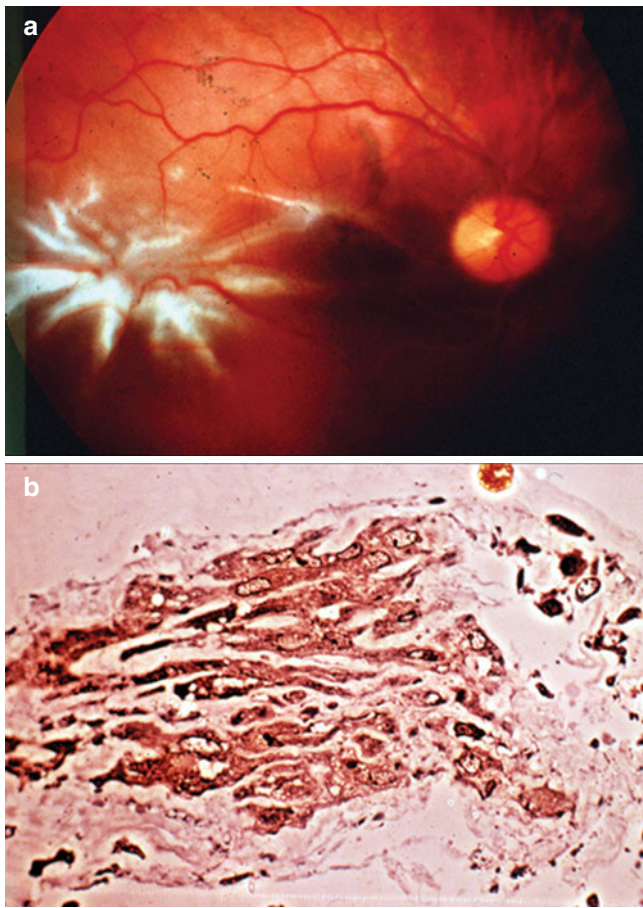


Figure III.J-9 (a) Clinical appearance of PVR causing fixed retinal folds, star folds, and a tractional retinal detachment. (b) Excised PVR membrane from patient shown in A demonstrates chord-like proliferations of cells that form gland-like structures in areas (H&E, 100×)

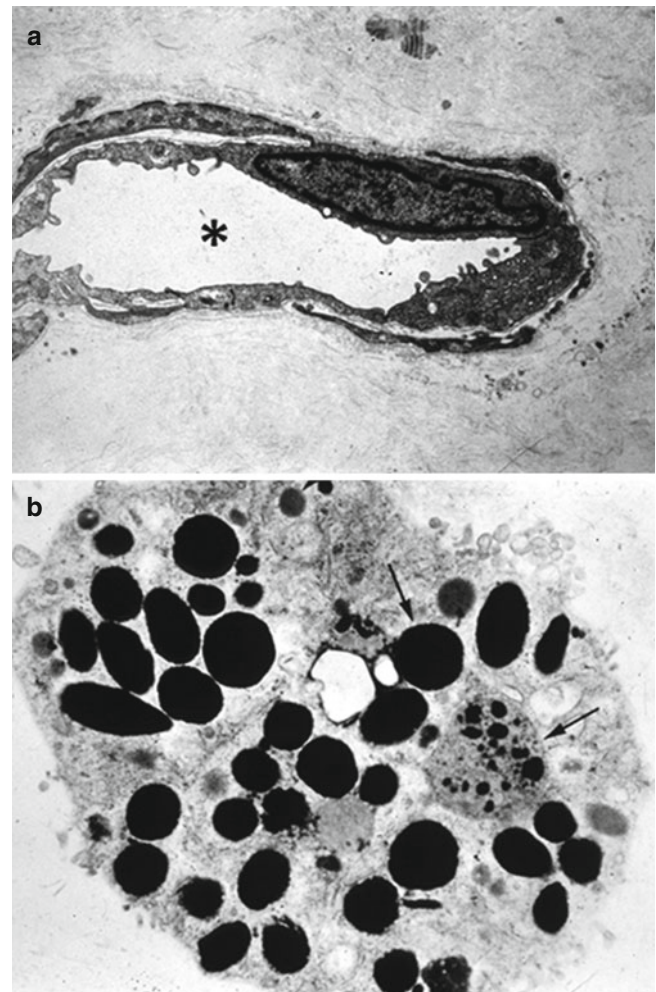


Figure III.J-11 (a) Endothelial-lined vascular channels surrounding a central lumen (*), sometimes surrounded by pericytes, may be found in PVR. (b) Macrophages may also be present in PVR. Macrophages contain intracytoplasmic inclusions of varying electron density (arrows) (uranyl acetate, lead citrate, 2,000×)

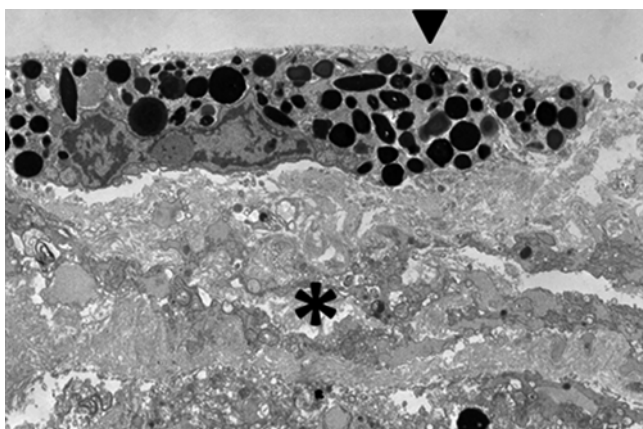


Figure III.J-10 Retinal pigment epithelium (RPE) is present on the surface of this PVR membrane. The RPE contains intracytoplasmic lancet-shaped melanin pigment granules and exhibits surface microvillous processes (black arrowhead). There are fibrocytes and collagen in the sub-RPE tissue (*) (uranyl acetate, lead citrate 2,000×)

the cell population that forms PVR membranes. The cytokines produced such as platelet-derived growth factor (PDGF) cause a change in the overall vitreous structure, leading to proteolysis and development of fibrous membranes [14]. The transformation of macrophages into fibroblast-like cells leads to further fibrosis and inflammatory changes within the vitreous.

c. Glial Cells

The glial cells mentioned above are actually activated Muller cells. The initial retinal break which triggers the proliferative and inflammatory response also activates Muller cells, the supporting cells of the retina. Activated Muller cells migrate into the vitreous and undergo proliferation and transformation at the vitreoretinal interface,

causing an increase in glial fibrillary acid protein (GFAP) and vimentin [22]. Activated Muller cells also have an increase in PDGFR- α production, a key cytokine in the pathogenesis process that will be discussed later. Muller cells have the plasticity and capacity to transform phenotypes, and this dedifferentiation and transformation helps to contribute to a change to the vitreous' overall environment and structure.

d. Myofibroblasts

Myofibroblasts also migrate into the vitreous following a break in the blood-retinal barrier. Possessing both contractile and fibroblast properties, myofibroblasts lead to an increase in the expression of α smooth muscle actin, imparting great contractile properties [23]. Myofibroblasts are also able to produce and secrete an extracellular matrix, especially collagen, that mediates the contractile properties within the proliferative membranes to the retina.

e. Immune Cells

There has, as it is basically an inflammatory response typically seen in wound repair also been speculation as to whether the immune system plays a role in PVR following injury anywhere in the body. However, studies using mouse models have found that PVR develops in mice in the absence of B or T cell immunity [24]. Thus, the immune system is not essential for the development of PVR, but the related cells and inflammatory/immune cytokines play essential roles.

2. Cytokines of PVR

The inciting event of the retinal break in PVR causes the retinal cell layer to come into contact with the vitreous, triggering RPE proliferation and migration into the vitreous. The transformation allows the activated RPE cells to secrete numerous proteins, components of the extracellular matrix, and cytokines. This different cytokines that are released into the vitreous and their roles in creating an inflammatory and fibrotic environment within the vitreous are discussed herein.

a. Tumor Necrosis Factor- α (TNF- α)

TNF- α is one of the cytokines released by the activated RPE cells and macrophages. Typically a marker in inflammation and wound healing, it activates the endothelial cells in the retina to produce leukocyte adhesion molecules, facilitating the influx of cells and the inflammatory response. Study has shown that TNF- α was found in the preretinal membrane of 22 out of 26 patients with PVR, and staining detected its presence within the extracellular matrix, showing its prominence and thus represents a potential subject for further research [25].

b. Transforming Growth Factor- β (TFG- β)

TFG- β is another cytokine that is found in elevated levels in the vitreous after retinal detachment. The second isoform TFG- β 2 is the most predominant form present and can elevate up to three times the normal amount in PVR. It is secreted into the vitreous by numerous cells, such as the ciliary body, macrophages, migrated RPE cells, and Muller cells [26]. TFG- β 2 helps to induce the epithelial-mesenchymal transformation of RPE cells into fibroblastic cells and also induces collagen synthesis in the transformed RPE cells. In addition, it increases RPE-mediated contraction leading to increase in fibrosis [15]. As discussed earlier, RPE cells play a crucial part in initiating fibrosis and formation of vitreoretinal membranes, and TFG- β 2 helps to induce RPE cells to take on fibroblastic characteristics and induce fibrosis.

c. Platelet-Derived Growth Factor Receptor- α (PDGFR- α)

PDGFR- α is garnering much attention in the field, since PDGFR- α is a key cytokine that is triggered in ocular injury. A chemoattractant and mitogen, it acts as a mediator of cellular contraction for RPE cells. There are 4 isoforms, with PDGFR- α C being the most predominant [27]. It is activated by PDGF but also by non-PDGR molecules such as insulin, epidermal growth factor (EGF), and hepatocyte growth factor (HGF). The activation of the receptor leads to suppression of P53, a key tumor suppressor gene, and increased proliferation, membrane formation, contraction, and survival. Research has shown that PDGFR- α is found in large quantities in rabbit models of PVR and that RPE and Muller cell interaction lead to a further upregulation of PDGFR- α and increased pathogenicity of Muller cells [28]. In addition, recent research has demonstrated that inhibition of PDGFR- α prevented PVR formation in a rabbit model [29]. Thus, targeting inhibition of PDGFR- α may lead to potential therapeutic agents in the future.

d. Miscellaneous Cytokines

Various other cytokines have also been shown to have roles in the proliferative and inflammatory processes. Activated RPE cells express *hepatocyte growth factor (HGF)*, which stimulates RPE migration [30]. Significantly elevated levels of *osteoponin*, *high-mobility group box-1 (HMBGB1)*, and *connective tissue growth factor (CTGF)* have also been found in PVR [31]. CTGF has been shown to be a potent stimulator of hyalocyte activity, particularly the induction of membrane contraction [see chapter II.D. Hyalocytes]. HMBGB1 has been shown to have angiogenic and fibrogenic effects. In vitro studies have shown that HMGB1 stimulated proliferation and migration of fibroblasts [32, 33]. CTGF is a downstream mediator of TGF- β and is a

mitogen and stimulated the formation of extracellular matrix. Potential therapeutic agents targeting this cytokine have also been found [34, 35]. Elevated levels of *pigment epithelium-derived factor (PEDF)* have also been found in the vitreous of patients with PVR compared to patients without PVR [31]. PEDF inhibits migration of endothelial cells which may account for the avascular nature of PVR membranes [31], a phenomenon observed in the human fetal vitreous during regression of the hyaloid vasculature [see chapter I.D. Vitreous proteomics and regression of the fetal hyaloid vasculature].

Monocyte chemoattractant protein-1 (MCP-1) has also been found at elevated levels in patients with PVR compared to no PVR [36–38]. Experimental retinal detachment induces increased MCP-1 expression in Müller cells and increased numbers of macrophages and microglial in detached retina [39]. MCP-1 also stimulates human RPE cell migration in vitro [40]. Mice with gene deficiencies in MCP-1 or the use of a MCP-1 blocking antibody greatly reduces macrophage and microglial response as well as photoreceptor apoptosis from the retinal detachment [39].

III. Treatment of PVR

A. Surgery of PVR

Currently the mainstay treatment for retinal detachment from PVR is surgery [see chapter V.B.5. Surgical management of retinal detachment with PVR]. Although successful reattachment occurs in 60–80 % of all cases, re-detachment is very common. [41] The main principles of treating recurrent retinal detachment from PVR include closing all retinal breaks, decreasing retinal traction, reattaching the retina, and minimizing recurrent traction. Decreasing traction on the retina can be achieved in several ways by membrane peeling, scleral buckling, debulking of the vitreous base, relaxing retinectomies [see chapter V.B.6. Retinectomy in recalcitrant retinal detachments], and internal tamponade. Often times, successful retinal reattachment requires a combination of the above techniques [see chapter V.B.5. Surgical management of retinal detachment with PVR].

B. Pharmacotherapy of PVR

Several studies are underway to identify patients at high risk for developing PVR so as to prevent PVR. Biomarkers are currently being utilized to study a myriad of disease processes. Studies have demonstrated that the use of a biomarker panel has the potential to predict PVR and having a favorable versus unfavorable outcome [42]. The panel of biomarkers

CCL22, IL-3, and MIF have been shown to have great potential in identifying patients at high risk for PVR with unfavorable outcomes [42]. Identifying high-risk groups is important, as early application of the agents discussed below to high-risk eyes may in fact prevent the development of PVR and subsequent need for multiple surgeries and visual compromise.

Several pharmacologic agents are being investigated in efforts to minimize recurrent retinal traction [see chapter IV.F. Pharmacotherapy of PVR]. Current research is being conducted to study potential targets in the inflammatory pathway, and different medications are being tested in animal trials and small human trials. Antibodies targeting the PDGFR pathway have been used in rabbit models, but yielding mixed results, as PDGF has been shown to be inhibited but not PVR [43]. However, *n-acetylcysteine (NAC)*, an antioxidant against reactive oxygen species, has been shown to prevent the activation of PDGFR in rabbit models and reduced the overall inflammatory response seen in prPVR [1]. Overall, results showed that NAC suppressed PDGFR receptor activation and retinal detachment, making it a potential candidate for pharmacological therapy.

Existing medications have also been studied for their potential in preventing or decreasing PVR. *5-FU (5-fluorouracil)*, a chemotherapy agent, has been shown to inhibit fibroblast formation. Human trials using 5-FU for PVR have yielded mixed results thus far [44]. The efficacy of *low-molecular-weight heparin (LMWH)* has also been studied [45]. LMWH has been shown to bind to fibronectin, FGF, and PDGFR. One study of 174 high-risk patients found the combination of 5-FU and LMWH reduced the incidence of PVR and reoperation rate, but had no change in overall visual acuity [44]. Although these results are very promising, the combination is currently not widely used in the clinical setting.

13-cis-retinoic acid is another agent currently being studied as a potential agent against PVR. In vitro studies have shown that 13-cis-retinoic acid is capable of inhibiting RPE proliferation [46]. A recent clinical trial of 35 patients showed that the use of retinoic acid in the treatment group resulted in significantly lower rates of macular traction and pucker and better visual acuity compared to the control group [47].

Nutlin 3 is another agent studied. This molecule is known to inhibit the MDM2/p53 interaction and thus preventing P53 decline [48]. Studies have shown that the application of nutlin to cells isolated from the PVR membranes of patients prevented cell contraction [29]. Suppression of P53 has been found to be required in the PDGFR- α activation, which results in contraction of cells and inflammatory changes. Thus, P53 is thought to be a checkpoint in PVR and is becoming an area of active research within the field.

Recent studies have also focused on new routes of delivery of medications and antimetabolites into the retina for prevention of PVR. A study using porcine eyes showed that the use of aerosolized nanoparticles during vitrectomy is a potential method for delivering antimetabolites to the retina in the future [49].

Abbreviations

5-FU	5-fluorouracil
CCL22	Chemokine cluster locus 22
CTGF	Connective tissue growth factor
ECM	Extracellular matrix
EGF	Epidermal growth factor
FGF	Fibroblastic growth factor
GFAP	Glial fibrillary acidic protein
HGF	Hepatocyte growth factor
HMBGB1	High-mobility group box-1
IGF1	Insulin-like growth factor 1
IL-3	Interleukin 3
LMWH	Low-molecular-weight heparin
MCP1	Monocyte chemotactic protein-1
MDM2	Mouse doubling minute homologue 2
NAC	n-acetylcysteine
PDGF	Platelet-derived growth factor
PDGFR- α	Platelet-derived growth factor alpha
PEDF	Pigment epithelium-derived factor
PVR	Proliferative vitreoretinopathy
RPE	Retinal pigment epithelium
RRD	Recurrent retinal detachment
TGF- β	Transforming growth factor beta
TNF- α	Tumor necrosis factor alpha

References

- Lei H, Velez G, Cui J, et al. N-acetylcysteine suppresses retinal detachment in an experimental model of proliferative vitreoretinopathy. *Am J Pathol.* 2010;177(1):132–40.
- Pastor JC. Proliferative vitreoretinopathy: an overview. *Surv Ophthalmol.* 1998;43(1):3–18.
- Aylward W. *Ophthalmology*, chapter 6.41. In: *Proliferative vitreoretinopathy*. 3rd ed. New York, NY: Elsevier Inc.;2009.
- Smiddy W, Michels R, Green R. Morphology, pathology, and surgery of idiopathic vitreoretinal macular disorders. *Retina.* 1990;10(4):288–96.
- Cowley M, Conway BP, Campochiaro PA, et al. Clinical risk factors for proliferative vitreoretinopathy. *Arch Ophthalmol.* 1989;107(8):1147–51.
- Lean JS, Stern WH, Irvine AR, et al. Classification of proliferative vitreoretinopathy used in the silicone study. *The Silicone Study Group. Ophthalmology.* 1989;96(6):765–71.
- Asaria RH, Kon CH, Bunce C, et al. How to predict proliferative vitreoretinopathy: a prospective study. *Ophthalmology.* 2001;108(7):1184–6.
- The Classification of retinal detachment with proliferative vitreoretinopathy. *Ophthalmology.* 1983;90(2):121–25.
- Schwartz D, De La Cruz ZC, Green WR, Michels RG. Proliferative vitreoretinopathy: ultrastructural study of 20 retroretinal membranes removed by vitreous surgery. *Retina.* 1988;8:275–81.
- Sadaka A, Giuliari GP. Proliferative vitreoretinopathy: current and emerging treatments. *Clin Ophthalmol.* 2012;6:1325–31.
- Machemer R, Aaberg TM, Freeman HM, et al. An updated classification of retinal detachment with proliferative vitreoretinopathy. *Am J Ophthalmol.* 1991;112(2):159–65.
- Campochiaro P, Kaden I, Vidaurri-Leal J, Glaser B. Cryotherapy enhanced intravitreal dispersion of viable retinal pigment epithelial cells. *Arch Ophthalmol.* 1985;103(3):434–6.
- Vinore SA, Campochiaro PA, Conway BP. Ultrastructural and electron- immunocytochemical characterization of cells in epiretinal membranes. *Invest Ophthalmol Vis Sci.* 1990;31(1):14–28.
- Muhar HS, Pollock RA, Wang C, et al. PDGF and its receptors in the developing rodent retina and optic nerve. *Development.* 1993;118(2):539–52.
- Yokoyama K, Kimoto K, Itoh Y, et al. The PI3K/Akt pathway mediates the expression of type I collagen induced by TGF- β 2 in human retinal pigment epithelial cells. *Graefes Arch Clin Exp Ophthalmol.* 2012;250(1):15–23.
- Du YH, Hirooka K, Miyamoto O, et al. Retinoic Acid suppresses the adhesion and migration of human retinal pigment epithelial cells. *Exp Eye Res.* 2013;109:22–30.
- Wiedemann P. Growth factors in retinal diseases: proliferative vitreoretinopathy, proliferative diabetic retinopathy, and retinal degeneration. *Surv Ophthalmol.* 1992;36(5):373–84.
- Umazume K, Barak Y, McDonald K, et al. Proliferative Vitreoretinopathy in the Swine- a new model. *Invest Ophthalmol Vis Sci.* 2012;53(8):4910–6.
- Bhutto I, Luttly G. Understanding age-related macular degeneration (AMD): relationships between the photoreceptor/retinal pigment epithelium/Bruch's membrane/choriocapillaris complex. *Mol Aspects Med.* 2012;33(4):295–317.
- Lin ML, Li YP, Li ZR, et al. Macrophages acquire fibroblast characteristics in a rat model of proliferative vitreoretinopathy. *Ophthalmic Res.* 2011;45(4):180–90.
- Kirchhof B, Sorgente N. Pathogenesis of proliferative vitreoretinopathy. Modulation of retinal pigment epithelial cell functions by vitreous and macrophages. *Dev Ophthalmol.* 1989;16:1–53.
- Okada M, Matsumura M, Ogino N, Honda Y. Muller cells in detached human retina express glial fibrillary acidic protein and vimentin. *Graefes Arch Clin Exp Ophthalmol.* 1990;228(5):467–74.
- Wynn TA. Cellular and molecular mechanisms of fibrosis. *J Pathol.* 2008;214(2):199–210.
- Zhang W, Tan J, Liu Y, et al. Assessment of the innate and adaptive immune system in proliferative vitreoretinopathy. *Eye.* 2010;26(6):872–81.
- Limb GA, Alam A, Earley O, et al. Distribution of cytokine proteins within epiretinal membranes in proliferative vitreoretinopathy. *Curr Eye Res.* 1994;13(11):791–8.
- Tanihara H, Yoshida M, Matsumoto M, Yoshimura N. Identification of transforming growth factor-beta expressed in cultured human retinal pigment epithelial cells. *Invest Ophthalmol Vis Sci.* 1993;34(2):413–9.
- Moysidis SN, Thanos A, Vavvas DG. Mechanisms of inflammation in proliferative vitreoretinopathy: from bench to bedside. *Mediators Inflamm.* 2012;2012:815937. doi:10.1155/2012/815937. Epub 2012 Sep 25.
- Velez G, Weingarden A, Tucker B, et al. Retinal pigment epithelium and muller progenitor cell interaction increase muller progenitor cell expression of PDGFR alpha and ability to induce proliferative vitreoretinopathy in a rabbit model. *Stem Cells Int.* 2012;2012:106486. doi:10.1155/2012/106486.

29. Lei H, Rheaume M, Cui J, et al. A novel function of P53, a gate-keeper of retinal detachment. *Am J Pathol.* 2012;181(3):866–74.
30. He P, He S, Garner J, et al. Retinal pigment epithelial cells secrete and respond to hepatocyte growth factor. *Biochem Biophys Res Commun.* 1998;249(1):253–7.
31. El-Asrar AM, Nawaz MI, Kangave D, et al. Osteopontin and other regulators of angiogenesis and fibrogenesis in the vitreous from patients with proliferative vitreoretinal disorders. *Mediators Inflamm.* 2010;2012:493043.
32. Yoshizaki A, Komura K, Iwata Y, et al. Clinical Significance of serum HMGB-1 and sRAGE levels in systemic sclerosis: association with disease severity. *J Clin Immunol.* 2009;29(2):180–9.
33. Ranzato E, Patrone M, Pedrazzi M, Burlando B. HMGB1 Promotes Wound healing of 3 T3 mouse fibroblasts via RAGE-dependent ERK1/2 activation. *Cell Biochem Biophys.* 2010;57(1):9–17.
34. Blom I, Goldschmeding R, Leask A. Gene regulation of connective tissue growth factor: new targets for antifibrotic therapy? *Matrix Biol.* 2002;21(6):473–82.
35. Shimo T, Nakanishi T, Nishida T, et al. Connective tissue growth factor induces the proliferation, migration, and tube formation of vascular endothelial cells in vitro, and angiogenesis in vivo. *J Biochem.* 1999;126(1):137–45.
36. Elner SG, Elner VM, Jaffe GJ, et al. Cytokines in proliferative diabetic retinopathy and proliferative vitreoretinopathy. *Curr Eye Res.* 1995;14(11):1045–53.
37. El-Asrar AM, Van Damme J, Put W, et al. Monocyte chemoattractant protein-1 in proliferative Vitreoretinal disorders. *Am J Ophthalmol.* 1997;123(5):599–606.
38. Capeans C, De Rojas MV, Lojo S, et al. C-C chemokines in the vitreous of patients with proliferative vitreoretinopathy and proliferative diabetic retinopathy. *Retina.* 1998;18(6):546–50.
39. Nakazawa T, Hisotomi T, Nakazawa C, et al. Monocyte chemoattractant protein 1 mediates retinal detachment-induced photoreceptor apoptosis. *Proc Natl Acad Sci U S A.* 2007;104(7):2425–30.
40. Han QH, Hui YN, Du HJ, et al. Migration of retinal pigment epithelial cells in vitro modulated by monocyte chemotactic protein-1: enhancement and inhibition. *Graefes Arch Clin Exp Ophthalmol.* 2001;239(7):531–8.
41. Capeans C, Lorenzo J, Santos L, et al. Comparative study of incomplete posterior vitreous detachment as a risk factor for proliferative vitreoretinopathy. *Graefes Arch Clin Exp Ophthalmol.* 1998;236(7):481–5.
42. Ricker LJ, Kessels AG, de Jager W, et al. Prediction of proliferative vitreoretinopathy after retinal detachment surgery: potential of biomarker profiling. *Am J Ophthalmol.* 2012;154(2):347–54.
43. Lei H, Velez G, Hovland P, et al. Growth factors outside the PDGF family drive experimental PVR. *Invest Ophthalmol Vis Sci.* 2009;50(7):3394–403.
44. Asaria R, Kon C, Bunce C, et al. Adjuvant 5-fluorouracil and heparin prevents proliferative vitreoretinopathy. *Ophthalmology.* 2001;108(7):1179–83.
45. Kumar A, Nainiwal S, Sreenivas B. Intravitreal low molecular weight heparin in PVR surgery. *Indian J Ophthalmol.* 2003;51(1):67–70.
46. Wu W, Hu D, Mehta S, Chang Y. Effects of retinoic acid on retinal pigment epithelium from excised membranes from proliferative vitreoretinopathy. *J Ocul Pharmacol Ther.* 2005;21(1):44–54.
47. Chang Y, Hu D, Wu W. Effect of oral 13-cis-retinoic acid treatment on postoperative clinical outcome of eyes with proliferative vitreoretinopathy. *Am J Ophthalmol.* 2008;146(3):440–6.
48. Prives C. Signaling to P53: breaking the MDM2-p53 circuit. *Cell.* 1998;95(1):5–8.
49. Zhang G, Feng X, Wabner K, et al. Intraocular nanoparticle drug delivery: a pilot study using an aerosol during pars plana vitrectomy. *Invest Ophthalmol Vis Sci.* 2007;48(11):5243–9.

Gabriele E. Lang

Outline

- I. **Introduction**
 - A. Retinal Vein Occlusion
 - 1. Definition
 - 2. Epidemiology
 - 3. Pathogenesis and Risk Factors
 - 4. Clinical Classification
 - 5. Symptoms
 - 6. Complications
 - B. Diabetic Macular Edema
 - 1. Definition
 - 2. Epidemiology
 - 3. Pathogenesis and Risk Factors
 - 4. Clinical Classification
 - 5. Symptoms
- II. **Role of Vitreous in RVO and DME**
 - A. Biochemical Role of Vitreous
 - 1. Inflammatory and Angiogenic Proteins in Vitreous
 - 2. Crystallin in Vitreous after Ischemia-Reperfusion Injury
 - B. Structural Role of Vitreous
 - 1. Vitreous Attachment in RVO
- III. **Role of Vitreous in Diabetic Macular Edema**
 - A. Structural
 - 1. Vitreous Detachment and Vitreoschisis in DME
 - 2. Vitreo-Retinal Interface in DME
 - B. Biochemistry of Vitreous in DME
 - 1. Advanced Glycation End Products in DME
 - 2. Inflammatory Factors in Vitreous of DME

References

G.E. Lang, MD
Department of Ophthalmology, University Eye Hospital Ulm,
Prittowitzstr. 43, Ulm, D-89075, Germany
e-mail: gabriele.lang@uniklinik-ulm.de

Keywords

Vitreous • Diabetes • Hypertension • Diabetic retinopathy • Diabetic vitreopathy • Retinal vein occlusions • Macular edema • Diabetic macular edema • Cytokines • Vitreoschisis

Key Concepts

1. Vitreous is a reservoir for different growth factors and cytokines involved in the development of macular edema in retinal vein occlusions and diabetic retinopathy. Pro-inflammatory factors are involved in the breakdown of the blood-retinal barrier. Growth factor and cytokine levels are increased in the vitreous of patients with macular edema due to retinal vein occlusions and diabetic retinopathy.
2. The structure of the vitreous plays a pathogenic role in the development of macular edema in diabetic retinopathy and retinal vein occlusion. There is evidence that vitreomacular adhesion is more common in those diseases in comparison to age-matched controls. In eyes with vitreomacular adhesion, the incidence of macular edema is higher.
3. In diabetic vitreopathy, advanced glycation end products cause cross-linking of collagen, increasing the adhesion of the posterior vitreous cortex to the inner limiting membrane, which can be associated with neurovascular injury and contribute to diabetic macular edema.

I. Introduction

A. Retinal Vein Occlusion

Retinal vein occlusion (RVO), the second most common retinal vascular disease after diabetic retinopathy, is a prevalent cause of vision loss.

1. Definition

Due to an obstruction of retinal veins and impaired blood outflow, vascular and tissue damage occurs upstream of the site of occlusion leading to retinal edema, hemorrhages, and ischemia. Depending on the occlusion site, central retinal vein occlusion (CRVO) (Figure III.K-1a), hemi-retinal vein occlusion (HRVO), and branch retinal vein occlusion

(BRVO) are differentiated. In CRVO the retinal tissue in all four quadrants and often the optic nerve are affected, while in BRVO only part of the venous circulation according to the occluded branch is compromised. Typical clinical findings are hemorrhages in the area of the occluded vessel, macular edema (Figure III.K-1b), and optic disc edema.

2. Epidemiology

Globally an estimated 2.5 million are affected by CRVO and 13.9 million by BRVO [1]. CRVO and BRVO occur in middle-aged and older people. The mean age of CRVO patients is 60–70 years. Males and females are equally affected. The prevalence of RVO in people over 40 years of age ranges from 0.3 to 2.1 %. RVO may occur in up to 5 % of individuals over 80 years of age [2]. The incidence of BRVO is 0.5–1.2 % [3].

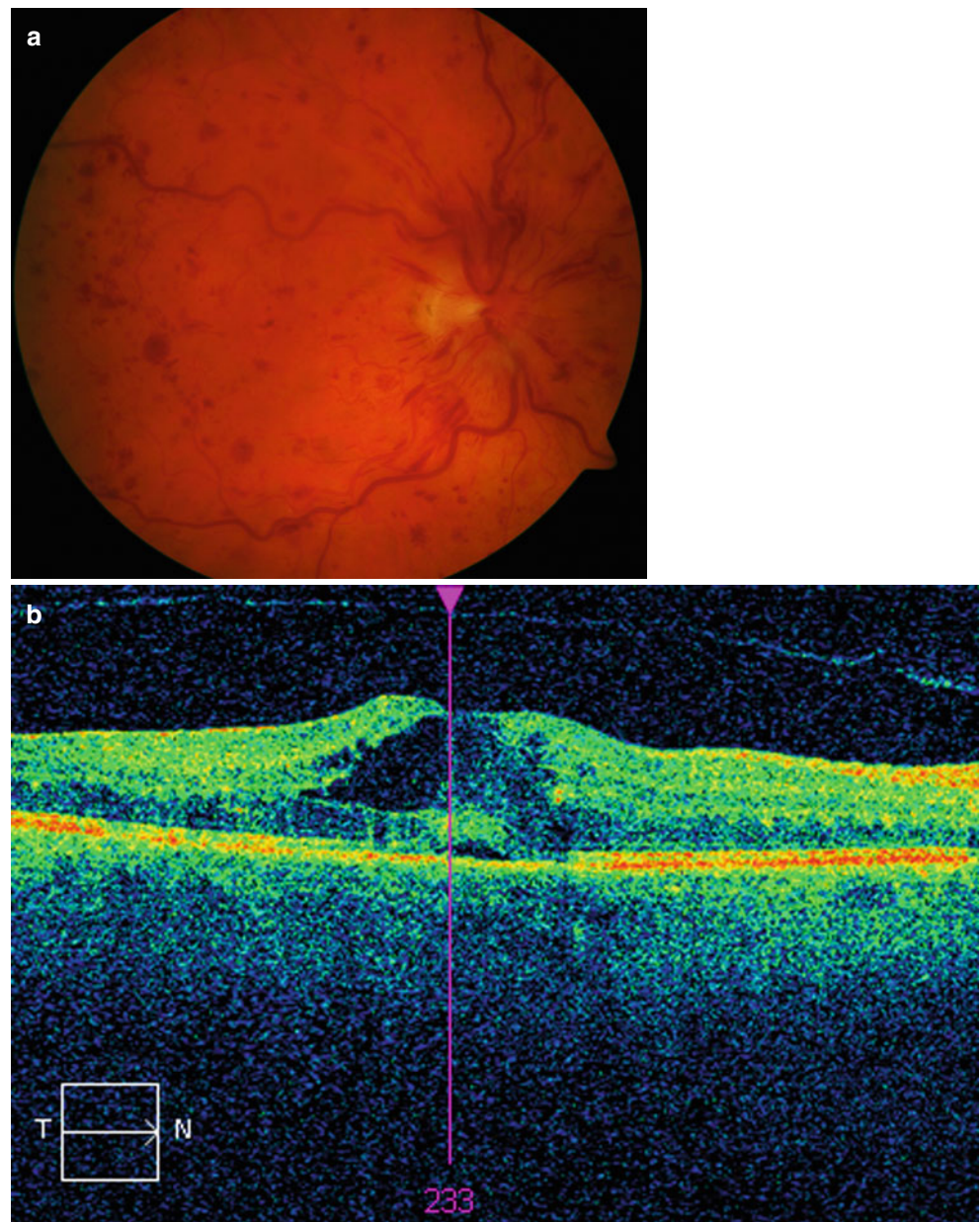


Figure III.K-1 (a) Central retinal vein occlusion with intraretinal hemorrhages and cystoid macular edema. (b) OCT: cystoid macular edema and posterior vitreous detachment

3. Pathogenesis and Risk Factors

The primary mechanisms which lead to RVO are compression of the vein by a sclerotic artery, degenerative changes of the vessel wall, glial cell proliferation, and hematological abnormalities. Numerous underlying diseases are known to be involved in the multifactorial pathogenesis of RVO, like arterial hypertension, cardiovascular diseases, diabetes mellitus, hyperlipidemia, hypercoagulation, thrombophilia, and inflammatory diseases. Systemic risk factors predisposing to RVO are independently associated with atherosclerosis [3, 4].

The initiating event of RVO is usually a thrombus formation in the vein, either resulting from compression by a sclerotic artery, degenerative or inflammatory alterations, or hemodynamic disorders. This leads to an increased intraluminal pressure resulting in extravasation of blood components. Secondary inflammatory processes and overexpression of cytokines play an important role in the course of the disease.

4. Clinical Classification

Two different types are distinguished angiographically, a perfused (non-ischemic) type and a non-perfused (ischemic) type. In CRVO the perfused type is any case which has less than 10 disc areas of non-perfusion, while in BRVO less than 5 disc areas of non-perfusion on fluorescein angiography is considered non-ischemic. If the area of non-perfusion is larger than 10 and 5 disc areas, respectively, it is considered a non-perfused type, according to the classification of the Central Retinal Vein Occlusion Study [5] and Branch Retinal Vein Occlusion Study [6].

5. Symptoms

The typical symptom is blurred vision most often caused by macular edema (Figure III.K-1b). Baseline visual acuity in CRVO and BRVO ranges on average from 20/40 to less than 20/200. In a recent study, the average visual acuity in ischemic BRVO is 20/50 and in non-ischemic types 20/60 [3].

6. Complications

The most common complications in RVO leading to visual deterioration are macular edema (Figure III.K-1b) and neovascularization. Macular edema is the most common reason for visual loss in BRVO [3] followed by neovascularization, neovascular glaucoma, vitreous hemorrhage, and tractional retinal detachment.

B. Diabetic Macular Edema

Diabetic macular edema (DME) is a common complication of diabetes mellitus. It is a chronic, progressive disease and leads to visual impairment (Figure III.K-2a, b).

1. Definition

DME is caused by accumulation of fluid in and under the neurosensory retina in the macular area (Figure III.K-2b). It is caused by the disruption of the blood-retinal barrier. The extracellular accumulation of fluid can lead to cystoid changes (Figure III.K-2b) especially in the chronic form of diabetic macular edema.

2. Epidemiology

It is estimated that up to 24 % of diabetic patients develop DME. According to the results of the Wisconsin Epidemiologic Study of Diabetic Retinopathy [7], the 25-year cumulative incidence of DME in type 1 diabetic patients is 29 %. Petrella et al. [8] found in a Canadian cohort a prevalence of DME of 15.7 % and prevalence of visual impairment due to DME of 2.56 %. The overall prevalence for any diabetic retinopathy is 34.6 %, for proliferative diabetic retinopathy 6.96 %, for DME 6.81 %, and for vision threatening diabetic retinopathy 10.2 %. Levels are higher in type 1 in comparison to type 2 diabetes [9].

3. Pathogenesis and Risk Factors

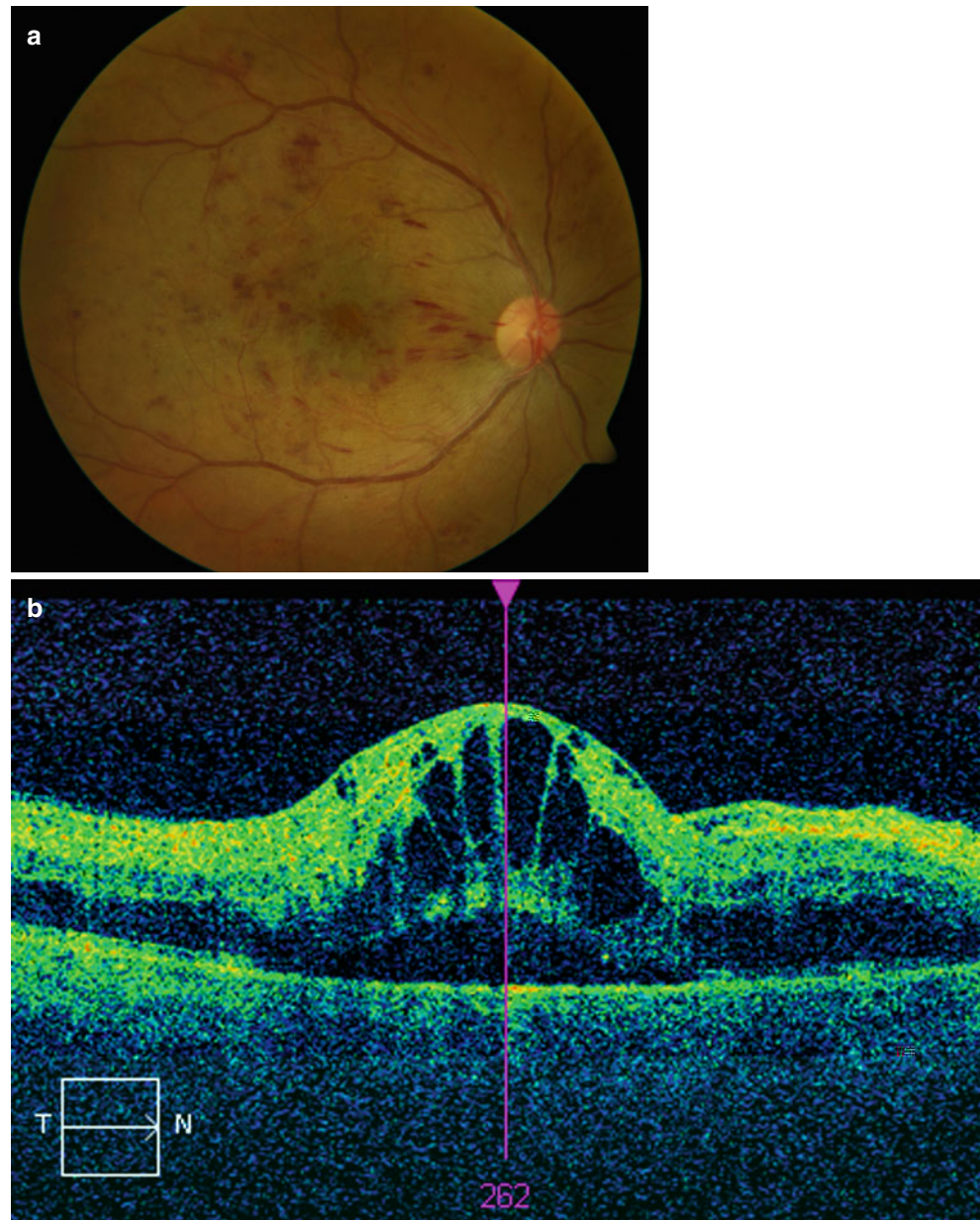
The pathogenesis of DME is rather complex. Several cellular pathways are activated which is mediated by hyperglycemia. This results in microvascular damage of the retina. The major causes are increased formation of advanced glycation end products, activation of polyol pathway and protein kinase C, and increased hexosamine pathway flux. Oxidative stress and inflammation also contribute to the development of diabetic retinopathy.

4. Clinical Classification

The most common classification of DME is focal and diffuse; however, the terms are used differently [10]. The most often used terminology worldwide is based on the source of fluorescein leakage. In the ETDRS, the source of fluorescein leakage was graded as *focal*, when ≥ 67 % of leakage was associated with microaneurysms, *intermediate* for 33–66 %, and *diffuse* for those with < 33 % [10]. Often the DME has features of both forms making a clear distinction difficult. Focal DME has been associated with better visual acuity, less macular thickening, and less severe diabetic retinopathy [10]. With respect to response to therapy, there are no differences between diffuse or focal DME in the subgroup analyses concerning laser or anti-VEGF treatment.

Other classifications based on ophthalmoscopy, fundus photography, fluorescein angiography, and optical coherence tomography are suggested by different groups; however, there is no broad consensus on these proposed classifications. However, with new treatment options, there may in the future need to be a new classification system based upon other criteria. The extent and location of retinal thickening (due to intraretinal and subretinal fluid accumulation and cystoid lesions) seem to be more meaningful than fluorescein

Figure III.K-2 (a) Diabetic retinopathy with cystoid macular edema. (b) OCT: cystoid macular edema, subretinal fluid, posterior vitreous attached, premacular membrane



angiographic findings. Another important factor is central macular involvement, which leads to visual impairment. The vitreoretinal interface also plays an important role, especially if vitreous detachment (Figure III.K-2b), vitreomacular traction, or premacular membranes (Figure III.K-3a–d) are involved in the pathogenesis of DME.

5. Symptoms

DME is often asymptomatic, as long as the center of the macula (fovea) is not involved. If central retinal thickening with intraretinal or subretinal fluid accumulation (Figure III.K-2a, b) develops, the patients become symptomatic. Typical symptoms are blurred vision, metamorphopsia, and if severe, central scotoma. Severe vision loss in DME can also be due to ischemic maculopathy. If massive diffuse DME is present, fibrosis and scarring can lead to permanent visual loss.

II. Role of Vitreous in RVO and DME

The role of the vitreous is getting increasingly into focus in the pathogenesis and course of retinal vein occlusions and diabetic macular edema and the development of complications in retinal vascular diseases.

A. Biochemical Role of Vitreous

Vitreous is a reservoir for different growth factors and cytokines. This knowledge is important to understand the role of the vitreous in the pathogenesis of macular edema in RVO as well as DME and for the development of new treatment strategies. For example, the upregulation of pro-inflammatory factors, which are found in the vitreous, are involved in the

leukocyte-endothelial interaction and the breakdown of the blood-retinal barrier. These factors are produced by retinal cells such as Müller cells and retinal pigment epithelial cells.

1. Inflammatory and Angiogenic Proteins in Vitreous

Inner retinal layers, which are supplied by the retinal arteries, show a high sensitivity to hypoxia. RVO and diabetic retinopathy are common causes of retinal hypoxia. The retinal tissue has protective mechanisms against ischemia like vessel dilation and angiogenesis. Under hypoxic condition, overexpressed soluble growth factors, cytokines, and chemokines

are secreted into the vitreous. Cytokines normally serve as signals between neighboring cells. They are involved in all biological processes including angiogenesis and inflammation. Chemokines are involved in the recruitment of leukocytes to inflammatory processes [11]. Therefore, research on the role of pro-inflammatory and angiogenic proteins in vitreous is becoming increasingly interesting in patients with RVO and DME.

Koss et al. [12] studied human vitreous fluids with cytometric bead array (CBA) technology that provides a quantitative analysis of multiple markers and requires smaller sample volume in contrast to enzyme-linked immunosorbent

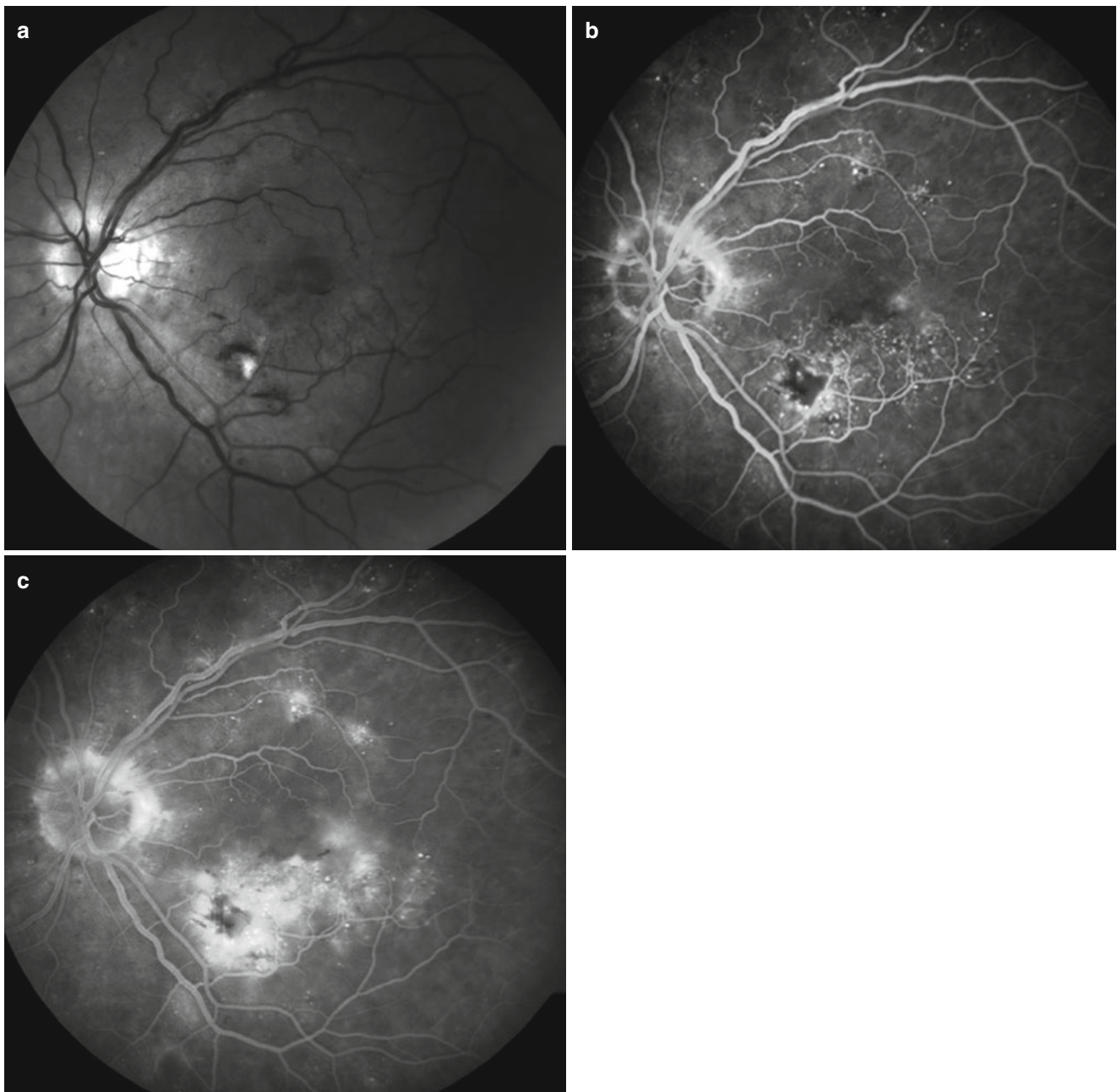


Figure III.K-3 (a) Diabetic retinopathy with cystoid macular edema. (b) Early frame fluorescein angiography diabetic retinopathy. (c) Late frame fluorescein angiography, dye leakage

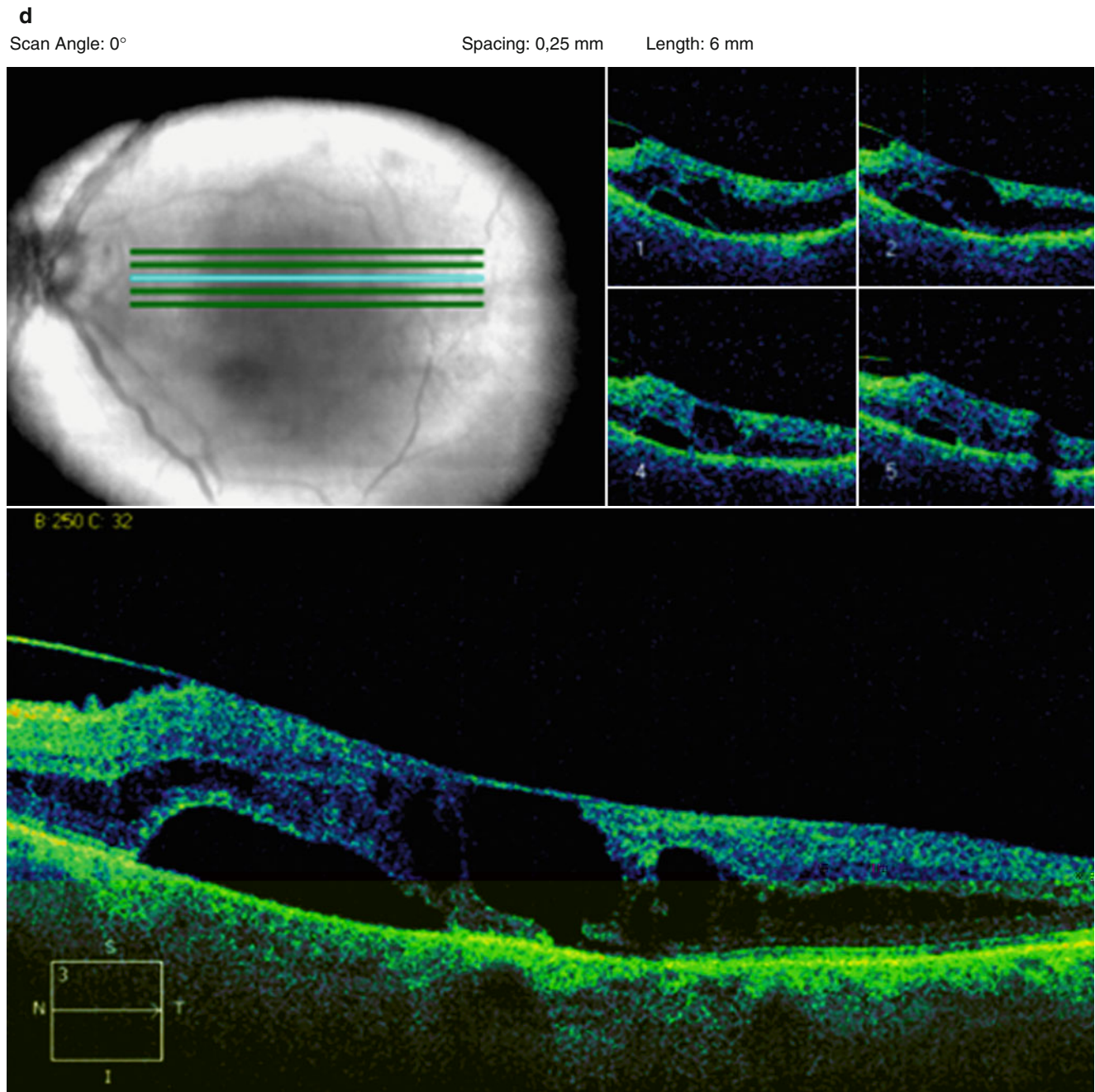


Figure III.K-3 (continued) (d) OCT: vitreomacular traction caused by premacular membrane

assay (ELISA). CBA is cost- and time-effective. It is an analytical tool that is based on flow cytometry and correlates well to ELISA. The non-diluted vitreous samples of three patients with CRVO with a history of 11 ± 3 weeks and mean central macular thickness of $557 \pm 125 \mu\text{m}$ and three patients with diabetic macular edema (DME) with a mean central macular thickness of $508 \pm 108 \mu\text{m}$ and six patients with age-related macular degeneration (AMD) with active occult choroidal neovascularization were studied. A core pars plana vitrectomy was performed for sample collection. A total of

0.6 ml mid- and posterior undiluted vitreous were aspirated for CBA analysis, half of it being analyzed fresh and half of it as frozen sample. The tested cytokines were interleukin 6 (IL-6), vascular endothelial growth factor (VEGF), and monocyte chemotactic protein 1 (MCP-1) [12]. In the fresh samples, IL-6 was highest in the CRVO group (median 55.8 pg/mL) followed by DME (50.6 pg/mL) and lowest in AMD (3.1 pg/mL). VEGF also was highest in CRVO (447.4 pg/mL), followed by DME (3.9 pg/mL) and AMD (2.0 pg/mL). MCP-1 again was highest in CRVO (595.7 pg/

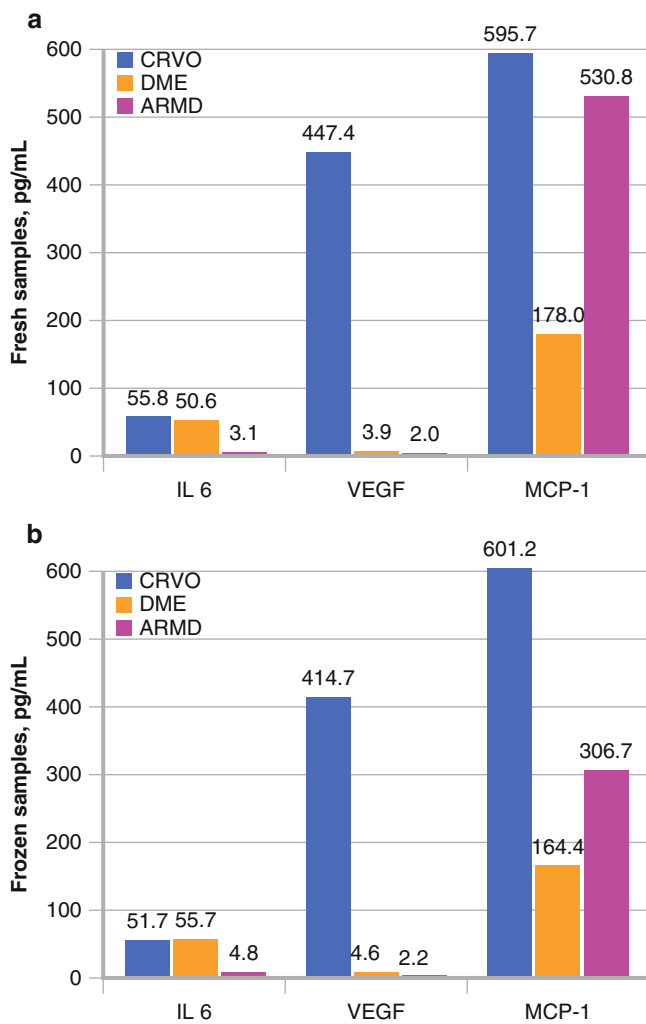


Figure III.K-4 Cytokine levels in human vitreous obtained from patients with age-related macular degeneration (ARMD), diabetic macular edema (DME), and central retinal vein occlusion (CRVO). The top graph (a) shows results for fresh vitreous samples, while the bottom graph (b) is data from frozen vitreous samples

mL) followed by AMD (530.8 pg/mL) and DME (178 pg/mL). In the frozen samples, IL-6 highest median levels were found in DME (55.7 pg/mL), followed by CRVO (51.7 pg/mL) and AMD (4.8 pg/mL). VEGF was highest in CRVO (414.7 pg/mL), followed by DME (4.6 pg/mL), and AMD (2.2 pg/mL). MCP-1 was highest in CRVO (601.2 pg/mL), followed by AMD (306.7 pg/mL) and DME (164.4 pg/mL). The study was primarily intended to evaluate the feasibility of CBA in the vitreous. The increased levels of VEGF, IL-6, and MCP-1 indicate their role in the pathogenesis of macular edema in RVO and DME [12].

Different molecules in the vitreous may influence the course of RVO. Molecules of interest are vascular endothelial growth factor (VEGF), soluble intercellular adhesion molecule 1 (sICAM-1), and pigment epithelial-derived factor (PEDF). Noma et al. [13] investigated the association

of inflammatory vitreous factors with macular edema in BRVO. They compared vitreous fluid levels of VEGF, soluble VEGF receptor 2 (sVEGFR-2), interleukin 6 (IL-6), pigment epithelial-derived factor (PEDF), sICAM-1, monocyte chemoattractant protein 1 (MCP-1), and pentraxin 3 (PTX-3) were measured by enzyme-linked immunosorbent assay from vitreous of patients with BRVO and compared to the vitreous of patients with macular hole. PEDF has anti-inflammatory and antiangiogenic properties in contrast to the other studied pro-inflammatory factors. The vitreous levels of VEGF, sVEGFR-2, IL-6, sICAM-1, MCP-1, and PTX-3 were significantly higher in the BRVO group compared to controls. PEDF, a protective growth factor, was significantly lower in comparison to the control group. Vitreous levels were all significantly correlated with the retinal thickness at the central foveal area measured by optical coherence tomography. This implies that these factors are correlated with the permeability of the retinal vessels and the severity of macular edema.

Noma et al. [14] also investigated whether vitreous fluid levels of sVEGFR-2, sICAM-1, and PEDF were associated with the occurrence of serous retinal detachment in CRVO. They compared 18 eyes with serous retinal detachment to 15 eyes with cystoids macular edema in CRVO and 18 controls with nonischemic ocular diseases. Retinal ischemia was significantly more common in the group with serous retinal detachment in comparison to cystoid macular edema. The vitreous fluid levels of sICAM-1 increased significantly across the three groups studied from 4.98 ng/ml in the control group to 15.4 ng/ml in the cystoid macular edema group to 21.7 ng/ml in the serous detachment group. The same was found for sVEGFR-2 showing significant increase across the groups. The vitreous fluid levels of PEDF, however, showed a significant decrease across the three groups (56.4 versus 24.3 and 16.4 ng/ml, respectively). These results indicate that inflammatory changes in the retina and vitreous play a significant role in the development of macular edema in CRVO. The authors also found that VEGF and IL-6 are involved in the development of serous detachment in CRVO and that ischemia was related to serous retinal detachment in CRVO. In addition findings related to sICAM-1 were increased vascular permeability and more severe ischemia.

Koss et al. [15] analyzed undiluted vitreous cytokine levels of untreated patients with CRVO, HRVO, and BRVO. 43 BRVO, 35 CRVO, and 16 HRVO patients underwent vitrectomy and application of bevacizumab and dexamethasone treatment for macular edema. IL-6, VEGF, and MCP-1 were measured with cytometric bead array (CBA). Vitreous samples from patients with premacular membranes and macular pucker served as control. The mean cytokine values (pg/ml) were highest in CRVO (IL-6 64.7, VEGF-A 211.5, MCP-1 1015.8) followed by HRVO (IL-6 59.9, VEGF-A 211.5, MCP-1 938.8) and BRVO (IL-6 23.3, VEGF 161.8, MCP-1 602.6). The values of VEGF-A and MCP-1 were significantly

higher in the CRVO or HRVO versus the BRVO group. All cytokine values were significantly higher than those of the control group (IL-6 6.2, VEGF-A 7, MCP-1 253). In RVO older than 7 months, only MCP-1 was significantly higher in CRVO or HRVO versus the BRVO. This indicates that monocyte recruitment to the vessel wall in tissue remodeling after RVO is important later in the course of disease. Inflammatory immune mediators in the vitreous body were also investigated by Yoshimura et al. [16] in 30 patients with BRVO and 13 patients with CRVO. 20 soluble factors in vitreous specimen were measured by multiplex bead analysis. IL-6, IL-8, and MCP-1 were significantly elevated in BRVO and CRVO. VEGF was significantly elevated only in CRVO.

Noma et al. [17] studied the correlation of inflammatory factors and electroretinographic findings in 19 patients with BRVO. During vitrectomy vitreous samples were obtained to measure VEGF, sICAM-1, IL-6, and MCP-1. The implicit time and amplitude of the a-wave cone, b-wave cone, and 30 Hz flicker were calculated and correlated to the four inflammatory factors. IL-6 and MCP-1 were significantly correlated with the implicit time of the b-wave cone. Vitreous levels of all four factors significantly correlated with the implicit time of the 30 Hz flicker, and the levels of all factors were significantly higher in patients with an implicit time ≥ 30 ms. The results suggest that the implicit times of the b-wave cone and 30 Hz flicker can detect patients with high risk of ischemia in BRVO.

Okunuki et al. [18] studied inflammatory aspects in patients with BRVO by measuring different inflammatory factors in the vitreous and aqueous humor using flow cytometry. In vitreous samples obtained during vitrectomy, they found high concentrations of VEGF, IL-8, and monokine induced by interferon γ (MIG) significantly correlated to macular thickness before and after surgery.

Noma et al. [19] evaluated the association between the levels of inflammatory factors in the vitreous fluid samples and macular edema measured by optical coherence tomography in 30 CRVO patients and compared it to vitreous samples of 29 controls with macular hole. Vitreous fluid levels of VEGF, soluble VEGF receptor 2, sICAM-1, IL-6, MCP-1, and pentraxin 3 (PTX3) were significantly higher in CRVO patients than in the control group. Vitreous levels of VEGF, sICAM-1, IL-6, MCP-1, and PTX3 significantly correlated with the central foveal thickness, indicating the importance of cytokines in the vitreous fluid in the mechanisms of macular edema development in CRVO patients.

Pfister et al. [20] assessed the levels of angiogenic and inflammatory cytokines in undiluted vitreous fluid from 43 treatment-naïve patients with macular edema due to non-ischemic BRVO with flow cytometric bead array (CBA). The results were correlated with SD-OCT parameters. The vitreous samples from 28 patients with idiopathic vitreous floaters served as controls. The BRVO eyes were divided into

a recent onset group (mean duration after onset 4.1 months) and an older group (mean duration 11.6 months). The mean IL-6 was 23.2 ± 48.8 pg/mL, MCP-1 602.9 ± 490.3 , and VEGF 161.8 ± 314.3 , and this was higher than in the control group (IL-6 6.2 ± 3.4 pg/mL ($p=0.17$), MCP-1 253.2 ± 73.5 ($p<0.0000001$), VEGF 7.0 ± 4.9 (0.003). VEGF was the only cytokine that correlated significantly with the SD-OCT thickness of the neurosensory retina ($r=0.31$). In the older BRVO group, there was a positive correlation between the cytokines IL-6, MCP-1, and VEGF, whereas in the fresh group, there was only a correlation of IL-6 with MCP-1. The assessed cytokines are elevated in the vitreous of patients with BRVO, and they correlate with each other. Only VEGF correlated with morphological changes.

Bertelmann et al. [21] examined intravitreal functional plasminogen in vitreous samples of 13 consecutive patients with recent onset of CRVO and compared it to 10 cases in whom vitrectomy was performed because of macular surgery or floater removal. Vitreous taps were extracted in the central vitreous body and plasminogen was determined in a new ultrasensitive p-nitroanilide reaction after activation with streptokinase. Patients with recent onset CRVO revealed significantly higher intravitreal plasminogen (2.19 ± 1.89 N) in comparison to controls (0.20 ± 0.21 %N) ($p<0.001$). Due to the significantly increased intravitreal plasminogen in patients with recent onset of CRVO, intravitreally administered tissue plasminogen activator might be an option to achieve enzymatic vitreolysis to induce posterior vitreous detachment in CRVO patients. This is interesting because the prevalence of vitreomacular adhesion is more common in retinal vascular diseases and might play a role in the development of macular edema.

2. Crystallin in Vitreous After Ischemia-Reperfusion Injury

Crystallins are major proteins in the vitreous body. Ischemia-reperfusion injury of the retina leads to apoptosis. Sudden hypoxic stress causes an increase in oxygen-free radicals. Crystallins have an antiapoptotic effect. Ischemia-reperfusion injury is a common pathogenic mechanism in ocular inflammation and in RVO, resulting in a damage of the blood-retinal barrier. Hong and Yang [22] studied ischemia-reperfusion injury in Sprague–Dawley rats by clamping the optic nerve for thirty minutes and then releasing it. The vitreous bodies of the study rats and a control group were obtained 24, 48, and 72 h after the injury. The total amount of α A and β crystallins and the phosphorylation of α B crystalline, as a type of heat shock protein, significantly increased 48 h after the ischemia-reperfusion injury, presumably to mediate pro- and anti-inflammatory reactions. Phosphorylation of ERK1/2 showed the greatest decrease at 48 h and then recovered. Damage to the ganglion cell layer of the retina was also most severe after 48 h after injury. However, there

was a subsequent recovery at 72 h. The results suggest that during ischemic and oxidative stress, phosphorylation of α B crystalline inhibits renin-angiotensin system (RAS), resulting in the inactivation of extracellular-regulated kinase 1 and 2 (ERK1/2). This may be associated with the inflammatory suppression in the vitreous via the ischemia-reperfusion injury and that this may play a role in retinal vein occlusions.

B. Structural Role of Vitreous

1. Vitreous Attachment in RVO

Jackson et al. [23] studied the role of vitreous attachment in retinal diseases. The prevalence of posterior vitreous detachment in CRVO was 30 %, in BRVO 31 % versus 25 % in controls. Observational studies suggest that in retinal vascular diseases, the prevalence of vitreomacular adhesion is more common than in age-matched controls.

Takahashi et al. [24] determined the relationship between macular edema associated with BRVO and the vitreous condition. They retrospectively studied 58 patients who underwent vitreous examination. The eyes were classified as having vitreomacular attachment (VMA) or vitreomacular separation (VMS) and were divided into two groups based on the mean age of the patients (group 1 ≤ 64 years of age, group 2 > 65 years of age). Macular edema was found in 39 (67 %) of the eyes. The prevalence of VMA was 81 % (22 of 27 eyes) in group 1 and 45 % (14 of 31 eyes) in group 2. Although no significant relationship was found, 77 % (17 of 22) of the eyes with VMA in group 1 had macular edema. The incidence of macular edema was significantly higher in eyes with VMA (93 %, 13 of 14) than in eyes with VMS (41 %, 7 of 17, $P = .009$) in group 2. The authors' findings suggest that VMA may influence the presence of macular edema associated with BRVO. Hikichi et al. [25] retrospectively investigated the role of the vitreous in eyes with central retinal vein occlusion, especially in relation to neovascularization and macular edema. They analyzed the vitreous condition of 150 patients (150 eyes) with CRVO. Based on fluorescein angiography findings and color photographs, eyes with CRVO were classified as ischemic or non-ischemic. In ischemic cases, retinal or optic disc neovascularization, or both, developed in eight (57 %) of 14 eyes without complete posterior vitreous detachment. The prevalence of neovascularization was significantly higher than in eyes with complete posterior vitreous detachment (0 %, 0/43) ($p < 0.01$). In non-ischemic cases, the prevalence of no posterior vitreous detachment or partial posterior vitreous detachment with vitreomacular adhesion was significantly higher in eyes with macular edema (76 %, 28/37) than in eyes without it (23 %, 13/56) ($p < 0.01$). Complete posterior vitreous detachment may protect against retinal or optic disc neovascularization in eyes with severe central retinal vein occlusion. Vitreomacular

adhesion may cause persistent macular edema in eyes with mild central retinal vein occlusion.

Ascaso et al. [26] investigated the role of vitreo-vascular traction in BRVO by SD-OCT in a case-control study. As the occlusion in BRVO typically occurs at an arteriovenous crossing site, the role of vitreoretinal traction at the obstruction site was studied prospectively in 32 consecutive patients. 25 % of the BRVO patient revealed traction at the point of the occlusion. An association with an adherence of the posterior vitreous cortex without traction was found in 44 %, whereas 31 % of eyes showed no vitreous adherence or traction. In the fellow eye at the corresponding vessel segment, no vitreo-vascular traction was found, and 37.5 % of the fellow eyes presented vitreoretinal adherence. Thus, vitreo-vascular traction in the occlusion site was significantly associated with BRVO. In addition ultrasonography B-scans revealed that the posterior vitreous cortex remains attached more frequently in BRVO eyes compared to healthy fellow eyes. Thus, vitreo-vascular traction and attached posterior vitreous cortex may play a role in the pathogenesis of BRVO.

III. Role of Vitreous in Diabetic Macular Edema

A. Structural

1. Vitreous Detachment and Vitreoschisis in DME

Posterior vitreous detachment (PVD) is an age-related process originating usually in the posterior pole (macula), progressing to the papilla and gradually extending up to the vitreous base in the late stage [see chapter II.C. Vitreous aging and PVD]. Processes that precede the PVD are progressive liquefaction and weakening of vitreoretinal adhesion. Anomalous PVD can occur in accelerated liquefaction of the gel vitreous without concurrent weakening of vitreoretinal adhesion. This may result in vitreoschisis caused by splitting of the multi-lamellar posterior vitreous cortex where firm vitreoretinal adherence undergoes traction by the detaching vitreous [see chapter III.B. Anomalous PVD and vitreoschisis]. This can lead to the development of premacular membranes [27] which in DME can result in cystoid formation primarily due to exudation but also as a consequence of tractional forces by the vitreoschisis membrane (Figure III.K-3a-d).

In cadaveric normal eyes, remnant of the posterior vitreous cortex was found in 44 % after spontaneous vitreous detachment including eyes that were clinically considered to have complete posterior vitreous detachment (Kishi et al. [28]). Vitreoschisis was found in 42 % of eyes with macular pucker by Sebag et al. [29]. In diabetic patients, vitreoschisis is one manifestation of diabetic vitreopathy. Vitreo-papillary

adhesion, which influences the vector of force on the macula, has a similarly high prevalence and may be involved in the development of diabetic macular edema [30]. Gaucher et al. [31] studied 49 eyes with and without DME aged 60 years or older and found a prevalence of completely attached posterior vitreous in 38.8 and 69.4 %, respectively. Incomplete posterior vitreous detachment was present in 55.0 and 22.4 %, respectively, and total posterior vitreous detachment in 6.2 % in both groups [31].

2. Vitreo-Retinal Interface in DME

There is evidence that the abnormalities in the vitreoretinal interface and vitreous changes might be involved in the pathogenesis of DME. In the macula, the inner limiting membrane, which is the basement membrane of the Müller cells, and vitreous have the tightest attachment [see chapter II.E. Vitreo-retinal interface and ILM]. The disrupted inner blood-retinal barrier plays an important role in the pathogenesis of DME [32]. However, altered vitreomacular interface may also contribute to the progression of DME. It might exacerbate due to accumulation of cytokines in the premacular vitreous.

Due to the infiltration of the posterior vitreous cortex with glial and inflammatory cells, the cortex thickens. A glistening, taut membrane can also occur over the macula in diabetic patients, which consists of a taut thick posterior vitreous cortex that is attached to the fovea and exerts horizontal and vertical traction. On fluorescein angiography, diffuse leakage is found in the late phases with diabetic macular edema. A thickened and taut posterior vitreous cortex may adhere to the inner limiting membrane in diabetic eyes and lead to traction and macular thickening. Since the diabetic retina is compromised due to microvascular damage, it may be particularly vulnerable to increased exudation caused by traction.

DME has a significantly higher prevalence in patients with attached posterior vitreous. There are reports that DME improves after spontaneous PVD. Before PVD, however, the posterior vitreous cortex induces vitreomacular traction. If vitreoschisis occurs, residual vitreous cortex persists after PVD [33]. After PVD a premacular membrane can develop leading to vitreomacular traction (Figure III.K-3d). Due to tractional forces, DME can deteriorate (Figure III.K-3a–d). The protein kinase C (PKC) pathways can enhance vitreous gel contraction [32].

In patients with diffuse diabetic macular edema, the posterior vitreous cortex removed at surgery showed on electron microscopy with immunocytochemical staining cytokeratin and glial fibrillary acidic protein in the premacular region [34]. Cytokeratin is usually found in the retinal pigment epithelial cells and glial fibrillary acidic protein in the astrocytes and Müller cells. In addition hyalocytes and macrophages were also found in the cortical vitreous.

B. Biochemistry of Vitreous in DME

Cytokines and chemokines play an important role in the development of DME. VEGF, fibroblast growth factor-2, and PKC pathways promote proliferation of hyalocytes and astrocytes that are found in the posterior vitreous cortex.

1. Advanced Glycation End Products in DME

Spontaneous PVD (Figure III.K-4) is caused by liquefaction of vitreous gel and dehiscence at the vitreoretinal interface. In diabetic patients, accumulation of advanced glycation end products (AGE) in vitreous leads to increased cross-linking of collagen and other proteins in the posterior vitreous cortex, inner limiting membrane of the retina, and intervening extracellular matrix. This increases the adhesion of the posterior vitreous to the inner limiting membrane and strengthens vitreomacular adhesion (Figure III.K-4) even if changes in vitreous lead to PVD. The vitreous cortex, however, can show a persistent attachment to the retina leading to vitreomacular traction and development or progression of DME [32].

Hyperglycemia can also contribute to the destabilization and liquefaction of the vitreous [see chapter I.E. Diabetic vitreopathy]. A posterior precortical vitreous pocket (Figure III.K-5) can occur within the temporal vascular arcades due to an incomplete PVD. The posterior wall consists of a thin layer of vitreous cortex closely adherent to the macula. This plays an important role in the formation of a fibrovascular ring found in the macular area and the vascular arcades with traction at the vitreomacular interface causing DME and tractional detachment of the retina in diabetic patients.

Accumulation of advanced glycation end products in the vitreous and at the vitreoretinal interface is associated with neurovascular injury in diabetic retinopathy. Indeed, the levels of AGE are 10–20 times more abundant in the vitreous of diabetic patients than of controls [35]. The removal of vitreous and associated AGEs may contribute to the improvement of ischemia and reduction of vasopermeability [36].

2. Inflammatory Factors in Vitreous of DME

There is a large body of evidence that pro-inflammatory factors contribute to the development of DME. Vitreous changes provide information on pathophysiological events and translational research of the key molecules that are involved in the development of diabetic retinopathy and DME. Diabetes causes inflammatory reactions. In the retina of diabetic patients, features of inflammation are found with an increase of inflammatory molecules also in the vitreous [37]. Inflammation involves multiple mediators like cytokines, chemokines, and adhesion molecules that initiate the interaction of leukocytes with

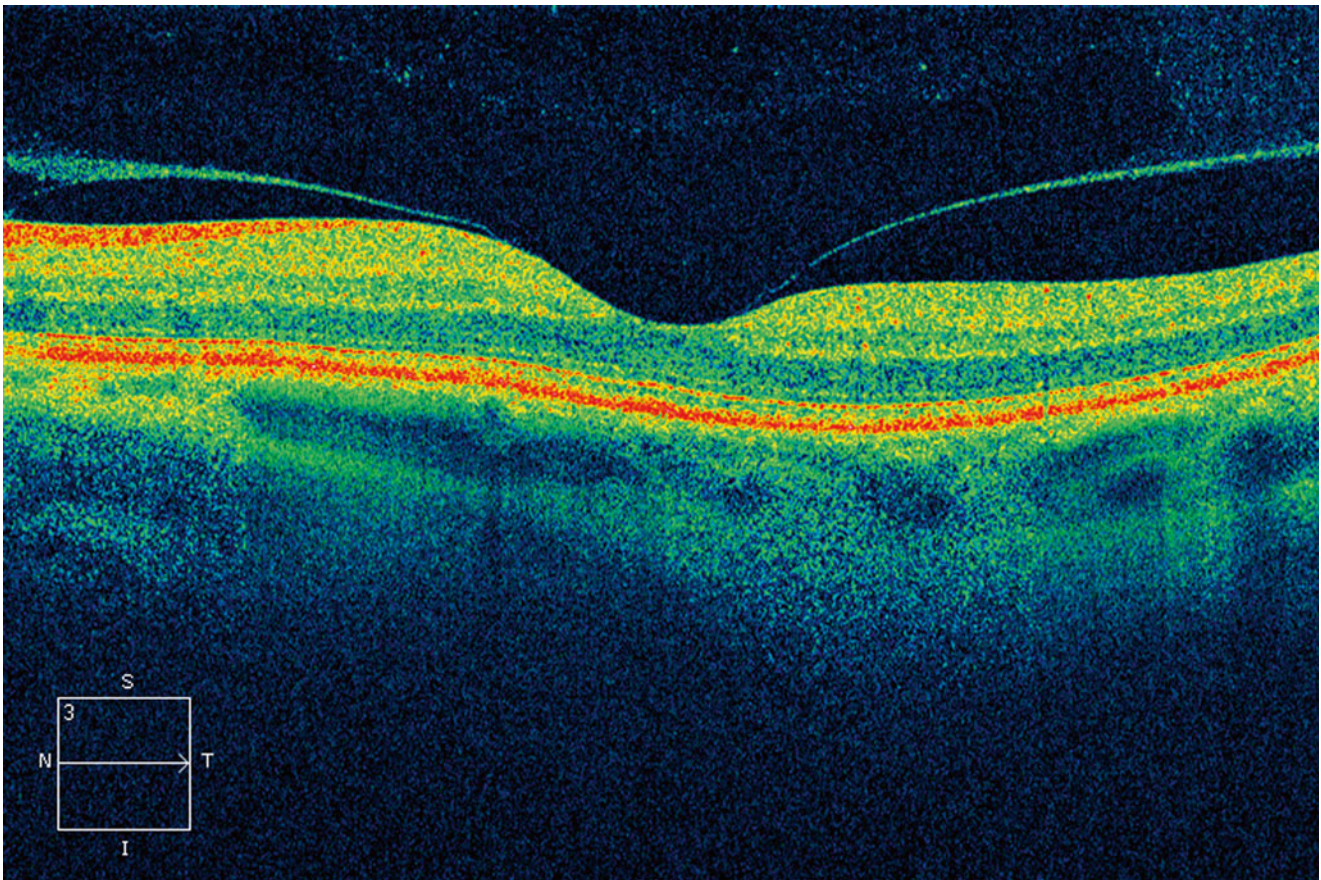


Figure III.K-5 Partial posterior vitreous detachment with vitreous adhesion and vitreous pocket/lacuna

endothelial cells [37]. Diabetic retinopathy is associated with the increase of pro-inflammatory cytokines and chemokines. IL-1 β , caspase 1, and chemokines are significantly increased in the vitreous. The number of neutrophils is elevated in retinal vessels and associated with capillary closure. In rodent diabetic models, there is an increase in leukocyte adherence to the retinal vasculature along with the progression of diabetic retinopathy. This might be due to increases in ICAM-1 and integrins in endothelial cells in leukocytes leading to leukostasis. There is evidence that low-grade chronic inflammation is part of the pathogenesis of diabetic macular edema leading to an increase in inflammatory molecules in the vitreous [37].

Factors secreted into the vitreous are associated with the pathologic processes and give insight in underlying biological mechanisms suggesting that common pathways are activated in different diseases. DME causes as secondary event a reactive local inflammation. A variety of factors, especially cytokines, are secreted in the vitreous. Inflammatory immune mediators in the vitreous body were investigated by Yoshimura et al. [16] in 92 patients with DME. Twenty soluble factors in vitreous including nine cytokines, six chemokines, and five growth fac-

tors were measured by multiplex bead analysis. IL-6, IL-8, and MCP-1 were significantly elevated in DME and correlated with each other. VEGF was not elevated in DME but in proliferative diabetic retinopathy in comparison to controls. In proliferative diabetic retinopathy, levels were higher than in DME. The multifunctional cytokine IL-6 induces the expression of VEGF. It may also directly increase the permeability of endothelial cells. IL-8 is produced in the ischemic retina by glial and endothelial cells. MCP-1 upregulation may stimulate the infiltration of inflammatory cells. VEGF is upregulated by hypoxia [16]. IL-1 β levels are higher in the vitreous of diabetic patients in comparison to nondiabetic patients. IL-6 can increase endothelial cell permeability in vitro. Stromal cell-derived factor 1 (SDF-1) concentration is increased in the vitreous of patients with DME suggesting that SDF-1 also plays a role in diabetic macular edema. TNF α is also elevated and known to increase retinal endothelial permeability [38].

Inflammatory cytokines are upregulated in the serum, vitreous, and aqueous humor of patients with diabetic retinopathy [39]. Key inflammatory molecules involved in the development of DME due to blood-retinal barrier breakdown

appear to be increased expression of endothelial adhesion molecules like ICAM1, VCAM1, platelet endothelial cell adhesion molecule 1 (PECAM-1), and P-selectin. Further events involved in the development of diabetic retinopathy are adhesion of leukocytes to the endothelium; infiltration of leukocytes into the neural retina; release of inflammatory cytokines, chemokines; and alteration of the tight junction proteins [40] of the retinal endothelial cells.

Abbreviations

AGE	Advanced glycation end products
ARM D	Age-related macular degeneration
BRVO	Branch retinal vein occlusion
CBA	Cytometric bead array
CRVO	Central retinal vein occlusion
DME	Diabetic macular edema
ELISA	Enzyme-linked immunosorbent assay
ERK1/2	Extracellular-regulated kinase 1 and 2
ETDRS	Early treatment diabetic retinopathy study
HRVO	Hemi-retinal vein occlusion
Hz	Hertz
ICAM-1	Intercellular adherence molecule 1
IL-6/8	Interleukins 6 and 8
MCP-1	Monocyte chemotactic protein 1
MIG	Monokine induced by interferon γ
ms	Millisecond
PECAM-1	Platelet endothelial cell adhesion molecule 1
PEDF	Pigment epithelial-derived growth factor
PKC	Protein kinase C
PTX-3	Pentraxin 3
PVD	Posterior vitreous detachment
RAS	Renin-angiotensin system
RVO	Retinal vein occlusion
SDF-1	Stromal cell-derived factor 1
SD-OCT	Spectral domain-optical coherence tomography
sICAM-1	Soluble intercellular adhesion molecule 1
sVEGFR-2	Soluble VEGF receptor 2
TNF α	Tumor necrosis factor 1
VEGF	Vascular endothelial growth factor
VMA	Vitreomacular adhesion
VMS	Vitreomacular separation

References

- Laouri M, Chen E, Looman M, Gallagher M. The burden of disease of retinal vein occlusion: review of the literature. *Eye*. 2011;25:981–8.
- Rogers S, McIntosh M, Cheung N, Lim L, Wang JJ, Mitchel P, Kowalski JW, Nquyen H, Wong TY. The international eye disease consortium: the prevalence of retinal vein occlusion: pooled data from population studies from the United States, Europe, Asia, and Australia. *Ophthalmology*. 2010;117:313–9.
- Jaulim A, Ahmed B, Khanam T, Chatziralli IP. Branch retinal vein occlusion: epidemiology, pathogenesis, risk factors, clinical features, diagnosis and complications. An update of the literature. *Retina*. 2013;33:901–10.
- Stern MS, Talwar N, Comer GM, Stein JD. A longitudinal analysis of risk factors associated with central retinal vein occlusion. *Ophthalmology*. 2013;120:362–70.
- The Central Vein Occlusion Study Group: baseline and early natural history report. *Arch Ophthalmol*. 1993;111:1087–95.
- The Branch Vein Occlusion Study Group. Argon laser photocoagulation for macular edema in branch vein occlusion. *Am J Ophthalmol*. 1984;98:271–82.
- Klein R, Knudtson K, Lee KA, Gangnon R, Klein BE. The Wisconsin epidemiologic study of diabetic retinopathy XXIII: the 25-year incidence of macular edema in persons with type 1 diabetes. *Ophthalmology*. 2009;116:497–503.
- Petrella RJ, Blouin J, Davies B, Barbeau M. Prevalence, demographics, and treatment characteristics of visual impairment due to diabetic macular edema in a representative Canadian cohort. *J Ophthalmol*. 2012;2012:159–67.
- Yau JW, Rogers SL, Kawasaki R, et al. Global prevalence and major risk factors of diabetic retinopathy. *Diabetes Care*. 2012;35:556–64.
- Browning DJ, Altawe MM, Bressler NM, Bressler SB, Scott IU. DRCR network: diabetic macular edema: what is focal and what is diffuse? *Am J Ophthalmol*. 2008;46:649–55.
- Dell’Omo R, Semeraro F, Bamonte G, Cirariello F, Romano MR, Costagliola C. Vitreous mediators in retinal hypoxic diseases. *Mediators Inflamm*. 2013;2013:935301.
- Koss MJ, Pfister M, Koch FH. Inflammatory and angiogenic protein detection in the human vitreous: cytometric bead assay. *J Ophthalmol*. 2011;2011:459251.
- Noma H, Mimura T, Eguchi S. Association of inflammatory factors with macular edema in branch retinal vein occlusion. *JAMA Ophthalmol*. 2013;131:160–5.
- Noma H, Funatsa H, Mimura T, Eguchi S. Vitreous inflammatory factors and serous retinal detachment in central retinal vein occlusion: a case control series. *J Inflamm*. 2011;8:38.
- Koss MJ, Pfister M, Rothweiler F, Michaelis M, Cinatl J, Schubert R, Koch FH. Comparison of cytokine levels from undiluted vitreous of untreated patients with retinal vein occlusion. *Acta Ophthalmol*. 2012;90:e98–103.
- Yoshimura T, Sonoda K-H, Sufahara M, Mochizuki Y, Enaida H, Oshima Y, Ueno A, Hata Y, Yoshida H, Ishibashi T. Comprehensive analysis of inflammatory immune mediators in vitreoretinal diseases. *PLoS One*. 2009;4:e8158.
- Noma H, Funatsa H, Mimura T. Association of electroretinographic parameters and inflammatory factors in branch retinal vein occlusion with macular oedema. *Br J Ophthalmol*. 2012;96:1489–93.
- Okunuki Y, Usui J, Katai N, Kezuka T, Takeuchi M, Goto H, Wakabayashi Y. Relation of intraocular concentrations of inflammatory factors and improvement of macular edema after vitrectomy in branch retinal vein occlusion. *Am J Ophthalmol*. 2011;151:610–6.
- Noma H, Mimura T, Masahara H, Shimada K. Pentraxin 3 an other inflammatory factors in central retinal vein occlusion and macular edema. *Retina*. 2014;34:352–9.
- Pfister M, Rothweiler F, Michaelis M, Cinatl Jr J, Schubert R, Koch FH, Koss MJ. Correlation of inflammatory and proangiogenic cytokines from undiluted vitreous samples with spectral domain OCT scans, in untreated branch retinal vein occlusion. *Clin Ophthalmol*. 2013;7:1061–7.
- Bertelmann T, Mennel S, Sekundo W, Strodthoff S, Witteborn MC, Stief T, Nguyen N, Koss MJ. Intravitreal functional plasminogen is

- elevated in central retinal vein occlusion. *Ophthalmic Res.* 2013;50:151–9.
22. Hong SM, Yang YS. A potential role of crystalline in the vitreous bodies of rats after ischemia-reperfusion injury. *Korean J Ophthalmol.* 2012;26:248–54.
 23. Jackson TL, Nicod E, Angelis A, Grimaccia F, Prevost AT, Simpson AR, Kanavos P. Vitreous attachment in age-related macular degeneration, diabetic macular edema, and retinal vein occlusion: a systematic review. *Retina.* 2013;33:1099–108.
 24. Takahashi MK, Hikichi T, Akiba J, Yoshida A, Trempe CL. Role of the vitreous and macular edema in branch retinal vein occlusion. *Ophthalmic Surg Lasers.* 1997;28(4):294–9.
 25. Hikichi T, Yoshida A, Konno S, Trempe CL. Role of the vitreous in central retinal vein occlusion. *Nihon Ganka Gakkai Zasshi.* 1996;100(1):63–8.
 26. Ascaso FJ, Huerva V. Vitreoretinal traction in impending branch retinal vein occlusion: a pathogenetic role? *Thromb Haemost.* 2012;108(2):208–9. doi: 10.1160/TH12-03-0190.
 27. Ophir A, Martinez MR. Epiretinal membranes and incomplete posterior vitreous detachment in diabetic macular edema, detected by spectral-domain optical coherence tomography. *Invest Ophthalmol Vis Sci.* 2011;52:6416–20.
 28. Kishi S, Demaia C, Shimizu K. Vitreous cortex remnants at the fovea after spontaneous vitreous detachment. *Int Ophthalmol.* 1986;9:253–60.
 29. Sebag J, Gupta P, Rosen R, Garcia P, Sadun AA. Macular holes and macular pucker: the role of vitreoschisis as imaged by optical coherence tomography/scanning laser ophthalmoscopy. *Trans Am Ophthalmol Soc.* 2007;105:121–31.
 30. Sebag J. Vitreoschisis in diabetic macular edema. *Invest Ophthalmol Vis Sci.* 2011;52:8455–6.
 31. Gaucher D, Tadayoni R, Erginay A, Haouchine B, Gaudric A, Massin P. Optical coherence tomography assessment of the vitreo-retinal relationship in diabetic macular edema. *Am J Ophthalmol.* 2005;139:807–13.
 32. Bhagat N, Grigorian RA, Tutela A, Zarbin MA. Diabetic macular edema: pathogenesis and treatment. *Surv Ophthalmol.* 2009;54:1–32.
 33. Romero-Aroca P. Managing diabetic macular edema: the leading cause of diabetes blindness. *World J Diabetes.* 2011;2:98–104.
 34. Jumper JM, Embasi SN, Toth CA, Mc Cuen II BW, Hatchell DL. Electron immunocytochemical analysis of posterior hyaloids associated with diabetic macular edema. *Retina.* 2000;20:63–8.
 35. Sebag J, Buckingham B, Charles MA, Reiser K. Biochemical abnormalities in vitreous of humans with proliferative diabetic retinopathy. *Arch Ophthalmol.* 1992;110:1472–6.
 36. Nguyen QD, Shah SM, Van Anden E, et al. Supplemental oxygen improved diabetic macular edema: a pilot study. *Invest Ophthalmol Vis Sci.* 2004;45:617–24.
 37. Zhang W, Liu H, Al-Shabraway M, Caldwell RW, Caldwell RB. Inflammation and diabetic retinal microvascular complications. *J Cardiovasc Dis Res.* 2011;2:96–103.
 38. Simó-Servat O, Hernández C, Simó R. Usefulness of the vitreous fluid analysis in the translational research of diabetic retinopathy. *Mediators Inflamm.* 2012;2012:872978.
 39. Rangasamy S, McGuire PG, DAS A. Diabetic retinopathy and inflammation: novel therapeutic targets. *Middle East Afr J Ophthalmol.* 2012;19:52–9.
 40. Deissler H, Deissler H, Lang S, Lang GE. VEGF-induced effects on proliferation, migration and tight junctions are restored by ranibizumab (Lucentis®) in microvascular retinal endothelial cells. *Br J Ophthalmol.* 2008;92:839–43.

Peter Kroll, Eduardo B. Rodrigues, and Carsten H. Meyer

Outline

I. Introduction

- A. Diabetes
- B. Diabetic Retinopathy
 1. Non-Proliferative Diabetic Retinopathy (NPDR)
 2. Proliferative Diabetic Vitreoretinopathy (PDVR)

II. Role of Vitreous in PDVR

- A. Classification of PDVR
 1. Airlie House Classification
 2. International Clinical Diabetic Retinopathy Severity Scale
 3. Kroll's Classification

III. Therapeutic Considerations

IV. Summary

References

Keywords

Vitreous • Retina • Diabetes • Diabetic vitreopathy • Proliferative diabetic vitreoretinopathy • Clinical staging • Neovascularization • Vascular endothelial growth factor

Key Concepts

1. Vitreous play a critical role in proliferative diabetic retinopathy, and thus, the appropriate term for this condition is proliferative diabetic vitreoretinopathy (PDVR).
2. A clinical classification of PDVR is proposed, which predicts surgical outcomes in advanced cases.
3. Treating diabetic vitreopathy may be a useful adjunct to treatments of diabetic retinopathy so as to mitigate the contribution of vitreous and improve long-term prognosis.

P. Kroll, MD (✉)
Department of Ophthalmology, Philipps-University,
Marburg, Germany
e-mail: phkkroll@yahoo.com

E.B. Rodrigues, MD
Department of Ophthalmology, Philipps-University,
Marburg, Germany

Department of Ophthalmology, Federal University of Sao Paulo,
Sao Paulo CH-5000, Brazil
e-mail: rodriguesretina@gmail.com

C.H. Meyer, MD, FEBO, FMH
Department of Ophthalmology, Philipps-University,
Marburg, Germany

Department of Ophthalmology, Pallas Clinic,
Aarau CH-5000, Switzerland
e-mail: meyer_eye@yahoo.com

I. Introduction

This chapter reviews the pathogenesis of proliferative diabetic vitreoretinopathy (PDVR) and presents recommendations for its clinical staging. Although numerous biochemical mediators may be responsible for the pathogenesis of PDVR, there is no consensus about the biochemical pathway(s) responsible for the progression of PDVR. Among the known and most studied mediators is vascular endothelial growth factor (VEGF) [18]. Since the thickened posterior vitreous cortex is one of the main components in proliferative diabetic retinopathy (PDR) causing the subsequent development of retinal proliferations, shrinkage of the diabetic posterior vitreous cortex leads to traction retinal detachment. Although several classifications are described in the literature, the

classification suggested herein is important in the clinical assessment of disease severity, communication about the disease state, and the evaluation of therapy. A new morphological classification of PDVR is presented which emphasizes the role of vitreous, hence the name PDVR. Moreover, this classification reliably predicts the surgical outcome in advanced stages of PDVR.

A. Diabetes

Diabetes is a metabolic disease that affects juvenile (type I) or adult patients (type II) throughout their lives, and is increasing worldwide [21, 22, 23, 36]. Several clinical trials in Europe and North America like EURODIAB Prospective Complication Study 1998; WESDR (*Wisconsin Epidemiological Study of Diabetic Retinopathy*) [27]; DCCT (*Diabetes Control and Complication Trial*) 1996, UKPDS (*United Kingdom Prospective Diabetes Study*) [62, 63]; ETDRS (*Early Treatment Diabetic Retinopathy Study*); and a Japanese group [39] demonstrated that the most important risk factor for the beginning and progression of diabetic retinopathy (DR) is the level and duration of hyperglycemia over years. Additional factors for the progression of DR are elevated blood pressure, especially an increased systolic blood pressure. Elevated lipids, microalbuminuria, and high ocular perfusion pressure also influence the progression of diabetic angiopathy [60]. Further, growth hormones stimulate the production of insulin-like growth factor, which may play a role in the pathogenesis of DR [5, 69].

At disease onset, diabetes remains predominantly a metabolic disease. However, after approximately five years, or in childhood after puberty, severe secondary changes in the vessels of the brain, heart, kidneys, inferior extremities, and especially in the eyes may occur, leading to dramatic complications either isolated or multiple in the affected organs [30, 31]. If the eyes of a diabetic patient become affected, the vascular changes start in the retina with signs of DR, less seldom are changes in the iris such as rubeosis iridis or iris neovascularization. However, vitreous changes occur even earlier in the natural history of disease [see chapter I.E. Diabetic vitreopathy].

B. Diabetic Retinopathy

The broad spectrum of clinical signs in diabetic retinopathy (DR) ranges from biomicroscopic changes of intraretinal

capillaries to severe proliferation of new vessels out of the retina into the vitreous, leading to vitreous hemorrhage and traction retinal detachments, which may cause severe loss of sight (Figure III.L-1). DR has traditionally been subdivided into nonproliferative diabetic retinopathy (NPDR) and proliferative diabetic retinopathy (PDR). While NPDR is characterized by a retinal microangiopathy with intraluminal, intramural, and extramural pathologies, PDR is predominantly characterized by proliferation of vessels onto the retinal surface and into the posterior vitreous cortex. Concurrent with these retinal changes is a separate set of pathologic changes in vitreous, known as diabetic vitreopathy [46] [see chapter I.E. Diabetic vitreopathy]. Since, PDR develops only if the vitreoretinal interface is partially or completely attached to the retinal surface to provide a scaffold for new vessel proliferation, we recommend including the impact of vitreous in clinical nomenclature and call this stage “proliferative diabetic vitreoretinopathy” (PDVR).

1. Nonproliferative Diabetic Retinopathy (NPDR)

NPDR usually appears 5 years after the beginning of the metabolic disorders, in juvenile diabetes mellitus typically shortly after puberty. Pathogenic mechanisms include increased aggregation of erythrocytes and platelets, elevated fibrinogen activity, and thickening of the retinal capillary basement membranes, presumably due to an accumulation of glycosylated proteins. Loss of pericytes outside and a loss of endothelial cells inside the retinal capillaries are the first changes in the retina weakening of the vessels wall, resulting in microaneurysms, venous abnormalities, intraretinal hemorrhages, and leakages of serum, leading to hard exudates and an accumulation of lipoproteins in retinal layers. Finally, there are so-called intraretinal microvascular abnormalities (IRMAs), characterized as arteriovenous shunts in areas of occluded retinal capillaries and early intraretinal neovascularization.

Clinical classification of these retinal abnormalities [7] is important for prognosis (45 % of patients with severe NPDR as defined by the University of Wisconsin 4:2:1 rule [9] progress to PDVR within one year) and to define indications for laser therapy [9]. It is currently not known whether diabetic vitreopathy plays a role in NPDR, but future research should be directed to address this question. It is suspected, however, that vitreoschisis [50] plays a role in diabetic macular edema [52], the most common cause of vision loss in diabetes [see chapter III.K. Vitreous in retino-vascular diseases and diabetic macular edema].

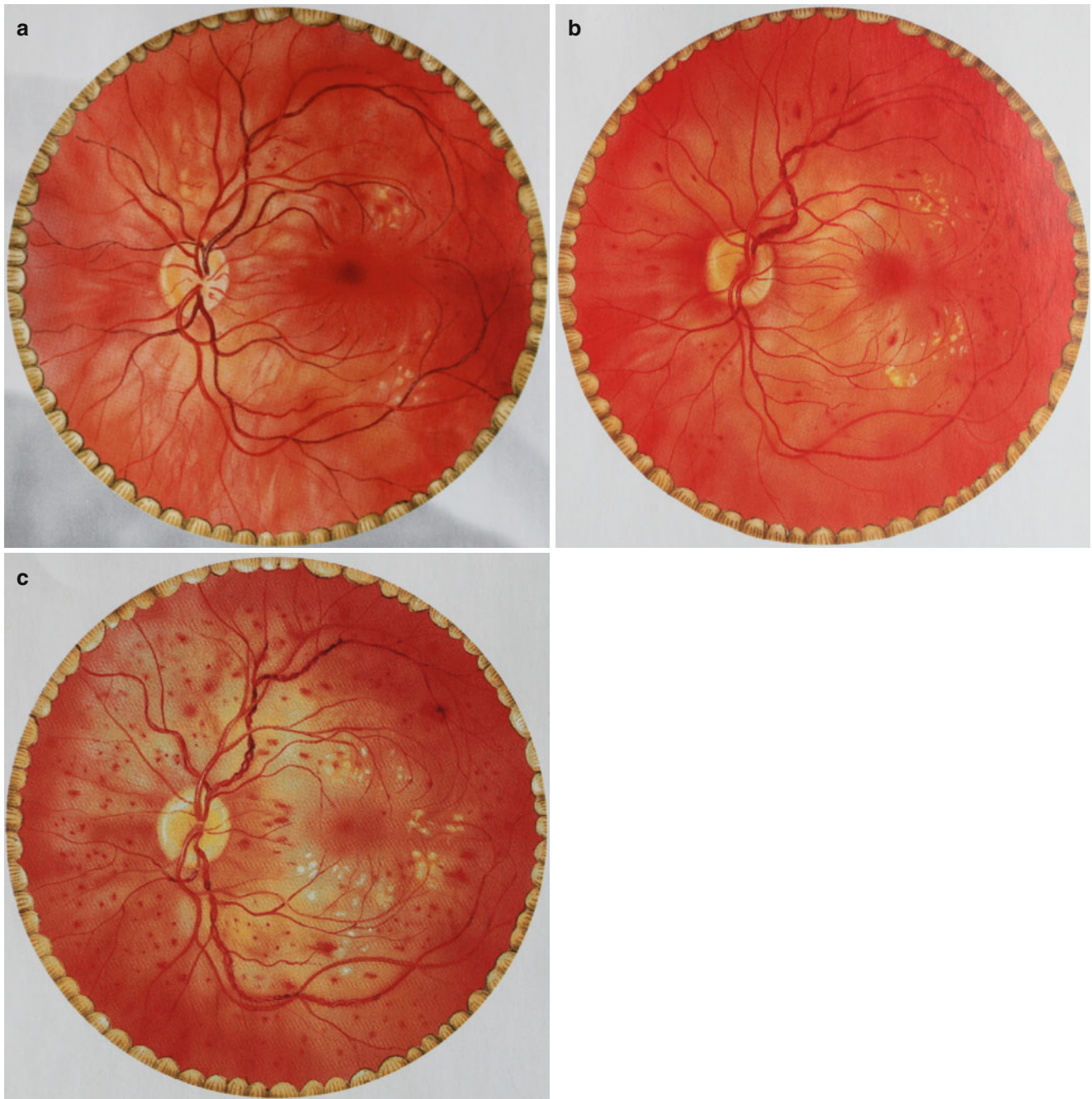


Figure III.L-1 (a) DR (diabetic retinopathy) mild; (b) DR moderate, (c) DR severe

2. Proliferative Diabetic Vitreoretinopathy (PDVR)

There is general agreement that the progression from NPDR to PDVR occurs approximately 15–20 years after the onset of uncontrolled diabetes, in 5–10 % of patients with type II diabetes and in 30 % of patients with type I diabetes [27]. Furthermore, diabetic patients with PDVR in one eye are at high risk of developing neovascularization in the second eye over a 5-year period, so close follow-up and early treatment are highly recommended [17, 65].

II. Role of Vitreous in PDVR

The progression from NPDR to PDVR is marked by two different processes:

- I. In early stages, there is thickening of the posterior vitreous cortex, a change seen only in diabetic eyes (Figure III.L-2) [19]. Since the healthy vitreous contains antiangiogenic properties, vessels are absent in health [40, 69]. Thickening of the posterior vitreous cortex is believed to alter these properties and promote the ingrowth of proliferating vessels out from the retinal surface into the thickened posterior vitreous cortex itself [11, 14, 29, 37].
- II. In a second set of events, the altered and thickened posterior vitreous cortex begins to shrink, possibly induced by factor 13 of the hematopoietic system [2], leading to traction and rupture of proliferating vessels inducing intravitreal hemorrhage or even traction retinal detachment.

The healthy posterior vitreous cortex consists of a dense matrix of collagen fibrils which are attached to the retina via

an extracellular matrix [42, 53] [see chapter II.E. Vitreoretinal interface and inner limiting membrane]. This tight attachment is mediated by extracellular matrix proteins, mainly fibronectin and laminin [20] (Figure III.L-2). Long-standing diabetes alters proteins throughout the entire body including in vitreous. Sebag et al. were the first to show the increased levels of advanced glycation end products in human diabetic vitreous as compared to controls [43, 45]. These biochemical abnormalities induce structural changes within the vitreous body [44] and likely at the vitreoretinal interface, perhaps similar to what has been identified during aging [42]. There is also a breakdown of the blood-retinal barrier. Serum proteins like fibronectin accumulate up to tenfold between the posterior cortex and the inner limiting membrane (ILM) of the retinal surface, especially in the temporal and nasal quadrants [20, 70]. At the same time, increased levels of laminin and type I and type IV collagen become apparent [4]. These accelerate the thickening of the vitreoretinal interface, leading to an additional metabolic barrier between retina and vitreous [see chapter IV.A. Vitreous physiology].

Several clinical and experimental investigations have clearly demonstrated that the thickened posterior vitreous cortex together with the thickened extracellular matrix at the vitreoretinal interface (see chapter II.E. Vitreoretinal interface and inner limiting membrane) plays a key role in angiogenic pathogenesis [10]. The first step involves angiogenic growth factors activating the endothelial cells to release specific protease enzymes, which promote the breakdown of basement membranes [66], allowing the endothelial cells to leave the vascular wall, migrate into the adjacent extracellular matrix where they proliferate, and build neovascular formations (Figure III.L-3). Initially, the endothelial cells of the

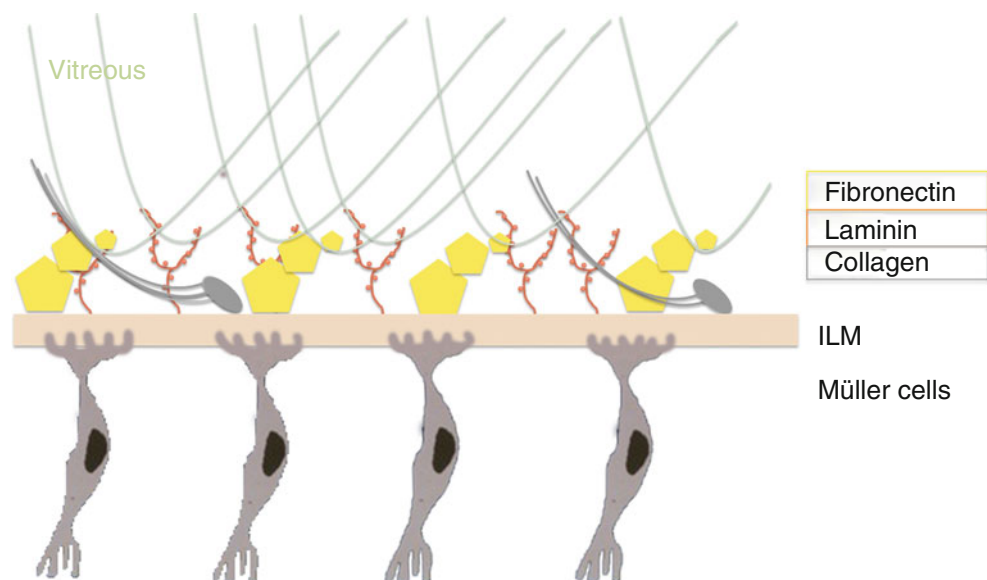


Figure III.L-2 Vitreoretinal interface: the vitreoretinal interface is believed to play a key role in the development of PDVR

retinal capillaries penetrate predominantly affected ischemic retinal areas mainly by the action of proteolytic enzymes upon the basal membrane of diabetic vessels. This early proteolytic process is followed by a proliferation through the ILM onto the retinal surface and further through the vitreoretinal interface into the posterior vitreous cortex, taking advantage of adhesive molecules, such as adjacent integrins. There are also many additional cofactors, which are responsible for this process such as growth factors, e.g., vascular endothelial growth factor (VEGF) [32, 33], transforming growth factor (TGF β), platelet-derived growth factor (PDGF), endothelial growth factor (EGF), interleukin 1 (IL-1), angiotensin II, or somatostatin [see chapter IV.C. Vitreous and iris neovascularization]. In this context, it has been demonstrated that Müller cells release a large amount of VEGF in ischemic areas [68] and in the presence of advanced glycation end products [12, 13, 43]. At this stage, the posterior vitreous cortex appears on biomicroscopy as a thickened preretinal membrane, especially around the optic disk and along the temporal retinal vessel arcades [70]. This scaffold facilitates additional formations of proliferating vessels in this ongoing PDVR process [10].

The second step in PDVR development starts with shrinkage of the altered posterior vitreous cortex, possibly via cross-linking of collagen fibrils. Akiba et al. [2] postulated that

factor 13 (transglutaminase) of the hematopoietic system might trigger this collagen cross-linking. These advanced changes of the vitreoretinal interface by means of thickening and shrinkage lead to a potentially fateful course for the diabetic eye: the shrinking vitreous induces traction on proliferating retinal vessels inducing severe hemorrhages into the vitreous body. Additionally, vitreous shrinkage in combination with firm vitreoretinal adhesions may induce vigorous forces leading to severe traction retinal detachments, vitreopapillary traction [25, 34], and foreshortening of retina leading to a proliferative vitreoretinopathy (PVR)-like configuration. The combination of firm vitreous traction and PVR may cause retinal tears and severe combined traction/rhegmatogenous retinal detachments.

To prevent progression from NPDR to PDVR, one can perform panretinal laser photocoagulation (PRP). One therapeutic effect of this treatment is the destruction of retinal cells in areas of retinal hypoxia, especially Müller cells which are responsible for upregulation of VEGF [57–59]. Another therapeutic effect of PRP laser therapy is the induction of posterior vitreous detachment (PVD). Clinical studies [41] have shown a higher incidence of PVD following PRP. Progression of PVD can be observed 3–6 months following PRP [28]. These benefits of PRP give further support to the concept that vitreous plays a

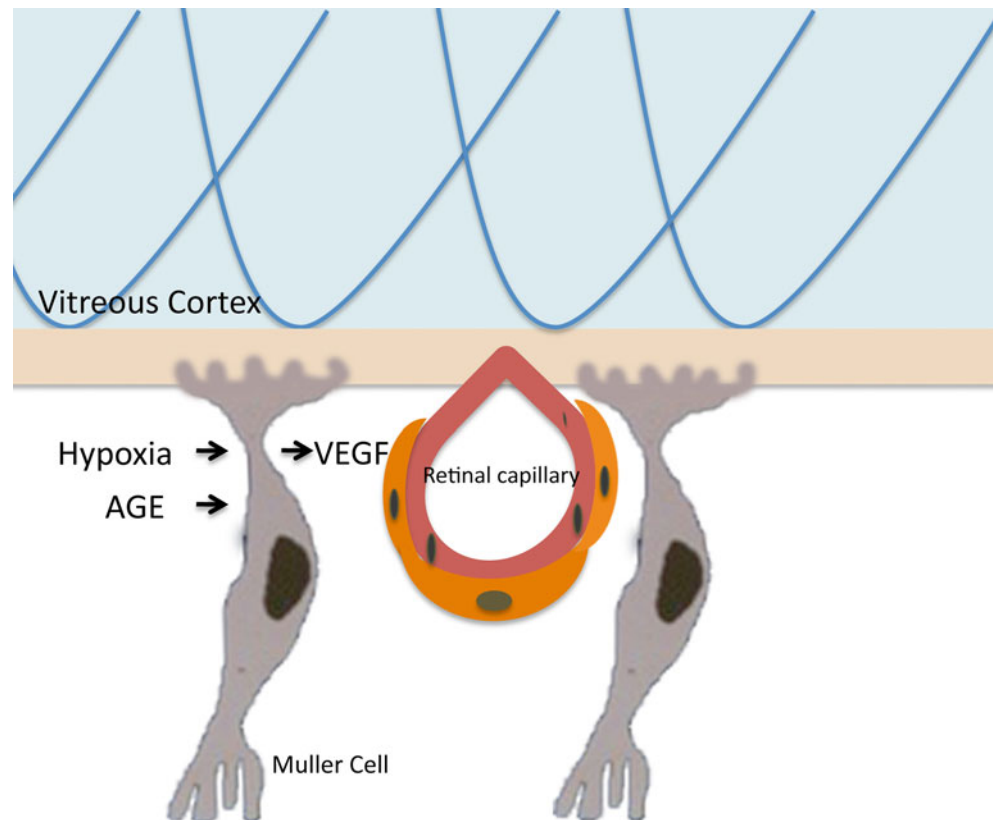


Figure III.L-3 Vascular endothelium crossing two basement membranes

role in the progression of severe NPDR to PDVR. It is of further interest to consider cases of NPDR that do not progress:

- Eyes with high myopia (>-10 diopters) rarely develop PDVR [70], since PVD frequently occurs long before diabetic retinopathy develops in elderly eyes with type II diabetes.
- Eyes with previous rhegmatogenous retinal detachment, usually due to PVD, do not develop PDVR. Conversely, diabetic patients with NPDR rarely develop rhegmatogenous retinal detachments, as their posterior vitreous frequently remains attached.
- Vitrectomized diabetic eyes rarely develop PDVR.

A. Classification of PDVR

1. Airlie House Classification

In the late 1960s, the first classification for diabetic retinopathy, the Airlie House Classification, was established [35]. Since vitrectomy was not yet introduced at that time, only the results of photocoagulation or laser coagulation therapy could be assessed by this classification. This as well as the classification of Sevin et al. [54] and the modified Airlie House Classification of the *Diabetic Retinopathy Study Research Group* [7] were only applied to diabetic eyes with vascular changes in or just outside the retina. All these classification systems were used for major multicenter studies in the 1970s and 1980s to evaluate the benefits mainly of laser coagulation treatments, primarily the *Diabetic Retinopathy Study (DRS)* and the *Early Treatment Diabetic Retinopathy Study (ETDRS)*. Vitreous abnormalities, however, were not considered in these classification systems. When vitrectomy became available, vitreous was indirectly taken into consideration when studies such as the *Diabetic Retinopathy Vitrectomy Study (DRVS)* and *ETDRS* evaluated the positive effect of this new surgical option [3]. However, both study groups, especially the *ETDRS* group, classified the proliferative form of DR only into early, high-risk, and severe proliferative diabetic retinopathy, based on the criteria of the Airlie House Classification. Different forms of retinal detachments, either traction or rhegmatogenous components, were considered during this classification. The *ETDRS* grouped all severe cases with retinal detachments, traction, iris neovascularization or fundus obscurations under “advanced PDR” without further subclassification. In 1983, Shea proposed the approach of an “early vitrectomy” in patients with diabetic retinopathy in order to improve surgical outcome and preservation of useful sight, without indicating the exact threshold for therapeutic intervention [8].

2. International Clinical Diabetic Retinopathy Severity Scale

At the turn of the century, Wilkinson et al. established another classification called the “International Clinical Diabetic Retinopathy Severity (ICDRS) Scale” during a workshop in 2003 [67]. A result of the American Academy of Ophthalmology Diabetes 2000 initiative, this classification system defined mild, moderate, and severe nonproliferative diabetic retinopathy (see Table III.L-1). There was also a stage for “no retinopathy” and a classification for “proliferative diabetic retinopathy.” Numerous studies used the ICDRS scale to report comparable results among different centers. Zehetner et al. [71] evaluated the reliability of this classification and correlated the stage of the diabetic retinopathy with the concentrations of glycosylated hemoglobin (HbA1c) and VEGF level in blood plasma samples. They determined that poor glycemic control was positively correlated with increased VEGF plasma levels in patients with type II diabetes. The highest individual VEGF measurements were found in patients with severe forms of proliferative DR. Quellec et al. [38] used a modified automated ICDRS scale algorithms and confirmed a high intraobserver agreement ($\kappa=0.769$) among young and experienced clinicians, making this classification reliable and applicable. However, this severity scale still did not propose subdividing proliferative disease into further subgroups for the proliferative diabetic retinopathy as diabetic vitreopathy was still not considered.

3. Kroll’s Classification

In 1987 Kroll first proposed a classification system with subdivision of proliferative diabetic retinopathy according to the proliferative vitreoretinopathy (PVR) classification. This was further specified in greater detail in 2007 (Figure III.L-4a–c). This classification is easy to understand, can be easily explained to patients and their relatives, and helps to communicate disease progression among retinal specialists. It also helps to define thresholds for therapeutic intervention, i.e., whether laser therapy is still indicated or if vitrectomy, especially an early vitrectomy, should be performed. It furthermore serves as a predictor of surgical outcomes and can be useful for evidence-based approaches to clinical research and care [15].

Since the thickened posterior vitreous plays an important role in the pathogenesis of the proliferating form of diabetic retinopathy, the term *proliferative diabetic retinopathy* has been modified into the more precise term *proliferative diabetic vitreoretinopathy (PDVR)* [24, 26, 47]. Four stages are defined: *Stage A* (Figure III.L-5a, b) denotes a completely attached retina, with a thickened posterior vitreous cortex. Remarkable in this stage are the proliferating vessels emanating from the retina into the posterior vitreous

Table III.L-1 Comparison of different classifications of nonproliferative and proliferative diabetic retinopathy and important studies with various stages for their inclusion criteria

International Clinical Diabetic Retinopathy Disease Scale according to AAO						
No retinopathy	Mild NPDR	Moderate NPDR	Severe NPDR	PDR		
Clinical disease severity scale of diabetic retinopathy according to ETDRS criteria						
No retinopathy	Mild NPDR	Moderate NPDR	Severe NPDR	Early PDR	High risk PDR	Severe PDR
Severity of PDVR according to Kroll						
No retinopathy	Mild NPDR	Moderate NPDR	Severe NPDR	PDVR A	PDVR Bt PDVR Bn	PDVR C1 - 4
DDCT type 1 DM			DRS			
UKPDS type 2 DM						
	ETDRS				DRVS	

PDVR proliferative diabetic vitreoretinopathy, *DM* diabetes mellitus

The upper part of the table shows three classification systems of diabetic retinopathy. The lower part lists important studies dealing with various stages of diabetic retinopathy. All studies have an evidence of 1b. The Diabetes Control and Comparison Trial (DCCT) and the United Kingdom Prospective Diabetes Study (UKPDS) investigated with mild and moderate cases of nonproliferative diabetic retinopathy (NPDR), the diabetic retinopathy study (DRS) with severe NPD to high-risk proliferative diabetic retinopathy (PDR). The Early Treatment Diabetic Retinopathy Study (ETDRS) on the other side investigated cases of mild, moderate, and severe NPDR and cases of early PDR. Finally the Diabetic Retinopathy Vitrectomy Study (DRVS) was performed on patients with high-risk and severe PDR

cortex, especially near the optic disk reaching to the nasal side of the posterior pole of the eye [26], but also in the area of the superior and inferior temporal arcade retinal vessels.

Stage B (Figure III.L-6a–c) is characterized by shrinking of the vitreous cortex and traction retinal detachments either in the nasal (n) (*stage B n*) or temporal side (t), in the area of the temporal arcade vessels, (*stage B t*) or at the optic

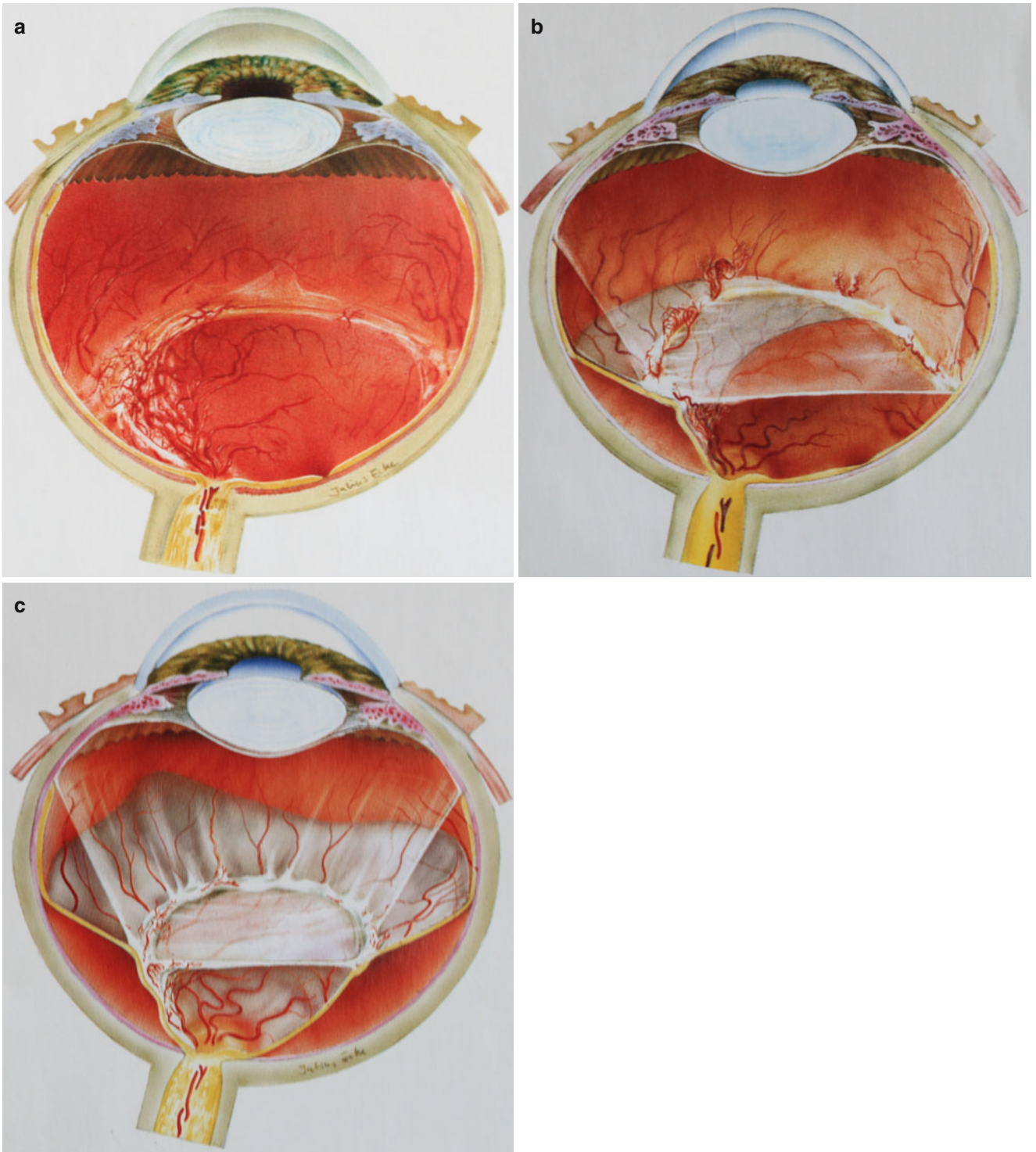


Figure III.L-4 (a–c) Stages A, B, C

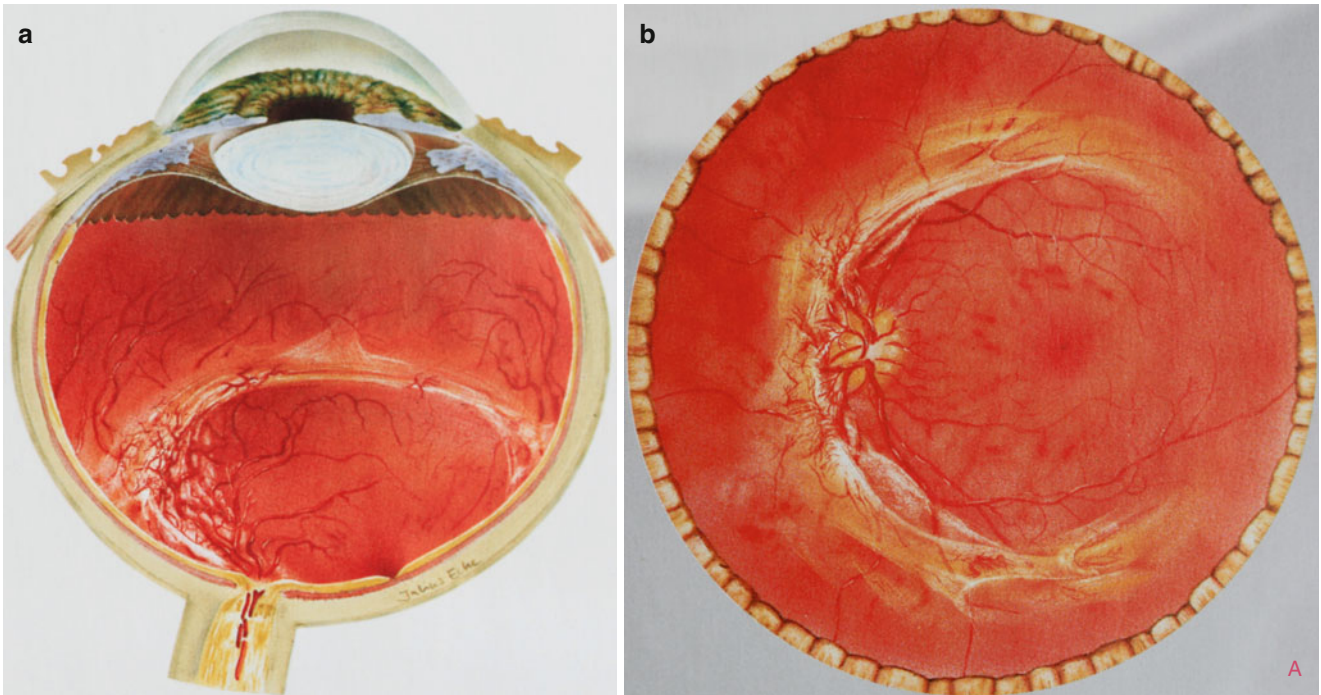


Figure III.L-5 (a, b) Stage A Figure III.L-2. PDVR, stage A: this stage is characterized by proliferative changes in vitreous and retina, especially around the optic disk and in the posterior vitreous cortex. The retina is still totally attached

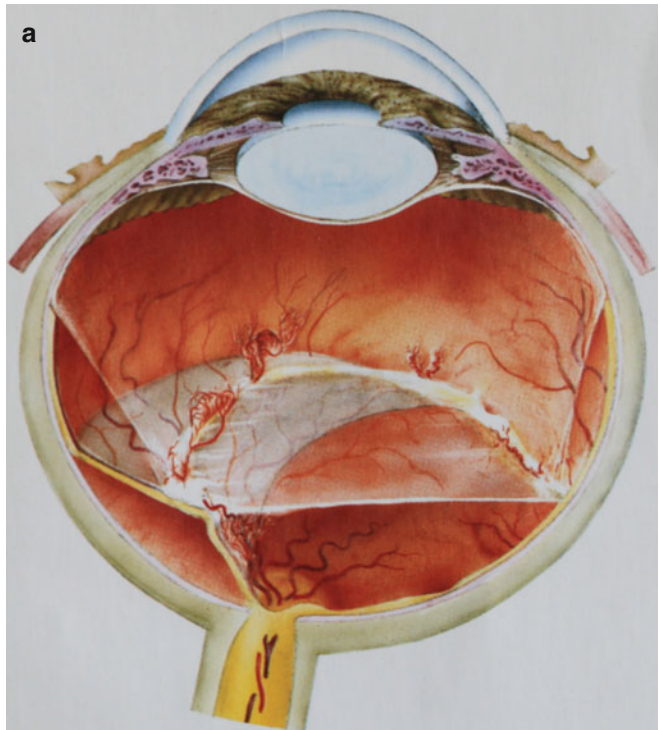


Figure III.L-6 PDVR, stage B: this (a) stage is characterized by shrinkage of the posterior vitreous cortex. In places where the vitreous adheres to the retina, circumscribed retinal detachments are found

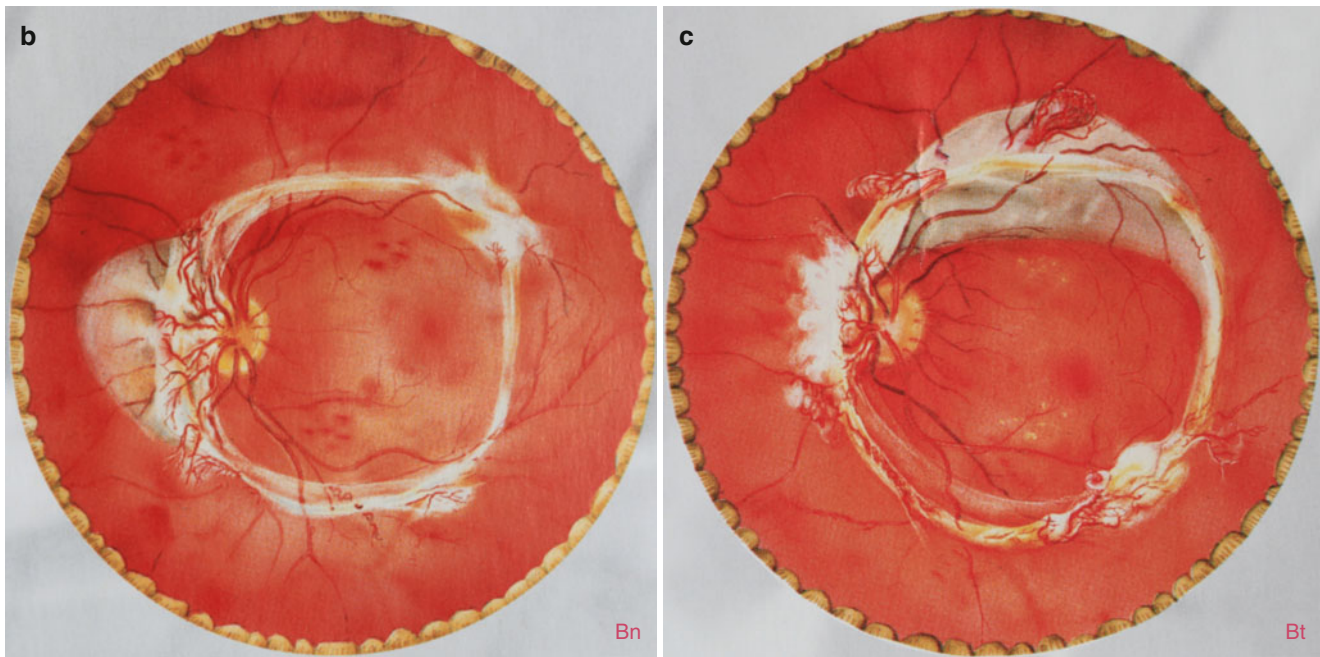


Figure III.L-6 (continued) (b) If a tractive detachment is *nasal* to the optic disc, this is described as stage Bn. (c) Proliferative and tractive changes in the area of the *temporal* superior and inferior vascular arcade, which may be followed by a macular detachment, are categorized as stage Bt

disk. Very important for the functional prognosis in this stage is the fact that the macula remains unaffected and the visual acuity, depending on additional diabetic changes in the macular area, may be normal.

Stage C (Figure III.L-7a–e): Increased shrinkage of vitreous induces vigorous traction leading to traction retinal detachment. With further progression, the macula becomes involved. Corresponding with the four quadrants of the fundus, this stage is divided into four subgroups: *stage C 1*, traction RD in one quadrant; *stage C 2*, traction RD in two quadrants; *stage 3*, traction RD in three quadrants; and *stage 4*, traction RD in all 4 quadrants. In stage C, visual acuity is dramatically decreased, since in all cases the macula is involved. In all stages, additional hemorrhages may occur, since vitreous traction can also rupture proliferating blood vessels.

III. Therapeutic Considerations

In a retrospective review of 563 patients, Hesse et al. [15] evaluated the prognostic value of Kroll's classification with respect to the postoperative visual outcome after vitreoretinal surgery. In 179 out of 563 eyes (31.7%), repeat vitrectomy (including silicone oil removal) was required, and in 51 eyes (9.1%), more than one reoperation was performed. Silicone oil tamponade was used in 22 out of 253 eyes

(8.7%) classified as *stage A*, in 27 out of 201 eyes (13.4%) of *stage B*, and in 17 out of 78 eyes (21.8%) of *stage C*. The mean postoperative visual acuity after vitreoretinal surgery was significantly better in *stage A* compared to *stage C* ($p < 0.01$). Postoperative increase of visual acuity of more than 3 lines was significantly less frequent in *stage B* ($p < 0.014$) and *stage C* ($p < 0.039$) as compared to *stage A*. The authors concluded that Kroll's classification for PDVR has a high prognostic value for postoperative visual outcome and the level of surgical risk management.

All of these clinical observations and experimental investigations point to the fact that the vitreous plays a key role in the development of a PVDR [6]. Therapeutic aims must therefore either prevent diabetic vitreopathy or eliminate vitreoretinal adhesion. As long as the retina is still attached, PRP may be effective if PVD can be achieved. However, PRP cannot often be administered early enough in the natural history of PDVR, and in other cases, PRP is simply not effective due to robust vitreoretinal adhesion and traction. In the presence of vitreous hemorrhage and traction retinal detachment, only the surgical release of traction via vitrectomy can save the diabetic eye. In recent years, the option of inducing PVD via pharmacologic vitreolysis [48, 49, 51, 56, 61, 64] has become available [see chapter VI.A. Pharmacologic vitreolysis]. A recent review outlines how pharmacologic vitreolysis can be used to treat diabetic retinopathy [6].

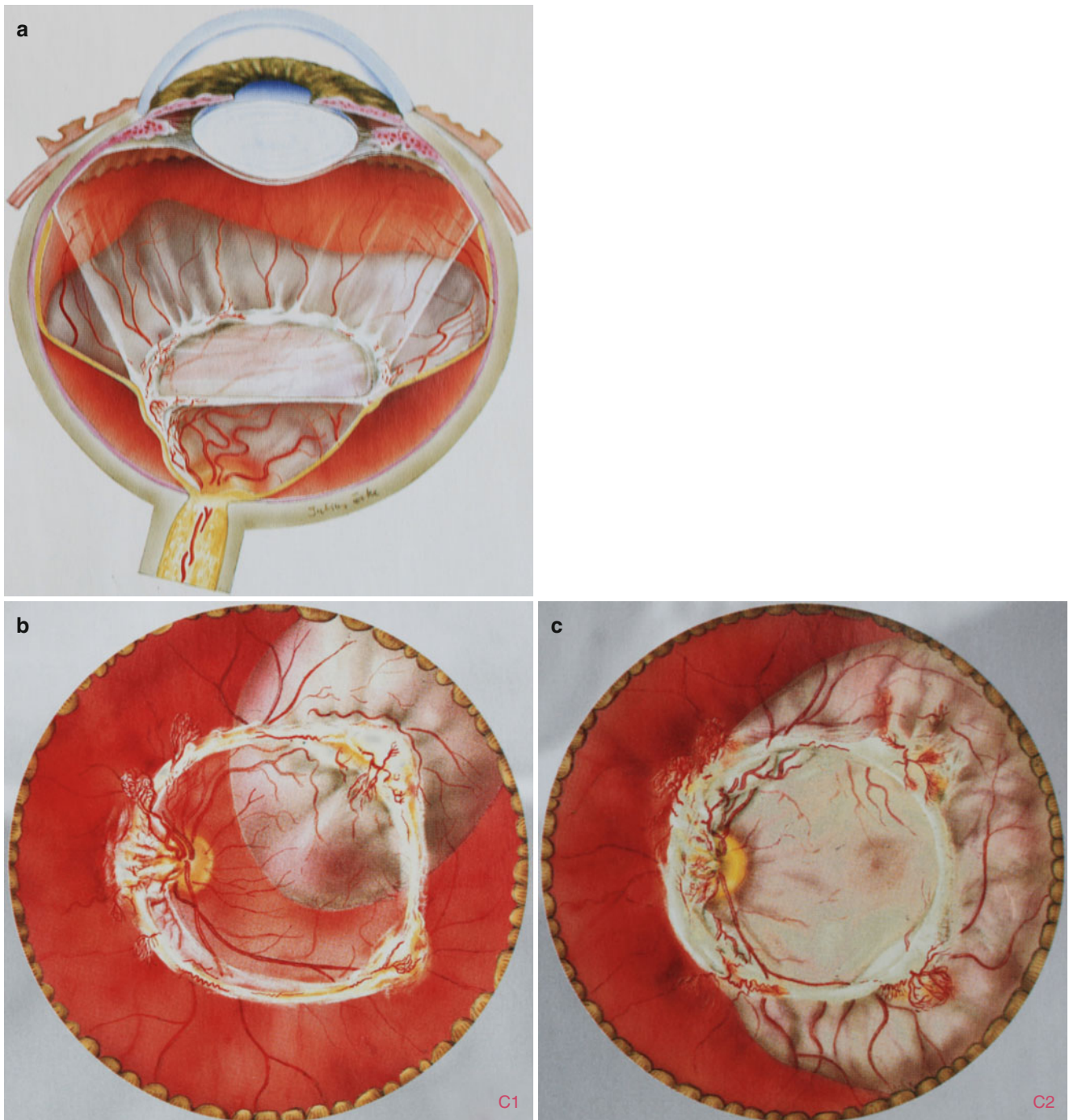


Figure III.L-7 (a–e) PDVR, stage C. Stage C is – similarly to the PVR classification – characterized by a traction retinal detachment, which includes the macula. PDVR, stage C. According to the number of quadrants involved, stages C1–C4 are distinguished

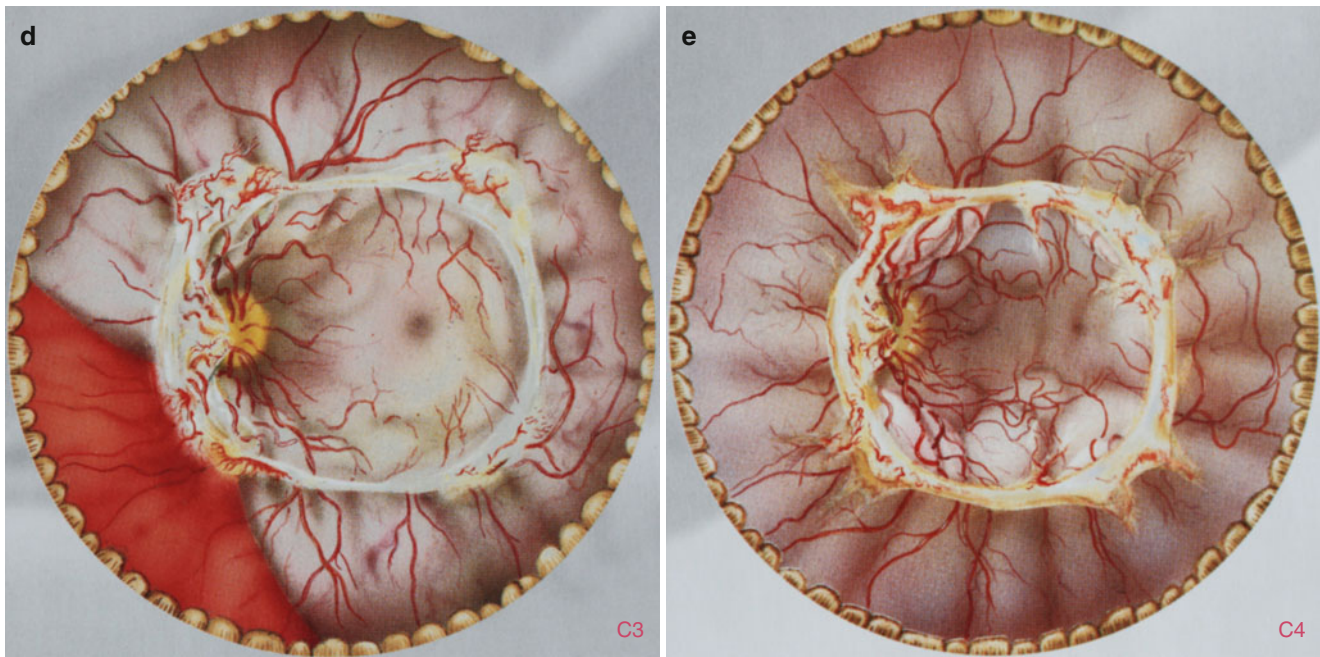


Figure III.L-7 (continued)

IV. Summary

While the underlying pathogenesis of NPDR has a multifactorial origin consisting of intraluminal and extraluminal factors of the retinal vessels and biochemical components of growth factors and especially advanced glycation end products, PDVR appears to reflect a different etiology. The vitreoretinal interface, especially the posterior vitreous cortex, plays a key role in the pathogenesis of PDVR. This vitreoretinal interface is thickened tenfold and becomes a metabolic barrier between retina and vitreous, leading to an accumulation of VEGF, expressed mainly by the Müller cells, which explains the proliferation of pathologic new vessels out of the retina into the posterior vitreous cortex. With progression toward PDVR, shrinkage of the posterior vitreous cortex with its tight adhesions to the retina results in the dramatic changes of traction retinal detachment. The classification for NPDR, established by the ETDRS in 1981 [7], has been confirmed by the International Clinical Diabetic Retinopathy Severity Scale in 2003. However, these classifications did not consider the role of diabetic vitreopathy [see chapter I.E. Diabetic vitreopathy] in the course of the proliferating forms of diabetic retinopathy and the status of the vitreoretinal interface [16]. Therefore, a morphological classification has been established, which combines the severity of the retinopathy with the status of diabetic vitreopathy. For this reason, the accurate and more precise term PDVR should be used instead of the more generalized term PDR. This classification system serves:

1. To document morphological fundus changes in PDVR
2. To grade the severity of the PDVR
3. To improve communication between ophthalmologists as well as patients
4. To indicate all forms of therapy: laser treatments, as long as the retina is attached; pars plana vitrectomy for removal of tractional vitreous, hemorrhages and attach the retina; and probably in the near future pharmacologic vitreolysis treatments
5. To predict the success of any treatment
6. To predict the further course of the diabetic fundus changes
7. To serve for retro- and prospective studies of any outcome of treatments or other defined studies of diabetic retinopathy

Abbreviations

AAO	American Academy of Ophthalmology
DCCT	Diabetes Control and Complication Trial
DM	Diabetes mellitus
DR	Diabetic retinopathy
DRVS	Diabetic Retinopathy Vitrectomy Study
EGF	Endothelial growth factor
ETDRS	Early Treatment Diabetic Retinopathy Study
ICDRS	International Clinical Diabetic Retinopathy Severity
ILM	Inner limiting membrane

IRMAs	Intraretinal microvascular abnormalities
NPDR	Nonproliferative diabetic retinopathy
PDGF	Platelet-derived growth factor
PDR	Proliferative diabetic retinopathy
PDVR	Proliferative diabetic vitreoretinopathy
PRP	Panretinal laser photocoagulation
PVD	Posterior vitreous detachment
PVR	Proliferative vitreoretinopathy
RD	Retinal detachment
TGF	Transforming growth factor
IL-1	Interleukin 1
UKPDS	United Kingdom Prospective Diabetes Study
VEGF	Vascular endothelial growth factor
WESDR	Wisconsin Epidemiological Study of Diabetic Retinopathy

References

- Akiba J, Ueno N, Chakrabarti B. Molecular mechanisms of posterior vitreous detachment. *Graefes Arch Clin Exp Ophthalmol*. 1993;231:408–12.
- Akiba J, Kakehashi A, Ueno N, Tano Y, Chakrabarti B. Serum-induced collagen gel contraction. *Graefes Arch Clin Exp Ophthalmol*. 1995;233:430–4.
- Blankenship GW, Machemer R. Long-term diabetic vitrectomy results. Report of 10 year follow-up. *Ophthalmology*. 1985;92:503–6.
- Casaroli Marano RP, Vilaró S. The role of fibronectin, laminin, vitronectin and their receptors on cellular adhesion in proliferative vitreoretinopathy. *Invest Ophthalmol Vis Sci*. 1994;35:2791–803.
- Chantelau E, Kohner EM, Seppel T, Schonau E, Althaus C. Elevation of serum IGF-1 precedes proliferative diabetic retinopathy in Mauriac's syndrome. *Br J Ophthalmol*. 1997;81:169–70.
- Costa Ede P, Rodrigues EB, Farah ME, Sebag J, Meyer CH. Novel vitreous modulators for pharmacologic vitreolysis in the treatment of diabetic retinopathy. *Curr Pharm Biotechnol*. 2011;12:410–22.
- Diabetic Retinopathy Study Research Group. Report 7: a modification of the Airlie-House-classification of diabetic retinopathy. *Invest Ophthalmol Vis Sci*. 1981;21:210–26.
- Diabetic Retinopathy Vitrectomy Study Research Group. Early vitrectomy for severe vitreous hemorrhage in diabetic retinopathy: two-year results of a randomized trial. *Diabetic Retinopathy Vitrectomy Study report 2*. *Arch Ophthalmol*. 1985;103:1644–52.
- Early Treatment Diabetic Retinopathy Study Research Group. Grading diabetic retinopathy from stereoscopic color fundus photographs—an extension of the modified Airlie-House-classification. ETDRS report No 10. *Ophthalmology*. 1991;98:786–806.
- Faulborn J, Bowald S. Microproliferations in proliferative diabetic retinopathy and their relationship to vitreous: corresponding light and electron microscopic studies. *Graefes Arch Clin Exp Ophthalmol*. 1985;223:130–8.
- Gentile RC, Milman T, Elliott D, Romero JM, McCormick SA. Taut internal limiting membrane causing diffuse diabetic macular edema after vitrectomy: clinicopathological correlation. *Ophthalmologica*. 2011;226:64–70.
- Hammes HP, Alt A, Niwa T, Clausen JT, Bretzel RG, Brownlee M, Schleicher ED. Differential accumulation of advanced glycation end products in the course of diabetic retinopathy. *Diabetologia*. 1999;42:728–36.
- Hammes HP, Kerner W, Hofer S, Kordonouri O, Raile K, Holl RW, DPV-Wiss Study Group. Diabetic retinopathy in type 1 diabetes—a contemporary analysis of 8,784 patients. *Diabetologia*. 2011;54:1977–84.
- Harbour JW, Smiddy WE, Flynn Jr HW, Rubsamen PE. Vitrectomy for diabetic macular edema associated with a thickened and taut posterior hyaloid membrane. *Am J Ophthalmol*. 1996;121:405–13.
- Hesse L, Heller G, Kraushaar N, Wesp A, Schroeder B, Kroll P. The predictive value of a classification for proliferative diabetic vitreoretinopathy. *Klin Monatsbl Augenheilkd*. 2002;219:46–9.
- Hörle S, Kroll P. Evidence-based therapy of diabetic retinopathy. *Ophthalmologica*. 2007;221:132–41.
- Hwang JC, Sharma AG, Elliott D. Fello eye vitrectomy for proliferative diabetic retinopathy in an inner city population. *Br J Ophthalmol*. 2013;97:297–301.
- Jain A, Saxena S, Khanna VK, Shukla RK, Meyer CH. Status of serum VEGF and ICAM-1 and its association with external limiting membrane and inner segment-outer segment junction disruption in type 2 diabetes mellitus. *Mol Vis*. 2013;19:1760–8.
- Khono T, Sorgente N, Ishibashi T, Goodnight R, Ryan SJ. Immunofluorescent studies of fibrinogen and laminin in the human eye. *Invest Ophthalmol Vis Sci*. 1987;28:506–14.
- Khono T, Sorgente N, Goodnight R, Ryan SJ. Alterations in the distribution of fibrinogen and laminin in diabetic human eye. *Invest Ophthalmol Vis Sci*. 1987;28:515–21.
- Klein R, Klein BEK, Moss SE, et al. The Wisconsin Epidemiological Study of Diabetic Retinopathy. IX. Four-year incidence and progression of diabetic retinopathy when age of diagnosis is less than 30 years. *Arch Ophthalmol*. 1989;107:237–43.
- Klein R, Myers CE, Lee KE, Klein BE. 15-year cumulative incidence and associated risk factors for retinopathy in nondiabetic persons. *Arch Ophthalmol*. 2010;128:1568–75.
- Klein R, Lee KE, Gangnon RE, Klein BE. The 25-year incidence of visual impairment in type 1 diabetes mellitus the wisconsin epidemiologic study of diabetic retinopathy. *Ophthalmology*. 2010;117:63–70.
- Kroll P, Meyer-Rüsenberg HW, Busse H. Recommendation for staging of proliferative diabetic retinopathy. *Fortschr Ophthalmol*. 1987;84:360–3.
- Kroll P, Wiegand W, Schmid J. Vitreopapillary traction in proliferative diabetic vitreoretinopathy. *Br J Ophthalmol*. 1999;83:261–4.
- Kroll P, Rodrigues EB, Hörle S. Pathogenesis and classification of proliferative diabetic vitreoretinopathy. *Ophthalmologica*. 2007;221:78–94.
- Lecaire TJ, Palta M, Klein R, Klein BE, Cruickshanks KJ. Assessing progress in retinopathy outcomes in type 1 diabetes: comparing findings from the Wisconsin Diabetes Registry Study and the Wisconsin Epidemiologic Study of Diabetic Retinopathy. *Diabetes Care*. 2013;36:631–7.
- Leuenberger S, Faulborn J, Gülecek O. Histologische Untersuchungen über die Auswirkung der Lichtkoagulation der Netzhaut auf den Glaskörper. *Klin Mbl Augenheilk*. 1985;186:272–4.
- Lewis H, Abrams GW, Blumenkranz MS, Campo RV. Vitrectomy for diabetic macular traction and edema associated with posterior hyaloidal traction. *Ophthalmology*. 1992;99:753–9.
- Meyer CH, Zaki NV, Mennel S, Schmidt JC, Kroll P. Verlauf der diabetischen Retinopathie bei einem Zwillingsspaar 5 Jahre nach Pankreas-Transplantation. *Spektrum der Augenheilkunde*. 2005;19:183–7.
- Meyer CH, Kroll P, Hammes HP. Does insulin glargine (lantus) lead to a progression in diabetic retinopathy? *Klin Monbl Augenheilkd*. 2005;222:353–4.

32. Meyer CH. Current treatment approaches in diabetic macular edema. *Ophthalmologica*. 2007;221:118–31.
33. Meyer CH, Rodrigues EB, Maia M, Farah ME, Penha FM, Holz FG. Emerging pharmacotherapies for diabetic macular edema. *Expert Opin Emerg Drugs*. 2007;12:591–603.
34. Meyer CH, Schmidt JC, Mennel S, Kroll P. Functional and anatomical results of vitreopapillary traction after vitrectomy. *Acta Ophthalmol Scand*. 2007;85:221–2.
35. Norton EWD, Davis MD, Fine SL. The Airlie classification of diabetic retinopathy, in Goldberg MF, Fine SL (eds): *Symposium on the Treatment of Diabetic Retinopathy*, publication 1890. Federal Security Agency, Public Health Service, 1968, pp 7–22.
36. Olafsdottir E, Andersson DK, Dedorsson I, Stefánsson E. The prevalence of retinopathy in subjects with and without type 2 diabetes mellitus. *Acta Ophthalmol*. 2013 Mar;4.
37. Pendergast SD, Hassan TS, Williams GA, Cox MS, Margherio RR, Ferrone PJ, Garretson BR, Trese MT. Vitrectomy for diffuse diabetic macular edema associated with a taut premacular posterior hyaloid. *Am J Ophthalmol*. 2000;130:178–86.
38. Quéllec G, Lamard M, Cazuguel G, Bekri L, Daccache W, Roux C, Cochener B. Automated assessment of diabetic retinopathy severity using content-based image retrieval in multimodal fundus photographs. *Invest Ophthalmol Vis Sci*. 2011;52:8342–8.
39. Sato Y, Lee Z. The subclassification and longterm prognosis of proliferative diabetic retinopathy. *Jpn J Ophthalmol*. 2002;46:323–9.
40. Schlingemann RO, Van Noorden CJ, Diekman MJ, Tiller A, Meijers JC, Koolwijk P, Wiersinga WM. VEGF Levels in plasma in relation to platelet activation, glycemic control, and microvascular complications in type 1 diabetes mellitus. *Diabetes Care*. 2013; 36:1629–34.
41. Sebag J, Buzney SM, Belyea DA, et al. Posterior vitreous detachment following panretinal laser photocoagulation. *Graefes Arch Clin Exp Ophthalmol*. 1990;228:5–8.
42. Sebag J. Age-related differences in the human vitreo-retinal interface. *Arch Ophthalmol*. 1991;109:966–71.
43. Sebag J, Buckingham B, Charles MA, Reiser K. Biochemical abnormalities in vitreous of humans with proliferative diabetic retinopathy. *Arch Ophthalmol*. 1992;110:1472–6.
44. Sebag J. Abnormalities of human vitreous structure in diabetes. *Graefes Arch Clin Exp Ophthalmol*. 1993;231:257–60.
45. Sebag J, Nie S, Reiser KA, Charles MA, Yu NT. Raman spectroscopy of human vitreous in proliferative diabetic retinopathy. *Invest Ophthalmol Vis Sci*. 1994;35:2976–80.
46. Sebag J. Diabetic vitreopathy. *Ophthalmology*. 1996;103:205–6.
47. Sebag J, Hageman GS. Interfaces. *Eur J Ophthalmol*. 2000;10: 1–3.
48. Sebag J. Is pharmacologic vitreolysis brewing? *Retina*. 2002;22: 1–3.
49. Sebag J. Molecular biology of pharmacologic vitreolysis. *Trans Am Ophthalmol Soc*. 2005;103:473–94.
50. Sebag J. Vitreoschisis. *Graefes Arch Clin Exp Ophthalmol*. 2008;246:329–32.
51. Sebag J. Pharmacologic vitreolysis – premise and promise of the first decade. *Retina*. 2009;29:871–4.
52. Sebag J. Vitreoschisis in diabetic macular edema. *Invest Ophthalmol Vis Sci*. 2011;52:8455–6.
53. Sebag J, Green WR. Vitreous and the vitreo-retinal interface. In: Ryan SJ, editor. *Retina*. St. Louis: Mosby; 2012.
54. Sévin R, Cuendet JF. Diabetic retinopathy and capillary resistance. Comparative study of various treatments. *Bibl Ophthalmol*. 1968;76:139–45.
55. Shea M. Early vitrectomy in proliferative diabetic retinopathy. *Arch Ophthalmol*. 1983;101:1204–5.
56. Stalmans P, Benz MS, Gandorfer A, Kampik A, Girach A, Pakola S, Haller J. Enzymatic vitreolysis with ocriplasmin for vitreomacular traction and macular hole. *N Engl J Med*. 2012;367(7): 606–15.
57. Stefánsson E, Landers III MB, Wolbarsht ML. Increased retinal oxygen supply following Pan-retinal photocoagulation and vitrectomy and lensectomy. *Trans Am Ophthalmol Soc*. 1981;79: 307–34.
58. Stefánsson E, Machermer R, de Juan Jr E, McCuen 2nd BW, Peterson J. Retinal oxygenation and laser treatment in patients with diabetic retinopathy. *Am J Ophthalmol*. 1992;113:36–8.
59. Stefánsson E. Microplasmin-induced posterior vitreous detachment affects vitreous oxygen levels. *Retina*. 2008;28:1175–6.
60. The Diabetes Control and Complications Trial Research Group. The effect of intensive treatment of diabetes on the development and progression of long-term complications in insulin-dependent diabetes mellitus. *N Engl J Med*. 1993;32:977–86.
61. Tozer K, Fink W, Sadun AA, Sebag J. Prospective three-dimensional analysis of structure and function in macular hole treated by pharmacologic vitreolysis. *Retin Cases Brief Rep*. 2013;7:57–61.
62. UK Prospective Diabetes Study (UKPDS) Group. Intensive blood-glucose control with sulphonylurease or insulin compared with conventional treatment and risk of complications in patients with type 2 diabetes (UKPDS 33). *Lancet*. 1998;352:837–53.
63. UK Prospective Diabetes Study Group. Tight blood pressure control and risk of macrovascular complications in type 2 diabetes: UKPDS 38. *BMJ*. 1998;317:703–13.
64. Verstraeten TC, Chapman C, Hartzler M, Winkler BS, Trese MT, Williams GA. Pharmacologic induction of posterior vitreous detachment in the rabbit. *Arch Ophthalmol*. 1993;111:849–54.
65. Vésteinsdóttir E, Björnsdóttir S, Hreidarsson AB, Stefánsson E. Risk of retinal neovascularization in the second eye in patients with proliferative diabetic retinopathy. *Acta Ophthalmol*. 2010;88: 449–52.
66. Vlodaysky I, Bar-Shavit R, Ishai-Michaeli R, Bashkin P, Fuks Z. Extracellular sequestration and release of fibroblast growth factor: a regulatory mechanism. *Trends Biochem Sci*. 1991;16: 268–71.
67. Wilkinson CP, Ferries 3rd FL, Klein RE, Lee PP, Agardh CD, Davis M, Dills D, Kampik A, Pararajasegaram R, Verdager JT, Global Diabetic Retinopathy Project Group. Proposed international clinical diabetic retinopathy and macular edema disease severity scales. *Ophthalmology*. 2003;110:1677–81.
68. Yang XM, Yafai Y, Wiedemann P, Kuhrt H, Wang YS, Reichenbach A, Eichler W. Hypoxia-induced upregulation of pigment epithelium-derived factor by retinal glial (Müller) cells. *J Neurosci Res*. 2012;90:257–66.
69. Yoshida S, Nakama T, Ishikawa K, Arima M, Tachibana T, Nakao S, Sassa Y, Yasuda M, Enaida H, Oshima Y, Kono T, Ishibashi T. Antiangiogenic shift in vitreous after vitrectomy in patients with proliferative diabetic retinopathy. *Invest Ophthalmol Vis Sci*. 2012;53:6997–7003.
70. Zhang ZY, Zhang XR. Effect of axial length on diabetic retinopathy. *Ophthalmology*. 2013;120:876–7.
71. Zehetner C, Kirchmair R, Kralinger M, Kieselbach G. Correlation of vascular endothelial growth factor plasma levels and glycemic control in patients with diabetic retinopathy. *Acta Ophthalmol*. 2013;91:e470–3.

Part IV

Physiology and Pharmacotherapy

Einar Stefánsson

Einar Stefánsson

Outline

- I. **Introduction**
- II. **Physiology**
 - A. Molecular Transport in the Vitreous
 - 1. Viscosity of Vitreous
 - B. Oxygen Physiology
- III. **Pathology**
 - A. Vitreous Aging
 - 1. Clearance of Molecules in the Vitreous
 - B. Iris Neovascularization
 - C. Retinal Neovascularization
 - D. Macular Edema
 - 1. Origins of Macular Edema
 - a. Increased Hydrostatic Pressure Gradient
 - b. Decreased Osmotic Pressure Gradient
 - 2. Diabetic Macular Edema
 - 3. Macular Edema in Retinal Vein Occlusions
 - 4. Vitreoretinal Traction and Edema
 - 5. Treating Macular Edema
 - a. Decreasing Hydrostatic Pressure Gradient
 - b. Increasing Osmotic Pressure Gradient
 - c. The Central Role of Oxygen
 - E. Age-Related Macular Degeneration (AMD)
 - F. Vitrectomy and Cataract
 - G. Vitrectomy and Glaucoma

References

Keywords

Vitreous • Physiology • Convection currents • Viscosity • Diffusion • Transport • Oxygen • Posterior vitreous detachment • Vitrectomy • Cataract • Neovascularization • Pharmacologic vitreolysis

Key Concepts

1. Vitreous gel modulates the transport of molecules through the vitreous body. The high viscosity of the gel reduces transport by convection currents and diffusion. With age, surgery, or pharmacologic vitreolysis, vitreous viscosity is reduced and the rate of transport of various molecules increases. This physiological change has various clinical consequences, some beneficial and others harmful.
2. Oxygen has been the prime molecule in the study of vitreous physiology and the effect of treatment. Changes in oxygen metabolism explain many of the clinical findings and correlate nicely with the effect of laser and other treatment modalities in the ischemic retinopathies.
3. Vitrectomy and pharmacologic vitreolysis stimulate nuclear sclerosis cataract formation. Posterior vitreous detachment and vitrectomy may protect against macular edema and neovascularization in diabetic and other ischemic retinopathies as well as age-related macular degeneration.

E. Stefánsson, MD, PhD
Department of Ophthalmology,
National University Hospital, University of Iceland,
Eiriksgata 37, 3.h., Reykjavik 101, Iceland
e-mail: einarste@landspitali.is

I. Introduction

Untouchable, Disposable and Invisible

Well into the twentieth century, most ophthalmologists considered the vitreous body to be sacred and that any interference with this structure would have serious consequences for the eye. The vitreous was *untouchable*. Pioneering researchers [1–7] changed this axiom, and towards the end of the century, vitreoretinal surgeons came to think of the vitreous gel almost as an inert substance, which could be freely operated, removed, and replaced for optical and structural reasons, with no consideration for any other functions of this tissue. It became *disposable*. At the same time the vitreous was practically *invisible*; visualizing vitreous detachment with slit lamp biomicroscopy was unreliable, but dramatically improved with ultrasound and optical coherence tomography (OCT). [see chapter II.F. To See the Invisible - the Quest of Imaging Vitreous]

Vitreous surgery and the removal and replacement of vitreous have physiological and clinical consequences for the eye, some beneficial and others detrimental. Several clinical effects have been recognized for decades, and while some of the physiological mechanisms were reported in the early 1980s, it is only recently that vitreoretinal surgeons have opened their eyes to the physiological consequences of vitreoretinal surgery.

This chapter explains the physiological consequences of vitreous surgery, some of which may be predicted from classical laws of physics and physiology. Understanding these physiological mechanisms allows a better rationale in the management of vitreous surgery and its combination with laser treatment and drug injections. Vitreous physiology has moved the vitreous gel to the center of ophthalmology and not just the eye.

II. Physiology

A. Molecular Transport in the Vitreous

The physiological consequences of vitreous gel removal, liquefaction, or replacement are predicted by classical theories of physics. They predict the effect vitrectomy has on transport of molecules within the vitreous chamber and the eye. Molecule transport within the vitreous is by two mechanisms: diffusion and convection currents. Diffusion may be described by the laws of Fick and Stokes–Einstein and fluid currents by the law of Hagen–Poiseuille [8]. Fick’s law describes the diffusion flux, J , in terms of the diffusion coefficient, D , and the concentration gradient of the molecule dC/dx :

$$J = D \, dC / dx$$

Stokes and Einstein described the diffusion coefficient, D , in terms of the molar gas constant, R ; the temperature in degrees Kelvin, T ; the viscosity of medium, η ; the radius of diffusing molecule, r ; and Avogadro’s number, N :

$$D = \frac{RT}{6\pi\eta rN}$$

The diffusion coefficient, D , is inversely related to the viscosity of the medium, η . Consequently, rate of diffusion is also inversely related to the viscosity of the medium.

The Hagen–Poiseuille law describes fluid currents, J , in terms of the pressure difference, ΔP ; the length, L ; and diameter, d , of a channel and the viscosity of medium, η .

$$J = \pi d^4 \Delta P / 8L\eta$$

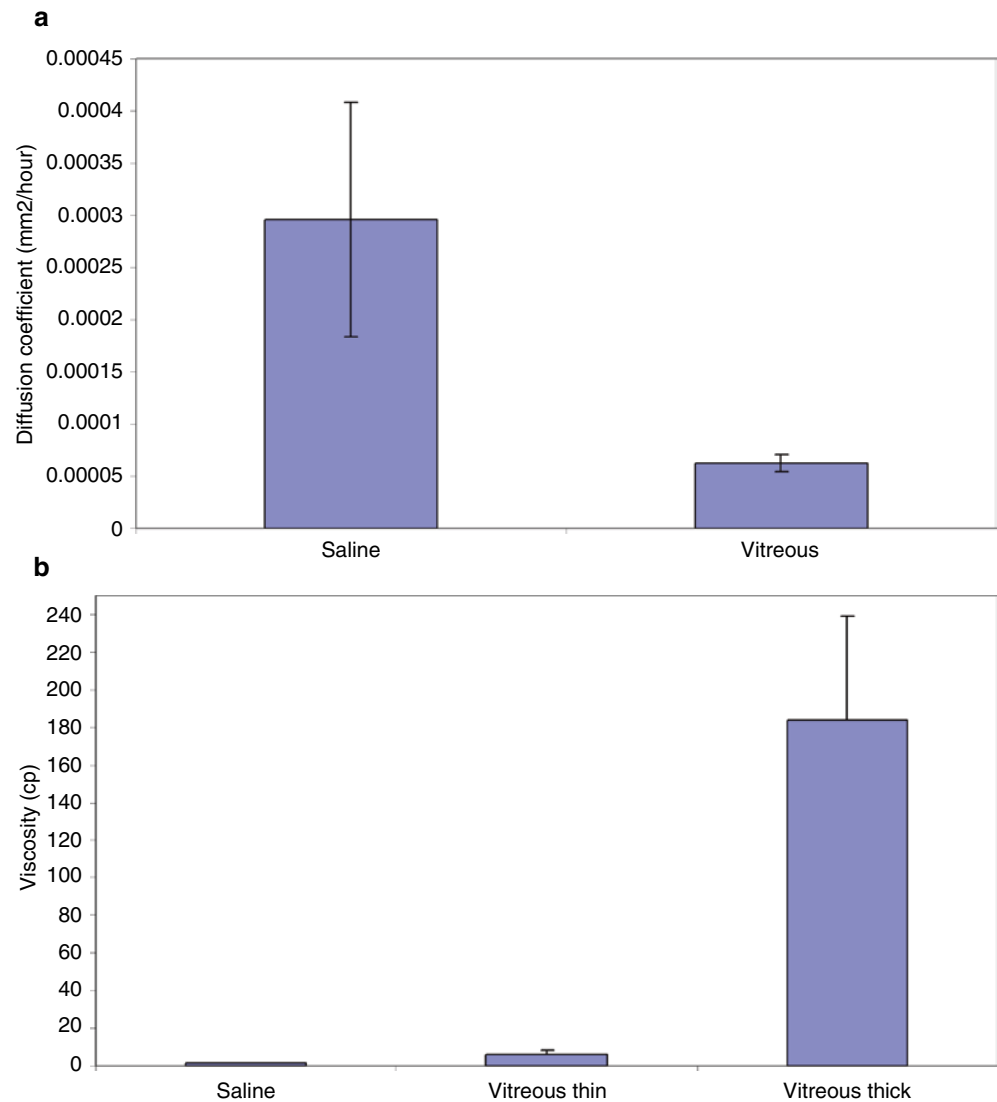
Note that convection currents, J , are inversely related to the viscosity of the medium, η .

It is important to note that both diffusion and convection currents are inversely related to the viscosity of the medium. This may be intuitively obvious: diffusion and fluid currents are slower in a highly viscous substance than in a less viscous medium. Since vitrectomy involves the replacement of the vitreous with substances that have different viscosity, this influences the transport of molecules in the vitreous cavity. It is important to keep in mind that this is a general principle that applies to all diffusing molecules, both beneficial and potentially harmful molecules including oxygen and other nutrients, drugs, growth factors, and other cytokines.

1. Viscosity of Vitreous

Ophthalmic surgeons know by experience that the vitreous gel is more viscous than the saline solution that replaces it or the aqueous humor that eventually fills the vitrectomized eye. At the same time the silicone oil, with which we sometimes fill the vitreous chamber has higher viscosity than both vitreous gel and water. The surgeons’ impression is confirmed by science [9–11]. While the viscosity of the vitreous gel is variable and depends on species and measurement techniques, it is many times more than water, balanced salt solution, or aqueous humor. Lee et al. [12] found the viscosity of human vitreous gel to be 300–2,000 cP, while the viscosity of water is 1 cP. Gisladottir et al. [13] used a kinetic viscosity meter to measure the viscosity of porcine vitreous and found this to be bimodal; the thinner phase had viscosity of about 5 cP and the thicker about 180 cP (Figure IV.A-1). Also, the diffusion of dexamethasone was found to be about five times greater in saline than in vitreous (Figure IV.A-1). Similarly, Sebag et al. [14] showed that pharmacologic vitreolysis with ocriplasmin increases vitreous diffusion coefficients *in vitro*. It is reasonable to assume that the vitreolysis breaks down vitreous macromolecules and reduces the viscosity of the vitreous gel, resulting in increased diffusion coefficients. Silicone oil that is used for vitreoretinal surgery

Figure IV.A-1 (a) Diffusion of dexamethasone through vitreous gel (b) Viscosity of porcine vitreous comparing saline to liquid vitreous (*thin*) and gel vitreous (*thick*) (From Gisladdottir et al. [13])



is available in several different viscosities, all of which are considerably more viscous than vitreous gel [15].

The relatively high viscosity of the vitreous gel modulates the transport of molecules within the vitreous body and keeps the rate of transport at a relative low level. This is important for the tissues surrounding the vitreous. With age, the viscosity changes as well as the transport characteristics, and this plays a role in some of the aging diseases in the lens and the retina.

B. Oxygen Physiology

The first studies of vitreous physiology were by-products of studies about oxygen physiology in the retina. In 1972, Alm and Bill [16] showed that oxygen tension in the cat vitreous falls gradually moving anteriorly from the surface of the retina to a minimum behind the crystalline lens. The first

physiological studies of vitreous surgery were published in the early 1980s. Stefansson et al. [17, 18] removed the vitreous gel and crystalline lens in cats and found that oxygen transport between the anterior and posterior segments of the eye was increased in the vitrectomized–lensectomized eye compared to the intact eye (Figure IV.A-2). Oxygen was transported at a faster rate from the anterior segment, resulting in a significantly lower PO₂ in the aqueous humor. If the retina was made ischemic and hypoxic with vascular occlusion, the oxygen tension in the anterior segment fell even more (Figure IV.A-2).

de Juan et al. [19] showed that silicone oil is the exception that proves the rule. Using silicone oil that is more viscous than the vitreous humor, they reported that anterior chamber hypoxia in the vitrectomized–lensectomized cat eye is prevented if the vitreous chamber is filled with silicone oil (Figure IV.A-3). The silicone oil is highly viscous, slows the transport of oxygen, and reestablishes a diffusion barrier,

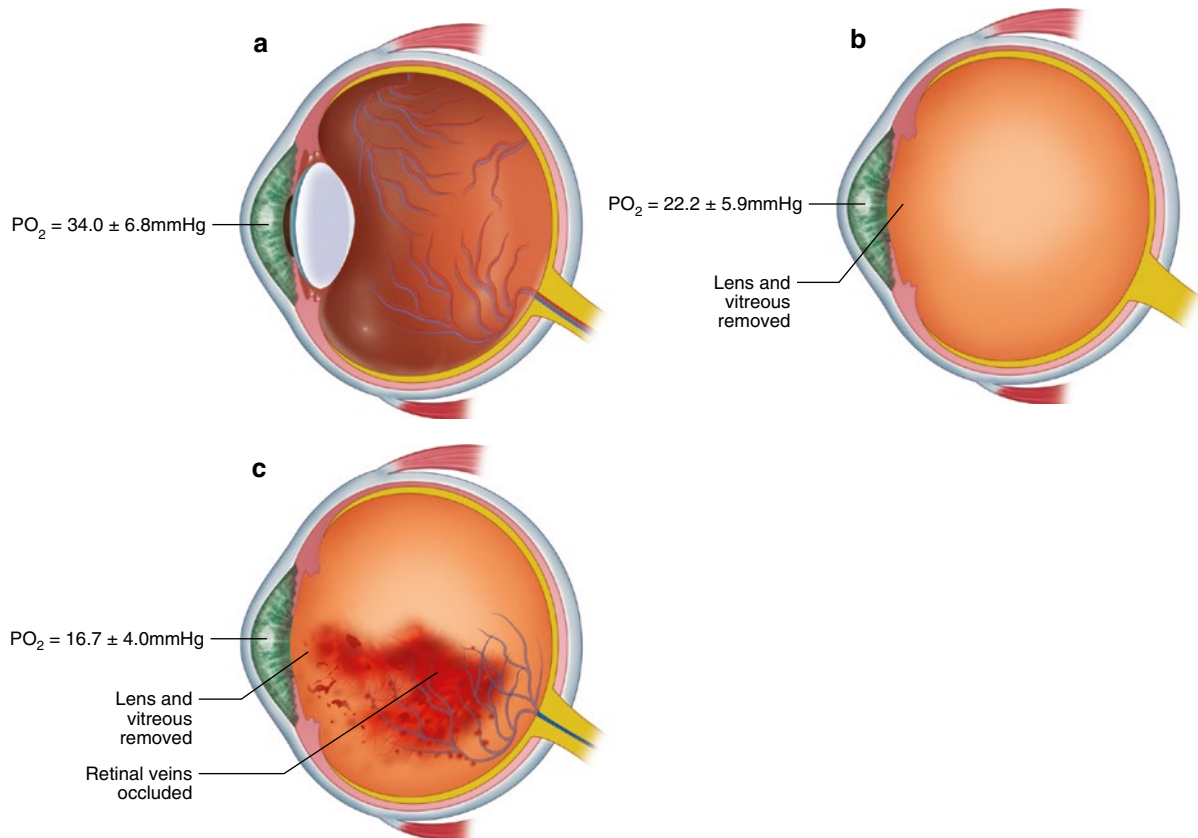


Figure IV.A-2 Stefánsson et al. (1981) reported the oxygen tension in the anterior chamber of cat eyes. The mean anterior chamber oxygen tension is 34 mmHg in the intact eye (a), 22 mmHg after vitrectomy and lens extraction (b), which is similar to the normal retinal oxygen

tension in cats. The anterior chamber oxygen tension falls to 17 mmHg if the retinal veins are occluded in the vitrectomized–lensectomized eye (c) (Published with permission from the American Ophthalmological Society)

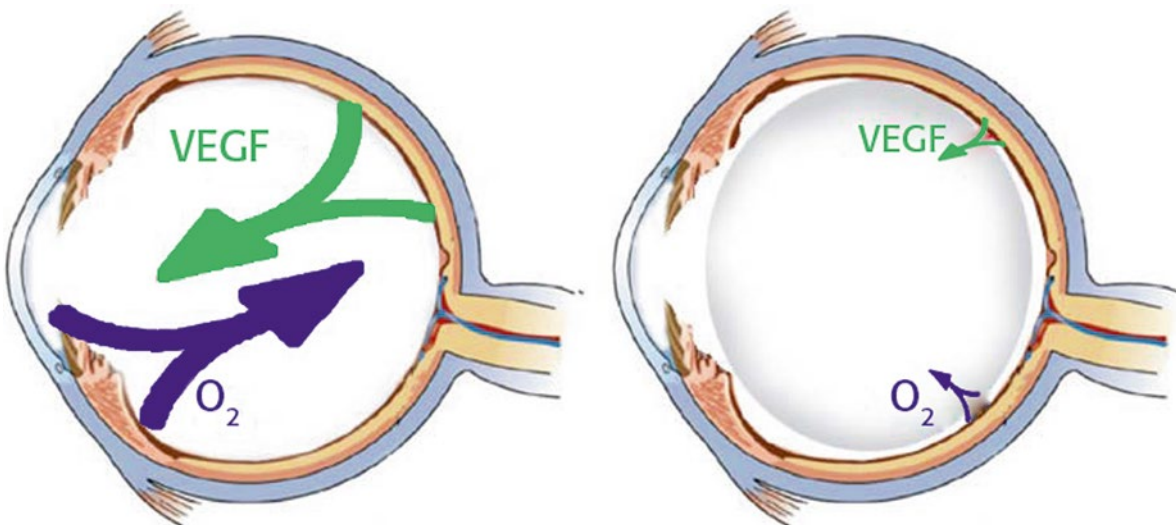


Figure IV.A-3 The schematic drawings show the theoretical fluxes of oxygen and vascular endothelial growth factor (VEGF; and any molecule) in the vitrectomized–lensectomized eye (left) and silicone oil-filled vitreous chamber (right). The low viscosity of the fluid in the vitrectomized eye increases diffusion and convection currents compared with the intact eye. Oxygen is transported from the anterior segment and well-perfused retinal areas to ischemic retinal areas. VEGF is cleared away from the ischemic retinal areas by diffusion and convec-

tion at a much higher rate than before vitrectomy. The retina receives oxygen and gets rid of VEGF, and the risk of retinal neovascularization decreases. At the same time, the iris loses oxygen and receives VEGF from the retina, and the risk of iris neovascularization is increased. Silicone oil is more viscous than the vitreous gel, and transport of all molecules is slowed accordingly. It reestablishes the diffusion barrier between the anterior and posterior segments and reduces the risk of iris neovascularization

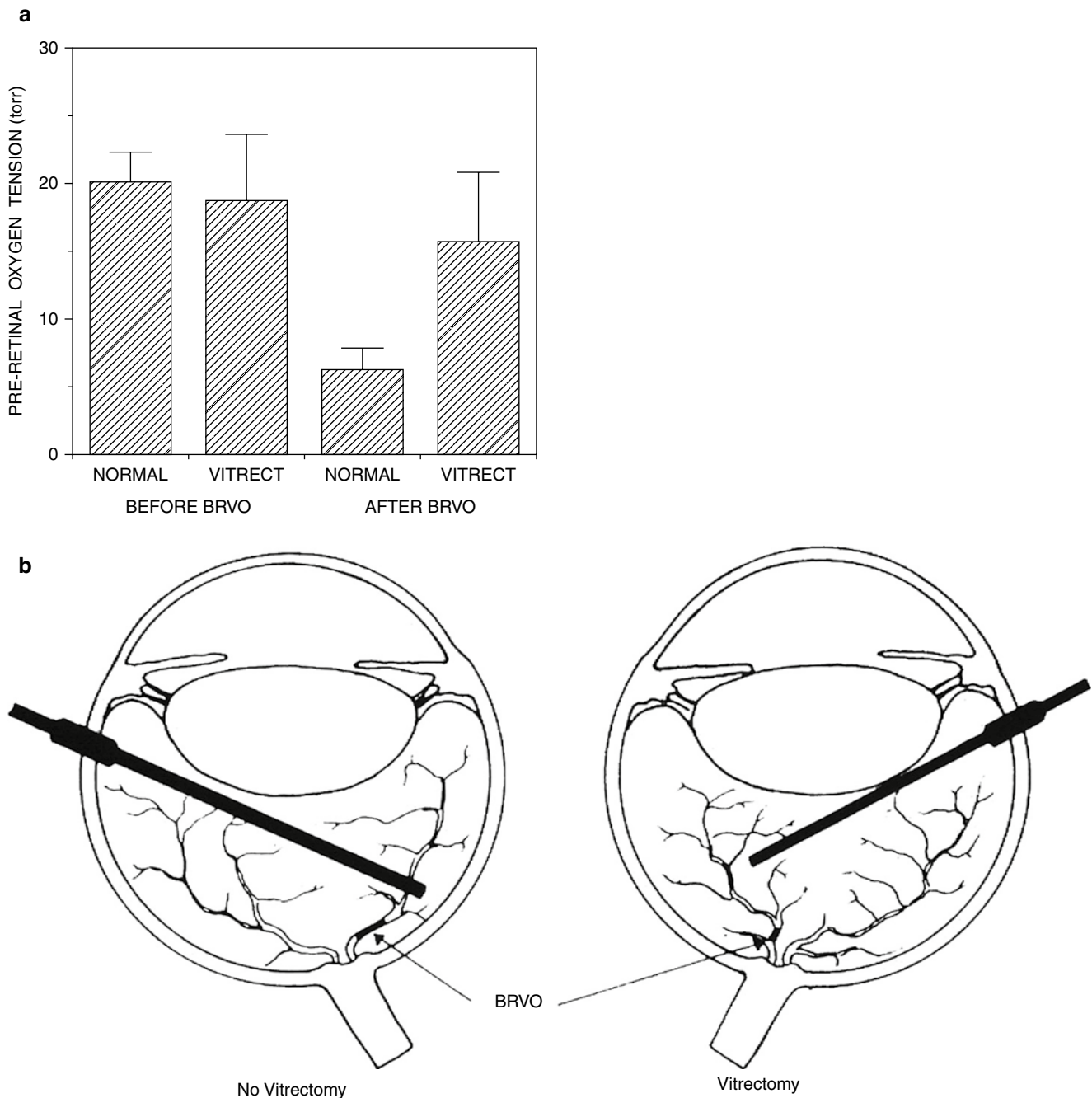


Figure IV.A-4 Stefánsson et al. [20] reported that preretinal oxygen tension falls with branch retinal vein occlusion (BRVO) in the intact eye, but vitrectomy prevents retinal hypoxia in this situation. (a) Shows

the oxygen tension measurements and figure (b) the experimental set-up (Reprinted with permission from IOVS)

compared to the situation in the vitrectomized eye with aqueous humor filling.

In the late 1980s, Stefánsson et al. [20] induced bilateral branch retinal vein occlusion (BRVO) in cats, where one eye had vitrectomy and the other eye not. BRVO leads to severe regional hypoxia in the retina in non-vitrectomized eyes, whereas vitrectomy reduces or prevents hypoxia in the ischemic retina (Figure IV.A-4). These studies clearly estab-

lished the physiological effect of vitreous surgery on increased oxygen transport in the eye (Figure IV.A-5).

Blair and colleagues [21, 22] demonstrated in cats that the retina may be oxygenated from the vitreous body by “vitroperfusion.” Maeda and Tano [23] measured oxygen tension in the human vitreous chamber before and after vitrectomy and concluded that “successful diabetic vitrectomy reduces the activity of the neovascular tissue and equalizes

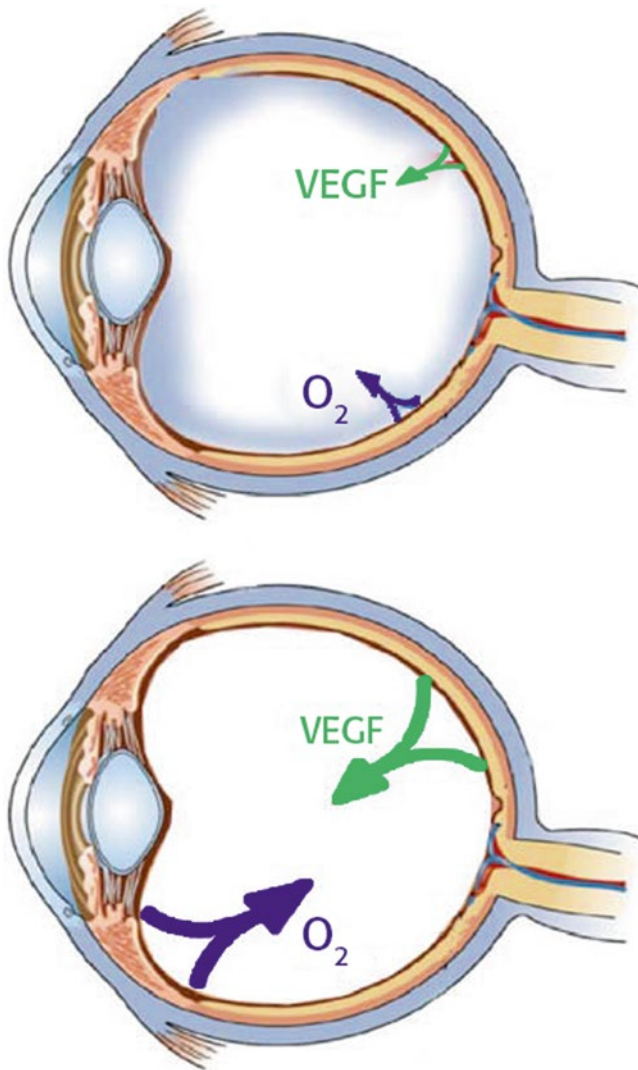


Figure IV.A-5 Schematic drawings showing the diffusion and convection fluxes of oxygen and VEGF (and any molecule) in the intact eye (*top*), vitrectomized eye (*bottom*). The transport of all molecules is relatively slow through the viscous vitreous in the intact eye and much faster when this is replaced with low-viscosity saline or aqueous. In the vitrectomized eye, oxygen diffuses from well-perfused to ischemic retinal areas, thus reducing hypoxia and VEGF production. At the same time, VEGF is cleared away from the retina at a faster rate. Both mechanisms combine to lower VEGF levels in the retina and inhibit neovascularization and edema

levels of oxygenation in vitreous.” Holekamp and Beebe et al. [24] have confirmed in the human eye that vitrectomy facilitates the diffusion of oxygen. In the vitrectomized eye, the oxygen tension gradients are flatter than in the normal eye, and the oxygen flux from the retina to the lens is increased. They have also suggested that oxygen consumption by ascorbic acid in the vitreous gel may play a role in increasing oxygen availability after vitrectomy [25] [see chapter IV.B. Oxygen in vitreo-retinal physiology and pathology]. Several investigators [26–30] have also dem-

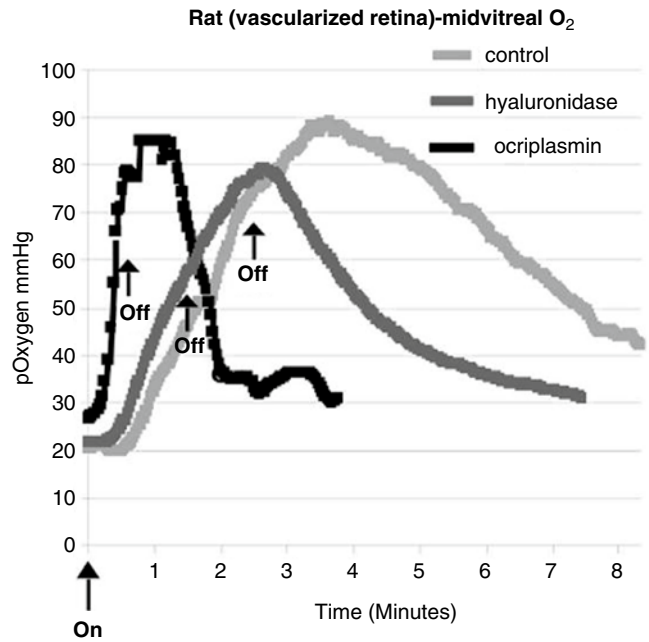


Figure IV.A-6 Comparison of mid-vitreous oxygen levels in control, ocriplasmin-, and hyaluronidase-treated rat eyes over time following exposure to 100 % oxygen. Arrows indicate start and stop of 100 % oxygen breathing. Reprinted with permission Quiram et al. [33]

onstrated oxygen delivery to the retina through the vitreous body.

Pharmacologic vitreolysis [31, 32] also creates a physiological situation with improved transport of molecules in the vitreous body. Sebag and colleagues [14, 31] demonstrated that ocriplasmin increased the diffusion coefficient of vitreous in a dose-dependent fashion, presumably via breakdown of the macromolecules of the vitreous. Quiram et al [33] showed that pharmacologic vitreolysis speeds oxygen diffusion within the vitreous body (Figure IV.A-6).

More recently, Petropoulos et al. [34] found that oxygen gradients in pig eyes were similar before and after vitrectomy and suggested that diffusion of oxygen was not changed by vitrectomy. They suggested that changes in oxygen transport after vitrectomy were predominantly due to convection currents, which are greater in low-viscosity fluids. Probably, convection currents are much more effective in transport than diffusion. In the completely still eye in an experimental setting, convection may be prevented. In the living mobile eye, convection currents are substantial, influenced by viscosity, and influence molecular transport within the vitreous body.

Simpson et al. [35] used magnetic resonance imaging to measure oxygen tension in the vitreous chamber before and after pars plana vitrectomy (Figure IV.A-7). They confirmed that oxygen tension in the mid-vitreous is significantly higher in vitrectomized eyes than normal. This confirms earlier invasive measurements in animals and humans.

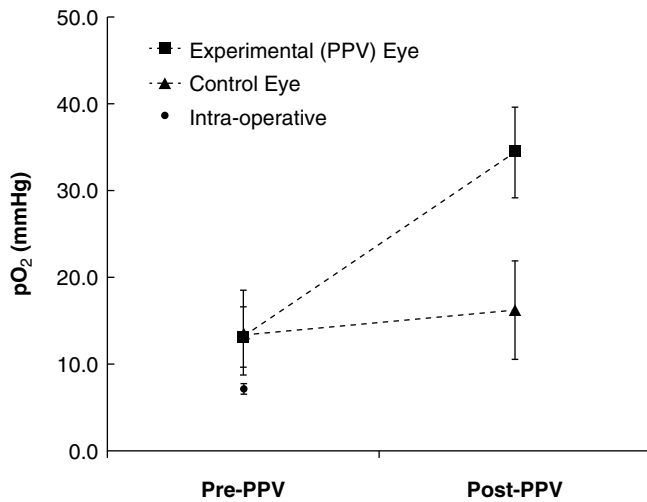


Figure IV.A-7 The effect of pars plana vitrectomy (PPV) on vitreous oxygenation measured with magnetic resonance imaging. Values are mean and error bars are SD. Reprinted with permission Simpson et al. [35]

Sín et al. [36] used noninvasive retinal oximetry (Figure IV.A-8) to measure oxygen saturation in retinal blood vessels before and after vitrectomy. They found higher oxygen saturation in retinal venules after vitrectomy compared to before (Figure IV.A-9). This shows that vitrectomy influences retinal oxygenation.

III. Pathology

When vitrectomy was first introduced, the rationale was entirely structural. Removal of bloody and opaque vitreous was intended solely to restore a clear visual pathway to improve patients' vision, for example, in cases of proliferative diabetic retinopathy. The long-term metabolic consequences came as a surprise – some good, some bad, but all unexpected. The following considers the metabolic effects of aging and various diseases, as well as the metabolic alterations introduced by therapeutic intervention of various types.



Figure IV.A-8 Pseudocolor retinal oximetry image (a) and spectrophotometric retinal oximeter (b). The oximetry image shows oxygen saturation in retinal vessels. The pseudocolor scale indicates oxygen saturation; red is 100 % saturation and violet is 0 %

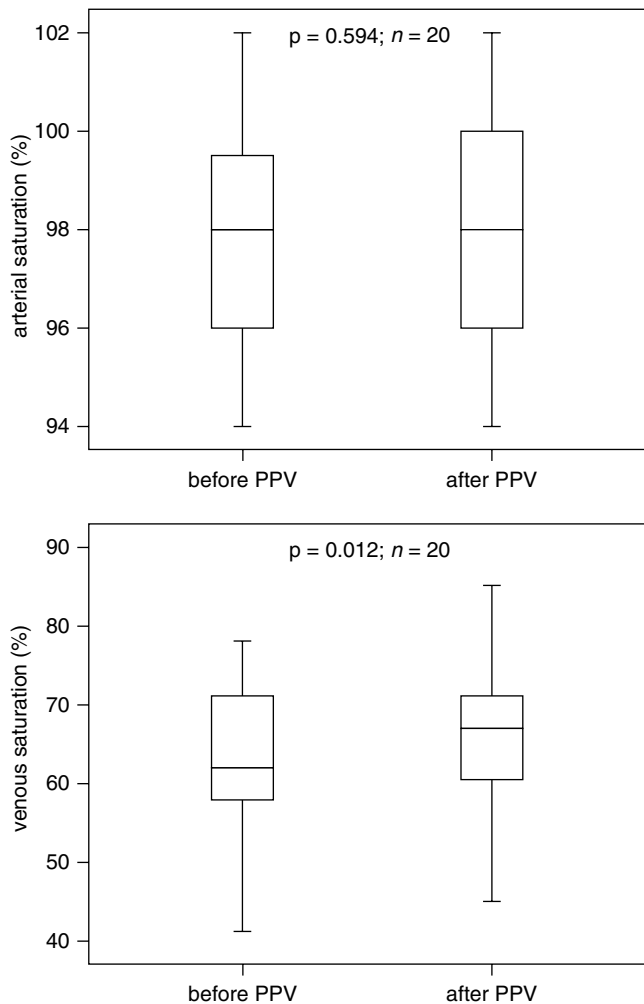


Figure IV.A-9 Box graphs comparing average arterial and venous saturation before and 45 days after pars plana vitrectomy (PPV) measured by automatic retinal oximetry. The box shows the distance between the quartiles, with the median marked as a line, and the whiskers show the maximum and the minimum. Paired t-tests were used for statistical analyses. Reprinted with permission Sín et al. [36]

A. Vitreous Aging

Changes in vitreous viscosity often result from natural degeneration [see chapter II.C. Vitreous aging and posterior vitreous detachment]. Sebag describes a *spectrum* from the fully attached, homogenous vitreous gel in a young healthy eye, through the various stages of vitreous liquefaction [37] and posterior vitreous detachment, partially vitrectomized eye, and pharmacologic vitreolysis to the totally vitrectomized eye on the other extreme [38]. Some of the same clinical consequences of vitrectomy may be seen in eyes with age-related vitreous liquefaction and posterior vitreous detachment. The development of posterior vitreous detachment in midlife may indeed reduce the risk of some aging diseases of the retina in older age, including exudative age-related macular degeneration and

diabetic retinopathy, while at the same time increase the risk of others, such as peripheral retinal tears and nuclear sclerotic cataract. These changes will be considered for a physiological perspective.

1. Clearance of Molecules in the Vitreous

The principle of increased transport with reduced viscosity of the medium applies to all molecules. It also applies to postoperative conditions following the replacement of the vitreous gel with saline, pharmacologic vitreolysis, and physiological degeneration of the vitreous gel and posterior vitreous detachment. This means that following vitrectomy, vitreolysis, or a posterior vitreous detachment, the transport of all molecules to and from the retina is increased (Figures IV.A-3 and IV.A-5). Molecules that are produced in the retina, such as vascular endothelial growth factor (VEGF), may be cleared into the fluid vitreous chamber at a higher rate following vitrectomy or posterior vitreous detachment. This serves to reduce the VEGF concentration in the retina (Figure IV.A-5) and may be helpful in several diseases. Obviously, the clearance of VEGF and other cytokines helps prevent macular edema and retinal neovascularization in ischemic retinopathies, such as diabetic retinopathy and retinal vein occlusions. The possible role of this phenomenon in age-related macular degeneration and diabetic macular edema will be discussed later. The positive or negative effect of clearance of molecules from the retina into the vitreous chamber following vitrectomy, vitreolysis, or posterior vitreous detachment needs further study in a variety of eye diseases.

Vitreous clearance of VEGF may have the same effect as the presence of VEGF antibodies in the vitreous body. VEGF, which is produced in the retina, diffuses from the retina into the vitreous body. If VEGF is constantly removed through clearance by diffusion, convection, binding with an antibody, or other mechanisms, the removal of VEGF from the retina will increase and the concentration of VEGF in (and under) the retina decrease.

B. Iris Neovascularization

Soon after the invention of vitrectomy, surgeons noticed increased risk of iris neovascularization following vitrectomy in diabetic retinopathy eyes, particularly if the lens had also been removed [39, 40]. In light of the previously described vitreous physiology, this is easy to understand [see chapter IV.C. Vitreous and iris neovascularization]. In the vitrectomized eye, and in particular in the vitrectomized–lensectomized eye, both oxygen and various growth [24] factors/cytokines are transported faster through the vitreous chamber (Figures IV.A-2 and IV.A-3). Oxygen is transported by diffusion and convection from the anterior chamber

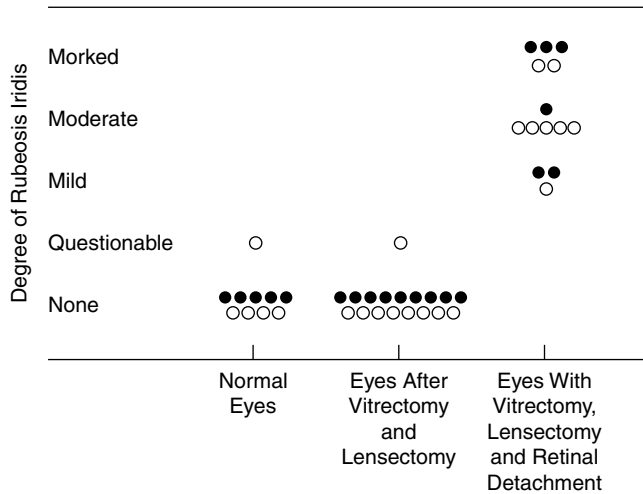


Figure IV.A-10 Vitrectomy, lens extraction, and retinal detachment create iris neovascularization in the cat. *Open circles* denote the clinical diagnosis made at the slit lamp 6–12 months after the onset of the experiments. The histologic diagnosis made by light microscopy of the enucleated eyes 6–12 months after the onset of the experiments is shown in *filled circles*. In both the clinical and histologic evaluation, an arbitrary scale of “no-questionable-mild-moderate-marked” rubeosis iridis was created. Reprinted with permission Stefansson et al. [41]

(where the PO_2 is normally higher than at the retina) to the posterior segment, resulting in anterior segment and iris hypoxia (Figures IV.A-2 and IV.A-3). At the same time, growth factors such as vascular endothelial growth factor (VEGF) are transported faster from the retina to the iris. Anterior segment hypoxia and additional VEGF from the retina will stimulate neovascularization on the iris. Experimentally, iris neovascularization could be induced in healthy cats by removing the vitreous gel and lens and creating a retinal detachment, which makes the retina hypoxic (Figure IV.A-10) [41].

Retinal laser therapy during vitreous surgery helped reduce iris neovascularization, as the photocoagulation reduced retinal hypoxia [42, 17, 43–51] and VEGF production, thus decreasing concentration gradients and transport of both oxygen and VEGF between anterior and posterior segments. Wakabayashi et al. [52] found a strong correlation between neovascular glaucoma and VEGF levels in the vitreous following diabetic vitrectomy. The same was true for vitreous hemorrhages after vitrectomy.

Silicone oil, which is highly viscous and reduces transport of oxygen and growth factors between anterior and posterior segments of the eye, reduces the risk of iris neovascularization in vitrectomized eyes (Figure IV.A-3). In 1986, de Juan et al. [19] showed that silicone oil filling of the vitreous chamber reestablishes a diffusion barrier between the anterior and posterior segments, thus reducing the exchange of oxygen and VEGF. Silicone oil filling also reduces the risk of iris neovascularization following vitrectomy.

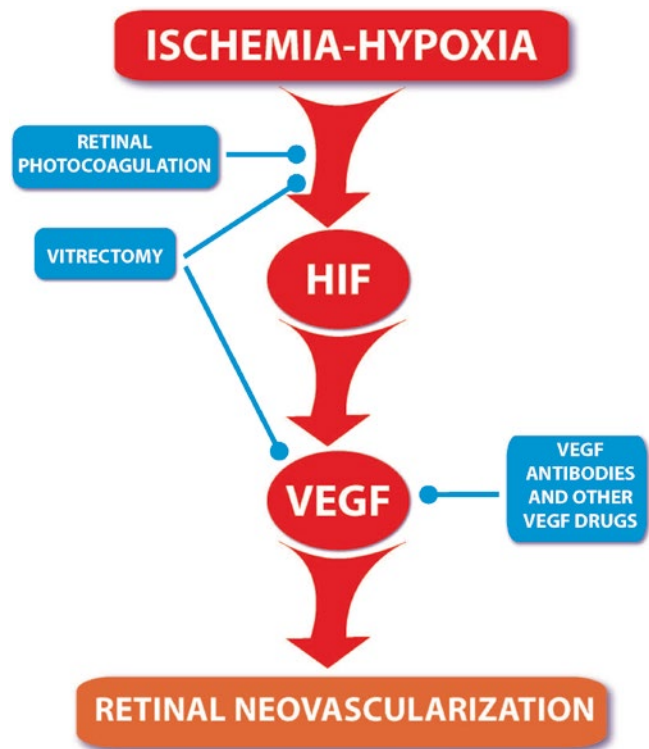


Figure IV.A-11 Vascular endothelial growth factor (VEGF) is a major stimulus for retinal neovascularization. VEGF production is controlled by oxygen tension, and therefore retinal photocoagulation, vitrectomy, and oxygen breathing can reduce VEGF production. VEGF can be cleared away from the retina into low-viscosity fluid in the vitrectomized eye or in an eye with posterior vitreous separation. VEGF antibodies in the vitreous gel will also remove VEGF from the solution and similarly clear it away from the retina. Hypoxia-inducible factor (HIF) allows the cell to sense hypoxia

C. Retinal Neovascularization

Machemer and Blankenship [53] observed that diabetic patients who underwent successful vitrectomy did not have recurrent retinal neovascularization. This can be explained by the physiological principles stated above. In vitrectomized eyes, oxygen is transported from well-perfused areas to ischemic zones [20, 24] reducing local hypoxia and decreasing VEGF production (Figure IV.A-5). VEGF and other cytokines will be cleared away from the ischemic retina faster than before. Consequently, VEGF levels will be reduced both from reduced production and increased clearance into the vitreous chamber (Figure IV.A-5). Retinal laser photocoagulation helps further by also relieving hypoxia of remaining retinal cells and thus reducing VEGF production [17, 23, 42–51]. The physiological principles provide a rational foundation to combine treatment, as laser treatment and vitrectomy have synergistic and similar effects on the ischemic retina (Figure IV.A-11). Vascular endothelial growth factor (VEGF) is an important (but not the only) stimulus for retinal neovascularization. VEGF production

is primarily controlled by oxygen tension, and therefore retinal photocoagulation, vitrectomy/vitreolysis, and oxygen breathing can reduce VEGF production. VEGF can be cleared away from the retina into low-viscosity fluid in the vitrectomized eye or in an eye with posterior vitreous detachment. VEGF antibodies in the vitreous gel also remove VEGF from the solution and similarly clear it away from the retina (Figure IV.A-11). Recent support for this thesis comes from experimental work in rats by Li et al. [54] who found that pharmacologic vitreolysis increases oxygen concentration in the vitreous and reduces expression of HIF-1 α and VEGF, thus alleviating the progression of diabetic retinopathy. Similarly, Lange et al. [55] found hypoxia in mid-vitreous in eyes with proliferative retinopathy, and these eyes also had high levels of several cytokines in the vitreous, including VEGF.

D. Macular Edema

Edema is swelling of soft tissues due to an abnormal accumulation of fluid, i.e., water. Edema may be cytotoxic or vasogenic in origin. In cytotoxic or ischemic edema, the abnormal water accumulation and swelling occurs within cells [56], whereas in vasogenic edema the water accumulates in the interstitial space between cells. While retinal edema may be either cytotoxic or vasogenic, Starling's law applies to the vasogenic edema, which presumably is the most frequent and important form of edema in vascular retinopathies. With abnormal accumulation of water in the retina, the tissue volume increases and the retina thickens. The thickening may be measured with optical coherence tomography (OCT) [57].

1. Origins of Macular Edema

To fully understand the effect of the vitreous on retinal edema, we must understand the pathophysiology of edema, which follows Starling's law [58]. The general law explaining the formation or disappearance of edema in any tissue of the body was formulated in the nineteenth century by Ernest Henry Starling (1866–1927). In 1896, Starling described the transport of fluid between the microcirculation and a tissue, including edema formation: "...there must be a balance between the hydrostatic pressure of the blood in the capillaries and the osmotic attraction of the blood for the surrounding fluids... and whereas capillary pressure determines transudation, the osmotic pressure of the proteins of the serum determines absorption." In other words, the hydrostatic pressure forcing fluids from the vessel into the tissue must be balanced by the osmotic pressure, generated by the colloidal protein solutions in the capillary, forcing absorption of the fluid from the tissues [59]. The four Starling's forces that govern the transport of water between the vascular compartment and the tissue compartment are:

- Hydrostatic pressure in the capillary (P_c)
- Hydrostatic pressure in the tissue interstitium (P_i)
- Osmotic (oncotic) pressure exerted by plasma proteins in the capillary (Q_c)
- Osmotic pressure exerted by proteins in the interstitial fluid (Q_i)

The balance of these forces allows the calculation of the net driving pressure for filtration:

$$\text{Net Driving Pressure} = (P_c - P_i) - (Q_c - Q_i)$$

The hydrostatic pressure, which originates in the heart, is higher in the vessel than in tissue, and this drives water from the vessel into the tissue. The hydrostatic pressure gradient, ΔP , must be balanced by the osmotic pressure gradient, ΔQ , where osmotic pressure is higher in blood than in interstitial fluid, and this pulls water back into blood vessels. If the hydrostatic pressure gradient and the osmotic pressure gradient are equal, no net transport of water takes place, and edema is neither formed nor resolved. Starling's law is frequently shown in this form as:

$$\Delta P - \Delta Q = 0$$

which describes the steady state of the equal and opposing hydrostatic, ΔP , and osmotic pressure, ΔQ , pressure gradients [59].

Starling's law has been generally accepted in medicine and physiology for more than a century as the fundamental rule governing the formation and disappearance of vasogenic edema in the body. It is reasonable to believe that the ocular tissues follow the same general laws of physiology and physics as the rest of the body, and those who believe otherwise should be burdened with the duty to disprove Starling's law in the eye [8, 60, 61]. According to Starling's law, edema will form if the hydrostatic pressure gradient between the vessel and tissue is increased or the osmotic pressure gradient is decreased. The hydrostatic gradient increases if the blood pressure in the microcirculation rises or the tissue pressure decreases. The osmotic pressure gradient decreases if proteins accumulate in the interstitium to increase the osmotic pressure in the tissue and also if the osmotic pressure in the blood goes down. Osmotic pressure changes in the retina as a result of increased vascular leakage, which allows macromolecules to escape from plasma into tissue interstitial space. VEGF is the main instigator of vascular leakage.

a. Increased Hydrostatic Pressure Gradient

The hydrostatic pressure in the microcirculation, capillaries, and venules is a function of the work of the heart, arterial blood pressure, and resistance and pressure fall in the arterioles. Arterial hypertension tends to increase the hydrostatic

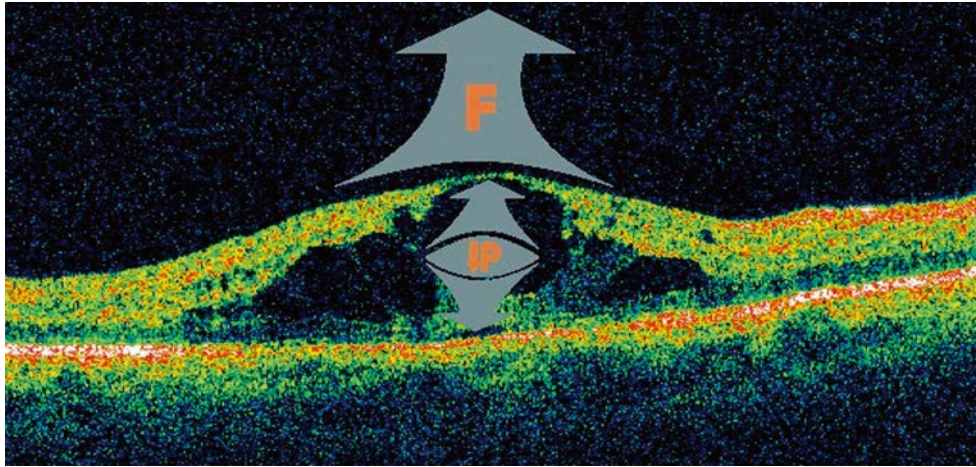


Figure IV.A-12 An axial vitreoretinal traction force (F) is indicated with the *large gray arrow*. Inside the retinal tissue, the two *smaller arrows* indicate force and counterforce according to Newton's third law. The counteracting forces result in lowering of the hydrostatic tissue

pressure, indicated by P . The lowered tissue pressure will increase the pressure gradient between vascular and tissue compartments and stimulate fluid flux from vessel to tissue resulting in edema accumulation according to Starling's law. F Force, P pressure

pressure in the capillaries and is a well-known risk factor for diabetic macular edema [62, 63]. Diabetic macular edema tends to improve if arterial hypertension is successfully treated [64]. The resistance in the retinal arterioles, and thereby the pressure drop in the arterioles, is a function of the diameter of the arterioles. The resistance to flow is described by the Hagen–Poiseuille law, where the resistance is inversely related to the fourth power of the vessel radius [59]. If the arterioles dilate, as they do in hypoxia, the resistance in the arterioles decreases, and the hydrostatic pressure in the capillary bed rises [8, 17, 65]. This is also seen in diabetic retinopathy, where progressive dilatation of the retinal blood vessels has been observed during the development of diabetic macular edema [41, 66].

The hydrostatic pressure gradient between the vessel and tissue is the difference between the hydrostatic pressure in the microcirculation and the intraocular pressure. In ocular hypotony, where the intraocular pressure is low, the hydrostatic pressure gradient in Starling's law will increase. Ocular hypotony is associated with retinal edema, which may improve if the intraocular pressure increases [67–69]. Hydrostatic pressure in the tissue also decreases if there is vitreous traction on the retina, which decreases the hydrostatic tissue pressure, according to Newton's third law (Figure IV.A-12). Relieving such traction will restore the tissue pressure to normal and decrease the hydrostatic pressure gradient between the vessel and tissue.

b. Decreased Osmotic Pressure Gradient

The traditional example of a decrease in the osmotic pressure in blood is in hypoalbuminemia, which may be seen in nephrotic syndrome or starvation with severe generalized

edema. A more frequent cause of decreased osmotic pressure gradients between the vessel and tissue comes from capillary leakage, where plasma proteins leak from the capillaries and venules into the tissue. The accumulation of plasma proteins in the tissue increases the osmotic pressure in the tissue and thereby decreases the osmotic pressure difference between the vessel and the tissue compartment. The reduction of the osmotic pressure gradient reduces water movement from the tissue into the vessel and leads to edema formation [8]. Funatsu et al. [70] demonstrated the close correlation between macular edema and VEGF, which is a potent stimulator of capillary leakage [71]. Retinal edema, such as in diabetic retinopathy and branch retinal vein occlusion, is highly associated with retinal capillary leakage [60, 72, 73]. Fluorescein angiography and fluorophotometry have shown a close association between retinal and macular edema formation and fluorescein leakage, and this has indeed been one of the most frequently used clinical tools to evaluate retinal edema [74–79]. It is the leakage of plasma proteins that matters, due to their effect on osmotic pressure. The leakage of fluorescein itself is naturally not involved in the pathophysiology of edema, and the capillaries are naturally permeable to water. It is important to realize that Starling's law takes into account both the osmotic pressure gradient and the hydrostatic pressure gradient. It is the balance between the two that governs water movement and the formation and disappearance of edema.

2. Diabetic Macular Edema

Vitreous physiology plays a significant role in the development of diabetic macular edema [see chapter III.K. Vitreous in retino-vascular diseases and diabetic macular edema]. Full understanding of the pathophysiology of diabetic macular

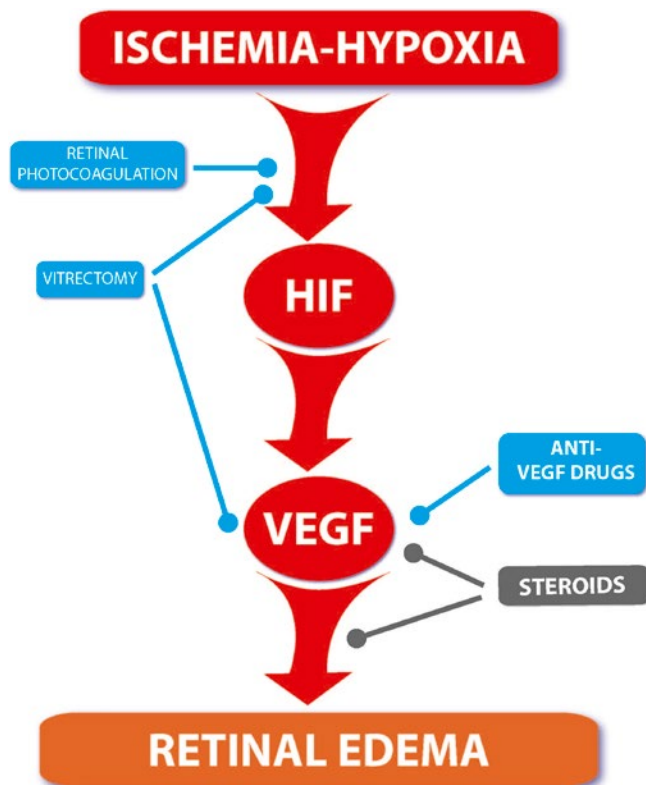


Figure IV.A-13 Ischemia leads to hypoxia. The cells sense hypoxia through hypoxia-inducible factor, HIF. Laser treatment reduces retinal hypoxia (through reduced consumption), and vitrectomy can also improve retinal oxygen supply in hypoxic areas. HIF activation promotes vascular endothelial growth factor (*VEGF*) formation, which increases vascular permeability and induces edema. Vitrectomy and vitreous detachment allows clearance of VEGF away from the retina into the vitreous chamber and VEGF antibodies have essentially the same effect. Corticosteroids reduce VEGF formation and also reduce their permeability effect

edema involves Starling's law, which is discussed above. Nasrallah et al. [80] reported that posterior vitreous adhesion plays a major role in the development of macular edema in diabetic retinopathy. We may deduce that a posterior vitreous detachment tends to prevent diabetic macular edema, in the same fashion as vitrectomy does (Figure IV.A-13). Similarly, Sivaprasad et al. [81] suggested that posterior vitreous detachment plays a role in reducing diabetic macular edema following intravitreal injections.

Lewis et al. [82, 83] were the first to note that vitrectomy is beneficial in diabetic macular edema. Thus they promoted the use of vitrectomy and membrane peeling in cases where vitreoretinal traction contributes to macular edema [see chapter V.A.5. Surgery of diabetic vitreo-retinopathy and diabetic macular edema]. While this issue is still controversial, other experts have since reported that vitrectomy also successfully decreases macular edema in cases where no vitreoretinal traction can be detected [71, 84–89]. Both the physiology of diabetic macular edema

with and without vitreoretinal traction are explained by principles described above (Figure IV.A-3). In the vitrectomized eye or eye with posterior vitreous detachment, oxygen is transported from well-perfused areas to ischemic retinal zones to reduce hypoxia and VEGF production (Figures IV.A-4, IV.A-5, IV.A-11, and IV.A-13) [20, 24]. At the same time, VEGF and other cytokines will be transported faster away from the hypoxic area (Figure IV.A-5). Improved oxygenation and reduced VEGF concentration will reduce stimulus for edema formation (Figures IV.A-4, IV.A-11, and IV.A-13).

This works both through the osmotic and hydrodynamic arms of Starling's law [8] [see chapter IV.B. Oxygen in vitreo-retinal physiology and pathology].

Hoerle et al. [90] reported therapeutic effects of vitrectomy on diabetic macular edema in patients with proliferative diabetic retinopathy. Terasaki et al. [91] found improved vision and electroretinographic activity as well as thinning of edematous and thickened retina following vitrectomy in patients with diabetic macular edema. Yamamoto et al. [92] proposed that the creation of a posterior vitreous detachment is critical in order to influence diabetic macular edema through vitreous surgery. In all reports there is structural improvement of macular edema following vitrectomy, but visual improvement is variable and in some cases either minimal or transient [71, 93, 94]. Vitrectomy clearly has effects on retinal edema in diabetes, but in many cases the treatment is instituted late in the disease, and permanent tissue damage prevents visual improvement, even though the retinal thickness and edema per se are reduced (Figure IV.A-13).

Retinal photocoagulation also reduces diabetic macular edema [95] and has to some degree similar physiological effects as vitrectomy. Photocoagulation improves retinal oxygenation [17, 42–51], reduces VEGF production, and constricts retinal arterioles to influence both the osmotic and hydrodynamic arms of Starling's law [72, 96–99].

3. Macular Edema in Retinal Vein Occlusions

Hikichi et al. [100] reported that partial posterior vitreous attachment contributes to edema development in patients with central retinal vein occlusion, while complete posterior vitreous detachment is protective. According to the laws of physics, posterior vitreous detachment should help to prevent macular edema and retinal neovascularization in all vein occlusions. Indeed, similar observation has been made in branch retinal vein occlusion [101], where the incidence of macular edema was significantly higher in eyes with vitreomacular adhesion (93 %) than in eyes with posterior vitreous detachment (41 %, $P = .009$).

Charbonnel et al. [102]) suggested that vitrectomy with posterior vitreous separation and sheathotomy [see chapter V.A.6. Vitreous surgery of arterial and venous retinovascular

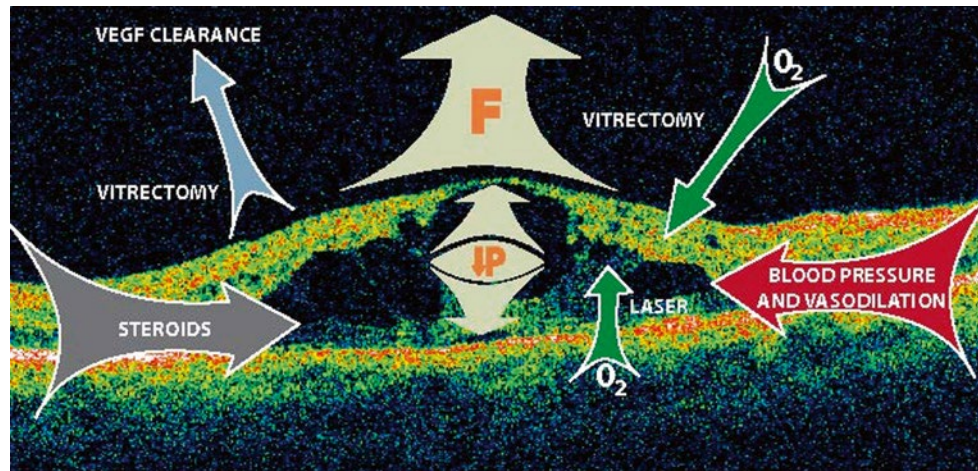


Figure IV.A-14 The figure indicates the several ways macular edema may be treated. Releasing vitreoretinal traction (F) will increase the tissue pressure (P), reduce the hydrostatic pressure gradient between the vessel and tissue, and reduce edema according to Starling's law. Vitrectomy (or posterior vitreous detachment) will increase oxygen delivery to the retina and reduce hypoxia and VEGF production (green upper right-hand arrow). Vitrectomy (or posterior vitreous detachment) will clear VEGF and other cytokines from the retina, due to increased diffusion and convection currents (blue upper left-hand arrow). VEGF antibodies in the vitreous would similarly increase VEGF clearance from the retina. Retinal

photocoagulation decreases outer retinal oxygen consumption, increases oxygen delivery to the inner retina, and reduces hypoxia and VEGF production (green lower arrow). Steroids reduce permeability of retinal blood vessels, reduce leakage of proteins into the tissue, and help restore the osmotic gradient between the blood and tissue, thus reducing edema (gray left horizontal arrow). Lowering of arterial blood pressure or constriction of retinal arterioles (oxygen, photocoagulation, vitrectomy) will reduce the hydrostatic pressure in the microcirculation, reduce hydrostatic pressure gradient between the vessel and tissue, and reduce edema according to Starling's law (red right horizontal arrow). F Force, P pressure

diseases] was helpful in reducing macular edema in branch retinal vein occlusion. It may be that the former is the actual therapeutic act as opposed to the sheathotomy. Indeed, Kumagai et al. [103] suggested that the vitrectomy is critical in treatment of branch retinal vein occlusion, and sheathotomy may or may not have an additional effect. Hvarfner and Larsson [104] observed that vitrectomy reduces macular edema in central retinal vein occlusion. All these observations agree with the physiological effect of posterior vitreous detachment in improving oxygen transport and cytokine clearance (Figure IV.A-13).

4. Vitreoretinal Traction and Edema

Vitreoretinal traction has been associated with macular edema in diabetic retinopathy (Figure IV.A-12 and IV.A-14) [84, 83, 82] and following complicated cataract surgery (Irvine–Gass syndrome). Removal of such traction through vitreoretinal surgery has been found to be useful. The effect of traction on retinal edema is understandable in light of Newton's third law [105]: *to any action (force) there is always an equal and opposite reaction (counterforce)*. In other words, a force is always met by an equal force, in the opposite direction. The force of vitreoretinal traction will be met by an equal and opposite force in the retina, and these tend to pull the tissue apart. This results in a lowering of the tissue pressure in the retina (Figure IV.A-14). The lowered tissue pressure increases the difference between the hydrostatic pressure in the blood vessels and the tissue and contributes to edema formation according to Starling's law [8, 58].

Releasing the traction will increase tissue pressure and thus lower the hydrostatic pressure gradient and reduce the water flux from blood vessels into retinal tissue and edema formation (see Starling's law above).

5. Treating Macular Edema

It should be obvious from the previous discussion that according to Starling's law retinal edema may be treated either by decreasing the hydrostatic pressure gradient between the vessel and tissue or by increasing/restoring the osmotic pressure gradient between the vessel and tissue (Figure IV.A-13).

a. Decreasing Hydrostatic Pressure Gradient

Treatment of arterial hypertension is a well-established method for treating diabetic macular edema and is certainly beneficial in some cases [64, 106]. Another way to reduce the hydrostatic pressure in the microcirculation is to constrict the arterioles. This may be done simply by breathing oxygen-enriched air, an approach that has been shown to constrict retinal blood vessels and reduce diabetic macular edema [107–110].

Retinal oxygenation may also be improved by scattered laser treatment, which destroys a part of the retina and thereby reduces its oxygen consumption and by vitrectomy [17]. Retinal laser treatment destroys some of the photoreceptors and allows oxygen to diffuse from the choroid through the laser scars into the inner retina, where it increases retinal

oxygen tension [17, 23, 42–47, 49–51, 111–113], and leads to constriction of retinal blood vessels [96–99]. Interestingly, intravitreal bevacizumab [114] and triamcinolone [115] have been reported to constrict retinal blood vessels, suggesting that these drugs may have a hemodynamic effect, in addition to their role of reducing VEGF-induced permeability. This is possibly related to the role of VEGF in inflammation, where the anti-VEGF drugs would decrease inflammation and therefore constrict the retinal blood vessels.

Retinal vein occlusions are an obvious case of elevated hydrostatic pressure, due to the occlusion of the central retinal vein or a branch retinal venule. The high hydrostatic pressure in the venule is obvious from the dilatation and tortuosity, which reflects the increased transmural pressure difference according to the law of Laplace [41, 116–118]. Laser treatment has been shown to reduce the vessel diameter in branch retinal vein occlusion and resolve the macular edema at the same time [96–98]. Presumably this involves a reduction in the intravascular hydrostatic pressure. It may be presumed that other methods to relieve the high intravascular pressure, such as the creation of shunt vessels or resolution of the occlusion, for example, with sheathotomy, would have the same effect [119–123]. [see chapter V.A.6. Vitreous surgery of arterial and venous retinovascular diseases].

Since the hydrostatic pressure gradient is the difference between the blood pressure in the microcirculation and the intraocular pressure, this is increased in ocular hypotony, which may be associated with retinal edema as was previously mentioned [69]. Such edema may be successfully treated simply by raising the intraocular pressure [124]. It is less clear whether intraocular pressure changes have a function when the intraocular pressure is in the normal range and whether the intraocular pressure should be considered in patients with macular edema and normal or high intraocular pressure. Vitreoretinal traction decreases tissue hydrostatic pressure (Figure IV.A-12), as discussed earlier, and increases the hydrostatic pressure difference between blood and tissue compartments. This stimulates water flux from the vessel to tissue and edema formation, and relieving the vitreoretinal traction reduces the water flux and retinal edema.

b. Increasing Osmotic Pressure Gradient

Leaking capillaries and venules in the retina are closely associated with retinal and macular edema [74–76, 78]. Fluorescein leakage has been used for diagnostic purposes in macular edema. The leaky blood vessels presumably leak plasma proteins from the blood into the interstitial tissue compartment, thus decreasing the osmotic pressure gradient between the two compartments. The protein leakage may be influenced by administering drugs that reduce vascular endothelial growth factor, which is one of the most powerful agents known to induce capillary leakage [125, 126].

Reducing hypoxia is a natural way to reduce VEGF production, and this may be achieved through retinal photocoagulation or vitrectomy (Figure IV.A-13). Corticosteroids such as triamcinolone and dexamethasone also stabilize capillaries and tend to reduce capillary leakage [127–130]. These treatment modalities will decrease the leakage of proteins into the interstitial tissue compartment and help to restore the osmotic gradient between blood and tissue compartments. This will resolve edema formation according to Starling's law [131–133] (Figure IV.A-13).

c. The Central Role of Oxygen

Oxygen plays an important role in influencing both the hydrostatic and the osmotic arms of Starling's equation. On one hand, oxygen controls the diameter of retinal arterioles and thereby the hydrostatic pressure in the microcirculation. On the other hand, oxygen is a major regulator of the production of vascular endothelial growth factor and other hypoxia-induced growth factors and exerts influence on capillary leakage. Vascular endothelial growth factor is produced in hypoxia, and oxygen is the natural anti-VEGF factor [134]. Retinal oxygenation may be improved by breathing oxygen. Retinal photocoagulation, as well as vitreous surgery, improves retinal oxygenation [17, 72]. Retinal photocoagulation and vitreous surgery improve oxygenation and thereby influence the hemodynamic consequences of hypoxia, as well as the hypoxia-induced VEGF. If these measures do not correct the hypoxia, it is possible to decrease the effect of the hypoxia with anti-VEGF drugs, and with corticosteroids, which decrease the permeability effect of VEGF. All these actions are easily understood in the light of Starling's law, keeping in mind the hydrodynamic and osmotic arms of the law (Figure IV.A-15) [see chapter IV.B. Oxygen in vitreo-retinal physiology and pathology].

E. Age-Related Macular Degeneration (AMD)

Based upon observations made during sub-macular surgery for AMD, Krebs et al. [135] suggested that vitreoretinal adhesion contributes to exudative AMD [see chapter III.G. Vitreous in age-related macular degeneration]. The physiological considerations above suggest a possible mechanism for this effect. VEGF and other cytokines are important in the development of exudative AMD, and the improved clearance of the cytokines following posterior vitreous detachment or vitrectomy would offer protection from the development or persistence of exudative AMD [136] (Figure IV.A-16). Adherent vitreous over the macula does not allow VEGF and other cytokines to be cleared away into the vitreous body (Figures IV.A-14 and IV.A-17). With a posterior vitreous detachment or vitrectomy, the clearance of the cytokines is increased and VEGF load in

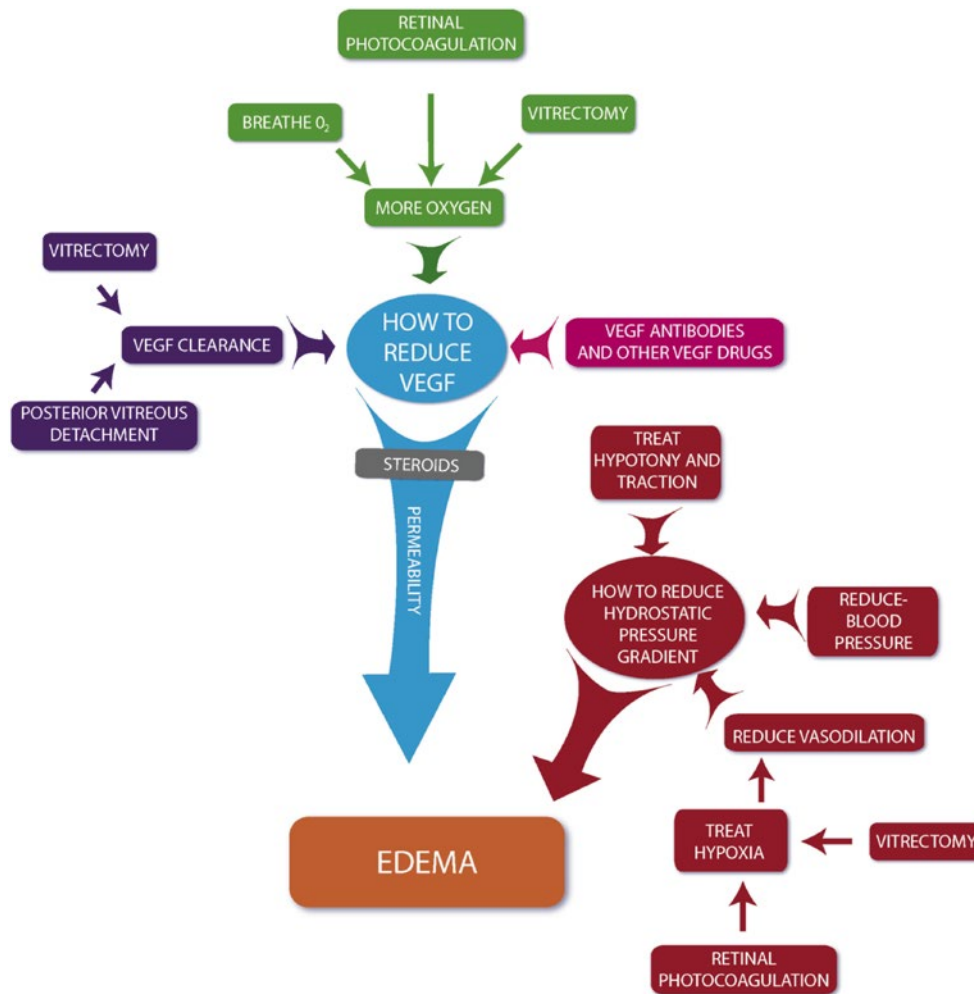


Figure IV.A-15 Physiological principles explain the combination of various treatment modalities, including vitrectomy, for diabetic macular edema and edema in other ischemic retinopathies, such as vein occlusions. Starling’s law governs the formation of vasogenic edema, based on osmotic and hydrostatic gradients between the microcirculation and tissue. The osmotic gradient is influenced by vascular endothelial growth factor (VEGF), which controls the leakage of osmotically active proteins into the tissue compartment (*blue balloon*). VEGF is controlled by oxygen tension. Laser treatment, vitrectomy, and oxygen breathing can increase retinal oxygen tension and thereby reduce VEGF production (*green arrows*). Vitrectomy and posterior vitreous detachment (*purple*) increase diffusion and convection in the vitreous chamber and increase clearance of VEGF (and other cytokines) from the retina, thus reducing VEGF concentration in the retina. VEGF antibodies in the vitreous also remove VEGF from the retinal surface and decrease VEGF concentra-

tion in the retina by clearance (*red arrows*). The permeability effect of VEGF can be reduced by the administration of steroids (*gray bar*). The hydrostatic arm of Starling’s law is indicated by the *dark red arrows*. The hydrostatic gradient between the microcirculation and tissue may be reduced through several mechanisms. Releasing vitreoretinal traction will increase the tissue pressure, reduce hydrostatic pressure gradient between the vessel and tissue, and reduce edema according to Starling’s law. Treating ocular hypotony by raising intraocular pressure will do the same. Reduction of arterial blood pressure will reduce hydrostatic pressure in the microcirculation and thus reduce the hydrostatic gradient between the vessel and tissue and reduce edema. Finally, improved retinal oxygenation through laser treatment or vitrectomy constricts the retinal arterioles, increases their resistance, and reduces hydrostatic pressure in the microcirculation, thus reducing the hydrostatic gradient between the vessel and tissue and edema

the macula decreased. Oxygenation would also improve and reduce VEGF production. Krebs et al. [135] found a close correlation between vitreoretinal adhesion on OCT and choroidal neovascularization in AMD. It is the experience of many experienced vitreoretinal surgeons that vitrectomized eyes do not as a rule develop exudative AMD. This clinical observation has not been studied systematically and must be taken with some caution. Nonetheless, physiological considerations suggest that such a mechanism may be present. Improved clear-

ance of growth factors from the retina after vitrectomy or posterior vitreous detachment, along with improved oxygenation, might help prevent exudative AMD. Recurrence of neovascularization after macular translocation surgery for exudative AMD [see chapter V.A.1. AMD Surgery] is an exception here, but may be a wound-healing response in severely diseased eyes and not representative of prevention in less advanced AMD. Schulze et al. (2008) reviewed the role of the vitreous in AMD and suggest that “incomplete or

Figure IV.A-16 The schematic drawing on top of an OCT image indicates that where the posterior vitreous cortex is attached, oxygen delivery from the vitreous body is slow and VEGF cannot easily escape. Conversely, where the posterior vitreous cortex is detached, oxygen supply to hypoxic retina is possible, and VEGF and other cytokines may be cleared into the vitreous body

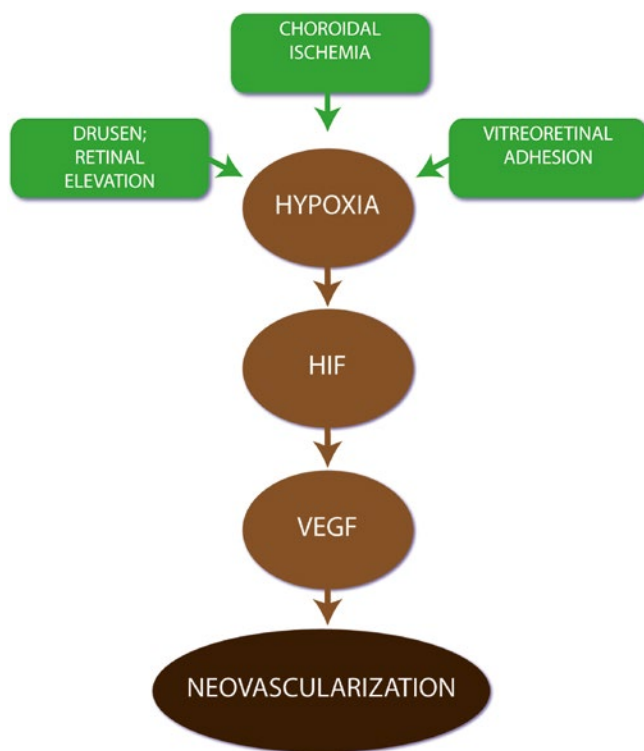
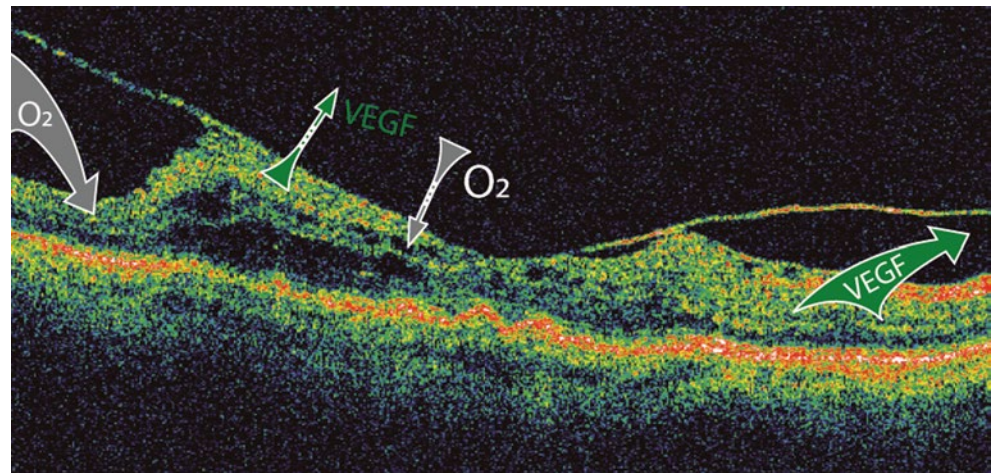


Figure IV.A-17 A schematic drawing showing how choroidal ischemia, drusen, and vitreoretinal adhesion can contribute to retinal hypoxia, resulting in VEGF accumulation and neovascularization (See Stefánsson et al. [136])

anomalous posterior vitreous detachment is suspected to play a crucial role in the pathogenesis of different forms of age-related macular degeneration.” They reviewed several studies that have found vitreoretinal adhesion in patients with AMD. Schulze et al. [137] went on to study patients who had unilateral vitrectomy. In 0 of 21 vitrectomized eyes, there were signs of early AMD, while in 5 of 21 non-vitrectomized eyes (24 %), there were AMD-like changes on angiography and slit-lamp examinations.

Some studies [138, 139] found a higher rate of posterior vitreous attachment in patients with AMD, and others [140] found vitreoretinal attachment in 80 % of patients undergoing vitrectomy for subretinal neovascularization in AMD. Schmidt et al. [141] reported a high incidence of vitreoretinal traction in recurrent subretinal neovascularization, suggesting that a complete posterior vitreous separation (or vitrectomy) would be protective in AMD. Schmidt et al. [141] and Meyer and Toth [142] suggested that vitreomacular traction might play a role in the development of pigment epithelial detachments, and Gross-Jendroska et al. [143] reported that pigment epithelial detachments flatten following an intravitreal gas bubble.

In summary, with a posterior vitreous detachment or vitrectomy, the clearance of cytokines from the retina is increased, and the oxygenation of the retina is improved (Figures IV.A-11, IV.A-12, IV.A-13, IV.A-14, and IV.A-15). Both mechanisms will reduce the concentration of VEGF and other cytokines in and under the retina, and this may reduce the development of neovascularization and edema. In addition, traction will reduce tissue pressure in the retina (Figures IV.A-12 and IV.A-14) and possibly also in a pigment epithelial detachment and contribute to edema formation and fluid accumulation. Release of such traction should reduce edema and fluid accumulation, for example, in a pigment epithelial detachment.

F. Vitrectomy and Cataract

The effect of vitreous gel on cataract formation is the subject of much research. Liang et al. [144] reported that vitrectomy may increase the oxygen delivery to the lens in the rabbit. Holekamp et al. [24, 145] have shown in the human eye that the transport of oxygen through the vitreous chamber to the lens is increased after vitrectomy, and the increased oxygen tension of the lens contributes to nuclear sclerosis cataract

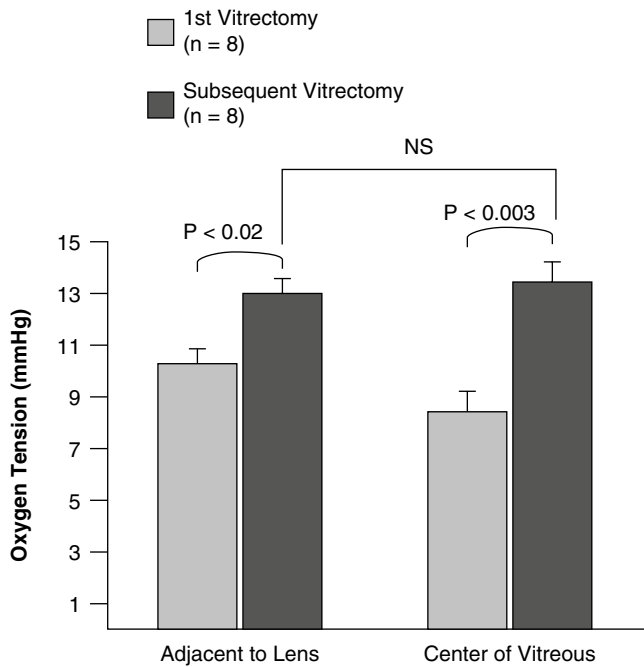


Figure IV.A-18 Oxygen tension measurements made before the first vitrectomy and before the subsequent surgery. Values adjacent to the lens and in the center of the vitreous body were significantly higher in eyes with a previous history of vitrectomy [24]

(Figure IV.A-18). Posterior vitreous detachment also increases pO_2 levels [see chapter IV.B. Oxygen in vitreoretinal physiology and pathology]. Another factor to consider is that the vitreous gel contains antioxidants that act as free radical scavengers mitigating the untoward effects of elevated oxygen levels. Thus, human studies employing minimally invasive vitrectomy without surgical induction of PVD have found a significantly lower incidence of postoperative cataract surgery [see chapter V.B.8. Floaters and vision – current concepts and management paradigms]. This fits perfectly with the physical and physiological principles stated above and confirms the principles previously demonstrated in animal studies (Figures IV.A-2, IV.A-3, IV.A-4, and IV.A-5) [17, 20]. It is likely that the nuclear sclerosis cataract frequently seen following trabeculectomy surgery for glaucoma may be of similar nature [146]. The increased flow rate of aqueous humor following glaucoma filtration surgery is very likely to increase the oxygen delivery to the lens and may contribute to nuclear sclerosis cataract formation [147–153].

G. Vitrectomy and Glaucoma

Studies [154] have suggested that there is an increased risk of open-angle glaucoma after vitrectomy, especially if the crystalline lens has also been removed, presumably via

oxidative stress in the trabecular meshwork as the pathogenesis. Koreen et al. [155] observed that 12 % of 285 vitrectomized eyes later developed open-angle glaucoma, and the incidence rose to 15 % in non-phakic eyes. However, these clinical findings have been disputed. Yu et al. [156] followed 441 eyes after vitrectomy for about 7 years and found only 4 % who developed glaucoma and 4 % ocular hypertension, which was not significantly different than the control group (3 % in both categories). Also, they found no effect from lens extraction. In another study, Lalezary et al. [157] audited 101 eyes after vitrectomy and did not see increased risk for glaucoma. Vitrectomized eyes may not have increased risks of glaucoma. On the other hand, Siegfried et al. [158] measured oxygen distribution with a fiberoptic probe beneath the central cornea, in the mid-anterior chamber, and in the anterior chamber angle. They found that eyes which had undergone both vitrectomy and previous cataract surgery had increased oxygen tension in the posterior chamber, anterior to the IOL, and in the anterior chamber angle compared with non-vitrectomized eyes. They concluded that vitrectomy and cataract surgery increase oxygen tension in the anterior chamber angle, potentially damaging trabecular meshwork cells. These findings are different from early measurements in cats [17, 43] where oxygen tension was found to be lower in the anterior chamber of cats following vitrectomy and lens extraction (Figure IV.A-2). Thus, the hypothesis, that vitrectomy leads to glaucoma, still enjoys some controversy, both clinically and experimentally. Thus, this question deserves further study, and other molecules that move freely from the retina towards the trabecular meshwork after vitrectomy may be worth exploring.

Abbreviations

AMD	Age-related Macular Degeneration
BRVO	Branch Retinal Vein Occlusion
HIF	Hypoxia inducible factor
OCT	Ocular coherence tomography
P_c	Hydrostatic pressure in the capillary
P_i	Hydrostatic pressure in the tissue interstitium
PO_2	Partial pressure of oxygen
PPV	Pars plana vitrectomy
PVD	Posterior vitreous detachment
Q_c	Osmotic (oncotic) pressure exerted by plasma proteins in the capillary
Q_i	Osmotic pressure exerted by proteins in the interstitial fluid
VEGF	Vascular endothelial growth factor

References

1. Dodo T, Okuzawa Y, Baba N. Trans-pupillary resection of vitreous body opacity. *Ganka*. 1969;11(1):38–44.
2. Kasner D, Miller GR, Taylor WH, Sever RJ, Norton EW. Surgical treatment of amyloidosis of the vitreous. *Trans Am Acad Ophthalmol Otolaryngol*. 1968;72(3):410–8.
3. Klöti R. Vitrectomy. I. A new instrument for posterior vitrectomy. *Albrecht Von Graefes Arch Klin Exp Ophthalmol*. 1973;187(2):161–70.
4. Klöti R. Pars plana vitrectomy with the vitreous stripper. *Mod Probl Ophthalmol*. 1975;15:246–52.
5. Machemer R, Buettner H, Norton EW, Parel JM. Vitrectomy: a pars plana approach. *Trans Am Acad Ophthalmol Otolaryngol*. 1971;75(4):813–20.
6. Machemer R, Parel JM, Norton EW. Vitrectomy: a pars plana approach. Technical improvements and further results. *Trans Am Acad Ophthalmol Otolaryngol*. 1972;76(2):462–6.
7. Machemer R. Pars plana vitrectomy. Summary. *Trans Sect Ophthalmol Am Acad Ophthalmol Otolaryngol*. 1976;81(3 Pt 1):431.
8. Stefánsson E, Loftsson T. The Stokes-Einstein equation and the physiological effects of vitreous surgery. *Acta Ophthalmol Scand*. 2006;84(6):718–9.
9. Boruchoff SA, Wooddin AM. Viscosity and composition of solutions derived from rabbit vitreous humour. *Br J Ophthalmol*. 1956;40(2):113–8.
10. Madinaveitia J, Quibell TH. Studies on diffusing factors: the action of testicular extracts on the viscosity of vitreous humour preparations. *Biochem J*. 1940;34(4):625–31.
11. Madinaveitia J, Quibell TH. Studies on diffusing factors: the reduction of the viscosity of vitreous humour preparations by ascorbic acid and some diazo compounds. *Biochem J*. 1941;35(4):453–5.
12. Lee B, Litt M, Buchsbaum G. Rheology of the vitreous body. Part I: viscoelasticity of human vitreous. *Biorheology*. 1992;29(5–6):521–33.
13. Gísladóttir S, Loftsson T, Stefánsson E. Diffusion characteristics of vitreous humour and saline solution follow the Stokes Einstein equation. *Graefes Arch Clin Exp Ophthalmol*. 2009;247(12):1677–84.
14. Sebag J, Ansari RR, Suh KI. Pharmacologic vitreolysis with microplasmin increases vitreous diffusion coefficients. *Graefes Arch Clin Exp Ophthalmol*. 2007;245(4):576–80.
15. Soman N, Banerjee R. Artificial vitreous replacements. *Biomed Mater Eng*. 2003;13(1):59–74.
16. Alm A, Bill A. The oxygen supply to the retina. I. Effects of changes in intraocular and arterial blood pressures, and in arterial P O₂ and P CO₂ on the oxygen tension in the vitreous body of the cat. *Acta Physiol Scand*. 1972;84(2):261–74.
17. Stefánsson E, Landers MB, Wolbarsht ML. Increased retinal oxygen supply following pan-retinal photocoagulation and vitrectomy and lensectomy. *Trans Am Ophthalmol Soc*. 1981;79:307–34.
18. Stefánsson E, Landers MB, Wolbarsht ML. Vitrectomy, lensectomy, and ocular oxygenation. *Retina*. 1982;2(3):159–66.
19. de Juan E, Hardy M, Hatchell DL, Hatchell MC. The effect of intraocular silicone oil on anterior chamber oxygen pressure in cats. *Arch Ophthalmol*. 1986;104(7):1063–4.
20. Stefánsson E, Novack RL, Hatchell DL. Vitrectomy prevents retinal hypoxia in branch retinal vein occlusion. *Invest Ophthalmol Vis Sci*. 1990;31(2):284–9.
21. Blair NP, Baker DS, Rhode JP, Solomon M. Vitreoperfusion. A new approach to ocular ischemia. *Arch Ophthalmol*. 1989;107(3):417–23.
22. Blair NP. Ocular oxygen consumption during vitreoperfusion in the cat. *Trans Am Ophthalmol Soc*. 2000;98:305–29.
23. Maeda N, Tano Y. Intraocular oxygen tension in eyes with proliferative diabetic retinopathy with and without vitreous. *Graefes Arch Clin Exp Ophthalmol*. 1996;234 Suppl 1:S66–9.
24. Holekamp NM, Shui YB, Beebe DC. Vitrectomy surgery increases oxygen exposure to the lens: a possible mechanism for nuclear cataract formation. *Am J Ophthalmol*. 2005;139(2):302–10.
25. Shui YB, Fu JJ, Garcia C, Dattilo LK, Rajagopal R, McMillan S, et al. Oxygen distribution in the rabbit eye and oxygen consumption by the lens. *Invest Ophthalmol Vis Sci*. 2006;47(4):1571–80.
26. Jampol LM. Oxygen therapy and intraocular oxygenation. *Trans Am Ophthalmol Soc*. 1987;85:407–37.
27. Ben-Nun J, Alder VA, Cringle SJ, Constable IJ. A new method for oxygen supply to acute ischemic retina. *Invest Ophthalmol Vis Sci*. 1988;29(2):298–304.
28. Wilson CA, Benner JD, Berkowitz BA, Chapman CB, Peshock RM. Transcorneal oxygenation of the preretinal vitreous. *Arch Ophthalmol*. 1994;112(6):839–45.
29. Wilson CA, Berkowitz BA, Srebro R. Perfluorinated organic liquid as an intraocular oxygen reservoir for the ischemic retina. *Invest Ophthalmol Vis Sci*. 1995;36(1):131–41.
30. Cringle SJ, Yu DY, Alder VA, Su EN. Intravitreal perfluorocarbon and oxygen delivery in induced retinal ischaemia. *Adv Exp Med Biol*. 1994;361:303–11.
31. Sebag J. Molecular biology of pharmacologic vitreolysis. *Trans Am Ophthalmol Soc*. 2005;103:473–94.
32. Gandorfer A. Experimental evaluation of microplasmin - an alternative to vital dyes. *Dev Ophthalmol*. 2008;42:153–9.
33. Quiram PA, Leverenz VR, Baker RM, Dang L, Giblin FJ, Trese MT. Microplasmin-induced posterior vitreous detachment affects vitreous oxygen levels. *Retina*. 2007;27(8):1090–6.
34. Petropoulos IK, Pournaras JA, Stangos AN, Pournaras CJ. Preretinal partial pressure of oxygen gradients before and after experimental pars plana vitrectomy. *Retina*. 2013;33(1):170–8.
35. Simpson AR, Dowell NG, Jackson TL, Tofts PS, Hughes EH. Measuring the effect of pars plana vitrectomy on vitreous oxygenation using magnetic resonance imaging. *Invest Ophthalmol Vis Sci*. 2013;54(3):2028–34.
36. Sín M, Sínová I, Chrapek O, Prachařová Z, Karhanová M, Langová K, et al. The effect of pars plan vitrectomy on oxygen saturation in retinal vessels - a pilot study. *Acta Ophthalmol*. 2014;92(4):328–31. doi: 10.1111/aos.12238. Epub 2013 Jul 15
37. Sebag J. Age-related changes in human vitreous structure. *Graefes Arch Clin Exp Ophthalmol*. 1987;225(2):89–93.
38. Sebag J. Anomalous posterior vitreous detachment: a unifying concept in vitreo-retinal disease. *Graefes Arch Clin Exp Ophthalmol*. 2004;242(8):690–8.
39. Laqua H. Rubeosis iridis following pars plana vitrectomy (author's transl). *Klin Monbl Augenheilkd*. 1980;177(1):24–30.
40. Rice TA, Michels RG, Maguire MG, Rice EF. The effect of lensectomy on the incidence of iris neovascularization and neovascular glaucoma after vitrectomy for diabetic retinopathy. *Am J Ophthalmol*. 1983;95(1):1–11.
41. Stefánsson E, Landers MB, Wolbarsht ML. Oxygenation and vasodilatation in relation to diabetic and other proliferative retinopathies. *Ophthalmic Surg*. 1983;14(3):209–26.
42. Diddie KR, Ernest JT. The effect of photocoagulation on the choroïdal vasculature and retinal oxygen tension. *Am J Ophthalmol*. 1977;84(1):62–6.
43. Landers MB, Stefánsson E, Wolbarsht ML. Panretinal photocoagulation and retinal oxygenation. *Retina*. 1982;2(3):167–75.
44. Molnar I, Poitry S, Tsacopoulos M, Gilodi N, Leuenberger PM. Effect of laser photocoagulation on oxygenation of the retina in miniature pigs. *Invest Ophthalmol Vis Sci*. 1985;26(10):1410–4.
45. Pournaras CJ, Ilic J, Gilodi N, Tsacopoulos M, Leuenberger MP. Experimental venous thrombosis: preretinal PO₂ before and

- after photocoagulation. *Klin Monbl Augenheilkd*. 1985;186(6):500–1.
46. Alder VA, Cringle SJ, Brown M. The effect of regional retinal photocoagulation on vitreal oxygen tension. *Invest Ophthalmol Vis Sci*. 1987;28(7):1078–85.
 47. Novack RL, Stefánsson E, Hatchell DL. The effect of photocoagulation on the oxygenation and ultrastructure of avascular retina. *Exp Eye Res*. 1990;50(3):289–96.
 48. Stefánsson E, Macherer R, de Juan E, McCuen BW, Peterson J. Retinal oxygenation and laser treatment in patients with diabetic retinopathy. *Am J Ophthalmol*. 1992;113(1):36–8.
 49. Funatsu H, Wilson CA, Berkowitz BA, Sonkin PL. A comparative study of the effects of argon and diode laser photocoagulation on retinal oxygenation. *Graefes Arch Clin Exp Ophthalmol*. 1997;235(3):168–75.
 50. Yu DY, Cringle SJ, Su E, Yu PK, Humayun MS, Dorin G. Laser-induced changes in intraretinal oxygen distribution in pigmented rabbits. *Invest Ophthalmol Vis Sci*. 2005;46(3):988–99.
 51. Budzynski E, Smith JH, Bryar P, Birol G, Linsenmeier RA. Effects of photocoagulation on intraretinal PO₂ in cat. *Invest Ophthalmol Vis Sci*. 2008;49(1):380–9.
 52. Wakabayashi Y, Usui Y, Okunuki Y, Ueda S, Kimura K, Muramatsu D, et al. Intraocular VEGF level as a risk factor for postoperative complications after vitrectomy for proliferative diabetic retinopathy. *Invest Ophthalmol Vis Sci*. 2012;53(10):6403–10.
 53. Blankenship GW, Macherer R. Long-term diabetic vitrectomy results. Report of 10 year follow-up. *Ophthalmology*. 1985;92(4):503–6.
 54. Li Q, Yan H, Ding TB, Han J, Shui YB, Beebe DC. Oxidative responses induced by pharmacologic vitreolysis and/or long-term hyperoxia treatment in rat lenses. *Curr Eye Res*. 2013;38(6):639–48.
 55. Lange CA, Stavarakas P, Luhmann UF, de Silva DJ, Ali RR, Gregor ZJ, et al. Intraocular oxygen distribution in advanced proliferative diabetic retinopathy. *Am J Ophthalmol*. 2011;152(3):406–12.e3.
 56. Bringmann A, Uckermann O, Pannicke T, Iandiev I, Reichenbach A, Wiedemann P. Neuronal versus glial cell swelling in the ischaemic retina. *Acta Ophthalmol Scand*. 2005;83(5):528–38.
 57. Massin P, Girach A, Erginay A, Gaudric A. Optical coherence tomography: a key to the future management of patients with diabetic macular oedema. *Acta Ophthalmol Scand*. 2006;84(4):466–74.
 58. Stefánsson E. Physiology of vitreous surgery. *Graefes Arch Clin Exp Ophthalmol*. 2009;247(2):147–63.
 59. Pocock G, Richards CD. Human physiology: the basis of medicine. 2nd ed. Oxford: Oxford University Press; 2004.
 60. Cunha-Vaz J. The blood-ocular barriers. *Surv Ophthalmol*. 1979;23(5):279–96.
 61. Cunha-Vaz JG, Travassos A. Breakdown of the blood-retinal barriers and cystoid macular edema. *Surv Ophthalmol*. 1984;28(Suppl):485–92.
 62. Klein R, Klein BE, Moss SE, Cruickshanks KJ. The Wisconsin epidemiologic study of diabetic retinopathy. XV. The long-term incidence of macular edema. *Ophthalmology*. 1995;102(1):7–16.
 63. Lopes de Faria JM, Jalkh AE, Trempe CL, McMeel JW. Diabetic macular edema: risk factors and concomitants. *Acta Ophthalmol Scand*. 1999;77(2):170–5.
 64. Matthews DR, Stratton IM, Aldington SJ, Holman RR, Kohner EM, Group UPDS. Risks of progression of retinopathy and vision loss related to tight blood pressure control in type 2 diabetes mellitus: UKPDS 69. *Arch Ophthalmol*. 2004;122(11):1631–40.
 65. Stefánsson E. The therapeutic effects of retinal laser treatment and vitrectomy. A theory based on oxygen and vascular physiology. *Acta Ophthalmol Scand*. 2001;79(5):435–40.
 66. Kristinsson JK, Gottfredsdóttir MS, Stefánsson E. Retinal vessel dilatation and elongation precedes diabetic macular oedema. *Br J Ophthalmol*. 1997;81(4):274–8.
 67. Kokame GT, de Leon MD, Tanji T. Serous retinal detachment and cystoid macular edema in hypotony maculopathy. *Am J Ophthalmol*. 2001;131(3):384–6.
 68. Schubert HD. Postsurgical hypotony: relationship to fistulization, inflammation, chorioretinal lesions, and the vitreous. *Surv Ophthalmol*. 1996;41(2):97–125.
 69. Stefánsson E. Ocular hypotony: what is the mechanism of effusion and oedema? *Acta Ophthalmol Scand*. 2007;85(6):584–5.
 70. Funatsu H, Yamashita H, Nakamura S, Mimura T, Eguchi S, Noma H, et al. Vitreous levels of pigment epithelium-derived factor and vascular endothelial growth factor are related to diabetic macular edema. *Ophthalmology*. 2006;113(2):294–301.
 71. Patel JI, Tombran-Tink J, Hykin PG, Gregor ZJ, Cree IA. Vitreous and aqueous concentrations of proangiogenic, antiangiogenic factors and other cytokines in diabetic retinopathy patients with macular edema: Implications for structural differences in macular profiles. *Exp Eye Res*. 2006;82(5):798–806.
 72. Stefánsson E. Ocular oxygenation and the treatment of diabetic retinopathy. *Surv Ophthalmol*. 2006;51(4):364–80.
 73. Knudsen ST, Bek T, Poulsen PL, Hove MN, Rehling M, Mogensen CE. Macular edema reflects generalized vascular hyperpermeability in type 2 diabetic patients with retinopathy. *Diabetes Care*. 2002;25(12):2328–34.
 74. Cunha-Vaz JG. Vitreous fluorophotometry recordings in posterior segment disease. *Graefes Arch Clin Exp Ophthalmol*. 1985;222(4–5):241–7.
 75. Krogsaa B, Lund-Andersen H, Mehlsen J, Sestoft L. Blood-retinal barrier permeability versus diabetes duration and retinal morphology in insulin dependent diabetic patients. *Acta Ophthalmol (Copenh)*. 1987;65(6):686–92.
 76. Phillips RP, Ross PG, Sharp PF, Forrester JV. Use of temporal information to quantify vascular leakage in fluorescein angiography of the retina. *Clin Phys Physiol Meas*. 1990;11(Suppl A):81–5.
 77. Ring K, Larsen M, Dalgaard P, Andersen HL. Fluorophotometric evaluation of ocular barriers and of the vitreous body in the aphakic eye. *Acta Ophthalmol Suppl*. 1987;182:160–2.
 78. Sander B, Larsen M, Moldow B, Lund-Andersen H. Diabetic macular edema: passive and active transport of fluorescein through the blood-retina barrier. *Invest Ophthalmol Vis Sci*. 2001;42(2):433–8.
 79. Smith RT, Lee CM, Charles HC, Farber M, Cunha-Vaz JG. Quantification of diabetic macular edema. *Arch Ophthalmol*. 1987;105(2):218–22.
 80. Nasrallah FP, Jalkh AE, Van Coppenolle F, Kado M, Trempe CL, McMeel JW, et al. The role of the vitreous in diabetic macular edema. *Ophthalmology*. 1988;95(10):1335–9.
 81. Sivaprasad S, Ockrim Z, Massautis P, Ikeji F, Hykin PG, Gregor ZJ. Posterior hyaloid changes following intravitreal triamcinolone and macular laser for diffuse diabetic macular edema. *Retina*. 2008;28(10):1435–42.
 82. Lewis H, Abrams GW, Blumenkranz MS, Campo RV. Vitrectomy for diabetic macular traction and edema associated with posterior hyaloidal traction. *Ophthalmology*. 1992;99(5):753–9.
 83. Lewis H. The role of vitrectomy in the treatment of diabetic macular edema. *Am J Ophthalmol*. 2001;131(1):123–5.
 84. Kaiser PK, Riemann CD, Sears JE, Lewis H. Macular traction detachment and diabetic macular edema associated with posterior hyaloidal traction. *Am J Ophthalmol*. 2001;131(1):44–9.
 85. Figueroa MS, Contreras I, Noval S. Surgical and anatomical outcomes of pars plana vitrectomy for diffuse nontraction diabetic macular edema. *Retina*. 2008;28(3):420–6.
 86. Hartley KL, Smiddy WE, Flynn HW, Murray TG. Pars plana vitrectomy with internal limiting membrane peeling for diabetic macular edema. *Retina*. 2008;28(3):410–9.
 87. Shimonagano Y, Makiuchi R, Miyazaki M, Doi N, Uemura A, Sakamoto T. Results of visual acuity and foveal thickness in diabetic macular edema after vitrectomy. *Jpn J Ophthalmol*. 2007;51(3):204–9.
 88. Yamamoto T, Takeuchi S, Sato Y, Yamashita H. Long-term follow-up results of pars plana vitrectomy for diabetic macular edema. *Jpn J Ophthalmol*. 2007;51(4):285–91.

89. Yanyali A, Horozoglu F, Celik E, Nohutcu AF. Long-term outcomes of pars plana vitrectomy with internal limiting membrane removal in diabetic macular edema. *Retina*. 2007;27(5):557–66.
90. Hoerle S, Poestgens H, Schmidt J, Kroll P. Effect of pars plana vitrectomy for proliferative diabetic vitreoretinopathy on preexisting diabetic maculopathy. *Graefes Arch Clin Exp Ophthalmol*. 2002;240(3):197–201.
91. Terasaki H, Kojima T, Niwa H, Piao CH, Ueno S, Kondo M, et al. Changes in focal macular electroretinograms and foveal thickness after vitrectomy for diabetic macular edema. *Invest Ophthalmol Vis Sci*. 2003;44(10):4465–72.
92. Yamamoto S, Yamamoto T, Ogata K, Hoshino A, Sato E, Mizunoya S. Morphological and functional changes of the macula after vitrectomy and creation of posterior vitreous detachment in eyes with diabetic macular edema. *Doc Ophthalmol*. 2004;109(3):249–53.
93. Shah SP, Patel M, Thomas D, Aldington S, Laidlaw DA. Factors predicting outcome of vitrectomy for diabetic macular oedema: results of a prospective study. *Br J Ophthalmol*. 2006;90(1):33–6.
94. Meyer CH. Current treatment approaches in diabetic macular edema. *Ophthalmologica*. 2007;221(2):118–31.
95. Soliman W, Sander B, Soliman KA, Yehya S, Rahamn MS, Larsen M. The predictive value of optical coherence tomography after grid laser photocoagulation for diffuse diabetic macular oedema. *Acta Ophthalmol*. 2008;86(3):284–91.
96. Arnarsson A, Stefánsson E. Laser treatment and the mechanism of edema reduction in branch retinal vein occlusion. *Invest Ophthalmol Vis Sci*. 2000;41(3):877–9.
97. Feke GT, Green GJ, Goger DG, McMeel JW. Laser Doppler measurements of the effect of panretinal photocoagulation on retinal blood flow. *Ophthalmology*. 1982;89(7):757–62.
98. Gottfredsdóttir MS, Stefánsson E, Jónasson F, Gíslason I. Retinal vasoconstriction after laser treatment for diabetic macular edema. *Am J Ophthalmol*. 1993;115(1):64–7.
99. Wilson CA, Stefánsson E, Klombers L, Hubbard LD, Kaufman SC, Ferris FL. Optic disk neovascularization and retinal vessel diameter in diabetic retinopathy. *Am J Ophthalmol*. 1988;106(2):131–4.
100. Hikichi T, Yoshida A, Konno S, Trempe CL. Role of the vitreous in central retinal vein occlusion. *Nihon Ganka Gakkai Zasshi*. 1996;100(1):63–8.
101. Takahashi MK, Hikichi T, Akiba J, Yoshida A, Trempe CL. Role of the vitreous and macular edema in branch retinal vein occlusion. *Ophthalmic Surg Lasers*. 1997;28(4):294–9.
102. Charbonnel J, Glacet-Bernard A, Korobelnik JF, Nyouma-Moune E, Pournaras CJ, Colin J, et al. Management of branch retinal vein occlusion with vitrectomy and arteriovenous adventitial sheathotomy, the possible role of surgical posterior vitreous detachment. *Graefes Arch Clin Exp Ophthalmol*. 2004;242(3):223–8.
103. Kumagai K, Furukawa M, Ogino N, Uemura A, Larson E. Long-term outcomes of vitrectomy with or without arteriovenous sheathotomy in branch retinal vein occlusion. *Retina*. 2007;27(1):49–54.
104. Hvarfner C, Larsson J. Vitrectomy for non-ischaemic macular oedema in retinal vein occlusion. *Acta Ophthalmol Scand*. 2006;84(6):812–4.
105. Newton IS, Cohen IB, Cohen IBGtNsP, Whitman AM. *The Principia: mathematical principles of natural philosophy*. Berkeley/London: University of California Press; 1999.
106. Stratton IM, Kohner EM, Aldington SJ, Turner RC, Holman RR, Manley SE, et al. UKPDS 50: risk factors for incidence and progression of retinopathy in Type II diabetes over 6 years from diagnosis. *Diabetologia*. 2001;44(2):156–63.
107. Averous K, Erginay A, Timsit J, Haouchine B, Gaudric A, Massin P. Resolution of diabetic macular oedema following high altitude exercise. *Acta Ophthalmol Scand*. 2006;84(6):830–1.
108. Nguyen QD, Shah SM, Van Anden E, Sung JU, Vitale S, Campochiaro PA. Supplemental oxygen improves diabetic macular edema: a pilot study. *Invest Ophthalmol Vis Sci*. 2004;45(2):617–24.
109. Kiryu J, Ogura Y. Hyperbaric oxygen treatment for macular edema in retinal vein occlusion: relation to severity of retinal leakage. *Ophthalmologica*. 1996;210(3):168–70.
110. Roy M, Bartow W, Ambrus J, Fauci A, Collier B, Titus J. Retinal leakage in retinal vein occlusion: reduction after hyperbaric oxygen. *Ophthalmologica*. 1989;198(2):78–83.
111. Stefánsson E, Hatchell DL, Fisher BL, Sutherland FS, Machemer R. Panretinal photocoagulation and retinal oxygenation in normal and diabetic cats. *Am J Ophthalmol*. 1986;101(6):657–64.
112. Pournaras CJ, Tsacopoulos M, Strommer K, Gilodi N, Leuenberger PM. Scatter photocoagulation restores tissue hypoxia in experimental vasoproliferative microangiopathy in miniature pigs. *Ophthalmology*. 1990;97(10):1329–33.
113. Jacobi KW, Kluge K. Measuring of oxygen partial pressure before the retina following photocoagulation. *Ber Zusammenkunft Dtsch Ophthalmol Ges*. 1972;71:397–401.
114. Soliman W, Vinten M, Sander B, Soliman KA, Yehya S, Rahman MS, et al. Optical coherence tomography and vessel diameter changes after intravitreal bevacizumab in diabetic macular oedema. *Acta Ophthalmol*. 2008;86(4):365–71.
115. Vinten M, Larsen M, Lund-Andersen H, Sander B, La Cour M. Short-term effects of intravitreal triamcinolone on retinal vascular leakage and trunk vessel diameters in diabetic macular oedema. *Acta Ophthalmol Scand*. 2007;85(1):21–6.
116. Christoffersen N, Larsen M. Unilateral diabetic macular oedema secondary to central retinal vein congestion. *Acta Ophthalmol Scand*. 2004;82(5):591–5.
117. Kylstra JA, Wierzbicki T, Wolbarsht ML, Landers MB, Stefánsson E. The relationship between retinal vessel tortuosity, diameter, and transmural pressure. *Graefes Arch Clin Exp Ophthalmol*. 1986;224(5):477–80.
118. Larsen M. Unilateral macular oedema secondary to retinal venous congestion without occlusion in patients with diabetes mellitus. *Acta Ophthalmol Scand*. 2005;83(4):428–35.
119. Sohn JH, Song SJ. Arteriovenous sheathotomy for persistent macular edema in branch retinal vein occlusion. *Korean J Ophthalmol*. 2006;20(4):210–4.
120. Wrigstad A, Algvere P. Arteriovenous adventitial sheathotomy for branch retinal vein occlusion: report of a case with long term follow-up. *Acta Ophthalmol Scand*. 2006;84(5):699–702.
121. Crafoord S, Karlsson N, la Cour M. Sheathotomy in complicated cases of branch retinal vein occlusion. *Acta Ophthalmol*. 2008;86(2):146–50.
122. Mandelcorn MS, Mandelcorn E, Guan K, Adatia FA. Surgical macular decompression for macular edema in retinal vein occlusion. *Can J Ophthalmol*. 2007;42(1):116–22.
123. Shimura M, Nakazawa T, Yasuda K, Kunikata H, Shiono T, Nishida K. Visual prognosis and vitreous cytokine levels after arteriovenous sheathotomy in branch retinal vein occlusion associated with macular oedema. *Acta Ophthalmol*. 2008;86(4):377–84.
124. Karasheva G, Goebel W, Klink T, Haigis W, Grehn F. Changes in macular thickness and depth of anterior chamber in patients after filtration surgery. *Graefes Arch Clin Exp Ophthalmol*. 2003;241(3):170–5.
125. Iturralde D, Spaide RF, Meyerle CB, Klancnik JM, Yannuzzi LA, Fisher YL, et al. Intravitreal bevacizumab (Avastin) treatment of macular edema in central retinal vein occlusion: a short-term study. *Retina*. 2006;26(3):279–84.
126. Mason JO, Albert MA, Vail R. Intravitreal bevacizumab (Avastin) for refractory pseudophakic cystoid macular edema. *Retina*. 2006;26(3):356–7.
127. Audren F, Erginay A, Haouchine B, Benosman R, Conrath J, Bergmann JF, et al. Intravitreal triamcinolone acetate for diffuse

- diabetic macular oedema: 6-month results of a prospective controlled trial. *Acta Ophthalmol Scand.* 2006;84(5):624–30.
128. Edelman JL, Lutz D, Castro MR. Corticosteroids inhibit VEGF-induced vascular leakage in a rabbit model of blood-retinal and blood-aqueous barrier breakdown. *Exp Eye Res.* 2005;80(2):249–58.
 129. Jonas JB. Intravitreal triamcinolone acetonide for treatment of intraocular oedematous and neovascular diseases. *Acta Ophthalmol Scand.* 2005;83(6):645–63.
 130. Sørensen TL, Haamann P, Villumsen J, Larsen M. Intravitreal triamcinolone for macular oedema: efficacy in relation to aetiology. *Acta Ophthalmol Scand.* 2005;83(1):67–70.
 131. Margolis R, Singh RP, Bhatnagar P, Kaiser PK. Intravitreal triamcinolone as adjunctive treatment to laser panretinal photocoagulation for concomitant proliferative diabetic retinopathy and clinically significant macular oedema. *Acta Ophthalmol.* 2008;86(1):105–10.
 132. Sivaprasad S, McCluskey P, Lightman S. Intravitreal steroids in the management of macular oedema. *Acta Ophthalmol Scand.* 2006;84(6):722–33.
 133. Wang L, Song H. Effects of repeated injection of intravitreal triamcinolone on macular oedema in central retinal vein occlusion. *Acta Ophthalmol.* 2009;87(3):285–9.
 134. Viores SA, Xiao WH, Aslam S, Shen J, Oshima Y, Nambu H, et al. Implication of the hypoxia response element of the Vegf promoter in mouse models of retinal and choroidal neovascularization, but not retinal vascular development. *J Cell Physiol.* 2006;206(3):749–58.
 135. Krebs I, Brannath W, Glittenberg C, Zeiler F, Sebag J, Binder S. Posterior vitreomacular adhesion: a potential risk factor for exudative age-related macular degeneration? *Am J Ophthalmol.* 2007;144(5):741–6.
 136. Stefansson E, Geirsdóttir A, Sigurdsson H. Metabolic physiology in age related macular degeneration. *Prog Retin Eye Res.* 2011;30(1):72–80.
 137. Schulze S, Hoerle S, Mennel S, Kroll P. Vitreomacular traction and exudative age-related macular degeneration. *Acta Ophthalmol.* 2008;86(5):470–81.
 138. Weber-Krause B, Eckardt U. Incidence of posterior vitreous detachment in eyes with and without age-related macular degeneration. An ultrasonic study. *Ophthalmologie.* 1996;93(6):660–5.
 139. Hayreh SS, Jonas JB. Posterior vitreous detachment: clinical correlations. *Ophthalmologica.* 2004;218(5):333–43.
 140. Lambert HM, Lopez PF. Surgical excision of subfoveal choroidal neovascular membranes. *Curr Opin Ophthalmol.* 1993;4(3):19–24.
 141. Schmidt JC, Mennel S, Hörle S, Meyer CH. High incidence of vitreomacular traction in recurrent choroidal neovascularisation after repeated photodynamic therapy. *Br J Ophthalmol.* 2006;90(11):1361–2.
 142. Meyer CH, Toth CA. Retinal pigment epithelial tear with vitreomacular attachment: a novel pathogenic feature. *Graefes Arch Clin Exp Ophthalmol.* 2001;239(5):325–33.
 143. Gross-Jendroska M, Flaxel CJ, Schwartz SD, Holz FG, Fitzke FW, Gabel VP, et al. Treatment of pigment epithelial detachments due to age-related macular degeneration with intra-ocular C3F8 injection. *Aust N Z J Ophthalmol.* 1998;26(4):311–7.
 144. Liang J, Zheng L, Yi C, Barbazetto I, Dillon J. Affection on oxygen tension of the lens after vitrectomy. *Yan Ke Xue Bao.* 2002;18(2):67–70.
 145. Holekamp NM, Shui YB, Beebe D. Lower intraocular oxygen tension in diabetic patients: possible contribution to decreased incidence of nuclear sclerotic cataract. *Am J Ophthalmol.* 2006;141(6):1027–32.
 146. Mathew RG, Murdoch IE. The silent enemy: a review of cataract in relation to glaucoma and trabeculectomy surgery. *Br J Ophthalmol.* 2011;95(10):1350–4.
 147. Chauvaud D, Clay-Fressinet C, Pouliquen Y, Offret G. Opacification of the crystalline lens after trabeculectomy. Study of 95 cases. *Arch Ophthalmol (Paris).* 1976;36(5):379–86.
 148. Daugeliene L, Yamamoto T, Kitazawa Y. Cataract development after trabeculectomy with mitomycin C: a 1-year study. *Jpn J Ophthalmol.* 2000;44(1):52–7.
 149. Popovic V, Sjöstrand J. Long-term outcome following trabeculectomy: I retrospective analysis of intraocular pressure regulation and cataract formation. *Acta Ophthalmol (Copenh).* 1991;69(3):299–304.
 150. Quigley HA, Buhrmann RR, West SK, Isseme I, Scudder M, Oliva MS. Long term results of glaucoma surgery among participants in an east African population survey. *Br J Ophthalmol.* 2000;84(8):860–4.
 151. Razzak A, al Samarrai A, Sunba MS. Incidence of posttrabeculectomy cataract among Arabs in Kuwait. *Ophthalmic Res.* 1991;23(1):21–3.
 152. Sihota R, Gupta V, Agarwal HC. Long-term evaluation of trabeculectomy in primary open angle glaucoma and chronic primary angle closure glaucoma in an Asian population. *Clin Experiment Ophthalmol.* 2004;32(1):23–8.
 153. Vesti E. Development of cataract after trabeculectomy. *Acta Ophthalmol (Copenh).* 1993;71(6):777–81.
 154. Chang S. LXII Edward Jackson lecture: open angle glaucoma after vitrectomy. *Am J Ophthalmol.* 2006;141(6):1033–43.
 155. Koreen L, Yoshida N, Escario P, Niziol LM, Koreen IV, Musch DC, et al. Incidence of, risk factors for, and combined mechanism of late-onset open-angle glaucoma after vitrectomy. *Retina.* 2012;32(1):160–7.
 156. Yu AL, Brummeisl W, Schaumberger M, Kampik A, Welge-Lüssen U. Vitrectomy does not increase the risk of open-angle glaucoma or ocular hypertension - a 5-year follow-up. *Graefes Arch Clin Exp Ophthalmol.* 2010;248(10):1407–14.
 157. Lalezary M, Kim SJ, Jiramongkolchai K, Recchia FM, Agarwal A, Sternberg P. Long-term trends in intraocular pressure after pars plana vitrectomy. *Retina.* 2011;31(4):679–85.
 158. Siegfried CJ, Shui YB, Holekamp NM, Bai F, Beebe DC. Oxygen distribution in the human eye: relevance to the etiology of open-angle glaucoma after vitrectomy. *Invest Ophthalmol Vis Sci.* 2010;51(11):5731–8.

Nancy M. Holekamp, David C. Beebe, and Ying-Bo Shui

Outline

- I. **Introduction**
 - A. The Oxygen Hypothesis
- II. **Intraocular Oxygen Tension**
 - A. Experimental Measurements
 1. Vitreous
 2. Lens
 3. Trabecular Meshwork
- III. **Intraocular Oxygen Tension Regulation**
 - A. Intraocular Oxygen Gradients
 - B. Vitreous Gel Regulates Intraocular Oxygen
 1. Vitreous Gel Metabolizes Oxygen
 2. Gel Vitreous Consumes Oxygen Better Than Liquid Vitreous
 3. Biophysical Properties of Gel Vitreous
- IV. **Vitreous Liquefaction or Vitrectomy Increases Oxygen**
- V. **Pathogenic Effects of Increased Intraocular Oxygen**
 - A. Nuclear Sclerotic Cataract
 1. Oxygen and Nuclear Sclerosis
 2. Role of Vitreous in Nuclear Sclerosis
 3. The “Oxygen Hypothesis” for Nuclear Sclerosis
 - B. Primary Open-Angle Glaucoma (POAG)
 1. Oxygen and POAG
 2. Role of Vitreous and Cataract Surgery in POAG
 3. The “Oxygen Hypothesis” for POAG
- VI. **Oxygen Ameliorates VEGF-Mediated Retinopathies**
 - A. Age-Related Macular Degeneration (AMD)
 - B. Diabetic Retinopathy
 - C. Retinal Vein Occlusions
- VII. **The Future**
- VIII. **Summary**

References

N.M. Holekamp, MD (✉)
Department of Ophthalmology and Visual Sciences,
Washington University, St. Louis, MO 63110, USA
e-mail: nholekamp@gmail.com

D.C. Beebe, PhD • Y.-B. Shui, MD, PhD
Department of Ophthalmology and Visual Sciences, Washington
University, St. Louis, MO, USA
e-mail: Beebe@wustl.edu; Shui@vision.wustl.edu

Keywords

Vitreous gel • Physiology • Vitreous degeneration • Oxygen • Ascorbate • Vitrectomy • Nuclear sclerotic cataract • Post-vitrectomy glaucoma • Diabetic retinopathy • Posterior vitreous detachment

Key Concepts

1. The intact vitreous gel and the high level of ascorbate in the vitreous protect the lens from exposure to excess oxygen arising from the retinal vasculature.
2. Age-related degeneration or destruction of the vitreous gel (vitrectomy) exposes the posterior lens to increased oxygen, leading to nuclear sclerotic cataract.
3. Lowering oxygen in the vitreous or restoring the structure of the vitreous gel could prevent nuclear sclerotic cataracts after vitrectomy and would decrease the risk of post-vitrectomy open-angle glaucoma.

I. Introduction

As recently as two decades ago, textbooks on vitreous taught students of ophthalmology that the vitreous gel had no real function in the adult eye other than to serve as a space-occupying, optically clear structure. In fact, one such textbook published in 1994 stated, “Apart from its role in oculogenesis, the vitreous has no well substantiated function so that an eye devoid of gel is not adversely affected” [1]. However, beginning in 2005 with published reports of oxygen tension measurements in the human vitreous gel before and after vitrectomy

surgery [2] and culminating with reports in 2009 that the human vitreous gel consumes oxygen in an ascorbate-dependent manner [3], a new understanding of the vitreous gel and its role in vitreoretinal physiology and pathology has emerged.

A. The Oxygen Hypothesis

The “Oxygen Hypothesis” challenges conventional thinking. This hypothesis contends that intraocular oxygen is low and that low oxygen is essential to the health of many tissues in the eye, as it prevents oxidation-induced ocular diseases such as nuclear cataract and some forms of primary open-angle glaucoma. The vitreous gel is principal (among other ocular tissues) in regulating intraocular oxygen tension and keeping it low. The vitreous gel biochemically eliminates the large amounts of molecular oxygen coming from the vascularized structures of the eye. The biophysical property of a gel vitreous is also critically important. The ability of the vitreous gel to consume oxygen diminishes as the vitreous gel liquefies with age or is removed surgically. Therefore, vertebrate evolution has led to a vitreous “gel” for a reason. The structure and function of an intact gel vitreous is central to the health of the human eye, protecting internal ocular structures from exposure to excess oxygen. Age-related liquefaction of the vitreous gel and subsequent loss of the gel’s biochemical and biophysical properties may be the initiating pathogenic step to oxidation-induced ocular disorders such as nuclear sclerotic cataract and some forms of primary open-angle glaucoma.

II. Intraocular Oxygen Tension

A. Experimental Measurements

1. Vitreous

In 1991, Eaton hypothesized that the human lens exists in a hypoxic state, thought necessary to preserve lens clarity [4]. In an article titled, “Is the lens canned?” Eaton suggested that the lens existed in a sterile, hypoxic state, ostensibly to avoid the damaging effects of oxidation much like a fruit or vegetable would be canned. Now, experimental data confirm that intraocular oxygen measurements near the human lens are below 1 % O₂, levels consistent with hypoxia. Figure IV.B-1 shows the results from a prospective, interventional consecutive case series of 69 eyes in which oxygen was measured using an optical oxygen sensor in patients undergoing vitrectomy surgery. Intraoperatively, oxygen measurements were taken before and after vitrectomy in two intraocular locations: adjacent to the lens and in the mid-vitreous. Prior to vitrectomy surgery, oxygen tension in the vitreous was low, measuring 8.7±0.6 mmHg adjacent to the lens and 7.1±0.5 mmHg in the mid-vitreous [2]. Atmospheric or

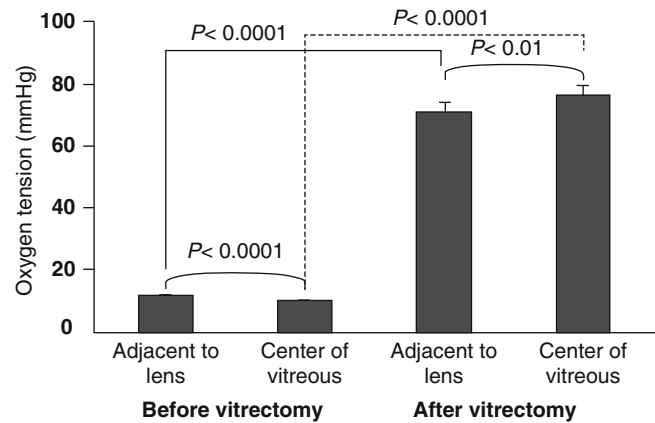


Figure IV.B-1 Oxygen tension (mmHg) in the human eye as measured in two locations before and immediately after vitrectomy surgery

inhaled oxygen tension is approximately 21 % or 156 mmHg. 1 % oxygen tension is approximately 7.6 mmHg. Thus, from these experimental data, it is presumed that in the healthy, normal eye, the lens and other interior structures of the eye exist under hypoxic conditions and are relatively protected from oxidative stress or oxidation-induced damage.

2. Lens

While Eaton hypothesized that the lens exists in a hypoxic state, human experimentation only allows for in vivo measurements of oxygen in the clear fluids surrounding the eye (i.e., an oxygen probe cannot be placed in the human lens for measurements during vitrectomy surgery). However, in 2004, Barbazetto et al. made seminal observations of oxygen tension in the rabbit lens before and after vitrectomy surgery [5]. Figure IV.B-2 shows the results of a consecutive series of 26 rabbit eyes undergoing vitrectomy surgery. Oxygen tension measurements were made in several locations within the eye, including within the lens itself, before and after vitrectomy surgery using an optical oxygen sensor. Prior to vitrectomy surgery, intraocular tension is low in both the vitreous and the lens. Thus, there is no barrier to diffusion of oxygen between the vitreous and the lens. In 2006, Shui et al. demonstrated by varying the amount of oxygen inhaled by rabbits between hypoxia and hyperoxia that the intraocular oxygen tension varied proportionally [6]. Thus, the amount of oxygen inhaled by a rabbit is reflected by the oxygen tension in the vitreous and the lens of the eye. This was confirmed by Holekamp et al. in humans when comparing oxygen tension measurements in the vitreous gel in patients undergoing vitrectomy surgery under local anesthesia and breathing 21 % oxygen to patients undergoing general anesthesia breathing 100 % oxygen [2]. The source of intraocular oxygen is inhaled air transmitted to the eye by the vasculature. Vitreous levels are reflective of the inhaled oxygen levels and vitreal oxygen diffuses into the lens of the eye from the posterior segment.

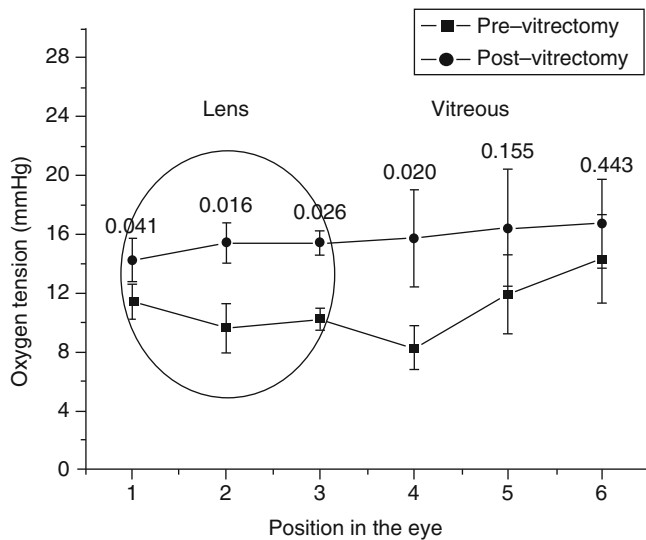


Figure IV.B-2 Oxygen tension (mmHg) in the rabbit eye measured throughout the lens and vitreous body before and after vitrectomy surgery (With permission from Barbazetto et al. [5])

3. Trabecular Meshwork

In the 2006 Jackson Memorial Lecture before the American Academy of Ophthalmology, Stanley Chang presented retrospective data from 453 patients who had undergone vitrectomy [7] and noted increased risk of developing open-angle glaucoma or increased intraocular pressure in operated eyes. The onset of glaucoma was accelerated by more than two years in patients who had previous cataract surgery before vitrectomy compared to those who had cataract surgery after vitrectomy. A more extensive follow-up study confirmed and extended these conclusions [8], but other studies dispute these findings (see chapter IV.A. Vitreous physiology). Based on these observations, Dr. Chang suggested that an oxygen metabolite could be responsible for damaging the outflow tissues. To examine the possible physiologic mechanism responsible for the increased risk of glaucoma after vitrectomy and cataract surgery, Siegfried et al. measured intraocular oxygen using an optical oxygen sensor in the anterior and posterior chambers of the eyes in a consecutive series of patients undergoing cataract or glaucoma surgery [9]. As seen in Figure IV.B-3, intraocular oxygen measurements in the anterior chamber angle were low, measuring 12 mmHg, which is less than 2% oxygen and is considered hypoxic. No statistically significant change in anterior chamber oxygen tension measurements were produced by vitrectomy or cataract surgery alone. However, following vitrectomy and cataract surgery, the mean oxygen level in the anterior chamber angle doubled to 25 mmHg, suggesting that oxidative damage to the outflow tissues could account for the increased risk of glaucoma after vitrectomy and cataract surgery.

III. Intraocular Oxygen Tension Regulation

There is now abundant experimental evidence that intraocular oxygen tension is low in the intraocular fluids of the human eye [2, 3, 9–11]. Remarkably, this finding is constant and conserved among hundreds of “normal” human eyes tested. Thus, it must be an important feature of the normal physiology of the eye—a feature overlooked by researchers until recently. Low intraocular oxygen tension also appears to be constant and conserved across mammalian species, with the rabbit eye having undergone the most rigorous scientific study [5, 6]. Shui and colleagues probed the rabbit eye extensively and found the following: Oxygen levels were highest near the retinal vasculature, the iris vasculature, and the inner surface of the central cornea. Compared with nearby regions, oxygen levels were decreased in the aqueous humor closest to the pars plicata of the ciliary body and near the anterior chamber angle. Oxygen levels were generally lower closer to the lens. The researchers concluded that, in the rabbit, intraocular oxygen is mostly derived from the retinal and iris vasculature and by diffusion across the cornea. Freshly secreted aqueous humor and the aqueous humor in the anterior chamber angle are relatively depleted of oxygen [6]. Intraocular oxygen tension in the eye is low and tightly regulated. Similar studies in human eyes confirmed this observation. The one major difference between oxygen distribution in the rabbit and human eyes was that oxygen levels were significantly lower in the human posterior chamber and near the anterior surface of the lens. Therefore, the human iris vasculature contributes little oxygen to the posterior chamber, and the human lens exists in a more hypoxic environment than the rabbit lens.

A. Intraocular Oxygen Gradients

Intraocular tissues appear to consume oxygen. Close inspection of Figures IV.B-1, IV.B-2, IV.B-3, and IV.B-4 in which intraocular oxygen tension measurements are made at different points within the anterior and posterior chambers of the eye reveals that oxygen gradients exist within these clear fluid spaces. For example, in Figure IV.B-1, measurements of oxygen tension before vitrectomy surgery were taken adjacent to the lens at 8.7 mmHg and in the center of the vitreous body at 7.1 mmHg. The probe adjacent to the lens was actually closer to the pars plana and the higher oxygen tension reflects oxygen coming from this tissue or the nearby peripheral retina. However, a more important yet subtle fact is that the difference in oxygen tension between the two locations is statistically significant ($p < 0.003$). The presence of a gradient suggests that the human vitreous gel consumes oxygen. This oxygen gradient in the vitreous is also seen in the rabbit eye in

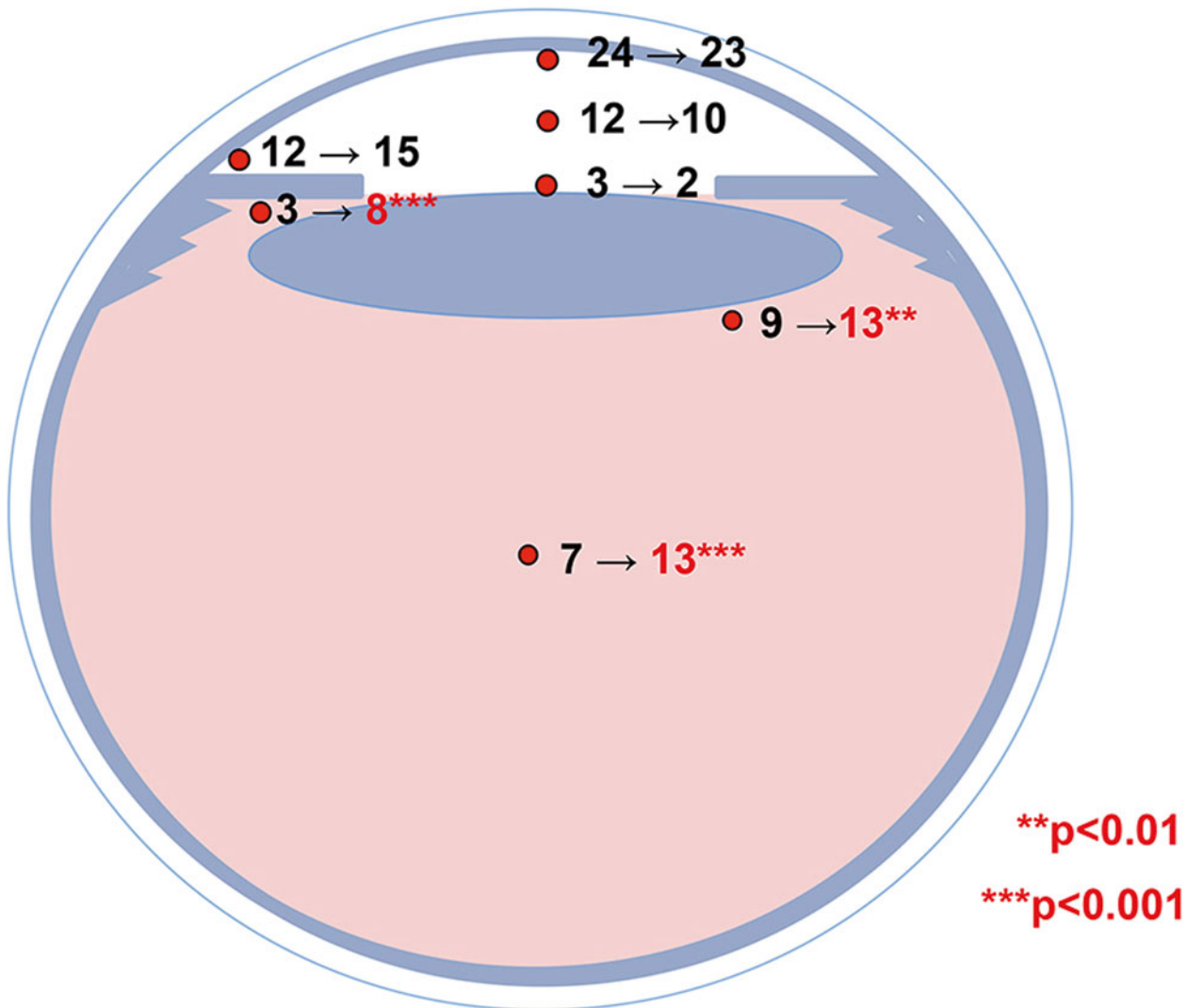


Figure IV.B-3 Oxygen tension (mmHg) in the human eye as measured before and after vitrectomy surgery. The number to the left of the arrow is before vitrectomy surgery. The number to the right of the arrow is after vitrectomy surgery. Numbers in red are statistically significantly elevated after vitrectomy surgery

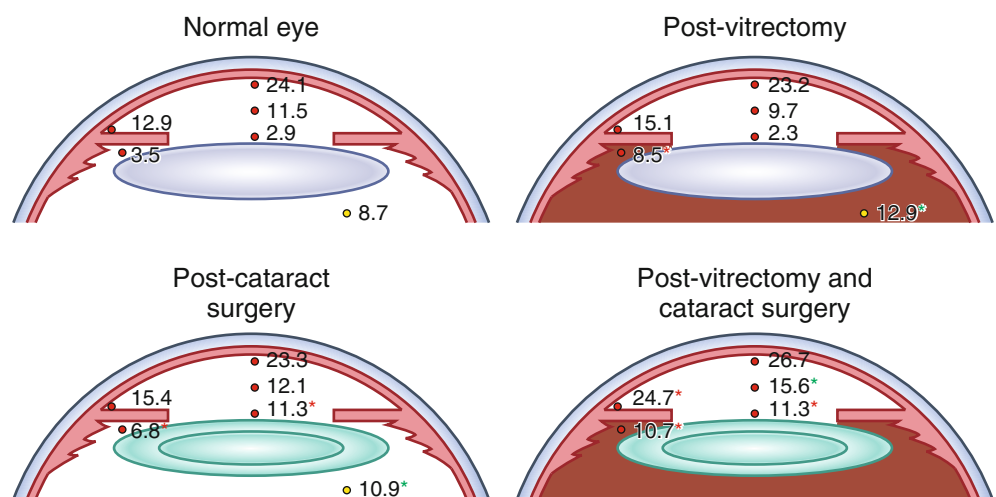


Figure IV.B-4 Oxygen tension (mmHg) in the human eye as measured before surgery (upper left) and after intraocular surgery (upper right and bottom)

* p<0.05
 * p<0.001

Figure IV.B-2. Thus, the rabbit vitreous gel consumes oxygen as well.

Figure IV.B-2 shows an intralenticular oxygen tension gradient. Barbazetto and colleagues found the lowest oxygen tension in the normal rabbit eye to be in the nucleus of the lens ($10.4 \text{ mmHg} \pm 3.0$). The presence of an oxygen gradient suggests that the lens consumes oxygen [9]. In fact, work by Shui and co-workers in rabbits calculated oxygen consumption by the posterior half of the lens to be $0.2\text{--}0.4 \text{ } \mu\text{L/h}$ under normoxic conditions. Oxygen consumption by the posterior half of the rabbit lens increased in proportion to the amount of oxygen supplied [6]. To corroborate the work of Shui et al. mentioned above, McNulty and colleagues found that the bovine crystalline lens consumed oxygen at a rate of $0.00003 \text{ cm}^3/\text{s}$. They also found a steep oxygen gradient within the lens, leading to $\text{PO}_2 < 2 \text{ mmHg}$ in the core. Lens fiber cells that contained mitochondria accounted for only 12 % of the oxygen consumed by the bovine lens, suggesting that another mechanism maintains the low oxygen levels in the lens core [12].

An oxygen gradient also exists in the anterior chamber. Figures IV.B-3 and IV.B-4 show that the anterior chamber oxygen tension in the normal eye is highest when measured just beneath the corneal endothelium at 24.1 mmHg and lowest when measured just above the anterior surface of the natural lens at 2.9 mmHg . Since oxygen levels in air are approximately 156 mmHg , oxygen is diffusing through the cornea and into the anterior chamber [9]. The corneal endothelium is highly concentrated with mitochondria that serve to consume molecular oxygen entering the eye. Dysfunction of the corneal endothelium, as in Fuchs' corneal endothelial dystrophy, leads not only to a clouded cornea but also an elevated anterior chamber oxygen tension (Andrew Hwang, MD PhD, personal communication). The presence of a gradient in the anterior chamber could suggest that aqueous consumes oxygen, but in this instance, it is the crystalline lens creating the gradient. As seen in Figure IV.B-4, after the crystalline lens is removed, post-cataract surgery measurements of oxygen tension anterior to the lens implant increase to 11.3 mmHg and the oxygen gradient in the anterior chamber is greatly diminished.

Figure IV.B-5 is a schematic representation of the ocular tissues that consume oxygen (marked in green): the corneal endothelium, the ciliary epithelium, the crystalline lens, and the vitreous gel. The vitreous gel, by virtue of its large size and central location within the eye, is important in regulating intraocular oxygen tension. In ocular tissues, mitochondrial abundance is a clue to oxygen consumption. As mentioned above, the normal corneal endothelium is replete with mitochondria. Also, the epithelium of the ciliary body has a high concentration of mitochondria. As a result, in spite of the rich vasculature of the ciliary body stroma, oxygen levels in the posterior chamber near the ciliary body of rabbits and humans are surprisingly low

when measured in vivo [6, 9]. Aqueous humor is produced depleted of oxygen.

B. Vitreous Gel Regulates Intraocular Oxygen

The importance of the vitreous gel in maintaining low intraocular oxygen tension is best illustrated by examining eyes in which the vitreous gel has been removed surgically. Post-vitreectomy eyes show markedly elevated intraocular oxygen tension at the time of vitrectomy surgery due to the highly oxygenated fluid being infused into the eye as the vitreous is removed, as seen in Figure IV.B-1. But, many months and even years later, the oxygen tension levels in a vitrectomized eye are significantly higher than in a non-vitrectomized eye. Holekamp and colleagues found that in eyes with a history of vitrectomy, the intraocular oxygen tension was significantly higher than in eyes with a formed vitreous gel undergoing a first vitrectomy ($P < .02$ when measured near the lens, $P < .003$ when measured in the mid-vitreous) [2]. More importantly, the intraocular oxygen gradient between measurements taken near the lens and in the mid-vitreous body was lost. Figure IV.B-3 shows that many months and years after vitrectomy surgery, the intraocular oxygen tension in either location was 13 mmHg . This is a significant elevation compared to pre-vitreectomy levels of 7 and 9 mmHg , and the oxygen gradient in the vitreous cavity is lost. Removal of the vitreous gel and its replacement with fluid (essentially aqueous) result in elevated intraocular oxygen tension and loss of intraocular oxygen tension regulation.

1. Vitreous Gel Metabolizes Oxygen

In 2009, Shui and co-workers published novel findings that human vitreous gel metabolizes molecular oxygen in an ascorbate-dependent manner [3]. A consecutive series of 62 small, undiluted human vitreous gel samples collected at the time of vitrectomy surgery were measured for oxygen consumption with a microrespirometer. Figure IV.B-6 shows the results typical for a human eye with a formed vitreous gel. Oxygen tension starts out very high due to exposure to atmospheric oxygen during the collection process. Generally within 2 h, the oxygen tension decreases to zero. The results are convincing: human vitreous gel metabolizes oxygen. Further laboratory analysis showed that vitreous actively consumes oxygen in an acellular, ascorbate-dependent fashion. Boiled vitreous retained the ability to consume oxygen. Vitreous humor exposed to oxygen and thereby depleted of ascorbate loses its ability to consume oxygen. Adding new ascorbate restores this ability. There is a catalyst in the vitreous that is required for this activity. Ascorbate in pure water does not consume oxygen. The vitreous is an essential component (Figure IV.B-7a). Further experiments with cadaver vitreous revealed that the rate at which vitreous consumed oxygen directly correlated with the amount of ascorbate present (Figure IV.B-7b).

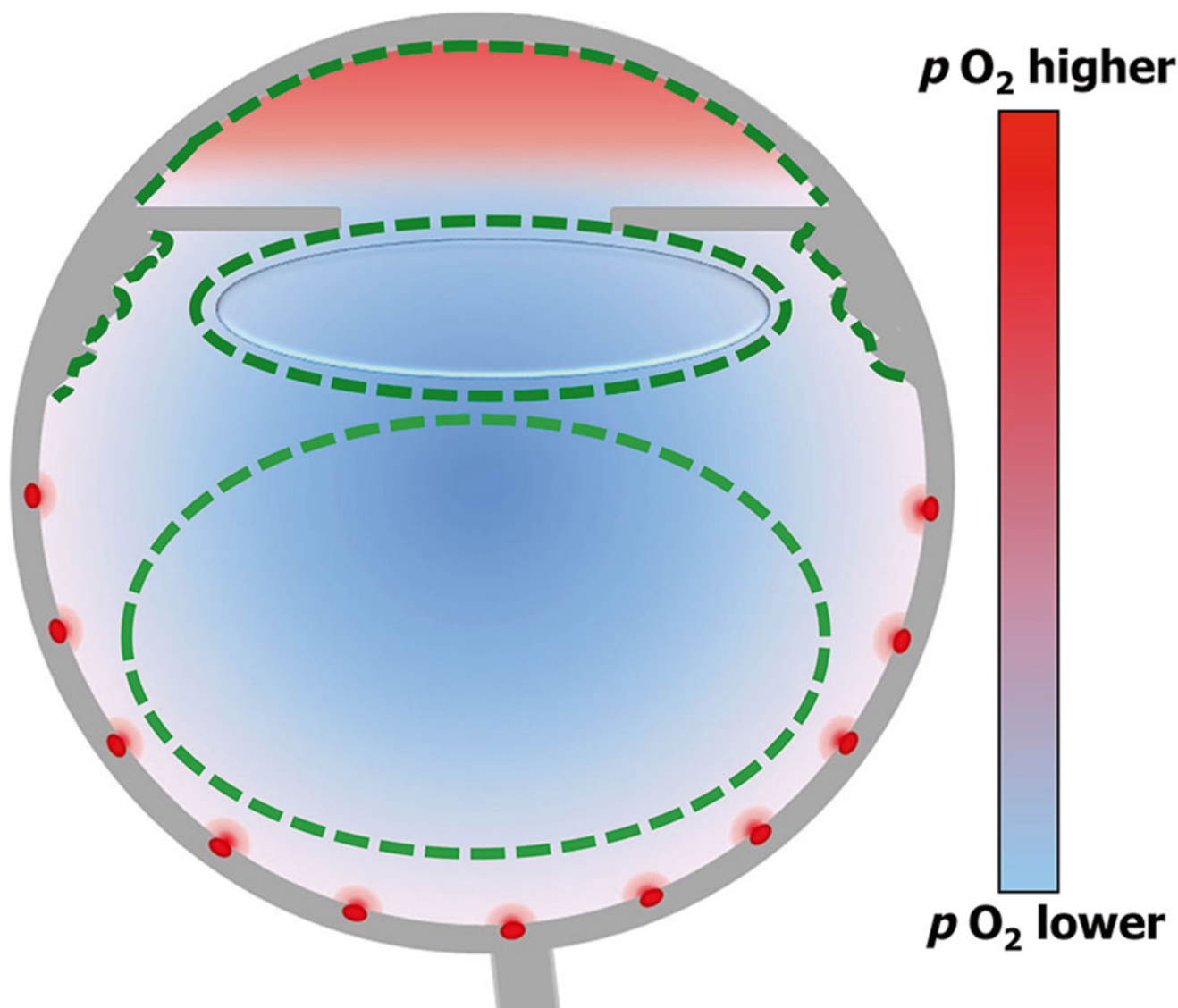


Figure IV.B-5 A schematic representation on oxygen distribution in the human eye. The structures outlined in green represent tissues that consume molecular oxygen

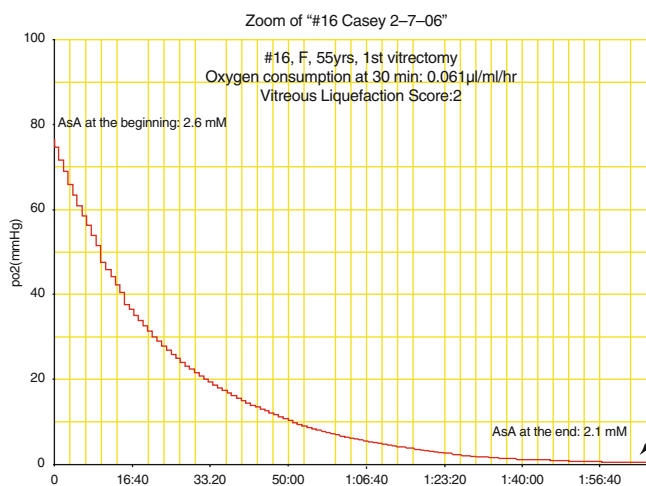


Figure IV.B-6 Oxygen consumption curve typical for vitreous removed from the eye during a first vitrectomy surgery. Note that both oxygen and ascorbate are consumed over time

The concentration of ascorbate in human vitreous is remarkably high. In eyes with an intact vitreous gel, the mean concentration of ascorbate is approximately 2 mM. Blood levels are only 50–60 μM, a 33- to 40-fold difference [13]. The high level of ascorbate in vitreous is maintained by a sodium-dependent ascorbate transporter (SLC23A2) in the pigmented layer of the ciliary epithelium [14]. The physiologic purpose of so much ascorbate in human vitreous has received past experimental investigation and speculation but has remained largely unexplained until now. Shui and co-workers propose the biochemical reaction in Figure IV.B-8 as the mechanism by which vitreous metabolizes oxygen. The reaction of ascorbate (AsA) with molecular oxygen (O₂) in the vitreous ultimately yields dehydroascorbate (dAsA; oxidized ascorbate), water, and half the initial amount of O₂. As this reaction cycles, oxygen (and ascorbate) are depleted. The catalyst for the second reaction is catalase. The catalyst for

Figure IV.B-7 (a) Oxygen consumption experiments with cadaver vitreous. (b) Ascorbate consumption which occurs is proportional to oxygen consumption

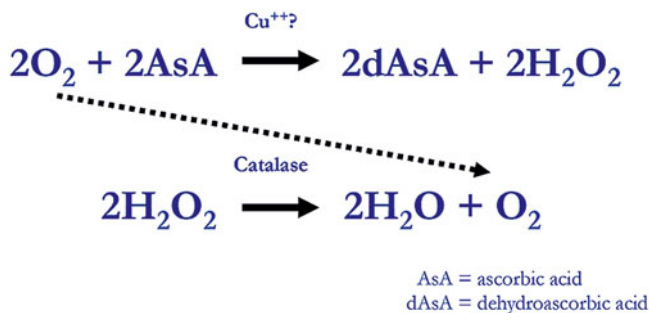
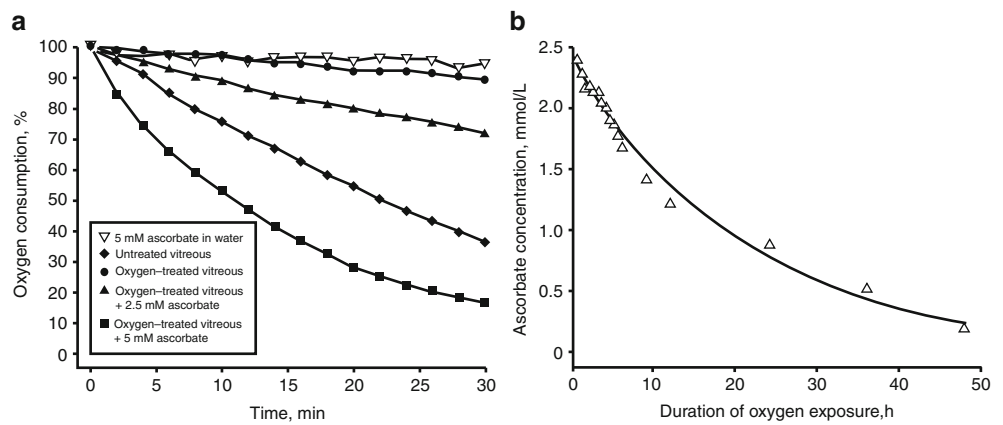


Figure IV.B-8 The proposed biochemical reaction by which oxygen is metabolized in the vitreous get. The metal ion catalyst in the first step is unknown but is found in vitreous. Note that both oxygen and ascorbate are consumed in the reaction. AsA ascorbic acid, dAsA dehydroascorbic acid

the first reaction has not yet been identified but is found in vitreous. It is important to note that in studies of nonhuman animals, ascorbate levels are uniformly higher in the aqueous than in the vitreous humor. In human eyes, ascorbate levels are higher in the vitreous. As will be discussed later in this chapter, this difference may partially explain why there is no good animal model of nuclear sclerotic cataract. Furthermore, animal studies led to the view that all ascorbate enters the eye in the aqueous humor [15] and then diffuses from the aqueous into the vitreous. Newer evidence suggests that human ascorbate enters across the RPE and into the vitreous (unpublished data, Ying-Bo Shui, MD PhD).

2. Gel Vitreous Consumes Oxygen Better Than Liquid Vitreous

Figure IV.B-9 shows the oxygen consumption of vitreous fluid removed from a 78-year-old woman who had undergone two prior vitrectomy surgeries for retinal detachment. In an eye with prior vitreous surgery, there was very little vitreous gel remaining in the posterior segment of the eye. The vitreous chamber was essentially filled with aqueous fluid [16]. Compared to Figure IV.B-6 showing oxygen consumption of formed vitreous gel, Figure IV.B-9 shows minimal if any consumption of oxygen by liquefied vitreous. It is important to note that in Figure IV.B-6, the ascorbate

concentration is high and that ascorbate is metabolized in the reaction that also metabolizes oxygen. In Figure IV.B-9, the ascorbate concentration is very low. The reaction to metabolize both ascorbate and oxygen occurs very slowly and little ascorbate or oxygen is consumed.

There exists no objective scale or measurement of vitreous liquefaction. Therefore, a subjective scale from 1–5 created by Shui and co-workers was used to grade the degree of vitreous liquefaction in a sample of vitreous being tested for oxygen consumption. A grade of 1 represented a fully gel-like vitreous. A grade of 5 represented a completely liquefied vitreous. Figure IV.B-6 notes a vitreous liquefaction score of 2. Figure IV.B-9 notes a vitreous liquefaction score of 5. In this way, it was noted that gel vitreous consumed oxygen more rapidly than liquefied vitreous when a large number of samples were studied. This result is seen in Figure IV.B-10a. Not unexpectedly, gel vitreous also has a higher concentration of ascorbate, as seen in Figure IV.B-10b.

3. Biophysical Properties of Gel Vitreous

Shui and co-workers found that, universally, gel vitreous has a higher concentration of ascorbate and consumes oxygen at a faster rate than liquid vitreous (i.e., vitreous gel that has undergone age-related liquefaction or surgical removal) [3]. Thus, the gel state of the vitreous is critical. Transvitreal movement of small molecules such as oxygen depends on several mechanisms including diffusion, hydrostatic pressure, osmotic pressure, convection, and active transport by surrounding tissues. Barton et al. have recently shown that the diffusion of small molecules through the vitreous gel occurs at the same rate as through a liquid [17]. The critical difference between oxygen movement in a gel and liquid lies in convection currents or “mixing” within the eye. When vitreous is mostly in the gel state, oxygen diffusing into the gel from retinal vessels is elevated only near the retinal tissue, as shown by oxygen microelectrode studies in experimental animals [18]. However, when the vitreous liquefies, oxygen from the retinal vessels can be carried away from the retina and distributed throughout the eye by fluid currents generated by movement of the eyes or head [19, 20]. The more that

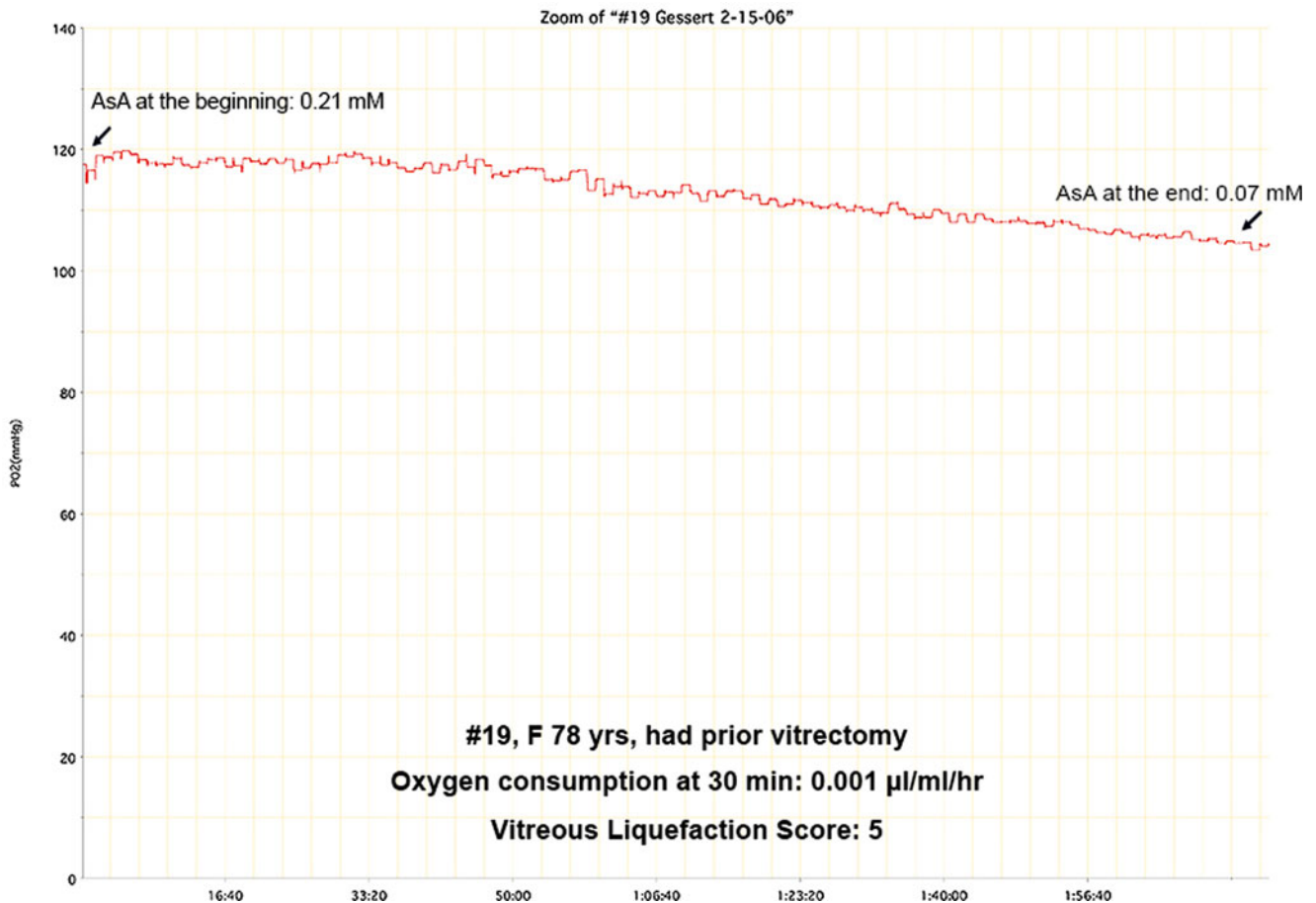


Figure IV.B-9 Oxygen consumption curve typical for vitreous removed from the eye during a second or third vitrectomy. Note the very low concentration of ascorbate at baseline

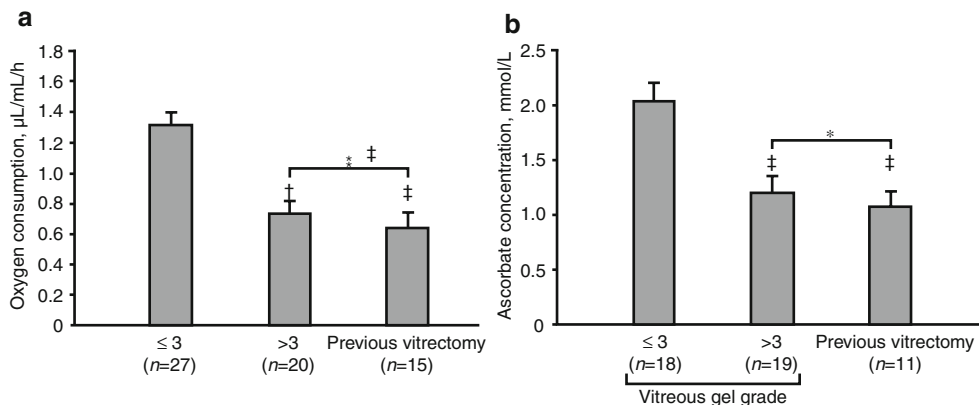


Figure IV.B-10 (a) Oxygen consumption rate varies with degree of vitreous liquefaction where a grade 1–3 is a gel vitreous and a grade greater than 3 is a liquified vitreous. Vitreous from an eye with previous

vitrectomy is purely liquid. **(b)** Similarly, ascorbate concentration varies with degree of vitreous liquefaction

oxygen mixes with the vitreous fluid, the more opportunity it will have to react with ascorbate. Both ascorbate and oxygen are consumed in this reaction. If the active transport of ascorbate into the eye is constant, the net effect of increased mixing with oxygen would be to lower the concentration of ascorbate in the vitreous fluid, slowing the consumption of

oxygen and raising intraocular oxygen tension. A recent publication presents a finite element model of oxygen distribution in the human eye [21]. The model is based on measurements of oxygen distribution and the function of the vitreous gel and vitreous ascorbate in regulating intraocular oxygen distribution. The model accurately predicts the

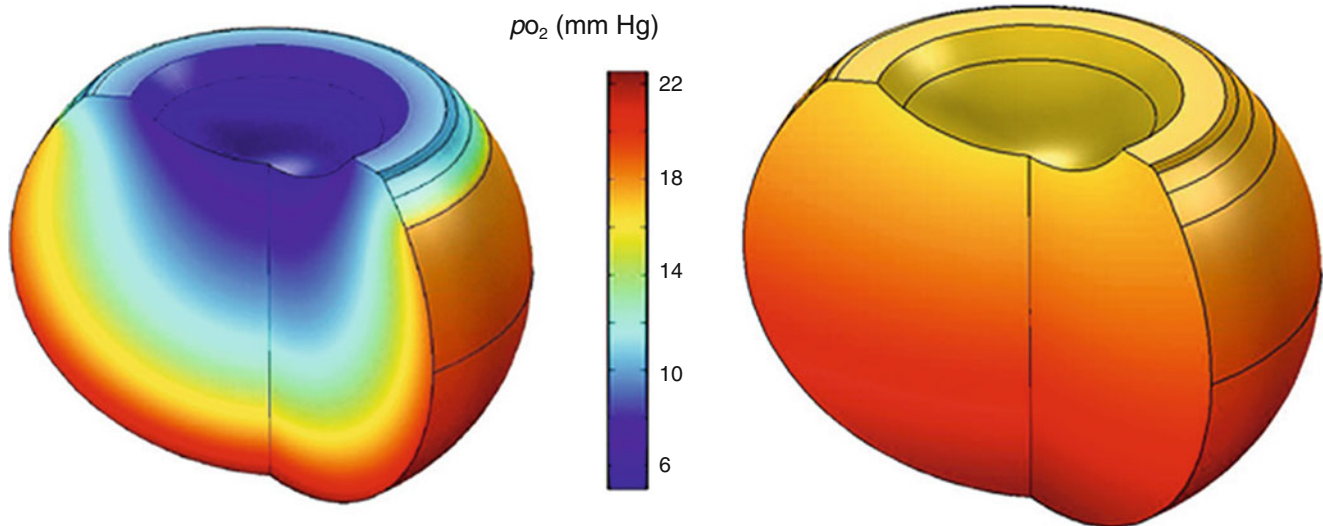


Figure IV.B-11 A finite element model can predict oxygen distribution in the human eye

distribution of oxygen in the eye pre-and post-vitrectomy (Figure IV.B-11). It also provides a means to determine the effects of vitreous-sparing surgery and may be useful for predicting the effectiveness of methods that preserve vitreous structure.

IV. Vitreous Liquefaction or Vitrectomy Increases Oxygen

Figure IV.B-3 demonstrates that intraocular oxygen tension increases after vitrectomy surgery in which the vitreous gel is surgically removed. Vitreous liquefaction or syneresis begins at approximately age 4 in humans and occurs very slowly throughout life. To better understand the “Oxygen Hypothesis,” it is useful to consider vitrectomy surgery tantamount to instantaneous vitreous liquefaction: the vitreous gel is surgically removed and is replaced with physiologic saline that rapidly becomes aqueous fluid. That post-vitrectomy eyes may mirror or simulate eyes with vitreous liquefaction can be seen clinically. Post-vitrectomy eyes are at higher risk for nuclear cataract [22–25]. Stickler syndrome includes both premature vitreous liquefaction and premature nuclear cataract. Recently, axial myopia, a condition associated with early-onset vitreous liquefaction, has been associated with earlier onset and denser nuclear cataract formation than emmetropic control eyes [26]. Furthermore, in patients who develop rapidly progressive post-vitrectomy nuclear cataract, the quality, character, color, hardness and opacity of the lens are identical to that seen in Stickler syndrome, high myopia, and typical age-related nuclear cataract (Figure IV.B-12). Age-related nuclear cataract and post-vitrectomy nuclear cataract differ only in the degree of oxidation. Thus, post-vitrectomy nuclear cataract appears to

be an accelerated form of age-related nuclear cataract. For research purposes, post-vitrectomy nuclear cataract is the perfect “experimental model” for age-related nuclear cataract.

It is important to note that the elevation of intraocular oxygen tension and the subsequent nuclear cataract following vitrectomy surgery are due to the removal of vitreous and not trauma associated with a surgical procedure. Work by Sawa et al. and Saito and colleagues has shown that vitrectomy surgery performed without infusion of a highly oxygenated balanced salt solution or removal of the vitreous gel does not cause post-vitrectomy nuclear cataract progression as measured by Scheimpflug photography, even after 5 years of follow-up [27–29]. Thus, either infusing a highly oxygenated fluid into the eye or removing the vitreous gel or both is likely to be responsible for post-vitrectomy nuclear cataract. Almony and colleagues found that small-gauge vitrectomy, with purportedly less surgical trauma and less fluid infusion into the eye, did not protect against post-vitrectomy nuclear cataract [33]. All eyes that develop post-vitrectomy nuclear cataract have the vitreous gel surgically removed. Interestingly, eyes that develop age-related nuclear cataract demonstrate increased vitreous liquefaction.

From these observations, the “Oxygen Hypothesis” predicts that intraocular oxygen tension increases slowly over time with age-related vitreous liquefaction, analogous to the increase in intraocular oxygen tension that immediately occurs following vitrectomy surgery with removal of the vitreous gel. More explicitly stated, the “Oxygen Hypothesis” contends that with every breath of air a human takes, a little bit of oxygen works its way from the retinal vasculature through the vitreous gel, reaching the lens. This process takes a lifetime. In older patients, it is aided by age-related

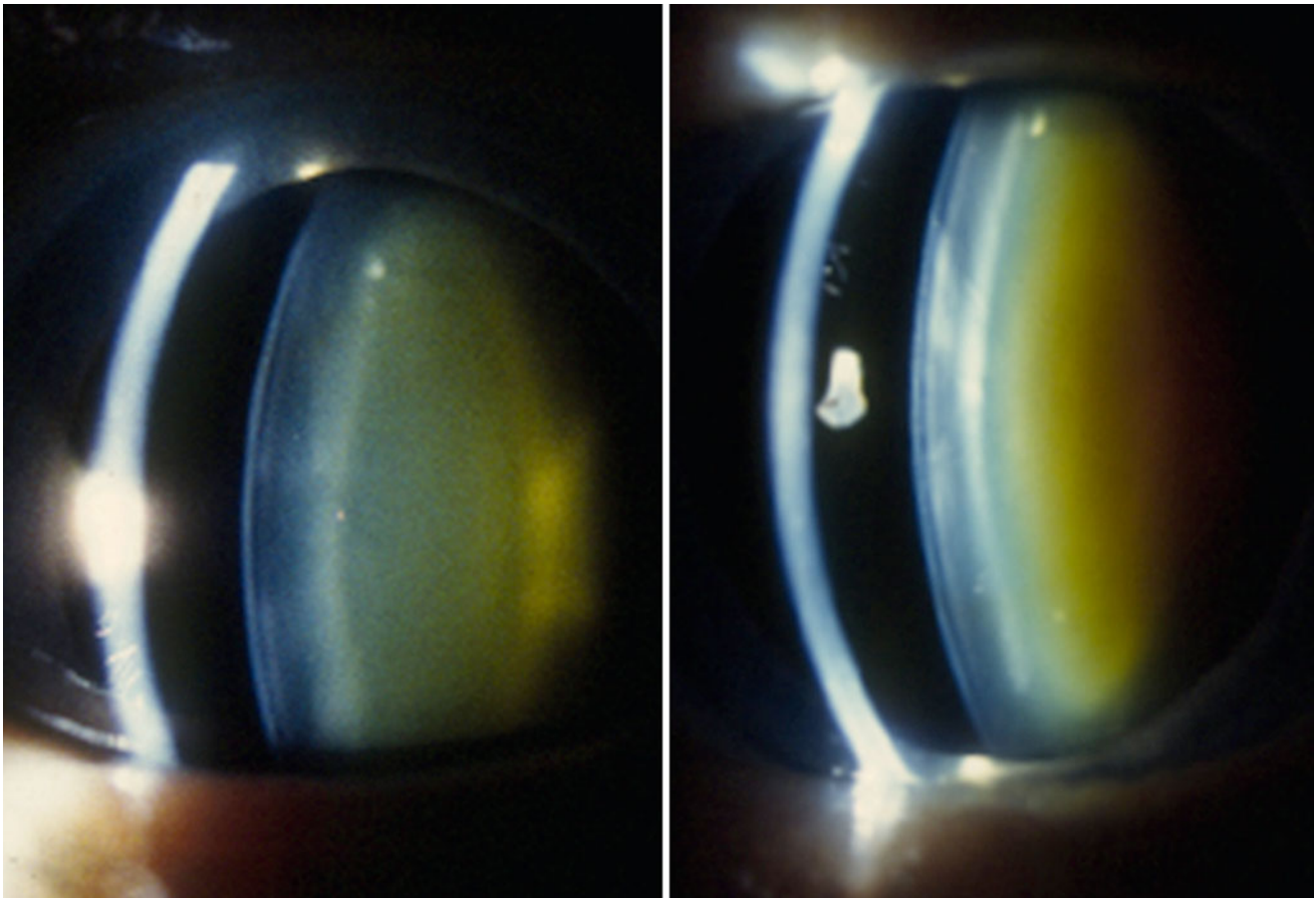


Figure IV.B-12 (Left) Normal age-related nuclear sclerosis in the right eye of a 75-year-old woman. (Right) Rapidly progressive nuclear sclerosis in the same patient's left eye following vitrectomy surgery 1 year earlier

vitreous liquefaction as liquefied vitreous has diminished capacity to metabolize oxygen diffusing from the retinal vasculature. Consequently, only older individuals manifest nuclear cataract. However, in eyes in which the vitreous gel has been surgically removed, oxygen passes freely from the retina to the lens, hastening nuclear cataract formation. Thus, the “Oxygen Hypothesis” is a unifying theory that potentially explains both age-related and post-vitrectomy nuclear cataract.

V. Pathogenic Effects of Increased Intraocular Oxygen

This section will present evidence to link vitreous liquefaction and/or surgical removal and the subsequent increase in intraocular oxygen tension with two common oxidation-induced ocular diseases: nuclear sclerotic cataract and some forms of primary open-angle glaucoma.

A. Nuclear Sclerotic Cataract

1. Oxygen and Nuclear Sclerosis

It is well accepted that nuclear sclerotic cataract is caused by the oxidation of proteins and lipids within the lens nucleus [13, 30]. Figure IV.B-12 shows opacity and yellowish discoloration of the nucleus of the lens caused by oxidation – similar to iron rusting or a cut apple turning brown. The source of oxidation has long been thought to be due to the activity of oxygen-free radicals. However, there is valid scientific rationale to propose that molecular oxygen is the initial insulting agent. Consider that hyperbaric oxygen therapy provides evidence that increased exposure of the lens to molecular oxygen can cause human nuclear sclerotic cataract. In a study by Palmquist et al., patients received between 150 and 850 treatments with 100 % inhaled oxygen delivered at 2–3 atm of pressure [14]. Seven of 15 patients developed nuclear sclerotic cataract. Fourteen of fifteen developed myopic shift, a change known to precede the opacity of nuclear cataract. All symptomatic patients were over

age 50. The one patient who did not develop symptoms was 24 years old. Similar to hyperbaric oxygen chambers, Japanese caisson workers are known to develop nuclear cataract with prolonged exposures to increased levels of oxygen [31]. These studies of nuclear sclerotic cataract associated with patients receiving hyperbaric oxygen treatments or caisson workers are corroborated by experimental work discussed earlier in this chapter. Holekamp and colleagues measured intraocular oxygen tension in patients undergoing vitrectomy surgery receiving general anesthesia with 100 % inhaled oxygen and found that intravitreal oxygen tension was immediately and significantly elevated [2]. Thus, high levels of inhaled oxygen are immediately reflected in the vitreous gel. Similar work by Barbazetto et al. in rabbits and later work by Giblin in rats demonstrated that the oxygen tension measured in vitreous increases the oxygen tension measured in the lens nucleus [5, 32]. There is no barrier to diffusion of oxygen between vitreous and the lens. Combining these observations suggests that molecular oxygen is implicated in the development of human nuclear sclerotic cataract.

2. Role of Vitreous in Nuclear Sclerosis

Experimental evidence has emerged that the extent of vitreous liquefaction correlates with the development of nuclear sclerotic cataract. In a study of 171 cadaver eyes, Harocopos and colleagues found that vitreous liquefaction was highly associated with nuclear sclerotic cataract. In fact, the state of the vitreous body was a better predictor of nuclear opacity than was age in subjects between 50 and 70 [19]. After age 70, vitreous liquefaction was so extensive that its association with cataract became nonsignificant. While numerous studies have attempted to correlate age-related nuclear sclerotic cataract with various factors such as smoking, diet, and socioeconomic status, one clinical observation given little attention remains constant: eyes with nuclear sclerotic cataract also demonstrate increased vitreous liquefaction. The corollary to this observation is an intact gel structure which appears to protect against nuclear sclerotic cataract.

Vitrectomy surgery offers compelling evidence that an intact vitreous gel protects against nuclear sclerotic cataract. The statistics are impressive: in patients over age 50, up to 60–95 % will develop nuclear sclerotic cataract requiring cataract surgery within 2 years after vitrectomy [22–25]. For eyes in patients under age 50, the percentage is less than 10 % [24]. This difference might be explained by the fact that the younger crystalline lens is more resistant to nuclear cataract, retaining its innate ability to metabolize oxygen and protect itself from oxidation, or that the younger gel structure just behind the lens not removed by vitrectomy retains a protective function.

3. The “Oxygen Hypothesis” for Nuclear Sclerosis

Both experimental and clinical observations suggest that an intact vitreous gel, with the full capacity to consume oxygen in an ascorbate-dependent manner, protects against nuclear cataract. The “Oxygen Hypothesis” proposes that if the vitreous gel structure and function are lost due to either surgery or age-related liquefaction, the resultant elevation in intraocular oxygen will lead to nuclear cataract – rapidly after vitrectomy surgery and slowly with age-related vitreous liquefaction (see chapter II.C. Vitreous aging and posterior vitreous detachment).

Figure IV.B-13a–c explains the “Oxygen Hypothesis” for nuclear cataract. In Figure IV.B-13a, when the normal eye has an intact vitreous gel, the oxygen exuding from the retinal vasculature is held close to the retinal surface, ultimately to be used by cells of the inner retina. It is not allowed to “mix” in the vitreous body. The vitreous gel metabolizes much of the excess molecular oxygen that escapes from the retina. Intraocular oxygen tension remains low. There is very little oxidation of the lens nucleus. In Figure IV.B-13b, when the aging eye undergoes vitreous liquefaction, the oxygen exuding from retinal capillaries can now “mix” in the vitreous body raising intraocular oxygen tension. The vitreous gel metabolizes oxygen in an ascorbate-dependent manner, but as the ascorbate is consumed by the chemical reaction, less oxygen is metabolized. Slowly over time, there is increased oxidation of the lens nucleus. In Figure IV.B-13c, surgical removal of vitreous and its replacement with aqueous fluid allows for convection currents with eye or head movement to carry oxygen from the retina throughout the vitreous chamber. In addition, the loss of the vitreous gel means there is complete mixing of oxygen with ascorbate, delivering oxygen to the posterior of the lens and reducing oxygen consumption by nearly half. The layer of vitreous immediately behind the lens and the lens itself are not sufficient to protect against the oxidative insult, especially in older eyes. Molecular oxygen passes unimpeded from the retinal vasculature to the lens. Oxidation of the lens nucleus occurs rapidly.

B. Primary Open-Angle Glaucoma (POAG)

1. Oxygen and POAG

Experimental evidence suggests that increased oxidative stress or oxidation-induced damage may contribute to the pathogenesis of primary open-angle glaucoma [34–41]. Antioxidant-protective mechanisms are decreased and enzymes induced by oxidative stress are increased in the aqueous humor of glaucoma patients compared to non-glaucoma patients undergoing

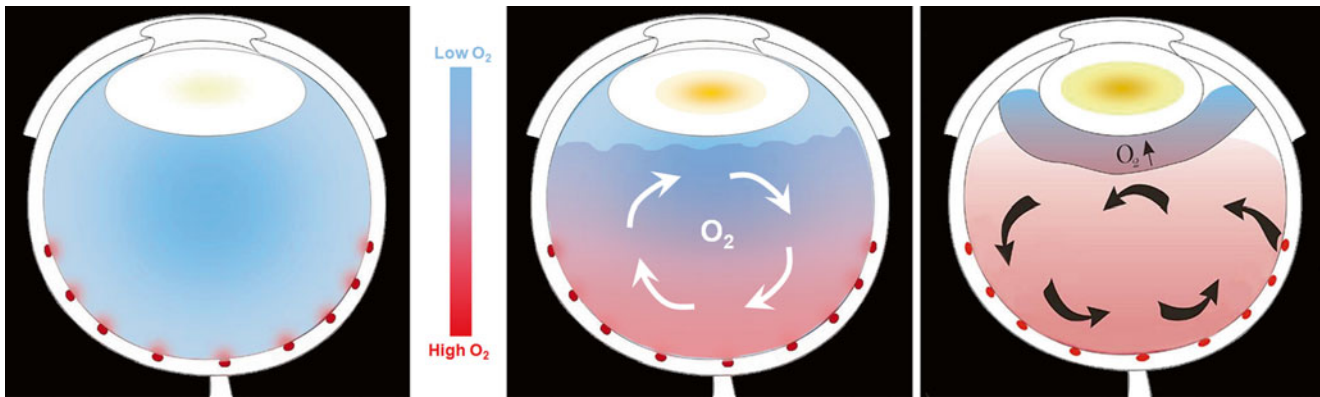


Figure IV.B-13 The “Oxygen Hypothesis” for nuclear sclerotic cataract. (a) When the normal eye has an intact vitreous gel, the oxygen exuding from the retinal vasculature is held close to the retinal surface, ultimately to be used by cells of the inner retina. It is not allowed to “mix” in the vitreous body. The vitreous gel metabolizes much of the excess molecular oxygen that escapes from the retina. Intraocular oxygen tension remains low. There is very little oxidation of the lens nucleus (b). When the aging eye undergoes vitreous liquefaction, the oxygen exuding from retinal capillaries can now “mix” in the vitreous body, raising intraocular oxygen tension. The vitreous gel metabolizes oxygen in an ascorbate-dependent manner, but as the ascorbate is con-

sumed by the chemical reaction, less oxygen is metabolized. Slowly over time, there is increased oxidation of the lens nucleus (c). Surgical removal of the vitreous and its replacement with aqueous fluid allow for convection currents to carry oxygen from the retina throughout the vitreous chamber. In addition, the loss of the vitreous gel means there is complete mixing of oxygen with ascorbate, delivering oxygen to the posterior of the lens. The layer of vitreous immediately behind the lens and the lens itself are not sufficient to protect against the oxidative insult. Molecular oxygen passes unimpeded from the retinal vasculature to the lens. Oxidation of the lens nucleus occurs rapidly

cataract surgery [36, 41]. Oxidative damage to DNA is increased in the trabecular meshwork cells of glaucoma patients. These cells are more susceptible to oxidative DNA damage than other cells in the anterior segment [37]. Glaucoma patients have pathogenic mutations in their mitochondrial DNA that are not present in non-glaucoma patients. These mutations may reduce the ability of cells to deal with oxidative damage [42]. Mitochondria of glaucoma patients also have significantly lower oxidative activity than controls. Despite this experimental evidence linking glaucoma pathogenesis to oxidative damage, the source of the oxidative stress in these patients is not known.

There is clinical evidence to suggest that the source of oxidative damage in primary open-angle glaucoma may be molecular oxygen. POAG is frequently seen in conditions that include premature vitreous liquefaction and/or the absence of a crystalline lens – altered anatomy now known to be associated with increased intraocular oxygen tension in the anterior segment. For example, age is an important independent risk factor for POAG, and the extent of vitreous liquefaction increases with age [16]. Myopia is a risk factor for glaucoma, although not a strong one. There is a higher incidence of vitreous liquefaction and even posterior vitreous detachment in myopia [2]. Aphakia is associated with POAG particularly refractory to treatment. The absence of a crystalline lens and the surgically induced vitreous liquefaction are likely contributing factors. Vitreous loss during cataract surgery in glaucoma patients adversely affects long-term control of intraocular pressure [43]. Finally, children often

develop glaucoma after surgery for congenital cataract, suggesting that the presence of the crystalline lens is protective [44]. Thus, an intact gel vitreous and crystalline lens, which both metabolize molecular oxygen, may have some function that protects against primary open-angle glaucoma.

2. Role of Vitreous and Cataract Surgery in POAG

When the gel is surgically removed and the lens is removed, a substantial percentage of eyes will show evidence of open-angle glaucoma if followed long term. Chang was the first to demonstrate an increased risk of open-angle glaucoma following vitrectomy surgery. He estimated the risk to be 15–20 % of eyes with long-term follow-up [7]. Chang’s observations have since been confirmed in one study but are disputed in other studies (see chapter IV.A. Vitreous physiology). With a mean follow-up of just 4 years, 8 (7.9 %) of 101 eyes developed open-angle glaucoma after vitrectomy surgery [45]. With longer follow-up, that percentage is likely to increase. Interestingly, it was also found that the presence of the crystalline lens is protective, since there was a delay in the onset of POAG until after the post-vitrectomy nuclear cataract was removed. These observations led Chang to propose that, after vitrectomy, metabolites of oxygen, like superoxide anion and hydrogen peroxide, might damage the tissues of the outflow pathway, contributing to the increased risk of glaucoma [7]. Since the presence of the natural lens reduced the risk of glaucoma, he proposed that the lens protected the anterior segment from oxygen or

oxygen metabolites. In 2010, Siegfried and co-workers provided experimental data in humans to confirm Chang's hypothesis: that oxygen is relatively low in the anterior segment of the unoperated eye, but increases after combined vitrectomy and cataract surgery [9].

Figure IV.B-4 shows that the oxygen tension in the anterior chamber angle of a "normal" eye undergoing cataract surgery is 12.9 mmHg. This represents less than 2 % oxygen and is considered hypoxia. After vitrectomy surgery, the oxygen tension in the anterior chamber angle goes up mildly to 15.1 mmHg. This was not a statistically significant elevation in this study group. After cataract surgery, the oxygen tension in the angle goes up mildly to 15.4 mmHg. Again, this was not a statistically significant elevation. However, after both vitrectomy surgery and cataract surgery, the oxygen tension in the anterior chamber angle goes up markedly to 24.7 mmHg. This is a statistically significant elevation in oxygen exposure, being almost a 100 % increase. If the cells of the trabecular meshwork are "adapted" to oxygen at 13 mmHg, increasing the oxygen tension to 25 mmHg could lead to oxygen toxicity: altered extracellular matrix accumulation, increased apoptosis, and decreased outflow facility. These oxidation-induced changes could lead to ocular hypertension and increased risk of glaucoma. The work of Siegfried and colleagues supports the Chang hypothesis that increased exposure to oxygen or its metabolites may cause open-angle glaucoma.

3. The "Oxygen Hypothesis" for POAG

Both experimental and clinical observations suggest that an intact vitreous gel and a native crystalline lens, both with the full capacity to metabolize molecular oxygen, protect against primary open-angle glaucoma. The "Oxygen Hypothesis" proposes that if vitreous gel and the crystalline lens are both surgically removed, the resultant elevation of oxygen at the anterior chamber angle will lead to oxidative damage of the trabecular meshwork and eventually POAG. Figure IV.B-14 is adapted from the work of Siegfried et al. and illustrates the "Oxygen Hypothesis" for POAG. (A) In the unoperated eye, oxygen enters from the retinal vasculature through the vitreous, across the ciliary epithelium from the ciliary body vasculature and into the anterior chamber across the cornea. Oxygen is consumed by the vitreous, lens, and the ciliary epithelium. A small amount of oxygen enters the anterior chamber angle by diffusing across the ciliary body and iris stroma (curved red arrow). (B) After vitrectomy, more oxygen reaches the posterior chamber. This supplies more oxygen to the "aqueous side" of the ciliary epithelium, reducing the amount of oxygen that the ciliary epithelium removes from the blood and slightly increasing the amount of oxygen available to enter the anterior chamber angle from the ciliary body stroma. (C) Cataract surgery reduces oxygen consumption by the lens, thereby increasing the pO_2 anterior to the lens and in the

posterior chamber. Again, the increased oxygen on the "aqueous side" of the ciliary epithelium reduces the amount of oxygen that the ciliary epithelium removes from the blood, thereby slightly increasing the amount of oxygen available to enter the anterior chamber angle from the ciliary body stroma. (D) After both vitrectomy and cataract surgery, significantly more oxygen is available on the "aqueous side" of the ciliary epithelium, resulting in the removal of significantly less oxygen from the blood. This increases the amount of oxygen available to diffuse from the ciliary body stroma, across the iris stroma, and into the anterior chamber angle, exposing the outflow system to a large excess of oxygen and/or oxygen metabolites.

VI. Oxygen Ameliorates VEGF-Mediated Retinopathies

An interesting corollary of the "Oxygen Hypothesis" is that vitreous liquefaction or surgical removal of the vitreous and the subsequent elevation in intraocular molecular oxygen may benefit ischemic retinal disease.

A. Age-Related Macular Degeneration (AMD)

Vascular endothelial growth factor (VEGF) has emerged as a predominant mediator of several retinal diseases, including choroidal neovascularization due to age-related macular degeneration. Because it suppresses VEGF gene expression, molecular oxygen is a potent anti-VEGF agent. In an experimental animal model, Quiram and colleagues showed that an enzymatically induced posterior vitreous detachment (PVD) in eyes with a vascularized retina will increase intraocular oxygen tension in vitreous [46]. Thus, PVD may increase intraocular oxygen tension and produce a sustained anti-VEGF effect. A retrospective study by Krebs and colleagues supports this hypothesis in AMD (see chapter III.G. Vitreous in AMD). They were able to show that eyes with a complete PVD had a lower incidence of exudative AMD than eyes without a PVD [47]. The "Oxygen Hypothesis" suggests that PVD allows for "mixing" of oxygen from the retinal vasculature in the vitreous body raising intraocular oxygen, reducing VEGF, and thereby reducing the VEGF stimulus for exudative AMD. The converse may also be true. Anomalous PVD with cortical vitreous remaining attached to the macula (see chapter III.B. Anomalous PVD and vitreoschisis) may keep intravitreal oxygen concentration low, allowing for permissive VEGF levels and a proangiogenic environment. Additional evidence for the possible beneficial effect of complete PVD on choroidal neovascularization (CNV) due to AMD can be found in The Submacular Surgery Trials Report No. 11 and in chapter III.G. Vitreous in

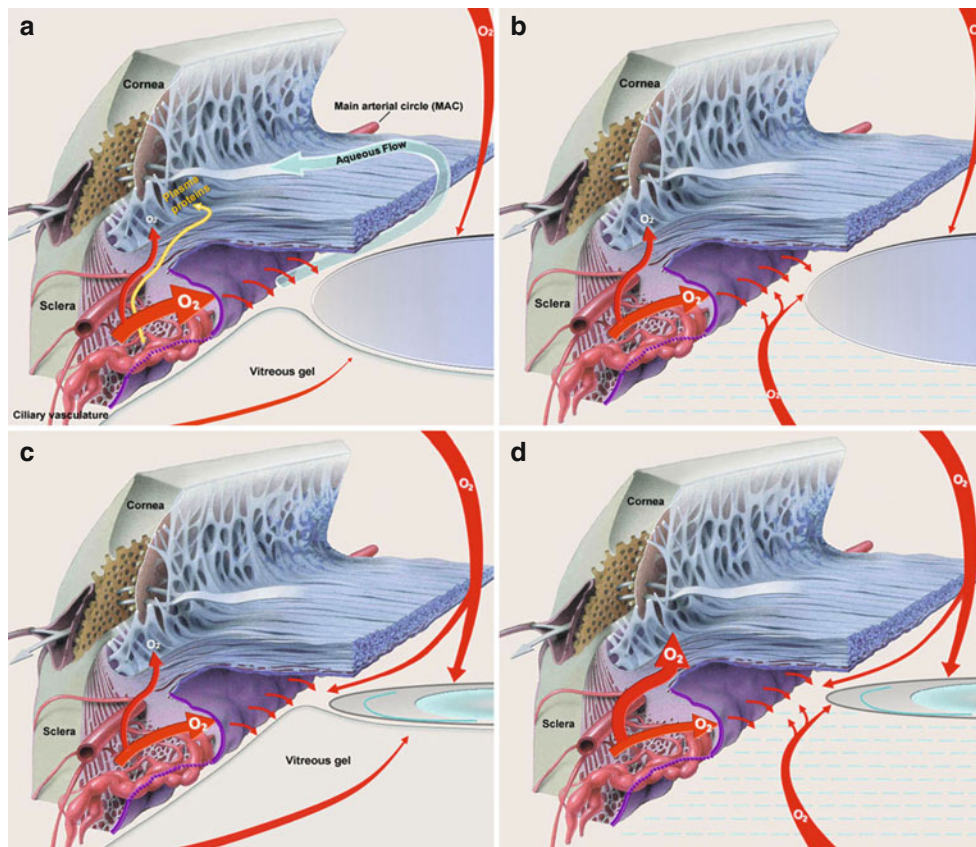


Figure IV.B-14 The “Oxygen Hypothesis” for primary open-angle glaucoma. (a) In the unoperated eye, oxygen enters from the retinal vasculature through the vitreous, across the ciliary epithelium from the ciliary body vasculature and into the anterior chamber across the cornea. Oxygen is consumed by the vitreous, lens, and the ciliary epithelium. A small amount of oxygen enters the anterior chamber angle by diffusing across the ciliary body and iris stroma (*curved red arrow*). (b) After vitrectomy, more oxygen reaches the posterior chamber. This supplies more oxygen to “aqueous side” of the ciliary epithelium, reducing the amount of oxygen that the ciliary epithelium removes from the blood and slightly increasing the amount of oxygen available to enter the anterior chamber angle from the ciliary body stroma. (c) Cataract surgery reduces oxygen consumption by the lens, thereby

increasing the pO_2 anterior to the lens and in the posterior chamber. Again, the increased oxygen on the “aqueous side” of the ciliary epithelium reduces the amount of oxygen that the ciliary epithelium removes from the blood, thereby slightly increasing the amount of oxygen available to enter the anterior chamber angle from the ciliary body stroma. (d) After both vitrectomy and cataract surgery, significantly more oxygen is available on the “aqueous side” of the ciliary epithelium, resulting in the removal of significantly less oxygen from the blood. This increases the amount of oxygen available to diffuse from the ciliary body stroma, across the iris stroma and into the anterior chamber angle, exposing the outflow system to a large excess of oxygen and/or oxygen metabolites (With permission from Siegfried et al. [9])

AMD. In the Submacular Surgery Trials, a thorough vitrectomy with complete PVD was performed prior to the extraction of the CNV. With 2-year follow-up, the recurrence rate of CNV in AMD was surprisingly low at 23 % after vitrectomy surgery. At 2-year follow-up, the rate of persistent or recurrent CNV in the observation arm was 66 % [48]. One possible explanation for this low recurrence rate after vitrectomy is that elevated intraocular oxygen tension may lower intraocular VEGF levels, thereby reducing pathologic neovascularization.

B. Diabetic Retinopathy

The cortical vitreous and vitreous gel also play key roles in the pathogenesis of proliferative diabetic retinopathy. Neovascularization of the disc or elsewhere is VEGF-mediated and occurs only in the presence of an attached

cortical vitreous. (See chapter IV.C. Vitreous and iris neovascularization.) Attached cortical vitreous implies a gel-like vitreous with low intraocular oxygen, allowing for VEGF levels to be high. Elevated new vessels do not grow after posterior vitreous detachment. Is this because the new vessels require the scaffold supplied by the cortical vitreous? The “Oxygen Hypothesis” suggests that PVD prevents new vessel growth by increasing intraocular oxygen that acts as an anti-VEGF agent. Consequently, some researchers have proposed intentional PVD as a way of preventing proliferative diabetic retinopathy (PDR) in high-risk eyes with severe preproliferative diabetic retinopathy [47, 49]. (See chapter VI.A. Pharmacologic vitreolysis.)

Holekamp and colleagues found that patients with ischemic diabetic retinopathy and low intraocular oxygen tension developed less post-vitrectomy nuclear cataract than patients without diabetes or to patients with diabetes but no ischemic retinopathy

[11]. Thus, ischemic diabetic retinopathy, but not diabetes without retinal ischemia, protected against post-vitreotomy nuclear cataract. Eyes with less intraocular molecular oxygen develop less post-vitreotomy nuclear cataract. These observations support the hypothesis that oxygen is implicated in nuclear cataract. It also supports the theory that the source of oxygen is the vasculature of the eye, which in the case of ischemic diabetic patients would constitute a reduced source of oxygen.

C. Retinal Vein Occlusions

Posterior vitreous detachment and the subsequent elevated intraocular oxygen may also be beneficial for retinal vein occlusions. (See chapter III.K. Vitreous in retino-vascular diseases and diabetic macular edema.) Murakami and colleagues examined the use of intravitreal tPA injection for the treatment of macular edema due to central retinal vein occlusions and found that the only statistically significant predictor of benefit was whether or not the injection created a PVD [50]. (See chapter VI.C. Pharmacologic vitreolysis with tPA.) PVD raises intraocular oxygen and acts as a potent, local anti-VEGF agent. Vitrectomy represents an immediate surgically induced PVD, and eyes with ischemic retinal vein occlusive disease often demonstrate postoperative clinical stabilization or improvement. In the past decade, there have been numerous reports of vitrectomy with some other surgical manipulation such as branch retinal vein sheathotomy, radial optic neurotomy, or retinal vascular endocanulation conferring benefit for branch or central retinal vein occlusion [51–53]. (See chapter V.A.6. Vitreous surgery of arterial and venous retino-vascular diseases.) All eyes had vitrectomy surgery, a procedure that increases intraocular oxygen tension long term and may have a clinically meaningful sustained anti-VEGF effect. Perhaps the proper conclusion from these studies is that vitrectomy surgery alone is beneficial in ischemic retinal disease.

VII. The Future

Currently, liquefaction of the vitreous gel is unavoidable in the aging human eye. The mechanism underlying this process is poorly understood and little studied. Unlike humans, very few mammals develop cataracts after vitrectomy, making it difficult to study post-vitreotomy cataracts with animal model [16]. Several breeds of dogs develop early vitreous degeneration, but there has been no study of the mechanism responsible and no studies have tested whether early vitreous degeneration in dogs is related to later nuclear cataract formation [54]. Currently, we know of no research efforts to prevent age-related vitreous liquefaction in any species, including humans, or to identify its causes. Alternatively, researchers have begun to explore the possibilities of a long-term, artificial vitreous substitute [55, 56]. (See chapter I.F. Vitreous biochemistry and

artificial vitreous.) Importantly, any future vitreous substitute will have to incorporate much of we have learned regarding the biochemical and biophysical properties of the gel vitreous. Any vitreous substitute will have to recreate the gel properties of the native vitreous and maintain close association with the retinal surface and be compatible with high ascorbate levels in order to effectively metabolize oxygen and regulate intraocular oxygen tension. As a final alternative, researchers have begun looking at interventions to restore the structure of the vitreous gel (personal communication, David Beebe, PhD). In the meantime, one aspect that can be controlled is the manner in which vitrectomy is performed. Preliminary findings suggest that performing minimally invasive 25 G vitrectomy that leaves the retrolental vitreous (containing endogenous antioxidants) undisturbed and that does include PVD induction surgically is associated with a significantly lower incidence of post-vitreotomy cataract formation requiring surgery [57]. (See chapter V.B.8. Floaters and vision – current concepts and management paradigms.)

VIII. Summary

An intact gel vitreous is central to a healthy human eye. The gel vitreous has the important biochemical and biophysical property of oxygen consumption and regulation of the distribution of intraocular molecular oxygen. This allows highly vascularized ocular structures such as the retina, choroid, and ciliary body to remain highly oxygenated while allowing ocular structures sensitive to oxidative damage such as the lens and trabecular meshwork to remain hypoxic. These functions of the vitreous gel diminish with age-related vitreous liquefaction. The “Oxygen Hypothesis” maintains that liquefaction of the vitreous gel may be the initiating pathologic step to oxidation-mediated ocular diseases such as nuclear cataract and some forms of primary open-angle glaucoma. Thus, perhaps current research efforts should be directed toward preventing vitreous liquefaction and posterior vitreous detachment. The goal would be to retain a healthy, formed vitreous gel indefinitely within the human eye.

Abbreviations

AMD	Age-related macular degeneration
AsA	Ascorbic acid
CNV	Choroidal neovascularization
dAsA	Dehydroascorbate
mmHg	Millimeters of mercury
O ₂	Oxygen
PO ₂	Partial pressure of oxygen
POAG	Primary open-angle glaucoma
PVD	Posterior vitreous detachment
tPA	Tissue plasminogen activator
VEGF	Vascular endothelial growth factor

References

- David M. Vitreous and vitreoretinal disorders. In: Spalton DJ, Hitchings RA, Hunter PA, editors. Atlas of clinical ophthalmology. 2nd ed. Philadelphia: Mosby-Year Book Europe Limited; 1994. Chapter 12. p. 122.
- Holekamp NM, Shui YB, Beebe DC. Vitrectomy surgery increases oxygen exposure to the lens: a possible mechanism for nuclear cataract formation. *Am J Ophthalmol.* 2005;139(2):302–10.
- Shui YB, Holekamp NM, Kramer BC, Crowley JR, Wilkins MA, Chu F, Malone PE, Mangers SJ, Hou JH, Siegfried CJ, Beebe DC. The gel state of the vitreous and ascorbate-dependent oxygen consumption: relationship to the etiology of nuclear cataract. *Arch Ophthalmol.* 2009;127(4):475–82.
- Eaton JW. Is the lens canned? *Free Radic Biol Med.* 1991;11(2):207–13.
- Barbazetto IA, Liang J, Chang S, Zheng L, Spector A, Dillon JP. Oxygen tension in the rabbit lens and vitreous before and after vitrectomy. *Exp Eye Res.* 2004;78(5):917–24.
- Shui YB, Fu JJ, Garcia C, Dattilo LK, Rajagopal R, McMillan S, Mak G, Holekamp NM, Lewis A, Beebe DC. Oxygen distribution in the rabbit eye and oxygen consumption by the lens. *Invest Ophthalmol Vis Sci.* 2006;47(4):1571–80.
- Chang S. LXII Edward Jackson Lecture: open angle glaucoma after vitrectomy. *Am J Ophthalmol.* 2006;141(6):1033.
- Koreen L, Yoshida N, Escario P, Niziol LM, Koreen IV, Musch DC, Chang S. Incidence of, risk factors for, and combined mechanism of late-onset open-angle glaucoma after vitrectomy. *Retina.* 2012;32(1):160–7.
- Siegfried CJ, Shui YB, Holekamp NM, Bai F, Beebe DC. Oxygen distribution in the human eye: relevance to the etiology of open angle glaucoma after vitrectomy. *IOVS.* 2010;2010(51):5731–8.
- Lange CA, Stavarakas P, Luhmann UF, de Silva DJ, Ali RR, Gregor ZJ, Bainbridge JW. Intraocular oxygen distribution in advanced proliferative diabetic retinopathy. *Am J Ophthalmol.* 2011;152(3):406–412.e3.
- Holekamp NH, Shui YB, Beebe DC. Lower intraocular oxygen tension in diabetics: possible contribution to decreased incidence of nuclear sclerotic cataract. *Am J Ophthalmol.* 2006;141(6):1027–32.
- McNulty R, Wang H, Mathias RT, Ortwerth BJ, Truscott RJ, Bassnett S. Regulation of tissue oxygen levels in the mammalian lens. *J Physiol.* 2004;559(Pt 3):883–98.
- Truscott RJW. Age-related nuclear cataract—oxidation is the key. *Exp Eye Res.* 2004;80(5):709–25.
- Palmquist BM, Philipson B, Barr PO. Nuclear cataract and myopia during hyperbaric oxygen therapy. *Br J Ophthalmol.* 1984;68(2):113–7.
- Tsukaguchi H, et al. A family of mammalian Na⁺-dependent L-ascorbic acid transporters. *Nature.* 1999;399(6731):70–5.
- Sebag, J. The vitreous in Adler's physiology of the eye. Hart WM (editor). 9th edition. St. Louis: Mosby. p. 268–347. 1992.
- Barton KA, Shui YB, Petrash JM, Beebe DC. Comment on: the Stokes-Einstein equation and the physiological effects of vitreous surgery. *Acta Ophthalmol Scand.* 2007;85:339–40.
- Buerk DG, Shonat RD, Riva CE, Cranstoun SD. O₂ gradients and countercurrent exchange in the cat vitreous humor near retinal arterioles and venules. *Microvasc Res.* 1993;45:134–48.
- Harocopos GJ, Shui Y-B, McKinnon M, Holekamp NM, Gordon MO, Beebe DC. Importance of vitreous liquefaction in age-related cataract. *Invest Ophthalmol Vis Sci.* 2004;45:77–85.
- Stefansson E, Novack RL, Hatchell DL. Vitrectomy prevents retinal hypoxia in branch retinal vein occlusion. *Invest Ophthalmol Vis Sci.* 1990;31:284–9.
- Filas BA, Shui Y, Beebe DC. Computational model for oxygen transport and consumption in human vitreous. *Invest Ophthalmol Vis Sci.* 2013;54(10):6549–59.
- Cherfan GM, Michels RG, de Bustros S, Enger C, Glaser BM. Nuclear sclerotic cataract after vitrectomy for idiopathic epiretinal membranes causing macular pucker. *Am J Ophthalmol.* 1991;111:434–8.
- de Bustros S, Thompson JT, Michels RG, Enger C, Rice TA, Glaser BM. Nuclear sclerosis after vitrectomy for idiopathic epiretinal membranes. *Am J Ophthalmol.* 1988;105:160–4.
- Melberg NS, Thomas MA. Nuclear sclerotic cataract after vitrectomy in patients younger than 50 years of age. *Ophthalmology.* 1995;102:1466–71.
- Thompson JT, Glaser BM, Sjaarda RN, Murphy RP. Progression of nuclear sclerosis and long-term visual results of vitrectomy with transforming growth factor beta-2 for macular holes. *Am J Ophthalmol.* 1995;119:48–54.
- Kubo E, Kumamoto Y, Tsuzuki S, Akagi Y. Axial length, myopia, and the severity of lens opacity at the time of cataract surgery. *Arch Ophthalmol.* 2006;124:1586–90.
- Sawa M, et al. Nonvitrectomizing vitreous surgery for epiretinal membrane: long-term follow-up. *Ophthalmology.* 2005;112(8):1402–8.
- Sawa M, et al. Assessment of nuclear sclerosis after nonvitrectomizing vitreous surgery. *Am J Ophthalmol.* 2001;132(3):356–62.
- Saito Y, et al. Nonvitrectomizing vitreous surgery: a strategy to prevent postoperative nuclear sclerosis. *Ophthalmology.* 1999;106(8):1541–5.
- Truscott RJ, Augusteyn RC. Oxidative changes in human lens proteins during senile nuclear cataract formation. *Biochim Biophys Acta.* 1977;492(1):43–52.
- Onoo A, et al. Development of myopia as a hazard for workers in pneumatic caissons. *Br J Ophthalmol.* 2002;86(11):1274–7.
- Giblin FJ, et al. Enzyme-induced posterior vitreous detachment in the rat produces increased lens nuclear pO₂ levels. *Exp Eye Res.* 2008;88(2):286–92.
- Almony A, Holekamp NM, Bai F, Shui YB, Beebe DC. Small-gauge vitrectomy does not protect against nuclear sclerotic cataract. *Retina.* 2012;32(3):499–505.
- Gabelt BAT, Kaufman PL. Changes in aqueous humor dynamics with age and glaucoma. *Prog Retin Eye Res.* 2005;24:612–37.
- Izzotti A, Bagnis A, Sacca SC. The role of oxidative stress in glaucoma. *Mutat Res.* 2006;612:105–14.
- Izzotti A, Sacca SC, Cartiglia C, De Flora S. Oxidative deoxyribo-nucleic acid damage in the eyes of glaucoma patients. *Am J Med.* 2003;114:638–46.
- Izzotti A, Sacca SC, Longobardi M, Cartiglia C. Sensitivity of ocular anterior-chamber tissues to oxidative damage and its relevance to glaucoma pathogenesis. *Invest Ophthalmol Vis Sci.* 2009;50(11):5251–8.
- Kumar DM, Agarwal N. Oxidative stress in glaucoma: a burden of evidence. *J Glaucoma.* 2007;16:334–43.
- Saccà SC, Izzotti A. Oxidative stress and glaucoma: injury in the anterior segment of the eye. In: Carlo Nucci LCNNO, Giacinto B, editors. Progress in brain research. Amsterdam/New York: Elsevier; 2008. p. 385–407.
- Sacca SC, Pascotto A, Camicione P, Capris P, Izzotti A. Oxidative DNA damage in the human trabecular meshwork: clinical correlation in patients with primary open-angle glaucoma. *Arch Ophthalmol.* 2005;123:458–63.
- Ferreira SM, Lerner SF, Brunzini R, Evelson PA, Llesuy SF. Oxidative stress markers in aqueous humor of glaucoma patients. *Am J Ophthalmol.* 2004;137:62–9.
- Abu-Amro KK, Morales J, Bosley TM. Mitochondrial abnormalities in patients with primary open-angle glaucoma 0.1167/iows.05-1639. *Invest Ophthalmol Vis Sci.* 2006;47:2533–41.

43. Sharma TK, Nessim M, Kyprianou I, Kumar V, Shah P, O'Neil E. Vitreous loss during phacoemulsification in glaucoma patients: long-term intraocular pressure control. *J Cataract Refract Surg.* 2008;34:831–4.
44. Kuhli-Hattenbach C, Luchtenberg M, Kohnen T, Hattenbach LO. Risk factors for complications after congenital cataract surgery without intraocular lens implantation in the first 18 months of life. *Am J Ophthalmol.* 2008;146:1–7.
45. Luk FO, Kwok AK, Lai TY, Lam DS. Presence of crystalline lens as a protective factor for the late development of open angle glaucoma after vitrectomy. *Retina.* 2009;29:218–24.
46. Quiram PA, Leverenz VR, Baker RM, Dang L, Giblin FJ, Trese MT. Microplasmin-induced posterior vitreous detachment affects vitreous oxygen levels. *Retina.* 2007;27:1090–6.
47. Krebs I, Brannath W, Glittenberg C, Zeiler F, Sebag J, Binder S. Posterior vitreomacular adhesion: a potential risk factor for exudative age-related macular degeneration? *Am J Ophthalmol.* 2007;144:741–6.
48. Submacular Surgery Trials Research Group. Surgery for subfoveal choroidal neovascularization in age-related macular degeneration: ophthalmic findings: SST report No. 11. *Ophthalmology.* 2004;111(11):1967–80.
49. Sebag J. Anomalous posterior vitreous detachment: a unifying concept in vitreo-retinal disease. *Graefes Arch Clin Exp Ophthalmol.* 2004;42(8):690–8.
50. Murakami T, Takagi H, Ohashi H, et al. Role of posterior vitreous detachment induced by intravitreal tissue plasminogen activator in macular edema with central retinal vein occlusion. *Retina.* 2007;27:1031–7.
51. Opremcak EM, Bruce RA. Surgical decompression of branch retinal vein occlusion via arteriovenous crossing sheathotomy: a prospective review of 15 cases. *Retina.* 1999;19:1–5.
52. Opremcak EM, Rehmar AJ, Ridenour CD, Kurz DE. Radial optic neurotomy for central retinal vein occlusion: 117 consecutive cases. *Retina.* 2006;26:297–305.
53. Weiss JN, Bynoe LA. Injection of tissue plasminogen activator into a branch retinal vein in eyes with central retinal vein occlusion. *Ophthalmology.* 2001;108:2249–57.
54. Labruyère JJ, Hartley C, Rogers K, Wetherill G, McConnell JF, Dennis R. Ultrasonographic evaluation of vitreous degeneration in normal dogs. *Vet Radiol Ultrasound.* 2008;49(2):165–71.
55. Soman N, Banerjee R. Artificial vitreous replacements. *Biomed Mater Eng.* 2003;13:59–74.
56. Ravi N, Swindle-Reilly KE, Shah M, Hamilton PD, Eskin TA, Kaushal S. Rabbit study of an in situ forming hydrogel vitreous substitute. *Invest Ophthalmol Vis Sci.* 2009;50(10):4840–6.
57. Sebag J, Yee KMP, Huang L, Wa C, Sadun AA. Vitrectomy for floaters – prospective efficacy analyses and retrospective safety profile. *Retina.* 2014;34(6):1062–8. PMID: 24296397.

David McLeod

Outline

- I. **Introduction**
- II. **Foundations of Vitreous Neovascular Pathology**
 - A. Biochemical Mediator Hypothesis
 - B. Clinical Pathology of Retinal Hypoxia
 - C. Experimental Retinal Hypoxia and Vitreous Neovascularization
- III. **Clinical Vitreous Neovascularization**
 - A. Retinal Vessel Occlusions
 - B. Spatial Characteristics of Intraocular Neovascularization
 - C. Temporal Characteristics of Intraocular Neovascularization
- IV. **Role of the Choroid in Intraocular Neovascularization**
 - A. A Graduated Metabolic Oxygen Barrier
 - B. Additional Oxygen Sources
- V. **Therapeutic Intervention and Intraocular Oxygen Physiology**
 - A. Modulating Intraocular Oxygenation by Laser Photocoagulation
 - 1. Targeting the Penumbra Obscura with Scatter (PRP) Photocoagulation
 - B. Vitreoretinal Surgery and Vitreous Neovascularization
 - 1. Anterior Vitreous Neovascularization
 - 2. Vitreous and Iris Neovascularization after Vitrectomy
 - 3. Vitreous and Iris Neovascularization after PVD
 - a. Peduncular Avulsion Induces Vitreous Hemorrhage
- VI. **Molecular Basis of Vitreous and Iris Neovascularization**
 - A. Identity of Michaelson's Biochemical Mediator
 - B. Extracellular Matrix Coupling Enables Rete Expansion
 - C. Sources of Michaelson's Biochemical Mediator

References

D. McLeod, MD
Manchester Royal Eye Hospital, University of Manchester,
Oxford Road, Manchester M13 9WL, England, UK
e-mail: david.mcleod@nhs.net

Keywords

Vitreous • Iris • Vitreous neovascularization • Iris neovascularization • Choroidal circulation • Intraocular oxygenation • Proliferative diabetic retinopathy • Retinal vein occlusions • Laser therapy • Vitrectomy

Key Concepts

1. The essential driver of vitreous and iris neovascularization is the choroidal circulation as this is the main source of marginal oxygenation to non-perfused inner retinal tissues. The principal mediators of budding and neovascular expansion from the retinal veins are soluble hypoxia-induced biochemicals and the collagenous component of the vitreous extracellular matrix to which the new vessels are coupled by integrins.
2. Posterior vitreous detachment uncouples endothelial cell interactions with the extracellular matrix of the posterior vitreous cortex, restricting post-basal preretinal angiogenesis to abortive neovascular outgrowths with no intrinsic extracellular matrix component.
3. In diabetic traction retinal detachment, the main source of proangiogenic proteins switches from a broad swathe of critically hypoxic inner retina (the penumbra obscura) to truncated tissue cylinders comprising full-thickness retina related to arteriovenous anastomoses. As well as being the source of optic disc and preretinal new vessels, retinal veins may thus become a source of marginal oxygenation to (detached) retinal photoreceptors, acting as drivers for further vitreous and iris neovascularization.

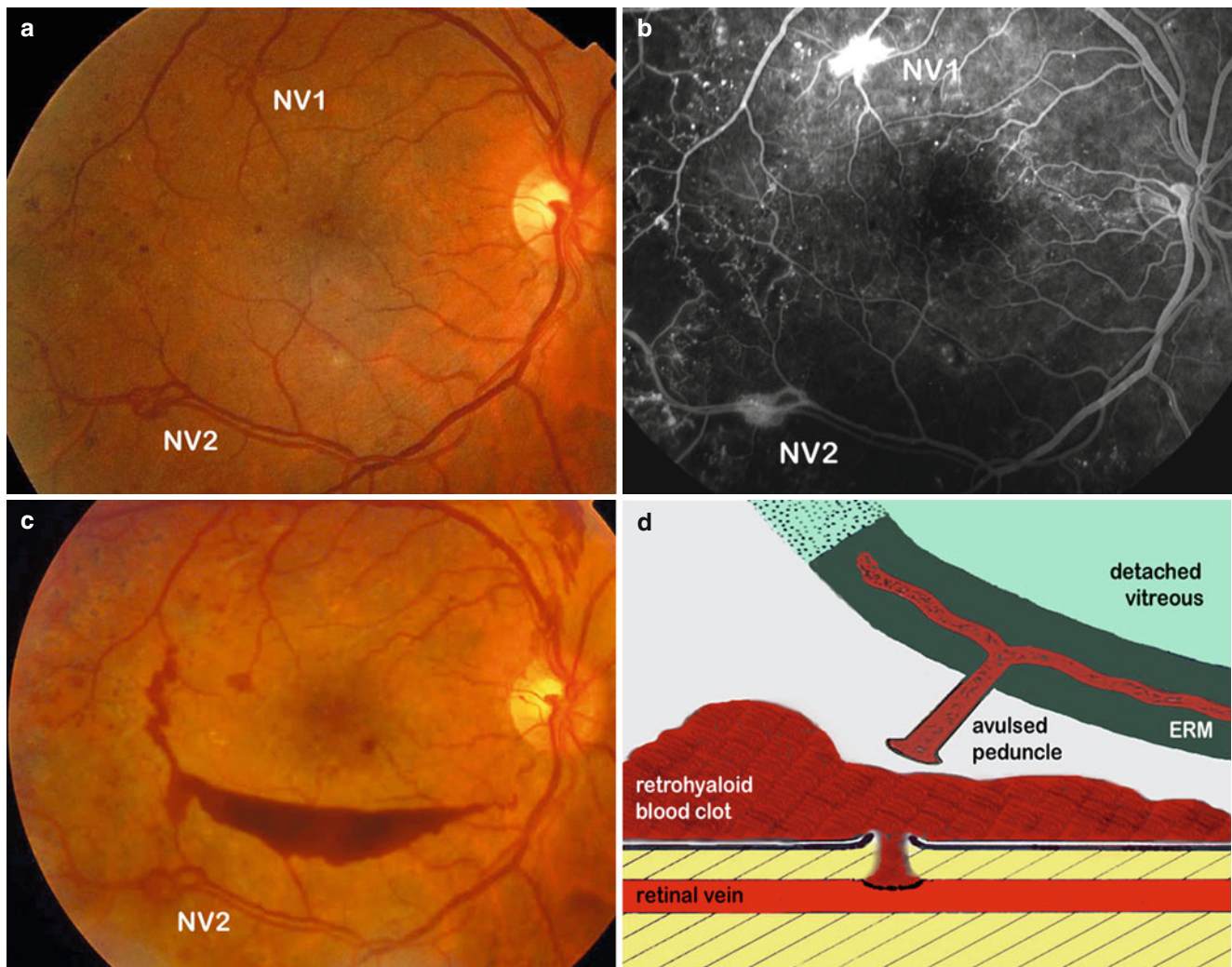


Figure IV.C-1 Diabetic vitreous hemorrhage. (a) Two focal fibrovascular outgrowths (NV1 and NV2). (b) Dye leakage from NV1 and NV2 in venous phase of fluorescein angiography, with capillary closure temporally. (c) Premacular retrohyaloid (behind the posterior vitreous cortex) lysed partially settled hemorrhage 2 weeks later; outgrowth

NV1 has disappeared. (d) Diagram showing mechanism of vitreous hemorrhaging through neovascular peduncular avulsion from an arterIALIZED retinal vein during posterior vitreous detachment; the fibrovascular epiretinal membrane (ERM) becomes a ghost membrane within detached vitreous cortex

I. Introduction

Until the 1940s, the growth of newly formed blood vessels into the vitreous was thought to be the *consequence* of vitreous hemorrhage, not its cause. The process appeared to represent “organization” (i.e., the invasion of a hematoma by macrophages, capillaries, and fibroblasts to form “granulation tissue”), eventually resulting a fibrous scar. However, serial examinations of eyes with “*rete mirabile*” (neovascular networks) and “*retinitis proliferans*” (fibrovascular membranes) showed that, except after severe trauma, neovascular invasion of the extracellular matrix invariably *precedes* vitreous hemorrhaging (Figure IV.C-1) [1]. Here, the evolution of theories of vitreous and iris neovascularization will be examined from within the perspectives of time and first-hand observations.

II. Foundations of Vitreous Neovascular Pathology

A revelatory hypothesis linking vitreous neovascularization (VNV) to disorders of the underlying retina arose during a study of embryonic retinal vascularization from the root of the regressing hyaloid vascular system. This coincided with the incipient inability of the choroid to meet the oxygen requirements of the rapidly growing retina.

A. Biochemical Mediator Hypothesis

Isaac Michaelson of the Tennent Institute of Ophthalmology in Glasgow was investigating the vascular supply to the

developing retina in cat and man using India ink injected via the heart or carotid artery. He was particularly struck by the pattern of vascularization of the retinal nerve fiber layer as revealed by the carbon particles filling the vessels. At this furthest point from the choroid, rete (neovascular complex) expansion to form a superficial capillary plexus followed budding from the endothelium of veins and not from arteries; also, budding only took place on the side of a vein remote from an artery and never at arteriovenous crossings [2]. Michaelson surmised that this pattern of capillary development must reflect the tissue distribution of a diffusible biochemical substance secreted in response to a local reduction in tissue oxygen tension (pO_2) should oxygen consumption outstrip supply. However, once the capillaries infiltrate the hypoxic parenchyma and the pO_2 rises, the concentration of the “vessel growth promoting factor” will fall and angiogenesis will cease. Nevertheless, as the retina continues to grow and metabolize, oxygenation of mid-retinal tissue by the choroid will become marginalized in its turn, hence the formation of a deep capillary plexus from the superficial plexus.

Although Michaelson did not report any ink injection studies of adult eyes with retino-vascular disease, he reasoned that his biochemical mediator hypothesis could be extrapolated to VNV associated with circulatory compromise within the mature retina. He had earlier demonstrated that preretinal new vessels bud from retinal veins in proliferative diabetic retinopathy (PDR), and he concluded that “*Just as the metabolic needs of embryonic retinal tissue demand closer proximity of capillary vessels, so does the disturbed metabolism of certain retinal diseases call for the accession of vessels to insufficiently or non-perfused situations, intraretinal, preretinal, or vitreous*” [2]. As the vessel growth-promoting factor accumulates in the vitreous after liberation from the hypoxic retina, he argued that retinal veins in the vicinity will somehow sense the concentration gradient and respond by budding, to be followed by new vessel growth towards its source. In the published discussion to his landmark 1948 paper, Michaelson also postulated that, following the buildup of the vessel growth-promoting factor in vitreous, its anterior diffusion into the aqueous will stimulate iris neovascularization (NVI) [2].

B. Clinical Pathology of Retinal Hypoxia

It fell to Norman Ashton, working in the newly established Institute of Ophthalmology in London, to demonstrate the nature of the retinal vascular disturbance underlying most instances of VNV and/or NVI. Ashton injected India ink directly into the central retinal artery of human globes excised postmortem. In patients with long-standing diabetes, the retina showed areas of “capillary closure” originating on the arterial side of the circulation. This was accompanied by

arteriovenous anastomoses and eventually resulted in a “*disastrous picture of...complete obliteration of the capillary blood supply to the retina*” [3]. In 1953, however, making the conceptual link between capillary closure and VNV was not straightforward. Eyes with such closure did not necessarily manifest VNV, so the arteriolar changes were thought to “*merely represent a late stage of development in the retinal disease*” [3]. Significantly, the effects of the capillary closure on parenchymal histology were not reported, although trypsin digestion and electron microscopy would later demonstrate that the capillaries were devoid of both endothelial cells and pericytes, with glial cell processes blocking the vessel lumen.

C. Experimental Retinal Hypoxia and Vitreous Neovascularization

Ashton was also intrigued by the burgeoning clinical problem of “retinopathy of prematurity” (ROP) in which oxygen was thought to play a key role. He devised an experiment that exploited the incomplete vascularization of the newborn kitten retina, administering oxygen at high concentration (60–80 % ambient levels) to mother cats and their litters [4]. This resulted in intense vasoconstriction and capillary closure in the kittens that involved the entire, or just the peripheral, retina (as judged by India ink injection). By contrast, the hyaloid vasculature and the choroidal vessels were unaffected, as was the mother’s retina. This “vaso-obliterative phase” of the ROP model was attributed to systemic hyperoxemia and oxygenation of the inner retina by the choroidal circulation (what Ashton called “*the increased nutritional range of the choroid*”); retinal ganglion cells within non-perfused areas had a normal histological appearance. Furthermore, in a separate experiment, detaching the kitten retina by vitreous aspiration prevented the vaso-obliterative response to hyperoxemia, ostensibly because the chorioretinal separation had attenuated inner retinal oxygenation from the choroid [5].

Returning kittens to room air resulted in rampant and disorderly revascularization of the non-perfused retina together with outgrowth of “glomerular tufts” and large neovascular networks into the vitreous (the “vaso-proliferative phase” of the ROP model) [4]. The vitreous new vessels, once filled with India ink, could be photographed en face after stripping the vitreous en bloc from the retina. Evidently, the points of attachment of the vitreous neovascularization to the intraretinal neovasculature from which it derived could be readily disconnected. Electron microscopy was later to show that as the new vessels penetrate the inner limiting membrane (ILM), they are often accompanied by glial cells and macrophages and become intimately associated with collagen fibrils in the vitreous extracellular matrix. Ashton felt that

the kittens' return to breathing room air had led to immediate withdrawal of the extended nutritional range of the choroid, but not so as to render the inner retina anoxic. This was confirmed by the continuing healthy state of most parenchymal cells on histology. Thus, marginal oxygenation of the inner retina by the choroid must have ensured its ongoing viability and its capability to secrete vessel growth-promoting factor. This fostered retinal revascularization and vitreous neovascularization that was excessive in degree and disorder due to the large volume of non-perfused inner retinal tissue that had been abruptly deprived of most of its (latterly choroid-derived) oxygen supply after restoration of normoxemia. The capability of the choroidal circulation to underpin retinal revascularization and vitreous neovascularization indicates that oxygen diffused across an immature photoreceptor layer that was later to become a significant "metabolic oxygen barrier" (by virtue of the huge energy expenditure and oxygen consumption of mature rods and cones) interposed between the choroid and inner retina.

III. Clinical Vitreous Neovascularization

Michaelson had drawn a developmental distinction between the retinal veins and their capillary extensions (the "vein-capillary unit") and the retinal arteries that he considered to be "supra-capillary." He proposed that, in the mature retina, disorders of the vein-capillary unit will include proliferative diabetic retinopathy and Eales' vasculitis, each giving rise to critical levels of inner retinal hypoxia and thus inducing vessel growth-promoting factor secretion [2].

A. Retinal Vessel Occlusions

In a similar vein, George Wise of New York felt that the tissue conditions producing the "relative anoxia" that stimulates production of vessel growth-promoting factor (or "factor X") will "almost exclusively follow capillary or venous obstruction" [6]. The common denominator was continuing but limited circulation through the inner retina as might typically follow central retinal vein occlusion (CRVO) or branch retinal vein occlusion (BRVO). Ashton was of similar mind in adducing that, in addition to a low tissue pO_2 to which viable tissue would respond by secreting vessel growth-promoting factor, poor venous drainage would encourage accumulation of this factor.

However, at this juncture, most investigators (including Michaelson, Ashton, and Wise) agreed that neither vitreous neovascularization nor iris neovascularization is a sequel to acute central retinal artery occlusion (CRAO) by virtue of the complete necrosis of the inner retina arising and its consequent inability to secrete vessel growth-promoting factor.

True, Wise felt that progressive retinal hypoperfusion from occlusion of proximal arteries will create appropriate conditions for vessel growth-promoting factor secretion, as in ocular ischemia from carotid stenosis, but such instances are rare. It thus appeared that "a critical degree of impairment of retinal blood flow" provides the stimulus for new vessel proliferation [6], whereas the role of irreversible capillary closure and of arterial occlusions in stimulating intraocular angiogenesis generally was not given much credence. In 1959, however, Lorenz Zimmerman from Washington argued that, from the pathologist's viewpoint, ocular neovascularization was indeed a potential complication of acute CRAO. He reviewed 26 previous reports of neovascular glaucoma following CRAO and added six new cases from the archives of the Armed Forces Institute of Pathology [7]. Clinical studies have since shown that 15–20 % of eyes with CRAO will progress to neovascular glaucoma, with or without vitreous neovascularization [8, 9], albeit the scientific basis for vitreous neovascularization or iris neovascularization after "isolated" CRAO (i.e., CRAO without associated CRVO or carotid stenosis) continues to be challenged to this day [9]. The majority of eyes with CRAO undergo spontaneous CRA recanalization within hours or days from CRAO onset. The reperfused microcirculation is usually somewhat attenuated, but the metabolic needs of inner retinal tissues that survived the CRAO are evidently satisfied. Eyes that develop rubeosis iridis after CRAO represent that small proportion in which CRA recanalization (or cilio-retinal collateral formation) fails to materialize in the aftermath of the occlusion [8, 10].

B. Spatial Characteristics of Intraocular Neovascularization

By 1963, Ashton had formed the opinion that in diabetic retinopathy "*areas of capillary closure ... provide the stimulus for the formation of rete mirabile*" (Figure IV.C-2a) [11]. However, even after the advent of fluorescein angiography (which provides *in vivo* delineation of capillary non-perfusion), the relationship of such closure to vitreous neovascularization and iris neovascularization was slow to become cemented in the minds of clinicians. Eventually, eyes with retinal vein occlusions were to prove instrumental in demonstrating that relationship unequivocally. In 1976, Eva Kohner from Moorfields in London showed, firstly, that eyes with vasodilatation and an increased dye transit time in the territory of an obstructed branch retinal vein were most unlikely to develop vitreous neovascularization, whereas, after BRVO with extensive retinal capillary closure, vitreous neovascularization regularly arose [12]. Thus, the effective stimulus for vitreous neovascularization is less a reduction in capillary perfusion and more the creation of regions of

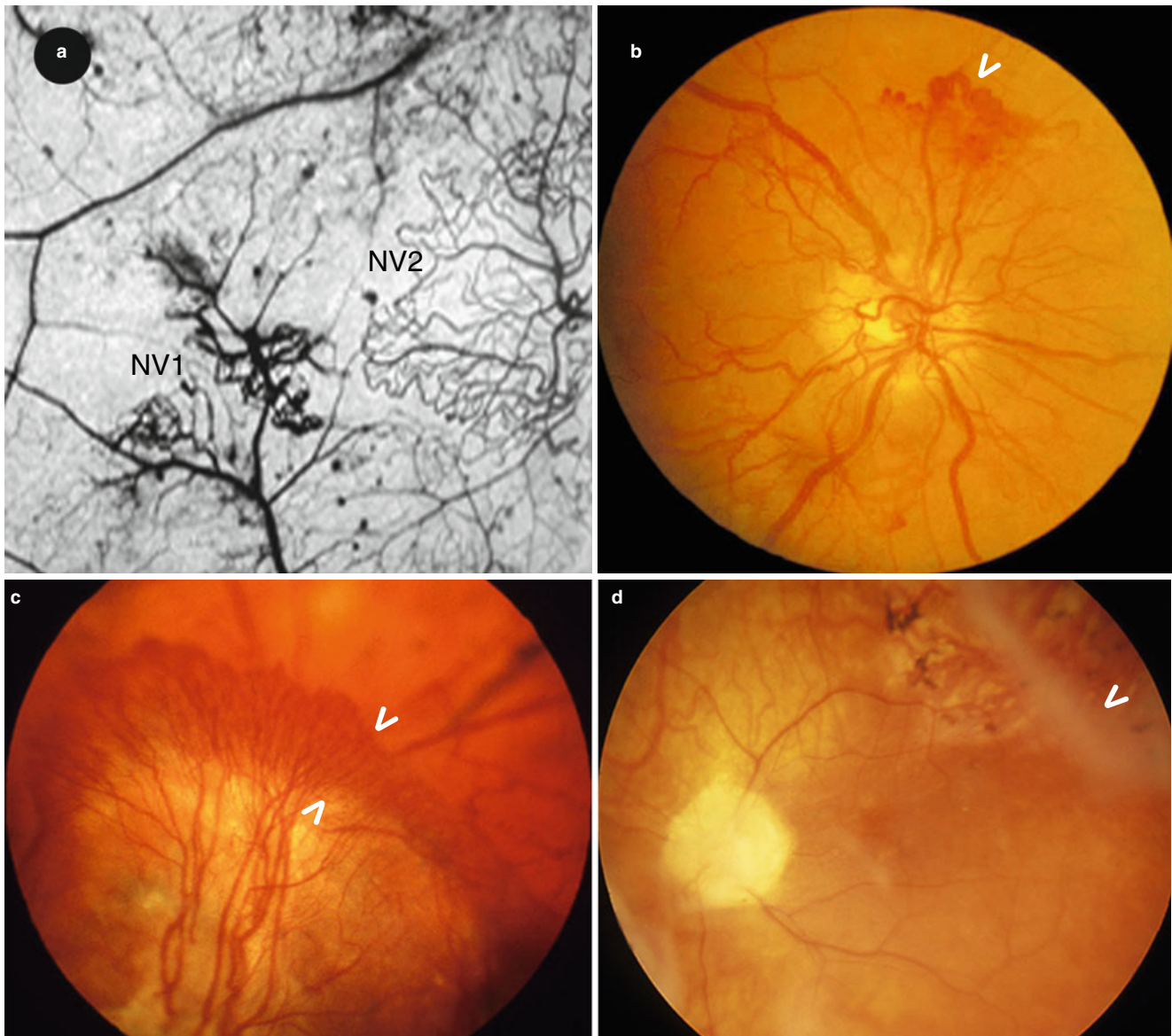


Figure IV.C-2 Diabetic vitreous neovascularization. (a) India ink-injected postmortem specimen showing two “flat” preretinal neovascular networks NV1 and NV2; microaneurysms and capillary closure in the underlying retina (courtesy of N Ashton). (b) Disc new vessels extending over the peripapillary retina; aneurysms and hemorrhages at the tips of the vessels (*arrowhead*). (c) Fibrovascular epiretinal membrane causing traction retinal detachment (*lower left half* of picture)

while attached retina in *upper right* half is out of focus; blush of active new vessels (between *arrowheads*) emanating from the membrane and growing forwards within the detached vitreous cortex. (d) Spontaneous involution of retinopathy and pale optic disc; pigmented area superotemporally with an overlying ghost membrane (*arrowhead*) indicating retinal reattachment. Note – no laser therapy was undertaken in this eye

complete capillary closure. Indeed, eyes with BRVO demonstrate a “cumulative” or quantitative relationship between vitreous neovascularization and the area of capillary closure (“proportionality”), but the iris neovascularization that frequently complicates CRVO does not occur after BRVO. This suggests that the threshold vitreous concentration of vessel growth-promoting factor required for stimulating iris neovascularization is not achievable as a result of the limited area of closure. Vitreous neovascularization typically takes origin from perfused venules located along the edge of the

areas of closure after BRVO (“proximity”) and extend thereafter towards the closure (“directionality”). This pattern of rete expansion is consistent with accumulation of, and diffusion gradients for, vessel growth-promoting factor and appears to be facilitated by the horizontal orientation of collagen fibrils within the cortical vitreous.

Kohner also demonstrated a clear relationship between the development of iris neovascularization after CRVO and extensive capillary closure on fluorescein angiography undertaken within 3 months of CRVO onset [13]. Such

closure, especially when located peripherally as well as centrally, was highly predictive for iris neovascularization, whereas vasodilatation, dye leakage, and an increased dye transit time were not. However, vitreous neovascularization from the retina or optic disc after CRVO was seen far less frequently than iris neovascularization, and it was also less prevalent than vitreous neovascularization after BRVO. This indicates that intravitreal vessel growth-promoting factor accumulation is not the sole determining factor in vitreous neovascularization. The extent of capillary closure that justifies attribution of the term “ischemic” CRVO, as distinct from “nonischemic” CRVO, has been much debated. Hayreh regards the minimum area of closure that brings a *significant risk* of neovascular glaucoma as 30 disc diameters, with a *high risk* in eyes with over 75 disc diameters of closure. Some 20 % of eyes with CRVO develop ischemic CRVO, of which 45 % progress to neovascular glaucoma [14]. With the eventual introduction of wide-angle fundus cameras, the closure-vitreous neovascularization relationship in proliferative diabetic retinopathy was also clarified. In 1981, using montages of such wide-angle photographs, Koichi Shimizu from Maebashi showed that extensive extramacular (or “mid-peripheral”) closure is the typical topographic pattern in proliferative diabetic retinopathy [15]. Eyes with optic disc new vessels tend to have more capillary closure than those with preretinal new vessels alone, and only those eyes with extensive closure develop “remote” iris neovascularization, again reflecting vessel growth-promoting factor accumulation and its anterior diffusion (as in CRVO).

Optic disc new vessels, although traditionally considered to represent “remote” vitreous neovascularization, are found in eyes with capillary closure in close proximity to the disc [15]. These vessels often extend meridionally for long distances over the peripapillary retina (albeit generally sparing the macula) without any connection to the underlying retinal vasculature. The tips of these vessels sometimes show aneurysmal dilatations, perhaps reflecting a paucity of intrinsic structural support (Figure IV.C-2b). Shimizu also confirmed the invariable presence of arteriovenous shunt vessels crossing the non-perfused retina and validated earlier reports indicating that the site on a retinal vein where vitreous neovascularization arises is usually at or near an arteriovenous crossing [16]. This suggests that the initiation of neovascular outgrowth in proliferative diabetic retinopathy is triggered biomechanically, perhaps by shear stress.

Profuse dye leakage from vitreous neovascularization on fluorescein angiography has drawn attention away from other attributes such as the slow progress of dye through the preretinal venovenous anastomosis. This contrasts with the rapid dye transit through, and limited dye leakage from, intraretinal arteriovenous shunt vessels. In proliferative diabetic retinopathy, such shunting contributes to the relatively high hydrostatic pressure and high oxygen saturation of

blood reaching the major retinal veins (“venous arterialization”) [17]. Vitreous neovascularization shares these properties including, somewhat paradoxically, relative venous hyperoxemia.

C. Temporal Characteristics of Intraocular Neovascularization

The time interval from capillary non-perfusion to overt vitreous neovascularization or iris neovascularization is variable, reflecting inter alia the volume of inner retina secreting vessel growth-promoting factor and thus the speed of its accumulation in the vitreous. Unlike embryonic retinal vascularization, vitreous neovascularization is futile in that it does not restore an oxygen supply to the vessel growth-promoting factor-producing tissue. In the kitten ROP model, however, retinal revascularization after vaso-obliteration takes 2–3 weeks to become established, but the associated vitreous neovascularization regresses once the retina is fully reperfused. Apart from ROP, the most rapid onset of vitreous neovascularization or iris neovascularization seen clinically is the 4–8-week interval to rubeosis iridis after CRAO [7]. In eyes with CRVO, the interval is significantly longer, in part due to the time for conversion from nonischemic to ischemic CRVO; even so, ischemic CRVO may eventually “burn itself out” [14]. Interestingly, a shorter interval to iris neovascularization is seen in eyes with nonischemic CRVO but with extensive cilioretinal infarction. In BRVO, by contrast, vitreous neovascularization is usually many months, if not a year, in the making.

The interval to overt vitreous neovascularization or iris neovascularization is difficult to estimate in proliferative diabetic retinopathy because the time of onset of capillary closure differs at different sites, as well as being asymptomatic. However, a rapid increase in vitreous neovascularization activity (Figure IV.C-2c) and/or an exacerbation of iris neovascularization sometimes heralds the onset of traction retinal detachment [18]. Eventually, some eyes with vitreous neovascularization, and even with traction retinal detachment, will undergo spontaneous neovascular regression and retinal reattachment (Figure IV.C-2d). This likely reflects a collapse in marginal inner retinal oxygenation owing to diabetic choroidopathy and shutdown of arteriovenous shunting [17].

IV. Role of the Choroid in Intraocular Neovascularization

As judged by the vitreous neovascularization and/or iris neovascularization arising, irreversible retinal capillary closure after CRVO and enduring occlusion of the central retinal

artery are equally capable of generating the critically hypoxic conditions within the inner retina that stimulate vessel production. This serves to underscore the principle that, in the absence of inner retinal perfusion from whatever cause, chorioidal oxygenation is the essential driver of vitreous neovascularization. That is to say, the inner retina will inevitably succumb to ischemic anoxia unless a marginal oxygen supply derives from blood circulating through the choroid.

A. A Graduated Metabolic Oxygen Barrier

Oxygenation of the inner retina from the choroid depends on (a) the “oxygen head pressure” (or the “ pO_2 maximum”) within the chorioidal circulation, (b) the diffusion distance for oxygen to the tissue under consideration (which depends in part on retinal thickness), and (c) oxygen consumption by the intervening tissues (reflecting the clustering of mitochondria within the rod inner segment ellipsoid and the number of rods per unit area) [10, 19]. A high pO_2 maximum is maintained throughout the choroid in normoxemia courtesy of its anatomy (e.g., the extraocular separation of its arterial supply and venous drainage) and its vascular physiology (i.e., the high volume flow rate and low oxygen extraction fraction). As such, the choroid as a whole has the oxygen physiology of a large artery. The pO_2 maximum can be elevated further by breathing a higher oxygen concentration or treating with hyperbaric oxygen [20]. By contrast, photoreceptor density changes significantly according to distance from the fovea (Figure IV.C-3). Beyond the “rod ring” at 10–20° eccentricity, rod density falls quickly such that a 50 % reduction is seen at about 50° eccentricity [21]. At normal ambient oxygen concentrations, therefore, non-perfused inner retina at the posterior pole will derive no oxygen from the choroid (and will thus become necrotic from ischemic anoxia) owing to the complete “metabolic oxygen barrier” presented by the photoreceptors. However, the *peripheral* inner retina will remain oxygenated (from the choroid) despite the absence of retinal capillary perfusion; here, the metabolic oxygen barrier imposed by the rods is lowered and the inner retina is thinner (Figure IV.C-3). Between the posterior and peripheral retina, there exists an annular zone or “swathe” of critical inner retinal hypoxia owing to marginal oxygenation from the chorioidal circulation [10].

Whereas it had been assumed that “relative anoxia” or critical hypoxia reflects a graduated reduction in tissue perfusion via the central retinal artery circulation [6], this is seldom the case. Oxygen movement across a graduated metabolic oxygen barrier, determined by a photoreceptor oxygen sink of progressively decreasing depth, is responsible for generating critically hypoxic conditions within non-perfused mid-peripheral inner retina (Figure IV.C-3). The

range of pO_2 values between the pO_2 thresholds for critical hypoxia and anoxia is narrow, but the diffusion distance for oxygen within this hypoxic zone is wide because of the reduced oxygen consumption of the hypoxic cells [19].

B. Additional Oxygen Sources

In proliferative diabetic retinopathy, inner retinal oxygenation from the choroid is overlaid by oxygenation from arteriovenous shunt vessels that have the choroid-like attributes of high flow and low oxygen extraction [17]. After central retinal artery occlusion, marginal oxygenation of the peripapillary and periarterial parenchyma may derive from residual circulation through the central retinal artery [10]. In both proliferative diabetic retinopathy and CRAO, histology will show a “mantle” of viable tissue surrounding the retinal vessels that provide the oxygen resource. The mantle around diabetic arteriovenous anastomoses will taper only slightly; the periarterial mantle after CRAO will taper rapidly as oxygen extraction reaches 100 %.

The tissue conditions developing in the inner retina after CRAO mirror those seen in the brain after middle cerebral artery occlusion. There, a zone of critically hypoxic tissue – the “ischemic penumbra” – surrounds a “core” of infarction, albeit the initially viable penumbral tissue rapidly succumbs and is incorporated into the infarct core. Prior to the penumbral conversion to umbra, however, the hypoxic tissue is sustained by collateral circulation via arterio-arterial anastomoses within the leptomeninges (or “soft” coverings) of the cerebrum. The vascular choroid is the ocular equivalent of these arachnoid and pial coverings, and critical hypoxia of penumbral tissue within non-perfused inner retina reflects marginal oxygenation from the corresponding collateral resource (Figure IV.C-3). Unlike cerebral cortex, however, penumbral inner retina can endure (and thus secrete vessel growth-promoting factor) indefinitely [10]. Its precise mid-peripheral location after CRAO and in proliferative diabetic retinopathy is uncertain in the absence of an *in vivo* hypoxia marker; so, this choroid-dependent swathe of viable inner retinal tissue has been dubbed “*the penumbra obscura*.”

V. Therapeutic Intervention and Intraocular Oxygen Physiology

A. Modulating Intraocular Oxygenation by Laser Photocoagulation

Laser photocoagulation of the fundus, which depends on local heat generation from light absorption by pigments such as melanin and hemoglobin, was originally directed at the new vessels themselves but they simply regrew, often with a

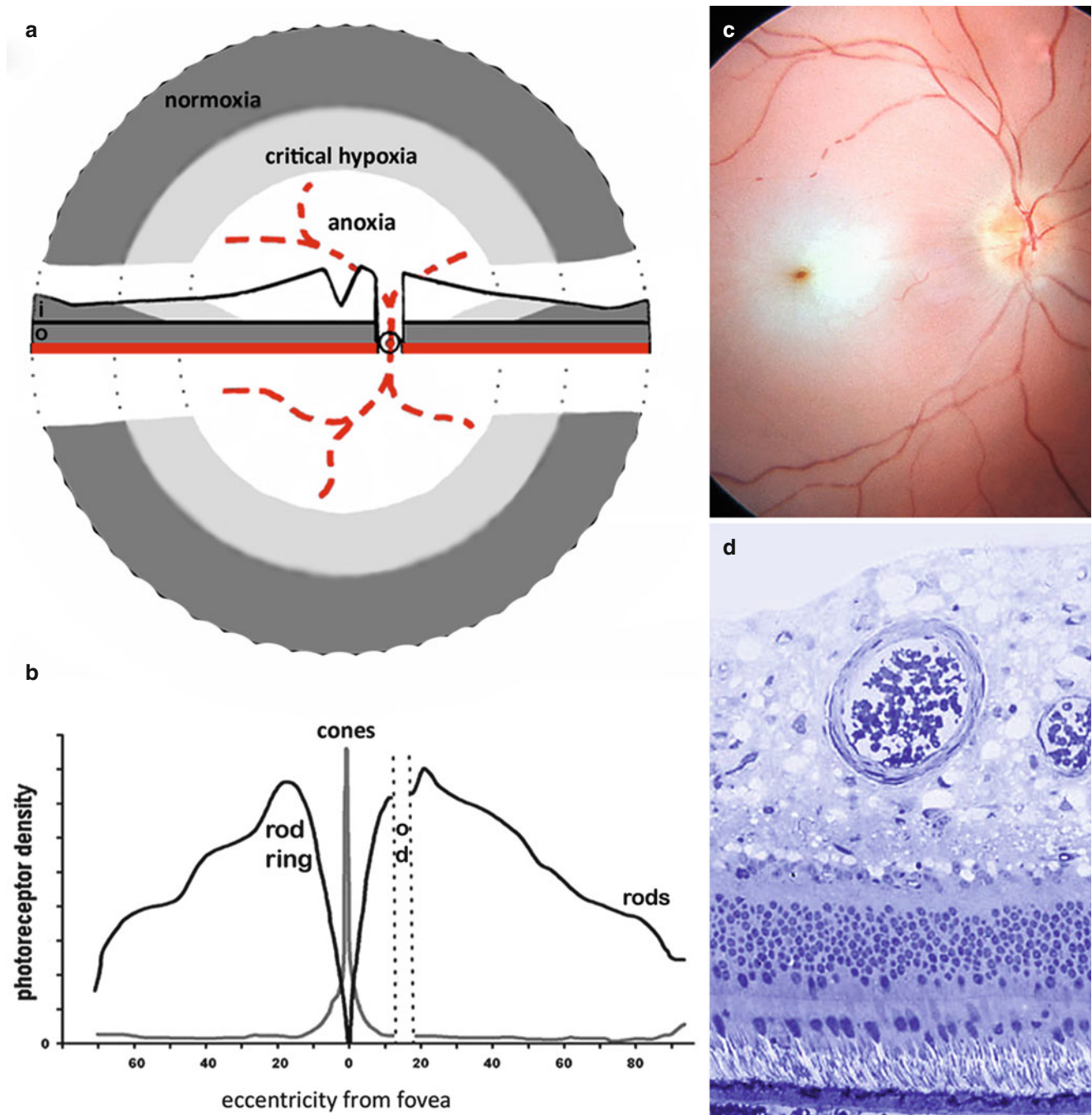


Figure IV.C-3 Central retinal artery occlusion. (a): Schematic diagram of inner retina *en face* showing oxygenation status of peripheral annulus (normoxia – dark shading), mid-peripheral annulus (critical hypoxia – light shading), and posterior pole (anoxia – no shading) some hours or days after the occlusion (dashed red lines are branch arteries). Centrally, a horizontal section through the optic disc and fovea shows variations in retinal thickness; the solid red line is the choroid, “o” is outer retina, and “i” is inner retina. The outer retina and peripheral inner retina are well oxygenated from the choroid whereas the mid-peripheral

inner retina is marginally oxygenated. (b) Graph of photoreceptor density (units not shown) versus horizontal eccentricity from the fovea (in degrees) for rods and cones (after Osterberg 1935). Rod density is a proxy for the height of the metabolic oxygen barrier interposed between the choroid and inner retina; “od” is the optic disc. (c) Fundus picture of foveal cherry red spot and cattle trucking 24 h after complaint of sudden visual loss. (d) Histological section through posterior retina from nonhuman primate eye 24 h after CRAO; anoxic necrosis (vacuolation) of most of the inner retina, whereas the outer retina is unaffected

fibrous component. Ironically, however, eyes in which the light energy had been applied less accurately showed lasting new vessel regression, leading to the eventual realization that

the new vessels need not be treated directly at all. Rather, a scattering of burns should be applied to the adjacent retina. Not only that, the intensity of the beam (and thus the extent

of thermal destruction after light absorption by the retinal pigment epithelium) need only be such as to damage the outer retina and not the inner retinal source of vessel growth-promoting factor, at least not directly.

1. Targeting the Penumbra Obscura with Scatter (PRP) Photocoagulation

Regression of vitreous neovascularization and iris neovascularization following scatter panretinal photocoagulation (PRP) is widely recognized as resulting from re-oxygenation of the hypoxic tissue instigating the angiogenic response [22]. PRP thus compounds the eccentricity-based attenuation of the metabolic oxygen barrier represented by the rod inner segments since these energy-expensive cells are replaced by less energetic glial cells. However, this will have no worthwhile effect other than within the penumbra obscura (which does not necessarily occupy the whole area of capillary closure) or around arteriovenous shunt vessels. PRP is unlikely to benefit from inner retinal tissue that is well-oxygenated despite the capillary non-perfusion; it will simply degrade peripheral visual fields unnecessarily. Nor will PRP benefit more posteriorly located non-perfused retina that is already necrotic for want of marginal oxygenation.

As long as the location of the penumbra obscura remains *obscure*, clinicians will have to rely on a standardized approach to PRP. George Blankenship showed that a distribution of PRP burns that includes the peripheral (post-equatorial) fundus as well as the mid-periphery is somewhat more efficacious in reversing diabetic vitreous neovascularization when compared with PRP that includes the area of the major temporal vascular arcades and the mid-periphery [23]. Latterly, automatic pattern laser techniques have become available that minimize the outer retinal destruction necessary to reverse vitreous neovascularization while maintaining or even improving visual fields [24]. The effectiveness of “minimally traumatic” laser, directed solely at the pigment epithelium, remains to be established.

B. Vitreoretinal Surgery and Vitreous Neovascularization

In addition to offering a means of addressing the hemorrhagic and tractional complications of vitreous neovascularization, the advent of closed intraocular microsurgery in the 1970s afforded new insights into the nature of vitreous neovascularization while providing opportunities to explore intravitreal pO₂ distribution and to collect intraocular tissue and fluid for laboratory analysis. Pars plana vitrectomy provides the surgeon with an astonishingly intimate means of visualizing and probing the posterior segment pathology of

vitreous neovascularization, not least in eyes with proliferative diabetic retinopathy. This has permitted histopathology-based concepts to be confirmed. For example, studies of early neovascular outgrowths (or “microproliferations”) in proliferative diabetic retinopathy indicate that, after penetrating the ILM, new vessel outgrowths incarcerate vitreous collagen fibers before extending horizontally within the posterior vitreous cortex as vascularized preretinal membranes with a variable fibrotic component [25]. Manipulation of the preretinal membranes confirms their incorporation of vitreous extracellular matrix, as does immunohistochemistry of excised preretinal membranes for collagen type II [26].

The process of vitreous incarceration results in a vitreoretinal adhesion that is primarily mediated via afferent and efferent vascular connections to the retinal veins within a so-called venous neovascular peduncle [17]. Accompanying glial outgrowth reinforces the membrano-retinal attachment (so-called glial nails) [27]. Myofibroblast contraction within the vascularized preretinal membrane then exerts tangential traction on the underlying retina, the tractional forces being transmitted via the neovascular peduncles and direct connections with the sustentacular glia of the retina. This results in fixed retinal folding and traction retinal detachment; the cellular contraction is thereafter “consolidated” by collagen type I secretion. The same tractional forces also result in posterior vitreous detachment (PVD) except at these points of membrano-retinal adhesion. As a result, previously “flat” new vessels within attached vitreous cortex become “forward” new vessels within detached vitreous cortex, albeit with retained attachment to the retina or optic disc at their base (“partial PVD”). Extensive rete expansion arising from the optic disc, for example, will separate from the peripapillary retina and contract, creating a narrow fibrovascular “stalk” that connects the otherwise detached vitreous to the disc [17]. Partial PVD was initially regarded as the vitreous conformation that most favored the onset of vitreous neovascularization. However, partial PVD is now recognized to be the *consequence* of retained membrano-retinal attachment, albeit a recrudescence of vitreous neovascularization may be seen if the retina itself begins to detach (Figure IV.C-2c). The onset of diabetic traction retinal detachment may also precipitate or exacerbate rubeosis iridis [18].

1. Anterior Vitreous Neovascularization

Fiberoptic endoscopic fluorescein angiography undertaken during vitrectomy for proliferative diabetic retinopathy has shown that, in eyes with extensive capillary closure and arteriovenous shunt vessels that reach beyond the equator, vitreous neovascularization can be found within the vitreous base in the form of an “oral ridge” [28]. Intraretinal new vessels breaking through the ILL and extending towards the posterior lens capsule have been identified pathologically (Figure IV.C-4a) [17].

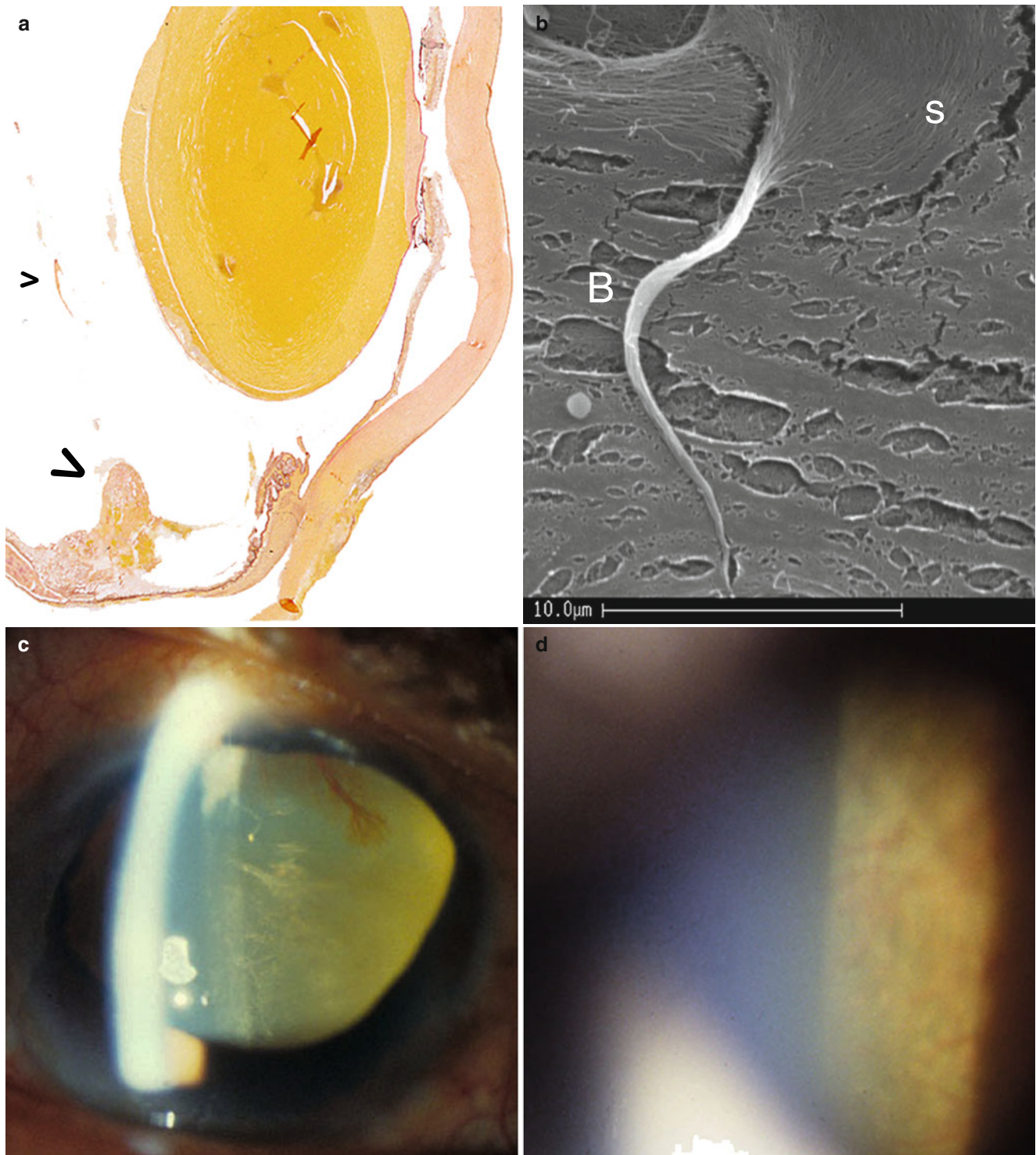


Figure IV.C-4 Anterior vitreous neovascularization. (a) Section through anterior half of an eye enucleated for diabetic rubeotic glaucoma (courtesy of R Bonshek); ridge of intraretinal and preretinal new vessels at ora serrata (*large arrowhead*) with anterior hyaloidal fibrovascular proliferation towards the lens (*small arrowhead*). (b) Scanning electron micrograph of digested undersurface of basal retina from normal postmortem eye; braid (*B*) and skein (*S*) of vitreous collagen

beneath the thin inner limiting membrane (splits are drying artifacts). Putative angiogenic substrate as fibrils from sublaminar skein penetrates the lamina and intermingle with prelaminar cortical vitreous (not shown). (c) Slit-lamp view of aphakic eye with rubeosis iridis after central retinal vein occlusion; iris new vessels extend onto anterior vitreous membrane substrate. (d) Slit-lamp view of clear lens and “retrolental neovascularization” 2 months after diabetic vitrectomy

A choroidal origin for this particular manifestation of vitreous neovascularization is a further possibility.

Collagen fibers are progressively secreted into the superficial reaches of the basal retina with increasing age, extruding into the cortical vitreous through breaks in the thin ILM (Figure IV.C-4b) [29]. This collagen framework, spanning the vitreoretinal interface, presumably serves as an initial substrate for intrabasal vitreous neovascularization which then uses the anterior vitreous cortex as a substrate (Figure IV.C-4c). The “anterior hyaloidal fibrovascular proliferation” or “retrolental neovascularization” eventually forms a cyclitic membrane (Figure IV.C-4d). This anterior pathology first came to attention as a complication of PDR vitrectomy in eyes with inadequate PRP and an encircling band *in situ* [30]. The scleral indent likely reduced the choroidal pO₂ maximum, causing the penumbra obscura to shift anteriorly.

2. Vitreous and Iris Neovascularization after Vitrectomy

Provided the cortical vitreous continuum is successfully removed at surgery for proliferative diabetic retinopathy, no re-proliferation of new vessels occurs on the post-basal retina nor on the optic disc post-vitrectomy. An exception to this rule is re-proliferation of preretinal new vessels following vitrectomy and silicone oil injection [17]. It may be, however, that retro-silicone oil neovascularization utilizes a *fibrin* matrix as a “substrate” in place of vitreous extracellular matrix (ECM). Indeed, following standard vitrectomy, the vitreous chamber fills with aqueous humor within which vessel growth-promoting factor and oxygen are dispersed. This contrasts with the putative pO₂ gradients and chemotactic gradients for vessel growth-promoting factor within intact vitreous body [31]. Thus, the vessel growth-promoting factor concentration in the anterior vitreous (relative to that in the non-vitrectomized eye) will likely increase, enhancing diffusion of vessel growth-promoting factor through the anterior vitreous cortex into the aqueous humor. Postoperative induction or exacerbation of iris neovascularization was frequently seen in the early days of vitreous surgery (before endolaser technology became available) and especially when the lens and anterior vitreous cortex had been removed via the pars plana along with the rest of the formed vitreous [18]. In some instances, the anterior vitreous cortex is disrupted incidentally at one or more pars plana entry sites during phakic vitrectomy, inducing “pseudo-aphakia.” Alternatively, the anterior vitreous cortex and Wieger’s ligament can be deliberately disrupted [32]. Free communication of molecules and cells between vitreous and the anterior chamber can be confirmed by comparing the density of the residual red cells suspended in these fluids immediately postoperatively. As in aphakic eyes, however, rapid clearance of resid-

ual blood risks clogging the trabecular meshwork. Nevertheless, the optimal surgical recourse in proliferative diabetic retinopathy is to combine anterior vitreous cortex disruption with endolaser photocoagulation so as to minimize the risk of postoperative iris neovascularization and anterior hyaloid vascular proliferation while achieving a low reoperation rate for post-vitrectomy hemorrhage clearance [32].

3. Vitreous and Iris Neovascularization after PVD

Complete posterior vitreous detachment (PVD) has a similar capability as vitrectomy in preventing rete expansion by removing the necessary extracellular matrix substrate from the retinal surface (except within the vitreous base). A PVD seemingly accounts for the paucity of vitreous neovascularization after CRAO and CRVO and explains the development of iris neovascularization in eyes with retinal ischemia but with no vitreous neovascularization. Many of the eyes with extensive diabetic capillary closure examined by Ashton [3] presumably had PVD to explain the absence of vitreous neovascularization.

The absence of cortical vitreous from the retinal surface precludes rete expansion for lack of a suitable substrate, but that is *not* to say that there can be no post-basal preretinal neovascularization after PVD. During vitrectomy for PDR, removal of lysed blood from the surface of the retina may reveal glomerulus-like nodules some 150–400 μm in diameter protruding into the red cell suspension behind the detached vitreous cortex [33]. Postoperative fluorescein angiography shows leaking dye forming a “smokestack” in the vitreous fluid, in contrast to relative confinement of dye to vitreous neovascularization within vitreous extracellular matrix, illustrating the operation of the Stokes-Einstein equation [31]. The convectional plume of dye on fluorescein angiography led to the discovery of identical pathology in nonoperated eyes with diabetic retinopathy and other ischemic retinopathies (not least RVO); all such eyes have preexisting PVD (Figure IV.C-5). The topographic distribution of these “abortive neovascular outgrowths” is similar to that of early vitreous neovascularization (i.e., in proximity to the margins of capillary closure). Abortive neovascular outgrowths in diabetic eyes also have a predilection for arteriovenous crossings, again raising the question of biomechanical stimulation of venous endothelial budding [33].

Histologically, an abortive neovascular outgrowth comprises a roughly spherical mass of contorted vessels forming a raspberry-like (or “*bosselated*”) structure [34]. It has a relatively narrow “neck” that contains the afferent (feeder) and efferent (draining) vessels connecting the nodule to a retinal vein (Figure IV.C-5). Similar vascular peduncles serving rounded aggregations of capillaries are characteristic of “glomeruloid microvascular proliferations,” a specific type

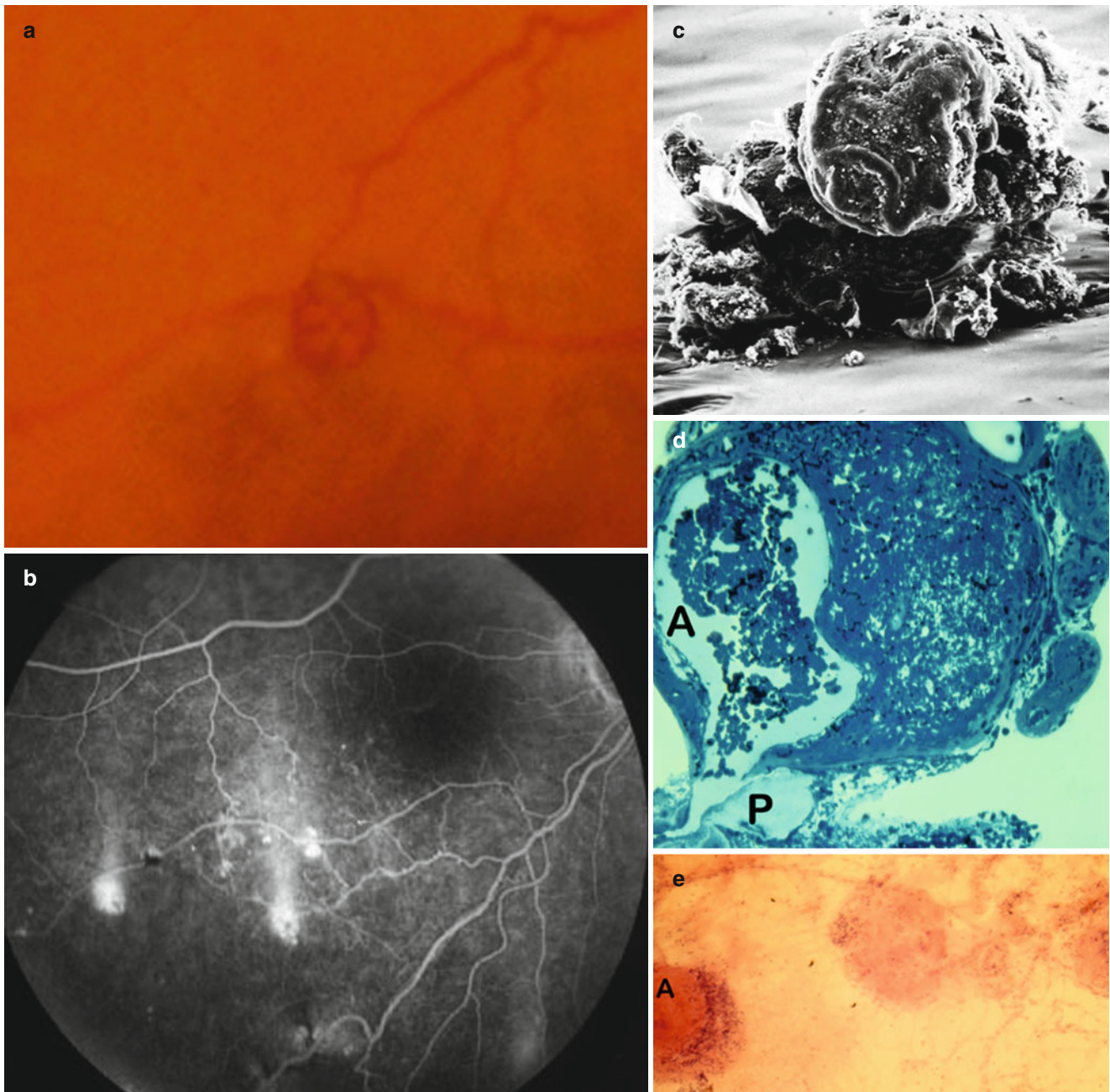


Figure IV.C-5 Abortive neovascular outgrowths. (a) A large raspberry-like nodule near an arteriovenous crossing is outlined with red cells from diabetic retrocortical (preretinal) hemorrhage (*arrowhead*). (b) Branch retinal vein occlusion with capillary closure inferotemporally on FFA and dye leakage from three abortive neovascular outgrowths in close proximity to the closure; convectional plumes of dye in fluid vitreous within retrocortical compartment. (c) Scanning electron micro-

graph of “bare” surface of inner limiting membrane and a protruding *glomerulus* of new vessels covered with hemorrhagic debris. (d) Light microscopic section of same lesion as in (c) showing that the “neck” of the lesion comprises a neovascular peduncle (*P*); there is an aneurysmal dilatation (*A*) within the nodule. (e) Surface view of digested retina showing three vascular nodules, one with an aneurysm (*A*). Material in (c–e) is from eyes with diabetic retinopathy and courtesy of P Hiscott

of hypoxia-induced angiogenesis found in tumors [35]. The walls of the endothelium-lined vessels within abortive neovascular outgrowths are grossly thickened owing to fibrin insudation (“hyaline sclerosis”), and the vessels sometimes undergo aneurysmal dilatation (Figure IV.C-5). These aneurysms and a putative bleeding potential may reflect the fact

that there are no pericytes within abortive neovascular outgrowths and minimal intrinsic extracellular matrix (e.g., no collagen type I) [34]. In fact, abortive neovascular outgrowths correspond to the initial neovascular outgrowths into the vitreous seen during the vaso-proliferative phase of Ashton’s kitten ROP model (so-called *glomerular tufts*) [4]

but without the subsequent horizontal extension. The biological inference to be drawn from the “natural experiment” created by PVD is that, while budding endothelial cells can dissolve the vein wall and the ILM at the onset of vitreous neovascularization, subsequent vessel growth-promoting factor-induced rete expansion (whether by sprouting or splitting angiogenesis) and intrinsic collagen type I production is dependent on the extrinsic substrate afforded by a vitreous ECM that is largely composed of collagen type II. At the optic disc, the equivalent abortive neovascular lesion takes the form of a network of new vessels that are confined to the disc with no peripapillary angiogenic amplification [17, 34]. Leaking dye forms a wide smokestack or plume on fluorescein angiography. The disc vessels presumably use ECM components at the base of the space of Martegiani (now detached) as a substrate for proliferation, a substrate that is not available on the surface of the peripapillary retina after PVD.

The tendency for vitreous neovascularization to spare the macula in eyes with proliferative diabetic retinopathy and an attached vitreous has been attributed to the presence of a fluid-filled “pocket” within the vitreous cortex (Worst’s premacular bursa). This pocket is thus thought to limit the substrate for premacular rete expansion [36]. An alternative or additional explanation is directional growth of new vessels away from the (perfused) macula and towards the mid-peripheral retinal capillary closure.

a. Peduncular Avulsion Induces Vitreous Hemorrhage

Scissors dissection of fibrovascular preretinal membranes during vitrectomy for proliferative diabetic retinopathy seldom results in significant bleeding provided the preretinal membrane is cleanly “segmented” (with vertical scissors) or “delaminated” (using horizontal scissors) [27]. Such careful dissection is thought to allow the myocytes or pericytes within the walls of the severed new vessels to contract, thus limiting any hemorrhaging. Serious intraoperative bleeding is generally the result of “membrane peeling” or preretinal membrane dragging during scissors cutting. By this means neovascular peduncles are avulsed from the retinal veins from which they initially budded. The retinal venous “puncturing” at the neovasculature’s most vulnerable point is readily observed during viscodelamination when a fluid such as Healon is injected beneath the preretinal membrane in order to elevate it from the retinal surface [17]. The puncturing of the vein can be visualized because the transparent viscoelastic confines the bleeding.

Peduncular avulsion also underlies spontaneous vitreous hemorrhage in proliferative diabetic retinopathy. During PVD, separation of a fibrovascular preretinal membrane from the underlying retina sometimes extends right through the points of peduncular attachment to the arterialized retinal

veins. The punctured vein releases blood into the preretinal (retro-cortical) compartment where it promptly clots and thereafter undergoes fibrinolysis (Figure IV.C-1). Thus, the vitreous neovascularization itself *is not* the source of the hemorrhage and, once a neovascular peduncle has been avulsed in this way, no more retinal bleeding is likely to arise at that location provided the puncture in the vein is successfully repaired. Vitreous hemorrhaging in proliferative diabetic retinopathy can therefore be regarded as a process of progressive preretinal membrane delamination that can potentially result in complete PVD, ghost preretinal membranes within the detached vitreous cortex, and freedom from further bleeding [17]. The process is akin to Ashton’s stripping the vitreous cortex from the revascularized retina of a kitten’s eye, yielding an intact *ex vivo* preparation of vitreous neovascularization [4].

Traditionally, diabetic vitreous hemorrhage has been attributed to the fragility of “naked” new vessels, but Ballantyne showed long ago that the vessels have their own intrinsic extracellular matrix support system (derived from myofibroblasts and pericytes) from the outset of rete expansion [1]. Moreover, PVD-induced bleeding typically occurs in association with vascularized preretinal membranes that already have a clinically obvious fibrous component and not from *rete mirabile*. However, minor hemorrhaging may arise from abortive neovascular outgrowths (given that they are truly “naked”) and from aneurysms at the tips of optic disc new vessels extending far and wide over the peripapillary retina (Figure IV.C-2b).

VI. Molecular Basis of Vitreous and Iris Neovascularization

The last 20 years have witnessed a huge expansion of knowledge concerning the biochemical and molecular biological components of vitreous neovascularization. Much of this knowledge has come on the heels of scientific progress in the field of solid tumor angiogenesis and has formed the basis for new therapeutic interventions.

A. Identity of Michaelson’s Biochemical Mediator

Of the large number of proteins discovered to be part of the angiogenic cascade, the candidate molecule satisfying the criteria for Michaelson’s vessel growth-promoting factor most closely is vascular endothelial growth factor (VEGF-A). One of its isoforms—VEGF₁₆₅ is a hypoxia-inducible, secreted, potent vascular endothelium-specific mitogen, as well as an endothelial permeability modulator and a neuro-protectant. Activation of its main receptor (VEGFR-2)

results in protease generation for basement membrane lysis (the first stage of angiogenesis) as well as initiation of endothelial cell migration and proliferation. Interruption of VEGF signaling using anti-VEGF agents is an important therapeutic strategy, therefore, but subject to similar strictures to those that applied to direct photocoagulation of vitreous neovascularization 50 years ago.

During embryonic development, physiological hypoxia stimulates secretion of VEGF by neuroglia and induces retinal vascularization thereby. In proliferative diabetic retinopathy, it is primarily hypoxic neurons that produce VEGF and induce vitreous neovascularization. VEGF is present in higher vitreous concentration in eyes with active vitreous neovascularization and in lower concentration in eyes with regressed vitreous neovascularization (such as after PRP) [37]. To date, establishing the presence of VEGF gradients within the vitreous extracellular matrix has proved problematic albeit the vitreous concentration of VEGF is higher than that in the aqueous in phakic eyes. More specifically, immunohistochemistry for VEGF protein in proliferative diabetic retinopathy eyes shows localization to the retinal veins and vitreous neovascularization in keeping “venous budding” while sparing the retinal arterial tree, but it provides little clue as to the protein’s source. Staining for VEGFR-1 (Figure IV.C-6) and VEGFR-2 shows a similar spatiotemporal pattern [38]. Inflammatory cytokines (such as interleukin-6) may also have a role in recruiting new vessels (i.e., independently of hypoxia sensing) [39], which is reminiscent of macrophage involvement in wound healing and granulation tissue formation.

Activation and involution of vitreous neovascularization is dependent on the balance between positive and negative endothelial regulators. As well as the Michaelson concept of growth factor downregulation, mechanisms contributing to neovascular inhibition and regression include (a) alternative splicing of VEGF-A to generate antiangiogenic molecules such as VEGF_{165b}; (b) alternative splicing of VEGF mRNA for endogenous production of soluble receptors such as sVEGFR-1 that act as decoys to inhibit ligand binding to signaling receptors; and (c) a role for pericytes (with which VEGF interacts negatively) in stabilizing new vessels. VEGF apart, proteins with proangiogenic roles (such as progenitor cell recruitment, vascular remodeling, and collagen type I secretion) include placenta growth factor, angiopoietin, and connective tissue growth factor, amongst many others [39].

B. Extracellular Matrix Coupling Enables Rete Expansion

Vitreous neovascularization depends on adhesive interaction between the integrins expressed on the surface of endothelial cells (specifically $\alpha 1\beta 1$ and $\alpha 2\beta 1$) and collagen type II fibers

within the vitreous extracellular matrix. Once the cells are thus “coupled” to the extracellular matrix, intracellular signaling pathways that regulate cell survival, migration, proliferation, and differentiation can be activated by proangiogenic proteins like VEGF. Integrins also localize enzymes such as metalloproteinases to advancing vessels in order to facilitate their invading the vitreous extracellular matrix. Antiangiogenic components of the vitreous include endostatin, pigment epithelium-derived factor, thrombospondin-1, and opticin [40] (see chapter I.D. Vitreous proteomics and regression of the fetal hyaloid vasculature). Opticin exerts its inhibitory effect by binding to various collagens, here to vitreous collagen type II. Because opticin alters their surface characteristics, therefore, the collagen fibers cannot support endothelial cell coupling and ensuing rete expansion [41]. In addition, vitreous collagen represents far more than a mere physical substrate for neovascularization. Prevention of rete expansion by PVD, and the “uncoupled angiogenesis” that abortive neovascular outgrowths symbolize, attests to the potential value of integrins as targets for antiangiogenic therapy [42]. Fibrin, an alternative proangiogenic substrate to collagen, interacts with endothelial $\alpha v\beta 3$ and $\alpha 5\beta 1$ integrins in granulation tissue and, possibly, in the space between injected silicone oil and ischemic retina.

C. Sources of Michaelson’s Biochemical Mediator

Retinal sites of VEGF production can be identified *ex vivo* by *in situ* hybridization for VEGF mRNA using freshly fixed tissue. This technique has been applied both to archival clinical material (e.g., eyes enucleated for iris neovascularization secondary to proliferative diabetic retinopathy or CRVO) [43] and to retinal tissue from experimental ischemia (e.g., multiple BRVOs in pig and primate eyes [44] and the rodent oxygen-induced retinopathy model) [45]. The latter differs from Ashton’s kitten ROP model in its superior reproducibility, in the peripapillary location of vaso-obliteration, and in the rapidity with which new vessels grow on return to normoxemia. All these resources show uniform patches of VEGF *in situ* hybridization signal within the inner nuclear and/or ganglion cell layer. In the oxygen-induced retinopathy model, increased VEGF message after 24 h of normoxemia correlates precisely with the area of vaso-obliteration, indicating diffusion of choroid-derived oxygen across immature photoreceptors and into the inner retina [45]. In proliferative diabetic retinopathy and CRVO, the signal was provisionally ascribed to “cells residing in a poorly perfused region” [43], but the signal pattern is consistent with a graduated metabolic oxygen barrier in the mature photoreceptor layer allowing marginal oxygenation of mid-peripheral inner retina from the choroid. To date, however, there is no report

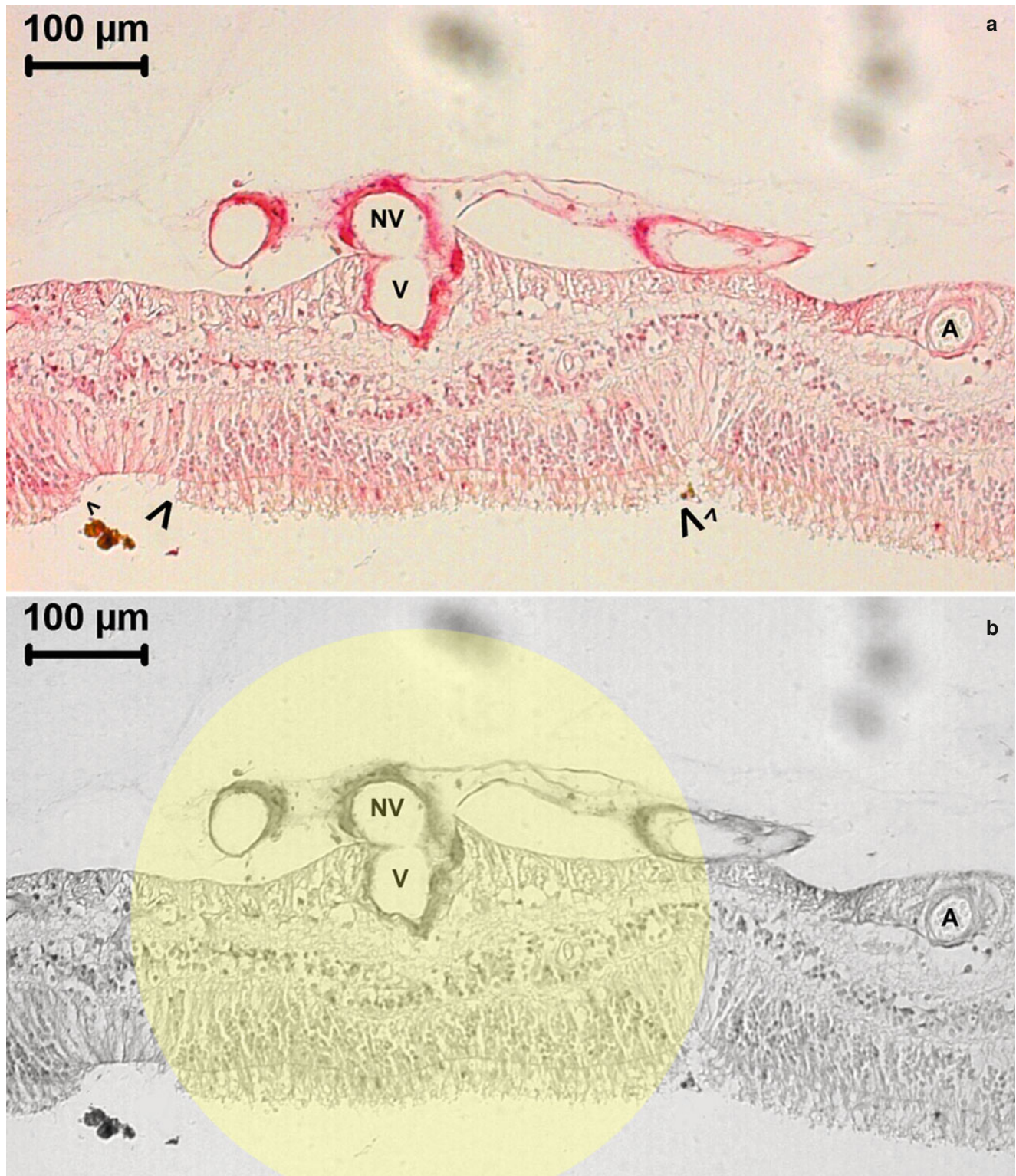


Figure IV.C-6 Marginal photoreceptor oxygenation from arteriovenous shunt vessels. **(a)** Light microscopic section of detached PDR retina immunostained for vascular endothelial growth factor receptor-1. A retinal vein (V) and associated preretinal neovascularity (NV) is heavily stained (red signal), unlike the retinal artery (A). Between the large black arrowheads, intact photoreceptor inner segments are evident on the outer aspect of the outer limiting membrane while corresponding photoreceptor cell nuclei are apparent on the inner aspect;

the outer segments have largely been shed. Small arrowheads point to the limits of similar "tissue cylinders" related to retinal arteries on each side of the vein; between the cylinders, the outer nuclear layer is absent and the outer limiting membrane is bare. **(b)** Grayscale image of the same section as in **(a)** in which a putative Krogh tissue cylinder, oxygenated by the retinal vein (V), has been highlighted in yellow; the photoreceptor inner segments are at or near the critical radius for oxygen diffusion from the vein

of VEGF in situ hybridization in an eye excised for neovascular glaucoma following CRAO.

In eyes with diabetic traction retinal detachment, VEGF in situ hybridization shows a strong signal from the outer nuclear layer (as well as from inner retina) in patches within the detached retina. This was provisionally attributed to photoreceptor hypoxia as a result of the chorioretinal separation [43]. However, histopathology of similar material has revealed collections of apparently viable cells that include photoreceptors whose inner segments are in geometrical relation to mid-sized extramacular arteries and veins [19]. By contrast, photoreceptors located outside the putative “Krogh tissue cylinders” had completely disappeared (Figure IV.C-6). Diabetic traction retinal detachment thus entails a switch from predominant marginal oxygenation of the inner retina by the choroidal circulation to predominant marginal oxygenation of the outer retina by inner retinal arteriovenous shunt vessels. This switch may be the mechanism whereby traction retinal detachment sometimes reignites vitreous neovascularization (Figure IV.C-2c) and iris neovascularization.

Abbreviations

BRVO	Branch retinal vein occlusion
CRA	Central retinal artery
CRAO	Central retinal artery occlusion
CRVO	Central retinal vein occlusion
ECM	Extracellular matrix
ILL	Internal limiting lamina
mRNA	Messenger ribonucleic acid
ILM	Inner limiting membrane
NVI	Iris neovascularization
pO ₂	Oxygen tension
PDR	Proliferative diabetic retinopathy
PRP	Panretinal retinal photocoagulation
PVD	Posterior vitreous detachment
PVP	Posterior vitreous pocket
ROP	Retinopathy of prematurity
VEGF	Vascular endothelial growth factor
VEGFR	Vascular endothelial growth factor receptor
VNV	Vitreous neovascularization

References

- Ballantyne AJ. The state of the retina in diabetes mellitus. *Trans Ophthalmol Soc U K.* 1946;66:503–43.
- Michaelson IC. The mode of development of the vascular system of the retina, with some observations on its significance for certain retinal diseases. *Trans Ophthalmol Soc U K.* 1948;68:137–80.
- Ashton N. Arteriolar involvement in diabetic retinopathy. *Br J Ophthalmol.* 1953;37:282–92.
- Ashton N, Ward B, Serpell G. Effect of oxygen on developing retinal vessels with particular reference to the problem of retrolental fibroplasia. *Br J Ophthalmol.* 1954;38:397–432.
- Ashton N, Cook C. Studies on developing retinal vessels – II. Influence of retinal detachment on oxygen vaso-obliteration. *Br J Ophthalmol.* 1954;39:457–62.
- Wise GN. Retinal neovascularisation. *Trans Am Ophthalmol Soc.* 1956;54:729–826.
- Perraut LE, Zimmerman LE. The occurrence of glaucoma following occlusion of the central retinal artery. *AMA Arch Ophthalmol.* 1959;61:845–65.
- Duker JS, Sivalingam A, Brown GC, et al. A prospective study of acute central retinal artery obstruction. The incidence of secondary ocular neovascularization. *Arch Ophthalmol.* 1991;109:339–42.
- Hayreh SS. Acute retinal arterial occlusive disorders. *Prog Retin Eye Res.* 2011;30:359–94.
- McLeod D. Letter to the editor: partial central retinal artery occlusion offers a unique insight into the ischaemic penumbra. *Clin Ophthalmol.* 2012;6:9–22.
- Ashton N. Studies of the retinal capillaries in relation to diabetic and other retinopathies. *Br J Ophthalmol.* 1963;47:521–38.
- Shilling JS, Kohner EM. New vessel formation in retinal branch vein occlusion. *Br J Ophthalmol.* 1976;60:810–5.
- Laatikainen L, Kohner EM. Fluorescein angiography and its prognostic significance in central retinal vein occlusion. *Br J Ophthalmol.* 1976;60:411–8.
- Hayreh SS. Neovascular glaucoma. *Prog Retin Eye Res.* 2007;26:470–85.
- Shimizu K, Kobayashi Y, Muraoka K. Mid-peripheral fundus involvement in diabetic retinopathy. *Ophthalmology.* 1981;88:601–12.
- Taylor E, Dobree JH. Proliferative diabetic retinopathy: site and size of initial lesions. *Br J Ophthalmol.* 1970;54:11–8.
- McLeod D. A chronic grey matter penumbra, lateral microvascular intussusception and venous peduncular avulsion underlie diabetic vitreous haemorrhage. *Br J Ophthalmol.* 2007;91:677–89.
- Michels R. *Vitreous surgery.* St. Louis: CV Mosby Co; 1981.
- McLeod D. Krogh cylinders in retinal development, panretinal hypoperfusion and diabetic retinopathy. *Acta Ophthalmol.* 2010;88:817–35.
- Dollery CT, Bulpitt CJ, Kohner EM. Oxygen supply to the retina from the retinal and choroidal circulations at normal and increased arterial oxygen tensions. *Invest Ophthalmol Vis Sci.* 1969;8:588–94.
- Osterberg G. Topography of the layer of rods and cones in the human retina. *Acta Ophthalmol.* 1935;6(Suppl):1–103.
- Stefánsson E. The therapeutic effects of retinal laser treatment and vitrectomy. A theory based on oxygen and vascular physiology. *Acta Ophthalmol Scand.* 2001;79:435–40.
- Blankenship GW. A clinical comparison of central and peripheral argon laser panretinal photocoagulation for proliferative diabetic retinopathy. *Ophthalmology.* 1988;95:170–7.
- Muqit MMK, Marcellino GR, Henson DB, et al. Pascal panretinal laser ablation and regression analysis in proliferative diabetic retinopathy. *Manchester Pascal Study Report 4.* *Eye.* 2011;25:1447–56.
- Faulborn J, Bouald S. Microproliferations in proliferative diabetic retinopathy and their relationship to the vitreous: corresponding light and electron microscopic studies. *Graefes Arch Clin Exp Ophthalmol.* 1985;23:130–8.
- Hosoda Y, Okada M, Matsumura M, et al. Epiretinal membrane of proliferative diabetic retinopathy: an immunohistochemical study. *Ophthalmic Res.* 1993;25:289–94.
- Charles S. *Vitreous microsurgery.* Baltimore: Williams and Wilkins; 1981.
- Terasaki H, Miyake Y, Mori M, et al. Fluorescein angiography of extreme peripheral retina and rubeosis iridis in proliferative diabetic retinopathy. *Retina.* 1999;19:302–8.

29. Wang J, McLeod D, Henson DB, Bishop PN. Age-dependent changes in the basal retinovitreal adhesion. *Invest Ophthalmol Vis Sci.* 2003;44:1793–800.
30. Lewis H, Abrams GW, Foos RY. Clinicopathological findings in anterior hyaloidal fibrovascular proliferation after diabetic vitrectomy. *Am J Ophthalmol.* 1987;104:614–8.
31. Stefánsson E, Loftsson T. Editorial: The Stokes-Einstein equation and the physiological effects of vitreous surgery. *Acta Ophthalmol Scand.* 2006;84:718–9.
32. McLeod D. Microsurgical management of neovascularisation secondary to posterior segment ischaemia. *Eye.* 1991;5:252–9.
33. Wong HC, Sehmi KS, McLeod D. Abortive neovascular outgrowths discovered during vitrectomy for diabetic vitreous haemorrhage. *Graefes Arch Clin Exp Ophthalmol.* 1989;27:237–40.
34. Hiscott P, Cooling RJ, Rosen P, et al. The pathology of abortive neovascular outgrowths from the retina. *Graefes Arch Clin Exp Ophthalmol.* 1992;30:531–6.
35. Sundberg C, et al. Glomeruloid microvascular proliferation follows adenoviral vascular permeability factor/vascular endothelial growth factor-164 gene delivery. *Am J Pathol.* 2001;158:1145–60.
36. Kishi S, Shimizu K. Clinical manifestations of posterior precortical vitreous pocket in proliferative diabetic retinopathy. *Ophthalmology.* 1993;100:225–9.
37. Aiello LP, Avery RL, Arrigg PG, et al. Vascular endothelial growth factor in ocular fluid of patients with diabetic retinopathy and other retinal disorders. *N Engl J Med.* 1994;331:1480–7.
38. Smith G, McLeod D, Foreman D, Boulton M. Immunolocalisation of the VEGF receptors FLT-1, KDR, and FLT-4 in diabetic retinopathy. *Br J Ophthalmol.* 1999;83:486–94.
39. Penn JS, Madan A, Caldwell RB, et al. Vascular endothelial growth factor in eye disease. *Prog Retin Eye Res.* 2008;27:331–71.
40. Reardon AJ, et al. Identification in vitreous and molecular cloning of opticin, a novel member of family of leucine-rich repeat proteins of the extracellular matrix. *J Biol Chem.* 2000;275:2123–9.
41. Le Goff MM, Sutton MJ, Slevin M, et al. Opticin exerts its anti-angiogenic activity by regulating extracellular matrix adhesiveness. *J Biol Chem.* 2012;287:28027–36.
42. Friedlander M, Theesfeld CL, Sugita M, et al. Involvement of integrins alpha v beta 3 and alpha v beta 5 in ocular neovascular diseases. *Proc Natl Acad Sci U S A.* 1996;93:9764–9.
43. Pe'er J, Folberg R, Itin A, et al. Upregulated expression of vascular endothelial growth factor in proliferative diabetic retinopathy. *Br J Ophthalmol.* 1996;80:241–5.
44. Pournaras CJ, Miller JW, Gragoudas ES, et al. Systemic hyperoxia decreases vascular endothelial growth factor gene expression in ischemic primate retina. *Arch Ophthalmol.* 1997;115:1553–8.
45. Pierce EA, Avery RL, Foley ED, et al. Vascular endothelial growth factor/vascular permeability factor expression in a mouse model of retinal neovascularization. *Proc Natl Acad Sci U S A.* 1995;92:905–9.

Physiology of Accommodation and Role of the Vitreous Body

IV.D.

D. Jackson Coleman, Ronald H. Silverman,
and Harriet Lloyd

Outline

- I. Introduction
 - II. Accommodation Theories
 - A. Lens Support of Accommodation (d'après Helmholtz)
 - B. Catenary Theory of Vitreous Support for Accommodation (d'après Coleman)
 - III. Imaging of Accommodation
 - IV. Observed Changes in Lens Shape During Accommodation
 - V. Summary
- ## References

Electronic supplementary material Supplementary material is available in the online version of this chapter at [10.1007/978-1-4939-1086-1_28](https://doi.org/10.1007/978-1-4939-1086-1_28). Videos can also be accessed at <http://www.springerimages.com/videos/978-1-4939-1085-4>.

D.J. Coleman, MD (✉)
Department of Ophthalmology, Edward S. Harkness
Eye Institute, College of Physicians and Surgeons,
Columbia University Medical Center,
635 West 165th Street, New York, NY 10032, USA
e-mail: djceye@gmail.com

R.H. Silverman, PhD
Department of Ophthalmology, College of Physicians
and Surgeons, Columbia University Medical Center,
New York, NY, USA

Biomedical Engineering Laboratory, Frederic L. Lizzi Center for
Biomedical Engineering, Riverside Research, New York, NY, USA

H. Lloyd, MS
Department of Ophthalmology, College of Physicians
and Surgeons, Columbia University Medical Center,
New York, NY, USA

Keywords

Vitreous • Accommodation • Lens support theory of Helmholtz • Vitreous catenary theory of Coleman • Presbyopia

Key Concepts

1. Accommodation is produced by contraction of the ciliary muscle producing a decreased diameter of the ciliary ring and a forward translational movement of the lens (owing to vitreous support) producing a steeper radius of curvature (catenary) of the anterior lens.
2. That the posterior zonules merge with the anterior vitreous cortex and the accessory zonules of the anterior vitreous argues against the horizontal capsular support required in the capsular model of accommodation and bolsters the concept of vitreous support (catenary theory).
3. The rapid advances in image resolution, depth of field, speed, and sensitivity that are occurring in ophthalmic imaging offer the prospect that the mysteries of accommodation will be subject to greater understanding and convergence of opinion in the near future.

I. Introduction

The eye is a three-chambered system, consisting of the anterior chamber, posterior chamber, and vitreous chamber. The anterior and posterior chambers are separated by the iris and filled with aqueous fluid produced by the ciliary epithelium and flowing from the posterior to the anterior chamber through the pupil. Fluid is constantly replenished and “turned over” in both the aqueous and the vitreous. The fluid “relief valve” is primarily movement of the aqueous from the eye

via the trabecular meshwork and Schlemm's canal, but also is transported from the eye via a secondary uveoscleral outflow route [1–3] involving the ciliary body, choroid, sclera, and episcleral tissues. The anterior and posterior chambers are normally in communication through the pupil and hence in pressure equilibrium. The vitreous is normally also in pressure equilibrium with the aqueous. Remarkably, this pressure equilibrium is maintained during growth and development when there are significant changes in anatomy.

Growth of the eye occurs primarily in the first one and one half decades of life [4–6]. The volume increases, but the pressure remains relatively constant throughout life unless disease or trauma intervenes. Normal growth maintains the optical cornea-lens-vitreous length relationships. The delicate but precise fluid production and turnover are basically a hydraulic function, i.e., a relatively constant support of the retina, choroid, and lens.

The vitreous compartment is the largest of the three chambers of the eye. A healthy young vitreous is an optically transparent gel that fills the posterior segment. Vitreous, like water, is incompressible, and maintenance of its volume and that of the anterior chamber is provided by choroidal and non-pigmented ciliary epithelial fluid production and turnover. The anterior vitreous cortex separates from the pars plana and comes into contact with the zonules and the posterior lens capsule. It is attached to the posterior lens capsule at the ligamentum hyaloidea capsulare (Weigert's ligament). The anterior vitreous cortex (hyaloid) thus constitutes the posterior limit of the posterior chamber as well as the anterior limit of the vitreous. It has a high collagen fibril density with fibers, sometimes termed accessory zonules, oriented parallel to the anterior hyaloid surface or face. Using either term ("hyaloid" or "face") to describe the posterior aspect of vitreous adjacent to the retina is incorrect [7]. Vitreous liquefaction increases throughout life, making up more than half its volume by the eighth decade. Concurrent weakening of the vitreoretinal interface and liquefaction of the gel result in posterior vitreous detachment (PVD) [see chapter II.C. Vitreous aging and posterior vitreous detachment]. Liquefaction without concurrent vitreoretinal dehiscence results in anomalous PVD and vitreoretinal traction [8] [see chapter III.B. Anomalous posterior vitreous detachment and vitreoschisis]. Despite liquefaction, the anterior vitreous maintains its fibrillar/gel composition, so that it and the lens act as a diaphragm between the aqueous and vitreous chambers.

This concept of the anterior cortical vitreous with the lens acting as a diaphragm is not universally accepted, but it is the basis for a different interpretation of the accommodative mechanism. The pressure within a closed, fluid-filled sphere such as the eye is uniformly distributed throughout the inner surface (Pascal's law). Vitreous pressure is generally assumed to be the same as the aqueous pressure except for transient

accommodative fluctuations. Intraocular pressure, normally 14–20 mmHg, has been measured directly by cannulation using intraocular manometers to rise to over 100 mmHg with voluntary squeezing of the lids or 30–50 mmHg with blinking [9]. In accommodation, the ciliary muscle, strategically positioned between the chambers, contracts and increases pressure in the vitreous and the choroid, producing a transient pressure differential with respect to the anterior/posterior chambers due to the presence of the anterior vitreous cortex (hyaloid face) diaphragm. With accommodation, lens position and shape are altered (no volume change), and aqueous chamber fluid is redistributed around the lens to relieve this pressure differential. This, according to the Coleman theory of accommodation described in more detail below, can provide a supporting pressure behind the lens contributing to accommodation. Differential pressure measurement has not yet been performed in humans but has been performed in primates [10].

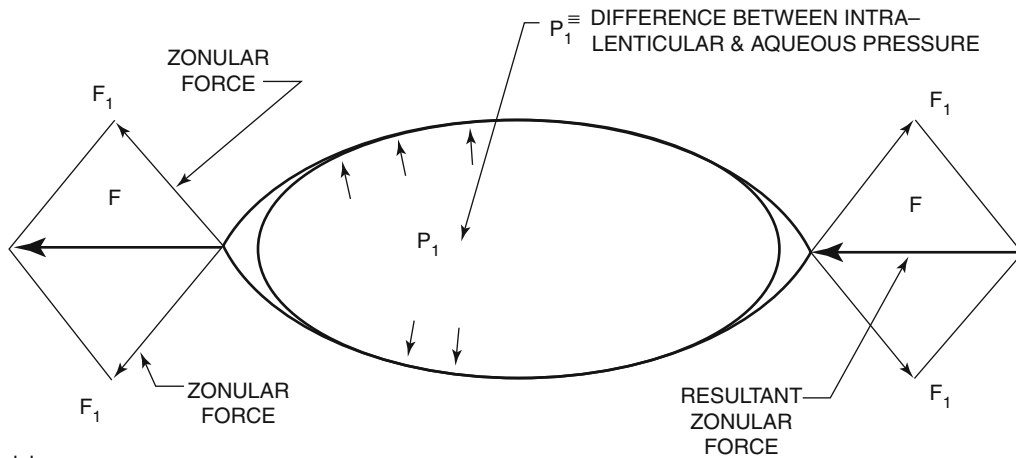
In 1970, Duke Elder summarized accommodative theories by stating: "*Every possible hypothesis has been put forward to explain the rationale of accommodation*" [11]. He was far too optimistic. There continue to be new observations and hypotheses explaining accommodation of the eye. In addition to reviewing alternative theories, this chapter will describe the vitreous physiology and its mechanical function during accommodation.

II. Accommodation Theories

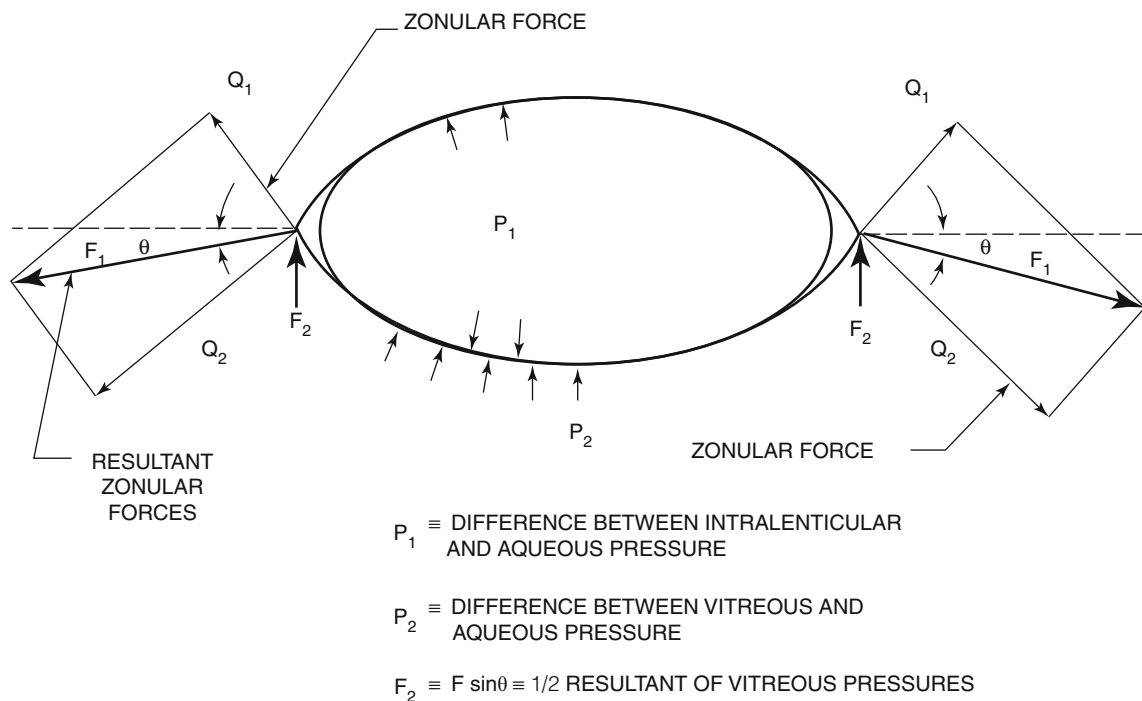
The theories of accommodation have largely coalesced into two general concepts: the Helmholtz capsular elasticity theory and the vitreous support or catenary theory.

A. Lens Support of Accommodation (d'après Helmholtz)

Hermann von Helmholtz proposed his capsular theory of accommodation in 1855 [12]. It is still the most widely held concept despite several challenges. The capsular theory, in brief, attributes an equatorial zonular force or traction via relaxation of the ciliary body to flatten the lens (disaccommodation) and a release of zonular force by contraction of the ciliary body to allow capsular elasticity to round up the lens (accommodation) (Figures IV.D-1 and IV.D-2). Cramer [13], Tscherning [14], von Pfugk [15], and more recently Coleman [10, 16] proposed vitreous support of the lens in accommodation. The earlier vitreous support proposals were discredited largely because of observations such as: the iris was felt to contribute to flattening of the peripheral anterior lens curvature, but it was shown that aniridia still has the



Helmholtz Model



Catenary Model

Figure IV.D-1 Top: free body diagram of Helmholtz model of accommodation showing zonular forces and resultant equatorial force in a system free from a vitreous-aqueous pressure gradient. Bottom: free body diagram of present model of accommodation showing combined

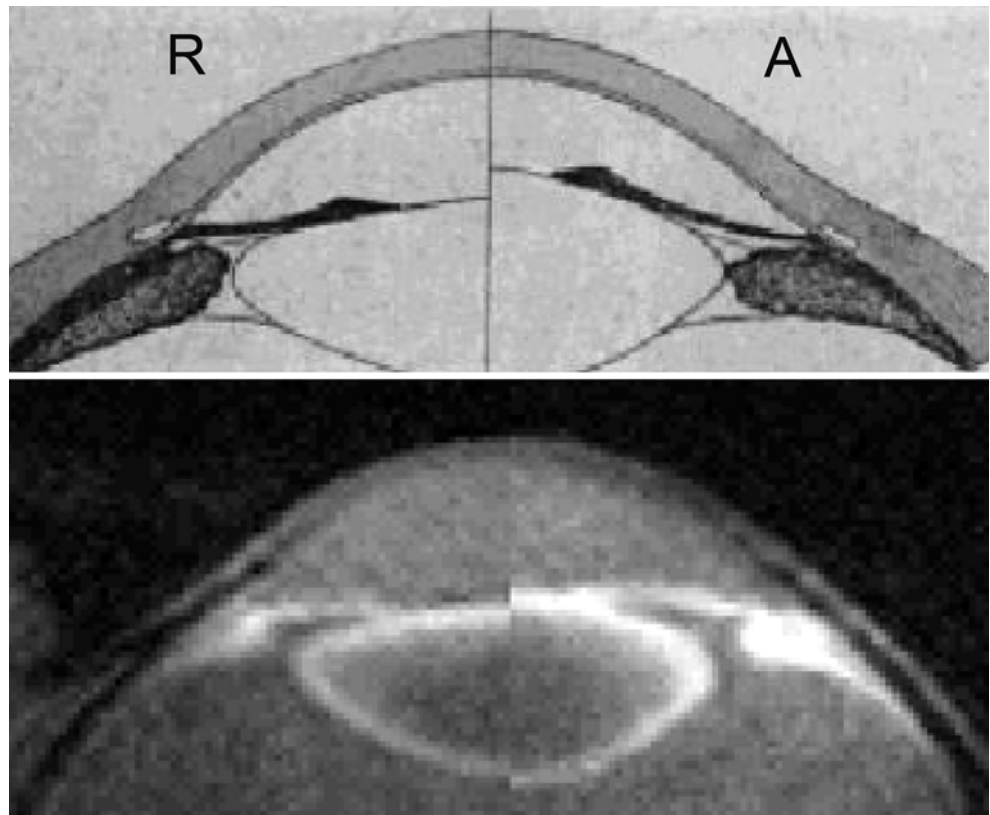
effects of a vitreous-aqueous pressure gradient and capsular forces in producing posteriorly directed zonular force. Components of vitreous forces are depicted counteracting lens forces (This figure was published in Coleman [16, p. 1072]. Copyright Elsevier (1970))

same lens shape, or a loose capsular bag was noted when a lens had absorbed post-injury [17] and thus indicated capsular relaxation in accommodation.

It is the incontrovertible appearance of a “relaxed zonule” in accommodation that is the most difficult for many observers to reconcile with vitreous support. It is due to a more posteriorly directed zonule force to the lens that allows the translational forward movement of the lens to have less

horizontal stability than in the tensed zonule disaccommodated state. The longer moment of force and gravity gives the appearance of a relaxed zonule. Vitreous support also explains why gravity can increase the accommodative state (it is easier to read looking lower), and convergence (with increased vitreous support by the medial rectus muscle contraction) can increase accommodative amplitude. While the contraction of the ciliary body could allow elastic lens

Figure IV.D-2 *Top:* Helmholtz's drawing demonstrating his theory of accommodation. The *left half* of the image shows relaxed accommodation (*R*). The *right half* shows the increase in lens thickness and decrease in equatorial diameter after ciliary muscle contraction (*A*). *Bottom:* a composite of two MRI images. The *left half* is an image acquired with relaxed accommodation, while the subject, a 26-year-old subject, views a far target. The *right half* is an image acquired during accommodation, while the subject views a near target. It shows an increase in lens thickness and a decrease in equatorial diameter upon ciliary muscle contraction (With permission from Strenk et al. [60])



properties to round up the lens, the weakness of the ciliary body zonule anatomy makes disaccommodation very questionable (Figure IV.D-3).

There have been many other theories over the years. Schachar [18] and Rohen [19] have also proposed theories that relate to zonular compression of the lens (Schachar) or to accessory attachments of the zonule to the ciliary body (Rohen). Fincham and Fisher have written extensive descriptions of the capsular mechanism. Fincham's monograph in the *British Journal of Ophthalmology* is a classic [20]. While supporting the capsular theory, he does, however, include vitreous support in his summary.

B. Catenary Theory of Vitreous Support for Accommodation (d'après Coleman)

The second general concept is that the vitreous body supports the lens in accommodation (Figure IV.D-1). The hydraulic theory proposed by Coleman attributes vitreous support of the lens to cause a forward translational movement of the lens and a reproducible "catenary" shape by molding the anterior lens surface in the zonule capsule sling (Figure IV.D-4, Video IV.D-1). This effect occurs instantly and provides an aspheric lens surface that can be documented

with ultrasound or optical techniques. A catenary is defined as the curvature assumed by a non-extensible cable suspended between two supports. Technically it is a graph of a hyperbolic cosine function. The shape is, in three dimensions, that of an aspheric lens. The posterior lens surface changes very little due to vitreous support and equal distribution of pressure from the vitreous (Pascal's law).

Pressure measurements demonstrating the difference (differential pressure) between the vitreous and aqueous described by Coleman in primates [10] prove the presence of a diaphragm effect of the lens-zonule and the anterior vitreous cortex (hyaloid face) (Figure IV.D-5). Croft et al. [21, 22] recently described peripheral anterior vitreous cortex backward movement with stimulus of the Edinger-Westphal nucleus in primates (Video IV.D-2, courtesy of MaryAnn Croft, MS) that indicates a diaphragm pressure gradient. This peripheral backward pressure can be interpreted as supporting the central lens since the vitreous is a noncompressible fluid. (If the periphery goes back, then the center has to come forward.) Earlier, van Alphen described a piston-like lens movement with Edinger-Westphal nucleus stimulation in cats [23]. Van Alphen noted that not only does the ciliary muscle contract the circular sphincter but also "leads to increased tension in any part of the choroid and that its tone affects part of the intraocular pressure."

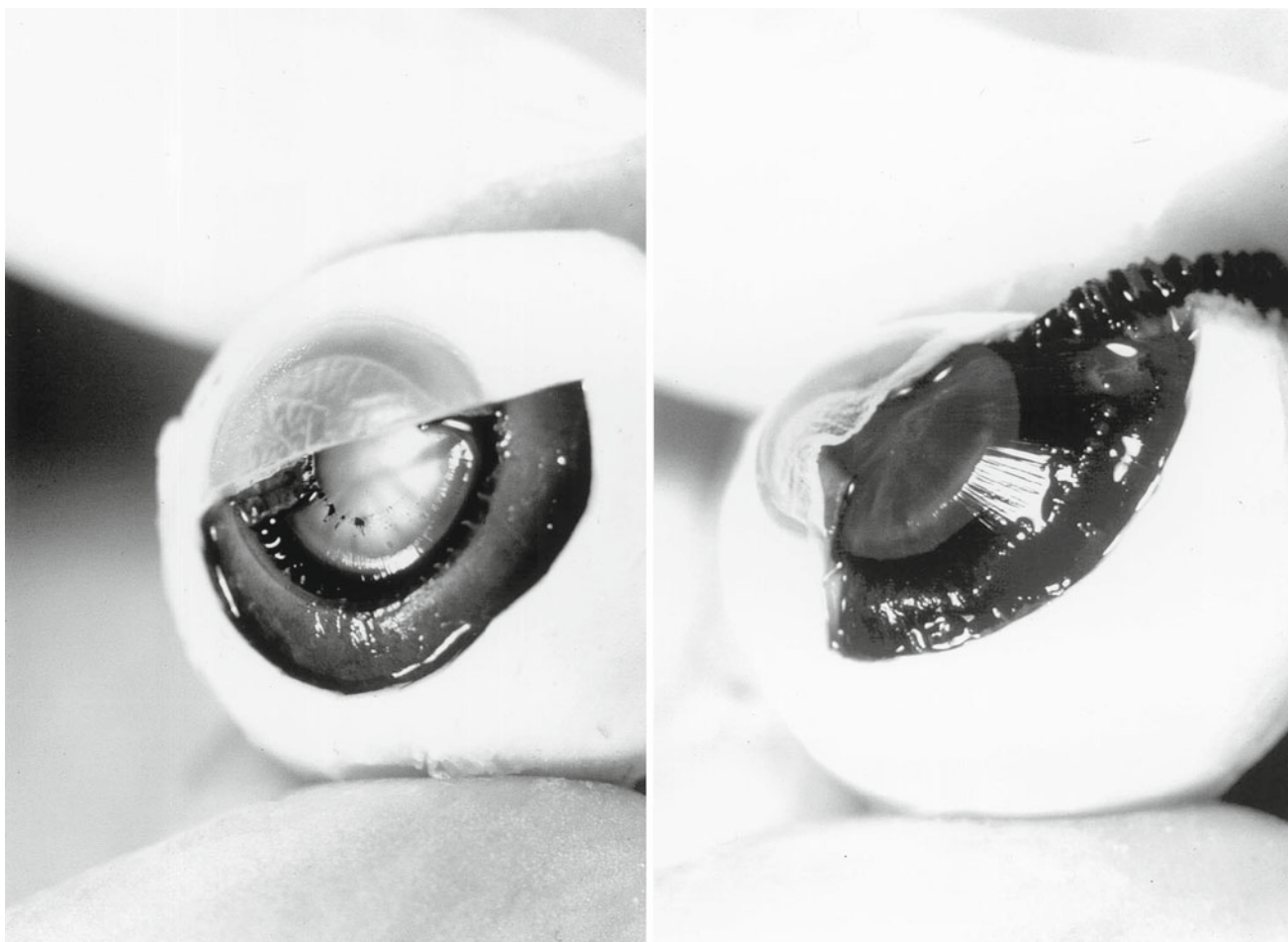


Figure IV.D-3 The integrity of the vitreous zonule-lens unit can be seen in the human eye by peeling away the ciliary body. This demonstrates that the ciliary body could produce an accommodated lens but

not a disaccommodated lens by the capsular (Helmholtz) theory (This figure was published in Coleman [51, p. 1545]. Copyright Elsevier (2001))

This observation also noted by Lutjen-Drecoll et al. [21] emphasizes vitreous support of accommodation. It is this diaphragm effect allowing the vitreous to support the lens and form the anterior catenary shape that is disputed by capsular theorists. There is an ever-increasing body of evidence, however, indicating that the anterior vitreous and the lens operate as a unit.

III. Imaging of Accommodation

Although the presence of the iris and sclera impedes visualization of the ciliary body and zonules, ultrasound and OCT have been applied in several studies of the accommodative process. While the recently developed anterior segment spectral domain OCTs operating in the 840 nm band cannot visualize the ciliary body due to scattering by the overlying sclera, the time-domain Visante (Carl Zeiss Meditec, Inc, Dublin, CA), operating at 1,310 nm, can often achieve sufficient pen-

etration to depict the ciliary muscles. Taking advantage of this capability, Lossing et al. [24] and Sheppard and Davies [25] used the Visante to visualize and measure the ciliary muscle in children and young adults under accommodative stimulus, documenting alterations in muscle configuration with accommodation. The Visante has also been used to study changes in anterior chamber depth during accommodation [26, 27]. Shen et al. [28] developed a spectral domain OCT system utilizing a custom spectrometer that provides extended focal depth, allowing simultaneous imaging of the cornea and both anterior and posterior lens surfaces (within the pupil), and an example of which is provided in Figure IV.D-6. This technology has allowed studies of anterior chamber and lens thickness during the accommodative process [29, 30] as well as ex vivo studies of the isolated lens during simulated accommodation [31]. Swept-source OCT systems operating at 1,050 nm have also been able to achieve greater depth of field, with images up to 12 mm in depth, and high sensitivity, enabling assessment of the posterior vitreous [32].



Figure IV.D-4 Very high-frequency ultrasound (35 MHz) demonstrating the congruence of an un-retouched Artemis image of the anterior lens shape and a catenary suspension bridge (The San Francisco Bay

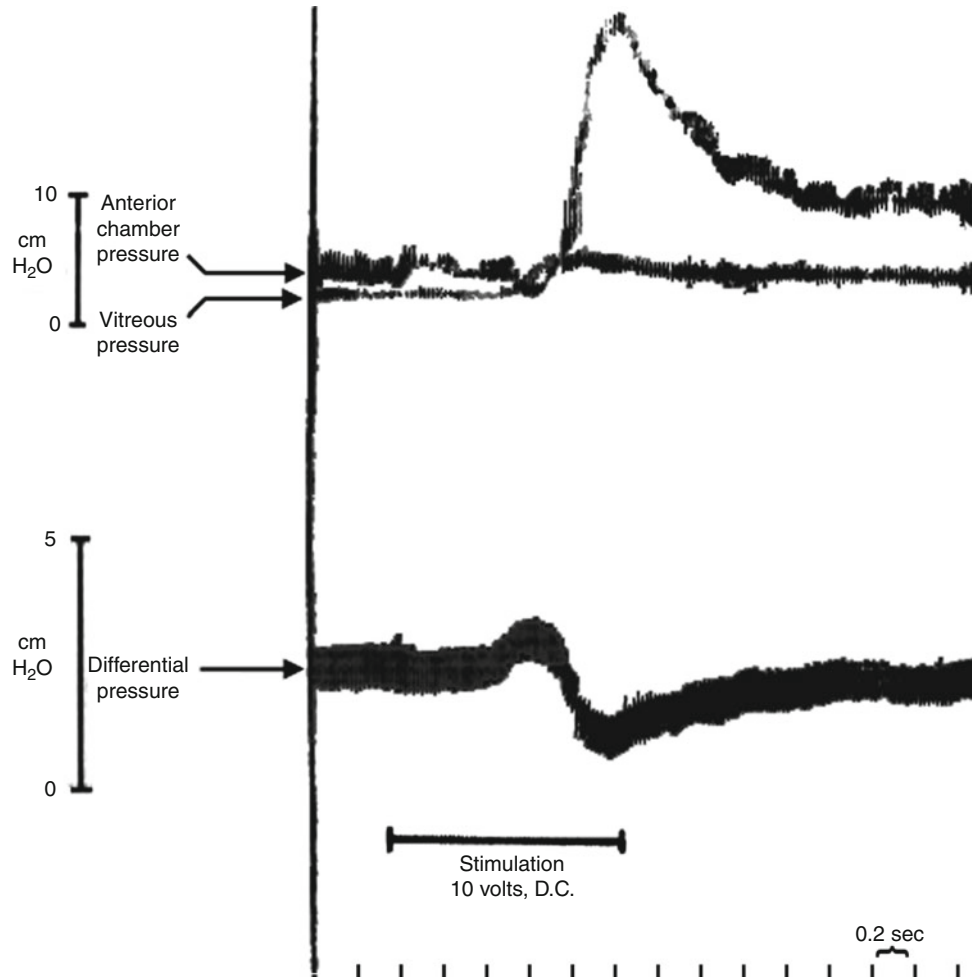
Bridge). The image is seen better on Video IV.D-1, also demonstrates the posterior direction of the zonules

We have made extensive use of B-scan high-frequency ultrasound to demonstrate changes in the lens as well as anterior vitreous zonules [33] (Figure IV.D-7). Ultrasound biomicroscopy (UBM) studies in primates were carried out by Glasser [34], by Schachar [35], and by Croft et al. [36]. Adam, Pavlin, and Ulanski described iris bowing in patients with pigmentary glaucoma during accommodation [37]. UBM-based clinical studies of ciliary body configuration in accommodation were carried out by Jeon et al. (in myopia) [38], Stachs et al. (in 3D) [39, 40], and by Park (pre- and post-cataract extraction) [41]. Modesti et al. [42] also imaged the eye pre- and post-cataract extraction, evaluating the configuration of the lens capsular bag with accommodative effort. UBM has also been used to study the zonules in relation to the lens and ciliary body during accommodation [21, 43, 44].

In addition to OCT and US, magnetic resonance imaging has also been used to visualize the accommodative process. Using a 1.5 tesla (T) field and surface coils, Kasthurirangan et al. [45] studied the refractive properties of the lens during the accommodative process in clinical subjects, acquiring images in slightly over 2 min with 0.15 mm in-plane resolu-

tion and 3 mm slice thickness. Jones et al. [46] also studied accommodation using a 1.5 T MRI, achieving 0.25 mm in-plane resolution in 3 mm slices with an acquisition time of about 3 min. Strenk et al. [47, 48] used a 1.5 T MRI with a custom eye coil and a T1-weighted, single-echo, multislice, spin-echo technique with 3 mm slices to study the eye and the ciliary body in accommodation (see Figure IV.D-2) in phakic and pseudophakic eyes, achieving 0.078 in-plane resolution. The large slice thickness and the long acquisition time of 1.5 T MRI make the images subject to degradation by eye motion and microsaccades. Richdale et al. [49] addressed these factors by using a 7 T MRI with a custom RF coil to achieve 3D resolution of $0.15 \times 0.25 \times 1.00 \text{ mm}^3$ or 0.0375 mm^3 per voxel, acquiring images in less than 30–40 s. Using signal processing and patient preparation techniques (such as taping the eyelids closed while fixating with the contralateral eye), the best signal-to-noise ratio and contrast were achieved with T1-weighted images that were characterized by low signal for the vitreous and anterior and posterior chambers and high signal for the lens and ciliary body.

Figure IV.D-5 Tracing of pressure fluctuations in a primate eye following electrical stimulation of ciliary body. A vitreous pressure rise occurs simultaneously with an aqueous drop in pressure. A subsequent "rebound" aqueous pressure rise is then seen without any corresponding drop in vitreous pressure. This aqueous pressure slowly drops back to prestimulus level (This figure is modified from Coleman [10, p. 855] and republished with permission of the American Ophthalmological Society)



IV. Observed Changes in Lens Shape During Accommodation

There is general agreement about many observations of the lens during accommodation:

1. The lens changes shape, with the anterior lens surface becoming steeper centrally and flattening toward the equator. Koretz described the shape as paraboloid [50]. Coleman terms it a catenary [51]. Both are similar polynomials. The posterior lens capsule is thin, and its curvature does not change appreciably (as expected by Pascal's law and vitreous support). The anterior lens capsule varies in thickness and is thicker in the periphery. The elastic modulus of the capsule has been estimated by several investigators, most thoroughly by Fincham [52] and by van Alphen [53] who also calculated the elasticity of all ocular tissues. The elastic modulus may be sufficient to mold the lens, but the question
2. Lens change in accommodation is rapid and reproducible, requiring approximately 300 μ s, more easily explained by molding than by elastic recovery.
3. Accommodation amplitudes are increased by convergence, i.e., medial rectus contraction will increase accommodation, explained by increased vitreous support.
4. The posterior capsule and the anterior vitreous cortex (hyaloid face) are attached to the lens at Weigert's ligament, a circular attachment outside the optical area of the

of the modulus being sufficient to rapidly and reproducibly mold the anterior and posterior curvatures of the lens is disputable, as is the elastic constant of the zonules. They are, however, suitable to support a catenary. The lens elongates axially in the accommodated state. The equator narrows. The posterior pole usually (but not always) moves back, but not as much as the anterior pole moves forward, thus indicating a translational forward movement of the lens [10].

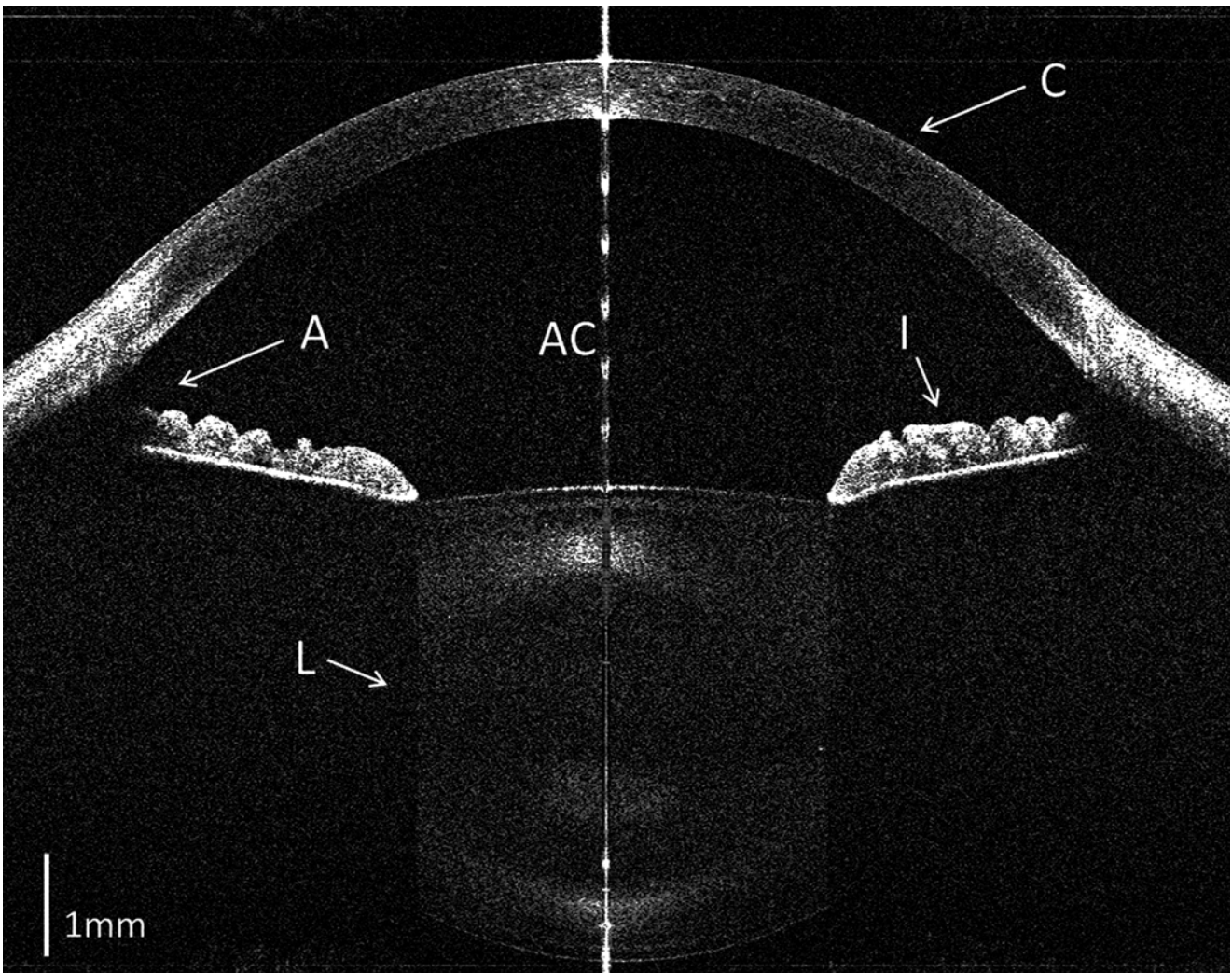


Figure IV.D-6 Cross-sectional image of the anterior segment of a 35-year-old human eye in the relaxed state acquired with extended depth spectral domain OCT at 840 nm. The axial resolution of the system is 8 μm in air. The main ocular structures are indicated: cornea (C), anterior chamber (AC), crystalline lens (L), iris (I), and angle (A). The image

consists of 1,000 A-lines of 2,556 (axial) pixels each. The size of the frame in the axial direction is 9.5 mm when the mean group refractive index of the anterior segment is taken to be 1.37 at 840 nm. The lateral scanning length was set to 16 mm (Image courtesy of Marco Ruggeri, Bascom Palmer Eye Institute, University of Miami, Miami, FL)

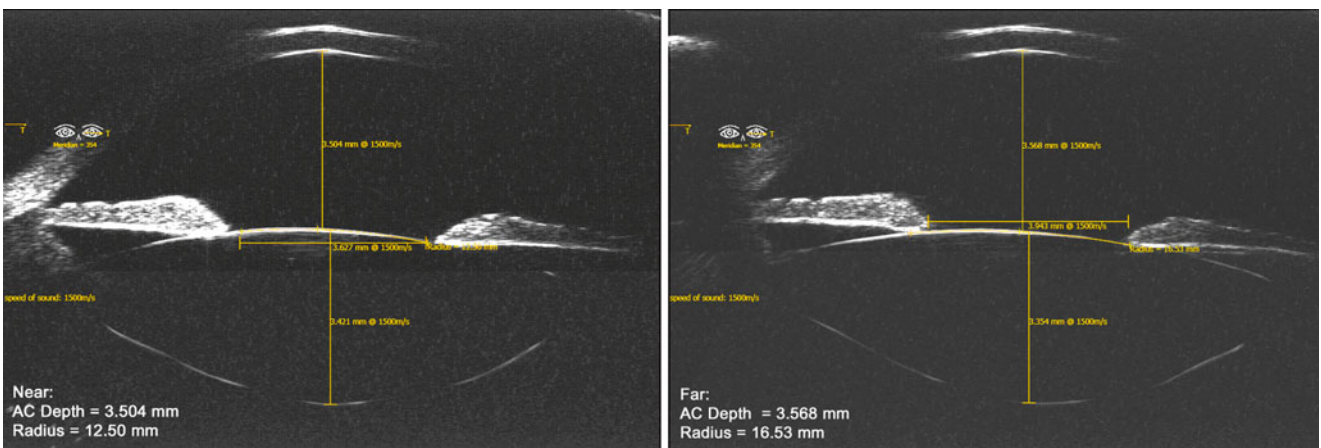


Figure IV.D-7 Artemis-3 very high-frequency ultrasonograms of the anterior segment of an eye demonstrating the iris and lens movement with accommodation and the radius change of the anterior capsule between near (*left image*) and far (*right image*)

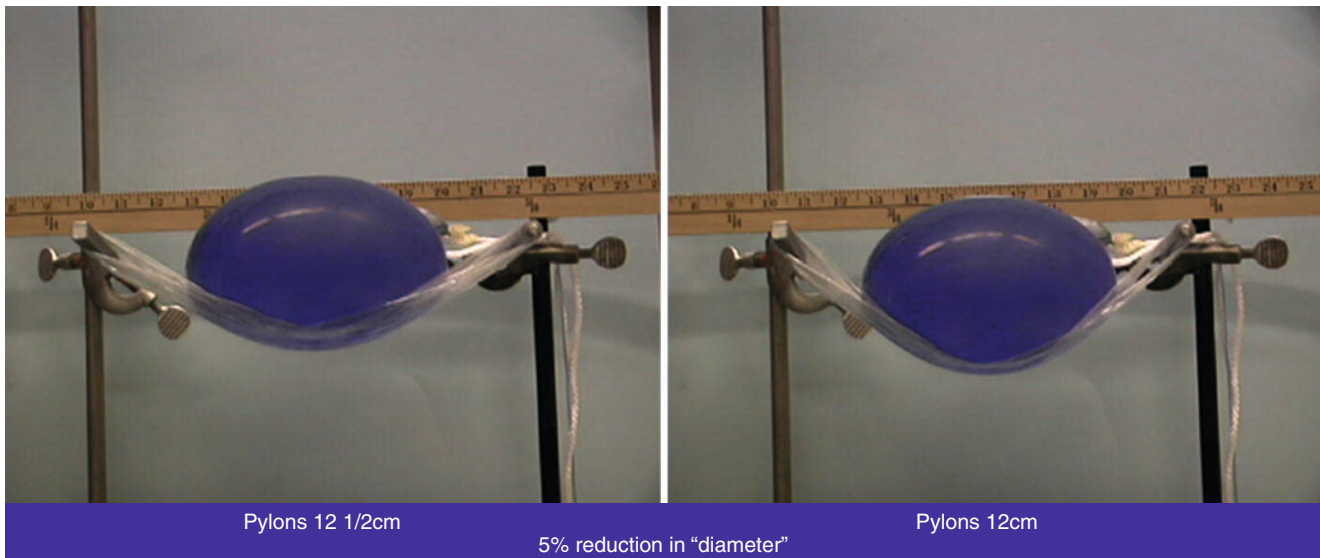


Figure IV.D-8 Five percent reduction in sphincter diameter produces dramatic change in suspension dynamics in order to produce steeper radius of curvature centrally in this paraboloid catenary diaphragm

model. This catenary lens shape is an aspheric lens, which helps explain the human eye's depth of field

posterior lens allowing the lens and anterior vitreous to function as a unit.

5. The equator of the lens may be molded by the reduction of the ciliary ring (Mueller's muscle) and displacement of Hannover's space [54]. (This is easily seen with a lens model that can reproduce all the lens features simply by vitreous support and constricting the ciliary opening [10].) (Figure IV.D-8)
6. Sagittal section of the lens shows uniform anterior and posterior optical lens curves, but coronal sections show a marked crenellation of the equator. This is unexplainable by a purely capsular mechanism, except as a local distortion produced by zonular insertion that inexplicably does not affect the optical surfaces.
7. Zonular anatomy is posteriorly directed from the lens to the origin at the suprachoroidal lamina at the ora serrata.
8. "Accessory zonules" in the anterior vitreous seen with ultrasound (Figure IV.D-9) tend to parallel the zonular alignment and argue for a posteriorly directed zonular lens force as well as an integrated lens, zonule, and anterior vitreous unit [21]. As declared by the Munich group, "The vitreous zonule system may help to smoothly translate to the lens the driving forces of accommodation and disaccommodation" [43].
9. Contraction of the ciliary muscle produces traction on the choroid [23].

V. Summary

In summary, if one accepts vitreous support of the lens during accommodation, then flattening of the lens (disaccommodation) is produced by a dilation of the ciliary muscle aperture and a posterior translational movement of the flattened lens. Accommodation is produced by a contraction of the ciliary muscle producing a decreased diameter of the ciliary ring, a forward translational movement of the lens producing a steeper radius of curvature (catenary) of the anterior lens (Figures IV.D-7 and IV.D-8). The anterior lens shape of paraboloid [55, 56] or catenary [51] is instantly reproducible. Redistribution of anterior chamber fluid reinforces equatorial lens diameter reduction [54]. Furthermore, as Armary and Burian have noted, increased outflow of aqueous would help sustain the accommodated state with less energy [57].

If one does NOT accept vitreous support, then (a) accommodation must be attributed to ciliary muscle contraction causing equatorial lens relaxation and zonule tension to allow the lens to move forward, as if on rollers, and (b) lens shape change is entirely due to lens capsular elasticity, with differences in thickness of the capsule responsible for the curvature differences. Vitreous support is not required or responsible for the change in lens shape. The strength of the zonular attachment to the ciliary processes is disputed (Figures IV.D-3 and IV.D-10).

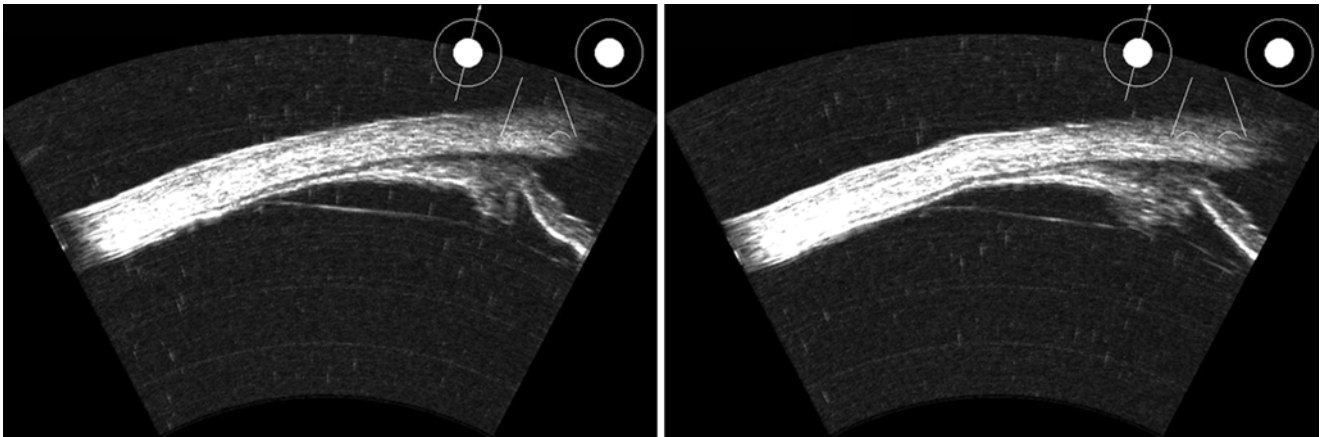


Figure IV.D-9 Ultrasound image demonstrating the accessory zonules in the anterior vitreous that parallel and support the concept of an anterior vitreous-zonule-lens unit

One argument commonly used by capsule theorists is that “vitrectomized eyes can still accommodate.” This result is to be expected, because in lens sparing vitrectomy surgeries, the anterior vitreous is not removed, leaving the anterior vitreous cortex diaphragm intact. Martin and Guthoff et al. [58] published an elegant finite element analysis comparing the “Helmholtz” and “Coleman” models and found that a greater change in anterior lens curvature is produced with the Helmholtz model than the Coleman model. Unfortunately, they used a horizontal zonular force for both computations, making the comparative observation of questionable value. They did, however, document that anterior lens shape changes are possible with either theory. The Coleman model requires a posteriorly directed zonular force. A video (Video IV.D-1) demonstrating the perfect correspondence of a catenary suspension and the anterior lens capsule by ultrasound further confirms the vitreous support of the lens into a shape consistent with all optical and ultrasound imaging. High-resolution ultrasound imaging also documents both the zonule direction and location as well as accessory zonules in the anterior vitreous (Figure IV.D-9). Parel [59] and also Lutjen-Drecoll et al. [21] have demonstrated that the posterior zonule merges with the anterior vitreous cortex, and they have shown the zonule passage through the ciliary processes back to the suprachoroidal lamina with elegant clarity (Figure IV.D-10). The strength of a ciliary body attachment is necessary for flattening of the lens, but is hard to justify. This and other ultrasound imaging of acces-

sory zonules in the anterior vitreous further argue against the horizontal capsular support required in the capsular model and justify the concept of vitreous support. Indeed, the preponderance of observations thus indicates vitreous support of the lens in accommodation to be capable of producing shaping of the lens. There is no question that further observations will lead to additional clarification about the mechanical interaction of ciliary body, lens vitreous unit, and relation of choroidal tension and movement to the accommodative process, but the body of evidence to support an anterior vitreous-lens unit is increasing and compelling. For example, measurement of lens and zonule dimensions during ciliary contraction and accommodation is of great importance. High-frequency ultrasound as well as other imaging techniques can show not only the lens shape but critical dimensions of ciliary body and the zonule relationships. The entire vitreous volume and changes during accommodation will also be measurable to further clarify our understanding of accommodative and physiologic functions of the eye.

The nature of the accommodative process has been subject to examination, speculation, and theory for well over a century, and controversy has not abated. The rapid advances in resolution, depth of field, speed, and sensitivity taking place in imaging technologies such as MRI, US, and OCT [see chapter II.F. To see the invisible – the quest of imaging vitreous] offer the prospect that the mysteries of accommodation will be subject to greater understanding and convergence of opinion in the near future.

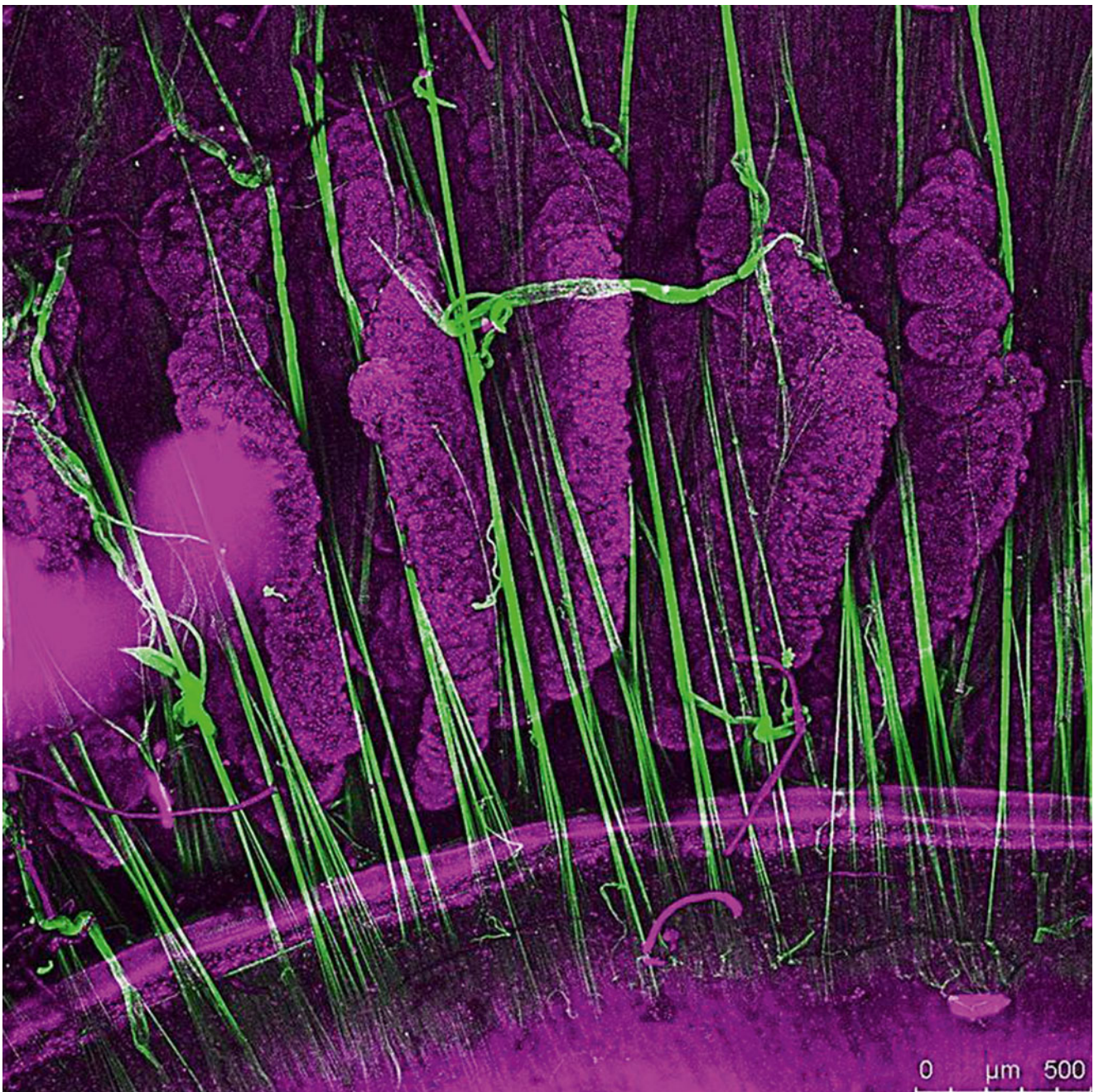


Figure IV.D-10 Attachment of zonule and passage between ciliary processes using confocal microscopy from a poster presented at the 2013 annual meeting of the Association for Research in Vision and

Ophthalmology by Heather Durkee, Steven Bassnett, Yanrong Shi, Esdras Arrieta, Sonia Yoo, and Jean-Marie Parel from the University of Miami School of Medicine (Courtesy of Jean Marie Parel, PhD)

References

1. Bill A, Hellsing K. Production and drainage of aqueous humor in the cynomolgus monkey (*Macaca irus*). *Invest Ophthalmol Vis Sci*. 1965;4:920–6.
2. Bill A. Conventional and uveo-scleral drainage of aqueous humour in the cynomolgus monkey (*Macaca irus*) at normal and high intra-ocular pressures. *Exp Eye Res*. 1966;5:45–54.
3. Bill A. The routes for bulk drainage of aqueous humour in the vervet monkey (*Cercopithecus ethiops*). *Exp Eye Res*. 1966;5:55–7.
4. Wilmer HA, Scammon RE. Growth of the components of the human eyeball; I. Diagrams, calculations, computation and reference tables. *Arch Ophthalmol*. 1950;43(4):599–619.
5. Scammon RE, Wilmer HA. Growth of the components of the human eyeball; II. Comparison of the calculated volumes of the eyes of the newborn and of adults, and their components. *Arch Ophthalmol*. 1950;43(4):620–37.

6. Oppel O. About some special aspects of the development of the human visual apparatus and its visual functions. *Klin Monbl Augenheilkd*. 1966;48(3):321–40.
7. Ruby AJ, Williams GA, Blumenkranz MS. Vitreous humor. In: Tasman W, Jaeger E, editors. *Duane's foundations of clinical ophthalmology*. Philadelphia: Lippincott Williams & Wilkins; 2000.
8. Sebag J. Anomalous posterior vitreous detachment: a unifying concept in vitreo-retinal disease. *Graefes Arch Clin Exp Ophthalmol*. 2004;42:690–8.
9. Coleman DJ, Trokel S. Direct-recorded intraocular pressure variations in a human subject. *Arch Ophthalmol*. 1969;85(2):637–40.
10. Coleman DJ. On the hydraulic suspension theory of accommodation. *Trans Am Ophthalmol Soc*. 1986;84:846–68.
11. Duke-Elder S. *System of ophthalmology. Ophthalmic optics and refraction*. St Louis: Mosby; 1970.
12. von Helmholtz H. Über die akkommodation des augues. *Albrecht Von Graefes Arch Klin Exp Ophthalmol*. 1855;1:1–89.
13. Cramer A. *Tijdschrift der maatshappij vor geneeskunde, Nederlandisch*. *Lancet*. 1851;1:529–41.
14. Tscherning M. *Physiologic optics, dioptrics of the eye, functions of the retina, ocular movements and binocular vision*. Philadelphia: C. Weiland; 1904.
15. von Pflugk A. Neve wege zur erforschung der lehre von der akkommodation, der glaskorper im akkommodierenden auge. *Albrecht Von Graefes Arch Klin Exp Ophthalmol*. 1935;133:454–571.
16. Coleman DJ. Unified model for accommodative mechanism. *Am J Ophthalmol*. 1970;69:1063–79.
17. Graves B. Changes of tension on the lens capsule during accommodation and under the influence of various drugs. *Br Med J*. 1926;9:46–50.
18. Schachar RA. Zonular function: a new hypothesis with clinical implications. *Ann Ophthalmol*. 1994;26:36–8.
19. Rohen JW. Experimental studies on the trabecular meshwork in primates. *Arch Ophthalmol*. 1963;69:335–49.
20. Fincham EF. The accommodation reflex and its stimulus. *Br J Ophthalmol*. 1951;35(7):381–93.
21. Lutjen-Drecoll E, Kaufman P, Wasielewski R, Lin TL, Croft MA. Morphology and accommodative function of the vitreous zonule in human and monkey eyes. *Invest Ophthalmol Vis Sci*. 2010;51(3):1554–64.
22. Croft MA, Nork TM, McDonald JP, Katz A, Lutjen-Drecoll E, Kaufman PL. Accommodative movements of the vitreous membrane, choroid, and sclera in young and presbyopic human and nonhuman primate eyes. *Invest Ophthalmol Vis Sci*. 2013;54(7):5049–58.
23. van Alphen GW. On emmetropia and ametropia. *Ophthalmologica*. 1961;142(S1):1–92.
24. Lossing LA, Sinnott LT, Kao CY, Richdale K, Bailey MD. Measuring changes in ciliary muscle thickness with accommodation in young adults. *Optom Vis Sci*. 2012;89:719–26.
25. Sheppard AL, Davies LN. In vivo analysis of ciliary muscle morphologic changes with accommodation and axial ametropia. *Invest Ophthalmol Vis Sci*. 2010;51:6882–9.
26. Baikoff G. *Measurement of accommodation. Anterior segment optical coherence tomography*. Thorofare: Slack; 2008.
27. Malyugin BE, Shpak AA, Pokrovskiy DF. Accommodative changes in anterior chamber depth in patients with high myopia. *J Cataract Refract Surg*. 2012;38:1403–7.
28. Shen M, Wang MR, Yuan Y, et al. SD-OCT with prolonged scan depth for imaging the anterior segment of the eye. *Ophthalmic Surg Lasers Imaging*. 2010;41:S65–9.
29. Du C, Shen M, Li M, Zhu D, Wang MR, Wang J. Anterior segment biometry during accommodation imaged with ultralong scan depth optical coherence tomography. *Ophthalmology*. 2012;119:2479–85.
30. Yuan Y, Chen F, Shen M, Lu F, Wang J. Repeated measurements of the anterior segment during accommodation using long depth optical coherence tomography. *Eye Contact Lens*. 2012;38:102–8.
31. Kim E, Ehrmann K, Uhlhorn S, Borja D, Arrieta-Quintero E, Parel JM. Semiautomated analysis of optical coherence tomography crystalline lens images under simulated accommodation. *J Biomed Opt*. 2011;16(5):056003-1-11.
32. Itakura H, Kishi S, Li D, Akiyama H. Observation of posterior pre-cortical vitreous pocket using swept source optical coherence tomography. *Invest Ophthalmol Vis Sci*. 2013;54(5):3102–7.
33. Coleman DJ, Silverman RS, Lizzi FL, Rondeau MJ, Reinstein DZ, Lloys H, Daly SW. *Ultrasonography of the eye and orbit*. Philadelphia: Lippincott Williams & Wilkins; 2006.
34. Glasser A, Kaufman PL. The mechanism of accommodation in primates. *Ophthalmology*. 1999;106:863–72.
35. Schachar RA, Kamangar F. Computer image analysis of ultrasound biomicroscopy of primate accommodation. *Eye*. 2006;20:226–33.
36. Croft MA, McDonald JP, Nadkarni NV, Lin TL, Kaufman PL. Age-related changes in centripetal ciliary body movement relative to centripetal lens movement in monkeys. *Exp Eye Res*. 2009;89:824–32.
37. Adam RS, Pavlin CJ, Ulanski LJ. Ultrasound biomicroscopic analysis of iris profile changes with accommodation in pigmentary glaucoma and relationship to age. *Am J Ophthalmol*. 2004;138(4):652–4.
38. Jeon S, Lee WK, Lee K, Moon NJ. Diminished ciliary muscle movement on accommodation in myopia. *Exp Eye Res*. 2012;105:9–14.
39. Stachs O, Martin H, Behrend D, Schnitz KP, Guthoff R. Three-dimensional ultrasound biomicroscopy, environmental and conventional scanning electron microscopy investigations of the human zonula ciliaris for numerical modelling of accommodation. *Graefes Arch Clin Exp Ophthalmol*. 2006;44:836–44.
40. Stachs O, Martin H, Kirchhoff A, Stave J, Terwee T, Guthoff R. Monitoring accommodative ciliary muscle function using three-dimensional ultrasound. *Graefes Arch Clin Exp Ophthalmol*. 2002;40:906–12.
41. Park KA, Yun JH, Kee C. The effect of cataract extraction on the contractility of ciliary muscle. *Am J Ophthalmol*. 2008;146:8–14.
42. Modesti M, Pasqualitto G, Appolloni R, Pecorella I, Sourdille P. Preoperative and postoperative size and movements of the lens capsular bag: ultrasound biomicroscopy analysis. *J Cataract Refract Surg*. 2011;37:1755–84.
43. Ludwig K, Wegscheider E, Hoops JP, Kampik A. In vivo imaging of the human zonular apparatus with high-resolution ultrasound biomicroscopy. *Graefes Arch Clin Exp Ophthalmol*. 1999;37:361–71.
44. Wasielewski R, McDonald JP, Heatley G, Lutjen-Drecoll E, Kaufman PL, Croft MA. Surgical intervention and accommodative responses, II: forward ciliary body accommodative movement is facilitated by zonular attachments to the lens capsule. *Invest Ophthalmol Vis Sci*. 2008;49:5495–502.
45. Kasthurirangan S, Markwell EL, Atchison DA, Pope JM. In vivo study of changes in refractive index distribution in the human crystalline lens with age and accommodation. *Invest Ophthalmol Vis Sci*. 2008;49:2531–40.
46. Jones CE, Atchison DA, Pope JM. Changes in lens dimensions and refractive index with age and accommodation. *Optom Vis Sci*. 2007;84(10):990–5.
47. Strenk SA, Strenk LM, Guo S. Magnetic resonance imaging of aging, accommodating, phakic and pseudophakic ciliary muscle diameters. *J Cataract Refract Surg*. 2006;32:1792–8.
48. Strenk SA, Strenk LM, Semmlow JL, DeMarco JK. Magnetic resonance imaging study of the effects of age and accommodation on

- the human lens cross-sectional area. *Invest Ophthalmol Vis Sci.* 2004;45(2):539–45.
49. Richdale K, Wassenaar P, Bluestein KT, et al. 7 Tesla MR imaging of the human eye in vivo. *J Magn Reson Imaging.* 2009;30:924–32.
 50. Koretz JF, Cook CA, Kaufman PL. Accommodation and presbyopia in the human eye: changes in the anterior segment and crystalline lens with focus. *Invest Ophthalmol Vis Sci.* 1997;38(3):569–78.
 51. Coleman DJ, Fish SK. Presbyopia, accommodation, and the mature catenary. *Ophthalmology.* 2001;108(9):1544–51.
 52. Fincham EF. The function of the lens capsule in the accommodation of the eye. *Trans Opt Soc.* 1928;30:101–37.
 53. van Alphen GW, Graebel WP. Elasticity of tissues involved in accommodation. *Vision Res.* 1961;31(7/8):1417–38.
 54. Croft MA, Glasser A, Kaufman PL. Accommodation and presbyopia. *Int Ophthalmol Clin.* 2001;41:33–46.
 55. Koretz JF, Handelman GH. Modeling age-related accommodative loss in the human eye. *Math Model.* 1986;7:1003–14.
 56. Koretz JF, Handelman GH. Model of accommodative mechanism in the human eye. *Vision Res.* 1982;22:917–27.
 57. Armaly MF, Burian HM. Changes in the tonogram during accommodation. *Arch Ophthalmol.* 1958;60(1):60–9.
 58. Martin H, Guthoff R, Terwee T, Schmitz KP. Comparison of the accommodation theories of Coleman and of Helmholtz by finite element simulations. *Vision Res.* 2005;45(22):2910–5.
 59. Nankivil D, Manns F, Arrieta-Quintero E, et al. Effect of anterior zonule transection on the change in lens diameter and power in cynomolgus monkeys during simulated accommodation. *Invest Ophthalmol Vis Sci.* 2009;50(8):4017–21.
 60. Strenk SA, Strenk LM, Koretz JF. The mechanism of presbyopia. *Prog Retin Eye Res.* 2005;24:379–93.

Phoebe Lin, Shivali Menda, and Eugene de Juan Jr.

Outline

- I. **Introduction**
- II. **Fundamental Principles of Intravitreal Drug Delivery**
- III. **The Practice of Intravitreal Injection of Drugs**
 - A. Technique for Intravitreal Drug Injection
 - B. Special Considerations in Infants
 - C. Complications
- IV. **Intravitreal Drug Therapy**
 - A. Short-Term Therapy
 - 1. Antibacterial Agents
 - 2. Antifungal Agents
 - 3. Antiviral Agents
 - 4. Steroids
 - 5. Anti-inflammatory/Antineoplastic Agents
 - 6. Anti-VEGF Agents
 - 7. Pharmacologic Vitreolysis
 - B. Sustained-Release Drug Delivery
 - 1. Implants
 - 2. Encapsulated Cell Technology
 - 3. Microspheres
 - 4. Porous Silicon Particles
 - 5. Liposomes
 - 6. Suprachoroidal Microinjection and Microneedles
- V. **Future Drug Delivery Approaches and Considerations**
 - A. Iontophoresis
 - B. Refillable Delivery Systems
 - C. Advances in Sustained-Release Intravitreal Injectables
 - D. Emerging Methods for Local Delivery
 - E. Vitreous Structure and Intravitreal Drug Delivery

References

P. Lin, MD, PhD (✉)
Division of Retina and Vitreous Diseases/Surgery,
Ocular Inflammation, Casey Eye Institute,
Oregon Health and Science University, Portland, OR, USA
e-mail: linp@ohsu.edu

S. Menda, MD
Department of Ophthalmology, USCF School of Medicine,
San Francisco, CA, USA

E. de Juan Jr., MD
ForSight Labs, Menlo Park, CA, USA

Keywords

Vitreous • Intravitreal injections • Drug delivery • Sustained drug release • Drug release implants • Microparticles • Nanoparticles • Uveitis • Age-related macular degeneration • Cystoid macular edema

Key Concepts

1. Intravitreal drug delivery provides a higher potency of drug to the retina and choroid, but is often short-lived, thus underscoring the need for sustained delivery methods.
2. There are advantages and disadvantages to biodegradable and nonbiodegradable sustained drug delivery devices.
3. New pharmacologic targets and methods of sustained drug delivery may transform the method of treatment of many retinal and choroidal diseases. Vitreous structural variations can influence pharmacokinetics and must be taken into consideration for new drug delivery systems to be effective at different ages and in different disease states.

I. Introduction

Over the last 10 years, the success of anti-vascular endothelial growth factor (VEGF) antibodies for the treatment of neovascular age-related macular degeneration (AMD) has made the use of intravitreal injections for the treatment of posterior segment disease commonplace. The application of drugs into vitreous, as either a direct intraocular injection or in the form of sustained-release devices, is currently the focus of many clinical studies to treat a number of retinal and choroidal diseases. The advantages of this approach are that local treatment bypasses the systemic side effects of a drug

and enables more direct control over the dose and duration of drug delivery to the target site. Furthermore, as we gain an increased understanding of the pathophysiological processes in diseases such as vitreomacular traction syndrome and diabetic retinopathy, new pharmacologic treatments have arisen that have the potential to obviate the need for surgical intervention or at least facilitate surgery [see chapter VI.A. Pharmacologic vitreolysis]. As technology and our understanding of disease processes evolve, these treatments will undoubtedly become more refined both in the way they are delivered and in the specificity of the pharmacologic target. This chapter reviews the principles of intravitreal drug delivery for both short-term and sustained-release formulations.

II. Fundamental Principles of Intravitreal Drug Delivery

The challenge of treating posterior segment disease resides in the obstacles encountered while trying to achieve therapeutic drug concentrations at the level of the retina and choroid. Topically administered drug that is not lost immediately to the systemic circulation (90–95 % is lost through nasal and conjunctival vessels into the systemic circulation) is absorbed through the cornea into the anterior chamber where it is eliminated through the trabecular meshwork. Drugs delivered to the sub-Tenon's space can penetrate the more permeable sclera to achieve higher concentrations in the retina and choroid. However, both the tight junctions of the retinal pigment epithelium (RPE) and dissipation of drug due to choroidal blood flow limit access of drugs to the retina, although lipophilic molecules may penetrate. Systemically administered (either intravenous or oral) drugs are one avenue to circumvent some of these barriers, especially if the drug is lipophilic and is therefore able to bypass the blood-retinal barrier. The systemic side effects from high enough concentrations of drug required to attain intraocular efficacy, however, limit the utility of many systemically administered drugs [1, 2]. Alternatively, drugs administered intravitreally can attain high enough concentrations for direct treatment of retinal conditions. Drugs delivered intravitreally are eliminated by outflow through either the anterior route, composed of the trabecular meshwork, or the posterior route, through the blood-retinal barrier, into the systemic circulation [1, 3].

The ideal drug formulation for intravitreal administration would require a number of qualifications. First, the drug should have a long enough half-life that does not mandate repeated injections and risk of complications. Anti-VEGF agents require repeated injections because they have short half-lives and first-order kinetics (Figure IV.E-1a, c) [4, 5]. Intravitreal steroids, such as triamcinolone, are biphasic, or follow a two-compartment model with exponential decline initially, followed by first-order kinetics after 1 month

(Figure IV.E-1a, b) [6]. Some of the newer sustained-release steroid devices can demonstrate zero-order kinetics (flat line shown in Figure IV.E-1a), thus releasing a constant amount of therapeutic level steroid for the lifespan of the implant (Figure IV.E-1d) [7]. Second, the ideal intravitreal drug formulation should not interfere with the transparency of the ocular media as not to interfere with vision. This is an important consideration for microsphere and nanosphere technology where a larger particle size or more numerous particles can cause visual obscuration. A third requisite for an intravitreally administered drug is that it should be delivered at a therapeutic dose that does not cause toxicity or impede normal cellular activity [3]. By providing a constant lower concentration of drug over time (zero order) rather than larger spurts of drug that decrease rapidly (first order), sustained-release devices are advantageous in that they provide therapeutic levels of drug without as much local and systemic toxicity.

Sustained-release devices now available or under investigation are shown in Figure IV.E-2. They include devices that are suspended in the vitreous cavity by fixation to the sclera, injected into the suprachoroidal space or into the vitreous cavity as a free-floating device, or placed underneath the conjunctiva or into the sclera.

III. The Practice of Intravitreal Injection of Drugs

A. Technique for Intravitreal Drug Injection

Topical proparacaine followed by 4 % lidocaine soaked into a cotton-tip applicator or subconjunctival 2 % lidocaine is commonly used over the injection site. The site is commonly located inferotemporally to avoid drug deposition into the visual axis by gravity or, alternatively, in the superotemporal quadrant to avoid contamination with the accumulation of bacteria in the tear lake of the inferior fornix. An eyelid speculum is placed in the eye to keep the eyelashes away from the injection site. A 5 % povidone-iodine solution is then applied to the eye and then irrigated. The pars plana is marked with an empty tuberculin syringe or calipers 3.5–4 mm behind the limbus. A half-inch 30 or 32 G needle on a tuberculin syringe containing 0.05–0.1 mL of the medication is then introduced into the mid-vitreous cavity. When the needle is removed, the site is tamponaded with a sterile cotton-tip applicator to prevent reflux of drug. Postinjection topical antibiotics are not required.

B. Special Considerations in Infants

Pars plana location varies with infant development and can be located 1–1.5 mm behind the limbus in premature infants,

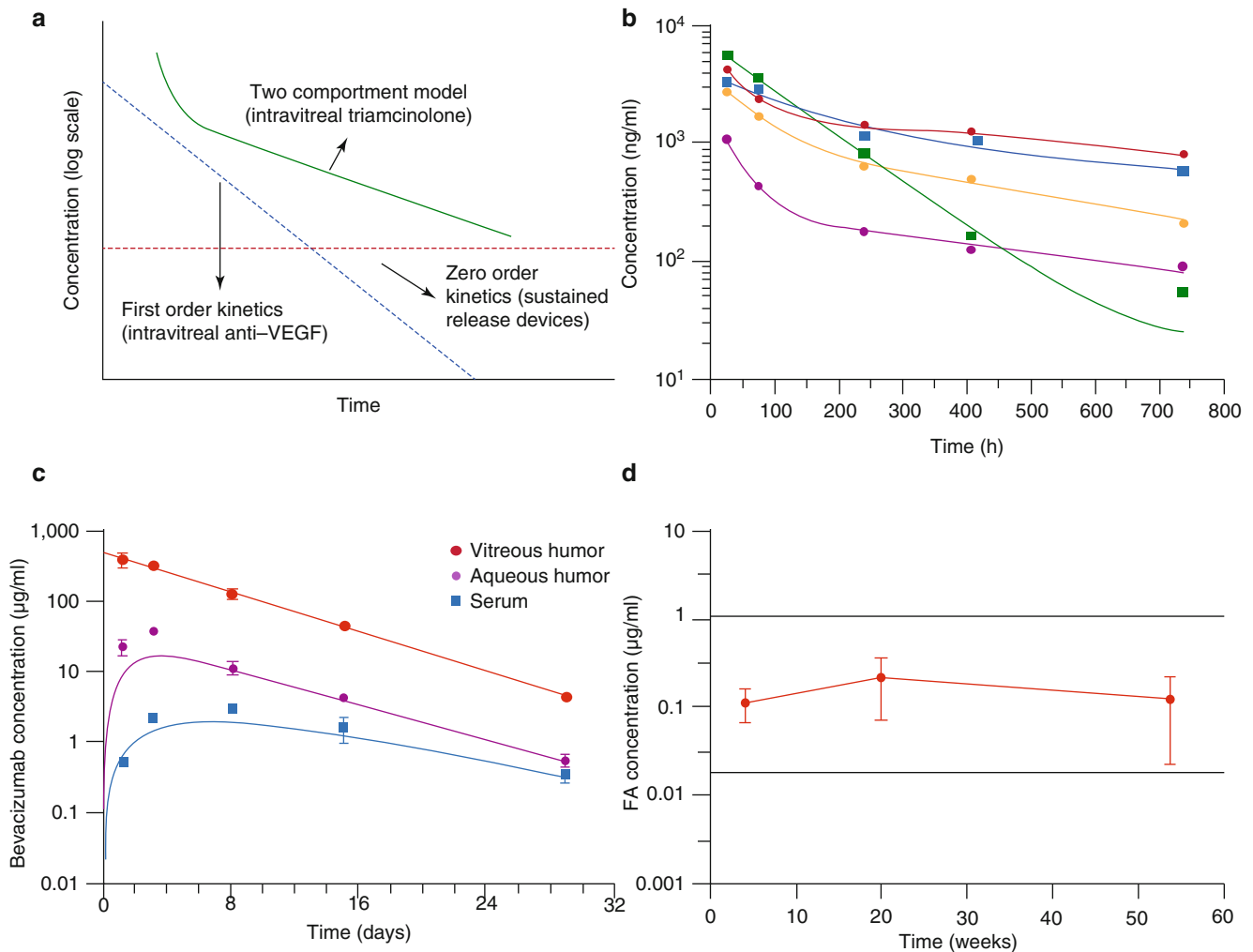


Figure IV.E-1 (a) First-order (blue dotted line), zero-order (red dashed line), and two-compartment model (green line) elimination kinetics shown in log scale. (b) Two-compartment model pharmacokinetics of triamcinolone in the vitreous cavity with different lines from different

patients. (c) First-order kinetics exhibited by bevacizumab given intravitreally. (d) Fluocinolone acetonide sustained delivery device (Retisert [4, 5]) exhibits zero-order kinetics (Jaffe et al. [7])

but is 2–3.5 mm from the limbus in full-term infants. This affects the approach to needle placement during intravitreal injections [8]. Accordingly, the vitreous volume in infants is approximately two-thirds to three-fourths that of adults, thus requiring adjustments in administered drug volume so as not to increase intraocular pressure too severely or cause drug toxicity to the retina.

C. Complications

Complications associated with intravitreal injections include pain, vitreous hemorrhage, subconjunctival hemorrhage, transient elevation of intraocular pressure, infectious endophthalmitis, uveitis, or sterile endophthalmitis. The rate of infectious endophthalmitis following intravitreal injections has been reported to be between 0.1 and 0.16 % per injection

and appears to be minimized using a standardized sterilization protocol including the use of povidone-iodine and eyelid specula [9] (see above). Sterile endophthalmitis was reported in 1–2 % of patients receiving intravitreal injection of non-preserved-free triamcinolone and can occur in patients receiving Avastin as well [10]. In a Medicare claims database case-control study, the rates per injection after anti-VEGF treatment of endophthalmitis (0.09 %), vitreous hemorrhage (0.23 %), and uveitis (0.11 %) were higher than in the control group [11]. Rates of rhegmatogenous retinal detachment and retinal tear do not appear to be significantly higher in patients who received intravitreal anti-VEGF agents than age-matched controls [11]. Furthermore, several reports have now shown that sustained elevation of intraocular pressure can occur in susceptible individuals who receive repeated injections of anti-VEGF agents [12–15]. In a head-to-head trial of ranibizumab with bevacizumab, two-year

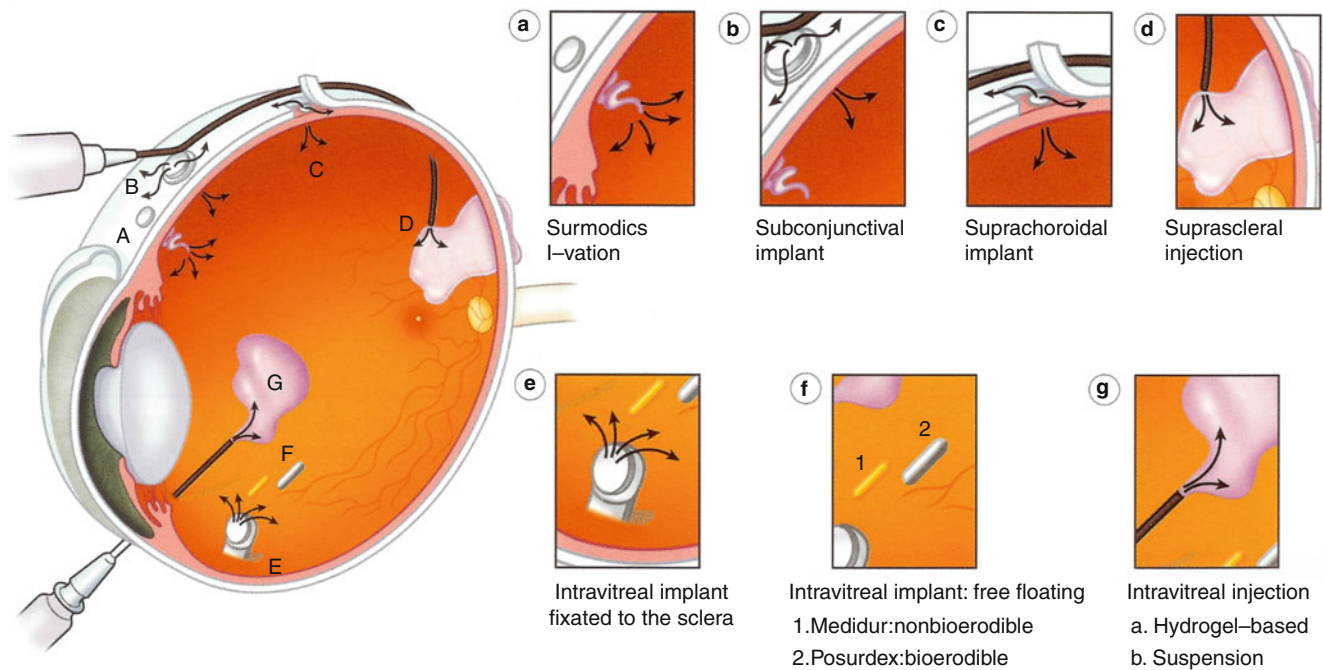


Figure IV.E-2 Drug delivery systems and their anatomical location (Adapted from Lee and Robinson [93]; Spaeth GL et al. [95])

data showed that overall systemic adverse events were low, but there appeared to be a slightly higher prevalence of overall systemic adverse events in patients treated with bevacizumab although there was no difference in arteriothrombotic events, and the events that were captured as differences have not been previously associated with anti-VEGF therapy [16]. Since then, a meta-analysis safety review of this issue has been unable to determine the relative safety of these drugs because most head-to-head studies were not designed to adequately monitor for systemic adverse events [17].

IV. Intravitreal Drug Therapy

A. Short-Term Therapy

1. Antibacterial Agents

The mainstay of empiric treatment for bacterial endophthalmitis employs the use of ceftazidime, a third-generation cephalosporin with increased activity against gram-negative organisms, and vancomycin, the drug of choice for methicillin-resistant *Staphylococcus aureus* and other gram-positive organisms [18]. Levofloxacin is a third-generation fluoroquinolone with activity against gram-positive and gram-negative bacteria. Rabbit models have shown similar antibacterial activity of 1.5 % levofloxacin against *Staphylococcus epidermidis*, *Staphylococcus aureus*, and *Pseudomonas aeruginosa* in comparison to standard intravitreal vancomycin and ceftazidime [19]. Recent evidence

supports the safety of intracameral moxifloxacin after anterior segment surgery [19], which can very likely be used safely in vitreous as well (Table IV.E-1).

2. Antifungal Agents

Fungal endophthalmitis is most commonly treated with intravitreal amphotericin B, which has been shown to be effective against most *Candida* species as well as *Aspergillus*, *Rhizopus*, and *Penicillium*. Doses up to 10 μg have been shown to be nontoxic, although there have been reports of retinal necrosis when injected too close to the retina [20]. The liposomal formulation of amphotericin B has been shown in animal models to have less toxicity to the retina. Koc and colleagues have reported a case of liposomal amphotericin B used after vitrectomy in the treatment of *Candida* endophthalmitis without any known ocular toxicity [21]. Among the newer generation triazoles (voriconazole, ravuconazole, posaconazole) that have broad antifungal coverage with relatively low toxicity, only voriconazole has been given intravitreally in humans. The short half-life of voriconazole results in the requirement for close observation with frequent repeated injections (Table IV.E-1). Sen et al. demonstrated in their case series that five patients who had fungal endophthalmitis resistant to fluconazole and amphotericin B responded to intravitreal voriconazole [22]. Although the echinocandin caspofungin does not appear to reach therapeutic levels in vitreous when given systemically, this agent shows promise as an intravitreal agent against *Candida* and *Aspergillus*. Kusbeci and colleagues demonstrated its

Table IV.E-1 Dosage and half-life of antibiotics given as intravitreal injections

Agent	Intravitreal dose	Half-life in vitreous (hours)	Coverage
Antibacterial			
Vancomycin	1 mg	30	Gram +, MRSA
Ceftazidime	2.25 mg	16	Gram +, gram –, anaerobes
Amikacin	0.4 mg	24	Gram +, gram –
Gentamicin	0.2 mg	12–35	Gram +, gram –
Gatifloxacin	0.4 mg ^a		Gram +, gram –, <i>Pseudomonas</i> , anaerobes
Moxifloxacin	0.05–0.16 mg ^a	1.72	Same as above
Antifungal			
Amphotericin B	5–10 µg	6.9–15.1	<i>Candida</i> , <i>Aspergillus</i> , <i>Penicillium</i> , <i>Rhizopus</i>
Fluconazole	100 µg	3.1	<i>Candida</i> , <i>Aspergillus</i> , <i>Histoplasma</i> , <i>Fusarium</i>
Itraconazole	10 µg		Same as above
Voriconazole	50–100 µg	2.5	Same as above
Antiviral			
Acyclovir	240 µg		HSV, VZV
Ganciclovir	2–5 mg	7–8	HSV, VZV, CMV
Foscarnet	1–2.4 mg	77	HSV, VZV, CMV
Cidofovir	20–100 µg	24.4	HSV, VZV, CMV

^aExtrapolated from animal studies

MRSA methicillin-resistant *Staphylococcus aureus*, HSV herpes simplex virus, VZV varicella zoster virus, CMV cytomegalovirus

effectiveness against *C. albicans* endophthalmitis in rabbits [23, 24]. While voriconazole can achieve therapeutic concentrations in the vitreous when given systemically, it is important to note that posaconazole and the echinocandins do not and therefore have limited use in the systemic treatment route for fungal endophthalmitis [25].

3. Antiviral Agents

Acyclovir is an antiviral that is effective against the herpes family of viruses. It becomes activated in virus-infected cells by a virally encoded enzyme and is therefore nontoxic to uninfected cells. Ganciclovir is a nucleoside analog of acyclovir with 10–100-fold increased activity against cytomegalovirus (CMV). Intravitreal ganciclovir can be used safely at 2–5 mg even as often as every week, and low-volume weekly ganciclovir (1.0 mg/0.02 ml) after an induction treatment may be an alternative to sustained-release implants in the treatment of CMV retinitis [26]. Foscarnet is effective against herpes simplex virus, varicella zoster virus, and CMV. Intravitreal foscarnet can be given intravitreally at a dose of 2.4 mg without causing toxicity (Table IV.E-1). Cidofovir is a nucleoside analog that has a longer duration of action due to prolonged clearance compared to ganciclovir or foscarnet. However, it causes a high rate of uveitis (26 %) and hypotony, although these complications can be prevented by prophylactically treating with probenecid and topical steroid [27, 28].

4. Steroids

Triamcinolone acetonide (TA) was first used as an intravitreal injection by Machemer in the attempt to prevent

proliferative vitreoretinopathy after retinal detachment repair [29]. It now has a variety of uses including the treatment of macular edema resulting from uveitis, diabetes, and retinal vein occlusion, as well as in pseudophakic cystoid macular edema (CME), radiation maculopathy, and CME related to retinitis pigmentosa (Table IV.E-2). In the treatment of macular edema following central retinal vein occlusion, patients treated with intravitreal triamcinolone acetonide (IVTA, 1 and 4 mg) were five times more likely to have a gain in visual acuity letter score of 15 or more letters at 1 year in comparison to observation alone [30, 31]. However, patients treated with 4 mg IVTA had higher rates of elevated IOP and cataract [30, 31]. Several studies have also shown that IVTA at doses of 2–4 mg is effective in the treatment of uveitic CME, but the effects of a single injection are temporary, lasting 3–7 months with a dose of 4 mg [32].

5. Anti-inflammatory/ Antineoplastic Agents

A prospective interventional case series reported on the use of intravitreal methotrexate in the treatment of uveitis and uveitic CME [33]. They found that 400 µg in 0.1 mL of methotrexate improved visual acuity over a 6-month follow-up period in 10 of 15 intermediate uveitis, panuveitis, or uveitic CME patients. No significant toxic effects were reported [33]. Intravitreal methotrexate has also been used for the treatment of vitreoretinal involvement in primary CNS lymphoma [34–36]. Complications in one series included cataract (73 %), corneal epitheliopathy (58 %), maculopathy (42 %), vitreous hemorrhage (8 %), optic atrophy (4 %), and sterile endophthalmitis (4 %) [37].

Table IV.E-2 Dosage and half-life of anti-inflammatory and anti-VEGF agents given intravitreally

Agent	Intravitreal dose	Half-life in vitreous	Clinical application
Anti-inflammatory			
Triamcinolone Acetonide	1–25 mg	For 4 mg dose: 18.6 days, non-vitreotomized 3.2 days, vitreotomized	Macular edema from uveitis, diabetes, vein occlusion, radiation, retinitis pigmentosa, pseudophakic CME
Methotrexate	400 µg	48 h	Uveitis, uveitic CME, intraocular lymphoma
Infliximab	1–2 mg	6.5 days	Neovascular AMD
Rituximab	1 mg	4.7 days	Intraocular lymphoma
Sirolimus	352 µg	NA	Noninfectious uveitis
Anti-VEGF			
Bevacizumab	1.25 mg	4.3 days	Neovascular AMD; macular edema in uveitis, diabetes, vein occlusion
Ranibizumab	0.5 mg	2.8 days	Same as above
Aflibercept	0.05–4 mg	4–5 days	Same as above
Pharmacologic Vitreolysis			
Ocriplasmin	125 µg	NA	Vitreomacular adhesion ± macular hole

CME cystoid macular edema, *AMD* age-related macular degeneration, *NA* not available [see chapter VI.E-1. Pharmacologic Vitreolysis with Ocriplasmin: Basic Science Studies]

Infliximab is a monoclonal antibody against tumor necrosis factor (TNF)-alpha used as a systemic treatment for rheumatologic conditions and the treatment of noninfectious ocular inflammatory disease. It has been applied at 1–2 mg doses intravitreally in the treatment of AMD [38–41]. After establishing a range of safe doses in an animal model, Theodossiadis et al. reported on three patients who received infliximab after failing to respond to intravitreal ranibizumab. All three patients had a reduction in central foveal thickness by optical coherence tomography as well as improvement in visual acuity [40]. Farvardin and colleagues described a decrease in mean central macular thickness and improvement in mean logMAR visual acuity after a single intravitreal injection of infliximab 1.5 mg/0.15 mL in ten eyes of seven patients who had refractory noninfectious uveitis, but the effects were temporary [42, 43]. Complications such as panuveitis and vitreous opacification after infliximab injection remain important concerns [42].

Adalimumab is a humanized antibody against the soluble and membrane-bound tumor necrosis factor (TNF), which has been studied for intravitreal injection in patients with uveitic CME but did not show improvement in vision or improvement in central macular thickness [44]. Rituximab, a humanized murine monoclonal antibody against the CD20 B-lymphocyte antigen used for the treatment of B cell lymphoma, is thought to be able to penetrate retinal tissue and has been studied for the treatment of intraocular lymphoma [45–47]. Santen Pharmaceutical is studying the efficacy and safety of intravitreally injected sirolimus, a T cell inhibitor that targets the intracellular protein mTOR (mammalian target of rapamycin), in a phase 3 study for the treatment of noninfectious posterior segment-involved uveitis (Table IV.E-2).

6. Anti-VEGF Agents

The anti-VEGF agents used for the treatment of neovascular AMD have revolutionized the use of intravitreal injections for posterior segment disease. Their use has since expanded to the treatment of macular edema due to diabetes, retinal vein occlusion, and uveitis. Ranibizumab is an Fab antibody fragment that binds to all isoforms of VEGF. Two large prospective, randomized controlled trials demonstrated the efficacy of ranibizumab in treating neovascular AMD compared to sham injections (MARINA), and when compared to PDT (ANCHOR), showing improvement in visual acuity in the anti-VEGF-treated patients [48, 49]. Bevacizumab (Avastin) is a full-length antibody against VEGF approved for systemic administration in the treatment of metastatic colorectal cancer. It has been used as an intravitreal injection for off-label treatment of neovascular AMD as well as for treatment of macular edema from retinal vein occlusion, diabetes, and uveitis. Two large trials, CATT and IVAN, have demonstrated lack of inferiority compared to ranibizumab at 24 and 12 months, respectively [50, 51]. The HORIZON study showed that long-term ranibizumab is well tolerated [52]. There have been concerns about higher rates of acute intraocular inflammation and outbreaks of infectious endophthalmitis for bevacizumab due to contamination during compounding into aliquots for intravitreal use [53, 54]. As mentioned in the complications section, several studies have also suggested a trend toward higher total systemic adverse events with bevacizumab compared to ranibizumab [16]. The use of ranibizumab has been expanded to the treatment of CME associated with retinal vein occlusions with improvements in visual acuity at 1 year in the BRAVO and CRUISE trials [55, 56]. Whether or not long-term repeated anti-VEGF

injections are required in vein occlusion patients with CME is a topic that requires further study.

Aflibercept is a chimeric fusion protein composed of an Fc fragment linked to the extracellular portions of VEGF receptors 1 and 2 that binds to all forms of VEGF as well as placental growth factor. The VIEW 1 and VIEW 2 studies demonstrated equivalency with monthly ranibizumab in maintaining vision at 1 year [57]. Additionally, the dosing regimen of 2 mg of aflibercept can be extended to every 2 months after the initial 3 monthly injections, decreasing the interval of monitoring and follow-up appointments. Ocular and systemic adverse events were similar between aflibercept and ranibizumab [57]. While aflibercept is FDA approved for use in AMD and CME related to CRVO, it is currently under active investigation for the treatment of diabetic macular edema (www.clinicaltrials.gov).

7. Pharmacologic Vitreolysis

Pharmacologic vitreolysis is a new treatment paradigm that can potentially replace vitreoretinal surgery for specific indications with pharmacotherapy [58, 59]. While several agents are under development [see references], the first to receive FDA and European approval is ocriplasmin (Jetrea®), a recombinant nonspecific protease [see chapter VI.E-1. Pharmacologic Vitreolysis with Ocriplasmin: Basic Science Studies and VI.E-2. Pharmacologic Vitreolysis with Ocriplasmin: Clinical Studies]. A single dose of 125 µg has been shown in phase III clinical trials to release vitreomacular adhesion and allowed for the nonsurgical closure of macular holes in 40.6 % vs. 10.6 % of placebo-injected eyes [60]. Additionally, there was improvement in best-corrected visual acuity of three or more lines in the ocriplasmin (12.3 %) group compared to placebo (6.4 %), $p=0.02$ [60]. Side effects were more common in the ocriplasmin group (68.4 % vs. 53.3 %, $p<0.001$) and most commonly included vitreous floaters, photopsia, eye pain, and subconjunctival hemorrhage [60]. Because of the pathological changes in the vitreoretinal interface found in diabetic retinopathy, this may be a condition that can be treated by pharmacologic vitreolysis, though further studies are warranted to determine whether this approach will be helpful [see chapters I.E. Diabetic vitreopathy; VI.A. Pharmacologic vitreolysis].

One limitation in the pharmacotherapeutic approach to vitreomacular disease is the lack of reproducible drug delivery to the site of interest, in this case the vitreomacular interface [see chapters II.E. Vitreo-retinal interface and inner limiting membrane; III.D. Vitreo-macular traction and holes (pseudo, lamellar and full thickness macular holes)]. Future developments should include improved drug delivery systems for pharmacologic vitreolysis. It is also plausible that combination therapy with more than one pharmacologic vitreolysis agent will yield better results [61].

B. Sustained-Release Drug Delivery

1. Implants

A shift from repeated intravitreal injections to sustained-release intraocular delivery devices in both implantable and injectable versions has recently occurred. These delivery devices can be classified into biodegradable and nonbiodegradable implants. The fluocinolone acetonide-releasing device or *Retisert* (Bausch & Lomb, Rochester, New York, USA), a nonbiodegradable steroid implant, has been FDA approved for the treatment of chronic, noninfectious posterior uveitis. It releases fluocinolone acetonide for approximately 30 months and is implanted through the pars plana through a scleral incision and secured using 8-0 Prolene suture (Figure IV.E-3a, d). In a 3-year clinical trial studying its efficacy in uveitis, Retisert was found by Callanan et al. to significantly reduce recurrences (from 62 to 4 %), and implanted eyes had improved visual acuity compared to non-implanted eyes ($p<0.01$) [62]. The MUST trial reported that after 24 months there was no statistical difference in visual acuity between systemic immunosuppression and the fluocinolone implant; it was successful in controlling 88 % of noninfectious uveitis [63]. Additionally, there was a higher rate of systemic complications with immunosuppression. On the other hand, ocular complications with the fluocinolone implant such as cataract (88–93 %) and glaucoma requiring surgery (21–40 %) [63, 64] limit its universal use and argue for combined cataract or glaucoma surgery in high-risk individuals [65]. Other reported side effects include hypotony, retinal detachment, endophthalmitis, and scleral thinning [62, 63].

Other sustained-release steroid-releasing implants that can be given through intravitreal injection in the clinic include a biodegradable dexamethasone implant (*Ozurdex*®, Allergan) (Figure IV.E-3c) and a nonbiodegradable fluocinolone acetonide insert (*Iluvien*®, Alimera Sciences) (Table IV.E-3). The advantage of biodegradable implants includes implantation without the need for extraction once drug elution terminates. However, biodegradable implants often have nonideal release kinetics and can have an uncontrolled burst of drug release at the end of their lifespan [1]. Nonbiodegradable implants, on the other hand, may require explantation once finished, but typically are longer lasting, and have closer to ideal drug-release kinetics (e.g., zero-order kinetics with Retisert, Figure IV.E-1). Ozurdex and Iluvien both have applicator systems that allow for outpatient placement through self-sealing, small gauge wounds (Figure IV.E-2, schematic). A phase III study that compared two doses (0.7 and 0.35 mg) of dexamethasone to sham treatment showed that both doses were effective in controlling inflammation and improving vision. However, the stronger dose had a longer duration of action and is now commercially available as Ozurdex. [66] While the incidences of

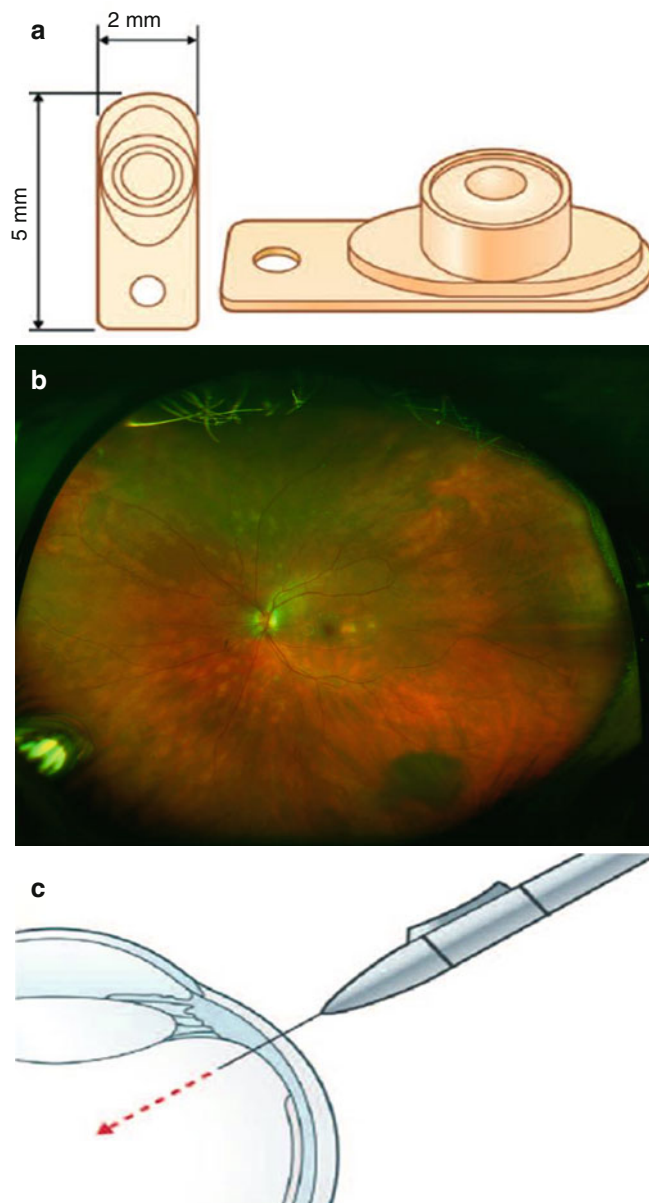


Figure IV.E-3 (a) Retisert® (Bausch & Lomb), fluocinolone acetonide, nonbiodegradable; (b) Retisert implanted into pars plana in patient with Birdshot chorioretinopathy; (c) Posurdex® (Allergan), now known as Ozurdex, dexamethasone ([93, 94])

cataract (26 %) and increased intraocular pressure were low, the effect of long-term use is unclear [66].

Iluvien is an injectable nonbiodegradable intravitreal insert that delivers sustained-release fluocinolone acetonide for 24–36 months at near zero-order kinetics. It is a 3.5 mm × 0.37 mm device that can be inserted in the office via a 25-gauge needle. The FAME study examined two doses of fluocinolone acetonide (0.5 µg/day vs. 0.2 µg/day) in patients with persistent diabetic macular edema despite one macular laser treatment. There was improvement in visual acuity by 1 month in comparison to controls, and this effect persisted through 36 months with 28.7 % (low dose) and 27.8 % (high-dose group) of patients maintaining an improvement of best-spectacle-corrected visual acuity of 15 letters or more in the two treatment groups [67, 68]. However, almost all patients required cataract surgery. Incisional glaucoma surgery was necessary more frequently in the high-dose group (8.1 % vs. 4.8 %) [67]. The *Iluvien* insert has been approved for use in diabetic macular edema in Europe. A fluocinolone acetonide insert (*pSivida*), similar to the *Iluvien*, lasts for up to 3 years after a single intravitreal injection and is currently undergoing phase I clinical trials for the treatment of noninfectious uveitis (www.clinicaltrials.gov).

The *Vitrasert*® implant is a polymeric (polyvinyl acetate) nonbiodegradable implant that releases 1 µg/h of ganciclovir with a duration of 8 months (Table IV.E-3). It was introduced in the 1990s to treat CMV retinitis in AIDS patients, but also has activity against herpes simplex virus. Studies have shown that the mean time to progression of CMV retinitis was 205 days with the ganciclovir implant which is approximately three times longer than with intravenous ganciclovir [69, 70]. The *Vitrasert* is no longer being produced and is not available for clinical use.

2. Encapsulated Cell Technology

Encapsulated cell technology is a method by which viable human cell lines that secrete a therapeutic protein are sequestered in a porous implant that allows for diffusion of the molecule out toward target tissues, while allowing for inward diffusion of oxygen and nutrients to maintain the health of live cells within the implant. This technology is being investigated for the treatment of retinitis pigmentosa and geographic atrophy (GA) in age-related macular degeneration.

Table IV.E-3 Intravitreal implants

Delivery system	Intravitreal dose released	Duration of action	Clinical application
<i>Implants or inserts</i>			
Retisert® (fluocinolone acetonide)	0.5 µg/day	30 months	Chronic noninfectious posterior segment uveitis
Iluvien® (fluocinolone acetonide)	0.2 or 0.5 µg/day	1.5 or 3 years	Same as above and CME due to RVO, uveitis, diabetes
Ozurdex® (dexamethasone; biodegradable)	350 or 700 µg	6 months	Same as above
^a Vitrasert®(ganciclovir)	1 µg/h	8 months	CMV, HSV, VZV

RVO retinal vein occlusion

^aNo longer available

The NT-501 Neurotech implant consists of a semipermeable outer membrane with 15 nm pores that allows for growth factors and oxygen to reach viable human retinal pigment epithelial cells that have been engineered to secrete ciliary neurotrophic factor (CNTF). This RPE cell line is maintained on a polyethylene terephthalate yarn scaffold inside the implant. The NT-501 implant is placed into the eye through a 2 mm incision through the pars plana. CNTF is a cytokine that binds to receptors found on Muller glial cells, rods, and cone photoreceptors [71]. It has been demonstrated to retard photoreceptor degeneration in animal models of retinitis pigmentosa [72]. Phase II data for the use of the CNTF implant for GA suggest dose-dependent changes in retinal thickness that is followed by visual stabilization in the high-dose group (96.3 %) and low-dose group (83.3 %) compared to the sham group (75 %) [73]. For retinitis pigmentosa, phase I study results have been published reporting three of seven implanted eyes that could be tracked by conventional reading charts with an improvement in acuity of 10–15 letters [74]. There were no serious complications in the ten eyes that were implanted. Neurotech has also developed encapsulated cell technology which has been designed with a cell line engineered to release a VEGF receptor Fc-fusion protein. This construct is 20-fold more efficient in neutralizing VEGF than ranibizumab, releases the fusion protein for up to 1 year in the rabbit vitreous, and is undergoing a phase 1 clinical trial for neovascular AMD outside of the United States (www.clinicaltrials.gov).

3. Microspheres

The concept of microspheres is to use biodegradable polymers such as polylactide and poly lactic-co-glycolic acid (PLGA) to suspend drugs into microparticles (1–1,000 μm) or nanoparticles (1–1,000 nm) resulting in controlled release of drugs [1]. They provide sustained drug release for weeks to months. Their advantage is that drug is released in a controlled fashion, minimizing the “burst” effect that biodegradable implants have at the end of their lifespan. Microspheres are injected into the vitreous cavity, and thus, the disadvantages are synonymous with the complication rates associated with any other intravitreal injection although drugs delivered in this method would need to be injected much less frequently. An additional complication is that nanoparticles may cause temporary clouding of the ocular media, although microspheres larger than 2 μm circumvent this problem because they sink to the bottom of the vitreous cavity due to gravity. However, head and body movement may cause upward displacement of the microspheres, blurring vision. This technology has been used to incorporate the pegylated anti-VEGF peptide, pegaptanib, into a vehicle that, when applied using a transscleral technique, released drug for up to 20 days, resulting in inhibition of VEGF-induced cell proliferation of human umbilical vein endothelial cells [75].

Cardillo et al. demonstrated in their case series that a microsphere preparation of triamcinolone acetonide was effective in reducing foveal thickness and improving visual acuity in patients with diabetic macular edema when compared to the conventional preparation of triamcinolone [76]. Microspheres may have a shorter half-life in eyes that have undergone vitrectomy.

4. Porous Silicon Particles

Micro-particulate photonic crystals made from porous silicon particles are now being studied as an intraocular sustained-release drug delivery system. The drug is chemically attached to the inner pores of the microparticle and released as the matrix dissolves. A recent *in vivo* study of covalently loaded daunorubicin, an antiproliferation medication with a short vitreous half-life formulated in oxidized porous silicon for the treatment of proliferative vitreoretinopathy, appears to be promising, with no toxicity at 6 months [77]. The microparticles were, on average, $30 \times 46 \times 15 \mu\text{m}$ with a pore size of 15 nm and a reddish color that decreased as the matrix degraded and daunorubicin was released [77]. Long-term and human studies are still required to establish efficacy and safety.

5. Liposomes

Liposomes are lipid vesicles made of phospholipids 25–10,000 nm in diameter that can be used to encapsulate both hydrophilic (in the core) and lipophilic (between the bilayer) drugs. They undergo phagocytosis by retinal pigment epithelial cells, thus allowing for targeted intracellular drug delivery. This technology has been utilized to create less toxic formulations of amphotericin B and gentamicin in animal models, although their utility in human intraocular disease is limited [78, 79]. Liposomes designed to release vasoactive intestinal peptide appear to have an anti-inflammatory effect in rats with endotoxin-induced uveitis [80]. Bevacizumab encapsulated into liposomes achieved higher concentrations in the rabbit vitreous at 28 and 42 days compared to soluble bevacizumab, although toxicity studies have not yet been conducted [81].

6. Suprachoroidal Microinjection and Microneedles

Microcannulation of drug delivery devices into the suprachoroidal space is a promising new technique that can potentially directly deliver drug to the macula, optic nerve, and posterior pole [82]. Advantages of this technique include higher drug levels to target tissues and decreased unintended exposure to nontarget tissues, which could decrease the incidence of cataract and increased IOP. One study used microneedles to inject the suprachoroidal space of rabbit eyes with fluorescently tagged dextrans and particles from 20 nm to 10 μm in size [83]. Patel et al. found that smaller molecules were cleared in hours, whereas suspensions of

nano- and microparticles remained in the suprachoroidal space for months [83]. Further research is required to improve access to the suprachoroidal space and study this system in human eyes. Phase 2 clinical trials for a microneedle device used to inject triamcinolone acetonide into the suprachoroidal space for the treatment of noninfectious uveitis affecting the posterior segment are underway.

V. Future Drug Delivery Approaches and Considerations

A. Iontophoresis

Iontophoresis is a nonsurgical technique that utilizes an applicator to deliver a weak electrical current to the sclera to drive ionically charged drug molecules across the sclera into the choroid, retina, and vitreous [84, 85]. This technique shows future promise for the delivery of sustained-release formulations with the ability to modulate dosage by altering the strength of current utilized. One study showed successful delivery of triamcinolone acetonide and ranibizumab through full-thickness rabbit ocular tissue [86]. Phase 2 clinical studies investigating the use of iontophoresis of dexamethasone phosphate for the treatment of anterior uveitis have been completed, and studies for this modality in the treatment of noninfectious non-necrotizing anterior scleritis are underway.

B. Refillable Delivery Systems

Refillable port-delivery systems (PDS, ForSight VISION4, Inc.) implemented by Genentech for delivery of ranibizumab may decrease the need for repeated intravitreal injections for wet AMD. The PDS is implanted surgically into the pars plana without scleral sutures and loaded with ranibizumab. Phase 1 data presented at the 2012 AAO meeting showed proof of concept for sustained release of ranibizumab with the PDS. At 12 months, most patients achieved significant gains in visual acuity from baseline, and 50 % gained 3 lines or more. Examination of devices explanted per protocol at 12 months, and observation of devices that remained in patients at month 36, indicated ongoing integrity and tolerability of the device. Alternatively, the microelectromechanical systems (MEMS) delivery device is a subconjunctival reservoir that forces drug through a cannula inserted into the anterior or posterior segment.

C. Advances in Sustained-Release Intravitreal Injectables

Tethadur (pSivida) is a nanostructured porous silicon microparticle that can be designed to release various peptides,

chemical molecules, therapeutic antibodies, and proteins in a sustained fashion. De Kozak et al. have used cyanoacrylate nanoparticles coated with polyethylene glycol to release tamoxifen to reduce inflammation in a rat model of uveitis [87]. The *Verisome* system (Icon Bioscience, Sunnyvale, CA) is an intravitreally injected liquid or viscous gel that is biodegradable and can be formulated to release small molecules, peptides, proteins, and monoclonal antibodies [87]. When injected via a 30-gauge needle into the vitreous cavity, it forms a spherule that can be assessed visually to monitor duration of action. A Verisome spherule designed to release a combination of triamcinolone and ranibizumab is being studied in phase 2 clinical trials for the treatment of neovascular AMD. It is expected to release drug for up to 1 year (www.clinicaltrials.gov). The *Cortiject* emulsion (NOVAA63035, Novagali, Pharma) is given as an intravitreal injection that provides sustained release of corticosteroid for 6–9 months. This is being tested in phase 1 studies for the treatment of diabetic macular edema, but has not yet been tested in uveitis.

D. Emerging Methods for Local Delivery

Small interfering RNA (siRNA) and microRNA technology can be designed to inhibit the expression of inflammatory cytokines. A phase 2 study of siRNA technology to treat AMD was terminated due to a company decision perhaps related to lower efficacy than ranibizumab. Other strategies such as designing viral vectors to sustain expression of antibodies that block inflammatory cytokines have yet to be fully developed but may represent an alternative sustained delivery method. Additionally, nonviral gene transfer techniques can be devised to deliver therapeutics to the eye. Behar-Cohen and colleagues have developed a recombinant protein ocular delivery system that utilizes an electrical current to transfer a plasmid encoding a soluble chimeric TNF α receptor directly to the ciliary muscle. This has achieved sustained local protein production for up to 3 months after introduction and appears to inhibit rat endotoxin-induced uveitis [88].

E. Vitreous Structure and Intravitreal Drug Delivery

It is important that all intravitreal drug delivery approaches take into consideration that vitreous is not a space or cavity, but a living tissue. Thus, except in the case of eyes that have undergone vitrectomy, all calculations of the pharmacokinetics of intravitreal drug therapy must be based on a more realistic approach than just assuming first-order kinetics. This consideration is further complicated by the fact that the molecular composition of vitreous changes with age [see chapters I.A. Vitreous proteins; I.F. Vitreous biochemistry

and artificial vitreous; II.C. Vitreous aging and PVD], refractive state [see chapter II.B. Myopic vitreopathy], and systemic disease such as diabetes [see chapter I.E. Diabetic vitreopathy]. Drug distribution following intravitreal administration *cannot* be the same in all of these circumstances, and there are many more such settings that are currently not receiving enough consideration. Furthermore, the particular site of injection will influence pharmacokinetics because vitreous structure is quite heterogeneous within the vitreous body, except in very young children. The heterogeneity of vitreous structure increases with age [89, 90] and different disease states, especially diabetes [91, 92]. That an injection into different locations within the vitreous body can have very different pharmacokinetics is considered elsewhere in this text [see chapter VI.A. Pharmacologic vitreolysis].

Abbreviations

AMD	Age-related macular degeneration
CME	Cystoid macular edema
CMV	Cytomegalovirus
CNS	Central nervous system
CNTF	Ciliary neurotrophic factor
CRVO	Central retinal vein occlusion
FDA	Food and Drug Administration
GA	Geographic atrophy
IOP	Intraocular pressure
IVTA	Intravitreal triamcinolone
PDS	Port-delivery system
PDT	Photodynamic therapy
PLGA	Poly lactic-co-glycolic acid
RPE	Retinal pigment epithelium
TA	Triamcinolone
TNF	Tumor necrosis factor
VEGF	Vascular endothelial growth factor

References

- Del Amo EM, Urtti A. Current and future ophthalmic drug delivery systems. A shift to the posterior segment. *Drug Discov Today*. 2008;13(3-4):135-43.
- Gaudana R, Jwala J, Boddu SH, Mitra AK. Recent perspectives in ocular drug delivery. *Pharm Res*. 2009;26(5):1197-216.
- Maurice D. Review: practical issues in intravitreal drug delivery. *J Ocul Pharmacol Ther*. 2001;17(4):393-401.
- Bakri SJ, Snyder MR, Reid JM, et al. Pharmacokinetics of intravitreal ranibizumab (Lucentis). *Ophthalmology*. 2007;114(12):2179-82.
- Bakri SJ, Snyder MR, Reid JM, et al. Pharmacokinetics of intravitreal bevacizumab (Avastin). *Ophthalmology*. 2007;114(5):855-9.
- Beer PM, Bakri SJ, Singh RJ, et al. Intraocular concentration and pharmacokinetics of triamcinolone acetonide after a single intravitreal injection. *Ophthalmology*. 2003;110(4):681-6.
- Jaffe GJ, Yang CH, Guo H, et al. Safety and pharmacokinetics of an intraocular fluocinolone acetonide sustained delivery device. *Invest Ophthalmol Vis Sci*. 2000;41(11):3569-75.
- Aiello AL, Tran VT, Rao NA. Postnatal development of the ciliary body and pars plana. A morphometric study in childhood. *Arch Ophthalmol*. 1992;110(6):802-5.
- Bhavsar AR, Googe Jr JM, Stockdale CR, et al. Risk of endophthalmitis after intravitreal drug injection when topical antibiotics are not required: the diabetic retinopathy clinical research network laser-ranibizumab-triamcinolone clinical trials. *Arch Ophthalmol*. 2009;127(12):1581-3.
- Sato T, Emi K, Ikeda T, et al. Severe intraocular inflammation after intravitreal injection of bevacizumab. *Ophthalmology*. 2010;117(3):512-6, 6 e1-2.
- Day S, Acquah K, Mruthyunjaya P, et al. Ocular complications after anti-vascular endothelial growth factor therapy in Medicare patients with age-related macular degeneration. *Am J Ophthalmol*. 2011;152(2):266-72.
- Abedi G, Adelman RA, Salim S. Incidence and management of elevated intraocular pressure with antivascular endothelial growth factor agents. *Semin Ophthalmol*. 2013;28(3):126-30.
- Adelman RA, Zheng Q, Mayer HR. Persistent ocular hypertension following intravitreal bevacizumab and ranibizumab injections. *J Ocul Pharmacol Ther*. 2010;26(1):105-10.
- Good TJ, Kimura AE, Mandava N, Kahook MY. Sustained elevation of intraocular pressure after intravitreal injections of anti-VEGF agents. *Br J Ophthalmol*. 2011;95(8):1111-4.
- Tseng JJ, Vance SK, Della Torre KE, et al. Sustained increased intraocular pressure related to intravitreal antivascular endothelial growth factor therapy for neovascular age-related macular degeneration. *J Glaucoma*. 2012;21(4):241-7.
- Martin DF, Maguire MG, Fine SL, et al. Ranibizumab and bevacizumab for treatment of neovascular age-related macular degeneration: two-year results. *Ophthalmology*. 2012;119(7):1388-98.
- Schmucker C, Ehlken C, Agostini HT, et al. A safety review and meta-analysis of bevacizumab and ranibizumab: off-label versus goldstandard. *PLoS One*. 2012;7(8):e42701.
- Hegazy HM, Kivilcim M, Peyman GA, et al. Evaluation of toxicity of intravitreal ceftazidime, vancomycin, and ganciclovir in a silicone oil-filled eye. *Retina*. 1999;19(6):553-7.
- Ferrer C, Rodriguez A, Abad JL, et al. Bactericidal effect of intravitreal levofloxacin in an experimental model of endophthalmitis. *Br J Ophthalmol*. 2008;92(5):678-82.
- Gupta A, Srinivasan R, Kaliaperumal S, Saha I. Post-traumatic fungal endophthalmitis—a prospective study. *Eye*. 2008;22(1):13-7.
- Koc A, Onal S, Yenice O, Kazokoglu H. Pars Plana Vitrectomy and Intravitreal Liposomal Amphotericin B in the Treatment of Candida Endophthalmitis. *Ophthalmic Surg Lasers Imaging*. 2010;1-3.
- Sen P, Gopal L, Sen PR. Intravitreal voriconazole for drug-resistant fungal endophthalmitis: case series. *Retina*. 2006;26(8):935-9.
- Goldblum D, Fausch K, Frueh BE, et al. Ocular penetration of caspofungin in a rabbit uveitis model. *Graefes Arch Clin Exp Ophthalmol*. 2007;245(6):825-33.
- Kusbeci T, Avci B, Cetinkaya Z, et al. The effects of caspofungin and voriconazole in experimental Candida endophthalmitis. *Curr Eye Res*. 2007;32(1):57-64.
- J R, Comer GM, Kauffman CA. Treatment of endogenous fungal endophthalmitis: focus on new antifungal agents. *Clin Infect Dis*. 2011;52(5):648-53.
- Teoh SC, Ou X, Lim TH. Intravitreal ganciclovir maintenance injection for cytomegalovirus retinitis: efficacy of a low-volume, intermediate-dose regimen. *Ophthalmology*. 2012;119(3):588-95.
- Chavez-de la Paz E, Arevalo JF, Kirsch LS, et al. Anterior non-granulomatous uveitis after intravitreal HPMPC (cidofovir) for the treatment of cytomegalovirus retinitis. Analysis and prevention. *Ophthalmology*. 1997;104(3):539-44.
- Rahhal FM, Arevalo JF, Munguia D, et al. Intravitreal cidofovir for the maintenance treatment of cytomegalovirus retinitis. *Ophthalmology*. 1996;103(7):1078-83.

29. Machemer R, Sugita G, Tano Y. Treatment of intraocular proliferations with intravitreal steroids. *Trans Am Ophthalmol Soc.* 1979;77:171–80.
30. Ip MS, Scott IU, VanVeldhuisen PC, et al. A randomized trial comparing the efficacy and safety of intravitreal triamcinolone with observation to treat vision loss associated with macular edema secondary to central retinal vein occlusion: the Standard Care vs Corticosteroid for Retinal Vein Occlusion (SCORE) study report 5. *Arch Ophthalmol.* 2009;127(9):1101–14.
31. Scott IU, Ip MS, VanVeldhuisen PC, et al. A randomized trial comparing the efficacy and safety of intravitreal triamcinolone with standard care to treat vision loss associated with macular edema secondary to branch retinal vein occlusion: the Standard Care vs Corticosteroid for Retinal Vein Occlusion (SCORE) study report 6. *Arch Ophthalmol.* 2009;127(9):1115–28.
32. Couch SM, Bakri SJ. Intravitreal triamcinolone for intraocular inflammation and associated macular edema. *Clin Ophthalmol.* 2009;3:41–7.
33. Taylor SR, Habet-Wilner Z, Pacheco P, Lightman SL. Intraocular methotrexate in the treatment of uveitis and uveitic cystoid macular edema. *Ophthalmology.* 2009;116(4):797–801.
34. Frenkel S, Hendler K, Siegal T, et al. Intravitreal methotrexate for treating vitreoretinal lymphoma: 10 years of experience. *Br J Ophthalmol.* 2008;92(3):383–8.
35. Hardwig PW, Pulido JS, Erie JC, et al. Intraocular methotrexate in ocular diseases other than primary central nervous system lymphoma. *Am J Ophthalmol.* 2006;142(5):883–5.
36. Velez G, Yuan P, Sung C, et al. Pharmacokinetics and toxicity of intravitreal chemotherapy for primary intraocular lymphoma. *Arch Ophthalmol.* 2001;119(10):1518–24.
37. Smith JR, Rosenbaum JT, Wilson DJ, et al. Role of intravitreal methotrexate in the management of primary central nervous system lymphoma with ocular involvement. *Ophthalmology.* 2002;109(9):1709–16.
38. Giansanti F, Ramazzotti M, Giuntoli M, et al. Intravitreal infliximab clearance in a rabbit model: different sampling methods and assay techniques. *Invest Ophthalmol Vis Sci.* 2009;50(11):5328–35.
39. Regatieri CV, Dreyfuss JL, Melo GB, et al. Dual role of intravitreal infliximab in experimental choroidal neovascularization. Effect on the expression of sulfated glycosaminoglycans. *Invest Ophthalmol Vis Sci.* 2009;50(11):5487–94.
40. Theodossiadis PG, Liarakos VS, Sfikakis PP, et al. Intravitreal administration of the anti-TNF monoclonal antibody infliximab in the rabbit. *Graefes Arch Clin Exp Ophthalmol.* 2009;247(2):273–81.
41. Theodossiadis PG, Liarakos VS, Sfikakis PP, et al. Intravitreal administration of the anti-tumor necrosis factor agent infliximab for neovascular age-related macular degeneration. *Am J Ophthalmol.* 2009;147(5):825–30, 30 e1.
42. Farvardin M, Afarid M, Mehryar M, Hosseini H. Intravitreal infliximab for the treatment of sight-threatening chronic noninfectious uveitis. *Retina.* 2010;30(9):1530–5.
43. Farvardin M, Afarid M, Shahrzad S. Long-term effects of intravitreal infliximab for treatment of sight-threatening chronic noninfectious uveitis. *J Ocul Pharmacol Ther.* 2012;28(6):628–31.
44. Androudi S, Tsironi E, Kalogeropoulos C, et al. Intravitreal adalimumab for refractory uveitis-related macular edema. *Ophthalmology.* 2010;117(8):1612–6.
45. Itty S, Pulido JS. Rituximab for intraocular lymphoma. *Retina.* 2009;29(2):129–32.
46. Kim H, Csaky KG, Chan CC, et al. The pharmacokinetics of rituximab following an intravitreal injection. *Exp Eye Res.* 2006;82(5):760–6.
47. Kitzmann AS, Pulido JS, Mohny BG, et al. Intraocular use of rituximab. *Eye.* 2007;21(12):1524–7.
48. Brown DM, Kaiser PK, Michels M, et al. Ranibizumab versus verteporfin for neovascular age-related macular degeneration. *N Engl J Med.* 2006;355(14):1432–44.
49. Rosenfeld PJ, Brown DM, Heier JS, et al. Ranibizumab for neovascular age-related macular degeneration. *N Engl J Med.* 2006;355(14):1419–31.
50. Chakravarthy U, Harding SP, Rogers CA, et al. Ranibizumab versus bevacizumab to treat neovascular age-related macular degeneration: one-year findings from the IVAN randomized trial. *Ophthalmology.* 2012;119(7):1399–411.
51. Martin DF, Maguire MG, Ying GS, et al. Ranibizumab and bevacizumab for neovascular age-related macular degeneration. *N Engl J Med.* 2011;364(20):1897–908.
52. Singer MA, Awh CC, Sadda S, et al. HORIZON: an open-label extension trial of ranibizumab for choroidal neovascularization secondary to age-related macular degeneration. *Ophthalmology.* 2012;119(6):1175–83.
53. Shah CP, Garg SJ, Vander JF, et al. Outcomes and risk factors associated with endophthalmitis after intravitreal injection of anti-vascular endothelial growth factor agents. *Ophthalmology.* 2011;118(10):2028–34.
54. Wickremasinghe SS, Michalova K, Gilhotra J, et al. Acute intraocular inflammation after intravitreal injections of bevacizumab for treatment of neovascular age-related macular degeneration. *Ophthalmology.* 2008;115(11):1911–5.
55. Brown DM, Campochiaro PA, Bhisitkul RB, et al. Sustained benefits from ranibizumab for macular edema following branch retinal vein occlusion: 12-month outcomes of a phase III study. *Ophthalmology.* 2011;118(8):1594–602.
56. Campochiaro PA, Brown DM, Awh CC, et al. Sustained benefits from ranibizumab for macular edema following central retinal vein occlusion: twelve-month outcomes of a phase III study. *Ophthalmology.* 2011;118(10):2041–9.
57. Heier JS, Brown DM, Chong V, et al. Intravitreal aflibercept (VEGF trap-eye) in wet age-related macular degeneration. *Ophthalmology.* 2012;119(12):2537–48.
58. Sebag J. Pharmacologic vitreolysis. *Retina.* 1998;18(1):1–3.
59. Sebag J. Pharmacologic vitreolysis—premise and promise of the first decade. *Retina.* 2009;29(7):871–4.
60. Stalmans P, Benz MS, Gandorfer A, et al. Enzymatic vitreolysis with ocriplasmin for vitreomacular traction and macular holes. *N Engl J Med.* 2012;367(7):606–15.
61. Sebag J. Is pharmacologic vitreolysis brewing? *Retina.* 2002;22(1):1–3.
62. Callanan DG, Jaffe GJ, Martin DF, et al. Treatment of posterior uveitis with a fluocinolone acetonide implant: three-year clinical trial results. *Arch Ophthalmol.* 2008;126(9):1191–201.
63. Kempen JH, Altaweel MM, Holbrook JT, et al. Randomized comparison of systemic anti-inflammatory therapy versus fluocinolone acetonide implant for intermediate, posterior, and panuveitis: the multicenter uveitis steroid treatment trial. *Ophthalmology.* 2011;118(10):1916–26.
64. Pavesio C, Zierhut M, Bairi K, et al. Evaluation of an intravitreal fluocinolone acetonide implant versus standard systemic therapy in noninfectious posterior uveitis. *Ophthalmology.* 2010;117(3):567–75, 75 e1.
65. Malone PE, Herndon LW, Muir KW, Jaffe GJ. Combined fluocinolone acetonide intravitreal insertion and glaucoma drainage device placement for chronic uveitis and glaucoma. *Am J Ophthalmol.* 2010;149(5):800–6 e1.
66. Lowder C, Belfort Jr R, Lightman S, et al. Dexamethasone intravitreal implant for noninfectious intermediate or posterior uveitis. *Arch Ophthalmol.* 2011;129(5):545–53.
67. Campochiaro PA, Brown DM, Pearson A, et al. Sustained delivery fluocinolone acetonide vitreous inserts provide benefit for at least 3 years in patients with diabetic macular edema. *Ophthalmology.* 2012;119(10):2125–32.

68. Campochiaro PA, Brown DM, Pearson A, et al. Long-term benefit of sustained-delivery fluocinolone acetonide vitreous inserts for diabetic macular edema. *Ophthalmology*. 2011;118(4):626–35 e2.
69. Martin DF, Parks DJ, Mellow SD, et al. Treatment of cytomegalovirus retinitis with an intraocular sustained-release ganciclovir implant. A randomized controlled clinical trial. *Arch Ophthalmol*. 1994;112(12):1531–9.
70. Musch DC, Martin DF, Gordon JF, et al. Treatment of cytomegalovirus retinitis with a sustained-release ganciclovir implant. The Ganciclovir Implant Study Group. *N Engl J Med*. 1997;337(2):83–90.
71. Beltran WA, Zhang Q, Kijas JW, et al. Cloning, mapping, and retinal expression of the canine ciliary neurotrophic factor receptor alpha (CNTFRalpha). *Invest Ophthalmol Vis Sci*. 2003;44(8):3642–9.
72. Tao W, Wen R, Goddard MB, et al. Encapsulated cell-based delivery of CNTF reduces photoreceptor degeneration in animal models of retinitis pigmentosa. *Invest Ophthalmol Vis Sci*. 2002;43(10):3292–8.
73. Zhang K, Hopkins JJ, Heier JS, et al. Ciliary neurotrophic factor delivered by encapsulated cell intraocular implants for treatment of geographic atrophy in age-related macular degeneration. *Proc Natl Acad Sci U S A*. 2011;108(15):6241–5.
74. Sieving PA, Caruso RC, Tao W, et al. Ciliary neurotrophic factor (CNTF) for human retinal degeneration: phase I trial of CNTF delivered by encapsulated cell intraocular implants. *Proc Natl Acad Sci U S A*. 2006;103(10):3896–901.
75. Carrasquillo KG, Ricker JA, Rigas IK, et al. Controlled delivery of the anti-VEGF aptamer EYE001 with poly(lactic-co-glycolic)acid microspheres. *Invest Ophthalmol Vis Sci*. 2003;44(1):290–9.
76. Cardillo JA, Souza-Filho AA, Oliveira AG. Intravitreal Bioerudivel sustained-release triamcinolone microspheres system (RETAAC). Preliminary report of its potential usefulness for the treatment of diabetic macular edema. *Arch Soc Esp Oftalmol*. 2006;81(12):675–7, 9–81.
77. Hartmann KI, Nieto A, Wu EC, et al. Hydrosilylated porous silicon particles function as an intravitreal drug delivery system for daunorubicin. *J Ocul Pharmacol Ther*. 2013;29(5):493–500.
78. Fishman PH, Peyman GA, Lesar T. Intravitreal liposome-encapsulated gentamicin in a rabbit model. Prolonged therapeutic levels. *Invest Ophthalmol Vis Sci*. 1986;27(7):1103–6.
79. Tremblay C, Barza M, Szoka F, et al. Reduced toxicity of liposome-associated amphotericin B injected intravitreally in rabbits. *Invest Ophthalmol Vis Sci*. 1985;26(5):711–8.
80. Haghjoun N, Soheilian M, Abdekhodaie MJ. Sustained release intraocular drug delivery devices for treatment of uveitis. *J Ophthalmic Vis Res*. 2011;6(4):317–29.
81. Abrishami M, Zarei-Ghanavati S, Soroush D, et al. Preparation, characterization, and in vivo evaluation of nanoliposomes-encapsulated bevacizumab (avastin) for intravitreal administration. *Retina*. 2009;29(5):699–703.
82. Olsen TW, Feng X, Wabner K, et al. Cannulation of the suprachoroidal space: a novel drug delivery methodology to the posterior segment. *Am J Ophthalmol*. 2006;142(5):777–87.
83. Patel SR, Berezovsky DE, McCarey BE, et al. Targeted administration into the suprachoroidal space using a microneedle for drug delivery to the posterior segment of the eye. *Invest Ophthalmol Vis Sci*. 2012;53(8):4433–41.
84. Myles ME, Neumann DM, Hill JM. Recent progress in ocular drug delivery for posterior segment disease: emphasis on transscleral iontophoresis. *Adv Drug Deliv Rev*. 2005;57(14):2063–79.
85. Singh RP, Mathews ME, Kaufman M, Riga A. Transcleral delivery of triamcinolone acetonide and ranibizumab to retinal tissues using macroesis. *Br J Ophthalmol*. 2010;94(2):170–3.
86. Halhal M, Renard G, Courtois Y, et al. Iontophoresis: from the lab to the bed side. *Exp Eye Res*. 2004;78(3):751–7.
87. de Kozak Y, Andrieux K, Villarroja H, et al. Intraocular injection of tamoxifen-loaded nanoparticles: a new treatment of experimental autoimmune uveoretinitis. *Eur J Immunol*. 2004;34(12):3702–12.
88. Touchard E, Omri S, Naud MC, et al. A peptide inhibitor of c-Jun N-terminal kinase for the treatment of endotoxin-induced uveitis. *Invest Ophthalmol Vis Sci*. 2010;51(9):4683–93.
89. Sebag J. Age-related changes in human vitreous structure. *Graefes Arch Clin Exp Ophthalmol*. 1987;225:89–93.
90. Sebag J, Balazs EA. Morphology and ultrastructure of human vitreous fibers. *Invest Ophthalmol Vis Sci*. 1989;30:1867–71.
91. Sebag J. Abnormalities of human vitreous structure in diabetes. *Graefes Arch Clin Exp Ophthalmol*. 1993;231:257–60.
92. Sebag J. Diabetic vitreopathy. *Ophthalmology*. 1996;103:205–6.
93. Lee SS, Robinson MR. Novel drug delivery systems for retinal diseases. A review. *Ophthalmic Res*. 2009;41:124–35.
94. Yasukawa T, Ogura Y. Medical devices for the treatment of eye diseases. *Handb Exp Pharmacol*. 2010;197:469–89.
95. Spaeth GL, Danesh-Meyer H, Goldberg I, et al. *Ophthalmic surgery: principles and practice*, 4th Edition, p 512; 2012.

Philip J. Banerjee, David G. Charteris, and David Wong

Outline

- I. **Introduction**
- II. **Clinical Classification of PVR**
- III. **Pathophysiology of PVR**
 - A. Blood-Retinal Barrier Breakdown
 - B. Cell Accumulation and Proliferation
 - C. Extracellular Matrix Production and Fibrin Deposition
 - D. Formed Membrane Contraction
- IV. **Adjunctive Agents and Target**
 - A. Anti-inflammatory Agents
 - 1. Corticosteroids
 - 2. Nonsteroidal Anti-inflammatory Agents
 - B. Inhibitors of Cell Proliferation
 - 1. Fluoropyrimidines
 - 2. Daunorubicin
 - 3. Retinoids
 - 4. Immunotoxins
 - 5. Colchicine
 - C. ECM Modifiers
 - 1. Cis-hydroxyproline
 - 2. Matrix Metalloproteinases
 - 3. Heparin/Low Molecular Weight Heparin (LMWH)
 - a. Clinical Evidence
 - i. High-Risk Retinal Detachments
 - ii. Established PVR
 - iii. Unselected Primary Retinal Detachments

References

P.J. Banerjee, MD • D.G. Charteris, MD
Vitreoretinal Department,
Moorfields Eye Hospital, London, England, UK

D. Wong, MD (✉)
Vitreoretinal Department, The Royal Liverpool University Hospital,
Liverpool, England, UK

Department of Ophthalmology,
LKS Faculty of Medicine, University of Hong Kong, Room 301,
Level 3, Block B, Cyberport 4, Pokfulam, Hong Kong, China
e-mail: shdwong@hku.hk

Keywords

Proliferative vitreoretinopathy • Vitreoretinal scarring • Pharmacologic adjuncts • Corticosteroids • Fluoropyrimidines • Retinoids • Chemotherapy • Immunotoxins • Heparins

Key Concepts

1. Despite numerous preclinical studies demonstrating potential pharmacologic candidates in the treatment of proliferative vitreoretinopathy (PVR), few have translated into clinical research.
2. The presence of PVR at the time of a recurrent detachment is a poor proxy for failing to adequately treat the detached retina at the time of initial surgery. The use of perioperative adjunctive agents may be effective at modifying the vitreoretinal scarring response, but in the presence of an untreated or inadequately treated retinal break, a recurrent detachment is likely to ensue.
3. Exploring new modes of local drug delivery in sustained-release preparations may provide sustained therapeutic levels over the crucial periods of vitreoretinal scarring, although as yet, no clinical trials have investigated this approach.

I. Introduction

Proliferative vitreoretinopathy (PVR) is the most common cause of late anatomic failure in retinal detachment surgery, with a reported incidence of 5–11 % of all rhegmatogenous retinal detachments [1]. PVR can be considered an exaggerated wound healing response in specialized tissue, resulting in the formation of complex fibrocellular membranes on both surfaces of the retina and the posterior vitreous cortex.

Contraction of these membranes then distorts the normal retinal architecture with resultant visually detrimental sequelae and/or traction retinal detachment, with re-opening of preexisting retinal breaks or the formation of new ones. Based on the premise that the primary pathology was centered in the vitreous, PVR was previously referred to as massive vitreous retraction syndrome (MVR) or massive preretinal retraction syndrome (MPR). However, to acknowledge the role of periretinal membrane formation and pigment epithelial cell proliferation, PVR later became known as massive periretinal proliferation (MPP) [2]. A unifying classification system was established in 1983 by the Retina Society Terminology Committee [1] coining the phrase proliferative vitreoretinopathy (PVR), which was later updated in 1991 to the current classification system in clinical practice today [3].

As is typical in medicine, the first treatments for PVR were surgical, an approach still practiced today [see chapter V.B.5. Management of PVR. However with expanding knowledge of the cells involved and the cytokine signaling that promotes PVR, surgery will be replaced, or at least augmented, by pharmacotherapy directed to the causative cells as well as the substrate upon which these cells migrate and proliferate – vitreous [see chapter VI.A. Pharmacologic vitreolysis]. Ultimately with sufficient knowledge, PVR will be preventable by pharmacotherapy, as will be described below.

II. Clinical Classification of PVR

Although the current classification system has served to standardize PVR terminology in clinical practice and research, it

remains limited. The number, location, and size of retinal breaks are not included, and many clinicians feel that grading the extent of PVR membranes in terms of clock hours limits their description to one circumferential meridian, e.g., when distinguishing linear subretinal bands from confluent sheets (Tables IV.F-1 and IV.F-2).

The following clinical illustrations provide examples of PVR and their corresponding grade: (Figures IV.F-1 and IV.F-2)

The grading of established PVR from photographic images may be limited by the field of exposure; however, below are examples of retinal detachments with Grade C PVR: (Figure IV.F-3)

III. Pathophysiology of PVR

The pathophysiology of PVR is a complex sequence of events that remain incompletely understood. A simplified overview is included in this chapter to aid the reader in identifying potential targets against which pharmacologic agents may be directed. Rhegmatogenous retinal detachment is conventionally viewed as the starting point for PVR development. Vitreoretinal scarring can be considered the result of the following components:

- Blood-retinal barrier (BRB) breakdown
- Cellular accumulation and proliferation [see chapter III.J. Cell proliferation at vitreo-retinal interface in PVR & related disorders]
- Extracellular matrix (ECM) production and fibrin deposition
- Formed membrane contraction

Table IV.F-1 Updated proliferative vitreo-retinopathy grade classification [3]

Grade	Features
A	Vitreous haze, vitreous pigment clumps, pigment clusters on inferior retina
B	Wrinkling of inner retinal surface, retinal stiffness, vessel tortuosity, rolled and irregular edge of retinal break, decreased mobility of vitreous
CP 1–12	Posterior to equator; focal, diffuse, or circumferential full-thickness folds, subretinal strands
CA 1–12	Anterior to equator; focal, diffuse, or circumferential full-thickness folds, subretinal strands, anterior displacement, condensed vitreous strands

Table IV.F-2 Updated proliferative vitreo-retinopathy contraction classification [3]

Type	Location (in relation to equator)	Features
Focal	Posterior	Starfold posterior to vitreous base
Diffuse	Posterior	Confluent starfolds posterior to vitreous base; optic disc may not be visible
Subretinal	Posterior/anterior	Proliferation under the retina; annular strand near disc; linear strands; moth-eaten-appearing sheets
Circumferential	Anterior	Contraction along posterior edge of vitreous base with central displacement of retina; peripheral retina stretched; posterior retina in radial folds
Anterior	Anterior	Vitreous base pulled anteriorly by proliferative tissue; peripheral retinal trough; displaced ciliary processes may be stretched, may be covered by membrane; iris may be retracted

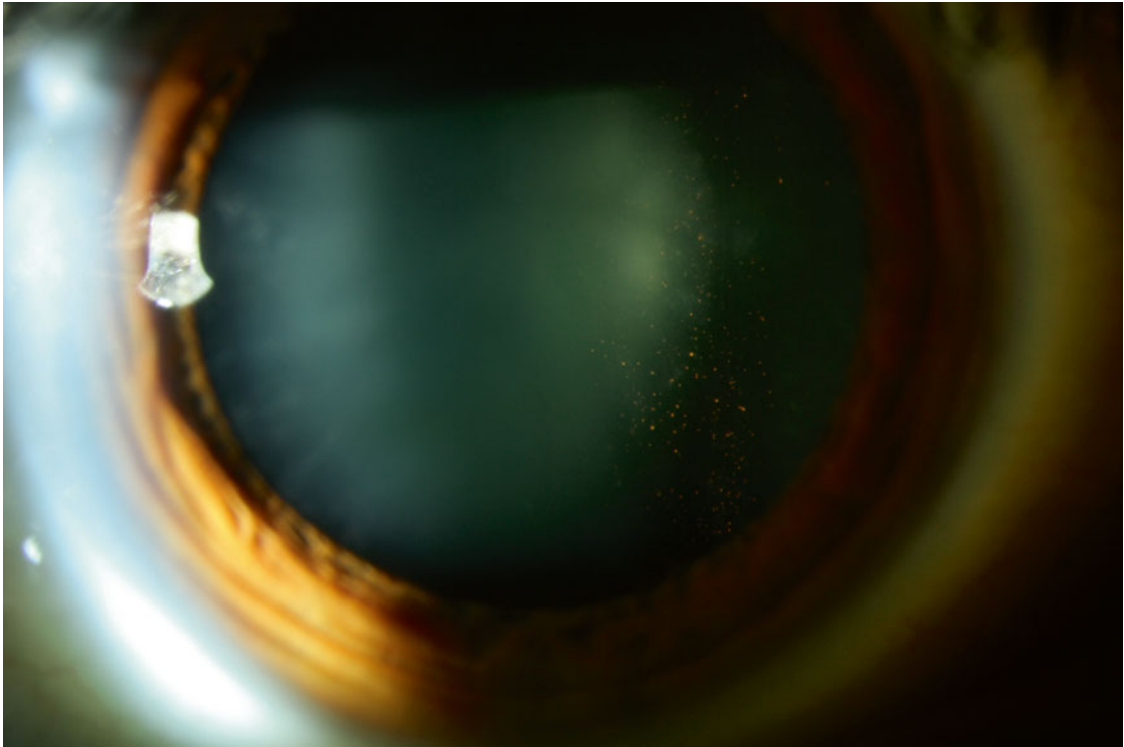


Figure IV.F-1 PVR *Grade A* – pigment clumping in the anterior vitreous

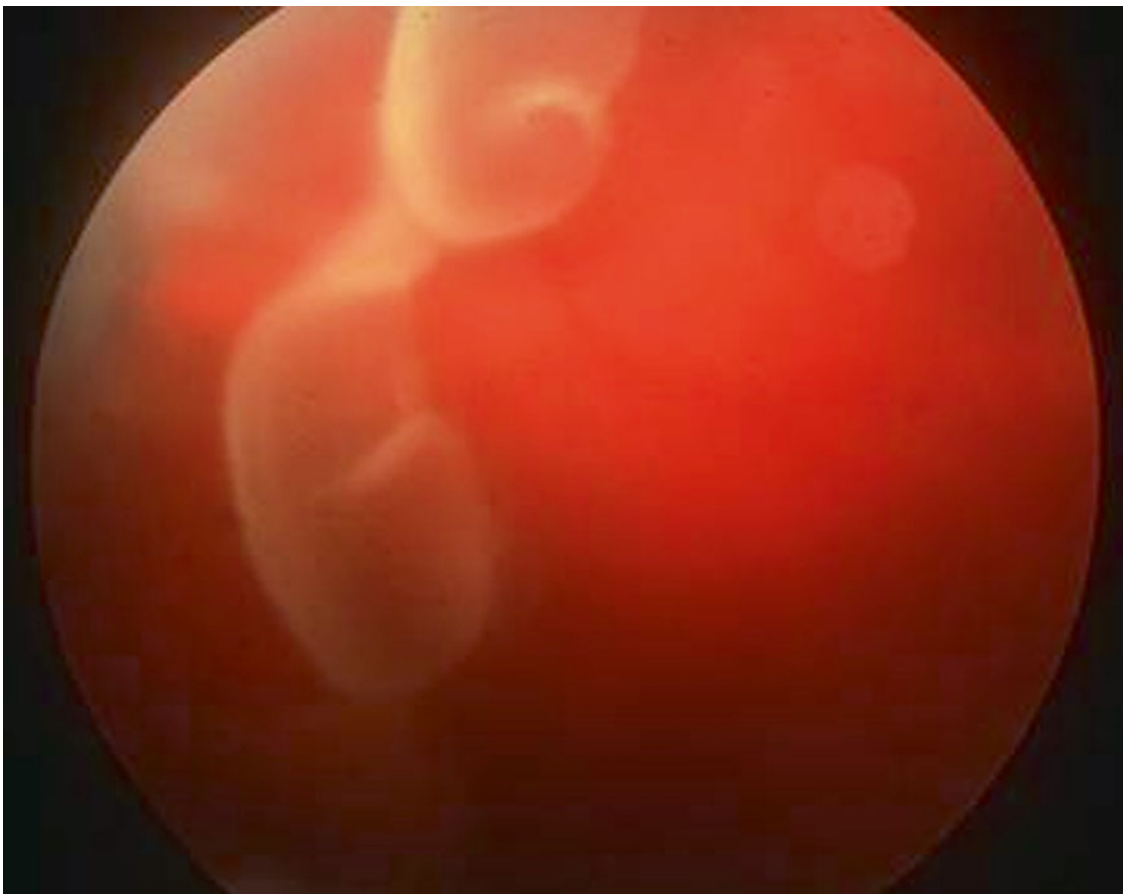


Figure IV.F-2 PVR *Grade B* – a rolled edge to a giant retinal tear (image reproduced courtesy of Lippincott, Williams and Wilkins)

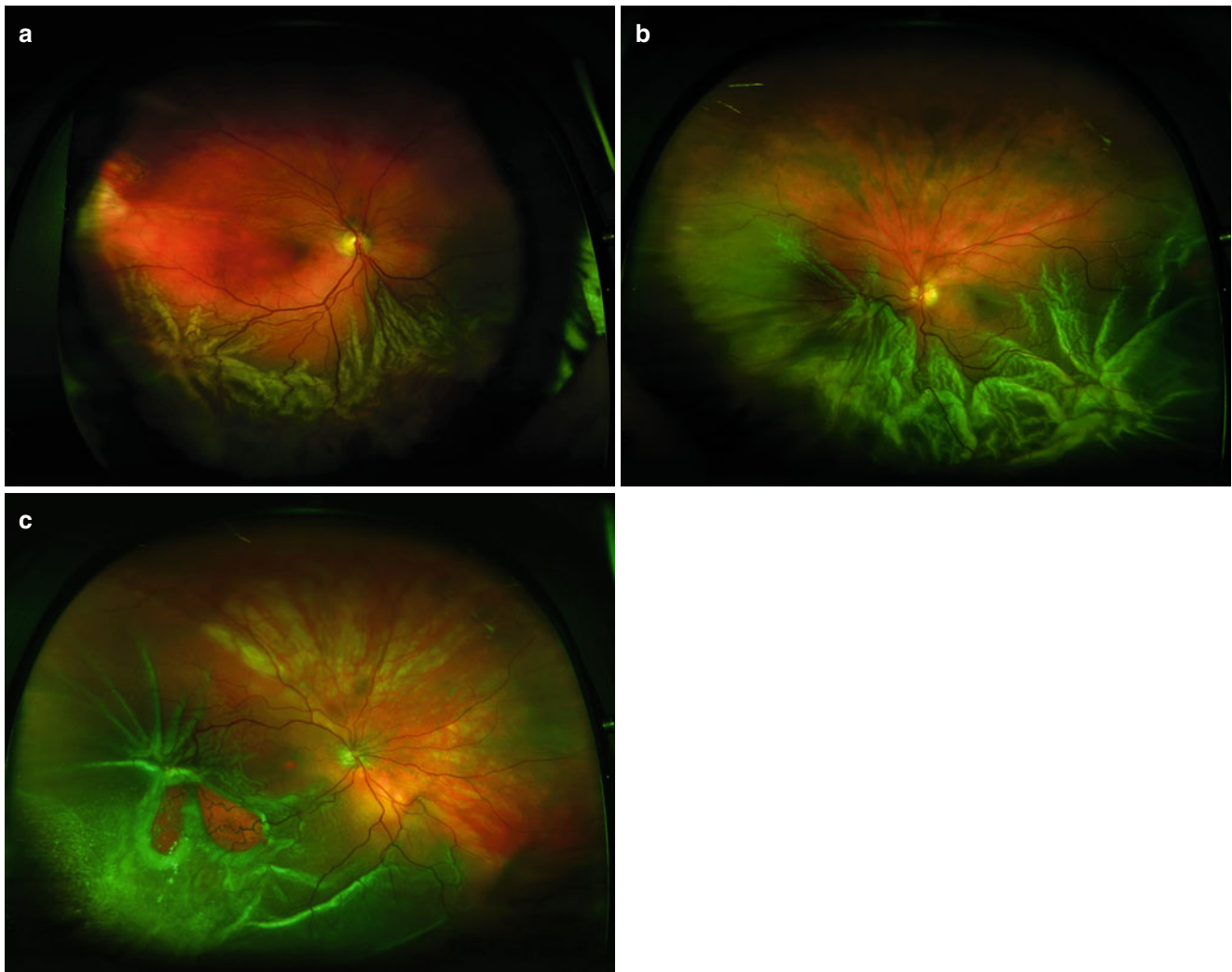


Figure IV.F-3 PVR Grade C – (a) anterior circumferential contraction with diffuse starfolds extending posteriorly, (b) multiple starfolds posterior to the equator with a full-thickness retinal tear temporally at

3 o'clock, and (c) a combined schisis-RD with a posterior starfold and inner leaf tear

A. Blood-Retinal Barrier Breakdown

In addition to allowing ingress of liquid vitreous into the sub-retinal space, a retinal tear results in the dispersion of retinal pigment epithelial (RPE) cells into the vitreous cavity. The blood-retinal barrier (BRB) breakdown which follows retinal detachment appears to have a central role in the dispersion of cells and growth factors which promote the further evolution of PVR [4].

B. Cell Accumulation and Proliferation

Analysis of excised tissue and animal models [see chapter III.J. Cell proliferation at the vitreo-retinal interface in PVR & related disorders] have identified four categories of cells in PVR membranes:

1. Retinal pigment epithelial cells (RPE) [5–14]
2. Glial cells [5, 10–18]

3. Fibroblasts [5–8, 19–23]

4. Inflammatory cells (macrophages [7, 9, 21, 22, 24, 25] and lymphocytes [26–28])

Experimental and clinical studies have identified the importance of RPE cell chemotaxis, proliferation, and metaplastic differentiation into fibroblast morphology under the effect of local growth factors/cytokines. Recent studies have demonstrated a central role of retinal glial cell activation and extension into periretinal membranes [29, 30]. Infiltrating inflammatory cells are also thought to play a role in membrane formation and contraction through growth factor production.

C. Extracellular Matrix Production and Fibrin Deposition

Collagen (predominantly types I and III) and fibronectin (a cell attachment protein), derived from RPE and glial cells, are key components in PVR membrane formation [9, 10, 31].

Fibrin deposition in the early phase of BRB breakdown may also provide a scaffold upon which complex fibrocellular PVR membranes may form [32].

D. Formed Membrane Contraction

Contraction of complex periretinal and vitreous membranes is responsible for the clinical picture of PVR. Membrane shortening may be mediated by intrinsic fibroblastic cells, some of which have been demonstrated to contain myofilaments [6, 8, 20]. However, alternative explanations suggest an RPE-collagen interaction via fibronectin bridges [33].

IV. Adjunctive Agents and Target

A wide variety of agents have been identified as potential adjuncts to modify the scarring response. Agents may either target a specific stage of the pathway or multiple stages, with the latter offering the advantage of monotherapy, where the former may require a combination of agents. The following section aims to provide an overview of the pharmacological agents that have been tested experimentally and is subdivided by their primary therapeutic target (summarized in Table IV.F-3). Selected agents which have been tested in clinical trials will be discussed in more detail thereafter under their relevant section (summarized in Table IV.F-4).

Table IV.F-3 Targets for adjunctive treatment

Pathological process	Strategy
Blood-retinal barrier breakdown	Anti-inflammatory treatment
Cellular activation	Antiproliferatives, growth factor manipulation
Cellular proliferation	Antiproliferatives – (a) cell specific (b) nonspecific
Fibrin formation	Decrease production/increase breakdown
Extracellular matrix formation	Inhibition of cellular activation, MMP/TIMP manipulation
Membrane contraction	Contraction inhibition

Table IV.F-4 Summary of adjunctive agents which have been investigated in clinical trials

Adjunct	Regime	Target	Study Population	Treatment Allocation	Outcome
Triamcinolone Acetonide ⁽⁴⁹⁾	4mg into oil filled eye at end of procedure	BRB breakdown, cellular proliferation, growth factors	75 eyes with established PVR undergoing vitrectomy with oil	38 patients adjunct 37 patients standard care	No difference in primary anatomical success, final VA or PVR recurrence
Prednisolone ⁽⁵⁰⁾	100mg PO od tapering to 12.5mg od for 15 days postoperatively	BRB breakdown, cellular proliferation, growth factors	220 consecutive patients with primary RD undergoing scleral buckle surgery	110 patients adjunct 110 patients placebo	Reduced cellophane maculopathy in steroid group (27%, 24%, 20% vs 42%, 47%, 39% control group at 1, 3, 6 months, respectively.
5FU and LMWH ⁽⁷⁰⁾	20ug/mL of 5FU with 5IU/mL of LMWH as 1hour intraoperative vitrectomy solution infusion	5FU – Cellular proliferation LMWH – Fibrin, fibronectin, cellular proliferation, growth factors	174 patients at high risk of PVR	87 patients adjunct 87 patients placebo	Reduction in postop PVR (12.6% treatment vs 26.4% control)
5FU and LMWH ⁽⁷¹⁾			157 patients with established PVR undergoing vitrectomy surgery with oil	73 patients adjunct 84 patients placebo	No difference in primary anatomical success (56% treatment vs 51% control) No difference in secondary outcome measures
5FU and LMWH ⁽⁷²⁾			641 consecutive unselected cases with primary RD undergoing vitrectomy surgery with gas tamponade	342 patients adjunct 299 patients placebo	No difference in primary anatomical success at 6 months (82.3% treatment vs 86.8% controls). Significantly worse final VA in patients with macula sparing RDs in treatment group
Daunorubicin ⁽⁸⁸⁾	7.5ug/mL of daunorubicin as 10 minute vitrectomy solution infusion upon retinal attachment	Cellular proliferation and migration	286 patients with established PVR undergoing vitrectomy with oil	145 patients adjunct 141 patients standard care	No difference in primary anatomical success at 6 months (62.7% treatment vs 54.1% controls). Significantly fewer reoperations in treatment group
13-cis-retinoic acid ⁽¹⁰⁰⁾	10mg oral 13-cis-retinoic acid bd for 8 weeks postoperatively	Cellular proliferation	35 patients with established PVR undergoing vitrectomy Surgery with oil	16 patients adjunct 19 patients standard care	Improved final reattachment rate at 1 year (93.8% treatment vs 63.2% controls). Reduced macula pucker 18.8% vs 78.9%) Greater rate of ambulatory VA (56.3% vs 10.5%)
Colchicine ⁽¹¹⁶⁾	0.6mg daily for 2weeks then 1.2mg daily of oral colchicine	Cellular proliferation and contractility	22 patients with PVR secondary to trauma or vascular disease	11 patients adjunct 11 patients standard care	No difference in reduction of PVR

A. Anti-inflammatory Agents

1. Corticosteroids

Corticosteroids emerged as the first pharmacological agent to be employed as an adjunctive agent to target the scarring response. Their anti-inflammatory properties and secondary reduction in blood-ocular barrier breakdown target a key component in the PVR process. A variety of modes of corticosteroid administration have been investigated: systemic (oral), periocular, and intraocular (by direct injection or via the infusate).

a. Preclinical Evidence

Intravitreal injection of corticosteroid was first reported to significantly reduce experimental PVR in rabbits by Tano et al. in 1980. Traction retinal detachment (TRD) in rabbits was significantly reduced from 57 to 24 % and from 84 to 34 % after a single injection of 1 mg dexamethasone or triamcinolone acetonide, respectively [34, 35]. This effect was later confirmed using 2 mg of intravitreal triamcinolone acetonide in a refined experimental PVR rabbit model, with a reduction in TRD rate from 90 to 56 % [36]. Periocular administration of methylprednisolone (10 mg) was shown to reduce experimental complicated RD from 87 to 14 %, also showing a reduction in cell proliferation within the vitreous microenvironment [37]. More recently, this antiproliferative effect has been confirmed by a significant reduction in human retinal pigment epithelial cell proliferation *in vitro* following a dose-dependent treatment of unpreserved triamcinolone acetonide [38].

b. Clinical Evidence

The clinical application of corticosteroids as adjuncts to vitreoretinal surgery was first reported by Koerner et al. in 1982 who concluded that the systemic effects of oral prednisolone on postoperative retinal fibrosis did not match that of experimental intravitreal triamcinolone [39]. An infusate containing dexamethasone showed a trend toward a reduction in PVR re-proliferation and a reduction in hypotony, but did not achieve statistical significance. Subconjunctival dexamethasone (10 mg) injected 5–6 h prior to scleral buckle surgery was reported to reduce blood-ocular barrier breakdown, postoperatively, as measured by laser flare photometry, but has not been investigated as an adjunctive agent in patients with PVR [40].

Jonas et al. opened the door to the clinical investigation of intravitreal triamcinolone in 2000 by reporting it to be non-toxic and of potential benefit through a reduction in postoperative intraocular inflammation [41], and this has since become the most widely clinically investigated adjunctive corticosteroid. Its clinical safety profile has been subsequently confirmed although its therapeutic benefit has yet to be consistently proven. Reduction in blood-ocular barrier breakdown [42] and a proposed benefit in established PVR

have been reported [43–46] although these studies were either retrospective or non-comparative. A large multicenter, prospective, quasi-randomized controlled trial investigating the use of varying doses of intravitreal triamcinolone acetonide as an adjunctive surgical tool to aid vitreous visualization showed a significant reduction in intraoperative complications [47] with fewer retinal breaks and intraoperative retinal detachments. However, 1-year follow-up failed to show a statistical difference in visual acuity or reoperation rate [48]. The absence of any long-term positive effect may be explained by its use as a surgical tool rather than as a therapeutic injection, as it is likely that negligible corticosteroid concentrations would have remained at the end of the procedure following its removal. To date, only one prospective randomized controlled clinical trial investigating the use of triamcinolone acetonide in the eyes with established PVR (Grade C) undergoing pars plana vitrectomy with silicone oil has been reported [49]. 75 eyes divided into two groups with a 1:1 treatment allocation ratio were investigated. The treatment group received 4 mg of intravitreal triamcinolone into the oil-filled eye at the end of the procedure. No statistical difference in primary anatomical success at 6 months was noted (84 and 78 % in the adjunct and control groups, respectively). Neither was there any statistical difference in any of the investigated secondary outcomes (visual acuity, reoperation rate, PVR recurrence, macula pucker, IOP rise). The authors acknowledge that a positive treatment effect may have been masked by a higher than expected primary success rate in the control group and a resultant underpowered study.

More recently, Koerner et al. have published earlier work on the use of systemic oral prednisolone [50] and its effect on cellophane maculopathy in 220 consecutive eyes undergoing scleral buckle surgery for primary RRD. They reported significantly fewer cases of cellophane maculopathy in the steroid group 27, 24, and 20 % compared with 42, 47, and 39 % in the control group at 1, 3, and 6 months, respectively. They concluded that oral corticosteroids have a prophylactic effect against the early stages of PVR, but affirm the need for larger randomized and controlled trials to confirm whether this effect is extended to advanced PVR. It should be noted, however, that local corticosteroid administration is preferable over systemic use, as it achieves significantly higher intraocular concentrations [51] and avoids systemic side effects. It is possible that previous clinical studies have been limited by the duration of action of the corticosteroid and that future success may be achieved by local slow release agents, thereby adequately covering the active PVR period, in addition to avoiding systemic side effects.

2. Nonsteroidal Anti-inflammatory Agents

Nonsteroidal agents, like corticosteroids, are of therapeutic value in vitreoretinal scarring through their anti-inflammatory

properties and subsequent reduction in blood-ocular barrier breakdown. They have been less widely investigated than corticosteroids due to their reduced potency.

a. Preclinical Evidence

Meclofenamate and indomethacin were first shown to inhibit cell proliferation in cell culture in 1984 [52], but were not subsequently investigated as single therapeutic agents, presumably due to their inability to compete with corticosteroids as realistic treatment options. However, in combination with 5-FU in a sustained-release preparation, a significant benefit was reported in posttraumatic experimental PVR in rabbits. A significant reduction in both the presence and severity of PVR was found in animals treated with the co-drug preparation [53].

b. Clinical Evidence

Topical indomethacin in combination with routine peroperative corticosteroids was found to significantly reduce blood-aqueous barrier breakdown in patients undergoing extracapsular cataract surgery [54] as well as decrease postoperative inflammation [55]. However, no clinical trials have investigated the use of nonsteroidal anti-inflammatory agents in patients with PVR.

B. Inhibitors of Cell Proliferation

1. Fluoropyrimidines

The fluoropyrimidines are a family of antimetabolites which modify protein synthesis by (a) binding to and inhibiting the enzyme thymidylate synthetase and (b) incorporation into RNA causing coding errors in protein translation, thus inhibiting cell proliferation. They are more commonly used as a chemotherapeutic agent in solid tumors, particularly of the gastrointestinal tract.

a. Preclinical Evidence

5-Fluorouracil (5-FU) was first reported to reduce experimental traction retinal detachment (TRD) in rabbits in 1982. In non-vitreotomized eyes, a TRD rate of 73.6 % in control animals was reduced to 31.5 % following a single intravitreal injection of 5-FU [56]. This effect was replicated in vitrectomized eyes with repeated daily intraocular injections 0.5 mg for 7 days [57] and found to be nontoxic at this dosing regimen [58] following initial toxicity concerns [59]. 5-FU may be converted to 5-fluorouridine (5-FUR), the latter offering the advantage of anti-contractile properties [60] and increased potency with a greater antiproliferative effect [61, 62]. However, 5-FUR was found to be significantly more toxic to retinal cells [63] and efforts to translate laboratory work to clinical trials have favored 5-FU. Use of a sustained-release preparation containing 1 mg of 5-FU was associated with a

reduction in TRD rates from 89 % in controls to 11 % in treated animals, in an experimental PVR model [64]. Sustained intravitreal concentrations of 5-FU of between 1 and 13 mg/L for at least 14 days were reported, with concentrations remaining above 0.3 microgram/mL for almost 21 days. No toxic effects were observed. Co-drug preparations containing 5-FU and either dexamethasone or triamcinolone have also been shown to reduce the severity and progression of experimental PVR in non-vitreotomized rabbits [65, 66]. When a co-drug containing 5-FU and fluocinolone was injected into the gas-filled eyes, intravitreal concentrations of the drug were unaffected, when compared with controls [67].

b. Clinical Evidence

In 1984, a prospective non-comparative pilot study was conducted in 22 patients undergoing surgery for established PVR who were treated intraoperatively with additional intraocular and periocular 5-FU. A final reattachment rate of 60 % was achieved at 6 months. The therapy was considered to be well tolerated, nontoxic, and superior to reported standard care at the time [68]. This was confirmed in a prospective randomized controlled trial using 10 mg of intravitreal 5-FU on completion of vitrectomy surgery [69]. A trend toward better vision was observed in the treatment group compared with controls, but with a lower macula reattachment rate (60 % vs 77 %). More recently, 5-fluorouracil has been investigated in combination with low molecular weight heparin in three prospective randomized controlled clinical trials [70–72]. These trials will be discussed in detail below.

2. Daunorubicin

Daunorubicin, or daunomycin, is a chemotherapeutic agent of the anthracycline family which was most commonly used in combination therapy to treat hematological malignancies. It inhibits cellular proliferation by inhibiting DNA replication.

a. Preclinical Evidence

Daunomycin was first tried intravitreally in experimental PVR in 1983, where it was shown to reduce dermal fibroblastic proliferation [73], and after initial concerns regarding its narrow safety margin [74], it later showed promise as a potential nontoxic and therapeutic adjunct [75–79]. The mode of administration of daunomycin has also been investigated, through drug delivery systems, and reports suggested a reduction in toxicity [80–83]; however, these preparations have yet to be tried clinically. In a staggered regime with intravitreal triamcinolone, it has been shown to significantly reduce experimental TRD in rabbits, with rates of 83.3 % in controls compared to 8.3 % in animals treated with combination therapy. This staggered combination was also found to be superior to monotherapy, with TRD rates of 33.3 and 16.1 %, in the eyes treated with only daunomycin or

triamcinolone, respectively. Human multidrug-resistant cells, via P-glycoprotein induction, have been found in excised premacular membranes, in the eyes treated with daunomycin, pushing it further down the list of preferred adjunctive agents [84]. More recently, doxorubicin, a close relative to daunorubicin, has been shown in addition to its antiproliferative properties, to attenuate the glial cell response and reduce the severity of experimental PVR [85], and may form the basis of future studies, either as a single agent or in combination therapy.

b. Clinical Evidence

Intravitreal daunorubicin was first shown to be safe and well tolerated when administered as a 7.5 µg/ml intravitreal 10 minute infusion in 15 posttraumatic eyes with PVR, prior to silicone oil injection [86]. A larger non-comparative study of 68 eyes with advanced PVR reported an eventual anatomic success rate of 73 % at 18 months, with 89 % achieving a final visual acuity of >20/800 [87]. A multicenter, prospective, randomized, controlled clinical trial studied 286 eyes of patients with PVR Grade C2 or greater undergoing vitrectomy and silicone oil exchange. Patients were randomized to treatment with or without a 10-minute intraoperative infusion of daunorubicin (7.5 µg/mL). The primary outcome measure used was primary anatomical success, with a rate of 62.7 % in the treatment group compared to 54.1 % in controls. It marginally failed to reach significance ($P=0.07$); however, the trial did demonstrate a statistically significant reduction in the number of vitreoretinal reoperations within 1 year ($P=0.005$) [88]. Further small-scale studies have since suggested a benefit [89], but daunorubicin has, like many other adjuncts, failed to gain widespread clinical acceptance.

3. Retinoids

Retinoids, or vitamin A compounds, have important roles in regulating the cell proliferation and differentiation of multiple cell types throughout the body by mediating gene transcription. They have been shown experimentally to inhibit RPE cell proliferation, as well as modify ECM and cell-mediated contraction.

a. Preclinical Evidence

Retinoic acid first emerged as a potential pharmacologic agent to prevent vitreoretinal scarring in 1991. Human RPE cell proliferation was significantly reduced when grown in the presence of 1 µm of retinoic acid. Cells were also found to maintain mature RPE cell morphology, rather than undergo the phenotypic changes associated with PVR retinal detachments [90]. This inhibitory effect on cell proliferation was subsequently confirmed [91], in addition to a reduction in cell-mediated contraction. Sustained drug delivery systems containing all-trans retinoic acid have been shown to reduce experimental PVR from 100 to 36 % in rabbit models [92],

but an associated foreign body reaction was reported. Doses of 605 micrograms and 1070 micrograms have since been found to be therapeutic and nontoxic [93, 94]. In an experimental PVR model in rabbits using silicone oil and heavy silicone oil, all-trans retinoic acid significantly reduced the severity of traction RDs at concentrations of 15 micrograms/ml and 10 micrograms/ml, respectively [95]. This was later confirmed with 13-cis-retinoic acid [96]. Both isomers of retinoic acid were shown to reduce proliferation of PVR membrane-derived human RPE cells [97]. This response was dose dependent at a variety of concentrations and found to be nontoxic. More recently, all-trans retinoic acid has been shown to significantly inhibit RPE cell extracellular matrix production (particularly laminin beta-1) and thereby reduce cell-mediated collagen contractility [98]. It therefore offers the advantage as a single therapeutic agent active against multiple steps in the PVR process.

b. Clinical Evidence

A small retrospective study compared the outcomes of 10 patients undergoing surgery for PVR who were additionally treated with 40 mg of oral 13-cis-retinoic acid twice daily for 4 weeks postoperatively, with 10 control patients. A trend toward a benefit was noted in the treatment group by a reduction in PVR recurrence, with anatomical success in 9 out of 10 patients at 8 months compared with 4 out of 10 in the control group ($P=0.061$) at 9 months [99]. A prospective randomized controlled clinical trial of 35 patients undergoing surgery for PVR compared the use of 20 mg of oral 13-cis-retinoic acid twice daily postoperatively for 8 weeks (16 patients) with no additional treatment (19 patients) [100]. Both anatomical and visual outcomes were superior in the treatment arm compared with the control arm, with reported final anatomical success rates of 93.8 and 63.2 % ($P=0.047$), respectively. Ambulatory vision was achieved in 56.3 % of patients in the treatment group, compared with only 10.5 % in the control arm ($P=0.009$). Fewer patients in the treatment group developed macula pucker (18.8 %) compared with the control group (78.9 %) ($P=0.001$). Despite this positive treatment effect, retinoic acid has not been universally adopted clinically. This may be due to the small sample size and lack of statistical power, in addition to concerns regarding systemic side effects of the treatment.

4. Immunotoxins

Immunotoxins are chimeric proteins consisting of a modified antibody or antibody fragment attached to a biological toxin fragment with its natural binding domain removed. The antibody is cell specific and hence, upon binding to its target, allows intracellular incorporation of the toxin and a resultant cytotoxic effect. Actively dividing RPE cells have been shown to abundantly express transferrin receptors and are thus targets for antiproliferative therapy [101, 102].

a. Preclinical Evidence

Transferrin ricin-A (Tfr-rRA) is an immunotoxin comprised of an antibody to the RPE transferrin receptor which is linked with the A chain of ricin, a potent toxin. It has been shown to significantly inhibit both RPE cell [103–105] and fibroblast proliferation [105, 106]. In an experimental PVR model in rabbits, only 10 % of the eyes developed traction retinal detachments when treated with an intravitreal injection of 2,000 ng of Tfr-rRA compared with 78 % of controls [107]. The VEGF receptors expressed by RPE cells have also been targeted using a combination of VEGF 165 and the diphtheria toxin (DT390-VEGF165). RPE cell survival was reduced when co-cultured with this immunotoxin in a dose-dependent response [108]. To date, no clinical studies have been conducted to investigate the use of immunotoxins as therapies for PVR.

5. Colchicine

Colchicine is a natural product sourced from the autumn crocus plant (*Colchicum autumnale*). Its use has been traced back to ancient Egypt when it may have been employed to treat rheumatism as early as 1500 BC. Today, it remains an alternative therapeutic agent in the treatment of gout, although its narrow therapeutic window limits its use. Colchicine prevents cell proliferation by inhibiting microtubule polymerization with a resultant inhibition of mitosis.

a. Preclinical Evidence

In 1985, colchicine was first shown to inhibit fibroblast growth in an experimental model *in vitro* [109] and later shown to be a potent inhibitor of RPE cell chemotaxis [110]. Its antiproliferative effects were subsequently confirmed in animal models, with inhibition of astrocyte and fibroblast and RPE cell proliferation and migration at concentrations well below levels of ocular toxicity [111] in cell culture. Experimental TRDs in rabbits was shown to be reduced from 74 to 29.6 % at 5 weeks in animals treated with oral colchicine [112]. In addition to its effect on proliferation, colchicine has also been shown to reduce RPE cell-mediated collagen gel contraction when human RPE cells were treated with 0.01–1 μm of colchicine [113]. More recently, therapies where colchicine has been combined with both methylprednisolone and sodium diclofenac [114] or 5-FU [115] have shown a significant reduction in experimental TRD rate and an inhibition of human glial cell proliferation, respectively.

b. Clinical Evidence

A small prospective controlled study in patients with PVR secondary to trauma or proliferative vascular disease compared the use of oral colchicine (1.2 mg daily) with controls (vitamin C 250 mg daily). It was concluded that the safe therapeutic dose of colchicine does not inhibit PVR [116]. No further clinical studies have been conducted since.

C. ECM Modifiers

Collagen (types 1 and 3), fibronectin, and deposited fibrin form key components to the extracellular matrix found in PVR membranes. Thus, drugs that affect their production, attachment, or contraction offer potential benefit as therapeutic agents against vitreoretinal scarring.

1. Cis-hydroxyproline

Hydroxyproline is a major constituent of collagen stability, and its synthesis can be inhibited by a proline analogue, cis-4-hydroxyproline.

a. Preclinical Evidence

Cis-hydroxyproline was shown to inhibit bovine RPE cell proliferation, collagen synthesis, attachment, and migration *in vitro*, in a dose-dependent manner [117]. More recently, when two sustained-release scleral implants were used in an experimental model of PVR, TRD were reduced from 89 % in controls to 57 % in treated animals at 1 month [118]. This adjunct has yet to be investigated clinically.

2. Matrix Metalloproteinases

Turnover and remodeling of extracellular matrix is regulated by a group of proteolytic enzymes known as matrix metalloproteinases (MMPs) and their natural inhibitors, tissue inhibitors of metalloproteinases (TIMPs). MMPs 1, 2, 3, and 9 and TIMPs 1, 2, and 3 have been demonstrated to be present in PVR membranes [119, 120]; thus it is reasonable to attempt modulating these factors.

a. Preclinical Evidence

Prinomastat (AG3340) is a synthetic inhibitor of MMPs that has been shown experimentally to reduce PVR in a rabbit model [121] and in posttraumatic rabbit eyes [122]. It has also been shown to reduce premacular membrane formation in rat eyes [123]. This treatment has yet to be investigated clinically in patients with PVR.

3. Heparin/Low Molecular Weight Heparin (LMWH)

Heparin has multiple cellular effects that can potentially inhibit PVR development. It inactivates thrombin by binding to antithrombin, promoting thrombin-antithrombin complex formation. In preclinical studies heparin has been shown to reduce fibrin formation and interfere with cell-substrate adhesion by binding fibronectin. It also binds fibrogenic growth factors (FGF, EGF, and PDGF) and inhibits cell proliferation, including scleral fibroblasts and RPE cells [124]. A prospective, randomized, controlled trial investigating the effect of heparin in the infusate on postoperative fibrin formation showed a positive effect using concentrations of 10 IU/ml, but a greater tendency to intraocular hemorrhage.

Lower concentrations were ineffective at reducing fibrin formation [125]. Combined heparin and dexamethasone in the infusate suggested a trend toward a reduction in postoperative PVR in treated patients, but again higher rates of intraocular hemorrhage were reported [126].

The low molecular weight fragments of heparin (LMWH) have less effect on the coagulation cascade or platelet function and thus reduce the risk of hemorrhagic complications compared with heparin but produce a comparable antithrombotic effect [124]. Intraocular fibrin formation was markedly reduced using an infusate containing LMWH in vitrectomy/lensectomy surgery in rabbits [127].

a. Clinical Evidence

The potential synergistic effect of combining LMWH with 5-FU to modify PVR development in eyes undergoing vitrectomy surgery has been investigated in three large prospective clinical trials [70–72]. The same adjunctive medication regime was used in the treatment arm of all three trials. An intraoperative vitrectomy infusion solution of Hartmann containing 5-FU at a concentration of 200 µg/ml and LMWH at a concentration of 5 IU/ml was used for 1 h. Control patients received plain Hartmann's solution as a placebo. The three studies investigated (i) high-risk retinal detachments undergoing vitrectomy and gas exchange [70], (ii) established PVR undergoing vitrectomy and silicone oil exchange [71], and (iii) unselected primary retinal detachments undergoing vitrectomy and gas exchange [72].

i. High-Risk Retinal Detachments

High-risk cases were identified using a previously published regression formula based in PVR risk factors [128]. 174 patients were studied, with PVR recurrence rates significantly lower in the treatment group at 12.6 % compared with 26.4 % in controls and fewer reoperations. In patients who developed recurrent PVR, visual outcomes were significantly better in the treatment group.

ii. Established PVR

A total of 157 patients with established PVR (Grade C) undergoing vitrectomy surgery with silicone oil tamponade were randomized to either receive the adjunctive regime or placebo in a 1:1 treatment allocation ratio. No benefit in primary anatomical success was found, and neither were there any significant differences in secondary outcome measures reported (complete or posterior retinal reattachment, visual acuity, hypotony, cataract, keratopathy).

iii. Unselected Primary Retinal Detachments

A total of 641 patients of unselected patients undergoing vitrectomy with gas tamponade were studied in a 1:1 treatment to control allocation ratio. No statistical difference was noted in primary anatomical success at 6 months with

rates of 82.3 and 86.8 % in the treatment and control groups, respectively. There was no significant difference in the proportion of patients who required reoperations due to PVR with 7.0 % in the treatment group, compared with 4.9 % of controls. However, patients with macula-sparing retinal detachments were found to have a significantly worse visual outcome at 6 months, thus raising concerns regarding toxicity.

Abbreviations

5-FU	5-Fluorouracil
5-FUR	5-Fluorouridine
BRB	Blood-retinal barrier
DNA	Deoxyribonucleic acid
ECM	Extracellular matrix
EGF	Epidermal growth factor
FGF	Fibroblast growth factor
IOP	Intraocular pressure
LMWH	Low molecular weight heparin
LWW	Lippincott, Williams and Wilkins
MMP	Matrix metalloproteinases
MPP	Massive periretinal proliferation
MPR	Massive preretinal retraction
MVR	Massive vitreous retraction
PDGF	Platelet-derived growth factor
PVR	Proliferative vitreo-retinopathy
RD	Retinal detachment
RNA	Ribonucleic acid
RPE	Retinal pigment epithelium
RRD	Rhegmatogenous retinal detachment
TIMPS	Tissue inhibitors of metalloproteinases
TRD	Tractional retinal detachment
VEGF	Vascular endothelial growth factor

References

1. The classification of retinal detachment with proliferative vitreo-retinopathy. *Ophthalmology*. 1983;90(2):121–5. Epub 1983/02/01.
2. Machemer R. Massive periretinal proliferation (MPP) I. Pigment epithelium proliferation. *Mod Probl Ophthalmol*. 1975;15:227. Epub 1975/01/01.
3. Machemer R, Aaberg TM, Freeman HM, Irvine AR, Lean JS, Michels RM. An updated classification of retinal detachment with proliferative vitreo-retinopathy. *Am J Ophthalmol*. 1991;112(2):159–65. Epub 1991/08/15.
4. Campochiaro PA, Bryan 3rd JA, Conway BP, Jaccoma EH. Intravitreal chemotactic and mitogenic activity. Implication of blood-retinal barrier breakdown. *Arch Ophthalmol*. 1986;104(11):1685–7. Epub 1986/11/01.
5. Clarkson JG, Green WR, Massof D. A histopathologic review of 168 cases of preretinal membrane. *Am J Ophthalmol*. 1977;84(1):1–17. Epub 1977/07/01.

6. Machemer R, van Horn D, Aaberg TM. Pigment epithelial proliferation in human retinal detachment with massive periretinal proliferation. *Am J Ophthalmol*. 1978;85(2):181–91. Epub 1978/02/01.
7. Kampik A, Kenyon KR, Michels RG, Green WR, de la Cruz ZC. Epiretinal and vitreous membranes. Comparative study of 56 cases. *Arch Ophthalmol*. 1981;99(8):1445–54.
8. Hiscott PS, Grierson I, McLeod D. Retinal pigment epithelial cells in epiretinal membranes: an immunohistochemical study. *Br J Ophthalmol*. 1984;68(10):708–15. Epub 1984/10/01.
9. Jerdan JA, Pepose JS, Michels RG, Hayashi H, de Bustros S, Sebag M, et al. Proliferative vitreoretinopathy membranes. An immunohistochemical study. *Ophthalmology*. 1989;96(6):801–10. Epub 1989/06/01.
10. Morino I, Hiscott P, McKechnie N, Grierson I. Variation in epiretinal membrane components with clinical duration of the proliferative tissue. *Br J Ophthalmol*. 1990;74(7):393–9. Epub 1990/07/01.
11. Wilkes SR, Mansour AM, Green WR. Proliferative vitreoretinopathy. Histopathology of retroretinal membranes. *Retina*. 1987;7(2):94–101. Epub 1987/01/01.
12. Trese MT, Chandler DB, Machemer R. Subretinal strands: ultrastructural features. *Graefes Arch Clin Exp Ophthalmol*. 1985;223(1):35–40. Epub 1985/01/01.
13. Schwartz D, de la Cruz ZC, Green WR, Michels RG. Proliferative vitreoretinopathy. Ultrastructural study of 20 retroretinal membranes removed by vitreous surgery. *Retina*. 1988;8(4):275–81.
14. Hiscott P, Morino I, Alexander R, Grierson I, Gregor Z. Cellular components of subretinal membranes in proliferative vitreoretinopathy. *Eye (Lond)*. 1989;3(Pt 5):606–10. Epub 1989/01/01.
15. Rodrigues MM, Newsome DA, Machemer R. Further characterization of epiretinal membranes in human massive periretinal proliferation. *Curr Eye Res*. 1981;1(6):311–5. Epub 1981/01/01.
16. Van Horn DL, Aaberg TM, Machemer R, Fenzl R. Glial cell proliferation in human retinal detachment with massive periretinal proliferation. *Am J Ophthalmol*. 1977;84(3):383–93. Epub 1977/09/01.
17. Hiscott PS, Grierson I, Trombetta CJ, Rahi AH, Marshall J, McLeod D. Retinal and epiretinal glia—an immunohistochemical study. *Br J Ophthalmol*. 1984;68(10):698–707. Epub 1984/10/01.
18. Foos RY. Vitreoretinal juncture—simple epiretinal membranes. *Albrecht Von Graefes Arch Klin Exp Ophthalmol*. 1974;189(4):231–50. Epub 1974/01/28.
19. Machemer R, Laqua H. Pigment epithelium proliferation in retinal detachment (massive periretinal proliferation). *Am J Ophthalmol*. 1975;80(1):1–23. Epub 1975/07/01.
20. Walshe R, Esser P, Wiedemann P, Heimann K. Proliferative retinal diseases: myofibroblasts cause chronic vitreoretinal traction. *Br J Ophthalmol*. 1992;76(9):550–2. Epub 1992/09/01.
21. Hiscott PS, Grierson I, McLeod D. Natural history of fibrocellular epiretinal membranes: a quantitative, autoradiographic, and immunohistochemical study. *Br J Ophthalmol*. 1985;69(11):810–23. Epub 1985/11/01.
22. Vinos SA, Van Niel E, Kim HJ, Campochiaro PA. Simultaneous expression of keratin and glial fibrillary acidic protein by the same cells in epiretinal membranes. *Invest Ophthalmol Vis Sci*. 1992;33(12):3361–6. Epub 1992/11/01.
23. Vinos SA, Campochiaro PA, McGehee R, Orman W, Hackett SF, Hjelmeland LM. Ultrastructural and immunocytochemical changes in retinal pigment epithelium, retinal glia, and fibroblasts in vitreous culture. *Invest Ophthalmol Vis Sci*. 1990;31(12):2529–45. Epub 1990/12/01.
24. Baudouin C, Fredj-Reygrobellet D, Gordon WC, Baudouin F, Peyman G, Lapalus P, et al. Immunohistologic study of epiretinal membranes in proliferative vitreoretinopathy. *Am J Ophthalmol*. 1990;110(6):593–8. Epub 1990/12/15.
25. Esser P, Heimann K, Wiedemann P. Macrophages in proliferative vitreoretinopathy and proliferative diabetic retinopathy: differentiation of subpopulations. *Br J Ophthalmol*. 1993;77(11):731–3. Epub 1993/11/01.
26. Charteris DG, Hiscott P, Grierson I, Lightman SL. Proliferative vitreoretinopathy. Lymphocytes in epiretinal membranes. *Ophthalmology*. 1992;99(9):1364–7. Epub 1992/09/01.
27. Limb GA, Franks WA, Munasinghe KR, Chignell AH, Dumonde DC. Proliferative vitreoretinopathy: an examination of the involvement of lymphocytes, adhesion molecules and HLA-DR antigens. *Graefes Arch Clin Exp Ophthalmol*. 1993;231(6):331–6. Epub 1993/06/01.
28. Charteris DG, Hiscott P, Robey HL, Gregor ZI, Lightman SL, Grierson I. Inflammatory cells in proliferative vitreoretinopathy subretinal membranes. *Ophthalmology*. 1993;100(1):43–6. Epub 1993/01/01.
29. Sethi CS, Lewis GP, Fisher SK, Leitner WP, Mann DL, Luthert PJ, et al. Glial remodeling and neural plasticity in human retinal detachment with proliferative vitreoretinopathy. *Invest Ophthalmol Vis Sci*. 2005;46(1):329–42. Epub 2004/12/30.
30. Charteris DG, Downie J, Aylward GW, Sethi C, Luthert P. Intraretinal and periretinal pathology in anterior proliferative vitreoretinopathy. *Graefes Arch Clin Exp Ophthalmol*. 2007;245(1):93–100. Epub 2006/04/14.
31. Scheiffarth OF, Kampik A, Gunther H, von der Mark K. Proteins of the extracellular matrix in vitreoretinal membranes. *Graefes Arch Clin Exp Ophthalmol*. 1988;226(4):357–61. Epub 1988/01/01.
32. Vidaurri-Leal JS, Glaser BM. Effect of fibrin on morphologic characteristics of retinal pigment epithelial cells. *Arch Ophthalmol*. 1984;102(9):1376–9. Epub 1984/09/01.
33. Glaser BM, Cardin A, Biscoe B. Proliferative vitreoretinopathy. The mechanism of development of vitreoretinal traction. *Ophthalmology*. 1987;94(4):327–32. Epub 1987/04/01.
34. Tano Y, Sugita G, Abrams G, Machemer R. Inhibition of intraocular proliferations with intravitreal corticosteroids. *Am J Ophthalmol*. 1980;89(1):131–6. Epub 1980/01/01.
35. Tano Y, Chandler D, Machemer R. Treatment of intraocular proliferation with intravitreal injection of triamcinolone acetonide. *Am J Ophthalmol*. 1980;90(6):810–6. Epub 1980/12/01.
36. Chandler DB, Rozakis G, de Juan Jr E, Machemer R. The effect of triamcinolone acetonide on a refined experimental model of proliferative vitreoretinopathy. *Am J Ophthalmol*. 1985;99(6):686–90. Epub 1985/06/15.
37. Rubsamens PE, Cousins SW. Therapeutic effect of periocular corticosteroids in experimental proliferative vitreoretinopathy. *Retina*. 1997;17(1):44–50. Epub 1997/01/01.
38. Kaczmarek R, Szurman P, Misiuk-Hojlo M, Grzybowski A. Antiproliferative effects of preservative-free triamcinolone acetonide on cultured human retinal pigment epithelial cells. *Medical Science Monitor: international medical journal of experimental and clinical research*. 2009;15(8):BR227–31. Epub 2009/08/01.
39. Koerner F, Merz A, Gloor B, Wagner E. Postoperative retinal fibrosis—a controlled clinical study of systemic steroid therapy. *Graefes Arch Clin Exp Ophthalmol*. 1982;219(6):268–71. Epub 1982/01/01.
40. Bali E, Feron EJ, Peperkamp E, Veckeneer M, Mulder PG, van Meurs JC. The effect of a preoperative subconjunctival injection of dexamethasone on blood-retinal barrier breakdown following scleral buckling retinal detachment surgery: a prospective randomized placebo-controlled double blind clinical trial. *Graefes Arch Clin Exp Ophthalmol*. 2010;248(7):957–62. Epub 2010/02/26.
41. Jonas JB, Hayler JK, Panda-Jonas S. Intravitreal injection of crystalline cortisone as adjunctive treatment of proliferative vitreoretinopathy. *Br J Ophthalmol*. 2000;84(9):1064–7. Epub 2000/09/01.
42. Sakamoto T, Miyazaki M, Hisatomi T, Nakamura T, Ueno A, Itaya K, et al. Triamcinolone-assisted pars plana vitrectomy improves the surgical procedures and decreases the postoperative blood-ocular barrier breakdown. *Graefes Arch Clin Exp Ophthalmol*. 2002;240(6):423–9. Epub 2002/07/11.
43. Munir WM, Pulido JS, Sharma MC, Buerk BM. Intravitreal triamcinolone for treatment of complicated proliferative dia-

- betic retinopathy and proliferative vitreoretinopathy. *Canadian Journal of Ophthalmology Journal Canadien d'ophtalmologie*. 2005;40(5):598–604. Epub 2006/01/05.
44. Cheema RA, Peyman GA, Fang T, Jones A, Lukaris AD, Lim K. Triamcinolone acetonide as an adjuvant in the surgical treatment of retinal detachment with proliferative vitreoretinopathy. *Ophthalmic Surg Lasers Imaging*. 2007;38(5):365–70. Epub 2007/10/25.
 45. Acar N, Kapran Z, Altan T, Unver YB, Pasaoglu E. Pars plana vitrectomy with and without triamcinolone acetonide assistance in pseudophakic retinal detachment complicated with proliferative vitreoretinopathy. *Jpn J Ophthalmol*. 2010;54(4):331–7. Epub 2010/08/12.
 46. Chen W, Chen H, Hou P, Fok A, Hu Y, Lam DS. Midterm results of low-dose intravitreal triamcinolone as adjunctive treatment for proliferative vitreoretinopathy. *Retina*. 2011;31(6):1137–42. Epub 2011/02/15.
 47. Yamakiri K, Sakamoto T, Noda Y, Nakahara M, Ogino N, Kubota T, et al. Reduced incidence of intraoperative complications in a multicenter controlled clinical trial of triamcinolone in vitrectomy. *Ophthalmology*. 2007;114(2):289–96. Epub 2007/02/03.
 48. Yamakiri K, Sakamoto T, Noda Y, Nakahara M, Ogino N, Kubota T, et al. One-year results of a multicenter controlled clinical trial of triamcinolone in pars plana vitrectomy. *Graefes Arch Clin Exp Ophthalmol*. 2008;246(7):959–66. Epub 2008/04/24.
 49. Ahmadieh H, Fegghi M, Tabatabaei H, Shoeibi N, Ramezani A, Mohebbi MR. Triamcinolone acetonide in silicone-filled eyes as adjunctive treatment for proliferative vitreoretinopathy: a randomized clinical trial. *Ophthalmology*. 2008;115(11):1938–43. Epub 2008/07/01.
 50. Koerner F, Koerner-Stiefbold U, Garweg JG. Systemic corticosteroids reduce the risk of cellophane membranes after retinal detachment surgery: a prospective randomized placebo-controlled double-blind clinical trial. *Graefes Arch Clin Exp Ophthalmol*. 2012;250(7):981–7. Epub 2012/01/25.
 51. Weijtens O, Schoemaker RC, Lentjes EG, Romijn FP, Cohen AF, van Meurs JC. Dexamethasone concentration in the subretinal fluid after a subconjunctival injection, a peribulbar injection, or an oral dose. *Ophthalmology*. 2000;107(10):1932–8. Epub 2000/10/03.
 52. Blumenkranz MS, Clafflin A, Hajek AS. Selection of therapeutic agents for intraocular proliferative disease. Cell culture evaluation. *Arch Ophthalmol*. 1984;102(4):598–604. Epub 1984/04/01.
 53. Cardillo JA, Farah ME, Mitre J, Morales PH, Costa RA, Melo LA, et al. An intravitreal biodegradable sustained release naproxen and 5-fluorouracil system for the treatment of experimental post-traumatic proliferative vitreoretinopathy. *Br J Ophthalmol*. 2004;88(9):1201–5. Epub 2004/08/20.
 54. Sanders DR, Kraff MC, Lieberman HL, Peyman GA, Tarabishy S. Breakdown and reestablishment of blood-aqueous barrier with implant surgery. *Arch Ophthalmol*. 1982;100(4):588–90. Epub 1982/04/01.
 55. Sanders DR, Kraff M. Steroidal and nonsteroidal anti-inflammatory agents. Effect on postsurgical inflammation and blood-aqueous humor barrier breakdown. *Arch Ophthalmol*. 1984;102(10):1453–6. Epub 1984/10/01.
 56. Blumenkranz MS, Ophir A, Clafflin AJ, Hajek A. Fluorouracil for the treatment of massive periretinal proliferation. *Am J Ophthalmol*. 1982;94(4):458–67. Epub 1982/10/01.
 57. Stern WH, Lewis GP, Erickson PA, Guerin CJ, Anderson DH, Fisher SK, et al. Fluorouracil therapy for proliferative vitreoretinopathy after vitrectomy. *Am J Ophthalmol*. 1983;96(1):33–42. Epub 1983/07/01.
 58. Stern WH, Guerin CJ, Erickson PA, Lewis GP, Anderson DH, Fisher SK. Ocular toxicity of fluorouracil after vitrectomy. *Am J Ophthalmol*. 1983;96(1):43–51. Epub 1983/07/01.
 59. Nao-i N, Honda Y. Toxic effect of fluorouracil on the rabbit retina. *Am J Ophthalmol*. 1983;96(5):641–3. Epub 1983/11/01.
 60. Hartzler MK, Blumenkranz MS, Hajek AS, Dailey WA, Cheng M, Margherio AR. Selection of therapeutic agents for intraocular proliferative disease 3. Effects of fluoropyrimidines on cell-mediated contraction of human fibroblasts. *Exp Eye Res*. 1989;48(3):321–8. Epub 1989/03/01.
 61. Blumenkranz MS, Hartzler MK, Hajek AS. Selection of therapeutic agents for intraocular proliferative disease. II. Differing antiproliferative activity of the fluoropyrimidines. *Arch Ophthalmol*. 1987;105(3):396–9. Epub 1987/03/01.
 62. Ward T, Hartzler M, Blumenkranz M, Lin LR. A comparison of 5-fluorouridine and 5-fluorouracil in an experimental model for the treatment of vitreoretinal scarring. *Curr Eye Res*. 1993;12(5):397–401. Epub 1993/05/01.
 63. Leon JA, Britt JM, Hopp RH, Mills RP, Milam AH. Effects of fluorouracil and fluorouridine on protein synthesis in rabbit retina. *Invest Ophthalmol Vis Sci*. 1990;31(9):1709–16. Epub 1990/09/01.
 64. Rubsamen PE, Davis PA, Hernandez E, O'Grady GE, Cousins SW. Prevention of experimental proliferative vitreoretinopathy with a biodegradable intravitreal implant for the sustained release of fluorouracil. *Arch Ophthalmol*. 1994;112(3):407–13. Epub 1994/03/01.
 65. Berger AS, Cheng CK, Pearson PA, Ashton P, Crooks PA, Cynkowski T, et al. Intravitreal sustained release corticosteroid-5-fluorouracil conjugate in the treatment of experimental proliferative vitreoretinopathy. *Invest Ophthalmol Vis Sci*. 1996;37(11):2318–25. Epub 1996/10/01.
 66. Yang CS, Khawly JA, Hainsworth DP, Chen SN, Ashton P, Guo H, et al. An intravitreal sustained-release triamcinolone and 5-fluorouracil codrug in the treatment of experimental proliferative vitreoretinopathy. *Arch Ophthalmol*. 1998;116(1):69–77. Epub 1998/01/28.
 67. Perkins SL, Gallemore RP, Yang CH, Guo H, Ashton P, Jaffe GJ. Pharmacokinetics of the fluocinolone/5-fluorouracil codrug in the gas-filled eye. *Retina*. 2000;20(5):514–9. Epub 2000/10/20.
 68. Blumenkranz M, Hernandez E, Ophir A, Norton EW. 5-fluorouracil: new applications in complicated retinal detachment for an established antimetabolite. *Ophthalmology*. 1984;91(2):122–30. Epub 1984/02/01.
 69. Blankenship GW. Evaluation of a single intravitreal injection of 5-fluorouracil in vitrectomy cases. *Graefes Arch Clin Exp Ophthalmol*. 1989;27(6):565–8. Epub 1989/01/01.
 70. Asaria RH, Kon CH, Bunce C, Charteris DG, Wong D, Khaw PT, et al. Adjuvant 5-fluorouracil and heparin prevents proliferative vitreoretinopathy: results from a randomized, double-blind, controlled clinical trial. *Ophthalmology*. 2001;108(7):1179–83. Epub 2001/06/27.
 71. Charteris DG, Aylward GW, Wong D, Groenewald C, Asaria RH, Bunce C. A randomized controlled trial of combined 5-fluorouracil and low-molecular-weight heparin in management of established proliferative vitreoretinopathy. *Ophthalmology*. 2004;111(12):2240–5. Epub 2004/12/08.
 72. Wickham L, Bunce C, Wong D, McGurn D, Charteris DG. Randomized controlled trial of combined 5-Fluorouracil and low-molecular-weight heparin in the management of unselected rhegmatogenous retinal detachments undergoing primary vitrectomy. *Ophthalmology*. 2007;114(4):698–704. Epub 2007/04/03.
 73. Kirmani M, Santana M, Sorgente N, Wiedemann P, Ryan SJ. Antiproliferative drugs in the treatment of experimental proliferative vitreoretinopathy. *Retina*. 1983;3(4):269–72. Epub 1983/01/01.
 74. Santana M, Wiedemann P, Kirmani M, Minckler DS, Patterson R, Sorgente N, et al. Daunomycin in the treatment of experimental proliferative vitreoretinopathy: retinal toxicity of intravitreal daunomycin in the rabbit. *Graefes Arch Clin Exp Ophthalmol*. 1984;221(5):210–3. Epub 1984/01/01.
 75. Verdoorn C, Renardel de Lavalette VW, Dalma-Weizhausz J, Orr GM, Sorgente N, Ryan SJ. Cellular migration, proliferation, and contraction. An in vitro approach to a clinical problem—proliferative vitreoretinopathy. *Arch Ophthalmol*. 1986;104(8):1216–9.

76. Weller M, Heimann K, Wiedemann P. Cytotoxic effects of daunomycin on retinal pigment epithelium in vitro. *Graefes Arch Clin Exp Ophthalmol*. 1987;225(3):235–8. Epub 1987/01/01.
77. Khawly JA, Saloupi P, Hatchell DL, Machemer R. Daunorubicin treatment in a refined experimental model of proliferative vitreoretinopathy. *Graefes Arch Clin Exp Ophthalmol*. 1991;229(5):464–7. Epub 1991/01/01.
78. Kumar A, Tewari HK, Bathwal DP, Khosla PK. Experimental inhibition of proliferative vitreoretinopathy in retinal detachment using daunorubicin. *Indian J Ophthalmol*. 1994;42(1):31–5. Epub 1994/03/01.
79. Wiedemann P, Sorgente N, Bekhor C, Patterson R, Tran T, Ryan SJ. Daunomycin in the treatment of experimental proliferative vitreoretinopathy. Effective doses in vitro and in vivo. *Invest Ophthalmol Vis Sci*. 1985;26(5):719–25. Epub 1985/05/01.
80. Rahimy MH, Peyman GA, Fernandes ML, el-Sayed SH, Luo Q, Borhani H. Effects of an intravitreal daunomycin implant on experimental proliferative vitreoretinopathy: simultaneous pharmacokinetic and pharmacodynamic evaluations. *J Ocul Pharmacol*. 1994;10(3):561–70. Epub 1994/01/01.
81. Hashizoe M, Ogura Y, Takanashi T, Kunou N, Honda Y, Ikada Y. Implantable biodegradable polymeric device in the treatment of experimental proliferative vitreoretinopathy. *Curr Eye Res*. 1995;14(6):473–7. Epub 1995/06/01.
82. Shinohara K, Tanaka M, Sakuma T, Kobayashi Y. Efficacy of daunorubicin encapsulated in liposome for the treatment of proliferative vitreoretinopathy. *Ophthalmic Surg Lasers Imaging*. 2003;34(4):299–305. Epub 2003/07/24.
83. Hueber A, Luke M, Esser PJ, Kirchoff B, Sickel W, Luke C. Effects of daunorubicin and CD95L on retinal function in superfused vertebrate retina. *J Ocul Pharmacol Ther*. 2005;21(2):133–8. Epub 2005/04/29.
84. Esser P, Tervooren D, Heimann K, Kociok N, Bartz-Schmidt KU, Walter P, et al. Intravitreal daunomycin induces multidrug resistance in proliferative vitreoretinopathy. *Invest Ophthalmol Vis Sci*. 1998;39(1):164–70. Epub 1998/01/16.
85. Kuo HK, Chen YH, Wu PC, Wu YC, Huang F, Kuo CW, et al. Attenuated glial reaction in experimental proliferative vitreoretinopathy treated with liposomal doxorubicin. *Invest Ophthalmol Vis Sci*. 2012;53(6):3167–74. Epub 2012/04/12.
86. Wiedemann P, Lemmen K, Schmiedl R, Heimann K. Intraocular daunorubicin for the treatment and prophylaxis of traumatic proliferative vitreoretinopathy. *Am J Ophthalmol*. 1987;104(1):10–4. Epub 1987/07/15.
87. Wiedemann P, Leinung C, Hilgers RD, Heimann K. Daunomycin and silicone oil for the treatment of proliferative vitreoretinopathy. *Graefes Arch Clin Exp Ophthalmol*. 1991;229(2):150–2. Epub 1991/01/01.
88. Wiedemann P, Hilgers RD, Bauer P, Heimann K. Adjunctive daunorubicin in the treatment of proliferative vitreoretinopathy: results of a multicenter clinical trial. Daunomycin Study Group. *Am J Ophthalmol*. 1998;126(4):550–9. Epub 1998/10/21.
89. Raczynska K, Gebka A, Iwaszkiewicz-Bilikiewicz B, Ciechanowski C. Vitrectomy with daunorubicin. *Klin Oczna*. 2004;106(3 Suppl):481–4. Epub 2005/01/08. Witrektomia z daunorubicyna.
90. Campochiaro PA, Hackett SF, Conway BP. Retinoic acid promotes density-dependent growth arrest in human retinal pigment epithelial cells. *Invest Ophthalmol Vis Sci*. 1991;32(1):65–72. Epub 1991/01/01.
91. Verstraeten T, Hartzler M, Wilcox DK, Cheng M. Effects of vitamin A on retinal pigment epithelial cells in vitro. *Invest Ophthalmol Vis Sci*. 1992;33(10):2830–8. Epub 1992/09/01.
92. Giordano GG, Refojo MF, Arroyo MH. Sustained delivery of retinoic acid from microspheres of biodegradable polymer in PVR. *Invest Ophthalmol Vis Sci*. 1993;34(9):2743–51. Epub 1993/08/01.
93. Yan XR, Dong XG, Chen N, Wang W. Antiproliferative effect of sustained drug delivery system of all-trans retinoic acid implant into rabbit's vitreous cavity for treatment of proliferative vitreoretinopathy. [Zhonghua yan ke za zhi] *Chinese Journal of Ophthalmology*. 2003;39(10):621–5. Epub 2004/02/10.
94. Dong X, Chen N, Xie L, Wang S. Prevention of experimental proliferative vitreoretinopathy with a biodegradable intravitreal drug delivery system of all-trans retinoic acid. *Retina*. 2006;26(2):210–3. Epub 2006/02/10.
95. Nakagawa M, Refojo MF, Marin JF, Doi M, Tolentino FI. Retinoic acid in silicone and silicone-fluorosilicone copolymer oils in a rabbit model of proliferative vitreoretinopathy. *Invest Ophthalmol Vis Sci*. 1995;36(12):2388–95. Epub 1995/11/01.
96. Veloso Jr AA, Kadrmas EF, Larrosa JM, Sandberg MA, Tolentino FI, Refojo MF. 13-cis-retinoic acid in silicone-fluorosilicone copolymer oil in a rabbit model of proliferative vitreoretinopathy. *Exp Eye Res*. 1997;65(3):425–34. Epub 1997/09/01.
97. Wu WC, Hu DN, Mehta S, Chang YC. Effects of retinoic acid on retinal pigment epithelium from excised membranes from proliferative vitreoretinopathy. *J Ocul Pharmacol Ther*. 2005;21(1):44–54. Epub 2005/02/19.
98. Chang YC, Kao YH, Hu DN, Tsai LY, Wu WC. All-trans retinoic acid remodels extracellular matrix and suppresses laminin-enhanced contractility of cultured human retinal pigment epithelial cells. *Exp Eye Res*. 2009;88(5):900–9. Epub 2008/12/20.
99. Fekrat S, De Juan Jr E, Campochiaro PA. The effect of oral 13-cis-retinoic acid on retinal redetachment after surgical repair in eyes with proliferative vitreoretinopathy. *Ophthalmology*. 1995;102(3):412–8. Epub 1995/03/01.
100. Chang YC, Hu DN, Wu WC. Effect of oral 13-cis-retinoic acid treatment on postoperative clinical outcome of eyes with proliferative vitreoretinopathy. *Am J Ophthalmol*. 2008;146(3):440–6. Epub 2008/07/05.
101. Weller M, Heimann K, Wiedemann P. Immunohistochemical findings in proliferative retinal diseases—on the significance of fibronectin, macrophages and transferrin. *Fortschr Ophthalmol*. 1989;86(2):121–3. Epub 1989/01/01. Immunohistochemische Befunde bei proliferativen Netzhauterkrankungen – zur Bedeutung von Fibronectin, Makrophagen und Transferrin.
102. Baudouin C, Brignole F, Fredj-Reygrobelle D, Negre F, Bayle J, Gastaud P. Transferrin receptor expression by retinal pigment epithelial cells in proliferative vitreoretinopathy. *Invest Ophthalmol Vis Sci*. 1992;33(10):2822–9. Epub 1992/09/01.
103. Davis AA, Whidby DE, Privette T, Houston LL, Hunt RC. Selective inhibition of growing pigment epithelial cells by a receptor-directed immunotoxin. *Invest Ophthalmol Vis Sci*. 1990;31(12):2514–9. Epub 1990/12/01.
104. Jaffe GJ, Earnest K, Fulcher S, Lui GM, Houston LL. Antitransferrin receptor immunotoxin inhibits proliferating human retinal pigment epithelial cells. *Arch Ophthalmol*. 1990;108(8):1163–8. Epub 1990/08/01.
105. Handa JT, Houston LL, Jaffe GJ. The antiproliferative effect of a transferrin-toxin on human retinal pigment epithelial cells and rabbit fibroblasts. *Invest Ophthalmol Vis Sci*. 1993;34(12):3419–28. Epub 1993/11/01.
106. Hermesen VM, Fulcher SF, Spiekerman AM, Phinizy JL, Di Tullio NW. Long-term inhibition of cellular proliferation by immunotoxins. *Arch Ophthalmol*. 1990;108(7):1009–11. Epub 1990/07/01.
107. Handa JT, Keithahn MA, Jaffe GJ. Transferrin-ricin A chain toxin limits the development of experimental proliferative vitreoretinopathy. *Exp Eye Res*. 1996;62(6):689–96. Epub 1996/06/01.
108. Hoffmann S, Masood R, Zhang Y, He S, Ryan SJ, Gill P, et al. Selective killing of RPE with a vascular endothelial growth factor chimeric toxin. *Invest Ophthalmol Vis Sci*. 2000;41(8):2389–93. Epub 2000/07/13.
109. van Bockxmeer FM, Martin CE, Constable IJ. Models for assessing scar tissue inhibitors. *Retina*. 1985;5(1):47–60. Epub 1985/01/01.

110. Campochiaro PA, Glaser BM. Mechanisms involved in retinal pigment epithelial cell chemotaxis. *Arch Ophthalmol.* 1986;104(2):277–80. Epub 1986/02/01.
111. Lemor M, de Bustros S, Glaser BM. Low-dose colchicine inhibits astrocyte, fibroblast, and retinal pigment epithelial cell migration and proliferation. *Arch Ophthalmol.* 1986;104(8):1223–5. Epub 1986/08/01.
112. Lemor M, Yeo JH, Glaser BM. Oral colchicine for the treatment of experimental traction retinal detachment. *Arch Ophthalmol.* 1986;104(8):1226–9. Epub 1986/08/01.
113. Raymond MC, Thompson JT. RPE-mediated collagen gel contraction. Inhibition by colchicine and stimulation by TGF-beta. *Invest Ophthalmol Vis Sci.* 1990;31(6):1079–86. Epub 1990/06/01.
114. Pastor JC, Rodriguez E, Marcos MA, Lopez MI. Combined pharmacologic therapy in a rabbit model of proliferative vitreoretinopathy (PVR). *Ophthalmic Res.* 2000;32(1):25–9. Epub 2000/02/05.
115. Cai J, Wei R, Ma X, Zhu H, Li Y. Cytotoxic effects of antiproliferative agents on human retinal glial cells in vitro. *Int Ophthalmol.* 2001;24(4):225–31. Epub 2003/04/08.
116. Berman DH, Gombos GM. Proliferative vitreoretinopathy: does oral low-dose colchicine have an inhibitory effect? A controlled study in humans. *Ophthalmic Surg.* 1989;20(4):268–72. Epub 1989/04/01.
117. Yoo JS, Sakamoto T, Spee C, Kimura H, Harris MS, Hinton DR, et al. cis-Hydroxyproline inhibits proliferation, collagen synthesis, attachment, and migration of cultured bovine retinal pigment epithelial cells. *Invest Ophthalmol Vis Sci.* 1997;38(2):520–8. Epub 1997/02/01.
118. Yasukawa T, Kimura H, Tabata Y, Miyamoto H, Honda Y, Ogura Y. Sustained release of cis-hydroxyproline in the treatment of experimental proliferative vitreoretinopathy in rabbits. *Graefes Arch Clin Exp Ophthalmol.* 2002;240(8):672–8. Epub 2002/08/23.
119. Kon CH, Occleston NL, Charteris D, Daniels J, Aylward GW, Khaw PT. A prospective study of matrix metalloproteinases in proliferative vitreoretinopathy. *Invest Ophthalmol Vis Sci.* 1998;39(8):1524–9. Epub 1998/07/11.
120. Salzmann J, Limb GA, Khaw PT, Gregor ZJ, Webster L, Chignell AH, et al. Matrix metalloproteinases and their natural inhibitors in fibrovascular membranes of proliferative diabetic retinopathy. *Br J Ophthalmol.* 2000;84(10):1091–6. Epub 2000/09/27.
121. Ozerdem U, Mach-Hofacre B, Cheng L, Chaidhawangul S, Keefe K, McDermott CD, et al. The effect of prinomastat (AG3340), a potent inhibitor of matrix metalloproteinases, on a subacute model of proliferative vitreoretinopathy. *Curr Eye Res.* 2000;20(6):447–53. Epub 2000/09/12.
122. Ozerdem U, Mach-Hofacre B, Keefe K, Pham T, Soules K, Appelt K, et al. The effect of prinomastat (AG3340), a synthetic inhibitor of matrix metalloproteinases, on posttraumatic proliferative vitreoretinopathy. *Ophthalmic Res.* 2001;33(1):20–3. Epub 2000/12/15.
123. El-Bradey MH, Cheng L, Bartsch DU, Niessman M, El-Musharaf A, Freeman WR. The effect of prinomastat (AG3340), a potent inhibitor of matrix metalloproteinase, on a new animal model of epiretinal membrane. *Retina.* 2004;24(5):783–9. Epub 2004/10/20.
124. Blumenkranz MS, Hartzler MK. Pharmacologic treatment of proliferative vitreoretinopathy: interrelationship with the coagulation cascade. In: Lewis HR, Ryan SJ, editors. *Medical and surgical retina, advances, controversies and management.* St Louis: Mosby; 1993. p. 172.
125. Johnson RN, Blankenship G. A prospective, randomized, clinical trial of heparin therapy for postoperative intraocular fibrin. *Ophthalmology.* 1988;95(3):312–7. Epub 1988/03/01.
126. Williams RG, Chang S, Comaratta MR, Simoni G. Does the presence of heparin and dexamethasone in the vitrectomy infusate reduce reepithelialization in proliferative vitreoretinopathy? *Graefes Arch Clin Exp Ophthalmol.* 1996;234(8):496–503. Epub 1996/08/01.
127. Iverson DA, Katsura H, Hartzler MK, Blumenkranz MS. Inhibition of intraocular fibrin formation following infusion of low-molecular-weight heparin during vitrectomy. *Arch Ophthalmol.* 1991;109(3):405–9. Epub 1991/03/01.
128. Kon CH, Asaria RH, Occleston NL, Khaw PT, Aylward GW. Risk factors for proliferative vitreoretinopathy after primary vitrectomy: a prospective study. *Br J Ophthalmol.* 2000;84(5):506–11. Epub 2000/04/27.

Ian Y. Wong, Ning Cheung, and David Wong

Outline

- I. **Introduction**
- II. **Short-Acting Vitreous Substitutes**
 - A. Aqueous Vitreous Substitutes
 - 1. Isotonic Saline
 - 2. Lactated Ringer's Solution
 - 3. Balanced Salt Solution
 - B. Gaseous Vitreous Substitutes
 - 1. Physical Properties of Intraocular Gases
 - a. Air
 - b. Long-Acting Gases
 - 2. Functional Properties of Intraocular Gases
 - a. Internal Tamponade
 - b. Flatten Folded Retina
 - c. Enable Visualization
 - d. Restore Globe Volume
 - e. Reduce Intraocular Fluid Currents
 - 3. Dynamic Properties of Gas Inside the Eye
 - a. Expansion
 - b. Equilibration
 - c. Dissolution
 - 4. Physiologic Changes of Gas in Special Circumstances
 - a. Interaction with General Anesthesia
 - b. Effects of Variations in Altitude

III. Long-Acting Vitreous Substitutes

- A. Perfluorocarbon Liquids
 - 1. Properties
 - 2. Retinal Toxicity
- B. Silicone Oil
 - 1. Chemical Properties of Silicone Oil
 - 2. Physical Properties of Silicone Oil
 - a. Specific Gravity
 - b. Buoyancy
 - c. Surface Tension and Interfacial Tension
 - d. Viscosity
 - e. Viscoelasticity

Conclusion

References

Keywords

Vitrectomy • Retinal detachment • Surgery • Vitreous substitutes • Internal tamponades • Perfluoropropane • Sulfur hexafluoride • Perfluorocarbon liquid • Silicone oil

Key Concepts

1. Gas as an internal tamponade agent offers a high tamponade force acting on the retina. However, this advantage is accompanied by the disadvantage of a relatively short intraocular life-span, which may not be sufficient in particular cases where prolonged tamponade is required.
2. Perfluorocarbon liquids are valuable intraoperative tools that offer numerous physical advantages in assisting unrolling of the retina and the displacement of subretinal fluid in retinal detachments.
3. Silicone oils of various viscosities offer different intraocular properties and can behave differently. With the refinement of small-gauge vitrectomy systems, the use of silicone oil has become more compatible.

I.Y. Wong, MD
Department of Ophthalmology, University of Hong Kong,
Hong Kong, China

N. Cheung, MD
Department of Ophthalmology, University of Hong Kong,
Hong Kong, China

Singapore Eye Research Institute, Singapore National Eye Centre,
Singapore

D. Wong, MD (✉)
Vitreous-Retinal Department, The Royal Liverpool
University Hospital, Liverpool, England, UK

Department of Ophthalmology, LKS Faculty of Medicine,
University of Hong Kong, Room 301, Level 3,
Block B, Cyberport 4, Pokfulam, Hong Kong, China
e-mail: shdwong@hku.hk

I. Introduction

Human vitreous is a natural intraocular polymeric hydrogel with distinct biochemical and physiological functions. Surgical removal of the vitreous, or vitrectomy, is now commonly performed for the treatment of many vitreoretinal diseases. This has led to the need for developing substances that can be used to replace vitreous. Although early attempts for vitreous transplantation have yielded little success [1], a range of other vitreous substitutes has been developed. An ideal substitute should have all the good qualities of the human vitreous, including transparency, elasticity, buffer capacity, and biocompatibility with surrounding ocular tissues. However, none of the currently available vitreous substitutes possesses all these qualities. In modern vitreoretinal surgery, both short-acting (e.g., air, balanced salt solutions, expansile gases) and long-acting vitreous substitutes (e.g., silicone oil) are used. All these substitutes have significant shortcomings, mostly related to the lack of local biocompatibility and inadequate physiological role. In this chapter, we discuss the biophysical, biochemical, and physiological properties of the available vitreous substitutes, as well as their clinical use, advantages, and limitations. A separate chapter addresses the future potential of an artificial vitreous [see chapter I.F. Vitreous biochemistry and artificial vitreous].

II. Short-Acting Vitreous Substitutes

During vitrectomy, an aqueous solution is infused. At the conclusion of surgery, this can be left in the eye or a short-acting vitreous substitute can be introduced.

A. Aqueous Vitreous Substitutes

Following vitrectomy, various aqueous substances, which approximate the human aqueous humor, are left inside the eye as a vitreous substitute, ranging from isotonic saline to lactated Ringer's solution and most recently a balanced salt solution (BSS), at times supplemented with various constituents (BSS Plus).

1. Isotonic Saline

Normal saline is an isotonic solution that has been used in the past as infusion fluid during vitrectomy. However, it is now rarely used due to its tendency to cause corneal edema even after short periods of infusion, limiting visualization of the posterior segment during vitrectomy as well as making it not suitable as a vitreous substitute after vitrectomy.

2. Lactated Ringer's Solution

Lactated Ringer's solution contains potassium, calcium, and a lactate buffer. These constituents make it more suitable as an irrigating solution because they slow down the onset of corneal edema. Nevertheless, lactated Ringer's solution is still not ideal due to its relative hypotonicity and acidity and also lack of energy source for cellular metabolism.

3. Balanced Salt Solution

Balanced salt solution (BSS) was introduced in the 1960s and is now the most commonly used aqueous vitreous substitute during or immediately after vitrectomy. Unlike normal saline or lactated Ringer's solutions, BSS contains magnesium and an acetate-citrate buffer. Subsequently, a further enhanced version of the solution called BSS Plus was developed, which includes other necessary electrolytes, glutathione, and bicarbonate as a buffer. Clinical studies have shown that BSS Plus causes less corneal edema and endothelial cell loss following vitrectomy than lactated Ringer's solution [2, 3]. It is frequently used as an irrigating solution to replace intraocular volume lost by vitreous removal intraoperatively. Moreover, it has also been used as vehicle to carry drugs for hemostasis, pupillary dilatation, and antiinflammatory effects [4]. Recently, low-molecular-weight heparin and 5-fluorouracil have been added to the infusion to prevent postoperative proliferative vitreoretinopathy [5] [see chapter IV.F. Pharmacotherapy of PVR].

B. Gaseous Vitreous Substitutes

Intraocular gas has been used in retinal detachment surgery for more than a century. However, its value was not widely appreciated until the 1930s, when Rosengren demonstrated improved retinal reattachment rates with the use of internal air tamponade [6]. In the 1960s, scleral buckling was coupled with intraocular gas injection in treating retinal detachments [7]. In the 1980s, pneumatic retinopexy was made possible with the use of expansile gases [8], although pure air was also very successful [9, 10] [see chapter V.B.7. Pneumatic retinopexy]. Subsequently, intraocular gas injection became an integral part of retinal detachment surgery using vitrectomy [11], resulting in better success rates of retinal reattachment, especially for more complicated cases such as those related to proliferative vitreoretinopathy (PVR) and giant retinal tears [see chapter V.B.5. Management of Proliferative Vitreo-Retinopathy]. Furthermore, indications for intraocular gas also extended to repair of macular hole and pneumatic displacement of submacular hemorrhage [see chapter V.A.1. Age-related macular degeneration Surgery].

Table IV.G-1 Commonly used intraocular gases and their physical properties

Gas ^a	Chemical formula	Molecular weight (g/mol)	Expansion (times original size)	Time to maximum expansion (hours)	Non-expansile concentration (%)	Longevity
Air	–	29	1.0	–	–	5–7 days
Sulfur hexafluoride	SF ₆	146	2.0	24–48	18	1–2 weeks
Perfluoroethane	C ₂ F ₆	138	3.3	36–60	15–16	4–5 weeks
Perfluoropropane	C ₃ F ₈	188	4.0	72–96	14	6–8 weeks

^aAll are odorless, colorless, inert, and inflammable

1. Physical Properties of Intraocular Gases

A variety of gaseous products have been investigated for intraocular use [12–15]. Rational choices should be made based on good understanding of the physical characteristics of the available products. Key characteristics with direct clinical relevance include longevity inside the eye, expansion ratio in pure form, and non-expansile concentration. Gases could be used in their pure forms, or as a mixture with air. Mixing the pure form with air in different proportions can adjust the expansile property of the gas (Table IV.G-1). Nowadays, three gases are most commonly used, including air, sulfur hexafluoride (SF₆), and perfluoropropane (C₃F₈) (Table IV.G-1).

a. Air

Air was the initial gas to be utilized in vitreoretinal surgery. Air is non-expansile at sea level and remains in the eye for around 5 days if the vitreous cavity is entirely filled. In Europe, air is often used in conventional scleral buckling surgery. McLeod and Chignell described the technique of sequential drainage of subretinal fluid, air injection, cryotherapy, and the application of explant in the same issue of the *British Journal of Ophthalmology* in 1985 [16, 17]. This surgical sequence, now known as the “D-ACE” technique, was designed for bullous superior retinal detachment associated with collapsed vitreous gel. The drainage of subretinal fluid, followed by the injection of air, effectively restores the anatomy in that the retina becomes re-apposed to the underlying retinal pigment epithelium and choroid. Precise and limited cryotherapy can then be applied, as there is no need for a large ice ball or to freeze through a depth of subretinal fluid. In addition, indentation by the scleral buckle needs only to be low profile as the retina is already mostly reattached [17]. Air injection is useful in 3 specific ways. Firstly, the intraocular pressure is restored after injection. Secondly, the surface tension of the air bubble keeps the retina apposed and reattached. Thirdly, the non-expansile nature of air is uniquely safe when combined with scleral buckling and in non-vitreotomized eyes. Unlike expansile gases, there is less concern of causing further collapse of the vitreous gel with trans-gel traction that can be transmitted to the vitreous base

inferiorly, giving rise to inferior retinal breaks [18, 19]. However, there are potential problems related to air injection in non-vitreotomized eyes. An example would be the breakup of the air bubble into “fish eggs” by poor injection techniques. The physics of air injection is complex involving not only buoyancy but also the rate of injection thus the rate of growth in size of the intraocular air bubble. The mechanics of “fish-egg” formation is well described by Aylward et al. who emphasized that the speed of injection is as important as keeping the needle in the uppermost part of the vitreous cavity. Sebag points out that this principle is also important when using pure air for office-based pneumatic retinopexy [9, 10] [see chapter V.B.7. Pneumatic retinopexy].

Air can also be used in combination with vitrectomy. The success of retinal detachment surgery relies on identifying and sealing all offending retinal breaks. With increasing use of endolaser coupled with vitrectomy, it is generally believed that chorioretinal adhesion can develop much quicker. Prolonged tamponade may therefore be unnecessary, as the duration of the tamponade effect from a gas bubble just needs to be long enough for chorioretinal adhesion around the breaks to develop. This is part of the rationale behind using very short-acting air as opposed to longer-acting SF₆ and C₃F₈ gases [9, 10]. Thus, in the absence of any risk factors for developing proliferative vitreoretinopathy and when causative retinal breaks are confined to one to three clock hours (depending upon the volume of air that is injected, since 0.8 ml bubble of air subtends an angle of 120°), air is a perfectly acceptable internal tamponade agent. The rapid absorption of air permits quicker visual rehabilitation and allows earlier air travel, if needed, for patients. It has also been suggested that the shorter duration of air mitigates against postoperative PVR and macular pucker [9].

b. Long-Acting Gases

Longer-acting internal tamponade might be required if retinal breaks are multiple and located widely apart from each other. For example, sulfur hexafluoride (SF₆) could be suitable in these cases. The non-expansile concentration of SF₆ is 20%. As a rule of thumb, if the vitreous cavity were totally filled, a bubble of 20% SF₆ (mixed with air) would last for about 2 weeks. The bubble would be relatively large for the

first few days to give adequately large area of tamponade to occlude widely separated retinal breaks. In addition, SF₆ is inert, nontoxic, and colorless and is five times heavier than air (relevant only intraoperatively during air-gas exchange).

Perfluorocarbon gases are similarly inert, odorless, and colorless. They have a generic chemical formula of C_xF_{2x+2} (x can be 1–4). Water solubility varies according to the carbon chain length. The longer the carbon chain, the lower the solubility in water; hence longer is the intraocular longevity. For instance, 1 ml of pure C₂F₆ expands approximately 3.3 times when injected into the eye and stays in the eye for 4–5 weeks; but for 1 ml of C₃F₈, the same volume expands 4 times and stays for 6–8 weeks. Both SF₆ and perfluorocarbon gases are heavier than air, which is relevant during intraoperative exchange of these expansile gases from an air-filled eye.

Two principal forces act on the gas bubble when it is injected into the eye: gravity-related downward and buoyancy-related upward forces. According to Archimedes' principle, any floating object displaces its own weight of fluid. For example, 1 ml of C₃F₈ weighs 0.001 g and displaces 1 ml of fluid that weighs 1 g (specific gravity of water is 1.0). Buoyancy is thus 1 g upward, and the net weight acting on the C₃F₈ bubble is 0.999 g (i.e., 1 g buoyancy minus 0.001 g gravity). The specific gravity of all gases is low, and buoyancy is for all intents and purposes the same for all the commonly used gases. The actual force depends on the amount of water the bubble displaces and thus on the size of the globe. The buoyancy force exerted is highest at the uppermost part of the eye cavity. For a normal-size eye of 2.3 cm diameter, it has been calculated that the force is 1.6 mmHg. Such a force pushes the bubble upward. The magnitude of this upward force for all gaseous tamponade is much larger than that of a silicone oil bubble, which has a specific gravity close to that of water or 1 g/ml. Perfluorocarbon liquid, on the other hand, can have a specific gravity up to and above 2 g/ml. Therefore, the buoyancy in the case of heavy liquids is negative or downward. If we assume the specific gravity to be 2 g/ml, the net downward force would be 1 g/ml. Note that this downward force exerted by the heavy liquids is exactly the same as the upward force exerted by air.

In principle, it is thought that a tamponade gas bubble works by making contact with retinal breaks, preventing fluid gaining access to subretinal space via the breaks. In the absence of fixed retinal folds, the risk of the bubble going through retinal breaks is minimal, because the high interfacial tension between water and gas keeps it as a single bubble. However, some surgeons believe that direct contact between bubble and retinal break might not be necessary. Clinical studies have demonstrated that inferior retinal breaks can be successfully treated with vitrectomy and gas tamponade, even without scleral buckling [20]. One theory is

that gas (or oil) bubbles may act as splints inside the eye, reducing intraocular fluid currents. This may allow the retina to reattach by itself. Nevertheless, assuming contact is important, the shape of the bubble determines the effectiveness of tamponade. Buoyancy has an important influence on the shape of an intraocular bubble. In the case of air, every molecule wants to float upward, and the bubble takes on the shape of a "spherical cap," that is, a bubble with a virtually flat bottom. Hence, most of the volume contributes to making contact with the retina. In contrast, small buoyancy occurs (e.g., silicone oil tamponade) when the shape of the bubble is rounded or spherical. In such case, less volume would contribute to making contact with the retina, as much of the bubble would go to form the meniscus, which is usually not in contact with the retina. An extreme example would be a spherical bubble inside a spherical cavity. The contact would go from none to total when it is 100 % filled. In reality, total tamponade is probably unachievable, and the volume of the bubble would in fact reduce further during the postoperative period. Nonetheless, most surgeons would use the non-expansile concentration of gases. The reason is that using "slightly expansile" concentration carries the serious risk of unpredictably high intraocular pressure as a result of the gas bubble, which completely fills the vitreous, exerting pressure anteriorly and leading to anterior chamber shallowing and secondary angle closure.

2. Functional Properties of Intraocular Gases

There are five major functions of a gas bubble inside the eye, which are to provide internal tamponade, flatten folded retina, enable visualization, replace globe volume, and reduce intraocular fluid currents.

a. Internal Tamponade

Providing internal tamponade for retinal detachments is usually the chief indication for use of intraocular gas [21]. The high surface tension between gas and fluid enables formation of an effective seal around retinal breaks, allowing retinal pigment epithelium to absorb any remaining subretinal fluid to facilitate retinal reattachment. The surface tension of gas is high compared to liquid tamponade agents such as silicone oil. Notably, the shape of a gas bubble varies with its volume. A small bubble takes on a rounded shape, as its shape is mainly determined by its high surface tension. With a bigger bubble, buoyancy becomes important. Every molecule of the bubble wants to float upward, resulting in a flattened bottom surface, which is used as a clinical marker for the size of gas bubble [22]. Upward force is greatest at the apex of the bubble, whereas it is near zero at the bottom. A relatively small bubble would provide a large arc of contact. As the bubble increases in size, the fill and contact is proportional. As the bubble approaches its maximal size within the eye, a slight

underfill would leave a large arc of retina not in contact with the bubble [23]. In clinical settings, inferior breaks are therefore difficult to tamponade, as complete gas fill is usually not achievable in reality. Furthermore, the sealing effect of gas bubbles on retinal breaks also prevents escape of cellular elements from under the retina into the vitreous cavity, thus reducing the risk of proliferative vitreoretinopathy [24] [see chapter III.J. Cell proliferation at vitreoretinal interface in PVR and related disorders].

b. Flatten Folded Retina

The surface tension and buoyancy force of the bubble can help unfold the retina. High radial buckles may sometimes cause circumferential retinal folds. These folds can be reduced by subretinal fluid drainage and air injection, as the air bubble pushes the retina to follow closely the contour of the indent. However, a large bubble coupled with incomplete subretinal fluid drainage could lead to the development of retinal fold, which may cause visual symptoms when the central macula is involved [25]. This complication could be prevented by complete drainage of subretinal fluid and judicious posturing immediately after surgery [26].

c. Enable Visualization

Looking through the gas bubble enables visualization after vitrectomy and gas tamponade. For looking at the upper retina, the surgeon should position lower than the patient, looking through the lower flat bottom surface of the bubble. Similarly, for looking at other parts of the fundus, the patient can be asked to lie on their side. If the vantage point is lower than the fluid level, the surgeon should easily see the nasal or temporal half of the retina. However, looking through the bubble, the retina often appears to be attached. This may simply be due to the buoyancy of the bubble displacing subretinal fluid laterally and posteriorly.

d. Restore Globe Volume

Globe volume restoration with air is often used in conventional scleral buckling surgery after the drainage of subretinal fluid. It prevents subretinal fluid from accumulating again, and importantly, it also raises intraocular pressure and restores the shape of the globe. Without subretinal fluid, cryotherapy would be limited and retinal break localization would be more accurate. Normal intraocular pressure also allows for safer placement of scleral sutures for external indentation.

e. Reduce Intraocular Fluid Currents

The presence of a gas bubble reduces intraocular fluid current, because the bubble usually occupies most of the volume of the globe. Such dampening of fluid current may minimize the chance of fluid movement into the subretinal space via retinal breaks, particularly the ones not covered by the bubble, i.e., inferior breaks.

3. Dynamic Properties of Gas Inside the Eye

Prior to complete resorption, an expansile gas bubble undergoes three phases after intraocular injection – expansion, equilibration, and dissolution.

a. Expansion

Pure SF₆, C₂F₆, and C₃F₈ will expand inside the eye because of their lower water solubility than nitrogen. Such expansion occurs due to nitrogen diffusion into the bubble at a rate that is higher than that of gas dissolving into surrounding tissue fluid compartment. During the initial 6 to 8 hours, expansion is rapid as the rate of expansion is mostly dependent on convection currents in the surrounding vitreous fluid [27]. Once the diffusion in and out of the bubble equilibrates, the bubble reaches its maximum size. This occurs around 1–2 days after injection for SF₆ and 3–4 days for C₃F₈ [28]. Thus, intraocular pressure (IOP) may rise if the outflow facility cannot cope with the rapid increase in intraocular volume. It has been shown that the eye may accommodate up to 1.2 ml of pure expansile gas injection (20–25 % of vitreous cavity volume) without significant changes in IOP [15, 28].

b. Equilibration

The equilibration phase starts when the partial pressure of nitrogen in the bubble equals that in the surrounding fluid compartment. There is a small net diffusion of expansile gas into the fluid compartment because the rate of equilibration of nitrogen is generally faster, due to its higher solubility, than that of other gases. As a result, the bubble decreases slightly in volume during this phase [28].

c. Dissolution

The dissolution phase commences when partial pressure of all gases within the bubble equals that in the fluid compartment. The volume of the gas bubble gradually reduces in size as gas dissolves into the fluid compartment, following the first-order exponential decay [29]. While it may take up to 6–8 weeks for a bubble to completely resorb, internal tamponade is effective during the initial 25 % of the bubble's life-span only, as it requires at least 50 % of the initial size to provide an effective tamponade. Internal tamponade is ineffective for a bubble smaller than 50 % or broken into a few smaller bubbles (i.e., fish eggs), even though it may still remain in the eye for a long time (Figure IV.G-1).

Unlike expansile gases, air does not expand and enters the dissolution phase immediately after injection. This is because the partial pressure of gases in air roughly equals that in the blood. In clinical practice, expansile gas is often mixed with air to create a “non-expansile” concentration. After injection of the gaseous mixture, the decrease in volume of the air compartment compensates for the increase in volume of the expansile gas compartment. With an appropriate ratio of

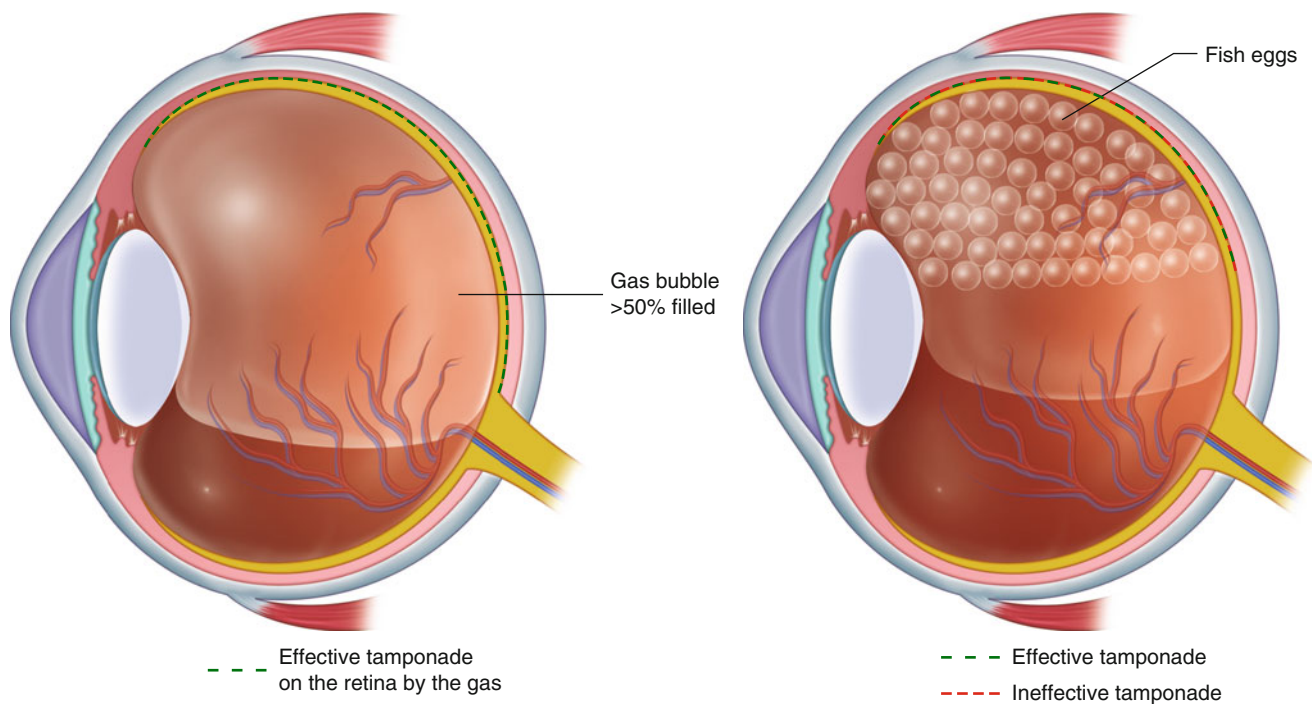


Figure IV.G-1 Fish-egg formation when gas volume reduces during gas resorption. Areas of the retina lying between the fish eggs are not supported by the gas bubbles

these two compartments, the overall gas compartment volume remains constant. Furthermore, the time taken for bubble resorption also depends on other factors, including lens status, aqueous turnover, presence of vitreous or periretinal membranes, ocular blood flow, and ocular elasticity [29]. For example, the life-span of SF₆ and C₃F₈ may be more than twice as long in phakic non-vitreotomized eyes than in aphakic vitreotomized eyes [30].

4. Physiologic Changes of Gas in Special Circumstances

a. Interaction with General Anesthesia

Inhalation of anesthetic gases during general anesthesia may affect intraocular gas volume. Nitrous oxide (N₂O) is 34 times and 117 times more water soluble than nitrogen and SF₆, respectively [30]. An intravitreal gas bubble would therefore increase in volume due to diffusion of nitrous oxide from the fluid compartment into the bubble. Such expansion in bubble volume would be threefold of its original size, leading to increased IOP (maximum IOP after 15 to 20 minutes of nitrous oxide use). IOP decreases once it is discontinued as it diffuses out of the body through ventilation. As the concentration of nitrous oxide in lung alveoli is reduced by 90% after it has been stopped for 10 minutes, nitrous oxide should be discontinued for at least 15 minutes prior to intraocular gas injection. This would prevent interference in the desired bubble volume. If it has been continued during gas

injection, the resultant bubble will be smaller than expected. Importantly, severe visual loss secondary to central retinal artery occlusion has been reported in patients with an intraocular gas in situ undergoing general anesthesia for non-ocular purposes [31, 32]. This was thought to be a result of uncompensated rapid rise in IOP during surgery due to nitrous oxide diffusion into the bubble.

b. Effects of Variations in Altitude

Another important consideration is variation in gas bubble size related to changing altitude during air travel and scuba diving. Airplane cabin pressure is only equal to atmospheric pressure at an altitude up to 8,000 feet. During airplane take-off, the climb rate is roughly 2,000–3,000 feet per minute, leading to rapid expansion in bubble size and subsequent IOP rise that may cause central retinal artery occlusion [33, 34]. To fully appreciate this consideration, it is important to understand the physics of bubble expansion.

We normally describe intraocular pressure in units of mmHg. A reading of 20 mmHg is actually 20 mmHg above atmospheric pressure. Given that atmospheric pressure at sea level is 760 mmHg, the actual intraocular pressure would therefore be 20 + 760 mmHg or 780 mmHg. In commercial airplanes, cabin pressure is around 580 mmHg (the equivalent of 8,000 feet). An intraocular bubble will expand according to gas law (Boyle's law). If there was 1 ml to begin with, the bubble will increase by a factor of 780/580, which is more than 1.3 times. The real question is

whether the eye has the capacity to accommodate the additional 0.3 ml. The normal human aqueous outflow rate is around 2.5–3 microliters per minute (normal range (95 %) is 1.8 to 4.3 microliters/min) [35]. With raised intraocular pressure, the outflow rate would increase in order to reduce intraocular pressure. The question really is whether the increased outflow can cope with the speed of expansion of the bubble. The rate of ascent is therefore important. It is not only with flying that could give rise to high intraocular pressure from gas expansion. Even rapid ascent by train has been associated with raised intraocular pressure [36]. The crux of the problem is that the outflow facility could vary from individual to individual and with the type of surgery performed. Although up to 1.0 ml of intraocular gas has been reported to be safe without significant IOP change during air travel [31], this is entirely dependent on outflow facility, and thus some surgeons feel that no volume is safe for air travel. Similarly, air bubble size may change during scuba diving [37], where gaseous equilibrium under atmospheric conditions may be altered by inhalation of oxygen from compressed air tanks. On returning to the surface, the bubble expands inside the eye and gives rise to an increase in IOP.

III. Long-Acting Vitreous Substitutes

Perfluorocarbon liquids and silicone oil are both liquid tamponades. The former is intended for short-term use but has been left inside the eye for days to weeks [38–40]. The latter is exclusively used for long-term internal tamponade.

A. Perfluorocarbon Liquids

1. Properties

Perfluorocarbon liquid (PFCL) was initially engineered as a blood substitute [41, 42]. Later, it was investigated by many either as an intraoperative tool or as a short-term internal tamponade after vitreous surgery [43–45]. Perfluorocarbon liquids (PFCLs) are synthetic fluorinated hydrocarbon containing carbon-fluorine bonds. Some incorporate components such as hydrogen, nitrogen, and bromide to form different chains. These chains form different shapes, such as straight chains or cylindrical chains. The molecular structure of straight chains contains carbon chains from C5 to C9, while that of a cylindrical chain is from C5 to C17.

Common PFCLs are colorless and odorless. They have low viscosities and higher specific gravities and are denser than water. Not only are they stable under high temperatures, they also do not absorb commonly used lasers. Frequently used PFCLs include perfluoro-n-octane (C_8F_{18}) [46], perfluoro-

romethylcyclohexane (C_8F_{16}) [47], perfluorodecaline ($C_{10}F_{18}$) [48, 49], perfluorooctylbromide ($C_8F_{17}Br$) [50], perfluorophenanthrene ($C_{14}F_{24}$) [51], perfluorotributylamine ($C_{12}F_{27}N$) [52], and perfluorotri-n-propylamine ($C_9F_{21}N$) [53]. Among these, C_8F_{18} was approved by the US Food and Drug Administration for intraocular use.

PFCL quickly became popular as an intraoperative tool during retinal surgery because it offers several advantages:

1. It is heavier than water. For instance, the specific gravity of C_8F_{18} is 1.76. This enables it to sink in the presence of water, or balanced salt solution. This property aids the displacement of subretinal fluid and flattening of the retina in detachments. It also enables the surgeon to unroll folded retina and avoids the need to perform posterior retinotomy to drain subretinal fluid.
2. It is immiscible in water. This property is very important as it does not mix with water and stays in two separate phases in the presence of water. It remains optically clear as it resists the incursion by saline or blood during operation and keeps the operating field clear.
3. The refractive indexes of PFCL and water are different; therefore, it is optically visible in the presence of saline, especially during removal one can clearly see if there are remaining globules that need removal.
4. It has a high boiling point. This allows endolaser photocoagulation to be performed under PFCL, and it would not vaporize [46].
5. It has a high interfacial tension. This property helps keep the PFCL bubble in one large globule and prevents breaking off of small droplets, reducing the risk of PFCL seeping under the retina through retinal breaks.
6. It has low viscosities. This allows ease of injection and removal.
7. It is immiscible with silicone oil. This allows direct PFCL-silicone oil exchange in difficult cases where retinal slippage is likely during PFCL-air exchange.

2. Retinal Toxicity

Ophthalmologists have long attributed the observed histological changes associated with the use of perfluorocarbon liquids as due to their weight. It stands to reason, however, that changes such as nuclear drop-down and loss of outer plexiform layers must be attributed to causes other than buoyancy forces. The changes are observed in the superior retina with silicone oil that we have demonstrated to have a low buoyancy force but not with gas that has a high buoyancy force [54]. Instead, such pathological changes are observed in the inferior retina with perfluorocarbons that have a high (negative) buoyancy force [54].

We speculated that the “toxic” effects of perfluorocarbon liquids and silicone oil on the retina might be due to the fact that they effectively exclude water from the retinal surface. In the case of silicone oil, the bubble of tamponade floats and

displaces water from the retina superiorly; likewise, perfluoro-carbon liquid sinks and displaces water from the retina inferiorly. There is likely to be a film of water on the surface of the retina. Winter et al. suggested that if the film of water is less than a given thickness, ionic exchange with the retinal cellular elements might be impaired, leading to a high concentration of potassium in the preretinal fluid, which in turn may give rise to excitotoxicity [54]. This is a plausible explanation of the toxic effects on the retina when liquid tamponades are used.

Thus, with multiple advantages and relatively minimal negative attributes, PFLC has been used extensively as an intraoperative tool to assist managing retinal problems. It has greatly improved the outcomes of complex retinal detachments associated with proliferative vitreoretinopathy. It has also made the life of the retinal surgeon much easier when handling other difficult scenarios. Although there are numerous precautions to take during its usage, it remains one of the indispensable tools in modern retinal surgery.

B. Silicone Oil

Silicone oil (SiO) was initially introduced in the 1960s not as a vitreous substitute, but rather to be injected in non-vitreotomized eyes [11]. Later, following the introduction of vitreous surgery in the 1970s, using SiO as a vitreous substitute in combination with vitrectomy has led to a surge in interest toward its use [55–60]. By the 1980s, SiO was successfully established in its role as a long-term internal tamponade agent in many European countries. Its use and potential risks have been further defined by the Silicone Oil Study [61, 62]. To date, SiO remains an indispensable tool in retinal surgery, especially in complicated retinal pathologies requiring a long-term vitreous substitute for internal tamponade.

1. Chemical Properties of Silicone Oil

To fully understand the physiology of intravitreal SiO use, one must first appreciate its chemical properties. Silicone oil is in the group of inert hydrophobic liquid polymers comprised of a backbone of siloxane. Silicone is made up of repeating units of siloxane, which is the backbone of all polymers in the silicone family, regardless of its form. The basic unit of siloxane is $[-Si-O-]$, which is capable of attaching to different organic or inorganic side chains to form polymers of different properties. Depending on the side chains attaching to the base unit, the polymers could be of different specific gravity, either lighter than water or heavier than water. By convention, lighter-than-water SiO polymers are usually called “SiO,” whereas heavier-than-water SiO is usually termed “heavy SiO.”

Most commonly, silicone oil consists of polydimethylsiloxane (siloxane with two attached methyl side chains), also known as PDMS. This has a specific gravity of 0.97, hence lighter than water. On the other hand, a methyl and a trifluoropropyl side chain could be added to the siloxane unit to form polytrifluoropropylmethylsiloxane, also known as fluorosilicone oils [63]. These have specific gravities from 1.25 to 1.3, hence heavier than water. The physiology of SiO in the vitreous cavity created after vitrectomy thus emerges from the varying specific gravities. (For details, refer to Table IV.G-2.)

2. Physical Properties of Silicone Oil

a. Specific Gravity

The specific gravity of a particular SiO not only determines whether it floats or sinks in the vitreous cavity but also governs its shape *in situ* [59]. The aqueous has a specific gravity around 1.01; hence it is usually considered the same as water. Most polydimethylsiloxanes (PDMS) have specific gravities of 0.97; this is due to the identical molecular densities; hence

Table IV.G-2 Chemical properties of silicone oil and other commonly used intraocular tamponade agents

Tamponade agent	Chemical composition	Specific gravity (g/cm ³ at 25 °C)	Viscosity (centistokes at 25 °C)
Silicone oil (1,000 cs)	PDMS – 100 %	0.97	1,000
Silicone oil (2,000 cs)	PDMS – 100 %	0.97	2,000
Silicone oil (5,000 cs)	PDMS – 100 %	0.97	5,000
C8F10	C8F10 – 100 %	1.94	0.69
C10F18	C10F18 – 100 %	1.76	2.7
F6H8	F6H8 – 100 %	1.35	3.44
Densiron 68®	F6H8 – 30.5 % PDMS (5,000 cs) – 69.5 %	1.06	1,349
Oxane HD®	RMN3 – 11.9 % Oxane 5700–88.1 %	1.02	3,300
HWS 46-3000®	F4H5 – 55 % PDMS (100,000 cs) – 45 %	1.118	2,903dv
Air	n/a	<0.0001	n/a
C3F8	n/a	<0.0001	n/a
SF6	n/a	<0.0001	n/a

PDMS polydimethylsiloxane, F4H5 perfluorobutylpentane, F6H8 perfluorohexyloctane, C8F10 perfluoro-n-octane, C10F18 perfluorodecalin

they float on water. For heavier SiOs, molecular density varies, so does specific gravity, but all are >1; hence all sink in the presence of water.

For heavy SiOs, the higher specific gravity has ignited a debate as to whether it would instill damage to the retina. Stolba and associates filled eyes with perfluorophenanthrene (specific gravity almost twice as that of vitreous) and found retinal damage in the inferior retina [64–67]. However, contradicting results have been produced by others [68, 69]. Some postulate that the force exerted on the retina with heavy SiOs is small when compared to the absolute intraocular pressure and its diurnal variation and may not be accountable for the observed retinal damage in some studies [68, 70]. Others attribute the damage to the thin layer of fluid between the heavy SiO and the retina. Winter and associates proposed that as the layer of fluid is so thin, it would not be enough for ionic exchange, and this may have affected the functions of the Muller cells [54]. This eventually may lead to excessive potassium buildup in situ and excitotoxicity when hyperpolarization takes place [54]. However, this theory is yet to be proven.

b. Buoyancy

As with intraocular gases, the law of buoyancy governs intravitreal SiO behavior. For any intravitreal SiO bubble, there are always two forces acting on it at any given time: one being the downward gravity pull and the other being the upward buoyancy push. Gravity equals the weight of the SiO bubble; e.g., for 1 ml of PDMS SiO with a specific gravity of 0.97, the gravity pull is 0.97 g. On the other hand, Archimedes' principle states that any floating object displaces its own weight of fluid. Hence, buoyancy for the same SiO bubble is the weight of 1 ml water that it has displaced, that is 1 g. Therefore, the net force acting on the 1 ml SiO bubble is

$$\text{Force} = (\text{Gravity}) + (\text{buoyancy}) = (0.97\text{g}) + (+1.0\text{g}) = +0.03\text{g}, \text{ where } + \text{ denotes upward and } - \text{ denotes downward force}$$

This force is very small when compared to that for intraocular gases, which in general have specific gravities of around 0.001:

$$\text{Force} = (\text{Gravity}) + (\text{buoyancy}) = (-0.001\text{g}) + (+1.0\text{g}) = +0.999\text{g}$$

This is why the tamponade effect of SiO is much weaker than that by intraocular gases.

The effectiveness of a vitreous substitute to act on the retina is governed by the size and shape of the substitute and

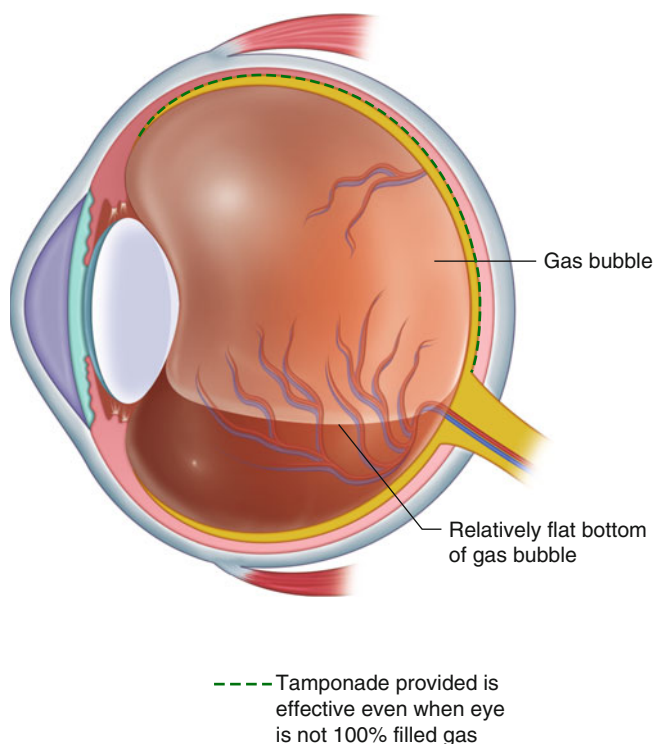


Figure IV.G-2 Gas is a better internal tamponade agent, and can provide more effective tamponade area, even if it is not completely filled

its area in contact with the retina. Buoyancy has a major role here: when the buoyancy is large, as in intraocular gases, the bubble takes on the shape of the superior part of the retina that comes into contact with its superior dome. The bottom of the bubble will be relatively flat. When buoyancy is small, as in SiOs, the bubble remains in a relatively spherical shape. Therefore, for an equivalent volume of SiO, the area in contact with the retina is much less than that for a gas bubble. It has been shown that a small gas bubble (as small as 0.28 ml) takes up 90 degrees of arc on the superior retina, but SiO bubbles almost do not come into contact with the retina other than the superior bit until its almost 100% filled [71, 72]. Figure IV.G-2 demonstrates how a gas bubble, even when not completely filled, provides a relative good tamponade to the superior retina, while the bottom of the bubble assumes a relatively flat shape. This is worse when scleral buckles are applied to the outside of the globe and recesses are created internally (Figure IV.G-3), hence the importance of achieving a near 100% fill when employing SiO as the vitreous substitute.

c. Surface Tension and Interfacial Tension

Surface tension refers to the ability of the surface of a fluid body to resist change, given the other phase being gaseous. This refers to the forces between like molecules (water-water)

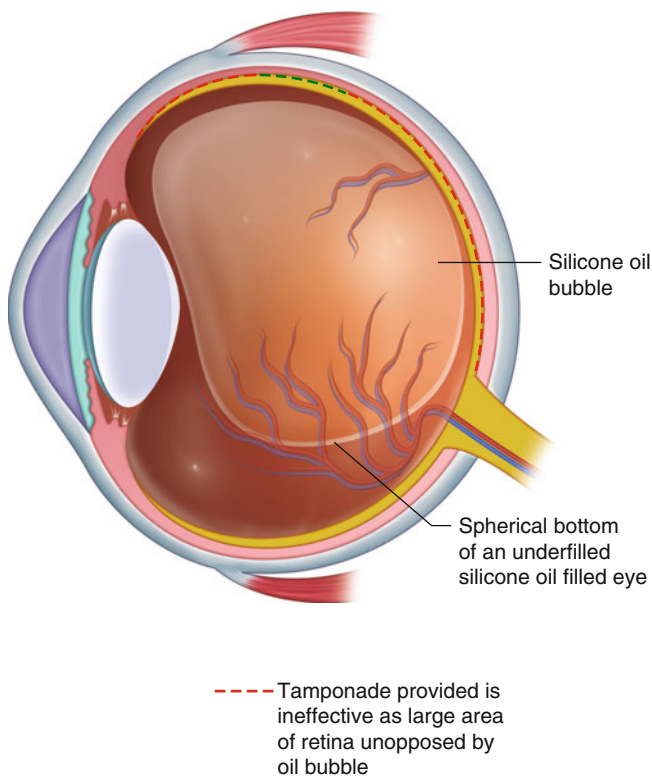


Figure IV.G-3 Slight underfilling of the vitreous cavity with silicone oil will much reduce the tamponade effect of it against the superior retina. This is due to the lower buoyancy of silicone oil as compared to that of an intraocular gas bubble

and unlike molecules (SiO-water). Equilibrium is attained when the free energy required to keep the interface stable is minimum. This is achieved by sorting all like molecules on one side and unlike molecules on the other side of the interface. When SiO is instilled in the eye, the other phase is usually fluid; hence interfacial tension effects should be applicable. The interface acts like a tough membrane across the two “compartments” and keeps the vitreous substitute, be it gaseous or SiO, intact [73]. Without impurities in the vitreous, a SiO bubble is able to hold itself in a single bubble as the interfacial tension is above what is required. However, in the presence of impurities such as proteins, lipids, or blood, the interfacial tension can be reduced to a level lower than what is required to keep the bubble intact as a whole [74]. Hence, breaking up may occur. Therefore, it is imperative to remove as much blood and residual fluid before instilling SiO. This reduces not only the risk of SiO bubble breakage but also the risk of developing proliferative vitreoretinopathy.

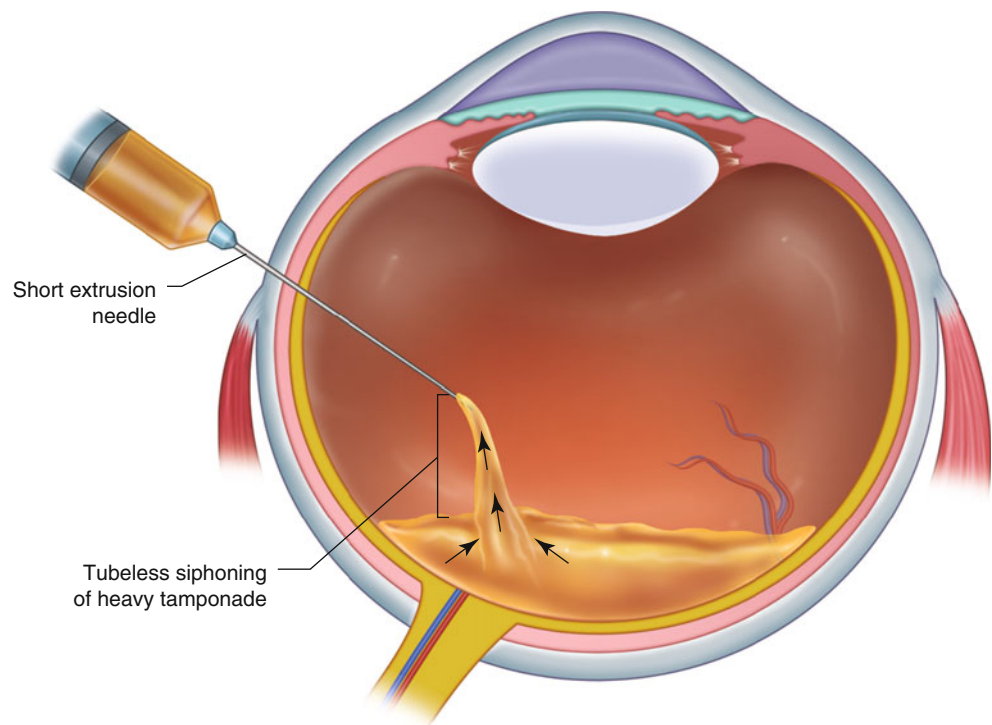
d. Viscosity

Viscosity, also known as shear viscosity, refers to the resistance of a fluid body to being deformed when put under shear

stress. It is a measure of the forces existing between molecules in close contact and the frictional force between molecular chains. From first principles, the higher the viscosity, the higher the force that is required to deform it. In practicality, this has to do with the ease of injection and removal of a SiO bubble from the vitreous cavity. The lower the viscosity, the easier it is to inject and remove and vice versa. Poiseuille’s law states that the flow of liquid in a tubular structure is in proportion to the fourth power of its radius and in inverse proportion to its length. Thus, to maximize efficiency during the injection of SiO, the length of the cannula has to be short, and the bore size has to be large. Therefore, we generally recommend using a 19 or 20 gauge angiocatheter as the injection cannula and making an oblique cut approximately 3 mm from its root. This length ensures penetration into the vitreous cavity while not compromising efficiency.

Another aspect of viscosity that concerns SiO as a vitreous substitute is the extensional viscosity. This measures the propensity of SiO to break up and is related to the proportion of low-molecular-weight components [75]. In practical terms, it measures the resistance of SiO to breakup when pulled into a strand and forming satellite droplets. If breaking up is easy, so is the likelihood of emulsification. The lower the viscosity of the SiO (i.e., 1,000 cs), the higher the risk of breaking up into satellite droplets, hence emulsification. To prevent this from happening, small amounts of polymers of higher molecular weights could be added. These additives have to be of identical chemical structures to the original SiO and will augment the extensional viscosity and prevent pinch-off droplets from forming [76]. Williams and associates added these high-molecular-weight polymers to low-viscosity silicone oil (1,000 cs) and produced equivalent extensional viscosity to that of SiO of 5,000 cs [77], thus producing SiO with high ease of injection and removal, yet low risk of emulsification. A randomized clinical trial comparing Siluron 2000 (1,000 cs standard PDMS with 5 % of 423,000 molecular weight PDMS) against silicone oil 5000 cs has been carried out and the results presented at the 2013 Euretina Meeting in Hamburg. The unique feature of the trial is that the oils were used for the treatment of full-thickness macular hole. In the past, the comparisons of oils had been difficult because it was difficult to control the many patient variables such as the degree of inflammation, the breakdown of blood-ocular barrier, the nature and complexity of rhegmatogenous retinal detachments, and the type and extent of surgery performed. In Leuven, there has long been a tradition of using silicone oil as the tamponade of choice for the treatment of full-thickness macular holes. All patients therefore had the same pathology and no inflammation and blood-ocular barrier breakdown; the surgery was fairly standard. The assessment includes clinical assessment with

Figure IV.G-4 “Tubeless siphoning” enables removal of a heavy silicone oil bubble using a shorter cannula and does not require the cannula to reach the bottom of the eye during removal



slit-lamp biomicroscopy and gonioscopy as well as special laboratory investigations using droplet counting using microscopy and ultrasonography. The results indicated that there was no significant difference between the oils in terms of emulsification. This is the first clinical trial that validated the design of the new oils.

e. Viscoelasticity

As with the removal of SiO, extraction of heavy SiO using long cannulas is not practical. However, due to its heavier-than-water nature, it sinks and potentially can pinch off from the tip of the cannula if suction is ineffective. Stappler and Wong have shown that it is possible to remove heavy SiO with a short and small-gauge cannula [78]. This is possible due to the viscoelasticity of heavy SiO, in which extensional flow occurs when it is aspirated. This allows the bubble to assume a conical shape, and thus removal in one go is feasible. The “tubeless siphoning” phenomenon aided the removal of heavy SiO with the use of a 20 gauge cannula cut to only 7 mm long [78]. Romano and colleagues have shown that it was even possible under the 23 gauge system [79]. Figures IV.G-4 outline how this is being carried out.

Conclusion

Both intraocular gas and silicone oil have proven to be invaluable vitreous substitutes in modern vitreoretinal surgery, especially in the management of complex

retinal detachments. In addition, their use has been extended to indications other than retinal detachment. The fundamental understanding of the physiological properties of these vitreous substitutes is important, as it would enable surgeons to make rational choice under different circumstances.

Abbreviations

BSS	balanced salt solution
C2F6	hexafluoroethane
C3F8	perfluoropropane
C8F18	perfluoro-n-octane
C8F17Br	perfluorooctylbromide
C8F16	perfluoromethylcyclohexane
C10F18	perfluorodecaline
C14F24	perfluorophenanthrene
C12F27N	perfluorotributylamine
C9F21N	perfluorotri-n-propylamine
D-ACE	drain-air-cryotherapy-explant
IOP	intraocular pressure
N2O	nitrous oxide
PDMS	polydimethylsiloxane
PFCL	perfluorocarbon liquid
PVR	proliferative vitreoretinopathy
SF6	sulfur hexafluoride
SiO	silicone oil

References

- Offret G, Pouliquen Y, Haut J. Transplantation of fresh vitreous humor as a treatment of posterior uveitis. *Bull Soc Ophthalmol Fr*. 1968;68(1):23–7.
- Benson WE, Diamond JG, Tasman W. Intraocular irrigating solutions for pars plana vitrectomy. A prospective, randomized, double-blind study. *Arch Ophthalmol*. 1981;99(6):1013–5.
- Matsuda M, Tano Y, Edelhauser HF. Comparison of intraocular irrigating solutions used for pars plana vitrectomy and prevention of endothelial cell loss. *Jpn J Ophthalmol*. 1984;28(3):230–8.
- de Bustros S, Glaser BM, Johnson MA. Thrombin infusion for the control of intraocular bleeding during vitreous surgery. *Arch Ophthalmol*. 1985;103(6):837–9.
- Asaria RH, Kon CH, Bunce C, et al. Adjuvant 5-fluorouracil and heparin prevents proliferative vitreoretinopathy: results from a randomized, double-blind, controlled clinical trial. *Ophthalmology*. 2001;108(7):1179–83.
- Rosengren B. Results of treatment of detachment of the retina with diathermy and injection of air into the vitreous. *Acta Ophthalmol*. 1938;16:573–9.
- Norton EW, Aaberg T, Fung W, Curtin VT. Giant retinal tears. I. Clinical management with intravitreal air. *Am J Ophthalmol*. 1969;68(6):1011–21.
- Hilton GF, Grizzard WS. Pneumatic retinopexy. A two-step outpatient operation without conjunctival incision. *Ophthalmology*. 1986;93(5):626–41.
- Sebag J, Tang M. Pneumatic retinopexy using only air. *Retina*. 1993;13(1):8–12.
- Yee KM, Sebag J. Long-term results of office-based pneumatic retinopexy using pure air. *Br J Ophthalmol*. 2011;95(12):1728–30.
- Machemer R, Buettner H, Norton EW, Parel JM. Vitrectomy: a pars plana approach. *Trans Am Acad Ophthalmol Otolaryngol*. 1971;75(4):813–20.
- Lincoff A, Lincoff H, Iwamoto T, Jacobiec F, Kreissig I. Perfluoro-n-butane. A gas for a maximum duration retinal tamponade. *Arch Ophthalmol*. 1983;101(3):460–2.
- Lincoff A, Lincoff H, Solorzano C, Iwamoto T. Selection of xenon gas for rapidly disappearing retinal tamponade. *Arch Ophthalmol*. 1982;100(6):996–7.
- Vyngantas CM, Peyman GA, Daily MJ, Ericson ES. Octafluorocyclobutane and other gases for vitreous replacement. *Arch Ophthalmol*. 1973;90(3):235–6.
- Killey FP, Edelhauser HF, Aaberg TM. Intraocular sulfur hexafluoride and octafluorocyclobutane. Effects on intraocular pressure and vitreous volume. *Arch Ophthalmol*. 1978;96(3):511–5.
- Stanford MR, Chignell AH. Surgical treatment of superior bullous rhegmatogenous retinal detachments. *Br J Ophthalmol*. 1985;69(10):729–32.
- Gilbert C, McLeod D. D-ACE surgical sequence for selected bullous retinal detachments. *Br J Ophthalmol*. 1985;69(10):733–6.
- Tornambe PE. Pneumatic retinopexy: the evolution of case selection and surgical technique. A twelve-year study of 302 eyes. *Trans Am Ophthalmol Soc*. 1997;95:551–78.
- Hilton GF, Tornambe PE. Pneumatic retinopexy. An analysis of intraoperative and postoperative complications. The Retinal Detachment Study Group. *Retina*. 1991;11(3):285–94.
- Sharma A, Grigoropoulos V, Williamson TH. Management of primary rhegmatogenous retinal detachment with inferior breaks. *Br J Ophthalmol*. 2004;88(11):1372–5.
- McCuen 2nd BW, Azen SP, Stern W, et al. Vitrectomy with silicone oil or perfluoropropane gas in eyes with severe proliferative vitreoretinopathy. Silicone Study Report 3. *Retina*. 1993;13(4):279–84.
- Chang S. Intraocular gases. In: Ryan SJ, editor. *Retina*. 4th ed. Philadelphia: Elsevier; 2006.
- Fawcett IM, Williams RL, Wong D. Contact angles of substances used for internal tamponade in retinal detachment surgery. *Graefes Arch Clin Exp Ophthalmol*. 1994;32(7):438–44.
- Charles S. *Vitreous surgery*. 2nd ed. Williams & Wilkins: Baltimore; 1987.
- van Meurs JC, Humalda D, Mertens DA, Peperkamp E. Retinal folds through the macula. *Doc Ophthalmol*. 1991;78(3–4):335–40.
- Hilton GF, Kelly NE, Salzano TC, Tornambe PE, Wells JW, Wendel RT. Pneumatic retinopexy. A collaborative report of the first 100 cases. *Ophthalmology*. 1987;94(4):307–14.
- Crittenden JJ, De Juan Jr E, Tiedeman J. Expansion of long-acting gas bubbles for intraocular use. Principles and practice. *Arch Ophthalmol*. 1985;103(6):831–4.
- Peters MA, Abrams GW, Hamilton LH, Burke JM, Schrieber TM. The nonexpansile, equilibrated concentration of perfluoropropane gas in the eye. *Am J Ophthalmol*. 1985;100(6):831–9.
- Thompson JT. Kinetics of intraocular gases. Disappearance of air, sulfur hexafluoride, and perfluoropropane after pars plana vitrectomy. *Arch Ophthalmol*. 1989;107(5):687–91.
- Wolf GL, Capuano C, Hartung J. Nitrous oxide increases intraocular pressure after intravitreal sulfur hexafluoride injection. *Anesthesiology*. 1983;59(6):547–8.
- Seaberg RR, Freeman WR, Goldbaum MH, Manecke Jr GR. Permanent postoperative vision loss associated with expansion of intraocular gas in the presence of a nitrous oxide-containing anesthetic. *Anesthesiology*. 2002;97(5):1309–10.
- Fu AD, McDonald HR, Elliott D, et al. Complications of general anesthesia using nitrous oxide in eyes with preexisting gas bubbles. *Retina*. 2002;22(5):569–74.
- Lincoff H, Weinberger D, Stergiu P. Air travel with intraocular gas. II. Clinical considerations. *Arch Ophthalmol*. 1989;107(6):907–10.
- Norton EWD, Fuller DG. The use of intraocular sulfur hexafluoride in vitrectomy. In: Irvine AR, O'Malley C, editors. *Advances in vitreous surgery*. Springfield: Charles C Thomas; 1976.
- Brubaker RF. Flow of aqueous humor in humans [The Friedenwald Lecture]. *Invest Ophthalmol Vis Sci*. 1991;32(13):3145–66.
- Levasseur SD, Rahhal FM. Travel to high mountain elevations following vitrectomy with intraocular gas. *Retina*. 2013;33(7):1456–61.
- Jackman SV, Thompson JT. Effects of hyperbaric exposure on eyes with intraocular gas bubbles. *Retina*. 1995;15(2):160–6.
- Drury B, Bourke RD. Short-term intraocular tamponade with perfluorocarbon heavy liquid. *Br J Ophthalmol*. 2011;95(5):694–8.
- Rush R, Sheth S, Surka S, Ho I, Gregory-Roberts J. Postoperative perfluoro-N-octane tamponade for primary retinal detachment repair. *Retina*. 2012;32(6):1114–20.
- Sigler EJ, Randolph JC, Calzada JI, Charles S. 25-gauge pars plana vitrectomy with medium-term postoperative perfluoro-n-octane tamponade for inferior retinal detachment. *Ophthalmic Surg Lasers Imaging Retina*. 2013;44(1):34–40.
- Clark Jr LC, Gollan F. Survival of mammals breathing organic liquids equilibrated with oxygen at atmospheric pressure. *Science*. 1966;152(3730):1755–6.
- Geyer RP. Fluorocarbon-polyol artificial blood substitutes. *N Engl J Med*. 1973;289(20):1077–82.
- Chang TM, Farmer M, Geyer RP, Moss G. Blood substitutes based on modified hemoglobin and fluorochemicals. *ASAIO Trans*. 1987;33(4):819–23.
- Chang S. Low viscosity liquid fluorochemicals in vitreous surgery. *Am J Ophthalmol*. 1987;103(1):38–43.
- Chang S, Ozmert E, Zimmerman NJ. Intraoperative perfluorocarbon liquids in the management of proliferative vitreoretinopathy. *Am J Ophthalmol*. 1988;106(6):668–74.

46. Bourke RD, Simpson RN, Cooling RJ, Sparrow JR. The stability of perfluoro-N-octane during vitreoretinal procedures. *Arch Ophthalmol*. 1996;114(5):537–44.
47. Sparrow JR, Matthews GP, Iwamoto T, Ross R, Gershbein A, Chang S. Retinal tolerance to intravitreal perfluoromethylcyclohexane liquid in the rabbit. *Retina*. 1993;13(1):56–62.
48. Azzolini C, Brancato R, Trabucchi G, Camesasca F, Codenotti M, Verdi M. Endophotocoagulation through perfluorodecalin in rabbit eyes. *Int Ophthalmol*. 1994;18(1):33–6.
49. Berglin L, Ren J, Algvere PV. Retinal detachment and degeneration in response to subretinal perfluorodecalin in rabbit eyes. *Graefes Arch Clin Exp Ophthalmol*. 1993;231(4):233–7.
50. Conway MD, Peyman GA, Karacorlu M, et al. Perfluorooctylbromide (PFOB) as a vitreous substitute in non-human primates. *Int Ophthalmol*. 1993;17(5):259–64.
51. Batman C, Cekic O. Effects of the long-term use of perfluoroperhydrophenanthrene on the retina. *Ophthalmic Surg Lasers*. 1998;29(2):144–6.
52. Chang S, Zimmerman NJ, Iwamoto T, Ortiz R, Faris D. Experimental vitreous replacement with perfluorotributylamine. *Am J Ophthalmol*. 1987;103(1):29–37.
53. Bryan JS, Friedman SM, Mames RN, Margo CE. Experimental vitreous replacement with perfluorotri-n-propylamine. *Arch Ophthalmol*. 1994;112(8):1098–102.
54. Winter M, Eberhardt W, Scholz C, Reichenbach A. Failure of potassium siphoning by Muller cells: a new hypothesis of perfluorocarbon liquid-induced retinopathy. *Invest Ophthalmol Vis Sci*. 2000;41(1):256–61.
55. Grey RHB, Leaver P. Results of silicone oil injection in massive preretinal retraction. *Trans Ophthalmol Soc UK*. 1977;97:238–41.
56. Grey RHB, Leaver P. Silicone oil in the treatment of massive preretinal retraction: I Results in 105 eyes. *Br J Ophthalmol*. 1979;63:345–50.
57. Haut J, Ullern M, Chermet M, et al. Complications of intraocular injections of silicone combined with vitrectomy. *Ophthalmologica*. 1980;180:29–35.
58. Leaver PK, Cooling R, Feretis EB, et al. Vitrectomy and fluid/silicone exchange for giant retinal tears: results at six months. *Br J Ophthalmol*. 1984;227:323–7.
59. Leaver PK, Garner A, Grey RHB. Effects of intraocular silicone oil. *Trans Ophthalmol Soc UK*. 1977;97:633.
60. Leaver PK, Grey R, Garner A. Complications following silicone oil injection. *Mod Probl Ophthalmol*. 1979;20:290–4.
61. Proliferative vitreoretinopathy. The Silicone Study Group. *Am J Ophthalmol*. 1985;99(5):593–595.
62. Azen SP, Boone DC, Barlow W, et al. Methods, statistical features, and baseline results of a standardized, multicentered ophthalmologic surgical trial: the Silicone Study. *Control Clin Trials*. 1991;12(3):438–55.
63. Wolf S, Schon V, Meier P, Wiedemann P. Silicone oil-RMN3 mixture (“heavy silicone oil”) as internal tamponade for complicated retinal detachment. *Retina*. 2003;23(3):335–42.
64. Stolba U, Krepler K, Velikay-Parel M, Binder S. The effect of specific gravity of perfluorocarbon liquid on the retina after experimental vitreous substitution. *Graefes Arch Clin Exp Ophthalmol*. 2004;242(11):931–6.
65. Velikay M, Wedrich A, Stolba U, Datlinger P, Li Y, Binder S. Experimental long-term vitreous replacement with purified and non-purified perfluorodecalin. *Am J Ophthalmol*. 1993;116(5):565–70.
66. Gonvers M, Hornung JP, de Courten C. The effect of liquid silicone on the rabbit retina. Histologic and ultrastructural study. *Arch Ophthalmol*. 1986;104(7):1057–62.
67. Eckardt C, Nicolai U, Winter M, Knop E. Experimental intraocular tolerance to liquid perfluorooctane and perfluoropolyether. *Retina*. 1991;11(4):375–84.
68. Wong D, Williams R, Stappler T, Groenewald C. What pressure is exerted on the retina by heavy tamponade agents? *Graefes Arch Clin Exp Ophthalmol*. 2005;243(5):474–7.
69. Mackiewicz J, Maaijwee K, Luke C, et al. Effect of gravity in long-term vitreous tamponade: in vivo investigation using perfluorocarbon liquids and semi-fluorinated alkanes. *Graefes Arch Clin Exp Ophthalmol*. 2007;245(5):665–75.
70. Doi M, Refojo M. Histopathology of rabbit eyes with intravitreous silicone-fluorosilicone copolymer oil. *Exp Eye Res*. 1994;59(6):737–46.
71. Parver LM, Lincoff H. Geometry of intraocular gas used in retinal surgery. *Mod Probl Ophthalmol*. 1977;18:338–43.
72. Parver LM, Lincoff H. Mechanics of intraocular gas. *Invest Ophthalmol Vis Sci*. 1978;17(1):77–9.
73. Feynman RP, Leighton R, Sands M. The Feynman lectures on physics. In: Feynman RP, Leighton R, Sands M, editors. *The Feynman lectures on physics*. Addison-Wesley; Boston. 1972.
74. Laqua H, Lucke K, Foerster M. Results of silicone oil surgery. *Jpn J Ophthalmol*. 1987;31(1):124–31.
75. Crisp A, De Juan Jr E, Tiedeman J. Effect of silicone oil viscosity on emulsification. *Arch Ophthalmol*. 1987;105(4):546–50.
76. Steinhaus B, Shen A, Sureshkumar R. Dynamics of viscoelastic fluid filaments in microfluidic devices. *Phys Fluids*. 2007;19:1–13.
77. Williams RL, Day M, Garvey MJ, English R, Wong D. Increasing the extensional viscosity of silicone oil reduces the tendency for emulsification. *Retina*. 2010;30(2):300–4.
78. Stappler T, Williams R, Gibran SK, Liazos E, Wong D. A guide to the removal of heavy silicone oil. *Br J Ophthalmol*. 2008;92(6):844–7.
79. Romano MR, Groenewald C, Das R, Stappler T, Wong D, Heimann H. Removal of Densiron-68 with a 23-gauge transconjunctival vitrectomy system. *Eye (Lond)*. 2009;23(3):715–7.

Part V.A.

Posterior Vitreo-Retinal Surgery

Susanne Binder

Susanne Binder and Lawrence P. Chong

Outline

I. Submacular Surgery

- A. History
 - 1. Trauma and PVR
 - 2. Choroidal Neovascular Membranes in AMD
- B. Instrumentation for Submacular Surgery
- C. Indications for Submacular Surgery
- D. Technique of Submacular Surgery
 - 1. Complications of Submacular Surgery
- E. Functional Results of Submacular Surgery

II. Macular Translocation in AMD

- A. History
- B. Surgical Technique
 - 1. Limited Translocation
 - a. Scleral Infolding
 - b. Outfolding Technique
 - 2. Full Macular Translocation (MTS 360)
- C. Complications
- D. Functional Results

III. RPE Transplantation

- A. Rationale
- B. History
 - 1. Transplantation of Ocular Tissues
 - 2. Retinal Pigment Epithelial Transplantation
 - 3. RPE Transplantation in Human Eyes

C. Surgical Techniques

- 1. Cell Suspensions
- 2. RPE/Bruch's Membrane/Choroid Patch

D. Functional Results

IV. Surgical Management of Submacular Hematoma

- A. History
- B. Surgery for Submacular Hematoma
 - 1. History
 - 2. Tissue Plasminogen Activator
 - 3. Surgery
 - a. Technique
 - b. Complications

References

Keywords

Exudative age-related macular degeneration • Vitrectomy
• Submacular surgery • Macular translocation
• Transplantation • Submacular hematoma surgery
• Tissue plasminogen activator

Electronic supplementary material Supplementary material is available in the online version of this chapter at [10.1007/978-1-4939-1086-1_32](https://doi.org/10.1007/978-1-4939-1086-1_32). Videos can also be accessed at <http://www.springerimages.com/videos/978-1-4939-1085-4>.

S. Binder, MD (✉)
Department of Ophthalmology,
Rudolph Foundation Hospital,
Vienna, Austria

The Ludwig Boltzmann Institute for Retinology and
Biomicroscopic Laser Surgery,
Vienna, Austria
e-mail: susanne@susannebinder.com

L.P. Chong, MD
Department of Ophthalmology,
Doheny Eye Institute,
Los Angeles, CA, USA

VMR Institute for Vitreous Macula Retina,
7677 Center Avenue, suite 400,
Huntington Beach, CA 92647, USA
e-mail: lchong@usc.edu

Key Concepts

1. Submacular surgery was introduced in the early 1990s as innovative treatment for subfoveal neovascularization. The submacular surgery trial demonstrated no benefit for eyes with subfoveal neovascularization related to AMD and only modest benefit for selected eyes with hemorrhagic subfoveal CNV in AMD. Today this technique is used very rarely.
2. Submacular surgery is effective for large hematomas of recent onset with dramatic results in a minority. Recurrent hematomas are the most frequent complication.
3. Macular translocation was developed to support the fovea with healthier pigment epithelium and thus restore or maintain vision. Results today are very good, indeed superior to PDT in a prospective randomized trial. The introduction of anti-VEGF therapy restricts surgical intervention to a second-line treatment for eyes not responding to therapy.
4. Retinal pigment epithelial transplantation has been supplanted by anti-VEGF injections, but may in the future find renewed interest because of stem cell therapies and viral or nonviral transfection of retinal cells to enhance survival. Thus, the expertise gained in the initial experience could be transferred to future applications.

I. Submacular Surgery

A. History

1. Trauma and PVR

For many years subretinal surgery has been performed in eyes with retinal detachments related to proliferative vitreoretinopathy (PVR) and severe trauma [1, 2]. Several techniques have been developed to achieve relaxation of the retina and prevent complications like subretinal silicone oil or perfluorocarbon displacement, enlargement of the retinotomy into the retinal center, as well as choroidal hemorrhage. Routine vitrectomy instruments were used at this time, which made subretinal strand removal quite adventurous, and enlargement of the retinotomy was often created due to mechanical manipulations. Large retinectomies were feared and only more frequently used in the late 1980s when Zivonovic actually showed that the retina could be purposefully cut to remove subretinal tissue and relax the retina [3]. With the introduction of liquid perfluorocarbons in 1986 to facilitate treatment of retinal detachments arising from giant retinal tears, these manipulations became easier to execute in PVR and other surgeries [4].

2. Choroidal Neovascular Membranes in AMD

Removal of a choroidal neovascular membrane (CNV) together with extensive hemorrhage in AMD patients was first described in 1988 by Machemer and Steinhilber [5], who considered this as a last attempt in hopeless cases. The removal of the subretinal membrane occurring in eyes with inflammatory disease, like presumed ocular histoplasmosis syndrome, was successfully performed by Thomas and Kaplan in 1991 [6]. Visual results were encouraging, and recurrences rare compared to other treatment modalities at that time. For several years subretinal techniques have been refined and special instrumentation designed allowing a much less traumatic and safer access to the subretinal space. Thus, submacular membrane removal in AMD patients evolved in an attempt to offer patients with subfoveal CNV an alternative treatment to observation or laser photocoagulation. In spite of this, visual results were generally disappointing when this surgery was performed in AMD patients.

B. Instrumentation for Submacular Surgery

As already mentioned special instruments are mandatory to perform subretinal surgery in the least traumatic way. The most important is a set of 70–90° angled instruments designed by Matthew Thomas in 1991 [7] which have a longer tip to firmly grasp a subfoveal membrane from an extrafoveal location. The microsurgical set consists of a vertical and horizontal forceps as well as a vertical and horizontal scissors and spatulas of different lengths. A tapered fluid needle with a long silicone end tip reaching under the retina to aspirate fluid actively or passively is helpful as well as a silicone tip forceps for gentle manipulation of the retina if it needs to be grasped.

C. Indications for Submacular Surgery

Current indications for subretinal surgery are large subretinal hematomas in AMD (below) and subretinal strands due to trauma and PVR, although most are managed by large retinectomies to allow direct access, better view, and more complete removal of this pathologic tissue [see chapter V.B.6. Retinectomy in recalcitrant retinal detachments]. Although small extrafoveal membranes are easy to remove and might do very well as far as visual acuity and recurrences are concerned, anti-VEGF injections, laser therapy, and PDT are the first treatments of choice for neovascularization of different origins, and surgery is considered as a last resort. Currently, subretinal surgery is a technique that augments the armamentarium of vitreous surgery allowing access and manipulations in the subretinal space to remove scar tissue, many types of CNV, and/or large hemorrhages. Whether subreti-

nal surgery for juxtafoveal membranes or juxtapapillary membranes is more successful than anti-VEGF treatment has never been compared. Still, there are small case series showing good results with subretinal membranectomy if the membrane itself has not yet grown under the fovea. However, due to the disappointing visual results of membrane excision in eyes with submacular involvement, anti-VEGF treatments are now preferentially administered in these patients [8]. On the other hand, knowledge about this technique might prove to become very useful for future treatment options in retinal degenerative disease amenable to subfoveal transplantation of retinal cells either as suspensions or sheets or retinal implants. Moreover, during the performance of this procedure for submacular CNV, there were important observations made regarding the frequency of an attached vitreous to the macula in these elderly patients. This led to studies that demonstrate a probable role for the vitreous in the pathophysiology of exudative AMD [see chapter III.G. Vitreous in age-related macular degeneration].

D. Technique of Submacular Surgery

Submacular surgery starts with a standard pars plana vitrectomy. Sclerotomy locations are chosen to enable easy access to the submacular pathology by the more dexterous hand of the surgeon. Small incision, trocar-guided systems can be used for vitreous removal, but in order to introduce the angled subretinal instruments for submacular manipulation, at least one self-retaining cannula needs to be removed and the incision enlarged. After core vitrectomy, the posterior vitreous cortex is lifted and removed if a posterior vitreous detachment is not present. Although AMD patients are elderly patients and thus one would expect that the posterior vitreous cortex is already detached, in more than 80 % of cases with neovascular AMD, the posterior vitreous is still attached [9]. Complete removal of the posterior vitreous cortex is mandatory in these cases.

The retinotomy site is chosen to be as far away from the foveola as possible, yet still allows the surgeon to reach the membrane with the 90° angled subretinal instruments. The retinotomy is best done by using a 130° angled pick to perforate the neurosensory retina. Endodiathermy can be used to facilitate perforation and will additionally improve visibility of a small retinotomy during later manipulations. Subretinal bleeding should be avoided as much as possible. If this occurs, intraocular pressure can be raised temporarily or a small liquid perfluorocarbon bubble can be placed over the posterior retina to stop or avoid bleeding.

Of paramount importance is that subretinal manipulations should be done with slow movements in a rather soft eye to avoid incarceration of tissue. —Professor Susanne Binder, 2013

A controlled retinal detachment is created to allow a working space for subretinal manipulation. With a bent cannula that is introduced through the retinotomy, balanced salt solution is

slowly injected into the subretinal space. A bullous configuration of the retinal detachment should be avoided because it reduces visibility of the subsequent subretinal maneuvers. The cannula is also used to gently loosen connective tissue around the membrane and to test for adhesions. If some hemorrhage becomes visible under the membrane, gentle pressure can be applied on the membrane with the cannula for some time to achieve hemostasis. If an extrafoveal retinal angiomatous proliferation is present with a vascular connection to the sensory retina, it must be treated with careful diathermy and then cut with horizontal subretinal scissors. The membrane must be completely separated from the retina to avoid tearing and hole formation during removal, and its edges should be freed to avoid unnecessary removal of adjacent RPE. Then, subretinal forceps are introduced, and an edge of the membrane is grasped and slowly removed in a rather horizontal or oblique direction but never in a vertical direction. Again, if bleeding occurs while the tissue is extracted, pressure increases, and perfluorocarbon will help to stop it. Since larger diffuse bleedings can occur after the tissue is removed from the eye and the sclerotomy is open, it is wiser to hold the membrane in the vitreous cavity or let it fall back on the retina for some time until bleeding has ceased. Then the membrane can be grasped again and safely removed from the eye, while the posterior retina is covered with perfluorocarbon liquid. As there is much elasticity of tissue, quite large membranes can be removed via a small retinotomy, if it is performed slowly. However if larger fibrotic choroidal neovascular membranes and organized blood complexes should be removed with the cutter, the size of the retinotomy needs to be adapted and sealed either with diathermy before removal or with laser after removal when the retina is reattached. Again the vitreous is cleaned from blood and tissue particles to reduce postoperative inflammation. The peripheral retina is indented to look for possible tear formation or tissue incarceration that can easily occur close to the sclerotomy site during tissue removal. The perfluorocarbon liquid is removed, and the surgery is completed with fluid gas exchange. If a large fibrohemorrhagic complex had to be removed via a large retinotomy, a silicone oil tamponade is preferable.

In elderly patients with some cataract, vitrectomy is usually preceded by phacoemulsification of the lens in combination with a posterior chamber lens implant.

1. Complications of Submacular Surgery

As with all types of vitreous surgery, there is a small chance of endophthalmitis, retinal detachment, and retinal tear formation in about 2–5 % of cases. In phakic eyes, cataracts will develop in more than 80 % of patients over 50 years of age. Related to the submacular surgery and retinotomy is insufficient closure of the retinotomy or a higher incidence of hemorrhage postoperatively which might clear within 1–3 weeks. While small retinotomies usually close even if not treated with laser coagulation, large retinotomies require careful laser treatment and a sufficient internal tamponade to permanently close [10]. The most common complication

during membrane removal in AMD is recurrent choroidal neovascularization that occurs in up to 32 % of cases [7].

E. Functional Results of Submacular Surgery

In younger patients with inflammatory neovascularization, the CNV is usually a classic type, i.e., well circumscribed (focal) and located anterior to the RPE, while in elderly patients with AMD, these membranes can be either classic, as described for younger patients, or occult, i.e., diffuse (non-focal) and located posterior to the RPE. Don Gass described classic membranes as type 2 membranes and the occult membranes as type 1 in his report about the rationale of subfoveal membrane excision [11]. In large studies of membrane excision in AMD patients, visual acuity improvement was reported between 0 and 33 % of patients [12–14]. This was much lower than the primary results in young patients with inflammatory disease, who attained postoperative visual acuity of 20/40 in 30–40 % [6]. The reason for this difference can be explained by two facts:

- Type one, occult, membranes located under the retinal pigment epithelium have worse outcomes because the overlying pigment epithelium is removed simultaneously during membrane excision leaving a larger defect of the RPE in comparison to type two classic membranes located anterior to the pigment epithelium where the membrane can be removed with much lesser mechanical damage to the RPE.
- In diffuse disease like AMD, the pigment epithelial defect created at surgery tends to enlarge over time, while in focal disease and young patients, the defect remains either stable or become smaller due to cell migration from its edges and a healthier Bruch's membrane/choriocapillaris complex than in elderly patients [15–17].

In a retrospective meta-analysis evaluating 26 different studies and a total of 647 cases of subretinal membrane excision in AMD patients, it was shown that improvement was achieved in about 33 %, but there was also deterioration in 27 %. Additionally, recurrence of CNV occurred in 25 % (0–55 %), which added to further visual loss in initially successful cases [18]. In a prospective multicenter study comparing submacular surgery with laser photocoagulation, the two treatment options were found to be equivalent. After 2 years, 65 % of laser-treated cases versus 50 % of surgically treated eyes had a visual acuity that was better than or no more than one line worse than baseline [19]. While in the early years of submacular surgery for AMD, small, classic membranes were removed surgically, but with the introduction of photodynamic therapy for small classic CNV this became the standard of care (later replaced by intravitreal anti-VEGF injections). Surgery was only performed for large occult hemorrhagic membranes with the worst prognosis [20].

II. Macular Translocation in AMD

The basic concept of macular translocation is to improve vision in patients with subfoveal choroidal neovascularization by relocating the macula away from the neovascular complex so that it enables the macula to receive nourishment from a healthier underlying RPE and choroid. For macular displacement an iatrogenic retinal detachment is created either partially or totally, and the retina is reattached by a tamponade.

A. History

The first who explored translocation of the retina experimentally was Linsey in 1983 [21]. In 1985 Tiedemann published their proposal for retinal translocation [22], and in 1993 Machemer and Steinhorst published their results in the first human surgical cases suffering from AMD [23]. Over the years the procedure has gone through multiple evolutionary iterations with major developments by Eckardt et al., Toth et al., and Tano et al. [24–26].

In 1996 translocation with partial retinotomy was described mainly to reduce surgical complications like PVR [27], and in 1998 de Juan invented a limited translocation technique combined with scleral infolding for smaller submacular membranes [28].

B. Surgical Technique

1. Limited Translocation

The original technique of limited translocation included primarily a crescent-shaped partial scleral resection which was subsequently followed by scleral infolding performed with 4–6 mattress sutures to reduce the complexity of the surgery [28]. A modified technique was to achieve scleral shortening by scleral outfolding with clips [29].

Essentially, the surgical procedure consists of four major steps:

1. Pars plana vitrectomy with posterior vitreous cortex removal
2. Iatrogenic retinal detachment
3. Scleral shortening
4. Partial fluid–air exchange

a. Scleral Infolding

In scleral infolding, rectus muscle traction sutures are placed first and 5–6 mattress sutures replaced through partial-thickness sclera starting 2 mm behind the temporal rectus muscle insertion and reaching upwards to the superior rectus muscle. Then, a standard 3-port pars plana vitrectomy is performed. By slowly injecting balanced saline solution into the subretinal space via a 39 or 41 gauge needle, a retinal detachment is created from the optic nerve to the ora serrata in

the temporal 180° of the globe. Following this, the scleral mattress sutures are secured to shorten the sclera, and the surgery is completed with a partial fluid–air exchange. Postoperatively the patient is positioned to attain a shift of the central retina away from the choroidal neovascular membrane.

b. Outfolding Technique

In the outfolding technique a pars plana vitrectomy is performed, and a retinal detachment is created. Then, titanium clips are applied to the sclera 2–2.5 mm wide and 10 mm long between the temporal lateral muscle and the oblique superior muscle. A fluid–air exchange and positioning are performed in a similar way to the aforementioned infolding technique [30].

2. Full Macular Translocation (MTS 360)

In this surgery phakic eyes undergo cataract surgery with implantation of a posterior chamber intraocular lens at the beginning of the procedure. After complete pars plana vitrectomy including posterior vitreous cortex removal and peripheral vitreous shaving under scleral depression, the retina is detached completely via a peripherally placed retinotomy and subretinal fluid injection. Then the retina is cut circumferentially as anterior as possible, while posteriorly placed perfluorocarbon liquid can help to stabilize the retina during this procedure for a short while. The retina is then reflected after the perfluorocarbon liquid is removed, and the subretinal membranous complex, if present, is carefully removed. Then the retina is gently translocated (mostly upwards) to cover the fovea with healthier retina using perfluorocarbon liquid placed on the posterior pole. When enough displacement is achieved (35–45°), the retina is completely reattached with additional perfluorocarbon liquid, and endolaser is applied at the edges of the retina. The perfluorocarbon liquid is immediately replaced by a silicone oil tamponade. To prevent visual distortion, extraocular muscle surgery needs to be performed in these eyes either simultaneously [24] or a few weeks after translocation surgery [25].

C. Complications

A large study cohort of 153 cases undergoing limited macular translocation showed at least one complication in 35 % of cases [31] including retinal tears, retinal detachments, macular holes, retinal folds affecting the fovea, neovascularization at the injection site, and subretinal and choroidal hemorrhages. The main problem with this surgery, however, was that the amount of translocation was small and insufficient for larger choroidal neovascular membranes, the amount of retinal shift was not predictable, and recurrences were frequent [32]. For MT360, retinal detachment was among the most common complications ranging from 7.8 % from reports by Cynthia Toth and her group [33] to 42.8 % in a

comparative study between different techniques by Ohji and coworkers [34]. Recurrent neovascularization was the second most common complication ranging from 3.3 % after an extremely long observation period of 90 months in a German study [35] to 27.8 % with a 36-month observation time in the comparative Japanese study [34]. Other complications were cystoid macular edema, preretinal membrane formation, macular hole or tear, hypotony, and keratopathy [36]. As frequently observed with complex surgery, the highest complication rates were reported with earlier cases than later because the learning curve is long.

Because of the large rotation performed in MTS 360, binocular vision is often not recovered, and extraocular muscle surgery is needed [37].

D. Functional Results

Functional assessment after limited macular translocation showed that after 6 months 48 % of patients gained two or more lines of visual acuity, and at 1 year 40 % gained two or more lines of visual acuity, while 31 % lost two or more lines [31, 32]. For MTS 360 the percentage of patients with improvement in distance visual acuity ranges between 43 and 66 % [24, 38], and gains of more than three lines range from 13 to 36 %. In contrast, the number of patients who were losing three or more lines after surgery is described between 6.6 and 56.2 % [24, 25]. Even more interesting, however, are the results in reading vision that have been reported to be larger than distance vision in two studies [39]. When compared with PDT in a prospective randomized trial, it was shown that macular translocation produced better visual results over 2-year observation [40].

III. RPE Transplantation

A. Rationale

The transplantation of RPE seemed to be a logical approach in restoring vision in patients with AMD. The disappointing visual results after membrane excision alone were explained by the mechanical removal of the RPE together with the membrane as well as the primary dysfunction of the RPE in these cases. Consequently, restoring RPE became an objective. Retinal rotation techniques (see above) have actually provided us with the proof of principle that this kind of *autotransplantation* can in fact restore useful vision and that reading visual acuity can be regained from an extrafoveal location. Thus, reconstituting central RPE structure and function via transplantation became a priority.

Following the path of successful experimental neuronal transplantation [41, 42], transplantation of retinal cells has been performed in animal and human eyes during the last

two decades. Despite evidence that transplantation was somewhat effective in animal models, efficacy in humans has been confounded by various difficulties. Indeed, successful transplantation requires the following:

- A viable source of cells
- A technique for safe delivery
- Survival of the transplanted cells within the host
- No transdifferentiation of the grafted cells from their normal RPE phenotype (i.e., ideally restoration of the retinal pigment epithelium monolayer)
- A restoration of normal retinal architecture
- A permanent stabilization or improvement in vision

B. History

Options for patients with exudative AMD and subfoveal choroidal neovascularization were subretinal membrane excision only, laser treatment, or observation. With the introduction of photodynamic therapy for classic choroidal neovascularization and limited lesion sizes, submacular surgery was only indicated for large or mainly occult lesions complicated by bleeding. With the introduction of anti-VEGF therapy as the first line of treatment in exudative AMD, retinal cell therapy came almost to a halt. It is only with several years of experience with anti-VEGF treatment that we have learned that this treatment delays but does not prevent further visual loss because of retinal atrophy. Consequently, there is and will continue to be a resurgence of interest in cell transplantation.

1. Transplantation of Ocular Tissues

The first experiments detailing the behavior of transplanted neural tissue were performed in 1946 by Tansley, who transplanted embryonic eyes into rat brains [43]. Although the use of the anterior chamber as a tissue culture chamber to observe the behavior and growth of various transplanted tissues had already been reported previously, the first transplantation of fetal retina into the anterior chamber of maternal eyes in rats was performed in 1959 by Royo and Quay [44]. No further experiments were reported for more than 20 years.

2. Retinal Pigment Epithelial Transplantation

The concept of retinal pigment epithelial (RPE) transplantation evolved from the successful culturing of RPE from donor eyes by Flood et al. in 1980 [45]. In 1984 and 1985, cultured human retinal cells were transplanted in the eyes of monkeys, first by open sky techniques and later with closed eye methods by Gouras and others [46–48]. Finally, the therapeutic potential of RPE transplantation was demonstrated in the Royal College of Surgeons (RCS) rat model when radiolabeled RPE suspension grafts delivered through a bleb detachment were fully capable of phagocytosing host outer segments [49, 50]. The retinal atrophy that occurred in the RCS rat within 2 months after birth as a result of the inher-

ited phagocytosis defect of the photoreceptor outer segment was therefore prevented [51–53].

The RPE is known to produce a variety of cytokines both *in vivo* and *in vitro* [54]. In addition to the expected rescue effects observed over areas with transplanted RPE cells, fine cellular processes extending from the transplanted RPE over long distances were observed with electron microscopy. This suggested that trophic factors secreted from the graft may be involved in rescue of the overlying retina as well [49]. It is well known that experimental debridement of Bruch's membrane in normal pigmented rabbits will lead to atrophy of the underlying choriocapillaris and the overlying neural retina [55, 56]. Interestingly, intravitreal administration of basic fibroblast growth factors (bFGF) in RCS rats also led to a transient effect of photoreceptor rescue, which therefore may support such a trophic factor interaction [57, 58].

3. RPE Transplantation in Human Eyes

RPE transplantation in humans was first performed by Peyman et al. in 1991 in two cases of terminal AMD [59]. Photoreceptor transplantation was attempted in human eyes in patients with retinitis pigmentosa by two groups: del Cerro and Das [60, 61]. Kaplan and his group treated two patients who were NLP preoperatively with outer retinal sheet transplants derived from adult cadaver eyes with no complications; however, no visual improvement was reported [62]. In 1994 Alverve and Gouras transplanted small patches as well as cell suspensions of previously cultured human fetal RPE into the foveal area after membrane excision [63]. Because of disappointing visual results, immune reaction to the homologous cells was considered as the main culprit in all the aforementioned experiments.

An interesting strategy to eliminate rejection has been the use of autografts of iris pigment epithelium (IPE) to replace defective RPE [64, 65]. Iris pigment epithelium cells have been used by groups in Japan and Germany [66, 67]. This concept is intriguing due to the ease by which the IPE can be harvested. The surgery can be performed in a one-step procedure or in two steps where iridectomy is performed in combination with cataract surgery and the IPE thereafter expanded in cell culture or transfected. Several investigators have shown the ability of IPE to phagocytose outer segments *in vitro* [68, 69]. However, when compared to the RPE, the IPE has been demonstrated to digest outer segments much more slowly and thus not as well as RPE [70]. It was thus reasonable to search for a safe way to harvest autologous RPE cells to transplant them subfoveally in eyes with subfoveal neovascularization related to AMD [71].

C. Surgical Techniques

1. Cell Suspensions (See Video V.A.1-1)

The technique we used was experimentally tested [72] and then used in a pilot study in humans and in a subsequent trial

comparing membrane excision with and without RPE transplantation [73, 74]. The procedure is as follows:

- After pars plana vitrectomy and careful removal of the posterior vitreous cortex, a bleb retinal detachment is created nasally from the optic disc via a small retinotomy.
- With a special instrument the RPE is gently harvested and aspirated in a tube and a microsyringe over an area of approximately 4–5 disc diameters.
- While these cells are counted and centrifuged by a surgical assistant, the subfoveal choroidal neovascular membrane is removed by the surgeon via a second retinotomy created away from the fovea but close enough to the lesion to grasp it with subretinal forceps (see above).
- A perfluorocarbon liquid bubble is used to cover the posterior pole and prevent bleeding.
- Now the RPE cell suspension prepared by the assistant is slowly injected into the subretinal space via a small cannula connected to a tuberculin syringe with the perfluorocarbon liquid still in place to avoid reflux of cells into the vitreous.
- The retinotomies are sealed with endolaser photocoagulation.
- PFCL is aspirated after some minutes to allow cells to settle and the vitreous cleaned from cellular debris.
- The retinal periphery is inspected carefully for retinal tears or vitreous incarceration.
- A fluid–air exchange is performed.
- The sclerotomy wounds are closed.

Postoperatively, the patient is asked to maintain a supine position for 1 h to further allow the cells to settle in the subretinal space and is then turned into a prone position until the next day. Complications with cell suspension transplantation were rather low and mainly related to vitrectomy. In a pilot study and in a trial, we reported about 8.7 % retinal detachment, all treatable [73, 74]. No recurrence of CNV was observed during the observation period of 17 months but reached 5–8 % after 2 years.

While the suspension technique bears the advantages of being technically easy and has complication rates close to standard vitrectomy, it bears the disadvantage that the cells are irregularly distributed on a defective or diseased Bruch's membrane which makes their survival difficult. This limitation is being addressed by experiments that are underway to create artificial basal lamina to provide better survival of these cells by improving this *cell culture* milieu from its diseased environment and by approaches using artificial laminas rather than cell suspensions.

2. RPE/Bruch's Membrane/Choroid Patch

Another strategy using autologous material is the transplantation of a full-thickness RPE–choroidal patch or sheet taken from the periphery of the same eye to cover the foveal defect. The first who performed full-thickness RPE patch transplantation that was taken from adjacent areas of the CNV in nine patients was Bill Awylard 1998 to 1999. Unfortunately these

flaps demonstrated sequestration after an observation period of 1–2 years [75], although some remaining functions were demonstrated by microperimetry [76]. As with retinal rotation, bleeding and inflammation need to be kept to a minimum to provide a basis for success with this surgery.

Over the following years full-thickness patch transplantation has gone through some technical changes with large contributions by Jan van Meurs and Drs. Pertile and Parolini [77–79]. As with full retinal rotation surgery, phakic patients undergo cataract surgery with lens implantation at the beginning of surgery. The classic transplantation consists of the following steps:

- A complete 3-port pars plana vitrectomy including anterior vitrectomy and removal of the posterior vitreous cortex.
- A retinotomy temporal from the lesion is created, and the fibromembranous complex is carefully removed under perfluorocarbon liquid.
- An area for the patch is identified nasal to the optic disc or inferior to the vascular arcade.
- Diathermy and/or laser is performed at the borders of the transplant which was chosen as large as possible, but in general 4×5 mm.
- With horizontal scissors the full-thickness patch is cut 90 % with the overlying retina left as long as possible to prevent damage to the RPE with instruments. If bleeding occurs from the choroid during cutting, this must be managed immediately with diathermy and transient intraocular pressure rise; otherwise, all manipulations are performed in a soft eye.
- Now some fluid is injected into the subretinal space to allow easier access with the patch.
- After the patch is freed completely and the overlying retina removed, it is grasped carefully at the edge and slowly transferred into the subfoveal space.
- Now the anterior vitreous is excised and the vitreous filled with perfluorocarbon liquid anterior from the equator.
- Addition laser treatment is applied to the retinotomies.
- A direct perfluorocarbon liquid–silicone oil exchange is performed, and the sclerotomy wounds are closed.

A variation mainly performed by Drs. Pertile and others is the following:

- After vitrectomy, a 180° retinotomy is created in the temporal periphery of the fundus, and the retina is detached and flapped nasally.
- PFCL is used to hold the retina in place when the neovascular complex and blood are removed.
- Bleeding vessels are treated with diathermy.
- The patch is prepared under perfluorocarbon liquid in a similar way as with the classic technique and then gently translocated over the foveal defect.
- A perfluorocarbon liquid “rock and roll” technique is used to allow this. The subretinal perfluorocarbon liquid is gently removed and the retina unrolled with new perfluorocarbon liquid.

- Laser photocoagulation is applied at the edges of the retinotomy.
- A direct perfluorocarbon liquid–silicone oil exchange is performed.

This technique has the clear advantage that it minimizes bleeding and provides better access to the neovascular lesion which tends to be quite large to justify surgical intervention and easier preparation of the patch. Whether a residual film of perfluorocarbon liquid around the transplant might reduce cell function has never been separately evaluated.

Complications with patch transplants were higher than cell suspension techniques, especially with the occurrence of proliferative vitreo-retinopathy in up to 45 % [76–80]. As already pointed out with MTS 360, complication rates were lower in reports from those groups who performed the surgery for several years in higher numbers [81–83]. Figures V.A.1-1, V.A.1-2, V.A.1-3, V.A.1-4, V.A.1-5, V.A.1-6, V.A.1-7, V.A.1-8, V.A.1-9, V.A.1-10, V.A.1-11, and V.A.1-12 show two cases of RPE–choroid patch transplantation performed by Dr. Binder. Both are last eye patients. Nr 1 (Case 2) turned out to be less successful (Figures V.A.1-1, V.A.1-2, V.A.1-3, V.A.1-4, V.A.1-5, V.A.1-6, and V.A.1-7), and Nr 2 (case 5) was indeed a permanent success (Figures V.A.1-8, V.A.1-9, V.A.1-10, V.A.1-11, and V.A.1-12).

D. Functional Results

While functional results in the pilot study of 14 cases with RPE suspensions were very promising since 57.5 % of cases gained two or more lines after 17 months of observation [73], later results were rather disappointing. When these experiments were started, PDT was not available, and

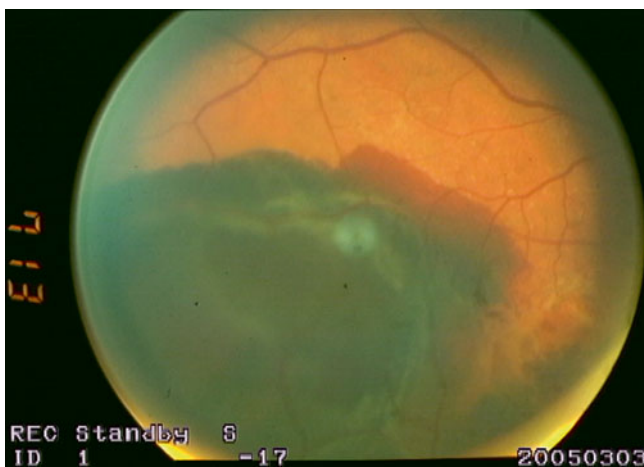


Figure V.A.1-1 Case Nr 1. Full-thickness RPE/Bruch's membrane choroidal patch transplantation. Case 2. A 76-year-old male. VA on admission=hand motions. History: Status post PDT Jan 2005. Massive subretinal hemorrhage from CNV. Other eye: end-stage AMD, VA=hand motions

patients with small foveal lesions were candidates for surgery. In the subsequent trial, however, patients who qualified for PDT were excluded from the surgery trial; thus, the patients who underwent surgery had larger lesions and more hemorrhage. In spite of that we saw a trend that was not statistically significant but suggested superiority in visual gain when cell suspension injection was compared with membrane removal alone. A significant difference, however, was observed in clinical tests like multifocal ERG and microperimetry [74]. Similar experiences have been reported also after iris pigment transplantation [67].

With patch transplantation significant improvement in distance and reading vision can be reached in a certain percentage of cases, but unfortunately due to the high number of complications, this advantage is lost (in a study). A mean gain of one line was described by Van Meurs and his group [83]. With the success of anti-VEGF therapy as first-line

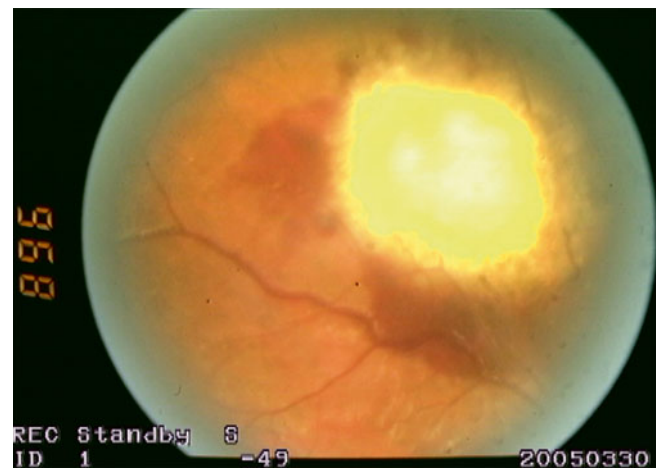


Figure V.A.1-2 Area where patch has been removed in superior quadrant

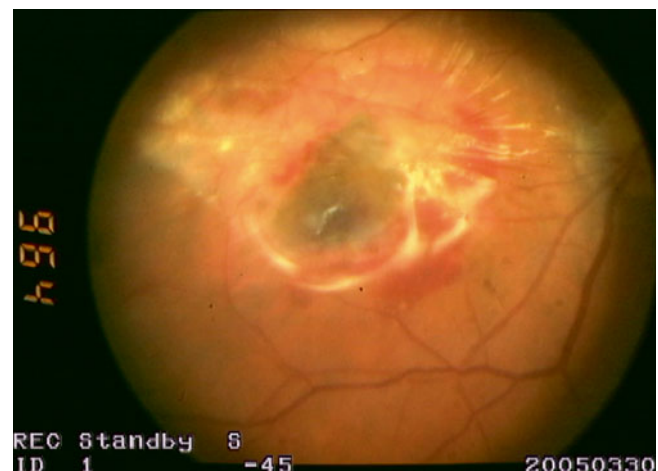


Figure V.A.1-3 One month postoperatively. Well-centered transplant patch that is perfused on fluorescein angiography. VA=0.05 (20/400)

Figure V.A.1-4 One month postoperatively. OCT of transplant shows cystic changes, intact retinal layers

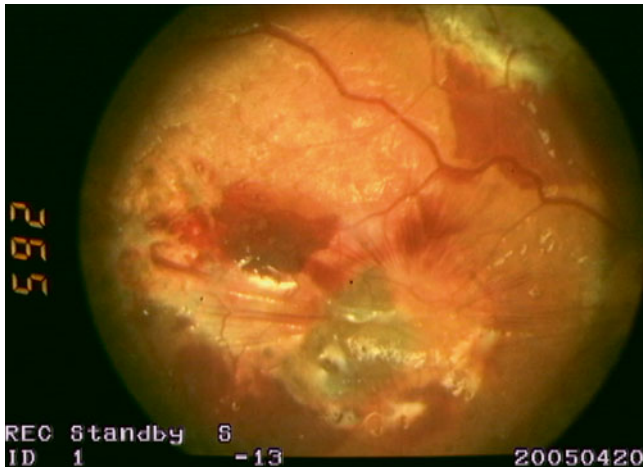
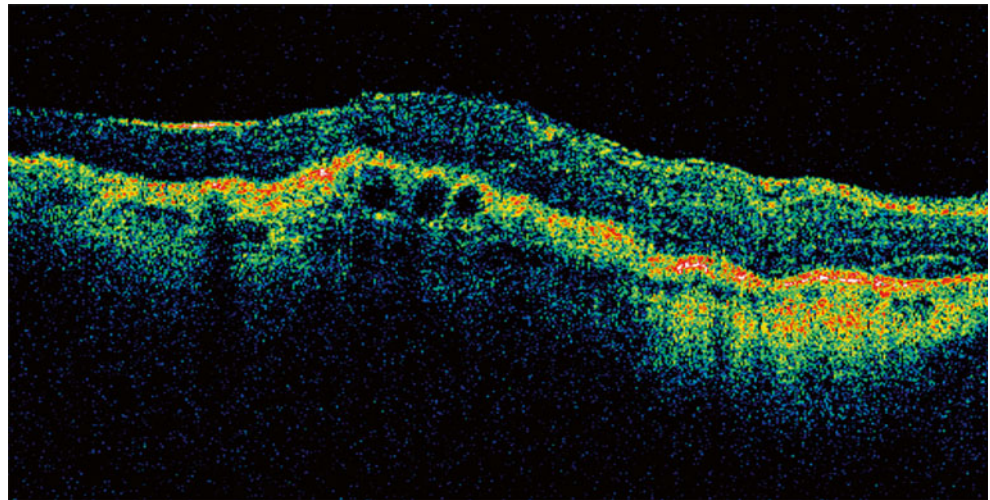


Figure V.A.1-5 Three months postoperatively. Central patch appears smaller and folded. VA=0.03 (20/400). Silicone oil removal planned

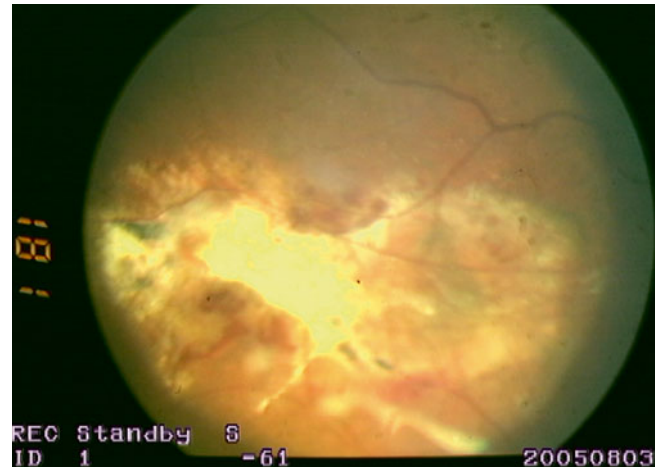


Figure V.A.1-6 Two months postoperatively. Silicone was removed uneventfully. Patch has lost pigmentation. VA=0.02 (20/800)

treatment in exudative AMD today, this surgery is only reserved as rescue therapy for isolated cases, but the experience that has been gained techniques that have been developed will be very useful for future therapies.

IV. Surgical Management of Submacular Hematoma

A. History

Submacular hematoma may be caused by a number of different conditions including exudative age-related macular degeneration and other causes of choroidal neovascular membrane, ruptured retinal macroaneurysm, complications of scleral buckle surgery, trauma, sickle cell disease, and retinal tears in primary rhegmatogenous retinal detachments. Systemic anticoagulants or antithrombotics may increase the

risk of submacular hemorrhage for exudative age-related macular degeneration [84, 85], and long-term anticoagulation or antiplatelet therapy may be associated with larger subretinal hemorrhages [86]. A variant of choroidal neovascular membrane, polypoidal choroidal vasculopathy, is also at increased risk of submacular hemorrhage [87]. Polypoidal choroidal vasculopathy is a common presentation of age-related macular degeneration in Asian patients [88].

Glatt and Machemer observed that in a rabbit model subretinal blood irreversibly damaged the outer retina within 24 h [89]. They hypothesized three mechanisms for this damage: thick subretinal blood created a diffusion barrier between the retinal pigment epithelium choroid and the photoreceptors, contraction of the blood clot caused mechanical damage, and/or iron toxicity. Fibrin was associated with tearing of sheets of photoreceptor inner and outer segments by 7–14 days in a cat model [90] supporting the concept of early therapeutic intervention.

Figure V.A.1-7 OCT 12 months postoperatively. Loss of intraretinal structure with fibrosis

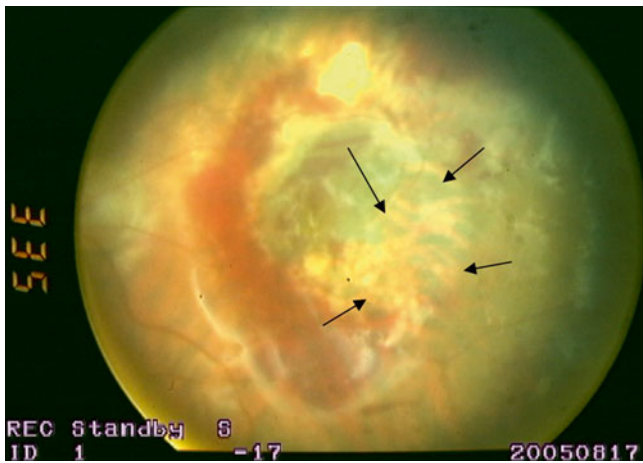
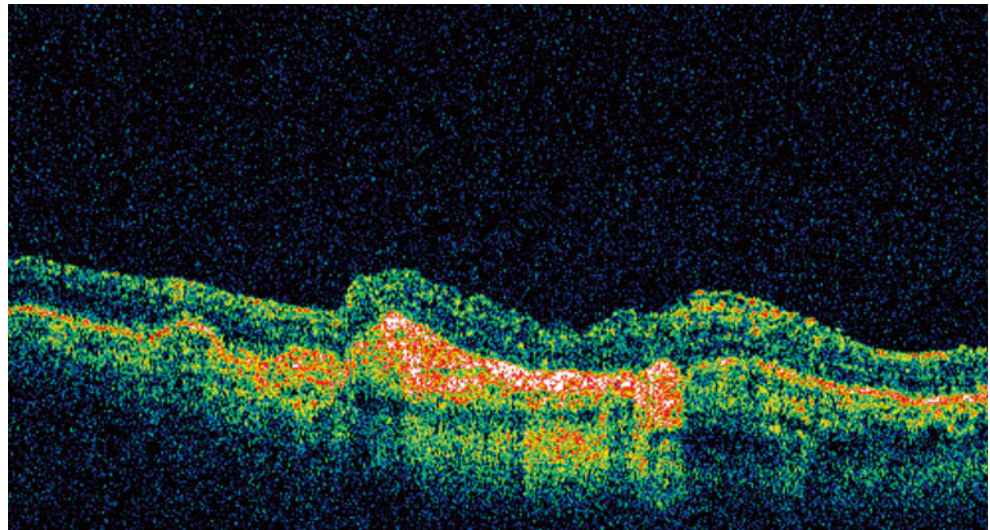


Figure V.A.1-8 Case Nr 2: 71-year-old female. History. Massive hemorrhage after PDT. VA=LP+, other eye enucleated after trauma in childhood. One month after surgery residual hemorrhage nasally from transplant. Good centration of transplant but surrounding rim of atrophic area (*black arrows*)

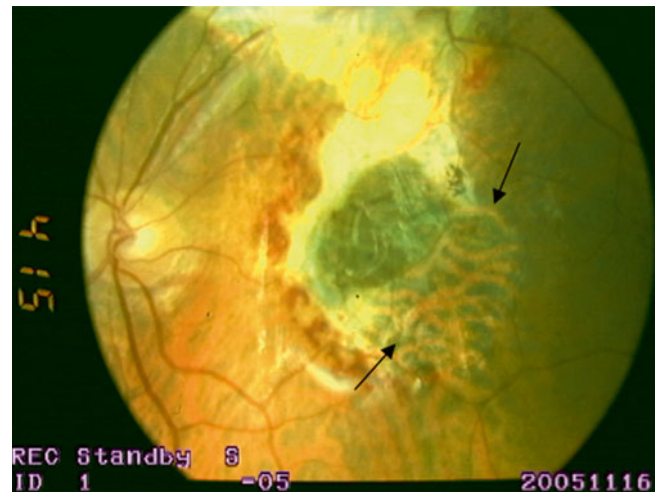


Figure V.A.1-9 Six months postop. VA=0.04 (20/400). Bridging between healthy pigment epithelium and transplant visible (*black arrows*)

The natural history of thick submacular hemorrhage in exudative macular degeneration is especially poor when compared to other etiologies without choroidal neovascular membranes such as choroidal rupture [91–93]. At 36 months 44 % of eyes with subfoveal blood had lost six or more lines of vision, and size and height of the subretinal blood were important factors [94]. Preexisting abnormalities of the photoreceptor and retinal pigment epithelium in age-related macular degeneration may lower the threshold to damage from subretinal blood. The results of anti-VEGF monotherapy for submacular hemorrhage due to AMD may be better than the natural history, but good visual acuity is rarely attained [95–97].

B. Surgery for Submacular Hematoma

1. History

In 1987 Hanscom and Diddie in California first reported the evacuation of subretinal hemorrhage of 1 week's duration from two patients (one with AMD and one with ruptured macroaneurysm) [98]. In 1988 de Juan and Machemer reported improvement in visual acuity after pars plana vitrectomy and removal of the subretinal clots in three of four patients with large submacular hemorrhage and AMD. Subsequent reports followed [93, 99, 100]. The surgeon waited for the submacular hemorrhage to hemolyze before performing pars plana vitrectomy. After pars plana

Figure V.A.1-10 Six months postoperatively. OCT shows nice integration of patch as well as a connection with healthy RPE

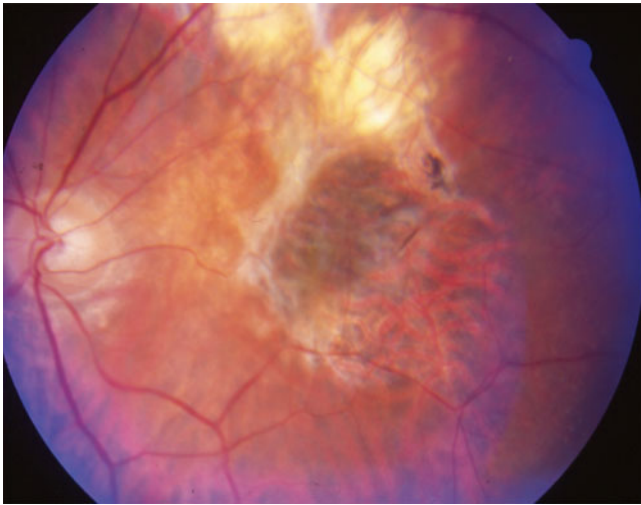
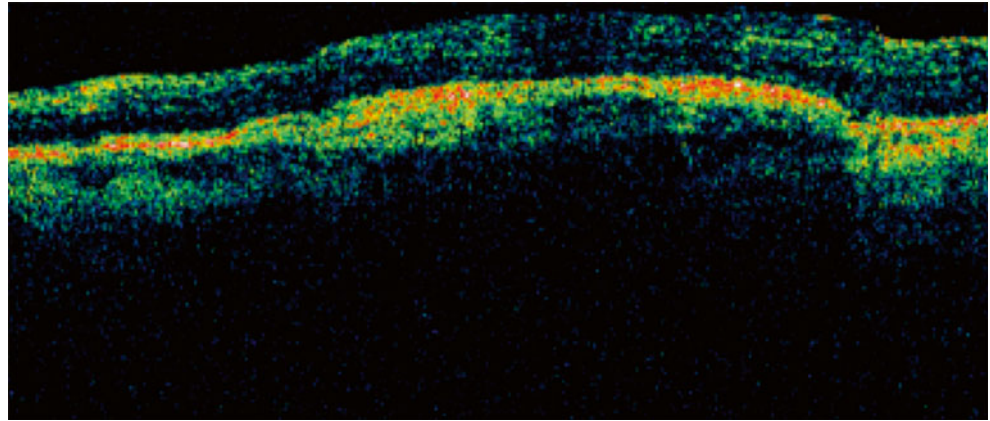


Figure V.A.1-11 Twenty-eight months postoperatively. Same clinical situation. VA improved to 0.1 (20/200) Jaeger 7

vitrectomy, a retinotomy was made through which intraocular forceps were introduced to grasp the clot and extract it or liquefied blood was lavaged. There was significant discussion about the timing of the intervention. Intervention too early could physically shear and damage the photoreceptors. A delay in intervention could result in an irreversibly damaged sensory retina.

2. Tissue Plasminogen Activator

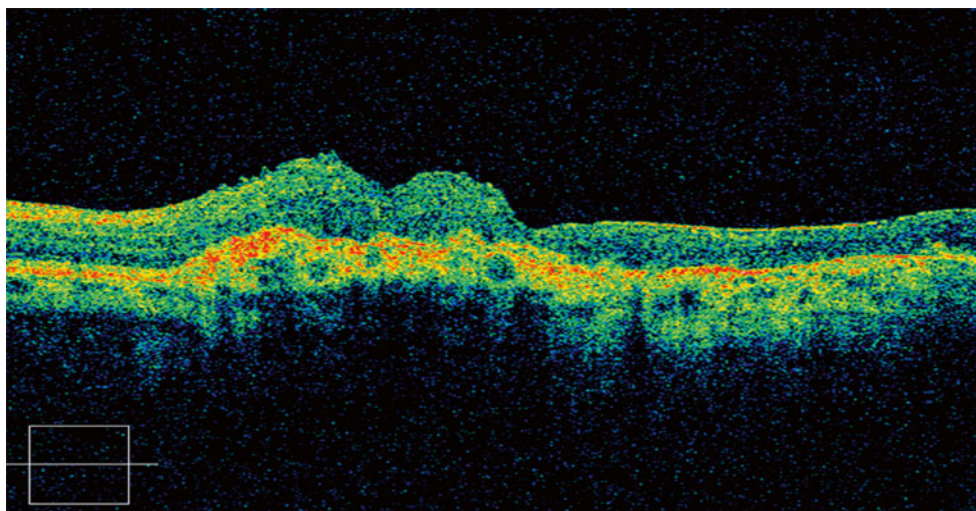
Tissue plasminogen activator (tPA) is a serine protease found on endothelial cells. It is an enzyme that catalyzes the conversion of plasminogen to plasmin, the major enzyme responsible for hemolysis [101]. It has advantages over other thrombolytic agents such as streptokinase and urokinase because its activity is enhanced in the presence of a fibrin clot, and a complex of fibrin, tissue plasminogen activator, and plasminogen is formed. These qualities make it fibrin specific and clot selective [102]. tPA available for clinical

use is manufactured using recombinant biotechnology and includes alteplase, reteplase, and tenecteplase. Alteplase is FDA approved for treatment of myocardial infarction with ST elevation, acute ischemic stroke, acute massive pulmonary embolism, and central venous access devices. Reteplase is FDA approved for acute myocardial infarction. Tenecteplase is indicated for acute myocardial infarction.

The introduction of subretinal injection of tPA allowed immediate surgical intervention of submacular hemorrhage. A number of animal studies established the retina toxicity profiles for intravitreal injection of tPA injected in the rabbit [103, 104], and cat [105–107]. In the rabbit eye, toxicity was not seen in doses up to 50 microgram/0.1 cc. Above 50 $\mu\text{g}/0.1$ cc, large necrotic retinal holes, bullous retinal detachment, and marked retinal vessel attenuation were seen. In the human, four patients developed exudative retinal detachment followed by hyperpigmentation after intravitreal injection of 100 μg of tPA [108]. The retinal toxicity of tPA has been attributed to L-arginine in the vehicle which prevents the self-degradation of tPA [106]. Hemolytic effects have been seen clinically with doses as low as 6 μg (delivered in 0.1 cc volume) injected into the vitreous [109] and 6 $\mu\text{g}/0.1$ cc injected into the subretinal space [110]. Clinically doses between 5 and 50 μg per 0.1 cc are used.

Early worries that tPA could not enter the subretinal space because of its large size (molecular weight of over 70 kD) were seemingly confirmed when labeled tPA injected into the vitreous could not be detected in the subretinal space of rabbits [111]. Yet intravitreally injected albumin at 69 kD diffused through the retina within 1 h in rabbit eyes [112], and subretinal clots were hemolyzed by intravitreal tPA compared to saline injections in rabbits [113] and pigs [114]. These worries were quickly dispelled by its clinical effectiveness. Kimura et al. found hemolyzed blood at time of vitrectomy 12–36 h after intravitreal injection of tPA [109]. More recently this discrepancy between failure of tPA to penetrate the rabbit retina and its clinical utility has been

Figure V.A.1-12 Twenty-eight months postoperatively. OCT shows well-integrated patch and development of foveal contour



attributed to species differences. A third-generation thrombolytic agent, a variation of native tPA produced by recombinant DNA technology with multiple point mutations, was shown to penetrate all layers of the pig eye after intravitreal injection [115]. Subretinal injection of tPA in experimental animal models enhanced the clearance of subretinal hemorrhage [104, 107], or facilitated surgical removal [116] and protected the outer retina.

3. Surgery

The use of subretinal tPA allowed earlier surgical intervention and the prospect of better visual outcome [110, 117–119]. Small gauge subretinal cannulas which had been developed to infuse fluid underneath the retina for excision of subfoveal choroidal neovascular membrane and macular translocation were adapted for injection of tPA (see Video V.A.1-2). Preoperative intravitreal injection of tPA also seemed to facilitate the removal of subretinal hemorrhage during pars plana vitrectomy a day later [109]. Perfluorocarbon liquids could be used to squeeze the liquefied blood into the vitreous cavity [110, 120]. To date published reports of surgical interventions for submacular hemorrhage have been retrospective, studying relatively few patients with variable follow-up and hemorrhage size. The SST Group B trial randomized 336 patients with relatively large hemorrhages (subfoveal choroidal neovascular lesions greater than 3.5 disc areas and composed of at least 50 % blood), but could not demonstrate any benefit to submacular surgery [121]. However, tPA was used in only 38 % of eyes, blood remained underneath the fovea in 62 % of eyes with greater than 4 disc areas of blood, and the duration of hemorrhage before intervention was not reported.

At the 1996 Vail Vitrectomy Meeting Heriot presented his success in displacing submacular hemorrhage from the fovea with intravitreal tPA, intravitreal gas injection, and facedown

positioning [122]. Other reports followed [108, 123–125]. One hundred micrograms of tPA was injected through the pars plana in a volume of 0.1 cc. A day later gas was injected into the eye. The patient was positioned in a prone position to localize the gas bubble to the macula to displace the hemolyzed blood. This captured the imagination of retinal surgeons around the world. There was discussion about how long to wait after tPA injection before gas should be injected. Submacular hemorrhage could be displaced even without tPA [126]. Surgeons soon adapted Heriot's idea of displacing submacular hemorrhage to the surgical management of this problem [127]. Eighty-seven percent of eyes had no subfoveal blood after this technique with 2 line visual acuity improvement in 59 % of eyes [128]. The risk of retinotomy-related complications was avoided. Direct injection of tPA into the subretinal space appeared to be more efficacious and predictable than intravitreal tPA.

a. Technique

The author (LPC) uses the following technique:

- Tissue plasminogen activator at a concentration of 25 $\mu\text{g}/0.1$ cc is prepared in the pharmacy and delivered to the operating room. The tPA is transferred to a 3 cc Luer-Lock syringe on the surgical field.
- A 39 or 41 gauge subretinal cannula is connected to the 3 cc syringe with a small length of intravenous tubing. This isolates movement at the syringe from inadvertently displacing the tip of the subretinal cannula at the time of tPA injection. All air in the tubing and cannula is carefully removed.
- After pars plana vitrectomy, the subretinal cannula is advanced to the surface of the retina until the choroid focally whitens. The view of a 68 diopter macula panoramic contact lens (Advanced Visual Instruments, Inc., New York, New York) provides both magnified detail as well as an arcade to arcade view of the macula.

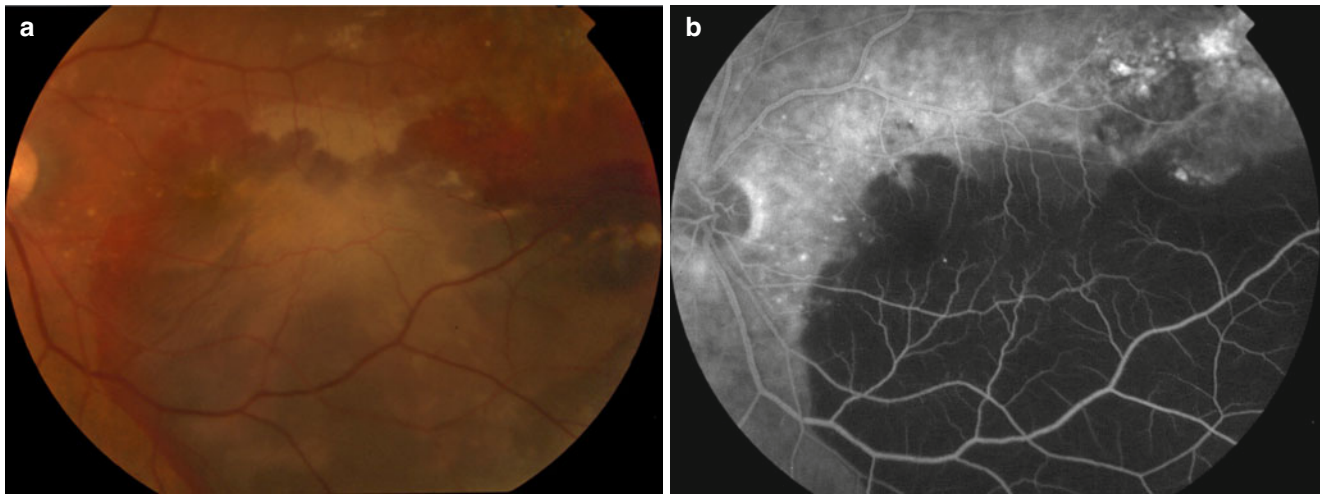


Figure V.A.1-13 (a) Preoperative photograph of the left eye in a 77-year-old man with exudative age-related macular degeneration and submacular hemorrhage lowering visual acuity to count fingers (Courtesy of J. Sebag, MD; VMR Institute for Vitreous Macula Retina).

(b) Preoperative fluorescein angiography of the same eye as in figure (a) demonstrating profound blocked fluorescence by the submacular hemorrhage (Courtesy of J. Sebag, MD; VMR Institute for Vitreous Macula Retina)

- The surgical assistant depresses the plunger on the syringe to inject the tPA into the subretinal space. These injections are made at the borders of the submacular hemorrhage and not over the clot itself. Injections made directly over the clot may result in failure at the retinotomy site from clot contraction or proliferation stimulated by the clot.
- Multiple injections are usually necessary to bathe the blood clot. The optic nerve limits the subretinal tPA from migrating to the nasal side.
- The induced detachment of the retina should be limited to the posterior pole just outside the temporal vascular arcades. Induction of retinal detachment beyond the equator increases the risk of postoperative rhegmatogenous retinal detachment.
- After subretinal tPA injection a small air bubble is injected into the subretinal space. This augments the displacement of the subfoveal blood to the periphery [129].
- In the recovery room, the patient is positioned supine for 1 h before positioning the head erect for 24 h.

Intraocular gas is not necessary to displace the blood or to tamponade the small retinotomies made by the 39 or 41 gauge subretinal cannulas. Therefore, I do not put any gas into the eye. Should gas be injected, then the head is conventionally positioned face down. Stopa et al. concluded that the head erect positioning is preferential to prone positioning because this maximizes the force of gravity force parallel to the subretinal space [130]. Foster and Chou demonstrated that a partial gas bubble has no buoyant force at the top in a vessel with gas in the upper portion and liquid in the lower portion [131]. This also favors head erect positioning without an intraocular gas bubble in the immediate postoperative period. The retina is usually completely attached after 24 h. This means that submacular hemorrhage is again locked into

place after 24 h, and further head erect positioning beyond this time is not useful. The submacular hemorrhage is most often displaced to just beyond the inferotemporal arcade and is a function of the volume of tPA injected into the subretinal space (Figures V.A.1-13 and V.A.1-14).

b. Complications

Complications include spontaneous rupture at the fovea with release of subretinal hemorrhage through the fovea during tPA injection, postoperative rhegmatogenous retinal detachment, inadequate displacement of hemorrhage, and breakthrough of submacular hemorrhage into the vitreous cavity. The fovea is the thinnest point of the sensory retina and therefore prone to spontaneous rupture. Despite this occurrence, the visual outcome remains good similar to successful macular hole repair. As mentioned, creation of retinal detachment beyond the equator increases the risk of rhegmatogenous retinal detachment. The subretinal blood can stimulate the development of proliferative vitreo-retinopathy. Inadequate displacement of hemorrhage may necessitate a repeat procedure to displace the remaining hemorrhage. Recurrent submacular hemorrhage is rarely seen after successful displacement of submacular hemorrhage secondary to exudative age-related macular degeneration. A definitive choroidal neovascular membrane is often not identifiable by fluorescein angiography.

Massive submacular hemorrhages for which displacement is ineffective are best managed with subretinal tPA and 360 retinotomy techniques. These techniques were described in the seminal report by Machemer and Steinhorst describing this approach in three eyes with severe and recent massive submacular hemorrhage [23] [see section II. Macular translocation in AMD].

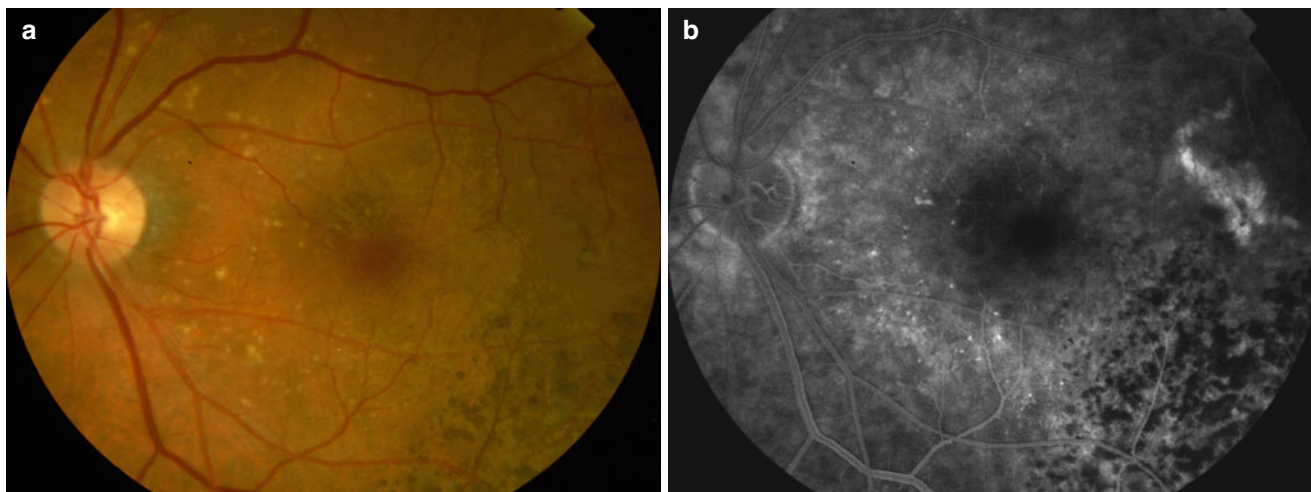


Figure V.A.1-14 (a) Postoperative photograph of the same eye as in Figure V.A.1-13 with successfully displaced submacular hemorrhage by vitrectomy with submacular tPA injection and perfluoropropane vitreous substitute. Drusen is noted nasally and RPE changes are seen inferotemporally. Visual acuity improved to 20/30 (0.67) [Courtesy of

J. Sebag, MD; VMR Institute for Vitreous Macula Retina]. (b) Postoperative fluorescein angiogram of the same eye as in figure (a) demonstrating that the source of the submacular hemorrhage was choroidal neovascularization in the distal temporal macula (Courtesy of J. Sebag, MD; VMR Institute for Vitreous Macula Retina)

Abbreviations

AMD	Age-related macular degeneration
bFGF	Basic fibroblast growth factor
CC	Cubic centimeter
CNV	Choroidal neovascularization
DNA	Deoxyribonucleic acid
ERG	Electroretinography
FDA	Food and Drug Administration
IPE	Iris pigment epithelium
kD	Kilodalton
MTS 360	Full macular translocation
NLP	No light perception
PDT	Photodynamic therapy
PFCL	Perfluorocarbon liquids
PVR	Proliferative vitreo-retinopathy
RCS	Royal College of Surgeons
RPE	Retinal pigment epithelium
SST	Submacular Surgery Trial
t-PA	Tissue plasminogen activator
VEGF	Vascular endothelial growth factor

References

- Machemer R. Surgical approaches to subretinal strands. *Am J Ophthalmol.* 1980;90:81–5.
- Lewis H, Aarberg TM, Abrams GW. Subretinal membranes in proliferative vitreoretinopathy. *Ophthalmology.* 1989;96:1403–14.
- Zivonovic R. Silicone oil in vitreoretinal surgery. Dordrecht, 1987, Martinus/Nijhoff/DW Junk.
- Chang S, Lincoff G, Zimmerman NJ. Giant retinal tears: surgical technique and results using perfluorocarbon liquids. *Arch Ophthalmol.* 1989;107:761–6.
- de Juan Jr E, Machemer R. Vitreous surgery for haemorrhagic and fibrous complications of age-related macular degeneration. *Am J Ophthalmol.* 1988;105:25–9.
- Thomas MA, Kaplan HJ. Surgical removal of subfoveal neovascularisation in the presumed ocular histoplasmosis syndrome. *Am J Ophthalmol.* 1991;111:1–7.
- Thomas MA, Grand MG, Williams DF. Surgical management of subfoveal choroidal neovascularisation. *Ophthalmology.* 1992;99:952–68.
- Binder S. Surgical treatment of peripapillary choroidal neovascularisation. *Br J Ophthalmol.* 2007;91:990–1. Editorial.
- Krebs I, Brannath W, Glittenberg C, Zeiler F, Sebag J, Binder S. Posterior vitreomacular adhesion: a potential risk factor for exudative age-related macular degeneration? *Am J Ophthalmol.* 2007;144(5):741–6.
- Bressler NM, Bressler SB, Childs AL, et al. Surgery for hemorrhagic choroidal neovascular lesion of age-related macular degeneration: ophthalmic findings: sst report No 13. *Ophthalmology.* 2004;111(11):1993–2006.
- Gass JDM. Biomicroscopic and histopathologic considerations regarding the feasibility of surgical excision of subretinal neovascular membranes. *Am J Ophthalmol.* 1994;118:285–98.
- Lambert HM, Capone Jr A, Aaberg T. Surgical excision of subfoveal neovascular membranes in age-related macular degeneration. *Am J Ophthalmol.* 1992;113:257–62.
- Berger AS, Kaplan HJ. Clinical experience with the surgical removal of subfoveal neovascular membranes: short term postoperative results. *Ophthalmology.* 1992;99:969–76.
- Thomas MA, Dickinson JD, Melberg NS, et al. Visual results after surgical removal of subfoveal neovascular membranes. *Ophthalmology.* 1994;101:1384–96.
- Scheider A, Gündisch O, Kampik A. Surgical extraction of subfoveal new vessels and submacular haemorrhage in AMD. Results of a prospective study. *Graefes Arch Clin Exp Ophthalmol.* 1998;237:10–5.
- Nasir MA, Sugino I, Zarbin MA. Decreased choriocapillaris perfusion following surgical excision of choroidal neovascular membranes in age-related macular degeneration. *Br J Ophthalmol.* 1997;81:481–9.
- Rabenlehner D, Stanzel BV, Krebs I, Binder S, Goll A. Reduction of iatrogenic RPE lesions in AMD patients: evidence for wound healing? *Graefes Arch Clin Exp Ophthalmol.* 2008;246(3):345–5.

18. Falkner CI, Leitich H, Frommelt F, Bauer P, Binder S. The end of submacular surgery for age-related macular degeneration? A meta-analysis. *Graefes Arch Clin Exp Ophthalmol*. 2007;245(4):490–501.
19. Bressler NM, et al. Submacular Surgery Trials Pilot Study Investigators. Submacular surgery trials randomized pilot trial of laser photocoagulation versus surgery for recurrent choroidal neovascularisation secondary to age-related macular degeneration: I. Ophthalmic outcomes. Submacular surgery trials pilot study report NR 1. *Am J Ophthalmol*. 2000;130:387–409.
20. Schachat AP. Should we recommend vitreous surgery for patients with choroidal neovascularisation? *Arch Ophthalmol*. 1994;112:459–61.
21. Lindey P, Finkelstein D, D'anna S. Experimental retinal translocation. *Invest Ophthalmol Vis Sci*. 1983;24:5242.
22. Tiedeman JS, de Juan JE, Machermer R, et al. Surgical rotation of the macula. *Invest Ophthalmol Vis Sci*. 1985;26:559.
23. Machermer R, Steinhilber UH. Retinal separation, retinotomy and macular relocation. II A surgical approach for age-related macular degeneration. *Graefes Arch Clin Exp Ophthalmol*. 1993;231:635–41.
24. Eckardt C, Eckardt U, Conrad HG. Macular rotation with and without counterrotation of the globe in patients with age-related macular degeneration. *Graefes Arch Clin Exp Ophthalmol*. 1999;237:313–25.
25. Toth CA, Freedman SF. Macular translocation with 360 degree peripheral retinectomy impact of technique and surgical experience on visual outcomes. *Retina*. 2001;21:293–303.
26. Tano Y. Pathologic myopia. Where are we now? *Am J Ophthalmol*. 2002;134:645–60.
27. Ninimya Y, Lewis JM, Hasegawa T, et al. Retinotomy and foveal translocation for surgical management of subfoveal choroidal neovascular membranes. *Am J Ophthalmol*. 1996;122:613–21.
28. De Juan Jr E, Loewenstein A, Bressler NM, et al. Translocation of the retina for management of subfoveal choroidal neovascularisation. II: a preliminary report in humans. *Am J Ophthalmol*. 1998;128:635–46.
29. Lewis H. Macular translocation with choriocleral outfolding: a pilot clinical study. *Am J Ophthalmol*. 2001;132:156–63.
30. Kamei M, Tano Y. Limited macular translocation. In: Alfaro V, Ligett P, Mieler WF, Qirioz Mercado H, Jager RD, Tano Y, editors. *Age-related macular degeneration. A comprehensive textbook*. Philadelphia: Lippincott Williams + Wilkins; 2006.
31. Fujii GY, Pieramici DJ, Humajun MS, et al. Complications associated with limited macular translocation. *Am J Ophthalmol*. 2000;130:751–62.
32. Fujii GY, de Juan Jr E, Pieramici DJ. Inferior limited macular translocation for subfoveal choroidal neovascularisation secondary to age-related macular degeneration: 1 year visual outcome and recurrence report. *Am J Ophthalmol*. 2002;34:69–74.
33. Mruthyunjaya P, Stinnett SS, Toth CA. Change in visual function after macular translocation surgery with 360 degree peripheral retinectomy for neovascular age-related macular degeneration. *Ophthalmology*. 2004;111(9):1715–24.
34. Ohji M, Fujicado T, Kusaka S, et al. Comparison of three techniques of foveal translocation in patients with subfoveal choroidal neovascularisation resulting from age-related macular degeneration. *Am J Ophthalmol*. 2001;132:88–96.
35. Aisenbrey S, Lafout BA, Szurman P, et al. Macular translocation with 360 degree retinotomy for exudative age-related macular degeneration. *Arch Ophthalmol*. 2002;120:451–9.
36. Ehlers JP, Toth CA. Macular translocation. In: *Retina*. 5th ed. Ryan SJ, Wilkinson CP, Wiedemann P, editors. Surgical retina, vol. 3. 1996–2009.
37. Fricke J, Neugebauer A, Nobis H, et al. Counterrotation of the globe in macular translocation. *Graefes Arch Clin Exp Ophthalmol*. 2000;238:664–8.
38. Pertile G, Claes C. Macular translocation with 360 degree retinectomy for management of age-related macular degeneration. *Am J Ophthalmol*. 2002;134:560–5.
39. Lai JC, Lapolice DJ, Stinnett SS. Visual outcome following macular translocation with 360-degree peripheral retinectomy. *Arch Ophthalmol*. 2002;120:1317–24.
40. Luke M, Ziemsen F, Völker M, et al. Full macular translocation (FMT) versus photodynamic therapy (PDT) with verteporfin in the treatment of neovascular age-related macular degeneration: 2 year results of a prospective, controlled randomized pilot trial (FMT-PDT). *Graefes Arch Clin Exp Ophthalmol*. 2009;247:745–54.
41. Björklund A, Stenevi U. Growth of central catecholamine neurons into smooth muscle grafts in the rat mesencephalon. *Brain Res*. 1971;31(1):1–20.
42. Widner H, Rhencrona S. Transplantation and surgical treatment of parkinsonian syndromes. *Curr Opin Neurol Neurosurg*. 1993;6:344–9.
43. Tansley K. The development of the rat eye in graft. *J Exp Biol*. 1946;22:221–3.
44. Royo PE, Quay WB. Retinal transplantation from fetal to maternal mammalian eye. *Growth*. 1959;23:313–36.
45. Flood MT, Gouras P, Kjeldbye H. Growth characteristics and ultrastructure of human retinal pigment epithelium in vitro. *Invest Ophthalmol Vis Sci*. 1980;19(11):1309–20.
46. Gouras P, Flood MT, Kjeldbye H, et al. Transplantation of cultured human retinal pigment epithelium to Bruch's membrane of the owl monkeys eye. *Curr Eye Res*. 1985;4:253–65.
47. Lopez R, Gouras P, Brittis M, et al. Transplantation of cultured rabbit retinal epithelium to rabbit retina using a closed eye method. *Invest Ophthalmol Vis Sci*. 1987;28:1131–7.
48. Li LX, Turner JE. Inherited retinal dystrophy in the RSC rat prevention of photoreceptor degeneration by pigment epithelial cell transplantation. *Exp Eye Res*. 1988;47:911–7.
49. Gouras P. Transplantation of retinal pigment epithelium. In: Marmor M, Wolfensberger TH, editor. *The retinal pigment epithelium*, vol. 25. Oxford University Press, Oxford, England; 1998. p. 492–507.
50. Das SR, Bhardwaj N, Gouras P. Synthesis of retinoids by human retinal epithelium and transfer to rod outer segments. *Biochem J*. 1990;268:201–6.
51. Gouras P, Lopez R, Brittis M, et al. Transplantation of cultured retinal epithelium. In: Agarath E, Ehinger B, editors. *Retinal signals system, degenerations and transplants*. Amsterdam: Elsevier; 1986. p. 271–86.
52. Repucci V, Goluboff E, Wapner F, et al. Retinal pigment epithelium transplantation in the RCS rat. *Invest Ophthalmol Vis Sci*. 1988;29 (ARVO) suppl 144.
53. Bourne M, Campell D, Tansley K. Hereditary degeneration of the rat retina. *Br J Ophthalmol*. 1938;22:613–23.
54. Mullen RJ, La Vail MM. Inherited retinal dystrophy: primary defect in retinal pigment epithelium determined with chimeric rats. *Science*. 1976;192:799–801.
55. Heron WL, et al. Retinal dystrophy in the rat. A pigment epithelial disease. *Invest Ophthalmol Vis Sci*. 1969;8:595–604.
56. Whiteley SJ, Lichfield TM, Tyers P, et al. Retinal pigment epithelium transplanted to the subretinal space improves the papillary light reflex in RCS rats. *Invest Ophthalmol Vis Sci*. 1995;36(4):212–9.
57. Factorovich EG, Steinberg RH, Tasumura D, et al. Photoreceptor degeneration in inherited retinal dystrophy delayed by basic fibroblast growth factor. *Nature*. 1990;347:83–6.
58. Perry J, Du J, Kjeldbye H, et al. The effects of bFGF on RSC rat eyes. *Curr Eye Res*. 1995;14:585–92.
59. Peyman GA, Blinder KJ, Paris KJ, et al. A technique for retinal pigment epithelial transplantation for age related macular degeneration secondary to extensive subfoveal scarring. *Ophthalmic Surg*. 1991;22:102–8.

60. del Cerro M, Das T, Reddy VI, et al. Human fetal neural cell transplantation in retinitis pigmentosa. *Vision Research*. 1995;35, suppl 140 (abstract).
61. Das T, del Cerro M, Jalali S, et al. The transplantation of human fetal neuroretinal cells in advanced retinitis pigmentosa: results of a long term safety study. *Exp Neurol*. 1999;157:58–68.
62. Kaplan HJ, Tezel TH, Berger AS, et al. Human photoreceptor transplantation in retinitis pigmentosa; a safety study. *Arch Ophthalmol*. 1997;115:1168–72.
63. Algere PV, Berglin L, Gouras P, et al. Transplantation of fetal retinal pigment epithelium in age-related macular degeneration with subfoveal neovascularisation. *Graefes Arch Clin Exp Ophthalmol*. 1994;232:707–16.
64. Rezaei KA, Kohan L, Wiedemann P, et al. Iris pigment epithelium transplantation. *Graefes Arch Clin Exp Ophthalmol*. 1997;235(9): 558–62.
65. Gelance M, Meneses P, Rosenfeld MR, et al. Long-term results of autologous transplantation of iris pigmented epithelial cells into the subretinal space. *Invest Ophthalmol Vis Sci*. 1997;38(4):334–42.
66. Tamai M, Abe T, Tomita H, et al. Autologous iris pigment transplantation in age related macular degeneration. In: Das T, editor. *Retina. Current practice and future trends*. Hyderabad: PARAS Publishing; 1999. p. 151–61.
67. Thumann G, Aisenbrey S, Schraemeyer U. Transplantation of autologous iris pigment epithelium after removal of choroidal neovascular membranes. *Arch Ophthalmol*. 2000;118(10):1350–5.
68. Thuman G, Heimann K, Schraemeyer U. Quantitative phagocytosis of rod outer segments by human and porcine iris pigment epithelial cells in vitro. *Invest Ophthalmol Vis Sci*. 1997;38(4):330.
69. Bisantis F, Fregona I, Mancini A. Is phagocytosis in iris pigmented (IPE) cultures by human iridectomies a self limited and dose dependant mechanism ? *Invest Ophthalmol Vis Sci*. 1997;38(4):5330.
70. Dintelman T, Heimann K, Kayatz P. Comparative study of ROS degradation by IPE and RPE cells in vitro. *Graefes Arch Clin Exp Ophthalmol*. 1999;237:830–9.
71. Binder S, Stolba U, Krebs I, et al. Zur Transplantation autologer Pigmentepithelzellen. *Spektrum Augenheilk*. 2000;14/5:249–53.
72. Assadolina A, Binder S, Stanzel B, et al. Harvesting efficacy and viability of retinal pigment epithelial cells in aspirates from posterior retinal areas – a study in human eyes. *Spektrum Augenheilk*. 2003;17/1:8–10.
73. Binder S, Stolba U, Krebs I, et al. Transplantation of autologous retinal pigment epithelium in eyes with foveal neovascularisation resulting from age-related macular degeneration: a pilot study. *Am J Ophthalmol*. 2002;133(2):215–25.
74. Binder S, Krebs I, Hilgrers HD, et al. Outcome after transplantation of autologous RPE in age related macular degeneration – a prospective trial. *Invest Ophthalmol Vis Sci*. 2004;45: 4151–60.
75. Awylard GW, Kyrchenthal A, Stanga PE, et al. RPE-transplantation. A new surgical technique for treatment of choroidal NV in AMD. 12th annual meeting of the Retinal Society, Regensburg; 1999.
76. Stanga PE, Kychenhal A, Fitzke F. Retinal pigment epithelium translocation after choroidal neovascular membrane removal in age-related macular degeneration. *Ophthalmology*. 2002;109: 1492–8.
77. Jousseaume AM, Heussen FM, Joeres S, et al. Autologous translocation of the choroid and retinal pigment epithelium in age-related macular degeneration. *Am J Ophthalmol*. 2006;142:17–30.
78. Mac Laren RE, Uppal GS, Balaggan KS, et al. Autologous transplantation of the retinal pigment epithelium and choroid in the treatment of neovascular age-related macular degeneration. *Ophthalmology*. 2007;114:561–70.
79. Falkner-Radler CI, Krebs I, Glittenberg C, Binder S. Human retinal pigment epithelium (RPE) transplantation: outcome after autologous RPE-choroid sheet and RPE cell suspension in a randomized clinical study. *Br J Ophthalmol*. 2011;95:370–5.
80. Mac Laren RE, Bird AC, Sathia PJ, et al. Long term results of submacular surgery combined with macular translocation of the retinal pigment epithelium in neovascular age-related macular degeneration. *Ophthalmology*. 2005;112:2081–7.
81. Cereda MG, Parolini B, Bellesini E, Pertile G. Surgery for CNV and autologous choroidal RPE patch transplantation: exposing the submacular space. *Graefes Arch Clin Exp Ophthalmol*. 2009;248:37–47.
82. van Zeeburg EJ, Cereda MG, van der Schoot J, Pertile G, van Meurs JC. Early perfusion of a free RPE-choroid graft in patients with exudative macular degeneration can be imaged with spectral domain OCT. *Invest Ophthalmol Vis Sci*. 2011;52(8):5881–6.
83. Van Meurs JC, Van Den Biesen PR. Autologous retinal pigment epithelium and choroid translocation in patients with exudative age-related macular degeneration: short term follow-up. *Am J Ophthalmol*. 2003;136:688–95.
84. El Baba F, Jarrett 2nd WH, Harbin Jr TS, Fine SL, Michels RG, Schachat AP, Green HR. Massive hemorrhage complicating age-related macular degeneration: clinicopathologic correlation and role of anticoagulants. *Ophthalmology*. 1986;93:1591–2.
85. Tilanus MA, Vaandrager W, Cuypers MH, Verbeek AM, Hoyng CB. Relationship between anticoagulant medication and massive intraocular hemorrhage in age-related macular degeneration. *Graefes Arch Clin Exp Ophthalmol*. 2000;238:482–5.
86. Kulli-Hattenbach C, Fischer IB, Schalnus R, Hattenbach LO. Subretinal hemorrhages associated with age-related macular degeneration in patients receiving anticoagulation or antiplatelet therapy. *Am J Ophthalmol*. 2010;149:316–21.
87. Yannuzzi LA, Wong DWK, Sforzolini BS, Goldbaum M, Tang KC, Spaide RF, Freund KB, Slakter JS, Guyer DR, Sorenson JA, Fisher Y, Maberley D, Orlock DA. Polypoidal choroidal vasculopathy and neovascularized age-related macular degeneration. *Arch Ophthalmol*. 1999;117:1503–10.
88. Uyama M, Matsubara T, Fukushima I, Matsunaga H, Iwashita K, Nagai Y, Takahashi K. Idiopathic polypoidal choroidal vasculopathy in Japanese patients. *Arch Ophthalmol*. 1999;117:1035–42.
89. Glatt H, Macherer R. Experimental subretinal hemorrhage in rabbits. *Am J Ophthalmol*. 1982;94:762–73.
90. Toth CA, Morse LS, Hjelmeland LM, Landers 3rd MB. Fibrin directs early retinal damage after experimental subretinal hemorrhage. *Arch Ophthalmol*. 1991;109:723–9.
91. Bennett SR, Folk JC, Blodi CF, Klugman M. Factors prognostic of visual outcome in patients with subretinal hemorrhage. *Am J Ophthalmol*. 1990;109:33–7.
92. Berrocal MH, Lewis ML, Flynn Jr HW. Variations in the clinical course of submacular hemorrhage. *Am J Ophthalmol*. 1996;122: 486–93 (published erratum appears in *Am J Ophthalmol* 1996;122:920).
93. Wade EC, Flynn Jr HW, Olsen KR, Blumenkrantz MS, Nicholson DH. Sub-retinal hemorrhage management by pars plana vitrectomy and internal drainage. *Arch Ophthalmol*. 1990;108:973–8.
94. Avery RL, Fekrat S, Hawkins BS, Bressler NM. Natural history of subfoveal subretinal hemorrhage in age-related macular degeneration. *Retina*. 1996;16:183–9.
95. Stifter E, Michels S, Prager F, Georgopoulos M, Polak K, Hirn C, Schmidt-Erfurth U. Intravitreal bevacizumab therapy for neovascular age-related macular degeneration with large submacular hemorrhage. *Am J Ophthalmol*. 2007;144:886–92.
96. Shienbaum G, Garcia Filho AA, Flynn HW, Nunes RP, Smiddy WE, Rosenfeld PJ. Management of submacular hemorrhage secondary to neovascular age-related macular degeneration with anti-vascular endothelial growth factor monotherapy. *Am J Ophthalmol*. 2013;155:1009–13.

97. Chang MA, Do DV, Bressler SB, Cassard SD, Gower EW, Bressler NM. Prospective one-year study of ranibizumab for predominantly hemorrhagic choroidal neovascular lesions in age-related macular degeneration. *Retina*. 2010;30:1171–6.
98. Hanscom TA, Diddie DR. Early surgical drainage of macular subretinal hemorrhage. *Arch Ophthalmol*. 1987;105:1722–3.
99. Vander JF, Federman JL, Greven C, Slusher MM, Gabel VP. Surgical removal of massive subretinal hemorrhage associated with age-related macular degeneration. *Ophthalmology*. 1991;98:23–7.
100. Mandelcorn MS, Menezes AV. Surgical removal of subretinal hemorrhage and choroidal neovascular membranes in acute hemorrhagic age-related macular degeneration. *Can J Ophthalmol*. 1993;28:19–23.
101. Collen D, Lijnen HR. Tissue-type plasminogen activator: mechanisms of action and thrombolytic properties. *Haemostasis*. 1986;16 suppl 3:25–32.
102. Holyaerts M, Rijken OC, Lijnen HR, Collen D. Kinetics of the activation of plasminogen by human tissue plasminogen activator. Role of fibrin. *J Biol Chem*. 1982;257:2912.
103. Irvine WD, Johnson MW, Hernandez E, Olsen KR. Retinal toxicity of human tissue plasminogen activator in vitrectomized rabbit eyes. *Arch Ophthalmol*. 1991;109:718–22.
104. Lewis H, Resnick SC, Flannery JG, Straatsma BR. Tissue plasminogen activator treatment of experimental subretinal hemorrhage. *Am J Ophthalmol*. 1991;111:197–204.
105. Benner JD, Morse LS, Toth CA, Landers MDIII, Hjelmeland LM. Evaluation of a commercial recombinant tissue-type plasminogen activator preparation in the subretinal space of the cat. *Arch Ophthalmol*. 1991;109:1731–6.
106. Hrach CJ, Johnson MW, Hassan AS, Lei B, Sieving PA, Elner VM. Retinal toxicity of commercial intravitreal tissue plasminogen activator solution in cat eyes. *Arch Ophthalmol*. 2000;128:650–63.
107. Johnson MW, Olsen DR, Hernandez E. Tissue plasminogen activator treatment of experimental subretinal hemorrhage. *Retina*. 1991;11:250–8.
108. Hesse L, Schmidt J, Kroll P. Management of acute submacular hemorrhage using recombinant tissue plasminogen activator and gas. *Graefes Arch Clin Exp Ophthalmol*. 1999;237:273–7.
109. Kimura AE, Reddy CV, Folk JC, Farmer SG. Removal of subretinal hemorrhage facilitated by preoperative intravitreal tissue plasminogen activator. *Retina*. 1994;14:83–4.
110. Lim JI, Drews-Botsch C, Sternberg Jr P, Capone Jr A, Aaberg Sr TM. Submacular hemorrhage removal. *Ophthalmology*. 1995;102:1393–9.
111. Kamei M, Misono K, Lewis H. A study of the ability of tissue plasminogen activator to diffuse into the subretinal space after intravitreal injection in rabbits. *Am J Ophthalmol*. 1999;128:739–46.
112. Takeuchi A, Kricorian G, Yao XY, Kenny JW, Marmor MF. The rate and source of albumin entry into saline-filled experimental retinal detachments. *Invest Ophthalmol Vis Sci*. 1994;35:3792–8.
113. Coll GE, Sparrow JR, Marinovic A, Chang S. Effect of intravitreal tissue plasminogen activator on experimental subretinal hemorrhage. *Retina*. 1995;15:319–26.
114. Boone DE, Boldt HC, Ross RD, Folk JC, Kimura AE. The use of intravitreal tissue plasminogen activator in the treatment of experimental subretinal hemorrhage in the pig model. *Retina*. 1996;16:518–24.
115. Kwan ASL, Vijaysekaran S, McAllister IL, Yu PK, Yu D. A study of retinal penetration of intravitreal tenecteplase in pigs. *Invest Ophthalmol Vis Sci*. 2006;47:2662–7.
116. Johnson MW, Olsen DR, Hernandez E. Tissue plasminogen activator thrombolysis during surgical evacuation of experimental subretinal hemorrhage. *Ophthalmology*. 1992;99:515–21.
117. Peyman GA, Nelson Jr NC, Alturki W, Blinder KJ, Paris CL, Desai UR, Harper 3rd CA. Tissue plasminogen activating factor assisted removal of subretinal hemorrhage. *Ophthalmic Surg*. 1991;22:575–82.
118. Lewis H. Intraoperative fibrinolysis for submacular hemorrhage with tissue plasminogen activator and surgical drainage. *Am J Ophthalmol*. 1994;118:559–68.
119. Ibanez HE, Williams DF, Thomas MA, Ruby AJ, Meredith TA, Boniuk I, Grand MG. Surgical management of submacular hemorrhage: a series of 47 consecutive cases. *Arch Ophthalmol*. 1995;113:62–9.
120. Kamei M, Tano Y, Maeno T, Ikuno Y, Mitsuda H, Yuasa T. Surgical removal of submacular hemorrhage using tissue plasminogen activator and perfluorocarbon liquid. *Am J Ophthalmol*. 1996;121:267–75.
121. Bressler NM, et al.; Submacular Surgery Trials (SST) Research Group. Surgery for hemorrhagic choroidal neovascular lesions of age-related macular degeneration: ophthalmic findings. SST report no. 13. *Ophthalmology*. 2004;111:1993–2006.
122. Heriot WJ. Intravitreal gas and TPA: an outpatient procedure for sub-retinal hemorrhage. Presented at Vail Vitrectomy meeting, Vail; Mar 1996.
123. Hassan AS, Johnson MW, Schneiderman TE, et al. Management of submacular hemorrhage with intravitreal tissue plasminogen activator injection and pneumatic displacement. *Ophthalmology*. 1999;106:1900–7.
124. Meier P, Zeumer C, Jochmann C, Wiedemann P. Management of submacular hemorrhage by tissue plasminogen activator and SF(6) gas injection. *Ophthalmologie*. 1999;96:643–7.
125. Karlsson E, Carlsson J, Crafoord S, Jemt M, Martensson PA, Stenkula S. Tissue plasminogen activator and expanding gas intravitreally in treatment of submacular hemorrhage. *Acta Ophthalmol Scand*. 1999;77:119.
126. Ohji M, Saito Y, Hayashi A, Lewis JM, Tano Y. Pneumatic displacement of subretinal hemorrhage without tissue plasminogen activator. *Arch Ophthalmol*. 1998;116:1326–32.
127. Hauptert CL, McCuen 2nd BW, Jaffe GJ, Steuer ER, Cox TA, Toth CA, Fekrat S, Postel EA. Pars plana vitrectomy, subretinal injection of tissue plasminogen activator, and fluid-gas exchange for displacement of thick submacular hemorrhage in age-related macular degeneration. *Am J Ophthalmol*. 2001;131:208–15.
128. Olivier S, Chow DR, Packo KH, MacCumber MW, Awh CC. Sub-retinal recombinant tissue plasminogen activator injection and pneumatic displacement of thick submacular hemorrhage in age-related macular degeneration. *Ophthalmology*. 2004;111:1201–8.
129. Martel JN, Mahmoud TH. Subretinal pneumatic displacement of subretinal hemorrhage. *JAMA Ophthalmol*. 2013;131:5464.
130. Stopa M, Lincoff A, Lincoff H. Analysis of forces acting upon submacular hemorrhage in pneumatic displacement. *Retina*. 2007;27:370–4.
131. Foster WJ, Chou T. Physical mechanisms of gas and perfluoron retinopexy and sub-retinal fluid displacement. *Phys Med Biol*. 2004;49:2989–97.

Marta S. Figueroa and Inés Contreras

Outline

- I. **Macular Pucker**
 - A. Prognostic Factors and Indications for Surgery
 - B. Surgical Technique
 1. Inner Limiting Membrane (ILM) Peeling with and without Chromodissection
 - C. Surgical Outcomes
 1. Complications
- II. **Macular Pseudoholes**
- III. **Lamellar Macular Holes**
 - A. Prognostic Factors and Indications for Surgery
 - B. Surgical Technique
 - C. Surgical Outcomes and Complications
- IV. **Full-Thickness Macular Hole (FTMH)**
 - A. Prognostic Factors
 - B. Surgical Technique
 1. Chromodissection
 2. Internal Tamponade
 3. Contemporaneous Cataract Surgery
 4. Pharmacologic Vitreolysis
 - C. Surgical Outcomes and Complications
- V. **Vitreomacular Traction (VMT)**
 - A. Surgical Technique and Outcomes

References

Electronic supplementary material Supplementary material is available in the online version of this chapter at [10.1007/978-1-4939-1086-1_33](https://doi.org/10.1007/978-1-4939-1086-1_33). Videos can also be accessed at <http://www.springerimages.com/videos/978-1-4939-1085-4>.

M.S. Figueroa, MD, PhD (✉)
Department of Ophthalmology, Hospital Universitario Ramón y Cajal, Instituto Ramón y Cajal de Investigaciones Sanitarias (IRYCIS), Madrid, Spain

Vissum Madrid, Madrid, Spain
e-mail: figueroa@servicom2000.com

I. Contreras, MD, PhD
Department of Ophthalmology, Hospital Universitario Ramón y Cajal, Instituto Ramón y Cajal de Investigaciones Sanitarias (IRYCIS), Madrid, Spain

Clínica Rementería, Madrid, Spain
e-mail: inescon3@yahoo.com

Keywords

Vitreous • Macula • Macular pucker • Pseudohole • Lamellar hole • Full-thickness macular hole • Vitreomacular traction • Vitrectomy • Chromodissection • Premacular (“epiretinal”) membrane • Macular pucker

Key Concepts

1. The optimum timing for macular pucker surgery is still uncertain. Surgery should be performed if there is progressive visual acuity loss or metamorphopsia or if there are signs on spectral-domain OCT of photoreceptor damage. Surgery should include core and peripheral vitrectomy with premacular membrane and inner limiting membrane (ILM) removal, in order to avoid recurrences.
2. Lamellar macular holes and macular pseudoholes are conditions that progress slowly, and surgery should be performed only in those cases in which there is deterioration on OCT with visual acuity loss. If performed, surgery should include premacular membrane and ILM removal with the use of a gas tamponade to ensure closure of the hole.
3. Full-thickness macular holes stages 2–4 should undergo surgery soon after diagnosis. Surgery should include ILM removal and a gas tamponade to ensure macular hole closure.
4. Vitrectomy in patients with vitreomacular traction should be performed at diagnosis if visual acuity is worse than 20/40 or if there is severe metamorphopsia. In patients presenting good visual acuity, surgery should be performed if there is a decrease in visual acuity with increased traction on OCT. It is important to proceed cautiously when inducing a posterior vitreous detachment surgically because vitreous may be firmly attached to the fovea, requiring sharp dissection.

I. Macular Pucker

Macular pucker results from a premacular membrane often referred to as an “epiretinal” membrane. However, the term “epi” means adjacent to, which could be subretinal. Furthermore, the membranes in question are attached to the macula; thus the term “premacular” is more precise for two reasons. This premacular membrane is a fibrocellular proliferation that grows on the inner limiting membrane of the macula [see chapter III.F. Vitreous in the pathobiology of macular pucker]. Premacular membrane contraction leads to progressive distortion of the macular structure, producing visual acuity loss and metamorphopsia (Figure V.A.2-1). Vitrectomy with membrane peeling has been shown to release the traction exerted on the macula, with an improvement in visual acuity and metamorphopsia. Since macular pucker is a very frequent pathology [1] that often progresses slowly, the optimum time for surgery remains unclear. Furthermore, in some cases in spite of an adequate removal of the premacu-

lar membrane, visual outcomes are unsatisfactory. In the last few years, several reports have focused on the prognostic factors that may help to determine when to recommend surgery to a specific patient.

Spectral-domain optical coherence tomography (SD-OCT) with its high scanning speed and its resolution of up to 3 μm allows a layer-by-layer analysis of the retina and is capable of detecting subtle pathologic changes of the retina. Four highly reflective bands are clearly depicted in the outer retina on a SD-OCT image of a healthy eye. Recently, the following consensus has been reached on what these lines represent and how to refer to them: the outermost line represents the retinal pigment epithelium (RPE) and Bruch’s membrane complex, and the innermost line represents the *external limiting membrane* (ELM), which consists of zonular adherence between photoreceptor inner segments and Müller cell processes. Posterior to the ELM is a band that has often been attributed to the boundary between the inner and outer segments of the photoreceptors but which actually aligns with the ellipsoid



Figure V.A.2-1 Fundus appearance of a premacular membrane

portion of the outer segments and will be referred to as the *ellipsoid zone*. Between this zone and the RPE is what has been previously referred to as the *COST line* or the *Verhoeff membrane*. This band was attributed to scattering from the tips of the cone outer segments. It actually seems to correspond to an ensheathment of these outer segments by apical processes of the RPE and is now called *interdigitation zone*. The ellipsoid zone reflects the integrity of the photoreceptor outer segments: a distinct and continuous line indicates normal alignment of the membranous discs in the photoreceptor outer segments. As alignment of the discs is necessary for normal functioning of the photoreceptors, the presence of a normal ellipsoid zone strongly suggests that the photoreceptors are functioning normally.

A. Prognostic Factors and Indications for Surgery

The main factors that have been associated with a better visual acuity after surgery are a shorter duration of symptoms, better baseline visual acuity, and pre- and postoperative photoreceptor integrity. Experience has taught us that structural changes are more easily reversible if not long-standing. However, in most cases patients are uncertain about the onset of symptoms, which would explain why some studies have found a significant correlation between the duration of symptoms with postoperative visual acuity [2], while others have not [3]. Better baseline visual acuity and photoreceptor integ-

rity are intimately related. The preservation of the ellipsoid and interdigitation lines has been shown in multiple reports to be correlated with visual outcomes [4–10] (Figure V.A.2-2). Damaged photoreceptors may recover with time after surgery (taking as much as 6 months for full recovery [7]), although this is not frequent [10] (Figure V.A.2-3). This suggests that prompt surgery is beneficial to prevent irreversible photoreceptor impairment. However, it is important to note that photoreceptor damage might also occur during surgery, leading to postoperative disruption of previously intact ellipsoid and interdigitation zones [10].

Premacular membrane contraction produces an increase in central retinal thickness, which has been found to be correlated with visual acuity [3, 6] if the photoreceptor layers are intact [10]. The restoration of the foveal contour after surgery has been associated with better functional outcomes [4] (Figure V.A.2-4). However, visual acuity improvement is often achieved without restoration of the foveal contour (Figure V.A.2-5). These results lead to speculation that the tractional force generated by a premacular membrane can alter the macular structure and the interface between the outer segment tips and the RPE without being sufficiently detrimental to severely damage the photoreceptor [9]. Thus, it would seem that photoreceptor integrity is the main prognostic factor.

Regarding metamorphopsia, it has been associated preoperatively with a greater central retinal thickness [3, 11] as well as with a greater disruption of the ellipsoid zone [11]. More specifically, metamorphopsia is correlated with edema in the inner nuclear layer [3, 8, 12]. Residual metamorphopsia

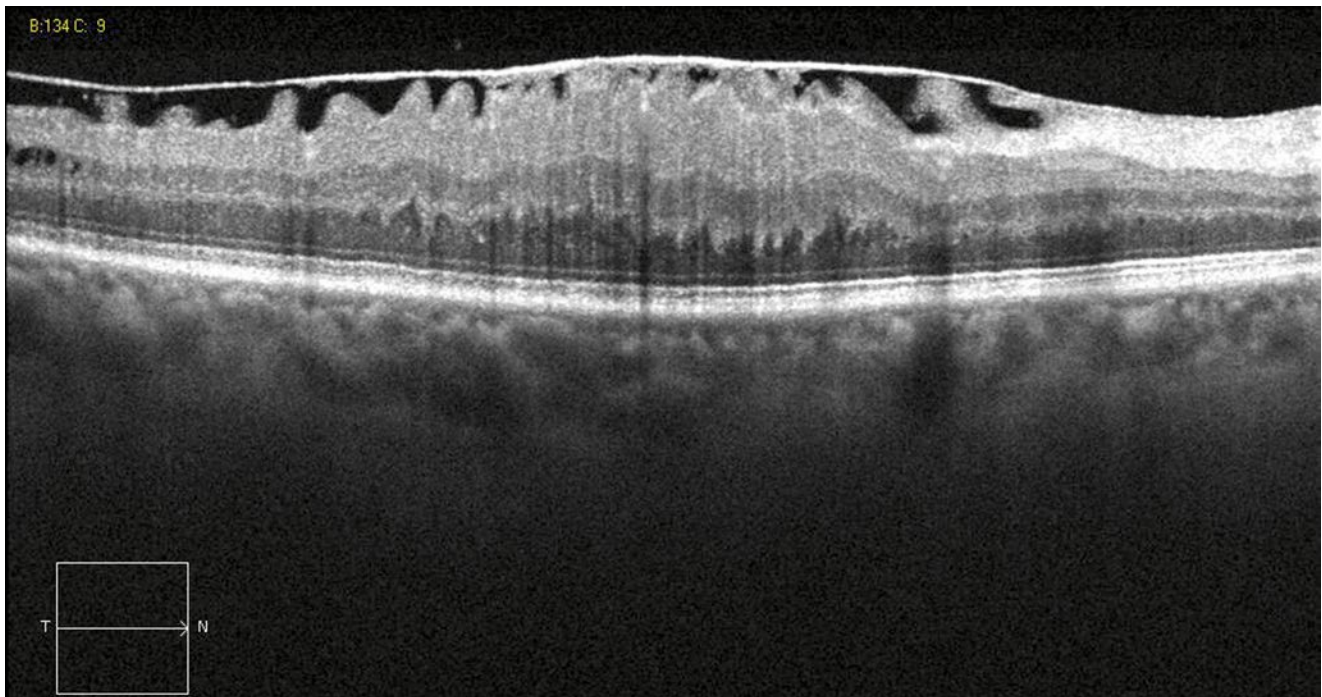


Figure V.A.2-2 Premacular membrane with preservation of the ellipsoid and interdigitation zones

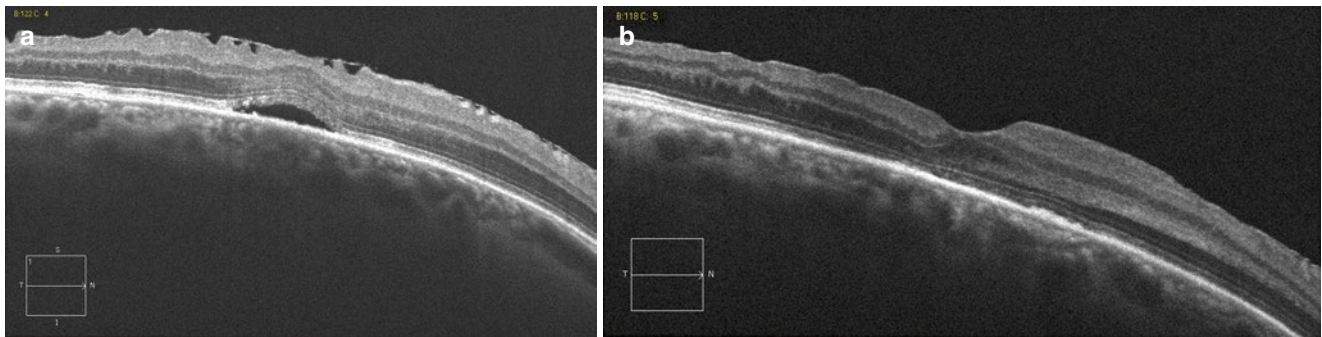


Figure V.A.2-3 (a) Premacular membrane causing foveal detachment and photoreceptor damage. (b) Recovery of damaged photoreceptors after surgery

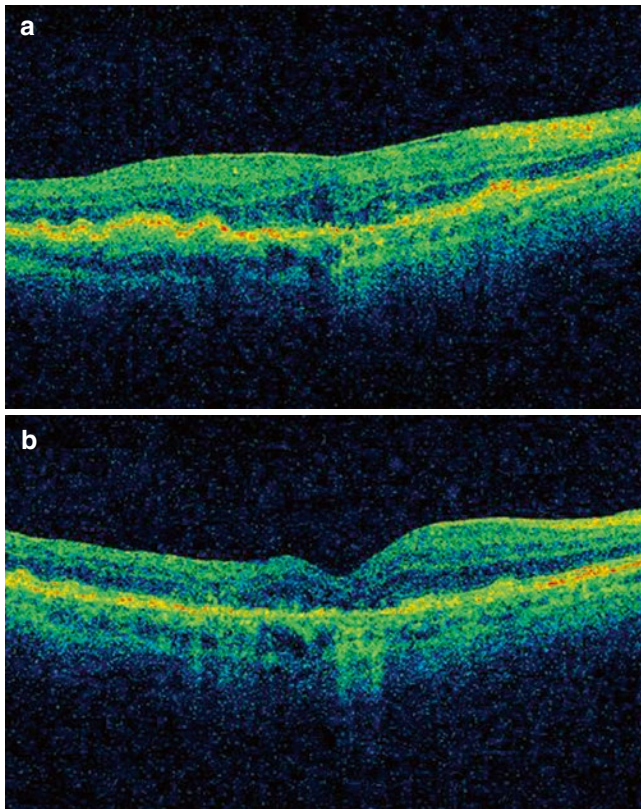


Figure V.A.2-4 (a) Premacular membrane contraction produces an increase in central retinal thickness. (b) Restoration of the foveal contour after surgery

after surgery is more frequent in eyes with intense metamorphopsia at baseline [3, 6, 11] and a greater disruption of the ellipsoid zone both at baseline and after surgery [11].

En face OCT imaging of macular pucker has revealed that there can be as many as four centers of retinal contraction [13]. The prognostic significance of this finding is considerable in that eyes with 3 or 4 pucker centers had a statistically significant higher incidence of intraretinal cysts and macular thickening than eyes with 1 or 2 foci of retinal contraction. This suggests that eyes with multiple foci of macular pucker

might benefit from surgery sooner than eyes with only one or two centers of retinal contraction. In another study using SD-OCT/SLO imaging, intraretinal cysts were also found much more frequently in eyes with macular pucker that had vitreo-papillary adhesion as compared to those with total PVD [14]. Fortunately, a total PVD is very common (up to 90 %) in eyes with macular pucker, lowering the risk of cysts and facilitating surgery.

B. Surgical Technique

For macular pucker surgery, 25G, 23G, or 27G valved canulas are usually employed (Video V.A.2-1). The conjunctiva is displaced approximately 2 mm with a cotton tip, and the sclera is penetrated by a trocar 3.5 mm posterior to the limbus, at an angle between 20° and 30°. Once reaching the trocar sleeve, the cannula is redirected toward the center of the globe. The cuff of the cannula is held in place by forceps, and the trocar removed. At the end of surgery, the cannulas are withdrawn from the sclera, and the conjunctiva is pushed laterally with a cotton tip. Pressure is applied over the sclera for a few seconds for wound closure. If there is any significant leakage, the scleral wound is closed with a Vicryl 8-0 suture through the conjunctiva. The suture is secured with a slipknot, so that it can be easily removed the following day in the office. Transient sutures should be performed whenever possible if there is leakage, since permanent transconjunctival sutures produce severe conjunctival inflammation. If it is impossible to locate the scleral wound through the conjunctiva, a small conjunctival incision should be performed, so that the sclera is closed with a standard suture, followed by suturing of the conjunctiva.

Our surgical approach for macular pucker surgery consists of three-port pars plana vitrectomy (Video V.A.2-1). Core vitrectomy is performed, followed by peripheral vitrectomy under indentation. This is to eliminate the possibility of vitreous incarceration when inserting and extracting instruments since vitreous traction may lead to iatrogenic retinal tears. If

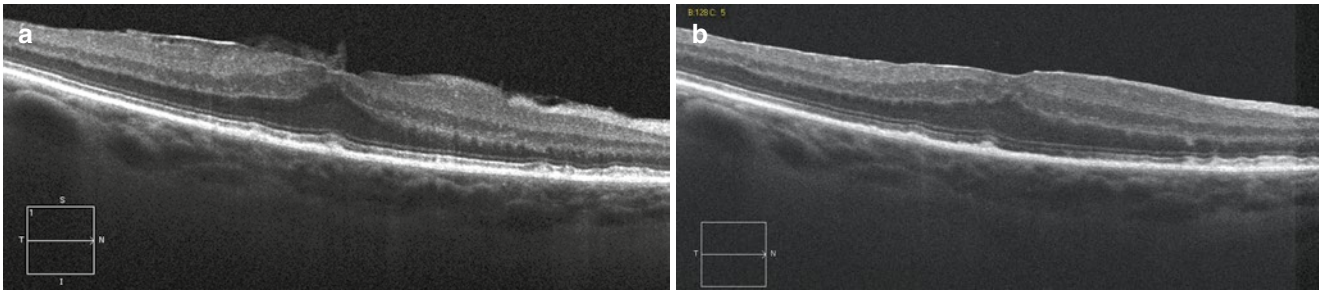


Figure V.A.2-5 (a) Premacular membrane with a preoperative VA of 20/40. (b) Postoperatively VA improved to 20/25 despite the absence of restoration of the foveal contour

necessary, a posterior vitreous detachment is induced by suction with the vitrectomy probe around the optic nerve head. In macular pucker, premacular membranes are usually visible enough to be grasped with forceps. They should be carefully removed by exerting traction tangential to the retina and avoiding anteroposterior traction that could lead to foveal retinal tears (Videos V.A.2-1 and V.A.2-2). At the end of the operation, a detailed examination of the peripheral retina with indentation is repeated. Retinal tears or holes are treated by endolaser.

1. Inner Limiting Membrane (ILM) Peeling with and without Chromodissection

Whether or not to peel the ILM in macular pucker surgery remains a controversial issue. When performed, our technique is to lower the infusion pressure, and brilliant blue G is carefully applied with a cannula over the posterior pole to stain the ILM. After 30 s, the dye is removed with the vitrectomy probe. The ILM is gripped with ILM forceps near the vascular arcades and peeled off with circular movements, in a capsulorhexis-style maneuver. (Video V.A.2-2) The rationale for ILM peeling is that removal of the ILM reduces the incidence of macular pucker recurrence by removing the scaffold upon which myofibroblasts would proliferate. Table V.A.2-1 shows some of the studies that have directly compared eyes with macular pucker operated with and without ILM peeling. In all these studies, ILM removal reduced or avoided recurrences [15–17]. Shimada et al. [17] performed a prospective study of macular pucker surgery with ILM peeling. Histopathological analysis of the ILM specimens indicated that a portion of the premacular membrane remained on the unpeeled ILM, probably as a result of vitreoschisis [18–20]. Fifteen ILM specimens were examined in detail, and residual premacular membrane was found on the ILM in 6 cases (40%). In the 6 eyes that underwent reoperation because of recurrent macular pucker, intraoperative staining with brilliant blue G identified partial ILM remaining in 2 eyes and total ILM remaining in 4 eyes [17].

Some studies have reported worse visual results, as well as the development of visual field defects, in patients in

which the ILM was removed [16, 21]. However, it seems that, in most cases, staining with indocyanine green (ICG) rather than the removal of the ILM per se might be responsible for these unfavorable outcomes. Indeed, in a study comparing the visual acuity of patients with macular pucker in which the ILM was removed with or without staining, Haritoglou et al. [22] found that visual outcomes were worse than expected only in eyes with ICG staining. No eye without ICG staining developed a visual field defect [22]. In their large prospective series including more than 200 eyes, Shimada et al. [17] did not find any difference in visual outcomes in patients with or without brilliant blue-assisted peeling. Although all dyes are potentially toxic to the retina [23, 24], brilliant blue does not appear to have any relevant toxicity at the dose and time exposure we propose [see chapter V.A.3. Chromodissection in vitreoretinal surgery]. One developing concern is the possibility that ILM removal may lead to some kind of damage to the inner retinal layers (Figure V.A.2-6). [see chapter V.A.4. Macular Hole & Macular Pucker Surgery with Special Emphasis on Re-Operations]. This issue will be discussed in further detail in the section treating full-thickness macular holes (below).

As regards the use of microincisional vitrectomy, several large prospective series have reported favorable outcomes with 27G, 25G, and 23G vitrectomy as compared with 20G. Microincisional vitrectomy achieves rapid and higher visual improvement and less postoperative inflammation than the 20 gauge vitrectomy in epiretinal membrane surgery [25]. A shorter duration of surgery and the absence of sutures (in most cases) contribute to the comfort of both the patient and the surgeon [26]. The incidence of complications (see below) appears to be similar or lower with microincisional vitrectomy [25, 26].

C. Surgical Outcomes

Table V.A.2-2 shows the results of some of the most recently published series of patients with macular pucker. Visual acuity improves by at least 2 lines in 48–80% of eyes. Worsening

Table V.A.2-1 Studies directly comparing outcomes after premacular membrane surgery with or without ILM peeling

Author, year [Ref] Type of study	Minimum follow-up	ILM removal (dye employed)	Eyes included	Preoperative BCVA	Postoperative BCVA	P value	Complications	P value
Kwok (2005) [15] Retrospective	18 months	Yes (ICG)	25 eyes	0.77±0.50	0.46±0.37	0.048	1 RD 0 % recurrence	0.030
		No	18 eyes	0.96±0.18	0.65±0.32		16.7 % recurrence 1 retinal detachment	
Park (2003) [16] Retrospective	3 months	Yes	20 eyes	–	Improved 100 %	0.01	0 % recurrence	NR
		No	24 eyes	–	Improved or unchanged 79 %		21 % recurrence	
Shimada (2009) [17] Prospective	12 months	Yes (BBG)	142 eyes			0.7681	0 % recurrence	<0.0001
		No PMM staining	46 eyes	0.57±0.31	0.29±0.28		0 % recurrence	
		PMM-TA staining	42 eyes	0.56±0.31	0.28±0.30		0 % recurrence	
		PMM-BBG staining	54 eyes	0.59±0.36	0.23±0.26		0 % recurrence	
		No	104 eyes	0.56±0.34	0.30±0.32		16.3 % recurrence	

Visual acuities are reported in LogMAR scale; mean and standard deviation or range

PMM premacular membrane, *BBG* brilliant blue G, *TA* triamcinolone acetonide, *ILM* inner limiting membrane, *ICG* indocyanine green, *BCVA* best-corrected visual acuity, *NR* not reported

of visual acuity is rare, ranging between 5 and 10 %. Central retinal thickness decreases significantly after surgery. Significant improvement of visual acuity and reduction of retinal thickness usually occur within 2 weeks after premacular membrane peeling, with 71.5 % of the total increase in best-corrected visual acuity and 61.3 % of the total reduction in central foveal thickness obtained at 1 month after surgery. However, visual acuity continues to improve up until 12 months after surgery [11]. The reduction of metamorphopsia is slower; complete regression of metamorphopsia has been reported in 33 % of eyes [11]. The degree of metamorphopsia has been shown to improve up until 12 months after surgery [6]. As described in the discussion of prognostic factors, better visual outcomes appear to be strongly correlated with the recovery of the photoreceptors after surgery, which may be identified in SD-OCT as an intact ellipsoid and interdigitation zones.

1. Complications

Macular pucker surgery with microincisional vitrectomy appears to have relatively few complications. The most frequent complication is the development of intra- or postoperative retinal tears, with a reported incidence that ranges between 2.2 and 8.4 %. Retinal tears seem to be significantly related to the induction of a posterior vitreous detachment [26]. A thorough examination of the peripheral retina at the end of surgery with scleral indentation should identify any breaks and allow intraoperative treatment, preventing postoperative retinal detachments, which appear after 0.5–1 % [25–27] of interventions. Intraocular pressure rises are present in 2–3.3 % [25, 26] of eyes and usually respond well to

topical treatment. Hypotony and postoperative leakage have been reported in 0.6–22 % eyes after vitrectomy [25–27]. The highest percentages correspond to sutureless 25G; in most cases hypotony resolved within 1 week after surgery. It is important to carefully check the sclerotomies at the end of surgery and to suture whenever any leakage is observed in order to avoid postoperative hypotony, which may lead to choroidal detachment. Endophthalmitis is rare, with reported incidence rates of 0–1.6 % [25–27]. The development of a full-thickness macular hole is also infrequent (1 % [25]). Premacular membrane recurrence rates are highly variable (between 1 and 20 % [2, 15–17]); the highest rates are reported in eyes without ILM peeling, as discussed above.

II. Macular Pseudoholes

Macular pseudoholes are caused by the centripetal contraction of a premacular membrane (Figure V.A.2-7). Publications on macular pseudoholes are scarce and must be interpreted with caution because in many cases the distinction between macular pseudohole and lamellar macular hole may not be completely correct, especially in reports previous to the development of OCT. García-Fernández et al. [28] analyzed the evolution of 25 eyes with macular pseudoholes. During a follow-up period that ranged between 12 and 84 months, they found that the visual acuity of eyes that did not develop cataracts was unchanged, at a mean of 0.18 LogMAR (range 0.00–0.7) [28].

There is only one report on the surgical results of macular pseudoholes in which the diagnosis was made with OCT

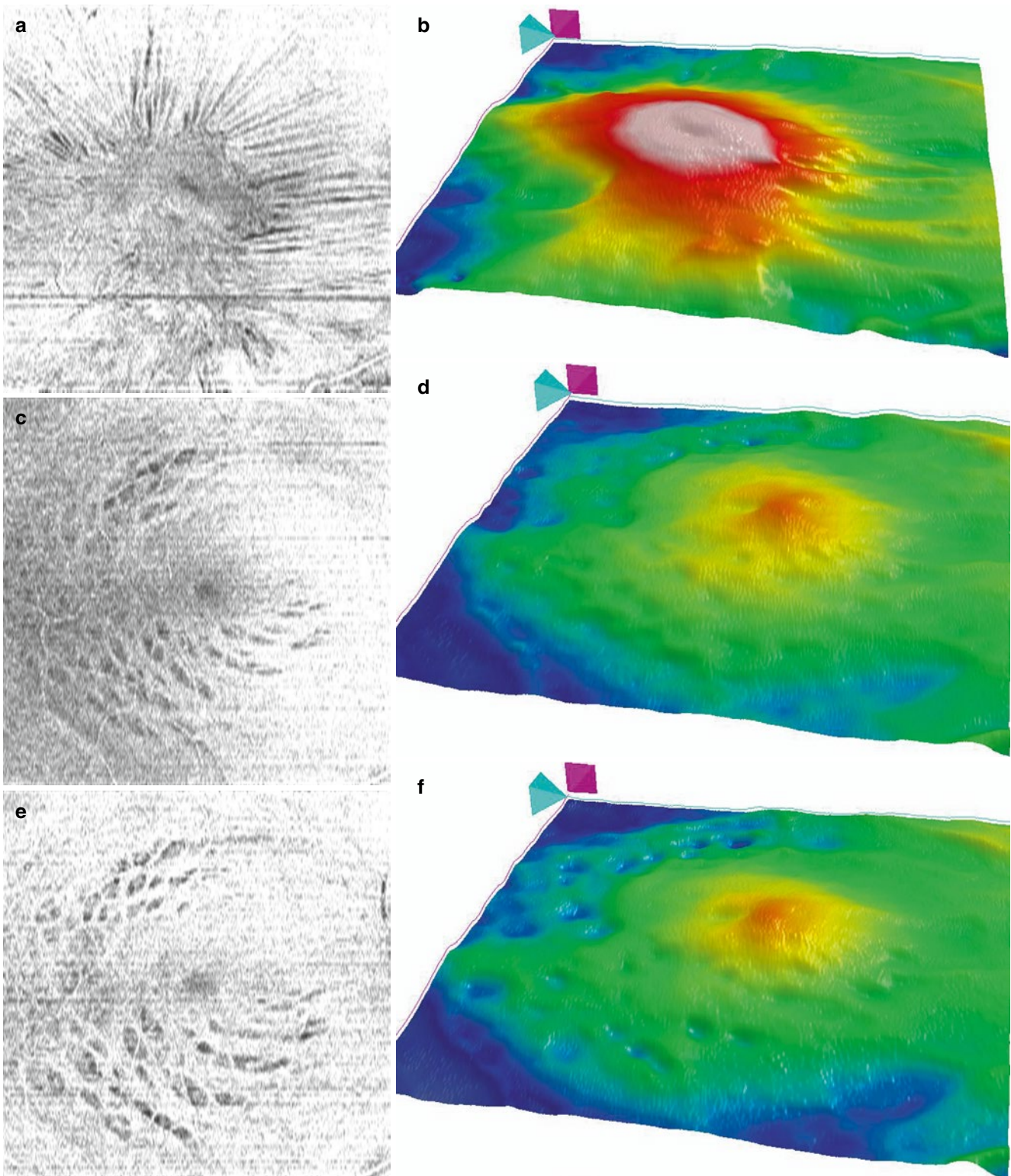


Figure V.A.2-6 Premacular membrane. OCT and topographic map. (a, b). Preoperative images. (c, d) Retinal dimples are visible in the area of ILM peeling 2 months after surgery. (e, f). Increase in the number of inner retinal defects 6 months after surgery

[29]. The authors of this study make a distinction between what they call macular pseudoholes with straight foveal edges and macular pseudoholes with stretched edges com-

bined with a partial cleavage between the inner and outer retina. We believe only the former group represents true macular pseudoholes and the latter lamellar macular holes.

Table VA.2-2 Studies reporting outcomes after premacular membrane surgery with or without ILM peeling

Author year [Ref] Type of study	Minimum follow-up	Number of eyes included ILM peeling performed	Vital dyes employed	Preoperative BCVA	Postoperative BCVA	Preoperative CRT or CFT (μm)	Postoperative CRT or CFT (μm)
Bae (2013) [11] Prospective	6 months	26 no ILM peeling 3 ILM peeling	TA for PMM	0.4 \pm 0.2	0.4 \pm 0.2	CRT 435.6 \pm 86.3	CRT 340.0 \pm 68.7
Falkner-Radler (2010) [4] Prospective	3 months	41 eyes ILM peeling	TB for PMM BBG or ICG \pm TB for ILM	0.56 \pm 0.21	0.39 \pm 0.24 46 % improved \geq 2 lines	CRT 436 \pm 105	CRT 380 \pm 76
Shimozono (2012) [9] Retrospective	3 months	43 eyes ILM peeling 7 eyes no ILM peeling	ICG for ILM	0.28 \pm 0.25	0.10 \pm 0.22	CFT 356 \pm 145	CFT 303 \pm 92
Suh (2009) [10] Prospective	3 months	38 eyes ILM peeling 63 eyes no ILM peeling	TA or ICG for ILM	Median 0.54 (range 0.1–1.3)	Median 0.18 (range –0.1–1) 80.2 % improved \geq 2 lines	CRT 426.8 \pm 186.0	CRT 327.4 \pm 94.1
Kinoshita (2012) [6] Prospective	12 months	49 eyes with ILM peeling	TA for ILM	0.38 \pm 0.03	VA (0.09 6 0.03) 67.3 % improved \geq 0.2 LogMAR units	CFT 418.2 \pm 19.2	
Kim (2012) [3] Prospective	6 months	ILM peeling	None or ICG for ILM	68.8 \pm 8.5 ETDRS	76.0 \pm 7.2	CFT 372.44 \pm 115.83	

Visual acuities are reported in LogMAR scale. Mean \pm standard deviations are provided unless otherwise stated

PMM premacular membrane, BBG brilliant blue G, TA triamcinolone acetamide, ILM inner limiting membrane, BCVA best-corrected visual acuity, CRT central retinal thickness, CFT central foveal thickness

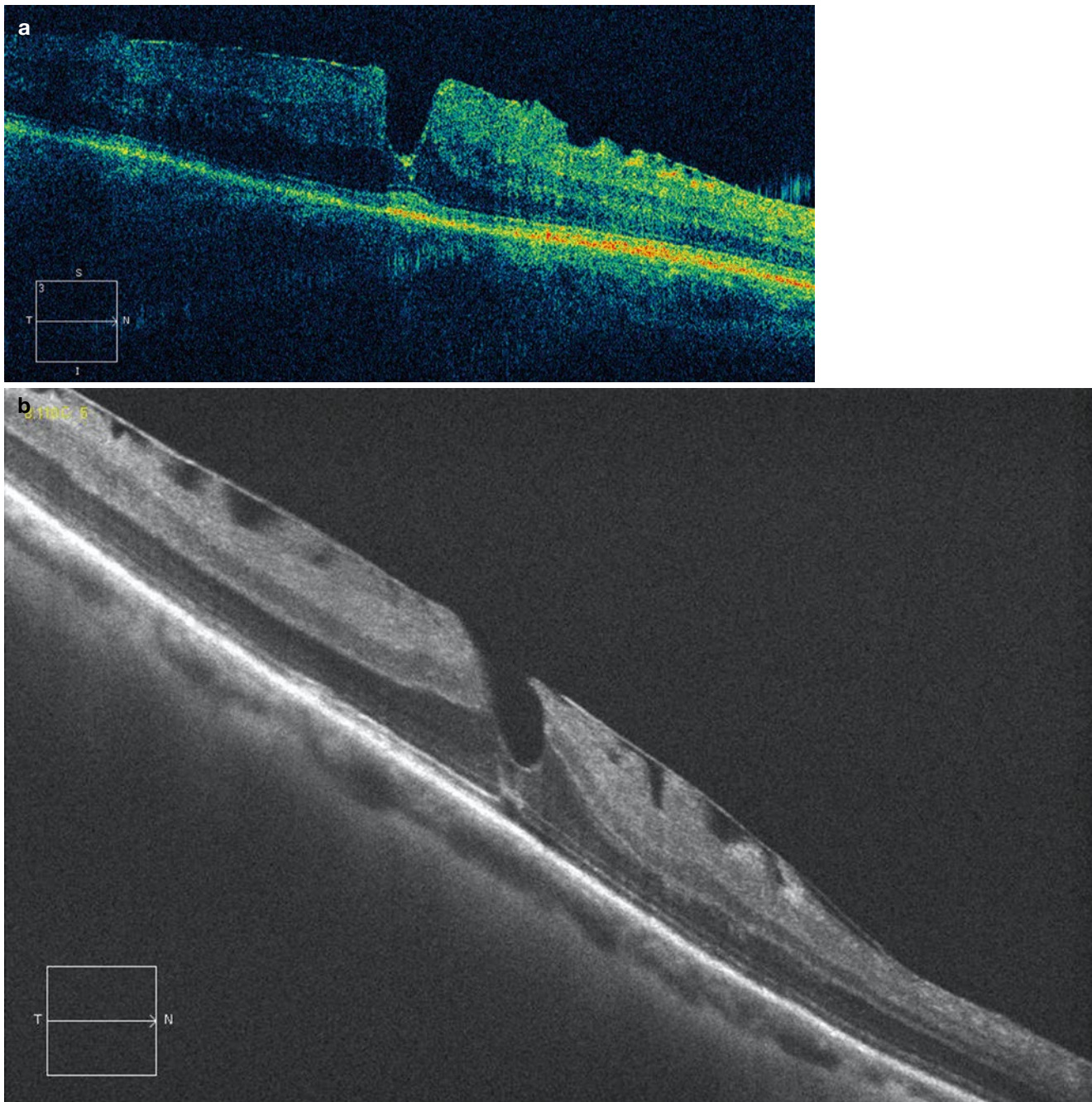


Figure V.A.2-7 (a, b) SD-OCT of a macular pseudohole showing verticalization of the foveal margin, a cylindrical appearance of the fovea, and a steepened foveal pit caused by the centripetal contraction of a premacular membrane

The surgical results of 14 eyes treated with pars plana vitrectomy, premacular membrane removal, and trypan blue-assisted ILM peeling were good, with visual acuity improvement from a mean of 0.41 (range 0.2–0.7) to 0.23 (0–0.6) LogMAR. No complications were described in this prospective series [29]. Thus, we believe that surgery in true macular pseudoholes should be performed only in cases with visual acuity deterioration and metamorphopsia. If vitreous surgery is performed, it should include ILM removal to avoid the risk of recurrence (Video V.A.2-3).

III. Lamellar Macular Holes

A. Prognostic Factors and Indications for Surgery

There are few reports on the natural evolution of lamellar macular holes. Theodossiadis et al. [30] followed 41 eyes diagnosed with lamellar macular holes for 3 years. Visual deterioration occurred in only 11 eyes (22 %); in the other 30 eyes (78 %), visual changes were minimal. The most

significant causes of visual deterioration were cystoid macular edema, an increase in the diameter of the foveal defect, or a reduction in foveal thickness [30]. García-Fernández et al. [28] analyzed the evolution of 83 eyes with lamellar macular holes. During a follow-up period that ranged between 12 and 84 months, they found that the visual acuity of eyes that did not develop cataracts was unchanged, at a mean of 0.24 LogMAR (range 0.00–1.30) [28]. Other studies have focused on factors associated with visual outcomes after surgery. In 2009 Sebag et al. reported that in eyes with lamellar macular holes and vitreo-papillary adhesion, intraretinal cysts were present in 75 % as compared to 43 % in eyes without vitreo-papillary adhesion [31]. Wang et al. identified that the prevalence of vitreo-papillary adhesion in eyes with lamellar macular holes and intraretinal cysts was 50 %, as compared to 20 % in eyes with lamellar macular holes but no cysts [14]. Three years later, Romano et al. [32] found that in eyes with lamellar holes with coexisting vitreo-papillary adhesion, the prevalence of vitreoretinal cysts increases to 46 %, as compared to 9.6 % without vitreo-papillary adhesion. Intraretinal cysts were significantly correlated with a poor functional prognosis [32]. Visual acuity gain after surgery has been found to be directly correlated with preoperative visual acuity [33, 34]. No correlation has been found between visual outcomes and the largest diameter of the hole, and results are unclear regarding the foveal thickness at the base of the hole [33, 34]. However, patients with a disrupted ellipsoid zone are less likely to gain visual acuity [34, 35]. The results of these studies suggest that surgical treatment should be proposed only in cases with progressive visual loss or metamorphopsia or in those eyes in which a disruption of the photoreceptors is detected on OCT.

B. Surgical Technique

The presence of a premacular membrane is a constant feature in both OCT and surgery in several series [34, 36–38] (Video V.A.2-4 and Figure V.A.2-8). Many of the premacular membranes associated with a lamellar macular hole have an unusual thickened appearance of moderate reflectivity on ultrahigh-resolution OCT [39] (Figure V.A.2-9). In our view, these premacular membranes cause a centrifugal traction, tearing the inner retina and leading to the intraretinal horizontal splits visible on OCT (Figure V.A.2-10). These splits always occur at the same level: between the outer plexiform layer and the outer nuclear layer, possibly due to lower resistance at this level. In fact, SD-OCT clearly shows the presence of remnants of tissue connecting the outer and inner retina in the intraretinal horizontal splits (Figure V.A.2-11). Since premacular membrane contraction appears to play a role in lamellar hole formation, removal of

the membrane is mandatory to improve surgical results (Video V.A.2-5). Even in cases in which the lamellar macular hole still persists after surgical intervention, the removal of the premacular membrane and ILM prevents further stretching of the retina and visual deterioration, and so even in these cases there is benefit to surgery. Although some authors now perform surgery with no internal tamponade (see Table V.A.2-3), we leave gas and request 1 week of face-down positioning because the margins of the hole are usually rigid, and we believe gas and positioning are necessary to allow the margins to reposition and to achieve complete closure of the hole.

C. Surgical Outcomes and Complications

Table V.A.2-3 provides the results of most published series reporting the outcomes of vitrectomy for lamellar macular holes. Early reports by Hirakawa [40] and Kokame [41] reported excellent anatomic and functional outcomes for vitrectomy with ILM peeling in patients with progressive visual loss. In the largest prospective series, Michalevskaya et al. [42] report complete normalization of the foveal contour in 50 % of cases (13 eyes). In 27 % (seven eyes) the foveal contour was slightly irregular. In another four eyes (15.3 %) a defect similar to a macular pseudohole was found, and in two eyes (7.7 %) a lamellar defect persisted [42]. In our experience, the process of retinal healing after surgery in lamellar holes starts in the inner retinal layers, proceeding progressively toward the outer layers. This would explain the frequent image of a retinal pseudocyst seen with spectral-domain OCT during follow-up. Visual acuity may improve in spite of the presence of this pseudocyst, which may take as long as 10 months to resolve (Figure V.A.2-12) [36].

Complications include not only those related to the removal of the premacular membrane but also the development of a full-thickness macular hole (Table V.A.2-3).

IV. Full-Thickness Macular Hole (FTMH)

A. Prognostic Factors

As has been previously described for macular pucker, one of the main factors associated with a better visual acuity after surgery is preoperative visual acuity [43–45]. Mean duration of macular hole prior to surgery has not been directly correlated to anatomic success, likely because patients are often unsure of the exact time of the onset of symptoms [44]. Recent reports have studied the characteristics of the macular hole in optical coherence tomography that are correlated with surgical outcomes. Base diameter [44, 46–48], macular



Figure V.A.2-8 Fundus appearance of a lamellar macular hole cause by a premacular membrane

hole inner opening [48], and minimum linear diameter [44, 46–48] are associated with both anatomical and visual success (Figure V.A.2-13). Although some groups have tried to calculate different indexes derived from these basic measurements, there appears to be no real advantage to be gained [48]. Preoperative base diameter is the most useful variable in this regard, as it has the strongest association with anatomical and visual outcome and is easily measured on an OCT scan. The choice of base diameter seems sensible when one considers that this parameter (the hole at the level of the RPE) is itself the basic retinal lesion being treated. Primary anatomic success rates of 100 % have been reported for macular holes of up to 500 μm in diameter [44]. The preoperative extent of the defect of the ellipsoid zone, which reflects photoreceptor damage, has also been shown to have a good predictive value for postoperative macular sensitivity [49] and visual acuity [50].

B. Surgical Technique

Very recently, the results of two randomized clinical trials have provided very interesting information on surgery for macular holes. The Full-Thickness Macular Hole and Internal Limiting Membrane Peeling Study (FILMS), a pragmatic clinical trial, included 127 eyes with stage 2 or 3 macular holes with a 6-month follow-up period [51]. All study eyes were randomized to undergo vitrectomy with or without trypan blue-assisted ILM peeling. Cataract surgery was performed simultaneously in all phakic eyes. At the 1-month follow-up visit, macular hole closure was observed in 56 (84 %) eyes in the ILM-peel group compared with 31 (48 %) in the no-ILM-peel group; this difference was statistically significant (odds ratio 6.23; $P < 0.001$). A substantial number of eyes (38 %) initially in the non-ILM-peeling group underwent repeat surgery during the 6-month follow-up period to

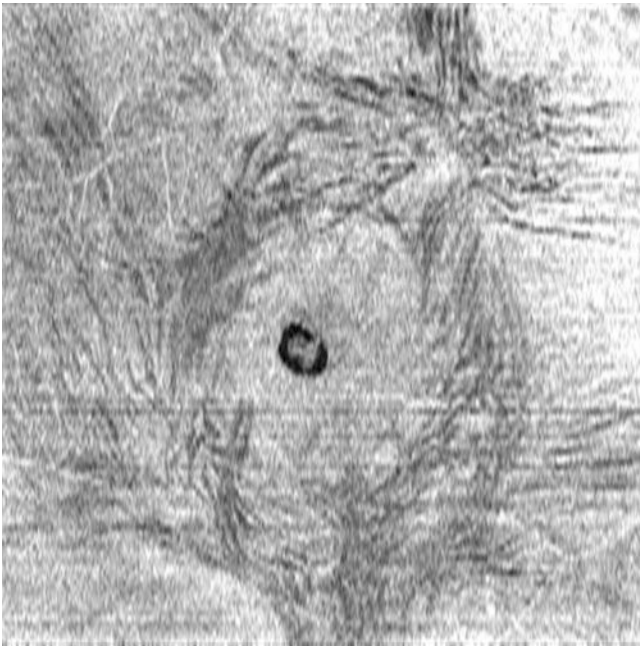


Figure V.A.2-9 Coronal OCT showing a lamellar macular hole and a premacular membrane with eccentric pucker

remove the ILM. With respect to visual outcome, the FILMS found no evidence of a difference between groups in distance visual acuity at the end of the follow-up period. However, there was a difference of 5 ETDRS letters favoring ILM peeling. This, together with the higher rates of macular hole closure and the corresponding fewer reoperations needed in the ILM-peel group, suggests that ILM peeling is the treatment of choice for patients with stage 2–3 macular holes [51] (see Video V.A.2-6).

1. Chromodissection

The use of dyes to stain the ILM, recently been termed “chromodissection” [see chapter V.A.3. Chromodissection in vitreoretinal surgery] has been increasingly used to treat eyes with macular holes [52]. Christensen et al. have reported the results of a clinical trial in which 78 eyes with macular holes with no evidence of premacular fibrosis were randomized to undergo vitrectomy alone without retinal surface manipulation, vitrectomy with ICG-assisted ILM peeling, or vitrectomy with trypan blue (TB)-assisted ILM peeling [53]. Primary anatomical closure was obtained in 11 of 25 eyes (44 %) in the non-peeling group, 32 of 34 (94 %) in the ICG chromodissection group,

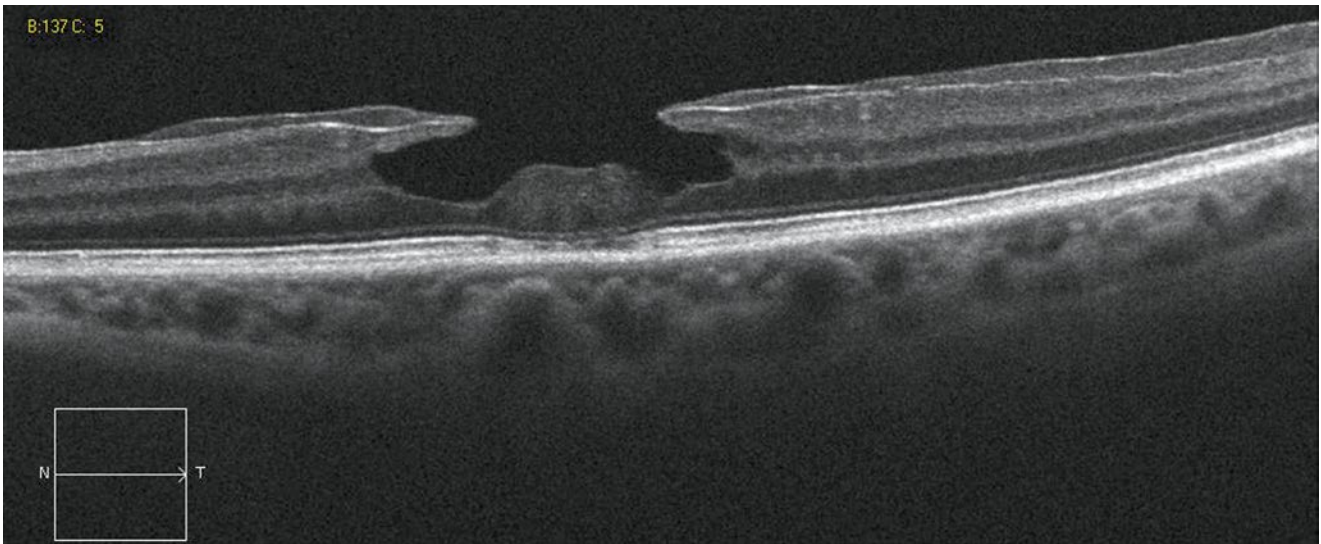


Figure V.A.2-10 Thick premacular membrane in a case of lamellar macular hole

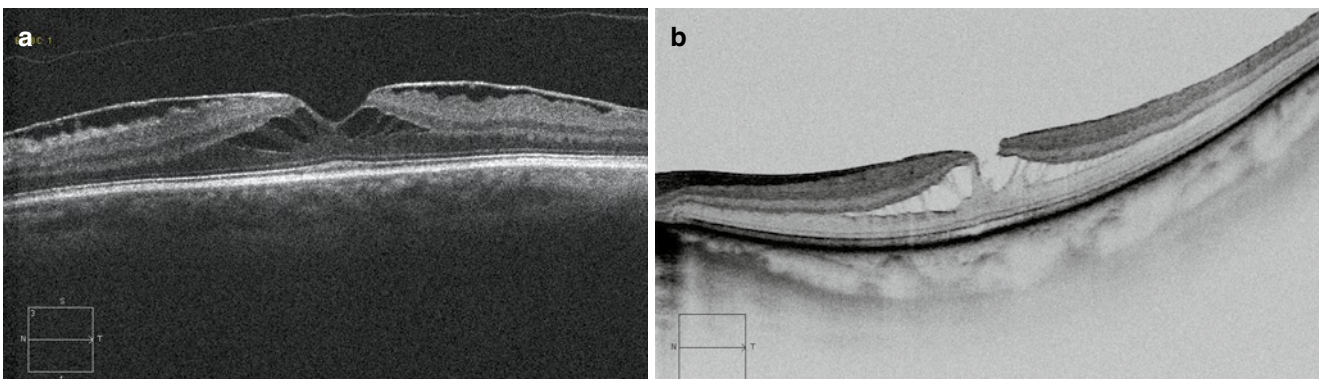


Figure V.A.2-11 (a, b) Lamellar macular hole. Premacular membrane causes a centrifugal traction, tearing the inner retina. Remnants of tissue connecting the outer and inner retina are visible on HD-OCT

Table V.A.2-3 Studies reporting outcomes after lamellar macular hole surgery

Author [Ref] Type of study	Surgery	Gas and positioning	Eyes included Minimum follow-up	Preoperative BCVA	Postoperative BCVA	Complications
Androudi [39] Prospective	25 G PM and TB or BBG- assisted ILM peeling	14 % C3F8 Avoid supine position for 1 week	20 eyes 12 months	-	BCVA improved in 85 % eyes Mean gain: 2.6 Snellen lines	Cataract progression in all phakic eyes 6 eyes incomplete closure
Figueroa [36] Retrospective	25 G PM and BBG-assisted ILM peeling	6 % C3F8 2 weeks face-down	12 eyes 6 months	0.34 (SD 0.14)	0.17 (SD 0.04) BCVA improved in 75 % eyes Mean gain: 2.08 Snellen lines	2 FTMH 4 pseudocysts
Casparis [33] Retrospective	20/23G PM and ILM peeling	Air or 20 % SF6 Prone positioning 12 h-6 days	45 eyes 1 month	0.4 Range 0.1-1.04	0.13 Range -0.1-1.04 93 % eyes ≥20/40 58 % gained ≥2 ETDRS lines Mean gain: 2.8 ETDRS lines	Cataract surgery in 53 % phakic eyes
Garretson [82] Retrospective	PM and ICG-assisted ILM peeling	Air/SF6/C3F8 Prone 1-7 days	27 eyes 2 months		BCVA improved in 93 % eyes Mean gain: 3.2 Snellen lines	1 FTMH 6 eyes cataracts 8 % incomplete closure
Hirakawa [40] Prospective	ILM peeling	20 % SF6 Face-down 7 days	2 eyes 12 months		20/25	
Lee [34] Retrospective	20/23G PM and ICG-assisted ILM peeling	Air/SF6/C3F8 Prone 1-7 days	30 eyes 3 months	0.51 (SD 1.6)	0.4 (SD 1.3) BCVA improved in 63 % eyes	-
Michaievska [42] Not specified	20 G TB-assisted PM and ILM peeling	Fluid No positioning	26 eyes 12 months	0.51 Range 0.16-1.00	0.2 Range 0.01-0.6 BCVA improved in 92.3 % eyes	5 eyes cataract surgery 1 case persistent LMH
Parolini [38] Prospective	PM and ILM peeling	Air No positioning	19 eyes 12 months		Mean gain: 2.1 Snellen lines	3 eyes (16 %) FTMH
Witkin [83] Retrospective	PM peeling ICG-assisted ILM peeling in 4 eyes	None 3 eyes; air 2 eyes; SF6 10 eyes; C3F8 1 eye 7 days face-down if gas	16 eyes 3 months	0.90	0.77 Comorbid ocular diseases present in 9 patients	2 eyes (13 %) FTMH 6 eyes (38 %) persist LMH 1 eye (6 %) CME

Visual acuities are reported in LogMAR scale; mean and standard deviation or range
 G gauge, PM premacular membrane, TB trypan blue, BBG brilliant blue G, ILM inner limiting membrane, ICG indocyanine green, FTMH full-thickness macular hole, LMH lamellar macular hole, CME cystoid macular edema, BCVA best-corrected visual acuity, SD standard deviation

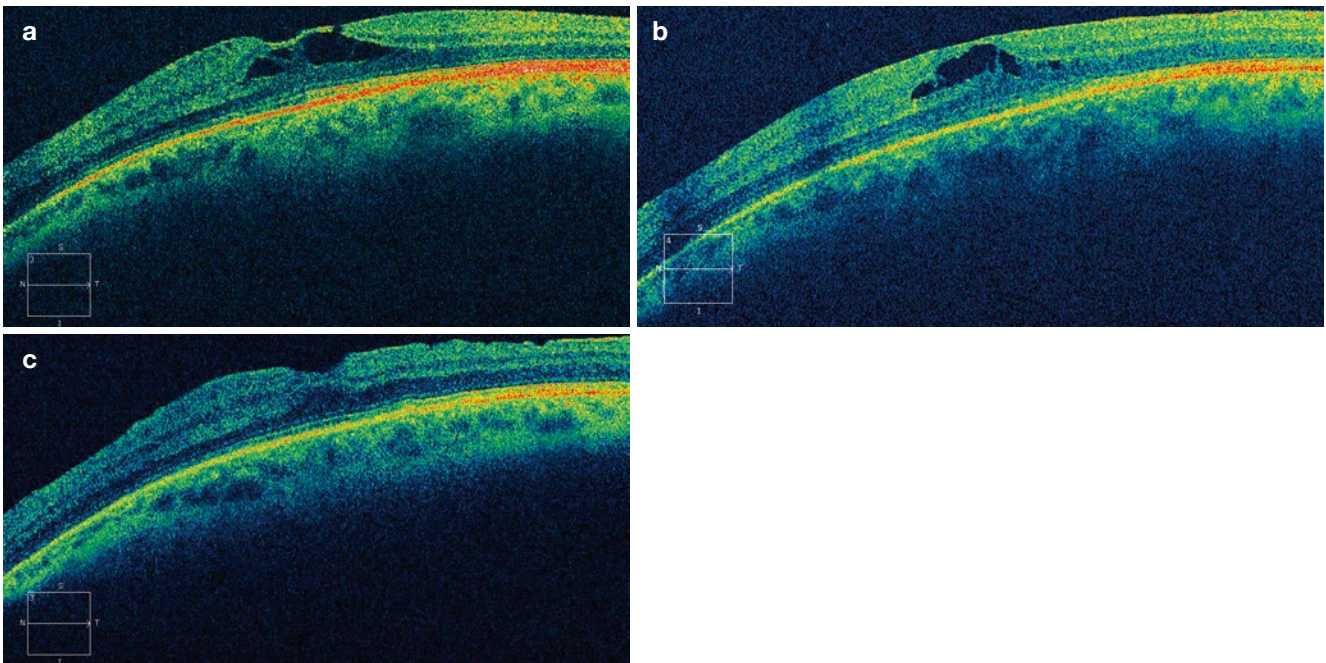


Figure V.A.2-12 Lamellar macular hole. (a) Preoperative OCT. VA of 20/40. (b) Three weeks after surgery showing a retinal pseudocyst. (c) One year after surgery. VA 20/30

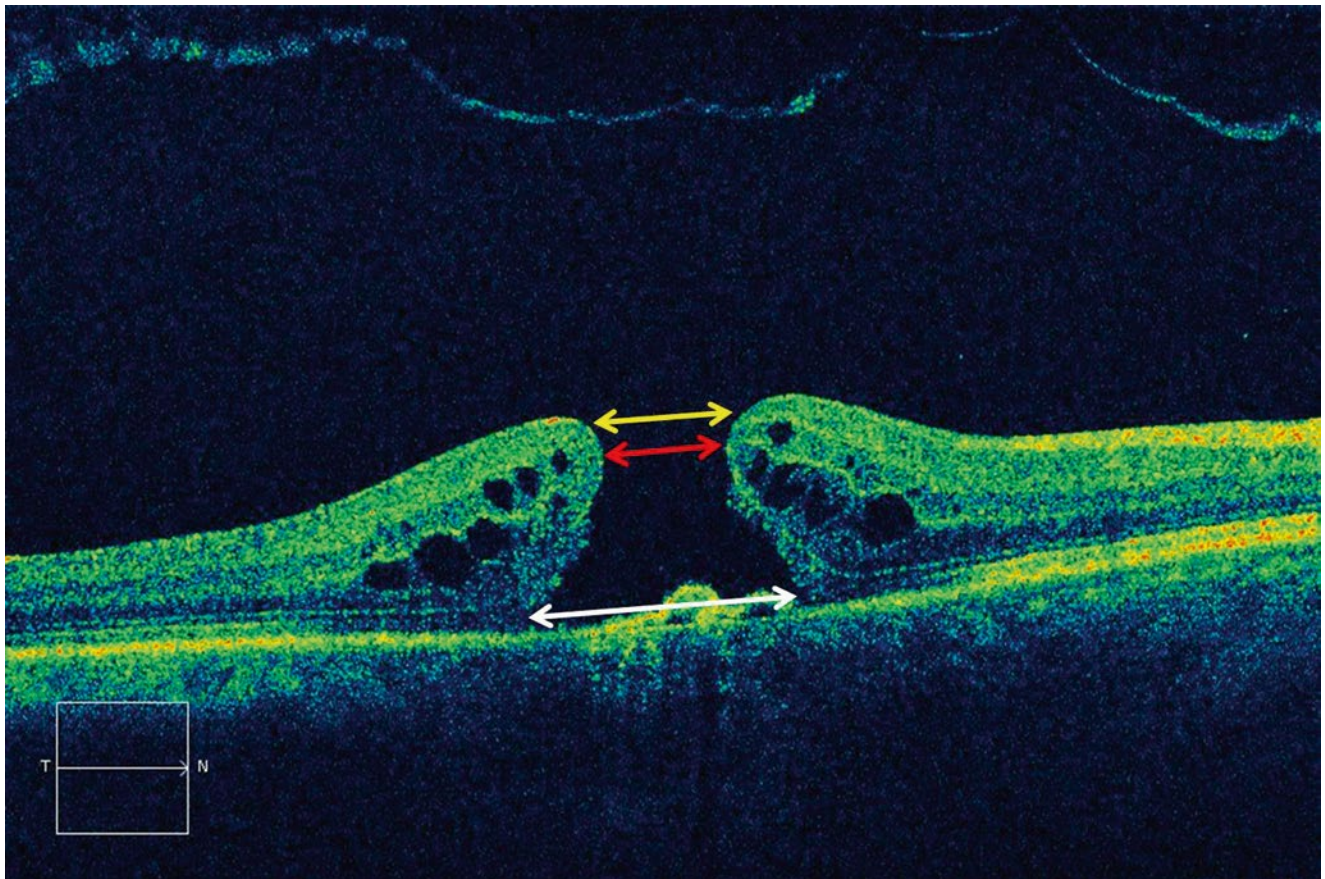


Figure V.A.2-13 SD-OCT of a full-thickness macular hole. Base diameter (white double-headed arrow), macular hole inner opening (yellow double-headed arrow), and minimum linear diameter (red double-headed arrow) are associated with both anatomic and visual success

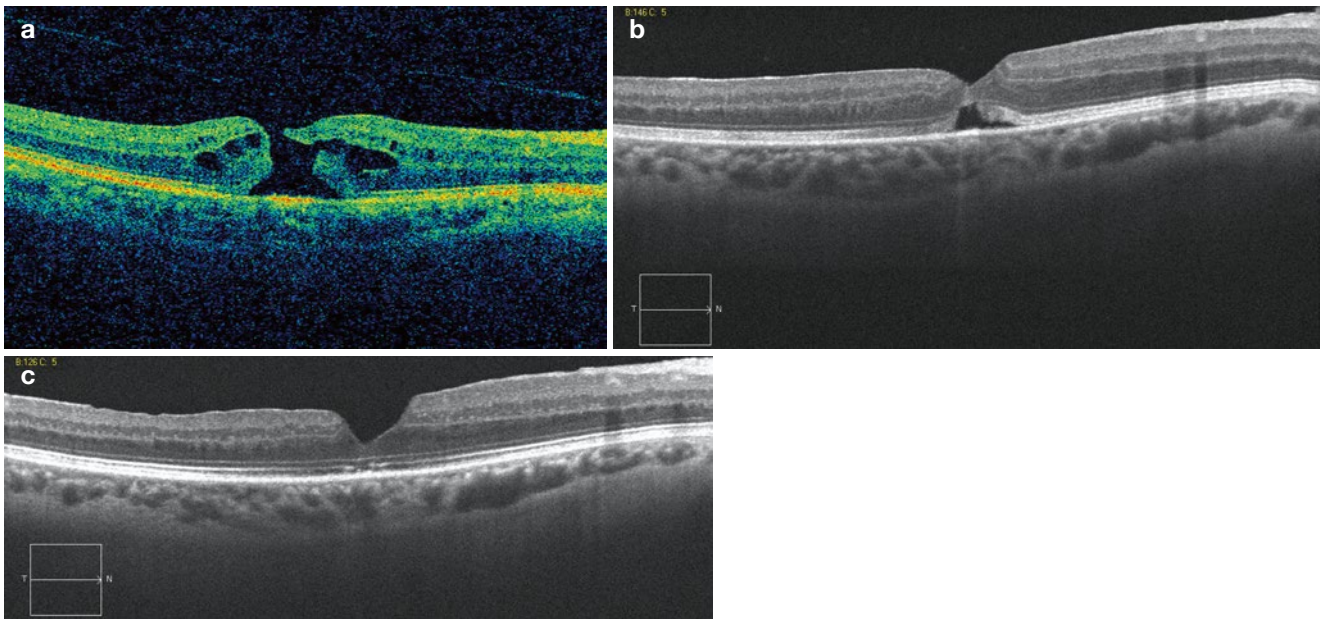


Figure V.A.2-14 Full-thickness macular hole. OCT. (a) Preoperative image. (b) Three weeks after surgery showing a closure of the hole which starts in the inner retina and progresses toward the external retina. (c) Complete closure of the macular hole 2 months after surgery

and 16 of 18 (89 %) in the TB chromodissection group ($P < 0.01$). Sixteen of the 18 patients without primary macular hole closure underwent a second surgery with additional ICG-assisted ILM peeling, one patient (ICG peeling group) declined reoperation, and one patient (TB peeling group) experienced late primary closure of the macular hole between 3 and 6 months of follow-up. Although the non-peeling group required a higher number of surgeries to achieve anatomic closure, no significant differences were found in visual outcomes at the end of follow-up between the three groups [53]. Thus, it would appear that for patients with stage 2 and 3 macular holes, the surgical procedure should include ILM removal in order to obtain a higher rate of primary closure (Video V.A.2-6) (Figure V.A.2-14). However, in 2001, Tadayoni et al. [54] described an anatomical feature after ILM removal that they termed dissociated optic nerve fiber layer (DONFL). It consisted of numerous arcuate striae within the posterior pole in the direction of the optic nerve fibers, slightly darker than the surrounding retina. This feature had no functional effect noticeable by the patient and did not preclude good visual recovery [54]. A DONFL has been observed in the macular region in as many as 42.9 % of eyes undergoing ILM peeling 12 months after surgery [43, 46], without producing a difference in visual acuity or in mean total deviation of sensitivity in the central 10° , as obtained from 30 to 2 automated perimetry. But the development of more advanced systems of scanning laser ophthalmoscopy (SLO) microperimetry combined with spectral-domain optical coherence tomography (SD-OCT) has shown that DONFL may lead to deterioration in visual function. In a retrospective, nonrandomized study of 16 eyes

of 16 consecutive patients who had experienced idiopathic macular hole closure, comparing 8 eyes with ILM peeling and 8 eyes without, Tadayoni et al. [55] found that mean retinal sensitivity was significantly lower (by about 3.4 dB) in eyes that underwent peeling than in those that did not. Postoperative microscotomas were also significantly more frequent in eyes that had undergone peeling. These abnormalities, which are difficult to detect, may reduce the quality of vision, even if they do not actually reduce visual acuity. The authors speculate that the retinal sensitivity deterioration and the development of a DONFL appearance might be due to deterioration of the retina, especially of the Müller cells, whose end-feet are closely connected to the ILM and may be affected by ILM peeling [55]. This same group, in a retrospective case series including 84 eyes and comparing eyes with and without ILM peeling, found that for macular holes $>400 \mu\text{m}$ in diameter, the primary closure rate was of 100 % with ILM peeling versus 73.3 % without ($p = 0.015$) [56]. However, for smaller macular holes, the rates were 100 % in both groups. Postoperative gain in visual acuity was not significantly different in eyes with ILM peeling and those without. Thus, they suggest that in view of the probable reduction in retinal sensitivity after ILM, this procedure should, in holes smaller than $400 \mu\text{m}$, be reserved for rare cases of first surgery failure or of recurrence, as this strategy would ensure the best quality of vision for the remaining large majority of these patients [56]. In a small series, Spaide [57] recently reported the appearance on SD-OCT of 25 eyes of 24 patients that had undergone macular surgery either for macular pucker or for full-thickness macular holes. Eighteen eyes had planned peeling of the ILM (assisted

in 15 eyes with brilliant blue chromodissection). Volume rendering showed that 13 of the eyes had pitting or dimples of the inner retinal surface that seemed to follow the course of the nerve fiber layer in the region of the macula. Close examination of the B-scans in regions of the dimples appeared to show thinning of the ganglion cell layer and also what may be a loss in reflectivity of the overlying nerve fibers. All 13 eyes with inner retinal dimpling had intentional ILM peeling, whereas 5

eyes with ILM peeling did not have inner retinal dimpling (chi-square test, $p=0.001$). None of the eyes without ILM peeling showed inner retinal dimpling [57] (Figure V.A.2-15).

2. Internal Tamponade

Gas tamponade plays an important role in hole closure following macular hole surgery, as the gas bubble keeps the edges of the macular hole dry, prevents entry of vitreous into the hole,

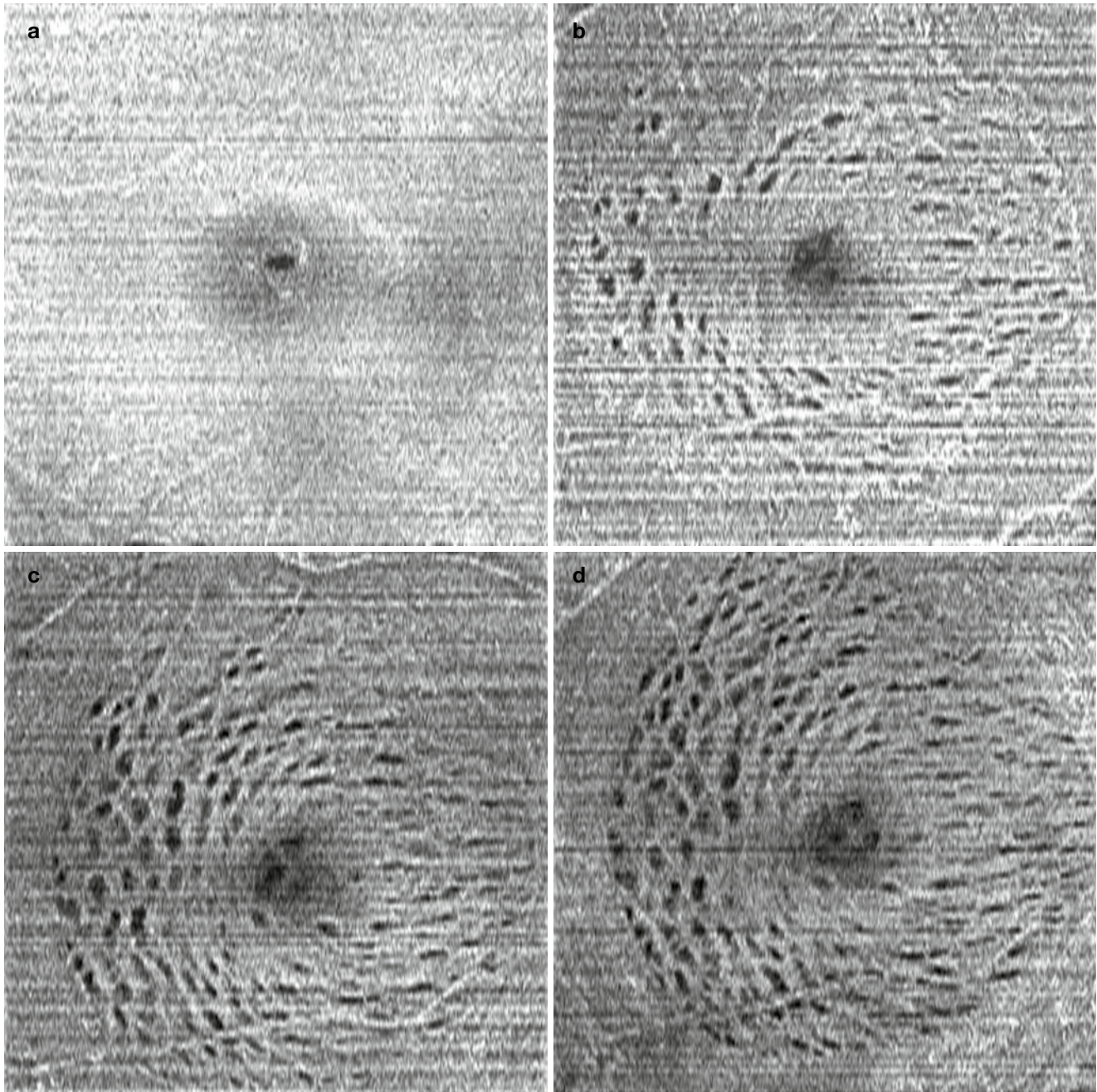


Figure V.A.2-15 OCT appearance of dissociated optic nerve fiber layers following vitrectomy and ILM peeling in a stage 1 macular hole with a preoperative VA of 20/70 and a severe metamorphopsia. (a) Preoperative coronal OCT. (b–f) Retinal dimples appeared as soon

as 15 days after surgery and progressed for the following 2 years. (g–l) Topographic map during the follow-up showing more dimples in the temporal macula

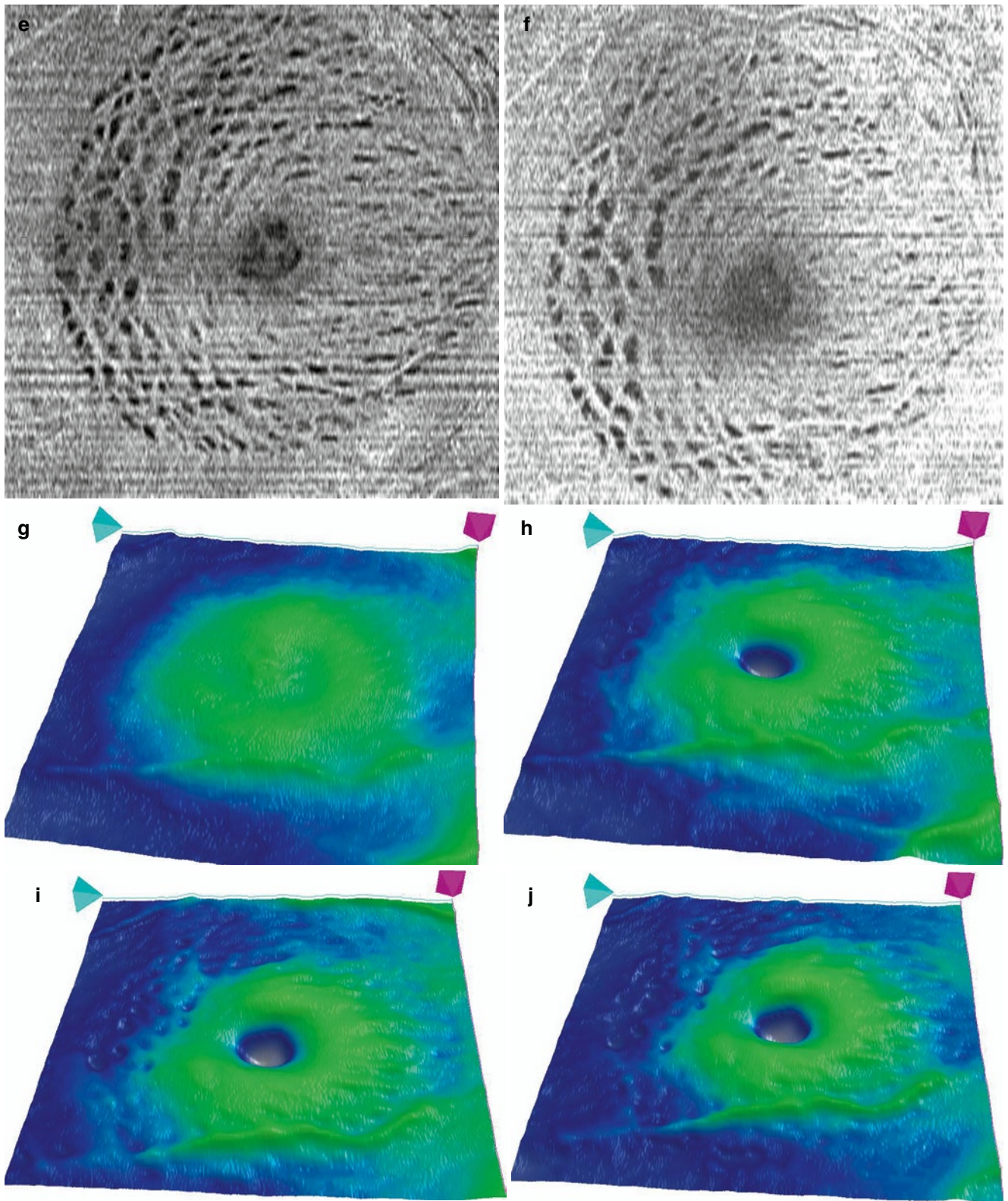


Figure V.A.2-15 (continued)

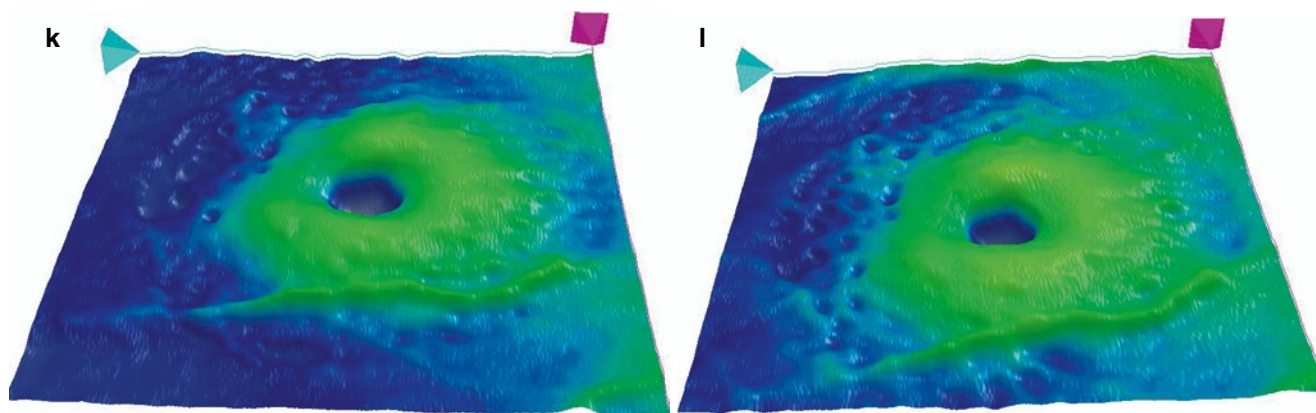


Figure V.A.2-15 (continued)

and provides a scaffold for glial cell proliferation. Additionally, the surface tension, which is constant around the bubble's interface with the retina, covers the macular hole as long as the volume of intraocular gas is sufficient (two-thirds to three-quarters of the vitreous volume). Face-down posturing is thought to aid macular hole closure by allowing the buoyant force of the intraocular gas bubble, which is maximal at the apex of the bubble, to be in contact with the macula. However, recent studies have suggested that prolonged face-down positioning may not be critical for achieving macular hole closure in all cases. In a prospective randomized study, Guillaubey et al. [58] found that the anatomical closure rate in idiopathic macular holes smaller than 400 μm was not influenced by the postoperative position. However, the anatomic success rate in holes larger than 400 μm was 79.5 % for those patients asked to keep seated and 95.1 % for patients instructed to keep face-down ($p=0.045$) [58]. A recent meta-analysis suggests slightly improved macular hole closure rates with 5–10 days of face-down posturing compared with posturing for 24 h or less, but the difference was not statistically significant [59].

3. Contemporaneous Cataract Surgery

Another controversial issue is whether cataract surgery should be combined with vitrectomy in phakic patients undergoing macular hole surgery. The advantage of combined surgery would be the possibility of performing a more thorough vitrectomy, which would allow a greater gas bubble to be introduced into the eye. Posturing would not be as critical, since the required level of gas to obtain macular hole closure would be maintained for longer, and there would be no risk of producing subcapsular posterior cataracts. The main disadvantage of combined surgery is that postoperative inflammation is often intense and may lead, among other complications, to the development of posterior iris synechiae. Christensen et al. [53] reported a 31.2 % incidence of posterior synechiae, even in cases in which cataract surgery was performed 1 month before vitrectomy. Delayed cataract surgery, if the crystalline is clear enough to allow a detailed view of the macula, would avoid this increased inflammation. Furthermore, recent studies have not found an increased risk of reopening of the macular hole with

delayed surgery [60]. A comparative case series found no differences in the rate of primary anatomic success between combined phacovitrectomy and vitrectomy followed by cataract surgery (100 % in combined surgery versus 96 % in the consecutive group), although patients in the consecutive group did not achieve a recovery of visual acuity similar to the combined surgery group until after cataract surgery was performed [61].

In summary and following the lessons learned from evidence-based medicine, in patients with macular hole we perform microincisional vitrectomy with brilliant blue chromodissection of the ILM. In patients with stage 2 macular holes, we employ 16 % SF6 as the internal tamponade agent and recommend face-down positioning for at least 3 days. In patients with stage 3 or 4 macular holes, we use SF6 16 % and 1 week of face-down positioning. We perform combined phacovitrectomy only in those eyes in which the lens opacity would preclude adequate viewing of the macula.

4. Pharmacologic Vitreolysis

Pharmacologic vitreolysis [62, 63] has been under development for the past decade [64] and offers a new approach to the treatment of symptomatic vitreomacular adhesion and vitreomacular traction [65], especially macular holes [66]. Very recently, the results of two phase III studies of the intravitreal injection of ocriplasmin for patients with macular holes have been published [67] [see chapter VI.E.2. Clinical studies of ocriplasmin pharmacologic vitreolysis]. In eyes with macular holes of less than 400 μm diameter, nonsurgical closure of the macular hole was achieved in 40.6 % of ocriplasmin-injected eyes, as compared with 10.6 % of placebo-injected eyes ($P<0.001$) [67]. Thus, ocriplasmin may represent an alternative for surgery in certain cases [see chapter VI.A. Pharmacologic vitreolysis].

C. Surgical Outcomes and Complications

Anatomic success rates vary among the series published (see Table V.A.2-4), probably because case series are highly prone to selection bias and often report better outcomes than

Table V.A.2-4 Studies reporting outcomes after full-thickness macular hole surgery

Author [Ref] Type of study	Surgery	Tamponade agent Positioning	Number of eyes Minimum follow-up	FTMH Stage	Preoperative BCVA	Postoperative BCVA	Primary closure rate	Complications
Xirou [45] Prospective	20 G BBG-assisted ILM peeling	20 % SF6 2 days face-down	23 eyes 6 months	Stage 2: 82.6 %	0.67±0.20	0.29±0.12 78 % eyes improved ≥3 lines	100 %	None
				Stage 3: 17.4 %				
				Stage 4: 0 %				
Wakely [48] Retrospective	23 G BBG-assisted ILM peeling	14 % C3F8 2 days face-down	23 eyes 6 months	Stage 2: 30.4 %	0.90±0.10	0.62±0.23 52 % eyes improved ≥3 lines	96 %	2 intraoperative retinal breaks
				Stage 3: 52.2 %				
				Stage 4: 17.4 %				
Almeida [84] Prospective	23 G BBG-assisted ILM peeling	20 % SF6 No positioning	50 eyes 3 months	Stage 2: 16 %	0.778±0.282	0.425±0.397 70 % eyes ≥ 6/12	84 %	
				Stage 3: 76 %				
				Stage 4: 8 %				
Salter [44] Retrospective	20 or 23G ICG-, TA-, or TB-assisted ILM peeling	20 % SF6 3 days face-down	50 eyes 1 month	Stage 2: 24 %	0.939±0.462	0.668±0.497 38 % ≥ 6/12	98 %	1 persistent CME 1 intraocular lens pupillary capture
				Stage 3: 76 %				
				Stage 4: 0 %				
Malik [68] Prospective	25G ILM peeling	14 % C3F8 7 days face-down	153 eyes 3 months	Stage 2: 8.5 %	-	-	93.5 %	4 eyes late reopening
				Stage 3 or 4: 91.5 %				
				Stage 4: 0 %				
Rhaman [85] Retrospective and prospective	23 G MB-assisted ILM peeling	20 % C2F6 1 day	14 eyes 6 months	Stage 2: 28.57 %	0.83 (range 0.5–1.3)	0.32 (range 0.2–0.6)	100 %	
				Stage 3: 50 %				
				Stage 4: 21.43 %				
	23 G BP-assisted ILM peeling	16 % C2F6	39 eyes 6 months	Stage 2: 13 %	0.81 (range 0.3–1.9)	0.44 (range 0–0.78)	89.7 %	4 pupillary capture
				Stage 3: 64 %				
				Stage 4: 23 %				
	23 G BP-assisted ILM peeling	20 % SF6	39 eyes 4 months	Stage 2: 16 %	0.78 (range 0.3–1.9)	0.38 (range 0–1)	87.2 %	1 tractional retinal detachment
				Stage 3: 74 %				
				Stage 4: 10 %				

Visual acuities are reported in LogMAR scale; mean ± standard deviation or range
 G gauge, TB trypan blue, BBG brilliant blue G, BP brilliant peel, MB membrane blue, ILM inner limiting membrane, ICG: indocyanine green, TA triamcinolone acetonide, FTMH full-thickness macular hole, CME cystoid macular edema, BCVA best-corrected visual acuity, SD standard deviation

those seen in clinical trials. Thus, success rates range between 84 and 100 % [44, 58, 68], where some of the lower success rates are reported in the clinical trials [51, 53]. As regards visual outcomes, Jackson et al. [69] in a review of the results reported in the United Kingdom's National Ophthalmology Database found that only 58.3 % (207 of 355 with recorded visual acuity) of eyes achieved visual success, defined as a 0.3 LogMAR improvement, 52 weeks after surgery. At 52 weeks, 8 % of eyes (29 eyes) had deteriorated by more than 0.30 LogMAR units [69]. Eyes that underwent ILM peel with primary surgery were more likely to achieve visual success ($p=0.027$) than eyes without ILM peel. Christensen et al. [53] report that 51 of 77 eyes (66.2 %) in their clinical trial reached a visual acuity $\geq 20/40$ and 60 of 77 (77.9 %) gained ≥ 3 lines on the ETDRS chart. Visual outcomes continued to improve up until 12 months after surgery [53]. The recovery of the ELM and of the ellipsoid zone after surgery have been associated with better visual outcomes [47, 50, 70]. The outer foveal thickness (the distance between the RPE and the ELM) is another parameter that reflects photoreceptor recovery and is also strongly correlated with visual acuity [47].

Some of the main intraoperative complications reported during macular hole surgery are iatrogenic retinal tears (6.9–32 %) [51, 53, 69], retinal trauma (1.7–13 %) [51, 69], and retinal hemorrhages (0.6–19 %) [51, 69] produced during the maneuvers to detach the posterior vitreous cortex and peel the ILM. In phakic eyes, there are also lens touch (1.1 %) and posterior capsular rupture (0.9 %) [69].

During the postoperative period, retinal detachment has been reported in 2.2–5 % [51, 53]. RPE changes (white-yellow or reddish lesions at the macula) are frequent (11–15 % [51, 53]), and they do not necessarily imply a worse visual outcome.

V. Vitreomacular Traction (VMT)

In contrast to the aforementioned conditions, where tangential traction is the pathogenic mechanism, anomalous PVD [see chapter III.B. Anomalous PVD and vitreoschisis] can exert anteroposterior traction upon the macula resulting in vitreomacular traction [see chapter III.D. Vitreo-macular adhesion/traction and macular holes: pseudo, lamellar and full-thickness]. There are few reports in the OCT era on the natural evolution of VMT and on the outcomes of surgery. Charalampidou et al. [71] followed 12 patients (15 eyes) with tractional cystoid macular edema presenting with good visual acuities (Snellen $\geq 20/40$). After a mean follow-up of 9.2 (± 7.4) months, 8 eyes (53 %) exhibited spontaneous and complete posterior vitreous detachment, with resolution of the tractional cystoid macular edema and restoration of normal foveal anatomy in 6 eyes and persistence of a single

foveal cyst in 2 eyes. Visual acuity in the eyes that underwent complete posterior vitreous detachment improved from Snellen 20/32 to Snellen 6/8 [71]. Thus, VMT may resolve spontaneously in a substantial proportion of cases within months of presentation. Why do some eyes develop complete posterior vitreous detachment while others show VMT? In 2004 Sebag proposed the unifying concept of anomalous PVD [72] wherein the principle of vitreoschisis was identified and later described in greater detail [18]. Four years later Chang et al. [73] performed histopathologic analysis of surgical specimens. Their findings suggested that in patients with vitreomacular traction, there is a splitting within the vitreous cortex, leaving remnants of vitreous on the foveal surface that act as scaffolding for cell proliferation (Video V.A.2-7). The corresponding side of the split vitreous cortex forms the outer surface of the cone of the detached vitreous. This portion of the vitreous cortex appears to be able to act as scaffolding for the proliferation of cells as well. This proliferation is identified on SD-OCT as areas of hyper-reflectivity on the posterior vitreous cortex (Figure V.A.2-16). The proliferating cells and their associated extracellular matrix may fortify the attachment strength of the vitreoretinal adhesion to the fovea, helping to prevent the ordinarily expected complete separation of the vitreous from the macular surface. Thus, persistent vitreomacular adhesion may be due to an exaggerated wound healing response [73].

Earlier reports described different patterns of vitreomacular traction that may be associated with different visual outcomes. Eyes with a VMT with a detached vitreous both temporal and nasal to the fovea (V-shaped pattern) seemed to have better visual outcomes than patients in which the vitreous remains attached nasally (J-shaped pattern) [74–76] (Figures V.A.2-17 and V.A.2-18). However, it seems that the diameter of the vitreoretinal adhesion may be the determining factor in the development of structural abnormalities in vitreomacular traction syndrome. In eyes with focal vitreomacular traction (1,500 μm or less), there is a high traction force per unit area. This leads to an intraretinal cavitation with no leakage on fluorescein angiography (Figure V.A.2-19). This cavitation may evolve to a lamellar macular hole if it is unroofed (Figure V.A.2-20) or to a full-thickness macular hole if the defect progresses toward the external layers of the retina (Figure V.A.2-21). Focal traction may also lead to a foveal detachment, although this appears to be less frequent (Figure V.A.2-22). If there is a broad vitreomacular traction (more than 1,500 μm), the traction force is spread out over a larger area. This is more likely to cause a diffuse macular thickening, loss of foveal contour, and occasionally diffuse edema and epiretinal membranes (Figure V.A.2-23). This distinction based upon the extent (greater or less than 1,500 μm) of vitreomacular adhesion was found to be a predictor of response to pharmacologic vitreolysis with ocri-

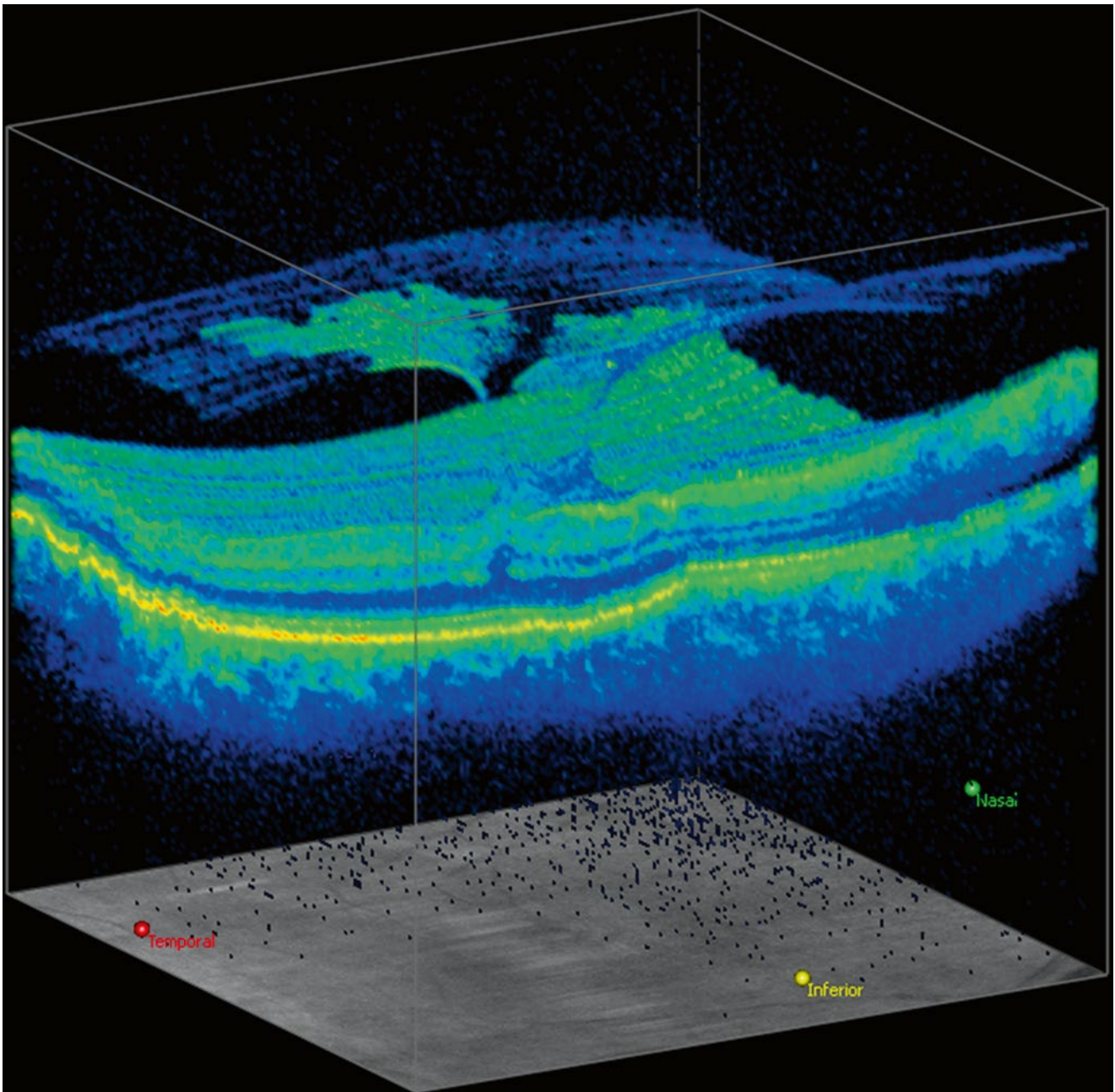


Figure V.A.2-16 3D OCT. Vitreomacular traction. Fibroglial proliferation on the posterior vitreous cortex identified on SD-OCT as a hyper-reflective plaque

plasmin [66] and has been recently incorporated into the new International Classification of VMT [77].

In their surgical series, Witkin et al. [75] found that patients with a lamellar separation of foveal layers or with subfoveal fluid had worse visual and anatomic results than patients with cystoid macular edema or perifoveal traction. They suggested that treatment of patients with the former OCT appearance should include surgical approaches more akin to macular hole treatment, including peeling of epiretinal membranes and possibly the internal limiting membrane,

as well as injection of a gas bubble [75]. As in other pathologies, final visual outcomes after surgery have been correlated with preoperative visual acuity [78] and with duration of symptoms [74]. Thus, vitrectomy in patients with vitreomacular traction should be performed at diagnosis if visual acuity is under 20/40 or if there is severe metamorphopsia. In patients presenting good visual acuity, surgery should be performed if there is a decrease in visual acuity with increased traction on OCT.

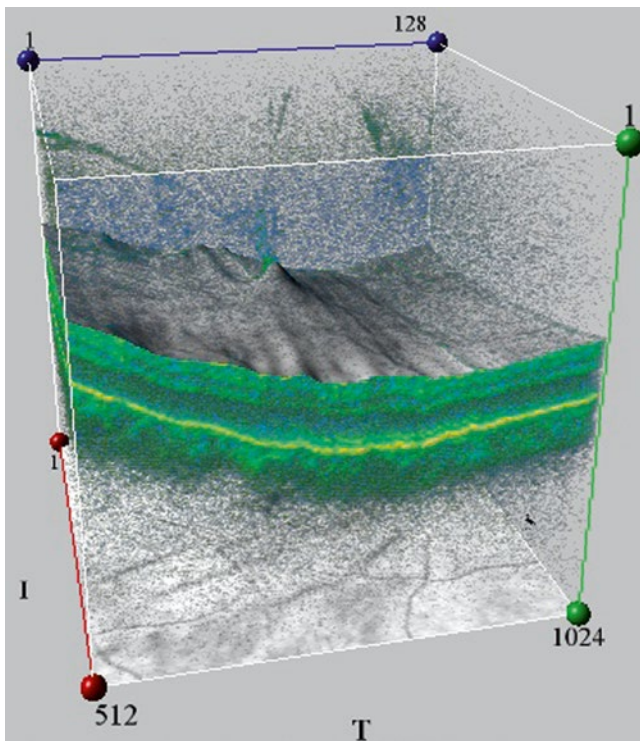


Figure V.A.2-17 Vitreomacular traction. V-shaped pattern

A. Surgical Technique and Outcomes

In patients with vitreomacular traction, we perform microincisional vitrectomy. It is important to proceed cautiously when inducing a posterior vitreous detachment because the vitreous may be firmly attached to the fovea, requiring sharp dissection (Video V.A.2-8). The ILM should be removed if there is a coexisting premacular membrane or a macular hole.

Reports on surgical outcomes are scarce (Table V.A.2-5). The rate of visual acuity improvement of two or more lines ranges between 45 and 91 % of eyes [74–81] (Figures V.A.2-24 and V.A.2-25). The studies that report worse outcomes are those that include eyes with coexisting pathologies. The

main complication of vitrectomy in vitreomacular traction is the development of lamellar or full-thickness macular holes. These complications are more frequent in eyes with more extended traction.

Abbreviations

BBG	Brilliant blue G
BCVA	Best-corrected visual acuity
CFT	Central foveal thickness
CME	Cystoid macular edema
CRT	Central retinal thickness
DONFL	Dissociated optic nerve fiber layer
ELM	External limiting membrane
ETDRS	Early Treatment Diabetic Retinopathy Study
FILMS	Full-Thickness Macular Hole and Inner Limiting Membrane Peeling Study
FTMH	Full-thickness macular hole
G	Gauge
ICG	Indocyanine green
ILM	Internal limiting membrane
LMH	Lamellar macular hole
LogMAR	Logarithm of the minimum angle of resolution
NR	Not reported
OCT	Optical coherence tomography
PMM	Premacular membrane
PVD	Posterior vitreous detachment
RPE	Retinal pigment epithelium
SD	Standard deviation
SD-OCT	Spectral-domain optical coherence tomography
SLO	Scanning laser ophthalmoscopy
TA	Triamcinolone acetonide
TB	Trypan blue
VA	Visual acuity
VMT	Vitreomacular traction

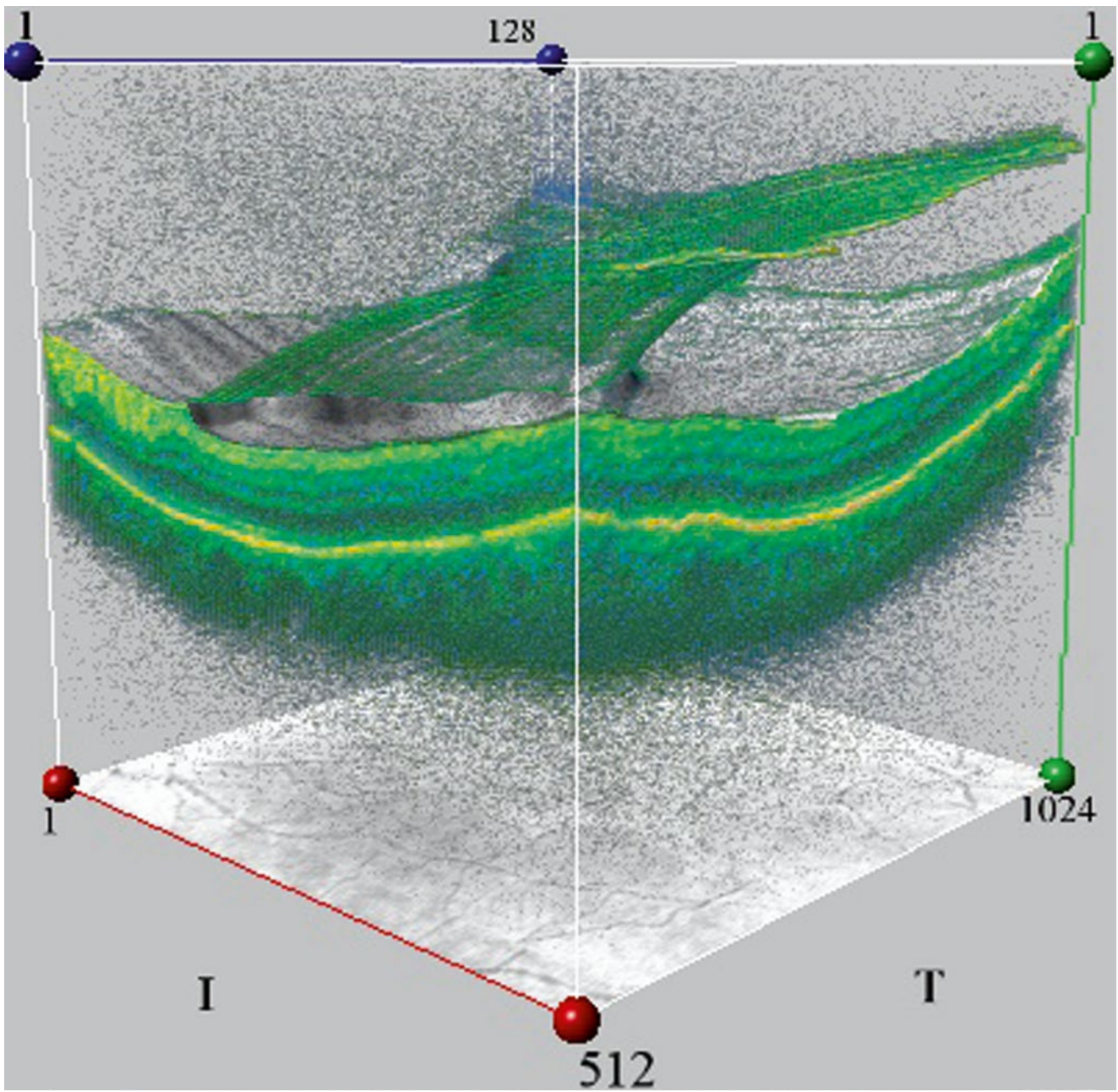


Figure V.A.2-18 Vitreomacular traction. J-shaped pattern

Figure V.A.2-19 Focal vitreo-macular traction with intraretinal cavitation

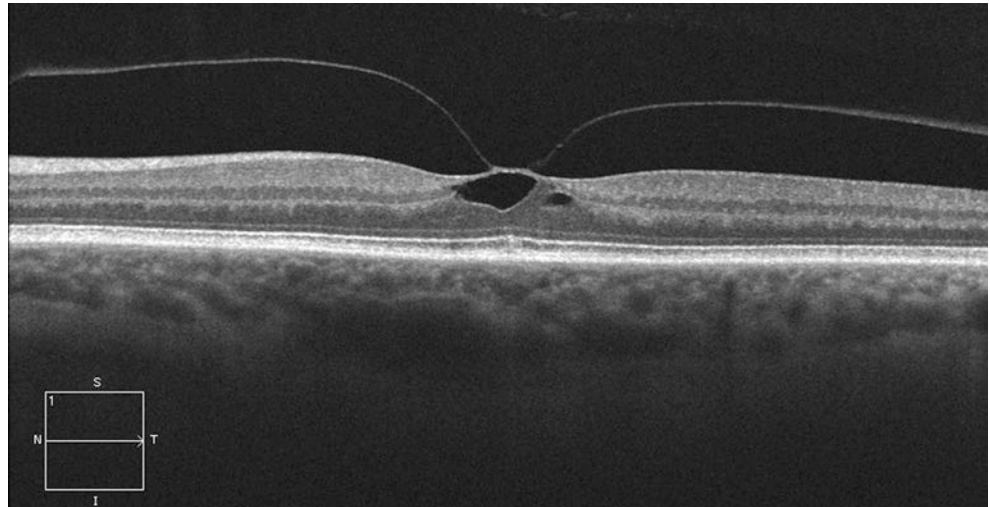


Figure V.A.2-20 Focal vitreo-macular traction. Intraretinal cavitation evolved to nearly a lamellar macular hole

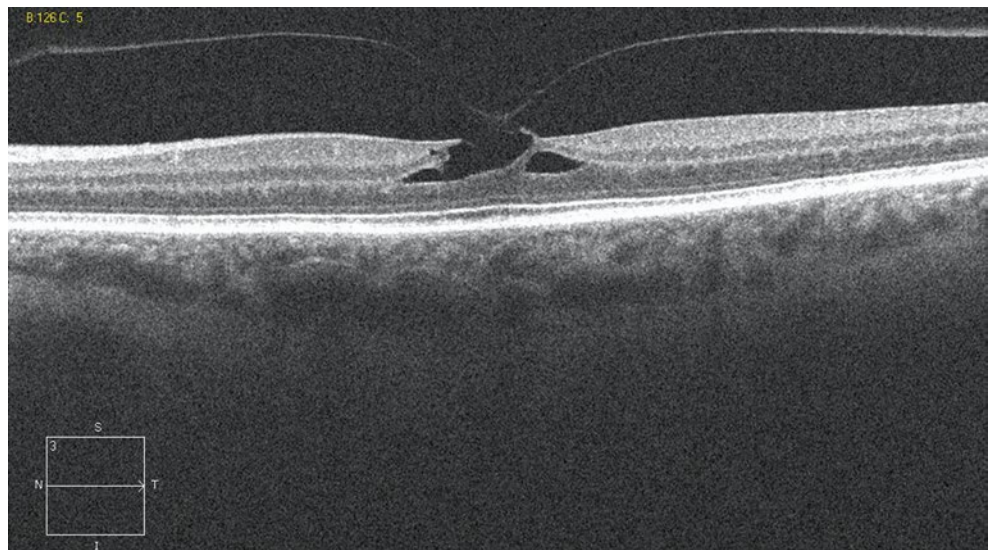


Figure V.A.2-21 Focal vitreo-macular traction. Intraretinal cavitation evolved to nearly a full-thickness macular hole

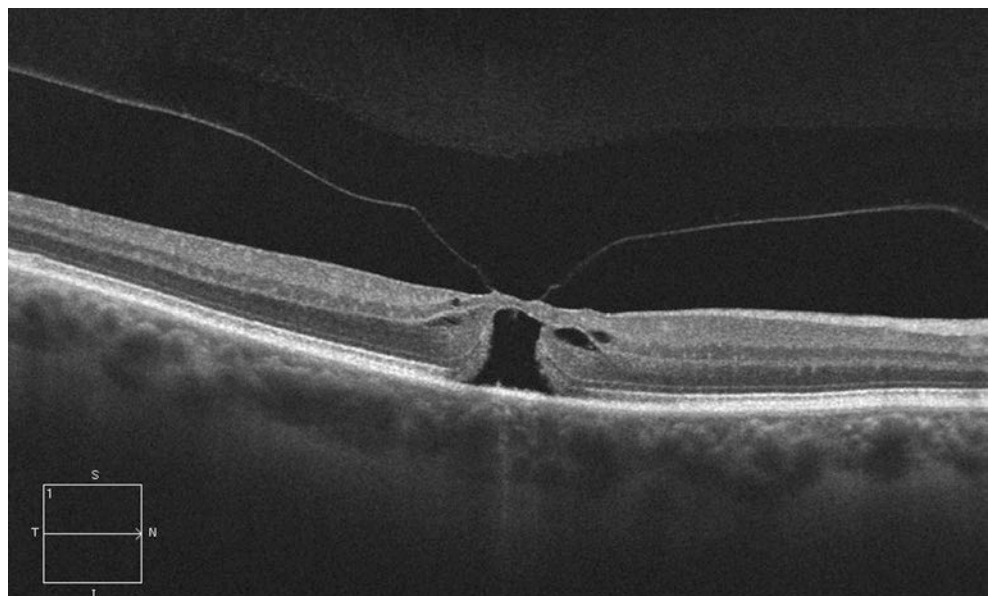


Figure V.A.2-22 Focal vitreomacular traction with foveal detachment

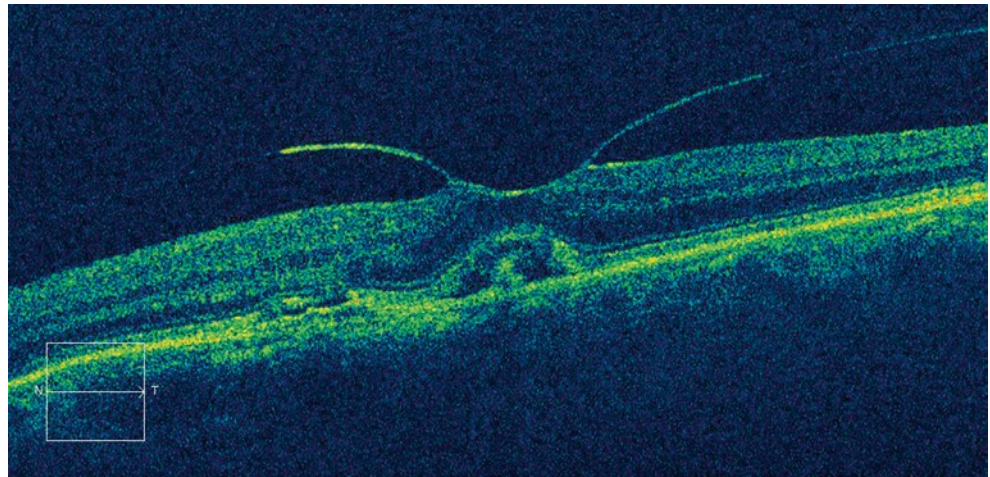


Figure V.A.2-23 Broad vitreomacular traction with loss of foveal contour

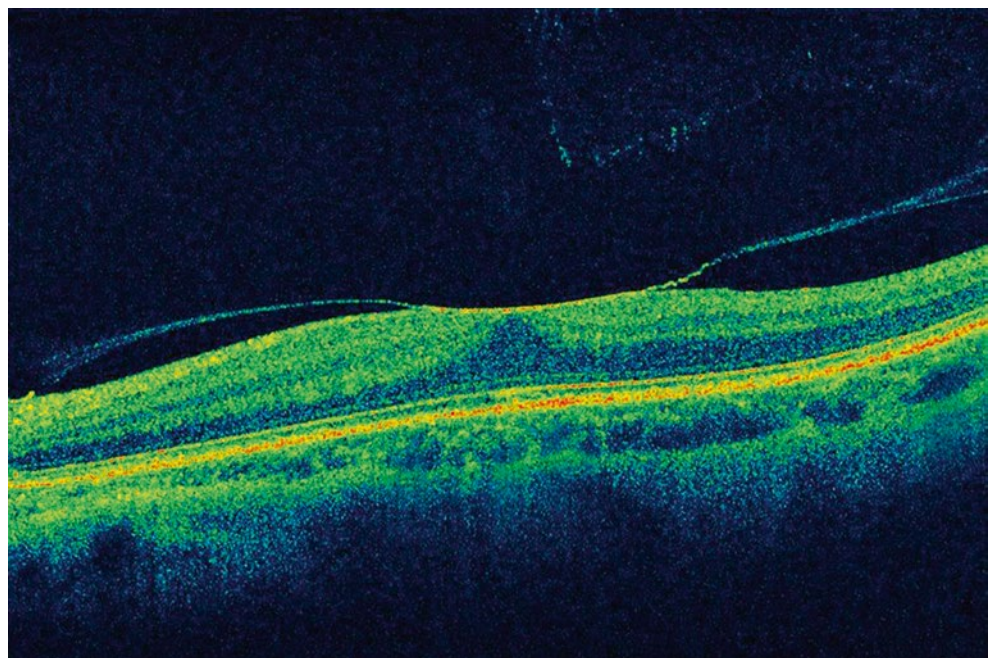


Table V.A.2-5 Studies reporting outcomes after vitreomacular traction surgery

Author [Ref] Type of study	Surgery	Tamponade agent	Eyes included Minimum follow-up	Preoperative BCVA	Postoperative BCVA	Comments/complications
Gandorfer [80] Prospective	Separation of posterior vitreous cortex; ICG-assisted ILM peeling (5 eyes)	Air	14 eyes 8 months	Range 1.3–0.18	Range 1.3–0.0 57 % improved ≥ 2 lines	In 5/6 eyes without visual improvement, ICG was used to stain the ILM
Chang [73] Retrospective	Separation of posterior vitreous cortex	None	6 eyes 8 months	0.59 (range 1.0–0.4)	0.43 (range 0.18–0.7)	SF6 employed in one eye with intraoperative tear
Chung [79] Retrospective	Separation of posterior vitreous cortex	None	6 eyes 1 month	0.7	0.1	
Larsson [78] Prospective	Separation of posterior vitreous cortex	None	11 eyes 6 months	0.7 (range 1.4–0.4)	0.4 (range 1–0.1) 91 % improved ≥ 2 lines	4/9 phakic eyes underwent surgery within 6 months
Sonmez [74] Retrospective	Separation of posterior vitreous cortex and PMM removal	None	24 eyes 6 months	–	54 % improved ≥ 2 lines	3 eyes (12 %) without restitution of the foveal pit
Toklu [81] Retrospective	Separation of posterior vitreous cortex	Air	13 eyes 6 months	1.3 \pm 0.4	0.5 \pm 0.3	None
Witkin [75] Retrospective	Separation of posterior vitreous cortex and PMM removal	SF6 in 6 eyes (30 %) and air in 1 eye (5 %)	20 eyes 3 months	0.784	0.532 45 % improved ≥ 2 lines	1 eye (5 %) FTMH 3 eyes (15 %) LMH 5 eyes (25 %) residual PM
Yamada [76] Prospective	Separation of posterior vitreous cortex ILM peeling in 4 eyes	SF6 in 3 eyes and air in 8 eyes	14 eyes 3 months	–	64 % improved ≥ 2 lines	1 eye FTMH; 1 impending macular hole; 1 persistent CME; 1 macular atrophy

Visual acuities are reported in LogMAR scale; mean and standard deviation or range
PMM premacular membrane, *ILM* inner limiting membrane, *ICG* indocyanine green, *FTMH* full-thickness macular hole, *LMH* lamellar macular hole, *CME* cystoid macular edema, *BCVA* best-corrected visual acuity, *SD* standard deviation

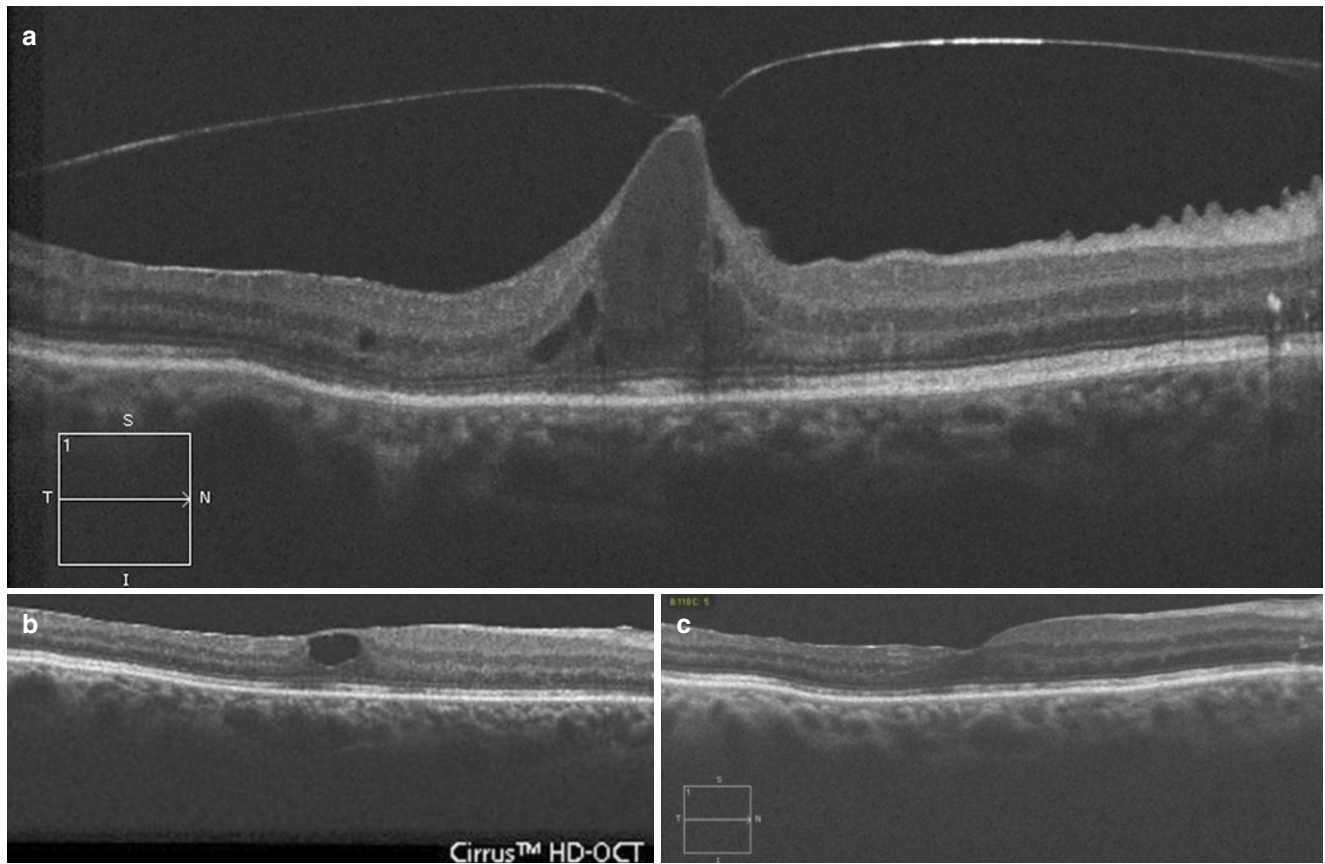


Figure V.A.2-24 Vitreomacular traction. (a) Preoperative OCT showing a severe intraretinal cavitation with a VA of 20/50. (b) Postoperative OCT 1 month after surgery. (c) Resolution of the intraretinal cavitation and improvement in VA to 20/30 3 months after surgery

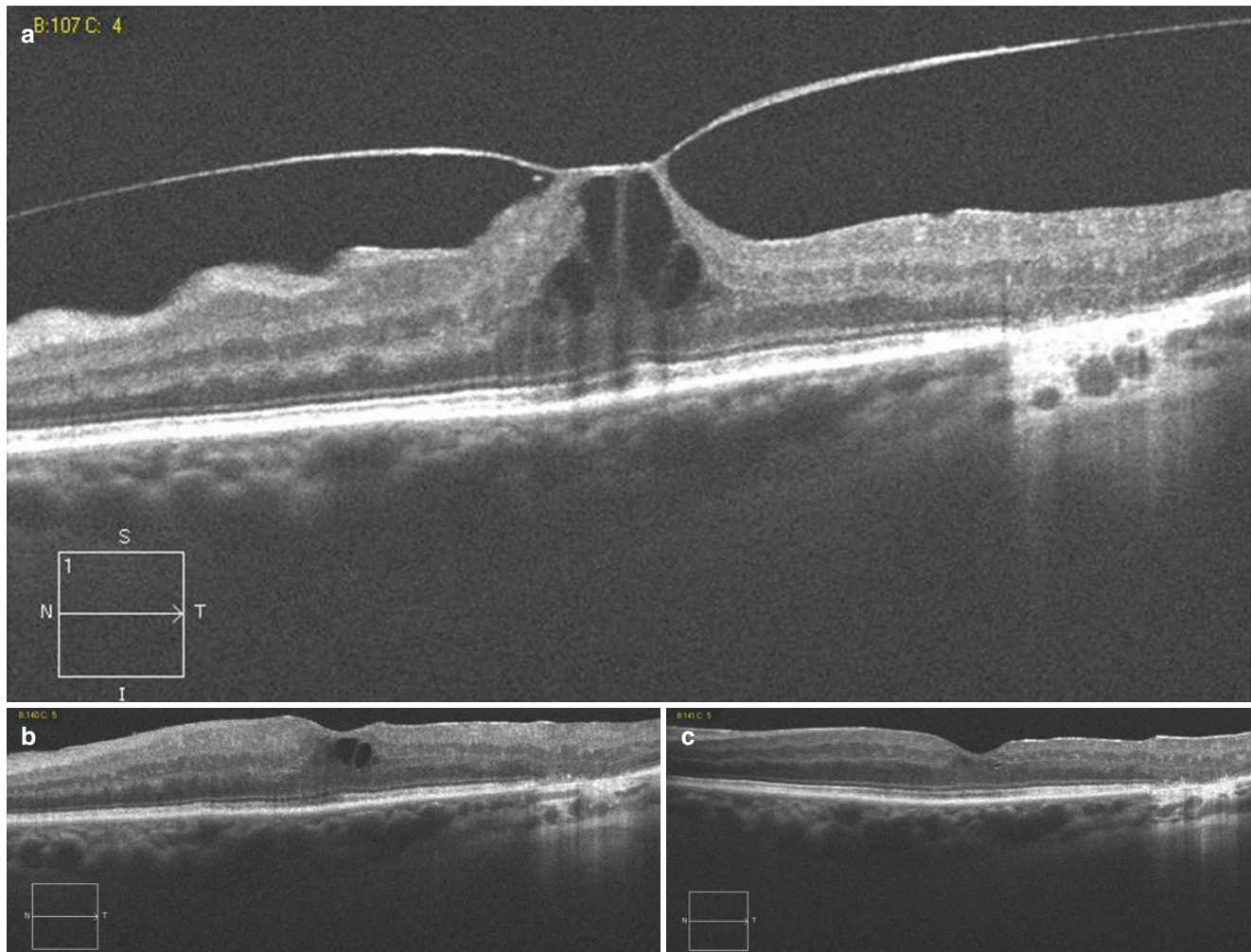


Figure V.A.2-25 Vitreomacular traction. (a) Preoperative OCT of a patient with severe metamorphopsia and a VA of 20/40. (b) Postoperative appearance 15 days after surgery. (c) Improvement in VA to 20/20 and resolution of metamorphopsia 4 months after surgery

References

- Contreras I, Noval S, Tejedor J. Use of optical coherence tomography to measure prevalence of epiretinal membranes in patients referred for cataract surgery. *Arch Soc Esp Ophthalmol*. 2008;83:89–94.
- Kim JH, Kim YM, Chung EJ, et al. Structural and functional predictors of visual outcome of epiretinal membrane surgery. *Am J Ophthalmol*. 2012;153:103–10.
- Kim JH, Kang SW, Kong MG, Ha HS. Assessment of retinal layers and visual rehabilitation after epiretinal membrane removal. *Graefes Arch Clin Exp Ophthalmol*. 2013;251:1055–64.
- Falkner-Radler CI, Glittenberg C, Hagen S, et al. Spectral-domain optical coherence tomography for monitoring epiretinal membrane surgery. *Ophthalmology*. 2010;117:798–805.
- Inoue M, Morita S, Watanabe Y, et al. Inner segment/outer segment junction assessed by spectral-domain optical coherence tomography in patients with idiopathic epiretinal membrane. *Am J Ophthalmol*. 2010;150:834–9.
- Kinoshita T, Imaizumi H, Okushiba U, et al. Time course of changes in metamorphopsia, visual acuity, and OCT parameters after successful epiretinal membrane surgery. *Invest Ophthalmol Vis Sci*. 2012;53:3592–7.
- Mitamura Y, Hirano K, Baba T, Yamamoto S. Correlation of visual recovery with presence of photoreceptor inner/outer segment junction in optical coherence images after epiretinal membrane surgery. *Br J Ophthalmol*. 2009;93:171–5.
- Okamoto F, Sugiura Y, Okamoto Y, et al. Associations between metamorphopsia and foveal microstructure in patients with epiretinal membrane. *Invest Ophthalmol Vis Sci*. 2012;53:6770–5.
- Shimozono M, Oishi A, Hata M, et al. The significance of cone outer segment tips as a prognostic factor in epiretinal membrane surgery. *Am J Ophthalmol*. 2012;153:698–704, 704.
- Suh MH, Seo JM, Park KH, Yu HG. Associations between macular findings by optical coherence tomography and visual outcomes after epiretinal membrane removal. *Am J Ophthalmol*. 2009;147:473–80.
- Bae SH, Kim D, Park TK, et al. Preferential hyperacuity perimeter and prognostic factors for metamorphopsia after idiopathic epiretinal membrane surgery. *Am J Ophthalmol*. 2013;155:109–17.
- Watanabe A, Arimoto S, Nishi O. Correlation between metamorphopsia and epiretinal membrane optical coherence tomography findings. *Ophthalmology*. 2009;116:1788–93.
- Gupta P, Sadun AA, Sebag J. Multifocal retinal contraction in macular pucker analyzed by combined optical coherence tomography/scanning laser ophthalmoscopy. *Retina*. 2008;28:447–52.

14. Wang MY, Nguyen D, Hindoyan N, Sadun AA, Sebag J. Vitreopapillary adhesion in macular hole and macular pucker. *Retina*. 2009;29:644–50.
15. Kwok AK, Lai TY, Yuen KS. Epiretinal membrane surgery with or without internal limiting membrane peeling. *Clin Experiment Ophthalmol*. 2005;33:379–85.
16. Park DW, Dugel PU, Garda J, et al. Macular pucker removal with and without internal limiting membrane peeling: pilot study. *Ophthalmology*. 2003;110:62–4.
17. Shimada H, Nakashizuka H, Hattori T, et al. Double staining with brilliant blue G and double peeling for epiretinal membranes. *Ophthalmology*. 2009;116:1370–6.
18. Sebag J, Gupta P, Rosen R, Garcia P, Sadun AA. Macular holes and macular pucker: The role of vitreoschisis as imaged by optical coherence tomography/scanning laser ophthalmoscopy. *Trans Am Ophthalmol Soc*. 2007;105:121–31.
19. Sebag J. Vitreoschisis. *Graefes Arch Clin Exp Ophthalmol*. 2008;246:329–32.
20. Gupta P, Yee KMP, Garcia P, et al. Vitreoschisis in macular diseases. *Br J Ophthalmol*. 2011;95:376–80.
21. Uemura A, Kanda S, Sakamoto Y, Kita H. Visual field defects after uneventful vitrectomy for epiretinal membrane with indocyanine green-assisted internal limiting membrane peeling. *Am J Ophthalmol*. 2003;136:252–7.
22. Haritoglou C, Gandorfer A, Gass CA, et al. The effect of indocyanine-green on functional outcome of macular pucker surgery. *Am J Ophthalmol*. 2003;135:328–37.
23. Farah ME, Maia M, Furlani B, et al. Current concepts of trypan blue in chromovitrectomy. *Dev Ophthalmol*. 2008;42:91–100.
24. Farah ME, Maia M, Rodrigues EB. Dyes in ocular surgery: principles for use in chromovitrectomy. *Am J Ophthalmol*. 2009;148:332–40.
25. Sayed KM, Naito T, Farouk MM, et al. Twenty five-gauge sutureless vitrectomy versus 20-gauge vitrectomy in epiretinal membrane surgery. *J Med Invest*. 2012;59:69–78.
26. Sandali O, El SM, Lecuen N, et al. 25-, 23-, and 20-gauge vitrectomy in epiretinal membrane surgery: a comparative study of 553 cases. *Graefes Arch Clin Exp Ophthalmol*. 2011;249:1811–9.
27. Haas A, Seidel G, Steinbrugger I, et al. Twenty-three-gauge and 20-gauge vitrectomy in epiretinal membrane surgery. *Retina*. 2010;30:112–6.
28. Garcia-Fernandez M, Navarro JC, Sanz AF, Castano CG. Long-term evolution of idiopathic lamellar macular holes and macular pseudoholes. *Can J Ophthalmol*. 2012;47:442–7.
29. Gaudric A, Aloulou Y, Tadayoni R, Massin P. Macular Pseudoholes with Lamellar Cleavage of Their Edge Remain Pseudoholes. *Am J Ophthalmol*. 2013;155:733–42.
30. Theodossiadis PG, Grigoropoulos VG, Emfietzoglou I, et al. Spontaneous closure of lamellar macular holes studied by optical coherence tomography. *Acta Ophthalmol*. 2012;90:96–8.
31. Sebag J, Wang M, Nguyen D, Sadun AA. Vitreo-papillary adhesion in macular diseases. *Trans Am Ophthalmol Soc*. 2009;107:35–46.
32. Romano MR, Vallejo-Garcia JL, Camesasca FI, et al. Vitreopapillary adhesion as a prognostic factor in pseudo- and lamellar macular holes. *Eye*. 2012;26:810–5.
33. Casparis H, Bovey EH. Surgical treatment of lamellar macular hole associated with epimacular membrane. *Retina*. 2011;31:1783–90.
34. Lee CS, Koh HJ, Lim HT, et al. Prognostic factors in vitrectomy for lamellar macular hole assessed by spectral-domain optical coherence tomography. *Acta Ophthalmol*. 2012;90:e597–602.
35. Reibaldi M, Avitabile T, Uva MG, et al. Ten Years of Severe Vitreomacular Traction Syndrome without Functional Damage Demonstrated by Optical Coherence Tomography. *Case Rep Ophthalmol Med*. 2011;931038.
36. Figueroa MS, Noval S, Contreras I. Macular structure on optical coherence tomography after lamellar macular hole surgery and its correlation with visual outcome. *Can J Ophthalmol*. 2011;46:491–7.
37. Michalewska Z, Michalewski J, Odrobina D, Nawrocki J. Non-full-thickness macular holes reassessed with spectral domain optical coherence tomography. *Retina*. 2012;32:922–9.
38. Parolini B, Schumann RG, Cereda MG, et al. Lamellar macular hole: a clinicopathologic correlation of surgically excised epiretinal membranes. *Invest Ophthalmol Vis Sci*. 2011;52:9074–83.
39. Androudi S, Stangos A, Brazitikos PD. Lamellar macular holes: tomographic features and surgical outcome. *Am J Ophthalmol*. 2009;148:420–6.
40. Hirakawa M, Uemura A, Nakano T, Sakamoto T. Pars plana vitrectomy with gas tamponade for lamellar macular holes. *Am J Ophthalmol*. 2005;140:1154–5.
41. Kokame GT, Tokuhara KG. Surgical management of inner lamellar macular hole. *Ophthalmic Surg Lasers Imaging*. 2007;38:61–3.
42. Michalewska Z, Michalewski J, Cisiecki S, et al. Correlation between foveal structure and visual outcome following macular hole surgery: a spectral optical coherence tomography study. *Graefes Arch Clin Exp Ophthalmol*. 2008;246:823–30.
43. Christensen UC, Kroyer K, Sander B, et al. Macular morphology and visual acuity after macular hole surgery with or without internal limiting membrane peeling. *Br J Ophthalmol*. 2010;94:41–7.
44. Salter AB, Folgar FA, Weissbrot J, Wald KJ. Macular hole surgery prognostic success rates based on macular hole size. *Ophthalmic Surg Lasers Imaging*. 2012;43:184–9.
45. Xirou T, Theodossiadis PG, Apostolopoulos M, et al. Macular hole surgery with short-acting gas and short-duration face-down positioning. *Clin Ophthalmol*. 2012;6:1107–12.
46. Christensen UC. Value of internal limiting membrane peeling in surgery for idiopathic macular hole and the correlation between function and retinal morphology. *Acta Ophthalmol*. 2009;87 Thesis 2:1–23.
47. Shimozono M, Oishi A, Hata M, Kurimoto Y. Restoration of the photoreceptor outer segment and visual outcomes after macular hole closure: spectral-domain optical coherence tomography analysis. *Graefes Arch Clin Exp Ophthalmol*. 2011;249:1469–76.
48. Wakely L, Rahman R, Stephenson J. A comparison of several methods of macular hole measurement using optical coherence tomography, and their value in predicting anatomical and visual outcomes. *Br J Ophthalmol*. 2012;96:1003–7.
49. Chen WC, Wang Y, Li XX. Morphologic and functional evaluation before and after successful macular hole surgery using spectral-domain optical coherence tomography combined with microperimetry. *Retina*. 2012;32:1733–42.
50. Inoue M, Watanabe Y, Arakawa A, et al. Spectral-domain optical coherence tomography images of inner/outer segment junctions and macular hole surgery outcomes. *Graefes Arch Clin Exp Ophthalmol*. 2009;247:325–30.
51. Lois N, Burr J, Norrie J, et al. Internal limiting membrane peeling versus no peeling for idiopathic full-thickness macular hole: a pragmatic randomized controlled trial. *Invest Ophthalmol Vis Sci*. 2011;52:1586–92.
52. Haritoglou C, Sebag J. Indications and considerations for chromodissection. *Retinal Physician* 2014;11(5):34–39.
53. Christensen UC, Kroyer K, Sander B, et al. Value of internal limiting membrane peeling in surgery for idiopathic macular hole stage 2 and 3: a randomised clinical trial. *Br J Ophthalmol*. 2009;93:1005–15.
54. Tadayoni R, Paques M, Massin P, et al. Dissociated optic nerve fiber layer appearance of the fundus after idiopathic epiretinal membrane removal. *Ophthalmology*. 2001;108:2279–83.
55. Tadayoni R, Svorenova I, Erginay A, et al. Decreased retinal sensitivity after internal limiting membrane peeling for macular hole surgery. *Br J Ophthalmol*. 2012;96:1513–6.
56. Tadayoni R, Gaudric A, Haouchine B, Massin P. Relationship between macular hole size and the potential benefit of internal limiting membrane peeling. *Br J Ophthalmol*. 2006;90:1239–41.

57. Spaide RF. "Dissociated optic nerve fiber layer appearance" after internal limiting membrane removal is inner retinal dimpling. *Retina*. 2012;32:1719–26.
58. Guillaubey A, Malvitte L, Lafontaine PO, et al. Comparison of face-down and seated position after idiopathic macular hole surgery: a randomized clinical trial. *Am J Ophthalmol*. 2008;146:128–34.
59. Tatham A, Banerjee S. Face-down posturing after macular hole surgery: a meta-analysis. *Br J Ophthalmol*. 2010;94:626–31.
60. Meng Q, Zhang S, Ling Y, et al. Long-term anatomic and visual outcomes of initially closed macular holes. *Am J Ophthalmol*. 2011;151:896–900.
61. Muselier A, Dugas B, Burelle X, et al. Macular hole surgery and cataract extraction: combined vs consecutive surgery. *Am J Ophthalmol*. 2010;150:387–91.
62. Sebag J. Pharmacologic vitreolysis. *Retina*. 1998;18:1–3.
63. Sebag J. Is Pharmacologic Vitreolysis Brewing? *Retina*. 2002;22:1–3.
64. Sebag J. Pharmacologic vitreolysis—premise and promise of the first decade. *Retina*. 2009;29:871–4.
65. Sebag J. The emerging role of pharmacologic vitreolysis. *Retinal Physician*. 2010;7:52–6.
66. Tozer K, Fink W, Sadun AA, Sebag J. Prospective three-dimensional analysis of structure and function in macular hole treated by pharmacologic vitreolysis. *Retin Cases Brief Rep*. 2013;7:57–61.
67. Stalmans P, Benz MS, Gandorfer A, et al. Enzymatic vitreolysis with ocriplasmin for vitreomacular traction and macular holes. *N Engl J Med*. 2012;367:606–15.
68. Malik A, Dooley I, Mahmood U. Single night postoperative prone posturing in idiopathic macular hole surgery. *Eur J Ophthalmol*. 2012;22:456–60.
69. Jackson TL, Donachie PH, Sparrow JM, Johnston RL. United Kingdom National Ophthalmology Database Study of Vitreoretinal Surgery: Report 2, Macular Hole. *Ophthalmology*. 2012. doi:10.1016/j.ophtha.2012.09.003. pii: S0161-6420(12)00862-7. [Epub ahead of print].
70. Ruiz-Moreno JM, Staicu C, Pinero DP, et al. Optical coherence tomography predictive factors for macular hole surgery outcome. *Br J Ophthalmol*. 2008;92:640–4.
71. Charalampidou S, Nolan J, Beatty S. The natural history of tractional cystoid macular edema. *Retina*. 2012;32:2045–51.
72. Sebag J. Anomalous PVD, – a unifying concept in vitreo-retinal diseases. *Graefes Arch Clin Exp Ophthalmol*. 2004;242:690–8.
73. Chang LK, Fine HF, Spaide RF, et al. Ultrastructural correlation of spectral-domain optical coherence tomographic findings in vitreomacular traction syndrome. *Am J Ophthalmol*. 2008;146:121–7.
74. Sonmez K, Capone Jr A, Trese MT, Williams GA. Vitreomacular traction syndrome: impact of anatomical configuration on anatomical and visual outcomes. *Retina*. 2008;28:1207–14.
75. Witkin AJ, Patron ME, Castro LC, et al. Anatomic and visual outcomes of vitrectomy for vitreomacular traction syndrome. *Ophthalmic Surg Lasers Imaging*. 2010;41:425–31.
76. Yamada N, Kishi S. Tomographic features and surgical outcomes of vitreomacular traction syndrome. *Am J Ophthalmol*. 2005;139:112–7.
77. Duker JS, Kaiser PK, Binder S, et al. The International Vitreomacular Traction Study Group Classification of Vitreomacular Adhesion, Traction, and Macular Hole. *Ophthalmology*. 2013. doi:10.1016/j.ophtha.2013.07.042. pii: S0161-6420(13)00682-9. [Epub ahead of print].
78. Larsson J. Vitrectomy in vitreomacular traction syndrome evaluated by ocular coherence tomography (OCT) retinal mapping. *Acta Ophthalmol Scand*. 2004;82:691–4.
79. Chung EJ, Lew YJ, Lee H, Koh HJ. OCT-guided hyaloid release for vitreomacular traction syndrome. *Korean J Ophthalmol*. 2008;22:169–73.
80. Gandorfer A, Rohleder M, Kampik A. Epiretinal pathology of vitreomacular traction syndrome. *Br J Ophthalmol*. 2002;86:902–9.
81. Toklu Y, Demirel S, Sarac O, et al. Anatomic and functional outcome of triamcinolone-assisted 23-gauge vitrectomy in vitreomacular traction syndrome. *Semin Ophthalmol*. 2012;27:73–7.
82. Garretson BR, Pollack JS, Ruby AJ, et al. Vitrectomy for a symptomatic lamellar macular hole. *Ophthalmology*. 2008;115:884–6.
83. Witkin AJ, Castro LC, Reichel E, et al. Anatomic and visual outcomes of vitrectomy for lamellar macular holes. *Ophthalmic Surg Lasers Imaging*. 2010;41:418–24.
84. Almeida DR, Wong J, Belliveau M, et al. Anatomical and visual outcomes of macular hole surgery with short-duration 3-day face-down positioning. *Retina*. 2012;32:506–10.
85. Rahman R, Madgula I, Khan K. Outcomes of sulfur hexafluoride (SF6) versus perfluoroethane (C2F6) gas tamponade for non-posturing macular-hole surgery. *Br J Ophthalmol*. 2012;96:185–8.

Christos Haritoglou, Arnd Gandorfer, and Anselm Kampik

Outline

- I. **Introduction**
 - A. Rationale: Why Chromodissection?
- II. **Chromodissection Techniques**
 - A. Staining Substances
 1. Indocyanine Green (ICG)
 2. Trypan Blue
 3. Brilliant Blue
 4. Other Experimental Dyes
 - B. Surgical Techniques
 1. Single Staining
 2. Double Staining
- III. **Tissue-Dye Interaction: Staining and Beyond**
- IV. **Clinicopathological Correlations**
- V. **Future Perspectives**

References

Electronic supplementary material Supplementary material is available in the online version of this chapter at [10.1007/978-1-4939-1086-1_34](https://doi.org/10.1007/978-1-4939-1086-1_34). Videos can also be accessed at <http://www.springerimages.com/videos/978-1-4939-1085-4>.

C. Haritoglou, MD (✉)
Department of Ophthalmology, Duke Carl Theodor
Eye Clinic, Ludwig Maximilian University,
Nymphenburger Str. 43, Munich 80335, Germany

Department of Ophthalmology, University Eye Hospital,
Ludwig-Maximilians-University, Munich, Germany
e-mail: christos.haritoglou@med.uni-muenchen.de

A. Gandorfer, MD
Department of Ophthalmology, MVZ Memmingen
and Ludwig Maximilian University, Munich, Germany

Department of Ophthalmology, University Eye Hospital,
Ludwig-Maximilians-University, Munich, Germany
e-mail: arnd.gandorfer@me.com

A. Kampik, MD
Department of Ophthalmology, Ludwig-Maximilians-University,
Mathildenstr. 8, Munich 80336, Germany

Department of Ophthalmology, University Eye Hospital,
Ludwig-Maximilians-University, Munich, Germany
e-mail: anselm.kampik@med.uni-muenchen.de

Keywords

Chromodissection • Vital dyes • Indocyanine green • Brilliant blue • Trypan blue • Inner limiting membrane • Macular hole • Macular pucker • Vitreo-macular traction • Posterior vitreous cortex • Vitreoschisis

Key Concepts

1. The use of staining substances in vitreoretinal surgery facilitates complex surgical procedures such as ILM peeling.
2. All staining substances need to be used with care regardless of which application technique is used, since the mechanisms of potential adverse effects are not completely understood.
3. There might be other relevant tissue-dye interactions besides the actual staining effect, such as in increase of the rigidity of the stained tissue, accounting in part for efficacy.

I. Introduction

The literature contains frequent reference to “epiretinal membranes (ERM).” This term is inaccurate for two reasons: The term “epi” refers to a location next to or beside a structure, in this case the retina. Thus, the term “epiretinal” could refer to a subretinal as well as preretinal location. In all of the situations discussed herein, the membrane location is in front of the retina; thus, the prefix “pre-” is more accurate and will be used instead of “epi.” Furthermore, all of the conditions discussed herein are maculopathies, not retinopathies. Thus, the term “premacular membrane” is the more precise terminology and will be employed herein to refer to what has previously been described as “ERM.” The term “macular pucker” will be used to refer to one clinical consequence of

an abnormal premacular membrane. Furthermore, the term “idiopathic ERM” is no longer an appropriate term to refer to macular pucker, since we now know that vitreous is the cause of this condition.

A. Rationale: Why Chromodissection?

The introduction of staining substances to visualize otherwise transparent and barely visible structures such as the vitreous, premacular membranes, and the inner limiting membrane (ILM) of the retina has greatly facilitated challenging surgical procedures such as ILM peeling during surgical interventions at the vitreoretinal interface. Today, there is common agreement that a crucial part for successful surgery for tractional vitreo-maculopathies is the dissection of the ILM from the underlying tissue using the retinal surface of the ILM as a cleavage plane in order to remove all cellular proliferations and vitreous collagen remnants and relieve all relevant tractional forces. The selective staining properties of the dyes currently being used allow for differentiation of tissues such as premacular proliferations or the ILM. While the unstained ILM can only be identified by a glistening reflex at the retinal surface, which turns into a slight whitening after removal of the ILM, the stained ILM can be removed more easily and in larger fragments. Furthermore, it is safe to assume that better visualization of this structure may help minimize surgical trauma to the underlying retinal nerve fibers. In addition, it appears easier to identify areas of unpeeled ILM. Therefore, this surgical technique has become workable even for the less trained surgeon.

Since the early reports on potential toxic effects of indocyanine green (ICG), one of the first dyes introduced for selective ILM staining, there is growing interest in the field of “chromodissection.” Several alternative and potentially safer dyes for ILM and also for premacular membrane removal are under investigation at present. The following will give an overview on the current “state of the art” in chromodissection, including some comments on specific dyes and surgical techniques, but will also discuss some relevant aspects with regard to tissue-dye interaction

and toxicity and will give a perspective on future concepts in this emerging field.

II. Chromodissection Techniques

A. Staining Substances

Several dyes are in clinical use to selectively visualize the target structure (Table V.A.3-1). The dyes are either injected into the fluid-filled or air-filled globe, and different concentrations are used. While the following substances represent true dyes with selective staining properties, triamcinolone acetonide represents more or less an adjunct to visualize the vitreous and facilitate the induction of a posterior vitreous detachment as the crystals of the suspension are entrapped between the collagen fibers of the vitreous. Fluorescein provides a slight staining of the vitreous, which can sometimes be noted if vitrectomy is performed shortly after angiography.

1. Indocyanine Green (ICG)

ICG is a near-infrared diagnostic tricarbocyanine dye with a molecular weight of 775.0 g/M, which was developed as a photographic dye. ICG typically has a maximum absorption peak at approximately 800 nm. However, it has been shown that the absorption qualities of ICG have significant variations depending on the solvent medium, for example, plasma or water, and the dye concentration. Another influence on the absorption spectrum results from progressive aggregate formation with increasing concentration [2].

This hydrophilic dye is delivered as a sterile powder and has been used in humans since 1956. The principal advantages were the confinement to the vascular compartment by binding to plasma proteins and rapid excretion almost exclusively into the bile. In 1959, it was approved by the FDA and became popular to record dilution curves in order to measure cardiac output or organ perfusion and was also used for liver function diagnosis following intravenous injection. Both absorption and fluorescence maximum of ICG are within the near-infrared spectral range, and human tissue is relatively transparent for near-infrared light, allowing for a noninvasive detection of the

Table V.A.3-1 Contrasting agents that are currently used for chromodissection during vitreoretinal surgery

Dye (concentration)	Premacular membrane	ILM	Vitreous	Mode of application ^a	Additional comments
ICG (0.5–0.05 %)	–	Selective +++	–	Usually fluid-filled globe	Question of toxicity, off-label
Brilliant blue (0.025 %)	–	Selective ++	–	Fluid-filled globe (if heavy BBG is used)	Approved in Europe
Trypan blue (0.15 %)	+++	(+)	(+)	Fluid- or air-filled globe	Approved in Europe
Triamcinolone acetonide	–	Nonselective (+)	+++	Fluid-filled globe	No dye, pharmacologic properties
Fluorescein	–	–	+	Intravitreal, intravenous, or peroral application	

^aSurgical techniques may vary depending on individual preference



Figure V.A.3-1 Indocyanine green-assisted ILM peeling (Courtesy of Dr. Henrich, Basel)

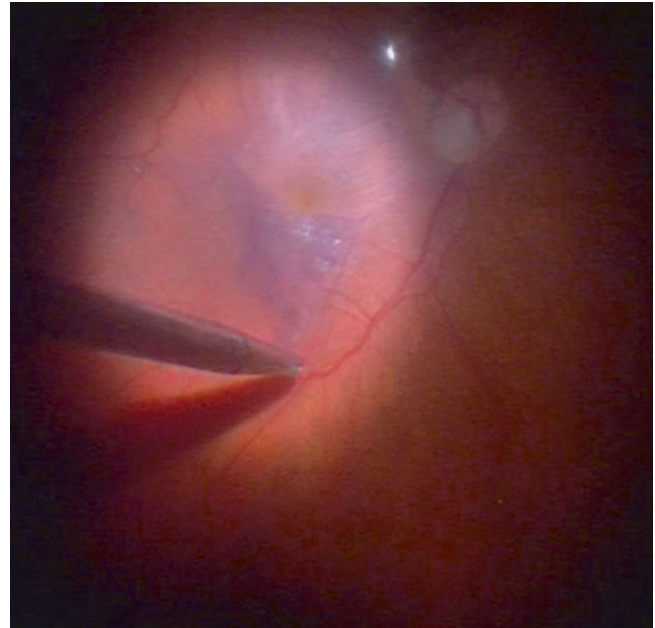


Figure V.A.3-2 Peeling of a premacular membrane after trypan blue staining

dye using absorption measurements or fluorescence imaging techniques. In ophthalmology, intravenous ICG has a long history of safety for choroidal angiography [3]. For diagnostic purposes such as choroidal angiography or cardiac diagnostics, the intravenous ICG dosage ranges between 0.1 and 0.3 mg/kg body weight.

Besides intravenous application, ICG can also be administered topically as a vital dye for donor corneal endothelium and to assist capsulorrhexis in eyes with mature cataract [4]. In addition, it was observed that ICG can also stain to some degree the vitreous cortex, especially the anterior vitreous base. The first description of ICG staining of the ILM was presented by Vivian Kim at the meeting of the American Academy of Ophthalmology (AAO) in 1999 (poster 349), followed by the first reports on ICG-assisted ILM peeling by Kadosono in the year 2000 [5] (Figure V.A.3-1). It was demonstrated that ICG selectively stains the ILM, as a staining effect could only be achieved when the vitreous cortex or premacular tissue had been thoroughly removed [6]. Several published studies have emphasized the obvious advantages of the dye in visualization and easier and more complete removal of the ILM [7–9]. ICG has not been approved for intraocular injection and represents an off-label use for this indication. The concentration typically injected into the vitreous chamber varies between 0.5 and 0.05 % (Video V.A.3-4).

2. Trypan Blue

Trypan blue is a large hydrophilic tetrasulfonated anionic dye with a large planar aromatic system and a lipophilic

domain sandwiched between sulfonated naphthyl end units [10]. The absorption maxima are 607 nm in methanol and 588 nm in water, and the emission when bound to protein is in the red; the solubilities are 1 % in water, 7.2 % in ethylene glycol, trivially in ethanol, and insoluble in xylene [10]. This dye has been commonly used as a vital stain. While trypan blue is excluded by most living cells, it can be taken into phagocytes and certain other cells. Therefore, current applications include a wide spectrum of viability testing such as frozen sperm [11] and aortic muscle cells [12]. In embryology the dye is used as a fluorescent tracer of cell populations [13]. After binding to proteins, mainly albumin, the resulting complex emits red fluorescence, a quality that has been used in studies on exudation from blood vessels in the injured nervous system [14]. Other applications include the assessment of arterial endothelial barrier dysfunction [15] and creatine kinase release as a sign of injured myocytes [16]. Trypan blue is used by oncologists as a tumor promoter modulating permeability of lysosomal membranes [17].

In ophthalmology, trypan blue is used in concentrations from 0.0125 to 0.1 % to stain the lens capsule to assist capsulorrhexis during surgery for mature cataract and for the evaluation of the corneal endothelium of donor tissue before penetrating keratoplasty [18–21]. In the posterior segment of the eye, trypan blue is mainly used to stain premacular membranes (Figure V.A.3-2). The staining of the ILM is weak compared to other selective ILM dyes [22]. There are no major concerns of trypan blue-related toxicity after vitreoretinal surgery. However, as long-term

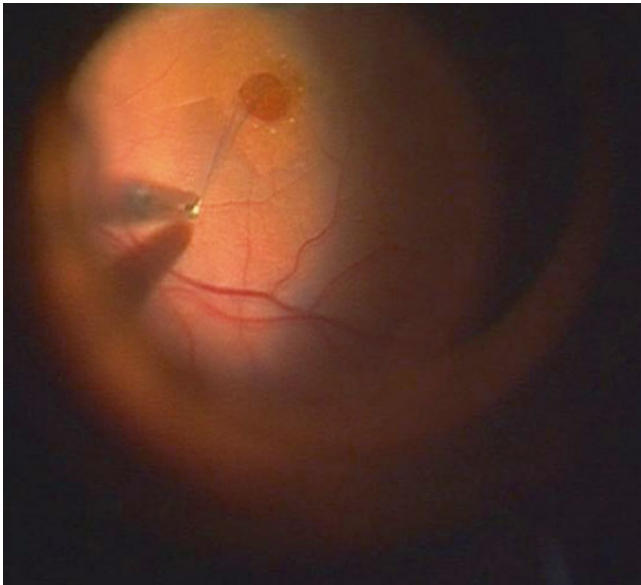


Figure V.A.3-3 Brilliant blue-assisted peeling of the ILM in a case of a traumatic macular hole

results are not yet available, trypan blue should be used with caution.

3. Brilliant Blue

Brilliant blue, or acid blue, or Coomassie, is a blue anionic amino triarylmethane dye and appears to be a promising new dye for ILM staining. Brilliant blue-assisted ILM staining (Figure V.A.3-3) was initially described by Enaida and coworkers [23–25]. Several experimental studies addressed the retinal toxicity of brilliant blue either in cell culture models or subretinal injections in animals as well as functional assessments including electrophysiological studies [26, 27]. They revealed a very good biocompatibility of BBG in contrast to control dyes including indocyanine green and trypan blue. An experimental study exposing glial cells to indocyanine green and brilliant blue disclosed ICG toxicity, as seen by the induction of apoptosis involving induction of the caspase cascade through p38 MAPK phosphorylation, while BBG did not cause apoptosis and therefore could be considered a safer adjuvant [28]. With regard to the excellent safety profile of other dyes of the same class of anionic triarylmethane dyes such as methylene blue or aniline blue, one may hypothesize that this class of dyes provides alternative candidate dyes to be used for ILM peeling [29]. Today, brilliant blue for ILM staining is approved in many European countries and commercially available in a concentration of 0.025 %. As the dye is usually injected into the fluid-filled globe, adjuncts such as deuterium oxide or polyethylene glycol have been added in order to create “heavier than water” solutions, which facilitate the application of the dye directly over the retinal surface without uncontrolled distribution within the vitreous chamber [30] but

do not further enhance the contrast obtained [31]. Similar to indocyanine green, brilliant blue can be considered a selective “ILM dye.” However, it has been shown that the contrast provided by brilliant blue is less remarkable compared to indocyanine green but still sufficient for ILM peeling [32].

4. Other Experimental Dyes

Chromodissection is an emerging field in vitreoretinal surgery, and therefore several other dyes are under investigation in experimental *in vivo* and *in vitro* studies. These include substances such as methyl violet, crystal violet, eosin Y, Sudan black B, methylene blue, toluidine blue, light green, indigo carmine, fast green, Congo red, Evans blue, brilliant blue, and bromophenol blue [29, 33–35]. Comparing the selective ILM dyes already used by vitreoretinal surgeons, a better contrast has been described for indocyanine green. Brilliant blue may provide a better safety profile [25, 26], yet the staining effect is weaker compared to indocyanine green [32]. In addition to the potential toxic effects of ICG and the narrow safety margin of this compound [36–39], ICG may not be an ideal candidate for ILM staining as its maximum absorption is in the near infrared and not within the spectral sensitivity of the human eye [40] (Figure V.A.3-4). This means that the majority of light absorption of ICG is useless or of low value during vitreoretinal surgery because it is in the invisible NIR and in the bathochromic region of the visible spectrum. As a consequence, relatively high dye concentrations are required to achieve a sufficient contrast at the vitreoretinal interface. In addition, the absorption spectrum of ICG overlaps with different types of illumination, posing the risk of phototoxicity to the retina [40–42]. Therefore, it seems that an ideal candidate dye would be a dye incorporating the excellent contrast provided by ICG and the high biocompatibility of brilliant blue (i.e., strongly absorbing at visible wavelengths, conveniently tissue binding, nontoxic, and physiologically degradable at a practical time scale). This may be reached by altering the molecular structure of ICG and thereby changing the absorption qualities and the affinity of the dye molecule (Figure V.A.3-5), resulting in improved absorption and fluorescent qualities. Compared to indocyanine green, the staining properties may be expected to be equal with an improved safety profile [43] as it is adapted to the spectral sensitivity of the human eye and to the standard illumination used during surgery. In addition, the dye implies both the blue absorption color and an even stronger purple fluorescence color which enhances the contrast obtained [43].

B. Surgical Techniques

Currently, chromodissection dyes are usually injected into the fluid-filled vitreous. Approved and commercially available brilliant blue solutions contain solutes being heavier than water allowing for a controlled application directly over the

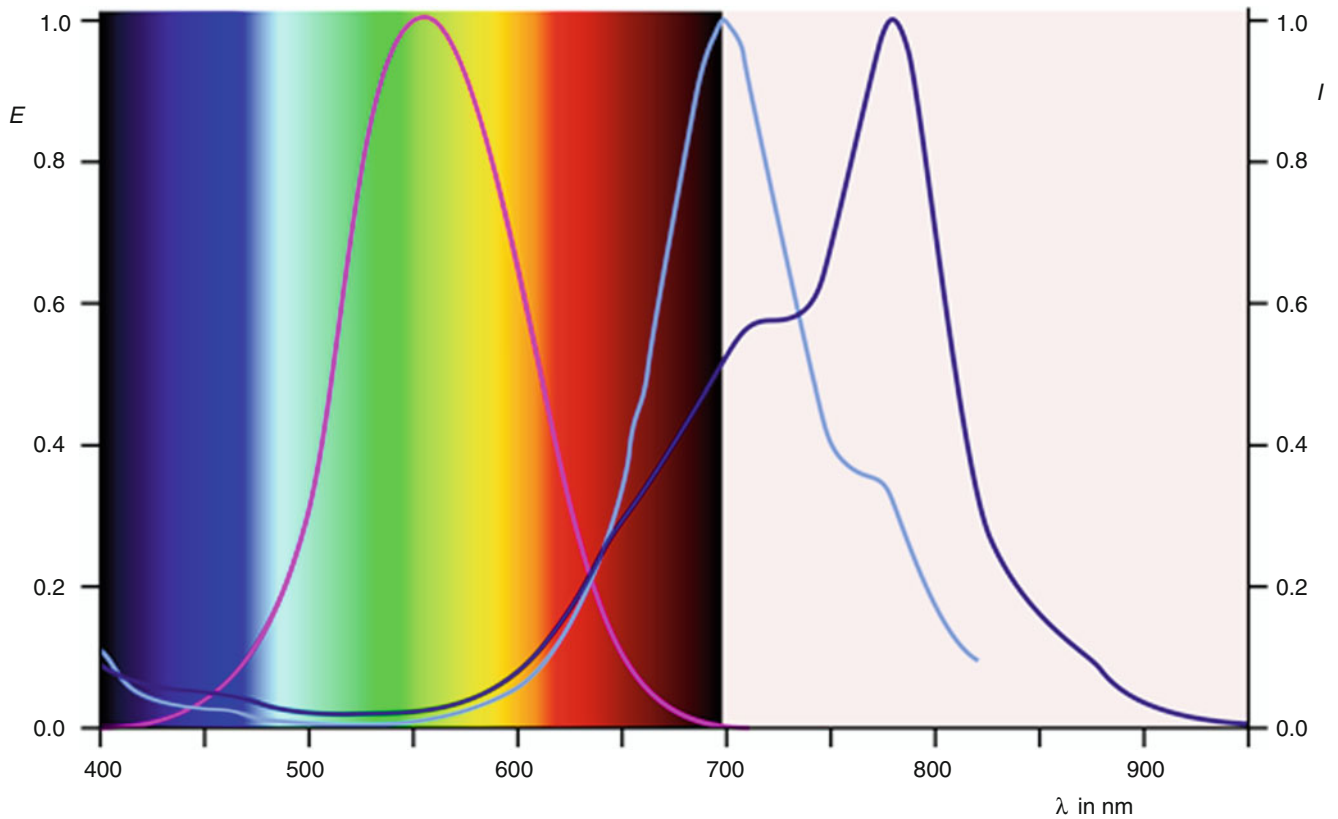


Figure V.A.3-4 Magenta line, spectral sensitivity of the eye; light blue line, aggregated ICG; dark blue line, ICG in solution. Note that the maximum absorption of ICG is in the NIR

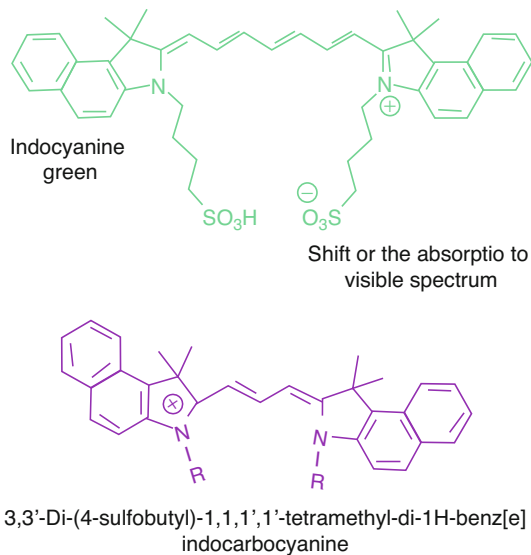


Figure V.A.3-5 Modification of the ICG molecule in order to optimize staining properties and safety profile

area of interest. Trypan blue may still be applied following fluid-air exchange, although this step is not mandatory. The choice of a visualizing agent depends on its staining characteristics (see Table V.A.3-1) and the underlying disease, espe-

cially the presence or absence of premacular cellular proliferations. In addition, some histopathological aspects should be considered in order to use these adjuncts in a reasonable fashion. Further, premacular membranes often represent multilayered structures with a vitreous collagen layer interspersed between the ILM and the cellular proliferation, most likely the result of vitreoschisis [44, 45]. Successful surgery requires complete removal of both the premacular membrane and the underlying ILM. In contrast, for the repair of a macular hole, usually a single layer, the ILM, needs to be peeled off as it represents the most relevant structure for the transmission of the underlying pathological tangential and anterior-posterior tractional forces and the amount of premacular proliferation is limited. The described selective staining properties of trypan blue for premacular membranes and brilliant blue and indocyanine green for the ILM in theory allow for a step-by-step removal of tissue at the vitreoretinal interface.

1. Single Staining

In the presence of a premacular membrane, trypan blue may be used to stain and peel the membrane. When using selective ILM dyes such as brilliant blue or indocyanine green during surgery for premacular membranes, it is a common observation that the presence of a premacular membrane impairs a sufficient visualization of the ILM. The premacular mem-

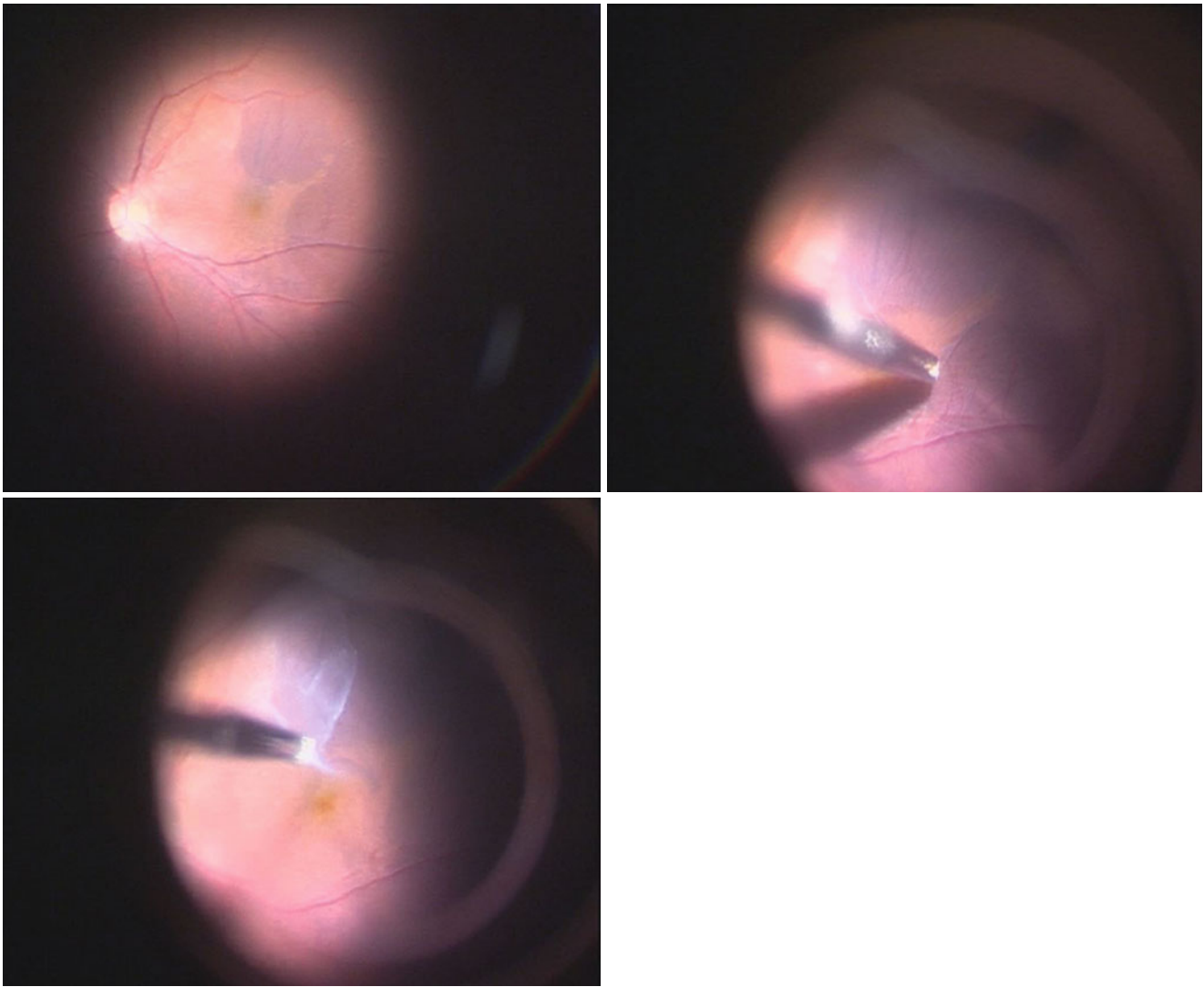


Figure V.A.3-6 After the injection and washout of brilliant blue, the ILM can be nicely visualized by its bluish appearance, surrounding the premacular proliferation that did not stain (“negative staining” of

the membrane). The unstained membrane is then peeled off using a forceps (*middle and bottom*)

brane does not stain using these dyes, and its borders can therefore be delineated intraoperatively as it is surrounded by bluish areas of stained ILM (Video V.A.3-3). Some authors have referred to this as a “negative staining” of premacular membranes (Figure V.A.3-6). Consequently, in the presence of a premacular membrane, the surgeon may either choose to peel off the premacular membrane first, followed by the injection of an ILM dye to identify ILM remnants (Figure V.A.3-7) which need to be additionally removed in order to prevent a re-proliferation of the premacular membrane (Video V.A.3-2). Should the application of the dye reveal that the ILM had already been removed along with the premacular membrane, no further manipulation is required (Figure V.A.3-8).

Alternatively, one might consider applying the dye before the removal of the premacular membrane. Then, the removal of the tissue can be initiated in an area of stained ILM, and

both tissue sheets may be removed together or one may peel the demarcated “negatively” stained premacular tissue followed by the removal of the ILM, which can be identified by the bluish contrast around the area of the removed premacular membrane (Video V.A.3-1).

However it may be achieved, sufficient ILM removal is crucial for successful premacular membrane surgery, as previous investigations have shown the ILM is often only partly removed along with a premacular membrane. Remaining ILM fragments have been associated with recurrent premacular membrane formation as there is an indeterminate extent of cells and collagen remaining on the vitreous side of the ILM which serves as a scaffold for cellular re-proliferations and leads to recurrence of disease. Therefore, a thorough removal of the ILM is crucial for anatomic and functional long-term success [46–50].

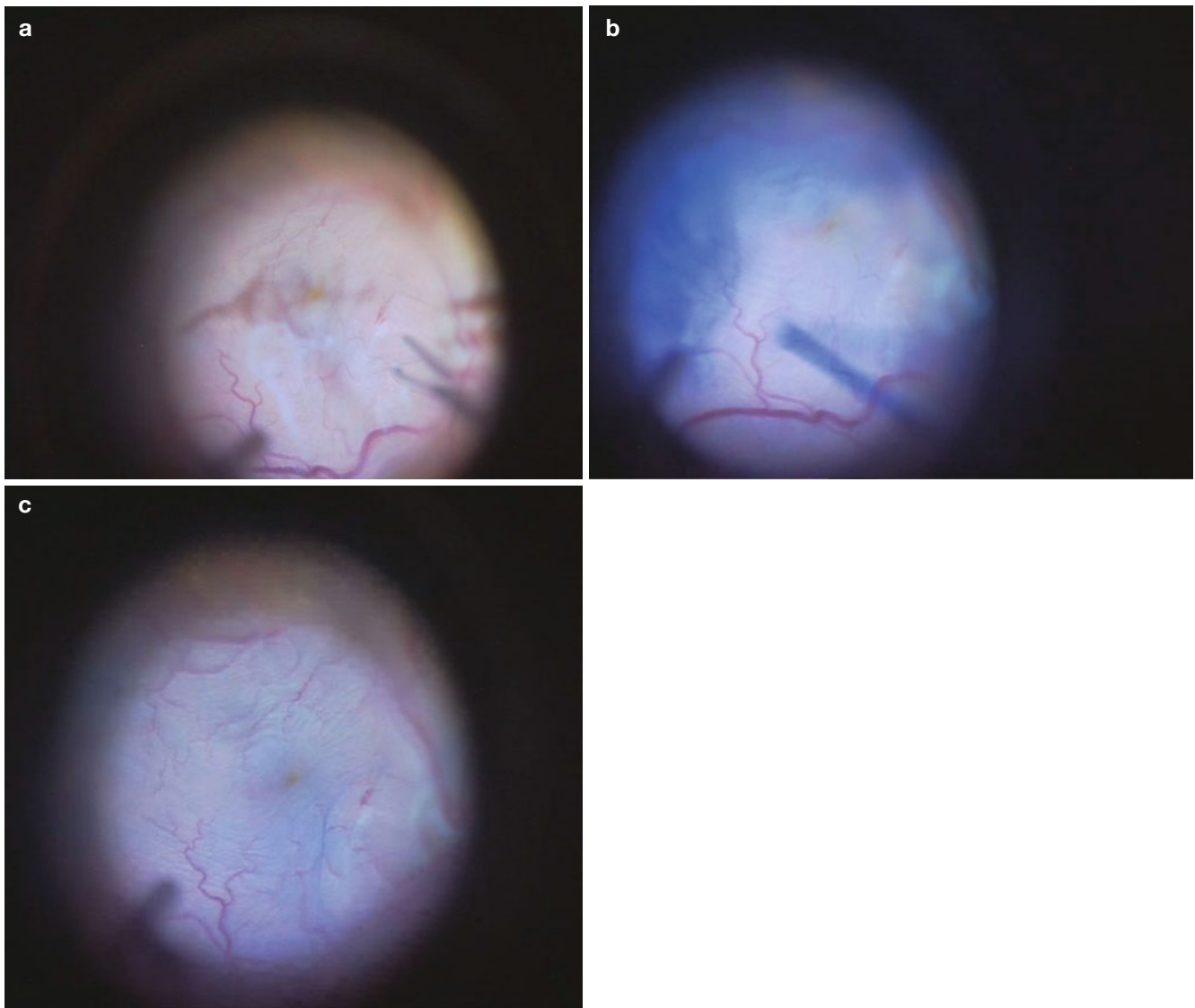


Figure V.A.3-7 Sequential peeling of the unstained premacular membrane (a), followed by an injection of brilliant blue in order to identify the remnant ILM (b). Note that the ILM is completely present in this case after the premacular membrane had been removed (c)

2. Double Staining

It has also been described in the literature to first inject trypan blue to stain and remove the premacular membrane, followed by a selective ILM dye to visualize the ILM. This technique is referred to as the “double staining technique” [51]. However, in most cases premacular membranes can be identified easily and be peeled off in a controlled fashion even without dye application. Therefore, one may question whether it is necessary to apply vital dyes to stain and remove premacular tissue in cases of macular pucker. It may well be sufficient to remove premacular tissue without dye assistance and limit the use of the dye to visualize ILM. As we do not completely understand the interactions of the dyes applied during surgery and the stained tissue as well as the underlying neurosensory retina, it seems advisable to use

these adjuncts carefully and limit their administration as much as possible with respect to potential toxic effects. In addition, as there is no standardized protocol for dye application at the vitreoretinal interface, modes of application, exposure times, and concentrations may vary and should also be taken into account.

III. Tissue-Dye Interaction: Staining and Beyond

The ILM is at present the most relevant target structure in vitreo-macular surgical interventions (see chapter II.E. Vitreoretinal interface and ILM). It is due to its high rigidity that this transparent and delicate structure of only 0.01–0.3 μm

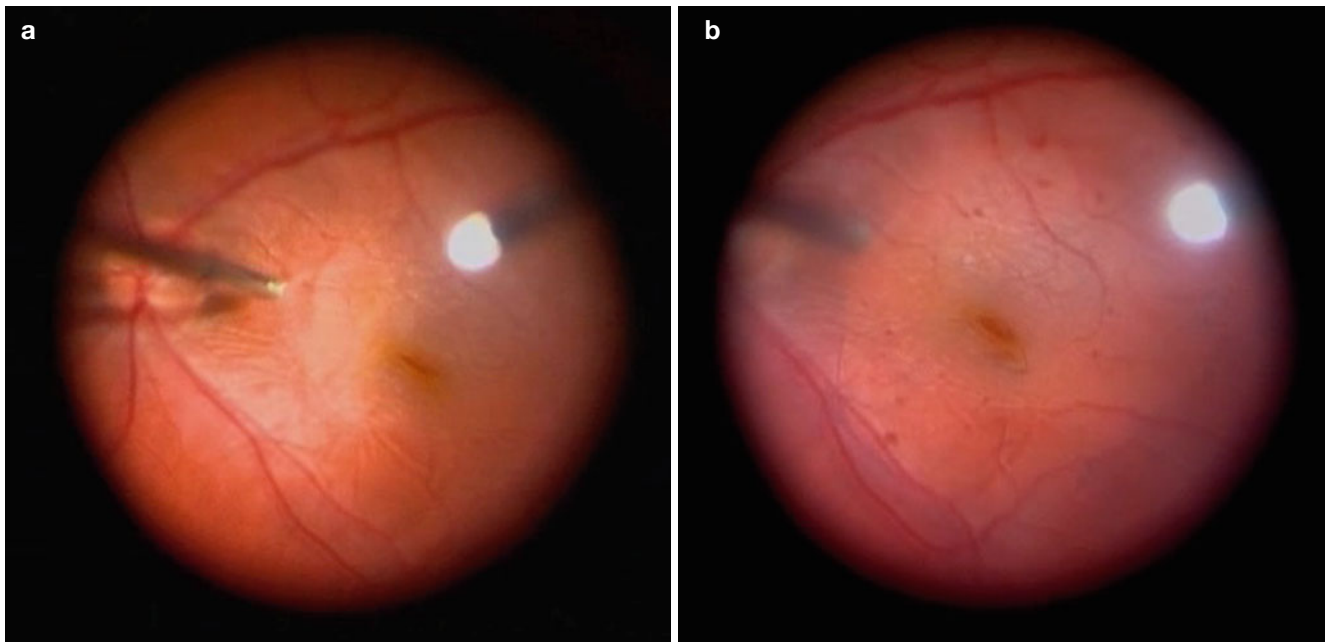


Figure V.A.3-8 Sequential peeling of the unstained premacular membrane (a). Note that the ILM has been completely removed along with the premacular tissue in this case. The borders of the area of peeled ILM can be nicely seen (b)

thickness [52] can be peeled using a forceps at all. Halfter and coworkers previously demonstrated that the mechanical strength of the ILM is very similar to articular cartilage [53–55]. It has also been reported that the retinal aspect of the ILM is approximately fivefold stiffer than the vitreous surface of the ILM, which explains why the ILM curls up toward the vitreous side during peeling [56, 57]. Interestingly, the stained ILM can be peeled off more easily and often in larger fragments compared to the unstained tissue. This observation holds true both for indocyanine green as well as brilliant blue. It is therefore obvious that there are other modes of interaction of the dyes and the tissue beyond the obvious better visualization. Ongoing studies using atomic force microscopy (AFM) have shown that both indocyanine green and brilliant blue significantly increase the stiffness of the ILM, an effect that was more pronounced for ICG [57]. It remains rather hypothetical what the underlying mechanism may be. Former studies focused on indocyanine green, a dye with known photosensitizing properties, which according to the present knowledge are likely to contribute to the adverse effects observed in experimental and clinical trials [42, 58]. Wollensak and coworkers reported an increased stiffness of the ICG-stained and illuminated porcine ILM, showing a significant increase in ultimate force and a decrease in ultimate elongation [59, 60]. They concluded that the stiffening effect of ICG is related to a photosensitizing effect of ICG by the formation of a triplet state of the ICG molecule and reactive oxygen species (type I reaction of photooxidation) [59, 61], which then lead to photooxidative damage of cells and

physical cross-linking of collagen fibers such as the type IV collagen of the ILM [59, 60]. However, other still unknown effects need to be considered, as increased rigidity is clinically also seen for brilliant blue, a triarylmethane dye without photosensitizing properties.

IV. Clinicopathological Correlations

ICG was the first dye to be introduced for ILM staining and soon became a subject of debate, as its administration appeared to be associated with peculiar alterations of the retinal pigment epithelium, less favorable functional outcome, and a high incidence of visual field defects, at least in some clinical studies as mentioned above. The underlying pathogenic mechanisms are somewhat hypothetical, but it seems very likely that adverse events are related to phototoxicity and the decomposition products of the ICG molecule after illumination as several studies have now indicated [62].

Histological evaluations of ILM specimens obtained during indocyanine green-assisted macular surgery revealed the presence of larger cellular fragments and greater amount of retinal debris as well as entire cell bodies adherent to the retinal surface of the ILM compared to unstained specimens. It was concluded that the use of indocyanine green resulted in an alteration of the cleavage plane from the retinal surface of the ILM to the innermost retinal layers [37, 63]. However, small cellular retinal fragments in a lesser

degree were also seen after conventional ILM peeling in microscopic studies as well as immunohistochemical studies [64] and appeared confined to areas of folded ILM in specimens obtained during surgery for premacular membranes [65]. These cellular fragments were attributed to glial cells and neuronal cell debris, in particular Müller cell end feet and cell fragments of the retinal nerve fiber layer. It was suggested that this observation might be on one hand somewhat inevitable due to the intimate association of the Müller cell end feet with the ILM, which represent their basal lamina. On the other hand, it was suggested that the increased rigidity of a multilayered structure such as a premacular membrane compared to the bare ILM may be accountable, and the presence of retinal debris was interpreted as the result of a mechanical trauma and disruption of cellular elements during peeling [65].

Recently, Kenawy et al. [66] confirmed that the plane of separation during ILM peeling for preretinal membrane surgery may be altered, although not related to the use of the dye, but should be interpreted as a result of the premacular membrane formation or of the macular pucker-inducing pathology such as the modulation of GFAP within Müller cells or the continuity between components of premacular membranes and the retina through pores of the ILM, which may increase the adhesion forces between these cells and the ILM [66, 67].

V. Future Perspectives

Looking at future trends in vitreo-macular surgery and the place of chromodissection within this field, the previous problem of whether to use ICG or not was actually solved by the introduction of alternative dyes such as brilliant blue, which are no longer off label, but commercially available in many countries. Although the concept of ILM peeling is currently widely accepted by vitreoretinal surgeons for successful treatment of tractional vitreo-maculopathies such as macular holes or macular pucker, there is growing evidence that we do not have to peel the ILM in all cases of macular holes, especially smaller macular holes which may be closed by a complete induction of a posterior vitreous detachment (PVD) and removal of preretinal tissue if present. In addition, the concept of pharmacologic vitreolysis has emerged and may help to relieve tractional forces and induce PVD by an intravitreal injection without further vitreoretinal surgery [68–70]. That notwithstanding, vital dyes will remain important adjuncts for vitreoretinal surgeons. Alternative dyes and dye classes are currently under investigation to better understand the effects of a dye on retinal tissue and function. In addition, new concepts of staining and absorption versus fluorescence are being evaluated.

Abbreviations

AFM	Atomic force microscopy
BB	Brilliant blue
FDA	Food and Drug Administration
GFAP	Glial fibrillary acidic protein
ICG	Indocyanine green
ILM	Inner limiting membrane
NIR	Near infrared
PVD	Posterior vitreous detachment
TB	Trypan blue

References

1. Haritoglou C, Sebag J. Indications and considerations for chromodissection. *Retinal Physician*. 2014;11(5):34–9.
2. Haritoglou C, Freyer W, Priglinger SG, Kampik A. Light absorbing properties of indocyanine green (ICG) in solution and after adsorption to the retinal surface: an ex-vivo approach. *Graefes Arch Clin Exp Ophthalmol*. 2006;244:1196–202.
3. Fineman MS, Maguire JL, Fineman SW, Benson WE. Safety of indocyanine green angiography during pregnancy: a survey of the retina, macula, and vitreous societies. *Arch Ophthalmol*. 2001;119:353–5.
4. Xiao Y, Wang YH, Fu ZY, Hong H. Staining the anterior capsule with indocyanine green or trypan blue for capsulorrhexis in eyes with white cataract. *Int Ophthalmol*. 2004;25:273–6.
5. Kadosono K, Itoh N, Uchio E, Nakamura S, Ohno S. Staining of the internal limiting membrane in macular hole surgery. *Arch Ophthalmol*. 2000;118:1116–8.
6. Gandorfer A, Messmer EM, Ulbig MW, Kampik A. Indocyanine green selectively stains the internal limiting membrane. *Am J Ophthalmol*. 2001;131:387–8.
7. Da Mata AP, Burk SE, Foster RE, Riemann CD, Petersen MR, Nehemy MB, Augsburger JJ. Long-term follow-up of indocyanine green-assisted peeling of the retinal internal limiting membrane during vitrectomy surgery for idiopathic macular hole repair. *Ophthalmology*. 2004;111:2246–53.
8. Hillenkamp J, Saikia P, Gora F, Sachs HG, Lohmann CP, Roeder J, Baumler W, Gabel VP. Macular function and morphology after peeling of idiopathic epiretinal membrane with and without the assistance of indocyanine green. *Br J Ophthalmol*. 2005;89:437–43.
9. Husson-Danan A, Glacet-Bernard G, Soubrane G, Coscas G. Clinical evaluation of the use of indocyanine green for peeling the internal limiting membrane in macular hole surgery. *Graefes Arch Clin Exp Ophthalmol*. 2006;244:291–7.
10. Horobin RW, Kiernan JA, editors. *Conn's biological stains*. 10th ed. Oxford: Published for the Biological Stain Commission by BIOS Scientific Publishers; 2002.
11. Sanchez R, Risopatron J, Sepulveda G, Pena P, Miska W. Evaluation of the acrosomal membrane in bovine spermatozoa – effects of proteinase inhibitors. *Theriogenology*. 2005;43:761–8.
12. Osaka K, Tyurina YY, Dubey PK, Tyurin VA, Ritov VB, Quinn PJ, Branch RA, Kagan VE. Amphotericin B as an intracellular antioxidant. Protection against 2,2-azobis (2,4-dimethylvaleronitrile) induced peroxidation of membrane phospholipids in rat aortic smooth muscle cells. *Biochem Pharmacol*. 1997;54:937–45.
13. Callebaut M, Vakaet L. Fluorescent yolk marking of the primary gonocytes in quail blastoderms by administration of trypan blue during late oogenesis. *ICRS Med Sci Biochem*. 1981;9:458.

14. Baskaya MK, Rao AM, Dogan A, Donaldson D, Dempsey RJ. The biphasic opening of the blood-brain barrier in the cortex and hippocampus after traumatic brain injury in rats. *Neurosci Lett*. 1997;226:33–6.
15. Berman RS, Martin W. Arterial endothelial barrier dysfunction: actions of homocysteine and the hypoxanthine-xanthine oxidase free radical generating system. *Br J Pharmacol*. 1993;108:920–6.
16. Huser M, Stegemann E, Kammermeier H. Is enzyme release a sign of irreversible injury of cardiomyocytes? *Life Sci*. 1996;58:545–50.
17. Kozłowska H, Drewa G, Grzanka A. Effect of trypan blue on the activity of lysosomal enzymes, tumor growth and cell ultrastructure in B16 melanotic melanoma in mice. *Neoplasma*. 1995;42:173–8.
18. Yetik H, Devranoglu K, Ozkan S. Determining the lowest trypan blue concentration that satisfactorily stains the anterior capsule. *J Cataract Refract Surg*. 2002;28:988–91.
19. Georgiadis N, Kardasopoulos A, Bufidis T. The evaluation of corneal graft tissue by the use of trypan blue. *Ophthalmologica*. 1999; 213:8–11.
20. Jacob S, Agarwal A, Agarwal S, Chowdhary S, Chowdhary R, Bagmar AA. Trypan blue as an adjunct for safe Phacoemulsification in eyes with white cataract. *J Cataract Refract Surg*. 2002;28:1819–25.
21. Melles GR, de Waard PW, Pameijer JH, Beekhuis WH. Staining the lens capsule with trypan blue for visualizing capsulorhexis in surgery of mature cataracts. *Klin Monatsbl Augenheilkd*. 1999;215: 342–4.
22. Perrier M, Sebag M. Trypan blue-assisted peeling of the internal limiting membrane during macular hole surgery. *Am J Ophthalmol*. 2003;135:903–5.
23. Ueno A, Hisatomi T, Enaida H, Kagimoto T, Mochizuki Y, Goto Y, Kubota T, Hata Y, Ishibashi T. Biocompatibility of brilliant blue G in a rat model of subretinal injection. *Retina*. 2007;27:499–504.
24. Enaida H, Hisatomi T, Hata Y, Ueno A, Goto Y, Yamada T, Kubota T, Ishibashi T. Brilliant blue G selectively stains the internal limiting membrane/brilliant blue G-assisted membrane peeling. *Retina*. 2006;26:631–6.
25. Enaida H, Hisatomi T, Goto Y, Hata Y, Ueno A, Miura M, Kubota T, Ishibashi T. Preclinical investigation of internal limiting membrane staining and peeling using intravitreal brilliant blue G. *Retina*. 2006;26:623–30.
26. Lüke M, Januschowski K, Beutel J, Lüke C, Grisanti S, Peters S, Jaissle GB, Bartz-Schmidt KU, Szurman P. Electrophysiological effects of Brilliant Blue G in the model of the isolated perfused vertebrate retina. *Graefes Arch Clin Exp Ophthalmol*. 2008;246(6):817–22.
27. Remy M, Thaler S, Schumann RG, May CA, Fiedorowicz M, Schüttauf F, Grüterich M, Priglinger SG, Nentwich M, Kampik A, Haritoglou C. An in-vivo evaluation of Brilliant Blue G in animals and humans. *Br J Ophthalmol*. 2008;92:1142–7.
28. Kawahara S, Hata Y, Miura M, Kita T, Sengoku A, Nakao S, Mochizuki Y, Enaida H, Ueno A, Hafezi-Moghadam A, Ishibashi T. Intracellular events in retinal glial cells exposed to ICG and BBG. *Invest Ophthalmol Vis Sci*. 2007;48:4426–32.
29. Haritoglou C, Priglinger SG, Eibl K, Liegl R, May CA, Thaler S, Kampik A, Schuettauf F. Experimental evaluation of aniline and methyl blue for intraocular surgery. *Retina*. 2009;29:166–73.
30. Haritoglou C, Schumann RG, Kampik A, Gandorfer A. Heavy brilliant blue G for internal limiting membrane staining. *Retina*. 2011;31(2):405–7.
31. Henrich PB, Valmaggia C, Lang C, Priglinger SG, Haritoglou C, Strauss RW, Cattin PC. Contrast recognizability during brilliant blue G – and heavier-than-water brilliant blue G-assisted chromovitrectomy: a quantitative analysis. *Acta Ophthalmol*. 2013;91(2):e120–4.
32. Henrich PB, Priglinger SG, Haritoglou C, Josifova T, Ferreira PR, Strauss RW, Flammer J, Cattin PC. Quantification of contrast recognizability during brilliant blue G (BBG) and indocyanine green (ICG) assisted chromovitrectomy. *Invest Ophthalmol Vis Sci*. 2011;52(7):4345–9.
33. Jackson TL, Griffin L, Vote B, Hillenkamp J, Marshall J. An experimental method for testing novel retinal vital stains. *Exp Eye Res*. 2005;81(4):446–54.
34. Rodrigues EB, Penha FM, de Paula Fiod Costa E, Maia M, Dib E, Moraes Jr M, Meyer CH, Magalhaes Jr O, Melo GB, Stefano V, Dias AB, Farah ME. Ability of new vital dyes to stain intraocular membranes and tissues in ocular surgery. *Am J Ophthalmol*. 2010; 149(2):265–77.
35. Haritoglou C, Strauss R, Priglinger SG, Kreutzer T, Kampik A. Delineation of the vitreous and posterior hyaloid using bromophenol blue. *Retina*. 2008;28:333–40.
36. Tsuiki E, Fujikawa A, Miyamura N, Yamada K, Mishima K, Kitaoka T. Visual field defects after macular hole surgery with indocyanine green-assisted internal limiting membrane peeling. *Am J Ophthalmol*. 2007;143(4):704–5.
37. Haritoglou C, Gandorfer A, Gass CA, Schaumberger M, Ulbig MW, Kampik A. Indocyanine green-assisted peeling of the internal limiting membrane in macular hole surgery affects visual outcome: a clinicopathologic correlation. *Am J Ophthalmol*. 2002;134(6): 836–41.
38. Rodrigues EB, Meyer CH. Meta-analysis of chromovitrectomy with indocyanine green in macular hole surgery. *Ophthalmologica*. 2008;222(2):123–9.
39. Yam HF, Kwok AKH, Chan KP, Lai TYY, Chu KY, Lam DSC, Pang CP. Effect of indocyanine green and illumination on gene expression in human retinal pigment epithelial cells. *Invest Ophthalmol Vis Sci*. 2003;44:370–7.
40. Langhals H, Haritoglou C. Chemical and spectroscopic aspects of the application of dyes in vitreoretinal surgery. *Ophthalmologie*. 2009;106(1):16–20.
41. Yip HK, Lai TY, So KF, Kwok AK. Retinal ganglion cells toxicity caused by photosensitizing effects of intravitreal indocyanine green with illumination in rat eyes. *Br J Ophthalmol*. 2006;90:99–102.
42. Sato T, Ito M, Ishida M, Karasawa Y. Phototoxicity of indocyanine green under continuous fluorescent lamp illumination and its prevention by blocking red light on cultured Müller cells. *Invest Ophthalmol Vis Sci*. 2010;51(8):4337–45.
43. Langhals H, Varja A, Laubichler P, Kernt M, Eibl K, Haritoglou C. Cyanine dyes as optical contrast agents for ophthalmological surgery. *J Med Chem*. 2011;54(11):3903–25.
44. Sebag J, Gupta P, Rosen R, Garcia P, Sadun AA. Macular holes and macular pucker: The role of vitreoschisis as imaged by optical coherence tomography/scanning laser ophthalmoscopy. *Trans Am Ophthalmol Soc*. 2007;105:121–31.
45. Gupta P, Yee KMP, Garcia P, Rosen RB, Parikh J, Hageman GS, Sadun AA, Sebag J. Vitreoschisis in macular diseases. *Br J Ophthalmol*. 2011;95(3):376–80.
46. Kampik A, Green WR, Michels RG, et al. Ultrastructural features of progressive idiopathic epiretinal membrane removed by vitreous surgery. *Am J Ophthalmol*. 1980;90:797–809.
47. Kwok AK, Lai TY, Yuen KS. Epiretinal membrane surgery with or without internal limiting membrane peeling. *Clin Exp Ophthalmol*. 2005;33:379–85.
48. Maguire AM, Smiddy WE, Nanda SK, et al. Clinicopathologic correlation of recurrent epiretinal membranes after previous surgical removal. *Retina*. 1990;10:213–22.
49. Shimada H, Nakashizuka H, Hattori T, et al. Double staining with brilliant blue G and double peeling for epiretinal membranes. *Ophthalmology*. 2009;116:1370–6.
50. Schumann RG, Gandorfer A, Eibl KH, Henrich PB, Kampik A, Haritoglou C. Sequential epiretinal membrane removal with internal limiting membrane peeling in brilliant blue G-assisted macular surgery. *Br J Ophthalmol*. 2010;94(10):1369–72.
51. Stalmans P, Freon EJ, Parys-Van Ginderdeuren R, et al. Double vital staining using trypan blue and infracyanine green in macular pucker surgery. *Br J Ophthalmol*. 2003;87:713–6.

52. Streeten BA. Disorders of the vitreous. In: Garner A, Klintworth GK, editors. Pathophysiology of ocular disease – a dynamic approach, part B. New York: Marcel Dekker; 1982. p. 1381–419.
53. Halfter W, Dong S, Dong A, Eller AW, Nischt R. Origin and turnover of ECM proteins from the inner limiting membrane and vitreous body. *Eye*. 2008;22(10):1207–13.
54. Candiello J, Balasubramani M, Schreiber EM, Cole GJ, Mayer U, Halfter W, Lin H. Biomechanical properties of native basement membranes. *FEBS J*. 2007;274(11):2897–908.
55. Halfter W, Candiello J, Hu H, Zhang P, Schreiber E, Balasubramani M. Protein composition and biomechanical properties of in vivo-derived basement membranes. *Cell Adh Migr*. 2013;7(1):64–71.
56. Henrich PB, Monnier CA, Halfter W, Haritoglou C, Strauss RW, Lim RY, Loparic M. Nanoscale topographic and biomechanical studies of the human internal limiting membrane. *Invest Ophthalmol Vis Sci*. 2012;53(6):2561–70.
57. Haritoglou C, Mauell S, Benoit M, Schumann RG, Henrich PB, Wolf A, Kampik A. Vital dyes increase the rigidity of the internal limiting membrane. *Eye (Lond)*. 2013;27(11):1308–15. doi:[10.1038/eye.2013.178](https://doi.org/10.1038/eye.2013.178).
58. Hillenkamp J, Dydykina S, Klettner A, Treumer F, Vasold R, Bäumler W, Roider J. Safety testing of indocyanine green with different surgical light sources and the protective effect of optical filters. *Retina*. 2010;30(10):1685–91.
59. Wollensak G. Biomechanical changes of the internal limiting membrane after indocyanine green staining. *Dev Ophthalmol*. 2008;42:82–90.
60. Wollensak G, Spoerl E, Wirbelauer C, Pham DT. Influence of indocyanine green staining on the biomechanical strength of porcine internal limiting membrane. *Ophthalmologica*. 2004;218(4):278–82.
61. Foote CS. Definition of type I and type II photosensitized oxidation. *Photochem Photobiol*. 1991;54:659.
62. Engel E, Schraml R, Maisch T, Kobuch K, König B, Szeimies RM, Hillenkamp J, Bäumler W, Vasold R. Light-induced decomposition of indocyanine green. *Invest Ophthalmol Vis Sci*. 2008;49(5):1777–83.
63. Gandorfer A, Haritoglou C, Gandorfer A, Kampik A. Retinal damage from indocyanine green in experimental macular surgery. *Invest Ophthalmol Vis Sci*. 2003;44:316–23.
64. Eckardt C, Eckardt U, Groos S, Luciano L, Reale E. Removal of the internal limiting membrane in macular holes. Clinical and morphological findings. *Ophthalmologe*. 1997;94(8):545–51.
65. Haritoglou C, Gandorfer A, Gass CA, Schaumberger M, Ulbig MW, Kampik A. The effect of indocyanine-green on functional outcome of macular pucker surgery. *Am J Ophthalmol*. 2003;135:328–37.
66. Kenawy N, Wong D, Stappler T, Romano MR, Das RA, Hebbar G, Prime W, Heimann H, Gibran SK, Sheridan CM, Cheung YH, Hiscott PS. Does the presence of an epiretinal membrane alter the cleavage plane during internal limiting membrane peeling? *Ophthalmology*. 2010;117(2):320–3.
67. Gandorfer A, Schumann R, Scheler R, Haritoglou C, Kampik A. Pores of the inner limiting membrane in flat-mounted surgical specimens. *Retina*. 2011;31(5):977–81.
68. Sebag J. Pharmacologic vitreolysis. *Retina*. 1998;18:1–3.
69. Sebag J. Is pharmacologic vitreolysis brewing? *Retina*. 2002;22:1–3.
70. Sebag J. Pharmacologic vitreolysis – premise and promise of the first decade. *Retina*. 2009;29:871–4.

Macular Hole and Macular Pucker Surgery with Special Emphasis on Reoperations*

V.A.4.

Billy X. Pan, Kenneth M.P. Yee, Fred N. Ross-Cisneros, Alfredo A. Sadun, and J. Sebag

Outline

- I. **Introduction**
- II. **Macular Hole**
 - A. Pathogenesis of Macular Hole
 - B. Therapy of Macular Hole
 - 1. Macular Hole Surgery
 - a. Benefits and Risks of ILM Chromodissection
 - C. Primary Failure Versus Macular Hole Reopening
- III. **Macular Pucker**
 - A. Pathogenesis of Macular Pucker
 - B. Macular Pucker Surgery
 - C. Primary Failure Versus Macular Pucker Recurrence
- IV. **Retreatment of Persistent/Recurrent Disease**
 - A. Retreatment Strategies
 - 1. Macular Hole Reoperations
 - 2. Macular Pucker Reoperations
 - B. Inner Retinal Optic Neuropathy (IRON)
 - C. Timing of Reoperations

References

* The original material in this chapter was accepted for publication by Investigative Ophthalmology and Visual Science on September 8, 2014.

B.X. Pan, MD • K.M.P. Yee, BS
J. Sebag, MD, FACS, FRCOphth, FARVO (✉)
VMR Institute for Vitreous Macula Retina,
7677 Center Avenue, suite 400,
Huntington Beach, CA 92647, USA

Doheny Eye Institute, Los Angeles, CA, USA
e-mail: kennethmpy@gmail.com; jsebag@VMRinstitute.com

F.N. Ross-Cisneros, BS • A.A. Sadun, MD, PhD, FARVO
Doheny Eye Institute/UCLA, Los Angeles, CA, USA
e-mail: alfredo.sadun@gmail.com

Keywords

Vitreous • Anomalous PVD • Vitreoschisis • Inner limiting membrane • Premacular membrane (PMM, previously ERM) • Macular hole • Macular pucker • Vitrectomy • Treatment failure • Disease recurrence • Re-Operation • Chromodissection • Inner retinal optic neuropathy

Key Concepts

1. Vitrectomy with membrane peeling for macular pucker and chromodissection for macular holes is a highly successful operation. Failures are typically due to persistent membranes related to vitreoschisis or recurrent membranes.
2. Reoperation is typically performed using inner limiting membrane peeling, typically with chromodissection and usually with good success. Rare cases of poor postoperative vision, either in primary procedures or more commonly in reoperations, are due to dissection that is too deep, injuring the retinal nerve fiber layer inducing a secondary optic neuropathy referred to as IRON (inner retinal optic neuropathy).
3. Reoperations performed later than 6 months following the initial procedure have a lower likelihood of retinal nerve fiber layer injury and IRON with a higher likelihood of good vision, probably due to an adequate enough time between the two operations for Müller cells to organize their fibrillar processes allowing the reformation of a protective tissue layer over the denuded retinal nerve fiber layer.

I. Introduction

Recent advances in the techniques of vitrectomy with membrane peeling [See chapter V.A.2. Vitreo-maculopathy surgery], at times with chromodissection [See chapter V.A.3. Chromodissection in vitreo-retinal surgery], have greatly improved patient outcomes. There are, however, risks associated with these procedures, and on rare occasions there can be much worse vision following surgery than preoperatively. This chapter will review the current concepts of pathogenesis and surgical management of macular holes and macular pucker. Special emphasis will be placed on failed cases and reoperations.

II. Macular Hole

A. Pathogenesis of Macular Hole

There are differing theories on the mechanism of macular hole formation, though central to all of them is the idea that tractional forces by vitreous induce structural defects in the macula. Anteroposterior traction can be exerted by a firmly attached posterior vitreous cortex (PVC) [1–3], and tangential traction can be induced by a premacular membrane (PMM) [4] that consists of the PVC plus cells and additional collagen synthesized by some of these cells. Under normal conditions, the central cone of Müller cells provides structural support and binds together foveal photoreceptor cells in the fovea centralis [5]. Tractional forces exerted by the PVC can dislodge the Müller cell cone from its photoreceptor attachments [1–3]. The formation of a foveal cyst progresses to a weakening of the roof of the cystic cavity and eventually to complete dehiscence [1]. The underlying neurosensory retina, now without Müller cell support, undergoes centrifugal expansion to form a full-thickness hole [5, 6]. There is elevation of the edges at times and almost always the appearance of pericentral cystoid spaces on optical coherence tomography (OCT) imaging [7, 8], previously believed to be retinal detachment. Macular holes are also no longer considered idiopathic as they are known to be caused by vitreous [9, 10], at times associated with high myopia, status post trauma (usually blunt force), or other retinal pathologies (tears, detachments), and rarely iatrogenic after posterior segment surgery [11] [See chapter III.C. Pathology of vitreo-maculopathies]. A new classification system of vitreo-macular traction and macular holes reflects the important role of vitreous [See chapter III.D. Vitreo-macular adhesion/traction and macular holes (Pseudo, Lamellar & Full-Thickness Holes)].

B. Therapy of Macular Hole

Until the 1990s, the only macular holes that were usually treated were those with retinal detachments. Meyer-Schwickerath, in 1961, utilized a combination of scleral

buckling, laser photocoagulation, and subretinal fluid drainage to flatten a macular hole retinal detachment [12]. Two decades later success was also attained without scleral buckling [13]. Early on, laser photocoagulation was attempted to treat macular holes even without retinal detachment [14–16], but this approach was never widely adopted and was subsequently abandoned when vitrectomy surgery proved to be the treatment of choice.

1. Macular Hole Surgery

In 1991 Neil Kelly and Rob Wendel published their initial experience with vitrectomy for macular hole closure [17], introducing for the first time a definitive treatment for a disease previously believed to be incurable [18]. Starting from an initial published cure rate of 58 %, the team was able to improve their success rates to 73 % after 2 years of practice [17, 19]. The initial procedure consisted of a pars plana vitrectomy with peeling of the PVC and any visible PMM to release vitreous traction that was thought to cause the macular hole. This was followed by a long-acting intraocular tamponade with prone positioning under the assumption that fluid was the cause and that this would keep the hole free of fluid, but also to allow apposition of the separated edges and provide structural bridging for fibrocellular proliferation [17, 19].

A number of randomized controlled trials have studied the natural history at different stages of macular holes. The primary aim of these studies was to determine whether observation alone would result in better outcomes compared to surgical management. The Vitrectomy for Prevention of Macular Hole (VPMH) study group looked at stage 1 macular holes and found that the benefit from a vitrectomy would likely be minimal as most do not progress to full-thickness holes. Indeed, many stage 1 holes self-resolve, particularly if smaller than 250 μm , thus making the case for conservative management [20]. The Moorfields Macular Hole Study (MMHS) studied stage 2, 3, and 4 holes and found an overall closure rate of 80.6 % in the surgical group versus 11.5 % in the observation alone group at 24 months follow-up. Additionally, eyes that underwent surgery had improved final Snellen visual acuity (6/36 to 6/18) compared to the group with observation alone, which had visual deterioration (6/36 to 6/60) [21]. The Vitrectomy for Treatment of Macular Hole Study (VMHS) investigated stage 3 and 4 holes and found a closure rate of 69 % in the surgical group versus 4 % in the observation alone group at 6 months. The final visual acuity from the surgical group was also statistically better than the observation alone group (20/115 versus 20/166 on an ETDRS chart, respectively) [22]. Thus, both the MMHS and VMHS studies showed clear benefit from surgical management of stage 3 and 4 holes [21, 22]. Furthermore, since the first published studies by Kelly and Wendel, vitreoretinal specialists have continued to refine the surgical technique resulting in closure rates that have continually increased over the years.

a. Benefits and Risks of ILM Chromodissection

Inner limiting membrane (ILM) peeling was introduced and hypothesized to assist in macular hole closure by ensuring complete removal of residual posterior vitreous cortex and subclinical PMMs [23]. Vitreoschisis, a common event that occurs in diabetic eyes, but also in at least half of eyes with macular holes and macular pucker [10, 24], may give the appearance of vitreous separation while tractional forces actually persist [10, 24–26]. The removal of a potential scaffold for contractile tissue to redevelop upon and once again exert tangential traction, as well as the micro-trauma induced by an ILM peel which is thought to enhance the localized fibrocellular proliferation needed for glial repair [27–29], is believed to prevent future macular hole reopening [30, 31]. Furthermore, the development of cystoid macular edema has been associated with the reopening of a macular hole, and the removal of the ILM can be prophylactic against edema formation [32, 33]. Finally, studies have shown that the duration of facedown positioning can be reduced or even eliminated in cases where an ILM peel is performed, an important consideration in patients who may have difficulty complying with a prone positioning regimen [34–37].

Mester and Kuln performed a meta-analysis of 1,654 macular holes and found that ILM peeling resulted in primary hole closure rates of 96 % versus 77 % in eyes without peeling [38]. Tognetto et al, in a multicenter retrospective study of 1,627 macular holes, found a 94 % primary closure rate in eyes undergoing an ILM peel, versus 89 % without peeling [39]. Kumagai et al. studied 877 eyes with macular hole and found a 0.39 % recurrence rate of holes after ILM peeling compared to a 7.2 % recurrence rate without peeling [40]. More recently, a number of randomized clinical trials have looked at the effects of ILM peeling on primary closure and subsequent reopening of the hole. A multicenter randomized clinical trial by Lois et al. (the FILMS group) looked at 141 eyes with stage 2 or 3 idiopathic full-thickness macular holes. The group found a significantly higher rate of primary hole closure in the ILM-peel group at 1 month follow-up (84 % vs. 48 %) and also fewer reoperations necessary at 6 months (12 % vs. 48 %) [41]. Two smaller such trials in China (49 patients) and Denmark (75 patients) found similar anatomic benefits from ILM peeling [35, 42].

While there are clear benefits to anatomical outcome in terms of improved primary closure and reduced chances for reopening, the effects on functional outcome are less well established. In a number of studies, an improvement in post-operative visual acuity has been described [38, 43–45], while in other studies, results were not statistically significant [39, 46–48]. It should be noted, however, that ILM peeling itself is a risky procedure which can result in complications such as the formation of micro-hemorrhages, defects in the retinal

pigment epithelium, damage to the neurosensory retina resulting in scotomata, phototoxicity from prolonged surgical manipulation, and possible toxic effects from dyes used to assist in the procedure [49, 50], known as chromodissection [51] [See chapter V.A.3. Chromodissection in vitreo-retinal surgery]. Furthermore, it has been suggested that multiple unsuccessful attempts at ILM peeling often lead to a poor functional outcome despite successful anatomic closure [52].

Because of the ILM's close proximity to the underlying neurosensory retina, inadvertent injury to the retinal nerve fiber layer (RNFL) is not uncommon [49, 52, 53]. To standardize the procedure and reduce possible trauma resulting from membrane peeling, vital dyes have been introduced to stain the ILM for better visibility. Indocyanine green (ICG) is the most commonly utilized vital dye for chromodissection of the ILM and has been shown to decrease the amount of time it takes to remove the membrane, as well as increase the ability to perform a thorough peel. However, the use of ICG is controversial as some studies have suggested potential side effects including worsening of the functional outcome despite enhanced rates of successful anatomic closure [54, 55]. The inconsistency of literature regarding the outcomes of ICG-assisted peels is likely related to the broad range of dye concentrations and durations of application used by different surgeons [56]. Though the exact dose and duration is surgeon-specific, it is agreed that the lowest concentration for the least amount of exposure time is ideal [57].

C. Primary Failure Versus Macular Hole Reopening

One of the complications associated with macular hole surgery is primary surgical failure, an event that has decreased in frequency with the progressive refinement of surgical techniques. The only preoperative factor that has been definitively shown to be predictive of primary failure is the size of the hole, where there is an inverse relationship between size and closure rates [21]. Rarely does surgery cure macular holes greater than 400 μm in diameter. Disease chronicity may also have an impact on closure success, with primary holes of <6 months' duration being easier to successfully treat [21]. Evidence for the importance of chronicity is not strong, however, as the duration of symptoms is a notoriously subjective measure. Furthermore, based on the aforementioned MMHS and VMHS studies, it is apparent that surgery is far superior to conservative management for stages 2–4 holes. Thus, in these cases, delaying intervention may result in a poorer prognosis [21, 22].

Failure to surgically close macular holes primarily is believed to be due an inability to form a stable glial plug. The reason for this may be due to incomplete peeling of

the PVC, the presence of a subclinical PMM resulting in residual traction at the hole, or inadequate gliosis [58, 59]. Schumann et al. studied the ILM and associated PMM removed after a second operation in 16 eyes with macular holes that had failed primary surgery. Ultrastructural analysis revealed a significant amount of fibrocellular proliferation on the vitreous side of the ILM in all specimens, supporting the hypothesis that residual ILM and remnant vitreous cortex may stimulate postoperative traction and surgical failure [60].

The reopening of a macular hole is another potential complication that most often occurs within months of initial successful closure, but can even present years later [43, 58, 61–64]. Just as a PMM can cause immediate surgical failure, its presence and progression has been correlated with a significant portion of recurrent macular holes. Similar to a primary macular hole with traction from the PVC, a PMM is thought to exert tangential traction and cause foveal dehiscence [58, 59]. Cystoid macular edema is also a significant factor associated with as much as a 7-fold increase in the risk of reopening of a previously closed macular hole [33]. The development of cystoid macular edema and the associated inflammatory fibrinolysis has also been proposed as a causative agent for hole reopening [33, 61]. Finally, Kumagai et al. proposed that surgeries complicated by intraoperative retinal tears and also eyes with high degrees of myopia both may be risk factors for macular hole reopening [40, 65].

A complication associated with pars plana vitrectomy is the development and/or progression of cataracts, occurring in up to 76 % of cases at 2 years post vitrectomy [66–70]. Although cataracts themselves are not a serious problem, the subsequent removal of cataracts after macular hole surgery has been associated with hole reopening, usually within 6 months of cataract extraction [33, 61, 63]. The hypothesis for this relates both the risk of developing cystoid macular edema and the risk of PMM formation after cataract surgery due to the same underlying cause – postoperative inflammatory mediators that break down the blood-retinal barrier. To avoid these complications, some retinal surgeons have elected to proceed with a combined macular hole surgery with phacemulsification. These combined surgeries have been shown to be effective and safe without increased risks of adverse events [71–73]. Another factor that has been implicated in the reformation of macular holes is Nd:YAG laser capsulotomy for treatment of posterior capsular opacification. The mechanism of action is thought to be related to perifoveal vitreous contraction associated with the laser pulse [74], but is more likely due to biochemical changes in the vitreous following capsulotomy after cataract surgery [75, 76]. Indeed, YAG capsulotomy has been shown to be associated with nearly a doubling in the incidence of PVD [77], due most likely to the same biochemical changes [78] [See chapters II.C. Vitreous aging and PVD; III.B. Anomalous PVD and Vitreoschisis].

III. Macular Pucker

A. Pathogenesis of Macular Pucker

Premacular membranes are avascular, fibrocellular membranes that develop anterior to the ILM [79, 80]. The literature refers to these membranes as “epiretinal”; however, this term is inappropriate because “epi” refers to a location next to or beside the retina. Thus, the term “epiretinal” could refer to a subretinal as well as preretinal location. In macular pucker, the pathologic membrane location is in front of the retina; thus, the prefix “pre” is more accurate than “epi.” Furthermore, since this membrane forms primarily in front of the macula, or at least is only relevant to vision in front of the macula, the term “premacular membrane” is a more precise term than “epiretinal membrane.” The former term will be used here and elsewhere.

Histopathological studies have shown a number of different cell types to be associated with PMMs depending on the etiology, including glial cells, retinal pigment epithelial cells, myofibroblasts, and macrophages [81–84]. When the proliferation occurs in the region of the macula, it can cause tangential traction and wrinkling of the underlying neurosensory retina, resulting in macular pucker and visual distortion [85–88]. The development of PMM can be primary, i.e., the result of anomalous PVD with vitreoschisis, or secondary, i.e., associated with a number of retinal diseases including retinal breaks, retinal detachment, retinal vascular diseases, diabetic retinopathy, inflammatory conditions, and others [89]. Anomalous PVD with vitreoschisis may indeed be an important mechanism in many of these conditions [See chapter III.B. Anomalous PVD and vitreoschisis].

In the setting of anomalous PVD, vitreoschisis produces a split between the anterior and posterior portions of the PVC, leaving the outermost (posterior) layer attached to the macula [9, 25]. If the vitreoschisis split occurs anterior to the level of hyalocytes (approximately 50–75 μm anterior to the ILM), the hyalocytes embedded in the outer layer can elicit monocyte migration from the circulation and/or undergo transdifferentiation into myofibroblasts as well as secrete collagen, a key component of PMM [90] [See chapter III.J. Cell Proliferation at vitreo-retinal interface in PVR and related disorders]. Based on the anomalous PVD theory proposed by Sebag, if vitreoschisis occurs at a level resulting in hyalocytes that remain attached to the macula, then there is considerable risk of contractile PMM formation and the development of macular pucker [9, 25] [See chapter III.F. Vitreous in the pathobiology of macular pucker].

B. Macular Pucker Surgery

The standard cure for macular pucker is surgical removal of the offending PMM, thus releasing the tangential traction, resulting in resolution of metamorphopsia in most cases

and, less frequently, visual acuity improvement. Prognostic factors associated with a better postoperative visual acuity include a better preoperative visual acuity, better preoperative photoreceptor integrity documented on OCT, and a shorter duration of symptoms [91–93]. Indeed, a number of studies have shown that earlier surgery results in better results postoperatively, perhaps due to a reduced duration of neurosensory disruption [94–96]. Studies employing coronal plane *en face* OCT/SLO imaging identified that there can be as many as 4 centers of retinal contraction in an eye with macular pucker [10, 97]. Cases with 3 or 4 centers had a higher incidence of retinal cysts and more macular thickening than cases with 1 or 2 centers of retinal contraction. Thus, it may be that eyes with more than 2 centers of retinal contraction should undergo surgery sooner.

Surgery involves vitrectomy followed by peeling of the PMM with or without the additional peeling of the ILM. Several studies have shown that PMM removal will concurrently result in unintentional ILM removal. However, the rates of inadvertent ILM stripping vary widely between studies, ranging from 27 to 77 % depending on surgical technique and use of chromodissection [98–102]. Ducournau and Ducournau found that cleavage planes between the ILM and the underlying retina could be easily induced in primary (post-anomalous PVD with vitreoschisis) PMMs, but that the ILM was more difficult to peel in secondary cases of PMM [103]. Thus, in cases of secondary PMM, more aggressive dissection may be required if the intention is to remove the ILM in addition to the PMM. There is some controversy in the literature, however, regarding postoperative visual acuity after ILM peeling in macular pucker surgery. Early papers described poor functional outcomes associated with ILM peeling [84, 104]; however, a considerable body of evidence has since been published that shows no adverse effects from ILM removal in PMM surgery, and indeed a number of studies demonstrate improved visual acuity with ILM removal [101, 105–108]. It is unclear why there is such a discrepancy between early reports and more recent literature on postoperative functional outcomes related to ILM removal, but it is at least partly due to improved surgical techniques, instrumentation, and development of vital dyes that can assist in tissue visualization [See chapter V.A.3. Chromodissection in vitreo-retinal surgery].

C. Primary Failure Versus Macular Pucker Recurrence

Immediate postsurgical failure to resolve metamorphopsia or improve visual acuity after macular pucker surgery is thought to relate to incomplete removal of the PMM, whereas delayed recurrence of symptoms is thought to be due to true disease recurrence. Incomplete removal is most likely due to the lamellar anatomy of the PVC [See chapter II.E. Vitreo-retinal interface and ILM], which can split during surgery

to peel the PMM and relieve the pucker, essentially *intra-operative vitreoschisis*. In this case, membranes are often transparent or semi-transparent [31, 109, 110]. If the PMM forms directly on the ILM and is tightly apposed to it, then it is more likely for both to be peeled together in a single dissection. However, if vitreoschisis occurs, surgical dissection may remove the PMM and inner (anterior) portions of the PVC, while sparing the ILM and residual cortical vitreous and cells. This is even more likely in the setting of an incomplete ILM peel [9, 25, 111]. Fortunately, this issue is currently not as common owing to the use of vital dyes during chromodissection [31, 102, 107, 112]. Furthermore, intraoperative OCT will likely be very useful in mitigating these circumstances [113, 114].

True recurrence, which in our experience only occurs about 10 % of the time, can develop after complete removal of the PMM as a result of cell (primarily glial) migration via breaks in the ILM that were induced during membrane peel surgery and subsequent proliferation of these cells on the anterior surface of the macula [102, 115]. In this regard, the issue of ILM peeling is important because the ILM can serve as a scaffold for the proliferation of another PMM. When the PMM is removed without attempts to further dissect the ILM, rates of recurrence have been reported to be as high as 56 % [101, 106, 115], although it is not known whether these studies distinguished between persistent and recurrent disease, as described above. However, when combined PMM and ILM removal is pursued, recurrence is observed to be less than 9 % [101, 106, 115], more consistent with our experience. The higher incidence of recurrence when PMM removal is performed in isolation may be due to a number of factors. One big risk is that residual ILM provides a scaffold for the re-proliferation of a PMM [100]. Haritoglou et al. found that there was a layer of collagen between the ILM and PMM which helps explain the high rate of PMM recurrence when ILM peeling is not undertaken [116]. Other studies found that recurrent PMMs had a higher frequency of myofibroblasts, supporting the theory that re-proliferation is an important mechanism for pucker recurrence [117]. Gandorfer et al. showed that residual ILM left on the macula contained cells that expressed alpha-smooth muscle actin and were capable of exerting continued tangential traction [100]. Park et al. showed that reformation of a PMM occurs directly on residual ILM [106]. Thus, by completely removing the ILM, one can eliminate a number of potential sources for treatment failure and/or disease recurrence. Complete ILM removal, however, places the patient at risk for inner retinal optic neuropathy (IRON; see below).

Shimada et al. [107] studied the effects of different types of staining and peeling patterns and its effect on PMM and ILM removal. They found that peeling without staining resulted in a high percentage (78 %) of residual ILM due to an unclear PMM-ILM border. They noted that without chromodissection, not only was it difficult to remove the PMM completely, but the ILM was left intact in the majority of

cases. When staining with Brilliant Blue G dye, they noted that a single episode of staining with a single episode of peeling resulted in reduced rates of residual ILM (39 %). Furthermore, they noted that restaining the peeled zone with a second course of Brilliant Blue G dye and re-peeling to ensure thorough removal of residual ILM helped to further reduce recurrence rates of PMM. Beyond studying the effects of staining, the group also demonstrated that grade 3 PMM cases had a much higher rate of total ILM remaining after a single peel attempt, indicating that the thicker the PMM, the more aggressive the initial peel may need to be [107] [See chapter V.A.3. Chromodissection in vitreo-retinal surgery].

The ILM is a multi-laminar structure [See chapter II.E. Vitreo-retinal interface and ILM]. Removal of the innermost layer(s) during ILM peeling is effective because it assures removal of all vitreous and pathologic cellular membranes attached to the anterior surface of the ILM. ILM peeling is safe because the posterior layers, which are adjacent to the RNFL and firmly adherent to the inner segment of Müller cells, are likely left undisturbed. In cases where there is no split in the ILM and full-thickness ILM peeling is performed, there is damage to the inner retina, at times severely affecting vision. This is especially true during reoperations when much of the inner ILM was removed at the first procedure.

IV. Retreatment of Persistent/Recurrent Disease

A. Retreatment Strategies

1. Macular Hole Reoperations

The approach to re-treating a macular hole largely depends on what was already performed during the primary surgery. If clinically apparent cystoid macular edema exists, then its resolution should be sought nonsurgically. If a PMM was missed during the initial procedure or formed postoperatively, then it should be removed. If an ILM peel was not performed initially, then ILM peel should be performed during reoperation to ensure that all traction is released and no future PMMs develop [31, 39, 114, 118]. However, the vast majority of failed surgeries and reopened macular holes do not have any obvious features that can be resolved with revised surgery [61]. To address this, different techniques have been described with varying degrees of success. Some surgeons have restained the macula to ensure that the ILM was adequately removed and subsequently pursue a further expansion of the original dissection [119]. Studies have also looked at the efficacy of an increased duration of tamponade using gases and oils. Heavy silicone oils, in particular, have gained popularity as an internal tamponade agent that can be used in noncompliant macular hole patients as it does not require patient positioning [120, 121].

Methods have also been described that attempt to enhance glial proliferation, which is thought to help bridge the hole and promote healing [27–29]. These include the use of adjuvants such as autologous platelets [122], autologous serum [123], transforming growth factor beta [124], as well as disruption of the underlying retinal pigment epithelium via photocoagulation [125]. These techniques, however, have not been studied in-depth and lack sufficient clinical evidence to be routinely recommended. There are also sporadic reports of spontaneous closure of macular holes (both primary and recurrent) that have been described in literature, though the incidence is very low [11, 126–131] and usually limited to small holes. These events are thought to be related to the self-resolution of an underlying inciting factor: resorption of cystoid macular edema [131], relief of vitreous traction [129], or the growth of a therapeutic PMM in a direction that relieves tension [124, 127, 128]. However, unless the macular hole is small (<250 μm), the chance for spontaneous resolution is low [20].

One prominent hypothesis of why macular holes close after surgery is that fibrocellular proliferation occurs, bridging the two separated retinal edges [27–29]. Indeed, there are scattered case reports of macular holes spontaneously closing, with the only evidence being the presence of a PMM that formed over the hole. However, the presence of a PMM has, more often than not, been the culprit underlying the formation or reformation of macular holes [28–31, 132–135], owing to its influence on cell organization into a therapeutic membrane. Indeed, histopathological analyses of PMMs associated with reformed macular holes have shown haphazard proliferation of fibrous astrocytes and Müller cells [60].

Hillenkamp et al. found that after a failed primary closure, a repeat surgery would be more likely to close if the hole had a cuff of elevation (claimed to be due to subretinal fluid) on OCT. The rationale is that the closure of a macular hole requires the displaced retinal tissue to reoccupy the fovea, and thus having a separation of the retinal tissue off of the underlying retinal pigment epithelium may facilitate the centripetal transition [136]. Interestingly, the hole size prior to repeat surgery was found not to be associated with either functional or anatomic success, unlike in cases of primary macular hole surgery.

2. Macular Pucker Reoperations

Much like reoperations for macular holes, retreatment for persistent/recurrent macular pucker depends largely on what was already performed during the first surgery. If the most likely cause for the persistence/recurrence of symptoms (reduced visual acuity, metamorphopsia) is incomplete removal of the PMM, then enhancement of PMM visualization can be performed with a number of staining methods during chromodissection, including ICG, trypan blue, triamcinolone acetonide, and Brilliant Blue G [98, 102, 103, 111]. If the ILM was not peeled initially, or if there was possibly inadequate ILM peeling, then staining for improved

visualization can be performed and further ILM removal attempted [98, 102, 103, 108, 111]. Finally, in cases where both adequate PMM and ILM peeling have been performed in the region of the macula, it has been suggested that further ILM removal toward the edges of the vascular arcades may be an option [106].

B. Inner Retinal Optic Neuropathy (IRON)

Abrupt optic neuropathy following any type of eye surgery is a well-known phenomenon that is often due to anterior ischemic optic neuropathy (AION) [137, 138]. In this setting, the patient usually describes the sudden onset of a scotoma that occurs hours, days or even weeks after cataract surgery. The ophthalmologist will note significant loss of visual acuity, an afferent pupillary defect (APD), and a visual field defect that is often altitudinal. The optic disc often appears hyperemic and edematous and then progresses, in about 2 months, to optic atrophy.

In contradistinction, inner retinal optic neuropathy (IRON) seems to occur specifically after vitrectomy with membrane peeling. As described, the patient notes a dark patch in the center of their vision hours or days after surgery. And, as in AION, there is an APD. However, unlike in AION, the visual field loss in IRON does not respect the horizontal raphe (it is not altitudinal). Furthermore, there is no disc edema. But like AION, there will be optic atrophy in about 2 months. The optic atrophy of IRON is more likely to be confined to the temporal aspects of the optic disc. In both AION and IRON, the condition is static with little likelihood of progression or resolution. Unfortunately, in both cases, there is no effective treatment [139].

C. Timing of Reoperations

Nakamura et al. looked at the effects of ILM peeling on the vitreoretinal interface. In their study, 10 monkey eyes underwent pars plana vitrectomy with ILM peeling assisted by ICG chromodissection. Eyes were enucleated at 3, 6, and 12 months post vitrectomy to evaluate the process of healing and regeneration. It was noted that 3 months following surgery there were regions of the retina where ILM peeling had been performed which had evidence of Müller cell fragmentation and exposed areas of the RNFL. At the 6- and 12-month time points, reactive gliosis from the remaining Müller cells formed a mesh-like network that expanded across the originally denuded surface. There was no evidence of complete ILM regeneration even at the 12-month time point [27].

Pan et al. studied the timing of repeat surgeries in 10 patients and found that patients who underwent reoperation at least 6 months after the primary surgery ($n=6$) had better functional outcomes [140] (Figure V.A.4-1). Reoperating too soon (<6 months) after an initial surgery was associated

with poor visual results (postoperative decimal visual acuity= 0.13 ± 0.19 ; equivalent to 20/800). On the other hand, waiting ≥ 6 months before reoperation was associated with excellent functional outcomes (postoperative decimal visual acuity= 0.45 ± 0.24 (equivalent to 20/50); $P=0.03$). The proposed explanation was that peeling of the ILM causes a significant amount of trauma to the underlying Müller cell foot processes that form the outer layers of the ILM. If a repeat peel was performed too soon (<6 months out from the primary), there would be a much greater chance to injure the underlying RNFL and neurosensory retina as the Müller cells would not have had enough time to reform a protective layer. This hypothesis was confirmed by studying OCT measurements of RNFL thickness and histopathological features of the inner retina in cases of membrane peel surgery.

RNFL thickness measurements were obtained after repeat operation in the study patients (Figure V.A.4-2). In the <6 month group, the average thickness and standard deviation of the temporal, inferior, superior, and nasal quadrants were $53.75\pm 8.42\ \mu\text{m}$, $80.50\pm 10.38\ \mu\text{m}$, $86.75\pm 27.20\ \mu\text{m}$, and $74.50\pm 8.06\ \mu\text{m}$, respectively, with an overall peripapillary thickness of $73.75\pm 7.41\ \mu\text{m}$. In the ≥ 6 month group, the measurements were $72.60\pm 13.26\ \mu\text{m}$, $87.80\pm 19.15\ \mu\text{m}$, $103.60\pm 7.02\ \mu\text{m}$, and $85.20\pm 24.69\ \mu\text{m}$, respectively, with an overall peripapillary thickness of $87.00\pm 14.95\ \mu\text{m}$. This difference in the temporal quadrant between groups was statistically significant ($P=0.04$). However, no such difference was detected in the inferior, superior, nasal, or overall thickness measurements.

Tissues removed from 6 eyes at the time of reoperation were processed for immunohistochemistry with antibodies targeting neurofilament, a component of the RNFL. This allowed for unmistakable identification of neurosensory retina in the tissue removed. In the early intervention group (<6 months), positive neurofilament staining was present in 2/2 (100 %) specimens (Figures V.A.4-3 and V.A.4-4). Transmission EM confirmed the presence of cellular debris (Figure V.A.4-5), ostensibly fragments of the RNFL. Postoperative vision in each subject was very poor. In the late (≥ 6 months) reoperation group, there was no evidence of neurofilament staining in 4/4 (100 %) of specimens (Figures V.A.4-3 and V.A.4-4). Postoperative vision was good in all cases. These findings suggest that in cases of reoperation, the risk of iatrogenic RNFL damage is heightened if the second operation is performed too soon (in this study before 6 months) after the first operation. The aforementioned experimental data suggest that this unfortunate consequence occurs when there has been too little time for reformation of a Müller cell barrier and the inner retinal surface is still exposed. During reoperation on an eye that has not reformed this “protective” barrier, membrane peeling, especially with chromodissection, risks damaging the RNFL, as found in this study. To reduce the risk of IRON following reoperation, a minimum duration of 6 months should be allowed between consecutive membrane peel operations.

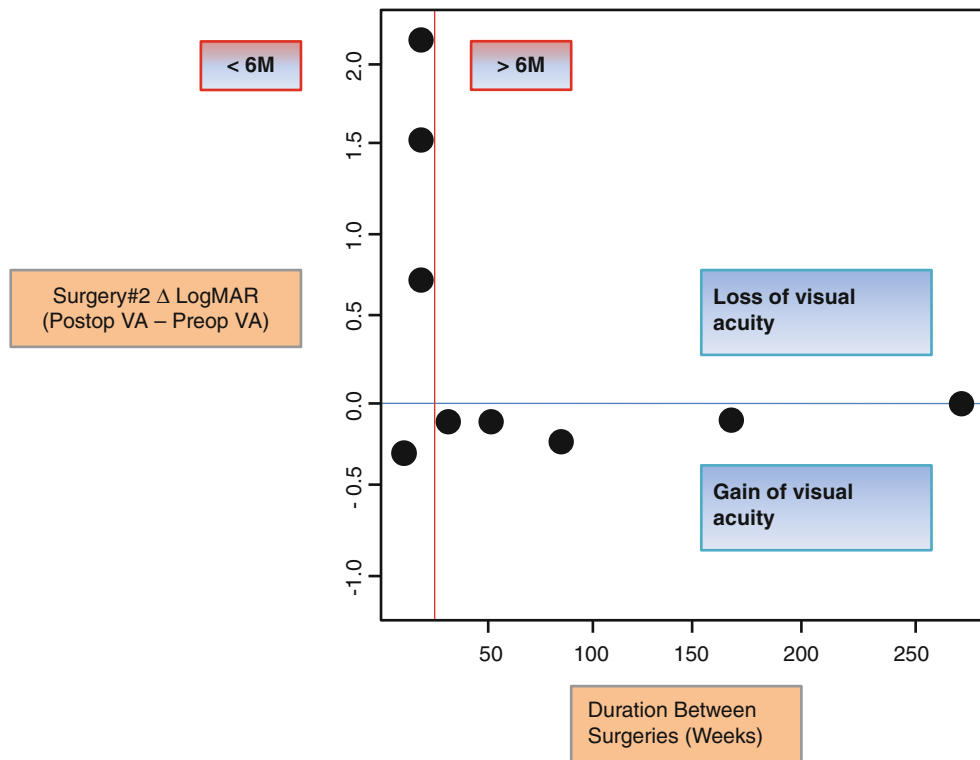


Figure V.A.4-1 Graphic presentation of visual acuity change after a repeat operation for macular hole/macular pucker. The *x*-axis represents the duration of time that elapsed between the first and the second surgeries, in weeks. The *vertical line* represents the 6-month demarcation. The *y*-axis represents the change in visual acuity (represented in LogMAR format) after the second surgery, calculated using the second surgery postoperative visual acuity minus the associated preoperative

visual acuity. The *horizontal line* demarcates loss of visual acuity (*above the line*), gain of visual acuity (*below the line*), and no change in visual acuity (*on the line*). It is notable that 3 of the 4 patients who received repeat surgeries before 6 months had elapsed between surgeries had worsening of visual acuity. In contrast, patients who received a repeat surgery after 6 months had elapsed between surgeries either had improved or stable visual acuities

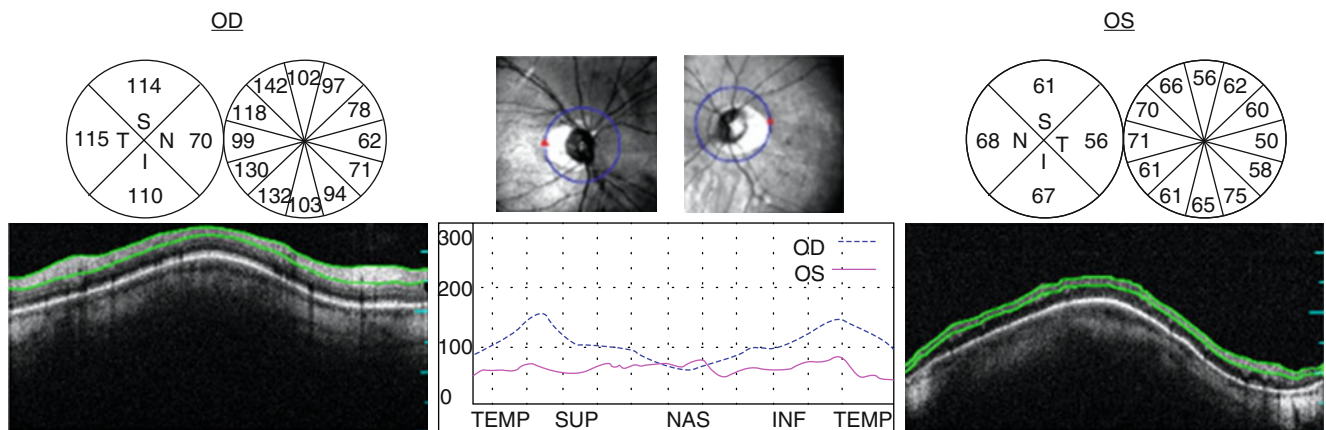


Figure V.A.4-2 Retinal nerve fiber thickness measured by optical coherence tomography demonstrates thinning in the superior, inferior, and temporal quadrants of the eye affected (*OS*) with inner retinal optic neuropathy (IRON) following membrane peeling with chromodissec-

tion during reoperation for macular pucker. Nasal fibers remain unaffected as the membrane peel is performed temporal to the optic nerve OD right eye, OS left eye

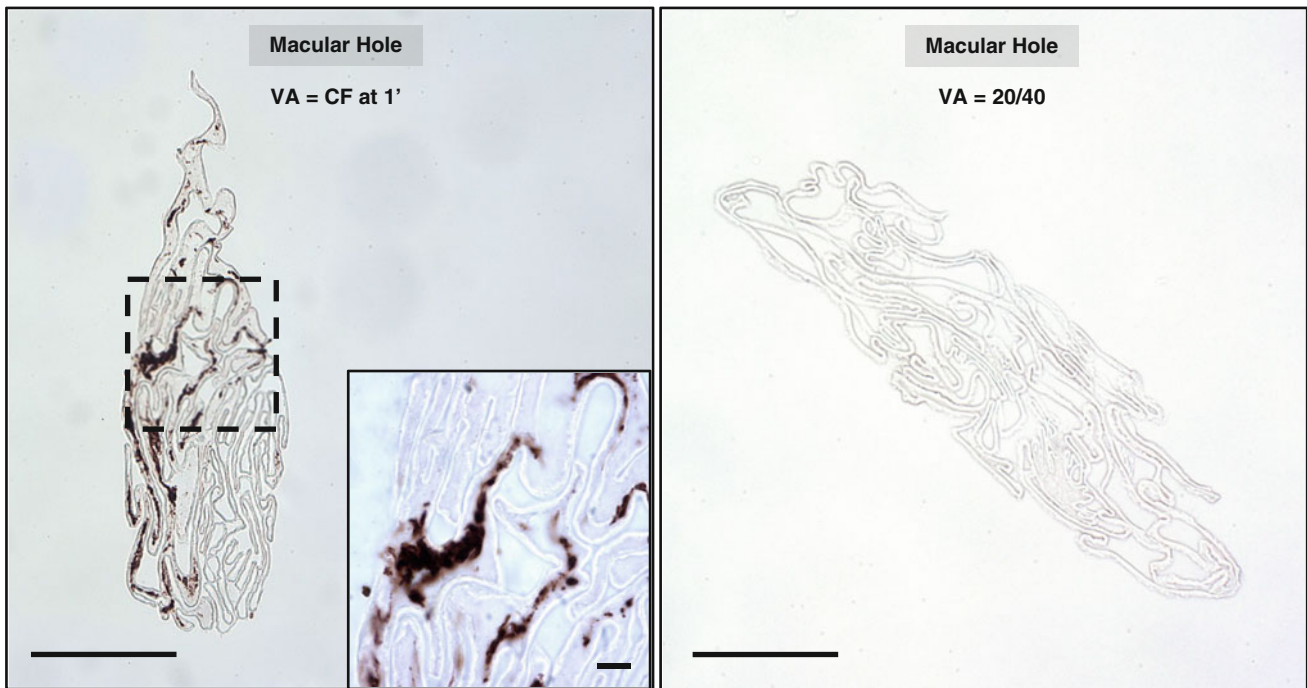


Figure V.A.4-3 Surgical specimens obtained from patients with macular hole. Specimens were processed for immunohistochemistry targeting neurofilament, a component of the retinal nerve fiber layer. *Brown staining* is indicative of neurosensory retina that was removed with the surgical specimen. Image on the left is from a patient who received a

repeat operation <6 months after the first, while the image on the right is from a patient who received a repeat operation >6 after the first operation. Postoperative vision was far better in the latter case (*right image*). VA visual acuity, CF count fingers. Large scale bar = 50 μ m; small scale bar = 5 μ m

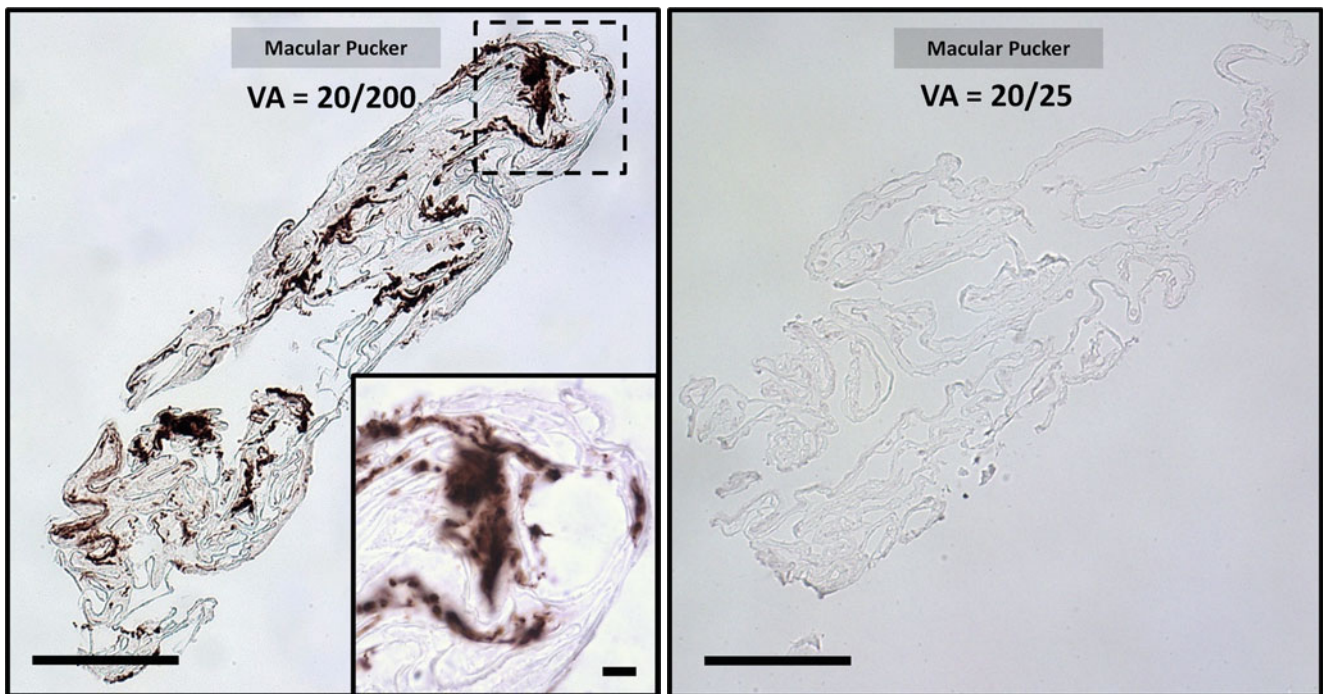
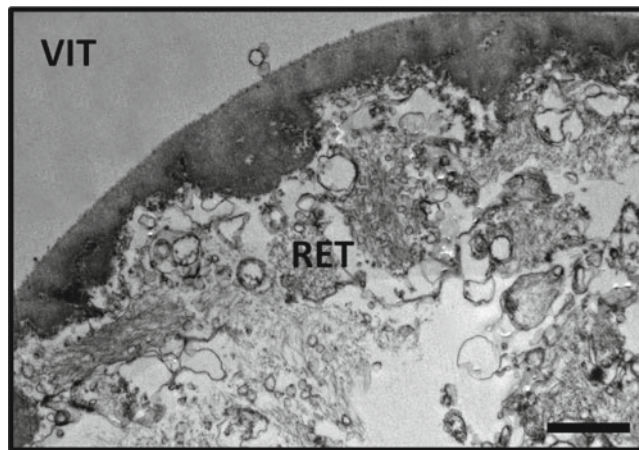


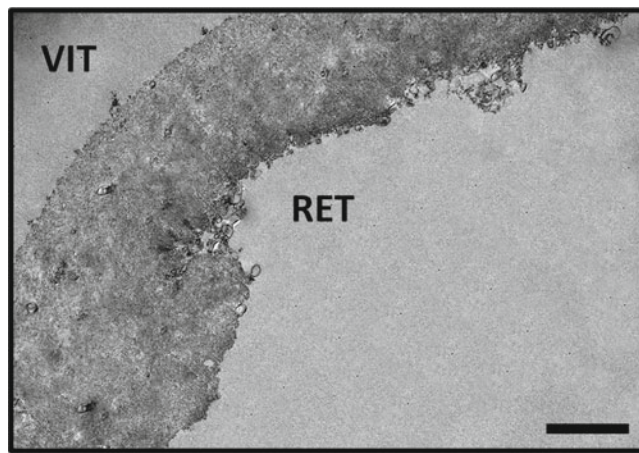
Figure V.A.4-4 Surgical specimens obtained from patients with macular pucker. Specimens were processed for immunohistochemistry targeting neurofilament, a component of the retinal nerve fiber layer. *Brown staining* is indicative of neurosensory retina that was removed with the surgical specimen. Image on the left is from a patient who

underwent a repeat operation < 6 months after the first, while the image on the right is from a patient who underwent reoperation >6 after the first surgery. Postoperative vision was far better in the latter case (*right image*). VA visual acuity. Large scale bar = 50 μ m; small scale bar = 5 μ m

Figure V.A.4-5 Ultrastructural analysis of tissues taken from patients who had repeat surgeries for macular hole. The *upper image* is taken from a patient who underwent reoperation <6 months after the primary surgery, whereas the *lower image* is taken from a patient who underwent reoperation >6 months after the first surgery. The upper image shows a significant amount of cellular tissue adherent to the retinal aspect of the inner limiting membrane, ostensibly fragments of the retinal nerve fiber layer. *VIT* vitreous, *RET* retina, *CF* count fingers, *Pos* positive, *Neg* negative, *NF* neurofilament, *IHC* immunohistochemistry. Scale bar=2 μ m



Snellen VA = CF 1 ft.
Pos (+) NF IHC



Snellen VA = 20/25
Neg (-) NF IHC

Abbreviations

AION	Anterior ischemic optic neuropathy
APD	Afferent pupillary defect
ICG	Indocyanine green
ILM	Inner limiting membrane
IRON	Inner retinal optic neuropathy
MMHS	Moorfields Macular Hole Study
OCT	Optical coherence tomography
PMM	Premacular Membrane (previously referred to as epiretinal membrane, or ERM)
PVC	Posterior vitreous cortex
RNFL	Retinal nerve fiber layer
VMHS	Vitrectomy for treatment of macular hole study
VPMH	Vitrectomy for Prevention of Macular Hole

References

- Gaudric A, Haouchine B, Massin P, Paques M, Blain P, Erginay A. Macular hole formation: new data provided by optical coherence tomography. *Arch Ophthalmol.* 1999;117(6):744–51. Available at: <http://www.ncbi.nlm.nih.gov/pubmed/10369584>. Accessed 15 Jan 2014.
- Azzolini C, Patelli F, Brancato R. Correlation between optical coherence tomography data and biomicroscopic interpretation of idiopathic macular hole. *Am J Ophthalmol.* 2001;132(3):348–55. Available at: <http://www.ncbi.nlm.nih.gov/pubmed/11530047>. Accessed 15 Jan 2014.
- Tanner V, Chauhan DS, Jackson TL, Williamson TH. Optical coherence tomography of the vitreoretinal interface in macular hole formation. *Br J Ophthalmol.* 2001;85(9):1092–7. Available at: <http://www.pubmedcentral.nih.gov/articlerender.fcgi?artid=1724123&tool=pmcentrez&rendertype=abstract>. Accessed 15 Jan 2014.
- Gass JD. Idiopathic senile macular hole. Its early stages and pathogenesis. *Arch Ophthalmol.* 1988;106(5):629–39. Available at: <http://www.ncbi.nlm.nih.gov/pubmed/3358729>. Accessed 15 Jan 2014.
- Gass JD. Müller cell cone, an overlooked part of the anatomy of the fovea centralis: hypotheses concerning its role in the pathogenesis of macular hole and foveomacular retinoschisis. *Arch Ophthalmol.* 1999;117(6):821–3. Available at: <http://www.ncbi.nlm.nih.gov/pubmed/10369597>. Accessed 15 Jan 2014.
- Tanner V, Williamson TH. Watzke-Allen slit beam test in macular holes confirmed by optical coherence tomography. *Arch Ophthalmol.* 2000;118(8):1059–63. Available at: <http://www.ncbi.nlm.nih.gov/pubmed/10922198>. Accessed 15 Jan 2014.
- Hee MR, Puliafito CA, Wong C, et al. Optical coherence tomography of macular holes. *Ophthalmology.* 1995;102(5):748–56. Available at: <http://www.ncbi.nlm.nih.gov/pubmed/7777274>. Accessed 15 Jan 2014.
- Hangai M, Ojima Y, Gotoh N, et al. Three-dimensional imaging of macular holes with high-speed optical coherence tomography. *Ophthalmology.* 2007;114(4):763–73. Available at: <http://www.ncbi.nlm.nih.gov/pubmed/17187861>. Accessed 15 Jan 2014.
- Sebag J. Anomalous posterior vitreous detachment: a unifying concept in vitreo-retinal disease. *Graefes Arch Clin Exp Ophthalmol.* 2004;242(8):690–8. Available at: <http://www.ncbi.nlm.nih.gov/pubmed/15309558>. Accessed 20 Apr 2012.

10. Sebag J, Gupta P, Rosen RR, Garcia P, Sadun AA. Macular holes and macular pucker: the role of vitreoschisis as imaged by optical coherence tomography/scanning laser ophthalmoscopy. *Trans Am Ophthalmol Soc.* 2007;105:121–9; discussion 129–31. Available at: <http://www.pubmedcentral.nih.gov/articlerender.fcgi?artid=2258095&tool=pmcentrez&rendertype=abstract>. Accessed 20 Apr 2012.
11. Cour M, Friis J, la Cour M. Macular holes: classification, epidemiology, natural history and treatment. *Acta Ophthalmol Scand.* 2002;80(6):579–87. Available at: <http://www.ncbi.nlm.nih.gov/pubmed/12485276>. Accessed 21 Apr 2012.
12. Meyer-Schwickerath G. Indications and limitations of light coagulation of the retina. *Trans Am Ophthalmol Soc.* 1959;63:725–38.
13. Harris MJ, de Bustros S, Michels RG. Treatment of retinal detachments due to macular holes. *Retina (Philadelphia, Pa).* 1984;4(3):144–7. Available at: <http://www.ncbi.nlm.nih.gov/pubmed/6494630>. Accessed 10 Feb 2014.
14. Hanselmayer H. Laser-photocoagulation of macular holes (author's transl). *Klin Monbl Augenheilkd.* 1976;169(2):231–4. Available at: <http://www.ncbi.nlm.nih.gov/pubmed/988419>. Accessed 10 Feb 2014.
15. Schocket SS, Lakhanpal V, Miao XP. Treatment of macular holes with the argon laser. *Trans Am Ophthalmol Soc.* 1987;85:159–75. Available at: <http://www.pubmedcentral.nih.gov/articlerender.fcgi?artid=1298771&tool=pmcentrez&rendertype=abstract>. Accessed 10 Feb 2014.
16. Schocket SS, Lakhanpal V, Miao XP, Kelman S, Billings E. Laser treatment of macular holes. *Ophthalmology.* 1988;95(5):574–82. Available at: <http://www.ncbi.nlm.nih.gov/pubmed/3174018>. Accessed 10 Feb 2014.
17. Kelly NE, Wendel RT. Vitreous surgery for idiopathic macular holes. Results of a pilot study. *Arch Ophthalmol.* 1991;109(5):654–9. Available at: <http://www.ncbi.nlm.nih.gov/pubmed/2025167>. Accessed 13 Aug 2012.
18. Sebag J. Indocyanine green-assisted macular hole surgery: too pioneering? *Am J Ophthalmol.* 2004;137(4):744–6. Available at: <http://www.ncbi.nlm.nih.gov/pubmed/15059715>. Accessed 25 Jan 2014.
19. Wendel RT, Patel AC, Kelly NE, Salzano TC, Wells JW, Novack GD. Vitreous surgery for macular holes. *Ophthalmology.* 1993;100(11):1671–6. Available at: <http://www.ncbi.nlm.nih.gov/pubmed/8233393>. Accessed 15 Jan 2014.
20. De Bustros S. Vitrectomy for prevention of macular holes. Results of a randomized multicenter clinical trial. *Vitrectomy for Prevention of Macular Hole Study Group.* *Ophthalmology.* 1994;101(6):1055–9; discussion 1060. Available at: <http://www.ncbi.nlm.nih.gov/pubmed/8008347>. Accessed 15 Jan 2014.
21. Ezra E, Gregor ZJ. Surgery for idiopathic full-thickness macular hole: two-year results of a randomized clinical trial comparing natural history, vitrectomy, and vitrectomy plus autologous serum: Morfields Macular Hole Study Group RAeport no. 1. *Arch Ophthalmol.* 2004;122(2):224–36.
22. Freeman WR, Azen SP, Kim JW, el-Haig W, Mishell DR, Bailey I. Vitrectomy for the treatment of full-thickness stage 3 or 4 macular holes. Results of a multicentered randomized clinical trial. *The Vitrectomy for Treatment of Macular Hole Study Group.* *Arch Ophthalmol.* 1997;115(1):11–21.
23. Eckardt C, Eckardt U, Groos S, Luciano L, Reale E. Removal of the internal limiting membrane in macular holes. Clinical and morphological findings. *Der Ophthalmologe.* 1997;94(8):545–51.
24. Gupta P, Yee KMP, Garcia P, et al. Vitreoschisis in macular diseases. *Br J Ophthalmol.* 2011;95(3):376–80. Available at: <http://www.ncbi.nlm.nih.gov/pubmed/20584710>. Accessed 13 Apr 2012.
25. Sebag J. Vitreoschisis. *Graefes Arch Clin Exp Ophthalmol.* 2008;246(3):329–32. Available at: <http://www.pubmedcentral.nih.gov/articlerender.fcgi?artid=2258312&tool=pmcentrez&rendertype=abstract>. Accessed 20 Apr 2012.
26. Sebag J. Vitreoschisis in diabetic macular edema. *Invest Ophthalmol Vis Sci.* 2011;52(11):8455–6; author reply 8456–7. Available at: <http://www.ncbi.nlm.nih.gov/pubmed/22042822>. Accessed 21 Apr 2012.
27. Nakamura T, Murata T, Hisatomi T, et al. Ultrastructure of the vitreoretinal interface following the removal of the internal limiting membrane using indocyanine green. *Curr Eye Res.* 2003;27(6):395–9. Available at: <http://www.ncbi.nlm.nih.gov/pubmed/14704923>.
28. Funata M, Wendel RT, de la Cruz Z, Green WR. Clinicopathologic study of bilateral macular holes treated with pars plana vitrectomy and gas tamponade. *Retina (Philadelphia, Pa).* 1992;12(4):289–98. Available at: <http://www.ncbi.nlm.nih.gov/pubmed/1485013>. Accessed 15 Jan 2014.
29. Madreperla SA, Geiger GL, Funata M, de la Cruz Z, Green WR. Clinicopathologic correlation of a macular hole treated by cortical vitreous peeling and gas tamponade. *Ophthalmology.* 1994;101(4):682–6. Available at: <http://www.ncbi.nlm.nih.gov/pubmed/8152763>. Accessed 15 Jan 2014.
30. Yooh HS, Brooks HL, Capone A, L'Hernault NL, Grossniklaus HE. Ultrastructural features of tissue removed during idiopathic macular hole surgery. *Am J Ophthalmol.* 1996;122(1):67–75. Available at: <http://www.ncbi.nlm.nih.gov/pubmed/8659600>. Accessed 15 Jan 2014.
31. Kwok AK, Li WW, Pang CP, et al. Indocyanine green staining and removal of internal limiting membrane in macular hole surgery: histology and outcome. *Am J Ophthalmol.* 2001;132(2):178–83. Available at: <http://www.ncbi.nlm.nih.gov/pubmed/11476676>. Accessed 21 Apr 2012.
32. Ameli N, Lashkari K. Macular hole following cataract extraction. *Semin Ophthalmol.* 2002;17(3–4):196–8. Available at: <http://www.ncbi.nlm.nih.gov/pubmed/12759850>. Accessed 15 Jan 2014.
33. Bhatnagar P, Kaiser PK, Smith SD, Meisler DM, Lewis H, Sears JE. Reopening of previously closed macular holes after cataract extraction. *Am J Ophthalmol.* 2007;144(2):252–9. Available at: <http://www.ncbi.nlm.nih.gov/pubmed/17543876>. Accessed 13 Apr 2012.
34. Tadayoni R, Gaudric A, Haouchine B, Massin P. Relationship between macular hole size and the potential benefit of internal limiting membrane peeling. *Br J Ophthalmol.* 2006;90(10):1239–41. Available at: <http://www.pubmedcentral.nih.gov/articlerender.fcgi?artid=1857449&tool=pmcentrez&rendertype=abstract>. Accessed 15 Jan 2014.
35. Kwok AKH, Lai TYY, Wong VWY. Idiopathic macular hole surgery in Chinese patients: a randomised study to compare indocyanine green-assisted internal limiting membrane peeling with no internal limiting membrane peeling. *Hong Kong Med J.* 2005;11(4):259–66. Available at: <http://www.ncbi.nlm.nih.gov/pubmed/16085942>. Accessed 15 Jan 2014.
36. Van De Moere A, Stalmans P. Anatomical and visual outcome of macular hole surgery with intracranial green-assisted peeling of the internal limiting membrane, endodrainage, and silicone oil tamponade. *Am J Ophthalmol.* 2003;136(5):879–87. Available at: <http://www.ncbi.nlm.nih.gov/pubmed/14597040>. Accessed 15 Jan 2014.
37. Hasler PW, Prunte C. Early foveal recovery after macular hole surgery. *Br J Ophthalmol.* 2008;92(5):645–9. Available at: <http://www.ncbi.nlm.nih.gov/pubmed/18296507>. Accessed 15 Jan 2014.
38. Mester V, Kuhn F. Internal limiting membrane removal in the management of full-thickness macular holes. *Am J Ophthalmol.* 2000;129(6):769–77. Available at: <http://www.ncbi.nlm.nih.gov/pubmed/10926987>. Accessed 21 Apr 2012.
39. Tognetto D, Grandin R, Sanguinetti G, et al. Internal limiting membrane removal during macular hole surgery: results of a multicenter retrospective study. *Ophthalmology.* 2006;113(8):1401–10. Available at: <http://www.ncbi.nlm.nih.gov/pubmed/16877079>. Accessed 15 Jan 2014.

40. Kumagai K, Furukawa M, Ogino N, Larson E. Incidence and factors related to macular hole reopening. *Am J Ophthalmol*. 2010;149(1):127–32. Available at: <http://www.ncbi.nlm.nih.gov/pubmed/19875088>. Accessed 15 Mar 2012.
41. Lois N, Burr J, Norrie J, et al. Internal limiting membrane peeling versus no peeling for idiopathic full-thickness macular hole: a pragmatic randomized controlled trial. *Invest Ophthalmol Vis Sci*. 2011;52(3):1586–92. Available at: <http://www.ncbi.nlm.nih.gov/pubmed/21051731>. Accessed 21 Apr 2012.
42. Christensen UC, Krøyer K, Sander B, et al. Value of internal limiting membrane peeling in surgery for idiopathic macular hole stage 2 and 3: a randomised clinical trial. *Br J Ophthalmol*. 2009;93(8):1005–15. Available at: <http://www.ncbi.nlm.nih.gov/pubmed/19028741>. Accessed 15 Jan 2014.
43. Brooks HL. Macular hole surgery with and without internal limiting membrane peeling. *Ophthalmology*. 2000;107(10):1939–48; discussion 1948–9. Available at: <http://www.ncbi.nlm.nih.gov/pubmed/11013203>.
44. Ben Simon GJ, Desatnik H, Alhalel A, Treister G, Moisseiev J. Retrospective analysis of vitrectomy with and without internal limiting membrane peeling for stage 3 and 4 macular hole. *Ophthalmic Surg Lasers Imaging*. 2004;35(2):109–15. Available at: <http://www.ncbi.nlm.nih.gov/pubmed/15088820>. Accessed 15 Jan 2014.
45. Sheidow TG, Blinder KJ, Holekamp N, et al. Outcome results in macular hole surgery: an evaluation of internal limiting membrane peeling with and without indocyanine green. *Ophthalmology*. 2003;110(9):1697–701. Available at: <http://www.ncbi.nlm.nih.gov/pubmed/13129864>. Accessed 15 Jan 2014.
46. Al-Abdulla NA, Thompson JT, Sjaarda RN. Results of macular hole surgery with and without epiretinal dissection or internal limiting membrane removal. *Ophthalmology*. 2004;111(1):142–9. Available at: <http://www.ncbi.nlm.nih.gov/pubmed/14711726>. Accessed 15 Jan 2014.
47. Ando F, Sasano K, Ohba N, Hirose H, Yasui O. Anatomic and visual outcomes after indocyanine green-assisted peeling of the retinal internal limiting membrane in idiopathic macular hole surgery. *Am J Ophthalmol*. 2004;137(4):609–14. Available at: <http://www.ncbi.nlm.nih.gov/pubmed/15059697>. Accessed 25 Apr 2012.
48. Kumagai K, Furukawa M, Ogino N, Uemura A, Demizu S, Larson E. Vitreous surgery with and without internal limiting membrane peeling for macular hole repair. *Retina*. 2004;24(5):721–7. Available at: <http://www.ncbi.nlm.nih.gov/pubmed/15492625>.
49. Tewari A, Almony A, Nudleman E, et al. Techniques, rationale, and outcomes of internal limiting membrane peeling. *Retina*. 2011. Available at: <http://www.ncbi.nlm.nih.gov/pubmed/22105502>. Accessed 20 Apr 2012.
50. Graham K, D'Amico DJ. Postoperative complications of epiretinal membrane surgery. *Int Ophthalmol Clin*. 2000;40(1):215–23. Available at: <http://www.ncbi.nlm.nih.gov/pubmed/10713927>. Accessed 22 Apr 2012.
51. Bababeygy SR, Sebag J. Chromodissection of the vitreo-retinal interface. *Retinal Physician*. 2009;6(3):16–21.
52. Smiddy WE, Feuer W, Cordahi G. Internal limiting membrane peeling in macular hole surgery. *Ophthalmology*. 2001;108(8):1471–6; discussion 1477–8. Available at: <http://www.ncbi.nlm.nih.gov/pubmed/11470703>.
53. Yamashita T, Uemura A, Kita H, Sakamoto T. Analysis of the retinal nerve fiber layer after indocyanine green-assisted vitrectomy for idiopathic macular holes. *Ophthalmology*. 2006;113(2):280–4. Available at: <http://www.ncbi.nlm.nih.gov/pubmed/16458094>. Accessed 27 Mar 2012.
54. Haritoglou C, Gandorfer A, Gass CA, Schaumberger M, Ulbig MW, Kampik A. Indocyanine green-assisted peeling of the internal limiting membrane in macular hole surgery affects visual outcome: a clinicopathologic correlation. *Am J Ophthalmol*. 2002;134(6):836–41. Available at: <http://www.ncbi.nlm.nih.gov/pubmed/12470751>. Accessed 21 Apr 2012.
55. Ando F, Sasano K, Ohba N, Hirose H, Yasui O. Anatomic and visual outcomes after indocyanine green-assisted peeling of the retinal internal limiting membrane in idiopathic macular hole surgery. *Am J Ophthalmol*. 2004;137(4):609–14. Available at: <http://www.ncbi.nlm.nih.gov/pubmed/15059697>. Accessed 15 Jan 2014.
56. Abdelkader E, Lois N. Internal limiting membrane peeling in vitreo-retinal surgery. *Surv Ophthalmol*. 2008;53(4):368–96. Available at: <http://www.ncbi.nlm.nih.gov/pubmed/18572054>. Accessed 18 Sept 2013.
57. Lai MM, Williams GA. Anatomical and visual outcomes of idiopathic macular hole surgery with internal limiting membrane removal using low-concentration indocyanine green. *Retina (Philadelphia, Pa)*. 2007;27(4):477–82. Available at: <http://www.ncbi.nlm.nih.gov/pubmed/17420702>. Accessed 15 Jan 2014.
58. Paques M, Massin P, Santiago PY, Spielmann AC, Le Gargasson JF, Gaudric A. Late reopening of successfully treated macular holes. *Br J Ophthalmol*. 1997;81(8):658–62. Available at: <http://www.pubmedcentral.nih.gov/articlerender.fcgi?artid=1722272&tool=pmcentrez&rendertype=abstract>.
59. Yoshida M, Kishi S. Pathogenesis of macular hole recurrence and its prevention by internal limiting membrane peeling. *Retina (Philadelphia, Pa)*. 2007;27(2):169–73. Available at: <http://www.ncbi.nlm.nih.gov/pubmed/17290198>. Accessed 20 Apr 2012.
60. Schumann RG, Rohleder M, Schaumberger MM, Haritoglou C, Kampik A, Gandorfer A. Idiopathic macular holes: ultrastructural aspects of surgical failure. *Retina (Philadelphia, Pa)*. 2008;28(2):340–9. Available at: <http://www.ncbi.nlm.nih.gov/pubmed/18301041>. Accessed 20 Apr 2012.
61. Christmas NJ, Smiddy WE, Flynn HW. Reopening of macular holes after initially successful repair. *Ophthalmology*. 1998;105(10):1835–8. Available at: <http://www.ncbi.nlm.nih.gov/pubmed/9787352>.
62. Scott IU, Moraczewski AL, Smiddy WE, Flynn HW, Feuer WJ. Long-term anatomic and visual acuity outcomes after initial anatomic success with macular hole surgery. *Am J Ophthalmol*. 2003;135(5):633–40. Available at: <http://www.ncbi.nlm.nih.gov/pubmed/12719070>. Accessed 15 Jan 2014.
63. Paques M, Massin P, Blain P, Duquesnoy AS, Gaudric A. Long-term incidence of reopening of macular holes. *Ophthalmology*. 2000;107(4):760–5; discussion 766. Available at: <http://www.ncbi.nlm.nih.gov/pubmed/10768340>.
64. Haritoglou C, Gass CA, Schaumberger M, Gandorfer A, Ulbig MW, Kampik A. Long-term follow-up after macular hole surgery with internal limiting membrane peeling. *Am J Ophthalmol*. 2002;134(5):661–6. Available at: <http://www.ncbi.nlm.nih.gov/pubmed/12429240>. Accessed 15 Jan 2014.
65. Kumagai K, Ogino N, Demizu S, et al. Incidence of reopening and variables that influence reopening after macular hole surgery. *Jpn J Ophthalmol*. 2001;45(1):112–3. Available at: <http://www.ncbi.nlm.nih.gov/pubmed/11341897>. Accessed 21 Apr 2012.
66. Sebag J, Yee KMP, Wa CA, Huang LC, Sadun AA. Vitrectomy for floaters: prospective efficacy analyses and retrospective safety profile. *Retina (Philadelphia, Pa)*. 2014;34:1062–8. Available at: <http://www.ncbi.nlm.nih.gov/pubmed/24296397>. Accessed 15 Jan 2014.
67. Cherfan GM, Michels RG, de Bustros S, Enger C, Glaser BM. Nuclear sclerotic cataract after vitrectomy for idiopathic epiretinal membranes causing macular pucker. *Am J Ophthalmol*. 1991;111(4):434–8. Available at: <http://www.ncbi.nlm.nih.gov/pubmed/2012145>. Accessed 15 Jan 2014.
68. Thompson JT. The role of patient age and intraocular gases in cataract progression following vitrectomy for macular holes and epiretinal membranes. *Trans Am Ophthalmol Soc*. 2003;101:485–98. Available at: <http://www.pubmedcentral.nih.gov/articlerender.fcgi?artid=1359001&tool=pmcentrez&rendertype=abstract>. Accessed 13 Aug 2012.
69. Thompson JT, Glaser BM, Sjaarda RN, Murphy RP. Progression of nuclear sclerosis and long-term visual results of vitrectomy with

- transforming growth factor beta-2 for macular holes. *Am J Ophthalmol*. 1995;119(1):48–54. Available at: <http://www.ncbi.nlm.nih.gov/pubmed/7825689>. Accessed 15 Jan 2014.
70. De Bustros S, Thompson JT, Michels RG, Enger C, Rice TA, Glaser BM. Nuclear sclerosis after vitrectomy for idiopathic epiretinal membranes. *Am J Ophthalmol*. 1988;105(2):160–4. Available at: <http://www.ncbi.nlm.nih.gov/pubmed/3341433>. Accessed 15 Jan 2014.
 71. Gottlieb CC, Martin JA. Phacovitrectomy with internal limiting membrane peeling for idiopathic macular hole. *Can J Ophthalmol*. 2002;37(5):277–82; discussion 282. Available at: <http://www.ncbi.nlm.nih.gov/pubmed/12322859>. Accessed 15 Jan 2014.
 72. Theocharis IP, Alexandridou A, Gili NJ, Tomic Z. Combined phacoemulsification and pars plana vitrectomy for macular hole treatment. *Acta Ophthalmol Scand*. 2005;83(2):172–5. Available at: <http://www.ncbi.nlm.nih.gov/pubmed/15799728>. Accessed 15 Jan 2014.
 73. Kotecha AV, Sinclair SH, Gupta AK, Tipperman R. Pars plana vitrectomy for macular holes combined with cataract extraction and lens implantation. *Ophthalmic Surg Lasers*. 2000;31(5):387–93. Available at: <http://www.ncbi.nlm.nih.gov/pubmed/11011707>. Accessed 15 Jan 2014.
 74. García-Arumí J, Palau MM, Espax AB, Martínez-Castillo V, Garrido HB, Corcóstegui B. Reopening of 2 macular holes after neodymium:YAG capsulotomy. *J Cataract Refract Surg*. 2006;32(2):363–6. Available at: <http://www.ncbi.nlm.nih.gov/pubmed/16565020>. Accessed 15 Jan 2014.
 75. Osterlin S. Vitreous changes after cataract extraction. In: Freeman H, Hirose T, Schepens C, editors. *Vitreous surgery and advances in fundus diagnosis and treatment*. New York: Appleton; 1977.
 76. Osterlin S. Macromolecular composition of the vitreous in the aphakic owl monkey eye. *Exp Eye Res*. 1978;26(1):77–84. Available at: <http://www.ncbi.nlm.nih.gov/pubmed/414928>. Accessed 25 Jan 2014.
 77. McDonnell PJ, Patel A, Green WR. Comparison of intracapsular and extracapsular cataract surgery. Histopathologic study of eyes obtained postmortem. *Ophthalmology*. 1985;92(9):1208–25. Available at: <http://www.ncbi.nlm.nih.gov/pubmed/4058884>. Accessed 25 Jan 2014.
 78. Larsson L, Osterlin S. Posterior vitreous detachment. A combined clinical and physiochemical study. *Graefes Arch Clin Exp Ophthalmol*. 1985;223(2):92–5. Available at: <http://www.ncbi.nlm.nih.gov/pubmed/4007512>. Accessed 25 Jan 2014.
 79. Hiscott PS, Grierson I, McLeod D. Natural history of fibrocellular epiretinal membranes: a quantitative, autoradiographic, and immunohistochemical study. *Br J Ophthalmol*. 1985;69(11):810–23. Available at: <http://www.pubmedcentral.nih.gov/articlerender.fcgi?artid=1040751&tool=pmcentrez&rendertype=abstract>. Accessed 15 Jan 2014.
 80. Foos RY. Vitreoretinal juncture; epiretinal membranes and vitreous. *Invest Ophthalmol Vis Sci*. 1977;16(5):416–22. Available at: <http://www.ncbi.nlm.nih.gov/pubmed/852943>. Accessed 13 Aug 2012.
 81. Kampik A, Green WR, Michels RG, Nase PK. Ultrastructural features of progressive idiopathic epiretinal membrane removed by vitreous surgery. *Am J Ophthalmol*. 1980;90(6):797–809. Available at: <http://www.ncbi.nlm.nih.gov/pubmed/7446667>. Accessed 15 Jan 2014.
 82. Gandorfer A, Rohleder M, Kampik A. Epiretinal pathology of vitreomacular traction syndrome. *Br J Ophthalmol*. 2002;86(8):902–9. Available at: <http://www.pubmedcentral.nih.gov/articlerender.fcgi?artid=1771255&tool=pmcentrez&rendertype=abstract>. Accessed 15 Jan 2014.
 83. Green WR, Kenyon KR, Michels RG, Gilbert HD, De La Cruz Z. Ultrastructure of epiretinal membranes causing macular pucker after retinal re-attachment surgery. *Trans Ophthalmol Soc U K*. 1979;99(1):65–77. Available at: <http://www.ncbi.nlm.nih.gov/pubmed/297384>. Accessed 15 Jan 2014.
 84. Smiddy WE, Maguire AM, Green WR, et al. Idiopathic epiretinal membranes. Ultrastructural characteristics and clinicopathologic correlation. *Ophthalmology*. 1989;96(6):811–20; discussion 821. Available at: <http://www.ncbi.nlm.nih.gov/pubmed/2740079>. Accessed 15 Jan 2014.
 85. Wilkins JR, Puliafito CA, Hee MR, et al. Characterization of epiretinal membranes using optical coherence tomography. *Ophthalmology*. 1996;103(12):2142–51. Available at: <http://www.ncbi.nlm.nih.gov/pubmed/9003350>. Accessed 15 Jan 2014.
 86. Sebag J, Wang MY, Nguyen D, Sadun AA. Vitreopapillary adhesion in macular diseases. *Trans Am Ophthalmol Soc*. 2009;107:35–44. Available at: <http://www.pubmedcentral.nih.gov/articlerender.fcgi?artid=2814571&tool=pmcentrez&rendertype=abstract>. Accessed 13 Apr 2012.
 87. Okamoto F, Sugiura Y, Okamoto Y, Hiraoka T, Oshika T. Associations between metamorphopsia and foveal microstructure in patients with epiretinal membrane. *Invest Ophthalmol Vis Sci*. 2012;53(11):6770–5. Available at: <http://www.ncbi.nlm.nih.gov/pubmed/22969078>. Accessed 15 Jan 2014.
 88. Niwa T, Terasaki H, Kondo M, Piao C-H, Suzuki T, Miyake Y. Function and morphology of macula before and after removal of idiopathic epiretinal membrane. *Invest Ophthalmol Vis Sci*. 2003;44(4):1652–6. Available at: <http://www.ncbi.nlm.nih.gov/pubmed/12657605>. Accessed 15 Jan 2014.
 89. Mitchell P, Smith W, Chey T, Wang JJ, Chang A. Prevalence and associations of epiretinal membranes. The Blue Mountains Eye Study, Australia. *Ophthalmology*. 1997;104(6):1033–40.
 90. Kohno R, Hata Y, Kawahara S, et al. Possible contribution of hyalocytes to idiopathic epiretinal membrane formation and its contraction. *Br J Ophthalmol*. 2009;93(8):1020–6. Available at: <http://www.ncbi.nlm.nih.gov/pubmed/19429593>. Accessed 15 Jan 2014.
 91. Kim JH, Kim YM, Chung EJ, Lee SY, Koh HJ. Structural and functional predictors of visual outcome of epiretinal membrane surgery. *Am J Ophthalmol*. 2012;153(1):103–10.e1. Available at: <http://www.ncbi.nlm.nih.gov/pubmed/21937015>. Accessed 15 Jan 2014.
 92. Christensen UC, Krøyer K, Sander B, Jorgensen TM, Larsen M, la Cour M. Macular morphology and visual acuity after macular hole surgery with or without internal limiting membrane peeling. *Br J Ophthalmol*. 2010;94(1):41–7. Available at: <http://www.ncbi.nlm.nih.gov/pubmed/19692379>. Accessed 15 Jan 2014.
 93. Salter AB, Folgar FA, Weissbrodt J, Wald KJ. Macular hole surgery prognostic success rates based on macular hole size. *Ophthalmic Surg Lasers Imaging*. 2012;43(3):184–9. Available at: <http://www.ncbi.nlm.nih.gov/pubmed/22320413>. Accessed 15 Jan 2014.
 94. De Bustros S, Thompson JT, Michels RG, Rice TA, Glaser BM. Vitrectomy for idiopathic epiretinal membranes causing macular pucker. *Br J Ophthalmol*. 1988;72(9):692–5. Available at: <http://www.pubmedcentral.nih.gov/articlerender.fcgi?artid=1041558&tool=pmcentrez&rendertype=abstract>. Accessed 15 Jan 2014.
 95. Rice TA, De Bustros S, Michels RG, Thompson JT, Debanne SM, Rowland DY. Prognostic factors in vitrectomy for epiretinal membranes of the macula. *Ophthalmology*. 1986;93(5):602–10. Available at: <http://www.ncbi.nlm.nih.gov/pubmed/3725320>. Accessed 15 Jan 2014.
 96. Wong JG, Sachdev N, Beaumont PE, Chang AA. Visual outcomes following vitrectomy and peeling of epiretinal membrane. *Clin Experiment Ophthalmol*. 2005;33(4):373–8. Available at: <http://www.ncbi.nlm.nih.gov/pubmed/16033349>. Accessed 15 Jan 2014.
 97. Gupta P, Sadun AA, Sebag J. Multifocal retinal contraction in macular pucker analyzed by combined optical coherence tomography/scanning laser ophthalmoscopy. *Retina (Philadelphia, Pa)*. 2008;28(3):447–52. Available at: <http://www.ncbi.nlm.nih.gov/pubmed/18327137>. Accessed April 20, 2012.
 98. Kampik A, Kenyon KR, Michels RG, Green WR, de la Cruz ZC. Epiretinal and vitreous membranes. Comparative study of 56 cases. *Arch Ophthalmol*. 1981;99(8):1445–54.

99. Kifuku K, Hata Y, Kohno R, et al. Residual internal limiting membrane in epiretinal membrane surgery. *Br J Ophthalmol*. 2009;93(8):1016–9. Available at: <http://www.ncbi.nlm.nih.gov/pubmed/19211605>. Accessed 15 Jan 2014.
100. Gandorfer A, Haritoglou C, Scheler R, Schumann R, Zhao F, Kampik A. Residual cellular proliferation on the internal limiting membrane in macular pucker surgery. *Retina* (Philadelphia, Pa). 2012;32(3):477–85. Available at: <http://www.ncbi.nlm.nih.gov/pubmed/22068175>. Accessed 13 Apr 2012.
101. Bovey EH, Uffer S, Achache F. Surgery for epimacular membrane: impact of retinal internal limiting membrane removal on functional outcome. *Retina*. 2004;24(5):728–35. Available at: <http://www.ncbi.nlm.nih.gov/pubmed/15492626>. Accessed 20 Apr 2012.
102. Gibran SK, Flemming B, Stappeler T, et al. Peel and peel again. *Br J Ophthalmol*. 2008;92(3):373–7. Available at: <http://www.ncbi.nlm.nih.gov/pubmed/18055573>. Accessed 20 Apr 2012.
103. Ducourneau Y, Ducourneau D. Aspects anatomopathologiques des membranes épiretiniennes idiopathiques et secondaires. Dans “La Chirurgie de la Macula.” *Bulletin des Sociétés d’Ophthalmologie de France, Rapport Annuel*. Nov 1996:87–119.
104. Sivalingam A, Eagle RC, Duker JS, et al. Visual prognosis correlated with the presence of internal-limiting membrane in histopathologic specimens obtained from epiretinal membrane surgery. *Ophthalmology*. 1990;97(11):1549–52. Available at: <http://www.ncbi.nlm.nih.gov/pubmed/2255528>. Accessed 7 Aug 2012.
105. Schadlu R, Tehrani S, Shah GK, Prasad AG. Long-term follow-up results of ilm peeling during vitrectomy surgery for premacular fibrosis. *Retina*. 2008;28(6):853–7. Available at: <http://www.ncbi.nlm.nih.gov/pubmed/18536602>. Accessed 21 Apr 2012.
106. Park DW, Dugel PU, Garda J, et al. Macular pucker removal with and without internal limiting membrane peeling: pilot study. *Ophthalmology*. 2003;110(1):62–4. Available at: <http://www.ncbi.nlm.nih.gov/pubmed/12511347>. Accessed 20 Apr 2012.
107. Shimada H, Nakashizuka H, Hattori T, Mori R, Mizutani Y, Yuzawa M. Double staining with brilliant blue G and double peeling for epiretinal membranes. *Ophthalmology*. 2009;116(7):1370–6. Available at: <http://www.ncbi.nlm.nih.gov/pubmed/19427701>. Accessed 15 Mar 2012.
108. Kwok AK, Lai TY, Yuen KS. Epiretinal membrane surgery with or without internal limiting membrane peeling. *Clin Experiment Ophthalmol*. 2005;33(4):379–85. Available at: <http://www.ncbi.nlm.nih.gov/pubmed/16033350>. Accessed 15 Jan 2014.
109. Margherio RR, Cox MS, Trese MT, Murphy PL, Johnson J, Minor LA. Removal of epimacular membranes. *Ophthalmology*. 1985;92(8):1075–83. Available at: <http://www.ncbi.nlm.nih.gov/pubmed/4047601>. Accessed 15 Jan 2014.
110. Wilkinson CP. Recurrent macular pucker. *Am J Ophthalmol*. 1979;88(6):1029–31. Available at: <http://www.ncbi.nlm.nih.gov/pubmed/517606>. Accessed 15 Jan 2014.
111. Sebag J. Vitreous: the resplendent enigma. *Br J Ophthalmol*. 2009;93(8):989–91. Available at: <http://www.ncbi.nlm.nih.gov/pubmed/19633281>.
112. Gandorfer A, Messmer EM, Ulbig MW, Kampik A. Indocyanine green selectively stains the internal limiting membrane. *Am J Ophthalmol*. 2001;131(3):387–8. Available at: <http://www.ncbi.nlm.nih.gov/pubmed/11239880>. Accessed 22 Apr 2012.
113. Binder S, Falkner-Radler CI, Hauger C, Matz H, Glittenberg C. Feasibility of intrasurgical spectral-domain optical coherence tomography. *Retina* (Philadelphia, Pa). 2011;31(7):1332–6. Available at: <http://www.ncbi.nlm.nih.gov/pubmed/21273942>. Accessed 25 Jan 2014.
114. Matz H, Binder S, Glittenberg C, et al. Intraoperative applications of OCT in ophthalmic surgery. *Biomedizinische Technik. Biomed Eng*. 2012;57 Suppl 1. Available at: <http://www.ncbi.nlm.nih.gov/pubmed/23096340>. Accessed 25 Jan 2014.
115. Kwok AKH, Lai TYY, Li WWY, Woo DCF, Chan NR. Indocyanine green-assisted internal limiting membrane removal in epiretinal membrane surgery: a clinical and histologic study. *Am J Ophthalmol*. 2004;138(2):194–9. Available at: <http://www.ncbi.nlm.nih.gov/pubmed/15289126>. Accessed 21 Apr 2012.
116. Haritoglou C, Gandorfer A, Schaumberger M, et al. Trypan blue in macular pucker surgery: an evaluation of histology and functional outcome. *Retina* (Philadelphia, Pa). 2004;24(4):582–90. Available at: <http://www.ncbi.nlm.nih.gov/pubmed/15300080>. Accessed 15 Jan 2014.
117. Maguire AM, Smiddy WE, Nanda SK, Michels RG, de la Cruz Z, Green WR. Clinicopathologic correlation of recurrent epiretinal membranes after previous surgical removal. *Retina* (Philadelphia, Pa). 1990;10(3):213–22. Available at: <http://www.ncbi.nlm.nih.gov/pubmed/2236947>. Accessed 15 Jan 2014.
118. Rezendes FA, Kapusta MA. Internal limiting membrane: ultrastructural relationships, with clinical implications for macular hole healing. *Can J Ophthalmol*. 2004;39(3):251–9. Available at: <http://www.ncbi.nlm.nih.gov/pubmed/15180142>. Accessed 15 Jan 2014.
119. Haritoglou C, Neubauer AS, Gandorfer A, Thiel M, Kampik A. Indocyanine green for successful repair of a long-standing macular hole. *Am J Ophthalmol*. 2003;136(2):389–91. Available at: <http://www.ncbi.nlm.nih.gov/pubmed/12888079>. Accessed 15 Jan 2014.
120. Lappas A, Foerster AMH, Kirchoff B. Use of heavy silicone oil (Densiron-68) in the treatment of persistent macular holes. *Acta Ophthalmol*. 2009;87(8):866–70. Available at: <http://www.ncbi.nlm.nih.gov/pubmed/18983619>. Accessed 13 Apr 2012.
121. Rizzo S, Genovesi-Ebert F, Vento A, Cresti F, Miniaci S, Romagnoli MC. Heavy silicone oil (Densiron-68) for the treatment of persistent macular holes: Densiron-68 endotamponade for persistent macular holes. *Graefes Arch Clin Exp Ophthalmol*. 2009;247(11):1471–6. Available at: <http://www.ncbi.nlm.nih.gov/pubmed/19649646>. Accessed 13 Apr 2012.
122. Kapoor KG, Khan AN, Tieu BC, Khurshid GS. Revisiting autologous platelets as an adjuvant in macular hole repair: chronic macular holes without prone positioning. *Ophthalmic Surg Lasers Imaging*. 2012;43(4):291–5. Available at: <http://www.ncbi.nlm.nih.gov/pubmed/22589336>. Accessed 15 Jan 2014.
123. Kung Y-H, Wu T-T. The effect of autologous serum on vitrectomy with internal limiting membrane peeling for idiopathic macular hole. *J Ocul Pharmacol Ther*. 2013;29(5):508–11. Available at: <http://www.ncbi.nlm.nih.gov/pubmed/23323888>. Accessed 15 Jan 2014.
124. Lansing MB, Glaser BM, Liss H, et al. The effect of pars plana vitrectomy and transforming growth factor-beta 2 without epiretinal membrane peeling on full-thickness macular holes. *Ophthalmology*. 1993;100(6):868–71; discussion 871–2. Available at: <http://www.ncbi.nlm.nih.gov/pubmed/8510899>. Accessed 15 Jan 2014.
125. Cho HY, Kim YT, Kang SW. Laser photocoagulation as adjuvant therapy to surgery for large macular holes. *Korean J Ophthalmol*. 2006;20(2):93–8. Available at: <http://www.pubmedcentral.nih.gov/articlerender.fcgi?artid=2908834&tool=pmcentrez&rendertype=abstract>. Accessed 15 Jan 2014.
126. Lo WR, Hubbard GB. Macular hole formation, spontaneous closure, and recurrence in a previously vitrectomized eye. *Am J Ophthalmol*. 2006;141(5):962–4. Available at: <http://www.ncbi.nlm.nih.gov/pubmed/16678522>. Accessed 20 Apr 2012.
127. Gross JG. Late reopening and spontaneous closure of previously repaired macular holes. *Am J Ophthalmol*. 2005;140(3):556–8. Available at: <http://www.ncbi.nlm.nih.gov/pubmed/16139019>.
128. Takahashi H, Kishi S. Optical coherence tomography images of spontaneous macular hole closure. *Am J Ophthalmol*. 1999;128(4):519–20. Available at: <http://www.ncbi.nlm.nih.gov/pubmed/10577602>. Accessed 15 Jan 2014.

129. Kokame GT, McCauley MB. Spontaneous reopening of a spontaneously closed macular hole. *Am J Ophthalmol.* 2002;133(2):280–2. Available at: <http://www.ncbi.nlm.nih.gov/pubmed/11812442>. Accessed 15 Jan 2014.
130. Menchini U, Virgili G, Giacomelli G, Cappelli S, Giansanti F. Mechanism of spontaneous closure of traumatic macular hole: OCT study of one case. *Retina (Philadelphia, Pa).* 2003;23(1):104–6. Available at: <http://www.ncbi.nlm.nih.gov/pubmed/12652242>. Accessed 15 Jan 2014.
131. Shaikh S, Garretson B. Spontaneous closure of a recurrent macular hole following vitrectomy corroborated by optical coherence tomography. *Ophthalmic Surg Lasers Imaging.* 2003;34(2):172–4. Available at: <http://www.ncbi.nlm.nih.gov/pubmed/12665236>. Accessed 15 Jan 2014.
132. Duker JS, Wendel R, Patel AC, Puliafito CA. Late re-opening of macular holes after initially successful treatment with vitreous surgery. *Ophthalmology.* 1994;101(8):1373–8. Available at: <http://www.ncbi.nlm.nih.gov/pubmed/8058282>. Accessed 13 Apr 2012.
133. Li J, Tang S, Luo Y, Zhang J, Lin S. The preliminary report of pathological changes of epiretinal membranes and internal limiting membrane removed during idiopathic macular hole surgery. *Yan Ke Xue Bao.* 2002;18(3):143–6. Available at: <http://www.ncbi.nlm.nih.gov/pubmed/15510742>. Accessed 15 Jan 2014.
134. Fekrat S, Wendel RT, de la Cruz Z, Green WR. Clinicopathologic correlation of an epiretinal membrane associated with a recurrent macular hole. *Retina (Philadelphia, Pa).* 1995;15(1):53–7. Available at: <http://www.ncbi.nlm.nih.gov/pubmed/7754248>. Accessed 20 Apr 2012.
135. Uemoto R, Yamamoto S, Takeuchi S. Epimacular proliferative response following internal limiting membrane peeling for idiopathic macular holes. *Graefes Arch Clin Exp Ophthalmol.* 2004;42(2):177–80. Available at: <http://www.ncbi.nlm.nih.gov/pubmed/14648135>. Accessed 20 Apr 2012.
136. Hillenkamp J, Kraus J, Framme C, et al. Retreatment of full-thickness macular hole: predictive value of optical coherence tomography. *Br J Ophthalmol.* 2007;91(11):1445–9. Available at: <http://www.pubmedcentral.nih.gov/articlerender.fcgi?artid=2095445&tool=pmcentrez&rendertype=abstract>. Accessed 13 Apr 2012.
137. Hayreh SS. Anterior ischemic optic neuropathy. IV. Occurrence after cataract extraction. *Arch Ophthalmol.* 1980;98(8):1410–6. Available at: <http://www.ncbi.nlm.nih.gov/pubmed/7417076>. Accessed 9 Feb 2014.
138. McCulley TJ, Lam BL, Feuer WJ. Incidence of nonarteritic anterior ischemic optic neuropathy associated with cataract extraction. *Ophthalmology.* 2001;108(7):1275–8. Available at: <http://www.ncbi.nlm.nih.gov/pubmed/11425687>. Accessed 9 Feb 2014.
139. Yee K, Pan B, Ross-Cisneros F, Chu E, Sadun A, Sebag J. Immunohistochemistry detects inner retina in excised membranes from vitreo-maculopathies with poor post-operative vision. In: *Association for Research in Vision and Ophthalmology.* Ft. Lauderdale, FL. 2012.
140. Pan B, Yee K, Sadun A, Sebag J. A longer time interval before re-operation is associated with less retinal damage and better visual acuity in macular hole and macular pucker. In: *Association for Research in Vision and Ophthalmology.* Seattle, WA. 2013.

Simon Brunner and Susanne Binder

Outline

I. Introduction

II. Indications and Timing of Surgery

- A. Cataract
- B. Vitreous Hemorrhage
- C. Diabetic Maculopathy
- D. Retinal Detachment
- E. Neovascular Glaucoma

III. Surgical Procedures

- A. Preparation and Anesthesia
- B. Modern Surgical Equipment
 - 1. Microscope
 - 2. Vitrectomy Machine
 - 3. Surgical Instruments
 - 4. Viewing Systems
 - 5. Chromodissection
 - 6. Internal Tamponade
- C. Cataract Surgery
- D. Glaucoma Surgery
 - 1. Aqueous Shunt Procedures
 - 2. Cyclodestruction
- E. Vitrectomy Surgery
 - 1. Sclerotomies
 - 2. Pars Plana Vitrectomy
 - a. Management of Incomplete Posterior Vitreous Cortex Separation
 - 3. Retinal breaks and Detachment
 - 4. Endolaser Photocoagulation
 - 5. Vitreous Substitutes
 - 6. Wound Closure

IV. Surgical Complications

- A. Intraoperative Complications
 - 1. Anterior Segment
 - a. Corneal Opacification
 - b. Small Pupil
 - c. Lens

- 2. Posterior Segment
 - a. Intraocular Hemorrhage
 - b. Subretinal Infusion
 - c. Retinal Breaks and Detachment
- B. Postoperative Complications
 - 1. Anterior Segment
 - a. Conjunctiva
 - b. Cornea
 - c. Uveitis or Iritis
 - d. Intraocular Pressure Elevation
 - 2. Vitreous Hemorrhage
 - 3. Fibrinoid Syndrome
 - 4. Anterior Hyaloidal Fibrovascular Proliferation

References

Keywords

Vitreous • Diabetic retinopathy • Proliferative diabetic vitreo-retinopathy • Vitreoretinal surgery • Vitreous hemorrhage • Diabetic macular edema • Neovascular glaucoma • Fibrinoid syndrome • Anterior hyaloidal fibrovascular proliferation • Complications in vitreous surgery

Key Concepts

1. Vitreo-retinal surgery plays a major role in treating diabetic vitreo-retinopathy by removing media opacities, relieving vitreo-retinal adhesion/traction, deactivating ischemic retina, and applying internal tamponades or intravitreal medications. Comprehensive equipment is necessary: coaxial microscope, wide-angle viewing, endolaser probe, diverse microinstruments, as well as different internal tamponades and dyes for chromodissection.

S. Brunner, MD (✉) • S. Binder, MD
Department of Ophthalmology, Rudolph Foundation Hospital,
Vienna, Austria

The Ludwig Boltzmann Institute for Retinology and
Biomicroscopic Laser Surgery, Vienna, Austria
e-mail: simon.brunner@wienkav.at; susanne.binder@wienkav.at

2. In diabetic maculopathy, it is not only necessary to know the different techniques of vitrectomy, but also to consider adjunctive therapies such as laser treatment and/or intravitreal anti-angiogenic injections prior to and/or during surgery to treat the non-tractional component of diabetic macular edema.
3. In complex cases with advanced retinal ischemia, endophotocoagulation, silicone oil tamponade, and the injection of anti-angiogenic drugs may inhibit propagation of angiogenesis. Combined vitrectomy and cataract extraction is recommended, especially in those cases, with posterior capsule preservation to mitigate iris neovascularization. Silicone IOLs must not be used, as they can swell and opacify when in contact with intravitreal oil.

I. Introduction

Intraocular surgery experienced a great revolution in the 1970s, when pars plana vitrectomy was developed. In the past decades, improvements in technique and instrumentation have broadened its use [1–3]. In recent times, it became an established tool in the management of the most severe complications of diabetic retinopathy [4]. Nonetheless, the decision for surgery of diabetic vitreoretinopathy depends on many factors and has to be carefully balanced against conservative treatments. The potential improvement of visual function or stabilization of anatomic structures has to be determined and compared with the patient's expectations and needs. All possible surgical side effects and benefits, as well as the consequences of alternative strategies, must be discussed in detail. Lastly, the timing of surgical intervention is an important consideration.

According to the natural history of disease, one of the milestones in the evolution of diabetic retinopathy is progressive retinal microvascular occlusion with consequent retinal ischemia. This is the main cause of chronic tissue hypoxia with subsequent development of retinal, optic disc, and and/or iris neovascularization. These changes are triggered by different proangiogenic factors, as insulin-like growth factor 1 (IGF-1), vascular endothelial growth factor (VEGF), basic fibroblast growth factor (bFGF), and others [5–7]. VEGF is suspected to mobilize and augment endothelial progenitor cells (EPC) from bone marrow to the sites of ischemia by acting as a chemoattractant protein [8–10]. In the final stages, these processes lead to the development of fibrovascular proliferations and membranes, proliferating in the space between vitreous and retina, thus bearing a high risk of vitreous hemorrhage, retinal tractional detachment, or

finally neovascular glaucoma. Surgery should be contemplated well before these advanced stages of disease. Lastly, the surgical principles and techniques described in this chapter may be applied to the treatment of other ischemic retinopathies as well (e.g., Coats' disease, retinal vascular occlusions, or retinopathy of prematurity).

II. Indications and Timing of Surgery

A. Cataract

Modern small-incision cataract surgery with implantation of an intraocular lens (IOL) is usually well tolerated even in advanced diabetic retinopathy as long as there is no severe anterior segment neovascularization [11]. In addition, lens removal allows for better fundus evaluation and/or further treatment, e.g., panretinal photocoagulation (PRP). However, any coexisting diabetic macular edema might progress after cataract surgery. There is some evidence that this progression might be lower when grid/focal laser is applied before cataract surgery or when PRP is applied after lens extraction instead of before [12]. Proliferative diabetic retinopathy should be still treated with PRP before cataract surgery, but it is also regarded as safe when PRP is applied at the time of surgery or shortly thereafter [13]. In recent times, an increasing trend for simultaneous cataract surgery and pars plana vitrectomy has been observed, following many considerable improvements in vitrectomy surgery techniques [14]. The advantage of a simultaneous cataract extraction and vitrectomy is a much better intraoperative view and access to the vitreous base, which is of great importance, especially in cases of diabetic fibrovascular proliferations. Following the observations of Schiff et al., reoperation rates seem to decrease when the lens has been removed during vitrectomy [15]. Accordingly, neovascularization of the anterior segment after combined surgery has become less hazardous when PRP and/or anti-VEGF drugs were carefully applied during surgery. However, in young diabetic patients with more or less clear lenses, the possible loss of accommodation has to be weighed against an earlier cataract formation after vitrectomy with the need of another surgical procedure [11, 15].

B. Vitreous Hemorrhage

Non-clearing vitreous hemorrhage from diabetic retinopathy is the still most common indication for vitrectomy for over 40 years, as there is a trend for an even earlier surgery in most institutions. In the past, patients were observed for many months together with head elevation during sleep, in

the hopes of spontaneous blood clearing, allowing for PRP to induce regression of active retinal neovascularization. However, early vitrectomy, defined by the Diabetic Retinopathy Vitrectomy Study (DRVS) as within 1–4 months from onset, usually results in earlier functional recovery and better outcome after 2 and 4 years [16]. This benefit was even greater in patients with type 1 diabetes, compared to type 2, perhaps due to a significantly higher incidence of diabetic macular edema, as well as preexisting posterior vitreous detachment in type 2 diabetic patients [17].

In cases with dense premacular hematoma, blood from fibrovascular proliferation is trapped either between the posterior vitreous cortex and the internal limiting membrane or within a posterior vitreoschisis cavity. Ultrasound and histopathology studies have shown that vitreoschisis is present in 80 % of cases with proliferative diabetic retinopathy [18]. In these cases the hemorrhage is generally well demarcated, leading to massive vision loss centrally. It may be associated with traction macular detachment, which is also a common indication for an early vitrectomy [19]. Other treatment options include short-term observation, laser membranotomy, or intravitreal injections with recombinant tissue plasminogen activator (r-tPA) with/without gas. Pharmacologic vitreolysis with hyaluronidase (Vitrace®) to clear vitreous hemorrhage failed clinical trials and never received FDA approval, most likely because too many type I patients were enrolled. These subjects were young and likely did not have PVD; thus, recurrent vitreous hemorrhage and traction retinal detachment necessitated vitrectomy [see chapter VI.F. Hyaluronidase as a vitreous liquefactant]. In the absence of spontaneous improvement, vitrectomy accelerates functional recovery or decreases the risk of complications [19, 20]. A longer delay than a few months at most for vitrectomy surgery is not advisable, as with disease progression, the surgical procedure and membrane dissection may become more difficult [21, 22]. In non-clearing vitreous hemorrhage together with rubeosis iridis and/or severe progressive proliferative diabetic retinopathy in the fellow eye, immediate vitrectomy is recommended, especially in eyes where no PRP has been applied before [16, 21].

C. Diabetic Maculopathy

The term “maculopathy” may include many different indications for vitreoretinal surgery: from classic macular pucker or macular holes to newer indications such as diabetic macular edema, vitreo-macular traction syndrome, or vitreo-papillary traction. All these entities have specific features in their clinical course and surgical management [23–25]. In diabetic patients, they may occur after premacular hemorrhage or even after extensive PRP [19]. Vitreo-macular traction may eventually result in tractional retinoschisis and is often associated with stronger vitreoretinal adhesions than in

nondiabetic patients [26]. Preretinal membrane formation with or without opacification of posterior vitreous cortex may result in severe visual loss, commonly associated with metamorphopsia [27]. Vitreo-papillary traction is suggested to play a causative role for diabetic macular edema as well; however, the benefit of vitrectomy for this rather rare indication has to be further elucidated [28].

In contrast to macular pucker, diabetic premacular membranes have an increased risk of proliferative activity and are more likely to have focal attachments to the macula [24]. In cases with tangential traction, diabetic macular edema, or after previous intravitreal surgery, macular holes may develop [23, 29].

The procedure to surgically induce vitreo-macular separation in cases with diabetic macular edema is based on the finding that a posterior vitreous detachment was less common in patients with diffuse diabetic macular edema than in diabetic controls without edema [30–32]. Unfortunately, the majority of studies lack homogenous definitions or inclusion criteria. Therefore, results show a large variety concerning the effects of vitrectomy. Even in those trials reporting both morphologic and functional improvements, the effects on morphology have been always more pronounced than the acuity gain. This could be caused by ischemia, subretinal exudates or fibrosis, previous focal/grid laser therapy, the presence of submacular fluid, or a longer duration of diabetic macular edema [33–36]. The effect of an additional inner limiting membrane peel is still not clear; potential benefits in releasing traction have to be weighed against surgical complications, as possible toxic effects of (indocyanine green) chromodissection [37, 38].

To prevent a rapid progression of diabetic macular edema, PRP (if necessary) can be divided into smaller sessions or be applied after intravitreal injections of anti-VEGF medication instead of before [39]. However, in most cases of diabetic macular disorders, the functional outcome is negatively associated with preoperative visual acuity and the degree of maculopathy [23]. As the gain in visual function might be rather small, these pathologies are indications for early, extensive, and careful surgical treatment, performed by experienced vitreoretinal surgeons – usually vitrectomy combined with membrane peeling [40]. It is important to note that diabetic macular edema can often have vitreoschisis [41], causing two or more membranes to be present on the macula. Thus, meticulous dissection of all membranes is important and this procedure can be monitored by pre- and postoperative serial high-resolution optical coherence tomography (hr-OCT) or experimental intraoperative OCT.

D. Retinal Detachment

In proliferative diabetic retinopathy, a progressive proliferation of fibrovascular preretinal tissue may occur despite PRP. Severe fibrovascular proliferations can finally lead to

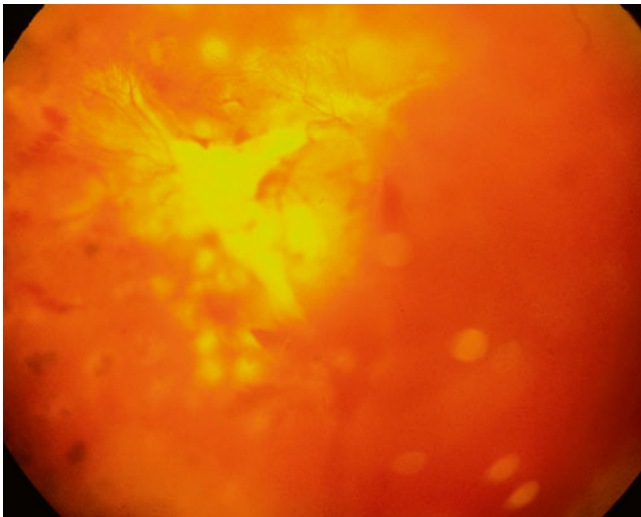


Figure V.A.5-1 Combined traction-rhegmatogenous detachment with dense fibrovascular proliferations over optic disc and arcades also causing tractional retinoschisis

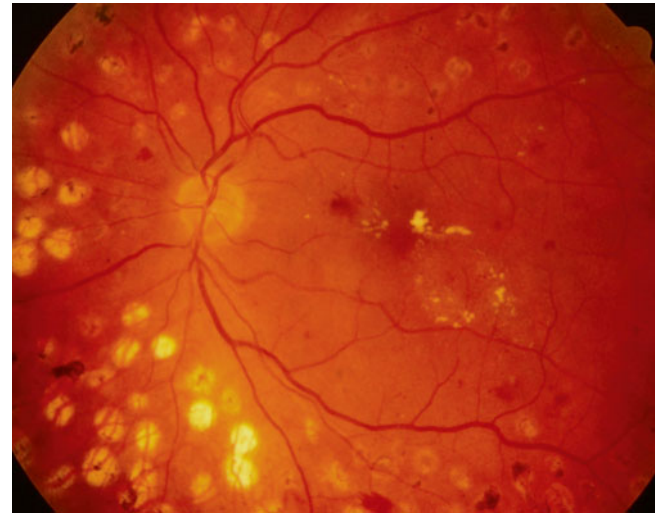


Figure V.A.5-2 Postoperative appearance after successful vitrectomy, membranectomy, endophotocoagulation, and silicone oil tamponade/removal

Table V.A.5-1 Vitrectomy for diabetic tractional retinal detachment: literature

Author, year	n =	Scl.Buck. (%)	Lensect. (%)	Gas/Sil.Oil (%)	Outcome					
					Retina attached (%)	≥5/200 (%)	≥20/200 (%)	Re-OP (%)	Improv. (%)	Phthisis (%)
Rice, 1983 [126]	197	>35	47	n.r./0	57	59	n.r.	29	57	9
Thompson, 1987 [127]	360	22	29	42/0	69	64	n.r.	24	48	11
Oldendoerp, 1989 [128]	100	39	0	65/9	81	77	47	9	71	4
Williams et al. 1989 [129]	69	17	7	51/0	83	71	n.r.	47	n.r.	6
Steinmetz, 2002 [44]	67	24	6	64/1	93	70	57	33	72	0

n number of cases in trials, *Scl.Buck.* Scleral Buckling procedure, *Lensect.* Lensectomy, *Gas/Sil.Oil* percentage of fluid/gas exchange or silicone oil instillation, *Ret.* Retina, *Re-OP* reoperations rate, *Improv.* percentage of functional (visual) improvement, *Phthisis* percentage of postoperative phthisis bulbi, *n.r.* not reported

profound loss of vision due to retinal detachment involving the macula and necessitate surgical intervention [11, 21] (Figures V.A.5-1 and V.A.5-2). Overall, the benefit of vitreoretinal surgery tends to increase with increasing severity of neovascularization. Eyes with a combination of severe fibrovascular proliferations and at least moderately severe neovascularization despite full-scatter PRP are definite indications for an early vitrectomy [4, 16]. On average, stable or even improved visual function may be achieved after surgery in 78 % of cases. Factors such as a better baseline visual acuity (>5/200), no iris neovascularization, or a younger age (<40 years), and complete preoperative PRP were found to be good prognostic factors [19, 21, 42] (Table V.A.5-1).

When neovascular membranes and fibrovascular proliferations grow into the cortical vitreous gel, forming firm vitreoretinal adhesion, contraction over time [25] results in traction retinal detachment [43]. Twenty years ago traction macular detachment in diabetics had been the most com-

mon indication for vitrectomy [21]. Nevertheless, patients showing severe macular traction detachment do still have poor functional results, even after successful vitrectomy [44, 45]. Accordingly, reoperation rates in diabetic traction detachment are higher than 24 % on average, reaching up to 47 % [34, 46] (Table V.A.5-1). In most severe proliferative diabetic cases, dense fibrovascular proliferation may cause traction and progressive membrane contraction, resulting in posterior retinal breaks, often combined with white hydration lines [47]. These holes are often located posteriorly or adjacent to vitreoretinal traction sites, sometimes combined with subretinal hemorrhage and retinal elevations [48]. In those desperate cases, the use of silicone oil may finally at least reduce the incidence of further complications, as neovascular glaucoma, and phthisis. Despite a generally high rate of reattachments, silicone oil cases usually obtain just a small to moderate functional improvement [48, 49].

E. Neovascular Glaucoma

In diabetic neovascular glaucoma, neovascularization or the growth of fibrovascular membranes in the chamber angle obstructs aqueous outflow so that the intraocular pressure rises. The ischemic retina is seen as the source of different vasoproliferative growth factors that diffuse into the anterior chamber [50]. Consequently, the first strategy is to reduce or even eliminate the ischemic neovascular stimulus by full-scatter PRP or cryotherapy. This can be combined with intravitreal or intracameral anti-VEGF medications as a short-term adjunct, especially when PRP fails to cause regression of rubeosis [51, 52]. In cases with opacified optical media, as cataract or vitreous hemorrhage, sufficient PRP can only be applied during or after vitrectomy with cataract extraction and a possible silicone oil tamponade. This procedure has been shown to reduce recurrent vitreous hemorrhage and rubeosis, thereby improving neovascular glaucoma [53]. Argon laser trabeculoplasty, as well as other non-penetrating glaucoma procedures are generally not recommended in diabetic neovascular glaucoma – as it has been shown that angle closure can even deteriorate after surgery [54].

Patients with progressive neovascular glaucoma or even synechial angle closure frequently need additional glaucoma surgery. Unfortunately, success rates for classic filtering surgery or the implantation of glaucoma-drainage tubes in diabetic neovascular glaucoma are much lower than surgery for primary or secondary open-angle glaucoma [54, 55]. To improve outcomes the intraoperative use of antimetabolites, such as mitomycin C, is strongly recommended, as well as an intensive anti-inflammatory treatment. Again, concomitant anti-VEGF injections and PRP, eventually combined with vitrectomy, can improve the outcome [52, 56, 57]. In advanced diabetic neovascular glaucoma with very low visual function, transscleral cryo- or diode-laser cyclocoagulation, is still a helpful, widely used method to control intraocular pressure [58, 59]. Desperate cases of painful, blind eyes may be treated with retrobulbar alcohol injections or finally, by enucleation as last resort [60].

III. Surgical Procedures

A. Preparation and Anesthesia

Before surgery, all patients should be referred to an internist to evaluate the medical and glycemic status, especially cardiovascular problems, since in the presence of advanced diabetic retinopathy, there is a much higher risk of coexistent macrovascular disease [10]. General medical findings may influence the decision for the timing and extent of surgery [61]. In addition, optimal diabetes management can be protective against perioperative wound healing dysfunction or

infection [62]. Patients should be well informed about prognosis, including all advantages and risks of surgery, and about necessary adjustments of medications.

In the operating room right before surgery, a 10 % polyvidone iodine solution is recommended to be applied on the eyelids and a 5 % solution in the conjunctival sac. To guarantee adequate disinfection, applied solutions should dry out for at least 3 min [63]. For optimal intraocular visualization, a combination of different mydriatic, cycloplegic, and sympathomimetic drops should be instilled repeatedly before surgery to allow for a maximal pupillary dilatation [61].

Surgery of diabetic vitreoretinopathy is sometimes performed under general anesthesia, which must be conducted by a specialized anesthesiologist. Alternatively, local anesthesia, sedoanalgesia, or a combination of those is possible [64]. The appropriate form of anesthesia depends on many factors, such as the patient's physical condition, the dimension and duration of surgery, diverging geographic and economic factors, or just the individual preference of the patient and/or surgeon.

B. Modern Surgical Equipment

Surgeons undertaking high-risk procedures as complicated as those for diabetic retinopathy require advanced skills and the use of highly developed equipment or instruments. Rapid advances in microsurgical techniques require regularly modernizing equipment and proper maintenance of all surgical instruments as well as frequent training of surgical skills to all operating room personnel [61].

1. Microscope

For modern vitreoretinal surgery, a binocular stereomicroscope with coaxial illumination (Halogen and/or Xenon) is needed, allowing for a 10–40× magnification. The microscope should be fitted with motorized power focusing, X-Y-positioning and a power zoom via foot pedals. It must be also equipped with different corresponding color laser filters to permit laser coagulation. To provide co-visualization of the operating personnel or live video recording, a beam splitter is necessary [65].

2. Vitrectomy Machine

The basic equipment for surgery of diabetic vitreoretinopathy consists of a modern vitrectomy cutter, combined with a suction unit. Furthermore, an air pump, a fiberoptic light probe, and an infusion of balanced salt solution are needed. Modern vitrectomy machine units usually provide all those basic functions in different combinations, with or without integrated endo-diathermy, endolaser photocoagulation, gas filling, or phacoemulsification modules.

The connected vitrectomy probe allows for cutting and dissecting diabetic membranes or fibrovascular proliferations. Newer probes, where the port is closer to the probe tip than in former constructions, facilitate and secure shaving of peripheral vitreous or membranous fibrovascular proliferations. Illuminators range from standard handheld single-function illumination probes to sophisticated multipurpose illuminated forceps, scissors, or even vitrectomy probes. In some cases of complex diabetic vitreoretinopathy, bimanual dissection with the use of a “chandelier” light illuminator, inserted manually or through additional sclerotomies, may be necessary [66, 67].

3. Surgical Instruments

Numerous types of surgical instruments have been created and further adapted over the past decades. Generally, there is a trend towards disposable single-use instruments for optimal aseptic conditions. For surgery in advanced diabetic retinopathy, 20-gauge vitrectomy systems were standard for many years and are still in use, as they offer the greatest diversity of instruments with minimal flex [61, 68]. In recent years, smaller gauge (23-, 25-, and 27-gauge) instruments have been developed, enabling sutureless sclerotomies, thereby reducing operating time and postoperative irritation to the patients [69–71]. However, in more complex cases, the efficiency of small-gauge vitrectomy is still a matter of debate. 23-gauge systems are mostly used today, showing safer and more reproducible results in cases of advanced diabetic retinopathy, compared to 25-gauge [69, 72].

There is also a great variety of tissue cutting or dissecting instruments. Many different scissors, forceps, or spatulas are available to cut, remove, or peel preretinal membranes. Picks or cannulas may be helpful for subretinal surgery. In complex fibrovascular proliferations, vertical scissors are used for tissue segmentation and horizontal scissors for delamination of the vitreous cortex from the retina [73, 74]. For retinal laser coagulation, retinotomy, or retinopexy procedures, scleral indentators, endo-diathermy, or endolaser probes for all incision sizes are available.

4. Viewing Systems

Noncontact wide-angle lens systems (130°) are another standard equipment and guarantee for optimal fundus visualization by neutralizing the cornea’s refractive power. They can be managed by the surgeon alone, offering a great depth of field and better visualization through media opacities [65, 75]. The additive use of methylcellulose gel or similar substances at the corneal surface during surgery is necessary for corneal clarity.

5. Chromodissection

Dyes are helpful to identify vitreous, retinal, and preretinal structures [see chapter V.A.3. Chromodissection in vitreoretinal surgery]. Various groups of dyes are in use for different

indications: corticosteroid crystals (e.g., triamcinolone acetonide) may be used for easier identification of the vitreous cortex, e.g., in diabetic vitreoretinopathy or retinal detachment surgery [63, 76]. In addition, corticosteroids have no toxic effects and help to prevent fibrin exudation in those cases due to their anti-inflammatory effects [65, 77]. For chromodissection of preretinal membranes in advanced diabetic retinopathy, dyes such as trypan blue are available, as all fibrovascular proliferations or preretinal membranes should be carefully removed to prevent proliferative vitreoretinopathy. Brilliant blue, infracyanine green, or indocyanine green are more specific for staining the inner limiting membrane, whereas preretinal membranes and other structures appear in negative contrast with those dyes [78, 79]. For infracyanine or indocyanine green dyes, surgeons must be aware of possible toxic retinal effects or peripheral visual field defects that could be time- and dose-dependent [79, 80].

6. Internal Tamponade

Various gases and liquids provide internal tamponade of the retina [chapter IV.G. Physiology of vitreous substitutes]. Perfluorocarbon liquid is frequently used as a short-term intraoperative instrument to reattach the retina or to protect the retina against damage from intraocular foreign bodies [81, 82]. Filtered air is useful as a short-term tamponade for several days. To provide a more prolonged tamponade in cases of diabetic vitreoretinopathy or retinal detachment, intraocular gases such as SF₆, C₂F₆, or C₃F₈ are available, providing tamponade times from 2 to 8 weeks. These gases are preferred in patients where some postoperative positioning is indicated, especially for superior or posterior pathologies [83]. In most complicated cases, however, silicone oil is still the instrument of choice, as it provides long-acting tamponade. Different types and brands of silicone oil from 1,000 to 10,000 centistokes are available. Silicone oil may also serve as a barrier to inhibit cytokines or growth factors from distributing to sensitive ocular tissues. To reduce the risk of silicone oil-related complications, these tamponade agents should be removed from the eye after about 3–6 months [84–86].

C. Cataract Surgery

In patients needing vitrectomy surgery for diabetic retinopathy, concomitant cataract surgery may be considered, since lens extraction provides much better intraoperative access to the anterior vitreous, which has a great importance for prognosis, especially in cases of proliferative diabetic vitreoretinopathy. Likewise, it was found that in aphakic or pseudophakic eyes, more complete PRP and resection of fibrovascular proliferations were possible [15]. There are different surgical options: cataract and vitrectomy surgery can be performed separately (by one or two surgeons) or be combined in one single

procedure [87]. Surgeons can start with cataract extraction, followed by vitrectomy and lens implantation at the end of surgery, but lens implantation may be done right after cataract surgery as well. In younger diabetic patients with clear crystalline lenses, patients should be informed that an earlier cataract formation is common after vitrectomy [11, 15].

In our center, combined phacoemulsification directly followed by implantation of a posterior chamber lens is performed in almost all patients undergoing vitrectomy for diabetic vitreoretinopathy, irrespective of the presence of significant cataract. It can be an issue to perform a capsulorhexis in an eye with a dense vitreous hemorrhage disabling the red fundus reflex. Thus, dying of the anterior capsule may be helpful, but the vitreous surgeon has to be an experienced cataract surgeon as well or at least be assisted by an experienced anterior segment specialist. In modern small-gauge vitrectomy, all sclerotomies are usually set and trocars inserted before cataract surgery to avoid hypotony or iris incarceration through the corneal incisions. For the same reason, the infusion line was preplaced and sutured but not connected before lens surgery in traditional 20-gauge vitrectomy.

D. Glaucoma Surgery

1. Aqueous Shunt Procedures

Management of advanced open-angle glaucoma or neovascular glaucoma in diabetic patients can be challenging. Most patients will ultimately need some sort of glaucoma surgery, depending on the stage of angle closure or functional prognosis. However, the outcome of invasive as well as noninvasive procedures is usually worse than in nondiabetics – despite the use of antimetabolites, usually due to an elevated risk for inflammation and hemorrhage in diabetic eyes [54, 56, 88].

Improved pressure control can be attained by intravitreal injections of bevacizumab combined with PRP, followed by glaucoma surgery 10–14 days later [89]. Another option are glaucoma-drainage tubes, such as Ahmed, Molteno or Baerveldt implants, which can be placed in the anterior chamber or in the sulcus ciliaris [88]. Nevertheless, functional results are not better than after standard trabeculectomy procedures, due to bleb formation, scarring of epibulbar tissue, or recurrent intracameral hemorrhages [55]. Other complications include decompensation of the corneal endothelium or exposure of tube material [89, 90]. In addition, vitrectomy surgery may be considered even at earlier stages of glaucoma in proliferative diabetic retinopathy, as it can be easily combined with full-scatter PRP ab interno or different glaucoma-drainage implants [57, 55].

2. Cyclodestruction

In eyes with end-stage neovascular glaucoma and poor visual prognosis, cyclodestructive procedures, such as transscleral

cryo- or diode-laser cyclocoagulation, can be a safe and helpful alternative [58, 59, 88]. Under these circumstances they have proven similar efficacy as trabeculectomy or drainage implant surgery [91]. The footplate of the diode-laser handpiece is placed along the limbus in order to concentrate the laser energy in the target tissue. Power is set between 1,500 and 2,500 mW with a pulse duration between 1.5 and 2.0 s. A total of 15–25 laser spots are applied to the full circumference, with sparing of the horizontal meridians [88]. Alternatively, cyclo-cryocoagulation of the ciliary body or cryocoagulation of the peripheral retina is performed in a similar way by indirect ophthalmoscopy. Cryocoagulation with no funduscopy control carries the risk of inducing choroidal neovascularization or overtreatment with resultant hypotension and phthisis [53].

Surgery is performed under retrobulbar local anesthesia, and after surgery, topical diclofenac, prednisolone, and atropine are given.

E. Vitrectomy Surgery

1. Sclerotomies

For many decades three-port vitrectomy has been used as a worldwide standard technique: one inferotemporal pars planar sclerotomy for intraocular infusion and two more incisions in the superotemporal and superonasal quadrants. All sclerotomies are prepared in a distance of 3.5–4.0 mm from the limbus. To reduce surgical trauma and postoperative discomfort, transconjunctival small-gauge trocar-guided systems (23-g and 25-g) are used with increasing frequency for almost all indications today, thereby replacing the classical 20-g system [68, 69, 72]. To assure optimal sclerotomy construction without intra- or postoperative wound dehiscence, all incisions should be oriented parallel to the limbus and trocars inserted 25° oblique to the scleral surface. To avoid suprachoroidal infusion and choroidal detachment, exact infusion cannula placement is critical (Figure V.A.5-3). In eyes with anterior retinal displacement, anterior fibrovascular proliferations, or obscured view, a 6-mm infusion cannula can be used instead of the standardized 4-mm cannula. In cases after silicone oil implantation, suturing of sclerotomies is always recommended to avoid subconjunctival extrusion of oil. In complicated cases of diabetic vitreoretinopathy, a 4-port vitrectomy allows for a safer bimanual dissection. For this purpose, a chandelier light probe is fixed between the two superior sclerotomies or in the nasal inferior quadrant.

2. Pars Plana Vitrectomy

The endo-illuminator and vitrectomy probes are first inserted through the upper sclerotomies and vitrectomy is started under microscopic view (Figure V.A.5-3). To avoid displacement of intraocular structures, infusion is turned on only

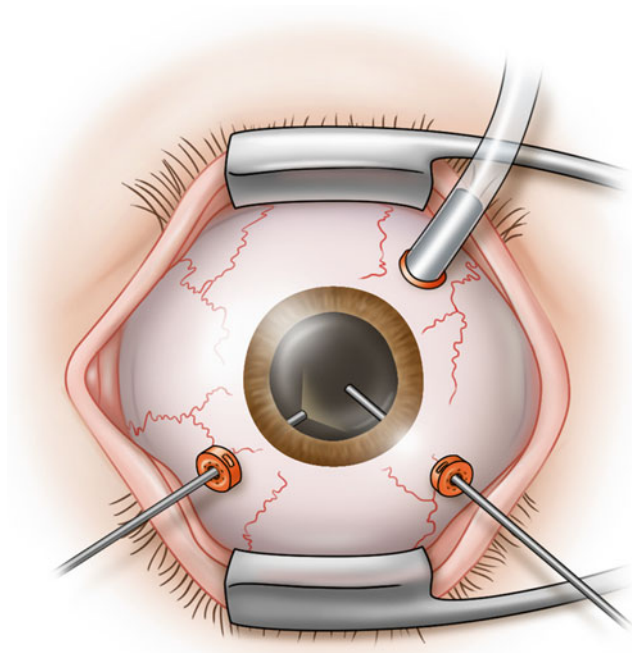


Figure V.A.5-3 Standard vitrectomy preparation: an infusion cannula is inserted in the inferotemporal pars plana sclerotomy. A fiberoptic illuminator and the vitreous cutter are positioned in the anterior vitreous cavity and visualized through the pupil

when the endo-illuminator and cutter probes are in the eye, ready to start vitreous removal. After removing the most anterior vitreous behind the lens, a noncontact wide-angle lens system, e.g., BIOM, is inserted to perform central (core) vitreous removal. For easier identification of the posterior vitreous cortex or vitreous remnants on the retina, 2–4 mg of triamcinolone acetonide will offer sufficient staining with no retinal toxicity [65, 76, 77]. Furthermore, the anti-inflammatory and antiangiogenic effects may prevent post-operative complications, especially in proliferative diabetic vitreoretinopathy.

In the presence of a complete or nearly complete posterior vitreous detachment, the posterior vitreous cortex is incised and the opening enlarged to improve visualization of the posterior pole and retina [7] (Figure V.A.5-4). However, surgeons should always be aware of *posterior vitreoschisis* that can mimic posterior vitreous separation in diabetic patients [92]. For the core vitrectomy, a higher cutting rate is used (3,000–5,000 cuts/min) and aspiration can be increased, but should be decreased again during removal of the posterior vitreous to reduce tractional forces to the retina. Pooled unclotted blood at the posterior pole can be aspirated with a soft-tipped fluid needle (Figure V.A.5-5). As soon as visualization of the retina is optimized, bleeding areas of (fibrovascular) neovascularization can be identified and treated with diathermy. In addition, dyes can be used to look for residual preretinal or premacular membranes or to remove the internal limiting membrane. Vitrectomy is fin-

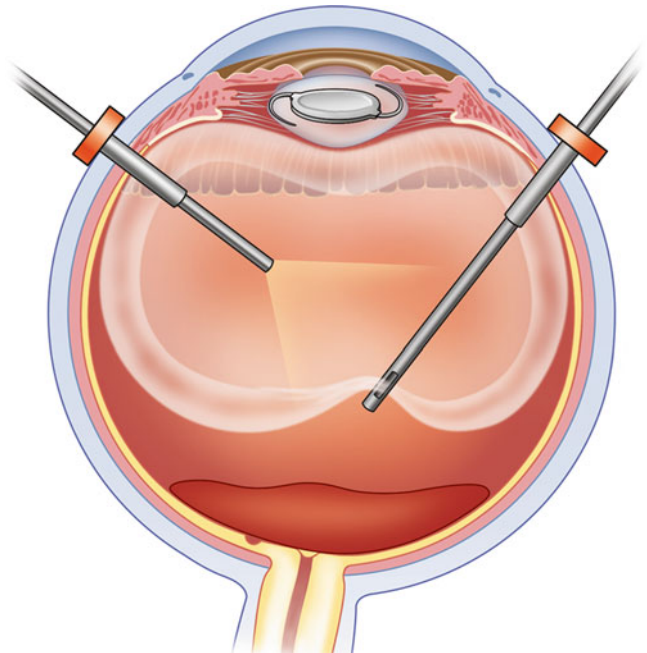


Figure V.A.5-4 Easy incision of the posterior vitreous cortex with the vitreous cutter, as a complete posterior vitreous detachment is present

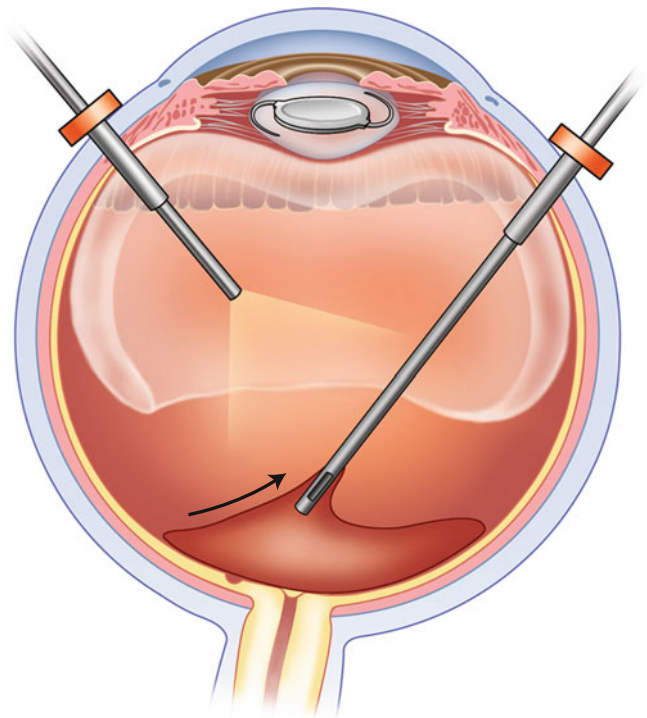


Figure V.A.5-5 Layered preretinal (retro-cortical) hemorrhage may be safely removed using a soft-tipped cannula

ished by removing all blood and vitreous remnants at the vitreous base under 360° indentation to prevent postoperative hemorrhage, tissue contraction, or neovascular glaucoma. However, in phakic eyes, usually more residual

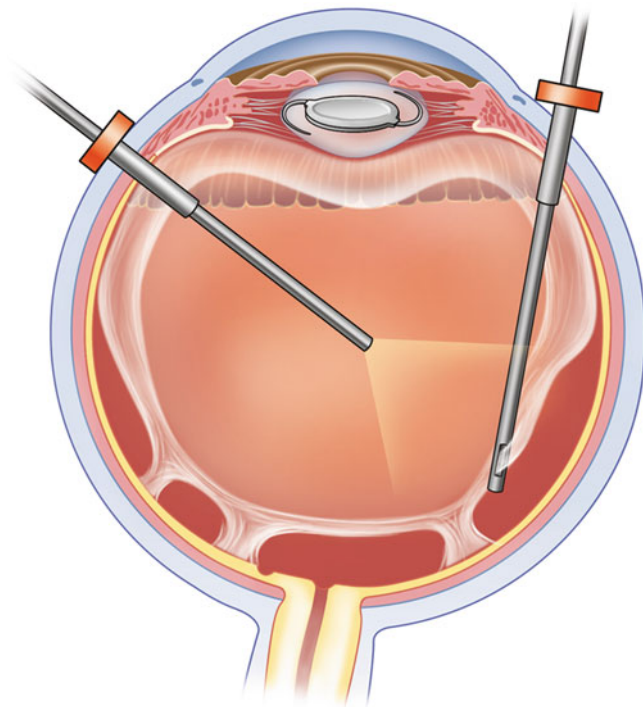


Figure V.A.5-6 Principle of incomplete posterior vitreous detachment with several focal vitreoretinal adhesions. To get access to the retro-cortical space, a hole is made in the outer cortical vitreous in an area of vitreoretinal separation. The port of the cutter is directed against the cortical vitreous and away from the retina

vitreous will remain than in pseudophakic eyes. For the same reason, full-scatter endolaser coagulation is now performed up to the retinal periphery. Finally, a fluid-air exchange can be performed to reduce the risk of postoperative hypotony and hemorrhage.

a. Management of Incomplete Posterior Vitreous Cortex Separation

In patients with incomplete separation of the posterior vitreous cortex, vitrectomy can be difficult even for experienced surgeons. Generally a core vitrectomy is performed first to get an overview of the areas of vitreoretinal adhesion or the tangential connections between them. Subsequently, anterior-posterior traction can be relieved with the vitreous cutter in all areas of existing vitreoretinal separation. In areas where the posterior vitreous is closely adjacent to the retina, gentle suction with the vitrector might be sufficient to provide a safe dissection of the vitreous from the retina (Figures V.A.5-5 and V.A.5-6). However, if the access to the subcortical (preretinal) space is more difficult, then gentle suction can be used to localize areas with less vitreoretinal adherence, e.g., areas of subcortical hemorrhage. A sharp blade may be used to create an access to the subcortical space, preferentially around the optic disc. Once any part of the posterior vitreous cortex is lifted

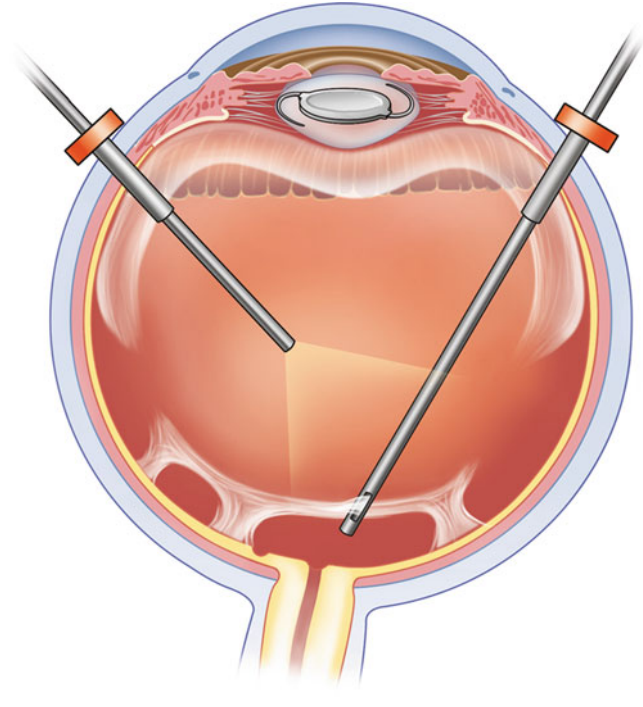


Figure V.A.5-7 The vitreous cutter is releasing tangential traction by excising remnants of the posterior vitreous cortex and fibrovascular tissue between areas of stronger vitreoretinal adhesion

up, relief of traction and separation of fibrovascular tissue is performed, usually centrifugally. Bleeding sources need to be cauterized immediately to maintain a controlled situation all the time.

3. Retinal breaks and Detachment

In cases of retinal breaks or detachment, the surrounding tissue must be carefully excised to eliminate residual traction. Other dissecting instruments, such as scissors or spatulas, might be needed to carefully separate the tissues, eventually with the injection of viscoelastic substances between the retina and posterior vitreous cortex [93–95]. Some perfluorocarbon might be useful to flatten out a localized retinal detachment and facilitate sufficient laser treatment of the holes. Several surgical techniques for removal of vitreoretinal adhesions or fibrovascular membranes have been developed. In *segmentation*, tangential tractions between centers of adhesions are removed [7, 96] (Figures V.A.5-7 and V.A.5-8), while in *delamination* the connections between the posterior vitreous cortex and the internal limiting membrane are cut [96, 97] (Figure V.A.5-9). The *en bloc technique* is designed to remove vitreous and associated vitreoretinal membranes [98] (Figure V.A.5-10). After core vitrectomy, the posterior vitreous cortex is opened in an area close to the optic nerve. Now it should be tried to gently loosen the connected fibrovascular tissue over the posterior pole in one piece. The remaining peripheral vitreous cortex will then lift the residual vitreous and membranes up into the mid-vitreous cavity, where it can

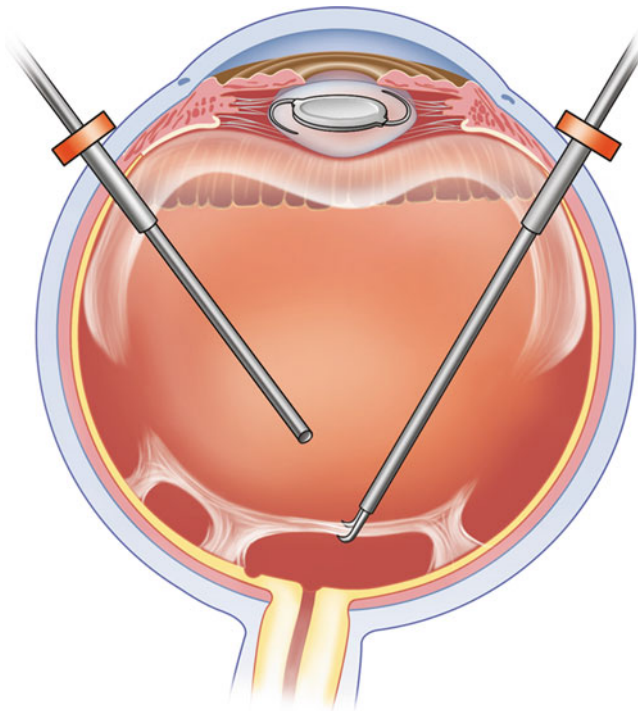


Figure V.A.5-8 In cases where posterior vitreous separation is not large enough to allow access of the vitreous cutter, the space between the posterior vitreous cortex and retina can be opened and augmented with vertical membrane peeler-cutter scissors

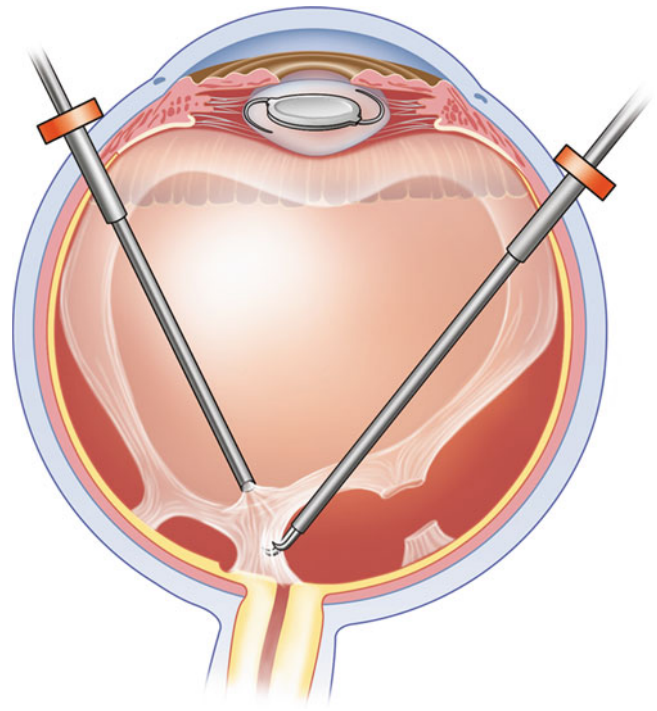


Figure V.A.5-10 En bloc vitrectomy. First, an opening is made into the posterior vitreous cortex adjoining tractional fibrovascular proliferations. Second, membrane peeler-cutter scissors enter the retro-cortical space separating the vitreous and fibrovascular tissue from the retina. The unremoved formed anterior vitreous provides anterior traction, which helps to identify and cut the sites of adhesion

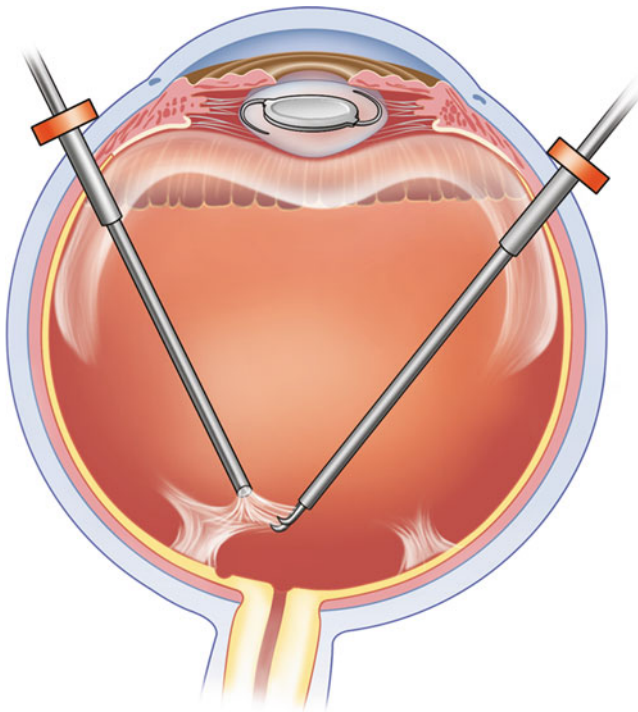


Figure V.A.5-9 Delamination: smaller fibrovascular adhesions to the posterior vitreous cortex are excised with horizontal scissors, mostly parallel to the retinal surface

be removed safely. If adhesions are too strong during the *en bloc technique*, a change to *delamination* or *segmentation* is advisable, although the current cutters of the 23-g systems have an opening close to the tip, allowing for segmentation of tissue without scissors or forceps. If all bleeding sources are cauterized and fibrovascular proliferations or membranes are cleaned up to the anterior retina, circular 360° laser coagulation treatment in multiple rows is performed up to the ora serrata under indentation. The tamponade of choice is either a long-acting gas tamponade or silicone oil.

For stabilization of the posterior pole during peripheral tissue removal, perfluorocarbon liquid can be used. However, the use of perfluorocarbon is not harmless if the retina is inelastic and shortened. Small retinal breaks can turn into a large holes and perfluorocarbon or silicone oil tamponade might glide into the subretinal space. Careful inspection of the retinal periphery during indentation is needed. Anteriorly dislocated retina must be freed from fibrotic tissue. Retinotomies and retinectomies cannot replace a careful membrane dissection and should be reserved only for selected cases, e.g., in eyes where reoperations become necessary or severe anterior hyaloid fibrovascular proliferations develop.

Diathermy must be applied to the margins of the intended retinotomy and surrounding vessels before the retina is cut. Sometimes, a shallow retinal detachment must be created in

order to cut without traumatizing the choroid. Retinotomies and retinectomies can be cut either with the vitrectomy cutter or scissors. They should be dimensioned to reach vital retinal tissue around the area of traction and to release all tractions around retinal holes, even in the anterior region. Surgeons must keep in mind that eyes requiring retinectomies have a much poorer outcome and visual prognosis than those not requiring [99].

In primary procedures, the retina is usually more elastic and an additional encircling band might make retinectomies unnecessary. It can also be useful in younger diabetics with sufficient central visual acuity in the presence of severe active fibrovascular proliferations and retinal detachment. In those cases combined surgery is started with the episcleral procedure. After a 360° dissection of the conjunctiva 1–2 mm behind the limbus, a Tenon's capsule peritomy is performed. All four rectus muscles are held with suture loops and four additional 5.0 nylon mattress sutures prepared intrasclerally in each quadrant to fix the encircling band. The distance between the sutures should be chosen 2 mm wider than the diameter of the silicone band to produce sufficient indentation, whereas the anterior suture is always placed 2–4 mm behind the rectus muscle insertions. The band is then placed under the muscles and the sutures that are fixed to secure the band. To reduce pressure during buckle placement and fixation, a paracentesis can be performed. However, a shallow buckle is usually enough to support the vitreous base. In eyes where lens surgery is planned, the infusion line is first prepared but not turned on. The anterior chamber is filled with viscoelastic through a small limbal incision, followed by standard phacoemulsification and intraocular lens implantation. To secure the cataract wound in complex diabetic vitrectomy with intra- and postoperative changes in intraocular pressure, a 10/0 nylon suture is advisable.

4. Endolaser Photocoagulation

Full-scatter PRP with an endolaser coagulation probe is a standard procedure today during vitrectomy surgery of diabetic vitreoretinopathy. The main goal is to achieve regression of neovascularization and to create adhesions around retinal breaks, retinotomies, and retinectomies [4, 25, 95, 100]. Additional photocoagulation is applied even in the presence of preexisting PRP, especially to the anterior retina and to areas around neovascularizations, eventually with the help of scleral depression. To get an adequate coagulation effect, the retina must be attached to the retinal pigment epithelium which might make it necessary to use internal tamponades with a high surface tension, as perfluorocarbon liquids [101]. To get sufficient gray-whitish laser effects, the power of the laser beam has to be adjusted continuously, depending on the clarity of media or the distance to the retina. Furthermore, the angle of the laser pipe in relation to the retinal plane will determine the intensity of

coagulation; anyway, hard hyperintense laser effects should be avoided [25, 102].

5. Vitreous Substitutes

To allow for adequate internal tamponade of the retina at the end of surgery, several liquids and gases are available. Heavy perfluorocarbon liquid is often used intraoperatively to reattach the retina or permit retinal laser coagulation. At the end of surgery, it must be removed to avoid retinotoxic effects [81, 82]. Perfluorocarbon can be replaced by fluid or filtered air that will be absorbed after a few days. To perform a fluid/air exchange, air from an air pump is supplied through the infusion port and BSS is stopped. To aspirate the fluid from the vitreous cavity, a fluted needle is used [7]. In cases of retinal breaks, hemorrhage, or detachment, different gases (SF₆, C₂F₆, C₃F₈) with more prolonged tamponade times (up to 8 weeks) are necessary, especially for posterior or superior pathologies [83]. After fluid/air exchange, the eye may be flushed with the gases in the desired non-expansive concentration (18 % for SF₆, 16 % for C₂F₆, and 14 % for C₃F₈) to minimize the risk of intraocular pressure elevation. If a longer tamponade is required in severe cases of PVR, after retinectomies, or severe hemorrhages or if positioning is difficult, silicone oil may be instilled after fluid/air exchange or in exchange to perfluorocarbon liquid. In aphakic eyes, an inferior iridectomy prevents silicone oil from entering the anterior chamber. To avoid late silicone-oil-related complications, such as glaucoma, optic disc atrophy, or keratopathy, the oil should be removed after 3–6 months on average [85, 86, 103, 104].

6. Wound Closure

After all silicone oil procedures, as well as in 20-gauge vitrectomies, all sclerotomies should be sutured with intrascleral 7.0 or 8.0 Vicryl sutures, starting with the superior sclerotomies. In small-gauge (23-g, 25-g, or 27-g) transconjunctival vitrectomies, intraocular pressure is slightly lowered before removal of the cannulas, and sclerotomies can remain unsutured or may be stabilized with an intravitreal air or gas bubble. However, delayed wound healing and higher risk of infections is often present in diabetic patients so suturing can be reasonable even after small-gauge surgery. Finally, sub-Tenon's injection of steroids as well as topical antibiotics, cycloplegics, and steroids are given together with a sterile dressing to prevent postoperative inflammation or infection [61, 72].

IV. Surgical Complications

As surgical techniques have continuously improved in conjunction with a better understanding of pathogenesis in diabetic eye disease, the frequency and severity of complications

have decreased dramatically. However, adequate and efficient management of all possible complications is still essential to optimize surgical results.

A. Intraoperative Complications

1. Anterior Segment

a. Corneal Opacification

Diabetic patients are generally predisposed to develop corneal edema intra- or postoperatively due to glycosylation-induced basement membrane disease, as occurs throughout the body, resulting in endothelial cell dysfunction [7, 105]. Corneal edema may occur in relation to an intraocular pressure elevation, the duration of surgery, or trauma to the endothelium [106]. To prevent its occurrence, the use of lubricants (e.g., methylcellulose) at the corneal surface or into the anterior chamber maintains a longer corneal integrity and clarity. If a corneal haze is developing, gentle wiping of the corneal surface with a cotton tip may help to reduce the edema. Mechanical debridement of the epithelium decreased with the use of noncontact wide-angle lens systems, as the BIOM, and should be avoided if possible [107]. If a corneal epithelial debridement is necessary, a bandage contact lens should be applied at the end of surgery to provide a fast and painless healing of the epithelial defect. Folds in Descemet's membrane (e.g., during fluid-air exchange) might also distort the fundus view and can be prevented by intracameral use of viscoelastics [7].

b. Small Pupil

Decreased pupil size or miosis hampers visualization of the fundus periphery. It may occur after hypotony, direct mechanical trauma, or prolonged surgery. Modern wide-angle lens systems usually allow for sufficient fundus visualization even with medium-sized pupils. To provide medical dilation, mydriatic drops or other agents might be used topically or injected into the anterior chamber. As a temporary mechanical option, flexible iris retractors or ring retractors are available [108].

c. Lens

As diabetic vitrectomies are increasingly combined with lens surgery and IOL implantations, the problem of intra- or postoperative cataract formation is becoming less significant. However, the incidence of postoperative lens opacification after vitrectomy surgery for diabetic eyes was reported to be from 17 to 37 % [7, 11, 109]. Lens opacities may develop from direct mechanical contact, fluctuations in serum glucose levels during surgery, or after prolonged surgery. The current concept of post-vitrectomy cataract pathogenesis relates to increased intravitreal oxygen levels and the effects of reactive oxygen species on lens proteins [see chapter IV.B. Oxygen in vitreo-retinal physiology and pathology].

Immediate cataract extraction during surgery can become necessary in cases of dense opacities; however, if there are only mild, peripheral opacities, cataract surgery can also be delayed. Lens touch may be prevented by careful dissection; eventually a thin layer of vitreous gel can be left behind the lens to protect it during surgery [109]. Given that vitreous is known to contain antioxidants, this protection is biochemical as well as mechanical. Lastly, some surgeons prefer to include high dose glucose in the infusate during vitrectomy to mitigate against cataract formation intraoperatively [109].

2. Posterior Segment

a. Intraocular Hemorrhage

Intraocular hemorrhage frequently occurs during surgery for diabetic vitreoretinopathy and poses a potential serious complication. Generally, all bleeding sources need to be controlled immediately to improve the surgical outcome. As a first step, transient elevation of intraocular pressure might be sufficient to stop the bleeding source. However, the elevated pressure must then be normalized soon to prevent ischemic damage to other ocular structures. The next option is a mechanical compression of the hemorrhage with a viscoelastic, such as perfluorocarbon liquid bubble directly applied with a silicone-tipped fluid needle. Larger hemorrhages or damage to choroidal vessels needs to be cauterized. Blood clots should be carefully removed in order not to provoke rebleeding. A small amount of fibrin can be left on site to support the hemostatic cascade. The preoperative intravitreal application of anti-VEGF medication (e.g., bevacizumab) might facilitate surgery and reduce intra- and postoperative complications, such as hemorrhage, in severe proliferative diabetic retinopathy [110, 111]. Before finishing surgery, intraocular pressure can be temporarily reduced to identify possible bleeding spots [7].

b. Subretinal Infusion

Infusion fluid, perfluorocarbon liquid, or silicone oil can enter the subretinal space under certain circumstances and pose a rather serious complication. If the infusion tip cannot be clearly visualized in cases of diabetic vitreous hemorrhage, the infusion fluid (BSS) can produce choroidal detachment with a rapidly enlarging indentation. In such cases, the infusion line must be removed. A new sclerotomy is then created in another quadrant, eventually using a longer (6 mm) infusion cannula. Perfluorocarbon or silicone oil can slip under the retina in severe cases of proliferative diabetic vitreoretinopathy, when the retina is atrophic or under traction. To remove these substances completely from the subretinal space can be challenging, but is necessary. In cases with subretinal perfluorocarbon, drainage can be tried through an existing retinal break with a fluted needle, or a new retinotomy can be created more posteriorly. Silicone oil is hard to remove from the subretinal space. Active aspiration with a 23-g cannula can be used for larger silicone bubbles;

however, a retinotomy or retinectomy often has to be created or enlarged for successful removal. This maneuver is sometimes also necessary for relaxation of the retina [see chapter V.B.6. Retinectomy in recalcitrant retinal detachments]. At the end of surgery, a new perfluorocarbon bubble is carefully injected and all retinotomies and breaks must be surrounded with dense photocoagulation. The perfluorocarbon is then exchanged with silicone oil.

c. Retinal Breaks and Detachment

In surgery for diabetic vitreoretinopathy, retinal breaks may occur more frequently than in other vitrectomies and represent a serious complication that has to be meticulously managed [93, 112]. Preexisting breaks may be hidden under fibrovascular tissue or hemorrhages and must be relieved from any traction around them. Iatrogenic breaks should be avoided; however, in atrophic tissue they may develop more easily, especially in the posterior pole in eyes with traction retinal detachments or massive fibrovascular proliferations [112]. After careful preparation the breaks can be marked with diathermy for easier identification and laser coagulation under perfluorocarbon. A detached retina is flattened by perfluorocarbon and all breaks or tears must be surrounded by laser coagulation. In the absence of more serious pathologies, a gas tamponade usually is sufficient to support the detached retina and the breaks [93]. To avoid postoperative entry-site-related retinal incarceration and re-detachment, residual vitreous or fibrovascular tissue around the sclerotomies must be carefully removed. With the use of modern vitreoretinal equipment and small-gauge trocar systems, the frequency of retinal incarceration or entry-side detachments has decreased considerably.

B. Postoperative Complications

1. Anterior Segment

a. Conjunctiva

To prevent conjunctivitis or scleritis from stitch infections or wound dehiscence, careful suturing with inverted knots is advisable, together with adequate postoperative local antibiotic therapy. In the case of infections or abscesses, a swab is taken to determine resistant germs, and local therapy should be continued until resorption of all sutures. Subconjunctival silicone oil can be the consequence of leaking or non-sutured sclerotomies [105].

b. Cornea

Due to neuropathy and pathologic changes in the basement membrane, corneal epithelial defects during or after vitrectomy are more common in diabetic patients. They are caused or increased by intraoperative debridement or a long operating time. Careful postoperative management is man-

datory due to a poorer wound healing in diabetics. Soft contact lenses in combination with lubricants and local antibiotics can reduce pain and accelerate epithelial closure to prevent keratitis or corneal scarring [106, 107, 113].

c. Uveitis or Iritis

These complications are usually mild after diabetic vitrectomy surgery. However, the accumulation of intraocular fibrin or an increasing, painful inflammation can be indicative of a beginning endophthalmitis. It should not be confused with chalk-white deposits of cortisone crystals that can also simulate an intraocular inflammation or hypopyon [25, 114].

d. Intraocular Pressure Elevation

Elevated intraocular pressure over 30 mmHg is a common early complication after vitrectomy for diabetic vitreoretinopathy [115, 116]. The incidence was reported to be around 35 % in the first 24 h after surgery. It can be caused by hemorrhage or significant postoperative inflammation or be related to gas or silicone oil tamponade. A stepwise treatment has shown to be most efficient, starting with topical or oral anti-glaucomatous drugs in addition to anti-inflammatory and mydriatic drops. When intraocular pressure does not normalize after resolution of inflammation or swelling of tissues, transscleral laser or cryocoagulation can be applied. In some cases with fair visual prognosis, glaucoma filtering surgery may become indicated. In eyes with an intraocular gas bubble, the tamponade may cause angle closure and has to be reduced by aspiration through a sclerotomy (or paracentesis in aphakic eyes), if facedown positioning is unsuccessful [117]. Angle closure may also be provoked by choroidal detachment or swelling after scleral buckling procedure which is treated by local corticosteroids and cycloplegics and systemic anti-inflammatory drugs [7].

2. Vitreous Hemorrhage

About two thirds of patients will suffer a mild postoperative vitreous hemorrhage, but in only one third this will occur repeatedly [118]. As it is often associated with retinal fibrovascular proliferations or anterior chamber neovascularization, a thorough intraoperative control of all bleeding sources and fibrovascular tissue may prevent further bleeding complications. If the postoperative hemorrhage clears within the first month, no additional surgery is necessary. In the case of recurrent bleeding with impaired funduscopy view, repeated ultrasound examinations are necessary. If the retinal anatomy is unclear, another vitrectomy procedure is mandatory to wash out the hemorrhage and remove eventual residual fibrovascular tissue. This procedure will become necessary in only 5–10 % of patients. An additional photocoagulation is then advisable, together with a longer acting gas or silicone oil tamponade [21, 97, 119].

3. Fibrinoid Syndrome

Vitreotomy surgery for diabetic vitreoretinopathy can provoke or increase a failure of the blood-retina barrier, which can lead to fibrin deposits in the anterior chamber or the vitreous cavity (the so-called fibrinoid syndrome), which was reported to occur in 5 % of patients [7, 120]. Risk factors include extensive prior surgery, lensectomy, buckle procedures, and a younger patient's age. Further complications may include an acute glaucoma due to a pupillary block, ciliary body or traction retinal detachment, hypotony, or finally neovascular glaucoma [120, 121]. Eyes with traction detachments have a poor functional prognosis with recurrent fibrin deposition and re-detachments. Prophylaxis and therapy consist of subconjunctival or peribulbar injections of dexamethasone and frequent topical application of steroids. In cases with massive fibrin formation in the vitreous cavity, an intracameral injection with recombinant tissue plasminogen activator can be given; however, additional vitrectomy with fibrin excision and silicone oil tamponade can sometimes become necessary [7, 122].

4. Anterior Hyaloidal Fibrovascular Proliferation (AHFVP)

This extremely severe complication has very poor functional outcome and affects up to 13 % of patients with severe proliferative diabetic retinopathy [25, 123]. AHFVP consists of the growth of fibrovascular membranes onto the peripheral retina, the vitreous base, and ciliary body up to the iris and lens capsule. Patients at higher risk are male, type I diabetics, phakic, with no or insufficient PRP, or had prior buckling surgery [123, 124]. The clinical picture of AHFVP may include rubeosis iridis, recurrent vitreous hemorrhage, peripheral traction retinal detachment, or hypotony [25]. Extensive treatment with the whole armamentarium can become necessary, as cataract extraction, scleral buckling, vitrectomy with extensive anterior dissection or retinectomy, and dense laser or cryocoagulation. Pre- and intraoperative injections of anti-VEGF (e.g., bevacizumab) can facilitate dissection of the vascularized tissues and reduce the risk of perioperative hemorrhage [125]. However, as the visual prognosis is usually poor, prevention and early treatment of AHFVP are essential [25, 123, 125].

Abbreviations

AHFVP	Anterior hyaloidal fibrovascular proliferation
bFGF	Basic fibroblast growth factor
BSS	Balanced salt solution
DRVS	Diabetic Retinopathy Vitrectomy Study
EPC	Endothelial progenitor cells
FDA	Food and Drug Administration
Hg	Mercury

hr-OCT	High-resolution optic coherence tomography
IGF-1	Insulin-like growth factor 1
IOL	Intraocular lens
mg	Milligram
min	Minute
mm	Millimeter
mW	Milliwatt
OCT	Optical coherence tomography
PRP	Panretinal photocoagulation
PVD	Posterior vitreous detachment
PVR	Proliferative vitreoretinopathy
rt-PA	Recombinant tissue plasminogen activator
SF6, C2F6, C3F8	(different intraocular gases)
VEGF	Vascular endothelial growth factor
23-g, 25-g	(g=gauge)

References

1. Aaberg TM, Abrams GW. Changing indications and techniques for vitrectomy in management of complications of diabetic retinopathy. *Ophthalmology*. 1987;94(7):775–9.
2. Michels RG. Vitrectomy for complications of diabetic retinopathy. *Arch Ophthalmol*. 1978;96(2):237–46.
3. Machemer R, Parel JM, Norton EW. Vitrectomy: a pars plana approach. Technical improvements and further results. *Trans Am Acad Ophthalmol Otolaryngol*. 1972;76(2):462–6.
4. Flynn Jr HW, Chew EY, Simons BD, Barton FB, Remaley NA, Ferris 3rd FL. Pars plana vitrectomy in the Early Treatment Diabetic Retinopathy Study. ETDRS report number 17. The Early Treatment Diabetic Retinopathy Study Research Group. *Ophthalmology*. 1992;99(9):1351–7.
5. Fong DS, Aiello LP, Ferris 3rd FL, Klein R. Diabetic retinopathy. *Diabetes Care*. 2004;27:2540–53. Review.
6. Calles-Escandon J, Cipolla M. Diabetes and endothelial dysfunction: a clinical perspective. *Endocr Rev*. 2001;22:36–52.
7. Elliott D, Lee MS, Abrams GW. Proliferative diabetic retinopathy: principles and techniques of surgical treatment. In: Ryan SJ, Hinton DR, Schachat AP, Wilkinson P, editors. *Retina*, vol. 142. 4th ed. Philadelphia: Mosby; 2006. p. 2413–49.
8. Asahara T, Masuda H, Takahashi T, et al. Bone marrow origin of endothelial progenitor cells responsible for postnatal vasculogenesis in physiological and pathological neovascularization. *Circ Res*. 1999;85(3):221–8.
9. Brunner S, Schernthaner GH, Satler M, Elhenicky M, Hoellerl F, Schmid-Kubista KE, Zeiler F, Binder S, Schernthaner G. Correlation of different circulating endothelial progenitor cells to stages of diabetic retinopathy: first in vivo data. *Invest Ophthalmol Vis Sci*. 2009;50(1):392–8.
10. Brunner S, Hoellerl F, Schmid-Kubista KE, Zeiler F, Schernthaner G, Binder S, Schernthaner GH. Circulating angiopoietic cells and diabetic retinopathy in type 2 diabetes mellitus, with or without macrovascular disease. *Invest Ophthalmol Vis Sci*. 2011;52:4655–62.
11. Hutton WL, Pesicka GA, Fuller DG. Cataract extraction in the diabetic eye after vitrectomy. *Am J Ophthalmol*. 1987;104(1):1–4.
12. Suto C, Hori S, Kato S. Management of type 2 diabetics requiring panretinal photocoagulation and cataract surgery. *J Cataract Refract Surg*. 2008;34(6):1001–6.

13. Menchini U, Cappelli S, Virgili G. Cataract surgery and diabetic retinopathy. *Semin Ophthalmol*. 2003;18:103–8. Review.
14. Demetriades AM, Gottsch JD, Thomsen R, Azab A, Stark WJ, Campochiaro PA, de Juan E, Haller Jr JA. Combined phacoemulsification, intraocular lens implantation, and vitrectomy for eyes with coexisting cataract and vitreoretinal pathology. *Am J Ophthalmol*. 2003;135(3):291–6.
15. Schiff WM, Barile GR, Hwang JC, Tseng JJ, Cekiç O, Del Priore LV, Chang S. Diabetic vitrectomy: influence of lens status upon anatomic and visual outcomes. *Ophthalmology*. 2007;114(3):544–50.
16. Early vitrectomy for severe vitreous hemorrhage in diabetic retinopathy. Two-year results of a randomized trial. Diabetic Retinopathy Vitrectomy Study report 2. The Diabetic Retinopathy Vitrectomy Study Research Group. *Arch Ophthalmol*. 1985;103(11):1644–52.
17. Ono R, Kakehashi A, Yamagami H, Sugi N, Kinoshita N, Saito T, Tamemoto H, Kuroki M, Lshikawa SE, Kawakami M. Prospective assessment of proliferative diabetic retinopathy with observations of posterior vitreous detachment. *Int Ophthalmol*. 2005;26(1–2):15–9.
18. Sebag J. Diabetic vitreopathy (Guest Editorial). *Ophthalmology*. 1996;103:205–6.
19. Two-year course of visual acuity in severe proliferative diabetic retinopathy with conventional management. Diabetic Retinopathy Vitrectomy Study (DRVS) report. *Ophthalmology*. 1985;92(4):492–502.
20. O'Hanley GP, Canny CL. Diabetic dense premacular hemorrhage. A possible indication for prompt vitrectomy. *Ophthalmology*. 1985;92(4):507–11.
21. Ho T, Smiddy WE, Flynn Jr HW. Vitrectomy in the management of diabetic eye disease. *Surv Ophthalmol*. 1992;37(3):190–202. Review.
22. Ramsay RC, Knobloch WH, Cantrill HL. Timing of vitrectomy for active proliferative diabetic retinopathy. *Ophthalmology*. 1986;93(3):283–9.
23. Kurihara T, Noda K, Ishida S, Inoue M. Pars plana vitrectomy with internal limiting membrane removal for macular hole associated with proliferative diabetic retinopathy. *Graefes Arch Clin Exp Ophthalmol*. 2005;243(7):724–6.
24. Mori K, Gehlbach PL, Sano A, Deguchi T, Yoneya S. Comparison of epiretinal membranes of differing pathogenesis using optical coherence tomography. *Retina*. 2004;24(1):57–62.
25. Pautler SE. Treatment of proliferative diabetic retinopathy. In: Browning DJ, editor. *Diabetic retinopathy – evidence-based management*. New York: Springer; 2010. p. 227–304.
26. Faulborn J, Ardjomand N. Tractional retinoschisis in proliferative diabetic retinopathy: a histopathological study. *Graefes Arch Clin Exp Ophthalmol*. 2000;238(1):40–4.
27. Packer AJ. Vitrectomy for progressive macular traction associated with proliferative diabetic retinopathy. *Arch Ophthalmol*. 1987;105(12):1679–82.
28. Meyer CH, Schmidt JC, Mennel S, Kroll P. Functional and anatomical results of vitreopapillary traction after vitrectomy. *Acta Ophthalmol Scand*. 2007;85(2):221–2.
29. Brazitikos PD, Stangos NT. Macular hole formation in diabetic retinopathy: the role of coexisting macular edema. *Doc Ophthalmol*. 1999;97(3–4):273–8.
30. Nasrallah FP, Van de Velde F, Jalkh AE, Trempe CL, McMeel JW, Schepens CL. Importance of the vitreous in young diabetics with macular edema. *Ophthalmology*. 1989;96:1511–6.
31. Lewis H. The role of vitrectomy in the treatment of diabetic macular edema. *Am J Ophthalmol*. 2001;131:123–5.
32. Hikichi T, Fujio N, Akiba J, Azuma Y, Takahashi M, Yoshida A. Association between the short-term natural history of diabetic macular edema and the vitreomacular relationship in type II diabetes mellitus. *Ophthalmology*. 1997;104:473–8.
33. Browning DJ, Fraser CM, Powers ME. Comparison of the magnitude and time course of macular thinning induced by different interventions for diabetic macular edema: implications for sequence of application. *Ophthalmology*. 2006;113:1713–9.
34. Parolini B, Panozzo G, Gusson E, Pinackatt S, Bertoldo G, Rottini S, Pignatto S. Diode laser, vitrectomy and intravitreal triamcinolone. A comparative study for the treatment of diffuse non tractional diabetic macular edema. *Semin Ophthalmol*. 2004;19:1–12.
35. Diabetic Retinopathy Clinical Research Network Writing Committee, Haller JA, Qin H, Apte RS, Beck RR, Bressler NM, Browning DJ, Danis RP, Glassman AR, Googe JM, Kollman C, Lauer AK, Peters MA, Stockman ME. Vitrectomy outcomes in eyes with diabetic macular edema and vitreomacular traction. *Ophthalmology*. 2010;117:1087–93.
36. Flaxel CJ, Edwards AR, Aiello LP, Arrigg PG, Beck RW, Bressler NM, Bressler SB, Ferris 3rd FL, Gupta SK, Haller JA, Lazarus HS, Qin H. Factors associated with visual acuity outcomes after vitrectomy for diabetic macular edema: diabetic retinopathy clinical research network. *Retina*. 2010;30:1488–95.
37. Radetzky S, Walter P, Fauser S, Koizumi K, Kirchhof B, Jousen AM. Visual outcome of patients with macular edema after pars plana vitrectomy and indocyanine green-assisted peeling of the internal limiting membrane. *Graefes Arch Clin Exp Ophthalmol*. 2004;242:273–8.
38. Gandorfer A, Haritoglou C, Kampik A. Toxicity of indocyanine green in vitreoretinal surgery. *Dev Ophthalmol*. 2008;42:69–81. Review.
39. Mason 3rd JO, Yunker JJ, Vail R, McGwin Jr G. Intravitreal bevacizumab (Avastin) prevention of panretinal photocoagulation-induced complications in patients with severe proliferative diabetic retinopathy. *Retina*. 2008;28(9):1319–24.
40. Chang PY, Yang CM, Yang CH, Chen MS, Wang JY. Pars plana vitrectomy for diabetic fibrovascular proliferation with and without internal limiting membrane peeling. *Eye (Lond)*. 2009;23(4):960–5.
41. Sebag J. Vitreoschisis in diabetic macular edema. *Invest Ophthalmol Vis Sci*. 2011;52(11):8455–6.
42. Favard C, Guyot-Argenton C, Assouline M, Marie-Lescure C, Pouliquen YJ. Full panretinal photocoagulation and early vitrectomy improve prognosis of florid diabetic retinopathy. *Ophthalmology*. 1996;103(4):561–74.
43. Ryan SJ. Traction retinal detachment. XLIX Edward Jackson Memorial Lecture. *Am J Ophthalmol*. 1993;115(1):1–20. Review.
44. Steinmetz RL, Grizzard WS, Hammer ME. Vitrectomy for diabetic traction retinal detachment using the multiport illumination system. *Ophthalmology*. 2002;109(12):2303–7.
45. La Heij EC, Tecim S, Kessels AG, Liem AT, Japing WJ, Hendrikse F. Clinical variables and their relation to visual outcome after vitrectomy in eyes with diabetic retinal traction detachment. *Graefes Arch Clin Exp Ophthalmol*. 2004;242(3):210–7.
46. Han DP, Murphy ML, Mieler WF. A modified en bloc excision technique during vitrectomy for diabetic traction retinal detachment. Results and complications. *Ophthalmology*. 1994;101(5):803–8.
47. Kakehashi A, Trempe CL, Fujio N, McMeel JW, Schepens CL. Retinal breaks in diabetic retinopathy: vitreoretinal relationships. *Ophthalmic Surg*. 1994;25:695–9.
48. Yang CM, Su PY, Yeh PT, Chen MS. Combined rhegmatogenous and traction retinal detachment in proliferative diabetic retinopathy: clinical manifestations and surgical outcome. *Can J Ophthalmol*. 2008;43:192–8.
49. Douglas MJ, Scott IU, Flynn Jr HW. Pars plana lensectomy, pars plana vitrectomy, and silicone oil tamponade as initial management of cataract and combined traction/rhegmatogenous retinal detachment involving the macula associated with severe proliferative diabetic retinopathy. *Ophthalmic Surg Lasers Imaging*. 2003;34:270–8.
50. Helbig H. Proliferative diabetic retinopathy. A surgical approach to proliferative diabetic retinopathy. In: Jousen AM, Gardner TW, Kirchhof B, Ryan SJ, editors. *Retinal vascular disease*. Berlin/Heidelberg: Springer; 2007. p. 330–41.
51. Avery RL, Pearlman J, Pieramici DJ, et al. Intravitreal bevacizumab (Avastin) in the treatment of proliferative diabetic retinopathy. *Ophthalmology*. 2006;113:1695–705.

52. Spiteri CK, Ramamurthi S, Saidkasimova S, Ramaesh K. Intravitreal bevacizumab and augmented trabeculectomy for neovascular glaucoma in young diabetic patients. *Eye*. 2008;23:979–81.
53. Jousseaume AM, Joeres S. Benefits and limitations in vitreoretinal surgery for proliferative diabetic retinopathy and macular edema. In: Lang GE (ed). *Diabetic Retinopathy*. Dev Ophthalmol. Basel, Karger; 2007;39:69–87.
54. Iliev ME, Wolf S. Management of neovascular glaucoma. In: Grieshaber LC, Orgül S, Flammer J, editors. *Glaucoma therapy – state of the art*. Basel: Grieshaber; 2009. p. 165–70.
55. Schlote T, Ziemssen F, Bartz-Schmidt KU. Pars plana-modified Ahmed Glaucoma Valve for treatment of refractory glaucoma: a pilot study. *Graefes Arch Clin Exp Ophthalmol*. 2006;244:336–41.
56. Miki A, Oshima Y, Otori Y, et al. Efficacy of intravitreal bevacizumab as adjunctive treatment with pars plana vitrectomy, endolaser photocoagulation and trabeculectomy for neovascular glaucoma. *Br J Ophthalmol*. 2008;92:1431–3.
57. Bartz-Schmidt KU, Thumann G, Psychias A, Kriegelstein GK, Heimann K. Pars plana vitrectomy, endolaser coagulation of the retina and the ciliary body combined with silicone oil endotamponade in the treatment of uncontrolled neovascular glaucoma. *Graefes Arch Clin Exp Ophthalmol*. 1999;237:969–75.
58. Iliev ME, Gerber S. Long-term outcome of trans-scleral diode laser cyclophotocoagulation in refractory glaucoma. *Br J Ophthalmol*. 2007;91:1631–5.
59. Murphy CC, Burnett CA, Spry PG, Broadway DC, Diamond JP. A two centre study of the dose-response relation for transscleral diode laser cyclophotocoagulation in refractory glaucoma. *Br J Ophthalmol*. 2003;87:1252–7.
60. Ehlers JP, Shah CP, Fenton G, Hoskins EN, Shelsta HN. *The Wills eye manual: office and emergency room diagnosis and treatment of eye disease*. 5th ed. Philadelphia: Lippincott Williams & Wilkins; 2008. p. 214–7.
61. Blankenship GW. Proliferative diabetic retinopathy: principles and techniques of surgical treatment. In: Ryan SJ, editor. *Retina*. Philadelphia (US): Elsevier Mosby; 2001. p. 515–39.
62. Moitra VK, Meiler SE. The diabetic surgical patient. *Curr Opin Anaesthesiol*. 2006;19:339–45.
63. Scott WJ. Povidone-iodine antiseptics for cataract surgery and ophthalmic procedures. *Am J Ophthalmol*. 2011;151:914; author reply 914–5.
64. Benatar-Haserfaty J, Puig Flores JA. Locoregional anesthesia in ophthalmology: update. *Rev Esp Anestesiol Reanim*. 2003;50:284–93; quiz 293–4, 8. Review.
65. Jousseaume AM, Kirshof B. Vitrectomy in retinal vascular disease: surgical principles. In: Jousseaume AM, Gardner TW, Kirshof B, Ryan SJ, editors. *Retinal vascular disease*. Berlin/Heidelberg: Springer; 2007. p. 260–73.
66. Chalam KV, Shah GY, Agarwal S, Gupta SK. Illuminated curved 25-gauge vitrectomy probe for removal of subsclerotomy vitreous in vitreoretinal surgery. *Indian J Ophthalmol*. 2008;56:331–4.
67. Oshima Y, Awh CC, Tano Y. Self-retaining 27-gauge transconjunctival chandelier endoillumination for panoramic viewing during vitreous surgery. *Am J Ophthalmol*. 2007;143:166–7.
68. Williams GA. 25-, 23-, or 20-gauge instrumentation for vitreous surgery? *Eye(Lond)*. 2008;22:1263–6.
69. Kellner L, Wimpfissinger B, Stolba U, Brannath W, Binder S. 25-gauge vs 20-gauge system for pars plana vitrectomy: a prospective randomised clinical trial. *Br J Ophthalmol*. 2007;91:945–8.
70. Oshima Y, Wakabayashi T, Sato T, Ohji M, Tano Y. A 27-gauge instrument system for transconjunctival sutureless microincision vitrectomy surgery. *Ophthalmology*. 2010;117:93–102.
71. Hubschman JP, Gupta A, Bourla DH, Culjat M, Yu F, Schwartz SD. 20-, 23-, and 25-gauge vitreous cutters: performance and characteristics evaluation. *Retina*. 2008;28:249–57.
72. Eckardt C. Transconjunctival sutureless 23-gauge vitrectomy. *Retina*. 2005;25:208–11.
73. Peyman GA, Lee KJ. New forceps for preretinal membrane removal. *Retina*. 1994;14:88–9.
74. Johnson TM, Glaser BM. Intraocular rake for removal of epiretinal membranes. *Am J Ophthalmol*. 2006;141:381–3.
75. Spitznas M. A binocular indirect ophthalmomicroscope (BIOM) for non-contact wide-angle vitreous surgery. *Graefes Arch Clin Exp Ophthalmol*. 1987;225:13–5.
76. Rodrigues EB, Meyer CH, Kroll P. Chromovitrectomy: a new field in vitreoretinal surgery. *Graefes Arch Clin Exp Ophthalmol*. 2005;243:291–3.
77. McCuen 2nd BW, Bessler M, Tano Y, Chandler D, Machemer R. The lack of toxicity of intravitreally administered triamcinolone acetonide. *Am J Ophthalmol*. 1981;91:785–8.
78. Farah ME, Maia M, Rodrigues EB. Dyes in ocular surgery: principles for use in chromovitrectomy. *Am J Ophthalmol*. 2009;148:332–40. Review.
79. Schmid-Kubista KE, Lamar PD, Schenk A, Stolba U, Binder S. Comparison of macular function and visual fields after membrane blue or infracyanine green staining in vitreoretinal surgery. *Graefes Arch Clin Exp Ophthalmol*. 2010;248:381–8.
80. von Jagow B, Höing A, Gandorfer A, Rudolph G, Kohnen T, Kampik A, Haritoglou C. Functional outcome of indocyanine green-assisted macular surgery: 7-year follow-up. *Retina*. 2009;29:1249–56.
81. Kobuch K, Menz IH, Hoerauf H, Dresch JH, Gabel VP. New substances for intraocular tamponades: perfluorocarbon liquids, hydrofluorocarbon liquids and hydrofluorocarbon-oligomers in vitreoretinal surgery. *Graefes Arch Clin Exp Ophthalmol*. 2001;239(9):635–42. Review.
82. Stolba U, Binder S, Velikay M, Datlinger P, Wedrich A. Use of perfluorocarbon liquids in proliferative vitreoretinopathy: results and complications. *Br J Ophthalmol*. 1995;79(12):1106–10.
83. Yang CM, Yeh PT, Yang CH. Intravitreal long-acting gas in the prevention of early postoperative vitreous hemorrhage in diabetic vitrectomy. *Ophthalmology*. 2007;114:710–5.
84. Scott IU, Flynn Jr HW, Murray TG, Smiddy WE, Davis JL, Feuer WJ. Outcomes of complex retinal detachment repair using 1000- vs 5000-centistoke silicone oil. *Arch Ophthalmol*. 2005;123(4):473–8.
85. Wong D, Van Meurs JC, Stappler T, Groenewald C, Pearce IA, McGalliard JN, Manousakis E, Herbert EN. A pilot study on the use of a perfluorohexyloctane/silicone oil solution as a heavier than water internal tamponade agent. *Br J Ophthalmol*. 2005;89(6):662–5.
86. Brunner S, Izay B, Weidinger B, Maichel B, Binder S. Chemical impurities and contaminants in different silicone oils in human eyes before and after prolonged use. *Graefes Arch Clin Exp Ophthalmol*. 2011;249:29–36.
87. Browning DJ. Cataract surgery and diabetic retinopathy. In: Browning DJ, editor. *Diabetic retinopathy - evidence-based management*. New York: Springer; 2010. p. 305–23.
88. Browning DJ, Rotberg MH. The relationship of diabetic retinopathy and glaucoma. In: Browning DJ, editor. *Diabetic retinopathy – evidence-based management*. New York: Springer; 2010. p. 325–46.
89. Kitnarong N, Chindasub P, Metheetrairut A. Surgical outcome of intravitreal bevacizumab and filtration surgery in neovascular glaucoma. *Adv Ther*. 2008;25:438–43.
90. Hille K, Hille A, Ruprecht KW. Drainage systems in glaucoma surgery. *Ophthalmologe*. 2002;99:902–16. Review. German.
91. Faghihi H, Hajizadeh F, Mohammadi SF, Kadkhoda A, Peyman GA, Riazi-Esfahani M. Pars plana Ahmed valve implant and vitrectomy in the management of neovascular glaucoma. *Ophthalmic Surg Lasers Imaging*. 2007;38:292–300.
92. Schwatz SD, Alexander R, Hiscott P, Gregor ZJ. Recognition of vitreoschisis in proliferative diabetic retinopathy. A useful land-

- mark in vitrectomy for diabetic traction retinal detachment. *Ophthalmology*. 1996;103:323–8.
93. Stirpe M, Orciuolo M. Pneumatic syringe used in fibrovascular membrane surgery. *Am J Ophthalmol*. 1985;99:729.
 94. McLeod D, James CR. Viscodelamination at the vitreoretinal juncture in severe diabetic eye disease. *Br J Ophthalmol*. 1988;72:413–9.
 95. Stenkula S. Photocoagulation in diabetic retinopathy. A multicentre study in Sweden. *Acta Ophthalmol Suppl*. 1984;162:1–100.
 96. Meredith TA, Kaplan HJ, Aaberg TM. Pars plana vitrectomy techniques for relief of epiretinal traction by membrane segmentation. *Am J Ophthalmol*. 1980;89:408–13.
 97. Mason 3rd JO, Colagross CT, Halem T, Fuller JJ, White MF, Feist RM, Emond TL, McGwin Jr G. Visual outcome and risk factors for light perception and no light perception vision after vitrectomy for diabetic retinopathy. *Am J Ophthalmol*. 2005;140:231–5.
 98. Abrams GW, Williams GA. “En bloc” excision of diabetic membranes. *Am J Ophthalmol*. 1987;103:302–8.
 99. Han DP, Lewis MT, Kuhn EM, Abrams GW, Mieler WF, Williams GA, Aaberg TM. Relaxing retinotomies and retinectomies. Surgical results and predictors of visual outcome. *Arch Ophthalmol*. 1990;108:694–7.
 100. Chaudhry NA, Lim ES, Saito Y, Mieler WF, Liggett PE, Filatov V. Early vitrectomy and endolaser photocoagulation in patients with type I diabetes with severe vitreous hemorrhage. *Ophthalmology*. 1995;102:1164–9.
 101. Imamura Y, Minami M, Ueki M, Satoh B, Ikeda T. Use of perfluorocarbon liquid during vitrectomy for severe proliferative diabetic retinopathy. *Br J Ophthalmol*. 2003;87:563–6.
 102. Fisher YL, Friedman R. Scleral depression to facilitate endophotocoagulation. *Arch Ophthalmol*. 1988;106:721.
 103. Kampik A, Höing C, Heidenkummer HP. Problems and timing in the removal of silicone oil. *Retina*. 1992;12:S11–6.
 104. Falkner CI, Binder S, Kruger A. Outcome after silicone oil removal. *Br J Ophthalmol*. 2001;85:1324–7.
 105. Oyakawa RT, Schachat AP, Michels RG, Rice TA. Complications of vitreous surgery for diabetic retinopathy. I. Intraoperative complications. *Ophthalmology*. 1983;90:517–21.
 106. Hiraoka M, Amano S, Oshika T, Kato S, Hori S. Factors contributing to corneal complications after vitrectomy in diabetic patients. *Jpn J Ophthalmol*. 2001;45:492–5.
 107. Garcia-Valenzuela E, Abdelsalam A, Elliott D, Pons M, Iezzi R, Puklin JE, McDermott ML, Abrams GW. Reduced need for corneal epithelial debridement during vitreo-retinal surgery using two different viscous surface lubricants. *Am J Ophthalmol*. 2003;136:1062–6.
 108. Chong LP. A disposable iris retractor for vitrectomy. *Am J Ophthalmol*. 1991;112:731–2.
 109. Haimann MH, Abrams GW. Prevention of lens opacification during diabetic vitrectomy. *Ophthalmology*. 1984;91:116–21.
 110. Smith JM, Steel DH. Anti-vascular endothelial growth factor for prevention of postoperative vitreous cavity haemorrhage after vitrectomy for proliferative diabetic retinopathy. *Cochrane Database Syst Rev*. 2011;(5):CD008214. Review.
 111. Yeh PT, Yang CM, Lin YC, Chen MS, Yang CH. Bevacizumab pretreatment in vitrectomy with silicone oil for severe diabetic retinopathy. *Retina*. 2009;29:768–74.
 112. Carter JB, Michels RG, Glaser BM, De Bustros S. Iatrogenic retinal breaks complicating pars plana vitrectomy. *Ophthalmology*. 1990;97:848–53.
 113. Schulze SD, Sekundo W, Kroll P. Autologous serum for the treatment of corneal epithelial abrasions in diabetic patients undergoing vitrectomy. *Am J Ophthalmol*. 2006;142:207–11.
 114. Roth DB, Flynn Jr HW. Distinguishing between infectious and non-infectious endophthalmitis after intravitreal triamcinolone injection. *Am J Ophthalmol*. 2008;146:346–7.
 115. Kangas TA, Bennett SR, Flynn Jr HW, Murray TG, Rubsamen PE, Han DP, Mieler WF, Williams DF, Abrams GW. Reversible loss of light perception after vitreoretinal surgery. *Am J Ophthalmol*. 1995;120:751–6.
 116. Anderson NG, Fineman MS, Brown GC. Incidence of intraocular pressure spike and other adverse events after vitreoretinal surgery. *Ophthalmology*. 2006;113:42–7.
 117. Barondes MJ, Davis MD, Myers FL. Acute glaucoma following fluid-gas exchange in a phakic patient. *Am J Ophthalmol*. 1989;108:738–40.
 118. Blankenship GW, Macheimer R. Long-term diabetic vitrectomy results. Report of 10 year follow-up. *Ophthalmology*. 1985;92:503–6.
 119. Brown GC, Tasman WS, Benson WE, McNamara JA, Eagle Jr RC. Reoperation following diabetic vitrectomy. *Arch Ophthalmol*. 1992;110:506–10.
 120. Sebestyen JG. Fibrinoid syndrome: a severe complication of vitrectomy surgery in diabetics. *Ann Ophthalmol*. 1982;14:853–6.
 121. Jaffe GJ, Schwartz D, Han DP, Gottlieb M, Hartz A, McCarty D, Mieler WF, Abrams GW. Risk factors for postvitrectomy fibrin formation. *Am J Ophthalmol*. 1990;109:661–7.
 122. Williams DF, Bennett SR, Abrams GW, Han DP, Mieler WF, Jaffe GJ, Williams GA. Low-dose intraocular tissue plasminogen activator for treatment of postvitrectomy fibrin formation. *Am J Ophthalmol*. 1990;109:606–7.
 123. Lewis H, Abrams GW, Williams GA. Anterior hyaloidal fibrovascular proliferation after diabetic vitrectomy. *Am J Ophthalmol*. 1987;104:607–13.
 124. West JF, Gregor ZJ. Fibrovascular ingrowth and recurrent haemorrhage following diabetic vitrectomy. *Br J Ophthalmol*. 2000;84:822–5.
 125. Eren E, Küçükerdönmez C, Yılmaz G, Akova YA. Regression of neovascular posterior capsule vessels by intravitreal bevacizumab. *J Cataract Refract Surg*. 2007;33:1113–5.
 126. Rice TA, Michels RG, Rice EF. Vitrectomy for diabetic traction retinal detachment involving the macula. *Am J Ophthalmol*. 1983;95:22–3.
 127. Thompson JD, de Bustros S, Michels RG, Rice TA. Results and prognostic factors in vitrectomy for diabetic traction-rhegmatogenous retinal detachment. *Arch Ophthalmol*. 1987;105:497–507.
 128. Oldendoerp J, Spitznas M. Factors influencing the results of vitreous surgery in diabetic retinopathy. I. Iris rubeosis and/or active neovascularization at the fundus. *Graefes Arch Clin Exp Ophthalmol*. 1989;227:1–8.
 129. Williams DF, Williams GA, Hartz A, et al. Results of vitrectomy for diabetic traction retinal detachments using the en bloc excision technique. *Ophthalmol*. 1989;96(6):752–8.

Jose Garcia-Arumi, Susanne Binder, Mahmoud Leila, and Miguel Angel Zapata Victori

Outline

- I. **Introduction**
- II. **Retinal Artery Occlusions**
 - A. Surgical Treatment of Non-arteritic Retinal Artery Occlusions
 - 1. Local Intra-arterial Fibrinolysis (LIF)
 - a. European Assessment Group for Lysis in the Eye (EAGLE) Study
 - 2. Surgical Embolectomy
 - a. Retinal Artery Occlusion Study (RAO)
- III. **Retinal Vein Occlusions**
 - A. Surgical Treatment of Central Retinal Vein Occlusion
 - 1. Radial Optic Neurotomy (RON)
 - a. Rationale
 - b. Technique
 - c. Results
 - i. Long-Term Results
 - d. Complications
 - 2. Comparing Surgery to Pharmacotherapy: The ROVO Study
 - a. Controversies
 - 3. Retina Endovascular Surgery (REVS) in CRVO
 - a. Vitreoretinal Approach
 - i. Concerns
 - b. Neuroradiological Approach
 - B. Surgical Treatment of Branch Retinal Vein Occlusion (BRVO)
 - 1. Rationale of Arteriovenous Adventitial Sheathotomy
 - 2. Technique
 - 3. Complications
 - 4. Results
 - 5. Controversies Regarding Sheathotomy

Conclusion

References

Electronic supplementary material Supplementary material is available in the online version of this chapter at [10.1007/978-1-4939-1086-1_37](https://doi.org/10.1007/978-1-4939-1086-1_37). Videos can also be accessed at <http://www.springerimages.com/videos/978-1-4939-1085-4>.

J. Garcia-Arumi (✉) • M. Leila, MD • M.A.Z. Victori
Department of Ophthalmology, Hospital Vall d'Hebron,
Paseo Vall Hebron, 119, Barcelona 08035, Spain
e-mail: jgarcia.arumi@gmail.com

Keywords

Retinal artery occlusions • Retinal vein occlusions • Vitrectomy • Embolectomy • Radial optic neurotomy • Sheathotomy • ROVO study

Key Concepts

1. Initial success of vitrectomy with surgical embolectomy for retinal arterial occlusions awaits corroborating evidence derived from well-designed clinical trials.
2. Vitrectomy with radial optic neurotomy or sheathotomy, either alone or in combination with other modalities, is a valid therapeutic option that should be reserved for selected patients with retinal vein occlusion seeking the advantage of a more permanent effect.
3. Intravitreal drugs for treating retinal vein occlusion (anti-VEGF/VEGF-Trap/Ozurdex) are superior to surgical treatment, but in most cases need repeated injections over a long period of time.

S. Binder, MD
Department of Ophthalmology, Rudolph Foundation Hospital,
Vienna, Austria

The Ludwig Boltzmann Institute for Retinology
and Biomicroscopic Laser Surgery, Vienna, Austria
e-mail: susanne.binder@wienkav.at

I. Introduction

Retinal vascular occlusions are traditionally considered major causes of ocular morbidity due to their drastic impact on central visual function. Modern ophthalmology has introduced an array of new therapeutic modalities that are being tested through clinical trials with promising results. Therapies such as anti-vascular endothelial growth factors, VEGF receptor binding agents, and steroid pharmacotherapy are rapidly evolving to replace traditional conservative treatment and laser therapy. While pharmacologic therapy will probably be the gold standard of practice in the near future, modern vitreoretinal surgery offers important treatment options that would complement pharmacotherapy. Surgical embolectomy for retinal arterial occlusions and radial optic neurotomy and sheathotomy for retinal vein occlusions are techniques that have long been regarded intimidating. Refined instrumentation and better vitrectomy viewing systems greatly reduce the surgical risk of these procedures and make them feasible for most vitreoretinal surgeons, thereby rendering them effective backup options in those patients in whom pharmacotherapy carries a guarded prognosis.

II. Retinal Artery Occlusions

The term *retinal artery occlusions* describes a group of diseases characterized by sudden obstruction of arterial blood flow in the retinal arterial circulation with consequent ischemic damage to the retina [1]. In terms of retinal survival time in ischemic states, an experimental study by Hayreh and Jonas [2] demonstrated that central retinal artery occlusion (CRAO) lasting for approximately 240 min results in massive, irreversible damage. The study therefore concluded that treatment should be instituted no later than 4 h after loss of vision. This experimental model, however, does not simulate most acute clinical situations because in the majority of eyes with CRAO, some residual retinal blood flow can be detected. Additionally, in the animal model the obstruction was created at the point of entrance of the central retinal artery into the optic nerve, while in humans the obstruction probably does not routinely occur at this location. Indeed, recovery of good vision has been noted to occur as long as 4 days after CRAO in humans [2, 3].

A. Surgical Treatment of Non-arteritic Retinal Artery Occlusions

It is noteworthy that the surgical options described below are meant to address non-arteritic forms of retinal artery occlusions. Arteritic retinal artery occlusions are associated with giant cell arteritis and almost invariably with arteritic anterior ischemic optic neuropathy. In these cases, immediate

intensive systemic corticosteroid therapy is of the essence to prevent further visual loss [4].

1. Local Intra-arterial Fibrinolysis (LIF)

In the early 1990s, Schmidt et al. [5] pioneered LIF as a treatment modality of CRAO. LIF involves super-selective administration of a thrombolytic agent directly into the ophthalmic artery. A range of outcomes was reported, from no improvement to complete restoration of visual acuity. Their work sparked interest in the use of LIF as treatment for CRAO, and several reports were released through the 1990s purporting favorable results of LIF. A meta-analysis summarized these studies and was reviewed by Beatty and Au Fong [6]. They identified 16 studies, all were retrospective and nonrandomized, and 100 subjects were analyzed. Mean delay between onset of symptoms and treatment was 11.6 h. They found that a final visual acuity of 20/20 or better was seen in 14 % of patients following LIF, and a visual acuity of 20/40 or better was seen in 27 % of subjects. A poor final visual acuity of 20/400 or worse was seen in 60.6 % of eyes treated with LIF. These results compared favorably with conventional forms of therapy. Potential serious complications were seen in four patients (hemiplegia with recovery and hypertensive crisis with recovery). They concluded that there may be a marginal visual benefit associated with LIF compared to conventional management, but stressed that in the absence of a randomized clinical trial, LIF for CRAO cannot be recommended.

Another systematic review of published literature about LIF was conducted by Noble et al. [7] who analyzed eight studies with 158 patients. Treatment was instituted within an average of 8.4 h of symptom onset. They found that visual improvement occurred on average in 93 % of patients with 13 % achieving 20/20 or better, 25 % achieving 20/40 or better, and 41 % achieving 20/200 or better. Complications occurred in 4.5 % of cases, including local hemorrhage, transient ischemic attack, hypertensive crisis, intracerebral hemorrhage, and stroke. They concluded that there was insufficient evidence to support the routine use of LIF to treat CRAO and recommended well-designed prospective randomized trials to be conducted.

a. European Assessment Group for Lysis in the Eye (EAGLE) Study

EAGLE is a prospective randomized multicenter clinical superiority trial comparing functional outcome following conservative standard treatment (CST) and LIF in acute non-arteritic CRAO. Patients were randomly assigned to CST or LIF. Data from 82 patients were analyzed, 40 patients in CST group, and 42 patients in LIF group. The mean interval between first symptoms and CST or LIF was 10.99 and 12.78 h respectively. Best-corrected visual acuity (BCVA) 1 month after treatment was the primary endpoint, whereas safety was the secondary endpoint. The authors found no sta-

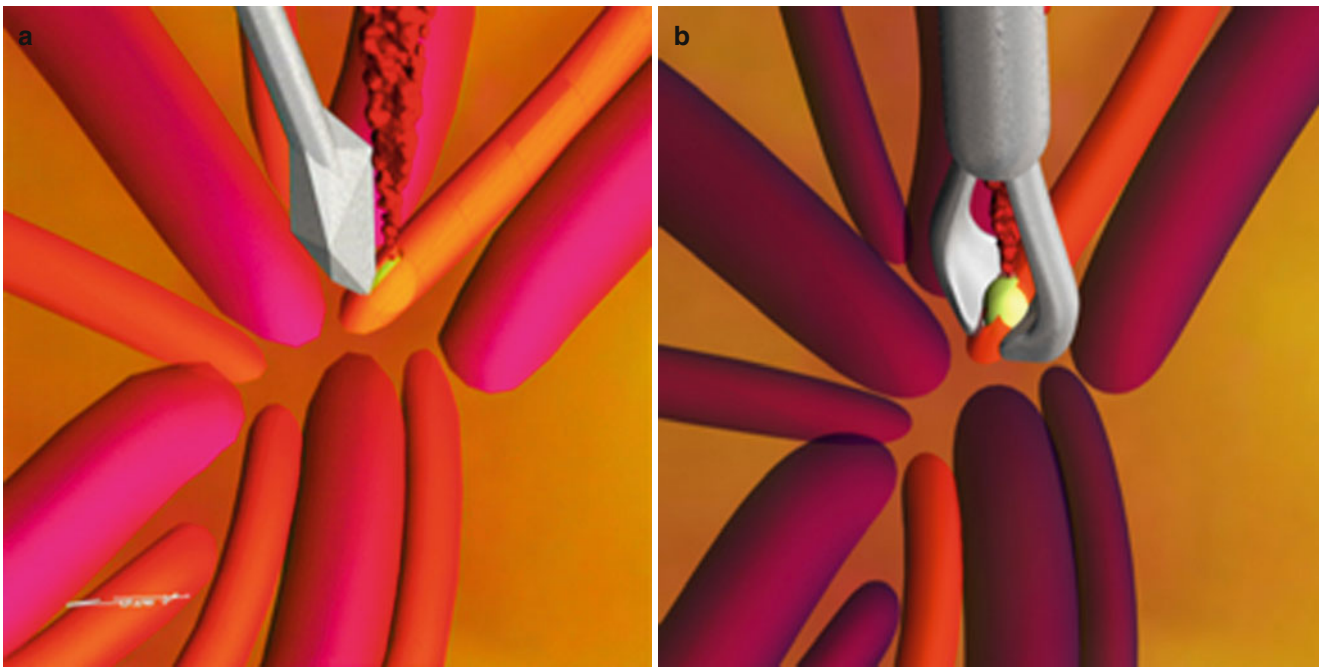


Figure V.A.6-1 (a) An MVR blade is used to penetrate the anterior arterial wall adjacent to the embolus, followed by a longitudinal incision. (b) Embolus expression and removal by microvitreoretinal forceps

tistically significant difference in mean BCVA between both groups and detected complications in 37.1 % in LIF group versus 4.3 % in CST group. The study was stopped at first interim analysis as per recommendation of the *data and safety monitoring committee* because of apparently similar efficacy of CST and LIF and higher rate of adverse reaction in the LIF group. Accordingly, the EAGLE study did not recommend LIF for the management of acute CRAO [8].

2. Surgical Embolectomy

Removal of the embolus through surgical arteriotomy was first reported by Peyman and Gremillion [9]. They presented a case with emboli in the superotemporal and inferotemporal branch retinal arteries of 60 h duration. Their technique consisted of standard pars plana vitrectomy (PPV) followed by dissection of the nerve fiber layer over the plaque using the bent tip of a 30-gauge needle and finally dislodging the embolus into the vitreous cavity. The artery underwent intense spasm with no bleeding encountered. The patient recovered 20/200 visual acuity from a baseline of counting fingers (CF) and remained stable for 3 months.

A histopathological study of BRAO demonstrated that though significant inner retinal damage occurred after 300 min, it is possible to maintain some retinal function past this time point as it was observed that only a small area surrounding the lesion was affected [10]. A prospective study by Garcia-Arumi et al. [11] included seven patients with retinal arterial occlusion of less than 36 h duration. Mean follow-up duration was 12 months. The incision in the affected artery was made using a 25-gauge microvitreoretinal (MVR)

blade. Tano asymmetrical vitreoretinal forceps were used to express the embolus outside the artery if it did not dislodge spontaneously. Surgical embolectomy succeeded in six patients (87.5 %). Reperfusion of the occluded artery was confirmed by fluorescein angiography in four out of these six cases. Median visual acuity improved to 20/40 from baseline median of 20/400 (Figures V.A.6-1a, b and V.A.6-2a–d).

A larger series of retinal arterial occlusion by Garcia-Arumi et al. [12] (unpublished data) included 19 patients (aforementioned 7 patients in addition to 12 new ones). Surgical embolectomy (see Video V.A.6-1) was partially or totally achieved in 84.2 % of cases; reperfusion of the occluded artery occurred in 73.6 % of cases. Statistically significant improvement in both visual acuity and visual field defects was noted in 68.4 % of cases. Thus, in our experience, surgical embolectomy for BRAO seems to be effective given the short postoperative time interval of visual recovery and restoration of visual field. This suggests that the classic dogma that irreversible damage to the retina occurs in 240 min might not hold true in cases of BRAO as the macula might receive some perfusion from the opposite temporal artery. Nevertheless, a randomized clinical trial is essential to provide evidence base for such intervention [11, 12].

a. Retinal Arterial Occlusion Study (RAO)

RAO is an ongoing prospective multicenter international study, looking at the efficacy and safety of surgical embolectomy in retinal arterial occlusions as compared to published natural history. The study is currently recruiting patients [12].

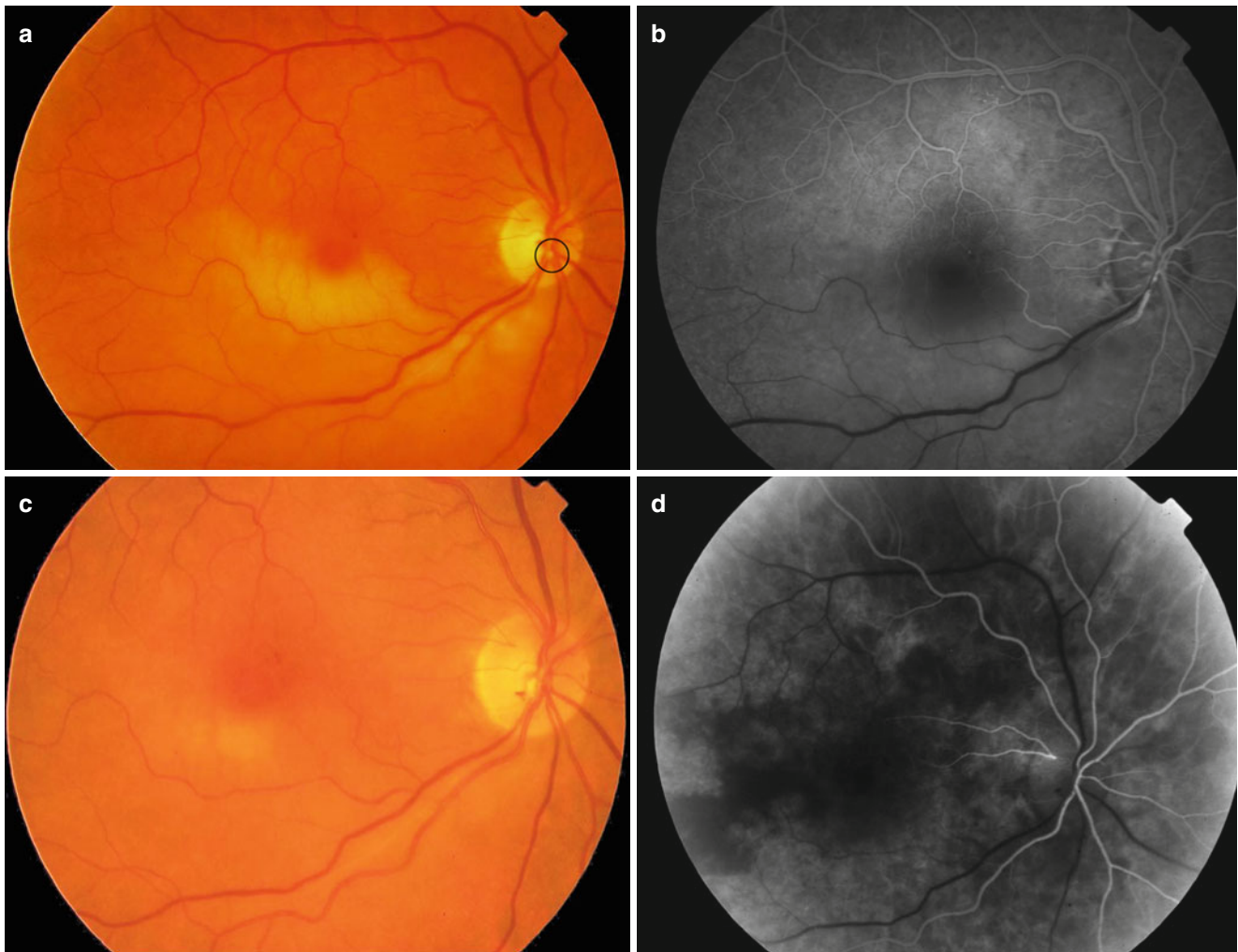


Figure V.A.6-2 (a) Inferotemporal BRAO in a 67-year-old female of 22 h duration and CF visual acuity. Note retinal whitening and cherry-red spot at the macular area. The embolus is located at the ONH (*circle*). (b) Fluorescein angiogram (40 s after intravenous injection), before embolus removal. (c) Forty-eight hours after surgery, retinal whitening

markedly decreased and visual acuity improved to 20/100. Two weeks later, visual acuity further improved to 20/30. (d) Fluorescein angiogram (28 s after intravenous injection) 48 h after embolus removal. Note reperfusion of the affected territory and absence of arterial wall staining

III. Retinal Vein Occlusions

Retinal vein occlusion is by far the most common retinal vascular occlusive disorder. It affects 0.7 % of the population according to one population-based study and 1.6 % according to another [13, 14]. The natural history of both central retinal vein occlusion (CRVO) and branch retinal vein occlusion (BRVO) causes significant ocular morbidity, which mandates prompt diagnosis and treatment to halt their potential drastic impact on central visual function. In addition to the classic laser therapy and, more recently, intravitreal injection of different therapeutic agents, vitreoretinal surgery offers important treatment options.

A. Surgical Treatment of Central Retinal Vein Occlusion

1. Radial Optic Neurotomy (RON)

a. Rationale

RON is based on the compartment syndrome theory of pathogenesis of CRVO. Compartment syndromes are conditions in which pressure within a confined space results in tissue ischemia and dysfunction. It is hypothesized that CRVO is a vascular compression syndrome resulting from increased pressure within the confined space of scleral outlet [15]. As it enters the globe, the optic nerve has a diameter of 3 mm and is comprised of myelinated optic nerve fibers, the central retinal artery (CRA), and central retinal vein (CRV).

The myelinated nerve fibers lose their myelin sheaths as they pass through the lamina cribrosa and share the available space with the CRA and the CRV within the scleral outlet whose internal diameter is 1.5 mm. This unique tissue architecture at the scleral outlet results in an anatomic bottleneck-like configuration. Contributions from several pathogenic mechanisms could increase pressure within this confined space and compress the lumen of the CRV triggering turbulent flow and vascular endothelial damage eventually leading to thrombus formation [15]. RON was therefore introduced to decompress the scleral outlet via an internal vitreoretinal approach (see Video V.A.6-2). The endpoint of the surgical procedure was to make a relaxing incision at the level of the cribriform plate, scleral ring, and adjacent sclera, thus relieving compression on the outflow of vessels [15]. Opremcak sought corroborating evidence for his theory from the histopathology study published by Green et al. [16], who demonstrated that the common finding in patients with terminal CRVO was a thrombus in the area of the lamina cribrosa. Other studies demonstrated that RON promotes and speeds up the development of retinochoroidal collateral vessels (RCVs), and established the protective effect of RCVs against poorer visual outcome through draining edema and hemorrhage. These vessels are a common finding after CRVO substantially draining the retinal venous circulation into the choroidal circulation and vortex veins. They usually develop after a mean time of 6.7 months. In RON, RCVs were reported to develop over a much shorter time period, ranging from 3 weeks to 3 months [17–19].

b. Technique

The surgical approach, originally described by Opremcak et al. [15], includes standard three-port vitrectomy followed by the use of an MVR blade to perform RON (see Video V.A.6-3). The tip of the blade is placed at the edge of the optic disc. The blade is then directed posteriorly into the optic nerve in a radial incision whose depth placed the blade just beyond the widest portion of the diamond-shaped tip. The incision is constructed radial to the optic disc and parallel to the nerve fiber pattern thus minimizing damage to the nerve fibers via separation rather than transection of neurons. Preoperative biomicroscopy and fluorescein angiography are done to assess the optic disc and its vascular pattern. The clock hour site of the incision is then carefully selected to avoid major retinal vessels and to allow access to the central-most portion of the optic disc. Intraoperative hemorrhage during RON can be controlled by raising the intraocular pressure (IOP) to 70–85 mmHg for 10–15 s along with gentle pressure by the tip of the microvitrectome. More recently a special CRVO blade was designed to maximize safety and accuracy of RON. The blade has a rounded edge to be placed toward the center of the disc reducing the risk of a razor-sharp edge accidentally lacerating the central retinal

vessels. The tip is blunted and the knife has a score mark to provide a depth guide [15, 20].

c. Results

The initial report of RON by Opremcak et al. [15] was a retrospective pilot study that included 11 cases: five had perfused CRVO and six had indeterminate CRVO. All patients had severe visual loss of 20/400 or worse. Average duration of the disease prior to RON was 4 months. Average follow-up period was 9 months. Postoperatively, the authors reported equal or better Snellen postoperative visual acuity in 9 patients (82 %). Eight patients (73 %) gained an average of 5 lines of vision. All patients had improvement of clinical picture in terms of retinal hemorrhage and venous congestion. There were no complications in any case. Opremcak et al. [20] reported another series of 117 consecutive cases that underwent RON for CRVO with severe visual loss (20/200 or worse). Sixty-four patients (55 %) had perfused CRVO, 28 patients (24 %) had non-perfused CRVO, while 15 patients (13 %) had indeterminate CRVO. The average duration of symptoms was 7 months, and the average follow-up period was 9 months. Analysis was made on 111 patients. The authors saw marked improvement of fundus appearance in 106 patients (95 %). In terms of visual acuity gain, 79 patients (71 %) gained an average of 2.5 lines. Two or more lines, ≥ 3 lines, ≥ 4 lines, and ≥ 6 lines were gained in 53 %, 41 %, 25 %, and 14 % of patients, respectively. RCVs developed in 8 % of patients at RON site. Complications included intraoperative bleeding and subretinal hemorrhage at the RON site, vitreous hemorrhage developing later during postoperative period, and cataract progression. Anterior segment neovascularization developed in 6 % of subjects. Persistent macular edema and macular pigmentation after resolution of CRVO correlated with poorer prognosis for central macular function.

Garcia-Arumi et al. [18] published a prospective study of 14 patients without controls. Recruited patients had RON for nonischemic CRVO with severe visual loss of less than 8 months' duration. Mean follow-up period was 9.6 months. The authors reported statistically significant improvement of visual acuity as compared to the baseline level: mean postoperative acuity was 20/80 whereas mean preoperative acuity was 20/250. Macular edema improved from a preoperative range of 418–1,000 μm to a postoperative range of 206–559 μm . Eight of their patients (57.1 %) gained one or more lines of vision, while six patients (42.9 %) gained two or more lines. RCVs developed in six patients (42.9 %) at the site of RON after a mean of 35 days and correlated with better visual acuity (median 20/60) as compared to patients who did not develop RCVs (median 20/110). The difference, however, was not statistically significant. The authors did not encounter major complications in their study (Figure V.A.6-3a–c).

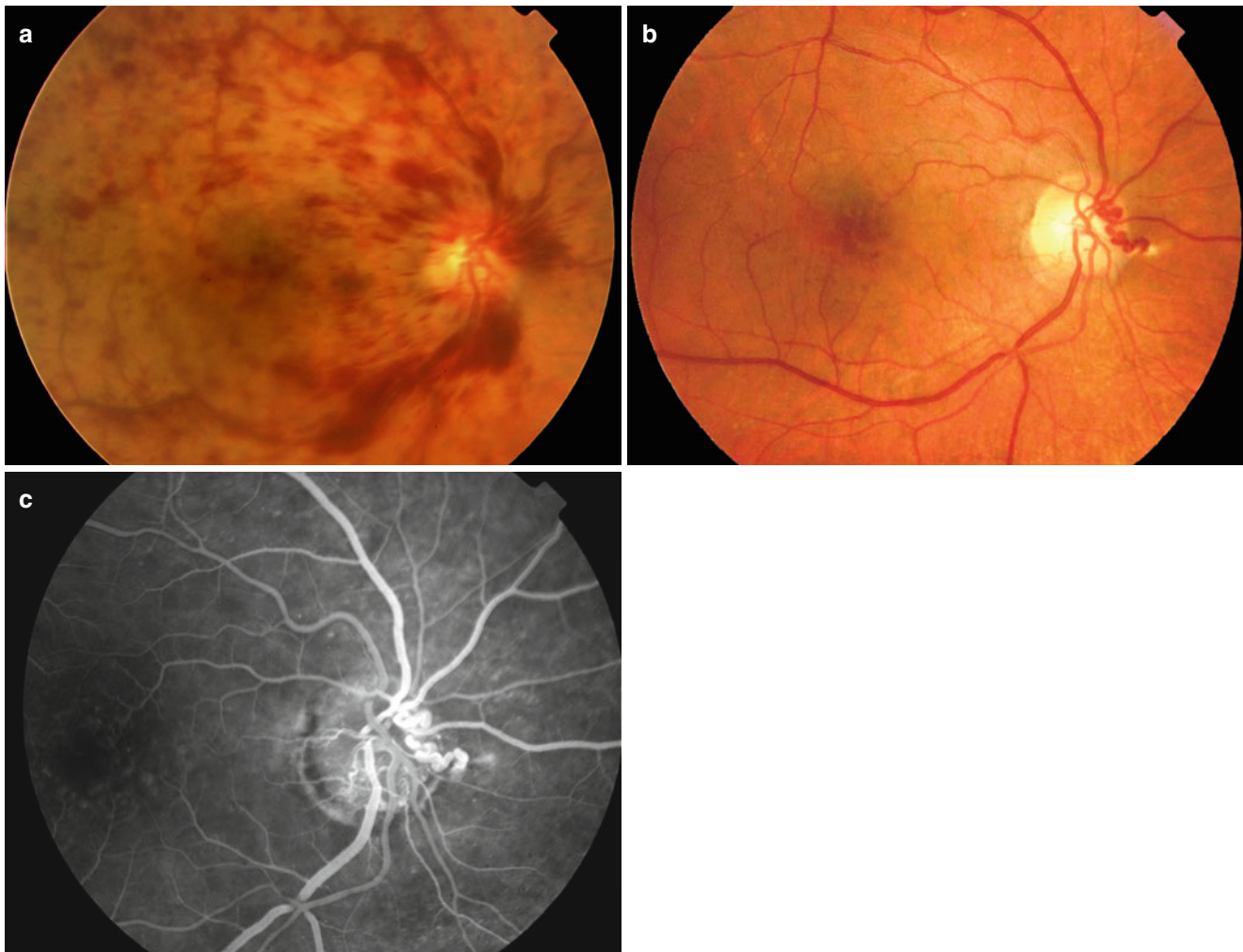


Figure V.A.6-3 (a) Color fundus photo of the right eye of a 60-year-old female with CRVO. Preoperative visual acuity was 20/400, while CFT was 666 μm as per OCT examination. (b) Fundus view 3 months after RON. Note that retinal hemorrhages and macular edema almost

disappeared and a chorioretinal anastomosis has developed at RON site. Visual acuity improved to 20/80. (c) Fluorescein angiography 3 months after RON showed residual macular edema and drainage of retinal veins into the chorioretinal anastomosis

Another prospective case series by Garcia-Arumi et al. [21] included 13 cases with hemi-central retinal vein occlusion (HCRVO) treated with RON. Duration of symptoms was less than 12 weeks. Median preoperative BCVA was 20/100 and median preoperative central foveal thickness (CFT) was 558 μm . Mean follow-up period was 8 months. The authors reported statistically significant improvement of median BCVA (20/50) and median CFT (252 μm) postoperatively. RCVs developed in six patients (46.1 %) and correlated with better visual outcome in patients who developed shunt vessels as compared to those who did not, though without statistical significance. Garcia-Arumi et al. [22] further compared the efficacy of RON in young and adult patients. In their prospective series they recruited 43 patients who had RON for CRVO. Patients were distributed into two groups according to their age. Group I (≤ 50 years) included 18 patients, whereas group II (≥ 50 years) included 25 patients. Mean preoperative

BCVA was 1.2 and 1.38 logMAR in groups I and II, respectively. Mean preoperative CFT was 731 and 646 μm in groups I and II, respectively. Mean time of CRVO onset was 16 and 22 weeks in groups I and II, respectively. Mean follow-up was 15 and 18 months in groups I and II, respectively. The authors reported statistically significant improvement of postoperative BCVA to mean values of 0.5 and 0.8 logMAR in groups I and II, respectively. Likewise, statistically significant improvement in CFT was noted in both groups postoperatively. Mean values were 318 and 326 μm in groups I and II, respectively. RCVs at RON site developed in 55.6 and 54.2 % in groups I and II, respectively and correlated significantly with better visual outcome. Their study revealed that RON was effective in both young and old populations, though better functional results were seen in patients aged 50 years or less, consistent with the greater capacity of retinal function recovery in younger patients.

In a retrospective study by Hasselbach et al. [23], 107 patients were recruited for RON. Sixty-five patients (60.7 %) had ischemic CRVO, whereas 42 patients (39.3 %) had non-ischemic CRVO. The median duration of CRVO prior to RON was 60 days. Median follow-up period was 6 months. Preoperatively, the authors classified patients on basis of peripapillary swelling into severe, moderate, and mild. They found that those patients who had severe preoperative peripapillary swelling derived most benefit from RON with a mean gain of 4.2 lines of vision at 6-month follow-up. They considered this finding as further corroborating evidence for the compartment syndrome theory. Among patients examined for the presence of RCVs, the authors verified development of shunt vessels in 54.1 and 70.4 %, at 3 and 6-month follow-up visits, respectively. In addition, they found that those patients who developed RCVs had significant better visual outcome with a mean gain of six lines, as compared to a mean gain of two lines in patients who did not develop RCVs. This finding provided further evidence of the favorable outcome associated with RCV's development at a RON site. In terms of complications, they had iatrogenic injury of CRA in one patient, visual field defects correlated with the site of RON in 25 % of patients who underwent visual field examination (68 patients), and choroidal neovascularization at the RON site in 5.6 %, 11.5, and 3.3 % of patients at 3-, 6-, and 12-month follow-up visits, respectively. The authors concluded that it was unclear whether the outcome of visual acuity was equivalent to the results of natural history of the CRVO, that the development of RCVs is a major factor influencing postoperative visual acuity, and that patients with pronounced peripapillary swelling and CRVO of less than 90 days' duration are more likely to benefit from RON.

i. Long-Term Results

Results of long-term follow-up following RON were provided by Binder et al. [24]. In an interventional case series including 14 patients who had RON for ischemic CRVO (43 %) and nonischemic CRVO (57 %), the authors had a minimum follow-up period of 24 months, range 24–48 months. Median duration of CRVO prior to RON was 9 months. They reported improvement of median postoperative visual acuity as compared to median baseline visual acuity at 24-month follow-up examination (1.005 logMAR as compared to 1.05 logMAR; $P = 0.013$). Six patients (43 %) gained one or more lines of vision, while four patients (29 %) gained three or more lines of vision. OCT study at 24-month examination revealed statistically significant reduction of median central thickness postoperatively (408 μm) compared to median preoperative value (627.5 μm) in 13 patients (93 %). Eyes with nonischemic CRVO demonstrated statistically significant better visual acuity and less macular edema than eyes with ischemic CRVO. RCVs developed in three patients with nonischemic CRVO at the site of RON between

4 and 12 months and correlated with better visual acuity than nonischemic CRVO eyes that did not develop RCVs.

d. Complications

The Pan-American Collaborative Retina Study (PACORES) is a multicenter, retrospective, interventional case series of 73 consecutive patients (without controls). The study's objective was to evaluate complications after RON for ischemic and nonischemic CRVO. The study found that following RON, 32 % of cases in ischemic CRVO group had better BCVA, 35.8 % had worse BCVA, and 32 % had their BCVA unchanged. In the nonischemic group 50 % had improved BCVA, 15 % had worse BCVA, and 35 % had the same BCVA postoperatively [25]. Such outcome did not differ substantially from the natural history of CRVO described by the Central Vein Occlusion Study Group (CVOSG) [26]. Complications were detected in 71.2 % of cases. The authors concluded that though RON may improve visual acuity in some eyes with CRVO, the procedure does not seem to improve the final outcome as compared to natural history of the disease, complications are common, and benefits of RON do not outweigh its risks [25]. It is noteworthy that the PACORES experienced an unmatched extremely high incidence of complications attributed to RON. It is difficult not to question such high complication rates given the relatively straightforward nature of the surgery. The retrospective study design and the fact that RON was performed by multiple surgeons with different surgical skills are other concerns. Prospective randomized controlled studies would provide more reliable data input than provided by PACORES.

2. Comparing Surgery to Pharmacotherapy: The ROVO Study

The Radial Optic Neurotomy for Central Vein Occlusion (ROVO) study is a prospective placebo-controlled randomized multicenter study comparing surgical outcome and efficacy of RON versus intravitreal triamcinolone injection (IVTA) in CRVO, along with comparison to natural history. The study included 83 patients randomized to receive a single IVTA injection 4 mg (25 patients), treatment with RON (38 patients), or placebo treatment (20 patients). Consecutive patients with history of CRVO less than 12 months and baseline acuity ≥ 0.3 logMAR were enrolled. Ischemic CRVO patients were included directly, whereas patients with nonischemic CRVO were only eligible if their baseline visual acuity was >1.0 logMAR. One year after RON, a statistically significant greater number of patients experienced visual acuity improvement compared to IVTA and placebo group (47 % versus 20 % versus 10 % respectively), though the difference in logMAR was not significant between the three groups. After 12 months, patients treated with RON improved from mean baseline logMAR 1.46 to mean 0.75

logMAR. In addition, RON patients showed statistically significant improvement of reading vision as compared to placebo. Three patients (8 %) in the RON group developed major complications related to surgery. The most threatening complications of CRVO, such as rubeosis iridis and neovascular glaucoma, occurred more often in the natural history group. The ROVO study concluded that RON offered significantly better long-term visual acuity than that of untreated patients. Also, significantly more untreated patients developed deterioration of visual acuity than those treated with RON [27].

It is noteworthy that ROVO demonstrated clear superiority in terms of visual outcome over the natural course of CRVO described by CVOSG [26], IVTA use in SCORE [28], and the laser chorioretinal anastomosis in central retinal vein bypass study [29]. Visual outcomes of CRUISE [30] and COPERNICUS [31] were superior to ROVO though with a narrow margin. Thus, in our opinion, the best candidates for RON would be those patients with CRVO duration less than 1 month, baseline visual acuity <20/60, and CFT >400 μm . In this group of patients, combined regimen of RON and anti-VEGF/Ozurdex, along with laser photocoagulation for peripheral ischemic areas to down-regulate VEGF production, would yield the best results.

a. Controversies

Hayreh considered that the histopathological study of enucleated eyes by Green et al. [16], demonstrating that the site of occlusion in CRVO was at the lamina cribrosa, was not representative of the entire population of CRVO eyes. Hayreh went on to state that the compartment syndrome theory was therefore a wrong assumption and accordingly RON an invalid procedure [32]. A reply to Hayreh's argument lies in a simple-logic question, "Why would a thrombus form within the CRV exiting from the globe unless there was anatomic predisposition such as compression of the vein within a scleral outlet and downstream turbulence?" The exact location of the thrombus would be irrelevant and the mainstay of RON would be reversing the hemodynamic abnormalities precipitated by bottleneck configuration of the scleral outlet [33]. Another concern raised by Hayreh regarding favorable functional outcome of RON was *inadvertent mixing* of ischemic and nonischemic CRVO subtypes. Such mixing has resulted from using the common criterion of 10-disc diameter capillary non-perfusion to differentiate both types, which Hayreh considered to be of poor reliability when used alone [32]. However, the use of angiographic criteria to assign patients to ischemic and nonischemic subtypes was not derived from sheer whim, but rather from solid evidence-based medicine provided by the Central Vein Occlusion Study Group (CVOSG) which is considered by most experts the gold standard of practice since the mid-1980s and remains the benchmark study against which all other studies concerning CRVO are compared. Moreover,

strict inclusion criteria and statistical analysis methodology in a prospective randomized controlled trial as ROVO indeed challenge the so-called inadvertent mixing of CRVO subgroups, which is the backbone of Hayreh's argument against favorable outcome of RON.

3. Retina Endovascular Surgery (REVS) in CRVO

REVS entails delivery of a bolus of a fibrinolytic agent directly into the thrombosed vein to induce thrombolysis and restore venous flow. Two approaches have been described, vitreoretinal and neuroradiological.

a. Vitreoretinal Approach

REVS with injection of recombinant tissue plasminogen activator (r-tPA) in patients with CRVO was described by Weiss et al. [34], in a prospective non-comparative interventional case series that included 28 patients with CRVO. The technique consisted of standard PPV followed by introduction of an angled glass cannula through a sclerotomy. IOP was lowered to 5 mmHg and a peripapillary branch retinal vein chosen for cannulation was pierced by the cannula. A bolus (average volume 3.4 ml of 200 $\mu\text{g}/\text{ml}$ r-tPA) was injected toward the optic nerve head. A pulsatile fluid wave through the blood vessel was visualized during infusion, consisting of injected r-tPA pushing the blood column toward the CRV. The authors proposed that since the flow rate achieved during retinal vein infusion is much higher than normal retinal venous blood flow, this procedure would combine both virtues of thrombolysis and flushing. The latter could have a positive effect especially in cases of CRVO with long duration. Average duration of CRVO prior to intervention was 4.9 months. Baseline BCVA was 20/63 or worse. Average follow-up period was 11.8 months. Twenty-two patients (79 %) experienced at least one line of visual improvement during the follow-up period, and the same number had this level of improvement at the last follow-up examination. Fifteen patients (54 %) gained ≥ 3 lines of vision within 3 months after the procedure, and 14 patients (50 %) had visual acuity at the last follow-up at least 3 lines better than baseline acuity. Ten patients (36 %) improved at least 5 lines of acuity at the last follow-up, and five patients improved at least 8 lines. Complications included vitreous hemorrhage occurring in seven patients and single case of retinal detachment from peripheral break. In a more recent case report of two patients by the same authors [35], they combined IVTA with REVS using r-tPA. They believed that this combination would promote visual recovery better than either treatment alone, in the sense that r-tPA would improve retinal perfusion whereas IVTA would improve macular edema. They reported an improvement of visual acuity of 8 lines in one patient and 11 lines in the other.

i. Concerns

Recombinant tissue plasminogen activator is a thrombolytic enzyme available through recombinant DNA technology [36]. Upon contact with fibrin, r-tPA converts plasminogen into plasmin, which then acts to degrade fibrin. It is presumed that intravitreal r-tPA might diffuse across the ILM and enter the retinal circulation through vessels damaged by breakdown of the blood-retina barrier (BRB) due to venous occlusion. The effectiveness of thrombolytic therapy for venous diseases is directly related to the age of the clot. In the case of mature thrombi, fibrin is cross-linked by factor XIII and becomes resistant to thrombolysis by r-tPA. In addition, in patients with extensive intraretinal hemorrhage, r-tPA may be bound up by fibrin in the intraretinal blood and hampered from reaching the clot [37].

There are serious concerns regarding r-tPA use. Injection of r-tPA could lead to lysis of smaller secondary fibrin clots at the retinal capillary level that are deposited in response to the damage caused by vein occlusion. A differential clot lysis could ensue in which secondary clot lysis occurs while lysis of the main clot does not. In such an instance, retinal venous pressure remains elevated, and increase in exudation could lead to macular edema and exudative retinal detachment. Another concern is that injecting thrombolytic agents into an eye with active bleeding may increase the risk of intraretinal or vitreous hemorrhage [37].

Our experience in REVS is limited to ten patients (unpublished data). All patients were young and had CRVO of less than 1 month's duration. The injected r-tPA bolus failed to induce thrombolysis and promote reperfusion of the occluded vein in all cases. Moreover, it was associated with retrograde flux that led to significant increase in macular edema postoperatively. Accordingly we abandoned REVS as treatment option for CRVO [12].

b. Neuroradiological Approach

Super-selective ophthalmic artery fibrinolytic therapy was described by Paques et al. [38] in a retrospective pilot study that included 26 patients. All patients underwent selective ophthalmic artery catheterization with injection of urokinase. The procedure was performed under local anesthesia by a neuroradiologist trained in the catheterization of intracranial vessels. The internal carotid artery (ICA) was catheterized via a femoral artery approach with a 5-Fr guide catheter. The catheter was positioned inside the proximal extracranial portion of the ICA. A 1.8/1.5-Fr flow guide microcatheter was advanced through the guide catheter to the ostium of the ophthalmic artery. Urokinase (300,000 IU pre-diluted with 0.9 % normal saline) was then perfused for 40 min through the microcatheter. The authors reported significant improvement of vision in six out of 26 patients included. Two patients developed vitreous hemorrhage. No extraocular complications were reported.

B. Surgical Treatment of Branch Retinal Vein Occlusion (BRVO)

1. Rationale of Arteriovenous Adventitial Sheathotomy

Sheathotomy derives its rationale from the pathogenic mechanisms that combine to precipitate BRVO through altering the anatomic configuration of the arteriovenous crossing sites normally present in the human retina. There are particular features of the vitreous interface with retinal blood vessels that differ from the rest of the vitreoretinal interface [see chapter II.E. Vitreo-retinal interface and inner limiting membrane]. Arteries cross anteriorly (innermost) over veins at 70–75 % of all arteriovenous intersections. At the point of crossing, the arterial adventitia and the venous glial coating fuse into one sheath, so that the only intervening structures between the lumens of the two vessels may be their own endothelial layer and basement membrane [39, 40]. Compression by an arteriosclerotic artery induces focal narrowing of the vein's lumen. Vascular narrowing will increase the velocity of blood flowing through the stenotic segment leading to turbulent flow. Along with eddies and local pockets of stasis, turbulence contributes to thrombosis by disrupting the laminar flow and bringing platelets in contact with damaged endothelium. Despite that organization and recanalization of BRVO, thrombi occur relatively rapidly and it seems that the vein's lumen does not fully reopen to its pre-morbid state. A narrow stricture often remains, inducing flow abnormality. The persistence of this stricture may lead to continued elevation of upstream venous pressure and edematous retinal changes. Continued compression of the retinal vein by the artery may perpetuate these flow abnormalities, which may not favor complete recanalization. Surgical division of the adventitial sheath around the artery and the vein at the arteriovenous crossing could release the compressive factor allowing the compromised lumen of the obstructed vein to expand, with consequent reversal of hemodynamic abnormalities and restoration of more normal venous return [41].

2. Technique (See Video V.A.6-4)

The original technique described by Osterloh and Charles [42] consisted of a vitrectomy and the use of 55° Sutherland scissors to cut across the glial tag that was associated with the compression of the vein. A bent MVR blade was then utilized to strip away the glial fibers between the artery and vein at their crossing and at the occlusion site. The original sheathotomy technique was practical only at arteriovenous crossings close to the optic disc where vessels seem to be sufficiently large and strong enough to tolerate this delicate manipulation.

Garcia-Arumi et al. [43] introduced a bimanual technique that would decrease the risk of lacerating the wall of the

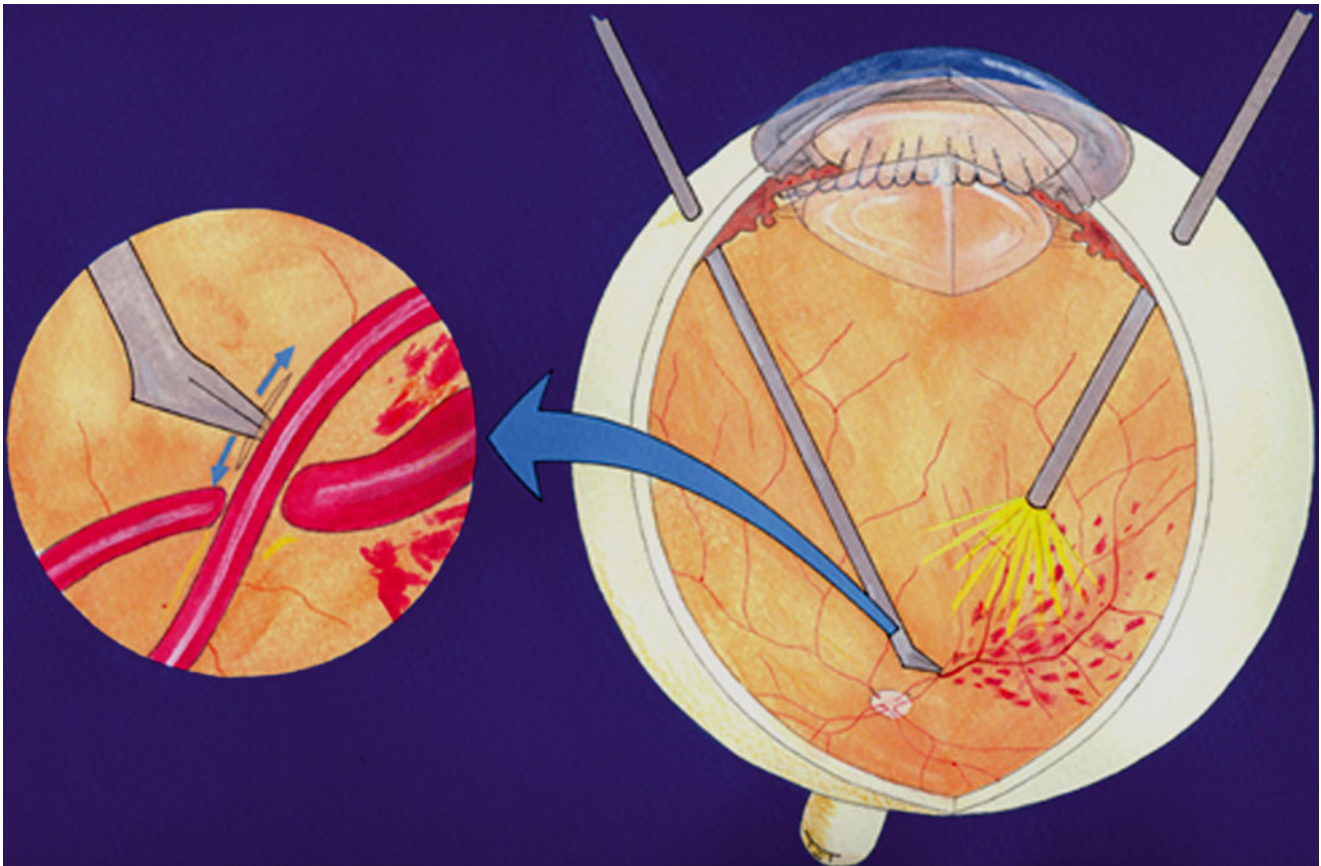


Figure V.A.6-4 Dissection of ILM and nerve fiber layer next to the artery 100–200 μm from the arteriovenous crossing using a bent MVR

arteriole or venule (see Video V.A.6-5). The technique consists of lifting and displacing the arteriole using a specially designed forceps, thereby allowing better visualization of the fibrous connections between the two vessels. A specially designed very thin microscissors then cuts off these connections (Figures V.A.6-4, V.A.6-5, V.A.6-6, and V.A.6-7).

3. Complications

Numerous possible complications could develop during performing sheathotomy. Retinal detachment could result from a full-thickness retinal tear produced during cutting the sheath connecting the artery and the vein. Vitreous hemorrhage could occur due to cutting either the artery or the vein. In the case of arterial laceration, a situation similar to a large BRAO could ensue. A small arcuate scotoma could develop by cutting through the nerve fiber layer at the site of the arteriovenous crossing. Postoperative gliosis could develop as the retina tries to heal the surgical wounds. This could lead to traction analogous to a macular pucker. Gliosis could also cause traction on the involved arteriovenous crossing that could further compromise the venous blood flow past this point. Vitrectomy imposes other potential complications that include cataract and retinal detachment, thus increasing the risk of the procedure [42, 44].

4. Results

Osterloh and Charles [42] were the first to report sheathotomy for BRVO. In their case they reported complete separation of the artery from the vein and did not encounter hemorrhage, arterial spasm, or other complications. The authors mentioned that at the time of surgery, no notable change was noticed in the caliber of the affected vein. Nonetheless, they had significant improvement of visual acuity from 20/200–2 to 20/25+1 during the 8 months following surgery.

Later, in a prospective review of 15 cases with BRVO, Opremcak and Bruce [44] reported successful decompression of arteriovenous crossing in all 15 cases, with clinical improvement in terms of intraretinal hemorrhage and edema in all patients. Baseline visual acuity was 20/70 or worse; the authors reported stabilization or improvement of visual acuity in 12 patients (80%). Moreover, 10 out of 15 eyes (67%) had a mean gain of four lines of vision. Fluorescein angiography demonstrated reperfusion of the retina drained by occluded vein within 24 h. The average duration of the disease was 3.3 months. Average follow-up period was 5 months.

Mester et al. [45] reported 43 cases of BRVO treated with sheathotomy, 16 of which had additional internal limiting

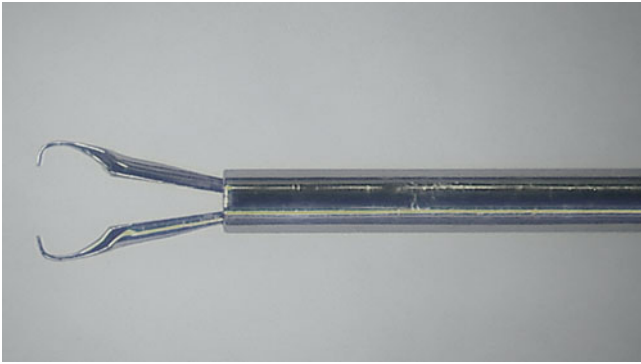


Figure V.A.6-5 Specially designed vitreoretinal microforceps allowing grasping and lifting of the artery without lacerating the arterial wall

membrane (ILM) peel. Mean duration of symptoms was 4.6 weeks. Fluorescein angiography revealed improved capillary perfusion in 93 % of all cases 6 weeks after surgery. Overall visual acuity improved at least two lines in 26 patients (60 %) and four lines or more in 12 patients (28 %). Mean visual acuity improved from 0.16 to 0.35. The authors proposed the possible beneficial effect of ILM peel, as they detected that 38 % of patients who were subjected to ILM peel gained ≥ 4 lines of vision as compared to 22 % of patients who did not have ILM peel. Denudation of the inner retinal surface by removal of the ILM might allow better oxygenation of the inner retina. It might also permit the congested, hemorrhagic retina to decompress by facilitating the release of extracellular fluid and blood into the vitreous [45, 46] [see chapters II.E. Vitreoretinal Interface and ILM; IV.A. Vitreous Physiology]. A less enthusiastic report came from Cahill et al. [47] in a retrospective review of 27 patients who had sheathotomy for BRVO of 7 months' median duration. Complete resolution of macular edema occurred in only 8 of 27 patients (29.6 %), and the overall improvement in median postoperative visual acuity was not statistically significant.

In a prospective randomized study of 36 patients comparing vitrectomy with and without sheathotomy, Kumagai et al. [48] reported no statistically significant difference in terms of improvement of macular edema and visual acuity between the two techniques, though there was a tendency toward better visual outcome in patients having sheathotomy for BRVO with duration of less than 1 month. Similarly, in a retrospective series of 20 patients with BRVO, Han et al. [49] reported improvement in visual acuity by at least two lines in 16 out of 20 eyes (80 %) though they were unable to separate the artery from the vein intraoperatively. They concluded that visual improvement may occur after PPV and arteriovenous crossing dissection without separation of the retinal vessels.

Chung et al. [50] concluded that sheathotomy is not the best option when compared to intravitreal steroids (IVTA). In a prospective randomized trial of 40 patients with BRVO,

they compared sheathotomy to IVTA and found that the latter provided better short-term outcomes in terms of improvement of macular edema and visual acuity. However, results of both approaches did not show statistically significant differences in the long term.

Garcia-Arumi et al. [43] reported the use of r-tPA in addition to sheathotomy in BRVO patients with persistent macular edema. In their prospective nonrandomized study of 40 patients, the authors reported an improvement in macular thickness by greater than 40 % from baseline in 31 patients (77.5 %) and visual acuity gain by an average of 4.5 lines in 34 patients (85 %) and 3 or more lines in 70 % of patients.

5. Controversies Regarding Sheathotomy

Several debates challenge the hypothesis that arteriovenous crossing sheathotomy can reverse the hemodynamic changes in the retina related to BRVO and allows reestablishment of retinal blood flow. Arteriovenous sheathotomy procedure incorporates vitrectomy and the surgical induction of posterior vitreous detachment, both known to promote better oxygenation of the retina and reduction of macular edema. In a study evaluating arteriovenous sheathotomy for BRVO patients, Charbonnel et al. [51] demonstrated postoperative reduction of macular edema using OCT, while only few changes have been observed at the level of the arteriovenous crossing. In particular, there was no hemodynamic improvement at the site of the occlusion or reperfusion of the preoperative ischemic territory, which suggested that postoperative reduction of macular edema was due to improved oxygenation following vitrectomy and the surgical induction of posterior vitreous detachment, rather than due to improvement of blood flow in the occluded territory [see chapter IV.B. Oxygen in vitreo-retinal physiology and pathology]. It is also a fact that microvascular changes secondary to vein occlusion involve complex evolutionary phenomena that continue to be vague. These changes may become relatively independent of blood flow after a short period of occlusion. Capillary closure may result from several factors including arterial perfusion changes, glial proliferation, ischemia-reperfusion lesions, intraluminal thrombosis, internal compression due to hemorrhage into the basal membrane, or VEGF-induced edema of endothelial cells. Even a brief occlusive event can trigger a cascade ending in extensive capillary non-perfusion despite recanalization of the occluded vein. Therefore, the benefits of arteriovenous sheathotomy will be limited unless surgery takes place very early [52].

To confirm the effectiveness of arteriovenous crossing sheathotomy, Opremcak et al. [44] reported improvement in venous perfusion intraoperatively and improvement of fluorescein angiography findings, but they did not quantitatively evaluate the improvement in perfusion. There are concerns

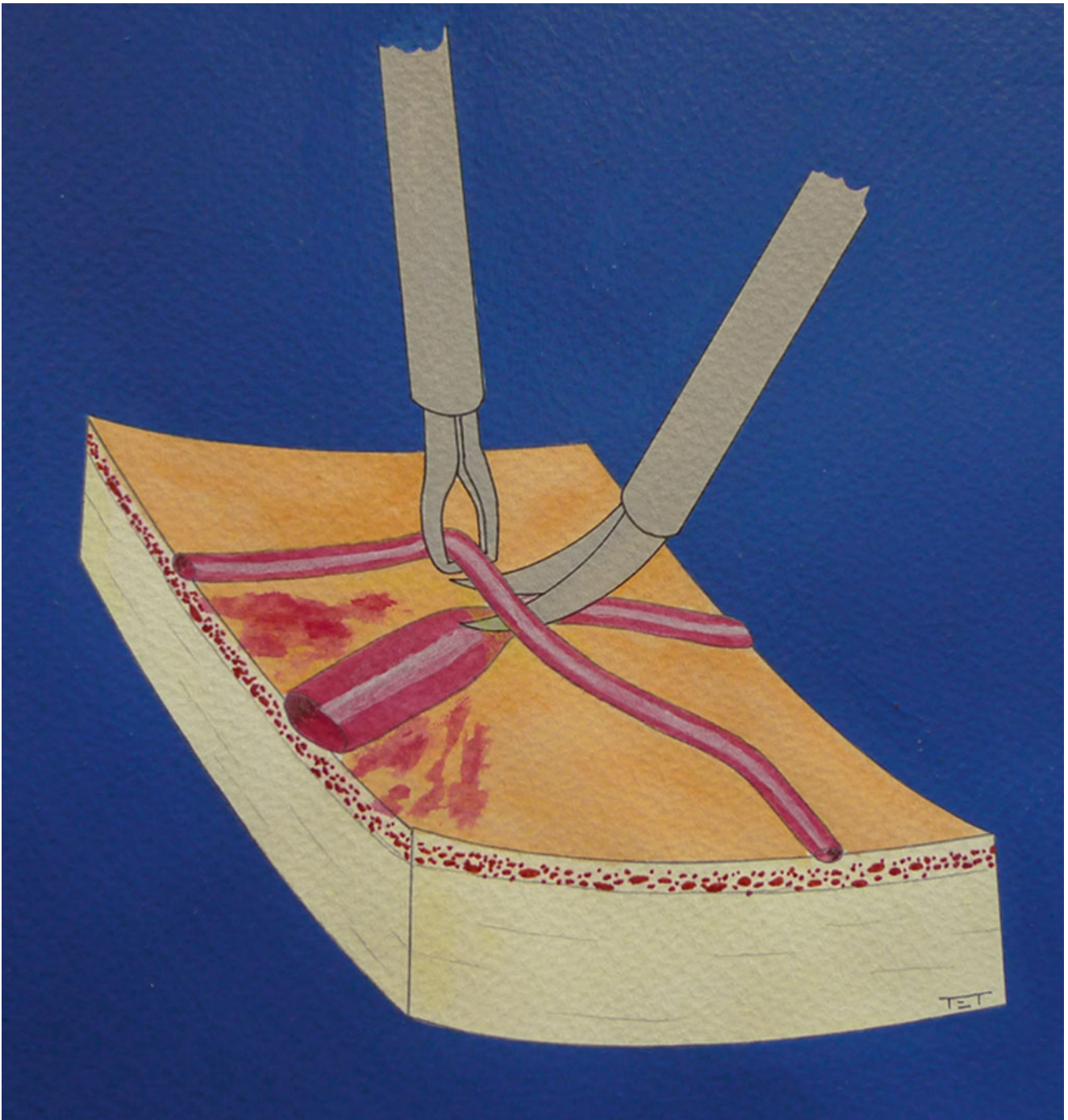


Figure V.A.6-6 Adventitial sheathotomy using bimanual surgery: the forceps displaces and lifts the arteriole, exposing the common sheath. Modified microscissors are then used to cut the sheath, separating the arteriole from the venule

that both intraoperative assessment and postoperative fluorescein angiography are falsely interpreted. The dilatation of the affected vein following arteriovenous dissection part of the procedure could represent reactive hyperemia induced by surgical manipulation rather than a lasting change in blood flow [49]. Moreover, fluorescein angiography is at best a semi-

quantitative measure of circulatory impairment providing a morphological description of the capillary bed that does not necessarily correspond to physiological function [53].

Yamaji et al. [54] published an interventional cases series including 18 patients in which they employed fluorescein videoangiography using a scanning laser ophthalmoscope

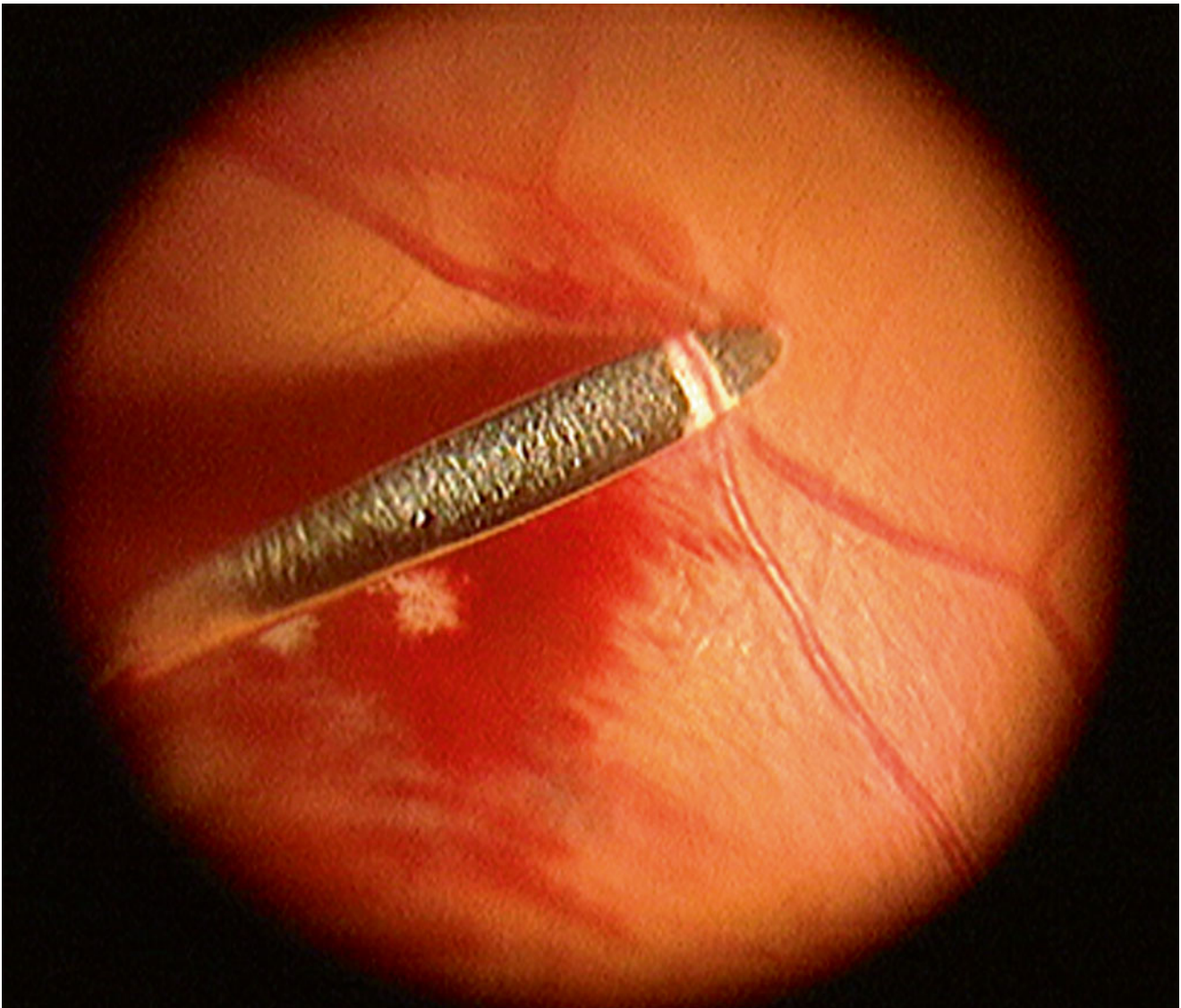


Figure V.A.6-7 Subretinal spatula used to ensure complete separation of the branch retinal arteriole

(SLO) and image analysis using dye dilution technique, for quantitative assessment of the effects of sheathotomy. They were able to demonstrate improved retinal circulation after surgery. Other techniques of evaluating blood flow such as fluorescein angiography, scanning laser ophthalmoscopy, of hypofluorescent clumps in the retinal veins, and laser Doppler flowmetry could be useful in quantifying retinal blood flow changes after such surgery [53, 55].

Despite these concerns regarding sheathotomy, our experience [43] with this procedure using refined instrumentation, substantially reduced the risks of the procedure. The combined effects of arteriovenous decompression and intravitreal r-tPA yielded a visual outcome superior to grid laser treatment in the BRVO Study [56], triamcinolone injection in SCORE [30], and ranibizumab injection in BRAVO [57].

In our experience, the best candidates for sheathotomy would be patients with baseline visual acuity <20/60 and CFT >400 μm , juxtapapillary arteriovenous crossing rather than peripheral one, and BRVO duration less than 1 month. Intraoperatively, the surgeon should attempt at complete separation of the artery from the vein, thrombus release, and confirm recanalization of the occluded vein by means of intraoperative fluorescein angiography.

Conclusions

Intra-arterial fibrinolytic therapy does not provide a better visual outcome than natural history and is associated with serious and perhaps life-threatening complications. Its use is therefore not recommended for treating retinal arterial occlusions. Initial success of surgical embolectomy

for retinal arterial occlusions awaits corroborating evidence derived from well-designed clinical trials. The collective body of evidence from clinical studies, along with benefits versus risks perspective, points out that intravitreal agents for treating retinal vein occlusion (anti-VEGF/VEGF-Trap/Ozurdex) are superior to surgical treatment and probably will be the gold standard in the near future. RON and sheathotomy, either alone or in combination with other modalities, are valid options that should be reserved for selected patients.

Abbreviations

BCVA	Best-corrected visual acuity
BRAO	Branch retinal artery occlusion
BRB	Blood-retina barrier
BRVO	Branch retinal vein occlusion
CF	Counting fingers
CFT	Central foveal thickness
CRA	Central retinal artery
CRAO	Central retinal artery occlusion
CRV	Central retinal vein
CRVO	Central retinal vein occlusion
CST	Conservative standard treatment
CVOSG	Central Vein Occlusion Study Group
DNA	Deoxyribonucleic acid
EAGLE study	European assessment group for lysis in the eye study
HCRVO	Hemi-central retinal vein occlusion
ICA	Internal carotid artery
ILM	Inner limiting membrane
IOP	Intraocular pressure
IU	International unit
IVTA	Intravitreal triamcinolone (injection)
LIF	Local intra-arterial fibrinolysis
logMAR	Logarithm of the minimum angle of resolution
MVR	Microvitreoretinal
µm	Micrometer
OCT	Optical coherence tomography
PACORES	Pan-American Collaborative Retina Study
RAO study	Retinal arterial occlusion study
RCVs	Retinochoroidal collateral vessels
REVS	Retina endovascular surgery
RON	Radial optic neurotomy
ROVO study	Radial Optic Neurotomy for Central Vein Occlusion study
r-tPA	Recombinant tissue plasminogen activator
SLO	Scanning laser ophthalmoscope
VEGF	Vascular endothelial growth factor

References

- Gass JDM. Obstructive retinal arterial diseases. In: Stereoscopic atlas of macular diseases. Diagnosis and treatment. 4th ed. St. Louis: Mosby; 1997. p. 444–66.
- Hayreh SS, Jonas JB. Optic disk and retinal nerve fiber layer damage after transient central retinal artery occlusion: an experimental study in rhesus monkeys. *Am J Ophthalmol.* 2000;129:786–95.
- Duker JS, Brown GC. Recovery following acute obstruction of the retinal and choroidal circulations. A case history. *Retina.* 1988;8:257–60.
- Hayreh SS, Podhajsky PA, Zimmerman B. Ocular manifestations of giant cell arteritis. *Am J Ophthalmol.* 1998;125:509–20.
- Schmidt D, Schumacher M, Wakhloo AK. Microcatheter urokinase infusion in central retinal artery occlusion. *Am J Ophthalmol.* 1992;113:429–34.
- Beatty S, Au Fong KG. Local intra-arterial fibrinolysis for acute occlusion of the central retinal artery: a meta-analysis of the published data. *Br J Ophthalmol.* 2000;84:914–6.
- Noble J, Weizblit N, Baerlocher MO, Eng KT. Intra-arterial thrombolysis for central retinal artery occlusion: a systematic review. *Br J Ophthalmol.* 2008;92:588–93.
- The EAGLE Study Group. Central retinal artery occlusion: local intra-arterial fibrinolysis versus conservative treatment, a multicenter randomized trial. *Ophthalmology.* 2010;117:1367–75.
- Peyman GA, Gremillion CM. Surgical removal of a branch retinal artery embolus: a case report. *Int Ophthalmol.* 1990;14:295–8.
- Carvalho AR, Zapata M, Distefano L, Salas A, Macià C, Garcia-Arumi J. Histological findings in a pig model of experimental branch retinal artery occlusion. Poster presented at: ARVO 2011, 1–5 May, Florida.
- Garcia-Arumi J, Martinez-Castillo V, Boixadera A, Fonollosa A, Corcostegui B. Surgical embolus removal in retinal artery occlusion. *Br J Ophthalmol.* 2006;90:1252–5.
- Garcia-Arumi J. Retinal vascular diseases: surgery, anti-VEGF, and steroid implants (unpublished lecture notes). Congress of the Ophthalmological Society of Valencia, Valencia, 2012.
- Klein R, Klein BEK, Moss SE, Meuer SM. The epidemiology of retinal vein occlusion: the Beaver Dam Eye Study. *Trans Am Ophthalmol Soc.* 2000;98:133–43.
- Mitchell P, Smith W, Chang A. Prevalence and associations of retinal vein occlusion in Australia. The Blue Mountains Eye Study. *Arch Ophthalmol.* 1996;114:1243–7.
- Opremcak EM, Bruce RA, Lomeo MD, Ridenour CD, Letson AD, Rehmar AJ. Radial optic neurotomy for central retinal vein occlusion. A retrospective pilot study of 11 consecutive cases. *Retina.* 2001;21:408–15.
- Green WR, Chan CC, Hutchins GM, Terry JM. Central retinal vein occlusion: a prospective histopathologic study of 29 eyes in 28 cases. *Trans Am Ophthalmol Soc.* 1981;79:371–422.
- Spaide RF, Klanchnik JM, Gross NE. Retinal choroidal collateral circulation after radial optic neurotomy correlated with the lessening of macular edema. *Retina.* 2004;24:356–9.
- Garcia-Arumi J, Boixadera A, Martinez-Castillo V, Castillo R, Dou A, Corcostegui B. Chorioretinal anastomosis after radial optic neurotomy for central retinal vein occlusion. *Arch Ophthalmol.* 2003;121:1385–91.
- Fuller JF, Mason III JO, White MF, McGwin G, Emond TL, Feist RM. Retinochoroidal collateral veins protect against anterior segment neovascularization after central retinal vein occlusion. *Arch Ophthalmol.* 2003;121:332–6.
- Opremcak EM, Rehmar AJ, Ridenour CD, Kurz DE. Radial optic neurotomy for central retinal vein occlusion. 117 consecutive cases. *Retina.* 2006;26:297–305.
- Garcia-Arumi J, Boixadera A, Martinez-Castillo V, Blasco H, Lavaque A, Corcostegui B. Radial optic neurotomy for management of hemicentral retinal vein occlusion. *Arch Ophthalmol.* 2006;124:690–5.

22. Garcia-Arumi J, Boixadera A, Martinez-Castillo V, Montolio M, Verdugo A, Corcostegui B. Radial optic neurotomy in central retinal vein occlusion: comparison of outcome in younger vs older patients. *Am J Ophthalmol.* 2007;143:134–40.
23. Hasselbach HC, Ruefer F, Feltgen N, Schneider U, Bopp S, Hansen LL, Hoerauf H, Bartz-Schmidt U, Roeder J. Treatment of central retinal vein occlusion by radial optic neurotomy in 107 cases. *Graefes Arch Clin Exp Ophthalmol.* 2007;245:1145–56.
24. Binder S, Aggermann T, Brunner S. Long-term effects of radial optic neurotomy for central retinal vein occlusion consecutive interventional case series. *Graefes Arch Clin Exp Ophthalmol.* 2007;245:1447–52.
25. The PACORES Study Group. Radial optic neurotomy for central retinal vein occlusion. Results of the Pan-American Collaborative Retina Study Group (PACORES). *Retina.* 2008;28:1044–52.
26. The central vein occlusion study group. Natural history and clinical management of central retinal vein occlusion. *Arch Ophthalmol.* 1997;115:486–91.
27. The ROVO study group. A prospective, randomized, multicenter trial for surgical treatment of central retinal vein occlusion: results of the Radial Optic Neurotomy for Central Vein Occlusion (ROVO) study group. *Graefes Arch Clin Exp Ophthalmol.* 2012. doi:10.1007/s00417-012-2134-1.
28. The SCORE Study Group. Baseline predictors of visual acuity and retinal thickness outcomes in patients with retinal vein occlusion: Standard Care versus Corticosteroid for RETinal vein occlusion study report 10. *Ophthalmology.* 2011;118:345–52.
29. McAllister IL, Gillies ME, Smithies LA, Rochtchina E, Harper CA, Daniell MD, Constable IJ, Mitchell P. The central retinal vein bypass study: a trial of laser-induced chorioretinal venous anastomosis for central retinal vein occlusion. *Ophthalmology.* 2010;117:954–65.
30. The CRUISE Study. Sustained benefits from ranibizumab for macular edema following central retinal vein occlusion: twelve-month outcomes of a phase III study. *Ophthalmology.* 2011;118:2041–9.
31. The COPERNICUS Study. Intravitreal aflibercept injection for macular edema secondary to central retinal vein occlusion: 1-year results from the phase 3 COPERNICUS study. *Am J Ophthalmol.* 2013;155:429–37.
32. Hayreh SS. Radial optic neurotomy for central retinal vein occlusion. *Retina.* 2002;22:374–7.
33. Opremcak EM, Bruce RA, Lomeo MD, Ridenour CD, Letson AD, Rehmar AJ. Radial optic neurotomy for central retinal vein occlusion. A retrospective pilot study of 11 consecutive cases (author's reply). *Retina.* 2002;22:377–9.
34. Weiss JN, Bynoe LA. Injection of tissue plasminogen activator into a branch retinal vein in eyes with central retinal vein occlusion. *Ophthalmology.* 2001;108:2249–57.
35. Bynoe LA, Weiss JN. Retinal endovascular surgery and intravitreal triamcinolone acetonide for central vein occlusion in young adults. *Am J Ophthalmol.* 2003;135:382–4.
36. Irvine WD, Johnson MW, Hernandez E, Olsen KR. Retinal toxicity of human tissue plasminogen activator in vitrectomized rabbit eyes. *Arch Ophthalmol.* 1991;109:718–22.
37. Lahey JM, Fong DS, Kearney J. Intravitreal tissue plasminogen activator for acute central retinal vein occlusion. *Ophthalmic Surg Lasers.* 1999;30:427–34.
38. Paques M, Vallée JN, Herbreteau D, Aymart A, Santiago PY, Campinchi-Tardy F, Payen D, Merlan JJ, Gaudric A, Massin P. Superselective ophthalmic artery fibrinolytic therapy for the treatment of central retinal vein occlusion. *Br J Ophthalmol.* 2000;84:1387–91.
39. Weinberg DV, Seddon JM, Albert DM, Jakobiec FA. Venous occlusive diseases of the retina. In: Albert & Jakobiec, Principles and practice of ophthalmology, Clinical practice, vol. 2. Philadelphia: W.B. Saunders Company; 1994. p. 735–46.
40. Staurenghi G, Lonati C, Aschero M, Orzalesi N. Arteriovenous crossing as a risk factor in branch retinal vein occlusion. *Am J Ophthalmol.* 1994;117:211–3.
41. Kumar B, Yu DY, Morgan WH, Barry CJ, Constable IJ, McAllister IL. The distribution of angioarchitectural changes within the vicinity of the arteriovenous crossing in branch retinal vein occlusion. *Ophthalmology.* 1998;105:424–7.
42. Osterloh MD, Charles S. Surgical decompression of branch retinal vein occlusions. *Arch Ophthalmol.* 1988;106:1469–71.
43. Garcia-Arumi J, Martinez-Castillo V, Boixadera A, Blasco H, Corcostegui B. Management of macular edema in branch retinal vein occlusion with sheathotomy and recombinant tissue plasminogen activator. *Retina.* 2004;24:530–40.
44. Opremcak EM, Bruce RA. Surgical decompression of branch retinal vein occlusion via arteriovenous crossing sheathotomy. A prospective review of 15 cases. *Retina.* 1999;19:1–5.
45. Mester U, Dillinger P. Vitrectomy with arteriovenous decompression and internal limiting membrane dissection in branch retinal vein occlusion. *Retina.* 2002;22:740–6.
46. Mandelcorn MS, Nrusimhadevara RK. Internal limiting membrane peeling for decompression of macular edema in retinal vein occlusion: A report of 14 cases. *Retina.* 2004;24:348–55.
47. Cahill MT, Kaiser PK, Sears JE, Fekrat S. The effect of arteriovenous sheathotomy on cystoid macular edema secondary to branch retinal vein occlusion. *Br J Ophthalmol.* 2003;87:1329–32.
48. Kumagai K, Furukawa M, Ogino N, Uemura A, Larson E. Long-term outcomes of vitrectomy with or without arteriovenous sheathotomy in branch retinal vein occlusion. *Retina.* 2007;27:49–54.
49. Han DP, Bennett SR, Williams DF, Dev S. Arteriovenous crossing dissection without separation of the retina vessels for treatment of branch retinal vein occlusion. *Retina.* 2003;23:145–51.
50. Chung EJ, Lee H, Koh HJ. Arteriovenous crossing sheathotomy versus intravitreal triamcinolone acetonide injection for treatment of macular edema associated with branch retinal vein occlusion. *Graefes Arch Clin Exp Ophthalmol.* 2008;246:967–74.
51. Charbonnel J, Glacet-Bernard A, Korobelnik JF, Nyouma-Moune E, Pourmaras CJ, Colin J, Coscas G, Soubrane G. Management of branch retinal vein occlusion with vitrectomy and arteriovenous adventitial sheathotomy, the possible role of surgical posterior vitreous detachment. *Graefes Arch Clin Exp Ophthalmol.* 2004;242:223–8.
52. Genevois O, Paques M, Simonutti M, Sercombe R, Seylaz J, Gaudric A, Brouland JP, Sahel J, Vicaut E. Microvascular remodeling after occlusion-recanalization of a branch retinal vein in rats. *Invest Ophthalmol Vis Sci.* 2004;45:594–600.
53. Fujio N, Fekke GT, Ogasawara H, Goger DG, Yoshida A, McMeel JW. Quantitative circulatory measurements in branch retinal vessel occlusion. *Eye.* 1994;8:324–8.
54. Yamaji H, Shiraga F, Tsuchida Y, Yamamoto Y, Ohtsuki H. Evaluation of arteriovenous crossing sheathotomy for branch retinal vein occlusion by fluorescein videoangiography and image analysis. *Am J Ophthalmol.* 2004;137:834–41.
55. Masaoka N, Nakaya K, Koura Y, Ohsaki M. Hemodynamic changes in two patients with retinal circulatory disturbances shown by fluorescein angiography using a scanning laser ophthalmoscope. *Retina.* 2001;21:155–60.
56. Branch vein occlusion study group. Argon laser photocoagulation for macular edema in branch vein occlusion. *Am J Ophthalmol.* 1984;98:271–82.
57. Brown DM, Campochiaro PA, Bhisitkul RB, Ho AC, Gray S, Saroj N, Adamis AP, Rubio RG, Murahashi WY. Sustained benefits from ranibizumab for macular edema following branch retinal vein occlusion: 12-month outcomes of a phase III study. *Ophthalmology.* 2011;118:1594–602.

Part V.B.

Peripheral Vitreo-Retinal Surgery

Lawrence P. Chong

The History of Vitrectomy Instrumentation: A Personal Account of a Transoceanic Australian-USA Collaboration

V.B.1.

Jean-Marie Parel

Outline

- I. Introduction
- II. Surgical R&D Down Under
- III. The Eye World Discovers
- IV. The Hard Work Begins
 - A. Prototype to Prodigious Innovation
 - B. Innovation Progresses to Benevolent Production
- V. Teach the World
- VI. Diversification

References

Keywords

Vitreous • Vitrectomy • Instruments • Microsurgery • Vitreous infusion suction cutter (VISC) • Operating microscope • Foot pedal • Endoillumination

Key Concepts

1. Prior to the collaborative efforts of Machemer Buettner, and Parel, there were no procedures to surgically remove vitreous, in part due to a lack of confidence that vitreous could be safely removed and in part due to the lack of instrumentation.
2. The first vitrectomy instruments were designed and fashioned based upon experience garnered from microvascular surgery.
3. The successful birth of vitrectomy depended upon the development of instrumentation illumination, and visualization equipment and methods.

Editor's Note

The section headings in this chapter were added for structure and the quotations were cited for embellishment of the author's original hand-written manuscript.

I. Introduction

The following presents a personal account of one man's journey through a once-in-a-lifetime experience that changed the world. Recounting the extraordinary events that led to the development of vitrectomy would not have been possible without the assistance of my long-time friend and indispensable colleague Dr. Helmut Buettner. In his endearing self-effacing manner, Helmut graciously insisted on not sharing authorship of this chapter, feeling that it was my story.

J.-M. Parel, IngETS-G, PhD, FARVO
Ophthalmic Biophysics Center, Bascom Palmer Eye Institute,
University of Miami Miller School of Medicine, Miami, MI, USA
e-mail: jmparel@med.miami.edu



Fig. V.B.1-1 Vitrectomy instrumentation R&D team planning the design of VISC II: Dr. Robert Machemer (seated to *right*), Dr. Helmut Buettner (seated to *left*), and Dr. Jean-Marie Parel (standing to *left*). Miami circa December 1970

I therefore dedicate this introduction to thanking him—for everything. Of course, words alone cannot express the gratitude and devotion I feel for the leadership of my mentors and friends, *the Chief*, EWD Norton and Robert Machemer, who shared in this adventure (Fig. V.B.1-1).

If your actions inspire others to dream more, learn more, do more and become more, you are a leader.

John Quincy Adams

II. Surgical R&D Down Under

The desire to reduce the size and improve the function of surgical instruments has always been strong in the field of ophthalmology—the first medical specialty to use the operating microscope instead of loupes. However, the move to motorization of microsurgical instruments came from vascular surgeons performing vessel microanastomosis during

limb reattachment procedures. It was quickly discovered that without proper reconnection of small blood vessels and nerves, reattachment failed. Collaborative efforts by engineers, chemists, and optical physicist were needed to solve these problems. While working at the University of Melbourne Department of Ophthalmology (MUDO) under Professor Gerald W Crock, I was introduced to Dr. Bernard O’Brien [1], a prominent microvascular surgeon, who headed a group of surgeons attempting to reattach severed limbs at St. Vincent Hospital in Melbourne.

Dr. O’Brien needed to solve several technical problems: finding sutures thin enough to anastomose vessels smaller than 1 mm. The thinnest suture material available at that time was 7-O. No more than four such sutures could be used to anastomose a blood vessel one millimeter in diameter without penetrating the vessel wall and causing intravascular blood clots. He needed smaller diameter sutures. With the help of a mechanical engineer and a polymer chemist, I

found a way to make thinner sutures by raising the nylon temperature just below melting point while applying a constant tension between the two ends of the suture. Of course, the large needles available severely traumatized the small vessels to be sutured. The problem was solved by electrodepositing metal on one end of the suture. Using a microscope and a ruby file, I gave them sharp edges [2]. Soon, our multidisciplinary team was able to produce sutures thinner than 10-0. Dr. O'Brien's goal was to anastomose vessels of 0.5 mm and smaller in diameter. To precisely reanastomose both ends of a severed blood vessel for suturing, the team designed a clamping device, which was finely adjustable to prevent traumatizing the delicate tissue [3].

Although using the most delicate needle holder available, Dr. O'Brien's first attempt at using the new sutures failed because the force he applied was much too great and he crushed the metallic needle. This problem was solved by motorizing the needle holder in such a manner that controlled pressure was applied, regardless of the surgeon's actions [4]. But this motorized system, that was perhaps one of the world's very first robotic surgical systems, was *bloody* (using an Aussie expression) expensive, so I searched for other endeavors. Vannas scissors as well as a nerve cutter for reliably making perpendicular cuts through nerve ends prior to suturing them together were developed. As both surgeons and scrub technician used both hands in the sterile field, a foot switch activating up to two motorized handles at the same time was designed (Fig. V.B.1-2). These motorized instruments and approaches lay the groundwork for modern ophthalmic surgical instrumentation, later used for vitrectomy, penetrating keratoplasty, and other delicate ophthalmic procedures.

Another problem was visualization of the surgical field. An operating microscope that would allow two surgeons to work together was needed. With the help of Professor Crock and optical physicist Hans Littmann at Carl Zeiss in Heidelberg, Germany, a microscope with a double-head (diploscope) was designed. By adding a biomicroscope head I had scavenged from an old slit lamp, the diploscope became a triploscope allowing the scrub nurse to view the surgical field as well (Fig. V.B.1-3).

In May 1968 a refugee from Czechoslovakia saw our motorized micro-instrument and mentioned that his father was sometimes cutting vitreous bands during cataract surgery. I had never seen such a case during my tenure at MUDO, but I thought this could be helpful and designed a vitreous band cutter tip (Fig. V.B.1-4) that could be plugged into the motorized handle. Arguably this was the world's first vitrectomy instrument, and I was very proud of this device. But when I showed it to Professor Crock, he looked at it and said, "*vitreous noli me tangere*" (vitreous touch not). This was the only microsurgical tip that was never used in MUDO's operating theaters.

III. The Eye World Discovers

I was given the opportunity to present these instruments at the 28th Annual Australian Ophthalmological Society in Hobart, Tasmania, on November 1, 1968. In contrast to the microanastomosis aficionados in vascular surgery, the eye surgeons looked at the instruments as if they were science fiction curios. They felt that the automated instruments were too slow, too delicate, and too expensive. Later, a paper written on the motorized instrument alluded to vitreous cutting [4], but it did not generate interest in the Australian ophthalmology community.

At that same time I was working on stereophotogrammetry of the fundus. Professor Crock was so impressed by the results that he urged me to present this work at the 2nd International Congress on Fluorescein Angiography organized by Pierre Amalric, Albi, France, in 1969. There I met Drs. Edward Norton and Donald Gass, who were particularly interested in the 4-frames/s stereo fluorescein angiographic and the stereo photogrammetric techniques I had developed for Professor Crock [5, 6] but not in the microsurgical instruments. Later on that day, Dr. Norton offered me a position at the Bascom Palmer Eye Institute to further develop the fluorescein stereo camera and stereophotogrammetry system under Dr. Donald Gass' guidance. Dr. Norton invited me to stop in Miami on this *around the world trip* and visit with several members of the Bascom Palmer Eye Institute faculty. He didn't mention Dr. Robert Machemer but serendipity decided otherwise, and I ran into him during my visit.

Dr. Machemer, wanting to know what I was doing at BPEI, looked at the work I had presented in Albi. Contrary to Drs. Gass and Norton, he exclusively focused on the motorized microsurgical instruments, especially the motorized vitreous band cutting tip. He showed me a manually operated vitreous cutter with a guillotine-like cutting tip made of two tubes (Fig. V.B.1-5). In retrospect, the action of Dr. Machemer's handheld instrument was similar to the tip of the vitreous cutter Dr. O'Malley later designed. Dr. Machemer mentioned this instrument had been made to his specifications by Leonard Klein of Germany, but then quickly added, "it doesn't work." He explained that the cutting edges were too far apart and would not cut vitreous; "the vitreous enters the tube but as the blades do not cut all vitreous strands, pulling the instrument out of the eye, pulls on the vitreous and that can rip the retina." Looking at my oscillating instrument, which had blade tension, he then said that with my instrument it would take him forever to cut the vitreous piece by piece and remove all of it. He also asked what I had come up with to maintain intraocular pressure during cutting and removal of vitreous from the eye. As my instrument had been designed to cut vitreous bands through an opened anterior segment during cataract surgery, I had not thought of it. He pointed out that the eye was always under

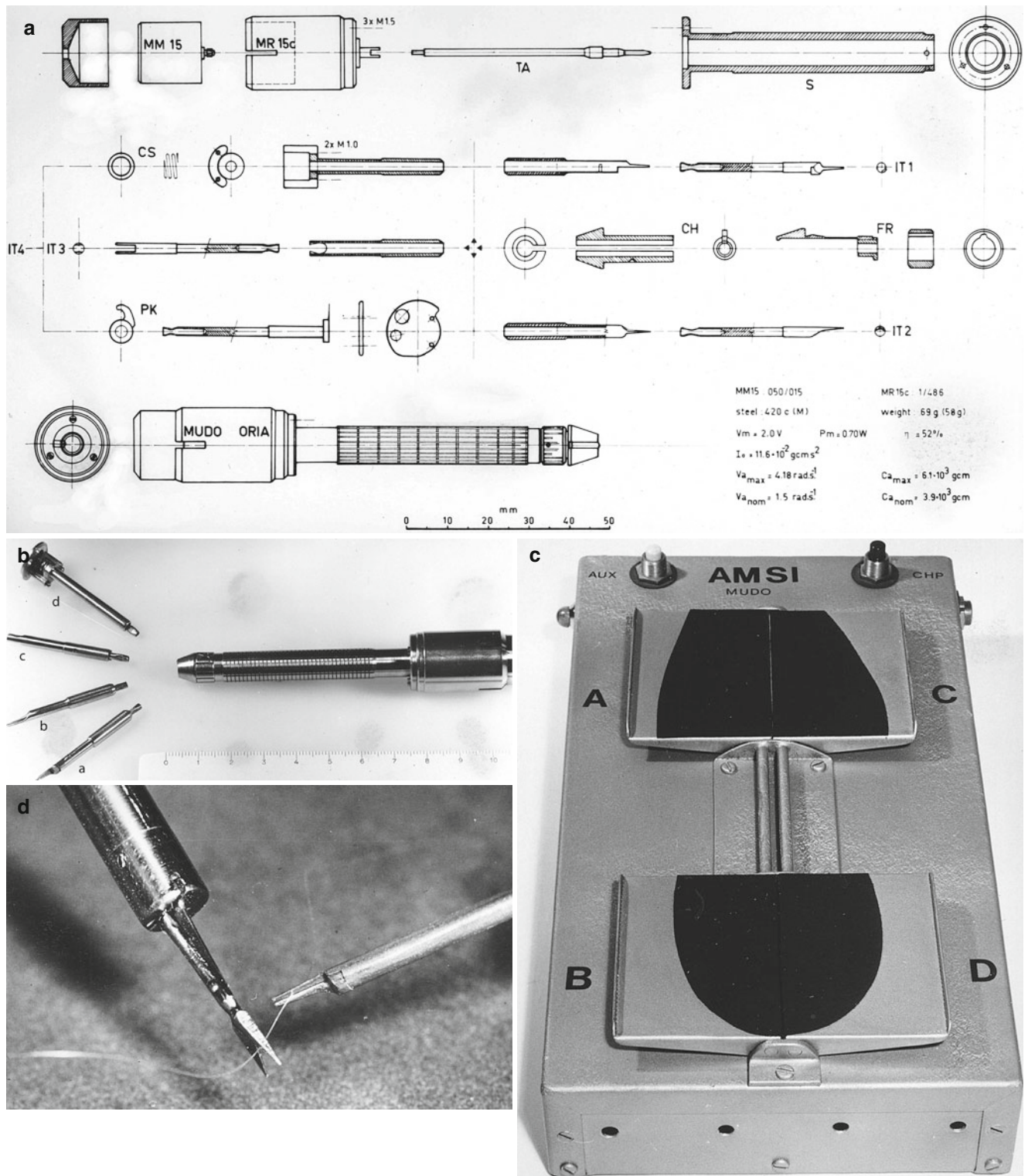


Fig.V.B.1-2 Design and assembly drawings (a) of the 1968 automated motorized surgical instruments (AMSI) with hand probe (b) accepting plug-in microsurgical tips (a) microscissors, (b) microneedle holder, (c)

vitreous band cutter, (d) nerve cutter), and a foot switch (c) designed to control two instruments, as shown in a bench test close-up (d)

pressure and it would collapse unless one maintained that intraocular pressure during surgery. My answer that Professor Crock was using a Flieringa ring to prevent collapse didn't satisfy him: "you need to add an infusion line." In addition he pointed out that the vitreous was not just made of a few bands but of millions of superfine crisscrossing fibrils attached to the retina and therefore a need of aspirating the cut vitreous with positive suction.

At lunch, Dr. Machemer and I kept exchanging ideas while I was sketching on paper napkins the design of different cutting tips, part of an instrument that would cut the vitreous while allowing for the cut pieces to be aspirated. The instrument would have a tube, coaxial to the cutter, which would infuse fluid to maintain intraocular pressure rather than having a handheld infusion cannula inserted in the opposite quadrant as Dr. Machemer had suggested. I believe that although not mentioned, he was already thinking of entering the globe through the pars plana and not through the anterior segment using, for instance, the open sky technique

practiced by Dr. David Kasner [7]. Dr. Machemer liked the idea of having all functions in a single instrument because it would free the other hand. I promised to keep working on that design and make the schematics necessary for a mechanic to fabricate a prototype. Cost was not discussed. We decided to communicate via post-mail, as the Internet and e-mail did not exist yet.

No problem can be solved from the same level of consciousness that created it.

Albert Einstein

IV. The Hard Work Begins

A. Prototype to Prodigious Innovation

Upon my return to Melbourne, I worked on drawings showing several cutting heads connected to a motor, activated with a foot switch with both infusion and suction lines

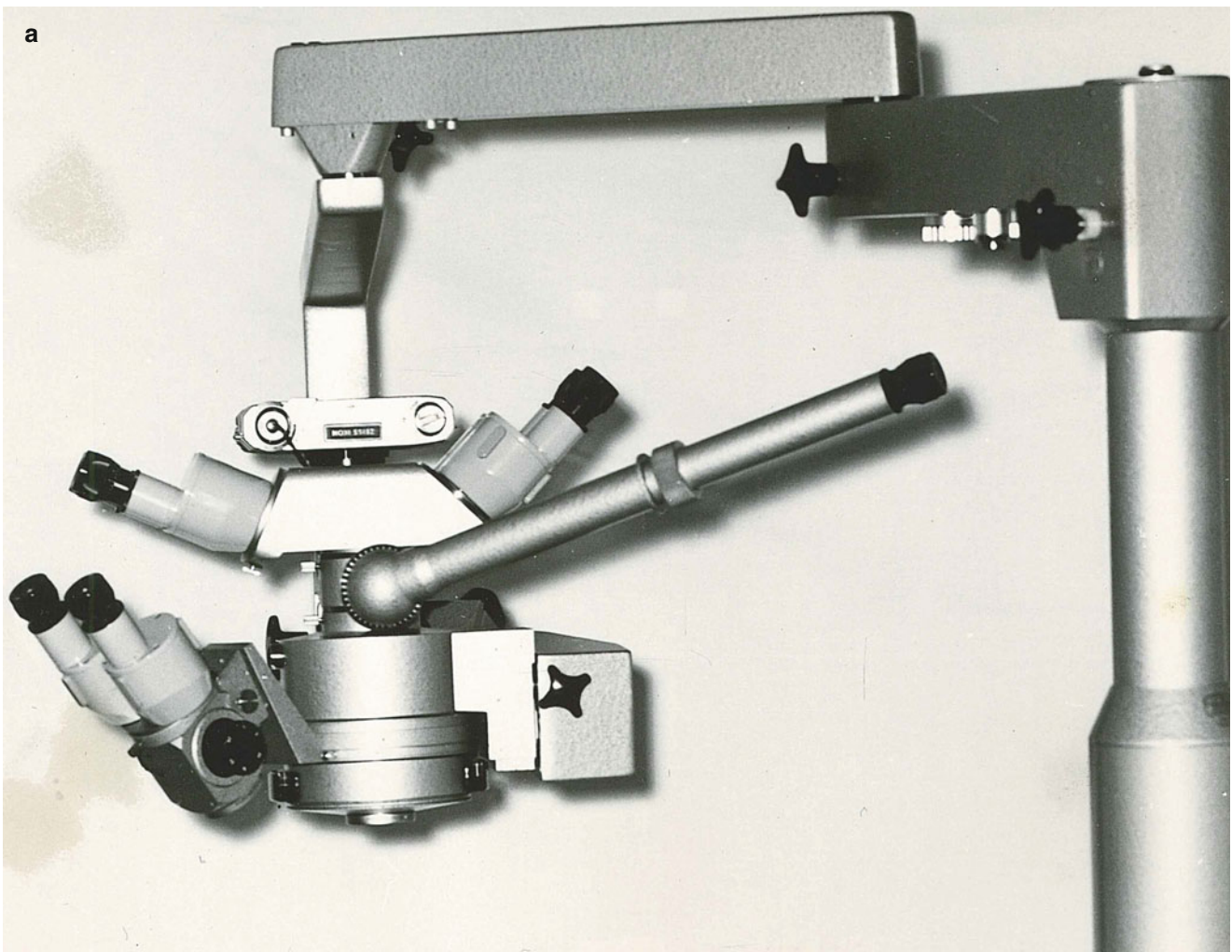


Fig.V.B.1-3 Photograph of diploscope modified in 1967 to accept a third stereomicroscope (a)

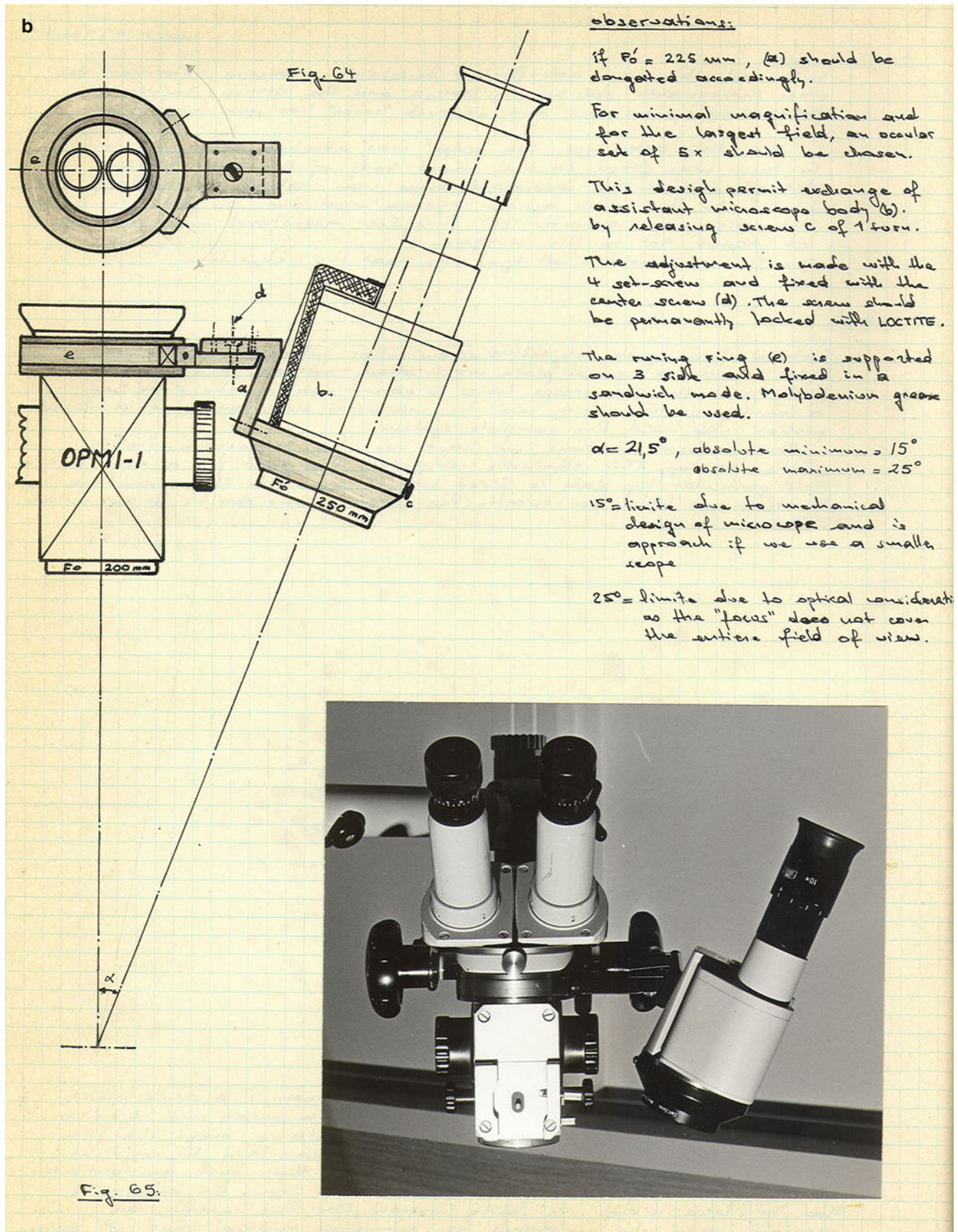


Fig.V.B.1-3 (continued) and its 1970 implementation to a more compact surgical microscope (b)

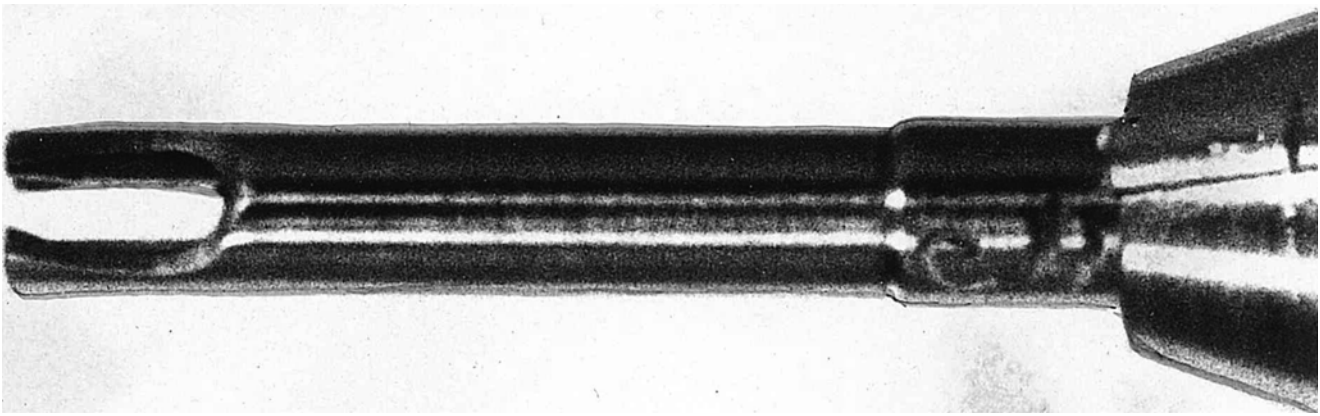


Fig. V.B.1-4 Melbourne vitreous band cutting tip fitting the AMSI hand probe

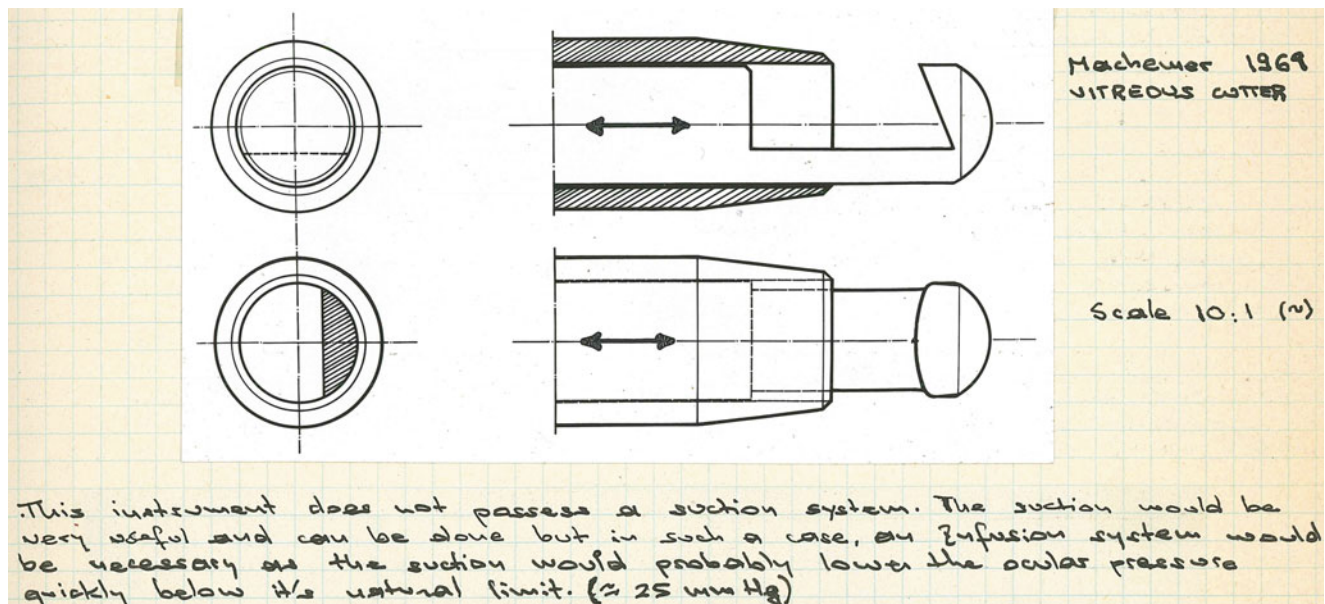


Fig. V.B.1-5 Schematic of Machemer's 1969 hand-activated vitreous band cutter

running all the way to the cutting tips which were exchangeable (Fig. V.B.1-6), and mailed these to Dr. Machemer. He answered promptly with new technical questions, which I answered with new, more refined drawings. At the time, a letter took well over a week to reach either continent, and it took me 3 months to finalize all the details. Finally I started to build the first prototype—the Australian vitreous infusion suction cutter (VISC), with my collaborator, mechanic Ljubomir Pericic.

In the meantime, however, after meeting Drs. Norton and Gass in Albi, I received a letter from the University of Miami with a student visa offering me to work for 1 year at Bascom Palmer Eye Institute. I was able to take a 1-year leave of absence from the University of Melbourne without losing my job nor my Australian visa. However, waiting for me to get the Australian VISC to Miami was too much for Dr. Machemer and his research fellow Dr. Helmut

Buettner. After testing the cutting efficacy of a drill rotating in a stationary tube on fresh eggs, they proceeded to build a vitreous cutting instrument. Using a 30 cc plastic syringe as the body of a handpiece that enclosed a small battery-driven DC motor, they connected a long aircraft drill inserted in a tube closed at the end except for a small hole at the side of the tip. The tube was connected with a Luer-Lock to the plastic syringe handpiece and motor. Suction was provided through a tube soldered to the stationary tube near the Luer-Lock. When suction was applied, tissue was aspirated into the hole near the tip and was then cut by the rotating drill. After trials on eye bank eyes, the instrument was improved by adding a coaxial tube for infusion to the cutting tip (Fig. V.B.1-7). After testing it on animal and eye bank eyes, this prototype instrument was used on a patient undergoing an open sky vitrectomy for vitreous amyloidosis in early 1970.

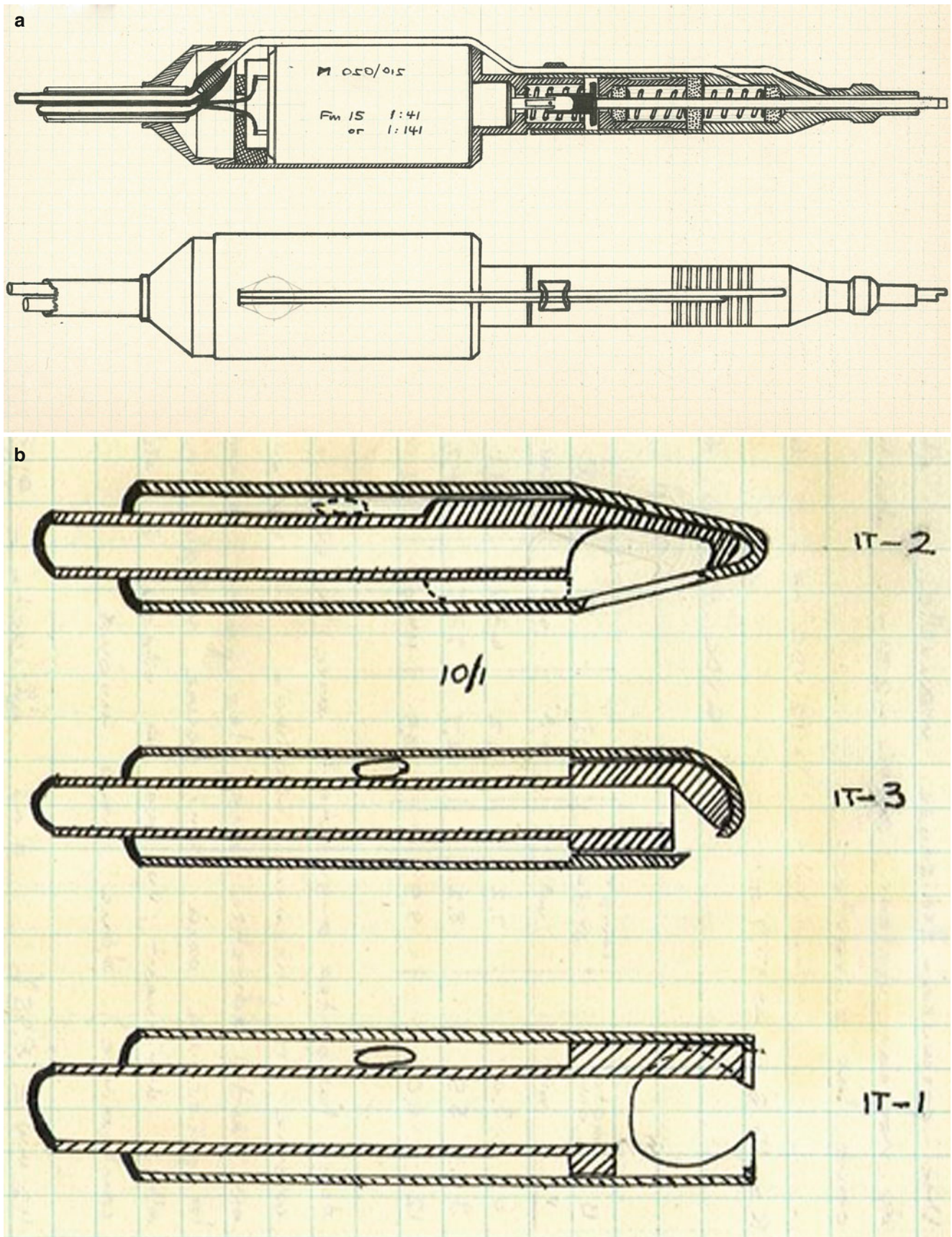


Fig.V.B.1-6 VISCI detailed hand probe drawings (a) and schematic views of three cutting tips (b)

When I arrived in Miami in April 1970, I presented Dr. Machemer the Australian vitrectomy instrument, which was tested 2 days later on donor and rabbit eyes as I watched. After successful testing of the Australian VISC (Fig. V.B.1-8),

the plastic syringe prototype developed by Buettner and Machemer was relegated to the museum. Ten days later, Dr. Machemer performed the first trans pars plana vitrectomy on a patient with diabetic retinopathy and non-clearing vitreous

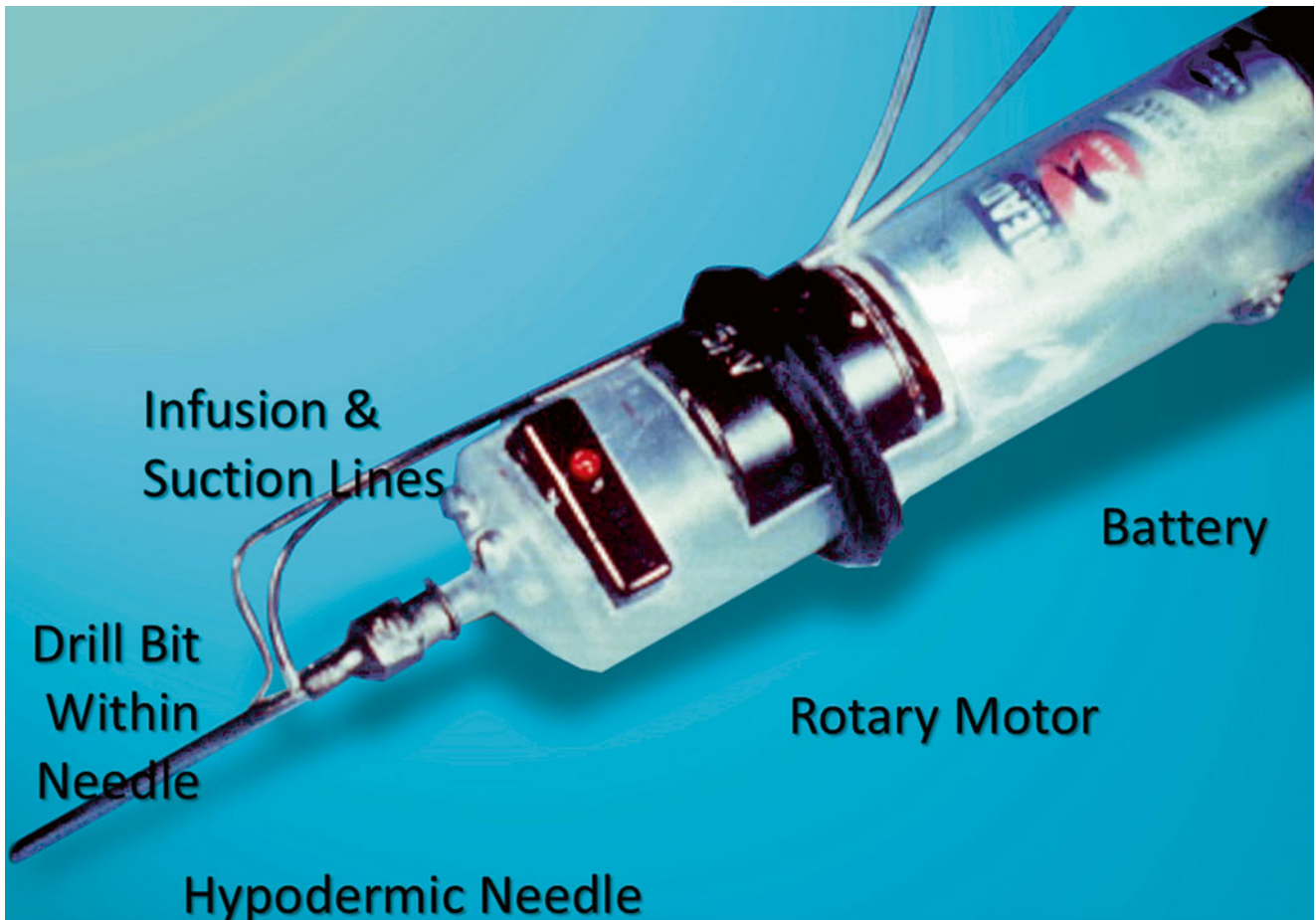


Fig.V.B.1-7 Robert and Helmut’s vitreous cutter fabricated in Robert’s garage on Key Biscayne

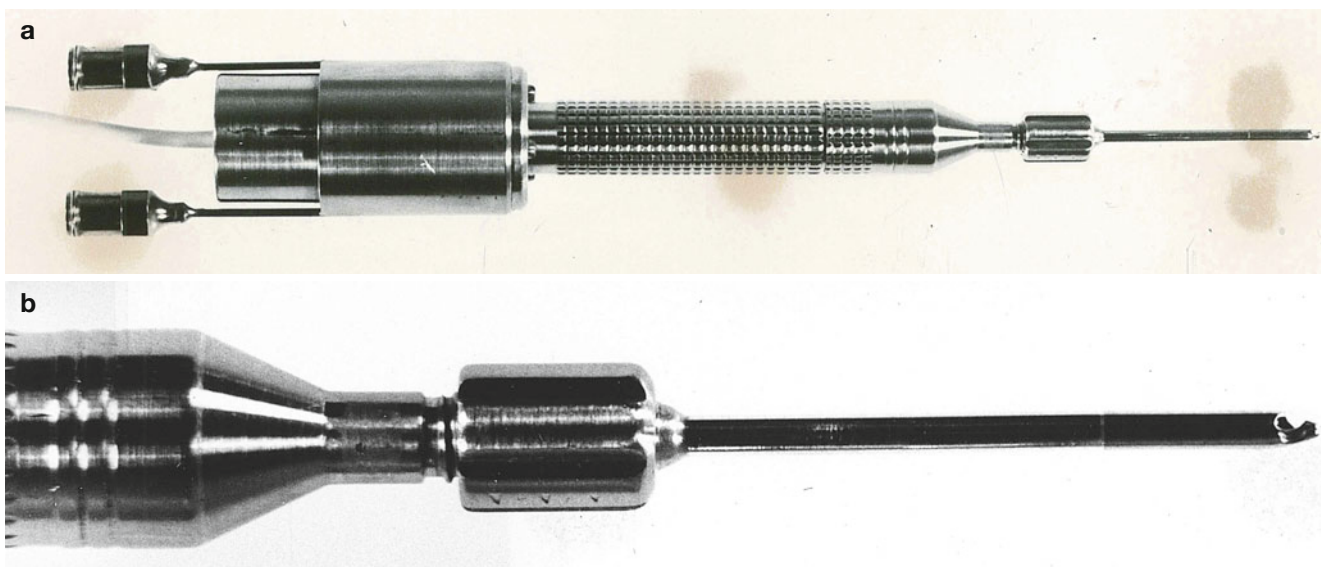


Fig.V.B.1-8 VISC I photographs of the hand probe (a) and magnified view of the cutting tip (b)

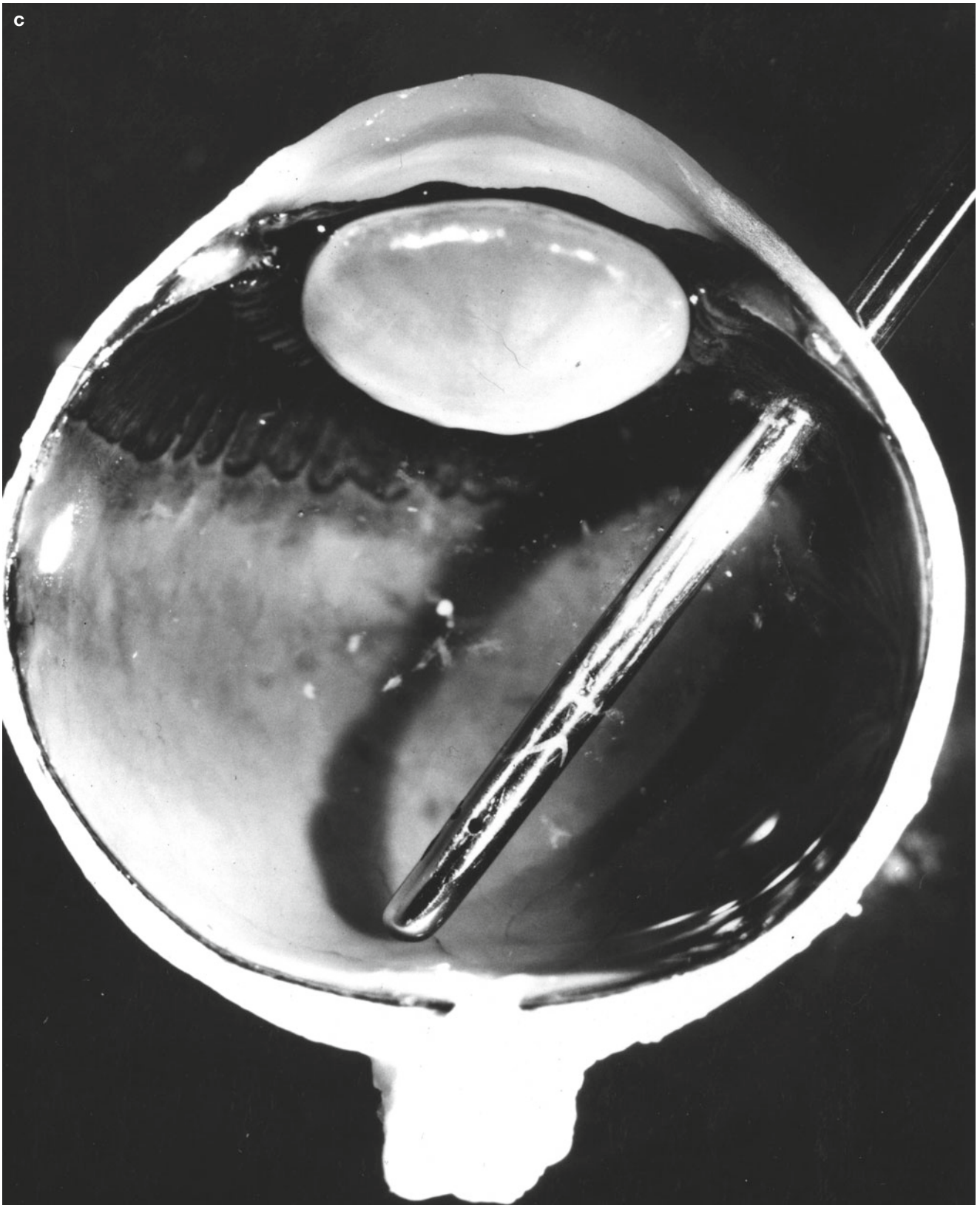


Fig. V.B.1-8 (continued) testing in an eye bank cadaver eye (**c**) and engineering details of the vitrectomy cutting tip (**d**) used during the first pars plana vitrectomy in the spring of 1970

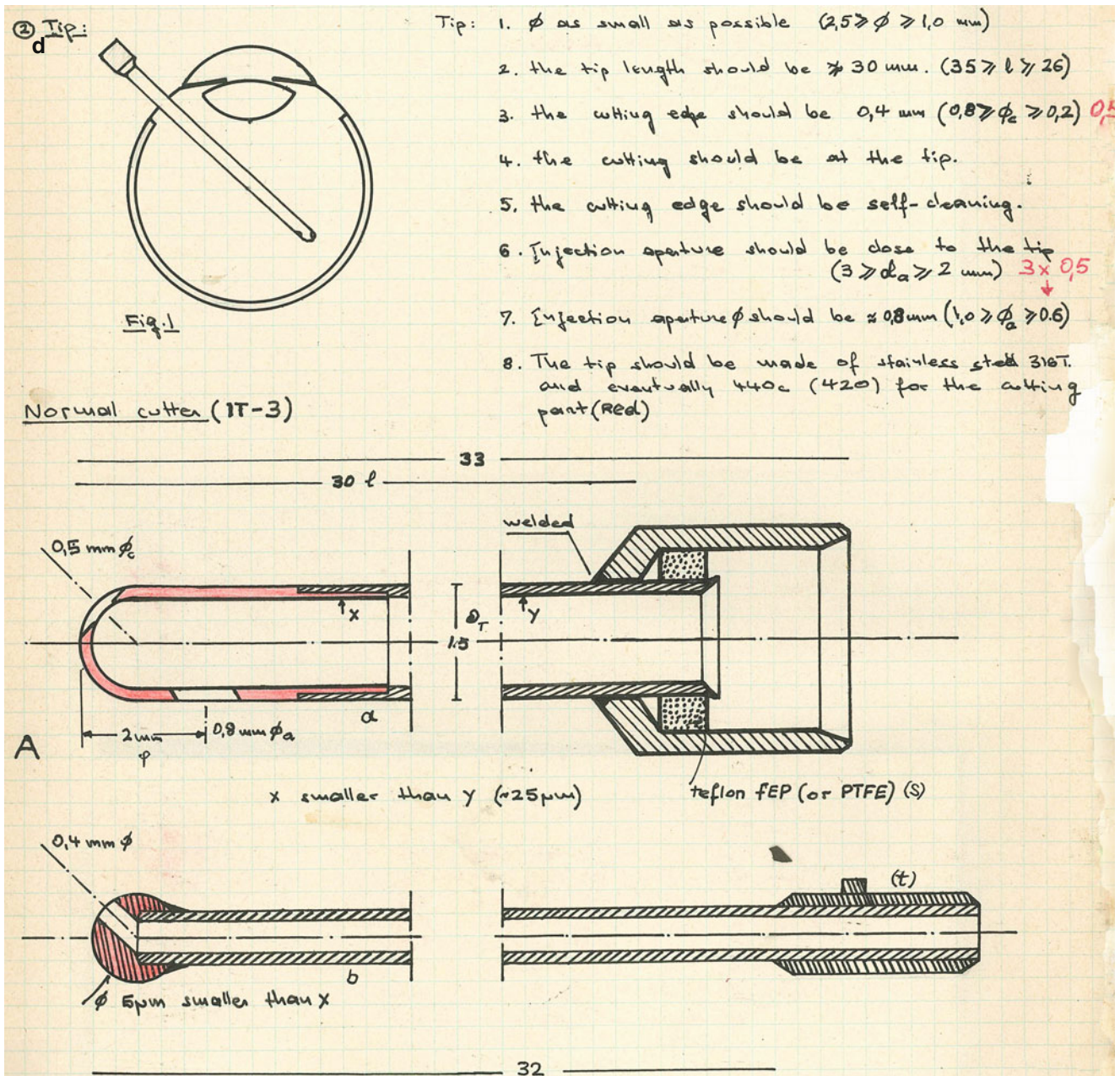


Fig.V.B.1-8 (continued)

hemorrhage at the Jackson Memorial Hospital in Miami. There were, however, some concerns regarding the self-sharpening action of the VISC tip, for it generated metal particles that could remain in the eye and induce metallosis (Fig. V.B.1-9). Through further design modification, this problem was resolved.

An invention has to make sense in the world in which it is finished, not the world in which it is started.

Ray Kurzweil (Director of Engineering, Google)

The summer and fall of 1970 were very productive times with regard to technical and surgical advances. Whenever Dr. Machemer performed a vitrectomy, Dr. Buettner and I were present to assist with the technical aspects of the procedure and to perform repairs of the Australian VISC as needed, often using tools and equipment provided by Dr. Steve Charles from the electrophysiology laboratory he had established and maintained. The limitations of this first VISC prototype quickly led to the development of the

Fig. 57

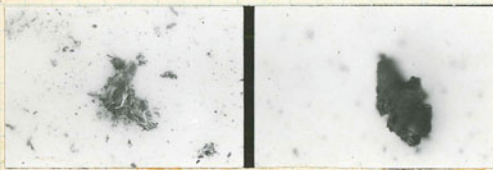
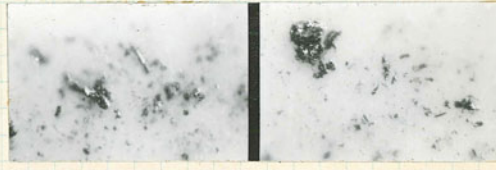


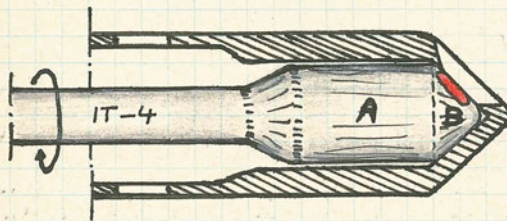
Fig. 58



.... after a vitrectomy, the large particles have a "diameter" of 60µm

The big problem is: why so many particles? and: why so large. If the particles are coming from the tip, then the cutting edges do not match perfectly! This means that we are tearing and not cutting. Two reasons may account for this: a) the s. steel edges are too soft. b) the eccentricity is very large and variable. It was found after many experimenting that the two phenomena are responsible for the large particles, as when the concentricity was practically inexistent, the particles were practically inexistent, and where hard edges (440c) could not produce many particles, an increase in eccentricity did not really increase the production of particles.

Fig. 59

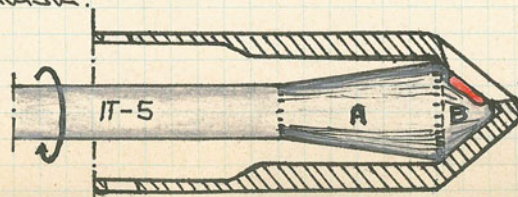


A and B are surfaces producing particles. It seems that the surface A produce more particles than surface B. This can be seen after having made the VISC working during 1h in a wet solution!

Logically the best concentricity will lower the number of particles to a minimum as in this case, the surface A will not touch the barrel.

If the concentricity can not be matched, the only solution will be our first attempt. (see page 1): a "ball" shaped cutter. In this case only surface B will touch, and by having a very hard material, the production of particles will be kept to a minimum.

Fig. 60



With such a tip, the production of particles will be reduced to a minimum if one considers only the factor of concentricity, only B they is producing particles.

Fig. V.B.1-9 Identifying and solving the problem of metal fragments created by the self-sharpening function of the VISC tip. Heat-hardened 440 °C stainless was used in later cutter design, but they still generated

microparticles. Dr. Harry Flynn found these being nontoxic to the retina (Harper et al. [41])

mechanically largely improved VISC II. At the same time, data were collected for Dr. Machemer's first presentation of pars plana vitrectomy at the 1970 meeting of the American Academy of Ophthalmology and Otolaryngology (AAOO) in Las Vegas. The first publication appeared in the Transactions of that meeting in 1971 [8]. By September 1970, the first coaxial fiberoptic endoilluminator fitting over the tip of VISC II was designed (Fig. V.B.1-10) and was also presented at the Academy meeting in Las Vegas. These presentations generated great interest in the budding field of vitreous surgery and were the beginning of a very fruitful

collaboration with retinal surgeons in the United States and abroad.

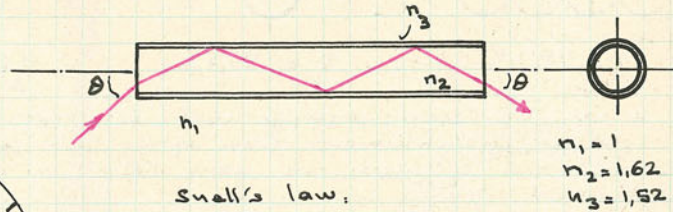
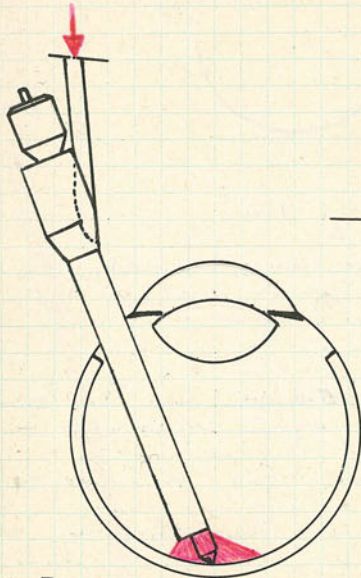
B. Innovation Progresses to Benevolent Production

The second-generation VISCII designed at BPEI (Fig. V.B.1-11) was also built by Ljubomir Pericic, the mechanic in my Melbourne lab. The slow process of communicating between continents far apart by post-mail and the VISC beginning to

③ Illuminated cutter: (1 October 1972)

a) as external illumination give poor contrast due to the high reflections of the contact lens or of the cornea, we experimented with optic fibers so as to conduct light in the vitreous. Cool light is a must in this technique.

fibers used: 55µm diameter ext. with approx 5.5µm coating of lower refractive index (n_3). (Scientific devices inc)



Snell's law:

$$NA = \text{Numerical aperture} = \sqrt{N_2^2 - N_3^2}$$

as $N.A. = \sin \theta \cdot n_0$ and as $n_0 = 1$

$$\rightarrow \sin \theta = \sqrt{N_2^2 - N_3^2}$$

in the above case, $NA = 0,566$ and $\theta = 34,5^\circ$

Fig. 5

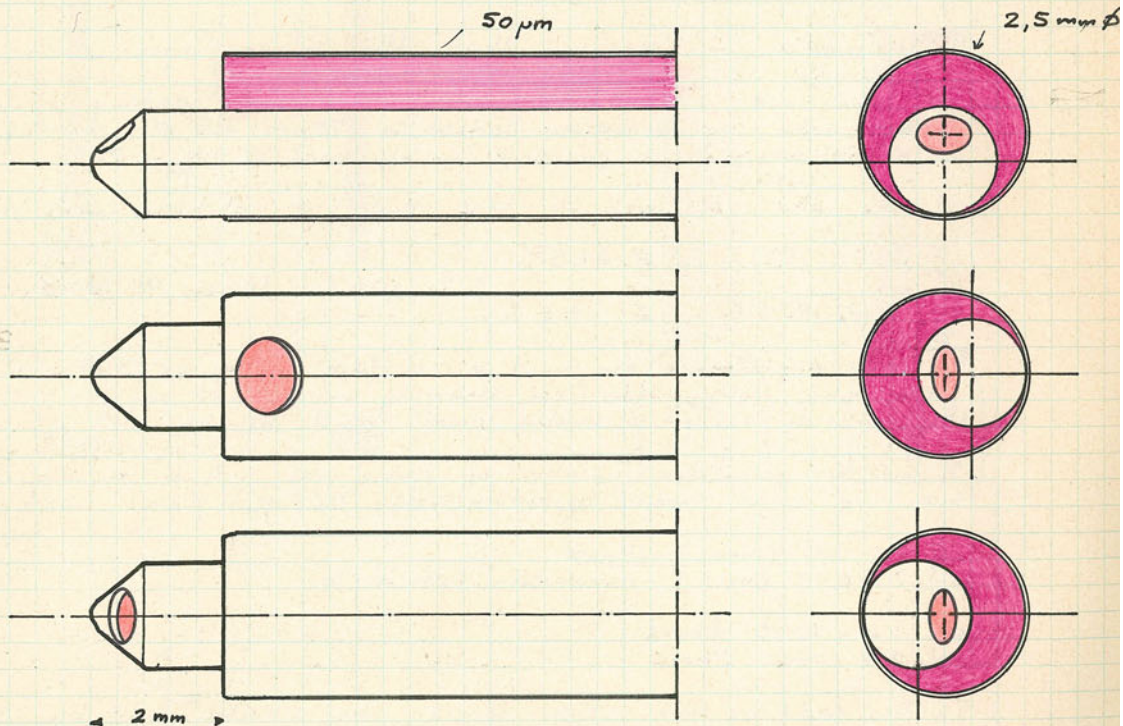


Fig. 6

Using IT-4 as the base. (using any other tip is possible)

Fig.V.B.1-10 Concept (a)

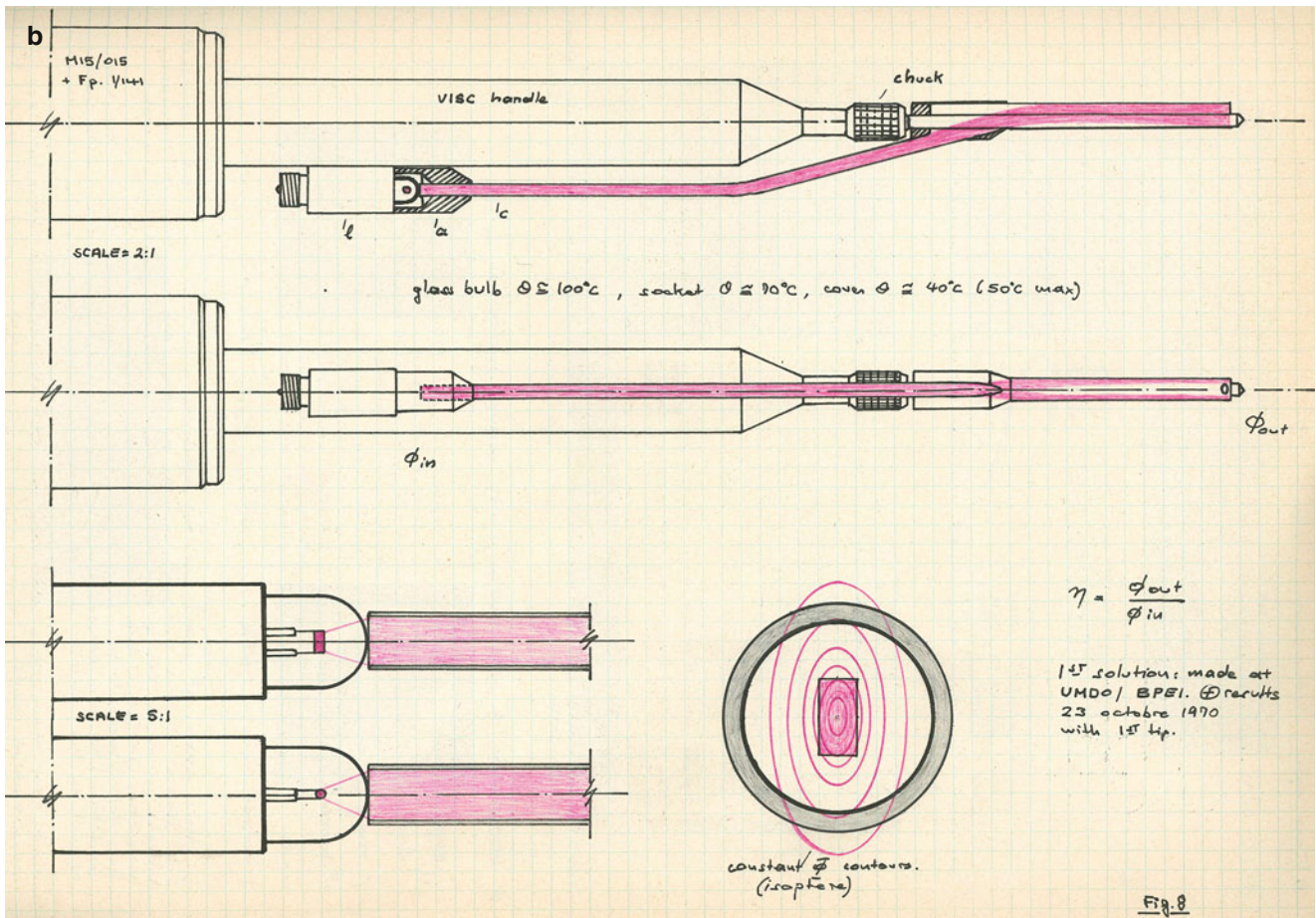
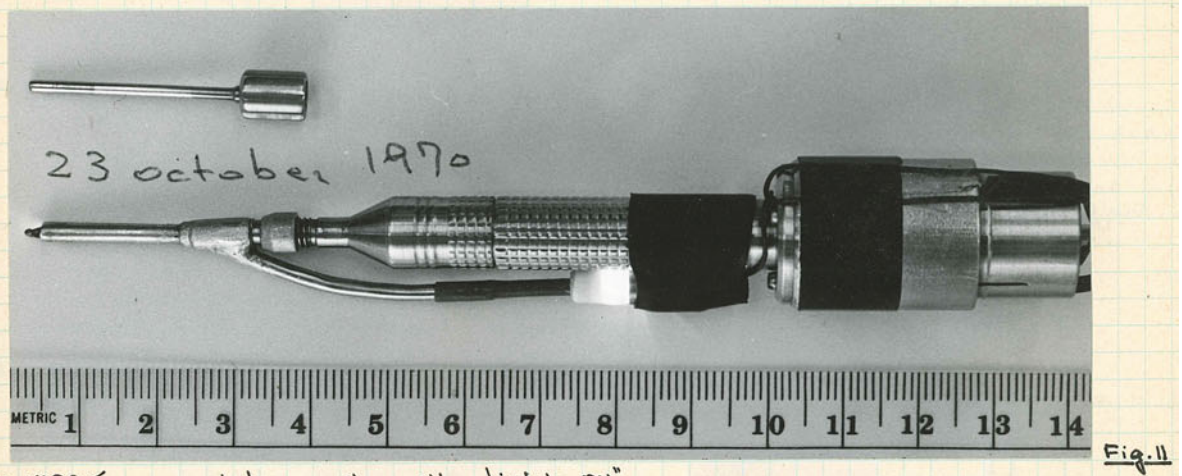
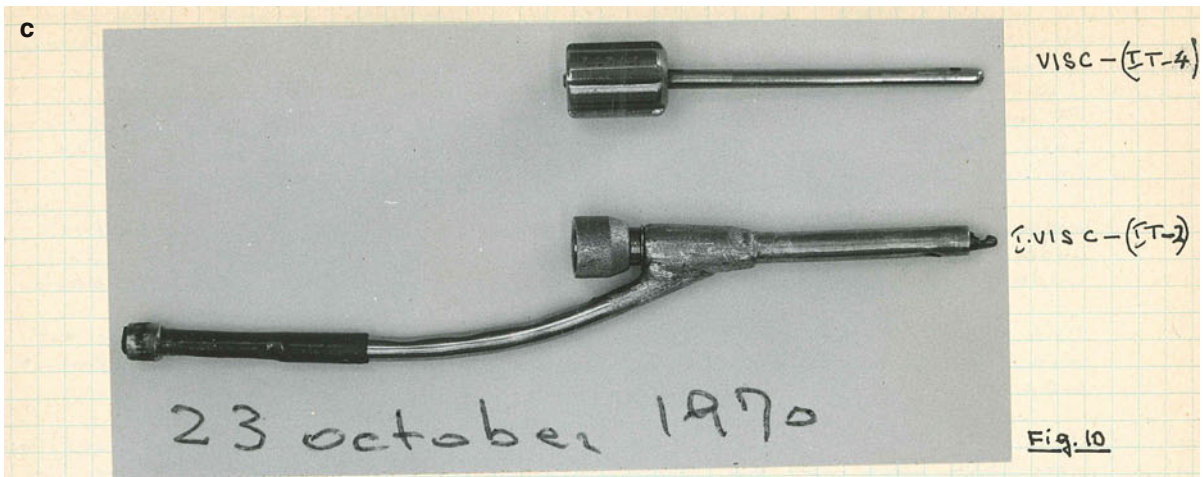
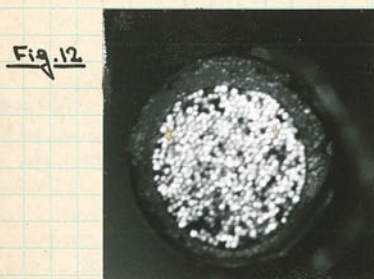


Fig.V.B.1-10 (continued) and design (b) of coaxial fiberoptic illumination added to the VISC I (c) in October 1970 to improve visualization of the vitreous and retinal structures

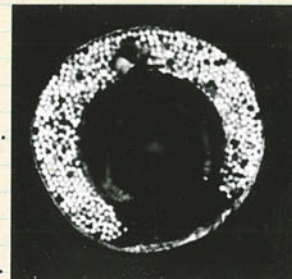


I. VISC.I complete unit with light "ON"



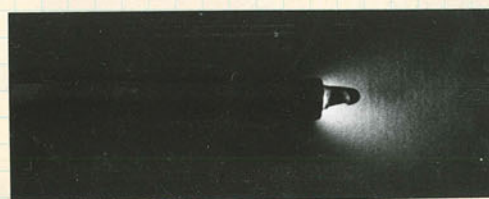
Input \approx 900 fibers

the non-symmetrical arrangement and the missing or broken fibers are well visible. lack of uniformity of the fibers is proof of the poor grinding and lack of polishing.



Output \approx 600 fibers

theo \rightarrow max: 1200 fibers in this model.



illuminated wall by the VISC.I (IT-2)

Fig. 14

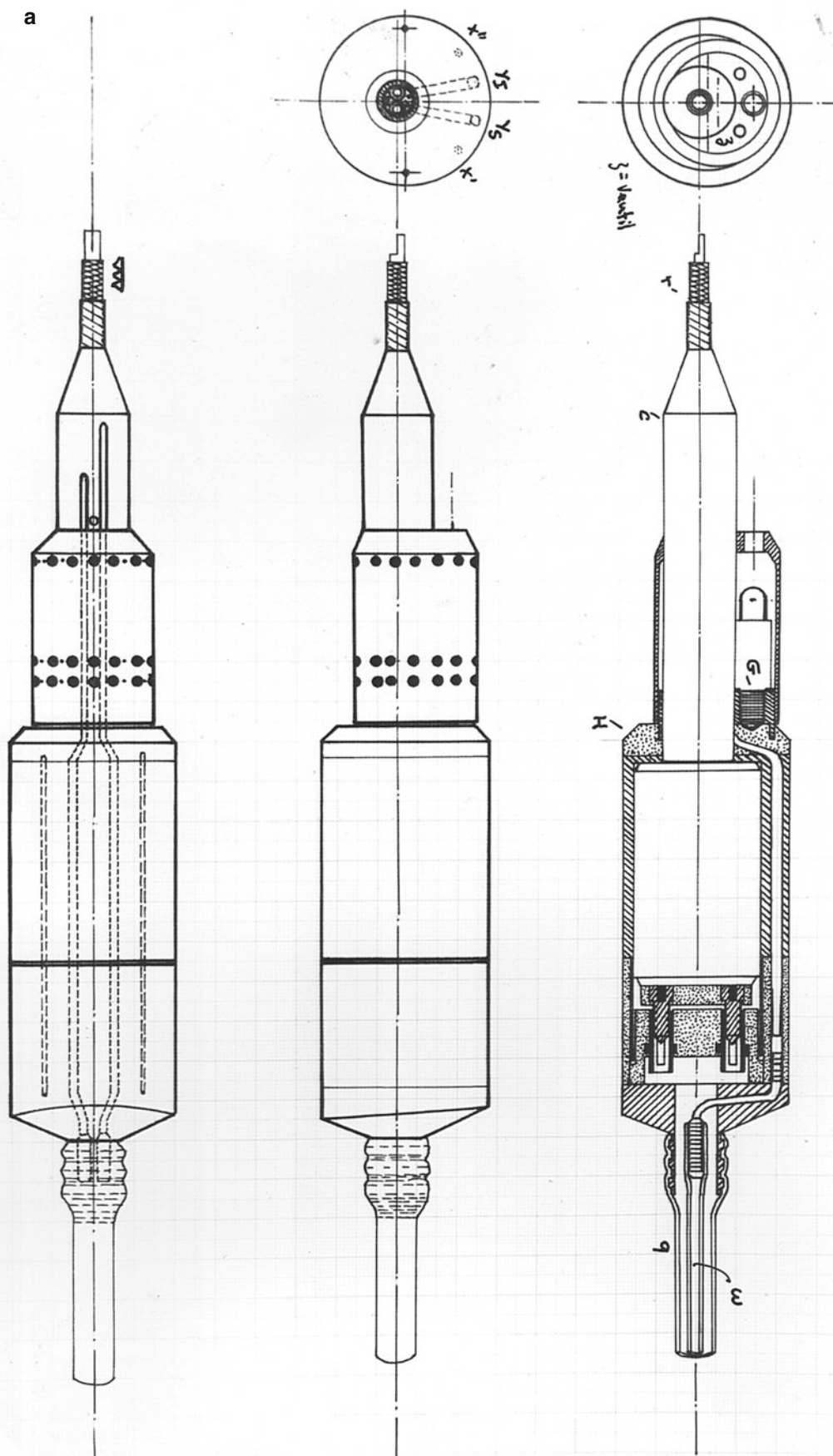


Fig.V.B.1-11 VISCO II design (a) and assembly (b)

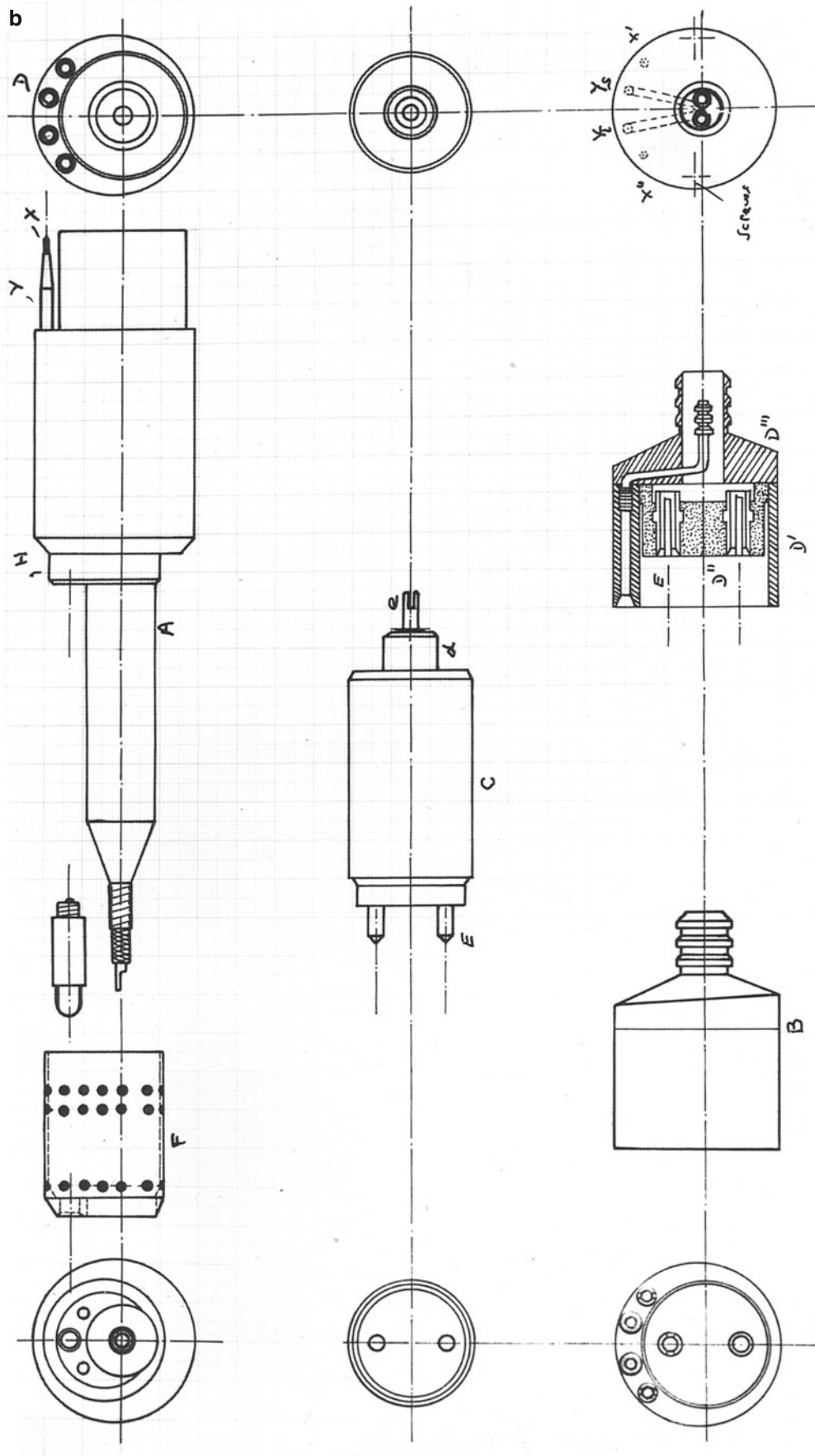


Fig.V.B.1-11 (continued)

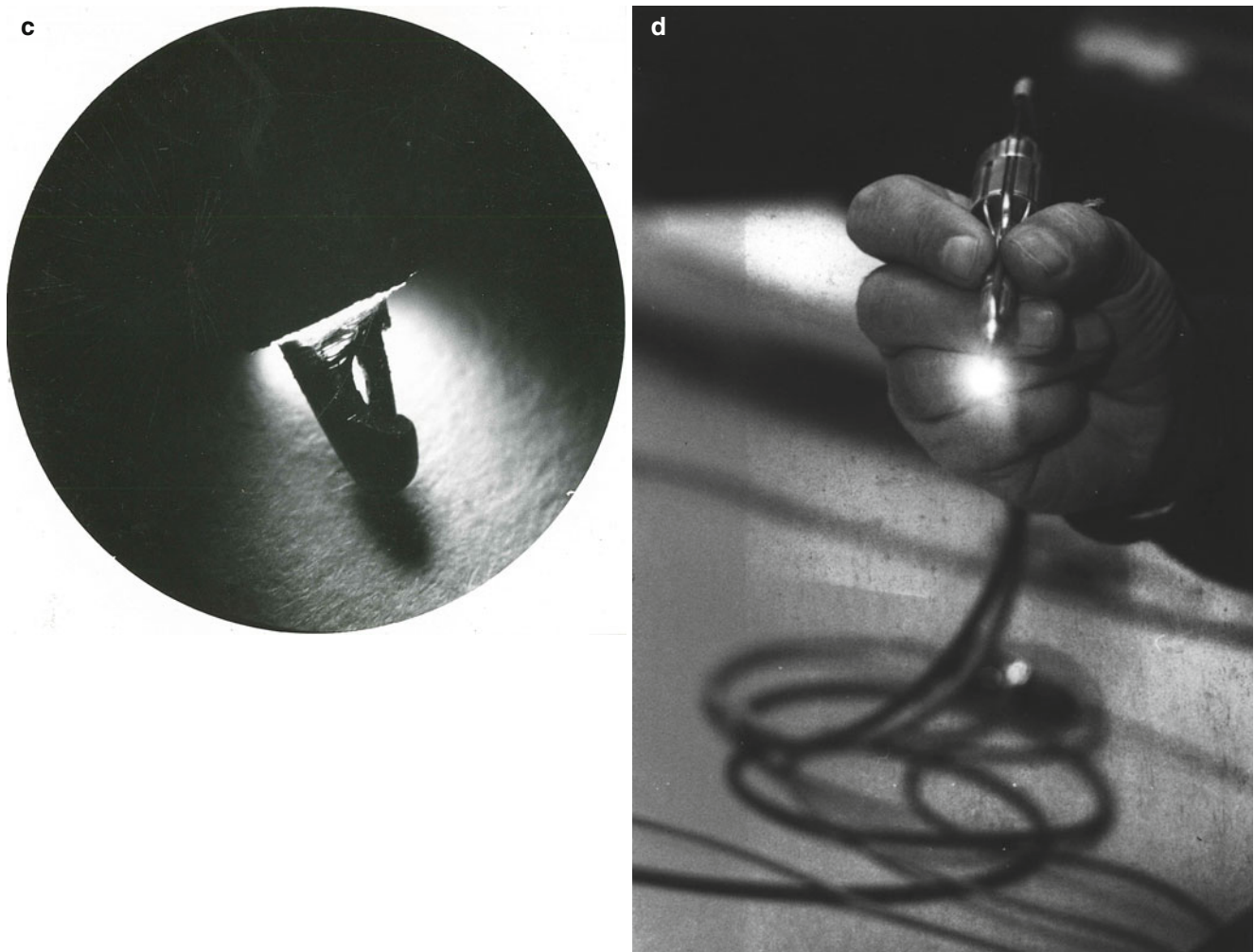


Fig. V.B.1-11 (continued) schematics with integral lamp on the body of the instrument. The light source was a miniature tungsten bulb mounted on the handle, but the illumination was insufficient (c). In

1971, a groove was made on the VISC body to accept a removable slip-on fiberoptic probe powered by a 100 W halogen lamp. This scheme was implemented in the VISC III (d) to VISC X designs

wear out with increasing use led to the decision to establish a laboratory in Miami, which became the Ophthalmic Biophysics Center. A Swiss mechanic, Hans-Jurg Vedder, joined me and started building vitrectomy instruments at the Bascom Palmer Eye Institute (Fig. V.B.1-12). Several generations of the VISC, each with some improvements, were built after the acquisition of a plastic injection machine, which greatly accelerated fabrication. By 1972, Austrian mechanic and mold maker Willi Aumayr had joined our team, and the seventh-generation vitrectomy instrument, which was duplicated by the dozen, had been produced (Fig. V.B.1-13). No attempts to patent these inventions were ever made. Dr. Norton felt strongly that the patenting process would slow down the rapid dissemination of knowledge and experience, which would foster healthy competition among different teams and which would ultimately improve patient care.

Science knows no country, because knowledge belongs to humanity, and is the torch which illuminates the world.

Louis Pasteur

As a result, improvements in the instrumentation [11, 12], surgical technique, and clinical results [13, 14] were rapidly published. Both the VISC VII and the microscope with x-y movement were displayed at the meeting of the Club Jules Gonin, on Key Biscayne in 1972, for which Dr. Machemer received the prestigious Wacker Prize, which he shared with his collaborators in Miami.

Dr. Helmut Buettner and I investigated the possibility of visualizing the intraocular surgical field endoscopically rather than with operating microscope using a corneal contact lens during vitrectomy was investigated (Fig. V.B.1-14). The smallest instrument at the time, a Storz pediatric endoscope measuring 3.5 mm in diameter, proved too large to be inserted through the pars plana without risking serious damage to the adjacent retina. The project ended up on the back burner. Instead the first operating microscope with foot switch-controlled x-y movement and motorized slit lamp powered by tungsten halogen and xenon flashlight sources [9] was developed. The team also continuously

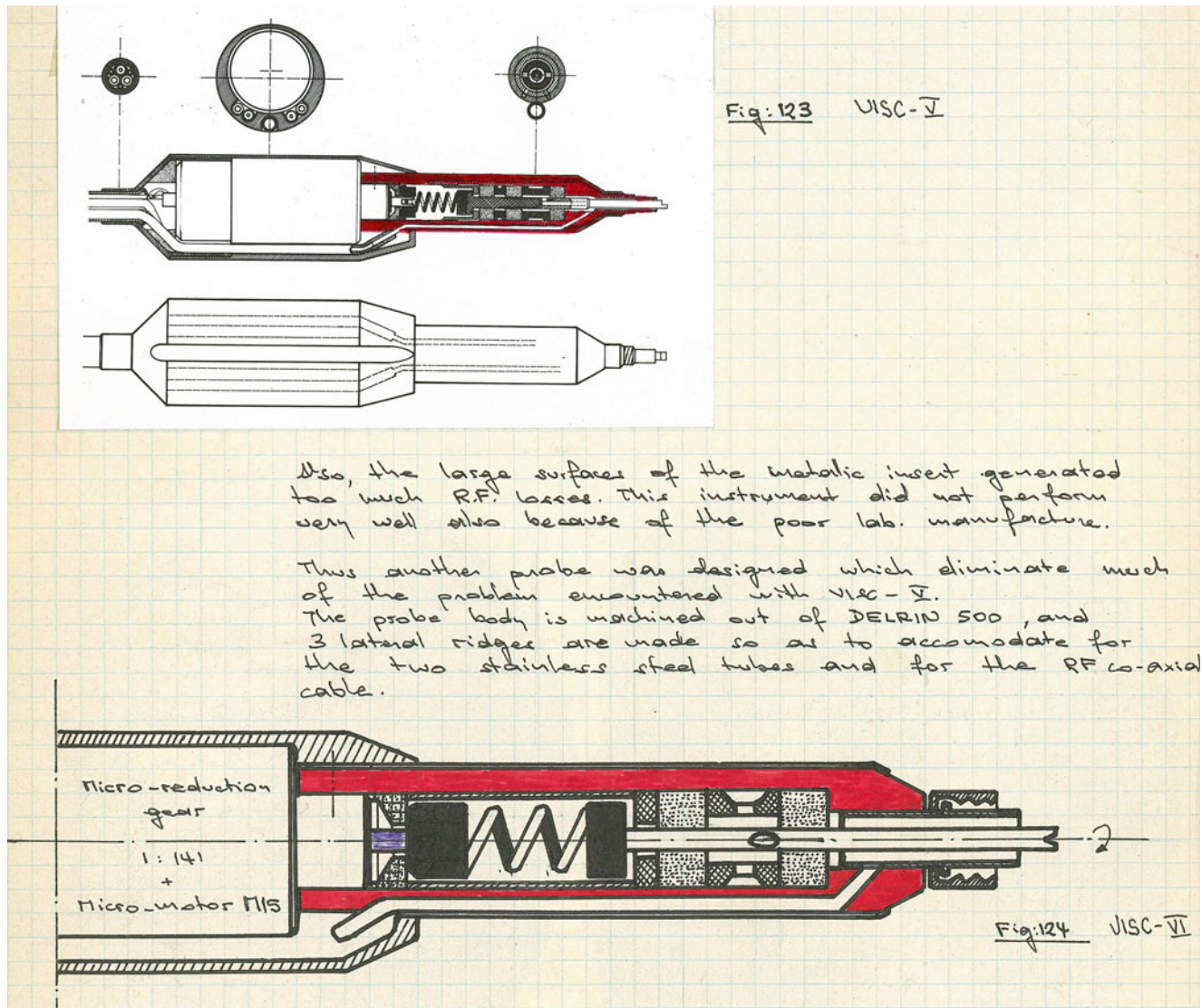


Fig. V.B.1-12 VISC V and VI with RF diathermy capability and groove to accept tungsten halogen and xenon-arc fiberoptic endoillumination. The instrument was connectable to a modified foot switch-con-

trolled RF generator for endodiathermy of bleeders. To prevent damage to surrounding tissues, the cutter was black Teflon coated except at its very tip

worked on improvements of the vitrectomy instrumentation [10]. Other developments included intraocular endodiathermy, bipolar diathermy, and a fiberoptic illuminated hook needle for peeling preretinal membranes [15].

V. Teach the World

The next *ordre de marche* Dr. Norton gave me was to make VISC VII for a dozen surgeons that included Steve Ryan in Los Angeles; Tom Aaberg in Milwaukee; Ron Michels at Wilmer; Klaus Heimann in Cologne, Germany; Peter Leaver at London's Moorfields Eye Hospital; and others—all became my friends whom I called them the *vitrectomy musketeers*. With the support of Dr. Norton, Dr. Machemer was able to organize courses to

disseminate the technique of vitrectomy through the pars plana with its problems and how best to prevent them. Dr. Norton rejected the idea of charging for the instruments, as he believed these surgeons would provide important feedback and suggestions for improvements of instrumentation, thus benefiting patient care. Shortly after the presentation of the vitrectomy experience from Miami at the 1970 AAOO meeting [15], other investigators presented their own vitreous cutter design; among them were Dr. Peyman [16], Dr. Kloti [17], Dr. Nick Douvas [18, 19], and Dr. O'Malley [20], who produced the very popular guillotine-type cutter that became known as the *microvit*, an instrument type that is still in use today being produced by several companies under various names.

In 1973, Robert gave my drawings (Fig. V.B.1-13) to Leonard Klein in Heidelberg, Germany, for the VISC VII to

be produced for all ophthalmologists. By then 3 years had passed and my student visa, already twice extended, was to expire. It was grand time for me to return to Australia to pay my dues to Professor Crock who had given me the opportunity to be part of what became a historical change in ophthalmology, to which I had simply contributed modern technologies for the development of ophthalmic surgical instrumentation. But my return at MUDO didn't stop my collaboration with BPEI. Professors Crock and Norton were not only colleagues, but very close friends and both had the same rule: *patient first*. I was thus given free reign to continue helping the Miami team in their quest to improve pars plana

vitrectomy. During my 3 short years in Miami, I had become a BPEI alumnus, thanks to Dr. Norton's mentoring and teachings. Owing to his endless generosity, I had been able to develop a second to none laboratory, something I sadly found Australia could not afford. Thus, I took the decision to emigrate again. The process took 1 year and by December 1974, I was back at BPEI and by end of 1975, the VISC X was born. It would be my last.

The OBC grew and mechanical engineer David Denham and electronic engineers Ronald Lashley and Izuru Nose were hired to develop more complex apparatuses including an integrated OR systems for intraocular surgery [21].

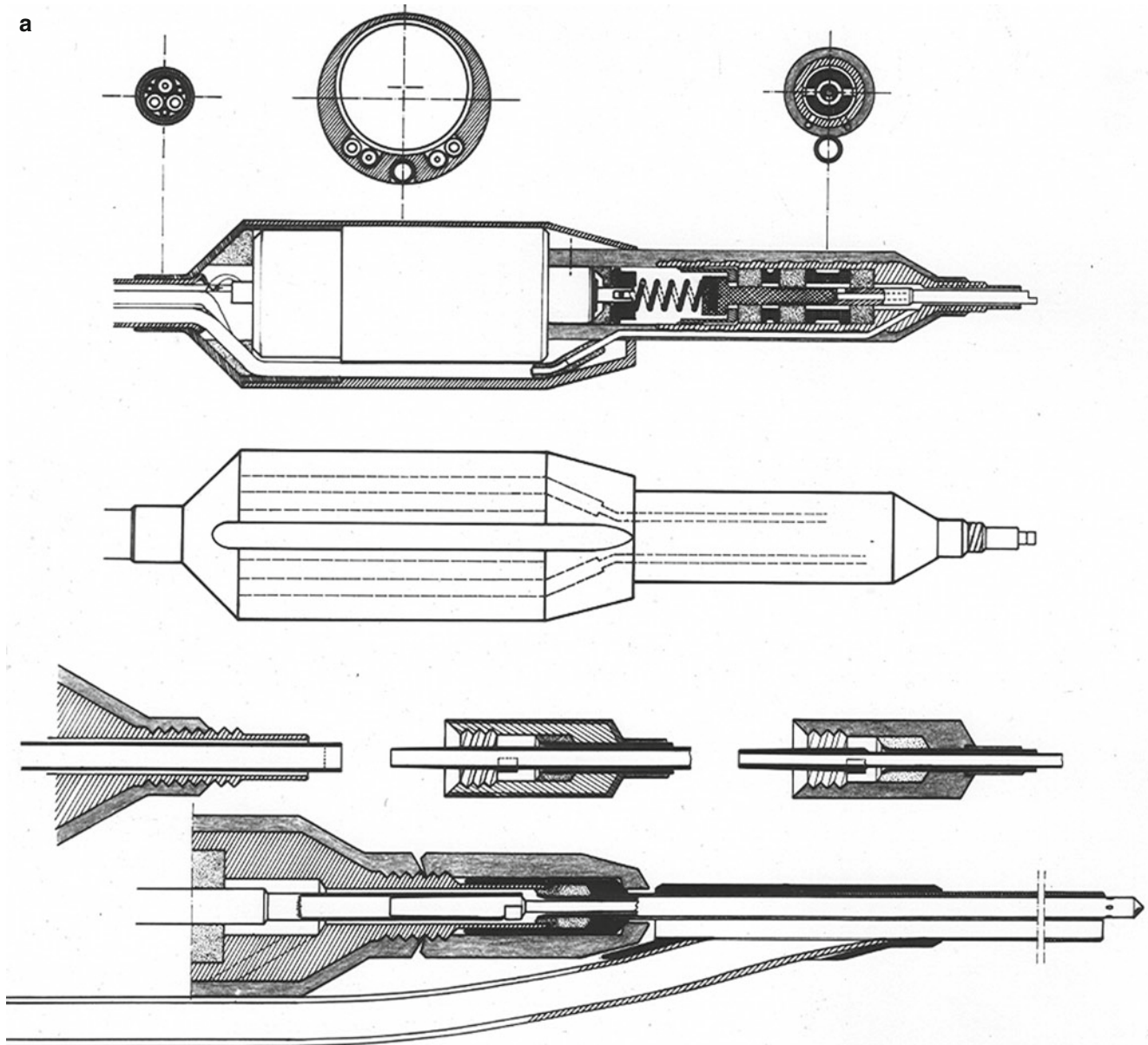


Fig.V.B.1-13 Design drawings of VISC VII (a), its endoillumination concept (b) and design (c)

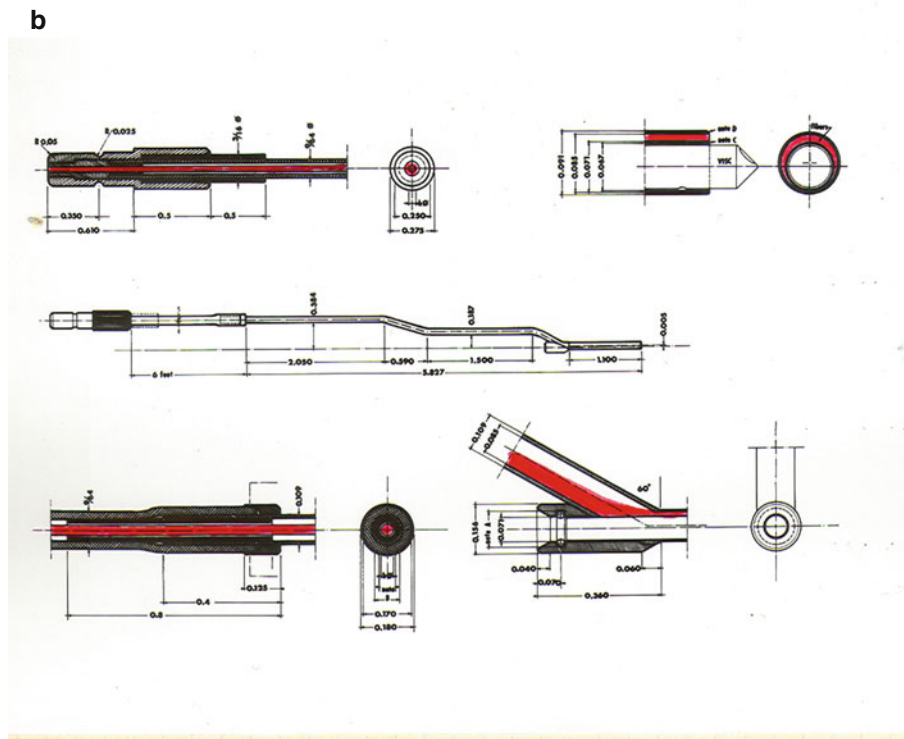


Fig:
 fibra optic attachment f
 the visc-VI.
 "O" ring is provided for
 outflow sealing.
 Silicon jacket give good
 flexibility and protection.
 The infusion flow is
 not impeded because
 of the special flat on
 the tip.

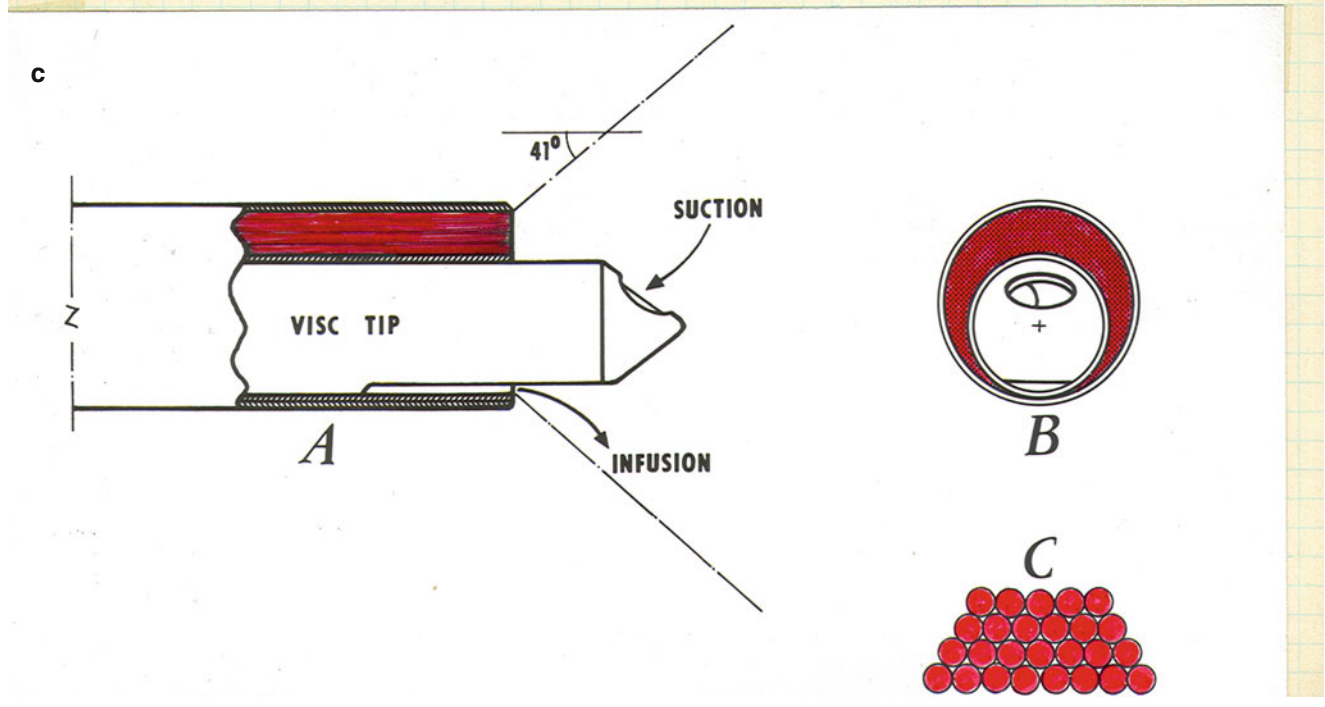


Fig.V.B.1-13 (continued)

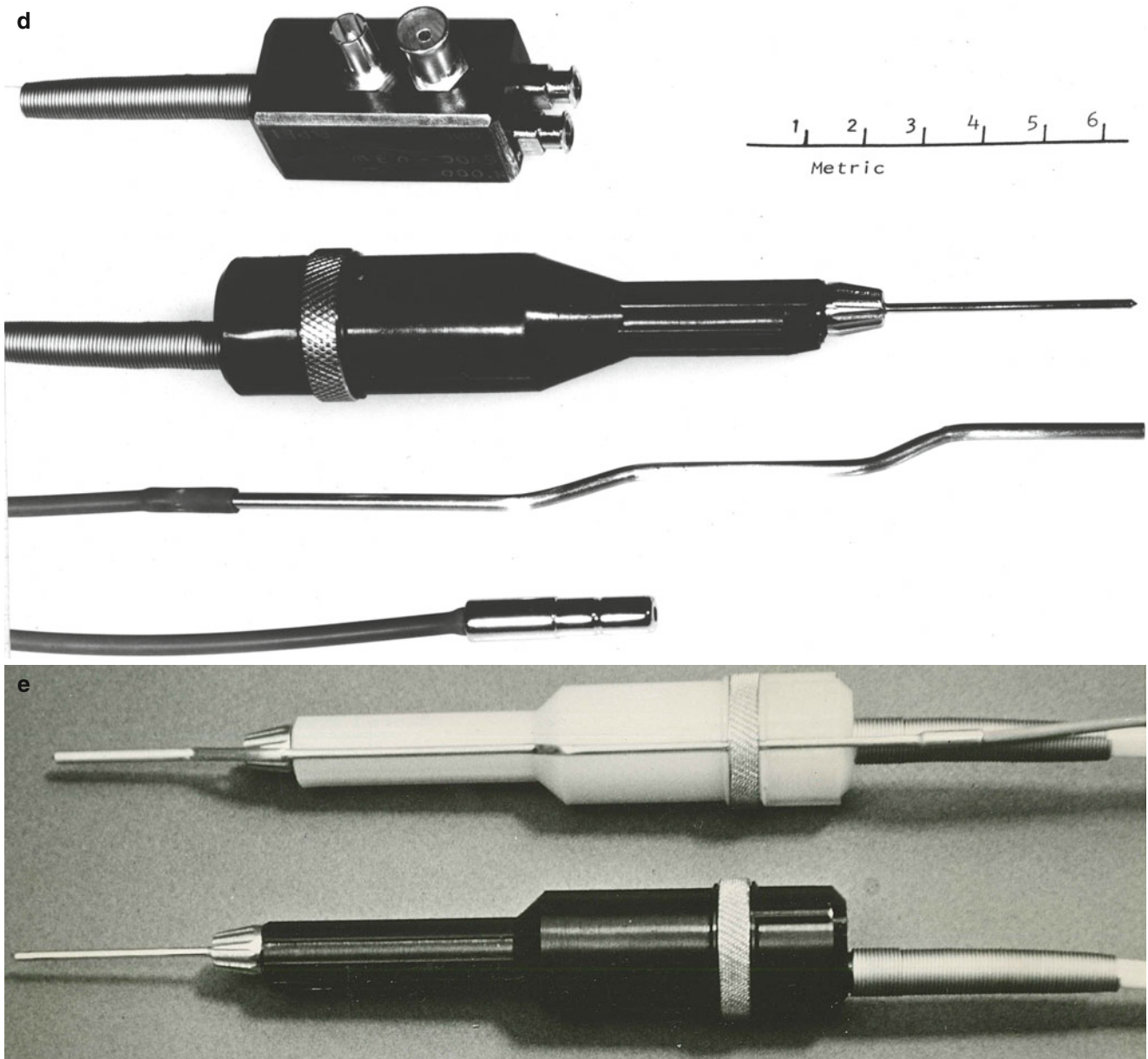


Fig. V.B.1-13 (continued) and the photograph of the instrument (d) built at Bascom Palmer Eye Institute. As each BPEI surgeon was responsible for the maintenance of his/her own instrument, the color of the injection molded plastic outer casing was individualized with the surgeon's preference (e)

Dr. Machemer's departure to become chair of the Department of Ophthalmology at Duke University didn't stop our close collaboration. I made monthly trips to Durham to help develop the Duke Ophthalmic Biophysics Center at Duke University Eye Center eventually led by the bright and inventive mechanical engineer Dyson Hickingbotham.

VI. Diversification

My OBC team not only kept collaborating with Dr. Machemer and Mr. Higginbotham developing the membrane peeler cutter (MPC) and transvitreal bipolar coagulator among other

instruments [22–27], but expanded collaboration with many BPEI clinical faculty members. In 1976 Dr. George Blankenship sparked the production of endophotocoagulation via fiberoptic initially connected to the Meyer-Schwickerath carbon arc photocoagulator, later to a small and portable xenon photocoagulator, which was used until argon lasers became widely available. Dr. Blankenship also took part in the conception of the rare-earth magnet [28] and the motorized infusion pole [29].

Dr. John Clarkson helped develop *Le System* [30], a modular console that with a single foot switch controlled infusion and suction, operated a motorized IV pole and intraocular probes for cryopexy, ultrasonic phacoemulsifi-

cation, and high-frequency bipolar diathermy. It also contained power supplies for several automated microsurgical instruments including the plasma membrane cutter developed with Dr. Mark Blumenkranz. At that same time, a battery-powered vitrectomy system was developed for field surgery [31], a pars plana phacoemulsifier [32], a subretinal fluid aspirator with Dr. Harry Flynn [33, 34], and an intraocular pressure monitor, with Dr. Richard Parrish [35], that allowed to quantify and correct severe fluctuations of intraocular pressure occurring during vitrectomy. This allowed us to improve the function of the aspiration module in *Le System*, which was clinically tested by Dr. Clarkson. Eventually the pressure monitoring system became a standard in all phacoemulsification and vitrectomy control modules.

Although this armamentarium had become quite sophisticated and surgical techniques had been refined, the cure of proliferative vitreo-retinopathy (PVR) remained largely elusive. Dr. Machemer often spoke about this problem, which used to generate heated discussions at the Vail vitrectomy meetings of vitreoretinal surgeons which I religiously attended [see chapters V.B.5. Surgical management of retinal detachment with PVR; V.B.6. Retinectomy in recalcitrant retinal detachments]. Dr. Machemer proposed the intraocular administration of triamcinolone, while Drs. Blankenship and Blumenkranz suggested injections of 5-fluorouracil (5-FU). Since both medications were retained in the vitreous for only short periods of time, the search for a controlled drug release implant began. With the help of polymer expert Frank Villain and Dr. Karl Skip Olsen, a metallic tack [36] was transformed

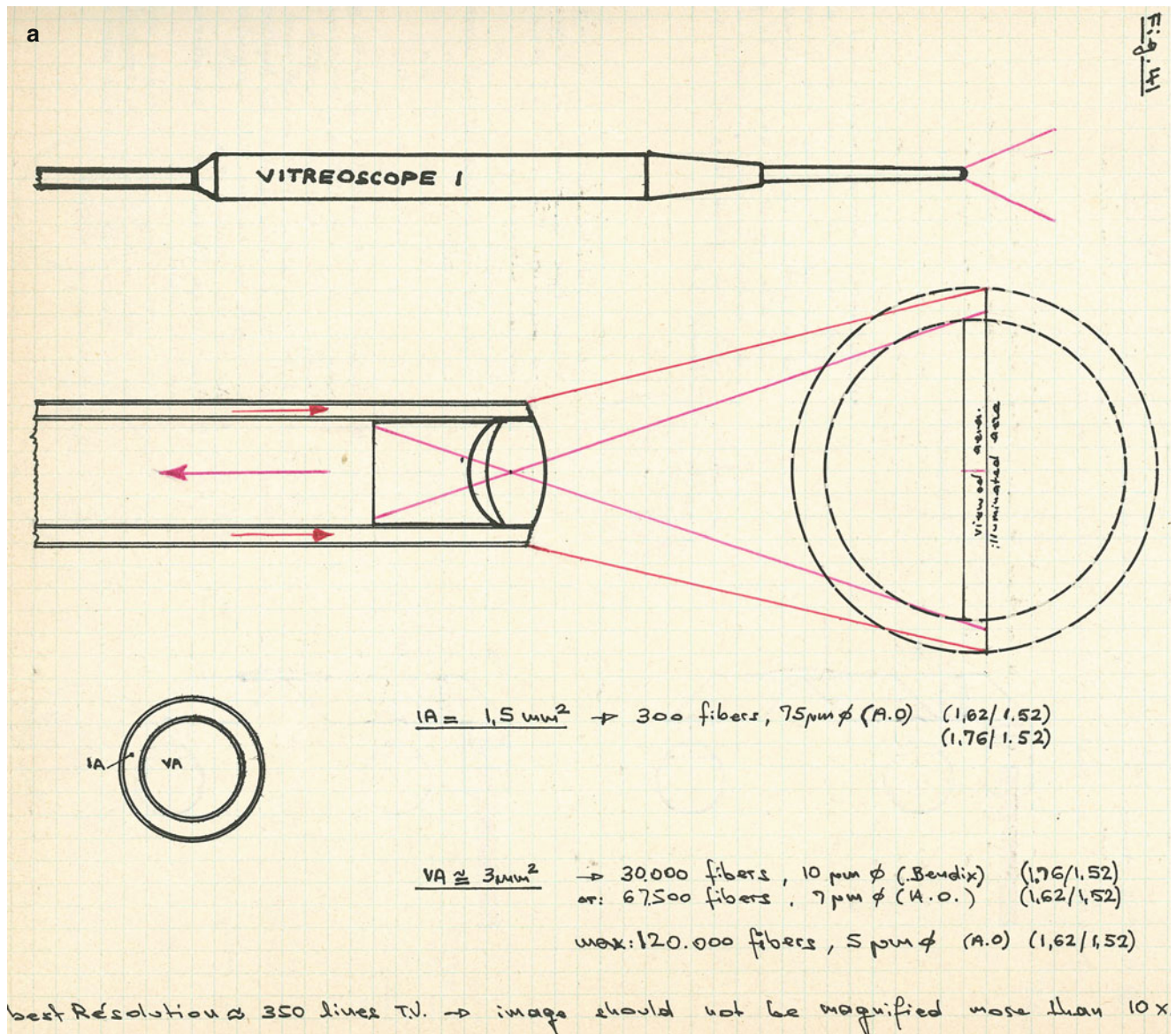


Fig. V.B.1-14 The Buettner vitreoscopy 1970 concept based on flexible fiberoptic bundles to image the vitreous and retina (a)

③ method:

b

The object is imaged (of retina and also) onto a fused end of a flexible fiber optic bundle and the image is transmitted from the fibers until the other end. At this point, reimaging is possible onto the observer eye or camera by proper optic objective.

The illumination is made by non-coherent fibers directly up to the lower end of the system. In this case, a very powerful light source should be used, such as hallogen lamp and arc lamp (Xenon); furthermore, for photographic purpose, a flash tube (Xenon) will be designed in the unit.

Fig. 40

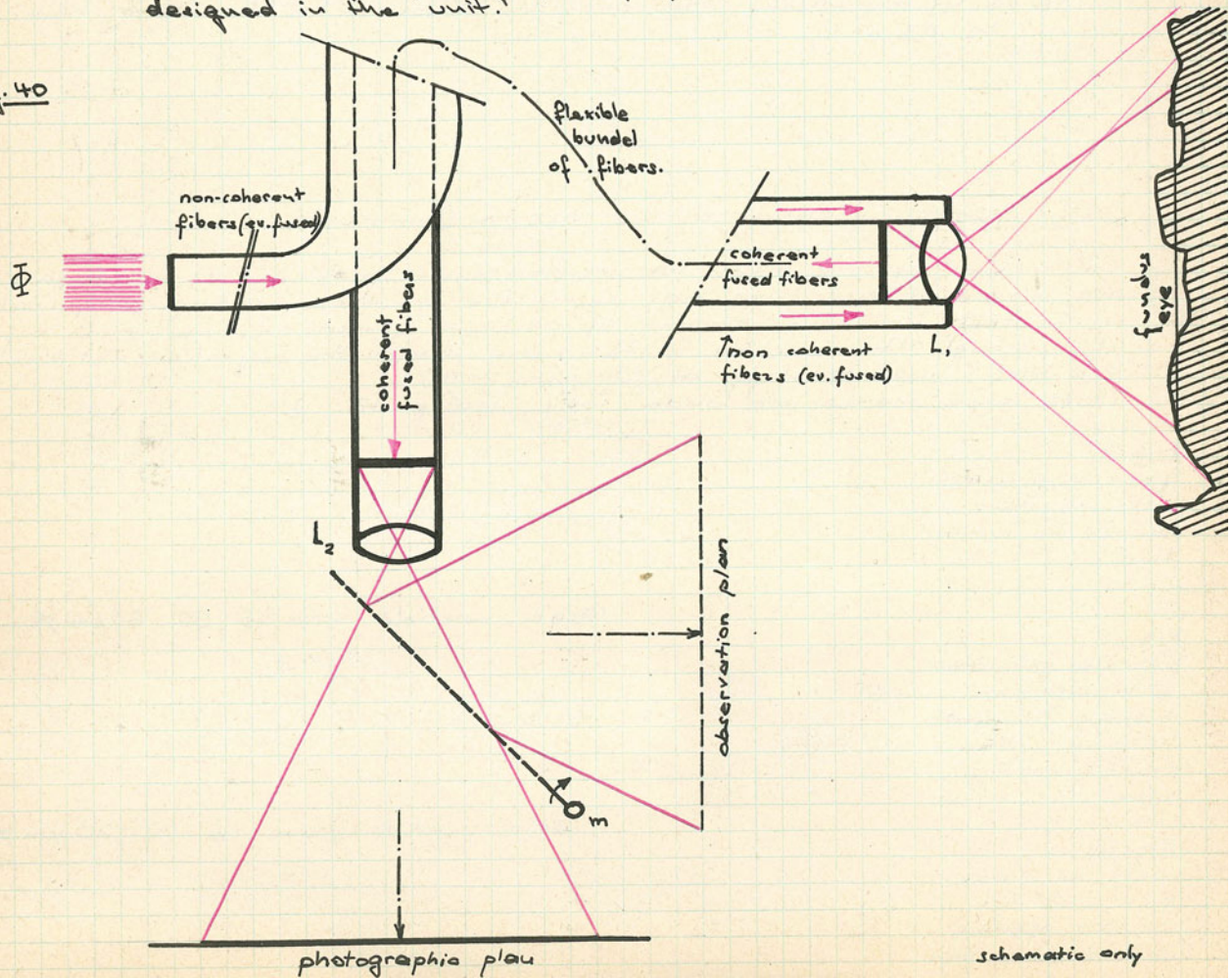


Fig.V.B.1-14 (continued) Illumination was produced by coaxial fibers surrounding the optical bundle that was fused at both ends, and a beam splitter allowed for photographic documentation of vitreoretinal surgery for teaching purposes (b). In another configuration, the endo-

scope's imaging bundle was linked to the optical path of the operation microscope via a rotating mirror allowing surgeons to switch between normal and endoscopic views (c)

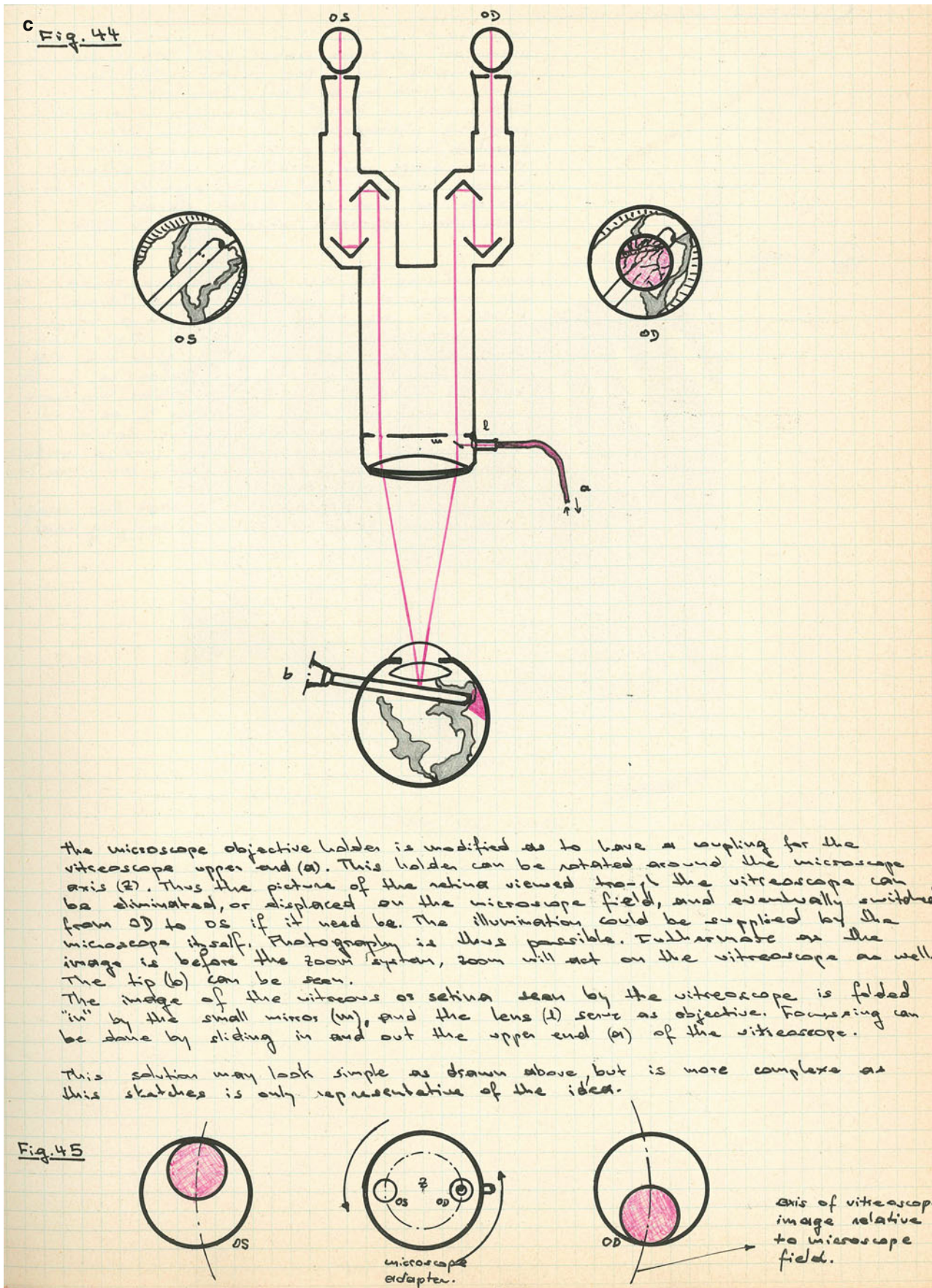


Fig.V.B.1-14 (continued)

into a biodegradable 5-FU implant [37, 38]. Although Dr. Scott Cousins demonstrated its efficacy in an animal model [39], the device never reached clinical trials because the Food and Drug Administration (FDA) ruled that 5-FU was not approved for use in ophthalmologic procedures. A French company, Corneal SA, was approached, but they were not interested in a study on the effect of 5-FU upon PVR, as the incidence had begun to decrease by this time. Nonetheless, they decided to conduct a European collaborative clinical trial on the effect of the 5-FU biodegradable implant in preventing scar tissue formation after trabeculectomy surgery.

As vitrectomy had become a well-established procedure and vitrectomy instrumentation was produced and further developed by many companies in the United States and abroad, the main interest of the Ophthalmic Biophysics Center focused on new intraocular drug delivery methods, including Coulomb-controlled iontophoresis that allows noninvasive transfer of many drugs into the retina-choroid [40] with the hope that one of them will be useful against PVR and other retinal diseases. The staff of the Ophthalmic Biophysics Center has increased to a dozen scientists and engineers and as many undergraduate and graduate students, all focused on developing new ophthalmic technologies. The laboratories of the Ophthalmic Biophysics Center have quadrupled in size. We are still happily doing what my mentors Professors Fankhauser, Crock, and Norton have taught me: helping physicians improve patient care. What life has taught me is to believe in serendipity, a force that had great influences on the adventure described above.

Most discoveries even today are a combination of serendipity and of searching.

Siddhartha Mukherjee

Abbreviations

AAOO	American Academy of Ophthalmology and Otolaryngology
BPEI	Bascom Palmer Eye Institute
cc	Cubic centimeter
DC	Direct current
IV	Intravenous
MPC	Membrane peeler cutter
MUDO	Melbourne University Department of Ophthalmology
OR	Operating room
PVR	Proliferative vitreo-retinopathy
VISC	Vitreous infusion suction cutter
5-FU	5-fluorouracil

References

- O'Brien BM. Neurovascular pedicle transfer in the hand. *Aust N Z J Surg.* 1965;35(1):1–11.
- O'Brien BM, Henderson PN, Crock GW. Metalized microsutures. *Med J Aust.* 1970;1(14):717–9.
- Henderson PO, O'Brien BM, Parel J-M. An adjustable double microvascular clamp. *Med J Aust.* 1970;1:715–7.
- Parel J-M, Crock GW, O'Brien BMC, Henderson PN, Galbraith JEK, Pericic L. Prototypal electromicrosurgical instruments. *Med J Aust.* 1970;1:709–14.
- Parel J-M, Crock GW, O'Day D, Wigley A. Automatic retinal camera for fluorescein angiography. *Med J Aust.* 1968;1:291–8.
- Crock GW, Parel J-M. Stereophotogrammetry of fluorescein angiographs in ocular biometrics. *Med J Aust.* 1969;2:586–90.
- Kasner D, Miller GR, Taylor WH, Sever RJ, Norton EWD. Surgical treatment of amyloidosis of the vitreous. *Trans Am Acad Ophthalmol Otolaryngol.* 1968;72:410–8.
- Machemer R, Buettner H, Norton EWD, Parel J-M. Vitrectomy: a pars plana approach. *Trans Am Acad Ophthalmol Otolaryngol.* 1971;75:813–20.
- Parel J-M, Machemer R, Aumayr W. A new concept for vitreous surgery. 5. An automated operation microscope. *Am J Ophthalmol.* 1974;77:161–8.
- Parel J-M, Machemer R, Aumayr W. A new concept for vitreous surgery. 4. Improvements in instrumentation and illumination. *Am J Ophthalmol.* 1974;77:6–12.
- Buettner H, Machemer R, Parel J-M. Vitrectomie. I. Instrumentarium und Operationstechnik. *Ber Deutscher Ophthalmol Ges Zusammenkunft.* 1971;71:424–8.
- Machemer R, Parel J-M, Buettner H. A new concept for vitreous surgery. I. Instrumentation. *Am J Ophthalmol.* 1972;73:1–8.
- Machemer R, Buettner H, Parel J-M. Vitrectomy: a pars plana approach. *Mod Probl Ophthalmol.* 1972;10:172–7.
- Machemer R, Norton EW. Vitrectomy, a pars plana approach. II. Clinical experience. *Mod Probl Ophthalmol.* 1972;10:178–85.
- Machemer R, Parel J-M, Norton EWD. Vitrectomy: a pars plana approach. Technical improvements and further results. *Trans Am Acad Ophthalmol Otolaryngol.* 1972;76(2):462–6.
- Peyman GA, Dodich NA. Experimental vitrectomy. Instrumentation and surgical technique. *Arch Ophthalmol.* 1971;86(5):548–51.
- Kloti R. Vitrectomy. I. A new instrument for posterior vitrectomy. *Albrecht Von Graefes Arch Klin Exp Ophthalmol.* 1973;187(2):161–70.
- Douvas NG. The cataract roto-extractor. A preliminary report. *Trans Am Acad Ophthalmol Otolaryngol.* 1973;77(6):OP792–800.
- Douvas NG. Microsurgical roto-extractor instrument for vitrectomy. *Mod Probl Ophthalmol.* 1975;15:253–60.
- O'Malley C, Heintz RM. Vitrectomy via the pars plana – a new instrument system. *Trans Pac Coast Otoophthalmol Soc Annu Meet.* 1972;53:121–37.
- Machemer R, Parel J-M. An improved microscope ceiling-mounted unit and an automated television. *Am J Ophthalmol.* 1978;85:205–9.
- Machemer R, Parel J-M, Hickingbotham D. Support and air supply tube for vitreous surgery. *Arch Ophthalmol.* 1980;98:154.
- Hickingbotham D, Parel J-M, Machemer R. Diamond coated all-purpose foreign body forceps. *Am J Ophthalmol.* 1981;91:267–8.
- Machemer R, Parel J-M, Hickingbotham D. The Membrane Peeler-Cutter. A new tool for vitreous surgery. *Arch Ophthalmol.* 1981;99:152–3.
- Parel J-M, Machemer R. Steam sterilizable fundus contact lenses. *Arch Ophthalmol.* 1981;99:151.

26. Parel J-M, O'Grady G, Machemer R. A bipolar coaxial microprobe for safe transvitreal diathermy. *Arch Ophthalmol*. 1981;99:494-7.
27. Parel J-M, Machemer R, O'Grady G, Crock GW, Nose I. Intraocular diathermy coagulation. *Graefes Arch Clin Exp Ophthalmol*. 1983;221:31-4.
28. Crock GW, Janakiraman P, Reddy P. Intraocular magnet of Parel. *Br J Ophthalmol*. 1986;70(12):879-85.
29. Blankenship G, Lee W, Parel J-M. An electronic infusion pole adjuster. *Ophthalmic Surg*. 1984;15(4):317-418.
30. Parel J-M. "Le System": a unified microsurgical center. In: Blankenship G, Gonvers M, Stripe M, editors. *Basic and advanced vitreous surgery*, Fidia research series, vol. 2. Padova: Liviana Press; 1986. p. 21-7.
31. May DR, Wang W-J, Yeh MH, Parel J-M. Results of 110 vitrectomies with VITAC: A portable system. *Am J Ophthalmol*. 1983;96:775-82.
32. Wilson DL, Parel J-M. Phacoexcavation: an alternative pars plana technique for lens removal. *Am J Ophthalmol*. 1985;100:528-33.
33. Flynn H, Blumenkranz M, Parel J-M, Lee W. Cannulated subretinal fluid aspirator for vitreoretinal surgery. *Am J Ophthalmol*. 1987;103:106-7.
34. Flynn HW, Davis JL, Parel J-M, Lee W. Applications of a cannulated extrusion needle during vitreoretinal microsurgery. *Retina*. 1988;8:42-9.
35. Parel J-M, Parrish RK, Nose I. An intraoperative intraocular pressure (IOP) monitor. *Ophthalmic Surg*. 1987;18:371-4.
36. O'Grady G, Parel J-M, Olsen K, Lee W, Blankenship G, Flynn H, Clarkson JG. Hypodermic stainless steel tacks and companion inserter designed for peripheral fixation of retina. *Arch Ophthalmol*. 1988;106:271-5.
37. Olsen K, Parel J-M, Lee W, Hernandez E. Biodegradable mechanical retinal fixation: a pilot study. *Arch Ophthalmol*. 1989;107:735-41.
38. Villain F, Davis P, Kiss K, Cousin SW, Parel JM, Parrish RK. A bioerodible intraocular implant for controlled drug release of 5-Fluorouracil. *ARVO Invest Ophthalmol Vis Sci*. 1992;33(4):230.
39. Rubsamén PE, Davis PA, Hernandez E, O'Grady GE, Cousins SW. Prevention of experimental proliferative vitreoretinopathy with a biodegradable intravitreal implant for the sustained release of fluorouracil. *Arch Ophthalmol*. 1994;112(3):407-13.
40. Behar-Cohen FF, Milne P, Parel J-M. Ocular iontophoresis. In: Edelhauser HF, Kompella UB, editors. *Drug product development for the back of the eye*, AAPS advances in the pharmaceutical sciences series 2. Arlington/New York: AAPS Press/Springer; 2011. p. 361-90. ISSN 2210-7371.
41. Harper TW, Flynn Jr HW, Berrocal A, Thompson JT, Parel J-M. Lack of toxicity during long-term follow-up of intraocular metallic fragments after Pars Plana Vitrectomy. *Ophthalm Surg Lasers Imaging*. 2008;39(4):319-22.

Modern Vitrectomy Cutters: An Improved Understanding of Vitreous Cutting

V.B.2.

Lawrence P. Chong

Outline

- I. Introduction
- II. Measuring Vitreous Flow and Cut Rates
 - A. Water Versus Vitreous
 - B. Vitreous Cutting Efficiency and Duty Cycle
 - C. Vitreous Flow Related to Cut Rate
- III. Traction Forces Transmitted to the Retinal Surface

References

Keywords

Vitreous • Vitrectomy • Instrumentation • Flow rate • Cutters • Cut rate • Retinal traction

Key Concepts

1. Maintaining high duty cycle at high cutting rates enhances vitreous removal.
2. High cutting rates are an easy way to improve rates of vitreous removal, because vitreous cutting is not efficient.
3. Retinal traction induced by a nearby vitreous cutter is dependent on vacuum rate and proximity to the retinal surface but is well below levels which can detach the retina.

Electronic supplementary material Supplementary material is available in the online version of this chapter at [10.1007/978-1-4939-1086-1_39](https://doi.org/10.1007/978-1-4939-1086-1_39). Videos can also be accessed at <http://www.springerimages.com/videos/978-1-4939-1085-4>.

L.P. Chong, MD
Doheny Retina Institute,
Los Angeles, CA, USA

VMR Institute for Vitreous Macula Retina,
Huntington Beach, CA, USA
e-mail: lchong@usc.edu

I. Introduction

Thirty-seven years have passed since Robert Machemer and Jean-Marie Parel (see chapter V.B.1. The History of Vitrectomy Instrumentation) developed a device and the technique for mechanized removal of vitreous from a closed eye. Over the past 37 years, vitrectomy has improved and is safer and more efficient [1]. We routinely operate not only on eyes with severe disease like complicated retinal detachment, penetrating ocular injury and diabetic retinopathy but also on eyes with less severe disease such as idiopathic pre-retinal membrane and even vitreous floaters. Instead of waiting until the vision declines to a low level, we are now operating on eyes before significant vision loss. This reflects the significant improvement in efficiency and safety of pars plana vitrectomy. Yet our understanding of the fundamental mechanisms of automated vitreous removal is incomplete. We must overcome this incomplete understanding if we are to achieve important breakthroughs in the design of vitreous

cutters. In this chapter, work is presented which was performed in the Eye Concepts Laboratory at the Doheny Eye Institute on the mechanics of automated vitrectomy.

II. Measuring Vitreous Flow and Cut Rates

A. Water Versus Vitreous

The efficiency of vitreous cutters has historically been evaluated by measuring water flow rates. Concerned that this method of measurement was misleading, we developed techniques to study vitreous flow rates. Vitreous cutters were suspended in vials of porcine vitreous, and the weight of the vials was constantly measured as the cutter was operated. For one particular cutter, data from water flow rates suggested a linear decrease of volume flow versus cut rate. However, the same cutter performing in vitreous demonstrated a different curve (Figure V.B.2-1). This convinced us that measuring vitreous flow rates rather than saline flow rates best assesses the efficiency of cutters [2].

B. Vitreous Cutting Efficiency and Duty Cycle

Studies in our “Eye Concepts Laboratory” showed that duty cycle is important in maximizing vitreous flow rate [3]. Duty cycle can be defined for vitreous cutters, as the ratio of the

time the cutter port is open to the time it is closed. By performing high-speed video analysis of the opening and closure of vitreous cutters, we confirmed that electric cutters have a constant duty cycle and that spring return pneumatic cutters have a variable duty cycle (see Video V.B.2-1). Electric cutters use an electric motor to open and close the port. Pneumatic cutters rely on pulsed air to close the port and a return spring to open the port. As the cutting rate increases, the spring constant behaves in a nonlinear fashion resulting in different duty cycles at different cut rates. At high cut rates, this can lead to the port being closed for most of the time and therefore dramatically affects the flow of vitreous (Figure V.B.2-2). The ports of some first-generation pneumatic cutters are completely closed at cutting rates of 2,400 cuts per minute.

Can this detrimental effect on duty cycle of pneumatic vitrectomy at high cutting rates be overcome by engineering?

We evaluated a second-generation pneumatic spring return vitreous cutter engineered to maintain a high duty cycle at a high cutting rate. A lowered pneumatic pulse pressure is used to drive the cutter, and the pulse itself has been shaped. The cutter was designed to operate at 2,500 cuts per minute, a rate far higher than commercially cutters available at that time. We confirmed not only the improved ability to move vitreous at higher cutting rates compared to first-generation cutters, but a 25-gauge version of this cutter was able to move more vitreous than some first-generation 20-gauge cutters (Figure V.B.2-3). Design improvements in duty cycle have been incorporated into all commercially available high-speed cutters [4–6].

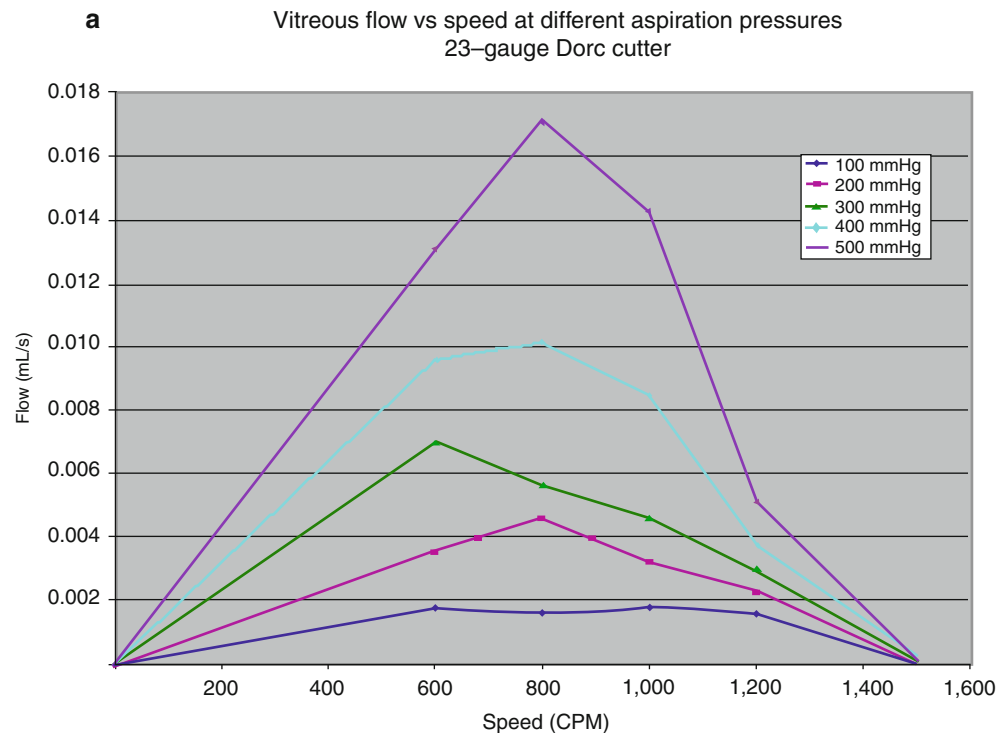


Figure V.B.2-1 (a, b) Water flow rates differ from vitreous flow rates for the same cutter

Figure V.B.2-1 (continued)

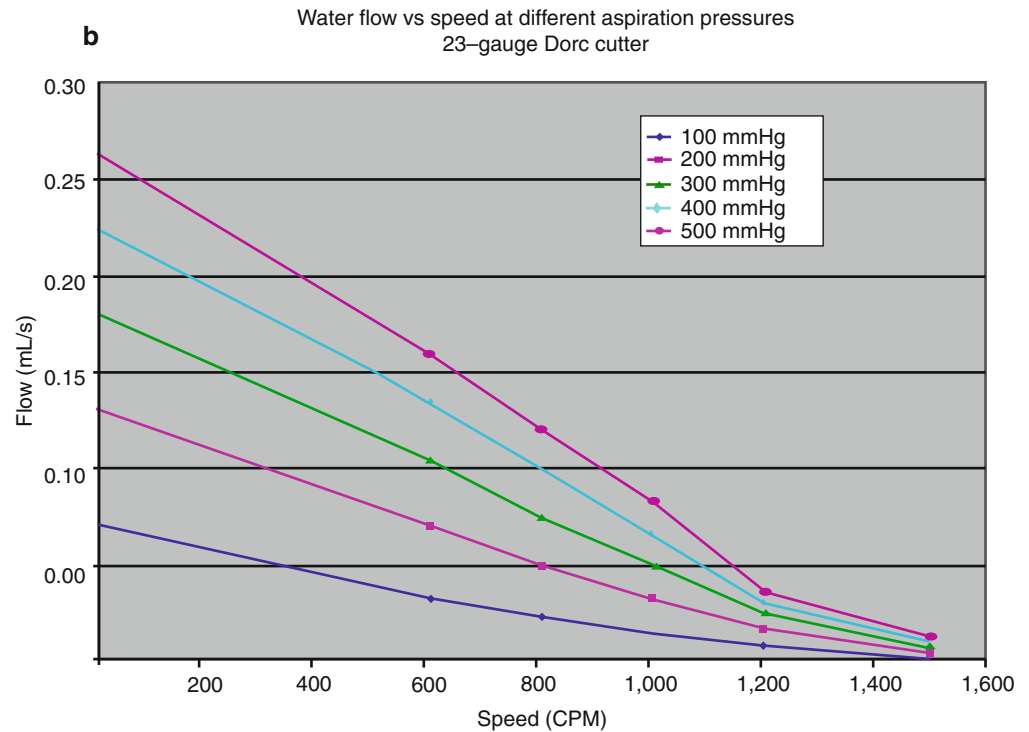
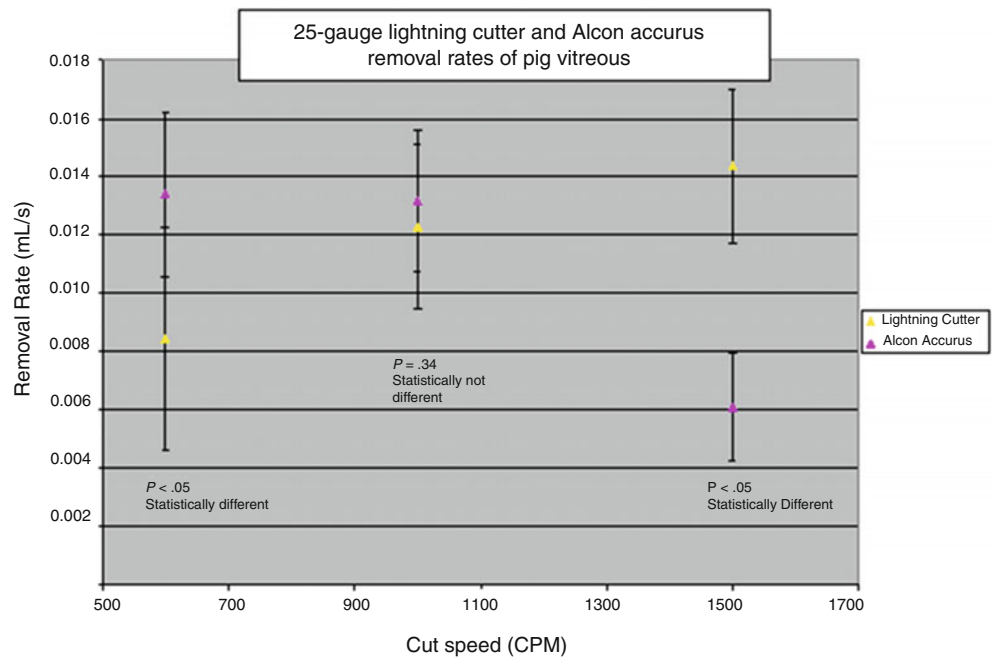


Figure V.B.2-2 At higher cutting rates, constant duty cycle electric cutter (Lightning) maintains flow rate in comparison to pneumatic cutter (Accurus) which loses efficiency as its duty cycle decreases



C. Vitreous Flow Related to Cut Rate

Increasing the cutting rate is another way to increase vitrectomy efficiency. Experimental work in our lab illustrated the dramatic effect of increasing cutting rate on increasing efficiency of cutting (Figure V.B.2-4). This is explained by the inefficiency of vitreous cutting as revealed by high-speed video analysis [7] (see Video V.B.2-1). We added triamcinolone acetate or microspheres to porcine vitreous

to enhance its visibility. We recorded the movement of vitreous at the tip of vitreous cutters using a high-speed camera capable of capturing 700 frames per second. Using this camera, each cut of a cutter run at 1,500 cuts per minute could be captured with 28 frames (Figure V.B.2-5). We observed that vitreous cutting is neither smooth nor efficient, but in fact, is a discontinuous process. There are times when the cutter is activated and no vitreous is moving into the port. At other times, there is even reversal of flow.

Figure V.B.2-3 Above 1,700 cpm, a high duty cycle 25-gauge cutter (MID Labs AVE) has greater flow than a 20-gauge first-generation pneumatic cutter (Accurus 2500)

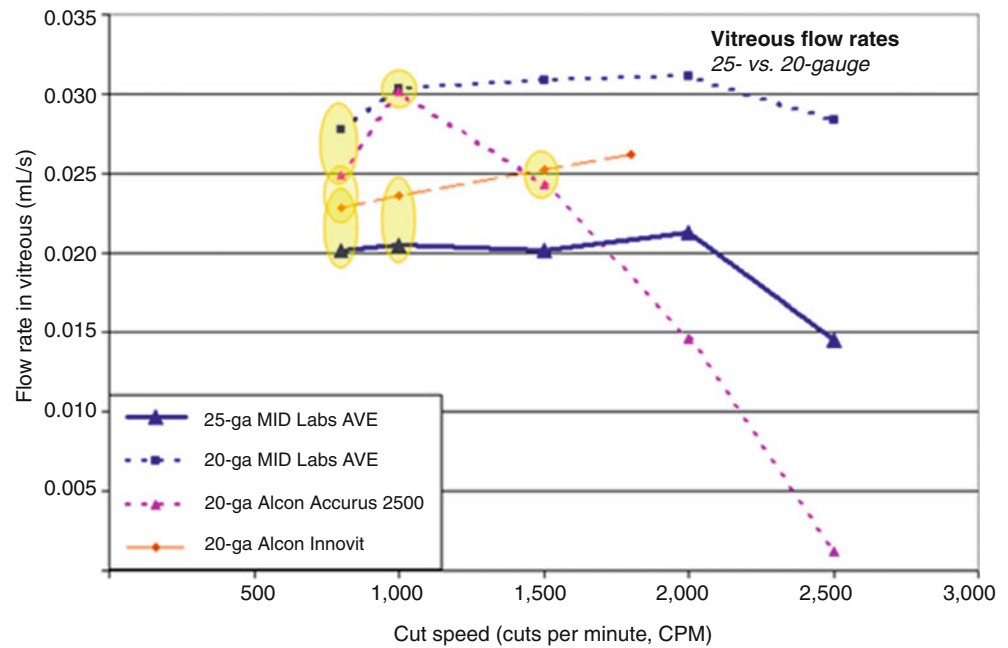
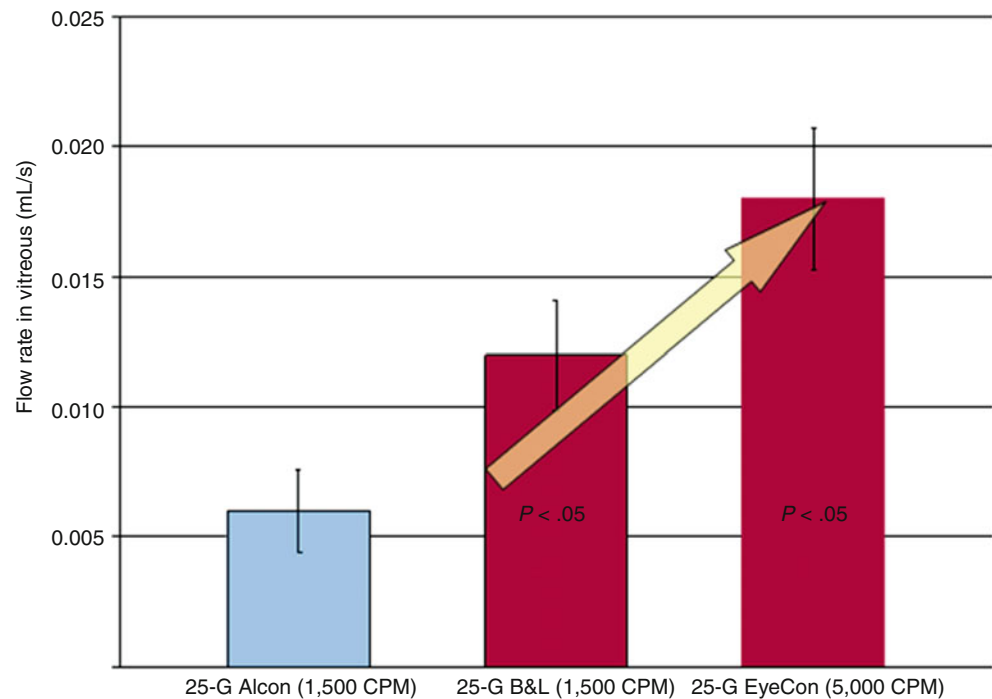


Figure V.B.2-4 An experimental 25-gauge cutter (stock cutter with a modified electric motor) demonstrates a dramatic increase in flow when the cut rate increased from 1,500–5,000 cpm



There are varying velocities of vitreous flow through the aperture within a single cycle. On opening of a pneumatic cutter, there is a slow movement of vitreous into the port, and as the port opens wider, there is a faster movement of vitreous. The effect of increasing cutting rate is similar to the effect of increasing the number of swings when using a dull axe. A computational study of the flow through a vitreous cutter by Juan et al. suggested that not only high duty cycle is important but that slow opening and closing transition also plays an important role in improving cutter efficiency and minimizing disturbance around the port [8].

III. Traction Forces Transmitted to the Retinal Surface

A technique to quantify vitreous traction created by vitreous cutters during vitrectomy was developed [9–11]. Prior to this measuring, these traction forces had never been achieved. Vitreous cutters used with conventional parameters have never induced retinal detachment by traction when near the attached retina. However, these traction forces become apparent when the cutter is near the detached retina. To find out why, a porcine eye was processed to attach a

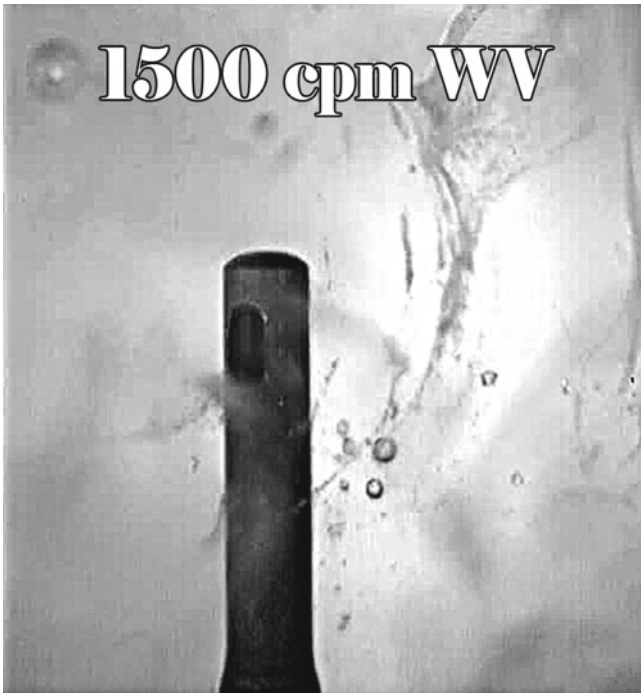


Figure V.B.2-5 Triamcinolone added to porcine vitreous enhances its visibility allowing high-speed video of vitreous movement around the cutting port

strain gauge to the retinal surface and place a vitreous cutter within the vitreous body in the following way:

- The sclera was trephined 4 mm from the limbus of fresh porcine eyes.
- The cornea, iris and crystalline lens were removed “en bloc”.
- The eye was positioned in a specially developed holder so that the trephined area was located at the most inferior part of the globe.
- On the most superior point of the positioned globe (180° to the trephined area), a 1 × 1 cm area of eye wall consisting of sclera, choroid and retina was removed using surgical scissors.
- The choroid and retina layer (exposed by scleral trephination) was then transfixed with a 0.15 mm stainless steel wire and fixed to the load cell of a strain gauge (Electroforce 3011 machine, Bose Corporation ElectroForce Systems Group, Eden Prairie, MN) (Figure V.B.2-6).
- Vitrectomy cutters were introduced into the eye by a micromanipulator at a 45-° angle adjacent to the choroid and retinal layer.

We found that 20-, 23- and 25-gauge pneumatic cutters have a respective range of traction between 2.06 and 37.22, 3.85 and 15.38 and 5.13 and 27.91 dyn. The 20- and 25-gauge electric cutters have a respective range of traction

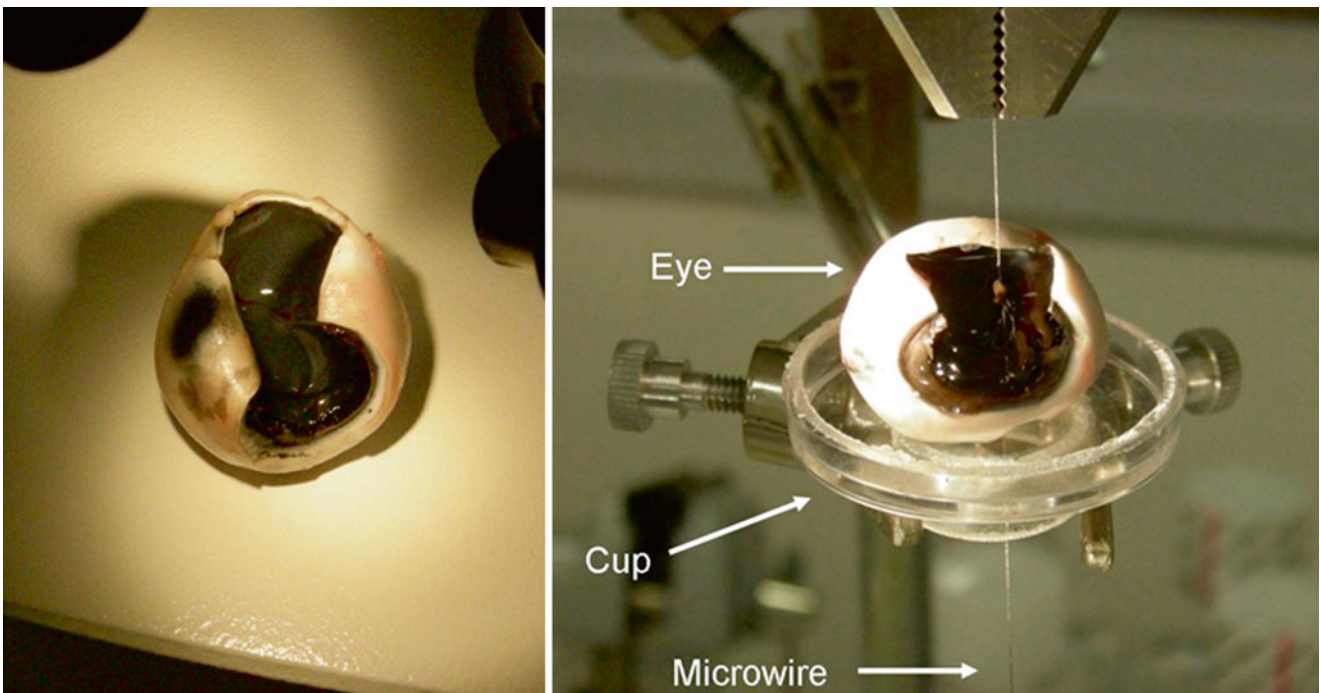


Figure V.B.2-6 A porcine eye is processed to allow the attachment of a strain gauge to the retina. The vitreous gel is left intact so the vitreous probe can enter it and be positioned at a set distance from the retina

of 3.60–41.78 and 5.28–27.91 dyn. These values are all under the threshold required to detach the retina as measured in previous models. Vitreoretinal traction increased by 3.14–7.89 dyn for each 100 mmHg increase in vacuum. Traction forces decreased by 2.51–5.71 dyn for each 500 cpm increase in cut rate. Traction force was greater when the cutter was 3 mm from the retina than when the cutter was 5 mm from the retina. While these findings are rather intuitive, they have now been quantified for the first time.

Further developments in vitrectomy instrumentation will be driven by both qualitative and quantitative techniques, examples of which have been presented in this chapter.

Abbreviations

cpm	cuts per minute
mm	millimeter
cm	centimeter
dyn	dyne

References

1. Machemer R, Buettner H, Parel JM. Vitrectomy, a pars plana approach. Instrumentation. *Mod Probl Ophthalmol*. 1972; 10:172–7.
2. Magalhaes Jr O, Chong LP, DeBoer C, Bhadri P, Kerns R, Barnes A, Fang S, Humayun M. Vitreous dynamics: vitreous flow analysis in 20, 23 and 25 gauge cutters. *Retina*. 2008;28:236–41.
3. Magalhaes Jr O, Barnes A, DeBoer C, Humayun M, Chong LP, Bhadri P, Fang S. Guillotine performance: duty cycle analysis of vitrectomy systems. *Ret Cases Brief Rep*. 2009;3:64–7.
4. Fang SY, DeBoer CM, Humayun MS. Performance analysis of new-generation vitreous cutters. *Graefes Arch*. 2008;246:61–7.
5. Matsuoka N, Texeira A, Lue JC, Fang SY, Kerns R, Bhadri P, Humayun M. Performance analysis of millennium vitreous enhancer™ system. *Ophthalmol Surg*. 2011;42:162–7.
6. Diniz B, Ribeiro RM, Fernandes RB, Lue JC, Teixeira AG, Maia M, Humayun MS. Fluidic in a dual pneumatic ultra high-speed vitreous cutter system. *Ophthalmologica*. 2013;229:15–20.
7. Magalhaes Jr O, Chong LP, Deboer C, Bhadri PR, Lescoulie J, McCormick J, Barnes A, Humayun M. Improved understanding of vitrectomy, qualitative high speed video analysis of vitreous movement around the aperture of vitreous cutters. *Invest Ophthalmol Vis Sci (ARVO Suppl)*. 2006;2688:127.
8. Juan T, Hubschman JP, Eldredge JD. A computational study of the flow through a vitreous cutter. *J Biomech Eng*. 2010;132(12):121005.
9. Texeira AG, Chong LP, Matsuoka N, Arana LA, Lue JC, McCormick M, Kerns R, Bhadri P, Humayun MS. An experimental protocol of the model to quantify traction applied to the retina by vitreous cutters. *Invest Ophthalmol Vis Sci*. 2010;51:4181–6.
10. Texeira AG, Chong LP, Matsuoka N, Arana L, Kerns R, Bhadri P, Humayun MS. Vitreoretinal traction created by conventional cutters during vitrectomy. *Ophthalmology*. 2010;117:138792.
11. Texeira AG, Chong LP, Matsuoka N, Rowley A, Lue JC, McCormick M, Kerns R, Humayun M. Novel method to quantify traction in a vitrectomy procedure. *Br J Ophthalmol*. 2010;94(9): 1226–9.

Jean-Pierre Hubschman, Sanket U. Shah,
and Vinod B. Voleti

Contents

- I. Introduction
- II. Improving Current Vitrectomy Technology
 - A. Improving the Vitrectomy Probe
 - 1. Size
 - 2. Cutting
 - 3. Aspiration
 - B. Improving Intraoperative Visualization
 - 1. Wide-Angle Viewing
 - 2. Illumination
- III. Future Vitreoretinal Surgery Approaches
 - A. Augmented Reality
 - 1. Supplementing Intraoperative Information
 - 2. Implementing Augmented Reality in Vitreoretinal Surgery
 - 3. Presenting Augmented Inputs to the Vitreoretinal Surgeon
 - B. Future Surgical Strategies
 - 1. Internal Tamponades
 - 2. Femtosecond Laser Surgery
 - 3. Robotic Vitreoretinal Surgery
 - 4. Retinal Prosthesis
 - C. Future Pharmacotherapies
 - 1. New Drug Delivery Systems
 - 2. Gene Therapy and Stem Cell-Based Therapies

References

Electronic supplementary material Supplementary material is available in the online version of this chapter at [10.1007/978-1-4939-1086-1_40](https://doi.org/10.1007/978-1-4939-1086-1_40). Videos can also be accessed at <http://www.springerimages.com/videos/978-1-4939-1085-4>.

J.-P. Hubschman, MD (✉)
Jules Stein Eye Institute at UCLA,
University of California Los Angeles,
200 Stein Plaza, Los Angeles, CA 90095, USA
e-mail: hubschman@jsei.ucla.edu

S.U. Shah, MD
Retina Division, Department of Ophthalmology,
Jules Stein Eye Institute, UCLA, Los Angeles, CA, USA

V.B. Voleti, MD
New Jersey Retina, Vauxhall, NJ, USA

Keywords

Vitreous • Vitrectomy • Vitreous fluidics • Small-gauge instrumentation • Task-specific features • Differentiated viewing • Augmented reality • Three-dimensional reconstruction • Femtosecond laser • Robotic vitrectomy

Key Concepts

1. Refinement of vitreous cutter size, cut rate, and aspiration systems to suit task-specific requirements will optimize vitreoretinal surgery. Wide-angle viewing and application of chromatic contrast for wavelength-specific visualization of intravitreal, retinal, and subretinal structures will improve intraoperative visualization.
2. Augmented reality will be incorporated as an intraoperative tool to assist the vitreoretinal surgeon with intraoperative access to multimodal imaging information providing both anatomical and functional status of the retina. This will facilitate planning of microsurgical maneuvers and continuous intraoperative monitoring and will improve the accuracy of vitreoretinal surgery.
3. Targeted delivery of pharmacologic agents, missing or defective genes, and stem cells using “intelligent hydrogels,” nanoparticles, and magnetically steered vehicles will usher in a new era in the management of vitreoretinal diseases.

I. Introduction

Entering into its fifth decade, vitrectomy continues to be an effective and safe solution for a myriad of vitreoretinal diseases. As knowledge about vitreous and the vitreoretinal interface continues to expand, vitrectomy technology and techniques have responsively evolved. The most recent innovations have included refinements of vitreous cutter and aspiration systems, improvements in illumination source and light delivery devices, and enhancements to intraoperative visualization systems. More excitingly, there are several emerging developments on the horizon, including the integration of augmented reality technology, robotic vitreoretinal surgery, gene and stem cell-based therapies, retinal prostheses, and novel drug delivery methods. This fantastic process of evolution continues to improve the safety and efficacy of vitrectomy, as well as expand its indications. As surgical outcomes continue to improve and complications are mitigated, new indications for vitrectomy have developed. Limited vitrectomy that involves removal of floaters or early preretinal membranes along with the posterior vitreous cortex and sparing the anterior vitreous may become the standard of care for certain indications, thereby reducing post-vitrectomy cataract development [see chapter V.B.8. Floaters and vision – current concepts and management paradigms]. With advanced imaging, such as spectral-domain OCT, we have identified new pathologies like vitreo-macular adhesion, which has been shown to play a role in diabetic retinopathy (DR) and exudative AMD. “Preventive surgery” for AMD and DR may become acceptable to arrest disease process early on. Such preemptive surgery may help to reduce blinding complications in their advanced stages. Application of pharmacologic vitreolysis before pars plana vitrectomy will encourage even more liberal use of vitrectomy for such “new indications” [see chapter VI.A. Pharmacologic vitreolysis].

II. Improving Current Vitrectomy Technology

Since the inception of the pars plana approach to closed-eye vitrectomy by Robert Machemer in 1971 [1], there has been continual refinement of the practice of excising the vitreous in various disease states. Parel, Buettner, and Machemer’s original vitreous infusion suction cutter (VISC) has continued to serve as the foundation of modern pars plana vitrectomy [see chapter V.B.1. History of vitrectomy instrumentation]. Today’s vitrectomy technology is a product of evolution on almost all fronts, including cutting, aspiration, illumination, visualization, and instrumentation.

A. Improving the Vitrectomy Probe

1. Size

A dramatic evolution in recent years has been a trend toward smaller-gauged cutters. Smaller-gauge instruments have gained popularity because they can be used transconjunctivally, obviating the need to perform a peritomy and/or suturing closed the sclerotomies. They also reduce the degree of surgical trauma, operative time, recovery time, and patient discomfort [2]. Multiple commercial platforms have adopted 23-, 25-, and 27-gauge vitrectomy systems and instruments [3, 4]. More recently, 29- and 30-gauge systems have been studied for pediatric vitreous surgery [5]. The concept of “smaller is better” does come with its own caveat, however. A smaller-gauged system is accompanied by increased resistance to flow, according to Poiseuille’s law ($R = 8\eta l / \pi r^4$), and higher flow velocities, according to the continuity equation ($Av = A'v'$) [6]. Increasing the cut rate overcomes these effects to some extent, by cutting the same volume of vitreous into smaller fragments that are less viscous and easier to aspirate and cause less surge [7]. Ultra high-speed cut rates can, however, limit the duty cycle, especially in the conventional spring-return pneumatic cutters. The newer dual-line and reciprocating-rotary pneumatic cutters are more suited to such high cut rates and deliver a high-performance duty cycle with optimized vitreous flow rate [8]. The effects of further increases in cut rate (to the order of 10,000 cuts/min) are still being studied, and the added benefit has not yet been quantified.

With respect to the vitreous cutter, an internal lumen area that is smaller than the cutting port surface area is a futile design [4], because the rate of vitreous flow reaches a plateau as the port size approaches the internal lumen area [9]. This limitation can be addressed by increasing the internal lumen area by reducing the wall thickness [8] or by reducing the overall length of the instrument. The challenge is to achieve these modifications without increasing the tendency to bend or deform the vitreous cutter, which can be addressed with using alternative materials with more rigidity [10, 11].

Adjusting the vitreous port size has also been explored over the last several decades. A large port allows higher vitreous flow, but can increase the risk of inadvertent retinal damage. A small port, on the other hand, can reduce these risks, but at the expense of increased surgical time [8]. Different surgical tasks demand different port functions [9]. Reduction in number of ports is becoming possible with changes in illumination mechanisms. Valved ports and self-sealing trocar systems that reduce wound leak, and vitreous incarceration will likely become more popular [5]. Pressurized infusion systems that can sense difference in inflow and outflow rates will gain popularity for automatic inflow adjustments [6, 7].

2. Cutting

The original VISC possessed electric motor-powered, non-disposable, rotating tubes with eccentric holes that would cut the vitreous as they spun [1]. This scheme was subject to wear with each surgical case, not to mention caused considerable vitreous and retinal traction [12]. Today's disposable axial (guillotine-like) cutters provide sharper shearing surfaces without the winding traction of rotary cutters. Additionally, the transition from electrodynamic actuators to the more efficient pneumatic actuators resulted in a dramatic reduction in the weight and size of cutters [12].

Going forward, customizing vitrectomy settings according to the various surgical steps and locations may help in achieving the best surgical outcomes. Furthermore, we can also envision a cutter-based device that is able to determine the viscosity, elasticity, and vitreoretinal adherent forces within an eye in real time and automatically respond to that local environment with adjustments to cutter settings in order to optimize performance. Additionally, the impact of transitional phases of a cutter during port opening and closing is critical in determining the flow dynamics [4]. Turbulence during cutting can be minimized by reducing the pressure waves created during the opening and closing phases of the guillotine by prolonging these transitions or by reducing the amplitude of guillotine while keeping the cut rate and duty cycles the same [8].

3. Aspiration

Modern vitrectomy systems combine the peristaltic and Venturi pump aspiration mechanisms to form a "hybrid" that utilizes the best of both technologies [7]. The peristaltic pump allows the surgeon to control flow rate with automatic control of negative pressure, while the Venturi pump allows the surgeon to control negative pressure with automatic control of flow rate depending on the fluid viscosity. The ideal system should produce smooth vitreous flow by minimizing traction, surge, and turbulence [8]. Peristaltic pump allows better control than the Venturi pump for less viscous media (air, gas, saline), but transition to more viscous media (peripheral vitreous) may be easier with the Venturi pump. In addition, the optimal aspiration flow rate is situation dependent – for example, a higher flow is desirable during core vitrectomy with an attached retina and a lower flow during vitreous shaving near detached retina [8].

B. Improving Intraoperative Visualization

1. Wide-Angle Viewing

Visualization of the vitreous and retina has been a significant optical challenge ever since the inception of pars plana vitrectomy. The original irrigating plano-concave contact lenses

permitted a narrow 20-degree view of the fundus even with a widely dilated pupil [13]. Biconcave lenses and prismatic lenses were adopted next to widen the view; however the prismatic effect interfered with stereopsis. The development of wide-angle viewing systems comprised of an aspheric indirect lens and a prismatic stereo re-inverter revolutionized vitreoretinal surgery in that they provided 130° of dynamic, stereoscopic, and high-resolution visualization of the retina [14]. Furthermore, adequate visualization can be achieved even in complex clinical situations, such as miotic pupils, lenticular opacities, and in air-filled eyes [14]. Noncontact wide-angle viewing systems have also gained popularity because they do not require an assistant; however they are accompanied with a slightly lower image resolution and narrower field of view [15].

2. Illumination

Illumination is just as important as resolution and field of view when it comes to safety and efficacy of vitrectomy. With regard to the illumination source, the challenge has always been to achieve the most effective lighting while minimizing phototoxicity and thermal damage. Current technology has evolved from the use of incandescent lamps to fiber-optic cables with high-intensity discharge lamps. More recently, we have begun to use lamps with shorter wavelengths, including metal halide lamps using mercury and argon (Millennium, Bausch & Lomb Inc., St. Louis, MO, USA; Oertli OS3 NovitreX 3000, Berneck, Switzerland) and high-pressure sodium lamps, using xenon, sodium, and mercury. Future systems are likely to feature high-intensity discharge (HID) lamps or semiconductor light-emitting diode (LED) lamps that produce a directed light with a narrow bandwidth of wavelength and are also longer lasting.

With the advent of small-gauge surgery, illumination requirements have changed. As the optical fiber core radius decreases with small-gauge surgery, the spot radius results in reduction of the coupled power proportional to the ratio of squared radii, thereby reducing the coupling efficiency. Future illumination systems are likely to use enhanced optical solutions, such as lens and reflector designs, to better suit the demands of small-gauge surgery. In addition to this new light source, a hands-free light allowing the second hand to be free for surgical maneuvers would be very appealing. Chandelier lights have become popular as they provide excellent panoramic illumination and freedom for bimanual surgery. Self-retaining 27-gauge chandelier illuminators are emerging in commercially available systems, making it easier to insert and remove during challenging cases [16]. There are, however, a few shortcomings with chandelier lights, such as suboptimal illumination of vitreous and retinal surface due to absence of focused illumination [17], as well as the potential of thermal damage from the chandelier tip after prolonged exposure to uveal tissue or blood [18]. Incorporating an illumination source into other vitrectomy instruments, such

as the infusion cannula or the vitreous probe, has also been explored as a means to achieving hands-free illumination. The use of more compact light sources, such as LED, may make this incorporation easier. Illuminated infusion chandeliers and endo-illuminating vitreous cutters are already available with some 25-gauge systems [19, 20].

Finally, the latest advancement regarding illumination during vitrectomy is the use of chromatic contrast. This concept is predicated on the fact that any particular tissue is best visualized if it is illuminated by a wavelength that is customized to its optical properties [21]. For instance, short wavelengths (490 nm) are most effective in highlighting premacular membranes in macular pucker, vitreoretinal traction, and macular edema; midrange wavelengths (585–610 nm) for deep retinal abnormalities like a retinal detachment surrounding a macular hole [22]; and longer wavelengths (795–895 nm) for subretinal deposits, retinal pigment epithelium, Bruch's membrane, and choroidal vessels [23]. The advantages of customized wavelength-specific visualization of intravitreal, retinal, and subretinal tissues are just beginning to be realized. New systems such as the Stellaris PC (Bausch & Lomb Inc., St. Louis, MO, USA) have already begun offering filters that can be interposed by the surgeon to emit specified wavelength of light [24].

III. Future Vitreoretinal Surgery Approaches

Several new approaches are being explored to further improve the vitreoretinal surgeon's ability to better manage vitreoretinal diseases.

A. Augmented Reality

Augmented reality (AR) refers to the real-time viewing of one's physical environment supplemented by computer-generated sound, video, tactile, or other sensory inputs. There are already numerous applications of AR to enhance real-life experiences, such as with sports, entertainment, advertising, marketing, and military training. In the healthcare sector, AR has been applied successfully in surgical fields such as urology, cardiothoracic surgery, and surgical oncology, providing surgeons with live dynamic intraoperative visual guidance [25–27]. For example, laparoscopic liver surgery can be performed with real-time instrument tracking on a three-dimensional (3D) volumetric computed tomography map [25]. This has been applied to other surgical sites, including the heart, pancreas, adrenal glands, kidneys, and parathyroid glands, with the goals of reducing invasiveness while improving outcomes [27, 28]. Vitreoretinal diseases present similar challenges to the above surgical subspecialties; however the fragile nature of the tissue and the cumbersome visualization

can make the surgery particularly demanding. The maneuverability and precision at a microscopic level could be enhanced by AR, and this potential has already been recognized and begun to be explored [29].

1. Supplementing Intraoperative Information

Currently, visualization through the surgical microscope is the only “live” input that the vitreoretinal surgeon receives intraoperatively. Additional intraoperative information that might be surgically relevant include 3D visualization, B-scan optical coherence tomography (OCT) at a desired site, retinal thickness, vascular permeability, structural and functional integrity of retina and vitreous, instrument location, and so on. Examples showing the use of intraoperative OCT to provide real-time retinal cross-sectional imaging and/or thickness mapping at specified retinal sites are shown (see Videos V.B.3-1 and V.B.3-2). An intriguing enhancement to intraoperative visualization in vitreoretinal surgery would be one that integrates anatomical information from OCT, fluorescein angiography and/or indocyanine green angiography (see Video V.B.3-3) and functional information from electroretinography with the surgical microscope. While many of these have been integrated for preoperative use in the clinic, most are unavailable in the operating room. The reason for interest in this real-time information is that any surgical maneuver can alter the anatomy and function of retinal tissue and, in turn, alter test results. Imaging data obtained days or weeks before the actual surgery may no longer be relevant. Relying on real-time testing data, on the other hand, would allow the surgeon to appreciate the dynamic state of the tissue as it is being manipulated and allow him/her make appropriate reformulations of the surgical plan based on this feedback. Initial steps toward integration of imaging platforms intraoperatively have already begun with an operating microscope-mounted OCT [30].

2. Implementing Augmented Reality in Vitreoretinal Surgery

The challenge with AR for vitreoretinal surgery is to be able to organize and present the data to the surgeon in manner that is easy to interpret and react to, since information could potentially be coming from multiple sources. The video signal from the surgical microscope can capture live two-dimensional (2D) (*X* and *Y* axes) information, while the OCT and/or a scanning laser ophthalmoscope can provide additional depth (*Z* axis) information in order to generate volumetric mapping. This 3D topographic mapping can be compared to preoperative maps and also serve as reference for successive steps. In addition to advanced imaging, AR could provide information about instrument location with relation to the vital tissue (e.g., distance from retina).

The next advance in AR for vitreoretinal surgery would be an attempt to supplement this anatomic mapping with

functional information. For instance, exact sites of fluorescein leakage could provide perfusion status, while electroretinography can help differentiate tissue that is salvageable from that which is not salvageable. Reinforcement with such functional data would allow the surgeon to adjust the surgical plan according to real-time information. Other functional data such as vitreous viscosity, elasticity, and traction during surgical maneuvers can be determined with instrument modifications. Yet another challenge with this advanced modality of surgery is the dynamic nature of vitreoretinal surgery, which would demand instantaneous registration so that functional and anatomic data is exactly matched up with real space tissue and instruments [28]. The interactive AR system could achieve 3D registration [31] by using anatomical landmarks, such as the optic disc, retinal vessels, arteriovenous crossings, other distinctive chorioretinal features, or even radio-opaque fiducials (applied to the instrument or to the sclera) [28]. Many of these features exist only as theoretical possibilities and there are significant obstacles, such as rapid data acquisition, computer processing, lag time, microscopic surgical space, and instrument/tissue interference, that will need to be addressed before these enhancements can become a reality.

3. Presenting Augmented Inputs to the Vitreoretinal Surgeon

Let us fast-forward to the time when all of the aforementioned technologies are available; the next question would be how would the data be presented to the vitreoretinal surgeon? AR

most commonly uses visual input to provide information to the operator. For example, surgeons refer to an image on a 2D (or coming soon 3D) video screen that is acquired by a hand-held camera within the surgical space. The vitreoretinal surgeon, however, requires microscopic binocular visualization in order to perform skilled maneuvers, such as membrane peeling. Thus, we are faced with the challenge of preserving the customary view through the microscope while supplementing it with the aforementioned augmented information. Potential solutions to this obstacle include video-based display, see-through display, and projection-based display (Figure V.B.3-1) [28]. However, the vitreoretinal scenario is complicated because superimposition of 3D augmented information onto a 3D surgical field can be very confusing for the surgeon. An alternative would be switching back and forth (by the surgeon) between separate “real” and “virtual” modes, or depending on a computer to augment choice anatomic and pathologic features, while masking other irrelevant details. Other informative pieces of data, such as the OCT thickness of the retina underneath the instrument or vitreous characteristics, could be displayed within a small window positioned adjacent to the area of interest.

Additionally, nonvisual feedbacks can also be explored to render AR, for example, instrument-to-instrument and instrument-to-tissue proximity via sound, flickering lights, or haptic feedback to the surgeon. The optimum vitrectomy settings may be announced periodically and could even be directly modified in an integrated fashion.



Figure V.B.3-1 Augmented reality in vitreoretinal surgery. Augmented reality can be provided to the vitreoretinal surgeon using video-based display, microscope-integrated see-through display, ophthalmoscope or goggles-integrated see-through display, or projection-based display

To put all of these possibilities together, let us consider what a standard vitrectomy with membrane peel for macular pucker might be like with the benefits of augmented reality:

The surgeon performs the vitrectomy, during which time vitrectomy settings and rheological characteristics of the vitreous (acquired from modified vitrector or light pipe) are reported to him within a window and/or via auditory prompts. While inducing a posterior vitreous detachment, a real-time OCT overlay is displayed at the bottom of the screen that allows him to visualize his instrument tip as well as the posterior vitreous cortex as it is lifted off the retina. Finally, during the membrane peel, instrument location and membrane features are displayed via OCT overlay, and the surgeon is notified of undue retinal damage via an auditory stimulus and/or flashing light. At the end of the case, the surgeon can evaluate function with ERG and/or anatomy with OCT and fluorescein angiogram.

Foreseeable challenges with AR rendering include type of information to present/hide, difference between virtual and real size, blocking of surgical view from augmented information, and surgeon learning curve. Despite these challenges, real-time feedback from such AR technology will be a boon to the vitreoretinal surgeon and could improve surgical and functional outcomes.

B. Future Surgical Strategies

1. Internal Tamponades

Retinal detachment continues to be a common condition and is a leading cause of visual deficit and morbidity in a vitreoretinal practice. Currently used gas and oil tamponade agents are imperfect because they are accompanied by postoperative positioning and mobility restrictions, delayed visual recovery, and cataract formation. The search for better tamponade agents led to the development of perfluorocarbon liquid (e.g., perfluoro-*n*-octane) although it has only been determined to be safe for short-term use [32]. Novel mixtures (heavy and light silicone oil, ether and silicone oil), suspensions (aspirin in silicone oil), and fluorinated ethers (decafluoro-di-*n*-pentylether) are being studied as new tamponade agents [33–35]. One group has investigated an inflatable foldable devices that can be filled with silicone oil or polyethylene glycol sol after implantation in the vitreous cavity [36], while another has developed an *in-situ*-formed cross-linked hydrogel composed of a biopolymer framework of polyvinyl alcohol, polyethylene glycol, or hyaluronic acid [35–38]. These innovations are designed to overcome the shortcomings of conventional gas and oil, although they still require extensive *in vivo* testing.

One revolutionary concept is to entirely remove the need for a tamponade agent and thus obviate the accumulation of proinflammatory cells and cytokines in a restricted meniscus close to the retina. The use of an adhesive biopolymeric hydrogel can function as a temporary retinal “patch” to

secure the retina in without the need of a tamponade agent, while conventional retinopexy (cryo or laser) develops into permanent scars. Gelatin-microbial transglutaminase complex has been shown to seal retinal tears and achieve retinal reattachment in rabbit eyes [39]. Such biopolymers could also serve as drug delivery mechanisms of anti-inflammatory drugs and thereby further reduce the risk of PVR. Another strategy would be to utilize magnetic forces to secure retinal breaks by strategically placing scleral magnets in conjunction with a silicone cobalt nanoparticle-bearing magnetic fluid or a ferrofluid within the vitreous cavity [40].

2. Femtosecond Laser Surgery

With increasing application to anterior segment procedures [41, 42], femtosecond lasers have gained increasing popularity—and we can envision that their precision, intricacy, and predictability would be applied to vitreoretinal surgery. For example, vitreo-macular adhesion and traction could be treated outside the operating room by creating customized incisions at tethered sites of strong vitreoretinal adhesion using the laser. Furthermore, femtosecond laser could be also be utilized intraoperatively in order to dissect and delaminate fibrotic tissue that is intricately adherent to the retina. It may even be possible to integrate the femtosecond laser with the abovementioned AR systems, which would provide 3D localization in order to achieve precise delivery. There are, however, many obstacles to the use of the femtosecond laser in the posterior segment, including intraoperative changes in tissue properties and relationships compared to preoperative measurements and potential collateral retinal toxicity. Until these issues are addressed, vitreoretinal surgery using femtosecond laser appears premature.

3. Robotic Vitreoretinal Surgery

Yet another adjuvant to vitreoretinal surgery that is likely to make strides in the near future is the introduction of robotic assistance. Robotic surgery can reduce invasiveness and minimize iatrogenic complications by either assisting the surgeon [43] or potentially independently performing automated surgery. A master-slave robotic system (Figures V.B.3-2 and V.B.3-3) has successfully been applied to various surgical maneuvers, including retinal vessel cannulation and injection, posterior vitreous detachment, and retinal vessel sheathotomy in a porcine animal model [44]. Recently, an intraocular robotic interventional system [45] has been prototyped to function in concert with the already existing da Vinci Surgical System (Intuitive Surgical, Inc., Sunnyvale, CA, USA). Delicate tissue manipulation with micrometer precision is facilitated with a surgical hook that has been outfitted with a microsensors, which can actively monitor membrane peeling forces and tremor and prevent inadvertent trauma [46].

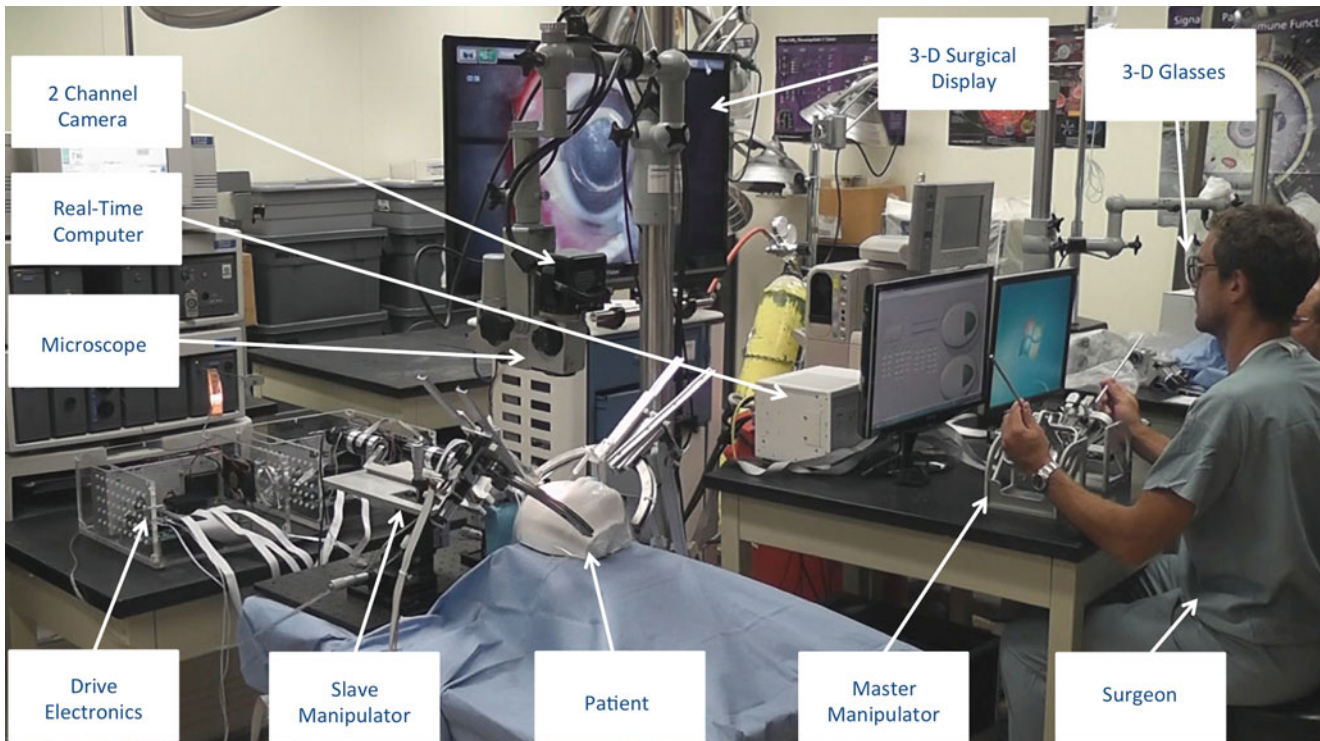


Figure V.B.3-2 Robotic vitreoretinal surgery setup. A robot-assisted vitreoretinal surgery setup shows how the surgeon will visualize the surgical scene using three-dimensional (3D) glasses and 3D display captured by the microscope and relayed after real-time computer pro-

cessing. The surgeon will use the master manipulator for performing surgical maneuvers that will then be reproduced in the patient via the slave manipulator with robust processing by the computer and the drive electronics

4. Retinal Prosthesis

Bioelectrical retinal prostheses have been implanted in pre-retinal (for direct ganglion cell stimulation by the prosthesis), subretinal (for stimulation of bipolar or middle retinal cells by the prosthesis), and suprachoroidal (for transchoroidal retinal stimulation) locations [47–49]. The Argus II preretinal implant (Figure V.B.3-4) is approved for surgical implantation in the USA and Europe. Its implantation involves suturing of an electronic stimulator and antenna to the sclera using an encircling silicone band, pars plana vitrectomy, and preretinal placement of the microelectrode array via a sclerotomy [47]. More recently, the Alpha IMS subretinal implant (Figure V.B.3-5) has also received approval for clinical use. It consists of a microchip placed in the subretinal space, and the photodiodes receive light and convert it to electrical impulses later transmitted to the optic nerve. A transmitter coil that is sutured subcutaneously behind the ear powers it [50]. Although currently indicated for patients with visual loss from retinitis pigmentosa (RP), retinal prostheses may soon be applied to other RP-like retinal degenerations and AMD. Its advantages include improved visual acuity, ability to read letters and words, assistance in mobility, and stable long-term functional vision in patients with profound visual loss and blindness [48].

C. Future Pharmacotherapies

1. New Drug Delivery Systems

Intraocular drug delivery via placement of intravitreal implants/devices, colloidal fluids, or other noninvasive techniques is a fast-developing area [51]. Emerging intravitreal medications include ciliary, brain, and glial-derived neurotrophic factors, angiostatin, endostatin, pigment epithelium-derived factors, integrin antagonists, complement inhibitors, and interleukins [52]. Drug delivery via biodegradable polymeric implants, microspheres, nanoparticles, and thermoplastic polymers has reached various stages of development [see chapter IV.E. Principles and practice of intravitreal application of drugs]. The ideal delivery mechanism would be one with low immunogenic potential that can cross-link to produce a flexible “mucoadhesive” 3D hydrogel [51]. These “intelligent hydrogels” could be used to switch on or off drug release via a nanochannel or micropump designs [53]. Other modifications to the actual drug can further enhance our abilities to control precise intravitreal delivery. For example, specific antigen/antibody ligands (endoglin, integrins, E-selectin, CCR3) fabricated onto the drug can promote drug movement toward the target. A drug tagged with a magnetic intraocular insert can be steered by electromagnetic control to reach the target [54, 55]. Colloidal intravitreal

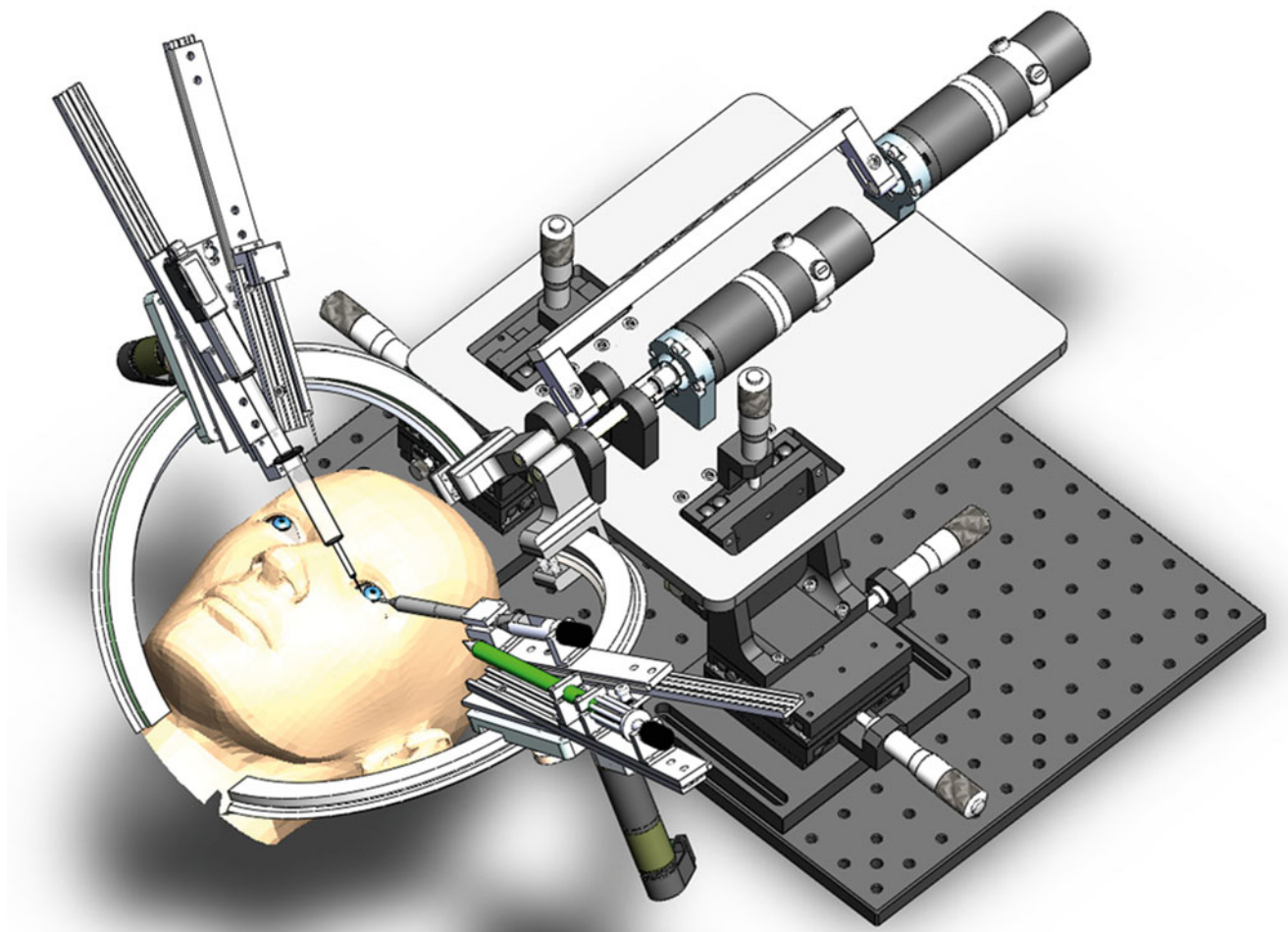


Figure V.B.3-3 A prototype for robotic vitreoretinal surgery. The robotic arms can be designed as shown in order to produce surgical maneuvers using standard vitrectomy ports after stabilization of

patient's head and registration of anatomical landmarks. Extensive engineering feedback controls are important for accurate spatial localization and error minimization

microspheres/nanoparticles may eliminate the need for multiple injections [51, 52, 56]. Antimetabolite drugs may possibly be delivered as microcapsules/nanocapsules as an adjunct during surgery [57].

Nanomaterials are promising drug delivery methods and it can be explored as an antiangiogenic platform on many fronts: (1) encapsulation of drugs inside nanoparticles for slow release after intravitreal injection; (2) encapsulation of plasmids that express antiangiogenic proteins inside nanoparticles for expression in the RPE after intravitreal administration; (3) encapsulation of RNA (short hairpin RNA or small interfering RNA) inhibiting neovascularization or DNA coding for an antiangiogenic protein inside nanoparticles; (4) nanoparticles like nanoceria, silver, gold, and silicate that demonstrate antiangiogenic properties from scavenging reactive oxygen species or suppressing vascular proliferation; and (5) fabrication into “functionalized nanoparticles” with specific surface ligands for targeted delivery [51, 58].

To date, its applications include prolonged ciliary neurotrophic factor delivery with encapsulated cell technology [52], dexamethasone delivery using cyclodextrins, vasoactive intestinal peptide delivery with pegylated liposomes, ganciclovir delivery with albumin nanoparticles, and tacrolimus delivery with reverse-phase evaporation vesicles [59]. Undoubtedly, this list will continue to grow as our understanding of nanotechnology evolves.

Other drug delivery developments on the horizon include sharp self-inserting delivery system that is able to make its own incision and insert itself; a multidrug delivery system that uses two or more co-assemblies for dispensing different drugs; and pulsatile release technology that responds to internal stimuli such as temperature, pH, pressure, and chemical changes or external stimuli such as light (laser), electric field, magnetic field [53, 56, 60]. Noninvasive methods of drug or gene delivery using trans-scleral iontophoresis have also been theorized as a potential delivery mechanism [59].

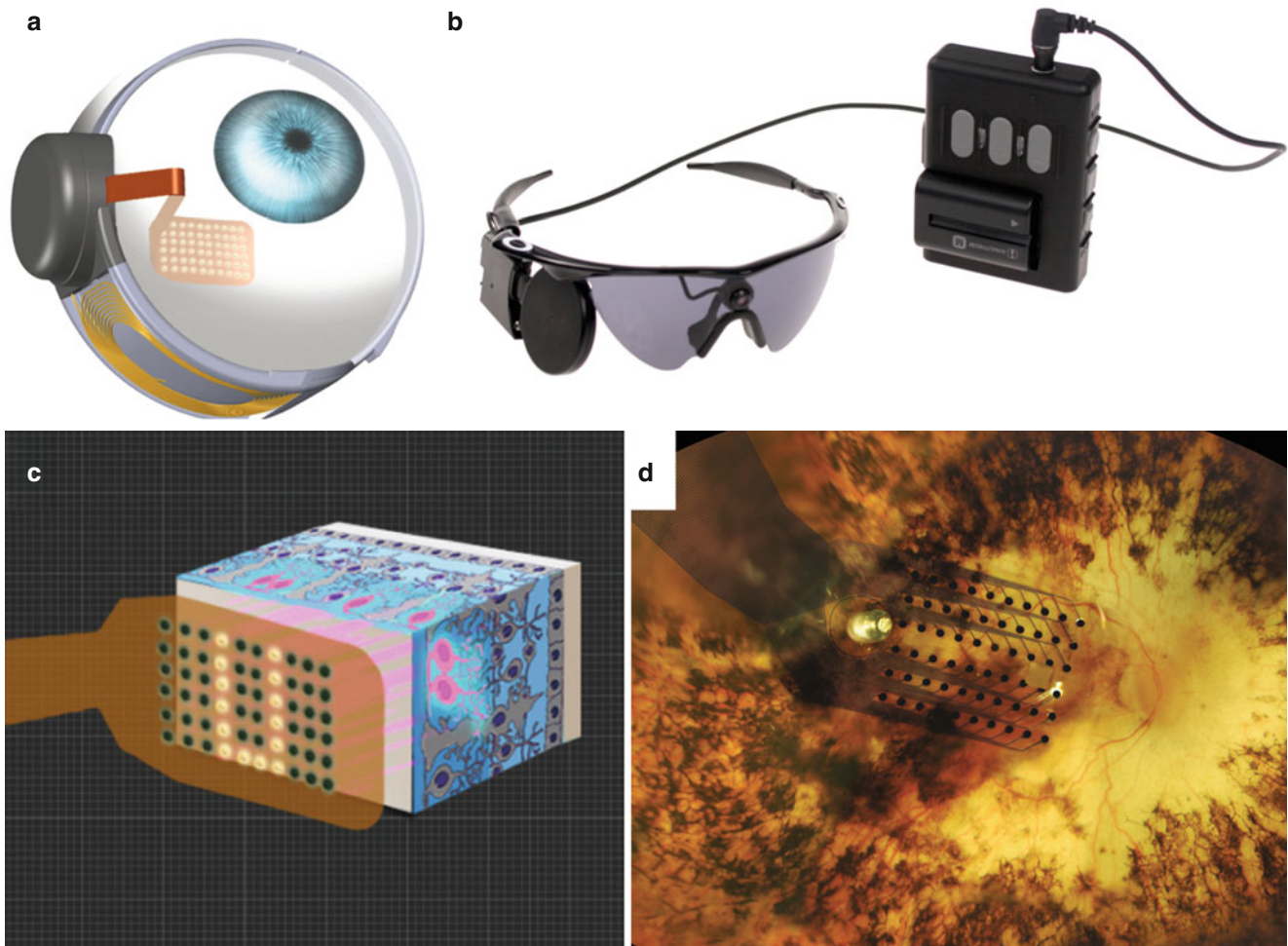


Figure V.B.3-4 Argus II retinal prosthesis. The Argus II Retinal Prosthesis System (Second Sight Medical Products Inc., Sylmar, CA, USA) is an epiretinal prosthesis that is currently approved for clinical use in the USA and Europe for retinitis pigmentosa. The system consists of intraocular and extraocular components. (a) The glasses with a mounted camera acquires the scene that is then processed by a video

processing unit (b) and transmitted wirelessly from the glasses coil to the receiver antenna, which is then transmitted to the electrode array (c) thereby stimulating retinal cells. The fundus photograph (d) shows the electrode array implanted anterior to the retina (Courtesy: Second Sight Medical Products Inc.)

2. Gene Therapy and Stem Cell-Based Therapies

Vitrectomy has recently become the vehicle for two exciting developments in the field of regenerative medicine: gene and stem cell therapy. The gene encoding a protein with isomero-hydrolase activity has been successfully replaced by introducing it with an adeno-associated viral (AAV) vector into the subretinal space in patients with RPE-65-associated Leber's congenital amaurosis, thus representing the first successful gene replacement experiment in humans [61]. Other gene therapy candidates include Leber's hereditary optic neuropathy [62], retinitis pigmentosa [63], and age-related macular degeneration (AMD) [64]. In addition to replacing defective genes, this type of therapy may enable us to modify

other proteins in order to slow photoreceptor degeneration and promote cone outer segment regeneration and outer nuclear layer preservation [52, 65]. Moreover, genes expressing VEGF inhibitor proteins for sustained therapeutic activity could be utilized as to create an "ocular biofactory" [64]. Gene delivery has also been accomplished by nonviral methods, such as encapsulated nanoparticles, magnetic cationic liposomes, subconjunctival injection of naked DNA plasmids, and electrical transfer of naked DNA into retinal cells [52, 59, 66]. Tools like small interfering RNA and zinc finger nucleases may become a common part of therapeutics in the future [65]. Modulation of gene expression in transfected RPE cells via antibiotics, hormones, Tet-on-Tet-off, or selective laser application may also be possible [67].

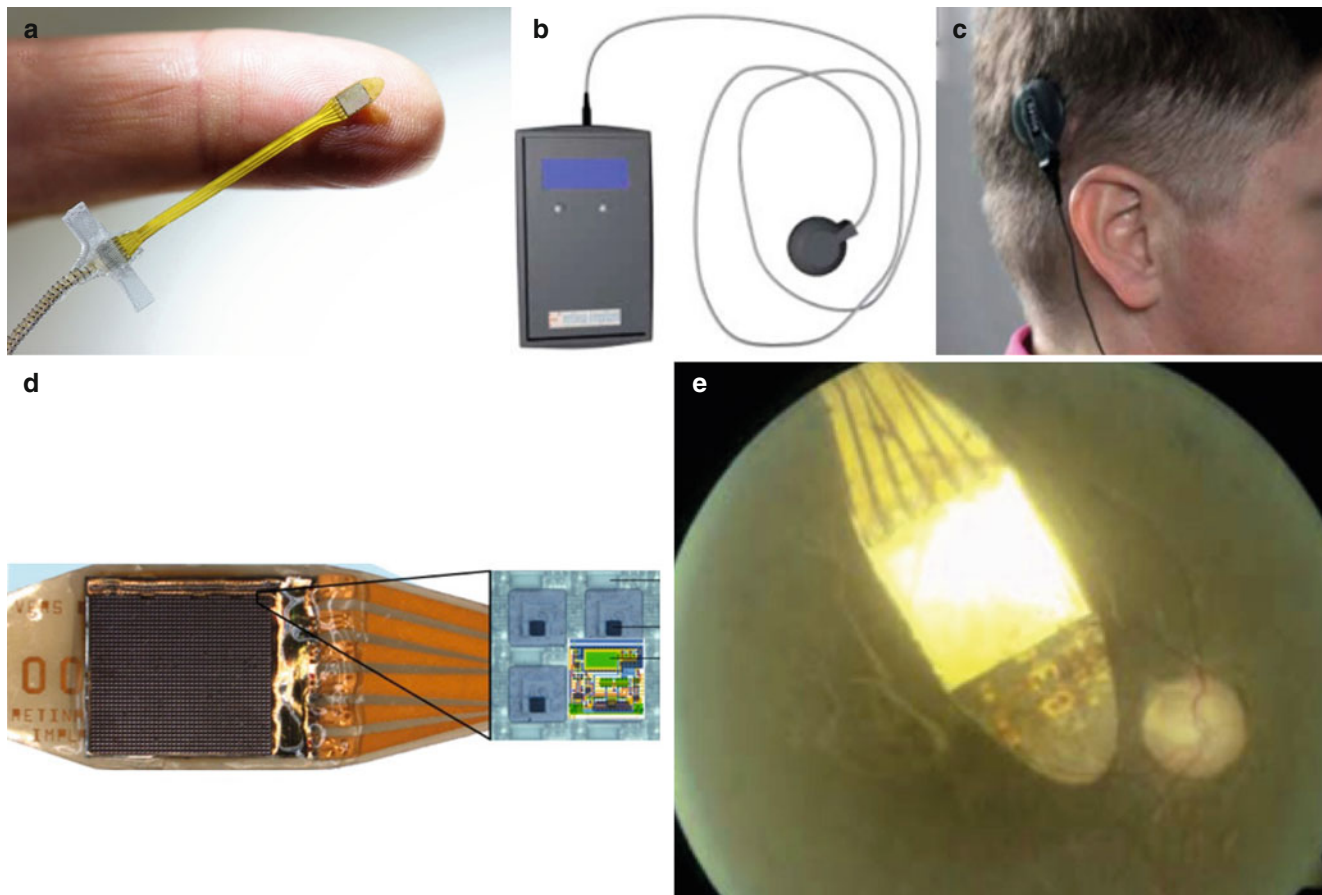


Figure V.B.3-5 Alpha IMS retinal prosthesis. The Alpha IMS (Retina Implant AG, Reutlingen, Germany) is a subretinal prosthesis that is currently approved for clinical use in Europe for retinitis pigmentosa. The system consists of a microchip (a) that is implanted in the subretinal space of the macula. It is connected via an orbital approach to the transmitter (secondary) coil that is implanted subcutaneously in the retroau-

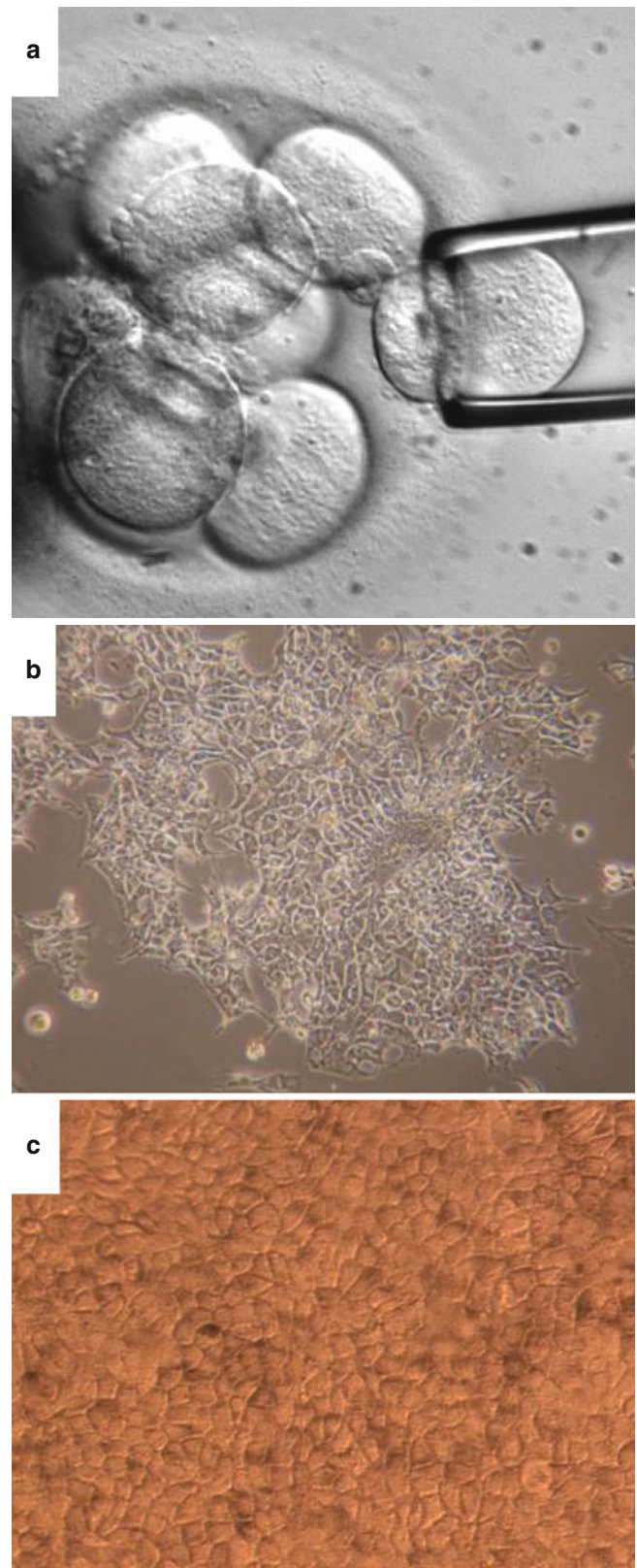
ricular location. The external power supply is connected to a primary coil (b), which is held close to the secondary coil (c) for electromagnetic induction and charging the microchip (d). The fundus photograph (e) shows microchip implanted in the subretinal space (Courtesy: Retina Implant AG)

Since degeneration and loss of outer retinal cells commonly precede that of inner retina, stem cells can potentially replace photoreceptors, reestablish synaptic connections, and ultimately restore vision [68]. Ongoing clinical trials using human embryonic stem cell-derived RPE (Figure V.B.3-6) in patients with Stargardt's macular dystrophy and dry AMD have shown encouraging results [69]. Such therapy has been well tolerated with an adequate differentiation into RPE and a modest visual recovery in patients [69]. Results from subretinal implantation of human induced pluripotent stem cells, neural progenitor cells, retinal progenitor cells, and homologous RPE cells in animal models are also promising. However, clinical application is challenging due to imperfect stem cell delivery techniques resulting in incorrect orientation, shortened survival, and failure of integration [68]. Potential solutions include the use of scaffolds instead of suspensions, hydrogel encapsulated ultrathin RPE carrier, and focused magnetic stem cell delivery [70, 71].

Abbreviations

3D	Three dimensional
AAV	Adeno-associated virus
AMD	Age-related macular degeneration
AR	Augmented reality
DNA	Deoxyribonucleic acid
DR	Diabetic retinopathy
HESC	Human embryonic stem cell
HID	High-intensity discharge
LED	Light-emitting diode
nm	Nanometer
OCT	Optical coherence tomography
PVR	Proliferative vitreo-retinopathy
RNA	Ribonucleic acid
RPE	Retinal pigment epithelium
VEGF	Vascular endothelial growth factor
VISC	Vitreous infusion suction cutter

Figure V.B.3-6 Stem cell therapy for retinal diseases. The first step in the application of stem cell therapy for retinal diseases involves a single cell biopsy (a) to derive a single cell from a human embryo, without destroying the embryo. The embryonic cell is cultured to produce a human embryonic stem cell (HESC) culture (b). This is followed by differentiation of stem cells into a sheet of human retinal pigment epithelial (RPE) cells, seen as a pigmented monolayer with cobblestone morphology (c). Such HESC-derived RPE is then transplanted via a subretinal injection in a selected macular location (Courtesy: Advanced Cell Technology Inc.)



References

- Machemer R, Buettner H, Norton EW, Parel JM. Vitrectomy: a pars plana approach. *Trans Am Acad Ophthalmol Otolaryngol.* 1971;75(4):813–20.
- Recchia FM, Scott IU, Brown GC, Brown MM, Ho AC, Ip MS. Small-gauge pars plana vitrectomy: a report by the American Academy of Ophthalmology. *Ophthalmology.* 2010;117(9):1851–7. Elsevier Inc.
- Oshima Y, Wakabayashi T, Sato T, Ohji M, Tano Y. A 27-gauge instrument system for transconjunctival sutureless microincision vitrectomy surgery. *Ophthalmology.* 2010;117(1):93–102. Elsevier Inc.
- Hubschman J-P, Bourges J-L, Tsui I, Reddy S, Yu F, Schwartz SD. Effect of cutting phases on flow rate in 20-, 23-, and 25-gauge vitreous cutters. *Retina.* 2009;29(9):1289–93.
- Binder S, Wimpfing B, Kellner L. Current clinical data and future (for small-gauge vitreoretinal surgery). In: Rizzo S, Patelli F, Chow DR, editors. *Vitreo-retinal surgery.* Berlin/Heidelberg: Springer; 2009. p. 213–22.
- Magalhães O, Maia M, Maia A, Penha F, Dib E, Farah ME, et al. Fluid dynamics in three 25-gauge vitrectomy systems: principles for use in vitreoretinal surgery. *Acta Ophthalmol.* 2008;86(2):156–9.
- Magalhães O, Maia M, Rodrigues EB, Machado L, Costa EF, Maia A, et al. Perspective on fluid and solid dynamics in different pars plana vitrectomy systems. *Am J Ophthalmol.* 2011;151(3):401–5. e1. Elsevier Inc.
- Steel DHW, Charles S. Vitrectomy fluidics. *Ophthalmologica.* 2011;226 Suppl 1:27–35.
- DeBoer C, Fang S, Lima LH, McCormick M, Bhadri P, Kerns R, et al. Port geometry and its influence on vitrectomy. *Retina.* 2008;28(8):1061–7.
- Barnes AC, Deboer CM, Bhadri PR, Magalhaes Jr O, Kerns RM, McCormick MT, et al. 25-gauge instrumentation: engineering challenges and tradeoffs. In: Rizzo S, Patelli F, Chow DR, editors. *Vitreo-retinal surgery.* Berlin/Heidelberg: Springer; 2009. p. 9–29.
- Chen C-J, Satofuka S, Inoue M, Ishida S, Shinoda K, Tsubota K. Suprachoroidal hemorrhage caused by breakage of a 25-gauge cannula. *Ophthalmic Surg Lasers Imaging.* 2008;39(4):323–4.
- Charles S. An engineering approach to vitreoretinal surgery. *Retina.* 2004;24(3):435–44.
- Tolentino FI, Freeman HM. A new lens for closed pars plana vitrectomy. *Arch Ophthalmol.* 1979;97(11):2197–8.
- Chalam KV, Shah VA. Optics of wide-angle panoramic viewing system-assisted vitreous surgery. *Surv Ophthalmol.* 2004;49(4):437–45.
- Spitznas M. A binocular indirect ophthalmomicroscope (BIOM) for non-contact wide-angle vitreous surgery. *Graefes Arch Clin Exp Ophthalmol.* 1987;225(1):13–5.
- Oshima Y, Chow DR, Awh CC, Sakaguchi H, Tano Y. Novel mercury vapor illuminator combined with a 27/29-gauge chandelier light fiber for vitreous surgery. *Retina.* 2008;28(1):171–3.
- Ohji M, Huang S, Kaiser P, Tornambe P, Gotzaris S. Pearls from experts. In: Rizzo S, Patelli F, Chow DR, editors. *Vitreo-retinal surgery.* Berlin/Heidelberg: Springer; 2009. p. 223–30.
- Mathias M, Ernst BJ, Pichi F, Torrazza C, Ciardella A, Oliver SCN. Thermal deformation of chandelier endoillumination probes exposed to uveal tissue and blood. *Retina.* 2012;32(4):773–5.
- Synergetics. Illuminated infusion chandeliers [Internet]. Available from: <http://synergeticsusa.com/products/standard/illumination>.
- Chalam KV, Shah GY, Agarwal S, Gupta SK. Illuminated curved 25-gauge vitrectomy probe for removal of subsclerotomy vitreous in vitreoretinal surgery. *Indian J Ophthalmol.* 2008;56(4):331–4.
- Oliveira TB, Trevelin LC, Moreira FMA, Bagnato VS, Schor P, de Carvalho LAV. Development and preliminary results of a chromatic illumination system for indirect ophthalmoscopes. *Arq Bras Oftalmol.* 2009;72(2):146–51.
- Ortiz RG, Lopez PF, Lambert HM, Sternberg P, Aaberg TM. Examination of macular vitreoretinal interface disorders with monochromatic photography. *Am J Ophthalmol.* 1992;113(3):243–7.
- Elsner AE, Burns SA, Weiter JJ, Delori FC. Infrared imaging of sub-retinal structures in the human ocular fundus. *Vision Res.* 1996;36(1):191–205.
- Stellaris PC. Brochure – Bausch + Lomb [Internet]. Available from: www.bausch.com/en/.../Stellaris-PC-ECP-Brochure.ashx.
- Shekhar R, Dandekar O, Bhat V, Philip M, Lei P, Godinez C, et al. Live augmented reality: a new visualization method for laparoscopic surgery using continuous volumetric computed tomography. *Surg Endosc.* 2010;24(8):1976–85.
- Nakamoto M, Ukimura O, Faber K, Gill IS. Current progress on augmented reality visualization in endoscopic surgery. *Curr Opin Urol.* 2012;22(2):121–6.
- Chu MWA, Moore J, Peters T, Bainbridge D, McCarty D, Guiraudon GM, et al. Augmented reality image guidance improves navigation for beating heart mitral valve repair. *Innovations (Phila).* 2012;7(4):274–81.
- Nicolau S, Soler L, Mutter D, Marescaux J. Augmented reality in laparoscopic surgical oncology. *Surg Oncol.* 2011;20(3):189–201. Elsevier Ltd.
- Greenberg K. Vantage Surgical Systems Joins Total Immersion's North America Partner Network, Seeks to Deploy Augmented Reality in Live Surgery [Internet]. Reuters. 2010 [cited 4 Apr 2013]. Available from: <http://www.reuters.com/article/2010/11/30/idUS106815+30-Nov-2010+BW20101130>.
- Ehlers JP, Tao YK, Farsi S, Maldonado R, Izatt JA, Toth CA. Integration of a spectral domain optical coherence tomography system into a surgical microscope for intraoperative imaging. *Invest Ophthalmol Vis Sci.* 2011;52(6):3153–9.
- Rohlfing T, Denzler J, Grässl C, Russakoff DB, Maurer CR. Markerless real-time 3-D target region tracking by motion backprojection from projection images. *IEEE Trans Med Imaging.* 2005;24(11):1455–68.
- Rush R, Sheth S, Surka S, Ho I, Gregory-Roberts J. Postoperative perfluoro-N-octane tamponade for primary retinal detachment repair. *Retina.* 2012;32(6):1114–20.
- Santos RAV, Keegan DJ, Fuchs BS, Song BJ, Avila MP, Simpson N, et al. DFPE, partially fluorinated ether: a novel approach for experimental intravitreal tamponade. *Retina.* 2013;33(1):120–7.
- Romano MR, Zenoni S, Arpa P, Mariotti C. Mixture of ether and silicone oil for the treatment of inferior complicated retinal detachment. *Eur J Immunol.* 2013;43(3):230–5.
- Kralinger MT, Stolba U, Velikay M, Egger S, Binder S, Wedrich A, et al. Safety and feasibility of a novel intravitreal tamponade using a silicone oil/acetyl-salicylic acid suspension for proliferative vitreoretinopathy: first results of the Austrian Clinical Multicenter Study. *Graefes Arch Clin Exp Ophthalmol.* 2010;248(8):1193–8.
- Chen H, Feng S, Liu Y, Huang Z, Sun X, Zhou L, et al. Functional evaluation of a novel vitreous substitute using polyethylene glycol sols injected into a foldable capsular vitreous body. *J Biomed Mater Res A.* 2013;28:1–10.
- Tao Y, Tong X, Zhang Y, Lai J, Huang Y, Jiang Y-R, et al. Evaluation of an in situ chemically crosslinked hydrogel as a long-term vitreous substitute material. *Acta Biomater.* 2013;9(2):5022–30. Acta Materialia Inc.
- Schramm C, Spitzer MS, Henke-Fahle S, Steinmetz G, Januschowski K, Heiduschka P, et al. The cross-linked biopolymer hyaluronic acid as an artificial vitreous substitute. *Invest Ophthalmol Vis Sci.* 2012;53(2):613–21.
- Yamamoto S, Hirata A, Ishikawa S, Ohta K, Nakamura K-I, Okinami S. Feasibility of using gelatin-microbial transglutaminase complex to repair experimental retinal detachment in rabbit eyes. *Graefes Arch Clin Exp Ophthalmol.* 2013;3:1109–14.

40. Holligan DL, Gillies GT, Dailey JP. Magnetic guidance of ferrofluidic nanoparticles in an in vitro model of intraocular retinal repair. *Nanotechnology*. 2003;14(6):661–6.
41. Farid M, Steinert RF. Femtosecond laser-assisted corneal surgery. *Curr Opin Ophthalmol*. 2010;21(4):288–92.
42. Abell RG, Kerr NM, Vote BJ. Toward zero effective phacoemulsification time using femtosecond laser pretreatment. *Ophthalmology*. 2013;25:1–7.
43. Nakano T, Sugita N, Ueta T, Tamaki Y, Mitsuishi M. A parallel robot to assist vitreoretinal surgery. *Int J Comput Assist Radiol Surg*. 2009;4(6):517–26.
44. Ueta T, Yamaguchi Y, Shirakawa Y, Nakano T, Ideta R, Noda Y, et al. Robot-assisted vitreoretinal surgery: development of a prototype and feasibility studies in an animal model. *Ophthalmology*. 2009;116(8):1538–43, 1543.e1–2. American Academy of Ophthalmology.
45. Rahimy E, Wilson J, Tsao T-C, Schwartz S, Hubschman J-P. Robot-assisted intraocular surgery: development of the IRISS and feasibility studies in an animal model. *Eye (Lond)*. 2013;27(8):972–8.
46. Gonenc B, Balicki MA, Handa J, Gehlbach P, Riviere CN, Taylor RH, et al. Evaluation of a micro-force sensing handheld robot for vitreoretinal surgery. *Rep U S*. 2012;2012:4125–30.
47. Humayun MS, Dorn JD, da Cruz L, Dagnelie G, Sahel J-A, Stanga PE, et al. Interim results from the international trial of Second Sight's visual prosthesis. *Ophthalmology*. 2012;119(4):779–88.
48. Da Cruz L, Coley BF, Dorn J, Merlini F, Filley E, Christopher P, et al. The Argus II epiretinal prosthesis system allows letter and word reading and long-term function in patients with profound vision loss. *Br J Ophthalmol*. 2013;20:1–5.
49. Fernandes RAB, Diniz B, Ribeiro R, Humayun M. Artificial vision through neuronal stimulation. *Neurosci Lett*. 2012;519(2):122–8. Elsevier Ireland Ltd.
50. Facts about alpha IMS retina implant [Internet]. Available from: <http://retina-implant.de/en/default.aspx>.
51. Achouri D, Alhanout K, Piccerelle P, Andrieu V. Recent advances in ocular drug delivery. *Drug Dev Ind Pharm*. 2013;39(11):1599–617.
52. El Sanharawi M, Kowalczyk L, Touchard E, Omri S, de Kozak Y, Behar-Cohen F. Protein delivery for retinal diseases: from basic considerations to clinical applications. *Prog Retin Eye Res*. 2010;29(6):443–65. Elsevier Ltd.
53. González-Alvarez M, González-Alvarez I, Bermejo M. Hydrogels: an interesting strategy for smart drug delivery. *Ther Deliv*. 2013;4(2):157–60.
54. Yasukawa T, Tabata Y, Kimura H, Ogura Y. Recent advances in intraocular drug delivery systems. *Recent Pat Drug Deliv Formul*. 2011;5(1):1–10.
55. Bergeles C, Kummer MP, Kratochvil BE, Framme C, Nelson BJ. Steerable intravitreal inserts for drug delivery: in vitro and ex vivo mobility experiments. *Med Image Comput Assist Interv*. 2011;14(Pt 1):33–40.
56. Conway BR. Recent patents on ocular drug delivery systems. *Recent Pat Drug Deliv Formul*. 2008;2(1):1–8.
57. Kuno N, Fujii S. Biodegradable intraocular therapies for retinal disorders: progress to date. *Drugs Aging*. 2010;27(2):117–34.
58. Jo DH, Kim JH, Lee TG, Kim JH. Nanoparticles in the treatment of angiogenesis-related blindness. *J Ocul Pharmacol Ther*. 2013;29(2):135–42.
59. Del Pozo-Rodríguez A, Delgado D, Gascón AR, Solinís MÁ. Lipid nanoparticles as drug/gene delivery systems to the retina. *J Ocul Pharmacol Ther*. 2013;29(3):173–88.
60. Kushwaha SK, Saxena P, Rai A. Stimuli sensitive hydrogels for ophthalmic drug delivery: a review. *Int J Pharm Investig*. 2012;2(2):54–60.
61. Jacobson SG, Cideciyan AV, Ratnakaram R, Heon E, Schwartz SB, Roman AJ, et al. Gene therapy for leber congenital amaurosis caused by RPE65 mutations: safety and efficacy in 15 children and adults followed up to 3 years. *Arch Ophthalmol*. 2012;130(1):9–24.
62. Lam BL, Feuer WJ, Abukhalil F, Porciatti V, Hauswirth WW, Guy J. Leber hereditary optic neuropathy gene therapy clinical trial recruitment: year 1. *Arch Ophthalmol*. 2010;128(9):1129–35.
63. Wert KJ, Davis RJ, Sancho-Pelluz J, Nishina PM, Tsang SH. Gene therapy provides long-term visual function in a pre-clinical model of retinitis pigmentosa. *Hum Mol Genet*. 2013;22(3):558–67.
64. Biotech A. The Avalanche approach: how it works [Internet]. Avalanchebiotech. 2012 [cited 4 Apr 2013]. Available from: <http://www.avalanchebiotech.com/how-it-works.php>.
65. Rossmiller B, Mao H, Lewin AS. Gene therapy in animal models of autosomal dominant retinitis pigmentosa. *Mol Vis*. 2012;18(February):2479–96.
66. Fujii Y, Kachi S, Ito A, Kawasumi T, Honda H, Terasaki H. Transfer of gene to human retinal pigment epithelial cells using magnetite cationic liposomes. *Br J Ophthalmol*. 2010;94(8):1074–7.
67. Lavinsky D, Chalberg TW, Mandel Y, Huie P, Dalal R, Marmor M, et al. Modulation of transgene expression in retinal gene therapy by selective laser treatment. *Invest Ophthalmol Vis Sci*. 2013;54(3):1873–80.
68. Hynes SR, Lavik EB. A tissue-engineered approach towards retinal repair: scaffolds for cell transplantation to the subretinal space. *Graefes Arch Clin Exp Ophthalmol*. 2010;248(6):763–78.
69. Schwartz SD, Hubschman J-P, Heilwell G, Franco-Cardenas V, Pan CK, Ostrick RM, et al. Embryonic stem cell trials for macular degeneration: a preliminary report. *Lancet*. 2012;379(9817):713–20. Elsevier Ltd.
70. Stanzel BV, Liu Z, Brinken R, Braun N, Holz FG, Eter N. Subretinal delivery of ultrathin rigid-elastic cell carriers using a metallic shooter instrument and biodegradable hydrogel encapsulation. *Invest Ophthalmol Vis Sci*. 2012;53(1):490–500.
71. Yanai A, Häfeli UO, Metcalfe AL, Soema P, Addo L, Gregory-Evans CY, et al. Focused magnetic stem cell targeting to the retina using superparamagnetic iron oxide nanoparticles. *Cell Transplant*. 2012;21(6):1137–48.

Prophylaxis and Cure of Rhegmatogenous Retinal Detachment

V.B.4.

C. Pat Wilkinson

Outline

- I. Introduction
- II. Prophylaxis of Retinal Detachment
 - A. Risk Factors for Retinal Detachment
 - B. Categories of Eyes and Lesions Considered for Preventative Therapy
 - 1. Eyes with Symptomatic PVD
 - a. Tears with Persistent Vitreoretinal Traction
 - b. Breaks and Precursors Unassociated with Vitreoretinal Traction
 - 2. Asymptomatic Vitreoretinal Lesions in Phakic Non-fellow Eyes
 - a. Retinal Lattice (Degeneration)
 - b. Cystic Retinal Tufts
 - c. Degenerative Retinoschisis
 - 3. Asymptomatic Retinal Breaks in Phakic Non-fellow Eyes
 - 4. Asymptomatic Vitreoretinal Lesions and Retinal Breaks in Non-phakic Non-fellow Eyes
 - 5. Asymptomatic Vitreoretinal Lesions and Retinal Breaks in Patients with a History of Retinal Detachment in the Fellow Eye
 - a. Phakic Fellow Eyes
 - i. Retinal Lattice
 - ii. Retinal Breaks
 - iii. Miscellaneous
 - b. Aphakic and Pseudophakic Fellow Eyes
 - C. Summary
- III. Repair of Retinal Detachment
 - A. Surgery for Uncomplicated Retinal Detachment
 - 1. Scleral Buckling
 - a. Advantages of Scleral Buckling
 - b. Disadvantages of Scleral Buckling
 - 2. Pneumatic Retinopexy
 - a. Advantages of Pneumatic Retinopexy
 - b. Disadvantages of Pneumatic Retinopexy

- 3. Vitrectomy
 - a. Advantages of Vitrectomy
 - b. Disadvantages of Vitrectomy
- B. Surgery for Complicated Retinal Detachments

Conclusions

References

Keywords

Vitreous • Posterior vitreous detachment • Vitreoretinal adhesion • Retinal tear • Retinal detachment • Prophylaxis Cure • Scleral buckle • Pneumatic retinopexy • Vitrectomy

Key Concepts

1. The pathogenesis of rhegmatogenous retinal detachment is intimately related to changes in vitreous, the nature of which influences decisions regarding both prevention and treatment.
2. As the posterior vitreous cortex detaches forward, inducing “flashes and floaters,” liquid vitreous gains access to retinal breaks and passes through them, creating the subretinal space. Any ocular condition associated with an increased vitreous liquefaction, PVD, and an increased vitreoretinal adhesion has a higher risk of retinal detachment.
3. “Atrophic” retinal holes, especially those within lattice lesions, have major vitreoretinal traction upon the edges of the lattice, and they therefore can behave as horseshoe tears. This and variables related to the state of the vitreous are of importance in considering methods to both prevent and repair retinal detachment.

C.P. Wilkinson, MD
Department of Ophthalmology, Greater Baltimore Medical Center,
6569 N Charles Street, suite 505, Baltimore, MD 21204, USA
e-mail: cwilkins@gbmc.org

I. Introduction

Rhegmatogenous retinal detachment (RRD) remains an important cause of reduced vision and blindness throughout the world. The pathogenesis of this important disorder is intimately related to changes in the vitreous gel and at the vitreoretinal interface. It is important to realize that the state of the vitreous influences decisions regarding both the prevention and treatment of RRD.

Essential elements for an RRD include some degree of vitreous liquefaction and a break (“tear” or “hole”) in the retina. In general, vitreous traction upon the edges of retinal break(s) or vitreoretinal adhesions associated with retinal break(s) are also necessary. The characteristic sequence of events leading to RRD begins with vitreous liquefaction leading to reduced vitreous stability and the development of fluid currents within the vitreous cavity which in turn result in increased mobility of the vitreous gel. The likelihood of posterior vitreous detachment (PVD) increases as these changes evolve [see chapter II.C. Vitreous aging and PVD]. Our understanding of PVD has recently been enhanced by ultrasound and optical coherence tomography (OCT) studies, and contemporary reports have demonstrated that this event usually begins slowly in the posterior pole [1] rather than suddenly, as previously believed. Still, it is the later rapid separation of much larger portions of the posterior vitreous cortex from the retina that typically causes symptoms of PVD (“flashes and floaters”) and retinal tears at sites of anomalous invisible or visible vitreoretinal adhesions [2] (Figure V.B.4-1). As the posterior cortical vitreous moves forward, liquid vitreous gains access to retinal breaks and passes through them, entering and creating the subretinal space. Vitreoretinal traction forces upon retinal breaks are augmented by eye movements causing increasing fluid currents in the vitreous, and progression of the RRD is accelerated by the momentum of increasing intravitreal and subretinal fluid currents (Figure V.B.4-2). Although a total PVD is usually present, many RRDs occur with only partial vitreous detachment, and evidence of PVD may not be observed. In addition, it should be noted that many so-called atrophic holes, especially those within lattice lesions, have major vitreoretinal traction upon the edges of the lattice, and they therefore behave in a manner similar to horseshoe tears (Figure V.B.4-3).

Any ocular condition associated with an increased prevalence of vitreous liquefaction, PVD, and an increased number or extent of visible and invisible vitreoretinal adhesions and traction is more likely to be associated with a higher incidence of subsequent RRD. All of these variables are of importance in considering methods to both prevent RRDs and repair them. This chapter will discuss retinal detachment prophylaxis and therapy, and the critical role of the state of the vitreous in both instances will be emphasized.

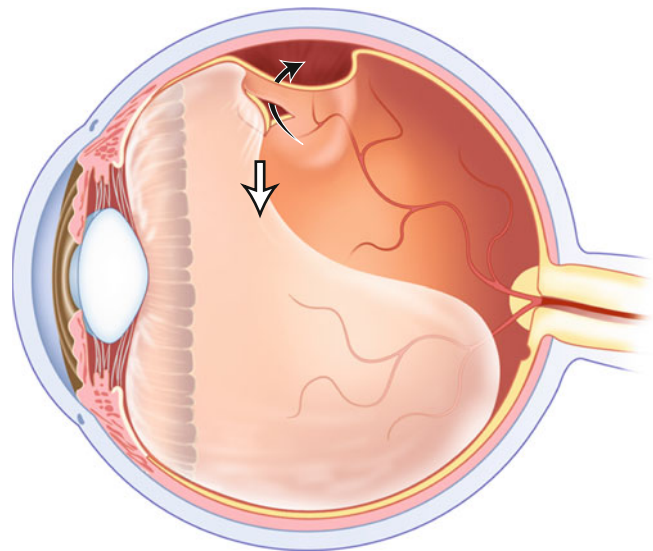


Figure V.B.4-1 During or following a posterior vitreous detachment, symptomatic retinal tears most commonly occur at locations of firm vitreoretinal adhesion. Traction (white arrow) from the detached posterior vitreous cortex upon the retina creates the retinal break(s). Liquid vitreous then passes through the tear(s) into the subretinal space (black arrow), resulting in a retinal detachment

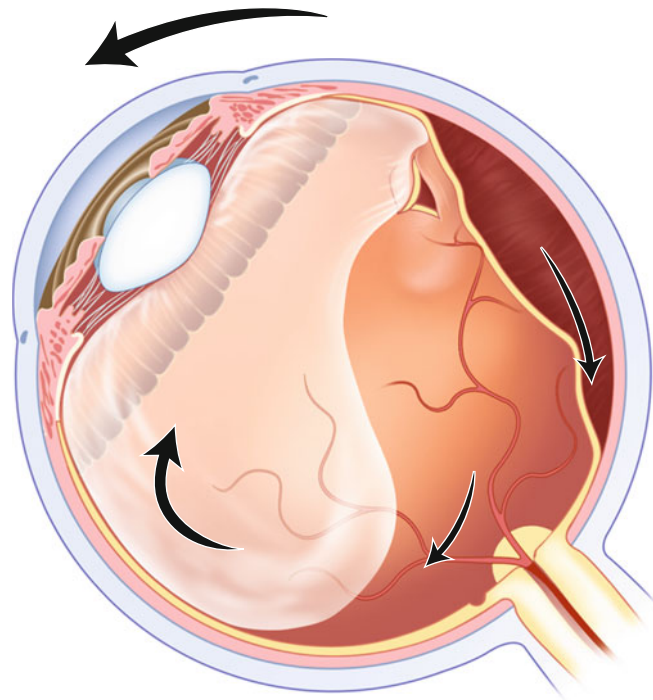
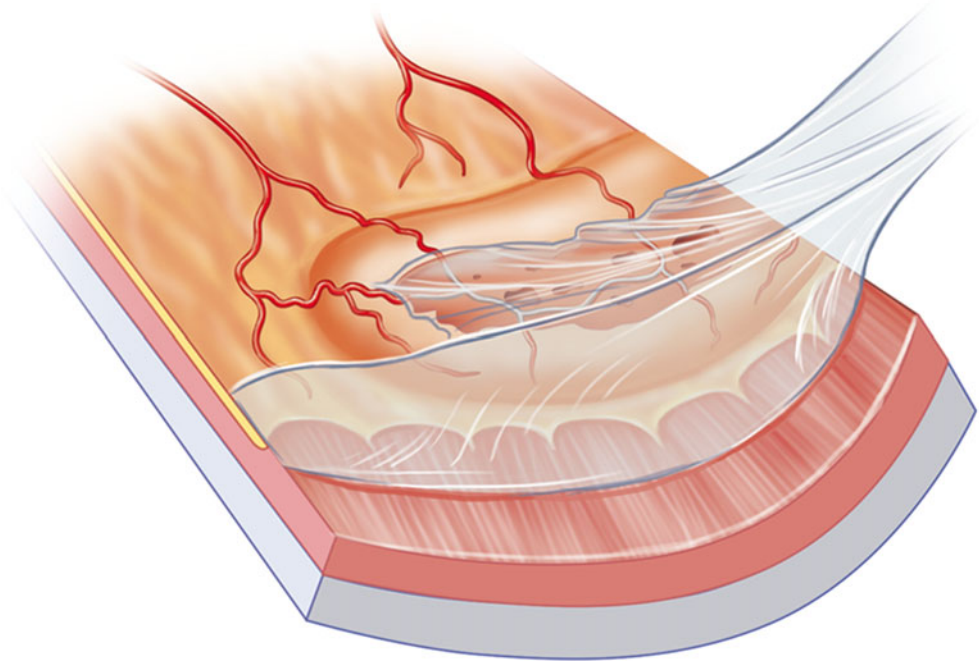


Figure V.B.4-2 Eye movements increase vitreoretinal traction forces. Rotation of the globe (upper large arrow) results in slightly delayed shifts (larger black arrow in vitreous body) in the vitreous gel which in turn result in more traction upon sites of vitreoretinal adhesion. In addition, movement of liquid currents within the vitreous cavity (smaller arrow) promotes increased vitreoretinal traction, whereas currents in the subretinal space (arrow) promote extension of subretinal fluid

Figure V.B.4-3 Although holes in lattice lesions are considered to be “atrophic,” they are associated with nearby vitreoretinal traction upon the margins of the lattice lesions, and this can facilitate passage of liquid vitreous into the subretinal space



II. Prophylaxis of Retinal Detachment

RRD is a relatively uncommon disease, affecting approximately 1 in 10,000 people in the general population per year. However, the prevalence of retinal breaks in the general population is relatively high, affecting 5–7 % of people. Obviously, many retinal breaks have minimal, if any, risk of progressing to a clinical RRD. These include typical macular holes and asymptomatic small round atrophic holes near the ora serrata. However, horseshoe tears that follow *symptomatic* PVD usually progress to clinical RRD [3]. Probably, all surgeons would agree that a horseshoe tear located near the equator in the superior temporal quadrant and associated with new symptoms of flashes and floaters and vitreous hemorrhage should be promptly treated to prevent RRD. In contrast, most would not advise treatment of a small, round atrophic hole near the inferior ora serrata in an asymptomatic patient with no history of prior detachment in the other (“fellow”) eye. Between these two obvious examples lies a broad spectrum of retinal breaks for which the surgeon must exercise judgment regarding instituting prophylactic therapy.

Most of the breaks reported in surveys of asymptomatic patients or in autopsy series are of the atrophic type, and only a small number are horseshoe tears. Although there are no specific rules for the selection of patients for treatment and while each case has to be judged on its own characteristics, the application of evidence-based medicine to this topic has modified the opinions of many regarding the genuine value of prophylactic therapy for most retinal breaks. The American Academy of Ophthalmology (AAO) has used this approach in developing a Preferred Practice Pattern (PPP) entitled “Posterior Vitreous Detachment, Retinal

Breaks, and Lattice Degeneration” [4]. The evidence described in this PPP will be employed in the following discussion.

A. Risk Factors for Retinal Detachment

Characteristics associated with a relatively high risk of RRD are listed in Table V.B.4-1). Symptoms and signs of PVD place an eye at particularly high risk. Additional factors include a variety of hereditary, congenital, acquired, and iatrogenic problems, all of which have in common an increased likelihood of premature vitreous liquefaction, early PVD, and subsequent vitreoretinal traction acting upon visible and invisible sites of vitreoretinal adhesion. The risk of RRD is substantially different among subgroups of eyes, a fact that influences interpretation of both natural history data and treatment results. For example, since an acute PVD is the primary cause of most RRDs and since most retinal tears occur during or soon after PVD, it is likely that eyes without a PVD have a higher risk of later RRD than eyes with a history of prior PVD unassociated with retinal breaks [5]. Similarly, vitreous liquefaction and PVD occur with greater frequency in older patients and in myopic and pseudophakic eyes. Thus, data regarding lesions in otherwise normal, young, non-myopic eyes are not comparable to statistics concerning cases that feature other risk factors that greatly increase the likelihood of PVD. Since more than one factor is often present, data analysis is difficult if all features are not recorded. For example, myopic pseudophakic eyes with retinal lattice (also called lattice degeneration) and with a history of retinal detachment in the fellow eyes of young male patients have a substantially greater risk of retinal detachment than otherwise normal eyes with retinal lattice.

As noted in the AAO PPP [4] and in a Cochrane Review [6], no prospective randomized trials of therapy to prevent RRD have been performed. The few meaningful published studies of treated and untreated comparable eyes have been retrospective, and most reports regarding prophylactic therapy have simply described results of a treatment series. This chapter briefly discusses published outcomes regarding both the natural course of lesions that predispose an eye to RRD and results of prophylactic therapy for these abnormalities, but a thorough review of treatment techniques is beyond the scope of this manuscript. Eyes with symptoms of PVD are much more likely to harbor retinal breaks than cases without such symptoms. Visible precursors of RRD also increase risk and have been considered for prophylactic therapy.

B. Categories of Eyes and Lesions Considered for Preventative Therapy

Cases potentially in need of prophylactic therapy can be arbitrarily grouped in a variety of ways, but eyes with symptoms and those with specific lesions and/or associated findings are at increased risk (Table V.B.4-1). Still, documenting increased risk does not necessarily mean that therapy is of value in preventing RRD [7].

1. Eyes with Symptomatic PVD

Approximately 5–20 % of eyes with an acute symptomatic PVD develop retinal tears of various types. The risk of retinal tears is directly related to the amount of vitreous hemorrhage, and the finding of many cells in the vitreous cavity is a sign associated with a particularly high chance of associated retinal tears. As noted above, symptomatic eyes with additional risk factors are more likely to have retinal breaks. In symptomatic eyes, retinal tears associated with persistent vitreoretinal traction are especially likely to cause RRD (Figure V.B.4-4) [2].

Retinal tears resulting from a symptomatic PVD should be distinguished from preexisting retinal breaks detected after the PVD but not caused by it. Thus, atrophic retinal holes within areas of retinal lattice are not considered “symptomatic,” even if they were first observed during an examination prompted by symptoms of an acute PVD. Symptomatic retinal tears are subdivided into those with persistent vitreoretinal traction and those in which all traction in the region of the retinal defect has resolved (Figure V.B.4-4).

a. Tears with Persistent Vitreoretinal Traction

Persistent vitreoretinal traction at or in the vicinity of retinal breaks is the most important factor leading to clinical RRD. Most symptomatic tears with persistent vitreoretinal traction are horseshoe shaped and have a high risk of causing

Table V.B.4-1 Risk factors for rhegmatogenous retinal detachment

Symptomatic posterior vitreous detachment (PVD)
Myopia
Lattice degeneration
Cystic retinal tuft
Degenerative retinoschisis
Retinal breaks
Male gender
Prior intraocular surgery
Aphakia/pseudophakia
Nd:YAG posterior capsulotomy
Other surgeries involving vitreous gel
Prior ocular trauma
Inflammation
CMV retinitis
Acute retinal necrosis
Others
Fellow eye non-traumatic retinal detachment
Hereditary vitreoretinopathies
Congenital/developmental/degenerative lesions

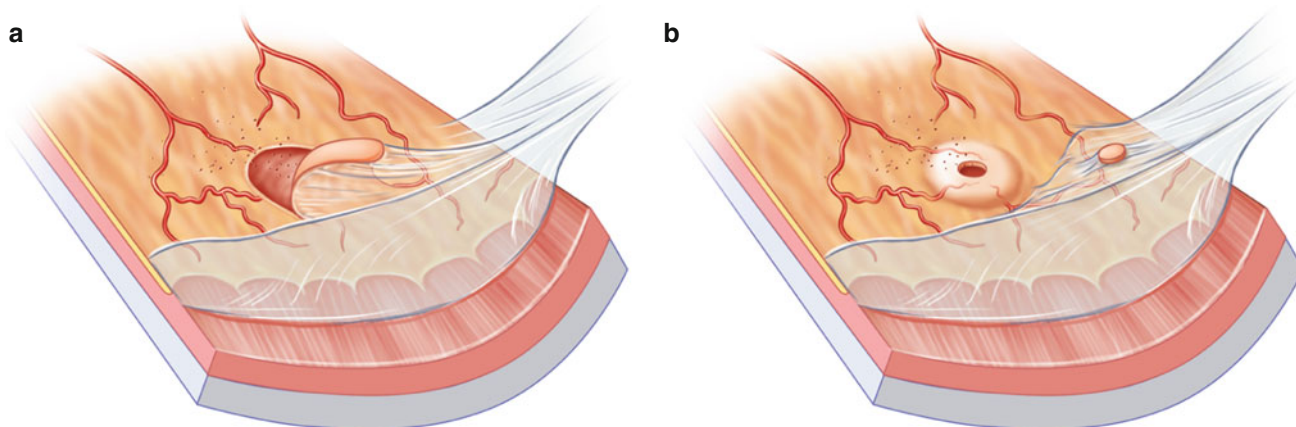
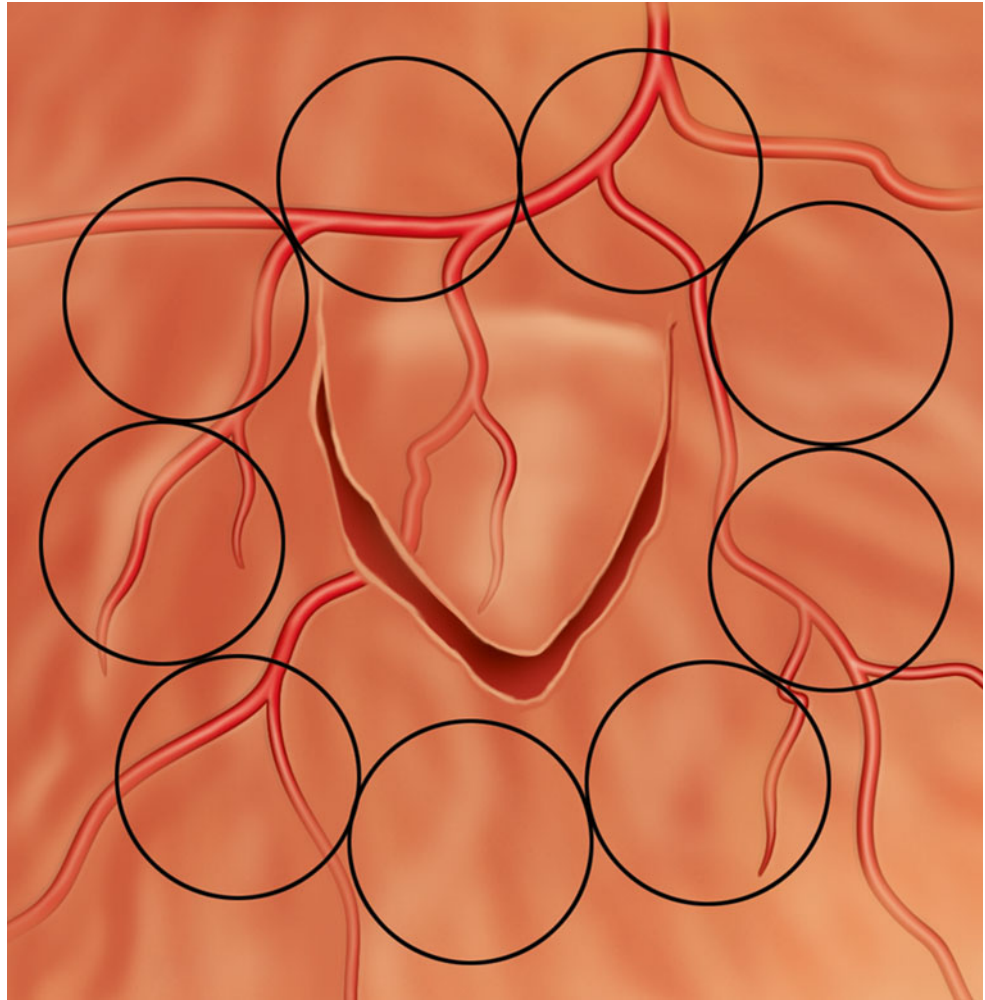


Figure V.B.4-4 Persistent traction on the retina (a) at a site of abnormal vitreoretinal adhesion has created a retinal break. Liquid vitreous posterior to the vitreous gel passes through the retinal break into the

subretinal space, creating a retinal detachment. Operculated tears (b) typically no longer have traction forces upon them unless there is a nearby vitreoretinal adhesion

Figure V.B.4-5 Acute symptomatic horseshoe tears should be treated by creating laser or cryotherapy burns immediately distal to the focal accumulation of subretinal fluid, and therapy should extend anterior to the flap of the tear and into the flat vitreous base



clinical RRD [2]. That risk has been reported to be in the range of 33–55 % of cases, but it may be higher, because most studied eyes were treated when progression of the RRD was observed. Treatment of this type of break substantially reduces the risk of RRD, and immediate prophylactic therapy for these lesions is indicated to prevent an accumulation of subretinal fluid (AAO PPP evidence level A:II [4]). A chorioretinal adhesion is created in flat retina immediately adjacent to localized subretinal fluid (Figure V.B.4-5).

Rarely, a retinal tear with a free operculum may have persistent vitreoretinal traction as a result of a residual vitreoretinal adhesion near the retinal break, most frequently at the location of a retinal blood vessel. Symptomatic operculated retinal breaks have extremely rarely been reported to progress from initial observation to clinical RRD, and these are typically associated with persistent vitreoretinal traction on nearby retinal vessels. In unusual cases in which an operculated retinal hole is the only retinal break associated with a clinical RRD, it is presumed that anomalous persistent vitreoretinal adhesions are located in the vicinity of the retinal tear. Treatment of operculated tears is frequently not nec-

essary, but it may be recommended if the presence of a nearby vitreoretinal adhesion cannot be ruled out (AAO PPP evidence level A:III [4]). Similarly, atrophic holes in zones of retinal lattice also have persistent nearby vitreoretinal traction upon the edges of the lattice, and they may behave as horseshoe tears (Figure V.B.4-3).

b. Breaks and Precursors Unassociated with Vitreoretinal Traction

Eyes with symptoms and signs of acute PVD frequently contain atrophic retinal breaks that are not due to acute vitreoretinal traction. For the purposes of this discussion, these lesions are considered to be preexisting and not symptomatic. Similarly, precursors of retinal breaks or detachment, including retinal lattice, cystic retinal tufts, and age-related retinoschisis, are managed as if they were originally discovered in asymptomatic eyes. Treatment of this type of retinal break appears to be unnecessary unless the possibility of persistent vitreoretinal traction cannot be excluded, as noted earlier, and it is rarely recommended (AAO PPP evidence level A:III [3]).

2. Asymptomatic Vitreoretinal Lesions in Phakic Non-fellow Eyes

Non-myopic phakic eyes in patients without a history of non-traumatic RRD are unlikely to develop RRD, regardless of the presence of vitreoretinal pathology. Nevertheless, prophylactic therapy has sometimes been recommended to treat visible precursors of RRD or retinal breaks. Precursors of retinal breaks and detachment include retinal lattice, cystic retinal tufts, and degenerative retinoschisis. Of these, retinal lattice is clearly the most important. Both retinal lattice and cystic retinal tufts can be sites of retinal tears resulting from vitreoretinal traction at the time of PVD (Figure V.B.4-1). Atrophic retinal holes commonly occur within areas of retinal lattice and also in the outer layer of degenerative retinoschisis.

a. Retinal Lattice (Degeneration)

Lattice degeneration is a commonly used term to refer to peripheral retinal pathology that features oval zones of linear hypo-pigmented structures in the peripheral fundus. The term implies that this lesion is the result of a degenerative process; however, it is more likely than not the manifestation of a dystrophy [see chapter III.H. Peripheral vitreoretinal pathology]. Thus, the term retinal lattice is probably a more accurate way to refer to this lesion.

Retinal lattice is present in approximately 30 % of RRDs, and approximately 94 % of these RRDs occur in primary (non-fellow) eyes [7]. Because lattice lesions are visible and occur in approximately 8 % of the population, they have commonly been considered as candidates for prophylactic therapy. However, an important natural history study [8] of 276 patients and 423 involved eyes, followed an average of almost 11 years, indicated that lattice lesions in phakic non-fellow eyes were not particularly dangerous. At the end of this follow-up period, atrophic retinal holes were present in 150 (35 %) eyes. Subclinical retinal detachments, defined as subretinal fluid extending more than one disc diameter from the break but not posterior to the equator, were observed in only ten of the eyes with holes. In six of these eyes, the subclinical retinal detachment developed during the observation period, whereas four eyes exhibited the changes at the initial examination. Only one subclinical retinal detachment was considered in need of treatment after a small asymptomatic posterior extension of subretinal fluid. Four asymptomatic tractional retinal tears were observed in 3 of these 423 eyes at the initial examination, and symptomatic tractional tears without clinical detachment developed in five additional eyes during follow-up periods of 1.5–18 years [8]. Three of five symptomatic and all asymptomatic breaks occurred adjacent to lattice lesions. All symptomatic breaks were successfully treated; no asymptomatic tractional tears were treated, and none changed over follow-up periods of 7, 10, and 15 years. Clinical RRDs developed in 3 of the 423 eyes.

Two were due to asymptomatic round retinal holes in lattice lesions of patients in their mid-twenties, and one was due to a symptomatic tractional tear. These figures clearly indicate that patients with retinal lattice in phakic non-fellow eyes should usually not be treated unless symptoms occur (AAO PPP evidence level A:III [4]).

b. Cystic Retinal Tufts

Retinal tears at sites of cystic retinal tufts may be responsible for as many as 10 % of clinical RRDs associated with PVD, and they are also associated with asymptomatic small horseshoe-shaped tears and minimal subretinal fluid in the absence of PVD. The chances of clinical RRDs in eyes with cystic retinal tufts have been estimated by one expert to be one in 357 [9], and these lesions are not worthy of prophylactic therapy in otherwise normal eyes.

c. Degenerative Retinoschisis

Clinical RRDs occur in association with degenerative retinoschisis in up to 6 % of consecutive detachment cases, and the presence of retinoschisis and outer layer breaks has sometimes been considered an indication for prophylactic therapy. However, a natural history course study [10] of 218 eyes in 123 patients demonstrated no clinical retinal detachments during a follow-up period averaging 9.1 years. The vast majority of small subclinical detachments that develop in association with outer layer breaks remain small, and prophylactic therapy is indicated only in the presence of obvious significant progression of subretinal fluid posterior to the equator.

3. Asymptomatic Retinal Breaks in Phakic Non-fellow Eyes

In phakic non-fellow eyes, asymptomatic retinal breaks that are discovered during a routine evaluation of the peripheral retina are extremely unlikely to lead to clinical RRD, even if they are flap tears and even if PVD occurs. In one study [11], during a follow-up period averaging 11 years, asymptomatic retinal breaks were detected in 235 eyes of 196 patients, and horseshoe-shaped tears were present in 45 cases. Acute PVDs occurred in nine eyes without adversely affecting the preexisting breaks, although new horseshoe-shaped tears developed in three cases, and these were promptly treated. Subclinical retinal detachments were observed in 19 (8 %) eyes. Modest extension of subretinal fluid required therapy in two of these cases, and in a third case a peripheral RRD slowly developed after 14 years of observation. Prophylactic therapy in these eyes is usually not recommended (AAO PPP evidence level A:III [4]). An occasionally observed exception to this rule is an inferior retinal dialysis. These breaks can cause slowly progressive RRDs that frequently become symptomatic only after macular involvement.

4. Asymptomatic Vitreoretinal Lesions and Retinal Breaks in Non-phakic Non-fellow Eyes

Regardless of the method of cataract surgery, removal of the crystalline lens is associated with a substantial increase in the rate of subsequent PVD and retinal tears and detachments [12], probably due to vitreous changes that follow cataract surgery [see chapter III.I. Role of vitreous in the pathogenesis of retinal detachment]. An intact posterior lens capsule appears to be associated with a reduced rate of retinal detachment following cataract surgery, whereas Nd:YAG capsulotomy is clearly associated with a small but significantly increased risk of subsequent detachment.

The natural history of retinal lattice, other precursors of RRD, and retinal breaks in non-phakic non-fellow eyes is not well documented, and appropriate studies of preventive treatment in these cases are not available. Therefore, treatment is usually not advised (AAO PPP level A:III [4]).

5. Asymptomatic Vitreoretinal Lesions and Retinal Breaks in Patients with a History of Retinal Detachment in the Fellow Eye

Pathologic vitreoretinal changes often occur bilaterally, and patients with retinal detachment in one eye have a significantly increased risk of retinal detachment in the other. This risk has been estimated as ranging from as low as 9 % to as high as 40 % [7]. Thus attempts to prevent retinal detachment in a “second eye” have received considerable attention. Prospective randomized studies have not been performed, but retrospective data regarding precursors of RRDs and asymptomatic retinal breaks have been published. These can be further categorized as phakic and non-phakic fellow eyes. Phakic fellow eyes have a lower risk of subsequent retinal detachment than comparable non-phakic eyes.

a. Phakic Fellow Eyes

i. Retinal Lattice

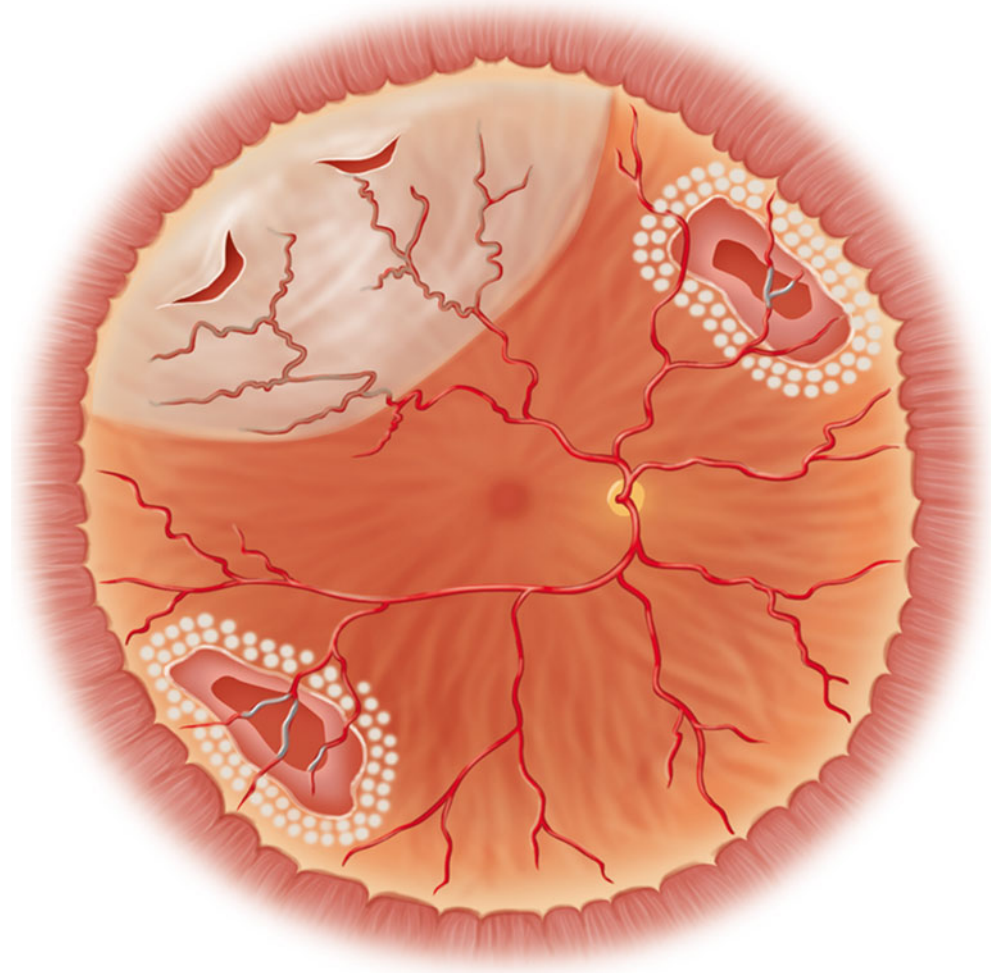
Retinal lattice is the most extensively studied indication for prophylactic therapy in fellow eyes. One widely quoted study [13] retrospectively evaluated 388 consecutive cases in which phakic retinal detachment associated with retinal lattice occurred in one eye and retinal lattice was present in the second eye. During an average follow-up period of over 7 years, new retinal breaks or detachments occurred in 31 (20 %) of 151 untreated eyes. New tears with retinal detachment developed in nine eyes, and new tears without retinal detachment developed in ten cases. In ten eyes, new holes developed within areas of retinal lattice, and atrophic retinal breaks occurred in areas distant from lattice lesions in the remaining two cases.

A reduction in the incidence of new retinal tears and detachments in eyes receiving prophylactic therapy for all lattice lesions was observed [13]. New tears without retinal detachment occurred in five (3.0 %) of these fully treated eyes. Retinal detachment occurred in three additional eyes (1.8 %), compared with 5.1 % in the 151 untreated phakic fellow eyes. The small beneficial effect of treating all lattice lesions was apparent when follow-up periods of 3, 5, and 7 years were analyzed separately. Importantly, the beneficial effect was statistically significant for all patient subgroups, *except* in eyes with myopia of six diopters or more and in eyes with both high myopia and more than 6 clock hours of lattice degeneration. Thus, in these subgroups with relatively increased risk, treatment did not reduce the chance of retinal tears or detachment. Conversely, no detachments occurred after full treatment in eyes with less than 6 clock hours of lattice degeneration or with less than 1.25 diopters of myopia. New horseshoe-shaped tears developed in areas unassociated with lattice degeneration in approximately 30 % of treated cases.

One expert [7] has estimated that as many as 58 % of retinal detachments in eyes with retinal lattice arise in areas that exhibit no visible vitreoretinal abnormalities (Figure V.B.4-6). Because of this reality, some surgeons have recommended prophylactic therapy featuring the production of laser or cryotherapy burns over 360° of the peripheral retina (Figure V.B.4-7). However, the precise indications, intraocular findings, long-term results, and complications of this form of therapy have not been thoroughly described, and remarkably different success rates have been reported. Studies of prophylactic therapy of retinal lattice, with and without holes, in phakic fellow eyes have been of limited value because they have not been prospective and because important information has been missing from available retrospective analyses. In particular, the outcomes have not been studied as a function of the presence of a PVD. It has been noted by several authors that retinal detachments are unusual in fellow eyes if a PVD was present at the time of the initial examination [5].

The relatively low incidence of retinal detachment in untreated cases, the frequency of new tears in normal-appearing retina, the apparent ineffectiveness of therapy in eyes with extensive retinal lattice and high myopia, and the known high success rate following treatment of acute symptomatic retinal tears and detachments indicate that prophylactic treatment is of limited value in these asymptomatic fellow eyes. The apparently modest benefit following treatment of all lattice lesions may be of value in selected patients, such as those with a poor surgical result in the first eye, patients who are incapable of recognizing symptoms of vitreous and/or retinal detachment, or those who live in areas with limited access to ophthalmologic care. In addition, as noted above, myopic patients with atrophic holes in lattice

Figure V.B.4-6 Adequate treatment of visible lattice lesions does not prevent new retinal tears from developing at invisible sites of vitreoretinal adhesion



lesions should be evaluated periodically and counseled about loss of peripheral vision (AAO PPP level: no consensus [4]).

ii. Retinal Breaks

Retinal breaks are frequently cited as an indication for prophylactic therapy in these phakic fellow eyes. Flap tears appear to be much more likely to cause retinal detachment than round or operculated retinal holes. In one study, retinal breaks were discovered in 186 (19 %) of 966 fellow eyes, 28 of which (15 %) later developed retinal detachment [14]. Horseshoe-shaped tears were the cause of the detachment in 20 (71 %) of the 28 eyes, whereas only 19 % of breaks were flap tears in the 158 eyes that did not progress to retinal detachment. However, another author followed ten untreated asymptomatic horseshoe-shaped tears in phakic fellow eyes, and no retinal detachments occurred [13]. Deficiencies in prior reports have made it difficult to assess both the natural course of asymptomatic retinal breaks that are discovered on an examination of a fellow eye and the results of treatment of these lesions. Most of these breaks are round and located within areas of retinal lattice, and these cases were discussed earlier. Data regarding therapy for asymptomatic horseshoe-shaped

tears in fellow eyes suffer from a lack of details, including the status of the vitreous and the relationship between the original retinal break and the cause of subsequent retinal detachment. Still, treatment of horseshoe-shaped tears that are discovered in asymptomatic fellow eyes is sometimes recommended despite the absence of optimal supportive data (AAO PPP level: no consensus [4]).

Prophylactic treatment is frequently recommended in phakic fellow eyes in which a non-traumatic giant retinal tear has occurred in the first eye. In one study, 321 cases were followed for 12 months to 29 years [14]. New giant retinal tears occurred in 14 (4.4 %) untreated eyes, 13 of which had developed “high-risk features” of high myopia, vitreous degenerative changes, and “white with pressure” that increased in extent (Figure V.B.4-8). In a more recent report [15], 48 patients were followed for a mean of 84 months after repair of a giant retinal tear in one eye and 360° cryotherapy of the second eye. During the follow-up period, retinal detachment developed in three patients, and a retinal tear alone was observed in the fourth. Giant retinal tears are particularly likely to occur in type 1 Stickler syndrome, and a relatively recent but retrospective study [16] provided

Figure V.B.4-7 Because of new retinal breaks developing in apparently “normal” peripheral retina, some surgeons have recommended 360° of laser photocoagulation



some compelling evidence that 360° cryotherapy of the anterior retina was of value in preventing subsequent RRD [see chapter I.C. Hereditary vitreo-retinopathies].

iii. Miscellaneous

Cystic retinal tufts are bilateral in only 6 % of cases, so they are not a common cause of bilateral retinal detachment, and there are no data supporting the value of prophylactic therapy.

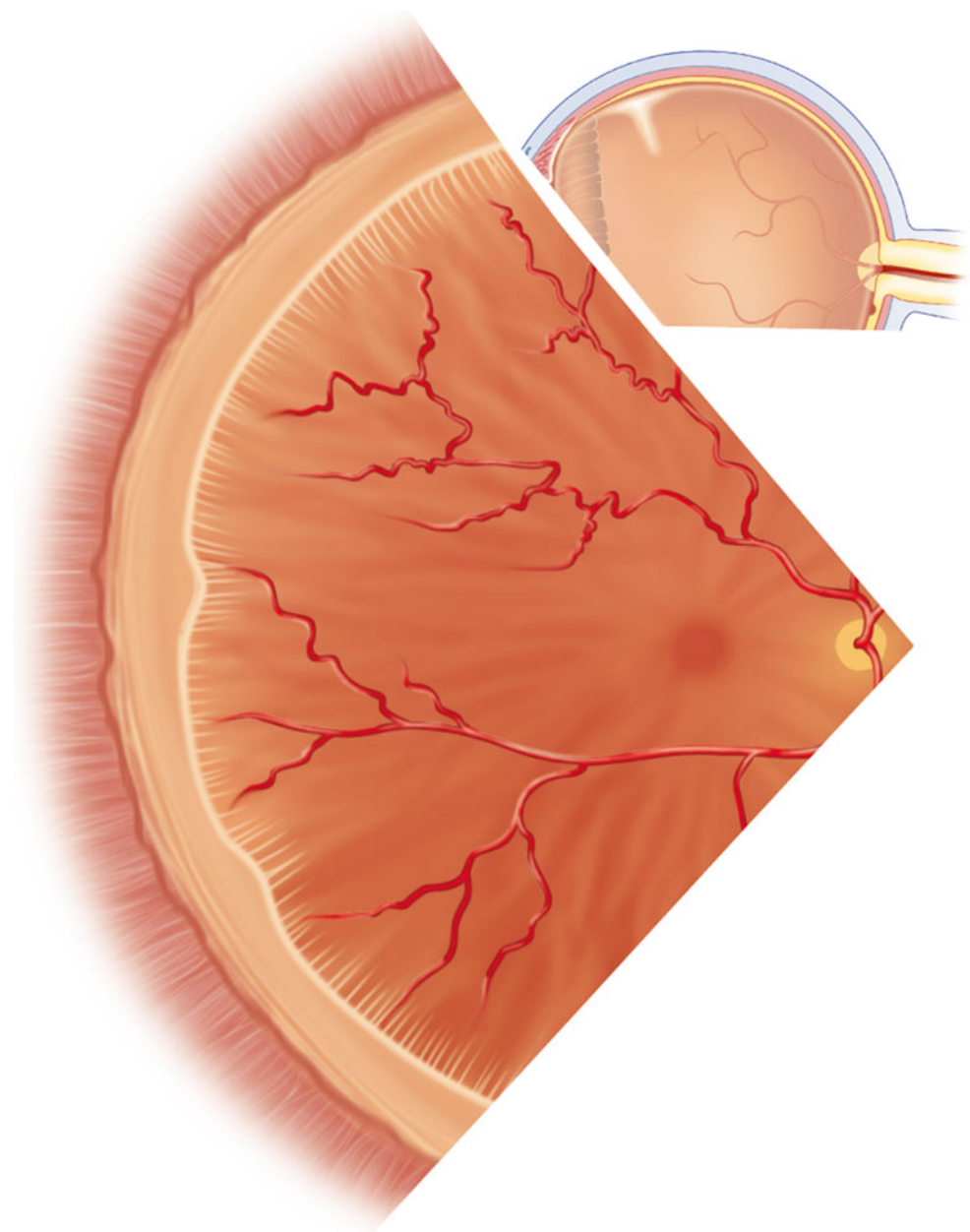
Degenerative retinoschisis is an unusual cause of progressive retinal detachment in these eyes, but retinoschisis is both common and frequently bilateral. Thus, patients with both retinal detachment and retinoschisis in one eye frequently have retinoschisis in the fellow eye. A review of the literature regarding prophylactic therapy for retinoschisis in phakic fellow eyes is very difficult because of a lack of complete information regarding the cases. In the unusual case in which outer layer retinal breaks have been responsible for retinal detachment in the first eye and outer layer breaks and retinoschisis are present in the fellow eye, prophylactic therapy is frequently recommended (AAO PPP level: no consensus [4]).

b. Aphakic and Pseudophakic Fellow Eyes

All eyes have an increased risk of retinal detachment after cataract extraction, and the post-cataract surgery risk for fellow eyes in patients with previous retinal detachment in the first eye has been estimated to be 14–41 % [7]. The chance of detachment appears to be higher if Nd:YAG capsulotomy was required. Thus, prophylactic therapy has frequently been recommended for vitreoretinal lesions in fellow eyes that are non-phakic or that are scheduled to undergo cataract extraction.

Retinal lattice is the most common precursors of retinal tears considered for prophylactic therapy before or after cataract extraction. However, no prospective randomized studies have compared the natural course in these cases with outcomes following preventive treatment [6]. As is true of phakic fellow eyes, a major problem in treating only visible pathology is the frequency of new retinal tears that develop in areas of the peripheral retina that appear normal. Although treatment of visible lesions appears to reduce the chances of retinal tears occurring at the treated site, the retinal detachments that frequently develop in these fellow eyes do not appear to be prevented by this focal therapy.

Figure V.B.4-8 A small traction ridge in the peripheral retina and an anterior band of “white without pressure” are seen in the fellow eye of a patient with non-traumatic giant tear in the other eye



Importantly, studies of prophylactic treatment of retinal lattice in fellow non-phakic eyes have not been stratified on the basis of PVD. In one important study [5], the critical importance of this variable was evaluated by studying aphakic eyes of patients with aphakic retinal detachment in the primary eye. Retinal detachment subsequently occurred in one (2.3 %) of 43 eyes with a PVD in the fellow eye. In the 40 eyes without a previous PVD, retinal detachment later occurred in eight eyes (21 %). Similarly, in another study [17], retinal detachments occurred in five (24 %) of 21 aphakic fellow eyes without PVD at the initial examination, but no detachments occurred in 15 additional cases in which a PVD was initially present.

Because of the tendency for new retinal breaks to develop in areas of the retina that appear normal, 360° treatment has been advocated, as noted earlier (Figure V.B.4-7). Although the evidence of this form of therapy is compelling in regard to patients with non-traumatic giant retinal tears, the risk-benefit ratio of this therapy remains unknown. Treatment of lattice lesions in non-phakic fellow eyes is frequently performed despite the lack of supportive data. In eyes in which a PVD has previously occurred, it is doubtful if therapy is particularly effective or necessary. The value of various forms of prophylactic treatment in eyes without PVD will remain debatable until appropriate trials are conducted.

Cystic retinal tufts and degenerative retinoschisis are unusual causes of bilateral retinal detachment, and data discussing the importance of these entities following cataract surgery are not available. They are managed as discussed under “asymptomatic phakic fellow eyes”. Retinal breaks in non-phakic fellow eyes of patients with a previous retinal detachment in the other eye may carry a higher chance of causing detachment than similar breaks in non-fellow eyes. One author [17] described asymptomatic retinal breaks in ten aphakic fellow eyes. Subsequent retinal detachments occurred in five of these cases. Four of the five breaks causing retinal detachment were horseshoe-shaped tears, and the type of the fifth break was not reported. The literature regarding the value of treating round holes unassociated with lattice lesions is not clear. Treatment usually can be expected to prevent retinal detachment resulting from the identified break but not detachment resulting from breaks in other areas of the retina. Treatment of asymptomatic horseshoe-shaped tears in aphakic fellow eyes and in fellow eyes scheduled to undergo cataract extraction is usually recommended despite the absence of supportive data (AAO PPP level: no consensus [4]).

C. Summary

Although prevention of retinal detachment is an important goal, the genuine value of prophylactic therapy for retinal breaks and most predisposing vitreoretinal lesions remains unknown because of a lack of appropriate trials. Treatment of symptomatic flap tears is an evidence-based and accepted method of preventing clinical retinal detachments, because the natural course of these breaks and the results of therapy are well documented. In most other instances, treatment of visible abnormal vitreoretinal adhesive lesions is of limited value, even in eyes with additional risk features such as high myopia, pseudophakia, and history of retinal detachment in the fellow eye. Specific decisions regarding prophylaxis for a given eye should be made on the basis of the features of the case and expanding medical knowledge. Patients with high-risk features should be made aware of symptoms of PVD and loss of visual field, and any patient with such symptoms should be promptly evaluated. In addition, periodic evaluations of these patients may be indicated.

III. Repair of Retinal Detachment

Rhegmatogenous retinal detachment (RRD) was regarded as incurable until the seminal work of Jules Gonin in the 1920s and Rosengren in the 1930s, when anatomic success rates approaching 50 % of selected cases were first described. Anatomic results for repair of routine RRDs further improved

Table V.B.4-2 Uncomplicated retinal detachments: relative indications (RI) and contraindication (RC)

Procedure	RI	RC
Scleral buckle	Cases without RC Inferior breaks	Opaque media Posterior break(s) Ultrathin sclera
Pneumatic	Break(s) localized Break(s) superior	Multiple separated breaks Breaks not superior Opaque media Incomplete PVD Inferior or extensive lattice
Vitrectomy	Opaque media Posterior break(s) Pseudophakia PVR	Relatively simple phakic RD Inferior retinal dialysis Obvious incomplete PVD

significantly when Charles Schepens introduced the binocular indirect ophthalmoscope and the techniques of encircling scleral buckle surgery in the 1950s and 1960s. Since then, techniques have slowly improved through decades, reaching the current 85–90 % single operation success rate for scleral buckling by the early 1980s. Unfortunately, a similar improvement in visual results has not occurred because of the profound influence of preoperative macular detachment and irreversible macular damage upon postoperative visual acuity.

As the anatomic success rates following repair of routine retinal detachments became relatively good and stable, increased attention was directed toward complications of routine scleral buckling, especially anisometropia, muscle imbalance, and pain. Thus, viable alternative techniques were developed in the 1980s, the most enduring being pneumatic retinopexy (PR) and vitrectomy. The former procedure evolved from initial experiences with intraoperative and postoperative gas injections associated with conventional scleral buckling surgery, whereas vitrectomies were originally reserved for only complicated detachments and became popular for more routine cases as experience and equipment improved. Today, scleral buckling, PR, and vitrectomy are all standards of care that are widely employed in the management of “routine” or “uncomplicated” RRD, and factors favoring one technique over another are based upon a number of considerations, many of which are sociological rather than medical. For instance, popularity of PR can be correlated with both physician age and geographical location, and scleral buckling appears to be much less popular in the hands of relatively young vitreoretinal surgeons.

Although it is quite clear that scleral buckling for uncomplicated cases has become less popular worldwide, it is appropriate to discuss objective clinical criteria that seem to favor one technique over another. Scleral buckling, PR, and vitrectomy have relative indications and contraindications (Table V.B.4-2) as well as limitations and complications.

Table V.B.4-3 Common types of *uncomplicated* retinal detachments

Horseshoe tears with complete or incomplete PVD
At margins of lattice lesions
Unassociated with lattice but posterior to vitreous base
Along posterior margin of vitreous base
Atrophic holes in lattice degeneration
Combinations of 1 and 2
Retinal dialyses

Table V.B.4-4 Variables associated with *uncomplicated* retinal detachments

Retinal break(s)
Type
Associated with persistent vitreoretinal traction on edge of break (“horseshoe”)
Associated with vitreoretinal traction near location of atrophic break
Unassociated with significant vitreoretinal traction upon breaks
Location: Quadrant
Distance from ora serrata
Distance from other breaks and degenerative lesions
Number
Posterior surface of cortical vitreous
Total PVD: vitreoretinal traction only at vitreous base and near break(s)
Incomplete PVD: Residual vitreoretinal apposition and/or traction
Vitreoretinal traction on breaks ± lattice lesions
Vitreoretinal traction at apparently normal sites
Location: Quadrant
Distance from ora serrata
Lens status
Clear crystalline lens
Cataract
Pseudophakic ± pupillary membranes
Clarity of vitreous body
Clear
Vitreous hemorrhage
Asteroid hyalosis
Vitreous opaque “debris”

In this portion of this chapter, clinical factors that may influence the choice of one technique over another, *for the types of cases in which scleral buckling, PR, and/or vitrectomy are neither mandatory nor contraindicated*, are discussed. However, it is obvious that opinions regarding the “best” operation for a given case will never be agreed upon universally, just as a single ice cream flavor will never be favored by all. Regardless of technique, if all retinal breaks are surgically closed and PVR or other more unusual complications do not develop, the procedure will almost always be anatomically successful.

Common types of uncomplicated RRDs are listed in Table V.B.4-3, and the variables regarding uncomplicated cases are contained in Table V.B.4-4. The relative indications

and contraindications in Table V.B.4-2 frequently dictate the selection of a specific reattachment procedure. The most important considerations include (1) the locations, numbers, and types of retinal breaks and vitreoretinal degenerative lesions; (2) the relationship between the posterior vitreous cortex and the retina; (3) the clarity of the vitreous body; and (4) the status of the crystalline lens.

A. Surgery for Uncomplicated Retinal Detachment

There are several relatively common types of uncomplicated retinal detachments (Table V.B.4-3) as well as numerous variables associated with all of them (Table V.B.4-4). Those that are genuinely complicated are usually routinely managed with vitrectomy techniques, whereas localized relatively simple cases are usually managed with a “walling-off” procedure employing laser or cryotherapy or with a small and localized scleral buckling procedure [18]. Between these two extremes are a large percentage of cases in which any of the three major options might be considered, and combinations of the three are also employed by many surgeons in selected situations. Regardless of technique, if all retinal breaks are surgically closed and PVR or other more unusual complications do not develop, the procedure will almost always be anatomically successful.

1. Scleral Buckling

As the only popular method of managing routine retinal detachments until the latter 1980s, scleral buckling can be employed in the vast majority of uncomplicated cases in which the retina can be adequately visualized. The diminished popularity of this technique is not primarily due to limitations in anatomical success but rather to the development of alternative techniques that provide acceptable reattachment rates, fewer or different complications, and additional advantages in selected cases.

In a non-drainage scleral buckle, functional closure of retinal breaks can result from several beneficial effects of a scleral buckle, including (1) alteration in the concave shape of the eyeball, resulting in a change in the effect of intraocular currents that encourage liquid vitreous to enter the subretinal space; (2) reduction of vitreoretinal traction by displacing the eye wall and retina centrally; (3) displacement of subretinal fluid away from the location of the retinal break and scleral buckle; (4) approximation of the retinal break to adjacent vitreous gel; and (5) postoperative increase in the height of the scleral buckle. All of these may promote an increase in resistance to fluid flow through the retinal break (Figure V.B.4-9), with consequent increase in the relative reattachment forces. These effects are probably synergistic, and they are also important in drainage cases. Although

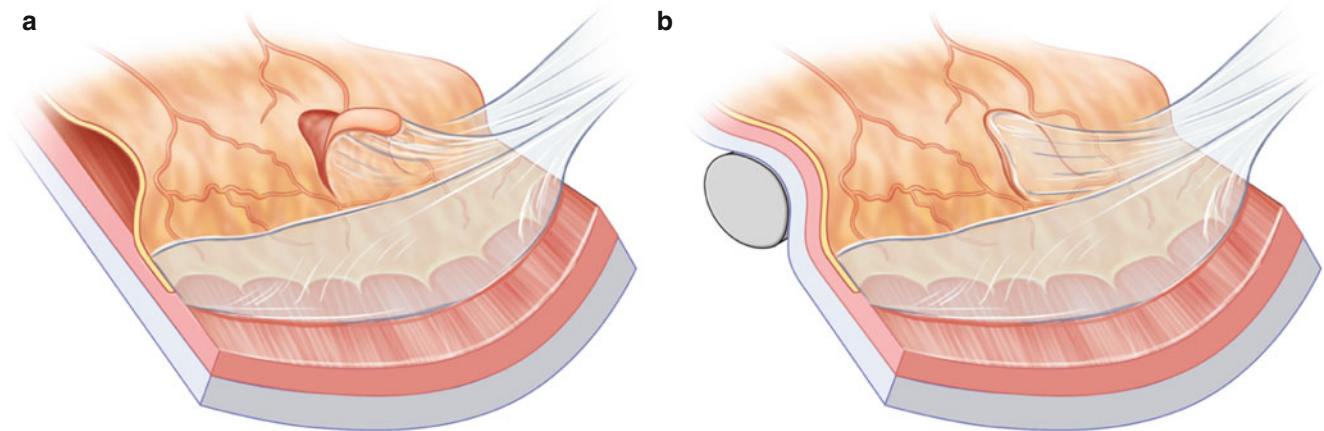


Figure V.B.4-9 Scleral buckling for retinal detachment. An open retinal tear (a) allows fluids to pass through the break into the subretinal space. Closure of the retinal tear with a scleral buckle (b) results in retinal reattachment

contemporary scleral buckling procedures routinely include the creation of a chorioretinal burn, such an adhesion is not always necessary to maintain retinal reattachment.

The most common complications of scleral buckling (other than anatomic failure) do not usually follow PR and vitrectomy without buckling. These are significant postoperative inflammation with swelling, discomfort, and blurred vision in most cases; induced myopia due to axial elongation in some cases; diplopia due to disturbance of extraocular muscles in a few cases; and subretinal hemorrhage or retinal incarceration in external drainage cases. In addition, PR offers additional advantages of an office procedure and reduced postoperative discomfort, whereas vitreous surgery provides a remedy for the most common relative contraindications of buckling, significant vitreous opacification, and posterior retinal breaks.

a. Advantages of Scleral Buckling

The primary advantage of scleral buckling is the fact that it has served as a standard of care for decades, and its indications and success and complication rates are therefore relatively well understood and acceptable. An additional important advantage is the fact that buckling is usually an extraocular procedure except for the important frequently optional steps of draining subretinal fluid and/or injecting gas. It therefore usually does not cause direct changes in the vitreous gel that routinely follow pneumatic procedures and vitrectomy. The costs of equipment and accessory materials are considerably less than for vitrectomy although much more than for PR. It is usually not associated with progressive cataract formation following surgery.

b. Disadvantages of Scleral Buckling

Compared to PR, important disadvantages of scleral buckling are the necessity of performing the operation in an operating room and the costs of this and additional equipment.

Increased patient morbidity usually occurs following scleral buckling than after PR and most vitrectomies without buckling. Compared to vitrectomy, significant disadvantages include increased difficulties in the management of very large and/or posterior retinal breaks and increased patient morbidity following repairs of relatively “difficult” cases. As mentioned earlier, postoperative muscle imbalance and altered refractive errors are important complications that are more commonly seen following scleral buckling than after PR or vitrectomy without buckling. A growing but relatively curious disadvantage is that many vitreoretinal training programs appear to be providing less extensive training in scleral buckling techniques than was true in years past.

2. Pneumatic Retinopexy

Pneumatic retinopexy (PR) was introduced in the United States by Hilton and Grizzard in the mid-1980s [19]. It is an office-based, sutureless alternative to scleral buckling and vitrectomy for the surgical repair of selected (superior) retinal detachments [see chapter V.B.7. Pneumatic retinopexy]. A bubble of pure air or an expansible, long-acting gas is injected into the vitreous, and the patient is positioned so that the bubble tamponades the retinal break(s), allowing endogenous resorption of subretinal fluid (Figure V.B.4-10). To form a permanent seal around responsible break(s), cryotherapy can be applied during the procedure, or laser photocoagulation can be administered after the retina becomes reattached. The “ideal” uncomplicated retinal detachment for a pneumatic procedure (PR) is one associated with a retinal break or closely localized group of breaks located between approximately 10:00 and 2:00 and extending no more than 1 clock hour in circumference, although RRDs from breaks between 8:00 and 4:00 are usually amenable to PR. Although the technique can be employed successfully when breaks are not located either superiorly or close together, fewer surgeons would select the procedure in these

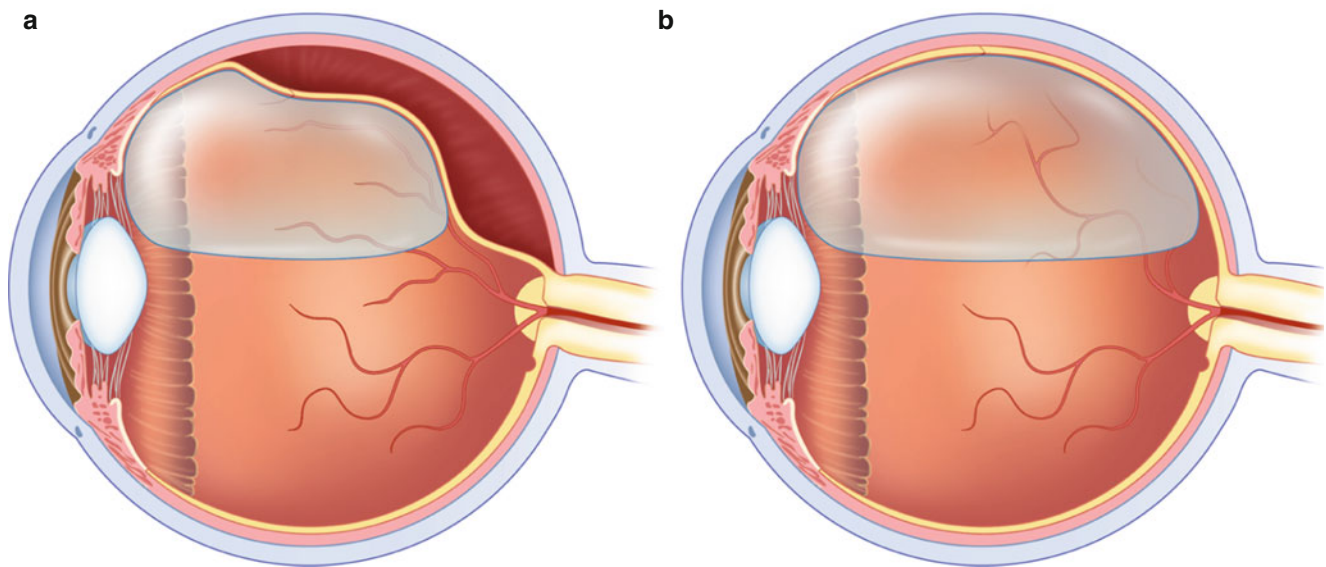


Figure V.B.4-10 Pneumatic retinopexy for retinal detachment. Injection of a gas bubble (a) internally closes the responsible retinal break. This allows the physiologic reattachment forces to remove the subretinal fluid and reattach the retina (b)

instances. Additional features that support the choice of PR include an apparently total PVD, the absence of retinal lattice and vitreous hemorrhage, and a phakic lens status.

PR is associated with approximately a 10 % reduction in single operation anatomical success rate when compared to scleral buckling [20], and the development of new inferior retinal breaks is a major cause of recurrent RRD [21], although it is very likely that many of these inferior breaks were not new, but missed retinal breaks [see chapter V.B.7. Pneumatic retinopexy]. Still, ultimate success following reoperation does not appear to be compromised. PR is therefore a procedure that represents a legitimate standard of care as an option to other forms of reattachment surgery. Interestingly, this operation is considerably more popular in the United States than in many parts of the world.

a. Advantages of Pneumatic Retinopexy

The primary advantages of PR are that it can be performed quickly in an office setting with modest local anesthesia and that it has an acceptable success rate. Patient morbidity is usually less than with alternative operations, and costs are considerably lower. Progressive cataract formation does not follow the procedure. Most importantly, perhaps, failed PR does not appear to compromise success with subsequent scleral buckling and/or vitrectomy [21].

b. Disadvantages of Pneumatic Retinopexy

The primary disadvantage of PR is that most surgeons limit its use to a relatively consistent subset of patients with single superior breaks and few signs of extensive vitreoretinal

degenerative disorders, and there are many common types of cases in which it should not be routinely employed (Table V.B.4-2). Additionally, even in carefully selected cases, the single operation anatomic success rate is approximately 10 % lower than for scleral buckling [20]. Still, there is no evidence that a failed PR procedure lowers the ultimate anatomic or visual success rate [21].

3. Vitrectomy

Retinal detachments that were initially managed with a “primary” vitrectomy were limited to relatively complicated cases with vitreous incarceration in cataract surgical wounds, severe vitreous hemorrhage, PVR, proliferative diabetic retinopathy (PDR), giant tears, etc., and the technique was not employed for more routine cases until the mid-1980s [22]. Since then this form of surgery has become tremendously popular, particularly in the management of pseudophakic cases.

The goals of vitrectomy for retinal detachment are to (1) remove media opacities such as vitreous hemorrhage or debris; (2) eliminate vitreoretinal (axial), preretinal (tangential), or subretinal traction; (3) identify and treat all retinal breaks; (4) internally reattach the retina; (5) facilitate placement of a large intraocular tamponade; and (6) avoid complications associated with scleral buckling surgery. The usual sequence of events includes removal of vitreous gel and preretinal membranes, identification of retinal breaks, internal drainage of subretinal fluid (via the retinal break(s) or a retinotomy), laser therapy to all responsible breaks and areas of significant vitreoretinal degeneration, and placement of an internal tamponade with gas or silicone oil (Figure V.B.4-11). Vitreous surgery is frequently combined

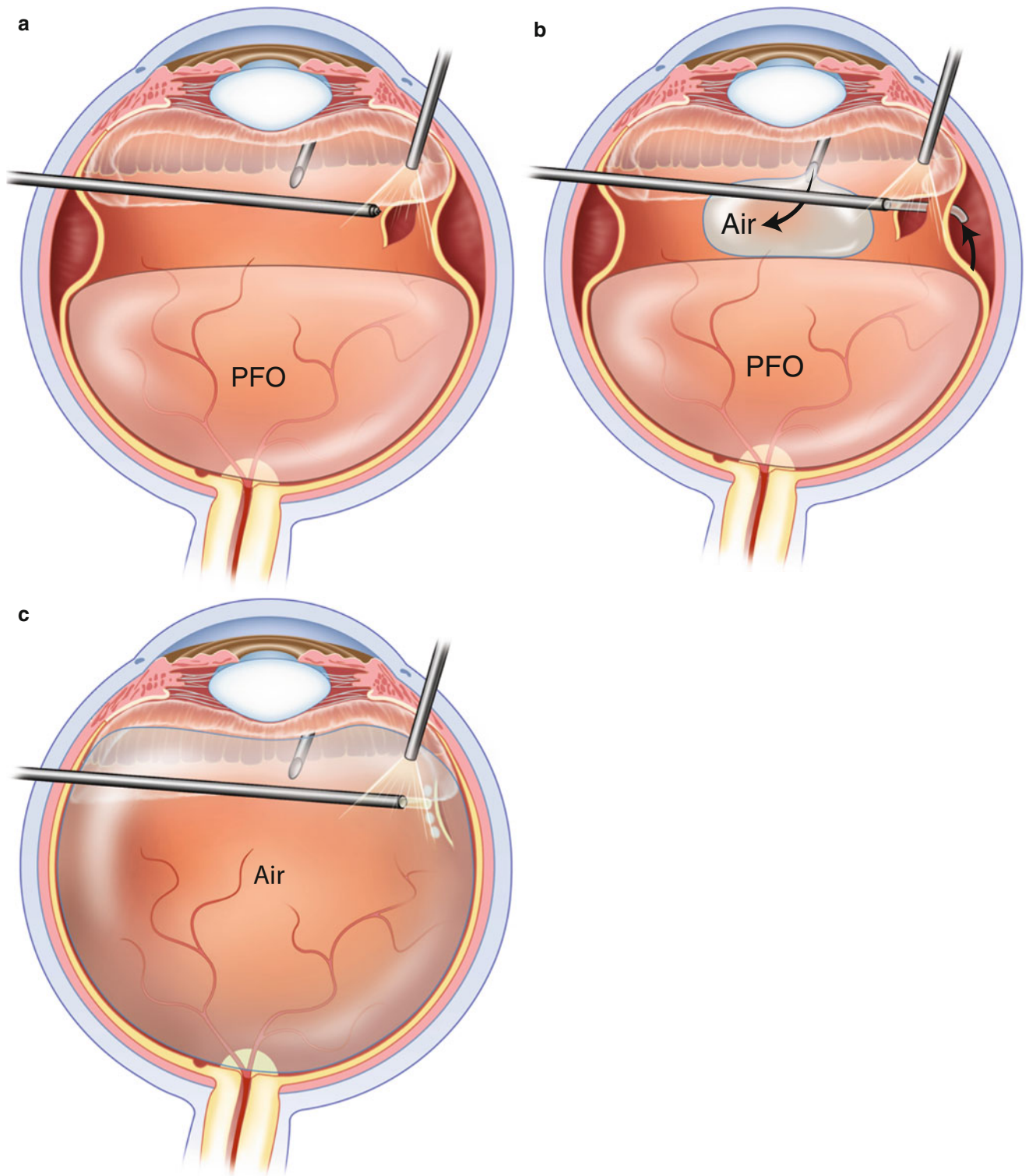


Figure V.B.4-11 Vitrectomy for retinal detachment. Perfluoro-octane has been injected to stabilize the posterior retina, and the vitreous is removed, eliminating traction forces upon the flap of the responsible horseshoe tear (**a**); subretinal fluid is removed internally (**b**) as air is injected. Perfluoro-octane is not routinely employed by many surgeons,

but if it is used, it is removed at this stage; following the air infusion, internal laser therapy (**c**) is then applied to surround all reattached retinal breaks. Non-expansile long-acting gases are exchanged for air in selected circumstances

with placement of a scleral buckle, although the pros and cons of this continue to be debated.

a. Advantages of Vitrectomy

The primary advantages of vitrectomy include the elimination of media opacities and transvitreal and periretinal membranous traction forces, improved visualization and localization of retinal breaks, internal intraoperative reattachment of the retina, and precise application of adhesive therapy. These steps can usually be accomplished without the complications that are relatively common following scleral buckling unless a buckling procedure is performed simultaneously with the vitrectomy.

b. Disadvantages of Vitrectomy

In phakic eyes, the routine development of postoperative nuclear sclerotic cataracts represents a major disadvantage, and there is some limited preliminary evidence that open-angle glaucoma may develop in pseudophakic vitrectomized eyes over decades following surgery [23]. The costs of vitrectomy are substantially higher than PR or scleral buckling. Failure of vitrectomy may be associated with the development of relatively severe forms of PVR, although considerably more research is needed to evaluate this phenomenon. A hopefully transient disadvantage is the lack of information regarding precise causes of failure following vitrectomy, and as additional data accumulate in regard to this relatively new technique, more answers will hopefully be forthcoming.

B. Surgery for Complicated Retinal Detachments

As mentioned above, scleral buckling was the only widely available method of retinal detachment repair for several decades through the 1980s. Vitreous surgery was introduced by Machemer in the early 1970s [24], and vitrectomy became increasingly employed in cases complicated by vitreous opacification, periretinal or transvitreal membrane formation, proliferative diabetic retinopathy, giant retinal tears, and other less common indications. A discussion of surgical techniques for these problems is beyond the scope of this chapter, but the management of PVR is discussed in chapter V.B.5 [Management of retinal detachment with PVR], and retinectomy techniques are presented in chapter V.B.6 [Retinectomy in recalcitrant retinal detachments].

IV. Conclusions

The fundamental goals of all forms of surgery for retinal detachment are the identification and closure of all responsible retinal breaks, and if these can be accomplished without complications and/or the development of PVR, the procedure will almost always be

successful. Currently, contemporary reattachment surgery is usually performed using one of the three techniques that have been described in this chapter or combinations thereof.

Although there is relative agreement among surgeons with regard to the use of vitrectomy for complicated retinal detachments, the management of less severe cases remains a most debatable topic but one that will hopefully become minimized by the development of more meaningful evidence bases in the future. In the meantime, surgeons will continue to select the procedure that they consider the best for a given case, and they will presumably be influenced in this regard by their training experiences, their observations of personal successes and failures, and their interpretations of data that continue to appear in the literature.

Abbreviations

AAO	American Academy of Ophthalmology
OCT	Optical Coherence Tomography
PDR	Proliferative Diabetic Retinopathy
PPP	Preferred Practice Pattern
PR	Pneumatic Retinopexy
PVD	Posterior Vitreous Detachment
PVR	Proliferative Vitreoretinopathy
RD	Retinal Detachment
RRD	Rhegmatogenous Retinal Detachment

References

1. Johnson M. Posterior vitreous detachment. Evolution and role in macular disease. *Retina*. 2012;32 Suppl 2:S174–8.
2. Sebag J. Anomalous posterior vitreous detachment: a unifying concept in vitreo-retinal disease. *Graefes Arch Clin Exp Ophthalmol*. 2004;242(8):690–8.
3. Shea M, Davis MD, Kamel I. Retinal breaks without detachment, treated and untreated. *Mod Probl Ophthalmol*. 1974;242(8):690–8.
4. American Academy of Ophthalmology Retina Preferred Practice Pattern Guidelines. Posterior vitreous detachment, retinal breaks, and lattice degeneration. San Francisco: American Academy of Ophthalmology; 2008. p. 1–24.
5. Hoveland KR. Vitreous findings in fellow eyes of aphakic retinal detachment. *Am J Ophthalmol*. 1978;86(3):350–3.
6. Wilkinson CP. Interventions for asymptomatic retinal breaks and lattice degeneration for preventing retinal detachment. *Cochrane Database Syst Rev*. 2012;3, CD003170. doi:10.1002/14651858.CD003170.pub3. Review.
7. Byer NE. Rethinking prophylactic therapy of retinal detachment. In: Stürpe M, editor. *Advances in vitreoretinal surgery*. New York: Ophthalmic Communications Society; 1992. p. 399–411.
8. Byer NE. Long-term natural history of lattice degeneration of the retina. *Ophthalmology*. 1989;96(9):1396–401.
9. Byer NE. Cystic tufts and their relationship to retinal detachment. *Arch Ophthalmol*. 1981;99(10):1788–90.

10. Byer NE. Long-term natural history study of senile retinoschisis with implications for management. *Ophthalmology*. 1986;93(9):1127–37.
11. Byer NE. What happens to untreated asymptomatic retinal breaks and are they affected by posterior vitreous detachment? *Ophthalmology*. 1998;105(6):1045–9.
12. Hikichi T. Time course of development of posterior vitreous detachment after phacoemulsification surgery. *Ophthalmology*. 2012;119(10):2102–7.
13. Folk JC, Arrindell EL, Klugman MR. The fellow eye of patients with phakic lattice retinal detachment. *Ophthalmology*. 1989;96(1):72–9.
14. Wilkinson CP. Prevention of retinal detachment. In: Ryan SJ, Wilkinson CP, Wiedemann P, editors. *Retina*. 5th ed. New York: Saunders/Elsevier; 2013. p. 1793–805.
15. Wolfensberger TJ, Aylward GW, Leaver PK. Prophylactic 360 degree cryotherapy in fellow eyes of patients with spontaneous giant retinal tears. *Ophthalmology*. 2003;110(6):1175–7.
16. Ang A, Poulson AV, Goodburn SF, et al. Retinal detachment and prophylaxis in type 1 stickler syndrome. *Ophthalmology*. 2008;115(1):164–8.
17. Davis MD. The natural course of retinal breaks without detachment. *Trans Am Ophthalmol Soc*. 1973;71:343–72.
18. Aylward GE. Optimal procedures for retinal detachment repair. In: Ryan SJ, Wilkinson CP, Wiedemann P, editors. *Retina*. 5th ed. New York: Saunders/Elsevier; 2013. p. 1784–92.
19. Hilton GF, Grizzard WS. Pneumatic retinopexy—a two-step outpatient operation without conjunctival incision. *Ophthalmology*. 1986;93(5):626–40.
20. Sharma S. Meta-analysis of clinical trials comparing scleral buckling surgery to pneumatic retinopexy. *Evid Base Eye Care*. 2002;3(1):125–8.
21. Mudvari SS, Ravage ZB, Rezaei KA. Retinal detachment after primary pneumatic retinopexy. *Retina*. 2009;29(10):1474–8.
22. Escoffery RE, Olk RJ, Grand MC, et al. Vitrectomy without scleral buckling for primary rhegmatogenous retinal detachment. *Am J Ophthalmol*. 1985;99(3):275–81.
23. Chang S. LXII Jackson lecture: open angle glaucoma after vitrectomy. *Am J Ophthalmol*. 2006;41(6):1033–43.
24. Machemer R, Buettner H, Norton EWD, et al. Vitrectomy: a pars plana approach. *Trans Am Acad Ophthalmol Otolaryngol*. 1971;75(4):813–20.

Ankur N. Mehta and Gary W. Abrams

Outline

- I. **Introduction**
- II. **Diagnosis and Classification**
 - A. Clinical Findings
 - B. Posterior PVR
 - C. Anterior PVR
- III. **Surgical Management**
 - A. Principles of Surgery
 - B. Techniques of Surgery
 1. Lens Removal
 2. Scleral Buckle
 3. Vitrectomy
 4. Membrane Peeling
 5. Relaxing Retinotomies and Retinectomies
 6. Reattachment of the Retina
 7. Laser Photocoagulation
 8. PFCL Removal
 9. Fluid or PFCL-Silicone Oil Exchange
 10. Intraocular Tamponade
 - C. Postoperative Management
- IV. **Prognosis and Results**

References

Keywords

Proliferative vitreoretinopathy • Rhegmatogenous retinal detachment • Surgical management • Preretinal membrane • Silicone oil

Key Concepts

1. The pathophysiology of proliferative vitreoretinopathy (PVR) is now better understood and there are effective strategies to prevent as well as treat PVR, based upon its diagnosis and classification.
2. The preoperative and postoperative management of PVR is as important as the surgery.
3. The surgical management of proliferative vitreoretinopathy includes relief of tractional forces, closure of retinal breaks and maintaining long-term stabilization of the retina.

I. Introduction

Proliferative vitreoretinopathy (PVR) is a term coined by the Retina Society Terminology Committee in 1983 to describe retinal detachment caused by contractile cellular membranes on the retina and vitreous following rhegmatogenous retinal detachment (RRD) [1]. Contraction of these membranes can lead to new retinal detachments (RD) or failure of surgically corrected detachments. PVR still remains the leading cause of failure in retinal detachment surgery, occurring in 5–10 % of all RRDs, and remains a major barrier to successful repair of RDs [2].

The events leading to the formation of PVR can be summarized as follows: First, a retinal break must be present that allows retinal glial cells and retinal pigment epithelium (RPE) cells into the vitreous cavity or on the surface of the

A.N. Mehta, MD • G.W. Abrams, MD (✉)
Department of Ophthalmology, Kresge Eye Institute/Wayne State
University School of Medicine, Detroit, MI, USA
e-mail: amehta@med.wayne.edu; gabrams@med.wayne.edu

inner or outer retina. At the same time, a breakdown in the blood-retinal barrier occurs which further enhances cell migration and proliferation, potentiated by the hyalocytes [see chapter II.D. Hyalocytes]. These cells then undergo transformation, attaining fibroblast-like qualities and proliferating in a membranous sheet. Various cytokines have been found in the retina and vitreous which play a role in the migration and proliferation of RPE cells [see chapter III.J. Cell proliferation at vitreo-retinal interface in PVR and related disorders]. The fibroblast-like cells, which have intrinsic contractile properties, then pull and contract collagen fibrils that lead to tractional forces on the vitreous and retina. This ultimately leads to tractional retinal detachments and RRDs due to the formation of new breaks. Finally, fixation of the contracted membranous sheets and bands and fixed folds of the retina occurs with deposition of new collagen. PVR involvement is most severe in the inferior retina. This is likely due to RPE cells settling on the inferior retina due to gravity and then proliferating.

Multiple studies have tried to identify risk factors for the development of PVR. These can be divided into pre- and postoperative risk factors. Preoperative risk factors include multiple and giant retinal tears, long duration of retinal detachment, aphakia, vitreous hemorrhage, presence of choroidal detachments, and the presence of uveitis [3, 4]. Postoperative risk of PVR is increased by the presence of preoperative PVR, intraocular hemorrhage, the use of air or gas in surgery, excessive cryotherapy, diathermy or photocoagulation, loss of vitreous during subretinal fluid drainage, the use of vitrectomy in the repair of RD, and repeated surgical procedures [5–7].

Vitreous plays a key role in PVR. It becomes hazy with pigment clusters and contains cells (hyalocytes), growth factors, and cytokines that stimulate proliferation of cellular membranes on the retina. Vitreous may become adherent to the retina and the preretinal membranes that are present as the PVR matures (see section III.B.3 below). Cellular contraction may also cause the vitreous body to contract when PVR matures as evidenced by the contraction of the vitreous base causing retinal foreshortening in anterior PVR. We have also found certain vitreous types more prone to PVR than others. Patients with vitreoretinal degenerations such as hereditary progressive arthro-ophthalmopathy (Stickler syndrome) are more prone to PVR because of abnormal and tightly adherent vitreoretinal adhesions [see chapter I.C. Hereditary vitreo-retinopathies]. During surgery, these adhesions are so strong that they may prevent separation of the vitreous and membranes from the retina. It may be necessary to section the vitreous at the retinal surface with scissors rather than peel the vitreous and membranes. Younger patients with RRDs are also more prone to develop PVR. Also, in our experience, patients with vitreoschisis

[see chapter III.B. Anomalous PVD and vitreoschisis] develop PVR more frequently than those without.

II. Diagnosis and Classification

A classification system developed by the Retina Society in 1983 was used to describe the extent and severity of PVR [1]. This system was broken down into four grades based on vitreous and retinal mobility, extent of fixed retinal folds, and configuration of the retinal detachment (Table V.B.5-1). This proved to be inadequate because it failed to characterize anterior PVR and did not characterize the different types of contraction. In 1991, this system was updated to include both anterior and posterior PVR and the different types of contraction in Grade C PVR [8]. Also, the extent of contraction

Table V.B.5-1 The Retina Society classification of retinal detachment with PVR

Grade	Clinical signs
A	Minimal vitreous haze Vitreous pigment clumps
B	Moderate wrinkling of the inner retinal surface Rolled edge of retinal break Retinal stiffness Vessel tortuosity
C	Marked full-thickness fixed retinal folds
C1	One quadrant
C2	Two quadrants
C3	Three quadrants
D	Massive fixed retinal folds in four quadrants
D1	Wide funnel shape
D2	Narrow funnel shape
D3	Closed funnel

Table V.B.5-2 Updated classification of PVR described by grade

Grade	Clinical signs
A	Vitreous haze Vitreous pigment clumps Pigment clusters on inferior retina
B	Wrinkling of the inner retinal surface Rolled and irregular edges of retinal break Retinal stiffness Vessel tortuosity Decreased mobility of vitreous
CP1-12^a	Posterior to equator Focal, diffuse, or circumferential full-thickness folds Subretinal strands
CA1-12	Anterior to equator Focal, diffuse, or circumferential full-thickness folds Subretinal strands Condensed vitreous with strands

^aExpressed in the number of clock hours involved

Table V.B.5-3 Grade C PVR described by contraction type

Type	Location	Features
Focal	Posterior	Star fold posterior to vitreous base
Diffuse	Posterior	Confluent star folds posterior to vitreous base Optic disc may not be visible
Subretinal	Posterior/anterior	Proliferations under retina “Napkin ring” around disc “Clothesline” Moth-eaten appearing sheets
Circumferential	Anterior	Contraction along posterior edge of vitreous base with central displacement of the retina Peripheral retina stretched Posterior retina in radial folds
Anterior displacement	Anterior	Vitreous base pulled anteriorly by proliferative tissue Peripheral retinal trough Ciliary processes may be stretched or may be covered by membrane Iris may be retracted

was defined according to the number of clock hours encompassed by PVR (Tables V.B.5-2 and V.B.5-3).

A. Clinical Findings

Grade A is the earliest phase and includes vitreous haze, pigment clumps, and pigment clusters, usually on the inferior retina. *Grade B* PVR involves superficial wrinkling of the retina and increased retinal stiffness. Retinal breaks develop rolled edges and there is an overall decrease in mobility of the vitreous and retina (Figure V.B.5-1). *Grade C* PVR is divided into anterior and posterior PVR and includes full-thickness retinal folds (Figure V.B.5-2). Posterior PVR consists of focal and diffuse contraction of the retina due to proliferation and contraction of preretinal and/or subretinal membranes posterior to the equator (Figure V.B.5-4), while anterior PVR encompasses focal or diffuse retinal contraction due to proliferation and contraction of preretinal and/or subretinal membranes at or anterior to the equator and includes anterior retinal displacement (Figure V.B.5-3).

B. Posterior PVR

In posterior PVR, the most common type of contraction is the star fold which is due to contraction of a focal cellular membrane on the retinal surface posterior to the vitreous base. The fixed retinal folds that develop radiate away from the epicenter of cellular proliferation, resulting in the star fold configuration (Figure V.B.5-4). Retinal contraction occurs in two varieties: focal and diffuse. A focal contraction is localized to less than four disc areas in size, while diffuse contraction involves four or more disk areas, often with multiple, confluent epicenters of proliferation. The optic disc

may be obscured by retinal contraction in diffuse posterior PVR. Also, subretinal membranes can develop due to cellular proliferation beneath the retina. Clinically, retinal contraction due to subretinal membranes can be seen as retinal folds without preretinal membranes or typical star fold configuration. Subretinal membranes can present as an annular constriction of the retina anterior to the optic disc (“napkin-ring” configuration), a linear fold with a strand of membrane beneath the retina (“clothesline” configuration), or as a diffuse membrane (“moth-eaten” appearance) (Figure V.B.5-5a-c).

C. Anterior PVR

Anterior PVR is due to cell proliferation and membrane contraction in the peripheral retina at or anterior to the equator and at the posterior vitreous base. The two main types of retinal contraction are circumferential contraction and anterior retinal displacement. In circumferential anterior PVR, the posterior edge of the vitreous base contracts causing circumferential shortening and displacement of the retina centrally toward the vitreous cavity. Radial retinal folds extend posterior to the vitreous base. Inward contraction of the vitreous base may cause stretching of the ciliary body substance leading to hypotony and further breakdown of the blood-aqueous barrier [9, 10].

III. Surgical Management

A. Principles of Surgery

The key principles in the management of PVR are preoperative management to reduce surgical inflammation, surgical relief of tractional forces, and closure of retinal

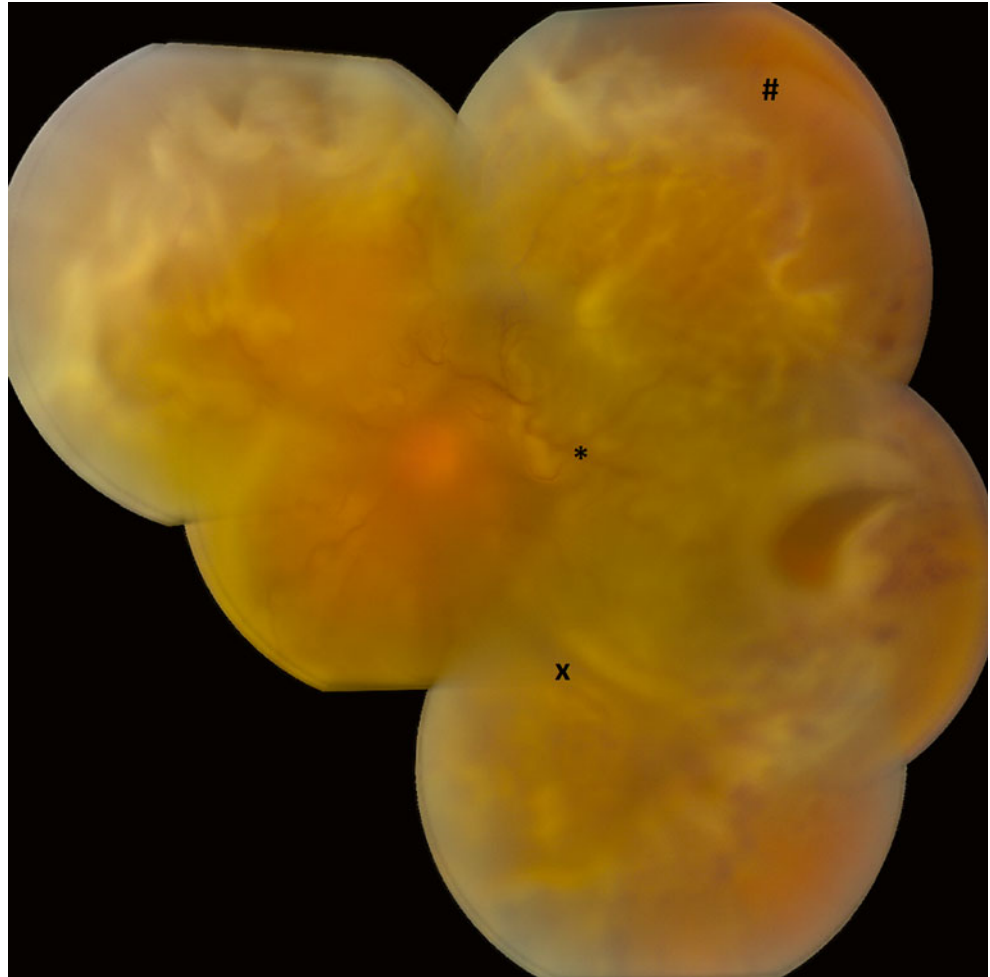


Figure V.B.5-1 Grade B PVR: wrinkling of the retinal surface and retinal stiffness

breaks [11]. Postoperative management is important for maintaining long-term stabilization of the retina. Studies of preoperative management of PVR have shown mixed results. A recent prospective placebo-controlled double-blind clinical trial by Jonas et al. [12] showed that 0.5 ml of subconjunctival dexamethasone 6 h preoperatively resulted in decreased laser flare measurements at 1 week postoperatively, suggesting that steroid priming might be useful.

Koerner and colleagues [13] randomized eyes with retinal detachments at high risk of PVR to systemic corticosteroids or placebo starting the day of surgery and continuing with taper for 15 days postoperatively. While there was no significant difference in visual acuity or the incidence of recurrent retinal detachment between the groups, corticosteroid-treated patients had significantly less premacular membrane formation in the operated eyes. We start patients

Figure V.B.5-2 Combined anterior C12 and posterior C12 PVR. Circumferential anterior contraction: contraction and inward displacement of posterior vitreous base with stretching of peripheral retina (#), radial fold extending from contracted vitreous base posteriorly (x), diffuse posterior contraction (*)



with no medical contraindications to corticosteroid therapy on oral prednisone 1.5 mg/kg beginning 2 days prior to complex PVR surgery and continue with tapering doses for 7–10 days postoperatively.

Visualization is paramount in order to perform effective surgery. Corneal opacities can arise from multiple reasons but are most commonly due to epithelial edema. If this limits adequate visualization, then the epithelium should be removed. Opacities deeper in the cornea, such as stromal opacities or corneal blood staining, may require intraoperative placement of a temporary keratoprosthesis followed by penetrating keratoplasty at the end of the case [14–17]. The temporary keratoprosthesis provides good intraoperative visualization of the posterior pole and peripheral retina.

If the pupil does not dilate adequately, we dilate and stretch the pupil mechanically using iris hooks [18]. First, all synechiae are lysed and capsular material removed. Then, a Ziegler-type blade is used to make limbal openings just anterior and parallel to the iris plane in 4 quadrants, typically 90°

apart. These are self-sealing wounds that do not need corneal sutures at the end of the case. The iris hooks are then passed through the limbal incisions and hooked on the edge of the pupillary border and retracted. The hooks are secured externally with a small plastic locking device.

Most phakic eyes will require removal of the lens, even if clear. Anterior membranes and the anterior vitreous cortex should be removed along with a complete vitreous base dissection during vitrectomy in PVR cases. Complete anterior dissection is not possible in the phakic eye. Failure to adequately remove peripheral vitreous can greatly increase the likelihood of recurrent anterior PVR. In addition, prolonged gas tamponade will almost always cause a cataract necessitating later lens removal. Management in the postoperative period, including the ability to do a fluid-gas exchange and to administer postoperative laser photocoagulation, is facilitated by lens removal. Strategies for lens management include lensectomy at the time of vitrectomy for PVR or phacoemulsification and placement of a posterior chamber intraocular lens (PCIOL) either prior to (at a separate

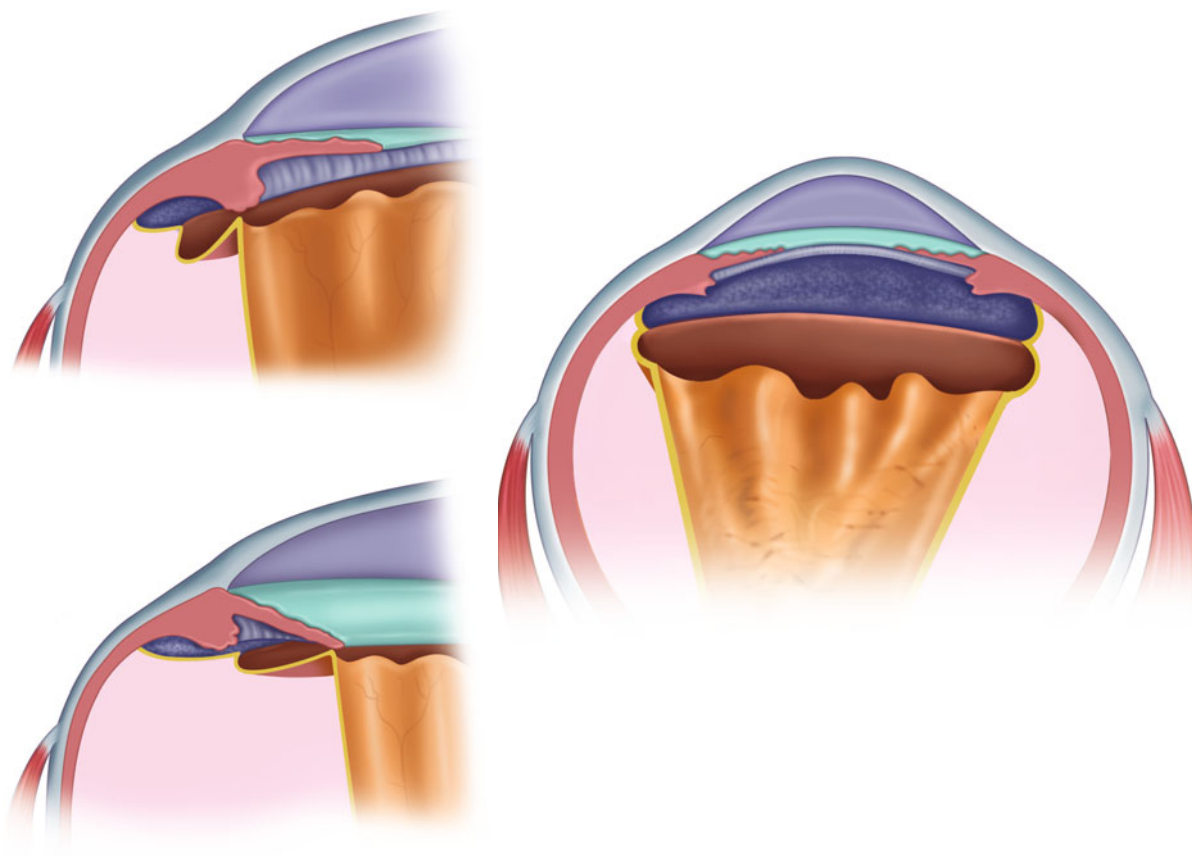


Figure V.B.5-3 Anterior PVR causes anterior retinal displacement (adapted from [27], reproduced with permission)

surgery) or at the time of surgery for PVR. We prefer to do cataract surgery 1–2 weeks prior to retinal surgery as there may be more breakdown of the blood-ocular barrier and fibrin formation when cataract surgery is done simultaneously. The risks and benefits of staged surgery should be weighed against the potential visual disadvantage of delaying repair of the retinal detachment. For most cases with advanced PVR, the 1- or 2-week delay for the retinal surgery will not likely affect the visual outcome. An existing PCIOL in a pseudophakic patient can usually be left in place as adequate dissection of the vitreous base and anterior membranes can still be achieved. If anterior proliferative tissue is adherent to the posterior capsule hindering visualization or if the PCIOL is unstable, then the IOL should be removed through the limbus. Anterior chamber intraocular lenses (ACIOL) are challenging because postoperative intraocular gas may push the ACIOL complex forward against the corneal endothelium increasing the chances of corneal decompensation and bullous keratopathy. Moreover, gas or silicone oil can easily prolapse around the ACIOL and touch the cornea

degrading the retinal view intraoperatively and postoperatively. If the ACIOL is unstable or poorly fixated, it is often best to remove the IOL through the limbus and leave the patient aphakic.

B. Techniques of Surgery

1. Lens Removal

The crystalline lens is removed through the pars plana, except in cases with extremely hard nuclei, in which case the nucleus may be best removed through the limbus. Following ultrasonic fragmentation of the nucleus and cortex, the vitrector is used to cut an opening in the anterior capsule. Forceps are then used to grasp the peripheral capsule and pull on it to expose the zonules. While retracting the capsule, the zonules can be cut by the vitrector or vertical scissors through the opposite sclerotomy site [19] (Figure V.B.5-6). We feel it is important to remove the capsule completely to decrease the likelihood of recurrent anterior PVR and to

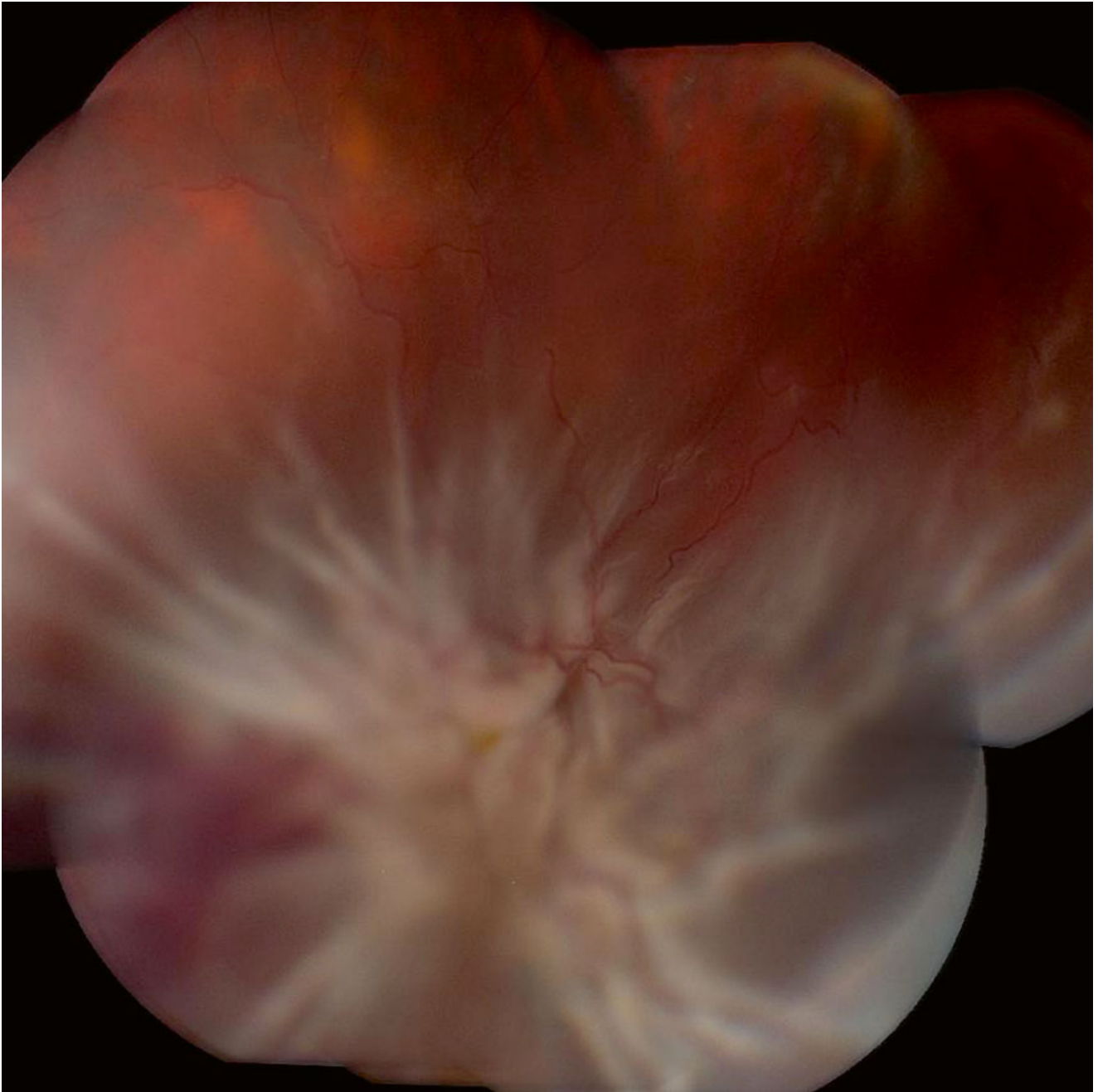


Figure V.B.5-4 Diffuse posterior PVR, star fold configuration

prevent synechiae of the iris to the lens capsule that can result in a distorted, fixed pupil.

2. Scleral Buckle

We recommend placement of a scleral buckle (if not already present) in most cases with PVR. Low-grade PVR (grade A or B and limited grade C) cases can often be managed with a scleral buckle alone. In many instances of retinal re-detachments with PVR, a scleral buckle is already present

from the initial surgery. These rarely need to be revised or replaced and can be left in place. At times, however, it is necessary to supplement an existing scleral buckle, especially inferiorly if adequate support is not present. Eyes with extensive retinectomies or giant tears, especially those greater than 180°, may not need a scleral buckle.

The goals of scleral buckling are to relieve traction and support the vitreous base and to facilitate closure of peripheral retinal breaks. The vitreous base should be supported

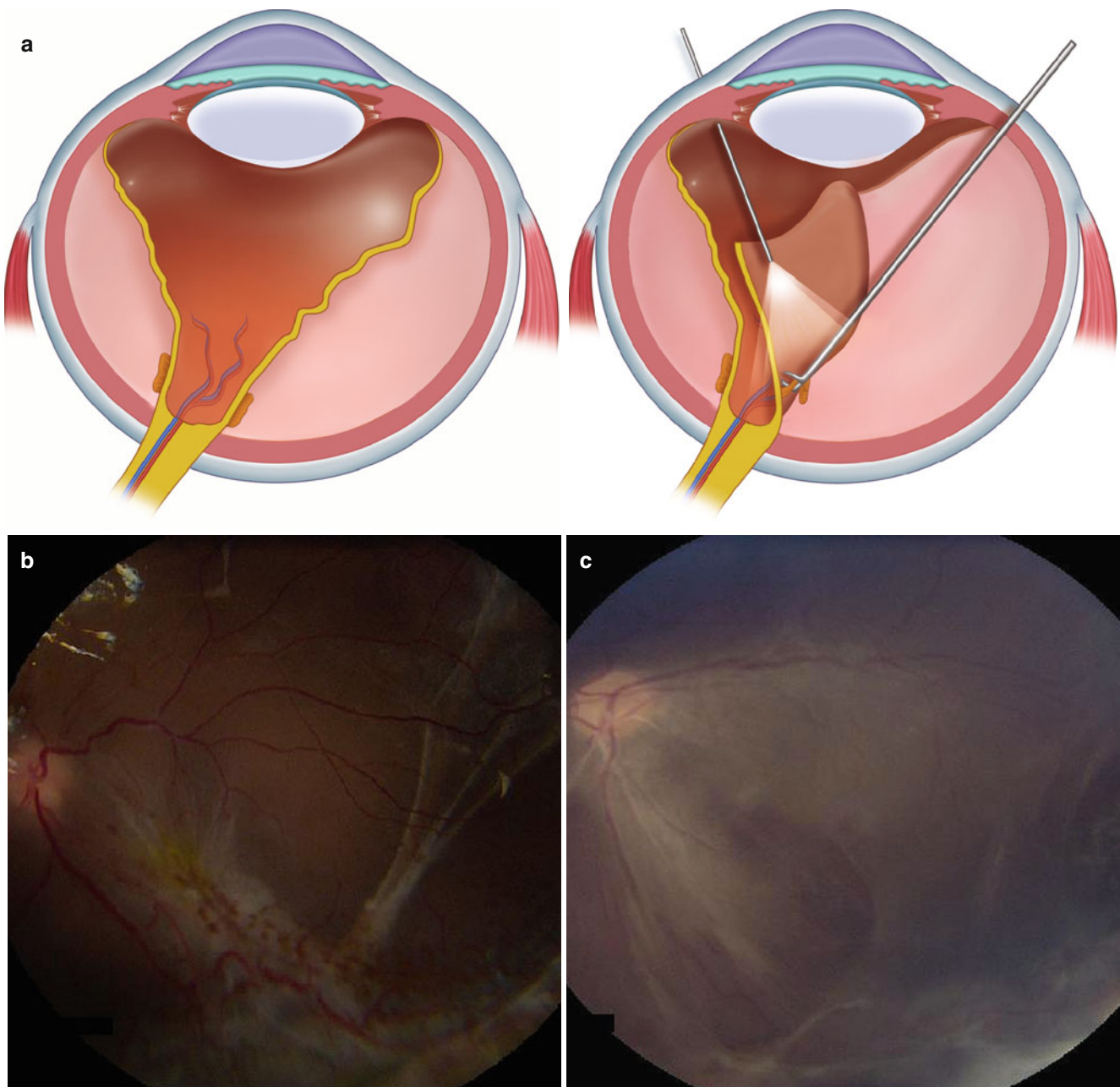


Figure V.B.5-5 (a) “Napkin-ring” configuration (from [49]. Reproduced with permission) (b) “clothesline configuration” with linear fold of subretinal membrane, and (c) “moth-eaten” appearance with diffuse membrane

for 360° by the element. A moderately high and broad indentation is ideal and helps to relieve anterior traction. The width of the scleral buckle will vary with the location of the breaks and the vitreous base. In most cases, we use a 4.5-mm-wide encircling band (42 band) with sutures placed 1.5 mm wider than the buckle (6 mm) to increase indentation and height. If the vitreous base extends more posterior, a silicone tire or sponge can be used. Placing the anterior suture for the sclera buckle approximately 2 mm posterior to the muscle

insertion ring usually places the buckle in a position to support the vitreous base and the retina just posterior to the vitreous base. In cases involving scleral buckle and vitrectomy, we prefer to pre-place the sutures for the buckle in each quadrant prior to creating sclerotomies for the vitrectomy. This is because the eye is firmer prior to making the sclerotomies, and it is easier to place the sutures safely. After the vitrectomy is completed, the buckling element is then placed around the eye.

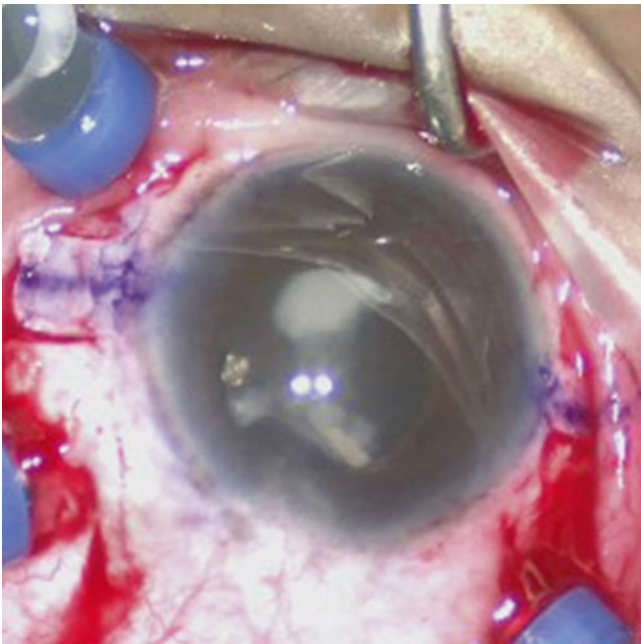


Figure V.B.5-6 Capsular removal using vitrector and forceps

3. Vitrectomy

A three-port pars plana vitrectomy system is used for surgery. Historically, complex PVR cases were performed using the larger bore 20-gauge system. More recently, microincisional vitrectomy surgery (MIVS) has supplanted larger gauge surgery. Studies have shown that surgical outcomes using MIVS are equal to and non-inferior to the standard 20-gauge system [20–22]. There are, however, distinct advantages and disadvantages to each system. An advantage of MIVS is that sutures are not required at the close of cases as long as the wound architecture is sound [23]. This confers the benefit for faster wound healing, reduced operative time, and less overall patient discomfort. However, in cases that have had previous vitrectomy, the wounds may not adequately seal due to thinning of the sclera and scarring. Thus, in cases with silicone oil, it may be best to always suture the sclerotomy sites to prevent subconjunctival silicone oil. Even if suturing the sclerotomy sites is necessary, there are other advantages to MIVS. The reduced infusion flow and the presence of cannulas, especially self-sealing cannulas, reduce the risk of incarceration of mobile retina in the sclerotomy sites. In addition, with self-sealing cannulas, there is reduced turbulence and, therefore, less of a chance of bubbles that can be retained beneath the retina when perfluorocarbon liquid is used.

A potential disadvantage of MIVS is reduced rigidity, causing increased flexibility that might make complex maneuvers and working in the far peripheral fundus more difficult. However, 23-gauge instruments and newly designed 25-gauge instruments maintain adequate rigidity so periph-

eral membrane dissection and shaving of the vitreous base can be easily performed. In 20-gauge surgery, the overall duration of vitrectomy is faster due to higher flow dynamics. However, compared to MIVS cases that do not require suturing of sclerotomy sites, this time benefit is lost when factoring in the time to suture wounds. Additionally, pars plana phacoemulsification currently requires 20-gauge instruments.

We prefer using a 23-gauge vitrectomy system. We first displace the conjunctiva using forceps and insert the cannula using a trocar and cannula system through the sclera 3.5 mm posterior to the limbus. In cases where anterior PVR pulls the retina anteriorly, the sclerotomies are made more anteriorly. After the cannula is well set, the trocar is removed. Cannulas are placed in the inferotemporal, superonasal, and superotemporal quadrants. The infusion cannula is placed in the inferotemporal quadrant and the tip is visualized prior to starting the infusion to make sure it has completely cleared the pars plana into the vitreous cavity to prevent subretinal or choroidal infusion. The risk of subretinal infusion is greatest in eyes with anterior PVR and anterior retinal displacement. A 4 mm infusion cannula is typically used; however, longer infusion cannulas can be used in cases with anterior membranes obstructing the surgeon's view.

Many lens systems have been developed to view the retina during surgery. Some surgeons prefer suturing a lens ring to the limbus in order to utilize plano-concave and prismatic lenses to view the posterior pole and periphery, respectively. We prefer using a non-contact wide-angle viewing system (BIOM, OCULUS Surgical Inc, Port St. Lucie, FL) that permits a viewing field of 130°. This allows for adequate visualization for peripheral vitrectomy and anterior dissection of membranes, often without the need for scleral depression. This system is also very useful for constricted views due to opacified capsules or small pupils. The major limitations of the wide-angle system are the reduction in stereopsis that makes fine membrane dissection difficult. For the posterior pole, a disposable plano-concave lens works well for membrane peeling and fine dissection, giving a 36° field of view and 1× magnification.

If there has been no previous vitrectomy, the core vitreous is removed first followed by removal of the peripheral vitreous. Posterior vitreous detachment (PVD) is usually present in cases of PVR. If separation has not occurred (sometimes seen in traumatic PVR, degenerative myopia, or vitreoretinal degenerations), a PVD must be induced using the cutter or a suction catheter at the disc. If the vitreous is strongly adherent to the retina, as can be seen in vitreoretinal degenerations such as Stickler or Wagner syndrome, the vitreous should be shaved and sectioned as close to the retina as possible. Next, vitrectomy proceeds with shaving the vitreous to the surface of the peripheral retina and to the vitreous base. Scleral depression by an assistant will help to visualize the vitreous base at this point; however, as mentioned before, the

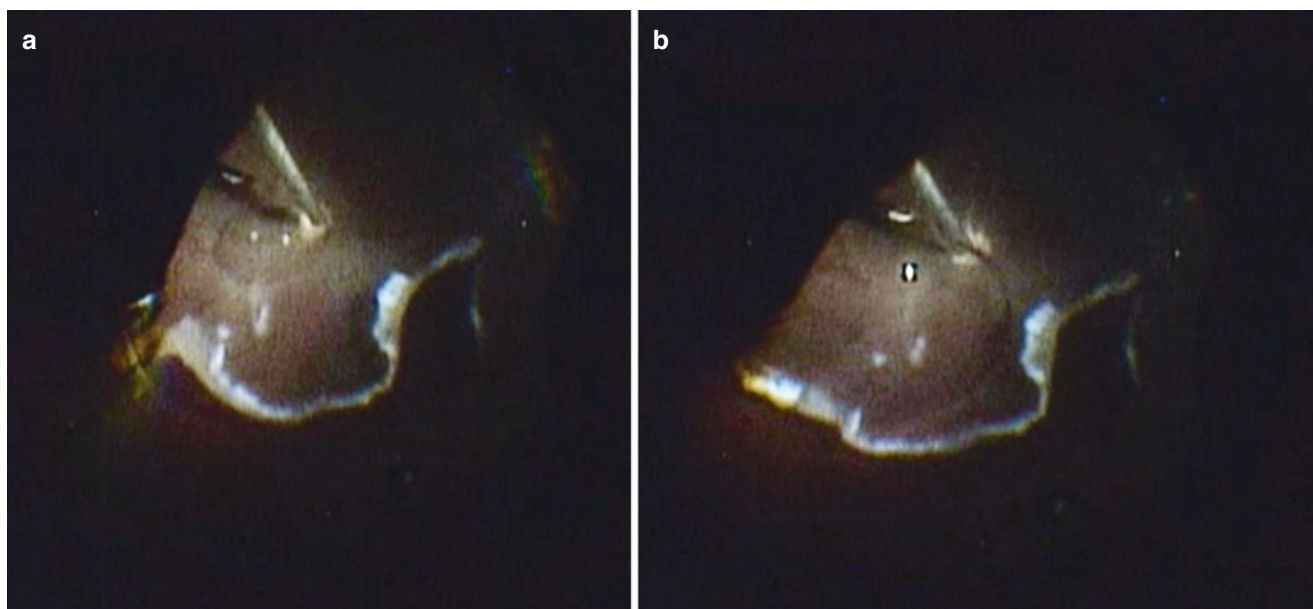


Figure V.B.5-7 Giant retinectomy with elevated, folded edges. (a) Perfluorocarbon liquid injected over optic disc. (b) Enlarging perfluorocarbon bubble unfolds and flattens edge of retinectomy

wide-angle viewing system may provide sufficient visualization. If significant anterior PVR is present, extensive shaving of the vitreous base and sectioning of anterior membranes should be delayed until removal of all posterior membranes [24]. Posterior and mid-peripheral membranes often extend anteriorly, and starting the peeling process posteriorly often facilitates anterior membrane removal. As the posterior membranes are removed, the retina may become more mobile and bullous. This may limit anterior dissection and increase the risk of peripheral retinal damage. Perfluorocarbon liquid (PFCL) can be used to stabilize the posterior retina to allow safe removal of peripheral vitreous and anterior membranes [25] (Figure V.B.5-7a, b). Only a small amount of PFCL is used during dissection so the PFCL does not compress peripheral vitreous and membranes.

The posterior cortical vitreous is often incorporated into the peripheral preretinal membranes when they form and contract, dragging the vitreous posterior to the vitreous base and sometimes even posterior to retinal tears. It is important to completely strip the posterior vitreous cortex anteriorly to the vitreous base. This is done by using forceps to grasp the edge of the adherent posterior vitreous cortex and lifting centrally while holding the retina back with the blunt surface of an illuminated pick to separate the vitreous cortex from the peripheral retina. Alternatively, the vitrectomy cutter set to suction-only mode can sometimes be used to grasp the posterior vitreous cortex edge and pulled centrally relieving any adherence and traction. An adjunct to help with visualization of the cortical vitreous and membranes is triamcinolone acetonide [26]. We use 0.1–0.2 ml of a suspension of triamcinolone acetonide 40 mg/cc diluted in balanced saline



Figure V.B.5-8 Illuminated pick and forceps used for membrane peeling

solution in a 1:5 ratio. This nicely highlights any remaining adherent cortical vitreous for removal.

4. Membrane Peeling

We prefer to use an illuminated pick and a vitreoretinal forceps for membrane peeling (Figure V.B.5-8). The illuminated pick should have a rounded, relatively blunt tip as

sharp tips will more likely perforate the retina. A good general-use forceps is the de Juan pick forceps (Synergetics, Inc, O'Fallon, MO) that has a pick for elevating membranes and a platform that grasps membrane well. However, sometimes a non-pick, end-grabbing forceps works best for grasping adherent membranes. Preretinal membranes at the posterior pole are best removed using a bimanual technique. Thicker membranes can be directly grasped by the forceps and stripped in a posterior to anterior fashion. Often, large membranes can be stripped off in a single sheet. If the membrane is thin and less distinct, the illuminated pick can be used to elevate it, then grasp with forceps and strip it. Posterior membranes usually can be easily identified, but extensive confluent membranes can obscure edges. To manage this, the illuminated pick or pick forceps can be placed in a retinal fold and dragged to the center of the fold to engage the membrane. Once it is engaged and an edge is created, a forceps can be used to grab the edge. As the forceps pulls the membrane centrally, the blunt portion of the pick is placed against the retina to give countertraction as the membrane is pulled centrally. The illuminated pick can be placed between the membrane and retina to completely separate the membrane. Another technique used for tightly adherent membranes is to use a barbed micro-vitreoretinal (MVR) blade to initially engage the membrane and then strip it using the technique described above.

If an excessively tight adhesion is found, aggressive force should not be applied because a retinal tear can occur. Instead, vertical cutting scissors or curved scissors can be used to segment the membrane from the retina to relieve traction. Very immature membranes are extremely friable and not easily grasped for removal. If left fragmented on the retinal surface, these can act as epicenters of re proliferation and therefore should be removed completely. In these situations, a backflush brush with a silicone tip can be used to gently "stroke" the immature membranes off the retinal surface and help remove any pigment dusting.

As mentioned previously, once all posterior and peripheral membranes are moved, the retina will become bullous and mobile. Prior to anterior membrane dissection and to facilitate peripheral membrane and vitreous removal, PFCL should be used to stabilize the posterior retina [25]. Initially, a small volume of PFCL is injected over the optic nerve so as not to cover any remaining vitreous. More is injected to flatten the retina further as the dissection is carried more anteriorly. PFCL should never be injected directly over a retinal break as it can go subretinal. Excessive traction on the retina in the presence of retinal breaks can cause PFCL to enter the subretinal space, but isolated, smaller posterior breaks not under traction are not a contraindication to the use of PFCL. Typically, PFCL is not used for dissection when large posterior retinal breaks are present. Instillation of PFCL may make subretinal membranes apparent if the posterior retina

does not flatten. This will necessitate removal of some of the PFCL for subretinal membrane removal (described later).

If anterior PVR is present, it must also be dissected and segmented [27]. Anterior focal and diffuse membranes are removed using the same techniques as in posterior membranes. Often, subretinal membranes become visible only after the preretinal membranes have been removed. Anterior retinal displacement is more difficult to manage. A circumferential retinal trough may be present at the vitreous base caused by the retina at the posterior aspect of the vitreous base being pulled anteriorly to the pars plana or more anterior structures. This can be difficult to visualize but telltale signs of anterior retinal displacement include obscuration of the ora serrata and a fibrous circumferential membrane attached to the pars plana, pars plicata, and/or ciliary processes.

A sharp-tipped MVR blade works well to open membranes bridging the anteriorly displaced retina to anterior structures. Once the membrane is opened, vertical cutting scissors can be used to section the membranes circumferentially. As this occurs, the anterior-posterior traction will be relaxed and the anteriorly displaced retina will fall posterior to its normal position. Any membrane remnants can exert traction and should be trimmed using the vitrectomy cutter or sectioned or amputated with scissors while countertraction is applied using the illuminated pick or forceps by bimanual technique. All membranes should be removed; however, if this is not possible due to tightly adherent membranes, they should be sectioned radially to eliminate circumferential traction. Any vitreous left in the trough should be shaved back as close to the peripheral retina as possible as well. Retinal breaks that are created during the sectioning process should be identified and all traction relieved around the breaks. In some instances, it is not possible to adequately relieve anterior contraction necessitating a peripheral circumferential relaxing retinectomy (see below).

Subretinal membranes can be present in up to half of PVR cases but rarely do they prevent retinal reattachment and need to be removed [28]. Sometimes, subretinal membranes that appear to be causing traction will relax after PFCL injection or fluid-gas exchange. In instances where they do not relax and preclude retinal reattachment, they must be removed. This should only be done after all posterior and anterior membranes have been dissected. Localized subretinal membranes and those having a "clothesline" configuration can often be removed through a small retinotomy. An adjacent retinotomy is created with diathermy that simultaneously marks the retinotomy for further laser and prevents bleeding. Then, forceps are inserted and the membrane is grasped with gentle traction applied in a back-and-forth motion to help loosen the adherent membrane. Frequent regripping of the membrane as it is pulled out will help prevent the membrane from breaking and from inadvertently enlarging the retinotomy. Sometimes

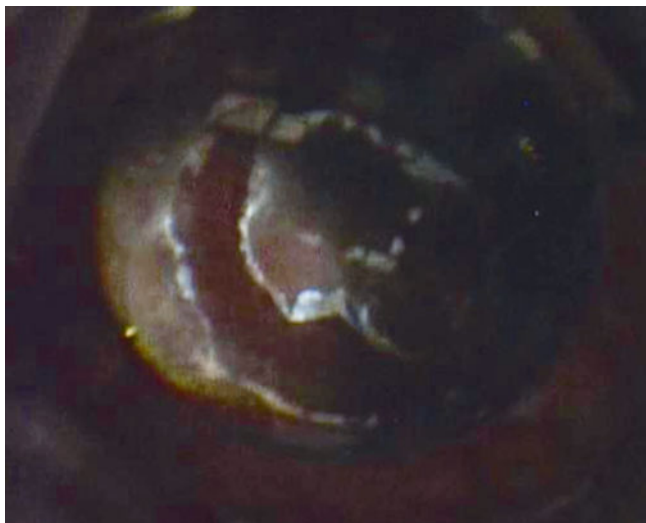


Figure V.B.5-9 Large circumferential peripheral retinectomy

the membrane is firmly adherent and aggressive pulling with forceps can risk creating retinal tears. In these cases, it is best to cut and segment the membrane using vertical scissors to relieve any traction. Extensive diffuse subretinal membranes and those with a “napkin-ring” configuration (whereby a circumferential subretinal membrane pulls the retina together anterior to the optic disc) require a large circumferential peripheral retinotomy for removal (Figure V.B.5-9). After creating a peripheral retinotomy of 90° or more, the retina is then folded over to access the subretinal space, and the membranes are removed completely using a bimanual technique. Sometimes a “napkin ring” membrane is best sectioned and left in place if tightly adherent to the posterior retina.

5. Relaxing Retinotomies and Retinectomies

Relaxing retinotomies (incision into the retina) and retinectomies (excision of the retina) are usually done when anterior PVR contracts causing retinal foreshortening that makes it impossible to reattach the retina [29]. This most commonly occurs in anterior retinal displacement in eyes that have had previous vitrectomy surgery. After all other membranes have been dissected, diathermy is applied in a double row posterior to the contracted retina. If a scleral buckle is present, the retinotomy is usually made just posterior to the scleral buckle. All vessels must be completely diathermized to achieve adequate hemostasis and to prevent hemorrhage (Figure V.B.5-10). The vitreous cutter or vertical cutting scissors are then used to create the circumferential retinotomy, and the retina anterior to the retinotomy is removed using the vitreous cutter (Figure V.B.5-11). A common mistake is to underestimate the needed size of the retinotomy which may leave traction at the ends of the retinotomy that can lead to re-detachment of the

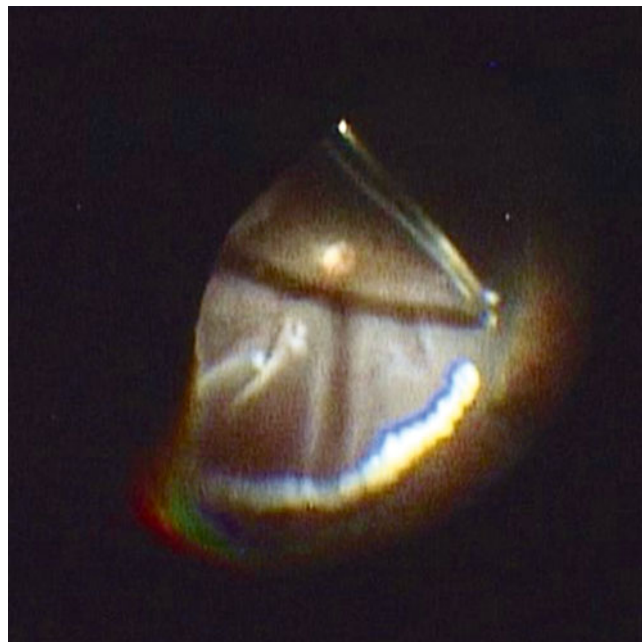


Figure V.B.5-10 Retinal diathermy in preparation for retinectomy



Figure V.B.5-11 Creation of a circumferential retinectomy

retina. The retinotomy should extend beyond the area of contraction into normal retina on each end and angled anteriorly toward the ora serrata. We usually avoid radial retinotomies as they tend to extend into the posterior pole and do not relieve traction well and, thus, are rarely indicated. A retinotomy greater than 90° in circumference will need to be managed like a giant retinal tear, usually with PFCL.

6. Reattachment of the Retina

If all traction has been relieved and no giant retinal tear or retinotomy created, the retina can be reattached with a fluid-air

exchange (described below). Surgery in most complex cases, however, will have used PFCL to stabilize the posterior retina during anterior membrane dissection. If PFCL was used, additional PCFL is injected to enlarge the existing bubble and reattach the retina. It is important to remove all retinal traction around breaks before raising the level of PFCL anterior to the retinal defects. If not, the PFCL can pass into the subretinal space, requiring further procedures to remove it. We prefer to inject the PFCL manually with a blunt, rigid cannula on a syringe and start the injection over the optic nerve. As described earlier, a small volume is injected initially, and once the bubble is large enough, the cannula can be placed into the PFCL bubble and injected to create a single, uniform bubble. As PCFL is injected, fluid is allowed to escape through the sclerotomy cannula. As the bubble increases in size, the retina will flatten and the choroidal pattern should become visible.

It is important to watch the peripheral retina flatten as the bubble enlarges. If a portion of the retina remains elevated under PFCL, the bubble should be removed until it is just posterior to the traction. Then the traction should be relieved (usually with membrane peeling or retinectomy) prior to restarting PFCL injection. PFCL should be injected until it is well anterior on the scleral buckle. However, try to avoid immersing the tip of the fluid infusion port in PFCL as many small bubbles can be produced. The turbulent flow can force some of these bubbles through anterior retinal breaks into the subretinal space. The use of MIVS with self-sealing cannulas will reduce turbulence and help prevent production of PFCL bubbles. Once the entire posterior and peripheral retina is attached, the retina should be examined. If areas are still elevated under PFCL, the traction should be relieved. Preretinal membranes can often be removed under PFCL. If further, more involved dissection is needed due to persistent membranes or subretinal membranes, the PFCL should be carefully aspirated out into a syringe for later use and the traction released.

If the decision is made to do a direct fluid-air exchange, retinal breaks should be marked using diathermy prior to the exchange so they are visible under air. Then, air is pumped into the eye through the infusion line from the vitrectomy machine while a silicone soft-tipped needle is placed over a retinal break and the subretinal fluid (SRF) is aspirated. Usually, a posterior or peripheral retinal break is present for SRF drainage; however, if no break is present, we create a drainage retinotomy with endodiathermy. This is best done in the mid-periphery, usually at least 5 disc diameters from the macula, preferably in the superior-temporal quadrant to minimize effects on the visual field. The drainage retinotomy can also be made even more peripherally so it is supported on the scleral buckle if the surgeon desires. Drainage through a peripheral break can be done using an extendable silicone soft-tipped cannula (extendable backflush brush, Dutch Ophthalmic Research Center, Netherlands) where the cannula can be passed through the peripheral break and extended

into the posterior subretinal space. Another technique for drainage of a peripheral break is to tilt the eye so the area of drainage is as posterior as possible to allow complete flattening of the retina while the fluid is aspirated. If draining peripherally, take care that the enlarging intravitreal air bubble does not cause a posterior retinal fold. If such a fold is seen, then the air should be removed and either a more posterior drainage retinotomy made or PFCL injected to reattach the retina.

It is not uncommon for the visibility to deteriorate dramatically after the fluid-air exchange is completed. This can be due to corneal striae or condensation of water vapor on the IOL. To help overcome this, applying dilute sodium hyaluronate onto the corneal endothelium or the posterior IOL can help improve the view. Also, the posterior surface of the IOL can be uniformly "wetted" using a soft-tipped cannula swept across the back surface. Because of their hydrophobic nature, silicone IOLs are notorious for having persistent lens condensation despite wiping the posterior surface. A technique to dry the posterior IOL surface involves torquing the infusion cannula toward the back surface of the silicone IOL and using the steady stream of air to help dry the condensation.

7. Laser Photocoagulation

Once the retina is attached, either under PFCL or under air, confluent endolaser photocoagulation is applied to surround all the retinal tears and the entire edge of any retinotomy. We usually apply laser 360° on the scleral buckle in a scatter pattern. Laser spots should be placed in two to three rows of moderate intensity burns placed about 1 burn width apart. Care should be taken not to create too intense burns as iatrogenic breaks can be created. If a laser spot is not visible despite adequate laser power and duration, SRF is likely present and should be removed in order to get proper retinal reattachment. Using a curved laser probe is helpful in treating the peripheral retina. Applying laser under PFCL affords excellent visualization and the level of PFCL can be raised anterior to the scleral buckle to assure no SRF is left and proper laser spots are made circumferentially. Laser treatment under air is more difficult due to the poor visualization that can occur. In these cases, diathermy of the retinal breaks prior to instillation of the air is useful to guide the location of treatment.

8. PFCL Removal

If PCFL was used to reattach the retina, it must be removed. This is best accomplished by using active suction with a silicone-tip cannula. Some surgeons prefer using passive extrusion through a backflush (Charles) silicone-tip cannula that works well but more slowly. The infusion line is switched from fluid to air, and the initial aspiration of PFCL and fluid is done immediately behind the lens and iris plane. Then the

cannula is directed toward the peripheral retina where the fluid is completely aspirated so that an air-PFCL interface is created. Anterior subretinal fluid can be removed by aspiration through breaks posterior to the fluid. The air forces the fluid posterior to the break. Once the retina is flat to the level of the most posterior break, the aspiration cannula is directed posteriorly over the optic nerve and the remaining PFCL is removed. As air is exchanged for the PFCL, a useful technique to assure the cannula is in fluid is the “dipping” maneuver. In this maneuver, the cannula is directed posterior toward the optic nerve until the reflex disappears (indicating the cannula tip is in fluid). Then aspiration is carried out until the reflex reappears, and the maneuver is carried out again until all fluid is removed. Finally, after all the fluid is aspirated, we prefer to inject approximately 0.25 ml of balanced saline solution onto the posterior retina to help identify any residual PFCL. The PFCL will coalesce in the saline solution and can then be aspirated with the soft-tip cannula.

If a giant retinotomy was created, there is a risk of retinal slippage that can occur during PFCL-air exchange. This occurs when fluid is left behind the edge of the retinotomy, and as the PFCL-air exchange proceeds, the residual fluid is forced posterior causing posterior slippage of the retina. This can be prevented by “drying” the edge of the retinotomy by filling the eye with air up to the anterior edge of the flap. Then the cannula is used to aspirate any residual fluid beneath the anterior retinotomy edge before posterior PFCL aspiration is carried out.

9. Fluid or PFCL-Silicone Oil Exchange

Some surgeons prefer to skip the step of exchanging either fluid or PFCL for air and go directly to silicone oil. In order to accomplish this, the silicone oil must be injected through the infusion port and a backflush brush used to passively extrude the fluid or PFCL out of the eye secondary to the increased pressure caused by the silicone oil infusion. The backflush brush is placed posterior over the optic nerve until all the PFCL or fluid is removed. Active aspiration should not be used at this point as the eye will collapse because the rate of injection of silicone oil is much lower than the rate of aspiration of fluid. For direct fluid-silicone oil exchange where a retinotomy or giant tear is present, the surgeon will need to bluntly position the flap of the tear and initially drain the fluid anteriorly at the retinotomy and then posterior over the optic nerve. This back-and-forth process is repeated until all the fluid has been removed and the eye filled with silicone oil. During the process, the flap of the retinotomy or giant tear may need to be repositioned if any posterior slippage occurs. This can be done by extruding the anterior edge of slipped retina into the orifice of the backflush brush and manually pulling the retina anteriorly to its proper anatomical position.

10. Intraocular Tamponade

The appropriate time length of tamponade in complex PVR cases is unknown, but the Silicone Study Group showed that long-term tamponade is more effective at retinal reattachment with better visual acuity outcomes compared to short-term tamponade [30]. Longer tamponade is achieved using perfluoropropane gas (C_3F_8) or silicone oil rather than sulfur hexafluoride gas (SF_6). The Silicone Study Group also showed that the anatomic and visual results were similar regardless of whether C_3F_8 gas or silicone oil was used [31, 32]. Gas may be favored over oil if there is risk of the silicone oil migrating into the anterior chamber and contacting the cornea or in the presence of vitreous or subretinal hemorrhage. Another advantage of gas is that it will disappear without the need for an additional surgery for its removal. A disadvantage of gas is that the tamponade is only temporary and the vision will be restricted while looking through the gas bubble. Oil may be preferred over gas in children and mentally handicapped patients who will have trouble positioning or in patients who must travel by air. Also, oil is preferred in most eyes with previously failed surgery for PVR and in eyes with large retinotomies or giant tears.

If C_3F_8 gas is used, the sclerotomy sites are sutured in 20-gauge cases. If MIVS is used, the cannulas are pulled out with pressure applied over the sclerotomy wounds using a cotton swab for 15 s. This will allow the sclera to slowly relax back to its normal anatomic shape and self-seal the wounds. If the wounds appear to be leaking, they will need to be sutured. Next, 40–45 ml of C_3F_8 gas in a concentration of 12–14 % is injected through the pars plana using a 30-gauge needle. A 27-gauge “chimney” (needle on a tuberculin syringe with the plunger removed) is placed 180° away through the pars plana to allow the gas/air mixture to escape until the air is completely replaced with C_3F_8 gas and then the needles are removed. We try to leave the intraocular pressure at 10 mmHg at the completion of the exchange. The intraocular pressure can be adjusted to the proper level by infusing or removing gas with a 30-gauge needle through the pars plana.

If silicone oil is used, an inferior iridectomy should be created in the aphakic eye using the vitreous cutter to prevent pupillary block and silicone oil migration into the anterior chamber [33]. In the pseudophakic eye, as long as the iris-capsular-IOL diaphragm is intact, an iridectomy is not necessary. Either 5,000 or 1,000 centistokes (CS) silicone oil can be used. The major difference between the two is that 5,000 CS oil has a higher viscosity. Studies have shown that the anatomic and visual acuity outcomes are similar regardless of which oil is used [34]. The higher viscosity oil does have less low molecular weight components and lower rates of emulsification and may be preferred if oil is to be left

in the eye for an extended time [35]. It is the surgeon's preference as to which type of oil to use, but 1,000 CS oil is faster and easier to inject and remove from the eye. 5,000 CS oil will require high-pressure tubing when injecting through the infusion port. If the MIVS system is used, 1,000 CS oil is much easier than 5,000 CS oil to pump through the smaller infusion ports using a silicone oil injection cannula.

Regardless of using large- or small-gauge vitrectomy systems, we advocate suturing all sclerotomies when using silicone oil. This is to assure that silicone oil does not leak into the subconjunctival space. The first step is to suture one of the sclerotomy sites (remove the cannula if the MIVS system is used). Next, the silicone oil is injected through the other sclerotomy site using a trimmed 20-gauge angiocath (5,000 CS oil) or the appropriate size infusion cannula for 1,000 CS oil for the MIVS system. The intraocular pressure is set at 15 mmHg but can be adjusted if needed. The oil is injected to the plane of the iris until it is barely visible in the infusion cannula. If the anterior chamber shallows, a small amount of oil can be removed and the chamber can be reformed with air injected through the limbus. After the eye is filled with silicone oil, the open sclerotomy site is sutured closed. The infusion cannula is then removed and the final sclerotomy site is closed. As the infusion cannula is removed, a small amount of oil will escape which will help ensure appropriate intraocular pressure and to prevent overfill. The intraocular pressure should be around 10 mmHg at the end of the case. After all the cannulas are removed and sclerotomies closed, the eye is copiously irrigated with saline solution to remove any residual oil before closure of the conjunctiva.

If the intraocular pressure and retina are stable, the oil can be left in the eye for 3 months or more. As long as the eye is not hypotonous, the retina is attached, and adequate time has elapsed to allow for appropriate laser-induced adhesion to maintain retinal reattachment, the oil can be removed [36]. Most surgeons remove oil 3–6 months after injection, but the duration of tamponade will vary on a case-by-case basis and if required, can be left indefinitely. If hypotony is present (IOP <7 mmHg), it is usually best not to remove the oil as these eyes may decompensate and become phthisical.

C. Postoperative Management

Generally, as long as a complete or near-complete silicone oil fill is present, prone positioning is not needed as the retinal breaks and laser treatment will be well tamponaded. The patient should avoid the supine position. Some surgeons do prefer facedown positioning for 24 h after surgery, however, to ensure a formed anterior chamber. Depending on the

location of the retinal breaks, positioning is more likely to be required with gas than with oil. If no inferior breaks are present, the patient can sleep on his or her side and be upright during the day. If inferior breaks are present, we prefer prone positioning with gas (but not for oil) for the first 2 weeks after surgery. If a large retinal break is present and gas was used, an appropriate position (upright, left or right tilt, face-down) can be used to ensure the bubble is apposed to the break.

At a minimum, the eye should have at least an 80 % gas fill in the immediate postoperative period. If this is not present, a fluid-gas exchange in the office can be done. If only a small amount of gas is needed (<0.2 ml), 14 % C₃F₈ can be injected through the pars plana followed by an anterior chamber paracentesis to normalize the pressure. If more gas is needed to achieve the appropriate gas fill, a two-needle technique can be used [37]. The patient is placed on his or her side with the operated eye down, and a 30-gauge needle attached to a 10 cc syringe filled with 14 % C₃F₈ is placed through the pars plana in the superior-most position (nasally). Then a 27-gauge needle on a 10 cc empty syringe is inserted through the pars plana in the inferior-most position (temporally). Simultaneously, as the gas is injected into the eye from the superior syringe, fluid is aspirated from the inferior syringe. This is done sequentially in 0.5 ml volumes until all the fluid has been aspirated and replaced with gas. It is helpful to slowly turn the head to a more prone position during the procedure as more fluid can be aspirated.

Intraocular pressure must be monitored carefully during the postoperative period. Patients with PVR have many possible risk factors for elevated IOP including scleral buckle, lensectomy, extensive laser photocoagulation, possible gas overfill, and development of a fibrin pupillary membrane causing pupillary block [38]. Management of IOP starts at the end of surgery. After normalizing the IOP during surgery, we administer topical IOP-lowering drops at the end of surgery. Pressure is then rechecked the following morning. Elevated pressure can usually be treated medically; however, if very high pressures persist, a fluid or gas paracentesis may be necessary to lower IOP.

Subconjunctival dexamethasone 5 mg at the end of surgery and topical corticosteroids every 1–2 h in the initial postoperative period may help decrease postoperative inflammation. Some surgeons inject intravitreal triamcinolone at the end of surgery. Animal studies have shown benefits to this as it decreases fibroblast proliferation; however, the evidence that this is beneficial in human studies is mixed when looking at prospective clinical trials [39–41]. As mentioned previously, if the patient's medical condition permits, we start them on prednisone 1.5 mg/kg 2 days prior to surgery and continue for 7–10 days postoperatively to reduce

inflammation and recurrent proliferation. A study by Hui et al. [42] suggests that preoperative administration of steroids may be more effective at reducing inflammation than postoperative administration, but the study by Koerner et al. [13] showed reduced macular preretinal membranes vs. control eyes in patients with retinal detachment with high-risk factors for PVR treated with prednisone 100 mg daily started the day of surgery and gradually tapered over 15 days.

In some situations, extensive postoperative fibrin can develop in the anterior chamber and around the pupil causing a pupillary block, occluding the iridectomy made in silicone-filled eyes and/or interfering with the posterior view making it impossible to evaluate the retina. In these situations, we lyse the fibrin with tissue plasminogen activator (tPA) [43, 44]. This is done 3–5 days post surgery to reduce the risk of an intraocular hemorrhage with earlier injection. We use 5 µg of tPA in 0.05 ml of BSS and inject into the anterior chamber through the limbus using a 30-gauge needle. It is particularly important to make sure fibrin does not occlude the peripheral iridectomy in silicone oil-filled eyes. The fibrin will lead to fibrosis and closure of the peripheral iridectomy that will cause silicone oil to migrate into the anterior chamber. Tissue plasminogen activator works well for fibrin membranes in gas-filled eyes. If both fibrin and hemorrhage are present, a fluid-gas exchange can be done to clear the hemorrhage and fibrin remnants after tPA injection.

We monitor patients closely following complex retinal detachment surgery, usually every 1–2 weeks, to look for complications and recurrent detachment. In a gas-filled eye, it is easiest to visualize the retina by looking around the bubble. If a retinal detachment is present, it is usually seen inferior to the gas or silicone oil and is usually due to an unrecognized and untreated retina tear and/or excessive retinal traction. The most common cause of a recurrent retinal detachment is anterior traction opening up an anterior break. Gas-filled eyes can sometimes be successfully treated by an in-office fluid-gas exchange. After the retina is flattened, laser treatment should be applied in several rows on the scleral buckle and posterior to the scleral buckle throughout the inferior 180°. If some residual retinal detachment is present anterior to the buckle, the fluid can be demarcated with laser and the retina monitored as the posterior retina will often remain attached. In some cases, however, the eye may become hypotonous. If posterior membranes exist (manifested by retinal folds) or extensive anterior membranes are still present, a fluid-gas exchange will not work and a reoperation is necessary. Recurrent retinal detachment in silicone oil-filled eyes requires a reoperation.

IV. Prognosis and Results

The surgical results of PVR management have steadily improved since vitreoretinal surgeons first attempted to treat the condition. Prior to 1970, the surgical reattachment rate was 15 % and consisted of external scleral buckling and resection as well as crude attempts to remove the vitreous through the limbus or pars plana with or without replacement (usually saline or air) [45]. In 1982, Grizzard and Hilton reported a 35 % retinal reattachment rate with a well-placed, high encircling scleral buckle alone supporting the retina [46]. However, it was not until Machemer's early pars plana vitrectomy (PPV) with the vitreous infusion suction cutter (VISC) in the 1970s that the rate of retinal reattachment began to improve. Despite this advancement, early surgical techniques by Machemer and Laqua that combined membrane peeling and vitrectomy only yielded a successful reattachment rate around 36 % [47]. This was because early PPV focused only on posterior membranes.

The description and surgical management of anterior PVR coupled with advancements in surgical techniques and instrumentation such as endoillumination, intraocular gas, silicone oil, and intraocular laser as well as intraocular irrigating solutions that preserve the cornea doubled the surgical success rate to 60 % [45]. In 1991, Lewis and Aaberg [9] reported a retinal reattachment rate of 81 % in eyes without previous vitrectomy for PVR and Lewis, Aaberg, and Abrams [10] a 70–80 % success rate in eyes that had undergone a previous vitrectomy for PVR. The addition of perfluoro-n-octane and widespread use of retinectomies increased the retinal reattachment rates even further. Currently, anatomic success rates in the range reported by Quiram et al. (93 %) are not unusual [48].

Even though the anatomic surgical success rates have drastically improved over the last 40 years, recurrent retinal detachments due to cellular proliferation and traction still remain a problem. Moreover, despite the anatomic success that surgery provides, many patients still lose significant functional vision as a result of recurrent retinal detachment. The "holy grail" in PVR management is the prevention and inhibition of cellular proliferation [see chapters II.D. Hyalocytes, III.J. Cell proliferation at the vitreo-retinal interface in PVR and related disorders]. The major areas of research include anti-inflammatory therapy, inhibition of cellular proliferation and contraction, prevention of attachment of proliferating cells, and downregulation of cytokines and angiogenic molecules that trigger proliferation [see chapter IV.F. Pharmacotherapy of PVR]. Thus far, the studies have not had as wide success in humans as they have in animal models. Likely, a multimodal approach will have to be developed to prophylactically treat PVR successfully. Until this is achieved, the surgical management of PVR will remain a mainstay in the surgeon's arsenal to treat this condition.

Abbreviations

ACIOL	Anterior chamber intraocular lens – A synthetic lens that is placed in the anterior chamber of the operated eye
C ₃ F ₈	Perfluoropropane gas – A type of long-acting gas used during retinal cases to tamponade the retina
MIVS	Micro-incisional vitrectomy surgery – Small-gauge vitrectomy surgery where the port size is usually 23-gauge or smaller
MVR	Micro-vitreoretinal blade – A type of ophthalmic knife used to make incisions
PCIOL	Posterior chamber intraocular lens – A synthetic lens that is placed in the posterior chamber of the operated eye
PFCL	Perfluorocarbon liquid – A colorless, odorless, high-density liquid used to stabilize the retina during surgery
PPV	Pars plana vitrectomy – A procedure to remove the vitreous gel and membranes through a pars plana incision
PVD	Posterior vitreous detachment – The separation of the posterior vitreous cortex from the retina anywhere posterior to the vitreous base
PVR	Proliferative vitreoretinopathy – Retinal detachment caused by contractile cellular membranes on the retina and vitreous following rhegmatogenous retinal detachment (RRD)
RPE	Retinal pigment epithelium – The pigmented cell layer just behind the neurosensory retina that nourishes retinal visual cells and is firmly attached to the underlying choroid and overlying retinal visual cells
RRD	Rhegmatogenous retinal detachment – Occurs when a tear in the retina leads to fluid accumulation with a separation of the neurosensory retina from the underlying retinal pigment epithelium
SF ₆	Sulfur hexafluoride gas – A type of shorter-acting gas used during retinal cases to tamponade the retina
tPA	Tissue plasminogen activator – A protein involved in the breakdown of blood clots systemically that is used to lyse fibrin in the eye after surgery

References

1. The Retinal Society Terminology Committee. The classification of retinal detachment with proliferative vitreoretinopathy. *Ophthalmology*. 1983;90:121–5.
2. Richardson EC, Verma S, Green WT, Woon H, Chignell AH. Primary vitrectomy for rhegmatogenous retinal detachment: an analysis of failure. *Eur J Ophthalmol*. 2000;10:160–6.
3. Cowley M, Conway BP, Campochiaro PA, Kaiser D, Gaskin H. Clinical risk factors for proliferative retinopathy. *Arch Ophthalmol*. 1989;107:1147–51.
4. Dumas C, Bonnet M. Choroidal detachment associated with rhegmatogenous retinal detachment: a risk factor for postoperative PVR. *J Fr Ophthalmol*. 1996;19:455–63.
5. Bonnet M, Fleury J, Guenon S, Yaniali A, Dumas C, Hajjar C. Cryopexy in primary rhegmatogenous retinal detachment: a risk factor for postoperative proliferative vitreoretinopathy? *Graefes Arch Clin Exp Ophthalmol*. 1996;234:739–43.
6. Kon CH, Asaria RH, Occeleston NL, Khaw PT, Aylward GW. Risk factors for proliferative vitreoretinopathy after primary vitrectomy: a prospective study. *Br J Ophthalmol*. 2000;84:506–11.
7. Nagasaki H, Shinagawa K, Mochizuki M. Risk factors for proliferative vitreoretinopathy. *Prog Retin Eye Res*. 1998;17:77–98.
8. Machemer R, Aaberg TM, Freeman HM, Irvine AR, Lean JS, Michels RM. An updated classification of retinal detachment with proliferative vitreoretinopathy. *Am J Ophthalmol*. 1991;112:159–65.
9. Lewis H, Aaberg TM. Causes of failure after initial vitreoretinal surgery for severe proliferative vitreoretinopathy. *Am J Ophthalmol*. 1991;111:8–14.
10. Lewis H, Aaberg TM, Abrams GW. Causes of failure after repeat vitreoretinal surgery for recurrent proliferative vitreoretinopathy. *Am J Ophthalmol*. 1991;111:15–9.
11. Pieramici D, Capone Jr A, Aaberg TM. Surgical management of proliferative vitreoretinopathy. In: Guyer D et al., editors. *Retina-vitreous-macula*. Philadelphia: W B Saunders; 1999. p. 1350–69.
12. Jonas JB, Hayler JK, Panda-Jonas S. Intravitreal injection of crystalline cortisone as adjunctive treatment of proliferative vitreoretinopathy. *Br J Ophthalmol*. 2000;84:1064–7.
13. Koerner F, Koerner-Stiefbold U, Garweg JG. Systemic corticosteroids reduce the risk of cellophane membranes after retinal detachment surgery: a prospective randomized placebo-controlled double-blind clinical trial. *Graefes Arch Clin Exp Ophthalmol*. 2012;250:981–7.
14. Landers 3rd MB, Foulks GN, et al. Temporary keratoprosthesis for use during pars plana vitrectomy. *Am J Ophthalmol*. 1981;91:615–9.
15. Eckardt C. A new temporary keratoprosthesis for pars plana vitrectomy. *Retina*. 1987;7:34–7.
16. Toth CA, Landers 3rd MB. A new wide-field temporary keratoprosthesis. *Retina*. 1993;13:353–5.
17. von Fischern T, Langefeld S, et al. The “Aachen” keratoprosthesis: a new approach towards successful keratoprosthesis surgery. *Int J Artif Organs*. 1999;22:52–7.
18. de Juan E, Hickingbotham Jr D. Flexible iris retractor. *Am J Ophthalmol*. 1991;111:776–7.
19. Lewis H, Aaberg TM, Abrams GW, Han DP, Kreiger AE. Management of the lens capsule during pars plana lensectomy. *Am J Ophthalmol*. 1987;103:109–10.
20. Lam DS, Yuen CY, Tam BS, Cheung BT, Chan WM. Sutureless vitrectomy surgery. *Ophthalmology*. 2003;110:2428–9.

21. Park KH, Woo SJ, Hwang JM, Kim JH, Yu YS, Chung H. Short-term outcome of bimanual 23-gauge transconjunctival sutureless vitrectomy for patients with complicated vitreoretinopathies. *Ophthalmic Surg Lasers Imaging*. 2010;41:207–14.
22. Sandali O, El Sanharawi M, Lecuen N, Barale PO, Bonnel S, Basli E, Borderie V, Laroche L, Monin C. 25-, 23-, and 20-gauge vitrectomy in preretinal membrane surgery: a comparative study of 553 cases. *Graefes Arch Clin Exp Ophthalmol*. 2011;249:1811–9.
23. Tewari A, Shah GK, Fang A. Visual outcomes with 23-gauge transconjunctival sutureless vitrectomy. *Retina*. 2008;28:258–62.
24. Aaberg TM. Management of anterior and posterior proliferative vitreoretinopathy. *Am J Ophthalmol*. 1988;106:519–32.
25. Capone Jr A, Lambert HM, Aaberg Sr TM, et al. Intravitreal use of perfluoro-n-octane in the management of retinal detachment with proliferative vitreoretinopathy. In: Franklin R, editor. *Retina and vitreous*. New York: Kugler Publications; 1993. p. 223–36.
26. Peyman GA, Cheema R, Conway MD, Fang T. Triamcinolone acetonide as an aid to visualization of the vitreous and the posterior hyaloid during pars plana vitrectomy. *Retina*. 2000;20:554–5.
27. Lewis H, Aaberg TM. Anterior proliferative vitreoretinopathy. *Am J Ophthalmol*. 1988;105:277–84.
28. Lewis H, Aaberg TM, Abrams GW, McDonald HR, Williams GA, Mieler WF. Subretinal membranes in proliferative vitreoretinopathy. *Ophthalmology*. 1989;96:1403.
29. Abrams GW, Garcia-Valenzuela E, Nanda S. Retinotomies and Retinectomies. In: Ryan SJ, Wilkinson CP, Wiedemann P, editors. *Retina*, vol. 3. 5th ed. London: Elsevier Limited; 2013. p. 1826–43. 108.
30. The Silicone Study Group. Vitrectomy with silicone oil or sulfur hexafluoride gas in eyes with severe proliferative vitreoretinopathy: results of a randomized clinical trial. *Silicone Study Report 1*. *Arch Ophthalmol*. 1992;110:770–9.
31. Silicone Study Group. Vitrectomy with silicone oil or perfluoropropane gas in eyes with severe proliferative vitreoretinopathy: results of a randomized clinical trial – Silicone Study report #2. *Arch Ophthalmol*. 1992;110:780–92.
32. Abrams GW, Azen SP, McCuen 2nd BW, Flynn Jr HW, Lai MY, Ryan SJ. Vitrectomy with silicone oil or long-acting gas in eyes with severe proliferative vitreoretinopathy: results of additional and long-term follow-up. *Silicone Study report 11*. *Arch Ophthalmol*. 1997;115:335–44.
33. Ando F. Usefulness and limit of silicone in management of complicated retinal detachment. *Jpn J Ophthalmol*. 1987;31:138–46.
34. Scott IU, Flynn Jr HW, Murray TG, Smiddy WE, Davis JL, Feuer WJ. Outcomes of complex retinal detachment repair using 1000- vs. 5000-centistoke silicone oil. *Arch Ophthalmol*. 2005;123:473–8.
35. Parel JM, Milne P, Sandrine G, Jallet V, Villain F. Silicone oils: physicochemical properties. In: Ryan SJ, Hinton DR, Schachat AP, Wilkinson CP, editors. *Retina*. 4th ed. Philadelphia: Elsevier; 2006. p. 2191–210.
36. Hutton WL, Azen SP, Blumenkranz MS, Lai MY, McCuen BW, Han DP, Flynn Jr HW, Ramsay RC, Ryan SJ, The Silicone Study Group. The effects of silicone oil removal: Silicone Study report #6. *Arch Ophthalmol*. 1994;112:778–85.
37. Lambrou FH, Devenyi RG, Han DP. Fluid-gas exchange after vitrectomy using long-acting gases in an outpatient setting. *Arch Ophthalmol*. 1988;106:1344.
38. Han DP, Lewis H, Lambrou Jr FH, Mieler WF, Hartz A. Mechanisms of intraocular pressure elevation after pars plana vitrectomy. *Ophthalmology*. 1989;96:1357–62.
39. Tano Y, Chandler D, Machermer R. Treatment of intraocular proliferation with intravitreal injection of triamcinolone acetonide. *Am J Ophthalmol*. 1980;90:810–6.
40. Ahmadi H, Feghhi M, Tabatabaei H, Shoeibi N, Ramezani A, Mohebbi MR. Triamcinolone acetonide in silicone-filled eyes as adjunctive treatment for proliferative vitreoretinopathy: a randomized clinical trial. *Ophthalmology*. 2008;115:1938–43.
41. Cheema RA, Peyman GA, Fang T, Jones A, Lukaris AD, Lim K. Triamcinolone acetonide as an adjuvant in the surgical treatment of retinal detachment with proliferative vitreoretinopathy. *Ophthalmic Surg Lasers Imaging*. 2007;38:365–70.
42. Hui YN, Liang HC, Cai YS, Kirchhof B, Heimann K. Corticosteroids and daunomycin in the prevention of experimental proliferative vitreoretinopathy induced by macrophages. *Graefes Arch Clin Exp Ophthalmol*. 1993;31:109–14.
43. MacCumber MW, McCuen BW, Toth CA, et al. Tissue plasminogen activator for preserving inferior peripheral iridectomy patency in eyes with silicone oil. *Ophthalmology*. 1996;103:269–73.
44. Williams DF, Bennett SR, Abrams GW, et al. Low dose intraocular tissue plasminogen activator for treatment of postvitrectomy fibrin formation. *Am J Ophthalmol*. 1990;109:606–7.
45. Aaberg Sr TM. Surgery as the primary management of proliferative vitreoretinopathy: a history reflecting my experiences and biases. *Arch Ophthalmol*. 2010;128:1068–70.
46. Grizzard WS, Hilton GF. Scleral buckling for retinal detachments complicated by periretinal proliferation. *Arch Ophthalmol*. 1982;100:419–22.
47. Machermer R, Laqua H. A logical approach to the treatment of massive periretinal proliferation. *Ophthalmology*. 1978;85:584–93.
48. Quiram PA, Gonzales CR, Hu W, et al. Outcomes of vitrectomy with inferior retinectomy in patients with recurrent rhegmatogenous retinal detachments and proliferative vitreoretinopathy. *Ophthalmology*. 2006;113:2041–7.
49. Abrams GW. Retinotomies and retinectomies. In: Ryan SJ, ed. *Retina*. St. Louis: CV Mosby; 1989;3:317–46.

Lawrence P. Chong

Outline

- I. **Introduction**
- II. **Pathophysiology**
- III. **Surgical Approach**
 - A. Retinotomy and Retinopexy
 - B. Vitreous Substitutes
 - C. Complications
- IV. **Future Developments**
 - A. Surgical
 - B. Pharmacologic

References

Keywords

Vitreous base • Retinal detachment • Proliferative vitreoretinopathy (PVR) • Vitrectomy • Retinectomy

Key Concepts

1. Anterior PVR membranes transmit traction to the retina and ciliary body via the arcuate fibers of the vitreous base, the “anterior loop”.
2. The firm adhesion of vitreous to peripheral retina makes it impossible to surgically separate the two structures.
3. Retinectomy is currently the treatment of choice for severe anterior PVR, although the future may see pharmacologic vitreolysis as adjunctive therapy to decrease vitreoretinal adhesion and facilitate removal of vitreous and PVR membranes.

I. Introduction

Anterior proliferative vitreoretinopathy (PVR) is the greatest challenge facing the surgeon attempting to repair recurrent retinal detachment [1]. The Retina Society recognized this and, to create a more prognostic classification, added anterior proliferation distinct from posterior proliferation (extensive macular pucker) to its ABCD classification of PVR [2] (Table V.B.6-1). The traction forces at the vitreous base were classified as circumferential or anterior (Figure V.B.6-1), acknowledging the complexity of contraction of fibrous tissue formation in this zone. Machemer first described retinotomy in 1981 [3] for incarcerated retina in a ruptured globe. Zivonovich described its application for severe traction membranes [4]. Subsequent reports followed [5–9] and emphasized the importance of removing retina anterior to the retinotomy

L.P. Chong, MD
Department of Ophthalmology, Doheny Eye Institute,
Los Angeles, CA, USA

VMR Institute for Vitreous Macula Retina,
Huntington Beach, CA, USA
e-mail: lchong@usc.edu

to prevent re-proliferation, extending the retinotomy to an adequate size, the importance of long-term tamponade, and the benefit of perfluorocarbon liquids. In the PVR Silicone Oil Study, retinotomy was performed in 29 % of cases [10].

Table V.B.6-1 Proliferative vitreoretinopathy described by contraction type and location

Grade C proliferative vitreoretinopathy		
Type	Location (in relation to equator)	Features
1. Focal	Posterior	Starfold posterior vitreous base
2. Diffuse	Posterior	Confluent starfolds posterior to vitreous base. Optic disk may not be visible
3. Subretinal	Posterior/ anterior	Proliferations under the retina: annular strand near disk; linear strands; moth-eaten-appearing sheets
4. Circumferential	Anterior	Contraction along posterior edge of vitreous base with central displacement of the retina; posterior retina in radial folds
5. Anterior displacement	Anterior	Vitreous base pulled anteriorly by proliferative tissue; peripheral retinal trough; ciliary processes may be stretched, may be covered by membrane; iris may be retracted

Proliferative vitreoretinopathy described by contraction type and location. (From page 161 Machemer et al. [2])

II. Pathophysiology

The cellular aspects of PVR pathogenesis are discussed in chapter III.J. Cell proliferation at the vitreoretinal interface in PVR and related disorders. It is important to appreciate that the proliferation of cells and formation of PVR membranes are influenced by the underlying structures of the vitreous cortex (see chapter II.E. Vitreoretinal interface and ILM) that creates surfaces upon which membranes form. The orientation of collagen fibrils within the vitreous base influences the vector of forces generated by contracting PVR membranes. The Retina Society classification of anterior traction being “circumferential” or “anterior” reflects the fact that the underlying structure of the vitreous base is an important component of the phenomenon. (see Table V.B.6-1) Circumferential traction arises from the entire vitreous base, a three-dimensional doughnut-like structure that straddles the ora serrata 360°. Within the vitreous base is a dense network of collagen fibrils that insert anterior and posterior to the ora serrata (Figure V.B.6-1). Because of the strong adherence of the vitreous to the retina in this area [11, 12], it is impossible to detach the vitreous at the vitreous base. Therefore, it is impossible to peel membranes in this area.

The collagen fibers of the vitreous base form a loop, called the “anterior loop” which connects the peripheral retina and the pars plana of the ciliary body (Figure V.B.6-2).

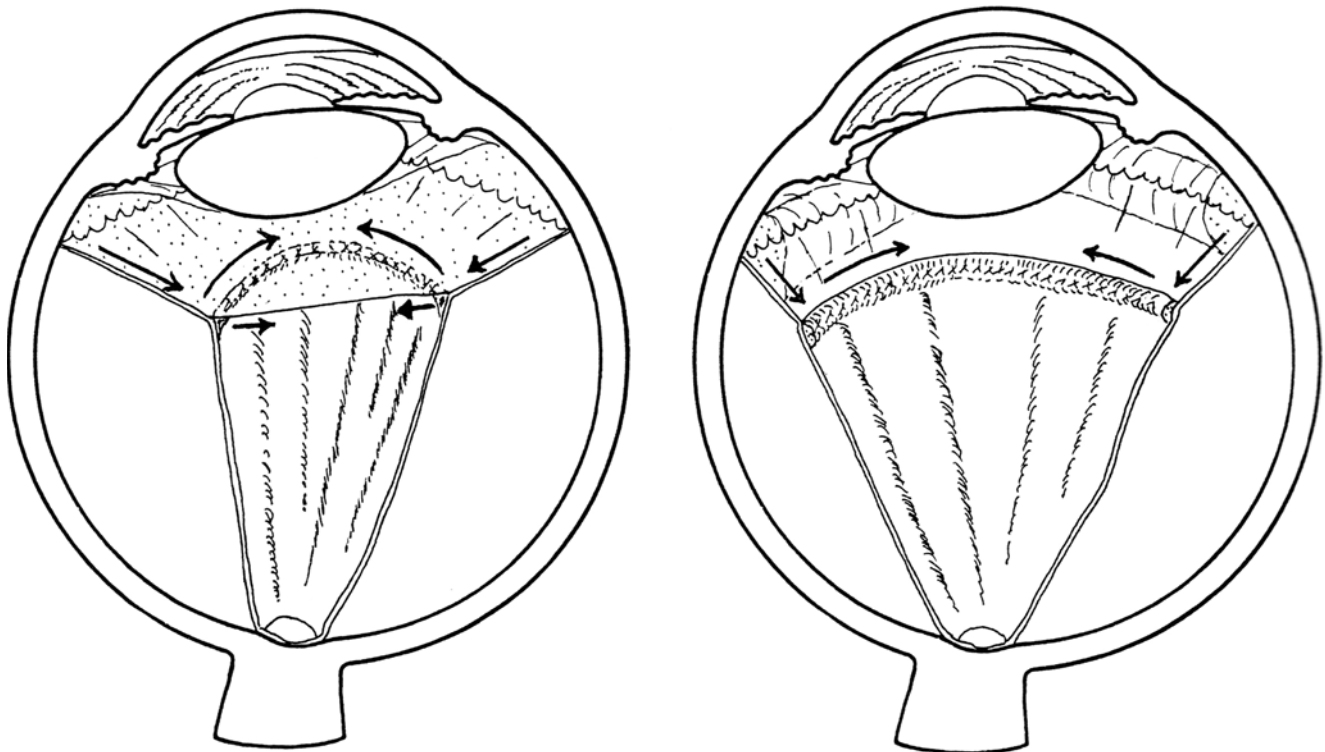


Figure V.B.6-1 Circumferential traction (From p 163 Machemer et al. [2])

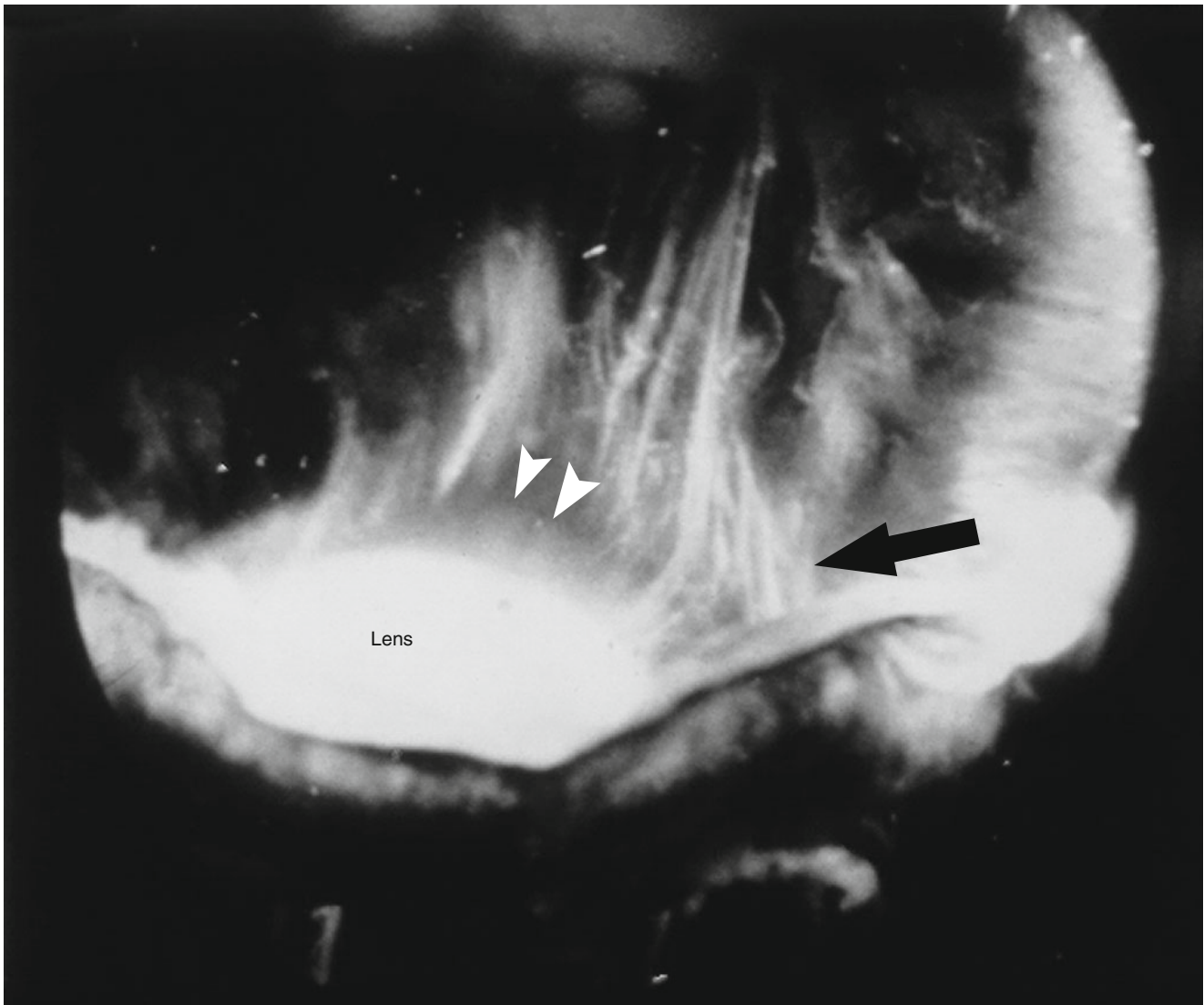


Figure V.B.6-2 Human vitreous base. After dissection of the sclera, choroid, and retina, the vitreous body of this 57-year-old man is left attached to the anterior segment, and the specimen is illuminated with dark-field slit microscopy. The vitreous base (*black arrow*) is seen sur-

rounding the lens and consists of a dense matrix of collagen fibrils that splay out to insert anterior and posterior to the ora serrata (*white arrowheads*) (courtesy of J. Sebag, MD of the VMR Institute for Vitreous Macula Retina)

Contraction of PVR membranes in the peripheral anterior vitreous thus transmits traction to adjacent structures. When the ciliary body detaches, it ceases to synthesize the aqueous and the result is hypotony. If traction is extensive, there can even be iris retraction. Perpendicular traction mediated by the anterior loop (Figure V.B.6-2) rolls the anterior retina forward onto the pars plana and foreshortens the retina usually inferiorly where retinal pigment epithelial cells preferentially settle and proliferate. For this reason, the retina can detach posterior to a broad and high inferior scleral buckle. Retinal reattachment rates improved when removal of crystalline lenses improved access to the vitreous base, and techniques were developed to better visualize this zone and to dissect membranes in this area thereby freeing up foreshortened retina.

III. Surgical Approach

In many cases, the retina remains foreshortened even after aggressive dissection, and the retina must be cut to allow the posterior retina to settle.

A. Retinotomy and Retinopexy

The location of the retinotomy should be posterior to all present and future contraction and therefore posterior to the vitreous base. Panoramic viewing systems provide an excellent view of the peripheral retina for this purpose. In the presence of a scleral buckle, the retinotomy can be made



Figure V.B.6-3 Anterior loop. Dark-field slit microscopy of the anterior vitreous in a 76-year-old man demonstrates the anterior loop of vitreous fibers (*arrow*) that traverse from the peripheral retina to the pars plana of the ciliary body. *L* lens (From Sebag and Balazs [20])

over the buckle posterior to the vitreous base, but if the retina is adherent over the buckle because of extensive retinopathy, then the retinotomy is made just posterior to the buckle. The extent of the retinotomy should allow complete relaxation of the inferior retina. An inferior 180° retinotomy is most common. Failure often occurs at the end of the retinotomy, and a 180° retinotomy places the ends more superiorly where there is less risk of re-proliferation and where there is superior tamponade especially with gas. Most relaxing retinotomies are circumferential, but occasionally a radial retinotomy may be indicated in cases of severe posterior foreshortening.

Prophylactic intraocular diathermy is applied to the area that will be cut to prevent bleeding and accumulation underneath the macula. The retina can be cut with scissors, but small incision high-speed vitreous cutters give superior control and safety (Figure V.B.6-4). For a more detailed discussion of the advantages of small incision high-speed vitreous cutters, see chapter V.B.2. Modern vitrectomy cutters. The vitreous can be cut in either a fluid-filled eye or a tamponade-filled eye. The latter is more common in a reoperation. The advantage of cutting in a fluid-filled eye is that traction is more easily evalu-

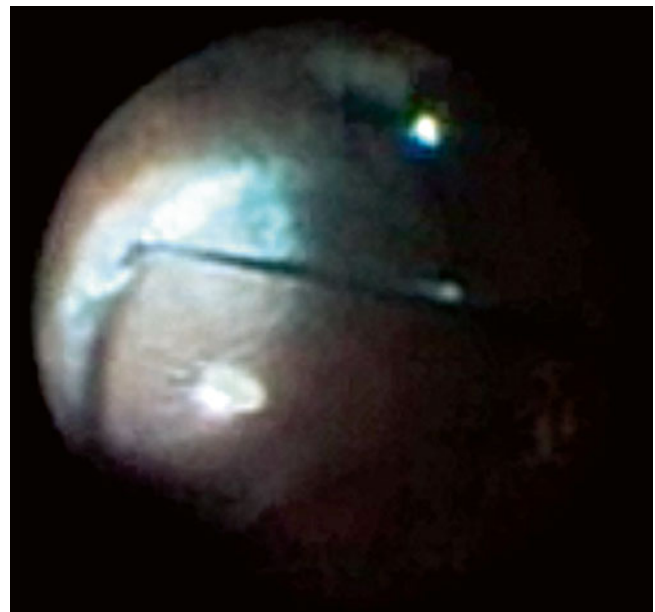


Figure V.B.6-4 Small-gauge vitrector is ideal for cutting the retina (screenshot of retinotomy video) see chapter V.B.5. Management of PVR

ated so the proper location and extent of the retinotomy can be optimized. Under oil, the retina can look artificially fine, even though there may be significant traction present. This occult inferior shortening of the retina manifests itself as recurrent retinal detachment after the oil is removed. An advantage of operating through tamponade is that the retina reattaches nicely as the retinotomy is performed, confirming that traction is relieved. However, any bleeding that may occur from inadequate prophylactic diathermy is trapped under the tamponade and requires that the tamponade be removed and the blood washed out. Blood trapped between the oil and retina induces re-proliferation, and the blood trapped between the gas and retina eventually diffuses into the vitreous chamber as the gas absorbs preventing postoperative evaluation of the retina. A successful inferior relaxing retinotomy should have good laser reaction around the margins and minimal fibrous re-proliferation and an attached retina.

B. Vitreous Substitutes

Perfluorocarbon liquid is used to reattach the retina. Laser retinopexy can be administered through the perfluorocarbon liquid or after a subsequent gas-fluid exchange. The

view to the periphery through a panoramic viewing system is expanded under gas which facilitates laser retinopexy. A directional laser probe is very useful in lasering the peripheral retinotomy. Laser retinopexy is preferred over cryoretinopexy because it has less effects on the blood-retinal barrier. The perfluorocarbon liquid (Figure V.B.6-5) is then removed and replaced with the final tamponade. Posterior slippage of the posterior edge of the retinotomy can occur at this point of the procedure. This is minimized by removing first all the irrigation fluid anterior to the perfluorocarbon liquid and then removing all subretinal fluid at the edges of the retinotomy before perfluorocarbon liquid posterior to the retinotomy (Figure V.B.6-6) is exchanged for air or oil.

Long-term tamponade can be provided by perfluoropropane gas or silicone oil. Silicone oil may be preferable because it can provide tamponade for several months outlasting the self-limited duration of PVR cellular activity but at the risk of perisilicone oil proliferation. Posterior slippage of the retinotomy which develops during direct exchange of perfluorocarbon liquid for silicone oil is caused by the small amount of infusion fluid trapped anterior to the sclerotomies when perfluorocarbon liquid is infused and the infusion line is open [13] (Figure V.B.6-7). This fluid

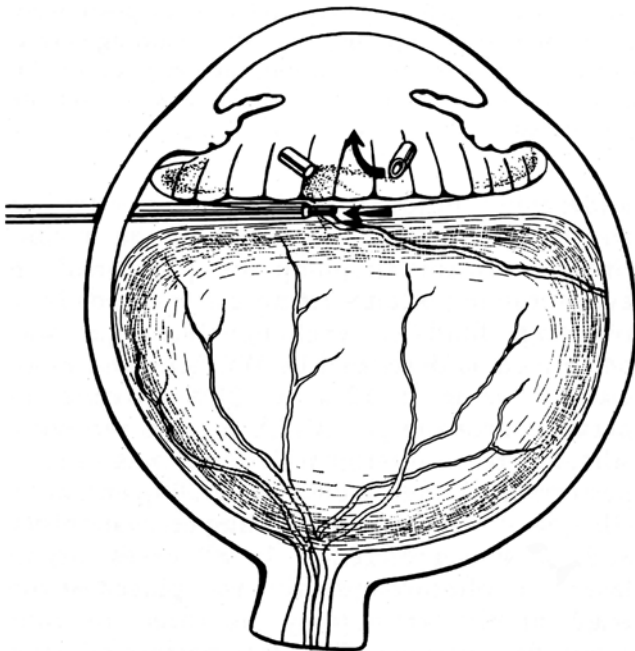


Figure V.B.6-5 Irrigation fluid anterior to the perfluorocarbon liquid bubble is aspirated first (Fig. 1 from page 25 Han et al. [9])

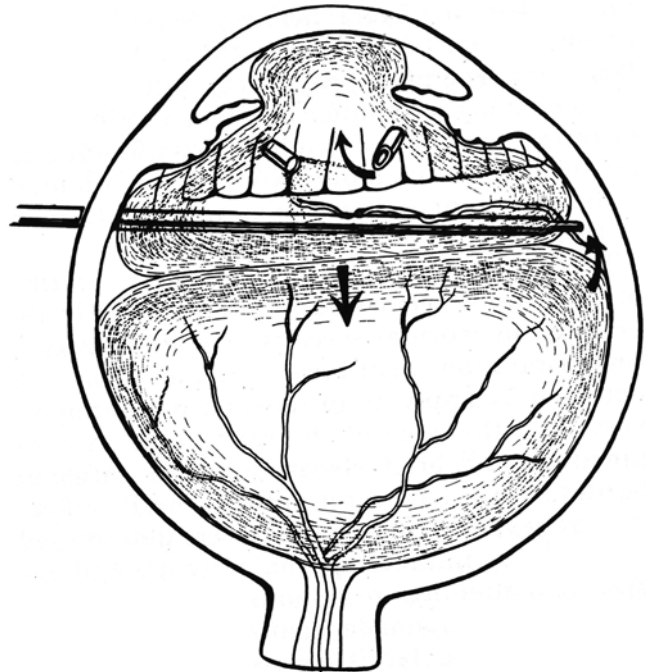


Figure V.B.6-6 After the irrigation fluid anterior to the perfluorocarbon liquid is removed, subretinal fluid at the edge of the retinotomy is meticulously removed before the perfluorocarbon liquid posterior to the retinotomy is exchanged for air or gas (Fig. 3 from page 26 Han et al. [9])

allows the retinotomy edge to slip posteriorly at the conclusion of the oil fill (Figure V.B.6-8). This is avoided by turning off the infusion and then filling the eye completely with perfluorocarbon liquid, pushing any remaining fluid

out through a superiorly positioned sclerotomy and making sure the perfluorocarbon liquid is seen in the infusion line. The perfluorocarbon liquid pushes the irrigation fluid anterior to the sclerotomies out through the open infusion

Figure V.B.6-7 Irrigation fluid is trapped anterior to the sclerotomies when perfluorocarbon liquid is injected into the eye and the infusion line is open (Fig. 1 from page 650 Li and Wong [13])

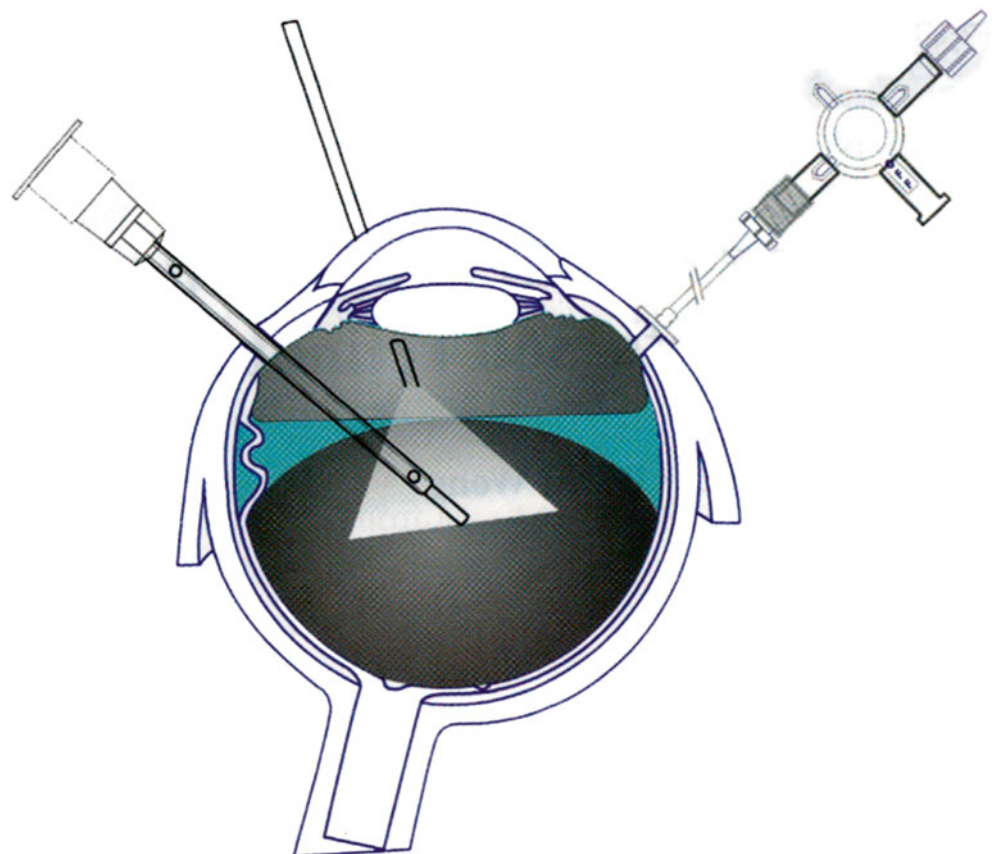
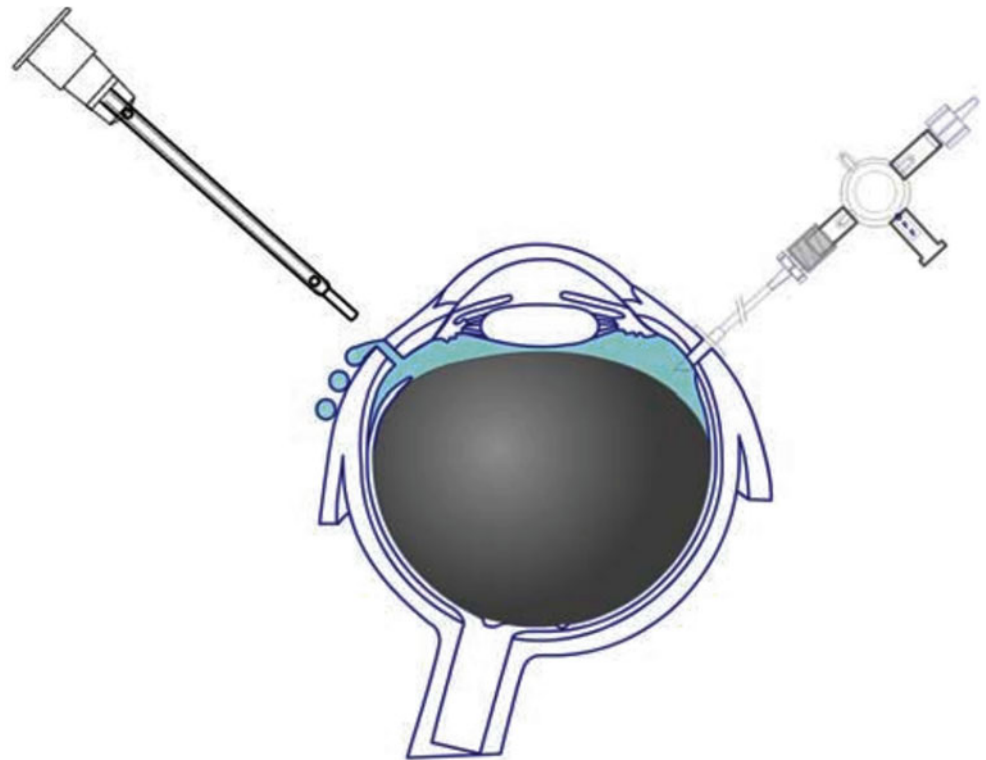
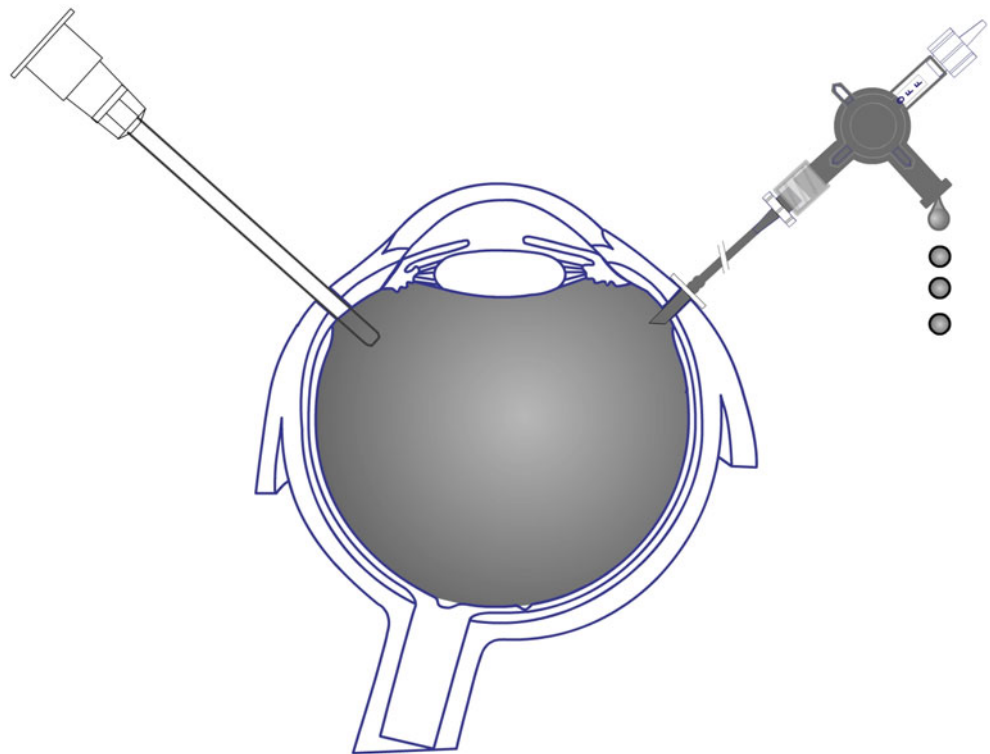


Figure V.B.6-8 The irrigation fluid which was trapped anterior to the sclerotomies, and the perfluorocarbon liquid later causes slippage of the posterior edge of the retinotomy after oil fill (Fig. 2 from page 650 Li and Wong [13])

line (Figure V.B.6-9). Postoperative positioning with oil is minimized when there is a good oil fill. Adequate tamponade with gas because of its diminishing volume may require alternating lateral sides or even a supine positioning. An inadequate gas bubble should be remedied on the first postoperative day by a gas-fluid exchange in the clinic. Oil is removed at 6 months when cellular activity of proliferative vitreoretinopathy is minimal. At the time of oil removal, the retina is examined carefully and prophylactic laser retinopexy or membrane peeling may be indicated (Figure V.B.6-10).

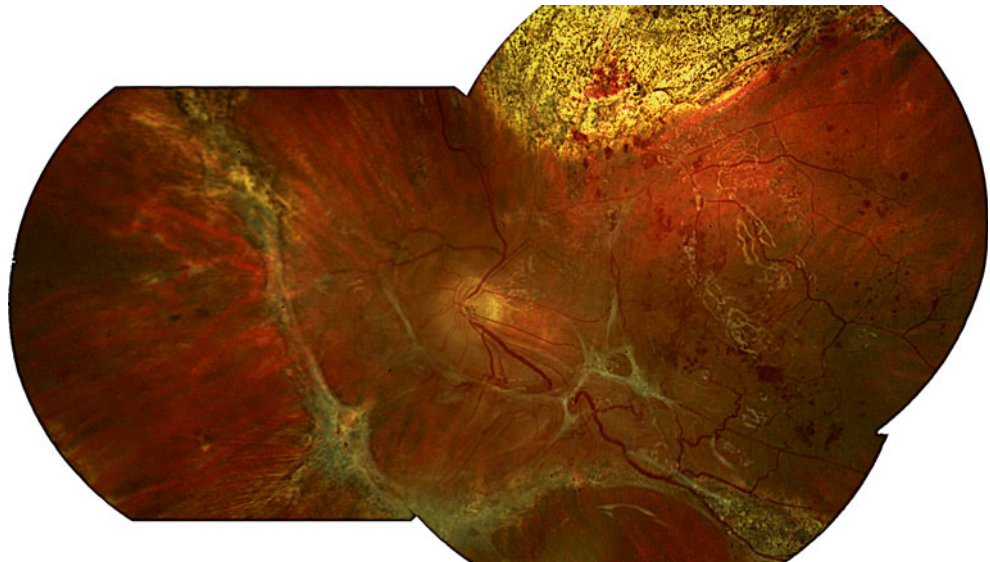
Figure V.B.6-9 To eliminate the trapped irrigation fluid anterior to the sclerotomy, the infusion line is turned off and perfluorocarbon liquid is pushed up the infusion line. At the same time, the trapped fluid simultaneously exits through a superiorly positioned sclerotomy. A total fill of perfluorocarbon liquid is achieved (Fig. 3 from page 650 Li and Wong [13])



C. Complications

Complications include retained subfoveal perfluorocarbon, macular pucker, hypotony, macular displacement, PVR re-proliferation at the retinotomy edges, corneal decompensation, emulsified silicone oil with or without glaucoma, and iris neovascularization. Retained perfluorocarbon liquid can be aspirated with a 39-gauge cannula [14] or displaced by injection of subretinal fluid and upright positioning. As discussed above, macular pucker is a risk of silicone oil tamponade and is addressed by repeat vitrec-

Figure V.B.6-10 Successful inferior relaxing retinotomy in an oil-filled eye. There is minimal re-proliferation at the retinotomy margins. The secondary macular pucker will be peeled at the time of oil removal (Courtesy of VMR Institute for Vitreous Macula Retina, Huntington Beach, California)



omy and membrane peeling. Internal limiting membrane peeling may prevent recurrences. Corneal decompensation is caused by oil migrating into the anterior chamber [15, 16]. Decreased aqueous production caused by PVR fibrosis of the ciliary body also contributes to corneal decompensation [17]. Emulsified oil, previously thought to be due to impurities in the oil, is now thought to be caused by emulsifiers in the oil such as blood and protein [18]. Therefore, preventing hemorrhage during retinotomy is important. Iris neovascularization is caused by fibrotic organization within the ciliary body and pars plana, and removal of the retina anterior to the retinotomy prevents this and consequent hypotony.

IV. Future Developments

A. Surgical

Twenty-seven-gauge vitrectomy instrumentation may be ideal for performing relaxing retinotomy. The inefficiency of such small-gauge instrumentation does not matter since the vitreous has already been removed. On the other hand, the precision and ability of the cutting port to be closer to the retinal pigment epithelium during the retinotomy should be an advantage [19]. There are significant challenges to the application of femtosecond laser to the posterior segment compared to its use in the anterior segment. However, the photodisruptive properties of femtosecond laser could be harnessed for the cutting of the retina [see chapter V.B.3. Future vitrectomy technologies].

B. Pharmacologic

Pharmacologic vitreolysis [see chapter VI.A. Pharmacologic vitreolysis] may provide useful adjuncts to surgery of anterior PVR by weakening the very strong vitreoretinal adhesion at the vitreous base. Indeed, studies in monkeys employing chondroitinase to perform pharmacologic vitreolysis found disinsertion of the vitreous base [see chapter VI.H. Chondroitinase as a vitreous interfactant – vitreous disinsertion in the human].

Abbreviations

PVR	proliferative vitreoretinopathy
ILM	inner limiting membrane
L	lens

References

- Lewis H, Aaberg TM. Anterior proliferative vitreoretinopathy. *Am J Ophthalmol.* 1988;105:277–84.
- Machemer R, Aaberg TM, Freeman HJM, et al. Updated classification of retinal detachment with proliferative vitreoretinopathy. *Am J Ophthalmol.* 1991;112:159–65.
- Machemer R. Retinotomy. *Am J Ophthalmol.* 1981;92(6):768–74.
- Zivojnovic R. *Silicone Oil in Vitreo-retinal Surgery.* Dardrecht: Martinus Nidjhoff Publishers; 1967. p. 142–3.
- Han D, et al. Relaxing retinotomy and retinectomy: surgical results and predetermining visual outcomes. *Arch Ophthalmol.* 1990;108(5):694–7.
- Morse L, McCuen BM, Machemer R. Relaxing retinotomy: analysis of anatomic and visual results. *Ophthalmology.* 1990;97(5):643–7.
- Iverson DA, et al. Indications and results of relaxing retinotomy. *Ophthalmology.* 1990;97(10):1298–304.
- Federman J, Eagle R. Extensive peripheral retinectomy combined with posterior 360 degree retinotomy for retinal reattachment in advanced proliferative vitreoretinopathy. *Ophthalmology.* 1990;97(10):1305–20.
- Han DP, et al. Management of complex retinal detachment with combined relaxing retinotomy and intravitreal perfluoro-n-octane injection. *Am J Ophthalmol.* 1994;118(1):24–32.
- Blumenkrantz M, et al. Relaxing retinotomy with silicone oil or long acting gas with severe proliferative vitreo retinopathy: Silicone Study report 5. The Silicone Study Group. *Am J Ophthalmol.* 1993;116(5):557–64.
- Hogan MJ. The vitreous. Its structure in relation to the ciliary body and retina. *Invest Ophthalmol.* 1963;2:418–45.
- Daicker B. Sind die symptom “Weiss mit Druck” und “Weiss ohne Druck” durch die periphere netzhautsklerose bedingt? *Mod Probl Ophthalmol.* 1975;15:82–90.
- Li KK, Wong D. Avoiding retinal slippage during macular translocation surgery with 360 retinotomy. *Graefes Arch Clin Exp Ophthalmol.* 2008;246:649–51.
- Roth DB, Sears JE, Lewis H. Removal of retained subfoveal perfluoro-n-octane liquid. *Am J Ophthalmol.* 2004;138(2):287–9.
- Liesenhoff HH, Schmitt J. Koplikationene durch flussiges silikon in der vorderkammer. *Berl Dtsch Ophthalmol Ges.* 1969;69:643–4.
- Sternberg Jr P, Hatchell DL, Foulks GN, et al. The effect of silicone oil on the cornea. *Arch Ophthalmol.* 1985;103:90–4.
- Zarbin MA, Michels RG, Green WR. Dissection of epicyliary tissue to treat chronic hypotony after surgery for retinal detachment with proliferative vitreoretinopathy. *Retina.* 1991;11:208–13.
- Bartov E, Pennarola F, Savion N, et al. A quantitative in vitro model for silicone oil emulsification. Role of blood constituents. *Retina.* 1992;12:523–7.
- Oshima Y, Wakabayashi T, Sato T, Ohji M, Tano Y. A 27-gauge instrument system for transconjunctival sutureless microincision vitrectomy surgery. *Ophthalmology.* 2010;117:93–102.
- Sebag J, Balazs EA. Pathogenesis of CME – an anatomic consideration of vitreoretinal adhesions. *Surv Ophthalmol.* 1984;28(Suppl):493–8.

Kenneth M.P. Yee and J. Sebag

Outline

- I. **History**
- II. **Clinical Considerations**
 - A. Case Selection
 - B. Expanded Indications for Pneumatic Retinopathy
 - C. Contraindications for Pneumatic Retinopathy
- III. **Methodology of In-Office Pneumatic Retinopathy**
 - A. Examination
 - B. Retinopathy
 - 1. Diathermy
 - 2. Cryopexy
 - 3. Laser Photocoagulation
 - C. Intravitreal Bubble Injection
 - 1. Pure Air
 - 2. Long-Acting Expansile Gases
 - a. Perfluorocarbons
 - b. Sulfur Hexafluoride
 - D. Post-Operative Positioning
 - E. Modified Pneumatic Retinopathy
- IV. **Outcomes**
 - A. Results
 - B. Complications
 - C. Benefits of Pneumatic Retinopathy

Conclusion

References

Keywords

Vitreous • Anomalous posterior vitreous detachment • Rhegmatogenous retinal detachment • Pneumatic retinopathy • Pure air • Sulfur hexafluoride • Perfluoropropane • Cryopexy • Laser photocoagulation • In-office repair

Key Concepts

1. Retinal detachments arising from anomalous PVD causing superior retinal breaks can be cured with in-office surgery called pneumatic retinopathy.
2. Pure air has the same success rate as long-acting expansile gases, perhaps with fewer complications.
3. Failure to reattach the retina with pneumatic retinopathy does not compromise the success of subsequent surgery by other methods.

I. History

Pneumatic retinopathy became popular in the late 1980s [1, 2]. However, Bengt Rosengren of Göteborg, Sweden, is perhaps the first to use an intravitreal air bubble to treat rhegmatogenous retinal detachment (RRD) [3]. In 1952, he reported his extensive experience [4] in a series of 300 cases treated between 1936 and 1950, in which he combined external diathermy with intravitreal air injection to treat RRD. Remarkably, the cure rate was 234/300 (78 %). Postoperative visual acuity of 20/40 or better was achieved in only 31 % of the first 100 cases but increased to 45 % of the last 100 cases. By 1957, Lister [5] wrote in the *British Journal of Ophthalmology* that “In retinal detachments, particularly those in the elderly when the tear is in the upper part of the eye, air seems to be the obvious choice, although this is not the view of everyone.” At the American Ophthalmological Society in 1969, Machemer [6] introduced

K.M.P. Yee • J. Sebag, MD, FACS, FRCOphth, FARVO (✉)
VMR Institute for Vitreous Macula Retina,
7677 Center Avenue, suite 400, Huntington Beach,
CA 92647, USA

Doheny Eye Institute, Los Angeles, CA, USA
e-mail: jsebag@VMRinstitute.com

the use of air to treat giant retinal tears, a technique that was further developed by Freeman and Schepens of Boston [7].

Expansile long-acting gases were first introduced in 1973 [8]. The term pneumatic retinopexy (PR) as a procedure to treat RRD without conjunctival incision was introduced and popularized by Hilton and Grizzard in 1986 [9]. Their procedure combined transconjunctival cryotherapy and intravitreal expansile gas injection with postoperative positioning. The first 100 cases reported had an 84 % rate of single-operation success (SOS), fewer complications than scleral buckling (SB), and reduced tissue trauma [10]. No hospitalization and reduced cost also made PR an attractive option for treating RRD. Although not yet FDA-approved, intraocular sulfur hexafluoride and perfluoropropane became widely used in North America by the late 1980s [11]. Successful retinal adhesion using laser photocoagulation made laser retinopexy a viable alternative to cryoretinopexy combined with intravitreal gas injection [12, 13]. Scleral buckling is preferred for inferior RRD in phakic eyes, vitrectomy in pseudophakic eyes, and both in failed/complicated cases. In recent years, PR has gained popularity especially among young surgeons [14–17]. Proven long-term efficacy [18], expanded indications, and novel techniques have broadened the usefulness of PR for retinal detachments.

II. Clinical Considerations

As extolled by Schepens, Lincoff, and others, the fundamental principle of successful RRD reattachment surgery is identifying the cause, i.e., the break(s) that caused the detachment and any other coexisting pathology. The Schepens binocular indirect ophthalmoscope made this possible in the office, clinic, and operating room. There is no setting where this principle is more vital than in the minimalist approach of PR, for an encircling scleral buckle can support breaks that are missed, while with PR a missed break will result in recurrent retinal detachment. This consideration along with patient understanding and compliance are keys to success and significantly influence proper case selection for PR.

A. Case Selection

Patient selection must involve a consideration of patient understanding, support and assistance from the family, physical ability to position properly and for the desired duration, and the particular attributes of the physical examination, particularly the fundus. Selecting the appropriate patient and properly motivating the patient and support group (family) to position correctly enable the use of short-acting gases such as SF₆ or air, for the retina often reattaches within a day or 2, obviating the need for long-acting gases.

It has been proposed [19] that the “classic” indications for combined laser or cryopexy with intravitreal air or gas injection in uncomplicated RRD are:

- Identification of all retinal breaks
- Retinal breaks limited to the superior 8 clock hours of the fundus
- Breaks within 1–2 clock hours of each other in the case of multiple breaks
- No signs of proliferative vitreoretinopathy
- A cooperative patient that can position
- Clear media

The presence of vitreous hemorrhage is considered by some to be a contraindication for PR [20, 21], primarily because adequate visualization of the inferior fundus is usually hampered by the blood. One study has shown that if adequate visualization of the peripheral retina is not impaired, then patients with vitreous hemorrhage have anatomic (72.2 %) and visual outcomes that are less than cases without vitreous hemorrhage (81 %) [22]. While the inferior retina is usually attached in these cases, there may nonetheless be retinal breaks inferiorly. Studies have shown that identifying inferior breaks and treating them prophylactically at the time of PR contributes to a high incidence of permanent retinal reattachment by decreasing the incidence of recurrent RRD due to missed breaks [7, 20]. Higher primary anatomic success rate has also been associated with the presence of complete posterior vitreous detachment (PVD) compared to partial PVD in phakic eyes with RD and flap tears [23]. Pseudophakic RRDs can also be successfully managed with PR [24]. Treated eyes with the classic indications for PR have a higher single-operation success rate and fewer complications than eyes with complicated retinal detachments [9, 10, 25, 26].

B. Expanded Indications for Pneumatic Retinopexy

Although PR is primarily indicated for uncomplicated RRDs with one or more breaks within 1 clock hour located in the superior fundus, some studies have proven the efficacy of PR for other indications. Multiple breaks in multiple quadrants, large tears up to 2.5 clock hours in size, and RRDs associated with a moderate degree of PVR have been successfully managed using PR with 75 % success [27], admittedly lower than in eyes with classic indications for PR but acceptable considering the complexity of the cases. Other studies have shown that PR can be used for complex detachments with breaks up to 180° apart, as intravitreal gas is not required to tamponade all breaks simultaneously [28, 29]. Indeed, intravitreal gas can be rotated from the position of tamponade for one break into a position where tamponade of the second break or groups of breaks is achieved [30]. Superior giant tears can

also be successfully managed with PR alone or followed by conventional scleral buckling procedures and cryopexy [31, 32]. Inferior RRDs resulting from inferior retinal breaks have also been successfully treated by PR with proper inverted head positioning and more attention to postoperative follow-up to ensure surgical success [33, 34]. One study found that eyes with vitreous hemorrhage that does not impede the thorough examination of the peripheral retina, macula-off detachments, and eyes with mild to extensive lattice degeneration can be treated successfully with PR [22].

Pneumatic retinopexy is also a feasible option for various other situations:

- Persistent or recurrent RRD, even long after initial repair by any technique (PPV and SB) [35–38].
- PR success rates for teens are comparable to adult success rates [39].
- PR is useful as an initial procedure in managing RD associated with hypotony, severe choroidal detachment, and vitritis. Subsequent surgical repair of complicated RDs can be facilitated by first resolving hypotony and choroidal detachments with PR, although PR alone achieved complete retinal reattachment in 33 % of cases [40].
- PR can also be used to delay surgical intervention in cases of RRD and concurrent cytomegalovirus infection with the causative break(s) located superiorly and in an area uninvolved with the infection [41].
- RRD following laser-assisted in situ keratomileusis can be managed with PR with high success rates and good visual outcome [42, 43].

C. Contraindications for Pneumatic Retinopexy

Patients who do not understand, cannot position correctly and/or adequately, and do not have adequate support at home are poor candidates for PR. Other identified risk factors for PR failure are location of retinal break(s) and extent of retinal detachment greater than two quadrants [37]. In patients with vitreous hemorrhage or RRD greater than 4.5 clock hours, PR success rates may be lower [21, 44]. Factors other than the extent of the RD that adversely affect PR success are lens status, number of breaks, and gender [45]. PR can be significantly less effective (as low as 43 % in one study [46]) in aphakic or pseudophakic patients with an absent or ruptured capsule [44, 46–49]. One study had a single-operation success rate of 92, 66, and 57 % for phakic, pseudophakic, and aphakic eyes, respectively [47]. Another also study showed phakic eyes fared better than non-phakic eyes for pneumatic retinopexy, with the single-operation successes of 71–84 % for the former and 41–67 % for the latter [1]. Furthermore, phakic eyes with partial PVD at the time of PR had lower primary anatomic success [23]. Poor visual acuity in cases of

attached macula and visual acuity worse than 20/50 are also risk factors for failed PR [44, 48]. A recent study found that the presence of inferior break(s) (even if treated with cryopexy or laser retinopexy at the time of PR) or visible vitreous traction causing a tear to gape open significantly reduces the success of PR to 28.6 and 50 %, respectively [22]. However, the former has not been our experience, as will be described below. The presence of additional pathologic findings in the same or fellow eye is also a risk factor for failed PR [44, 48]. Lastly, some studies show that being male correlates with primary PR failure [48, 50], perhaps due to lack of patient compliance. PR usually fails in RRD following vitrectomy for posteriorly dislocated lens fragments and requires subsequent scleral buckling [51]. PR has also been reported to cause anterior displacement of Artisan intraocular lenses [52].

III. Methodology of In-Office Pneumatic Retinopexy

A. Examination

As is the case in all of medicine, the success of PR depends upon proper case selection. A meticulous examination of the peripheral fundus, preferably with scleral depression, is critical in identifying the number, size, and location of all retinal breaks. Studies have shown that treating all breaks, both those involved in the RRD as well as those in attached retina (usually inferiorly), at the time of PR is associated with a very low incidence of PR failure [18, 20].

B. Retinopexy

1. Diathermy

Choroidal coagulation for the treatment of RRD by surface diathermy cauterization was first described by Marshall in 1933 [53]. Rosengren later described the use of diathermy and light coagulation to induce retinohoroidal contact in detachment surgery [54–56]. Schepens also described the use of diathermy for the treatment of small posterior retinal breaks [57, 58] and popularized the use of diathermy in scleral buckling when scleral flaps encased the buckling element and diathermy treatment was applied to the bed of the dissected scleral flap.

2. Cryopexy

First described in the 1970s by Lincoff et al. [59], retinal adhesion can also be achieved by creating a chorioretinal scar using extreme cold. The rate of single-operation success of PR combined with transconjunctival cryoretinopexy has been shown to be significantly higher than with laser photocoagulation in pseudophakic or aphakic eyes [24].

Caution should be exercised to limit the amount of cryopexy performed, as studies have shown that excess cryopexy is associated with migration of viable retinal pigment epithelial cells [60] (via the retinal breaks) and breakdown of the blood-ocular barrier which are thought to increase the risk of postoperative proliferative vitreoretinopathy (PVR), macular pucker, and cystoid macular edema. Cryopexy is not a promoter of postoperative PVR in primary RRDs that are due to atrophic holes in lattice, macular holes, oral dialyses, or horseshoe tears with mobile posterior edges. In contrast, cryopexy is a stimulating factor for postoperative PVR in detachments due to retinal tears that are 180° or more or horseshoe tears with curled posterior edges [61]. These among other reasons have led many to prefer laser over cryopexy.

3. Laser Photocoagulation

Both argon and krypton laser photocoagulation have been shown to achieve early adhesion of the neurosensory retina to the retinal pigment epithelium soon after retinal reattachment with PR [12, 13]. Retinal adhesion occurs within 24 h, and the retina remains attached even if surrounding untreated areas detach [13]. Laser retinopexy allows for faster recovery of visual acuity with fewer postoperative complications than cryopexy [62]. Cryopexy has been significantly associated with long-term failure of pneumatic retinopexy, and laser photocoagulation may be indicated in these cases [49]. Schepens considered laser photocoagulation the best option for the treatment of posterior retinal breaks [63]. The advent of the indirect ophthalmoscope laser delivery system has improved the use of laser photocoagulation in PR as it facilitates laser treatments of the peripheral fundus.

C. Intravitreal Bubble Injection

It has been proposed that paracentesis should be performed before the gas injection to reduce the chance of intravitreal gas migrating into the anterior chamber [64]. This technique especially applies to pseudophakic eyes with an open posterior capsule, either due to intraoperative incision or postoperative YAG laser capsulotomy. In aphakic or pseudophakic patients, the injection site is placed 3–3.5 mm posterior to the limbus and 4 mm if the patient is phakic. A slow gas injection through a shallowly inserted needle (1 mm) can prevent the formation of multiple small bubbles or “fish-egg” bubbles [65]. It is desirable to inject a single large bubble so as to reduce the risk of air or gas entering the subretinal space via the retinal break(s). The gas should also be injected away from any larger retinal break(s) to mitigate the risk of subretinal gas migration [1] (Figure V.B.7-1).

1. Pure Air

If all holes or breaks are closed, the retina usually reattaches within 24 h which makes the use of pure air a practical

alternative to expansile gases [18, 20, 66]. The use of pure air rather than long-acting expansile gases has many benefits including a larger initial tamponade, shortened postoperative positioning, reduced retinal toxicity, the ability to treat RDs in-office, lower cost, and higher accessibility [18, 20].

Some advocate that in cases of bullous detachments, 1–3 ml of pure air should be injected through the pars plana [67]. Obviously, this causes significant elevation of intraocular pressure, and either aqueous, liquid vitreous, or both must be released to lower the pressure. Other studies have shown that 0.8 cc can be very effective [18, 20]. This approach employs a single paracentesis of aqueous to lower intraocular pressure. As an example, consider that this technique was employed in a 74-year-old white man with a macula-on bullous RRD extending from 1 to 4:30 arising from a retinal break at 2:00 (Figure V.B.7-2). This patient was pseudophakic with an open capsule and had a PVD at the time of PR. Retinal cryopexy was administered at 1:30, a paracentesis was performed before the intravitreal injection, and then 0.8 ml of filtered air was injected at the 4:00 meridian, 3.5 mm posterior to the limbus. In this case, the retina was attached 2 days post PR (Figure V.B.7-3). By 5 days post injection, the bubble was completely gone, and the retina was attached and has remained attached since.

The non-expansile nature of pure air requires a larger initial volume of gas injection. An injection of 0.8 cc of air subtends an angle of 120° enabling tamponade of breaks within 3 clock hours apart. The duration of intravitreal air is 5–7 days [68], often less than 5 days. Histopathological examination after pure air PR reveals no abnormalities in the retina, ciliary body, or blood-ocular barrier [69].

2. Long-Acting Expansile Gases

There are many options available for long-acting expansile gases to use in PR. Several perfluorocarbons, the most widely used being perfluoropropane, and sulfur hexafluoride (SF₆) can be used for internal tamponade of RRD. Each gas has different expansile properties as well as different absorption rates, which should be considered when choosing the appropriate gas for PR. Lens and vitreous status are also considerations, as one study has shown that the intraocular half-life of both SF₆ and C₃F₈ is two to three times shorter in vitrectomized aphakic rabbit eyes than in phakic eyes with intact vitreous [70]. One study has shown that expansion of some intravitreal gases can cause reversible and irreversible damage to the retina and ciliary body. Also, the duration of exposure and the gas concentration determine the degree of damage or toxicity [69].

a. Perfluorocarbons

Perfluorocarbons persist for 6–28 days on average before being absorbed in the blood [71, 72]. One study of three different perfluorocarbon gases (perfluoromethane (CF₄), perfluoroethane (C₂F₆), and perfluoropropane (C₃F₈)) showed that the expansion and intraocular longevity of

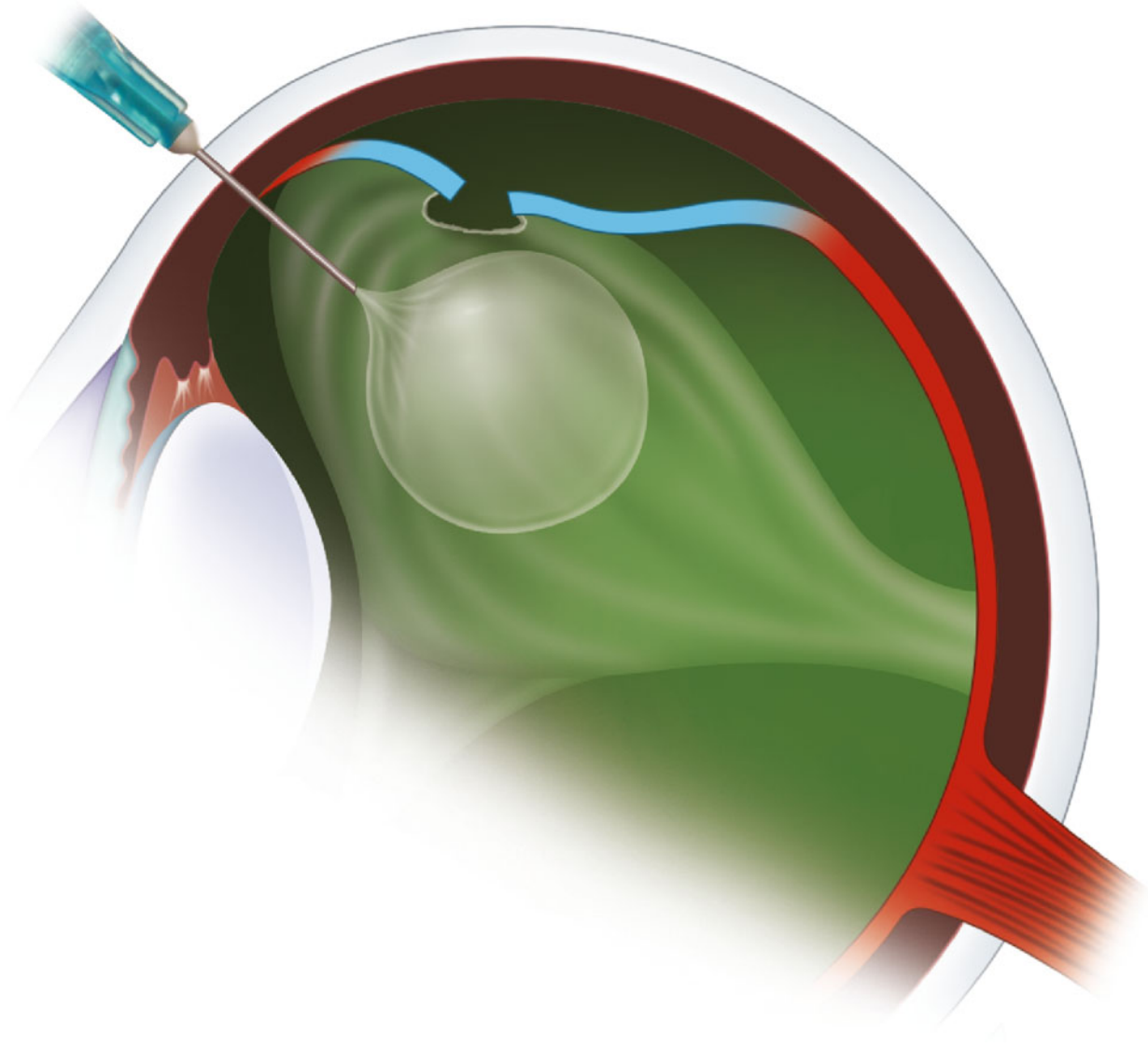


Figure V.B.7-1 Artist's rendition of intravitreal bubble injection for the treatment of superior rhegmatogenous retinal detachments. A bubble is injected into the vitreous body using a slow and shallow injection in order to avoid the formation of small bubbles. The intravitreal bubble

is placed over the break(s) by postoperative positioning in order to tamponade the break and mitigate any further accumulation of subretinal fluid (Courtesy of Merlin Hall)

the gases increase with the length of the carbon chain [72]. Perfluoropropane (C_3F_8) is the most common expansile long-acting gas used for internal tamponade of RRD. Perfluoropropane has been shown to expand up to four times its original volume and remain for up to 6–8 weeks [68]. Perfluoromethane and perfluoroethane are used much less and persist for 6 days and 2–5 weeks, respectively [68, 72]. Perfluoroethane expands to 3.3 times the original injection volume [68].

b. Sulfur Hexafluoride

Sulfur hexafluoride (SF_6) is a nonpolar gas that is inert in the vitreous. SF_6 is used for internal tamponade of RRD in

all surgeries, including PR. SF_6 doubles its volume during the initial 24–48 h and then is absorbed into the blood over 5–14 days [68, 71, 73]. Sulfur hexafluoride remains in the vitreous for as little as a quarter of the time as does perfluoropropane [72].

D. Post-Operative Positioning

One of the most important keys to success in PR is postoperative positioning. This is an arduous experience for patients especially considering that the recommendation is to maintain the specified head position for 16 h/day for 5 days [74],

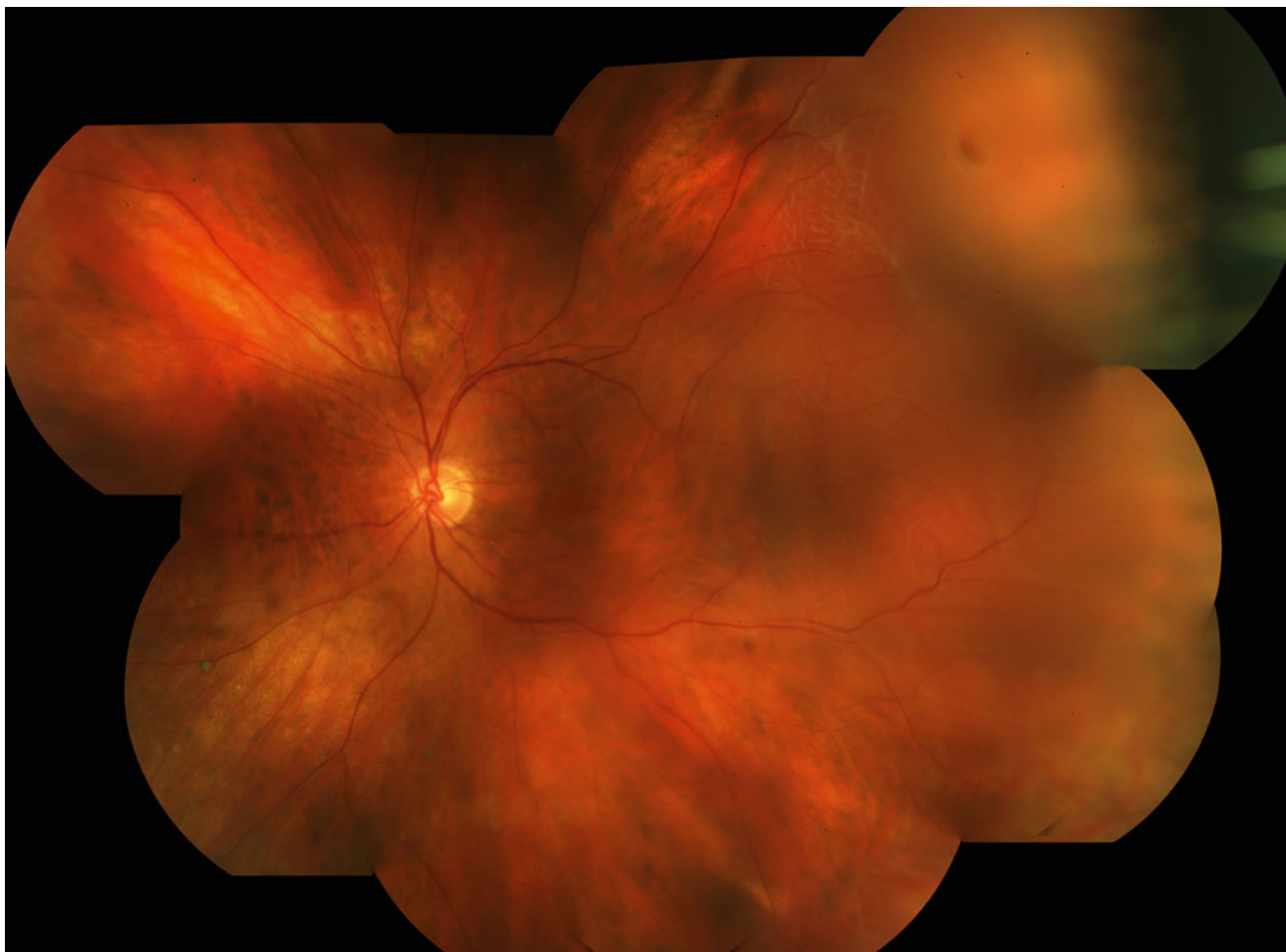


Figure V.B.7-2 Fundus photograph collage of a superior macula-on retinal detachment in the left eye extending from 1 to 4:30 arising from a retinal break located at 1:30. Subretinal fluid extended posteriorly to the temporal macula

although many recommend far longer periods of positioning. Shortening the duration of positioning by using shorter-acting gases like SF₆ or air can increase compliance and the likelihood of success. Immediately after the gas injection, the patient's head is positioned so that the bubble directly apposes the break(s). In cases where the macula is involved or threatened, a "steamroller" technique can be used. In this technique, the patient is positioned facedown after gas injection, and over a period of 10–15 min, the position is gradually changed so that the break is at the 12 o'clock position. This allows the bubble to roll toward the break displacing any subretinal fluid away from the macula and into the vitreous cavity. Basic and "steamroller" techniques have comparable risks for PVR development and appear to be equally safe and effective in PR for primary RRD [75].

E. Modified Pneumatic Retinopexy

Modifications of PR have been introduced, but it is not clear that these improve outcomes and reduce postoperative com-

plications. When combined with microscope-assisted subretinal fluid drainage, PR has been shown to be effective and safe in 86 % of phakic RRDs from breaks within the upper 60° of the fundus [76, 77]. Although this is not truly PR, one study of combined intravitreal bubble injection with drainage of subretinal fluid had 100 % single-operation success and no occurrences of extension of the detachment, persistence of subretinal fluid or subretinal gas, or reopening of retinal breaks [77]. This procedure, however, requires the use of an operating room, which limits access to care, raises costs substantially, reduces the rapidity of intervention afforded by PR in an office setting, and significantly decreases the applicability of PR to a broad global population.

Some studies have shown that mixing expansile gases can reduce incidences of elevated postoperative IOP [78]. In this regard, a mixture of 40 % SF₆ and 60 % air combined with subretinal fluid drainage can have favorable results [79]. Perfluoroethane (C₂F₆) gas has comparable success and complication rates as conventional gases [80]. Extensive studies have shown the efficacy and benefits of PR using pure air

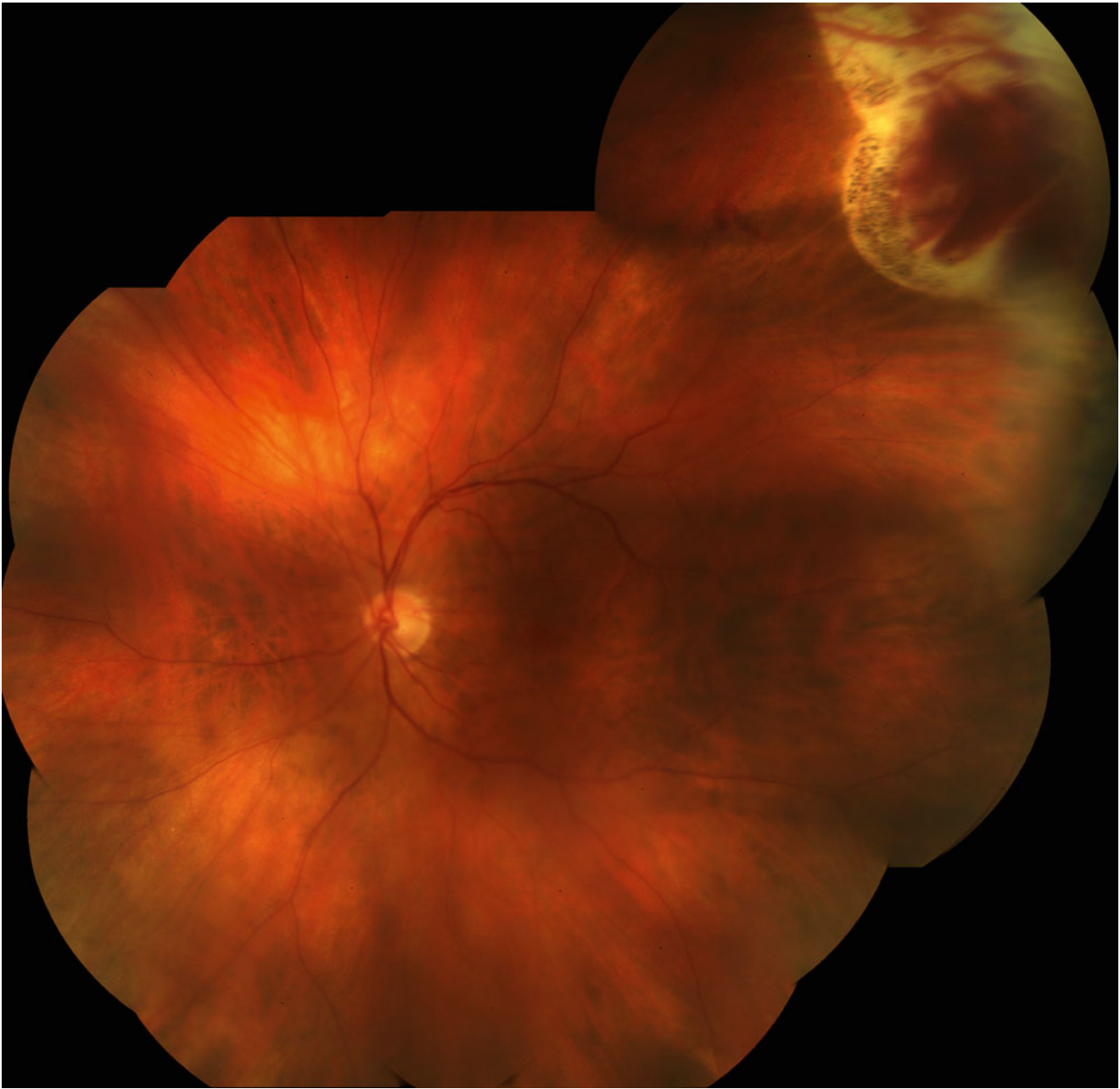


Figure V.B.7-3 Same eye as shown in Figure V.B.7-2, now healed 1 month after in-office pneumatic retinopexy. Pure air (0.8 ml) was injected after cryopexy was applied to the retinal break at 1:30, and a paracentesis was performed at the limbus to lower IOP

only [18, 20, 81]. Pure air PR achieves a high rate of reattachment and good visual outcome [18, 20]. Pure air PR can also have lower incidences of PVR, PMM, and new or missed breaks. The recovery period is also greatly reduced, and accessibility to pure air is universal as compared to expansile gases [20]. Long-term efficacy has also been shown to be comparable to other options for RD management [18]. Neodymium-doped yttrium aluminum garnet (Nd:YAG) laser augmented PR has also had good results with laser disruption of vitreous bands inducing traction via vitreoretinal adhesion [82].

IV. Outcomes

A. Results

Nonclassical (see above) indications have PR success rates that vary between 72 and 100 % (Table V.B.7-1).

In eyes with uncomplicated superior RRD without significant PVR, the single-operation success varies from 61 % to as high as 90 % [1, 9, 10, 22, 23, 45, 46, 48–50, 71, 73, 83–92]. Studies have shown that the single-operation success rate of PR (73 %) is comparable to that of SB (82 %) but lower than

PPV (94 %) after 6 months and there is a similar risk of late re-detachment after 2 years of follow-up [93, 94, 97]. Reoperation rates are higher after PR than PPV or SB although PPV results in more adverse outcomes [84]. In cases of primary PR failure, most are reattached with one additional procedure and have good visual outcome [93]. Despite the increased need for reoperation after PR, the final anatomic results do not differ compared to SB, and PR has less morbidity and better postoperative visual acuity [19, 95]. Following PR, PVR developed in 0–16 % [1, 18, 20, 85, 87, 90, 96] compared to an incidence of 5–10 % following SB and 29.4 % after PPV [97–99]. In other studies, the rate of postoperative PVR does not differ significantly between SB and PR [91, 100].

Most cases of primary failure can be reattached with one additional PR procedure [101]. In eyes with classic indications (see above), the final anatomical reattachment rates were similar to pars plana vitrectomy (PPV) and scleral buckle (SB) [102]. Postoperative visual acuity at 1 year does not differ

among these three treatment options to repair RRD [103]. Long-term efficacy of PR has been proven to be as high as 98.7 % up to 6.4 years postoperatively and to be even better than SB after 2 years with less cataract incidence, better visual outcome, and faster recovery [104, 105]. Final anatomic success after subsequent therapy following failed primary PR has been reported to be as high as 100 % [9, 10, 44, 45, 47, 48, 71, 73, 86, 89–91, 106], and repeat operation by PR, PPV, or SB does not negatively impact visual acuity at final follow-up [107].

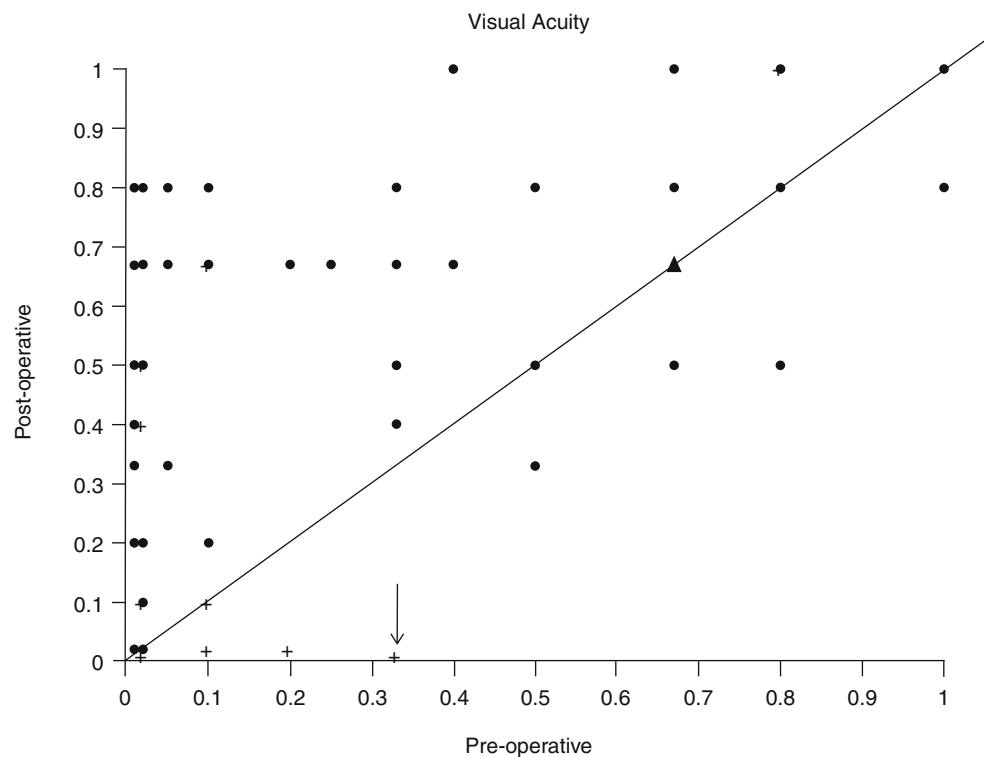
Scleral buckle or vitrectomy or a combination of both has slightly better initial anatomic success than PR, but postoperative visual acuity does not differ among the various techniques at 1 year [95]. Eyes treated with PR for RRD post PPV to remove posteriorly dislocated lens material require secondary SB to achieve reattachment in 63 % of cases [51]. Macular pucker develops in 3 % [85]. Given the limited support provided by the iris after cataract surgery, the presence of intravitreal gas has been shown to cause anterior displacement of Artisan intraocular lenses [52].

In a long-term study (6–186 months' follow-up), pure air PR achieved a single-operation success rate of 80.5%, that increased to 85.7 % reattachment after repeat PR. A final reattachment rate of 100 % was eventually achieved when failed cases underwent PPV or SB [18]. These success rates are comparable to the rates of PR using expanding gases. Eighty-six percent of patients treated with pure air PR had the same or better visual acuity postoperatively, and nearly two-thirds attained visual acuity $\geq 20/40$ [18] (Figure V.B.7-4). In this study, no patients

Table V.B.7-1 Non-classical indications for PR

	% Anatomic success
Multiple breaks	75 [22, 27]
Giant tears	89–100 [31, 32]
Inferior RD	77–91 [33, 34]
Macula off	81 [22]
Retinal lattice (<i>degeneration</i>)	77 [22]
Vitreous hemorrhage	72 [22]
Adolescents	84 [39]

Figure V.B.7-4 Scattergram of Snellen visual acuity (VA) pre- and postoperatively following pure air pneumatic retinopexy in 77 subjects [18]. The points above the sloped line represent improvement in VA, and points below the line represent worsened VA. The arrow represents a single patient who required a secondary scleral buckle with vitrectomy due to a new inferior break. The triangle marker indicates the only case that developed postoperative premacular membrane formation with macular pucker. The plus signs indicate all cases that required repeat pneumatic retinopexy procedures [18]



developed postoperative PVR and only 1/77 (1.3 %) developed macular pucker. This is lower than previous studies which showed that as many as 10 % of patients developed PVR and 3 % macular pucker after PR with expanding gases [1].

B. Complications

Although the success rate of PR in the management of superior RRD is high, there are some complications that should be considered. Following PR, 31 % of eyes showed one or more early complications such as the rare development of cataract due to impaling with the needle, choroidal detachment, endophthalmitis, vitreous hemorrhage, and peripheral subretinal hemorrhage or the much more common issues of delayed reabsorption of subretinal fluid and gas entrapment in the anterior chamber (between the pars plana and the lens) or in the subconjunctival space, the most common acute complication [108]. Late onset of these complications was observed in 7 % of eyes [49].

Most retinal complications develop in the inferior fundus [83–92]. New or missed breaks occur from 7 to 22 % [1, 10, 22, 27, 30, 47, 84, 85, 87, 90, 104, 109] of cases, and 83 % of these occur in pseudophakic or aphakic eyes [47]. PR has been implicated as the cause of new retinal tears and RRD in previously uninvolved quadrants, presumably due to vitreous condensation and traction [110, 111]. While possible, this is less likely than re-detachment with a new inferior RD caused by a missed break. Studies have shown that meticulous preoperative fundus examination with scleral depression can identify inferior breaks in attached retina that are treatable at the time of PR, resulting in a lower incidence of inferior RRD following PR [18, 20]. In other studies, the rates of missed or new retinal breaks after PR are higher than following SB [101].

Three complications reported with PR but not with scleral buckling are subretinal gas, gas entrapment at the pars plana, and subconjunctival gas [104, 112]. Postoperative elevation in intraocular pressure (IOP) has been associated with PR, especially with perfluoropropane [78]. Pressure-reducing medication is not usually indicated in these eyes because IOP returns to baseline 30–60 min after injection and does not increase during the subsequent 5 postinjection days [113]. Cystoid macular edema (CME) may develop in as many as 8 % of patients following PR and may deteriorate the final visual outcome [90]. Rates of CME after PR are similar to CME rates following SB, and previous cataract surgery or macular detachment may increase the CME rates following PR [114]. Central retinal artery occlusion is also a potential complication after PR and patients should be advised that flying or being at altitudes higher than 2,000 ft may cause expansion of intraocular gas in accordance with Boyle's law [115]. A rare complication of PR is delayed subretinal fluid absorption, shown to persist for more than 2 years which ultimately is spontaneously reabsorbed [116–118]. Delayed subretinal

fluid absorption can occur as often as 21–37 % of the time and can be associated with small subretinal pigment precipitates [49, 119]. Extensive cryotherapy and the presence of subretinal precipitates are factors that are significantly associated with delayed subretinal fluid absorption [119]. In cases where the macula is not involved, final visual acuity is not impaired [118]. Despite these possible complications of PR, many rhegmatogenous retinal detachments can be successfully managed with good anatomic and visual outcomes [120].

C. Benefits of Pneumatic Retinopexy

Pneumatic retinopexy (PR) for the treatment of uncomplicated superior RRDs has an anatomic success rate similar to conventional RRD surgery. Functional results appear to be better after PR than other interventions with low risks of subretinal gas, PVR, macular pucker, or infection [121]. Although the anatomic success rate of PR is comparable to SB, PR has less morbidity and better postoperative visual acuity [19]. In cases of macula-off detachments for less than 2 weeks, the visual results are significantly better with PR than SB [73]. Two-year outcomes are better for PR than SB with better visual outcome and faster recovery [98]. Two years after intervention, cataract incidence was less with PR than SB, and temporary gas tamponade for PR is not associated with permanent changes in lens transparency [97, 122]. PR does not cause strabismus or extraocular muscle imbalance like encircling bands, although PR strabismus rates are comparable to radial buckles [123]. The shape of the cornea is not altered after PR like after scleral buckling [124]. PR achieves similar success rates as SB and PPV in pseudophakic retinal detachments following cataract surgery [125].

Access where resources are scarce, good cost-effectiveness, ease of procedure, reasonable patient comfort, and early functional rehabilitation make PR a good choice for managing primary RRD [102, 126]. PR in an ambulatory facility was found to be 37.9 and 48.6 % less expensive than scleral buckling and vitrectomy, respectively. If done in-office without a facility fee, costs are 50.9 and 59.4 % lower than scleral buckling and vitrectomy, respectively [22]. The use of pure air lowers costs further. Thus, the theoretical average annual savings to Medicare are between \$6 million and \$30 million if PR utilization were increased to 20–35 % compared to the current usage rate of 15 % [22]. Another study found the cost of scleral buckle surgery to be as much as four to five times that of PR [73].

V. Conclusion

Considering the single-operation success, final anatomic outcome, and functional success, pneumatic retinopexy (PR) can be considered a primary option for a large number of rhegmatogenous retinal detachments (RRD). PR is a safe and effective option for the management of supe-

rior RRD and the related breaks in eyes with little to no signs of PVR. Laser or cryoretinopexy in conjunction with intravitreal gas tamponade can effectively reattach the retina with a single procedure in 60–90 % of cases. Final reattachment is achieved in 98–99 % of cases. Some factors such as lens status, preoperative visual acuity, macula status, and gender influence the final outcome. The most common complications resulting from PR are new or missed retinal breaks or delayed absorption of subretinal fluid though the rates of these complications are similar to SB and PPV. Complications unique to PR such as gas entrapment are acceptably infrequent. PR does not require surgical facilities, can be as much as ten times less expensive than scleral buckle or vitrectomy, and has shorter recovery than these surgeries. The need for postoperative positioning is an important consideration in PR, although this is often needed following SB and PPV as well. Modified and improved techniques for PR can improve efficacy, reduce postoperative complications, and expand the indications for PR.

Abbreviations

C ₃ F ₈	Perfluoropropane Gas
CME	Cystoid Macular Edema
FDA	Food and Drug Administration
IOP	Intraocular Pressure
Nd:YAG	Neodymium-doped yttrium aluminum garnet
PR	Pneumatic Retinopexy
RRD	Rhegmatogenous Retinal Detachment
SB	Scleral Buckle
SF ₆	Sulfur Hexafluoride Gas
PMM	Premacular Membrane
PPV	Pars Plana Vitrectomy
PVD	Posterior Vitreous Detachment
PVR	Proliferative Vitreoretinopathy
VA	Visual Acuity

References

- Chan KC, Lin SG, Nuthi AS, Salib DM. Pneumatic retinopexy for the repair of retinal detachments: a comprehensive review (1986–2007). *Surv Ophthalmol*. 2008;53(5):443–78.
- Barr CC. Pneumatic retinopexy and balloon buckles as alternatives to conventional scleral buckling surgery. *Semin Ophthalmol*. 1995;10(1):2–8.
- Rosengren B. Cases of retinal detachment treated with diathermy and injections of air into the vitreous body. *Acta Ophthalmol*. 1938;16:177.
- Rosengren B. 300 cases operated upon for retinal detachment; method and results. *Acta Ophthalmol*. 1952;30(1):117–22.
- Lister A. Air in the eye. *Br J Ophthalmol*. 1957;41(2):115–9.
- Machemer R, Aaberg TM, Norton EW. Giant retinal tears. II. Experimental production and management with intravitreal air. *Trans Am Ophthalmol Soc*. 1969;67:394–414.
- Freeman HM, Schepens CL, Couvillion GC. Current management of giant retinal breaks. II. *Trans Am Acad Ophthalmol Otolaryngol*. 1970;74(1):59–74.
- Vyngantas CM, Peyman GA, Daily MJ, Ericson EW. Octafluorocyclobutane and other gases for vitreous replacement. *Arch Ophthalmol*. 1973;90(3):235–6.
- Hilton GF, Grizzard WS. Pneumatic retinopexy. A two-step outpatient operation without conjunctival incision. *Ophthalmology*. 1986;93(5):626–41.
- Hilton GF, Kelly NE, Salzano TC, Tornambe PE, Wells JW, Wendel RT. Pneumatic retinopexy. A collaborative report of the first 100 cases. *Ophthalmology*. 1987;94(4):307–14.
- Ai E, Gardner TW. Current patterns of intraocular gas use in North America. *Arch Ophthalmol*. 1993;111(3):331–2.
- Friberg TR, Eller AW. Pneumatic repair of primary and secondary retinal detachments using a binocular indirect ophthalmoscope laser delivery system. *Ophthalmology*. 1988;95(2):187–93.
- Folk JC, Sneed SR, Folberg R, Coonan P, Pulido JS. Early retinal adhesion from laser photocoagulation. *Ophthalmology*. 1989;96(10):1523–5.
- Snyder WB, Bloome MA, Birch DG. Pneumatic retinopexy versus scleral buckle. Preferences of Vitreous Society members, 1990. *Retina*. 1992;12(1):43–5.
- Benson WE, Chan P, Sharma S, Snyder WB, Bloome MA, Birch DG. Current popularity of pneumatic retinopexy. *Retina*. 1999;19(3):238–41.
- Wild MR, Ruby AJ, Rosenshein J. Pneumatic retinopexy: a survey of current practice patterns among the vitreous society members. *Ophthalmic Surg Lasers*. 2000;31(1):76–81.
- Assi AC, Charteris DG, Gregor ZJ. Practice patterns of pneumatic retinopexy in the United Kingdom. *Br J Ophthalmol*. 2001;85(2):238.
- Yee KMP, Sebag J. Long-term results of office-based pneumatic retinopexy using pure air. *Br J Ophthalmol*. 2011;95(12):1728–30.
- Tornambe PE, Hilton GF. Pneumatic retinopexy: a multicenter randomized controlled clinical trial comparing pneumatic retinopexy with scleral buckling. The Retinal Detachment Study Group. *Ophthalmology*. 1989;96(6):772–83.
- Sebag J, Tang M. Pneumatic retinopexy using only air. *Retina*. 1993;13(1):8–12.
- Davis MJ, Mudvari SS, Shott S, Rezaei KA. Clinical characteristics affecting the outcome of pneumatic retinopexy. *Arch Ophthalmol*. 2011;129(2):163–6.
- Goldman DR, Shah CP, Heier JS. Expanded criteria for pneumatic retinopexy and potential cost savings. *Ophthalmology*. 2014;121(1):318–26.
- Rezende FA, Kapusta MA, Burnier MN, Costa RA, Scott IU. Preoperative B-scan ultrasonography of the vitreoretinal interface in phakic patients undergoing rhegmatogenous retinal detachment repair and its prognostic significance. *Graefes Arch Clin Exp Ophthalmol*. 2007;245(9):1295–301.
- Kleinmann G, Rechtman E, Pollack A, Schechtman E, Bukelman A. Pneumatic retinopexy: results in eyes with classic vs relative indications. *Arch Ophthalmol*. 2002;120(11):1455–9.
- Ross WH, Lavina A. Pneumatic retinopexy, scleral buckling, and vitrectomy surgery in the management of pseudophakic retinal detachments. *Can J Ophthalmol*. 2008;43(1):65–72.
- Jenzeri S, Yahia SB, Jelliti B, Ammari W, Attia S, Messaoud R, Khairallah M. Treatment of rhegmatogenous retinal detachment by pneumatic retinopexy: a review of 50 patients. *J Fr Ophtalmol*. 2009;32(10):715–20.
- Tornambe PE, Hilton GF, Kelly NF, Salzano TC, Wells JW, Wendel RT. Expanded indications for pneumatic retinopexy. *Ophthalmology*. 1988;95(5):597–600.

28. Tornambe PE. Bilateral retinal detachment repaired with bilateral pneumatic retinopathy. Case report. *Arch Ophthalmol*. 1987; 105(11):1489.
29. Irvine AR, Lahey JM. Pneumatic retinopathy for giant retinal tears. *Ophthalmology*. 1994;101(3):524–8.
30. McAllister IL, Zegarra H, Meyers SM, Gutman FA. Treatment of retinal detachments with multiple breaks by pneumatic retinopathy. *Arch Ophthalmol*. 1987;105(7):913–6.
31. Ando F, Hirose H, Nagasaka T, Takahashi K, Sekiryu T. Treatment of retinal detachment with giant tear by pneumatic retinopathy. *Eur J Ophthalmol*. 1993;3(4):201–6.
32. Melgen SE, Michels M. Pneumatic retinopathy for the treatment of giant retinal dialyses. *Am J Ophthalmol*. 1994;118(6):762–5.
33. Hwang JF, Chen SN, Lin CJ. Treatment of inferior rhegmatogenous retinal detachment by pneumatic retinopathy technique. *Retina*. 2011;31(2):257–61.
34. Chang TS, Pelzek CD, Nguyen RL, Purohit SS, Scott GR, Hay D. Inverted pneumatic retinopathy: a method of treating retinal detachments associated with inferior retinal breaks. *Ophthalmology*. 2003;110(3):589–94.
35. Friberg TR, Eller AW. Laser pneumatic retinopathy for repair of recurrent retinal detachment after failed scleral buckle – ten years experience. *Ophthalmic Surg Lasers*. 2001;32(1):13–8.
36. Levkovitch-Verbin H, Treister G, Moisseiev J. Pneumatic retinopathy as supplemental therapy for persistent retinal detachment after scleral buckling operation. *Acta Ophthalmol Scand*. 1998;76(3):353–5.
37. Sharma T, Badrinath SS, Mukesh BN, Gopal L, Shanmugam MP, Bhende P, Bhende M, Shetty NS, Agrawal R. A multivariate analysis of anatomic success of recurrent retinal detachment treated with pneumatic retinopathy. *Ophthalmology*. 1997;104(12):2014–7.
38. Weinberger D, Stiebel-Kalish H, Crystal O, Axer-Siegel R, Mosseive Y, Yassur Y. Pneumatic retinopathy for late-onset recurrent retinal detachment. *Ophthalmic Surg Lasers*. 1998;29(1):43–7.
39. Chen SN, Hwang JF. Treatment of rhegmatogenous retinal detachment in teenagers by pneumatic retinopathy technique. *Am J Ophthalmol*. 2007;143(2):217–21.
40. Yeung L, Kokame GT, Brod RD, Lightman DA, Lai JC. Pneumatic retinopathy for retinal detachment associated with severe choroidal detachment. *Retina*. 2001;31(1):87–92.
41. McAuliffe PF, Heinemann MH. The use of pneumatic retinopathy to delay surgical repair of a retinal detachment associated with the ganciclovir intraocular device. *Ophthalmic Surg Lasers*. 1998;29(3):244–6.
42. Arevalo JF, Ramirez E, Suarez E, Cortez R, Antzoulatos G, Morales-Stopello J, Ramirez G, Torres F, Gonzalez-Vivas R. Rhegmatogenous retinal detachment in myopic eyes after laser in situ keratomileusis. Frequency, characteristics, and mechanism. *J Cataract Refract Surg*. 2001;27(5):674–80.
43. Arevalo FJ, Ramirez E, Suarez E, Antzoulatos G, Torres F, Cortez R, Morales-Stopello J, Ramirez G. Rhegmatogenous retinal detachment after laser-assisted in situ keratomileusis (LASIK) for the correction of myopia. *Retina*. 2000;20(4):338–41.
44. Böker T, Schmitt C, Mougharbel M. Results and prognostic factors in pneumatic retinopathy. *Ger J Ophthalmol*. 1994;3(2):73–8.
45. Tornambe PE. Pneumatic retinopathy: The evolution of case selection and surgical technique. A twelve-year study of 302 Eyes. *Trans Am Ophthalmol Soc*. 1997;95:551–78.
46. McAllister IL, Meyers SM, Zegarra H, Gutman FA, Zakov ZN, Beck GJ. Comparison of pneumatic retinopathy with alternative surgical techniques. *Ophthalmology*. 1988;95(7):877–83.
47. Lowe MA, McDonald HR, Campo RV, Boyer DS, Schatz H. Pneumatic retinopathy. Surgical results. *Arch Ophthalmol*. 1988;106(12):1672–6.
48. Grizzard WS, Hilton GF, Hammer ME, Taren D, Brinton DA. Pneumatic retinopathy failures. Cause, prevention, timing, and management. *Ophthalmology*. 1995;102(6):929–36.
49. Abecia E, Pinilla I, Oliván JM, Larrosa JM, Polo V, Honrubia FM. Anatomic results and complications in a long-term follow-up of pneumatic retinopathy cases. *Retina*. 2000;20(2):156–61.
50. Kulkarni KM, Roth DB, Prenner JM. Current visual and anatomic outcomes of pneumatic retinopathy. *Retina*. 2007;27(8):1065–70.
51. Salam GA, Greene JM, Deramo VA, Tibrewala RK, Ferrone PJ, Fastenberg DM. Retinal tears and retinal detachment as factors affecting visual outcome after cataract extraction complicated by posteriorly dislocated lens material. *Retina*. 2005;25(5):570–5.
52. Van der Meulen I, Gunning F, Henry Y, deVries-Knopfert W, Gortzak-Moorstein N, deSmet MD. Management of retinal detachments in pseudophakic patients with artisan lenses. *J Cataract Refr Surg*. 2002;28(10):1804–8.
53. Marshall JC. Safar's method for treatment of detachment of the retina by diathermy. *Proc Royal Soc Med*. 1933;26(6):755–9.
54. Rosengren B, Sourander P, Törnquist R. Studies on the histology of tissue destruction produced by surface diathermy and psychrodiathermy in the rabbit eye. *Acta Ophthalmol (Copenh)*. 1969;47(5):1156–62.
55. Rosengren B. Chapter XIV: Diathermy and light coagulation in detachment surgery. *Acta Ophthalmol*. 1966;44(S84):121–33.
56. Rosengren B, Törnquist R. Chapter XVI: Methods for inducing retinohoroidal contact. *Acta Ophthalmol*. 1966;44(S84):143–61.
57. El-Mofty AA, Schepens CL. An insulated diathermy electrode. *Arch Ophthalmol*. 1980;98(6):1115–6.
58. Saran BR, Brucker AJ, Maguire AM. Drainage of subretinal fluid in retinal detachment surgery with the El-Mofty insulated diathermy electrode. *Retina*. 1994;14(4):344–7.
59. Lincoff H, O'Connor P, Kreissig I. Retinal adhesion after cryopexy. *Klin Monbl Augenheilkd*. 1970;156(6):771–83.
60. Hackett SF, Conway BP, Campochiaro PA. Subretinal fluid stimulation of retinal pigment epithelial cell migration and proliferation is dependent on certain features of the detachment or its treatment. *Arch Ophthalmol*. 1989;107(3):391–4.
61. Bonnet M, Fleury J, Guenoun S, Yaniali A, Dumas C, Hajjar C. Cryopexy in primary rhegmatogenous retinal detachment: a risk factor for postoperative proliferative vitreoretinopathy? *Graefes Arch Clin Exp Ophthalmol*. 1996;234(12):739–43.
62. Lira RP, Takasaka I, Arieta CE, Nascimento MA, Caldato R, Panetta H. Cryotherapy vs laser photocoagulation in scleral buckle surgery: a randomized clinical trial. *Arch Ophthalmol*. 2010; 128(12):1519–22.
63. Schepens CL. Management of retinal detachment. *Ophthalmic Surg*. 1994;25(7):427–31.
64. Ryan SJ, Schachat A, Wilkinson CP, Hinton DR, Saddy SR, Wiedemann P. Pneumatic retinopathy. In: *Retina*. 5th ed. London: Elsevier Health Sciences; 2013. p. 1723–34.
65. Bourla DH, Gupta A, Hubschman JP, Bourla N, Yu F, Schwartz SD. The slower the better: on the instability of gas jets in a model of pneumatic retinopathy. *Invest Ophthalmol Vis Sci*. 2007;48(6):2734–7.
66. Mudvari SS, Ravage ZB, Rezaei KA. Retinal detachment after primary pneumatic retinopathy. *Retina*. 2009;29(10):1474–8.
67. Chawla HB, Birchall CH. Intravitreal air in retinal detachment surgery. *Br J Ophthalmol*. 1973;57(1):60–70.
68. Mohamed S, Lai TYY. Intraocular gas in vitreoretinal surgery. *HK J Ophthalmol*. 2010;14(1):8–13.
69. Juzoji H, Iwasaki T, Usui M, Hasemi M, Yamakawa N. Histological study of intraocular changes in rabbits after intravitreal gas injection. *Jpn J Ophthalmol*. 1997;41(5):278–83.
70. Wong RF, Thompson JT. Prediction of the kinetics of disappearance of sulfur hexafluoride and perfluoropropane intraocular gas bubbles. *Ophthalmology*. 1988;95(5):609–13.
71. Thomas EL. Pneumatic retinopathy. *West J Med*. 1988;148(6):695.
72. Lincoff H, Mardirossian J, Lincoff A, Liggett P, Iwamoto T, Jakobiec F. Intravitreal longevity of three perfluorocarbon gases. *Arch Ophthalmol*. 1980;98(9):1610–1.

73. Hilton GF, Das T, Majji AB, Jalali S. Pneumatic retinopathy: principles and practice. *Indian J Ophthalmol*. 1996;44(3):131–43.
74. Tornambe PE. Pneumatic retinopathy. *Surv Ophthalmol*. 1988;32(4):270–81.
75. Yanyali A, Horozoglu F, Bayrak YI, Celik E, Nohutcu AF. Steamroller versus basic technique in pneumatic retinopathy for primary rhegmatogenous retinal detachment. *Retina*. 2007;27(1):74–82.
76. Algere P, Gjöetterberg M, Olivestedt G, Fituri S. Results of pneumatic retinopathy with air. *Acta Ophthalmol*. 1992;70(5):632–6.
77. Gündüz K, Günalp I. Pneumatic retinopathy with drainage of subretinal fluid. *Int Ophthalmol*. 1994;18(3):143–7.
78. Hutter JC, Luu HMD, Schroeder LW. A biological model of tamponade gases following pneumatic retinopathy. *Curr Eye Res*. 2002;25(4):197–206.
79. Baltatzis S, Djacos MC, Micha M. Treatment of retinal detachment by pneumatic retinopathy. *J Fr Ophtalmol*. 1989;12(6–7):441–4.
80. Bochow TW, Olk RJ, Hershey JM. Pneumatic retinopathy perfluoroethane (C₂F₆) in the treatment of rhegmatogenous retinal detachment. *Arch Ophthalmol*. 1992;110(12):1723–4.
81. Sinawat S, Ratanapakorn T, Sanguansak T, Prompol S, Laopaiboon M, Yospaiboon Y. Air vs perfluoropropane gas in pneumatic retinopathy: a randomized noninferiority trial. *Arch Ophthalmol*. 2010;128(10):1243–7.
82. Fleck BW, Dhillon BJ, Khanna V, McConnell JM, Chawla HB. Nd:YAG laser augmented pneumatic retinopathy. *Ophthalmic Surg*. 1988;19(12):855.
83. Freyler H, Radax U. Pneumatic retinopathy – a study of 7 years experience. *Klin Monbl Augenheilkd*. 1993;202(3):212–7.
84. Chen JC, Robertson JE, Coonan P, Blodi CF, Klein ML, Watzke RC, Folk JC, Weingeist TA. Results and complications of pneumatic retinopathy. *Ophthalmology*. 1988;95(5):601–6.
85. Algere P, Hallnäs K, Palmqvist BM. Success and complications of pneumatic retinopathy. *Am J Ophthalmol*. 1988;106(4):400–4.
86. Skoog KO, Textorius O, Wrigstad A. Pneumatic retinopathy in 50 patients. *Acta Ophthalmol*. 1989;67(1):103–5.
87. Berrod JP, Bazard MC, Bodart E, Noye JF, Raspiller A. Pneumatic retinopathy using SF₆ or C₃F₈. Results and complications apropos of 56 patients. *Bull Soc Ophtalmol Fr*. 1990;90(1):117–21.
88. Trillo M, Facino M, Terrile R, Corazza M, Mosci C, Baldi F, Trillo CA. Treatment of uncomplicated cases of rhegmatogenous retinal detachment with an expanding gas bubble. *Ophthalmologica*. 1993;207(3):140–3.
89. Mulvihill A, Fulcher T, Datta V, Acheson R. Pneumatic retinopathy versus scleral buckling: a randomised controlled trial. *Ir J Med Sci*. 1996;165(4):274–7.
90. Lisle C, Mortensen KK, Sjølie AK. Pneumatic retinopathy: a long term follow-up study. *Acta Ophthalmol Scand*. 1998;76(4):486–90.
91. Han DP, Mohsin NC, Guse CE, Hartz A, Tarkanian CN. Comparison of pneumatic retinopathy and scleral buckling in the management of primary rhegmatogenous retinal detachment. Southern Wisconsin Pneumatic Retinopathy Study Group. *Am J Ophthalmol*. 1998;126(5):658–68.
92. Assi AC, Charteris DG, Pearson RV, Gregor ZJ. Pneumatic retinopathy in the treatment of primary rhegmatogenous retinal detachment. *Eye (Lond)*. 1999;13(6):725–8.
93. Saw SM, Gazzard G, Wagle AM, Lim J, Au Eong KG. An evidence-based analysis of surgical interventions for uncomplicated rhegmatogenous retinal detachment. *Acta Ophthalmol Scand*. 2006;84(5):606–12.
94. Brazitikos PD, Androudi S, Christen WG, Stangos NT. Primary pars plana vitrectomy versus scleral buckle surgery for the treatment of pseudophakic retinal detachment: a randomized clinical trial. *Retina*. 2005;25(8):957–64.
95. Thapa R, Shrestha MK, Gurung R, Ruit S, Paudyal G. Outcome of pneumatic retinopathy at a tertiary eye care centre in Nepal. *Kathmandu Univ Med J*. 2008;6(24):466–71.
96. Charteris DG, Sethi CS, Lewis GP, Fisher SK. Proliferative vitreoretinopathy-developments in adjunctive treatment and retinal pathology. *Eye (Lond)*. 2002;16(4):369–74.
97. Hilton GF, Tornambe PE. Pneumatic retinopathy. An analysis of intraoperative and postoperative complications. The Retinal Detachment Study Group. *Retina*. 1991;11(3):285–94.
98. Macherer R, Aaberg TM, Freeman HM, Irvine AR, Lean JS, Michels RM. An updated classification of retinal detachment with proliferative vitreoretinopathy. *Retina*. 1992;12(1):73.
99. Kon CH, Asaria RH, Occeleston NL, Khaw PT, Aylward GW. Risk factors for proliferative vitreoretinopathy after primary vitrectomy: a prospective study. *Br J Ophthalmol*. 2000;84(5):506–11.
100. Heimann H, Bartzschmidt K, Bornfeld N, Weiss C, Hilgers R, Foerster M. Scleral buckling versus primary vitrectomy in rhegmatogenous retinal detachment: a prospective randomized multicenter clinical study. *Ophthalmology*. 2007;114(12):2142–54.
101. Fabian ID, Kinori M, Efrati M, Alhalel A, Desatnik H, Hai OV, Katz G, Platner E, Moisseiev J. Pneumatic retinopathy for the repair of primary rhegmatogenous retinal detachment: a 10-year retrospective analysis. *JAMA Ophthalmol*. 2013;131(2):166–71.
102. Mortensen KK, Sjølie AK. Retinal detachment treated by pneumatic retinopathy. *Acta Ophthalmol*. 1988;66(2):187–9.
103. Schaal S, Sherman MP, Barr CC, Kaplan HJ. Primary retinal detachment repair: comparison of 1-year outcomes of four surgical techniques. *Retina*. 2011;31(8):1500–4.
104. Eter N, Böker T, Spitznas M. Long-term results of pneumatic retinopathy. *Graefes Arch Clin Exp Ophthalmol*. 2000;238(8):677–81.
105. Tornambe PE, Hilton GF, Flood TP, Green S, Grizzard WS, Hammer ME, Leff SR, Masciulli L, Morgan CM, Brinton DA. Pneumatic retinopathy. A two-year follow-up study of the multicenter clinical trial comparing pneumatic retinopathy with scleral buckling. *Ophthalmology*. 1991;98(7):1115–23.
106. Purohit SS, Matthews GP, Zakov ZN. Pneumatic buckle for the repair of primary rhegmatogenous retinal detachment. *Ophthalmic Surg Lasers*. 1999;30(7):509–12.
107. Zaidi AA, Alvarado R, Irvine A. Pneumatic retinopathy: success rate and complications. *Br J Ophthalmol*. 2006;90(4):427–8.
108. Hilton GF, Tornambe PE, Flood TP, Brinton DA, Green S, Grizzard WS, Hammer ME, Leff SR, Masciulli L, Morgan CM. The complication of pneumatic retinopathy. *Trans Am Ophthalmol Soc*. 1990;88:191–207.
109. Freeman WR, Lipson BK, Morgan CM, Liggett PE. New posteriorly located retinal breaks after pneumatic retinopathy. *Ophthalmology*. 1988;95(1):14–8.
110. Poliner LS, Grand MG, Schoch LH, Olk RJ, Johnston GP, Okun E, Boniuk I, Escoffery RF. New retinal detachment after pneumatic retinopathy. *Ophthalmology*. 1987;94(4):315–8.
111. Yeo JH, Vidaurri-Leal J, Glaser BM. Extension of retinal detachments as a complication of pneumatic retinopathy. *Arch Ophthalmol*. 1986;104(8):1161–3.
112. McDonald HR, Abrams GW, Irvine AR, Sipperley JO, Boyden BS, Fiore Jr JV, Zegarra H. The management of subretinal gas following attempted pneumatic retinal reattachment. *Ophthalmology*. 1987;94(4):319–26.
113. Coden DJ, Freeman WR, Weinreb RN. Intraocular pressure response after pneumatic retinopathy. *Ophthalmic Surg*. 1988;19(9):667–9.
114. Tunc M, Lahey JM, Kearney JJ, Lewis JM, Francis R. Cystoid macular oedema following pneumatic retinopathy vs scleral buckling. *Eye*. 2007;21(6):831–4.
115. Polk JD, Rugaber C, Kohn G, Arenstein R, Fallon Jr WF. Central retinal artery occlusion by proxy: a cause for sudden blindness in an airline passenger. *Aviat Space Environ Med*. 2002;73(4):385–7.
116. Desatnik H, Alhalel A, Treister G, Moisseiev J. Management of persistent loculated subretinal fluid after pneumatic retinopathy. *Br J Ophthalmol*. 2001;85(2):189–92.

117. Ambler JS, Zegarra H, Meyers SM. Chronic macular detachment following pneumatic retinopathy. *Retina*. 1990;10(2):125–30.
118. Böker T, Koch F, Spitznas M. Delayed resorption of subretinal fluid after pneumatic retinopathy. *Fortschr Ophthalmol*. 1991;88(4):354–7.
119. Chan CK, Wessels IF. Delayed subretinal fluid absorption after pneumatic retinopathy. *Ophthalmology*. 1989;96(12):1691–700.
120. Wirostko WJ, Han DP, Perkins SL. Complications of pneumatic retinopathy. *Curr Opin Ophthalmol*. 2000;11(3):195–200.
121. Termote H. Pneumatic retinopathy. Analysis of the first 20 cases. *Bull Soc Belge Ophtalmol*. 1989;231:107–16.
122. Mougharbel M, Koch FH, Böker T, Spitznas M. No cataract two years after pneumatic retinopathy. *Ophthalmology*. 1994;101(7):1191–4.
123. Smiddy WE, Loupe D, Michels RG, Enger C, Glaser BM, deBustros S. Extraocular muscle imbalance after scleral buckling surgery. *Ophthalmology*. 1989;96(10):1489–90.
124. Weinberger D, Lichter H, Loya H, Axer-Siegel R, Muzmacher L, Gabbay U, Yassur Y. Corneal topographic changes after retinal and vitreous surgery. *Ophthalmology*. 1999;106(8):1521–4.
125. Wong D, Lois N. Pseudophakic retinal detachment. *Surv Ophthalmol*. 2003;48(5):467–87.
126. Gribomont AC, Rolland F. Efficacy of pneumatic retinopathy: 7 year retrospective study. *Bull Soc Belge Ophtalmol*. 1996;263:131–5.

Vitreous Floaters and Vision: Current Concepts and Management Paradigms

V.B.8.

Laura C. Huang, Kenneth M.P. Yee, Christianne A. Wa,
Justin N. Nguyen, Alfredo A. Sadun, and J. Sebag

Outline

- I. **Introduction**
- II. **Background**
 - A. Etiology of Floaters
- III. **Diagnostic Considerations**
 - A. Clinical Presentation
 - B. Clinical Characterization of Floaters
 - 1. Structural Assessment of Floaters
 - a. Ultrasonography
 - b. Combined OCT/SLO
 - c. Dynamic Light Scattering
 - 2. Effects of Floaters on Vision
 - a. Straylight
 - b. Contrast Sensitivity Function
- IV. **Therapeutic Considerations**
 - A. Vitrectomy
 - 1. Efficacy of Vitrectomy for Floaters
 - 2. Safety of Vitrectomy for Floaters
 - a. Endophthalmitis
 - b. Retinal Tears and Retinal Detachment
 - c. Cataracts

Conclusions

References

Keywords

Vitreous • Floaters • Posterior vitreous detachment • Myopic vitreopathy • Asteroid hyalosis • Light scattering • Straylight glare • Contrast sensitivity • VFQ quality of life • Vitrectomy • Retinal detachment • Oxygen • Cataracts

Key Concepts

1. Floaters result from structural abnormalities in vitreous. They are a more common complaint than previously known and have a more negative impact on the quality of life than previously appreciated.
2. Vision is adversely affected by vitreous light scattering causing straylight glare and degradation of contrast sensitivity. This explains the considerable degree of unhappiness experienced by patients suffering from floaters.
3. The only proven and safe treatment that effectively cures floaters and improves vision as well as patient well-being is limited vitrectomy.

L.C. Huang, BA
VMR Institute for Vitreous Macula Retina,
7677 Center Avenue, suite 400,
Huntington Beach, CA 92647, USA

Doheny Eye Institute, Department of Ophthalmology,
Los Angeles, CA, USA

University of Miami Miller School of Medicine, Miami, FL, USA
e-mail: lchuang@med.miami.edu

K.M.P. Yee, BS • C.A. Wa, BA
J. Sebag, MD, FACS, FRCOphth, FARVO (✉)
VMR Institute for Vitreous Macula Retina,
7677 Center Avenue, suite 400,
Huntington Beach, CA 92647, USA

Doheny Eye Institute, Department of Ophthalmology,
Los Angeles, CA, USA
e-mail: kennethmpy@gmail.com;
cwa@usc.edu; jsebag@VMRinstitute.com

J.N. Nguyen, BA
VMR Institute for Vitreous Macula Retina,
7677 Center Avenue, suite 400,
Huntington Beach, CA 92647, USA

A.A. Sadun, MD, PhD, FARVO
Doheny Eye Institute/UCLA,
Los Angeles, CA, USA
e-mail: alfredo.sadun@gmail.com

I. Introduction

Floater most commonly occur in middle age due to age-related changes in vitreous structure and light scattering by the posterior vitreous cortex after collapse of the vitreous body during posterior vitreous detachment (PVD). In youth, floaters are most often due to myopic vitreopathy. Vitreous floaters can have a negative impact on visual function and in turn the quality of life. Techniques to characterize floaters clinically include ultrasound imaging, optical coherence tomography, and dynamic light scattering for structural characterization. Functional impact can be assessed by straylight measurements, as well as contrast sensitivity testing. When the severity of floater symptomatology is significant, commonly used therapies include neodymium:yttrium-aluminum-garnet (YAG) laser and limited 25-gauge vitrectomy. While the former is of unproven efficacy, the latter has been shown to be a safe, effective, and definitive cure that improves patients' quality of life and eradicates symptomatology produced by light scattering and diffraction. It is thus reasonable to offer limited vitrectomy to individuals who have attempted to cope unsuccessfully and in whom functional deficit can be objectively demonstrated by testing contrast sensitivity, an important aspect of vision.

II. Background

Over a century ago, Duke Elder described vitreous as a structure composed of "loose and delicate filaments surrounded by fluid" [1]. Throughout the eighteenth century, the composition and structure of vitreous mystified early theorists, spawning four different theories regarding vitreous structure. In 1741, Demours advocated the "alveolar theory" [2] in which membranes oriented in many directions enclosed compartments, or alveoli, containing the fluid portion of vitreous. Pathologists such as Virchow supported this concept [3]. In 1780, Zinn postulated that vitreous is arranged in a concentric, lamellar orientation such as the "layers of an onion" [4]. This then constituted the "lamellar theory" and subsequently gained support from fellow theorists such as von Pappenheim [5] and Brucke [6]. In 1845, Hannover proposed the "radial sector theory" where he postulated that vitreous was composed in sectors that were radially oriented around the central anteroposterior core containing Cloquet's canal, similar in appearance to a "cut orange" [7]. Lastly, in 1848, Sir William Bowman introduced the "fibrillar theory" based upon a technique in which he utilized microscopy to show "nuclear granules" of fine fibrils that formed bundles [8].

Changes during life from the clear, gel-like structure led Szent-Gyorgi to be the first to propose that vitreous structure changes with age [9]. Duke Elder elaborated upon this with his first description of "floaters" as "the passive

reaction of the vitreous body to disturbances that create liquefaction with the separation of part of its colloid basis (the residual protein) to form appearances evident clinically as opacities" [10]. This description holds true today as it is quite consistent with the prevailing theory of the mechanism by which vitreous undergoes structural changes with age.

A. Etiology of Floaters

The etiology of floaters is believed to relate to macromolecular changes that alter vitreous organization present during youth, when hyaluronan (HA) interacts with vitreous collagen fibrils to stabilize the gel and keep collagen separated far enough to allow light to pass through vitreous with minimal or no light scattering, thereby achieving transparency [11]. The vitreous gel structure is maintained by thin, unbranched, heterotypic collagen fibrils composed of collagen types II, V/XI, and IX [12] and HA that fill the space in between the fibrils [13]. Liquid vitreous forms as HA dissociates from collagen and retains water molecules, sometimes forming pools or "lacunae." No longer separated by HA, vitreous collagen fibrils cross-link and aggregate [14, 15]. Studies have further shown that type IX collagen, most likely due to its chondroitin sulfate side chains, shields type II collagen from exposure on the collagen fibril surface. Type IX proteoglycan diminishes with age, further exposing type II collagen and predisposing vitreous collagen fibrils to lateral fusion. This additionally contributes to liquefaction [16]. Through these mechanisms, the human vitreous body undergoes two morphological changes with age that create further light diffraction: an increase in the volume of liquefied spaces (synchysis) [17] and an increase in optically dense areas due to collagen cross-linking [18] (Figure V.B.8-1) [see chapter II.C. Vitreous aging and PVD].

This macromolecular inhomogeneity scatters light and creates diffraction. Electron microscopy of vitreous opacities demonstrates collagen fibrils and cellular debris that contribute to light scattering and visual disturbances [19] (Figure V.B.8-2a). Another contributing factor to the development of opacities is separation of vitreous away from the retina that follows gel liquefaction and weakening of vitreoretinal adhesion, commonly referred to as posterior vitreous detachment (PVD) [20]. The dense collagen fibril matrix in the posterior vitreous cortex (Figure V.B.8-2b) causes significant light scattering. Thus, the combination of vitreous synchysis and syneresis with PVD, which is reported in 53 % of patients older than 50 years and 65 % in patients older than 65 years [20], results in the light scattering that causes the visual perception of "floaters." Indeed, the most common etiologies of floaters are posterior vitreous detachment (PVD), followed by myopic vitreopathy, and asteroid hyalosis [21–23]. Other pathologies such as Marfan's syndrome,

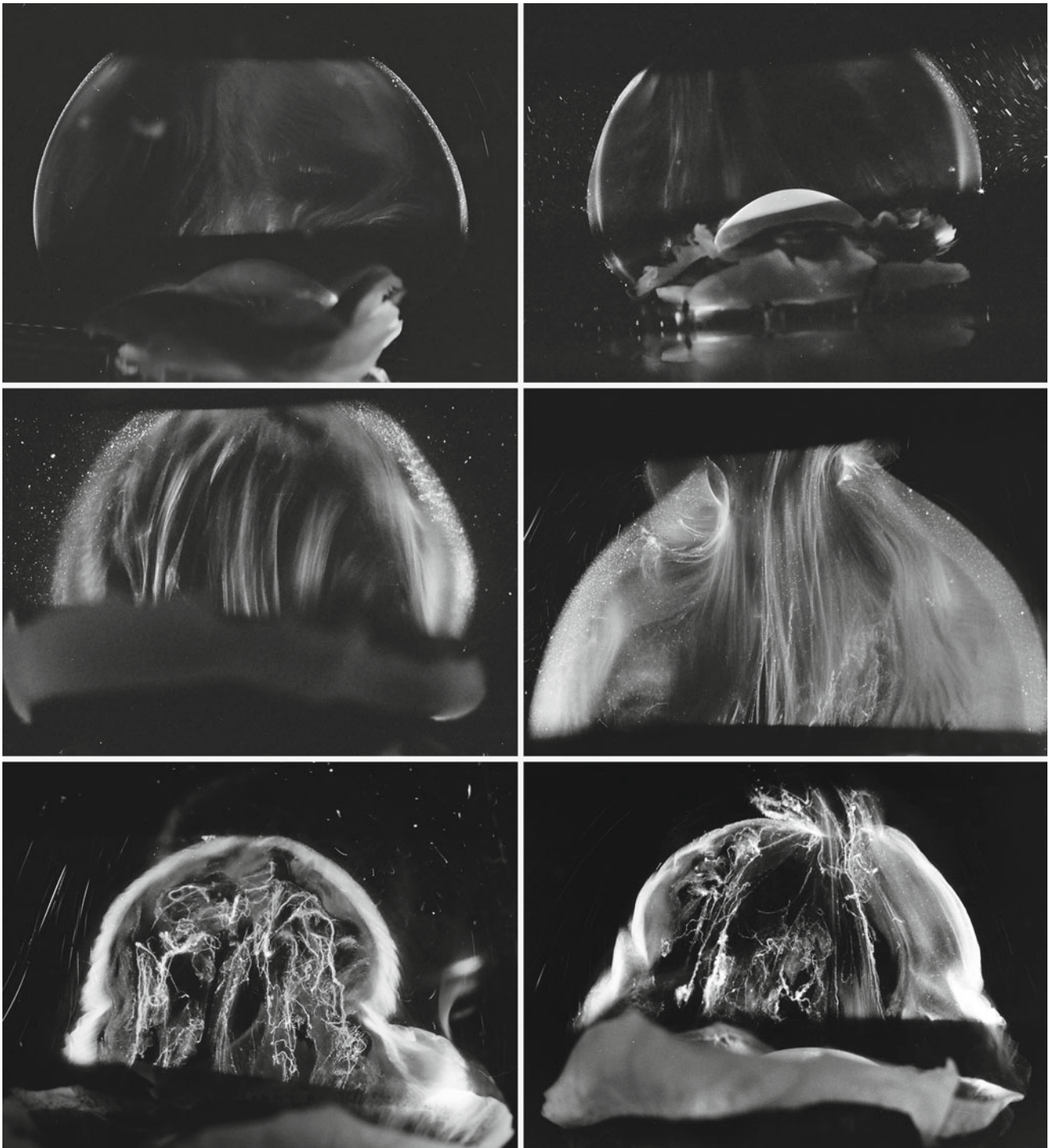


Figure V.B.8-1 Aging changes in human vitreous structure. Dark-field slit microscopy of fresh unfixed whole human vitreous with the sclera, choroid, and retina dissected off the vitreous body, which remains attached to the anterior segment. A slit lamp beam illuminates from the side, creating a horizontal optical section with an illumination-observation angle of 90° , maximizing the Tyndall effect. The anterior segment is below and the posterior pole is above in all specimens. *Top row:* The vitreous bodies of an 11-year-old girl (*left*) and a 14-year-old boy (*right*) demonstrate a homogeneous structure with no significant light scattering within the vitreous body, only at the periphery where the vitreous cortex is comprised of a dense matrix of collagen fibrils. The

posterior aspect of the lens is visible at the bottom of each image. *Middle row:* Vitreous structure in a 56-year-old (*left*) and a 59-year-old (*right*) subject features macroscopic fibers in the central vitreous body with an anteroposterior orientation. These form when hyaluronan molecules no longer separate collagen fibrils, allowing cross-linking and aggregation of collagen fibrils into visible fibers which scatter light, inducing floaters and degrading contrast sensitivity. *Bottom row:* In old age, the fibers of the central vitreous become significantly thickened and tortuous, as demonstrated in the two eyes of an 88-year-old woman. Adjacent to these large fibers are areas of liquid vitreous, at times forming pockets, called lacunae

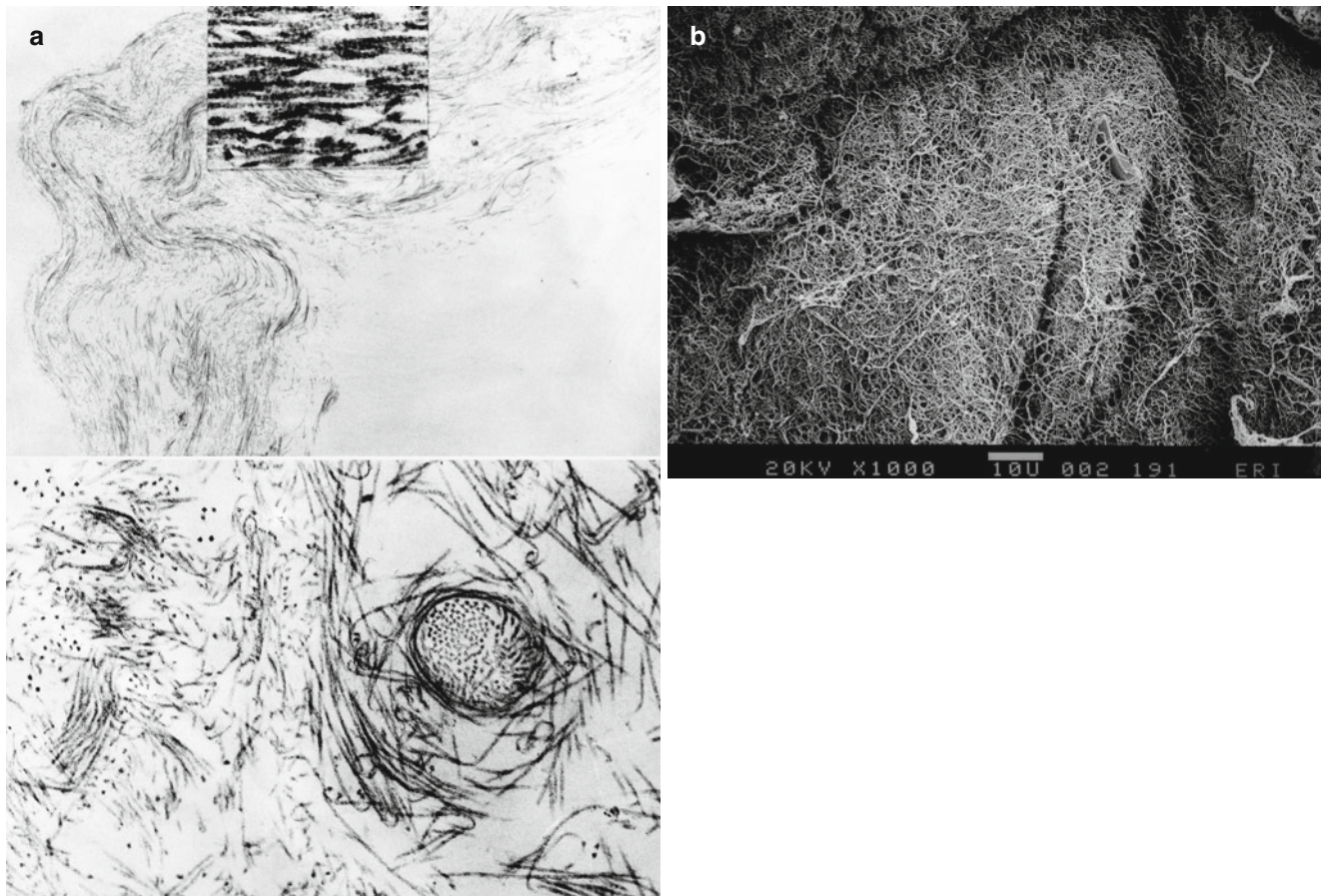


Figure V.B.8-2 (a) Ultrastructure of human vitreous fibers. Transmission electron microscopy of human vitreous-detected bundles of collagen fibrils shown longitudinally in the upper image and in cross section in the lower image. The inset in the upper image is a high magnification view of the bundle of fibrils demonstrating their collagenous nature. While these fibers form universally with aging, their formation is accelerated in myopia, constituting the second most common cause of floaters (From Sebag and Balazs [125]). (b) Ultrastructure of posterior vitreous cortex.

Scanning electron microscopy of the outer surface of the human posterior vitreous cortex after dissection and peeling away of the retina. The dense matrix of collagen fibrils is apparent, albeit somewhat exaggerated by the dehydration prep for electron microscopy. Nonetheless, it is apparent that when detached away from the retina, this structure will interfere with photon passage to the retina. The consequent light scattering will induce floaters and degrade contrast sensitivity (Courtesy of the Eye Research Institute of Retina Foundation, Boston, MA)

Ehlers-Danlos syndrome, and diabetic vitreopathy [see chapter I.E. Diabetic vitreopathy] also feature aggregation of vitreous collagen fibers resulting in glare due to light scattering.

above age 50), this may simply be the result of selection bias since younger individuals are more likely to respond to surveys on smartphones than older individuals.

III. Diagnostic Considerations

Recent studies have found that floaters are more prevalent than previously appreciated. An electronic survey recently administered to 603 people via a smartphone application has demonstrated that 76 % of individuals report seeing floaters and 33 % report impairment in vision due to floaters [24]. Additionally, myopes were 3.5 times more likely to report moderate or severe floaters compared to those with normal vision. While this study suggests a significant prevalence of floaters in younger individuals (< 5 % of participants were

A. Clinical Presentation

The clinical presentation of a patient with floaters includes visual symptoms often described as gray, linear, hair-like structures with round points that appear more prominent against bright backgrounds (a white wall or clear sky), translucent strings, or a “spider web-like” image. The perception of these objects floating occurs during head or eye movements with an overdamping effect. To date, floaters have been viewed by the medical profession as an innocuous and benign process that will improve over time. Recent studies

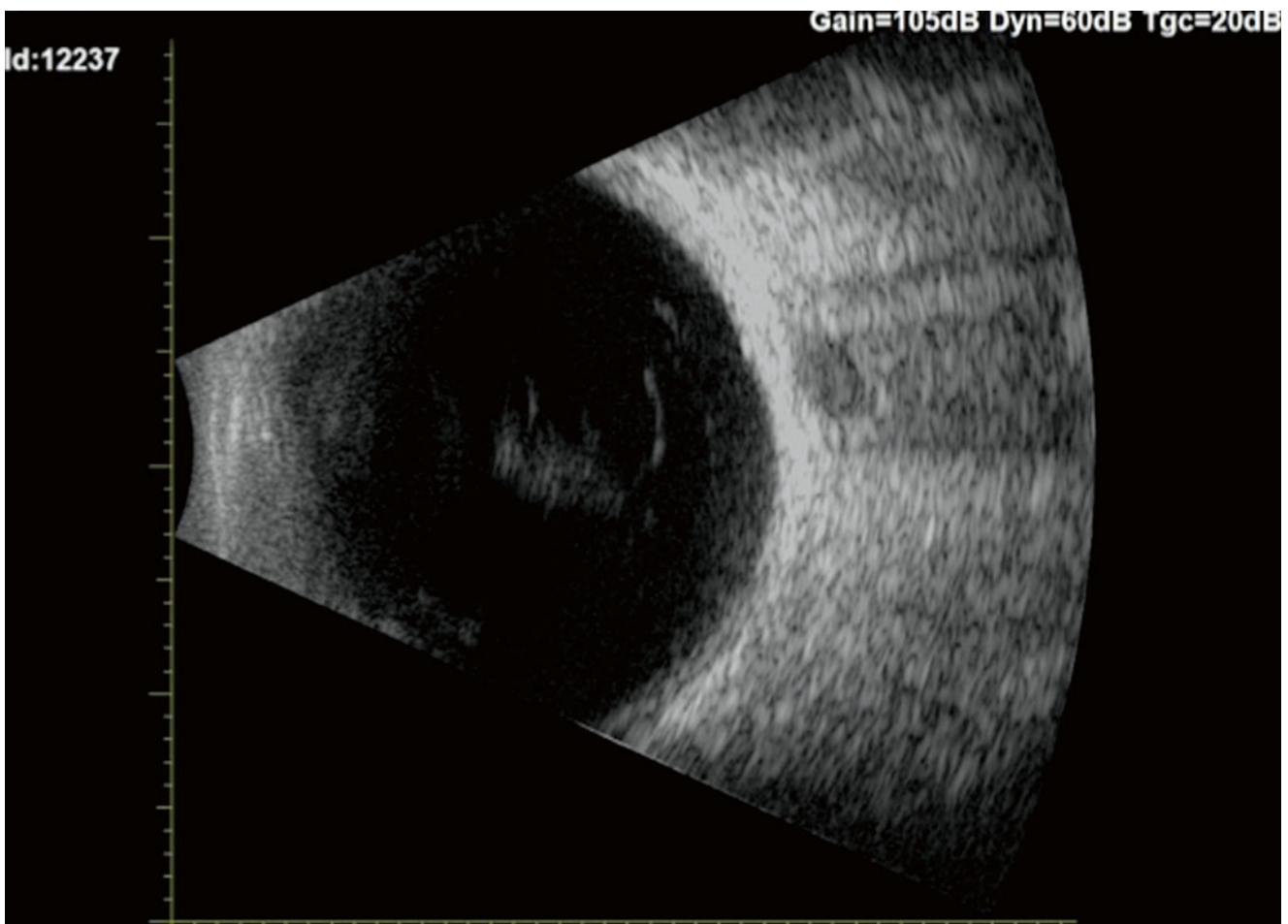


Figure V.B.8-3 B-scan ophthalmic ultrasound image of a patient demonstrating prominent echodensities in the vitreous body

have begun to dismiss this notion of floaters as a benign and innocuous process [25, 26]. These studies employed utility value analysis to determine that floaters have a significantly negative impact upon quality of life and symptoms can be much more disturbing than previously appreciated [27]. In one such study [25], researchers demonstrated that the degree to which floaters lower the visual quality of life is equivalent to age-related macular degeneration and greater than diabetic retinopathy and glaucoma, as well as mild angina, mild stroke, and colon cancer. Additionally, the perceived negative impact of floaters is underscored by the fact that patients would be willing to take an 11 % risk of death and a 7 % risk of blindness and would be willing to trade 1.1 years out of every 10 years remaining in their lives to eradicate floaters.

B. Clinical Characterization of Floaters

One of the contributing factors to clinicians' perception of floaters as a benign condition and not a disease is the

lack of a clinical approach to characterize floaters both in terms of structure as well as the impact on visual function. Beyond visual acuity, the evaluation of the impact of floaters on vision is lacking, since rarely do such vitreous opacities affect visual acuity, the most common method for assessing visual function. Thus, both structural [see chapter II.F. To See the Invisible – the Quest of Imaging Vitreous] and functional assessments of floaters are needed.

1. Structural Assessment of Floaters

a. Ultrasonography

Ultrasonography may be used to image opacities within the vitreous body. Ultrasound measures differences in acoustic impedance generated by echoes produced at tissue interfaces between structures of different densities. Ultrasonography imaging within the frequencies of 8–10 MHz can produce wavelengths as small as 0.2 mm to determine pathologies such as PVD, asteroid hyalosis, vitreous hemorrhage, and large foreign bodies [28, 29] (see Figure V.B.8-3). As the vitreous ages, inhomogeneities in density develop via the aforementioned biochemical changes and echoes become

more prominent. Acoustic changes or echoes in the vitreous also occur when there is persistence of primary vitreous (vascular) structures, changes induced by myopic vitreopathy, or the presence of intraocular foreign bodies [30]. An advantage of vitreous imaging by ultrasound is the ability to visualize posterior structures regardless of media opacification anteriorly (primarily lens) and the ability to estimate lacunar size and collagen fibril density [31].

Many studies have utilized ultrasonography to image the topography of the vitreous body. In patients being considered for vitrectomy surgery, rapid B-scan imaging is the most useful technique to investigate vitreoretinal pathology [30]. Static A-scan ultrasound demonstrated an 80 % incidence of acoustic interfaces in patients 60 years old and greater, which differed drastically from the 5 % incidence in patients 21–40 years old [32]. This demonstrates the decrease in acoustic homogeneity as the vitreous ages. Additionally, kinetic B-scan ultrasonography was utilized to quantify the vitreous of aged eyes with PVD compared to younger eyes [33]. The speckle density, referring to areas of acoustic hyper-reflectivity in areas of greater acoustic impedance, is increased in older subjects due to aggregation of collagen fibrils. Furthermore, chirp pulse encoding and synthetic focusing with an annular array was utilized to provide imaging of the vitreous with higher resolution and sensitivity through a 20-MHz ultrasound probe [34].

Recently, quantitative ultrasonography was used to analyze increased vitreous echodensity and correlate the findings with contrast sensitivity in patients with floaters of varying severity [35]. Investigators found that quantitative ultrasonography taken at nasal longitudinal, inferotemporal longitudinal, and inferotemporal transverse positions correlated strongly with contrast sensitivity ($R=0.82$, $P<0.001$) [35]. Quantitative ultrasonography should therefore have great utility to assess the severity of vitreous degeneration and aid in clinical decision-making regarding therapy of floaters.

b. Combined OCT/SLO

Time-domain OCT was previously used to extensively analyze the vitreoretinal interface [36], but utility was limited and fine details of the posterior vitreous were lacking. SD-OCT possesses inherent image resolution enhancement over time domain but also provides advantages in comparison to ultrasound with a greater horizontal resolution as well as better imaging of the vitreoretinal interface [37]. Combined SD-OCT and scanning laser ophthalmoscopy (SLO) provides further insight on vitreous structure and evolving physiologic and pathologic vitreoretinal changes. In one study [31], SD-OCT/SLO imaging examined 202 eyes and demonstrated a high correlation between diagnosis of complete PVD found by both clinical examination and OCT.

Additionally, high correlation was found between ultrasound and SD-OCT/SLO results for complete and incomplete PVD. Due to excellent depth of field during coronal plane imaging with the SLO, central vitreous opacities can be very well visualized (see Figure V.B.8-4). Note how the central darkness (umbra) is surrounded by an area of lighter shadow (penumbra) for both floaters. The umbra is the innermost and darkest part of a shadow, while the penumbra is where only part of the light is obscured, resulting in a partial shadow.

Furthermore, with longitudinal OCT imaging, the floater-induced attenuation of incident light transmission to the fundus results in shadowing and poor resolution of fundus structure, in particular, the retinal pigment epithelium/Bruch's membrane complex, that maps the floater shadow upon the fundus and may serve as a means of quantifying the density of these structures (see Figure V.B.8-5).

c. Dynamic Light Scattering

Dynamic light scattering (DLS) is a laser-based nanodetector that can measure the size of particles from 3 nm to 3 μ m in the cornea, lens, aqueous, and vitreous [38], thus enabling the mapping of three-dimensional distribution of vitreous macromolecules [39]. Ophthalmic usages of DLS include characterizing diabetic vitreopathy by detecting aggregation of vitreous collagen fibrils in diabetes [40–43], identifying patients at high risk for cataracts by detecting a decreased alpha-crystallin index [44], monitoring inflammatory processes following refractive surgery [45], and evaluating the molecular effects of pharmacologic vitreolysis [46]. In a comprehensive study of the last mentioned [43], DLS reproducibility demonstrated a coefficient of variance less than 3.3 % in all but one specimen. Thus, DLS was utilized to measure vitreous macromolecule sizes before, during, and after injection of ocriplasmin, hyaluronidase, and collagenase into solutions of respective substrates as well as whole bovine vitreous. This was made possible by measuring the diffusion coefficients of the molecules to determine size and detecting the increase in Brownian motion produced when the particle size decreased following pharmacologic vitreolysis. Therefore, the use of DLS in pharmacologic vitreolysis may play a paramount role in the future of vitreoretinal pharmacotherapy of various types, especially pharmacologic vitreolysis [see chapter VI.A. Pharmacologic vitreolysis].

2. Effects of Floaters on Vision

a. Straylight

Light scattering produced by opacities within the vitreous body can be quantified by the use of the C-quant (C-Quant; Oculus Optikgeräte, Wetzlar-Dutenhofen, Germany) straylight meter [47, 48]. Straylight, or disability glare, refers to a perceived spreading of light around a bright light source. Straylight was first described by Cobb in the early 1900s as “equivalent veiling luminance” (*Leq*), the

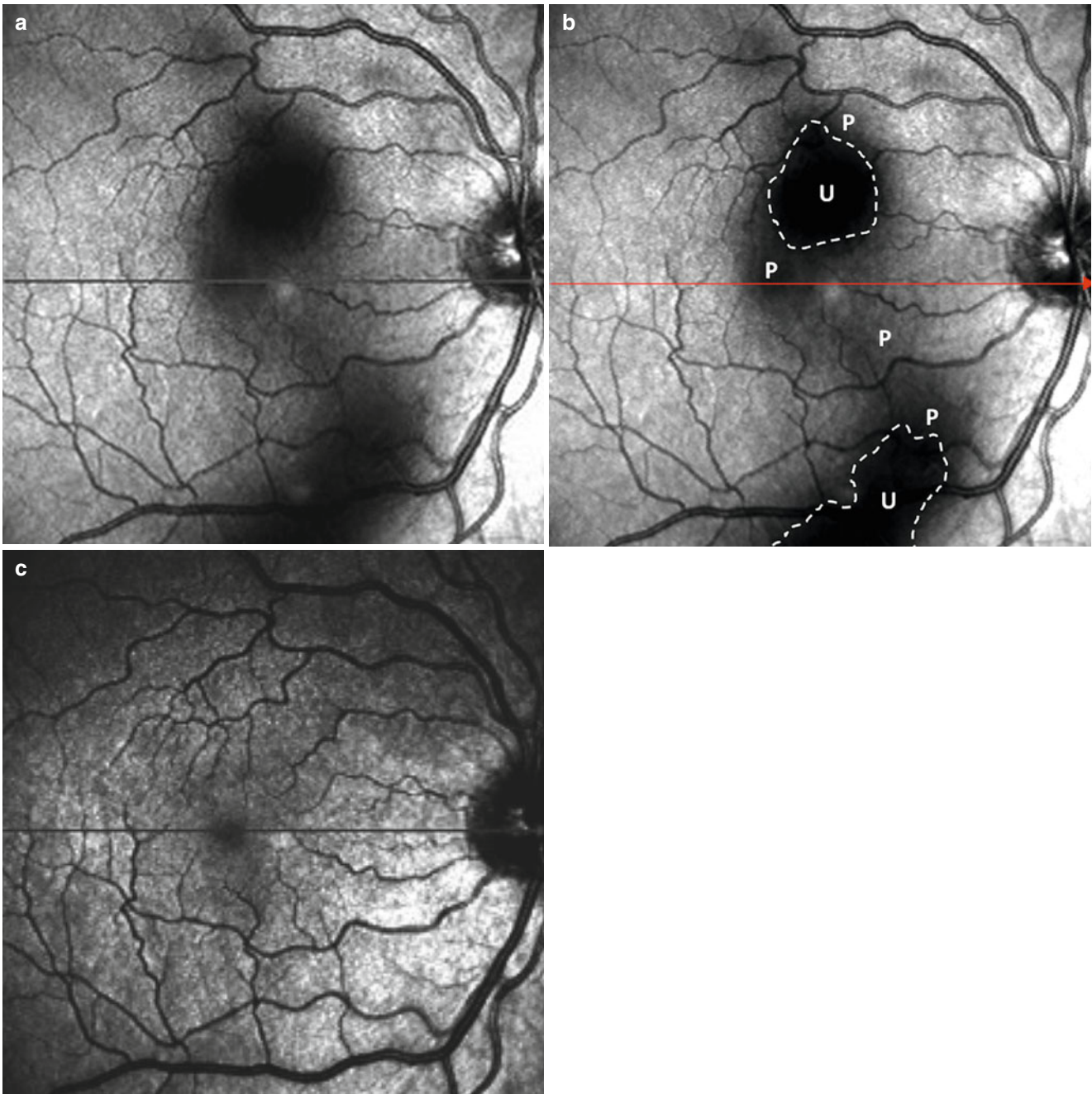


Figure V.B.8-4 (a) Scanning laser ophthalmoscope image of the same patient as in Figure V.B.8-3 with two large pre-macular opacities. (b) The central darkness (umbra) is surrounded by an area of lighter shadow

(penumbra) for both floaters. (*U* umbra, *P* penumbra). (c) Following limited vitrectomy, the central vitreous is clear with complete disappearance of both the umbras and penumbras

external luminance that has the same visual effect as the glare source [24]. Symptoms of straylight appear to the patient as haziness, decreased color and contrast, difficulty recognizing faces, and glare hindrance. Factors affecting straylight in normal patients include age (2× increased straylight values at 65 years old and 3× increased straylight values at 77 years old) [44, 49] and pigmentation – blue-eyed Caucasians had increased values 0.1–0.4 log

units higher compared to pigmented non-Caucasians [50]. One study [51] recommended the utilization of the C-quant straylight meter to assess long-term effect of surgical procedures on quality of vision based on its high reproducibility. The C-quant straylight meter thus provides a functional measure for the intensity of light spreading seen by the patient and demonstrates the increasing role of glare and contrast sensitivity in impairing vision.

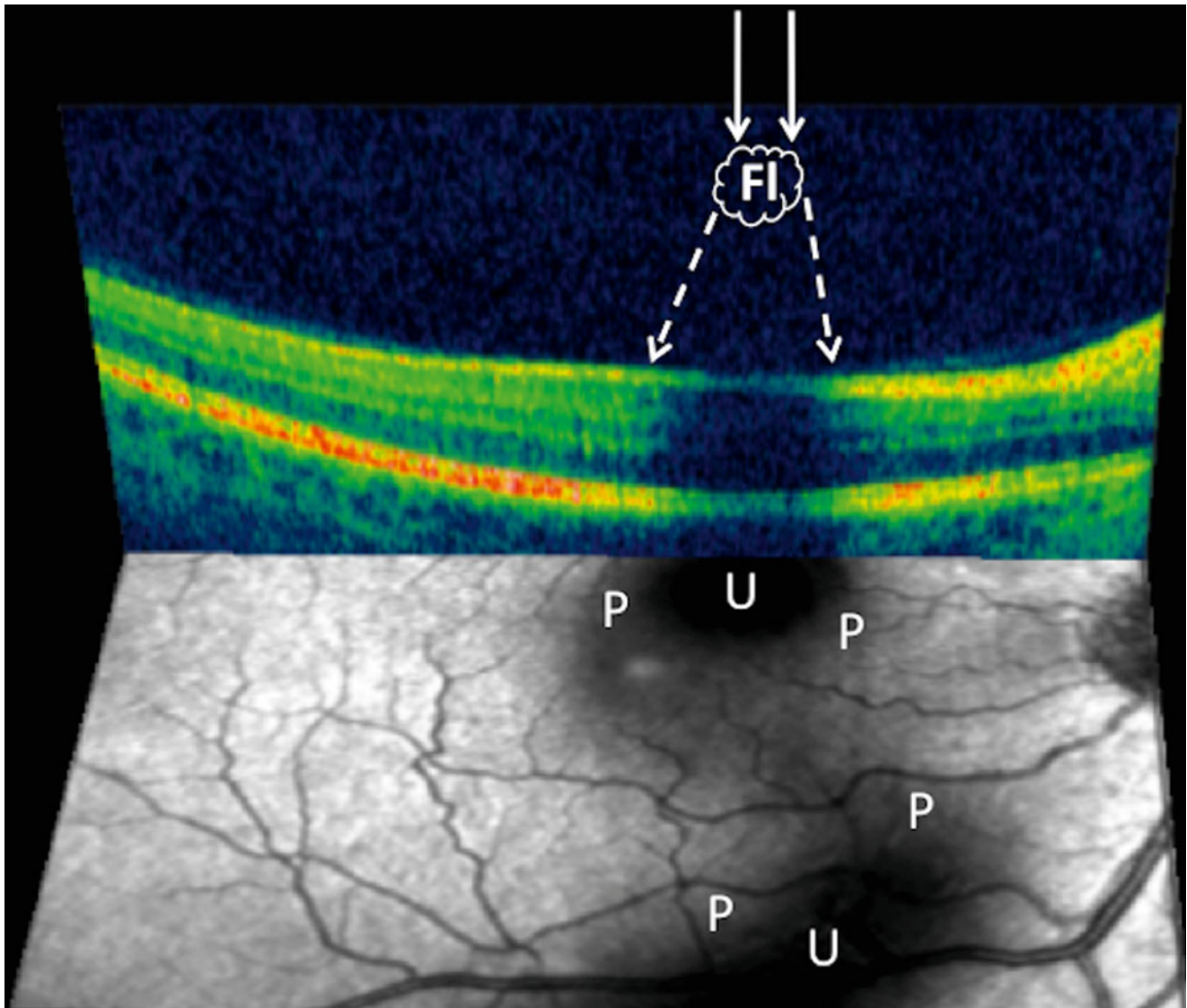


Figure V.B.8-5 OCT of the same patient as in Figure V.B.8-3 demonstrating floater-induced attenuation of imaging, especially at the retinal pigment epithelium/Bruch's membrane complex. *Solid arrows* repre-

sent incident light rays, while *dashed arrows* represent scattered light. (*FI* floater, *U* umbra, *P* penumbra)

b. Contrast Sensitivity Function

Measuring contrast sensitivity function (CSF) provides a useful method to quantify floaters and the impact on vision. The measure of CSF is often used to supplement visual acuity measurements in evaluating posterior capsular opacification after cataract surgery [52] as well as demonstrate reduced visual function in patients with cataracts whose acuity is only slightly impaired [53, 54]. In one study, multiple logistic regression analysis demonstrated that reduced contrast sensitivity was independently associated with a vision disability score affecting tasks such as judging distance, night driving, and mobility issues [55]. In addition to anterior ocular media opacities, vitreous opacities may also degrade CSF.

This hypothesis was tested in a study [56] at the VMR Institute for Vitreous Macula Retina in California, that

utilized computer-based Freiburg Acuity Contrast test (FrACT) to evaluate CSF [57–59]. This CSF testing method had a reproducibility of 92.1% when employing the Weber index ($\%W = (\text{Luminance}_{\text{max}} - \text{Luminance}_{\text{min}}) / \text{Luminance}_{\text{max}}$) [52, 60] as the outcome measure. Studies have previously demonstrated that FrACT yields results similar to those of Pelli-Robson and is not significantly affected by group differences in visual acuity [61]. Patients with bothersome floaters have been reported to have CSF that is diminished by 67.4% ($4.0 \pm 2.3\%W$; $N=16$) compared to age-matched controls ($2.4 \pm 0.9\%W$; $N=16$; $P < 0.01$). Since publication of these preliminary findings, this study has continued with increased enrollment ($n=38$) obtaining similar results: in floater patients, CSF is degraded by 72.3% ($4.14 \pm 1.95\%W$) compared to controls ($P < 0.01$).

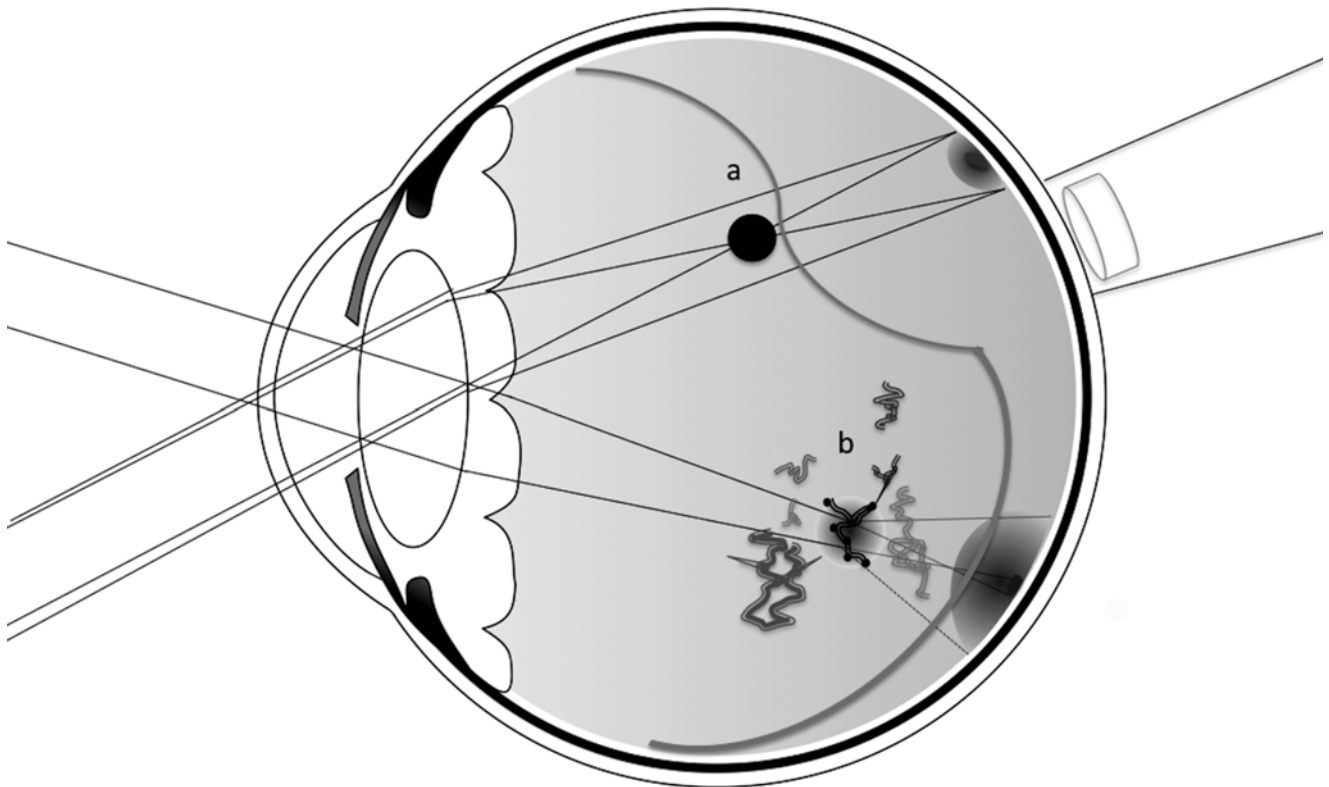


Figure V.B.8-6 Schematic diagram of the umbra and penumbra effect of floaters. (a) Shows how the convergence of light on a smooth body results in a small umbra and a penumbra. (b) Shows how the diffraction

and scatter of light on a floater of the same size but with uneven edges results in a smaller umbra and a larger penumbra

As demonstrated in Figure V.B.8-6, diminished contrast sensitivity is often a clinically significant consequence of light scattering by ocular media opacities. An opaque object with a smooth surface (e.g., an asteroid hyalosis body) will block light rays that create an umbra and a penumbra (see “a” in Figure V.B.8-6). A floater of the same size but with uneven surfaces and edges will scatter more light rays, creating a smaller umbra and a larger penumbra than a smooth body (see “b” in Figure V.B.8-6). Although the objects are of the same size, the uneven surface of a floater will scatter more light, and the larger penumbra will degrade contrast sensitivity. As light interacts with collagen fibers in the vitreous (Figure V.B.8-7), the spacing of the collagen fibrils, or interfibrillar distance, can influence the transmission of light to the retina. When the interfibrillar distance is decreased as in aged vitreous with syneresis (b in Figure V.B.8-7), increased scattered light will create a larger penumbra and degrade contrast sensitivity.

IV. Therapeutic Considerations

To date, treatment options for patients with bothersome floaters have been limited. Because floaters are generally viewed by doctors as benign and innocuous, patients are often told

to cope with symptoms and hope for either improvement via settling inferiorly or acceptance over time. For patients unwilling to accept this advice, eyedrops and Nd:YAG (neodymium:yttrium-aluminum-garnet (YAG) laser) are sometimes offered as therapies, though efficacy has never been demonstrated and reports are conflicting [62–64]. In one study, Nd:YAG vitreolysis eradicated floater symptoms in only 1/3 of patients with moderate clinical improvement and worsened symptoms in 7.7 % of patients [62]. As a result, the authors concluded that Nd:YAG vitreolysis provided a safe, but only mildly if at all effective, treatment for the eradication of floater symptoms. Additionally, posteriorly located vitreous opacities, which often cause the most disturbing symptoms, cannot be safely treated by YAG laser [64].

A. Vitrectomy

Pars plana vitrectomy (PPV) provides the most effective treatment for floaters as it offers a definitive cure with complete resolution of symptoms. However, this procedure is invasive with the possibility of complications such as endophthalmitis, retinal tears and detachments, cataract formation, glaucoma, vitreoretinal hemorrhage, and macular edema [65]. Therefore, it is important to only advocate

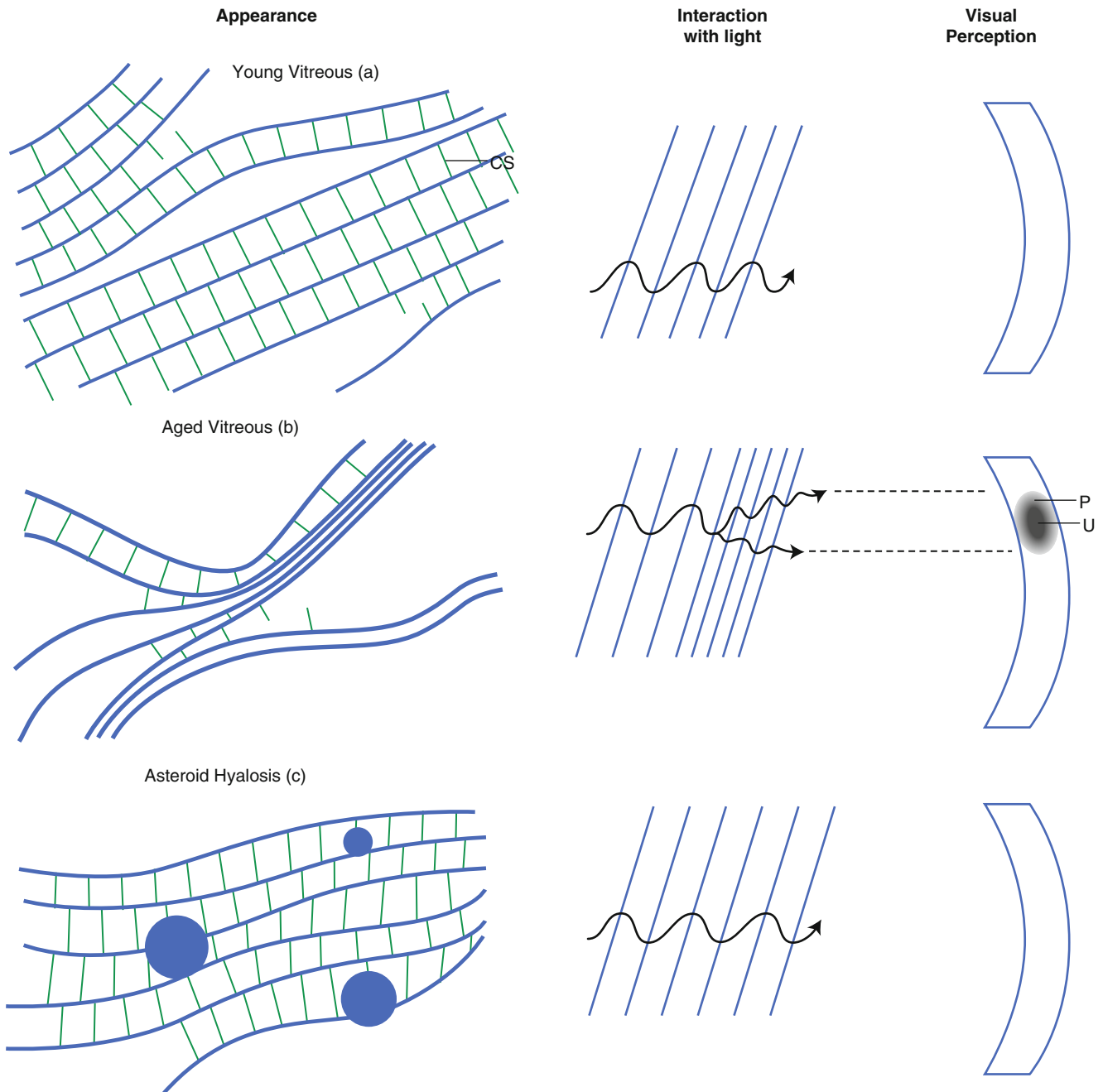


Figure V.B.8-7 Schematic representing how light is transmitted to the retina through normal vitreous (a), aged vitreous (b), and asteroid hyalosis (c). Thin green lines connecting the large collagen fibrils represent chondroitin sulfate (CS) chains of type IX collagen. In normal vitreous (a), light passes through unaltered since the interfibrillar distance between the collagen fibrils remains constant and unaltered. In aged vitreous (b), the fibrils have aggregated and collapsed, resulting in a

decreased interfibrillar distance. Thus, light rays are now scattered and diffracted creating an umbra and a penumbra on the retina. In asteroid hyalosis (c), the collagen fibrils are not affected, yet there are smooth focal opacities. The light rays should still pass through, perhaps back-scattered but otherwise mostly unaltered without significant shadows on the retina from the asteroid hyalosis bodies, since the interfibrillar distance remains constant and unaltered

vitrectomy to cure floaters for patients who understand the desired surgical goal and accept the risks, albeit minimal, and who have objective findings of visual dysfunction, such as contrast sensitivity or, if sufficiently severe, visual acuity.

With the use of 25-gauge instruments and sutureless, technique with limited vitrectomy, postoperative complications can be diminished significantly to provide a safe and effective cure for clinically significant floaters [56, 65].

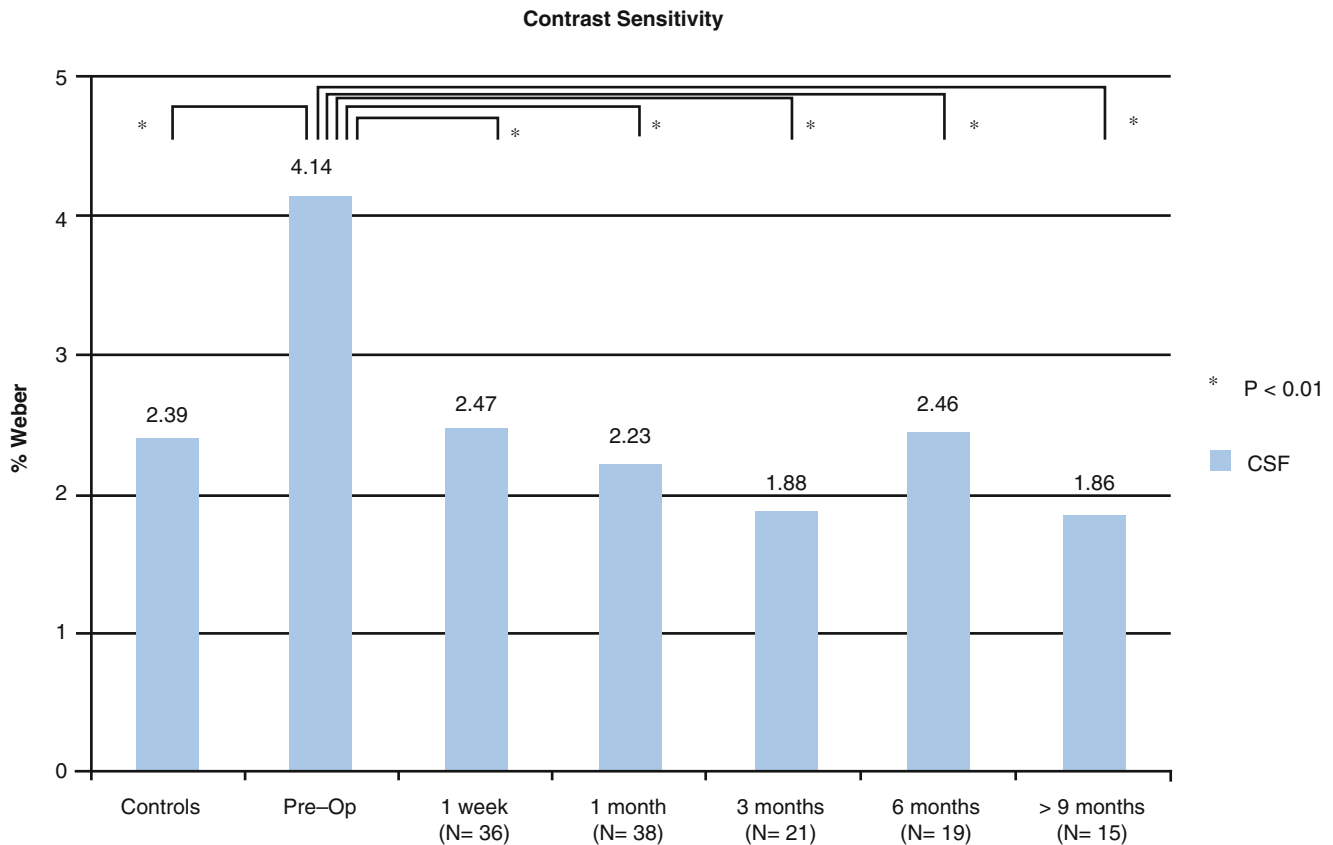


Figure V.B.8-8 Preoperative contrast sensitivity function (CSF) was 67 % worse in floater subjects (3.97 ± 1.95 %W) compared with age-matched control subjects (2.39 ± 0.92 %W, $P < 0.003$). After vitrectomy,

CSF normalized at 1 week (2.36 ± 1.53 %W, $P < 0.0001$) and remained normal 1 month (2.17 ± 1.11 %W, $P < 0.0001$) and 3–9 months postoperatively

1. Efficacy of Vitrectomy for Floaters

Vitrectomy can cure floaters by decreasing light scattering and thus decrease straylight, increase contrast sensitivity function (CSF), and improve the quality of life. It has been demonstrated that straylight measurements improve following vitrectomy [66]. Improvement in recognizing faces and glare hindrance occurred in 38 of 39 cases (97 %) with a statistically significant decrease in straylight glare measurements post vitrectomy, with 69 % of cases having straylight values within the normal range compared to 21 % preoperatively. The overall improvement, however, was only 18.2 % in the 39 floater cases of that study, perhaps related to the fact that 21 % of the cases had preoperative straylight measurements that were within the normal range.

Light scattering also degrades contrast sensitivity [47] underscoring that floaters negatively impact patients' vision in more than one way. In the aforementioned prospective study of 16 cases [56], investigators at the VMR Institute in Huntington Beach, California, found that patients with floaters had a 67 % diminution in CSF when compared to age-matched controls ($P < 0.013$). Following limited vitrectomy, CSF normalized at 1 week ($P < 0.01$) and remained normal at 1 month ($P < 0.003$) and at greater than 3 months ($P < 0.018$).

Following publication in 2013, this study has been continued with enrollment now up to 38 subjects. CSF improved in every single subject at 1 week ($P = 1.4 \times 10^{-6}$; $N = 36$), 1 month ($P < 0.0001$; $N = 38$), 3 months ($P = 1.07 \times 10^{-5}$; $N = 21$), 6 months ($P = 0.008$; $N = 19$), and >9 months ($P = 0.009$; $N = 15$) after limited vitrectomy (Figure V.B.8-8).

Given the aforementioned impacts of floaters on vision and patient well-being, it is reasonable to expect that following vitrectomy, patients would perceive an improvement in their quality of life. One study [67] of 110 patients who underwent vitrectomy to cure bothersome floaters demonstrated 85 % patient satisfaction. Additionally, 84 % of patients were completely cured of floaters, while 9.3 % of patients were less troubled by floaters. Several studies have utilized the National Eye Institute Visual Function Questionnaire (NEI VFQ-39) to quantify patients' improved visual quality of life following surgery. In the aforementioned prospective study at the VMR Institute in Huntington Beach, California [56], VFQ testing in the original 16 cases demonstrated VFQ improvement of 29.2 % ($P < 0.001$) at 1 month postoperatively that was sustained at 3–9 months following surgery. Continued study at the VMR Institute in Huntington Beach has increased this

series and found an average postoperative improvement in the composite index of NEI VFQ-36 of 32 % ($P < 0.001$). Similar improvements have been demonstrated in other studies utilizing the NEI VFQ [68–70] and other methods [71, 72] to assess patient visual quality of life before and after vitrectomy.

2. Safety of Vitrectomy for Floaters

As described above, vitrectomy offers an effective cure of floaters that improves vision and quality of life for patients who cannot cope with the symptoms of floaters, presumably because of profound diminution in contrast sensitivity. As an invasive procedure, however, vitrectomy has known potential complications [73–76]. Fortunately, a study by Delaney et al. [62] demonstrated a lower postoperative complication rate associated with vitrectomy for floaters as opposed to other vitreoretinal diseases. In a study of 31 patients (42 eyes) who underwent either Nd:YAG vitreolysis or pars plana vitrectomy for floaters, the authors compared the efficacy of the two treatments to eradicate floater symptomatology. Of these, 15 eyes underwent vitrectomy for floaters: 4 eyes underwent vitrectomy as a primary treatment for floaters, while 11 patients had vitrectomy subsequent to Nd:YAG laser treatment for floaters. In this admittedly small and limited study, 93.3 % of patients demonstrated complete resolution of floaters following vitrectomy with an average follow-up post vitrectomy of 31.5 months (range 6–108 months). Reported complications included postoperative cataract development that underwent successful phacoemulsification surgery and postoperative retinal detachment occurring 7 weeks after a combined vitrectomy with phacoemulsification. Another study found a relatively low rate of immediate post-floater vitrectomy retinal detachment with a slightly increased risk during long-term follow-up [77]. Out of 73 eyes that underwent vitrectomy for severe and persistent floaters ≥ 6 months' duration, a total of five (6.8 %) developed retinal detachments, four occurring 24–44 months after vitrectomy.

The current approach to curing floaters with vitrectomy must take into consideration the following specific risks and incorporate measures to mitigate these risks.

a. Endophthalmitis

Endophthalmitis is a rare but severe complication of vitrectomy [78]. However, instrument size (microincisional 23- or 25-gauge vs. conventional 20-gauge), beveled entry technique, and cannula removal with a blunt probe have all been demonstrated to lower the risk of this postsurgical complication. Recent literature has reported that there is inconclusive evidence that 25-gauge PPV has a higher rate of endophthalmitis than 20-gauge PPV [79–82]. The one exception is the use of a straight approach to cannula

insertion, which has an increased risk for endophthalmitis as compared to a beveled approach [83, 84]. This probably relates to a reduction of vitreous incarceration, which will not only mitigate endophthalmitis [85, 86] but also peripheral retinal tears [87–89] and fibrovascular proliferation in diabetic patients [90]. Regarding endophthalmitis, incisional vitreous incarceration is believed to improve postoperative sclerotomy closure, preventing the entry of bacteria into vitreous via an incisional vitreous wick [85]. Cannula removal at the end of surgery also influences the risk of postoperative endophthalmitis. In a prospective study of 118 cadaveric pig eyes that underwent vitrectomy with 23-gauge transconjunctival sclerotomies, two techniques of cannula removal were employed: the superior cannula was extracted with the illumination probe inserted through it and the other cannula was removed with a cannula plug inserted [86]. Postoperative incisional vitreous entrapment was subsequently evaluated and demonstrated vitreous entrapment in 95.8 % of entry sites whose cannulas were extracted with the plug inserted, whereas incarceration only occurred in 93.2 % of incisions whose cannulas were extracted with the light probe inside. While this was not a big difference, the authors report that this difference may be due to the peripheral vitreous being displaced to the inner face of sclerotomies when a plug is inserted, thus leading to a greater degree of vitreous incarceration. The use of non-hollow probes for cannula extraction may have contributed to the safety profile observed in the ongoing study at the VMR Institute in Huntington Beach, California [56], that employs 25-gauge vitrectomy with beveled incisions and illumination probe insertion for cannula removal at the end of the case. In 98 eyes with severe floaters, there have been no cases of endophthalmitis. Additionally, a reduction in vitreous incarceration may also decrease post-vitrectomy retinal detachment rate [89].

b. Retinal Tears and Retinal Detachment

Retinal tears and detachments occurring intraoperatively or postoperatively are well-documented potential complications [91, 92]. However, smaller instrument size (microincisional 23- or 25-gauge vs. conventional 20-gauge), avoiding surgical induction of PVD, and performing cannula removal as described above can decrease the incidence of retinal tears and detachment.

The use of 25-gauge vitrectomy instruments allows for an incision with an oblique scleral tunnel that can be self-sealing without any sutures, decreasing operating time and hastening postoperative recovery [93–95]. Furthermore, the use of self-retaining cannulas preserves the edge of the incisions during instrument insertion and removal and allows more effective self-sealing during sutureless surgery [96, 97]. Iatrogenic intraoperative peripheral retinal break

incidence during 23-gauge vitrectomy was compared to conventional 20-gauge vitrectomy, and retinal breaks occurred significantly less often during 23-gauge (16 of 973 cases, 1.6 %) compared to conventional vitrectomy (25 of 402 cases, 6.2 %) [98]. This is consistent with another study that found a 4.9 % retinal detachment rate 14 months after vitreomacular surgery with 20-gauge instruments versus a 1.1 % retinal detachment rate with 23-gauge instruments [99].

Additionally, the use of 360° indirect ophthalmoscopy with scleral depression to identify retinal breaks or tears for prophylactic treatment prior to or during surgery has also been shown to decrease the incidence of postoperative retinal detachments [100]. In a study of 415 eyes of 381 patients that underwent primary, standard, three-port vitrectomy, 65 retinal breaks were found in 48/415 eyes (11.6 %) that were treated perioperatively. Of 366 eyes in which no breaks were identified during vitrectomy, postoperative retinal detachment occurred in 8 (2.2 %) eyes; all occurring at least 3 months following vitrectomy. This demonstrates the importance of avoiding, detecting, and treating breaks during surgery to decrease the incidence of postoperative RD. In a study performed by Sebag et al. [56], 24/98 (24.5 %) cases received localized prophylactic laser or cryopexy to peripheral retinal breaks a minimum of 3 months prior to vitrectomy for floaters. This further contributed to the safety profile of the procedure, with no cases of retinal detachment occurring at a mean follow-up of 16.2 months (range=3–51 months).

Lastly, avoiding the induction of PVD during vitrectomy will also help decrease the incidence of intraoperative or postoperative retinal breaks. A study of 311 patients undergoing vitrectomy for treatment of premacular membrane with macular pucker or macular hole demonstrates a decreased incidence of retinal tears when surgical PVD was avoided in both groups [101]. For patients undergoing vitrectomy for macular pucker, 32.1 % had retinal breaks with induction of PVD compared to 2.1 % that had retinal breaks without induction of PVD ($P=0.006$). For patients undergoing vitrectomy for macular hole, 12.7 % had retinal breaks with induction of PVD while only 3.1 % had breaks without induction of PVD ($P=0.008$). Additionally, in a previous study that induced PVD during vitrectomy for floaters, retinal breaks occurred in 9/30 (30.5 %) cases [102], compared to 0/60 (0 %) that developed retinal breaks or detachments without induction of PVD ($P<0.007$) [56]. Since that publication, a total of 98 cases have been performed at the VMR Institute in Huntington Beach without PVD induction. There have been no cases of retinal breaks or detachment.

c. Cataracts

Increased risk of cataract formation due to increased intravitreal levels of oxygen following vitrectomy [103–108] may be mitigated by leaving the anterior vitreous and

posterior vitreous intact to protect the lens against oxygen free radicals. Previous studies [103, 106] have demonstrated that vitreous maintains an intraocular oxygen concentration gradient from the retina to the vitreous gel [see chapter IV.B. Oxygen in vitreo-retinal physiology and pathology]. Following vitrectomy, the oxygen gradient no longer exists due to the removal of the vitreous. One study demonstrated that the difference in oxygen tension pre- and post vitrectomy is statistically significant with oxygen tension levels in the mid-vitreous and near the lens increasing greatly, remaining elevated, and becoming more uniform in distribution in patients who had previous removal of vitreous gel [103]. This led to the conclusion that vitrectomy significantly increases intraocular oxygen tension after surgery causing exposure of the crystalline lens to reactive oxygen species that contribute to cataract formation. Similar reports of vitrectomy in animal models have further confirmed that oxygen measurements taken in the nucleus of the lens post vitrectomy had increased oxygen levels due to diffusion from elevated oxygen tension in the vitreous [106].

Beebe et al. [104] further elucidated the concept of oxidative damage and its role in cataract formation. They demonstrated that patients with ischemic diabetic retinopathy had lower oxygen levels in the vitreous and thus had partial protection from nuclear cataract development within the first year after vitrectomy. Other studies have also suggested that the rate of cataract extraction following vitrectomy in diabetic patients is lower than in nondiabetic patients undergoing vitrectomy [108]. Additionally, PVD has been implicated in possible acceleration of nuclear cataract formation due to increased oxygen tension levels following PVD. Pharmacologic vitreolysis induction of posterior vitreous detachment with ocriplasmin has also been demonstrated to increase vitreous oxygen concentration in comparison to control eyes and hyaluronidase-injected (without PVD) eyes [109]. In another study, intravitreal ocriplasmin injection that produced liquefaction and PVD was associated with a 68 % increase in lens nuclear oxygen tension compared to intravitreal hyaluronidase that only produced liquefaction and not PVD [110].

Thus, based on the strong association between increased oxygen levels and nuclear cataract formation [103, 111, 112], age-related PVD may be related to an acceleration of nuclear cataract development. Due to the increased oxygen tension levels that occur with induction of PVD and removal of the vitreous in vitrectomy, this suggests that leaving the anterior and posterior vitreous intact during surgery may result in decreased cataract formation postoperatively. In the VMR Institute study of 98 eyes with limited vitrectomy for clinically significant floaters, only 14/60 phakic eyes (23 %) needed cataract surgery, all in patients with a mean age 64.1 years and average time between vitrectomy and cataract

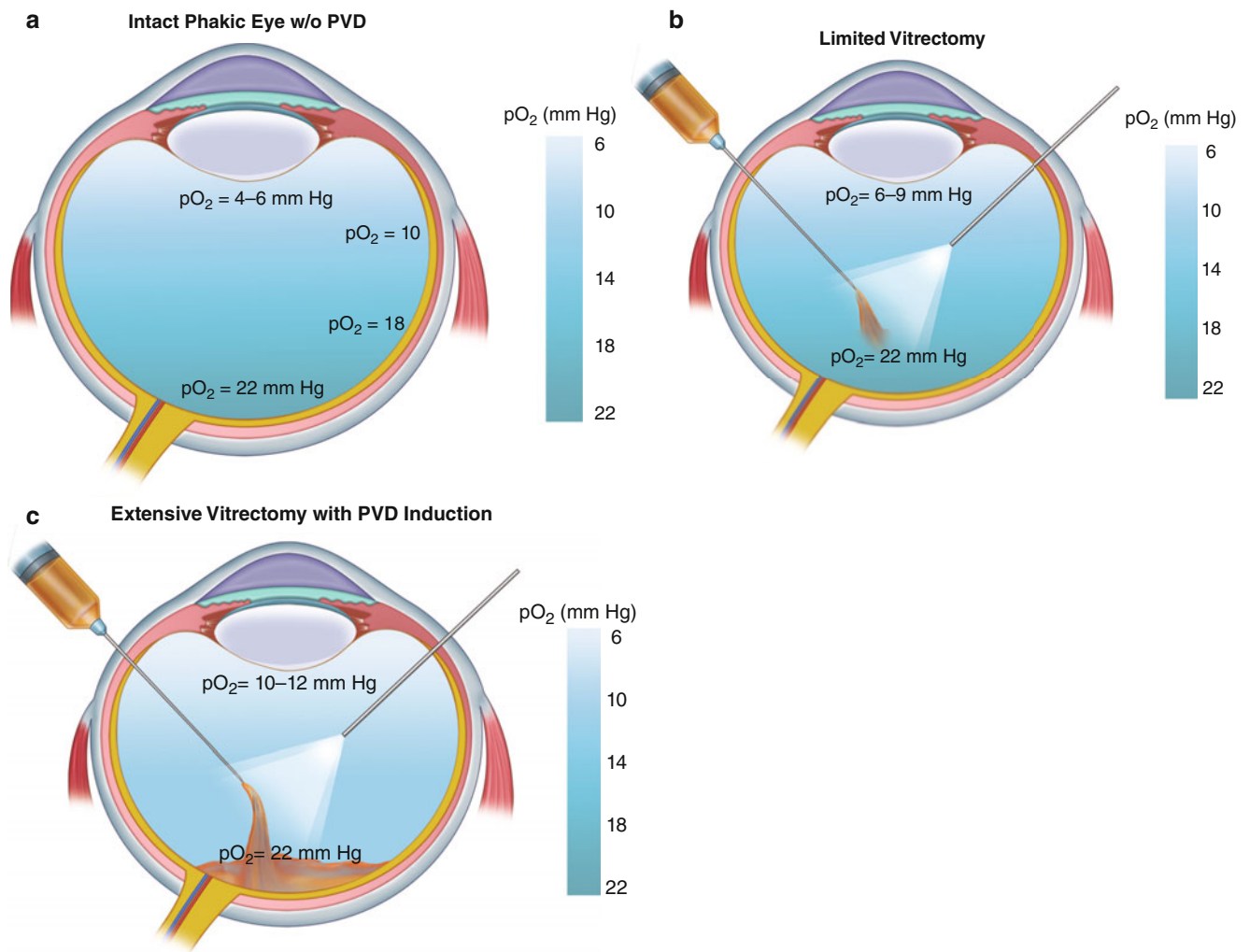


Figure V.B.8-9 The effects of limited vitrectomy on oxygen distribution. Intravitreal oxygen arises from the retina/choroid circulation posteriorly as well as from the ciliary body anteriorly. Vitrectomy increases convective motion and fluid circulation in the vitreous chamber, which increases oxygen levels behind the lens. (a) Intact eye. The pO_2 gradient ranges from 22 mmHg at the posterior pole to 8 mmHg at the equator and 10 mmHg peripherally in front of the ciliary body. pO_2 levels are 4–6 mmHg behind the lens. (b) Limited vitrectomy. Leaving the anterior

vitreous intact and not inducing a PVD results in increased retrolental oxygen levels of only 6–9 mmHg. This may account for the relatively low (23 %) incidence of cataract formation observed with limited vitrectomy. (c) Extensive vitrectomy with PVD induction. Following extensive vitrectomy with surgical induction of PVD, retrolental oxygen levels increase to 10–12 mmHg, twofold above those in the intact eye. These elevated levels may account for the 50–76 % incidence of cataract formation following extensive vitrectomy

surgery of 13 months. No patients under 53 years of age required cataract surgery. These findings support the concept of cataract mitigation by not inducing PVD and leaving vitreous (and its constituent antioxidants) intact behind the lens (see Figure V.B.8-9).

Conclusions

Patients are disturbed by floaters due to a reduction in contrast sensitivity, an important, albeit underappreciated, aspect of vision. As the medical community begins to better understand the impact of floaters on patients' vision and the impact on quality of life, it is advisable to consider

the treatment that has proven to be most effective and safe. Today, for patients who are unable to cope with chronically symptomatic vitreous opacities, the use of sutureless, limited vitrectomy using small-gauge instrumentation can safely eradicate symptoms, improve vision, and increase quality of life. Future directions to help patients with floaters include the use of optical methods to counteract or neutralize the visual effects, improved surgical instrumentation to further decrease risks, and pharmacologic vitreolysis (see Part VII. Pharmacologic vitreolysis) to obviate the need for vitrectomy and minimize the invasive nature of the treatment by

pharmacologically breaking down vitreous macromolecules, especially the aggregates of collagen that underlie the formation of floaters [46, 113–123].

It is important that the medical profession heed the cry of reasonable patients afflicted with clinically significant floaters, defined by quantitative ultrasound and contrast sensitivity testing, to achieve the goal of modern medicine [124]:

To help people die young, as late in life as possible

Ernst L. Wynder MD

Founding President of the American Health Foundation

Abbreviations

CSF	Contrast sensitivity function
DLS	Dynamic light scattering
FrACT	Freiburg acuity contrast test
HA	Hyaluronan
Leq	Equivalent veiling luminance
mmHg	Millimeters of mercury
Nd:YAG	Neodymium:yttrium-aluminum-garnet
NEI VFQ-39	National Eye Institute visual function questionnaire
pO ₂	Partial pressure of oxygen
PPV	Pars plana vitrectomy
PVD	Posterior vitreous detachment
RD	Retinal detachment
SD-OCT	Spectral-domain optical coherence tomography
SLO	Scanning laser ophthalmoscopy

References

- Duke-Elder WS. The nature of the vitreous body. *Br J Ophthalmol.* 1930;14(Suppl):6.
- Demours F. Observations anatomiques sur la structure cellulaire du corps vitre. *Memoires de Paris.* 1741.
- Virchow H. Die morphologische Natur des Glaskörpergebens. *Ophthalmol Gesellsch Heidelberg.* 1885; *Klin Monatsbl Augenheilkd.*
- Zinn. *Descriptio anatomica oculi humani.* Goettingen. 1780.
- Von Pappenheim A: Die spezielle gewebelehre des auges. 1842: 179–184; as cited by Redflob E: *Le Corps Vitre.* Paris: Masson et Cie, 1932:160–217
- Brucke E. Ueber den innern Bau des Glaskörpers. *Arch Anal Physiol Wissensch Med (Mueller)* 1843.
- Hannover A. Entdeckung des baues des glaskörpers. *Müller Archiv* 1845;467–77.
- Bowman W. Observations on the structure of the vitreous humor. *Dublin Quart J Med Sci.* 1848;6:102–18.
- Szent-Györgyi A. Untersuchungen über die Struktur des Glaskörpers des Menschen. *Arch f Mikroskop Anat.* 1917;89.
- Duke-Elder WS. The physico-chemical properties of the vitreous body. *J Physiol (Lond).* 1929;68(2):155–65.
- Sebag J, Yee K. Vitreous – from biochemistry to clinical relevance. In: Tasman W, Jaeger EA, editors. *Duane's foundation of clinical ophthalmology*, vol. 1. Philadelphia: Lippincott Williams & Wilkins; 1998. p. 1–34.
- Bishop PN. Structural macromolecules and supramolecular organisation of the vitreous gel. *Prog Retin Eye Res.* 2000; 19(3):323–44.
- Snowden JM, Eyre DR, Swann DA. Vitreous structure. VI. Age-related changes in the thermal stability and crosslinks of vitreous, articular cartilage and tendon collagens. *Biochim Biophys Acta.* 1982;706(2):153–7.
- Los LI, Van der Worp RJ, Van Luyn MJ, Hooymans JM. Age-related liquefaction of the human vitreous body: LM and TEM evaluation of the role of proteoglycans and collagen. *Invest Ophthalmol Vis Sci.* 2003;44(7):2828–33.
- Van Deemter M, Kuijter R, Pas HH, van der Worp RJ, Hooymans JM, Los LI. Trypsin-mediated enzymatic degradation of type II collagen in the human vitreous. *Mol Vis.* 2013;19:1591–9.
- Bishop PN, Holmes DF, Kadler KE, McLeod D, Bos KJ. Age-related changes on the surface of vitreous collagen fibrils. *Invest Ophthalmol Vis Sci.* 2004;45(4):1041–6.
- Foos RY, Wheeler NC. Vitreoretinal juncture. Synchysis senilis and posterior vitreous detachment. *Ophthalmology.* 1982; 89(12):1502–12.
- Sebag J. Age-related changes in human vitreous structure. *Graefes Arch Clin Exp Ophthalmol.* 1987;225(2):89–93.
- Hong PH, Han DP, Burke JM, Wiostko WJ. Vitrectomy for large vitreous opacity in retinitis pigmentosa. *Am J Ophthalmol.* 2001;131(1):133–4.
- Sebag J. The vitreous—structure, function and pathobiology. New York: Springer; 1989.
- Murakami K, Jalkh AE, Avila MP, Trempe CL, Schepens CL. Vitreous floaters. *Ophthalmology.* 1983;90(11):1271–6.
- Nguyen N, Sebag J. Myopic vitreopathy – significance in anomalous PVD and vitreo-retinal disorders. In: Midena E, editor. *Myopia and related diseases.* New York: Ophthalmic Communications Society; 2005. p. 137–45.
- Balazs EA, Denlinger JL. Aging changes in the vitreous. In: Sekuler R, Kline D, Dismukes K, editors. *Aging and human visual function*, vol. 2. New York: Alan R. Liss; 1982. p. 45–57.
- Webb BF, Webb JR, Schroeder MC, North CS. Prevalence of vitreous floaters in a community sample of smartphone users. *Int J Ophthalmol.* 2013;6(3):402–5.
- Wagle AM, Lim W-Y, Yap T-P, Neelam K, Au Eong K-G. Utility values associated with vitreous floaters. *Am J Ophthalmol.* 2011; 152(1):60–5.
- Sebag J. Floaters and the quality of life [editorial]. *Am J Ophthalmol.* 2011;152(1):3–4.
- Zou H, Liu H, Xu X, Zhang X. The impact of persistent visually disabling vitreous floaters on health status utility values. *Qual Life Res.* 2013;22:1507–14.
- Sebag J. Seeing the invisible: the challenge of imaging vitreous. *J Biomed Opt.* 2004;9(1):38–46.
- Coleman DJ, Daly SW, Atencio A, Lloyd HO, Silverman RH. Ultrasonic evaluation of the vitreous and retina. *Semin Ophthalmol.* 1998;13(4):210–8.
- McLeod D, Restori M, Wright JE. Rapid B-scanning of the vitreous. *Br J Ophthalmol.* 1977;61(7):437–45.
- Mojana F, Kozak I, Oster SF, Cheng L, Bartsch DU, Brar M, et al. Observations by spectral-domain optical coherence tomography combined with simultaneous scanning laser ophthalmoscopy: imaging of the vitreous. *Am J Ophthalmol.* 2010; 149(4):641–50.
- Oksala A. Ultrasonic findings in the vitreous body at various ages. *Albrecht Von Graefes Arch Klin Exp Ophthalmol.* 1978;207:275–80.

33. Walton KA, Meyer CH, Harkrider CJ, Cox TA, Toth CA. Age-related changes in vitreous mobility as measured by video B scan ultrasound. *Exp Eye Res.* 2002;74(2):173–80.
34. Silverman RH, Ketterling JA, Mamou J, Lloyd HO, Filoux E, Coleman DJ. Pulse-encoded ultrasound imaging of the vitreous with an annular array. *Ophthalmic Surg Lasers Imaging.* 2012;43(1):82–6.
35. Wa CA, Yee KM, Mamou J, Silverman R, Gale J, Ganti AK, et al. Quantitative ultrasonography of vitreous correlates with contrast sensitivity in patients with floaters. Paper presented at: the Association for Research in Vision and Ophthalmology (ARVO), Orlando, 4–8 May 2014.
36. Mirza RG, Johnson MW, Jampol LM. Optical coherence tomography use in evaluation of the vitreoretinal interface: a review. *Surv Ophthalmol.* 2007;52(4):397–421.
37. Coleman DJ, Silverman RH, Chabi A, Rondeau MJ, Shung KK, Cannata J, et al. High-resolution ultrasonic imaging of the posterior segment. *Ophthalmology.* 2004;111(7):1344–51.
38. Sebag J. Vitreous anatomy, aging, and anomalous posterior vitreous detachment. In: Dartt DA, editor. *Encyclopedia of the eye.* Oxford: Academic; 2010. p. 307–15.
39. Ansari RR, Suh KI, Dunker S, Kitaya N, Sebag J. Quantitative molecular characterization of bovine vitreous and lens with non-invasive dynamic light scattering. *Exp Eye Res.* 2001;73(6):859–66.
40. Rovati L, Fankhauser F, Docchio F, Van Best J. Diabetic retinopathy assessed by dynamic light scattering and corneal autofluorescence. *J Biomed Opt.* 1998;3(3):357–63.
41. Fankhauser F. Dynamic light scattering in ophthalmology: results of in vitro and in vivo experiments. *Technol Health Care.* 2006;14(6):521–35.
42. Fankhauser F. Analysis of diabetic vitreopathy with dynamic light scattering spectroscopy—problems and solutions related to photon correlation. *Acta Ophthalmol.* 2012;90(3):173–8.
43. Sebag J. To see the invisible: the quest of imaging vitreous. *Dev Ophthalmol.* 2008;42:5–28.
44. Datiles MB, Ansari RR, Suh KI, Vitale S, Reed GF, Zigler JS, et al. Clinical detection of precataractous lens protein changes using dynamic light scattering. *Arch Ophthalmol.* 2008;2008(126):12.
45. Fankhauser F. Postoperative follow up by dynamic light scattering: detection of inflammatory molecular changes in the cornea, the vitreous and the lens. *Technol Health Care.* 2007;15(4):247–58.
46. Sebag J. Molecular biology of pharmacologic vitreolysis. *Trans Am Ophthalmol Soc.* 2005;103:473–94.
47. Van den Berg T, Franssen L, Coppens JE. Ocular media clarity and straylight. In: Dartt D, Besharse J, Dana R, editors. *Encyclopedia of the eye.* Oxford: Academic; 2010. p. 173–83.
48. Van den Berg TJ, Franssen L, Kruijt B, Coppens JE. History of ocular straylight measurement: a review. *Z Med Phys.* 2012;23(1):6–20.
49. Rozema JJ, Van den Berg T, Tassignon MJ. Retinal straylight as a function of age and ocular biometry in healthy eyes. *Invest Ophthalmol Vis Sci.* 2010;51(5):2795–9.
50. IJspeert JK, de Waard PW, van den Berg TJ, de Jong PT. The intraocular straylight function in 129 healthy volunteers; dependence on angle, age and pigmentation. *Vision Res.* 1990;30:699–707.
51. Guber I, Bachmann LM, Guber J, Bochmann F, Lange AP, Thiel MA. Reproducibility of straylight measurement by C-Quant for assessment of retinal straylight using the compensation comparison method. *Graefes Arch Clin Exp Ophthalmol.* 2011;249(9):1367–71.
52. Tan JC, Spalton DJ, Arden GB. The effect of neodymium:YAG capsulotomy on contrast sensitivity and the evaluation of methods for its assessment. *Ophthalmology.* 1999;4:703–9.
53. Adamsons I, Rubin GS, Vitale S, Taylor HR, Stark WJ. The effect of early cataracts on glare and contrast sensitivity. A pilot study. *Arch Ophthalmol.* 1992;110(8):1081–6.
54. Mäntyjärvi M, Tuppurainen K. Cataract in traffic. *Graefes Arch Clin Exp Ophthalmol.* 1999;237(4):278–82.
55. Rubin GS, Roche KB, Prasada-rao P, Fried LP. Visual impairment and disability in older adults. *Optom Vis Sci.* 1994;71(12):750–60.
56. Sebag J, Yee KMP, Wa CA, Huang LC, Sadun AA. Vitrectomy for floaters – prospective efficacy analysis and retrospective safety profile. *Retina.* 2014;34:1062–8. PMID: 24296397.
57. Bach M. The Freiburg Visual Acuity Test – variability unchanged by post-hoc re-analysis. *Graefes Arch Clin Exp Ophthalmol.* 2007;245(7):965–71.
58. Nielsen E, Hjortdal J. Visual acuity and contrast sensitivity after posterior lamellar keratoplasty. *Acta Ophthalmol.* 2012;90(8):756–60.
59. Dennis RJ, Beer JM, Baldwin JB, Ivan DJ, Lorusso FJ, Thompson WT. Using the Freiburg Acuity and Contrast Test to measure visual performance in USAF personnel after PRK. *Optom Vis Sci.* 2004;81(7):516–24.
60. Woods RL, Tregear SJ, Mitchell RA. Screening for ophthalmic disease in older subjects using visual acuity and contrast sensitivity. *Ophthalmology.* 1998;12:2318–26.
61. Nearing SA, Stone ER, Cronin-golomb A, Oross S. The impact of acuity on performance of four clinical measures of contrast sensitivity in Alzheimer's disease. *J Gerontol B Psychol Sci Soc Sci.* 2003;58(1):54–62.
62. Delaney YM, Oyinloye A, Benjamin L. Nd:YAG vitreolysis and pars plana vitrectomy: surgical treatment for vitreous floaters. *Eye (Lond).* 2002;16(1):21–6.
63. Tsai WF, Chen YC, Su CY. Treatment of vitreous floaters with neodymium YAG laser. *Br J Ophthalmol.* 1992;77(8):485–8.
64. Toczolowski J, Katski W. Use of Nd:YAG laser in treatment of vitreous floaters. *Klin Oczna.* 1998;100(3):155–7.
65. Wilkinson CP. Safety of vitrectomy for floaters – how safe is safe? [editorial]. *Am J Ophthalmol.* 2011;151(6):919–20.
66. Mura M, Engelbrecht LA, de Smet MD, Papadaki TG, van den Berg TJ, Tan HS. Surgery for floaters. *Ophthalmology.* 2011;118:1894.
67. De Nie KF, Crama N, Tilanus MA, Klevering BJ, Boon CJ. Pars plana vitrectomy for disturbing primary vitreous floaters: clinical outcome and patient satisfaction. *Graefes Arch Clin Exp Ophthalmol.* 2013;251(5):1373–82.
68. Martínez-Sanz F, Velarde JI, Casuso P, Fernández-Cotero JN. Surgical solution to vitreous floaters visual problem. *Arch Soc Esp Oftalmol.* 2009;84(5):259–62.
69. Schiff WM, Chang S, Mandava N, Barile GR. Pars plana vitrectomy for persistent, visually significant vitreous opacities. *Retina.* 2000;20(6):591–6, forthcoming.
70. Okamoto F, Okamoto Y, Fukuda S, Hiraoka T, Oshika T. Vision-related quality of life and visual function after vitrectomy for various vitreoretinal disorders. *Invest Ophthalmol Vis Sci.* 2010;51(2):744–51.
71. Stoffelns BM, Vetter J, Keicher A, Mirshahi A. Pars plana vitrectomy for visually disturbing vitreous floaters in pseudophacic eyes. *Klin Monbl Augenheilkd.* 2011;228(4):293–7.
72. Hoerauf H, Müller M, Laqua H. Vitreous body floaters and vitrectomy with full visual acuity. *Ophthalmologie.* 2003;100(8):639–43.
73. Bansal AS, Hsu J, Garg SJ, Sivalingam A, Vander JF, Moster M, et al. Optic neuropathy after vitrectomy for retinal detachment: clinical features and analysis of risk factors. *Ophthalmology.* 2012;119(11):2364–70.
74. Gonzalez MA, Flynn HW, Smiddy WE, Albin TA, Berrocal AM, Tenzel P. Giant retinal tears after prior pars plana vitrectomy: management strategies and outcomes. *Clin Ophthalmol.* 2013;7:1687–91.
75. Hasegawa Y, Okamoto F, Sugiura Y, Okamoto Y, Hiraoka T, Oshika T. Intraocular pressure elevation after vitrectomy for various vitreoretinal disorders. *Eur J Ophthalmol.* 2014;24:235–41.
76. Shousha MA, Yoo SH. Cataract surgery after pars plana vitrectomy. *Curr Opin Ophthalmol.* 2010;21(1):45–9.

77. Schulz-Key S, Carlsson JO, Crafoord S. Longterm follow-up of pars plana vitrectomy for vitreous floaters: complications, outcomes and patient satisfaction. *Acta Ophthalmol.* 2011;89(2):159–65.
78. Chiang A, Kaiser RS, Avery RL, Dugel PU, Elliott D, Shah SP, et al. Endophthalmitis in microincision vitrectomy: outcomes of gas-filled eyes. *Retina.* 2011;31(8):1513–7.
79. Bahrani HM, Fazelat AA, Thomas M, et al. Endophthalmitis in the era of small gauge transconjunctival sutureless vitrectomy—meta analysis and review of literature. *Semin Ophthalmol.* 2010; 25(5–6):275–82.
80. Scott IU, Flynn HW, Acar N, et al. Incidence of endophthalmitis after 20-gauge vs 23-gauge vs 25-gauge pars plana vitrectomy. *Graefes Arch Clin Exp Ophthalmol.* 2011;249(3):377–80.
81. Hu AY, Bourges JL, Shah SP, et al. Endophthalmitis after pars plana vitrectomy a 20- and 25-gauge comparison. *Ophthalmology.* 2009;116(7):1360–5.
82. Wu L, Berrocal MH, Arévalo JF, et al. Endophthalmitis after pars plana vitrectomy: results of the Pan American Collaborative Retina Study Group. *Retina.* 2011;31(4):673–8.
83. Govetto A, Virgili G, Menchini F, Lanzetta P, Menchini U. A systematic review of endophthalmitis after microincisional versus 20-gauge vitrectomy. *Ophthalmology.* 2013;120:2286–91.
84. Kaiser RS, Prenner J, Scott IU, et al. The Microsurgical Safety Task Force: evolving guidelines for minimizing the risk of endophthalmitis associated with microincisional vitrectomy surgery. *Retina.* 2010;30(4):692–9.
85. Chen SD, Mohammed Q, Bowling B, Patel CK. Vitreous wick syndrome—a potential cause of endophthalmitis after intravitreal injection of triamcinolone through the pars plana. *Am J Ophthalmol.* 2004;137:1159–60.
86. Benitez-Herreros J, Lopez-Guajardo L, Camara-Gonzalez C, Silva-Mato A. Influence of the interposition of a non-hollow probe during cannula extraction on sclerotomy vitreous incarceration in sutureless vitrectomy. *Invest Ophthalmol Vis Sci.* 2012; 53(11):7322–6.
87. Buettner H, Machermer R. Histopathologic findings in human eyes after pars plana vitrectomy and lensectomy. *Arch Ophthalmol.* 1977;95(11):2029–33.
88. Gosse E, Newsom R, Lochhead J. The incidence and distribution of iatrogenic retinal tears in 20-gauge and 23-gauge vitrectomy. *Eye (Lond).* 2012;26(1):140–3.
89. Tan HS, Mura M, De Smet MD. Iatrogenic retinal breaks in 25-gauge macular surgery. *Am J Ophthalmol.* 2009;148(3): 427–30.
90. Hotta K, Hirakata A, Ohi Y, et al. Ultrasound biomicroscopy for examination of the sclerotomy site in eyes with proliferative diabetic retinopathy after vitrectomy. *Retina.* 2000;20(1):52–8.
91. Rahman R, Murray CD, Stephenson J. Risk factors for iatrogenic retinal breaks induced by separation of posterior hyaloid face during 23-gauge pars plana vitrectomy. *Eye (Lond).* 2013;27(5):652–6.
92. Al-harhi E, Abboud EB, Al-dhibi H, Dhindsa H. Incidence of sclerotomy-related retinal breaks. *Retina.* 2005;25(3):281–4.
93. López-guajardo L, Pareja-esteban J, Teus-guezala MA. Oblique sclerotomy technique for prevention of incompetent wound closure in transconjunctival 25-gauge vitrectomy. *Am J Ophthalmol.* 2006;141(6):1154–6.
94. Shimada H, Nakashizuka H, Mori R, Mizutani Y, Hattori T. 25-gauge scleral tunnel transconjunctival vitrectomy. *Am J Ophthalmol.* 2006;142(5):871–3.
95. Keshavamurthy R, Venkatesh P, Garg S. Ultrasound biomicroscopy findings of 25 G Transconjunctival Sutureless (TSV) and conventional (20G) pars plana sclerotomy in the same patient. *BMC Ophthalmol.* 2006;6:7.
96. Eckardt C. Transconjunctival sutureless 23-gauge vitrectomy. *Retina.* 2005;25(2):208–11.
97. Schweitzer C, Delyfer MN, Colin J, Korobelnik JF. 23-Gauge transconjunctival sutureless pars plana vitrectomy: results of a prospective study. *Eye (Lond).* 2009;23(12):2206–14.
98. Cha DM, Woo SJ, Park KH, Chung H. Intraoperative iatrogenic peripheral retinal break in 23-gauge transconjunctival sutureless vitrectomy versus 20-gauge conventional vitrectomy. *Graefes Arch Clin Exp Ophthalmol.* 2013;251(6):1469–74.
99. Le Rouic JF, Becquet F, Ducourneau D. Does 23-gauge sutureless vitrectomy modify the risk of postoperative retinal detachment after macular surgery? A comparison with 20-gauge vitrectomy. *Retina.* 2011;31(5):902–8.
100. Moore JK, Kitchens JW, Smiddy WE, Mavrofrides EC, Gregorio G. Retinal breaks observed during pars plana vitrectomy. *Am J Ophthalmol.* 2007;144(1):32–6.
101. Chung SE, Kim KH, Kang SW. Retinal breaks associated with the induction of posterior vitreous detachment. *Am J Ophthalmol.* 2009;147(6):1012–6.
102. Tan HS, Mura M, Lesnik Oberstein SY, Bijl HM. Safety of vitrectomy for floaters. *Am J Ophthalmol.* 2011;151(6):995–8.
103. Holekamp NM, Shui YB, Beebe DC. Vitrectomy surgery increases oxygen exposure to the lens: a possible mechanism for nuclear cataract formation. *Am J Ophthalmol.* 2005;139(2):302–10.
104. Beebe DC, Holekamp NM, Siegfried C, Shui YB. Vitreoretinal influences on lens function and cataract. *Philos Trans R Soc B Biol Sci.* 2011;366(1568):1293–300.
105. Pardo-Muñoz A, Muriel-Herrero A, Abraira V, Muriel A, Munoz-Negrete FJ, Murube J, et al. Phacoemulsification in previously vitrectomized patients: an analysis of the surgical results in 100 eyes as well as the factors contributing to the cataract formation. *Eur J Ophthalmol.* 2006;16(1):52–9.
106. Barbazetto IA, Liang J, Chang S, Zheng L, Spector A, Dillon JP. Oxygen tension in the rabbit lens and vitreous before and after vitrectomy. *Exp Eye Res.* 2004;78:917–24.
107. Van Effenterre G, Ameline B, Campinchi F, et al. Is vitrectomy cataractogenic? Study of changes of the crystalline lens after surgery of retinal detachment. *J Fr Ophthalmol.* 1992;15(8–9):449–54.
108. Smiddy WE, Feuer W. Incidence of cataract extraction after diabetic vitrectomy. *Retina.* 2004;24(4):574–81.
109. Quiram PA, Leverenz VR, Baker RM, Dang L, Giblin FJ, Trese MT. Microplasma-induced posterior vitreous detachment affects vitreous oxygen levels. *Retina.* 2007;27(8):1090–6.
110. Giblin FJ, Quiram PA, Leverenz VR, Baker RM, et al. Enzyme-induced posterior vitreous detachment in the rat produces increased lens nuclear pO₂ levels. *Exp Eye Res.* 2009;88(2):286–92.
111. Palmquist BM, Philipson B, Barr PO. Nuclear cataract and myopia during hyperbaric oxygen therapy. *Br J Ophthalmol.* 1984;68(2):113–7.
112. Simpanya MF, Ansari RR, Suh KI, Leverenz VR, Giblin FJ. Aggregation of lens crystallins in an in vivo hyperbaric oxygen guinea pig model of nuclear cataract: dynamic light-scattering and HPLC analysis. *Invest Ophthalmol Vis Sci.* 2005; 46(12):4641–51.
113. Sebag J. Pharmacologic vitreolysis. *Retina.* 1998;18(1):1–3.
114. Sebag J, Kitaya N, Ansari RR, Karagozian H, Yoshida A. Preliminary findings using dynamic light scattering to study vitreous effects of Pharmacologic Vitreolysis. *Proc SPIE.* 2000;3908:69–77.
115. Sebag J. Is pharmacologic vitreolysis brewing? *Retina.* 2002;22(1):1–3.
116. Sebag J. Vitreous pathobiology and pharmacologic vitreolysis. In: Binder S, editor. *The macula – diagnosis, treatment, and future trends.* Wein/New York: Springer; 2004. p. 171–80.
117. Sebag J, Ansari RR, Suh KI. Pharmacologic vitreolysis with microplasma increases vitreous diffusion coefficients. *Graefes Arch Clin Exp Ophthalmol.* 2007;245(4):576–80.

118. Sebag J. Pharmacologic vitreolysis—premise and promise of the first decade. *Retina*. 2009;29(7):871–4.
119. Sebag J. The emerging role of pharmacologic vitreolysis. *Retinal Physician*. 2010;7(2):52–6.
120. Costa Ede P, Rodrigues EB, Farah ME, Sebag J, Meyer CH. Novel vitreous modulators for pharmacologic vitreolysis in the treatment of diabetic retinopathy. *Curr Pharm Biotechnol*. 2011;12(3):410–22.
121. Tozer K, Fink W, Sadun AA, Sebag J. Prospective three-dimensional analysis of structure and function in macular hole treated by pharmacologic vitreolysis. *Retinal Cases & Brief Reports*. 2013;7:57–61.
122. Sebag J, Tozer K. Vitreous biochemistry and pharmacologic vitreolysis. In: Hartnett ME, editor. *Pediatric retina*. 2nd ed. Philadelphia: Lippincott Williams & Wilkins; 2013.
123. Stalmans P, Duker JS, Kaiser PK, Heier JS, Dugel PU, Gandorfer A, et al. Oct-based interpretation of the vitreomacular interface and indications for pharmacologic vitreolysis. *Retina*. 2013;33:2003–11.
124. Sebag J. The diagnosis of health. First prize, national essay competition. *Prev Med*. 1979;8:76–8.
125. Sebag J, Balazs EA. Morphology and ultrastructure of human vitreous fibers. *Invest Ophthalmol Vis Sci*. 1989;30:1867–71.

Rare Indications for Vitrectomy: Tumor Excision, Optic Nerve Pits, and Malignant Glaucoma

V.B.9.

Lawrence P. Chong

Outline

- I. Introduction
 - II. Tumors
 - A. Retinoblastoma
 - B. Malignant Melanoma
 - C. Vascular Tumors
 - III. Optic Nerve Pits
 - IV. Malignant Glaucoma
- References

Keywords

Vitrectomy • Tumors • Retinoblastoma • Von Hippel-Lindau • Coat's disease • Malignant melanoma • Optic pits • Malignant glaucoma

Key Concepts

1. Endoresection of choroidal malignant melanoma is highly controversial. A significant period of tumor inactivity is required before pars plana vitrectomy should be performed in an eye previously treated for retinoblastoma. Endoresection of retinal capillary hemangioblastoma is technically feasible.
2. Recent observations suggest that the retinoschisis associated with optic nerve pits may be a result of vitreous traction in the peripapillary region.
3. The most effective therapy for malignant glaucoma may be pars plana vitrectomy and the creation of a tunnel through the peripheral iris and underlying zonules.

L.P. Chong, MD
VMR Institute for Vitreous Macula Retina,
Huntington Beach, CA, USA

Doheny Eye Institute,
Los Angeles, CA, USA
e-mail: lchong@usc.edu

I. Introduction

These rare indications for pars plana vitrectomy are related in that highly novel techniques have evolved to either achieve the therapeutic goal or to improve our understanding of the pathophysiology. Even then, the merits of the procedures continue to be debated as in the case of optic nerve pit and malignant glaucoma. In these conditions, we await a more definitive understanding of their pathophysiology before the proper approach to therapy can be determined. Until such time, however, the following describes the current vitrectomy approaches to tumors, optic pits, and malignant glaucoma.

II. Tumors

A. Retinoblastoma

Vitrectomy for retinoblastoma may be fraught with hazards. It has been reported that inadvertent vitrectomy in an eye with an unsuspected retinoblastoma could potentially seed the orbit with tumor and cause metastases [1]. Clusters of tumor cells were identified in the 25 gauge biopsy needle tracks in an experimental model involving eyes enucleated for retinoblastoma [2]. Three cases of local extraocular extension of retinoblastoma following intraocular surgery via a transscleral approach were reported from a single center [3].

Currently, the most common indications for elective pars plana vitrectomy in eyes which have been treated for retinoblastoma include cataract after external beam radiation, vitreous hemorrhage secondary to radiation retinopathy, and retinal detachment after cataract surgery. In the literature, 70 eyes have been reported which underwent pars plana vitrectomy after treatment for retinoblastoma. The indications were radiation-related cataract in 42 [4, 5]. In the remaining 28 eyes, the indications were radiation retinopathy causing vitreous hemorrhage in 12, retinal detachment in 15, and endophthalmitis in 1 [6–11]. There were 2 recurrent tumors in the 42 eyes that underwent procedures related to cataract and 7 recurrent tumors in the remaining 28 eyes. The median interval between completion of treatment for retinoblastoma and intraocular surgery was 26 months in patients with a favorable outcome versus 6 months in those with unfavorable outcome [9]. A minimal tumor-free interval of 12–18 months has been suggested before intraocular intervention, although this may not always be practical when the vision in the only remaining eye is threatened.

When the fellow eye has good vision, it is not a difficult decision to enucleate an eye which has been previously treated for retinoblastoma and has now a serious indication for pars plana vitrectomy. However, when the involved eye is the only functional eye, the decision is more difficult and surgical intervention may be considered.

B. Malignant Melanoma

Peyman first developed techniques to perform endoresection [12] and others soon reported their experience [13, 14]. After pars plana vitrectomy and induction of posterior vitreous detachment, the margins of the melanoma are treated with laser photocoagulation and/or endodiathermy. An anterior retinal flap is made through which the vitreous cutter is introduced to remove the melanoma. The retina is then reattached, and the eye is filled with silicone oil. If the retina is invaded by the melanoma, then the retina and the melanoma are

removed together. Variations on this technique include the use of hypotensive anesthesia, preoperative [15–18] or post-operative radiation therapy [19], intraoperative laser and/or diathermy to the tumor surface, intraoperative endodiathermy or cryoablation to tumor margins, photocoagulation to the bare scleral bed, incising the choroid before removing the tumor, cryotherapy to the sclerotomy sites, and simultaneous lens removal.

The major concerns of this technique include incomplete resection, residual intrascleral melanoma, intraretinal invasion, and irretrievable dissemination and implantation of malignant cells in the vitreous [20]. Eight of 12 eyes that were enucleated after endoresection had recurrence at the site of the primary tumor. One of these eyes had vitreous seeding [21]. Intrascleral recurrence of a uveal melanoma was reported after endoresection and laser photocoagulation to the tumor margins [22].

The most serious perioperative complication of endoresection is retinal detachment (9.4–32 %). Other complications include cataract, macular traction, premacular macular proliferation, bleeding, ocular hypertension, local recurrence, or systemic dissemination. Concerning the two last mentioned complications, all of the large reported series of endoresection have been single-center retrospective studies [13, 14, 18, 19, 23–25]. Local recurrence ranged between 0 % [14] and 15 % [24]. Death from metastatic disease ranged between 0 % [14] and 5 % [24]. The small numbers of patients and limited follow-up preclude conclusive interpretation of the data. The case-controlled series suggested a trend for a lower incidence of metastasis in patients who underwent endoresection compared to those who underwent brachytherapy [19].

Visual acuity preservation is the *raison d'être* for this procedure, and between 9.2 and 32 % of eyes have 20/200 or better vision after surgery. One center reported a remarkable 92 % of patients achieving 20/200 or better vision after endoresection as primary treatment [14]. However the same center subsequently reported that only 18.2 % of patients achieved 20/200 or better vision after endoresection for recurrence after conventional treatment [25].

In summary, endoresection of choroidal malignant melanoma is an alternative to enucleation for tumors that are small, but thick, and located in close proximity to the optic nerve. Vision loss is common because radiation must be delivered close to the optic nerve and at a high dose. There is an active debate over the merits of this procedure [20, 26–28].

C. Vascular Tumors

Macular pucker is a complication of progressive vitreoretinal interface disease [see chapter III.F. Vitreous in the pathobiology of macular pucker] resulting from anomalous

PVD with vitreoschisis [see Chapter III.B. Anomalous PVD and vitreoschisis]. It is also associated with high-flow retinal vascular pathology and is an indication for pars plana vitrectomy and membrane peeling [29]. The majority of these patients have attached vitreous. Spontaneous peeling of the macular pucker occurs in eyes that have a partial posterior vitreous detachment which progresses to complete posterior vitreous detachment [30]. In addition to macular pucker, fibrotic organization can occur directly over the vascular abnormality. Machemer [31] described a sequence of events that culminated in what he termed “proliferative vasculopathy.” He performed pars plana vitrectomy and membrane peeling for traction retinal detachment in 2 eyes with von Hippel-Lindau retinal hemangioblastomas, 2 eyes with exudative vitreo-retinopathy, and 2 eyes with Coat’s disease. He observed resolution of exudates when traction was relieved, but exudate would recur and traction would return if the vascular abnormality continued to leak. These observations led him to conclude that chronic leakage from diseased vessels stimulates the infiltration of cells derived from the retina and their proliferation. These cells produce collagen and form the bands and strands, resulting in traction on the retina. This traction in turn induces more leakage. This cycle continues until there is frank traction retinal detachment. At this point, treatment with anti-VEGF, pan-retinal or focal laser with or without dye enhancement, transpupillary thermal therapy, photodynamic therapy, cryoablation, or brachytherapy is ineffective. Surgical relief of this traction is necessary to break this cycle of traction and leakage. Retinal interface pathology associated with the high-flow vascular shunts is seen in retinopathy of prematurity, sickle retinopathy, Coat’s disease, and retinal angioma. The pathology of these different diseases shows similar findings at the vitreoretinal interface over the abnormal leaking vasculature.

Schlesinger and colleagues have described internal en bloc resection of retinal capillary hemangioblastoma [32]. After pars plana vitrectomy is performed, the feeder vessel is ligated. The area to be excised is cauterized, and the retina along with the tumor is excised with scissors. The eye is then filled with gas tamponade. Collagenous tissue adherent to the vitreous side of the excised area correlated to the area of traction retinal detachment.

III. Optic Nerve Pits

Optic nerve pit was first described in 1882 by Wieth [33] as a congenital optic nerve abnormality that can be associated with serous detachment of the macula [34–36]. The cause of the retinal detachments was debated. Early observations of contrast media migrating from spinal fluid to the macula [37] and of silicone oil in the vitreous migrating to the macula [38] suggested communications through the optic nerve pit

between either the cerebrospinal fluid and the subretinal space or the vitreous body and the subretinal space. Careful examination of the macula in these eyes by Lincoff [39] led him to conclude that fluid was accumulating in the retinoschisis cavity and not in the subretinal space. This was later corroborated by optical coherence tomography [40].

The long-term visual prognosis of serous retinal detachment of the macula associated with optic nerve pits is poor [36]. Interventional techniques have included barrier laser to the borders of the optic nerve [41, 42], macular scleral buckling [43], gas injections [44] and pars plana vitrectomy, and gas fluid exchange with [45] or without [46] barrier laser. Pars plana vitrectomy and induction of posterior vitreous detachment without gas tamponade or barrier laser were successful in complete retinal reattachment in 7 of 8 eyes [47]. This suggests that removal of traction on the surface of the optic nerve pit may be the most important mechanism for resolution of the macular retinoschisis and that gas or laser is unnecessary. At the time of surgery, a sharp retinal elevation adjacent to the optic disc and inner retinoschisis-like separation immediately decreased after surgery. This suggested that traction on the peripapillary retina may be a factor in the migration of fluid from the vitreous body into the macular retinoschisis. Vitreo-macular traction and vitreous strands over the optic disc have been observed by OCT in this condition [48]. Intraoperative OCT imaging of another case treated at the same institution demonstrated the collapse of the macular retinoschisis during air-fluid exchange and aspiration over the optic nerve pit [49].

Histopathologic studies of optic disc pits showed poorly differentiated retinal tissue combined with collagen herniating into the subarachnoid space [50]. This observation and their surgical experience led Hirakota and colleagues [47] to conclude that there is communication between the subarachnoid space and the vitreous body through this porous, poorly differentiated retina and the lamina cribrosa. Depending on the balance between intraocular pressure and intracranial pressure and traction on the surface of the optic pit, eddy currents may cause fluid migration into the retinoschisis cavity from either the subarachnoid space or vitreous body.

IV. Malignant Glaucoma

Malignant glaucoma was first described by von Graefe in 1869 as occurring after glaucoma surgery [51]. It is characterized by a very shallow anterior chamber (axially), the presence of a patent peripheral iridectomy or iridotomy, and the absence of suprachoroidal effusion or hemorrhage [52]. Malignant glaucoma has been reported with the use of miotics [53, 54] and after the following procedures: filtration surgery [55–57], cataract surgery with and without

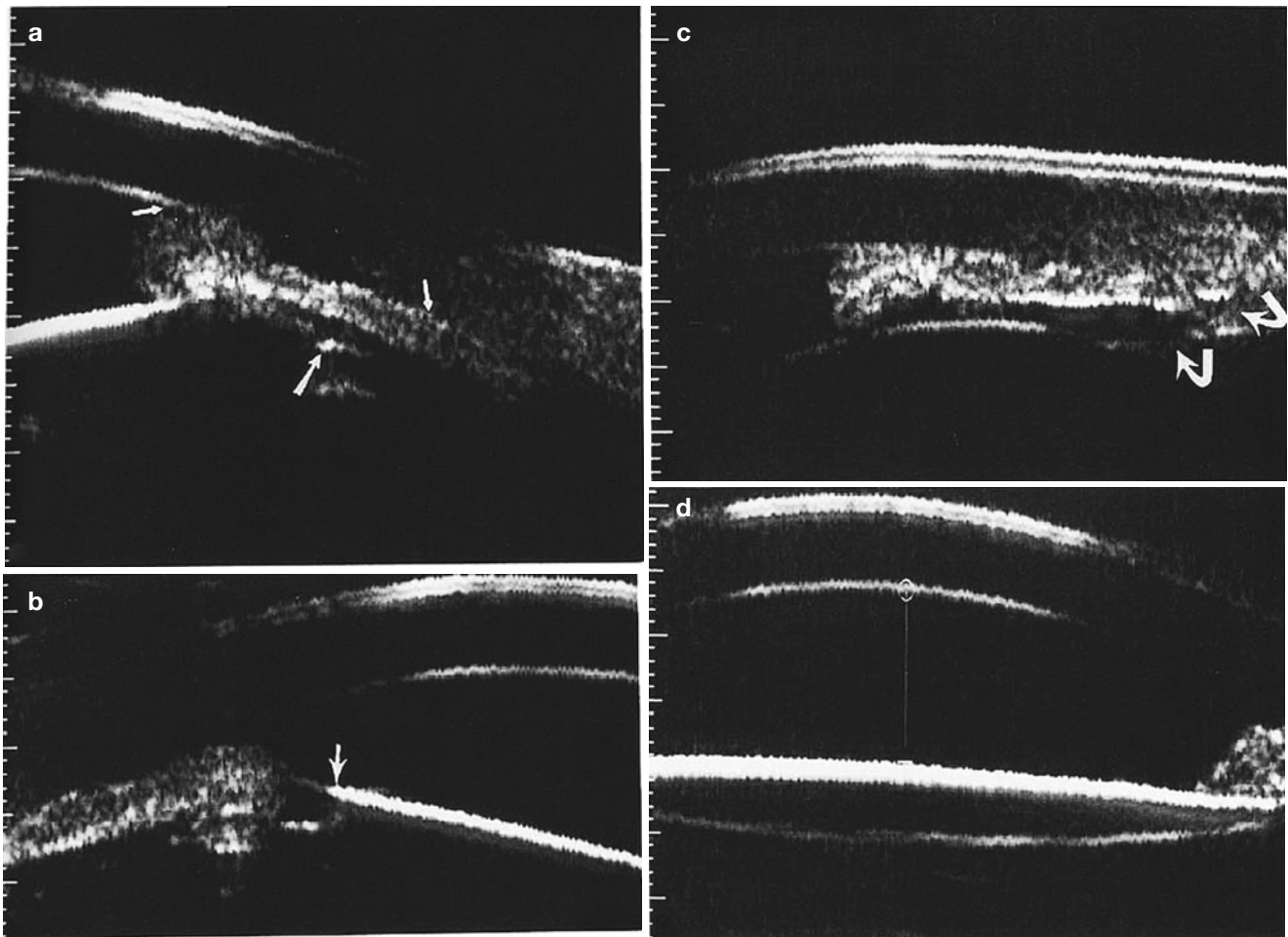


Figure V.B.9-1 Ultrasound biomicroscopy of pseudophakic malignant glaucoma. (a) in the temporal angle, peripheral iridocorneal apposition is present (small arrows). The haptic is visible beneath the iris

(large arrow). (b) the nasal portion of the optic (arrow) is anterior to the iris. (c) anterior rotation of the ciliary body (arrows), in apposition to the peripheral iris. (d) the central anterior chamber is shallow

intraocular lens implantation [58], glaucoma drainage device implantation [59], laser suture lysis of a trabeculectomy flap suture [60], laser iridotomy [61–63], Nd:YAG laser posterior capsulotomy [64], cyclophotocoagulation [65, 66], and pars plana vitrectomy [67]. The fellow eye is at risk for malignant glaucoma. These eyes tend to be axially short and hyperopic. Early theories of the mechanism of malignant glaucoma included aqueous misdirection due to an abnormally impermeable anterior vitreous face [68] and choroidal swelling which leads to forward lens movement [69]. Ultrasound biomicroscopy was performed in a case of pseudophakic malignant glaucoma which resolved after Nd:YAG photodisruption of the anterior vitreous face [70]. There was anterior rotation of the ciliary body and a forward displacement of the posterior chamber IOL and ciliary body. This was compatible with an abnormality of the vitreo-ciliary anatomic relationship blocking access of aqueous to the anterior chamber

(Figure V.B.9-1). Accumulation of aqueous volume in the vitreous body pushed the iris against the trabecular meshwork. These findings were reversed after the anterior vitreous face was disrupted. Adhesions can develop between the ciliary body and iris, lens equator, lens capsule, or the vitreous which would explain why a variety of techniques have been partially successful in treating this condition. These include medical treatment with cycloplegics [71], aqueous suppressants, and hyperosmotics [72] and the following procedures: cryotherapy [73], photocoagulation of the ciliary processes [74], contact transscleral cyclophotocoagulation [75], disruption of the anterior vitreous face by knife or needle (with or without aspiration of vitreous fluid) [68, 76–78], Nd:YAG laser [79, 80], anterior vitrectomy [81–83], pars plana needle aspiration of vitreous fluid [77], and pars plana vitrectomy [58]. Medical treatment may be effective in up to 50 % of the cases. Core vitrectomy alone is effective in

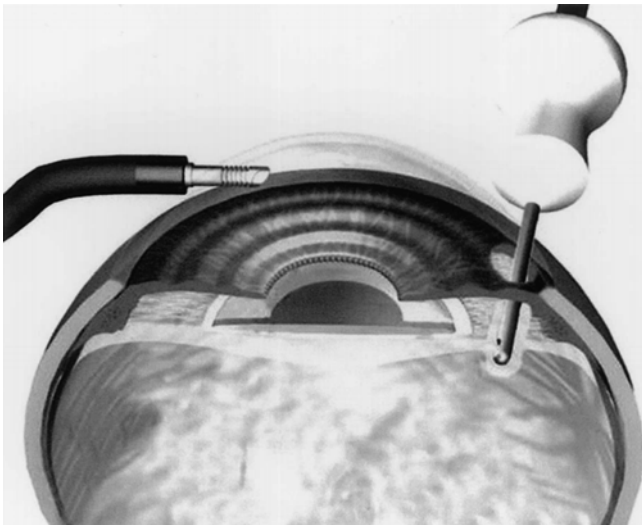


Figure V.B.9-2 The vitreous cutter is introduced into the anterior chamber and then through the peripheral iridotomy to remove zonules, anterior hyaloid face, and the anterior vitreous [Reprinted with permission from Lois et al. [84] (figure 1, page 781)]

25–65 % of the cases, with higher success in aphakic patients. Currently the treatment of choice is zonulohyaloido-vitrectomy by an anterior approach through a peripheral iridectomy in pseudophakic eyes [84] or vitrectomy-phacoemulsification-vitrectomy in phakic eyes [85]. Both procedures create a peripheral tunnel through which aqueous from the vitreous body gains unobstructed access to the anterior chamber. In the pseudophakic eye, the procedure involves zonulectomy, hyaloidectomy, and anterior vitrectomy through a peripheral iridectomy or iridotomy through the anterior chamber (Figure V.B.9-2). In phakic eyes, the operation is performed in three steps: A pars plana vitrectomy is first performed to debulk the vitreous and soften the eye. Then phacoemulsification of the lens is performed. Finally the residual vitrectomy, zonulohyaloidectomy, and peripheral iridectomy are performed (Figures V.B.9-3, V.B.9-4, and V.B.9-5). Prophylactic pars plana vitrectomy may be indicated in a fellow eye undergoing surgery [86].

Figure V.B.9-3 Core vitrectomy deepens the anterior chamber, and viscoelastic is injected into the anterior chamber [Reprinted with permission from Sharma et al. [85] (figure 1, page 3)]

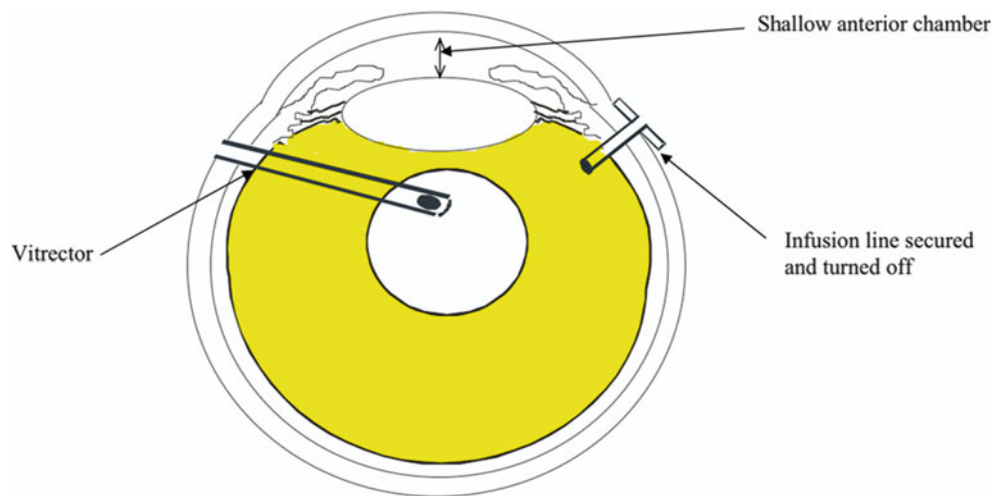


Figure V.B.9-4 Phacoemulsification is performed through the deepened anterior chamber [Reprinted with permission from Sharma et al. [85] (figure 2, page 3)]

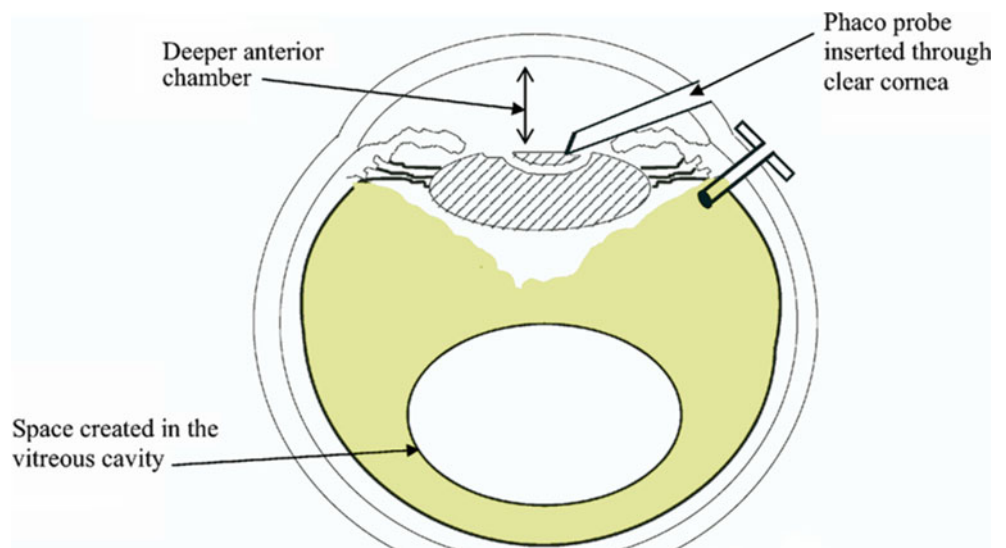
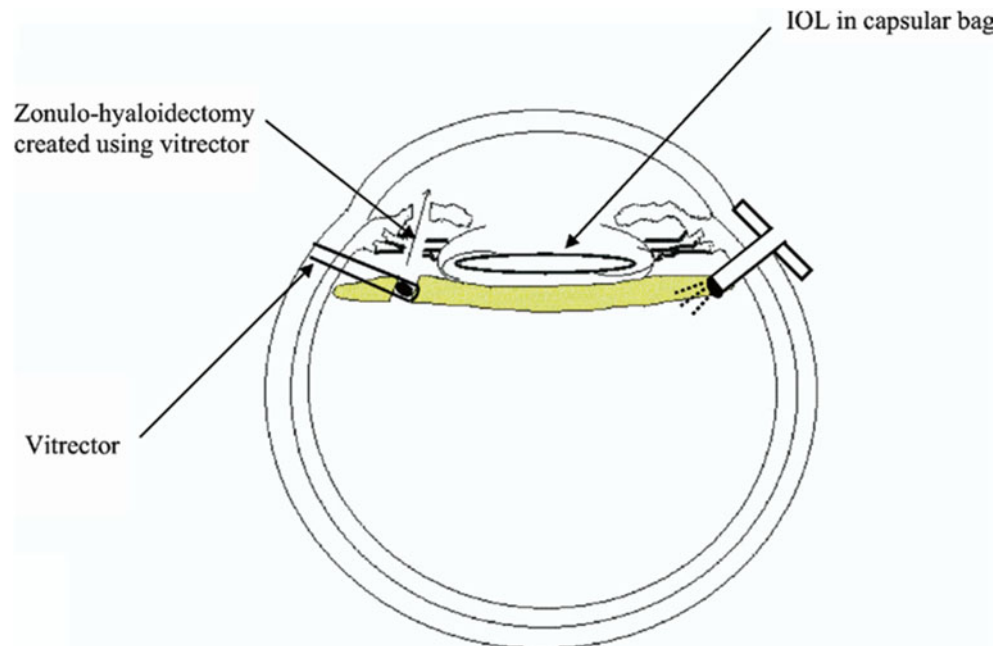


Figure V.B.9-5 After posterior chamber intraocular lens implantation in the bag, a complete pars plana vitrectomy is performed. Then the vitreous cutter is used to perform a peripheral iridectomy and remove adjacent zonules [Reprinted with permission from Sharma et al. [85] (figure 3, page 3)]



Abbreviations

IOL	Intraocular lens
Nd:YAG	Neodymium:yttrium-aluminum-garnet laser
OCT	Optical coherence tomography
PVD	Posterior vitreous detachment
VEGF	Vascular endothelial growth factor

References

- Shields CL, Honavar S, Shields JA, Demirci H, Meadows AT. Vitrectomy in eyes with unsuspected retinoblastoma. *Ophthalmology*. 2000;107:2250–5.
- Karcioglu ZA, Gordon RA, Karcioglu GL. Tumor seeding in ocular fine needle aspiration biopsy. *Ophthalmology*. 1985;92:1763–7.
- Stevenson KE, Hungerford J, Garner A. Local extraocular extension of retinoblastoma following intraocular surgery. *Br J Ophthalmol*. 1989;73:730–42.
- Brooks Jr HL, Meyers D, Shields JA, Balas AG, Nelson LR, Fontanesi J. Removal of radiation-induced cataracts in patients treated for retinoblastoma. *Arch Ophthalmol*. 1990;108:1701–8.
- Portellos M, Buckley EG. Cataract surgery and intraocular lens implantation in patients with retinoblastoma. *Arch Ophthalmol*. 1998;116:449–52.
- Monge DR, Flage T, Hatlevoll R, Vermund H. Sightsaving therapy in retinoblastoma: experience with external megavoltage radiotherapy. *Acta Ophthalmol*. 1986;64:414–20.
- Baumal CR, Shields CL, Shields JA, Tasman WS. Surgical repair of rhegmatogenous detachment after treatment for retinoblastoma. *Ophthalmology*. 1998;105:2134–9.
- Madreperla SA, Hungerford JL, Cooling RJ, Sullivan P, Gregor Z. Repair of late retinal detachment after successful treatment of retinoblastoma. *Retina*. 2000;20:28–32.
- Honavar SG, Shields CL, Shields JA, Demirci H, Naduvilath TJ. Intraocular surgery after treatment of retinoblastoma. *Arch Ophthalmol*. 2001;119:1613–21.
- Moshfeghi DM, Wilson MW, Grizzard S, Haik BG. Intraocular surgery after treatment of germline retinoblastoma. *Arch Ophthalmol*. 2005;123:1008–12.
- Warden SM, Mukai S. Pars plana vitrectomy in eyes treated for retinoblastoma. *Retina*. 2006;26:S53–6.
- Peyman GA, Cohen SB. Ab interno resection of uveal melanoma. *Int Ophthalmol*. 1986;9:29–36.
- Damato B, Gorenwald C, McGalliard J, Wond D. Endoresection of choroidal melanoma. *Br J Ophthalmol*. 1998;82:213–8.
- Garcia-Arumi J, Sarorls L, Martinez V, Corcostegui B. Vitreoretinal surgery and endoresection in high posterior choroidal melanomas. *Retina*. 2001;21:445–52.
- Bechrakis NE, Hocht S, Martus P, et al. Endoresection following proton beam irradiation of large uveal melanomas. *Ophthalmologie*. 2004;101:370–6.
- Bechrakis NE, Petousis V, Krause L, et al. Surgical treatment modalities in uveal melanomas. *Klin Monbl Augenheilkd*. 2009;226:921–6.
- Bechrakis NE, Forester MH. Neoadjuvant proton beam radiotherapy combined with subsequent endoresection of choroidal melanomas. *Int Ophthalmol Clin*. 2006;46:95–107.
- Schilling H, Bornfeld N, Talies S, et al. Endoresection of large uveal melanomas after pretreatment by single-dose stereotactic convergence irradiation with the leksell gamma knife- First experience on 46 cases. *Klin Monatsbl Augenheilkd*. 2006;223:513–20.
- Caminal JM, Mejia K, Masuet-Aumadell C, Arias L, Piulats JM, Gutierrez C, Pera J, Catala J, Rubio M, Arruga J. Endoresection versus iodine-125 plaque brachytherapy for the treatment of choroidal melanoma. *Am J Ophthalmol*. 2013;156:334–42.
- Robertson DM. Melanoma endoresection: a perspective. *Retina*. 2001;21:403–7.
- Hadden PW, Hiscott PS, Damato BE. Histopathology of eyes enucleated after endoresection of choroidal melanoma. *Ophthalmology*. 2004;111:154–60.
- Damato B, Wong D. Intrasclear recurrence of uveal melanoma after transretinal “endoresection.”. *Br J Ophthalmol*. 2001;84:114–5.

23. Kertes PJ, Johnson JC, Peyman GA. Internal resection of posterior uveal melanomas. *Br J Ophthalmol*. 1998;82:1147–53.
24. Karkaneh R, Chams H, Amoli FA, Riazi-Esfahani M, Ahmadabadi MN, Mansouri MR, Nouri K, Karkahaneh A. Long-term surgical outcome of posterior choroidal melanoma treated by endoresection. *Retina*. 2007;27:908–14.
25. Garcia-Arumi J, Zapata MA, Fonollosa A, Boixadera A, Martinez-Castillo V. Endoresection in high posterior choroidal melanomas: long term outcome. *Br J Ophthalmol*. 2008;92:1040–5.
26. Rennie IG. From the outside in, or the inside out. Resecting uveal melanomas. *Br J Ophthalmol*. 1998;82:209.
27. Singh AD, Triozzi PL. Endoresection for choroidal melanoma: palliative or curative intent? *Br J Ophthalmol*. 2008;92:1015–6.
28. Damato B. Choroidal melanoma endoresection, dandelions and allegory-based medicine. *Br J Ophthalmol*. 2008;92:1013–4.
29. McDonald HR, Schatz H, Johnson RN, Abrams GW, Brown GC, Brucker AJ, Han DP, Lewis H, Mieler WF, Meyers S. Vitrectomy in eyes with peripheral retinal angioma associated with traction macular detachment. *Ophthalmology*. 1996;103(2):329–35.
30. Schwartz PL, Fastenberg DM, Shakin JL. Management of macular puckers associated with retinal angiomas. *Ophthalmic Surg*. 1990;21:550–6.
31. Macherer R, Williams JM Sr. Pathogenesis and therapy of traction retinal detachment in various retinal vascular diseases (published erratum appears in *Am J Ophthalmol*. 1988 Jun 15;104:714). *Am J Ophthalmol*. 1988;105:170–81.
32. Schlesinger T, Appukuttan B, Hwang T, Atchaneeyakul L, et al. Internal en bloc resection and genetic analysis of retinal capillary hemangioblastoma. *Arch Ophthalmol*. 2007;125(9):1189–93.
33. Wiethe T. Ein Fall von angeborener Difformitat der Sehnervierpapille. *Arch Augenheilkd*. 1882;11:14–9.
34. Kranenburg EW. Crater-like holes in the optic disc and central serous retinopathy. *Arch Ophthalmol*. 1960;64:912–24.
35. Brown GC, Shields JA, Goldberg RE. Congenital pits of the nerve head: II. Clinical studies in humans. *Ophthalmology*. 1980;87:551–65.
36. Cobol WM, Blodi CF, Folk JC, Weingeist TA. Long-term visual outcome in patients with optic nerve pit and serous retinal detachment of the macula. *Ophthalmology*. 1990;97:1539–42.
37. Chang S, Haik BG, Ellsworth RM, St Louis L, Berrocal JA. Treatment of total retinal detachment in morning glory syndrome. *Am J Ophthalmol*. 1984;97:596–600.
38. Dithmar S, Schuett F, Voelcker HE. Delayed sequential occurrence of perfluorodecalin and silicone oil in the subretinal space following retinal detachment surgery in the presence of an optic disc pit. *Arch Ophthalmol*. 2004;122(3):409–11.
39. Lincoff H, Lopez R, Kreissig I, et al. Retinoschisis associated with optic nerve pits. *Arch Ophthalmol*. 1988;106:61–7.
40. Rive D, Gentile R, Lineman JM, Stedman Z, Walsh JB, Retch R. Imagine congenital optic disc pits and associated maculopathy using optical coherence tomography. *Arch Ophthalmol*. 1996;114:165–70.
41. Brochures RJ. Optic pits and posterior retinal detachment. *Trans Am Ophthalmol Soc*. 1975;73:264–91.
42. Mustonen E, Varonen T. Congenital pit of the optic nerve head associated with serous detachment of the macula. *Acta Ophthalmol*. 1972;50:689–98.
43. Theodossiadis GP. Treatment of maculopathy associated with optic disc pit by sponge explant. *Am J Ophthalmol*. 1996;121:630–7.
44. Lincoff H, Yanuzzi L, Singerman L, et al. Improvement in visual function after displacement of the retinal elevations emanating from optic pits. *Arch Ophthalmol*. 1993;111:1071–9.
45. Schatz H, McDonald HR. Treatment of sensory retinal detachment associated with optic nerve pit or coloboma. *Ophthalmology*. 1988;95:178–86.
46. Hirakata A, Okada AA, Hida T. Long-term results of vitrectomy without laser treatment for macular detachment associated with an optic disc pit. *Ophthalmology*. 2005;112:1430–5.
47. Hiraoka A, Inoue M, Hiraoka T, McCuen II BW. Vitrectomy without laser treatment or gas tamponade for macular detachment associated with an optic disc pit. *Ophthalmology*. 2012;119:810–8.
48. Theodossiadis PG, Grigoropoulos VG, Emfietzoglou J, Theossiadi GP. Vitreous finding in optic disc pit maculopathy based on optical coherence topography. *Graefes Arch Clin Exp Ophthalmol*. 2007;245:1311–8.
49. Ehlers JP, Kernstine K, Farsiu S, Sarin N, Maldonado R, Toth CA. Analysis of pars plana vitrectomy for optic pit-related maculopathy with intraoperative optical coherence tomography. A possible connection with the vitreous cavity. *Arch Ophthalmol*. 2011;129(11):1483–6.
50. Irvine AR, Crawford JB, Sullivan JH. The pathogenesis of retinal detachment with morning glory disc and optic pit. *Retina*. 1986;6:146–50.
51. Von Graefe A. Beitragezurpathologie und therapie des glaucoms. *Archiv fur Ophthal*. 1869;15(3):108–252.
52. Epstein DL. The malignant glaucoma syndromes. In: Epstein DL, Allingham RR, Schuman JS, editors. *Chandler and Grant's glaucoma*. 45th ed. Baltimore: Williams & Wilkins; 1997. p. 285–303.
53. Levene R. A new concept of malignant glaucoma. *Arch Ophthalmol*. 1972;87:497–506.
54. Rieser JC, Schwartz B. Miotic-induced malignant glaucoma. *Arch Ophthalmol*. 1972;87:706–12.
55. Harbour JW, Rubsamen PE, Palmberg P. Pars plana vitrectomy in the management of phakic and pseudophakic malignant glaucoma. *Arch Ophthalmol*. 1996;114:1073–8.
56. Byrnes GA, Leen MM, Wong TP, Benson WE. Vitrectomy for ciliary block (malignant glaucoma) glaucoma. *Ophthalmology*. 1995;102:1308–11.
57. Tomey KF, Senft SH, Antonios SR, et al. Aqueous misdirection and flat chamber after posterior chamber implants with and without trabeculectomy. *Arch Ophthalmol*. 1987;105:770–3.
58. Lynch MG, Brown RH, Michels RG, et al. Surgical vitrectomy for pseudophakic malignant glaucoma. *Am J Ophthalmol*. 1986;102:149–53.
59. Melamed S, Cahane M, Gutman I, Blumenthal M. Postoperative complications after Molteno implant surgery. *Am J Ophthalmol*. 1991;111:319–22.
60. Macken P, Buys Y, Trope GE. Glaucoma laser suture lysis. *Br J Ophthalmol*. 1996;80:398–401.
61. Cashwell LF, Martin TJ. Malignant glaucoma after laser iridotomy. *Ophthalmology*. 1992;99:651–9.
62. Robinson A, Prialnic M, Deutsch D, Savir H. The onset of malignant glaucoma after prophylactic laser iridotomy. *Am J Ophthalmol*. 1990;110:95–6.
63. Brooks AMV, Harper CA, Gillies WE. Occurrence of malignant glaucoma after laser iridotomy. *Br J Ophthalmol*. 1989;73:617–20.
64. Mastropasqua L, Ciancaglini M, Carpineto P, et al. Aqueous misdirection syndrome: a complication of YAG posterior capsulotomy. *J Cataract Refract Surg*. 1994;20:563–5.
65. Hardten DR, Brown JD. Malignant glaucoma after Nd-YAG cyclophotocoagulation (letter). *Am J Ophthalmol*. 1991;111:245–7.
66. Azuara-Blanco A, Dua HS. Malignant glaucoma after diode laser cyclophotocoagulation. *Am J Ophthalmol*. 1999;127:467–9.
67. Massicotte EC, Schuman JS. A malignant glaucoma-like syndrome following pars plana vitrectomy. *Ophthalmology*. 1999;106:1375–9.
68. Shaffer RN. The role of vitreous detachment in aphakic and malignant glaucoma. *Trans Am Acad Ophthalmol Otolaryngol*. 1954;58:217–28.
69. Chandler PA. Malignant glaucoma. *Am J Ophthalmol*. 1950;34:993–1000.
70. Tello C, Chi T, Shepps G, Liebmann J, Ritch R. Ultrasound biomicroscopy in pseudophakic malignant glaucoma. *Ophthalmology*. 1993;100:1330–4.

71. Chandler PA, Grant WM. Mydriatic-cycloplegic treatment in glaucoma. *Arch Ophthalmol*. 1962;68:353.
72. Weiss DI, Shaffer RN, Harrington DO. Treatment of malignant glaucoma with intravenous mannitol infusion. *Arch Ophthalmol*. 1963;69:154.
73. Benefice O. Einneuesopertivesverfahrenzurbehandlung des malignenglaukoms. *Klin Monatsbl augenheilkd*. 1977;170:665.
74. Herschler J. Laser shrinkage of the ciliary processes. A treatment for malignant (ciliary block) glaucoma. *Ophthalmology*. 1980;87:1155.
75. Carissa RG, Bettin P, Fiori M, Brancato R. Treatment of malignant glaucoma with contact transscleral cyclophotocoagulation. *Arch Ophthalmol*. 1999;117:688–90.
76. Shaffer RN, Hoskins Jr HD. Ciliary block (malignant) glaucoma. *Trans Am Acad Ophthalmol Otolaryngol*. 1978;85:215.
77. Simmons RJ. Malignant glaucoma. *Br J Ophthalmol*. 1972;57:263.
78. Chandler PA. A new operation for malignant glaucoma. A preliminary report. *Trans Am Ophthalmol Soc*. 1964;62:408.
79. Shrader CE, Belcher CD, Thomas JV, Simmons RJ, Murphy EB. Pupillary and iridovitreous block in pseudophakic eyes. *Ophthalmology*. 1984;91:831.
80. Epstein DL, Steinert RF, Puliafito CA. Neodymium-YAG laser therapy to the anterior hyaloid in aphakic malignant (ciliovitreal block) glaucoma. *Am J Ophthalmol*. 1984;98(2):137–43.
81. Irvine RA. Pars plana vitrectomy for malignant and aphakic pupillary block glaucoma. *Tran Pac Coast Oto Ophthalmol Soc*. 1977;58:189.
82. Koerner FH. Anterior pars plana vitrectomy in ciliary and iris block glaucoma. *Albrecht Von Graefes Arch Klin Exp Ophthalmol*. 1980;214:119.
83. Weiss H, Shin DH, Kollarits CR. Vitrectomy for malignant (ciliary block) glaucomas. *Int Ophthalmol Clin*. 1981;21:113.
84. Lois N, Wong D, Groenewald C. New surgical approach in the management of pseudophakic malignant glaucoma. *Ophthalmology*. 2001;108:780–3.
85. Sharma A, Sii F, Shah P, Kirkby GR. Vitrectomy-phacoemulsification-vitrectomy for the management of aqueous misdirection syndromes in phakic eyes. *Ophthalmology*. 2006;113:1968–73.
86. Chaudhry NA, Flynn HW, Murray TG, Nicholson D, Palmberg PF. Pars plana vitrectomy during cataract surgery for prevention of aqueous misdirection in high-risk fellow eye. *Am J Ophthalmol*. 2000;129(3):387–8.

Part VI

Pharmacologic Vitreolysis

J. Sebag

J. Sebag

Outline

- I. **Introduction**
- II. **Classification of Approaches to Pharmacologic Vitreolysis**
 - A. Chemical Action of Pharmacologic Vitreolysis Agents
 - B. Biological Action of Pharmacologic Vitreolysis Agents
- III. **Pharmacologic Vitreolysis Agents**
 - A. Agents with Failed or Discontinued Development
 1. Hyaluronidase (Vitrase®)
 2. Chondroitinase
 3. Nattokinase
 4. Vitreosolve®
 5. RGD Peptides
 - B. Agents Under Development
 1. Dispase (Vitreolysin™)
 - C. Agents Approved for Pharmacologic Vitreolysis
 1. Ocriplasmin
 - a. Case Study
 - b. Case Selection
- IV. **Future Considerations**
 - A. Enhancing Drug Delivery
 - B. Improving Vision Outcome Measures
 - C. Combination Therapy
 - D. Prevention
 1. Prophylactic Posterior Vitreous Detachment
 2. Anomalous PVD Prevention

References

Electronic supplementary material Supplementary material is available in the online version of this chapter at [10.1007/978-1-4939-1086-1_47](https://doi.org/10.1007/978-1-4939-1086-1_47). Videos can also be accessed at <http://www.springerimages.com/videos/978-1-4939-1085-4>.

J. Sebag is a past or present consultant to Advanced Corneal Systems/ ISTA Pharmaceuticals, Storz/B & L, ThromboGenics, ALCON

J. Sebag, MD, FACS, FRCOphth, FARVO
VMR Institute for Vitreous Macula Retina,
7677 Center Avenue, suite 400,
Huntington Beach, CA 92647, USA

Doheny Eye Institute, Los Angeles, CA, USA
e-mail: jsebag@VMRinstitute.com

Keywords

Vitreous • Vitreoretinal interface • Hyaluronan • Collagen Extracellular matrix • Pharmacologic vitreolysis
Posterior vitreous detachment (PVD) • Anomalous PVD
Liquefactant • Interfactant

Key Concepts

1. Vitreous and the vitreoretinal interface are comprised of molecules that dictate structure and function as well as underlie the changes that result in posterior vitreous detachment (PVD) in most cases and anomalous PVD in some individuals.
2. Pharmacologic vitreolysis, which is the molecular manipulation of vitreous to induce liquefaction via *liquefactant* agents and dehiscence at the vitreoretinal interface via *interfactant* activity, is destined to replace the surgical cure of various pathologies of anomalous PVD.
3. The failures and success of different pharmacologic vitreolysis agents under development hold important lessons for future progress that may include combination therapy but should also emphasize improved drug delivery to the target tissues.

I. Introduction

Vitreous constitutes about 80 % of the volume of the human eye. It is an extended extracellular matrix that is composed of collagen, hyaluronan, and other extracellular matrix molecules but is 98 % water. In both health as well as disease, the molecular composition and organization of vitreous dictate the structure and function of the vitreous body as well as the status of the vitreoretinal interface. During aging, there is

reorganization of vitreous macromolecules resulting in gel liquefaction and structural changes that destabilize the vitreous body. Molecular changes at the vitreoretinal interface, whose components are the retinal inner limiting membrane (ILM), the posterior vitreous cortex, and the intervening extracellular matrix (ECM), usually weaken vitreoretinal adhesion and allow the collapsing destabilized vitreous to separate from the retina, a condition called posterior vitreous detachment (PVD) [see chapter II.C. Vitreous Aging and Posterior Vitreous Detachment]. When there is insufficient weakening of vitreoretinal adherence, anomalous PVD occurs with various pathologic effects on both vitreous and retina [see chapter III.B. Anomalous PVD and Vitreoschisis]. To date, these pathologies have been treated with surgery.

Throughout the history of medicine, therapeutics have evolved as a direct result of advances in our basic understanding of disease pathogenesis. This has led to less invasive yet increasingly effective therapeutics. At first, when little is known, little, if anything, is done. As recognition and understanding of anatomic pathology increases, surgery is employed. With increasing knowledge about the cause(s) of disease, surgery is supplemented with and eventually replaced by pharmacotherapy. When we fully understand a disease, we develop ways to prevent it, obviating the need for both surgery and pharmacotherapy. Consider, for example, that the treatment of severe infections by surgical drainage of an abscess has been to a great extent replaced by the use of antibiotics. Peptic ulcers, for many years a surgical disease believed to be caused by stress, had high mortality. Antacids, antihistamines, and proton pump inhibitors as well as good gastroscopies made huge improvements. The breakthrough came with the discovery of *Helicobacter pylori* as the underlying cause in the vast majority, and now, antibiotic therapy has largely eliminated surgery in many settings. Cervical cancer, once treated with hysterectomy, was increasingly recognized to arise from subtle dysplastic changes in the epithelium. A population level screening program and development of less invasive biopsies and surgical procedures made a huge difference in survival. Recognition of a papilloma virus as the underlying cause has led to widespread vaccination programs, which may prevent the vast majority of cases with this disease.

This type of evolution is now occurring in the discipline of vitreoretinal diseases and surgery. Laser surgery for exudative maculopathies due to diabetic retinopathy, vein occlusions, and age-related macular degeneration (AMD) has been largely replaced by intravitreal anti-VEGF pharmacotherapy. Another recent development is “*pharmacologic vitreolysis*,” a term that was coined in 1998 to refer to the use of drugs to alter the molecular structure of vitreous and the vitreoretinal interface [23]. The objective of this therapy is to pharmacologically induce an innocuous PVD and thus mitigate any untoward effects of vitreous on the retina that

cause or worsen pathology. Furthermore, a variety of physiologic effects are introduced, which are, in some settings, very beneficial.

The foregoing chapters of this book are witness to the expansion of our knowledge about vitreous and its role in disease. Various predisposing genetic factors and congenital anomalies, contributing systemic diseases, anomalous aging effects, and ocular conditions have been described. A few good examples are chapters I.C. [Hereditary Vitreo-Retinopathies], III.A. [Congenital Vascular Vitreo-Retinopathies], I.E. [Diabetic Vitreopathy], III.K. [Vitreous in Retino-Vascular Diseases and Diabetic Macular Edema], III.B. [Anomalous PVD and Vitreoschisis], III.G. [Vitreous in AMD], III.I. [Role of Vitreous in the Pathogenesis of Retinal Detachment], and II.B. [Myopic Vitreopathy]. The surgical management of these conditions has also been discussed at length (see chapters V.A.1. to V.A.6. and V.B.1. to V.B.9.). However, owing to the significantly expanded fund of knowledge related to vitreous and its role in retinal disorders, nonsurgical therapies are being developed, initially to augment but eventually to replace surgery. The following reviews these approaches to the future. Of note is the fact that of the seven major pharmacologic vitreolysis modalities that have been undertaken to date, one has been approved for clinical use, one is currently under development, and five have either failed or been disbanded. All seven research and development programs will be critically reviewed below and presented in greater detail in the remaining chapters of this section.

II. Classification of Approaches to Pharmacologic Vitreolysis

The first retrievable publication on pharmacologic vitreolysis appeared 65 years ago in the British Journal of Ophthalmology [17]. Since this and other initial approaches all used enzymes as adjuncts to surgery, the term “*enzymatic vitreolysis*” was prevalent in the early literature [see chapter VI.B. History of pharmacologic vitreolysis]. However, in 1998, the term “*pharmacologic vitreolysis*” replaced the older term, so that vitreolytic agents could be grouped according to more than just an enzymatic mechanism of action [23]. The following presents two different classifications based upon the actions of the various pharmacologic vitreolysis agents.

A. Chemical Action of Pharmacologic Vitreolysis Agents

In 1998, pharmacologic vitreolysis was viewed in terms of the chemical activity of the various agents under development [23]. Thus, the two broad classes of drugs were

Table VI.A-1 Classification of pharmacologic vitreolysis agents by chemical activity

Enzymatic	Nonenzymatic
Substrate specific	
Chondroitinase	Urea/vitreosolve
Hyaluronidase	RGD peptides
Dispase	
Nonspecific	
tPA	
Plasmin	
Ocriplasmin	
Nattokinase	

Table VI.A-2 Pharmacologic vitreolysis classification based on biologic action

Liquefactants (agents that liquefy the gel vitreous)
Nonspecific:
tPA, plasmin, ocriplasmin, nattokinase, Vitreosolve ^a
Substrate-specific:
Hyaluronidase
Interfactants (agents that weaken vitreo-retinal adhesion)
Nonspecific:
tPA, plasmin, microplasmin, nattokinase, Vitreosolve ^a
Substrate-specific:
Dispase, chondroitinase, RGD peptides ^a

tPA, plasmin, microplasmin, nattokinase, and vitreosolve are believed to be both liquefactants and interfactants

tPA tissue plasminogen activator

^aNonenzymatic agents

enzymatic or *nonenzymatic* agents (Table VI.A-1). Within the larger enzymatic group of agents, there was further subdivision into *substrate-specific* and *nonspecific* agents.

Although logical, this classification of the various approaches to pharmacologic vitreolysis based on chemical activity did not seem useful from the clinical standpoint. Thus, an alternative approach was sought a decade later.

B. Biological Action of Pharmacologic Vitreolysis Agents

In 2009, the various pharmacologic vitreolysis agents under development were reclassified in terms of their biological activity. Central to the biological classification system is the fact that posterior vitreous detachment (PVD) results from concurrent liquefaction of the gel vitreous and weakening of vitreoretinal adhesion [see chapter II.C. Vitreous aging and posterior vitreous detachment]. Thus, these two components of PVD were considered important in classifying agents for pharmacologic vitreolysis [25]. Those agents that primarily liquefy the gel vitreous are referred to a *liquefactants*, while those that induce dehiscence at the vitreoretinal interface are called *interfactants*. As can be seen in Table VI.A-2,

however, the chemical and biological classification systems are not mutually exclusive, since there can be further subdivisions based upon chemical activity (enzymatic vs. nonenzymatic) and substrate specificity. Of further note is that several agents are considered to have both liquefactant and interfactant effects.

The following will consider the various agents that are being developed or already approved for use in clinical pharmacologic vitreolysis. Of considerable interest are those agents whose development has been discontinued, as there are lessons to be learned from their failure or discontinuation.

III. Pharmacologic Vitreolysis Agents

A. Agents with Failed or Discontinued Development

1. Hyaluronidase (Vitrase®)

[See chapter VI.F. Hyaluronidase]

This substrate-specific liquefactant targets hyaluronan, which is a glycosaminoglycan composed of repeating disaccharide units of *N*-acetyl glucosamine glycosidically linked to glucuronic acid [see chapter I.F. Vitreous biochemistry and artificial vitreous]. Hyaluronidase (Hase) has a number of natural biological functions including fertilization and preserving mobility in human body tissues. Hase can also enhance pathologic processes such as bacterial virulence and the spread of cancer cells [7, 18].

Hase has been used in ophthalmology to facilitate the periocular distribution of retrobulbar injection of anesthetics. The first use of Hase for pharmacologic vitreolysis was by Pirie [17] who employed it in the rabbit vitreous. Foulds then reported that Hase induces significant vitreous liquefaction [see chapter VI.B. History of pharmacologic vitreolysis]. Much later, ovine testicular Hase was developed for pharmacologic vitreolysis. Preclinical studies demonstrated efficacy in animal models, so clinical studies were undertaken, including a phase 3 trial to assess the efficacy of Hase in accelerating the clearance of vitreous hemorrhage [see chapter VI.F. Hyaluronidase as a vitreous liquefactant]. While Hase was able to clear vitreous hemorrhage more rapidly than saline, the phase 3 results did not provide sufficient evidence to demonstrate efficacy and warrant approval as a commercial product.

The underlying reasons for this failure convey important lessons. Firstly, study subjects with vitreous hemorrhage were predominantly patients with proliferative diabetic retinopathy. It is therefore relevant that none of the preclinical animal studies were performed in diabetic animals, although it is well known that diabetes alters vitreous on a biochemical [27, 28] as well as structural [22] level [see chapter I.E.

Diabetic vitreopathy]. Thus, to extrapolate from nondiabetic animal studies to the diabetic human vitreous is fraught with hazard, especially when dealing with a biochemical phenomenon like pharmacologic vitreolysis, for in diabetes, the substrate of vitreous molecules (especially collagen) is not the same due to glycation and the formation of advanced glycation end products.

Another explanation for the failure of Vitrase relates to the fact that HASE is not an interfactant, only a liquefactant (Table VI.A-2). Because HA does not play a significant role in mediating vitreoretinal adhesion [see chapter II.E. Vitreoretinal interface and inner limiting membrane], the action of HASE is limited to gel liquefaction. While HASE will liquefy gel vitreous, it will not induce vitreoretinal dehiscence and PVD [8, 36]. In proliferative diabetic retinopathy, this will result in persistent traction upon neovascular complexes that have grown into the posterior vitreous cortex with recurrent vitreous hemorrhage and vision loss. This is particularly hazardous in patients with type I diabetes who are younger and have more firm and extensive vitreoretinal adherence. In these individuals, HASE will risk inducing traction retinal detachment, as was the experience of this author during the clinical trials. Thus, not only is Vitrase® not approved for use as an intravitreal injection, it should not be used off-label for pharmacologic vitreolysis, except perhaps in the setting of existing PVD.

2. Chondroitinase

[See chapter VI.H. Chondroitinase]

Chondroitinase is an enzyme complex that cleaves and fragments chondroitin-sulfate-containing glycosaminoglycan (GAG) side chains of proteoglycan “core” molecules [see chapter I.F. Vitreous biochemistry and artificial vitreous]. Given the importance of GAGs at the vitreoretinal interface [see chapter II.E. Vitreoretinal interface and inner limiting membrane], chondroitinase has potential to be a potent interfactant. Chondroitinase specifically cleaves and degrades only bonds between and within the disaccharide *N*-acetylgalactosamine glucuronic acid. As formulated for human clinical trials, chondroitinase is a biological agent that consists of a mixture of two enzymes, Chondroitinase I and II. Chondroitinase I (110 kDa) is a lyase that attacks chondroitin sulfate in endolytic fashion, breaking the polymeric structure into oligosaccharides and disaccharides. Chondroitinase II (112 kDa) has no activity against the intact polymer, but can digest tetrasaccharides produced by the Chondroitinase I-catalyzed reaction. The combined activity of these two enzymes results in more rapid degradation than the use of Chondroitinase I alone.

In human, primate, and pig eye sections exposed to chondroitinase, adhesion between the collagen of the vitreous cortex and the retina, optic disc, and lens was markedly reduced [11, 12]. This effect was greater with chondroitinase

than trypsin, hyaluronidase, dispase, heparinase, and others. Follow-on studies demonstrated that exposure of the human vitreoretinal interface to chondroitinase resulted in complete disruption of the adhesion, a process Russell and Hageman termed “dis-insertion.” Unlike known proteolytic enzymes, chondroitinase resulted in complete, rather than incomplete, separation of the vitreous from the primate retina, but did not liquefy vitreous [1].

The results of phase I/II FDA testing are described in chapter VI.H. [Chondroitinase as a Vitreous Interfactant – Vitreous Dis-insertion in the Human]. Although this was primarily a safety study that found no untoward effects, there was some evidence of efficacy. Nonetheless, there have been no further clinical trials with chondroitinase. In the words of the principal investigator Dr. Stephen Russell, “*Despite the initial discovery and testing of chondroitinase as a pharmacologic vitreolysis agent that began nearly three decades ago, contractual restrictions in the initial years and intellectual drift in more recent years have limited the peer-reviewed publication of most of the animal (monkey) and human studies that evaluated this promising agent.*” Moreover, the procurement process employed for chondroitinase was expensive, far more than a recombinant enzyme. Also, during the 1980s, the chondroitinase project was handled by four different corporate development teams: Storz, American Cyanamid, American Home Products, and Bausch and Lomb. By the time a decision was made for a Phase III trial, none of the early advocates of chondroitinase were managing the project. Since chondroitinase did not originate in their pipeline and the phase I/II data (not powered for efficacy) appeared to be insufficient [see details in chapter VI.H. Chondroitinase as a vitreous interfactant: vitreous disinsertion in the human], chondroitinase did not undergo further study [21]. While this may have made sense in a corporate context, the scientific and clinical perspectives appear to suggest that further research and development is warranted, perhaps with a less expensive recombinant form of chondroitinase.

3. Nattokinase

Nattokinase is an enzyme extracted from natto, a Japanese food made from soybeans fermented by the bacteria *Bacillus subtilis natto*. This popular breakfast food in Japan has a cheese-like smell, a nutty/salty flavor, and a sticky consistency. The dietary supplement of nattokinase is purified from natto and made into tablets and capsules, so it does not have the strong smell or taste as the food. It is a popular supplement because nattokinase is thought to dissolve abnormal blood clots.

Medical research with this substance is limited and relatively recent. Indeed, the first nattokinase publication listed on PubMed dates back no earlier than 1987. This study describes nattokinase as an enzyme with a molecular

weight=20,000 and strong fibrinolytic activity, especially to the plasmin substrate H-D-Val-Leu-Lys-pNA (S-2251) [30]. A more recent study [38] identified that nattokinase promoted the release of tissue plasminogen activator from vascular endothelial cells and HeLa cells. This finding may explain nattokinase's ability to promote pharmacologic vitreolysis [see chapter VI.C. Pharmacologic vitreolysis with tissue plasminogen activator].

The first and, to this author's knowledge, only study of nattokinase in the eye demonstrated the efficacy of this serine protease to induce PVD in rabbits, as determined by scanning electron microscopy [31]. Clinical examination, ERG testing, and light microscopy identified toxicity at a dose ten-fold greater than the dose that was able to induce PVD. Remarkably, PVD was induced within 30 min after injecting nattokinase. In recent years, there have been no further publications on the subject of nattokinase pharmacologic vitreolysis. The chairman of Ophthalmology at Kumamoto University in Japan, Professor Hidenobu Tanihara, describes that this is primarily due to the fact that the producers of nattokinase are producers of food, not pharmaceuticals (personal communication, 2014).

4. Vitreosolve®

Vitreosolve® is a nonenzymatic agent for pharmacologic vitreolysis that is comprised of urea, which "unravels" collagen fibers and purportedly induces both liquefaction and vitreoretinal dehiscence, making it both a liquefactant and interfactant. Following animal studies, this drug has been evaluated in Phase III clinical trials conducted at multiple sites in the United States, India, and Mexico. The objective of the clinical trials was to evaluate the safety and efficacy of intravitreal injections of Vitreosolve® to induce a PVD (as determined by ultrasound) in patients with nonproliferative diabetic retinopathy (NPDR). This prospective, randomized, double-masked, placebo-controlled study enrolled approximately 400 patients with NPDR in the United States and India and 150 in Mexico. The study design involved monthly intravitreal injections for 3 months. The results showed that while Vitreosolve® did induce a PVD in 50 % of cases, PVD also occurred in 36 % of controls ([13]; V. Karageozian, MD, personal communication, 2013). This difference was not statistically significant and all clinical research with Vitreosolve® has been terminated.

While this is disappointing, there may be valuable lessons to be learned. The importance that clinical trials be designed with sufficiently large subject groups to assure statistically significant results is underscored. Although the Vitreosolve® trials involved over 500 subjects, these were apparently not sufficiently large numbers, perhaps suggesting a lack of drug potency, as well as a surprisingly high efficacy (36 %) of placebo injections. Secondly, no preclinical studies were done with Vitreosolve® in diabetic animals. Studies have

previously shown that the vitreous gel and vitreoretinal interface in diabetic patients are quite different from nondiabetic individuals [see chapter I.E. Diabetic vitreopathy]. Thus, future investigators are well advised to research the effects of agents for pharmacologic vitreolysis (or any drug to be injected intravitreally in diabetic patients) in appropriate models of the ultimate disease application, in this case to induce PVD in subjects with diabetic vitreopathy and diabetic retinopathy. As mentioned above, this shortcoming was also a factor in the failure of the liquefactant Vitrase® (hyaluronidase) to induce beneficial effects in diabetic patients and obtain FDA approval.

5. RGD Peptides

The rationale for using RGD peptides in pharmacologic vitreolysis derives from their interaction with integrins. Many adhesive proteins present in extracellular matrices contain the tripeptide arginine-glycine-aspartic acid (RGD) as their cell recognition site. Identified nearly three decades ago [20], the RGD sequences of each of the adhesive proteins are recognized by at least one member of a family of structurally related receptors, integrins, which are heterodimeric proteins with two membrane-spanning subunits. These transmembrane receptors mediate the attachment of a cell to other cells or the extracellular matrix (ECM). Integrins are also known to play a critical role in cell signaling [10]. Therefore, in addition to transmitting mechanical forces across otherwise vulnerable membranes, integrins are involved in the regulation of cell cycle, shape, and motility. The specific binding complex "RGD" (a term referring to the amino acid sequence arginine-glycine-aspartate) is important as it is present in various ECM components including laminin, fibronectin, and certain collagens, thereby playing a potentially important role at the vitreoretinal interface [see chapter II.E. Vitreoretinal interface and the ILM]. Indeed, immunolocalization studies have identified integrins on the surface of the ILM [2]. Because synthetic RGD peptides compete for integrin-binding sites, they could disrupt integrin-ECM interaction with subsequent loosening of interface attachments, in this case at the vitreoretinal interface. Thus, it may be possible to disrupt vitreoretinal adhesion and induce PVD via pharmacologic vitreolysis with RGD analogues.

Studies [16] in a rabbit model found that after 24-h incubation of intravitreal RGD peptides, limited vitrectomy (30-core vitrectomy with attempted PVD induction at low aspiration ≤ 30 mmHg) resulted in a significantly greater extent of PVD in treated eyes compared with controls. Although retinal edema was noted in half of the treated eyes, no toxicity was detected on clinical examination, electron microscopy, or TUNEL (terminal deoxynucleotidyl transferase dUTP nick end labeling) apoptosis assay. Despite the solid rationale and these encouraging initial findings, no further studies have been published in the past 12 years. The reasons are unknown.

B. Agents Under Development

1. Dispase (Vitreolysin™)

[See chapter VI.G. Dispase]

Dispase is being developed under the proprietary name Vitreolysin™ as a purified 35.9 kDa extracellular neutral protease produced by *Paenibacillus polymyxa*. It selectively cleaves the attachment of the posterior vitreous cortex to the inner limiting membrane (ILM) by degrading type IV collagen and fibronectin, which contribute to the attachment between these two structures [see chapter II.E. Vitreoretinal interface and the ILM]. The low affinity of Vitreolysin™ for type II collagen allows it to induce a posterior vitreous detachment (PVD) without disrupting the macromolecular structure of the vitreous body. This *direct* enzymatic action on the posterior vitreous cortex-ILM interface prevents vitreous liquefaction and resultant vitreoretinal traction which is a common way to induce PVD with many *indirectly* acting enzymes [6]. There are several other advantages of Vitreolysin™, such as lack of a known natural inhibitor, which insures sustained enzyme activity even in complex vitreoretinal diseases where several enzyme inhibitors circulating within the serum may leak into the eye. Vitreolysin™'s activity can be quenched by its own titratable autolysis that ensures fine control on its degradation and removal. Vitreolysin™ is a highly stable molecule with a long shelf life in lyophilized form. Early preclinical studies also revealed high rates (80–100 %) of PVD induction at picomolar concentrations.

Whereas early studies demonstrated retinal and optic nerve toxicity in animal models, these effects were attributable to bacterial contaminants. Other studies [15] employed commercially available dispase and found efficacy in young pigs with no evidence of toxicity. Synthesized using recombinant technology, Vitreolysin™ pharmacologic vitreolysis has not been associated with untoward effects [see chapter VI.G. Pharmacologic vitreolysis with dispase (vitreolysin™)]. To date, however, there have been no presentations or publications of human studies investigating the safety and efficacy of pharmacologic vitreolysis with Vitreolysin™.

C. Agents Approved for Pharmacologic Vitreolysis

1. Ocriplasmin [see chapter VI.E.1.

Pharmacologic vitreolysis with ocriplasmin: basic science studies and VI.E.2. Pharmacologic vitreolysis with ocriplasmin: clinical studies]

Ocriplasmin (des-kringle 1–5 plasmin) is a truncated recombinant form of plasmin. Formerly called microplasmin, this recombinant 27 kDa serine protease contains the catalytic

domain of plasmin but none of the 5 kringle located as extensions towards the C-terminal end of the larger of its two chains [37]. These kringles normally serve as binding sites for substrates, regulatory molecules, and inhibitors [33, 37]. As a result, ocriplasmin has a more potent effect on thrombin than is observed with plasmin but binds to its primary inhibitor with less affinity. Ocriplasmin has a well-characterized enzyme activity profile that is stable for several days in an acidic environment. Highly active in neutral pH, inactivation follows second-order kinetics (autolysis), so that when Ocriplasmin is placed in a vitreous substrate, only 25 % of the activity remains at 24 h. However, as a member of the plasminogen family of proteins, ocriplasmin regulates a number of pathways including proinflammatory cytokines and matrix metalloproteinases that help to extend its mode of action and define its secondary clinical manifestations. For maximal effect, it requires injection close to the site of intended activity, which can also limit any adverse effect on adjacent structures such as zonules. Nonetheless, preclinical studies found efficacy without toxicity [see chapter VI.E.1. Pharmacologic Vitreolysis with Ocriplasmin: Basic Science Studies].

The efficacy and safety of ocriplasmin versus placebo for the treatment of vitreo-macular traction (VMT) in humans has been demonstrated in a clinical trial program that includes eight phase 2 studies, two phase 3 studies, and two phase 3b studies. The pivotal phase 3 Microplasmin Intravitreal Injection–Traction Release without Surgical Treatment (MIVI-TRUST) study demonstrated superiority of a single intravitreal injection of 125 µg ocriplasmin versus placebo in pharmacologic resolution of VMA and total induction of PVD. Pharmacologic closure of full-thickness macular hole (FTMH, ≤400 µm and with VMA) was achieved in a higher percentage of patients with FTMH at baseline in the ocriplasmin group compared with placebo and was highest among patients with small FTMH (≤250 µm). On this basis, ocriplasmin was approved by the US Food and Drug Administration for the treatment of symptomatic vitreo-macular adhesion (sVMA) in October 2012 and by the European Medicines Agency for the treatment of vitreo-macular traction (VMT), including when associated with macular hole less than or equal to 400 µm, in February 2013. The details of all study results are reviewed elsewhere in this book [see chapter VI.E.2. Pharmacologic vitreolysis with ocriplasmin: clinical studies]. The following is the story of one of the patients in this clinical research program.

a. Case Study

SC is a 62-year-old white woman who presented with the chief complaint of distortions and vision loss in the right eye of 3 months' duration. Visual acuity was 20/50+3. Three-dimensional threshold Amsler grid testing (3D-TAG; [5, 11, 19, 34]) demonstrated a cylindrical central visual field defect with 1.16 % volume lost relative to the hill of vision

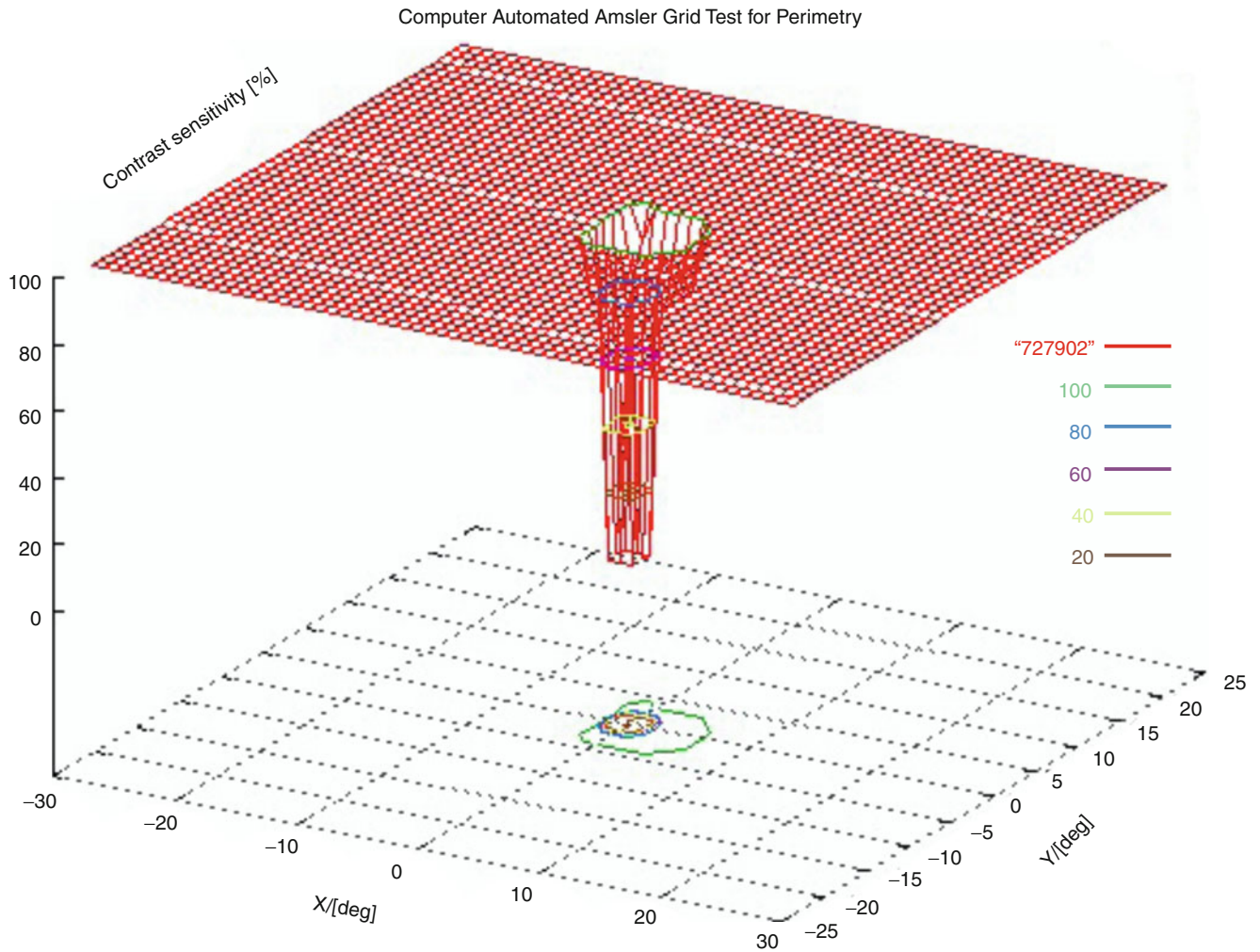


Figure VI.A-1 3D threshold Amsler Grid plot demonstrates the central visual field abnormality on presentation. The x - and y -axes display the area of distortion as drawn by the patient onto a touch screen computer monitor.

This was repeated five times at contrast levels ranging from 5 to 100 % contrast. The vertical z -axis stacks the five sets of test results, thus creating a 3-dimensional representation of the central visual field abnormality

(Figure VI.A-1). Combined optical coherence tomography/scanning laser ophthalmoscopy (OCT/SLO) demonstrated anomalous PVD with persistent adhesion of the posterior vitreous cortex to the fovea and an underlying macular cyst (Figure VI.A-2). This constituted focal, isolated vitreo-macular traction (VMT), according to the new IVTS classification system [3] and made the patient eligible for pharmacologic vitreolysis. The patient elected to consider enrolling in the phase II FDA trial of microplasmin pharmacologic vitreolysis (MIVI III) [see chapter VI.E.2. Clinical studies of ocriplasmin pharmacologic vitreolysis].

Six weeks later, she returned with decreased vision and increased distortions. Visual acuity measured 20/200 (previously 20/50). 3D-TAG detected a worsening of the central visual field abnormality, which increased from 1.16 % volume lost to 2.24 % volume lost (Figure VI.A-3). Combined OCT-SLO demonstrated a full-thickness macular hole (Figure VI.A-4), which on 3D OCT imaging clearly

demonstrated a membrane attached to both the edge of the elevated macular hole and the temporal margin of the optic disc (Figure VI.A-5), constituting vitreo-papillary adhesion (VPA), a finding present in 87.5 % of all eyes with macular holes [29, 35]. The linear distance of vitreo-macular adhesion (VMA) was 515 μm in the horizontal and 525 μm in the vertical axis. Central macular volume (central \equiv 1 mm Early Treatment Diabetic Retinopathy Study region) measured 0.32 ml (normal = 0.16 mL; [4]). The patient enrolled in the MIVI III study and received an injection of 125 μg of ocriplasmin (masked at the time of injection).

One week after injection, the distortions were much reduced and vision had subjectively improved. Visual acuity was 20/40 (pre-injection VA = 20/200). 3D-TAG demonstrated diminution of the central visual field abnormality with a reduction from 2.24 to 0.66 % volume lost (Figure VI.A-6). Combined OCT/SLO demonstrated PVD with closure of the macular hole and no evidence of cysts



Figure VI.A-2 Combined OCT/SLO imaging of the patient demonstrating vitreo-foveal adhesion with an underlying central cyst. By the IVTS classification, this constitutes focal, isolated vitreo-macular

traction (VMT) [see chapter III.D. Vitreo-Macular Adhesion/Traction & Macular Holes - Pseudo, Lamellar & Full-Thickness]

(Figure VI.A-7). There was, however, elevation of the fovea, which is seen following surgical closure of macular holes. During the ensuing 15 months, the foveal elevation slowly disappeared (Video VI.A-1), with complete restoration of normal foveal anatomy and attainment of VA=20/20 (Figure VI.A-8). At 6 months after injection, the macular volume was decreased to 0.21 mL (pre-injection=0.32 mL), and 3D-TAG measured an absolute percent volume lost of 0.65 %. At 15 months, macular volume improved to 0.15 uL, within the normal range. The patient is still very happy.

b. Case Selection

Retrospective analyses of the clinical trial data have resulted in a very interesting set of observations. Certain pre-injection factors were found to be associated with a higher success rate of inducing PVD and relieving VMT. If the extent of VMA was less than 1,500 μm , the success rate increased from 27.1 to 34.7 %. The aforementioned case has about 500 μm of VMA. The absence of a premacular membrane (PMM) with pucker (so-called ERM) was associated with a success rate of 37.4 %. The case study above had no PMM. If the patient had VMA <1,500 μm , had no PMM, and was phakic, the success rate increased to 44.7 %. The aforementioned patient was phakic. If in addition to these factors the patient were younger than 65 years of age, the success rate was an impressive 68.4 %. The case study was a 62-year-old woman.

The resolution of macular holes following a single injection of ocriplasmin was similarly associated with certain clin-

ical features. If the macular hole were smaller than 250 μm in diameter, the closure rate was 58 %. In similar fashion to the release of VMT, the closure rate for macular holes increased if the patient was younger than 65, had no PMM with pucker (“ERM”), and had VMA less than 1,500 μm in extent. In such cases, the closure rate was a striking 80 %. It is interesting to note that the case study described above meets these criteria, perhaps explained the very favorable response to pharmacologic vitreolysis with ocriplasmin.

IV. Future Considerations

A. Enhancing Drug Delivery

Preclinical studies with ocriplasmin demonstrated that for maximal drug effect, the drug should be injected close to the site of intended action [see chapter VI.E.1. Pharmacologic Vitreolysis with Ocriplasmin: Basic Science Studies]. Presently, all drugs are injected into the mid-vitreous without very much concern or control over the direction of drug delivery. Further, it is not known whether or not following injection, a drug could be directed posteriorly by having the patient lie supine for a period of time or whether iontophoresis forces could be employed to direct drug distribution posteriorly. Of course, the former maneuver would only be effective if the specific gravity of the drug solution is greater than vitreous. Special needles have been discussed, such as

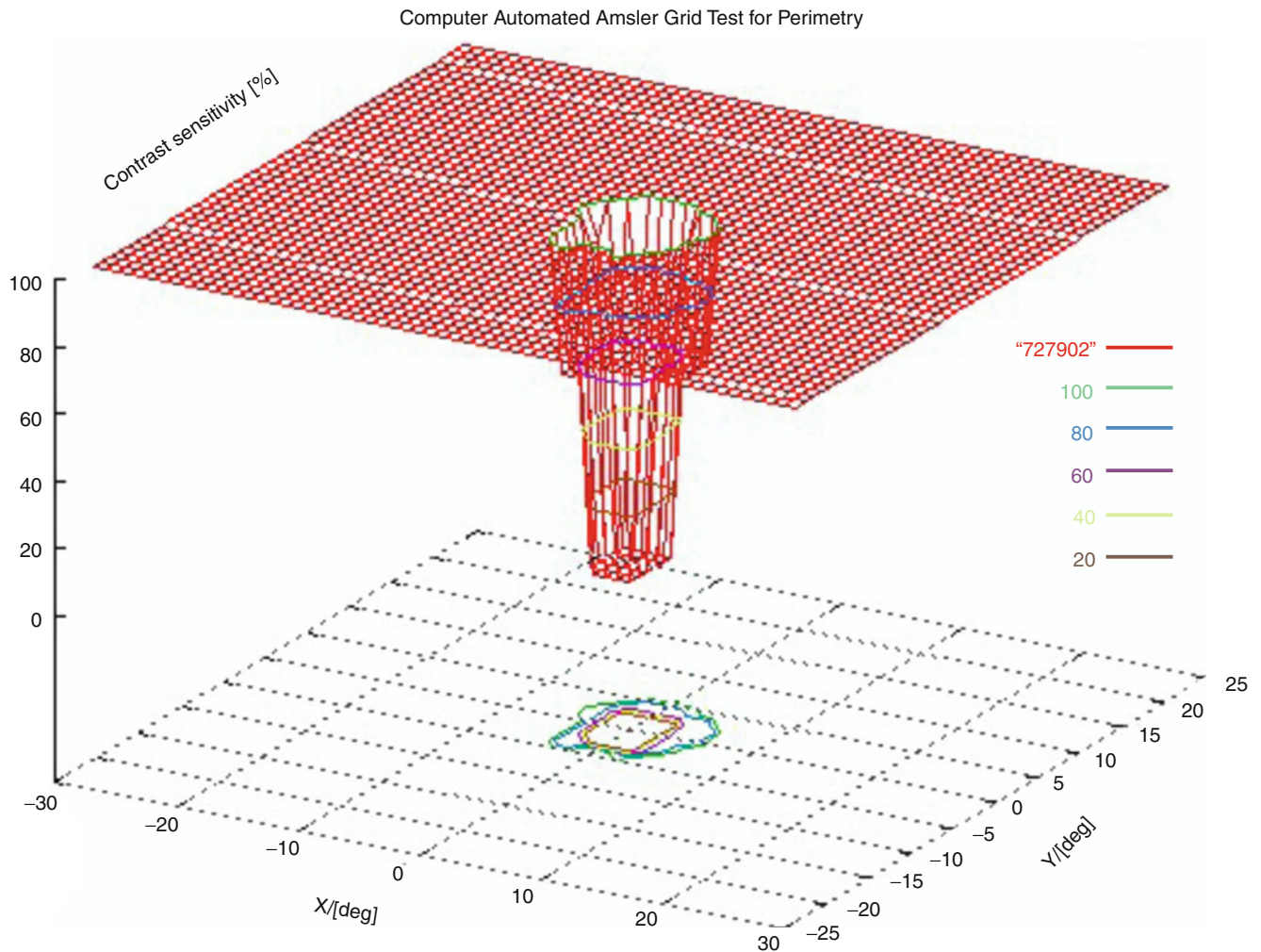


Figure VI.A-3 3D threshold Amsler Grid plot demonstrates the central visual field abnormality 6 weeks after presentation. Visual acuity was reduced to 20/200 and the central visual field abnormality worsened

from 1.16 % volume lost to 2.24 % volume lost, as a percent of the total hill of vision (Reprinted with permission from Tozer et al. [32])

the “quadrant” tip, but none has been adopted for routine use. Clearly, this is an area that would benefit greatly from enhanced intravitreal drug delivery systems [see chapter IV.E. Principles and Practice of Intravitreal Application of Drugs].

A potentially important aspect that has not been considered in this or any clinical setting of intravitreal drug therapy is vitreous structure. It is well known that vitreous structure is very different at different ages (Figure VI.A-9) and in different ocular conditions and disease states [see chapters II.C. Vitreous Aging and Posterior Vitreous Detachment; II.B. Myopic Vitreopathy; I.E. Diabetic Vitreopathy]. These and other influences create topographic heterogeneity in vitreous structure that could influence drug distribution and delivery to the target following intravitreal injection. In the elderly, this is particularly relevant since there can be profound variability of vitreous structure from one part of the vitreous body to another. It is plausible, if not probable, that drug distribution would be very different if an injection were placed

into a lacuna of liquid vitreous as opposed to an injection into the adjacent gel vitreous (Figure VI.A-10). There is currently no way to control for this variable. Thus, future approaches should strive to enhance drug delivery for pharmacologic vitreolysis as well as other forms of intravitreal pharmacotherapy by achieving therapeutic drug levels at the desired site of action taking into consideration the particular biochemical and structural attributes of the eye being treated. This type of individualized therapeutic approach, however, will require enhanced ways to evaluate the biochemical composition and structure of vitreous and adjacent tissues, ideally on a molecular level.

Indeed, one of the most significant limitations facing ophthalmology today is the lack of adequate diagnostic approaches to evaluate both the structure and function of the eye on more fundamental levels. While OCT imaging of the posterior pole has certainly been a very useful diagnostic tool from a structural standpoint (Videos VI.A-2 and



Figure VI.A-4 Combined OCT/SLO imaging of the patient 6 weeks after presentation. The macular cyst is now a full-thickness macular hole, classified as primary (initiated by VMT), small (<250 μm)

full-thickness macular hole [see chapter III.D. Vitreo-Macular Adhesion/Traction & Macular Holes – Pseudo, Lamellar & Full-Thickness] [3]

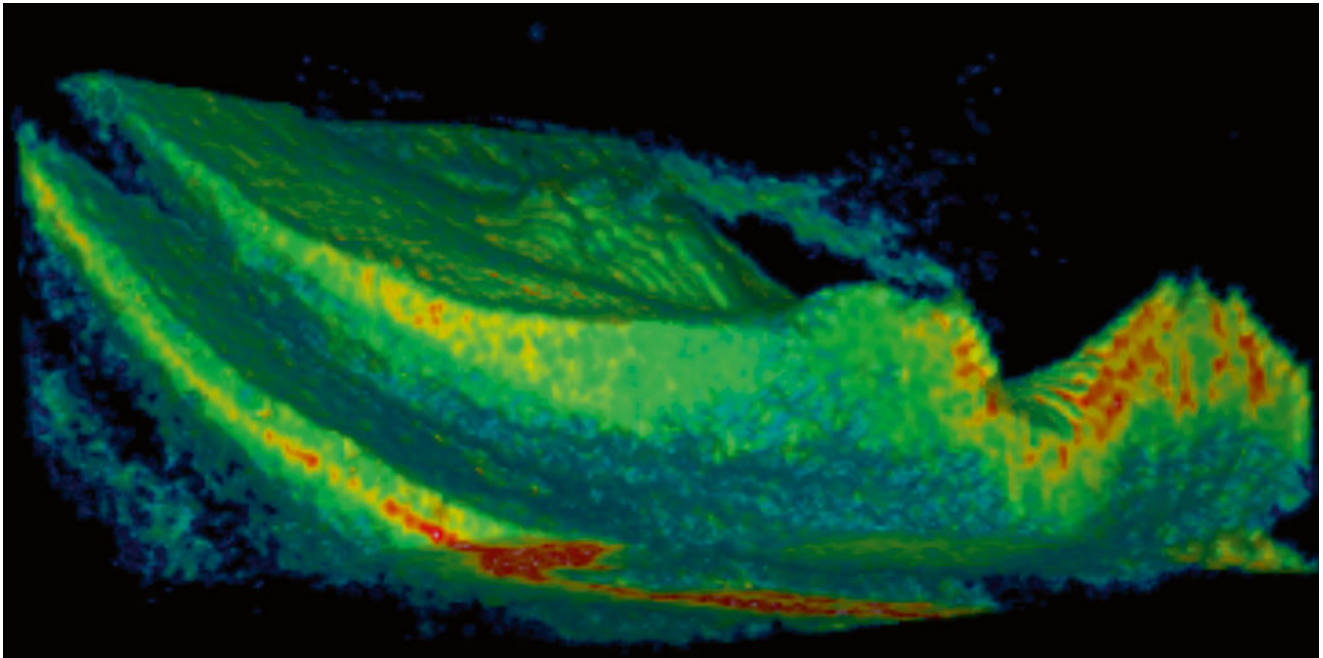


Figure VI.A-5 3D Combined OCT/SLO imaging demonstrates the “erupted volcano” appearance of the macular hole in this patient with the central macula being lifted anteriorly and retracted nasally by a

vitreous membrane (posterior vitreous cortex) attached to the temporal margin of the optic disc

Computer Automated Amsler Grid Test for Perimetry

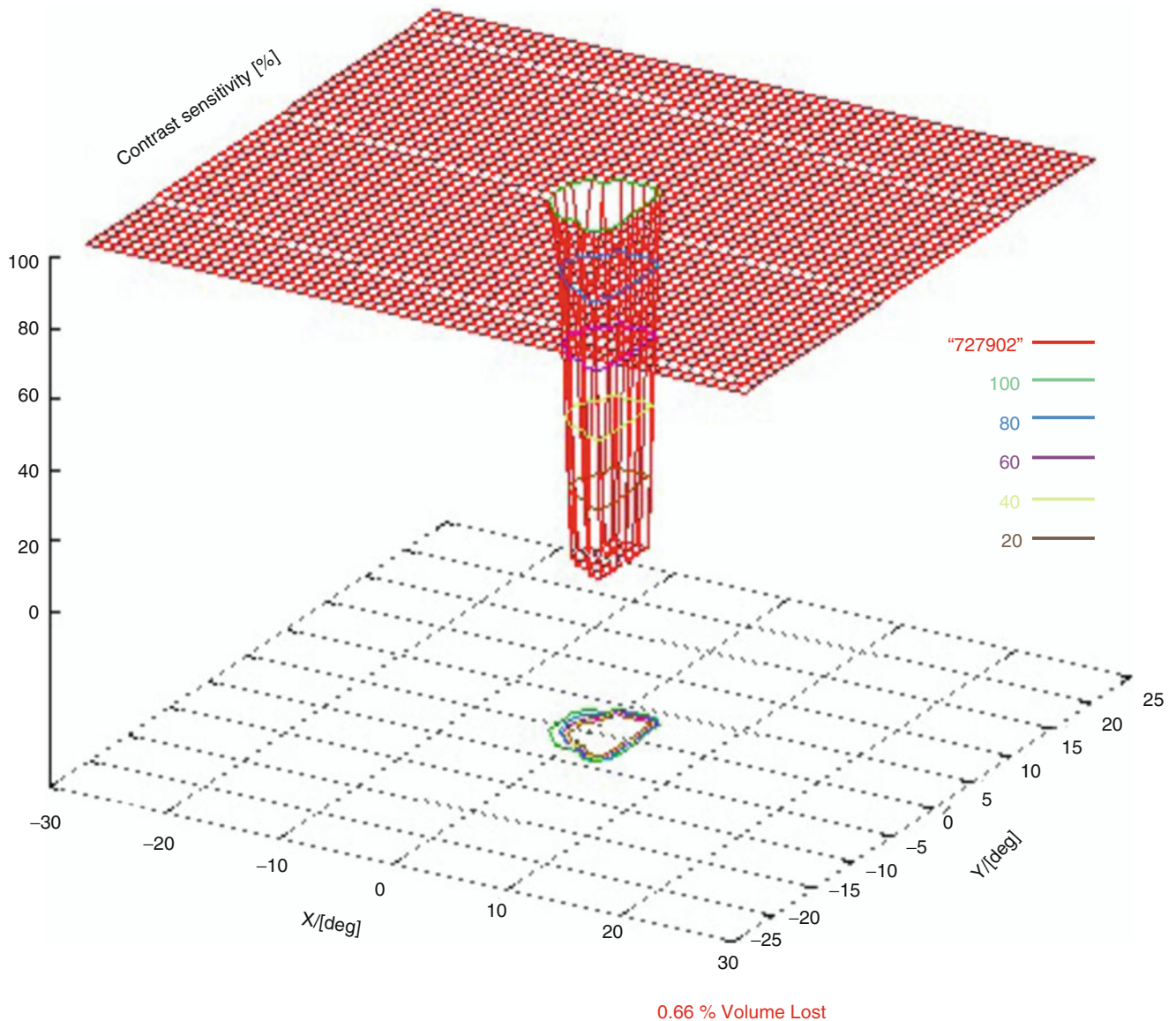


Figure VI.A-6 3D threshold Amsler Grid testing demonstrating a marked reduction in the area of the central visual field abnormality at all contrast levels 1 week after pharmacologic vitreolysis. Quantitatively,

the degree of abnormality decreased from 2.24 % (pre-injection) to 0.66 % volume lost (Reprinted with permission from Tozer [32])

VI.A-3), it does not represent a paradigm shift, which is vital to progress. The fundamental reason for our lack of powerful and innovative diagnostic approaches is surprisingly the ophthalmoscope, the very instrument that spawned our field. When introduced by Helmholtz in 1857 (based on earlier designs by Purkinje), the ophthalmoscope revolutionized ophthalmology. While imaging technologies have since advanced, our concept of disease has not substantially changed for more than a century. We are still “laden” with the notion that until structural abnormalities are detected, there is no disease. Thus, for example, we await the appearance of visible abnormalities such as retinal microaneurysms and microhemorrhages before diagnosing diabetic

retinopathy. Although the disease actually begins long before the development of such structural changes, these early changes are not diagnosed by today’s imaging technologies. What is needed, therefore, is a new generation of diagnostic technologies that evaluate the eye on a molecular level—nanotechnologies, for lack of a better term. These new approaches are already in development [see chapters IV.A. Vitreous Physiology; II.F. To See the Invisible - The Quest of Imaging Vitreous] and will have great impacts on our understanding of disease pathogenesis, as well as our ability to diagnose abnormalities early in the natural history of disease when there is a greater likelihood of reversibility and more potential for preventing further progression.



Figure VI.A-7 Combined OCT/SLO imaging of the patient 1 week after pharmacologic vitreolysis demonstrating release of vitreo-macular traction and detachment of the posterior vitreous cortex away from the retina.

There is closure of the macular hole with elevation of the foveal region, an appearance that is very similar to what is often seen following surgical closure of macular hole (Reprinted with permission from Sebag [26])

B. Improving Vision Outcome Measures

As a corollary to the aforementioned needs for enhanced imaging on a molecular level and for methodologies to assess ocular physiology in health rather than just pathology in disease, there is a similar need for improved measures of visual function. This will not only enable earlier diagnosis in some cases but also provide improved outcome measures of therapy. At the present time, there is great emphasis on visual acuity. However, this is only one aspect of visual function. Contrast sensitivity, another very important component of the phenomenon of vision, has recently been shown to be severely reduced (on average by over 60 %) in many patients with floaters [see chapter V.B.8 Floaters and Vision – Current Concepts and Treatment Paradigms]. Remarkably, this normalizes in every single case (now a series of over 50 patients) within a week of minimally invasive vitrectomy. Recent studies [14] have quantified similar reduction of contrast sensitivity in patients with macular pucker, which also normalized after vitrectomy with membrane peeling.

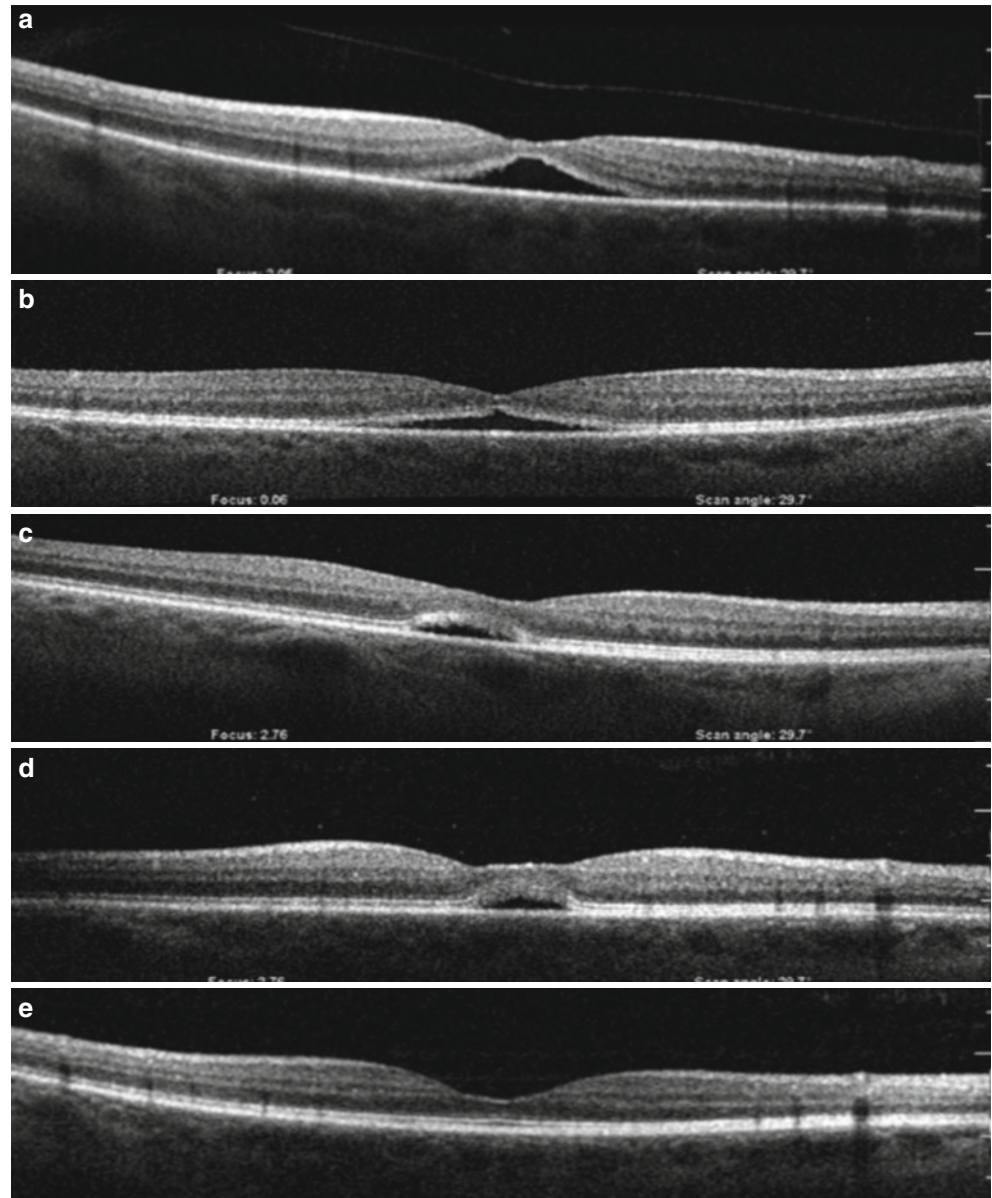
Metamorphopsia is a significant complaint of patients with vitreo-maculopathy [see chapters III.B. Anomalous PVD and Vitreoschisis; III.C. Pathology of Vitreomaculopathies; III.F. Vitreous in the Pathobiology of Macular Pucker; V.A.2. Vitreomaculopathy Surgery]. Nevertheless, we do not routinely quantify this aspect of vision. The case study described above features the use of Three-dimensional Threshold

Amsler Grid testing to quantitate central visual dysfunction induced by anomalous PVD with vitreo-macular traction (VMT) and macular hole. This prototype diagnostic technology was in fact able to quantitate worsening of central vision during disease progression and improvement following pharmacologic vitreolysis. This type of diagnostic assessment would be very useful as a quantitative measure of vision to supplement visual acuity in two regards: it could help determine the degree of disease severity [11] and thus be useful for case selection. As described above, it could also find great utility as an outcome measure of the efficacy of pharmacologic vitreolysis as well as other therapies of eye disease. Lastly, it could help new drug development.

C. Combination Therapy

The theoretical superiority of combination therapy over monotherapy has previously been postulated for pharmacologic vitreolysis [24]. Initially, combination pharmacologic vitreolysis involved the use of intravitreal drug and gas injection. While hyaluronidase alone was unable to induce PVD in rabbits [8], the addition of perfluoropropane gas injection was able to induce PVD [12]. A similar phenomenon was observed in rabbits where the effect of plasmin was augmented by sulfur hexafluoride gas [9]. Thereafter, combination therapy involved the use of two different drugs.

Figure VI.A-8 Time course of normalization in foveal anatomy following successful closure of macular hole with pharmacologic vitreolysis. Closure of the macular hole after pharmacologic vitreolysis was followed by persistent elevation of the central macula with gradual resolution over the ensuing 15 months. There was ultimately complete restoration of normal macular anatomy with visual acuity of 20/20 and normal 3D threshold Amsler Grid test results. (a) one week, (b) one month, (c) six months, (d) nine months, (e) fifteen months post-injection



Studies on diabetic rats found that neither hyaluronidase nor plasmin alone achieved effective pharmacologic vitreolysis, yet the combination of the two agents induced a total PVD in 8/10 (80 %) eyes. The fact that other studies were able to induce PVD with plasmin alone yet this one did not might relate to the fact that this study employed diabetic animals whose vitreous is very likely very different from nondiabetic animal models [see chapter I.E. Diabetic vitreopathy]. A plausible explanation for why the combination of hyaluronidase and plasmin yielded superior results to either agent alone could be that the liquefactant hyaluronidase induced gel liquefaction while the interfactant properties of plasmin induced sufficient dehiscence at the vitreoretinal interface to induce total PVD in a much higher percentage of cases.

Future clinical development should consider combination therapy as a means of increasing the efficacy of pharmacologic vitreolysis. It is, in fact, unlikely that a single agent will meet the needs of all patients at all ages with different systemic conditions and a variety of ocular diseases at various stages of severity. Rather, the future will most likely see the use of a mixture of agents whose selection will be based upon the results of basic and clinical experimentation to determine which combination will have the highest likelihood of inducing a salubrious PVD in different clinical settings. It is furthermore likely that the concentrations of the various ingredients will be varied depending upon various clinical criteria. What seems quite important, however, is that vitreoretinal dehiscence should

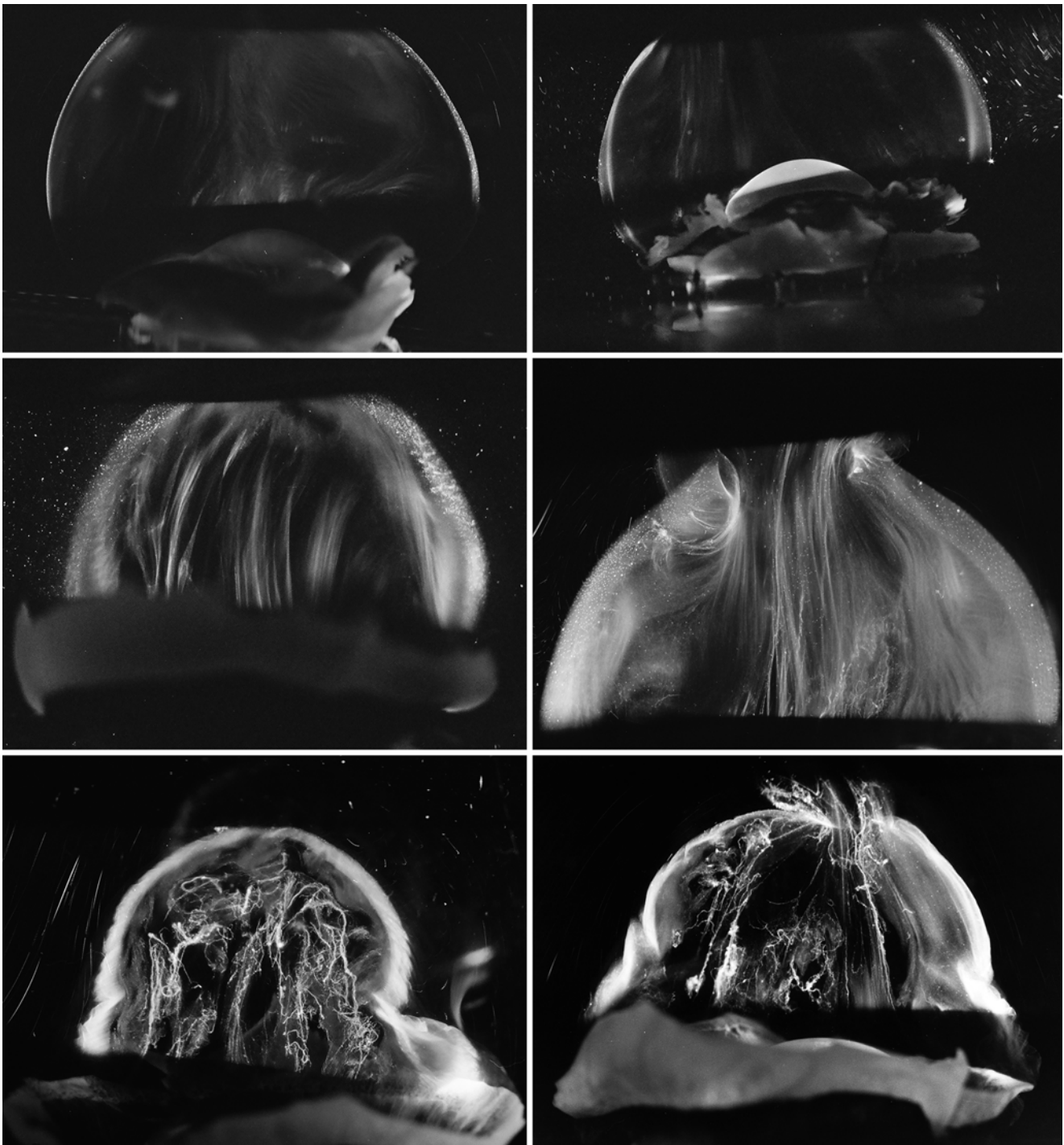


Figure VI.A-9 Age-related differences in human vitreous structure. Dark-field slit microscopy of fresh unfixed whole human vitreous with the sclera, choroid and retina dissected off the vitreous body, which remains attached to the anterior segment. A slit lamp beam illuminates from the side, creating a horizontal optical section with an illumination-observation angle of 90° , maximizing the Tyndall effect. The anterior segment is below and the posterior pole is above in all specimens. *Top row:* The vitreous bodies of an 11-year-old girl (*left*) and a 14-year-old boy (*right*) demonstrate a homogeneous structure with no significant light scattering within the vitreous body, only at the periphery where the vitreous cortex is comprised of a dense matrix of collagen fibrils.

The posterior aspect of the lens is visible at the bottom of each image. *Middle row:* Vitreous structure in a 56-year-old (*left*) and a 59-year-old (*right*) subject features macroscopic fibers in the central vitreous body with an anteroposterior orientation. These form when hyaluronan molecules no longer separate collagen fibrils, allowing cross-linking and aggregation of collagen fibrils into visible fibers. *Bottom row:* In old age, the fibers of the central vitreous become significantly thickened and tortuous, as demonstrated in the two eyes of an 88-year-old woman. Adjacent to these large fibers are areas of liquid vitreous, at times forming pockets, called lacunae



Figure VI.A-10 Heterogeneous vitreous structure in old age. Intravitreal injection of any drug could have variable drug distribution and thus efficacy, depending upon whether the drug is injected into a lacuna of liquefied vitreous or into an area of gel vitreous. The syringe on the lower left is injecting into a lacuna (see *arrows at the top* indicating other lacunae)

of liquid vitreous. The syringe on the lower right is injecting into gel vitreous. The pharmacokinetics and pharmacodynamics will likely be very different for any drug injected into such very different areas within the vitreous body. Such heterogeneity of vitreous structure is significant in older individuals and less prominent in youth

be induced before gel liquefaction to avoid causing an iatrogenic anomalous PVD [see chapter III.B. Anomalous PVD and Vitreoschisis].

D. Prevention

The foregoing has presented considerable information regarding the use of pharmacologic vitreolysis to treat existing diseases. The true promise of this approach, however, lies with implementation in patients at risk of anomalous PVD who would likely benefit greatly from prophylactic pharmacologic vitreolysis. Alternatively, the future may see the development of ways to inhibit the molecular changes that underlie anomalous PVD and prevent this fundamental cause of various vitreoretinopathies.

1. Prophylactic Posterior Vitreous Detachment

As has been extensively discussed in this book, vitreous plays an important role in a variety of retinal diseases. Thus, while the foregoing has focused on the use of pharmacologic vitreolysis to treat existing vitreoretinal disorders, it is reasonable to consider the induction of PVD as prophylaxis in situations that are known to be high risk. Fellow eyes of rhegmatogenous retinal detachments (especially from giant tears), macular holes, and perhaps macular pucker may be good candidates for prophylactic PVD induction. Two clinical conditions would seem very amenable to this approach—diabetic retinopathy and age-related macular degeneration.

Diabetes has significant biochemical, structural, and physiologic effects upon vitreous [see chapter I.E. Diabetic Vitreopathy]. Vitreous plays a particularly important role in

proliferative diabetic retinopathy as well as in diabetic macular edema (DME). [see chapter III.K. Vitreous in Retinovascular Diseases and Diabetic Macular Edema]. As many studies have shown that PVD is associated with a much better prognosis in diabetic retinopathy, it would seem advantageous to prevent advanced stages of disease and vision loss by inducing a prophylactic PVD. To this end, ocriplasmin is being tested in a multicenter, randomized, double-masked, sham-controlled, ascending-dose trial. This study of 60 patients with vitreo-macular adhesion (VMA) and concomitant advanced DME is complete, but data are not yet published.

Vitreous may also play an important role in the pathogenesis of exudative age-related macular degeneration [see chapter III.G. Vitreous in AMD]. Thus, a clinical trial was undertaken to test the hypothesis that ocriplasmin pharmacologic vitreolysis can induce an innocuous PVD and that this will have salubrious effects on the course of the wet AMD. This phase 2 study was a multicenter, randomized, double-masked, sham-controlled trial of 100 patients with VMA and concomitant exudative AMD who were randomized 3:1 to receive a single intravitreal injection of 125 μ g ocriplasmin or sham treatment. Eyes that had previously undergone vitrectomy or received more than 9 injections of bevacizumab and/or ranibizumab were excluded. The primary end point was pharmacologic resolution of VMA at day 28 after injection. Selected secondary end points included resolution of VMA at all other study visits, PVD status, macular thickness, area of vascular leakage, change in visual acuity (ETDRS letters) from baseline, requirement for additional therapy, and number of bevacizumab and/or ranibizumab injections required over the course of study. The study is complete, but data are not yet published.

2. Anomalous PVD Prevention

With further evolution in our understanding of the mechanisms that underlie vitreous liquefaction and dehiscence at the vitreoretinal interface, new treatment paradigms may be developed to prevent these changes and thus prevent anomalous PVD [see chapter III.B. Anomalous PVD and Vitreoschisis]. Such an approach might not only obviate the untoward effects of anomalous PVD on the retina, optic disc, and macula but also promote healthier intraocular physiology, since age-related macular degeneration and diabetic retinopathy are known to be aggravated by unhealthy vitreous physiology [see chapter IV.A. Vitreous Physiology]. Given that cataracts are at least in part related to dysfunction of intravitreal oxygen physiology, it may also be determined that treatments to prevent vitreous degeneration and promote its various physiologic functions will mitigate against cataract formation [see chapter IV.B. Oxygen in Vitreoretinal Physiology and Pathology].

Abbreviations

AMD	Age-related macular degeneration
APVD	Anomalous posterior vitreous detachment
DME	Diabetic macular edema
ECM	Extracellular matrix
ERG	Electroretinography
ETDRS	Early Treatment Diabetic Retinopathy Study
FDA	US Food & Drug Administration
FTMH	Full-thickness macular hole
GAG	Glycosaminoglycans
HA	Hyaluronan
Hase	Hyaluronidase
HeLa	Henrietta Lack's immortal cell line
ILM	Inner limiting membrane
kDa	Kilodalton
MIVI-TRUST	Microplasmin Intravitreal Injection–Traction Release without Surgical Treatment
mL	Milliliter
NPDR	Nonproliferative diabetic retinopathy
OCT/SLO	Combined optical coherence tomography/scanning laser ophthalmoscopy
PMM	Premacular membrane
PVD	Posterior vitreous detachment
PVR	Proliferative vitreoretinopathy
RGD	The amino acid sequence arginine-glycine-aspartate (RGD)
sVMA	Symptomatic vitreo-macular adhesion
tPA	Tissue plasminogen activator
TUNEL	Terminal deoxynucleotidyl transferase nick end labeling
μ L	Microliter
μ m	Micrometer
VA	Visual acuity
VMA	Vitreo-macular adhesion
VMT	Vitreo-macular traction
VPA	Vitreo-papillary adhesion
3D-TAG	Three-dimensional threshold Amsler Grid test

References

1. Bishop P, McLeod D, Reardon A. Effects of hyaluronan lyase, hyaluronidase, and chondroitin ABC lyase on mammalian vitreous gel. *Invest Ophthalmol Vis Sci.* 1999;40(10):2173–8.
2. Brem RB, Robbins SG, Wilson DJ, O'Rourke LM, Mixon RN, Robertson JE, Planck SR, Rosenbaum JT. Immunolocalization of integrins in the human retina. *Invest Ophthalmol Vis Sci.* 1994; 35(9):3466–74.

3. Duker JS, Kaiser PK, Binder S, de Smet MD, Gaudric A, Reichel E, Sadda SR, Sebag J, Spaide RF, Stalmans P. The International Vitreomacular Traction Study (IVTS) group classification of vitreomacular adhesion, traction, and macular hole. *Ophthalmology*. 2013;120(12):2611–9.
4. El-Ashry M, Hegde V, James P, Pagliarini S. Analysis of macular thickness in British population using optical coherence tomography (OCT) - an emphasis on interocular symmetry. *Curr Eye Res*. 2008;33:693–9.
5. Fink W, Sadun AA. 3D computer-automated threshold Amsler grid test. *J Biomed Opt*. 2004;9(1):149–53.
6. Gandorfer A. Enzymatic vitreous disruption. *Eye (Lond)*. 2008;22(10):1273–7.
7. Girish KS, Kemparaju K. The magic glue hyaluronan and its eraser hyaluronidase: a biological overview. *Life Sci*. 2007;80:1921–43.
8. Hikichi T, Kado M, Yoshida A. Intravitreal injection of hyaluronidase cannot induce posterior vitreous detachment in the rabbit. *Retina*. 2000;20(2):195–8.
9. Hikichi T, Yangiya N, Kado M, Akiba J, Yoshida A. Posterior vitreous detachment induced by injection of plasmin and sulfur hexafluoride in the rabbit vitreous. *Retina*. 1999;19:55–8.
10. Hynes RO. Integrins: versatility, modulation, and signaling in cell adhesion. *Cell*. 1992;69(1):11–25.
11. Jivrajka RV, Kim JK, Fink W, Sadun AA, Sebag J. Quantitative analysis of central visual field defects in macular edema using three-dimensional computer-automated threshold Amsler grid testing. *Graefes Arch Clin Exp Ophthalmol*. 2009;247:165–70.
12. Kang SW, Hyung S-M, Choi MY, Lee J. Induction of vitreolysis and vitreous detachment with hyaluronidase and perfluoropropane gas. *Korean J Ophthalmol*. 1995;9:69–78.
13. Karageozian HL. Determine the safety and efficacy of Vitreosolve® administered intravitreally to induce a complete posterior vitreous detachment (PVD) in non proliferative diabetic retinopathy human subjects. *Invest Ophthalmol Vis Sci (ARVO)*. 2005;46:5453.
14. Nguyen J, Yee KM, Wa C, Sadun A. Macular pucker lowers contrast sensitivity which improves after surgery. *Invest Ophthalmol Vis Sci*. 2014 (ARVO).
15. Oliveira LB, Tatebayashi M, Mahmoud TH, Blackmon SM, Wong F, McCuen 2nd BW. Dispace facilitates posterior vitreous detachment during vitrectomy in young pigs. *Retina*. 2001;21(4):324–31.
16. Oliveira LB, Meyer CH, Kumar J, Tatebayashi M, Toth CA, Wong F, Epstein DL, McCuen 2nd BW. RGD peptide-assisted vitrectomy to facilitate induction of a posterior vitreous detachment: a new principle in pharmacological vitreolysis. *Curr Eye Res*. 2002;25(6):333–40.
17. Pirie A. Effect of hyaluronidase injection on vitreous humor of rabbit. *Br J Ophthalmol*. 1949;33:678–84.
18. Robert L, Robert AM, Renard G. Biological effects of hyaluronan in connective tissues, eye, skin, venous wall. Role in aging. *Pathol Biol (Paris)*. 2010;58:187–98.
19. Robison CD, Jivrajka RV, Bababegy SR, Fink W, Sadun AA, Sebag J. Distinguishing wet from dry age-related macular degeneration using three-dimensional computer-automated threshold Amsler grid testing. *Br J Ophthalmol*. 2011;95(10):1419–23.
20. Ruoslahti E, Pierschbacher MD. New perspectives in cell adhesion: RGD and integrins. *Science*. 1987;238(4826):491–7.
21. Russell SR. What we know (and don't know) about the vitreoretinal interface. *Retina*. 2012;32(Suppl):S181–6.
22. Sebag J. Abnormalities of human vitreous structure in diabetes. *Graefes Arch Clin Exp Ophthalmol*. 1993;231:257–60.
23. Sebag J. Pharmacologic vitreolysis. *Retina*. 1998;18(1):1–3.
24. Sebag J. Is pharmacologic vitreolysis brewing? *Retina*. 2002;22(1):1–3.
25. Sebag J. Pharmacologic vitreolysis—premise and promise of the first decade. *Retina*. 2009;29(7):871–4.
26. Sebag J. The emerging role of pharmacologic vitreolysis. *Retin Physician*. 2010;7(2):52–6.
27. Sebag J, Buckingham B, Charles MA, Reiser K. Biochemical abnormalities in vitreous of humans with proliferative diabetic retinopathy. *Arch Ophthalmol*. 1992;110:1472–9.
28. Sebag J, Nie S, Reiser KA, Charles MA, Yu NT. Raman spectroscopy of human vitreous in proliferative diabetic retinopathy. *Invest Ophthalmol Vis Sci*. 1994;35:2976–80.
29. Sebag J, Wang M, Nguyen D, Sadun AA. Vitreo-papillary adhesion in macular diseases. *Trans Am Ophthalmol Soc*. 2009;107:35–46.
30. Sumi H, Hamada H, Tsushima H, Mihara H, Muraki H. A novel fibrinolytic enzyme (nattokinase) in the vegetable cheese Natto; a typical and popular soybean food in the Japanese diet. *Experientia*. 1987;43(10):1110–1.
31. Takano A, Hirata A, Ogasawara K, Sagara N, Inomata Y, Takahiro K, Tanihara H. Posterior vitreous detachment induced by nattokinase (Subtilisin NAT): a novel enzyme for pharmacologic vitreolysis. *Invest Ophthalmol Vis Sci*. 2006;47(5):2075–9.
32. Tozer KR, Fink W, Sadun AA, Sebag J. Prospective three-dimensional analysis of structure and function in vitreo-macular adhesion cured by pharmacologic vitreolysis. *Retin Cases Brief Rep*. 2013;7:57–61.
33. Turner RB, Liu L, Sazonova IY, Reed GL. Structural elements that govern the substrate specificity of the clot-dissolving enzyme plasmin. *J Biol Chem*. 2002;277:33068–74.
34. Wall M, Sadun AA. Threshold amsler grid testing: cross-polarizing lenses enhance yield. *Arch Ophthalmol*. 1986;104:520–3.
35. Wang MY, Nguyen D, Hindoyan N, Sadun AA, Sebag J. Vitreo-papillary adhesion in macular hole and macular pucker. *Retina*. 2009;29:644–50.
36. Wang ZL, Zhang X, Xu X, Sun XD, Wang F. PVD following plasmin but not hyaluronidase: implications for combination pharmacologic vitreolysis therapy. *Retina*. 2005;25(1):38–43.
37. Wu HL, Shi GY, Bender ML. Preparation and purification of microplasmin. *Proc Natl Acad Sci U S A*. 1987;84:8292–5.
38. Yatagai C, Maruyama M, Kawahara T, Sumi H. Nattokinase-promoted tissue plasminogen activator release from human cells. *Pathophysiol Haemost Thromb*. 2008;36(5):227–32.

Wallace S. Foulds

Outline

- I. Introduction
 - II. Pharmacologic Vitreolysis Approaches
 - A. Hyaluronidase
 - B. Collagenases
 - C. Management of Intraocular Hemorrhage
 - D. Induction of Posterior Vitreous Detachment
 - E. Physiologic Effects of Pharmacologic Vitreolysis
 - III. Targeting Specific Disease States
 - IV. Summary
- References

Keywords

Vitreous • Pharmacologic vitreolysis • History • Hyaluronan • Hyaluronidase • Collagen • Collagenases • Tissue plasminogen activator • Dispase • Plasmin • Ocriplasmin

Key Concepts

1. Pharmacologic vitreolysis has been attempted for only about 65 years.
2. The majority of agents that have been investigated have largely failed, and the only one that has been approved for clinical application in the EU and the USA has limited efficacy.
3. A better understanding of vitreous is needed before highly effective agents are developed for pharmacologic vitreolysis.

W.S. Foulds, MD, ChM, FRCS
Singapore Eye Research Institute (Retina Research),
University of Glasgow (Emeritus),
Kinnoul Place, 68, Dowanside Road,
Glasgow G12 9DL, Scotland, UK
e-mail: wallace.stewart.foulds@seri.com.sg

I. Introduction

Pharmacologic vitreolysis is an evolving therapeutic modality with increasing actual or potential applications and a relatively short history. Prior to the introduction of vitrectomy in the early 1970s [1], the vitreous was regarded by most ophthalmologists as sacrosanct and not amenable to therapeutic intervention. However, owing to the expansion of our understanding of the composition and organization of the vitreous on a molecular level and how aging as well as disease affect this delicate homeostasis, we now have enough information to broach this subject.

II. Pharmacologic Vitreolysis Approaches

A. Hyaluronidase

During the period 1961–1964, the author, while developing an animal model of retinal detachment [2–4], investigated the effect of a variety of enzymes on the vitreous of rabbits. A retinal break in the presence of an intact vitreous failed to result in a retinal detachment, while the intravitreal injection of bovine testicular hyaluronidase and a retinal break caused a widespread detachment of the retina that subsequently underwent spontaneous resolution over a period of 6 weeks or so (Figure VI.B-1). This latter development was considered to be the result of replacement of depolymerized hyaluronan by new hyaluronan secreted by hyalocytes, previously shown to be the source of vitreous hyaluronan [5]. As the author was aware [6, 7] that vitreous syneresis and posterior vitreous detachment were known to play an etiological role in human retinal detachment, it appeared that destruction of the collagen network of the posterior vitreous might be necessary for the creation of a permanent retinal detachment experimentally.

B. Collagenases

To induce pharmacologic vitreolysis experimentally, a variety of collagenases were investigated on their own or in conjunction with hyaluronidase. These included pronase (a mixture of collagenases derived from the supernatant of cultured streptococci), bromelain (a collagenase extracted from the stems of pineapple plants), and a commercially available collagenase. The results were disappointing. At a dose low enough to avoid retinal toxicity, there was a failure to induce vitreolysis, while in a dosage sufficient to liquefy the vitreous, there was evidence of retinal toxicity and the development of retinal hemorrhages. As it was found that collagen fibrils adhered to a needle inserted into the vitreous for an intravitreal injection of hyaluronidase and that adherent collagen fibrils could be removed from the posterior vitreous by rotation of the needle (Figure VI.B-2) and that this combined with a retinal hole resulted in a permanent experimental retinal detachment (Figure VI.B-1), no further attempt was made to induce vitreolysis with collagenases.

C. Management of Intraocular Hemorrhage

An early use of vitrectomy was in the management of vitreous hemorrhage, but during the 1970s there were reports of the use of intravitreal enzymes and other agents to accelerate the absorption of intravitreal blood both as an aid to vitrectomy or as a nonsurgical treatment for vitreous hemorrhage. Injected agents included those inducing fibrinolysis in clotted

blood such as urokinase [7–11]. Intravitreal interleukin-1 (IL-1) to induce macrophage recruitment and increase phagocytosis of red cells was also investigated for efficacy and safety [12, 13]. The results showed that intravitreal human IL-1 was well tolerated and sped the absorption of vitreous hemorrhage with or without accompanying cryotherapy [12], while recombinant IL-1 β caused an inflammatory response with vascular changes and vitreous veils [13]. Conversely, inhibition of IL-1 β -induced fibrinolysis delayed the absorption of experimental vitreous hemorrhage in rabbits [13]. This was thought to be due to a loss of fibrin chemotaxis that might have promoted the incursion of macrophages into the vitreous and their phagocytosis of red cells [14]. Thus, trans-scleral cryotherapy that was thought to accelerate the clearance of vitreous hemorrhage by activation of plasminogen and resulting fibrinolysis continued to be used for the treatment of vitreous hemorrhage [15].

In the 1990s and subsequently, pharmacologic vitreolysis with intravitreal tissue plasminogen activator (tPA) combined with intravitreal gas was extended to the treatment of subretinal hemorrhage both experimentally [16] and clinically [17–19]. Intravitreal tPA was found to be useful in the management of submacular hemorrhage associated with AMD, with around half of treated patients gaining vision [18] [see chapter V.A.1. AMD surgery]. Although recombinant tPA produced a similar visual improvement in patients with submacular hemorrhage, a temporary exudative retinal detachment was frequently seen as was a temporary opacification of the vitreous [19].

D. Induction of Posterior Vitreous Detachment

Initially the aim for pharmacologic vitreolysis was as an adjunct to vitrectomy [20, 21], the aim at that time being the creation of a posterior vitreous detachment (PVD) to aid the clearance of the cortical vitreous during vitrectomy. Relief of vitreoretinal traction was another recognized use for vitreolysis as was the management of vitreous hemorrhage. Early work on vitreolysis was largely experimental, assessing the effects on the vitreous and the safety of a variety of agents that might be used clinically. The agents investigated included hyaluronidase initially claimed to induce a PVD [22] but not subsequently confirmed [23, 24], chondroitinase [25] (which cleaves proteoglycans), dispase [26] (a protease that cleaves fibronectin and collagen IV), streptokinase [27] (a collagenase), and plasmin [26–32] (a serine protease that induces fibrinolysis, activates collagenases, and cleaves fibrin, fibronectin, thrombospondin, and laminin). Among the agents investigated, intravitreal plasmin was reported to effectively cause a PVD experimentally and to eliminate cortical vitreous remnants [33]. Electron microscopy showed that plasmin caused cleavage between the vitreous cortex and the ILM

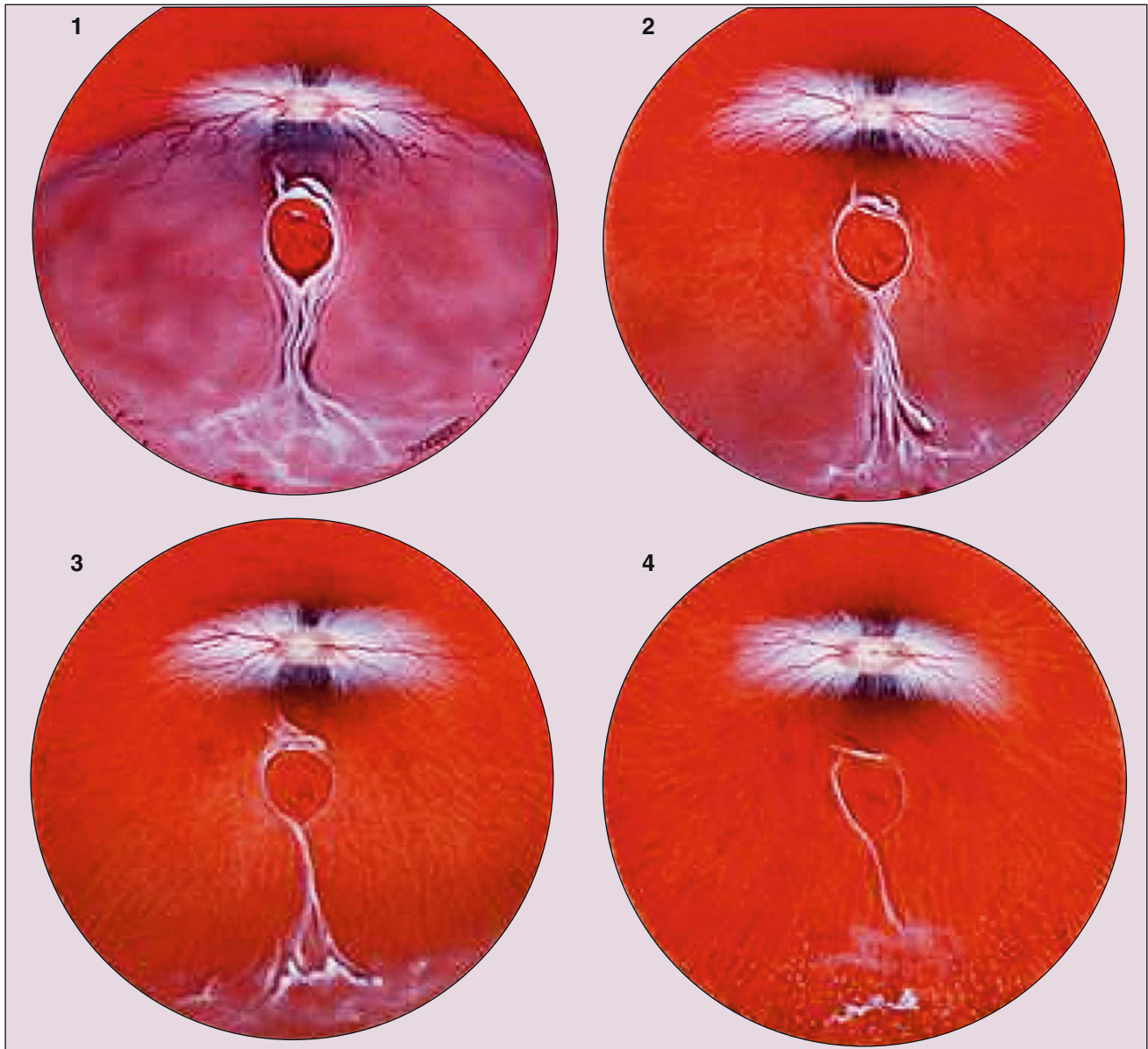


Figure VI.B-1 History of pharmacologic vitreolysis. In a rabbit eye, following temporary vitreolysis induced by the intravitreal injection of hyaluronidase, and in the presence of a retinal hole, an extensive retinal detachment develops but

undergoes spontaneous resolution over a period of 6 weeks as the depolymerized hyaluronan regenerates. Appearance at 1 week (1), at 2 weeks (2), at 4 weeks (3), and at 6 weeks (4)

without morphological change in the retina [34]. Plasmin can also be made available through activation of plasminogen by tissue plasminogen activator (tPA) or by urokinase plasminogen activator (uPA). A combination of recombinant lysine-plasminogen and recombinant urokinase together with intravitreal sulfur hexafluoride was reported as causing a PVD in 75 % of a large number of rabbits in which it was tested [35]. Following the investigation of a wide range of agents potentially suitable for pharmacologic vitreolysis, attention was gradually focused on plasmin as the best agent

for this purpose. In clinical practice, various methods were used to obtain a therapeutic level of plasmin within the vitreous including the injection into the vitreous of human or bovine plasmin. Owing to its relative instability, however, human plasmin had to be generated from autologous plasminogen a short time prior to its injection into the vitreous [36]. Thus, the introduction of recombinant human plasmin and particularly recombinant microplasmin (ocriplasmin) greatly facilitated the use of plasmin for pharmacologic vitreolysis. This truncated form of plasmin retains the vitreolytic

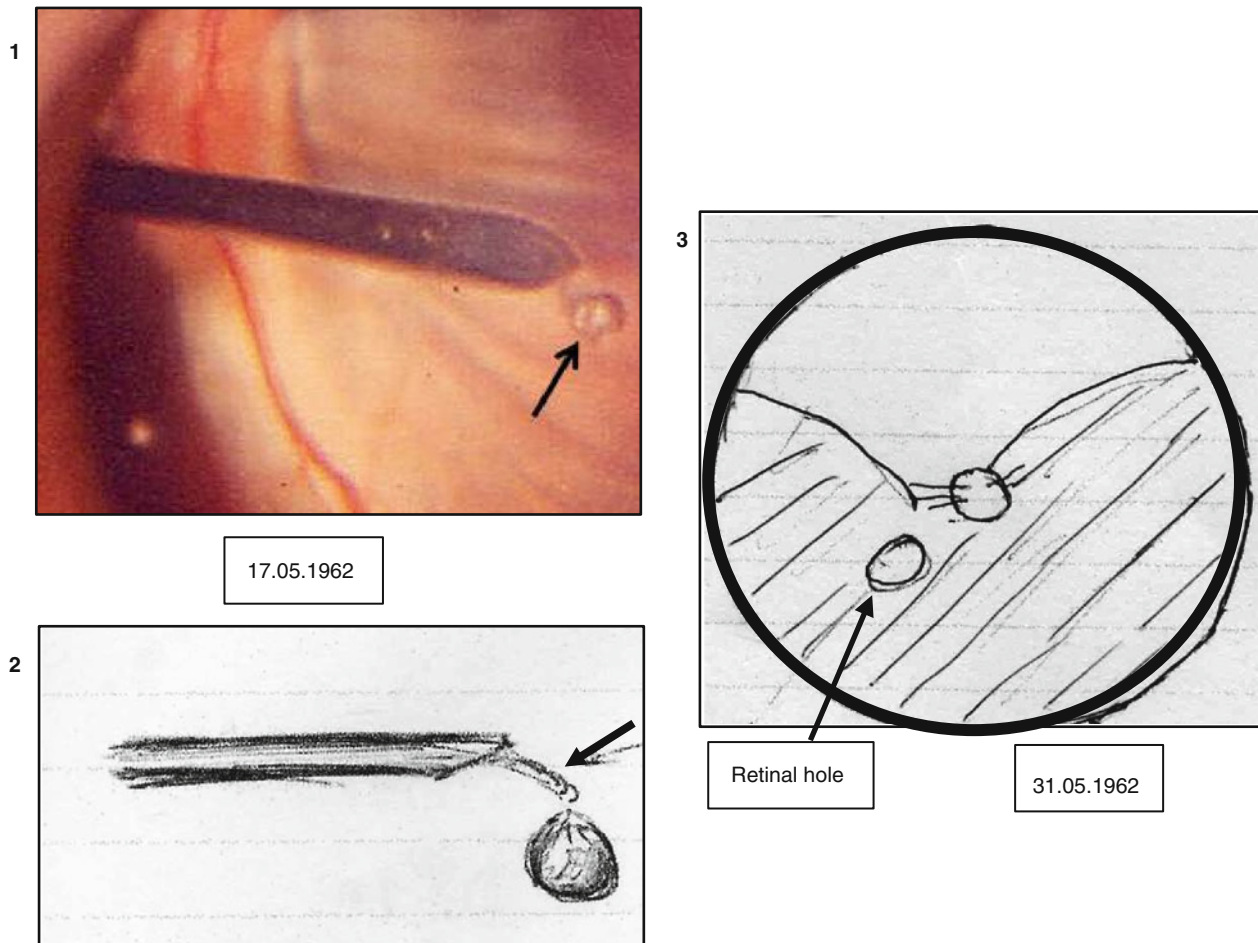


Figure VI.B-2 Following the intravitreal injection of hyaluronidase, as shown (1) in a photograph of 1962, rotation of the injecting needle causes intravitreal collagen fibrils to aggregate into a small mass (arrow) adherent to the needle. A laboratory sketch (2) shows that the aggregated collagen fibrils are attached to the

needle by a rope-like aggregation of fibrils (arrow). Withdrawal of the needle and the attached collagen fibrils, results in a permanent mechanical vitreolysis and in the presence of a retinal hole, a long-lasting retinal detachment as shown (3) in a lab book sketch 3 weeks after the withdrawal of aggregated fibrils

capability of plasmin and has the advantages of ready availability, stability, and smaller molecular size than plasmin, thus aiding its penetrance into ocular tissues and dispersion within the vitreous. Ocriplasmin received FDA approval for the treatment of symptomatic vitreo-macular adhesion in October 2012. Approval followed the experimental assessment of its mode of action and safety [37–39] and a number of clinical trials [40–43] together with the combined opinion of a panel of experts based on their own interpretation of current clinical data and their experience [44]. It was recorded that symptomatic vitreo-macular adhesion represented a substantial burden of illness that could be reduced by ocriplasmin pharmacologic vitreolysis [45, 46]. It was rapidly confirmed that intravitreal ocriplasmin not only relieved vitreo-macular traction but also induced a PVD as confirmed clinically by OCT [47, 48]. The use of microplasmin for the

relief of vitreo-macular traction was then extended to the treatment of macular holes associated with vitreo-macular traction [43], but not macular holes associated with premacular membranes and macular pucker.

E. Physiologic Effects of Pharmacologic Vitreolysis

As pharmacologic vitreolysis increases molecular movement within the vitreous and molecular exchange with neighboring tissues [49–51], it is reasonable to consider that vitreolysis might have a role to play in intravitreal drug delivery and have beneficial effects other than the mechanical relief of vitreous traction. This has yet to be further explored and developed. It has further been shown that vitreolysis increases

oxygen concentration in the vitreous and in the retina [52, 53], and thus it has been proposed that vitreolysis could alleviate the progression of diabetic retinopathy through deactivation of the hypoxia-inducible factor 1 α (HIF-1 α) pathway [54] that, in this condition, is activated by hypoxia.

III. Targeting Specific Disease States

There was already evidence that intravitreal plasmin could reduce central retinal thickness in diabetic macular edema [55–57] and was useful as an adjunct in the surgical treatment of proliferative diabetic retinopathy [58, 59]. Separation of the cortical vitreous from the inner limiting membrane in the treatment of diabetic retinopathy could be obtained by a variety of vitreous modulators and most promisingly with ocriplasmin [60, 61]. Not surprisingly, it has been suggested that pharmacologic vitreolysis might also have beneficial effects on other retinal disorders in which hypoxia plays a role, including the macular edema resulting from retinal vein occlusion [62] and the retinopathy of prematurity (ROP) [63]. An additional mechanism that was recognized in plasmin-induced pharmacologic vitreolysis was activation of matrix metalloproteinase-2 (MMP-2) [64–67] that with MMP-9 may play a part in diabetic retinopathy [68].

The role of pharmacologic vitreolysis was further expanded by the discovery that vitreo-macular traction (VMT) appears to be a risk factor for age-related macular degeneration (AMD) including choroidal neovascularization (CNV) in exudative AMD [69–72] [see chapter III.G. Vitreous in AMD], and thus PVD induced by pharmacologic vitreolysis might be protective against CNV [73]. The presence of vitreo-macular traction adversely influenced surgical results in the treatment of CNV in AMD [74] and had an adverse effect on anti-VEGF treatment for CNV [75].

IV. Summary

In summary, the current indications for pharmacologic vitreolysis have expanded to include intravitreal drug delivery, the management and possible prevention of the ocular complications of diabetes, the treatment and possible retardation of CNV in AMD, and the management of central or branch retinal vein occlusions and retinopathy of prematurity in addition to its original approved use in the relief of symptomatic vitreo-macular adhesion and traction. With increasing indications for pharmacologic vitreolysis, it is unlikely that the history of pharmacologic vitreolysis has reached its final conclusion. Pharmacologic vitreolysis has been shown to have benefit in a large and increasing number of sight-threatening conditions with few adverse effects, and it seems likely that further advances in its use will see an evolving future history.

Abbreviations

AMD	Age-related macular degeneration
CNV	Choroidal neovascularization
FDA	Food and Drug Administration
HIF-1 α	Hypoxia-inducible factor 1 α
IL-1/1 β	Interleukin 1 and 1 β
ILM	Internal limiting membrane
MMP-2/9	Matrix metalloproteinase-2 and -9
OCT	Optical coherence tomography
PVD	Posterior vitreous detachment
ROP	Retinopathy of prematurity
tPA	Tissue plasminogen activator
uPA	Urokinase plasminogen activator
VEGF	Vascular endothelial growth factor
VMT	Vitreo-macular traction

References

1. Machemer R, Buettner H, Norton EW, Parel JM. Vitrectomy: a pars plana approach. *Trans Am Acad Ophthalmol Otolaryngol.* 1971;75:813–20.
2. Foulds WS. Experimental detachment of the retina. *Mod Probl Ophthalmol.* 1961;4:233–3.
3. Foulds WS. Experimental retinal detachment. *Trans Ophthalmol Soc U K.* 1963;83:153–70.
4. Foulds WS. Experimental detachment of the retina and its effect on the intraocular fluid dynamics. *Mod Probl Ophthalmol.* 1969;8:51–63.
5. Balazs EA. Molecular morphology of the vitreous body. In: Smelser GK, editor. *Structure of the eye.* New York: Academic Press Inc; 1961. p. 293–310.
6. Foulds WS. Aetiology of retinal detachment. *Trans Ophthalmol Soc U K.* 1975;95:118–27.
7. Foulds WS. The vitreous in retinal detachment. *Trans Ophthalmol Soc U K.* 1975;95:412–6.
8. Williamson J, Forrester JV. Urokinase in the treatment of vitreous haemorrhage. *Lancet.* 1972;2(7775):488.
9. Forrester J, Williamson J. Resolution of intravitreal clots by urokinase. *Lancet.* 1973;2(7822):179–81.
10. Dugmore WN, Raichand M. Intravitreal urokinase in the treatment of vitreous hemorrhage. *Am J Ophthalmol.* 1973;75:779–81.
11. Forrester JV, Williamson J. Lytic therapy in vitreous haemorrhage. *Trans Ophthalmol Soc U K.* 1974;94:583–6.
12. Pastor JC, Fernandez C. Efficacy of intravitreal interleukin-1 in the reabsorption of experimental vitreous hemorrhage in rabbits. *Ophthalmic Res.* 1993;25:302–6.
13. Pastor JC, González O, Saavedra JA, Guerra A, Angulo S. Tolerance of intravitreal interleukin-1 beta in the treatment of experimental vitreous hemorrhage. *Ophthalmic Res.* 1995;27:37–41.
14. Forrester JV, Edgar W, Prentice CR, Forbes CD, Williamson J. The effect of fibrinolytic inhibition in the resolution of experimental vitreous hemorrhage. *Am J Ophthalmol.* 1977;84:810–4.
15. Guerra A, Pastor JC. Retinal cryoapplication and fibrinolysis in experimental vitreous hemorrhage. *Curr Eye Res.* 1991;10:697–701.
16. Coll GE, Sparrow JR, Marinovic A, Chang S. Effect of intravitreal tissue plasminogen activator on experimental subretinal hemorrhage. *Retina.* 1995;15:319–26.
17. Hassan AS, Johnson MW, Schneiderman TE, Regillo CD, Tornambe PE, Poliner LS, Blodi BA, Elner SG. Management of submacular hemorrhage with intravitreal tissue plasminogen

- activator injection and pneumatic displacement. *Ophthalmology*. 1999;106:1900–6.
18. Hattenbach LO, Klais C, Koch FH, Gümbel HO. Intravitreal injection of tissue plasminogen activator and gas in the treatment of submacular hemorrhage under various conditions. *Ophthalmology*. 2001;108:1485–92.
 19. Hesse L, Schmidt J, Kroll P. Management of acute submacular hemorrhage using recombinant tissue plasminogen activator and gas. *Graefes Arch Clin Exp Ophthalmol*. 1999;237:273–7.
 20. Trese MT. Enzymatic-assisted vitrectomy. *Semin Ophthalmol*. 2000;15:116–21.
 21. Trese MT. Enzymatic-assisted vitrectomy. *Eye (Lond)*. 2002;16:365–8.
 22. Narayanan R, Kuppermann BD. Hyaluronidase for pharmacologic vitreolysis. *Dev Ophthalmol*. 2009;44:20–5.
 23. Hikichi T, Kado M, Yoshida A. Intravitreal injection of hyaluronidase cannot induce posterior vitreous detachment in the rabbit. *Retina*. 2000;20:195–8.
 24. Wang ZL, Zhang X, Xu X, Sun XD, Wang F. PVD following plasmin but not hyaluronidase: implications for combination pharmacologic vitreolysis therapy. *Retina*. 2005;25:38–43.
 25. Staubach F, Nober V, Janknecht P. Enzyme-assisted vitrectomy in enucleated pig eyes: a comparison of hyaluronidase, chondroitinase, and plasmin. *Curr Eye Res*. 2004;29:261–8.
 26. Tezel TH, Del Priore LV, Kaplan HJ. Posterior vitreous detachment with dispase. *Retina*. 1998;18:7–15.
 27. Baha E, Abou-Nazel MW, Idriss HF, Abdel-Megeed AS. The role of streptokinase in induction of posterior detachment: a scanning and transmission electron microscopic study of the retina in rabbits. *Retina*. 2003;23:698–704.
 28. Hermel M, Schrage NF. Efficacy of plasmin enzymes and chondroitinase ABC in creating posterior vitreous separation in the pig: a masked, placebo-controlled in vivo study. *Graefes Arch Clin Exp Ophthalmol*. 2007;245:399–406.
 29. Verstraeten TC, Chapman C, Hartzler M, Winkler BS, Trese MT, Williams GA. Pharmacologic induction of posterior vitreous detachment in the rabbit. *Arch Ophthalmol*. 1993;111:849–54.
 30. Hikichi T, Yanagiya N, Kado M, Akiba J, Yoshida A. Posterior vitreous detachment induced by injection of plasmin and sulfur hexafluoride in the rabbit vitreous. *Retina*. 1999;19:55–8.
 31. Wang LF, Ma JX, Liu JZ, Cai SZ, Lu LC, Wang ZD. An experimental study on dissolving and detaching vitreoretinal interface with enzymes. *Zhonghua Yan Ke Za Zhi*. 2004;40:459–64.
 32. Li X, Shi X, Fan J. Posterior vitreous detachment with plasmin in the isolated human eye. *Graefes Arch Clin Exp Ophthalmol*. 2002;240:56–62.
 33. Gandorfer A, Ulbig M, Kampik A. Plasmin-assisted vitrectomy eliminates cortical vitreous remnants. *Eye (Lond)*. 2002;16:95–7.
 34. Gandorfer A, Putz E, Welge-Lüssen U, Grüterich M, Ulbig M, Kampik A. Ultrastructure of the vitreoretinal interface following plasmin assisted vitrectomy. *Br J Ophthalmol*. 2001;85:6–10.
 35. Men G, Peyman GA, Genaidy M, Kuo PC, et al. The role of recombinant lysine-plasminogen and recombinant urokinase sulphur hexafluoride combination in inducing posterior vitreous detachment. *Retina*. 2004;24:199–209.
 36. Rizzo S, Pellegrini G, Benocci F, Belting C, Baicchi U, Vispi M. Autologous plasmin for pharmacologic vitreolysis prepared 1 hour before surgery. *Retina*. 2006;26:792–6.
 37. Sakuma T, Tanaka M, Mizota A, Inoue J, Pakola S. Safety of in vivo pharmacologic vitreolysis with recombinant microplasmin in rabbit eyes. *Invest Ophthalmol Vis Sci*. 2005;46:3295–9.
 38. Gandorfer A. Experimental evaluation of microplasmin – an alternative to vital dyes. *Dev Ophthalmol*. 2008;42:153–9.
 39. Chen W, Mo W, Sun K, Huang X, Zhang YL, Song HY. Microplasmin degrades fibronectin and laminin at vitreoretinal interface and outer retina during enzymatic vitrectomy. *Curr Eye Res*. 2009;34:1057–64.
 40. de Smet MD, Gandorfer A, Stalmans P, Veckeneer M, Feron E, Pakola S, Kampik A. Microplasmin intravitreal administration in patients with vitreomacular traction scheduled for vitrectomy: the MIVI I trial. *Ophthalmology*. 2009;116:1349–55.
 41. Benz MS, Packo KH, Gonzalez V, et al. A placebo-controlled trial of microplasmin intravitreal injection to facilitate posterior vitreous detachment before vitrectomy. *Ophthalmology*. 2010;117:791–7.
 42. Stalmans P, Delaey C, de Smet MD, van Dijkman E, Pakola S. Intravitreal injection of microplasmin for treatment of vitreomacular adhesion: results of a prospective, randomized, sham-controlled phase II trial (the MIVI-IIT trial). *Retina*. 2010;30:1122–7.
 43. Stalmans P, Benz MS, Gandorfer A, Kampik A, Girach A, Pakola S, Haller JA, MIVI-TRUST Study Group. Vitreolysis with ocriplasmin for vitreomacular traction and macular holes. *N Engl J Med*. 2012;367:606–15.
 44. Kuppermann BD. Ocriplasmin for pharmacologic vitreolysis. *Retina*. 2012;32 Suppl 2:S225–8.
 45. Jackson TL, Nicod E, Simpson A, Angelis A, Grimaccia F, Kanavos P. Symptomatic vitreomacular adhesion. *Retina*. 2013;33:1503–11.
 46. Kim BT, Schwartz SG, Smiddy WE, Doshi RR, et al. Initial outcomes following intravitreal ocriplasmin for treatment of symptomatic vitreomacular adhesion. *Ophthalmic Surg Lasers Imaging Retina*. 2013;44:334–43.
 47. Folgar FA, Toth CA, DeCroos FC, Girach A, Pakola S, Jaffe GJ. Assessment of retinal morphology with spectral and time domain OCT in the phase III trials of enzymatic vitreolysis. *Invest Ophthalmol Vis Sci*. 2012;53:7395–401.
 48. Stalmans P, Duker JS, Kaiser PK, Heier JS, Dugel PU, Gandorfer A, Sebag J, Haller JA. OCT-based interpretation of the vitreomacular interface and indications for pharmacologic vitreolysis. *Retina*. 2013;33(10):2003–11.
 49. Sebag J. Molecular biology of pharmacologic vitreolysis. *Trans Am Ophthalmol Soc*. 2005;103:473–94.
 50. Sebag J, Ansari RR, Suh KI. Pharmacologic vitreolysis with microplasmin increases vitreous diffusion coefficients. *Graefes Arch Clin Exp Ophthalmol*. 2007;245:576–80.
 51. Goldenberg DT, Trese MT. Pharmacologic vitreodynamics and molecular flux. *Dev Ophthalmol*. 2009;44:31–6.
 52. Quiram PA, Leverenz VR, Baker RM, Dang L, Giblin FJ, Trese MT. Microplasmin-induced posterior vitreous detachment affects vitreous oxygen levels. *Retina*. 2007;27:1090–6.
 53. Gandorfer A. Objective of pharmacologic vitreolysis. *Dev Ophthalmol*. 2009;44:1–6.
 54. Li C, Chen P, Zhang J, Zhang L, Huang X, Yao Y, Che X, Fan X, Ge S, Wang Z. Enzyme-induced vitreolysis can alleviate the progression of diabetic retinopathy through the HIF-1 α pathway. *Invest Ophthalmol Vis Sci*. 2013;54:4964–70.
 55. Azzolini C, D'Angelo A, Maestranzi G, et al. Intraoperative plasmin enzyme in diabetic macular edema. *Am J Ophthalmol*. 2004;138:560–6.
 56. Asami T, Terasaki H, Kachi P, et al. Ultrastructure of internal limiting membrane removed during plasmin-assisted vitrectomy from eyes with diabetic macular edema. *Ophthalmology*. 2004;111:231–7.
 57. Elsayy MF. Intravitreal autologous plasmin as a therapeutic modality for diffuse diabetic macular edema. *Clin Ophthalmol*. 2012;6:2063–8.
 58. Hesse L, Kroll P. Enzymatically induced posterior vitreous detachment in proliferative diabetic vitreoretinopathy. *Klin Monbl Augenheilkd*. 1999;214:84–9.
 59. Williams JG, Trese MT, Williams GA, Hartzler MK. Autologous plasmin enzyme in the surgical management of diabetic retinopathy. *Ophthalmology*. 2001;108:1902–5.
 60. Costa Ede P, Rodrigues EB, Farah ME, Sebag J, Meyer CH. Novel vitreous modulators for pharmacologic vitreolysis in the treatment of diabetic retinopathy. *Curr Pharm Biotechnol*. 2011;12:410–22.

61. Lopez-Lopez F, Rodriguez-Blanco M, Gomez Ulla F, Marticorena J. Enzymatic vitreolysis. *Curr Diab Rev.* 2009;5:57–62.
62. Udaondo P, Díaz-Llopis M, García-Delpech S, Salom D, Romero FJ. Intravitreal plasmin without vitrectomy for macular edema secondary to branch retinal vein occlusion. *Arch Ophthalmol.* 2011;129(3):283–7.
63. Wu WC, Drenser KA, Lai M, Capone A, Trese MT. Plasmin enzyme-assisted vitrectomy for primary and reoperated eyes with stage 5 retinopathy of prematurity. *Retina.* 2008;28:S75–80.
64. Brown DJ, Bishop P, Hamdi H, Kenney MC. Cleavage of structural components of mammalian vitreous by endogenous matrix metalloproteinase-2. *Curr Eye Res.* 1996;15:439–45.
65. Monea S, Lehti K, Keski-Oja J, Mignatti P. Plasmin activates pro-matrix metalloproteinase-2 with a membrane-type 1 matrix metalloproteinase-dependent mechanism. *J Cell Physiol.* 2002;192:160–70.
66. Takano A, Hirata A, Inomata Y, et al. Intravitreal plasmin injection activates endogenous matrix metalloproteinase-2 in rabbit and human vitreous. *Am J Ophthalmol.* 2005;140:654–60.
67. Gandorfer A, Kampik A. Intravitreal plasmin injection activates endogenous matrix metalloproteinase-2 in rabbit and human vitreous. *Am J Ophthalmol.* 2006;141:784–5.
68. Jin M, Kashiwagi K, Lizuka Y, et al. Matrix metalloproteinases in human diabetic and nondiabetic vitreous. *Retina.* 2001;21:28–33.
69. Mennel S, Meyer CH, Schmidt JC. The role of vitreous in the pathogenesis of age-related macular degeneration. *Klin Monbl Augenheilkd.* 2011;228:460–4.
70. Krebs I, Brannath W, Glittenberg C, Zeiler F, Sebag J, Binder S. Posterior vitreomacular adhesion: a potential risk factor for exudative age-related macular degeneration? *Am J Ophthalmol.* 2007;144:741–6.
71. Robison CD, Krebs I, Binder S, Barbazetto IA, Kotsolis AI, Yannuzzi LA, Sadun AA, Sebag J. Vitreomacular adhesion in active and end-stage age-related macular degeneration. *Am J Ophthalmol.* 2009;148:79–82.
72. Lee SJ, Lee CS, Koh HJ. Posterior vitreomacular adhesion and risk of exudative age-related macular degeneration: paired eye study. *Am J Ophthalmol.* 2009;147:621–6.
73. Simpson AR, Petrarca R, Jackson TL. Vitreomacular adhesion and neovascular age-related macular degeneration. *Surv Ophthalmol.* 2012;57:498–509.
74. Mojana F, Cheng L, Bartsch DU, Silva GA, et al. The role of abnormal vitreomacular adhesion in age-related macular degeneration: spectral optical coherence tomography and surgical results. *Am J Ophthalmol.* 2008;146(2):218–27.
75. Lee SJ, Koh HJ. Effects of vitreomacular adhesion on anti-vascular endothelial growth factor treatment for exudative age-related macular degeneration. *Ophthalmology.* 2011;118:101–10.

Peter Kroll and Lutz Hesse

Outline

- I. **Introduction**
- II. **Properties of Tissue Plasmin Activator**
 - A. Biochemical
 - B. Methods of Generating Intravitreal tPA
 - C. Clearance of tPA
 - D. Toxicity of tPA
- III. **Ophthalmic Indications and Applications of tPA**
 - A. Submacular Hematoma
 - B. Induction of Posterior Vitreous Detachment (PVD)
 - C. Proliferative Diabetic Vitreoretinopathy
 - D. Retinal Vein Occlusions
 - E. Age-Related Macular Degeneration (AMD)
 - F. Miscellaneous Conditions

References

Keywords

Vitreous • Pharmacologic vitreolysis • Tissue plasminogen activator (tPA) • Subretinal hemorrhage • Vitreous liquefaction • Posterior vitreous detachment

Key Concepts

1. In the presence of fibrin, tissue plasminogen activator transforms the circulating inactive proenzyme plasminogen into the active protease plasmin.
2. Tissue plasminogen activator was the first enzyme clinically used in ophthalmology for diseases of the posterior segment, available for clinical use through recombinant DNA technology.
3. Tissue plasminogen activator is able to induce posterior vitreous detachment, which provides benefits in the course of many other diseases of the posterior segment.

P. Kroll, MD (✉)
Department of Ophthalmology, Philipps-University,
Marburg, Germany
e-mail: phkkroll@yahoo.de

L. Hesse, MD
Augenlinik der SLK-Kliniken,
Am Gesundbrunnen 20-26, Heilbronn 74076, Germany
e-mail: lutz.hesse@slk-kliniken.de

I. Introduction

In the late 1980s and early 1990s, it was assumed that vitrectomy is a perfect tool to handle most vitreoretinal diseases even in cases of vitreo-macular traction. However, vitrectomy surgery includes risks like retinal detachment, hemorrhages, cataract formation, and infections. To avoid these problems, there is a need for a pharmacologic approach called pharmacologic vitreolysis. The use of enzymes in ophthalmology has a long history, as some of these enzymes, like hyaluronidase [1] and collagenase [2], were investigated long before vitrectomy was introduced. Further investigations for liquefaction and posterior vitreous detachment were undertaken in the early 1990s with different types of enzymes.

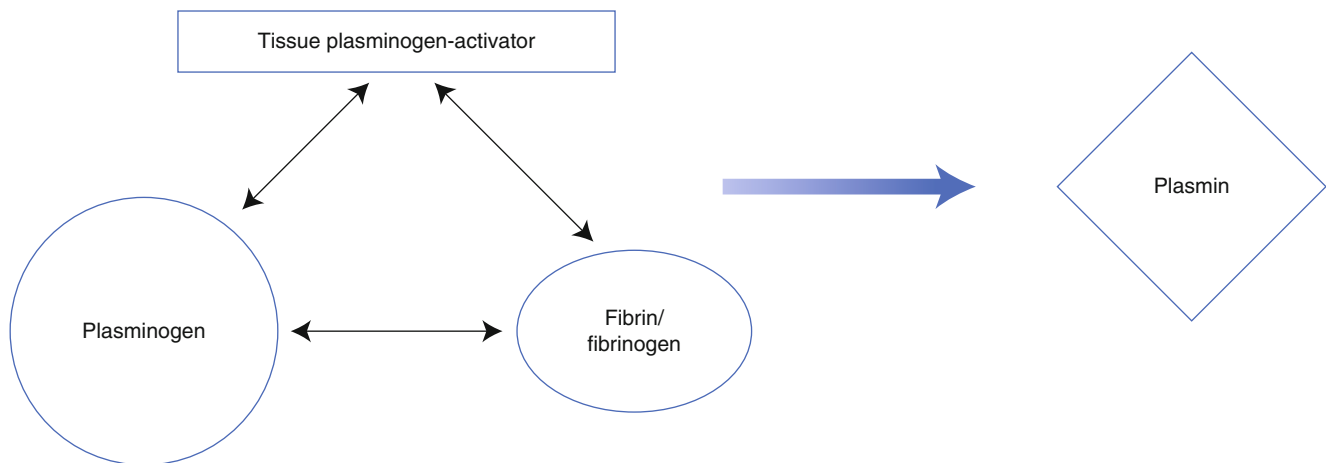


Figure VI.C-1 The fibrinolytic cascade. Protease plasmin is catalyzed in the presence of tissue plasminogen activator (*tPA*) and fibrin, forming a ternary complex. The presence of fibrin increases the enzymatic activity of *tPA* and thereby the proteolytic activity of plasmin

Streptokinase [3], hyaluronidase [4, 5], nattokinase [6], and chondroitinase [4, 7–9] were investigated but had significant side effects or insufficient clinical efficacy.

Verstraeten and colleagues first demonstrated in 1993 [10] that a posterior vitreous detachment in rabbit eyes could be achieved after intravitreal injection of plasmin. In 1999, Hikichi and coworkers [11] confirmed the finding of a complete PVD after injecting 1U plasmin and 0.5 cc SF6 gas into the vitreous of rabbits. However, for clinical use, plasmin must be prepared from autologous blood, a tricky and expensive laboratory technique.

In 1995 at the Vail Vitrectomy Meeting, Wilson Heriot [12] from Australia surprised all in attendance with a case series of four patients with submacular hemorrhages, which he treated successfully with an intravitreal injection of tissue plasmin activator (*tPA*) to liquefy the submacular blood clot and co-injection of SF6 gas to displace the hemorrhage out of the macular area through prone positioning of the patient. His exceptional results based on a minimally invasive procedure were confirmed by Hesse in 1997 [13]. This subject is extensively discussed in chapter V.A.1. AMD surgery.

increased three-fold. Plasmin is insufficiently produced in the presence of fibrinogen, which is the soluble precursor of fibrin. Plasmin itself is a trypsin-like serine protease, which activates the degradation of fibrin but also of fibronectin, laminin, and other peptides [14, 15]. Although plasmin is known as a key enzyme in blood clot lysis, it displays a broad-spectrum activity. It degrades extracellular matrix as well as fibrin and activates other proteinases such as pro-metalloproteinases (MMP-1, MMP-3, and MMP-9). Plasmin can also activate or release growth factors from the extracellular matrix including latent transforming growth factor (TGF- β), basic fibroblast growth factor (bFGF), and VEGF. This function supports cell movement, proliferation, inflammation, and invasive growth of cancer cells. Today *tPA* is available for clinical use through recombinant technology. It is also known by the names alteplase, reteplase, and tenecteplase, substances with FDA approval for the treatment of myocardial infarction, acute ischemic stroke, acute massive pulmonary embolism, and central venous access device occlusion. Desmoteplase, an additional recombinant *tPA*, is still under clinical investigation. All these activators have in common that their enzymatic activity increases up to the 100-fold in the presence of fibrin [16].

II. Properties of Tissue Plasmin Activator

A. Biochemical

The main component of the fibrinolytic cascade is plasminogen, which circulates as an inactive proenzyme in the human blood (200 mg/L). Plasminogen activator, which is generated either in the human blood (intrinsic) or in the tissue (extrinsic), mediates the circulating proenzyme plasminogen into the fibrinolytic effective protease plasmin (Figure VI.C-1). *tPA* is fibrin specific that means *tPA* has a high affinity to fibrin. *tPA*, plasminogen, and fibrin form a ternary complex; thereby the catalytic efficiency of plasmin activation is

B. Methods of Generating Intravitreal *tPA*

An intravitreal injection of *tPA* is the most simple and effective technique to achieve high intraocular concentrations of the enzyme. Today ophthalmologists are experienced in this technique, but three decades earlier, most ophthalmic surgeons mistrusted intravitreal injections. Thus, *tPA* was given via intravenous route [17], transretinal route via placement onto the retinal surface during vitrectomy [18, 19], or via transscleral route by introduction into the choroid [20]. However, these alternative techniques resulted in incomplete

liquefaction of subretinal hemorrhage due to ineffective tissue levels of tPA (intravenous administration) or limited time and thereby incomplete clot lysis during vitrectomy [21].

Peyman generated tPA by injecting plasminogen and urokinase separately and allowing their interaction to create tPA. Studies [22] showed that this was nontoxic to the retina at plasminogen concentrations of 2.0 CU or less and could induce PVD in rabbits. Subsequent studies [23] showed that recombinant lysine-plasminogen and recombinant urokinase with the addition of an intravitreal injection of sulfur hexafluoride gas induced a PVD in 75 % of rabbits tested. To our knowledge, no human studies were ever undertaken.

C. Clearance of tPA

After intravitreal injection, the clearance of tPA depends on three factors: the presence of (1) fibrin, (2) vitreous, and (3) plasminogen activator inhibitors. Following intravitreal injection, the peak concentration of tPA in vitreous will be achieved after approximately 6 h [24]. Therefore, it is recommended that in cases of submacular hemorrhage tPA should be injected intravitreally as a first step and between 12 and 24 h later the gas to displace the liquefied blood clot should be introduced in a second step. A simultaneous injection of tPA and gas is possible and widely used, but prone position should be avoided in the first hours because the surface of the gas bubble may cover the subretinal hemorrhage, thereby preventing tPA from crossing the retina and entering the clot.

D. Toxicity of tPA

Toxic side effects after intravitreal tPA are well known. The cause of retinal damage is not the tPA protein itself but L-arginine, an added stabilizer of the formulation [18]. Pure tPA (50 µg intravitreal or 20 µg subretinal) has no toxic effect on the retina [13, 18]. One reported patient [13] received a high dose of 100 µg and developed a serous retinal detachment in the lower part of the eye, which recovered after one and a half months, leaving an irregular pigmentation in the area of the previously detached retina. The visual field recovered and the visual acuity was not affected, albeit limited by underlying AMD. Further reports confirmed that a safe intravitreal dose was 40–50 µg, with toxic side effects to the retina occurring with doses of 50 µg and more [25].

III. Ophthalmic Indications and Applications of tPA

In 1988 Williams et al. [26] were the first to report on three patients with intraocular fibrin formation after pars plana vitrectomy and their successful treatment with tPA,

injected into the anterior chamber of the eye. Thereafter, tPA was mentioned as a standard treatment for anterior segment disorders like fibrin or fibrin membrane formation after cataract surgery [27], fibrin or blood-induced ocular hypertension after glaucoma surgery or keratoplasty [28, 29], and fibrin-induced blockage of a basal iridectomy after silicone oil surgery [30]. For the posterior segment inflammatory conditions after vitrectomy with fibrin formation or even with an endophthalmitis [31], tPA is a further option for treatment. With more knowledge about tPA in ophthalmology, these therapeutic options became standard, without being further mentioned in the ophthalmic literature. However, experimental studies to resolve vitreous hemorrhage with tPA failed [32], because of its less convincing therapeutic effect.

A. Submacular Hematoma

See chapter V.A.1. AMD surgery.

B. Induction of Posterior Vitreous Detachment (PVD)

A new application for tPA appeared in 1993 with the landmark paper of Verstraeten et al. [10] which demonstrated that as a protease, plasmin is able to split the extracellular matrix proteins fibronectin and laminin at the vitreoretinal interface, which normally glue the vitreous cortex to the retina. The consequence of this enzymatic effect of tPA leads to a dissolution of fibronectin and laminin, resulting in a posterior vitreous detachment (PVD). In 1995, after Heriot's presentation, Hesse et al. [33] published the first study about an enzymatically induced PVD in diabetic patients. With this idea of an easy method to create a pharmacologic PVD without or in combination with a vitrectomy, a new concept for pharmacologic treatment of vitreoretinal diseases without the demanding production of autologous plasmin became inaugurated, named pharmacologic vitreolysis by Sebag in 1998 [34]. Other reports [35, 36] with different indications described the benefit of intravitreal tPA and the induction of posterior vitreous detachment. In rabbits, a PVD was induced by combining cryopexy and intravitreal injection of tPA. The effect is based on plasminogen which enters the vitreous after breakdown of the blood-retinal barrier through cryopexy [37].

Knowing that depending on the amount of attendant fibrin, the half-life of tPA is between 5.8 and 11.8 h and that the generated peak for the active agent plasmin is about 6 h, it is recommended that for a striking effect of pharmacologic vitreolysis, tPA should be injected 24 h before a surgical intervention. This would guarantee a tPA effect, since Le Mer et al. [38] were not convinced by the pharmacologic

effect of tPA during vitrectomy in diabetic patients, injecting the agent only 15 min before the surgical intervention.

C. Proliferative Diabetic Vitreoretinopathy

In 1995, Hesse et al. [33] published the first study about pharmacologic vitreolysis induction of PVD in diabetic patients. The first clinical reports about autologous plasmin appeared later by Williams et al. [39] in the treatment of diabetic retinopathy. In both case series, they observed posterior vitreous detachment, which facilitated the surgical intervention [see chapter VI.D.1. Pharmacologic vitreolysis with plasmin: basic science experiments, VI.D.2. Pharmacologic vitreolysis with plasmin: clinical studies]. The encouraging results of Hesse et al. [33] and Hesse [40] in treating proliferative diabetic vitreoretinopathy (PDVR) with tPA, which facilitates vitrectomy, would justify further studies with tPA, to verify the effectiveness of pharmacologic PVD induction in comparison with other agents, like autologous plasmin, which is not easy to produce, or ocriplasmin which has been recently approved by the EU and FDA [41], but has not been applied yet to PDVR [see chapter VI.E.2. Pharmacologic vitreolysis with ocriplasmin: clinical studies].

With the knowledge that in diabetic patients, the posterior vitreous cortex plays an important role in the development of neovascularization into the vitreous, a PVD seems to be an effective treatment to prevent this pathology [see chapter III.L. Proliferative diabetic vitreo-retinopathy]. A thickened vitreoretinal interface and a thickened posterior vitreous cortex represent a metabolic barrier [see chapter IV.A. Vitreous physiology] that promotes proliferation of new retinal vessels into the attached posterior vitreous cortex that also serves as a scaffold for the proliferating vessels. Therefore, in cases of severe diabetic retinopathy that are not yet proliferative, panretinal photocoagulation is routinely employed throughout the world. However, the beneficial effect of panretinal photocoagulation is not understood, although one theory is that this induces PVD [42]. Thus, combining laser coagulation with an intravitreal injection of tPA might increase the likelihood of PVD. The additional effect of the retinal laser photocoagulation would be the breakdown of the blood-ocular barrier with influx of fibrin into the vitreous, which will promote the efficacy of tPA induction of PVD. With this treatment, effective prophylaxis of this challenging disease could be achieved. This hypothetical treatment should be investigated in the future.

D. Retinal Vein Occlusions

As early as 1989, Peyman [43] experimented with tPA in the treatment of experimental branch retinal vein occlusion in

rabbit eyes. Garcia-Arumi subsequently used tPA as an adjunct to vitrectomy surgery for retinal vein occlusions in humans [see chapter V.A.6. Vitreous surgery of arterial and venous retino-vascular diseases]. The rationale for intravitreal injection of tPA derives from the fact that due to breakdown of the blood-ocular barrier in eyes with retinal vein occlusion, a large amount of plasmin is generated after injection of tPA. This could induce PVD that might be therapeutic with respect to the macular edema. Indeed, resolution of macular edema following tPA injection has been reported in patients with retinal vein occlusions [36, 44, 45] and is believed to be due to the induction of PVD. This supports the theory that the posterior vitreous cortex plays a role in the pathogenesis of macular edema following retinal vein occlusion [see chapter III.K. Vitreous in retino-vascular diseases and diabetic macular edema]. A similar mechanism has been implicated in diabetic macular edema where the condition improved after tPA-induced PVD [46].

E. Age-Related Macular Degeneration (AMD)

In recent years, wet AMD is treated worldwide by intravitreal anti-VEGF injections to stop leakage and further proliferation of vessels into submacular membranes. Vitreoretinal surgeons treating AMD by extracting subretinal membranes or performing macular translocations [see chapter V.A.1. AMD surgery] reported strong adhesion of the posterior vitreous cortex to the retina from the macula to the midperiphery [47]. Perichon et al. [48], Krebs et al. [49], and Lee et al. [50] confirmed these findings and determined that complete PVD was much more common in dry AMD, while persistent vitreo-macular adhesion was more common in wet AMD. These observations suggest that the posterior vitreous cortex has a pathogenic effect in AMD [see chapter III.G. Vitreous in AMD]. Hypothetically one may suppose that a permanent traction of the tight adhesive vitreous cortex in the macular area may lead to a slow destruction of the subjacent pigment epithelium. This mechanical stress to the underlying retinal pigment epithelium may release higher levels of VEGF, inducing angiogenesis from the choroid into the submacular space with membrane formation [51]. A chronic vitreo-macular traction may also lead to a continuous exposure of free radicals and cytokines or both, inducing a low-grade inflammation as cause for an AMD [52]. Just recently, Schulze et al. [53] described that a previous (at least 8 years before) vitrectomy with a complete removal of the posterior vitreous cortex for different indications has a protective effect against wet AMD. These considerations should be taken into account, to induce PVD in patients with an AMD in one eye, either via vitrectomy or even better by pharmacologic vitreolysis. tPA or ocriplasmin

could be the agent of choice, depending on various clinical considerations.

F. Miscellaneous Conditions

Only one paper by Diaz-Llopis et al. [54] of unsuccessful treatment with autologous plasmin in four patients with premacular membranes and macular pucker has been published. The lack of efficacy probably relates to the fact that most cases of macular pucker already have a PVD. Indeed, anomalous PVD with vitreoschisis [see chapter III.B. Anomalous PVD and vitreoschisis] is believed to be pathogenic in this condition [see chapter III.F. Vitreous in the pathobiology of macular pucker].

Peyman tested intravenous tPA in experimental suprachoroidal hemorrhage [17] and subsequently tested subconjunctival hemorrhage to treat this condition in humans, with negative results [55]. This group has also tested intravitreal tPA to treat experimental bacterial endophthalmitis [56] and premacular retrocortical hemorrhage in shaken baby and battered child syndrome [57].

There are no reports in the literature about the use of tPA alone or in combination with vitrectomy in the therapy of vitreo-macular traction, macular hole, PVR, or retinopathy of prematurity, although the last mentioned has indeed been treated with plasmin [see chapter VI.D.2. Pharmacologic vitreolysis with plasmin: clinical studies].

Abbreviations

AMD	Age-related macular degeneration
bFGF	Basic fibroblast growth factor
cc	Cubic centimeters
DNA	Deoxyribonucleic acid
EU	European Union
FDA	US Food and Drug Administration
L	Liter
mg	Milligrams
MMP	Matrix metalloproteinase
PVD	Posterior vitreous detachment
SF6	Sulfur hexafluoride gas
tPA	Tissue plasminogen activator
U	Units
VEGF	Vascular endothelial growth factor

References

- Pirie A. Ox vitreous humor, hyaluronic acid relationships. *Br J Ophthalmol.* 1949;33(5):271–83.
- O'Neil R, Shea M. The effects of bacterial collagenase in rabbit vitreous. *Can J Ophthalmol.* 1973;8(2):366–70.
- Cherfan GM, el Maghraby A, Tabbara KF, Nasr Y, Hassan H. Dissolution of intraocular fibrinous exudate by streptokinase. *Ophthalmology.* 1991;98(6):870–4.
- Bishop PN, McLeod D, Reardon A. Effects of hyaluronan lyase, hyaluronidase, and chondroitin ABC lyase on mammalian vitreous gel. *Invest Ophthalmol Vis Sci.* 1999;40(10):2173–8.
- Gottlieb JL, Antoszyk AN, Hatchell DL, Saloupis P. The safety of intravitreal hyaluronidase. A clinical and histologic study. *Invest Ophthalmol Vis Sci.* 1990;31(11):2345–52.
- Takano A, Hirata A, Ogasawara K, Sagara N, Inomata Y, Kawaji T, Tanihara H. Posterior vitreous detachment induced by nattokinase (subtilisin NAT); a novel enzyme for pharmacologic vitreolysis. *Invest Ophthalmol Vis Sci.* 2006;47(5):2075–9.
- Hageman GS, Russel SR. Chondroitinase-mediated disinsertion of primate vitreous body. *Invest Ophthalmol Vis Sci.* 1994;35(4):1260.
- Hermel M, Schrage NF. Efficacy of plasmin enzymes and chondroitinase ABC in creating posterior vitreous separation in the pig: a masked, placebo-controlled in vivo study. *Graefes Arch Clin Exp Ophthalmol.* 2007;245(3):399–406.
- Staubach F, Nöber V, Janknecht P. Enzyme-assisted vitrectomy in enucleated pig eyes: a comparison of hyaluronidase, chondroitinase, and plasmin. *Curr Eye Res.* 2004;29(4–5):261–8.
- Verstraeten TC, Chapman C, Hartzler M, Winkler BS, Trese MT, Williams GA. Pharmacological induction of posterior vitreous detachment in the rabbit. *Arch Ophthalmol.* 1993;111(6):849–54.
- Hikichi T, Nomiyama G, Ikeda H, Yoshida A. Posterior vitreous detachment induced by injection of plasmin and sulfur hexafluoride in the rabbit vitreous. *Retina.* 1999;19(1):55–8.
- Heriot WJ. Intravitreal gas and TPA: an outpatient procedure for submacular hemorrhage. 1996, Vail Vitrectomy Meeting, 10–15 March, Vail.
- Hesse L, Schmidt J, Kroll P. Management of acute submacular hemorrhage using recombinant tissue plasmin activator and gas. *Graefes Arch Clin Exp Ophthalmol.* 1999;237:273–7.
- Donaldson VH. Effect of plasmin in vitro on clotting factors in plasma. *J Lab Clin Med.* 1960;56:644–51.
- Garcia-Arumi J, Martinez-Castillo V, Boixadera A, Blasco H, Corcostegui B. Management of macular edema in branch retinal vein occlusion with sheathotomy and recombinant tissue plasmin activator. *Retina.* 2004;24(4):530–40.
- Hoylaerts M, Rijkem DC, Lijnen HR, Collen D. Kinetics of the activation of plasminogen by human tissue plasmin activator. *J Biol Chem.* 1982;257:2912–9.
- Liu JC, Peyman GA, Oncel M. Treatment of experimental suprachoroidal hemorrhage with intravenous tissue plasminogen activator. *Int Ophthalmol.* 1990;14(4):267–70.
- Johnson MW, Olsen KR, Hernandez E, Irvine WD, Johnson RN. Retinal toxicity of recombinant tissue plasmin activator in the rabbit. *Arch Ophthalmol.* 1990;108:259–63.
- Peyman G, Nelson N, Alturki W, Blinder K, Paris C, Desai U, Harper C. Tissue plasminogen activating factor assisted removal of subretinal hemorrhage. *Ophthalmic Surg.* 1991;22:575–81.
- Lewis H, Resnick SC, Flannery JG, Straatsma BR. Tissue plasminogen activator treatment of experimental subretinal hemorrhage. *Am J Ophthalmol.* 1991;111:197–204.
- Hesse L, Meitingner D, Schmidt J. Little effect of tissue plasminogen activator in subretinal surgery for acute hemorrhage in age-related macular degeneration. *Ger J Ophthalmol.* 1997;5:479–83.
- Unal M, Peyman GA. The efficacy of plasminogen-urokinase combination in inducing posterior vitreous detachment. *Retina.* 2000;20(1):69–75.
- Men G, Peyman GA, Genaidy M, Kuo PC, Ghahramani F, Blake DA, Bezerra Y, Naaman G, Figueiredo E. The role of recombinant lysine-plasminogen and recombinant urokinase and sulfur hexafluoride combination in inducing posterior vitreous detachment. *Retina.* 2004;24(2):199–209.

24. Jaffe GJ, Green GDJ, McKay BS, Hartz A, William GA. Intravitreal clearance of tissue plasmin activator in the rabbit. *Arch Ophthalmol*. 1988;106:969–72.
25. Chen SN, Yang TC, Ho CL, Kuo YH, Yip Y, Chao AN. Retinal toxicity of tissue plasmin activator: case report and literature review. *Ophthalmology*. 2003;110(4):704–8.
26. Williams GA, Lambrou FH, Jaffe GA, Snyder RW, Green GD, Devenyi RG, Abrams GW. Treatment of postvitrectomy fibrin formation with intraocular tissue plasmin activator. *Arch Ophthalmol*. 1988;106(8):1055–8.
27. Schmitz K, Greite HJ, Bartenschläger EM. Tissue plasminogen activator for the treatment of postoperative intraocular fibrinous membranes following Cataract surgery. *German J Ophthalmol*. 1995;4:75–9.
28. Lundy DC, Sidoti P, Winarko T, Minckler D, Heuer DK. Intracameral tissue plasmin activator after glaucoma surgery. Indications, effectiveness, and complications. *Ophthalmology*. 1996;103(2):274–82.
29. Starck T, Hopp L, Held KS, Marouf LM, Yee RW. Low-dose intraocular tissue plasmin activator treatment for traumatic total hyphema, postcataract, and penetrating keratoplasty fibrinous membranes. *J Cataract Refract Surg*. 1995;21(2):219–26.
30. MacCumber MW, McCuen 2nd BW, Toth CA, Ferrone PJ, Jaffe GJ. Tissue plasmin activator for preserving inferior peripheral iridectomy patency in eyes with silicone oil. *Ophthalmology*. 1996;103(2):269–73.
31. Ryan EH, Mizener JB. Tissue plasmin activator and Staphylococcus epidermidis endophthalmitis. *Arch Ophthalmol*. 1993;111(8):1117–22.
32. Johnson RN, Olsen KR, Hernandez E. Intravitreal tissue plasmin activator treatment of experimental vitreous hemorrhage. *Arch Ophthalmol*. 1989;107(6):891–4.
33. Hesse L, Chofflet J, Kroll P. Tissue plasminogen activator as a biochemical adjuvant in vitrectomy for proliferative diabetic vitreoretinopathy. *Ger J Ophthalmol*. 1995;4(6):323–7.
34. Sebag J. Pharmacologic vitreolysis. *Retina*. 1998;18:1–3.
35. Glacet-Bernard A, Kuhn D, Vine AK, Oubranam H, Coscas G, Soubrane G. Treatment of recent onset central retinal vein occlusion with intravitreal tissue plasmin activator: a pilot study. *Br J Ophthalmol*. 2000;84(6):609–13.
36. Murakami T, Takagi H, Kita M, Nishiwaki H, Miyamoto K, Ohashi H, Watanabe D, Yoshimura N. Intravitreal tissue plasmin activator to treat macular edema associated with branch retinal vein occlusion. *Am J Ophthalmol*. 2006;142(2):318–20.
37. Hesse L, Nebeling B, Schroeder B, Heller G, Kroll P. Induction of posterior vitreous detachment in rabbits by intravitreal injection of tissue plasmin activator following cryopexy. *Exp Eye Res*. 2000;70(1):31–9.
38. Le Mer Y, Korobelnik JF, Morel C, Ullern M, Berrod JP. TPA-assisted vitrectomy for proliferative diabetic retinopathy: results of a double masked, multicenter trial. *Retina*. 1999;19(5):378–82.
39. Williams JG, Trese MT, Williams GA, Hartzler MK. Autologous plasmin enzyme in the surgical management of diabetic retinopathy. *Ophthalmology*. 2001;108(10):1902–5.
40. Hesse L. Gewebe-Plasmin Activator. Ein vielfältig einsetzbares Enzym in der Augenheilkunde. *Ophthalmologie*. 1997;94:366–71.
41. Stalmans P, Benz MS, Gandorfer A, Kampik A, Girach A, Pakola S. Enzymatic vitreolysis for vitreomacular traction and macular holes. *N Engl J Med*. 2012;367:606–15.
42. Sebag J, Buzney SM, Belyea DA, et al. Posterior vitreous detachment following panretinal laser photocoagulation. *Graefes Arch Clin Exp Ophthalmol*. 1990;228:5–8.
43. Oncel M, Peyman GA, Khoobei B. Tissue plasminogen activator in the treatment of experimental retinal vein occlusion. *Retina*. 1989;9(1):1–7.
44. Murakami T, Takagi H, Ohashi H, Kita M, Nishiwaki H, Miyamoto K, Watanabe D, Sakamoto A, Yamaike N, Yoshimura N. Role of posterior vitreous detachment induced by intravitreal tissue plasmin activator in macular edema with central retinal vein occlusion. *Retina*. 2007;27(8):1031–7.
45. Tagami M, Kusuhara S, Imai H, Honda S, Tsukahara Y, Negi A. Impact of intravitreal injection of tissue plasmin activator on full-field electroretinogram in patients with macular edema secondary to retinal vein occlusion. *Ophthalmologica*. 2011;226(2):81–6.
46. Abrishami M, Moosavi MN, Shoeibi N, Hosseini SS. Intravitreal tissue plasmin activator to treat refractory diabetic macular edema by induction of posterior vitreous detachment. *Retina*. 2011;31(10):2065–70.
47. Schmidt JC, Mennel S, Hörle S, Meyer CH. High incidence of vitreomacular traction in recurrent choroidal neovascularisation after repeated photodynamic therapy. *Br J Ophthalmol*. 2006;90:1361–2.
48. Perichon JY, Brasseur G, Uzzan J. Etudes échographiques du décollement postérieur du vitré chez l'emmétrope (Ultrasound study of posterior vitreous detachment in emmetropic eyes). *J Fr Ophthalmol*. 1993;16:538–44.
49. Krebs I, Brannath W, Glittenberg C, Zeiler F, Sebag J, Binder S. Posterior macular adhesion: a potential risk factor for exudative age-related macular degeneration? *Am J Ophthalmol*. 2007;144:741–6.
50. Lee SJ, Lee CS, Koh HJ. Posterior vitreomacular adhesion and risk of exudative age-related macular degeneration: Paired eye study. *Am J Ophthalmol*. 2009;147:621–6.
51. Seko Y, Seko Y, Fujikura H, Pang J, Tokoro T, Shimakawa H. Induction of vascular endothelial growth factor after application of mechanical stress to retinal pigment epithelium of the rat in vitro. *Invest Ophthalmol Vis Sci*. 1999;40:3287–91.
52. Schulze S, Hörle S, Mennel S, Kroll P. Vitreomacular traction and exudative age-related macular degeneration. *Acta Ophthalmol*. 2008;86(5):470–81.
53. Schulze S, Neugebauer A, Kroll P. Appearance of age-related macular degeneration in vitrectomized and nonvitrectomized eyes: an intraindividual case study. *Acta Ophthalmol*. 2012;90:244–7.
54. Diaz-Llopis M, Udaondo P, Cervera E, Garcia-Delpech S, Salom D, Quijada A, Romero FJ. Enzymatic vitrectomy by intravitreal autologous plasmin injection as initial treatment for macular epiretinal membranes and vitreomacular traction syndrome. *Arch Soc Esp Ophthalmol*. 2009;84(2):91–100.
55. Liu JC, Peyman GA, Oncel M. Treatment of experimental suprachoroidal hemorrhage with subconjunctival injection of tissue plasminogen activator: a negative report. *Ophthalmic Surg*. 1990;21(9):641–3.
56. Baziuk N, Fang T, Peyman GA, Gremillion Jr CM. Intravitreal recombinant tissue plasminogen activator in the treatment of experimentally induced bacterial endophthalmitis. *Int Ophthalmol*. 1991;15(2):79–86.
57. Conway MD, Peyman GA, Recasens M. Intravitreal tPA and SF6 promote clearing of premacular subhyaloid hemorrhages in shaken and battered baby syndrome. *Ophthalmic Surg Lasers*. 1999;30(6):435–41.

Pharmacologic Vitreolysis with Plasmin: Basic Science Experiments

VI.D.1.

Thierry C. Verstraeten

Outline

- I. **Introduction**
- II. **Plasmin**
 - A. Biochemistry
 - B. Plasmin Procurement
- III. **Experimental Models**
 - A. Animals
 - 1. Rabbit Model
 - a. Efficacy
 - b. Safety
 - 2. Other Experimental Models and Considerations
 - B. *Ex Vivo* Human Experimental Models
- IV. **Future Considerations**

References

Keywords

Vitreous • Vitreoretinal interface • Pharmacologic vitreolysis • Plasmin • Electron microscopy • Electrophysiology

Key Concepts

1. Vitreous and the vitreoretinal interface can be altered experimentally using a nonspecific serine protease derived from blood, called plasmin.
2. Plasmin effaces the retinal surface of all vitreous collagen in experimental models.
3. There are no untoward effects of plasmin pharmacologic vitreolysis as assessed ultrastructurally and by electrophysiology.

I. Introduction

Unmet needs in the treatment of vitreoretinal (VR) disorders provide the impetus to explore new pharmacologic treatments to complement the ever-improving quality and miniaturization of mechanical surgical tools [1, 2]. This is true today as it was 20 years ago when we undertook a novel exploration in biochemical manipulation of the VR interface. Plasmin, a nonspecific serine protease, was first used in 1990 in an experimental animal model to assess its potential to cleave the VR interface [1]. The physiologic adhesion between the inner retina and the posterior vitreous cortex is primarily attributed to glycoproteins, including laminin and fibronectin [see chapter II.E. Vitreoretinal interface and the ILM]. These molecules interact with the internal limiting membrane (ILM) of the retina and the posterior vitreous cortex collagens [3, 4], which over the posterior pole are mostly running parallel to the ILM, whereas perpendicular insertion of vitreous

T.C. Verstraeten, MD
Department of Ophthalmology,
Allegheny General Hospital,
Drexel University College of Medicine,
420 East North Ave, Pittsburgh, PA15212, USA
e-mail: verstraeten3@comcast.net

collagen fibrils is seen at the vitreous base [5]. Laminin is primarily located in the basement membrane and attached to collagen type IV. Fibronectin is seen preferentially around blood vessels, in the basement membrane of most cells, and in the extracellular matrix. In the eye, it is present in the vitreous and in the ILM. These glycoproteins are also present in lens zonules, the lamina cribrosa, and the ciliary body. Variations in the distribution of laminin and fibronectin may underlie variability in the strength of the VR adhesion. Some pathologic conditions, like diabetes, can lead to a buildup of laminin and fibronectin at the VR interface [6, 7].

Clinical observations led to the choice of plasmin as a candidate for pharmacologic vitreolysis of the VR interface. In diabetic patients in particular, the presence of neovascularization with preretinal hemorrhage in the absence of a posterior vitreous detachment (PVD) often leads to localized areas of PVD, unless fibrosis is present with resulting increased VR adhesion. It was therefore hypothesized that a blood-derived molecule may alter the VR interface and contribute to the onset of a PVD. *In vitro* studies in the early 1980s were published in cancer research and demonstrated the degradation of basement membrane components, i.e., laminin and fibronectin, by plasmin [8]. Plasmin was thought to be a candidate worthy of further study [8].

II. Plasmin

A. Biochemistry

Plasmin is a two-chain serine endopeptidase (MW=83 kDa) linked by a disulfide bond. It contains 1 heavy chain with 5 kringles and 1 light chain, which holds its active site. Plasmin is prepared from Glu-plasminogen using urokinase, streptokinase, or tissue plasminogen activator (tPA). Its main role in blood is lysis of fibrin clots. Plasmin has been shown to break down fibronectin and laminin into degradation products that can be chemoattractive to polymorphonuclear leukocytes [9]. These cells can, in turn, release elastase that degrades collagen type IV [10], even though plasmin does not cleave collagen type IV. Plasmin can cleave collagen type V, which is not thought to be present at the VR interface, but there is no experimental evidence to support that claim. Plasmin can also activate progelatinase A, a matrix metalloproteinase-2 (MMP-2) [11] which in turn can cleave collagen type IV. In planning our experiments 20 years ago, we hypothesized that plasmin may indirectly cause the release of various enzymes believed to contribute to the onset of PVD in addition to its direct effect on the breakdown of laminin and fibronectin [1].

B. Plasmin Procurement

Lyophilized human plasmin was obtained (Calbiochem, La Jolla, CA) and stored at -20°C . It was then reconstituted in BSS at room temperature and used immediately at the concentration of 1 U per 0.1 ml for pars plana injection. Autologous plasminogen can be isolated from a patient's plasma by affinity chromatography. One can obtain plasmin by adding streptokinase [12], but this has been found to lead to increased proteolytic activity on fibronectin and laminin *in vitro*. A lower ratio of streptokinase-activated plasminogen (1:10) can generate increasing amounts of free plasmin [13]. The same authors have raised a valid caution when one compares the activity of a particular dose or unit of plasmin, as there exists a level of variability in calibrating the particular molecule in the absence of a uniform standard [13]. They concluded that one should test plasmin activity against a uniform standard based on the 3rd International Reference Preparation (IRP). Finally tPA at a dose of 25 micrograms has been tried in combination with transscleral cryopexy to induce a breakdown of the blood-retinal barrier with presumed release of plasminogen [see chapter VI.C. Pharmacologic vitreolysis with tissue plasminogen activator]. In rabbit eyes, this technique has been shown to produce a PVD [14] as well as in diabetic human eyes [15]. Similar results have been achieved by pairing recombinant lysine-plasminogen with recombinant urokinase [16] or pairing recombinant microplasminogen with tPA [17]. Both techniques can induce PVD in the rabbit.

III. Experimental Models

A. Animals

1. Rabbit Model

a. Efficacy

The experimental model chosen in 1990 was the rabbit because of its availability and low maintenance as well as its known strong VR adhesion without any evidence of spontaneous PVD. Some shortcomings, however, include the presence of a constant ILM thickness as well as the absence of vitreous collagen fibrils inserting onto the lamina densa of the ILM, which makes this a standout difference from the human eye [6]. The rabbit, furthermore, has a particular feature that significantly differs from the human, the presence of a medullary ray with the emergence of blood vessels at 3 and 9 o'clock along the horizontal raphe. Here the nerve fiber layer is myelinated and exhibits extremely strong adhesions to the vitreous with perpendicular insertion of collagen fibrils very similar to that of the human vitreous base [6]. In the original experiments, 1 IU of lyophilized human plasmin

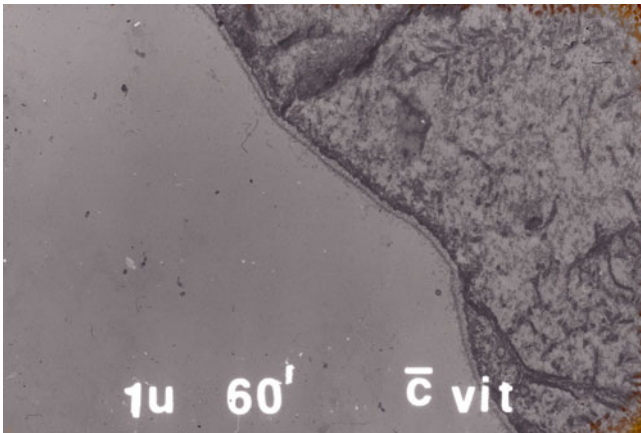


Figure VI.D.1-1 Transmission electron micrograph of the rabbit retina in an eye injected with plasmin followed by vitrectomy at 60 min. Note smooth ILM surface. Original magnification $\times 11,500$

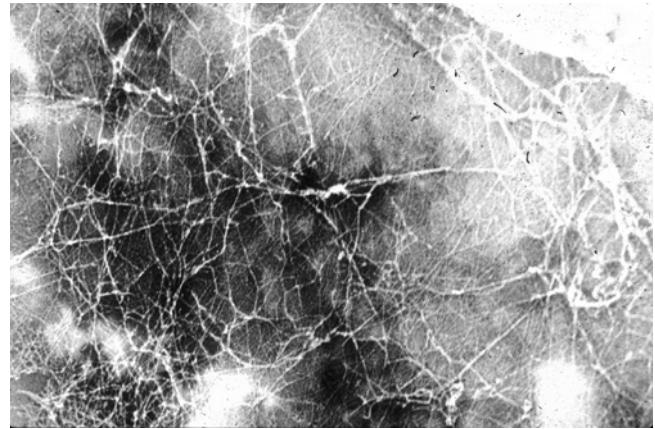


Figure VI.D.1-2 Scanning electron micrograph of the rabbit retina in an eye injected with plasmin without vitrectomy. Note sparse collagen fibrils over ILM. Original magnification $\times 2,500$

(Calbiochem, La Jolla, CA) was injected in live rabbits' eyes and allowed to remain for varying lengths of time before sacrifice or performing vitrectomy. The first and almost immediate effect observed with indirect ophthalmoscopy at the time of plasmin injection was the appearance of a vitreous haze and a "schlieren" effect in the vitreous at the tip of the injecting needle. That observation formed this author's opinion that plasmin exerts an immediate biologic effect that includes a certain degree of liquefaction (synchysis) in addition to its activity on the VR interface. Following vitrectomy, the rabbits were sacrificed and the VR interface was studied histologically. Plasmin was found to have increasing efficacy with longer exposure time in the rabbit vitreous. Increasing the time interval between plasmin injection and performing vitrectomy from 5 to 60 min led to a smoother, cleaner retinal surface, constituting either vitreous separation or degradation of the posterior vitreous cortex. This was observed by light (LM), scanning electron (SEM), and transmission electron (TEM) microscopy, all showing bare ILM by 60 min of exposure. In the absence of vitrectomy, however, the PVD was partial, and it was only in combination with a vitrectomy that a complete PVD was observed on TEM (Figure VI.D.1-1) and SEM (Figure VI.D.1-2). In control eyes injected with balanced salt solution (BSS), vitrectomy alone resulted in a retinal surface still covered with dense collagen fibers (Figure VI.D.1-3).

b. Safety

To assess the health of the retina in these rabbits, dark-adapted electroretinography (ERG) was performed at intervals ranging from 1 h to 7 days after plasmin injection. Different surgical combinations were also tested. Vitrectomy was not found to affect the recorded amplitudes compared to controls. However, when ERGs were measured 1 h after plasmin injection, a transient 50 % decreased b wave ampli-

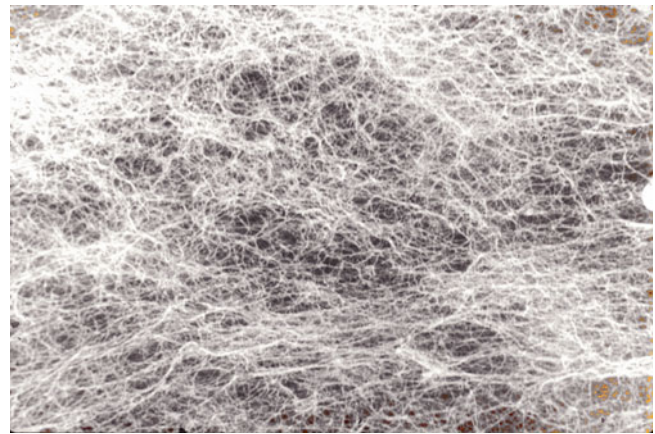


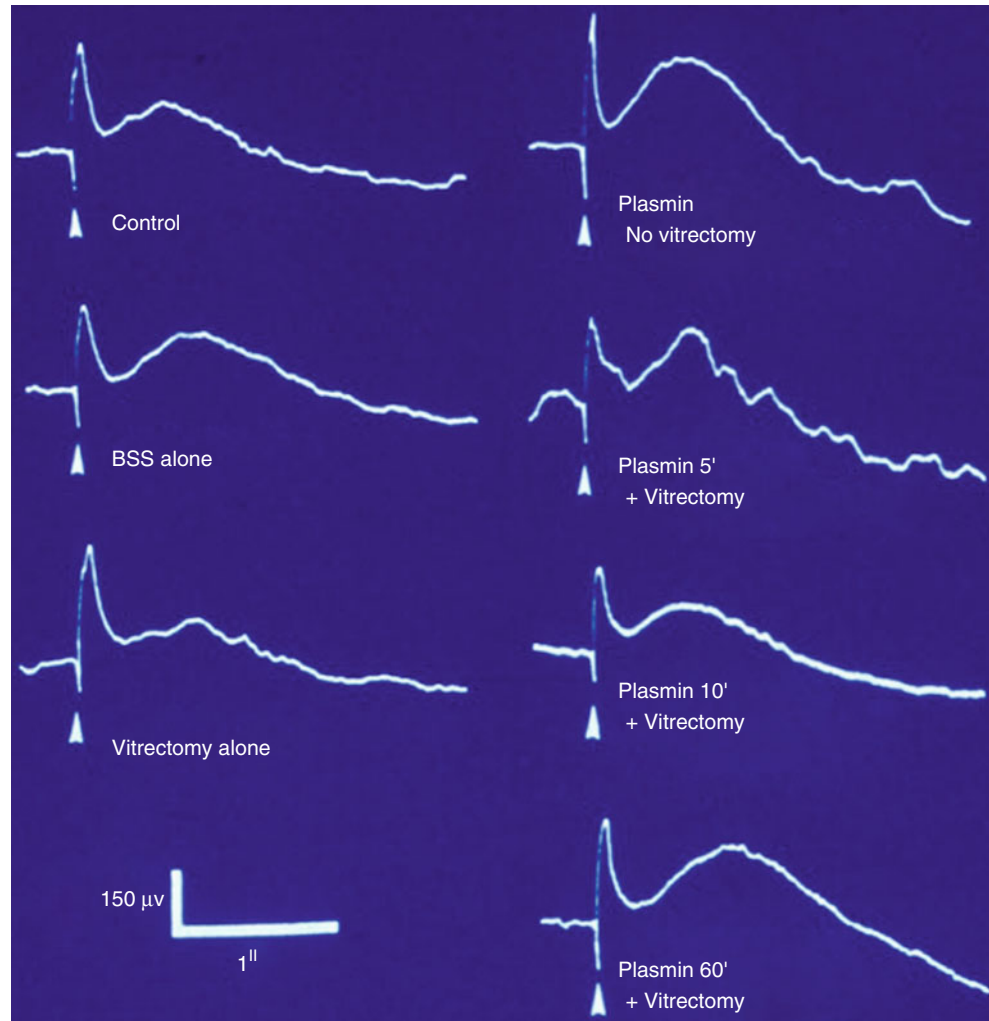
Figure VI.D.1-3 Scanning electron micrograph of the rabbit retina in an eye injected with BSS followed by vitrectomy. Note dense collagen of cortical vitreous. Original magnification $\times 4,200$

tude was measured in 70 % of eyes and found to recover by day 3 (Figure VI.D.1-4). A possible explanation for this finding is the high osmolarity of the plasmin solution. Full recovery of normal ERG amplitude was always noted. Extensive histology studies by LM, TEM, and SEM have consistently shown absence of retinal toxicity not only in our rabbit model [1] but subsequently in the rat, pig [10], and monkey.

2. Other Experimental Models and Considerations

In diabetic rats, it has been shown that it is harder to create a PVD than in normal rats, due most likely to the effects of diabetic vitreopathy [see chapter I.E. Diabetic vitreopathy]. In normal rats, plasmin alone was able to achieve a PVD whereas hyaluronidase was not. Diabetic rats required not only the use of plasmin but also hyaluronidase to achieve a complete PVD [18]. In other models, plasmin autologous to the species injected was used [19–21]. This may alleviate

Figure VI.D.1-4
Electroretinograms taken on day 7 after different combinations of plasmin injection with or without vitrectomy. Note good b wave amplitude



some cross-species specificity concerns and potential lack of activity. In these models, plasmin has been shown to be able to produce a PVD by simply injecting it in the vitreous and not subjecting the eye to a surgical vitrectomy. Indeed, our own model used human plasmin in a rabbit model, and a smooth retinal surface was best achieved when plasmin was followed by a vitrectomy. More recently, in another rabbit model, plasmin was injected in combination with an SF6 gas injection [20, 21]. In these eyes, a total PVD was achieved whereas residual collagen fibrils and incomplete PVD was discovered in eyes injected with plasmin alone. In the pig eye model, porcine plasmin was able to achieve a clean retinal surface with total PVD within one hour of administration [19]. The investigators found a direct correlation between exposure time as well as concentration of plasmin and the degree of VR separation assessed by SEM and TEM. Postmortem human eyes were also used in this model, and a total PVD was observed after 30 min of incubation with plasmin at 37 ° C [22]. Histology revealed a smooth retinal surface in this model [23]. Interestingly, not incubating at this temperature failed to produce a PVD. Indeed a few

experiments of pharmacologic vitreolysis are conducted at body temperature, an important consideration when dealing with enzymes whose activities can differ at different temperatures. This issue was raised in an experiment that found mid-vitreous and retinal temperatures dropped by about 9 ° C during vitrectomy [24]. Furthermore raising the vitreous temperature from 37 to 44 ° C for 1 min in ex vivo porcine eyes greatly facilitated the onset of an atraumatic PVD with no apparent retinal damage [25].

B. Ex Vivo Human Experimental Models

Postmortem human eyes were used to study the degradation of fibronectin and laminin after 60 min of exposure to plasmin [23]. Using an elegant technique with Western blot analysis of anti-laminin and anti-fibronectin antibodies, human ILM samples retrieved at the time of vitrectomy for macular hole or cystoid macular edema were tested. Some of these eyes were treated with pre-vitrectomy administration of plasmin. In these vitreous samples, fibronectin was degraded

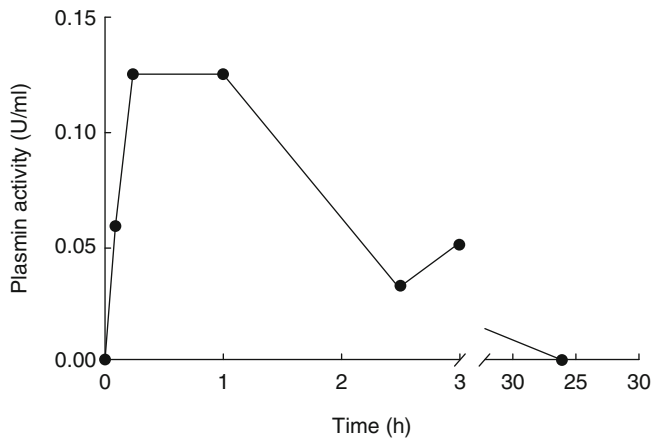


Figure VI.D.1-5 Plasmin activity in the rabbit vitreous over time after a single 1 U injection. Note total loss of activity by 24 h

in fragments of 30,000 Da, and laminin was degraded in fragments of 13,000 Da. This demonstrates the level of activity of plasmin and its capacity to break down fibronectin and laminin. Additionally, the investigators tested plasmin *in vitro* on commercially available laminin and showed no additional degradation beyond 2 h of exposure [23]. Against fibronectin, the activity of plasmin increased and peaked by 1 h of exposure. These results confirmed and validated our initial observations that seemed to indicate peak activity after 1 h of exposure to plasmin in the vitreous (Figure VI.D.1-5). Furthermore, we also found that plasmin displayed a rapid drop of activity beyond 3 h after injection in the rabbit vitreous. An *in vitro* caseinolytic chromogenic assay against D-Val-Leu-Lys-pNA (Sigma-Aldrich) allowed us to test undiluted vitreous samples retrieved at various time intervals following plasmin injection. It demonstrated the complete loss of activity of plasmin by 24 h (Figure VI.D.1-5). Another study looking at human donor eyes, which were injected with plasmin, showed reduced immunoreactivity for laminin and fibronectin at the vitreoretinal interface when studied histologically [26].

IV. Future Considerations

With increased understanding of the basic science factors governing a healthy vitreoretinal interface, we will be able to measure the variations present in different disease states. This will lead to the development of specific agents to target the abnormal molecules. It may turn out that as originally proposed by Sebag in 2002, the best treatment may be offered by a combination of more than one agent or enzyme acting on several key targets [27]. Likely the first step would involve the use of a “liquefying” agent followed by a second agent administered later. This second molecule would be injected right over the posterior pole with the patient in

supine position, thereby avoiding loss of biologic activity caused by it being trapped in an intact vitreous gel some distance from the macula. This should lead to increasing efficacy, lower morbidity, and better adjunct therapy for diseases that still often require surgical treatment today.

Abbreviations

C	Centigrade
ERG	Electroretinogram
ILM	Inner limiting membrane
MW	Molecular weight
PVD	Posterior vitreous detachment
SEM	Scanning electron microscopy
TEM	Transmission electron microscopy
VR	Vitreoretinal

References

- Verstraeten T, Chapman C, Hartzler M, et al. Pharmacologic induction of posterior vitreous detachment in the rabbit. *Arch Ophthalmol*. 1993;111:849–54.
- Sebag J. Pharmacologic vitreolysis (guest editorial). *Retina*. 1998;18:1–3.
- Jerdan J, Kao L, Glaser B. The inner limiting membrane: a modified membrane? *Invest Ophthalmol Vis Sci*. 1986;27(Suppl):230. ARVO abstracts.
- Bishop P. Structural macromolecules and supramolecular organization of the vitreous gel. *Prog Retin Eye Res*. 2000;19:323–44.
- Sebag J, Balazs A. Morphology and ultrastructure of human vitreous fibers. *Invest Ophthalmol Vis Sci*. 1989;30:1867–71.
- Matsumoto B, Blanks J, Ryan S. Topographic variations in the rabbit and primate internal limiting membrane. *Invest Ophthalmol Vis Sci*. 1984;25:71–82.
- Khono T, Sorgente N, Ishibashi T, et al. Immunofluorescent studies of fibronectin and laminin in the human eye. *Invest Ophthalmol Vis Sci*. 1987;28:506–14.
- Liotta L, Goldfarb R, Brundage R, et al. Effect of plasminogen activator (urokinase), plasmin, and thrombin on glycoprotein and collagenous components of basement membrane. *Cancer Res*. 1981;41:4629–36.
- Wachtfogel Y, Abrams W, Kucich U, et al. Fibronectin degradation products containing the cytoadhesive tetrapeptide stimulate human polymorphonuclear leucocyte granules. *J Clin Invest*. 1988;81:1310–6.
- Mainardi C, Dixit S, Kang A. Degradation of (type IV) basement membrane collagen by a proteinase isolated from human polymorphonuclear leucocyte granules. *J Biol Chem*. 1980;255:5435–41.
- Takano A, Hirata A, Inomata Y, et al. Intravitreal plasmin injection activates endogenous matrix metalloproteinase-2 in rabbit and human vitreous. *Am J Ophthalmol*. 2005;140(4):654–6.
- Rizzo S, Pellegrini G, Benocci F, et al. Autologous plasmin for pharmacologic vitreolysis prepared 1 hour before surgery. *Retina*. 2006;26(7):792–6.
- Hermel M, Dailey W, Hartzler M. Efficacy of plasmin, microplasmin, and streptokinase-plasmin complex for the *In Vitro* degradation of fibronectin and laminin - implications for vitreoretinal surgery. *Curr Eye Res*. 2010;35(5):419–24.

14. Hesse L, Nebeling B, Schroeder B, et al. Induction of posterior vitreous detachment in rabbits by intravitreal injection of tissue plasminogen activator following cryopexy. *Exp Eye Res.* 2000;70(1):31–9.
15. Le Mer Y, Korobelnik JF, Morel C, et al. TPA-assisted vitrectomy for proliferative diabetic retinopathy: results of a double-masked, multicenter trial. *Retina.* 1999;19(5):378–82.
16. Men G, Peyman G, Genaidy M, et al. The role of recombinant lysine-plasminogen and recombinant urokinase and sulfur hexafluoride combination in inducing posterior vitreous detachment. *Retina.* 2004;24:199–209.
17. Chen W, Huang X, Ma XW, et al. Enzymatic vitreolysis with recombinant microplasminogen and tissue plasminogen activator. *Eye.* 2008;22:300–7.
18. Wang ZL, Shi WD, Luo M, et al. Pharmacologic vitreolysis with plasmin and hyaluronidase in diabetic rats. *Retina.* 2009;29(2):269–74.
19. Gandorfer A, Putz E, Welge-Lussen U, et al. Ultrastructure of the vitreoretinal interface following plasmin assisted vitrectomy. *Br J Ophthalmol.* 2001;85:6–10.
20. Hikichi T, Yanagiya N, Kado M, et al. Posterior vitreous detachment induced by injection of plasmin and sulfur hexafluoride in the rabbit vitreous. *Retina.* 1999;19:55–8.
21. Wu WC, Liu CH, Chen CC, et al. Efficient vitreolysis by combining plasmin and sulfur hexafluoride injection in a preclinical study in rabbit eyes. *Mol Vis.* 2012;18:2361–70.
22. Gandorfer A, Ulbig M, Kampik A. Plasmin-assisted vitrectomy eliminates cortical vitreous remnants. *Eye.* 2002;16:95–7.
23. Uemura A, Nakamura M, Kachi S, et al. Effect of plasmin on laminin and fibronectin during plasmin-assisted vitrectomy. *Arch Ophthalmol.* 2005;123:209–13.
24. Landers M, Watson J, Ulrich J, et al. Determination of retinal and vitreous temperature in vitrectomy. *Retina.* 2012;32(1):172–6.
25. Chen K, Weiland J. Relationship between vitreous temperature and posterior vitreous detachment. *J Mech Behav Biomed Mater.* 2013;26:54–8.
26. Li X, Shi X, Fan J. Posterior vitreous detachment with plasmin in the isolated human eye. *Graefes Arch Clin Exp Ophthalmol.* 2002;240:56–62.
27. Sebag J. Is pharmacologic vitreolysis brewing? (guest editorial). *Retina.* 2002;22:1–3.

Hiroko Terasaki and Tetsu Asami

Outline

- I. **Introduction**
- II. **Plasmin Procurement**
 - A. Activation of Plasminogen into Plasmin Enzyme
 - B. Preparation of Autologous Plasmin Enzyme
 - 1. Standard Purification System
 - 2. Rapid Purification System
- III. **Clinical Application of Autologous Plasmin Enzyme**
 - A. Macular Hole
 - B. Diabetic Macular Edema
 - C. Retinopathy of Prematurity
 - D. Retinal Vein Occlusion (RVO)

Conclusions

References

Keywords

Vitreous • Vitreoretinal interface • Pharmacologic vitreolysis • Plasmin enzyme • Macular hole • Diabetic macular edema • Retinopathy of prematurity • Retinal vein occlusion • Laminin • Fibronectin

Key Concepts

1. Plasmin can induce posterior vitreous detachment by hydrolyzing molecules, such as fibronectin and laminin, which link between vitreous and retina.
2. Western blot analysis demonstrated that autologous plasmin enzyme (APE) degraded laminin and fibronectin in the inner limiting membrane (ILM), indicating that APE had hydrolyzed the two proteins.
3. An electron microscopy study revealed that APE cleaved the vitreous cortex from the surface of ILM in eyes with diabetic macular edema.

I. Introduction

Various retinal disorders, e.g., vitreo-macular traction syndrome, macular hole, macular pucker, and diabetic macular edema, have been attributed to changes at the vitreoretinal interface that result from traction caused by an anomalous posterior vitreous detachment [1, 2]. The purpose of vitreous surgery is to break the links between the vitreous and the retina at the macula to relieve vitreous traction and restore normal foveal configuration.

Pharmacologic vitreolysis is a nonsurgical method to break down vitreous macromolecules into smaller particles and induce vitreoretinal dehiscence so as to facilitate PVD [3]. Several enzymes have been used for this, including

H. Terasaki, MD, PhD (✉) • T. Asami, MD, PhD
Department of Ophthalmology, Nagoya University School of
Medicine, 65 Tsuruma-cho, Showa-ku, Nagoya 466-8550, Japan
e-mail: terasaki@med.nagoya-u.ac.jp

Table VI.D.2-1 Pharmacologic vitreolysis classification based on biological activity (d'après Sebag [4])

Liquefactants		Interfactants	
Nonspecific	Substrate specific	Nonspecific	Substrate specific
tPA, plasmin	Chondroitinase	tPA, plasmin	Dispase, chondroitinase
Vitreosolve	Hyaluronidase	Microplasmin	RGD-peptides
Microplasmin		Nattokinase	
Nattokinase		Vitreosolve	

plasmin, tissue plasminogen activator, hyaluronidase, chondroitinase, collagenase, dispase, and nattokinase. Recently, Sebag [4] proposed a new classification of pharmacologic vitreolysis agents based on their different biological effects: liquefactants are agents that induce liquefaction of the vitreous, and interfactants induce cleavage at the vitreoretinal interface. The different pharmacologic compounds and their properties are shown in Table VI.D.2-1. Among these agents, a most promising enzyme for inducing a PVD is plasmin, which is both a liquefactant and an interfactant. Plasmin is a serine protease that hydrolyses glycoproteins such as laminin, fibronectin, and fibrin. By liquefying the gel vitreous and cleaving the links at the vitreoretinal interface enzymatically, PVD induction should be easier and safer. In 1993, Verstraeten et al. [5] reported that an intravitreal injection of plasmin in rabbits facilitated the detachment of the vitreous from the retina during vitrectomy. Since then, there have been many reports on the effects of plasmin on the vitreoretinal interface in animal models [6–10] and human cadaver eyes [11, 12]. In addition, there have been clinical studies on the use of APE in humans [13–26]. In this chapter, we shall discuss our studies on the effects of APE at the vitreoretinal interface and clinical applications of APE.

II. Plasmin Procurement

A. Activation of Plasminogen into Plasmin Enzyme

Plasminogen is a serine protease with a molecular weight of about 88,000 Da. It is a single-strand glycoprotein consisting of 5 kringle domains and active sites. Plasminogen is cleaved at the Arg 560-Val 561 peptide bond by tPA or urokinase to become a double-strand plasmin. Plasminogen is also activated by a 1:1 complex with streptokinase, a streptokinase-plasminogen complex. This complex is then converted to a streptokinase-plasmin complex which also activates plasminogen into free plasmin. [27]

B. Preparation of Autologous Plasmin Enzyme

1. Standard Purification System

The original procedure of purifying APE was introduced by Margherio et al. [13] Thirty-five milliliters of blood is drawn from the patient's antecubital vein 3 days before surgery. Autologous plasminogen is extracted from the plasma and purified by affinity chromatography on a lysine-sepharose column. The plasminogen is eluted from the column with 15 mmol/L ϵ -aminocaproic acid. The aminocaproic acid is removed by overnight dialysis. The plasminogen is concentrated to a volume of 0.5 mL, converted to plasmin by the addition of 50,000 IU of streptokinase, and then sterilized by passing the solution through a 0.22 μ m filter. Plasmin activity is determined spectrophotometrically by measuring the change in absorbance at 405 nm after cleavage of the D-Val-Leu-Lys-*p*-nitroaniline substrate. The plasmin is stored at 4 °C until used. An aliquot is sent for sterility testing, and the culture is examined for 48 h.

2. Rapid Purification System

The standard purification procedure usually requires about 7 h and is expensive. Several attempts have been made to reduce the time and procedures for purification. Rizzo et al. [28] modified the standard method by collecting 7 ml of autologous whole blood 1 h before surgery. The blood is centrifuged, and 1.5 mL of the plasma is added to 750,000 IU of streptokinase that had been incubated for 15 min at 37 °C. The mixture is gently agitated for 3–5 min. Then, the solution is incubated for 10 min at 37 °C, and 0.2 mL of the plasmin can be used for intravitreal injections. Udaondo et al. [29] modified the Rizzo method to try to reduce the toxicity derived from the streptokinase. A 750,000 IU vial of streptokinase is added to 12 mL of the patient's serum and incubated at 37 °C for 15 min. Then, 7 mL of the venous blood is centrifuged, and 4 mL of the separated plasma is mixed with 1 mL of diluted streptokinase (62,500 IU) and agitated slowly for several minutes and incubated again for 10 min at 37 °C. After an injection of this preparation, Díaz-Llopis et al. [30] found some inflammation in the eyes injected with the plasmin activated by streptokinase, and they attributed this to the streptokinase. Thus, urokinase was used to activate plasminogen, and they found urokinase-activated plasmin had the same clinical efficacy as the streptokinase-activated plasmin and no intraocular adverse inflammation developed.

Hermel et al. [31, 32] developed a disposable rapid purification kit (NuVue, Keene, NH, USA, US Patent No. 6,183,692; 6,207,066) to minimize the time for the purification process. Human plasmin was obtained by affinity chromatography using this kit and activated by adding 6,250 U of streptokinase for 10 min at 20 °C. The preparation time with this kit was about 30 min.

All of these experiments used different doses of streptokinase or urokinase. Hermel et al. [31] determined that as the dose

of streptokinase used for plasminogen activation is increased, the proteolysis rate decreases. This inverse dose-dependent relationship might be due to the decreasing content of free plasmin with increasing amounts of streptokinase. Therefore, careful interpretation of the results of earlier studies is necessary.

III. Clinical Application of Autologous Plasmin Enzyme

A. Macular Hole

Since Kelly and Wendel [33] first reported their successful results in surgically closing idiopathic macular holes in 1991, the main purpose of vitreous surgery has been to break the vitreoretinal attachment at the fovea and remove vitreous cortex including ILM. Because laminin and fibronectin are involved in the attachment of vitreous to ILM [see chapter II.E. Vitreoretinal interface and ILM], it was assumed that APE might have the ability to close macular holes with its cleaving effect on the vitreoretinal interface. At Nagoya University in Japan, ILMs were removed from the eyes with MH and eyes with cystoid macular edema associated with RVO that underwent APE-assisted vitrectomy, and Western

blot analysis was performed with anti-laminin or anti-fibronectin antibodies on the ILM specimens. The results showed that laminin and fibronectin in the ILM were degraded to several fragments of lower MW, indicating that APE had hydrolyzed two proteins (Figure VI.D.2-1). In addition, *in vitro* experiments were conducted to determine if commercially available human plasmin could degrade human laminin and fibronectin. The results showed that the laminin and fibronectin were degraded to several fragments of lower MW that were the same results as that obtained in the *in vivo* experiments using APE, leading to the conclusion that APE degraded laminin and fibronectin in the ILMs clinically [26] (Figures VI.D.2-2 and VI.D.2-3).

Margherio et al. [13] and Chow et al. [14] described their experiences with the use of APE as an adjuvant to vitrectomy in cases of traumatic pediatric MHs. These cases are generally considered difficult because of strong adherence of posterior vitreous cortex to the ILM as is the case in children [34]. They reported that the induction of PVD became easier with APE. In addition, Wu et al. [15] summarized their experience in treating traumatic pediatric MHs. APE-assisted vitrectomy was performed in 13 cases, in which the MHs in 12 cases were successfully closed with PVD induction, membrane peeling, and gas or silicone oil tamponade. After the

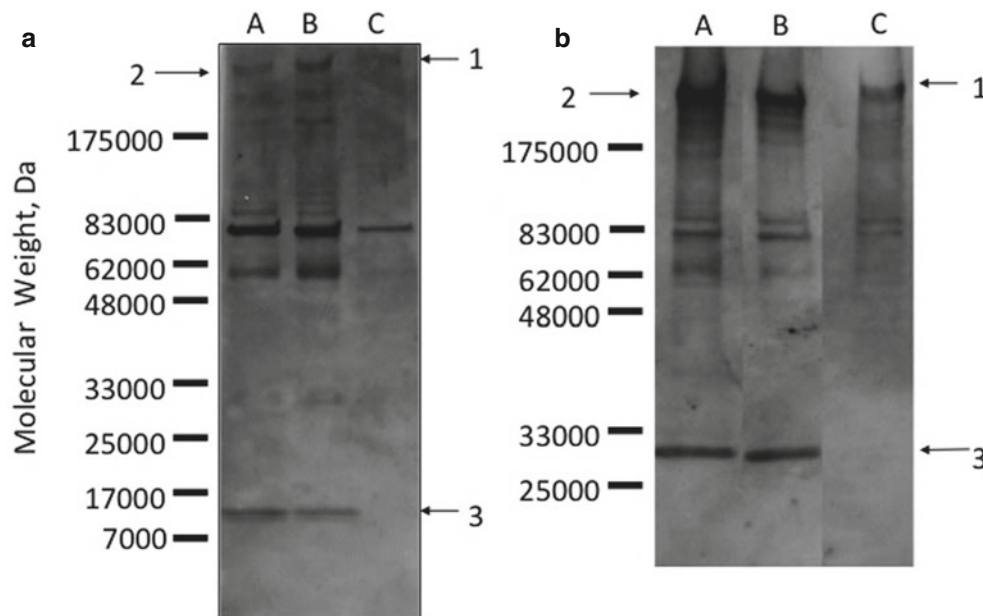


Figure VI.D.2-1 Western blot analysis of ILM specimens from patients with macular holes. ILM was collected during vitrectomy and processed for immunoblotting using anti-laminin antibody (a) and anti-fibronectin antibody (b). Lanes A and B, ILMs collected during APE-assisted vitrectomy. Lane C, ILM collected during conventional vitrectomy without plasmin (a). A large MW fragment can be seen in lane C (arrow 1). The MW of the band was approximately 400,000 Da which corresponds to α -chain of laminin. In the APE-treated ILMs, a band with slightly lower MW is detected in lanes A and B (arrow 2),

and several new bands with lower MWs can be seen including a fragment of 13,000 Da in lanes A and B (arrow 3). (b) A 400,000 to 450,000 Da band was identified in the control ILM (without plasmin) (lane C, arrow 1). This band corresponds to the MW of fibronectin dimer. In the APE-treated ILMs, a new band with a MW of 30,000 Da can be seen in lanes A and B (arrow 3). The 400,000–450,000 Da band appeared to have been degraded to lower MW components (lanes A, B, arrows 2 and 3)

Figure VI.D.2-2 Sodium dodecyl sulfate polyacrylamide gel electrophoresis of plasmin-digested laminin stained with Coomassie blue. Lanes A through E, results of incubating human laminin with human plasmin for 0, 15, 30, 60, and 120 min. Lane F, results with plasmin alone. At 0 min, several bands possibly derived from laminin are seen (lane A, *arrowheads*). At 15 min, 4 new bands were found (*arrows*), while the other bands are still present. One of the new bands has a MW of about 13,000 Da (lane B, *arrow 1*). There was little change in the patterns between 15 and 120 min (lanes B–E)

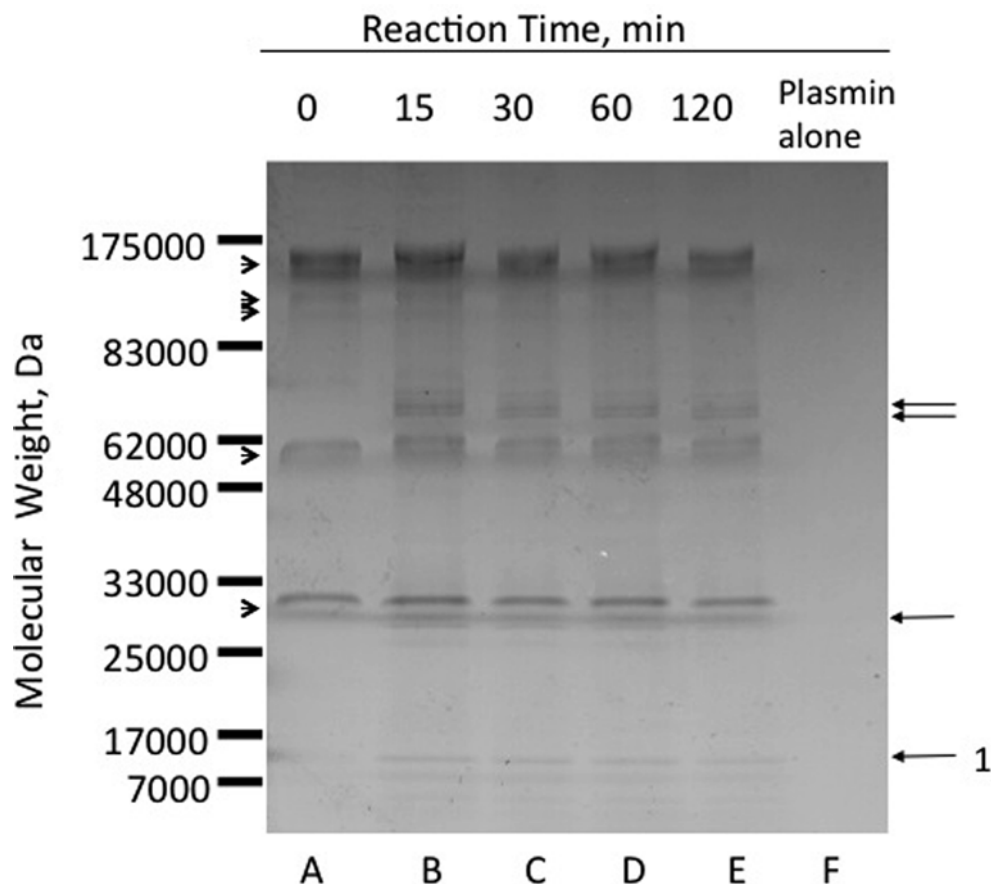
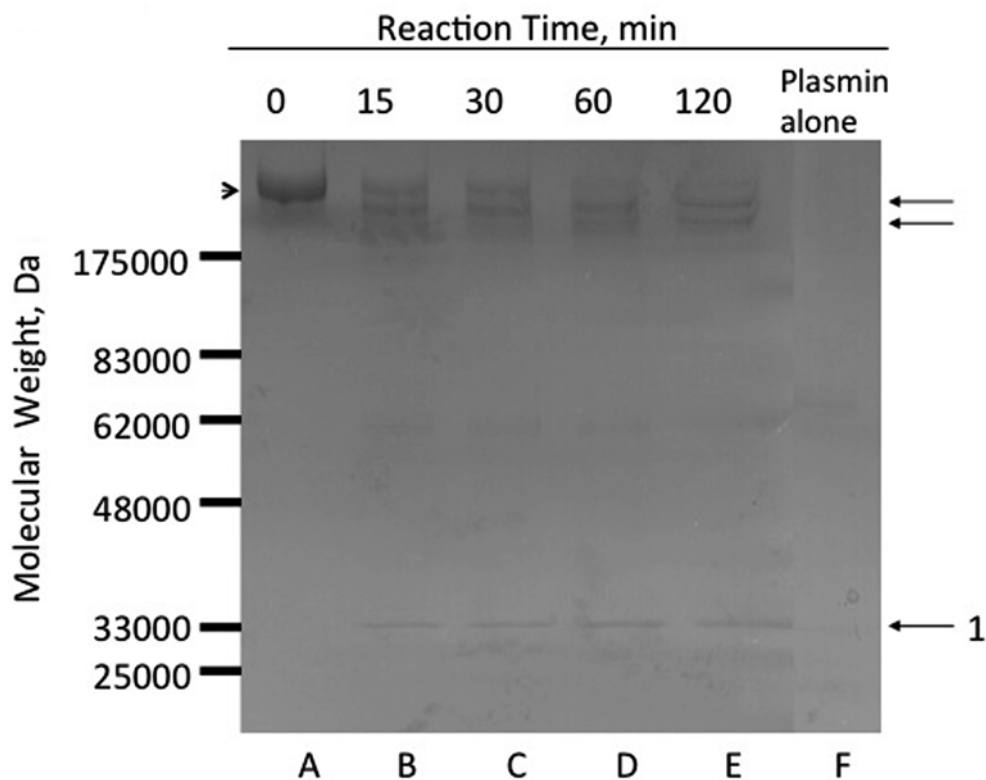


Figure VI.D.2-3 Sodium dodecyl sulfate polyacrylamide gel electrophoresis of plasmin-digested fibronectin, stained with Coomassie blue. Lanes A through E, results of incubating human fibronectin with human plasmin for 0, 15, 30, 60, and 120 min. Lane F, results with plasmin alone. At 0 min, a band with a large MW about 450,000 Da was detected (lane A, *arrowhead*), which corresponds to the MW of fibronectin dimer. At 15 min, the 450,000 Da band had been degraded to several new fragments (*arrows*), one of which had a MW of 30,000 Da (lane B, *arrow 1*). There was little difference in the appearance of the gels for exposure times of 15 and 30 min (lanes B, C). After 60 min, all of the bands appeared to have reached an equilibrium and showed no remarkable change thereafter



injection of APE, complete PVDs were created in 3 eyes and partially in 2 eyes. From the same group, Trese et al. [16] also used APE and showed its promising effect in cases of idiopathic stage 3 MHs, which had an anomalous vitreous detachment with persistent vitreous attachment to the disc. These findings indicated that plasmin might be a useful adjunct to vitrectomy for eyes with MH.

B. Diabetic Macular Edema

Diabetic macular edema is the most common cause of visual impairment in patients with diabetes. Since Nasrallah et al. [35] first reported in 1988 that the eyes of diabetic patients without DME had a significantly higher rate of PVD than those with DME, it was generally assumed that the vitreous plays an important role in the pathogenesis of DME. It is furthermore known that eyes with DME have increased levels of laminin and fibronectin that act as adhesion molecules at the vitreoretinal interface. In addition, accumulated serum-derived chemoattractants stimulate the migration of hyalocytes and glial cells to the posterior vitreous cortex. [36] Contraction of these cells could then lead to traction on the macula. Nonenzymatic glycation of collagen occurs in the vitreous of diabetic patients, which leads to advanced glycation end products (AGEs) [37], altering structure in the vitreous body [38] and at the vitreoretinal interface. Here, AGEs are mainly accumulated along the posterior vitreous cortex and the ILM, which then promotes collagen cross-linking [39]. All of these factors may contribute to anomalous PVD and tangential or anterior-posterior traction, which exacerbate DME.

Clinical studies have shown that the eyes with PVD had a higher prevalence of spontaneous resolution of DME than in eyes without PVD [40]. In addition, vitrectomy with the creation of PVD can resolve diffuse macular edema and improve visual acuity [41, 42]. Therefore, plasmin enzyme might be a reasonable treatment to induce PVD in DME which would also remove the tissue scaffold for neovascularization as well as eliminate tractional forces on the fovea. It might also prevent the diabetic retinopathy from progressing to the proliferative stage. Given that plasmin enzyme has a proteolytic effect on laminin and fibronectin which links the vitreous to the ILM which then creates PVD, we studied the effects of APE in eyes with DME [25]. We recruited 20 patients with DME who were scheduled to undergo vitreous surgery and divided them into two groups randomly: an APE group and a control group. The APE group received an intravitreal injection of 0.4–0.8 IUs of APE about 45 min prior to vitreous surgery. During surgery, both groups underwent chromodissection [43] with indocyanine dye staining and peeling of the ILM [see chapter V.A.3. Chromodissection in vitreoretinal surgery]. The

excised ILMs were examined by scanning and transmission electron microscopy, and the ease of PVD induction during the vitrectomy was also compared in the two groups. The number of eyes with vitreous cortex remnants on the surface of ILM was compared between the 2 groups. The results showed that remnants of the vitreous cortex were observed in 7 of 10 eyes in the control group but only 2 of 10 eyes in the APE group (Figure VI.D.2-4). At the beginning of vitrectomy, a spontaneous PVD was present in 2 eyes in the APE group, while none of the eyes in the control group had a spontaneous PVD. In addition, we found that the creation of the PVD seemed to be easy in 1 of 10 in the control group and 7 of 10 eyes in the APE group. These results indicated that APE was effective in cleaving vitreous from the retinal surface in DME patients.

In 2001, APE was first used as an adjunct to vitreous surgery in eyes with advanced diabetic retinopathy [17]. The removal of posterior vitreous cortex was purportedly easier with APE even in eyes with the vitreous firmly attached to the retina, such as eyes with macular tractional retinal detachment. Azzolini et al. [18] conducted a similar comparative study in eyes with DME using 0.8–1.2 IU of APE 25 min prior to vitreous surgery. In APE-treated group, the separation of the posterior vitreous was achieved more easily than in non-APE group. However, in eyes with DME associated with vitreo-macular traction, the extent of the attachment of vitreous differs in individual cases. Elbendary et al. [20] investigated the relationship of the posterior vitreous cortex thickness and degree of reflectivity with the ease of creating a PVD in diabetic eyes with vitreo-macular traction. They reported that eyes with thinner and less reflective posterior vitreous face had a higher rate of PVD development.

The activity of APE injected into the mid-vitreous peaks around 15–60 min and then gradually decreases to almost zero after 24 h [5]. So the effect of leaving APE in the vitreous without vitrectomy for an induction of a PVD might be more effective than the removal of APE by vitrectomy. Diaz-Llopis et al. [19] performed a prospective comparative study in which APE was injected intravitreally without vitrectomy in 16 eyes with refractory diffuse diabetic macular edema. They compared the results to that of eyes that did not receive APE. After intravitreal APE injection, there was a reduction in the central macular thickness and improvement of the visual acuity, with no adverse effects in all cases.

C. Retinopathy of Prematurity

ROP is a leading cause of childhood blindness [see chapter III.A. Congenital vascular vitreo-retinopathies]. Initially, scleral buckling surgery was the major treatment in eyes with retinal detachment at stages 4A, 4B, and 5 ROP. However, lens-sparing vitrectomy at an early stage

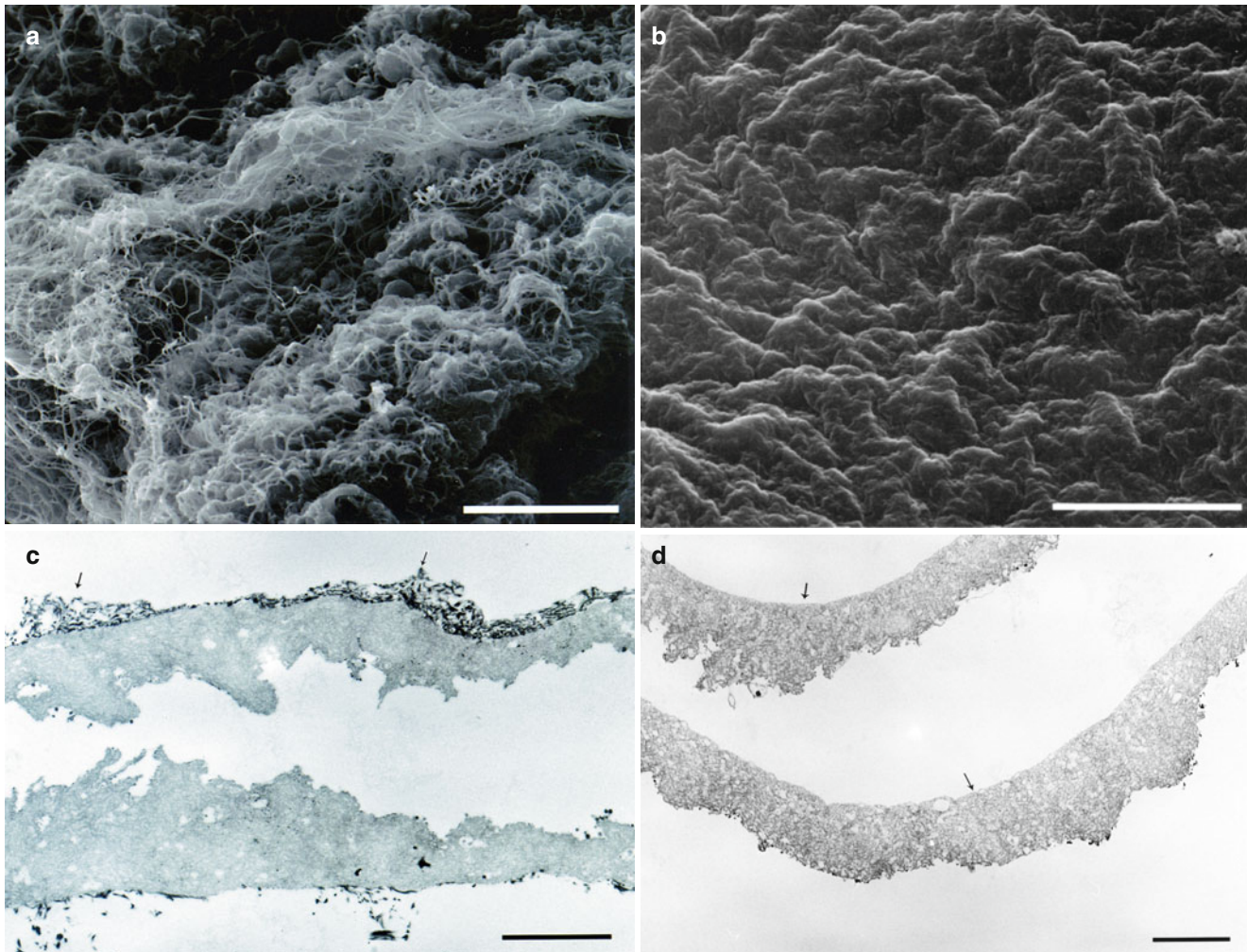


Figure VI.D.2-4 Scanning (SEM) and transmission electron microscopy (TEM) of ILM specimens removed from eyes with diabetic macular edema during vitreous surgery. (a) SEM of ILM removed from eyes undergoing vitrectomy without APE as the control group. The SEM micrograph shows a dense network of collagen fibers on the ILM. (b) SEM of ILMs from eyes that had an APE injection before the vitrec-

tomy (APE group) shows smooth ILM surface (a, b: original magnification, $\times 10,000$; bars = $3.0\ \mu\text{m}$). (c) TEM of ILM from the control group shows that the collagen fibrils are attached to the surface of the ILM without a cellular component (arrows). (d) TEM of ILM in APE group shows a smooth surface (arrows) (c, d: original magnification, $\times 3,500$; bars = $2.8\ \mu\text{m}$)

has become the main treatment paradigm. The purpose of the surgery is to relieve the tractional force of proliferative tissue on the surface of retina where vitreoretinal interface is firmly attached by laminin and fibronectin. Thus, it was assumed that plasmin enzyme might be beneficial in cleaving or at least weakening the vitreoretinal juncture and make the vitreous surgery easier. At present, there are several reports on the use of APE in ROP cases. Tsukahara et al. [21] injected 0.03–0.22 IUs of APE, purified from the patients' plasma, into 6 eyes at stage 5 ROP before vitrectomy. The membranes were removed successfully and a complete reattachment of the posterior retina was achieved in all eyes. Wu et al. [22] reported the results from 80 eyes of 68 patients who were treated with or without APE prior

to vitrectomy. They reported that 68.8 % of the treated eyes had anatomical success. APE appeared to have positive effects on the vitreoretinal interface even in the severe stages of ROP.

D. Retinal Vein Occlusion (RVO)

APE was used in eyes with macular edema associated with branch RVO in two studies. Sakuma et al. [23] injected 1 IU of APE into vitreous without vitrectomy, and a total PVD was observed at 1 week in 23 of 26 eyes. Udaondo et al. [24] confirmed the effects and safety of APE in a small case series with branch RVO.

Conclusions

The accumulated results of animal and clinical experiments suggest that plasmin is a useful adjunct to vitrectomy in eyes with vitreo-macular adhesion such as MHs, vitreo-macular traction syndrome, and DME. Plasmin might reduce the risk of iatrogenic damage to the fovea during vitrectomy and reduce the number of indications for vitrectomy.

Abbreviations

APE	Autologous plasmin enzyme
DME	Diabetic macular edema
ILM	Inner limiting membrane
MH	Macular hole
MW	Molecular weight
PVD	Posterior vitreous detachment
RVO	Retinal vein occlusion
ROP	Retinopathy of prematurity
SEM	Scanning electron microscopy
tPA	Tissue plasminogen activator
TEM	Transmission electron microscopy

References

- Sebag J. Anomalous PVD – a unifying concept in vitreo-retinal diseases. *Graefes Arch Clin Exp Ophthalmol.* 2004;242:690–8.
- Sebag J. Vitreous anatomy, aging, and anomalous posterior vitreous detachment. In: Dartt DA, Besharse JC, Dana R, editors. *Encyclopedia of the eye*, vol. 4. Oxford: Elsevier; 2010. p. 307–15.
- Sebag J. Pharmacologic vitreolysis (guest editorial). *Retina.* 1998;18:1–3.
- Sebag J. Pharmacologic vitreolysis- premise and promise of the first decade. *Retina.* 2009;29:871–4.
- Verstraeten TC, Chapman C, Hartzler M, Winkler BS, Trese MT, Williams GA. Pharmacologic induction of posterior vitreous detachment in the rabbit. *Arch Ophthalmol.* 1993;111:849–54.
- Hikichi T, Yanagiya N, Kado M, Akiba J, Yoshida A. Posterior vitreous detachment induced by injection of plasmin and sulfur hexafluoride in the rabbit vitreous. *Retina.* 1999;19:55–8.
- Gandorfer A, Putz E, Welge-Lüssen U, Grüterich M, Ulbig M, Kampik A. Ultrastructure of the vitreoretinal interface following plasmin assisted vitrectomy. *Br J Ophthalmol.* 2001;85:6–10.
- Kim NJ, Yu HG, Yu YS, Chung H. Long-term effect of plasmin on the vitreolysis in rabbit eyes. *Korean J Ophthalmol.* 2004;18:35–40.
- Wang ZL, Zhang X, Xu X, Sun XD, Wang F. PVD following plasmin but not hyaluronidase: implications for combination pharmacologic vitreolysis therapy. *Retina.* 2005;25:38–43.
- Hermel M, Mahgoub M, Youssef T, Azrak MI, Raza H, Alldredge C, Trese M, Williams GA, Hartzler M. Safety profile of the intravitreal streptokinase-plasmin complex as an adjunct to vitrectomy in the rabbit. *Graefes Arch Clin Exp Ophthalmol.* 2006;244:996–1002.
- Gandorfer A, Priglinger S, Schebitz K, Hoops J, Ulbig M, Ruckhofer J, Grabner G, Kampik A. Vitreoretinal morphology of plasmin-treated human eyes. *Am J Ophthalmol.* 2002;133:156–9.
- Li X, Shi X, Fan J. Posterior vitreous detachment with plasmin in the isolated human eye. *Graefes Arch Clin Exp Ophthalmol.* 2002;240:56–62.
- Margherio AR, Margherio RR, Hartzler M, Trese MT, Williams GA, Ferrone PJ. Plasmin enzyme-assisted vitrectomy in traumatic pediatric macular holes. *Ophthalmology.* 1998;105:1617–20.
- Chow DR, Williams GA, Trese MT, Margherio RR, Ruby AJ, Ferrone PJ. Successful closure of traumatic macular holes. *Retina.* 1999;19:405–9.
- Wu WC, Drenser KA, Trese MT, Williams GA, Capone A. Pediatric traumatic macular hole: results of autologous plasmin enzyme-assisted vitrectomy. *Am J Ophthalmol.* 2007;144:668–72.
- Trese MT, Williams GA, Hartzler MK. A new approach to stage 3 macular holes. *Ophthalmology.* 2000;107:1607–11.
- Williams JG, Trese MT, Williams GA, Hartzler MK. Autologous plasmin enzyme in the surgical management of diabetic retinopathy. *Ophthalmology.* 2001;108:1902–5.
- Azzolini C, D'angelo A, Maestranzi G, Codenotti M, Valle PD, Prati M, Brancato R. Intravitreal plasmin enzyme in diabetic macular edema. *Am J Ophthalmol.* 2004;138:560–6.
- Diaz-Llopis M, Udaondo P, Arevalo F, Salom D, Garcia-Delpech S, Quijada A, Romero FJ. Intravitreal plasmin without associated vitrectomy as a treatment for refractory diabetic macular edema. *J Ocular Pharmacol Therapeutics.* 2009;25:379–84.
- Elbendary AM, Elwan MM, Azzam HA, Eldeeb DR. Predictability of vitreous detachment following intravitreal plasmin injection in diabetic macular edema associated with vitreomacular traction. *Curr Eye Res.* 2011;36:534–9.
- Tsukahara Y, Honda S. Autologous plasmin-assisted vitrectomy for stage 5 retinopathy of prematurity: A preliminary trial. *Am J Ophthalmol.* 2007;144:139–41.
- Wu WC, Drenser KA, Lai M, Capone A, Trese MT. Plasmin enzyme-assisted vitrectomy for primary and reoperated eyes with stage 5 retinopathy of prematurity. *Retina.* 2008;28:S75–80.
- Sakuma T, Mizota A, Inoue J, Tanaka M. Intravitreal injection of autologous plasmin enzyme for macular edema associated with branch retinal vein occlusion. *Am J Ophthalmol.* 2010;150:876–82.
- Udaondo P, Diaz-Llopis M, Garcia-Delpech S, Salom D, Romero FJ. Intravitreal plasmin without vitrectomy for macular edema secondary to branch retinal vein occlusion. *Arch Ophthalmol.* 2011;129:283–7.
- Asami T, Terasaki H, Kachi S, Nakamura M, Yamamura K, Nabeshima T, Miyake Y. Ultrastructure of internal limiting membrane removed during plasmin-assisted vitrectomy from eyes with diabetic macular edema. *Ophthalmology.* 2004;111:231–7.
- Uemura A, Nakamura M, Kachi S, Nishizawa Y, Asami T, Miyake Y, Terasaki H. Effect of plasmin on laminin and fibronectin during plasmin-assisted vitrectomy. *Arch Ophthalmol.* 2005;123:209–13.
- Young KC, Shi GY, Wu DH, et al. Plasminogen activation by streptokinase via a unique mechanism. *J Biol Chem.* 1998;273:3110–6.
- Rizzo S, Pellegrini G, Benocci F, Belting C, Baicchi U, Vispi M. Autologous plasmin for pharmacologic vitreolysis prepared 1 hour before surgery. *Retina.* 2006;26:792–6.
- Udaondo P, Diaz-Llopis M, Garcia-Delpech S, Cervera E, Salom D. Autologous plasmin for intravitreal injection without associated vitrectomy: a simple preparation method with streptokinase. *Arch Soc Esp Oftalmol.* 2008;83:153–4.
- Díaz-Llopis M, Udaondo P, Salom D, García-Delpech S, Romero FJ. Intravitreal autologous plasmin without associated-vitrectomy. Pharmacological vitreolysis, a perfeccionated method using urokinase. *Arch Soc Esp Oftalmol.* 2008;83:291–2.
- Hermel M, Dailey W, Hartzler MK. Efficacy of plasmin, microplasmin, and streptokinase-plasmin complex for the in vitro degradation of fibronectin and laminin- implications for vitreoretinal surgery. *Curr Eye Res.* 2010;35:419–24.

32. Hermel M, Dailey W, Trese M, Hartzler MK. A disposable system for rapid purification of autologous plasmin as an adjunct to vitrectomy - performance and safety profile. *Graefes Arch Clin Exp Ophthalmol*. 2011;249:37–46.
33. Kelly NE, Wendel RT. Vitreous surgery for idiopathic macular holes. Results of a pilot study. *Arch Ophthalmol*. 1991;109:654–9.
34. Sebag J. Age-related differences in the human vitreoretinal interface. *Arch Ophthalmol*. 1991;109:966–71.
35. Nasrallah FP, Jalkh AE, Van Coppenolle F, Kado M, Trempe CL, McMeel JW, Schepens CL. The role of the vitreous in diabetic macular edema. *Ophthalmology*. 1988;95:1335–9.
36. Gandorfer A. Role of vitreous in diabetic macular edema. *Retina*. 2012;32:S211–5.
37. Sebag J, Buckingham B, Charles MA, Reiser K. Biochemical abnormalities in vitreous of humans with proliferative diabetic retinopathy. *Arch Ophthalmol*. 1992;110:1472–9.
38. Sebag J. Abnormalities of human vitreous structure in diabetes. *Graefes Arch Clin Exp Ophthalmol*. 1993;231:257–60.
39. Sebag J, Nie S, Reiser K, Charles MA, Yu NT. Raman spectroscopy of human vitreous in proliferative diabetic retinopathy. *Invest Ophthalmol Vis Sci*. 1994;35:2976–80.
40. Hikichi T, Fujio N, Akiba J, Azuma Y, Takahashi M, Yoshida A. Association between the short-term natural history of diabetic macular edema and the vitreomacular relationship in type II diabetes mellitus. *Ophthalmology*. 1997;104:473–8.
41. Tachi N, Ogino N. Vitrectomy for diffuse macular edema in cases of diabetic retinopathy. *Am J Ophthalmol*. 1996;122:258–60.
42. Lopes de Faria JM, Jalkh AE, Trempe CL, McMeel JW. Diabetic macular edema: risk factors and concomitants. *Acta Ophthalmol Scand*. 1999;77:170–5.
43. Bababegy SR, Sebag J. Chromodissection of the vitreo-retinal interface. *Retin Physician*. 2009;6(3):16–21.

Pharmacologic Vitreolysis with Ocriplasmin: Basic Science Studies

VI.E.1.

Marc D. de Smet and Bart Jonckx

Outline

- I. Introduction
 - II. Structural and Physiologic Characteristics
 - III. Pharmacokinetics of Ocriplasmin
 - IV. Pharmacodynamics of Ocriplasmin
 - A. Effects on Vitreous
 - B. Toxicology
 - V. Future Directions
- ## References

Keywords

Vitreous • Pharmacologic vitreolysis • Ocriplasmin • Microplasmin • Pharmacodynamics • Pharmacokinetics

Key Concepts

1. Ocriplasmin is a recombinant serine protease with a well-characterized enzymatic activity profile that is stable for several days in an acidic environment. Highly active in neutral pH, inactivation follows second-order kinetics (autolysis), so that when placed in a vitreous substrate only 25 % of the activity remains in 24 h.
2. A protein of 27 kDA, ocriplasmin is subject to steric hindrance also in the vitreous. For maximal effect, it requires injection close to the site of intended activity, which can also limit any adverse effect on adjacent structures such as zonules.
3. As a member of the plasminogen family of proteins, ocriplasmin regulates a number of pathways including proinflammatory cytokines and matrix metalloproteinases that help to extend its mode of action and define its secondary clinical manifestations.

M.D. de Smet, MDCM, PhD, FRCSC, FRCOphth, FMH (✉)
Department of Retina and Inflammation,
Specialized Eye Clinic in Uveitis and Retina,
MIOS sa, Lausanne, Switzerland
e-mail: mddesmet1@mac.com

B. Jonckx, PhD
Department in vivo pharmacology,
Thrombogics nv, Leuven, Belgium

I. Introduction

Pharmacologic vitreolysis is an important new avenue of ophthalmic therapeutics, representing a paradigm shift from surgical to pharmacologic therapy of vitreoretinal diseases [24, 26, 27]. Ocriplasmin (des-kringle 1-5 plasmin), formerly called microplasmin, is a truncated recombinant form of plasmin. Originally shown to form upon autolytic degradation of plasmin at high pH, it contains the catalytic domain of plasmin but without associated kringles [38]. In ophthalmology, ocriplasmin was initially studied as a

possible alternative to plasmin enzyme (desirable because of the difficulties with plasmin preparation) and was found to be a stable, well-characterized, clinical grade product, which was notable given its highly autolytic nature [34].

Plasmin enzyme had been envisioned as a therapeutic agent in humans since the 1950s. It was first considered for ocular use in retinal vein occlusion [5, 18]. Plasmin was first studied as a vitreolytic agent in 1993 using a rabbit model [35]. Subsequently its potential as an adjunct to vitreoretinal surgery was confirmed, as was its ability to facilitate the formation of a posterior vitreous detachment even in premature infants [11, 17, 20, 32] [see chapter VI.D.2. Pharmacologic vitreolysis with plasmin: clinical studies].

Ocriplasmin has been studied in a number of preclinical models, and its mode of action on the vitreous gel and at the vitreoretinal interface is at least partially established. The known chemical behavior of ocriplasmin helps to understand some of the observed biologic activity useful to define some of the observed effects in humans. It may also help to orient future research to enhance its current level of clinical efficacy. This chapter will review the basic science investigations that led to this knowledge, while clinical studies are summarized elsewhere [see chapter VI.E.2. Pharmacologic vitreolysis with ocriplasmin: clinical studies].

II. Structural and Physiologic Characteristics

Ocriplasmin is a 27.3 kDA serine protease, consisting of 2 polypeptide chains of 19 and 230 residues linked by 2 disulfide bonds joining residues 6 and 124, 16 and 24. The 230-residue polypeptide is stabilized by 4 intra-chain

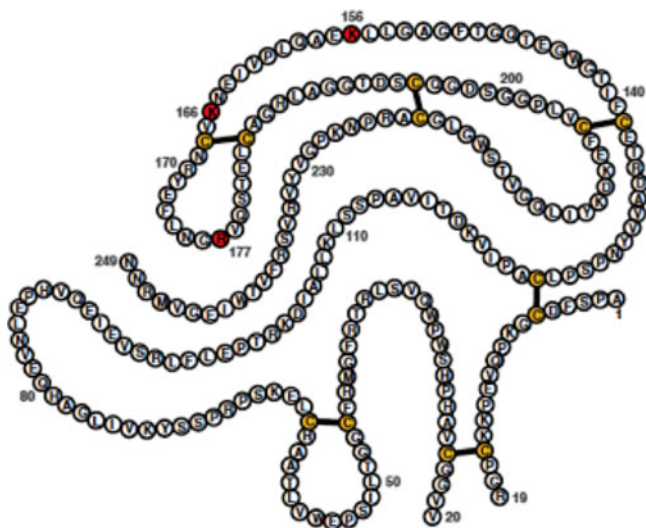


Figure VI.E.1-1 Amino acid composition of ocriplasmin and its primary structure [1]

disulfide bonds (Figure VI.E.1-1). Ocriplasmin contains the catalytic domain of plasmin but none of the 5 kringles located as extensions toward the C-terminal end of the larger of its two chains. These kringles normally serve as binding sites for substrates, regulatory molecules, and inhibitors [31, 38]. As a result, ocriplasmin has a more potent effect on thrombin than is observed with the native molecule, but binds to its primary inhibitor with less affinity [36, 22]. It is unclear if this translates to a more potent activity in the eye, though diffusion through the vitreous proper is enhanced by its smaller size [13, 28]. Inhibition occurs preferentially with serpin proteins such as $\alpha(2)$ -antiplasmin in addition to other serum components such as antithrombin III and $\alpha(1)$ -antitrypsin [9, 21, 31]. Inhibition likely occurs within the eye via a similar mechanism, particularly in the presence of a breakdown in the blood-ocular barrier.

Ocriplasmin is a recombinant human microplasmin produced as microplasminogen in the yeast *Pichia pastoris*, stabilized with a dilute citrate buffer at pH 3.1, and converted to the active form with recombinant staphylokinase [21]. Microplasmin catalyzes the cleavage of peptide bonds on the COOH-terminal side of lysine and arginine residues embedded in proteins and peptide substrates [38]. Typical targets include thrombin, plasminogen, and a number of extracellular matrix proteins such as laminin and fibronectin [4, 6, 16]. While not clearly demonstrated for microplasmin itself, plasmin-like proteases have a number of non-fibrinolytic functions such as directional cell migration, tissue remodeling, and the activation of other proteases within the matrix metalloproteinase (MMP) family [23]. Analogous to other members of the plasminogen family, ocriplasmin is likely to regulate the expression or activity of cytokines involved in various inflammatory processes. Plasmin can cause the release of IL-1 from macrophages and activate transforming growth factor- β , while degradation products of fibrin are chemoattractant for leukocytes [3]. This may explain why in experimental models and in some patients, a transient low-grade inflammatory response is observed shortly after the injection of plasmin or ocriplasmin into the vitreous body [7, 29, 35].

III. Pharmacokinetics of Ocriplasmin

The inactivation of ocriplasmin in both neutral-pH buffer and porcine vitreous is mostly due to autolytic degradation. The activity of ocriplasmin is temperature and pH dependent. At $-20\text{ }^{\circ}\text{C}$, the product is stable for 24 months or more [7]. At room temperature, in an acidic environment, it is stable for at least 2 h [12, 13]. No studies have looked at its stability in multiple refreezing cycles, which therefore should be avoided. Although stable in its formulation buffer, it has limited stability when diluted to a neutral pH (as with balanced salt solution (BSS)) or following injection into the vitreous

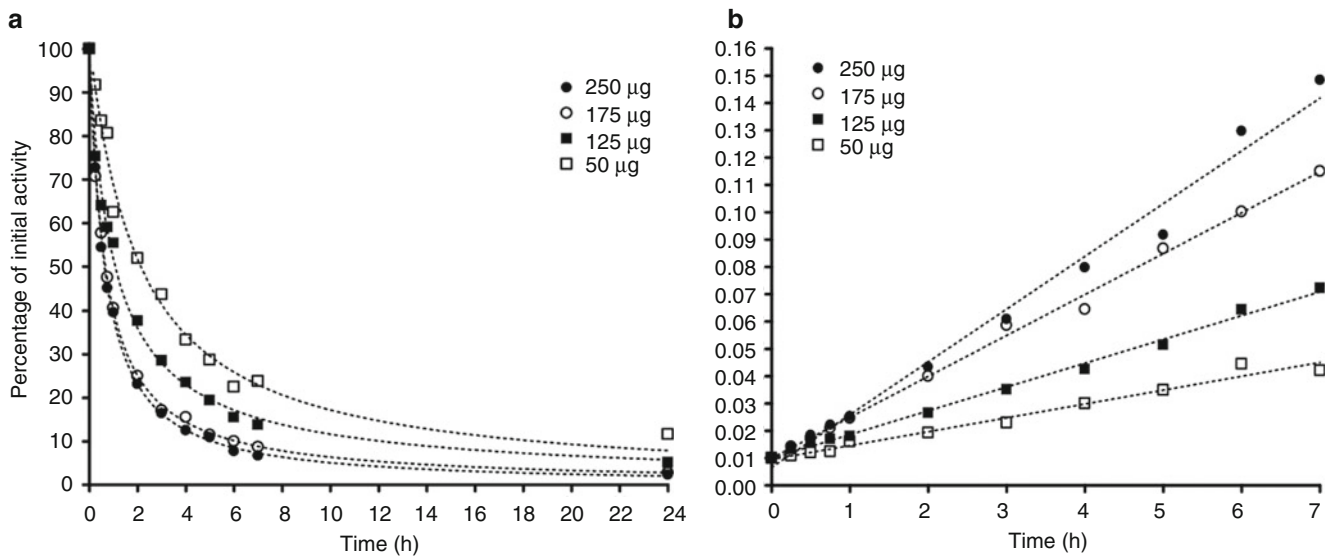


Figure VI.E.1-2 Ocriplasmin inactivation in a neutral-pH buffer (PBS). (a) Different doses of ocriplasmin were diluted in PBS, and the autolytic activity was measured at various time points. In panel (b), the data was linearized, assuming second-order enzymatic reaction [1]

body [12, 13]. Under these circumstances, within 1 h, 50 % of the biologic activity is lost. In an acid environment, serine de-protonation is prevented, which in turn limits interactions with potential substrates [2].

The *in vitro* pharmacokinetics of ocriplasmin are similar in porcine and human vitreous extracts. Ocriplasmin is stable in vitreous at a pH of 3.1 for over 13 weeks at -20°C and 3 days at 4°C , while it loses its activity at room temperature within half a day. At a neutral pH, a slower inactivation rate is observed in vitreous ($k=81\text{ M}^{-1}\text{ s}^{-1}$) as compared to phosphate buffered saline ($k=176\text{ M}^{-1}\text{ s}^{-1}$) [1, 9]. Hence, the residual activity after 24 h of incubation is in the range of 1–4 % in saline and 8–24 % in vitreous.

The inactivation of ocriplasmin follows second-order kinetics as predicted for an autolytic process. Inactivation is therefore concentration dependent, with faster inactivation observed at higher doses (Figure VI.E.1-2). As a consequence, ocriplasmin will more rapidly inactivate itself when injected into gel vitreous, while it will retain activity for a longer time when injected in liquefied vitreous (a consequence of faster diffusion and more accessible substrate). Uptake into the systemic circulation results in inactivation by numerous inhibitors present in blood [7]. Inhibitors of serine proteases were identified in human vitreous, including $\alpha(1)$ -antitrypsin, $\alpha(2)$ -antiplasmin, antithrombin III, C1 esterase inhibitor, and $\alpha 2$ -macroglobulin [9, 15, 37]. The ability of these inhibitors to effectively inhibit ocriplasmin activity has not been assessed so far. Samples from patients with well-characterized retinal pathologies would be required to assess the level of inhibition.

Of all the inhibitors mentioned above, only $\alpha(2)$ -antiplasmin is known to effectively and completely inhibit

ocriplasmin [22]. To date, detected levels in vitreous are low, sufficient to inhibit only about 4 % of the amount injected [9]. Other inhibitors are described as slow (progressive) inhibitors of plasmin; while sufficient to inhibit a large portion of the administered enzyme, they do not seem to contribute significantly to inhibition as one is able to recover high levels of enzymatically active ocriplasmin after *in vitro* incubation in vitreous [9]. Studies so far have been carried out in pooled vitreous from a variety of patients undergoing surgery. As new indications are developed, particularly for interface diseases such as diabetic retinopathy or vein occlusion, it will be necessary to study the possible influence of these inhibitors on the action of ocriplasmin at the vitreoretinal interface.

IV. Pharmacodynamics of Ocriplasmin

A. Effects on Vitreous

Ocriplasmin was tested in several animal models. Initial studies were carried out in an *ex vivo* porcine model [8, 10, 34] demonstrating an ability to break down the vitreous structure as well as cause a separation of the posterior vitreous cortex from the retinal surface. The action of ocriplasmin is concentration and time dependent, as was shown in a number of experiments using light and electron microscopy [8, 10, 12, 13]. Following an intraocular injection into *ex vivo* porcine eyes at room temperature and a 1-h incubation, complete vitreoretinal separation is seen with 125 µg of ocriplasmin in the posterior pole and partial separation from the peripheral retina. At 37°C , the same incubation leads to a complete

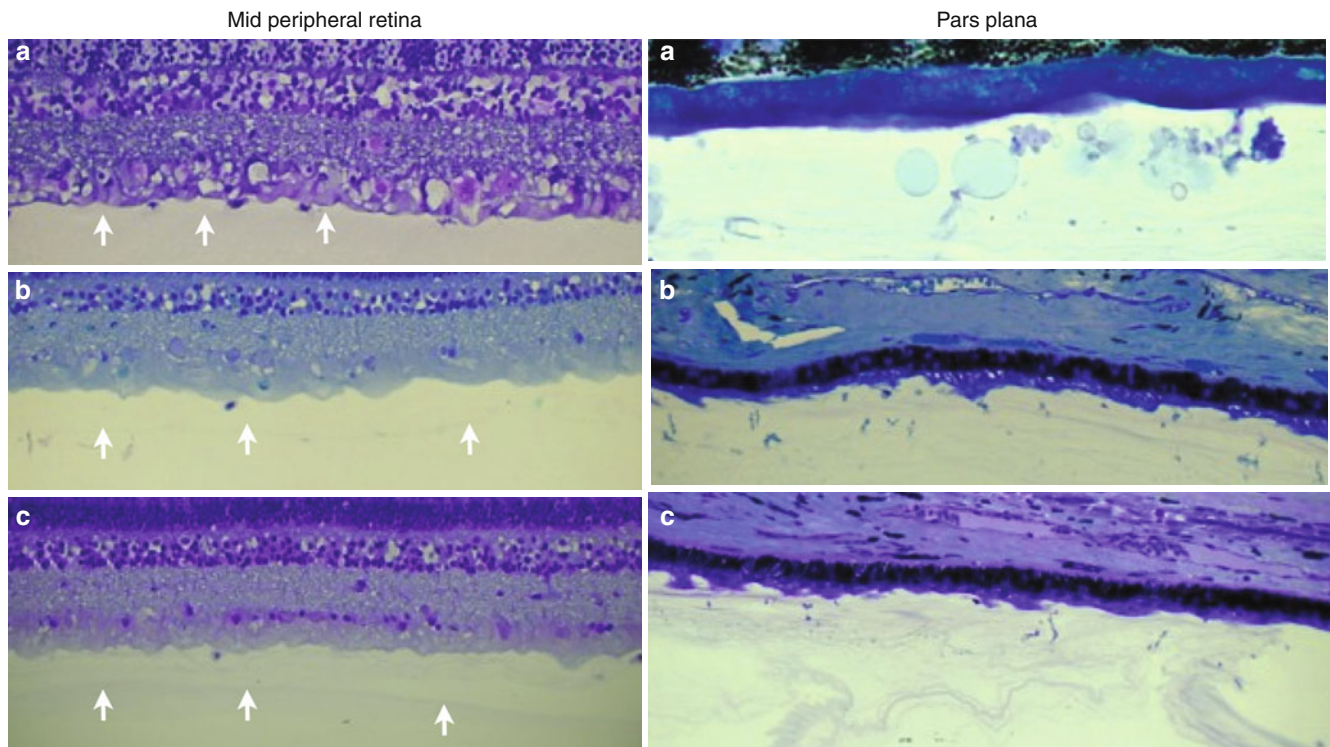


Figure VI.E.1-3 Effect of concentration on the degree of vitreous separation following a 2-h incubation at 37 °C with different concentrations of ocriplasmin injected in the mid-vitreous or the pars plana (**a**, 62.5 µg;

b, 125 µg; **c**, 250 µg). Arrows indicate the location of the posterior vitreous cortex

separation up to the ora serrata (Figure VI.E.1-3). At 250 µg and above, in the midperiphery, vitreous separation is present, but proteinaceous material is often visible close to the retinal surface, suggesting that an anomalous posterior vitreous detachment [25] may have taken place (Figure VI.E.1-3). This has been observed clinically as part of the MIVI I trial [8, 10]. Concentrations up to 400 µg have been tested. None have led to vitreous detachment overlying the ora serrata. At 400 µg, following a 2-h exposure at room temperature, circular elevations of the RPE were observed. These were not seen at lower concentrations. This may indicate an upper limit to the concentrations of ocriplasmin that can be tolerated within the vitreous and the eye.

Electron microscopy of specimens taken proximal to the site of injection showed a retinal surface with either sparse or absent collagen fibers as opposed to control eyes (Figure VI.E.1-4) [8, 10, 14]. Condensed vitreous, present close to the site of injection, takes on a coarse granular appearance. Biopsies from areas more distant to the site of injection show that the vitreous resumes a more normal structure [8, 10]. From these and similar experiments, it is clear that ocriplasmin is capable of inducing a posterior vitreous detachment but is also able to alter the structure of the vitreous. This therefore qualifies this drug as both an interfactant and a liquefactant agent [27] [see chapter VI.A. Pharmacologic vitreolysis]. Concerning the latter, dynamic light scattering experiments have shown a dose-dependent

effect on vitreous diffusion coefficients with a near doubling of the diffusional capacity within 30 min of exposure to 800 µg of ocriplasmin [28]. Experiments conducted with fluorescein further support these findings yet indicate that the alteration of the vitreous is not homogeneous but proceeds by extension around the site of injection [12, 13].

A mouse model has been established to further study the effects of ocriplasmin *in vivo*. When injected into the vitreous body of the mouse, 0.5 µg of ocriplasmin can reproducibly induce a partial PVD after 3–5 days. OCT allows the animals to be monitored in a noninvasive manner (Figure VI.E.1-5). A good correlation between OCT findings and histology has been demonstrated and shows the extent of the PVD (Figure VI.E.1-5). This model has allowed better elucidation of the effect of ocriplasmin on laminin and fibronectin, important because several lines of evidence have implicated laminin and fibronectin as important at the vitreoretinal interface [see chapter II.E. Vitreoretinal interface and ILM].

It is possible to study variations in the expression of extracellular matrix proteins at the vitreoretinal interface using immunofluorescent dual stains. Laminin is restricted primarily to basement membranes and is likely produced by the Mueller cell footplates. Fibronectin is found at the surface of many cell types and in most extracellular matrices. It binds with high affinity to collagen, proteoglycans, and hyaluronan [4, 19, 33]. Expression of laminin and fibronectin varies with age and tends to increase in older individuals

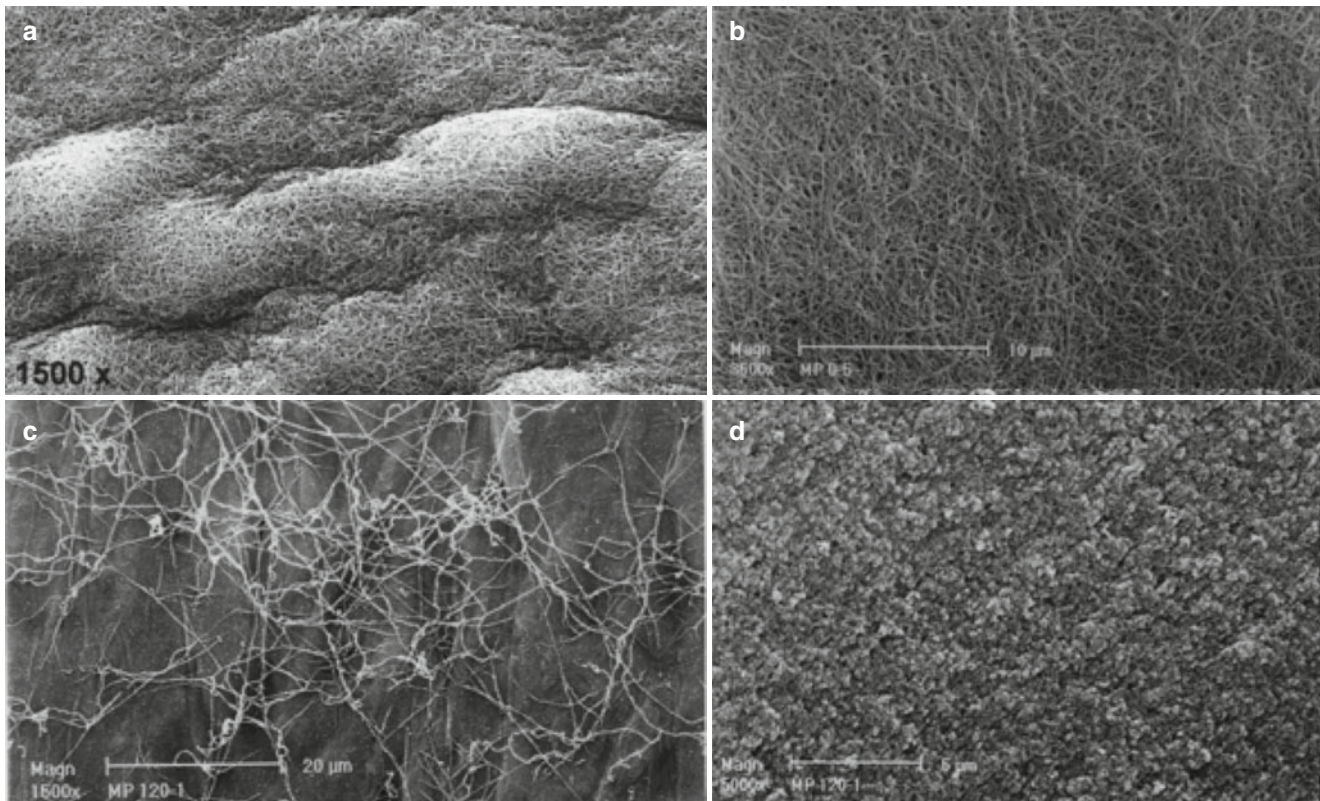


Figure VI.E.1-4 Electron microscopy of porcine eyes following incubation with 125 μg ocriplasmin at room temperature for 2 h. (a) control eye in the equatorial region showing the presence of a dense network of fibers (1,500 \times); (b) ocriplasmin injected eye at time 0 taken in the mid-periphery showing a similar pattern of fibers; (c) equatorial region of a

ocriplasmin injected eye after 2 h incubation. Sparse fibers are present overlying the retina (1,500 \times); (d) ocriplasmin treated eye. Vitreous condensation adjacent to the area in (c) showing a coarse granular structure (5,000 \times)

(Figure VI.E.1-6). In the presence of a PVD, fibronectin is expressed on the posterior surface of the vitreous but not at the anterior surface of the retina, where only collagen is present. Where the posterior vitreous cortex is intact, one additionally finds the presence of laminin (Figure VI.E.1-7). Following the intravitreal injection of ocriplasmin, fibronectin and laminin are degraded both at the vitreoretinal interface as well as in the outer retina [4]. There appears to be a predilection for the intraretinal laminin to be degraded preferentially, an effect that was not seen with fibronectin. Recovery of both proteins requires a prolonged period of time. At 1 week, there does not appear to be any significant evidence of recovery. A possible correlation between the loss of intraretinal laminin and fibronectin and the observed transient ERG changes has been suggested [4].

B. Toxicology

Toxicology studies were carried out in Dutch belted rabbits, cynomolgus monkeys, and Goettingen mini-pigs [7]. In both rabbits and monkeys, vitreous inflammation was seen in over 50 % of eyes but was variable in extent and persistence, eventually resolving over time. Anterior segment

involvement was seen as early as day 2 in monkeys but also resolved. Lens subluxation was observed in rabbits and monkeys but was observed in only one treated pig. Needle size and positioning of the injection and dose were determined to be important elements influencing the risk of a lens luxation and may explain why the risk is higher in rabbits with a smaller eye and a larger lens. Transient ERG changes were seen in rabbits at doses of 50 μg and more. At the higher doses (substantially above the clinical dose), changes were still present following 8 weeks of recovery. In monkeys, transient ERG changes were seen at all doses above 1.5 μg . Recovery was present in all cases but was only partial by the end of follow-up at the highest dose (200 $\mu\text{g}/\text{eye}$). No ERG changes were observed in the mini-pig.

V. Future Directions

Clinical studies have demonstrated the clinical efficacy of ocriplasmin in symptomatic vitreo-macular adhesion and traction [see chapter VI.E.2. Pharmacologic vitreolysis with ocriplasmin: clinical studies]. However, the rate of success remains limited. Several pathways can be explored to enhance the efficacy of ocriplasmin: improving drug delivery

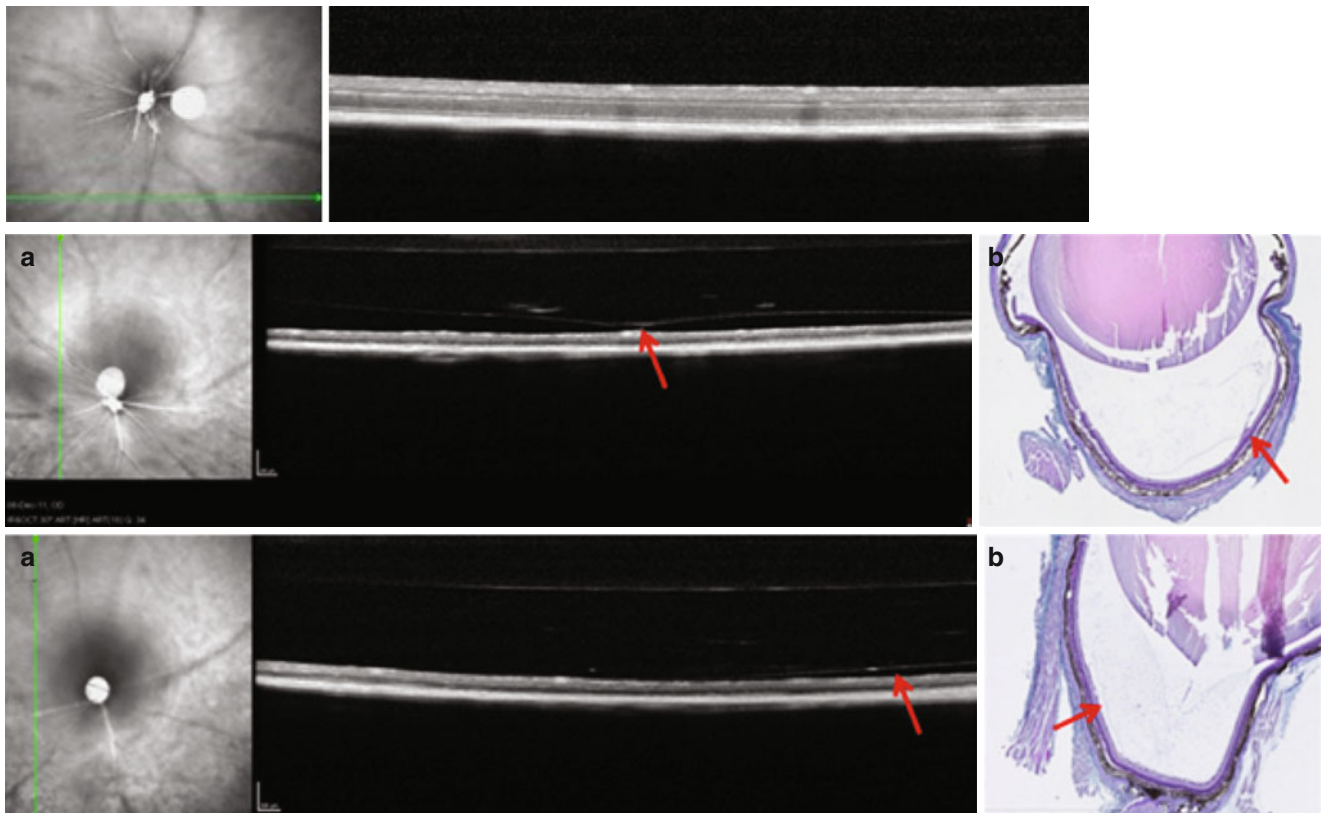


Figure VI.E.1-5 OCT images of ocriplasmin-treated mice using a modified Heidelberg Spectralis OCT (a). Upper panel shows a normal mouse eye. Middle panel shows an ocriplasmin-treated eye after 7 days. An extensive posterior vitreous detachment is present (arrow). The site of adhesion to the retina is confirmed by histology (arrow in b of middle panel). Inferior panel shows an ocriplasmin-treated eye after 3 days. The PVD is much less prominent, as confirmed in the histologic insert (b)

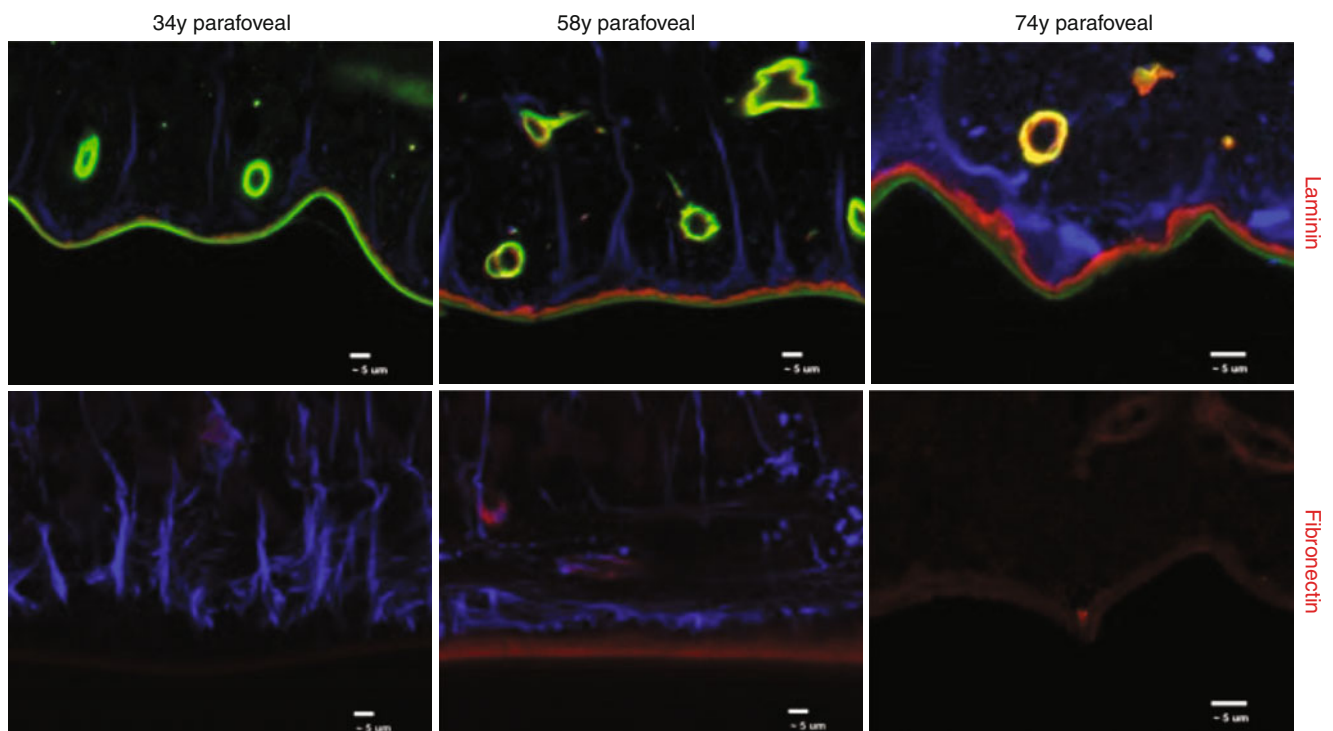


Figure VI.E.1-6 Expression of laminin and fibronectin varies in human donor eyes with age as seen on confocal microscopy using monoclonal stains. Collagen type IV in green, vimentin in blue

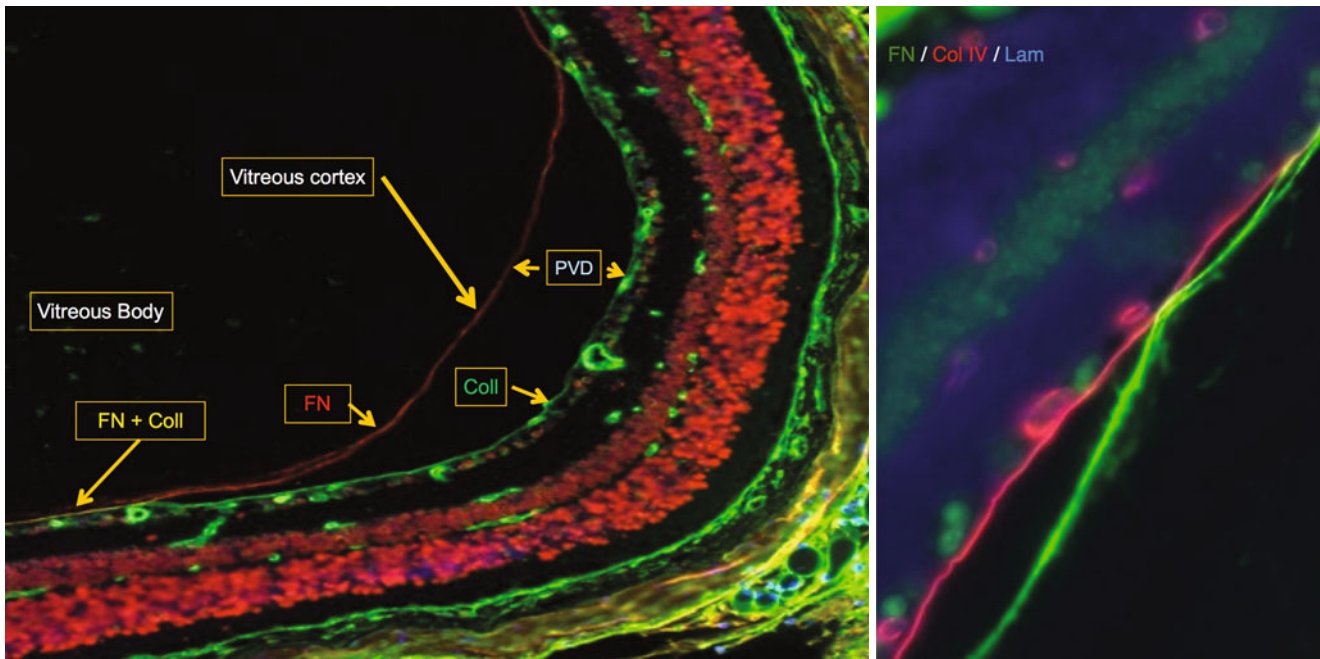


Figure VI.E.1-7 Confocal microscopy of laminin, fibronectin (FN), and collagen (Coll) type IV co-stained in mouse eyes treated with ocriplasmin. PVD, posterior vitreous detachment

(see chapter IV.E. Principles and practice of intravitreal application of drugs) to the mid-vitreous or deeper depending on the structure of the vitreous gel, repeating the injection to achieve a better induction of a PVD or vitreous liquefaction, and/or controlling or enhancing downstream pathways that are activated by ocriplasmin. These include the activation of matrix metalloproteinases, in particular MMP2 and MMP9 [30]. While unlikely to be a cause for concern in symptomatic vitreo-macular adhesion, inhibitors present in the vitreous may present a challenge when the indications are expanded to diabetes and macular degeneration. Indeed in circumstances where the blood-ocular barrier is incompetent, the likelihood of having inhibitors present in vitreous increases. Another challenge and unanswered question is the reason for the observed ERG changes in some species, including man. If indeed they are caused by changes in surface proteins within the retinal structure, this may be amenable to therapy or at the very least monitoring. Challenges enough, but in a new era of pharmacologic vitreolysis, answers to some of these questions will certainly extend the use of this and other therapies.

Abbreviations

µg	Micrograms
BSS	Balanced salt solution
C	Centigrade
COOH	Carboxyl
ERG	Electroretinography
IL	Interleukin

kDA	Kilodalton
MIVI	Microplasmin Intravitreal Injection Trial
MMP	Matrix metalloproteinase
PVD	Posterior vitreous detachment
RPE	Retinal pigment epithelium

References

1. Aerts F, Noppen B, Fonteyn L, et al. Mechanism of inactivation of ocriplasmin in porcine vitreous. *Biophys Chem.* 2012;165–166:30–8.
2. Banacky P, Linder B. Model of serine proteases charge relay system - PCILO study. *Biophys Chem.* 1981;13:223–31.
3. Castellino FJ, Ploplis VA. Structure and function of the plasminogen/plasmin system. *Thromb Haemost.* 2005;93:647–54.
4. Chen WL, Mo W, Sun K, et al. Microplasmin degrades fibronectin and laminin at vitreoretinal interface and outer retina during enzymatic vitrectomy. *Curr Eye Res.* 2009;34:1057–64.
5. Clifton EE. The use of plasmin in humans. *Ann N Y Acad Sci.* 1957;68:209–29.
6. Collen D. Natural inhibitors of fibrinolysis. *J Clin Pathol.* 1980;33:24–30.
7. Committee for Medicinal Products for Human Use: Assessment report of Jetea. 2013; European Medicines Agency. Accessed Sept 2013. www.ema.europa.eu/docs/en_GB/document_library/EPAR_-_Public_assessment_report/human/002381/WC500142228.pdf.
8. de Smet MD, Valmaggia C, Zarrantz J, et al. Microplasmin: ex vivo characterization of its activity in porcine vitreous. *Invest Ophthalmol Vis Sci.* 2009;50:814–9.
9. de Smet MD, Jonckx B, Vanhove M, et al. Pharmacokinetics of ocriplasmin in vitreous. *Invest Ophthalmol Vis Sci.* 2012; 53:8208–13.

10. de Smet MD, Gandorfer A, Stalmans P, et al. Microplasmin intravitreal administration in patients with vitreomacular traction scheduled for vitrectomy: the MIVI I trial. *Ophthalmology*. 2009;116:1349–55.
11. Diaz-Llopis M, Udaondo P, Cervera E, et al. Vitrectomia enzimática por inyección intravítrea de plasmina autóloga como tratamiento inicial de las membranas epirretinianas maculares y el síndrome de tracción vitreomacular. *Arch Soc Esp Ophthalmol*. 2009;84:91–100.
12. Gad El Kareem A, Willikens B, Vanhove M, et al. Characterization of a stabilized form of microplasmin for the induction of a posterior vitreous detachment. *Curr Eye Res*. 2010;35:909–15.
13. Gad El Kareem AM, Willikens B, Stassen JM, et al. Differential vitreous dye diffusion following microplasmin or plasmin pre-treatment. *Curr Eye Res*. 2010;35:235–41.
14. Gandorfer A, Rohleder M, Sethi C, et al. Posterior vitreous detachment induced by microplasmin. *Invest Ophthalmol Vis Sci*. 2004;45:641–7.
15. Gao BB, Chen X, Timothy N, et al. Characterization of the vitreous proteome in diabetes without diabetic retinopathy and diabetes with proliferative diabetic retinopathy. *J Proteome Res*. 2008;7:2516–25.
16. Hermel M, Dailey W, Hartzer M. Efficacy of plasmin, microplasmin, and streptokinase-plasmin complex for the in-vitro degradation of fibronectin and laminin-implications for vitreoretinal surgery. *Curr Eye Res*. 2011;35:419–24.
17. Hikichi T, Yanagiya N, Kado M, et al. Posterior vitreous detachment induced by injection of plasmin and sulfur hexafluoride in the rabbit vitreous. *Retina*. 1999;19:55–8.
18. Howden GD. The successful treatment of a case of central retinal vein thrombosis with intravenous fibrinolysin. *Can J Ophthalmol*. 1959;81:382–4.
19. Kohno T, Sorgente N, Ishibashi T, et al. Immunofluorescent studies of fibronectin and laminin in the human eye. *Invest Ophthalmol Vis Sci*. 1987;28:506–14.
20. Margherio AR, Margherio RR, Hartzer M, et al. Plasmin enzyme-assisted vitrectomy in traumatic pediatric macular holes. *Ophthalmol*. 1998;105:1617–20.
21. Nagai N, Demarsin E, van Hoef B, et al. Recombinant human microplasmin: production and potential therapeutic properties. *J Thromb Haemost*. 2003;1:307–13.
22. Pakola S, Cahillane G, Stassen J, et al. Neutralization of anti-plasmin by microplasmin: a randomized, double-blind, placebo-controlled, ascending-dose study in healthy male volunteers. *Clin Ther*. 2009;31:1688–706.
23. Ploplis VA, Castellino FJ. Nonfibrinolytic functions of plasminogen. *Methods*. 2000;21:103–10.
24. Sebag J. Pharmacologic vitreolysis. *Retina*. 1998;18:1–3.
25. Sebag J. Anomalous PVD – a unifying concept in vitreo-retinal diseases. *Graefes Arch Clin Exp Ophthalmol*. 2004;42:690–8.
26. Sebag J. Molecular biology of pharmacologic vitreolysis. *Trans Am Ophthalmol Soc*. 2005;103:473–94.
27. Sebag J. Pharmacologic vitreolysis – premise and promise of the first decade. *Retina*. 2009;29:871–4.
28. Sebag J, Ansari R, Suh K. Pharmacologic vitreolysis with microplasmin increases vitreous diffusion coefficients. *Graefes Arch Clin Exp Ophthalmol*. 2007;45:576–80.
29. Stalmans P, de Laey C, de Smet M, et al. Intravitreal injection of microplasmin for treatment of vitreomacular adhesion: results of a prospective, randomized, sham-controlled phase II trial (the MIVI-IIT trial). *Retina*. 2010;30:1122–7.
30. Takano A, Hirata A, Inomata Y, et al. Intravitreal plasmin injection activates endogenous matrix metalloproteinase-2 in rabbit and human vitreous. *Am J Ophthalmol*. 2005;140:654–60.
31. Turner RB, Liu L, Sazonova IY, Reed GL. Structural elements that govern the substrate specificity of the clot-dissolving enzyme plasmin. *J Biol Chem*. 2002;277:33068–74.
32. Udaondo P, Diaz-Llopis M, Garcia-Delpech S, et al. Intravitreal plasmin without vitrectomy for macular edema secondary to branch retinal vein occlusion. *Arch Ophthalmol*. 2011;129:283–7.
33. Uemura A, Nakamura M, Kachi S, et al. Effect of plasmin on laminin and fibronectin during plasmin-assisted vitrectomy. *Arch Ophthalmol*. 2005;123:209–13.
34. Valmaggia C, Willekens B, de Smet MD. Microplasmin induced vitreolysis in porcine eyes. *Invest Ophthalmol Vis Sci*. 2003;44:E Abstract 3050.
35. Verstraeten TC, Chapman C, Hartzer M, et al. Pharmacologic induction of posterior vitreous detachment in the rabbit. *Arch Ophthalmol*. 1993;111:849–54.
36. Wang X, Lin X, Loy J, et al. *Science*. 1998;281:1662–5.
37. Wu CW, Sauter JL, Johnson PK, et al. Identification and localization of major soluble vitreous proteins in human ocular tissue. *Am J Ophthalmol*. 2004;137:655–61. doi:10.1016/j.ajo.2003.11.009.
38. Wu HL, Shi GY, Bender ML. Preparation and purification of microplasmin. *Proc Natl Acad Sci U S A*. 1987;84:8292–5.

Peter Stalmans

Outline

- I. **Introduction**
- II. **Clinical Trials with Ocriplasmin for sVMA and VMT**
 - A. Summary
 - B. Phase 2 Trials
 1. Intravitreal Microplasmin During Surgical Vitrectomy (MIVI-I) (TG-MV-001)
 2. Multi-dosing in Patients with Vitreomacular Traction (MIVI-IIT) (TG-MV-004)
 3. Safety and Efficacy of Inducing PVD (MIVI-III) (TG-MV-003)
 - C. Phase 3 Trials
 1. Background and Study Design
 2. Efficacy Findings
 3. Safety Findings
- III. **Phase 2 Trials of Ocriplasmin in Patients with VMA and Concomitant Retinal Disease**
 - A. Diabetic Macular Edema [MIVI-II-DME (TG-MV-002)]
 - B. Age-Related Macular Degeneration [MIVI-V (TG-MV-005)]

Conclusions

References

Keywords

Vitreous • Full-thickness macular hole • MIVI-TRUST • Pars plana vitrectomy • Vitreomacular adhesion • Vitreomacular interface • Vitreomacular traction • Premacular (epiretinal) membrane • Intravitreal injection • Ocriplasmin • Posterior vitreous detachment

Key Concepts

1. Ocriplasmin is a pharmacologic vitreolysis agent approved by the US Food and Drug Administration for the treatment of symptomatic vitreomacular adhesion (VMA) and by the European Medicines Agency for the treatment of vitreomacular traction (VMT), including when associated with macular hole less than or equal to 400 microns.
2. The efficacy and safety of ocriplasmin versus placebo for the treatment of VMT has been demonstrated in a clinical trial program funded by ThromboGenics, Inc, that, as of publication, includes eight phase 2 studies, two phase 3 studies, and two phase 3b studies.
3. The pivotal phase 3 Microplasmin for Intravitreal Injection–Traction Release Without Surgical Treatment (MIVI-TRUST) study demonstrated superiority of a single intravitreal injection of 125 µg ocriplasmin versus placebo in pharmacologic resolution of VMA and total induction of posterior vitreous detachment. Pharmacologic closure of full-thickness macular hole (FTMH, ≤400 microns and with VMA) was achieved in a higher percentage of patients with FTMH at baseline in the ocriplasmin group compared with placebo and was highest among patients with small FTMH (≤250 microns).

P. Stalmans, MD, PhD
Department of Ophthalmology, Universitaire Ziekenhuizen
Leuven, Herestraat 49, Leuven 3000, Belgium
e-mail: peter.stalmans@uzleuven.be

I. Introduction

The natural vitreous aging process involves liquefaction of the gel and separation of the posterior vitreous cortex from the retina [1–3] [see chapter II.C. Aging and PVD]. In some eyes, however, the adhesion between the vitreous cortex and the macular surface does not weaken sufficiently to allow complete posterior vitreous detachment (PVD), leading to persistent attachment at the macular surface, or vitreomacular adhesion (VMA) [see chapter III.B. Anomalous PVD and vitreoschisis]. The diagnosis of VMA is based on the analysis of optical coherence tomography (OCT) imaging and is, by definition, an asymptomatic non-pathologic state. Persistent VMA can progress to pathologic conditions, such as vitreomacular traction (VMT), that disturb the vitreomacular interface (VMI) and can cause visual symptoms. A classification system of VMA, VMT, and full-thickness macular holes has been developed by an international consensus panel [see chapter III.D. Vitreo-macular traction and holes] [4]. For objectivity and uniformity, this system is based on findings and not symptoms.

Patients with VMT typically present with decreased vision and varying degrees of metamorphopsia. Even patients with well-preserved visual acuity may experience disturbances in the quality of vision or daily visual functioning. In a retrospective study of 53 consecutive eyes with VMT that were followed for a median study period of 60 months (range 6–110 months), 64 % experienced a decrease in best-corrected visual acuity (BCVA) of at least two lines from baseline, and only 11 % ended with complete PVD [5]. Persistent VMT can progress to increasingly severe conditions, such as full-thickness macular hole (FTMH). If left untreated, disorders of the VMI can lead to irreversible macular damage, progressive deterioration of vision, and increasingly difficult surgeries [5–9].

In cases where symptoms are not sufficiently severe to warrant surgical intervention, a physician may decide to watch and wait for the vitreous traction to spontaneously resolve. In several cases, watchful waiting can have a deleterious effect on outcomes, as chronic VMT can stress the macula and lead to irreversible damage. Only approximately 20 % of eyes with unresolved VMA will spontaneously detach and not need vitrectomy [5, 10]. In the remaining majority of eyes, persistent VMA progresses in 30 % to the point where intervention with vitrectomy is required [10]. Surgical success rates decrease the longer vitrectomy is delayed, and patients with greater losses at the beginning of treatment tend to have worse surgical prognoses.

Vitrectomy, like any surgery, carries the risk of complications, both during and after the procedure. As is the case with many other surgeries, vitrectomy imposes a significant treatment burden on patients and their families. Complications that have been associated with vitrectomy include retinal tear and detachment, iatrogenic damage to ocular structures, cataracts, hemorrhage, vitreous hemorrhage, and endophthalmitis [11–22]. Even when vitrectomy is successful, patients must wait several weeks before returning to work, with some patients having to spend at least a week in a “head-down” prone position [23].

The risks and burdens associated with watchful waiting or vitrectomy underlie the need for a pharmacologic treatment option for patients with VMT, including when associated with macular hole [see chapter VI.A. Pharmacologic vitreolysis] [10]. Moreover, non-surgical release of VMT induces better visual acuity outcome. After extensive testing in experimental animal models [see chapter VI.E.1. Basic science of ocriplasmin pharmacologic vitreolysis], ocriplasmin underwent clinical trials whose results are summarized below. Based on these trials, ocriplasmin therapy, in the form of an intravitreal injection, was approved by the US Food and Drug Administration (FDA) in October 2012 for the treatment of symptomatic VMA and by the European Medicines Agency (EMA) in March 2012 for the treatment of VMT, including when associated with macular hole of diameter less than or equal to 400 microns. To date, ocriplasmin is the only pharmacologic treatment option approved by the FDA and the EMA for the treatment of patients with this sight-threatening condition that includes VMT, with or without macular hole. Several phase 2 and pivotal phase 3 trials demonstrated that ocriplasmin is superior to placebo or sham injection in the pharmacologic resolution of VMA [24–27]. Funded by ThromboGenics, Inc, the ocriplasmin clinical development program led to the following findings in support of ocriplasmin as a pharmacologic vitreolytic agent for the treatment of patients with VMA and associated symptomatology.

II. Clinical Trials with Ocriplasmin for sVMA and VMT

A. Summary

1. *Ocriplasmin effectively resolves VMA.* Ocriplasmin successfully treats VMT and averts the need for vitrectomy in many patients. In addition, patients with FTMH (≤ 400 microns and with VMA) in the MIVI-TRUST clinical trial program had a nearly 4-fold increase in the rate of pharmacologic hole closure after a single injection of ocriplasmin compared with placebo.
2. *Ocriplasmin does not interfere with surgical outcomes in cases where vitrectomy is still required.* In some patients, treatment with ocriplasmin may even support improved vitrectomy outcomes.
3. *Ocriplasmin is well tolerated.* Suspected drug-related ocular adverse events tend to be nonserious, transient, and mild in severity. Twelve studies comprise the ocriplasmin clinical development program to date, including eight phase 2 studies, two phase 3 studies that together comprised the Microplasmin for Intravitreal Injection–Traction Without Surgical Treatment (MIVI-TRUST) program, and two phase 3b studies, amounting up to more than 1000 patients (Table VI.E.2-1).

Table VI.E.2-1 Ocriplasmin clinical development program

Study ID	Indication, design, and control	Ocriplasmin groups	Enrollment
<i>Phase II trials</i>			
MIVI-I (TG-MV-001)	VMT patients scheduled for vitrectomy Multicenter, open-label, dose-escalation trial Uncontrolled	25 µg/1–2 h 25 µg/24 h 25 µg/7 days 50 µg/24 h 75 µg/24 h 125 µg/24 h	60
MIVI-II-DME (TG-MV-002)	Patients with VMA and concomitant advanced DME Multicenter, randomized, double-masked trial Sham-controlled	50 µg 75 µg 125 µg	51
MIVI-III (TG-MV-003)	VMT patients scheduled for vitrectomy Multicenter, randomized, double-masked trial Placebo-controlled	25 µg 75 µg 125 µg	125
MIVI-IIT (TG-MV-004)	Patients with VMT Multicenter, randomized, double-masked trial Sham-controlled	75 µg 125 µg 175 µg 125 µg ^a	60
MIVI-V (TG-MV-005)	Patients with VMA and concomitant exudative AMD Multicenter, randomized, double-masked trial Sham-controlled	125 µg	100
MIVI-VIII (TG-MV-008)	Patients with symptomatic VMA Single-center, open-label trial Uncontrolled	125 µg	30
MIC (TG-MV-009)	Pediatric patients scheduled for vitrectomy Single-center, randomized, double-masked trial Placebo-controlled	175 µg	24
MIVI-X (TG-MV-010)	VMT patients scheduled for vitrectomy Single-center, open-label, pharmacokinetic trial	125 µg/5–30 min 125 µg/31–60 min 125 µg/2–4 h 125 µg/24 ± 2 h 125 µg/7 ± 1 days	38
<i>Phase III trials</i>			
MIVI-VI (TG-MV-006)	Patients with symptomatic VMA Multicenter, randomized, double-masked trial Placebo-controlled	125 µg	326
MIVI-VII (TG-MV-007)	Patients with symptomatic VMA Multicenter, randomized, double-masked trial Placebo-controlled	125 µg	326
<i>Phase IIIb trials</i>			
MIVI-XII (TG-MV-012)	Long-term follow-up of patients from phase III trials	125 µg	20
OASIS (TG-MV-014)	patients with symptomatic VMA including FTMH Multicenter, randomized, double-masked trial Sham-controlled	125 µg	220

^aPatients eligible for up to two subsequent doses in absence of VMA resolution

Abbreviations: AMD age-related macular degeneration, DME diabetic macular edema, FTMH full-thickness macular hole, VMA vitreomacular adhesion, VMT vitreomacular traction

B. Phase 2 Trials

1. Intravitreal Microplasmin During Surgical Vitrectomy (MIVI-I) (TG-MV-001)

This phase 2 study was the first reported use of ocriplasmin administered as an intravitreal injection in humans. MIVI-I was a prospective, multicenter, non-controlled, dose-

escalation trial consisting of 60 patients with VMT or FTMH without PVD who were scheduled to undergo vitrectomy. Study participants were 18 years or older and divided into 6 groups of 9–11 patients each. In all patients, surgery was performed at a predetermined time after the drug was injected into the vitreous. The study was performed in two parts: The first part involved an ascending-exposure series in which a fixed dose of ocriplasmin (25 µg) was injected at specific

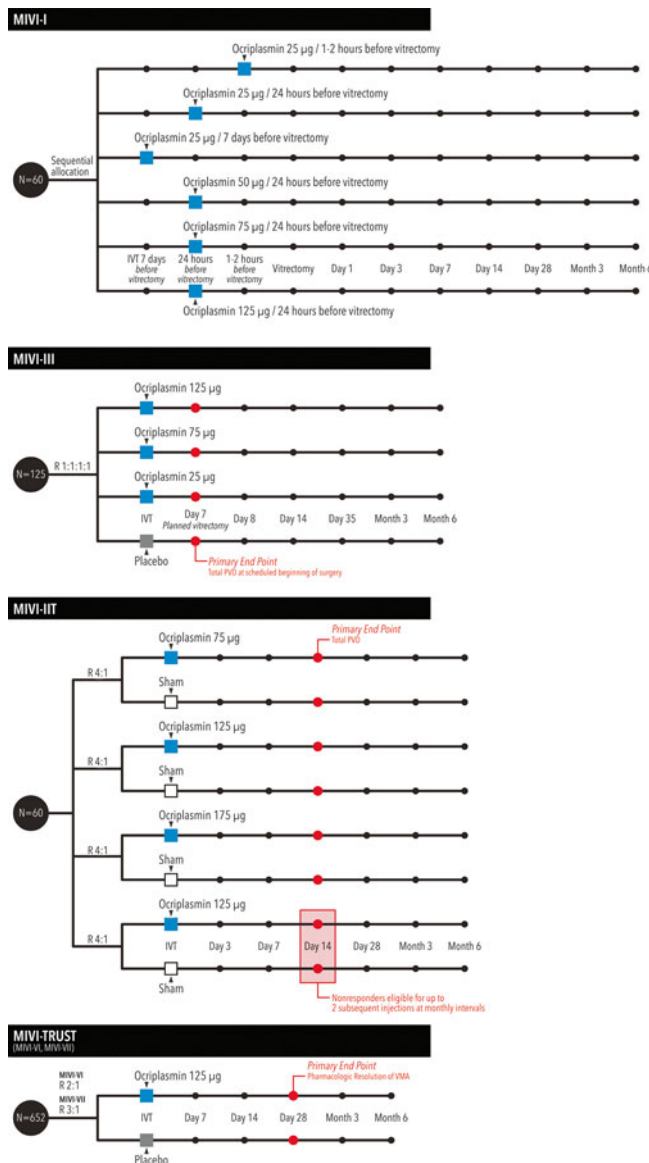
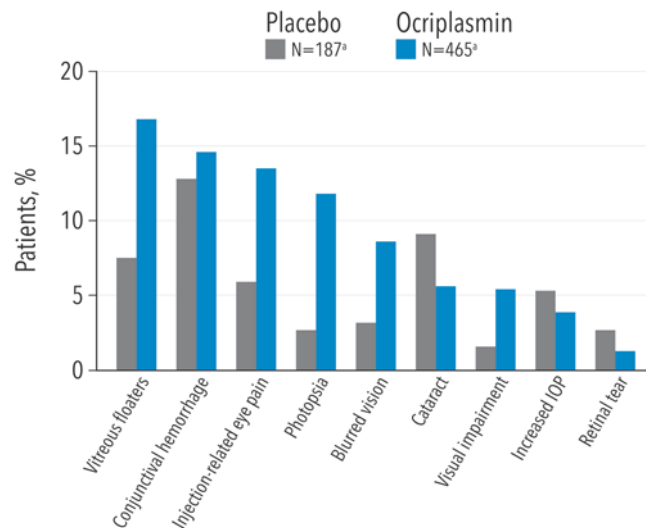


Figure VI.E.2-1 Ocriplasmin clinical development program: study designs. Diagrams show the study designs of the phase 2 MIVI-I, MIVI-III, and MIVI-IIT trials and the phase 3 MIVI-TRUST clinical trial program. *Abbreviations:* BCVA best-corrected visual acuity, FTMH full-thickness macular hole, PVD posterior vitreous detachment, VMA vitreomacular adhesion, VFQ-25 25-item Visual Function Questionnaire

times before surgery (1–2 h, 24 h, or 7 days). The second part involved a dose-escalation series (50, 75, and 125 µg) in which ocriplasmin was injected 24 h before surgery for all doses (Figure VI.E.2-1) [25].

MIVI-I assessed the safety and preliminary efficacy of a single intravitreal injection over a range of doses and exposure times. Results showed that intravitreal ocriplasmin was well tolerated up to the maximum study dose of 125 µg and was capable of inducing preoperative PVD in some patients. In general, MIVI-I served as a proof-of-principle trial for the



¹ One patient who was randomized to the placebo group inadvertently received treatment with ocriplasmin; this patient was included in the ocriplasmin group for the purposes of safety analysis.

Figure VI.E.2-2 Pharmacologic resolution of vitreomacular adhesion (VMA) over the course of the phase 3 MIVI-TRUST clinical trial program. *Line graph* shows the proportion of patients in each treatment group with pharmacologic resolution of VMA at each study visit over the course of the phase 3 MIVI-TRUST clinical trial program. Among the 26.5 % of patients in the ocriplasmin group with pharmacologic resolution of VMA at day 28 (primary end point), 73 % had already achieved resolution by day 7

use of ocriplasmin in pharmacologic vitreolysis. The study showed that increasing lengths of exposure to ocriplasmin led to progressively higher incidences of preoperative PVD induction and that ocriplasmin led to pharmacologic induction of total PVD in some patients [25].

Overall, ocriplasmin was well tolerated in this trial. Adverse events included vitreous floaters and photopsia, all cases of which developed within 6 h of injection. Transient rises in intraocular pressure were observed in 14 patients. All cases responded to standard pressure-reducing strategies [25].

2. Multi-dosing in Patients with Vitreomacular Traction (MIVI-IIT) (TG-MV-004)

MIVI-IIT was a phase 2, multicenter, randomized, double-masked, sham-controlled trial. Sixty patients with VMT, including some with macular hole, were randomized into one of four cohorts. In the first 3 cohorts, patients were randomized 4:1 to receive a single intravitreal injection of ocriplasmin (75, 125, or 175 µg, depending on the cohort) or a sham injection. Patients in the fourth cohort were randomized to receive a single intravitreal injection of 125 µg ocriplasmin or placebo but were eligible to receive up to 2 subsequent injections of 125 µg ocriplasmin at monthly intervals if resolution of VMA was not achieved (Figure VI.E.2-2) [27].

The primary end point of MIVI-IIT was total PVD at 14 days after intravitreal injection with ocriplasmin. Secondary end points included total PVD at other time points (3, 7, and 28 days after injection), pharmacologic resolution of VMA, progression of PVD, need for vitrectomy, resolution of macular edema (if relevant), and changes in best-corrected visual acuity (BCVA, measured as ETDRS letter score) from baseline [27].

Findings from the MIVI-IIT trial demonstrated the following [27]:

- At 14 days after injection, total PVD was observed in 16 % of all patients treated with ocriplasmin in the first 3 cohorts compared with 0 % of patients who received a sham injection in these same cohorts.
- On day 90, total PVD was observed in a higher proportion of patients in the 125 µg ocriplasmin group (third cohort) compared to the sham group ($P=0.046$).
- In the cohort eligible to receive repeat injections (fourth cohort), 58 % of patients eventually achieved pharmacologic resolution of VMA by study end.

3. Safety and Efficacy of Inducing PVD (MIVI-III) (TG-MV-003)

MIVI-III was a phase 2, multicenter, randomized, double-masked, placebo-controlled, dose-ranging clinical trial. The trial included 125 patients 18 years or older with VMT, including some with FTMH, who were scheduled to undergo vitrectomy. Patients were randomized 1:1:1:1 to receive a single intravitreal injection of 25, 75, or 125 µg ocriplasmin or placebo (Figure VI.E.2-3) [24].

The primary end point of MIVI-III was pharmacologic induction of total PVD by the scheduled beginning of surgery. The study also assessed progression of PVD at 7 days after injection, the proportion of participants achieving pharmacologic resolution of VMT, the proportion of patients achieving pharmacologic closure of FTMH, and the proportion of patients with BCVA that increased from baseline (regardless of whether vitrectomy was performed) [24].

Results of the MIVI-III trial [24] demonstrated several efficacy points, including:

- At the scheduled beginning of surgery, rates of total PVD increased in accordance with increasing doses of ocriplasmin.
- Higher doses of ocriplasmin were associated with greater rates of pharmacologic VMT resolution.
- Pharmacologic closure of FTMH was observed in a larger proportion of patients in the ocriplasmin group compared with placebo.
- By the end of the study (6 months), 17.0 % of patients treated with ocriplasmin (any dose) avoided vitrectomy compared to 3.2 % of those treated with placebo.
- Among patients who proceeded with scheduled vitrectomy, mean maximum suction and mean surgical time required to

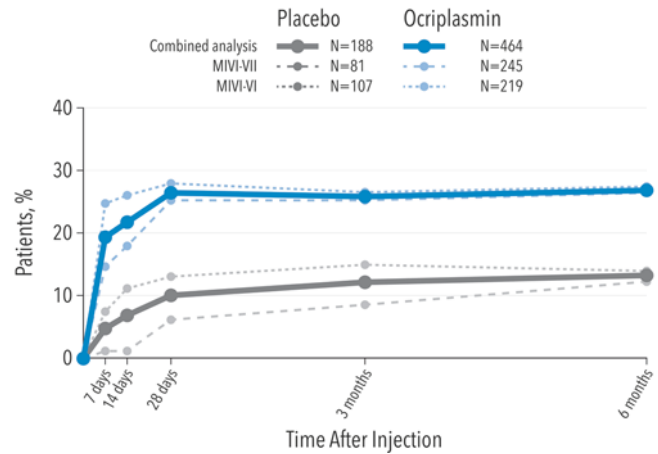


Figure VI.E.2-3 Incidence of ocular adverse events in the phase 3 MIVI-TRUST clinical trial program. Bar graph shows the proportion of patients in each treatment group that reported an ocular adverse event (by type) over the course of the phase 3 MIVI-TRUST clinical trial program. The proportion of patients who reported at least one ocular adverse event was 68.4 % in the ocriplasmin group and 53.5 % in the placebo group. Most reported ocular adverse events were transient and mild in severity. Abbreviation: IOP intraocular pressure

induce total PVD were less for patients who received an injection of ocriplasmin versus placebo. Results were consistent with a potential dose-dependent effect, as increasing doses of ocriplasmin corresponded to greater reductions in mean maximum suction and mean surgical time.

C. Phase 3 Trials

1. Background and Study Design

The ocriplasmin phase 3 MIVI-TRUST program included the MIVI-006 and MIVI-007 trials, which were designed in collaboration with the FDA over a 5-month period after the completion of several phase 2 studies. These pivotal phase 3 studies depended on the interpretation of data derived from OCT visualization and, as such, used a masked central reading center (CRC) to ensure consistent interpretation of OCT readings and a data monitoring committee to oversee all safety aspects of the program. The resulting study design was implemented at major eye clinics across the United States and Europe.

MIVI-006 and MIVI-007 were multicenter, randomized, double-masked, placebo-controlled, 6-month studies designed to determine the safety and efficacy of a single intravitreal injection of 125 µg ocriplasmin in patients with OCT-confirmed VMA with associated symptomatology. The 2 trials were identical in design except for (1) the randomization of ocriplasmin to placebo (injection of same volume of saline), with an allocation ratio of 2:1 in MIVI-006 and 3:1 in MIVI-007, and (2) the geography of the study sites, with MIVI-006 conducted in the United States and MIVI-007 in the United States and European

Union. Total combined patient enrollment was 652 patients with VMT, including 153 with FTMH. All patients were randomized to receive a single intravitreal injection of 125 µg ocriplasmin ($N=464$) or placebo ($N=188$). Participants were then examined for follow-up at days 7, 14, 28, 90, and 180 after injection (Figure VI.E.2-1) [26].

The primary efficacy end point was the proportion of patients with pharmacologic resolution of VMA at 28 days after injection, as determined by masked CRC OCT evaluation [26]. Patients who developed an anatomic defect (i.e., retinal break or retinal detachment) that resulted in loss of vision or that required additional intervention were not counted as success on the primary end point.

Secondary efficacy end points included the following [26]:

- Total PVD at 28 days after injection, as determined by masked investigator-certified assessment of B-scan ultrasound
- Pharmacologic closure of FTMH
- Avoidance of vitrectomy
- Achievement of at least 2- or 3-line increase in BCVA (without vitrectomy)
- Improvement in mean BCVA ETDRS letter score
- Improvement in the 25-item Visual Function Questionnaire (VFQ-25) score (composite and subscales)

2. Efficacy Findings

The results of MIVI-006 and MIVI-007 were analyzed separately and for the combined phase 3 population. Specific references to data in the following discussion are derived from the combined analysis. Success on the primary efficacy end point, pharmacologic resolution of VMA at 28 days after injection, was observed in a significantly greater proportion of patients treated with ocriplasmin (26.5 %) versus placebo (10.1 %, $P<0.001$) (Table VI.E.2-2) [24]. Notably, most cases of pharmacologic resolution occurred within 7 days of injection. Among those in the ocriplasmin group with pharmacologic resolution of VMA at day 28, 73 % had already achieved resolution by 7 days after injection (Figure VI.E.2-2). The area of vitreous attachment appears to be an important factor in the achievement of successful anatomic outcomes after treatment with ocriplasmin. Pharmacologic resolution of VMA at day 28 was observed in more than twice the proportion of patients with focal VMA (diameter $\leq 1,500$ microns) when treated with ocriplasmin (34.7 %) compared with placebo (14.6 %, $P<0.001$). For patients with broad VMA (diameter $>1,500$ microns), pharmacologic resolution of VMA at day 28 occurred in only 5.9 % of patients treated with ocriplasmin and none in the placebo group ($P=0.113$) [28].

Success on all secondary end points was observed in larger proportions of the ocriplasmin group compared with placebo in the combined analysis of both trials (Table VI.E.2-2). Total PVD at day 28 after injection was

observed in a significantly larger proportion of the ocriplasmin group (13.4 %) compared with the placebo group (3.7 %, $P<0.001$). Pharmacologic closure of FTMH at day 28 also occurred at a higher rate among patients treated with ocriplasmin (40.6 %) versus placebo (10.6 %, $P<0.001$) [26]. This effect of ocriplasmin on closure of FTMH was also deemed to be rapid, being observed by day 7 in almost 70 % of patients who achieved this outcome at day 28. The rate of pharmacologic closure of FTMH differed according to the size of the hole at baseline. Small holes (narrowest linear width ≤ 250 microns, not counting the inner limiting membrane) had the highest rates of pharmacologic closure of FTMH at day 28 after treatment with ocriplasmin (58.3 % versus 16.0 % in the placebo group, $P<0.001$). Pharmacologic closure of FTMH at day 28 was observed at lower rates in both treatment groups among patients with medium holes (>250 to ≤ 400 microns) but was still higher after treatment with ocriplasmin (36.8 %) versus placebo (5.3 %, $P=0.009$). Patients with large holes (>400 microns) were excluded from the study based on predefined exclusion criteria; however, 22 patients with large holes at baseline were inadvertently enrolled in the study. None of these patients, in either group, had pharmacologic closure of FTMH at day 28 [26, 28].

A subgroup analysis was performed to analyze the efficacy of ocriplasmin in patients with or without presence of an epiretinal (“premacular” is the preferred term) membrane (ERM) with macular pucker at baseline. Among patients with a premacular ERM at baseline, only 8.7 % of those treated with ocriplasmin had pharmacologic resolution of VMA at day 28. Despite this low rate, success was still higher after treatment with ocriplasmin when compared with placebo (1.5 %, $P=0.046$). Rates of successful VMA resolution were higher in both treatment groups among patients who did not have a premacular ERM at baseline. Primary end point success was observed in 37.4 % of the ocriplasmin group versus 14.3 % of the placebo group ($P<0.001$) [26, 29]. Analysis of post-marketing injections, excluding patients with concomitant ERM showed VMT success rates of up to 78 %.

Vitrectomy by the end of study was required less often in the ocriplasmin group (17.7 %) compared to the placebo group (26.6 %), suggesting that the availability of ocriplasmin as a treatment option for VMA-associated disorders of the VMI may help to reduce the overall surgical volume [26]. In patients with FTMH at baseline who ended up requiring vitrectomy, the rate of postoperative hole closure remained high and was nearly the same for patients treated with ocriplasmin (93.1 %) and those receiving placebo (92.3 %), suggesting that treatment with ocriplasmin before surgery does not hinder the chances of achieving anatomic success after surgery [28].

Treatment with ocriplasmin was also associated with promising visual outcomes. The mean change in BCVA from baseline was higher in the ocriplasmin group (+3.6 letters) versus placebo (+2.5 letters), and the achievement ≥ 2 or 3

Table VI.E.2-2 Summary of efficacy findings from the ocriplasmin phase III MIVI-TRUST program (MIVI-VI, MIVI-VII, and combined analysis)

End point	Study	Ocriplasmin 125 µg, %	Placebo, %	p value
Pharmacologic resolution of VMA, day 28	MIVI-VI	27.9	13.1	0.003
	MIVI-VII	25.3	6.2	<0.001
	Combined analysis	26.5	10.1	<0.001
Pharmacologic inducement of total PVD, day 28	MIVI-VI	16.4	6.5	0.010
	MIVI-VII	10.6	0.0	<0.001
	Combined analysis	13.4	3.7	<0.001
Pharmacologic closure of FTMH, day 28	MIVI-VI	43.9	12.5	0.002
	MIVI-VII	36.7	6.7	0.030
	Combined analysis	40.6	10.6	<0.001
Need for vitrectomy, month 6	MIVI-VI	20.5	29.0	0.100
	MIVI-VII	15.1	23.5	0.090
	Combined analysis	17.7	26.6	0.020
Achievement of ≥2-line BCVA increase, month 6 (without vitrectomy)	MIVI-VI	25.6	11.2	0.002
	MIVI-VII	22.0	11.1	0.035
	Combined analysis	23.7	11.2	<0.001
Achievement of ≥3-line BCVA increase, month 6 (without vitrectomy)	MIVI-VI	10.5	6.5	0.310
	MIVI-VII	9.0	0.0	0.002
	Combined analysis	9.7	3.7	0.008
Mean change in VFQ-25 composite score, month 6	MIVI-VI	+3.5	+1.2	0.094
	MIVI-VII	+3.3	-0.1	0.013
	Combined analysis	+3.4	+0.7	0.004

Abbreviations: BCVA best-corrected visual acuity, FTMH full-thickness macular hole, PVD posterior vitreous detachment, VMA vitreomacular adhesion, VFQ-25 25-item Visual Function Questionnaire

lines BCVA from baseline was observed in larger proportions of the ocriplasmin group (28.0 % ≥2 lines and 12.3 % ≥3 lines) compared to the placebo group (17.1 % ≥2 lines and 6.4 % ≥3 lines) [26, 28].

Analysis of the VFQ-25 results indicated that treatment with ocriplasmin also led to significant improvements in visual function and vision-related quality of life. Mean improvement from baseline in the overall VFQ-25 composite score was higher in the ocriplasmin group (3.4) compared to the placebo group (0.7, $P=0.007$). Individual VFQ-25 subscales that showed significant improvement in patients treated with ocriplasmin versus placebo included general vision ($P=0.006$), distance vision ($P=0.03$), dependency ($P=0.009$), and driving ($P=0.03$) [26].

3. Safety Findings

Findings from the phase 3 MIVI-TRUST trials showed that ocriplasmin was well tolerated and that most suspected drug-related adverse events were nonserious, transient, and mild in severity. The percentage of patients experiencing at least one ocular adverse event was 68.4 % in the ocriplasmin group and 53.5 % in the placebo group. Common ocular adverse events included vitreous floaters (16.8 % ocriplasmin versus 7.5 % placebo), conjunctival hemorrhage (14.6 % versus 12.8 %), injection-related eye pain (13.5 % versus 5.9 %), photopsia (11.8 % versus 2.7 %), blurred vision (8.6 % versus 3.2 %), cataract (5.6 % versus 9.1 %), visual

impairment (5.4 % versus 1.6 %), and intraocular pressure increase (3.9 % versus 5.3 %) (Figure VI.E.2-3). Most adverse events were of mild or moderate intensity and reported between days 0 and 7 after injection. The overall incidence of serious ocular adverse events in the study eye was higher in the placebo group (7.7 %) than the ocriplasmin group (10.7 %) [26].

Only three non-ocular adverse events were reported by at least 2 % of the study population. These included nausea, bronchitis, and headache. With the exception of nausea, the incidence of each of these adverse events was similar between the ocriplasmin and placebo groups. Overall, the non-ocular events reported during these clinical studies were consistent with an elderly population with underlying medical conditions followed for a 6- to 12-month period [26].

Most cases of retinal breaks (tears and/or detachments) were iatrogenic. The incidence of nonsurgical retinal breaks was 0.4 % in the ocriplasmin group (2 cases) and 0.5 % in the placebo group (1 case). All nonsurgical breaks were successfully corrected after vitrectomy [28].

Cataract progression was observed in similar proportion of phakic eyes in the ocriplasmin (8.2 %) and placebo (11.9 %) groups. These rates were lower in patients who did not require vitrectomy by the end of study (4.8 % ocriplasmin versus 5.2 % placebo) [26].

No cases of endophthalmitis were reported in any of the phase 2 and phase 3 trials [24–27].

III. Phase 2 Trials of Ocriplasmin in Patients with VMA and Concomitant Retinal Disease

The phase 3 trials were designed to address the effectiveness of ocriplasmin in patients with isolated VMA and associated symptomatology. Enrollment criteria excluded patients with the presence of concomitant retinal diseases known to affect visual function, including proliferative diabetic retinopathy, exudative age-related macular degeneration (AMD), and retinal vein occlusion [26]. To date, there are two studies in the ocriplasmin clinical trial program to address efficacy and safety of ocriplasmin in patients with VMA and concomitant retinal disease: MIVI-II-DME and MIVI-V.

A. Diabetic Macular Edema [MIVI-II-DME (TG-MV-002)]

Diabetes has significant biochemical, structural, and physiologic effects upon the vitreous [see chapter I.E. Diabetic vitreopathy]. The role of vitreous in diabetic macular edema (DME) specifically is discussed in chapter III.K. [Vitreous in retino-vascular diseases and diabetic macular edema]. With this knowledge, ocriplasmin pharmacologic vitreolysis was tested in this clinical setting. MIVI-II-DME was a multicenter, randomized, double-masked, sham-controlled, ascending-dose trial. Sixty patients with VMA and concomitant advanced diabetic macular edema (DME) were assigned to 1 of 3 cohorts and, within each cohort, randomized 3:1 to receive a single intravitreal injection of ocriplasmin or sham treatment. Patients randomized to the ocriplasmin group in the first cohort received a single 25 µg dose. Corresponding patients in the second and third cohorts received 75 and 125 µg doses, respectively. Patients in the first or second cohort were eligible to receive an additional injection at the next-highest dose if the investigator deemed necessary and safety of the first dose had been demonstrated [28].

The primary end point was total PVD at day 14 after injection. The study is complete but data are not yet published [28].

B. Age-Related Macular Degeneration [MIVI-V (TG-MV-005)]

The vitreous may play an important role in the pathogenesis of exudative age-related macular degeneration [see chapter III.G. Vitreous in AMD]. Thus, a clinical trial was undertaken to test the hypothesis that ocriplasmin pharmacologic vitreolysis can induce an innocuous PVD and that this will have salubrious effects on the course of the disease. This phase 2 study was a multicenter, randomized, double-

masked, sham-controlled trial. One hundred patients with VMA and concomitant exudative AMD were randomized 3:1 to receive a single intravitreal injection of 125 µg ocriplasmin or sham treatment. To qualify for enrollment, primary or recurrent subfoveal choroidal neovascularization covering at least half of the total lesion area must have been present in the study eye at baseline. In addition, the study eye needed to have previously received at least three injections of bevacizumab and/or ranibizumab. Eyes that had previously undergone vitrectomy or received more than nine injections of bevacizumab and/or ranibizumab were excluded [28].

Patients were assessed on the day of injection and at days 7, 14, and 28 and months 3, 6, and 12 after injection. The primary end point was pharmacologic resolution of VMA at day 28 after injection. Selected secondary end points included resolution of VMA at all other study visits, PVD status, macular thickness, area of vascular leakage, change in visual acuity (ETDRS letters) from baseline, requirement for additional therapy, and number of bevacizumab and/or ranibizumab injections required over the course of study. The study is complete but data are not yet published [28].

Conclusions

Twelve studies comprise the ocriplasmin clinical trial program to date, including eight phase 2 studies, two phase 3 studies, and two phase 3b studies, with the pivotal phase 3 MIVI-TRUST program demonstrating efficacy and safety of a single intravitreal injection of ocriplasmin for the treatment of patients with symptomatic VMA or VMT including when associated with macular hole of diameter less than or equal to 400 microns. MIVI-II-DME and MIVI-V are phase 2 studies that have been completed with ongoing data analysis that may soon show efficacy of ocriplasmin in the treatment of patients with VMT and concomitant retinal diseases, such as DME and exudative AMD. Ocriplasmin was well tolerated in all clinical studies to date, and no cases of endophthalmitis have been reported thus far. The approval of ocriplasmin by the FDA and the EMA means that vitreoretinal specialists now have a pharmacologic option for appropriate patient types who may benefit from early intervention but do not yet have symptoms that are sufficiently severe to warrant the risks and burden of vitrectomy. Successful anatomic outcomes, such as resolution of VMA or closure of macular hole, were associated with successful visual outcomes. Patient-reported visual function and related quality-of-life scores were higher in patients after treatment with ocriplasmin compared to placebo, with improvements specifically noted in general vision, distance vision, vision-related dependency, and driving capabilities.

Many questions remain, and future studies are needed to determine whether ocriplasmin is a safe and effective treatment option for pediatric patients with VMI disorders,

whether administration of multiple doses over defined intervals is safe and effective for the treatment of resistant cases, and whether injection of ocriplasmin before surgery can function as an adjunct that improves postoperative outcomes. The role of patient selection in ocriplasmin treatment outcomes has yet to be fully explored, and a greater understanding of features that may predict response can help physicians choose the most appropriate treatment strategy for each unique case [30].

Abbreviations

AMD	Age-related macular degeneration
BCVA	Best-corrected visual acuity
CRC	Central reading center
DME	Diabetic macular edema
EMA	European Medicines Agency
ERM	Epiretinal (“premacular” is the preferred term) membrane
FDA	Food and Drug Administration (USA)
FTMH	Full-thickness macular hole
OCT	Optical coherence tomography
PVD	Posterior vitreous detachment
sVMA	Symptomatic vitreomacular adhesion
VFQ	Visual Function Questionnaire
VMA	Vitreomacular adhesion
VMI	Vitreomacular interface
VMT	Vitreomacular traction

References

- Larsson L, Osterlin S. Posterior vitreous detachment. A combined clinical and physiochemical study. *Graefes Arch Clin Exp Ophthalmol.* 1985;223(2):92–5.
- Sebag J. Anomalous posterior vitreous detachment: a unifying concept in vitreo-retinal disease. *Graefes Arch Clin Exp Ophthalmol.* 2004;242(8):690–8.
- Uchino E, Uemura A, Ohba N. Initial stages of posterior vitreous detachment in healthy eyes of older persons evaluated by optical coherence tomography. *Arch Ophthalmol.* 2001;119(10):1475–9.
- Duker JS, Kaiser PK, Binder S, et al. The international vitreomacular traction study group classification of vitreomacular adhesion, traction, and macular hole. *Ophthalmol.* 2013;120(12):2611–9.
- Hikichi T, Yoshida A, Trempe CL. Course of vitreomacular traction syndrome. *Am J Ophthalmol.* 1995;119(1):55–61.
- Ezra E, Fariss RN, Possin DE, et al. Immunocytochemical characterization of macular hole opercula. *Arch Ophthalmol.* 2001;119(2):223–31.
- Kim JW, Freeman WR, Azen SP, et al. Prospective randomized trial of vitrectomy or observation for stage 2 macular holes. *Vitrectomy for Macular Hole Study Group.* *Am J Ophthalmol.* 1996;121(6):605–14.
- Sonmez K, Capone Jr A, Trese MT, Williams GA. Vitreomacular traction syndrome: impact of anatomical configuration on anatomical and visual outcomes. *Retina.* 2008;28(9):1207–14.
- Thompson JT, Sjaarda RN, Lansing MB. The results of vitreous surgery for chronic macular holes. *Retina.* 1997;17(6):493–501.
- Peter Stalmans. Retrospective cohort study in patients with tractional diseases of the vitreomacular interface (ReCoVit). *Retina.* submitted.
- Banker AS, Freeman WR, Kim JW, et al. Vision-threatening complications of surgery for full-thickness macular holes. *Vitrectomy for Macular Hole Study Group.* *Ophthalmology.* 1997;104(9):1442–52; discussion 1452–1443.
- Chen CJ. Glaucoma after macular hole surgery. *Ophthalmology.* 1998;105(1):94–9; discussion 99–100.
- Cheng L, Azen SP, El-Bradey MH, et al. Duration of vitrectomy and postoperative cataract in the vitrectomy for macular hole study. *Am J Ophthalmol.* 2001;132(6):881–7.
- Freeman WR, Azen SP, Kim JW, et al. Vitrectomy for the treatment of full-thickness stage 3 or 4 macular holes. Results of a multi-centered randomized clinical trial. *The Vitrectomy for Treatment of Macular Hole Study Group.* *Arch Ophthalmol.* 1997;115(1):11–21.
- Guillaubey A, Malvitte L, Lafontaine PO, et al. Incidence of retinal detachment after macular surgery: a retrospective study of 634 cases. *Br J Ophthalmol.* 2007;91(10):1327–30.
- Kunimoto DY, Kaiser RS, Wills Eye Retina Service. Incidence of endophthalmitis after 20- and 25-gauge vitrectomy. *Ophthalmology.* 2007;114(12):2133–7.
- Park SS, Marcus DM, Duker JS, et al. Posterior segment complications after vitrectomy for macular hole. *Ophthalmology.* 1995;102(5):775–81.
- Ramkissoon YD, Aslam SA, Shah SP, et al. Risk of iatrogenic peripheral retinal breaks in 20-G pars plana vitrectomy. *Ophthalmology.* 2010;117(9):1825–30.
- Recchia FM, Scott IU, Brown GC, et al. Small-gauge pars plana vitrectomy: a report by the American Academy of Ophthalmology. *Ophthalmology.* 2010;117(9):1851–7.
- Rizzo S, Belting C, Genovesi-Ebert F, di Bartolo E. Incidence of retinal detachment after small-incision, sutureless pars plana vitrectomy compared with conventional 20-gauge vitrectomy in macular hole and epiretinal membrane surgery. *Retina.* 2010;30(7):1065–71.
- Scott IU, Flynn Jr HW, Dev S, et al. Endophthalmitis after 25-gauge and 20-gauge pars plana vitrectomy: incidence and outcomes. *Retina.* 2008;28(1):138–42.
- Thompson JT, Sjaarda RN, Glaser BM, Murphy RP. Increased intraocular pressure after macular hole surgery. *Am J Ophthalmol.* 1996;121(6):615–22.
- Ip MS, Baker BJ, Duker JS, et al. Anatomical outcomes of surgery for idiopathic macular hole as determined by optical coherence tomography. *Arch Ophthalmol.* 2002;120(1):29–35.
- Benz MS, Packo KH, Gonzalez V, et al. A placebo-controlled trial of microplasmin intravitreal injection to facilitate posterior vitreous detachment before vitrectomy. *Ophthalmology.* 2010;117(4):791–7.
- de Smet MD, Gandorfer A, Stalmans P, et al. Microplasmin intravitreal administration in patients with vitreomacular traction scheduled for vitrectomy: the MIVI I trial. *Ophthalmology.* 2009;116(7):1349–55, 1355.e1341–2.
- Stalmans P, Benz MS, Gandorfer A, et al. Enzymatic vitreolysis with ocriplasmin for vitreomacular traction and macular holes. *N Engl J Med.* 2012;367(7):606–15.
- Stalmans P, Delaey C, de Smet MD, et al. Intravitreal injection of microplasmin for treatment of vitreomacular adhesion: results of a prospective, randomized, sham-controlled phase II trial (the MIVI-IIT trial). *Retina.* 2010;30(7):1122–7.
- Novack RL. Ocriplasmin In Exudative AMD: Results of a prospective randomized clinical trial. *AAO Annual Meeting, New Orleans, Nov 16, 2013.*
- Koen W, Luís AP, Evelien V, et al. Efficacy of ocriplasmin as treatment for vitreomacular traction in carefully selected patients and ultrastructural findings at the optic disc. *Retina.* submitted
- Stalmans P, Duker JS, Kaiser PK, et al. Oct-based interpretation of the vitreomacular interface and indications for pharmacologic vitreolysis. *Retina.* 2013;33(10):2003–11.

Hyaluronidase as a Vitreous Liquefactant

VI.F.

Marc D. de Smet and Lisa Grillone

Outline

- I. **Introduction**
- II. **Mechanism of Action and Pharmacodynamics**
 - A. Hyaluronidase Enzyme Activity
 - B. Biological Activity
- III. **Clinical Experience**
 - A. Study Design
 - B. Results
 - C. Complications
 - D. Conclusions
- IV. **Future Directions and Applications**

References

Keywords

Vitreous • Pharmacologic vitreolysis • Hyaluronidase • Spreading • Hyaluronan • Liquefactant • Inflammation • Vitreous hemorrhage

Key Concepts

1. Hyaluronidase is a vitreous liquefactant with rapid onset and short duration of action. Within 3 days, the bulk of the activity is gone.
2. Ovine hyaluronidase and most formulations purified from animal material cause inflammation. This does not seem to be the case with human recombinant hyaluronidase rHuPH20, but this formulation has not been tested in eyes.
3. Intravitreal injection of ovine testicular hyaluronidase cleared vitreous hemorrhage in humans, but the clinical effect was insufficient to warrant FDA approval for this indication.
4. Excluding inflammation, hyaluronidase injections in humans were well tolerated with no significant differences from vehicle placebo injections regarding the incidence of retinal detachment or lenticular changes.

M.D. de Smet, MDCM, PhD, FRCSC, FRCOphth (✉)
Department of Retina and Inflammation,
Specialized Eye Center for Uveitis and Retina,
MIOS sa, Lausanne, Switzerland
e-mail: mddesmet1@mac.com

L. Grillone, PhD
PharmaQuest Associates LLC, San Diego, CA, USA

I. Introduction

Hyaluronan (HA) is a member of the glycosaminoglycan (GAG) family of polysaccharides, which are composed of repeating disaccharide units, each consisting of hexosamine (usually *N*-acetylglucosamine or *N*-acetylgalactosamine) glycosidically linked to either uronic (glucuronic or iduronic) acid or galactose. The nature of the predominant repeating unit is characteristic for each GAG, and the relative

amount, molecular size, and type of GAG are said to be tissue specific. GAGs do not normally occur *in vivo* as free polymers but are covalently linked to a protein core, the ensemble called a proteoglycan [see chapter I.F. Vitreous biochemistry and artificial vitreous]. HA is a GAG that plays an important role as a structural macromolecule in the vitreous. HA is a long, unbranched polymer of the repeating disaccharide glucuronic acid beta 1,3 *N*-acetylglucosamine, linked by beta 1,4 bonds. Its interactions with collagen and other molecular components of the vitreous account for the gel state of the transparent extracellular matrix that is the vitreous [see chapter I.F. Vitreous biochemistry and artificial vitreous], although HA does not likely play a role in mediating vitreoretinal adhesion [see chapter II.E. Vitreo-retinal interface and ILM].

All three forms of human hyaluronidases are capable of degrading hyaluronan and to a lesser extent chondroitin, two major components of the vitreous matrix [7, 33]. They have a number of natural biologic functions including fertilization, preserving mobility in human body tissues, and also enhancing pathologic processes such as bacterial virulence and the spread of cancer cells [14, 27]. Vertebrate hyaluronidases share considerable homology, and the testis provides an easy source of one of the most commonly used hyaluronidases (PH20) in experimental and clinical settings.

Bovine hyaluronidase has been widely used in ophthalmology to facilitate the periocular dispersal of anesthetic agents injected into the retrobulbar space. As initially reported by Foulds, hyaluronidase induces significant vitreous liquefaction [see chapter VI.B. The history of pharmacologic vitreolysis]. Therefore, testicular hyaluronidase was tested and developed as a vitreous liquefactant. Following preclinical studies that demonstrated efficacy in animal models, clinical studies were undertaken, including a phase 3 trial to assess its clinical potential in accelerating the clearance of vitreous hemorrhage [11, 15, 20, 21]. While ovine testicular hyaluronidase was able to clear vitreous hemorrhage more rapidly than saline, the phase 3 results did not provide sufficient evidence to demonstrate efficacy and to warrant approval as a commercial product. Vitrase® is currently used as a spreading agent mainly in dermatology and esthetic surgery [22].

II. Mechanism of Action and Pharmacodynamics

A. Hyaluronidase Enzyme Activity

Hyaluronidase cleaves β 1,4 glycosaminidic bonds (between glucosamine and glucuronic acid) within hyaluronan in a random catalytic attack along the glycosaminoglycan chain [23]. A similar mechanism is probably operative upon chondroitin but is only efficient in regions of limited

or low sulfation. The kinetics of hyaluronan hydroxylation by testicular hyaluronidase has been studied *in vitro* [1]. In low concentrations, the kinetics follows a Michaelis-Menten behavior, but as the concentration or viscosity of solution increases, a nonlinear model applies in which electrostatic charges, viscosity, and steric orientation play an increasing role. Half-life in the eye is between 60 and 112 h based on preclinical studies carried out in rabbits using radio-labeled Vitrase® (ovine testicular hyaluronidase) [5, 20]. In the skin, the duration of action has been demonstrated to be between 24 and 48 h [6, 22].

Some of the breakdown products from the hydrolysis of hyaluronan can cause inflammation [33]. In studies carried out using Vitrase in Dutch-belted rabbits, vitreous haze and fluffy white deposits were frequently seen between day 4 and day 28 postinjection [5]. On histologic examination, cellular infiltrates were seen consisting of activated macrophages, T- and B-lymphocytes. They were most numerous between day 4 and 15 and subsequently decreased. Similar findings were observed in cynomolgus monkeys. Repeat injections of Vitrase given at 4-week intervals after the initial injection led to the reemergence of the inflammatory response which was more intense and prolonged. By the third such injection the inflammation persisted for 45 days with several animals (5 of 8 animals) developing vitreous membranes and/or retinal detachments. The putative mechanism for this inflammation is thought to arise through the hyaluronan receptor CD44 and/or TLR2 and TLR4 or possibly the presence of protein contaminants left after the purification process [2, 25].

B. Biological Activity

Hyaluronidase causes significant vitreous liquefaction and has a rapid onset. Foulds et al. studied the diffusion of $^3\text{H}_2\text{O}$ in eyes treated with hyaluronidase or saline. He reported that after 60 min, the rabbit's vitreous was difficult to handle because it contained considerable fluid [11]. Boruchoff reported that this effect reached its peak within a few days and the effect was sustained for a month, as eyes harvested at 4 or 30 days after mid-vitreous injection of hyaluronidase where hydrolyzed to a similar extent [3]. Compared to plasmin enzyme and chondroitinase, the degree of liquefaction per unit time is higher with hyaluronidase, but this difference is not statistically significant [32]. On the other hand, less retinal damage is noted with hyaluronidase (100 U) as compared to the other enzymes tested using an *ex vivo* porcine model. A 3-h incubation with 1,000 U of hyaluronidase leads to a 20 % reduction in vitreous weight as compared to a 9 % increase in eyes injected with an equivalent volume of saline [32].

Since hyaluronan has a considerable effect upon the resistance to flow of solutes and cells through connective tissues [9, 26], it was felt that altering this property offered an

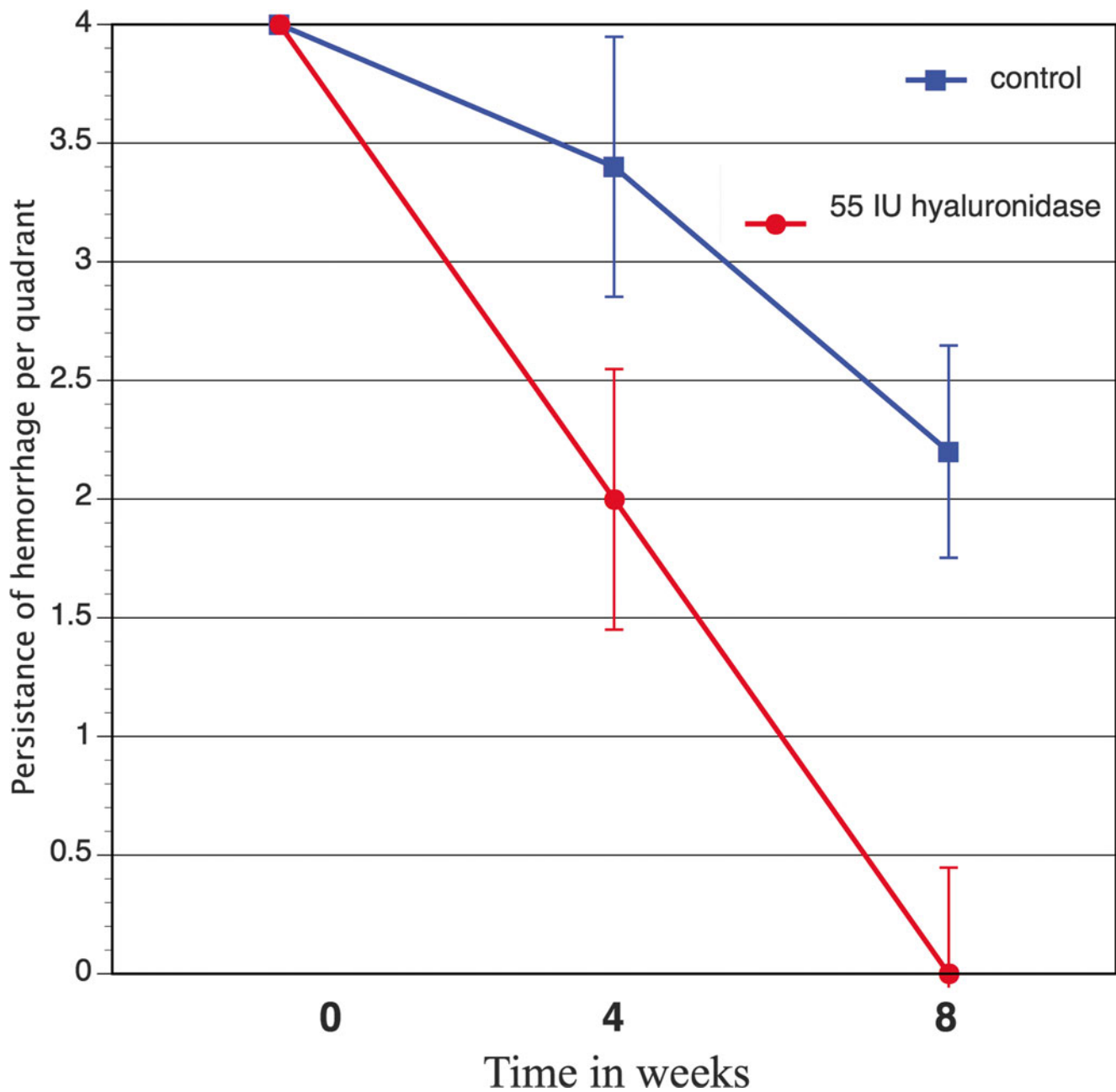


Figure VI.F-1 Presence of residual vitreous hemorrhage per quadrant examined by indirect ophthalmoscopy (20 D lens) (error bars represent 2 SD)

opportunity for pharmacologic vitreolysis in various clinical settings. In particular, the absence of significant fibrinolytic activity and the macromolecular structure of the vitreous, which is rich in mucopolysaccharides, significantly delays reabsorption of blood [8, 10, 24]. Breakdown of hyaluronan accelerates the clearance of both large and small molecules including water [4, 11]. Thus, it was felt that clearance of vitreous hemorrhage could be enhanced with the introduction of hyaluronidase, as was first proposed in 1950 by von Sallmann [34]. Indeed, studies in animal models showed that

ovine testicular hyaluronidase induced efficient clearance of blood from the vitreous body of rabbits [13]. In this model, visualization of the posterior pole was not possible after the introduction of blood into the vitreous body. Within 1 month of hyaluronidase injection, most rabbit eyes could be examined in all but 1 quadrant (Figure VI.F-1). By 8 weeks, all eyes were cleared of vitreous hemorrhage. Interestingly, none had developed a posterior vitreous detachment (PVD), consistent with the lack of an interfactant effect by hyaluronidase [see chapter VI.A. Pharmacologic vitreolysis].

Despite its impressive liquefactant abilities, hyaluronidase is limited in its capacity to induce a PVD [13, 17], most likely because HA does not play an important role in promoting vitreoretinal adhesion [see chapter II.E. Vitreo-retinal interface and inner limiting membrane]. It is possible that its potent liquefactant properties combined with its inability to weaken the vitreoretinal interface leaves an insufficient central support to exert mechanical traction on the posterior vitreous cortex as is required to induce a PVD. For a PVD to occur, one needs to increase vitreoretinal traction in conjunction with the injection of hyaluronidase such as can be provided by a perfluorinated gas [18]. Alternatively, time may weaken the interface by repeat ocular movements leading to a PVD in 5 or more weeks following injection [16]. Similar results were observed in a clinical setting.

III. Clinical Experience

A. Study Design

Ovine testicular hyaluronidase (Vitrase®) was tested in two phase 3 trials. In the US trial, patients were randomly assigned to either an intravitreal injection of Vitrase® (7.5, 55, or 75 IU) or a saline control injection [21]. In the ex-US trial, only 55 and 75 IU units of Vitrase® were compared to a saline injection. A pooled analysis of results was conducted on 1,125 patients having received an injection of saline or Vitrase® at a dose of 55 or 75 IU. Clinical assessments were carried out at day 1, week 1, and months 1, 2, and 3. Safety was assessed during the clinical visits and then at month 6 and every 6 months thereafter. The primary efficacy endpoint was defined as clearance of vitreous hemorrhage sufficient to see the underlying pathology and to complete treatment, when indicated, by the month 3 visit. Secondary endpoints included 3-line improvement in best-corrected visual acuity (BCVA), reduction of vitreous hemorrhage density, and a clinical assessment of medical utility by the attending ophthalmologist.

B. Results

The results of the trial were as follows: a total of 330 (90.4 %), 355 (94.2 %), and 361 (94.3 %) patients in the 55, 75 IU, and saline groups, respectively, completed the month 3 visit. Baseline characteristics were similar between the two studies. A statistically significant proportion of patients in the 55 IU dose group achieved the primary efficacy endpoint by months 1 and 2 (adjusted P -value: $P=0.001$ and $P=0.002$, respectively). By month 2, 25.5 % of patients treated with 55 IU and 21.2 % of patients treated with 75 IU achieved the primary endpoint compared with 16.2 % in the saline group

($P=0.002$, $P=0.083$). Similarly, the primary endpoint was statistically significant by month 3 for patients in the 55 IU group (32.9 %) compared with the saline group (25.6 %) with a $P=0.025$. The 75 IU group did not reach statistical significance at this time point compared with saline: 30.5 % versus 25.6 %, $P=0.144$.

Vision improvement by 3 lines paralleled these results. By month 1, 30.7 and 27.9 % of patients in the 55 and 75 IU groups, respectively, had a 3-line or greater improvement in BCVA compared with 20.1 % of patients in the saline group ($P=0.001$ and $P=0.013$, respectively, vs saline). For patients in the 55 and 75 IU groups, improvement in BCVA of at least 3 lines by month 2 was achieved for 41.1 and 38.2 % of patients, respectively, compared with 27.4 % of patients in the saline group ($P=0.001$ and $P=0.002$). By month 3, 44.9 % (55 IU) and 43.5 % (75 IU) of patients had at least a 3-line improvement in BCVA compared with 34.5 % of patients in the saline group ($P=0.004$ and $P=0.011$).

Investigator-graded reduction in vitreous hemorrhage showed a statistically significant difference compared to the saline group for both the 55 IU and the 75 IU at months 1, 2, and 3. By month 3, 38.6 % (55 IU) and 38.2 % (75 IU) of patients compared with 28.5 % of patients in the saline group attained a reduction in vitreous hemorrhage versus saline ($P=0.003$ and $P=0.005$, respectively). The clinical assessment of therapeutic utility (clearance of hemorrhage sufficient to diagnose the underlying pathology) paralleled these results.

C. Complications

Among the safety parameters followed in the course of this study, iritis was the most common ocular adverse event, occurring in 33.3, 62.1, 58.9, and 62.1 % of the saline group, 7.5, 55, and 75 IU treated subjects [20]. In eyes with moderate to severe iritis, a dose response was observed: 8.0, 20.2, 33.7, and 39.7 % of saline, 7.5, 55, and 75 IU treated subjects, respectively. A transient noninfectious hypopyon was seen in 0, 0.5, 1.6, and 5.4 % of patients given saline, 7.5, 55, and 75 IU, respectively. These were not associated with pain, hyperemia, and chemosis. They cleared spontaneously. As indicated above, the presence of transient inflammation may be a sign of therapeutic effect. Unfortunately, no analysis was carried out to correlate the presence of an inflammatory response with the rate of therapeutic success. A number of patients reported transient eye pain or discomfort following the injection (22–41 %). This was not dose related and reported in 22–29 % of control eyes. Retinal detachments (RD) were reported in 9.5 % of study eyes: 26 (6.9 %), 22 (11.1 %), 35 (9.3 %), and 45 (11.5 %) in the saline group, 7.5, 55, and 75 IU treated subjects. Most were tractional in nature and likely related to the underlying disease process rather than the injection of the drug. Overall, 1.8 % of study

eyes had rhegmatogenous RD: 1.1, 2.5, 1.6, and 2.3 % of the saline group, 7.5, 55, and 75 IU treated subjects. Over 90 % of these developed within the first 30 days following the injection of Vitrase™ or saline.

D. Conclusions

When the data was reviewed by the FDA, the safety/efficacy profile for Vitrase® was inadequate to support approval of the drug for the treatment of vitreous hemorrhage. The natural history of vitreous hemorrhage is such that the majority of patients clear within 3–4 months. The increased risk of retinal complications from watchful waiting was not felt to warrant the early use of this drug in patients with vitreous hemorrhage. Nevertheless, Vitrase® (hyaluronidase injection) ovine, 200 USP units/mL, is indicated as an adjuvant to increase the absorption and dispersion of other injected drugs, for hypodermoclysis, and as an adjunct in subcutaneous urography for improving resorption of radiopaque agents (Valeant/Bausch + Lomb).

IV. Future Directions and Applications

Experimental data has shown that hyaluronidase is a powerful liquefactant. However, the clinical effect in humans and animals was associated with some ocular inflammation. While the inflammation may be inherent to the action of hyaluronidase, it is also possible that it is the result of by-products remaining in the preparation following the purification process. Human recombinant hyaluronidase (rHuPH20) has been developed since the Vitrase® trial and has been found to be particularly well tolerated, as it is currently used in a number of subcutaneous drug delivery systems. Repeat subcutaneous administration at doses up to 38,800 U over 28 days did not lead to the development of a cellular or humoral response [2, 12]. Periocular administration was also free of inflammation. rHuPH20 might be a better choice for intraocular use both to disperse vitreous hemorrhage or opacities and as an adjunct to pharmacologic vitreolysis with an interfactant in combination therapy [29].

Pharmacologic vitreolysis requires both liquefaction of the vitreous as well as separation of the posterior vitreous cortex (PVD) [28, 30]. As discussed in the chapter on ocriplasmin [see chapter V.I.E.2. Pharmacologic vitreolysis with ocriplasmin – clinical studies], a PVD is achieved in about 1/3 of patients overall. Combining hyaluronidase and plasmin enzyme was shown in a diabetic rat model to significantly enhance the incidence of a PVD, which also appeared earlier than after single-agent administration: 1 week versus 1 month [35, 36]. The authors postulated that the improved performance of the combined therapy was a result of hyaluronidase

facilitating the diffusion of plasmin to the interface between the retina and the vitreous. An alternative explanation suggests that the hyaluronidase was a more effective agent at causing vitreous liquefaction—a prerequisite for an efficient PVD. Indeed, the combination of hyaluronidase with perfluoropropane is also capable of inducing a PVD [18].

The treatment of vitreous floaters is a subject receiving increasing attention. Current treatment modalities include the use of a Nd:YAG laser or vitrectomy. In a recent paper, Sebag has achieved excellent results without the induction of a PVD at the time of surgery and limiting the vitreous aspiration to the central vitreous [31]. The use of a liquefactant in this particular setting, particularly if it is noninflammatory, might in the future become an acceptable alternative but will require significant development.

Finally, it is worth remembering that bovine hyaluronidase was widely used in ophthalmology to facilitate the periocular dispersion of anesthesia. It may also enhance the transscleral penetration of drugs such as dexamethasone [19]. With the availability of rHuPH20 or newer compounds that can minimize the inflammatory response previously seen, it may be time to reexplore its use in enhancing external drug delivery to the eye.

Abbreviations

BCVA	Best-corrected visual acuity
FDA	US Food and Drug Administration
GAG	Glycosaminoglycans
HA	Hyaluronan
HAse	Hyaluronidase
IU	International units
Nd:YAG	Neodymium-doped yttrium aluminum garnet
PVD	Posterior vitreous detachment
RD	Retinal detachment
U	Units
USP	United States Pharmacopeia

References

1. Asteriou T, Vincent JC, Tranchepain F, et al. Inhibition of hyaluronan hydrolysis catalysed by hyaluronidase at high substrate concentration and low ionic strength. *Matrix Biol.* 2006;25:166–74.
2. Bookbinder LH, Hofer A, Haller MF, et al. A recombinant human enzyme for enhanced interstitial transport of therapeutics. *J Control Release.* 2006;114:230–41.
3. Boruchoff SA, Woodin AM. Viscosity and composition of solutions derived from rabbit vitreous humour. *Br J Ophthalmol.* 1956;40:113–8.
4. Comper WD, Laurent TC. Physiological function of connective tissue polysaccharides. *Physiol Rev.* 1978;58:255–315.
5. Center for Drug Evaluation and Research. Application number 21-640. Pharmacology review. 2004. <http://www.accessdata.fda>

- [gov/drugsatfda_docs/nda/2004/21-640_Vitraxe_Pharmr.pdf](http://www.accessdata.fda.gov/drugsatfda_docs/nda/2004/21-640_Vitraxe_Pharmr.pdf). Accessed 27 Mar 2014.
6. Center for Drug Evaluation and Research. Application number 21-640. Medical review. 2004. http://www.accessdata.fda.gov/drugsatfda_docs/nda/2004/21-640_Vitraxe_Medr.pdf. Accessed 27 Mar 2014.
 7. de Smet M, Gad El Kareem A, Zwinderman AH. The vitreous, the retinal interface in ocular health and disease. *Ophthalmologica*. 2013;230:165–78.
 8. Fatt I. Flow and diffusion in the vitreous body of the eye. *Bull Math Biol*. 1975;37:85–90.
 9. Forrester JV, Wilkinson PC. Inhibition of leukocyte locomotion by hyaluronic acid. *J Cell Sci*. 1981;48:315–31.
 10. Forrester JV, Edgar W, Millar W, et al. Enhancement of vitreous clot lysis by urokinase: mode of action. *Exp Eye Res*. 1982;34:895–907.
 11. Foulds WS, Allan D, Moseley H, et al. Effect of intravitreal hyaluronidase on the clearance of tritiated water from the vitreous of the choroid. *Br J Ophthalmol*. 1985;69:529–32.
 12. Frost GI. Recombinant human hyaluronidase (rHuPH20): an enabling platform for subcutaneous drug and fluid administration. *Expert Opin Drug Deliv*. 2007;4:427–40.
 13. Gad Elkareem AM, de Smet MD. Effect of microplasmin on the clearance of vitreous haemorrhage from an experimental model in rabbits. *Acta Ophthalmol*. 2012. doi:10.1111/j.1755-3768.2012.02568.x.
 14. Girish KS, Kemparaju K. The magic glue hyaluronan and its eraser hyaluronidase: a biological overview. *Life Sci*. 2007;80:1921–43.
 15. Gottlieb JL, Antoszyk A, Hatchell DL, et al. The safety of intravitreal hyaluronidase. A clinical and histologic study. *Invest Ophthalmol Vis Sci*. 1990;31:2345–52.
 16. Harooni M, McMillan T, Refojo M. Efficacy and safety of enzymatic posterior vitreous detachment by intravitreal injection of hyaluronidase. *Retina*. 1998;18:16–22.
 17. Hikichi T, Kado M, Yoshida A. Intravitreal injection of hyaluronidase cannot induce posterior vitreous detachment in the rabbit. *Retina*. 2000;20:195–8.
 18. Kang SW, Hyung SM, Choi MY, et al. Induction of vitreolysis and vitreous detachment with hyaluronidase and perfluoropropane gas. *Korean J Ophthalmol*. 1995;9:69–78.
 19. Kozak I, Kayikcioglu OR, Cheng L, et al. The effect of recombinant human hyaluronidase on dexamethasone penetration into the posterior segment of the eye after sub-tenon's injection. *J Ocular Pharm Ther*. 2006;22:362–9.
 20. Kuppermann BD, Thomas EL, de Smet M, et al. Safety results of two phase III trials of an intravitreal injection of highly purified ovine hyaluronidase (Vitraxe) for the management of vitreous hemorrhage. *Am J Ophthalmol*. 2005;140:585–7.
 21. Kuppermann BD, Thomas EL, de Smet MD, et al. Pooled efficacy results from two multinational randomized controlled clinical trials of a single intravitreal injection of highly purified ovine hyaluronidase (Vitraxe→) for the management of vitreous hemorrhage. *Am J Ophthalmol*. 2005;140:573–84.
 22. Lee A, Grummer SE, Kriegel D, et al. Hyaluronidase. *Dermatol Surg*. 2010;36:1071–7.
 23. Ludowieg J, Venneqland B, Dorfman A. The mechanism of action of hyaluronidases. *J Biol Chem*. 1961;236:333–9.
 24. Maberley AL, Chisholm LDJ. The effect of a fibrinolytic agent on the vitreous haemorrhage in rabbits. *Can J Ophthalmol*. 1970;4:55–64.
 25. McKee CM, Penno MB, Cowman M, et al. Hyaluronan (HA) fragments induce chemokine gene expression in alveolar macrophages. *J Clin Invest*. 1996;98:2403–13.
 26. Ogston AG, Sherman TF. Effects of hyaluronic acid upon diffusion of solutes and flow of solvent. *J Physiol*. 1961;156:67–74.
 27. Robert L, Robert AM, Renard G. Biological effects of hyaluronan in connective tissues, eye, skin, venous wall. Role in aging. *Pathol Biol (Paris)*. 2010;58:187–98.
 28. Sebag J. Pharmacologic vitreolysis. *Retina*. 1998;18:1–3.
 29. Sebag J. Is pharmacologic vitreolysis brewing? *Retina*. 2002;22:1–3.
 30. Sebag J. Pharmacologic vitreolysis – premise and promise of the first decade. *Retina*. 2009;29:871–4.
 31. Sebag J, Yee KMP, Wa CA, et al. Vitrectomy for floaters. Prospective efficacy analyses and retrospective safety profile. *Retina* 2014;34:1062–8. PMID: 24296397.
 32. Staubach F, Nober V, Janknecht P. Enzyme-assisted vitrectomy in enucleated pig eyes: a comparison of hyaluronidase, chondroitinase, and plasmin. *Curr Eye Res*. 2004;29:261–8.
 33. Stem R, Jdrzejewski MJ. Hyaluronidases: their genomics, structures, and mechanisms of action. *Chem Rev*. 2006;106:818–39.
 34. von Sallmann L. Experimental study on the vitreous. II. Experiments on disappearance of red blood cells from the vitreous. *Arch Ophthalmol*. 1950;43:638–52.
 35. Wang Z-LM, Zhang XM, Xu XM, et al. PVD following plasmin but not hyaluronidase: implications for combination pharmacologic vitreolysis therapy. *Retina*. 2005;25:38–43.
 36. Zhi-Liang W, Wo-Dong S, Min L, et al. Pharmacologic vitreolysis with plasmin and hyaluronidase in diabetic rats. *Retina*. 2009;29:269–74.

Pharmacologic Vitreolysis with Purified Dispase (Vitreolysin™)

VI.G.

Tongalp H. Tezel, Lucian V. Del Priore,
and Henry J. Kaplan

Contents

- I. **Introduction**
- II. **Chemistry and Mechanism of Action**
 - A. Substrate Specificity
 - B. Structure
 - C. Inhibition
 - D. Pharmacokinetics and Pharmacodynamics
- III. **Potential Applications**
 - A. Induce Posterior Vitreous Detachment
 - B. Facilitate the Surgical Removal of Pathologic Preretinal Membranes
- IV. **Drug Development**
 - A. Purification and Toxicity
 - B. Stability
 - C. Potential Advantages
- V. **Safety and Efficacy**
 - A. *In Vitro* Studies
 - 1. Efficacy
 - 2. Effect on Retinal Cell Viability and Structure
 - 3. Effect on Mechanical Properties of the Sensory Retina
 - B. *In Vivo* Studies
 - 1. PVD Induction
 - 2. Effect on Retinal Electrophysiology

References

Keywords

Vitreous • Vitreoretinal interface • Inner limiting membrane • Pharmacologic vitreolysis • Dispase® • Vitreolysin™ • Interfactant • Type IV collagen • Fibronectin • Posterior vitreous detachment

Key Concepts

1. Dispase degrades type IV collagen, a major component of the inner limiting membrane of the retina, and fibronectin. It thus has selective action at the vitreoretinal interface as an interfactant with little effect as a liquefactant of the gel vitreous.
2. Previous crude enzyme preparations contained raw bacterial contaminants that have been eliminated in the purified form of Vitreolysin™, effective in picomolar concentrations without retinal toxicity.
3. Dispase is able to induce PVD without significant risks of retinal tears and detachment.

T.H. Tezel, MD (✉)
Department of Ophthalmology, Columbia University College
of Physicians and Surgeons, Edward S. Harkness Eye Institute,
635 West 165th Street, 38, New York, NY 10032, USA
e-mail: tht2115@cumc.columbia.edu

L.V. Del Priore, MD, PhD
Department of Ophthalmology and Visual Sciences,
Medical University of South Carolina,
167 Ashley Avenue; Room 829, Charleston, SC, USA
e-mail: ldelpriore@yahoo.com

H.J. Kaplan, MD
Department of Ophthalmology and Visual Sciences, University of
Louisville, School of Medicine, University of Louisville School of
Medicine, Kentucky Lions Eye Center,
301 E. Muhammad Ali Blvd., Louisville, KY 40202, USA

Department of Microbiology and Immunology, University of
Louisville, School of Medicine, University of Louisville School of
Medicine, Kentucky Lions Eye Center,
301 E. Muhammad Ali Blvd., Louisville, KY 40202, USA
e-mail: hank.kaplan@louisville.edu

I. Introduction

Vitreolysin™ is a purified 35.9 kDa extracellular neutral protease produced by *Paenibacillus polymyxa*. It can selectively cleave the attachment of the posterior vitreous cortex from the inner limiting membrane (ILM) due to its high affinity for type IV collagen and fibronectin, which contributes to the attachment between these two structures [see chapter II.E. Vitreo-retinal interface and inner limiting membrane]. The low affinity of Vitreolysin™ for vitreous type II collagen allows it to induce a posterior vitreous detachment (PVD) without disrupting the delicate macromolecular structure of the vitreous (Figure VI.G-1). This *direct* enzymatic action on the posterior vitreous cortex-ILM interface prevents vitreous liquefaction and resultant vitreoretinal traction which is a common way of PVD induction for many *indirectly* acting enzymes [1]. There are several other advantages of Vitreolysin™, such as lack of a known natural inhibitor, which insures reliable enzymatic activity even in complex vitreoretinal diseases where several enzyme inhibitors within



Figure VI.G-1 Two weeks after the injection of 0.05 units of Vitreolysin™ into the domestic pig's eye, the animal was sacrificed and the globe was enucleated. Removal of the anterior segment reveals a complete PVD. Note that vitreous structure was not disrupted; however, strong vitreoretinal adhesions were released

the serum may leak into the eye. Vitreolysin™'s activity can be quenched by its own titratable autolysis, which ensures a fine control on its degradation and removal. Vitreolysin™ is a highly stable molecule with a long shelf life in lyophilized form. Early preclinical studies also revealed high rates (80–100 %) of PVD induction at picomolar concentrations.

The crude form of the *Paenibacillus polymyxa* extract (Dispase®, Gibco, Invitrogen, Grand Island, NY) has been available for many years and has been used for cell harvesting and tissue culture purposes. This product contains minute amounts of the active enzyme but high amounts of bacterial debris and endotoxin. Although initial *in vitro* and *ex vivo* studies for PVD induction were conducted using this crude extract, its *in vivo* use was limited due to a high endotoxin content. Efforts to purify the active enzyme have recently been finalized, and studies to develop it as a pharmacologic vitreolysis [2, 3] agent for PVD induction are currently under way.

II. Chemistry and Mechanism of Action

A. Substrate Specificity

Vitreolysin™ is the purified form of the 35.9 kDa neutral amino-endopeptidase produced by *Paenibacillus polymyxa* (Protein Accession Number: P29148.1; <http://www.ncbi.nlm.nih.gov/protein/P29148>). This exoenzyme has a substrate specificity to two major components of the inner limiting membrane-posterior vitreous cortex interface: fibronectin and collagen type IV. It also exerts a negligible effect on collagen I; however, it does not cleave collagen type II, V, elastin, or laminin [4]. Vitreolysin™ hydrolyzes the N-terminal peptide bonds of hydrophobic amino acid residues, such as alanine, valine, leucine, isoleucine, proline, and phenylalanine, and, thus, can selectively act on exposed nonpolar residues of amphiphilic basement membrane proteins. *Paenibacillus polymyxa* secretes this neutral protease to degrade extracellular proteins and peptides for nutrition, particularly prior to sporulation.

B. Structure

Vitreolysin™ is a product of the *npr* gene (GenBank Accession Number: GenBank: D00861.1) which spans 2.4 Kbp and contains one large open reading frame composed of 1,770 bp (<http://www.ncbi.nlm.nih.gov/nuccore/216307>) [5]. It is synthesized as a proenzyme composed of 590 amino acids and becomes active after the cleavage of the 264 amino acid long autoinhibitory pro-sequence which also assists in the folding of the protein. The first 23 amino acids at the N-terminal serve as a signal sequence for secretion and target the remaining 303 amino acid long active enzyme for exocytosis. The amino acid

composition of Vitreolysin™ does not resemble any other *Bacillus* proteases but reveals some homology (54.8 %) with *Bacillus* neutral metalloproteases, such as thermolysin, and the M4 family of peptidases, such as protealysin and aureolysin [5]. It has two domain structures with the active site between these domains. The C-terminal domain exhibits an alpha-helical structure, whereas the N-terminal domain contains the His-Glu-Xaa-Xaa-His (HEXXH) zinc-binding motif and exhibits a beta structure. Apart from the catalytic zinc-binding domain, the Vitreolysin™ molecule contains four calcium-binding sites which play a role in the stabilization of its tertiary structure. In its active form, the enzyme is highly stable and functions within a pH range of 4.0–9.0 and at temperatures between 20 and 60 °C [6].

C. Inhibition

There are no naturally occurring inhibitors for Vitreolysin™. Its activity can be quenched by keeping it at a pH below 3.0 or by heating at 65 °C for 10 min. [6] The enzymatic activity of Vitreolysin™ is highly dependent on the concentration of the divalent cations in the medium. Chelating calcium with ethylenediaminetetraacetic (EDTA) at concentrations higher than 20 μM significantly reduces the activity of Vitreolysin™. Paradoxically, enzyme activity can also be decreased by elevating the calcium concentration above 15 mM [7]. Optimum enzymatic activity is achieved within the physiological range of calcium concentration (5.0–10 mM) in the human vitreous [8]. Tetracycline and its analogs can partially inhibit the enzymatic activity of Vitreolysin™ by chelating calcium [9]. The major limitation for continuous enzymatic activity in the eye is the autodigestion of the enzyme itself. At physiological conditions Vitreolysin™ loses its proteolytic activity due to autodigestion that yields several smaller fragments some of which may still exhibit proteolytic activity. Its autolysis is temperature dependent and completely halts at temperatures below 0 °C [9].

D. Pharmacokinetics and Pharmacodynamics

Intravitreally injected Vitreolysin™ diffuses within the eye following Fick's second law of diffusion and creates a concentration gradient inversely proportional to the distance from the injection site [10]. The inner limiting membrane-posterior vitreous cortex interface constitutes the first target for the enzyme due to its high fibronectin and type IV collagen content. During its diffusion within the vitreous, it cannot digest vitreous collagen due to its inability to digest type II collagen; thus, it does not induce vitreous collapse and resultant vitreoretinal traction that can result in peripheral retina breaks and retinal detachment. Also, due to its well-

characterized autolytic properties, the enzymatic activity can be titrated to cleave the posterior vitreous cortex from the inner limiting membrane and then lose its enzymatic activity.

III. Potential Applications

A. Induce Posterior Vitreous Detachment

The high specificity of Vitreolysin™ for type IV collagen and fibronectin makes it an ideal enzyme to cleave the attachment of the ILM to the posterior vitreous cortex. Vitreolysin™ acts on type IV collagen which constitutes the main framework of the middle layer of the ILM, the *lamina densa*, and the radially oriented fibronectin molecules [11, 12] that anchor the innermost layer of the ILM, the *lamina rara interna* to the rhomboid type IV collagen framework [see chapter II.E. Vitreo-retinal interface and inner limiting membrane]. As a result, the posterior vitreous cortex-*lamina rara interna* complex separates from the *lamina densa* of the ILM similar to a natural posterior vitreous detachment [13] [see chapter II.C. Vitreous aging and PVD].

Due to the high specificity of Vitreolysin™ for type IV collagen and fibronectin, PVD induction occurs rapidly (~15 min) with picomolar concentrations of the enzyme and at a high frequency (80–100 %). Vitreolysin™ can be used to induce PVD in two different settings: (1) *To facilitate removal of the posterior vitreous cortex during vitreoretinal surgery*: For this purpose, relatively high doses (2.5 IU) can be injected 15 min before surgery and residual active enzyme will be washed out during surgery. (2) *To induce a therapeutic PVD eliminating the need for surgery*. There are a rapidly growing number of vitreoretinal interface pathologies that can benefit from a therapeutic PVD by removal of the vitreoretinal traction [see chapter III.D. Vitreo-macular adhesion/traction and macular holes], elimination of a scaffold for fibrovascular growth [see chapter I.E. Diabetic vitreopathy] removal of debris and cytokines from the retinal surface [14], and/or facilitation of ionic oxygen transport [15] [see chapter IV.B. Oxygen in vitreo-retinal physiology and pathology]. For this purpose, relatively small doses of Vitreolysin™ (0.05 U) are sufficient and they will induce PVD within 2 weeks. The enzymatic activity of such smaller doses of Vitreolysin™ is terminated by autodigestion.

B. Facilitate the Surgical Removal of Pathologic Preretinal Membranes

The increased expression of fibronectin and type IV collagen within pathologic preretinal membranes [16–19] makes

these structures a good target for Vitreolysin™ and may facilitate their surgical peeling [see chapter V.A.2. Vitreomaculopathy surgery]. It may also be used as an adjuvant in proliferative diabetic retinopathy [18] or proliferative vitreoretinopathy [19] to decrease the complication rates associated with membrane peeling as well as shorten surgical time [see chapter V.B.5. Management of PVR].

The therapeutic impact of PVD induction has only recently been recognized in many retinal diseases. Complete removal of the posterior vitreous cortex appears beneficial in age-related macular degeneration, diabetic retinopathy, diabetic macular edema, retinal vein occlusion, and cystoid macular edema. The fast, accurate, and safe induction of PVD with Vitreolysin™ will find many applications regardless whether its therapeutic effect is mediated by increased convectional oxygen currents, alleviation of vitreoretinal traction, or removal of hyalocytes and the posterior vitreous cytokine load.

IV. Drug Development

A. Purification and Toxicity

The idea of using the neutral protease from *Paenibacillus polymyxa* extract to induce a PVD was initially recognized in 1995, and the first patent was granted in 1998 (Tezel & Kaplan, United States Patent 5,722,428, <http://patft.uspto.gov>). Early studies were conducted using the commercially available

crude enzyme product (Dispase®, Gibco, Invitrogen, Grand Island NY) still in the market today for cell harvesting. This raw form of the enzyme is made from *Paenibacillus polymyxa* extract and contains high amounts of bacillus protein and endotoxin. Although this crude form of the enzyme was sufficient initially to demonstrate the *in vitro* [11], and even short-term *in vivo*, efficacy, its use for a long term for *in vivo* studies was limited due to endotoxin and bacterial protein contamination (Figure VI.G-2). Injection of the high-dose crude enzyme extract into the vitreous of mice [20] and rabbits [21, 22] results in the infiltration of inflammatory cells and the development of proliferative vitreoretinopathy within 2 weeks [23]. Early animal experiments in domestic pig confirmed that these detrimental effects of the crude enzyme were seen at high doses, but intravitreal injection of lower doses induced a PVD without any significant complications [24, 25]. Another problem with the crude enzyme is the inconsistency of enzyme activity with each batch. Detailed analysis revealed that only 2.4 % of the total mass of the lyophilized powder was protein, and active enzyme constituted 49 % of the total protein – thus, only 1.2 % of the marketed product was active enzyme. Attempts to purify the crude enzyme were initiated earlier by Roche Applied Sciences (Mannheim, Germany) and yielded a purer form of the enzyme marketed as Dispase® II. However, our analysis of this product still revealed unacceptably high amounts of *Bacillus* contaminants and paradoxically low enzymatic activity due to loss (84.4 %) of the active enzyme during the purification process.

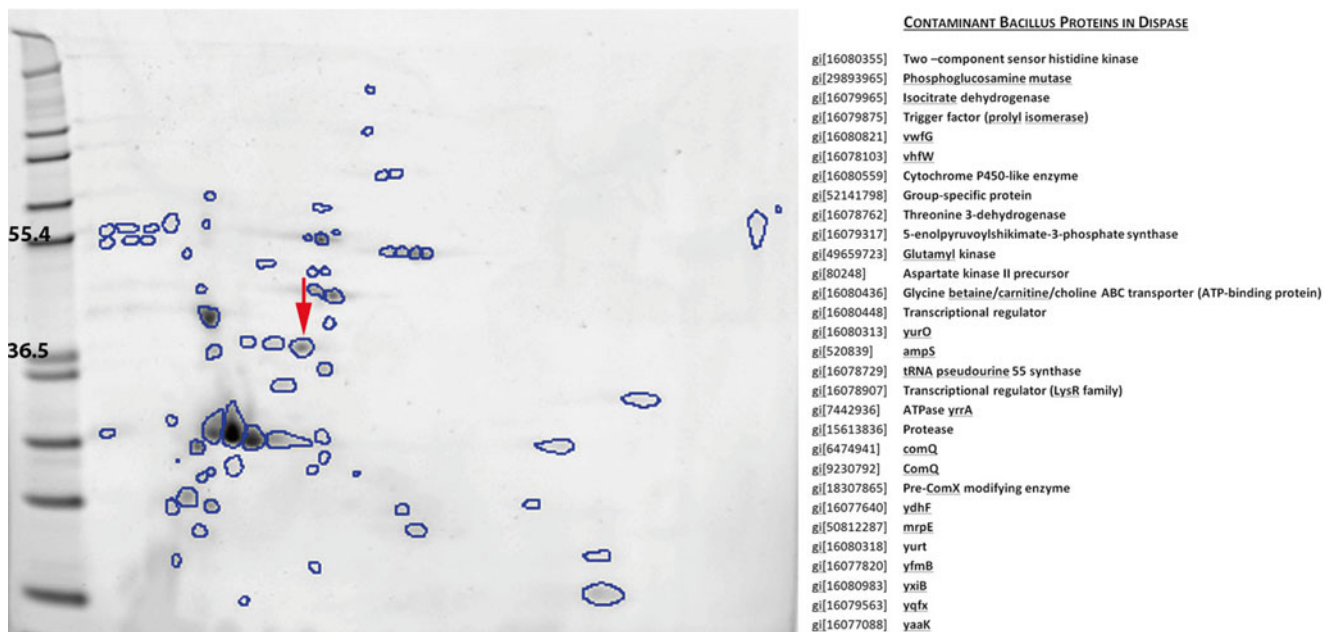


Figure VI.G-2 2D gel separation of the proteins within the commercially available crude *Paenibacillus polymyxa* extract (Dispase®) reveals several protein contaminants. Mass spectrometry identifies

majority of these contaminants as bacillus proteins. Active enzyme (red arrow, MW=35.9 kDa; pI=5.14) constitutes only 1.2 % of the total mass of the lyophilized powder

B. Stability

Vitreolysin™ is the purified 35.9 kDa neutral aminopeptidase produced by *Paenibacillus polymyxa*. By weight it is >92 % pure active neutral protease (Figure VI.G-3a). Most of the impurities within Vitreolysin™ are characterized as breakdown products of the enzyme created by autodigestion and reveal similar catalytic activity (Figure VI.G-3b). Due to its high purity and high enzymatic activity, Vitreolysin™ yields a higher rate of PVD compared with Dispase® (Figure VI.G-4) and only requires picomolar doses to achieve reproducible results. Vitreolysin™ is prepared in a lyophilized form and can stay at –20 °C for 9–12 months without losing its activity. After reconstitution the enzyme retains its activity for up to 48 h at 4 °C.

C. Potential Advantages

Vitreolysin™ carries certain advantages over plasmin and ocriplasmin for the induction of PVD (Table VI.G-1). Unlike ocriplasmin, Vitreolysin™ is a matrix metalloprotease that acts directly on the ILM-posterior vitreous cortex interface. It does not liquefy the vitreous, so it does not induce vitreoretinal traction with the potential to cause peripheral retinal tears. Vitreolysin™ is a highly stable molecule and has no

known inhibitors, such as α 2-antiplasmin in the case of ocriplasmin [26] [see chapter VI.E.1. Pharmacologic vitreolysis with ocriplasmin – basic science studies]. Its activity is quenched by autolysis that allows the reproducible induction of a PVD without retinal toxicity or development of proliferative vitreoretinopathy. This property is a major advantage over ocriplasmin, since breakdown of the blood-retinal barrier with intravitreal leakage of α 2-antiplasmin is associated with many vitreoretinal diseases, such as diabetic retinopathy, proliferative vitreoretinopathy, and age-related macular degeneration. Early animal studies with the intravitreal injection of 0.05 U of Vitreolysin™ did not reveal any toxic effects on the retina or other ocular structures (Figure VI.G-5).

V. Safety and Efficacy

A. In Vitro Studies

1. Efficacy

The efficacy of *Paenibacillus polymyxa* neutral protease to induce a PVD was assessed in freshly enucleated pig and human cadaver eyes [11]. Two different scenarios were tested: (1) *Induction of PVD within 15 min of vitrectomy*: The rationale for this experimental design is that the injection of a high dose of the enzyme just before vitrectomy surgery would facilitate removal of the posterior vitreous cortex at the time of surgery. After the induction of a PVD, the injected enzyme would be cleared from the vitreous chamber by irrigation during the vitrectomy. For this purpose, a total dose of 0.5–12.5 U of the enzyme was injected intravitreally in 3-month-old domestic pig eyes incubated at 37 °C for 15 min. The anterior segment of the globe was then removed and the extent of PVD graded. In 30 % of PBS-injected control eyes, a partial (20 %) or complete (10 %) PVD was seen, whereas a dose-related increase in PVD was observed with the neutral protease injection (0.5 and 1.0 U: 40 % complete, 30 % partial; 2.5 U: 60 % complete, 20 % partial; 5 U: 80 % complete, 10 % partial; 12.5 U: 50 % complete, 10 % partial; Figure VI.G-6a). The paradoxical decrease in the incidence of PVD at the highest dose was due to the weakening of the RPE-Bruch's membrane attachment by the neutral protease that created a false-negative grading of PVD. The lowest concentration of the enzyme that yielded a statistically significant high rate of PVD compared to control was 2.5 U ($p=0.03$). The ability of this dose to induce a PVD was then tested on 20 human cadaver eyes. Globes from young donors (mean: 39.1 ± 13.2 years, range: 18–61) were used to decrease the likelihood of a naturally occurring PVD. The mean death-to-experiment time was 23 h. Nineteen of twenty (95 %) eyes developed a complete PVD, and the remaining eyes (5 %) had a partial PVD within 15 min. None of the

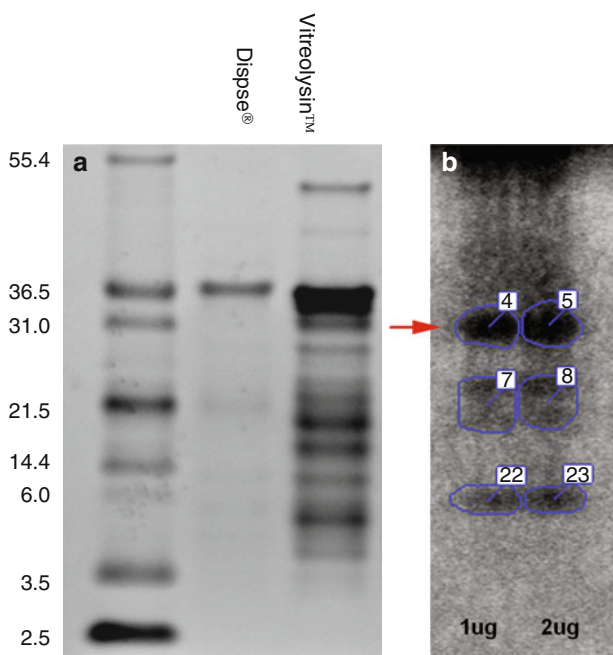


Figure VI.G-3 (a) SDS-PAGE gels loaded with equal protein amounts of Vitreolysin™ and Dispase® shows more active enzyme in Vitreolysin™. Due to its higher catalytic activity there are more breakdown products with Vitreolysin™. (b) Zymogram of Vitreolysin™ shows the active enzyme (red arrow) and its autolytic breakdown products. Note that breakdown fragments also exert enzymatic activity

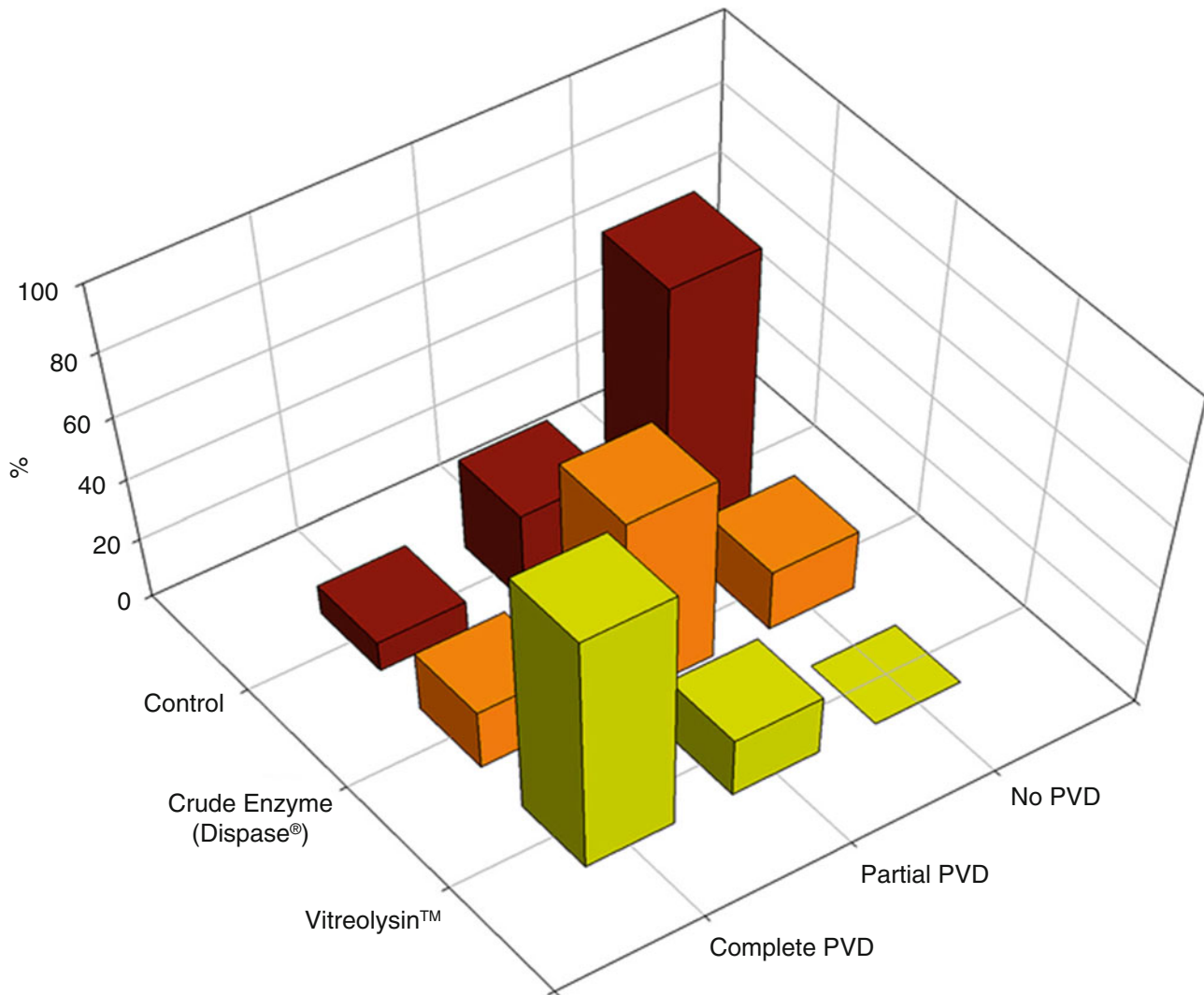


Figure VI.G-4 Vitreolysin™ is the purified neutral protease from *Paenibacillus polymyxa*. It contains >92 % pure enzyme. Intravitreal injection of Vitreolysin™ equivalent to 2.5 U of Dispase® II results in 80 % complete and 20 % incomplete PVD in 15 min. In crude enzyme (30 % complete, 60 % incomplete, 10 % no PVD) and PBS injection (10 % complete, 20 % incomplete, and 70 % no PVD), these rates remain lower

Table VI.G-1 Major differences between *Vitreolysin™* and *Ocriplasmin*: Vitreolysin has a target specificity to type IV collagen and fibronectin and selectively cleaves the attachment of ILM to the posterior vitreous cortex. It does not induce vitreous collapse and exert traction on the retina. Its enzymatic effect is predictable and can be titrated resulting in more reproducible PVD induction

	Vitreolysin™	Ocriplasmin
Target specificity	Specific to type IV collagen and fibronectin which is responsible for the attachment of posterior vitreous cortex to the ILM	Nonspecific; through activation of several proteases including MMPs
Mode of action	Matrix metalloprotease; Induces separation of posterior vitreous cortex from ILM without liquefying the vitreous gel. Thus, does not collapse the gel and exert traction on the retina	Serine protease; Results in vitreous gel collapse which exerts traction on the retina and may result in peripheral retinal tears and detachment
Inhibitors	No known natural inhibitors; thus its action is reproducible and cannot be inhibited with any natural chemicals	Can be inhibited with $\alpha 2$ -antiplasmin which is abundant in the vitreous of patients with different vitreoretinal diseases
Efficacy	Results in complete dehiscence of cortical vitreous	Often results in remnant patches of cortical vitreous which may act as a scaffold for subsequent glial proliferation and pucker formation
Stability	Has a long shelf half-life and known to be thermodynamically stable	Unstable with a very short half-life

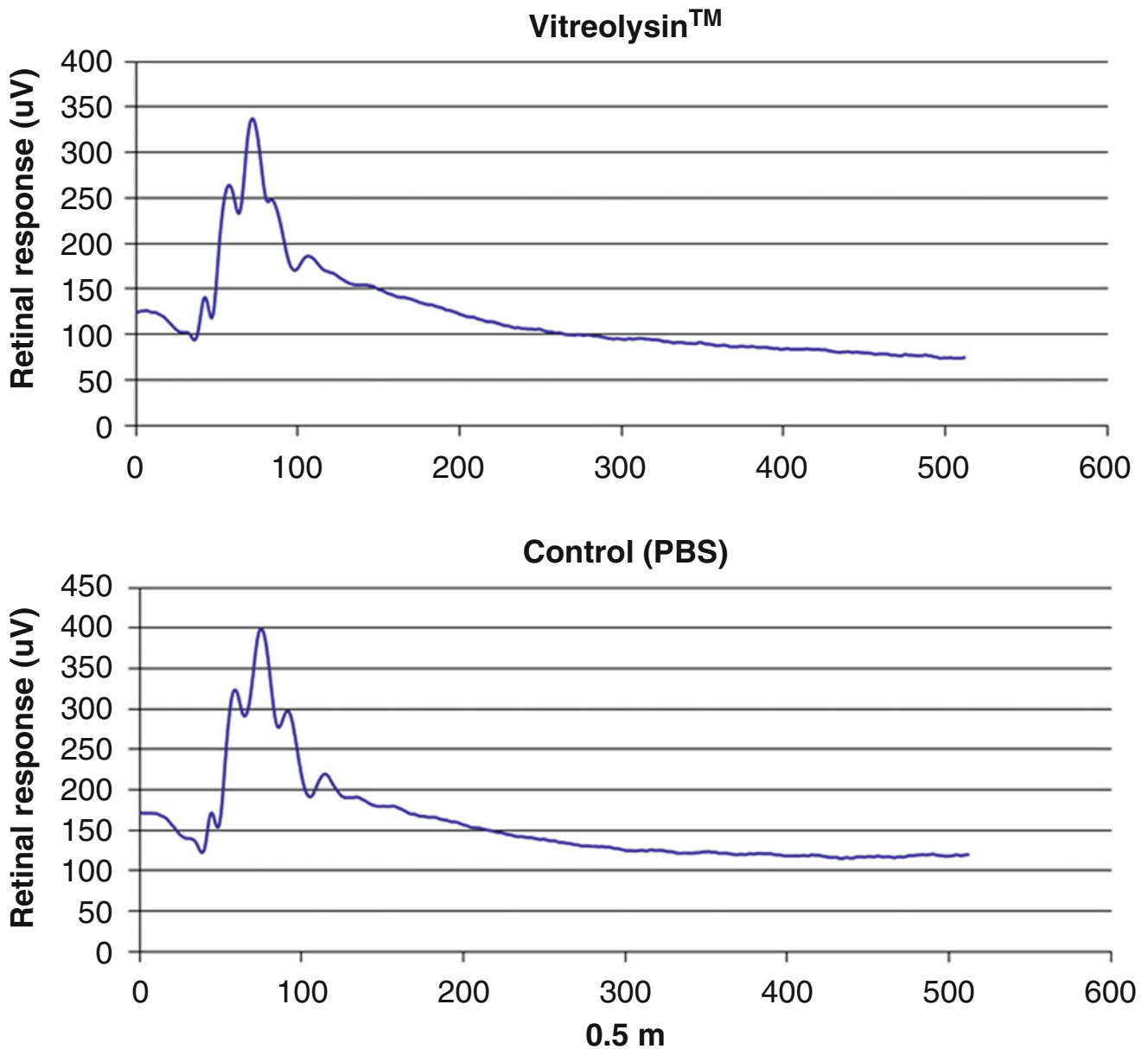


Figure VI.G-5 Two weeks after injection of 0.05 U of Vitreolysin™ into the vitreous of adult domestic pig flash ERG shows no difference in response to -10 dB flash between the PVD-induced eye and the control PBS-injected eye

PBS-injected control eyes had a complete PVD. Only one control eye (5 %) developed a partial PVD with no PVD in the remaining 19 (95 %) (Figure VI.G-6b). (2) *PVD induction over a longer term (2 h) using a lower dose of the enzyme*: This experimental design was used to determine the lowest dose of the enzyme required to induce a PVD without the need of removing the residual enzyme from the vitreous. Varying concentrations of the neutral protease (total dose: 0.025–2.0 U) were injected into the vitreous body of 3-month-old domestic pig eyes and the induction of PVD was assessed after 2 h of incubation at 37 °C. 0.05 U was the lowest dose that created a statistically significantly higher

rate of PVD (80 % complete and 10 % partial) compared to control (10 % complete and 10 % partial, $p=.0003$, Figure VI.G-6c). In all of these studies, the vitreous remained as an intact gel after neutral protease treatment (Figure VI.G-1).

2. Effect on Retinal Cell Viability and Structure

No adverse effect of the neutral protease was detected on retinal cell viability (96.2 ± 2.3 % vs. 97.3 ± 1.5 %, $p=0.74$) with an ethidium bromide-calcein-based dye (Live-Dead Assay, Invitrogen, Grand Island, NY). The retinal structure,

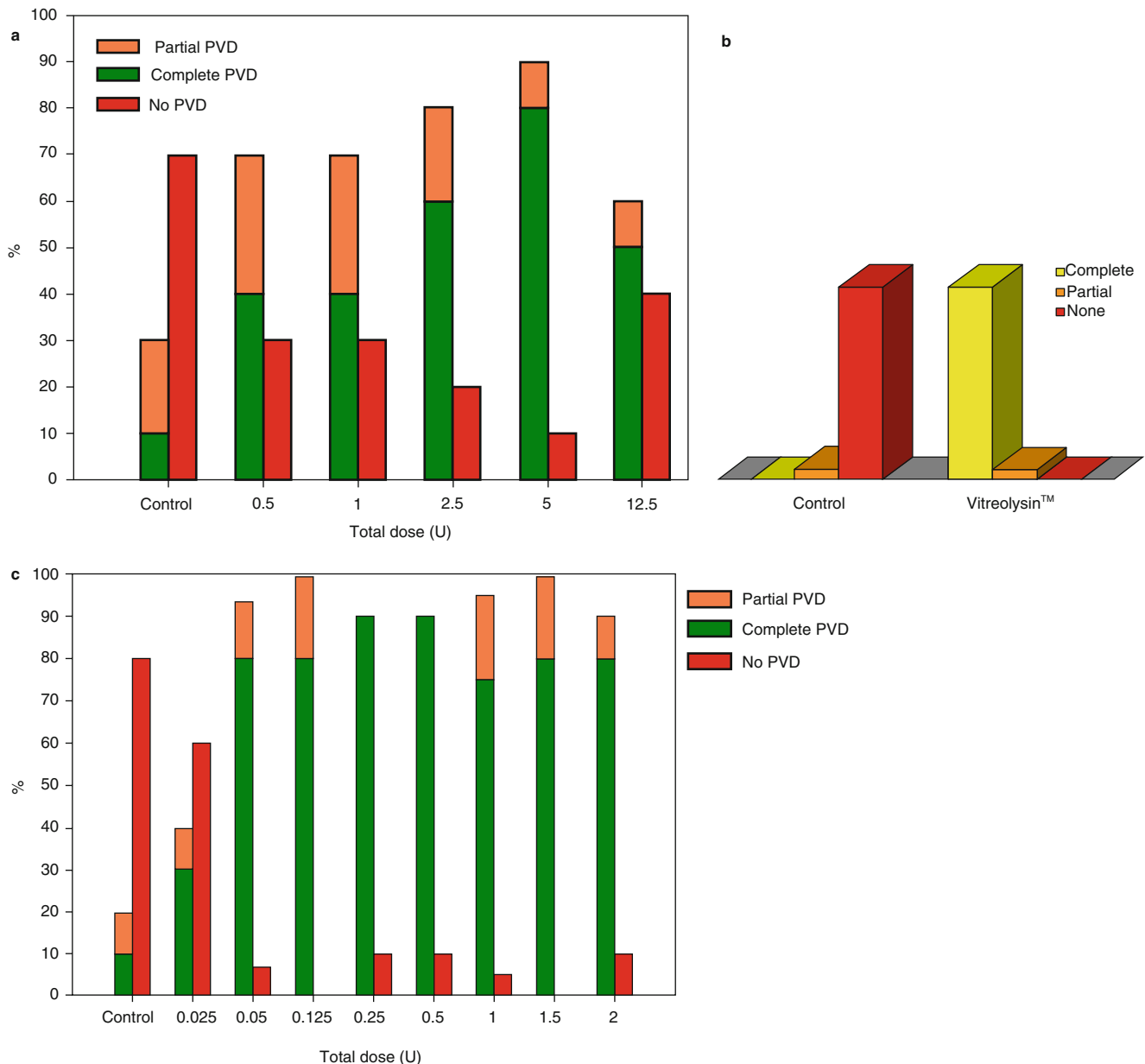


Figure VI.G-6 (a) PVD induction after 15 min in freshly enucleated porcine eyes with high-dose crude neutral protease: A total dose of 2.5 U is the lowest dose that induces a statistically higher rate of PVD ($p=0.03$). (b) PVD induction in young human donor eyes: Intravitreal injection of 2.5 U of the crude neutral protease results in a complete

PVD in 95 % of the eyes within 15 min. (c) PVD induction in a longer duration with a lower dose of the crude *Paenibacillus polymyxa* neutral protease: 0.05 U is the lowest total dose of the enzyme that induced a statistically higher rate of PVD in 2 h ($p=0.0003$)

including the retinal vessels, were intact on light microscopy; no hemorrhage was noticed (Figure VI.G-7, top row). On transmission electron microscopy, collagen fibrils of the posterior vitreous cortex disappeared along with the *lamina rara externa* of the ILM after enzyme injection. Also, the *lamina densa* lost its distinct borders and became an amorphous granular structure (Figure VI.G-7, middle row). Scanning electron microscopy revealed the mosaic pattern of the inner retinal surface after the Muller cell end plates were exposed following enzymatic digestion of the ILM-

posterior vitreous cortex interface. No cortical remnants were observed on the inner surface of the sensory retina (Figure VI.G-7, bottom row).

3. Effect on Mechanical Properties of the Sensory Retina

The effects of the *Paenibacillus polymyxa* neutral protease on the biomechanical properties of the sensory retina were also tested. Enzyme treatment did not alter the elastic constant (2.5 ± 0.3 % vs. 2.2 ± 0.4 %, $p=0.71$) and the maximal

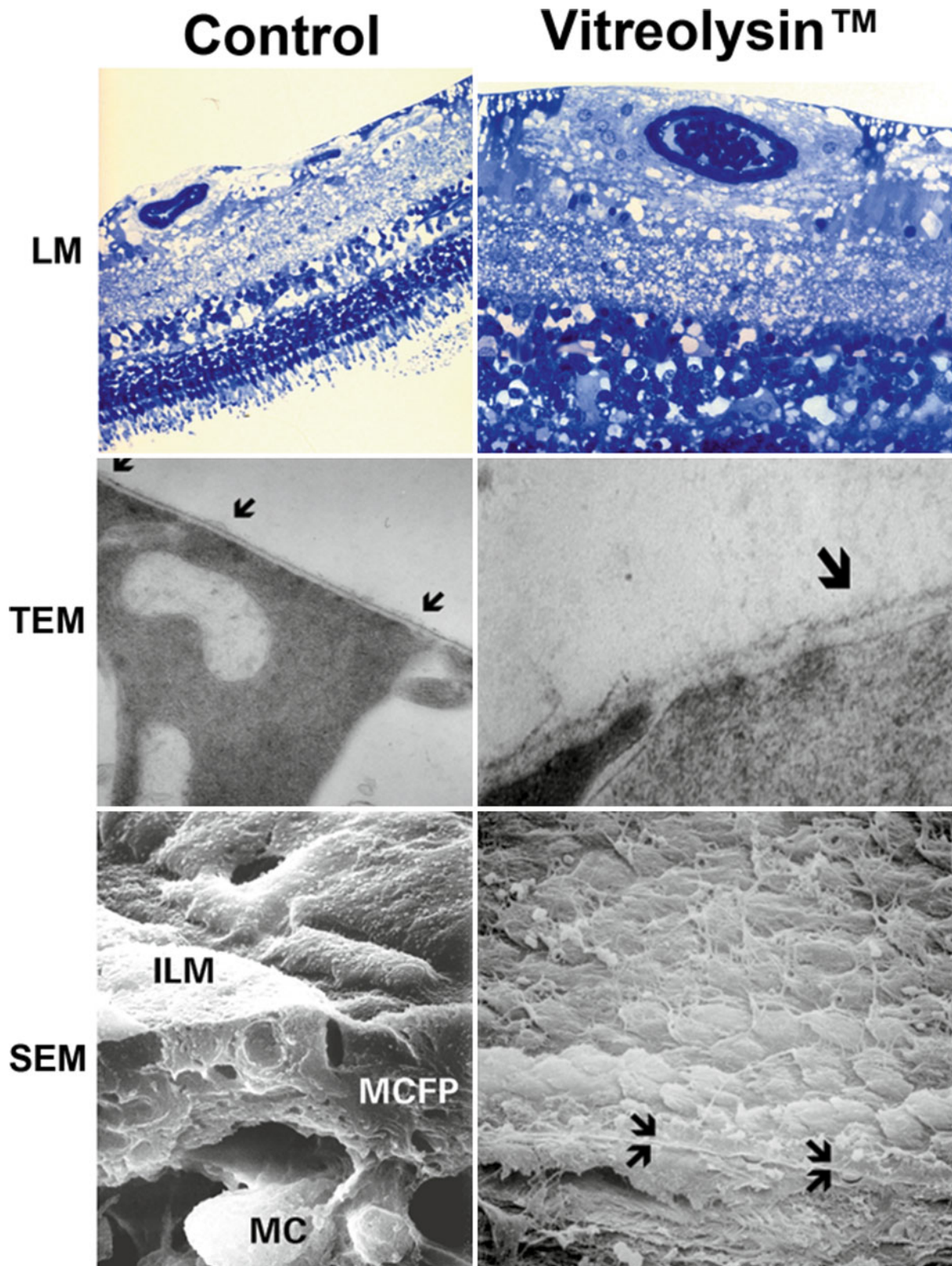


Figure VI.G-7 Top row: Treatment with 2.5 U of crude *Paenibacillus polymyxa* neutral protease does not alter the retinal architecture on light microscopy. Note that retinal vessel walls are intact and no hemorrhage is visible. Middle row: Transmission electron microscopy of the vitreoretinal interface reveals the digestion of the cortical posterior vitreous cortex collagen (right, arrows) along with the lamina rara interna of

the ILM. Note that the lamina densa became an amorphous granular structure after enzyme treatment (left, arrows). Bottom row: Freeze-fracture SEM shows the impression of the exposed Muller cell (MC) foot-plates (MCFP) after enzyme treatment (left). Note that no cortical remnant is left on the inner surface of the sensory retina after treatment

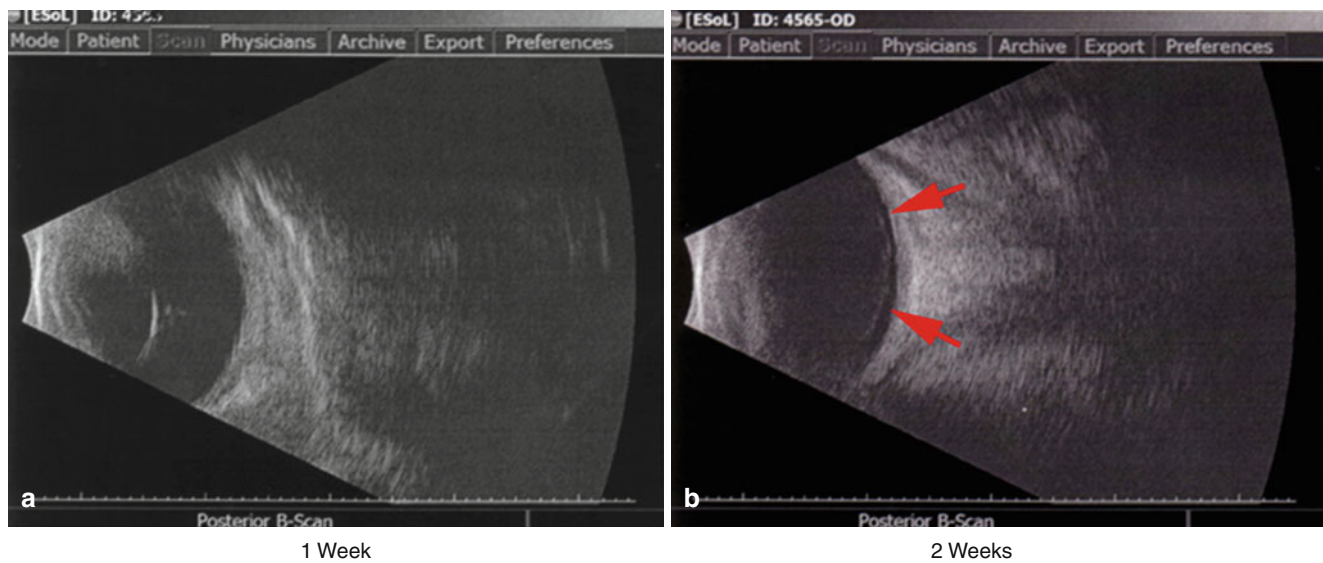


Figure VI.G-8 B-scan ultrasound exam shows induction of PVD (red arrows) 2 weeks after intravitreal injection of 0.05 U of Vitreolysin™ in the albino rabbit

retinal stretching ($2.3 \pm 1.0 \text{ Nm}^{-1}$ vs. $2.0 \pm 0.7 \text{ Nm}^{-1}$, $p=0.46$) of the sensory retina.

B. In Vivo Studies

1. PVD Induction

Crude neutral protease from *Paenibacillus polymyxa* has been used to induce a PVD in albino rabbits and domestic pigs. In an early experiment with albino rabbits, 4 rabbits received a total dose of 2.5 U and were sacrificed in 30 min, whereas another 6 animals received 0.05 U of the crude enzyme and were sacrificed 2 h later. Initial results did not reveal any toxicity from the crude enzyme (Dispase®) (B-wave amplitude electroretinogram (ERG), $p=0.972$; latency, $p=0.285$) if used as an adjunct to vitrectomy during peeling of the posterior vitreous cortex. However, keeping the crude enzyme in the eye resulted in endotoxin-induced inflammation in all animals within the first 24 h. In three animals the vitritis partially resolved at the end of the 1-week observation period. ERG readings reflect the course of the endotoxin-induced uveitis. In three animals, amplitudes of all ERG components decreased along with prolongation of implicit times on the first day after injection followed by recovery at 1 week. In 2/6 animals, however, ERG readings remained depressed (PBS vs. Dispase® for day 1, amplitude, $p=0.373$; latency, $p=0.723$; PBS vs. Dispase® for day 7, amplitude, $p=0.783$; latency, $p=0.671$). None of the animals developed a corneal melt or lenticular opacities or lens dislocation [9].

The ability of crude enzyme (Dispase®) to induce a PVD was also tested in pig eyes *in vivo* [24]. Twenty-four eyes were injected with 50 µg of crude enzyme followed 15 min

later with vitrectomy surgery to assess the ease of peeling the posterior vitreous cortex. A higher incidence of PVD (7 total, 5 partial vs. 2 total, 7 partial, and 3 none in the control group, $p=0.029$) was observed in eyes injected with the crude enzyme. Clinical exam, ERG, and light and transmission electron microscopy did not show any evidence of toxicity. In a similar experiment, after the core vitrectomy was done, 0.025 U of Dispase® was injected into the remaining cortical vitreous. Fifteen minutes of incubation caused a complete PVD in 6/8 animals while the remaining two had a partial PVD. However, 3/8 animals had a temporary vitreous haze and one animal had a spot of preretinal hemorrhage. None of these complications were serious and the investigators concluded that there was no structural damage to the retina [25].

2. Effect on Retinal Electrophysiology

These experiments clearly showed that the long-term use of the crude enzyme was unsafe due to several contaminants within the crude product, including endotoxin. These early studies resulted in attempts to purify the active enzyme and remove endotoxin; as a result the pure enzyme (Vitreolysin™) has been produced. The safety and efficacy of Vitreolysin™ was studied using 12 pigs that received 0.05 and 0.5 U of the purified enzyme. The 0.5 U group had a vitrectomy almost immediately after injection. Animals were sacrificed at 2 weeks. Induction of a PVD was assessed during the follow-up period with B-scan ultrasonography and at the time of sacrifice by direct observation. All the animals developed PVD (Figure VI.G-8) without any structural defects in the eye. Full-field ERG remained within normal limits [9].

Abbreviations

C	Centigrade
EDTA	Ethylenediaminetetraacetic
ERG	Electroretinogram
ILM	Inner limiting membrane
kDa	KiloDalton
mM	Millimoles
PBS	Phosphate buffered saline
PVD	Posterior vitreous detachment
U	Units

References

- Gandorfer A. Enzymatic vitreous disruption. *Eye (Lond)*. 2008;22(10):1273–7.
- Sebag J. To see the invisible: the quest of imaging vitreous. *Dev Ophthalmol*. 2008;42:5–28.
- Sebag J. Pharmacologic vitreolysis—premise and promise of the first decade. *Retina*. 2009;29(7):871–4.
- Griffin PJ, Fogarty WM. Physicochemical properties of the native, zinc- and manganese-prepared metalloprotease of *Bacillus polymyxa*. *Appl Microbiol*. 1973;26(2):191–5.
- Takekawa S, Uozumi N, Tsukagoshi N, Udaka S. Proteases involved in generation of beta- and alpha-amylases from a large amylase precursor in *Bacillus polymyxa*. *J Bacteriol*. 1991;173(21):6820–5.
- Matsudo Y. Neutral protease useful for animal tissue and cell culture. In: Office USP, editor. United States Patent and Trademark Office: Godo Shusei Kabushiki Kaisha, vol 3. p. 930–54; 1976.
- Tang D, Del Priore LV, Kaplan HJ, Tezel T. Factors modulating the matrix metalloprotease (MMP) activity of dispase. *IOVS (ARVO)*. 2007;48:259.
- Jashnani KD, Kale SA, Rupani AB. Vitreous humor: biochemical constituents in estimation of postmortem interval. *J Forensic Sci*. 2010;55(6):1523–7.
- Tezel TH: unpublished data
- Tojo K. A pharmacokinetic model for ocular drug delivery. *Chem Pharm Bull (Tokyo)*. 2004;52(11):1290–4.
- Tezel TH, Del Priore LV, Kaplan HJ. Posterior vitreous detachment with dispase. *Retina*. 1998;18(1):7–15.
- Matsumoto B, Blanks JC, Ryan SJ. Topographic variations in the rabbit and primate inner limiting membrane. *Invest Ophthalmol Vis Sci*. 1984;25(1):71–82.
- Snead MP, Snead DR, Richards AJ, et al. Clinical, histological and ultrastructural studies of the posterior hyaloid membrane. *Eye*. 2002;16(4):447–53.
- Barile GR, Pachydaki SI, Tari SR, et al. The RAGE axis in early diabetic retinopathy. *Invest Ophthalmol Vis Sci*. 2005;46(8):2916–24.
- Stefansson E. Physiology of vitreous surgery. *Graefes Arch Clin Exp Ophthalmol*. 2009;247(2):147–63.
- Scheiffarth OF, Kampik A, Gunther H, von der Mark K. Proteins of the extracellular matrix in vitreoretinal membranes. *Graefes Arch Clin Exp Ophthalmol*. 1988;226(4):357–61.
- Kritzenberger M, Junglas B, Framme C, et al. Different collagen types define two types of idiopathic epiretinal membranes. *Histopathology*. 2011;58(6):953–65.
- George B, Chen S, Chaudhary V, et al. Extracellular matrix proteins in epiretinal membranes and in diabetic retinopathy. *Curr Eye Res*. 2009;34(2):134–44.
- Casaroli Marano RP, Vilaro S. The role of fibronectin, laminin, vitronectin and their receptors on cellular adhesion in proliferative vitreoretinopathy. *Invest Ophthalmol Vis Sci*. 1994;35(6):2791–803.
- Canto Soler MV, Gallo JE, Dodds RA, Suburo AM. A mouse model of proliferative vitreoretinopathy induced by dispase. *Exp Eye Res*. 2002;75(5):491–504.
- Frenzel EM, Neely KA, Walsh AW, et al. A new model of proliferative vitreoretinopathy. *Invest Ophthalmol Vis Sci*. 1998;39(11):2157–64.
- Kralinger MT, Kieselbach GF, Voigt M, et al. Experimental model for proliferative vitreoretinopathy by intravitreal dispase: limited by zonulolysis and cataract. *Ophthalmologica*. 2006;220(4):211–6.
- Tan J, Liu Y, Li W, Gao Q. Ocular pathogenesis and immune reaction after intravitreal dispase injection in mice. *Mol Vis*. 2012;18:887–900.
- Oliveira LB, Tatebayashi M, Mahmoud TH, et al. Dispase facilitates posterior vitreous detachment during vitrectomy in young pigs. *Retina*. 2001;21(4):324–31.
- Ivastinovic D, Langmann G, Aigelsreiter A, et al. Dispase-assisted vitrectomy for epiretinal prostheses implantation. *Acta Ophthalmol*. 2012;90(2):e163–5.
- de Smet MD, Jonckx B, Vanhove M, et al. Pharmacokinetics of ocriplasmin in vitreous. *Invest Ophthalmol Vis Sci*. 2012;53(13):8208–13.

Chondroitinase as a Vitreous Interfactant: Vitreous Disinsertion in the Human

VI.H.

Stephen R. Russell and Gregory S. Hageman
Chondroitinase Study Group (Addendum 1)

Outline

- I. **Introduction**
- II. **Biochemistry**
 - A. Proteoglycans and the Vitreoretinal Interface
 - B. Biochemistry of Chondroitinase Enzymes and Substrates
- III. **Chondroitin Sulfate at the Vitreoretinal Interface**
- IV. **Chondroitinase Pharmacologic Vitreolysis**
 - A. Preliminary Monkey Studies
 - B. Human Proof-of-Concept Study
 - C. FDA Phase I/II Study and its Implications
 - 1. Efficacy
 - a. Proliferative Diabetic Retinopathy
 - b. Macular Hole
 - 2. Safety

Conclusions

References

S.R. Russell, MD (✉)
Department of Ophthalmology and Visual Sciences,
The University of Iowa Carver College of Medicine,
200 Hawkins Drive, Iowa City, IA 52242, USA

Carver Center for Macular Degeneration, Institute of Visual
Research, Carver College of Medicine, University of Iowa,
Iowa City, IA USA
e-mail: stephen-russell@uiowa.edu

G.S. Hageman, PhD
Department of Ophthalmology and Moran Eye Institute,
University of Utah Health Care, Salt Lake City, UT, USA
Laboratory of Ocular Cell Biology, Salt Lake City, UT, USA

Funding/Support

Supported by the Dina J. Schrage Professorship for Macular
Degeneration, University of Iowa (SRR) and the John A. Moran
Presidential Professorship, Department of Ophthalmology and Visual
Sciences, University of Utah School of Medicine (GSH).

Keywords

Vitreous • Pharmacologic vitreolysis • Chondroitinase •
Posterior vitreous detachment • Vitreous disinsertion •
Monkey • Electrophysiology • Ultrastructure • Human
vitrectomy

Key Concepts

1. Studies in monkeys have demonstrated that chondroitinase disinserts the posterior vitreous cortex from the ILM, the vitreous base from the peripheral fundus, and the anterior vitreous cortex from the lens. It has thus been found to be an effective interfactant agent for pharmacologic vitreolysis, but does not induce liquefaction.
2. Proof-of-principle studies in human brain-dead patients demonstrated efficacy as an interfactant without any untoward effects upon ocular morphology, in particular retinal ultrastructure.
3. Phase I/II FDA trials demonstrated safety and efficacy as a surgical adjunct in treating macular holes and proliferative diabetic retinopathy.

Financial Disclosure
Gregory S. Hageman, P.

Addendum 1. Participants in the Chondroitinase Study Group
Emory University
Principal Investigator: Paul Sternberg, MD
Co-Investigators: David A. Saperstein, MD, Timothy W. Olsen, MD,
Scott Lambert, MD (ERG)
Johns Hopkins University/Wilmer Eye Institute
Co-Principal Investigator: Peter Campochiaro, MD PhD,
Julia Allison Haller, MD
Co-Investigators: Janet S. Sunness, MD (ERG)
VMR Institute for Vitreous Macula Retina
Principal Investigator: J. Sebag, MD, FACS, FRCOphth, FARVO
Study Coordinator: Sherry Christofferson

I. Introduction

Despite the initial discovery and testing of chondroitinase as a pharmacologic vitreolysis agent that began nearly three decades ago, contractual restrictions in the initial years and intellectual drift in more recent years have limited the peer-reviewed publication of most of the animal (monkey) and human studies that evaluated this promising agent. Detailed investigator, institutional, corporate, and registered FDA regulatory documents that are available to us provided the basis for the majority of this chapter. Two devastating floods of Dr. Gregory Hageman's data room at the University of Iowa, however, reduced the number and variety of images available from which to provide supplementary visual illustration of the human results that will be discussed.

II. Biochemistry

A full appreciation of the rationale and initial results of chondroitinase pharmacologic vitreolysis requires an understanding of the localization of the proteoglycans substrate within the vitreous body and at the vitreoretinal interface as well as the biochemical properties and mechanism of action of chondroitinase.

A. Proteoglycans and the Vitreoretinal Interface

Proteoglycans are complex macromolecules found in all extracellular matrices including the vitreoretinal interface (Figure VI.H-1). Proteoglycans' function in basement membranes is to hydrate and resist compression, constrain diffusion by anionic charge, and provide mechanical adhesion between tissues [1]. They are identified by their core protein sequence and many, but not all, have been sequenced, characterized, and named, as for example decoran, versican, and perlecan [2]. Chondroitin sulfate proteoglycans have been previously shown to provide adhesion between basement membranes and adjacent extracellular matrices within the eye and other tissues. For instance, inhibiting the secretion of chondroitin sulfate proteoglycans within the insoluble interphotoreceptor matrix has been shown to result in reduction of adhesion between the retina and the retinal pigment epithelium [3–6].

As target substrates, proteoglycans consist of proteins that are heavily glycosylated by the attachment of linear glycosaminoglycan (GAG) polymer side chains attached via a serine (Ser) residue through which the GAG is attached by a tetrasaccharide bridge (i.e., <chondroitin sulfate>-glucose-galactose-galactose-xylose-serine) (Figure VI.H-1) [1]. In addition to their sequence, proteoglycans are characterized

by the predominant saccharide dimer-pair that makes up the GAG side chains. For instance, a proteoglycan is called a chondroitin sulfate proteoglycan if the majority of the GAGs consist of alternating N-acetylgalactosamine and glucuronic acid.

In earlier sections of this book, the localization and significance of vitreous attachment(s) in development and disease have been documented [see chapters II.A. Vitreous Embryology; II.E. Vitreo-retinal interface & ILM; III.B. Anomalous PVD & vitreoschisis; III.C. Pathology of vitreomaculopathies]. The vitreous fibrillar structure can be clinically appreciated in aging [see chapter II.C. Vitreous aging & posterior vitreous detachment] and may be histologically visualized with a variety of particulates, stains, and probes. An illustration of the relative orientation and density of this fibrillar architecture is given in Figure VI.H-2. Regional differences in the adherence of the vitreous to the neural retina correspond to the density of the fibrillar vitreous structure, particularly to the density of fibrils orthogonal to the vitreoretinal surface. Central portions of the vitreous fibrillar material co-localize with collagen II [7]. However, our understanding of the terminations of the fibrillar structure and its insertions remains incomplete. Other fibrillar proteins and/or proteoglycans contribute to the vitreous and to retinal linkage as has been confirmed by Paul Bishop and colleagues [8–10] [see chapter I.A. Vitreous proteins].

Several mechanisms of adhesion of the vitreous fibrils are clinically known. These include the constitutive attachments found in younger humans and other primates. In addition, however, attachments of a pathologic nature may also add to or replace the constitutive adhesive mechanisms. For instance the development of retinal neovascularization onto or into the posterior vitreous cortex in proliferative diabetic vitreoretinopathy or the formation of organized tissue may complicate the attachment paradigm. Differing models of the constitutive attachments incorporate data derived from transmission electron microscopy, immunohistochemistry, and enzymatic response of the vitreoretinal interface. Based upon our observations of the behavior of the primate and human vitreoretinal interface to chondroitinase, we conclude that a structurally significant, omnipresent layer exists between the normal fibrillar/lamellar vitreous cortex and the neural retina (as suggested in the schematic representation of the vitreoretinal interface shown in Figure VI.H-3) [see "ECM" in chapter II.E. Vitreo-retinal interface & ILM]. The orientation and attachment site(s) of the chondroitin sulfate proteoglycan core protein has not been established.

We have previously shown that an incompletely identified, chondroitin sulfate-containing proteoglycan (core size approx. 240KDa) is associated with regions of strong adhesion between the vitreous and the retina, with the proteoglycan being localized to the vitreoretinal interface (a human example illustrating these adhesions in retinopathy of prematurity is

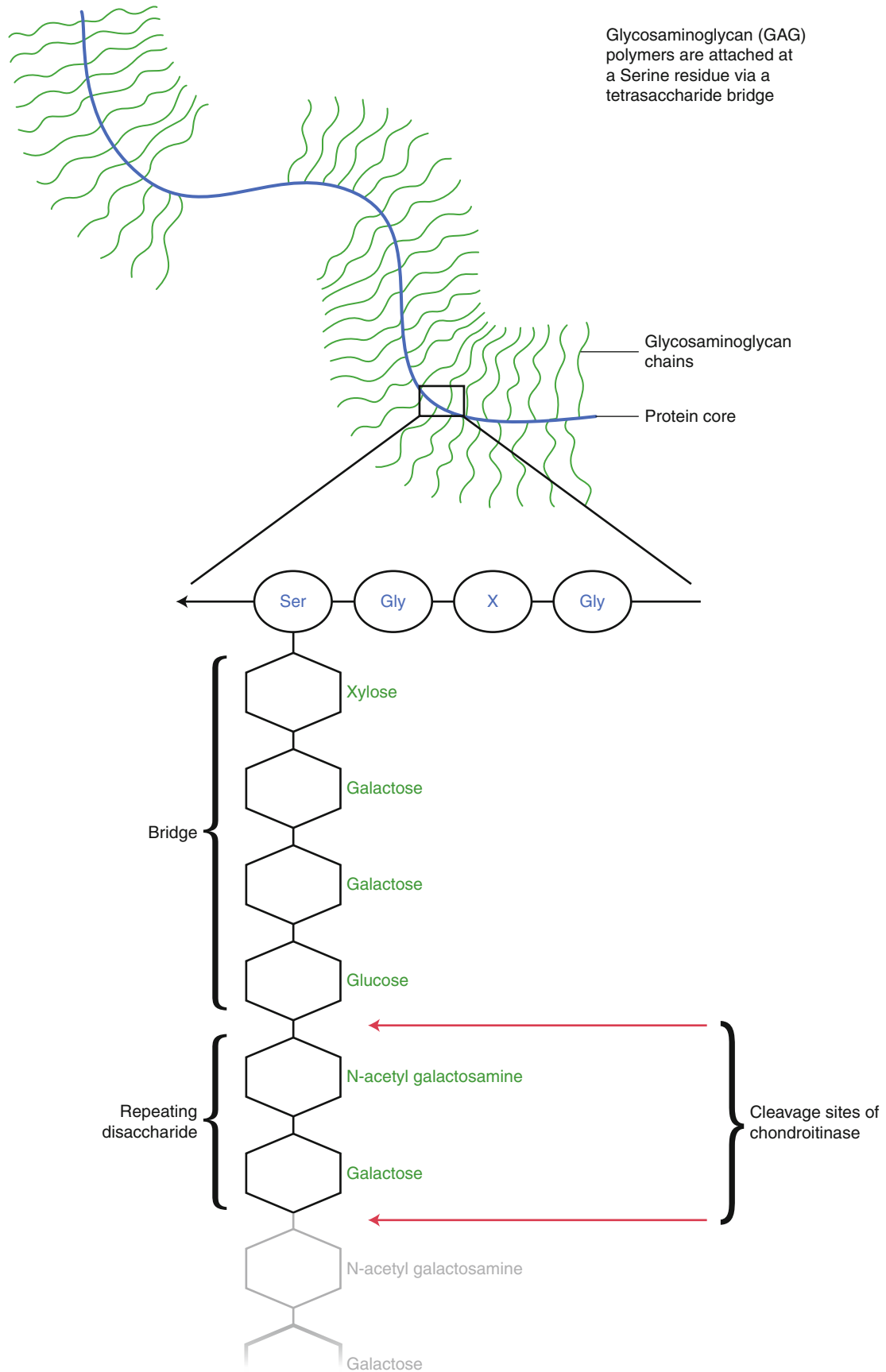


Figure VI.H-1 Proteoglycan structure and relationship of glycosaminoglycan (GAG) attachments. Glycosaminoglycan polymers are attached to a core protein via a serine residue (“O-linked”) and a tetrasaccharide bridge. Exposure of the disaccharide repeats within the

GAGs to chondroitinase facilitates isolation of the protein core, which may be adherent or covalently attached to other structural proteins at one or more sites

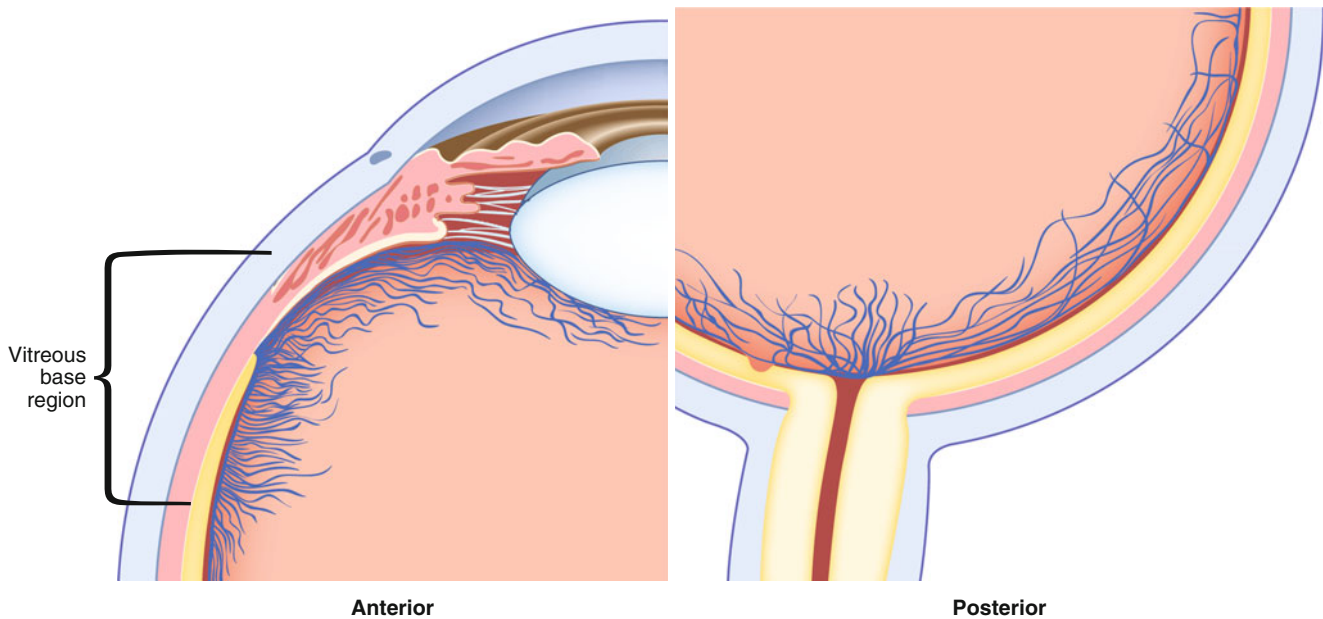


Figure VI.H-2 Schematic illustration of the fibrillar anatomy of the human vitreous. Vitreous adhesion and fibrillar density co-localize and are highest where the fibrils are dense and orthogonal to the vitreous base (region anterior and posterior to the ora serrata), intermediate in

adhesion where there is intermediate orthogonal fibrillar density at the inner optic disk and lowest in adhesion and density where the fibers are sparsely distributed over the posterior inner retinal surface

shown in Figure VI.H-4) [11]. In the case of the incompletely identified vitreoretinal interface proteoglycan, the lectin peanut agglutinin or PNA binds with highest affinity to its glycosaminoglycans or GAGs which contain chondroitin-4-sulfate and/or chondroitin-6-sulfate. Subsequently we developed an antibody to the proteoglycan that facilitated more specific identification of this molecule associated with vitreous/retinal adhesion [12]. In a series of pilot experiments using commercially available chondroitinase, cynomolgus monkeys were treated with various doses of chondroitinase for varying time (incubation) periods prior to vitrectomy in order to determine if the enzyme could facilitate disinsertion of the vitreous from the neural retina [11, 13].

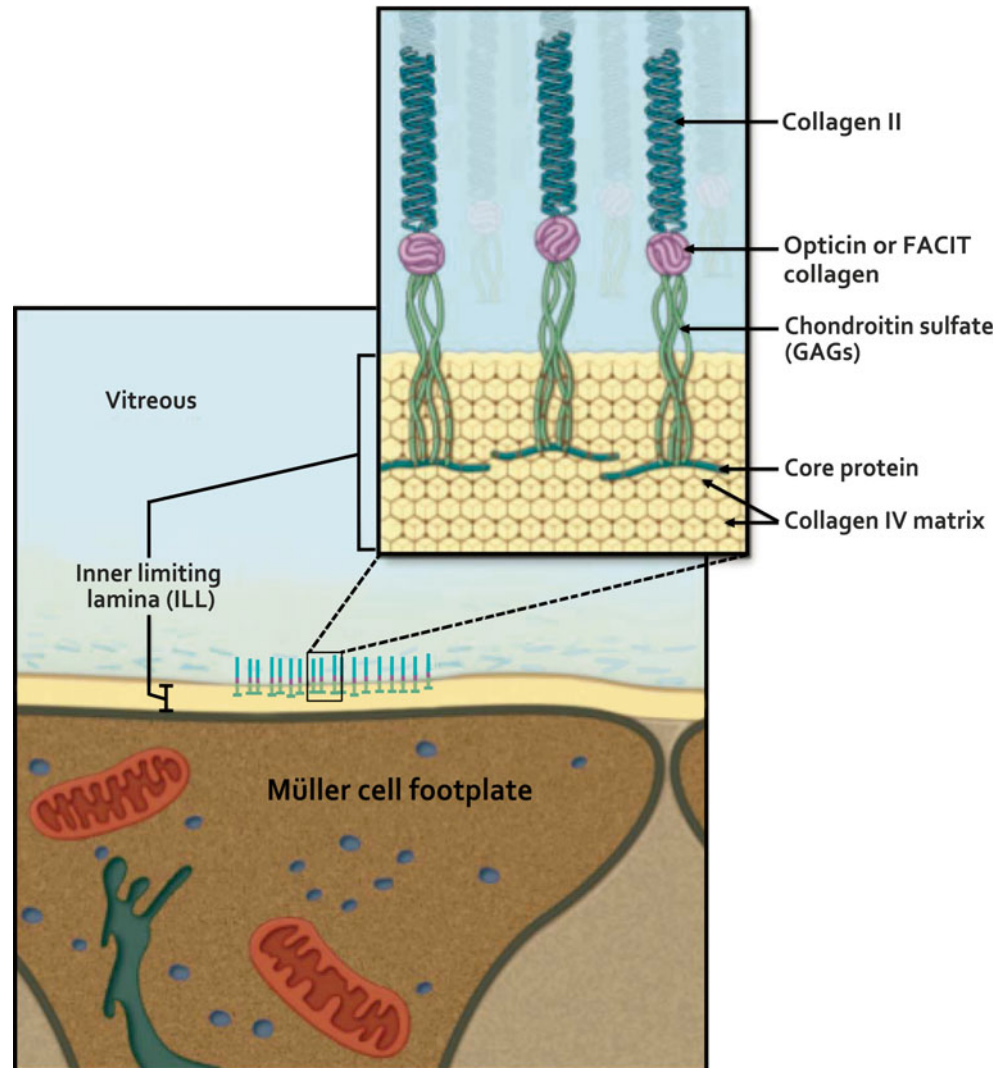
B. Biochemistry of Chondroitinase Enzymes and Substrates

Chondroitinase is an enzyme complex that acts to cleave and fragment chondroitin-sulfate-containing glycosaminoglycan (GAG) side chains of proteoglycan “core” molecules [12]. Chondroitinase demonstrates a specificity to cleave and degrade only bonds between and within the disaccharide N-acetylgalactosamine-glucuronic acid. As formulated for human clinical trials, chondroitinase is a biologic agent that consists of a mixture of two enzymes, chondroitinase I and chondroitinase II [12]. Chondroitinase I (110 KDa) is a lyase that attacks chondroitin sulfate in an endolytic fashion, breaking the polymeric structure into oligosaccharides and disaccharides [12]. The second enzyme, chondroitinase II (112

KDa), has no activity against the intact polymer but can digest tetrasaccharides produced by the chondroitinase I-catalyzed reaction [12]. The combined activity of these two enzymes results in a more rapid degradation than use of chondroitinase I alone. This type of depolymerization activity utilizing more than one enzyme to attack a large polymeric substance is analogous to many other enzymatic systems among microorganisms capable of degrading such polymers. The amino acid sequences of the chondroitinase enzymes are known [12].

Chondroitinase is produced by *Proteus vulgaris* bacteria, which can be induced to produce high concentrations of chondroitinase when incubated on a carbon diet consisting exclusively of chondroitin sulfate, such as shark cartilage. When other bacterially derived enzymes, secreted products, and waste are removed, the purified chondroitinase is a white, lyophilized powder that can be reconstituted with balanced salt solution. Purification methods often inactivate the enzymatic active sites or otherwise modify their protein structure, conformation, or glycosylation. Collaboration with Storz/American Cyanamid Company resulted in developing batch-produced, incubation product that was physically and chemically purified to acceptably low concentrations of endotoxins and pyrogens and achieved physiologic stoichiometry of chondroitinase I and II that permitted human FDA IND approval of a pharmacologically purified and biologically active chondroitinase in 1994 [12]. Multiple attempts to develop recombinant forms of chondroitinase I and chondroitinase II were unsuccessful, which may have led to elevated production cost estimates and ultimate discontinuance of human testing after completion of the FDA phase I/II study. Difficulty or failure to purify enzymes

Figure VI.H-3 Schematic illustration of the human vitreoretinal interface. The inner limiting membrane (lamina) is represented by the yellow structure. Note the layer of chondroitin sulfate GAGs within the vitreoretinal interface. Cleavage or disruption of the saccharide layer (chondroitinase) or degradation of the fibrillar proteins or basement membrane (proteases) may result in weakening or separation of the vitreous from the inner limiting membrane of the retina (Reprinted from the journal *Retina*, reference [11], courtesy of Wolters Kluwer Health)



in an experimental setting commonly results in residual contamination by other enzymes that may have different substrates and/or activities. Chondroitinase contamination found in off-the-shelf enzyme formulations, which may be of adequate purity for biochemical purposes but insufficient for pharmacologic testing, has resulted in unexpected inflammation due to breakdown of unintended structures and/or reaction to degradation products [14].

III. Chondroitin Sulfate at the Vitreoretinal Interface

As previously mentioned, Dr. Greg Hageman and I began our collaboration in 1988 to evaluate the potential usefulness of chondroitinase for human application, a project which preceded the development of plasmin by years [11]. Preliminary survey studies of lectin binding on transverse primate globe sections revealed that fluorescein-conjugated peanut agglutinin or PNA, a marker for chondroitin sulfate linkages, localized to

the vitreoretinal interface, posterior lens capsule, and surface of the optic disk (Figure VI.H-4) [11, 12, 15]. Further, the intensity of PNA binding and the width of binding by immunofluorescence microscopy corresponded to the strength or degree of vitreoretinal adhesion. For instance, the PNA binding was expressed as most intensely overlying the vitreous base region, less intensely adjacent to the optic disk and posterior lens capsule, and finely in a linear binding pattern to the majority of the remaining vitreoretinal interface (Figure VI.H-4). In human, primate, and pig eye sections exposed to chondroitinase, PNA binding was extinguished, and adhesion between the vitreous collagen network and the retina/optic nerve head/lens could be appreciated by separation with minimal effort or force [11, 12]. Comparison to other enzymatic degradation agents such as trypsin, hyaluronidase, dispase, heparinase, and others confirmed that the most complete loss of PNA binding signal and reduction in adhesion could be obtained with chondroitinase.

Follow-on studies demonstrated that exposure of the human vitreoretinal interface to chondroitinase resulted in complete disruption of the adhesion, a process we termed

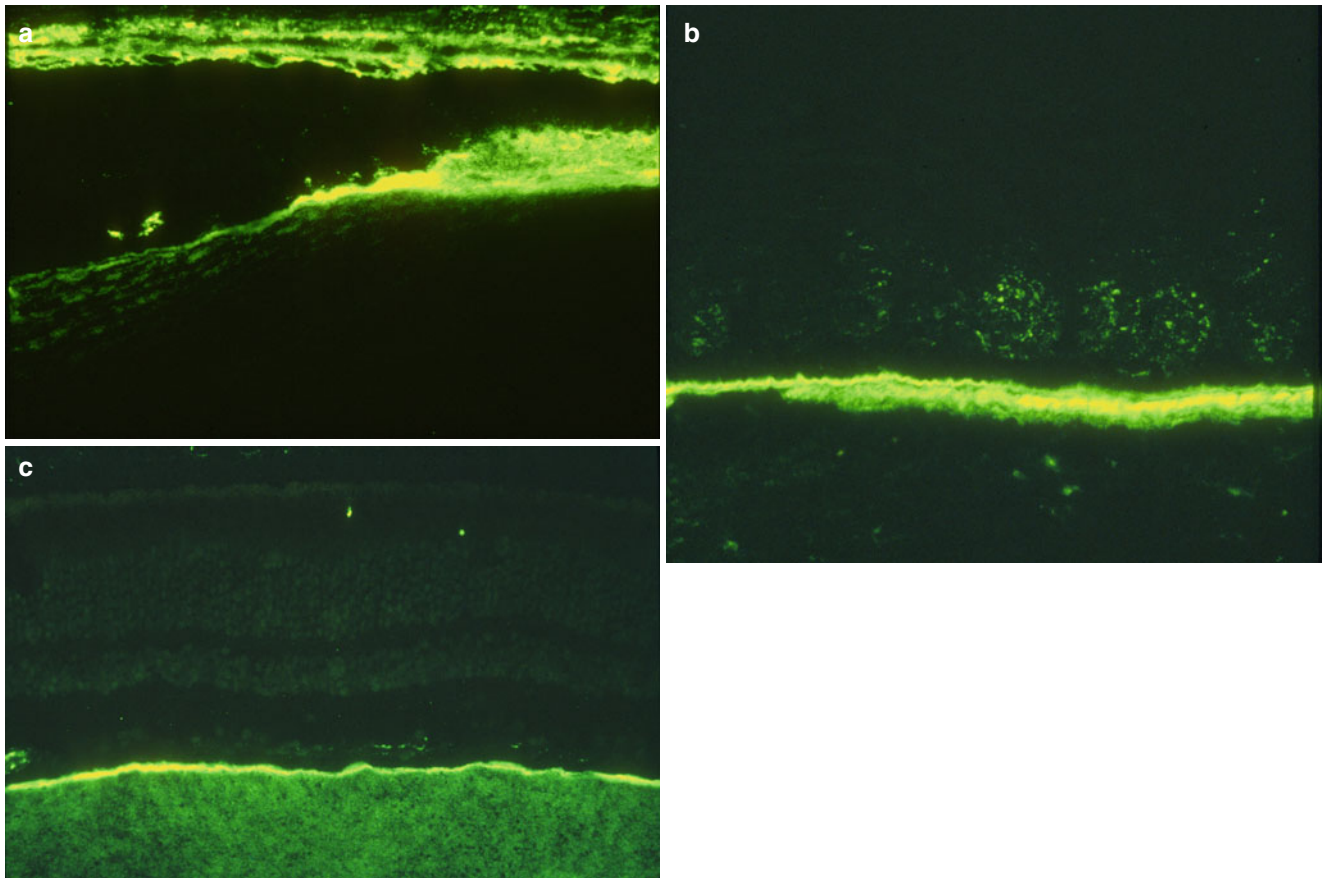


Figure VI.H-4 Epifluorescence microscopy of fluorescein-labeled anti-CS proteoglycan antibody binding at human vitreoretinal interface in retinopathy of prematurity. In this 17-week-old premature human donor, the localization of the proteoglycan core is demonstrated by the

intensity and distribution of the antibody binding. Note the intense binding in the region of the vitreous base (a), intermediate density in the region of the inner optic disk (b), and lesser density in the other regions of the vitreo-retinal interface (c)

disinsertion. We argued for several weeks over what was the best term to use when describing this unique and characteristic effect of exposing chondroitinase to the human vitreoretinal, vitreopapillary, and vitreolenticular interfaces. Unlike known proteolytic enzymes, chondroitinase exposure resulted in complete, rather than incomplete, separation of the vitreous from the primate retina and did not liquefy the vitreous as might be suggested by the term “pharmacologic vitreolysis.” The absence of vitreous liquefaction by chondroitinase has since been confirmed [16]. As illustrated in cynomolgus eyes during preclinical testing (Figure VI.H-5), “complete” disinsertion refers to the mechanical separation of the vitreous from the inner limiting membrane, optic disk, vitreous base, and posterior lens attachments. We refer to “incomplete” separation as effecting separation only in regions of relatively weaker adhesion that corresponds to regions of less PNA binding (i.e., posterior pole and optic disk). Phylogenetic analysis showed that complete vitreous cleavage or “disinsertion” was only observed in higher primates and pigs. Extensive testing of chondroitinase on mice, rats, and rabbits showed no effect on vitreous attachment strength [12].

IV. Chondroitinase Pharmacologic Vitreolysis

As mentioned above, Dr. Hageman and I published very few peer-reviewed publications on this topic from 1988 to 2012. However we did publish on related issues such as the generation of preretinal membranes that resulted from chondroitin sulfate injection into rabbit vitreous and the outcome of the control arm of one of our primate studies [15, 17, 18]. A few representative observations were reported by Sebag based upon interim discussions [13]. Since that first publication, Sebag proposed a classification system for pharmacologic vitreolysis agents based on biological activity [19]. Whereas he described chondroitinase as both a *liquefactant* (agent that liquefies the gel vitreous) and an *interfactant* (agent that induces vitreoretinal dehiscence), it is now clear that the former is not an effect of chondroitinase [16].

A. Preliminary Monkey Studies

After determining that lower primates and non-primates failed to show the same degree and type of response to chon-

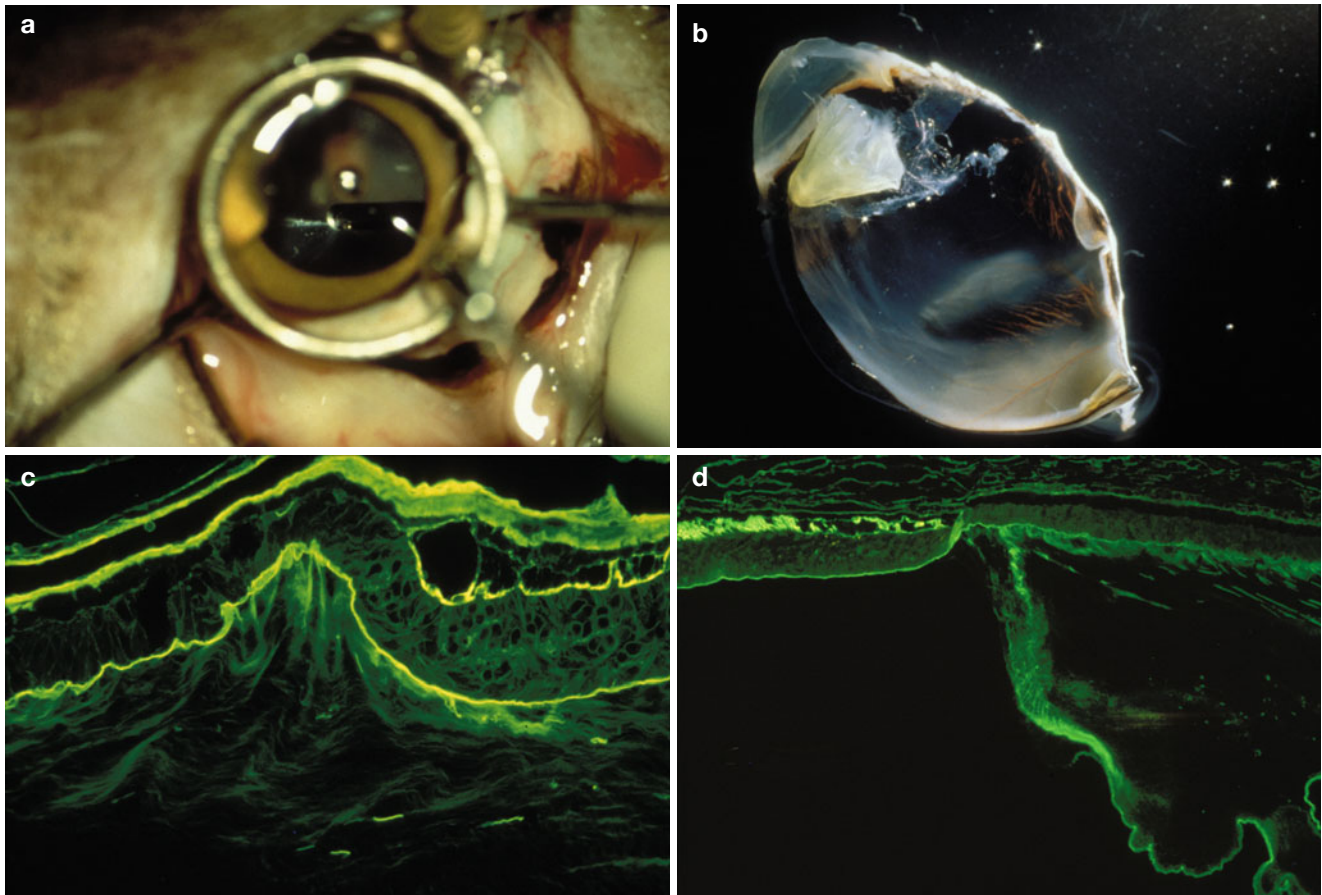


Figure VI.H-5 Disinsertion of vitreoretinal adhesion by chondroitinase in the cynomolgus monkey (a) Intraoperative photograph illustrates that traction applied to the illuminated vitreous following chondroitinase treatment reveals that the residual vitreous attachment is anterior to the crystalline lens. (b) The companion gross anatomical section depicts fixed visible vitreous (translucent white) unattached to the retina or ciliary body but maintaining connection to the zonules. (c) Epifluorescence microscopy of cynomolgus globe sections treated with fluorescein-linked PNA that bisects the ora serrata. In the left panel is a

control untreated eye. In the right panel is a chondroitinase-treated eye. Under normal conditions the adhesion of the vitreous to the retina in this region is stronger than either the vitreous or retinal tissue. The separation of the vitreous from the retina in the region of the vitreous base supports the contention that all regions of constitutive vitreoretinal adhesion are mediated by the same, chondroitinase-sensitive mechanism (Reprinted from reference [11], courtesy of Wolters Kluwer Health)

droitinase as in higher primates, we completed a series of studies which evaluated the efficacy, safety, and toxicology of exposing cynomolgus and rhesus monkey vitreous to chondroitinase. Although these studies go beyond the scope of this chapter, an enumeration of a subset of these may be illustrative of the extent of preclinical data that were collected. We initially conducted a non-survival study on 6 animals to determine approximate concentrations and exposure times for effectiveness. We then performed a short- and long-term treatment trial (one eye treated, one eye control) to evaluate for efficacy and longer-term side effects. In a third study we evaluated whether chondroitinase was effective in facilitating the removal of preretinal membranes. These were generated in primates by vitreous injection of chondroitin sulfate GAGs, a technique we had demonstrated to successfully generate preretinal membranes in rabbits [17]. We also examined a number of human postmortem specimens to

determine whether the chondroitinase-sensitive (constitutive) vitreoretinal mechanism was recapitulated between human preretinal membranes and the inner limiting membrane. We subsequently performed non-survival studies on a number of batches of recombinant chondroitinase. We evaluated supra-threshold doses in 12 animals for evidence of toxicity or inflammation. Once we determined that the Storz-produced incubation product would be used for clinical trial, we performed an extended short-term survival study utilizing radioactive enzyme to trace its metabolism and excretion.

However, because this chapter focuses on the effects of chondroitinase on the human vitreoretinal interface and because our primate testing of chondroitinase went well beyond the scope of this chapter, these data will be summarized and published elsewhere (Russell SR and Hageman GS, American Ophthalmological Society, thesis in preparation).

B. Human Proof-of-Concept Study

In 1992, Dr. Hageman and I undertook a key proof-of-concept human study. We decided that to accelerate our understanding of the value of chondroitinase, we needed to determine whether this agent could “disinsert” the vitreous *in vivo* in the human. Until then all of our testing *in vivo* had been on rhesus and cynomolgus monkeys, as described above. Since testing in living humans was impossible, as the agent had not received an FDA Investigational New Drug approval (IND), Dr. Hageman approached the Missouri Eye Bank and affiliated organ transplant collection agencies for access to brain-dead organ donors. Following delicate negotiations with donor groups and our institutional human subjects and ethics committees, we obtained permission to perform vitrectomy and place chondroitinase into two eyes of subjects who had been declared brain-dead and were undergoing multiple organ donation (liver, kidney, and heart harvest). Both subjects were young males (22 and 30 years old), unlikely to have spontaneous vitreous separation. One died from a motor vehicle accident and the other from a non-ocular gunshot wound. Fundus evaluations revealed normal fundi, retinal vessels, optic nerves, and peripheral retinal vessels in the gunshot victim. In the subject who succumbed to motor vehicle accident, the fundus examination revealed scattered intraretinal hemorrhages, judged to be a result of the trauma. The retinal vessels in this subject were otherwise normal as were the optic nerves.

Vitrectomy surgery was performed on one eye of each subject using a method similar to that used for the monkey and subsequent human studies. In the first study, a 500-unit dose of chondroitinase (pharmaceutical grade chondroitinase ABC, Seikagaku Corporation, Tokyo, Japan) was placed for a treatment period of 35–40 min. In the second study 600 units were used for a treatment period of 15–18 min. In each case, both the treated and untreated eyes were enucleated following the vitrectomy procedure and portions of the eyes were fixed for histology, immunohistochemistry, and transmission electron microscopy. In addition, the anterior segment was fixed for routine histologic evaluation of the lens, posterior lens capsule, cornea, iris, and ciliary body. Based on the impression of the surgeon and the gross observation of the enucleated eye, the vitreous appeared to be disinserted in the chondroitinase-treated eye. Histology, immunohistochemistry, and TEM confirmed that the vitreous was disinserted from the inner limiting membrane of the neural retina and the posterior lens in the chondroitinase-treated eye but not in the control eye (Figure VI.H-6). All other ocular structures (i.e., retina, RPE, optic nerve, ciliary body, lens, iris, and cornea) appeared normal in both eyes. These two experiments indicated that the human vitreous could be disinserted using chondroitinase and revealed no acute adverse effects resulting from chondroitinase-mediated surgery.

Analysis of the surgical procedures showed spontaneous separation of the posterior vitreous from the optic disk and

retina. No posterior vitreous detachment was present in the untreated eyes of either brain-dead donor. Sectioning the treated eyes showed disinsertion of the vitreous from the anterior retina and posterior lens surface, with residual vitreous attached where zonules passed through the formed vitreous gel [see chapter IV.D. Physiology of accommodation & role of vitreous].

Light-level immunofluorescence microscopy demonstrated loss of PNA binding along the inner limiting membrane and within the vitreous gel. PNA binding was reduced but not extinguished over the pars plana and pars ciliaris. Transmission electron microscopy demonstrated that the ILM was intact and smooth, suggesting that no proteoglycan remnants remained attached to the ILM surface (Figure VI.H-6). The eyes from both brain-dead donors demonstrated similar features (although only those of the 22-year-old donor are shown in Figure VI.H-6). No inflammation was noted on light-level microscopy, immunofluorescence, or electron microscopy.

C. FDA Phase I/II Study and its Implications

Subsequent to FDA IND approval, twenty-five subjects enrolled in a registered FDA phase I/II dose-ranging trial conducted by the Chondroitinase Study Group (see Addendum 1) between August and December 1995. The study was sponsored by Storz (later American Cyanamid and subsequently American Home Products) and utilized the batch-produced chondroitinase derived and purified from a 1,000 l incubation of *P. vulgaris* on shark cartilage (see above) [12]. Subjects were assigned into one of three escalating-dose treatment groups, 500 units, 1,000 units, or 1,500 units (reconstituted in 300 μ l of balanced salt solution, respectively). The starting dose of 500 units of chondroitinase was selected based upon the effectiveness of vitreous disinsertion in our human brain-dead study. For each of the three study sites, the indication for surgery and entry criteria for surgery differed.

Drs. Peter Campochiaro and Julia Haller (co-principal investigators) at Wilmer Eye Institute of Johns Hopkins University enrolled 10 subjects with stage II to IV full-thickness macular hole (Protocol DP-123-1). Dr. Jerry Sebag at the VMR Institute in Huntington Beach enrolled 6 subjects with proliferative diabetic retinopathy, macular edema, and vitreomacular traction (Protocol DP-123-2). Dr. Paul Sternberg at Emory University enrolled 9 subjects with proliferative diabetic retinopathy and macular tractional retinal detachment with or without vitreous hemorrhage (Protocol DP-123-2). Subjects were followed up to 1 year. Summary data are shown in Table VI.H-1.

Subjects ranged in age from 36 to 81 years old and included 16 women and 9 men. Within the trial, one subject died of a stroke, unrelated causally or temporally to chon-

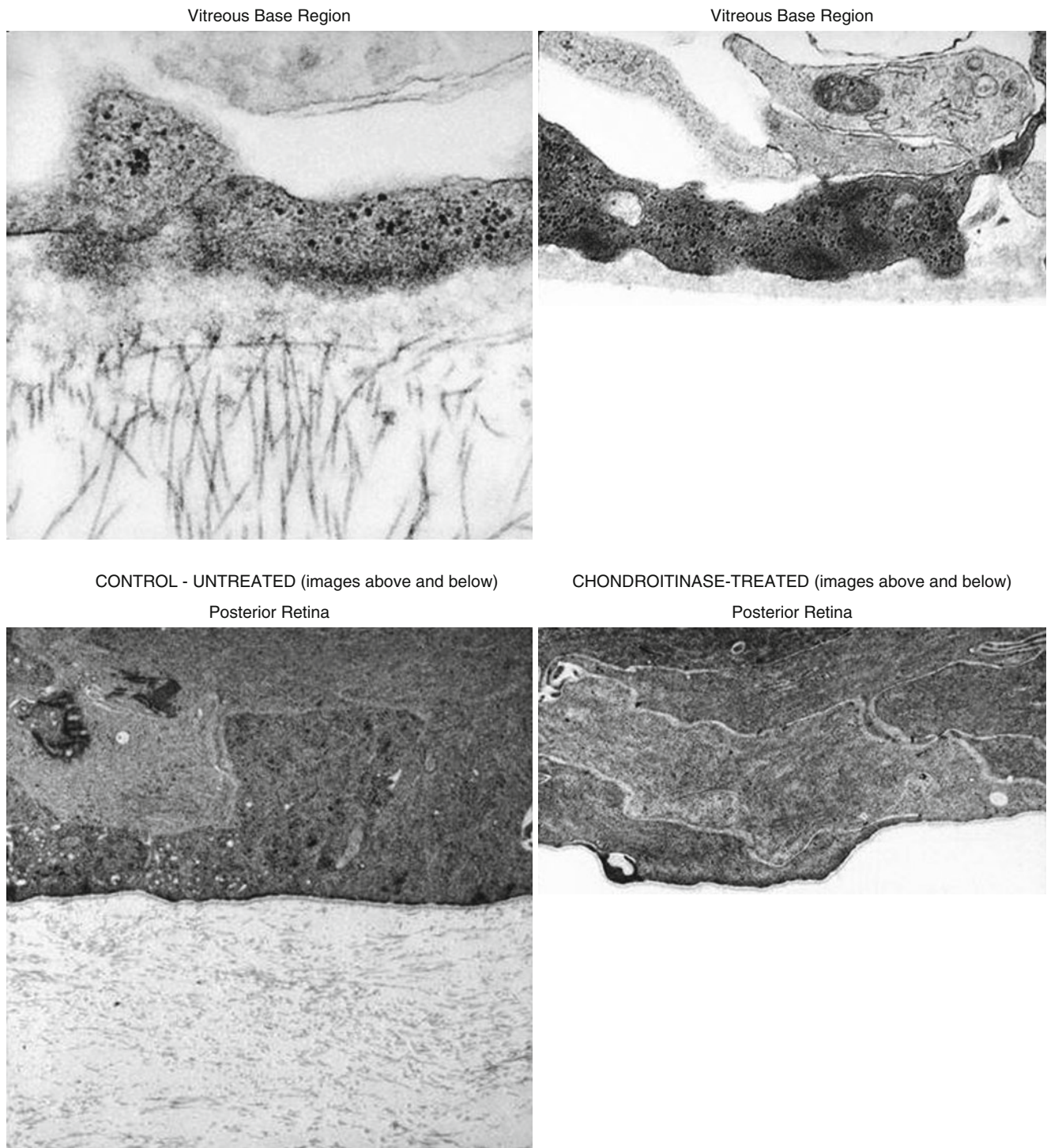


Figure VI.H-6 Transmission electron micrographs (TEMs) of chondroitinase-treated and control eyes from brain-dead human study. Eyes were fixed in half-strength Karnovsky fixative, pH 7.4 for 2–4 h followed by secondary fixation with 2.0 % osmium tetroxide for 1–2 h. Sections were imaged on a JEOL 1200EX TEM. In this subject, 600 units of chondroitinase were applied for 15–18 min. In left panels, vitreous fibrils can be seen to insert or attach to the inner limiting mem-

brane (ILM) or basement membrane of the retina (Muller cells). In the right panels, the vitreous fibrils have been entirely disinserted without evidence of residual fibrillar attachments. Ultrastructurally, the ILM is undisrupted. Note the complete separation of the vitreous fibrils from the ILM in the region of the vitreous base, a region in which vitreoretinal adhesive strength exceeds the strength of either the ILM or vitreous fibrils [20]

Table VI.H-1 Summary of FDA phase I/II chondroitinase-treated subjects

Subject #	Indication	(Stage)	Dose	Age/ gender	Pre op VA	Op time	Resid vit att	PVD ease	MP ease NV	MP ease NV	MP ease NoV	Comment	Post op VA	Late compl
1	PDR OS	TRD	500 u	50 F	1/200	3:30	Ant to equ	Easy	Difficult	Difficult	Easy	Drug assisted vitreous removal but not membrane peel	20/100	Stroke unrelated to drug
2	PDR OS	TRD	500 u	46 F	2/200	2:00	Ant to equ	Easy	Difficult	Difficult	Easy	No drug effect noted	20/63	Pneumonia unrelated to drug
3	PDR OD	VH	500 u	62 F	20/HM	2:30	Ant to equ	Easy	Easy	Easy	Easy	No drug effect noted	20/32	None
4	PDR OS	VH	1,000 u	55 M	CF	2:36	NA	Easy	Difficult	Difficult	Easy	Drug facilitated complex procedure	20/63	None
5	PDR OS	VH/ TRD	1,000 u	36 M	20/100	1:35	Equ	Easy	Difficult	Difficult	Difficult	Equivocal effect of drug	20/16	None
6	PDR OD	TRD	1,000 u	44 F	20/HM	1:05	NA	Easy	Easy	Easy	Easy	Felt vitreous largely separated preop	20/100	None
7	PDR OS	VH/ TRD	1,500 u	36 F	20/200	1:38	NA	Easy	Difficult	Difficult	Difficult	Drug did not facilitate surgery	20/25	None
8	PDR OS	VH	1,500 u	73 F	5/200	1:08	Ant to equ	Easy	Easy	Easy	Easy	Minimal premacular membrane and vitreous attachments	20/100	None
9	PDR OD	T/RRD	1,500 u	61 M	6/200	2:02	Ant to equ	Easy	Easy	Easy	Easy	Drug may have effect, membranes peeled easily	20/100	None
10	FTMH OD	Stage III	500 u	78 F	20/70	2:05	Ant to equ	Easy				Posterior vitreous cortex came up within 30 secs of aspiration	20/40	None
11	FTMH OS	Stage III	500 u	62 F	20/100	1:35	Ant to equ	Easy				Easy as any with normal aspiration	20/30	None
12	FTMH OS	Stage III	500 u	75 M	20/70	1:13	Ant to equ	Easy				Spontaneous vitreous separation to equator	20/25	None
13	FTMH OD	Stage III	500 u	69 F	20/80	1:27	Ant to equ	Easy				Lens opacity, cleared post op	20/40	None, mild lens feathering post op
14	FTMH OS	Stage IV	1,000 u	63 F	20/400	1:30	Ant to equ	Easy				Posterior vitreous cortex separated within 5 sec of aspiration	20/40	None
15	FTMH OS	Stage II	1,000 u	68 M	20/50	1:20	Equator	Difficult				No effect noted by surgeon	20/25	None
16	FTMH OS	Stage III	1,000 u	66 F	20/160	2:25	Ant to equ	Unable				Temporal limited choroidal hemorrhage	20/63	RD repaired with SBP
17	FTMH OS	Stage III	500 u	81 F	20/80	2:16	Ant to equ	Easy				Posterior vitreous cortex separated within 5 sec of aspiration	20/20	None

Subject #	Indication	(Stage)	Dose	Age/ gender	Pre op VA	Op time	Resid vit att	PVD ease	MP ease	MP ease NV	MP ease No V	Comment	Post op VA	Late compl
18	FTMH OD	Stage III	1,500 u	65 F	20/400	1:20	Ant to equ	Easy				No perceived effect by surgeon	20/400	hole remained open
19	FTMH OS	Stage III	1,500 u	37 F	20/100	1:38	Ant to equ	Easy				Bubble came around lens into anterior chamber	20/40	None
20	PDR OS		1,000 u	64 M	20/100	1:05	NA	Easy	NA	NA	NA		20/80	None
21	PDR OD		1,000 u	74 M	CF	1:30	NA	Easy	Easy	Difficult	Easy	Tears near sclerotomy in pars plana	20/200	MI 4 months post op
22	PDR OD		1,000 u	34 M	20/100	1:15	PP	Difficult	Difficult	Difficult	Difficult	Agent did not alter surgery as usual	20/30	Periph ring RD
23	PDR OS		1,500 u	54 F	CF 5'	1:45	NA	Easy	NA	Easy	Easy	Vitreous gel remained formed	HM	VH last visit
24	PDR OS		1,500 u	75 F	CF	1:15	NA	Difficult	NA	NA	NA	Agent did not alter surgery as usual	20/70	None
25	PDR OS		1,500 u	52 M	CF	1:15	Ant to equ	Easy	Difficult	Difficult	Easy	Agent did not alter surgery as usual	CF	None

droitinase treatment. One subject withdrew with nonsurgically related pneumonia. Two of 25 subjects developed retinal detachment (one a peripheral “ring” detachment outside of the peripheral scatter photocoagulation and one successfully repaired with a scleral buckle). One macular hole failed to close in an eye in which the surgeon did not appreciate any chondroitinase effects. Other complications included limited choroidal hemorrhage (subject 16), transitory crystalline lens opacification (subject 13), intraretinal hemorrhage (subjects 2, 4, 7, 22, and 25), and retinal tears (subjects 1, 3, 4, 7, and 21), although most hemorrhages and tears developed in subjects that underwent membrane peeling for proliferative diabetic retinopathy.

1. Efficacy

Vision improved in 23 of 25 subjects but remained stable at counting fingers in one subject and was reduced from counting fingers to hand motions in one subject (due to non-clearing vitreous hemorrhage, patient lost to follow-up). Because this was an unmasked trial, the effectiveness of chondroitinase was assessed by the ease of vitreous separation from the retina (iatrogenic or surgical posterior vitreous detachment) and ease of delaminating nonvascularized preretinal membranes. In 21 subjects vitreous separation was assessed by the operating surgeon as easy and in three as difficult. In one subject who developed a temporal choroidal hemorrhage, the macular hole was later found to be closed and vision improved to 20/25 (Subject 16). In seven subjects the operating surgeon could not determine the location of the anterior insertion of the vitreous. In two subjects the residual vitreous was inserted at the equator and in 16 subjects vitreous was inserted anterior to the equator or pars plana (complete disinsertion including vitreous base, similar to Figure VI.H-4, top left panel).

a. Proliferative Diabetic Retinopathy

Among the 15 subjects with proliferative diabetic retinopathy, in whom retinal neovascularization could confound recognition or effectiveness of chondroitinase application, the operating surgeon reported that surgical separation of the vitreous from the retina was easy. In only 2 cases was this process described as difficult. However, when peeling preretinal membranes, only 5 were described as easy and 7 were difficult (as might be anticipated).

b. Macular Hole

The effects of chondroitinase were most easily recognized in the macular hole group. Of the 9 subjects in whom vitreous separation could be assessed, 8 were recognized as easy, and in 4 of these, the vitreous separated within 5 to 30 s of gentle aspiration. The vitreous was found to be inserted anterior to the equator (i.e., residual attachment to zonules) in 9 of 10 subjects. In one phakic patient intraocular gas migrated around the crystalline lens, which did not affect long-term visual outcome (20/40).

2. Safety

Electroretinograms (ERGs) were obtained from 23 subjects. Two subjects with normal pre-chondroitinase treatment ERGs refused posttreatment ERGs. In one subject, the posttreatment ERG improved but remained abnormal. In the remaining subjects (12 with abnormal and 8 with normal pretreatment ERGs), the posttreatment ERGs remained unchanged.

Conclusions

Chondroitinase remains an intriguing agent as an adjunct in the vitreoretinal surgeons’ armamentarium. Even after extensive testing, the limits of use and potential benefits remain incompletely determined. Development of recombinant or altered enzyme may prove more potent and appealing than our current offerings for “vitrealysis” given the demonstrated potential of chondroitinase to disinsert the vitreous from the retina especially in the region of the vitreous base and posterior lens capsule.

Recent regulatory and marketing developments continue to highlight the attraction of pharmacological separation of the loose connective tissue within the eye, the vitreous, from its adjacent basement membranous attachments of the optic disk, retina, uvea, and lens capsule. Controlling or restricting enzymatic activity in topography, degree of cleavage, and effect on surrounding tissues will likely require further assessment of the expected and potential unanticipated effects of pharmacologically breaking these and similar physiological attachments.

Abbreviations

AC	Anterior chamber
Asp	Aspiration
CF	Count fingers
CS	Chondroitin sulfate
Complic	Complication
ECM	Extracellular matrix
equ	Equator
ERG	Electroretinography
F	Female
FDA	US Food and Drug Administration
FTMH	Full-thickness macular hole
GAG	Glycosaminoglycans
hemor	Hemorrhage
HM	Hand motions
ILM	Inner limiting membrane
IND	Investigational new drug
kDa	KiloDalton
M	Male
MI	Myocardial infarction
OD	Right eye

Op Time	Operative time
OS	Left eye
PDR	Proliferative diabetic retinopathy
periph	Peripheral
PNA	Peanut agglutinin
post op	Postoperative
PP	Pars plana
Pre Op	Preoperative
PVD	Posterior vitreous detachment
RD	Retinal detachment
ResidVitAtt	Residual vitreous attachment location
RRD	Rhegmatogenous retinal detachment
SBP	Scleral buckle procedure
sec	Seconds
TEM	Transmission electron microscopy
TRD	Traction retinal detachment
u	Units
VA	Visual acuity
VH	Vitreous hemorrhage
vit	Vitreous

References

- Hardingham TE, Fosang AJ. Proteoglycans: many forms and many functions. *FASEB J.* 1992;6(3):861–70.
- Keenan T, Clark S, Unwin R, Ridge L, Day A, Bishop P. Mapping the differential distribution of proteoglycan core proteins in the adult human retina, choroid and sclera. *Invest Ophthalmol Vis Sci.* 2012;53(12):7528–38.
- Hageman GS, Marmor MF, Yao XY, Johnson LV. The interphotoreceptor matrix mediates primate retinal adhesion. *Arch Ophthalmol.* 1995;113(5):655–60.
- Lazarus HS, Hageman GS. Xyloside-induced disruption of interphotoreceptor matrix proteoglycans results in retinal detachment. *Invest Ophthalmol Vis Sci.* 1992;33(2):364–76.
- Yao XY, Hageman GS, Marmor MF. Retinal adhesiveness is weakened by enzymatic modification of the interphotoreceptor matrix in vivo. *Invest Ophthalmol Vis Sci.* 1990;31(10):2051–8.
- Yao XY, Hageman GS, Marmor MF. Recovery of retinal adhesion after enzymatic perturbation of the interphotoreceptor matrix. *Invest Ophthalmol Vis Sci.* 1992;33(3):498–503.
- Bos K, Holmes D, Meadows R, Kadler K, McLeod D, Bishop P. Collagen fibril organisation in mammalian vitreous by freeze etch/rotary shadowing electron microscopy. *Micron.* 2001;32(3):301–6.
- Bishop P. Structural macromolecules and supramolecular organisation of the vitreous gel. *Prog Retin Eye Res.* 2000;19(3):323–44.
- Hindson H, Gallagher J, Halfter W, Bishop P. Opticin binds to heparan and chondroitin sulfate proteoglycans. *Invest Ophthalmol Vis Sci.* 2005;46(12):4417–23.
- Reardon A, LeGoff M, Briggs M, McLeod D, Sheehan J, Thornton D, Bishop P. Identification in vitreous and molecular cloning of opticin, a novel member of the family of leucine-rich repeat proteins of the extracellular matrix. *J Biol Chem.* 2000;275(3):2123–9.
- Russell SR. What we know (and don't know) about the vitreoretinal interface. *Retina.* 2012;32(Suppl):S181–6.
- Storz Ophthalmics Corporation. Investigational New Drug Application U.S. Food: Drug Administration. Chondroitinase, vol. 186,566. Submitted Dec 20, 1994.
- Sebag J. Pharmacologic vitreolysis. *Retina.* 1998;18(1):1–3.
- Sawaguchi S, Yue BY, Yey P, Tso MO. Effects of intracameral injection of chondroitinase ABC in vivo. *Arch Ophthalmol.* 1992;110(1):110–7.
- Russell SR, Shepherd JD, Hageman GS. Distribution of glycoconjugates in the human retinal internal limiting membrane. *Invest Ophthalmol Vis Sci.* 1991;32(7):1986–95.
- Bishop P, McLeod D, Reardon A. Effects of hyaluronan lyase, hyaluronidase, and chondroitin ABC lyase on mammalian vitreous gel. *Invest Ophthalmol Vis Sci.* 1999;40(10):2173–8.
- Russell SR, Hageman GS. Chondroitin sulfate-induced generation of epiretinal membranes. *Arch Ophthalmol.* 1992;110(7):1000–6.
- Russell SR, Hageman GS. Optic disc, foveal, and extrafoveal damage due to surgical separation of the vitreous. *Arch Ophthalmol.* 2001;119(11):1653–8.
- Sebag J. Pharmacologic vitreolysis – premise and promise of the first decade. *Retina.* 2009;29:871–4.
- Sebag J. Age-related differences in the human vitreo-retinal interface. *Arch Ophthalmol.* 1991;109:966–71.

Erratum

Vitreous Floaters and Vision: Current Concepts and Management Paradigms

Laura C. Huang, Kenneth M.P. Yee, Christianne A. Wa, Justin N. Nguyen, Alfredo A. Sadun, and J. Sebag

DOI 10.1007/978-1-4939-1086-1_45

The online version of the original book can be found under
DOI 10.1007/978-1-4939-1086-1_45

L.C. Huang, BA
VMR Institute for Vitreous Macula Retina,
7677 Center Avenue, suite 400,
Huntington Beach, CA 92647, USA

Doheny Eye Institute, Department of Ophthalmology,
Los Angeles, CA, USA

University of Miami Miller School of Medicine, Miami, FL, USA
e-mail: lchuang@med.miami.edu

K.M.P. Yee, BS • C.A. Wa, BA
J. Sebag, MD, FACS, FRCOphth, FARVO (✉)
VMR Institute for Vitreous Macula Retina,
7677 Center Avenue, suite 400,
Huntington Beach, CA 92647, USA

Doheny Eye Institute, Department of Ophthalmology,
Los Angeles, CA, USA
e-mail: kennethmpy@gmail.com;
cwa@usc.edu; jsebag@VMRinstitute.com

J.N. Nguyen, BA
VMR Institute for Vitreous Macula Retina,
7677 Center Avenue, suite 400,
Huntington Beach, CA 92647, USA

A.A. Sadun, MD, PhD, FARVO
Doheny Eye Institute/UCLA,
Los Angeles, CA, USA
e-mail: alfredo.sadun@gmail.com

The Figure V.B.8-9 in chapter V.B.8. is incorrect. The correct figure and its legend are given below:

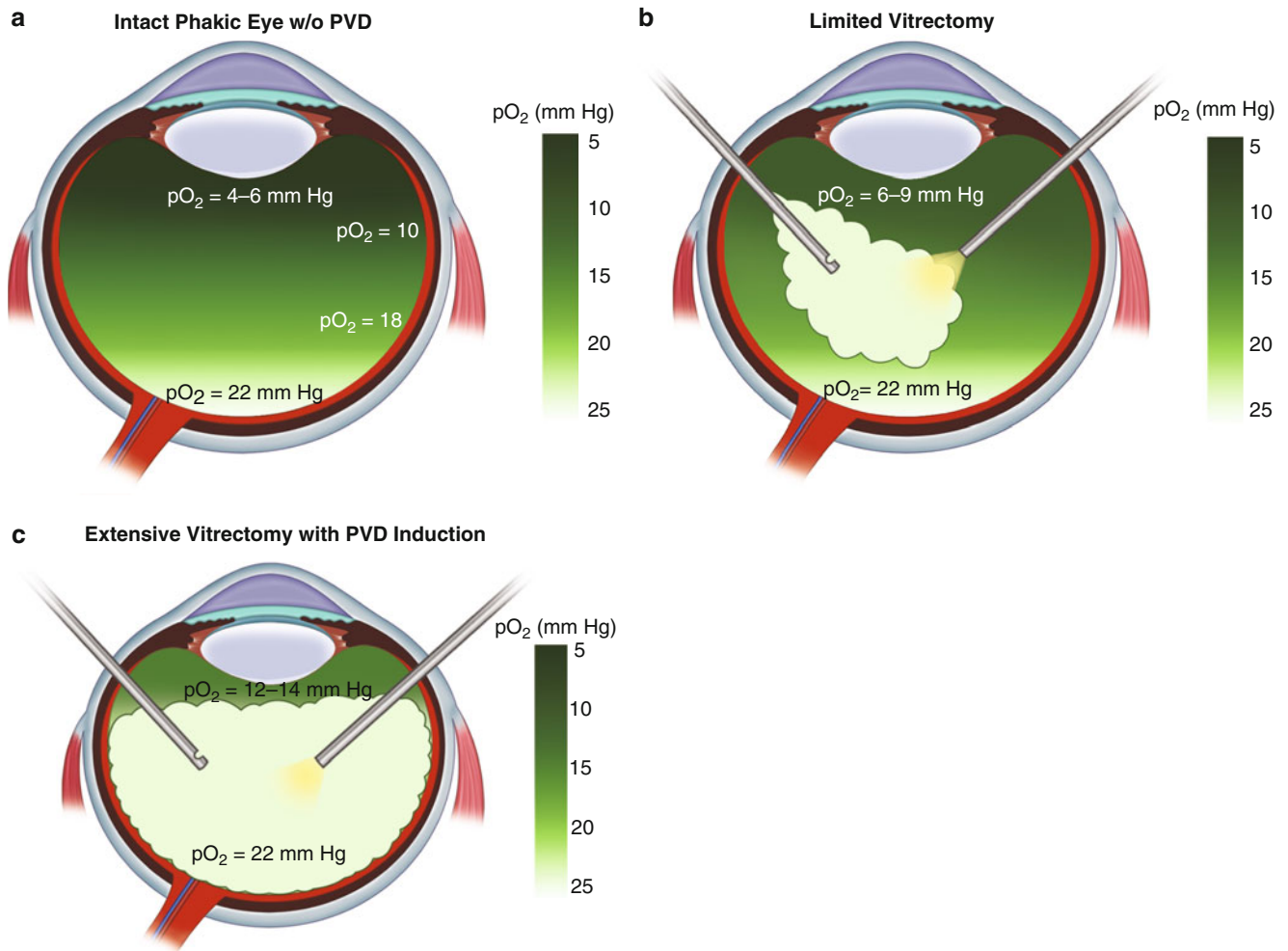


Figure V.B.8-9 The effects of limited vitrectomy on oxygen distribution. Intravitreal oxygen arises from the retina/choroid circulation posteriorly as well as from the ciliary body anteriorly. Vitrectomy increases convective motion and fluid circulation in the vitreous chamber, which increases oxygen levels behind the lens. (a) **Intact eye.** The pO_2 gradient ranges from 22 mmHg at the posterior pole to 18 mmHg at the equator and 10 mmHg peripherally in front of the ciliary body. pO_2 levels are 4–6 mmHg behind the lens. (b) **Limited vitrectomy.** Leaving the anterior vitreous intact and not inducing a PVD results in increased

retrolental oxygen levels of only 6–9 mmHg. This may account for the relatively low (23 %) incidence of cataract formation observed with limited vitrectomy. (c) **Extensive vitrectomy with PVD induction.** Following extensive vitrectomy with surgical induction of PVD, retrolental oxygen levels increase to 12–14 mmHg, approaching three-fold above those in the intact eye. These elevated levels may account for the 50–76 % incidence of cataract formation following extensive vitrectomy. (Adapted from Beebe, Holekamp, et al.)

Index

- A**
- Aaberg, T., 182, 683
- Aaberg, T.M., 746
- Abrams, G.W., 731–746
- Accessory zonules, 496, 503
- Accommodation
- B-scan high-frequency ultrasound, 500, 502
 - changes, lens shape, 501, 503–505
 - ciliary ring, 503
 - equatorial lens relaxation and zonule tension, 503
 - high-resolution ultrasound imaging, 504
 - lens support, 496–499
 - lens thickness and anterior chamber, 499
 - mechanical interaction, 504
 - MRI, 500
 - OCTs, 499
 - vitreous support, 498–501
- ACIOL. *See* Anterior chamber intraocular lens (ACIOL)
- Acoustic imaging
- A-and B-mode system, 208
 - advantages, 208
 - attenuation, 208
 - B-scan ultrasonography, 211
 - ‘chirp’ excitation, 210–211
 - disadvantages, 208
 - inhomogeneities/interfaces, 208–209
 - OCT, 208
 - opacification, 208
 - posterior vitreous cortex, 208, 209
 - QUS parameters, 213
 - saccade-induced vitreous motion, 213
 - solid and fluid components, 212
 - ultrasound, 208, 209
 - vitreoschisis, 212
 - vitreous echodensities, 213
- Activating protein 2 (AP-2), 97
- Activin receptor-like kinase (Alk-1), 45
- Acute PVD, 358
- Adams, A.P., 357
- Adam, R.S., 500
- Adeno-associated virus (AAV), 707
- Advanced glycation end product (AGE), 132, 141, 416
- alagebrium, 72
 - collagen cross-linking, 64
 - in diabetic vitreous, 64
 - and DME, 841
 - extracellular, 62
 - formation, 59, 62, 65, 66, 71, 72
 - glycation of proteins, 75
 - non-enzymatic glycation and, 66
 - paracrine signals, 70
- ADVIRC. *See* Autosomal dominant vitreo-choroidopathy (ADVIRC)
- AGE, Advanced glycation end product (AGE)
- Age-related macular degeneration (AMD), 187, 288, 343, 413
- afibercept, 515
 - anti-VEGF agents, 514
 - B-scan ultrasound, 330
 - exudative, 444, 450, 451
 - exudative AMD (*see* Exudative AMD)
 - hypoxia, 344
 - infliximab, 514
 - low grade inflammation, 343–344
 - macular cytokine load, 344
 - macular translocation (*see* Macular translocation)
 - ocriplasmin, 860
 - OCT, 330
 - posterior vitreous cortex, 330
 - posterior vitreous detachment/vitreotomy, 450–452
 - “preventive surgery”, 700
 - PVD, 471, 472
 - ranibizumab, 514
 - RPE transplantation, 557–561
 - and RP-like retinal, 705
 - sub-macular hematoma, 562–563
 - submacular surgery (*see* Submacular surgery)
 - Submacular Surgery Trials, 471–472
 - synthetic gels, 84
 - and tPA, 828–829
 - traction, 343
 - VEGF, 471
 - vitreo-macular interface, 330
 - vitreo-retinal adhesion, 450
 - vitreous, 343
- Aging
- biochemical manifestations, 242
 - increase in thickness, 172, 175
 - laminin and collagen IV, 170, 172–173
 - peripheral vitreo-retinal, 357
 - vitreo-retinal diseases, 166
 - vitreous body (*see* Vitreous body aging)
- Agripin and type XVIII collagen, 9
- AHFVP. *See* Anterior hyaloidal fibrovascular proliferation (AHFVP)
- Aiello, L.P., 41–52, 57–75
- AION. *See* Anterior ischemic optic neuropathy (AION)
- Airlie House classification, 426
- Akiba, J., 118, 425
- Algere, P.V., 558
- Allen, R.A., 352, 358
- Alm, A., 439
- Alme, A.M., 229
- Almony, A., 467
- Alpha-SMA-mediated contraction, 280, 281

- AMD, Age-related macular degeneration (AMD)
- American Academy of Ophthalmology (AAO), 228, 715–722
- American Academy of Pediatrics (AAP), 228
- Amino-(N-), 4–7, 9, 10
- Andre, J.C., 155
- Angiogenesis
- leucine-rich alpha-2 glycoprotein (LRG1), 11
 - opticin, 9–10
 - PEDF, 11
 - thrombospondins, 11
- Angiopoietin (Ang), 47
- Angiopoietin-2 (Ang-2), 102
- Anomalous PVD (APVD), 267, 271, 288, 316, 317, 329, 616
- and vitreoschisis (VS), 242
 - acute PVD, 358
 - age-related vitreous degeneration and detachment, 148
 - avulsion, 358
 - clinical sign, 357
 - complications, 148
 - echography, 358
 - El Bayadi-Kajiura aspherical lens, 358
 - etiology, 251–253
 - floaters, 358
 - gel dehiscence, 146
 - liquefaction, 146, 813
 - Marfan's Syndrome or high myopia, 146
 - myopic vitreopathy, 118–119
 - pathologic effects, 800
 - persistent gel adhesion, location, 146
 - posterior vitreous cortex, 804
 - prevention, 814
 - retinal detachment, 120
 - retinal effects, 253–259
 - and retinal tears, 120
 - rhegmatogenous retinal detachment, 375
 - static and dynamic forces, 146
 - vitreoretinal adherence and traction, 251
 - vitreoretinopathies, 800
 - vitreoschisis, 146
 - vitreous cortex, structural integrity, 146
 - vitreous traction, peripheral retina (*see* Vitreous traction)
 - VMT (*see* Vitreoretinal traction (VMT))
 - and VMT, 810
- Anterior chamber-associated immune deviation (ACAID), 155–156
- Anterior chamber intraocular lens (ACIOL), 736
- Anterior hyaloidal fibrovascular proliferation (AHFVP), 642
- Anterior ischemic optic neuropathy (AION), 619
- Anterior Persistent Fetal Vasculature
- iridohyaloid blood vessels, 232
 - Mittendorf's dot, 232
 - muscae volitantes, 232–233
 - persistent pupillary membrane, 232
 - retrolental membrane, 233
- Anterior vitreous cortex, 496, 498, 504
- Anterior vs. posterior split, 255–256, 258
- Anti-angiogenesis
- inhibitors, 48
 - promoters, 47–48
- Antigen-presenting cells (APCs), 155–156
- Anti-inflammatory agents
- corticosteroids, 528
 - dosage and half-life, 514
 - non-steroidal, 528–529
- Antioxidant therapies, 228
- Anti-VEGF agents, 237, 513–514
- Aphakic and pseudophakic fellow eyes
- cataract extraction, 721
 - cystic retinal tufts and degenerative retinoschisis, 723
 - “normal” peripheral retina, 721, 722
 - retinal lattice, 721–722
- Apoptosis
- autophagy, 48
 - endothelial cells, 43
 - fetal vessel regression, 44–46
 - hyaloid vascular endothelial cells, 47
 - hyaloid vasculature, regression, 44
 - macrophage-induced, 47
 - macrophagy, 46–47
 - PGD 16, proteins upregulated, 44
 - protein ubiquitination pathway, 44
 - reactive oxygen species (ROS), 43
 - APVD. *See* Anomalous PVD
- Aquaporin (AQP), 47
- Aqueous vitreous substitutes
- BSS, 538
 - isotonic saline, 538
 - lactated ringer's solution, 538
- AR. *See* Augmented reality (AR)
- Aretz, S., 3
- Armaly, M.F., 503
- Arrieta, E., 505
- Artificial vitreous
- aging, 82
 - drug vehicle, 84
 - free radical scavenger, 84
 - hemostasis, 84, 85
 - in vitro* experimental model, 87–89
 - in vivo* experimental model, 86–87
 - optical clarity, 84, 85
 - pars plana vitrectomy, 82
 - properties, 85
 - tamponade, 84
 - volume filler, 84
- Artist's rendition
- Cloquet's canal and hyaloid artery, 232
 - traction retinal detachment, 227
- Asami, T., 837–843
- Ascaso, F.J., 415
- Ascorbate, 459–460, 463–466, 469, 470, 473
- Ashton, N., 479–480, 487, 489, 490
- Aspiration (asp), 892
- Asteroid hyalosis
- indirect ophthalmoscopy, 199
 - interfibrillar distance, 780
 - pathologies, 775
 - profound entities, 211
- Asymptomatic vitreoretinal lesions, phakic non-fellow eyes, 718
- Atomic force microscopy (AFM), 172
- Augmented reality (AR)
- applications, 702
 - augmented inputs, 703–704
 - implementation, 702–703
 - supplementing intraoperative information, 702
 - surgical sub-specialties, 702
 - in vitreoretinal surgery, 703
- Aumayr, W., 682
- Autologous plasmin enzyme (APE)
- and diabetic macular edema, 841
 - in humans, 838
 - and macular hole, 839–841
 - plasminogen activation, 838
 - rapid purification system, 838–839

- and retinal vein occlusion, 842
 - and retinopathy of prematurity, 841–842
 - standard purification system, 838
 - Autophagy, 48
 - Autosomal dominant vitreo-choroidopathy (ADVIRC), 32
 - Ayad, S., 184
 - Azzolini, C., 841
- B**
- Badr, I.A., 120
 - Balanced salt solution (BSS), 538, 846–847
 - Balazs, E., 195
 - Balazs, E.A., 13–19, 82, 152, 169, 182, 184, 316, 348
 - Banerjee, P.J., 523–532
 - Barbazetto, I.A., 460, 461, 463, 469
 - Barishak, Y.R., 357
 - Barton, K.A., 465
 - Basement membrane (BM), 169–171
 - Basic fibroblast growth factor (b-FGF), 157, 826
 - Bassnett, S., 505
 - Baum, G., 208
 - BCVA. *See* Best-corrected visual acuity (BCVA)
 - Beebe, D., 473
 - Beebe, D.C., 442, 459–473, 783
 - Behar-Cohen, F.F., 518
 - Beighton scoring system, 25, 33
 - Benson, W.E., 235, 253, 360, 361
 - Bergmeister's papilla, 103–106, 233, 388
 - Berman, E.R., 118
 - Bertelmann, T., 414
 - Best-corrected visual acuity (BCVA), 866
 - MIVI-IIT trial, 857
 - PVD, 857
 - VMT, 857
 - Bevacizumab, 229–230
 - Bilateral Rhegmatogenous Retinal Detachment (BRRD), 22, 33
 - Bill, A., 439
 - Bim (hyaloid vessel regression), 44
 - Binder, S., 329–344, 553–566, 629–642, 647–660
 - Bio-Alcamid[®], 87, 89
 - Biochemical mediator, 478–479. *See also* Michaelson's biochemical mediator
 - Biochemistry
 - amino and fatty acids, 84
 - ascorbic acid, 84
 - basement membrane, 169–171
 - cDNA cloning, 170
 - GAGS, 82–83
 - HA-collagen interaction, 83–84
 - in situ* hybridization, 171–172
 - integrin family and dystroglycan, 171
 - metabolites and enzymes, 84
 - Müller cells, 171
 - ocular and retinal development, 14–15
 - ocular embryogenesis, 172
 - polymerization, 170
 - prostaglandins, 84
 - proteins, 83, 170
 - regeneration, 172
 - retinal phenotypes, mutations, 172
 - Bishop, P., 882
 - Bishop, P.N., 3–11
 - Blackwell, J., 83
 - Blair, N.P., 441
 - Blankenship, G., 686, 687
 - Blankenship, G.W., 445, 485
 - Bleckmann, H., 183
 - Blood retinal barrier (BRB) breakdown, 524, 526, 527
 - Blumenkranz, M., 686–687
 - Blunt trauma, 251
 - B-mode OCT scan, 253
 - Boldrey, E.E., 357–358
 - Boniuk, M., 357
 - Boruchoff, S.A., 864
 - Borzacchiello, A., 15
 - Bowald, S., 187
 - Bowman, W., 194, 772
 - Branch retinal vein occlusion (BRVO)
 - angiography, 657
 - and APE, effects and safety, 842
 - bimanual technique, 655–656
 - cats, 441
 - complications, 351
 - outcomes, 657
 - Scanning Laser Ophthalmoscopy, 658–659
 - sheathotomy, 655
 - vitreous neovascularization, 480–482
 - BRB. *See* Blood retinal barrier (BRB)
 - Brilliant blue, 604
 - Britt, M.T., 228
 - Bronson, N.R., 208
 - Bruce, R.A., 656
 - Bruch's membrane/choroid patch, 559–560
 - Brucke, E., 772
 - Brunner, S., 629–642
 - BRVO. *See* Branch retinal vein occlusion (BRVO)
 - B-scan image, 145, 249, 288
 - Buettner, H., 665, 671, 673, 675, 682, 700
 - Buettner, M., 665
 - Burian, H.M., 503
 - Butler, F.C., 357
 - Byer, N.E., 253, 353–355, 360, 361
- C**
- Cahill, M.T., 657
 - Callanan, D.G., 515
 - Campochiaro, P., 888
 - Carbon dioxide (CO₂), 49
 - Carboxy-(C-), 5, 6, 9
 - Cardillo, J.A., 517
 - Carlin, B.A., 208
 - Cataract, 124
 - age-related nuclear cataract, 467
 - concentration gradient, 783
 - decreased alpha-crystallin, 776
 - diabetic patients, 783
 - nuclear sclerotic, 444, 460, 465, 468–469
 - oxygen distribution, 784
 - oxygen tension, anterior chamber angle, 471
 - phakic eyes, 783–784
 - reactive oxygen species, 783
 - surgery, 250–251, 470–471, 634–635
 - and vitrectomy, 452–453
 - Catenary theory of Coleman, 498–501
 - CBA. *See* Cytometric bead array (CBA)
 - Cell proliferation inhibitors
 - colchicine, 531
 - daunorubicin, 529–530
 - fluoropyrimidines, 529
 - immunotoxins, 530–531
 - retinoids, 530
 - Celorio, J.M., 119

- Central nervous system (CNS), 513
- Central reading center (CRC)
OCT, 857
vitreo-macular adhesion, 857
- Central retinal artery (CRA)
recanalization, 480
- Central retinal artery occlusion (CRAO), 480, 482–484, 487, 492, 648
- Central retinal vein occlusion (CRVO), 307, 515
cystoid macular edema, 413
cytokine levels, 413
iris neovascularization, 481
ischemic, 482
non-ischemic, 482
occlusion site, RVO, 408
OCT, 413
PVD, 415
serous retinal detachment, 413
VEGF, 412
visual acuity, 409
vitreous neovascularization, 482
- Chang, L.K., 590
- Chang, S., 461, 470, 471
- Charbonnel, J., 448, 657
- Charles, S., 208, 655, 675
- Charteris, D.G., 523–532
- Chatzoulis, D., 362
- Chemotherapy, 369, 403, 529
- Cheng, C.Y., 116
- Chen, T., 318
- Cheung, N., 537–547
- Chignell, A.H., 539
- Chi, H.H., 248
- Chinn, S.R., 203
- Chondroitinase, 802
chondroitin sulfate, at vitreo-retinal interface, 885–886
enzymes and substrates, biochemistry, 884–885
pharmacologic vitreolysis (*see* Pharmacologic vitreolysis)
proteoglycans and vitreo-retinal interface, 882–884
- Chondroitin sulfate (CS), 83, 132, 135, 885–886
- Chong, L.P., 553–566, 693–698, 749–756, 789–794
- Choroidal neovascularization (CNV), 121
dry AMD, 338
removal, membrane, 554
submacular, 555
Submacular Surgery Trials Report No. 11, 471–472
vitreo-macular adhesion, 329
- Choroid, intraocular neovascularization, 482–483
- Chou, T., 565
- Chow, D.R., 839
- Chow, L.C., 228
- Christensen, U.C., 582, 588, 590
- Chromodissection
benefits and risks, 615
DONFL, 585
ICG, 619
ILM, 575, 615
staining methods, 618
- Chromodissection vital dyes
brilliant blue, 604
clinico-pathological correlations, 608–609
double staining, 607
ERM, 601
fluorescein, 602
human eye, 604
ICG, 602
indocyanine green, 604
premacular membranes, 605
single staining, 605–606
staining substances, 602
trypan blue, 603–604
- Chronic intraocular inflammation, 16–17
- Chung, E.J., 657
- Cibis, G.W., 305
- Cicatricial contraction, proliferative membranes
hyalocytes, 157–158
PDR/PVR-induced collagen gel contraction, 157
 α -SMA expression, 157
traction retinal detachment, 157
- Ciliary neurotrophic factor (CNTF)
description, 517
implant, 517
- Cis-hydroxyproline, 531
- Clarkson, J.G., 686, 687
- Classification system, PVR
anterior, 733, 736
combined anterior C12 and posterior C12, 733, 735
diffuse posterior, 733, 737, 738
grade B, 733, 734
grade C PVR, contraction type, 732–733
The Retina Society classification, 732
updated classification, 732–733
- Clinical staging, PDVR, 421
- Cloquet's canal (*cc*), 98, 99, 101, 103–6, 231
- Clusterin (Apolipoprotein J), 50
- Cluster of differentiation (CD), 50
- CME. *See* Cystoid macular edema (CME)
- CMV. *See* Cytomegalovirus (CMV)
- CNS. *See* Central nervous system (CNS)
- CNV. *See* Choroidal neovascularization (CNV)
- Coat's disease, 364, 366–368, 791
- Coats, G., 364
- Cogan, D.G., 185
- COL9A1 gene, 8
- COL2A1 related disorders
Kniest Dysplasia, 27, 28, 33
Knobloch syndrome, 30, 31, 33
Marfan syndrome, 30–31, 33
Marshall syndrome, 24, 29–30, 33, 36
SEDC, 27–29, 33
V-PED, 28–30
- Colchicine
clinical evidence, 531
description, 531
preclinical evidence, 531
- Coleman, D., 208
- Coleman, D.J., 193–217, 495–505
- Collagen (COL)
abnormalities, 25
AGEs, 132, 141
aging, 8–9
bovine vitreous collagen fibril, 7
 α -chain composition, 5
concentration, 4
cortical vitreous, 65–66
cross-linking, 4–5, 60
destruction, 818
extracellular matrix, 800
fibrillar, 33, 34
fibrils, 4, 8–9, 22, 59, 83
and fibronectin, 804, 818
gene, 104
heterotypic collagen fibrils, vitreous, 6–7

- lamellae, 105
 - “mature”, 4
 - mutations, 4
 - post-translational modifications, 4
 - PVD, 803
 - structure, 4–6, 59
 - synthesis and turnover, 7–8
 - tripe helical domain, 29, 30
 - type II, 5, 26, 27, 33, 34, 36, 132, 135, 140, 146
 - type V, 27
 - type V/XI, 5–6, 132
 - type VI, 6, 7
 - type IX, 5–6, 132, 137, 140
 - type XI, 24, 26, 27
 - vitreous collagen fibrils, 6, 7
 - vitreous cortex, 802
 - Collagenases, 818
 - Collagen type XVIII (Col18), 48
 - Colloid osmotic pressure, 383
 - Colyear, B.H., 361
 - Combs, J.L., 253, 361
 - Comper, W.D., 83
 - Complication (complic), 882, 892
 - Computerized tomography (CT), 30
 - Concomitant retinal disease
 - AMD, 860
 - diabetic macular edema, 860
 - retinal vein occlusion, 860
 - Confidence interval (CI), 37
 - Congenital vitreo-retinopathy. *See* Vitreo-retinopathies
 - Connective tissue growth factor (CTGF), 157, 317
 - Constable, I.J., 357
 - Contact lens biomicroscopy, 202
 - Contrast sensitivity function (CSF), 778–779, 781
 - Contreras, I., 571–598
 - Convection currents, 438, 440, 442, 449
 - COOH-terminal, 846
 - Corticosteroids
 - clinical evidence, 528
 - preclinical evidence, 528
 - Count finger (CF), 891
 - Cousins, S.W., 690
 - Crafoord, S., 81–89
 - Cramer, A., 496
 - CRAO. *See* Central retinal artery occlusion (CRAO)
 - Criswick, V.G., 234
 - Crock, G.W., 666, 667, 669, 684
 - Croft, M.A., 498, 500
 - Cross-linked hyaluronic acid hydrogel, 85, 86
 - CRVO. *See* Central retinal vein occlusion (CRVO)
 - Cryopexy
 - blood-retinal barrier, 827
 - chorioretinal scar, 759
 - combined laser, 758
 - intraocular probes, 686
 - laser retinopexy, 759
 - long-term failure, pneumatic retinopexy, 760
 - PVR, 760
 - retinal pigment epithelial cells, 760
 - and scleral buckling procedures, 759
 - Cryotherapy, 229, 399
 - Cryotherapy for Retinopathy of Prematurity (CRYO-ROP) study, 225
 - CTGF. *See* Connective tissue growth factor (CTGF)
 - Cunningham, E.T. Jr., 165–188
 - Cure of RRD. *See* Rhegmatogenous retinal detachment (RRD)
 - Curtin, B.J., 117, 119, 121
 - Cut rate. *See* Vitreous flow and cut rates
 - Cutters. *See* Vitrectomy
 - Cystic retinal tufts
 - bilateral retinal detachment, 721
 - and degenerative retinoschisis, 723
 - in phakic non-fellow eyes, 718
 - Cystoid macular edema (CME), 289
 - adalimumab, 514
 - afibercept, 515
 - intravitreal methotrexate, 513
 - ranibizumab, 514
 - triamcinolone acetonide (TA), 513
 - Cytokines, 399, 402
 - angiogenic and inflammatory, 414
 - DME, 416
 - miscellaneous cytokines, 402–403
 - retinal vein occlusion, 409
 - TNF α , 402
 - TNF β , 402
 - VEGF, 416
 - vitreous, 411
 - Cytomegalovirus (CMV), 513, 516
 - Cytometric bead array (CBA), 413, 414
- D**
- Daicker, B., 356
 - Dark-filed slit microscopy
 - application, 193
 - diabetic vitreopathy *in vitro*, 200
 - human vitreous, 195, 196
 - posterior and central vitreous, 198, 199
 - Das, T., 558
 - Daunorubicin/daunomycin
 - clinical evidence, 530
 - preclinical evidence, 529–530
 - Davies, L.N., 499
 - Davis, M.D., 361
 - Days of gestation (DG), 96, 97
 - de Bustros, S., 361
 - Degenerative retinoschisis
 - and cystic retinal tufts, 723
 - in phakic non-fellow eyes, 718
 - progressive retinal detachment, 721
 - Dehydroascorbate (dAsA), 464, 465
 - de Juan, E., 439, 445
 - de Juan, E. Jr., 509–519, 556, 562
 - De Kozak, Y., 518
 - Delaney, Y.M., 782
 - del Cerro, M., 558
 - Del Priore, L.V., 869–879
 - Demours, F., 772
 - Denham, D., 684
 - Denlinger, J.L., 13–19
 - Deoxyribonucleic acid (DNA)
 - cloning, 170
 - fragmentation, 89
 - macrophage-vascular endothelial cell adhesion, 47
 - minigenes, splicing reporters, 35
 - neovascularization, 706
 - oxidative damage, 470
 - replication inhibition, 529
 - sequence variation databases, 36
 - sequencing technologies, 36
 - subconjunctival injection, naked, 707
 - variant, 34

- de Smet, M.D., 845–851, 863–867
- Development, ILM, 172, 174–175
- Diabetes. *See also* Diabetic macular edema (DME)
- advanced glycation end products, 59–60
 - aldose reductase, 60
 - clinical trials, 422
 - diabetic angiopathy, 422
 - diabetic retinopathy, 422
 - hexosamine, 60
 - oxidative stress, 60
 - pathological pathways, 58
 - protein kinase C, 60
 - type I and type II, 422
 - vascular changes, 422
- Diabetes Control and Complication Trial (DCCT), 422
- Diabetic macular edema (DME), 60, 72, 73, 253, 288
- advanced glycation end products, 416
 - and AGEs, 841
 - cataract surgery, 630
 - clinical classification, 409
 - component, 630
 - definition, 409
 - diabetic retinopathy, 841
 - epidemiology, 409
 - inflammatory and angiogenic proteins, 411–414
 - inflammatory factors, vitreous, 416–418
 - macular holes, 631
 - MIVI-II-DME and MIVI-V, 860
 - pathogenesis, 409, 841
 - PVD induction, vitrectomy, 841
 - risk factors, 409
 - symptoms, 410
 - tissue scaffold, neovascularization, 841
 - visual impairment, 841
 - vitreo-macular adhesion, 856
 - vitreo-macular traction, 841
 - vitreoretinal interface, 416
 - vitreous detachment and vitreoschisis, 415–416
- Diabetic maculopathy
- diabetic macular edema, 631
 - premacular membranes, 631
 - vitrectomy, 631
 - vitreo-macular traction, 631
- Diabetic retinopathy (DR), 409–411
- characterization, 422
 - clinical signs, 422, 423
 - cortical vitreous and vitreous gel, 472
 - diabetic retinal vasculopathy, 62–63
 - epidemiology, 61
 - evolution, 630
 - exudative AMD, 700
 - human vitreoretinal interface, neovascularization, 64–65
 - ischemic, 473
 - low intraocular oxygen tension, 472
 - and neurosensory retina, 61–62
 - NPDR, 422
 - PDVR (*see* Proliferative diabetic vitreoretinopathy (PDVR))
 - proliferative, 640
 - vascular and neuronal elements, feedback cycle, 62
 - VEGF, 61
 - vitreoretinal complications, 63
 - vitreoschisis in nonproliferative, 67
 - vitreous hemorrhage, 630–631
- Diabetic retinopathy clinical research network (DRCR.net), 72
- Diabetic vitreopathy, 416
- collagen, 64
 - elements, 71
 - extracellular matrix constituents, 65
 - glucose, 63
 - hyaluronan, 64–65
 - oxygen physiology, 69–70
 - paracrine depot, 70–71
 - PDR, 63
 - pharmacotherapy, 71–72
 - structural manifestations, 68
 - surgery, 72–73
 - vitreoretinal interface, 65–66
 - vitreous body, 66–69
- Diabetic vitreous hemorrhage, 478
- Diacyl glycerol (DAG), 58, 60
- Diagnosis, PVD
- OCT (*see* Optical coherence tomography (OCT))
 - ultrasound, 249
- Diaz-Llopis, M., 829, 838, 841
- Diddie, D.R., 562
- Differentiated viewing, 701
- Diffusion, 438–440, 442, 444, 445, 449
- Disease
- diabetes, 173, 176, 177
 - proliferative diseases, 176
 - recurrence, 617
 - tractional disorders, 179
 - uveitis and vitreoretinal interface, 180–181
- Dispase®, 818. *See also* Vitreolysin™
- Dissociated optic nerve fiber layer (DONFL), 585
- Distortions, 318, 320, 325
- DME. *See* Diabetic macular edema (DME)
- Dobbie, G., 356
- Dominant Rhegmatogenous Retinal Detachment (DRRD), 33
- DONFL. *See* Dissociated optic nerve fiber layer (DONFL)
- Douvas, N.G., 683
- DR. *See* Diabetic retinopathy (DR)
- Drain-Air-Cryo-Endotamponade (D-ACE) technique, 539
- Drug delivery, intravitreal drug. *See* Intravitreal drug therapy
- Drug-release implants
- fluocinolone acetonide-releasing device/Retisert®, 515, 516
 - Illuvien, 516
 - intravitreal implants, 516
 - Ozurdex®, 515–516
 - Vitrasert®, 516
- 3D-TAG. *See* Three-dimensional threshold Amsler grid (3D-TAG)
- Ducournau, D., 617
- Ducournau, Y., 617
- Duke-Elder, W.S., 194, 772
- Duker, J.S., 287–295
- Dunker, S., 347–369
- Durkee, H., 505
- Dynamic light scattering (DLS), 216–217
- biophysical properties, 217
 - diabetic vitreopathy, 776
 - laser-based nanodetector, 776
 - microscopic particles measurement, 216
 - pharmacologic vitreolysis, 776
 - probe, 217
- Dystroglycan, 49
- E**
- Early Treatment Diabetic Retinopathy Study (ETDRS), 409, 422, 426
- The Early Treatment for Retinopathy of Prematurity (ETROP) study, 226
- Eaton, J.W., 460
- Eckardt, C., 556
- ECM. *See* Extracellular matrix (ECM)

- Edema. *See* Macular edema
- EDTA. *See* Ethylenediaminetetraacetic (EDTA)
- Ethylenediaminetetraacetic (EDTA), 871
- Eisner, G., 16, 195, 201, 202, 356
- El-Bayadi, G., 202
- El Bayadi-Kajiura aspherical lens, 358
- Elbendary, A.M., 841
- Elder, D., 496
- Electron microscopy (EM), 47, 833
- Electrophysiology, 831
- Electroretinogram (ERG), 32, 875, 878, 892
- Electroretinography (ERG), 85, 87, 849
- ELISA. *See* Enzyme-linked immunosorbent assay (ELISA)
- Embolectomy
 - BRAO, 649
 - pars plana vitrectomy (PPV), 649
 - retinal artery occlusion, 648–650
- Embryogenesis, 44
- Embryology, vitreous
 - primary vitreous, 97–98
 - secondary vitreous, 98–101
- Embryonic day (ED), 43
- Emmetropization
 - and axial length, 114–115
 - myopia, 114, 115
- Enaida, H., 604
- Encapsulated cell technology, 516–517
- Endoillumination, 683
- Endophthalmitis
 - fibrovascular proliferation, 782
 - postsurgical complication, 782
 - vitrectomy, 779
- Endostatin, 48
- Englander, M., 287–295
- Enzyme-linked immunosorbent assay (ELISA), 412
- Epidermal growth factor (EGF), 531
- Epiretinal membrane (ERM), 158, 160, 601, 858
- Equator (equ), 892
- ERG. *See* Electroretinography (ERG)
- ERK1/2. *See* Extracellular-regulated kinase 1 and 2 (ERK1/2)
- Erosive vitreoretinopathy, 388
- Erythroid-2-related factor 2 (NRF2), 60
- ETDRS. *See* Early Treatment Diabetic Retinopathy Study (ETDRS)
- European Assessment Group for Lysis in the Eye (EAGLE), 648–649
- European Medicines Agency (EMA)
 - ocriplasmin, 853
 - vitrectomy, 660
 - VMT treatment, 853
- European Union (EU)
 - autologous plasmin, 827
 - and FDA, 828
- External limiting membrane (ELM), 491, 572–573
- Extracapsular cataract extraction (ECCE), 120, 126
- Extracellular matrix (ECM), 95, 99, 103, 134–135, 141, 169
 - adhesive proteins, 803
 - agrins and type XVIII collagen, 9
 - coupling, 490
 - fibrillins, 9
 - fibrils and ageing changes, 8–9
 - fibulins, 9
 - heterotypic collagen fibrils, 6–7
 - ILM & posterior vitreous cortex, 312
 - interactions, cell receptors, 59
 - modifiers, 531–532
 - posterior vitreous cortex, 800
 - PVD, 316
 - structure, 4–6
 - synthesis and turnover, 7–8
 - transmembrane receptors, 803
 - versican and link proteins, 9
 - vitreo-retinal interface, 312
 - vitreous, 487, 490
- Extracellular-regulated kinase 1 and 2 (ERK1/2), 415
- Exudative age-related macular degeneration. *See* Age-related macular degeneration (AMD)
- Exudative AMD
 - AREDS study, 338
 - dry AMD cases, 340
 - etiology, 329
 - non-responders, 341–342
 - pharmacologic vitreolysis, 343
 - polypoidal choroidal vasculopathy and retinal angiomatous proliferation, 342
 - spontaneous PVD, 340, 341
 - vitrectomy, 342–343
- Exudative retinal detachment
 - blood retinal barrier, 375
 - choroidal melanomas, 384
 - colloid osmotic pressure, 383
 - hydrostatic pressure, 384
 - posterior blood retinal barrier, 383
 - rhegmatogenous, 384
 - subretinal fluid, 384
- Eye development
 - embryonic origin, 96–97
 - optic vesicle, cup and fissure, 97
- F**
- FACIT. *See* Fibril-associated collagens with interrupted triple (FACIT)
- Familial exudative vitreo-retinopathy (FEVR), 32, 388–389
 - classification, 235
 - clinical presentation, 234–235
 - genetics, 235–236
 - ROP in children and adolescents, 234
 - treatment, 236–237
- Fan, Q., 116
- Farvardin, M., 514
- Faulborn, J., 187
- FDA. *See* Food and Drug Administration (FDA)
- Feener, E.P., 41–52
- Femtosecond laser surgery, 704
- Fercher, A.F., 203
- Fetal hyaloid vasculature, 11
- Fetal vasculature, 231
- Fibril-associated collagens with interrupted triple (FACIT), 5
- Fibrillins, 9
- Fibrils and aging changes, 8–9
- Fibrinoid syndrome, 642
- Fibroblast, 185
- Fibroblast growth factor (FGF), 48, 531
- Fibrocytes, 267, 268
- Fibronectin
 - adhesion molecules, vitreo-retinal interface, 841
 - ILM, 839
 - PVD, 841
 - type IV collagen, 870, 871, 874
- Fibrous aggregation, 140
- Fibrous astrocytes, 267, 273
- Fibulins, 9
- Fierce* (frc), 51
- Figuerola, M.S., 571–598
- Fincham, E.F., 501
- Flatten folded retina, 541

- Floater, 145
 clinical presentation, 774–775
 CSF, 778–779
 etiology, 772–774
 Nd:YAG vitreolysis, 779
 straylight, 776–777
 structural assessment, 775–776
 vitrectomy (*see* Vitrectomy)
- Flood, M.T., 558
- Flow conductivity, 383
- Flow rate. *See* Vitreous flow and cut rates
- Fluorescein angiogram, 236
- Fluoropyrimidines
 clinical evidence, 529
 description, 529
 preclinical evidence, 529
- 5-Fluorouracil (5-FU)
 co-drug preparations, 529
 with low MW heparin combination, 532
 TRD in rabbits, 529
- 5-Fluorouridine (5-FUR), 529
- Flynn, H., 676, 687
- Food and Drug Administration (FDA), 18, 867
 aflibercept, 515
 chondroitinase, 881, 882, 884, 888
 ocriplasmin, 515, 860
 Retisert®, 515
 vitreo-macular adhesion, 854
- Foos, R.Y., 186, 271, 273, 352–355, 357–359
- Foot pedal, 633
- Forkhead box C1 (FoxC1), 102
- Foster, C.S., 369
- Foster, F., 208
- Foster, W.J., 565
- Foulds, W.S., 375–391, 817–821, 864
- Fraser, J.R., 82
- Freeman, H.M., 356, 758
- Frizzled protein (Fzd), 102, 104
- FTMH. *See* Full-thickness macular hole (FTMH)
- Fujimoto, J.G., 203
- Full-thickness macular hole (FTMH), 291–294, 888
 cataract surgery, 581–582
 chromodissection, 582
 ocriplasmin effect, 858
 persistent VMT, 854
 pharmacologic vitreolysis, 588
 preoperative base diameter, 580–581
 surgical outcomes and complications, 588, 590
 tamponade, 588
- Funatsu, H., 447
- G**
- GA. *See* Geographic atrophy (GA)
- GAG. *See* Glycosaminoglycan (GAG)
- Gale, J., 57–75, 113–125
- Gandorfer, A., 265–285, 601–609, 617
- Ganley, J.P., 360
- Gao, B., 41–52
- Gao, Q., 85
- García-Arumi, J., 647–660, 828
- García-Fernández, M., 576, 580
- Gärtner, J., 143, 185, 248, 348, 356
- Gas inside eye
 dissolution, 341–342
 equilibration, 541
 expansion, 541
- Gass, C.A., 257
- Gass, D., 667, 671
- Gaseous vitreous substitutes
 dynamic properties, 541–542
 functional properties, 540–541
 physical properties, 539–540
 physiologic changes, 542–543
- Gass, J.D.M., 179, 291, 292, 324, 386
- Gaucher, D., 416
- Gauge (G), 85
- Gaze-evoked amaurosis (GEA), 307–308
- Gelman, R.A., 83
- Gel vitreous. *See also* Liquid vitreous
 human vitreous, 17
 hyaluronan concentration, 18
- Gene and stem cell-based therapies
 for retinal diseases, 708, 709
 transfected RPE cells, 707
 vitrectomy, 707
- Genetics
 candidate genes, 36
 COL2A1, complete exon skipping, 34
 collagen molecules and exon, 34
 minigene model, 34
 missense mutations, 27, 34–36
 mosaicism, 36
 nonsense associated exon skipping, 34
 pre-mRNA processing, 34
 single gene disorder, 22, 23, 33
 whole genome sequencing and exome sequencing, 36
- Geographic atrophy (GA), 516–517
- GFAP. *See* Glial fibrillary acidic protein (GFAP)
- Ghosh, F., 81–89
- Giant retinal tear (GRT), 28, 36
- Giblin, F.J., 469
- Gisladottir, S., 438, 439
- Glasser, A., 500
- Glatt, H., 561
- Glaucoma surgery
 aqueous shunt procedures, 635
 cyclodestruction, 635
- Glial fibrillary acidic protein (GFAP), 87, 103, 106, 153, 159, 277, 280, 314, 317
- Glittenberg, C., 329–344
- Globe volume restoration, 541
- Gloor, B.P., 155, 357
- Glyceraldehyde-3-phosphate dehydrogenase (GAPDH)
 advanced glycation end products, 59
 inhibition, 60
 protein kinase C, 60
 superoxide causes inhibition, 58
- Glycoprotein
 definition, 2
 endogenous, 2
 fibulins, extracellular matrix, 9
 leucine-rich alpha-2 glycoprotein (LRG1), 11
 opticin, homodimeric, 9–10
 thrombospondins, 11
- Glycosaminoglycan (GAG), 82–83, 103, 118, 132, 135, 141, 168
 chondroitinase, 882–884, 887
 chondroitin sulfate (CS), 83
 heparan sulfate (HS), 83
 hyaluronan, 82–83
 hyaluronidase, 863–864
- Goldberg, M., 103–104

Goldmann–Favre syndrome/enhanced S-cone dystrophy, 32
 Gonin, J., 682, 723
 Gouras, P., 558
 Granath, K.A., 83
 Green fluorescent protein (GFP), 154
 Green, R., 347–369
 Green, W.R., 651, 654
 Gremillion, C.M., 649
 Grillone, L., 863–867
 Grizzard, W.S., 725, 746
 Gross-Jendroska, M., 452
 Grossniklaus, H.E., 395–404
 GRT. *See* Giant retinal tear (GRT)
 Grulkowski, I., 204
 Guggenheim, J.A., 116
 Guillaubey, A., 588
 Gullstrand, A., 195
 Guthoff, R., 504

H

Haddad, A., 155
 Hageman, G.S., 881–893
 Halfter, W., 165–188, 608
 Haller, J., 888
 Halpern, J.I., 360
 Hammond, C.J., 116
 Han, D.P., 657
 Hannover, A., 194, 772
 Hanscom, T.A., 562
 Haouchine, B., 291
 Haritoglou, C., 265–285, 575, 601–622
 Harocopos, G.J., 469
 Hartmann, 532 (Not listed in the reference)
 Hartnett, M.E., 223–237
 Hasselbach, H.C., 653
 Hayreh, S.S., 251, 648
 Hazard ratio (HR), 37
 Healaflo[®], 86, 89
 Heegaard, S., 167
 Heimann, K., 118–119, 683
 Helmholtz capsular elasticity theory, 496–499
 Hemi-retinal vein occlusion (HRVO), 408, 413–414
 Hemorrhage
 choroidal, 892
 intra-retinal, 892
 vitreous, 892
 Heparan sulfate (HS), 82, 83, 132
 Heparins. *See* Low molecular weight heparin (LMWH)
 Hepatocyte growth factor (HGF), 157
 Heriot, W.J., 826
 Hermel, M., 838
 Hersh, P.S., 362
 Hesse, L., 430, 825–829
 Heterotypic collagen fibrils, 6–7
 Hexafluoroethane (C₂F₆), 539–541
 Hickingbotham, D., 686
 HID. *See* High intensity discharge (HID) lamps
 HIF. *See* Hypoxia inducible factor (HIF)
 High intensity discharge (HID) lamps, 701
 Hikichi, T., 415, 448, 826
 Hillenkamp, J., 618
 Hilton, G.F., 725, 746
 Hirakata, A., 308
 Hirakawa, M., 580
 Hiraoka, A., 791
 Hiscott, P., 315

Histopathology, 267, 399
 History, pharmacologic vitreolysis, 818, 819
 Hobbs, R.P., 223–237
 Hoerle, S., 448
 Hoffman, K., 184
 Hogan, M.J., 153
 Holekamp, N.M., 442, 452, 459–473
 Hong, S.M., 414
 Hoornaert, K.P., 24
 Hoyt, W.F., 305
 HRVO. *See* Hemi-retinal vein occlusion (HRVO)
 Huang, L.C., 771–785
 Hubschman, J.-P., 699–709
 Hughes, W., 208
 Hui, Y.N., 746
 Hu, J., 229
 Human embryonic stem cell (HESC), 709
 Human vitrectomy, 888
 Human vitreous
 age-related differences, 197
 alveolar theory, 194
 cisternal systems, 202
 dark field slit microscopy, *in vitro*, 195, 196
 extracellular matrix, 195
 fibrillar theory, 194
 imaging, 194
 ocular disorders, 193
 slit-lamp biomicroscopy, 195
 structure, 201
 Hvarfner, C., 449
 Hwang, A., 463
 Hyalocytes, 268, 273, 277, 280
 cell density, quantitative studies, 183
 cell surface antigenic characteristics, 153–154
 collagen, 158–159, 184
 definition, 152, 155, 162
 during development, 155
 existence and distribution, 152–153
 extracellular matrix, synthesis, 103
 fibrinolytic activity, 155
 glial cell migration, 318
 glycoproteins, 184
 HA synthesis, 183–184
 hyaloid vasculature, regression, 103
 intraocular immune system, VCAID, 155–156
 leukocyte-associated antigens, 103
 macrophage-like characteristics, 103
 membrane contraction, 317
 mononuclear phagocytes, 255
 morphological characteristics, 153
 origin, 154–155
 oval-shaped mononuclear phagocytes, 312
 PDR and PVR, 156–160
 phagocytic activity/capacity, 155, 184
 pharmacotherapy, 161–162
 posterior vitreous cortex, 182, 312, 315
 structure, 100–101
 surgical approach, 160–161
 TGF- β 2, 317
 tissue regression, 155
 in vitreoretinal interface pathology, 156–160
 vitreoschisis, 255
 vitreous chamber (VC), 162
 on vitreous gel surface, 153
 vitreous ground substance, 155
 Hyaloid artery, 42, 233
 Hyaloid capillary network, 155

- Hyaloid vascular system
 Bergmeister's papilla, 105–106
 hyaloid regression, 102
 Mittendorf's dot, 105
 persistent hyaloid artery, 105
 persistent pupillary membranes, 106, 107
 primary vitreous, 97, 99
 pro-and anti-angiogenic proteins, 102
 regression of hyaloid cells
 structure, 100–102
 VEGF-A, 102
 vitreous cyst, 106
 Wnt signaling pathway, 102, 116
- Hyaloid vasculature, 102
 absence of veins, 42
 fetal, 41–52
 genetic influences, 51–52
 humans, 43
 lower mammals, 42–43
 regression effect, 44–45
 structure, 42
- Hyaloid vessels, 99–100, 102
- Hyaluronan (HA), 82–84, 99, 103, 132, 137, 140, 799, 801, 812
 average molecular weight, 14
 concentration gradient, 15
 connective tissue compartments, 15
 depolymerization, 75
 diabetic vitreopathy, 64–65
 glycosaminoglycans (GAG) family, 863–864
 in humans and animals, 15
 hyalocytes, 818
 synthesis, 183–184
 turnover time (half-life), 15
 viscoelasticity, 14, 18–19
 vitreous, “mimic” rheological properties, 15
 vitreous, physical properties, 15
- Hyaluronidase (HAse), 801–802, 814
 biological activity, 864–866
 bovine, 864, 867
 complications, 866–867
 enzyme activity, 864
 graded reduction in vitreous hemorrhage, 866
 human, 864
 human recombinant hyaluronidase (rHuPH20), 867
 as liquefactant, 864, 866
 Nd:YAG laser, 867
 pharmacologic vitreolysis, 864, 865
 study design, 866
 vision improvement, 866
- Hyams, S., 253
 Hyams, S.W., 120
 Hydrodissection, 143
 Hydrogels
 hyaluronic, 86, 89
 smart, 85–86
 synthetic, 85–86
- Hydrostatic pressure, 378, 384
 in capillary (P_c), 446
 in tissue interstitium (P_i), 446
- Hypertension, 409
 Hypoxia inducible factor (HIF), 445, 446, 448
 Hypoxia inducible factor-1 (HIF-1), 157
- I**
 ICAM-1. *See* Intercellular adhesion molecule 1 (ICAM-1)
 Idiopathic intracranial hypertension (IIH), 307
 Ikeda, T., 236
 Ikuno, Y., 113–125
 IL-6. *See* Interleukin 6 (IL-6)
 ILM. *See* Inner limiting membrane (ILM)
 Imaging
 Cirrus OCT, 332
 single scans, 332
 Spectralis OCT, 332
 Stratus OCT, 332
 three dimensional OCT, 333–335
 vitreo-macular interface in AMD, 336
- Immunocytochemistry
 alphaSMA-positive cells, 280, 281
 cell morphology, 279
 continuous layer, vitreous collagen type II, 284
 expression, contractile filaments, 281
 GFAP and hyalocyte cell, 277, 280
 myofibroblast-like transdifferentiation, 280, 281
 PVD, 281
 vitreomaculopathies pathophysiology, 281
- Immunohistochemistry, 50
- Immunotoxins
 description, 530
 preclinical evidence, 531
- Implants. *See* Drug-release implants
- IND. *See* Investigational new drug (IND)
- Indocyanine green (ICG), 575
 description, 602
 hydrophilic dye, 602
 and ILM, 603
- Inflammation, 72
 hyaluronan hydrolysis, 864
 ocular, 867
- Ingenuity Pathways Bioinformatic Analysis, 43, 44
- Inherited vitreo-retinopathies
 COL2A1 related disorders, 27–31
 Stickler syndromes, 23–27
 vitreo-retinal surgeon, 22
- Inner limiting membrane (ILM), 70–72, 85, 99, 134, 142, 147, 575, 613, 615
 aging, 172–173
 anti-fibronectin antibodies, 839
 biophysical properties, 179–180
 biosynthesis and assembly, 170–172
 brilliant blue, 604
 cell adhesion, 179
 cell locations, 269, 270
 definition, 165–166
 detachment, 122–123
 diabetes, 173, 176, 177
 fetal human, 167
 human embryonic eye, immunohistochemistry, 173
 hyalocytes, 312
 ICG staining, 603
 laminae, 167
 laminin and fibronectin, 839
 macular hole eyes, 273–275
 Mueller cells, 167
 in ocular development, 172, 174–175
 peeling, 160–161
 pharmacologic vitreolysis, 870
 posterior vitreous cortex, 839
 premacular fibrocellular tissue, 267
 premacular (epiretinal) membranes, 178, 605
 proliferating glial cells, 273
 proliferative diseases, 176
 retina, 166, 602
 staining, 602
 structure, 167–168

- topographic variations, 168–170
- traction, 266
- tractional disorders, 179
- trans-ILM diffusion, 187–188
- type IV collagen, 288
- uveitis and vitreo-retinal interface, 180–181
- vitrectomy, 123
- vitreomacular attachment, 267
- vitreoretinal attachment, 839
- vitreo-retinal interface, 300
- Inner retinal optic neuropathy (IRON)
 - afferent pupillary defect, 619
 - AION, 619
- Inner segment-outer segment (IS/OS) junction, 122, 319, 320
- In-office repair. *See* Pneumatic retinopexy (PR)
- Inomata, H., 353
- Instrumentation, vitrectomy, 698
- Instruments. *See* Vitrectomy
- Insulin-like growth factor-1 (IGF-1), 157, 161
- Intercellular adhesion molecule 1 (ICAM-1), 66, 417
- Interfactant
 - H₂Ase, 801
 - liquefactant, 799–800
 - plasmin, 802–803
 - vitreo-retinal interface, 799
- Interleukin (IL)
 - macrophage recruitment, 818
 - plasmin, 846
- Interleukin 6 (IL-6), 412, 413
- Interleukin 1-beta (IL-1 β), 66
- Internal limiting lamina (ILL), 479, 485, 487, 489
- Internal limiting membrane (ILM). *See* Inner limiting membrane (ILM)
- Internal tamponades
 - air, 539
 - intraocular gases, 540–541
 - longer-acting, 539
 - SiO₂, 544
 - vitreo-retinal surgery, 704
- International Classification of Retinopathy of Prematurity (ICROP), 224, 235
- International Clinical Diabetic Retinopathy Severity (ICDRS) Scale, 426, 427
- International vitreo-macular traction (IVTS) classification, 295
- Interphotoreceptor matrix (IPM), 376
- Intraocular fluid current, 540, 541
- Intraocular gases
 - dynamic properties, 541–542
 - functional properties, 540–541
 - physical properties, 539–540
 - physiologic changes, 542–543
- Intraocular neovascularization
 - choroid, 482–483
 - spatial characteristics, 480–482
 - temporal characteristics, 482
- Intraocular oxygen physiology
 - laser photocoagulation, 483–485
 - vitreo-retinal surgery and vitreous neovascularization, 485–489
- Intraocular oxygen tension
 - gradients, 461–463
 - lens, 460–461
 - oxygen distribution, human eye, 463, 464
 - trabecular meshwork, 461, 462
 - vitreous, 460
 - vitreous gel, 463–467
- Intraocular pressure (IOP), 117, 513, 517, 528
 - air travel, 543
 - central retinal artery occlusion, 542
 - expansile gas injection, 541
 - intraocular triamcinolone treated patients, 513
 - nitrous oxide diffusion, 542
- Intraocular tamponade
 - advantages and disadvantages, 744
 - iridectomy, 744
 - longer, 744
 - sclerotomy, 744, 745
 - vitrectomy systems, 745
- Intraoperative visualization, vitrectomy
 - illumination, 701–702
 - wide-angle viewing, 701
- Intraretinal cysts, 300, 305, 306
- Intra-retinal microvascular abnormalities (IRMAs), 422
- Intravitreal bubble injection
 - drainage, subretinal fluid, 762
 - long-acting expansile gases, 760
 - pure air, 760
 - treatment, superior rhegmatogenous retina, 761
- Intravitreal drug therapy
 - anti-bacterial agents, 512, 513
 - anti-fungal agents, 512–513
 - anti-inflammatory/anti-neoplastic agents, 513–514
 - anti-VEGF agents, 514–515
 - anti-viral agents, 513
 - delivery systems and anatomical location, 510, 512
 - encapsulated cell technology, 516–517
 - implants, 515–516
 - injection (*see* Intravitreal injection)
 - liposomes, 517
 - microspheres, 517
 - pharmacologic vitreolysis, 515
 - porous silicon particles, 517
 - principles, 510, 511
 - steroids, 513
 - suprachoroidal micro-injection, 517–518
- Intravitreal injection
 - complications, 511–512
 - Cortiject emulsion, 518
 - dosage and half-life of antibiotics, 513
 - in humans, 855
 - infants, 510–511
 - pressure-reducing strategies, 856
 - safety and preliminary efficacy, 856
 - technique, 510
 - Tethadur, 518
 - Verisome system, 518
- Intravitreal triamcinolone (IVTA), 513
- Intravitreal membrane (*Ivm*), 99
- Investigational new drug (IND), 884, 888
- In vitro* imaging, 195–198
- In vivo* imaging
 - acoustic imaging (*see* Acoustic imaging)
 - anterior segment, 198
 - direct ophthalmoscopy, 198–199
 - indirect ophthalmoscopy, 199
 - light-based imaging (*see* Light-based imaging)
 - MRI spectroscopy, 213–215
 - slit-lamp biomicroscopy (*see* Slit-lamp biomicroscopy)
 - Tyndall effect, 198
- Iontophoresis, 518
- IOP. *See* Intraocular pressure (IOP)
- Iridohyaloid blood vessels, 232
- Iris neovascularization
 - after CRVO, 481, 482
 - after PVD, 487–489
 - after vitrectomy, 487
 - healthy cats, 445

- Iris neovascularization (*cont.*)
 non-ischemic CRVO, 482
 proliferative diabetic retinopathy, 482
 regression, 485
 Ishibashi, T., 151–162
 IS/OS junction. *See* Inner segment-outer segment (IS/OS) junction
 Itakura, H., 17, 204, 250
 Iwanoff, A., 311
- J**
 Jackson, D.S., 83
 Jackson, T.L., 415, 590
 Jaffe, N.S., 142, 202, 316
 Jeon, S., 500
 Johnson, M.W., 131–148
 Johnson, R.N., 257
 Jokl, A., 99
 Jonas, J.B., 251, 258, 648, 734
 Jonckx, B., 845–851
 Jones, C.E., 500
 Juan, T., 696
- K**
 Kadosono, K., 603
 Kaiser, P.K., 287–296
 Kampik, A., 265–285, 601–609
 Kaplan, H.J., 554, 558, 869–878
 Karlin, D.B., 119, 121
 Kasner, D., 669
 Kasthurirangan, S., 500
 Katz, B., 305, 307
 Katzin, K.M., 357
 Katz, L., 208
 Kelly, N.E., 614, 839
 Kenawy, N., 609
 Ketterling, J., 210
 Kiefer, A.K., 116
 KiloDalton (kDa), 6, 9–11, 16, 87, 188, 846
 Kim, J.H., 48
 Kimura, A.E., 563
 Kingston, Z.S., 95–108
 Kinsey, V.E., 224
 Kishi, S., 142, 195, 316, 415
 Kita, T., 151–162
 Kloti, R., 141, 683
 Kniest dysplasia, 27, 28, 33
 Knobloch syndrome, 30, 31, 33
 Koerner, F., 528, 734, 746
 Kohner, E.M., 480, 481
 Kohno, R., 317
 Kokame, G.T., 580
 Konig, W., 208
 Koreen, L., 453
 Koretz, J.F., 501
 Koss, M., 413
 Koss, M.J., 241–259, 411
 Koutsandrea, C.N., 362
 Krebs, I., 253, 329–344, 450, 451, 471, 828
 Kroll, P., 421–432, 825–829
 Kroll's classification, 426–431
 Kuhn, F., 615
 Kumagai, K., 449, 615, 616, 657
 Kurz, G.H., 359
 Kusbeci, T., 512–513
 Kuwabara, T., 185
- L**
 Lacqua, H., 200
 Lacquer cracks, 121
 Lalezary, M., 453
 Lamellar hole (LH), 291, 292
 prognostic factors and indications, 579–580
 surgical technique, 580
 VPA, 303–304
 Laminin
 adhesion molecules, vitreo-retinal interface, 841
 ILM, 841
 PVD, 841
 Laminin alpha-2 subunit gene (LAMA2), 116
 Lange, C.A., 446
 Lang, G.E., 407–418
 Laqua, H., 746
 Larsson, J., 449
 Laser *in situ* keratomileusis (LASIK), 120
 Laser photocoagulation, 229, 743
 argon, 342
 avascular retina, 229
 intraocular oxygenation, 483–485
 macular holes, 614
 in pseudophakic/aphakic eyes, 759
 retinal adhesion, 760
 retinopexy, 758
 submacular surgery, 556
 treatment, posterior retinal breaks, 760
 Lashley, R., 684
 Laurent, T.C., 83
 Laurent, U.B., 83
 Leaver, P., 683
 Leber, T., 364
 LED. *See* Light-emitting diode (LED) lamps
 Lee, B., 438
 Lee, S.J., 331, 828
 Leila, M., 647–660
 Le Mer, Y., 827
 Lensectomy, 236
 Lens placode (*lp*), 96
 Lens removal, 736, 751
 Lens-sparing vitrectomy, 230
 Lens support theory of Helmholtz, 496–498
 Lens vesicle (*lv*), 97
 Leucine-rich alpha-2 glycoprotein (LRG1), 11
 Lewis, H., 448, 746
 Liang, J., 452
 LIF. *See* Local intra-arterial fibrinolysis (LIF)
 Light-based imaging
 OCT, 203–208
 SLO, 203
 Light-emitting diode (LED) lamps, 701
 Light scattering
 analysis, vitreous structure *in vitro*, 216
 DLS, 776
 'floaters', 772
 ocular media opacities, 779
 and visual disturbances, 772
 Lim, H., 203
 Lincoff, H., 308, 361, 758, 759, 791
 Lindey, P., 556
 Lindner, K., 143, 387
 Lin, P., 509–519
 Li, Q., 446
 Liquefactant
 abilities, 866
 agents, 800

- hyaluronan, 801
 hyaluronidase, 801–802 (*see also* Hyaluronidase (Hase))
 and interfacant, 801
 Vitreosolve®, 803
 vitreous, 864
- Liquefaction**
 age-related vitreous, 249
 APVD, 251
 collagen aggregation, 140
 collagen disorders, 137
 dark-field slit microscopy, 137–140
 gel vitreous, 136
 HA, 137, 140
 lacunae, 137
 liquid vitreous, 136
 optical coherence tomography, 137
 pathogenesis, 242–244
 Stickler's syndromes, 253
 synchysis senilis, 136
 type IX collagen, 140
- Liquid vitreous**
 adult human vitreous, 14
 after birth, 14
 formation, 14
 hyaluronan, 14
 proteoglycans, 16
 viscoelastic, 14, 18–19
 volume, 16
- Littmann, H., 667
 Lloyd, H., 495–505
 LMWH. *See* Low molecular weight heparin (LMWH)
 Local intra-arterial fibrinolysis (LIF), 648
 Loeys–Dietz syndrome (LDS), 31
 Lois, N., 615
 Long-acting expansile gases
 perfluorocarbons, 760
 sulfur hexafluoride, 760, 761
 Long-acting vitreous substitutes
 perfluorocarbon liquids, 543–544
 silicone oil (*see* Silicone oil (SiO))
- Lossing, L.A., 499
 Low molecular weight heparin (LMWH)
 established PVR, 532
 high risk retinal detachments, 532
 preclinical studies, 531
 unselected primary retinal detachments, 532
- LPA. *See* Lysophosphatidic acid (LPA)
 LRG1. *See* Leucine-rich alpha-2 glycoprotein (LRG1)
 Lucier, A.C., 355
 Lutjen-Drecoll, E., 499, 504
 Luty, G.A., 48
 Lymphatic vessel endothelial receptor 1 (LYVE-1), 102
 Lysophosphatidic acid (LPA), 48
- M**
 Machemer, R., 158, 200, 445, 554, 556, 561, 562, 565, 666, 667, 669, 671, 673, 676, 682, 683, 686, 687, 693, 700, 728, 746, 749, 757, 791
- Macrophage**
 ablation transgenic mice, 155
 antigen-pulsed, 156
 definition, 153
 hyalocytes, 153, 155
 premacular membranes, 160
 tissue, 155
 vitreous, 154
- Macrophagy, 44, 46
- Macula**
 cysts, 254
 FTMH (*see* Full-thickness macular hole (FTMH))
 macular pseudoholes (*see* Macular pseudoholes)
 macular pucker (*see* Macular pucker)
- Macular diseases, 303–304
- Macular edema**
 diabetic, 447–448
 DME (*see* Diabetic macular edema (DME))
 hydrostatic pressure gradient, 446–447
 osmotic pressure gradient, 450
 oxygen, 450
 retinal vein occlusions, 448–449
 RVO, 408
 and Starling's law, 446
 treatment, 449–450
 vitreo-retinal traction, 449
- Macular hole (MH)**, 257, 259, 888, 892
 anomalous PVD, 160
 capsulotomy, 616
 cell clusters, 275
 collagen type II, 275
 cystoid macular edema, 615
 fibrocellular proliferation, 274
 foveal dehiscence, 275, 277
 FTMH, 291–294
in vitro cicatricial contraction model, 157
 ILM, 273, 274, 609, 615
 immunocytochemistry (*see* Immunocytochemistry)
 lamellar hole, 291, 292
 meta-analysis, 615
 Müller cell, 614
 myofibroblastic differentiation, 160
 myopic maculopathy, 25
 NVC, 274
 and PMMs, 160, 615–616
 posterior vitreous cortex, 614
 premacular cell proliferation, 275
 premacular membranes, 160
 primary surgical failure, 615
 pseudohole, 290–291
 PVD, 275
 re-opening, 615–616
 re-operations, 618
 retinal detachment, 24
 retinal nerve fiber layer, 615
 retinoschisis, 125
 rim flat mount, 275, 276
 SDS-PAGE, 839, 840
 therapy, 614
 treatment, 614
 vitreo-macular traction, 614
 vitreo-papillary adhesion, 300, 302–303
 western blot analysis of ILM, 839
- Macular pseudoholes**, 576, 579
- Macular pucker (MP)**, 148, 254, 255, 259
 anatomy, 312–314
 anomalous macular conditions, 288
 anomalous PVD, 316, 317, 320
 The Blue Mountain Eye Study, 320
 cannulas, 564
 cell locations, 269–272
 cellophane macular reflex, 320
 cell origins, 273, 274
 cell types, 267–268
 connective tissue growth factor, 317

- Macular pucker (MP) (*cont.*)
 description, 311–312
 ellipsoid and interdigitation lines, 573
 ELM, 572–573
 epidemiology, 312
 ERM, 158
 foveal contour, 573
 GFAP and α -SMA immunopositive cells, 159
 grading systems, 320
 hyalocytes, 317
 ICG, 575
 ILM, 575
 ILM removal, 617
 impacts vision, 325
 intraretinal cysts, 319
 metamorphopsia, 576
 microincisional vitrectomy, 576
 OCT, 321, 574
 pathology, 314–316
 PDFG, 317
 photoreceptors, 573
 PMM and ILM removal, 617
 post-operative functional outcomes, 617
 post-surgical failure, 617
 premacular membrane, 158, 267, 320, 572, 592, 609, 616
 PVD, 159, 316–318, 616
 re-operations, 618
 retinal breaks, 316
 ROCK, 317
 SD-OCT, 572
 secondary premacular membranes, 321
 staining and peeling patterns, 617
 TGF- β , 158
 TGF- β 2, 317
 visual acuity, 573
 vitrectomy, 158, 575
 vitreo-macular traction syndrome, 324–325
 vitreo-papillary adhesion, 300, 303–304
 vitreoschisis, 316, 616
- Macular translocation
 complications, 557
 concept, 556
 description, 556
 full macular translocation, 557
 limited translocation, 556
 outcomes, 560
 unfolding technique, 557
 scleral infolding, 556–557
- Madigan, M.C., 41–52, 95–108
- Maeda, N., 441
- Magnetic resonance imaging (MRI), 30
 hydrogen nuclei, 213
 hyperintense characteristic, 215
 longitudinal relaxation time, 214
 NMR signal, 214
 noninvasive method, 193, 214
 pre-retinal oxygen tension changes, 215
 transverse relaxation time, 214
 ultrasound and OCT, 214
- Malignant glaucoma
 aqueous misdirection, 792
 core vitrectomy, 793
 description, 791
 intraocular lens placement, 793, 794
 iridectomy/iridotomy, 791
 phacoemulsification, 793
 phakic eyes, 793
 ultrasound biomicroscopy, 792
 vitreous cutter, 793
 zonulohyaloido-vitrectomy, 793
- Malignant melanoma, 790
- Malignant peripheral nerve sheath (MPNST), 48
- Malinowski, S.M., 369
- Mann, I.C., 42
- Marfan/high myopia, 146
- Marfan syndrome, 30–31, 33
- Margherio, A.R., 838, 839
- Marshall, J.C., 759
- Marshall syndrome, 24, 29–30, 33, 36
- Martin, H., 504
- Massive periretinal proliferation (MPP), 524
- Massive preretinal retraction (MPR), 524
- Massive vitreous retraction (MVR), 524. *See also* Proliferative vitreoretinopathy (PVR)
- Matrix metalloproteinase (MMP), 531, 846
- McLeod, D., 477–492, 539
- McNulty, R., 463
- MCP-1. *See* Monocyte chemoattractant protein-1 (MCP-1)
- Mehta, A.N., 731–746
- Mehta, S., 395–404
- Membrane peeler cutter (MPC), 686
- Membrane peeling
 barbed micro-vitreoretinal (MVR) blade, 741
 illuminated pick and forceps, 740
 large circumferential peripheral retinectomy, 742
 PCFL, 741
 subretinal membranes, PVR, 741
- Menda, S., 509–519
- Mesoderm (*mes*), 96–98
- Messenger ribonucleic acid (mRNA), 490
 alternative splicing, 5, 6
 cells expression, 35
 mutant, 26
 pre-mRNA processing, 34
 splicing, 32
 tissue-dependent splicing variation, 27
 transcript, 32
- Mester, U., 656–657
- Mester, V., 615
- Meurs, J.C., 154
- Meyer, C.H., 307, 421–432, 452
- Meyer, E., 359
- Meyer, K., 14, 82
- Meyer-Schwickerath, G., 614
- mfERG. *See* Multifocal electroretinography (mfERG)
- Michaelson, I.C., 118, 478–480, 490
- Michaelson's biochemical mediator
 inflammatory cytokines, 490
 sources, 490, 492
 VEGF, 489–491
 vitreous neovascularization, 490
- Michalewska, Z., 580
- Micro-incisional vitrectomy surgery (MIVS)
 advantages and disadvantages, 739
 PFCL bubbles production, 743
- Microparticles, 517, 518
- Microplasmin
 recombinant form, plasmin, 845
 vitreous chamber, 846
 yeast *Pichia pastoris*, 846
- Microplasmin intravitreal injection trial (MIVI), 848
- Microsurgery, 665

- Micro-vitreo-retinal blade (MVR)
 adherent membranes, 741
 anteriorly displaced retina to structures, 741
- MIG. *See* Monokine induced by interferon γ (MIG)
- Miller, B., 251
- Miller, J.W., 357
- Milligrams (mg), 14
- Milliliters (mL), 14, 17
- Millimeters of mercury (mm Hg), 460–464, 471
- Mittendorf's dot, 103, 105, 232, 233
- MIVI-TRUST
 drug-related adverse events, 859
 efficacy end point, 858
 MIVI-006 and MIVI-007 trials, 857
 nonsurgical retinal breaks, 859
- MIVS. *See* Micro-incisional vitrectomy surgery (MIVS)
- Miyakubo, H., 235
- Miyamoto, T., 32
- MMP. *See* Matrix metalloproteinase (MMP)
- Modarres, M., 307
- Modesti, M., 500
- Mojana, F., 250, 336, 337
- Molecular movement within and from vitreous
 collagen and hyaluronan, 376
 colloid osmotic pressure, 378–379
 depolymerization, 378
 diffusion, 379–380
 fluid movement, 378
 hydrostatic pressure, 378
 tritiated water ($^3\text{H}_2\text{O}$) injection, 376, 377
- Monkey, pharmacologic vitreolysis, 886–887
- Monnier, V.M., 64
- Monocyte chemoattractant protein-1 (MCP-1), 157
 bevacizumab and dexamethasone, 413
 CRVO, 412
 cytokines, 413
 IL-6, 417
 vitrectomy vitreous samples, 417
- Monokine induced by interferon γ (MIG), 414
- Moore's light flashes, 145
- Morita, H., 118
- Morse, P.H., 355
- Müller cells, 99, 103, 141, 142, 153, 157, 277, 425
- Multifocal electroretinography (mfERG), 61
- Multiple epiphyseal dysplasia (MED), 27
- Mundt, G., 208
- Murakami, K., 358
- Murakami, T., 473
- MVR. *See* Micro-vitreo-retinal blade (MVR)
- Myocardin-related transcription factors A and B, 51
- Myofibroblast, 267, 268, 280, 281
 cells, 159–161
 transdifferentiation, 157, 159–160
- Myopia, 251
 accommodation, 117
 animal studies, 116–117
 and cataract, 124
 classification, 114
 definition, 114
 education and urbanization, 117
 emmetropization, 114–115
 extracellular matrix proteins, mutations, 116
 eye size and axial length, 116
 familial high myopia, 116
 genome-wide association studies, 116
 heritability, 116
 prevalence, 115
 PVD (*see* Posterior vitreous detachment (PVD))
 refractive error, 115
 retina and choroid, 119–120
 scleral changes and axial length, 117–118
 staphyloma, 125
 syndromes, 115
 twin studies, 116
 vitreopathy (*see* Myopic vitreopathy)
 vitreous factors, 117
- Myopic foveoschisis, 119–123
- Myopic macular degeneration. *See* Myopic maculopathy
- Myopic maculopathy
 choroidal neovascularization, 121
 diffuse atrophy, 121
 foveoschisis, 121–123
 lacquer cracks, 121
 macular hole, 123
 paravascular retinal microholes, 123–124
 patchy atrophy, 120–121
 premacular membrane formation, 123
- Myopic vitreopathy
 anomalous PVD, 118–120
 and asteroid hyalosis, 772–773
 cataract, 124
 in chicks, 118
 floaters, 772
 gel vitreous, 118
 hyaluronate concentrations, 118
 intraocular foreign bodies, 776
 myopic maculopathy, 120
 premature synchysis and PVD, 118
 premature vitreous liquefaction, 118–119
 retinal detachment, 120
 vitreo-retinal interactions, 118
- Myosin light chain (MLC), 157, 161
- N**
- Nagpal, K.C., 356
- NAION. *See* Non-arteritic anterior ischemic optic neuropathy (NAION)
- Nakamura, T., 619
- Nanoparticles
 cyanoacrylate, 518
 temporary clouding, ocular media, 517
- Nasrallah, F.P., 448, 841
- Native vitreous collagen, 267
- Nattokinase, 802–803
- Neodymium-doped yttrium aluminum garnet (Nd:YAG) laser, 867
- Neoplastic diseases, 200
- Neovascular glaucoma
 antimetabolites, 633
 neovascularization, 632
- Neovascularization
 high risk, PDVR, 424
 retinal, 445–446
 rubeosis iridis/iris, 422, 444–445
- Nerve injury-induced protein (Ninj1), 47
- Neumann, E., 120, 253
- Neural cadherin (N-Cadherin, Cadherin-2), 50–51
- Neural ectoderm (*ne*)Lens placode 96, 97
- Neurosensory retina (*nr*), 97
- New drug delivery systems
 antimetabolite drugs, 706
 flexible “mucoadhesive” 3D hydrogels, 705

- New drug delivery systems (*cont.*)
 intravitreal medications, 705
 nanomaterials, 706
 non-invasive methods, 706
- Newsome, D.A., 184
- Nguyen, J.N., 771–785
- Nicotinamide adenine dinucleotide phosphate (NADPH), 60
- Niemeyer, M., 241–259
- Ninjurin 1, 47
- Nitrogen (N₂), 49
- Nitrous oxide (N₂O), 542
- Niwa, T., 319
- Noble, J., 648
- Noma, H., 413, 414
- Non-arteritic anterior ischemic optic neuropathy (NAION), 307
- Non-collagenous
 telopeptides, 5
 vitreous, extracellular matrix components (*see* Extracellular matrix, vitreous)
- Non-inflammatory fraction of sodium hyaluronate (NIF-NaHA), 18
- Non-proliferative diabetic retinopathy (NPDR), 422
- Non-steroidal anti-inflammatory agents
 clinical evidence, 529
 pre-clinical evidence, 529
 vitreoretinal scarring, 528
- Norrie disease, 234
- Norrie disease protein (Ndp), 102
- Norrin, 47
- Norton, E.W.D., 361, 667, 671, 682–684
- Nose, I., 684
- Noulas, A.V., 16
- Novak, M.A., 358
- Nuclear factor kappa-B (NF-κB), 58–60, 62
- Nuclear sclerotic cataract
 oxygen and nuclear sclerosis, 468–469
 vitreous, nuclear sclerosis, 469
- O**
- O'Brien, B.M., 666, 667
- Ocriplasmin, 230
 Amsler Grid testing, 805, 806
 case selection, 806
 clinical trial program, 860
 concomitant retinal disease, 860
 diabetic retinopathy, 821
 3D threshold Amsler Grid plot, 805
 efficacy and safety, 804
 krinkles, 804
 macular cyst, 805, 808
 microplasmin, 804
 OCT/SLO detection of effects, 804–805
 pharmacodynamics, 847–849
 pharmacokinetics, 846–847
 pre-clinical models, 846
 structural and physiologic characteristics, 846
 surface proteins, retinal structure, 851
 symptomatic VMA & VMT, 854–859
 vitreo-foveal adhesion, 806
 vitreo-macular adhesion (VMA), 805
 vitreo-macular traction, 804
- OCT. *See* Optical coherence tomography (OCT)
- OCT/SLO coronal plane imaging
 macular pucker *in vivo*, 206
 posterior vitreoschisis *in vivo*, 207
 vitreo-papillary adhesion *in vivo*, 208
- Ocular hypotony, 447, 450, 451
- Odds ratio (OR), 116, 120, 124
- OIR. *See* Oxygen-induced ischemic retinopathy (OIR)
- Oksala, A., 211, 249
- Okun, E., 357
- Okunuki, Y., 414
- Oldendoerp, J., 632
- Olsen, K., 690
- O'Malley, C., 667, 683
- Ondes, F., 330
- ONL. *See* Outer nuclear layers (ONL)
- Operating microscope, 666, 667, 682
- OPL. *See* Outer plexiform (OPL)
- Opremcak, E.M., 651, 656, 657
- Opsin melanopsin gene (Opn4), 49, 52
- Optical coherence tomography (OCT), 33, 61, 66, 67, 121–125, 266, 288, 438, 446, 451, 452
 age-related PVD, 306
 anatomical changes, photoreceptors, 319
 Cirrus OCT, 332
 confocal microscopy, 203
 coronal plane imaging, 205
 detachments, 330
 disadvantages, 204
ex vivo retina, 203
 full-thickness MH, 291–294
 Huang's implementation, 203
 interference fringes, 203
 intraoperative, 702
 intraretinal cysts, 208
 IS/OS junction, 319, 320
 lamellar macular, 291
 monochromatic light source, 203
 ophthalmology, clinical applications, 203
 pivotal phase 3 studies, 857
 premacular membrane (PMM), 290
 PVD, 146, 147, 288
 SLO image, 204
 spectral-domain, 203
 Spectralis OCT, 332
 Stratus OCT, 331
 swept-source imaging, 204
 three dimensional, 333–335
 time-domain systems, 203
 and ultrasound, 714
 visualization, vitreo-papillary interface, 301
 vitreo-macular adhesion, 700
 vitreo-macular interface, 205
 vitreo-macular morphology, 321
 vitreo-papillary adhesion, 205, 208
 vitreo-retinal interface, 250
 vitreoschisis, 316
 vitreous body imaging, 250
 VMA, 288, 854
 VMT, 289
- Optic fissure (*of*), 97
- Opticin
 anti-angiogenic actions, 10
 Coomassie Blue stained SDS-PAGE gel, 9–10
 description, 50
 immunohistochemistry demonstrates, 10
 recombinant, 10
 small leucine-rich repeat proteoglycan (SLRP) family, 9–10
- Optic nerve, 225
- Optic nerve pit, 308

- Optic neuropathies
GEA, 307–308
- Optic pits
detachment, macula, 791
histopathologic studies, 791
long-term visual prognosis, 791
vitreo-macular traction, 791
- Optic stalk (*os*), 97
- Ora bays, 350
- Osgood Schlatter's disease, 26
- Osmotic pressure, 378–380
exerted by plasma proteins in the capillary (Qc), 446
exerted by proteins in the interstitial fluid (Qi), 446
- Osterlin, S., 251
- Osterloh, M.D., 655, 656
- Oster, S.F., 319
- Outer nuclear layers (ONL), 291
- Outer plexiform (OPL), 291
- Oxygen (O₂), 47, 48, 50. *See also* Intraocular oxygen physiology
cat vitreous, 439
and glaucoma, 469–470
human eye, 442
intraocular oxygen tension (*see* Intraocular oxygen tension)
“metabolic oxygen barrier”, 483
and nuclear sclerosis, 469
physiology, 439–443
pig eyes, 442
sources, intraocular neovascularization, 483
tension, 479
tension measurements, cataract, 453
VEGF-mediated retinopathies, 471–473
vitreo-retinal physiology (*see* Vitreo-retinal physiology)
vitreous liquefaction/vitreotomy, 467–468
- Oxygen hypothesis
age-related and post-vitreotomy nuclear cataract, 468
age-related liquefaction, 465
glaucoma, 471, 472
intraocular oxygen, 461, 463
nuclear sclerosis, 469, 470
vitreous gel, 460
- Oxygen-induced ischemic retinopathy, 50
- P**
- Palmer, J., 14
- Palmer, J.W., 82
- Palmquist, B.M., 468
- Pan, B.X., 613–622
- Panretinal retinal photocoagulation (PRP), 485
- Paques, M., 655
- Paravascular retinal lattice, 24
- Parel, J-M, 504, 505, 665–690, 693, 700
- Park, D.W., 617
- Parolini, B., 559
- Parrish, R.K., 687
- Pars plana vitrectomy (PPV), 442–444
floaters, 779
posterior membranes, 740
vitrectomy (*see* Vitrectomy)
- Pars planitis
anatomical region, 365
epidemiology and clinical presentation, 366–367, 369
fibrovascular layer, 365
peripheral uveitis/chronic cyclitis, 365
sequelae, 367, 369
SUN terminology, 365
systemic disease, absence, 365
therapy, 369
- Partial pressure of oxygen (pO₂), 83, 439, 440, 445, 453, 463, 471, 472
- Patellar fossa, 348
- Patel, S.R., 517
- Pathology
AMD, 450–452
iris neovascularization, 444–445
macular edema (*see* macular edema)
retinal neovascularization, 445–446
vitrectomy, 452–453
vitreous aging, 444
- Pathophysiology, PVR
BRB breakdown, 526
cell accumulation and proliferation, 526
cell types, 399
collagen and fibronectin, 399
cytokines, 399, 401
development and progression, 399
ECM production and fibrin deposition, 526–527
formed membrane contraction, 527
glial cells, 401–402
immune cells, 401
macrophages/hyalocytes, 400–401
miscellaneous cytokines, 402–403
myofibroblasts, 401
PDGFR α , 401
rhegmatogenous RD, 524
RPE cells, 400
scleral depression and cryotherapy, 399
TNF α , 401
TNF β , 401
vitreo-retinal interface, 399–400
vitreoretinal scarring, 524
- Patz, A., 224
- Pau, H., 99
- Pavlin, C., 208
- Pavlin, C.J., 500
- Paysse, E.A., 229
- PBS. *See* Phosphate buffer solution (PBS)
- PCIOL. *See* Posterior chamber intraocular lens (PCIOL)
- p53 deficiency, 45
- PDGF. *See* Platelet-derived growth factor (PDGF)
- PDMS. *See* Poly-dimethylsiloxane (PDMS)
- PDR. *See* Proliferative diabetic retinopathy (PDR)
- PDS. *See* Port delivery system (PDS)
- PDT. *See* Photodynamic therapy (PDT)
- PECAM-1. *See* Platelet endothelial cell adhesion molecule 1 (PECAM-1)
- PEDF. *See* Pigment epithelium-derived factor (PEDF)
- Pendergast, S.D., 235
- Penetrating trauma, 251
- Pentraxin 3 (PTX-3), 413, 414
- Perfluorocarbon liquid (PFCL)
anterior membrane dissection, 741
fluid/PFCL-silicone oil exchange, 744
giant retinectomy with elevated, folded edges, 740
injection/fluid-gas exchange, 741
peripheral vitreous and anterior membranes, 740
posterior retina stabilization, 740, 741
scleral buckle, 737–738
subretinal membrane removal, 741
- Perfluorocarbon liquid (PFCL)
properties, 543
retinal toxicity, 543–544

- Perfluorodecaline (C₁₀F₁₈), 543
- Perfluoroethylcyclohexane (C₈F₁₆), 543
- Perfluoro-n-octane (C₈F₁₈), 543
- Perfluorooctylbromide (C₈F₁₇Br), 543
- Perfluorophenanthrene (C₁₄F₂₄), 543
- Perfluoropropane (C₃F₈)
- gas/silicone oil, 753
 - intraocular tamponade, 744–745
 - long-acting gas, 761
 - sclerotomy sites, 744
 - submacular tPA injection, 566
 - tamponade, 791
- Perfluoropropane (C₃F₈)
- buoyancy, 540
 - expansion, 540, 541
 - phakic non-vitreomized eyes, 542
- Perfluorotributylamine (C₁₂F₂₇N), 543
- Perfluorotri-n-propylamine (C₉F₂₁N), 543
- Perichon, J.Y., 828
- Periostin (POSTN), 47
- Peripheral fundus lesions, 354
- Peripheral vitreo-retinal
- aging, 357
 - anatomic, 347
 - anterior loop, 349
 - dark-field slit microscopy, 348
 - indirect ophthalmoscopy, 347
 - meridional complexes, 351
 - meridional folds, 350–351
 - ora bays, 350
 - pars planitis (*see* Pars planitis)
 - patellar fossa, 348
 - post-traumatic retinal healing, 357
 - PVD, 357–358
 - retinal excavations, 351
 - retinal lattice, 354–355
 - retinal tufts (*see* Retinal tufts)
 - spiculate and nodular pigment epithelial hyperplasia, 354
 - traction, 356–357
 - vasculopathies (*see* Vasculopathies)
 - verruca, 356
 - vitreous, 347–349
 - white-with and without-pressure, 355–356
- Persistent fetal vasculature (PFV), 103–104
- abnormal regression, 232
 - ancillary tests, 232
 - anterior PFV (*see* Anterior PFV)
 - genetics, 234
 - gestation, 231
 - hyaloid vasculature, 230
 - individual components, fetal vasculature, 232
 - posterior PFV (*see* Posterior PFV)
 - treatment, 234
 - tunica vasculosa lentis, 231
 - vasa hyaloidea propria, 230, 231
- Persistent hyaloid artery, 104, 105
- Persistent hyperplastic primary vitreous (PHPV), 103–105
- Persistent pupillary membrane (PPM), 106, 107
- Pertile, G., 559
- Petrella, R.J., 409
- Petropoulos, I.K., 442
- Peyman, G.A., 558, 649, 683, 790, 827–829
- PFCL. *See* Perfluorocarbon liquid (PFCL)
- Pfister, M., 140
- Phacoemulsification, 633
- Phakic fellow eyes
- aphakic and pseudophakic fellow eyes, 721–723
 - cystic retinal tufts, 718, 721, 723
 - degenerative retinoschisis, 718, 721
 - retinal breaks, 720–721
 - retinal lattice, 719–720
- Phakic non-fellow eyes
- asymptomatic retinal breaks, 718
 - asymptomatic vitreo-retinal lesions, 718, 720
- Pharmacodynamics, ocriplasmin, 847–849
- Pharmacokinetics, ocriplasmin
- diabetic retinopathy/vein occlusion, 847
 - inactivation, autolytic degradation, 846
 - porcine and human vitreous extracts, 847
 - second order kinetics, 847
 - serine protease inhibitor, 847
- Pharmacologic adjuncts
- anti-inflammatory agents, 528–529
 - cell proliferation inhibitors, 529–531
 - clinical trials, 527
 - extracellular matrix modifiers, 531–532
 - targets, 527
- Pharmacologic vitreolysis, 230, 293, 294, 438, 442, 444, 446
- biological action, 801
 - case selection, 806
 - chemical action, 800–801
 - classification, biologic activity, 838
 - collagenases, 818
 - combination therapy, 810–813
 - dispase (*see* Vitreolysin™)
 - distortions and vision loss, 804
 - drug delivery, 806–807, 810, 812, 813
 - eyes form brain dead human, transmission EM, 889
 - failed/discontinued agents, 801–803
 - FDA phase I/II study and its implications, 888, 890–891
 - human proof-of-concept study, 888
 - hyaluronan, 864–865
 - hyaluronidase, 818
 - intraocular hemorrhage management, 818
 - ocriplasmin, 804–806, 845
 - OCT-SLO, 805
 - ophthalmic therapeutics, 845
 - physiologic effects, 820–821
 - plasmin (*see* Plasmin)
 - plasmin enzyme, 846
 - preliminary monkey studies, 886–887
 - prevention, 813–814
 - PVD, 818–820
 - tPA (*see* Tissue plasminogen activator (tPA))
 - vision outcome measures, 810
 - visual acuity, 805
 - vitreous liquefaction, 867
- Pharmacotherapy, 229–230, 403–404
- Phosphate buffer solution (PBS), 87, 873, 874, 878
- Photodynamic therapy (PDT), 514
- Photopsia, 145
- Physical examination
- direct ophthalmoscopy, 198–199
 - indirect ophthalmoscopy, 199
 - optical transparency, 198
 - slit-lamp biomicroscopy (*see* Slit-lamp biomicroscopy)
 - Tyndall effect, 198
- Physiology. *See also* Vitreo-retinal physiology
- molecular transport, 438
 - oxygen, 439–443
- Pierre Robin sequence (PRS), 22
- Pierro, L., 119

- Pigment epithelium-derived factor (PEDF), 10, 11, 102, 413
- Pirie, A., 801
- Pischel, D.K., 361
- PKC. *See* Protein kinase C (PKC)
- Plasmin
 - affinity chromatography, 832
 - APE (*see* Autologous plasmin enzyme (APE))
 - biochemistry, 832
 - blood-derived molecule, 832
 - bovine, 819
 - diabetic macular edema, 821
 - ex-vivo* human experimental models, 834–835
 - hyaluronidase, 833
 - intravitreal, 818–819
 - lyophilized human plasmin, 832
 - rabbit model, 832–833
 - streptokinase-activated plasminogen, 932
 - tPA, 819
 - truncated form, 819–820
- Platelet-derived growth factor (PDGF), 47, 155, 157, 161, 162, 317, 531
- Platelet-derived growth factor-BB (PDGF-BB), 155
- Platelet derived growth factor receptor α (PDGFR α), 402
- Platelet endothelial cell adhesion molecule (PECAM), 50
- Platelet endothelial cell adhesion molecule 1 (PECAM-1), 418
- PLGA. *See* Poly lactic co-glycolic acid (PLGA)
- Plus disease, 225
- PMM. *See* Premacular membrane (PMM)
- Pneumatic retinopathy (PR)
 - advantages and disadvantages, 726
 - benefits, 765
 - complications, 765
 - contraindication, 759
 - description, 725
 - examination, 759
 - intravitreal bubble injection, 760–761
 - lattice degeneration, 759
 - modifications, 762–763
 - non-classical indications, 764
 - patient selection, 758
 - post-operative positioning, 761–762
 - and PVD, 758
 - reattachment rate, 764
 - for retinal detachment, 725, 726
 - retinal detachments, 758
 - retinopathy (*see* Retinopathy)
 - and rhegmatogenous RD, 757
 - Schepens binocular indirect ophthalmoscope, 758
 - scleral buckle and vitrectomy, 396
 - single operation anatomical success rate, 726
 - SOS and SB, 758
 - uncomplicated retinal detachment, 715, 758
 - and vitrectomy, 725
 - vitreal hemorrhage, 758
- PO₂. *See* Partial pressure of oxygen (PO₂)
- Polyalkylimide, 86–89
- Poly-dimethylsiloxane (PDMS), 544–546
- Polyethylene glycol (PEG), 87
- Poly lactic co-glycolic acid (PLGA), 517
- Ponsioen, T.L., 8
- Port delivery system, 518
- Posterior chamber intraocular lens (PCIOL), 735–736
- Posterior PFV
 - Bergmeister's papilla, 233
 - macular abnormalities, 233
 - malformations, 233
 - optic nerve head abnormalities, 234
 - persistent hyaloid artery, 233
 - retina and retinal detachment, 233
- Posterior subcapsular cataract (PSC), 124
- Posterior tunica lentis (ttl)*, 97
- Posterior vitreous cortex (PVC), 181, 266, 312, 609, 614
 - anterior vitreous cortex, 132
 - collagen fibrils, matrix, 133
 - fibroblasts, 185
 - hyalocytes, 182–185
 - lamellar organization, 133
 - structure, 181–185
 - vitroschisis, 133
- Posterior vitreous detachment (PVD), 118, 159–160, 176, 182–183, 187–188, 384, 609
 - acute, 715
 - aging, 16, 248–249, 306, 316
 - and AMD, 450–452
 - anomalous, 146, 148, 471, 882
 - “atrophic holes”, 714
 - blunt trauma, 251
 - cadaveric normal eye remnants, 415
 - cataract surgery, 250–251
 - CD68, 281
 - central vitreous liquefaction, 65
 - clearance of molecules, 444
 - clinical presentation, 144–146
 - collagen, 64
 - cutter/suction catheter at disc, 739
 - diabetes, 64
 - diabetic macular edema, 448
 - diabetic vitreopathy, 71
 - diagnosis (*see* Diagnosis, PVD)
 - early stages, OCT, 146, 147
 - enzymatically-induced, 471
 - enzymatic vitreolysis, 414
 - epidemiology, 141
 - etiologies, floaters, 772–774
 - exudative AMD, 471
 - eyes with symptomatic, 716–717
 - GEA, 307–308
 - 20G vitrectomy, 87
 - hyaluronidase, 865–867
 - idiopathic, 320
 - induced bleeding, 489
 - induction, 71, 870–876, 878
 - intraocular oxygen, 471, 473
 - last stages, schematic representation, 145
 - liquefaction, 801
 - macular edema, 65, 449
 - macular surface attachment, 854
 - mid-life, 444
 - MIVI-IIT, 857
 - myopia, 251
 - neovascularization and aggressive PDR, 65
 - non-ischemic cases, 415
 - ocriplasmin, 783
 - oxygen transport, 445, 449
 - partial, 485
 - pathophysiology, 141–144, 288, 316–318
 - penetrating trauma, 251
 - phakic eyes, 758, 759
 - pharmacologic vitreolysis, 73
 - pO₂ levels, cataract, 453
 - premacular membranes, 281
 - preoperative PVD induction, 856

- Posterior vitreous detachment (PVD) (*cont.*)
- preset lens biomicroscopy, 144
 - prevalence, 415
 - prophylactics, 813
 - “pseudopapilledema”, 302
 - pseudophakic patient, 759
 - retinal vein occlusions, 473
 - safety and efficacy, 857
 - stage IV macular holes, 274
 - symptoms, 714
 - time course, 146
 - tPA, 827–828
 - in type 1 Stickler syndrome, 26
 - VEGF clearance, 445
 - vitreo-macular traction, 73
 - vitreo-papillary adhesion, 302
 - vitreoretinal adhesion, 772
 - vitreo-retinal adhesion and vitreous liquefaction, 248
 - vitreo-retinal traction, 870
 - Vitreosolve[®], 803
 - and vitreous aging, 84 (*see also* Vitreous aging)
 - vitreous and iris neovascularization, 487–489
 - vitreous collagen, 271
 - vitreous cortex and ILM adhesion, 301
 - vitreous liquefaction, 714
 - vitreous type II collagen, 870
- Post gestational day (PGD), 43, 44
- Postmenstrual age (PMA), 228
- Post-operative complications
- AHFVP, 642
 - conjunctiva, 641
 - cornea, 641
 - fibrinoid syndrome, 642
 - intraocular pressure elevation, 641
 - uveitis/iritis, 641
 - vitreous hemorrhage, 641
- PPV. *See* Pars plana vitrectomy (PPV)
- PR. *See* Pneumatic retinopexy (PR)
- Predominantly effusive detachment, 226
- Predominantly tractional detachment, 226
- Preferred practice pattern (PPP)
- phakic non-fellow eyes, 718
 - prevent rhegmatogenous RD, 716
- Premacular membrane (PMM), 123, 158–160, 858
- central retinal thickness, 573
 - centripetal contraction, 579
 - complex, 314
 - definition, 312
 - formation and retinal thickening, 123
 - hyalocytes, 315
 - idiopathic macular holes, 160
 - and ILM, 580, 596
 - ILM specimens, 575
 - internal limiting membrane, 636
 - laminocytes, 314
 - macular pucker, 314–316
 - OCT, 591
 - posterior vitreous cortex, 316
 - preretinal macular fibrosis, 320
 - visual acuity, 320
- Premature infant
- stage 2 ROP, 225
 - stage 3 ROP, 225
- Premature synchysis, 118
- Preretinal membrane
- bimanual technique, 741
 - removed under PFCL, 743
 - typical star fold configuration, 733
 - vitreous, 740
- Preretinal PVR membranes
- contraction, 400
 - transformed RPE cells, 400
- Preset lens biomicroscopy, 202
- Prethreshold ROP, 225
- Primary open angle glaucoma (POAG)
- oxygen and, 469–470
 - vitreous and cataract surgery, 470–471
- Primary vitreous
- mesodermal cells, 97–98
 - monocyte-lineage hyalocytes, 97
 - optic cup and lens vesicle, 97
 - persistent primary vitreous, 103
 - PHPV/PFV, 103–104
 - primordial vitreous, 97
 - regression of hyaloid vasculature, 98
- Prinomastat (AG3340), 531
- Pro-apoptotic proteins (Bax and Bak), 44
- Profilin-1, 50
- Prolactin (PRL), 45
- Proliferative diabetic retinopathy (PDR), 152, 156–161, 888, 892
- complications, 63, 65, 75, 487
 - detached PDR retina, 491
 - florid neovascularization and aggressive, 65
 - and LPA, 48
 - retinal detachments, 726
 - vitrectomy, 487
 - vitreoschisis, 66
- Proliferative diabetic vitreo-retinopathy (PDVR), 828
- adhesive molecules, 425
 - Airlie House classification, 426
 - angiogenic growth factors, 424, 425
 - biochemical abnormalities, 424
 - classifications, 421–422
 - clinical and experimental investigations, 424
 - diabetes, 424
 - endothelial cells, 424–425
 - hematopoietic system, 424, 425
 - ICDRS Scale, 426, 427
 - Kroll’s classification, 426–431
 - Müller cells, 425
 - and NPDR, 425–426
 - panretinal photocoagulation, 425
 - pathogenesis, 421, 432
 - posterior vitreous cortex, 424
 - serum proteins, 424
 - therapeutic considerations, 430
 - thickening, 424
 - tPA, 828
- Proliferative vitreoretinal diseases
- cicatricial contraction, 157–158
 - macular holes, 160
 - Macular Pucker, 158–160
 - proliferative membranes, formation, 157
- Proliferative vitreoretinopathy (PVR), 152, 156–161, 176, 185
- adjunctive agents, 527–532
 - anterior and posterior proliferation, 749
 - anterior loop, 750, 752
 - anti-inflammatory agents, 528–529
 - biopolymers, 704
 - cell proliferation inhibitors, 529–531
 - cell types, 396
 - classification, 524 (*see also* Classification system, PVR)

- clinical signs and staging, 396–399
 - complications, 755–756
 - contractile cellular membranes, 731
 - contraction type and location, 749, 750
 - cytokines, 395
 - description, 524
 - extracellular matrix modifiers, 531–532
 - fibrous contractile membranes, 395
 - formation of, 731–732
 - grades, 524–526
 - histopathology, 399
 - human vitreous base, 750, 751
 - pathophysiology, 750–751 (*see also* Pathophysiology, PVR)
 - pharmacologic vitreolysis, 756
 - pharmacotherapy, 403–404
 - post-operative, 539
 - pre-and post-operative risk factors, 732
 - retinal detachments, 726
 - retinal pigment epithelial cells, 395
 - retinotomy and retinopexy, 751–753
 - rhegmatogenous RD, 396
 - risk factors, 396
 - small-gauge vitrector, 752
 - surgical, 403, 756 (*see also* Surgical management, PVR)
 - vitrectomy failure, 728
 - vitreous, 740
 - vitreous substitutes (*see* Vitreous substitutes)
 - Prophylactic retinopexy, 36–37
 - Prophylaxis
 - The American Academy of Ophthalmology (AAO), 715
 - asymptomatic patients/autopsy series, 715
 - asymptomatic retinal breaks, 718
 - asymptomatic vitreo-retinal lesions, 718
 - eyes with symptomatic PVD, 716–717
 - prevalence of retinal breaks, 715
 - risk factors, 715–716
 - Protein. *See also* Collagen
 - extracellular matrix proteins (*see* Extracellular matrix)
 - glycoproteins, 9–11
 - plasma, 3
 - in vitreous (*see* Vitreous)
 - Protein kinase C (PKC), 416
 - activated, 60
 - diabetes, pathological pathways, 58
 - physiologic activator, 60
 - Protein kinase C diabetic retinopathy study (PKC-DRS), 60
 - Proteoglycan
 - chondroitin sulphate, 9
 - heparan sulphate, 9
 - type IX collagen, 6
 - and vitreo-retinal interface, 882–884
 - vitreous, 16
 - Proteomics
 - acellular collagenous secondary vitreous, 43
 - connective tissue pathway, 45–46
 - embryonic human vitreous, 48
 - IPA bioinformatic analysis, 44
 - murine model of vitreous embryogenesis, 44–46
 - reactive oxygen species, 43
 - small molecule-dependent regulation, 43
 - Provis, J.M., 95–108
 - Pseudohole, 290–291
 - lamellar macular holes, 577
 - macular pseudoholes (*see* Macular pseudoholes)
 - PTX-3. *See* Pentraxin 3 (PTX-3)
 - Pupillary membrane (*pm*), 97–99, 102
 - endothelial cells, 47
 - hyaloid vasculature, 46–47
 - lens and tunica vasculosa lentis, 42
 - regression, 42, 47
 - tunica vasculosa lentis extension, 42
 - vasa hyaloidea propia and, 42
 - Pure air
 - bullous detachments therapy, 760
 - long-acting gas, 725
 - lower incidences, PVR and PMM, 763
 - non-expansile nature, 760
 - office-based, 539
 - PVC. *See* Posterior vitreous cortex (PVC)
 - PVD. *See* Posterior vitreous detachment (PVD)
 - PVR. *See* Proliferative vitreoretinopathy (PVR)
- Q**
- Quay, W.B., 558
 - Quellic, G., 426
 - Quinn, G.E., 117
 - Quiram, P.A., 442, 471, 746
- R**
- Radial optic neurotomy (RON)
 - central foveal thickness, 652
 - compartment syndromes, 650
 - complications, 653
 - CRVO, 650
 - long-term follow-up, 653
 - macular edema, 652
 - pre-operative biomicroscopy, 651
 - retinochoroidal collaterals, 651
 - shunt vessels, 652
 - Radial optic neurotomy for central vein occlusion (ROVO), 653–654
 - Raman spectroscopy, 215–216
 - Ranchod, T.M., 234, 235
 - RAS. *See* Renin-angiotensin system (RAS)
 - RBX. *See* Ruboxistaurin (RBX)
 - RD. *See* Retinal detachment (RD)
 - Reactive oxygen species (ROS)
 - apoptosis, 43
 - cell defenses, 60
 - Receptor for advanced glycation end products (RAGE)
 - activation, 60
 - expression, 59
 - in ILM, 65
 - pathway blockage, 71
 - Redslob, E., 194, 195
 - Reese, A.B., 324, 364
 - Reeser, F.H., 182
 - Refillable delivery systems, 518
 - Renin-angiotensin system (RAS), 415
 - Re-operation
 - cellular tissue, 622
 - macular hole, 619, 620
 - Müller cells, 619
 - retinal nerve fiber layer, 619–621
 - timing, 619
 - Retina
 - and ciliary body, 349
 - excavation, 351
 - posterior indentation, 350
 - vitreous base, 350

- Retina endovascular surgery (REVS)
 - neuro-radiologic approach, 654
 - tissue plasminogen activator, 655
 - vitreoretinal approach, 654
- Retinal adhesion
 - flow conductivity, 383
 - measurement, 380–381
 - in vivo* and post-enucleation, 381
- Retinal artery occlusions (RAO)
 - CRAO, 648
 - EAGLE study, 648–649
 - embolectomy, 649–650
 - local intra-arterial fibrinolysis, 648
 - non-arteritic retinal artery occlusions, 648
- Retinal detachment (RD). *See also* Rhegmatogenous retinal detachment (RRD)
 - age-related changes, 376
 - anomalous PVD and retinal tears, 120
 - bilateral total, 32
 - blood-retinal barrier breakdown, 526
 - clear lens extraction, 119–120
 - congenital myopia and visual loss, 22, 24
 - developmental abnormalities, 388–389
 - DRRD/BRRD, 33
 - exudative (*see* Exudative retinal detachment)
 - fibrovascular proliferations, 631–632
 - with grade C PVR, 524, 526
 - high risk, 361, 532
 - hyaluronidase enzyme activity, 864, 866
 - inferior shortening of, 753
 - inherited, 22
 - macular hole, 119, 120
 - male patients, 364
 - mechanisms, 226–227
 - mediate retinal attachment, 375
 - molecular movement (*see* Molecular movement within and from vitreous)
 - neovascular membranes, 632
 - ocular tissues, 389–391
 - pathogenesis, 361, 375
 - pH, 381–382
 - phacoemulsification technology, 120
 - prophylaxis, 36–37
 - PRP, 632
 - PVR, 530
 - rate of RRD, 120
 - refractive corneal surgery & RD, 120
 - retinal adhesion (*see* Retinal adhesion)
 - rhegmatogenous, 28, 32, 355, 362, 524 (*see also* Rhegmatogenous retinal detachment)
 - risk, 24, 27
 - RPE, 376, 382–383
 - silicone oil, 632
 - Stickler syndromes, 23
 - structural factors, 376, 377
 - surface energy and electrostatic forces, 383
 - surgery, 524
 - traction RD, 528, 529, 531
 - traction retinoschisis, 358
 - treatment, 230
 - unselected primary, 532
 - vitreoretinopathy and, 31
- Retinal disorders
 - intraretinal cysts, 305, 306
 - macular diseases, 303–304
 - vascular disorders, 305–307
- Retinal folds, 358
- Retinal hypoxia
 - choroidal ischemia, drusen, and vitreoretinal adhesion, 452
 - clinical pathology, 479
 - and vitreous neovascularization, 479–480
- Retinal lattice, 119–120, 354–355
- Retinal microfolds, 122
- Retinal nerve fiber layer (RNFL), 615
- Retinal pigment epithelial transplantation
 - Bruch's membrane/choroid patch, 559–560
 - cell suspensions, 558–559
 - cytokines, 558
 - in human eyes, 558
 - ocular tissues, 558
 - outcomes, 560, 561
 - rationale, 557–558
 - subfoveal choroidal neovascularization, 558
- Retinal pigment epithelium (RPE), 30, 50, 97, 152, 153, 156–158, 267, 273, 288, 289, 293, 510, 517
 - actively dividing RPE cells, 530
 - after intravitreal administration, 706
 - apical RPE, 376
 - associated Leber's congenital amaurosis, 707
 - baso-lateral membranes, 383
 - cell proliferation, 530, 531
 - chemotaxis, 526, 531
 - circular elevations, 848
 - collagen and fibronectin, 526
 - dispersion, 526
 - HCO₃ transporters, 383
 - inhibition, 383
 - loss of adhesion, 381
 - migration and proliferation, 732
 - photoreceptor OS, 376
 - and retina, 375
 - trans-cellular water movement, 382
 - trans-RPE fluid movement, 383
 - VEGF receptors, 531
- Retinal pits, 359
- Retinal prosthesis
 - alpha IMS, 705, 708
 - Argus II, 705, 707
 - bioelectrical, 705
- Retinal tags, 358
- Retinal tear, 359–361
 - acute symptomatic PVD development, 716
 - anomalous persistent vitreo-retinal adhesions, 717
 - lattice and cystic tufts, 718
 - prophylactic therapy, 719, 721
- Retinal tear and detachment
 - indirect ophthalmoscopy, 783
 - intraoperatively/postoperatively, 782
 - intraoperative/postoperative retinal breaks, 783
 - myopic individuals, 146
 - prophylactic treatment, 719
 - PVD, 719
 - self-retaining cannulas, 782
- Retinal toxicity, 543–544
- Retinal traction, 698
- Retinal tufts
 - cystic retinal tufts, 352–353
 - non-cystic retinal tufts, 351–352
 - zonular traction tufts, 353–354
- Retinal vein occlusion (RVO), 288
 - and autologous plasmin enzyme, 842
 - classification, 409
 - complications, 409
 - crystallins, 414

- definition, 408
 - description, 650
 - epidemiology, 408
 - inflammatory and angiogenic proteins, 411–414
 - pathogenesis and risk factors, 409
 - RON (*see* Radial optic neurotomy (RON))
 - symptoms, 409
 - tPA, 828
 - Retinoblastoma
 - diagnosis, 364
 - FEVR, 234
 - pars plana vitrectomy, 790
 - treatment, 790
 - vitrectomy, 790
 - Retinoids
 - cell proliferation regulation, 530
 - clinical evidence, 530
 - preclinical evidence, 530
 - Retinopathy of prematurity (ROP)
 - and autologous plasmin enzyme, 841–842
 - childhood blindness in the United States, 224
 - classification, 224–226
 - kitten ROP model, 482, 488, 490
 - oxygen, 224, 479
 - pathophysiology, 226–227
 - preterm infant, 224
 - prevention, 228
 - retinal re-vascularization, 482
 - risk factors, 227
 - treatment, 226–228
 - “vaso-obliterative phase”, 479
 - Retinopexy
 - cryopexy, 759–760
 - diathermy, 759
 - laser photocoagulation, 760
 - and retinotomy, 751–753
 - Retinoschisis, 122–125
 - Retrolental membrane, 233
 - Reverse transcription polymerase chain reaction (RT-PCR), 35, 36
 - Rhegmatogenous retinal detachment (RRD), 22, 28, 32, 33, 120, 396, 524. *See also* Pneumatic retinopexy (PR)
 - atrophic, 714, 715
 - binocular indirect ophthalmoscope, 723
 - considerations, 724
 - eye movements, vitreoretinal traction forces, 714
 - fibrous tissue formation, 384
 - inferior retinal breaks, 759
 - internal tamponade, 760
 - intravitreal air bubble, 757
 - pathogenesis, 714
 - in phakic eyes, 758
 - posterior vitreous detachment (PVD), 714
 - PR (*see* Pneumatic retinopexy (PR))
 - prophylaxis (*see* Prophylaxis)
 - pseudophakic, 758
 - PVR development, 732
 - reattachment surgery, 758
 - scleral buckling (*see* Scleral buckle (SB))
 - surface diathermy cauterization, 759
 - surgery for complicated, 728
 - synchisis, syneresis and vitreous currents, 387–388
 - and tractional, 732
 - treatment, 759
 - uncomplicated, 723–724
 - vitrectomy (*see* Vitrectomy)
 - vitreous, 384
 - vitreous degeneration, 384–386
 - vitreous liquefaction, 714
 - vitreous traction (*see* Vitreous traction)
 - Rhodes, R.H., 184
 - Rho kinase (ROCK), 157, 161, 317
 - Ribonucleic acid (RNA)
 - coding errors, 529
 - encapsulation of, 706
 - zinc finger nucleases, 707
 - Rice, T.A., 632
 - Richards, A.J., 21–37
 - Richdale, K., 500
 - Rizzo, S., 838
 - Robertson, D.M., 361
 - Robison, C.D., 254
 - Robotic vitreo-retinal surgery
 - invasiveness and iatrogenic complications, 704
 - prototype for, 704, 706
 - setup, 704, 705
 - ROCK. *See* Rho kinase (ROCK)
 - Rodrigues, E.B., 421–433
 - Rohen, J.M., 498
 - Romano, M.R., 304, 547, 580
 - ROP. *See* Retinopathy of prematurity (ROP)
 - ROS. *See* Reactive oxygen species (ROS)
 - Rosengren, B., 538, 723, 757, 759
 - Ross-Cisneros, F., 613–622
 - Rossi, T., 212
 - Royo, P.E., 558
 - RPE. *See* Retinal pigment epithelium (RPE)
 - RRD. *See* Rhegmatogenous retinal detachment (RRD)
 - RT-PCR. *See* Reverse transcription polymerase chain reaction (RT-PCR)
 - Ruboxistaurin (RBX), 60
 - Russell, S.R., 135, 188, 802, 881–893
 - Rutnin, U., 253, 353, 355, 360, 361
 - RVO. *See* Retinal vein occlusion (RVO)
 - Ryan, S., 683
- S**
- Sadun, A.A., 41–52, 299–308, 613–622, 771–785
 - Saito, Y., 467
 - Sakaguchi, H., 119
 - Sakamoto, T., 151–162
 - Sakuma, T., 842
 - Salzmann, J., 167
 - Sandoval, M., 228
 - Sawa, M., 467
 - Saw, S.M., 119
 - Scanning electron microscopy (SEM), 49
 - Scanning laser ophthalmoscope (SLO), 203, 658–659
 - Schachar, R.A., 498, 500
 - Scheie, H.G., 355
 - Schepens, C.L., 202, 234, 316, 353, 355, 356, 360, 361, 758–760
 - Schiff, W.M., 630
 - Schlesinger, T., 791
 - Schmidt, D., 648
 - Schmidt, J.C., 452
 - Schulze, S., 451, 452, 828
 - Schumann, R.G., 265–285
 - Schwalbe, G., 182
 - Schwartz, D., 399
 - Scleral buckle (SB), 230
 - advantages and disadvantages, 725
 - description, 714

- Scleral buckle (SB) (*cont.*)
 functional closure, retinal breaks, 724
 and PPV, 763–764
 and reduced tissue trauma, 758
 for retinal detachment, 724, 725
 surgical management, PVR, 736–738
 Scleral depression, 399
 SDF-1. *See* Stromal cell-derived factor 1 (SDF-1)
 SD-OCT. *See* Spectral-domain optical coherence tomography (SD-OCT)
 SDS-PAGE. *See* Sodium dodecyl sulfate-polyacrylamide gel electrophoresis (SDS-PAGE)
 Sebag, J., 14, 41–52, 57–75, 81–89, 131–148, 160, 165–188, 193–217, 241–259, 267, 299–308, 311–325, 330–331, 347–369, 415, 424, 438, 442, 444, 539, 580, 590, 613–622, 757–766, 771–785, 799–814, 827, 835, 838, 886, 888
 Secondary vitreous
 bundle of Druault or “*faisceau isthmique*”, 100
 continuous and gradual remodeling method, 99
 intravitreal membrane (*ivm*), 98, 99
 syndromic disorders, 104–105
 zonular system, 101
 SEDC. *See* Spondyloepiphyseal dysplasia congenita (SEDC)
 Seltner, R.L., 117
 SEM. *See* Scanning electron microscopy (SEM)
 Sequelae, 367–369
 Serum response factor (SRF), 51
 Sévin, R., 426
 Shah, S.U., 699–709
 Shaken Baby Syndrome, 251
 Sheathotomy, 655
 Shen, M., 499
 Sheppard, A.L., 499
 Sherar, M., 208
 Shimada, H., 575, 617
 Shimizu, K., 195, 482
 Shi, Y., 505
 Short-acting vitreous substitutes
 aqueous, 538
 gaseous (*see* Gaseous vitreous substitutes)
 Shui, Y.-B., 459–473
 Shukla, D., 235
 sICAM-1. *See* Soluble intercellular adhesion molecule 1 (sICAM-1)
 Siegfried, C.J., 453, 461, 471, 472
 Silicone oil (SiO)
 ACIOL, 736
 buoyancy, 545
 chemical properties, 544
 fluid/PFCL-silicone oil exchange, 744
 intraocular tamponade, 744–745
 peripheral iridectomy, 746
 recurrent retinal detachment, 746
 sclerectomies, 745
 specific gravity, 544–545
 surface tension and interfacial tension, 545–546
 viscoelasticity, 547
 viscosity, 546–547
 Silverman, R.H., 193–217, 249, 495–505
 Simpson, A.R., 215, 442, 443
 Sín, M., 437, 444
 Sivaprasad, S., 448
 Slit-lamp biomicroscopy
 anterior vitreous, 200
 contact lens, 202
 neoplastic diseases, 200
 posterior pathology, 200
 preset lens, 202
 Tyndall effect, 200
 vitreous transparency, 200
 SLRP. *See* Small leucine-rich repeat proteoglycan (SLRP)
 Small gauge instrumentation, 700
 Small leucine-rich repeat proteoglycan (SLRP) family, 9–10
 Smiddy, W.E., 257, 361
 Smith, R.E., 360
 α -Smooth muscle actin (α -SMA), 157, 159, 161, 317
 Snead, D., 314, 315
 Snead, M.P., 21–37
 Snowflake vitreo-retinal degeneration (SVD), 32
 Sodium dodecyl sulfate-polyacrylamide gel electrophoresis (SDS-PAGE), 9–10
 Sodium hyaluronate acid hydrogel, 86
 Soluble intercellular adhesion molecule 1 (sICAM-1), 413
 Soluble VEGF receptor 2 (sVEGFR-2), 413
 Spaide, R.F., 585
 Spectral-domain optical coherence tomography (SD-OCT), 411, 415, 572
 anterior segment *in vivo*, 205
 grating-based, 203
 posterior precortical vitreous pocket *in vivo*, 204
 posterior vitreous detachment *in vivo*, 204
 reference mirror and sample, 203
 and SLO, 776
 time-domain OCT, 776
 Spencer, L.M., 186, 350, 351, 357, 359
 Spondyloepiphyseal dysplasia congenita (SEDC), 27–29, 33
 Spreading, agent, 864
 Srinivasan, V.J., 203–204
 Stachs, O., 500
 Stalmans, P., 853–861
 Stambolian, D., 116
 Starling, E.H., 446
 Stefánsson, E., 437–453
 Steinhilber, U.H., 554, 556, 565
 Steinmetz, R.I., 632
 Stein, R., 357
 Sternberg, P., 888
 Stickler syndrome, 253, 388
 diagnosis and differential diagnosis, 23–24
 epidemiology, 23
 gene selection and mutation analysis, clinical algorithm, 24
 hearing loss, 25
 inherited retinal detachment, 22
 joint hypermobility and dysplasia, 26
 musculoskeletal features, 25–26
 “ocular-only” Stickler syndrome, 27
 ophthalmologic features, 24
 oro-facial features, 24–25
 posterior vitreous detachment in type 1, 26
 profound deafness, 27
 type 1, 26
 type 2, 26
 type 3 “non-ocular”, 27
 type 4, 5 and 6 Stickler syndrome, 27
 unresolved, 27
 vitreous phenotypes, schematic illustration, 25
 Stürpe, M., 118–119
 Stolba, U., 545
 Stopa, M., 565
 Straatsma, B.R., 354, 355
 Straylight glare, 781
 Strenk, S.A., 498, 500
 Stromal cell-derived factor 1 (SDF-1), 417

- Subconjunctival hemorrhage, 829
- Submacular hematoma, 827
- Submacular hematoma surgery
 complications, 565
 description, 561
 intraocular gas bubble, 565–566
 subretinal cannulas, 564
 techniques, 564–565
 tPA, 563–564
- Submacular surgery
 CNV, 554–555
 complications, 555–556
 indications, 554–555
 instrumentation, 554
 outcomes, 556
 perfluorocarbon liquid, 555
 retinal detachment, 555
 retinotomy, 555
 trauma and PVR, 554
- Subretinal fibrosis, 396
- Subretinal hemorrhage, 826–827
- Sulfur hexafluoride (SF₆), 758, 760, 761
 expansion, 541
 intraocular tamponade, 744–745
 intravitreal injection, 827
 macular area, 826
 non-expansile concentration, 539
 nonpolar gas, 761
 and perfluoropropane, 756
 phakic non-vitreomized eyes, 542
 physical properties, 539
 silicone oil, 744
 vitreous, rabbits, 826
- Sullu, Y., 181
- Supplemental Therapeutic Oxygen for Prethreshold ROP (STOP-ROP) study, 228
- Surface ectoderm (*se*), 96
- Surgical complications
 corneal opacification, 640
 intraocular hemorrhage, 640
 lens, 640
 pupil size/miosis hampers, 640
 retinal breaks and detachment, 641
 subretinal infusion, 640–641
- Surgical management, PVR
 anterior membranes and vitreous cortex, 735
 corneal opacities, 735
 fluid/PFCL-silicone oil exchange, 744
 iris hooks, 735
 lens removal, 736–737, 739
 PCIOL and ACIOL, 736
 PFCL removal, 743–744
 post-operative management, 745–746
 pre-and post-operative management, 734
 prognosis, 746
 relaxing retinotomies and retinectomies, 742
 retina reattachment, 742–743
 scleral buckle, 737–738
 vitrectomy, 739–740
- Surgical procedures
 chromodissection, 634
 equipment, 633–634
 instruments, 634
 internal tamponade, 634
 microscope, 633
 preparation and anesthesia, 633
 vitrectomy machine, 633–634
 wide-angle lens systems, 634
- Sustained drug release
 encapsulated cell technology, 516–517
 implants, 515–516
 intravitreal injectables, 518
 iontophoresis, 518
 liposomes, 517
 microspheres, 517
 porous silicon particles, 517
 suprachoroidal micro-injection and microneedles, 517–518
- SVD. *See* Snowflake vitreo-retinal degeneration (SVD)
- sVEGFR-2. *See* Soluble VEGF receptor 2 (sVEGFR-2)
- Swann, D.A., 83, 184
- Swanson, E.A., 203
- Symptomatic vitreo-macular adhesion (sVMA)
 MIVI-I, 855–856
 MIVI-III, 857
 MIVI-IIT, 856–857
 phase 3 trials, 857–859
- Synchysis, 387–389
- Synchysis senilis*, 132, 136
- Syneresis, 140, 387–388
- Szent-Györgi, A., 194
- T**
- Tadayoni, R., 585
- Tai, H., 86
- Takahashi, M.K., 415
- Tanenbaum, H.L., 316
- Tano, Y., 441, 528, 556
- Tansley, K., 558
- Task-specific features, 700
- Tasman, W., 360
- TEM. *See* Transmission electron microscopy (TEM)
- Teng, C.C., 248, 357
- Terasaki, H., 448, 837–843
- Terminal deoxynucleotidyl transferase (TUNEL), 89
- Tertiary vitreous, 95
- Tezel, T.H., 869–878
- TGF-β2. *See* Transforming growth factor beta-2 (TGF-β2)
- Theodossiadis, G.P., 361, 362
- Theodossiadis, P.G., 514, 579
- Thomas, M.A., 554
- Thompson, J.D., 632
- Three-chambered system, 495
- Three dimensional (3D)
 flexible “mucoadhesive” hydrogel, 705
 interactive AR system, 703
 localization, 704
 volumetric computed tomography map, 702
- Three-dimensional threshold Amsler grid (3D-TAG), 325
- Threshold ROP, 225
- Thrombospondin-1 (TSP-1), 11
- Thrombospondin (TSP/THBS), 11, 48
- Tiedeman, J.S., 556
- Tillery, W.V., 355
- Time autocorrelation function (TCF), 217
- Tissue-dye interaction, 607–608
- Tissue inhibitors of metalloproteases (TIMPs), 118, 531
- Tissue plasminogen activator (tPA)
 biochemical, 826
 description, 563
 enzymes, ophthalmology, 825
 extensive post-operative fibrin, 746

- Tissue plasminogen activator (tPA) (*cont.*)
 intravitreal gas, 818
 intravitreal injection, 826–827
 ophthalmic indications and applications, 827–829
 plasmin, 819
 retinal toxicity, 563
 SF6 gas co-injection, 826
 submacular blood clot, 826
 submacular hemorrhage, 818
 subretinal hemorrhage, 826–827
 subretinal injection, 563
 toxic side effects, 827
- TNF. *See* Tumor necrosis factor (TNF)
 TNF α . *See* Tumor necrosis factor 1 (TNF α)
 Tognetto, D., 615
 Toth, C.A., 452, 556
 Tozer, K., 131–148, 309–322
 tPA. *See* Tissue plasminogen activator (tPA)
 Tractional retinal detachment (TRD)
 rabbits, 528, 529, 531
 Traction vs. adhesion, 336–337
 Transferrin ricin-A (Tfr-rRA), 531
 Transforming growth factor- β (TGF- β), 11, 44, 155, 157–159, 161
 Transforming growth factor beta-2 (TGF- β 2), 317
 Trans-ILM diffusion
 cell migration, 187
 from chorio-retinal compartment to vitreous, 187
 viral penetration into retina, 187
 vitreous-ILM adhesion, 187–188
 from vitreous to retina and choroid, 187
 Transmission electron microscopy (TEM), 49, 167–168, 889
 Transplantation
 human eyes, RPE, 558
 ocular tissues, 558
 RPE (*see* Retinal pigment epithelial transplantation)
 Transport
 molecular transport, vitreous, 438–439
 molecules, vitreous cavity, 442
 oxygen, eye, 439, 441
 VEGF, 445
 water, vascular and tissue compartment, 446
 Treatment failure, 229, 617
 Trese, M.T., 235, 841
 Triamcinolone acetonide, 513, 514, 517, 518
 and ranibizumab combination, 518
 sterile endophthalmitis, 511
 Tricarboxylic acid (TCA), 58
 Trypan blue, 603–604
 Tscherning, M., 496
 Tsukahara, Y., 842
 Tumor
 malignant melanoma, 790
 retinoblastoma, 790
 suppressor proteins p16, 51
 vascular tumors, 790–791
 Tumor necrosis factor 1 (TNF α), 417
 Tumor necrosis factor (TNF), 514
 Tumor necrosis factor- α (TNF- α), 157, 161, 402
 Tumor necrosis factor- β (TNF- β), 402
 Tunica vasculosa lentis (TVL), 42–43, 99–101, 155
 Turner, F.T., 208
 Type 1 ROP, 225
 Type 2 ROP, 226
 Type IV collagen
 fibronectin and, 870, 871, 874
 ILM, 870
- U**
 Udaondo, P., 838, 842
 UK Genetic Testing Network, 23
 Ulanski, L.J., 500
 Ultrasonography. *See* Acoustic imaging
 Ultrasound imaging
 incomplete posterior vitreous detachment, 213
 PVD, 249
 SD-OCT, 210
 Ultrastructure, ILM
 AFM, 167–168
 basement membrane (BM), 167
 central meniscus of Kuhnt, 169
 confocal microscopy, 168
 glycosaminoglycans of proteoglycans, 168
 membrana limitans interna, 167
 TEM, 169
 Ultraviolet (UV), 65, 117
 Urokinase-type plasminogen activator (uPA), 155
 Uveitis
 Cidofovir, 513
 intravitreal methotrexate, 513
 macular edema, 513
 noninfectious, 514
- V**
 van Alphen, G.W., 498, 501
 VanderVeen, D.K., 228
 Van Meurs, J.C., 559, 560
 van Nouhuys, C.E., 235
Vasa hyaloidea propia (*vhp*), 42, 97, 98, 230, 231
 Vascular cell adhesion molecule 1 (VCAM-1), 66
 Vascular disorders, retinal disorders
 central retinal vein occlusion, 307
 diabetic vitreo-retinopathy, 306
 peripapillary, subretinal and intrapapillary
 hemorrhage, 305, 306
 Vascular endothelial growth factor (VEGF), 47, 48, 50, 85, 121, 157,
 161, 187, 226
 abnormal new vessel proliferation, 62
 accumulation and neovascularization, 452
 activated PKC, 60
 and AMD, 828
 angiogenic growth factor, 344
 antibodies, vitreous gel, 445
 anti-VEGF agents, 510, 511, 514–515
 anti-VEGF therapy, 341, 342
 blood plasma, 426
 BRVO eyes, 414
 clearance, 444
 CRVO, 412
 cytokines, 413
 diabetes, pathological pathways, 58
 in diabetic eye, 61
 diabetic vitreopathy, 63–64
 DR, 61, 66
 exudative AMD, 450
 hyaluronan, 64
 hypoxia, 417
 inflammation, 450
 inhibitor proteins, 707
 ischemic areas, 425
 and macular edema, 447
 mediated retinopathies, 471–473
 oxygenation, 451

- and photocoagulation, 448
- production, 61, 342
- retina, 442
- retinal neovascularization, 445
- retinal pigment epithelium, 828
- RPE cells expressed, 531
- serous detachment, CRVO, 413
- signalling, 490
- vascular leakage, 446
- VEGF₁₆₅, 489
- VEGF-A, 102
- vitrectomized eyes, 445, 448
- vitreous concentration, eyes, 490
- Vascular endothelial growth factor receptor (VEGFR), 489, 490
- Vascular regression, 102
 - anti-angiogenesis, 48–49
 - apoptosis, 43–46
 - autophagy, 48
 - external stimuli, 49
 - hyaloid, 43, 44
 - macrophagy, 46–47
- Vascular stages, ROP, 224–225
- Vascular tumors, 790–791
- Vasculopathies
 - Coat's disease, 364, 366–368
 - indirect ophthalmoscopy, 361
 - sickle cell, 362–364
 - three-mirror Goldmann contact lens, 361
 - tractional avulsion, 361–362
- Vedder, H.-J., 682
- VEGF. *See* Vascular endothelial growth factor (VEGF)
- VEP. *See* Visual evoked potential (VEP)
- Verhoeven, V.J.M., 116
- Versican and link proteins, 9
- Verstraeten, T.C., 826, 827, 831–835, 838
- VFQ quality of life questionnaire, 782
- VHP. *See* *Vasa hyaloidea propia* (*vhp*)
- Victori, M.A.Z., 647–660
- Villain, F., 687
- Vine, A.K., 362
- Virchow, H., 772
- Virchow, R., 14
- Viscosity
 - rate of diffusion is, 438
 - vitreous, 438–439, 444
- Visual evoked potential (VEP), 306
- Visual Function Questionnaire (VFQ-25) score
 - secondary efficacy end points, 858
 - vision-related quality-of-life, 860
- Vitrectomy, 158, 160, 230, 236, 655
 - advantages and disadvantages, 728
 - aspiration, 701
 - biomicroscope, 667
 - blood vessel, 666
 - cannula placement, 739
 - and cataract, 452–453
 - cataracts, 783–784
 - cataract surgery, 576, 667
 - contrast sensitivity, 781–782
 - cutting, 701
 - decrease, light scattering, 781
 - endolaser photocoagulation, 639
 - endophthalmitis, 782
 - flow and cut rates
 - cutting efficiency and duty cycle, 694
 - retinal surface, 696–697
 - velocities, 696
 - water vs. vitreous, 694
 - giant retinectomy with elevated, folded edges, 740
 - and glaucoma, 453
 - instrumentation, 680
 - and internal drainage, 562
 - intraocular oxygen tension, 467, 643
 - intraoperative visualization, 701–702
 - lamellar macular holes, 580
 - larger bore 20-gauge system, 739
 - macular hole, 614
 - macular pucker surgery, 576
 - and membrane peeling, 620, 755–756, 791
 - microincisional, 576
 - microsurgical instruments, 686
 - “microvit”, 683
 - MIVS, disadvantages, 739
 - MPC, 686
 - Nd:YAG laser treatment, 782
 - NEI VFQ-39, 781
 - ocular injury and diabetic retinopathy, 693
 - open angle glaucoma, 470
 - ophthalmic surgical instrumentation, 684
 - oxygen hypothesis, 467–468
 - oxygen level, 461
 - oxygen tension, anterior chamber angle, 471
 - pars plana phacoemulsifier, 687
 - pars plana vitrectomy, 635–636
 - pathophysiology, 789
 - perfluorcarbon, 639, 740
 - plastic syringe prototype, 673
 - posterior cortical vitreous, 740
 - posterior vitreous, 556, 636
 - posterior vitreous cortex, 555
 - post-vitrectomy eyes, 467
 - post-vitrectomy nuclear cataract, 467, 468, 470, 472, 473
 - preventive surgery, 700
 - proliferative vitreo-retinopathy (PVR), 687
 - prototype instrument, 671
 - PVD, 739
 - quality of life, 782
 - rabbit, 460
 - retinal breaks and detachments, 637–639, 726, 727, 782–783
 - retinal surgeons, 676
 - retinoblastoma, 790
 - safety and efficacy, 700
 - sclerotomies, 635
 - size, 700
 - stereophotogrammetry, 667
 - straylight values, 781
 - subconjunctival silicone oil prevention, 739
 - Submacular Surgery Trials, 472
 - subretinal cannula, 564
 - therapeutic goal, 789
 - thinnest suture material, 666
 - treatment, floaters, 779
 - tungsten halogen and xenon flash light sources, 682
 - VISC, 671
 - wound closure, 639
- Vitrectomy for prevention of macular hole study, 614
- Vitreo-foveal traction syndrome, 324
- Vitreolysin™
 - adult domestic pig flash ERG, 875
 - domestic pig's eye, 870
 - efficacy, 873–875

- Vitreolysin™ (*cont.*)
 extracellular neutral protease, 870
 induce posterior vitreous detachment, 871
 inhibition, 871
 and Ocriplasmin, 874
Paenibacillus polymyxa extract, 870, 872
 pharmacokinetics & pharmacodynamics, 871
 potential advantages, 873
 purification and toxicity, 872
 PVD induction, 878
 retinal cell viability effect and structure, 875, 876
 retinal electrophysiology, 878
 SDS-PAGE gels loaded, 873
 sensory retina mechanical properties, 876, 878
 stability, 873
 structure, 870–871
 substrate specificity, 870
 surgical removal, pathologic preretinal membranes, 871–872
- Vitreomacular adhesion (VMA)
 adherences and neovascular complex, 335
 adhesion vs. traction, 336–337
 concomitant retinal disease, 860
 definition and classification, 288, 289
 imaging (*see* Imaging)
 juxtafoveal adhesions, 335
 neovascularization, 336
 OCT imaging, 854
 PVD, 330, 331
 Spectralis OCT, 335
 and traction, 329, 338, 415
 vitreo-retinal adhesion, 289
 vitreous in unilateral exudative, 330, 331
- Vitreomacular interface (VMI), 288, 858
- Vitreomacular separation (VMS), 415
- Vitreomacular traction (VMT)
 age-related macular degeneration, 253–254, 821
 anomalous PVD., 293
 anterior vs. posterior split, 255–256
 B-mode OCT scan, 253, 581
 classification, 289, 290
 CME and macular cysts, 254
 definition, 253, 289, 290
 diabetic macular edema, 254
 focal traction, 590
 full-thickness macular hole surgery, 589
 irreversible damage, 854
 lamellar macular hole surgery, 582, 583
 macular hole, 257, 259, 810
 macular pucker, 256, 257, 259
 MIVI-I, 855–856
 MIVI-III, 857
 MIVI-IIT, 856–857
 outcomes, 593–598
 pharmacologic resolution, 857
 premacular membrane, 592, 606
 PVD, 609
 tangential traction, 590
 treatment, 609
 vitrectomy, 591, 854
 vitreoschisis, 255
 vitreous cortex, 596
- Vitreomacular traction syndrome (VMTS), 146, 302, 316, 324–325
 cell proliferation, 267, 268
in situ arrangement, cellular proliferation, 267, 269
 premacular fibrocellular tissue, 267, 270
 ultrastructural analysis, 267
 vitreoschisis, 267
- Vitreomaculopathies
 collagen fibrils dense network, 266
 epiretinal membranes (ERM), 266–267
 imaging techniques, 266
 macular hole (*see* Macular hole (MH))
 macular pucker, 267–273
 traction arising, 266
 traction syndrome (*see* Vitreo-macular traction syndrome (VMTS))
 vitreous cortex, ILM, 266
- Vitreopapillary adhesion (VPA), 255–257, 259, 291, 337, 338, 343
 CRVO, 307
 definition, 302, 303
 macular pucker, 305
 non-arteritic AION, 307
 optic nerve, 307
 papillo-foveal traction, 304
 prevalence, 303
- Vitreopapillary interface, 301
- Vitreopapillary separation, 146, 148
- Vitreopapillary traction, 302–303
- Vitreoretinal adhesion
 operculated tears treatment, 717
 symptoms of PVD, 714
- Vitreoretinal dehiscence, 251
- Vitreoretinal interface, 82, 247–248, 300–301, 870–871
 abnormal molecules, 835
 age-related differences, 142–143
 in animal models, 838
 chondroitinase, 802
 cortical vitreous fibers, 136
 cystic degeneration, 186–187
 extracellular matrix (ECM), 135
 gel liquefaction, 838
 glycosaminoglycans, 141, 802
 ILM, 141
 immunoreactivity, 835
 interfactants, 801
 laminin and fibronectin, 839, 841
 molecular structure, 800
 Müller cells, 140–141
 neovascularization, 186, 187
 optic disc, 135–136
 paravascular rarefaction, 187
 PVD, 140
 retinal dystrophy, 186
 retinal ILM, 800
 spider-like bodies, peripheral retina, 185
 type XVIII collagen, 141
 vitreoretinal adhesion, 166
 vitreo-retino-vascular bands, 186
 vitreous body, 799–800
 vitreous liquefaction, 814
 weakening, 140–141
 Weiss ring, 135, 136
- Vitreoretinal physiology
 intraocular oxygen tension (*see* intraocular oxygen tension)
 nuclear sclerotic cataract, 468–469
 oxygen hypothesis, 460
 primary open angle glaucoma, 469–471
 VEGF-mediated retinopathies, 471–473
 vitreous liquefaction, 467–468
- Vitreoretinal scarring
 corticosteroids, 528–529
 retinoic acid, 530
 therapeutic agents, 531
- Vitreoretinal surgery, 634
 AR (*see* Augmented reality (AR))

- femtosecond laser surgery, 704
- internal tamponades, 704
- retinal prosthesis (*see* Retinal prosthesis)
- robotic (*see* Robotic vitreo-retinal surgery)
- Vitreo-retinopathies
 - autosomal dominant vitreo-choroidopathy (ADVIRC), 32
 - brachydactyly, 30
 - COL2A1 related disorders, 27–31
 - corneal changes, 32–33
 - dominant and/or bilateral rhegmatogenous retinal detachment (DRRD / BRRD), 33
 - familial exudative vitreo-retinopathy, 32
 - Goldmann–Favre syndrome/enhanced S-cone dystrophy, 32
 - idiosyncratic alternative splicing, 22
 - Knobloch syndrome, 31
 - prophylaxis, 36–37
 - screening and ancillary investigations, 33
 - skeletal abnormalities, 23
 - Stickler syndrome (*see* Stickler syndrome)
 - Wagner vitreo-retinopathy/erosive vitreo-retinopathy, 31–32
- Vitreo-retinopathy with phalangeal epiphyseal dysplasia (V-PED), 28–30
- Vitreoschisis (VS), 119–123, 132, 146, 289–290, 338, 605, 616
 - Anomalous PVD theory, 316, 317
 - definition, 252
 - description, 267
 - DME, 415–416
 - OCT documentation, 316
 - partial-thickness vitreo-macular traction (*see* Vitreo-macular traction)
 - posterior vitreous cortex, 316
 - PVD, 316, 320
 - splitting, vitreous cortex, 271, 321
 - thickness posterior vitreous cortex, 324
- Vitreosolve[®], 803
- Vitreous. *See also* Posterior vitreous detachment (PVD); Vitreo-maculopathies; Vitreous hemorrhage
 - accommodation (*see* Accommodation)
 - advanced glycation end products, DME, 416
 - aging, 444
 - aqueous pressure, 496
 - attachment in retinal vein occlusion, 415
 - band cutter, 667
 - biochemistry, 64, 242 (*see also* Biochemistry, vitreous)
 - body, 66–69
 - body of rabbits, 865
 - cataract surgery, 719
 - characteristics, 703
 - chondroitinase, as vitreous interfactant (*see* Chondroitinase)
 - collagen fibrils, 831–32
 - collagens (*see* Collagen)
 - condensation and traction, 765
 - cortex, 867
 - crystallin, 414
 - cutter and aspiration systems, 700
 - degeneration, 473
 - description, 288, 772
 - detachment, 415–416, 575, 631
 - developmental stages, 97, 98
 - diabetic vitreopathy (*see* Diabetic vitreopathy)
 - diabetic vitreo-retinopathy, 306
 - dis-insertion, 888
 - diabetic retinopathy, 63
 - dyes, 634
 - ECM and PVD, 800
 - embryology, 22 (*see also* Embryology, vitreous)
 - factors, myopia, 117
 - fibrocellular proliferation, 616
 - fibrovascular proliferations, 631–632
 - fluid portion, 772
 - formation, 101
 - foveal configuration, 837
 - gel liquefaction, 802
 - genetic factors, 800
 - glycoproteins, 831
 - hemorrhage, 630–631, 758–759
 - human/bovine plasmin, 819
 - human eye, 799
 - human vitreous, 17, 70
 - hyaluronan, 818
 - hyaluronic hydrogels, 85
 - ichthyosan V, 17–18
 - ILM, 615
 - infants, 511
 - inflammatory and angiogenic proteins, 411–414
 - inflammatory factors, DME, 416–418
 - instrument, 667
 - intraocular oxygen tension, 460
 - laser surgery, 800
 - liquefaction, 760, 864, 866
 - macular pucker (*see* Macular pucker (MP))
 - membranes, 864
 - microspheres, 517
 - molecular composition, 132
 - molecular level, 817
 - myopic and pseudophakic eyes, 715
 - natural and semisynthetic polymers, 85
 - non-collagenous extracellular matrix components, 9
 - nonpolar gas, 761
 - ocriplasmin, pharmacokinetics, 846–847
 - opacification, 514
 - optic disc, 302, 305
 - pathogenesis, 800
 - pathological paracrine signals, 70
 - pediatric surgery, 700
 - peptic ulcers, 800
 - perifoveal vitreous cortex detachment, 289
 - phakic eyes, 760
 - pharmacologic vitreolysis, 73, 230, 314, 438, 756, 813, 837, 882
 - physiology (*see* Physiology)
 - plasmin injection, 833
 - porcine animal model, 704
 - port size, 700
 - posterior cortex (*see* Posterior vitreous cortex)
 - posterior vitreous cortex, 85
 - prevention and treatment, rhegmatogenous RD, 714
 - PVD, 136, 714, 758
 - rabbit, 517
 - of rabbits, 818
 - and retina, 630
 - retinal disorders, 837
 - and retinal traction, 701
 - in retino-vascular diseases and diabetic macular edema, 63
 - rhegmatogenous RD, 759
 - structure and intravitreal drug delivery, 518–519, 832–833
 - subsequent retinal detachment, 720
 - sulfate-free chondroitin proteoglycan, 17
 - synthetic and smart hydrogels, 85–86
 - three chambers of eye, 496
 - traction, 289
 - veils, 105
 - vitreo-papillary adhesion, 289
 - vitreoretinal interface, 247–248
 - vitreoretinal interface, DME, 416

- Vitreous (*cont.*)
- vitreoschisis, DME, 415–416
 - VMT (*see* Vitreo-macular traction (VMT))
 - voriconazole, 513
- Vitreous aging
- fibrous aggregation, 140
 - gel liquefaction, 854
 - liquefaction, 136–140
 - vitreo-retinal interface weakening, 140–141
 - vitreous base migration, 140
 - VMA (*see* Vitreo-macular adhesion (VMA))
 - VMI (*see* Vitreo-macular interface (VMI))
 - VMT (*see* Vitreo-macular traction (VMT))
- Vitreous base
- circumferential/anterior, 749, 750
 - collagen fibrils, 750
 - scleral buckle, 751
- Vitreous body aging
- “lacunae”, 242
 - liquefaction, 242, 244
 - structural changes, 244–247
- Vitreous catenary theory of Coleman, 498–501
- Vitreous cavity-associated immune deviation (VCAID), 156, 162
- Vitreous congenital disorders, 103–107
- Vitreous development
- cells, 102–103
 - disorders, 103–107
 - hyaloid vascular system, structure, 102
 - hyaloid vasculature, molecular factors, 102
 - molecular changes, 103
- Vitreous fluidics
- intraocular drug delivery, 705
 - magnetic forces, retinal breaks, 704
- Vitreous gel
- age-related liquefaction, 460
 - biophysical properties, 465–467
 - intraocular oxygen tension, 460
 - and liquid vitreous, 465, 466
 - oxygen metabolization, 463–466
- Vitreous hemorrhage
- clearance, 864–866
 - diabetic retinopathy, 630
 - investigator-graded reduction, 866
 - membrane dissection, 638
 - premacular hematoma, 631
 - residual, 865
 - treatment, 866
- Vitreous in AMD. *See* Age-related macular degeneration (AMD)
- Vitreous infusion suction cutter (VISC), 700
- Vitreous liquefaction, 226
- age-related nuclear cataract, 467, 468
 - enzyme types, 825–826
 - grading degree, 465
 - post-vitrectomy nuclear cataract, 467
- Vitreous neovascularization
- activation and involution, 490
 - after PVD, 487–489
 - anterior, 485–487
 - choroidal oxygenation, 483
 - extracellular matrix coupling, 490
 - intraocular neovascularization, 482–483
 - Michaelson’s biochemical mediator, 477–479
 - partial PVD, 485
 - retinal hypoxia, experimental, 479–480
 - retinal vessel occlusions, 480
 - VEGF, 490
 - and vitreoretinal surgery, 485–489
- Vitreous neovascular pathology
- biochemical mediator hypothesis, 478–479
 - experimental retinal hypoxia, 479–480
 - retinal hypoxia, 479
- Vitreous structure
- dark-field slit microscopy, 137–140
 - posterior vitreous cortex, 132–133
 - vitreo-retinal interface, 134–136
 - vitreous base, 133–134
 - vitreous body, 132
- Vitreous substitutes
- after irrigation fluid anterior to perfluorocarbon liquid, 753
 - circumferential traction, 750
 - description, 753
 - inferior relaxing retinotomy, oil-filled eye, 753, 755
 - irrigation fluid trapped anterior to sclerotomies, 753–755
 - long-acting (*see* Long-acting vitreous substitutes)
 - perfluorocarbon fluid, irrigation fluid anterior to, 753
 - short-acting (*see* Short-acting vitreous substitutes)
- Vitreous traction
- cystic degeneration and peripheral retinoschisis, 358–359
 - etiological factor, 385
 - firm vitreo-retinal adhesion, 358
 - macular holes, 386
 - posterior vitreous, 385
 - retinal breaks, 386–387
 - retinal folds, 358
 - retinal pits, 359
 - retinal tags, 358
 - retinal tears, 359–361
 - volume reducing surgery, 386
- VMA. *See* Vitreo-macular adhesion (VMA)
- VMI. *See* Vitreo-macular interface (VMI)
- VMS. *See* Vitreomacular separation (VMS)
- VMT. *See* Vitreo-macular traction (VMT)
- VMTS. *See* Vitreo-macular traction syndrome (VMTS)
- Voleti, V.B., 699–709
- von Graefe, A., 791
- von Helmholtz, H., 496, 497
- von Hippel Lindau, 791
- von Pappenheim, A., 772
- von Pflugk, A., 496
- VPA. *See* Vitreo-papillary adhesion (VPA)
- V-PED. *See* Vitreo-Retinopathy with phalangeal epiphyseal dysplasia (V-PED)
- VPMH. *See* Vitrectomy for prevention of macular hole (VPMH)
- W**
- Wa, C.A., 771–785
- Wagner’s disease, 388
- Wagner syndrome, 9, 31, 32
- Wagner vitreo-retinopathy/erosive vitreo-retinopathy, 31–32
- Wakabayashi, Y., 445
- Wang, J., 248
- Wang, M.Y., 299–308, 580
- Watzke, R.C., 356
- Weber-Krause, B., 330
- Weeks of gestation (WG), 96, 97
- cytoplasmic proteins, 43
 - human embryonic vitreous, 42, 43
- Weiss, J.B., 136, 145, 184
- Weiss, J.N., 654
- Welch, R.B., 253, 358, 361
- Wendel, R.T., 614, 839

Wiethe, T., 791
Wilkinson, C.P., 426, 713–728
Wilkinson, J.L., 117
Williams, G.A., 632, 827
Williams, J.G., 828
Williams, R.L., 546
Winter, M., 544
Wisconsin Epidemiologic Study of Diabetic
Retinopathy (WESDR), 422
Wise, G.N., 480
Witkin, A.J., 591
Wnt signaling pathway, 102, 116, 234
Wollensak, G., 608
Wolter, J.R., 358
Wong, D., 523–532, 537–547
Wong, I.Y., 537–547
Worst, J., 137, 195, 198
Wound repair, 402
Wu, W.C., 839, 842
Wynder, E.L., 785

Y

Yamaji, H., 658
Yamamoto, S., 448
Yang, Y.S., 414
Yee, K.M.P., 41–52, 613–622, 757–766, 771–785
Yoo, S., 505
Yoshimura, T., 414, 417
Yu, A.L., 453
Yura, T., 119

Z

Zehetner, C., 426
Zhang, R., 395–404
Zhao, F., 256
Zimmerman, L.E., 480
Zimmerman, R.L., 249
Zinn, K., 194
Zivojnovic, R., 749
Zonular anatomy, 503